Scientific and Technical Aerospace Reports

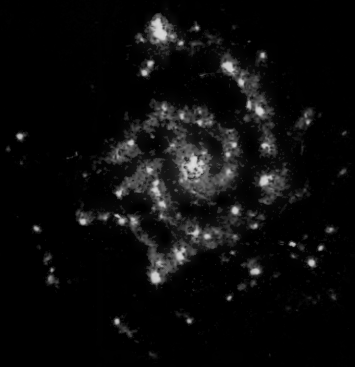

An Abstract Journal

NASA

Volume 33, Number 5
May 1995
N95-17934 to N95-19882

The NASA STI Office ... in Profile

Since its founding, NASA has been dedicated to the advancement of aeronautics and space science. The NASA Scientific and Technical Information (STI) Office plays a key part in helping NASA maintain this important role.

The NASA STI Office provides access to the NASA STI Database, the largest collection of aeronautical and space science STI in the world. The Office is also NASA's institutional mechanism for disseminating the results of its research and development activities.

Specialized services that help round out the Office's diverse offerings include creating custom thesauri, translating material to or from 34 foreign languages, building customized databases, organizing and publishing research results ... even providing videos.

For more information about the NASA STI Office, you can:

- **Phone** the NASA Access Help Desk at (301) 621-0390
- **Fax** your question to the NASA Access Help Desk at (301) 621-0134
- **E-mail** your question via the **Internet** to help@sti.nasa.gov
- **Write** to:

NASA Access Help Desk
NASA Center for AeroSpace Information
800 Elkridge Landing Road
Linthicum Heights, MD 21090-2934

Scientific and Technical Aerospace Reports

Scientific and Technical Aerospace Reports (STAR), is published each month as a major product of the NASA Scientific and Technical Information (STI) Office.

Inside this issue you will find:

- **Front Matter** containing a typical citation and abstract sample explaining the standard format, including codes for ordering reports
- **An Abstract Section** containing citations and abstracts of reports and publications that provide comprehensive coverage of worldwide aerospace-related topics including aeronautics and space science technology. *STAR* lists published and publicly available reports entered into the NASA STI Database during the four weeks preceding publication of this issue. These citations and abstracts are listed by subject categories.
- **An Index Section**
  - Subject
  - Personal author
  - Corporate source
  - Contract number
  - Report number
- **An Appendix** containing a guide for ordering cited reports, registering with the NASA STI Office, and using the available products and services. Additionally, price schedules, phone numbers, and addresses are included in this information packed section.

NASA also sponsors the companion journal, *NASA Open Volumes on Aerospace (NOVA)*, which lists abstracts of the open literature on aerospace subjects available worldwide. *NOVA* is for internal NASA use only, available from the NASA Center for AeroSpace Information (CASI).

Entries found in *STAR* are available through the NASA online retrieval service, RECON, and through DIALOG as the Aerospace Database.

The NASA STI Office gathers information through national and international agreements and exchanges and makes this information available to the NASA community and to the public in many forms through various outlets.

For additional information on the NASA STI Office, call the NASA Access Help Desk at (301) 621-0390, or write to:

NASA Center for AeroSpace Information
800 Elkridge Landing Road
Linthicum Heights, Maryland 21090-2934

US ISSN 0036-8741

This publication was prepared by the NASA Center for AeroSpace Information,
800 Elkridge Landing Road, Linthicum Heights, MD 21090-2934, (301) 621-0390.

Volume 33 Number 5 / May 1995

TABLE OF CONTENTS

AERONAUTICS For related information see also *Astronautics.*

01 AERONAUTICS (GENERAL) **927**

02 AERODYNAMICS **928**
Includes aerodynamics of bodies, combinations, wings, rotors, and control surfaces; and internal flow in ducts and turbomachinery. For related information see also *34 Fluid Mechanics and Heat Transfer.*

03 AIR TRANSPORTATION AND SAFETY **933**
Includes passenger and cargo air transport operations; and aircraft accidents. For related information see also *16 Space Transportation* and *85 Urban Technology and Transportation.*

04 AIRCRAFT COMMUNICATIONS AND NAVIGATION **940**
Includes digital and voice communication with aircraft; air navigation systems (satellite and ground based); and air traffic control. For related information see also *17 Space Communications, Spacecraft Communications, Command and Tracking* and *32 Communications and Radar.*

05 AIRCRAFT DESIGN, TESTING AND PERFORMANCE **941**
Includes aircraft simulation technology. For related information see also *18 Spacecraft Design, Testing and Performance* and *39 Structural Mechanics.* For land transportation vehicles see *85 Urban Technology and Transportation.*

06 AIRCRAFT INSTRUMENTATION **947**
Includes cockpit and cabin display devices; and flight instruments. For related information see also *19 Spacecraft Instrumentation* and *35 Instrumentation and Photography.*

07 AIRCRAFT PROPULSION AND POWER **947**
Includes prime propulsion systems and systems components, e.g., gas turbine engines and compressors; and onboard auxiliary power plants for aircraft. For related information see also *20 Spacecraft Propulsion and Power, 28 Propellants and Fuels,* and *44 Energy Production and Conversion.*

08 AIRCRAFT STABILITY AND CONTROL **956**
Includes aircraft handling qualities; piloting; flight controls; and autopilots. For related information see also *05 Aircraft Design, Testing and Performance.*

09 RESEARCH AND SUPPORT FACILITIES (AIR) **958**
Includes airports, hangars and runways; aircraft repair and overhaul facilities; wind tunnels; shock tubes; and aircraft engine test stands. For related information see also *14 Ground Support Systems and Facilities (Space).*

ASTRONAUTICS For related information see also *Aeronautics.*

12 ASTRONAUTICS (GENERAL) **961**
For extraterrestrial exploration see *91 Lunar and Planetary Exploration.*

13 ASTRODYNAMICS **961**
Includes powered and free-flight trajectories; and orbital and launching dynamics.

14 GROUND SUPPORT SYSTEMS AND FACILITIES (SPACE) ..... **N.A.**
Includes launch complexes, research and production facilities; ground support equipment, e.g., mobile transporters; and simulators. For related information see also *09 Research and Support Facilities (Air).*

15 LAUNCH VEHICLES AND SPACE VEHICLES **962**
Includes boosters; operating problems of launch/space vehicle systems; and reusable vehicles. For related information see also *20 Spacecraft Propulsion and Power.*

16 SPACE TRANSPORTATION **963**
Includes passenger and cargo space transportation, e.g., shuttle operations; and space rescue techniques. For related information see also *03 Air Transportation and Safety* and *18 Spacecraft Design, Testing and Performance.* For space suits see *54 Man/System Technology and Life Support.*

17 SPACE COMMUNICATIONS, SPACECRAFT COMMUNICATIONS, COMMAND AND TRACKING ..... **N.A.**
Includes telemetry; space communications networks; astronavigation and guidance; and radio blackout. For related information see also *04 Aircraft Communications and Navigation* and *32 Communications and Radar.*

N.A.—No abstracts were assigned to this category for this issue.

18 SPACECRAFT DESIGN, TESTING AND PERFORMANCE **963**
Includes satellites; space platforms; space stations; spacecraft systems and components such as thermal and environmental controls; and attitude controls. For life support systems see *54 Man/System Technology and Life Support.* For related information see also *05 Aircraft Design, Testing and Performance*, *39 Structural Mechanics*, and *16 Space Transportation.*

19 SPACECRAFT INSTRUMENTATION **966**
For related information see also *06 Aircraft Instrumentation* and *35 Instrumentation and Photography.*

20 SPACECRAFT PROPULSION AND POWER **966**
Includes main propulsion systems and components, e.g., rocket engines; and spacecraft auxiliary power sources. For related information see also *07 Aircraft Propulsion and Power*, *28 Propellants and Fuels*, *44 Energy Production and Conversion*, and *15 Launch Vehicles and Space Vehicles.*

CHEMISTRY AND MATERIALS

23 CHEMISTRY AND MATERIALS (GENERAL) **969**

24 COMPOSITE MATERIALS **969**
Includes physical, chemical, and mechanical properties of laminates and other composite materials. For ceramic materials see *27 Nonmetallic Materials.*

25 INORGANIC AND PHYSICAL CHEMISTRY **973**
Includes chemical analysis, e.g., chromatography; combustion theory; electrochemistry; and photochemistry. For related information see also *77 Thermodynamics and Statistical Physics.*

26 METALLIC MATERIALS **977**
Includes physical, chemical, and mechanical properties of metals, e.g., corrosion; and metallurgy.

27 NONMETALLIC MATERIALS **983**
Includes physical, chemical, and mechanical properties of plastics, elastomers, lubricants, polymers, textiles, adhesives, and ceramic materials. For composite materials see *24 Composite Materials.*

28 PROPELLANTS AND FUELS **990**
Includes rocket propellants, igniters and oxidizers; their storage and handling procedures; and aircraft fuels. For related information see also *07 Aircraft Propulsion and Power*, *20 Spacecraft Propulsion and Power*, and *44 Energy Production and Conversion.*

29 MATERIALS PROCESSING **990**
Includes space-based development of products and processes for commercial application. For biological materials see *55 Space Biology:*

ENGINEERING For related information see also *Physics.*

31 ENGINEERING (GENERAL) **991**
Includes vacuum technology; control engineering; display engineering; cryogenics; and fire prevention.

32 COMMUNICATIONS AND RADAR **994**
Includes radar; land and global communications; communications theory; and optical communications. For related information see also *04 Aircraft Communications and Navigation* and *17 Space Communications, Spacecraft Communications, Command and Tracking.* For search and rescue see *03 Air Transportation and Safety*, and *16 Space Transportation.*

33 ELECTRONICS AND ELECTRICAL ENGINEERING **1007**
Includes test equipment and maintainability; components, e.g., tunnel diodes and transistors; microminiaturization; and integrated circuitry. For related information see also *60 Computer Operations and Hardware* and *76 Solid-State Physics.*

34 FLUID MECHANICS AND HEAT TRANSFER **1014**
Includes boundary layers; hydrodynamics; fluidics; mass transfer and ablation cooling. For related information see also *02 Aerodynamics* and *77 Thermodynamics and Statistical Physics.*

35 INSTRUMENTATION AND PHOTOGRAPHY **1031**
Includes remote sensors; measuring instruments and gauges; detectors; cameras and photographic supplies; and holography. For aerial photography see *43 Earth Resources and Remote Sensing.* For related information see also *06 Aircraft Instrumentation* and *19 Spacecraft Instrumentation.*

36 LASERS AND MASERS **1036**
Includes parametric amplifiers. For related information see also *76 Solid-State Physics.*

37 MECHANICAL ENGINEERING **1040**
Includes auxiliary systems (nonpower); machine elements and processes; and mechanical equipment.

38 QUALITY ASSURANCE AND RELIABILITY **1043**
Includes product sampling procedures and techniques; and quality control.

39 STRUCTURAL MECHANICS **1044**
Includes structural element design and weight analysis; fatigue; and thermal stress. For applications see *05 Aircraft Design, Testing and Performance* and *18 Spacecraft Design, Testing and Performance.*

GEOSCIENCES For related information see also *Space Sciences.*

42 GEOSCIENCES (GENERAL) **1049**

43 EARTH RESOURCES AND REMOTE SENSING **1049**
Includes remote sensing of earth resources by aircraft and spacecraft; photogrammetry; and aerial photography. For instrumentation see *35 Instrumentation and Photography.*

44 ENERGY PRODUCTION AND CONVERSION **1052**
Includes specific energy conversion systems, e.g., fuel cells; global sources of energy; geophysical conversion; and windpower. For related information see also *07 Aircraft Propulsion and Power, 20 Spacecraft Propulsion and Power,* and *28 Propellants and Fuels.*

45 ENVIRONMENT POLLUTION **1056**
Includes atmospheric, noise, thermal, and water pollution.

46 GEOPHYSICS **1063**
Includes aeronomy; upper and lower atmosphere studies; ionospheric and magnetospheric physics; and geomagnetism. For space radiation see *93 Space Radiation.*

47 METEOROLOGY AND CLIMATOLOGY **1066**
Includes weather forecasting and modification.

48 OCEANOGRAPHY **1073**
Includes biological, dynamic, and physical oceanography; and marine resources. For related information see also *43 Earth Resources and Remote Sensing.*

LIFE SCIENCES

51 LIFE SCIENCES (GENERAL) **1076**

52 AEROSPACE MEDICINE **1077**
Includes physiological factors; biological effects of radiation; and effects of weightlessness on man and animals.

53 BEHAVIORAL SCIENCES **1088**
Includes psychological factors; individual and group behavior; crew training and evaluation; and psychiatric research.

54 MAN/SYSTEM TECHNOLOGY AND LIFE SUPPORT **1090**
Includes human engineering; biotechnology; and space suits and protective clothing. For related information see also *16 Space Transportation.*

55 SPACE BIOLOGY **1092**
Includes exobiology; planetary biology; and extraterrestrial life.

MATHEMATICAL AND COMPUTER SCIENCES

59 MATHEMATICAL AND COMPUTER SCIENCES (GENERAL) ..... **N.A.**

60 COMPUTER OPERATIONS AND HARDWARE **1092**
Includes hardware for computer graphics, firmware, and data processing. For components see *33 Electronics and Electrical Engineering.*

61 COMPUTER PROGRAMMING AND SOFTWARE **1093**
Includes computer programs, routines, algorithms, and specific applications, e.g., CAD/CAM.

62 COMPUTER SYSTEMS **1108**
Includes computer networks and special application computer systems.

63 CYBERNETICS **1112**
Includes feedback and control theory, artificial intelligence, robotics and expert systems. For related information see also *54 Man/System Technology and Life Support.*

64 NUMERICAL ANALYSIS **1116**
Includes iteration, difference equations, and numerical approximation.

65 STATISTICS AND PROBABILITY **1120**
Includes data sampling and smoothing; Monte Carlo method; and stochastic processes.

66 SYSTEMS ANALYSIS ..... **N.A.**
Includes mathematical modeling; network analysis; and operations research.

67 THEORETICAL MATHEMATICS **1121**
Includes topology and number theory.

PHYSICS For related information see also *Engineering.*

70 PHYSICS (GENERAL) **1122**
For precision time and time interval (PTTI) see *35 Instrumentation and Photography*; for geophysics, astrophysics or solar physics see *46 Geophysics, 90 Astrophysics*, or *92 Solar Physics.*

71 ACOUSTICS **1123**
Includes sound generation, transmission, and attenuation. For noise pollution see *45 Environment Pollution.*

72 ATOMIC AND MOLECULAR PHYSICS **1129**
Includes atomic structure, electron properties, and molecular spectra.

73 NUCLEAR AND HIGH-ENERGY PHYSICS **1135**
Includes elementary and nuclear particles; and reactor theory. For space radiation see *93 Space Radiation.*

74 OPTICS **1138**
Includes light phenomena and optical devices. For lasers see *36 Lasers and Masers.*

75 PLASMA PHYSICS **1145**
Includes magnetohydrodynamics and plasma fusion. For ionospheric plasmas see *46 Geophysics.* For space plasmas see *90 Astrophysics.*

76 SOLID-STATE PHYSICS **1148**
Includes superconductivity. For related information see also *33 Electronics and Electrical Engineering* and *36 Lasers and Masers.*

77 THERMODYNAMICS AND STATISTICAL PHYSICS **1155**
Includes quantum mechanics; theoretical physics; and Bose and Fermi statistics. For related information see also *25 Inorganic and Physical Chemistry* and *34 Fluid Mechanics and Heat Transfer.*

SOCIAL SCIENCES

80 SOCIAL SCIENCES (GENERAL) **1157**
Includes educational matters.

81 ADMINISTRATION AND MANAGEMENT **1170**
Includes management planning and research.

82 DOCUMENTATION AND INFORMATION SCIENCE **1172**
Includes information management; information storage and retrieval technology; technical writing; graphic arts; and micrography. For computer documentation see *61 Computer Programming and Software.*

83 ECONOMICS AND COST ANALYSIS ..... **N.A.**
Includes cost effectiveness studies.

84 LAW, POLITICAL SCIENCE AND SPACE POLICY ..... **N.A.**
Includes NASA appropriation hearings; aviation law; space law and policy; international law; international cooperation; and patent policy.

85 URBAN TECHNOLOGY AND TRANSPORTATION ..... **N.A.**
Includes applications of space technology to urban problems; technology transfer; technology assessment; and surface and mass transportation. For related information see *03 Air Transportation and Safety, 16 Space Transportation,* and *44 Energy Production and Conversion.*

SPACE SCIENCES For related information see also *Geosciences.*

88 SPACE SCIENCES (GENERAL) ..... **N.A.**

89 ASTRONOMY **1177**
Includes radio, gamma-ray, and infrared astronomy; and astrometry.

90 ASTROPHYSICS **1178**
Includes cosmology; celestial mechanics; space plasmas; and interstellar and interplanetary gases and dust. For related information see also *75 Plasma Physics.*

91 LUNAR AND PLANETARY EXPLORATION **1194**
Includes planetology; and manned and unmanned flights. For spacecraft design or space stations see *18 Spacecraft Design, Testing and Performance.*

92 SOLAR PHYSICS **1195**
Includes solar activity, solar flares, solar radiation and sunspots. For related information see also *93 Space Radiation.*

93 SPACE RADIATION **1197**
Includes cosmic radiation; and inner and outer earth's radiation belts. For biological effects of radiation see *52 Aerospace Medicine.* For theory see *73 Nuclear and High-Energy Physics.*

GENERAL

Includes aeronautical, astronautical, and space science related histories, biographies, and pertinent reports too broad for categorization; histories or broad overviews of NASA programs.

99 GENERAL **1198**

SUBJECT INDEX **I-1**

PERSONAL AUTHOR INDEX **I-117**

CORPORATE SOURCE INDEX **I-129**

CONTRACT NUMBER INDEX **I-149**

REPORT NUMBER INDEX **I-153**

APPENDIX **A-1**

TYPICAL CITATION AND ABSTRACT

NASA SPONSORED — ON MICROFICHE

ACCESSION NUMBER → **N95-10148*#** National Aeronautics and Space Administration. Lewis Research Center, Cleveland, OH. ← CORPORATE SOURCE

TITLE → **EFFECTS OF A FORWARD-SWEPT FRONT ROTOR ON THE FLOWFIELD OF A COUNTERROTATION PROPELLER**

AUTHORS → M. Nallasamy (NYMA, Inc., Brook Park, OH.) and Gary G. Podboy Aug. 1994 19 p Presented at the 30th Joint Propulsion Conference, Indianapolis, IN, 27-29 Jun. 1994; sponsored by AIAA, ASME, SAE, and ASEE ← PUBLICATION DATE

CONTRACT OR GRANT → (Contract NAS3-27186; RTOP 538-03-11)

REPORT NUMBERS → (NASA-TM-106671; E-8994; NAS 1.15:106671; AIAA Paper 94-2694) Avail: CASI HC A03/MF A01; 6 functional color pages ← AVAILABILITY SOURCE AND PRICE CODE

The effects of a forward-swept front rotor on the flowfield of a counterrotation model propeller at takeoff conditions at zero degree angle of attack are studied by solving the unsteady three-dimensional Euler equations. The configuration considered is an uneven blade count counterrotation model with twelve forward-swept blades on the fore rotor and ten aft-swept blades on the aft rotor. The flowfield is compared with that of a reference aft-swept counterrotation geometry and Laser Doppler Velocimeter (LDV) measurements. At the operating conditions considered, the forward-swept blade experiences a higher tip loading and produces a stronger tip vortex compared to the aft-swept blade, consistent with the LDV and acoustic measurements. Neither the solution nor the LDV data indicated the formation of a leading edge vortex. The predicted radial distribution of the circumferentially averaged axial velocity at the measurement station agreed very closely with LDV data, while crossflow velocities showed poor agreement. The discrepancy between prediction and LDV data of tangential and radial velocities is due in part to the insufficient mesh resolution in the region between the rotors and in the tip region to track the tip vortex. The vortex is diffused by the time it arrives at the measurement station. The uneven blade count configuration requires the solution to be carried out for six blade passages of the fore rotor and five passages of the aft rotor, thus making grid refinement prohibitive.

Author

VOLUME 33 NUMBER 5 / May 1995

Scientific and Technical Aerospace Reports

A Monthly Publication of the National Aeronautics and Space Administration

01 AERONAUTICS (GENERAL)

N95-18044*# Rocket Research Corp., Redmond, WA.
ARCJET THRUSTER RESEARCH AND TECHNOLOGY, PHASE 2 Final Report, Mar. 1987 - Feb. 1990
Steve E. Yano Cleveland, OH NASA Mar. 1991 254 p
(Contract NAS3-24631; RTOP 506-42-31)
(NASA-CR-182276; E-9332; NAS 1.26:182276; Rept-91-R-1475) Avail: CASI HC A12/MF A03

The principle objective of Phase 2 was to produce an engineering model N2H4 arcjet system which met typical performance, lifetime, environmental, and interface specifications required to support a 10-year N-S stationkeeping mission for a communications spacecraft. The system includes an N2H4 arcjet thruster, power conditioning unit (PCU), and the interconnecting power cable assembly. This objective was met with the successful conclusion of an extensive system test series.
Derived from text

N95-18197*# National Aeronautics and Space Administration. Lewis Research Center, Cleveland, OH.
MICROGRAVITY ISOLATION SYSTEM DESIGN: A MODERN CONTROL SYNTHESIS FRAMEWORK
R. D. Hampton (McNeese State Univ., Lake Charles, LA.), C. R. Knospe (Virginia Univ., Charlottesville, VA.), P. E. Allaire (Virginia Univ., Charlottesville, VA.), and C. M. Grodsinsky Dec. 1994 34 p Sponsored by Commonwealth of Virginia's Center for Innovative Technology
(Contract NCC3-365; RTOP 963-70-OH)
(NASA-TM-106805; E-9283; NAS 1.15:106805) Avail: CASI HC A03/MF A01

Manned orbiters will require active vibration isolation for acceleration-sensitive microgravity science experiments. Since umbilicals are highly desirable or even indispensable for many experiments, and since their presence greatly affects the complexity of the isolation problem, they should be considered in control synthesis. A general framework is presented for applying extended H2 synthesis methods to the three-dimensional microgravity isolation problem. The methodology integrates control and state frequency weighting and input and output disturbance accommodation techniques into the basic H2 synthesis approach. The various system models needed for design and analysis are also presented. The paper concludes with a discussion of a general design philosophy for the microgravity vibration isolation problem. Author

N95-18486*# National Aeronautics and Space Administration. Lewis Research Center, Cleveland, OH.
MICROGRAVITY ISOLATION SYSTEM DESIGN: A MODERN CONTROL ANALYSIS FRAMEWORK
R. D. Hampton (McNeese State Univ., Lake Charles, LA.), C. R. Knospe (Virginia Univ., Charlottesville, VA.), P. E. Allaire (Virginia Univ., Charlottesville, VA.), and C. M. Grodsinsky Dec. 1994 36 p Sponsored by Commonwealth of Virginia's Center for Innovative Technology
(Contract NCC3-365; RTOP 963-70-OH)
(NASA-TM-106803; E-9281; NAS 1.15:106803) Avail: CASI HC A03/MF A01

Many acceleration-sensitive, microgravity science experiments will require active vibration isolation from the manned orbiters on which they will be mounted. The isolation problem, especially in the case of a tethered payload, is a complex three-dimensional one that is best suited to modern-control design methods. These methods, although more powerful than their classical counterparts, can nonetheless go only so far in meeting the design requirements for practical systems. Once a tentative controller design is available, it must still be evaluated to determine whether or not it is fully acceptable, and to compare it with other possible design candidates. Realistically, such evaluation will be an inherent part of a necessary iterative design process. In this paper, an approach is presented for applying complex mu-analysis methods to a closed-loop vibration isolation system (experiment plus controller). An analysis framework is presented for evaluating nominal stability, nominal performance, robust stability, and robust performance of active microgravity isolation systems, with emphasis on the effective use of mu-analysis methods. Author

N95-18606# National Aerospace Lab., Bangalore (India). Structural Integrity Div.
AGEING NUCLEAR POWER PLANT MANAGEMENT: AN AERONAUTICAL VIEWPOINT
R. Sunder Oct. 1993 15 p Presented at the 77th Meeting of the AGARD Structures and Materials Panel, Bordeaux, France, Sep. 1993
(NAL-PD-SN-9306) Avail: CASI HC A03/MF A01

Aircraft like nuclear power plants are extremely safety critical. Aircraft development programs have evolved over many decades and the standards governing their evolution are reasonably well established. This paper attempts to describe ASIP (Aircraft Structural Integrity Program) and ENSIP (Engine Structural Integrity Program) standards for airframes and aeroengines and how their background may interest specialists in the design, development and operation of nuclear power plant facilities including the management of ageing plants. The accent of ASIP ENSIP is on inspectability and fail-safety to enable maintenance on condition. Author

N95-19168* National Aeronautics and Space Administration, Washington, DC.
AERONAUTICAL ENGINEERING: A CONTINUING BIBLIOGRAPHY WITH INDEXES (SUPPLEMENT 313)
Jan. 1995 76 p
(NASA-SP-7037(313); NAS 1.21:7037(313)) Avail: CASI HC A05

This bibliography lists 179 reports, articles, and other documents introduced into the NASA scientific and technical information system in Jan. 1995. Subject coverage includes: engineering and theoretical aspects of design, construction, evaluation, testing, operation, and performance of aircraft (including aircraft engines) and associated components, equipment, and systems. It also includes research and development in aerodynamics, aeronautics, and ground support equipment for aeronautical vehicles.
CASI

N95-19357* National Aeronautics and Space Administration, Washington, DC.
AERONAUTICAL ENGINEERING: A CONTINUING BIBLIOGRAPHY WITH INDEXES (SUPPLEMENT 314)
Feb. 1995 71 p
(NASA-SP-7037(314); NAS 1.21:7037(314)) Avail: CASI HC A04

This bibliography lists 144 reports, articles, and other documents introduced into the NASA scientific and technical information system in Feb. 1995. Subject coverage includes: design, construction and testing of aircraft and aircraft engines; aircraft components, equipment, and systems; ground support systems; and theoretical and applied aspects of aerodynamics and general fluid dynamics. Author

02 AERODYNAMICS

Includes aerodynamics of bodies, combinations, wings, rotors, and control surfaces; and internal flow in ducts and turbomachinery.

For related information see also *34 Fluid Mechanics and Heat Transfer.*

N95-18101*# National Aeronautics and Space Administration. Ames Research Center, Moffett Field, CA.

PARAMETRIC STUDY ON LAMINAR FLOW FOR FINITE WINGS AT SUPERSONIC SPEEDS

Joseph Avila Garcia Dec. 1994 101 p

(RTOP 537-07-00)

(NASA-TM-108852; A-94146; NAS 1.15:108852) Avail: CASI HC A06/MF A02

Laminar flow control has been identified as a key element in the development of the next generation of High Speed Transports. Extending the amount of laminar flow over an aircraft will increase range, payload, and altitude capabilities as well as lower fuel requirements, skin temperature, and therefore the overall cost. A parametric study to predict the extent of laminar flow for finite wings at supersonic speeds was conducted using a computational fluid dynamics (CFD) code coupled with a boundary layer stability code. The parameters investigated in this study were Reynolds number, angle of attack, and sweep. The results showed that an increase in angle of attack for specific Reynolds numbers can actually delay transition. Therefore, higher lift capability, caused by the increased angle of attack, as well as a reduction in viscous drag, due to the delay in transition, can be expected simultaneously. This results in larger payload and range.

Author

N95-18337 Department of the Navy, Washington, DC.

CORNER VORTEX SUPPRESSOR Patent

Promode R. Bandyopadhyay, inventor (to Navy) 19 Apr. 1994 6 p Filed 22 Feb. 1993. Supersedes AD-D015772

(AD-D016423; US-Patent-5,303,882; US-Patent-Appl-SN-020940; US-Patent-Class-244-130) Avail: US Patent and Trademark Office

A corner vortex forms at the corners of a square or rectangular wind tunnel or water tunnel and disrupts the flow and creates excessive drag, turbulence, noise and wake. The corners defined by a wing/fuselage interface creates the same type of situation. The suppressor provides many small corners to prevent forming of the single large vortex. A honeycomb or mesh provides parallel passageways, each having a size that is a fraction (1/5th to 1/10th) of the depth of the boundary layer (defined as that point in the fluid flow where the velocity is 99% of free stream velocity. DTIC

N95-18340# Army Natick Research and Development Command, MA. Engineering Center.

PARACHUTE INFLATION: A PROBLEM IN AEROELASTICITY Final Report

Keith R. Stein and Richard J. Benney Aug. 1994 86 p

(DA Proj. 1L1-62786-D-283; DA Proj. 1L1-61102-AH-52)

(AD-A284375) Avail: CASI HC A05/MF A01

In parachute research, canopy inflation is the least understood and most complex process to model. Unfortunately, it is during the opening process that the canopy experiences the largest deformations and loadings. The complexity of modeling the opening process stems from the coupling between the structural dynamics of the canopy, lines plus payload and the aerodynamics of the surrounding fluid medium. The addition of a computational capability to model the coupled opening behavior would greatly assist in understanding the canopy inflation process. Ongoing research at the U.S. Army Natick Research, Development and Engineering Center (Natick) focuses on this coupled problem. The solution to this problem will assist in the development of future U.S. Army airdrop systems, which include the capability of deploying at low altitudes and high speeds. This report describes research at Natick that currently involves coupling a computational fluid dynamics (CFD) code to a mass spring damper (MSD) parachute structural code. The model is described and results are presented. DTIC

N95-18380 Lockheed Corp., Fort Worth, TX.

OVERVIEW OF UNSTEADY TRANSONIC WIND TUNNEL TEST ON A SEMISPAN STRAKED DELTA WING OSCILLATING IN PITCH Final Report, Mar. 1989 - Dec. 1993

Atlee M. Cunningham, Jr. and Ruud G. Den Boer Aug. 1994 57 p Limited Reproducibility: More than 20% of this document may be affected by microfiche quality

(AF Proj. 2401)

(AD-A284097; WL-TR-94-3017) Avail: Issuing Activity (Defense Technical Information Center (DTIC))

A wind tunnel investigation was conducted in 1992 to investigate the unsteady aerodynamic aspects of transonic high incidence flows over a simple straked wing model. This test was designed to show how low speed vortex type flows evolve into complicated shock vortex interacting flows at transonic speeds. Requirements for this test were based on a low speed test conducted in 1986 on a full span model in the NLR Low Speed Tunnel. The transonic model was a semispan version of the low speed model with some modifications. It was equipped with a three-component semispan balance to measure total wing loads, seven rows of high response pressure transducers to measure unsteady pressures and 15 vertical accelerometers to measure model motion and vibrations. The model was oscillated sinusoidally in pitch at various amplitudes and frequencies for mean model incidences varying from 4 deg to 48 deg. In addition, maneuver type transient motions of the model were tested with amplitudes of 16 deg and 30 deg total rotation at various starting angles. The test was conducted in the NLR HST in the Mach range of 0.225 to 0.90 with some preliminary vapor screen flow visualization data taken at M=0.6 and 0.9. DTIC

N95-18457*# National Aeronautics and Space Administration. Lewis Research Center, Cleveland, OH.

MEASUREMENT OF GUST RESPONSE ON A TURBINE CASCADE

A. P. Kurkov and B. L. Lucci Jan. 1995 12 p Presented at the Turbo Expo 1995, Houston, TX, 5-8 Jun. 1995; sponsored by the ASME

(RTOP 505-63-5B)

(NASA-TM-106776; E-9227; NAS 1.15:106776) Avail: CASI HC A03/MF A01

The paper presents benchmark experimental data on a gust response of an annular turbine cascade. The experiment was particularly designed to provide data for comparison with the results of a typical linearized gust-response analysis. Reduced frequency, Mach number, and incidence were varied independently. Except for the lowest reduced frequency, the gust velocity distribution was nearly sinusoidal. For the high inlet-velocity series of tests, the cascade was near choking. The mean flow was documented by measuring blade surface pressures and the cascade exit flow. High-response pressure transducers were used to measure the unsteady pressure distribution. Inlet-velocity components and turbulence parameters were measured using hot wire. In addition to the synchronous time-average pressure spectra, typical power spectra are included for several representative conditions. Author

N95-18503 National Aerospace Lab., Amsterdam (Netherlands).

SECTIONAL PREDICTION OF 3D EFFECTS FOR SEPARATED FLOW ON ROTATING BLADES

H. Snel, R. Houwink, and W. J. Piers 1992 31 p Limited Reproducibility: More than 20% of this document may be affected by microfiche quality

(PB94-201696; NLR-TP-92409-U) Avail: Issuing Activity (National Technical Information Service (NTIS))

A method is presented which allows the computation of air load coefficients for rotor blade sections at attached and separated flow conditions, including leading effects of blade rotation. The method consists of an existing computer code for 2D unsteady flow with strong viscous-inviscid interaction, in which the turbulent boundary layer integral method has been modified by including leading terms for steady 3D effects on a high aspect ratio rotating blade. A summary is presented of the approach made, and a first set of results are compared with wind-tunnel data for a wind-turbine model. Computed 2D polars and corresponding pressure distributions for a nonrotating and rotating blade section appear to be qualitatively similar to experimental data, including high values of the lift coefficient measured at 30% of the tip radius. For sufficient accuracy in practice, however, various aspects of the method need further analysis and improvement. NTIS

N95-18539 Advisory Group for Aerospace Research and Development, Neuilly-Sur-Seine (France). Fluid Dynamics Panel.
A SELECTION OF EXPERIMENTAL TEST CASES FOR THE VALIDATION OF CFD CODES. SUPPLEMENT: DATASETS A-E (Diskette Supplement)
Aug. 1994 See also N95-14201 and N95-17846 Diskette supplement: nine 3.5-inch DSHD diskettes
(AGARD-AR-303-Suppl; NONP-AGARD-Suppl-VT-95-38380) Copyright Avail: CASI DK A18

Relevant data of all 39 test cases for the validation of Computational Fluid Dynamics (CFD) codes by Working Group 14 of the AGARD Fluid Dynamics Panel is compiled on these 9 diskettes to accompany Volumes 1 and 2 of the report. The test cases cover the subsonic, transonic, and supersonic flow regimes. CASI

N95-18565*# National Aeronautics and Space Administration. Hugh L. Dryden Flight Research Facility, Edwards, CA.
IN-FLIGHT LIFT-DRAG CHARACTERISTICS FOR A FORWARD-SWEPT WING AIRCRAFT AND COMPARISONS WITH CONTEMPORARY AIRCRAFT)
Edwin J. Saltzman (PRC Kentron, Inc., Edwards, CA.), John W. Hicks, and Sue Luke, ed. Washington Dec. 1994 61 p
(RTOP 505-68-50)
(NASA-TP-3414; H-1913; NAS 1.60:3414) Avail: CASI HC A04/MF A01

Lift (L) and drag (D) characteristics have been obtained in flight for the X-29A airplane (a forward swept-wing demonstrator) for Mach numbers (M) from 0.4 to 1.3. Most of the data were obtained near an altitude of 30,000 ft. A representative Reynolds number for M = 0.9, and a pressure altitude of 30,000 ft, is 18.6 x 10(exp 6) based on the mean aerodynamic chord. The X-29A data (forward-swept wing) are compared with three high-performance fighter aircraft: the F-15C, F-16C, and F/A18. The lifting efficiency of the X-29A, as defined by the Oswald lifting efficiency factor, e, is about average for a cantilevered monoplane for M = 0.6 and angles of attack up to those required for maximum L/D. At M = 0.6 the level of L/D and e, as a function of load factor, for the X-29A was about the same as for the contemporary aircraft. The X-29A and its contemporaries have high transonic wave drag and equivalent parasite area compared with aircraft of the 1940's through 1960's. Author

N95-18611# Army Research Lab., Aberdeen Proving Ground, MD.
STATIC AERODYNAMICS CFD ANALYSIS FOR 120-mm HYPERSONIC KE PROJECTILE DESIGN Final Report, Sep. 1992 - Apr. 1994
Bernard J. Guidos Sep. 1994 37 p
(DA Proj. 1L1-62618-AH-80)
(ARL-MR-184) Avail: CASI HC A03/MF A01

Computational fluid dynamics (CFD) predictions of static aerodynamic coefficients for large caliber (120 mm) M829-like come-cylinder-flare kinetic energy (KE) projectile shapes are presented. Zero-yaw drag and static pitch-plane aerodynamic coefficients are presented for velocities in the range 1.5 to 3.0 km/sec for several flare angles. The aerodynamic coefficients are required to assess the velocity retardation and static stability of candidate configurations that use the M829 projectile as a basis for design. Comparisons of the aerodynamic coefficients are made with those of the fielded M829 projectile, and a preliminary evaluation is made of the performance of these shapes in hypersonic flight. Author

N95-18624# Federal Aviation Administration, Cambridge, MA. National Transportation Systems Center.
AIRCRAFT WAKE VORTEX TAKEOFF TESTS AT O'HARA INTERNATIONAL AIRPORT Final Report, Feb. - May 1992
J. Yarmus, D. Burnham, A. Wright, and T. Talbot Aug. 1994 88 p
(AD-A283828; DOT-VNTSC-FAA-94-12; DOT/FAA/RD-94-25) Avail: CASI HC A05/MF A01

Three wake vortex measurement systems (anemometer, acoustic doppler, and laser doppler) were used to collect wake vortex data from aircraft departing Runway 22L at Chicago's O'Hare Airport for nine months in 1980. The data were analyzed to determine vortex decay and vortex transport probabilities. The results support the classification of all B-707 and DC-8 aircraft in the large wake vortex class. The acoustic doppler system was found to be significantly more sensitive than the ground anemometer system to vortices transported long distances laterally by a crosswind. The most efficient lateral transport was noted for crosswinds greater than seven knots. The horizontal and vertical ground wind signatures of a wake vortex are compared. DTIC

N95-18645# National Renewable Energy Lab., Golden, CO.
WIND TURBINE BLADE AERODYNAMICS: THE COMBINED EXPERIMENT
M. C. Robinson (Colorado Univ., Boulder, CO.), M. W. Luttges (Colorado Univ., Boulder, CO.), M. S. Miller (Colorado Univ., Boulder, CO.), D. E. Shipley (Colorado Univ., Boulder, CO.), and T. S. Young (Colorado Univ., Boulder, CO.) Aug. 1994 10 p Presented at the Windpower 1993, San Francisco, CA, 12-16 Jul. 1993
(Contract DE-AC36-83CH-10093)
(DE94-011866; NREL/TP-441-7107; CONF-930726-8) Avail: CASI HC A02/MF A01

Data obtained from the National Renewable Energy Laboratory site test of a wind turbine (The Combined Experiment) was analyzed specifically to capture information regarding the aerodynamic loading experienced by such machines. The analysis showed that inflow conditions were extremely variable and that these inflows yielded three different operational regimes. Each regime produces very different aerodynamic loading conditions that must be tolerated by the turbine. The two conditions not predicted from wind tunnel data are being subjected to further analyses to provide new guidelines for both designers and operators. Author

N95-18646# National Renewable Energy Lab., Golden, CO.
WIND TURBINE BLADE AERODYNAMICS: THE ANALYSIS OF FIELD TEST DATA
M. W. Luttges (Colorado Univ., Boulder, CO.), M. S. Miller (Colorado Univ., Boulder, CO.), M. C. Robinson (Colorado Univ., Boulder, CO.), D. E. Shipley (Colorado Univ., Boulder, CO.), and T. S. Young (Colorado Univ., Boulder, CO.) Aug. 1994 8 p Presented at the 13th Energy-Sources Technology Conference and Exhibition (ETCE) on Wind Energy, New Orleans, LA, 23-26 Jan. 1994
(Contract DE-AC36-83CH-10093)
(DE94-011867; NREL/TP-441-7108; CONF-940113-11) Avail: CASI HC A02/MF A01

Data obtained from the National Renewable Energy Laboratory site test of a wind turbine (The Combined Experiment) was analyzed specifically to capture information regarding the aerodynamic loading experienced by the machine rotor blades. The inflow conditions were shown to be extremely variable. These inflows yielded three different operational regimes about the blades. Each regime produced very different aerodynamic loading conditions. Two of these regimes could not have been readily predicted from wind tunnel data. These conditions are being subjected to further analyses to provide new guidelines for both designers and operators. The roles of unsteady aerodynamics effects are highlighted since periods of dynamic stall were shown to be associated with brief episodes of high aerodynamic forces. Author

N95-18663 Arnold Engineering Development Center, Arnold AFS, TN.
HYPERSONIC WIND TUNNEL TEST TECHNIQUES Final Report, Jul. 1992 - May 1993
R. K. Matthews and R. W. Rhudy Aug. 1994 57 p Limited Reproducibility: More than 20% of this document may be affected by microfiche quality
(AD-A284057; AEDC-TR-94-6) Avail: CASI HC A04

This report describes the procedures used in the continuous flow hypersonic tunnels of the AEDC for static stability, pressure, heat transfer, materials/structures, boundary-layer transition, and electromagnetic wave testing. Particular emphasis is placed on heat-transfer techniques because of the importance of defining the thermal environment of hypersonic vehicles. An overview of the materials/structures test methodology used in the development of hypersonic vehicle components is presented. Unfortunately the methodology to predict transition has eluded the aerodynamicist for over three decades, and there are still many unanswered questions. This report briefly touches on the many parameters that affect transition and provides numerous references for those who are interested in specializing in this topic. The methodology of using trip spheres is discussed, and illustrative data are presented. Electromagnetic wave testing represents a relatively new test technique that involves the union of several disciplines: aerothermodynamics, electromagnetics, materials/structures, and advanced diagnostics. The essence of this new technique deals with the transmission

and possible distortion of electromagnetic waves (RF or IR) as they pass through the bow shock, flow field, and electromagnetic (EM) window of a missile flying at hypersonic speeds. DTIC

N95-18669 Naval Postgraduate School, Monterey, CA.
INTERACTION, BURSTING AND CONTROL OF VORTICES OF A CROPPED DOUBLE-DELTA WING AT HIGH ANGLE OF ATTACK M.S. Thesis
Abdullah M. Alkhozam Mar. 1994 224 p Limited Reproducibility: More than 20% of this document may be affected by microfiche quality
(AD-A283656) Avail: CASI HC A10

A flow visualization study of the vortical flow over a cropped double-delta wing model with sharp leading edges and its three derivatives with small geometric modifications (fillets) at the strake wing junction was conducted in the Naval Postgraduate School water tunnel using the dye-injection technique. The fillets increased the wing area of the baseline model by 1%. The main focus of this study was to evaluate the effect of fillets on vortex core trajectories, interactions and breakdown on the leeward surface at high angle of attack (AOA) with zero sideslip angle. Comparison of test results for different fillet shapes indicates delay in both vortex interaction and breakdown at high AOA, particularly for the diamond fillet shapes. The vortex breakdown data implies lift augmentation for both static and dynamic case, with the static data correlating well with recently published numerical data. DTIC

N95-18670 Army Research Lab., Aberdeen Proving Ground, MD.
NUMERICAL COMPUTATIONS OF SUPERSONIC BASE FLOW WITH SPECIAL EMPHASIS ON TURBULENCE MODELING Final Report, Dec. 1991 - Dec. 1992
Jubaraj Sahu Jun. 1994 39 p Supersedes BRL-IMR-971 Limited Reproducibility: More than 20% of this document may be affected by microfiche quality
(DA Proj. 1L1-61102-AH-43)
(AD-A283688; ARL-TR-438; BRL-IMR-971) Avail: CASI HC A03

A zonal, implicit, time-marching Navier-Stokes computational technique has been used to compute the turbulent supersonic base flow over cylindrical afterbodies. A critical element of calculating such flows is the turbulence model. Various eddy viscosity turbulence models have been used in the base region flow computations. These models include two algebraic turbulence models and a two-equation k-epsilon model. The k-epsilon equations are developed in a general coordinate system and solved using an implicit algorithm. Calculations with the k-epsilon model are extended up to the wall. Flow field computations have been performed for a cylindrical afterbody at M = 2.46 and at angle of attack alpha = 0. The results are compared to the experimental data for the same conditions and the same configuration. Details of the mean flow field as well as the turbulence quantities have been presented. In addition, the computed base pressure distribution has been compared with the experiment. In general, the k-epsilon turbulence model performs better in the near wake than the algebraic models and predicts the base pressure much better. DTIC

N95-18674 Arnold Engineering Development Center, Arnold AFS, TN.
HYPERSONIC FLOW-FIELD MEASUREMENTS: INTRUSIVE AND NONINTRUSIVE Final Report, Jul. 1992 - Jul. 1993
R. K. Matthews and W. D. Williams Aug. 1994 54 p Limited Reproducibility: More than 20% of this document may be affected by microfiche quality
(AD-A283867; AEDC-TR-94-5) Avail: CASI HC A04

Flow-field measurement techniques that require a probe or other device to be inserted into the flow are classified as intrusive. In general, these intrusive techniques are currently viewed as inferior to the more popular nonintrusive techniques. However, it should be remembered that in general these intrusive techniques have evolved over several decades while the flow-field experience of nonintrusive techniques is relatively limited. Included in the intrusive classification are pitot tubes, total temperature probes, Mach/angularity probes, static pressure devices, and others. For many years nonintrusive diagnostics have also been under development to meet the demands of hypersonic testing. Today, a large number of nonintrusive techniques at various levels of maturity and complexity are available for application. These techniques provide measurement of species number density, rotational and vibrational temperatures, static pressure, flow velocity, and visualization of flow structure. DTIC

N95-18904# National Aerospace Lab., Bangalore (India). Computer Supports and Services.
SOLUTION OF FULL POTENTIAL EQUATION ON AN AIRFOIL BY MULTIGRID TECHNIQUE
C. Srinivasa Apr. 1993 17 p
(NAL-TM-CSS-9303) Avail: CASI HC A03/MF A01

Multigrid technique is a method which accelerates the convergence and hence reduces the CPU time for a given flow problem. This technique has been used to solve the full potential equation for an airfoil in cartesian grid. This report describes the multigrid technique solutions obtained for two to three grid levels and for an angle of attack of zero degree and one degree. This report also gives the grid size details for various levels. Author

N95-18910# Deutsche Forschungsanstalt fuer Luft- und Raumfahrt, Brunswick (Germany). Inst. fuer Entwurfsaerodynamik.
THEORETICAL INVESTIGATIONS OF SHOCK/BOUNDARY LAYER INTERACTIONS ON A Ma(INFINITY) = 8 WAVERIDER [THEORETISCHE UNTERSUCHUNGEN UEBER STOSS-GRENZSCHICHT-WECHSELWIRKUNGEN AN EINEM MA(INFINITY) = 8 WELLENRITER]
Michael Waibel 1994 149 p In GERMAN
(ISSN 0939-2963)
(DLR-FB-94-12) Avail: CASI HC A07/MF A02

Shock/boundary layer interactions are investigated on a Ma(sub infinity) = 8 waverider, which has a sharp leading edge. This is done by comparing Euler and Navier-Stokes calculations at the design point and at higher angles of attack. The original waverider configuration was modified with a blunt leading edge to investigate the influence of leading edge bluntness. This comparison is made at the design point and higher angles of attack using Euler calculations. Author

N95-18933*# National Aeronautics and Space Administration. Lewis Research Center, Cleveland, OH.
ENHANCED CAPABILITIES AND MODIFIED USERS MANUAL FOR AXIAL-FLOW COMPRESSOR CONCEPTUAL DESIGN CODE CSPAN
Arthur J. Glassman (Toledo Univ., OH.) and Thomas M. Lavelle Jan. 1995 24 p
(RTOP 505-69-50)
(NASA-TM-106833; E-9394; NAS 1.15:106833) Avail: CASI HC A03/MF A01

Modifications made to the axial-flow compressor conceptual design code CSPAN are documented in this report. Endwall blockage and stall margin predictions were added. The loss-coefficient model was upgraded. Default correlations for rotor and stator solidity and aspect-ratio inputs and for stator-exit tangential velocity inputs were included in the code along with defaults for aerodynamic design limits. A complete description of input and output along with sample cases are included. Author

N95-19041*# National Aeronautics and Space Administration. Ames Research Center, Moffett Field, CA.
AN ASSESSMENT OF THE ADAPTIVE UNSTRUCTURED TETRAHEDRAL GRID, EULER FLOW SOLVER CODE FELISA
M. Jahed Djomehri (Calspan Corp., Moffett Field, CA.) and Larry L. Erickson Dec. 1994 37 p
(RTOP 505-59-20)
(NASA-TP-3526; A-94147; NAS 1.60:3526) Avail: CASI HC A03/MF A01

A three-dimensional solution-adaptive Euler flow solver for unstructured tetrahedral meshes is assessed, and the accuracy and efficiency of the method for predicting sonic boom pressure signatures about simple generic models are demonstrated. Comparison of computational and wind tunnel data and enhancement of numerical solutions by means of grid adaptivity are discussed. The mesh generation is based on the advancing front technique. The FELISA code consists of two solvers, the Taylor-Galerkin and the Runge-Kutta-Galerkin schemes, both of which are spacially discretized by the usual Galerkin weighted residual finite-element methods but with different explicit time-marching schemes to steady state. The solution-adaptive grid procedure is based on either remeshing or mesh refinement techniques. An alternative geometry adaptive procedure is also incorporated. Author

N95-19042*# National Aeronautics and Space Administration. Langley Research Center, Hampton, VA.
STATIC INVESTIGATION OF TWO FLUIDIC THRUST-VECTORING CONCEPTS ON A TWO-DIMENSIONAL CONVERGENT-DIVERGENT NOZZLE
David J. Wing Dec. 1994 203 p
(RTOP 505-62-30-01)
(NASA-TM-4574; L-17350; NAS 1.15:4574) Avail: CASI HC A10/MF A03

A static investigation was conducted in the static test facility of the Langley 16-Foot Transonic Tunnel of two thrust-vectoring concepts which utilize fluidic mechanisms for deflecting the jet of a two-dimensional convergent-divergent nozzle. One concept involved using the Coanda effect to turn a sheet of injected secondary air along a curved sidewall flap and, through entrainment, draw the primary jet in the same direction to produce yaw thrust vectoring. The other concept involved deflecting the primary jet to produce pitch thrust vectoring by injecting secondary air through a transverse slot in the divergent flap, creating an oblique shock in the divergent channel. Utilizing the Coanda effect to produce yaw thrust vectoring was largely unsuccessful. Small vector angles were produced at low primary nozzle pressure ratios, probably because the momentum of the primary jet was low. Significant pitch thrust vector angles were produced by injecting secondary flow through a slot in the divergent flap. Thrust vector angle decreased with increasing nozzle pressure ratio but moderate levels were maintained at the highest nozzle pressure ratio tested. Thrust performance generally increased at low nozzle pressure ratios and decreased near the design pressure ratio with the addition of secondary flow. Author

N95-19109# University of Southern California, Los Angeles, CA. Dept. of Aerospace Engineering.
HYPERVELOCITY AIR FLOWS WITH FINITE RATE CHEMISTRY Annual Technical Report, 1 Jul. 1993 - 30 Jun. 1994
I. Boyd, R. Hanson, M. Holden, J. Kunc, and E. P. Muntz 1 Jul. 1994 82 p
(Contract F49620-93-1-0373)
(AD-A284727; AFOSR-94-0579TR) Avail: CASI HC A05/MF A01

In the first year of this program the foundation for a productive collaboration has been laid. Using the CUBRC experiments as a focus detailed design calculation for LENS flow fields about a sphere cone have been completed and reported. Considerations of PLIF and PEBF measurements have been made for LENS as preliminary studies for this program. Very encouraging results have been obtained and reported on the efficient calculation of state and energy dependent vibrational transition probabilities. Initial PLIF measurements in a small shock tunnel have been made and reported. DTIC

N95-19110 Air Force Inst. of Tech., Wright-Patterson AFB, OH.
NUMERICAL SIMULATION OF DYNAMIC-STALL SUPPRESSION BY TANGENTIAL BLOWING Ph.D. Thesis
Matthew C. Towne Jul. 1994 164 p Limited Reproducibility: More than 20% of this document may be affected by microfiche quality
(AD-A284887; AFIT/DS/AA/94-4) Avail: CASI HC A08

The use of tangential blowing to suppress the dynamic stall of a pitching airfoil is investigated numerically. The laminar two-dimensional, compressible Navier-Stokes equations are solved time-accurately using a Beam-Warming algorithm. A slot is located at four different positions along the surface of a NACA 0015 airfoil and air is injected in a nearly tangential sense along the upper surface. Suction control is also employed at one of these slot locations to directly compare with tangential-blowing control. Solution sensitivity to grid refinement, time-step size, numerical smoothing, and initial conditions is investigated at a Reynolds number of 2.4*10(exp 4). Initial-condition and initial-airfoil-acceleration effects are analyzed for various pitch rates. Compressibility of M infinity = 0.2 solutions is investigated. Numerical simulation uncertainties of jet-orientation angle and jet velocity profile are investigated. Studies are conducted to establish the effects of slot position, slot width, blowing-initiation angle, blowing velocity, pulsed blowing, and blowing at different pitch rates. DTIC

N95-19114*# National Aeronautics and Space Administration. Langley Research Center, Hampton, VA.
NAVIER-STOKES, FLIGHT, AND WIND TUNNEL FLOW ANALYSIS FOR THE F/A-18 AIRCRAFT
Farhad Ghaffari Dec. 1994 67 p Original contains color illustrations
(RTOP 505-68-30-03)
(NASA-TP-3478; L-17336; NAS 1.60:3478) Avail: CASI HC A04/MF A01; 5 functional color pages

Computational analysis of flow over the F/A-18 aircraft is presented along with complementary data from both flight and wind tunnel experiments. The computational results are based on the three-dimensional thin-layer Navier-Stokes formulation and are obtained from an accurate surface representation of the fuselage, leading-edge extension (LEX), and the wing geometry. However, the constraints imposed by either the flow solver and/or the complexity associated with the flow-field grid generation required certain geometrical approximations to be implemented in the present numerical model. In particular, such constraints inspired the removal of the empennage and the blocking (fairing) of the inlet face. The results are computed for three different free-stream flow conditions and compared with flight test data of surface pressure coefficients, surface tuft flow, and off-surface vortical flow characteristics that included breakdown phenomena. Excellent surface pressure coefficient correlations, both in terms of magnitude and overall trend, are obtained on the forebody throughout the range of flow conditions. Reasonable pressure agreement was obtained over the LEX; the general correlation tends to improve at higher angles of attack. The surface tuft flow and the off-surface vortex flow structures compared qualitatively well with the flight test results. To evaluate the computational results, a wind tunnel investigation was conducted to determine the effects of existing configurational differences between the flight vehicle and the numerical model on aerodynamic characteristics. In most cases, the geometrical approximations made to the numerical model had very little effect on overall aerodynamic characteristics. Author

N95-19119*# National Aeronautics and Space Administration. Ames Research Center, Moffett Field, CA.
2-D AND 3-D OSCILLATING WING AERODYNAMICS FOR A RANGE OF ANGLES OF ATTACK INCLUDING STALL
R. A. Piziali (Army Aviation Systems Command, Moffett Field, CA.) Sep. 1994 570 p Prepared in cooperation with Army Aviation Systems Command, Moffett Field, CA
(RTOP 505-59-52)
(NASA-TM-4632; A-94053; NAS 1.15:4632; USAATCOM-TR-94-A-011)
Avail: CASI HC A24/MF A04

A comprehensive experimental investigation of the pressure distribution over a semispan wing undergoing pitching motions representative of a helicopter rotor blade was conducted. Testing the wing in the nonrotating condition isolates the three-dimensional (3-D) blade aerodynamic and dynamic stall characteristics from the complications of the rotor blade environment. The test has generated a very complete, detailed, and accurate body of data. These data include static and dynamic pressure distributions, surface flow visualizations, two-dimensional (2-D) airfoil data from the same model and installation, and important supporting blockage and wall pressure distributions. This body of data is sufficiently comprehensive and accurate that it can be used for the validation of rotor blade aerodynamic models over a broad range of the important parameters including 3-D dynamic stall. This data report presents all the cycle-averaged lift, drag, and pitching moment coefficient data versus angle of attack obtained from the instantaneous pressure data for the 3-D wing and the 2-D airfoil. Also presented are examples of the following: cycle-to-cycle variations occurring for incipient or lightly stalled conditions; 3-D surface flow visualizations; supporting blockage and wall pressure distributions; and underlying detailed pressure results. Author

N95-19546# Aircraft Research Association Ltd., Bedford (England).
AN INVESTIGATION OF DRAG REPEATABILITY IN HALF MODEL TESTING IN THE ARA TRANSONIC WIND TUNNEL
I. F. Burns, J. E. Green, and D. R. Stanniland Oct. 1993 28 p Presented at the 80th STA Meeting, Koeln, Germany, 17-19 Oct. 1993
(ARA-Memo-392) Avail: CASI HC A03/MF A01

In 1990 the variability of drag measurements on a half model in the ARA Transonic Tunnel increased from the usual one drag count to between two and three drag counts. An investigation showed the primary source of the variability to be a damaged balance, with a possible air leak into the tunnel plenum chamber as an additional contributor. When these sources had been eliminated, drag repeatability was restored to approximately one count. It was found however that this was mainly a systematic, diurnal

variation, caused by cyclic variation of the heat exchange between the tunnel airflow and the plenum chamber structure. A procedure was established, using measured sidewall pressures, to correct for this effect and thereby reduce drag variability within a test series to rather less than one count. As a further improvement to the tunnel for half model testing, the test section has been modified to extend the region of uniform flow and improve the aerodynamics of the diffuser. Initial results of the commissioning trials with this modification are reported. Author

N95-19574# Aircraft Research Association Ltd., Bedford (England).
EVALUATION OF THREE TURBULENCE MODELS FOR AFTERBODY/JET FLOWS, INCLUDING REYNOLDS STRESS CLOSURE
N. E. May Oct. 1993 123 p Prepared for British Aerospace (Military Aircraft) Limited
(Contracts SMD113325; SPO-S-0020536)
(ARA-90) Avail: CASI HC A06/MF A02

Turbulent, Navier-Stokes solutions for axisymmetric, transonic afterbody/jet flows are presented. The predictive capabilities of three different turbulence models, namely a zero-equation model, a two-equation model and an algebraic Reynolds stress model are compared by comparison with experiment. the algebraic Reynolds stress model gives superior predictions, particularly for separated flow regions. However, this improvement must be weighed against the reduced robustness of the algebraic Reynolds stress model and increased computer run-times. Author

N95-19623*# National Aeronautics and Space Administration. Marshall Space Flight Center, Huntsville, AL.
AN OIL FLOW STUDY OF THE REFERENCE SHUTTLE-C CONFIGURATION
Darlene C. Pokora and Anthony M. Springer Oct. 1994 107 p Original contains color illustrations
(NASA-RP-1352; M-766; NAS 1.61:1352) Avail: CASI HC A06/MF A02; 95 functional color pages

An oil flow study of the reference Shuttle-C configuration is presented. The Shuttle-C vehicle was a proposed shuttle derived vehicle where the orbiter was to be replaced by an unmanned cargo carrier element. Oil flows are shown for the range of Mach numbers from Mach 1.10 to 3.48 at various angles-of-attack and roll angles. The major flow field phenomena over the Shuttle-C reference configuration are shown in these oil flows. Using the oil flows, a qualitative understanding of the flow around the vehicle can be determined, aiding the quantitative definition of aerodynamic data from theoretical analyses and test results. The oil flows presented in this study were obtained from configurations tested in the NASA Marshall Space Flight Center's 14-Inch Trisonic Wind Tunnel from October 1988 through February 1989. Author

N95-19772# Aircraft Research Association Ltd., Bedford (England).
MULTIPORT PRESSURE MEASUREMENTS ON CONTINUOUSLY MOVING WIND TUNNEL MODELS
David G. Coulton Sep. 1993 10 p Presented at the ICIASF 1993, St. Louis, France, 20-23 Sep. 1993
(ARA-Memo-391) Avail: CASI HC A02/MF A01

Tests have been performed in the large Transonic Wind Tunnel at the Aircraft Research Association Limited, Bedford, England, to investigate the possibility of improving productivity by acquiring pressure data from continuously moving models. The experimental work has been centered around the use of Electronically Scanned Pressure (ESP) Modules and has been restricted to the measurement of pressures whose absolute value has been changing relatively smoothly with model attitude. The paper shows that good agreement has been obtained between data acquired whilst the model was moving continuously and when measured in the traditional move and pause mode of operation. The recording of pressure data whilst the model incidence is continually moving permits wind tunnel testing to be performed more efficiently with a subsequent reduction in energy and overall costs. Author

N95-19863 Naval Research Lab., Washington, DC.
WIND TUNNEL TESTS OF A 42 INCH DIAMETER SELF-STARTING AUTOGYRO ROTOR Interim Report
Steven K. Tayman 31 May 1994 19 p Limited Reproducibility: More than 20% of this document may be affected by microfiche quality
(AD-A279922; NRL/MR/5710-94-7485) Avail: Issuing Activity (Defense Technical Information Center (DTIC))

The autogyro is being investigated for potential use as a small unmanned air vehicle for Navy electronic warfare missions. This paper presents wind tunnel test results for a 42 inch diameter unpowered rotor with coupling between feathering and flapping that allows for self-starting from a vertical descent. Aerodynamic performance is given for several blade pitch angles and angles of attack. DTIC

N95-18604# De Havilland Aircraft Co. of Canada Ltd., Downsview (Ontario).
A REVIEW OF GUST LOAD CALCULATION METHODS AT DE HAVILLAND
John Glaser *In* AGARD, Aircraft Loads due to Turbulence and their Impact on Design and Certification Dec. 1994 9 p (For primary document see N95-18597 05-08)
Copyright Avail: CASI HC A02/MF A01

N95-19259# Technische Univ., Delft (Netherlands). High Speed Aerodynamics Lab.
THE UTILIZATION OF A HIGH SPEED REFLECTIVE VISUALIZATION SYSTEM IN THE STUDY OF TRANSONIC FLOW OVER A DELTA WING
S. R. Donohoe and W. J. Bannink *In* AGARD, Wall Interference, Support Interference and Flow Field Measurements Jul. 1994 13 p (For primary document see N95-19251 05-34)
Copyright Avail: CASI HC A03/MF A04

N95-19260# British Aerospace Aircraft Group, Preston (England). Aerodynamics Dept.
TRANSONIC AND SUPERSONIC FLOWFIELD MEASUREMENTS ABOUT AXISYMMETRIC AFTERBODIES FOR VALIDATION OF ADVANCED CFD CODES
Martin Burt, Philip Miller (Miller and Wilson Aerodynamics Research, Bath, England.), and Johan Agrell (Aeronautical Research Inst. of Sweden, Bromma.) *In* AGARD, Wall Interference, Support Interference and Flow Field Measurements Jul. 1994 28 p Sponsored by Swedish Ministry of Defence (For primary document see N95-19251 05-34)
Copyright Avail: CASI HC A03/MF A04

N95-19261# Technische Univ., Munich (Germany). Lehrstuhl fuer Fluidmechanik.
VELOCITY MEASUREMENTS WITH HOT-WIRES IN A VORTEX-DOMINATED FLOWFIELD
Christian Breitsamter and Boris Laschka *In* AGARD, Wall Interference, Support Interference and Flow Field Measurements Jul. 1994 13 p Sponsored by MBB Original contains color illustrations (For primary document see N95-19251 05-34)
Copyright Avail: CASI HC A03/MF A04

N95-19268*# Georgia Inst. of Tech., Atlanta, GA. Aerospace Lab.
DEVELOPMENT OF PNEUMATIC TEST TECHNIQUES FOR SUBSONIC HIGH-LIFT AND IN-GROUND-EFFECT WIND TUNNEL INVESTIGATIONS
Robert J. Englar *In* AGARD, Wall Interference, Support Interference and Flow Field Measurements Jul. 1994 11 p Sponsored by NASA. Langley Research Center (For primary document see N95-19251 05-34)
Copyright Avail: CASI HC A03/MF A04

N95-19270*# National Aeronautics and Space Administration. Ames Research Center, Moffett Field, CA.
WALL INTERACTION EFFECTS FOR A FULL-SCALE HELICOPTER ROTOR IN THE NASA AMES 80- BY 120-FOOT WIND TUNNEL
Patrick M. Shinoda *In* AGARD, Wall Interference, Support Interference and Flow Field Measurements Jul. 1994 14 p Prepared in cooperation with Army Aviation Research and Development Command, Moffett Field, CA (For primary document see N95-19251 05-34)
Copyright Avail: CASI HC A03/MF A04

N95-19278# Institute for Aerospace Research, Ottawa (Ontario). High Speed Aerodynamics Lab.
EVALUATION OF COMBINED WALL- AND SUPPORT-INTERFERENCE ON WIND TUNNEL MODELS
M. Mokry *In* AGARD, Wall Interference, Support Interference and Flow

Field Measurements Jul. 1994 11 p (For primary document see N95-19251 05-34)
Copyright Avail: CASI HC A03/MF A04

N95-19279# Aerospatiale, Toulouse (France).
INTERACTION OF A THREE STRUT SUPPORT ON THE AERODYNAMIC CHARACTERISTICS OF A CIVIL AVIATION MODEL [INTERACTION D'UN SUPPORT DE TYPE 3 MATS SUR LES CARACTERISTIQUES AERODYNAMIQUES D'UNE MAQUETTE D'AVION CIVIL]
J. Willaume, C. Quemard (Office National d'Etudes et de Recherches Aerospatiales, Toulouse, France.), and A. Bonnet (Ecole Nationale Superieure de l'Aeronautique et de l'Espace, Toulouse, France.) *In* AGARD, Wall Interference, Support Interference and Flow Field Measurements Jul. 1994 25 p In FRENCH (For primary document see N95-19251 05-34)
Copyright Avail: CASI HC A03/MF A04

N95-19280# De Havilland Aircraft Co. of Canada Ltd., Downsview (Ontario). Aerodynamic Research and Development.
INTERFERENCE CORRECTIONS FOR A CENTRE-LINE PLATE MOUNT IN A POROUS-WALLED TRANSONIC WIND TUNNEL
Richard J. D. Poole and Robin D. Galway (Institute for Aerospace Research, Ottawa, Ontario.) *In* AGARD, Wall Interference, Support Interference and Flow Field Measurements Jul. 1994 10 p Sponsored by Industry, Science and Technology Canada and Inst. for Aerospace Research (For primary document see N95-19251 05-34)
Copyright Avail: CASI HC A02/MF A04

N95-19281# German-Dutch Wind Tunnel, North East Polder (Netherlands).
CORRECTION OF SUPPORT INFLUENCES ON MEASUREMENTS WITH STING MOUNTED WIND TUNNEL MODELS
D. Eckert *In* AGARD, Wall Interference, Support Interference and Flow Field Measurements Jul. 1994 11 p (For primary document see N95-19251 05-34)
Copyright Avail: CASI HC A03/MF A04

N95-19282# Analytical Methods, Inc., Redmond, WA.
CALCULATION OF SUPPORT INTERFERENCE IN DYNAMIC WIND-TUNNEL TESTS
D. Almosnino *In* AGARD, Wall Interference, Support Interference and Flow Field Measurements Jul. 1994 6 p (For primary document see N95-19251 05-34)
Copyright Avail: CASI HC A02/MF A04

N95-19457# National Aerospace Lab., Bangalore (India). Computational and Theoretical Fluid Dynamics Div.
VISCOUS FLOW PAST AEROFOILS AXISYMMETRIC BODIES AND WINGS
S. S. Desai *In its* CFD: Advances and Applications, 1994 Oct. 1994 p 43-76 (For primary document see N95-19455 05-34)
Avail: CASI HC A03/MF A04

N95-19464# National Aerospace Lab., Bangalore (India). Computational and Theoretical Fluid Dynamics Div.
PARABOLIZED NAVIER-STOKES SOLUTION OF SUPERSONIC/HYPERSONIC FLOWS
Dinesh K. Prabhu *In its* CFD: Advances and Applications, 1994 Oct. 1994 p 321-371 (For primary document see N95-19455 05-34)
Avail: CASI HC A04/MF A04

03 AIR TRANSPORTATION AND SAFETY

Includes passenger and cargo air transport operations; and aircraft accidents.

For related information see also *16 Space Transportation* and *85 Urban Technology and Transportation.*

N95-18507 Naval Air Warfare Center, Patuxent River, MD. Aircraft Div.
DEVELOPMENT OF A BULK CURRENT INJECTION DIRECT-DRIVE SYSTEM TO TEST SYSTEM LEVEL COMPONENTS WITH STRESS WAVEFORMS THAT ARE ENCOUNTERED DURING FULL THREAT INDIRECT EFFECTS LIGHTNING
Sam Frazier and Kurt Sebacher 1994 7 p Limited Reproducibility: More than 20% of this document may be affected by microfiche quality (AD-A284160) Avail: Issuing Activity (Defense Technical Information Center (DTIC))

The NAWCAD has developed an effective lightning BCI direct drive system that can be used to inject indirect effects waveforms onto test point cables. The amplitude and shapes of these waveforms correspond to what would be seen caused by indirect effect lightning with a 6 odB margin. The waveform normalization and the load impedance normalization processes mentioned in the text have allowed near exact replication of waveforms. This BCI direct drive ability has allowed the Navy to test aircraft to indirect effects lightning and define strength levels well above the 200 kA threat. DTIC

N95-18582*# National Aeronautics and Space Administration. Lewis Research Center, Cleveland, OH.
COLLECTION EFFICIENCY AND ICE ACCRETION CALCULATIONS FOR A SPHERE, A SWEPT MS(1)-317 WING, A SWEPT NACA-0012 WING TIP, AN AXISYMMETRIC INLET, AND A BOEING 737-300
Colin S. Bidwell and Stanley R. Mohler, Jr. (NYMA, Inc., Brook Park, OH.) Jan. 1995 45 p Presented at the 33rd Aerospace Sciences Meeting and Exhibit, Reno, NV, 9-12 Jan. 1995; sponsored by AIAA
(Contract NAS3-27186; RTOP 505-68-10)
(NASA-TM-106831; E-9381; NAS 1.15:106831; AIAA Paper 95-0755)
Avail: CASI HC A03/MF A01

Collection efficiency and ice accretion calculations have been made for a sphere, a swept MS(1)-317 wing, a swept NACA-0012 wing tip, an axisymmetric inlet, and a Boeing 737-300 inlet using the NPARC flow solver and the NASA Lewis LEWICE3D grid based ice accretion code. Euler flow solutions for the geometries were generated using the NPARC flow solver. The LEWICE3D grid based ice accretion program was used to calculate the impingement efficiencies and ice shapes. Ice shapes specifying rime and mixed icing conditions were generated for a 30 minute hold condition. All calculations were performed on an SGI Model Power Challenge Computer. The results have been compared to experimental flow and impingement data. In general, the calculated flow and collection efficiencies compared well with experiment, and the ice shapes looked reasonable and appeared representative of the rime and mixed icing conditions for which they were calculated. Author

N95-19132# National Transportation Safety Board, Washington, DC.
SAFETY STUDY: COMMUTER AIRLINE SAFETY
Nov. 1994 134 p
(PB94-917004; NTSB/SS-94/02) Avail: CASI HC A07/MF A02

The commuter airline industry has grown dramatically and has experienced significant changes in operating characteristics in the past 15 years. In response to safety recommendations issued by the National Transportation Safety Board and through other initiatives taken by government and industry, regulatory revisions and other actions have resulted in an improved safety record for commuter airlines and conducting operations under title 14 Code of Federal Regulations Part 135. However, despite efforts to bring about safety improvements, accident rates for commuter airlines continue to be higher than the rates for domestic Part 121 airlines. The higher accident rate, the difference in regulatory standards between Parts 135 and 121, and findings of the Safety Board's investigations of recent accidents prompted the Board to initiate this study of commuter airline safety. The safety issues discussed in the study are: (1) the need for sweeping regulatory action; (2) the adequacy of Part 135 regulations concerning flight time limits and rest requirements; (3) the need for licensed dispatch personnel; (4) the adequacy of Part 135 pilot training; (5) the

adequacy of flight attendant training practices; (6) the need for mandated safety programs at commuter airlines and for operational oversight by major air carrier code-sharing partners; (7) the training of Federal Aviation Administration inspectors; and (8) the certification of airports served by scheduled passenger operations. As a result of the safety study, recommendations concerning these issues were made to the Federal Aviation Administration, the U.S. Department of Transportation, major U.S. domestic air carriers, and the Regional Airline Association. Author

N95-19284*# National Aeronautics and Space Administration. Lewis Research Center, Cleveland, OH.

METHODS FOR SCALING ICING TEST CONDITIONS

David N. Anderson Jan. 1995 11 p Presented at the 33rd Aerospace Sciences Meeting and Exhibit, Reno, NV, 9-12 Jan. 1995; sponsored by AIAA

(RTOP 505-68-10)

(NASA-TM-106827; E-9376; NAS 1.15:106827; AIAA Paper 95-0540)

Avail: CASI HC A03/MF A01

This report presents the results of tests at NASA Lewis to evaluate several methods to establish suitable alternative test conditions when the test facility limits the model size or operating conditions. The first method was proposed by Olsen. It can be applied when full-size models are tested and all the desired test conditions except liquid-water content can be obtained in the facility. The other two methods discussed are: a modification of the French scaling law and the AEDC scaling method. Icing tests were made with cylinders at both reference and scaled conditions representing mixed and glaze ice in the NASA Lewis Icing Research Tunnel. Reference and scale ice shapes were compared to evaluate each method. The Olsen method was tested with liquid-water content varying from 1.3 to .8 g/m(exp3). Over this range, ice shapes produced using the Olsen method were unchanged. The modified French and AEDC methods produced scaled ice shapes which approximated the reference shapes when model size was reduced to half the reference size for the glaze-ice cases tested. Author

N95-19285*# National Aeronautics and Space Administration. Lewis Research Center, Cleveland, OH.

ICE ACCRETION WITH VARYING SURFACE TENSION

Alan J. Bilanin (Continuum Dynamics, Inc., Princeton, NJ.) and David N. Anderson Jan. 1995 13 p Presented at the 33rd Aerospace Sciences Meeting and Exhibit, Reno, NV, 9-12 Jan. 1995; sponsored by AIAA

(RTOP 505-68-10)

(NASA-TM-106826; E-9375; NAS 1.15:106826; AIAA Paper 95-0538)

Avail: CASI HC A03/MF A01

During an icing encounter of an aircraft in flight, super-cooled water droplets impinging on an airfoil may splash before freezing. This paper reports tests performed to determine if this effect is significant and uses the results to develop an improved scaling method for use in icing test facilities. Simple laboratory tests showed that drops splash on impact at the Reynolds and Weber numbers typical of icing encounters. Further confirmation of droplet splash came from icing tests performed in the NaSA Lewis Icing Research Tunnel (IRT) with a surfactant added to the spray water to reduce the surface tension. The resulting ice shapes were significantly different from those formed when no surfactant was added to the water. These results suggested that the droplet Weber number must be kept constant to properly scale icing test conditions. Finally, the paper presents a Weber-number-based scaling method and reports results from scaling tests in the IRT in which model size was reduced up to a factor of 3. Scale and reference ice shapes are shown which confirm the effectiveness of this new scaling method. Author

N95-19468*# National Aeronautics and Space Administration. Langley Research Center, Hampton, VA.

FAA/NASA INTERNATIONAL SYMPOSIUM ON ADVANCED STRUCTURAL INTEGRITY METHODS FOR AIRFRAME DURABILITY AND DAMAGE TOLERANCE, PART 2

Charles E. Harris, ed. Sep. 1994 572 p Symposium held at Hampton, VA, 4-6 May 1994; sponsored by NASA and FAA

(RTOP 538-02-10-01)

(NASA-CP-3274-Pt-2; L-17432-Pt-2; NAS 1.55:3274-Pt-2) Avail: CASI HC A24/MF A04

The international technical experts in the areas of durability and damage tolerance of metallic airframe structures were assembled to present and discuss recent research findings and the development of advanced design and analysis methods, structural concepts, and advanced materials. The principal focus of the symposium was on the dissemination of new knowledge and the peer-review of progress on the development of advanced methodologies. Papers were presented on the following topics: structural concepts for enhanced durability, damage tolerance, and maintainability; new metallic alloys and processing technology; fatigue crack initiation and small crack effects; fatigue crack growth models; fracture mechanics failure criteria for ductile materials; structural mechanics methodology for residual strength and life prediction; development of flight load spectra for design and testing; and corrosion resistance. For individual titles, see N95-19469 through N95-19500.

N95-19469*# Systems and Electronics, Inc., Elk Grove Village, IL.

FLIGHT PARAMETERS MONITORING SYSTEM FOR TRACKING STRUCTURAL INTEGRITY OF ROTARY-WING AIRCRAFT **c05**

Jamshid Mohammadi and Craig Olkiewicz *In* NASA. Langley Research Center, FAA/NASA International Symposium on Advanced Structural Integrity Methods for Airframe Durability and Damage Tolerance, Part 2 Sep. 1994 p 505-516 (For primary document see N95-19468 05-03)

Avail: CASI HC A03/MF A04

Recent developments in advanced monitoring systems used in conjunction with tracking structural integrity of rotary-wing aircraft are explained. The paper describes: (1) an overview of rotary-wing aircraft flight parameters that are critical to the aircraft loading conditions and each parameter's specific requirements in terms of data collection and processing; (2) description of the monitoring system and its functions used in a survey of rotary-wing aircraft; and (3) description of the method of analysis used for the data. The paper presents a newly-developed method in compiling flight data. The method utilizes the maneuver sequence of events in several pre-identified flight conditions to describe various flight parameters at three specific weight ranges. Author

N95-19470*# Rockwell International Corp., Downey, CA. Space Sytems Div.

FATIGUE LOADS SPECTRA DERIVATION FOR THE SPACE SHUTTLE: SECOND CYCLE **c39**

Raphael Ortasse *In* NASA. Langley Research Center, FAA/NASA International Symposium on Advanced Structural Integrity Methods for Airframe Durability and Damage Tolerane, Part 2 Sep. 1994 p 517-545 (For primary document see N95-19468 05-03)

Avail: CASI HC A03/MF A04

Some of the environments and loads experienced by the Space Shuttle or future reusable space vehicles are unique, while others are similar to those encountered by commercial and/or military aircraft. Prior to the Space Transportation System (STS) flights, fatigue loads spectra were generated for the Space Shuttle based on anticipated environments and assumptions that were shown not to be applicable to the actual flight environments the vehicle experienced. This resulted in the need to generate a new cycle of fatigue loads spectra, which was based on measured flight data as well as mission profiles, reflecting the various types of service and operations the vehicle and payloads experienced. Author

N95-19471*# Laboratory for Strength of Materials Components and Structures, Puspiptek (Indonesia).

PREDICTION OF FATIQUE CRACK GROWTH UNDER FLIGHT-SIMULATION LOADING WITH THE MODIFIED CORPUS MODEL **c39**

U. H. Padmadinata and J. Schijve (Technische Hogeschool, Delft, Netherlands.) *In* NASA. Langley Research Center, FAA/NASA International Symposium on Advanced Structural Integrity Methods for Airframe Durability and Damage Tolerance, Part 2 Sep. 1994 p 547-562 (For primary document see N95-19468 05-03)

Avail: CASI HC A03/MF A04

The CORPUS (Computation Of Retarded Propagation Under Spectrum loading) crack growth prediction model for variable-amplitude loading, as introduced by De Koning, was based on crack closure. It includes a multiple-overload effect and a transition from plane strain to plane stress. In the modified CORPUS model an underload affected zone (ULZ) is introduced, which is significant for flight-simulation loading in view of the once per flight compressive ground load. The ULZ is associated with

reversed plastic deformation induced by the underloads after crack closure has already occurred. Predictions of the crack growth fatigue life are presented for a large variety of flight-simulation test series on 2024-T3 sheet specimens in order to reveal the effects of a number of variables: the design stress level, the gust spectrum severity, the truncation level (clipping), omission of small cycles, and the ground stress level. Tests with different load sequences are also included. The trends of the effects induced by the variables are correctly predicted. The quantitative agreement between the predictions and the test results is also satisfactory. Author

N95-19472*# National Aeronautics and Space Administration. Langley Research Center, Hampton, VA.

THE CHARACTERIZATION OF WIDESPREAD FATIGUE DAMAGE IN FUSELAGE STRUCTURE **c39**

Robert S. Piascik, Scott A. Willard (Lockheed Engineering and Sciences Co., Hampton, VA.), and Matthew Miller (Boeing Commercial Airplane Co., Seattle, WA.) *In its* FAA/NASA International Symposium on Advanced Structural Integrity Methods for Airframe Durability and Damage Tolerance, Part 2 Sep. 1994 p 563-579 (For primary document see N95-19468 05-03)

Avail: CASI HC A03/MF A04

The characteristics of widespread fatigue damage (WSFD) in fuselage riveted structure were established by detailed nondestructive and destructive examinations of fatigue damage contained in a full size fuselage test article. The objectives of this work were to establish an experimental data base for validating emerging WSFD analytical prediction methodology and to identify first order effects that contribute to fatigue crack initiation and growth. Detailed examinations were performed on a test panel containing four bays of a riveted lap splice joint. The panel was removed from a full scale fuselage test article after receiving 60,000 full pressurization cycles. The results of in situ examinations document the progression of fuselage skin fatigue crack growth through crack linkup. Detailed tear down examinations and fractography of the lap splice joint region revealed fatigue crack initiation sites, crack morphology and crack linkup geometry. From this large data base, distributions of crack size and locations are presented and discussions of operative damage mechanisms are offered. Author

N95-19473*# Georgia Inst. of Tech., Atlanta, GA. Computational Modeling Center.

DISCRETE CRACK GROWTH ANALYSIS METHODOLOGY FOR THROUGH CRACKS IN PRESSURIZED FUSELAGE STRUCTURES **c39**

David O. Potyondy, Paul A. Wawrzynek (Cornell Univ., Ithaca, NY.), and Anthony R. Ingraffea (Cornell Univ., Ithaca, NY.) *In* NASA. Langley Research Center, FAA/NASA International Symposium on Advanced Structural Integrity Methods for Airframe Durability and Damage Tolerance, Part 2 Sep. 1994 p 581-601 (For primary document see N95-19468 05-03)

(Grant NAG1-1184)

Avail: CASI HC A03/MF A04

A methodology for simulating the growth of long through cracks in the skin of pressurized aircraft fuselage structures is described. Crack trajectories are allowed to be arbitrary and are computed as part of the simulation. The interaction between the mechanical loads acting on the superstructure and the local structural response near the crack tips is accounted for by employing a hierarchical modeling strategy. The structural response for each cracked configuration is obtained using a geometrically nonlinear shell finite element analysis procedure. Four stress intensity factors, two for membrane behavior and two for bending using Kirchhoff plate theory, are computed using an extension of the modified crack closure integral method. Crack trajectories are determined by applying the maximum tangential stress criterion. Crack growth results in localized mesh deletion, and the deletion regions are remeshed automatically using a newly developed all-quadrilateral meshing algorithm. The effectiveness of the methodology and its applicability to performing practical analyses of realistic structures is demonstrated by simulating curvilinear crack growth in a fuselage panel that is representative of a typical narrow-body aircraft. The predicted crack trajectory and fatigue life compare well with measurements of these same quantities from a full-scale pressurized panel test. Author

N95-19474*# Victoria Univ. (British Columbia).

A NEW STOCHASTIC SYSTEMS APPROACH TO STRUCTURAL INTEGRITY **c39**

James W. Provan and Khalil Farhangdoost (McGill Univ., Montreal, Quebec.) *In* NASA. Langley Research Center, FAA/NASA International Symposium on Advanced Structural Integrity Methods for Airframe Durability and Damage Tolerance, Part 2 Sep. 1994 p 603-619 (For primary document see N95-19468 05-03)

Avail: CASI HC A03/MF A04

This paper develops improved stochastic models for the description of a large variety of fatigue crack growth phenomena that occur in components of considerable importance to the functionality and reliability of complex engineering structures. In essence, the models are based on the McGill-Markov and Closure-Lognormal stochastic processes. Not only do these models have the capability of predicting the statistical dispersion of crack growth rates, they also, by incorporating the concept of crack closure, have the capability of transferring stochastic crack growth properties measured under ideal laboratory conditions to situations of industrial significance, such as those occurring under adverse loading and/or environmental conditions. The primary data required in order to be in a position to estimate the pertinent parameters of these stochastic models are obtained from a statistically significant number of replicate tests. In this paper, both the theory and the experimental technique are illustrated using a Ti-6Al-4V alloy. Finally, important structural integrity, reliability, availability and maintainability concepts are developed and illustrated. Author

N95-19475*# Central Aerohydrodynamics Inst., Zhukovsky (Russia).

FATIGUE AND DAMAGE TOLERANCE SCATTER MODELS **c39**

Veniamin L. Raikher *In* NASA. Langley Research Center, FAA/NASA International Symposium on Advanced Structural Integrity Methods for Airframe Durability and Damage Tolerance, Part 2 Sep. 1994 p 621-633 (For primary document see N95-19468 05-03)

Avail: CASI HC A03/MF A04

Effective Total Fatigue Life and Crack Growth Scatter Models are proposed. The first of them is based on the power form of the Wohler curve, fatigue scatter dependence on mean life value, cycle stress ratio influence on fatigue scatter, and validated description of the mean stress influence on the mean fatigue life. The second uses in addition are fracture mechanics approach, assumption of initial damage existence, and Paris equation. Simple formulas are derived for configurations of models. A preliminary identification of the parameters of the models is fulfilled on the basis of experimental data. Some new and important results for fatigue and crack growth scatter characteristics are obtained. Author

N95-19476*# Purdue Univ., West Lafayette, IN. School of Mechanical Engineering.

A PROBABILISTIC FATIGUE ANALYSIS OF MULTIPLE SITE DAMAGE **c39**

S. M. Rohrbaugh, D. Ruff, B. M. Hillberry, G. McCabe, and A. F. Grandt, Jr. *In* NASA. Langley Research Center, FAA/NASA International Symposium on Advanced Structural Integrity Methods for Airframe Durability and Damage Tolerance, Part 2 Sep. 1994 p 635-651 (For primary document see N95-19468 05-03)

(Contract F49620-93-1-0377)

Avail: CASI HC A03/MF A04

The variability in initial crack size and fatigue crack growth is incorporated in a probabilistic model that is used to predict the fatigue lives for unstiffened aluminum alloy panels containing multiple site damage (MSD). The uncertainty of the damage in the MSD panel is represented by a distribution of fatigue crack lengths that are analytically derived from equivalent initial flaw sizes. The variability in fatigue crack growth rate is characterized by stochastic descriptions of crack growth parameters for a modified Paris crack growth law. A Monte-Carlo simulation explicitly describes the MSD panel by randomly selecting values from the stochastic variables and then grows the MSD cracks with a deterministic fatigue model until the panel fails. Different simulations investigate the influences of the fatigue variability on the distributions of remaining fatigue lives. Six cases that consider fixed and variable conditions of initial crack size and fatigue crack growth rate are examined. The crack size distribution exhibited a dominant effect on the remaining fatigue life distribution, and the variable crack growth rate exhibited a lesser effect on the distribution. In addition, the probabilistic model predicted that only a small percentage of the life remains after a lead crack develops in the MSD panel. Author

N95-19477*# Foster-Miller Associates, Inc., Waltham, MA.
EVALUATION OF THE FUSELAGE LAP JOINT FATIGUE AND TERMINATING ACTION REPAIR **c39**
Gopal Samavedam, Douglas Thomson, and David Y. Jeong (Department of Transportation, Cambridge, MA.) *In* NASA. Langley Research Center, FAA/NASA International Symposium on Advanced Structural Integrity Methods for Airframe Durability and Damage Tolerance, Part 2 Sep. 1994 p 653-663 Sponsored by FAA (For primary document see N95-19468 05-03)
Avail: CASI HC A03/MF A04

Terminating action is a remedial repair which entails the replacement of shear head countersunk rivets with universal head rivets which have a larger shank diameter. The procedure was developed to eliminate the risk of widespread fatigue damage (WFD) in the upper rivet row of a fuselage lap joint. A test and evaluation program has been conducted by Foster-Miller, Inc. (FMI) to evaluate the terminating action repair of the upper rivet row of a commercial aircraft fuselage lap splice. Two full scale fatigue tests were conducted on fuselage panels using the growth of fatigue cracks in the lap joint. The second test was performed to evaluate the effectiveness of the terminating action repair. In both tests, cyclic pressurization loading was applied to the panels while crack propagation was recorded at all rivet locations at regular intervals to generate detailed data on conditions of fatigue crack initiation, ligament link-up, and fuselage fracture. This program demonstrated that the terminating action repair substantially increases the fatigue life of a fuselage panel structure and effectively eliminates the occurrence of cracking in the upper rivet row of the lap joint. While high cycle crack growth was recorded in the middle rivet row during the second test, failure was not imminent when the test was terminated after cycling to well beyond the service life. The program also demonstrated that the initiation, propagation, and linkup of WFD in full-scale fuselage structures can be simulated and quantitatively studied in the laboratory. This paper presents an overview of the testing program and provides a detailed discussion of the data analysis and results. Crack distribution and propagation rates and directions as well as frequency of cracking are presented for both tests. The progression of damage to linkup of adjacent cracks and to eventual overall panel failure is discussed. In addition, an assessment of the effectiveness of the terminating action repair and the occurrence of cracking in the middle rivet row is provided, and conclusions of practical interest are drawn. Author

N95-19478*# Technische Hogeschool, Delft (Netherlands). Dept. of Aerospace Engineering.
FATIGUE LIFE UNTIL SMALL CRACKS IN AIRCRAFT STRUCTURES: DURABILITY AND DAMAGE TOLERANCE **c05**
J. Schijve *In* NASA. Langley Research Center, FAA/NASA International Symposium on Advanced Structural Integrity Methods for Airframe Durability and Damage Tolerane, Part 2 Sep. 1994 p 665-681 (For primary document see N95-19468 05-03)
Avail: CASI HC A03/MF A04

Crack initiation in notched elements occurs very early in the fatigue life. This is also true for riveted lap joints, an important fatigue critical element of a pressurized fuselage structure. Crack nucleation in a riveted lap joint can occur at different locations, depending on the riveting operation. It can occur at the edge of the rivet hole, at a small distance away from the hole, but still with subsequent crack growth through the hole, and ahead of the hole with a crack no longer passing through the hole. Moreover, crack nucleation can occur in the top row at the countersunk holes (outer sheet) or in the bottom row at the non-countersunk holes. Fractographic evidence is shown. The initial growth of the small cracks occurs as an (invisible) part through crack. As a consequence, predictions on the crack initiation life are problematic. After a though crack is present, the major part of the fatigue life has been consumed. There is still an apparent lack of empirical data on crack growth and residual strength of riveted lap joints, five years after the Aloha accident. Such data are very much necessary for further developments of prediction models. Some test results are presented. Author

N95-19479*# Deutsche Airbus G.m.b.H., Hamburg (Germany). Dept. of Fatigue and Fracture Mechanics.
DEVELOPMENT OF LOAD SPECTRA FOR AIRBUS A330/A340 FULL SCALE FATIGUE TESTS **c05**
H.-J. Schmidt and Thomas Nielsen *In* NASA. Langley Research Center, FAA/NASA International Symposium on Advanced Structural Integrity Methods for Airframe Durability and Damage Tolerance, Part 2 Sep. 1994 p 683-697 (For primary document see N95-19468 05-03)
Avail: CASI HC A03/MF A04

For substantiation of the recently certified medium range Airbus A330 and long range A340 the full scale fatigue tests are in progress. The airframe structures of both aircraft types are tested by one set of A340 specimens. The development of the fatigue test spectra for the two major test specimens which are the center fuselage and wing test and the rear fuselage test is described. The applied test load spectra allow a realistic simulation of flight, ground and pressurization loads and the finalization of the tests within the pre-defined test period. The paper contains details about the 1 g and incremental flight and ground loads and the establishment of the flight-by-flight test program, i.e., the definition of flight types, distribution of loads within the flights and randomization of flight types in repeated blocks. Special attention is given to procedures applied for acceleration of the tests, e.g. omission of lower spectrum loads and a general increase of all loads by ten percent. Author

N95-19480*# Southwest Research Inst., San Antonio, TX. Structural Engineering Dept.
AIRCRAFT STRESS SEQUENCE DEVELOPMENT: A COMPLEX ENGINEERING PROCESS MADE SIMPLE **c05**
K. H. Schrader, D. G. Butts, and W. A. Sparks *In* NASA. Langley Research Center, FAA/NASA International Symposium on Advanced Structural Integrity Methods for Airframe Durability and Damage Tolerance, Part 2 Sep. 1994 p 699-701 (For primary document see N95-19468 05-03)
Avail: CASI HC A01/MF A04

Development of stress sequences for critical aircraft structure requires flight measured usage data, known aircraft loads, and established relationships between aircraft flight loads and structural stresses. Resulting cycle-by-cycle stress sequences can be directly usable for crack growth analysis and coupon spectra tests. Often, an expert in loads and spectra development manipulates the usage data into a typical sequence of representative flight conditions for which loads and stresses are calculated. For a fighter/trainer type aircraft, this effort is repeated many times for each of the fatigue critical locations (FCL) resulting in expenditure of numerous engineering hours. The Aircraft Stress Sequence Computer Program (ACSTRSEQ), developed by Southwest Research Institute under contract to San Antonio Air Logistics Center, presents a unique approach for making complex technical computations in a simple, easy to use method. The program is written in Microsoft Visual Basic for the Microsoft Windows environment. Derived from text

N95-19481*# College of New Jersey, Pomona, NJ.
THE LOAD SEPARATION TECHNIQUE IN THE ELASTIC-PLASTIC FRACTURE ANALYSIS OF TWO- AND THREE-DIMENSIONAL GEOMETRIES **c39**
Monir H. Sharobeam *In* NASA. Langley Research Center, FAA/NASA International Symposium on Advanced Structural Integrity Methods for Airframe Durability and Damage Tolerance, Part 2 Sep. 1994 p 703-724 (For primary document see N95-19468 05-03)
Avail: CASI HC A03/MF A04

Load separation is the representation of the load in the test records of geometries containing cracks as a multiplication of two separate functions: a crack geometry function and a material deformation function. Load separation is demonstrated in the test records of several two-dimensional geometries such as compact tension geometry, single edge notched bend geometry, and center cracked tension geometry and three-dimensional geometries such as semi-elliptical surface crack. The role of load separation in the evaluation of the fracture parameter J-integral and the associated factor eta for two-dimensional geometries is discussed. The paper also discusses the theoretical basis and the procedure for using load separation as a simplified yet accurate approach for plastic J evaluation in semi-elliptical surface crack which is a three-dimensional geometry. The experimental evaluation of J, and particularly J(sub pl), for three-dimensional geometries is very challenging. A few approaches have been developed in this regard and they are either complex or very approximate. The paper also presents the load separation as a mean to identify the blunting and crack growth regions in the experimental test records of precracked specimens. Finally,

load separation as a methodology in elastic-plastic fracture mechanics is presented. Author (revised)

N95-19482*# Alcoa Technical Center, Alcoa Center, PA.
AN ARTIFICAL CORROSION PROTOCOL FOR LAP-SPLICES IN AIRCRAFT SKIN **c26**
Bevil J. Shaw *In* NASA. Langley Research Center, FAA/NASA International Symposium on Advanced Structural Integrity Methods for Airframe Durability and Damage Tolerance, Part 2 Sep. 1994 p 725-739 Sponsored in part by Boeing Co. (For primary document see N95-19468 05-03)
(Contract F34601-90-C-1336)
Avail: CASI HC A03/MF A04

This paper reviews the progress to date to formulate an artificial corrosion protocol for the Tinker AFB C/KC-135 Corrosion Fatigue Round Robin Test Program. The project has provided new test methods to faithfully reproduce the corrosion damage within a lap-splice by accelerated means, the rationale for a new laboratory test environment, and a means for corrosion damage quantification. The approach is pragmatic and the resulting artificial corrosion protocol lays the foundation for future research in the assessment of aerospace alloys. The general means for quantification of corrosion damage has been presented in a form which can be directly applied to structural integrity calculations. Author

N95-19483*# Boeing Commercial Airplane Co., Seattle, WA.
THE APPLICATION OF NEWMAN CRACK-CLOSURE MODEL TO PREDICTING FATIGUE CRACK GROWTH **c39**
Erjian Si (Shanghai Aircraft Research Inst., Shanghai, China.) *In* NASA. Langley Research Center, FAA/NASA International Symposium on Advanced Structural Integrity Methods for Airframe Durability and Damage Tolerance, Part 2 Sep. 1994 p 741-753 (For primary document see N95-19468 05-03)
Avail: CASI HC A03/MF A04

Newman crack-closure model and the relevant crack growth program were applied to the analysis of crack growth under constant amplitude and aircraft spectrum loading on a number of aluminum alloy materials. The analysis was performed for available test data of 2219-T851, 2024-T3, 2024-T351, 7075-T651, 2324-T39, and 7150-T651 aluminum materials. The results showed that the constraint factor is a significant factor in the method. The determination of the constraint factor is discussed. For constant amplitude loading, satisfactory crack growth lives could be predicted. For the above aluminum specimens, the ratio of predicted to experimental lives, Np/Nt, ranged from 0.74 to 1.36. The mean value of Np/Nt was 0.97. For a specified complex spectrum loading, predicted crack growth lives are not in very good agreement with the test data. Further effort is needed to correctly simulate the transition between plane strain and plane stress conditions, existing near the crack tip. Author (revised)

N95-19484*# Bahrain Univ., Issa Town (Bharain). College of Engineering.
FATIGUE CRACK GROWTH UNDER VARIABLE AMPLITUDE LOADING **c39**
Jihad A. Sidawi *In* NASA. Langley Research Center, FAA/NASA International Symposium on Advanced Structural Integrity Methods for Airframe Durability and Damage Tolerance, Part 2 Sep. 1994 p 755-770 (For primary document see N95-19468 05-03)
Avail: CASI HC A03/MF A04

Fatigue crack growth tests were conducted on an Fe 510 E C-Mn steel and a submerged arc welded joint from the same material under constant, variable, and random loading amplitudes. Paris-Erdogan's crack growth rate law was tested for the evaluation of m and C using the stress intensity factor K, the J-integral, the effective stress intensity factor K(sub eff), and the root mean square stress intensity factor K(sub rms) fracture mechanics concepts. The effect of retardation and residual stresses resulting from welding was also considered. It was found that all concepts gave good life predictions in all cases. Author

N95-19485*# Georgia Inst. of Tech., Atlanta, GA. FAA Center of Excellence for Computational Modeling of Aircraft Structures.
RESIDUAL LIFE AND STRENGTH ESTIMATES OF AIRCRAFT STRUCTURAL COMPONENTS WITH MSD/MED **c05**
Ripudaman Singh (Indian Inst. of Science, Bangalore.), Jai H. Park (Chungbuk National Univ., Republic of Korea.), and Satya N. Atluri *In* NASA. Langley Research Center, FAA/NASA International Symposium on Advanced Structural Integrity Methods for Airframe Durability and Damage Tolerance, Part 2 Sep. 1994 p 771-783 Sponsored by FAA (For primary document see N95-19468 05-03)
Avail: CASI HC A03/MF A04

Economic and safe operation of the flight vehicles flying beyond their initial design life calls for an in-depth structural integrity evaluation of all components with potential for catastrophic damages. Fuselage panels with cracked skin and/or stiffening elements is one such example. A three level analytical approach is developed to analyze the pressurized fuselage stiffened shell panels with damaged skin or stiffening elements. A global finite element analysis is first carried out to obtain the load flow pattern through the damaged panel. As an intermediate step, the damaged zone is treated as a spatially three-dimensional structure modeled by plate and shell finite elements, with all the neighboring elements that can alter the stress state at the crack tip. This is followed by the Schwartz-Neumann alternating method for local analysis to obtain the relevant crack tip parameters that govern the onset of fracture and the crack growth. The methodology developed is generic in nature and aims at handling a large fraction of problem areas identified by the Industry Committee on Wide-Spread Fatigue Damage. Author

N95-19486*# Battelle Columbus Labs., OH.
ULTRASONIC TECHNIQUES FOR REPAIR OF AIRCRAFT STRUCTURES WITH BONDED COMPOSITE PATCHES **c05**
S. H. Smith, N. Senapati, and R. B. Francini *In* NASA. Langley Research Center, FAA/NASA International Symposium on Advanced Structural Integrity Methods for Airframe Durability and Damage Tolerance, Part 2 Sep. 1994 p 785-800 (For primary document see N95-19468 05-03)
Avail: CASI HC A03/MF A04

This is a paper on a research and development project to demonstrate a novel ultrasonic process for the field application of boron/epoxy (B/Ep) patches for repair of aircraft structures. The first phase of the project was on process optimization and testing to develop the most practical ultrasonic processing techniques. Accelerated testing and aging behavior of precured B/Ep patches, which were ultrasonically bonded to simulated B-52 wing panel assemblies, were performed by conducting flight-by-flight spectrum loading fatigue tests. The spectrum represented 2340 missions/flights or 30 years of service. The effects of steady-state applied temperature and prior exposure of the B/Ep composite patches were evaluated. Representative experimental results of this phase of the project are presented. Author

N95-19487*# Agency for the Assessment and Application of Technology (Indonesia).
NEAR TIP STRESS AND STRAIN FIELDS FOR SHORT ELASTIC CRACKS **c39**
A. H. Soediono, G. A. Kardomateas (Georgia Inst. of Tech., Atlanta, GA.), and R. L. Carlson (Georgia Inst. of Tech., Atlanta, GA.) *In* NASA. Langley Research Center, FAA/NASA International Symposium on Advanced Structural Integrity Methods for Airframe Durability and Damage Tolerance, Part 2 Sep. 1994 p 801-828 (For primary document see N95-19468 05-03)
(Contract F09603-85-G-3104)
Avail: CASI HC A03/MF A04

Recent experimental fatigue crack growth studies have concluded an apparent anomalous behavior of short cracks. To investigate the reasons for this unexpected behavior, the present paper focuses on identifying the crack length circumstances under which the requirements for a single parameter (K(sub I) or delta K(sub I) if cyclic loading is considered) characterization are violated. Furthermore, an additional quantity, the T stress, as introduced by Rice, and the related biaxiality ratio, B, are calculated for several crack lengths and two configurations, the single-edge-cracked and the centrally-cracked specimen. It is postulated that a two-parameter characterization by K and T (or B) is needed for the adequate description of the stress and strain field around a short crack. To further verify the validity of this postulate, the influence of the third term of the Williams series on the stress, strain and displacement fields around the crack tip and in particular on the B parameter is also examined. It is found that the biaxiality ratio would be more negative if the third term effects are included in both geometries. The study is conducted using the finite element method with linearly elastic material and isoparametric elements and axial (mode I)

loading. Moreover, it is clearly shown that it is not proper to postulate the crack size limits for 'short crack' behavior as a normalized ratio with the specimen width, a/w; it should instead be stated as an absolute, or normalized with respect to a small characteristic dimension such as the grain size. Finally, implications regarding the prediction of cyclic (fatigue) growth of short cracks are discussed. Author

N95-19488*# Federal Aviation Administration, Long Beach, CA.
WIDESPREAD FATIGUE DAMAGE MONITORING: ISSUES AND CONCERNS **c05**
T. Swift *In* NASA. Langley Research Center, FAA/NASA International Symposium on Advanced Structural Integrity Methods for Airframe Durability and Damage Tolerance, Part 2 Sep. 1994 p 829-870 Presented at 5th International Conference on Structural Airworthiness of New and Aging Aircraft, Hamburg, Germany, 16-18 Jun. 1993 (For primary document see N95-19468 05-03)
Avail: CASI HC A03/MF A04

This paper is intended to illustrate the considerable effect that small in-service undetectable multi-site-damage (MSD) can have on the residual strength capability of aging aircraft structures. In general, very few people in the industry believe that tiny cracks of undetectable size are a problem because they know that many aircraft have been able to survive much larger damage. In fact they have been certified for this large damage capability. However, this is not the issue. The real issue is the effect the tiny cracks, at multiple sites, have on the large damage capability which the industry has become accustomed to expect and which the aircraft have been certified to sustain. The concern is that this message does not appear to be fully understood by many people outside the fracture community. The prime purpose of this paper, therefore, has been to convey this message by describing in simple terms the net section yielding phenomenon in ductile materials which causes loss in lead crack residual strength in the presence of MSD. The explanation continues with a number of examples on complex stiffened structures, using the results of previous finite element analyses, which illustrate that the effect of MSD is extremely sensitive to structural configuration. It is hoped that those members of the aviation community who believe that tiny cracks are not a problem will read this paper very carefully. Author

N95-19489*# Utah Univ., Salt Lake City, UT. Quality and Integrity Design Engineering Center.
MICROSTRUCTURALLY BASED VARIATIONS ON THE DWELL FATGUE LIFE OF TITANIUM ALLOY IMI 834 **c26**
Mark L. Thomsen and David W. Hoeppner *In* NASA. Langley Research Center, FAA/NASA International Symposium on Advanced Structural Integrity Methods for Airframe Durability and Damage Tolerance, Part 2 Sep. 1994 p 871-889 (For primary document see N95-19468 05-03)
Avail: CASI HC A03/MF A04

An experimental study was undertaken to determine the role of microstructure on the fatigue life reduction observed in titanium alloy IMI 834 under dwell loading conditions. The wave forms compared were a trapezoid with 15 and 30 second hold times at the maximum test load and a baseline, 10 Hertz, haversine. The stress ratio for both loading wave forms was 0.10. The fatigue loading of each specimen was conducted in a vacuum within a scanning electron microscope chamber which minimized the possibility that the laboratory environment would adversely affect the material behavior. Two microstructural conditions were investigated in the experimental program. The first involved standard 'disk' material with equiaxed alpha in a transformed beta matrix. The second material was cut from the same disk forging as the first but was heat treated to obtain a martensitic alpha prime microstructure. Tensile tests were performed prior to the onset of the fatigue loading portion of the study, and it was determined that the yield strengths of the specimens from both material conditions were within ten percent. The maximum fatigue loads were chosen to be 72 percent of the average yield strength for both materials as determined from the tensile tests. It was found that the cycles to failure from the 10 Hertz loading wave form were reduced by a factor of approximately five when the loading was changed to the trapezoidal wave form for the standard 'disk' material. The fatigue life reduction for the martensitic structure under identical test conditions was approximately 1.75. The improvement observed with the martensitic structure also was accompanied by an increase in overall fatigue life for the wave forms tested. This paper will review the results and conclusions of this effort. Author

N95-19490*# Cornell Univ., Ithaca, NY. Dept. of Theoretical and Applied Mechanics.
FATIGUE CRACK GROWTH IN 2024-T3 ALUMINUM UNDER TENSILE AND TRANSVERSE SHEAR STRESSES **c26**
Mark J. Viz and Alan T. Zehnder *In* NASA. Langley Research Center, FAA/NASA International Symposium on Advanced Structural Integrity Methods for Airframe Durability and Damage Tolerance, Part 2 Sep. 1994 p 891-910 (For primary document see N95-19468 05-03)
(Grant NAG1-1311)
Avail: CASI HC A03/MF A04

The influence of transverse shear stresses on the fatigue crack growth rate in thin 2024-T3 aluminum alloy sheets is investigated experimentally. The tests are performed on double-edge cracked sheets in cyclic tensile and torsional loading. This loading generates crack tip stress intensity factors in the same ratio as the values computed for a crack lying along a lap joint in a pressurized aircraft fuselage. The relevant fracture mechanics of cracks in thin plates along with the details of the geometrically nonlinear finite element analyses used for the test specimen calibration are developed and discussed. Preliminary fatigue crack growth data correlated using the fully coupled stress intensity factor calibration are presented and compared with fatigue crack growth data from pure delta K(sub I)fatigue tests. Author

N95-19491*# National Aerospace Lab., Amsterdam (Netherlands).
RESULTS OF UNIAXIAL AND BIAXIAL TESTS ON RIVETED FUSELAGE LAP JOINT SPECIMENS **c05**
H. Vlieger *In* NASA. Langley Research Center, FAA/NASA International Symposium on Advanced Structural Integrity Methods for Airframe Durability and Damage Tolerance, Part 2 Sep. 1994 p 911-931 (For primary document see N95-19468 05-03)
Avail: CASI HC A03/MF A04

As part of an FAA-NLR collaborative program on structural integrity of aging aircraft, NLR carried out uniaxial and biaxial fatigue tests on riveted lap joint specimens being representative for application in a fuselage. All tests were constant amplitude tests with maximum stresses being representative for fuselage pressurization cycles and R-values of 0.1. The parameters selected in the testing program were the stress level (sigma(sub max) = 14 and 16 ksi) and the rivet spacing (0.75 and 1.0 inch). All specimens contained 3 rows of countersunk rivets, the rivet row spacing was 1 inch and the rivet orientation continuous. Author

N95-19492*# Open Univ., Milton Keynes (England). Fracture Research Group.
ON THE MEASUREMENT OF THE CRACK TIP STRESS FIELD AS A MEANS OF DETERMINING DELTA K(SUB eff) UNDER CONDITIONS OF FATIGUE CRACK CLOSURE **c39**
Ian R. Wallhead, Lyndon Edwards, and Peter Poole (Defence Research Agency, Farnborough, Hampshire, England.) *In* NASA. Langley Research Center, FAA/NASA International Symposium on Advanced Structural Integrity Methods for Airframe Durability and Damage Tolerance, Part 2 Sep. 1994 p 933-946 Sponsored by Dept. of Trade and Industry (For primary document see N95-19468 05-03)
Avail: CASI HC A03/MF A04

The optical method of caustics has been successfully extended to enable stress intensity factors as low as 1MPa square root of m to be determined accurately for central fatigue cracks in 2024-T3 aluminium alloy test panels. The feasibility of using this technique to study crack closure, and to determine the effective stress intensity factor range, Delta K(sub eff), has been investigated. Comparisons have been made between the measured values of stress intensity factor, K(sub caus), and corresponding theoretical values, K(sub theo), for a range of fatigue cracks grown under different loading conditions. The values of K(sub caus) and K(sub theo) were in good agreement at maximum stress, where the cracks are fully open, while K(sub caus) exceeded K(sub theo) at minimum stress, due to crack closure. However, the levels of crack closure and values of Delta K(sub eff) obtained could not account for the variations of crack growth rate with loading conditions. It is concluded that the values of Delta K(sub eff), based on caustic measurements in a 1/square root of r stress field well outside the plastic zone, do not fully reflect local conditions which control crack tip behavior. Author

N95-19493*# Southwest Research Inst., San Antonio, TX. Aerospace and Reliability Engineering Dept.

ANALYSIS OF COLD WORKED HOLES FOR STRUCTURAL LIFE EXTENSION **c39**

David H. Wieland, Jon T. Cutshall, O. Hal Burnside, and Joseph W. Cardinal *In* NASA. Langley Research Center, FAA/NASA International Symposium on Advanced Structural Integrity Methods for Airframe Durability and Damage Tolerance, Part 2 Sep. 1994 p 947-961 (For primary document see N95-19468 05-03)

Avail: CASI HC A03/MF A04

Cold working holes for improved fatigue life of fastener holes are widely used on aircraft. This paper presents methods used by the authors to determine the percent of cold working to be applied and to analyze fatigue crack growth of cold worked fastener holes. An elastic, perfectly-plastic analysis of a thick-walled tube is used to determine the stress field during the cold working process and the residual stress field after the process is completed. The results of the elastic/plastic analysis are used to determine the amount of cold working to apply to a hole. The residual stress field is then used to perform damage tolerance analysis of a crack growing out of a cold worked fastener hole. This analysis method is easily implemented in existing crack growth computer codes so that the cold worked holes can be used to extend the structural life of aircraft. Analytical results are compared to test data where appropriate. Author

N95-19494*# National Inst. of Standards and Technology, Gaithersburg, MD. Mechanical Properties and Performance.

FRACTURE BEHAVIOR OF LARGE-SCALE THIN-SHEET ALUMINUM ALLOY **c26**

Roland deWit, Richard J. Fields, Leonard Mordfin, Samuel R. Low, and Donald Harne *In* NASA. Langley Research Center, FAA/NASA International Symposium on Advanced Structural Integrity Methods for Airframe Durability and Damage Tolerance, Part 2 Sep. 1994 p 963-983 (For primary document see N95-19468 05-03)

(Contract DTFA03-92-Z-00018)

Avail: CASI HC A03/MF A04

A series of fracture tests on large-scale, pre-cracked, aluminum alloy panels is being carried out to examine and to characterize the process by which cracks propagate and link up in this material. Extended grips and test fixtures were specially designed to enable the panel specimens to be loaded in tension, in a 1780-kN-capacity universal testing machine. Twelve panel specimens, each consisting of a single sheet of bare 2024-T3 aluminum alloy, 3988 mm high, 2286 mm wide, and 1.016 mm thick are being fabricated with simulated through-cracks oriented horizontally at mid-height. Using existing information, a test matrix has been set up that explores regions of failure that are controlled by fracture mechanics, with additional tests near the boundary between plastic collapse and fracture. In addition, a variety of multiple site damage (MSD) configurations have been included to distinguish between various proposed linkage mechanisms. All tests but one use anti-buckling guides. At this writing seven specimens have been tested. Three were fabricated with a single central crack, three others had multiple cracks on each side of the central crack, and one had a single crack but no anti-buckling guides. Each fracture event was recorded on film, video, computer, magnetic tape, and occasionally optical microscopy. The visual showed the crack tip with a load meter in the field of view, using motion picture film for one tip and SVHS video tape for the other. The computer recorded the output of the testing machine load cell, the stroke, and twelve strain gages at 1.5 second intervals. A wideband FM magnetic tape recorder was used to record data from the same sources. The data were analyzed by two different procedures: (1) the plastic zone model based on the residual strength diagram; and (2) the R-curve. The first three tests were used to determine the basic material properties, and these results were then used in the analysis of the two subsequent tests with MSD cracks. There is good agreement between measured values and results obtained from the model. Author

N95-19495*# Tennessee Technological Univ., Cookeville, TN.

FATIGUE AND RESIDUAL STRENGTH INVESTIGATION OF ARALL(R) -3 AND GLARE(R) -2 PANELS WITH BONDED STRINGERS **c05**

Ming Wu, Dale A. Wilson, and S. V. Reddy (Textron Aerostructures, Nashville, TN.) *In* NASA. Langley Research Center, FAA/NASA International Symposium on Advanced Structural Integrity Methods for Airframe Durability and Damage Tolerance, Part 2 Sep. 1994 p 985-998 (For primary document see N95-19468 05-03)

Avail: CASI HC A03/MF A04

Stiffened panels were fabricated from ARALL-3 and GLARE-3 laminates for the purpose of providing improved structural performance of lower wing panels for aircraft. To verify the designs fatigue crack growth and residual strength tests were conducted and compared to those for conventional monolithic aluminum panels. Author

N95-19496*# Aluminum Co. of America, Alcoa Center, PA.

PREDICTION OF R-CURVES FROM SMALL COUPON TESTS **c39**

J. R. Yeh, G. H. Bray, R. J. Bucci, and Y. Macheret *In* NASA. Langley Research Center, FAA/NASA International Symposium on Advanced Structural Integrity Methods for Airframe Durability and Damage Tolerance, Part 2 Sep. 1994 p 999-1013 (For primary document see N95-19468 05-03)

Avail: CASI HC A03/MF A04

R-curves were predicted for Alclad 2024-T3 and C188-T3 sheet using the results of small-coupon Kahn tear tests in combination with two-dimensional elastic-plastic finite element stress analyses. The predictions were compared to experimental R-curves from 6.3, 16 and 60-inch wide M(T) specimens and good agreement was obtained. The method is an inexpensive alternative to wide panel testing for characterizing the fracture toughness of damage-tolerant sheet alloys. The usefulness of this approach was demonstrated by performing residual strength calculations for a two-bay crack in a representative fuselage structure. C188-T3 was predicted to have a 24 percent higher load carrying capability than 2024-T3 in this application as a result of its superior fracture toughness. Author

N95-19497*# Textron Bell Helicopter, Fort Worth, TX.

AIRCRAFT FATIGUE AND CRACK GROWTH CONSIDERING LOADS BY STRUCTURAL COMPONENT **c05**

J. D. Yost *In* NASA. Langley Research Center, FAA/NASA International Symposium on Advanced Structural Integrity Methods for Airframe Durability and Damage Tolerance, Part 2 Sep. 1994 p 1015-1028 (For primary document see N95-19468 05-03)

Avail: CASI HC A03/MF A04

The indisputable 1968 C-130 fatigue/crack growth data is reviewed to obtain additional useful information on fatigue and crack growth. The proven Load Environment Model concept derived empirically from F-105D multichannel recorder data is refined to a simpler method by going from 8 to 5 variables in the spectra without a decrease in accuracy. This approach provides the true fatigue/crack growth and load environment by structural component for both fatigue and strength design. Methods are presented for defining fatigue scatter and damage at crack initiation. These design tools and criteria may be used for both metal and composite aircraft structure. Author

N95-19498*# National Aeronautics and Space Administration. Langley Research Center, Hampton, VA.

STRESS INTENSITY FACTORS FOR SURFACE AND CORNER CRACKS EMANATING FROM A WEDGE-LOADED HOLE **c39**

W. Zhao (South Carolina Univ., Columbia, SC.), M. A. Sutton (South Carolina Univ., Columbia, SC.), K. N. Shivakumar (North Carolina Agricultural and Technical State Univ., Greensboro, NC.), and J. C. Newman, Jr. *In its* FAA/NASA International Symposium on Advanced Structural Integrity Methods for Airframe Durability and Damage Tolerance, Part 2 Sep. 1994 p 1029-1043 (For primary document see N95-19468 05-03)

(Grant NAG1-1489)

Avail: CASI HC A03/MF A04

To assist analysis of riveted lap joints, stress intensity factors are determined for surface and corner cracks emanating from a wedge-loaded hole by using a 3-D weight function method in conjunction with a 3-D finite element method. A stress intensity factor equation for surface cracks is also developed to provide a closed-form solution. The equation covers commonly-encountered geometrical ranges and retains high accuracy over the entire range. Author

N95-19499*# National Aeronautics and Space Administration. Langley Research Center, Hampton, VA.

NONLINEAR ANALYSIS OF DAMAGED STIFFENED FUSELAGE SHELLS SUBJECTED TO COMBINED LOADS **c05**

James H. Starnes, Jr., Vicki O. Britt, Richard D. Young (Lockheed Engineering and Sciences Co., Hampton, VA.), Charles C. Rankin (Lockheed Missiles and Space Co., Palo Alto, CA.), Charles P. Shore, and Jane C. Bains *In its* FAA/NASA International Symposium on Advanced Structural Integrity Methods for Airframe Durability and Damage Tolerance, Part 2 Sep. 1994 p 1045-1075 (For primary document see N95-19468 05-03)
Avail: CASI HC A03/MF A04

The results of an analytical study of the nonlinear response of stiffened fuselage shells with long cracks are presented. The shells are modeled with a hierarchical modeling strategy that accounts for global and local response phenomena accurately. Results are presented for internal pressure and mechanical bending loads. The effects of crack location and orientation on shell response are described. The effects of mechanical fasteners on the response of a lap joint and the effects of elastic and elastic-plastic material properties on the buckling response of tension-loaded flat panels with cracks are also addressed. Author

N95-19500*# West Coast Industries, Inc., Seattle, WA.
SPLIT MANDREL VERSUS SPLIT SLEEVE COLDWORKING: DUAL METHODS FOR EXTENDING THE FATIGUE LIFE OF METAL STRUCTURES **c39**
Geoffrey A. Rodman and Matthew Creager (Structural Integrity Engineering, Chatsworth, CA.) *In* NASA. Langley Research Center, FAA/NASA International Symposium on Advanced Structural Integrity Methods for Airframe Durability and Damage Tolerance, Part 2 Sep. 1994 p 1077-1086 (For primary document see N95-19468 05-03)
Avail: CASI HC A02/MF A04

It is common practice to use split sleeve coldworking of fastener holes as a means of extending the fatigue life of metal structures. In search of lower manufacturing costs, the aerospace industry is examining the split mandrel (sleeveless) coldworking process as an alternative method of coldworking fastener holes in metal structures. The split mandrel process (SpM) significantly extends the fatigue life of metal structures through the introduction of a residual compressive stress in a manner that is very similar to the split sleeve system (SpSl). Since the split mandrel process is significantly less expensive than the split sleeve process and more adaptable to robotic automation, it will have a notable influence upon other new manufacture of metal structures which require coldworking a significant number of holes, provided the aerospace community recognizes that the resulting residual stress distributions and fatigue life improvement are the same for both processes. Considerable testing has validated the correctness of that conclusion. The findings presented in this paper represent the results of an extensive research and development program, comprising data collected from over 400 specimens fabricated from 2024-T3 and 7075-T651 aluminum alloys in varied configurations, which quantify the benefits (fatigue enhancement and cost savings) of automating a sleeveless coldworking system. Author

N95-19720# Federal Aviation Administration, Washington, DC.
FEDERAL AVIATION REGULATIONS, PART 91. GENERAL OPERATING AND FLIGHT RULES. CHANGE 8
21 Jun. 1994 12 p See also PB94-194883
(PB94-217445) Avail: CASI HC A03/MF A01

This change to Part 91, General Operating and Flight Rules, incorporates two amendments: Amendment 91-241, Special Visual Flight Rules (SVFR), Denver, CO which delays the effective date of May 15, 1994 indefinitely; and Amendment 91-242, Emergency Locator Transmitters, effective June 21, 1994. This amendment affects Section 91.207. NTIS

N95-19793# National Transportation Safety Board, Washington, DC.
SPECIAL INVESTIGATION REPORT: MAINTENANCE ANOMALY RESULTING IN DRAGGED ENGINE DURING LANDING ROLLOUT. NORTHWEST AIRLINES FLIGHT 18, BOEING 747-251B, N637US, NEW TOKYO INTERNATIONAL AIRPORT, NARITA, JAPAN, 1 MAR. 1994
20 Dec. 1994 67 p
(PB94-917006; NTSB/SIR-94/02) Avail: CASI HC A04/MF A01

This special investigation report addresses the maintenance activity at Northwest Airlines that led to the accident involving Northwest Airlines flight 18, a B-747, during the airplane's intermediate stop at Narita, Japan, while it was flying from Hong Kong to John F. Kennedy International Airport, Jamaica, New York, on March 1, 1994. Safety issues in the report focused on maintenance operations and maintenance work environments. Safety recommendations concerning these issues were made to the Federal Aviation Administration and to Northwest Airlines. Author

N95-19805 Galaxy Scientific Corp., Pleasantville, NJ.
ROTORCRAFT DITCHINGS AND WATER-RELATED IMPACTS THAT OCCURRED FROM 1982 TO 1989, PHASE 1 Final Report
Charles C. Chen, M. Muller, and K. M. Fogarty Oct. 1993 116 p
Limited Reproducibility: More than 20% of this document may be affected by microfiche quality
(Contract DTFA03-89-C-00043)
(AD-A279164; DOT/FAA/CT-92/13) Avail: Issuing Activity (Defense Technical Information Center (DTIC))

This report documents Phase 1 of a two-phase program that investigates ditchings and water-related impacts for rotorcraft that occurred during the years 1982-1989. The main sources of accident data were the National Transportation Safety Board and the U.S. Army Safety Center. Data from a total of 89 accidents were obtained and examined for this study. Of these, 77 cases satisfied the criteria for inclusion into the database, 67 from the NTSB and 10 from the U.S. Army. In this report the impact and post-impact conditions were categorized to assess rotorcraft behavior and occupant survivability. Three impact scenarios and two post-impact scenarios were established. Special emphasis was placed on examining rotorcraft flotation equipment performance and post-impact survivability. Six representative case studies are presented to demonstrate aspects peculiar to the rotorcraft water impact and postimpact sequence that could not be adequately covered by the statistical categorizations alone. Recommended areas requiring enhancement of occupant survivability are presented. DTIC

N95-19167# National Research Council of Canada, Ottawa (Ontario). Structures and Materials Lab.
SPECTROGRAM DIAGNOSIS OF AIRCRAFT DISASTERS
F. W. Slingerland *In* AGARD, Impact of Acoustic Loads on Aircraft Structures Sep. 1994 6 p Original contains color illustrations (For primary document see N95-19142 05-71)
Copyright Avail: CASI HC A02/MF A03

04 AIRCRAFT COMMUNICATIONS AND NAVIGATION

Includes digital and voice communication with aircraft; air navigation systems (satellite and ground based); and air traffic control.

For related information see also *17 Space Communications, Spacecraft Communications, Command and Tracking* and *Communications and Radar.*

N95-18059# Systems Control Technology, Inc., Arlington, VA.
HELIPORT/VERTIPORT MLS PRECISION APPROACHES Final Report
Deborah Peisen and Brian Sawyer Jul. 1994 68 p
(AD-A283505; Rept-92RR-28; DOT/FAA/RD-94/23) Avail: CASI HC A04/MF A01

In the early 1990's, the Federal Aviation Administration initiated an effort to answer certain questions on precision approaches to heliports and vertiports. Of particular interest were issues of economic justification and available airspace. Among the tasks included in this effort were the following: (1) Develop a criteria of what is required to establish an instrument approach at a heliport or vertiport. (2) Develop a selection process to qualify potential IFR heliport and vertiport candidates. is effort was focused on MLS. The implementation of GPS instrument approaches has required us to re-focus our thinking. This re-focusing is now well underway as evidenced with the commissioning of the Chattanooga hospital heliport GPS nonprecision approach. The publication of this report is not likely to have broad implications regarding the implementation of GPS instrument approaches. However, some portions of the work may have application to GPS instrument approaches and this document is published with this in mind. DTIC

N95-18088# Federal Aviation Administration, Atlanta, GA.
OPERATIONAL AND SUPPORTABILITY IMPLEMENTATION SYSTEM (OASIS) TEST AND EVALUATION MASTER PLAN
William E. Benner and James A. McCullough Sep. 1994 83 p
(AD-A284765; DOT/FAA/CT-TN94/6) Avail: CASI HC A05/MF A01

This Test and Evaluation Master Plan (TEMP) is for the Operational And Supportability Implementation System (OASIS) and describes the Test and Evaluation (T&E) processes that ensure the system meets the requirements allocated to the project in the NAS-SS-1000, volumes 1 and 2, and the NAS-SR-1000. The document defines test strategy, test requirements, and organizational roles and responsibilities. The purpose of the plan is to define the overall T&E phases necessary to ensure the integration of the OASIS within the environment of the National Airspace System (NAS). The OASIS will replace the Model 1 Full Capacity (M1FC) work station position equipment, located at the 61 Automated Flight Service Stations (AFSS) and provide a planned capability for new Flight Service Automation System (FSAS) AFSS state-of-the-art work station equipment which can be logistically supported. The hardware and software will mainly be comprised of commercial-off-the-shelf (COTS) and/or nondevelopmental item (NDI) acquisitions. The capability will include functionality to store, retrieve, display, highlight, zoom, and transfer information applying to any set of weather conditions, route of flight, or aircraft type. Weather and flight route information will be displayed simultaneously. The specialist will review visual notification of flight route problems including severe weather, and other safety concerns. DTIC

N95-18347* National Aeronautics and Space Administration. Ames Research Center, Moffett Field, CA.
VSTOL SYSTEMS RESEARCH AIRCRAFT (VSRA) HARRIER (Videotape)
Dec. 1994 Videotape: 9 min. 30 sec. playing time, in color, with sound
(NASA-TM-110117; NONP-NASA-VT-95-37002) Avail: CASI VHS A02/BETA A22

NASA's Ames Research Center has developed and is testing a new integrated flight and propulsion control system that will help pilots land aircraft in adverse weather conditions and in small confined ares (such as, on a small ship or flight deck). The system is being tested in the V/STOL (Vertical/Short Takeoff and Landing) Systems research Aircraft (VSRA), which is a modified version of the U.S. Marine Corps's AV-8B Harrier jet fighter, which can take off and land vertically. The new automated flight control system features both head-up and panel-mounted computer displays and also automatically integrates control of the aircraft's thrust and thrust vector control, thereby reducing the pilot's workload and help stabilize the aircraft for landing. Visiting pilots will be encouraged to test the new system and provide formal evaluation flights data and feedback. An actual flight test and the display panel of control system are shown in this video. CASI

N95-18927# Advisory Group for Aerospace Research and Development, Neuilly-Sur-Seine (France). Guidance and Control Panel.
ON-LINE HANDLING OF AIR TRAFFIC: MANAGEMENT, GUIDANCE AND CONTROL [CONDUITE EN LIGNE DU TRAFIC AERIEN: GESTION, GUIDAGE, AND PILOTAGE]
Andre Benoit, ed., C. Garcia-Avello, J. Lemaitre, M. Pelegrin, E. Petre, and S. Swiertra Nov. 1994 220 p Original contains color illustrations
(AGARD-AG-321; ISBN-92-835-0758-4) Copyright Avail: CASI HC A10/MF A03

Following a summary of the activities of the Guidance and Control Panel of AGARD in the field of Air Traffic Handling, this volume constitutes essentially an introduction for those new to the Air Traffic Control Research and Development community, offering, on the one hand, a broad view of the present situation and actual limitations, on the other hand, some precise idea of a long term system objective. It is composed of a preface, a general introduction and ten chapters, each constituting an introduction to the corresponding topics, successively entitled: the air transport system, air traffic complexity, traffic evolution, electronic aids to controllers, arrivals management systems, decision making aids, a look further into the future, towards global optimization, systems evaluation facilities, and the airport of the future. Author

N95-19810 MiTech, Inc., Pleasantville, NJ.
RESEARCH REQUIREMENTS FOR FUTURE VISUAL GUIDANCE SYSTEMS Final Report
Harold W. Olson and Thomas H. Paprocki Feb. 1994 101 p Limited Reproducibility: More than 20% of this document may be affected by microfiche quality
(AD-A279188; DOT/FAA/CT-93/49) Avail: Issuing Activity (Defense Technical Information Center (DTIC))

Airport visual aids provide essential information to pilots to facilitate their tasks of taking off, landing, and maneuvering the aircraft on the airport surfaces. Application of state-of-the-art technology can significantly improve the design and performance of the lighting, marking, and signage visual aids that provide the pilots with essential air and ground movement guidance. This study was undertaken to identify deficiencies in existing visual guidance systems and to forecast or project needs of the future. It also describes possible applications of new technology for resolving existing deficiencies and developing state-of-the-art visual guidance systems of the future. The study report identifies a number of potential research areas and new technologies of potential benefit to visual guidance. The recommended research areas are grouped by category according to phase of operation. DTIC

05 AIRCRAFT DESIGN, TESTING AND PERFORMANCE

Includes aircraft simulation technology.

For related information see also *18 Spacecraft Design, Testing and Performance* and *39 Structural Mechanics*.For land transportation vehicles see *85 Urban Technology and Transportation*.

N95-17953 Naval Air Warfare Center, Patuxent River, MD. Aircraft Div.
FLIGHT TESTING HIGH LATERAL ASYMMETRIES ON HIGHLY AUGMENTED FIGHTER/ATTACK AIRCRAFT
G. D. Dungan and C. M. Clark 23 Jun. 1994 13 p Presented at the Seventh Biennial AIAA Flight Test Conference, Colorado Springs, CO, 20-23 Jun. 1994 Limited Reproducibility: More than 20% of this document may be affected by microfiche quality
(AD-A284206) Avail: CASI HC A03

The F/A-18's flight control system (FCS) is highly augmented to tailor flying qualities, increase departure resistance, and help protect the airframe structure throughout the flight envelope. Since the F/A-18 flight control laws were designed primarily for the symmetrically loaded airplane, the effects of the high lateral asymmetries represent a significant off-design condition where control margins may be substantially reduced. Adequately defining the flight envelope limits requires a flight test program that addresses the stability and control, structural, and mission suitability issues associated with these large lateral weight asymmetries. This paper will address the risk reduction techniques, test methodologies, and real-time analysis tools that have been used in the past or are planned to be used in an ongoing flight test program to expand the lateral asymmetry limit of the F/A-18. DTIC

N95-18008# Naval Postgraduate School, Monterey, CA.
WIND TUNNEL PERFORMANCE COMPARATIVE TEST RESULTS OF A CIRCULAR CYLINDER AND 50 PERCENT ELLIPSE TAILBOOM FOR CIRCULATION CONTROL ANTITORQUE APPLICATIONS M.S. Thesis
David T. Fisher Mar. 1994 115 p
(AD-A283335) Avail: CASI HC A06/MF A01

A low speed wind tunnel study to quantitatively evaluate the performance (lift and drag) of a circular cylinder and comparable 50% ellipse was conducted. Circular cylinder performance was evaluated at slot positions of 80 deg to 135 deg, measured relative to freestream; 50% ellipse performance was measured for angles of attack between -5 deg and 30 deg. Tests were conducted at three blowing coefficients, 0.3, 0.4 (optimal historically) and 0.5, to evaluate tailboom performance sensitivity. Circulation control test results revealed optimal c1 values at an approximate 116 deg slot position, corresponding to cd values no greater than that of a smooth cylinder. The 50% ellipse results revealed optimal c1 values at approximately 18 deg AOA, though associated with considerable drag. For all three blowing coefficients, the circular cylinder L/D values were consistently three

to four times greater than their 50% ellipse counterparts. Recommendations for future NOTAR(TM) tailboom design modifications and later research are made. DTIC

N95-18090*# Mississippi State Univ., Mississippi State, MS. Dept. of Aerospace Engineering.
WING DESIGN FOR A CIVIL TILTROTOR TRANSPORT AIRCRAFT Performance Report, 25 Jan. - 24 Nov. 1994
Masoud Rais-Rohani 24 Nov. 1994 6 p
(Grant NAG1-1571)
(NASA-CR-197523; NAS 1.26:197523) Avail: CASI HC A02/MF A01

The goal of this research is the proper tailoring of the civil tiltrotor's composite wing-box structure leading to a minimum-weight wing design. With focus on the structural design, the wing's aerodynamic shape and the rotor-pylon system are held fixed. The initial design requirement on drag reduction set the airfoil maximum thickness-to-chord ratio to 18 percent. The airfoil section is the scaled down version of the 23 percent-thick airfoil used in V-22's wing. With the project goal in mind, the research activities began with an investigation of the structural dynamic and aeroelastic characteristics of the tiltrotor configuration, and the identification of proper procedures to analyze and account for these characteristics in the wing design. This investigation led to a collection of more than thirty technical papers on the subject, some of which have been referenced here. The review of literature on the tiltrotor revealed the complexity of the system in terms of wing-rotor-pylon interactions. The aeroelastic instability or whirl flutter stemming from wing-rotor-pylon interactions is found to be the most critical mode of instability demanding careful consideration in the preliminary wing design. The placement of wing fundamental natural frequencies in bending and torsion relative to each other and relative to the rotor 1/rev frequencies is found to have a strong influence on the whirl flutter. The frequency placement guide based on a Bell Helicopter Textron study is used in the formulation of frequency constraints. The analysis and design studies are based on two different finite-element computer codes: (1) MSC/NASATRAN and (2) WIDOWAC. These programs are used in parallel with the motivation to eventually, upon necessary modifications and validation, use the simpler WIDOWAC code in the structural tailoring of the tiltrotor wing. Several test cases were studied for the preliminary comparison of the two codes. The results obtained so far indicate a good overall agreement between the two codes. Derived from text

N95-18097# Sydney Univ. (Australia). Dept. of Aeronautical Engineering.
SIX DEGREE OF FREEDOM FLIGHT DYNAMIC AND PERFORMANCE SIMULATION OF A REMOTELY-PILOTED VEHICLE
D. M. Newman and K. C. Wong Jun. 1993 57 p
(Aero-TN-9301) Avail: CASI HC A04/MF A01

The purpose of this technical note is to describe the aerodynamic, propulsive and inertial data on which the remotely piloted vehicle (RPV) simulation is based, the limits of applicability of the data, and the analytic modelling techniques used in the simulation process. The note also acts as a user guide for other simulation programs and for post-processing of simulation histories. A full performance and flight dynamic simulation of the RPV was developed in Fortran 77, using the Lahey F77L-EM/32 Version 5.01 compiler to run on IBM-compatible 386/486 personal computers with numeric coprocessors. The main Fortran simulation called several locally-developed PC-specific assembly language interface routines for control input via mouse or other hardware device and graphics output to screen. The input/output routines were not considered part of the simulation proper. The simulation was designed to be applicable to all gross weights, center of gravity positions, power settings and flight conditions throughout the normal operating envelope of the RPV as shown in Appendix A. Computational model characteristics were derived from wind tunnel testing, engine manufacturer's data and computational aerodynamic and inertial data. Post-stall behavior was incompletely modelled. The model extended to flight conditions beyond the normal operating envelope in several areas. Atmospheric conditions used were those of the International Standard Atmosphere (ISA), and wind shear and turbulence models were derived from those of MIL-F-8785C. All work was performed in SI units, with inputs and outputs transformed where necessary to ICAO-approved forms. A series of test maneuvers and performance data points were run to examine the simulation validity. Results were compared to classical small-perturbation theory. As the RPV first prototype was under construction during the period when this simulation was developed, simulator validation against flight test data was not possible. The simulation was performed by repeated numerical integration of the non-linear equations of motion for a rigid aircraft with time-varying control inputs, using aircraft characteristic data based on experiment and analysis. The aircraft database consisted of an aerodynamic model, a propeller and engine model, an inertial model, and a control actuator model. Derived from text

N95-18162# Dayton Univ. Research Inst., OH.
CONFERENCE ON AEROSPACE TRANSPARENT MATERIALS AND ENCLOSURES. VOLUME 2: SESSIONS 5-9 Interim Report, 9 Aug. - 13 Aug. 1993
Samuel A. Marolo Mar. 1994 563 p Conference held in San Diego, CA, 9-13 Aug. 1993 See also AD-A283925
(Contract F33615-92-C-3400)
(AD-A283926; WL-TR-94-4084-Vol-2) Avail: CASI HC A24/MF A04

The purpose of this report is to make available the technical papers presented at the Sixteenth Conference on Aerospace Transparent Materials and Enclosures. Sixty-seven technical papers are presented in nine sessions that address transparent material for enclosures, coatings for transparencies, transparency design; bird impact resistance; human factors and optics; operational problems; design criteria on transparent plastics, glasses and elastomers; aircraft-structural integration of windshields and canopies; computed design; testing techniques; and cost of ownership reduction. The papers contained herein have been reproduced directly from the original manuscripts. DTIC

N95-18198*# National Aeronautics and Space Administration. Langley Research Center, Hampton, VA.
MICROBURST VERTICAL WIND ESTIMATION FROM HORIZONTAL WIND MEASUREMENTS
Dan D. Vicroy Dec. 1994 83 p Sponsored in part by FAA Original contains color illustrations
(RTOP 505-64-13-01)
(NASA-TP-3460; L-17376; NAS 1.60:3460; DOT/FAA/RD-94/7) Avail: CASI HC A05/MF A01; 32 functional color pages

The vertical wind or downdraft component of a microburst-generated wind shear can significantly degrade airplane performance. Doppler radar and lidar are two sensor technologies being tested to provide flight crews with early warning of the presence of hazardous wind shear. An inherent limitation of Doppler-based sensors is the inability to measure velocities perpendicular to the line of sight, which results in an underestimate of the total wind shear hazard. One solution to the line-of-sight limitation is to use a vertical wind model to estimate the vertical component from the horizontal wind measurement. The objective of this study was to assess the ability of simple vertical wind models to improve the hazard prediction capability of an airborne Doppler sensor in a realistic microburst environment. Both simulation and flight test measurements were used to test the vertical wind models. The results indicate that in the altitude region of interest (at or below 300 m), the simple vertical wind models improved the hazard estimate. The radar simulation study showed that the magnitude of the performance improvement was altitude dependent. The altitude of maximum performance improvement occurred at about 300 m. Author

N95-18381 Army Research Lab., Aberdeen Proving Ground, MD.
HELICOPTER PERFORMANCE EVALUATION (HELPE) COMPUTER MODEL Final Report, Sep. 1992 - Oct. 1993
Abdul R. Kiwan Jul. 1994 54 p Limited Reproducibility: More than 20% of this document may be affected by microfiche quality
(DA Proj. 1L1-62618-AH-80)
(AD-A284319; ARL-TR-489) Avail: CASI HC A04

A HELicopter Performance Evaluation (HELPE) computer model has been developed. The model is empirically based on the energy balance method. For a helicopter at a given mission, the model computes for a helicopter at given weight and flight conditions, the maximum possible level speed, its maneuverability in a turn, and its hover and climb capabilities in the in-ground and out-of-ground effects modes. The code also computes the speeds of maximum endurance in the air and of maximum range for the helicopter. DTIC

N95-18398 Aeronautical Systems Div., Wright-Patterson AFB, OH.
KC-135 COCKPIT MODERNIZATION STUDY. PHASE 1: EQUIPMENT EVALUATION Final Report, 1 Feb. - 31 May 1994

John E. Ehrhart, Jr. and Thomas C. Hughes Jul. 1994 100 p Limited Reproducibility: More than 20% of this document may be affected by microfiche quality
(AD-A284099; ASC-TR-94-5026-Phase-1) Avail: Issuing Activity (Defense Technical Information Center (DTIC))

Future KC-135 missions will require significant increases in aircraft flexibility to respond to the Air Force vision of 'Global Reach, Global Power.' Such flexibility typically translates into advanced avionics systems and system and capabilities; however, a large percentage of the avionics systems currently installed on the KC-135 are late 1950s and 1960s technology which has degraded the efficiency, reliability, maintainability and safety of the KC-135 mission. Strategic Air Command (SAC), now Air Mobility Command (AMC) issued a statement of need (SON, 1987) addressing the need to modernize the KC-135 cockpit avionics to attend to these problems. This report documents the evaluation of the Phase 1 modification plan as proposed by HQ/AMC. The evaluation of the reduced crew consisted of a comparison of crew workload and performance across three missions: Minot, Castle and McChord. Based on crew workload, safety of flight issues and crew interviews, study results did not support the two-person (No Nav) cockpit, given the Phase 1 modifications. Based on these results, the CSEF recommended that the feasibility of the Phase 1 modification plan be re-assessed prior to installation into the KC-135. Recommendations are based upon using the final design, identical in system capabilities, as evaluated at the Crew Station Evaluation Facility. DTIC

N95-18407 Naval Air Development Center, Warminster, PA. Systems Dept.
PRELIMINARY EVALUATION OF THE F/A-18 QUANTITY/MULTIPLE ENVELOPE EXPANSION
Win Everett and John Oster 1994 40 p Limited Reproducibility: More than 20% of this document may be affected by microfiche quality
(AD-A284119; NAWCAD-SA80) Avail: CASI HC A03

Currently the F/A-18 Hornet has restrictions on performing ripple salvo (quantity greater than multiple, multiple greater than 1) releases when Vertical Ejection Racks (VER) or Canted Vertical Ejection Racks (CVER) are loaded on (the inboard) wing stations 3 and 7 due to bomb to bomb collisions upon release. Hornet test pilots assigned to the Ordnance System Department of the Flight Test and Evaluation Group (NAWCAD) located at Patuxent River MD, sought to remedy this restriction. As Strike Leaders in the fleet, we recognized the need to eliminate these release restrictions. By testing a representative sample of weapons loadouts, we sought to increase the Hornet's weapon delivery options. DTIC

N95-18415 Naval Air Warfare Center, Patuxent River, MD. Aircraft Div.
TILT ROTOR UNMANNED AIR VEHICLE SYSTEM (TRUS) DEMONSTRATOR FLIGHT TEST PROGRAM
Michael J. Meyers 10 Mar. 1994 28 p Limited Reproducibility: More than 20% of this document may be affected by microfiche quality
(AD-A284151) Avail: Issuing Activity (Defense Technical Information Center (DTIC))

The Tilt Rotor UAV System flight demonstration program commenced in July 1993 and concluded with conversion to airplane mode and a level flight speed of 160 kts in February 1994. The purpose of the flight tests was to evaluate the utility of Tilt Rotor UAV technology in order to develop requirements for a Government maritime system. The TRUS program was divided into three test phases: Ground, Helicopter Mode, and Conversion to Airplane Mode. Helicopter Mode testing occurred at the contractor's facilities in Fort Worth, TX over two periods and consisted of fourteen flights totaling 3.0 flight-hours. During phase 2, the aircraft conducted IGE (In Ground Effect) and OGE (Out Ground Effect) hovers, longitudinal and lateral translations at up to 20 kts, as well as pitch, roll, and yaw control response testing. Handling qualities during the takeoff and landing flight regimes were also assessed. DTIC

N95-18417 Naval Air Warfare Center, Patuxent River, MD. Aircraft Div.
APPLICATION OF PHOTOGRAMMETRY OF F-14D STORE SEPARATION
Chris J. Ferguson and E. S. Getson 20 May 1994 32 p Limited Reproducibility: More than 20% of this document may be affected by microfiche quality
(AD-A284154) Avail: Issuing Activity (Defense Technical Information Center (DTIC))

Conceived in the 1960's as a replacement for the F-4 Phantom, the 'A' variant of the F-14 Tomcat was first deployed as an air superiority fighter in the early 1970's. Designed as a follow-on to the F-14A, the F-14D was introduced to the U.S. Navy in 1990. Improvements were manifold and included addition of the A/N-AAS-429 Infrared Search and Track Set (IRSTS) to the 'chin' pod located beneath the radome forward of the nose landing gear. This chin pod, which was smaller and housed only the A/N AXX-1 Television Camera Set (TCS) in the F-14A variant, was postulated to adversely affect air-to-air and air-to-ground weapon separation from the aircraft fuselage stations. This warranted additional testing to validate the separation envelope previously tested and authorized on the F-14A. In an attempt to bring state-of-the-art separation prediction techniques to the F-14D weapon certification program, the Navy's flight clearance authority mandated the use of wind tunnel generated predictions to minimize program risk. Validation of the air-to-ground predictions, performed at the Naval Air Warfare Center - Aircraft Division, NAS Patuxent River, MD required a precise method by which store six-degree-of-freedom motion could be determined. Several methods of obtaining this quantitative data were evaluated with photogrammetric analysis selected as the most suitable. While tailored for the particular application detailed in this paper, photogrammetry may be used wherever precise position and orientation of objects in three-dimensional space is a requirement. DTIC

N95-18483# McDonnell-Douglas Corp., Saint Louis, MO.
AEROMECHANICS TECHNOLOGY, VOLUME 1. TASK 1: THREE-DIMENSIONAL EULER/NAVIER-STOKES AERODYNAMIC METHOD (TEAM) ENHANCEMENTS Final Report, Jul. 1991 - Feb. 1992
R. K. Agarwal and T. P. Gielda 26 Jul. 1994 22 p
(Contract F33617-91-C-3004; AF Proj. 2404)
(AD-A285713; WL-TR-93-3010-Vol-1) Avail: CASI HC A02/MF A01

McDonnell Douglas has implemented a Johnson-King turbulence model into the Wright Laboratory TEAM code. Solutions were obtained for several test cases using the standard Baldwin-Lomax model and the incorporated Johnson-King model. Comparisons with experimental data were made where possible. General agreement was seen between the two turbulence models; however, poor agreement with the experimental data was noted for the Onera M6 wing test case. Grid sensitivity studies and further calibration of the TEAM code are needed. DTIC

N95-18504 Naval Air Warfare Center, Patuxent River, MD. Aircraft Div.
KC-130 ANVIS/HUD ASSESSMENT AND SYMBOLOGY RATIONALE
Lakaszow 25 Feb. 1994 24 p Limited Reproducibility: More than 20% of this document may be affected by microfiche quality
(AD-A284155) Avail: Issuing Activity (Defense Technical Information Center (DTIC))

Naval Air Systems Command (AIR5117D) tasked the Flight Test Engineering Group (FTEG) of the Naval Air Warfare Center Aircraft Division (NAWCAD) to conduct a technical analysis of the Blue night vision device (NVD) Lighting Kit as installed on the KC-130 aircraft. As a part of this analysis FTEG was additionally tasked to prove a quick look evaluation of a manufacturer installed, ANVIS compatible, Head Up Display (HUD). The HUD was provided through an unsolicited proposal by Elbit Corp. of Israel. On 15 Dec 1993 a follow up meeting was conducted regarding aircraft installation, concurrently a symbology review occurred. Several subtle symbology and logic changes were made based on experience gained while flying other platforms with a similar HUD installed. DTIC

N95-18505 Naval Air Warfare Center, Patuxent River, MD. Aircraft Div.
V-22 SIMULATOR EVALUATION FOR SHIPBOARD OPERATIONS
William D. Reddy 1994 17 p Limited Reproducibility: More than 20% of this document may be affected by microfiche quality
(AD-A284156) Avail: Issuing Activity (Defense Technical Information Center (DTIC))

In June 1990, a preliminary evaluation of the Naval Air Warfare Center Aircraft Division (NAWCAD) Patuxent River's Manned Flight Simulator (MFS) motion base was performed to assess its value for pilot training and task familiarization for Dynamic Interface (DI) testing. Since that time, MFS engineers have made significant improvements in the areas of ship airwake and turbulence modelling, ship visual elements, and motion cueing. In early 1993, the DI department was tasked to perform an evaluation with a duel purpose. The first was to evaluate and document the fidelity of the V-22 flight simulator for the shipboard operations flight tests. The second

was to identify the critical elements required to adequately perform various shipboard compatibility analyses and prepare project pilots for shipboard DI testing. The test consisted of 220 shipboard landings, 8 short take off's, and comprised a total of 16 flight hours. DTIC

N95-18616# Naval Postgraduate School, Monterey, CA.
COURSE MODULE FOR AA201: WING STRUCTURAL DESIGN PROJECT M.S. Thesis
Stephen A. Burris Mar. 1994 132 p
(AD-A283618) Avail: CASI HC A07/MF A02

This thesis defined a fundamental approach for aircraft wingbox design appropriate for an introductory course in aircraft structures based upon material strength and stiffness requirements. The process developed sought to encompass major conceptual engineering design considerations that ranged from load estimation at various points in the subsonic flight envelope, to initial structural sizing and layout. The goal was to present a process that could be readily conducted via hand calculations and applied by any student entering basic aircraft structures design. The sequence of analysis began with application of a comprehensive panel code method developed by NASA Ames Research Center known as PMARC. Loads obtained from the code were then used to formulate a strength of materials study of the structure subjected to combined bending, shear and torsion. The static load approach allowed initial estimation of component sizing based upon material or buckling allowable stress selection. Finally, the study demonstrated a strength to weight ratio comparison. Several calculation examples and computer-based spreadsheets were prepared for rapid analysis of multiple option design scenarios. Since the study employed analysis methods that could be performed without the aid of a finite element routine or extensive computer programming knowledge, it serves as a good introduction for the entry and intermediate level structural engineer. DTIC

N95-18621# Naval Postgraduate School, Monterey, CA.
PLANT AND CONTROLLER OPTIMIZATION BY CONVEX METHODS Ph.D. Thesis
Robert J. Niewoehner, Jr. Jun. 1994 283 p
(AD-A283700) Avail: CASI HC A13/MF A03

This report presents results of a three phase effort to demonstrate the use of convex control design techniques in aeronautical applications. The first phase was the demonstration of a methodology by which classical aircraft controller design requirements could be translated into the weighting matrices for H infinity controller synthesis. The second phase extended that methodology to the design of mixed H2 / H infinity controllers. The third phase considered the problem of minimizing the size of aircraft control surfaces while meeting closed-loop dynamic performance requirements. Control sizing is a critical element in the design of Reduced Static Stability (RSS) aircraft. Inadequate control power places the vehicle in peril, while too much control power forfeits the benefits of RSS, resulting in poorer performance, increased weight, increased cost, increased drag, and increased observability. Non-heuristic methods have been required by which the physical configuration and the accompanying controller can be designed directly from the flying qualities specifications. The optimization of the surfaces should be done while searching over the set of all controllers which, together in closed-loop, satisfy the flying qualities requirements. This report presents a methodology which simultaneously optimizes both the physical configuration and the control system of a rigid body, using performance requirements which can be posed as Linear Matrix Inequalities. DTIC

N95-18677 Dayton Univ., OH.
CONFERENCE ON AEROSPACE TRANSPARENT MATERIALS AND ENCLOSURES, VOLUME 1 Interim Report, 9-13 Aug. 1993
Samuel A. Marolo Mar. 1994 647 p Conference held in San Diego, CA, 9-13 Aug. 1993 Limited Reproducibility: More than 20% of this document may be affected by microfiche quality
(Contract F33615-92-C-3400; AF Proj. 1926)
(AD-A283925; WL-TR-94-4083-Vol-1) Avail: CASI HC A99

The purpose of this report is to make available the technical papers presented at the Sixteenth Conference on Aerospace Transparent Materials and Enclosures. Sixty-seven technical papers are presented in nine sessions that address transparent materials for enclosures, coatings for transparencies, transparency design; bird impact resistance; human factors and optics; operational problems; design criteria on transparent plastics, glasses and elastomers; aircraft-structural integration of windshields and canopies; computed design; testing techniques; and cost of ownership reduction. The papers contained herein have been reproduced directly from the original manuscripts. DTIC

N95-18723 Naval Air Warfare Center, Patuxent River, MD. Aircraft Div.
F/A-18 SIMULATION VALIDATION AND VERIFICATION: MAKING A GOOD PRODUCT EVEN BETTER
S. Whitley and R. Traven 1993 14 p Limited Reproducibility: More than 20% of this document may be affected by microfiche quality
(AD-A283995) Avail: Issuing Activity (Defense Technical Information Center (DTIC))

The Naval Air Warfare Center Aircraft Division (NAWCAD) F/A-18 flight simulator has numerous uses in the Test and Evaluation and fleet communities which include flight test risk reduction, pilot proficiency training, mishap investigation, and basic research. It is imperative that the simulation accurately model the F/A-18 airplane for valid training or efficient flight testing. To ensure that the F/A-18 simulation properly models the aircraft in flight, it was necessary to collect dynamic data across the entire flight envelope of the F/A-18 airplane in several weapon loadings. This paper discusses the results of a flight test program that will improve the fidelity of the F/A-18 simulation by providing the necessary flight data to update its aerodynamic data base throughout the flight envelope. Specific topics to be addressed include scope of the test conducted, test methodology used, and instrumentation systems developed specifically for this flight test program. DTIC

N95-18726 Naval Air Warfare Center, Patuxent River, MD. Aircraft Div.
ASSESSING AIRCRAFT SURVIVABILITY TO HIGH FREQUENCY TRANSIENT THREATS
Samuel J. Frazier, Edward M. Parimuha, William Prather, Michael Antley, and Donald McLemore 1994 7 p Limited Reproducibility: More than 20% of this document may be affected by microfiche quality
(AD-A283999) Avail: CASI HC A02

Throughout the United States Department of Defense (DOD), the need exists to assess and characterize aircraft system survivability to High Frequency (HF) electromagnetic (EM) transient threats. These threats include the HF Electromagnetic Pulse (EMP) and other ultra wideband (UWB) transient environments. The Navy recognizes this need and is taking the initiative to investigate the feasibility of a realistic, low-cost test methodology to assess, characterize and validate aircraft survivability to threats that may range from a few hundred Kilohertz to the low Gigahertz region. The proposed Navy technical approach is based on established system-level RDT&E technology using existing high frequency test laboratories and equipment. The approach will be validated using a combination of High Level Pulse (HLP) testing at the Naval Air Warfare Center Aircraft Division Patuxent Rivers Horizontally Polarized Dipole (HPD) and Vertically Polarized Dipole (VPD) free-field EMP simulators, electromagnetic effects generating equipment to simulate the carrier shipboard environment free-field low-level continuous wave (LLCW) testing to acquire the stress response data, and wideband direct-drive tests to characterize system strength. The Navy is developing a new wideband (up to 1 GHz) direct-drive technology and waveform combination techniques using stress response data to develop worst-case stress envelopes to be used during the direct-drive tests. DTIC

N95-18891 Arnold Engineering Development Center, Arnold AFS, TN.
HYPERSONIC FLIGHT TESTING Final Report, Jul. 1992 - Jul. 1993
V. K. Smith, R. K. Matthews, and J. R. Maus Aug. 1994 37 p Limited Reproducibility: More than 20% of this document may be affected by microfiche quality
(AD-A283981; AEDC-TR-94-7) Avail: CASI HC A03

The challenges of hypersonic system development require a combination of integrated ground testing, flight testing, and computational/simulation approaches. This report addresses the role of flight testing in the triad of development approach and is sub-divided into three parts: Propulsion, Aerothermal and Extrapolation of ground test data to flight. The reasons for propulsion flight test are illustrated by specific mini-case studies. The second part reviews some of the fundamental issues of flight testing and provides an overview of the aerothermal techniques. Specific examples include heat-transfer gage measurements and some of the common problems that have been encountered. The third part of this report discusses the

initial flights of the Space Shuttle which uncovered a number of differences between preflight aerodynamic predictions and actual flight data. Most notable among these discrepancies was for longitudinal trim during high-speed re-entry. To investigate these differences, several computer codes were applied to a modified Space Shuttle Orbiter to determine aerodynamic parameters over a wide range of conditions. Computations were carried out for wind tunnel conditions and flight conditions to assess Mach number, real gas, and viscous effects on the reentry aerodynamics of the orbiter. DTIC

N95-19044*# National Aeronautics and Space Administration. Hugh L. Dryden Flight Research Facility, Edwards, CA.

DETERMINATION OF STORES POINTING ERROR DUE TO WING FLEXIBILITY UNDER FLIGHT LOAD

William A. Lokos, Catherine M. Bahm, and Robert A. Heinle Washington Jan. 1995 25 p Presented at the 7th Biennial Flight Test Conference, Colorado Springs, CO, 20-23 Jun. 1994

(NASA-TM-4646; H-2022; NAS 1.15:4646; AIAA Paper 94-2112) Avail: CASI HC A03/MF A01

The in-flight elastic wing twist of a fighter-type aircraft was studied to provide for an improved on-board real-time computed prediction of pointing variations of three wing store stations. This is an important capability to correct sensor pod alignment variation or to establish initial conditions of iron bombs or smart weapons prior to release. The original algorithm was based upon coarse measurements. The electro-optical Flight Deflection Measurement System measured the deformed wing shape in flight under maneuver loads to provide a higher resolution database from which an improved twist prediction algorithm could be developed. The FDMS produced excellent repeatable data. In addition, a NASTRAN finite-element analysis was performed to provide additional elastic deformation data. The FDMS data combined with the NASTRAN analysis indicated that an improved prediction algorithm could be derived by using a different set of aircraft parameters, namely normal acceleration, stores configuration, Mach number, and gross weight. Author

N95-19067 Naval Air Warfare Center, Patuxent River, MD. Aircraft Div.

E-6A HARDNESS ASSURANCE, MAINTENANCE AND SURVEILLANCE PROGRAM

Joel Haines, Mark Mallory, William DePasquale, and Bernd Lubosch 1994 14 p Limited Reproducibility: More than 20% of this document may be affected by microfiche quality

(AD-A283994) Avail: CASI HC A03

The challenge facing aircraft program managers and the Fleet is to ensure that the electromagnetic hardness of design is maintained throughout the aircraft life-cycle. The electromagnetic pulse (EMP) community must work closely with aircraft program managers and aircraft design contractors to properly integrate the logistics elements necessary to accomplish this effort. This process must begin early in the acquisition phase and be dynamic enough to evolve as changes in life-cycle mission requirements occur. This paper identifies the Hardness Assurance, Maintenance, and Surveillance Program for the U.S. Navy's E-6A aircraft. The program includes various test techniques that are used to monitor aircraft hardness integrity and maintenance procedures to direct the hardness critical process. A database was also developed which integrates all test and maintenance data to aid aircraft hardness surveillance. DTIC

N95-19130*# California Univ., Los Angeles, CA.

THE ACCURACY OF PARAMETER ESTIMATION IN SYSTEM IDENTIFICATION OF NOISY AIRCRAFT LOAD MEASUREMENT Ph.D. Thesis

Jeffrey Kong 1994 138 p

(Contract NCC2-374)

(NASA-CR-197516; NAS 1.26:197516) Copyright Avail: CASI HC A07/MF A02

This thesis focuses on the subject of the accuracy of parameter estimation and system identification techniques. Motivated by a complicated load measurement from NASA Dryden Flight Research Center, advanced system identification techniques are needed. The objective of this problem is to accurately predict the load experienced by the aircraft wing structure during flight determined from a set of calibrated load and gage response relationship. We can then model the problem as a black box input-output system identification from which the system parameter has to be estimated. Traditional LS (Least Square) techniques and the issues of noisy data and model accuracy are addressed. A statistical bound reflecting the change in residual is derived in order to understand the effects of the perturbations on the data. Due to the intrinsic nature of the LS problem, LS solution faces the dilemma of the trade off between model accuracy and noise sensitivity. A method of conflicting performance indices is presented, thus allowing us to improve the noise sensitivity while at the same time configuring the degredation of the model accuracy. SVD techniques for data reduction are studied and the equivalence of the Correspondence Analysis (CA) and Total Least Squares Criteria are proved. We also looked at nonlinear LS problems with NASA F-111 data set as an example. Conventional methods are neither easily applicable nor suitable for the specific load problem since the exact model of the system is unknown. Neural Network (NN) does not require prior information on the model of the system. This robustness motivated us to apply the NN techniques on our load problem. Simulation results for the NN methods used in both the single load and the 'warning signal' problems are both useful and encouraging. The performance of the NN (for single load estimate) is better than the LS approach, whereas no conventional approach was tried for the 'warning signals' problems. The NN design methodology is also presented. The use of SVD, CA and Collinearity Index methods are used to reduce the number of neurons in a layer. Author

N95-19517# Wright Lab., Wright-Patterson AFB, OH.

PROCEEDINGS OF THE USAF STRUCTURAL INTEGRITY PROGRAM CONFERENCE Final Report, 30 Nov. - 2 Dec. 1993

Thomas D. Cooper, John W. Lincoln, and James L. Rudd Aug. 1994 646 p Conference held in San Antonio, TX, 30 Nov. - 2 Dec. 1993

(AF Proj. 2418)

(AD-A285684; WL-TR-94-4079) Avail: CASI HC A99/MF A06

The purpose of this 1993 Conference was to bring together technical personnel in DOD and the aerospace industry who are involved in the various technologies required to ensure the structural integrity of aircraft gas turbine engines, airframes and other mechanical systems. It provided a forum to exchange ideas and share new information relating to the critical aspects of durability and damage tolerance technology for aircraft systems. DTIC

N95-19693# Naval Postgraduate School, Monterey, CA.

AUTOMATION OF HARDWARE-IN-THE-LOOP TESTING OF CONTROL SYSTEMS FOR UNMANNED AIR VEHICLES M.S. Thesis

Michael L. Moats Sep. 1994 109 p

(AD-A284833) Avail: CASI HC A06/MF A02

Modern computing advances allow the aerospace controls engineer the ability to design, test, and implement automatic control systems for air vehicles with breath taking speed and accuracy. This work examines the automation of the hardware-in-the-loop testing and implementation of autonomous controllers for unmanned air vehicles. Extraordinary interest is generated in this subject considering automation results in hardware-in-the-loop testing within days of completing a controller design. The entire automation process is presented, from design of the controller to implementation on a particular control platform to hardware-in-the-loop testing of the controller. This accomplishes control design and implementation in a matter of months compared to a few years or more before automation. DTIC

N95-19731 Naval Air Warfare Center, Patuxent River, MD. Aircraft Div.

AIRSHIP APPLICATIONS OF MODERN FLIGHT TEST TECHNIQUES

Sean Brennan and Michael McDaniel 1994 19 p Limited Reproducibility: More than 20% of this document may be affected by microfiche quality

(AD-A284253) Avail: CASI HC A03

This viewgraph presentation covers the application of modern flight tests techniques to airships. Four airships were flow for a total of 19.7 flight hours. The airships ranged in size from 90 to 200 feet, and in gross weight from 1200 to 12,000 lbs. Single and twin-engine airships were flown. It was found that while the basic scientific test method works, many of the conventional test methods did not work on airships. In particular, new methods had to be developed for some dynamics and most stability characteristics. Further work is needed to refine stability and pressure system test techniques. Testing indicated that irreversible flight control systems and vectored thrust both enhance flying qualities. CASI

N95-19789# Aircraft Research Association Ltd., Bedford (England).
THE AERODYNAMIC DESIGN OF AN INTEGRATED WING LOWER SURFACE AND PYLONS FOR REDUCED DRAG
Dennis R. Stanniland and Dian F. M. MacDonald-Smith May 1994 11 p Presented at the 19th Congress of the International Council of the Aeronautical Sciences, Anaheim, CA, Sep. 1994 Sponsored by Ministry of Defence
(ARA-Memo-406) Avail: CASI HC A03/MF A01

The aerodynamic design of the wing for a military aircraft frequently concentrates on the clean wing performance, particularly the development of the upper surface flow at moderate and high incidence. The addition of underwing pylons and stores can cause a significant increase in drag, especially at the high subsonic Mach numbers and low incidences typical of 1-g flight at low altitude. This paper describes the design modifications to the wing lower surface and pylons of a military aircraft research model, aimed at reducing the installed drag of the pylons and stores. The redesign was carried out using the ARA Multiblock/Euler code to compute the flow around the fuselage/wing/pylon/store configuration. Geometric changes were specified using a simple relationship between the local surface curvature and the required change in surface pressure. Since the flow in the vicinity of the pylons and stores is highly viscous, the inviscid Euler code could not be relied upon to predict the drag differences between alternative designs. The success of the design modifications was therefore judged by the changes in surface pressure distributions, notably in the reduction in the shock strength on the wing lower surface. The redesigned wing/pylon combination has been tested in the ARA Transonic Wind Tunnel in conjunction with various store installations. The results demonstrate that a significant drag reduction can be achieved by redesigning the wing lower surface and pylons and a comparison with the predicted pressures shows that the CFD method has been successful in predicting the flow features accurately. Author

N95-18599# Aerospatiale, Toulouse (France). Dept. Etudes Generales-Structures.
GYROSCOPIC AND PROPELLER AERODYNAMIC EFFECTS ON ENGINE MOUNTS DYNAMIC LOADS IN TURBULENCE CONDITIONS [EFFETS GYROSOPIQUES ET AERODYNAMIQUES DES PROPULSEURS SUR LES CHARGES DES MOTEURS D'AVIONS EN CONDITIONS TURBULENTES]
J. M. Saucray *In* AGARD, Aircraft Loads due to Turbulence and their Impact on Design and Certification Dec. 1994 12 p In FRENCH (For primary document see N95-18597 05-08)
Copyright Avail: CASI HC A03/MF A01

N95-18601# Construcciones Aeronauticas S.A., Madrid (Spain). Structural Dynamics Dept.
A STUDY OF THE EFFECT OF STORE UNSTEADY AERODYNAMICS ON GUST AND TURBULENCE LOADS
M. Oliver, J. Casalengua, C. Maderuelo, Y. Camacho, and H. Climent *In* AGARD, Aircraft Loads due to Turbulence and their Impact on Design and Certification Dec. 1994 12 p (For primary document see N95-18597 05-08)
Copyright Avail: CASI HC A03/MF A01

N95-18602# McDonnell-Douglas Aerospace, Long Beach, CA. Transport Aircraft.
COMPARISON OF STOCHASTIC AND DETERMINISTIC NONLINEAR GUST ANALYSIS METHODS TO MEET CONTINUOUS TURBULENCE CRITERIA
Patrick J. Goggin *In* AGARD, Aircraft Loads due to Turbulence and their Impact on Design and Certification Dec. 1994 12 p (For primary document see N95-18597 05-08)
Copyright Avail: CASI HC A03/MF A01

N95-18603# Cessna Aircraft Co., Wichita, KS. Aircraft Structural Integrity Dept.
DESIGN LIMIT LOADS BASED UPON STATISTICAL DISCRETE GUST METHODOLOGY
D. L. Hull *In* AGARD, Aircraft Loads due to Turbulence and their Impact on Design and Certification Dec. 1994 8 p (For primary document see N95-18597 05-08)
Copyright Avail: CASI HC A02/MF A01

N95-18605*# National Aeronautics and Space Administration. Langley Research Center, Hampton, VA.
SPECIAL EFFECTS OF GUST LOADS ON MILITARY AIRCRAFT
John C. Houbolt *In* AGARD, Aircraft Loads due to Turbulence and their Impact on Design and Certification Dec. 1994 7 p (For primary document see N95-18597 05-08)
Copyright Avail: CASI HC A02/MF A01

N95-19151# Wright Lab., Wright-Patterson AFB, OH.
NONLINEAR DYNAMIC RESPONSE OF AIRCRAFT STRUCTURES TO ACOUSTIC EXCITATION
H. F. Wolfe and R. G. White (Southampton Univ., England.) *In* AGARD, Impact of Acoustic Loads on Aircraft Structures Sep. 1994 10 p (For primary document see N95-19142 05-71)
Copyright Avail: CASI HC A02/MF A03

N95-19154# Wright Lab., Wright-Patterson AFB, OH.
MODELLING STRUCTURALLY DAMAGING TWIN-JET SCREECH
Mary Kae Lockwood, Steven H. Walker, and Alan B. Cain (McDonnell-Douglas Corp., Saint Louis, MO.) *In* AGARD, Impact of Acoustic Loads on Aircraft Structures Sep. 1994 8 p (For primary document see N95-19142 05-71)
Copyright Avail: CASI HC A02/MF A03

N95-19469*# Systems and Electronics, Inc., Elk Grove Village, IL.
FLIGHT PARAMETERS MONITORING SYSTEM FOR TRACKING STRUCTURAL INTEGRITY OF ROTARY-WING AIRCRAFT
Jamshid Mohammadi and Craig Olkiewicz *In* NASA. Langley Research Center, FAA/NASA International Symposium on Advanced Structural Integrity Methods for Airframe Durability and Damage Tolerance, Part 2 Sep. 1994 p 505-516 (For primary document see N95-19468 05-03)
Avail: CASI HC A03/MF A04

N95-19478*# Technische Hogeschool, Delft (Netherlands). Dept. of Aerospace Engineering.
FATIGUE LIFE UNTIL SMALL CRACKS IN AIRCRAFT STRUCTURES: DURABILITY AND DAMAGE TOLERANCE
J. Schijve *In* NASA. Langley Research Center, FAA/NASA International Symposium on Advanced Structural Integrity Methods for Airframe Durability and Damage Tolerane, Part 2 Sep. 1994 p 665-681 (For primary document see N95-19468 05-03)
Avail: CASI HC A03/MF A04

N95-19479*# Deutsche Airbus G.m.b.H., Hamburg (Germany). Dept. of Fatigue and Fracture Mechanics.
DEVELOPMENT OF LOAD SPECTRA FOR AIRBUS A330/A340 FULL SCALE FATIGUE TESTS
H.-J. Schmidt and Thomas Nielsen *In* NASA. Langley Research Center, FAA/NASA International Symposium on Advanced Structural Integrity Methods for Airframe Durability and Damage Tolerance, Part 2 Sep. 1994 p 683-697 (For primary document see N95-19468 05-03)
Avail: CASI HC A03/MF A04

N95-19480*# Southwest Research Inst., San Antonio, TX. Structural Engineering Dept.
AIRCRAFT STRESS SEQUENCE DEVELOPMENT: A COMPLEX ENGINEERING PROCESS MADE SIMPLE
K. H. Schrader, D. G. Butts, and W. A. Sparks *In* NASA. Langley Research Center, FAA/NASA International Symposium on Advanced Structural Integrity Methods for Airframe Durability and Damage Tolerance, Part 2 Sep. 1994 p 699-701 (For primary document see N95-19468 05-03)
Avail: CASI HC A01/MF A04

N95-19485*# Georgia Inst. of Tech., Atlanta, GA. FAA Center of Excellence for Computational Modeling of Aircraft Structures.
RESIDUAL LIFE AND STRENGTH ESTIMATES OF AIRCRAFT STRUCTURAL COMPONENTS WITH MSD/MED
Ripudaman Singh (Indian Inst. of Science, Bangalore.), Jai H. Park (Chungbuk National Univ., Republic of Korea.), and Satya N. Atluri *In* NASA. Langley Research Center, FAA/NASA International Symposium on Advanced Structural Integrity Methods for Airframe Durability and Damage Tolerance,

Part 2 Sep. 1994 p 771-783 Sponsored by FAA (For primary document see N95-19468 05-03)
Avail: CASI HC A03/MF A04

N95-19486*# Battelle Columbus Labs., OH.
ULTRASONIC TECHNIQUES FOR REPAIR OF AIRCRAFT STRUCTURES WITH BONDED COMPOSITE PATCHES
S. H. Smith, N. Senapati, and R. B. Francini *In* NASA. Langley Research Center, FAA/NASA International Symposium on Advanced Structural Integrity Methods for Airframe Durability and Damage Tolerance, Part 2 Sep. 1994 p 785-800 (For primary document see N95-19468 05-03)
Avail: CASI HC A03/MF A04

N95-19488*# Federal Aviation Administration, Long Beach, CA.
WIDESPREAD FATIGUE DAMAGE MONITORING: ISSUES AND CONCERNS
T. Swift *In* NASA. Langley Research Center, FAA/NASA International Symposium on Advanced Structural Integrity Methods for Airframe Durability and Damage Tolerance, Part 2 Sep. 1994 p 829-870 Presented at 5th International Conference on Structural Airworthiness of New and Aging Aircraft, Hamburg, Germany, 16-18 Jun. 1993 (For primary document see N95-19468 05-03)
Avail: CASI HC A03/MF A04

N95-19491*# National Aerospace Lab., Amsterdam (Netherlands).
RESULTS OF UNIAXIAL AND BIAXIAL TESTS ON RIVETED FUSELAGE LAP JOINT SPECIMENS
H. Vlieger *In* NASA. Langley Research Center, FAA/NASA International Symposium on Advanced Structural Integrity Methods for Airframe Durability and Damage Tolerance, Part 2 Sep. 1994 p 911-931 (For primary document see N95-19468 05-03)
Avail: CASI HC A03/MF A04

N95-19495*# Tennessee Technological Univ., Cookeville, TN.
FATIGUE AND RESIDUAL STRENGTH INVESTIGATION OF ARALL(R) -3 AND GLARE(R) -2 PANELS WITH BONDED STRINGERS
Ming Wu, Dale A. Wilson, and S. V. Reddy (Textron Aerostructures, Nashville, TN.) *In* NASA. Langley Research Center, FAA/NASA International Symposium on Advanced Structural Integrity Methods for Airframe Durability and Damage Tolerance, Part 2 Sep. 1994 p 985-998 (For primary document see N95-19468 05-03)
Avail: CASI HC A03/MF A04

N95-19497*# Textron Bell Helicopter, Fort Worth, TX.
AIRCRAFT FATIGUE AND CRACK GROWTH CONSIDERING LOADS BY STRUCTURAL COMPONENT
J. D. Yost *In* NASA. Langley Research Center, FAA/NASA International Symposium on Advanced Structural Integrity Methods for Airframe Durability and Damage Tolerance, Part 2 Sep. 1994 p 1015-1028 (For primary document see N95-19468 05-03)
Avail: CASI HC A03/MF A04

N95-19499*# National Aeronautics and Space Administration. Langley Research Center, Hampton, VA.
NONLINEAR ANALYSIS OF DAMAGED STIFFENED FUSELAGE SHELLS SUBJECTED TO COMBINED LOADS
James H. Starnes, Jr., Vicki O. Britt, Richard D. Young (Lockheed Engineering and Sciences Co., Hampton, VA.), Charles C. Rankin (Lockheed Missiles and Space Co., Palo Alto, CA.), Charles P. Shore, and Jane C. Bains *In its* FAA/NASA International Symposium on Advanced Structural Integrity Methods for Airframe Durability and Damage Tolerance, Part 2 Sep. 1994 p 1045-1075 (For primary document see N95-19468 05-03)
Avail: CASI HC A03/MF A04

06 AIRCRAFT INSTRUMENTATION

Includes cockpit and cabin display devices; and flight instruments.

For related information see also *19 Spacecraft Instrumentation* and *35 Instrumentation and Photography.*

N95-18164# Burnette Engineering, Fairborn, OH.
AN EVALUATION OF AIRCRAFT CRT AND DOT-MATRIX DISPLAY LEGIBILITY REQUIREMENTS Interim Report, 17 Apr. 1985 - 25 Jun. 1991
Keith T. Burnette Jun. 1994 73 p
(Contract F33615-84-C-3627)
(AD-A283933; WL-TR-91-7020) Avail: CASI HC A04/MF A01

Pilot satisfaction with the legibility performance of the absorption bandpass filtered green P-43 phosphor cathode ray tube (CRT) electronic displays employed in the F-15, F-16 and F-18 aircraft, prior to 1980 has been used in this report as a basis for establishing minimum luminance and contrast requirements for both CRT and dot-matrix electronic aircraft displays. The data drawn on and the methods used to derive the alphanumeric, graphic and video information legibility requirements that should as a minimum be met by aircraft electronic display portrayals under direct sunlight, glare source and other high ambient viewing conditions are described. The sunlight readability/legibility requirements and tests of the night vision imaging system (NVIS) compatibility specification MIL-L-85762 were in part founded on the data contained in this report. DTIC

07 AIRCRAFT PROPULSION AND POWER

Includes prime propulsion systems and systems components, e.g., gas turbine engines and compressors; and onboard auxilliary power plants for aircraft.

For related information see also *20 Spacecraft Propulsion and Power, 28 Propellants and Fuels,* and *44 Energy Production and Conversion.*

N95-18133*# National Aeronautics and Space Administration. Lewis Research Center, Cleveland, OH.
NUMERICAL MIXING CALCULATIONS OF CONFINED REACTING JET FLOWS IN A CYLINDRICAL DUCT
Victor L. Oechsle (Allison Engine Co., Indianapolis, IN.) and J. D. Holdeman Jan. 1995 46 p Presented at the 33rd Aerospace Sciences Meeting and Exhibit, Reno, NV, 9-12 Jan. 1995; sponsored by AIAA Original contains color illustrations
(Contract NAS3-25950; RTOP 537-02-21)
(NASA-TM-106736; E-9349; NAS 1.15:106736; AIAA Paper 95-0733)
Copyright Avail: CASI HC A03/MF A01; 22 functional color pages

The results reported in this paper describe some of the main flow characteristics and NOx production results which develop in the mixing process in a constant cross-sectional cylindrical duct. A 3-dimensional numerical model has been used to predict the mixing flow field and NOx characteristics in a mixing section of an RQL combustor. Eighteen configurations have been analyzed in a circular geometry in a fully reacting environment simulating the operating condition of an actual RQL gas turbine combustion liner. The evaluation matrix was constructed by varying three parameter: (1) jet-to-mainstream momentum-flux ration (J), (2) orifice shape or orifice aspect ratio, and (3) slot slant angle. The results indicate that the mixing flow field and NOx production significantly vary with the value of the jet penetration and subsequently, slanting elongated slots generally improve the NOx production at high J conditions. Round orifices produce low NOx at low J due to the strong jet penetration. The NOx production trends do not correlate with the mixing non-uniformity parameters described herein. Author

N95-18383 Naval Air Warfare Center, Trenton, NJ. Aircraft Div.
UNMANNED AERIAL VEHICLE HEAVY FUEL ENGINE TEST Final Report, Apr. 1992 - Jan. 1993
Robert Brucato, Joseph Lawton, and Anthony Maggio Oct. 1993 129 p
Limited Reproducibility: More than 20% of this document may be affected by microfiche quality

(AD-A284332; NAWCADTRN-PE-261) Avail: Issuing Activity (Defense Technical Information Center (DTIC))

This report documents the test results of three heavy fuel engines designed to demonstrate that Unmanned Aerial Vehicle operational requirements can feasibly be met utilizing heavy fuels (JP-5, JP-8 and Diesel) versus gasoline. The three engines included rotary engines delivered by AA-I Corporation and Defense Group Industries Incorporated and a two cylinder, two stroke engine delivered by Southwest Research Institute. The testing was conducted at the Naval Air Warfare Center Aircraft Division Trenton during the period of 17 April 1992 through 22 January 1993.

DTIC

N95-18911# Deutsche Forschungsanstalt fuer Luft- und Raumfahrt, Cologne (Germany). Inst. fuer Antriebstechnik.

ONE-DIMENSIONAL FLOW DESCRIPTION FOR THE COMBUSTION CHAMBER OF A SCRAMJET Ph.D. Thesis [EINDIMENSIONALE BRENNKAMMERBETRACHTUNGEN FUER EIN STAUSTRAHLTRIEBWERK MIT UEBERSCHALLVERBRENNUNG]

Frans G. J. Kremer 1994 171 p In GERMAN

(ISSN 0939-2963)

(DLR-FB-94-06) Avail: CASI HC A08/MF A02

A theoretical calculation model for the determination of the one-dimensional flow data in the combustion chamber of a scramjet is established. This model serves to improve the physical understanding of such flows in order to enable a more profound design of a scramjet combustor. It is shown, that the analytic notation of the continuity, momentum and energy equation of the non-constant area combustor is not useful to describe the physical relations. This is due to the unknown wall pressure integral, for which usually the formulation of the pressure-area power family, introduced by Crocco, is assumed. Therefore a model is established, which bases on the differential notation of the laws of conservation. This is solved using distribution functions and verified with experimental data. The model is used to quantify the influence of several parameters on the flow data. Finally design considerations for flight Mach number 15 and off-design considerations for flight Mach numbers 5, 10 and 15 are performed.

Author

N95-19017# Advisory Group for Aerospace Research and Development, Neuilly-Sur-Seine (France). Propulsion and Energetics Panel.

MATHEMATICAL MODELS OF GAS TURBINE ENGINES AND THEIR COMPONENTS [LES MODELES MATHEMATIQUES DES TURBOMOTEURS ET DE LEURS ORGANES]

Dec. 1994 183 p Lecture series held in Cleveland, OH, 7-8 Dec. 1994, in Wessling, Germany, 12-13 Dec. 1994 and in Paris, France, 15-16 Dec. 1994

(AGARD-LS-198; ISBN-92-836-1008-3) Copyright Avail: CASI HC A09/MF A02

This Lecture Series will present and discuss the scientific problems of modern mathematical simulation of gas turbine engines and their components. Some peculiarities of complex multicomponent and multidisciplinary models for whole flow passage of bypass gas turbine engine, core, multistage compressors and turbines, and other engine components will be studied. Solutions of steady and unsteady problems are given using high efficiency monotone numerical methods and the theoretical bases of these methods are presented. Many practical results of aerodynamic and thermostress simulations for engine components are shown. These results are compared widely with experimental data for accurate verification of developing computational codes. This Lecture Series, endorsed by the Propulsion and Energetics Panel of AGARD, has been implemented by the Technology Cooperation Program. For individual titles, see N95-19018 through N95-19026.

N95-19018# Central Inst. of Aviation Motors, Moscow (Russia).

ON THE CFD MONOTONE HIGH ACCURACY METHODS **c34**

Mikhail J. Ivanov, Vladislav G. Krupa, and Ravil Z. Nigmatullin *In* AGARD, Mathematical Models of Gas Turbine Engines and their Components Dec. 1994 19 p (For primary document see N95-19017 05-07)

Copyright Avail: CASI HC A03/MF A02

Some theoretical fundamentals of monotone high accuracy methods are presented. The conditions for the construction of monotone, total variation diminishing (TVD) and following difference schemes are described. The peculiarities of high accuracy and implicit methods design are given. The typical results of numerical solutions illustrate the principle features of developed computational techniques.

Author

N95-19019# Central Inst. of Aviation Motors, Moscow (Russia).

SOLUTION OF NAVIER-STOKES EQUATIONS USING HIGH ACCURACY MONOTONE SCHEMES **c34**

Vladislav G. Krupa and Mikhail J. Ivanov *In* AGARD, Mathematical Models of Gas Turbine Engines and their Components Dec. 1994 16 p (For primary document see N95-19017 05-07)

Copyright Avail: CASI HC A03/MF A02

Numerical monotone methods for integration of the Reynolds averaged Navier-Stokes equations are presented. These methods employ finite volume formulation, implicit high-order accuracy Godunov type scheme and two-equation (q - omega) turbulence model, based on integration up to the wall. To illustrate the typical peculiarities of these methods the computations of viscous flows in curvilinear ducts, around 2D airfoils and 3D shock-wave boundary layer interaction are considered. Available experimental data are used for verification of the computed results.

Author

N95-19020# Central Inst. of Aviation Motors, Moscow (Russia).

THE MATHEMATICAL MODELS OF FLOW PASSAGE FOR GAS TURBINE ENGINES AND THEIR COMPONENTS

Ravil Z. Nigmatullin and Mikhail J. Ivanov *In* AGARD, Mathematical Models of Gas Turbine Engines and their Components Dec. 1994 28 p (For primary document see N95-19017 05-07)

Copyright Avail: CASI HC A03/MF A02

Mathematical models for gas turbine engines and installation component flow passages based on real 3D geometry of flow passages, in particular spatial shape of blades, are considered. The models are based on numerical solving of unsteady Euler equations and so it allows simulation of some unsteady transitional functioning regimes of engines and installations together with steady ones. The models take into consideration the viscous losses, leakage in axial gaps and tip clearances, cooling air injection and selection. The first level mathematical models are based on 2D steady and unsteady methods on S(sub 1) and S(sub 2) surfaces. Some features of numerical algorithms based on these methods are considered. The second level models are based on 3D approaches anywhere in computational domains excluding the middles of axial gaps between neighboring blade rows where for the simplification of the problem the averaging in angular direction is fulfilled.

Author (revised)

N95-19021# Central Inst. of Aviation Motors, Moscow (Russia).

SIMULATION OF MULTIDISCIPLINARY PROBLEMS FOR THE THERMOSTRESS STATE OF COOLED HIGH TEMPERATURE TURBINES

Valerey K. Kostege, V. A. Halturin, and V. G. Sundurin *In* AGARD, Mathematical Models of Gas Turbine Engines and their Components Dec. 1994 15 p (For primary document see N95-19017 05-07)

Copyright Avail: CASI HC A03/MF A02

Numerical models for the thermostress state analysis of turbine rotor elements are discussed. Steady and unsteady temperature fields are calculated and result in solution of conjugate heat and hydraulic problems for blades (quasi three-dimensional model) for disk (two-dimensional model) and for the whole cooled rotor (three-dimensional model). A lot of attention is given to mass flow calculation in blade passages and turbine circumferential disk cavities. They are determined by using experimental data for pressure loss and generalized dependencies for friction and heat transfer coefficients on stators and rotors surfaces. On external blade surfaces the boundary conditions are defined from the solution of two-dimensional and three-dimensional gas dynamics problems and corrected from experimental data base for film cooling. The thermostress state is calculated by a finite element method for realistic geometry using common equations of elasticity theory.

Author

N95-19022# Central Inst. of Aviation Motors, Moscow (Russia).

APPLICATION OF MULTICOMPONENT MODELS TO FLOW PASSAGE SIMULATION IN MULTISTAGE TURBOMACHINES AND WHOLE GAS TURBINE ENGINES

Ravil Z. Nigmatullin *In* AGARD, Mathematical Models of Gas Turbine Engines and their Components Dec. 1994 17 p (For primary

document see N95-19017 05-07)
Copyright Avail: CASI HC A03/MF A02

Some features of used numerical algorithms for gas turbine engines components flow simulation are considered. Among them are topology of computational grids in 2D and 3D cases for flow passages of complex geometry, details of realization of conservative scheme at joints of different grids. In S(sub 2)-calculations it is necessary to consider the problem of inlet and outlet angles; in Euler calculation the ways of accounting for viscous loss effects are briefly described. Examples of calculations of flow through by-pass engine components are presented. Author

N95-19023# Central Inst. of Aviation Motors, Moscow (Russia).
SIMULATION OF STEADY AND UNSTEADY VISCOUS FLOWS IN TURBOMACHINERY
Vladislav G. Krupa *In* AGARD, Mathematical Models of Gas Turbine Engines and their Components Dec. 1994 39 p (For primary document see N95-19017 05-07)
Copyright Avail: CASI HC A03/MF A02

A Navier-Stokes code has been used to compute the viscous turbulent cascade flows. The numerical method employs implicit high-order accurate Godunov scheme and a two equation (q - omega) turbulence model based on the integration to the wall. The generation of the O-H grid system for viscous cascade flow simulations is discussed. Numerical solutions were obtained for 2D and 3D turbine cascade flows and 2D unsteady rotor-stator interactions. Available experimental data are used for verification of the computed results. Author

N95-19024# Central Inst. of Aviation Motors, Moscow (Russia).
APPLICATION OF MULTIDISCIPLINARY MODELS TO THE COOLED TURBINE ROTOR DESIGN
Valery K. Kostege, V. D. Venediktov, and A. V. Granovskii *In* AGARD, Mathematical Models of Gas Turbine Engines and their Components Dec. 1994 10 p (For primary document see N95-19017 05-07)
Copyright Avail: CASI HC A02/MF A02

A computer program for designing turbine vane and blade cooling systems is discussed. This program is based on the complex use of 2D and 3D gas dynamic, heat-transfer and thermostress models. FEM Thermostress models are formatted based on geometry data from the computer design system. One-dimensional mass flow and conjugate thermal models are quickly created by using graphic dialogue regimes for different cooling systems. Quasi-3D and 3D thermostress models are used to carry out cooling system optimization or comparison of alternative cooling systems. Author

N95-19025# Central Inst. of Aviation Motors, Moscow (Russia).
VERIFICATION OF MULTIDISCIPLINARY MODELS FOR TURBOMACHINES
Valerey K. Kostege *In* AGARD, Mathematical Models of Gas Turbine Engines and their Components Dec. 1994 7 p (For primary document see N95-19017 05-07)
Copyright Avail: CASI HC A02/MF A02

Accurate prediction of the temperature distribution in rotating blades is an important and difficult task. An approach for the verification of hydraulic and thermal models in real blades is discussed in the lecture. For static conditions, predicted local internal convective heat transfer coefficients on blades are corrected using a quasi-3D thermal-hydraulic model with the blade unsteady surface temperatures measured by the Thermovision system. External boundary conditions are corrected using the blade base surface temperatures measured by thermocouples on a hot static rig. The final identification of the models is carried out using measurements of the gas temperature distribution within the rotating blade passage, and the measured blade external surface temperature in the engine. Author

N95-19026# Central Inst. of Aviation Motors, Moscow (Russia).
PERSPECTIVE PROBLEMS OF GAS TURBINE ENGINES SIMULATION
Mikhail J. Ivanov *In* AGARD, Mathematical Models of Gas Turbine Engines and their Components Dec. 1994 19 p (For primary document see N95-19017 05-07)
Copyright Avail: CASI HC A03/MF A02

The purpose of the last lecture is to present the activity of CIAM in the field of the development of Computer Turbojet Test Technology based on aero-engine models of high 3D level. Using this technology the aero-engine design may be transformed into new quality. It's the predictions of steady and transient working processes, performance and efficiency on the first stage of engine design (without the real metal engine testing). These aero-engine models must accompany the whole engine life - from design to production and use on aircraft. Author

N95-19380*# National Aeronautics and Space Administration. Lewis Research Center, Cleveland, OH.
NASA LEWIS RESEARCH CENTER WORKSHOP ON FORCED RESPONSE IN TURBOMACHINERY
George L. Stefko, comp., Durbha V. Murthy, comp. (Toledo Univ., OH.), Michael Morel, comp. (NYMA, Inc., Brook Park, OH.), Dan Hoyniak, comp., and Jim W. Gauntner, comp. Dec. 1994 135 p Workshop held in Cleveland, OH, 11 Aug. 1993
(RTOP 505-63-5B)
(NASA-CP-10147; E-9111; NAS 1.55:10147) Avail: CASI HC A07/MF A02

A summary of the NASA Lewis Research Center (LeRC) Workshop on Forced Response in Turbomachinery in August, 1993 is presented. It was sponsored by the following NASA organizations: Structures, Space Propulsion Technology, and Propulsion Systems Divisions of NASA LeRC and the Aeronautics and Advanced Concepts & Technology Offices of NASA Headquarters. In addition, the workshop was held in conjunction with the GUIde (Government/Industry/Universities) Consortium on Forced Response. The workshop was specifically designed to receive suggestions and comments from industry on current research at NASA LeRC in the area of forced vibratory response of turbomachinery blades which includes both computational and experimental approaches. There were eight presentations and a code demonstration. Major areas of research included aeroelastic response, steady and unsteady fluid dynamics, mistuning, and corresponding experimental work. For individual titles, see N95-19381 through N95-19383.

N95-19381*# United Technologies Research Center, East Hartford, CT.
UNSTEADY AERODYNAMIC ANALYSES FOR TURBOMACHINERY AEROELASTIC PREDICTIONS
Joseph M. Verdon, M. Barnett, and T. C. Ayer *In* NASA. Lewis Research Center, NASA Lewis Research Center Workshop on Forced Response in Turbomachinery Dec. 1994 p 13-36 (For primary document see N95-19380 05-07)
Avail: CASI HC A03/MF A02

Applications for unsteady aerodynamics analysis in this report are: (1) aeroelastic: blade flutter and forced vibration; (2) aeroacoustic: noise generation; (3) vibration and noise control; and (4) effects of unsteadiness on performance. This requires that the numerical simulations and analytical modeling be accurate and efficient and contain realistic operating conditions and arbitrary modes of unsteady excitation. The assumptions of this application contend that: (1) turbulence and transition can be modeled with the Reynolds averaged and using Navier-Stokes equations; (2) 'attached' flow with high Reynolds number will require thin-layer Navier-Stokes equations, or inviscid/viscid interaction analyses; (3) small-amplitude unsteady excitations will need nonlinear steady and linearized unsteady analyses; and (4) Re to infinity will concern inviscid flow. Several computer programs (LINFLO, CLT, UNSVIS, AND SFLOW-IVI) are utilized for these analyses. Results and computerized grid examples are shown. This report was given during NASA LeRC Workshop on Forced Response in Turbomachinery in August of 1993. CASI

N95-19382*# National Aeronautics and Space Administration. Lewis Research Center, Cleveland, OH.
STEADY POTENTIAL SOLVER FOR UNSTEADY AERODYNAMIC ANALYSES
Dan Hoyniak *In its* NASA Lewis Research Center Workshop on Forced Response in Turbomachinery Dec. 1994 p 37-49 (For primary document see N95-19380 05-07)
Avail: CASI HC A03/MF A02

Development of a steady flow solver for use with LINFLO was the objective of this report. The solver must be compatible with LINFLO, be composed of composite mesh, and have transonic capability. The approaches used were: (1) steady flow potential equations written in nonconservative form; (2) Newton's Method; (3) implicit, least-squares, interpolation method to obtain finite difference equations; and (4) matrix

inversion routines from LINFLO. This report was given during the NASA LeRC Workshop on Forced Response in Turbomachinery in August of 1993. CASI

N95-19383*# Michigan Univ., Ann Arbor, MI.
FORCED RESPONSE OF MISTUNED BLADED DISKS
Christophe Pierre *In* NASA. Lewis Research Center, NASA Lewis Research Center Workshop on Forced Response in Turbomachinery Dec. 1994 p 95-120 (For primary document see N95-19380 05-07)
Avail: CASI HC A03/MF A02

Small mistuning can cause large, catastrophic changes in blade vibrational response whereby the amplitudes of vibration of some blades may increase by several hundred percent. This can produce 'rogue' blades and HCF failure. The free and forced responses may be highly sensitive to mistuning, and the tuned system predictions may be qualitatively in error and grossly underestimate blade forced response and overestimate fatigue life. Manufacturing tolerances, material non-uniformities, nonidentical root fixtures, and in-service degradation result in blade-to-blade differences that destroy cyclic symmetry in bladed discs. Therefore, a credible forced response prediction system for turbomachinery vibration must take mistuning into account. This report addresses these problems, states several objectives, and introduces NASA research program thrusts concerning this problem. This report was given during the NASA LeRC Workshop on Forced Response in Turbomachinery in August of 1993. CASI

N95-19595# Naval Postgraduate School, Monterey, CA.
AN ANALYSIS OF THE COSTS AND BENEFITS IN IMPROVING F402-RR-406A HIGH PRESSURE TURBINE, SECOND STAGE BLADES UNDER THE AIRCRAFT ENGINE COMPONENT IMPROVEMENT PROGRAM (CIP) M.S. Thesis
Donald Alan Walter Sep. 1994 82 p
(AD-A285127) Avail: CASI HC A05/MF A01

This thesis is part of a continuing project at the Naval Postgraduate School attempting to validate the cost effectiveness of the Aircraft Engine Component Improvement Program. It focuses on the costs and benefits derived from Power Plant Change 159 which improved High Pressure Turbine, Second Stage blades on the Harrier (AV-8B) aircraft's Rolls-Royce Pegasus (F402-RR-F406A) engine. Because sufficient failure rate data for the improved blades was not available, the analysis considers a range of costs/benefits based on two different projected blade reliabilities. The improvement to the High Pressure Turbine, Second Stage blades was found to be cost-effective from both a financial break-even point, in that the cost to produce the improvement will be recovered by the end of 1996 for the full range of projected blade reliabilities and from a Net Present Value analysis which shows that this improvement will save the Department of the Navy between $17,192,827 and $38,639,494 (in 1992 dollars) over the projected life cycle of the engine. DTIC

N95-19651*# NYMA, Inc., Brook Park, OH. Engineering Services Div.
PREDICTION OF WIND TUNNEL EFFECTS ON THE INSTALLED F/A-18A INLET FLOW FIELD AT HIGH ANGLES-OF-ATTACK Final Report
Crawford F. Smith Cleveland, OH NASA Jan. 1995 55 p
(Contract NAS3-27186; RTOP 505-68-30)
(NASA-CR-195429; E-9416; NAS 1.26:195429) Avail: CASI HC A04/MF A01

NASA Lewis is currently engaged in a research effort as a team member of the High Alpha Technology Program (HATP) within NASA. This program utilizes a specially equipped F/A-18A, the High Alpha Research Vehicle (HARV), in an ambitious effort to improve the maneuverability of high performance military aircraft at low subsonic speed, high angle of attack conditions. The overall objective of the Lewis effort is to develop inlet technology that will ensure efficient airflow delivery to the engine during these maneuvers. One part of the Lewis approach utilizes computational fluid dynamics codes to predict the installed performance of inlets for these highly maneuverable aircraft. Wind tunnel tests were a major component of the Lewis program. Since the available wind tunnel was small (9 x 15 ft) as compared to the scale of the model of the F/A-18A (19.78 percent), there were questions about the capability to obtain useful inlet performance data. The blockage effects were expected to be very large. This report represents the results of an analysis to determine how the wind tunnel walls effect inlet performance at several angles of attack. The predictions for the external particle traces along the fuselage indicate the influence of the wind tunnel side wall under the model is greater at 30 deg angle of attack than at 50 deg angle of attack on the under Leading Edge Extension (LEX) vortex trajectory. The side wall above the model appears to have negligible influence on the under LEX vortex. This may be due to the LEX acting as 'shield' to the upper wall effects. As expected, the wind tunnel has a significant influence on the external forces. The lift and drag coefficients increase significantly for the wind tunnel model as compared to free stream conditions. The wind tunnel had a small effect on the inlet recovery and on inlet total pressure distortion patterns. The predicted recoveries for the wind tunnel model are within one percentage point of the model recoveries in free stream conditions. Author

N95-19653# Advisory Group for Aerospace Research and Development, Neuilly-Sur-Seine (France). Propulsion and Energetics Panel.
EROSION, CORROSION AND FOREIGN OBJECT DAMAGE EFFECTS IN GAS TURBINES [LES CONSEQUENCES DE L'ENDOMMAGEMENT DES TURBINES A GAZ PAR EROSION, CORROSION ET OBJETS ETRANGERS]
Nov. 1994 338 p In ENGLISH and FRENCH Symposium held in Rotterdam, Netherlands, 25-28 Apr. 1994 Original contains color illustrations
(AGARD-CP-558; ISBN-92-836-0005-3) Copyright Avail: CASI HC A15/MF A03

The Conference Proceedings contains 31 papers presented at the Propulsion and Energetics Panel Symposium on Erosion, Corrosion and Foreign Object Damage Effects in Gas Turbines which was held from 25-28th April 1994, in Rotterdam, The Netherlands. The Technical Evaluation Report and the Keynote Address are included at the beginning and discussions follow most papers. The Symposium was arranged in the following Sessions: Operational Experience and Requirements (7); Deposition and Erosion (7); Foreign Object Damage (5); Coatings, Repairs and Materials Aspects - 1 (4); Coatings, Repairs and Materials Aspects - 2 (7); and Testing and Certification Procedures (1). For individual titles, see N95-19654 through N95-19684.

N95-19654# Rolls-Royce Ltd., Bristol (England).
OUT OF AREA EXPERIENCES WITH THE RB199 IN TORONTO
M. G. Down and M. J. Williams *In* AGARD, Erosion, Corrosion and Foreign Object Damage Effects in Gas Turbines Nov. 1994 7 p (For primary document see N95-19653 05-07)
Copyright Avail: CASI HC A02/MF A03

The Turbo Union RB 199 engine was developed during the late 1960's / early 1970's to meet a specification requirement aimed at defense of the Western European NATO alliance countries against the (then) perceived threat. During the latter part of the 1980's Tornado aircraft were delivered to the Royal Saudi Air Force and, supplemented by deployed units from the Royal Air Force, were engaged in an operational role during 1990 / 1991. Aircraft operations in the Saudi Arabia climates and natural environment created problems with engine life, hitherto not encountered in the European area of operation, nor during many RAF overseas deployments, including North America. These problems, mainly concerned with turbine blade contamination from airborne sand, were alleviated by the introduction of unique engine maintenance management techniques and eliminated by design changes. Author

N95-19655# Defence Research Agency, Farnborough, Hampshire (England). Air Vehicle Performance Dept.
THE OPERATION OF GAS TURBINE ENGINES IN HOT AND SANDY CONDITIONS: ROYAL AIR FORCE EXPERIENCES IN THE GULF CONFLICT
R. C. Sirs *In* AGARD, Erosion, Corrosion and Foreign Object Damage Effects in Gas Turbines Nov. 1994 8 p (For primary document see N95-19653 05-07)
Copyright Avail: CASI HC A02/MF A03

During the initial phase of the Gulf Crisis, the principal instrument at the disposal of the British Government which could respond in time was air power. This situation continued, and throughout the period of military build up and subsequent conflict air power remained a dominant factor. During the period, many equipment modifications were incorporated to increase both performance and reliability, and the gas turbine engines

which powered the RAF's aircraft were no exception. However in some cases, engines were operated at a much increased flying rate in harsh operating conditions in standard configuration. This paper reviews the operating experiences and some of the modifications incorporated, including the subsequent effect on aero-engine reliability trends. Author

N95-19656# Army Aviation Systems Command, Saint Louis, MO. Directorate for Engineering.

US ARMY ROTORCRAFT TURBOSHAFT ENGINES SAND AND DUST EROSION CONSIDERATIONS

Vernon R. Edwards and Peter L. Rouse *In* AGARD, Erosion, Corrosion and Foreign Object Damage Effects in Gas Turbines Nov. 1994 10 p (For primary document see N95-19653 05-07)

Copyright Avail: CASI HC A02/MF A03

The impact of operating in a sand and dust environment on U.S. Army rotorcraft turbine engines has been a major concern since the first turbine powered UH-1 Iroquois (Huey) helicopter was fielded in the early 1960s. The implication on turbine engine performance and durability had not sufficiently been recognized, or addressed, in early engine designs. Early engine military specifications had been primarily concerned with U.S. Air Force 'jet' engines for fixed wing aircraft. Although these early specifications included sand and dust requirements relative to ingestion capability and test substantiation, actual rotorcraft field experience was not considered, nor, in fact, was actual data available. This paper provides a brief history of the impact of operation in sand and dust and operational considerations on U.S. Army rotorcraft turbine engines. The general effects of sand and dust erosion, compaction, deformation, glassing, etc., on engine turbomachinery will be discussed. Finally, the results of operation in Southeast Asia, and during Desert Shield/Desert Storm, possibly the worse case operational environment encountered to date, will be presented. Author

N95-19657# Rolls-Royce Ltd., Bristol (England).

FUTURE DIRECTIONS IN HELICOPTER PROTECTION SYSTEM CONFIGURATION

Darrell L. Mann and Gordon D. Warnes *In* AGARD, Erosion, Corrosion and Foreign Object Damage Effects in Gas Turbines Nov. 1994 12 p (For primary document see N95-19653 05-07)

Copyright Avail: CASI HC A03/MF A03

Recent events have highlighted the fact that none of the currently available turboshaft intake protection systems, whether they be the permanent fit IPS or mission specific vortex pack types, have an adequate sand/dust separation capability. Evidence has been amply provided by low engine life, consequent support logistics problems and the necessity for development of short term emergency measures. The paper seeks to quantify the extent of the problem and define the solutions which will be required if a repeat of past experiences is to be avoided. The paper describes the directions which particles separator technology must take in order to meet future requirements. A further important aspect of future directions is the drive for an increase in an engine's ability to resist damage; the paper identifies those areas of the engine which are most prone to damage, comments on the need to strike the right balance between resistance and removal, and discusses the increasing value of sophisticated computer based design methodologies. Author

N95-19658# Naval Air Warfare Center, Trenton, NJ. Aircraft Div.

NAVY FOREIGN OBJECT DAMAGE AND ITS IMPACT ON FUTURE GAS TURBINE ENGINE LOW PRESSURE COMPRESSION SYSTEMS

Peter Charles DiMarco *In* AGARD, Erosion, Corrosion and Foreign Object Damage Effects in Gas Turbines Nov. 1994 9 p (For primary document see N95-19653 05-07)

Copyright Avail: CASI HC A02/MF A03

Foreign Object Damage (FOD), Domestic Object Damage (DOD), bird ingestion, and ice ingestion are all necessary factors to be considered in the design of reliable and maintainable fan systems for future U.S. Navy aircraft applications. The high rate of fan damage reported in U.S. Navy engines and its impact on repair and maintenance requirements such as engine down time, level of repair, and number of spares have caused the Navy in recent years to scrutinize the requirements which must be met in order to design a more reliable and rugged yet highly maintainable fan system for future aircraft. This paper reports the results of an investigation into the occurrences of Foreign Object Damage in several U.S. Navy aircraft, the repair approaches presently used by the U.S. Navy, and investigates the implications which these considerations present to the design of more damage tolerant fan systems. It further investigates the trade-offs in future turbomachinery design which balance gas turbine engine performance payoff against supportability and maintainability onboard ship. Author

N95-19659# Scandinavian Airlines System, Oslo (Norway).

SCANDINAVIAN AIRLINES SYSTEMS EXPERIENCE ON EROSION, CORROSION AND FOREIGN OBJECT DAMAGE EFFECTS ON GAS TURBINES

P. Stokke *In* AGARD, Erosion, Corrosion and Foreign Object Damage Effects in Gas Turbines Nov. 1994 10 p (For primary document see N95-19653 05-07)

Copyright Avail: CASI HC A02/MF A03

This article summarizes SAS' experience on engine FOD and compressor erosion. It will mainly focus on type of damages, debris sources, modifications developed, development of maintenance and inspection method to cope with the problem, revision of operational procedures etc. In addition the added maintenance costs implied by FOD and erosion will be discussed, as also will be the special considerations to be used for cold winter operations. Author

N95-19660# General Electric Co., Cincinnati, OH. Aircraft Engines Div.

MODERN TRANSPORT ENGINE EXPERIENCE WITH ENVIRONMENTAL INGESTION EFFECTS

T. L. Alge and J. T. Moehring *In* AGARD, Erosion, Corrosion and Foreign Object Damage Effects in Gas Turbines (SEE N95-19653 05-07) Nov. 1994 (For primary document see N95-19653 05-07)

Copyright Avail: CASI HC A02/MF A03

Modern propulsion engines have achieved a high level of reliability while manufacturers and users are always striving to further improve the safety record. The drive for safety in single-engine aircraft has resulted in safer multiple-engine applications. In modern turbofan-powered transports it is extremely unlikely that a failure intrinsic to an engine would initiate a sequence of events which could result in loss of capability for continued safe flight and landing. These rare events are limited to uncontained rotor disk fracture or uncontrolled fire. Of greater concern today are the non-intrinsic, common-cause events which involve power loss of more than one engine. These are externally-inflicted occurrences such as ingestion events or common-cause maintenance events resulting in simultaneous loss of power on more than one engine. The most frequent are those ingestion events involving products of the flying environment - flocking birds, ice, volcanic ash and extreme inclement weather. This environmental ingestion hazard viewed in overview is the primary subject of this paper. There is a body of knowledge on each of these subjects. Data from field operations and engine experience have provided guidelines for recognition of an occurrence and the proper action response. The primary precaution however remains - be aware, prevent, communicate and avoid. Author

N95-19661# Oxford Univ., Oxford (England). Dept. of Engineering Science.

PARTICLE DEPOSITION IN GAS TURBINE BLADE FILM COOLING HOLES

V. H. M. Kuk, P. T. Ireland, T. V. Jones, and M. G. Rose (Rolls-Royce Ltd., Derby, England.) *In* AGARD, Erosion, Corrosion and Foreign Object Damage Effects in Gas Turbines Nov. 1994 18 p Original contains color illustrations (For primary document see N95-19653 05-07)

Copyright Avail: CASI HC A03/MF A03

The aerodynamic processes leading to film cooling hole blockage have been investigated experimentally in large scale models of idealized internal cooling passages. The experimental scaling included reproducing engine cooling passage and hole Reynolds numbers together with a new dimensionless group which was matched experimentally to ensure that the measured particle trajectories were engine representative. It has been possible to achieve correct dimensional scaling with particles one thousand times larger than engine size. Simple visualization of the particle trajectories showed concentrations of impact locations inside holes normal to and inclined to the cooling passage surface. No attempt was made to model interaction between the particles and the passage walls. A new instrument has been developed to measure the concentration of particle impacts. Use of the device provides a fast and convenient way of measuring particle

impact distributions. The regions of high impact concentration are consistent with blockage structures found in engines after service. The process of internal blockage of film cooling holes has been shown to be due to inertia driven particles of the order of 1 micron in diameter. Flow conditions immune from impact concentration and hence the blockage process have been identified for the inclined film cooling hole. Author

N95-19662# Cincinnati Univ., OH. Dept. of Aerospace Engineering and Engineering Mechanics.

EXPERIMENTAL AND NUMERICAL SIMULATIONS OF THE EFFECTS OF INGESTED PARTICLES IN GAS TURBINE ENGINES

A. Hamed and W. Tabakoff *In* AGARD, Erosion, Corrosion and Foreign Object Damage Effects in Gas Turbines Nov. 1994 13 p (For primary document see N95-19653 05-07)

Copyright Avail: CASI HC A03/MF A03

Particles ingested in gas turbine engines follow trajectories that generally deviate from the flow streamlines and impact the component surfaces causing erosion damage. This paper deals with the experimental and numerical simulations of particle dynamics including surface interactions and the associated blade erosion in gas turbine engines. The experimental studies of particle surface impacts include the nonintrusive measurements of particle bounce conditions and the erosion testing of blade materials and blade coatings. Data obtained in the University of Cincinnati's high temperature erosion test facility at temperatures up to 1500 F for different alloys and coatings are presented. The numerical studies to simulate the particle dynamics in the turbomachines are described. Results of combined experimental and computational modeling are presented for the particle dynamics, the associated turbomachinery blade erosion, and performance loss. The probabilistic modeling of the experimentally measured variance in the particle bounce conditions and the loss of performance associated with particle ingestion are discussed. Author

N95-19663# Cranfield Univ., Bedford (England). School of Mechanical Engineering.

PARTICLE TRAJECTORIES IN GAS TURBINE ENGINES

S. C. Tan, R. L. Elder, and P. K. Harris *In* AGARD, Erosion, Corrosion and Foreign Object Damage Effects in Gas Turbines Nov. 1994 13 p (For primary document see N95-19653 05-07)

Copyright Avail: CASI HC A03/MF A03

This paper describes the technique of particle trajectory modeling in gas turbine engines with applications in helicopter inertial particle separator, axial ad centrifugal compressor. The model can be used with most CFD codes which utilize the finite volume (or element) techniques. Some qualitative validations were carried out using a laser transit anemometer in a particle separator and results show good comparison with predictions. The anemometer was also used to obtain restitution data for several target materials using quartz particle of different sizes at a range of impact velocities and angles. Author

N95-19664# Defence Research Agency, Farnborough, Hampshire (England).

THE CALCULATION OF EROSION IN A GAS TURBINE COMPRESSOR ROTOR

G. C. Horton, H. Vignau (Turbomeca S.A. - Brevets Szydlowski, Bordes, France.), and G. Leroy (Turbomeca S.A. - Brevets Szydlowski, Bordes, France.) *In* AGARD, Erosion, Corrosion and Foreign Object Damage Effects in Gas Turbines Nov. 1994 14 p (For primary document see N95-19653 05-07)

Copyright Avail: CASI HC A03/MF A03

Erosion of the turbomachinery and other components in helicopter gas turbines operating in a sandy environment is a significant problem. In order to better understand the mechanics of such erosion, and to enable the design of components better able to withstand it, a means of modelling erosion is needed. Such a method has been developed at Turbomeca. It consists of a method of predicting the trajectories of the particles within the component, on the basis of a prescribed aerodynamic field and taking into account rebounds from the walls, together with correlations for the erosion caused by impacts of the particles with the walls. The various aspects of the method have been validated by comparison with available experimental data and these comparisons are presented. Predictions of particle trajectories in two types of particle separator and in two gas turbine compressors (axial and centrifugal) are also presented, together with some comparisons with experiment. Author

N95-19665# Motoren- und Turbinen-Union Muenchen G.m.b.H., Munich (Germany).

PERFORMANCE DETERIORATION OF AXIAL COMPRESSORS DUE TO BLADE DEFECTS

J. Schmuecker and A. Schaeffler *In* AGARD, Erosion, Corrosion and Foreign Object Damage Effects in Gas Turbines Nov. 1994 6 p (For primary document see N95-19653 05-07)

Copyright Avail: CASI HC A02/MF A03

During flight operation the engine swallows sand or other hard particles usually from the runway. Passing through the compressors they will damage the blades, erode the coating and deteriorate seals. The submitted paper presents some measurements, which show the effect on compressor performance due to the most important and frequent defects. The investigation - conducted at high pressure compressors - includes tests with reworked blades at leading and trailing edges, rounded rotor tips and increased tip clearances. The results are summarized in easy to handle correlations, which enables the user to estimate the deterioration and to fix repair rules within the allowed performance loss range. Author

N95-19666# National Research Council of Canada, Ottawa (Ontario). Inst. for Aerospace Research.

EROSION OF T56 5TH STAGE ROTOR BLADES DUE TO BLEED HOLE OVERTIP FLOW

B. C. Barry and T. C. Currie *In* AGARD, Erosion, Corrosion and Foreign Object Damage Effects in Gas Turbines Nov. 1994 10 p (For primary document see N95-19653 05-07)

Copyright Avail: CASI HC A02/MF A03

Severe trailing edge erosion of ALLISON T56 gas turbine 5th and 10th stage compressor blades has been observed in Field Service Evaluations and sand ingestion tests. The erosion typically occurs within 3 mm of the blade tip and has been attributed to overtip flow produced by the bleed holes present over the 5th and 10th stage rotors. The overtip flow through the 5th stage bleed holes of an operating T56 has been surveyed with a laser two-focus (L2F) velocimeter in order to identify the features of the flow field responsible for the tip erosion. Two-dimensional measurements were made at 4 spanwise locations in the outer 25 percent of the span. Three-dimensional measurements were made at three spanwise stations within 7 mm of the blade tip (15 percent of span). The flow was found to be unaffected by the bleed holes beyond 3-4 mm from the blade tip. This result is consistent with erosion patterns observed on service-exposed blades and blades subjected to accelerated erosion in sand ingestion tests. Author

N95-19667# National Technical Univ., Athens (Greece). Thermal Engineering Section.

INVESTIGATION OF MECHANICAL EROSION IN FUEL PIPELINES c37

M. Founti and A. Klipfel *In* AGARD, Erosion, Corrosion and Foreign Object Damage Effects in Gas Turbines Nov. 1994 7 p (For primary document see N95-19653 05-07)

Copyright Avail: CASI HC A02/MF A03

The aim of this work is to investigate the characteristics of mechanical erosion in a vertical sudden expansion turbulent two-phase flow. The flow field in an axisymmetric sudden expansion flow laden with round glass particles at 3 percent per volume and flowing in the direction of gravity was examined both experimentally and computationally. Velocities of particles and fluid were simultaneously measured at Re = 6 x 10(exp 4) using a single component laser Doppler anemometer and a burst peak detector which discriminates the amplitude of the Doppler bursts resulting from the two discrete phases. The test facility was refractive index matched, allowing measurement of the bar-U, V, sq bar-u, sq v and sq w components throughout the whole velocity flow field. Computations were performed using a Eulerian/Langrangian approach considering drag, lift and gravity forces acting on a particle as well as modelling of particle-dispersion by turbulence, particle-wall and particle-particle collisions. Mechanical erosion of the pipe wall was determined via an empirical formula, using the predicted impact velocities and angles. Author

N95-19668# Palermo Univ. (Italy). Dipt. di Meccanica e Aeronautica.
AN AIRBORNE MONITORING SYSTEM FOR FOD AND EROSION FAULTS
Giuseppe Lombardo and Giovanni Torella (Italian Air Force Academy, Naples, Italy.) *In* AGARD, Erosion, Corrosion and Foreign Object Damage Effects in Gas Turbines Nov. 1994 12 p (For primary document see N95-19653 05-07)
Copyright Avail: CASI HC A03/MF A03

FOD and erosion are the events causing the most part of accidental damages in gas turbine engines. When FOD is not destroying or when erosion is in progress the performance level decreases and the necessity of unscheduled maintenance actions becomes quite real. Moreover when there is a light FOD, or the erosion process is constant in time, it may be difficult to detect the exact cause of performance decrease and to plan the most effective maintenance action. This paper deals with the results of a study carried out for developing an Engine Condition Monitoring system particularly suitable for detecting the MicroFOD and erosion effects in gas turbines. The developed numerical code has been applied to a single spool turboshaft engine with free power turbine. The obtained results are presented and discussed. Author

N95-19669# Societe Nationale d'Etude et de Construction de Moteurs d'Aviation, Moissy-Cramayel (France).
DESIGN OF FAN BLADES SUBJECTED TO BIRD IMPACT [CONCEPTION DES AUBES FAN SOUMISES A L'IMPACT D'OISEAUX]
P. Vignolles, P. X. Bussonnet, and J. Talbotec *In* AGARD, Erosion, Corrosion and Foreign Object Damage Effects in Gas Turbines Nov. 1994 11 p In FRENCH Original contains color illustrations (For primary document see N95-19653 05-07)
Copyright Avail: CASI HC A03/MF A03

The quality of fan blades in terms of behavior is one of the major parameters affecting the safety of modern aircraft driven by engines with strong by-pass ratio. The reinforcements defined as necessary in certain areas of the profiles of the fan blades must be a compromise between the objectives of mechanical resistance and aerodynamic performance. SNECMA developed a methodology to forecast the impact behavior of the fan blades based on a mathematical model. In parallel, the progress made in aerodynamics made it possible to predict the consequences of these stresses related to ingestion on aerodynamic performance and still maintain high levels of performance. Author

N95-19670# Motoren- und Turbinen-Union Muenchen G.m.b.H., Munich (Germany).
IMPACT LOADING OF COMPRESSOR STATOR VANES BY HAILSTONE INGESTION
J. Frischbier *In* AGARD, Erosion, Corrosion and Foreign Object Damage Effects in Gas Turbines Nov. 1994 12 p (For primary document see N95-19653 05-07)
Copyright Avail: CASI HC A03/MF A03

Impacts of 1 inch diameter ice bullets onto stator vanes of the first stage of an axial compressor were investigated at an impact velocity of v = 257 m/s. The analytical and experimental simulations of typical hailstone ingestions were performed with special emphasis on damage effects of the thin leading edges of the hidden titanium vanes. The paper includes a comprehensive overview of the ice properties used in the analytical model regarding elastic constants, strain rate dependent strength and crack propagation under compression. The influence of different impact positions and ice properties was investigated in the analytical simulations. In all cases the highest stresses occur at the leading edge of the hidden vane. When the center of impact is placed on the leading edge plastic deformations are expected and localized microcracks cannot be excluded. When the target point is positioned on the suction side of the vane (air foil flank) the energy transfer and the loading is high, but the deformations remain elastic. For verification shooting tests of ice bullets on a complete stator were performed. The ice balls were made by freezing water in liquid nitrogen and the impacts were recorded with a high speed camera. The observed leading edge deflections are in good agreement with the calculated values, but in no case plastic deformations or cracks were detected. Author

N95-19671# Oxford Univ., Oxford (England). Dept.of Engineering Science.
SOFT BODY IMPACT ON TITANIUM FAN BLADES
D. A. Hughes, I. Martindale (Rolls-Royce Ltd., Derby, England.), and C. Ruiz *In* AGARD, Erosion, Corrosion and Foreign Object Damage Effects in Gas Turbines Nov. 1994 5 p (For primary document see N95-19653 05-07)
Copyright Avail: CASI HC A01/MF A03

The strength of titanium fan blades under soft body impact has been studied by means of panel tests. The panels, representing blades with various leading edge profiles, were exposed to oblique impact in a gas gun facility by launching a block of gelatine at speeds of up to 600 m/s. High speed photography, at 100,000 f.p.s. and strain gauges provide a record of the deformation. Failure occurred either as a result of the deformation or localized tearing. Tearing was taken as determining the limiting strength of the blade, which was found to be strongly dependent on the leading edge profile. Author

N95-19672*# National Aeronautics and Space Administration. Lewis Research Center, Cleveland, OH.
ICE-IMPACT ANALYSIS OF BLADES
C. C. Chamis, P. L. N. Murthy, S. N. Singhal (NYMA, Inc., Brook Park, OH.), and E. S. Reddy (NYMA, Inc., Brook Park, OH.) *In* AGARD, Erosion, Corrosion and Foreign Object Damage Effects in Gas Turbines Nov. 1994 12 p (For primary document see N95-19653 05-07)
Copyright Avail: CASI HC A03/MF A03

A computational capability is described for evaluating the ice-impact on engine blades made from composites. The ice block is modeled as an equivalent spherical object and has the velocity opposite to that of the aircraft with direction parallel to the engine axis. A finer finite element mesh is used for a portion of the blade near the impact region compared to the course mesh for the rest of the blade. The effects of ice size and velocity on the average leading edge strain are evaluated for a simulated unswept composite propfan blade. Parametric studies are performed to assess the blade structural responses due to the ice-impact at various locations along the span. It is found that: (1) for a given engine speed, a critical ice speed exists that corresponds to the maximum strain; and (2) the tip bending type frequencies increase after impact while the torsion frequencies decrease. Author

N95-19673# Motoren- und Turbinen-Union Muenchen G.m.b.H., Munich (Germany).
DAMAGE OF HIGH TEMPERATURE COMPONENTS BY DUST-LADEN AIR
P. Koenig, T. Miller, and A. Rossmann *In* AGARD, Erosion, Corrosion and Foreign Object Damage Effects in Gas Turbines Nov. 1994 12 p Original contains color illustrations (For primary document see N95-19653 05-07)
Copyright Avail: CASI HC A03/MF A03

Turbine engine operators are familiar with damage to components due to dust-laden air in the compressor, but they are less aware that such damage can also occur to high temperature components, especially turbine rotor blades. Nevertheless, the frequency of occurrence of this type of damage as well as the related costs and effects on turbine performance are also of major concern. Author

N95-19674# Liege Univ. (Belgium). Dept. Metallurgie et Science des Materiaux.
ANALYSIS OF THE EROSION OF CUBIC CENTERED AND FACE CENTERED METALLIC MATERIALS [ANALYSE DE L'EROSION DE MATERIAUX METALLIQUES DE STRUCTURES CUBIQUES CENTREE ET FACE CENTREE] **c26**
A. Magnee *In* AGARD, Erosion, Corrosion and Foreign Object Damage Effects in Gas Turbines Nov. 1994 13 p In FRENCH (For primary document see N95-19653 05-07)
Copyright Avail: CASI HC A03/MF A03

A generalized law of erosion, in nondimensional form, is proposed. The aforementioned explicitly gives an account of the nature and the microstructure of the material impacted, the angle of impact of the particles, and their hardness. The erosion behavior of various steels, pig iron, and cast iron is examined as well as the behavior of new ordered intermetallic materials, Fe-25 percent Al-(Zr, Cr, B). The concern of such alloys in an erosion-corrosion environment is shown. Author

N95-19675# Liburdi Engineering Ltd., Hamilton (Ontario).
PROTECTIVE COATINGS FOR COMPRESSOR GAS PATH COMPONENTS
D. R. Nagy, V. R. Parameswaran (National Research Council of Canada, Ottawa, Ontario.), J. D. MacLeod (National Research Council of Canada, Ottawa, Ontario.), and J. P. Immarigeon (National Research Council of Canada, Ottawa, Ontario.) *In* AGARD, Erosion, Corrosion and Foreign Object Damage Effects in Gas Turbines Nov. 1994 10 p (For primary document see N95-19653 05-07)
Copyright Avail: CASI HC A02/MF A03

The blades and vanes in gas turbine compressors operating in dusty environments are prone to degradation by solid particle erosion, which causes surface roughening and changes in airfoil geometry. This results in decreased compressor performance, and higher specific fuel consumption, leading to significantly increased operational cost. Erosion damage is more prominent in flight engines without air inlet filter protection. Application of a thin ceramic titanium nitride (TiN) coating to improve the erosion resistance of compressor airfoils was thoroughly investigated. Coatings were applied to engine hardware by a Reactive Ion Coating (RIC) process and optimized to produce a very adherent erosion resistant coating. Computer modeling of the erosion process occurring on coated and uncoated airfoils suggested that the operational life of the compressor can be enhanced by a factor of two. A complete set of compressor blades and vanes for an Allison T56 turboprop engine was coated for engine qualification tests. Laboratory tests showed that the thin coating had no significant influence on either the resonant frequency or the fatigue resistance of the blades and the instrumented engine tests confirmed that the performance was typical of overhauled engines, with no aerothermodynamic loss. Therefore, titanium nitride coatings are suitable for service and can be used on existing engines to improve the life of the compressors. Author

N95-19676# Societe Nationale d'Etude et de Construction de Moteurs d'Aviation, Evry (France). Materials and Process Dept.
NEW TRENDS IN COATINGS DEVELOPMENTS FOR TURBINE BLADES: MATERIALS PROCESSING AND REPAIR
S. Alperine, R. Martinou, R. Mevrel (Office National d'Etudes et de Recherches Aeronautiques, Paris, France.), and J. P. Huchin (Sochata, Chatellerault, France.) *In* AGARD, Erosion, Corrosion and Foreign Object Damage Effects in Gas Turbines Nov. 1994 10 p (For primary document see N95-19653 05-07)
Copyright Avail: CASI HC A02/MF A03

Turbine engines for aeronautic applications now have to face strenuous requirements concerning not only operating performances but also reliability and repairability. This evolution of the specifications induces important consequences regarding the choice and the design of turbine blade protective coatings. This paper presents several key features concerning the deposition techniques and the real-life behavior of such coatings: (1) complex aluminides well suited to the protection against high temperature oxidation and hot corrosion of directionally solidified nickel-base superalloy turbine blades; (2) ceramic coatings used as thermal barriers - they have to exhibit both high resistance to thermomechanical fatigue and adequate smoothness; (3) processing techniques for thermal barriers, including plasma spraying, electron beam physical vapor deposition and plasma enhanced chemical vapor deposition; and (4) blades and coatings repair techniques. Author

N95-19677# Interturbine Holding B.V., Lomm (Netherlands).
BRAZE REPAIR POSSIBILITIES FOR HOT SECTION GAS TURBINE PARTS
G. Marijnissen and R. vanGestel (Elbar B.V., Lomm, Netherlands.) *In* AGARD, Erosion, Corrosion and Foreign Object Damage Effects in Gas Turbines Nov. 1994 5 p (For primary document see N95-19653 05-07)
Copyright Avail: CASI HC A01/MF A03

Overlay braze repair is a good technique for restoring aircraft vanes and industrial blades and vanes. The negative effects of the intermetallic phase, formed during the overlay braze process, can be reduced in such a way that the mechanical properties - creep rupture, strength and ductility - can be achieved close to the properties of the base materials. The elimination of the negative effects can be achieved by a combination of careful selection of the chemistries of the repair materials and the application of the correct procedures for cleaning and heat cycle. Author

N95-19678# National Aerospace Lab., Amsterdam (Netherlands).
GAS TURBINE COMPRESSOR CORROSION AND EROSION IN WESTERN EUROPE
H. J. Kolkman *In* AGARD, Erosion, Corrosion and Foreign Object Damage Effects in Gas Turbines Nov. 1994 7 p (For primary document see N95-19653 05-07)
Copyright Avail: CASI HC A02/MF A03

It is shown that for gas turbines in the West European environment: (1) during operation hygroscopic salts - notably ammonium sulphate (originating from manure) and sodium and magnesium chloride (from sea salt) - are deposited on compressor components and (2) during shutdowns these wet deposits acidify owing to the absorption of the air pollutants NO2 and SO2. The response of the compressor metals can be broadly categorized as follows. Different steels show different degrees of corrosion. Especially pitting corrosion can lead to component rejection and compressor disintegration. This necessitates frequent washing and/or corrosion resistant coatings. Modern cleaners are environmentally friendly and contain a corrosion inhibitor. The performance of cleaners and coatings is discussed. Nickel-based superalloys and titanium alloys are not prone to corrosion in compressor applications. In order to avoid problems these materials should be used even for secondary components. This is exemplified by a crash due to stress corrosion of a component costing only a few dollars. Compressor erosion as such is not a major problem in Western Europe. However, corrosion resistant coatings usually have a poor erosion resistance. Moreover, engine manufacturers and users prefer a general compressor coating for use in both corrosive and erosive environments. Developments with respect to compressor cleaners and coatings are discussed. Author

N95-19679# Turbomeca S.A. - Brevets Szydlowski, Bordes (France).
MULTILAYER ANTI-EROSION COATINGS [REVETEMENTS ANTI-EROSION MULTICOUCHES]
P. Monge-Cadet, F. Pellerin, C. Farges (Etablissement Technique Central de l'Armement, Arcueil, France.), D. Rickerby (Rolls-Royce Ltd., Derby, England.), and E. Quesnel (Nuclear Research Center of Grenoble, Grenoble, France.) *In* AGARD, Erosion, Corrosion and Foreign Object Damage Effects in Gas Turbines Nov. 1994 8 p In FRENCH (For primary document see N95-19653 05-07)
Copyright Avail: CASI HC A02/MF A03

Gas turbines for helicopters are prone to high degradations by abrasive particle ingestion when taking off, landing or during low altitude flights. Multilayer coatings have been developed to protect critical compressor components. After a presentation of the relevant parameters for conception and achievement of erosion resistant coatings, the most promising systems will be described. They are based on stacking arrangement of ductile layers (tungstene) and hard layers (solid solution of carbon or nitrogen into tungstene, titanium diboride). These multilayer coatings exhibit an erosion resistance improved by more than two orders of magnitude compared with that of uncoated Ti6Al4V alloy. Author

N95-19680# Turbine Support Europa, Tilburg (Netherlands).
HIGH VELOCITY OXYGEN FUEL SPRAYING OF EROSION AND WEAR RESISTANT COATINGS ON JET ENGINE PARTS
A. T. J. Verbeek *In* AGARD, Erosion, Corrosion and Foreign Object Damage Effects in Gas Turbines Nov. 1994 10 p (For primary document see N95-19653 05-07)
Copyright Avail: CASI HC A02/MF A03

High velocity oxygen fuel (HVOF) spraying is the most recent development in the field of thermal spraying. The importance of this technique for the repair and new part manufacturing of jet engine parts is rapidly increasing. The HVOF uses a supersonic oxygen-fuel flame to heat and accelerate the powder particles that form the coating. The high particle velocity results in a high density and a low porosity, a high bond strength, and a high macro and micro hardness of the coating. The high quality of the HVOF coatings makes it possible to use these coatings on high loaded, rotating parts in jet engines. This paper will highlight the use of HVOF processes to apply erosion resistant cermet coatings to high pressure compressor blades. These blades are exposed to severe erosion. Next to the D-gun process, HVOF spraying is the only nonproprietary technique that can be used to apply these high performance coatings. Also the use of the HVOF process to apply wear resistant coatings and superalloys to jet engine parts will be discussed. The difference between HVOF coatings

and plasma sprayed coatings will be highlighted. During HVOF spraying, the parts are exposed to a high heat flow. Solutions to avoid overheating, especially of titanium parts, will be presented. Author

N95-19681# Centro Sviluppo Materiali S.p.A., Trento (Italy).
THERMAL TESTING OF HIGH PERFORMANCE THERMAL BARRIER COATINGS FOR TURBINE BLADES
L. Bertamini and A. DiGianfrancesco (Centro Sviluppo Materiali S.p.A., Rome, Italy.) *In* AGARD, Erosion, Corrosion and Foreign Object Damage Effects in Gas Turbines Nov. 1994 11 p (For primary document see N95-19653 05-07)
Copyright Avail: CASI HC A03/MF A03

A 350 micron thick 7 wt percent Y2O3-ZrO2 (7YSZ) ceramic Thermal Barrier Coating (TBC) was manufactured in an argon atmosphere and with a strictly controlled substrate temperature on flat IN 600 samples and on IN 100 aircraft turbine blades. This new atmosphere and temperature controlled spraying (ATCS) allows the reduction of the residual stresses and an improvement in the microstructure and in the mechanical properties of the coating. The good performance of these new TBC's was assessed in thermal fatigue and in thermal shock tests carried out in air at 1100 C and at 1280 C respectively. The oxidation rate of the metal-ceramic interface was measured at 1100 C. Failure of the TBC's was induced only by the deterioration (like oxidation, cracking) of the uncoated parts of the samples, as testing temperature was too severe for the base metals. Spalling was thereafter driven by compressive stresses near the aluminum oxide layer at the metal-ceramic interface. The results of these tests underline the good quality of the ceramic coating manufactured by the new ATCS technology. Author

N95-19682# La Sapienza Univ., Rome (Italy). Dipt. di Chimica.
X-RAY ABSORPTION SPECTROSCOPY IN HIGH TEMPERATURE OXIDATION OF METALS AND ALLOYS **c26**
Daniele Gozzi and Massimo Tomellini (Tor Vergata Univ., Rome, Italy.) *In* AGARD, Erosion, Corrosion and Foreign Object Damage Effects in Gas Turbines Nov. 1994 8 p Sponsored by Centro Sviluppo Materiali and Lab. Nazionali di Frascati (For primary document see N95-19653 05-07)
Copyright Avail: CASI HC A02/MF A03

An experimental technique is described that allows for the joint study of the kinetics and of the oxide structure during the high temperature oxidation of metal surfaces. Oxygen is supplied at the metal through an electrochemical oxygen pump and the oxygen pressure, at the metal surface, is measured during oxidation by a YSZ (yttria stabilized zirconia) oxygen sensor. XAS (x-ray absorption spectroscopy) is performed in fluorescence mode at the cation K edge and after each oxidation step. An appropriate analysis of the XAS spectra could provide information on both the oxidation kinetics and oxide structure. Experimental data on the high temperature oxidation of nickel, cobalt, and Fe(64%)Ni(36%) alloy, at low oxygen pressure, are reported and analyzed according to the proposed data reduction. These results indicate the presented technique to be particularly suitable for studying the hot corrosion of oxide film too thick for common surface spectroscopy (AUGER, ESCA) and too thin for conventional thermogravimetric technique. Author

N95-19683*# National Aeronautics and Space Administration. Lewis Research Center, Cleveland, OH.
RESISTANCE OF SILICON NITRIDE TURBINE COMPONENTS TO EROSION AND HOT CORROSION/OXIDATION ATTACK
Thomas E. Strangmen (Garrett Turbine Engine Co., Phoenix, AZ.) and Dennis S. Fox *In* AGARD, Erosion, Corrosion and Foreign Object Damage Effects in Gas Turbines Nov. 1994 11 p (For primary document see N95-19653 05-07)
Copyright Avail: CASI HC A03/MF A03

Silicon nitride turbine components are under intensive development by AlliedSignal to enable a new generation of higher power density auxiliary power systems. In order to be viable in the intended applications, silicon nitride turbine airfoils must be designed for survival in aggressive oxidizing combustion gas environments. Erosive and corrosive damage to ceramic airfoils from ingested sand and sea salt must be avoided. Recent engine test experience demonstrated that NT154 silicon nitride turbine vanes have exceptional resistance to sand erosion, relative to superalloys used in production engines. Similarly, NT154 silicon nitride has excellent resistance to oxidation in the temperature range of interest - up to 1400 C. Hot corrosion attack of superalloy gas turbine components is well documented. While hot corrosion from ingested sea salt will attack silicon nitride substantially less than the superalloys being replaced in initial engine applications, this degradation has the potential to limit component lives in advanced engine applications. Hot corrosion adversely affects the strength of silicon nitride in the 850 to 1300 C range. Since unacceptable reductions in strength must be rapidly identified and avoided, AlliedSignal and the NASA Lewis Research Center have pioneered the development of an environmental life prediction model for silicon nitride turbine components. Strength retention in flexure specimens following 1 to 3300 hour exposures to high temperature oxidation and hot corrosion has been measured and used to calibrate the life prediction model. Predicted component life is dependent upon engine design (stress, temperature, pressure, fuel/air ratio, gas velocity, and inlet air filtration), mission usage (fuel sulfur content, location (salt in air), and times at duty cycle power points), and material parameters. Preliminary analyses indicate that the hot corrosion resistance of NT154 silicon nitride is adequate for AlliedSignal's initial engine applications. Protective coatings and/or inlet air filtration may be required to achieve required ceramic component lives in more aggressive environments. Author

N95-19684# Naval Air Warfare Center, Trenton, NJ. Aircraft Div.
TESTING CONSIDERATIONS FOR MILITARY AIRCRAFT ENGINES IN CORROSIVE ENVIRONMENTS (A NAVY PERSPECTIVE)
Frank T. Carroll and Deborah R. Parish *In* AGARD, Erosion, Corrosion and Foreign Object Damage Effects in Gas Turbines Nov. 1994 13 p Original contains color illustrations (For primary document see N95-19653 05-07)
Copyright Avail: CASI HC A03/MF A03

This paper describes the considerations given to the testing of aircraft engines intended for use by the United States military (primarily the Navy) in potentially corrosive environments. The origins and intent of the Navy's full-scale corrosion susceptibility test are explored, and the evolution of the test from its early form to the present 1,200-hour program is described in detail. Sample results illustrating the effectiveness of the current test procedure are presented. Also noted are the activities currently underway to improve the test's effectiveness in the face of advancing engine and test equipment technologies. Author

N95-19769*# NYMA, Inc., Cleveland, OH.
ON SUPERSONIC-INLET BOUNDARY-LAYER BLEED FLOW Final Report
Gary J. Harloff and Gregory E. Smith Cleveland, OH NASA Jan. 1995 17 p
(Contract NAS3-27186; RTOP 505-62-20)
(NASA-CR-195426; E-9393; NAS 1.26:195426; AIAA Paper 95-0038)
Copyright Avail: CASI HC A03/MF A01

Boundary-layer bleed in supersonic inlets is typically used to avoid separation from adverse shock-wave/boundary-layer interactions and subsequent total pressure losses in the subsonic diffuser and to improve normal shock stability. Methodologies used to determine bleed requirements are reviewed. Empirical sonic flow coefficients are currently used to determine the bleed hole pattern. These coefficients depend on local Mach number, pressure ratio, hole geometry, etc. A new analytical bleed method is presented to compute sonic flow coefficients for holes and narrow slots and predictions are compared with published data to illustrate the accuracy of the model. The model can be used by inlet designers and as a bleed boundary condition for computational fluid dynamic studies. Author

N95-19864 Purdue Univ., West Lafayette, IN. School of Mechanical Engineering.
AERO-THERMODYNAMIC DISTORTION INDUCED STRUCTURED DYNAMIC RESPONSE Final Report, 1 Jun. 1991 - 31 Dec. 1993
Sanford Fleeter 4 May 1994 101 p Limited Reproducibility: More than 20% of this document may be affected by microfiche quality
(Grant AF-AFOSR-0251-91)
(AD-A279931; AFOSR-94-0338TR) Avail: Issuing Activity (Defense Technical Information Center (DTIC))

This final report summarizes the results obtained on Grant AFOSR-91-025. The overall objective of this basic research program was the quantitative investigation of the fundamental phenomena relevant to

aero-thermodynamic distortion induced structural dynamic blade responses in multistage gas turbine engines and the study of the fundamental unsteady aerodynamics and heat transfer phenomena inherent in turbines. The technical approach involved unique benchmark experiments and also analyses. In particular, the flow physics of multistage blade row interactions were investigated, with unique unsteady aerodynamic data obtained and analyses developed to understand, quantify, and discriminate the fundamental flow phenomena as well as to direct the modeling of advanced analyses. DTIC

08 AIRCRAFT STABILITY AND CONTROL

Includes aircraft handling qualities; piloting; flight controls; and autopilots.

For related information see also *05 Aircraft Design, Testing and Performance.*

N95-18553 Department of the Navy, Washington, DC.
FLUID DYNAMIC LINEAR ACCELEROMETER Patent
David R. Keyser, inventor (to Navy) 8 Mar. 1994 7 p Filed 17 May 1993
(AD-D016413; US-Patent-5,291,784; US-Patent-Appl-SN-063844; US-Patent-Class-73-516) Avail: US Patent and Trademark Office

A linear acceleration sensing device operates through a fluid medium. A fluid signal output represents a differential pressure from the elastic deformation of a fluid-filled diaphragm or bellows assembly. A pair of fluid proximity sensors operate differentially in a fluid control network and detect the elastic deformation of the diaphragm assembly caused by increased hydrostatic pressure resulting from a change in acceleration, or 'g' force. DTIC

N95-18567*# Rockwell International Corp., Downey, CA. Space Systems Div.
STRATEGIC AVIONICS TECHNOLOGY DEFINITION STUDIES. SUBTASK 3-1A3: ELECTRICAL ACTUATION (ELA) SYSTEMS TEST FACILITY
J. P. Rogers, K. L. Cureton, and J. R. Olsen 30 Sep. 1994 53 p (Contract NAS9-18880)
(NASA-CR-188360; NAS 1.26:188360; SSD94D0298) Avail: CASI HC A04/MF A01

Future aerospace vehicles will require use of the Electrical Actuator systems for flight control elements. This report presents a proposed ELA Test Facility for dynamic evaluation of high power linear Electrical Actuators with primary emphasis on Thrust Vector Control actuators. Details of the mechanical design, power and control systems, and data acquisition capability of the test facility are presented. A test procedure for evaluating the performance of the ELA Test Facility is also included. Author

N95-18597# Advisory Group for Aerospace Research and Development, Neuilly-Sur-Seine (France). Structures and Materials Panel.
AIRCRAFT LOADS DUE TO TURBULENCE AND THEIR IMPACT ON DESIGN AND CERTIFICATION [EFFORTS AVION DUS A LA TURBULENCE ATMOSPHERIQUE ET LEURS IMPACTS SUR LA CONCEPTION ET LA CERTIFICATION]
Dec. 1994 93 p In ENGLISH and FRENCH Workshop held in Lillehammer, Norway, 5 May 1994
(AGARD-R-798; ISBN-92-836-0002-9) Copyright Avail: CASI HC A05/MF A01

The AGARD Structures and Materials Panel has always been heavily involved in the field of the effects of atmospheric disturbances on the behavior of aircraft. The Panel organized a Workshop on the theme 'Aircraft Loads due to Turbulence and their Impact on Design and Certification'. This Workshop was held on 5 May 1994. This document reproduces the papers presented. For individual titles, see N95-18598 through N95-18605.

N95-18598# British Aerospace Airbus Ltd., Bristol (England).
THE IMPACT OF NON-LINEAR FLIGHT CONTROL SYSTEMS ON THE PREDICTION OF AIRCRAFT LOADS DUE TO TURBULENCE
R. M. Warman *In* AGARD, Aircraft Loads due to Turbulence and their Impact on Design and Certification Dec. 1994 8 p (For primary document see N95-18597 05-08)
Copyright Avail: CASI HC A02/MF A01

During the past ten years the extensive use of electronic flight control systems has introduced a high level of non-linearity, to the behavior of civil transport aircraft, in response to both pilot inputs and external influences such as turbulence. These systems that control, protect, and, in some instances, alleviate the loads experienced by the aircraft have had a significant impact on the prediction of aircraft loads. There is an increasing need both to model control system non-linearity to avoid designing control systems that degrade structural performance, and to demonstrate the effectiveness of alleviation systems for aircraft certification. The introduction of non-linear flight control systems presents little problem when using time-based simulations to predict aircraft loads due to discrete gusts. Frequency domain, Power-Spectral Density (PSD), analysis used to predict aircraft loads due to Continuous Turbulence (CT), however, is severely restrictive, requiring a linear mathematical model of both the aircraft and control systems. Over the past ten-to-fifteen years various analysis techniques have been developed that provide time-based interpretations of the CT atmosphere and, therefore, means by which loads due to CT can be predicted for aircraft with non-linear flight control systems. Recent involvement in the design of Airbus aircraft has led to British Aerospace Airbus Limited taking an active role in both developing and using these non-linear analysis techniques. By drawing on experience gained during the design of recent Airbus aircraft, the impact of non-linear flight control systems on the prediction of aircraft loads due to turbulence is discussed. Author

N95-18599# Aerospatiale, Toulouse (France). Dept. Etudes Generales-Structures.
GYROSCOPIC AND PROPELLER AERODYNAMIC EFFECTS ON ENGINE MOUNTS DYNAMIC LOADS IN TURBULENCE CONDITIONS [EFFETS GYROSOPIQUES ET AERODYNAMIQUES DES PROPULSEURS SUR LES CHARGES DES MOTEURS D'AVIONS EN CONDITIONS TURBULENTES] c05
J. M. Saucray *In* AGARD, Aircraft Loads due to Turbulence and their Impact on Design and Certification Dec. 1994 12 p In FRENCH (For primary document see N95-18597 05-08)
Copyright Avail: CASI HC A03/MF A01

This paper deals with the problem of calculating loads on engines and their supporting structures when inertial characteristic, high engine speeds, large displacements, imposed by extreme atmospheric disturbances, give an important impact of gyroscopic effect. A direct method integrating the gyroscopic action in Lagrange's equations as a function of the polar moment of inertia, engine revolution speed and precession speed is presented and compared to the more common practice of superimposing gyroscopic effects on the basis of the angular speed calculated at the engine center of gravity. The results establish a good correlation between the two method on pitch and yaw moments on engine. On the other hand, transfer function modifications due to gyroscopic effects generate an increase of other loads for the direct method calculations, for both the turboprop and the turbojet aircraft. Effects of the aerodynamic force of the propeller due to the engine response are also examined. Author

N95-18600# Deutsche Airbus G.m.b.H., Hamburg (Germany). Structural Dynamics.
TREATMENT OF NON-LINEAR SYSTEMS BY TIMEPLANE-TRANSFORMED CT METHODS: THE SPECTRAL GUST METHOD
H. Lusebrink and J. Brink-Spalink *In* AGARD, Aircraft Loads due to Turbulence and their Impact on Design and Certification Dec. 1994 8 p (For primary document see N95-18597 05-08)
Copyright Avail: CASI HC A02/MF A01

The present paper discusses the problems which occur when PSD/Continuous Turbulence (C.T.) gust methods, originally developed for linear dynamic gust analysis in the frequency plane, are applied to modern transport A/C with flight control systems, containing a variety of nonlinearities for signal shaping. Power spectral density (PSD) gust velocity intensities are defined by the von Karman power spectrum in the frequency plane, scaled by the design gust intensity U(sub sigma) (RMS). This definition of gust in the frequency plane causes the basic problems for nonlinear dynamic analysis, in contrary to the timeplane defined Tuned Discrete Gusts. Discrete Gust calculations show that aircraft nonlinearities cannot be neglected. To

treat nonlinearities for C.T. there are basically three approaches (apart from linearization methods): (1) (SSB) Stochastic Simulation Based Methods (timeplane stochastic simulation), usually in combination with exceedance rate based design load definition; (2) MFB) Matched Filter Based Methods ('Worst Case Gusts'): for each load station, a search within a class of shape functions of prescribed 'spectral energy' is necessary to find that shape giving the highest load; and (3) (SG) Spectral Gust Method: uses discrete gusts having exactly the von karman spectrum, and computes the energy norm of the loadtime history. A practical method for nonlinear C.T. method should have the following characteristics: give loads consistent to existing requirements (for linear aircraft); give correlated (balanced) loads; and be straight-forward and economical, when applied for a large number of design cases to be calculated. Since the SSB methods need long simulation times and give no balanced loads (together with exceedance rate counting), and the MFB methods are very expensive, the present paper proposes the SG method. It needs only one step to derive design loads, is consistent to Design Envelope Analysis and provides correlated loads. Author

N95-18601# Construcciones Aeronauticas S.A., Madrid (Spain). Structural Dynamics Dept.

A STUDY OF THE EFFECT OF STORE UNSTEADY AERODYNAMICS ON GUST AND TURBULENCE LOADS **c05**

M. Oliver, J. Casalengua, C. Maderuelo, Y. Camacho, and H. Climent *In* AGARD, Aircraft Loads due to Turbulence and their Impact on Design and Certification Dec. 1994 12 p (For primary document see N95-18597 05-08)

Copyright Avail: CASI HC A03/MF A01

Gust and turbulence loads are the most severe conditions for some parts of the aircraft, especially in the outboard wing region. The addition of external stores usually alleviates the gust/turbulence loads on the wing but becomes critical for other components as pylons and wing/pylon attachments. Safety implications and all-weather envelope of current fighters force an accurate study of the gust/turbulence response of the aircraft for each store configuration. Inertia is the most important contribution of the store to the gust/turbulence loads. Nevertheless, store unsteady aerodynamics should be included if significantly changes the results of the gust/turbulence response. This paper is devoted to the analytical study of the effect of store unsteady aerodynamics on gust/turbulence response. A large number of configurations have been included in the study. Several regulations to define the gust/turbulence excitation have been used. Author

N95-18602# McDonnell-Douglas Aerospace, Long Beach, CA. Transport Aircraft.

COMPARISON OF STOCHASTIC AND DETERMINISTIC NONLINEAR GUST ANALYSIS METHODS TO MEET CONTINUOUS TURBULENCE CRITERIA **c05**

Patrick J. Goggin *In* AGARD, Aircraft Loads due to Turbulence and their Impact on Design and Certification Dec. 1994 12 p (For primary document see N95-18597 05-08)

Copyright Avail: CASI HC A03/MF A01

Current continuous turbulence Power Spectral Density (PSD) gust analysis methods are valid only for linear aircraft. In the past, many methods for the analysis of nonlinear aircraft to meet the current PSD gust criteria have been proposed. In this paper, three stochastic simulation based and one deterministic function based methods are compared and evaluated for the compliance of nonlinear aircraft to the current continuous turbulence gust criteria. The aircraft configurations analyzed in this paper include a symmetric aircraft model coupled to a nonlinear gust load alleviation (GLA) system and an anti-symmetric aircraft model coupled to a nonlinear yaw damper system. Results from these four nonlinear methods are compared to linear closed and open-loop results as well as currently used linear approximation methods. Computing performance issues are addressed to provide the reader with a complete picture of the trade-off between the analysis' accuracy and computing cost. Author

N95-18603# Cessna Aircraft Co., Wichita, KS. Aircraft Structural Integrity Dept.

DESIGN LIMIT LOADS BASED UPON STATISTICAL DISCRETE GUST METHODOLOGY **c05**

D. L. Hull *In* AGARD, Aircraft Loads due to Turbulence and their Impact on Design and Certification Dec. 1994 8 p (For primary document see N95-18597 05-08)

Copyright Avail: CASI HC A02/MF A01

Statistical Discrete Gust (SDG) methodology for extreme turbulence provides the basis of a design criterion that accounts for: (1) the statistical nature of design level turbulence; (2) the effects of lightly damped aircraft responses; (3) critical responses that may have significant frequency separation; and (4) the effects of nonlinear control systems. The criterion would eliminate the need for multiple design criteria and could increase the structural efficiency of new aircraft. The increased efficiency would be the result of having equally probable design limit loads for all gust critical components of the aircraft. Author

N95-18604# De Havilland Aircraft Co. of Canada Ltd., Downsview (Ontario).

A REVIEW OF GUST LOAD CALCULATION METHODS AT DE HAVILLAND **c02**

John Glaser *In* AGARD, Aircraft Loads due to Turbulence and their Impact on Design and Certification Dec. 1994 9 p (For primary document see N95-18597 05-08)

Copyright Avail: CASI HC A02/MF A01

The development of an analysis system for the routine calculation of gust response loads is reviewed in some detail in this report. While the system provides adequate design strength margins, a more robust and effective system would reduce user workload, computer costs and analysis time. it is suggested that other analysis systems could benefit similarly, particularly when considering the demands imposed by highly nonlinear aircraft systems, the trend toward full finite element structural dynamic models and the relentless quest for structural efficiency. It is proposed that improvements in analysis systems could evolve from the collective experience in gust loads methodologies acquired within the aeronautical community. To capitalize on that collective experience, it is recommended that a working group of gust load specialists be formed to assemble and evaluate current and promising methods for calculating gust loads and to recommend standardized airplane test cases, both rigid and elastic, for validating analysis methods and results. Author

N95-18605*# National Aeronautics and Space Administration. Langley Research Center, Hampton, VA.

SPECIAL EFFECTS OF GUST LOADS ON MILITARY AIRCRAFT **c05**

John C. Houbolt *In* AGARD, Aircraft Loads due to Turbulence and their Impact on Design and Certification Dec. 1994 7 p (For primary document see N95-18597 05-08)

Copyright Avail: CASI HC A02/MF A01

In the operation of airplanes, atmospheric turbulence creates a broad spectrum of problems. The nature of these problems is presented in this paper. Those that are common to both the commercial carriers and to the military fleet are discussed first. Attention is then focused on the problems that are of special concern in military operations. An aim is to bring out the need for continued effort in the gust research area. Author

N95-18641# Wright Lab., Wright-Patterson AFB, OH.

PRESSURE MEASUREMENTS ON AN F/A-18 TWIN VERTICAL TAIL IN BUFFETING FLOW. VOLUME 4, PART 2: BUFFET CROSS SPECTRAL DENSITIES Final Report, 15 Apr. 1993 - 15 Aug. 1994

Chris Pettit, Michael Banford, Dansen Brown, and Ed Pendleton Aug. 1994 693 p See also AD-A279126, AD-A281581 and AD-A281444 (AF Proj. 2401)

(AD-A285555; WL-TM-94-3132-Vol-4-Pt-2) Avail: CASI HC A99/MF A06

Buffeting pressure measurements were made on the vertical tail surface of a full scale F/A-18 aircraft model in the National Full Scale Aerodynamics Complex at NASA Ames Research Center. Test variables included angle-of-attack, aircraft sideslip angle, and dynamic pressure. Accelerometers were used to obtain vertical tail accelerations. Pressure transducers were mounted on the starboard vertical tail. Steady and unsteady pressures were obtained. Unsteady pressure data were reduced to PSD and CSD forms. Both steady and unsteady RMS pressure coefficients are also presented. Volume 1 contains the general description of the model, the test program, and highlights of the reduced data. Volume 2 contains steady and unsteady RMS data. Volume 3 contains unsteady PSD results. Volume 4 contains unsteady CSD results. DTIC

N95-18902 Stanford Univ., CA.
DESIGN AND FLIGHT TEST OF A SIMPLIFIED CONTROL SYSTEM FOR A TRANSPORT HELICOPTER Ph.D. Thesis
Christopher Reece Purvis 1994 230 p
Avail: Univ. Microfilms Order No. DA9414640

Helicopter transport pilots must give priority to aircraft control tasks when flying in a high-workload cockpit. To test a control system that would enhance safety and expedite pilot training in high-workload cockpits, the investigator test flew on the NASA CH-47 variable-stability helicopter a command-and-hold control system that required only constant inputs by the pilot to generate ramp responses in groundspeed, heading, and altitude. If undelayed, these ramp responses are ideal for simplified control, but in practice each controlled output, particularly groundspeed, experiences a distracting time lag. This distraction can be eliminated by presenting the integral of the pilot's output-rate commands on a cockpit display. Distractions caused by overshoots in pitch and roll following each command change are minimized by employing the dynamic feedforward of asymptotic model following (AMF), which generates in real time attitude commands correct to fly a constant velocity rate. Tailored to be well-damped, these feedforward attitude commands are particular solutions, or forced responses, that can be tracked asymptotically by a stabilized aircraft. In the baseline control logic these attitude commands were tightly tracked using the stabilization of the linear quadratic regulator. Because the attitude feedback is relatively noise free and not subject to drop-outs, tight tracking of attitude instead of velocity commands not only minimizes the control distraction of pitch and roll overshoots but also minimizes feedback noise on the aircraft controls. After the pilot releases his controls, the distraction of having to monitor and correct the groundspeed response during velocity-hold flight is removed through use of integral-error feedback on the controlled outputs. Turns were coordinated by gain-scheduling the lateral-directional compensation. Turn coordination was also evaluated using an alternative design that employed nonlinear cancellation compensation in translation. During flight the groundspeed, heading, and altitude for both the baseline and alternative designs tracked their particular solutions with small errors, and both designs achieved satisfactory handling qualities in pitch. Handling only one control at a time and using simple, pulse-like inputs, the pilot was able to change and hold groundspeed, heading, and altitude. The two designs were exercised using various maneuvers; among these were longitudinal dash/quickstops, lateral sidesteps, bobups, pedal turns, coordinated slalom turns, and a climbing/descending 180 degree course reversal.
Dissert. Abstr.

N95-19029* National Aeronautics and Space Administration. Ames Research Center, Moffett Field, CA.
NASA DEVELOPS NEW DIGITAL FLIGHT CONTROL SYSTEM
Michael Mewhinney 12 Dec. 1994 2 p
(NASA-News-Release-94-47) Avail: CASI HC A04

This news release reports on the development and testing of a new integrated flight and propulsion automated control system that aerospace engineers at NASA's Ames Research Center have been working on. The system is being tested in the V/STOL (Vertical/Short Takeoff and Landing) Systems Research Aircraft (VSRA).
CASI

N95-19576*# West Virginia Univ., Morgantown, VA. Dept. of Mechanical and Aerospace Engineering.
DETERMINATION OF STABILITY AND CONTROL DERIVATIVES FROM THE NASA F/A-18 HARV FROM FLIGHT DATA USING THE MAXIMUM LIKELIHOOD METHOD Progress Report
Marcello R. Napolitano Jan. 1995 101 p
(Contract NCC2-759)
(NASA-CR-197320; NAS 1.26:197320) Avail: CASI HC A06/MF A02

This report is a compilation of PID (Proportional Integral Derivative) results for both longitudinal and lateral directional analysis that was completed during Fall 1994. It had earlier established that the maneuvers available for PID containing independent control surface inputs from OBES were not well suited for extracting the cross-coupling static (i.e., C(sub N beta)) or dynamic (i.e., C(sub Npf)) derivatives. This was due to the fact that these maneuvers were designed with the goal of minimizing any lateral directional motion during longitudinal maneuvers and vice-versa. This allows for greater simplification in the aerodynamic model as far as coupling between longitudinal and lateral directions is concerned. As a result, efforts were made to reanalyze this data and extract static and dynamic derivatives for the F/A-18 HARV (High Angle of Attack Research Vehicle) without the inclusion of the cross-coupling terms such that more accurate estimates of classical model terms could be acquired. Four longitudinal flights containing static PID maneuvers were examined. The classical state equations already available in pEst for alphadot, qdot and thetadot were used. Three lateral directional flights of PID static maneuvers were also examined. The classical state equations already available in pEst for betadot, p dot, rdot and phi dot were used. Enclosed with this document are the full set of longitudinal and lateral directional parameter estimate plots showing coefficient estimates along with Cramer-Rao bounds. In addition, a representative time history match for each type of meneuver tested at each angle of attack is also enclosed.
Derived from text

09 RESEARCH AND SUPPORT FACILITIES (AIR)

Includes airports, hangars and runways; aircraft repair and overhaul facilities; wind tunnels; shock tubes; and aircraft engine test stands.

For related information see also *14 Ground Support Systems and Facilities (Space).*

N95-18054*# National Aeronautics and Space Administration. Lewis Research Center, Cleveland, OH.
BACKGROUND NOISE LEVELS MEASURED IN THE NASA LEWIS 9-BY 15-FOOT LOW-SPEED WIND TUNNEL
Richard P. Woodward, James H. Dittmar, David G. Hall (NYMA, Inc., Brook Park, OH.), and Bonnie Kee-Bowling Dec. 1994 17 p Presented at the 33d Aerospace Sciences Meeting and Exhibit, Reno, NV, 9-12 Jan. 1995; sponsored by AIAA
(Contract NAS3-27186; RTOP 538-03-11)
(NASA-TM-106817; E-9356; NAS 1.15:106817; AIAA Paper 95-0720)
Copyright Avail: CASI HC A03/MF A01

The acoustic capability of the NASA Lewis 9 by 15 Foot Low Speed Wind Tunnel has been significantly improved by reducing the background noise levels measured by in-flow microphones. This was accomplished by incorporating streamlined microphone holders having a profile developed by researchers at the NASA Ames Research Center. These new holders were fabricated for fixed mounting on the tunnel wall and for an axially traversing microphone probe which was mounted to the tunnel floor. Measured in-flow noise levels in the tunnel test section were reduced by about 10 dB with the new microphone holders compared with those measured with the older, less refined microphone holders. Wake interference patterns between fixed wall microphones were measured and resulted in preferred placement patterns for these microphones to minimize these effects. Acoustic data from a model turbofan operating in the tunnel test section showed that results for the fixed and translating microphones were equivalent for common azimuthal angles, suggesting that the translating microphone probe, with its significantly greater angular resolution, is preferred for sideline noise measurements. Fixed microphones can provide a local check on the traversing microphone data quality, and record acoustic performance at other azimuthal angles.
Author

N95-18087# Federal Aviation Administration, Atlanta, GA.
EVALUATION OF AN UNLIGHTED SWINGING AIRPORT SIGN
Eric S. Katz Aug. 1994 13 p
(AD-A284763; DOT/FAA/CT-TN94/29) Avail: CASI HC A03/MF A01

An unlighted swinging airport sign was evaluated at the Federal Aviation Administration Technical Center. The purpose of the evaluation was to determine the readability of the sign under varying wind and jet blast conditions. Results indicate that the sign is readable under all of the test conditions except when subjected to wind speeds of approximately 35 to 40 knots with gusts produced by the additive effect of the ambient winds and the jet blast. Even under this condition, readability of the sign remained adequate except at the most extreme angular displacement.
DTIC

N95-18405 Naval Air Warfare Center, Patuxent River, MD. Aircraft Div.
COMPARISON OF FREQUENCY RESPONSE AND PERTURBATION METHODS TO EXTRACT LINEAR MODELS FROM A NONLINEAR SIMULATION
Keith A. Balderson and Jeffrey T. Weathers 1994 14 p Limited Reproducibility: More than 20% of this document may be affected by

microfiche quality
(AD-A284115) Avail: CASI HC A03

The purpose of this paper is to compare two distinct methods to extract a linear state-space model about a reference flight condition from a nonlinear simulation. The frequency response method uses a time history input which contains the frequencies of interest to drive the simulation. The frequency response method uses a time history input which contains the frequencies of interest to drive the simulation frequency input and the output of the simulation are transformed to the frequency domain, and the desired frequency responses of the simulation are calculated. A linear model is then fit to the frequency responses using system identification techniques. The perturbation method extracts a linear model by perturbing the model states and inputs from the reference flight condition and calculating the resulting model coefficients. Both methods were used to extract a fourth order longitudinal state-space model from the V-22 full nonlinear simulation. The time history responses and system matrices of the extracted model were compared. The comparison showed that both methods are effective means to reduce a nonlinear simulation to a linear state-space model. DTIC

N95-18508 Naval Air Warfare Center, Patuxent River, MD. Aircraft Div.
VIRTUAL REALITY, AN AIR COMBAT T AND E PERSPECTIVE
R. R. Smullen, Jr. and R. E. Nowak 1994 10 p Limited Reproducibility: More than 20% of this document may be affected by microfiche quality
(AD-A284161) Avail: Issuing Activity (Defense Technical Information Center (DTIC))

The exponential increase in the complexity of modern aircraft and aircraft systems has made it extremely difficult to assess the mission effectiveness of Naval aviation weapons systems against new threats. Flight testing has historically been the primary source of data on the effectiveness of our aircraft and weapons, but flight testing is expensive and limited in the questions it can answer. For this reason, the U.S. Naval Air Warfare Center has embarked on the development of a fully integrated,. multi-spectral ground test facility called the Air Combat Environment Test and Evaluation Facility (ACETEF) which is capable of creating a virtual test environment for testing advanced weapon systems. DTIC

N95-18586*# National Aeronautics and Space Administration. Lewis Research Center, Cleveland, OH.
USERS GUIDE FOR NASA LEWIS RESEARCH CENTER DC-9 REDUCED-GRAVITY AIRCRAFT PROGRAM
John S. Yaniec Jan. 1995 78 p
(RTOP 694-03-0C)
(NASA-TM-106755; E-9175; NAS 1.15:106755) Avail: CASI HC A05/MF A01

The document provides guidelines and information for users of the DC-9 Reduced-Gravity Aircraft Program. It describes the facilities, requirements for test personnel, equipment design and installation, mission preparation, and in-flight procedures. Those who have used the KC-135 reduced-gravity aircraft will recognize that many of the procedures and guidelines are the same, to ensure a commonality between the DC-9 and KC-135 programs. Author

N95-18724 Naval Air Warfare Center, Patuxent River, MD. Aircraft Div.
THE GENERIC SIMULATION EXECUTIVE AT MANNED FLIGHT SIMULATOR
James Nichols 1994 9 p Limited Reproducibility: More than 20% of this document may be affected by microfiche quality
(AD-A283997) Avail: Issuing Activity (Defense Technical Information Center (DTIC))

The Manned Flight Simulator (MFS) at the Naval Air Warfare Center Aircraft Division (formerly the Naval Air Test Center) was created to provide rapid response to a wide range of US Navy simulation requirements. The necessity to simulate any aircraft in the US Navy inventory stimulated the idea of creating 'roll-in, roll-out' simulation bays that would accept any cockpit having standard geometric and electrical interfaces. The capability to use any cockpit at any simulation bay in turn led to the need for a flexible and generic software package for simulating any airframe. The Controls Analysis and Test Loop Environment (CASTLE) executive allows the user to easily generate and operate an aircraft simulation, while also providing a very powerful set of tools for simulation development and engineering analysis. Although the CASTLE package was originally designed to operate on Digital Equipment Corporation (DEC) machines using the VMS operating system and DEC screen management software, recent developments include a MOTIF-based window interface environment and compatibility with the UNIX operating system. The CASTLE package is being proposed as a starting point for a standard airframe simulation package to satisfy US Navy requirements. DTIC

N95-18725 Naval Air Warfare Center, Patuxent River, MD. Aircraft Div.
HELICOPTER IN-FLIGHT SIMULATION DEVELOPMENT AND USE IN TEST PILOT TRAINING
R. V. Miller and L. A. Khinoo 1994 15 p Limited Reproducibility: More than 20% of this document may be affected by microfiche quality
(AD-A283998) Avail: CASI HC A03

The U.S. Naval Test Pilot School (USNTPS) trains pilots, flight officers and engineers in the technical and managerial skills necessary to conduct aircraft and airborne systems test and evaluation. An integral part of this training is the use of ground and in-flight simulators to demonstrate the effects of varying aircraft flying qualities parameters. The USNTPS has developed specialized simulation facilities to meet the unique training requirements. This paper describes the development of a Variable Stability and Control (VSC) system installed in an SH-60B helicopter as a specialized training aid for use at the USNTPS. The development of the VSC system is traced from requirements through syllabus introduction. DTIC

N95-18903 Georgia Inst. of Tech., Atlanta, GA.
A LINEAR SYSTEM IDENTIFICATION AND VALIDATION OF AN AH-64 APACHE AEROELASTIC SIMULATION MODEL Ph.D. Thesis
Selwyn Howard Sturisky 1993 269 p
Avail: Univ. Microfilms Order No. DA9415668

This study addresses a linear math model validation of a global, nonlinear real-time rotary wing flight simulator at hover and 130 knots. The simulation is the AH-64 attack helicopter with a rotor blade element model. The main rotor dynamics have been formulated to provide a consistent matching between structural and aerodynamic theory. The structural model is a representation of the flexible blade based on a priori mode shape data. The dynamic inflow model is an adaptation of the Peters/He theory. Frequency response testing of the simulation model permits an evaluation of the mid to high frequency range. The Comprehensive Identification from Frequency Responses (CIFER) program is used to (1) extract a complete set of nonparametric input-to-output frequency responses that fully characterize the coupled helicopter dynamics, and (2) conduct a nonlinear search for a state space model that matches the frequency response data set. CIFER is used to extract state space stability derivative models from both flight test data and simulator generated responses. These linear models are compared with the vehicle response in both the frequency domain and in the time domain to confirm predictive capabilities to dissimilar input forms. The hover results obtained showed that a high fidelity identification of the state space linear models was achieved. Both linear models proved an excellent match with the frequency response set and demonstrated excellent predictive capabilities. The six-DOF model fit was significantly improved by inclusion of the higher order rotor terms. The effects of these higher order terms were most apparent on the pitch rate, roll rate, and collective response of the aircraft. The forward flight data set was not as high quality as the hover data set and low signal to noise ratios hindered the identification process. Nevertheless, it was possible to identify a six-DOF model that matched the aircraft frequency response set quite closely. Of extreme significance is confirmation that the FLIGHTLAB solution technique used to model the Apache correctly predicts the off-axis response of the aircraft. The methodology described herein explores a new approach to the rotorcraft system identification problem, simplifying the selection of model parameters to be changed and aiding in determining an adequate model form and structure. Dissert. Abstr.

N95-18942 Materials Research Labs., Ascot Vale (Australia).
CALIBRATION AND TESTING OF A LARGE-SCALE ELECTRIC GUN FOR SHOCK HUGONIOT MEASUREMENTS
David J. Hatt and Philip F. X. Ryan Oct. 1993 37 p
(MRL-TR-93-24) Copyright Avail: Issuing Activity

This report presents further work on the MRL large-scale electric gun facility including the use of a screened room and a purpose-built safety interlock system, calibration of an electric gun using a VISAR velocity interferometer, and tests on two laser break-beam arrangements for

measuring flyer velocity. The VISAR was also used for making velocity measurements during some impact experiments on several materials to test the suitability of the facility for obtaining Hugoniot and spall strength data. The materials were Perspex and Lexan (polymethyl methacrylate and polycarbonate) and aluminium alloy 3105. The flyer velocities measured using the break-beam arrangements were compared with those measured by the VISAR. The agreement between the two methods was found to be poor and inconsistent. High-speed photographs show leakage of plasma past the flyer. Interruption of the laser beams by the plasma instead of the flyer seems to be the reason for the poor agreement. The Hugoniot and spall strength data were in general agreement with published data.

Author

N95-18961* National Aeronautics and Space Administration. Langley Research Center, Hampton, VA.

METHOD AND DEVICE FOR DETERMINING BOND SEPARATION STRENGTH USING INDUCTION HEATING Patent

Robert H. Coultrip, inventor (to NASA), Samuel D. Johnson, inventor (to NASA), Carl E. Copeland, inventor (to NASA), W. Morris Phillips, inventor (to NASA), and Robert L. Fox, inventor (to NASA) 20 Dec. 1994 14 p Filed 23 Jun. 1993

(NASA-Case-LAR-14678-1; US-Patent-5,374,808; US-Patent-Appl-SN-083402; US-Patent-Class-219-633; US-Patent-Class-219-635; US-Patent-Class-219-659; US-Patent-Class-219-665; US-Patent-Class-73-827; Int-Patent-Class-H05B-6/10) Avail: US Patent and Trademark Office

An induction heating device includes an induction heating gun which includes a housing, a U-shaped pole piece having two spaced apart opposite ends defining a gap there between, the U-shaped pole piece being mounted in one end of the housing, and a tank circuit including an induction coil wrapped around the pole piece and a capacitor connected to the induction coil. A power source is connected to the tank circuit. A pull test machine is provided having a stationary chuck and a movable chuck, the two chucks holding two test pieces bonded together at a bond region. The heating gun is mounted on the pull test machine in close proximity to the bond region of the two test pieces, whereby when the tank circuit is energized, the two test pieces are heated by induction heating while a tension load is applied to the two test pieces by the pull test machine to determine separation strength of the bond region.

Official Gazette of the U.S. Patent and Trademark Office

N95-19286*# National Aeronautics and Space Administration. Lewis Research Center, Cleveland, OH.

OPERATING CAPABILITY AND CURRENT STATUS OF THE REACTIVATED NASA LEWIS RESEARCH CENTER HYPERSONIC TUNNEL FACILITY

Scott R. Thomas, Charles J. Trefny, and William D. Pack Jan. 1995 13 p Presented at the 6th International Aerospace Planes and Hypersonics Technologies Conference, Chattanooga, TN, 3-7 Apr. 1995; sponsored by AIAA

(RTOP 505-70-62)

(NASA-TM-106808; E-9294; NAS 1.15:106808; AIAA Paper 95-6146)

Copyright Avail: CASI HC A03/MF A01

The NASA Lewis Research Center's Hypersonic Tunnel Facility (HTF) is a free-jet, blowdown propulsion test facility that can simulate up to Mach-7 flight conditions with true air composition. Mach-5, -6, and -7 nozzles, each with a 42 inch exit diameter, are available. Previously obtained calibration data indicate that the test flow uniformity of the HTF is good. The facility, without modifications, can accommodate models approximately 10 feet long. The test gas is heated using a graphite core induction heater that generates a nonvitiated flow. The combination of clean-air, large-scale, and Mach-7 capabilities is unique to the HTF and enables an accurate propulsion performance determination. The reactivation of the HTF, in progress since 1990, includes refurbishing the graphite heater, the steam generation plant, the gaseous oxygen system, and all control systems. All systems were checked out and recertified, and environmental systems were upgraded to meet current standards. The data systems were also upgraded to current standards and a communication link with NASA-wide computers was added. In May 1994, the reactivation was complete, and an integrated systems test was conducted to verify facility operability. This paper describes the reactivation, the facility status, the operating capabilities, and specific applications of the HTF. Author

N95-19848 Aeronautical Research Labs., Melbourne (Australia).

PROGRAMMABLE COCKPIT RESEARCH SIMULATOR

M. Iob, A. G. Page, and D. A. Craven Mar. 1994 27 p Limited Reproducibility: More than 20% of this document may be affected by microfiche quality

(AD-A279219; ARL-TN-49; DODA-AR-008-375) Avail: Issuing Activity (Defense Technical Information Center (DTIC))

The 'Programmable Cockpit' is a low-cost facility to be used for study and development of the aircrew-vehicle interface for future aircraft systems. It was designed so that instrument layouts and display formats could be reconfigured rapidly and tested in a realistic aircraft representation or emulation, with the pilot under representative workload conditions. It is not intended to be used for pilot training and/or evaluation. It uses personal computers and computer graphics workstations linked together to represent the aircraft displays, and includes representative flight dynamic models for fixed-wing aircraft. Controls include a sidestick, rudder pedals, throttle, and touch sensitive screens. DTIC

N95-19150# Industrieanlagen-Betriebsgesellschaft m.b.H., Ottobrunn (Germany).

DESIGN AND OPERATION OF A THERMOACOUSTIC TEST FACILITY

G. Bayerdoerfer and L. Freyberg *In* AGARD, Impact of Acoustic Loads on Aircraft Structures Sep. 1994 5 p Sponsored in cooperation with BMFT and the Deutsche Agentur fuer Raumfahrtangelegenheite G.m.b.H., Bonn, Germany (For primary document see N95-19142 05-71)

Copyright Avail: CASI HC A01/MF A03

N95-19267# Naples Univ. (Italy). Inst. di Aerodinamica.

ADAPTIVE WIND TUNNEL WALLS VERSUS WALL INTERFERENCE CORRECTION METHODS IN 2D FLOWS AT HIGH BLOCKAGE RATIOS

G. P. Russo, G. Zuppardi, and M. Basciani *In* AGARD, Wall Interference, Support Interference and Flow Field Measurements Jul. 1994 12 p Sponsored by Ministry of University and Scientific and Technological Research (For primary document see N95-19251 05-34)

Copyright Avail: CASI HC A03/MF A04

N95-19269# City Univ., London (England). Center for Aeronautics.

INTERFERENCE DETERMINATION FOR WIND TUNNELS WITH SLOTTED WALLS

M. M. Freestone and S. R. Mohan *In* AGARD, Wall Interference, Support Interference and Flow Field Measurements Jul. 1994 12 p Sponsored by Dept. of Trade and Industry (For primary document see N95-19251 05-34)

Copyright Avail: CASI HC A03/MF A04

N95-19271# McDonnell-Douglas Aerospace, Saint Louis, MO.

TRANSONIC WIND TUNNEL BOUNDARY INTERFERENCE CORRECTION

M. L. Rueger, R. C. Crites, R. F. Weirich, F. Creasman, R. K. Agarwal, and J. E. Deese *In* AGARD, Wall Interference, Support Interference and Flow Field Measurements Jul. 1994 14 p (For primary document see N95-19251 05-34)

Copyright Avail: CASI HC A03/MF A04

N95-19272# British Columbia Univ., Vancouver (British Columbia). Dept. of Mechanical Engineering.

UNSTEADY FLOW TESTING IN A PASSIVE LOW-CORRECTION WIND TUNNEL

L. Kong and G. V. Parkinson *In* AGARD, Wall Interference, Support Interference and Flow Field Measurements Jul. 1994 7 p Sponsored by Natural Sciences and Engineering Research Council (For primary document see N95-19251 05-34)

Copyright Avail: CASI HC A02/MF A04

12 ASTRONAUTICS (GENERAL)

For extraterrestrial exploration see *91 Lunar and Planetary Exploration.*

N95-18568* National Aeronautics and Space Administration. Lyndon B. Johnson Space Center, Houston, TX.
STS-68 MISSION HIGHLIGHTS RESOURCE TAPE (Videotape)
22 Dec. 1994 Videotape: 58 min. 45 sec. playing time, in color, with sound
(NASA-TM-110049; NONP-NASA-VT-95-38127) Avail: CASI VHS A02/BETA A22

VJSC1440 contains important visual events including Space Radar Laboratory-2, Get Away Special canisters, Commercial Protein Crystal Growth, Biological Research in Canisters, Cosmic Radiation Effects and Activation Monitor, Military Applications of Ship Tracks, other onboard activities, earth views, and landing. Also includes Air-to-ground transmission between the crew and Mission control. Author

N95-19040* National Aeronautics and Space Administration. Lyndon B. Johnson Space Center, Houston, TX.
SKYLAB: THE FIRST 40 DAYS (Videotape)
1973 Videotape: 22 min. 30 sec. playing time, in color, with sound
(NASA-TM-110491; NONP-NASA-VT-95-39136) Avail: CASI VHS A02/BETA A22

This video records the launch of unmanned Skylab-1 on May 14, 1973 and the major problems resulting from the loss of the meteoroid heat shield. Also shown is the fabrication of materials and the equipment used in the repair operation, followed by the installation of the parasol after the launch and docking of the manned SL-2 with the SL-1 workshop. The onboard sequences of daily work routines and some of the experiments are included. JSC

N95-19058* National Aeronautics and Space Administration. Lyndon B. Johnson Space Center, Houston, TX.
LEGACY OF GEMINI (Videotape)
1967 Videotape: 28 min. running time, in color, with sound Awards: Golden Eagle Council on International Nontheatrical Events (CINE), 1968; Silver Metal, Atlanta International Festival, 1968; Chris Award, Columbus Film Festival, 1968; Award of Merit, American Film Festival, 1968; and Diploma, 6th Internation
(NASA-TM-110486; NONP-NASA-VT-95-39131) Avail: CASI VHS A02/BETA A22

In the perspective of a single composite mission, this documentary illustrates the major accomplishments of the Gemini two man space flights and the significance of these flights to the Apollo Program. This film includes outstanding photography of the Earth and man in space. JSC

N95-19059* National Aeronautics and Space Administration. Lyndon B. Johnson Space Center, Houston, TX.
SKYLAB: THE SECOND MANNED MISSION. A SCIENTIFIC HARVEST (Videotape)
1974 Videotape: 36 min. 30 sec. playing time, in black and white, no sound
(NASA-TM-110487; NONP-NASA-VT-95-39132) Avail: CASI VHS A02/BETA A22

This black and white video presentation covers the Skylab launch activities and docking with unmanned SL-1 workshop. Included are observations of student experiments (the Minchmog minnows and Arabella, the spider), observations of student experiments, exercise routines, and the enabling of the Earth Resources Experiments Package. Also shown is planet Earth documentation, manned operation of the Apollo Telescope Mount for observations of the Sun and beyond, outside EVA activity, testing of the Astronaut Maneuvering Unit, experiments to explore industrial uses of space, and the Skylab living routine. JSC

N95-19060* National Aeronautics and Space Administration. Lyndon B. Johnson Space Center, Houston, TX.
TIME OF APOLLO (Videotape)
1975 Videotape: 29 min. playing time, in color, with sound
(NASA-TM-110488; NONP-NASA-VT-95-39133) Avail: CASI VHS A02/BETA A22

In the year 1961, President John F. Kennedy set forth the task that...'This nation should commit itself to achieving the goal, before this decade is out, of landing a man on the Moon and returning him safely tio Earth'. The decade is over and the task has been accomplished. Project Apollo has been achieved. This video documentary is a tribute to the historical accomplishments of the Apollo program. JSC

N95-19191*# Tokyo Univ., Sagamihara (Japan). Inst. of Space and Aeronautical Science.
SCIENTIFIC OBJECTIVES OF THE PRIMITIVE BODY SAMPLE RETURN MISSIONS: AN APPROACH FROM THE LIGHT-INDUCED EFFECT ON WATER VAPOR Abstract Only
Mikio Shimizu *In* Lunar and Planetary Inst., Workshop on Particle Capture, Recovery and Velocity/Trajectory Measurement Technologies 1994 p 76-77 (For primary document see N95-19172 05-90)
Avail: CASI HC A01/MF A02

13 ASTRODYNAMICS

Includes powered and free-flight trajectories; and orbital and launching dynamics.

N95-18900 Texas Univ., Austin, TX.
OPTIMAL TRANSFER AND SWING-BY ORBITS IN THE TWO- AND THREE-BODY PROBLEMS Ph.D. Thesis
Antonio Fernando BertachiniDeAlmeidaPrado 1993 253 p
Avail: Univ. Microfilms Order No. DA9413442

This dissertation deals with the general topic of transfer orbits in the two- and three-body problems. To begin with, we study what is called Henon's problem. It is the problem of transferring a spacecraft from one body back to the same body, after a certain time. We also generalize to the problem of transferring to the corresponding Lagrangian points L4 or L5. This problem is solved first by using two-body equations and the Lambert problem. Families of transfers with small Delta V are found. Next, this problem is studied using the planar restricted circular three-body problem with the global Lamaitre's regularization as the model for the simulations. Transfers with near-zero Delta V to the Lagrangian points exist in this model. Next, we study the swing-by maneuvers. The fundamentals of the theory and some practical applications are presented, including a classification of Jupiter or moon swing-bys. The effect of the atmospheric drag is later included, and we study aerobraking in swing-by-maneuvers. We also study the effect of a swing-by with Jupiter on comets. A large range of initial conditions has been used for the incoming comets. The main questions considered are: the probability of capture of a comet in the solar system; the distribution of captured comets according to pericenter distance and semimajor axis; and the percentage of captured comets that will have a short period. Another important problem is the question of time-free minimum Delta V transfers between any two elliptical coplanar orbits. A set of analytical equations to solve this problem for a multi-impulsive maneuver is derived and solved. Comparisons between those maneuvers are made. Then, the Lambert problem is studied. We define and solve a new version of the problem, where the transfer is time-free, but has to be completed with minimum Delta V. Dissert. Abstr.

14 GROUND SUPPORT SYSTEMS AND FACILITIES (SPACE)

Includes launch complexes, research and production facilities; ground support equipment, e.g., mobile transporters; and simulators.

For related information see also *09 Research and Support Facilities (Air).*

N95-19180*# Kent Univ., Canterbury (England). Unit for Space Sciences.
THE HYPERVELOCITY IMPACT FACILITIES AT THE UNIVERSITY OF KENT AT CANTERBURY, UK Abstract Only
Mark J. Burchell, J. A. M. McDonnell, M. J. Cole, and P. R. Ratcliff *In* Lunar and Planetary Inst., Workshop on Particle Capture, Recovery and

Velocity/Trajectory Measurement Technologies 1994 p 32-35 (For primary document see N95-19172 05-90)
Avail: CASI HC A01/MF A02

N95-19183*# Tokyo Univ., Sagamihara (Japan). Inst. of Space and Astronautical Science.
LABORATORY SIMULATION OF INTACT CAPTURE OF COMETARY AND ASTEROIDAL DUST PARTICLES IN ISAS Abstract Only
A. Fujiwara, A. Nakamura, and T. Kadono *In* Lunar and Planetary Inst., Workshop on Particle Capture, Recovery and Velocity/Trajectory Measurement Technologies 1994 p 38-39 (For primary document see N95-19172 05-90)
Avail: CASI HC A01/MF A02

N95-19184*# Perkin-Elmer Corp., Pomona, CA. Applied Science Operation.
TECHNIQUES FOR IN SITU COLLECTION AND MEASUREMENT OF VOLATILES RELEASED DURING HYPERVELOCITY IMPACT Abstract Only
R. A. Heppner, William Niu, and Carl R. Maag (Science Applications International Corp., Glendora, CA.) *In* Lunar and Planetary Inst., Workshop on Particle Capture, Recovery and Velocity/Trajectory Measurement Technologies 1994 p 39-42 (For primary document see N95-19172 05-90)
Avail: CASI HC A01/MF A02

15 LAUNCH VEHICLES AND SPACE VEHICLES

Includes boosters; operating problems of launch/space vehicle systems; and reusable vehicles.

For related information see also *20 Spacecraft Propulsion and Power.*

N95-18045*# Cincinnati Univ., OH. Dept. of Electrical and Computer Engineering.
LVQ AND BACKPROPAGATION NEURAL NETWORKS APPLIED TO NASA SSME DATA Final Report
Timothy F. Doniere and Atam P. Dhawan Jun. 1993 79 p
(Contract NCC3-308; RTOP 584-03-11)
(NASA-CR-195418; E-9348; NAS 1.26:195418; TR-156/6/93/ECE) Avail: CASI HC A05/MF A01

Feedfoward neural networks with backpropagation learning have been used as function approximators for modeling the space shuttle main engine (SSME) sensor signals. The modeling of these sensor signals is aimed at the development of a sensor fault detection system that can be used during ground test firings. The generalization capability of a neural network based function approximator depends on the training vectors which in this application may be derived from a number of SSME ground test-firings. This yields a large number of training vectors. Large training sets can cause the time required to train the network to be very large. Also, the network may not be able to generalize for large training sets. To reduce the size of the training sets, the SSME test-firing data is reduced using the learning vector quantization (LVQ) based technique. Different compression ratios were used to obtain compressed data in training the neural network model. The performance of the neural model trained using reduced sets of training patterns is presented and compared with the performance of the model trained using complete data. The LVQ can also be used as a function approximator. The performance of the LVQ as a function approximator using reduced training sets is presented and compared with the performance of the backpropagation network. Author

N95-18150* National Aeronautics and Space Administration. Goddard Space Flight Center, Greenbelt, MD.
METEOR 3/TOMS LAUNCH OF 15 AUGUST 1991 IN PLESETSK, USSR (Videotape)
3 Aug. 1994 Videotape: 11 min. 34 sec. playing time, in color, with sound
(NASA-TM-110115; NONP-NASA-VT-95-37004) Avail: CASI VHS A02/BETA A22

The TOMS launch of August 15, 1991, was a joint effort between the U.S.S.R. and the United States. The pre-launch briefing, a tour of the TOMS storage site, it's delivery and setup at the launch site, and the actual launch were viewed in this video, along with a post-launch conference and a dinner. The launch occurred in Plesetsk, U.S.S.R., with the TOMS payload being launched on a Soviet Meteor. Officials from NASA were present for the launch. CASI

N95-18387*# National Aeronautics and Space Administration. Lewis Research Center, Cleveland, OH.
APPLICATIONS CATALOG OF PYROTECHNICALLY ACTUATED DEVICES/SYSTEMS
Thomas L. Seeholzer, Floyd Z. Smith (Analex Corp., Brook Park, OH.), Charles W. Eastwood (Analex Corp., Brook Park, OH.), and Paul R. Steffes (Analex Corp., Brook Park, OH.) Jan. 1995 324 p
(Contract NAS3-25776; RTOP 323-17-07)
(NASA-TM-106810; E-9297; NAS 1.15:106810) Avail: CASI HC A14/MF A03

A compilation of basic information on pyrotechnically actuated devices/systems used in NASA aerospace and aeronautic applications was formatted into a catalog. The intent is to provide (1) a quick reference digest of the types of operational pyro mechanisms and (2) a source of contacts for further details. Data on these items was furnished by the NASA Centers that developed and/or utilized such devices to perform specific functions on spacecraft, launch vehicles, aircraft, and ground support equipment. Information entries include an item title, user center name, commercial contractor/vendor, identifying part number(s), a basic figure, briefly described purpose and operation, previous usage, and operational limits/requirements. Author

N95-18467*# Cincinnati Univ., OH. Dept. of Electrical and Computer Engineering.
RADIAL BASIS FUNCTION NEURAL NETWORKS APPLIED TO NASA SSME DATA Final Report
Kevin R. Wheeler and Atam P. Dhawan Jun. 1993 63 p
(Contract NCC3-308; RTOP 584-03-11)
(NASA-CR-195417; E-9347; NAS 1.26:195417; TR-154/6/93/ECE) Avail: CASI HC A04/MF A01

This paper presents a brief report on the application of Radial Basis Function Neural Networks (RBFNN) to the prediction of sensor values for fault detection and diagnosis of the Space Shuttle's Main Engines (SSME). The location of the Radial Basis Function (RBF) node centers was determined with a K-means clustering algorithm. A neighborhood operation about these center points was used to determine the variances of the individual processing notes. Author

N95-18932*# National Aeronautics and Space Administration. Marshall Space Flight Center, Huntsville, AL.
SYSTEM ENGINEERING TOOLBOX FOR DESIGN-ORIENTED ENGINEERS
B. E. Goldberg, K. Everhart (Sverdrup Technology, Inc., Huntsville, AL.), R. Stevens (Sverdrup Technology, Inc., Huntsville, AL.), N. Babbitt, III (Sverdrup Technology, Inc., Huntsville, AL.), P. Clemens (Sverdrup Technology, Inc., Huntsville, AL.), and L. Stout (Sverdrup Technology, Inc., Huntsville, AL.) Washington Dec. 1994 300 p
(NASA-RP-1358; M-768; NAS 1.61:1358) Avail: CASI HC A13/MF A03

This system engineering toolbox is designed to provide tools and methodologies to the design-oriented systems engineer. A tool is defined as a set of procedures to accomplish a specific function. A methodology is defined as a collection of tools, rules, and postulates to accomplish a purpose. For each concept addressed in the toolbox, the following information is provided: (1) description, (2) application, (3) procedures, (4) examples, if practical, (5) advantages, (6) limitations, and (7) bibliography and/or references. The scope of the document includes concept development tools, system safety and reliability tools, design-related analytical tools, graphical data interpretation tools, a brief description of common statistical tools and methodologies, so-called total quality management tools, and trend analysis tools. Both relationship to project phase and primary functional usage of the tools are also delineated. The toolbox also includes a case study for illustrative purposes. Fifty-five tools are delineated in the text. Author

N95-19648*# National Aeronautics and Space Administration. Marshall Space Flight Center, Huntsville, AL.

A 20k PAYLOAD LAUNCH VEHICLE FAST TRACK DEVELOPMENT CONCEPT USING AN RD-180 ENGINE AND A CENTAUR UPPER STAGE

Ronald Toelle, comp. Washington Jan. 1995 80 p
(NASA-TM-108475; NAS 1.15:108475) Avail: CASI HC A05/MF A01

A launch vehicle concept to deliver 20,000 lb of payload to a 100-nmi orbit has been defined. A new liquid oxygen/kerosene booster powered by an RD-180 engine was designed while using a slightly modified Centaur upper stage. The design, development, and test program met the imposed 40-mo schedule by elimination of major structural testing by increased factors of safety and concurrent engineering concepts. A growth path to attain 65,000 lb of payload is developed. Author

N95-18993*# State Univ. of New York, Oneonta, NY. Dept. of Physics and Astronomy.

A CMC DATABASE FOR USE IN THE NEXT GENERATION LAUNCH VEHICLES (ROCKETS)

Kamala Mahanta *In* Alabama Univ., Research Reports: 1994 NASA/ASEE Summer Faculty Fellowship Program Oct. 1994 6 p (For primary document see N95-18967 05-80)
Avail: CASI HC A02/MF A03

16 SPACE TRANSPORTATION

Includes passenger and cargo space transportation, e.g., shuttle operations; and space rescue techniques.

For related information see also *03 Air Transportation and Safety* and *18 Spacecraft Design, Testing and Performance.* For space suits see *54 Man/System Technology and Life Support.*

N95-18047*# National Aeronautics and Space Administration. John F. Kennedy Space Center, Cocoa Beach, FL.

DEBRIS/ICE/TPS ASSESSMENT AND INTEGRATED PHOTOGRAPHIC ANALYSIS OF SHUTTLE MISSION STS-68 Final Report, 29 Sep. - 13 Oct. 1994

Jorge E. Rivera, Barry C. Bowen, J. Bradley Davis, and Robert F. Speece Nov. 1994 120 p Original contains color illustrations
(NASA-TM-109207; NAS 1.15:109207) Avail: CASI HC A06/MF A02; 50 functional color pages

A debris/ice/thermal protection system assessment and integrated photographic analysis was conducted for Shuttle mission STS-68. Debris inspections of the flight elements and launch pad were performed before and after launch. Icing conditions on the External Tank were assessed by the use of computer programs, nomographs, and infrared scanner data during cryogenic loading of the vehicle followed by on-pad visual inspection. High speed photography of the launch was analyzed to identify ice/debris sources and evaluate potential vehicle damage and/or in-flight anomalies. This report-documents the ice/debris/thermal protection system conditions and integrated photographic analysis of Shuttle mission STS-68, and the resulting effect on the Space Shuttle Program. Author

N95-18610*# Lockheed Engineering and Sciences Co., Houston, TX. Flight Evaluation Office.

STS-65 SPACE SHUTTLE MISSION REPORT

Robert W. Fricke, Jr. Sep. 1994 64 p Sponsored by NASA. Johnson Space Center
(NASA-CR-197598; NAS 1.26:197598; NSTS-08292) Avail: CASI HC A04/MF A01

The STS-65 Space Shuttle Program Mission Report summarizes the Payload activities as well as the Orbiter, External Tank (ET), Solid Rocket Booster (SRB), Redesigned Solid Rocket Motor (RSRM), and the Space Shuttle main engine (SSME) systems performance during the sixty-third flight of the Space Shuttle Program and the seventeenth flight of the Orbiter vehicle Columbia (OV-102). In addition to the Orbits the flight vehicle consisted of an ET that was designated ET-64; three SSME's that were designated as serial numbers 2019, 2030, and 2017 in positions 1, 2, and 3, respectively; and two SRB's that were designated BI-066. The RSRM's that were installed in each SRB were designated as 360P039A for the left SRB, and 360W039 for the right SRB. The primary objective of this flight was to complete the operation of the second International Microgravity Laboratory (IML-2). The secondary objectives of this flight were to complete the operations of the Commercial Protein Crystal Growth (CPCG), Orbital Acceleration Research Experiment (OARE), and the Shuttle Amateur Radio Experiment (SAREX) II payloads. Additional secondary objectives were to meet the requirements of the Air Force Maui Optical Site (AMOS) and the Military Application Ship Tracks (MAST) payloads, which were manifested as payloads of opportunity. Derived from text

N95-19790*# National Aeronautics and Space Administration. John F. Kennedy Space Center, Cocoa Beach, FL.

DEBRIS/ICE/TPS ASSESSMENT AND INTEGRATED PHOTOGRAPHIC ANALYSIS OF SHUTTLE MISSION STS-66 Final Report, 1-16 Nov. 1994

Gregory N. Katnik, Barry C. Bowen, and J. Bradley Davis Jan. 1995 107 p Original contains color illustrations
(NASA-TM-110141; NAS 1.15:110141) Avail: CASI HC A06/MF A02; 46 functional color pages

A debris/ice/thermal protection system assessment and integrated photographic analysis was conducted for Shuttle mission STS-66. Debris inspections of the flight elements and launch pad were performed before and after launch. Icing conditions on the External Tank were assessed by the use of computer program nomographs, and infrared scanner data during cryogenic loading of the vehicle followed by on-pad visual inspection. High speed photography of the launch was analyzed to identify ice/debris sources and evaluate potential vehicle damage and/or in-flight anomalies. This report documents the ice/debris/thermal protection system conditions and integrated photographic analysis of Shuttle mission STS-66, and the resulting effect on the Space Shuttle Program. Author

17 SPACE COMM., SPACECRAFT COMM., COMMAND & TRACKING

Includes telemetry; space communications networks; astronavigation and guidance; and radio blackout.

For related information see also *04 Aircraft Communications and Navigation* and *32 Communications and Radar.*

N95-18998*# Tuskegee Inst., AL. Dept. of Electrical Engineering.

ERROR CODING SIMULATIONS IN C

Viveca K. Noble *In* Alabama Univ., Research Reports: 1994 NASA/ASEE Summer Faculty Fellowship Program Oct. 1994 5 p (For primary document see N95-18967 05-80)
Avail: CASI HC A01/MF A03

18 SPACECRAFT DESIGN, TESTING AND PERFORMANCE

Includes satellites; space platforms; space stations; spacecraft systems and components such as thermal and environmental controls; and attitude controls.

For life support systems see *54 Man/System Technology and Life Support.* For related information see also *05 Aircraft Design, Testing and Performance, 39 Structural Mechanics,* and *16 Space Transportation.*

N95-18098# Naval Postgraduate School, Monterey, CA.

THE CURRENT STATUS OF RUSSIAN/CIS COMMUNICATION SATELLITES M.S. Thesis

Larry E. Ninas Sep. 1994 78 p
(AD-A285526) Avail: CASI HC A05/MF A01

As part of a Memorandum of Understanding (MOU) signed by U.S. President George Bush and Russian President Mikhail Gorbackev during a July 1991 summit meeting, the U.S. agreed to expand civil space cooperation with the Russian Federation and the Commonwealth of Independent States (CIS). The goal of the MOU was to increase the technical capabilities of both sides to respond to both natural and man-made disasters and top benefit from the capabilities and involvement of international and non-government organizations. This summit agreement has allowed the Russian Federation to offer unprecedented commercial and emergency

relief access to their on-orbit communications satellites. This thesis presents a brief history of the Soviet/Russian communication satellite program, and an examination of current systems as well as future and on-order systems. Simulations were conducted to determine the useability of the major systems (Gorizont, Ekran, Molniya, and Raduga) from 17 geographic locations. This is concluded with an introduction to the Telemedicine Space-bridge Project that is a direct result of the Bush-Gorbachev summit, and a shining example of Russian/U.S. cooperation in the satellite communication arena. DTIC

N95-18105*# Lockheed Engineering and Sciences Co., Hampton, VA.
MODAL IDENTIFICATION EXPERIMENT ACCOMMODATIONS REVIEW
Phillip J. Klich, Frederic H. Stillwagen, and Philip Mutton Dec. 1994 39 p
(Contract NAS1-19000; RTOP 963-89-00-01)
(NASA-CR-195009; NAS 1.26:195009) Avail: CASI HC A03/MF A01

The Modal Identification Experiment (MIE) will monitor the structure of the Space Station Freedom (SSF), and measure its response to a sequence of induced disturbances. The MIE will determine the frequency, damping, and shape of the important modes during the SSF assembly sequence including the Permanently Manned Configuration. This paper describes the accommodations for the proposed instrumentation, the data processing hardware, and the communications data rates. An overview of the MIE operational modes for measuring SSF acceleration forces with accelerometers is presented. The SSF instrumentation channel allocations and the Data Management System (DMS) services required for MIE are also discussed. Author

N95-18163# Naval Postgraduate School, Monterey, CA.
ELECTRODYNAMIC BEHAVIOR OF PMG-DELTA M.S. Thesis
Chung-Jen Chang Jun. 1994 73 p
(AD-A283930) Avail: CASI HC A04/MF A01

The PMG-Delta experiment was launched on 26 June 1993 to test basic tether electrodynamic principles. The 500 m conducting tether deployed from the second stage of a Delta-rocket, and provided approximately 3 orbits of useful information. The tether was equipped at both ends with xenon hollow cathodes. With both cathodes operating, currents up to 0.3A could be driven in either direction. Plasma impedances outside the tether were as low as a few hundred ohms at peak current during daytime/perigee(200km). Large impedances (10-100 kohms) occurred at night/apogee(900km), or when cathode cycled off. DTIC

N95-18362# Naval Postgraduate School, Monterey, CA.
ISSUES IN MILITARY USE OF COMMERCIAL SATELLITES M.S. Thesis
Frank A. Kunst Jun. 1994 87 p
(AD-A283707) Avail: CASI HC A05/MF A01

The purpose of this thesis is to identify some of the issues to be considered for evaluating the suitability of commercial satellites to supplement the Department of Defense space communications segment. Specifically, the European Telecommunications Satellite (EUTELSAT) System is used as a case study. The thesis identifies current, unclassified military satellite communications resources and provides a measure of satellite communications requirements. Additionally, this thesis discusses the armed forces' satellite communications doctrine and equipment, and policy considerations for military use of commercial satellites. Conclusions reveal that EUTELSAT would be suitable for use in a future integrated military/commercial satellite communications architecture. The information in this thesis may be useful for personnel involved with planning and implementing communications architectures at the CINC-level and above. DTIC

N95-18495*# Texas A&M Univ., College Station, TX. Dept. of Nuclear Engineering.
DESIGN CONSIDERATIONS FOR A SPACE STATION RADIATION SHIELD FOR PROTECTION FROM BOTH MAN-MADE AND NATURAL SOURCES Final Report
Wesley E. Bolch, K. Lee Peddicord, Harry Felsher, and Simon Smith Dec. 1994 87 p
(Grant NAG3-944; RTOP 488-10-12)
(NASA-CR-195298; E-8680; NAS 1.26:195298) Avail: CASI HC A05/MF A01

This study was conducted to analyze scenarios involving the use of nuclear-power vehicles in the vicinity of a manned Space Station (SS) in low-earth-orbit (LEO) to quantify their radiological impact to the station crew. In limiting the radiant dose to crew members, mission planners may (1) shut the reactor down prior to reentry, (2) position the vehicle at a prescribed parking distance, and (3) deploy radiation shield about the shutdown reactor. The current report focuses on the third option in which point-kernel gamma-ray shielding calculations were performed for a variety of shield configurations for both nuclear electric propulsion (NEP) and nuclear thermal rocket (NTR) vehicles. For a returning NTR vehicle, calculations indicate that a 14.9 MT shield would be needed to limit the integrated crew exposure to no more than 0.05 Sv over a period of six months (25 percent of the allowable exposure to man-made radiation sources). During periods of low vehicular activity in LEO, the shield may be redeployed about the SS habitation module in order to decrease crew exposures to trapped proton radiations by approximately a factor of 10. The corresponding shield mass required for deployment at a returning NEP vehicle is 2.21 MT. Additional scenarios examined include the radioactivation of various metals as might be found in tools used in EVA activities. Author

N95-18580*# Harris Corp., Melbourne, FL.
STREAMLINED DESIGN AND SELF RELIANT HARDWARE FOR ACTIVE CONTROL OF PRECISION SPACE STRUCTURES Report, 30 Jan. 1989 - 31 Aug. 1994
David C. Hyland, James A. King, and Douglas J. Phillips Hampton, VA NASA Dec. 1994 154 p
(Contract NAS1-19372; RTOP 233-01-01-06)
(NASA-CR-4637; NAS 1.26:4637) Avail: CASI HC A08/MF A02

Precision space structures may require active vibration control to satisfy critical performance requirements relating to line-of-sight pointing accuracy and the maintenance of precise, internal alignments. In order for vibration control concepts to become operational, it is necessary that their benefits be practically demonstrated in large scale ground-based experiments. A unique opportunity to carry out such demonstrations on a wide variety of experimental testbeds was provided by the NASA Control-Structure Integration (CSI) Guest Investigator (GI) Program. This report surveys the experimental results achieved by the Harris Corporation GI team on both Phases 1 and 2 of the program and provides a detailed description of Phase 2 activities. The Phase 1 results illustrated the effectiveness of active vibration control for space structures and demonstrated a systematic methodology for control design, implementation test. In Phase 2, this methodology was significantly streamlined to yield an on-site, single session design/test capability. Moreover, the Phase 2 research on adaptive neural control techniques made significant progress toward fully automated, self-reliant space structure control systems. As a further thrust toward productized, self-contained vibration control systems, the Harris Phase II activity concluded with experimental demonstration of new vibration isolation hardware suitable for a wide range of space-flight and ground-based commercial applications.The CSI GI Program Phase 1 activity was conducted under contract NASA1-18872, and the Phase 2 activity was conducted under NASA1-19372. Author

N95-18639# Los Alamos National Lab., NM.
ON ORBIT PERFORMANCE OF THE ALEXIS EUV TELESCOPES
J. Bloch, B. Edwards, and W. Priedhorsky et al 1994 14 p Presented at the Annual Meeting of the Society of Photo-Optical Instrumentation Engineers, San Diego, CA, 24-29 Jul. 1994
(Contract W-7405-eng-36)
(DE94-016197; LA-UR-94-2612; CONF-940723-9) Avail: CASI HC A03/MF A01

The Array of Low Energy X-ray Imaging Sensors (ALEXIS) satellite is Los Alamos' first attempt at building and flying a low cost, rapid development, technology demonstration and scientific space mission. The ALEXIS satellite contains the two experiments: the ALEXIS telescope array, (which consists of six EUV/ultrasoft x-ray telescopes utilizing multilayer mirrors, each with a 33 degree field-of-view), and a VHF ionospheric experiment called Blackbeard. A ground station located at Los Alamos exclusively controls the spacecraft. The 248 pound ALEXIS satellite was launched by a Pegasus booster into a 400 (times) 450 nautical mile, 70 degree inclination orbit on April 25, 1993. Images from a video system on the rocket indicated that ALEXIS had been severely damaged during launch with one of the 4 solar panels breaking away from its mounting. (It later turned out that the solar paddle was still attached to the spacecraft but only through cable bundles.)

Attempts at communicating with the satellite were unsuccessful until a surprised ground crew received a short transmission on June 2. By mid July, ground station operators had regained full control of the satellite and began to initiate scientific operations with both the telescope array and the VHF experiment. In this paper we will discuss a preliminary analysis of the on-orbit performance of EUV telescopes on ALEXIS. DOE

N95-19039* National Aeronautics and Space Administration. Lyndon B. Johnson Space Center, Houston, TX.
GEMINI 8, THIS IS HOUSTON, FLIGHT (Videotape)
1966 Videotape: 25 min. 30 sec. playing time, in color, with sound (NASA-TM-110490; NONP-NASA-VT-95-39135) Avail: CASI VHS A02/BETA A22

The historic first docking in space with the Agena is completed. Camaras record the harrowing experiences of the astronauts as Gemini VIII wildly gyrates through space following a malfunction. The spacecraft is separated from the Agena, brought under control and reentry is achieved. JSC

N95-19131# General Accounting Office, Washington, DC. National Security and International Affairs Div.
SPACE STATION: PLANS TO EXPAND RESEARCH COMMUNITY DO NOT MATCH AVAILABLE RESOURCES. REPORT TO THE RANKING MINORITY MEMBER, SUBCOMMITTEE ON OVERSIGHT OF GOVERNMENT MANAGEMENT, COMMITTEE ON GOVERNMENT AFFAIRS, US SENATE
Nov. 1994 28 p
(GAO/NSIAD-95-33; B-259020) Avail: CASI HC A03/MF A01; GAO, PO Box 6015, Gaithersburg, MD 20884-6015

The National Aeronautics and Space Administration's (NASA) goal is to launch, assemble, and operate an earth-orbiting microgravity and life sciences research laboratory - International Space Station Alpha - starting in 1997. We reviewed (1) what NASA is doing to assess the required size of the research community needed for the space station and to ensure that such a community will be available, (2) how NASA will ensure that the research selected for the space station will be the best possible, and (3) whether a recently cancelled Shuttle research flight adversely affected NASA's efforts to develop a research community for the space station. NASA has taken an initial step to assess the size of the space station's research community, but it is not intending to develop this community by directly soliciting proposals to do research on the space station. Instead, NASA is focusing on developing a comprehensive research program that emphasizes more ground-based research and uses space flight only for research efforts that require a microgravity environment in space. Author

N95-19237*# National Aeronautics and Space Administration. Lyndon B. Johnson Space Center, Houston, TX.
DOCUMENTATION AND ARCHIVING OF THE SPACE SHUTTLE WIND TUNNEL TEST DATA BASE. VOLUME 1: BACKGROUND AND DESCRIPTION
Paul O. Romere and Steve Wesley Brown (Lockheed Engineering and Sciences Co., Houston, TX.) Jan. 1995 191 p
(NASA-TM-104806-Vol-1; S-786-Vol-1; NAS 1.15:104806-Vol-1) Avail: CASI HC A09/MF A02

Development of the space shuttle necessitated an extensive wind tunnel test program, with the cooperation of all the major wind tunnels in the United States. The result was approximately 100,000 hours of space shuttle wind tunnel testing conducted for aerodynamics, heat transfer, and structural dynamics. The test results were converted into Chrysler DATAMAN computer program format to facilitate use by analysts, a very cost effective method of collecting the wind tunnel test results from many test facilities into one centralized location. This report provides final documentation of the space shuttle wind tunnel program. The two-volume set covers evolution of space shuttle aerodynamic configurations and gives wind tunnel test data, titles of wind tunnel data reports, sample data sets, and instructions for accessing the digital data base. Author

N95-19377# Institut des Hautes Etudes Scientifiques, Bures-sur-Yvette (France).
ORBITAL TESTS OF RELATIVISTIC GRAVITY USING ARTIFICIAL SATELLITES
T. Damour and G. E. Farese (Centre National de la Recherche Scientifique, Marseilles, France.) Apr. 1994 17 p Submitted for publication
(PB94-217239; IHES/P/94/22) Avail: CASI HC A03/MF A01

We reexamine non-Einsteinian effects observable in the orbital motion of low-orbit artificial Earth satellites. Our analysis suggests that such data could measure two independent combinations of the Eddington parameters bar-beta identically equal to beta - 1 and bar-gamma identically equal to gamma - 1 at the 10(exp -4) level and probe the time variability of Newton's 'constant' at the (G dot)/G approximately 10(exp -13)/yr level. These tests would provide well-needed complements to the results of the Lunar Laser Ranging experiment, and of the presently planned experiments aiming at measuring gamma bar. In view of the strong demands they make on the level of non-gravitational perturbations, these tests might require a dedicated mission consisting of an optimized passive drag-free satellite. NTIS

N95-19571# Naval Postgraduate School, Monterey, CA.
A SYSTEMS ANALYSIS AND PROJECT MANAGEMENT PLAN FOR THE PETITE AMATEUR NAVY SATELLITE (PANSAT) M.S. Thesis
Markham K. Rich Sep. 1994 154 p
(AD-A285968) Avail: CASI HC A08/MF A02

The Petite Amateur Navy Satellite (PANSAT) is a communications satellite being developed at the Naval Postgraduate School by the Space Systems Academic Group. This thesis is the result of an investigation into all aspects of the project. Research, analyses, and recommendations were concentrated in the areas of engineering design, testing, orbital operations, and organization and management. The study identified the upcoming Shuttle to Mir flights as providing the most attractive orbital parameters for PANSAT operations. A systems analysis was conducted that attempted to develop and prioritize engineering design issues requiring more thorough investigation. The chief problem area discovered by this analysis was in the power production aspect of the Electrical Power System (EPS). PANSAT was determined to have a negative power margin under certain conditions, and an even lower power margin than previously believed under most conditions. It is recommended that the project make satellite development its principal objective (over education) to maximize the likelihood of success. Student participation in the project is the single greatest asset of the project, and it remains largely untapped. Reorganizing the project to increase student involvement, within the constraints of the Space Systems curricula, will improve efficiency by easing extraneous requirements on an over-tasked engineering staff, and thereby improve overall productivity. DTIC

N95-19624*# National Aeronautics and Space Administration. Lyndon B. Johnson Space Center, Houston, TX.
DOCUMENTATION AND ARCHIVING OF THE SPACE SHUTTLE WIND TUNNEL TEST DATA BASE. VOLUME 2: USER'S GUIDE TO THE ARCHIVED DATA BASE Technical Report, 1969-1994
Paul O. Romere and Steve Wesley Brown Jan. 1995 186 p
(NASA-TM-104806-Vol-2; S-786-Vol-2; NAS 1.15:104806-Vol-2) Avail: CASI HC A09/MF A02

Development of the Space Shuttle necessitated an extensive wind tunnel test program, with the cooperation of all the major wind tunnels in the United States. The result was approximately 100,000 hours of Space Shuttle wind tunnel testing conducted for aerodynamics, heat transfer, and structural dynamics. The test results were converted into Chrysler DATAMAN computer program format to facilitate use by analysts, a very cost effective method of collecting the wind tunnel test results from many test facilities into one centralized location. This report provides final documentation of the Space Shuttle wind tunnel program. The two-volume set covers the evolution of Space Shuttle aerodynamic configurations and gives wind tunnel test data, titles of wind tunnel data reports, sample data sets, and instructions for accessing the digital data base. Author

N95-19780*# National Aeronautics and Space Administration. Marshall Space Flight Center, Huntsville, AL.
SPACECRAFT ENVIRONMENTS INTERACTIONS: PROTECTING AGAINST THE EFFECTS OF SPACECRAFT CHARGING
J. L. Herr (Sverdrup Technology, Inc., Huntsville, AL.) and M. B. McCollum Washington Nov. 1994 21 p Original contains color illustrations
(NASA-RP-1354; M-767; NAS 1.61:1354) Avail: CASI HC A03/MF A01; 5 functional color pages

The effects of the natural space environments on spacecraft design, development, and operation are the topic of a series of NASA Reference Publications currently being developed by the Electromagnetics and

Environments Branch, Systems Analysis and Integration Laboratory, Marshall Space Flight Center. This primer, second in the series, describes the interactions between a spacecraft and the natural space plasma. Under certain environmental/spacecraft conditions, these interactions result in the phenomenon known as spacecraft charging. It is the focus of this publication to describe the phenomenon of spacecraft charging and its possible adverse effects on spacecraft and to present the key elements of a Spacecraft Charging Effects Protection Plan. Author

N95-18168*# Jackson State Univ., Jackson, MS. Dept. of Technology.
SPACE STATION RACKS WEIGHT AND CG MEASUREMENT USING THE RACK INSERTION END-EFFECTOR
William V. Brewer *In* Univ. of Central Florida, NASA/ASEE Summer Faculty Fellowship Program. 1994 Research Reports Oct. 1994 p 31-60 (For primary document see N95-18166 05-80)
Avail: CASI HC A03/MF A04

N95-18976*# University of Southern Illinois, Carbondale, IL. Dept. of Mechanical Engineering and Energy Processes.
COMPOSITE STRUCTURES FOR MAGNETOSPHERE IMAGER SPACECRAFT
Tsuchin Chu *In* Alabama Univ., Research Reports: 1994 NASA/ASEE Summer Faculty Fellowship Program Oct. 1994 6 p (For primary document see N95-18967 05-80)
Avail: CASI HC A02/MF A03

19 SPACECRAFT INSTRUMENTATION

For related information see also *06 Aircraft Instrumentation* and *35 Instrumentation and Photography.*

N95-18196*# Lockheed Sanders, Inc., Nashua, NH. Engineering Div.
NEW TECHNOLOGIES FOR SPACE AVIONICS Final Report, 1994
David W. Aibel, Peter Dingus, Mark Lanciault, Debra Hurdlebrink, Inna Gurevich, and Lydia Wenglar Dec. 1994 85 p
(Contract NAS9-18873)
(NASA-CR-197574; NAS 1.26:197574) Avail: CASI HC A05/MF A01

This report reviews a 1994 effort that continued 1993 investigations into issues associated with the definition of requirements, with the practice concurrent engineering and rapid prototyping in the context of the development of a prototyping of a next-generation reaction jet driver controller. This report discusses lessons learned, the testing of the current prototype, the details of the current design, and the nature and performance of a mathematical model of the life cycle of a pilot operated valve solenoid. Author

N95-18994*# Vanderbilt Univ., Nashville, TN. Dept. of Mechanical Engineering.
LEAN SPACECRAFT AVIONICS TRADE STUDY
John A. Main *In* Alabama Univ., Research Reports: 1994 NASA/ASEE Summer Faculty Fellowship Program Oct. 1994 6 p (For primary document see N95-18967 05-80)
Avail: CASI HC A02/MF A03

N95-19178*# A & M Associates, Lanham, MD.
HIGHLY TRANSPARENT AND RUGGED SENSOR FOR VELOCITY DETERMINATIONS OF COSMIC DUST PARTICLES Abstract Only
Siegfried Auer and F. O. vonBun *In* Lunar and Planetary Inst., Workshop on Particle Capture, Recovery and Velocity/Trajectory Measurement Technologies 1994 p 25-29 (For primary document see N95-19172 05-90)
(Contract NAS9-18368)
Avail: CASI HC A01/MF A02

N95-19189*# Search for Extraterrestrial Intelligence Inst., Mountain View, CA.
SPICE: AN INNOVATIVE, FLEXIBLE INSTRUMENT CONCEPT Abstract Only
Kenji Nishioka, D. P. Cauffman (Lockheed Missiles and Space Co., Palo Alto, CA.), B. Jurcevich (Lockheed Missiles and Space Co., Palo Alto, CA.), David J. Mendez (Lockheed Missiles and Space Co., Palo Alto, CA.), and James T. Ryder (Lockheed Missiles and Space Co., Palo Alto, CA.) *In* Lunar and Planetary Inst., Workshop on Particle Capture, Recovery and Velocity/Trajectory Measurement Technologies 1994 p 61-64 (For primary document see N95-19172 05-90)
Avail: CASI HC A01/MF A02

N95-19196*# Chicago Univ., Chicago, IL. Lab. for Astrophysics and Space Research.
PVDF FLUX/MASS/VELOCITY/TRAJECTORY SYSTEMS AND THEIR APPLICATIONS IN SPACE Abstract Only
Anthony J. Tuzzolino *In* Lunar and Planetary Inst., Workshop on Particle Capture, Recovery and Velocity/Trajectory Measurement Technologies 1994 p 89-94 (For primary document see N95-19172 05-90)
(Contracts NAGw-3078; JPL-959531; N00014-91-J-1716)
Avail: CASI HC A02/MF A02

20 SPACECRAFT PROPULSION AND POWER

Includes main propulsion systems and components, e.g., rocket engines; and spacecraft auxilliary power sources.

For related information see also *07 Aircraft Propulsion and Power, 28 Propellants and Fuels, 44 Energy Production and Conversion,* and *15 Launch Vehicles and Space Vehicles.*

N95-17997# Los Alamos National Lab., NM.
LUNAR SURFACE FISSION POWER SUPPLIES: RADIATION ISSUES
M. G. Houts and S. K. Lee 1994 7 p Presented at the 29th Intersociety Energy Conversion Engineering Conference, Monterey, CA, 7-12 Aug. 1994
(Contract W-7405-eng-36)
(DE94-014439; LA-UR-94-1958; CONF-940812-11) Avail: CASI HC A02/MF A01

A lunar space fission power supply shield that uses a combination of lunar regolith and materials brought from earth may be optimal for early lunar outposts and bases. This type of shield can be designed such that the fission power supply does not have to be moved from its landing configuration, minimizing handling and required equipment on the lunar surface. Mechanisms for removing heat from the lunar regolith are built into the shield, and can be tested on earth. Regolith activation is greatly reduced compared with a shield that uses only regolith, and it is possible to keep the thermal conditions of the fission power supply close to these seen in free space. For a well designed shield, the additional mass required to be brought from earth should be less than 1000 kg. Detailed radiation transport calculations confirm the feasibility of such a shield. DOE

N95-18192*# GenCorp Aerojet, Sacramento, CA. Propulsion Div.
ADVANCED SMALL ROCKET CHAMBERS. BASIC PROGRAM AND OPTION 2: FUNDAMENTAL PROCESSES AND MATERIAL EVALUATION Final Report
Donald M. Jassowski Sep. 1993 367 p
(Contract NAS3-25646)
(NASA-CR-195349; NAS 1.26:195349) Avail: CASI HC A16/MF A03

Propellants, chamber materials, and processes for fabrication of small high performance radiation cooled liquid rocket engines were evaluated to determine candidates for eventual demonstration in flight-type thrusters. Both storable and cryogenic propellant systems were considered. The storable propellant systems chosen for further study were nitrogen tetroxide oxidizer with either hydrazine or monomethylhydrazine as fuel. The cryogenic propellants chosen were oxygen with either hydrogen or methane as fuel. Chamber material candidates were chemical vapor deposition (CVD) rhenium protected from oxidation by CVD iridium for the chamber hot section, and film cooled wrought platinum-rhodium or regeneratively cooled stainless steel for the front end section exposed to partially reacted propellants. Laser diagnostics of the combustion products near the hot chamber surface and measurements at the surface layer were performed in a collaborative program at Sandia National Laboratories, Livermore, CA. The Material Sample Test Apparatus, a laboratory system to simulate the combustion environment in terms of gas and material temperature, composition, and pressure up to 6 Atm, was developed for these studies. Rocket engine simulator studies were conducted to evaluate the materials under simulated combustor flow conditions, in the diagnostic test chamber. These tests

used the exhaust species measurement system, a device developed to monitor optically species composition and concentration in the chamber and exhaust by emission and absorption measurements. Author

N95-18195*# Rocket Research Corp., Redmond, WA. Defense Systems Group.
HIGH PERFORMANCE STORABLE PROPELLANT RESISTOJET Final Technical Report
C. E. Vaughan 17 Jan. 1992 314 p
(Contract NAS3-24652; RTOP 242-70-02)
(NASA-CR-191128; E-7825; NAS 1.26:191128; Rept-91-R-1553) Avail: CASI HC A14/MF A03

From 1965 until 1985 resistojets were used for a limited number of space missions. Capability increased in stages from an initial application using a 90 W gN2 thruster operating at 123 sec specific impulse (Isp) to a 830 W N2H4 thruster operating at 305 sec Isp. Prior to 1985 fewer than 100 resistojets were known to have been deployed on spacecraft. Building on this base NASA embarked upon the High Performance Storable Propellant Resistojet (HPSPR) program to significantly advance the resistojet state-of-the-art. Higher performance thrusters promised to increase the market demand for resistojets and enable space missions requiring higher performance. During the program three resistojets were fabricated and tested. High temperature wire and coupon materials tests were completed. A life test was conducted on an advanced gas generator. Author

N95-18570*# National Aeronautics and Space Administration. Lewis Research Center, Cleveland, OH.
SOLAR-ELECTROCHEMICAL POWER SYSTEM FOR A MARS MISSION
Colleen A. Withrow and Nelson Morales Dec. 1994 13 p
(RTOP 233-03-05)
(NASA-TM-106606; E-8885; NAS 1.15:106606) Avail: CASI HC A03/MF A01

This report documents a sizing study of a variety of solar electrochemical power systems for the intercenter NASA study known as 'Mars Exploration Reference Mission'. Power systems are characterized for a variety of rovers, habitation modules, and space transport vehicles based on requirements derived from the reference mission. The mission features a six-person crew living on Mars for 500 days. Mission power requirements range from 4 kWe to 120 kWe. Primary hydrogen and oxygen fuel cells, regenerative hydrogen and oxygen fuel cells, sodium sulfur batteries advanced photovoltaic solar arrays of gallium arsenide on germanium with tracking and nontracking mechanisms, and tent solar arrays of gallium arsenide on germanium are evaluated and compared. Author

N95-18571*# National Aeronautics and Space Administration. Lewis Research Center, Cleveland, OH.
FINAL RESULTS OF THE ADVANCED PHOTOVOLTAIC EXPERIMENT FLIGHT TEST
David J. Brinker and John R. Hickey (Eppley Lab., Inc., Newport, RI.) Jan. 1995 6 p Presented at the 1st World Conference on Photovoltaic Energy Conversion, Waikoloa, HI, 5-9 Dec. 1994; sponsored by IEEE, PVSEC-Japan, PVSEC-Europe
(RTOP 233-01-0A)
(NASA-TM-106828; E-9377; NAS 1.15:106828) Avail: CASI HC A02/MF A01

The Advanced Photovoltaic Experiment was designed to generate laboratory reference standards as well as to explore the durability of a wide variety of space solar cells. In addition to the cells, it was equipped with an absolute cavity radiometer to measure solar intensity, a spectroradiometer to measure the spectral content of this radiation and a sun angle sensor. Data from the solar cells and various sensors was obtained on a daily basis during the first eleven months of the 69 month flight. In this paper pre-flight and post-flight laboratory measurements are compared with on-orbit calibration data. Pre-flight and post-flight calibration data of the cavity radiometer as well as on-orbit data demonstrated the accuracy and durability of the Eppley instrument flown on APEX. Author

N95-18632 Department of the Navy, Washington, DC.
FLAME POSITION ULTRASONIC INTERFEROMETER Patent
David A. Soss, inventor (to Navy) 28 Dec. 1993 8 p Filed 6 Feb. 1990
(AD-D016235; US-Patent-5,272,908; US-Patent-Appl-SN-474695; US-Patent-Class-73-35) Avail: US Patent and Trademark Office

A sensitive instrument system for determining the position of the burn front in a rocket motor is disclosed. Separate adjacent transmitter and receiver elements are attached to the rocket motor casing to form an ultrasonic interference system. An ultrasound beam is transmitted to the motor's interior and the reflected beam from the propellant gas burn front is captured by the receiver. The received signal is processed to determine the distance to the propellant-gas interface. DTIC

N95-18720# Instituto de Pesquisas Espaciais, Sao Paulo (Brazil).
REGENERATIVE COOLING FOR LIQUID PROPELLANT ROCKET THRUST CHAMBERS M.S. Thesis [REFRIGERACAO REGENERATIVA PARA CAMARAS DE EMPUXO DE MOTORES FOGUETE A PROPELENTES LIQUIDOS]
Rafael Levy Rubin Apr. 1994 121 p In PORTUGESE
(INPE-5565-TDI/540) Avail: CASI HC A06/MF A02

This work describes a calculation model for regeneratively cooled rocket thrust chambers. A computational program, based on a one-dimensional coolant pressure drop in the cooling channels. Radiation is included in the model. The channels have rectangular cross sections, the dimensions being determined during the calculations in order to maintain the wall temperature distributions at tolerable levels, with a minimum channel pressure drop. Several wall materials were investigated, as well as the employment of the hydrocarbon fuels JP-4 and JP-5 and Aerozine 50 as coolants. The influence of many design parameters on the cooling system performance is verified for the analysis of the system capabilities and limitations. Author

N95-18743*# Praxair, Inc., Tonawanda, NY.
AIRBORNE ROTARY SEPARATOR STUDY Final Report
R. F. Drnevich and J. J. Nowobilski Dec. 1992 141 p
(Contract NAS3-25560)
(NASA-CR-191045; E-9387; NAS 1.26:191045) Avail: CASI HC A07/MF A02

Several air breathing propulsion concepts for future earth-to-orbit transport vehicles utilize air collection and enrichment, and subsequent storage of liquid oxygen for later use in the vehicle mission. Work performed during the 1960's established the feasibility of substantially reducing weight and volume of a distillation type air separator system by operating the distillation elements in high 'g' fields obtained by rotating the separator assembly. The purpose of this study was to evaluate various fuels and fuel combinations with the objective of minimizing the weight and increase the ready alert capability of the plane. Fuels will be used to provide energy as well as act as heat sinks for the on-board heat rejection system. Fuel energy was used to provide power for air separation as well as to produce refrigeration for liquefaction of oxygen enriched air, besides its primary purpose of vehicle propulsion. The heat generated in the cycle was rejected to the fuel and water which is also carried on board the vehicle.The fuels that were evaluated include JP4, methane, and hydrogen. Hydrogen served as a comparison to the JP4 and methane cases. Author (revised)

N95-19073 Department of the Navy, Washington, DC.
INTEGRATED AERODYNAMIC FIN AND STOWABLE TVC VANE SYSTEM Patent
Arnold O. Danielson, inventor (to Navy) 16 Jun. 1994 11 p Filed 15 Mar. 1991
(AD-D016457; US-Patent-5,320,304; US-Patent-Appl-SN-666104; US-Patent-Class-244-3.22) Avail: US Patent and Trademark Office

An aerodynamic fin and stowable jet vane system preferably for rocket motor missile applications to control roll, pitch, and yaw, in either the aerodynamic or thrust flight control conditions, has a retractable and stowable aerodynamic vane integrated with a stowable aerodynamic vane integrated with a stowable thrust vector reaction steering system on a common support. The integrated aerodynamic fins and thrust vector control reduce the overall missile mainframe dimensions and are mounted on a single, space saving support. DTIC

N95-19566*# Mississippi State Univ., Mississippi State, MS. Dept. of Chemical Engineering.
NOZZLE INITIATIVE INDUSTRY ADVISORY COMMITTEE ON STANDARDIZATION OF CARBON-PHENOLIC TEST METHODS AND SPECIFICATIONS Final Report

William B. Bull, comp., Pat C. Pinoli, comp. (Lockheed Missiles and Space Co., Palo Alto, CA.), Cindy G. Upton, comp. (National Aeronautics and Space Administration. Marshall Space Flight Center, Huntsville, AL.), Tony Day, comp. (Thiokol Corp., Brigham City, UT.), Keith Hill, comp. (Hercules, Inc., Magna, UT.), Frank Stone, comp. (Quality Data Analysis, Inc., Baton Rouge, LA.), and William B. Hall 31 Dec. 1994 410 p Meeting held in Mississippi State, MS, 18-20 May 1994
(Grant NAG8-936)
(NASA-CR-197529; NAS 1.26:197529) Avail: CASI HC A18/MF A04

This report is a compendium of the presentations of the 12th biannual meeting of the Industry Advisory Committee under the Solid Propulsion Integrity Program. A complete transcript of the welcoming talks is provided. Presentation outlines and overheads are included for the other sessions: SPIP Overview, Past, Current and Future Activity; Test Methods Manual and Video Tape Library; Air Force Developed Computer Aided Cure Program and SPC/TQM Experience; Magneto-Optical mapper (MOM), Joint Army/NASA program to assess composite integrity; Permeability Testing; Moisture Effusion Testing by Karl Fischer Analysis; Statistical Analysis of Acceptance Test Data; NMR Phenolic Resin Advancement; Constituent Testing Highlights on the LDC Optimization Program; Carbon Sulfur Study, Performance Related Testing; Current Rayon Specifications and Future Availability; RSRM/SPC Implementation; SRM Test Methods, Delta/Titan/FBM/RSRM; and Open Forum on Performance Based Acceptance Testing -- Industry Experience. CASI

N95-19795*# National Aeronautics and Space Administration. Lewis Research Center, Cleveland, OH.
CENTRIFUGAL AND AXIAL PUMP DESIGN AND OFF-DESIGN PERFORMANCE PREDICTION
Joseph P. Veres Feb. 1995 24 p Presented at the 1994 Joint Subcommittee and User Group Meetings, Sunnyvale, CA, 17-21 Oct. 1994; sponsored by the Joint Army-Navy-NASA-Air Force Interagency Propulsion Committee
(RTOP 505-62-5J)
(NASA-TM-106745; E-9157; NAS 1.15:106745) Avail: CASI HC A03/MF A01

A meanline pump-flow modeling method has been developed to provide a fast capability for modeling pumps of cryogenic rocket engines. Based on this method, a meanline pump-flow code PUMPA was written that can predict the performance of pumps at off-design operating conditions, given the loss of the diffusion system at the design point. The design-point rotor efficiency and slip factors are obtained from empirical correlations to rotor-specific speed and geometry. The pump code can model axial, inducer, mixed-flow, and centrifugal pumps and can model multistage pumps in series. The rapid input setup and computer run time for this meanline pump flow code make it an effective analysis and conceptual design tool. The map-generation capabilities of the code provide the information needed for interfacing with a rocket engine system modeling code. The off-design and multistage modeling capabilities of PUMPA permit the user to do parametric design space exploration of candidate pump configurations and to provide head-flow maps for engine system evaluation. Author

N95-19877# Oak Ridge Y-12 Plant, TN.
THE METALLURGICAL INTEGRITY OF THE FRIT VENT ASSEMBLY DIFFUSION BOND
G. B. Ulrich Jun. 1994 22 p
(Contract DE-AC05-84OS-21400)
(DE95-000610; Y/DV-1321) Avail: CASI HC A03/MF A01

Iridium alloy clad vent sets (CVS's) are now being made by Energy Systems at the Oak Ridge Y-12 Plant. These CVS's are being made for the US Department of Energy's (NE-53) General Purpose Heat Source-Radioisotope Thermoelectric Generator (GPHS-RTG) program, which is to supply electrical power for the National Aeronautics and Space Administration's Cassini mission to Saturn. A GPHS-RTG has 72 CVS'. Each CVS encapsulates one (238)PuO2 fuel pellet. The helium gas produced from the alpha decay of the (238)Pu is vented through a nominal 0.45-mm-diam hole in the vent cup of each CVS. A frit vent assembly that is electron beam welded over the vent hole allows helium gas to escape but prevents plutonia fines from exiting. The metallurgical integrity of frit vent assemblies produced by Martin Marietta Energy Systems, Inc. (Energy Systems) were compared with those produced earlier by EG&G-Mound Applied Technology, Inc. (EG&G-MAT). Scanning electron microscope (SEM) photographs were taken (at magnifications of from 126x to 1,000x) of the starting frit vent powder and the diffusion-bonded powder in finished frit vent assemblies produced by Energy Systems and EG&G-MAT. Frit vent assemblies also were metallographically prepared and visually examined/photographed at magnifications of from 50x to 1,000x. The SEM and metallographic examinations of the particle-to-particle and particle-to-foil component diffusion bonds indicated that the Energy Systems-produced and EG&G-MAT-produced frit vent assemblies have comparable metallurgical integrity. Statistical analysis of the Energy Systems production data shows that the frit vent manufacturing yield is 91%. DOE

N95-18979*# Alabama Univ., Huntsville, AL. Dept. of Mechanical and Aerospace Engineering.
OPTICAL MEASUREMENTS IN ROCKET ENGINE LIQUID SPRAYS
Douglas A. Feikema *In* Alabama Univ., Research Reports: 1994 NASA/ASEE Summer Faculty Fellowship Program Oct. 1994 6 p (For primary document see N95-18967 05-80)
Avail: CASI HC A02/MF A03

N95-18980*# Ohio Univ., Athens. Dept. of Industrial and Systems Engineering.
DATA DRIVEN PROPULSION SYSTEM WEIGHT PREDICTION MODEL
Richard J. Gerth *In* Alabama Univ., Research Reports: 1994 NASA/ASEE Summer Faculty Fellowship Program Oct. 1994 6 p (For primary document see N95-18967 05-80)
Avail: CASI HC A02/MF A03

N95-18982*# Auburn Univ., AL. Dept. of Aerospace Enginerring.
STEADY AND UNSTEADY BLADE STRESSES WITHIN THE SSME ATD/HPOTP INDUCER
R. Steven Gross *In* Alabama Univ., Research Reports: 1994 NASA/ASEE Summer Faculty Fellowship Program Oct. 1994 6 p (For primary document see N95-18967 05-80)
Avail: CASI HC A02/MF A03

N95-18987*# Auburn Univ., AL. Dept. of Aerospace Engineering.
A PRELIMINARY ANALYSIS OF LOW FREQUENCY PRESSURE OSCILLATIONS IN HYBRID ROCKET MOTORS
Rhonald M. Jenkins *In* Alabama Univ., Research Reports: 1994 NASA/ASEE Summer Faculty Fellowship Program Oct. 1994 6 p (For primary document see N95-18967 05-80)
Avail: CASI HC A02/MF A03

N95-18988*# North Carolina Agricultural and Technical State Univ., Greensboro, NC. Dept. of Mechanical Engineering.
DEVELOPMENT OF CFD MODEL FOR AUGMENTED CORE TRIPROPELLANT ROCKET ENGINE
Kenneth M. Jones *In* Alabama Univ., Research Reports: 1994 NASA/ASEE Summer Faculty Fellowship Program Oct. 1994 6 p (For primary document see N95-18967 05-80)
Avail: CASI HC A02/MF A03

N95-18989*# Alabama Univ., Huntsville, AL. Dept. of Mechanical and Aerospace Engineering.
COMPUTATIONAL SIMULATION OF LIQUID FUEL ROCKET INJECTORS
D. Brian Landrum *In* Alabama Univ., Research Reports: 1994 NASA/ASEE Summer Faculty Fellowship Program Oct. 1994 6 p (For primary document see N95-18967 05-80)
Avail: CASI HC A02/MF A03

N95-19002*# Christian Brothers Coll., Memphis, TN. Dept. of Mechanical Engineering.
EVALUATION OF SSME TEST DATA REDUCTION METHODS
L. Michael Santi *In* Alabama Univ., Research Reports: 1994 NASA/ASEE Summer Faculty Fellowship Program Oct. 1994 6 p (For primary document see N95-18967 05-80)
Avail: CASI HC A02/MF A03

23 CHEMISTRY AND MATERIALS (GENERAL)

N95-18448*# National Aeronautics and Space Administration. Lewis Research Center, Cleveland, OH.
TRIBOLOGY AND MICROSTRUCTURE OF PS212 WITH A Cr2O3 SEAL COAT
Harold E. Sliney, Patricia A. Benoy (Saint Louis Univ., MO.), Andras Korenyi-Both (Calspan Corp., Fairview Park, OH.), and Christopher DellaCorte Dec. 1994 17 p
(Contract NAS3-25685; RTOP 505-63-5A)
(NASA-TM-106768; E-9211; NAS 1.15:106768) Avail: CASI HC A03/MF A01

PS212 is a plasma sprayed metal bonding chrome carbide coating with solid lubricant additives which has lubricating properties at temperatures up to about 900 deg C. The coating is diamond ground to achieve an acceptable tribological surface. But, as with many plasma spray coatings, PS212 is not fully-dense. In this study, a chromium oxide base seal coating is used in an attempt to seal any porosity that is open to the surface of the PS212 coating, and to study the effect of the sealant on the tribological properties of PS212. The results indicate that the seal coating reduces friction and wear when it is applied and then diamond ground leaving a thin layer of seal coating which fills in the surface pits of the PS212 coating. Author

N95-19822# Brigham Young Univ., Provo, UT. Dept. of Chemistry.
ENANTIOMERIC SEPARATION OF CHIRAL ALPHA-(1-NAPHTHYL)ETHYL AMMONIUM PERCHLORATE BY SILICA GEL-BOUND CHIRAL PYRIDINO-18-CROWN-6 LIGANDS
Peter Huszthy, Jerald S. Bradshaw, A. V. Bordunov, and Reed M. Izatt 11 May 1994 9 p
(Contract N00014-91-J-1710)
(AD-A280156; TR-27) Avail: CASI HC A02/MF A01

The separation of (alpha-(L-naphthyl)ethyl) ammonium perchlorate (NapEt) into its (R) and (S) forms using silica gel-bound dimethylpyridino-18-crown-6 ligand (S,S)-1 with methanol as an element is reported. We also report the synthesis of a new silica gel-bound diphenyl-substituted pyridino-18-crown-6 ligand (R,R)-2 by the following reactions. Dimethyl chelidamate (7) was first alkylated with 11-iodoundec-1-ene (6) on the phenolic oxygen and the resulting ether diester was reduced to form 4-undecenyloxy-2,6-pyridinedimethanol (8). Tosylation of 8 gave ditosylate 9 which was cyclized with (R,R)-diphenyl-substituted tetraethylene glycol (R,R)-10 to form crown (R,R)-11. Ligand (R,R)-11 was treated with triethoxysilane using a platinum catalyst. The resulting chiral crown-substituted triethoxysilane, (R,R)-12, was reacted with silica gel in toluene at 90 deg to attach the ligand to silica gel. The results of the separation of (R)- and (S)-NapEt using new silica gel-bound crown (R,R)-2 with methanol as the eluent are also presented. DTIC

N95-19823# Brigham Young Univ., Provo, UT. Dept. of Chemistry.
MOLECULAR RECOGNITION AS SHOWN BY THE SOLVENT EXTRACTION OF (R)- AND (S)-ALPHA-(1-NAPHTHYL)ETHYL AMMONIUM PICRATE OR ORANGE 2 BY CHIRAL PYRIDINO-CROWN ETHERS
Alexander Y. Nazaraenko, Peter Huszthy, Jerald S. Bradshaw, John D. Lamb, and Reed M. Izatt 12 May 1994 8 p
(Contract N00014-91-J-1710)
(AD-A280157; TR-29) Avail: CASI HC A02/MF A01

A solvent extraction technique was used to determine equilibrium constants for the reaction of (alpha-(1-naphthyl)ethyl)ammonium ions (R)- and (S)-isomers with chiral substituted pyridino- 18-crown-6 ligands in a water-chloroform system. Selectivity coefficients and stability constants for the interaction in chloroform solutions were calculated. The selectivity patterns are similar to those found by the 1H NMR technique. Thus, this method may be a simple and rapid way to determine enantiomeric recognition. DTIC

24 COMPOSITE MATERIALS

Includes physical, chemical, and mechanical properties of laminates and other composite materials.

For ceramic materials see *27 Nonmetallic Materials.*

N95-17941 Pennsylvania State Univ., University Park, PA. Dept. of Chemistry.
FABRICATION OF BIOMIMETIC MOLECULAR LEVEL COMPOSITES Annual Report, 1 Jun. 1993 - 31 May 1994
Patricia A. Bianconi 31 May 1994 13 p Limited Reproducibility: More than 20% of this document may be affected by microfiche quality
(Contract F49620-92-J-0296)
(AD-A284204; AFOSR-94-0502TR) Avail: CASI HC A03

This report describes development of the chemistry and applications of a new biomimetic in situ synthetic system for the fabrication of inorganic/organic composite materials. The major findings involve understanding the mechanisms of the solid-state syntheses which give rise to composites in which the crystals of the inorganic phase are identical in size, morphology, and crystallographic orientation, the determining characteristics of naturally-formed biological composites. Synthetic control over the morphology and therefore of the material properties of both the organic and inorganic phases of these new materials, as well as the mixing of the two disparate phases on the molecular level, is found to be affected primarily by (1) general factors controlling the crystallization of CdS in polymers, (2) surfactant effects on crystal growth and organization, and (3) matrix effects on crystal growth and organization. DTIC

N95-18021 Naval Postgraduate School, Monterey, CA.
SODIUM SULFATE CORROSION OF SILICON CARBIDE FIBER-REINFORCED CALCIUM ALUMINOSILICATE GLASS-CERAMIC MATRIX COMPOSITES M.S. Thesis
Peter J. Newton Mar. 1994 81 p Limited Reproducibility: More than 20% of this document may be affected by microfiche quality
(AD-A283703) Avail: CASI HC A05

Hot corrosion effects of Sodium Sulfate (NaSO4) coated Calcium Aluminosilicate (CAS)/Silicon Carbide (SiC) reinforced glass-ceramic matrix composite were investigated using Scanning Electron Microscopy (SEM), Energy Dispersive X-ray Analysis (EDX) and X-ray Diffraction (XRD). The samples provided by the Naval Air Warfare Center (NAWC) were unidirectional SiC/CAS as follows: (1) as received; (2) uncoated in air; (3) Na2SO4; coated in air; and (4) Na2SO4 coated in argon. A heat treatment was conducted at 900 C for 100 hours. Experimental observations indicated that the Na2S04 coating in an oxidizing environment had severely corroded the silicon fiber resulting in a silica rich, Nepheline (NaAlSi04), Wollastonite (CaSiO3), Rankinite (CaSi2O7), Albite (NaAlSi3O8 and glassy phases. In the argon atmosphere fiber degradation was present although less severe than in the oxygen environment. Similar phases of silica rich, Nepheline, Albite, Rankinite, Mullite (Al6Si2O13), Pseudo-Wollastonite (CaSiO3) and a glassy region were present. Minimal fiber and matrix degradation was observed in the uncoated sample beat treated in air. DTIC

N95-18028# Naval Postgraduate School, Monterey, CA.
STUDY OF FAILURE IN FIBROUS COMPOSITES SUBJECTED TO BENDING LOADS M.S. Thesis
Shih-Ting Ying Jun. 1994 77 p
(AD-A283330) Avail: CASI HC A05/MF A01

This study investigates the failure modes, failure strengths and failure criteria of laminated composite plates with stress concentration and subjected to bending loading. Graphite/epoxy composites are used for the present study. Lamina material properties, such as stiffness and strength, of the composite are obtained by experiments. A series of bending tests are conducted for laminated, graphite/epoxy composite plate with and without a hole to investigate their failure modes and strengths. In addition, finite element analyses are performed to compute stress distributions around holes of the composite plates subjected to bending loading. Based on the stress computation, a couple of failure criteria are examined to predict the failure strengths of composite plates with stress concentration. DTIC

N95-18135*# Alabama Univ., Huntsville, AL. Materials Processing Lab.
ACOUSTIC METHOD OF DAMAGE SENSING IN COMPOSITE MATERIALS Final Report

Gary L. Workman, James Walker, and Matthew Lansing 20 Oct. 1994 39 p
(Contract NAS8-38609)
(NASA-CR-196538; NAS 1.26:196538) Avail: CASI HC A03/MF A01

The use of acoustic emission and acousto-ultrasonics to characterize impact damage in composite structures is being performed on both graphite epoxy and kevlar bottles. Further development of the acoustic emission methodology to include neural net analysis and/or other multivariate techniques will enhance the capability of the technique to identify failure mechanisms during fracture. The acousto-ultrasonics technique will be investigated to determine its ability to predict regions prone to failure prior to the burst tests. The combination of the two methods will allow for simple nondestructive tests to be capable of predicting the performance of a composite structure prior to being placed in service and during service. Author

N95-18466*# Analytical Services and Materials, Inc., Hampton, VA.
TEXCAD: TEXTILE COMPOSITE ANALYSIS FOR DESIGN. VERSION 1.0: USER'S MANUAL Final Report
Rajiv A. Naik Dec. 1994 42 p
(Contract NAS1-19708; RTOP 510-02-11-07)
(NASA-CR-4639; NAS 1.26:4639) Avail: CASI HC A03/MF A01

The Textile Composite Analysis for Design (TEXCAD) code provides the materials/design engineer with a user-friendly desktop computer (IBM PC compatible or Apple Macintosh) tool for the analysis of a wide variety of fabric reinforced woven and braided composites. It can be used to calculate overall thermal and mechanical properties along with engineering estimates of damage progression and strength. TEXCAD also calculates laminate properties for stacked, oriented fabric constructions. It discretely models the yarn centerline paths within the textile repeating unit cell (RUC) by assuming sinusoidal undulations at yarn cross-over points and uses a yarn discretization scheme (which subdivides each yarn not smaller, piecewise straight yarn slices) together with a 3-D stress averaging procedure to compute overall stiffness properties. In the calculations for strength, it uses a curved beam-on-elastic foundation model for yarn undulating regions together with an incremental approach in which stiffness properties for the failed yarn slices are reduced based on the predicted yarn slice failure mode. Nonlinear shear effects and nonlinear geometric effects can be simulated. Input to TEXCAD consists of: (1) materials parameters like impregnated yarn and resin properties such moduli, Poisson's ratios, coefficients of thermal expansion, nonlinear parameters, axial failure strains and in-plane failure stresses; and (2) fabric parameters like yarn sizes, braid angle, yarn packing density, filament diameter and overall fiber volume fraction. Output consists of overall thermoelastic constants, yarn slice strains/stresses, yarn slice failure history, in-plane stress-strain response and ultimate failure strength. Strength can be computed under the combined action of thermal and mechanical loading (tension, compression and shear). Author (revised)

N95-18471*# Massachusetts Inst. of Tech., Cambridge. Dept. of Materials Science and Engineering.
COMPOSITES RESEARCH IN SUPPORT OF THE NASP INSTITUTE FOR COMPOSITES (NIC) Final Report, 1 Jun. 1991 - 31 Aug. 1994
R. M. Pelloux 29 Nov. 1994 52 p Prepared for Ohio Aerospace Inst., Cleveland, OH
(Contract NCC3-218)
(NASA-CR-197580; NAS 1.26:197580) Avail: CASI HC A04/MF A01

The main goal was to measure the elevated temperature tensile and creep properties of a SiC fiber-reinforced titanium metal matrix composite. Author

N95-18612# Army Research Lab., Watertown, MA.
A REAL-TIME VISION SYSTEM TO MONITOR/ANALYZE THE CHANGES IN COMPOSITE SPECIMENS DURING MECHANICAL TESTING Final Report
James D. Kleinmeyer and Gary B. White Apr. 1994 12 p Presented at the 48th Meeting of the Mechanical Failure Prevention Group, 19-21 Apr. 1994
(ARL-TR-344; AD-A280114) Avail: CASI HC A03/MF A01

Research has demonstrated the feasibility of using digital image processing techniques to determine dimensional changes and analyze qualitative and quantitative fracture processes in fiber-reinforced composite material test specimens that have experienced environmentally and mechanically induced stresses. The application of image analysis techniques during mechanical testing has been shown to facilitate test automation and to provide information essential to interpretation and quantification of mechanical test data. Since fracture is a dynamic process, real-time image acquisition and special image processing techniques are needed to determine specimen size and shape changes, identify where fracture is initiated, and describe how fracture develops in specimens during mechanical testing. Images must be classified and interpreted in terms of appropriate fracture models to facilitate the analysis of mechanical test data and provide a quantitative assessment of damage. Author

N95-18629 Department of the Navy, Washington, DC.
COMPOSITE STRUCTURES HAVING ORGANIC MATRICES AND DUPLEX ZINC/CERAMIC FIRE BARRIERS Patent
Usman A. Sorathia, inventor (to Navy) and Roger M. Crane, inventor (to Navy) 8 Feb. 1994 11 p Filed 13 Aug. 1992
(AD-D016232; US-Patent-5,284,697; US-Patent-Appl-SN-929212; US-Patent-Class-428-213) Avail: US Patent and Trademark Office

A process is described for forming a duplex coating as a fire barrier on a composite structure comprising organic matrices so that the structure shows reduced flammability, less smoke, higher ignition resistance, and more residual flexural strength after exposure to fire. A thin layer of a metal such as zinc is arc wire sprayed onto a surface of the structure to form a bonding and heat-diffusing coating, and a stabilized zirconia coating is then plasma sprayed onto the metal coating to form a thermal barrier coating. DTIC

N95-18920 Virginia Univ., Charlottesville, VA.
OPTIMIZATION OF LAYERED METAL MATRIX COMPOSITE CYLINDERS Ph.D. Thesis
Robert Scott Salzar 1994 202 p
Avail: Univ. Microfilms Order No. DA9415582

An analytical method that exactly satisfies the equations of the boundary-value problem for the inelastic response of laminated metal matrix composite tubes on a point-wise basis is presented. Because of the lack of a generally accepted constitutive relation for the inelastic behavior of metal matrix composites, the micromechanics relations known as 'the method of cells' are used to compute the effective elastic composite behavior as well as the incremental inelastic response of the individual plies. The method of successive elastic approximations is then used in an iterative process to obtain the effective plastic strain distributions in the individual layers of the laminated tube. The model can be subjected to a variety of thermomechanical loadings. In addition to a classical incremental plasticity theory, a viscoplastic model is included in the analysis to simulate the time-dependent effects of a composite tube under load. The developed analytical scheme is subsequently incorporated into an optimization algorithm, resulting in a design tool for the optimization of arbitrarily layered metal matrix composite tubes in the presence of inelastic effects. Representative tubes are optimized with respect to a user-defined objective function by varying ply thickness and orientation, as well as the laminate's fiber volume fraction. Dissert. Abstr.

N95-18940*# Northwestern Univ., Evanston, IL. School of Engineering and Applied Science.
CHARACTERIZATION OF METAL MATRIX COMPOSITES Final Report, 15 Nov. 1988 - 31 Mar. 1993
I. M. Daniel, H. J. Chun, and D. Karalekas Cleveland, OH NASA Nov. 1994 338 p
(Grant NAG3-950; RTOP 505-63-5B)
(NASA-CR-195381; E-9121; NAS 1.26:195381) Avail: CASI HC A15/MF A03

Experimental methods were developed, adapted, and applied to the characterization of a metal matrix composite system, namely, silicon carbide/aluminim (SCS-2/6061 Al), and its constituents. The silicon carbide fiber was characterized by determining its modulus, strength, and coefficient of thermal expansion. The aluminum matrix was characterized thermomechanically up to 399 C (750 F) at two strain rates. The unidirectional SiC/Al composite was characterized mechanically under longitudinal, transverse, and in-plane shear loading up to 399 C (750 F). Isothermal and non-isothermal creep behavior was also measured. The applicability of a proposed set of multifactor thermoviscoplastic nonlinear constitutive

relations and a computer code was investigated. Agreement between predictions and experimental results was shown in a few cases. The elastoplastic thermomechanical behavior of the composite was also described by a number of new analytical models developed or adapted for the material system studied. These models include the rule of mixtures, composite cylinder model with various thermoelastoplastic analyses and a model based on average field theory. In most cases satisfactory agreement was demonstrated between analytical predictions and experimental results for the cases of stress-strain behavior and thermal deformation behavior at different temperatures. In addition, some models yielded detailed three-dimensional stress distributions in the constituents within the composite. Author

N95-19043*# Old Dominion Univ., Norfolk, VA.
EXPERIMENTAL VERIFICATION OF A PROGRESSIVE DAMAGE MODEL FOR COMPOSITE LAMINATES BASED ON CONTINUUM DAMAGE MECHANICS M.S. Thesis Final Report
Timothy William Coats Dec. 1994 122 p
(Contract NAS1-19858; RTOP 505-63-50-04)
(NASA-CR-195020; NAS 1.26:195020) Avail: CASI HC A06/MF A02

Progressive failure is a crucial concern when using laminated composites in structural design. Therefore the ability to model damage and predict the life of laminated composites is vital. The purpose of this research was to experimentally verify the application of the continuum damage model, a progressive failure theory utilizing continuum damage mechanics, to a toughened material system. Damage due to tension-tension fatigue was documented for the IM7/5260 composite laminates. Crack density and delamination surface area were used to calculate matrix cracking and delamination internal state variables, respectively, to predict stiffness loss. A damage dependent finite element code qualitatively predicted trends in transverse matrix cracking, axial splits and local stress-strain distributions for notched quasi-isotropic laminates. The predictions were similar to the experimental data and it was concluded that the continuum damage model provided a good prediction of stiffness loss while qualitatively predicting damage growth in notched laminates. Author

N95-19123 Department of the Navy, Washington, DC.
SUPERSTRENGTH METAL COMPOSITE MATERIAL AND PROCESS FOR MAKING THE SAME Patent
Norman P. Louat, inventor (to Navy), Virgil Provenzano, inventor (to Navy), M. A. Imam, inventor (to Navy), and Kuntimaddi Sadananda, inventor (to Navy) 2 Aug. 1994 9 p Filed 31 Jan. 1992
(AD-D016555; US-Patent-5,333,667; US-Patent-Appl-SN-828630;
US-Patent-Class-164-97) Avail: US Patent and Trademark Office

A metal composite material provides improved strength at all temperatures, in particular at those temperatures greater half the melting point of its matrix. The metal composite material is at least 50 volume percent hard particulate material in a matrix which is significantly more ductile than the hard particulate material. At or above 50 volume percent hard particulate material, each particle is surrounded by a thin film of the matrix material. This thin film resists deformation by converting sliding motion between particles into the rotational motion of the particles about each other. The matrix may be made by infiltrating a powder of the particulate material with a charge of the matrix material, for example, by hot isostatically pressing the matrix material into the powder or by melting a block of matrix material on top of the powder and thus infiltrating the powder by gravitational flow of the melted matrix material into the powder. DTIC

N95-19386# Rhode Island Univ., Kingston, RI. Dept. of Chemical Engineering.
A MECHANISM FOR BLISTERING OF CARBON FIBER COMPOSITES Annual Report
S. K. Miriyala, T. J. Rockett, W. C. Tucker, and R. Brown 3 Nov. 1994 14 p
(Contract N00014-91-J-1328)
(AD-A286252) Avail: CASI HC A03/MF A01

Blisters containing fluid with a high pH were induced in a carbon fiber vinyl ester polymer matrix composite by cathodic polarization in a sodium chloride solution. The oxygen content of the solution was varied in order to determine the effect of oxygen on the blister process. It was found that increasing the oxygen content in solution decreased the time for blister initiation, indicating that the reduction of oxygen to form hydroxyl ions was an important reaction. Calculations indicated that a similar cumulative charge density was required for blister initiation for the different oxygen contents, confirming the importance of oxygen to the blister process. A mechanism for blister formation dependent upon oxygen reduction to hydroxyl ions and the subsequent formation of an osmotic cell is outlined from the results of this study. DTIC

N95-19467 Aeronautical Research Labs., Melbourne (Australia).
DAMAGE MONITORING IN METALLIC AND COMPOSITE STRUCTURES USING PIEZOELECTRIC THIN FILM SENSORS
W. K. Chiu and S. C. Galea May 1993 22 p
(ARL-RR-4; AR-008-342) Copyright Avail: Issuing Activity (Aeronautical Research Labs., Melbourne, Australia)

The increasing emphasis on intelligent material systems and structures has resulted in a significant research effort in the areas of embedded and bonded sensors and actuators. Piezoelectric film are one of the many sensing materials available. The piezoelectric sensor output is proportional to changes in surface displacement and can be used to interpret variations in structural and material properties, e.g., the compliance of the structure. The aim of this paper is to demonstrate the use of piezoelectric film sensors as a structural integrity monitoring device for detecting damage in fiber reinforced composites, and crack growth in aluminum alloy specimens. Author

N95-19579# Sandia National Labs., Albuquerque, NM.
ENVIRONMENTAL EFFECTS ON COMPOSITE AIRFRAMES: A STUDY CONDUCTED FOR THE ARM UAV PROGRAM (ATMOSPHERIC RADIATION MEASUREMENT UNMANNED AEROSPACE VEHICLE)
R. A. Noguchi Jun. 1994 49 p
(Contract DE-AC04-94AL-85000)
(DE94-015351; SAND-94-8210) Avail: CASI HC A03/MF A01

Composite materials are affected by environments differently than conventional airframe structural materials are. This study identifies the environmental conditions which the composite-airframe Atmospheric Radiation Measurement Unmanned Aerospace Vehicle (ARM UAV) may encounter, and discusses the potential degradation processes composite materials may undergo when subjected to those environments. This information is intended to be useful in a follow-on program to develop equipment and procedures to prevent, detect, or otherwise mitigate significant degradation with the ultimate goal of preventing catastrophic aircraft failure. DOE

N95-19650*# Drexel Univ., Philadelphia, PA. Dept. of materials Engineering.
UNIT CELL GEOMETRY OF MULTIAXIAL PREFORMS FOR STRUCTURAL COMPOSITES Final Report
Frank Ko, Charles Lei, Anisur Rahman, G. W. Du, and Yun-Jia Cai Nov. 1993 201 p
(Contract NCC1-138)
(NASA-CR-197294; NAS 1.26:197294) Avail: CASI HC A10/MF A03

The objective of this study is to investigate the yarn geometry of multiaxial preforms. The importance of multiaxial preforms for structural composites is well recognized by the industry but, to exploit their full potential, engineering design rules must be established. This study is a step in that direction. In this work the preform geometry for knitted and braided preforms was studied by making a range of well designed samples and studying them by photo microscopy. The structural geometry of the preforms is related to the processing parameters. Based on solid modeling and B-spline methodology a software package is developed. This computer code enables real time structural representations of complex fiber architecture based on the rule of preform manufacturing. The code has the capability of zooming and section plotting. These capabilities provide a powerful means to study the effect of processing variables on the preform geometry. the code also can be extended to an auto mesh generator for downstream structural analysis using finite element method. This report is organized into six sections. In the first section the scope and background of this work is elaborated. In section two the unit cell geometries of braided and multi-axial warp knitted preforms is discussed. The theoretical frame work of yarn path modeling and solid modeling is presented in section three. The thin section microscopy carried out to observe the structural geometry of the preforms is the subject in section four. The

structural geometry is related to the processing parameters in section five. Section six documents the implementation of the modeling techniques into the computer code MP-CAD. A user manual for the software is also presented here. The source codes and published papers are listed in the Appendices. Author

N95-19702# Dayton Univ. Research Inst., OH.
CVD SILICON CARBIDE CHARACTERIZATION Final Report, Aug. 1992 - Oct. 1993
G. A. Graves, Jr. and D. Iden Aug. 1994 51 p
(Contract F30602-90-D-0105)
(AD-A285667; UDR-TR-93-122; RL-TR-94-122) Avail: CASI HC A04/MF A01

Chemically vapor deposited (CVD) silicon carbide is a candidate material for high quality ground and space-based mirror substrates and high quality reflective optics. Statistically valid material property data has not been available, however, to make durability and lifetime predictions for such optics. The primary purpose of this study was to determine the Weibull and slow crack growth parameters for CVD silicon carbide. Specimens were cut from various locations in a 25 mm thick, 50 cm diameter piece of SiC to analyze bulk material property homogeneity. Flexural strength was measured using a four-point bend technique. In addition to mechanical testing for strength, hardness, and fracture toughness, the material crystallography and microstructure were studied. Thermal expansion, thermal diffusivity, specific heat, optical absorption, and infrared reflectivity measurements were also conducted. Raman spectroscopy was used to check for any residual stress. Test results show this CVD silicon carbide is a high-purity, homogeneous, fine-grained substrate material with very good mechanical, optical, and thermal properties. DTIC

N95-19782*# National Aeronautics and Space Administration. Lewis Research Center, Cleveland, OH.
DRIVING FORCE ANALYSIS IN AN INFINITE ANISOTROPIC PLATE WITH MULTIPLE CRACK INTERACTIONS
Wieslaw K. Binienda and Steven M. Arnold (Akron Univ., Akron, OH.) Jan. 1995 40 p
(Grant NAG3-1223; RTOP 505-63-12)
(NASA-TM-106838; E-9401; NAS 1.15:106838) Avail: CASI HC A03/MF A01

The methodology and a rigorous solution formulation are presented for stress intensity factors (SIF's, k) and total strain energy release rates (SERR, G(sub T)) of a multicracked plate, that has fully interacting cracks and is subjected to a far-field arbitrary stress state. The fundamental perturbation problem is derived, and the steps needed to formulate the system of singular integral equations whose solution gives rise to the evaluation of the SIF's are identified. Parametric studies are conducted for two, three, and four crack problems. The sensitivity and characteristics of the model is demonstrated. Author

N95-19814 Missouri Univ., Rolla, MO. Dept. of Chemistry.
USE OF TITANATE COUPLING AGENTS IN KEVLAR (TRADE NAME)/PHENOLIC COMPOSITES Technical Report, 1 Jan. 1993 - 1 Apr. 1994
Nalini Menon, Frank D. Blum, and Lokesh R. Dharani 2 Apr. 1994 28 p Submitted for publication Limited Reproducibility: More than 20% of this document may be affected by microfiche quality
(Contract N00014-91-J-1274)
(AD-A279200; UMR-FDB-37) Avail: Issuing Activity (Defense Technical Information Center (DTIC))

Surface modification of Kevlar(R) fibers with titanate coupling agents for improved adhesion of the fiber and resin in Kevlar(R)/phenolic composites has been attempted to explore the possibility of enhancement in adhesion and bulk properties of composites for friction materials. Titanate coupling agents were used and flexural properties of the Kevlar(R)-fiber reinforced composites determined. A study of different amounts of the coupling agents at the fiber-matrix interface suggested that 2% by weight of fiber was the optimum amount, in terms of improvement in flexural properties. The composite samples with the coupling agents, showed an increase in flexural strength, over the untreated samples with the maximum increase being approx. 18% over the control. Water absorption studies were conducted on Kevlar(R)/phenolic composites treated with organotitanates to determine the effectiveness of these coupling agents in improving resistance to moisture attack. The treated Kevlar(R)/phenolic composite samples exhibited greater resistance to moisture-ingress over the untreated samples. The control samples showed a decrease of 17% in flexural strength. The largest decrease in strength was 14% for the treated samples containing coupling agent tetrakis(2-ethylhexyl)titanate (TYZOR TOT). Recovery in strength on reconditioning, was also greater for treated samples over control. A recovery in strength of ca. 94% was seen for some treated samples. DTIC

N95-19851 Army Research Lab., Watertown, MA. Materials Directorate.
BARIUM STRONTIUM TITANATE AND NON-FERROELECTRIC OXIDE CERAMIC COMPOSITES FOR USE IN PHASED ARRAY ANTENNAS Final Report
L. C. Sengupta, S. Stowell, E. Ngo, M. ODay, and R. Lancto Apr. 1994 19 p Presented at the Intergrate Ferroelectrics Meeting, Monterey, CA, 14-16 Mar. 1994 Limited Reproducibility: More than 20% of this document may be affected by microfiche quality
(AD-A279225; ARL-TR-342) Avail: Issuing Activity (Defense Technical Information Center (DTIC))

A ceramic ferroelectric phase shifting device has been demonstrated using Ba(1-x)Sr(x)TiO3 (BSTO) ceramics. As part of an effort to optimize the electronic device performance in the phase shifter, various composites of BSTO combined with other nonelectrically active oxide ceramics have been formulated. In general the composites have reduced dielectric constants, Epsilon,' where epsilon = epsilon'-i epsilon' and loss tangents tan delta. The low dielectric constant and low loss tangent reduce the overall impedance mismatch and insertion loss of the device. In addition, the overall tunability, change in the dielectric constant with applied voltage, is maintained at a relatively high level (15% with an applied electric field of 1.5 V/microns) for dielectric constants of 200. The combination of electronic properties of these materials offer substantially higher operating frequencies, 10 GHz and above. The microstructures including grain size and phase analysis have been examined using SEM and EDX. X ray diffraction has been used to identify compositions of any secondary phases formed in the composites. The analysis of the phase formation and compositional variations will be related to the electronic properties of the materials. DTIC

N95-18184*# North Carolina Univ., Charlotte, NC. Dept. of Engineering Tech.
OUTGASSING OF SOLID MATERIAL INTO VACUUM THERMAL INSULATION SPACES
Pao-Lien Wang *In* Univ. of Central Florida, NASA/ASEE Summer Faculty Fellowship Program. 1994 Research Reports Oct. 1994 p 509-520 (For primary document see N95-18166 05-80)
Avail: CASI HC A03/MF A04

N95-18973*# Union Coll., Schenectady, NY. Dept. of Mechanical Engineering.
FOREIGN BODY IMPACT EVENT DAMAGE FORMATION IN COMPOSITE STRUCTURES
Ronald B. Bucinell *In* Alabama Univ., Research Reports: 1994 NASA/ASEE Summer Faculty Fellowship Program Oct. 1994 6 p (For primary document see N95-18967 05-80)
Avail: CASI HC A02/MF A03

N95-18981*# Kansas Univ., Lawrence, KS. Dept. of Mechanical Engineering.
REAL-TIME THICKNESS MEASUREMENT OF MCC ABLATOR MATERIAL
R. Bryan Greenway, Jr. *In* Alabama Univ., Research Reports: 1994 NASA/ASEE Summer Faculty Fellowship Program Oct. 1994 6 p (For primary document see N95-18967 05-80)
Avail: CASI HC A02/MF A03

25 INORGANIC AND PHYSICAL CHEMISTRY

Includes chemical analysis, e.g., chromatography; combustion theory; electrochemistry; and photochemistry.

For related information see also *77 Thermodynamics and Statistical Physics.*.

N95-17966 Virginia Commonwealth Univ., Richmond, VA.
ENHANCEMENT OF FLUORESCENCE DETECTION IN CHROMATOGRAPHIC METHODS BY COMPUTER ANALYSIS OF SECOND ORDER DATA
S. C. Rutan 1993 8 p Limited Reproducibility: More than 20% of this document may be affected by microfiche quality
(Contract DE-FG05-88ER-13833)
(DE94-014682; DOE/ER-13833/19) Avail: CASI HC A02

Two types of experiments were studied during the course of this project. The first was liquid chromatographic separation of polyaromatic hydrocarbons (PAH's) followed by detection with full-spectrum fluorescence spectroscopy using an intensified diode array detector. Methods such as generalized rank annihilation and adaptive Kalman filtering were developed and evaluated. The second was the use of a thin-layer chromatographic or planar electrophoretic separation of analytes (amino acids or enzymes). The analytes are then reacted with a reagent or enzyme substrate; the reaction is followed by fluorescence intensity versus time and migration distance, and kinetic analysis is used to quantify the component species. DOE

N95-17975# Stanford Univ., CA. Dept. of Chemistry.
AASERT-93: NEW HIGH-PRESSURE DIAGNOSTIC TECHNIQUE Annual Report, 1 Aug. 1993 - 31 Jul. 1994
Richard N. Zare 31 Jul. 1994 4 p
(Contract F49620-93-1-0442)
(AD-A284943; AFOSR-94-0568TR) Avail: CASI HC A01/MF A01

As we outlined in our submitted proposal, progress towards making DFWM spectroscopy quantitative has been achieved. This work makes explicit how the magnitude of the DFWM signal depends on the polarizations of the three incident beams under the weak and strong-field limits. We have been using DFWM to investigate acetylene (C2H2) and methyl radical (CH3) molecules in an atmospheric pressure flame and in a low-pressure hot-filament reactor. To calibrate the measurement, acetylene is measured in the free flow of a C2H2/O2 mixture, and also in the pre-reaction zone of a C2H2/O2 flame-both with a fast flow rate of 40-50 m/s at the nozzle outlet of the mixture. The DFWM signal falls in the weak field limit (far from saturation), which means the DFWM signal is proportional to the products of the three incident beam intensities (IfIbIp). DTIC

N95-17982# Eltron Research, Inc., Boulder, CO.
METHANE CONVERSION BY SOLID ELECTROLYTE MEMBRANES Final Report, 1 Jan. 1989 - 31 Aug. 1993
A. F. Sammells, M. Schwartz, R. L. Cook, and J. H. White Mar. 1994 133 p See also PB93-127041 Sponsored by Gas Research Inst., Chicago, IL
(Contract GRI-5089-260-1824)
(PB94-191781; GRI-94/0081) Avail: CASI HC A07/MF A02

This program is focusing on solid-state fuel cells which operate in the same temperature range as molten carbonate fuel cells. One approach involves selecting new solid electrolytes with high ionic conductivity at approximately 600 C. Experimentally determined activation energies for ionic transport in perovskite solid electrolytes have been found related to lattice and thermodynamic parameters. Using this approach, we have identified solid electrolytes having high ionic and low electronic conductivity. These electrolytes have been incorporated in small unoptimized laboratory fuel cells that may perform better at 600 C than zirconia based SOFC's at 1000 C, assuming that many other issues can be resolved. These issues include the chemical and physical stability of cell components, including electrocatalysts for each respective half-cell reaction and the development of multicell designs and fabrication procedures. Progress has been made in identifying anode electrocatalysis towards promoting partial and complete CH4 oxidation. New fuel cell structures are being defined using thin-film techniques involving metalloorganic chemical vapor deposition (MOCVD) of solid electrolytes. Author

N95-17991 Quaid-i-Azam Univ., Islamabad (Pakistan).
PREPARATION AND SURFACE CHARACTERIZATION OF METAL DOPED ALUMINA CATALYST Thesis
H. Tahir 1993 149 p Sponsored by Direction des Recherches, Etudes et Techniques, Paris (France) Limited Reproducibility: More than 20% of this document may be affected by microfiche quality
(PB94-175296) Avail: Issuing Activity (National Technical Information Service (NTIS))

Alumina was doped with divalent metals such as nickel, cobalt, manganese, zinc, and copper by method of impregnation techniques. Thermal analysis techniques were used for their surface characterization. Absorption of dye such as Acid Red 4 on pure alumina and alumina supported metals was studied as a function of temperature. Spectrophotometric techniques were used for measuring the extent of adsorption. The data were fitted in Langmuir, Freundlich and Dubinin-Radushkevic isotherm equations and their corresponding constants were determined from the slope and intercepts of their respective lines. Thermodynamic parameters such as enthalpy (delta H), free energy (delta G), and entropy (delta S) of adsorption were calculated by using Langmuir constant K. Sorption mean free energy (E) for each system was calculated by using (D-R) equation and interpreted. Author

N95-17994# National Inst. of Standards and Technology, Gaithersburg, MD. Office of Measurement Services.
STANDARD REFERENCE MATERIALS: GLASS FILTERS AS A STANDARD REFERENCE MATERIAL FOR SPECTROPHOTOMETRY. SELECTION, PREPARATION, CERTIFICATION AND USE OF SRM 930 AND SRM 1930 Final Report
Radu Mavrodineanu, Robert W. Burke, John R. Baldwin, Melody V. Smith, and Jerry D. Messman Mar. 1994 207 p See also PB-246437
(PB94-188844; NIST/SP-260/116) Avail: CASI HC A10/MF A03; SOD HC

This publication describes the various factors that can affect the proper functioning of a spectrophotometer and suggests procedures to assess and control these factors. Particular consideration is given to the long and short-term stability of a spectrophotometer, wavelength accuracy, spectral bandpass, stray radiation, and the accuracy of the transmittance or absorbance scale. A description is given of the Standard Reference Materials (SRM's) that can be used to control these factors. The methods for the preparation, certification, and use of two such material (SRM 930 and SRM 1930) are also presented. The results obtained in the actual use of the SRM's are examined in some detail. An Appendix contains the reproduction of several publications and certificates relevant to the subject discussed in this publication. Author

N95-18377 Selskapet for Industriell og Teknisk Forskning, Trondheim (Norway). Dept. for Materials Technology.
PALLADIUM-BASED MEMBRANES FOR HYDROGEN SEPARATION
R. Bredesen 22 Dec. 1993 15 p See also PB93-201671
(PB94-207156; STF28-A93087) Avail: Issuing Activity (National Technical Information Service (NTIS))

The report describes the work during the last part of the SPUNG Program on Palladium based membranes for hydrogen separation. The main result is that a successful method for preparation of thin defect-free Pd-30%Ag membranes has been developed (membrane thickness approx. 1 micrometer). The Pd-Ag membranes are supported on porous ceramic substrates developed in the project. The membranes have been tested in N2+H2 mixtures and in pure hydrogen at temperatures between 200-260 C. They show 100% selectivity and very high hydrogen permeability. The results suggest that the transport of hydrogen from the feed to the permeate side is not limited by the hydrogen diffusion through the membrane. It is suggested that the flux rate is limited by the permeability of the porous ceramic support. NTIS

N95-18410 Princeton Univ., NJ. Dept. of Mechanical and Aerospace Engineering.
STUDIES ON HIGH PRESSURE AND UNSTEADY FLAME PHENOMENA Annual Report, 15 Apr. 1993 - 14 Apr. 1994
C. K. Law 20 Jun. 1994 55 p Limited Reproducibility: More than 20% of this document may be affected by microfiche quality
(Contract F49620-92-J-0227)

(AD-A284126; AFOSR-94-0501TR) Avail: Issuing Activity (Defense Technical Information Center (DTIC))

The objective of the present program is to study the structure and response of steady and unsteady laminar premixed and nonpremixed flames in reduced and elevated pressure environments through: (1) non-intrusive experimentation; (2) computational simulation using detailed flame and kinetic codes; and (3) asymptotic analysis with reduced kinetic mechanisms. During the reporting period progress has been made in the following projects: (1) a theoretical and experimental study of unsteady diffusion flames; (2) a computational and experimental study of hydrogen/air diffusion flames at sub- and super-atmospheric pressures; (3) an asymptotic analysis of the structure of premixed flames with volumetric heat loss; (4) asymptotic analyses of ignition in the supersonic hydrogen/air mixing layer with reduced mechanisms; (5) a new numerical algorithm for generating the ignition-extinction S-curves. A total of three reprints are appended. DTIC

N95-18412 Tennessee Univ., Knoxville, TN. Dept. of Chemistry.
SPECTROELECTROCHEMICAL INVESTIGATIONS OF MOLTEN HALIDE SOLUTIONS Annual Technical Report No. 2, 1 May - 30 Apr. 1993
Gleb Mamantov 16 Jun. 1994 5 p Limited Reproducibility: More than 20% of this document may be affected by microfiche quality
(Contract F49620-92-J-0222)
(AD-A284147; AFOSR-94-0500TR) Avail: Issuing Activity (Defense Technical Information Center (DTIC))

The main objective of this research, performed by Ellen Kurt Hondrogiannis, a graduate student at the University of Tennessee, is to investigate the utility of the combination of spectroscopy and electrochemistry, or spectroelectrochemistry (SEC), for studies of redox processes in molten halides. The initial studies involved the use of UV-visible, Raman, and electron spin resonance SEC to identify the radical anion intermediate formed during the electrochemical reduction of tetrachloro-p-benzoquinone, or chloranil, in the basic (50 mole percent AlCl3) molten sodium chloroaluminate melt at 175 C. This anion intermediate had not been detected in this melt previously, since cyclic voltammetry shows only one wave which had previously been attributed to a single two electron reduction to the dianion. DTIC

N95-18514 Tennessee Univ., Knoxville, TN. Dept. of Chemistry.
ELECTROCHEMICAL AND SPECTROSCOPY STUDIES OF SELECTED INORGANIC AND ORGANIC SYSTEMS IN MOLTEN HALIDES Annual Report, 15 Feb. 1993 - 14 Feb. 1994
Gleb Mamantov 14 Feb. 1994 43 p Limited Reproducibility: More than 20% of this document may be affected by microfiche quality
(Contract F49620-93-1-0129)
(AD-A284171; AFOSR-94-0496TR) Avail: Issuing Activity (Defense Technical Information Center (DTIC))

The research during the past year has concentrated on the photochemistry of anthracene and 9-methylanthracene in molten aluminum chloride-1-ethyl-3-methylimidazolium chloride (AlCl3/EMIC), looking in particular for photoinduced electron transfer reactions. Several such reactions have been found. Experiments demonstrate that this chemistry was initiated by electron transfer from the excited state of 9-methylanthracene to EMI+. The difference in behavior of anthracene and 9-methylanthracene in the basic melt can be attributed to the difference in the rate of electron transfer to EMI+: for anthracene, the electron transfer is endothermic and slow, while for 9-methylanthracene, the electron transfer is exothermic and fast. Irradiation of anthracene in oxygenated basic medium afforded several products including 9-chloranthracene. Although the formation of 9-chloranthracene can be envisioned to arise by electron transfer from the excited state of anthracene to O2, additional work will be required to prove that this assumption is correct. DTIC

N95-18637# Purdue Univ., West Lafayette, IN.
THE SOLVENT ABSORPTION-EXTRACTIVE DISTILLATION (SAED) PROCESS FOR ETHANOL RECOVERY FROM GAS/VAPOR STREAMS
M. C. Dale 1993 14 p Presented at the American Institute of Chemical Engineers (AICHE) Conference, Chicago, IL, Mar. 1993
(Contract DE-FG02-85CE-40772)
(DE94-013112; CONF-9303281-1) Avail: CASI HC A03/MF A01

A low energy system for ethanol recovery and dehydration has been developed. This system utilizes a solvent for (1) absorption of ethanol vapors, and then the same solvent for (2) extractive distillation. The ideal solvent for this process would have a high affinity for ethanol, and no affinity for water. Heavy alcohols such as dodecanol, and tridecanol, some phosphorals, and some fatty acids have been determined to meet the desired specifications. These solvents have the effect of making water more volatile than ethanol. Thus, a water stream is taken off initially in the dehydration column, and a near anhydrous ethanol stream is recovered from the ethanol/solvent stripper column. Thus the solvent serves dual uses (1) absorption media, and (2) dehydration media. The SAED process as conceptualized would use a solvent similar to solvents used for direct extractive separation of ethanol from aqueous ethanol solutions. DOE

N95-18744*# Nebraska Univ., Lincoln, NE. Dept. of Physics.
A PHOTOIONIZATION STUDY OF OH AND OD FROM 680A TO 950A: AN ANALYSIS OF THE RYDBERG SERIES
J. N. Cutler, Z. X. He, and J. A. R. Samson 1994 30 p
(Grants NAGw-1751; NSF OMR-92-12658)
(NASA-CR-196970; NAS 1.26:196970) Avail: CASI HC A03/MF A01

The photoionization spectra of OH(+) and OD(+) have been reported from 680 to 950 A (18.23 to 13.05 eV) at a wavelength resolution of 0.07 A. Through interpretation of both spectra, the Rydberg series and their higher vibrational members have been reported for three of the excited ionic states, a(sup 1)Delta, A(sup 3)Pi(i), and b(sup 1) Sigma(sup +). A vibrational progression has also been observed in both OH(+) and OD(+) which is apparently related to a fourth excited ionic state, c(sup 1)Pi. Finally, the dissociative ionization limits, corrected to 0 K,for H2O AND D2O have been measured to be 18.11+/-0.01 and 18.21+/-0.01 eV, respectively, and shown to be in good agreement with previously reported results. Author

N95-19066 Florida Univ., Gainesville, FL. Dept. of Chemistry.
MASS SPECTROMETRIC STUDIES OF CLUSTERS AND SURFACES Final Report, Oct. 1990 - Jun. 1994
John R. Eyler 29 Aug. 1994 14 p Limited Reproducibility: More than 20% of this document may be affected by microfiche quality
(Contract N00014-87-J-1248)
(AD-A283992) Avail: Issuing Activity (Defense Technical Information Center (DTIC))

Fourier transform ion cyclotron resonance (FTICR) mass spectrometry was used to obtain information about the reactivity and physical properties of gaseous cluster ions, and to develop various mass spectrometric surface and bulk analysis techniques. New values for electron affinities and ionization potentials of many different semiconductor clusters were determined. Ultra-high resolution glow discharge FTICR mass spectrometry was developed to better characterize solid materials. Author (DTIC)

N95-19170 Battelle Memorial Inst., Columbus, OH.
THEORETICAL INTERPRETATION OF THE FLUORESCENCE SPECTRA OF TOLUENE AND p-CRESOL Final Report, Apr. - Aug. 1993
James O. Jensen and Hendrik F. Hameka Jul. 1994 24 p Limited Reproducibility: More than 20% of this document may be affected by microfiche quality
(Contract DAAL03-91-C-0034; DA Proj. 1O1-62622-A-553)
(AD-A284314; ERDEC-CR-144) Avail: CASI HC A03

The fluorescence spectra of toluene and p-cresol from ab initio calculations were interpreted on the ground states and the lowest excited singlet states of the two molecules. Determination was made on the energy minima and the optimized geometries of the ground states and the lowest excited singlet states from 4 in 4 CASSCF computations using 6-31G basis set. Also computed was the vibrational frequencies of both molecules in the two states. It is believed that this work constitutes the first complete calculation of the vibrational spectra of both ground and excited states of aromatic molecules. DTIC

N95-19515# Davidson Coll., NC. Dept. of Chemistry.
DEVELOPMENT OF A COLLOIDAL REDOX SYSTEM CONTAINING A SMECTITE CLAY FOR CONTROL OF REACTIVITY AND REACTION SELECTIVITY Final Report, 1 Nov. 1993 - 30 Sep. 1994
David N. Blauch 26 Sep. 1994 4 p
(Contract N00014-94-1-0072)
(AD-A285958) Avail: CASI HC A01/MF A01

This project is directed towards the development of colloidal redox systems involving smectite clays:. Two polypyridylosmium(II) complexes

containing ligands bearing anionic pendant groups have been synthesized. Each complex has been successfully incorporated into stable montmorillonite colloids. Approximately 96% - 99% of the complex adsorbs onto the colloidal montmorillonite for loadings up to 1 mmole/g. These findings demonstrate the utility of adding a negatively charged side group to a complex to prevent simultaneous adsorption of the complex on two clay particles, which produces flocculation. Electrochemical studies of these colloidal redox systems indicate that at least part of the clay-adsorbed complex is accessible for electron transfer. These properties are prerequisites for the development of new catalytic systems based upon the incorporation of transition-metal catalysts into clay colloids. In order to develop such a system, two bipolar aquaruthenium(II) catalysts have been synthesized. These aquaruthenium(II) catalysts can also be incorporated into stable montmorillonite colloids. Characterization of clay colloids containing these catalysts is in progress. DTIC

N95-19550# Universidad Autonoma del Estado de Mexico, Toluca. Facultad de Quimica.
STUDY OF THE EFFECT OF IONIZING RADIATION ON THE STRUCTURE OF NATURAL RUBBER LATEX BY POSITRON ANNIHILATION TECHNIQUE Ph.D. Thesis
I. R. LopezSaldana 1993 99 p
(DE94-631466; INIS-mf-13925) Avail: CASI HC A05/MF A02 (US Sales Only)

At the present research, were studied the changes in natural rubber latex structure, due to electron beam by a 3 MeV, 25 m A Dynamitron electron accelerator. The natural rubber latex was irradiated at 30, 40 and 50 kGy/s dose rate, over a total dose range from 150 to 250 kGy, for each dose rate used. From natural rubber latex irradiated films were prepared by casting with 0.7 mm. thickness. In the main part, the study was made by positron annihilation lifetime (PAL), this technique is unique in the determination of free-volume properties due to the fact that positronium atom (Ps) is found to be preferentially localized in the free-volume region of polymeric materials. The positron lifetime measurements were performing using a gamma-gamma coincidence system. These results were analyzed by PATFIT-88 program computer into three components, the long-lived component for orthopositronium (o-Ps) with parameters lifetime ((tau)(sub 3)) and formation intensity (I(sub 3)), were plotted and analyzed for each dose rate and total dose used. Besides with (tau)(sub 3) were calculated the mean free-volume size based on the spherical model for the free-volume bubble, found that the free-volume decrease slightly with the total dose due to the crosslinking of natural rubber latex. Besides was studied the effect of dose rate on tensile strength, the tensile strength is increased with the total dose although there was not a clear effect due to the dose rate. Also the films were subjected to aging in order to determined the thermal stability of natural rubber latex irradiated, the results show that the films have good stability. Besides was used the infrared spectroscopy to determine the changes due to the crosslinking by variations in the characteristically absorption bands for cis 1,4-polyisoprene. DOE

N95-19559# Sandia National Labs., Albuquerque, NM.
USING ELECTROCHEMISTRY IN DEVICE PROCESSING ON POLY(TETRAFLUOROETHYLENE) SUBSTRATES
A. J. Howard, R. R. Rye, A. J. Ricco, D. J. Rieger, M. L. Lovejoy, L. R. Sloan, and M. A. Mitchell 1994 6 p Presented at the 186th Meeting of the Electrochemical Society, Miami, FL, 9-14 Oct. 1994
(Contract DE-AC04-94AL-85000)
(DE95-000541; SAND-94-1172C; CONF-941063-6) Avail: CASI HC A02/MF A01

By combining electrochemical and electroless metal deposition processes with standard optical lithography and wet chemical etching, the authors have developed techniques for the fabrication of fine (less than 20 (mu)m), adherent, conducting features on poly(tetrafluoroethylene) (PTFE) substrates. These techniques are less expensive and have demonstrated resolution of at least a factor of five better than existing printed wiring board-based processes. Using these PTFE-based processes, the authors have fabricated (approximately) 10 GHz coupled-line quadrature (Lange) couplers, for which test results will be presented. DOE

N95-19616# California Univ., Berkeley. Lawrence Berkeley Lab, CA.
TRANSITION METAL OXIDES DEPOSITED ON RHODIUM AND PLATINUM: SURFACE CHEMISTRY AND CATALYSIS Ph.D. Thesis
A. B. Boffa Jul. 1994 202 p
(Contract DE-AC03-76SF-00098)
(DE95-000793; LBL-35954) Avail: CASI HC A10/MF A03

The surface chemistry and catalytic reactivity of transition metal oxides deposited on Rh and Pt substrates has been examined in order to establish the role of oxide-metal interactions in influencing catalytic activity. The oxides investigated included titanium oxide (TiOx), vanadium oxide (VOx), iron oxide (FeOx), zirconium oxide (ZrOx), niobium oxide (NbOx), tantalum oxide (TaOx), and tungsten oxide (WOx). The techniques used to characterize the sample included AES, XPS, LEED, TPD, ISS, and STM. After characterization of the surface in UHV, the sample was enclosed in an atmospheric reaction cell to measure the influence of the oxide deposits on the catalytic activity of the pure metal for CO and CO2 hydrogenation. The oxide deposits were found to strongly enhance the reactivity of the Rh foil. The rates of methane formation were promoted by up to 15 fold with the maximum in rate enhancement occurring at oxide coverages of approximately 0.5 ml. TiOx TaOx, and NbOx were the most effective promoters and were stable in the highest oxidation states during both reactions (compared to VOx, WOx, and FeOx). The trend in promoter effectiveness was attributed to the direct relationship between oxidation state and Lewis acidity. Bonding at the metal oxide/metal interface between the oxygen end of adsorbed CO and the Lewis acidic oxide was postulated to facilitate C-O bond dissociation and subsequent hydrogenation. DOE

N95-19618# Argonne National Lab., IL. Analytical Chemistry Lab.
[ACTIVITIES OF THE ANALYTICAL CHEMISTRY LABORATORY] Progress Report, FY 1993
Dec. 1993 66 p
(Contract W-31-109-eng-38)
(DE95-000834; ANL/ACL-93/2) Avail: CASI HC A04/MF A01

The purpose of this report is to summarize the activities of the Analytical Chemistry Laboratory (ACL) at Argonne National Laboratory (ANL) for Fiscal Year (FY) 1993 (October 1992 through September 1993). This annual report is the tenth for the ACL and describes continuing effort on projects, work on new projects, and contributions of the ACL staff to various programs at ANL. The Analytical Chemistry Laboratory is a full-cost-recovery service center, with the primary mission of providing a broad range of analytical chemistry support services to the scientific and engineering programs at ANL. The ACL also has research programs in analytical chemistry, conducts instrumental and methods development, and provides analytical services for governmental, educational, and industrial organizations. The ACL handles a wide range of analytical problems. Some routine or standard analyses are done, but it is common for the Argonne programs to generate unique problems that require development or modification of methods and adaption of techniques to obtain useful analytical data. The ACL is administratively within the Chemical Technology Division (CMT), its principal ANL client, but provides technical support for many of the technical divisions and programs at ANL. The ACL has four technical groups--Chemical Analysis, Instrumental Analysis, Organic Analysis, and Environmental Analysis--which together include about 45 technical staff members. Talents and interests of staff members cross the group lines, as do many projects within the ACL. DOE

N95-19699# Materials Research Labs., Ascot Vale (Australia).
ON THE CONDUCT OF FAST COOKOFF TESTS IN AUSTRALIA
L. M. Barrington and K. J. Schebella Apr. 1994 33 p
(AD-A284260; MRL-TN-664; DODA-AR-008-640) Avail: CASI HC A03/MF A01

The conduct of full scale fast cookoff or liquid fuel fire tests in Australia is becoming increasingly important as Australia moves to adopt and implement an official policy on insensitive munitions. EOD-Salisbury has considerable experience in the development and conduct of these tests, and some relevant findings are summarized here. This report is presented in five Sections: Section 1 introduces the official Australian insensitive munitions policy; Section 2 discusses the various fast cookoff test specifications which exist both internationally and in Australia; Section 3 describes the results of a number of trials conducted to measure the spatial distribution of temperature within a liquid fuel fire, in order to firstly establish an upper wind limit for such tests, and secondly to locate the 'hottest' region of the fire; Section 4 examines meteorological (wind) conditions at three potential fast cookoff test sites in Australia; and Section 5 briefly summarizes the report's findings. DTIC

N95-19729 Army Research Lab., Aberdeen Proving Ground, MD.
FLAMESPREADING IN GRANULAR SOLID PROPELLANT: INITIAL RESULTS Final Report, Oct. 1991 - Oct. 1993
Douglas E. Kooker, Stephen L. Howard, and Lang-Mann Chang Jun. 1994 40 p Limited Reproducibility: More than 20% of this document may be affected by microfiche quality
(AD-A284245; ARL-TR-446) Avail: CASI HC A03

This study is an experimental investigation into fundamental aspects of ignition and flamespreading in compacted granular solid propellant. The 76-mm-diameter dual-chamber laboratory apparatus was designed as a closed-volume simulator with an ignition source at one end to generate a gas-phase planar wave. Diagnostics include wall-mounted pressure gages to monitor the time-history of the pressure field, and fast-response Type S thermocouples mounted in special hollow steel holders. Concern about adequacy of the thermocouple response time in this transient flow field is addressed by comparing data from 1-mil, 2-mil, and 3-mil-diameter thermocouples. The simulator is loaded with two granular solid propellants: the triple-base M30A1 and the LOVA nitramine composite M43. Under certain conditions, the granular bed of 'insensitive' M43 ignites more readily than the granular bed of M30A1, which emphasizes an important concept: Time to ignition is determined by competition between the 'flow residence time' and the 'characteristic time for chemical reaction.' For M43, chamber diagnostics indicate pressure of 2-3 MPa and gas-phase temperatures in the range of 800 to 1200 K before combustion runs away. These conditions are compatible with speculation that 'dark zone' flame chemistry is controlling delayed ignition in LOVA propellant. Author (DTIC)

N95-19785# SRI International Corp., Menlo Park, CA.
NOVEL CATALYSTS FOR METHANE ACTIVATION
A. S. Hirschon, H. J. Wu, R. Malhotra, and R. B. Wilson 24 May 1994 13 p
(Contract DE-AC22-92PC-92112)
(DE95-001179; DOE/PC-92112/T5) Avail: CASI HC A03/MF A01

Fullerenes are a recently discovered allotrope of carbon that have been found to possess unusual properties, some of which may be ideal for methane activation. This project is designed to evaluate these carbon based materials for conversion of methane into higher hydrocarbons. The project is divided into three technical tasks. Task 1 deals with the synthesis and characterization of the fullerenes and fullerene soots, Task 2 with the testing of the catalysts, and Task 3 with the evaluation of the results and technical reporting requirements. The results and accomplishments for this quarter are as follows: A fullerene soot (obtained from Ulvick Labs) and an extracted soot (obtained from MER) were treated with carbon dioxide to obtain high surface area soots of greater than 600 sq m)/g; A palladium-C60 complex was synthesized and characterized by a surface analysis by laser ionization (SALI) instrument; Fullerene soot and Norit-A carbon were tested as catalysts for methane activation and the order of reactivity was found to be Soot(greater than) Norit-A(greater than) no catalyst; Increases in surface area of the soot did not significantly alter the methane conversion activity; Hydrogen and helium were tested as diluents, with helium causing an increase in selectivity towards C2 hydrocarbons for the fullerene soot catalyzed reactions; and The MER extracted soot was found to be more reactive towards methane conversion, but less selective towards C2 hydrocarbons than the Ulvick fullerene soot. DOE

N95-19824# Wisconsin Univ., Madison, WI. Dept. of Chemistry.
DIRECT DIMER-BY-DIMER IDENTIFICATION OF CLEAN AND MONOHYDRIDE DIMERS ON THE Si(001) SURFACE BY SCANNING TUNNELING MICROSCOPY Interim Report, 1 Jun. 1993 - 31 May 1994
Y. Wang, M. Bronikowski, and R. J. Hamers 27 May 1994 28 p
(Contract N00014-91-J-1629)
(AD-A280158; TR-15) Avail: CASI HC A03/MF A01

Atomic resolution images of clean Si(001)-(2x1) and the mono-hydride phase, Si(001)-(2xl)H were investigated using scanning tunneling microscopy at various sample-tip bias voltages. At a sample-tip bias of -1.9 V, each dimer of the monohydride phase show two protrusions 3.3 A apart separated by a minimum 0.11 A deep for a sample bias of -1.9 Volt, while clean dimers show a single protrusion per unit cell. Monohydride dimers appear lower than clean dimers, with apparent height differences ranging from 1.9 A at -1.6 V to 0.65 A at -3.0 V sample bias. An analysis of the apparent height and spatial distribution of tunneling current within each dimer can be used to unambiguously discriminate between clean dimers, monohydride dimers, and vacancy defects. This methodology is applied to study the distribution using disilane, revealing segregation of the monohydride into nearly isotropic islands. DTIC

N95-19825# Wisconsin Univ., Madison, WI. Dept. of Chemistry.
AN ATOMIC-RESOLUTION STUDY OF OVERLAYER FORMATION AND INTERFACIAL MIXING IN THE INTERACTION OF PHOSPHORUS WITH Si(001) Interim Report, 1 Jun. 1993 - 31 May 1994
Y. Wang, X. Chen, and R. J. Hamers 27 May 1994 45 p
(Contract N00014-91-J-1629)
(AD-A280159; TR-16) Avail: CASI HC A03/MF A01

Scanning tunneling microscopy (STM), tunneling spectroscopy, and Auger electron spectroscopy have been used to study the formation of phosphorus-terminated silicon(001) surfaces by the thermal decomposition of phosphine (PH3). The STM images show that surface phosphorus atoms readily displace Si from the substrate, dramatically changing the overall surface morphology through the formation of large numbers of islands and an extreme roughening of step edges. The surfaces are terminated with P-P dimers, but also contain large numbers of line defects which act as a strain relief mechanism. STM images are used to determine the symmetry of these line defects and are compared with model defect structures. Line defects in the phosphorus-terminated surface both nucleate islands and also constrain their growth in one dimension, such that the phosphorus-terminated surfaces contain large numbers of extremely anisotropic islands and very rough step edges. At lower phosphorus coverage, the STM experiments are able to identify Si and P atoms individually, revealing the formation of large numbers of Si-P heterodimers and the simultaneous disappearance of the strain-induced line defects. Counting statistics are used to study the equilibrium between Si=Si, Si-P, and P-P dimers, showing that the surface is a near random alloy with a slight non-statistical preference for formation of the Si-P heterodimer. DTIC

N95-19830# Bowling Green State Univ., OH. Center for Photochemical Sciences.
REACTION CHANNEL COMPETITION IN VIBRATIONAL OVERTONE ACTIVATION: 1-METHYLCYCLOPROPENE Technical Report, Sep. 1993 - Jun. 1994
Deanne Snavely, Oleg Grinevich, and Salah Hassoon 3 Jun. 1994 14 p
(Contract N00014-91-J-4130)
(AD-A280185; TR-15) Avail: CASI HC A03/MF A01

Laser vibrational overtone activation has been used to investigate the reaction channel competition in the isomerization of 1-methylcyclopropene (MCPene). The vibrational overtone activation of three types of CH stretches (methyl, methylenic and olefinic) in the 6vCH transition was initiated and all three products (2-butyne. 1,3-butadiene and 1,2-butadiene) were detected by gas chromatography. Stern-Volmer plots have been constructed for the appearance of each individual product and the derived experimental specific rate coefficients compared to those of RRKM theory. Product ratios of 1,3-butadiene to 2-butyne were independent of pressure. These ratios were compared to the RRKM ratios. The product yield ratio for the methylenic photolysis compared well with the RRKM ratio but the olefinic product yield ratio was approximately 40% lower than the RRKM ratio. The implications of these comparisons are discussed. DTIC

N95-19836 California Univ., Berkeley. Lawrence Berkeley Lab, CA.
CHARACTERIZATION OF INACTIVE CARBON IN GaAs
A. J. Moll, E. E. Haller, J. W. Ager, III, K. M. Yu, and W. Walukiewicz Jul. 1994 6 p Presented at the 21th International Symposium on Compound Semiconductors, San Diego, CA, 18-22 Sep. 1994 Limited Reproducibility: More than 20% of this document may be affected by microfiche quality
(Contract DE-AC03-76SF-00098)
(DE95-002352; LBL-35433; CONF-940981-3) Avail: CASI HC A02

Independent of the doping technique, the electrical efficiency of C-doped GaAs is less than 100%. We have shown that Raman spectroscopy provides direct evidence for the formation of C precipitates in GaAs. GaAs samples doped with C and annealed at various temperatures exhibit two broad peaks in the Raman spectra at 1585 cm(sup -1) and 1355 cm(sup -1) which are characteristic of two sp(sup 2) bonded C atoms. Photoluminescence of annealed C-doped GaAs indicates the presence of

compensating defects as well. Both precipitation of C and compensation due to native defects play a role in the reduction of the electrical activity of C-doped GaAs. DOE

N95-19839 North Carolina Univ., Chapel Hill, NC.
EXCITED STATE PROCESSES IN TRANSITION METAL COMPLEXES. REDOX SPLITTING IN SOLUBLE POLYMERS
Thomas J. Meyer Jul. 1994 6 p Limited Reproducibility: More than 20% of this document may be affected by microfiche quality
(Contract DE-FG05-86ER-13633)
(DE95-002690; DOE/ER-13633/12) Avail: CASI HC A02

In the past grant period, this DOE supported work has progressed considerably in the rational design of polypyridyl complexes of ruthenium(II), osmium(II), and rhenium(I) that exhibit predetermined photochemical, photophysical, and redox properties. The exploration of molecular design has moved forward along four fronts. The author's have developed a synthetic strategy for the preparation of heteroleptic complexes based on ruthenium(II) that contain three different bidentate ligands. Second, the authors are utilizing this synthetic procedure to prepare complexes with broad band absorbance throughout the UV and visible regions of the spectrum, so called 'black absorbers.' Third, the authors have utilized more traditional synthetic procedures to prepare an extended series of nitro and nitrosyl containing complexes that could provide the basis for emission-based pH determination. Fourth, the controlled immobilization of the d(sup 6) chromophores on soluble styrenic polymers is under investigation in an attempt to study long range electron and energy transfer. Additionally, the authors have established protocols for the elucidation of excited state dynamics by utilizing time-resolved resonance Raman and transient infrared spectroscopies, as well as emission spectral fitting techniques. These studies have lead to the publication or submission of nine manuscripts during the budget period. DOE

N95-19840 Texas A&M Univ., College Station, TX. Dept. of Chemistry.
DEVELOPMENT OF LASER-ION BEAM PHOTODISSOCIATION METHODS Progress Report, Dec. 1991 - Nov. 1994
D. H. Russell Jun. 1994 12 p Limited Reproducibility: More than 20% of this document may be affected by microfiche quality
(Contract DE-FG05-85ER-13434)
(DE95-002800; DOE/ER-13434/T2) Avail: CASI HC A03

This project emphasizes the development of laser mass spectrometry methods for fundamental and applied studies of gas-phase processes. The current studies are focussed on the photochemistry and photophysics of peptides and other biological molecules. Matrix-assisted laser desorption ionization (MALDI) is used to produce ions that are subsequently subjected to photoexcitation and dissociation. MALDI is still very much in the developmental stages, thus a significant portion of this research focuses on fundamental studies of the MALDI ion formation/energy transfer process. The authors' view is that excited state H(+)-transfer reactions play an important role in MALDI, consequently a significant portion of research activities are focussed on such studies. Fundamental studies of the role of the matrix in MALDI are an integral part of this project. A new MALDI experiment, MALDI of aerosol particles generated from solutions, has been demonstrated and new developmental research in this area is planned. The authors are also actively pursuing a research program on gas-phase H(+) transfer processes that mimic the MALDI process. In addition, the authors are developing photodissociation experiments, based on tandem time-of-flight mass spectrometers, for structural characterization of complex organic molecules. The photodissociation studies use MALDI as the ionization method. These research areas involve the development of new instrumentation, new instrument methodologies, and data processing. DOE

N95-19868 Phillips Lab., Hanscom AFB, MA.
THERMOCHEMICAL IR SOURCES: COCHISE AND FACELIF EXPERIMENTS Final Report
S. M. Miller, W. A. Blumberg, W. T. Rawlins, M. E. Fraser, and C. P. Fell 14 Mar. 1994 39 p Limited Reproducibility: More than 20% of this document may be affected by microfiche quality
(AD-A279940; PL-TR-94-2086; PSRP-670) Avail: Issuing Activity (Defense Technical Information Center (DTIC))

Each of the experiments performed in the COCHISE facility has measured a fundamental chemical quantity such as a relative branching ratio, a quenching rate coefficient, or developed a new detection technique. These measurements are then provided for incorporation into the various atmospheric radiation codes, such as NORSE and SHARC, where they provide a solid experimental footing for modeling the complex chemical system of the upper atmosphere. The following papers provide the details of these experiments: (1) Branching Ratios for Infrared Vibrational Emission from NO(X2Pi,v'=2-13); (2) Ro-vibrational Excitation of Carbon Monoxide by Energy Transfer from Metastable Nitrogen; (3) Quenching of N (2D) by 0(3P); and (4) Detection of N(4S) by Resonantly Enhanced Multi-photon Ionization Spectroscopy. DTIC

N95-18170*# Randolph-Macon Coll., Ashland, VA. Dept. of Chemistry.
EVALUATION OF INORGANIC ZINC-RICH PRIMERS USING ELECTROCHEMICAL IMPEDANCE SPECTROSCOPY (EIS) IN COMBINATION WITH ATMOSPHERIC EXPOSURE
Luz M. Calle *In* Univ. of Central Florida, NASA/ASEE Summer Faculty Fellowship Program. 1994 Research Reports Oct. 1994 p 91-112 (For primary document see N95-18166 05-80)
Avail: CASI HC A03/MF A04

N95-18175*# California State Polytechnic Univ., Pomona, CA. Dept. of Chemical and Materials Engineering.
INVESTIGATION OF NEW HYPERGOL SCRUBBER TECHNOLOGY
Barbara H. Glasscock *In* Univ. of Central Florida, NASA/ASEE Summer Faculty Fellowship Program. 1994 Research Reports Oct. 1994 p 235-262 (For primary document see N95-18166 05-80)
Avail: CASI HC A03/MF A04

N95-19012*# Alabama A & M Univ., Huntsville, AL. Dept. of Physics.
NUMERICAL FORMULATION OF COMPOSITION SEGREGATION AT CURVED SOLID-LIQUID INTERFACE DURING STEADY STATE SOLIDIFICATION PROCESS
Jai-Ching Wang *In* Alabama Univ., Research Reports: 1994 NASA/ASEE Summer Faculty Fellowship Program Oct. 1994 6 p (For primary document see N95-18967 05-80)
Avail: CASI HC A02/MF A03

26 METALLIC MATERIALS

Includes physical, chemical, and mechanical properties of metals, e.g., corrosion; and metallurgy.

N95-17962# Lawrence Livermore National Lab., Livermore, CA.
PHASE TRANSFORMATIONS AND PHASE RELATIONS IN Ti(50)Pd(50-x)TM(x) ALLOYS
Adam J. Schwartz, Marcel H. Sluiter, Bruce N. Harmon, and Lee E. Tanner 15 Jul. 1994 8 p Presented at the International Conference on Solid-to-solid Phase Transformations in Organic Materials, Pittsburgh, PA, 17-22 Jul. 1994
(Contract W-7405-eng-48)
(DE94-018999; UCRL-JC-116385; CONF-940704-3) Avail: CASI HC A02/MF A01

The effect of transition metal (TM) substitution for Pd in Ti(50)Pd(50-x)TM(x) alloys with x between 5 and 37.5 at. percent and TM = V, Cr, Mn and Fe are being characterized by transmission electron microscopy and First-Principles Alloy Theory modeling. The goal is to obtain detailed structural information related to the ternary phase relations and transformations that are necessary for effective shape-memory alloy development. Thus far, the authors have found that they tend to have pseudobinary eutectoid-like configurations with a terminal TiPd and a non-close-packed long period ordered structure related to beta2 (B2, CsCl-type crystal structure) based on the stoichiometry Ti2PdTM. The systems exhibit a conventional martensitic transformation, as well as a new type of displacive transformation that shear-modulates B2 to produce a periodically distorted, but non-close-packed metastable product phase. DOE

N95-17968# Sandia National Labs., Albuquerque, NM.
ION BEAM SURFACE TREATMENT: A NEW CAPABILITY FOR SURFACE ENHANCEMENT
R. W. Stinnett, D. C. McIntyre, R. G. Buchheit, E. L. Neau, J. B. Greenly

(Cornell Univ., Ithaca, NY.), M. O. Thompson (Cornell Univ., Ithaca, NY.), and G. P. Johnston (New Mexico Univ., Albuquerque, NM.) 1994 8 p Presented at the 10th International Conference on High Power Particle Beams, San Diego, CA, 20-24 Jun. 1994
(Contract DE-AC04-94AL-85000)
(DE94-014663; SAND-93-2775C; CONF-940634-9) Avail: CASI HC A02/MF A01

The emerging capability to produce high average power (5-350 kW) pulsed ion beams at 0.2-2 MeV energies is enabling the authors to develop a new, commercial-scale thermal surface treatment technology called Ion Beam Surface Treatment (IBEST). This new technique uses high energy, pulsed (less than or equal 250 ns) ion beams to directly deposit energy in the top 2-20 micrometers of the surface of any material. The depth of treatment is controllable by varying the ion energy and species. Deposition of the energy with short pulses in a thin surface layer allows melting of the layer with relatively small energies and allows rapid cooling of the melted layer by thermal diffusion into the underlying substrate. Typical cooling rates of this process (10(exp 9)-10(exp 10) K/sec) cause rapid resolidification, resulting in the production of non-equilibrium microstructures (nano-crystalline and metastable phases) that have significantly improved corrosion, wear, and hardness properties. The authors conducted IBEST feasibility experiments with results confirming surface hardening, noncrystalline grain formation, metal surface polishing, controlled melt of ceramic surfaces, and surface cleaning using pulsed ion beams. DOE

N95-18027# Connecticut Univ., Storrs, CT. Inst. of Materials Science.
NANOSTRUCTURED BEARING ALLOY STUDIES Quarterly Report, 1 Apr. - 30 Jul. 1994
30 Jul. 1994 11 p
(AD-A283328) Avail: CASI HC A02/MF A01

A variation of the method reported previously for the synthesis of M50 type steel was made. Iron pentacarbonyl (liquid) was mixed with vanadium carbonyl (solid), bis(ethylbenzene) chromium (liquid) and bis(ethylbenzene) molybdenum (liquid) in dry decalin. The mixture was maintained under an inert argon atmosphere and stirred at 85-90 C for 24 hrs and then at 150 C for another 12 hrs. A black solid precipitated and the reaction was concluded at the end of approx. 36 hrs. when a clear top layer of the solvent resulted. The solvent was then distilled off under reduced pressure, and the black shiny solid maintained under an argon atmospher, was sealed and delivered to Pratt & Whitney for consolidation. The powders were provided to Pratt & Whitney without any organic protective coating. This is a significant departure from the previously reported synthesis and consolidation. These powders are being analyzed for their respective elemental composition. Derived from text

N95-18046*# Washington Univ., Saint Louis, MO.
INFLUENCE OF HIGH PRESSURE HYDROGEN ENVIRONMENT ON CREEP DEFORMATION OF Mo-Re, HAYNES 188, AND NARloy-Z ALLOYS Annual Technical Report
S. M. L. Sastry, Charles C. Yang, Shewang Ouyang, K. L. Jerina, and D. S. Schwartz (McDonnell-Douglas Corp., Saint Louis, MO.) 27 Nov. 1994 35 p Original contains color illustrations
(Grant NAG2-865)
(NASA-CR-197572; NAS 1.26:197572) Avail: CASI HC A03/MF A01; 1 functional color page

The present study focuses on the investigation of the influence of hydrogen on the mechanical properties of three types of alloys at elevated temperatures. The reasons for the consideration of hydrogen effects are the potential use of hydrogen as a coolant in gas-cooled reactors and fuel in advanced hypersonic vehicles. The materials used in hydrogen atmosphere must not be embrittled by hydrogen at ambient temperature and should have good strength in hydrogen atmosphere at elevated temperature. The paucity of information concerning the mechanical performance in hydrogen atmosphere at elevated temperature has been a limiting factor in the selection and design of structural components for operation in hydrogen environment. Derived from text

N95-18068# Pratt and Whitney Aircraft, West Palm Beach, FL. Government Engines and Space Propulsion.
FATIGUE IN SINGLE CRYSTAL NICKEL SUPERALLOYS Progress Report, 16 Oct. 1993 - 15 Oct. 1994
Daniel P. DeLuca and Charles Annis 15 Oct. 1994 33 p
(Contract N00014-91-C-0124)
(AD-A285727) Avail: CASI HC A03/MF A01

This program investigates the seemingly unusual behavior of single crystal airfoil materials. The fatigue initiation processes in single crystal (SC) materials are significantly more complicated and involved than fatigue initiation and subsequent behavior of a (single) macrocrack in conventional, isotropic, materials. To understand these differences is the major goal of this project. DTIC

N95-18121# Oak Ridge National Lab., TN.
ALLOYING EFFECTS ON THE HIGH-TEMPERATURE OXIDATION RESISTANCE OF Cr-Cr2Nb
P. F. Tortorelli and J. H. DeVan 1994 10 p Presented at the 8th Annual Conference on Fossil Energy Materials, Oak Ridge, TN, 10-12 May 1994
(Contract DE-AC05-84OR-21400)
(DE94-018146; CONF-9405143-6) Avail: CASI HC A02/MF A01

Alloying effects on the high-temperature oxidation resistance of Cr-Cr2Nb were examined on the basis of isothermal exposures to air at 950 C. Additions of either Re and Al or Fe, Ni, and Al had relatively little effect on weight gains relative to the Cr-6% Nb binary alloy. One alloying element that improved the mechanical behavior of Cr-Cr2Nb alloys substantially increased the oxidation rates and spallation susceptibilities of Cr-6 and -12% Nb alloys. However, the addition of another element completely offset these deleterious effects. The presence of this latter element resulted in the best overall oxidation behavior (in terms of both weight gains and spallation tendencies) of all Cr-Cr2Nb compositions. Its beneficial effect can be attributed to improvement in the oxidation resistance of the Cr-rich phase. DOE

N95-18128# Oak Ridge National Lab., TN.
ON THE CRACK GROWTH RESISTANCE AND STRENGTH OF THE B2 IRON ALUMINIDES Fe-40Al, Fe-45Al, AND Fe-10Ni-40Al (AT. %)
J. H. Schneibel and P. J. Maziasz 1994 10 p Presented at the Metallurgical Society Annual Meeting, San Francisco, CA, 27 Feb. - 3 Mar. 1994
(Contract DE-AC05-84OR-21400)
(DE94-017857; CONF-940286-4) Avail: CASI HC A02/MF A01

The crack growth resistance and yield strength of the B2 iron aluminides Fe-40Al, Fe-45Al, are Fe-10Ni-40Al (at. %) have been investigated at room temperature laboratory air. After fast cooling from 1273 K, Fe-45Al and Fe-10Ni-40Al are much stronger than Fe-40Al, and exhibit considerably lower crack growth resistance. The crack growth resistance decreases with decreasing crack propagation velocity. Low crack propagation velocities favor intergranular fracture, whereas high velocities can lead to significant contributions from transgranular fracture. Boron additions to Fe-40Al and Fe-10Ni-40Al improve the crack growth resistance, reduce its dependence on the crack propagation velocity, and cause the path to be predominantly transgranular. In a plot of fracture toughness versus yield strength, the properties of the iron aluminides are similar to those of typical aluminum alloys. DOE

N95-18332 Department of the Navy, Washington, DC.
TRIVALENT CHROMIUM CONVERSION COATINGS FOR ALUMINUM Patent
Fred Pearlstein, inventor (to Navy) and S. Agarawala, inventor (to Navy) 19 Apr. 1994 6 p Filed 27 Sep. 1993
(AD-D016274; US-Patent-5,304,257; US-Patent-Appl-SN-126869) Avail: US Patent and Trademark Office

Corrosion resistant coatings are formed on aluminum by immersion in aqueous solutions containing chromic salts, a fluoride ion from compounds such as a fluosilicate with an alkali added near or slightly beyond the precipitation of the insoluble basic compounds. Trivalent chromium films formed on the aluminum surface when tested in 5% NaCl salt spray chamber showed corrosion resistance in excess of 96 hours. After a posttreatment with peroxide or permanganate solutions, the corrosion resistance for the aluminum substrates exceeded 168 hours. Trivalent chromium coated aluminum serves as an effective base for paint primers. Anodized aluminums were also afforded excellent corrosion resistance, after being treated in dilute/basic chromic sulfate solutions and post-treated with peroxide. DTIC

N95-18358# Cornell Univ., Ithaca, NY. Dept. of Materials Science and Engineering.
SURFACE PHASES, SURFACE DEFECTS AND THE INITIAL STAGES OF OXIDATION
J. Blakely Mar. 1994 6 p
(Contract DE-FG02-87ER-45328)
(DE94-016947; DOE/ER-45328/8) Avail: CASI HC A02/MF A01

The 2-D system S + O on Ni(111) has been studied. Results show that S, which initially bonds strongly to Ni, remains concentrated at the interface even after many monolayers of oxide have grown. During this period, studies were carried out on the breakup of Fe oxide layers under S exposure in an Environmental Scanning Electron Microscope. The oxide layers were grown on a (100) surface of Fe40(minus)Ni60 alloy. At low temperatures, S (from H2S) had no effect on the oxide layer, but at 500 C, the oxide layer broke up. Atomic force microscopic study was also carried out. DOE

N95-18458# Department of the Navy, Washington, DC.
TRIVALENT CHROMIUM SOLUTIONS FOR SEALING ANODIZED ALUMINUM Patent Application
Fred Pearlstein, inventor (to Navy) and Vinod S. Agarwala, inventor (to Navy) 1 Oct. 1993 26 p Continuation-in-part of co-pending application Navy-Case-74766
(AD-D016472; US-Patent-Appl-SN-134762; Navy-Case-75647; Navy-Case-74766) Avail: CASI HC A03/MF A01

Corrosion resistant seal-coatings are formed on anodized aluminum by immersion in aqueous solutions containing trivalent chromic compounds with an alkali added near or slightly beyond the precipitation of insoluble basic compounds. Trivalent chromium seals formed on the anodized aluminum when tested in 5 percent NaCl salt spray chamber showed improved corrosion resistance. After a post-treatment in a peroxide or permanganate solution, the corrosion resistance for the anodized aluminum showed even greater improvement in the salt chamber. DTIC

N95-18630 Department of the Navy, Washington, DC.
METHOD FOR MAKING A NON-MAGNETIC ALLOY Patent
Joseph L. Abita, inventor (to Navy) 15 Mar. 1994 5 p Filed 2 Dec. 1992
(AD-D016233; US-Patent-5,294,268; US-Patent-Appl-SN-984637; US-Patent-Class-148-432) Avail: US Patent and Trademark Office

A method for making a non-magnetic alloy structure. Alloy samples are formed by taking three volumes V1 of host matrix material having a first susceptibility X1 and adding to each of them one of three volumes V2, V3 and V4 of a magnetically compensating material having a second opposite susceptibility X2. The volume V3 is chosen so that (V1)(X1) = (V3X)(X2). The volumes V2 and V4 are chosen so that V3/V1 - V2/V1 is equal to 0.299% and V4/V1 -V3/V1 is equal to 0.531%. The magnetizations of the alloy samples are determined and plotted as a function of their volume percentages. A volume percentage V5/VI is determined from the plot, such that the volume percentage, V5/V1, has zero magnetization. This volume percentage V5/V1 is used to make nonmagnetic alloy structures having this volume percentage V5/V1. DTIC

N95-18934# General Electric Co., Schenectady, NY. Atomic Power Lab.
J-INTEGRAL CHARACTERIZATION OF THE NOZZLE STEELS FROM INTERMEDIATE TEST VESSELS IV-5 AND IV-9
T. A. Auten, B. D. Macdonald, D. W. Scavone, and D. Bozik [1994] 61 p
(Contract DE-AC12-76SN-00052)
(DE95-001066; KAPL-4744; DOE/TIC-4500-R74) Avail: CASI HC A04/MF A01

Reported here are the results of elastic-plastic fracture toughness tests performed on low alloy steels from the nozzles of the intermediate test vessels IV-5 and IV-9 from the Heavy Steel Section Technology Program at Oak Ridge National Laboratory. These vessels had been given prototypic nozzle corner flaw tests prior to the development of the ASTM E-813 standard test procedure for J-integral testing. The objective of this work is to provide J-integral material test support for future elastic-plastic fracture mechanics analysis of the nozzles. J-integral tests at 88 deg C (190 deg F) of the IV-5 nozzle material produced stable ductile tearing. The tearing resistance data are expected to support analysis of the observed similar stable tearing response of the nozzle corner flaw. J-integral tests at 24 deg C (75 deg F) of the IV-9 nozzle produced elastic-plastic fracture instability preceded by stable tearing. A similar response was observed in the IV-9 nozzle corner flaw test. It will be a major and important challenge to develop a fracture mechanics rationale that reconciles these small specimen and nozzle corner flaw test results. These test results are being made available to allow their use by a wide variety of organizations in developing such a rationale, which would be a significant contribution to quantifying the flaw tolerance of reactor pressure vessels. Author

N95-18939# Army Research Lab., Watertown, MA.
DEVELOPMENT OF AN IMPROVED BALLISTIC ACCEPTANCE TEST FOR HIGH HARD ARMOR STEEL PLATE: MIL-A-46100 Final Report
Richard John Squillacioti Sep. 1994 35 p Sponsored by Army Tank-Automotive Command
(ARL-TR-509) Avail: CASI HC A03/MF A01

This report is one of three reports generated as a subtask under the project entitled 'Development of Improved High Hard Armor Steel (MIL-A-46100)' funded by the PM, Survivability (TACOM). This report investigates ballistic acceptance tests for MIL-A-46100 plate. Ballistic test results for MIL-A-46100 armor plate with the 20mm M602 projectile show a high level of scatter in V(sub 50) values. The V(sub 50) is used as the criterion for acceptance/rejection of MIL-A-46100 armor plate. Furthermore, the M602 projectile produces a shatter gap phenomenon when tested versus high hardness plate near the 1.1 inch thickness. The shatter gap results in two V(sub 50) values with a spread of approximately 180 - 200 ft./sec. Reasons for the high failure rate of 20 percent for MIL-A-46100 plate can, in part, be attributed to a combination of shatter gap phenomenon and scatter in V(sub 50) measurements. ARL/MD heats of MIL-A-46100 armor plate were processed and tested with the 20mm M602 projectile and a 1/2 scale 30mm APDS tungsten projectile. Results of ballistic testing show that the 1/2 scale 30mm APDS projectile exhibits minimal scatter in V(sub 50) values with no shatter gap and therefore is considered to be a superior round for testing and qualifying MIL-A-46100 steel armor. Author

N95-18948# Northwestern Univ., Evanston, IL.
DESIGN OF ADVANCED STEELS FOR ARMOR APPLICATIONS Final Report, 30 Aug. 1991 - 30 Jul. 1993
Gregory B. Olson and Timothy A. Stephenson Watertown, MA Army Research Lab. Aug. 1994 47 p
(Contract DAAL04-91-C-0073)
(ARL-CR-175) Avail: CASI HC A03/MF A01

An interdisciplinary research effort has addressed the fundamental principles for the design of fracture-tough, stress-corrosion resistant, ultrahigh-strength martensitic steels for advanced armor applications. Three alloy compositions, designated MTL1, MTL2, and MTL3 were derived from thermodynamics-based computer-aided design using the THERMOCALC thermochemical database and software system. Hardness and K(IC) fracture toughness were measured as a function of solution treatment temperature and tempering time at 482 deg C, and undissolved carbides were examined by analytical electron microscopy. Although the as-received carbon contents for alloys MTL2 and MTL3 exceeded the design carbon content by .03 wt. pct., optimum heat treatment for alloy MTL2 produced R(C)56.2 with 69.4 ksi square root of in toughness, and R(C)56.4 with 66.3 ksi square root of in for MTL3. The carbon content of MTL1 fell short by .06 wt. pct., producing a hardness of R(C)55.2 at 82.2 ksi square root of in. Despite the low carbon content, the hardness achieved in the latter case demonstrates the effectiveness of small V additions in enhancing strength in these alloys. Ballistic testing is recommended. Based on the prototype alloy evaluations, iterative design calculations predict improved compositions. Further toughness enhancement should be achievable with a carbon content of 0.25 wt. pct., and by exploitation of multistep tempering treatments to achieve transforming toughening. Author

N95-19093# California Univ., Berkeley. Lawrence Berkeley Lab, CA.
NONSTOICHIOMETRY OF Al-Zr INTERMETALLIC PHASES
V. Radmilovic and G. Thomas Jun. 1994 8 p Presented at the 4th International Conference of Aluminum Alloys, Atlanta, GA, 11-16 Sep. 1994
(Contract DE-AC03-76SF-00098)
(DE94-016877; LBL-35725; CONF-9409179-2) Avail: CASI HC A02/MF A01

Nonstoichiometry of metastable cubic (beta)(prime) and equilibrium

tetragonal (beta) Al-Zr intermetallic phases of the nominal composition Al3Zr in Al-rich alloys has been extensively studied. It is proposed that the 'dark contrast' of (beta) (prime) core in (beta)(prime)/(sigma)(prime) complex precipitates, in Al-Li-Zr based alloys, is caused by incorporation of Al and Li atoms into the (beta)(prime) phase on Zr sublattice sites, forming nonstoichiometric Al-Zr intermetallic phases, rather than by Li partitioning only. (beta)(prime) particles contain very small amounts of Zr, approximately 5 at.%, much less than the stoichiometric 25 at.% in the Al3Zr metastable phase. These particles are, according to simulation of high resolution images, of the Al3(Al(0.4)Li(0.4)Zr(0.2)) type. Nonstoichiometric particles of average composition Al4Zr and Al6Zr are observed also in the binary Al-Zr alloy, even after annealing for several hours at 600 deg C. DOE

N95-19111# Michigan Univ., Ann Arbor, MI.
ATOMISTIC AND ELASTIC ANALYSES OF DEFECTS AND SMALL STRUCTURES
1994 9 p
(Contract DE-FG02-88ER-45367)
(DE94-017047; DOE/ER-45367/6) Avail: CASI HC A02/MF A01

Focus was on interfacial segregation and its effect on interfacial phase stability. A method for performing atomistic simulations in alloys was developed which accounts for equilibrium solute redistribution and allows determination of all thermodynamic properties. Segregation was shown to be strongly correlated with interfacial stresses on an atomic site-by-site basis and to greatly reduce the atomic level stresses, homogenizing the boundary. Differences in interfacial energies between elements plays a more important role than atomic size in predicting the dominant segregant. Effect of segregation on interfacial cohesive energies/ideal fracture toughness was examined in order to see how tight existing theoretical bounds on these quantities are. Small atomic cluster methods were used to determine average surface properties and to develop stereographic maps of surface energy, stress and segregation tendency for all surface orientations. Equilibrium Wulff plots (surface energy vs misorientation) for both elemental metal and binary alloys. Segregation significantly increases the order- disorder transformation temperatures at (001) surfaces in Ni-Pt and Cu-Pd alloys and steps on these surfaces resulted in transformation temperatures which were even higher near the steps. (Other alloys are covered, such as Ag-Cu, Ni-Cu, Ag-Au, Au-Pd). DOE

N95-19395# Sandia National Labs., Albuquerque, NM.
AN ATOMIC VIEW OF SURFACE DIFFUSION ON METAL SURFACES
G. L. Kellogg 1994 14 p Presented at the North Atlantic Treaty Organization (NATO) Advanced Research Workshop on the Energy Between Dynamics and Reactivity, Drymen, Scotland, 3-8 Jul. 1994
(Contract DE-AC04-94AL-85000)
(DE94-016150; SAND-94-1804C; CONF-9407108-1) Avail: CASI HC A03/MF A01

Investigations of surface diffusion and cluster nucleation by field ion microscopy have provided a considerable amount of physical insight concerning the fundamental interactions that control dynamical processes on surfaces. The investigations rely not only on the FIM's ability to resolve and track individual atoms on a surface, but also its ability to manipulate the number of adatoms and the size of clusters by the process of field desorption. Results of the investigations are surprising. Whereas metal atom diffusion was once thought to be a simple hopping process, FIM experiments have revealed new mechanisms for atom transport. Whereas cluster nucleation was once thought to be an aggregation process dependent only upon pairwise interactions between atoms, FIM investigations have shown that long-range and many body interactions can make non-negligible contributions to the overall process. By providing a brief overview of the experimental methods used in FIM surface diffusion studies and discussing a few selected applications, I hope to have conveyed some of the rich history as well as the current excitement associated with FIM investigations of dynamical processes on surfaces. DOE

N95-19396# Lawrence Livermore National Lab., Livermore, CA.
WARM FORMABILITY OF ALUMINUM-MAGNESIUM ALLOYS
E. M. Taleff (Stanford Univ., CA.), G. A. Henshall, D. R. Lesuer, and T. G. Nieh 27 May 1994 8 p Presented at the 4th International Conference of Aluminum Alloys, Atlanta, GA, 11-16 Sep. 1994
(Contract W-7405-eng-48)
(DE94-016170; UCRL-JC-117528; CONF-9409179-1) Avail: CASI HC A02/MF A01

Manufacturers have become increasingly interested in near-net-shape forming of aluminum alloys as a means to reduce production costs and the weight of aircraft and automotive structures. To achieve the ductilities required for this process, we have examined extended ductility of Al-Mg alloys in the warm forming, or Class I creep, regime. We have studied a high-purity, binary alloy of Al-2.8Mg and ternary alloys of Al-(x)Mg-0.5Mn with Mg concentrations from 1.0 to 6.6 wt. %. Tensile tests, including strain rates-change tests, have been performed with these materials at temperatures of 300 and 400 C over a range 10(sup -4) to 2 x 10(sup -2) s(sup-1). A maximum tensile failure strain of 325% for the binary alloy and a maximum of 125% in the ternary alloys have been measured. The experimental results have been used to evaluate the effects of solute concentration, microstructure, temperature, and strain rate on flow stress ((sigma)), elongation to failure (e(sub f)), and strain-rate sensitivity (m) of these alloys. DOE

N95-19400# Oak Ridge National Lab., TN.
DEFORMATION TEXTURE STUDIES IN Fe3Al ALLOYS
B. K. Kad (California Univ., San Diego, La Jolla, CA.), S. E. Schoenfeld (California Univ., San Diego, La Jolla, CA.), R. J. Asaro (California Univ., San Diego, La Jolla, CA.), and C. G. McKamey 1994 9 p Presented at the Metallurgical Society Annual Meeting, San Francisco, CA, 27 Feb. - 3 Mar. 1994
(Contract DE-AC05-84OR-21400)
(DE94-017709; CONF-940286-2) Avail: CASI HC A02/MF A01

Fe3Al alloys currently targeted for commercial manufacture are generally thermo-mechanically processed in a 600-1000 C. In this temperature range, large scale strains are produced, either solely or by a combination of group of zone axes (111)zone axes(100), group of zone axes(100)zone axes(011), and groups of zone axes(100)zone axes(001) slip systems. The texture is derived from the dominant slip system operating under a specific set of processing variables (i.e., deformation temperature, rate, etc.). In this report, numerical means have been employed to predict deformation textures in Fe3Al alloys produced entirely by crystallographic shears on the group of zone axes(111)zone axes(110), group of zone axes(100)zone axes(011), and group o f zone axes(100)zone axes(001) slip systems. It is shown that both group of zone axes(111)zone axes(110) and group of zone axes(100)zone axes(011) slip systems produce a reasonably strong texture, while group of zone axes(100)zone axes(001) induces no texture over the initial random configuration. Experimental texture measurements, for samples deformed approximately 70% by rolling at 650 K agree well with the predictions for the group of zone axes(111)zone axes(110) slip system activation. These results appear to be in disagreement with transmission electron microscopy observations reported in the literature. Possible sources of discrepancies are discussed. DOE

N95-19401# Du Pont de Nemours (E. I.) and Co., Wilmington, DE.
EVALUATION OF POWDER METALLURGY PLATES MADE BY SYLVANIA ELECTRIC PRODUCTS, INCORPORATED
1994 4 p
(Contract DE-AC09-76SR-00001)
(DE94-017911; DPW-56-321; SR/H-789) Avail: CASI HC A01/MF A01

These plates, numbered 13129, 13130, 13133, 13137, and 13146 were fabricated by Sylvania Electric Products, Inc., and were received at the Savannah plant in February, 1956. All of the plates were of the wide, ribless design. A summary of the data obtained by Sylvania on these and on 'companion' plates is given in Table I, and a summary of the data obtained upon examining the plates at the Savannah River Laboratory is contained in Table II. DOE

N95-19539# Naval Surface Warfare Center, Bethesda, MD.
MODIFIED Cu-Mn-Al HIGH DAMPING ALLOYS
C. R Wong and R. S. Venkatachalam Sep. 1994 17 p
(AD-A285460; CARDIVNSWC-TR-61-94-06) Avail: CASI HC A03/MF A01

Zirconium and erbium modified Cu-Mn-Al was spray formed in an effort to increase homogeneity and damping capacity and decrease impurity levels. Although the microstructure revealed that the optimum spray forming parameters have not yet been achieved, the modified alloys showed both

high damping and resistance to losing that damping over time. The elemental additions also accelerated the formation of alpha manganese at the grain boundaries during aging. DTIC

N95-19568# Oak Ridge National Lab., TN.
WELDABILITY OF IRON ALUMINIDES
G. M. Goodwin, P. J. Maziasz, C. J. McKamey, J. H. DeVan, and V. K. Sikka 1994 5 p Presented at the 8th Annual Conference on Fossil Energy Materials, Oak Ridge, TN, 10-12 May 1994
(Contract DE-AC05-84OR-21400)
(DE95-000686; CONF-9405143-7) Avail: CASI HC A01/MF A01

Corrosion-resistant weldable iron aluminide alloys are being developed for weld overlay cladding of conventional steels and alloys and possible structural applications. Weld hot cracking can be minimized by careful choice of alloying additions, and hot cracking resistance equivalent to commercial austenitic stainless steels has been achieved. Hydrogen-induced cold cracking, however, continues to be a problem with these alloys, both in monolithic weldments and weld overlay cladding applications. The authors have found that preheat and postweld heat treatment can reduce hydrogen cracking, and that composition is also an important variable. Experiments in controlled atmospheres have confirmed that a major source of hydrogen is provided by the reduction of water vapor from the environment, and that oxygen helps reduce cracking sensitivity. Concurrently, they are developing filler metals using the aspiration-casting process, for use both as filler metals with the gas tungsten arc process, and as core wire for the production of shielded metal arc electrodes. DOE

N95-19610# Lehigh Univ., Bethlehem, PA.
CORROSION FATIGUE OF IRON-CHROMIUM-NICKEL ALLOYS: FRACTURE MECHANICS, MICROSTRUCTURE AND CHEMISTRY
R. P. Wei Jan. 1994 9 p
(Contract DE-FG02-88ER-45354)
(DE95-000909; DOE/ER-45354/6) Avail: CASI HC A02/MF A01

A multi-disciplinary research program was undertaken to address certain fundamental issues relating to corrosion fatigue crack growth in structurally important alloys in aqueous solutions. Focus was placed on austenitic iron-chromium-nickel alloys. DOE

N95-19611# Los Alamos National Lab., NM.
PHASE STABILITY AND ELASTIC PROPERTIES OF C15 COMPOUNDS HfV2+Nb
F. Chu, T. E. Mitchell, and D. P. Pope 1994 9 p Presented at The Metallurgical Society (TMS) Conference on High Performance Composites, Rosemont, IL, 10-15 Oct. 1994
(Contract W-7405-eng-36)
(DE95-000940; LA-UR-94-3247; CONF-9410184-2) Avail: CASI HC A02/MF A01

The ternary phase diagram of Hf-V-Nb system has been established and the C15 and C14 Laves phase regions located. The structural stability of the cubic Laves phase HfV2+Nb was examined using heat capacity measurements and transmission electron microscopy. It is found that the binary C15 has a martensitic transformation at 115K and that Nb addition can eliminate the martensitic transformation and stabilize the C15 structure. The elastic properties vs. temperature of the C15 HfV2+Nb were studied using the resonant ultrasound technique. It is observed that the shear and Young's moduli increase abnormally with increasing temperature, the bulk modulus is virtually constant, and the Poisson's ratio is very high and decreases abnormally with increasing temperature. The elastic properties of the C15 compound can be qualitatively understood using the electronic structure obtained from ab initio calculations. The relation between the phase stability and anomalous elastic properties is discussed based on these results. DOE

N95-19652*# National Aeronautics and Space Administration. Lewis Research Center, Cleveland, OH.
THERMO-OXIDATIVE STABILITY OF GRAPHITE/PMR-15 COMPOSITES: EFFECT OF FIBER SURFACE MODIFICATION ON COMPOSITE SHEAR PROPERTIES
Madhu S. Madhukar (Tennessee Univ., Knoxville, TN.), Kenneth J. Bowles, and Demetrios S. Papadopolous (Case Western Reserve Univ., Cleveland, OH.) Sep. 1994 26 p Presented at the International Conference on Composites Engineering, New Orleans, LA, 28-31 Aug. 1994
(RTOP 510-01-50)
(NASA-TM-4608; E-8953; NAS 1.15:4608) Avail: CASI HC A03/MF/A01

Experiments were conducted to establish a correlation between the weight loss of a polyimide (PMR- 15) matrix and graphite fibers and the in-plane shear properties of their unidirectional composites subjected to different isothermal aging times up to 1000 hr at 316 C. The role of fiber surface treatment on the composite degradation during the thermo-oxidative aging was investigated by using A4 graphite fibers with three surface modifications: untreated (AU-4), surface treated (AS-4), and surface treated and sized with an epoxy-compatible sizing (AS-4G). The weight loss of the matrix fibers, and composites was determined during the aging. The effect of thermal aging was seen in all the fiber samples in terms of weight loss and reduction in fiber diameter. Calculated values of weight loss fluxes for different surfaces of rectangular unidirectional composite plates showed that the largest weight loss occurred at those cut surfaces where fibers were perpendicular to the surface. Consequently, the largest amount of damage was also noted on these cut surfaces. Optical observation of the neat matrix and composite plates subjected to different aging times revealed that the degradation (such as matrix microcracking and void growth) occurred in a thin surface layer near the specimen edges. The in-plane shear modulus of the composites was unaffected by the fiber surface treatment and the thermal aging. The shear strength of the composites with the untreated fibers was the lowest and it decreased with aging. A fracture surface examination of the composites with untreated fibers suggested that the weak interface allowed the oxidation reaction to proceed along the interface and thus expose the inner material to further oxidation. The results indicated that the fiber-matrix interface affected the composite degradation process during its thermal aging and that the the weak interface accelerated the composite degradation. Author

N95-19703# National Inst. of Standards and Technology, Gaithersburg, MD.
STUDY OF LASER RESONANCE IONIZATION MASS SPECTROMETRY USING A GLOW DISCHARGE SOURCE
X. Xiong (Eastern Analytical, Inc., College Park, MD.), J. M. R. Hutchinson, J. D. Fassett, T. B. Lucatorto, F. J. Schima, W. A. Bowman, and K. R. Hess (Franklin and Marshall Coll., Lancaster, PA.) 1994 5 p
(Contract DE-AI05-86ER-60447)
(DE94-018566; DOE/ER-60447/T6) Avail: CASI HC A01/MF A01

The mass spectra of a metal alloy sample consisting of Al, Cu and Fe were studied using both glow discharge mass spectrometry (GDMS) and resonance ionization mass spectrometry (RIMS). Particular emphasis was placed on the reduction of isobaric interferences and discrimination between those ions formed by the discharge and those formed by the laser radiation. DOE

N95-19707# Allied-Signal Aerospace Co., Kansas City, MO.
CHARACTERIZATION OF THE DEFORMATION AND ANNEALING OF 304L STAINLESS STEEL
W. H. Smith Aug. 1994 99 p
(Contract DE-AC04-76DP-00613)
(DE94-018584; KCP-613-5471) Avail: CASI HC A05/MF A02

Stainless steel, type 304L, was deformed at room temperature using the two processes of semi-piercing and cold-rolling and then annealed at various temperatures and times. The three metallurgical areas of work hardening, age hardening, and anneal softening were observed and characterized using metallography techniques of macrohardness, optical and transmission electron microscopy, and X-ray diffraction. DOE

N95-19723# Oak Ridge National Lab., TN.
PROCEEDINGS OF THE EIGHTH ANNUAL CONFERENCE ON FOSSIL ENERGY MATERIALS
N. C. Cole, comp. and R. R. Judkins, comp. Aug. 1994 451 p Conference held in Oak Ridge, TN, 10-12 May 1994
(Contract DE-AC05-84OR-21400)
(DE95-001055; ORNL/FMP-94/1; CONF-9405143) Avail: CASI HC A20/MF A04

Objective of the meeting was to conduct R and D on materials for longer-term fossil energy applications as well as for generic needs of various fossil fuel technologies. The work is divided into ceramics, new alloys, corrosion, and technology assessment/transfer. The 39 papers are

arranged under the session headings: ceramics, ceramics and new alloys, and intermetallics and advanced austenitics; a workshop on new materials development and applications is summarized briefly. The papers are processed separately for the data base. DOE

N95-19725# Argonne National Lab., IL.
STATUS OF VANADIUM ALLOY DEVELOPMENT FOR FUSION FIRST WALL/BLANKET APPLICATIONS
D. L. Smith, H. M. Chung, B. A. Loomis, E. E. Bloom (Oak Ridge National Lab., TN.), M. L. Grossbeck (Oak Ridge National Lab., TN.), J. H. Jones (Pacific Northwest Lab., Richland, WA.), and F. Wiffen Aug. 1994 17 p Presented at the 15th International Conference on Plasma Physics and Controlled Nuclear Fusion Research, Seville, Spain, 26 Sep. - 1 Oct. 1994 (Contract W-31-109-eng-38)
(DE95-001067; ANL/TD/CP-82851; CONF-940933-7) Avail: CASI HC A03/MF A01

Vanadium alloys exhibit important advantages as a candidate structural material for fusion first wall/blanket applications. These advantages include fabricability, favorable safety and environmental features, high temperature and high wall load capability, and long lifetime under irradiation. Major concerns regarding the use of vanadium alloys for fusion applications relate to cost, reactivity with air/oxygen, and the limited data base. Vanadium alloys with (3-5)% chromium and (3-5)% titanium appear to offer the best combination of properties for first wall/blanket applications. A V-4Cr-4Ti alloy is currently considered as the leading candidate composition. DOE

N95-19743 Virginia Univ., Charlottesville, VA. Dept. of Physics.
SYNTHESIS AND STRUCTURAL PROPERTIES OF NEW METALLIC PHASES EXHIBITING NON-CRYSTALLOGRAPHIC SYMMETRIES
S. J. Poon and G. J. Shiflet 15 Aug. 1994 7 p Limited Reproducibility: More than 20% of this document may be affected by microfiche quality (AD-A284882) Avail: CASI HC A02

In carrying out research on aluminum-glasses (Al-glasses), several unusual results are found: (1) Submillimeter dutile glassy ribbons are obtained. (2) Significant enhancement in the tensile strength is measured in Al-glass ribbons with Al nanocrystallites embedded in them. (3) Deformation induced crystallization within the shear bands is observed for the first time. (4) Strong Al-transition metal interaction is inferred from x-ray and neutron diffraction measurements. These results have added to our understanding of formation and microstructure-mechanical effect relationships of metal glasses, and also to the technological values of these materials. We have begun to apply our findings to the synthesis and studies of bulk metallic-glass and nanocrystalline alloys. Thus far, we have succeeded in making subcentimeter glasses based on rare-earths and magnesium-tin, nanocrystalline alloys based on refractory metals via conventional casting, and centimeter Al-glass button via consolidation of amorphous powders obtained by ball-milling. A method for obtaining two-dimensional atomic pair distribution is developed to unravel the structure of decagonal crystals. DTIC

N95-19792*# Tennessee Univ., Knoxville, TN.
NiAl AND NiAl-BASED COMPOSITES DIRECTIONALLY SOLIDIFIED BY A CONTAINERLESS ZONE PROCESS Ph.D. Thesis
Steven M. Joslin Cleveland, OH NASA Feb. 1995 264 p (Grant NAG3-876; RTOP 505-63-52)
(NASA-CR-195430; E-9422; NAS 1.26:195430) Avail: CASI HC A12/MF A03

A containerless electromagnetically levitated zone (CELZ) process has been used to directionally solidify NiAl and NiAl-based composites. The CELZ processing results in single crystal NiAl (HP-NiAl) having higher purity than commercially pure NiAl grown by a modified Bridgman process (CP-NiAl). The mechanical properties, specifically fracture toughness and creep strength, of the HP-NiAl are superior to binary CP-NiAl and are used as a base-line for comparison with the composite materials subsequently studied. Two-phase composite materials (NiAl-based eutectic alloys) show improvement in room temperature fracture toughness and 1200 to 1400 K creep strength over that of binary HP-NiAl. Metallic phase reinforcements produce the greatest improvement in fracture toughness, while intermetallic reinforcement produces the largest improvement in high temperature strength. Three-phase eutectic alloys and composite materials were identified and directionally solidified with the intent to combine the improvements observed in the two-phase alloys into one alloy. The room temperature fracture toughness and high temperature strength (in air) serve as the basis for comparison between all of the alloys. Finally, the composite materials are discussed in terms of dominant fracture mechanism observed by fractography. Author

N95-18180*# Puerto Rico Univ., Mayaguez. Dept. of Mechanical Engineering.
MECHANICAL BEHAVIOR OF PRECIPITATION HARDENABLE STEELS EXPOSED TO HIGHLY CORROSIVE ENVIRONMENT
Ferdinand Rosa *In* Univ. of Central Florida, NASA/ASEE Summer Faculty Fellowship Program. 1994 Research Reports Oct. 1994 p 379-417 (For primary document see N95-18166 05-80)
Avail: CASI HC A03/MF A04

N95-19007*# Wichita State Univ., Wichita, KS. Dept. of Mechanical Engineering.
MICROSTRUCTURAL ANALYSIS OF CRACKS GENERATED DURING WELDING OF 2195 ALUMINUM-LITHIUM ALLOY
George E. Talia *In* Alabama Univ., Research Reports: 1994 NASA/ASEE Summer Faculty Fellowship Program Oct. 1994 6 p (For primary document see N95-18967 05-80)
Avail: CASI HC A02/MF A03

N95-19011*# California Polytechnic State Univ., San Luis Obispo, CA. Dept. of Materials Engineering.
THE EFFECT OF FABRICATION ON CORROSION IN ALUMINUM 2195: ENVIRONMENTAL AND MICROSTRUCTURAL CONSIDERATIONS
Daniel W. Walsh *In* Alabama Univ., Research Reports: 1994 NASA/ASEE Summer Faculty Fellowship Program Oct. 1994 6 p (For primary document see N95-18967 05-80)
Avail: CASI HC A02/MF A03

N95-19482*# Alcoa Technical Center, Alcoa Center, PA.
AN ARTIFICAL CORROSION PROTOCOL FOR LAP-SPLICES IN AIRCRAFT SKIN
Bevil J. Shaw *In* NASA. Langley Research Center, FAA/NASA International Symposium on Advanced Structural Integrity Methods for Airframe Durability and Damage Tolerance, Part 2 Sep. 1994 p 725-739 Sponsored in part by Boeing Co. (For primary document see N95-19468 05-03)
(Contract F34601-90-C-1336)
Avail: CASI HC A03/MF A04

N95-19489*# Utah Univ., Salt Lake City, UT. Quality and Integrity Design Engineering Center.
MICROSTRUCTURALLY BASED VARIATIONS ON THE DWELL FATGUE LIFE OF TITANIUM ALLOY IMI 834
Mark L. Thomsen and David W. Hoeppner *In* NASA. Langley Research Center, FAA/NASA International Symposium on Advanced Structural Integrity Methods for Airframe Durability and Damage Tolerance, Part 2 Sep. 1994 p 871-889 (For primary document see N95-19468 05-03)
Avail: CASI HC A03/MF A04

N95-19490*# Cornell Univ., Ithaca, NY. Dept. of Theoretical and Applied Mechanics.
FATIGUE CRACK GROWTH IN 2024-T3 ALUMINUM UNDER TENSILE AND TRANSVERSE SHEAR STRESSES
Mark J. Viz and Alan T. Zehnder *In* NASA. Langley Research Center, FAA/NASA International Symposium on Advanced Structural Integrity Methods for Airframe Durability and Damage Tolerance, Part 2 Sep. 1994 p 891-910 (For primary document see N95-19468 05-03)
(Grant NAG1-1311)
Avail: CASI HC A03/MF A04

N95-19494*# National Inst. of Standards and Technology, Gaithersburg, MD. Mechanical Properties and Performance.
FRACTURE BEHAVIOR OF LARGE-SCALE THIN-SHEET ALUMINUM ALLOY
Roland deWit, Richard J. Fields, Leonard Mordfin, Samuel R. Low, and Donald Harne *In* NASA. Langley Research Center, FAA/NASA International Symposium on Advanced Structural Integrity Methods for Airframe Durability and Damage Tolerance, Part 2 Sep. 1994 p 963-983 (For primary

document see N95-19468 05-03)
(Contract DTFA03-92-Z-00018)
Avail: CASI HC A03/MF A04

N95-19674# Liege Univ. (Belgium). Dept. Metallurgie et Science des Materiaux.
ANALYSIS OF THE EROSION OF CUBIC CENTERED AND FACE CENTERED METALLIC MATERIALS [ANALYSE DE L'EROSION DE MATERIAUX METALLIQUES DE STRUCTURES CUBIQUES CENTREE ET FACE CENTREE]
A. Magnee *In* AGARD, Erosion, Corrosion and Foreign Object Damage Effects in Gas Turbines Nov. 1994 13 p In FRENCH (For primary document see N95-19653 05-07)
Copyright Avail: CASI HC A03/MF A03

N95-19682# La Sapienza Univ., Rome (Italy). Dipt. di Chimica.
X-RAY ABSORPTION SPECTROSCOPY IN HIGH TEMPERATURE OXIDATION OF METALS AND ALLOYS
Daniele Gozzi and Massimo Tomellini (Tor Vergata Univ., Rome, Italy.) *In* AGARD, Erosion, Corrosion and Foreign Object Damage Effects in Gas Turbines Nov. 1994 8 p Sponsored by Centro Sviluppo Materiali and Lab. Nazionali di Frascati (For primary document see N95-19653 05-07)
Copyright Avail: CASI HC A02/MF A03

27 NONMETALLIC MATERIALS

Includes physical, chemical, and mechanical properties of plastics, elastomers, lubricants, polymers, textiles, adhesives, and ceramic materials.

For composite materials see *24 Composite Materials.*

N95-17942# Universidad Autonoma del Estado de Mexico, Toluca. Facultad de Quimica.
OBTENTION OF CATIONIC POLYMERIC MEMBRANES BY RADIATION-INDUCED GRAFTING METHOD Ph.D. Thesis [OBTENCION DE MEMBRANAS POLIMERICAS CATIONICAS POR EL METODO DE INJERTO POR RADIACION]
H. MarinH E 1994 61 p In SPANISH
(DE94-629193; INIS-MF-13928) Avail: CASI HC A04/MF A01 (US Sales Only)

Radiation-induced grafting of LDPE with the monomers, acrylic acid and methacrylic acid, has been studied. The grafting was made with several presentations of LDPE (foil, powder and pellets) by direct method using a Co(sup 60) gamma rays. The irradiation was carried out in vacuum at room temperature at different doses (0.02 kGy - 0.2 kGy) with a rate dose of 0.8632 kGy/h. The graft yield was measured by the relation of initial and final weights. The variations of the LDPE structure was followed by infrared absorption spectroscopy and the results showed that there was important variations in LDPE structure when the dose increases. The tensile strong properties of the copolymers were investigated and it was found that the structure of LDPE was modified by the presence of chains of poly (acrylic) and poly (methacrylic) acid and this was reflected in the tensile properties of the polymer. A trial has been made in order to use the powder presentation of the copolymer like ion exchange resin first we measured volumetrically the quantity of milliequivalents per gram of carboxylic groups by titration 5 ml. of a solution 0.1 N of NaOH, which was 48 h. in contact with the copolymer, with a solution 0.1 N of HCl and we found that the quantity of milliequivalents enhance according with the irradiation dose. Finally, we made ion exchange experiments by passing a solution containing Ca (+2) ions through ion exchange columns packed with the copolymer the results showed that these copolymers has good properties in retaining Ca(+2) ions. We conclude that these copolymers can be used for ion exchange process however final conditions must be improved. DOE

N95-17957 Washington State Univ., Pullman, WA. Dept. of Physics.
POLYMER FIBERS FOR NONLINEAR OPTICS Annual Report, 1 May 1993 - 30 Apr. 1994
Mark G. Kuzyk 30 Apr. 1994 6 p Limited Reproducibility: More than 20% of this document may be affected by microfiche quality
(Contract F49620-93-1-0255)
(AD-A284216; AFOSR-94-0499TR) Avail: CASI HC A02

The goal of our research is to build an ultrafast all-optical switching device. Such a device would be the first step towards ultrafast switching-systems for the information highway and all-optical computing applications. Our work is motivated by the demonstration of an all-optical switch in a silica optical fiber. While this device displays all essential switching functions, the small material nonlinearity requires fibers of 1 km lengths, resulting in long latency periods. Because we have the ability to make polymer fibers with optical nonlinearities that are three orders of magnitude larger, we can make sub-meter length devices. In our first year, we have worked out the preliminaries required to make such a device which includes optimization of the fiber drawing process, characterization of crucial material properties, and the design of optical switches that take advantage of the polymer fiber's nonlinearity. We have demonstrated the fabrication of fibers with cores that are less than 10 micrometers in diameter, have shown that these can support single mode light-guiding (required for optimum device operation), and have designed and build a Sagnac interferometer experiment that is being used to characterize material nonlinearity. This experiment will be eventually converted to an all-optical switch by replacing bulk components with fibers. DTIC

N95-18016 Naval Postgraduate School, Monterey, CA.
A CONSTANT-DEPTH SCRATCH TEST FOR THE MEASUREMENT OF ADHESION AT FILM-SUBSTRATE INTERFACES M.S. Thesis
E. D. Secor Mar. 1994 93 p Limited Reproducibility: More than 20% of this document may be affected by microfiche quality
(AD-A283660) Avail: Issuing Activity (Defense Technical Information Center (DTIC))

This thesis reviews the development of the constant-depth Scratch Test for determining the adhesive shear strength of thin film-substrate interfaces, and proposes refinements to the theoretical analyses and experimental approach which were developed earlier. Modifications were made to incorporate a change in indenter orientation (for a Vicker's pyramidal indenter) as a measure to minimize damage during scratching. Additionally, the model was expanded to include the use of a conical indenter. A review of film failure modes was conducted, and the damage mechanism of forward lateral flaking was incorporated into the model. The data acquisition program was changed to reflect these modifications. Improvements were added to the previously constructed apparatus. Preliminary tests were conducted on chromium-on-glass samples, the results of which are also presented. DTIC

N95-18019 Fluorochem, Inc., Azusa, CA.
DIFUNCTIONAL MONOMERS BASED ON PERFLUOROPROPYLENE TELOMERS Technical Report No. 2
K. Baum and A. A. Malik 19 Aug. 1994 18 p Limited Reproducibility: More than 20% of this document may be affected by microfiche quality
(Contract N00014-91-C-0007)
(AD-A283677) Avail: CASI HC A03

Telomers of perfluoropropylene with alpha,omega- diiodoperfluoroalkanes were converted to branched-chain difunctional condensation monomers. The reaction of ethylene with the telomers gave alpha,omega-bis (iodoethyl)perfluoroalkanes, which were converted to the corresponding diols by reaction with fuming sulfuric acid. The reaction of the branched-chain alpha,omega-bis (iodoethyl)-perfluoroal with sodium azide gave the corresponding on of the alpha,omega-bis (azidoethyl)-perfluoroalkanes gave diamines. Phosgenation of the amino groups gave diisocyanates. DTIC

N95-18134* National Aeronautics and Space Administration. Lyndon B. Johnson Space Center, Houston, TX.
METHOD OF MAKING A MEMBRANE HAVING HYDROPHILIC AND HYDROPHOBIC SURFACES FOR ADHERING CELLS OR ANTIBODIES BY USING ATOMIC OXYGEN OR HYDROXYL RADICALS Patent
Steven L. Koontz, inventor (to NASA) and Glenn F. Spaulding, inventor (to NASA) 29 Nov. 1994 12 p Filed 26 Mar. 1992 Supersedes N92-30100 (30 - 20, p 3427)
(NASA-Case-MSC-21529-1; US-Patent-5,369,012;
US-Patent-Appl-SN-857901; US-Patent-Class-435-7.92;
US-Patent-Class-435-180; US-Patent-Class-435-181;

US-Patent-Class-435-240.23; US-Patent-Class-435-240.243; US-Patent-Class-436-531; US-Patent-Class-436-532) Avail: US Patent and Trademark Office

A portion of an organic polymer article such as a membrane is made hydrophilic by exposing a hydrophobic surface of the article to a depth of about 50 to about 5000 angstroms to atomic oxygen or hydroxyl radicals at a temperature below 100C., preferably below 40 C, to form a hydrophilic uniform surface layer of hydrophilic hydroxyl groups. The atomic oxygen and hydroxyl radicals are generated by a flowing afterglow microwave discharge, and the surface is outside of a plasma produced by the discharge. A membrane having both hydrophilic and hydrophobic surfaces can be used in an immunoassay by adhering antibodies to the hydrophobic surface. In another embodiment, the membrane is used in cell culturing where cells adhere to the hydrophilic surface. Prior to adhering cells, the hydrophilic surface may be grafted with a compatibilizing compound. A plurality of hydrophilic regions bounded by adjacent hydrophobic regions can be produced such that a maximum of one cell per each hydrophilic region adheres. Official Gazette of the U.S. Patent and Trademark Office

N95-18320 Department of the Navy, Washington, DC.
POLYURETHANE SELF-PRIMING TOPCOATS Patent
Charles R. Hegedus, inventor (to Navy), Donald J. Hirst, inventor (to Navy), and Anthony T. Eng, inventor (to Navy) 1 Mar. 1994 6 p Filed 16 Apr. 1993
(AD-D016264; US-Patent-5,290,599; US-Patent-Appl-SN-054497) Avail: US Patent and Trademark Office

A corrosion-resistant coating which can be applied directly to a surface as a self-priming topcoat comprising a polyurethane resin binder and a combination of pigments consisting essentially of an alkaline earth metal metaborate, zinc salts of benzoic acids, and an alkaline earth metal phosphate such as zinc-barium phosphate. In addition, the coating contains from 5-40 parts by weight of a titanium dioxide pigment, up to about 3.0 parts by weight of an oil soluble dispersant and up to about 50 parts by weight of at least one organic solvent. DTIC

N95-18321* National Aeronautics and Space Administration. Lewis Research Center, Cleveland, OH.
ION EXCHANGE POLYMERS AND METHOD FOR MAKING Patent
Warren H. Philipp, inventor (to NASA) and Kenneth W. Street, Jr., inventor (to NASA) 6 Dec. 1994 5 p Filed 21 Jun. 1993 Supersedes N93-31316 (31 - 12, p 3709)
(NASA-Case-LEW-15576-1; US-Patent-5,371,110; US-Patent-Appl-SN-081910; US-Patent-Class-521-28; US-Patent-Class-521-25; US-Patent-Class-521-27; US-Patent-Class-521-31; US-Patent-Class-525-154; US-Patent-Class-525-330.2; US-Patent-Class-525-383) Avail: US Patent and Trademark Office

An ion exchange polymer comprised of an alkali metal or alkaline earth metal salt of a poly(carboxylic acid) in a poly(vinyl acetal) matrix is described. The polymer is made by treating a mixture made of poly(vinyl alcohol) and poly(acrylic acid) with a suitable aldehyde and an acid catalyst to cause acetalization with some cross-linking. The material is then subjected to an alkaline aqueous solution of an alkali metal salt or an alkali earth metal salt. All of the film forming and cross-linking steps can be carried out simultaneously, if desired.
Official Gazette of the U.S. Patent and Trademark Office

N95-18336 Department of the Navy, Washington, DC.
POLYURETHANE SELF-PRIMING TOPCOATS Patent
Charles R. Hegedus, inventor (to Navy), Donald J. Hirst, inventor (to Navy), and Anthony T. Eng, inventor (to Navy) 3 May 1994 6 p Filed 14 May 1993 Supersedes AD-D016205
(AD-D016420; US-Patent-5,308,903; US-Patent-Appl-SN-062864; US-Patent-Class-524-204) Avail: US Patent and Trademark Office

A corrosion-resistant coating which can be applied directly to a surface as a self-priming topcoat comprising a polyurethane resin binder and a combination of pigments consisting essentially of a molybdate-modified zinc phosphate, zinc salts of benzoic acids, and an alkaline earth metal phosphate such as zinc-barium phosphate is described. In addition, the coating contains up to about 35 parts by weight of a titanium dioxide pigment, up to about 3.0 parts by weight of an oil soluble dispersant agent and up to about 50 parts by weight of at least one organic solvent. DTIC

N95-18339# Imperial Coll. of Science and Technology, London (England).
INTERNATIONAL CONFERENCE ON DEFORMATION, YIELD AND FRACTURE OF POLYMERS
1994 572 p The 9th Conference was held in Cambridge, England, on 11-14 April 1994
(Contract N68171-94-M-5109)
(AD-A284354; R/D-7341-MS-02) Avail: CASI HC A24/MF A04

The Churchill conferences on deformation, yield and fracture of polymers, held triennially since 1970, have established this event as the leading conference on its subject worldwide. The 1994 conference reviews developments and identifies trends in the scientific understanding of the deformation, yield and fracture of polymeric materials. DTIC

N95-18348# Pacific Northwest Lab., Richland, WA.
APPLICATION OF CONDUCTING POLYMERS TO ELECTROANALYSIS
M. A. Josowicz Apr. 1994 24 p Presented at the International Symposium on Electroanalysis, Cardiff, England, 6-8 Apr. 1994
(Contract DE-AC06-76RL-01830)
(DE94-015204; PNL-SA-23945; CONF-9404190-1) Avail: CASI HC A03/MF A01

Conducting polymers can be used as sensitive layers in chemical microsensors leading to new applications of theses devices. They offer the potential for developing material properties that are critical to the sensor sensitivity, selectivity and fabrication. The advantages and limitations of the use of thin polymer layers in electrochemical sensors are discussed.
DOE

N95-18355# Tennessee Univ., Knoxville, TN.
POLYMER-BASED SEPARATIONS: SYNTHESIS AND APPLICATION OF POLYMERS FOR IONIC AND MOLECULAR RECOGNITION
S. D. Alexandratos Apr. 1994 11 p
(Contract DE-FG05-86ER-13591)
(DE94-016427; DOE/ER-13591/8) Avail: CASI HC A03/MF A01

During this period, focus was on design and synthesis of bifunctional polymers for complexing metal ions from aqueous solutions; this could provide a means for separating radioactive and toxic metal ions from contaminated waste water as well as valuable metals from dilute ore processing streams. The synthesis of bifunctional polymers required a new preparative technique; bifunctional interpenetrating polymer networks (IPN) was an important part of the studies. In the preparation, a pre-formed crosslinked polymer is contacted with a solution of monomers, and a second network was polymerized within the first. Imidazole ligands were used. A new resin, prepared with a macrocyclic sorbed within polystyrene beads modified with sulfonic acid ligands, extracted Cu(II) 10--100-fold. Maximum metal ion complexation rates depend on a balance between chemical interactions and physical parameters (matrix porosity, rigidity). A novel ion exchange resin (Diphonix(trademark)) has been produced which displays both ionic selectivity (diphosphonic acid ligands) and rapid complexation rates (sulfonicacid ligands). DOE

N95-18402 Texas Univ., Austin, TX. Dept. of Chemistry.
ELEMENTAL FLUORINE BASED SYNTHESES OF PENTAFLUORO PHENLY AND OTHER AROMATIC PERFLUOROPOLYETHER POLYMERS Annual Report, 1 Feb. 1993 - 31 Jan. 1994
Richard J. Lagow 31 Jan. 1994 31 p Limited Reproducibility: More than 20% of this document may be affected by microfiche quality
(Contract F49620-92-J-0104)
(AD-A284102; AFOSR-94-0511TR) Avail: Issuing Activity (Defense Technical Information Center (DTIC))

Since we successfully obtained a fused perfluoro (benzofuran) from perfluoro (dicyclohexyl ether), reductive defluorination of the perfluorinated ethers containing three perfluoro (cyclohexyl) groups would be interesting. The three isomers of o-, m-, and p-perfluoro (dicyclohexanoxyl cyclohexane) were prepared by liquid-phase direct fluorination of o-, m-, and p-diphenoxyl benzene. After several runs of liquid-phase direct fluorination, enough amount of o-perfluoro (dicyclohexanoxyl cyclohexane) was collected to carry out the following reductive defluorination. The reductive defluorination was carried out from -70 to 70 deg for 2 days, but the ortho-ether, however, kept unreacted. One of the reasons for that is perhaps steric hindrance. Reductive defluorination of the meta- and para- ethers are under investigation. DTIC

N95-18430 Department of the Navy, Washington, DC.
METHOD OF LOWERING THE REACTION EXOTHERM IN THERMALLY POLYMERIZED ACETYLENE TERMINATED RESINS Patent
Thomas Diberardino, inventor (to Navy) 25 Jan. 1994 4 p Filed 10 Sep. 1992
(AD-D016276; US-Patent-5,281,672; US-Patent-Appl-SN-942912) Avail: US Patent and Trademark Office

A method for producing acetylide polymers substantially without charring or decomposition comprises heating a mixture comprising an acetylene terminated monomer and a prepolymer of said monomer, resulting in a lower reaction exotherm. DTIC

N95-18442 Clark Univ., Worcester, MA.
ADHEREND SURFACE EFFECTS ON EPOXY CURE BY NMR Final Technical Report, Sep. 1991 - Sep. 1993
Paul T. Inglefield 11 May 1994 12 p Limited Reproducibility: More than 20% of this document may be affected by microfiche quality
(Contract DAAL03-91-G-0333)
(AD-A284774) Avail: CASI HC A03

A solid state NMR investigation is undertaken to characterize at the molecular level the structure and dynamic nature of epoxy resin systems cured in the presence of an active surface intended to represent an adherend surface. Comparison is made with the cure reaction in the bulk phase in the absence of a surface. This comparison focuses both on the different products and different kinetics which result from the presence of an active surface. The major system considered is that based on the diglycidyl ether of bisphenol A cured with primary amines, in particular 4,4' diaminodiphenyl sulfone. Aluminum oxide is used as a high surface area model of aluminum adherend surfaces. The NMR experiments utilize line narrowing techniques to yield resolved spectra of the solid materials. 13C and 15N NMR are used to identify the structures, with various relaxation experiments being employed to aid in the assignments and to characterize the mobility of the cured resin. This represents a new and powerful probe of surface adhesion and the understanding achieved can hopefully yield benefit in terms of improved understanding of adhesive joint performance. Author

N95-18510 Massachusetts Univ., Amherst, MA. Dept. of Polymer Science and Engineering.
MULTI-FUNCTIONAL PI-CONJUGATED MACROMOLECULES BASED ON POLY (PHENYLENE VINYLENE) Annual Report, 15 Mar. 1993 - 14 Mar. 1994
Frank E. Karasz 14 Mar. 1994 22 p Limited Reproducibility: More than 20% of this document may be affected by microfiche quality
(Contract F49620-93-1-0178)
(AD-A284163; AFOSR-94-0507TR) Avail: Issuing Activity (Defense Technical Information Center (DTIC))

This report is for the period 15 Mar. 93 to 14 Mar. 94 and covers all AFOSR supported research under the P.I.'s direction. The principal thrusts of the research are in four relatively disparate areas related only by a polymeric theme: conjugated macromolecules; thermodynamics of inorganic-organic block copolymers; hyperbranched (dendritic) macromolecules; theoretical dielectric strength of polymers. However, because the present grant was the successor to a series of more widely focused AFOSR funding periods the opportunity was taken to complete numerous projects which originated earlier. As a result some forty-six AFOSR-supported manuscripts were published or were in press during the grant period. The focus of attention with respect to conjugated macromolecules was their electroluminescent (EL) properties. The fact that poly-p-phenylene vinylene (PPV) displayed EL has been known since 1992, and in the present work, based on many years of AFOSR-supported PPV research, derivatives of PPV were synthesized and characterized in terms of their electro-optical properties. In particular a series of conjugated-nonconjugated multi-block copolymer with extremely promising EL properties were studied and EL devices constructed. In these materials the hard blocks were short, monodisperse, phenylene vinylene oligomers, or derivatives thereof, while the soft block were oligomethylene spacer units designed to impart solubility and film formation to the materials. By varying the nature of the hard block EL emission throughout the visible spectral range was achieved. DTIC

N95-18513 Cincinnati Univ., OH. Dept. of Chemistry.
NOVEL POLYMERIC COMPOSITES THROUGH MOLECULAR ENGINEERING Annual Report, 1 Jul. 1993 - 30 Jun. 1994
James E. Mark 30 Jun. 1994 7 p Limited Reproducibility: More than 20% of this document may be affected by microfiche quality
(Contract F49620-92-J-0322)
(AD-A284168; AFOSR-94-0493TR) Avail: Issuing Activity (Defense Technical Information Center (DTIC))

Some final studies during this period were carried out in collaboration with Wright-Patterson AFB. They were based on some benzoxazole copolymers of good thermo-oxidative stability and solubility in tetrahydrofuran. The hydroxypolybenzoxazoles employed were reacted with an isocyanatosilane coupling agent and the hybrid consequently with in-situ produced silica. The resulting hybrid films containing one third silica were transparent. The mechanical properties of the hybrid materials were highly dependent on the nature of the organic polymers. In general, the tensile modulus of the hybrid materials increased with addition of silica but, as in the case of the polyamides, the elongation at break decreased at higher silica contents. Future work will focus on new polymers, additional physical properties, and new processing techniques. The new polymers will include benzoxazole polymers being prepared at Wright-Patterson AFB with structural changes to improve tractability and alternative functional groups to improve bonding to ceramic phases. Examples of new physical properties of importance are thermal expansion coefficients and impact strengths. New processing techniques to be sought include methods for densifying cameras prepared from glassy polymers such as poly(methyl methacrylate), and preparing organic-inorganic aerogels by supercritically drying some of the hybrid composites from the gel state. DTIC

N95-18631 Department of the Navy, Washington, DC.
POLYURETHANE SELF-PRIMING TOPCOATS Patent
Charles R. Hegedus, inventor (to Navy), Donald J. Hirst, inventor (to Navy), and Anthony T. Eng, inventor (to Navy) 1 Mar. 1994 7 p Filed 25 Aug. 1992
(AD-D016234; US-Patent-5,290,839; US-Patent-Appl-SN-936983; US-Patent-Class-124-204) Avail: US Patent and Trademark Office

A corrosion-resistant coating which can be applied directly to a surface as a self-priming topcoat comprising a polyurethane resin binder and a combination of pigments consisting essentially of a molybdate-modified zinc phosphate, zinc salts of benzoic acids, and an alkaline earth metal phosphate such as zinc-barium phosphate. In addition, the coating contains up to about 35 parts by weight of a titanium dioxide pigment, up to about 3.0 parts by weight of an oil soluble dispersant agent and up to about 50 parts by weight of at least one organic solvent. DTIC

N95-18636 Massachusetts Inst. of Tech., Cambridge. Dept. of Chemistry.
LARGE AMPLITUDE MOTIONS, ESPECIALLY ISOMERIZATION AND TUNNELING IN POLYATOMIC MOLECULE SPECTRA: NOVEL EXPERIMENTAL, PATTERN RECOGNITION, AND THEORETICAL METHODS Final Report, 1 Nov. 1990 - 31 Oct. 1993
Robert W. Field and Robert J. Silbey 29 Jul. 1994 23 p Limited Reproducibility: More than 20% of this document may be affected by microfiche quality
(Grant AF-AFOSR-0079-91)
(AD-A284194; Rept-3; AFOSR-94-0479TR) Avail: CASI HC A03

Stimulated Emission Pumping (SEP) spectra of HCP imply surprisingly regular dynamics for a rigid molecule undergoing up to 300 deg bending vibrations. Optical Optical Double Resonance (OODR) spectra characterize corresponding (pi* squared reversing pi squared) doubly excited (predissociated) states of HCP and HCCH. The factors governing intensities of nominally forbidden transitions in bent yielding linear SEP spectra are analyzed; this analysis forces the conclusion that transitions into excited CH stretching levels are absent from the A (tilde)-X(tilde) SEP spectra of HCN and HCCH. All mystery transitions in Wodtke's SEP spectra of HCN are assigned. An OODR scheme has been devised for distinguishing electric dipole from magnetic dipole transitions. DTIC

N95-18638# Rensselaer Polytechnic Inst., Troy, NY. Dept. of Nuclear Engineering and Engineering.
DEVELOPMENT OF RADIATION-HARDENED CERAMIC COMPOSITES FOR FUSION APPLICATIONS

M. C. Osborne, D. Steiner, and L. L. Snead (Oak Ridge National Lab., TN.) May 1994 18 p
(Contract DE-FG02-92ER-54181)
(DE94-016182; DOE/ER-54181/2) Avail: CASI HC A03/MF A01

The strength and toughness of continuous fiber reinforced ceramic composites (CFCC) are highly dependent on the fiber strength distribution. To first order, weaker fibers lead to low strength but higher toughness while stronger fibers lead to high strength composites of relatively low toughness. Toughness is associated with pullout of the fibers from the ceramic matrix. It has been shown previously that both strength and toughness of SiC/Nicalon(sup TM) composites are drastically changed following irradiation. This paper will present and discuss results for low oxygen Nicalon fibers irradiated at three damage levels; 0.013 dpa, 0.13 dpa, and 0.32 dpa. Single fibers were tensile tested and analyzed, using Weibull statistics, for mean strength and distribution. Tensile modulus was also determined. Using a diffractometer, the fiber grain size and percent crystallinity were determined. The initial results of these low level neutron irradiations exhibit no substantial degradation of the properties investigated. Therefore, continued research at higher doses is recommended. DOE

N95-18648# Pacific Northwest Lab., Richland, WA.
HETEROGENEOUS NUCLEATION OF CALCIUM OXALATE ON NATIVE OXIDE SURFACES
L. Song, M. J. Pattillo, G. L. Graff, A. A. Campbell, and B. C. Bunker Apr. 1994 6 p Presented at the Monitored Retrievable Storage Spring Meeting, San Francisco, CA, 4-8 Apr. 1994 Prepared in cooperation with Washington State Univ., Pullman, WA
(Contracts DE-AC06-76RL-01830; DE-FG06-89ER-75522)
(DE94-018725; PNL-SA-23282; CONF-9404213-1) Avail: CASI HC A02/MF A01

The aqueous deposition of calcium oxalate onto colloidal oxides has been studied as a model system for understanding heterogeneous nucleation processes of importance in biomimetic synthesis of ceramic thin films. Calcium oxalate nucleation has been monitored by measuring induction times for nucleation using Constant Composition techniques and by measuring nucleation densities on extended oxide surfaces using an atomic force microscope. Results show that the dependence of calcium oxalate nucleation on solution supersaturation fits the functional form predicted by classical nucleation theories. Anionic surfaces appear to promote nucleation better than cationic surfaces, lowering the effective energy barrier to heterogeneous nucleation. DOE

N95-18651# Sandia National Labs., Albuquerque, NM.
COMPLEX OXIDATION EFFECTS IN POLYMER DEGRADATION
R. L. Clough, K. T. Gillen, and J. Wise 1994 4 p Presented at the European Polymer Federation Meeting, Basel, Switzerland, 9-12 Oct. 1994
(Contract DE-AC04-94AL-85000)
(DE94-018903; SAND-94-2233C; CONF-9410200-1) Avail: CASI HC A01/MF A01

The authors are working to understand why predictions of degradation behaviors and rates, based on accelerated thermal aging experiments, often fail to match with aging of polymers under service conditions. A main goal of these studies is to develop more reliable lifetime prediction methodologies. DOE

N95-18678 Naval Surface Warfare Center, Bethesda, MD. Survivability Structures and Materials Directorate.
THERMOELECTRIC PROPERTIES OF CONDUCTING POLYMERS Technical Report, Sep. 1991 - Jun. 1994
Barbara Howell Jul. 1994 41 p Limited Reproducibility: More than 20% of this document may be affected by microfiche quality
(AD-A284058; CARDIVNSWC-SSM-64-94/12) Avail: CASI HC A03

Development of an inexpensive thermoelectric material which has a better cooling capacity than any currently available would have many practical advantages. On board ships or submarines it would allow a quiet, decentralized cooling architecture, it would reduce usage of chlorofluorocarbons, and would provide less expensive and lighter weight cooling systems. To this end a number of organic materials have been obtained and tested for thermoelectric properties. These include conductive vinyl elastomer, conductive nylon 12, and conductive polyphenylene sulfide, all of which are made conductive by addition of carbon. Polymers made conductive in this way do not have a high Seebeck coefficient. other polymers tested include polyaniline, a Schiff's base polymer laniline)), TTF-TCNQ (tetrathiafulvalinium tetracyanoquinodimethanide), D(sub S)(TCNQ)2 (1,2-bis(4-N-methylpyridylium-TCNQ)ethane), and polyoctylthiophene (POT) doped (separately) with 33% of the following substances: iodine, tetraethylamineammonium tetrafluoroborate, potassium persulfate, and ferric chloride. Ferric chloride doped POT was found to have a high Seebeck coefficient (1800 gV/deg C), but the conductivity (0.0074 S/cm) is not high enough to provide a good figure of merit. DTIC

N95-18918 Pennsylvania State Univ., University Park, PA.
COUPLED FINITE ELEMENT ANALYSIS OF DECOMPOSING POROELASTIC POLYMERIC COMPOSITES AND STRUCTURES WITH SUBSEQUENT THERMAL AND GAS DIFFUSION Ph.D. Thesis
Sunpyo Lee 1993 170 p
Avail: Univ. Microfilms Order No. DA9414327

A theory for axisymmetric problems which involves thermal and gas diffusion in anisotropic poroelastic composites has been developed. The derived governing equations couple material deformation with temperature and internal pore pressure and strongly couple gas diffusion and heat transfer in the porous body. Hence the theory accounts for the interactions between conductive heat transfer in the porous body and convective heat carried by the mass flux through the pores. The Bubnov-Galerkin finite element method is applied to the governing equations to transform them into a semidiscrete finite element system. A numerical procedure is developed to solve the coupled equations in the space and time domains. The method is applied to thermalchemical decomposition of carbon-phenolic composites. The effect of the pressure-stress coupling factor on the numerical solution for thermochemically decomposing carbon-phenolic is investigated. As a result, hypotheses to explain the variation of the pressure-stress coupling factor are introduced. Using the varying pressure-stress coupling factor, better correlations with experimental data are achieved. A thermal insulation liner in the cowl region under typical operating conditions is analyzed. The numerical solution is qualified by convergence tests and then critical time step and element sizes are suggested. The numerical solution shows that the effect of the coupling between heat transfer and gas diffusion is considerable. The results from the structural analysis show across-ply failure in the cowl zone. The delamination mechanism is hypothesized as a sequential procedure: (1) the across-ply failure which is the precursor to plylift and (2) the local fiber buckling caused by generation of excessive in-plane compressive stress. To prevent plylift, the across-ply stress can be reduced by using appropriate material ply angles in cowl zone design. Dissert. Abstr.

N95-18923 Cornell Univ., Ithaca, NY.
FRACTURE TOUGHNESS OF POLYMER/POLYMER BIMATERIAL INTERFACE REINFORCED WITH BLOCK COPOLYMERS Ph.D. Thesis
Fei Xiao 1994 218 p
Avail: Univ. Microfilms Order No. DA9416684

The effect of phase angle Psi on the bimaterial interface fracture toughness G(sub c) has been investigated in this work. The asymmetric double cantilever beam (ADCB) specimen used for the interface fracture test was calibrated. A boundary element method (BEM) program was developed to compute energy release rate G and phase angle Psi using the crack closure method and crack opening displacement method. Craze initiation ahead of a bimaterial interface crack was studied utilizing a dislocation model. Experimental results of G(sub c) as functions of Psi, block copolymer areal chain density Sigma and polymerization index N were obtained for the polystyrene/poly(2 vinylpyridine) (PS/PVP) system. The dependence of G(sub c) on Psi of this particular system was explained using micromechanics models. Dissert. Abstr.

N95-19064 Army Research Lab., Fort Monmouth, NJ.
LITHIUM ELECTRODE/POLYACRYLONITRILE BASED POLYMER ELECTROLYTE INTERFACE Technical Report, Jul. - Oct. 1993
Steve Slane Aug. 1994 15 p Limited Reproducibility: More than 20% of this document may be affected by microfiche quality
(AD-A283947; ARL-TR-73) Avail: CASI HC A03

Preparation of solid-state polymer lithium electrolytes based on polyacrylonitrile (PAN) have achieved room temperature conductivities equal to that of liquid organic electrolytes. Polymer films of ethylene carbonate, propylene carbonate, PAN, and lithium salts have yielded conductivities as

high as 0.004 S/cm at 25 deg C. These high conductivities make the use of polymer electrolytes a viable possibility in advanced lithium batteries. Besides a high ionic conductivity, chemical stability of the polymer with lithium is another consequential property to make an electrolyte successful in a practical battery configuration. It is shown that the growth of the interfacial resistance between lithium and the solid polymer electrolyte (SPE) can be reduced by the addition of dimethyl carbonate, or ground molecular sieves, or by reducing the solvent to salt ratio. Reported here are the film preparation technique, conductivities from -70 to +70 deg C, and the time evolution of the impedance responses of Li/SPE/Li cells. DTIC

N95-19095# Pennsylvania State Univ., University Park, PA. Dept. of Materials Science and Engineering.

FUNDAMENTAL STUDIES OF PASSIVITY AND PASSIVITY BREAKDOWN

Digby D. Macdonald and Mima Urquidi-Macdonald 21 Feb. 1994 33 p
(Contract DE-FG02-91ER-45461)
(DE94-016954; DOE/ER-45461/T1) Avail: CASI HC A03/MF A01

Purpose is to understand the mechanisms for growth and breakdown of passive films on metal and alloy surfaces in aqueous medium; a secondary goal is to devise methods for predicting localized corrosion damage in industrial systems. Tasks currently being studied are: (1) formation of bilayer structures in passive films on metals and alloys; passivity breakdown on solid vs. liquid gallium; (2) roles of alloying elements in passivity breakdown; (3) electrochemical impedance spectroscopy of passive films; (4) electronic structure of passive oxide films; (5) photoelectrochemical impedance spectroscopy of passive films; and (6) kinetics of localized attack. DOE

N95-19102 Case Western Reserve Univ., Cleveland, OH. Dept. of Physics.

THERMAL RELAXATION PROCESSES AND STABILITY IN POLED ELECTRO-OPTIC POLYMERS Annual Report, 1 Jul. 1993 - 30 Jun. 1994

Kenneth D. Singer 30 Jun. 1994 8 p Limited Reproducibility: More than 20% of this document may be affected by microfiche quality
(Contract F49620-93-1-0202)
(AD-A283948; AFOSR-94-0543TR) Avail: CASI HC A02

We have made important progress in the last year in modeling the decay of molecular orientation in poled electro-optic materials in order to more accurately predict the evolution of the nonlinear optical response over time and are approaching a predictive description of the long time scale orientational decay of poled polymer systems. The most remarkable feature of decay measurements of the nonlinear optical response is that it appears similar over so many time scales. The breadth of the time scales involved can exceed those normally measured in dielectric relaxation measurements. Models have been developed in the dielectric literature to describe relaxation processes measured over many decades of time (or frequency). These models describe the dispersive and fractal time nature of these processes, and involve an extra parameter beyond that of a stretched exponential. Thus, one parameter defines an average time (frequency), and two describe the shape of the distribution of relaxation time (frequencies) above and below the average. An example of these models includes the Havriliak-Nagami model. We have begun to analyze our current data in light of these new models, and are developing programs to take transforms between the time and frequency domain to relate dielectric measurements to nonlinear optical. DTIC

N95-19227# Lawrence Livermore National Lab., Livermore, CA.

INVESTIGATION OF THE MICROSTRUCTURE OF COATINGS FOR HIGH POWER LASERS BY NON-OPTICAL TECHNIQUES

R. J. Tench, M. R. Kozlowski, and R. Chow Jun. 1994 9 p Presented at the International Symposium on Optical Interference Coatings, Grenoble, France, 6-14 Jun. 1994
(Contract W-7405-eng-48)
(DE94-017697; UCRL-JC-117438; CONF-9406168-3) Avail: CASI HC A02/MF A01

The microstructure of optical coatings strongly influence their resistance to high fluence laser, scatter properties, as well as, their mechanical and environmental stability. The relative merits of non-optical techniques, such as: scanning electron microscopy, transmission electron microscopy, atomic force microscopy, and focused ion beam, are discussed as they apply to optical multilayer coatings. The combination of these techniques provides a unique method to analyze defects in coatings. The long term objective of this work is to: (1) understand the initiation and growth mechanisms of defects in optical coatings; (2) investigate failure mechanisms of laser coatings; and (3) suggest methods for reducing the number of defects during the deposition process. To date, our defect analysis using non-optical techniques has focused on hafnia/silica multilayers for high power lasers. In summary, the information we have compiled about the defect seeds indicates that seed size has an influence upon the mechanical stability of the whole defect, indicates that seed shape and chemical composition reveal potential seed sources in the coating system, and demonstrates that defects can be initiated either as a single event or continuously during the deposition process. Also, it is shown that different vendors have characteristic defects and seeds. DOE

N95-19399# Oak Ridge National Lab., TN.

ENHANCEMENT OF CREEP RESISTANCE OF A SINTERED Si3N4 CERAMIC BY MICROWAVE ANNEALING

K. C. Liu, C. O. Stevens, C. R. Brinkman, K. L. More, J. D. Kiggans, and T. N. Tiegs 1994 5 p Presented at the Science and Technology Materials Conference, Greensboro, NC, 27-29 Oct. 1993
(Contract DE-AC05-84OR-21400)
(DE94-017688; CONF-9310328-2) Avail: CASI HC A01/MF A01

Creep behavior was investigated for a sintered Si3N4 Ceramic microwave annealing at 1400 and 1500 C for 20 h. Results of creep tests at 1200 C showed that microwave annealing can enhance the creep resistance in terms of lowering creep rate and, hence, extending creep rupture life, but the 1400 C annealing was most effective. X-ray diffraction analyses showed that the crystalline second phase was transformed as a result of microwave annealing from single phase Y10Al2Si3O18N4 to several different phases. The situation was further complicated by evolution of additional phases during high temperature creep experiments. DOE

N95-19520# Massachusetts Inst. of Tech., Cambridge. Dept. of Materials Science and Engineering.

WORKSHOP ON SYNTHESIS OF MACROMOLECULES WITH PRECISELY CONTROLLED STRUCTURE FOR NEW MATERIALS Final Report, 1 Mar. 1993 - 28 Feb. 1994

Edwin L. Thomas 28 Feb. 1994 4 p
(Contract F49620-93-1-0175)
(AD-A285321; AFOSR-94-0631TR) Avail: CASI HC A01/MF A01

Recent development on the theoretical and synthetic experimental fronts mean that we can better tailor, characterize and understand materials based on macromolecule. Macromolecules can now be prepared by a wide range of synthetic techniques that result in polymers with very well-defined composition, architecture and molecular weight. A variety of theories, including those describing melt dynamics, liquid crystallinity and microphase organization, are sufficiently well-developed to enable prediction of particular polymer compositions are chain structures exhibiting unique properties. Theories are just starting to possess sufficient molecular detail such that they are synthetically suggestive, thereby enabling chemists to translate the parameters into actual substances. New experimental techniques permit critical testing of theories on small-scale quantities of model materials. Computer simulations and molecular modeling are increasingly powerful tools to guide us in polymer design. However, with these new capabilities arise questions of how best to implement and exploit them. The capabilities on both the chemical & physical communities are now such that specific collaborations will certainly bear fruit. The interplay of theory & experiment, as well as physics & chemistry, is leading to mutual inspiration, providing a better tie between the predictive power of theory and materials synthesis. DTIC

N95-19544# California Univ., Irvine, CA.

ARYL GELS AND RELATED MATERIALS. SYNTHESIS AND CHARACTERIZATION OF A NEW CLASS OF MICROPOROUS MATERIALS Annual Report, Jul. 1992 - Jul. 1994

Kenneth J. Shea 16 Aug. 1994 17 p
(Contract F49620-92-J-0379)
(AD-A285044; AFOSR-94-0557TR) Avail: CASI HC A03/MF A01

The objective of this program is the synthesis and characterization of new families of optically responsive materials for use in optical device fabrication. The materials that have been developed are polysilsesquioxanes, hybrids of organic network polymers and inorganic oxides. The materials

are prepared by sol-gel techniques employing molecular building blocks that contain a variable organic component and an inorganic oxide precursor. The resulting materials are molecular composites with no phase boundary between the organic and inorganic domains. Where the organic component of the molecular building block contains a chromophore with known NLO properties, optically responsive materials can be produced. In our efforts we have produced optical quality thin films by a combined sol-gel/electric field poling technique. The resulting poled thin films exhibit d(sub 33) and r(sub 33) figures of merit of 35-37(pm/V) and 9-10 (pm/V). These values are comparable to that of lithium niobate. Work is continuing to enhance the d(sub 33) and r(sub 33) values as well as to improve the optical stability at elevated temperatures. Author (DTIC)

N95-19558# Sandia National Labs., Albuquerque, NM.
FERROELECTRIC THIN FILM BISMUTH TITANATE PREPARED FROM ACETATE PRECURSORS
Yanxia Lu (Alfred Univ., NY.), D. T. Hoelzer (Alfred Univ., NY.), W. A. Schulze (Alfred Univ., NY.), B. A. Tuttle, and B. G. Potter 1994 13 p Presented at the 9th International Symposium on the Application of Ferroelectrics, University Park, PA, 7-10 Aug. 1994
(Contract DE-AC04-94AL-85000)
(DE95-000538; SAND-94-2276C; CONF-940839-1) Avail: CASI HC A03/MF A01

Bismuth titanate Bi4Ti3O12 thin films were fabricated by spin coat deposition followed by rapid thermal processing (RTP). Acetate derived solutions for deposition were synthesized by blending bismuth acetate in aqueous acetic acid and then adding titanium acetate. A series of electrically insulating, semiconducting and conducting substrates were evaluated for Bi4Ti3O12 film deposition. While x ray diffraction and TEM analyses indicated that the initial perovskite crystallization temperature was 500 deg C or less for these Bi4Ti3O12 films, a 700 deg C crystallization treatment was used to obtain single phase perovskite films. Bi4Ti3O12 film crystallographic orientation was shown to depend on three factors: substrate surface morphology, the number of coating layers and thermal processing. While preferred c-direction orientation was observed for Bi4Ti3O12 films deposited on silver foil substrates, preferred a-direction orientation was obtained for films deposited on both Si and Pt coated Si wafers. The films were dense, smooth, crack free, and had grain sizes ranging from 20 nm to 100 nm. Film thickness and refractive index were determined using a combination of ellipsometry, waveguide refractometry and TEM measurements. Both low field dielectric and ferroelectric properties were measured for an 800 nm thick film deposited on a Pt coated MgO substrate. A remanent polarization of 38 (mu)C/sq cm and a coercive field of 98 kV/cm were measured for this film that was crystallized at 700 deg C. DOE

N95-19580# Ceramics and Materials Processing, Inc., Clarence, NY.
RECENT PROGRESS ON ECVD PROJECT Report, 15 Apr. 15 Jul. 1994
1994 7 p
(Contract DE-FG42-93R2-15556)
(DE94-016773; DOE/R2-15556/T1) Avail: CASI HC A02/MF A01

Recent experimental results obtained for enhanced chemical vapor deposition (ECVD) are reported. These experiments included: (1) the distribution of deposition rates of various powders on the substrate in the reactor; (2) comparison of deposition rates of CVD and enhanced CVD; and (3) evaluation of the mechanical properties of ECVD with commercial powders and ultra fine powders produced by plasma vapor deposition method. Particles are introduced from an external source into the reaction chamber. This permits better control of particle feed rates and also allows a variety of different powders to be used. The feed mechanism is entrainment from a fluidized bed of fine particles. DOE

N95-19614# Foster-Miller Associates, Inc., Waltham, MA.
NOVEL e-o POLYMERS: NLO MATERIALS WITH SUPERIOR TEMPORAL STABILITY Final Technical Report, Jul. 1993 - Jul. 1994
M. Druy Sep. 1994 24 p
(Contract F49620-93-C-0053)
(AD-A285872; NAS-3988-FM-94101-839; AFB-0053-FM-9740-841; AFOSR-94-0626TR) Avail: CASI HC A03/MF A01

This report contains experimental results on a comprehensive study of the second order nonlinear optical (NLO) properties of a molecularly doped polymer system. A second-order NLO chromophore, 4-morpholino-4'nitrostilbene (MNS) was synthesized which possesses a large molecular first hyperpolarizability and dipole moment. The chromophore was doped into a polymer matrix with a high glass transition temperature and subsequently poled by a strong electric field to induce noncentrosymmetry required for second-order nonlinear optical behavior. An in situ poling technique was employed to determine the processing and poling parameters in order to obtain high and stable nonlinearities. Detailed information on the synthesis, processing, characterization, and results on a series of samples is presented. DTIC

N95-19691# Nebraska Univ., Lincoln, NE.
INVESTIGATION OF MICROSCOPIC MECHANISMS OF FAILURE OF ELECTRONIC SMART MATERIALS/SYSTEMS Letter Report, 1 Oct. 1993 - 30 Sep. 1994
Qing Jiang 30 Sep. 1994 9 p
(Contract N00014-94-1-5300)
(AD-A284830) Avail: CASI HC A02/MF A01

The objectives of this investigation are the following: (1) understand the microscopic mechanism of formation of microcracks in these ferroelectric ceramics; (2) quantify the dependence of the strength of these ceramics upon their microstructural parameters, that can be controlled through the manufacturing processes; and (3) tailor these ceramics for maximum strength by optimizing the microstructural parameters. DTIC

N95-19696# State Univ. of New York, Stony Brook, NY. Dept. of Chemistry.
MACROMOLECULAR CHARACTERIZATION AND SOLUTION BEHAVIOR OF POLYMER ADDITIVES Final Report
Ben Chu 10 Jun. 1994 7 p
(Contract DAAL03-91-G-0040)
(AD-A284845) Avail: CASI HC A02/MF A01

Several aspects of polymer rheology and microstructures were investigated by using a variety of physical techniques, including the development of a new magnet-enhanced optical falling needle/sphere rheometer. From studies of rheological properties and association behavior of mixtures of poly(isobutyl methacrylate-tert-butyl aminoethyl methacrylate) and an ionomer in solution, and of random copolymers of styrene with sodium-2-acrylamido-2-methylpropane sulphonate, it becomes clear that structures of associative polymers can best be approached by using well-defined block copolymers. Furthermore, the ionic interactions deserve special examination in view of ion cluster formation and long-range inhomogeneities which are present often because of processing procedures. A series of studies of block copolymers, including lightly sulfonated polystyrene-b-poly(tert butylstyrene) and triblock poly(oxyethylene-oxypropylene-oxyethylene) in nonpolar (xylene), polar (water), and water/o-xylene mixtures, were performed. The size, shape, and aggregation number were determined by using laser light scattering, small angle x ray scattering, and transient electric birefringence techniques. DTIC

N95-19721# Los Alamos National Lab., NM.
GLOBAL EQUATION OF STATE FOR A GLASSY MATERIAL: FUSED SILICA
J. C. Boettger Sep. 1994 12 p
(Contract W-7405-eng-36)
(DE94-018598; LA-12841-MS) Avail: CASI HC A03/MF A01

A new SESAME equation of state (EOS) for fused silica has been generated using the computer program GRIZZLY and will be added to the SESAME library as material number 7387. This new EOS provides better agreement with experimental data than was achieved by all previous SESAME EOSs for fused silica. Material number 7387 also constitutes the most realistic SESAME-type EOS generated for any glassy material thus far. DOE

N95-19745# Toranaga Technologies, Inc., Carlsbad, CA.
POLYMER BASED MATERIALS FOR ADDITIVE PROCESSING OF HIGH TEMPERATURE ELECTRONICS PACKAGING Annual Progress Report No. 1, 1-30 Sep. 1994
Michael Todd 3 Oct. 1994 3 p
(Contract F49620-94-C-0074)
(AD-A285962; AFOSR-94-0672TR) Avail: CASI HC A01/MF A01

Work under Task 1 has begun on the evaluation of candidate high temperature transient liquid phase sintering (TLPS) systems as well as

candidate high temperature polymer materials. In evaluating candidate metal and alloy systems, binary and available ternary phase diagrams are being reviewed to identify alloy systems that could be used in a high temperature application. The goal is to find a combination of metals and alloys that will go through TLPS at a temperature compatible with the polymer processing and that will form products that will be able to withstand the proposed high operating temperatures. DSC studies of some of these combinations have been done to confirm their potential. Metal powders studied so far include copper and various low melting point metals and alloys to ascertain the products formed by TLPS. DTIC

N95-19783*# National Aeronautics and Space Administration. Lewis Research Center, Cleveland, OH.

ADHESION, FRICTION, AND WEAR BEHAVIOR OF CLEAN METAL-CERAMIC COUPLES

Kazuhisa Miyoshi Feb. 1995 8 p Presented at the International Tribology Conference, Yokohama, Japan, 29 Oct. - 2 Nov. 1995; sponsored by the Japanese Society of Tribologists

(RTOP 505-63-5A)

(NASA-TM-106815; E-9341; NAS 1.15:106815) Avail: CASI HC A02/MF A01

When a clean metal is brought into contact with a clean, harder ceramic in ultrahigh vacuum, strong bonds form between the two materials. The interfacial bond strength between the metal and ceramic surfaces in sliding contact is generally greater than the cohesive bond strength in the metal. Thus, fracture of the cohesive bonds in the metal results when shearing occurs. These strong interfacial bonds and the shearing fracture in the metal are the main causes of the observed wear behavior and the transfer of the metal to the ceramic. In the literature, the surface energy (bond energy) per unit area of the metal is shown to be related to the degree of interfacial bond strength per unit area. Because the two materials of a metal-ceramic couple have markedly different ductilities, contact can cause considerable plastic deformation of the softer metal. It is the ductility of the metal, then, that determines the real area of contact. In general, the less ductile the metal, the smaller the real area of contact. The coefficient of friction for clean surfaces of metal-ceramic couples correlates with the metals total surface energy in the real area of contact gamma A (which is the product of the surface energy per unit area of the metal gamma and the real area of contact (A)). The coefficient of friction increases as gamma A increases. Furthermore, gamma A is associated with the wear and transfer of the metal at the metal-ceramic interface: the higher the value of gamma A, the greater the wear and transfer of the metal. Author

N95-19826# Southwest Research Inst., San Antonio, TX. Belvoir Fuels and Lubricants Research Facility.

TECHNOLOGY DEMONSTRATION OF SINGLE HYDRAULIC FLUID FOR ARMORED GROUND VEHICLE SYSTEMS Interim Report, Oct. 1992 - Dec. 1993

Bernard R. Wright, Ruben A. Alvarez, and Paul I. Lacey Dec. 1993 55 p

(Contract DAAK70-92-C-0059)

(AD-A280170; BFLRF-298) Avail: CASI HC A04/MF A01

The primary hydraulic fluids used today by the U.S. Army are MIL-H-6083 and MIL-H-46170. MIL-H-6083 is a petroleum-base, low flash point fluid, and MIL-H-46170 is a synthetic fluid with a higher flash point but extremely high viscosity at lower temperatures. This new fluid, referred to as single hydraulic fluid (SHF), is a synthetic-base fluid with improved flammability and low-temperature viscosity characteristics. This report discusses the SHF characteristics, laboratory evaluations, and initiation of pilot field demonstration and preliminary results. DTIC

N95-19861 Edgerton, Germeshausen and Grier, Inc., Idaho Falls, ID.

ALTERNATIVE SOLVENTS/TECHNOLOGIES FOR PAINT STRIPPING: PHASE 1 Final Report, Mar. 1991 - Sep. 1992

M. N. Tsang, E. J. Mommens, P. M. Wikoff, T. L. Harris, B. D. Lee, D. F. Suciu, A. L. Schulz, and J. L. Scott Mar. 1994 258 p Prepared for AF Civil Engineering Center, Tyndall AFB, FL Limited Reproducibility: More than 20% of this document may be affected by microfiche quality

(Contracts DE-AC07-76ID-01570; DE-GM07-87ID-11026; AF Proj. 0702)

(AD-A279918; EGG-WTD-10299; AFCESA/ESL-TR-89-62) Avail: CASI HC A12

This report presents the results of an extensive investigation of possible alternative solvents and technologies that may be safely applied to some Air Force paint-stripping operations. The objective of the Alternative Solvents/Technologies Program is to minimize hazardous waste by eliminating toxic chemicals in the maintenance and repair processes. Three phases of study are defined: Phase 1, identify alternate solvents/strippers and screen them; Phase 2, field test solvent/strippers; and Phase 3, implement alternate solvents and technologies as approved. A list of potential alternate solvents and paint systems were identified and carried into Phase 2. Both immersion and spray/brush-on application methods were studied. DTIC

N95-19866 Defence Research Establishment Ottawa, Ottawa (Ontario).

A REVIEW OF FOOTWEAR FOR COLD/WET SCENARIOS. PART 2: SOCKS, LINERS, AND INSOLES

Walter Dyck Dec. 1993 26 p Limited Reproducibility: More than 20% of this document may be affected by microfiche quality

(AD-A279937; DREO-TN-93-28-Pt-2) Avail: Issuing Activity (Defense Technical Information Center (DTIC))

Presented herein is the second of a proposed multi-part review on footwear. This report deals mostly with the materials and their properties making up the layer or layers of footwear between the skin and the boot, i.e. socks and removable insoles and liners. Aspects of these elements of footwear are related to various military requirements, and as in the first part of the review, attention is drawn to the f act that in meeting these requirements, solutions conflict. A discussion on possible compromises follows, leading to the recommendation that in order to develop proper footwear for the military, a very carefully written statement of requirement is necessary. DTIC

N95-19867 Defence Research Establishment Ottawa, Ottawa (Ontario).

DIFFUSION OF WATER VAPOUR THROUGH COLD GORE-TEX (TRADEMARK)

Randall J. Osczevski Jul. 1993 22 p Limited Reproducibility: More than 20% of this document may be affected by microfiche quality

(AD-A279939; DREO-1202) Avail: Issuing Activity (Defense Technical Information Center (DTIC))

A simple gravimetric procedure was devised to measure the water vapour diffusion resistance of waterproof, water vapour permeable textiles at temperatures below freezing. The apparent resistance of a hydrophilic film, part of a Gore-Tex(TM) laminate, increased exponentially with a decrease in temperature. At sub-zero temperatures, water vapour transfer through this film was only a few percent of what it is at room temperature. The diffusion process in such materials is discussed. other hydrophilic films are likely to be similarly affected. DTIC

N95-19000*# University of Western Kentucky, Bowling Green, KY. Dept. of Chemistry.

GROWTH OF THIN FILMS OF DICYANOVINYLANISOLE ON QUARTZ AND TEFLON-COATED QUARTZ BY PHYSICAL VAPOR TRANSPORT

Earl F. Pearson *In* Alabama Univ., Research Reports: 1994 NASA/ASEE Summer Faculty Fellowship Program Oct. 1994 7 p (For primary document see N95-18967 05-80)

Avail: CASI HC A02/MF A03

N95-19008*# State Univ. of New York, Farmingdale, NY. Mfg. and Mechanical Research Div.

QUALITY OPTIMIZATION OF THERMALLY SPRAYED COATINGS PRODUCED BY THE JP-5000 (HVOF) GUN USING MATHEMATICAL MODELING

Hazem Tawfik *In* Alabama Univ., Research Reports: 1994 NASA/ASEE Summer Faculty Fellowship Program Oct. 1994 9 p (For primary document see N95-18967 05-80)

Avail: CASI HC A02/MF A03

N95-19197*# National Aeronautics and Space Administration. Lyndon B. Johnson Space Center, Houston, TX.

THE USE OF SILICA AEROGEL TO COLLECT INTERPLANETARY DUST IN SPACE Abstract Only

Michael E. Zolensky, Ruth A. Barrett (Lockheed Engineering and Sciences Co., Houston, TX.), and F. Hoerz *In* Lunar and Planetary Inst., Workshop on Particle Capture, Recovery and Velocity/Trajectory Measurement

Technologies 1994 p 94-98 (For primary document see N95-19172 05-90)
Avail: CASI HC A01/MF A02

28 PROPELLANTS AND FUELS

Includes rocket propellants, igniters, and oxidizers; their storage and handling procedures; and aircraft fuels.

For related information see also *07 Aircraft Propulsion and Power, 20 Spacecraft Propulsion and Power,* and *44 Energy Production and Conversion.*

N95-19090 Department of the Navy, Washington, DC.
SOLID FUEL RAMJET COMPOSITION Patent
George W. Burdette, inventor (to Navy) and Gary W. Meyers, inventor (to Navy) 14 Jun. 1994 3 p Filed 25 Nov. 1981
(AD-D016458; US-Patent-5,320,692; US-Patent-Appl-SN-329621; US-Patent-Class-149-19.9) Avail: US Patent and Trademark Office

A ramjet solid fuel composed of Hydroxyl terminated polybutadiene aluminum, magnesium, and boron carbide is described. The high volumetric heating value fuel of the present invention significantly increases the distance range of missiles. DTIC

N95-19100# Sandia National Labs., Albuquerque, NM.
EVALUATION OF SCANNERS FOR C-SCAN IMAGING IN NONDESTRUCTIVE INSPECTION OF AIRCRAFT
J. H. Gieske Apr. 1994 60 p
(Contract DE-AC04-94AL-85000)
(DE94-012473; SAND-94-0945) Avail: CASI HC A04/MF A01

The goal of this project was to produce a document that contains information on the usability and performance of commercially available, fieldable, and portable scanner systems as they apply to aircraft NDI inspections. In particular, the scanners are used to generate images of eddy current, ultrasonic, or bond tester inspection data. The scanner designs include manual scanners, semi-automated scanners, and fully automated scanners. A brief description of the functionality of each scanner type, a sketch, and a list of the companies that support the particular design are provided. Vendors of each scanner type provided hands-on demonstrations of their equipment on real aircraft samples in the FAA Aging Aircraft Nondestructive Inspection Validation Center (AANC) in Albuquerque, NM. From evaluations recorded during the demonstrations, a matrix of scanner features and factors and ranking of the capabilities and limitations of the design, portability, articulation, performance, usability, and computer hardware/software was constructed to provide a quick reference for comparing the different scanner types. Illustrations of C-scan images obtained during the demonstration are shown. DOE

N95-19505 Materials Research Labs., Ascot Vale (Australia).
MIXED HIGH EXPLOSIVES FOR INSENSITIVE BOOSTER COMPOSITIONS
Ian J. Dagley, Robert P. Parker, Lucianna Montelli, and Craig N. Louey Jul. 1993 23 p
(MRL-TR-92-22; AR-006-903) Copyright Avail: Issuing Activity

Three series of candidate insensitive booster compositions based on RDX (Grade A)/Elvax 210, and incorporating various amounts of PETN, DATB, and TATB (ranging from 5 to 35 percent) have been prepared and characterized for impact sensitiveness (Rotter F of I), shock sensitivity (SSGT), and cookoff behavior (SSCB). The RDX/PETN/Elvax 210 compositions are generally more impact sensitive than RDX, have shock sensitivities between those of tetryl and PBXW-7 Type 2, and give less violent cookoff responses than RDX/Elvax 210 (95:5) at the slow heating rate but more violent responses at the fast heating rate. All the RDX/DATB/Elvax 210 and RDX/TATB/Elvax 210 compositions had acceptable impact sensitiveness, but most were extremely shock insensitive. Use of finer particle size RDX led to increase in both the impact sensitiveness and shock sensitivity of RDX/TATB/Elvax 210 (75:20:5) composition. The compositions generally gave less violent reactions than RDX/Elvax 210 (95:5) at both fast and slow heating rates. The RDX/TATB/Elvax 210 (65:30:5) composition was the best of those examined, giving mild explosions or deflagrations in most tests; however, further reduction of cookoff violence is still required to give an acceptable insensitive booster composition. Author

29 MATERIALS PROCESSING

Includes space-based development of products and processes for commercial applications.

For biological materials see *55 Space Biology.*

N95-17973 National Aerospace Lab., Amsterdam (Netherlands).
MICROGRAVITY FLUID SCIENCE RESEARCH IN EUROPE
J. P. B. Vreeburg 1992 29 p Limited Reproducibility: More than 20% of this document may be affected by microfiche quality
(PB94-201720; NLR-TP-92426-U) Avail: CASI HC A03

The activities in Europe related to fluid science research in microgravity are discussed. After a short historical introduction, the general organizational traits and operational modes are described. The available facilities and those under development are surveyed, with the flight opportunities that exist. Fluid science research subjects are introduced under four main headings: molecular physics; thermodynamic properties and transport coefficients; heat and mass transfer processes; and mechanics and statics of liquids. A list of research institutes is provided and their main fields of interest are indicated. NTIS

N95-18082*# Colorado Univ., Boulder, CO. Center for Combustion Research.
IGNITION AND COMBUSTION OF BULK METALS IN A MICROGRAVITY ENVIRONMENT Final Technical Report
Melvyn C. Branch, J. W. Daily, and Angel Abbud-Madrid 15 Dec. 1994 14 p
(Grant NAG3-1257)
(NASA-CR-197519; NAS 1.26:197519; CCR-94-08) Avail: CASI HC A03/MF A01

Knowledge of the oxidation, ignition, and combustion of bulk metals is important for fire safety in the production, management, and utilization of liquid and gaseous oxygen for ground based and space applications. This report summarizes research under NASA support to investigate the ignition and combustion characteristics of bulk metals under varying gravity conditions. Metal ignition and combustion have not been studied previously under these conditions and the results are important not only for improved fire safety but also to increase knowledge of basic ignition and combustion mechanisms. The studies completed to date have led to the development of a clean and reproducible ignition source and diagnostic techniques for combustion measurements and have provided normal gravity combustion data on ten different pure metals. Metal specimens were ignited using a xenon short-arc lamp and measurements were made of the radiant energy flux, surface temperature history, spectroscopy of surface and gas products, and surface morphology and chemistry. Elevated gravity was provided by the University of Colorado Geotechnical Centrifuge. Author

N95-18211*# National Aeronautics and Space Administration. Lewis Research Center, Cleveland, OH.
OBSERVATIONS OF METHANE AND ETHYLENE DIFFUSION FLAMES STABILIZED AROUND A BLOWING POROUS SPHERE UNDER MICROGRAVITY CONDITIONS
Arvind Atreya (Michigan Univ., Ann Arbor, MI.), Sanjay Agrawal (Michigan Univ., Ann Arbor, MI.), Kurt Sacksteder, and Howard R. Baum (National Inst. of Standards and Technology, Gaithersburg, MD.) Nov. 1994 11 p Presented at the 32nd Aerospace Sciences Meeting and Exhibit, Reno, NV, 10-13 Jan. 1994; sponsored by AIAA Original contains color illustrations
(RTOP 656-61-23)
(NASA-TM-106766; E-9209; NAS 1.15:106766; AIAA Paper 94-0572)
Avail: CASI HC A03/MF A01; 1 functional color page

This paper presents the experimental and theoretical results for expanding methane and ethylene diffusion flames in microgravity. A small porous sphere made from a low-density and low-heat-capacity insulating material was used to uniformly supply fuel at a constant rate to the expanding diffusion flame. A theoretical model which includes soot and gas radiation is formulated but only the problem pertaining to the transient expansion of the flame is solved by assuming constant pressure infinitely

fast one-step ideal gas reaction and unity Lewis number. This is a first step toward quantifying the effect of soot and gas radiation on these flames. The theoretically calculated expansion rate is in good agreement with the experimental results. Both experimental and theoretical results show that as the flame radius increases, the flame expansion process becomes diffusion controlled and the flame radius grows as gamma t. Theoretical calculations also show that for a constant fuel mass injection rate a quasi-steady state is developed in the region surrounded by the flame and the mass flow rate at any location inside this region equals the mass injection rate. Author

N95-18326* National Aeronautics and Space Administration. Pasadena Office, CA.

PLASMA HEATING FOR CONTAINERLESS AND MICROGRAVITY MATERIALS PROCESSING Patent

Emily W. Leung, inventor (to NASA) (Jet Propulsion Lab., California Inst. of Tech., Pasadena, CA.) and Kin F. Man, inventor (to NASA) (Jet Propulsion Lab., California Inst. of Tech., Pasadena, CA.) 20 Dec. 1994 9 p Filed 15 Nov. 1993 Supersedes N94-29371 (32 - 8, p 3229)
(NASA-Case-NPO-18819-1-CU; US-Patent-5,374,801;
US-Patent-Appl-SN-153933; US-Patent-Class-219-121.36;
US-Patent-Class-219-123; US-Patent-Class-219-121.52;
US-Patent-Class-219-121.59; US-Patent-Class-361-144;
Int-Patent-Class-B23K-10/00) Avail: US Patent and Trademark Office

A method for plasma heating of levitated samples to be used in containerless microgravity processing is disclosed. A sample is levitated by electrostatic, electromagnetic, aerodynamic, or acoustic systems, as is appropriate for the physical properties of the particular sample. The sample is heated by a plasma torch at atmospheric pressure. A ground plate is provided to help direct the plasma towards the sample. In addition, Helmholtz coils are provided to produce a magnetic field that can be used to spiral the plasma around the sample. The plasma heating system is oriented such that it does not interfere with the levitation system.
Official Gazette of the U.S. Patent and Trademark Office

N95-18913*# Naval Surface Warfare Center, Bethesda, MD. Ship Systems and Programs Directorate.

MARANGONI CONVECTION IN A GRAVITY-FREE SILICON FLOAT ZONE Final Report

Hans J. Lugt and Samuel Ohring Apr. 1994 52 p
(NASA Order C-32007-M)
(NASA-CR-197600; NAS 1.26:197600; CARDIVNSWC-94/003;
AD-A280187) Avail: CASI HC A04/MF A01

The onset of Marangoni convection in the float zone of liquid silicon is studied from a state at rest in the absence of gravity. This time-dependent flow problem is solved numerically with the aid of the Navier-Stokes equations for an axisymmetric flow with nonlinear free surface conditions. On this free surface the temperature gradient is generated by heat transfer and radiation from a heater, which is symmetrically located between the two walls of the float zone. After a certain time, the flow is asymmetrically disturbed by moving the heat for a short time away from its symmetric position and back. Three different Marangoni numbers (based on the temperature difference between heater and melting point of silicon) are computed: 10,400, 30,255, and 50,050. The results show that for Ma = 10,400 the flow is steady and stable. For the two higher Marangoni numbers, however, the disturbed flows become unstable, and persistent oscillatory modes of 0.22 Hz for Ma = 30,225 and 0.27 Hz for Ma = 50,050 develop. The free surface itself is little deformed by computation with a flat surface confirms Kazarinoff and Wilkowski's 1989 result that the flat surface suppresses instability. It is conjectured that the flat surface imposes a strong local flow symmetry, which has a damping effect, and that, in the case of a deformable free surface, instability and maintenance of oscillation occur when the two rolls attached to the corners, which are formed by the wall and the free surface, separate and become vortices with extremal vorticity. these two vortices interact rhythmically by alternating build-up and decay. Author

N95-19076# Oak Ridge National Lab., TN.

GENERAL INFORMATION FOR OPERATION OF THE HIGH-TEMPERATURE ELECTROMAGNETIC CONTAINERLESS VACUUM INDUCTION FURNACE

C. A. Hahs and R. J. Fox Jun. 1994 13 p
(Contract DE-AC05-84OR-21400)
(DE94-017170; ORNL/M-3595) Avail: CASI HC A03/MF A01

The High-Temperature Electromagnetic Containerless Vacuum Induction Furnace was developed at Oak Ridge National Laboratory for the National Aeronautics and Space Administration (NASA), Marshall Space Flight Center, Alabama. The high-efficiency radio-frequency system developed for the conceptual design of the Modular Electromagnetic Levitator was created to evaluate this hardware on the KC135 microgravity airplane operated by NASA. Near-future KC135 flights are being planned to levitate, melt, and undercool 5-mm samples of niobium. General information on the operation of this hardware is included. DOE

N95-19788*# National Aeronautics and Space Administration. Lewis Research Center, Cleveland, OH.

SUMMARY REPORT OF MISSION ACCELERATION MEASUREMENTS FOR STS-60, SPACEHAB2, LAUNCHED 11 FEBRUARY 1994

Melissa J. B. Rogers (Tal-Cut Co., Beachwood, OH.) and Richard DeLombard Dec. 1994 171 p Original contains color illustrations
(RTOP 963-60-OD)
(NASA-TM-106797; E-9267; NAS 1.15:106797) Avail: CASI HC A08/MF A02; 44 functional color pages

The STS-60 mission, which launched on 11 February 1994, carried seven accelerometer systems. This report describes the configuration of each of these systems, where they were located on the Orbiter and the name of a contact person for each system. The Space Acceleration Measurement System (SAMS) was one of the accelerometer systems on-board and this mission marked its eighth successful flight. Acceleration data are provided here for SAMS which flew under an agreement between the NASA Microgravity Science and Applications division and the NASA office of Advanced Concepts and Technology. Acceleration data for the other accelerometer systems are not presented here. SAMS was located in the commercial SPACEHAB laboratory, on its second flight. The SAMS system was configured with three triaxial sensor heads with filter cut-offs of 5, 10, and 50 Hz. The acceleration environment related to an experiment centrifuge, an experiment refrigerator freezer unit, a SAMS sensor head rotation, an Orbiter shudder, and payload deploy activities are discussed. In the Appendices, all of the data from SAMS Head B (10 Hz) are plotted to provide an overview of the environment during the majority of the STS-60 mission. An evaluation form is included at the end of the report to solicit users' comments about the usefulness of this series of reports.
Author

N95-18970*# Tennessee Univ. Space Inst., Tullahoma, TN. Dept. of Engineering Science and Mechanics.

BUBBLE FORMATION IN MICROGRAVITY

Basil N. Antar *In* Alabama Univ., Research Reports: 1994 NASA/ASEE Summer Faculty Fellowship Program Oct. 1994 6 p (For primary document see N95-18967 05-80)
Avail: CASI HC A02/MF A03

N95-19013*# Alabama Univ., Huntsville, AL.

EFFECTS OF VIBRATION (G-JITTERS) ON CONVECTION IN MICRO-GRAVITY

Francis C. Wang *In* Alabama Univ., Research Reports: 1994 NASA/ASEE Summer Faculty Fellowship Program Oct. 1994 9 p (For primary document see N95-18967 05-80)
Avail: CASI HC A02/MF A03

31 ENGINEERING (GENERAL)

Includes vacuum technology; control engineering; display engineering; cryogenics; and fire prevention.

N95-17934 Newcastle-upon-Tyne Univ., Newcastle (England). Dept. of Computing Science.

REQUIREMENTS ANALYSIS FOR SAFETY-CRITICAL SYSTEMS: A CHEMICAL BATCH PROCESSING EXAMPLE

R. deLemos, A. Saeed, and T. Anderson Jan. 1994 36 p See also PB94-201555

(PB94-201563; TRS-469) Copyright Avail: Issuing Activity (National Technical Information Service (NTIS))

An essential basis for the development of software for safety-critical systems is to establish high-quality requirements specifications. In the paper the authors present a methodology for requirements analysis that consists of: a framework which facilitates the systematic analysis of the safety requirements, a graph which records the safety specifications and their relationships, and a set of procedures for the quality analysis of the safety specifications. To illustrate the approach a case study, based on chemical batch processing, is presented. NTIS

N95-18165# Naval Postgraduate School, Monterey, CA. Dept. of Physics.

IMPROVED EFFICIENCY AND POWER DENSITY FOR THERMOACOUSTIC COOLERS Annual Report, 1 Oct. 1992 - 30 Sep. 1993

Thomas J. Hofler Jun. 1994 128 p

(AD-A283946) Avail: CASI HC A07/MF A02

Research on improving the efficiency, cooling power, and cooling power density of thermoacoustic refrigerators is described. A heuristic analysis of short thermoacoustic heat exchangers in a high amplitude sound field is given. A heat exchanger experiment, utilizing a very high amplitude thermoacoustic prime-mover, shows some agreement with the heuristic analysis. This indicates that acoustic losses in the heat exchanger can be drastically reduced in high amplitude engines, while maintaining good thermal effectiveness. Other related, but more applied, research is briefly discussed. This includes the design and construction of a compact, portable, air-cooled, thermoacoustic refrigerator for the purpose of producing frost at a lecture demonstration. This design has roughly the same temperature span (40 deg C) as required by shipboard applications. Also, two new electrodynamic acoustic drivers have been designed and one design has been constructed. These designs offer high efficiency, good power density, and low cost and are probably scalable up to significantly higher acoustic power levels. DTIC

N95-18431 Department of the Navy, Washington, DC.

CENTRIFUGAL CASTING OF REINFORCED ARTICLES Patent

Amarnath P. Diyecha, inventor (to Navy), Subhash D. Karmarkar, inventor (to Navy), William A. Ferrando, inventor (to Navy), and Scott M. Hoover, inventor (to Navy) 22 Mar. 1994 6 p Filed 17 May 1991

(AD-D016277; US-Patent-5,295,528; US-Patent-Appl-SN-704563; US-Patent-Class-164-75) Avail: US Patent and Trademark Office

A reinforcement made of a composite material is positioned inside of a centrifugal casting mold. Molten matrix metal is then introduced into the mold while being rotated about its longitudinal axis until the molten metal completely encapsulates the reinforcement. DTIC

N95-18533 British Broadcasting Corp., Tadworth (England). Research and Development Dept.

THE SOUND INSULATIONS OF METAL-FRAMED PARTITIONS HAVING STRUCTURAL LOADBEARING PROPERTIES

G. D. Plumb 1994 12 p

(BBC-RD-1994/8) Copyright Avail: Issuing Activity (BBC, Kingswood Warren, Tadworth, Surrey, England)

The sound insulations were measured of several single and double leaf partitions. The partitions had metal frames and were capable of supporting significant structural loads. The purpose of the work was to design structural partitions that were cheaper to build than the existing masonry walls used for the construction of large studios. For some of the double leaf tests, one of the leaves was blockwork and the other was metal-framed, for the remainder of the double leaf tests, both leaves were metal-framed. Each of the partitions tested was suitable for use in different types of studio construction. The addition of glass wool insulation batts to the cavities of the partitions resulted in large increases in the measured sound insulations. The glass wool damps the motion of the boards and absorbs sound that has been transmitted into the cavities. The levels of sound insulation achieved from the partitions should be adequate for certain types of low cost studio construction. The partitions are considerably lighter than masonry walls. Therefore, the loadbearing requirements of the surrounding building will be reduced. Provided that the reductions in sound insulations are acceptable, the potential cost savings resulting from the use of lightweight structural partitions rather than masonry walls are very large. Author

N95-18567 Selskapet for Industriell og Teknisk Forskning, Trondheim (Norway). Div. of Refrigeration Engineering.

NORWEGIAN HEAT PUMP STATUS AND POLICY REVIEW

J. Stene, G. Eggen, R. Aarlien, and K. Evenmo 18 Feb. 1994 39 p

(PB94-206992; STF11-A94005) Avail: Issuing Activity (National Technical Information Service (NTIS))

This report is the Norwegian National Position Paper on heat pumps prepared for the IEA Heat Pump Centre's 1994 analysis, 'International Heat Pump Status and Policy Review'. The main objectives of this analysis is to provide an authoritative assessment of: the achievements of policy measures regarding heat pumps, the current and expected penetration of heat pumps in all market segments, and the technological status of various heat pumping technologies. NTIS

N95-18684 New Mexico Univ., Albuquerque, NM. Engineering Research Inst.

HANDHELD DELIVERY SYSTEM FOR MODIFIED BORON-TYPE FIRE EXTINGUISHMENT AGENT Final Report, 30 Jul. 1987 - 31 May 1988

Michael E. Lee and Robert E. Tapscott Nov. 1993 110 p Limited Reproducibility: More than 20% of this document may be affected by microfiche quality

(Contract F29601-84-C-0080)

(AD-A283955; NMERI-WA3-53(3.29); ESL-TR-88-46) Avail: CASI HC A06

A handheld, portable extinguisher was developed for Boralon, a modified Boron-type Class D fire extinguishing agent. The development of this unit progressed through the design, prototype, and final product stages. Two prototypes were designed as valved, stored-pressure types using Boralon compatible materials in critical areas exposed to the agent. The units were tested at an operating pressure of 200 lbf/sq in and an agent capacity of 2 to 3 gallons to determine the optimum application rate, throw range and throw pattern. The most favorable unit was tested for reliability. The information obtained in the prototype testing was developed further into a final design. This design specified a stored-pressure type that was sealed with a frangible plug or splined rupture disk and was activated by depressing the handle and removing the seal. Further requirements of a fill ratio of 75 percent agent to 25 percent pressure head at 200 lbf/sq in and an agent fill capacity of at least 2 gallons were also specified. Two manufactured units were found that met the criteria. An extinguisher with a frangible plug seal was successfully tested against 30- and 50-pound magnesium fires. Both the frangible plug and splined rupture disk designs satisfy the final design requirements of the handheld Boralon extinguisher. Both types are recommended for use in the Draft Military Specification for this unit. DTIC

N95-18738* National Aeronautics and Space Administration. Lyndon B. Johnson Space Center, Houston, TX.

GAS STORAGE AND RECOVERY SYSTEM Patent

Joseph S. Cook, Jr., inventor (to NASA) 29 Nov. 1994 8 p Filed 23 Mar. 1993 Supersedes N93-28136 (31 - 10, p 3021)

(NASA-Case-MSC-22091-1; US-Patent-5,368,067; US-Patent-Appl-SN-039602; US-Patent-Class-137-485; US-Patent-Class-137-549; US-Patent-Class-137-571; US-Patent-Class-137-587; US-Patent-Class-220-581; US-Patent-Class-220-901; US-Patent-Class-141-114) Avail: US Patent and Trademark Office

A system for recovering and recycling gases is disclosed. The system is comprised of inlet and outlet flow lines, controllers, an inflatable enclosure, and inflatable rib stiffeners which are inflatable by the gas to be stored. The system does not present gas at an undesirable back pressure to the gas source. A filtering relief valve is employed which prevents environmental airborne contamination from flowing back into the system when the relief valve is closing. The system is for storing and re-using helium.

Official Gazette of the U.S. Patent and Trademark Office

N95-18745*# Jet Propulsion Lab., California Inst. of Tech., Pasadena, CA.

METROLOGY: CALIBRATION AND MEASUREMENT PROCESSES GUIDELINES

Howard T. Castrup, Woodward G. Eicke, Jerry L. Hayes, Alexander Mark,

Robert E. Martin, and James L. Taylor Jul. 1994 342 p
(Contract NAS7-918; RTOP 323-36-02)
(NASA-RP-1342; NAS 1.61:1342) Avail: CASI HC A15/MF A03

The guide is intended as a resource to aid engineers and systems contracts in the design, implementation, and operation of metrology, calibration, and measurement systems, and to assist NASA personnel in the uniform evaluation of such systems supplied or operated by contractors. Methodologies and techniques acceptable in fulfilling metrology quality requirements for NASA programs are outlined. The measurement process is covered from a high level through more detailed discussions of key elements within the process, Emphasis is given to the flowdown of project requirements to measurement system requirements, then through the activities that will provide measurements with defined quality. In addition, innovations and techniques for error analysis, development of statistical measurement process control, optimization of calibration recall systems, and evaluation of measurement uncertainty are presented. Author

N95-19036 Rensselaer Polytechnic Inst., Troy, NY.
REPRESENTING VISIBILITY FOR SITING PROBLEMS M.S. Thesis
Clark K. Ray Apr. 1994 165 p Limited Reproducibility: More than 20% of this document may be affected by microfiche quality
(AD-A284076) Avail: Issuing Activity (Defense Technical Information Center (DTIC))

Many siting and other terrain analysis problems require the determination of the visibility from large numbers of observer locations over their surrounding terrain. The computational costs of existing visibility algorithms often require serious compromises on the fidelity, accuracy, or scope of analysis in real world settings. A highly accurate viewshed determination Algorithm, R2, is presented that executes in O(R2) time (where R is proportional to the number of points along the radius of the potential viewshed) and does not suffer from numerical problems, complex special cases, or high constant factors. Since the size of the output in viewshed determination is also O(R2), that time complexity of R2 is within a constant factor of optimality. The R2 algorithm is used to verify a fast and effective visibility index estimation procedure, WeightF. WeightF has time complexity O(R) and produces visibility index estimates with a correlated variation to R2 in excess of 0.9 on a variety of terrain datasets and problem settings. These visibility indexes can be used to select points with best aggregate visibility in an area. On real terrain, analysis using WeightF shows that points with significantly above average visibility index values are only a very small number of the total observer points. This property and the fast execution time of WeightF makes it useful for identifying high visibility points for use in siting algorithms, and to produce a viewable visibility index image that can display a large amount of visibility information in an intuitive fashion. DTIC

N95-19053 British Broadcasting Corp., Tadworth (England). Research Dept.
OPTIMUM DIMENSION RATIOS FOR STUDIOS, CONTROL ROOMS AND LISTENING ROOMS
R. Walker 1993 12 p
(BBC-RD-1993/8) Copyright Avail: Issuing Activity (BBC, Kingswood Warren, Tadworth, Surrey, England)

Most control rooms, listening rooms and small studios have dimensions that become comparable with the wavelength of the sound within the normally accepted audio range. Standing waves, where one of the room dimensions is an integer multiple of half the wavelength of the sound energy, result in irregular frequency responses. The response will also be a strong function of position of both the listener and the sound source because of the changing coupling to the spatial distribution of the modes. This behavior is fundamental to sound in enclosed spaces and is accentuated if the room proportions cause clustering of the modes. For practical purposes, it is necessary to define a range of acceptable room proportions from which selections may be made to suit particular cases. This requires the derivation of some form of criterion identifying regions of 'good' and 'poor' room proportions. This report describes the development of a computer program to produce plots of the distribution of an index of room 'quality' for rectangular rooms with different proportions. From these plots, regions of 'good' and 'poor' rooms were identified. A general design criterion was derived to restrict room proportions to those giving rooms with more even distributions of low frequency modes. Author

N95-19137 British Broadcasting Corp., Tadworth (England). Research Dept.
METAL-FRAMED PARTITIONS WITH REDUCED THICKNESSES. PART 2: BUILT-IN ACOUSTIC TREATMENT
G. D. Plumb 1993 16 p
(BBC-RD-1993/6-Pt-2) Copyright Avail: Issuing Activity (BBC, Kingswood Warren, Tadworth, Surrey, England)

Laboratory measurements were made of the sound insulations and absorption coefficients of a range of metal-framed partitions having built-in acoustic treatment. The optimum contructions for single and double leaf absorbent partitions had marginally lower sound insulations (approximately 1dB) than those of comparable single and double metal-framed Camdens. The effective absorption coefficient curves of the new partitions were reasonably flat between 50 Hz and 10 kHz. Savings in studio floor areas of up to 25% should be possible by using the new partitions rather than metal-framed Camdens fitted with conventional modular acoustic treatment. The partitions should have similar construction costs and weights to those of metal-framed Camdens. An initial assessment was made of the expected structural loadbearing performances and fire resistance of these partitions. However, a further assessment by specialists will be necessary before the partitions can be recommended for use in studio construction. Author

N95-19138 British Broadcasting Corp., Tadworth (England). Research Dept.
METAL-FRAMED PARTITIONS WITH REDUCED THICKNESSES. PART 1: NARROWER STUDS AND CAVITIES
G. D. Plumb 1993 14 p
(BBC-RD-1993/5-Pt-1) Copyright Avail: Issuing Activity (BBC, Kingswood Warren, Tadworth, Surrey, England)

The sound insulations were measured, in the Research Department Transmission Suite, of ten different metal-framed partitions. These partitions had narrower cavities and metal studs than those of the conventional thickness metal-framed Camden. Mineral wool had been installed in the cavities of some of the partitions and some partitions had double plasterboard skins rather than plasterboard-fiberboard skins. The sound insulations of these narrow partitions were generally comparable with, or marginally higher than, those of similar partitions, having stud and cavity widths equal to those in the conventional thickness metal-framed Camden. However, the loadbearing capabilities must be investigated before these narrow partitions can be recommended as alternatives to the conventional thickness metal-framed Camden. The use of these narrow partitions should result in average increases, of approximately 8%, in the available floor areas of typical studios. Author

N95-19402# National Inst. of Standards and Technology, Gaithersburg, MD. Building and Fire Regulations Lab.
VENTCF2: AN ALGORITHM AND ASSOCIATED FORTRAN 77 SUBROUTINE FOR CALCULATING FLOW THROUGH A HORIZONTAL CEILING/FLOOR VENT IN A ZONE-TYPE COMPARTMENT FIRE MODEL
L. Y. Cooper Aug. 1994 71 p
(PB94-210127; NISTIR-5470) Avail: CASI HC A04/MF A01

An algorithm and associated FORTRAN 77 subroutine, called VENTCF2, is presented for calculating the effects on two-layer compartment fire environments of the quasi-steady flow through a circular, shallow (i.e., small ratio of depth to diameter), horizontal vent connecting two spaces. The two spaces can be either two inside rooms of a multi-room facility or one inside room and the outside ambient environment local to the vent. The description of the flow through the vent is determined by combining considerations of the uni-directional-type of flow driven by a cross-vent pressure difference and, when appropriate, the combined pressure- and buoyancy-driven flows which occur when the density configuration across the vent is unstable, i.e., a relatively cool, dense gas in the upper space overlays a less dense gas in the lower space. In the algorithm, calculation of the rates of flow exchange between the two spaces is based on previously reported model equations. Characteristics of the geometry and the instantaneous environments of the two spaces are assumed to be known and specified as inputs. The outputs calculated by the algorithm/subroutine are the rates and the properties of the vent flow at the elevation of the vent as it enters the top space from the bottom space and/or as it enters the bottom space from the top space. Rates of

mass, enthalpy, and products of combustion extracted by the vent flows from upper and lower layers of inside room environments and from outside ambient spaces are determined explicitly. NTIS

N95-18975*# Marquette Univ., Milwaukee, WI. Dept. of Mechanical and Industrial Engineering.
CONCEPT OF USING A BENCHMARK PART TO EVALUATE RAPID PROTOTYPE PROCESSES
Vikram Cariapa *In* Alabama Univ., Research Reports: 1994 NASA/ASEE Summer Faculty Fellowship Program Oct. 1994 6 p (For primary document see N95-18967 05-80)
Avail: CASI HC A02/MF A03

32 COMMUNICATIONS AND RADAR

Includes radar; land and global communications; communications theory; and optical communications.

For related information see also *04 Aircraft Communications and Navigation* and *17 Space Communications, Spacecraft Communications, Command and Tracking.* For search and rescue see *03 Air Transportation and Safety,* and *16 Space Transportation.*

N95-17954 Boston Univ., MA. Coll. of Engineering.
GEOMETRICAL AND TOPOLOGICAL METHODS IN TIME DOMAIN ANTENNA SYNTHESIS Final Report, 1 Dec. 1991 - 30 Apr. 1994
P. R. Kotiuga 30 Apr. 1994 32 p Limited Reproducibility: More than 20% of this document may be affected by microfiche quality
(Contract F49620-92-J-0056)
(AD-A284208; AFOSR-94-0517TR) Avail: CASI HC A03

The nonlinear version of Lorentz reciprocity cannot be articulated in terms of frequency domain concepts. Similarly, the fact that a Fourier transform relates an antenna's far field to its sources cannot be used to explain why electromagnetic bullets or missiles cannot exist since, by construction, there is no far field for a bullet. Over the last year it has become clear that one has to deal with Maxwell's equations as a system of hyperbolic partial differential equations and avoid the temptation of using elliptic theory which is applicable when taking a Fourier transform (as engineers are trained to do) and playing with Helmholtz's equation. The way to achieve these goals is to reexamine the 'raison d'etre' for the use of the Radon transform in these hyperbolic problems. DTIC

N95-17958 Kaman Sciences Corp., Utica, NY.
FUSION OF CORRELATED SENSOR OBSERVATIONS Final Report
Robert Vienneau Aug. 1994 102 p Limited Reproducibility: More than 20% of this document may be affected by microfiche quality
(Contract F30602-93-C-0006)
(AD-A284224; RL-TR-94-134) Avail: CASI HC A06

Kaman Sciences Corporation has designed and implemented a graphical user interface-based fourth generation system for analyzing the algorithms developed for the Multichannel Signal Processing Simulation System (MSPSS). The MSPSS is comprised of two major subsystems, a menu-based subsystem and the user front-end interface (UFI) based subsystem. The menu-based subsystem interacts with the user by a series of menus and prompts that can be displayed on a line-oriented glass terminal. It is implemented as a collection of Fortran programs providing the desired signal processing capabilities. Multichannel data is passed between these programs by user-defined files. The menus themselves are Unix c-shells where the bottom-level menu automatically compiles, links, and executes the desired program. DTIC

N95-17964 Naval Command, Control and Ocean Surveillance Center, San Diego, CA. Research, Development, Technology and Evaluation Div.
LONG WAVELENGTH PROPAGATION CAPACITY, VERSION 1.1 (COMPUTER DISKETTE)
May 1994 2 p Supersedes AD-B147582
(AD-M200254; NRAD-TD-2394-CD; NONP-DTIC-DK-94-15236) Avail: Issuing Activity (Defense Technical Information Center (DTIC))

File Characteristics: software and data file. (72 files); ASCII character set. Physical Description: 2 computer diskettes; 3 1/2 in.; high density; 1.44 MB. System Requirements: PC compatible; Digital Equipment Corp. VMS; PKZIP (included on diskette). This report describes a revision of the Naval Command, Control and Ocean Surveillance Center RDT&E Division's Long Wavelength Propagation Capability (LWPC). The first version of this capability was a collection of separate FORTRAN programs linked together in operation by a command procedure written in an operating system unique to the Digital Equipment Corporation (Ferguson & Snyder, 1989a, b). A FORTRAN computer program named Long Wavelength Propagation Model (LWPM) was developed to replace the VMS control system (Ferguson & Snyder, 1990; Ferguson, 1990). This was designated version 1 (LWPC-1). This program implemented all the features of the original VMS plus a number of auxiliary programs that provided summaries of the files and graphical displays of the output files. This report describes a revision of the LWPC, designated version 1.1 (LWPC-1.1) DTIC

N95-18024# Ohio State Univ., Columbus. Electroscience Lab.
METHOD OF MOMENTS ANALYSIS OF ARTIFICIAL MEDIA COMPOSED OF DIELECTRIC WIRE OBJECTS
M. E. Peters and E. H. Newman Jul. 1994 157 p
(Contract N00014-89-J-1007)
(AD-A283318; ESL-721566-3) Avail: CASI HC A08/MF A01

The problem considered is an integral equation and periodic method of moments (PMM) solution determining the effective permittivity and permeability of an artificial medium. The artificial medium is composed of a 3D periodic array of identical arbitrarily-shaped thin conductive or dielectric wire objects arranged in a homogeneous host medium. In general, the artificial medium is anisotropic, in which case the effective permittivity and permeability tensors are determined. The method is based upon finding the complex wavenumber and the eigenfunction currents and fields, for a plane wave propagating in the artificial medium. Three methods are presented for determining the complex effective constitutive parameters of the artificial medium, all using various results of the PMM solution. The PMM solution solves for the currents induced in or on the wire objects. Mutual coupling between the wire objects is included in the PMM formulation. This mutual coupling affects the eigenfunction currents in the wire objects, the average eigenfunction fields in the artificial medium, and hence the effective permittivity and permeability tensors for the artificial medium. All fields are expressed as spectral summations of propagating and evanescent plane waves. Sample results are included to illustrate the method of the PMM solution, and to present some interesting points and characteristics of the periodic artificial media treatable by the solution. It is shown that for a given direction of propagation through the artificial medium, there are in general two distinct modes of plane wave propagation. These plane wave modes of propagation, as well as the eigenfunction currents in the wire objects, can change with the direction of propagation. DTIC

N95-18058# Naval Postgraduate School, Monterey, CA.
PERSONAL COMMUNICATIONS SERVICES: IMPROVING THEATER DEPLOYABLE COMMUNICATIONS FOR THE 21ST CENTURY M.S. Thesis
Ronald C. Cournoyer, Jr. Jun. 1994 80 p
(AD-A283465) Avail: CASI HC A05/MF A01

Personal Communications Services (PCS) may be the key ingredient for vastly improved military communications capabilities at the turn of the century. The Federal Communications Commission (FCC) defines PCS as a family of mobile or portable radio communications services which could provide services to individuals and businesses and be integrated with a variety of competing networks ... the primary focus of PCS will be to meet communications requirements of people on the move. Today's generation of Theater Deployable Communications, which provides joint tactical communications to deployed forces, is the Tri-Service Tactical Communications (TRI-TAC) system. A description of TRITAC's family of equipment, network topology, typical employment, and critical limitations is presented in this thesis. Five commercial Mobile Satellite Services (MSS) are described as viable candidates for augmenting existing communications systems. Cellular design principles such as frequency reuse, cell splitting, channel access methods, and propagation factors are also addressed. Finally, a framework for comparison of the candidate MSS systems is proposed as a baseline for further studies into the most beneficial implementation of PCS into theater deployable communications systems for the future. DTIC

N95-18066# SRI International Corp., Menlo Park, CA.
ALTERNATIVE VOLUME INTEGRAL EQUATION FORMULATIONS APPLIED TO DIELECTRIC CYLINDERS Final Report, Sep. 1992 - Sep. 1993
Rose W. Wang Aug. 1994 52 p
(Contract F30602-91-D-0001; AF Proj. 2304)
(AD-A285537; RL-TR-94-100) Avail: CASI HC A04/MF A01

A new volume-surface integral equation method is used for evaluating the bistatic scattering from dielectric cylinders with high dielectric constants. The kernel of this alternate volume-surface integral equations is less singular than the original volume integral equation because it does not require the computation of the double derivative in the highly singular dyadic Green's function. Numerical results indicate that there is a significant improvement in performance by using this new volume-surface integral formulation. We can achieve better accuracy, and require fewer cells per wavelength in the computations than with the original volume integral equation. DTIC

N95-18116# Rome Lab., Griffiss AFB, NY.
NUMERICALLY EFFICIENT USE OF FREQUENCY DOMAIN MoM CODES FOR WIDEBAND RADIATION AND SCATTERING PROBLEMS. AN APPLICATION: SCATTERING FROM A MICROSTRIP PATCH Report, Feb. 1992 - Sep. 1993
H. Steyskal and R. C. Hall Oct. 1993 34 p
(AF Proj. 2304)
(AD-A284561; RL-TR-93-221) Avail: CASI HC A03/MF A01

A concise and numerically efficient method for the wide band or transient characterization of three-dimensional antennas or scatterers is presented. Assuming a situation where a frequency domain method of moment code already exists for the particular structure of interest, we extend the code to accept complex frequencies and use it to compute the natural resonances and modes. The desired wide-band spectrum is then expanded in terms of these modes, and the unknown expansion coefficients (the crux in any application of the singularity expansion method) are determined by a least mean square match to a known reference case, also obtained with the existing code. The computational issues involved in using this approach are discussed. As an example, an analytic approximation for the radar cross section of a microstrip patch valid over the 1-18 Ghz range is derived, which uses only 15 natural modes. DTIC

N95-18136 Army Research Lab., Aberdeen Proving Ground, MD.
MULTIPATH-INDUCED, LOW-ANGLE TRACKING ERROR AT 140 GHz Final Report, 3-19 Sep. 1991
Suzanne R. Stratton, Donald G. Bauerle, and H. B. Wallace Jul. 1994 78 p Limited Reproducibility: More than 20% of this document may be affected by microfiche quality
(DA Proj. 1L1-61102-AH-43)
(AD-A283630; ARL-MR-140) Avail: Issuing Activity (Defense Technical Information Center (DTIC))

This report describes a measurement program to characterize multipath-induced errors which can affect missile guidance. Measurements of angular position errors were made using a 140-GHz amplitude monopulse radar and a vertical probe. Data was collected at ranges out to 4.8 km. The longest ranges give propagation geometries that are typical for a missile trajectory in close proximity to the earth. Angular positioning errors due to diffuse multipath, specular multipath, and atmospheric-induced noise were measured. DTIC

N95-18139 Naval Postgraduate School, Monterey, CA.
PERFORMANCE EVALUATION OF GROUND BASED RADAR SYSTEMS M.S. Thesis
Stanley E. Grant Jun. 1994 121 p Limited Reproducibility: More than 20% of this document may be affected by microfiche quality
(AD-A283654) Avail: CASI HC A06

Ground based radar systems are a critical resource to the command, control, and communications system. This thesis provides the tools and methods to better understand the actual performance of an operational ground based radar system. This thesis defines two measurable performance standards: (1) the baseline performance, which is based on the sensor's internal characteristics, and (2) the theoretical performance, which considers not only the sensor's internal characteristics, but also the effects of the surrounding terrain and atmosphere on the sensor's performance. The baseline radar system performance, often used by operators, contractors, and radar modeling software to determine the expected system performance, is a simplistic and unrealistic means to predict actual radar system performance. The theoretical radar system performance is more complex; but, the results are much more indicative of the actual performance of an operational radar system. The AN/UPS-1 at the Naval Postgraduate School was used as the system under test to illustrate the baseline and theoretical radar system performance. The terrain effects are shown by performing a multipath study and producing coverage diagrams. The key variables used to construct the multipath study and coverage diagrams are discussed in detail. The atmospheric effects are illustrated by using the Integrated Refractive Effects Prediction System (IREPS) and the Engineer's Refractive Effects Prediction System (EREPS) software tools to produce propagations conditions summaries and coverage displays. DTIC

N95-18187*# National Aeronautics and Space Administration. Langley Research Center, Hampton, VA.
FINITE ELEMENT METHOD FOR EIGENVALUE PROBLEMS IN ELECTROMAGNETICS
C. J. Reddy, Manohar D. Deshpande (Vigyan Research Associates, Inc., Hampton, VA.), C. R. Cockrell, and Fred B. Beck Dec. 1994 37 p
(RTOP 505-64-52-04)
(NASA-TP-3485; L-17392; NAS 1.60:3485) Avail: CASI HC A03/MF A01

Finite element method (FEM) has been a very powerful tool to solve many complex problems in electromagnetics. The goal of the current research at the Langley Research Center is to develop a combined FEM/method of moments approach to three-dimensional scattering/radiation problem for objects with arbitrary shape and filled with complex materials. As a first step toward that goal, an exercise is taken to establish the power of FEM, through closed boundary problems. This paper demonstrates the developed of FEM tools for two- and three-dimensional eigenvalue problems in electromagnetics. In section 2, both the scalar and vector finite elements have been used for various waveguide problems to demonstrate the flexibility of FEM. In section 3, vector finite element method has been extended to three-dimensional eigenvalue problems. Author

N95-18314 Department of the Navy, Washington, DC.
MODULAR SIGNAL PROCESSING UNIT Patent
Alan J. Davis, inventor (to Navy) and Walter T. Schneider, inventor (to Navy) 1 Mar. 1994 6 p Filed 23 Apr. 1991
(AD-D016258; US-Patent-5,291,611; US-Patent-Appl-SN-693106; US-Patent-Class-395-800) Avail: US Patent and Trademark Office

A modular signal processing unit capable of being connected in series, parallel or combinations thereof, is provided. Each modular unit is a parallel signal processor that receives input data on a plurality of parallel-signal input lines and sends processed data on the same number of parallel-signal output lines. Each modular signal processing unit has an input gate array for distributing the input data, a plurality of current state-of-the-art single chip, digital signal processors (DSP) to process the distributed data, and an output gate array to organize the processed data onto the parallel-signal output lines. The modular signal processing unit is easily upgraded by replacing the single chip DSP's as such technology improves. DTIC

N95-18315 Department of the Navy, Washington, DC.
SIGNAL PROCESSOR HAVING MULTIPLE DISTRIBUTED DATA BUFFERS Patent
Victor A. Andersen, inventor (to Navy) 1 Mar. 1994 33 p Filed 7 May 1993
(AD-D016259; US-Patent-5,291,459; US-Patent-Appl-SN-059770; US-Patent-Class-367-134) Avail: US Patent and Trademark Office

A hydrophone analog signal data acquisition, A/D conversion and data transmission system includes a first-stage signal processing subsystem which provides digital representations of the hydrophone analog signal, which in turn are signal processed for transmission in the form of data packets by a second stage signal processing subsystem. Subsystem 40 includes a plurality of Data Multiplexer/FIFO units, including corresponding selectively acting data unit accumulators, each accumulator having a plurality of inputs coupled to output channels of the first-stage signal processing subsystem for receiving digital representations of hydrophone analog signals. Each data unit accumulator includes a first buffer for storing information that includes a digital representation of the analog hydrophone signal, an

identification of a hydrophone that generated the acoustic information, and a time that the acoustic information is received from the hydrophone.
DTIC

N95-18331# Instituto de Fisica Teorica, Sao Paulo (Brazil).
THE GREEN'S FUNCTION IN THE BLOCH-NORDSIECK MODEL FOR QED3
B. M. Pimentel and J. L. Tomazelli Jan. 1994 8 p
(DE94-626680; IFT-P-004/94) Avail: CASI HC A02/MF A01 (US Sales Only)

The electron Green's function is obtained in the Bloch-Nordsieck approximation of three-dimensional QED. Dimensional regularization is used in the intermediate stages of calculation. DOE

N95-18341# Naval Command, Control and Ocean Surveillance Center, San Diego, CA. RDT and E Div.
HIGH-FREQUENCY SKYWAVE SIGNAL POWER MEASUREMENT SYSTEM Preliminary Report, Oct. 1993 - Jul. 1994
Richard Sprague and William Moison Jul. 1994 29 p
(AD-A284382; NRAD-TD-2664) Avail: CASI HC A03/MF A01

The objective of this study was to verify high-frequency (HF) models for prediction of signal strength, signal-to-noise ratio, and circuit reliability. We derived a model of the short-term variability of signal strength. We established a transmission path for making high time resolution measurements of received power and transmission loss and used collected data to verify current models and develop new models. A transmission circuit was established between Forsyth, Montana, and Imperial Beach, California. Transmitting and receiving systems were designed and built. Software was developed for computer control of both transmitting and receiving systems. Measurements of received power at three selected frequencies in the HF band was begun in late December 1993. DTIC

N95-18359# Naval Postgraduate School, Monterey, CA.
US NAVY SHF SATCOM: PAST, PRESENT AND FUTURE M.S. Thesis
Christopher J. Bushnell Jun. 1994 156 p
(AD-A283704) Avail: CASI HC A08/MF A02

This thesis discusses the Navy's Super High Frequency Satellite Communications (SHF SATCOM) capabilities prior to Desert Shield/Desert Storm, and the requirements for future systems that were generated due to Navy SATCOM shortcomings during the Gulf War. The four-phased evolutionary approach the Navy has designed (based on post-war requirements) to provide itself with a medium for SHF SATCOM into the 21st Century, as well as the Defense Satellite Communications Systems (DSCS), are examined in detail. Decreasing defense budgets have begun to have a significant impact on future military satellite communication (MILSATCOM) systems. A cost comparison between utilization of DSCS III satellites and the INMARSAT commercial SATCOM system is presented. Recommended improvements to current MILSATCOM procedures and training practices are proposed that could improve operational C4I capabilities. Finally, this study determines that future SATCOM architectures should include a mixture of commercial systems and MILSATCOM systems to provide both cost savings and command and control protection. DTIC

N95-18367# Joint Inst. for Nuclear Research, Dubna (USSR). Lab. of Theoretical Physics.
He-4 ELECTROMAGNETIC STRUCTURE IN UNITARY AND ANALYTIC VMD MODEL WITH STRICT OZI RULE
P. Strizenec (Slovak Academy of Sciences, Bratislava, Czechoslovakia.) 1993 6 p Submitted for publication
(DE94-626716; JINR-E-2-93-432) Avail: CASI HC A02/MF A01 (US Sales Only)

We present the results of a new analysis of He-4 electromagnetic form factor data, based on the unitary and analytic VMD model with the OZI rule to be taken strictly into account. DOE

N95-18386 Georgia Inst. of Tech., Atlanta, GA. Computer Engineering Research Lab.
GUIDANCE, NAVIGATION AND CONTROL DIGITAL EMULATION TECHNOLOGY LABORATORY Annual Report, 28 Sep. 1993 - 27 Sep. 1994
Cecil O. Alford, J. I. Chamdani, T. C. Huang, T. Kubota, and F. Ghannadian 12 Sep. 1994 19 p Limited Reproducibility: More than 20% of this document may be affected by microfiche quality
(Contract DASG60-89-C-0142)
(AD-A284339) Avail: Issuing Activity (Defense Technical Information Center (DTIC))

The contract began with seven tasks: (1) Digital Emulation Facility; (2) FPA Seeker Emulator Development; (3) Special Studies; (4) Software Development; (5) Automated Input; (6) PFP Technology; and (7) GN and C Processor Development. These tasks were developed through the first two years of the contract when virtually all funding was removed. Two additional tasks have been developed since the funding cut. The first was a speed test on the rad-hard FPU chip developed by Harris. A summary of this testing and the associated report is given in Section 2. The second task is the development of an FPA Test System. DTIC

N95-18411 Missouri Univ., Columbia, MO. Dept. of Physics and Astronomy.
WAVELETS AND SCATTERING Final Report, 1 Jun. 1990 - 31 May 1994
Grant V. Welland and Brian DeFacio 29 Jul. 1994 17 p Limited Reproducibility: More than 20% of this document may be affected by microfiche quality
(Grant AF-AFOSR-0307-90)
(AD-A284131; AFOSR-94-0476TR) Avail: Issuing Activity (Defense Technical Information Center (DTIC))

During this project wavelets were used to analyze several problems in signal processing, quantum optics, elastic wave nondestructive evaluation, electromagnetic scattering and the dielectric response of water. A number of research papers were published including the first calculation of p-wavelets. Another publication shows the scale change of wavelet theory corresponds to the squeezing operation in quantum optics. A wavelet approach to visual recognition of faces was completed and has been submitted for publication. The Calderon-Grossmann-Morlet reproducing formula was shown to hold for the two-sided ideal of Hilbert-Schmidt operators. In elastic wave NDE, the frequency scales in phase space for the front face echo were shown to require a very different compression from the other scales. New results on Maxwell's equations in regions with Lipschitz boundaries were published. DTIC

N95-18429 Department of the Navy, Washington, DC.
RADAR SECTOR BLANKER Patent
Roger B. Hall, inventor (to Navy) 15 Mar. 1994 7 p Filed 7 Jun. 1993
(AD-D016275; US-Patent-5,294,936; US-Patent-Appl-SN-074100; US-Patent-Class-342-175) Avail: US Patent and Trademark Office

A radar sector blanker comprises in analog-to-digital converter and a sector controller unit. The analog-to-digital converter receives the analog synchro voltages describing the positioning of a radar antenna and changes these voltages into binary-coded decimal (BCD) information. The sector controller unit comprises a portable housing, a controller system, and a power supply. The controller system includes an OFF comparator circuit, an ON comparator circuit, an S-R latch, and a solid-state switch. Each comparator circuit comprises three cascaded transistor-transistor logic (TTL) integrated chips. The power supply gives a direct-current voltage to the solid-state switch and the TTL chips. The sector blanker blocks transmission for a predetermined rotational region or sector of a radar system. DTIC

N95-18436 Federal Aviation Administration, Cambridge, MA. National Transportation Systems Center.
AN ANALYSIS OF TOWER (LOCAL) CONTROLLER-PILOT VOICE COMMUNICATIONS Final Report
Kim M. Cardosi Jun. 1994 28 p Limited Reproducibility: More than 20% of this document may be affected by microfiche quality
(AD-A283718; DOT-VNTSC-FAA-94-11; DOT/FAA/RD-94/15) Avail: Issuing Activity (Defense Technical Information Center (DTIC))

The purpose was to examine current pilot-controller communication practices in the terminal environment. Forty-nine hours of voice tapes from local positions in ten air traffic control towers (ATCTs) were examined. There were 8444 controller-to-pilot messages (e.g., clearances to takeoff or land, instructions to hold short or change radio frequencies, etc.) examined. The complexity of the controller's message (i.e., the number of pieces of information) was examined and the number of erroneous readbacks and pilot requests for repeats were analyzed as a function of message

complexity. Pilot acknowledgements were also analyzed; the numbers of full and partial readbacks and acknowledgements only (i.e., 'roger') were tallied. Fewer than one percent of the messages resulted in communications errors. Among the error factors examined were: complexity of the message, type of acknowledgement, use of call sign in the acknowledgement, type of information in error, and whether or not the controller responded to the readback error. Instances in which the controller contacted the aircraft with one call sign and the pilot acknowledged the transmission with another call sign were also examined. The report concludes with recommendations to further reduce the probability of communication errors. DTIC

N95-18462# Department of the Navy, Washington, DC.
COMMUNICATION WITH REENTRY VEHICLE THROUGH MODULATED PLASMA Patent Application
Philip W. Hesse, inventor (to Navy), Han S. Uhm, inventor (to Navy), and Joon Choe, inventor (to Navy) 23 May 1994 12 p
(AD-D016476; US-Patent-Appl-SN-247827; Navy-Case-75471) Avail: CASI HC A02/MF A01

Signal antennae are mounted on the casing wall between forward nose and rear tail ends of an aerospace launched vehicle for radio communication through a conducting sheath of plasma formed thereon by atmospheric ionization during descent of the vehicle along a non-gliding reentry path. The reentry path is maintained by vehicle guidance at a steep angle in response to data transmitted to the antennae through the plasma of the conducting sheath which is thereby maintained in complete surrounding relation to the vehicle and modulated to enhance data transmission during the entire duration of vehicle descent. DTIC

N95-18475# Naval Undersea Warfare Center, New London, CT.
DETECTION PERFORMANCE OF GENERALIZED LIKELIHOOD RATIO PROCESSORS FOR RANDOM SIGNALS OF UNKNOWN LOCATION, STRUCTURE, EXTENT, AND STRENGTH Progress Report
Albert H. Nuttall Aug. 1994 163 p
(Contract PE0601152)
(AD-A285589; NUWC-NPT-TR-10739) Avail: CASI HC A08/MF A01

A signal (if present) is located somewhere in a band of frequencies characterized by a total of N search bins. The signal occupies an arbitrary set of M of these bins, where not only is M unknown, but also, the locations of the particular M occupied bins are unknown. Also, the signal strength is unknown. The generalized likelihood ratio (GLR) method furnishes an approach for estimating all the unknown parameters and for testing for presence or absence of the signal in an observation of the outputs of the N search bins. However, there is nothing guaranteed optimum about the GLR approach. Also, the optimum (likelihood ratio) processor cannot be constructed or realized, due to all the unknowns and the voluminous amount of searching required for this scenario. These deleterious conditions force adoption of some suboptimum processing techniques, guided by the GLR and likelihood ratio results. DTIC

N95-18481# Naval Postgraduate School, Monterey, CA.
THE FUTURE USE OF DSCS AND COMMERCIAL SATELLITES IN THE US NAVY M.S. Thesis
Robert J. Zoppa Sep. 1994 109 p
(AD-A285707) Avail: CASI HC A06/MF A01

This thesis considers the Navy's use of the Defense Satellite Communications System (DSCS), International Maritime Satellite (INMARSAT) network, and the International Telecommunications Satellite (INTELSAT) system with emphasis on the future utilization of C, X, and Ku-band Super High Frequency (SHF) communications in the Navy's satellite communications (SATCOM) architecture. It evaluates all three systems addressing critical issues such as anti-jamming capability, survivability, timeliness, availability, interoperability, and capacity. All three satellite systems currently have a place in the Navy's SATCOM architecture. This thesis focuses on the advantages and disadvantages that the DSCS satellite network offers the Navy and recommends using DSCS for low capacity protected circuits and high capacity unprotected service in the future. Additionally, a recommendation is made for a future high capacity DSCS follow-on satellite. This thesis also addresses the advantages and disadvantages that INMARSAT and INTELSAT offer the Navy and recommends that these systems be used as surge communication mediums in the future. DTIC

N95-18494 British Broadcasting Corp., Tadworth (England). Research Dept.
THE DEVELOPMENT OF THE SWITCHED-HORN RADIO-CAMERA SYSTEM
R. H. Evans, C. E. Melvin, and J. T. Zubrzycki 1993 16 p Original contains color illustrations
(BBC-RD-1993/13) Copyright Avail: Issuing Activity (BBC, Kingswood Warren, Tadworth, Surrey, England)

Radio-cameras are now well established at outside broadcast events (OB's) but conventional circularly polarized antennas and electromechanical tracking systems still leave considerable room for improvement. A new radio-camera system is described which uses a cluster of six directional transmitting antennas, with each antenna pointing in a different direction. Test signals inserted into the video during the field blanking interval are transmitted through each antenna in turn, and are then analyzed at the receiving base station to determine which horn is transmitting the best signal. The result of this analysis is used to select the best horn for the following frame of video, and the result is updated 25 times each second. Both the level of the received signal strength and the degree of multipath distortion are analyzed to determine the best horn. This report describes the development of a prototype switched-horn system and also describes two field trials, one of which took place during a live program transmission. The results of the trials showed that the switched-horn system suffers from far less multipath distortion than conventional omnidirectional circularly-polarized antennas, and does not have any of the drawbacks of electromechanical systems. Author

N95-18506 Naval Air Warfare Center, Patuxent River, MD. Aircraft Div.
HIGH FREQUENCY DIRECT DRIVE GENERATION USING WHITE NOISE SOURCES
S. Frazier, K. Sebacher, D. Lawry (Phillips Lab., Kirtland AFB, NM.), W. Prather (Phillips Lab., Kirtland AFB, NM.), and G. Hoffer (Kaman Sciences Corp., Santa Monica, CA.) 1994 15 p Limited Reproducibility: More than 20% of this document may be affected by microfiche quality
(AD-A284158) Avail: Issuing Activity (Defense Technical Information Center (DTIC))

Damped sinusoid direct drive injection on interconnecting cable bundles between subsystems has long been used as a technique for determining susceptibility to electromagnetic transients in military weapon systems. Questions arise, however, about the adequacy of this method of individually injected, single sinusoids in assuring subsystem strength against broad band threats. This issue has recently been raised in the latest revision of MIL-STD-461 that requires subsystems exhibit no malfunctions when subjected to a repetitive square wave pulse with fast rise and fall time (CS115). An extension to this approach would be to test subsystems using arbitrary waveforms. In recent years arbitrary waveform generators (AWG's) have been used to duplicate, with a high degree of fidelity, the waveforms measured on cable bundles in a system illuminated by fields in a system-level EMP simulator. However, the operating speeds of present AWG's do not allow the extension of this approach to meet new threats such as MIL-STD-2169A. A novel alternative approach for generation of the required signals, being developed in a cooperative effort between the Naval Air Warfare Center and Phillips Laboratory, is the use of white noise signals conditioned in such a manner to produce the desired direct drive waveforms. DTIC

N95-18516 Department of the Navy, Washington, DC.
COMBINER FOR TWO DIMENSIONAL ADAPTIVE INTERFERENCE SUPPRESSION SYSTEM Patent
Thomas W. Schlosser, inventor (to Navy) 22 Feb. 1994 14 p Filed 25 Jun. 1992
(AD-D016272; US-Patent-5,289,194; US-Patent-Appl-SN-904109; US-Patent-Class-342-378) Avail: US Patent and Trademark Office

A multisignal combiner is provided for weighting the best performing signal of an amplitude transform signal and a phase difference transform signal produced by a processor which receives a two dimensional signal and has intermediate signals which are a variance of the amplitude and a variance of the phase difference of the received signal. A device is provided for receiving the variance of the amplitude and the variance of the phase difference for producing a pair of weighting factors, each of which is inversely proportional to the size of the variances of the respective values,

and a third weighting factor which is 1 - the weighting factor of the signal which has the smallest variance. DTIC

N95-18520 Army Research Lab., Adelphi, MD.
RADIATION-INDUCED NOISE IN UMPC-TYPE CURRENT PROBES: IEMP RESPONSE OF THE CURRUENT MEASUREMENT SYSTEM Final Report, Jun. 1992 - Aug. 1993
James C. Blackburn Aug. 1994 43 p Limited Reproducibility: More than 20% of this document may be affected by microfiche quality
(AD-A284176; ARL-TR-366) Avail: Issuing Activity (Defense Technical Information Center (DTIC))

The purpose of these tests was to determine the radiation-induced noise response of the probes in fluences up to the maximum obtainable from our high-intensity flash x ray (HIFX), somewhat above 2 x 10 to the 11th power rads(Si)/s. This noise level determines the signal-to-noise ratio that can be obtained in low level current measurements in the pulsed radiation environment, such as input photocurrents to silicon-on-sapphire devices. The UMPC probes themselves are a significant issue because they are at present the most satisfactory way of measuring currents in pulsed radiation; in spite of their limitations a better means is not available. Not only is the internal electromagnetic pulse (IEMP) response of the probe itself presented, but also that of unavoidably related structures is addressed, such as the circuit conductors connecting to the probes. It is found that these connections typically are the limiting factor in determining the measurement system noise level. The lowest noise level attained, about 2.5 mA at 3 x 10 to the 11th power, was with a two-core transformer. DTIC

N95-18522 Naval Postgraduate School, Monterey, CA.
A TRIANGULATION METHOD FOR PASSIVE RANGING M.S. Thesis
Gerasimos Pelegris Jun. 1994 118 p Limited Reproducibility: More than 20% of this document may be affected by microfiche quality
(AD-A284180) Avail: Issuing Activity (Defense Technical Information Center (DTIC))

A method for passive ranging based on the principle of triangulation is considered. In the basic triangulation scheme that is a single baseline model the precision in the bearing readings can be related to the precision in the range estimation. For some target orientations the precision in the triangulated target is completely lost. This phenomenon is known as geometric dilution. A proposed orthogonal dual baseline scheme eliminates the geometric dilution effect. The performance of each of the two orthogonal baselines depends on the orientation. For specific target orientations the triangulation range measurements for the two baselines are equivalent. The dual baseline scheme would require smart electronics which would switch between baselines at crossover points in the range estimation precision. It is shown that the crossover points depend primarily on the ratio of the two baselines. A general expression for the maximum triangulation range consistent with limitations in minimum tolerance precision in range estimation is derived. The dependency between maximum range and target orientation are presented in polar form. Limitations in the dual baseline model due to physical limitation created by the optical horizon are also considered. DTIC

N95-18534 British Broadcasting Corp., Tadworth (England). Research and Development Dept.
FURTHER MEASUREMENTS OF THE SOUND INSULATIONS OF METAL-FRAMED PARTITIONS
G. D. Plumb 1994 11 p
(BBC-RD-1994/7) Copyright Avail: Issuing Activity (BBC, Kingswood Warren, Tadworth, Surrey, England)

The sound insulations were measured of a number of single and double leaf metal-framed partitions. The purpose of the work was to develop alternative designs for partitions to that of the Camden. The Camden contains fiberboard as one of its constituent elements. The new partitions used plasterboard as the sole board material. Therefore, the new partitions were heavier than the comparable metal-framed partitions. The levels of sound insulation achieved from the new partitions were generally slightly higher than those of comparable metal-framed Camdens. However, the greater masses of the new partitions may rule out their use in certain circumstances because of the loadbearing requirements of the surrounding building. The installation of glass wool insulation batts in the cavities of the new partitions resulted in large increases in the measured sound insulations. The glass wool damps the motion of the boards and absorbs sound that has been transmitted into the cavities. Author

N95-18535 British Broadcasting Corp., Tadworth (England). Research and Development Dept.
MULTI-CHANNEL SOUND FOR HDTV: SUBJECTIVE TESTS ON SOUND CHANNEL CONFIGURATION
J. A. Fletcher 1994 23 p
(BBC-RD-1994/4) Copyright Avail: Issuing Activity (BBC, Kingswood Warren, Tadworth, Surrey, England)

This Report describes subjective tests carried out as part of the Eureka 95 project to compare different multi-channel sound systems being considered for use with HDTV. In the tests, the number of sound channels varied from one (mono) to five (three front channels and two surround channels). The improvement in quality obtained by increasing the number of front channels from two to three (adding a center-front channel) was often similar to that obtained by increasing the number of front channels from one to two. Two-channel stereo was in one case found inferior to mono, presumably because of mislocation of central sound images for off-center listeners, but three-channel stereo was always preferred to two-channel stereo (and to mono). The improvement obtained by adding one or two surround channels was about half that obtained by adding a center-front channel. On most program items the use of two surround channels, rather than one, gave a small improvement but only on one program item was this significant. Author

N95-18536 British Broadcasting Corp., Tadworth (England). Research and Development Dept.
IMPLEMENTATION OF AMPLITUDE MODULATION COMPANDING USING A DIGITAL SIGNAL PROCESSOR
C. R. Nokes 1994 11 p
(BBC-RD-1994/1) Copyright Avail: Issuing Activity (BBC, Kingswood Warren, Tadworth, Surrey, England)

BBC Amplitude Modulation (AM) radio transmissions have for some time been using amplitude modulation companding (AMC) - a method of companding whose purpose is to reduce the costs of transmission while maintaining, as far as possible, the audibility of the radio service. AMC is one form of compression of AM transmissions more generally called dynamic carrier control (DCC). The BBC has undertaken a feasibility study to examine the possibility of implementing DCC by means of a Digital Signal Processor (DSP). The study has shown that a DSP implementation of DCC would be entirely feasible, providing a stable and reliable means of realizing the compression algorithms and the potential for greater sophistication in control. Author

N95-18537 British Broadcasting Corp., Tadworth (England). Research Dept.
RACE PROJECT 1036: WTDM BROADBAND CUSTOMER PREMISES NETWORK Final Report, 1988 - 1993
A. Oliphant and C. D. Mathers et al 18 Feb. 1993 28 p Original contains color illustrations
(BBC-RD-1993/15) Copyright Avail: Issuing Activity (BBC, Kingswood Warren, Tadworth, Surrey, England)

Discussions in 1985 with BBC Television showed that signal routing in broadcasting centers presented two problems which would become more severe in the future: first, the increasing requirement for all sources to be available at all destinations, and second, the impending proliferation of signal standards (e.g. digital component signals, HDTV). The solution proposed by Research Department was the use of both wavelength and time division multiplexing (WTDM) over an optical fiber network; this inherently distributes all signals to all destinations, and with suitable terminal equipment can carry any signal format. To develop the required optical and electronic technology, a consortium of European firms was set up; at just this time, the EC launched its RACE initiative; after some negotiation, the work was accepted as Project R2001, and carried out with EC support. Author

N95-18538 British Broadcasting Corp., Tadworth (England). Research Dept.
RINSE: A DIGITALLY IMPLEMENTED FLYWHEEL SYNC REGENERATOR FOR IMPROVED VIDEO SYNCHRONISER PERFORMANCE
Richard H. Evans 1993 15 p Original contains color illustrations
(BBC-RD-1993/14) Copyright Avail: Issuing Activity (BBC, Kingswood Warren, Tadworth, Surrey, England)

Microwave links are widely used at live outside broadcast events for carrying video signals from mobile cameras such as those carried on the shoulder or fitted to vehicles. A digital frame store synchronizer is required when using a remote radio-camera and this has caused additional problems with variable quality signals. During moments of weak signal strength when threshold noise appears in the picture, a video synchronizer may lose synchronization and produce an unnatural freeze-frame effect. A new device called RINSE (Regeneration and Insertion of New Sync Equipment) is described which replaces the old variable quality syncs with 'flywheel' regenerated syncs. When connected between the microwave receiver and the synchronizer, it cleans up the syncs and allows the synchronizer to pass the video without the freeze frame artifacts which would further degrade the picture. By operating the synchronizer with an external sync input from RINSE it will carry any video signal transparently for a short time irrespective of the noise level. Author

N95-18540 British Broadcasting Corp., Tadworth (England). Research Dept.
PREDICTED COVERAGE OF A COFDM SINGLE FREQUENCY NETWORK FOR UHF DIGITAL TERRESTRIAL TV BROADCASTING
M. B. R. Lee 1993 18 p Original contains color illustrations
(BBC-RD-1993/12) Copyright Avail: Issuing Activity (BBC, Kingswood Warren, Tadworth, Surrey, England)

The Coded Orthogonal Frequency Division Multiplex (COFDM) transmission system provides a very high degree of tolerance towards multipath interference. Three factors contribute towards this tolerance: the inclusion of a guard interval, coding to provide error correction and the division of the digital data amongst a very large number of low bit rate carriers. It follows from this that a national network of co-channel transmitters can be developed such that not only do neighboring transmitters not cause mutual interference but can combine in a constructive manner. This is the principle of the Single Frequency Network, or SFN. Experience with Digital Audio Broadcasting (DAB) suggests that an SFN could be utilized for Digital Video Broadcasting (DVB). Such a system would make very efficient use of the available UHF channels. The Report presents the results of coverage predictions performed for a network of 128 transmitters sited at the locations of existing high and medium power UK UHF broadcast transmitters. Predictions were carried out for a range of values of guard interval, and for both directional and omnidirectional receiving antennas. Use of COFDM and the latest data compression techniques allows a High Definition Television (HDTV) program to be transmitted in a standard UHF channel. However it will require a higher-order modulation scheme than is used for DAB. This will reduce the tolerance towards noise and interference. The guard interval may therefore have to be lengthened so that signals from more distant transmitters within the network arrive within the guard interval. The results of the predictions show that the ad hoc transmitter network examined will serve 90 percent or more of the UK population, using the same guard interval as has been chosen for Mode 1 of the Eureka DAB system, provided that a directional antenna is used. The directional antenna provides most of the extra protection required against interfering signals. The same coverage can be obtained using an omnidirectional antenna if the guard interval is doubled. Alternatively, the data could be coded in such a way that a standard definition picture is produced if the level of interference is too high for HDTV. Author

N95-18545 Department of the Navy, Washington, DC.
MULTI-CHANNEL, COVERT, NON-LINE-OF-SIGHT UV COMMUNICATION Patent
Myer Geller, inventor (to Navy) 5 Apr. 1994 8 p Filed 8 Mar. 1988
(AD-D016269; US-Patent-5,301,051; US-Patent-Appl-SN-165207) Avail: US Patent and Trademark Office

A system enables omnidirectional non-line-of-sight simultaneous communications in a number of frequency separated channels in the ultraviolet spectrum. A plurality of discharge lamps each has at least a single different isotope of mercury for each omnidirectionally radiating a discrete line in the ultraviolet spectrum. Each of the discrete lines in the ultraviolet spectrum is modulated by an on-off sequence generator so that modulated discrete lines transmit communications to a number of receivers randomly disposed in a non-line-of-sight relationship to the discharge lamps. Absorption filters at each receiver contain a quenching gas and all the other isotopes of mercury except the one which generated the modulated discrete line of interest. DTIC

N95-18558 Oak Ridge National Lab., TN.
COMPARISON OF THE FOLDED STRIPLINE AND STACKED STRIPLINE CONCEPTS TO THE FOLDED WAVEGUIDE LAUNCHER
W. L. Gardner, J. B. O. Caughman, D. J. Hoffman, and P. H. Probert (Wisconsin Univ., Madison, WI.) 1993 5 p Presented at the 10th Topical Conference on Radio Frequency Power in Plasmas, Boston, MA, 1-3 Apr. 1993 Limited Reproducibility: More than 20% of this document may be affected by microfiche quality
(Contract DE-AC05-84OR-21400)
(DE94-018951; CONF-9304112-27) Avail: CASI HC A01

Two new concepts are being developed as possible upgrades to the folded waveguide launcher. The folded stripline is a folded waveguide with an additional conductor positioned inside. The term stripline refers to the resemblance of the design to microwave microstrip line. The conductor provides support for TEM mode propagation, which eliminates cutoff and the nonlinear frequency dependence of the waveguide impedance and phase velocity. A natural extension to the folded stripline is the stacked stripline, which comprises several stacked, independent TEM waveguides. Initial measurements indicate that both concepts have better magnetic flux coupling than the folded waveguide. DOE

N95-18561 Department of the Navy, Washington, DC.
METHOD AND SYSTEM FOR INFERRING THE RADIO REFRACTIVE INDEX STRUCTURE OF THE ATMOSPHERE FROM RADIO MEASUREMENTS Patent
Herbert V. Hitney, inventor (to Navy) 5 Jul. 1994 6 p Filed 24 Sep. 1992
(AD-D016436; US-Patent-5,327,359; US-Patent-Appl-SN-950569;
US-Patent-Class-364-550) Avail: US Patent and Trademark Office

A system and method are provided for determining in real time, the radio refractive index structure of the atmosphere. The method may be characterized as comprising the steps of transmitting a radio frequency signal over a predetermined path; receiving the radio frequency signal; detecting the strength of the radio frequency signal; determining a radio propagation factor from the strength of the radio frequency signal; determining a base height function of the atmosphere; and employing the radio propagation factor in the base height function to determine a trapping layer base height of the atmosphere which represents the radio refractive index structure of the atmosphere. DTIC

N95-18619# Naval Undersea Warfare Center, New London, CT.
IONCAP PREDICTION-BASED AUTOMATIC LINK ESTABLISHMENT (ALE) FREQUENCY SELECTION FOR A TEN-NODE AUSTRALIAN HIGH-FREQUENCY NETWORK Final Report
J. R. Katan and R. I. Desourdis 11 Jul. 1994 260 p
(AD-A283698) Avail: CASI HC A12/MF A03

This report presents the results of a high-frequency (HF) propagation analysis performed to a ten-node Australian HF network using the IONCAP computer program. This analysis was performed for months in different seasons and sunspot numbers. The ten-node network locations are listed in table 1 and are plotted on the map in figure 1. The objective of this effort was to establish a preliminary approach for automatic link establishment (ALE) frequency-set selection. A tacit objective of this analysis was to determine the fewest number of frequencies that would provide the greatest network connectivity. This analysis is based only on predicted propagation connectivity with no consideration of link and network communication protocols or operation. In addition, it was assumed that a single frequency set would be employed over a 24-hour period in a single month. DTIC

N95-18657 Army Topographic Engineering Center, Fort Belvoir, VA.
INTERFEROMETRIC SYNTHETIC APERTURE RADAR AND THE DATA COLLECTION SYSTEM DIGITAL TERRAIN ELEVATION DEMONSTRATION

Robert Heidelbach, R. Bolus, and J. Chadwick 1 Aug. 1994 9 p Limited Reproducibility: More than 20% of this document may be affected by microfiche quality
(AD-A284024; USATEC-R-237) Avail: Issuing Activity (Defense Technical Information Center (DTIC))

Digital Terrain Elevations (DTE) that can be rapidly generated, and that have better fidelity and accuracy than Digital Terrain Elevation Data (DTED) Levels 1 or 2, would be extremely beneficial to Department of Defense (DOD) military operations, civil works programs, and various commercial applications. As a result, the Advanced Research Projects Agency (ARPA), along with the U.S. Army Topographic Engineering Center (TEC), are developing an Interferometric Synthetic Aperture Radar (IFSAR) elevation mapping capability. This system, the Interferometric Synthetic Aperture Radar for Digital Radar Elevations (IFSARE), is capable of collecting and providing data in all weather (reasonable), in day or night scenarios, and where obscurants are present. The IFSARE, which is currently undergoing Integration and Test, will allow for rapid on-line automatic processing of the collected digital radar data into DTE and high quality imagery. The prime contractor is the Environmental Research Institute of Michigan (ERIM). This paper addresses the proof of concept for civil works applications by analyzing a data set taken by the Wright Labs/ERIM Data Collection System (DCS). The objective was to demonstrate the capability of an IFSAR system to provide high fidelity, fine resolution DTE that can be employed in hydraulic models of the Mississippi River watershed. The demonstration was sponsored by ARPA and TEC. DTIC

N95-18671 Naval Postgraduate School, Monterey, CA.
COMPUTER SIMULATION OF WAVE PROPAGATION THROUGH TURBULENT MEDIA Ph.D. Thesis
Charles A. Davis Jun. 1994 185 p Limited Reproducibility: More than 20% of this document may be affected by microfiche quality
(AD-A283695) Avail: Issuing Activity (Defense Technical Information Center (DTIC))

This research used Huygens-Fresnel wave optics computer simulations to investigate the effects of high turbulence strength and inner scale on the normalized irradiance variance and coherence length of electromagnetic waves propagating through a turbulent atmosphere. These investigations developed several guidelines for validity of propagation simulations employing a numerical, split-step, Huygens-Fresnel, method, and within these guidelines, considered five types of turbulence spectrum inner scale: (1) zero inner scale; (2) Gaussian inner scale; (3) Hill's; (4) Frehlich's viscous-convective enhancement inner scales; and (5) turbulence spectrum truncation from the discrete grid representation. The simulation results showed that the normalized irradiance variance generally decreased (-30%) below the zero inner scale values in the Rytov regime with increasing inner scale size, but increased monotonically in the saturation regime, and agreed within 2% of the Rytov-Tatarski predictions at low turbulence strengths. The E-field coherence length in a spatially confined beam, with either spherical or plane wave divergence and zero inner scale, followed the Rytov-Tatarski-Fried predictions in the Rytov regime, but departed from the theory in the saturation regime. Increasing inner scale size modified this finite beam behavior by raising the coherence length (up to -50%) in the saturation regime. DTIC

N95-18686 Federal Aviation Administration, Atlantic City, NJ. Technical Center.
THE 23 GIGAHERTZ (GHz) DIGITAL LOW DENSITY RADIO COMMUNICATIONS LINK (LDRCL) OPERATIONAL TEST AND EVALUATION (OT/E) INTEGRATION AND OT/E OPERATION Final Test Report
Michael R. Melilio Aug. 1994 35 p Limited Reproducibility: More than 20% of this document may be affected by microfiche quality
(AD-A283963; DOT/FAA/CT-TN94/27) Avail: Issuing Activity (Defense Technical Information Center (DTIC))

This report contains the results of the Operational Test and Evaluation (OT&E) Integration and OT&E Operational Testing of the Commercial-Off-The-Shelf (COTS) Low Density Radio Communications Link's (LDRCL) 23-gigahertz (GHz) digital radio system. The OT&E testing was accomplished by first testing the LDRCL equipment against its equipment specification (FAA-E-2853A), and then performing OT&E Operational Testing at the key site (Keller, Texas). These tests proved that the 23-GHz LDRCL equipment can fulfill its mission in the National Airspace System (NAS) and that it is suitable and effective. Based on the test results, it is concluded that the 23-GHz LDRCL equipment is qualified for operational deployment. DTIC

N95-18727 Mitre Corp., Bedford, MA.
SYNTHESIS OF NOTCHED ANTENNA PATTERNS FOR WIDE BANDWIDTH PROCESSING
T. P. Guella and R. M. Davis Aug. 1994 24 p Limited Reproducibility: More than 20% of this document may be affected by microfiche quality
(Contract DAAB07-94-C-H601)
(AD-A284004; Mitre-MP-94B000007) Avail: Issuing Activity (Defense Technical Information Center (DTIC))

Antenna patterns can be designed to have broad notches in regions where clutter and jamming are expected to be received. A number of narrowband synthesis techniques exist to design notched antenna patterns, but they break down in the presence of wideband signals on arrays which employ a combination of phase and time steering. The authors derive definitions for wideband antenna patterns and present a new synthesis procedure which can be used to design notched patterns for signals having specified bandwidths on any type of array. DTIC

N95-18733*# National Aeronautics and Space Administration. Lewis Research Center, Cleveland, OH.
EEsoF MICAD AND ACADEMY MACRO FILES FOR COPLANAR WAVEGUIDE AND FINITE GROUND PLAN COPLANAR WAVEGUIDE
George E. Ponchak Jan. 1995 107 p
(RTOP 235-01-08)
(NASA-TM-106800; E-9276; NAS 1.15:106800) Avail: CASI HC A06/MF A02

A collection of macro files is presented which when appended to either the EEsoF MICAD.ELE or EEsoF ACADEMY.ELE file permits the layout of coplanar waveguide and finite ground plane coplanar waveguide circuits. Author

N95-18960* National Aeronautics and Space Administration. Pasadena Office, CA.
DOUBLE-LOOP FREQUENCY SELECTIVE SURFACES FOR MULTI FREQUENCY DIVISION MULTIPLEXING IN A DUAL REFLECTOR ANTENNA Patent
Te-Kao Wu, inventor (to NASA) (Jet Propulsion Lab., California Inst. of Tech., Pasadena, CA.) 13 Dec. 1994 16 p Filed 23 Sep. 1993 Continuation of abandoned US-Patent-Appl-SN-909501, filed 24 Jun. 1992
(NASA-Case-NPO-18701-2-CU; US-Patent-5,373,302;
US-Patent-Appl-SN-126144; US-Patent-Appl-SN-909501;
US-Patent-Class-343-781P; US-Patent-Class-343-781CA;
US-Patent-Class-343-909; Int-Patent-Class-H01Q-19/14) Avail: US Patent and Trademark Office

A multireflector antenna utilizes a frequency-selective surface (FSS) in a subreflector to allow signals in two different RF bands to be selectively reflected back into a main reflector and to allow signals in other RF bands to be transmitted through it to the main reflector for primary focus transmission. A first approach requires only one FSS at the subreflector which may be an array of double-square-loop conductive elements. A second approach uses two FSS's at the subreflector which may be an array of either double-square-loop (DSL) or double-ring (DR). In the case of DR elements, they may be advantageously arranged in a triangular array instead of the rectangular array for the DSL elements.
Official Gazette of the U.S. Patent and Trademark Office

N95-19035 Naval Air Warfare Center, Patuxent River, MD. Aircraft Div.
WAVEFORM BOUNDING AND COMBINATION TECHNIQUES FOR DIRECT DRIVE TESTING
Samuel Frazier, Edward Parimuha, Murali Tummala, and Thomas F. Winnenberg 1994 8 p Limited Reproducibility: More than 20% of this document may be affected by microfiche quality
(AD-A284075) Avail: Issuing Activity (Defense Technical Information Center (DTIC))

This paper presents various methods to combine a set of measured test signals into a composite signal. The composite signal represents the set of measured test signals by retaining the significant attributes of the original set of measured test data. The composite waveforms are generated

to obtain rigorous direct drive waveforms used during aircraft lightning and EMP assessments. Here we propose two techniques and a hybrid method to synthesize the composite waveforms. DTIC

N95-19047 British Broadcasting Corp., Tadworth (England). Research and Development Dept.
DIGITAL VIDEO COMPRESSION: STANDARDISATION OF SCALABLE CODING SCHEMES
P. N. Tudor and N. D. Wells 1994 14 p
(BBC-RD-1994/10) Copyright Avail: Issuing Activity (BBC. Kingswood Warren, Tadworth, Surrey, England)

Scalable coding schemes for bit-rate reduction of digital TV, including HDTV, are being considered in order to provide for compatibility with lower resolution scanning formats and to provide for graceful degradation of the picture quality in the presence of transmission errors. This Report describes some of the scalable coding schemes considered within the Moving Pictures Expert Group (MPEG) of the International Standards Organization (ISO) and discusses the advantages and disadvantages of the different schemes which may be classified as frequency scalable, spatial scalable and SNR scalable. The reasons for selecting particular scalable schemes for inclusion in the MPEG-2 standard are described. Author

N95-19049 British Broadcasting Corp., Tadworth (England). Research and Development Dept.
MAXIMAL-LENGTH SEQUENCE METHODS: ACOUSTIC MEASUREMENTS IN THE PRESENCE OF HIGH LEVELS OF EXTRANEOUS NOISE
R. Walker 1994 17 p
(BBC-RD-1994/5) Copyright Avail: Issuing Activity (BBC, Kingswood Warren, Tadworth, Surrey, England)

The use of the maximal-length sequence method to measure acoustic responses in the presence of high levels of extraneous noise is described. Direct and reliable measurements of time and frequency response functions down to a signal-noise ratio of 0 dB are possible. With modest amounts of signal-averaging, response functions down to S/N ratios of -20 dB can also be measured with errors of the order of 1 dB. Further extension of the averaging process is possible but has not been investigated The results are described with special reference to the measurement of high values of sound insulation. The results of a brief experiment to verify the performance are presented and some examples field measurements using the method are discussed. Author

N95-19050 British Broadcasting Corp., Tadworth (England). Research and Development Dept.
DAB: MULTIPLEX AND SYSTEM SUPPORT FEATURES
J. L. Riley 1994 19 p
(BBC-RD-1994/9) Copyright Avail: Issuing Activity (BBC, Kingswood Warren, Tadworth, Surrey, England)

This Report describes the multiplex and system support features of the Eureka 147/DAB digital audio system. It sets out the requirements of all users along the broadcast chain from service providers and broadcaster through to the listener. The contents of the transmission frame are examined drawing the distinction between the main service multiplex and the provision of control information in a separate fast data channel. The concept of the DAB service structure is introduced and the inherent system flexibility for altering the service arrangement is explained. A wide range of service information features builds on those provided in earlier systems, such as RDS (Radio Data System) and is intended to make it easier for a listener to find any required service and to add a further dimension to audio broadcasting. The choices available to users in all of these areas are examined. Author

N95-19051 British Broadcasting Corp., Tadworth (England). Researh and Development Dept.
MEASUREMENTS OF WIDEBAND MULTIPATH PROPAGATION AT 531 MHz AND 1.265 GHz
C. P. Bell, P. J. Brightwell, N. J. Misson, R. F. Rudd, and W. F. Williams 1994 16 p
(BBC-RD-1994/3) Copyright Avail: Issuing Activity (BBC, Kingswood Warren, Tadworth, Surrey, England)

Multipath propagation measurements and their analyses are described. The work was carried out by the BBC over the period 1988-1990 as a contribution to the Eureka 147 Project, with the aim of providing statistical data required in the configuration of a Digital Audio Broadcast system. Two different areas were chosen for the tests, one considered as representative of a generally built-up area with varying degrees of urbanization, the other on the fringe of a relatively hilly area. In the first area two widely separated frequencies in the UHF band were used to enable estimates to be made of frequency dependence. The results are compared with those of other similar measurement programs in both Europe and the USA available prior to 1991. In general a somewhat lower incidence of long-delay multipath was observed in the BBC results, especially in the case of the hilly area. Author

N95-19052 British Broadcasting Corp., Tadworth (England). Research and Development Dept.
BIT-RATE REDUCTION OF DIGITAL TELEVISION FOR TRANSMISSION: AN INTRODUCTORY REVIEW
N. D. Wells 1994 40 p
(BBC-RD-1994/2) Copyright Avail: Issuing Activity (BBC, Kingswood Warren, Tadworth, Surrey, England)

This Report is based on a BBC tutorial paper describing several bit-rate-reduction techniques which have been studied at the BBC and which are used for the transmission of digital television signals. The techniques described are Sample-Rate Reduction, Differential Pulse Code Modulation (DPCM) coding - including a review of linear prediction theory and quantizations Transform Coding (DCT), Entropy Coding and Vector Quantization. The text of the tutorial was first prepared in 1986 before some of the recent advances in low bit-rate coding for television involving techniques such as motion compensated interframe prediction and subband coding However, the material presented here continues to prove itself to be a useful introduction to the subject and therefore it has been reprinted in the hope that it will give useful insights to engineers requiring a reasonably detailed introduction to bit-rate reduction of television signals. Author

N95-19055 British Broadcasting Corp., Tadworth (England). Research and Development Dept.
ENGINEERING REVIEW, JANUARY 1993 - MARCH 1994
1994 39 p
Copyright Avail: Issuing Activity (BBC, Kingswood Warren, Tadworth, Surrey, England)

R & D Department, along with Transmission, Telecommunications and the Technical Operations Centre, are in Engineering Division, part of the BBC's Resources Directorate. The Directorate provides a comprehensive range of resources across the BBC for both Radio and Television, from studio facilities to building services. Research & Development Department is responsible for innovating and assessing new broadcasting systems and techniques, and for providing the engineering specialist and operational departments with technical advice based on theoretical studies and experiments. Projects undertaken by the Department impinge upon all the technical aspects of broadcasting, including: television cameras, recording, video, audio and optical systems, signal processing, acoustics, transmission systems, service planning, antennas and propagation. Many of the projects are undertaken in collaboration with external organizations, either for research purposes or by joint development of broadcast equipment. Equipment designs are licensed to manufacturers for further development and marketing, thus giving the BBC valuable royalty income. Derived from text

N95-19069 Naval Air Warfare Center, Patuxent River, MD. Aircraft Div.
PROCESSING MULTILEVEL SECURE TEST AND EVALUATION INFORMATION
George Hurlburt, Bradley Hildreth, and Teresa Acevedo 31 Jul. 1994 11 p Presented at the ITEA Symposium on Testing the Global Village, Baltimore, MD, 3-6 Oct. 1994 Limited Reproducibility: More than 20% of this document may be affected by microfiche quality
(AD-A284073) Avail: Issuing Activity (Defense Technical Information Center (DTIC))

The Test and Evaluation Community Network (TECNET) is building a Multilevel Secure (MLS) system. This system features simultaneous access to classified and unclassified information and easy access through widely availabie communications channels. It provides the necessary separation of classification levels, assured through the use of trusted system design techniques, security assessments and evaluations. This system enables cleared T&E users to view and manipulate classified and unclassified

information resources either using a single terminal interface or multiple windows in a graphical user interface. TECNET is in direct partnership with the National Security Agency (NSA) to develop and field the MLS TECNET capability in the near term. The centerpiece of this partnership is a state-of-the-art Concurrent Systems Security Engineering (CSSE) process. In developing the MLS TECNET capability, TECNET and NSA are providing members, with various expertise and diverse backgrounds, to participate in the CSSE process. The CSSE process is founded on the concepts of both Systems Engineering and Concurrent Engineering. Systems Engineering is an interdisciplinary approach to evolve and verify an integrated and life cycle balanced set of system product and process solutions that satisfy customer needs (ASD/ENS-MIL STD 499B 1992). Concurrent Engineering is design and development using the simultaneous, applied talents of a diverse group of people with the appropriate skills. Harnessing diverse talents to support CSSE requires active participation by team members in an environment that both respects and encourages diversity. DTIC

N95-19072 Department of the Navy, Washington, DC.
DIGITAL MONOPULSE Patent
Sam Ghaleb, inventor (to Navy) and Michael Stokes, inventor (to Navy) 24 May 1994 11 p Filed 2 Jul. 1993
(AD-D016447; US-Patent-5,315,304; US-Patent-Appl-SN-086424; US-Patent-Class-342-165) Avail: US Patent and Trademark Office

A digitally formed monopulse radar employing dynamic real-time calibration during operation is described. The invention has a transmitter section, timing circuit, RF section, IF section, in-phase and quadrature section and a digital signal processor. A portion of the transmit signal is diverted from the transmitter section for preparation of calibration factors during the calibration period between receive signals. The calibration factors prepared by the digital signal processor are applied by the processor to antenna received signals during the receive mode and to produce the corrected sum and delta pitch, and delta yaw signals and the tracking errors Ey. DTIC

N95-19084# Naval Postgraduate School, Monterey, CA.
HIGH RADAR RANGE RESOLUTION WITH THE STEP FREQUENCY WAVEFORM M.S. Thesis
Abraham Paulose Jun. 1994 104 p
(AD-A284611) Avail: CASI HC A06/MF A02

High range resolution can be obtained using a number of methods including ultra-wideband radar, intrapulse pulse compression, and super-resolution techniques. This thesis investigates the achievement of high radar range resolution by means of the step frequency waveform. The key advantage of the step frequency approach compared to other methods is the wide total bandwidth resulting in high range resolution while still maintaining a narrow instantaneous bandwidth which eases A/D sampling requirements. The effects of various waveform parameters on the high resolution range profile are determined for both noise and clutter limited environments. A novel technique is developed which enhances the resolution of moving targets in clutter and estimates the target velocity. This method consists of clutter cancellation followed by successive velocity compensations. Finally, design methods are developed to optimize system performance in a low PRF mode for both noise and clutter limited environments. DTIC

N95-19087# Coast Guard Research and Development Center, Groton, CT.
AN/APS-137 FORWARD LOOKING AIRBORNE RADAR (FLAR) EVALUATION Final Report, May 1991 - May 1994
R. Q. Robe, D. L. Raunig, and R. L. Marsee May 1994 181 p
(AD-A284672; CGR/DC-19/94; USCG-D-18-94) Avail: CASI HC A09/MF A02

During April 1992, September and October 1992, and May 1993, the U.S. Coast Guard R&D Center conducted experiments to determine the sweep width for the AN/APS-137 Forward Looking Airborne Radar (FLAR) when searching for 4-, 6- and 10-person life rafts and small recreational boats. Workboats used to deploy the life rafts during the Fall 1992 and Spring 1993 experiments were used as targets of opportunity. The experiments were conducted in the coastal waters off the west coast of Florida from Wacussa Bay to Gasparilla Island and on Lake Erie. Realistic radar searches to collect data used unalerted sensor operators and standard search patterns for small waterborne targets. Aircraft and target positions were recorded using a Differential Global Positioning System (DGPS). Target detections were recorded by observers and by computers onboard the aircraft. Environmental conditions were recorded by observers on the workboats. In addition, MINIMETM environmental buoys recorded the sea and wind conditions in the search areas. Environmental conditions represented in the data set included 0.3- to 3.6-foot significant sea heights and 1.0- to 15.2-knot winds. Analysis of the data confirmed sweep width to be largely determined by range scale, lateral range and wind speed for the life rafts. Lateral range, radar range scale, boat size and wind speed determined the sweep width for small boats. Recommended sweep width values and AN/APS-137 FLAR search guidance are presented. DTIC

N95-19097# Wisconsin Univ., Madison, WI. Dept. of Electrical and Computer Engineering.
HIGH-POWER MICROWAVE TRANSMISSION AND MODE CONVERSION PROGRAM
R. J. Vernon and J. A. Lorbeck Jun. 1994 10 p
(Contract DE-FG02-85ER-52122)
(DE94-017046; DOE/ER-52122/10) Avail: CASI HC A02/MF A01

This report briefly discusses the following topics: (1) Quasi-optical converter design for Varian gyrotron SN 4.1; (2) Quasi-optical converter cold-test measurement; (3) Modification of geometrical-optics synthesized surfaces; (4) Diffraction synthesis; (5) Tapered dimpled launcher; (6) Work on Vlasov converter system for Varian gyrotron SN 4.1R; (7) Analysis of gyrotron spurious modes; (8) MIT code benchmarking; (9) Development of low-power efficiency test for Vlasov converters; (10) Investigation of optimal beam waist size and mode content for injection into a circular and rectangular corrugated waveguides; (11) The effect of corrugations on reduction of the fields at the wall of waveguides; (12) Shipping of a microwave scanner to Varian and further microwave scanner development; and (13) Code transferred to Varian. DOE

N95-19103 Florida Inst. of Tech., Melbourne, FL. Dept. of Electrical and Computer Engineering.
PHASE AND AMPLITUDE CONTROLLED MICROPATCH ANTENNA Final Technical Report, 1 Apr. 1993 - 31 Mar. 1994
Michael H. Thursby 28 Jul. 1994 8 p Limited Reproducibility: More than 20% of this document may be affected by microfiche quality
(Contract F49620-93-1-0286)
(AD-A284191; ASL-94-001; AFOSR-94-0521TR) Avail: Issuing Activity (Defense Technical Information Center (DTIC))

As the wireless communications industry in the U.S. stands poised for an explosion of new commercial and military applications (e.g. the Radio Mall, the Airlink), reducing the high cost of phased array antennas becomes ever more important. Reducing these antenna costs is the primary objective of this research. We will describe an effort that to date has produced a working prototype of a micropatch antenna incorporating a single dollar per bit phase shifter. Since 1987, when we have been involved in designing antenna systems using micropatch elements, early work led to our discovery of the Smart Electromagnetic Structure concept which resulted in the development of a neural controlled, frequency agile antenna element capable of following the frequency of incoming radiation, and tuning the antenna center frequency to that of the incoming signal. This can be applied to systems like frequency-hop radios. In this paper we will describe a method of controlling a micropatch antenna to provide phase only variation of the antenna characteristics using a similar device to that used for the frequency control experiments. We have successfully varied the phase of the antenna element without significantly changing the operating frequency. This work has led us to pursue further the design and fabrication of an array of such phase adjustable element to test the hypothesis that such phase controlled micropatch elements can be used to fabricate a low cost phased array antenna. DTIC

N95-19135 British Broadcasting Corp., Tadworth (England). Research Dept.
DIGITAL AUDIO BROADCASTING: COMPARISON OF COVERAGE AT DIFFERENT FREQUENCIES AND WITH DIFFERENT BANDWIDTHS
M. C. D. Maddocks and I. R. Pullen 1993 25 p Original contains color illustrations
(BBC-RD-1993/11) Copyright Avail: Issuing Activity (BBC, Kingswood Warren, Tadworth, Surrey, England)

A Digital Audio Broadcasting (DAB) system capable of reliable reception

in vehicles and portables has been developed by the Eureka 147 project. This Report describes a set of experiments performed to investigate the effect on the coverage area by changing the bandwidth of the DAB signal and its transmit frequency band. It is concluded that the choice of a bandwidth for the DAB signal of approximately 1.5 MHz is suitable. This is because it is sufficiently wideband to provide a significant benefit in reducing the location variation of the total received signal power, while being narrow enough to allow suitable channelization within the existing frequency bands. It is also concluded that a frequency allocation below Band IV would be more suitable in order to provide satisfactory coverage for all types of reception from terrestrial DAB transmitters. Above this frequency, the effects of clutter and terrain undulations appear to significantly increase the problems of providing uniform coverage at low antenna heights. Author

N95-19136 British Broadcasting Corp., Tadworth (England). Research Dept.

ALLEVIATION OF CO-CHANNEL INTERFERENCE AT POOLE RELAY STATION

J. H. Moore and A. I. E. Booker 1993 19 p Original contains color illustrations

(BBC-RD-1993/4) Copyright Avail: Issuing Activity (BBC, Kingswood Warren, Tadworth, Surrey, England)

The Rowridge UHF television transmitting station, situated on the Isle of Wight, radiates the four principal UK domestic television channels to the south coast of England, and provides an off-air feed to a number of dependent relays. At one relay station (Poole), occasional Co-channel Interference (CCI) is known to occur. It is particularly noticeable during the summer and autumn periods. Large numbers of domestic viewers along the south coast (receiving Rowridge directly) are also affected by CCI. The dominant source of interference on the Re-broadcast Link (RBL) from Poole had been shown from previous investigations to be the French TV station at Lille Bouvigny, which is co-channel with three of the Rowridge channels (BBC-2, ITV and Channel 4); BBC-1 is virtually free of CCI. The bearings from Poole to Rowridge and Lille Bouvigny differ by only 3.5 degrees; far too small a value for the Poole receiving antennas to provide any discrimination between these two stations - unimportant when tropospheric conditions are not favoring anomalous UHE propagation, but a significant weakness when such conditions do pertain. Of several possible solutions for reducing the CCI along the south coast, that of providing precision offset of the affected channels' RF carriers was the one chosen. The Lille Bouvigny transmitter already employed such carrier offsets. Only BBC-2 was dealt with, so that comparisons with the other two affected channels could be made. This report gives the details of the tests that were carried out, the selection of the method for producing an improvement to TV reception from Rowridge, and the notable benefits achieved.

Author

N95-19411 Selskapet for Industriell og Teknisk Forskning, Oslo (Norway). Div. for Informatics.

ODP BASED UPT MODEL

A. J. Berre, T. Handegard, K. Loevnes, B. Skjellaug, and J. O. Aagedal 21 Jan. 1994 65 p

(PB94-215589; STF33-A94007) Avail: Issuing Activity

The report documents the experiments with object oriented modelling of Universal Personal Telecommunication (UPT) in a telecommunication environment based on the basic principles of open distributed processing (ODP). Through the object-oriented analysis and design technique Object Modelling Technique (OMT) the service is modelled as a collection of software objects distributed across multiple network nodes. A software platform provides the mechanisms for application objects to interact. The platform builds on the basic facilities in the native computing and communication environments, but hides the heterogeneity of these environments and provides distribution transparency at the application programmer's interface. The report closes with some thoughts about applying the paradigm of ODP to intelligent networks (IN), and the experience with OMT as a modelling technique for real time distributed applications. NTIS

N95-19510# Denver Univ., Denver, CO. Coll. of Engineering.

SIGNAL PROCESSING VIA FOURIER-BESSEL SERIES EXPANSION Final Report

Jim Schroeder 31 May 1994 37 p

(Contract F49620-93-1-0271)

(AD-A285316; AFOSR-94-0630TR) Avail: CASI HC A03/MF A01

In many cases it may not be desirable or even practical to represent a signal by its sample values directly or by an analytical function if a suitable function is available. For example, a signal may be determined by time domain sample values when the parameters of interest are more compact within the frequency domain. Many practical signals are highly redundant, both image and speech signals fall into this category, and it may be desirable and possibly necessary to represent the signal with a fewer number of samples for economy of storage and/or transmission bandwidth limitations. Whatever the desired goal the processing of signals can often be carried out more efficiently in another domain than that of the original signal. An obvious example here with the advent of hardware Fast Fourier Transform (FFT) devices is the widespread frequency domain processing of naturally occurring time domain signals. Pattern recognition techniques rely on the ability to generate a set of coefficients from the raw data (time domain samples) that are more compact (i.e. fewer samples) and we hope, are more closely related to the signal characteristics of interest. Clearly, if one is interested in frequency content, a Fourier series representation packs the frequency information in to fewer samples (Fourier series coefficients) than a time domain representation. DTIC

N95-19516# Essex Corp., Columbia, MD.

TRUE TIME DELAY BEAMFORMING Final Report, Feb. 1992 - Feb. 1994

Leslie H. Gesell and Richard E. Feinleib Aug. 1994 105 p

(Contract F30602-92-C-0018)

(AD-A285683; RL-TR-94-104) Avail: CASI HC A06/MF A02

Wide aperture arrays for transmitting and receiving wideband signals suffer beam broadening when steered away from the array normal using phase delays between the array elements. This beam dispersion is eliminated if time delays instead of phase shifts are used between antenna array elements. This report represents the results of a project to demonstrate the proof-of-principle of an acousto-optic signal processing concept that generates and controls, with a single tone, the set of time delays required for linear antenna array beamforming. This acousto-optic concept allows an array to scan a beam rapidly over a continuum of angles. In the approach described in this report, the time delays between elements are generated by using an acousto-optic Bragg cell as a continuous delay line, and indirectly tapping selected points in the Bragg cell to the output. This optical tapping is controlled with a second Bragg cell and other standard passive optical elements. Included in this concept is a passive optical element to ensure that the phase shifts of the carrier of the time delayed signals will be correct at the RF of the array. The time-delay controller also provides the proper relative phases between the carriers of the time delayed signals at the RF of the antenna array. A proof-of-principle breadboard of the time delay controller was assembled. Results of the demonstration of the breadboard are described. DTIC

N95-19525# Naval Postgraduate School, Monterey, CA. Dept. of Electrical and Computer Engineering.

MULTICAST TREE CONSTRUCTION IN NETWORK TOPOLOGIES WITH ASYMMETRIC LINK LOADS Final Report

Shridhar B. Shukla, James E. Klinker, and Eric B. Boyer 30 Sep. 1994 30 p

(AD-A285679; NPS-EC-94-012) Avail: CASI HC A03/MF A01

This report addresses the problem of constructing multicast trees with reservation of resources. The main features of the approach described are that it tolerates asymmetric traffic loads on network links and algorithmically locates data distribution centers for every multiparticipant interaction. A fast and scalable algorithm for locating distribution centers based on the network load and a priori knowledge of participant's locations and resource requirements is given. To explicitly handle cases of disjoint send and receive paths between two nodes, a protocol to build separate send-trees and receive-trees around the centers located in the manner above is given. Simulation results on various topologies are presented showing that, with the above center location mechanism, center-specific trees yield lower tree cost than source-specific trees for many concurrent senders without increasing the average path length significantly. The use of distribution centers, a priori information, and sensitivity to load asymmetry permit effective combination of center-specific and source-specific trees for an interaction

and eliminate the need for symmetry checks during resource reservation. DTIC

N95-19534# Army Missile Command, Redstone Arsenal, AL. Advanced Sensors Directorate.

DESIGN OF A RADIO FREQUENCY DATA LINK FOR THE UNMANNED GROUND VEHICLE TECHNOLOGY TEST BED DEMONSTRATION PROGRAM Final Report

Keith D. Hilliard and Tom Barr Sep. 1994 42 p

(AD-A284997; AMSMI-TR-RD-AS-94-23) Avail: CASI HC A03/MF A01

A description of the design of an L-Band Radio Frequency data link for the Unmanned Ground Vehicle Technology Test Bed Program conducted by Research, Development, and Engineering Center, MICOM is presented. This report describes the command and control data link design. The system provides remote operator control communications for a robotic HMMWV. The data link utilizes a bidirectional RF system with a relay station to provide non-line-of-sight operations. The report details the design and expected performance of the data link. DTIC

N95-19535# Physics and Electronics Lab. TNO, The Hague (Netherlands).

ANALYSIS AND SYNTHESIS OF (SAR) WAVEGUIDE PHASED ARRAY ANTENNAS

H. J. Visser Feb. 1994 116 p

(AD-A285336; FEL-94-B062; TDCK-94-0176) Avail: CASI HC A06/MF A02

This report describes work performed due to ESA contract No. 101 34/93/NL/PB. Started is with a literature study on dual polarized waveguide radiators, resulting in the choice for the open ended square waveguide. After a thorough description of the mode matching infinite waveguide array analysis method - including finiteness effects - that forms the basis for all further described analysis and synthesis methods, the accuracy of the analysis software is validated by comparison with measurements on two realized antennas. These antennas have centered irises in the waveguide apertures and a dielectric wide angle impedance matching sheet in front of the antenna. A synthesis method, using simulated annealing and downhill simplex, is described next and different antenna designs, based on the analysis of a single element in an infinite array environment, are presented. Next, designs of subarrays are presented. Shown is the paramount importance of including the array environment in the design of a subarray. A microstrip patch waveguide exciter and subarray feeding network are discussed and the depth of the waveguide radiator is estimated. Chosen is a rectangular grid array with waveguides of 2.5 cm depth without irises and without dielectric sheet, grouped in linear 8 elements subarrays. DTIC

N95-19547*# California Univ., San Diego, CA. Dept. of Electrical and Computer Engineering.

SIMULATION OF WAVE PROPAGATION IN THREE-DIMENSIONAL RANDOM MEDIA

William A. Coles, J. P. Filice, R. G. Frehlich (Colorado Univ., Boulder, CO.), and M. Yadlowsky (Colorado Univ., Boulder, CO.) 16 Dec. 1993 31 p

(Grant NAG8-253)

(NASA-CR-197605; NAS 1.26:197605) Avail: CASI HC A03/MF A01

Quantitative error analysis for simulation of wave propagation in three dimensional random media assuming narrow angular scattering are presented for the plane wave and spherical wave geometry. This includes the errors resulting from finite grid size, finite simulation dimensions, and the separation of the two-dimensional screens along the propagation direction. Simple error scalings are determined for power-law spectra of the random refractive index of the media. The effects of a finite inner scale are also considered. The spatial spectra of the intensity errors are calculated and compared to the spatial spectra of intensity. The numerical requirements for a simulation of given accuracy are determined for realizations of the field. The numerical requirements for accurate estimation of higher moments of the field are less stringent. Author

N95-19555# Sandia National Labs., Albuquerque, NM.

SANDIA NATIONAL LABORATORIES' HIGH POWER ELECTROMAGNETIC IMPULSE SOURCES

L. F. Rinehart, M. T. Buttram, G. J. Denison, J. M. Lundstrom, W. R. Crowe, J. F. Aurand, and P. E. Patterson 1994 7 p Presented at the International Symposium on Electromagnetic Environments and Consequences, Bordeaux, France, 30 May - 3 Jun. 1994

(Contract DE-AC04-94AL-85000)

(DE95-000423; SAND-93-2743C; CONF-940531-3) Avail: CASI HC A02/MF A01

Three impulse sources have been developed to cover a wide range of peak power, bandwidth and center frequency requirements. Each of the sources can operate in single shot, rep-rate, or burst modes. These devices are of rugged construction and are suitable for field use. This paper will describe the specifications and principals of operation for each source. The sources to be described are: SNIPER (Sub-Nanosecond ImPulsE Radiator), a coaxial Blumlein pulser with an in-line (series) peaking switch; EMBL (EnantioMorphic BLurfflein), a bipolar parallel plate Blumlein with a crowbar type (parallel) peaking switch; and the LCO (L-C Oscillator) a spark-switched L-C oscillator with damped sinusoidal output. SNIPER and EMBL are ultra-wideband (UWB) sources which produce a very fast high voltage transition. When differentiated by the antenna, an impulse whose width corresponds to the transition time is radiated. The LCO operates with a center frequency up to 800 MHz and up to 100 MHz bandwidth. Because the LCO output is relatively narrow band, high gain antennas may be employed to produce very high radiated field strengths. DOE

N95-19565# Massachusetts Inst. of Tech., Lexington. Lincoln Lab.

SIGNAL ENHANCEMENT IN AM-FM INTERFERENCE

Thomas F. Quantieri, Robert B. Dunn, and Robert J. McAulay 17 May 1994 77 p

(Contract F19628-90-C-0002)

(AD-A285114; TR-993; ESC-TR-93-328) Avail: CASI HC A05/MF A01

A new approach to interference suppression is developed to enhance the audibility of signals corrupted by amplitude-modulated (AM) and frequency-modulated (FM) tonal interference. The suppression algorithm uses a short-time, least-squares estimation of the parameters of an AM-FM model of the time-varying tonal interference. The method, developed in a sine-wave analysis/synthesis framework, can be integrated with time and frequency modifications for further signal enhancement. Suppression is applied to single and multitone synthetic and actual AM-FM interference, the latter including man-made signals (e.g., siren interference) and those that occur naturally (e.g., biologic interference). The relative advantages and disadvantages of the sine-wave framework in contrast to a short-time Fourier transform overlap-add framework are described. The enhancement techniques are robust in a large range of environments and can be designed to preserve a random noise background. Finally, it is shown that interference suppression on multichannels prior to beamforming enhances beamformer performance. DTIC

N95-19594# Massachusetts Inst. of Tech., Lexington. Lincoln Lab.

ADAPTIVE DETECTION AND COPY OF COHERENT NARROWBAND WAVEFORMS WITH UNCALIBRATED ARRAYS

Keith W. Forsythe 20 Jun. 1994 60 p

(Contract F19628-90-C-0002)

(AD-A285125; TR-994; ESC-TR-93-292) Avail: CASI HC A04/MF A01

Adaptive detection and copy of temporally coherent narrowband waveforms with multiple sensors is discussed. Unlike related problems treated in the radar literature, the sensor response to the coherent signal of interest is assumed unknown. Thus the techniques presented can be used with uncalibrated sensor arrays. The signal processing takes advantage of the sensor array as well as the signal coherence in order to form an adaptive spatial beam that suppresses cochannel interference. More general signal models involving partial coherence are also considered. DTIC

N95-19600# University of Southern California, Marina del Rey, CA.

ZONED ANALOG PERSONAL TELECONFERENCING (ZAPT) Final Report

Joseph D. Touch Dec. 1993 23 p

(Contract DABT63-91-C-0001)

(AD-A285877; ISI/SR-93-374) Avail: CASI HC A03/MF A01

ZAPT is a desktop multiparty audio/video teleconferencing system at ARPA, based on Bellcore's Touring Machine ZAPT supports one multiparty call (up to 4 parties), and any number of point-to-point calls, with analog multimedia. ZAPT supports automated remote operation and conference

'joint' requests. ZAPT provides interoffice conferencing at ARPA, and manual cross-connect to Internet-style conferencing tools. DTIC

N95-19622 Defence Science and Technology Organization, Melbourne (Australia). Aeronautical and Maritime Research Lab.
HANDBOOK FOR THE EXTREMELY LOW FREQUENCY (ELF) DATA ACQUISITION AND ANALYSIS SYSTEM
J. Vrbancich, S. Valentine-Flint, and R. Wong Oct. 1994 93 p
(DSTO-GD-0021; AR-008-932) Copyright Avail: Issuing Activity (Defence Science and Technology Organization, Melboure, Australia)

This handbook describes the digital data acquisition system built to record data in the 1 Hz to 600 Hz bandwidth from the portable underwater extremely low frequency (ELF) electromagnetic sensor unit. The sensors supported by the acquisition system are three-axis alternating magnetic field detection coils, three-axis alternating electric field sensors (electrodes) and three-axis seismic sensors; plus ancillary sensors such as pressure-depth, inclination and compass heading. The data acquisition system consists of the wet-end electronics package incorporating the controller board, 16 bit analog to digital converter, low noise preamplifiers etc. and the dry-end electronics unit incorporating the power supply and computer. The data acquisition software for remote control of the total system and the analysis software which is linked to the data acquisition system is also presented. The analysis software which is purposely designed as an integral part of the acquisition system provides frequency domain spectral information (via the fast Fourier transform algorithm) from the raw time series data and may be used both for quick look analysis during the data acquisition phase and for full analysis of data in slow time. Author

N95-19694 Naval Research Lab., Washington, DC.
RADAR ANTENNA CHARACTERIZATION USING POLARIZATION MEASUREMENTS Report, Aug. 1992 - Aug. 1993
Elaine Chincheck 8 Aug. 1994 71 p Limited Reproducibility: More than 20% of this document may be affected by microfiche quality
(AD-A284840; NRL/FR/5730-94-9588) Avail: CASI HC A04

The Naval Research Laboratory (NRL) is investigating polarization features of antennas to determine if they can be used for radar identification. This report presents the results of a test under this program whose main objective was to use existing polarization measuring hardware to examine the mainlobe and sidelobe antenna polarization characteristics of different navigation radars and to evaluate how this information can be used for radar identification. A theoretical model was generated to plot the polarization characteristics of slotted waveguide arrays, the type of arrays used in navigation radars. A comparison between theory and real-time measurements was made with encouraging results. This report shows that radars belonging to the same 'class' with the same antenna polarization can be distinguishable when comparing their mainlobe and sidelobe antenna polarization characteristics. DTIC

N95-19730 Naval Postgraduate School, Monterey, CA.
INBAND RADAR CROSS SECTION OF PHASED ARRAYS WITH PARALLEL FEEDS M.S. Thesis
Vassilios Flokas Jun. 1994 66 p Limited Reproducibility: More than 20% of this document may be affected by microfiche quality
(AD-A284249) Avail: CASI HC A04

Approximate formulas for the inband radar cross section of arrays with parallel feeds are presented. To obtain the formulas, multiple reflections are neglected, and devices of the same type are assumed to have identical electrical performance. The approximate results were compared to the results obtained using a scattering matrix formulation. Both methods were in agreement in predicting RCS lobe positions, levels, and behavior with scanning. The advantages of the approximate method are its computational efficiency and its flexibility in handling an arbitrary number of coupler levels. DTIC

N95-19736 Naval Undersea Warfare Center, Newport, RI.
THE USE OF TWO-STATION IONOSONDE DATA FOR IONCAP/ASAPS MODEL VALIDATION ON TRANSPOLAR TWO-HOP, HIGH-FREQUENCY SKYWAVE RADIO LINKS Final Report
Joseph R. Katan and Robert I. Desourdis 8 Aug. 1994 127 p Limited Reproducibility: More than 20% of this document may be affected by microfiche quality
(AD-A284270; NUWC-NPT-TR-10689) Avail: CASI HC A07

Ionosonde data were taken from two high-latitude Arctic radio links in order to investigate two-hop high-frequency (HF) polar propagation. A comparison of the two-hop data measurements with both IONCAP and ASAPS predictions has validated the accuracy of the model for complex skywave radio links. DTIC

N95-19744# Mitre Corp., Bedford, MA.
MEASUREMENT AND PROPER EQUALIZATION OF RANGE SIDELOBES USING A SPHERICAL SATELLITE AS A REFLECTOR Final Report
A. G. Kramer Aug. 1994 30 p
(Contract F19628-94-C-0001)
(AD-A285955; MTR-11162; ESC-TR-94-196) Avail: CASI HC A03/MF A01

We have investigated the problems of measuring range sidelobes by using a small sphere (ka 15) as a target. This measurement scheme requires coherent integration to increase the signal-to-noise ratio at the sidelobes to a level where accurate estimation is possible. We determined that two pathologic coherent responses can occur in this situation. A wave creeping around the sphere causes the formation of an asymmetric range sidelobe that lags the main response. We find that the relative level of coherent errors, whose magnitude is below the noise on a single plus basis, is invariant with coherent integration. DTIC

N95-19771 Materials Research Labs., Ascot Vale (Australia).
POTENTIAL DISTRIBUTIONS FOR ELLIPSOIDAL BODIES IN UNIFORM FIELDS
G. D. Furnell Mar. 1994 59 p
(MRL-TR-92-48; AR-008-245) Copyright Avail: Issuing Activity

Details are given of analytic expressions for the induced magnetostatic and electrostatic potential distributions arising when ellipsoidal bodies are immersed in a uniform field. Both multi-layered and homogeneous bodies are considered, and purely spherical and spheroidal body geometries are treated separately as special cases. To provide results which may be used by other researchers for checking purposes, numerical tables and constant potential contour plots are presented for a set of representative example problems. Author

N95-19781*# National Aeronautics and Space Administration. Langley Research Center, Hampton, VA.
RADAR CROSS-SECTION MEASUREMENTS AND SIMULATION OF A TETHERED SATELLITE. THE SMALL EXPENDABLE DEPLOYER SYSTEM END-MASS PAYLOAD
Robin L. Cravey, Dion T. Fralick (Lockheed Engineering and Sciences Co., Hampton, VA.), and Erik Vedeler Feb. 1995 22 p
(RTOP 505-64-70-01)
(NASA-TM-4613; L-17410; NAS 1.15:4613) Avail: CASI HC A03/MF A01

The first Small Expendable Deployer System (SEDS-1), a tethered satellite system, was developed by NASA and launched March 29, 1993 as a secondary payload on a United State Air Force (USAF) Delta-2 launch vehicle. The SEDS-1 successfully deployed an instrumented end-mass payload (EMP) on a 20-km nonconducting tether from the second stage of the Delta 2. This paper describes the effort of NASA Langley Research Center's Antenna and Microwave Research Branch to provide assistance to the SEDS Investigators Working Group (IWG) in determining EMP dynamics by analyzing the mission radar skin track data. The radar cross section measurements taken and simulations done for this study are described and comparisons of the measured data with the simulated data for the EMP at 6 GHz are presented. Author

N95-19796*# Michigan Univ., Ann Arbor, MI. Radiation Lab.
SIMULATION OF THIN SLOT SPIRALS AND DUAL CIRCULAR PATCH ANTENNAS USING THE FINITE ELEMENT METHOD WITH MIXED ELEMENTS Semiannual Progress Report, period ending Jan. 1995
Jian Gong, John L. Volakis, and Michael W. Nurnberger Jan. 1995 91 p
(Grant NAG1-1478)
(NASA-CR-197671; NAS 1.26:197671; UMICH-030601-4-T) Avail: CASI HC A05/MF A01

This semi-annual report describes progress up to mid-January 1995. The report contains five sections all dealing with the modeling of spiral

and patch antennas recessed in metallic platforms. Of significance is the development of decomposition schemes which separate the different regions of the antenna volume. Substantial effort was devoted to improving the feed model in the context of the finite element method (FEM). Finally, an innovative scheme for truncating finite element meshes is presented. For individual titles, see N95-19797 through N95-19801.

N95-19797*# Michigan Univ., Ann Arbor, MI. Radiation Lab.
SLOT SPIRAL ANTENNA MODELING USING HYBRID/MIXED FE-BI TECHNIQUE
Jian Gong and John L. Volakis *In its* Simulation of Thin Slot Spirals and Dual Circular Patch Antennas Using the Finite Element Method with Mixed Elements Jan. 1995 p 1-20 (For primary document see N95-19796 05-32)
Avail: CASI HC A03/MF A01

This report is concerned with the numerical simulation of the printed slot spiral antenna (SSA) using the finite element - boundary integral (FE-BI) analysis. It has been reported that the FE-BI technique is suited for modeling microstrip patch antennas of any shape, printed on layered planar structure or cylindrical platform and fed with a coaxial cable or a microstripline network underneath the radiating elements. However, direct application of the hybrid FE-BI technique to thin slot spirals requires excessive sampling rates to accurately simulate the geometry. To alleviate the meshing/modeling difficulties encountered with cavity-backed slot antennas, we describe a mixed finite element-boundary integral formulation. As in the past, the boundary integral is used to describe the radiation of the slot above the cavity. However the cavity is now modeled using a suitable mix of edge and node elements. The latter are used only at the aperture of the thin slot so that the nodes follow the center line of the slot. In this manner, regular size elements can be used regardless of the slot's width and any meshing restrictions are substantially relaxed. The proposed mixed element FE-BI formulation introduces three different computational regions and as expected this complicates the generation of the discrete system.
Derived from text

N95-19798*# Michigan Univ., Ann Arbor, MI. Radiation Lab.
DESIGN CONSIDERATIONS FOR AN ARCHIMEDEAN SLOT SPIRAL ANTENNA
Michael W. Nurnberger and John L. Volakis *In its* Simulation of Thin Slot Spirals and Dual Circular Patch Antennas Using the Finite Element Method with Mixed Elements Jan. 1995 p 21-46 (For primary document see N95-19796 05-32)
Avail: CASI HC A03/MF A01

The design goal is to develop a 118-157 MHz, vertically polarized, low-profile (or conformal) antenna as a replacement for VHF AM blade antennas on aircraft. This design is to be arrived at by scaling the dimensions of an antenna designed for a center frequency of 1.1 GHz. The design prior to scaling may have the following maximum dimensions: diameter less than 3.70 in. and thickness less than 0.50 in. Although a four-arm spiral design was originally suggested, a two-arm spiral may also be used, as both mode-1 and mode-2 (sum and difference) radiation patterns aren't required. While a four-arm spiral can easily be designed should both sum and difference patterns be required, the two-arm design will provide the required sum pattern and simplify the design problem somewhat: only one feed is required, and the feed area geometry is more straightforward. Polarization requirements dictate that a slot spiral be used, as opposed to a wire spiral. Two similar radiating structures were considered. The first is the standard archimedean spiral antenna. The second is a hollow archimedean spiral antenna, essentially a standard archimedean spiral with the inner portion removed.
Derived from text

N95-19799*# Michigan Univ., Ann Arbor, MI. Radiation Lab.
AN EFFICIENT AND ACCURATE MODEL OF THE COAX CABLE FEEDING STRUCTURE FOR FEM SIMULATIONS
Jian Gong and John L. Volakis *In its* Simulation of Thin Slot Spirals and Dual Circular Patch Antennas Using the Finite Element Method with Mixed Elements Jan. 1995 p 47-57 (For primary document see N95-19796 05-32)
Avail: CASI HC A03/MF A01

An efficient and accurate coax cable feed model is proposed for microstrip or cavity-backed patch antennas in the context of a hybrid finite element method (FEM). A TEM mode at the cavity-cable junction is assumed for the FEM truncation and system excitation. Of importance in this implementation is that the cavity unknowns are related to the model fields by enforcing an equipotential condition rather than field continuity. This scheme proved quite accurate and may be applied to other decomposed systems as a connectivity constraint. Comparisons of our predictions with input impedance measurements are presented and demonstrate the substantially improved accuracy of the proposed model.
Author

N95-19800*# Michigan Univ., Ann Arbor, MI. Radiation Lab.
ARBITRARILY SHAPED DUAL-STACKED PATCH ANTENNAS: A HYBRID FEM SIMULATION
Jian Gong and John L. Volakis *In its* Simulation of Thin Slot Spirals and Dual Circular Patch Antennas Using the Finite Element Method with Mixed Elements Jan. 1995 p 58-76 (For primary document see N95-19796 05-32)
Avail: CASI HC A03/MF A01

A dual-stacked patch antenna is analyzed using a hybrid finite element - boundary integral (FE-BI) method. The metallic patches of the antenna are modeled as perfectly electric conducting (PEC) plates stacked on top of two different dielectric layers. The antenna patches may be of any shape and the lower patch is fed by a coaxial cable from underneath the ground plane or by an aperture coupled microstrip line. The ability of the hybrid FEM technique for the stacked patch antenna characterization will be stressed, and the EM coupling mechanism is also discussed with the aid of the computed near field patterns around the patches.
Author

N95-19801*# Michigan Univ., Ann Arbor, MI. Radiation Lab.
PERFORMANCE OF AN ARTIFICIAL ABSORBER FOR TRUNCATING FEM MESHES
Jian Gong and John L. Volakis *In its* Simulation of Thin Slot Spirals and Dual Circular Patch Antennas Using the Finite Element Method with Mixed Elements Jan. 1995 p 77-87 (For primary document see N95-19796 05-32)
Avail: CASI HC A03/MF A01

We investigate the effectiveness of an artificial absorber for truncating finite element (FE) meshes. Specifically, we present the implementation of a novel mesh truncation approach using a perfectly matched anisotropic absorber for waveguides and stripline circuits. This truncation scheme is useful in many applications, including antennas, scattering, and microwave circuits.
Author

N95-19833 Lawrence Livermore National Lab., Livermore, CA.
HIGH SPEED OPTICAL LINKS BETWEEN LLNL AND BERKELEY
W. J. Lennon and R. L. Thombley Aug. 1994 14 p Presented at the SPIE International Symposium on Photonic Sensors and Controls for Commercial Applications, Boston, MA, 31 Oct. - 4 Nov. 1994 Limited Reproducibility: More than 20% of this document may be affected by microfiche quality
(Contract W-7405-eng-48)
(DE95-000552; UCRL-JC-118154; CONF-9410154-2) Avail: CASI HC A03

The Advanced Telecommunications Program at Lawrence Livermore National Laboratory, in collaboration with Pacific Bell, is developing an experimental high speed, four wavelength, protocol independent optical link for evaluating wide area networking interconnection schemes and the use of fiber amplifiers. Lawrence Livermore National Laboratory, as a super-user, supercomputer, and super-application site, is anticipating the future bandwidth and protocol requirements to connect to other such sites as well as to connect to remote sited control centers and experiments. In this paper we discuss our vision of the future of Wide Area Networking and describe the plans for the wavelength division multiplexed link between Livermore and the University of California at Berkeley.
DOE

N95-18185*# Southern Coll. of Technology, Marietta, GA. Dept. of Electrical and Computer Engineering Technology.
FEASIBILITY STUDY OF TRANSMISSION OF OTV CAMERA CONTROL INFORMATION IN THE VIDEO VERTICAL BLANKING INTERVAL
Preston A. White, III *In* Univ. of Central Florida, NASA/ASEE Summer Faculty Fellowship Program. 1994 Research Reports Oct. 1994 p 521-543 (For primary document see N95-18166 05-80)
Avail: CASI HC A03/MF A04

N95-18968*# Alabama Univ., Huntsville, AL. Dept. of Computer Science.
MSFC INSTITUTIONAL AREA NETWORK AND ATM TECHNOLOGY
Ashok T. Amin *In* Alabama Univ., Research Reports: 1994 NASA/ASEE Summer Faculty Fellowship Program Oct. 1994 6 p (For primary document see N95-18967 05-80)
Avail: CASI HC A02/MF A03

33 ELECTRONICS AND ELECTRICAL ENGINEERING

Includes test equipment and maintainability; components, e.g., tunnel diodes and transistors; microminiaturization; and integrated circuitry.

For related information see also *60 Computer Operations and Hardware* and *76 Solid-State Physics.*

N95-17959 Naval Surface Warfare Center, Silver Spring, MD. Weapons Research and Technology Dept.
CHARACTERIZATION OF RECHARGEABLE LITHIUM CELLS. PART 1: LITHIUM/NIOBIUM TRISELENIDE CHEMISTRY
T. C. Murphy, D. M. Cason-Smith, P. H. Smith, and S. D. James 16 Aug. 1994 29 p Limited Reproducibility: More than 20% of this document may be affected by microfiche quality
(AD-A284229; NSWCDD/TR-92/298) Avail: CASI HC A03

The Naval Surface Warfare Center is evaluating industry's emerging lithium rechargeable battery technology for use in underwater vehicle applications. The battery industry typically characterizes cells for consumer applications requiring low rate cycling at room temperature and rarely provides high rate, low temperature data. High rate and low temperature performance of AT&T's lithium/niobium triselenide (Li/NbSe3) AA cells is reported here. At 25 C and 10 mA/sq cm (approximately the 3C rate), delivered energy densities were as high as 30 Wh/lb. However, these lithium cells proved vulnerable to performance loss in low temperature (0 deg C), high discharge rate cycling. DTIC

N95-17961 Argonne National Lab., IL.
ELECTRONICS FOR THE SI DETECTORS IN APEX
P. R. Wilt, R. R. Betts, M. Freer, Th. Happ, M. R. Maier (Michigan State Univ., East Lansing, MI.), P. A. A. Perara (Rochester Univ., NY.), M. D. Rhein, M. Robertson (Michigan State Univ., East Lansing, MI.), D. Sowinski, and F. L. H. Wolfs (Rochester Univ., NY.) 1994 11 p Presented at the LeCroy Conference on Electronics for Future Colliders, Montvale, NJ, 10-11 May 1994 Sponsored in part by NSF Limited Reproducibility: More than 20% of this document may be affected by microfiche quality
(Contracts W-31-109-eng-38; DE-AC03-76SF-00098)
(DE94-015078; ANL/PHY/CP-83448; CONF-9405199-1) Avail: CASI HC A03

APEX (ATLAS Positron EXperiment), a collaborative effort of ANL, FSU, MSU/NSCL, Princeton, Queen's, Rochester, Washington, and Yale, is an experiment to study positron and electron production in very heavy ion collisions. The electrons and positrons are detected with two detector arrays, each consisting of 216 1 mm thick Si PIN diodes, and their energy and time-of-flight are measured. The number of detectors and limited space made it necessary to develop a system that could efficiently process and transfer signals from the detectors to the charge sensing ADC's and data readout electronics as well as monitor the condition of the detectors. The discussion will cover the electronics designed for the Si detectors, including the charge amplifier, 'Mother board' for the charge amplifiers, eight channel shaper, 16 channel constant fraction discriminator (CFD), 16 channel peak-to-FERA (PTF), and the integration of the CFD and PTF with charge sensing ADC's. Function and performance of the individual modules as well as the system as a whole will be discussed. DOE

N95-17984# National Inst. of Standards and Technology, Gaithersburg, MD. Semiconductor Electronics Div.
SEMICONDUCTOR MEASUREMENT TECHNOLOGY: DESIGN AND TESTING GUIDES FOR THE COMOS AND LATERAL BIPOLAR-ON-SOI TEST LIBRARY
J. C. Marshall and M. E. Zaghloul (George Washington Univ., Washington, DC.) Mar. 1994 142 p See also PB93-152106 and PB94-163458
(PB94-178019; NIST/SP-400-93) Avail: CASI HC A07/MF A02; SOD HC

Design and testing guides have been developed for the test library from which test chip NIST8 and test wafer NIST9 were derived. They were designed for use in process monitoring and device parameter extraction to evaluate and compare CMOS (Complementary Metal-Oxide-Semiconductor) test structures, including devices and circuits, fabricated on both bulk silicon and SOI (Silicon-on-Insulator), specifically SIMOX (Separation by the IMplantation of OXygen), wafers. The test library consists of both CMOS-on-SOI and lateral bipolar-on-SOI modules. From it, 20 modules were assembled to create CMOS test chip NIST8 that was fabricated using a standard bulk CMOS foundry through the MOSIS service. SOI/SIMOX test wafer NIST9 contains approximately 1000 modules and was also assembled from modules in this test library. Fourteen processing masks are used to fabricate depletion-mode MOSFET's, lateral bipolar devices, and CMOS MOSFET's with source-to-channel ties. The SOI/SIMOX technology file used with the Magic VLSI layout editor was modified to include the layers necessary to generate these 14 processing masks. This modification is discussed, and unique test structure designs are presented. Author

N95-17999# Carnegie-Mellon Univ., Pittsburgh, PA. Dept. of Social Science.
TECHNOLOGICAL AND ORGANIZATIONAL DIVERSITY AND TECHNICAL ADVANCE IN THE EARLY HISTORY OF THE AMERICAN SEMICONDUCTOR INDUSTRY
W. Cohen, D. Holbrook, and S. Klepper Jun. 1994 240 p
(Contract SBA-5648-OA-90)
(PB94-175700) Avail: CASI HC A11/MF A03

This study examines the early years of the semiconductor industry and focuses on the roles played by different size firms in technologically innovative processes. A large and diverse pool of firms participated in the growth of the industry. Three related technological areas were chosen for in-depth analysis: integrated circuits, materials technology, and device packaging. Large business producing vacuum tubes dominated the early production of semiconductor devices. As the market for new devices grew during the 1950's, new firms were founded and existing firms from other industries, e.g. aircraft builders and instrument makers, began to pursue semiconductor electronics. Small firms began to cater to the emerging industry by supplying materials and equipment. These firms contributed to the development of certain aspects of one thousand firms that were playing some part in the semiconductor industry. Author (revised)

N95-18037 Helsinki Univ. of Technology, Espoo (Finland).
DC-CONDUCTIVITY AND MAGNETORESISTANCE OF INHERENTLY CONDUCTING POLYMERS. POLYACETYLENE AND POLY(3-ALKYLTHIOPHENES) Ph.D. Thesis
K. Vaekiparta 1993 126 p Limited Reproducibility: More than 20% of this document may be affected by microfiche quality
(PB94-184587; ISBN-951-22-1760-0) Avail: Issuing Activity (National Technical Information Service (NTIS))

Inherently conducting polymers with optimal charge transport properties lie in the vicinity of the M-I transition. The most powerful demonstration of this is potassium-doped highly conducting polyacetylene (room temperature dc-conductivity 3000-4000 S/cm), the dc-conductivity of which shows a temperature dependence (power law) in perfect accordance with the theory for a material in the critical intermediate regime of the M-I transition. As suggested by earlier research, iodine doped polyacetylene (doped to the maximum of room temperature conductivity, 1 to 100,000 S/cm) is on the metallic side of the M-I transition. Based on de-conductivity and magnetoresistance measurements, this work confirms the dominating role of weak localization effects on the charge transport in the temperature regime 2-60 K, and suggest that electron-electron interactions play an important role below 2 K. Ferric chloride doped poly(3-alkylthiophenes) (P3OT and P3HT, with room temperature conductivities 30-160 S/cm) show a temperature behavior of dc-conductivity due to localized charge carriers and are therefore on the insulating side of the M-I transition. Author

N95-18052# Naval Command, Control and Ocean Surveillance Center, San Diego, CA. RDT and E Div.

METAL/HYDROGEN ENERGY STORAGE: SELECTED TECHNICAL ISSUES Final Report

P. A. Mosier-Boss and S. J. Szpak Jun. 1994 40 p

(AD-A283355; NRAD-TR-1657) Avail: CASI HC A03/MF A01

The report illustrates a rational approach for modeling and characterizing porous electrodes. Although the authors selected the metal hydride system for this purpose, such an approach is applicable to other systems as well and is an example of current trends in the development of electrochemical cells. DTIC

N95-18103# California Univ., Berkeley, CA. Dept. of Electrical Engineering and Computer Science.

SUPERCONDUCTIVE SIGNAL-PROCESSING CIRCUITS Final Report, Aug. 1990 - Oct. 1993

Theodore VanDuzer Aug. 1994 76 p Sponsored by Ballistic Missile Defence Organization

(Contract F19628-90-K-0037; AF Proj. R381)

(AD-A285533; RL-TR-94-140) Avail: CASI HC A05/MF A01

This work addresses new signal processing circuits using the special features of superconductivity. A novel flash-type analog-to-digital converter based on a comparator invented in the preceding contract period was demonstrated. The comparator was shown to be useful as a logic gate and an encoder was designed with it. A high-resolution delta-sigma analog-to-digital converter was devised with superconductive components in spite of the lack of an analog integrator in this technology. Positive theoretical results are being followed up experimentally. A simple flux-shuttle single-flux-quantum shift register was devised and several different readout schemes were studied. A six-bit-long version was successfully tested at 1 GHz. A decoder that takes in a five-bit word to select one of 32 output lines was completed. The design involved very tight limitations on current and power. The decoder was combined with a serial-to-parallel converter and operated at 2 GHz. A study of the appropriate architectures for various types of superconductive or Josephson digital technology was developed: an inductance-extraction program. DTIC

N95-18143# Sandia National Labs., Albuquerque, NM.

USING FEDERAL TECHNOLOGY POLICY TO STRENGTH THE US MICROELECTRONICS INDUSTRY

J. E. Gover and C. W. Gwyn Jul. 1994 128 p

(Contract DE-AC04-94AL-85000)

(DE94-017293; SAND-94-1681) Avail: CASI HC A07/MF A02

A review of US and Japanese experiences with using microelectronics consortia as a tool for strengthening their respective industries reveals major differences. Japan has established catch-up consortia with focused goals. These consortia have a finite life targeted from the beginning, and emphasis is on work that supports or leads to product and process-improvement-driven commercialization. Japan's government has played a key role in facilitating the development of consortia and has used consortia promote domestic competition. US consortia, on the other hand, have often emphasized long-range research with considerably less focus than those in Japan. The US consortia have searched for and often made revolutionary technology advancements. However, technology transfer to their members has been difficult. Only SEMATECH has assisted its members with continuous improvements, compressing product cycles, establishing relationships, and strengthening core competencies. The US government has not been a catalyst nor provided leadership in consortia creation and operation. We propose that in order to regain world leadership in areas where US companies lag foreign competition, the US should create industry-wide, horizontal-vertical, catch-up consortia or continue existing consortia in the six areas where the US lags behind Japan -- optoelectronics, displays, memories, materials, packaging, and manufacturing equipment. In addition, we recommend that consortia be established for special government microelectronics and microelectronics research integration and application. We advocate that these consortia be managed by an industry-led Microelectronics Alliance, whose establishment would be coordinated by the Department of Commerce. We further recommend that the Semiconductor Research Corporation, the National Science Foundation Engineering Research Centers, and relevant elements of other federal programs be integrated into this consortia complex. DOE

N95-18156# Army Communications-Electronics Command, Fort Belvoir, VA. Night Vision and Electronics Sensors Directorate.

IMAGE INTENSIFIER SYSTEM RESOLUTION BASED ON LABORATORY MEASURED PARAMETERS Final Report, Jun. 1980 - Apr. 1993

Raymond J. Stefanik Aug. 1994 63 p

(AD-A283917; AMSEL-NV-TR-0112) Avail: CASI HC A04/MF A01

Suitability of any analytical model is entirely dependent on how well the model prediction fits the actual measured data under real conditions. The primary intent of formulating this laboratory version of an image intensifier performance model considered the following premise. If an image intensifier model cannot accurately predict laboratory measured performance (where all test conditions and parameters are controlled and known), then it cannot be viable for predicting field performance (where conditions cannot be controlled nor are well known). The report details the basis of the model and its complete derivation. The Appendix presents numerous examples that compare the model's output with actual performance data measured by observers. The reader is referred to a planned update of the NVESD Image Intensifier Performance Model to be released in early calendar year 1994. The revised performance model will include this work on limiting resolution and establish the link between limiting resolution and the traditional Minimum Resolvable Contrast utilized for the prediction of observer performance in field conditions. DTIC

N95-18318 Department of the Navy, Washington, DC.

PREPARATION OF AN ELECTROCATALYTIC CATHODE FOR AN ALUMINUM-HYDROGEN PEROXIDE BATTERY Patent

Catherine L. Marsh, inventor (to Navy), Gerald L. Seebach, inventor (to Navy), John W. VanZee, inventor (to Navy), Russell R. Bessette, inventor (to Navy), and Hubert G. Meunier, inventor (to Navy) 22 Mar. 1994 5 p Filed 21 Aug. 1992

(AD-D016262; US-Patent-5,296,429; US-Patent-Appl-SN-931467) Avail: US Patent and Trademark Office

An electrocatalytic cathode that will allow hydrogen peroxide, H2O2, to behave electrochemically within an Al-H2O2 battery system is provided. The electrocatalytic cathode is comprised of nickel specially coated with one or a combination of the following six metals: platinum, ruthenium, rhodium, osmium, palladium, and iridium. The use of nickel coated with the appropriate combination of metals reduces the problems of excessive peroxide decomposition, thereby producing a battery that can operate efficiently by producing a high voltage at a high current density. The electrocatalytic cathode is produced by pretreating a nickel electrode with a hydrochloric acid bath and then by applying the metal coating by plating methods. DTIC

N95-18338# Warsaw Technical Univ. (Poland).

MIKON 94. INTERNATIONAL MICROWAVE CONFERENCE. INVITED PAPERS, VOLUME 3

Roman Dufrene 1994 187 p The 10th Conference was held in Ksiaz (Poland, 30 May - 2 Jun. 1994

(AD-A284353; R/D-7346-EE-02-Vol-3) Avail: CASI HC A09/MF A02

The following topics are discussed: (1) New trends and ideas in the fields of microwave technology; (2) Development of dual-reflector feed for the arecibo radio telescope, an overview; (3) Advanced microwave technology in modern communication satellites; (4) Differential methods of signal selection in microwave polarimetry; (5) Anticollision car radar in the mm-wave range with pseudo-noise code modulation and digital angle evaluation; (6) Industrial microwave sensors; Theory and applications of polarimetry in radar; (7) Basic theory of radar polarimetry-an engineering approach; (8) Microwave research in agriculture; (9) Wave approach to CAD noise analysis, modeling and measurement of microwave networks; (10) Advances in technology of microwave submicrometer devices and integrated circuits; (11) Recent advances in power amplifier design methodologies; (12) Chiral media: theory and applications for microwaves; (13) State and trends in time domain electromagnetic modelling using the TLM method; and (14) Microwave remote sensing of road surface during winter time. DTIC

N95-18378# Army Research Lab., Adelphi, MD.

SILICON CARBIDE PHOTOCONDUCTIVE SWITCHES Final Report, Oct. 1992 - Dec. 1993

Stephen E. Saddow Sep. 1994 26 p

(AD-A284310; ARL-TR-388) Avail: CASI HC A03/MF A01

The optoelectronic properties of p-type 6-H silicon carbide (6H-SiC) have been investigated in an experiment that used lateral and vertical photoconductive (PC) switches. Both photovoltaic and photoconductive effects are reported, which were observed on switches using both geometries and measured at several wavelengths near the 6H-SiC absorption edge. PC techniques were employed to measure the surface and bulk carrier lifetimes of 40 and 200 ns, respectively. The switches displayed a high-speed photovoltaic response to picosecond laser excitations in the UV and visible spectral regions. In particular, efficient subnanosecond optical absorption processes were observed in the visible region. The photovoltage was measured as a function of both laser wavelength (and hence absorption depth) and laser beam position within the switching gap. The switch response to picosecond laser pulses in the UV, violet, green, and red spectral regions was shown to have subnanosecond photovoltaic response times. Finally, since the optical absorption coefficient had not been well established for device-grade 6H-SiC, the optical absorption coefficient near the 6H-SiC bandgap energy (Eg) was also measured, and the bandgap was determined to be approximately 3.1 eV. DTIC

N95-18418# National Semiconductor Corp., Santa Clara, CA.
RELIABILITY WITHOUT HERMETICITY (RWOH) FOR INTEGRATED CIRCUITS (IC) Final Technical Report
Mar. 1994 212 p
(Contract F33615-90-C-5009)
(AD-A284340; WL-TR-94-4086) Avail: CASI HC A10/MF A03

This effort establishes baseline performance data for an inorganic (ceramic) protective coating over integrated circuits in plastic packages. Severe and differentiating environmental stress testing demonstrated protection against humidity beginning to approach the protection offered by hermetic packaging. Advantages in size and weight are inherent in the technology. DTIC

N95-18425# Warsaw Technical Univ. (Poland).
MIKON 94. INTERNATIONAL MICROWAVE CONFERENCE. VOLUME 1: CONFERENCE PROCEEDINGS
Roman Dufrene 1994 335 p The 10th Conference was held in Ksiaz, Poland, on 30 May - 2 Jun. 1994
(AD-A284351; R/D-7346-EE-02-Vol-1) Avail: CASI HC A15/MF A03

The following topics are discussed: (1) Semiconductor Devices; (2) Passive Devices and Components; (3) Active Devices and Components; (4) Integrated Circuits-Hybrid and Monolithic; (5) Millimeter Technology; (6) Radar Technology; (7) CAD Methods; Antennas and Propagation; Radar Polarimetry; (8) Field Theory; (9) Measurements; and (10) Industrial, Agricultural, Environmental and Medical Applications. DTIC

N95-18426# Warsaw Technical Univ. (Poland).
MIKON 94. INTERNATIONAL MICROWAVE CONFERENCE. CONFERENCE PROCEEDINGS, VOLUME 2
Roman Dufrene 1994 371 p The 10th Conference was held in Ksiaz, Poland, on 30 May - 2 Jun. 1994
(AD-A284352; R/D-7346-EE-02-Vol-2) Avail: CASI HC A16/MF A03

The following topics are discussed: (1) Semiconductor Devices; (2) Passive Devices and Components; (3) Active Devices and Components; (4) Integrated Circuits-Hybrid and Monolithic; (5) Millimeter Technology; (6) Radar Technology; (7) CAD Methods; (8) Antennas and Propagation; (9) Radar Polarimetry; (10) Field Theory; (11) Measurements; and (12) Industrial, Agricultural, Environmental and Medical Applications. DTIC

N95-18432 Department of the Navy, Washington, DC.
HIGH CURRENT AMPLIFIER UTILIZING A JOSEPHSON JUNCTION SCHOTTKY DIODE THREE TERMINAL DEVICE Patent
Bruce J. Dalrymple, inventor (to Navy), Arnold H. Silver, inventor (to Navy), and Randy W. Simon, inventor (to Navy) 26 Apr. 1994 6 p Filed 15 Aug. 1991
(AD-D016278; US-Patent-5,306,927; US-Patent-Appl-SN-745315) Avail: US Patent and Trademark Office

A high current amplifier, three terminal device, comprising a Josephson tunnel junction and a Schottky diode is configured so that the Josephson junction and Schottky diode share a common base electrode which is made very thin. Electrons which cross the Schottky barrier are supplied to the Josephson junction to obtain the amplified output current. DTIC

N95-18433 Department of the Navy, Washington, DC.
SUPERCONDUCTOR MICROELECTRONIC DEVICES AND CIRCUITS AND A METHOD OF FABRICATING THEREFOR Patent
Ted G. Berlincourt, inventor (to Navy) 22 Mar. 1994 6 p Filed 5 Feb. 1992
(AD-D016280; US-Patent-5,296,749; US-Patent-Appl-SN-831582) Avail: US Patent and Trademark Office

Magnetic flux concentrating materials are introduced in superconducting microelectronic devices and circuits as a method and means for fabrication of more compact, higher speed superconducting microelectronic devices and circuits. DTIC

N95-18455# Department of the Navy, Washington, DC.
FAULT PROTECTION CIRCUIT FOR POWER SWITCHING DEVICE Patent Application
John R. Raposa, inventor (to Navy) 5 Apr. 1994 19 p
(AD-D016466; US-Patent-Appl-SN-223346; Navy-Case-74453) Avail: CASI HC A02/MF A01

A fault protection circuit for a power switching device. The circuit comprises a driver circuit electrically connected to the power switching device, a saturation comparator electrically connected to the collector of the switching device to determine if the switching device is switching an excessive voltage, and two undervoltage comparators to determine if the gate is receiving sufficient voltage. If the gate is oversaturated the saturation comparator enables the gate of a field effect transistor which drains the gate of the switching device, and the saturation comparator also disables the driver circuit. The undervoltage detectors detect insufficient voltage to the driver circuit and disable the driver circuit. Once the driver circuit is disabled the control circuitry can take corrective action. DTIC

N95-18485# Texas Technological Univ., Lubbock, TX. Dept. of Computer Science.
LOCALLY CONNECTED ADAPTIVE GABOR FILTER FOR REAL-TIME MOTION COMPENSATION Quarterly Progress Report No. 4, 20 Jul. - 19 Oct. 1994
Hua Li 19 Oct. 1994 84 p
(Contract N00014-94-1-0077)
(AD-A285726) Avail: CASI HC A05/MF A01

We have conducted extensive research work on the design and simulation of electronic analog circuits as basic building blocks for the VLSI implementation. This phase of the work is a little bit ahead of the schedule (about 1 month) than we originally planned in the proposal. This hardware design phase concurrent with the algorithm analysis and verification provided coherent work and ensured the quality of the analog VLSI design. In order to benchmark the VLSI chips, a hardware prototype board is under design and construction. This board will be used to compare the performance of digital approach vs. analog approach, analog approach based on the standard off-the shelf components vs. analog customer-design VLSI approach. The board is now operating and it is under calibration. The board is designed with a 486 machine as a host. DTIC

N95-18501 Technische Univ., Delft (Netherlands).
PARTITION METHOD FOR THE DETERMINATION OF MULTIPLE DC OPERATING POINTS Ph.D. Thesis [PARTITIE METHODE TER BEPALENVAN MEERVOUDIGE DC INSTLPUNTEN]
L. A. Sarmiento Reyes 2 May 1994 220 p
(PB94-201480; ISBN-90-6275-974-2) Copyright Avail: Issuing Activity

A topological description of transistor circuits is used to determine an upper bound on the number of DC operating points along with the calculation of these operating points. This leads to a method useful for a class of transistor circuits. In Chapter 1, the phenomenon of multiple DC solutions in electronic circuits is outlined. In chapter 2, some fundamentals of graph theory and circuit topology which are applicable to circuit analysis are presented. There is also a review of the most commonly used network analysis methods. In Chapter 3, the formulation of the equilibrium equations for DC analysis for the modified nodal analysis representation is explained. In Chapter 4, the problem of finding multiple solutions is formulated from a point of view which takes into account the topology of the circuit. In Chapter 5, the characteristics of both matrices are widely analyzed and a first main result is achieved. In Chapter 6, the method is tested by several examples. Among these, typical benchmarks used by various authors are

treated. Finally, the conclusions of the present work are given in Chapter 7, as well as some recommendations for future research. NTIS

N95-18523 Department of the Navy, Washington, DC.
POWER CONVERSION SYSTEM MODIFICATION TO PERMIT USE OF DC POWER SOURCE Patent
Thomas A. Frank, inventor (to Navy) and Claude D. Michel, inventor (to Navy) 7 Jun. 1994 5 p Filed 7 Aug. 1992 Supersedes AD-D015409
(AD-D016421; US-Patent-5,319,249; US-Patent-Appl-SN-926112; US-Patent-Class-307-66) Avail: US Patent and Trademark Office

In an electrical power conversion system designed to operate on three-phase AC voltage generated by a motor generator, a modification is provided to permit the use of a DC power source to operate same. The power conversion system has a plurality of AC-to-DC conversion means for converting the generated three-phase AC voltages. The first specified DC voltage is supplied to a voltage reduction means and the second specified DC voltage is supplied to a control logic circuit of the power' source and means, utilizing power from said DC power source, for supplying DC voltages equivalent to the first and second specified DC voltages. The supplying means is isolated from the generated three-phase voltage such that the power conversion system can operate on: three-phase AC voltage generated by the motor generator, DC voltages equivalent to the first and second specified DC voltages from the supplying means, or a combination of the three-phase AC voltage generated by the motor generator and the DC voltages from the supplying means. DTIC

N95-18528# Department of the Navy, Washington, DC.
SYNCHRONIZATION OF NONAUTONOMOUS CHAOTIC SYSTEMS Patent Application
Thomas L. Carroll, inventor (to Navy) and Louis M. Pecora, inventor (to Navy) 29 Jun. 1994 67 p
(AD-D016440; US-Patent-Appl-SN-267696; Navy-Case-75496) Avail: CASI HC A04/MF A01

A cascaded synchronized system includes a nonlinear transmitter, a nonlinear cascaded receiver, a phase-detector/controller coupled to the receiver, and a signal generator also coupled to the receiver. The transmitter is responsive to an externally generated transmitter forcing signal for producing and transmitting a chaotic communications signal containing phase information. The cascaded receiver is responsive to a receiver forcing signal and to the chaotic communications signal for producing a chaotic receiver output signal containing phase information. The phase-detector/controller is responsive to the chaotic communications signal and to the receiver output signal for producing a correction signal. The signal generator is responsive to the correction signal for producing the receiver forcing signal in phase with and having the same frequency as the transmitter forcing signal. DTIC

N95-18546 Department of the Navy, Washington, DC.
METHOD FOR FABRICATING COMPLEMENTARY ENHANCEMENT AND DEPLETION MODE FIELD EFFECT TRANSISTORS ON A SINGLE SUBSTRATE Patent
Randy L. Shimabukuro, inventor (to Navy), Michael E. Wood, inventor (to Navy), and Oswald I. Csanadi, inventor (to Navy) 5 Apr. 1994 11 p Filed 30 Jun. 1993
(AD-D016270; US-Patent-5,300,443; US-Patent-Appl-SN-094541; US-Patent-Class-437-34) Avail: US Patent and Trademark Office

A method for fabricating complementary enhancement and depletion mode field effect transistors on a single substrate comprises the steps of: (1) patterning a structure of a layer of silicon formed on an insulating substrate to form first, second, third, and fourth silicon islands; (2) doping the second island with a n-type dopant; (3) doping the third island with a n-type dopant; (4) doping the fourth island with an n-type dopant; (5) forming a first electrically insulating gate layer on the third and fourth islands; (6) forming a second electrically insulating gate on the first and second islands; (7) forming an electrically conductive gate over the first and second electrically insulating gate layers; (8) doping the second island with an n-type dopant; (9) doping the fourth island with an n-type dopant; (10) doping the first and third islands with a n-type dopant: and (11) doping the first and third islands with a n-type dopant to transform the first island into a n-type enhancement mode field effect transistor, the second island into a n-type enhancement mode field effect transistor, the third island into a n-type depletion mode field effect transistor, and the fourth island into an n-type depletion mode field effect transistor. DTIC

N95-18625 Stanford Univ., CA. Center for Integrated Systems.
LOW VOLTAGE ELECTRON BEAM LITHOGRAPHY Monthly Report, Jul. 1994
R. Browning and R. F. Pease 29 Aug. 1994 2 p Limited Reproducibility: More than 20% of this document may be affected by microfiche quality
(Contract N00014-92-J-1996)
(AD-A284181) Avail: Issuing Activity (Defense Technical Information Center (DTIC))

The contract has three parts covering aspects of high precision electron beam lithography: (1) Comprehensive computer modeling of the electron beam tools; (2) Experimental determination of the properties of sources, columns, and targets; and (3) The use of silicon single crystals as straightness and orthogonality standards using orientation dependent etching techniques. DTIC

N95-18660 Johnson Controls, Inc., Milwaukee, WI. Battery Group.
DEVELOPMENT OF A BIPOLAR LEAD/ACID BATTERY FOR THE MORE ELECTRIC AIRCRAFT Interim Report, 1 Sep. 1991 - 1 Mar. 1993
Douglas C. Pierce Mar. 1994 43 p Limited Reproducibility: More than 20% of this document may be affected by microfiche quality
(Contract F33615-91-C-2142)
(AD-A284050; WL-TR-94-2025) Avail: Issuing Activity (Defense Technical Information Center (DTIC))

This report summarizes the development work completed under contract F33615-91-C-2142 for the time period of September 1991 through March 1993. The focus of the work was on the development of a filled polymeric composite substrate for use in a true bipolar lead acid battery. The contract goals for the development of the substrate material are as follows: Resistivity: less than or equal to 2 ohm-cm; Thickness: less than or equal to 0.064 cm; Weight: less than or equal to 150 mg/sq cm; Area: more than or equal to 400 sq cm. This report presents information towards achieving those goals. DTIC

N95-18662 Martin Marietta Labs., Baltimore, MD.
WAVEGUIDE SWITCHES USING ASYMMETRIC COUPLED QUANTUM WELLS Final Report, Dec. 1989 - Dec. 1993
Kenneth J. Ritter and Scott C. Horst Jul. 1994 79 p Limited Reproducibility: More than 20% of this document may be affected by microfiche quality
(Contract F19628-90-C-0028)
(AD-A284056; RL-TR-94-92) Avail: CASI HC A05

This report contains the results of a three-year effort to investigate the use of Asymmetric Coupled Quantum Well in optical waveguide cross bar switches. The two types of devices investigated are the standard delta beta switch and the delta alpha switch. The delta alpha switch uses the imaginary part of the refractive index to modulate the intensity along different waveguide paths in the switch structure. Both types of switch were fabricated and tested. The delta beta switches produced are suitable as 1-input 2-output devices. The delta alpha switches were demonstrated as 2 by 2 cross bar switches with up to 40% throughput. To compensate for losses in the switches the use of amplifying elements was investigated. To provide gain at a longer wavelength than that of the excitons in the modulation waveguides, the quantum wells in the modulation waveguides were blue shifted using vacancy induced disordering (VID). The VID shifted quantum wells showed less Stark shift than the unshifted quantum wells. This effect is explained by the nearly parabolic shape of the disordered wells. Coupled quantum wells can be used to create a structure that will maintain a strongly Stark shifted spatially indirect transition even after VID. Modeling of the various waveguide structures used is also discussed. DTIC

N95-18925*# Alabama Univ., Huntsville, AL. Dept. of Physics.
COMPUTATIONAL MODELING OF PROPERTIES Final Report, 12 Mar. 1993 - 11 Jul. 1994
Judy R. Franz 11 Jul. 1994 51 p
(Contract NAS8-38609)
(NASA-CR-197558; NAS 1.26:197558) Avail: CASI HC A04/MF A01

A simple model was developed to calculate the electronic transport

parameters in disordered semiconductors in strong scattered regime. The calculation is based on a Green function solution to Kubo equation for the energy-dependent conductivity. This solution together with a rigorous calculation of the temperature-dependent chemical potential allows the determination of the dc conductivity and the thermopower. For wide-gap semiconductors with single defect bands, these transport properties are investigated as a function of defect concentration, defect energy, Fermi level, and temperature. Under certain conditions the calculated conductivity is quite similar to the measured conductivity in liquid 2-6 semiconductors in that two distinct temperature regimes are found. Under different conditions the conductivity is found to decrease with temperature; this result agrees with measurements in amorphous Si. Finally the calculated thermopower can be positive or negative and may change sign with temperature or defect concentration. Author

N95-18959* National Aeronautics and Space Administration. Ames Research Center, Moffett Field, CA.
CONSTANT CURRENT LOOP IMPEDANCE MEASURING SYSTEM THAT IS IMMUNE TO THE EFFECTS OF PARASITIC IMPEDANCES Patent
Karl F. Anderson, inventor (to NASA) 6 Dec. 1994 11 p Filed 16 Feb. 1993
(NASA-Case-ARC-11988-1; US-Patent-5,371,469;
US-Patent-Appl-SN-018128; US-Patent-Class-324-705;
US-Patent-Class-324-706; US-Patent-Class-324-713;
US-Patent-Class-324-601; US-Patent-Class-324-130;
US-Patent-Class-73-862.628; Int-Patent-Class-G01R-27/02) Avail: US Patent and Trademark Office

A constant current loop measuring system is provided for measuring a characteristic of an environment. The system comprises a first impedance positionable in the environment, a second impedance coupled in series with said first impedance and a parasitic impedance electrically coupled to the first and second impedances. A current generating device, electrically coupled in series with the first and second impedances, provides a constant current through the first and second impedances to produce first and second voltages across the first and second impedances, respectively, and a parasitic voltage across the parasitic impedance. A high impedance voltage measuring device measures a voltage difference between the first and second voltages independent of the parasitic voltage to produce a characteristic voltage representative of the characteristic of the environment. Official Gazette of the U.S. Patent and Trademark Office

N95-18962* National Aeronautics and Space Administration. Langley Research Center, Hampton, VA.
INDUCTION HEATING COUPLER AND ANNEALER Patent
Robert L. Fox, inventor (to NASA), Samuel D. Johnson, inventor (to NASA), Carl E. Copeland, inventor (to NASA), Robert H. Coultrip, inventor (to NASA), W. Morris Phillips, inventor (to NASA), David F. Johnston, inventor (to NASA), Robert J. Swaim, inventor (to NASA), and James R. Dinkins, inventor (to NASA) 20 Dec. 1994 14 p Filed 12 May 1993
(NASA-Case-LAR-14277-1; US-Patent-5,374,809;
US-Patent-Appl-SN-060947; US-Patent-Class-219-633;
US-Patent-Class-219-634; US-Patent-Class-219-635;
US-Patent-Class-219-659; US-Patent-Class-148-573;
Int-Patent-Class-H05B-6/14) Avail: US Patent and Trademark Office

An induction heating device includes a handle having a hollow interior and two opposite ends, a wrist connected to one end of the handle, a U-shaped pole piece having- two spaced apart ends, a tank circuit including an induction coil wrapped around the pole piece and a capacitor connected to the induction coil, a head connected to the wrist and including a housing for receiving the U-shaped pole piece, the two spaced apart ends of the pole piece extending outwardly beyond the housing, and a power source connected to the tank circuit. When the tank circuit is energized and a susceptor is placed in juxtaposition to the ends of the U-shaped pole piece, the susceptor is heated by induction heating due to a magnetic flux passing between the two ends of the pole piece.
Official Gazette of the U.S. Patent and Trademark Office

N95-19089# Oregon State Univ., Corvallis, OR. Dept. of Electrical and Computer Engineering.
THE 3D INTERNATIONAL WORKSHOP ON COMPUTATIONAL ELECTRONICS Final Report
Stephen M. Goodnick 15 Sep. 1994 7 p Workshop held in Portland, OR, 18-20 May 1994
(AD-A284678) Avail: CASI HC A02/MF A01

The Third International Workshop on Computational Electronics (IWCE) was held at the Benson Hotel in downtown Portland, Oregon, on May 18, 19, and 20, 1994. The workshop was devoted to a broad range of topics in computational electronics related to the simulation of electronic transport in semiconductors and semiconductor devices, particularly those which use large computational resources. The workshop was supported by the National Science Foundation (NSF), the Office of Naval Research and the Army Research Office, as well as local support from the Oregon Joint Graduate Schools of Engineering and the Oregon Center for Advanced Technology Education. There were over 100 participants in the Portland workshop, of which more than one quarter represented research groups outside of the United States from Austria, Canada, France, Germany, Italy, Japan, Switzerland, and the United Kingdom. There were a total 81 papers presented at the workshop, 9 invited talks, 26 oral presentations and 46 poster presentations. The emphasis of the contributions reflected the interdisciplinary nature of computational electronics with researchers from the Chemistry, Computer Science, Mathematics, Engineering, and Physics communities participating in the workshop. DTIC

N95-19120 Department of the Navy, Washington, DC.
POWER TERMINAL PROTECTION DEVICE Patent
Yung K. Yi, inventor (to Navy) 5 Jul. 1994 5 p Filed 9 Oct. 1990 Supersedes AD-D014747
(AD-D016528; US-Patent-5,327,316; US-Patent-Appl-SN-594751;
US-Patent-Class-361-56) Avail: US Patent and Trademark Office

Metal oxide varistors are connected in parallel with grounded capacitors to load outlet terminals coupled to a power source through inductor coils forming a low pass filter with the capacitors to delay propagation of a voltage increasing transient pulse to the power source until ground shunting paths of low resistance are developed in the varistors. Electromagnetic shielding partitions the inductor from the capacitors and varistors within a power outlet box mounting the load outlet terminals to prevent interference with absorption of transient energy by the varistors during the delay in establishing the ground shunting paths. DTIC

N95-19171 Department of the Navy, Washington, DC.
DIGITAL CIRCUIT FOR THE INTRODUCTION AND LATER REMOVAL OF DITHER FROM AN ANALOG SIGNAL Patent
Gary S. Borgen, inventor (to Navy) 10 May 1994 20 p Filed 15 Jan. 1993
(AD-D016462; US-Patent-5,311,180; US-Patent-Appl-SN-004004;
US-Patent-Class-341-131) Avail: US Patent and Trademark Office

An electronics circuit is presented for accurately digitizing an analog audio or like data signal into a digital equivalent signal by introducing dither into the analog signal and then subsequently removing the dither from the digitized signal prior to its conversion to an analog signal which is a substantial replica of the incoming analog audio or like data signal. The electronics circuit of the present invention is characterized by a first pseudo-random number generator which generates digital random noise signals or dither for addition to the digital equivalent signal and a second pseudo-random number generator which generates subtractive digital random noise signals for the subsequent removal of dither from the digital equivalent signal prior its conversion to the analog replica signal. DTIC

N95-19200# Los Alamos National Lab., NM.
THE US 100 T MAGNET PROJECT
L. J. Campbell, D. M. Parkin, D. G. Rickel, J. B. Schillig, Y. Eyssa (Florida State Univ., Tallahassee, FL), P. Gilmore (Florida State Univ., Tallahassee, FL), P. Pernambuco-Wise (Florida State Univ., Tallahassee, FL), and H. J. Schneider-Muntau (Florida State Univ., Tallahassee, FL) 1994 11 p Presented at the 4th International Symposium on Research in High Magnetic Fields, Nijmegen, Netherlands, 29-31 Aug. 1994
(Contract W-7405-eng-36)
(DE94-016099; LA-UR-94-2576; CONF-940831-1) Avail: CASI HC A03/MF A01

A design is presented of a 100 T research magnet to generate high field pulses having lengths of more than 20 ms at field levels of above 80 T. The magnet is designed to be non-destructive, have a bore of 24 mm and a repetition rate of less than one hour. It consists of a 50 T outsert

magnet, constructed of five concentric, mechanically independent coils, powered from a motor-generator, and a self-supporting 50 T insert magnet, which is energized from a capacitor bank. The design is based on commercially available materials. The magnet has an overall diameter and total length of approximately 1 m. DOE

N95-19230# Allied-Signal Aerospace Co., Kansas City, MO.
PRECISION GOLD CONDUCTORS FOR HMCs
M. R. Widmer Aug. 1994 15 p
(Contract DE-AC04-76DP-00613)
(DE94-018558; KCP-613-5376) Avail: CASI HC A03/MF A01

Ti/Pd/Au multiple code coded switch (MCCS) networks were built and compared to Cr/Au MCCS networks. The data showed no measurable difference between the two systems. Interface resistance of both types of networks was measured as a diagnostic aid to determine if hydrogen was affecting the Ti/Pd/Au MCCS networks. The data showed that although hydrogen does affect Ti/Pd/Au, the changes are not significant with respect to MCCS environments. An evaluation of several proprietary gold electroplating solutions for use in the production of Ti/Pd/Au conductors was performed. All the testing results were comparable to the current product requirements. DOE

N95-19231# Allied-Signal Aerospace Co., Kansas City, MO.
DEVELOPMENT OF HIGH RELIABILITY PLANAR CHIP INDUCTORS
H. W. Swanson, Jr. Aug. 1994 9 p
(Contract DE-AC04-76DP-00613)
(DE94-018589; KCP-613-5482) Avail: CASI HC A02/MF A01

A process for fabrication of multilayer planar chip inductors on ceramic wafers has been developed. This paper will summarize the progress made in the use of step-and-repeat print processes to fabricate a family of high reliability planar chip inductors for surface mount RF applications. Experimental data on thick-film gold and plated-copper windings are presented. In addition, the development of an automated RF probe station and waferized calibration standards are discussed. DOE

N95-19240# Sandia National Labs., Albuquerque, NM.
RESONATOR/OSCILLATOR RESPONSE TO LIQUID LOADING
J. J. Spates (Ktech Corp., Albuquerque, NM.), S. J. Martin, K. O. Wessendorf, and R. J. Huber (Utah Univ., Salt Lake City, UT.) 1994 11 p Presented at the 186th Meeting of the Electrochemical Society, Miami, FL, 9-14 Oct. 1994
(Contract DE-AC04-94AL-85000)
(DE94-013442; SAND-94-1310C; CONF-941063-2) Avail: CASI HC A03/MF A01

A thickness-shear mode (TSM) resonator typically consists of a thin disk of AT-cut quartz with circular electrodes patterned on both sides. When connected to appropriate circuitry, the quartz crystal resonates at a frequency determined by the crystal thickness. Originally used to measure metal deposition in vacuum, the device has recently been used for measurements in liquid. Since the mass sensitivity of the resonator is nearly the same in liquids as in air or vacuum, the device can be used as a sensitive solution-phase microbalance. In addition, the sensitivity of the TSM resonator to contacting fluid properties enables it to function as a monitor for these properties. Under liquid loading, the change in frequency of the resonator/oscillator combination differs from the change in resonant frequency of the device. Either of these changes can be determined from an appropriate application of an equivalent-circuit model that describes the electrical characteristics of the liquid-loaded resonator. DOE

N95-19246# Argonne National Lab., IL.
REAL TIME SIMULATOR WITH TI FLOATING POINT DIGITAL SIGNAL PROCESSOR
K. Razazian, J. P. Bobis, S. L. Dieckman, and A. C. Raptis 1994 9 p Presented at the Texas Instruments TMS320 Conference, Houston, TX, 5-7 Aug. 1994
(Contract W-31-109-eng-38)
(DE94-016372; ANL/ET/CP-83611; CONF-9408130-1) Avail: CASI HC A02/MF A01

This paper describes the design and operation of a real time simulator using Texas Instruments TMS320C30 digital signal processor. This system operates with two banks of memory which provide the input data to digital signal processor chip. This feature enables the TMS320C30 to be utilized in variety of applications for which external connections to acquire input data is not needed. In addition, some practical applications of this real time simulator are discussed. DOE

N95-19519# Army Lab. Command, Fort Monmouth, NJ. Electronics Technology and Devices Lab.
QUARTZ CRYSTAL RESONATORS AND OSCILLATORS FOR FREQUENCY CONTROL AND TIMING APPLICATIONS. A TUTORIAL
John R. Vig Aug. 1994 280 p Revised
(DA Proj. 1L1-62705-AH-94)
(AD-A284995; SLCET-TR-88-1-Rev-7.0) Avail: CASI HC A13/MF A03

Subjects covered include: applications of frequency standards; types of oscillators (quartz and atomic); quartz resonator properties; quartz growing, sweeping, and material characteristics; Q and its significance; resonator and oscillator stability, including aging, short-term instability, frequency vs. temperature characteristics, oscillator circuit caused instabilities, frequency vs. drive level effects, acceleration effects, the effect of shock, and radiation effects emerging technologies; atomic frequency standards; comparison of the major oscillator types; oscillator specifications and selection guidelines; time and timekeeping; clock errors; relativistic time; time transfer; time and frequency subsystem; and other applications of quartz resonators. The goal of this document is to assist in presenting to the nonspecialist the most frequently encountered concepts in frequency control and timing. The document originated as a set of hard copies' of presentation visuals (i.e., vugraphs.) DTIC

N95-19548# National Inst. for Fusion Science, Nagoya (Japan).
IMPROVEMENT OF A HIGH CURRENT DC POWER SUPPLY SYSTEM FOR TESTING THE LARGE SCALED SUPERCONDUCTING CABLES AND MAGNETS
Shuichi Yamada, Hirotaka Chikaraishi, and Shugo Tanahashi et al Nov. 1993 23 p
(DE94-770767; NIFS-256) Avail: CASI HC A03/MF A01

A dc 75 kA power supply system was constructed to test the superconducting (SC) R and D cables and magnets for the Large Helical Device. It consists of three 25 kA unit banks. A unit bank has two double-star-rectifier connections with the inter-phase reactors. A digital feedback control method is applied to the automatic current regulation (ACR) in each unit bank. For shortening the dead time of the feedback process, a new algorithm of a digital phase controller for the ACR is investigated. A Bode diagram of the feedback process is directly measured. It is confirmed that the dead time of the feedback process is reduced to one sixth, and that the feedback gain of PID compensation is improved by a factor of two from the original method. DOE

N95-19573# Naval Postgraduate School, Monterey, CA.
MITIGATION OF EMI GENERATED BY A VARIABLE-FREQUENCY-DRIVE CONTROLLER FOR AN AC INDUCTION MOTOR M.S. Thesis
Philip E. VanWiltenburg Sep. 1994 59 p
(AD-A286045) Avail: CASI HC A04/MF A01

In recent years a significant number of digital devices and systems have been added to receiving and data-processing sites. These additions have enhanced the ability of the sites to accomplish their mission. They have also introduced new kinds of electromagnetic interference (EMI) into these sites along with accompanying performance degradation problems. In this thesis one specific case of EMI is considered. It is EMI from a digital climate-control system of a building housing a data-processing facility. The digital system generated excessive amounts of EMI. The EMI was conducted throughout the site over power and control conductors. Electromagnetic fields from EMI current flowing in these conductors coupled the EMI into other nearby conductors. Integrated barrier, filter, and ground techniques were used to reduce the conducted and radiated EMI to harmless levels. DTIC

N95-19606# University of Southern California, Marina del Rey, CA. Information Sciences Inst.
AUTO: AUTOMATIC SCRIPT GENERATION SYSTEM
John Granacki, Ivan Hom, and Tauseef Kazi 17 Nov. 1993 28 p
(AD-A285897; ISI/TM-93-389) Avail: CASI HC A03/MF A01

This technical manual describes an automatic script generation system (Auto) for guiding the physical design of a printed circuit board. Auto

accepts a printed circuit board design as specified in a netlist and partslist and returns a script to automatically provide all the necessary commands and file specifications required by Harris EDA's Finesse CAD system for placing and routing the printed circuit board. Auto insulates the designer from learning the details of commercial CAD systems, allows designers to modify the script for customized design entry, and performs format and completeness checking of the design files. This technical manual contains a complete tutorial/design example describing how to use the Auto system and also contains appendices describing the format of files required by the Finesse CAD system. DTIC

N95-19687# California Univ., Santa Barbara, CA. Dept. of Electrical and Computer Engineering.

VACUUM MICROELECTRONIC EMITTERS AND THEIR APPLICATIONS USING COMPOUND SEMICONDUCTOR TECHNOLOGY Final Report, 1 Jun. 1991 - 31 May 1994

David Holcombe, Wei-Nan Jiang, and Umesh K. Mishra 16 Jul. 1994 29 p

(Contract DAAL03-91-G-0161)

(AD-A284811) Avail: CASI HC A03/MF A01

Vacuum microelectronic devices (VMDs) are a class of devices in which electron transport occurs both in semiconductors and in vacuum. They have the potential of combining the advantages of vacuum tube based devices with those of modern semiconductor devices. The key to the success of VMDs is fabricating reliable solid state electron emitters with high emission efficiency and high emission current density. This report will present the design, growth, fabrication, and characterization of planar-doped-barrier electron emitters (PDBEEs) made of compound semiconductor AlGaAs/GaAs. In PDBEEs, electrons, as majority carriers, are injected over a triangular barrier into a high field region accelerated towards the surface. Injected electrons gain kinetic energy from the field and lose kinetic energy through scattering processes. Those electrons with enough energy to overcome the surface barrier upon reaching the surface could be emitted into vacuum. The surface work function of semiconductors (GaAs in this work) is lowered by cesiation. An emission efficiency of 4.2% and an emission current density of 5.8 A/sq cm have been obtained from Al(0.3)Ga(0.7)As/GaAs PDBEEs. Author (DTIC)

N95-19741 Case Western Reserve Univ., Cleveland, OH. Dept. of Chemistry.

ELECTROCHEMICAL INTERFACES AND ELECTRODE PROCESSES: ELECTROCHEMICAL OXIDATION OF SMALL ORGANISMS Final Report, 1 Oct. 1989 - 30 Sep. 1993

Ernest B. Yeager 1 Sep. 1994 24 p Limited Reproducibility: More than 20% of this document may be affected by microfiche quality

(Contract N00014-90-J-1212)

(AD-A284873) Avail: CASI HC A03

This report summarizes research involving mechanistic studies of the oxidation of small hydrocarbons and carbon monoxide on platinum in aqueous electrolytes, transition metal oxides as electrocatalysts for O2 reduction and as supports for dispersed platinum, and transition metal complexes exhibiting high catalytic activity for O2 reduction on graphite. Author (DTIC)

N95-19842 Sandia National Labs., Albuquerque, NM. Dept. of Electromechanical Components.

CHARACTERISTICS AND DEVELOPMENT REPORT FOR THE MC3994 AND MC3994A RELAYS

W. R. Nance, J. P. Young, and D. P. Wrobel Nov. 1994 31 p Limited Reproducibility: More than 20% of this document may be affected by microfiche quality

(Contract DE-AC04-94AL-85000)

(DE95-002952; SAND-93-1531) Avail: CASI HC A03

This report gives a brief description of the development activities for the MC3994 and MC3994A relays, including their mechanical and electrical characteristics. The basic details of the design were presented in SAND85-1288, 'Characteristics and Development Report for the MC3593 and MC3594 Relays.' This report also summarizes test results and describes the tests that were performed to ensure that the MC3994 and MC3994A had adequate design margin in accordance with the capability drawing requirements. DOE

N95-19849 Virginia Univ., Charlottesville, VA. Dept. of Electrical Engineering.

SECOND INTERNATIONAL SEMICONDUCTOR DEVICE RESEARCH SYMPOSIUM (ISDRS-1993) Final Report, 1 Nov. 1993 - 28 Feb. 1994 Abstract Only

Michael Shur and John M. Money Apr. 1994 8 p Symposium held in 1993; sponsored by NASA. Ames Research Center, ARO, ONR, and the Soros International Science Foundation Limited Reproducibility: More than 20% of this document may be affected by microfiche quality

(Contract N00014-94-1-0167)

(AD-A279221; UVA/525486/EE94/101) Avail: Issuing Activity (Defense Technical Information Center (DTIC))

The goal of this second biannual international meeting was to provide a congenial forum for the exchange of information and new ideas for researchers from university, industry and government laboratories in the field of semiconductor devices and device physics. To this end, we have an unusually short period between the submission of papers and the conference, a speedy publication of the proceedings, poster sessions, panel discussions, and a wide dissemination of the conference proceedings. Our other goal is to make this conference truly international. To achieve this, the symposium has sub-committees in Asia, Europe and the former Soviet Union. This conference is organized in cooperation with the IEEE MTT Society, the European Physical Society, the United States National Committee of URSI and the Russian Physical Society. Generous financial support has been provided by the Army Research Office, the Office of Naval Research, the NASA Ames Research Center and the Soros International Science Foundation. Papers cover a broad range of topics, including novel and ultrasmall devices, photonics and optoelectronics, heterostructure and cryogenic devices, wide band gap semiconductors, thin film transistors, MOSFET technology and devices, carrier transport phenomena, materials and device characterization, simulation and modeling. It is hoped that such a broad range of topics will foster a cross-fertilization of the different fields related to semiconductor materials and devices. DTIC

N95-19865 SRI International Corp., Menlo Park, CA.

FIELD-EMITTER ARRAYS FOR RF VACUUM MICROELECTRONICS Quarterly Technical Report No. 9, 1 Sep. - 31 Dec. 1993

C. A. Spindt 27 May 1994 46 p Limited Reproducibility: More than 20% of this document may be affected by microfiche quality

(Contract MDA972-91-C-0029; ARPA Order 8162)

(AD-A279932) Avail: Issuing Activity (Defense Technical Information Center (DTIC))

SRI International has completed the ninth quarter of a program to develop field-emitter arrays for vacuum microelectronics. We have met the first-phase program goals of 5 mA total emission, with a current density of 5 A/sq cm for at least 2 hours and demonstrated modulation of the emission current at a frequency of 1 GHz. An evaluation was made of deposition processes and cone materials that could lead to improved (tall and sharp) cone geometries for low-capacitance cathode fabrication. Principal efforts involved investigation of the limited emission of high-frequency cathode samples, continued stability tests on high-frequency cathodes to determine the effectiveness of processes designed to avoid contamination, and capacitance measurements on cathode samples incorporating an electrostatic shield designed to prevent fringing fields from the base electrode from influencing the trajectories of emitted electrons. DTIC

N95-19872# Sandia National Labs., Albuquerque, NM.

BATTERY AND CHARGE CONTROLLER EVALUATIONS IN SMALL STAND-ALONE PV SYSTEMS

J. R. Woodworth, M. G. Thomas, J. W. Stevens, J. L. Dunlop (Florida Solar Energy Center, Cape Canaveral, FL.), M. R. Swamy (Florida Solar Energy Center, Cape Canaveral, FL.), L. Demetrius (Florida Solar Energy Center, Cape Canaveral, FL.), and S. R. Harrington (Ktech Corp., Albuquerque, NM.) 1994 5 p Presented at the 1st World Conference on Photovoltaic Energy Conversion, Waikoloa, HI, 5-9 Dec. 1994

(Contract DE-AC04-94AL-85000)

(DE94-014252; SAND-94-1560C; CONF-941203-2) Avail: CASI HC A01/MF A01

We report the results of two separate long-term tests of batteries and charge controllers in small stand-alone PV systems. In these experiments, seven complete systems were tested for two years at each of two locations:

Sandia National Laboratories in Albuquerque and the Florida Solar Energy Center in Cape Canaveral, Florida. Each system contained a PV array, flooded-lead-acid battery, a charge controller and a resistive load. Performance of the systems was strongly influenced by the difference in solar irradiance at the two sites, with some batteries at Sandia exceeding manufacturer's predictions for cycle life. System performance was strongly correlated with regulation reconnect voltage (R(sup 2) correlation coefficient = 0.95) but only weakly correlated with regulation voltage. We will also discuss details of system performance, battery lifetime and battery water consumption. DOE

N95-19881# National Renewable Energy Lab., Golden, CO.
CURRENT HYBRID ELECTRIC VEHICLE PERFORMANCE BASED ON TEMPORAL DATA FROM THE WORLD'S LARGEST HEV FLEET
K. Wipke Sep. 1994 11 p Presented at the 12th International Electric Vehicle Symposium, Anaheim, CA, 5-7 Dec. 1994
(Contract DE-AC36-83CH-10093)
(DE94-011859; NREL/TP-473-7260; CONF-941221-2) Avail: CASI HC A03/MF A01

The United States Department of Energy (DOE) procured new data collection equipment for the 42 vehicles registered to compete in the 1994 Hybrid Electric Vehicle (HEV) Challenge, increasing the amount of information gathered from the worlds largest fleet of HEVs. Data were collected through an on-board data storage device and then analyzed to determine effects of different hybrid control strategies on energy efficiency and driving performance. In this paper, the results of parallel hybrids versus series hybrids with respect to energy usage and acceleration performance are examined, and the efficiency and performance of the power-assist types are compared to that of the range-extender types. Because on-board and off-board electrical charging performance is critical to an efficient vehicle energy usage cycle, charging performance is presented and changes and improvements from the 1993 HEV Challenge are discussed. Peak power used during acceleration is presented and then compared to the electric motor manufacturer ratings. Improvements in data acquisition methods for the 1995 HEV Challenge are recommended. DOE

N95-18974*# Alabama Univ., Huntsville, AL. Dept. of Civil and Environmental Engineering.
A FINITE ELEMENT CODE FOR ELECTRIC MOTOR DESIGN
C. Warren Campbell *In* Alabama Univ., Research Reports: 1994 NASA/ASEE Summer Faculty Fellowship Program Oct. 1994 6 p
(For primary document see N95-18967 05-80)
Avail: CASI HC A02/MF A03

N95-18983*# Oregon Graduate Center for Study and Research, Beaverton, OR. Dept. of Electrical Engineering and Applied Physics.
SPECIAL RELATIVITY EFFECTS FOR SPACE-BASED COHERENT LIDAR EXPERIMENTS
V. S. RaoGudimetla *In* Alabama Univ., Research Reports: 1994 NASA/ASEE Summer Faculty Fellowship Program Oct. 1994 6 p
(For primary document see N95-18967 05-80)
Avail: CASI HC A02/MF A03

N95-18985*# Catawba Coll., Salisbury, NC. Dept. of Chemistry.
PROBING THE CHEMISTRY OF NICKEL/METAL HYDRIDE BATTERY CELLS USING ELECTROCHEMICAL IMPEDANCE SPECTROSCOPY
Bryan J. Isaac *In* Alabama Univ., Research Reports: 1994 NASA/ASEE Summer Faculty Fellowship Program Oct. 1994 6 p (For primary document see N95-18967 05-80)
Avail: CASI HC A02/MF A03

N95-19634*# Tennessee Technological Univ., Cookeville, TN.
DEVELOPMENT OF AN EXPERT SYSTEM FOR POWER QUALITY ADVISEMENT USING CLIPS 6.0
A. Chandrasekaran, P. R. R. Sarma, and Ashok Sundaram (Electric Power Research Inst., Palo Alto, CA.) *In* NASA. Johnson Space Center, Third CLIPS Conference Proceedings, Volume 1 Nov. 1994 p 61-66 (For primary document see N95-19625 05-61)
Avail: CASI HC A02/MF A03

34 FLUID MECHANICS AND HEAT TRANSFER

Includes boundary layers; hydrodynamics; fluidics; mass transfer; and ablation cooling.

For related information see also *02 Aerodynamics* and *77 Thermodynamics and Statistical Physics.*

N95-18036*# National Aeronautics and Space Administration. Lewis Research Center, Cleveland, OH.
THE SPACE-TIME SOLUTION ELEMENT METHOD: A NEW NUMERICAL APPROACH FOR THE NAVIER-STOKES EQUATIONS
James R. Scott and Sin-Chung Chang Jan. 1995 21 p Presented at the 33rd Aerospace Sciences Meeting and Exhibit, Reno, NV, 9-12 Jan. 1995, sponsored by AIAA
(RTOP 505-62-52)
(NASA-TM-106818; E-9357; NAS 1.15:106818; AIAA Paper 95-0763)
Copyright Avail: CASI HC A03/MF A01

This paper is one of a series of papers describing the development of a new numerical method for the Navier-Stokes equations. Unlike conventional numerical methods, the current method concentrates on the discrete simulation of both the integral and differential forms of the Navier-Stokes equations. Conservation of mass, momentum, and energy in space-time is explicitly provided for through a rigorous enforcement of both the integral and differential forms of the governing conservation laws. Using local polynomial expansions to represent the discrete primitive variables on each cell, fluxes at cell interfaces are evaluated and balanced using exact functional expressions. No interpolation or flux limiters are required. Because of the generality of the current method, it applies equally to the steady and unsteady Navier-Stokes equations. In this paper, we generalize and extend the authors' 2-D, steady state implicit scheme. A general closure methodology is presented so that all terms up through a given order in the local expansions may be retained. The scheme is also extended to nonorthogonal Cartesian grids. Numerous flow fields are computed and results are compared with known solutions. The high accuracy of the scheme is demonstrated through its ability to accurately resolve developing boundary layers on coarse grids. Finally, we discuss applications of the current method to the unsteady Navier-Stokes equations. Author

N95-18042*# College of William and Mary, Williamsburg, VA. Program in Applied Science.
A SPECTRALLY ACCURATE BOUNDARY-LAYER CODE FOR INFINITE SWEPT WINGS Interim Report
C. David Pruett Dec. 1994 36 p
(Contract NAS1-19656; RTOP 505-59-50-02)
(NASA-CR-195014; NAS 1.26:195014) Avail: CASI HC A03/MF A01

This report documents the development, validation, and application of a spectrally accurate boundary-layer code, WINGBL2, which has been designed specifically for use in stability analyses of swept-wing configurations. Currently, we consider only the quasi-three-dimensional case of an infinitely long wing of constant cross section. The effects of streamwise curvature, streamwise pressure gradient, and wall suction and/or blowing are taken into account in the governing equations and boundary conditions. The boundary-layer equations are formulated both for the attachment-line flow and for the evolving boundary layer. The boundary-layer equations are solved by marching in the direction perpendicular to the leading edge, for which high-order (up to fifth) backward differencing techniques are used. In the wall-normal direction, a spectral collocation method, based upon Chebyshev polynomial approximations, is exploited. The accuracy, efficiency, and user-friendliness of WINGBL2 make it well suited for applications to linear stability theory, parabolized stability equation methodology, direct numerical simulation, and large-eddy simulation. The method is validated against existing schemes for three test cases, including incompressible swept Hiemenz flow and Mach 2.4 flow over an airfoil swept at 70 deg to the free stream. Author

N95-18092*# Wisconsin Univ., Milwaukee, WI. Dept. of Mechanical Engineering.
REWETTING OF MONOGROOVE HEAT PIPE IN SPACE STATION RADIATORS Annual Status Report, 15 Dec. 1993 - 14 Dec. 1994
S. H. Chan 1994 30 p

(Grant NAG3-1381)
(NASA-CR-197579; NAS 1.26:197579) Avail: CASI HC A03/MF A01

This annual report summarizes the work accomplished on rewetting of monogroove heat pipe in space station. Specifically, theoretical and experimental investigations of the rewetting characteristics of thin liquid films over unheated and heated capillary grooved plates were performed. To investigate the effect of gravity on rewetting, the grooved surface was placed in upward and downward facing positions. Profound gravitational effects were observed as the rewetting velocity was found to be higher in the upward than in the downward facing orientation. The difference was even greater with higher initial plate temperatures. With either orientation, it was found that the rewetting velocity increased with the initial plate temperature. But when the temperature was raised above a rewetting temperature, the rewetting velocity decreased with the initial plate temperature. Hydrodynamically controlled and heat conduction controlled rewetting models were then presented to explain and to predict the rewetting characteristics in these two distinct regions. The predicted rewetting velocities were found to be in good agreement with experimental data with elevated plate temperatures. Author

N95-18107*# NYMA, Inc., Brook Park, OH. Engineering Services Div.
AN APPLICATION OF A TWO-EQUATION MODEL OF TURBULENCE TO THREE-DIMENSIONAL CHEMICALLY REACTING FLOWS Final Report
J. Lee Cleveland, OH NASA Dec. 1994 16 p Presented at the 33rd Aerospace Sciences Meeting and Exhibit, Reno, NV, 9-12 Jan. 1995; sponsored by AIAA Original contains color illustrations
(Contracts NAS3-25266; NAS3-27186; RTOP 505-62-52)
(NASA-CR-195411; E-9278; NAS 1.26:195411; AIAA Paper 95-0734)
Avail: CASI HC A03/MF A01; 5 functional color pages

A numerical study of three dimensional chemically reacting and non-reacting flowfields is conducted using a two-equation model of turbulence. A generalized flow solver using an implicit Lower-Upper (LU) diagonal decomposition numerical technique and finite-rate chemistry has been coupled with a low-Reynolds number two-equation model of turbulence. This flow solver is then used to study chemically reacting turbulent supersonic flows inside combustors with synergetic fuel injectors. The reacting and non-reacting turbulent combustor solutions obtained are compared with zero-equation turbulence model solutions and with available experimental data. The hydrogen-air chemistry is modeled using a nine-species/eighteen reaction model. A low-Reynolds number k-epsilon model was used to model the effect of turbulence because, in general, the low-Reynolds number k-epsilon models are easier to implement numerically and are far more general than algebraic models. However, low-Reynolds number k-epsilon models require a much finer near-wall grid resolution than high-Reynolds number models to resolve accurately the near-wall physics. This is especially true in complex flowfields, where the stiff nature of the near-wall turbulence must be resolved. Therefore, the limitations imposed by the near-wall characteristics and compressible model corrections need to be evaluated further. The gradient-diffusion hypothesis is used to model the effects of turbulence on the mass diffusion process. The influence of this low-Reynolds number turbulence model on the reacting flowfield predictions was studied parametrically. Author

N95-18111*# Foster-Miller Associates, Inc., Waltham, MA.
LUNAR BASE HEAT PUMP, PHASE 1 Final Report, 20 Jan. - 18 May 1993
Jeffrey H. Goldman, A. Harvey, T. Lovell, and David H. Walker Jul. 1994 62 p
(Contract NAS9-18819; FMI PROJ. NAS-9614)
(NASA-CR-188300; NAS 1.26:188300; NAS-8819-FM-9614-820; FMI-NAS-9614-4) Avail: CASI HC A04/MF A01

This report describes the Phase 1 process and analysis used to select a refrigerant and thermodynamic cycle as the basis of a vapor compression heat pump requiring a high temperature lift, then to perform a preliminary design to implement the selected concept, including major component selection. Use of a vapor compression heat pump versus other types was based on prior work performed for the Electric Power Research Institute. A high lift heat pump is needed to enable a thermal control system to remove heat down to 275 K from a habitable volume when the external thermal environment is severe. For example, a long-term lunar base habitat will reject heat from a space radiator to a 325 K environment. The first step in the selection process was to perform an optimization trade study, quantifying the effect of radiator operating temperature and heat pump efficiency on total system mass; then, select the radiator operating temperature corresponding to the lowest system mass. Total system mass included radiators, all heat pump components, and the power supply system. The study showed that lunar night operation, with no temperature lift, dictated the radiator size. To operate otherwise would require a high mass penalty to store power. With the defined radiation surface, and heat pump performances assumed to be from 40 percent to 60 percent of the Carnot ideal, the optimum heat rejection temperature ranged from 387 K to 377 K, as a function of heat pump performance. Refrigerant and thermodynamic cycles were then selected to best meet the previously determined design conditions. The system was then adapted as a ground-based prototype lifting temperature to 360 K (versus 385 K for flight unit) and using readily available commercial-grade components. Over 40 refrigerants, separated into wet and dry compression behavioral types, were considered in the selection process. Refrigerants were initially screened for acceptable critical temperature. The acceptable refrigerants were analyzed in ideal single and two-stage thermodynamic cycles. Top candidates were analyzed assuming realistic component limits and system pressure drops, and were evaluated for other considerations such as safety, environmental impact, and commercial availability. A maximum coefficient of performance (COP) of 56 percent of the Carnot ideal was achievable for a three-stage CFC-11 cycle operating under the flight conditions above. The program was completed by defining a control scheme and by researching and selecting the major components, compressor and heat exchangers, that could be used to implement the thermodynamic cycle selected. Special attention was paid to using similar technologies for the SIRF and flight heat pumps resulting in the commercially available equivalent of the flight unit. A package concept was generated for the components selected and mass and volume estimated. Author

N95-18112 Department of the Navy, Washington, DC.
METHOD AND FLOWMETER FOR UNSTEADY FLUID FLOW STUDY Patent
Paul J. Lefebvre, inventor (to Navy) 3 May 1994 6 p Filed 24 Dec. 1990
(AD-D016432; US-Patent-5,307,688; US-Patent-Appl-SN-632872; US-Patent-Class-73-861.16) Avail: US Patent and Trademark Office

An electromagnetic flowmeter and a method for measurement of the rate of flow of a fluid under unsteady conditions are described. It uses fluid steady-state flowmeter technology and a new algorithm to measure transient rate of flow of a fluid such as water. The algorithm teaches (1) measuring the e.m.f. generated due to the rate of flow of the fluid under test moving through a tube placed in an area with uniform magnetic flux, and (2) comparing it to a simultaneously generated reference signal which is a measure of the magnetic flux density generated when an electromagnetic flowmeter is energized due to the fluid flow rate at the instant of taking the flow rate data of the fluid. DTIC

N95-18149*# National Aeronautics and Space Administration. Lewis Research Center, Cleveland, OH.
EVALUATION OF BOUNDARY CONDITIONS FOR COMPUTATIONAL AEROACOUSTICS
R. Hixon, S.-H. Shih, and Reda R. Mankbadi 1995 23 p Presented at the 33d Aerospace Sciences Meeting, Reno, NV, 5-12 Jan. 1995; sponsored by AIAA
(NASA-TM-109989; NAS 1.15:109989; AIAA Paper 95-0160) Copyright Avail: CASI HC A03/MF A01

The performance of three boundary conditions for aeroacoustics were investigated, namely, (1) Giles-1990; (2) Tam and Webb-1993, and (3) Thompson-1987. For each boundary condition, various implementations were tested to study the sensitivity of their performance to the implementation procedure. Details of all implementations are given. Results are shown for the acoustic field of a monopole in a uniform freestream. Author (revised)

N95-18188*# Institute for Computer Applications in Science and Engineering, Hampton, VA.
TIME-EVOLVING BUBBLES IN TWO-DIMENSIONAL STOKES FLOW Final Report
Saleh Tanveer (Ohio State Univ., Columbus.) and Giovani L. Vasconcelos (Ohio State Univ., Columbus.) Nov. 1994 31 p Submitted for

publication
(Contracts NAS1-19480; RTOP 505-90-52-01; DE-FG02-92ER-14270)
(NASA-CR-194998; NAS 1.26:194998; ICASE-94-90) Avail: CASI HC A03/MF A01

A general class of exact solutions is presented for a time evolving bubble in a two-dimensional slow viscous flow in the presence of surface tension. These solutions can describe a bubble in a linear shear flow as well as an expanding or contracting bubble in an otherwise quiescent flow. In the case of expanding bubbles, the solutions have a simple behavior in the sense that for essentially arbitrary initial shapes the bubble will asymptote an expanding circle. Contracting bubbles, on the other hand, can develop narrow structures ('near-cusps') on the interface and may undergo 'break up' before all the bubble-fluid is completely removed. The mathematical structure underlying the existence of these exact solutions is also investigated. Author

N95-18190*# Institute for Computer Applications in Science and Engineering, Hampton, VA.
THE STABILITY OF TWO-PHASE FLOW OVER A SWEPT-WING Final Report
Adrian Coward (Manchester Univ., England.) and Philip Hall (Manchester Univ., England.) Oct. 1994 44 p Submitted for publication Sponsored by Science Research Council
(Contract NAS1-19480; RTOP 505-90-52-01)
(NASA-CR-194994; NAS 1.26:194994; ICASE-94-86) Avail: CASI HC A03/MF A01

We use numerical and asymptotic techniques to study the stability of a two-phase air/water flow above a flat porous plate. This flow is a model of the boundary layer which forms on a yawed cylinder and can be used as a useful approximation to the air flow over swept wings during heavy rainfall. We show that the interface between the water and air layers can significantly destabilize the flow, leading to traveling wave disturbances which move along the attachment line. This instability occurs for lower Reynolds numbers than in the case of the absence of a water layer. We also investigate the instability of inviscid stationary modes. We calculate the effective wavenumber and orientation of the stationary disturbance when the fluids have identical physical properties. Using perturbation methods we obtain corrections due to a small stratification in viscosity, thus quantifying the interfacial effects. Our analytical results are in agreement with the numerical solution which we obtain for arbitrary fluid properties. Author

N95-18191*# Institute for Computer Applications in Science and Engineering, Hampton, VA.
ON THE LIGHTHILL RELATIONSHIP AND SOUND GENERATION FROM ISOTROPIC TURBULENCE Final Report
Ye Zhou, Alexander Praskovsky (National Center for Atmospheric Research, Boulder, CO.), and Steven Oncley (National Center for Atmospheric Research, Boulder, CO.) Nov. 1994 19 p Submitted for publication Sponsored by NSF
(Contract NAS1-19480; RTOP 505-90-52-01)
(NASA-CR-195005; NAS 1.26:195005; ICASE-94-92) Avail: CASI HC A03/MF A01

In 1952, Lighthill developed a theory for determining the sound generated by a turbulent motion of a fluid. With some statistical assumptions, Proudman applied this theory to estimate the acoustic power of isotropic turbulence. Recently, Lighthill established a simple relationship that relates the fourth-order retarded time and space covariance of his stress tensor to the corresponding second-order covariance and the turbulent flatness factor, without making statistical assumptions for a homogeneous turbulence. Lilley revisited Proudman's work and applied the Lighthill relationship to evaluate directly the radiated acoustic power from isotropic turbulence. After choosing the time separation dependence in the two-point velocity time and space covariance based on the insights gained from direct numerical simulations, Lilley concluded that the Proudman constant is determined by the turbulent flatness factor and the second-order spatial velocity covariance. In order to estimate the Proudman constant at high Reynolds numbers, we analyzed a unique data set of measurements in a large wind tunnel and atmospheric surface layer that covers a range of the Taylor microscale based on Reynolds numbers 2.0 x 10(exp 3) less than or equal to R(sub lambda) less than or equal to 12.7 x 10(exp 3). Our measurements demonstrate that the Lighthill relationship is a good approximation, providing additional support to Lilley's approach. The flatness factor is found between 2.7 - 3.3 and the second order spatial velocity covariance is obtained. Based on these experimental data, the Proudman constant is estimated to be 0.68 - 3.68. Author

N95-18193*# Institute for Computer Applications in Science and Engineering, Hampton, VA.
EFFECT OF CROSSFLOW ON GOERTLER INSTABILITY IN INCOMPRESSIBLE BOUNDARY LAYERS Final Report
Y. H. Zurigat (Jordan Univ., Amman.) and M. R. Malik (High Technology Corp., Hampton, VA.) Nov. 1994 20 p Submitted for publication
(Contracts NAS1-19480; NAS1-19299; RTOP 505-90-52-01)
(NASA-CR-195007; NAS 1.26:195007; ICASE-94-94) Avail: CASI HC A03/MF A01

Linear stability theory is used to study the effect of crossflow on Goertler instability in incompressible boundary layers. The results cover a wide range of sweep angle, pressure gradient, and wall curvature parameters. It is shown that the crossflow stabilizes Goertler disturbances by reducing the maximum growth rate and shrinking the unstable band of spanwise wave numbers. On the other hand, the effect of concave wall curvature on crossflow instability is destabilizing. Calculations show that the changeover from Goertler to crossflow instabilities is a function of Goertler number, pressure gradient, and sweep angle. The results demonstrate that Goertler instability may still be relevant in the transition process on swept wings even at large angles of sweep if the pressure gradient is sufficiently small. The influence of pressure gradient and sweep can be combined by defining a crossflow Reynolds number. Thus, the changeover from Goertler to crossflow instability takes place at some critical crossflow Reynolds number whose value increases with Goertler number. Author

N95-18200*# National Aeronautics and Space Administration. Lewis Research Center, Cleveland, OH.
A THREE-DIMENSIONAL STRUCTURED/UNSTRUCTURED HYBRID NAVIER-STOKES METHOD FOR TURBINE BLADE ROWS
F.-L. Tsung, J. Loellbach, O. Kwon (NYMA, Inc., Brook Park, OH.), and C. Hah Dec. 1994 12 p Presented at the 30th Joint Propulsion Conference and Exhibit, Indianapolis, IN, 27-29 Jun. 1994; sponsored by AIAA, ASME, SAE and ASEE
(Contracts NAS3-27186; NCC3-233; RTOP 505-90-5K)
(NASA-TM-106813; ICOMP-94-31; E-9339; NAS 1.15:106813; AIAA Paper 94-3369) Avail: CASI HC A03/MF A01

A three-dimensional viscous structured/unstructured hybrid scheme has been developed for numerical computation of high Reynolds number turbomachinery flows. The procedure allows an efficient structured solver to be employed in the densely clustered, high aspect-ratio grid around the viscous regions near solid surfaces, while employing an unstructured solver elsewhere in the flow domain to add flexibility in mesh generation. Test results for an inviscid flow over an external transonic wing and a Navier-Stokes flow for an internal annular cascade are presented. Author

N95-18212*# National Aeronautics and Space Administration. Lewis Research Center, Cleveland, OH.
A NOTE ON THE WAVE ACTION DENSITY OF A VISCOUS INSTABILITY MODE ON A LAMINAR FREE-SHEAR FLOW
Thomas F. Balsa (Arizona Univ., Tucson, AZ.) Nov. 1994 15 p
(Contract NCC3-233; RTOP 505-90-5K)
(NASA-TM-106771; ICOMP-94-27; E-9219; NAS 1.15:106771) Avail: CASI HC A03/MF A01

Using the assumptions of an incompressible and viscous flow at large Reynolds number, we derive the evolution equation for the wave action density of an instability wave traveling on top of a laminar free-shear flow. The instability is considered to be viscous; the purpose of the present work is to include the cumulative effect of the (locally) small viscous correction to the wave, over length and time scales on which the underlying base flow appears inhomogeneous owing to its viscous diffusion. As such, we generalize our previous work for inviscid waves. This generalization appears as an additional (but usually non-negligible) term in the equation for the wave action. The basic structure of the equation remains unaltered. Author

N95-18323* National Aeronautics and Space Administration. Lyndon B. Johnson Space Center, Houston, TX.

GEOMETRICAL VAPOR BLOCKER FOR PARALLEL CONDENSATION TUBES REQUIRING SUBCOOLING Patent

Eugene K. Ungar, inventor (to NASA), John D. Cornwell, inventor (to NASA), and William D. Harwell, inventor (to NASA) 29 Nov. 1994 9 p Filed 3 Sep. 1993 Supersedes N94-15962 (32 - 3, p 1022)

(NASA-Case-MSC-22090-1; US-Patent-5,368,090; US-Patent-Appl-SN-115832; US-Patent-Class-165-1; US-Patent-Class-165-110; US-Patent-Class-165-174; US-Patent-Class-165-913; US-Patent-Class-29-890.037; Int-Patent-Class-F28B-11/00) Avail: US Patent and Trademark Office

An apparatus and method is disclosed for regulating flow of working fluid through parallel condensation tubes requiring subcooling. The apparatus provides an elongated restriction element extending into the outlet of the respective condensation tubes to the approximate point of onset of subcooling. The elongated restriction element is braced externally to the condensation tube with a support that is used for positioning and maintaining the elongated restriction element in the correct position. The elongated restriction element has a pentagonal cross-section and is slightly undersized with respect to the working fluid passageways through the condensation tubes. The restriction member significantly restricts flow of partially vaporized working fluid but does not significantly affect the flow of fully liquid working fluid. Official Gazette of the U.S. Patent and Trademark Office

N95-18327*# NYMA, Inc., Cleveland, OH.

OBSERVATION OF FLOW AND TEMPERATURE OSCILLATIONS AROUND A BUBBLE ON A SOLID SURFACE SUBJECT TO A VERTICAL TEMPERATURE GRADIENT

Nasser Rashidnia 1995 12 p Presented at the 33d Aerospace Sciences Meeting and Exhibit, Reno, NV, 9-12 Jan. 1995; sponsored by AIAA

(Contract NAS3-27186)

(NASA-CR-197593; NAS 1.26:197593; AIAA Paper 95-0880) Copyright Avail: CASI HC A03/MF A01

In space and many industrial cases on earth which involve materials processing, manufacturing, and storage and management of liquids, the interaction between gas and vapor bubbles with the surrounding is of great interest. Study of thermocapillary motions near bubbles attached to a heated or cooled wall in conjunction with the space experiments has received considerable attention in recent years. We present results of preliminary experimental observations which have indicated that when the Marangoni number is increased beyond a critical value, a series of oscillatory modes develop in the vicinity of the bubble. The oscillations have been detected in both the basic flow induced by combined Marangoni and buoyancy effects, by using a laser sheet for tracing particles, and in the temperature field visualized by interferometry techniques. The influence of the Marangoni and Prandtl numbers and bubble geometry on the oscillations are indicated. Author

N95-18396 Royal Netherlands Meteorological Inst., De Bilt.

SEARCHING FOR STATIONARY STABLE SOLUTIONS OF EULER'S EQUATION

Roger Salden 1993 23 p

(ISSN 0169-1651)

(KNMI-WR-93-01; ISBN-90-369-2035-3) Copyright Avail: Issuing Activity

In this paper an attempt of finding new stationary stable solutions of the Euler equation is presented. We will look into solutions of the sinh-Poisson equation, which lead to stationary stable solutions of the Euler equation. New solutions can be generated by applying a Backlund transformation method on known solutions of the sine-Gordon equation which is related to the sinh-Poisson equation. This method is applied to a circular symmetric solution. Unfortunately we're not able to present any new circular symmetric solutions. Author

N95-18397*# Institute for Computer Applications in Science and Engineering, Hampton, VA.

A NOTE ON SINGULARITIES OF THE 3-D EULER EQUATION Final Report

S. Tanveer Nov. 1994 14 p Submitted for publication

(Contracts NAS1-19480; RTOP 505-90-52-01; DE-FG02-92ER-14270) (NASA-CR-195006; NAS 1.26:195006; ICASE-94-93) Avail: CASI HC A03/MF A01

In this paper, we consider analytic initial conditions with finite energy, whose complex spatial continuation is a superposition of a smooth background flow and a singular field. Through explicit calculation in the complex plane, we show that under some assumptions, the solution to the 3-D Euler equation ceases to be analytic in the real domain in finite time. Author

N95-18406 Naval Air Warfare Center, Patuxent River, MD. Aircraft Div.

PARALLELIZATION OF THE FLUID DYNAMICS EQUATIONS ON UNSTRUCTURED GRIDS

Christopher W. Bruner 1994 4 p Limited Reproducibility: More than 20% of this document may be affected by microfiche quality

(AD-A284116) Avail: CASI HC A01

The objective of this research is to investigate the parallelization properties of different time-integration algorithms for Computational Fluid Dynamics (CFD) on unstructured grids, i.e., to compare the scalability of several commonly-used algorithms on distributed-memory parallel processors. The author is developing a parallel Euler solver, PUE3D, on the Intel Paragon at WPAFB. This machine is a distributed-memory machine based on the Intel i860 processor. Several different implicit and one explicit algorithm have been implemented, and encouraging preliminary results have been obtained for the Symmetric Successive Over-relaxation (SSOR) algorithm. This research effort is being funded through the Office of Naval Research (ONR) Independent Laboratory In-house Research (ILIR) program, which does not cover computer charges; therefore, the availability of the DOD HPC SRC makes this research possible. DTIC

N95-18434# DynaFlow, Inc., Fulton, MD.

EVOLUTION OF A COLLECTION OF BUBBLES WITH APPLICATION TO WAKES, BUBBLE SCREENS, AND CLOUD NOISE Final Report

Georges L. Chahine Aug. 1994 476 p

(Contract N00014-89-C-0025)

(AD-A283597) Avail: CASI HC A21/MF A04

Content include: Bubble Dynamics and Cavitation Inception in Nonuniform Flow Fields; Bubble Interactions with Vortices; Cavitation Dynamics at Microscale Level; Viscous Interaction Between Bubble and Line Vortex; The Motion of a Spherical Body Below a Free Surface; Study of Jet Instability Formation on Free Surfaces; The Final Stage of the Collapse of a Cavitation Bubble Near a Rigid Wall; Study of the Interaction Between a Bubble and a Vortical Structure; Asymptotic Study of Bubble Dynamics in a Nonuniform Potential Flow; Analytical study of the Interaction a Gas Bubble and a Line Vortex; Analytical and Numerical Study of Large Bubble/Bubble and Bubble/Flow Interaction; Asymptotic Study of Bubble Dynamics in a Slightly Compressible Flow; Asymptotic Study of Bubble Cloud Dynamics in the Proximity of a Body in Potential Flow; Dynamical Interactions in a Bubble Cloud; and, Dynamics of the Interaction of Nonspherical Cavities. Author (DTIC)

N95-18443# Argonne National Lab., IL.

NUMERICAL PREDICTIONS OF TURBULENT FLOW AROUND A CUBE VIA THE k-EPSILON MODEL

C. P. Tzanos 1994 26 p

(Contract W-31-109-eng-38)

(DE94-018361; ANL/RE/PP-79251) Avail: CASI HC A03/MF A01

Turbulent air flows around structures are of importance in many engineering applications. Such flows can also have a significant impact on the thermal performance of the reactor vessel auxiliary cooling system of advanced liquid-metal reactor designs. The objective of the work presented in this paper was to evaluate the adequacy of the high-Reynolds-number form of the k-(epsilon) model in analyzing turbulent air flow around structures. An experiment of simulated atmospheric turbulent flow around a cube, performed by Castro and Robins, was analyzed with the computer code COMMIX and numerical predictions for pressure and velocity distributions were compared with experimental measurements. Considering the complexity of the problem and the approximations involved in the k-(epsilon) model, the overall agreement between numerical predictions and measurements of pressure coefficients and velocities was good. The largest discrepancies between predictions and measurements were in the pressure coefficient at the sections of the top and side cube surfaces very close to the upwind

edges, and in the span wise velocity distribution downstream from the cube. DOE

N95-18469# Arizona Univ., Tucson, AZ. Coll. of Engineering and Mines.
REAL-TIME ADAPTIVE CONTROL OF MIXING IN A PLANE SHEAR LAYER Final Technical Report, 15 Jul. 1989 - 14 Dec. 1993
Ari Glezer (Georgia Inst. of Tech., Atlanta, GA.) and Frank H. Champagne 14 Dec. 1993 225 p
(Grant AF-AFOSR-0465-89; AF Proj. 2307)
(AD-A285541; AFOSR-94-0628) Avail: CASI HC A10/MF A01

A control system for the enhancement and regulation of mixing in a nonreactive plane shear layer has been developed in a two-stream closed-return water facility. Mixing of a passive scalar is estimated using a thermal analog in which the two streams have uniform, steady temperatures differing by 3 C. Control is effected via an array of surface heaters flush-mounted on the flow partition and cross-stream temperature distributions are measured with a resolution of 0.03 C using an array of closely-spaced cold wire sensors. Open-loop forcing is used for the enhancement of mixing in a nonreactive plane shear layer. Mixing of a passive scalar is estimated using a thermal analog to species concentration. From the temperature distributions, a number of mixing performance measures can be calculated to describe the development of mixing with downstream distance. Further, phase-locked measurements are used to study the spatial and temporal structure of the flow and in particular the overall mixedness and composition of the flow as a function of phase in the forcing cycle. In closed-loop experiments, the position of the temperature interface between the two streams is measured in the plane of its cross stream Schlieren image by an optical sensor which is placed upstream of the rollup of the primary vortices. The output from the interface position sensor is fed back to the surface heaters. A transfer function has been developed to predict the effect of feedback on the interface motion. The dependence of various measures of mixing on the feedback gain k and the total delay time delta between the actuators and the sensors is studied. DTIC

N95-18477 Technical Univ. of Lisbon (Portugal).
7TH INTERNATIONAL SYMPOSIUM ON APPLICATIONS OF LASER TECHNIQUES TO FLUID MECHANICS, VOLUME 2
14 Jul. 1994 659 p Symposium held at Lisbon, Portugal, 11-14 Jul. 1994 See also AD-A285685 Limited Reproducibility: More than 20% of this document may be affected by microfiche quality
(Contract N68171-94-M-6048)
(AD-A285685; R/D-7414-AN-02-Vol-2) Avail: CASI HC A99

The proceedings volumes 1 and 2 comprise the papers that were accepted for presentation at the Seventh International Symposium on Applications of Laser Techniques to Fluid Mechanics held at The Calouste Gulbenkian Foundation in Lisbon, during the period of July 11 to 14, 1994. The prime objective of this Seventh Symposium is to provide a forum for the presentation of the most advanced research on laser techniques for flow measurements, and reveal significant results to fluid mechanics. The applications of laser techniques to scientific and engineering fluid flow research is emphasized, but contributions to the theory and practice of laser methods are also considered where they facilitate new improved fluid mechanic research. Attention is focused on laser-Doppler anemometry, particle sizing and other methods for the measurement of velocity and scalars such as particle image velocimetry and laser induced fluorescence. DTIC

N95-18488*# Institute for Computer Applications in Science and Engineering, Hampton, VA.
LOW-DISSIPATION AND -DISPERSION RUNGE-KUTTA SCHEMES FOR COMPUTATIONAL ACOUSTICS Final Report
F. Q. Hu (Old Dominion Univ., Norfolk, VA.), M. Y. Hussaini, and J. Manthey (Old Dominion Univ., Norfolk, VA.) Dec. 1994 26 p Submitted for publication
(Contract NAS1-19480; RTOP 505-90-52-01)
(NASA-CR-195022; NAS 1.26:195022; ICASE-94-102) Avail: CASI HC A03/MF A01

In this paper, we investigate accurate and efficient time advancing methods for computational acoustics, where non-dissipative and non-dispersive properties are of critical importance. Our analysis pertains to the application of Runge-Kutta methods to high-order finite difference discretization. In many CFD applications multi-stage Runge-Kutta schemes have often been favored for their low storage requirements and relatively large stability limits. For computing acoustic waves, however, the stability consideration alone is not sufficient, since the Runge-Kutta schemes entail both dissipation and dispersion errors. The time step is now limited by the tolerable dissipation and dispersion errors in the computation. In the present paper, it is shown that if the traditional Runge-Kutta schemes are used for time advancing in acoustic problems, time steps greatly smaller than that allowed by the stability limit are necessary. Low-Dissipation and -Dispersion Runge-Kutta (LDDRE) schemes are proposed, based on an optimization that minimizes the dissipation and dispersion errors for wave propagation. Order optimizations of both single-step and two-step alternating schemes are considered. The proposed LDDRK schemes are remarkably more efficient than the classical Runge-Kutta schemes for acoustic computations. Moreover, low storage implementations of the optimized schemes are discussed. Special issues of implementing numerical boundary conditions in the LDDRK schemes are also addressed. Author (revised)

N95-18525 Department of the Navy, Washington, DC.
METHOD AND SYSTEM FOR IDENTIFYING THE ONSET OF A TURBULENT BOUNDARY LAYER INDUCED BY A BODY MOVING THROUGH A FLUID MEDIUM Patent
Richard A. Katz, inventor (to Navy) 7 Jun. 1994 15 p Filed 2 Sep. 1993
(AD-D016434; US-Patent-5,319,608; US-Patent-Appl-SN-117514; US-Patent-Class-367-1) Avail: US Patent and Trademark Office

A method of detect the onset of turbulence in connection with a body moving through a fluid medium. First, the body is supplied with sensors each for generating a signal suitable for measuring amplitude of pressure fluctuations of the medium proximate a region of said sidewall of the body in at least a region of the body in which turbulence is expected to occur. During a reference stage during which the body moves through the fluid medium when it is known that turbulence is occurring around at least a portion of said body, the sensors each generate reference temporal pressure data representing fluctuations in pressure of the fluid medium around said body. In response to reference temporal pressure data generated by sensors in a turbulence zone at which turbulence is occurring and sensors in a transition zone between the turbulence zone and a laminar flow zone, a method-of-delay phase portrait is generated for each of a progression of selected delay intervals. DTIC

N95-18549# Argonne National Lab., IL.
SLOSHING ROOF IMPACT TESTS OF A RECTANGULAR TANK
Chikahiro Minowa (National Research Inst. for Earth Science and Disaster Prevention, Tsukuba, Japan.), Nobuyuki Ogawa (National Research Inst. for Earth Science and Disaster Prevention, Tsukuba, Japan.), Iki Harada (Bridgestone Corp., Yokohama, Japan.), and David C. Ma 1994 9 p Presented at the Pressure Vessel and Piping Conference, Minneapolis, MN, 19-23 Jun. 1994
(Contract W-31-109-eng-38)
(DE94-012462; ANL/RE/CP-82360; CONF-940613-13) Avail: CASI HC A02/MF A01

Some tanks have been damaged at the roofs due to sloshing impact caused by strong earthquakes. It is, therefore, necessary to consider the impact force in the aseismic design code for tank roofs. However, there are few studies on the earthquake responses of storage and process tank roofs. As a first step to investigate the effects of sloshing impact a series of the shaking table tests of a rectangular tank have been conducted at the National Research Institute for Earth Science and Disaster Prevention (NIED). The results of these shaking table tests are presented in the paper. The test tank is rectangular in shape having dimensions of 5 m x 3 m x 2 m (length x width x height). The tank was constructed of glass-fiber reinforced plastic panels. Every panel had a flange on four edges, and each panel was connected by bolts along the flange. The test tank was set on the NIED shaking table (15 m by 15 m). Two types of liquid were used, water and a viscous liquid (water mixed with polymeric powders). The roof impact pressures and other quantities were measured. During the tests using the 400 pi El-Centro excitation, the roof deformation sensor steel beam was damaged. The response of side walls with different rigidity were measured in the wall bulging tests. The measured vibrations within the panel plates were larger than those in the panel flanges. The viscous liquid of 100 cp had little influence on wall bulging responses. However,

the viscous effects on sloshing responses were observed in the sloshing tests. Approximate analyses of rectangular tanks, considering the influence of static water pressure, are also presented in this paper. DOE

N95-18562# Air Force Inst. of Tech., Wright-Patterson AFB, OH.
A NUMERICAL ANALYSIS OF SMOOTHED PARTICLE HYDRODYNAMICS Ph.D. Thesis
David A. Fulk Sep. 1994 352 p
(AD-A284698; AFIT/DS/ENC-94-1) Avail: CASI HC A16/MF A03

This dissertation studies the numerical method of Smoothed Particle Hydrodynamics (SPH) as a technique for solving systems of conservation equations. The research starts with a detailed consistency analysis of the method. Higher dimensions and non-smooth functions are considered in addition to the smooth one dimensional case. A stability analysis is then performed. Using a linear technique, an instability is found. Solutions are proposed to resolve the instability. Also a total variation stability analysis is performed leading to a monotone form of SPH. The concepts of consistency and stability are then used in a convergence proof. This proof uses lemmas derived from the Lax-Wendroff theorem in finite differences. The numerical analysis of the method is concluded with a study of the SPH kernel function. Measures of merit are derived for SPH kernels and these are used to show bell-shaped kernels to be superior over other shaped kernels. Three second-order time schemes are applied to SPH to provide a full discretization of the problem; these are Lax-Wendroff, central, and Shu schemes. In addition a lower-order SPH Lax-Friedrichs type form is developed. This method is used in proposing the use of flux-limited hybrid methods in SPH to resolve shocks. DTIC

N95-18609# Deutsche Forschungsanstalt fuer Luft- und Raumfahrt, Goettingen (Germany). Inst. fuer Stroemungsmechanik.
NUMERICAL SIMULATION OF SHOCK/SHOCK AND SHOCK/BOUNDARY-LAYER INTERACTIONS IN CHEMICALLY REACTING HYPERSONIC FLOWS Ph.D. Thesis - Technische Hochschule [NUMERISCHE SIMULATION VON WECHSELWIRKUNGEN ZWISCHEN STOESSEN UND GRENZSCHICHTEN IN CHEMISCH REAGIERENDEN HYPERSCHALLSTROEMUNGEN]
Gunther Brenner 1994 108 p In GERMAN
(ISSN 0939-2963)
(DLR-94-04) Avail: CASI HC A06/MF A02

The shock/shock and shock/boundary-layer interactions in the laminar, hypersonic flowfield are investigated by means of a finite-difference method. Special attention is paid to the influence of the high temperature effects in air on the local topology of the flow near to the interactions. The simulation is based on the integration of the time-dependent Navier-Stokes equations to describe the flow of a chemically reacting gas employing different reaction-kinetic models. The present numerical results are validated by comparison with experimental results. A hyperboloid with flare is used as the model configuration to investigate the shock/shock and shock/boundary-layer interactions. This configuration represents the windward centerline of HERMES 1.0. It is shown that the reactions exhibit a significant influence on the flow properties. Comparable inexpensive simulations comprising only chemical equilibrium appear not to be suitable to describe the structure of the interactions correctly. Thus, the kinetics of the chemical reactions have to be considered to achieve a realistic prediction. Author

N95-18634 Department of the Navy, Washington, DC.
STRATIFIED CARRIER ELECTROVISCOUS FLUIDS AND APPARATUS Patent
Ronald P. Reitz, inventor (to Navy) 22 Mar. 1994 9 p Filed 24 Jan. 1992
(AD-D016238; US-Patent-5,296,155; US-Patent-Appl-SN-826202; US-Patent-Class-252-73) Avail: US Patent and Trademark Office

An improved electroviscous fluid formulated with discrete fluids of diverse densities, characterized in that settling of aggregate in functional apparatus is diminished. Aggregate particles having a density between the density of two fluids migrate to the boundary layer of the fluids when the fluids are at rest. By appropriately selecting the volume of the fluids in functional apparatus, the electroviscous fluid aggregate is placed in position for more immediate response when the apparatus is activated by electrical energy. DTIC

N95-18898*# National Aeronautics and Space Administration. Lewis Research Center, Cleveland, OH.
ON THE CONVERGENCE OF LOCAL APPROXIMATIONS TO PSEUDODIFFERENTIAL OPERATORS WITH APPLICATIONS
Thomas Hagstrom (New Mexico Univ., Albuquerque, NM.) Nov. 1994 12 p
(Contract NCC3-233; RTOP 505-90-5K; NSF DMS-93-04406)
(NASA-TM-106792; ICOMP-94-29; E-9253; NAS 1.15:106792) Avail: CASI HC A03/MF A01

We consider the approximation of a class pseudodifferential operators by sequences of operators which can be expressed as compositions of differential operators and their inverses. We show that the error in such approximations can be bounded in terms of L(1) error in approximating a convolution kernel, and use this fact to develop convergence results. Our main result is a finite time convergence analysis of the Engquist-Majda Pade approximants to the square root of the d'Alembertian. We also show that no spatially local approximation to this operator can be convergent uniformly in time. We propose some temporally local but spatially nonlocal operators with better long time behavior. These are based on Laguerre and exponential series. Author (revised)

N95-18921 California Univ., San Diego, CA.
THE EFFECT OF STABLE STRATIFICATION ON THREE-DIMENSIONAL STRUCTURE IN SHEAR LAYERS Ph.D. Thesis
David Gregg Schowalter 1993 135 p
Avail: Univ. Microfilms Order No. DA9414748

The existence of an organized streamwise vortical structure, which is superimposed on the well known coherent spanwise vorticity in nominally two-dimensional free shear layers, has been studied extensively. In the presence of stratification, however, buoyancy forces contribute to an additional mechanism for the generation of streamwise vorticity. As the spanwise vorticity layer rolls up and pulls high density fluid above low density fluid, a local instability results. The purpose of the current investigation is to force the three-dimensional instability in the stratified shear layer. In this manner, one experimentally observes the effect of buoyancy on the streamwise vortex tube evolution, the evolution of the buoyancy-induced instability, and the interaction between these two vortical structures. A simple numerical model is proposed which captures the relevant physics of the flow evolution. It is found that, depending on the location, streamwise vortices resulting from vortex stretching may be weakened or enhanced by the stratification. Buoyancy-induced vortex structures are shown to form where the unstable part of the interface is tilted by the streamwise vortex tubes. These vortices strengthen initially, then weaken downstream, the time scale for this process depending upon the degree of stratification. For initial Richardson numbers larger than about 0.03, the baroclinically weakened vortex tubes eventually disappear as the flow evolves downstream and the baroclinically generated vortices dominate the three-dimensional flow structure. Dissert. Abstr.

N95-18941*# National Aeronautics and Space Administration. Lewis Research Center, Cleveland, OH.
PARALLEL NAVIER-STOKES COMPUTATIONS ON SHARED AND DISTRIBUTED MEMORY ARCHITECTURES
M. Ehtesham Hayder, D. N. Jayasimha (Ohio Aerospace Inst., Cleveland, OH.), and Sasi Kumar Pillay Jan. 1995 15 p Presented at the 33rd Aerospace Sciences Meeting and Exhibit, Reno, NV, 9-12 Jan. 1995; sponsored by AIAA
(Contract NCC3-233; RTOP 505-90-5K)
(NASA-TM-106823; ICOMP-94-32; E-9369; NAS 1.15:106823; AIAA Paper 95-0577) Avail: CASI HC A03/MF A01

We study a high order finite difference scheme to solve the time accurate flow field of a jet using the compressible Navier-Stokes equations. As part of our ongoing efforts, we have implemented our numerical model on three parallel computing platforms to study the computational, communication, and scalability characteristics. The platforms chosen for this study are a cluster of workstations connected through fast networks (the LACE experimental testbed at NASA Lewis), a shared memory multiprocessor (the Cray YMP), and a distributed memory multiprocessor (the IBM SPI). Our focus in this study is on the LACE testbed. We present some results for the Cray YMP and the IBM SP1 mainly for comparison purposes. On the LACE testbed, we study: (1) the communication characteristics of Ethernet, FDDI, and the ALLNODE networks and (2) the

overheads induced by the PVM message passing library used for parallelizing the application. We demonstrate that clustering of workstations is effective and has the potential to be computationally competitive with supercomputers at a fraction of the cost. Author

N95-18955*# Eidetics International, Inc., Torrance, CA.
DEVELOPMENT OF A MULTICOMPONENT FORCE AND MOMENT BALANCE FOR WATER TUNNEL APPLICATIONS, VOLUME 1
Carlos J. Suarez, Gerald N. Malcolm, Brian R. Kramer, Brooke C. Smith, and Bert F. Ayers Washington NASA Dec. 1994 103 p Original contains color illustrations
(Contract NAS2-13571; RTOP 505-59-53)
(NASA-CR-4642-Vol-1; H-2030-Vol-1; NAS 1.26:4642-Vol-1) Avail: CASI HC A06/MF A02; 3 functional color pages

The principal objective of this research effort was to develop a multicomponent strain gauge balance to measure forces and moments on models tested in flow visualization water tunnels. An internal balance was designed that allows measuring normal and side forces, and pitching, yawing and rolling moments (no axial force). The five-components to applied loads, low interactions between the sections and no hysteresis. Static experiments (which are discussed in this Volume) were conducted in the Eidetics water tunnel with delta wings and a model of the F/A-18. Experiments with the F/A-18 model included a thorough baseline study and investigations of the effect of control surface deflections and of several Forebody Vortex Control (FVC) techniques. Results were compared to wind tunnel data and, in general, the agreement is very satisfactory. The results of the static tests provide confidence that loads can be measured accurately in the water tunnel with a relatively simple multicomponent internal balance. Dynamic experiments were also performed using the balance, and the results are discussed in detail in Volume 2 of this report. Author

N95-18956*# Eidetics International, Inc., Torrance, CA.
DEVELOPMENT OF A MULTICOMPONENT FORCE AND MOMENT BALANCE FOR WATER TUNNEL APPLICATIONS, VOLUME 2
Carlos J. Suarez, Gerald N. Malcolm, Brian R. Kramer, Brooke C. Smith, and Bert F. Ayers Washington NASA Dec. 1994 131 p Original contains color illustrations
(Contract NAS2-13571; RTOP 505-59-53)
(NASA-CR-4642-Vol-2; H-2030-Vol-2; NAS 1.26:4642-Vol-2) Avail: CASI HC A07/MF A02; 2 functional color pages

The principal objective of this research effort was to develop a multicomponent strain gauge balance to measure forces and moments on models tested in flow visualization water tunnels. Static experiments (which are discussed in Volume 1 of this report) were conducted, and the results showed good agreement with wind tunnel data on similar configurations. Dynamic experiments, which are the main topic of this Volume, were also performed using the balance. Delta wing models and two F/A-18 models were utilized in a variety of dynamic tests. This investigation showed that, as expected, the values of the inertial tares are very small due to the low rotating rates required in a low-speed water tunnel and can, therefore, be ignored. Oscillations in pitch, yaw and roll showed hysteresis loops that compared favorably to data from dynamic wind tunnel experiments. Pitch-up and hold maneuvers revealed the long persistence, or time-lags, of some of the force components in response to the motion. Rotary-balance experiments were also successfully performed. The good results obtained in these dynamic experiments bring a whole new dimension to water tunnel testing and emphasize the importance of having the capability to perform simultaneous flow visualization and force/moment measurements during dynamic situations. Author

N95-18958*# Institute for Computer Applications in Science and Engineering, Hampton, VA.
ACTIVE CONTROL OF INSTABILITIES IN LAMINAR BOUNDARY-LAYER FLOW. PART 1: AN OVERVIEW Final Report
Ronald D. Joslin (National Aeronautics and Space Administration. Langley Research Center, Hampton, VA.), Gordon Erlebacher, and M. Yousuff Hussaini Dec. 1994 16 p Submitted for publication
(Contract NAS1-19480; RTOP 505-90-52-01)
(NASA-CR-195016-Pt-1; NAS 1.26:195016-Pt-1; ICASE-94-97-Pt-1) Avail: CASI HC A03/MF A01

This paper (the first in a series) focuses on using active-control methods to maintain laminar flow in a region of the flow in which the natural instabilities, if left unattended, lead to turbulent flow. The authors review previous studies that examine wave cancellation (currently the most prominent method) and solve the unsteady, nonlinear Navier-Stokes equations to evaluate this method of controlling instabilities. It is definitely shown that instabilities are controlled by the linear summation of waves (i.e., wave cancellation). Although a mathematically complete method for controlling arbitrary instabilities has been developed (but not yet tested), the review, duplication, and physical explanation of previous studies are important steps for providing an independent verification of those studies, for establishing a framework for subsequent work which will involve automated transition control, and for detailing the phenomena by which the automated studies can be used to expand knowledge of flow control. Author

N95-19098# Argonne National Lab., IL.
FREE VIBRATION ANALYSIS OF PARTIALLY FILLED LIQUID STORAGE TANKS
Yu Tang and Y. W. Chang 1994 9 p Presented at the Pressure Vessel and Piping Conference, Minneapolis, MN, 19-23 Jun. 1994
(Contract W-31-109-eng-38)
(DE94-012456; ANL/RE/CP-82143; CONF-940613-20) Avail: CASI HC A02/MF A01

A study on the free vibration analysis of partially filled liquid storage tanks is presented. The tanks considered are the upright circular cylindrical tanks that are rigidly supported at the base. The top of the tanks are either free or constrained. Two types of constraints are considered, namely, hinged and roller support. The governing differential equations for the tank-liquid system are obtained by application of the Rayleigh-Ritz procedure in combination with Lagrange's equation. The response functions examined include the frequency of the fundamental mode of vibration of the tank-liquid system and the associated modal pressure. DOE

N95-19099# Argonne National Lab., IL.
SSI EFFECTS FOR A TANK CONTAINING TWO LIQUIDS
Yu Tang 1994 5 p Presented at the Pressure Vessel and Piping Conference, Minneapolis, MN, 19-23 Jun. 1994
(Contract W-31-109-eng-38)
(DE94-012457; ANL/RE/CP-82146; CONF-940613-12) Avail: CASI HC A01/MF A01

Following a brief review of a mechanical model which permits consideration of the flexibility of the tank wall and the supporting medium, the effects of the soil-structure interaction on the dynamic response of a laterally excited tank that contains two liquids are examined. The quantities examined include the hydrodynamic pressure, base shear and moments. The results are compared with those obtained with no soil-structure interaction. Only the impulsive component of response is examined; the convective component is for all practical purposes unaffected by soil-structure interaction. It is shown that for the conditions considered, soil-structure interaction reduces the peak response of the tank-liquid system. DOE

N95-19139 Materials Research Labs., Ascot Vale (Australia).
DATA ACQUISITION FROM BLAST OVERPRESSURE TRIALS
D. R. Kirk Mar. 1993 22 p
(MRL-TN-628; AR-008-234) Copyright Avail: Issuing Activity

A Macintosh computer has been used to acquire data from blast overpressure trials on various weapons. The computer is connected to a multiple channel FM data recorder via a MacSCS1488 bus controller, allowing the computer to control the recorder and to acquire data from it through an analog to digital converter. Detailed instructions are given for connecting the hardware and operating the software involved. Author

N95-19251# Advisory Group for Aerospace Research and Development, Neuilly-Sur-Seine (France). Fluid Dynamics Panel.
WALL INTERFERENCE, SUPPORT INTERFERENCE AND FLOW FIELD MEASUREMENTS [LES EFFETS DE PAROI ET DE SUPPORT ET LES MESURES DES CHAMPS D'ECOULEMENT]
Jul. 1994 439 p In ENGLISH and FRENCH Symposium held in Brussels, Belgium, 4-7 Oct. 1993 Original contains color illustrations
(AGARD-CP-535; ISBN-92-835-0756-8) Copyright Avail: CASI HC A19/MF A04

The 31 papers prepared for the AGARD Fluid Dynamics Panel (FDP)

Symposium on 'Wall Interference, Support Interference, and Flow Field Measurements' are contained in this report. In addition, a Technical Evaluator's Report assessing the success of the Symposium in meeting its objectives, and an edited transcript of the General Discussion held at the end of the meeting are also included. The primary objective of this Symposium was to report on recent developments from research and technology programs aimed at reducing test data errors caused by wind tunnel walls, model supports, and intrusive flow field measurement devices. The scope of papers included wall interference correction methods based on measured data at the walls and methods to eliminate wall interference through adaptive and/or ventilated walls, support interference calculations and correction methods, and recent advances in flow field measurement techniques. For individual titles, see N95-19252 through N95-19282.

N95-19252# McDonnell-Douglas Aerospace, Long Beach, CA. Transport Aircraft.

THE CRUCIAL ROLE OF WALL INTERFERENCE, SUPPORT INTERFERENCE AND FLOW FIELD MEASUREMENTS IN THE DEVELOPMENT OF ADVANCED AIRCRAFT CONFIGURATIONS

F. T. Lynch, R. C. Crites (McDonnell-Douglas Aerospace, Saint Louis, MO.), and F. W. Spaid (McDonnell-Douglas Aerospace, Saint Louis, MO.) *In* AGARD, Wall Interference, Support Interference and Flow Field Measurements Jul. 1994 38 p (For primary document see N95-19251 05-34)

Copyright Avail: CASI HC A03/MF A04

The requirements, current technology status, and future needs for methodologies to assess wall and support interference effects, and for flow field measurement capabilities, are addressed from an aircraft industry perspective. The requirement for higher Reynolds number testing, especially for transport aircraft, places a much greater burden on the development of the respective technologies. Accurate wall interference estimation methods, including modeling of the tunnel wall flow, are required to assure that models are sized such that wall effects are correctable. Limitations of wall-interference correction methodologies, which occur as a consequence of current CFD inadequacies, are addressed. Flow field correction methods, as well as surface pressure correction methods, are covered. Three techniques for estimating model support interference are reviewed, namely, the use of dummy stings in experimental tests, use of empirically-based methods for similar installations, and use of CFD-based methods. The need to design support system concepts that minimize interference, and, in the process, permit the effective application of CFD-based methods, is highlighted. Flow diagnostic techniques needed to permit extrapolation of sub-scale wind-tunnel-measured aerodynamic characteristics to full-scale conditions, and to provide the understanding to allow deficiencies to be addressed and corrected, or to guide the design of improved-performance concepts, are reviewed. Both surface flow measurement/visualization and off-body measurements are considered. Noteworthy results obtained with current intrusive devices are reviewed, but the emphasis for the future is clearly shown to reside with optical, non-intrusive techniques such as pressure sensitive paint, infrared imaging, particle image velocimetry, and Doppler global velocimetry. Author

N95-19253# Von Karman Inst. for Fluid Dynamics, Rhode-Saint-Genese (Belgium).

PARTICLE IMAGE VELOCIMETRY: PRINCIPLES, CURRENT APPLICATIONS AND FUTURE PROSPECTS **c74**

M. L. Riethmuller *In* AGARD, Wall Interference, Support Interference and Flow Field Measurements Jul. 1994 12 p (For primary document see N95-19251 05-34)

Copyright Avail: CASI HC A03/MF A04

The basic principle of the technique of Particle Image Velocimetry is presented. The different methods available are discussed and advantages of each of them are exposed. The latest fully optical processing methods are compared to recent video based techniques. The extension of the measurements technique to 3D and the suppression of the directional ambiguity are presented. Examples of application in a variety of domains are discussed. Author

N95-19254# Coimbra Univ. (Portugal). Grupo de Mecanica dos Fluidos.

CALIBRATION AND USE OF A NON-NULLING SEVEN-HOLE PRESSURE PROBE **c35**

M. C. G. Silva and D. X. Viegas *In* AGARD, Wall Interference, Support Interference and Flow Field Measurements Jul. 1994 7 p (For primary document see N95-19251 05-34)

Copyright Avail: CASI HC A02/MF A04

The calibration and the measuring methods associated with the use of a non-nulling seven-hole pressure probe are exposed. A detailed analysis of the error associated with the fitting process used in the calibration is presented. Some results related with the use of the probe for the determination of average local flow properties (incidence angles and dynamic pressure coefficient) in wind tunnel tests are presented. Author

N95-19255# Institute for Aerospace Research, Ottawa (Ontario).

APPLICATIONS OF THE FIVE-HOLE PROBE TECHNIQUE FOR FLOW FIELD SURVEYS AT THE INSTITUTE FOR AEROSPACE RESEARCH **c35**

L. H. Ohman (De Havilland Aircraft Co. of Canada Ltd., Downsview, Ontario.) and V. D. Nguyen *In* AGARD, Wall Interference, Support Interference and Flow Field Measurements Jul. 1994 15 p Original contains color illustrations (For primary document see N95-19251 05-34)

Copyright Avail: CASI HC A03/MF A04

This paper deals with calibrations and uses of the five-hole probes for flow field survey. Two applications are given: one in transonic regime in the near slipstream of a powered propfan mounted on a half-model wing configuration and the other behind a generic submarine model at subsonic speeds. The acquired data have been analyzed in terms of flow angles, total and dynamic pressures and Mach number and velocity vector in a probe fixed coordinate system. These parameters were necessary in determining the flow field characteristics of the studied configurations which are presented and discussed. Author

N95-19256# Von Karman Inst. for Fluid Dynamics, Rhode-Saint-Genese (Belgium).

IMPROVEMENT AND VALIDATION OF AN LDV SYSTEM TO PERFORM MEASUREMENTS IN LAMINAR SUPERSONIC FLOWS **c35**

Luca Bertuccioli and Gerard Degrez *In* AGARD, Wall Interference, Support Interference and Flow Field Measurements Jul. 1994 8 p (For primary document see N95-19251 05-34)

(Contracts CEC-Aero-0027-C; CEC-ERB-CHBI-CT-92049)

Copyright Avail: CASI HC A02/MF A04

This paper describes the optimization and systematic testing of a single component LDV system developed to perform measurements on the tests carried out to validate the performance of the system and on issues which are particular to high speed LDV applications. Particular emphasis is given to issues connected to the seeding of the flow such as the constraints on the selection of a seeding material and its sizing. Oblique shock wave traverses were performed to validate the selected seeding material and the developed seeding delivery system. These tests confirmed the monodispersity of the seeding in the wind tunnel test section and showed a reasonable particle response. The oblique shock traverse results are also compared to various particle dynamics models though the comparison is inconclusive. A series of supersonic laminar boundary layer traverses were also performed. These profiles are compared to the compressible flat plate boundary layer theory of Chapman and Rubesin and the validity of this theory in the current test conditions is demonstrated. The boundary layer measures are in good agreement with the theory, show good repeatability and do not display any signs of particle lag errors. Collectively, these experimental results clearly demonstrate the ability of the LDV system to perform accurate measurements in complex compressible flowfields. Author

N95-19257# Von Karman Inst. for Fluid Dynamics, Rhode-Saint-Genese (Belgium). Turbomachinery Dept.

AERODYNAMIC INVESTIGATION OF THE FLOW FIELD IN A 180 DEG TURN CHANNEL WITH SHARP BEND

Guido Rau and Tony Arts *In* AGARD, Wall Interference, Support Interference and Flow Field Measurements Jul. 1994 8 p (For primary document see N95-19251 05-34)

Copyright Avail: CASI HC A02/MF A04

The internal cooling of gas turbine blades is generally ensured by secondary air flowing through narrow passages existing inside the airfoils. These internal channels are usually connected by 180 deg turns with sharp bends. The aerodynamic and associated convective heat transfer characteristics observed in this type of geometry are significantly influenced

by strong secondary flows and flow separations. The purpose of the present experimental effort is to give a detailed description of some aerodynamic aspects of this particular flow pattern. Detailed measurements of the three-dimensional velocity field were performed by means of a two-component Laser Doppler Velocimeter. The third velocity component was obtained by repeating the measurements at two different orientations of the emitting optics with respect to the test section. Author

N95-19258# Centre d'Etudes et de Recherches, Toulouse (France). Dept. d'Etudes et de Recherches en Aero-Thermodynamique.

EXPERIMENTAL TECHNIQUES FOR MEASURING TRANSONIC FLOW WITH A THREE DIMENSIONAL LASER VELOCIMETRY SYSTEM. APPLICATION TO DETERMINING THE DRAG OF A FUSELAGE [TECHNIQUE EXPERIMENTALE DE MESURE EN ECOULEMENT TRANSSONIQUE AVEC UN SYSTEME DE VELOCIMETRIE LASER TRIDIMENSIONNEL. APPLICATION A LA DETERMINATION DE LA TRAINEE D'UN FUSELAGE] **c36**

A. Seraudie, A. Mignosi, J. B. Dor, and S. Prudhomme *In* AGARD, Wall Interference, Support Interference and Flow Field Measurements Jul. 1994 6 p In FRENCH Original contains color illustrations (For primary document see N95-19251 05-34)

Copyright Avail: CASI HC A02/MF A04

Recent developments in laser anemometry have been used to design a three dimensional laser system which has been in operation at the CERT ONERA's T2 wind tunnel since December 1989: fiber optics (to lead the light between the source and the emitting optics), Fast FOURIER Transfer Doppler processors (to analyze the Doppler signals), high power transmission system (to provide color separation), digital control of displacement motors and real time operation (to move the measuring point during the run). This device works well for the short run times of the T2 wind tunnel, providing a good accuracy which allows 30 to 50 measurement points during 60 to 120 seconds of the test. After a complete description of the 3D laser velocimetry system, the present paper will develop some typical measurements which have been performed. For each case we will present some test results obtained under transonic conditions: shock wave probing (shape and location on the upper side of a 2D transonic model); and 3D velocity measurements in forward and backward scatter configurations with the wall approach for areas without good accessibility. In order to obtain the drag of a fuselage, a vertical plane located downstream of the model was measured with two devices: laser velocimetry in order to obtain the three components of velocity; and a pressure rake providing the static and total pressures. The combination of these measurements (pressure and velocity) allowed the calculation of the total drag of the 3D model. Author

N95-19259# Technische Univ., Delft (Netherlands). High Speed Aerodynamics Lab.

THE UTILIZATION OF A HIGH SPEED REFLECTIVE VISUALIZATION SYSTEM IN THE STUDY OF TRANSONIC FLOW OVER A DELTA WING **c02**

S. R. Donohoe and W. J. Bannink *In* AGARD, Wall Interference, Support Interference and Flow Field Measurements Jul. 1994 13 p (For primary document see N95-19251 05-34)

Copyright Avail: CASI HC A03/MF A04

An experimental study was conducted to examine the flow over a non-cambered 65 deg swept delta wing with a sharp leading edge in high subsonic compressible flow at various angles of attack. This flow is known to be highly three dimensional. At certain combinations of Mach number and high angle of attack, an unsteady and often non axial symmetric phenomenon known as vortex breakdown is found to occur above the wing. The present experimental study includes both visualizations of the flow over the model surface and of the flow field itself. The surface flow visualization study is done using a conventional oil-flow visualization technique. Flow field visualizations are done using both a traditional transmission visualization system as well as a newly developed Surface Reflective Visualization (SRV) technique. The development and application of this SRV system will be the main topic addressed in the current report. The SRV technique provides a new perspective on the compressible flow over wings. This technique incorporates a specially designed model with a reflective surface to enable visualization of the flow over the wing in plan view. The technique has been developed and applied to the transonic flow over a delta wing presently under investigation in a vortex breakdown research program. The plan view perspective makes it possible to visualize the span-wise distribution of the shock system present in the flow field and provides confirmation of the existence of cross flow shocks for certain combinations of Mach number and angle of attack. Combining this technique with the use of a high-speed camera enables the high speed shock fluctuations associated with this flow to be assessed for the first time. The SRV system, thus, allows insight to be gained into the time scales associated with these shock fluctuations and the vortex breakdown phenomenon in general. Author

N95-19260# British Aerospace Aircraft Group, Preston (England). Aerodynamics Dept.

TRANSONIC AND SUPERSONIC FLOWFIELD MEASUREMENTS ABOUT AXISYMMETRIC AFTERBODIES FOR VALIDATION OF ADVANCED CFD CODES **c02**

Martin Burt, Philip Miller (Miller and Wilson Aerodynamics Research, Bath, England.), and Johan Agrell (Aeronautical Research Inst. of Sweden, Bromma.) *In* AGARD, Wall Interference, Support Interference and Flow Field Measurements Jul. 1994 28 p Sponsored by Swedish Ministry of Defence (For primary document see N95-19251 05-34)

Copyright Avail: CASI HC A03/MF A04

Two axisymmetric afterbody experimental programs, aimed at providing necessary and sufficient data for CFD code validation, were conducted in the FFA S5 suckdown wind-tunnel. Flow conditions covered the range of transonic to supersonic. Mean and fluctuating flowfield velocities in a single longitudinal plane were measured using LDA along many traverses, both over the afterbody and in the jet and mixing regions. Flow separated on the boattail of the AGARD 10 and 15 degree geometries at all conditions tested. Separation also occurred on a conical afterbody at supersonic Mach number. Comprehensive sets of boundary condition data were also recorded, through a wide variety of techniques. Extensive error analyses have been undertaken to evaluate the accuracy of all data. Transonic Navier-Stokes computations on the configurations were performed and showed the benefit of having static pressure information along the slotted tunnel roof. An algebraic stress model of turbulence returned predictions of afterbody surface pressures superior to two more simple models, in both attached and separated flow. Author

N95-19261# Technische Univ., Munich (Germany). Lehrstuhl fuer Fluidmechanik.

VELOCITY MEASUREMENTS WITH HOT-WIRES IN A VORTEX-DOMINATED FLOWFIELD **c02**

Christian Breitsamter and Boris Laschka *In* AGARD, Wall Interference, Support Interference and Flow Field Measurements Jul. 1994 13 p Sponsored by MBB Original contains color illustrations (For primary document see N95-19251 05-34)

Copyright Avail: CASI HC A03/MF A04

Selected results from a quantitative experimental investigation documenting the low-speed flow environment over a 75 deg swept delta wing and over a delta-canard-configuration are presented. The hot-wire measurement techniques using cross-wire and triple-wire probes are described. Results obtained include detailed flowfields of the time-dependent velocity components for angles of attack from 12.5 deg to 31.5 deg at a test Reynolds number of 1.0 x 10(exp 6). The structure of the highly turbulent vortex dominated flow is clearly shown by time-averaged, root-mean-square and spectral distributions. Thus the delta wing vortex substructure organized by discrete vortices and vortex breakdown characteristics are analyzed. With increasing incidence both the wing and the canard leading-edge vortices move inboard resulting in increase of the velocity fluctuations due to the bursting of these vortices. At the delta-canard configuration strong interference effects between the canard and the wing vortex systems are found. Peaked velocity spectra are detected in the vorticity sheets at burst flow conditions related to a narrow-band concentration of kinetic turbulent energy in the flow of the wing/canard vortex sheets. Author

N95-19262# Defence Research Agency, Bedford (England).

BOUNDARY-FLOW MEASUREMENT METHODS FOR WALL INTERFERENCE ASSESSMENT AND CORRECTION: CLASSIFICATION AND REVIEW

P. R. Ashill *In* AGARD, Wall Interference, Support Interference and

Flow Field Measurements Jul. 1994 21 p Sponsored by Dept. of Trade and Industry (For primary document see N95-19251 05-34)
Copyright Avail: CASI HC A03/MF A04

The development of methods of determining wind-tunnel wall interference from measurements of the flow at a boundary adjacent to the wind-tunnel walls has required the collaboration of theoreticians and experimenters. After these methods are classified and reviewed, techniques for making the measurements are discussed and the concept of correcting wind-tunnel flows to equivalent free-air conditions is examined. Three classes of method are identified, two needing a model representation ('one-variable' and 'wall-signature' types) and a third needing no simulation of the flow around the model ('two-variable' methods). All three classes are related and the need for accuracy in the model representation in 'one-variable' methods can be relaxed by a suitable choice of 'mixed' boundary conditions. Further work is needed to establish non-intrusive techniques and to develop improved methods for determining the normal component of velocity at or just away from the measurement surface. The need for research to establish allowable limits on variations in wall-induced velocity in the region of the model is highlighted. Author

N95-19263# Deutsche Forschungsanstalt fuer Luft- und Raumfahrt, Brunswick (Germany).
WALL CORRECTION METHOD WITH MEASURED BOUNDARY CONDITIONS FOR LOW SPEED WIND TUNNELS
A. Kuepper *In* AGARD, Wall Interference, Support Interference and Flow Field Measurements Jul. 1994 10 p (For primary document see N95-19251 05-34)
Copyright Avail: CASI HC A02/MF A04

In the wind tunnel division of DLR in Braunschweig a wall correction method based on measured boundary conditions was developed. The verification of the method was made with theoretically calculated boundary conditions and with experimental test data. The calculation of the wall interferences from theoretical boundary conditions are in good agreement with exact reference data of the wall interferences. The advantage of the wall pressure correction method is shown by the results of the experimental tests where the measured coefficients of the force and the moments are compared with the corrected coefficients and the coefficients of free-flight. In this comparison the classical correction method is shown too. The wall correction method is easy to use because no information of the model is required and can be applied into an on-line processing. Particular attention should be paid to the wall pressure measurement system because wrong wall pressure data can have an influence on the calculated wall interferences. Author

N95-19264# Aeronautical Research Inst. of Sweden, Bromma. Aerodynamics Dept.
COMPUTATIONAL SIMULATIONS FOR SOME TESTS IN TRANSONIC WIND TUNNELS
Nada Agrell *In* AGARD, Wall Interference, Support Interference and Flow Field Measurements Jul. 1994 13 p Sponsored by FFV and Defence Material Dept. (For primary document see N95-19251 05-34)
Copyright Avail: CASI HC A03/MF A04

Two large models with swept wings have been investigated in two rather similar tunnels, whose cross sectional areas differ by a factor of 9. The tunnels are configured with slotted walls. The larger of the tunnels has a ventilation of 8.3 percent, while the ventilation of the smaller tunnel has been varied between 4.2 percent and 8.3 percent for this investigation. The blockage of the tested models in the tunnels varied from approximately 0.2 percent to 1.7 percent. For the case with blockage of 1.7 percent the ratio of span to the width (equals to the height) of the tunnel was 0.8. For the configuration blocking 0.6 percent in the larger of the two wind tunnels the comparison of Mach number signatures on the tunnel walls between experiments and computations is very good at both Mach numbers, 0.9 and 0.95, and both angles of attack, 0 and 10 degrees. The position of the 'shock' is very well predicted in the computations. Most of the computational simulations for the model blocking 1.7 percent in the smaller of the two tunnels have so far been performed at Mach number 0.8 and at angles of attack of 0 and 2 degrees. This presentation has been concentrated on Mach number 0.8 and angle of attack of 2 degrees. However, a limited number of comparisons is given for other cases, like Mach number 0.8 with angle of attack 5 degrees and Mach number 0.95 with angle of attack 2 degrees. As can be seen the agreement is excellent for all Mach numbers and related angles of attack that have been investigated. Author

N95-19265# Nangia Associates, Bristol (England).
ESTIMATING WIND TUNNEL INTERFERENCE DUE TO VECTORED JET FLOWS
R. K. Nangia *In* AGARD, Wall Interference, Support Interference and Flow Field Measurements Jul. 1994 14 p Sponsored by Defence Research Agency (For primary document see N95-19251 05-34)
Copyright Avail: CASI HC A03/MF A04

An important consideration in the testing of aircraft models with vectored jets is the allowance to be made for wind tunnel interference on jet flows. Depending on the cross-section dimensions, the wind tunnel interference, can be particularly severe at high incidences or for high jet velocities and large jet deflections. For assessment of these effects, either 'Wall pressure signature' or 'Direct' methods can be used. The wall pressure methods, although requiring dedicated instrumentation, have the advantage that model flow simulation is not required. The direct methods allow calculations of interference prior to the tests and can therefore assist in optimization of model geometry for a particular wind tunnel. A 'Direct' method for estimating wind tunnel interference due to jet flows is described. A semi-empirical model of the jet plume, imaged in walls has been used to represent the tunnel constraint. Comparisons with results from a 'wall pressure signature' method are very encouraging. The results emphasize the large magnitudes of effects which can arise, particularly in experiments with 2, 3 or 4 vectoring nozzles on multi-surface aircraft configurations. For 4 nozzles with jet velocity ratio near 10, the vertical velocity flow angle can be near 6 - 8 degrees. The present technique offers the capability of guiding the design of acceptable experiments, or for checking the validity of existing information. Several aspects of future work have been proposed. Author

N95-19266*# Wright Lab., Wright-Patterson AFB, OH. Aero-Instrumentation Group.
DETERMINATION OF SOLID/POROUS WALL BOUNDARY CONDITIONS FROM WIND TUNNEL DATA FOR COMPUTATIONAL FLUID DYNAMICS CODES
Thomas J. Beutner, Zeki Z. Celik (Stanford Univ., CA.), and Leonard Roberts (Stanford Univ., CA.) *In* AGARD, Wall Interference, Support Interference and Flow Field Measurements Jul. 1994 19 p (For primary document see N95-19251 05-34)
(Contract NCC2-55)
Copyright Avail: CASI HC A03/MF A04

A computational and experimental study has been undertaken to investigate methods of modelling solid and porous wall boundary conditions in computational fluid dynamics (CFD) codes. The procedure utilizes experimental measurements at the walls to develop a flow field solution based on the method of singularities. This flow field solution is then imposed as a pressure boundary condition in a CFD simulation of the internal flow field. The effectiveness of this method in describing the boundary conditions at the wind tunnel walls using only sparse experimental measurements has been investigated. Verification of the approach using computational studies has been carried out using an incompressible flow solver. The current work demonstrates this technique for low speed flows and compares the result with experimental data obtained from a heavily instrumented variable porosity test section. Position and refinement of experimental measurements required to describe porous wall boundary conditions have also been considered for application to other porous wall wind tunnels. The approach developed is simple, computationally inexpensive, and does not require extensive or intrusive measurements. It may be applied to both solid and porous wall wind tunnel tests. Some consideration is given to the extension of this method to three dimensions. Author

N95-19267# Naples Univ. (Italy). Inst. di Aerodinamica.
ADAPTIVE WIND TUNNEL WALLS VERSUS WALL INTERFERENCE CORRECTION METHODS IN 2D FLOWS AT HIGH BLOCKAGE RATIOS c09
G. P. Russo, G. Zuppardi, and M. Basciani *In* AGARD, Wall Interference, Support Interference and Flow Field Measurements Jul. 1994 12 p Sponsored by Ministry of University and Scientific and Technological Research (For primary document see N95-19251 05-34)
Copyright Avail: CASI HC A03/MF A04

The aim of the present work is to compare the effectiveness of adaptive-wall approach with the capabilities of WIAC (wall interference assessment and correction) methods in reducing wall interference effects in wind tunnel testing. Tests have been made in the 20 cm x 20 cm subsonic Adaptive Walls Wind Tunnel in Naples. Three different models having a chord of 100 mm, 150 mm and 200 mm have been used. The corresponding blockage ratios at alpha = 0 degrees are 6 percent, 9 percent and 12 percent, respectively. Results of the tests show that wall adaptation and measured boundary condition WIAC methods are equivalent in correcting wall interference at moderate angles of incidence and/or with medium size models (i.e. at moderate blockage ratios). Furthermore adaptive walls wind tunnels can give data correctable with a WIAC method also at very large blockage ratios as high as 4 times the blockage ratio used in conventional wind tunnels. Author

N95-19268*# Georgia Inst. of Tech., Atlanta, GA. Aerospace Lab.
DEVELOPMENT OF PNEUMATIC TEST TECHNIQUES FOR SUBSONIC HIGH-LIFT AND IN-GROUND-EFFECT WIND TUNNEL INVESTIGATIONS **c02**
Robert J. Englar *In* AGARD, Wall Interference, Support Interference and Flow Field Measurements Jul. 1994 11 p Sponsored by NASA. Langley Research Center (For primary document see N95-19251 05-34)
Copyright Avail: CASI HC A03/MF A04

Wind tunnel evaluations of two-dimensional high-lift airfoils and of vehicles operating in ground effect near the tunnel floor require special test facilities and procedures. These are needed to avoid errors caused by proximity to the walls and interference from the wall boundary layers. Pneumatic test techniques and facilities were developed for GTRI aerodynamic research tunnels and calibrated to verify that these wall effects had been removed. The modified facilities were then employed to evaluate the aerodynamic characteristics of blown very-high-lift airfoils and of racing hydroplanes operating in ground effect at various levels above the floor. The pneumatic facilities, techniques and calibrations are discussed and typical aerodynamic data recorded both with and without the test-section blowing systems are presented. Author

N95-19269# City Univ., London (England). Center for Aeronautics.
INTERFERENCE DETERMINATION FOR WIND TUNNELS WITH SLOTTED WALLS **c09**
M. M. Freestone and S. R. Mohan *In* AGARD, Wall Interference, Support Interference and Flow Field Measurements Jul. 1994 12 p Sponsored by Dept. of Trade and Industry (For primary document see N95-19251 05-34)
Copyright Avail: CASI HC A03/MF A04

The effectiveness of a 'two-variable' scheme, for evaluating wall interference with slotted liners installed, is assessed. Test data from transonic wind tunnel tests with a two-dimensional model geometry are utilized. In these tests untypically high levels of wall interference are produced. In the first tests, solid wall liners were used, in order to establish a standard. Selected results from two further series of tests, in which slotted roof and floor liners were fitted, are then presented and analyzed. In the first of these, divergent liners were used, and it was found that the slot flows generated large disturbances in the wall shear region, causing the normal velocity of the equivalent inviscid flow to be amplified in relation to the normal velocity in the slot. An allowance therefore had to made in the proposed interference scheme to account for this amplification. With convergent wall liners, large disturbances were avoided, and no such allowance was needed. Implications of the investigation for tests in large slotted liner wind tunnels are discussed. Author

N95-19270*# National Aeronautics and Space Administration. Ames Research Center, Moffett Field, CA.
WALL INTERACTION EFFECTS FOR A FULL-SCALE HELICOPTER ROTOR IN THE NASA AMES 80- BY 120-FOOT WIND TUNNEL **c02**
Patrick M. Shinoda *In* AGARD, Wall Interference, Support Interference and Flow Field Measurements Jul. 1994 14 p Prepared in cooperation with Army Aviation Research and Development Command, Moffett Field, CA (For primary document see N95-19251 05-34)
Copyright Avail: CASI HC A03/MF A04

A full-scale helicopter rotor test was conducted in the NASA Ames 80- by 120-Foot Wind Tunnel with a four-bladed S-76 rotor system. This wind tunnel test generated a unique and extensive data base covering a wide range of rotor shaft angles-of-attack and rotor thrust conditions from 0 to 100 knots. Three configurations were tested: (1) empty tunnel; (2) test stand body (fuselage) and support system; and (3) fuselage and support system with rotor installed. Empty tunnel wall pressure data are evaluated as a function of tunnel speed to understand the baseline characteristics. Aerodynamic interaction effects between the fuselage and the walls of the tunnel are investigated by comparing wall, ceiling, and floor pressures for various tunnel velocities and fuselage angles-of-attack. Aerodynamic interaction effects between the rotor and the walls of the tunnel are also investigated by comparing wall, ceiling, and floor pressures for various rotor shaft angles, rotor thrust conditions, and tunnel velocities. Empty tunnel wall pressure data show good repeatability and are not affected by tunnel speed. In addition, the tunnel wall pressure profiles are not affected by the presence of the fuselage apart from a pressure shift. Results do not indicate that the tunnel wall pressure profiles are affected by the presence of the rotor. Significant changes in the wall, ceiling, and floor pressure profiles occur with changing tunnel speeds for constant rotor thrust and shaft angle conditions. Significant changes were also observed when varying rotor thrust or rotor shaft angle-of-attack. Other results indicate that dynamic rotor loads and blade motion are influenced by the presence of the tunnel walls at very low tunnel velocity and, together with the wall pressure data, provide a good indication of flow breakdown. Author

N95-19271# McDonnell-Douglas Aerospace, Saint Louis, MO.
TRANSONIC WIND TUNNEL BOUNDARY INTERFERENCE CORRECTION **c09**
M. L. Rueger, R. C. Crites, R. F. Weirich, F. Creasman, R. K. Agarwal, and J. E. Deese *In* AGARD, Wall Interference, Support Interference and Flow Field Measurements Jul. 1994 14 p (For primary document see N95-19251 05-34)
Copyright Avail: CASI HC A03/MF A04

A continuous effort in the area of transonic boundary interference correction has been underway at McDonnell Douglas Aerospace for over 6 years. A method of interference correction based on force and moment increments computed from CFD solutions was proposed in 1986. An extensive validation database has been acquired of transonic wind tunnel data for a set of geometrically similar models of different sizes. An empirical model of the flow at a porous transonic wind tunnel wall has been used in conjunction with panel codes and Euler solvers to yield corrections at a variety of conditions in both the MDA Polysonic Wind Tunnel (PSWT) and the MDA Trisonic Wind Tunnel (TWT). Author

N95-19272# British Columbia Univ., Vancouver (British Columbia). Dept. of Mechanical Engineering.
UNSTEADY FLOW TESTING IN A PASSIVE LOW-CORRECTION WIND TUNNEL **c09**
L. Kong and G. V. Parkinson *In* AGARD, Wall Interference, Support Interference and Flow Field Measurements Jul. 1994 7 p Sponsored by Natural Sciences and Engineering Research Council (For primary document see N95-19251 05-34)
Copyright Avail: CASI HC A02/MF A04

A passive low-correction wind tunnel designed for two-dimensional testing has a test section consisting of transverse airfoil-slatted side walls separating it from outer plenum chambers. The uniform spacing of the airfoil slats determines the open-area ratio (OAR). The tests described were on two sizes of NACA 0015 airfoil in plunging oscillation, and instantaneous pressure distributions were measured for different values of airfoil reduced amplitude and frequency, and over a full range of tunnel OAR. It was found that, despite the relatively large sizes of test airfoil, values of pressure, lift, and moment coefficient close to theoretical free-air values were obtained for 0.6 less than OAR less than 0.8, whereas values were much too high in the presence of solid walls and much too low in open-jet testing. Test Reynolds numbers were in the range (2.5-8.0) x 10(exp 5). Author

N95-19273# Aeronautical Research Inst. of Sweden, Bromma.
CALCULATION OF LOW SPEED WIND TUNNEL WALL INTERFERENCE FROM STATIC PRESSURE PIPE MEASUREMENTS
Lars Fernkrans *In* AGARD, Wall Interference, Support Interference and Flow Field Measurements Jul. 1994 7 p Sponsored by FMV (For primary document see N95-19251 05-34)
Copyright Avail: CASI HC A02/MF A04

A wall interference prediction tool based on a boundary condition method

is developed. The correction method, based on Green's theorem, gives the interference velocity potential field in the control volume from the velocities on a control surface around the model of interest without the need to model the flow field. The boundary velocities around separated wake flows are measured with static pressure pipes. This is done with both solid and partially open test section walls. The results are used for validation of the tool and to evaluate the possibilities to use static pressure pipes in low speed flows as a means to get the perturbation velocities needed to calculate blockage effects in nonsolid walls cases. This paper also describes some problems in estimating flow properties that are not measured. The results presented show that if the static pressure measurements are made carefully it is possible to resolve small cross flow velocities with the necessary accuracy for the correction method. Author

N95-19274# Central Aerohydrodynamics Inst., Zhukovsky (Russia).
OPTICAL SURFACE PRESSURE MEASUREMENTS: ACCURACY AND APPLICATION FIELD EVALUATION **c74**
A. Bukov, V. Mosharov, A. Orlov, V. Pesetsky, V. Radchenko, S. Phonov, S. Matyash, M. Kuzmin (Moscow M. V. Lomonosov Inst. of the Technology of Fine Chemicals, USSR.), and N. Sadovskii (Moscow M. V. Lomonosov Inst. of the Technology of Fine Chemicals, USSR.) *In* AGARD, Wall Interference, Support Interference and Flow Field Measurements Jul. 1994 9 p (For primary document see N95-19251 05-34)
Copyright Avail: CASI HC A02/MF A04

Optical pressure measurement (OPM) is a new pressure measurement method rapidly developed in several aerodynamic research centers: TsAGI (Russia), Boeing, NASA, McDonnell Douglas (all USA), and DLR (Germany). Present level of OPM-method provides its practice as standard experimental method of aerodynamic investigations in definite application fields. Applications of OPM-method are determined mainly by its accuracy. The accuracy of OPM-method is determined by the errors of three following groups: (1) errors of the luminescent pressure sensor (LPS) itself, such as uncompensated temperature influence, photo degradation, temperature and pressure hysteresis, variation of the LPS parameters from point to point on the model surface, etc.; (2) errors of the measurement system, such as noise of the photodetector, nonlinearity and nonuniformity of the photodetector, time and temperature offsets, etc.; and (3) methodological errors, owing to displacement and deformation of the model in an airflow, a contamination of the model surface, scattering of the excitation and luminescent light from the model surface and test section walls, etc. OPM-method allows getting total error of measured pressure not less than 1 percent. This accuracy is enough to visualize the pressure field and allows determining total and distributed aerodynamic loads and solving some problems of local aerodynamic investigations at transonic and supersonic velocities. OPM is less effective at low subsonic velocities (M less than 0.4), and for precise measurements, for example, an airfoil optimization. Current limitations of the OPM-method are discussed on an example of the surface pressure measurements and calculations of the integral loads on the wings of canard-aircraft model. The pressure measurement system and data reduction methods used on these tests are also described. Author

N95-19275# Tsentralni Aerogidrodinamicheskii Inst., Moscow (USSR). Aerodynamics Dept.
THE TRADITIONAL AND NEW METHODS OF ACCOUNTING FOR THE FACTORS DISTORTING THE FLOW OVER A MODEL IN LARGE TRANSONIC WIND TUNNELS
V. M. Neyland *In* AGARD, Wall Interference, Support Interference and Flow Field Measurements Jul. 1994 10 p (For primary document see N95-19251 05-34)
Copyright Avail: CASI HC A02/MF A04

The report presents a brief review of the investigation methods and results obtained for the key problems of the test procedure in the industrial sub- and transonic TSAGI wind tunnels. Among these are the flow calibration in 'empty wind tunnels', the wall interference minimization, and the interference with supporting devices. These problems can be solved only in the combination of the calculation and theoretical investigations with the tests carried out first in pilot facilities and then in large wind tunnels. As examples are given the results of the flow calibration both in the conventional conditions of a uniform test section flow and in a flow with the side wall boundary layer suction which is typical for two-dimensional model tests. The flow boundary influence is investigated by the calculation and experimental method of corrections which works well at angles of attack up to 50 degrees at M = 0.9. Good results are also obtained owing to the application of the adaptive perforation to reduce the wall interference on a large-scale civil plane model (blockage is 3.16 percent). The introduction of corrections for the sting-induced flow distortion over the model afterbody is discussed shortly. Author

N95-19276# Centre d'Etudes et de Recherches, Toulouse (France). Dept. d'Etudes et de Recherches en Aero-Thermodynamique.
ANALYSIS OF TEST SECTION SIDEWALL EFFECTS ON A TWO DIMENSIONAL AIRFOIL: EXPERIMENTAL AND NUMERICAL INVESTIGATIONS [EFFETS LATERAUX DANS UNE VEINE D'ESSAIS AUTOUR D'UN PROFIL D'AILE BIDIMENSIONNEL: ETUDES EXPERIMENTALE ET NUMERIQUE]
J. P. Archambaud, J. F. Michonneau, and A. Mignosi *In* AGARD, Wall Interference, Support Interference and Flow Field Measurements Jul. 1994 8 p In FRENCH (For primary document see N95-19251 05-34)
Copyright Avail: CASI HC A02/MF A04

Sidewall effects affect the pressure field around a 2D airfoil tested in wind tunnel, even on its central section. First, laser measurement results show the 3D boundary condition near sidewalls. Then, another experimental investigation points out on the model the perturbation due to sidewall effects. In the second part a numerical method is described (coupling between inviscid flow and sidewall boundary layer computations) which allows taking into account sidewall effects. Comparisons with experiments are shown. Finally, the numerical method is used to estimate the Mach number correction due to sidewall effects. Author

N95-19277# Office National d'Etudes et de Recherches Aerospatiales, Modane (France). Centre d'Essais de Modane-Avrieux.
CALCULATION OF WALL EFFECTS OF FLOW ON A PERFORATED WALL WITH A CODE OF SURFACE SINGULARITIES [CALCULS DES EFFETS DE PAROIS DANS DES VEINES A PAROIS PERFOREES AVEC UN CODE DE SINGULARITIES SURFACIQUES]
J. F. Piat *In* AGARD, Wall Interference, Support Interference and Flow Field Measurements Jul. 1994 12 p In FRENCH (For primary document see N95-19251 05-34)
Copyright Avail: CASI HC A03/MF A04

Simplifying assumptions are inherent in the analytic method previously used for the determination of wall interferences on a model in a wind tunnel. To eliminate these assumptions, a new code based on the vortex lattice method was developed. It is suitable for processing any shape of test sections with limited areas of porous wall, the characteristic of which can be nonlinear. Calculation of wall effects in S3MA wind tunnel, whose test section is rectangular 0.78 m x 0.56 m, and fitted with two or four perforated walls, have been performed. Wall porosity factors have been adjusted to obtain the best fit between measured and computed pressure distributions on the test section walls. The code was checked by measuring nearly equal drag coefficients for a model tested in S3MA wind tunnel (after wall corrections) and in S2MA wind tunnel whose test section is seven times larger (negligible wall corrections). Author

N95-19278# Institute for Aerospace Research, Ottawa (Ontario). High Speed Aerodynamics Lab.
EVALUATION OF COMBINED WALL- AND SUPPORT-INTERFERENCE ON WIND TUNNEL MODELS **c02**
M. Mokry *In* AGARD, Wall Interference, Support Interference and Flow Field Measurements Jul. 1994 11 p (For primary document see N95-19251 05-34)
Copyright Avail: CASI HC A03/MF A04

Coupled interference effects of model support systems and ventilated test section walls on stream parameters at the model are calculated using a subsonic source panel method. The configurations discussed are the movable sting support system and the model plate mount in the IAR 1.5 m x 1.5 m perforated-wall wind tunnel, and an automobile model in the DSMA slotted-wall wind tunnel. Author

N95-19279# Aerospatiale, Toulouse (France).
INTERACTION OF A THREE STRUT SUPPORT ON THE AERODYNAMIC CHARACTERISTICS OF A CIVIL AVIATION MODEL [INTERACTION D'UN SUPPORT DE TYPE 3 MATS SUR LES CARACTERISTIQUES AERODYNAMIQUES D'UNE MAQUETTE D'AVION CIVIL] **c02**
J. Willaume, C. Quemard (Office National d'Etudes et de Recherches Aerospatiales, Toulouse, France.), and A. Bonnet (Ecole Nationale Superieure de l'Aeronautique et de l'Espace, Toulouse, France.) *In* AGARD, Wall Interference, Support Interference and Flow Field Measurements Jul. 1994 25 p In FRENCH (For primary document see N95-19251 05-34)
Copyright Avail: CASI HC A03/MF A04

The interference effects of a three strut support system on the longitudinal aerodynamic characteristics of a model is mainly due to the guards. Our purpose is to describe two theoretical methods allowing to gain access to the level of correction to apply to the wind tunnel gross measurements. The first one is a well known panel method which provides a global correction of the forces; the second one is a simplified method which calculates separately both the displacement effect (thickness) of the guards and the mutual lift effect between them and the wing. The validity of these theoretical results has been checked by specific tests in wind tunnel F1 (ONERA) on a model of the AIRBUS A310. The experimental interference due to the struts and the influence of the model on the strut tares are also discussed. Author

N95-19280# De Havilland Aircraft Co. of Canada Ltd., Downsview (Ontario). Aerodynamic Research and Development.
INTERFERENCE CORRECTIONS FOR A CENTRE-LINE PLATE MOUNT IN A POROUS-WALLED TRANSONIC WIND TUNNEL **c02**
Richard J. D. Poole and Robin D. Galway (Institute for Aerospace Research, Ottawa, Ontario.) *In* AGARD, Wall Interference, Support Interference and Flow Field Measurements Jul. 1994 10 p Sponsored by Industry, Science and Technology Canada and Inst. for Aerospace Research (For primary document see N95-19251 05-34)
Copyright Avail: CASI HC A02/MF A04

A program of collaborative research between the National Research Council of Canada, Institute for Aerospace Research (IAR), and de Havilland Inc. included the design and manufacture of a slim center-line plate mount model support for installation in the IAR 1.5 m Trisonic Wind Tunnel. The primary objective of the collaborative research program was to provide a mounting method suitable for accurate measurement of the drag increments resulting from configuration changes on typical transport aircraft models. The secondary objective was to derive the tare effect of the model mounting plate so that datum aerodynamic parameters could be measured. To obtain the tare effect of the mounting plate on a model, an alternative mount from the tunnel ceiling was designed and built. The 'Y-Mount' allowed the model to be held in close proximity to a dummy plate and also to be tested without the plate in the tunnel. Comparative plate in and plate out measurements were made for a range of Mach numbers and model incidences to obtain the plate tares. Author

N95-19281# German-Dutch Wind Tunnel, North East Polder (Netherlands).
CORRECTION OF SUPPORT INFLUENCES ON MEASUREMENTS WITH STING MOUNTED WIND TUNNEL MODELS **c02**
D. Eckert *In* AGARD, Wall Interference, Support Interference and Flow Field Measurements Jul. 1994 11 p (For primary document see N95-19251 05-34)
Copyright Avail: CASI HC A03/MF A04

The structures of wind tunnel model supports always penetrate the so-called near field of the flow around the model. Therefore, support corrections of aerodynamic coefficients, evaluated either by measurement or by calculation, depend on the specific configuration of the model and of the model/support intersection. As a consequence support influences known for the correction of a wind tunnel measurement with one model are, in general, not transferrable to another configuration. Nevertheless, such a generalization, at least between models of the same aircraft family, would in principle be very helpful in avoiding the time consuming measurements or the viscous flow calculations necessary for the evaluation of support corrections. To this end, at DNW a comprehensive data-base of measured influences of three sting support types on different low-speed aircraft models was analyzed. The aim was to split up the total support effects in terms representing the effect of support volumes located in the far field of the model and in terms representing the effect of support elements located in the near field of the model. The data-base has been analyzed with the aid of a physical model which interprets support influences as flow perturbations relevant for the wing, the fuselage, and the tail of the model. This analysis showed that for some fuselage/sting arrangements the near field effects may be considered small compared with the far field effects and independent of the wing's slat/flap configuration. These findings offered the important possibility of using near field dependent correction terms known for one model configuration for measurements with new configurations (e.g. new wing slat/flap combination). In order to determine the far field influence on new configurations, the physical model mentioned before is used in DNW's on-line data processing system to calculate the support corrections by combining previously determined flow perturbations with the actual measurements during routine tests. Examples show the successful application of the method to measurements with different models. Author

N95-19282# Analytical Methods, Inc., Redmond, WA.
CALCULATION OF SUPPORT INTERFERENCE IN DYNAMIC WIND-TUNNEL TESTS **c02**
D. Almosnino *In* AGARD, Wall Interference, Support Interference and Flow Field Measurements Jul. 1994 6 p (For primary document see N95-19251 05-34)
Copyright Avail: CASI HC A02/MF A04

An unsteady, subsonic flow panel method is applied to predict the support interference effects in dynamic wind tunnel test simulation. Interference effects are calculated by simulating the unsteady flow around the aircraft model, both in the presence and absence of the support system, unlike common experimental techniques that try to measure these effects. The present study uses the standard dynamics model (SDM) in pitch oscillations as a test case. Calculated results for free flight conditions are compared with results obtained when simulating the presence of an existing side-wall-mounted support system in a dynamic wind-tunnel test facility. The calculated results are also compared with experimental data available from different dynamic wind tunnel test facilities. Author

N95-19444# National Aerospace Lab., Bangalore (India). Computational and Theoretical Fluid Dynamics Div.
CFD: ADVANCES AND APPLICATIONS, PART 1
Oct. 1993 216 p Lecture series held in Bangalore, India, 19-21 Oct. 1993
(NAL-SP-9322-Pt-1) Avail: CASI HC A10/MF A03

The important topics covered in this series of lectures include governing equations for aerodynamic flow, grid generation techniques, potential flow methods, accurate high resolution discretization schemes for hyperbolic conservation laws, principle and application of multigrid techniques for convergence acceleration, and finally the efficient and robust finite-volume algorithms for computation of high speed flows in complex aerodynamic configurations. For individual titles, see N95-19445 through N95-19454.

N95-19445# National Aerospace Lab., Bangalore (India). Computational and Theoretical Fluid Dynamics Div.
BASIC EQUATIONS OF FLUID DYNAMICS
M. D. Deshpande *In its* CFD: Advances and Applications, Part 1 Oct. 1993 p 1-18 (For primary document see N95-19444 05-34)
Avail: CASI HC A03/MF A03

We assume that the Navier-Stokes equations along with the continuity and energy equations govern the fluid motion irrespective of the fact that the flow is laminar or turbulent. These equations are well established and are well known. But because of the difficulty in solving them a variety of approaches and approximations have been tried. That is the reason why including some of these formulations and approximations here becomes appropriate. At the beginning of this century the boundary layer concept emerged and a major effort in fluid mechanics was to understand fluid motion through these equations. During the last two to three decades the emergence of high speed computers and the consequent development of efficient numerical algorithms have led to a vigorous activity to understand complex flows through computation. Interestingly, this has an impact on the form of the equations and even the boundary conditions. Some popular boundary conditions at infinity when analytical tools were used may not be

convenient when computers are used. We give below a summary of these equations including some special forms of these equations. Time averaged and mass weighted averaged equations which are useful in dealing with turbulent flows are also included. No attempt has been made to deal with the boundary conditions. Also, we are not dealing with any turbulence models here, since it needs detailed separate attention. Author (revised)

N95-19446# National Aerospace Lab., Bangalore (India). Computational and Theoretical Fluid Dynamics Div.

COMPUTATION OF INVISCID FLOWS: VARIOUS APPROXIMATIONS

U. N. Sinha *In its* CFD: Advances and Applications, Part 1 Oct. 1993 p 19-22 (For primary document see N95-19444 05-34)

Avail: CASI HC A03/MF A03

The Navier-Stokes equations describe the fluid motion in its utmost generality: the flow could be transient, three dimensional, rotational, and turbulent. In practice it is not possible to solve this system of equations corresponding to any given flow situation especially when the geometry is complex (for example the flow past a cylinder, sphere, or an airfoil of an aircraft). Because of tremendous growth in computing resources in recent years, it has been possible to try direct simulation of Navier-Stokes equations for a very simple geometry or try Reynolds averaged Navier-Stokes equations for a geometry of medium complexity. However, certain aspects of flow fields can be examined by simplifying the governing equations. These simplifying assumptions idealize the flow and are described in sequence.

Derived from text

N95-19447# National Aerospace Lab., Bangalore (India). Computational and Theoretical Fluid Dynamics Div.

COMPUTATION OF INVISCID FLOWS: FULL POTENTIAL METHOD

R. Rangarajan *In its* CFD: Advances and Applications, Part 1 Oct. 1993 p 23-50 (For primary document see N95-19444 05-34)

Avail: CASI HC A03/MF A03

Various forms of FP (full potential) equation, spatial differencing schemes, and iterative schemes are briefly discussed. The finite difference method of solution of FP equation in cartesian coordinates is discussed in some detail. Applications of this code to a variety of flow situations like those on airfoils, axisymmetric bodies, wing, and wing-body combinations are presented. The note concludes with some general remarks on the state-of-the-art in this field. Derived from text

N95-19448# National Aerospace Lab., Bangalore (India). Computational and Theoretical Fluid Dynamics Div.

PANEL METHODS

Ashok Srivastava *In its* CFD: Advances and Applications, Part 1 Oct. 1993 p 51-75 (For primary document see N95-19444 05-34)

Avail: CASI HC A03/MF A03

A comprehensive description of panel methods has been given to enable an understanding of the underlying theory and the basic structure of the panel codes for aerodynamic applications. Panel methods have seen peak activity in the industry and remain as yet the sole technique for efficient and practical computations on complex-aircraft configurations. The method of the linearized approach of solving flow problems is well proven and till the turn of the century panel methods will continue to remain as the workhorse for computing aerodynamic characteristics of aircraft shapes in the industry. The alternative Euler and Navier-Stokes solvers have yet to mature for applications to complex shapes, hence panel methods will be in the light for at least another decade. Derived from text

N95-19449# National Aerospace Lab., Bangalore (India). Computational and Theoretical Fluid Dynamics Div.

NUMERICAL GRID GENERATION

J. S. Mathur *In its* CFD: Advances and Applications, Part 1 Oct. 1993 p 77-106 (For primary document see N95-19444 05-34)

Avail: CASI HC A03/MF A03

The solution of problems in Computational Fluid Dynamics (CFD), using finite difference, finite volume, or finite element techniques, requires the discretization of the computational domain into a set of points at which flow quantities are calculated. This set of points is called the computational grid, and the generation of such a grid is now an important activity in CFD. Experience has shown that the accuracy of numerical computations is influenced to a large extent by the grid used. Hence, grid generation techniques should allow some control over positioning of the grid points, in order to allow the generation of a suitable grid for a particular flow problem. We look at grid generation in two dimensions. Some of the techniques for three dimensional grid generation are discussed, but a discussion of grid generation methods for complex three dimensional shapes is beyond the scope of this course. The methods discussed are those with which the author has had some experience. Derived from text

N95-19450# National Aerospace Lab., Bangalore (India). Computational and Theoretical Fluid Dynamics Div.

DIFFERENCE SCHEMES FOR HYPERBOLIC SYSTEM OF CONSERVATION LAWS

K. S. Ravichandran *In its* CFD: Advances and Applications, Part 1 Oct. 1993 p 107-131 (For primary document see N95-19444 05-34)

Avail: CASI HC A03/MF A03

Conservation laws are a time dependent system of partial differential equations that define a set of relationships between the conserved variables (denoted by u) and the flux of these variables (denoted by f or F). It turns out that the conservation laws of mathematical physics are hyperbolic in the sense that the Jacobian matrix of the flux vector is diagonalizable with real eigenvalues and a complete set of eigenvectors. This mathematical property when interpreted physically means that signals propagate in the form of waves with finite speed and hence given initial data with compact support the solution for any finite t also has compact support. It is then conceptually apparent that given the data at any time t, it is in principle possible to compute the solution u(t + Delta t, x) and thus proceed indefinitely. The task of computing solutions therefore comes down to deriving suitable algorithms that do not break down during the computation and produce physically valid solutions of acceptable quality.

Derived from text

N95-19451# National Aerospace Lab., Bangalore (India). Computational and Theoretical Fluid Dynamics Div.

FINITE VOLUME METHOD USING RUNGE-KUTTA TIME-STEPPING FOR SOLUTION OF EULER EQUATIONS

Anand Kumar *In its* CFD: Advances and Applications, Part 1 Oct. 1993 p 133-173 (For primary document see N95-19444 05-34)

Avail: CASI HC A03/MF A03

Potential flow methods have proved very useful in aerodynamics design. Nevertheless their applications is limited by the assumption of potential flow. On the other hand Euler equations provide correct description of inviscid subsonic, transonic, and supersonic flows. Other motivations for the development of Euler codes are that unlike potential flow models vortex sheets are obtained as part of the solution and in regions where shocks are present conservation of mass, momentum, and energy is maintained. Further, Euler codes are easily extended to solve Reynolds averaged Navier-Stokes equations. Jameson et al. proposed a method for the solution of Euler equations. The method uses a semidiscretization approach where spatial discretization is delinked from time integration. Features of the method are: a finite volume spatial discretization for treatment of complex geometry, controlled addition of artificial dissipation, a new class of multistage schemes, and techniques to accelerate solution convergence to steady state. The development of this method for the solution of Euler equations is described. Derived from text

N95-19452# National Aerospace Lab., Bangalore (India). Computational and Theoretical Fluid Dynamics Div.

COMPUTATION OF COMPRESSIBLE FLOWS: IMPLICIT METHODS

Vimala Dutta *In its* CFD: Advances and Applications, Part 1 Oct. 1993 p 175-203 (For primary document see N95-19444 05-34)

Avail: CASI HC A03/MF A03

The present lecture is mainly concerned with the implicit finite difference technique of Beam and Warming and some of the many variants of this popular and widely used implicit method. The Euler and Navier-Stokes equations for 2-D compressible flows and the implicit time differencing formulae are presented in sections 2 and 3. The implicit, noniterative, approximate factorization, central difference algorithm in delta form is derived in section 4 while section 5 deals with stability and convergence considerations. Next, some salient features of implicit upwind schemes based on flux-vector splitting,and TVD schemes are discussed in section 6. The unfactored implicit relaxation method due to Hanel et al is outlined in section 7. Finally, an implicit finite volume nodal point scheme is presented

in section 8. Section 9 presents some examples and results for certain flow problems while section 10 contains some concluding remarks.
Author

N95-19453# National Aerospace Lab., Bangalore (India). Computational and Theoretical Fluid Dynamics Div.
INTRODUCTION TO MULTIGRID METHODS
K. S. Ravichandran *In its* CFD: Advances and Applications, Part 1 Oct. 1993 p 205-217 (For primary document see N95-19444 05-34)
Avail: CASI HC A03/MF A03

The principal aim of computational fluid dynamics is to compute flows in multicomponent 3-D geometries using accurate and reliable mathematical models. A major or perhaps even the single most important parameter governing fluid flow is the Reynolds number Re = UL/nu where U is the typical flow speed, L is a length (of an aircraft, say), and nu is the kinematic viscosity. Typical Reynolds numbers encountered in airflow range from 10(exp 5) for flow past a flat plate to 10(exp 7) for flow past an aircraft. It is well known that for high Reynolds number flow becomes chaotic and turbulent and energy transfer processes take place through the large eddies and dissipation through the small eddies. The ratio of the sizes of the small and large eddies is given by eta/L = O(Re(exp -3/4)). If one intends to resolve the smallest eddies then the mesh size is of the order of eta and to cover the entire flow domain with such a mesh in three dimensions, we require (L/eta)(exp 3) grid points. In other words the number of mesh points required to resolve the flow fully is O(Re(exp 9/4)) and for a Reynolds number of one million, the computing resource required is certainly beyond current projections. Consequently, even if the task is scaled down to the computation of averaged flow with turbulence modeling for the small eddies, one needs to approach steady states rather efficiently. Typically, as Brandt quantifies it, we need methods that would solve a problem of N unknowns with O(N) work and storage. Multigrid offers a way of doing this for different problems. We explain the multigrid principle and technique beginning with simple linear problems and two grid levels.
Author

N95-19454# National Aerospace Lab., Bangalore (India). Computational and Theoretical Fluid Dynamics Div.
APPLICATIONS OF MULTIGRID METHODS TO PROBLEMS IN CFD
J. P. Singh *In its* CFD: Advances and Applications, Part 1 Oct. 1993 p 219-243 (For primary document see N95-19444 05-34)
Avail: CASI HC A03/MF A03

The discipline where multigrid methods have found extensive applications with remarkable success is computational fluid dynamics. The impact of this method on the practical use of various codes based on highly nonlinear differential equations describing the complexity of the fluid flow phenomena has been revolutionary. It is not very long ago that the Navier-Stokes solutions of simple problems took 100 hours and more of CPU time. The independent tremendous revolution taking place in the area of faster chips, on one hand, and the development in multigrid methods, on the other, have brought even the 3-D Navier-Stokes solutions for full aircraft configuration on the threshold of routine computation. Focus will be on the application of multigrid methods to a couple of specific problems, although some essential elements of background are presented. Derived from text

N95-19455# National Aerospace Lab., Bangalore (India). Computational and Theoretical Fluid Dynamics Div.
CFD: ADVANCES AND APPLICATIONS, 1994
Oct. 1994 402 p Lecture series held in Bangalore, India, 26-28 Oct. 1994
(NAL-SP-9412) Avail: CASI HC A18/MF A04

This special publication contains the notes of the lectures delivered under the NAL - UNI series program entitled 'GFD - Advances and Applications - 1994' held at NAL during October 26 - 28, 1994 and coordinated by Dr. S.M. Majumdar and Dr. M.D. Deshpande of CTFD Division, NAL. The topics covered in this series include finite volume algorithm for inviscid gas dynamics, viscous-inviscid interactive methods, turbulence modelling, spectral methods, discrete vortex method for computation of viscous flows, vortex breakdown, hypersonic viscous flows, parabolized N-S equations and CFD on parallel computers. For individual titles, see N95-19456 through N95-19466.

N95-19456# National Aerospace Lab., Bangalore (India). Computational and Theoretical Fluid Dynamics Div.
FINITE-VOLUME UPWIND SCHEMES FOR INVISCID GAS DYNAMICS
K. S. Ravichandran *In its* CFD: Advances and Applications, 1994 Oct. 1994 p 1-4 (For primary document see N95-19455 05-34)
Avail: CASI HC A03/MF A04

In the present notes we shall describe in detail a finite-volume formulation of Osher's upwind scheme for 2-D flow governed by the unsteady compressible Euler equations. The material to be presented has the added advantage of almost being in an algorithm i.e form so that coding of the same for test problems is relatively straightforward. The justification for our choice of Osher scheme for presentation in these lectures is (1) unlike schemes based on linearized approximate Riemann solvers, such as that of Roe, Osher scheme is known to be entropy consistent and not susceptible to some of the defects mentioned above (2) an unified approach to the interior scheme and boundary scheme is possible, and (3) the resulting algorithm therefore is expected to be more robust than other comparable upwind schemes.
Author

N95-19457# National Aerospace Lab., Bangalore (India). Computational and Theoretical Fluid Dynamics Div.
VISCOUS FLOW PAST AEROFOILS AXISYMMETRIC BODIES AND WINGS **c02**
S. S. Desai *In its* CFD: Advances and Applications, 1994 Oct. 1994 p 43-76 (For primary document see N95-19455 05-34)
Avail: CASI HC A03/MF A04

A brief outline is given here of computing viscous flow past aerospace components such as aerofoils, bodies of revolution and wings, based on a coupling of potential flow computations and integral boundary layer calculations. Direct and semi-inverse procedures for viscous-inviscid coupling are described. Keeping in mind transonic and high Reynolds number flows, only turbulent flow computations are considered; laminar and transitional flows are not covered here.
Author

N95-19458# National Aerospace Lab., Bangalore (India). Computational and Theoretical Fluid Dynamics Div.
TURBULENCE MODELING FOR CFD, PART 1
Sekhar Majumdar *In its* CFD: Advances and Applications, 1994 Oct. 1994 p 77-121 (For primary document see N95-19455 05-34)
Avail: CASI HC A03/MF A04

The present lecture is divided into two parts. The first part introduces the fundamental ideas, goals and limitations of turbulence models for numerical prediction of turbulent flows, the eddy viscosity based models used in practice including the special treatment of the near wall zones. The second part discusses the two equation models based on non-linear constitutive relations, the Reynolds stress transport equation-based models and also the engineering turbulence modeling of compressible flows. The capability of different existing models are demonstrated in a few application examples and the future direction of research is also highlighted. Author

N95-19459# National Aerospace Lab., Bangalore (India). Computational and Theoretical Fluid Dynamics Div.
SPECTRAL METHODS FOR FLUID FLOW
A. J. Basu *In its* CFD: Advances and Applications, 1994 Oct. 1994 p 123-129 (For primary document see N95-19455 05-34)
Avail: CASI HC A02/MF A04

Spectral schemes are part of the Methods of Weighted Residuals (MWR), of which even the finite-difference method forms a part. The two key elements of MWR are the trial and the test functions. The trial functions are the basis for the truncated series expansion of the solution. These are infinitely differentiable global functions. The choice of trial functions differentiate spectral methods from finite-difference or finite-element methods (in the finite-difference method, for example, trial functions are local in character). The test functions are used to ensure that the differential equation is satisfied as closely as possible by the truncated series expansion. This is achieved by minimizing the residual (error between truncated series expansion solution and the exact solution). Typical basis functions used in spectral method are the Fourier, the Chebychev and the Legendre series. Of these, Fourier series can only be used in periodic geometries. Most spectral schemes use either Fourier or Chebychev basis functions because of the availability of fast transforms for these two. The choice of test

functions differentiates between the three most commonly used spectral schemes, namely, the Galerkin, the Collocation and the Tau methods.

Author

N95-19460# National Aerospace Lab., Bangalore (India). Computational and Theoretical Fluid Dynamics Div.

DISCRETE VORTEX METHOD FOR COMPUTATION OF VISCOUS INCOMPRESSIBLE FLOWS

P. K. Dutta *In its* CFD: Advances and Applications, 1994 Oct. 1994 p 131-204 (For primary document see N95-19455 05-34)

Avail: CASI HC A04/MF A04

The discrete vortex method has certain advantages over its counterparts, namely, finite difference, finite volume and finite element methods. Since the method is grid-free, the problems of grid generation for complex configurations and requirement of large number of grid points for resolution of fine scale structure do not arise here. Similarly, the far field boundary condition is here satisfied exactly, while in the other methods, the outer domain has to be extended to large distances from the region of interest so as to satisfy this condition. The most important feature of this method, however, consists of its close and direct link with many of the physical mechanisms that govern viscous flows. Quite often, the results from this method can be directly compared with the experimental flow visualization pictures so that the effectiveness of the method in a particular situation can be addressed very quickly. However, the method is not completely free from certain difficulties. To resolve fine structures at high Reynolds numbers, one here needs to use vortices with very small core. For a given finite domain, this implies that the number of vortices required to represent this region accurately is also very large. Since the computation time to calculate the convection velocities of the vortices is proportional to square of the number of vortices, a reasonable computation often requires a computing system with a large core and speed. This situation is further aggravated by the requirement of large number of vortices for simulation of viscous effect. Notwithstanding all its problems, the discrete vortex method has proved to be very successful in recent years in computing complex two-dimensional flows at high Reynolds numbers which are not easily tractable by other methods. The main aim of the present work is to describe this method in as much detail as possible keeping in mind the need of those who wish to step into this area. No attempt is made here to review the method critically, since the usefulness and limitations of the method are already well described in a number of reviews. Author

N95-19461# National Aerospace Lab., Bangalore (India). Computational and Theoretical Fluid Dynamics Div.

PRESSURE BASED FINITE VOLUME ALGORITHM FOR VISCOUS FLOW COMPUTATION

Sekhar Majumdar *In its* CFD: Advances and Applications, 1994 Oct. 1994 p 205-239 (For primary document see N95-19455 05-34)

Avail: CASI HC A03/MF A04

The present lecture deals with issues related mainly to the geometric and algorithmic complexities, i.e. how to handle irregular shaped arbitrary geometry and how a generalized pressure-based algorithm is developed which can, in principle, compute flows at all speeds ranging from incompressible to hypersonic. The pressure-based method is emphasized since it is not covered in details in most of the currently available textbooks and the methodology has reached a certain maturity during the last three decades so that it can adequately handle many issues encountered in flow problems of engineering interest. Section 2 discusses the different possibilities and provides some strategies for the development of general, accurate and efficient pressure-based finite volume algorithms for prediction of flow in complex configurations. Section 3 provides the detailed formulation of a particular pressure-based algorithm developed by the author and his colleagues at the University Karlsruhe, Germany and NAL, Bangalore. Some interesting application examples of incompressible and compressible flow are illustrated in Section 4 to demonstrate the universality and capability of the algorithm whereas, Section 5 presents a few concluding remarks.

Author

N95-19462# National Aerospace Lab., Bangalore (India). Computational and Theoretical Fluid Dynamics Div.

COMPUTATION OF VORTEX BREAKDOWN

Vidyadhar Y. Mudkavi *In its* CFD: Advances and Applications, 1994 Oct. 1994 p 241-280 (For primary document see N95-19455 05-34)

Avail: CASI HC A03/MF A04

Vortex breakdown is a deceptively simple looking, complex and poorly understood phenomenon. According to Benjamin (1962), vortex breakdown or bursting is an abrupt and drastic change of structure which sometimes occurs in swirling flows. This phenomenon is commonly found to occur on leading edge vortices over delta wings and on trailing vortices in aircraft wakes. While it is necessary to prevent vortex breakdown over a delta wing, since it results in loss of lift, it is desirable to allow vortices to burst in aircraft wakes since it reduces hazard to follower aircraft. Vortex breakdown is also useful in chemically reacting flows where it is employed as a flame holder. But, more than anything, this phenomenon is studied because it is one of the basic problems in fluid dynamics. What follows is the authors own limited perspective of the problem. The reader will find that he/she is not introduced to the problem directly. Instead, a whole lot of material is devoted to the development of the equations of vortex dynamics with special emphasis on the motion of a vortex filament. The intention here is to motivate the reader about the merits of describing fluid flows using vortex elements as building blocks rather than velocity and pressure. Model equations of vortex breakdown are derived next using these equations. Other theoretical descriptions of the phenomenon are also stated, Benjamin's theory being of prime importance. Author

N95-19463# National Aerospace Lab., Bangalore (India). Computational and Theoretical Fluid Dynamics Div.

HYPERSONIC VISCOUS FLOW COMPUTATIONS

S. K. Saxena *In its* CFD: Advances and Applications, 1994 Oct. 1994 p 281-319 (For primary document see N95-19455 05-34)

Avail: CASI HC A03/MF A04

This section aims at providing the participants with some essential but bare minimum background information on hypersonic gas dynamics before introducing the subject of hypersonic flow computations. It is hoped that this would help them to have better appreciation of the main topic of this lecture. Author

N95-19464# National Aerospace Lab., Bangalore (India). Computational and Theoretical Fluid Dynamics Div.

PARABOLIZED NAVIER-STOKES SOLUTION OF SUPERSONIC/HYPERSONIC FLOWS **c02**

Dinesh K. Prabhu *In its* CFD: Advances and Applications, 1994 Oct. 1994 p 321-371 (For primary document see N95-19455 05-34)

Avail: CASI HC A04/MF A04

In this lecture we will (1) develop the governing PNS (Parobolized Navier-Stokes) equations for ideal gas, equilibrium air and nonequilibrium air, (2) develop the numerical algorithm to solve these equations, (3) apply the algorithm to compute the hypersonic flow past a simple geometrical shape such as a sharp cone at zero incidence, and (4) discuss the results in terms of the various gas models. Some of the expressions in this lecture have been derived in detail for the ideal/equilibrium model only.

Author

N95-19465# National Aerospace Lab., Bangalore (India). Computational and Theoretical Fluid Dynamics Div.

CFD ON PARALLEL COMPUTERS

A. J. Basu *In its* CFD: Advances and Applications, 1994 Oct. 1994 p 373-377 (For primary document see N95-19455 05-34)

Avail: CASI HC A01/MF A04

CFD or Computational Fluid Dynamics is one of the scientific disciplines that has always posed new challenges to the capabilities of the modern, ultra-fast supercomputers, and now to the even faster parallel computers. For applications where number crunching is of primary importance, there is perhaps no escaping parallel computers since sequential computers can only be (as projected) as fast as a few gigaflops and no more, unless, of course, some altogether new technology appears in future. For parallel computers, on the other hand, there is no such limit since any number of processors can be made to work in parallel. Computationally demanding CFD codes and parallel computers are therefore soul-mates, and will remain so for all foreseeable future. So much so that there is a separate and fast-emerging discipline that tackles problems specific to CFD as applied to parallel computers. For some years now, there is an international conference on parallel CFD. So, one can indeed say that parallel CFD has arrived. To understand how CFD codes are parallelized, one must understand

a little about how parallel computers function. Therefore, in what follows we will first deal with parallel computers, how a typical CFD code (if there is one such) looks like, and then the strategies of parallelization. Author

N95-19466# National Aerospace Lab., Bangalore (India). Computational and Theoretical Fluid Dynamics Div.

TURBULENCE MODELING FOR CFD, PART 2

Sekhar Majumdar *In its* CFD: Advances and Applications, 1994 Oct. 1994 p 379-403 (For primary document see N95-19455 05-34)

Avail: CASI HC A03/MF A04

This part of the lecture first explains the limitations of the Boussinesq Eddy Viscosity hypothesis which forms the basis of all the algebraic and transport equation-based models discussed in Part 1. Unlike laminar viscosity, the eddy viscosity is affected by the shape and nature of the solid boundaries, freestream turbulence intensity and most significantly by the flow history effects. The linear stress-strain relationship is therefore not likely to predict a satisfactory description of a complex turbulent flow situation. Two basic approaches to remove the limitations of the Boussinesq approximation are to use either a Nonlinear Constitutive Relation or a Second Moment Closure based Model. These modeling techniques expected to provide more accurate prediction of complex flows are presented in Sections 2 and 3. Section 4 addresses some important issues in constructing turbulence models for application to compressible flows. A few examples on application of second moment closure and models for compressible flows are demonstrated in Section 5, followed by some concluding remarks. Author

N95-19506# Aircraft Research Association Ltd., Bedford (England).

GENERAL PROCEDURES EMPLOYED IN THE GENERATION OF THREE-DIMENSIONAL HYBRID STRUCTURED/UNSTRUCTURED MESHES

Jonathon A. Shaw, Jeanette M. Georgala, and Paul N. Childs (INTERA Information Technologies Ltd., Abingdon, England.) Apr. 1994 12 p Presented at the Fourth International Conference on Numerical Grid Generation in Computational Fluid Dynamics and Related Fields, Swansea, England, 6-8 Apr. 1994 Sponsored by Ministry of Defence

(ARA-Memo-400) Avail: CASI HC A03/MF A01

An overview is given of the procedure pursued for the generation of meshes composed of both block-structured hexahedral elements and irregularly connected tetrahedral elements. Algorithms are identified that have been instrumental in the development of a mesh generation facility that allows high quality hybrid meshes to be formed efficiently for geometrically complex domains. Examples of the application of the algorithms are given in a companion paper within the same conference proceedings. Author

N95-19578# Cornell Univ., Ithaca, NY. School of Mechanical and Aerospace Engineering.

EXPERIMENTAL STUDIES OF REYNOLDS NUMBER DEPENDENCE OF TURBULENT MIXING AND TRANSPORT

Z. Warhaft 1994 24 p

(Contract DE-FG02-88ER-13929)

(DE94-015338; DOE/ER-13929/5) Avail: CASI HC A03/MF A01

Predicting turbulent mixing and transport remains a critical problem in industrial flows (combustion chambers, mixers, ventilation systems, etc.) and in the environment (smoke plumes, etc.). The mixing and transport processes are often a strong function of Reynolds number (Re) and yet there is a paucity of information on their Re dependence. We propose experiments of passive scalar mixing in isotropic grid turbulence whereby the Taylor Reynolds number (R(sub lambda)) will be varied from 30 to over 400 (60 less than R(sub l) less than 10,000). We will achieve the high R(sub lambda) by means of an active grid, which consists of grid bars with small wings that rotate and flap in a random way. We propose to study basic statistics (pdf, spectra, etc). of a homogeneous passive scalar (linear mean profile), as well as of an inhomogeneous scalar (passive line source) as a function of Re. There are many problems concerning the nature of the fine scale structure of a scalar (e.g., the existence of derivative skewness, the relation of the scalar spectrum to the velocity spectrum, and the rate of spreading of a contaminant plume), placing the similarity theory developed over the past 40 years in doubt, yet there is no information concerning its Reynolds number dependence in isotropic turbulence. The passive scalar will be temperature, although some experiments will be done using helium (which has a Schmidt number of 0.23). Particular emphasis will be placed on higher order statistics of both the signal and its derivative. Our experiments will be related to theory and modeling and to recent advances in direct numerical simulations. We will also do further work on mixing in a jet (also as a function of Re) and will relate this work to the (shearless) grid turbulence. DOE

N95-19607# Rutgers - The State Univ., Piscataway, NJ. Dept. of Mechanical and Aerospace Engineering.

PARALLEL COMPUTATIONS IN HYDRO ACOUSTICS Final Report, 1 Dec. 1988 - 8 Aug. 1993

Richard B. Pelz 25 Oct. 1994 16 p

(Contract N00014-89-J-1320)

(AD-A285900) Avail: CASI HC A03/MF A01

This research concerns the algorithmic development, computer implementation and direct numerical simulation of incompressible and compressible flow of naval relevance. Calculations were executed on a class of current generation multiprocessors. Pseudospectral methods were used exclusively. Lack of parallel algorithms critical to the effective implementation of spectral methods on parallel computers necessitated the need for the development of parallel FFT algorithms for real, conjugate symmetric and real symmetric sequences. These algorithms are applied to spectral methods, but also in many areas of scientific computing. The last algorithm, the parallel fast discrete cosine transform, is used extensively in image and signal processing. The parallel Fourier pseudospectral method for the incompressible Navier-Stokes equations was developed and implemented on many multiprocessors. Reconnection of orthogonally interacting vortex tubes was then investigated using the algorithm on parallel computers as well as vector supercomputers. The parallel Fourier pseudospectral method for the compressible Navier-Stokes equations was also developed. Shock/vortex interactions in two dimensions were investigated. DTIC

N95-19716# Naval Academy, Annapolis, MD.

INCOMPRESSIBLE FLOW OF A NEWTONIAN FLUID PAST A VERTICAL PLATE WITH THERMAL AND MAGNETIC STRESSES

David W. Fink 19 May 1994 66 p

(AD-A284856; USNA-TSPR-213) Avail: CASI HC A04/MF A01

This paper analyzes incompressible flow of a Newtonian fluid past a vertical, flat plate with thermal and magnetic stresses. This analysis will include deriving the equations governing the fluid velocity and the temperature distribution. The equations governing fluid velocity will be derived from a force balance approach. We shall consider the forces that act on a differentially small parcel of fluid to determine its behavior. The equations governing temperature will be derived from the principle of conservation of energy. Energy and temperature are closely related. In fact, in an incompressible fluid, temperature is a direct measurement of internal energy. These equations will then be programmed to provide a computer simulation for predicting velocity and temperature fields for various parameters. These simulations will tell us whether or not it is possible to 'shape' velocity and temperature distributions using magnetic fields. Possible applications include heat exchanges and any transfer process using fluid flow as a transport medium. DTIC

N95-19774# Aircraft Research Association Ltd., Bedford (England).

VALIDATION AND EVALUATION OF THE ADVANCED AERONAUTICAL CFD SYSTEM SAUNA: A METHOD DEVELOPER'S VIEW

J. A. Shaw, A. J. Peace, J. M. Georgala, and P. N. Childs Sep. 1993 44 p Presented at the Recent Developments and Applications in Aeronautical CFD, Bristol, England, 1993 Sponsored by United Kingdom Ministry of Defence

(ARA-Memo-390) Avail: CASI HC A03/MF A01

This paper is concerned with a detailed validation and evaluation of the SAUNA CFD system for complex aircraft configurations. The methodology of the complete system is described in brief, including its unique use of differing grid generation strategies (structured, unstructured or both) depending on the geometric complexity of the configuration. A wide range of configurations and flow conditions are chosen in the validation and evaluation exercise to demonstrate the scope of SAUNA. A detailed description of the results from the method is preceded by a discussion on the philosophy behind the strategy followed in the exercise, in terms of equality assessment and the differing roles of the code developer and the

code user. It is considered that SAUNA has grown into a highly usable tool for the aircraft designer, in combining flexibility and accuracy in an efficient manner. Author

N95-19775# Aircraft Research Association Ltd., Bedford (England).
APPLICATION OF THREE-DIMENSIONAL HYBRID STRUCTURED/UNSTRUCTURED GRIDS TO LAND, SEA AND AIR VEHICLES
Jonathon A. Shaw, Jeanette M. Georgala, Nicholas E. May, and Mark F. Pocock Apr. 1994 17 p Presented at the 4th International Conference on Numerical Grid Generation in Computational Fluid Dynamics and Related Fields, Swansea, Wales, 6-8 Apr. 1994 Sponsored by United Kingdom Ministry of Defence
(ARA-Memo-399) Avail: CASI HC A03/MF A01

The use of a numerical grid generation facility capable of forming unstructured meshes, block-structured meshes and a hybrid combination of these alternative mesh types is described. Examples of meshes created for cars, submarines, missiles and powered civil and military aircraft are given. The motives for choosing a particular type of mesh for each applied configuration are covered, with grid related data given which includes the amount of user effort required to attain the grids. Throughout the paper, algorithms are referred to which have been invoked in the creation of the meshes. These algorithms are introduced in a companion paper within the same conference proceedings. Author

N95-19776# Aircraft Research Association Ltd., Bedford (England).
VERIFICATION OF THE CFD SIMULATION SYSTEM SAUNA FOR COMPLEX AIRCRAFT CONFIGURATIONS
Jonathon A. Shaw, Andrew J. Peace, Nicholas E. May, and Mark F. Pocock Apr. 1994 19 p Presented at the 32nd Aerospace Sciences Meeting, Reno, NV, 10-13 Jan. 1994 Sponsored by United Kingdom Ministry of Defence
(ARA-Memo-401; AIAA Paper 94-0393) Avail: CASI HC A03/MF A01

This paper is concerned with the verification for complex aircraft configurations of an advanced CFD simulation system known by the acronym SAUNA. A brief description of the complete system is given, including its unique use of differing grid generation strategies (structured, unstructured or both) depending on the geometric complexity of the addressed configuration. The majority of the paper focuses on the application of SAUNA to a variety of configurations from the military aircraft, civil aircraft and missile areas. Mesh generation issues are discussed for each geometry and experimental data are used to assess the accuracy of the inviscid (Euler) model used. It is shown that flexibility and accuracy are combined in an efficient manner, thus demonstrating the value of SAUNA in aerodynamic design. Author

N95-19777# Aircraft Research Association Ltd., Bedford (England).
INVISCID AND VISCOUS FLOW MODELLING OF COMPLEX AIRCRAFT CONFIGURATIONS USING THE CFD SIMULATION SYSTEM SAUNA
Andrew J. Peace, Nicholas E. May, Mark F. Pocock, and Jonathon A. Shaw Apr. 1994 14 p Presented at the 19th Congress of the International Council of the Aeronautical Sciences, Anaheim, CA, 18-23 Sep. 1993 Sponsored by United Kingdom Ministry of Defence
(ARA-Memo-403) Avail: CASI HC A03/MF A01

This paper is concerned with the flow modelling capabilities of an advanced CFD simulation system known by the acronym SAUNA. This system is aimed primarily at complex aircraft configurations and possesses a unique grid generation strategy in its use of block-structured, unstructured or hybrid grids, depending on the geometric complexity of the addressed configuration. The main focus of the paper is in demonstrating the recently developed multi-grid, block-structured grid, viscous flow capability of SAUNA, through its evaluation on a number of configurations. Inviscid predictions are also presented, both as a means of interpreting the viscous results and with a view to showing more completely the capabilities of SAUNA. It is shown that accuracy and flexibility are combined in an efficient manner, thus demonstrating the value of SAUNA in aerodynamic design. Author

N95-19778# Aircraft Research Association Ltd., Bedford (England).
THE APPLICATION OF THE SAUNA CFD SYSTEM TO HIGH AND LOW SPEED VEHICLES
Nicholas E. May, Andrew J. Peace, and Jonathon A. Shaw Apr. 1994 20 p Presented at the 1st I Mech E Seminar on The Validation of Computational Techniques in Vehicle Design - Stage One: Computational Fluid Dynamics (CFD), 18 Apr. 1994 Sponsored by United Kingdom Ministry of Defence and British Aerospace, (Military Aircraft)
(ARA-Memo-402) Avail: CASI HC A03/MF A01

The SAUNA grid generation and flow simulation system is applied to a variety of vehicles flows. The basic features and problems associated with predicting high speed external flows are discussed and contrasted with those associated with typical internal flows. Particular attention is paid in the discussion to turbulence modelling requirements. General descriptions of the grid generation philosophy adopted within the SAUNA system (structured, unstructured, hybrid) and the flow solution methodology are given. It is explained how the compressible flow algorithm may be modified to enable efficient calculation of low speed flows, thus extending the range of application of the SAUNA system to include conventional ground and sea vehicles. The grid generation capabilities of SAUNA are illustrated by showing examples of grids generated around configurations of a complete aircraft, a submarine and an automobile. The flow simulations are evaluated by comparison with experiment for several external high speed flows and a lower speed internal flow. Author

N95-18996*# Texas Christian Univ., Fort Worth, TX. Dept. of Engineering.
DESIGN OF HIGH PRESSURE WATERJET NOZZLES
Andre P. Mazzoleni *In* Alabama Univ., Research Reports: 1994 NASA/ASEE Summer Faculty Fellowship Program Oct. 1994 6 p
(For primary document see N95-18967 05-80)
Avail: CASI HC A02/MF A03

N95-19018# Central Inst. of Aviation Motors, Moscow (Russia).
ON THE CFD MONOTONE HIGH ACCURACY METHODS
Mikhail J. Ivanov, Vladislav G. Krupa, and Ravil Z. Nigmatullin *In* AGARD, Mathematical Models of Gas Turbine Engines and their Components Dec. 1994 19 p (For primary document see N95-19017 05-07)
Copyright Avail: CASI HC A03/MF A02

N95-19019# Central Inst. of Aviation Motors, Moscow (Russia).
SOLUTION OF NAVIER-STOKES EQUATIONS USING HIGH ACCURACY MONOTONE SCHEMES
Vladislav G. Krupa and Mikhail J. Ivanov *In* AGARD, Mathematical Models of Gas Turbine Engines and their Components Dec. 1994 16 p (For primary document see N95-19017 05-07)
Copyright Avail: CASI HC A03/MF A02

N95-19153# Science Applications International Corp., Fort Washington, PA.
PREDICTION OF FLUCTUATING PRESSURE AND POWER SPECTRA IN ATTACHED AND SEPARATED COMPRESSIBLE FLOW
A. L. Laganelli, K. R. Wentz (Rohr Industries, Inc., Chula Vista, CA.), and H. F. Wolfe (Rohr Industries, Inc., Chula Vista, CA.) *In* AGARD, Impact of Acoustic Loads on Aircraft Structures Sep. 1994 12 p (For primary document see N95-19142 05-71)
(Contract F33615-87-C-3227)
Copyright Avail: CASI HC A03/MF A03

35 INSTRUMENTATION AND PHOTOGRAPHY

Includes remote sensors; measuring instruments and gages; detectors; cameras and photographic supplies; and holography.

For aerial photography see *43 Earth Resources and Remote Sensing*. For related information see also *06 Aircraft Instrumentation*, and *19 Spacecraft Instrumentation*.

N95-17963# Lawrence Livermore National Lab., Livermore, CA.
THE LINEAR DYNAMICS OF A MICROSENSOR ACCELEROMETER MODELED AS A CANTILEVER BEAM WITH AN END MASS
C. L. Lee Aug. 1994 21 p
(Contract W-7405-eng-48)
(DE94-019108; UCRL-ID-118367) Avail: CASI HC A03/MF A01

Two classes of accelerometers are being developed using silicon microsensor technology. One class of accelerometers will be used to measure accelerations on the order of 10(exp -6)g range. A dynamic

model of these devices is derived in order to aid in their design and characterization. Both types of accelerometers axe modeled as a flexible cantilever beam that is fixed at one end and has a mass attached to the free end. Linear motion about a (straight) horizontal equilibrium shape is considered. The natural frequencies and mode shapes of the model are calculated in terms of the system geometry and material properties. With these results, the continuum model is discretized into a set of modal equations. The responses of the discrete model subject to an impulsive force, a step force, and a single-frequency harmonic external excitation are determined. A comparison between the characteristics of a lumped mass model and a one-degree-of-freedom modal model is presented. Finally, numerical values are given for an example case of a beam without the end mass. DOE

N95-17970 Department of the Navy, Washington, DC.
JUNCTION FIELD EFFECT TRANSISTOR WITH LATERAL GATE VOLTAGE SWING (GVS-JFET) Patent
Galina Kelner, inventor (to Navy) and Michael Shur, inventor (to Navy) 3 May 1994 5 p Filed 30 Sep. 1991
(AD-D016353; US-Patent-5,309,007; US-Patent-Appl-SN-767952; US-Patent-Class-257-286) Avail: US Patent and Trademark Office

A field effect transistor is described having a buried gate and one or more gates disposed along the channel between the source and drain, which cooperate to cause the electric field within the channel along its length to be more uniform and have a lower field maximum. The geometry and/or doping of the channel can be varied to selectively vary the channel resistivity along its length, which also makes the field more uniform. Because of the more uniform field, electrons are exposed to a higher field strength nearer the source, and are accelerated to higher velocities more quickly, reducing the response time and increasing the frequency range of the transistor. Because the peak field is reduced, the transistor can carry more power without reaching breakdown potential within the channel. DTIC

N95-18065 Electronics Research Lab., Salisbury (Australia).
MODULAR IMPLEMENTATION OF FEATURE EXTRACTION AND MATCHING ALGORITHMS FOR PHOTOGRAMMETRIC STEREO IMAGERY
James Kershaw and Garry Hamlyn Jun. 1994 100 p Limited Reproducibility: More than 20% of this document may be affected by microfiche quality
(AD-A285422; ERL-0800-RR; DODA-AR-008-839) Avail: CASI HC A05

This paper describes the implementation of algorithms for automatically extracting and matching features in stereo pairs of images. The implementation has been designed to be as modular as possible to allow different algorithms for each stage in the matching process to be combined in the most appropriate manner for each particular problem. The modules have been implemented in the AVS environment but are designed to be portable to any platform. This work has been undertaken as part of task DEF 93/1 63 'Intelligence Analysis of Imagery', and forms part of ITD's contribution to the Visual Processing research program in the Centre for Sensor System and Information Processing. A major aim of both the task and the research program is to produce software to assist intelligence analysts in extracting three dimensional shape from imagery: the algorithms and software described here will form the first part of a module for automatically extracting depth information from stereo image pairs. DTIC

N95-18130# Los Alamos National Lab., NM.
NONLINEAR RESPONSE OF THE PHOTOCATHODE OF AN X-RAY STREAK CAMERA TO UV LIGHT
G. A. Kyrala, D. M. Oro, J. K. Studebaker, W. M. Wood, G. T. Schappert, S. Watts, and R. D. Fulton 1994 8 p Presented at the Annual Meeting of the Society of Photo-Optical Instrumentation Engineers, San Diego, CA, 24-29 Jul. 1994
(Contract W-7405-eng-36)
(DE94-018073; LA-UR-94-2696; CONF-940723-19) Avail: CASI HC A02/MF A01

We have found that a potassium-iodide photocathode of an x-ray streak camera responds to UV light at lambda = 308 nm. The photocathode surface work function, 6.5 eV, is larger than the 4 eV energy of the UV photon, hence the source of the response is interesting. We will present results on the response of a transmission type potassium-iodide photocathode to the UV light from a lambda = 308 nm, subpicosecond XeCl laser and from a lambda = 326 nm HeCd laser. We will test for the nonlinearity of the yield to measure of the number of photons that are needed to be absorbed before a signal is recorded. We will present data on the effect of the UV irradiance on the yield, as well as on the temporal width of the recorded signal. We will give an explanation of the observation and its effect on the dynamic-range response of the streak-camera. We will show that the response is linear with the incident irradiance, up to an incident irradiance of 10(exp 8) W/cm(exp 2) and we will explain the observation. DOE

N95-18194*# National Aeronautics and Space Administration. Langley Research Center, Hampton, VA.
A SPECTRAL STUDY OF A RADIO-FREQUENCY PLASMA-GENERATED FLUX OF ATOMIC OXYGEN
Carmen E. Batten, Kenneth G. Brown (Old Dominion Univ., Norfolk, VA.), and Beverley W. Lewis (Old Dominion Univ., Norfolk, VA.) Dec. 1994 14 p
(RTOP 307-51-12-04)
(NASA-TM-4612; L-17351; NAS 1.15:4612) Avail: CASI HC A03/MF A01

The active environment of a radio-frequency (RF) plasma generator, with and without low-pressure oxygen, has been characterized through the identification of emission lines in the spectral region from 250 to 900 nm. The environment is shown to be dependent on the partial pressure of oxygen and the power applied to the RF generator. Atomic oxygen has been found in significant amounts as well as atomic hydrogen and the molecular oxygen species O2((sup 1)Sigma). The only charged species observed was the singly charged molecular ion O2(+). With a polymer specimen in the plasma chamber, carbon monoxide was also observed. The significance of these observations with respect to previous studies using this type of generator to stimulate material degradation in space is discussed. The possibility of using these generators as atomic oxygen sources in the development of oxygen atom fluorescence sensors is explored. Author

N95-18316* National Aeronautics and Space Administration. Langley Research Center, Hampton, VA.
TWO-STAGE GAS MEASUREMENT SYSTEM Patent
Danny R. Sprinkle, inventor (to NASA), Tony T. D. Chen, inventor (to NASA), and Sushil K. Chaturvedi, inventor (to NASA) 20 Dec. 1994 4 p Filed 7 May 1992 Supersedes N93-31297 (31 - 12, p 3729)
(NASA-Case-LAR-14791-1; US-Patent-5,374,400; US-Patent-Appl-SN-879480; US-Patent-Class-422-94; US-Patent-Class-204-426; US-Patent-Class-422-88; US-Patent-Class-422-98; Int-Patent-Class-G01N-27/12) Avail: US Patent and Trademark Office

A quick-response, real-time gaseous measurement system allows for the continuous sampling of a low pressure gaseous environment. A sample of test gas from the low pressure gaseous environment is continuously extracted and pumped to a structural tee joint which is open to the atmosphere at one end to maintain the test gas at a constant pressure. The structural tee joint communicates at the other end with a heater for maintaining the test gas at a constant temperature. From the heater, the test gas is sent to a sensor which develops a voltage that is proportional to the partial pressure of the gaseous component to be measured in the test gas, a constant flow rate of test gas being provided through the heater and sensor. Since test gas pressure, temperature, and flow rate are being held constant, changes in sensor voltage are attributable only to changes in the concentration of the measured gas component. Official Gazette of the U.S. Patent and Trademark Office

N95-18319 Department of the Navy, Washington, DC.
FIXTURE FOR PRESSURE TESTING SIGHT GLASSES Patent
Earl S. Nickerson, Jr., inventor (to Navy) 22 Feb. 1994 7 p Filed 19 Jun. 1992
(AD-D016263; US-Patent-5,287,727; US-Patent-Appl-SN-901286) Avail: US Patent and Trademark Office

A fixture for pressure testing sight glasses includes a base having a recessed pressure chamber therein, a peripheral seal ring in the pressure chamber and a supply passage for supplying a pressurized fluid to the pressure chamber. The test fixture is operable by securing a sight glass

on the fixture so that the sight glass is received in sealing engagement with the seal ring above the pressure chamber in order to apply a predetermined fluid pressure to the sight glass. DTIC

N95-18461# Department of the Navy, Washington, DC.
HYDROFOIL FORCE BALANCE Patent Application
Paul J. Lefebvre, inventor (to Navy) and William P. Barker, inventor (to Navy) 20 Jul. 1994 22 p
(AD-D016475; US-Patent-Appl-SN-279037; Navy-Case-74885) Avail: CASI HC A02/MF A01

The present invention relates to a measuring device for measuring a component of a force acting on a test body, such as a hydrofoil, positioned within a testing apparatus. The measuring device has a test body formed by a foil shaped center section and two adjacent end sections. Each end section is joined to the center section by a flexure member having sufficient stiffness so that there is negligible relative motion between the center section and the end sections as a fluid medium flows past the center section. At least one strain gauge is mounted to at least one flexure member to measure the forces acting on the center section. A method for measuring the load on a test body is also described. DTIC

N95-18524 Department of the Navy, Washington, DC.
CORROSIVITY SENSOR Patent
Vinod S. Agarwala, inventor (to Navy) and Fred Pearlstein, inventor (to Navy) 10 May 1994 6 p Filed 10 Sep. 1992
(AD-D016422; US-Patent-5,310,470; US-Patent-Appl-SN-942914; US-Patent-Class-204-404) Avail: US Patent and Trademark Office

A lightweight corrosivity sensor is provided which is thin enough to be embedded between the layers of a composite structure or placed on a surface beneath a coating. It comprises a thin non-conductive base and two electrically isolated conductive elements fixed to the surface thereof. Each conductive element comprises a bus bar and a plurality of strips extending from the bus bar and interdigitated with the strips of the other conductive element. The corrosivity sensor is connectable to a current measuring means for measuring the current across the two conductive elements as an indicator of the presence of a corrosive environment. A masking method of manufacturing such a sensor is also provided. DTIC

N95-18555# Lawrence Livermore National Lab., Livermore, CA.
IMPLEMENTATION OF 40-ps HIGH-SPEED GATED-MICROCHANNEL-PLATE BASED X-RAY FRAMING CAMERAS ON REENTRANT SIM'S FOR NOVA
P. M. Bell, J. D. Kilkenny, O. Landen, D. K. Bradley (Rochester Univ., NY.), R. Watt (Los Alamos National Lab., NM.), and J. Oertel (Los Alamos National Lab., NM.) 28 Jul. 1994 13 p Presented at the Annual Meeting of the Society of Photo-Optical Instrumentation Engineers, San Diego, CA, 24-29 Jul. 1994
(Contract W-7405-eng-48)
(DE94-018597; UCRL-JC-117193; CONF-940723-25) Avail: CASI HC A03/MF A01

Gated framing cameras used in diagnosing laser produced plasmas have been used on the Nova laser system since 1987. There have been many variations of these systems implemented. All of these cameras have been ultimately limited in response time for two reasons. One being the electrical gating amplitude verses the gate width, this has always limited the detectable gain in the system. The second being the length to diameter (l/d) ratio of standard off the shelf microchannel plates (MCP). This sets the minimum electrical gate pulse that will give detectable gain from a given microchannel plate. The authors have implemented two different types of 40 ps framing camera configurations on the Nova laser system. They will describe the configurations of both systems as well as discuss the advantages of each. DOE

N95-18620# Army Research Lab., Aberdeen Proving Ground, MD.
THERMOCOUPLES FOR INTERIOR BALLISTIC TEMPERATURE MEASUREMENTS Final Report, Oct. 1991 - Sep. 1993
Stephen L. Howard, Lang-Mannn Chang, and Douglas E. Kooker Aug. 1994 51 p
(DA Proj. 1L1-61102-AH-43)
(AD-A283699; ARL-MR-146) Avail: CASI HC A04/MF A01

Flamespreading processes during the ignition of ballistic events have long been studied by pressure measurements and visual records from high-speed film. While optical temperature measurements have been utilized, they are not useful much below 1500 K. This report describes a fine-wire thermocouple probe designed to measure gas temperature in a propellant bed over the range from the initial propellant bed temperature to over 2000 K. Several diameters of thermocouple wire are tested for survivability and time response in the simulated pressure-wave environment of ignition of a propellant bed. Examples of temperature histories during ignition of M30A1 and M43 propellants are also included. DTIC

N95-18735*# National Aeronautics and Space Administration. Hugh L. Dryden Flight Research Center, Edwards, CA.
CURRENT LOOP SIGNAL CONDITIONING: PRACTICAL APPLICATIONS
Karl F. Anderson Washington Jan. 1995 22 p Presented at the 1995 Measurement Science Conference, Anaheim, CA, 26-27 Jan. 1995
(RTOP 505-63-50)
(NASA-TM-4636; H-2026; NAS 1.15:4636) Avail: CASI HC A03/MF A01

This paper describes a variety of practical application circuits based on the current loop signal conditioning paradigm. Equations defining the circuit response are also provided. The constant current loop is a fundamental signal conditioning circuit concept that can be implemented in a variety of configurations for resistance-based transducers, such as strain gages and resistance temperature detectors. The circuit features signal conditioning outputs which are unaffected by extremely large variations in lead wire resistance, direct current frequency response, and inherent linearity with respect to resistance change. Sensitivity of this circuit is double that of a Wheatstone bridge circuit. Electrical output is zero for resistance change equals zero. The same excitation and output sense wires can serve multiple transducers. More application arrangements are possible with constant current loop signal conditioning than with the Wheatstone bridge. Author

N95-18929 Stanford Univ., CA.
THE GRAVITY PROBE B NIOBIUM BIRD EXPERIMENT: EXPERIMENTAL VERIFICATION OF A DATA REDUCTION SCHEME WITH A PROTOTYPICAL DC SQUID READOUT SYSTEM Ph.D. Thesis
Hirohiko Uematsu 1994 256 p
Avail: Univ. Microfilms Order No. DA9414670

This dissertation describes the concept and the latest results from the niobium bird experiment, which is an integrated, end-to-end test environment for the data reduction scheme and the readout system designed for the Gravity Probe B program (GP-B). The Gravity Probe B program is a relativity gyroscope experiment begun at Stanford University in 1960 and supported by NASA since 1963. This experiment, for the first time, will check the relativistic precession of an Earth-orbiting gyroscope that was predicted by Einstein's General Theory of Relativity, to an accuracy of 1 milliarcsecond per year or better. A drag-free satellite will carry four gyroscopes in a polar orbit to observe their relativistic precession. The primary sensor for measuring the direction of the gyroscope spin axis is the SQUID (superconducting quantum interference device) magnetometer. The data reduction scheme designed for the GP-B program processes the signal from the SQUID magnetometer and estimates the relativistic precession rates. I reformulated the two-step Kalman filters, originally developed by J. V. Breakwell and X. Qin, and designed the niobium bird experiment to verify the performance of the data reduction scheme experimentally with SQUID readout hardware within the test loop. The niobium bird experiment comprised three major components: a truth model, Kalman filters, and a SQUID readout system. The truth model simulated the science signal, which was injected into the SQUID readout system. The SQUID output was then fed into the two-step Kalman filters as a measurement, and the true values and the estimates by the filters were compared to evaluate the filter performance. The latest results from the niobium bird experiment showed that the temperature-dependent bias drift in a commercially available dc SQUID was about twenty times larger than what I assumed in the simulation and was too large to achieve the required estimation accuracy. For the GP-B science mission, the bias drift in the SQUID readout can be reduced to meet the requirement by implementing a temperature regulation system and designing a SQUID controller with a smaller temperature coefficient. Dissert. Abstr.

N95-18938*# McDonnell-Douglas Aerospace, Saint Louis, MO.
FIBER OPTIC CONTROL SYSTEM INTEGRATION FOR ADVANCED AIRCRAFT. ELECTRO-OPTIC AND SENSOR FABRICATION, INTEGRATION, AND ENVIRONMENTAL TESTING FOR FLIGHT CONTROL SYSTEMS: LABORATORY TEST RESULTS Final Report
Bradley L. Kessler Nov. 1994 388 p
(Contract NAS3-25796; RTOP 505-62-50)
(NASA-CR-195408; E-9265; NAS 1.26:195408) Avail: CASI HC A17/MF A04

This report presents the data obtained in laboratory testing of the optical sensors and multiplexing architecture developed for flight testing in the NASA F-18 systems research aircraft. Author

N95-19071 Naval Air Warfare Center, Patuxent River, MD. Aircraft Div.
NAWCAD PHOTOGRAMMETRICS: METHODS AND APPLICATIONS FOR AVIATION TEST AND EVALUATION
John J. Shields, Alec E. Forsman, and Robert F. Stancil 1994 7 p
Limited Reproducibility: More than 20% of this document may be affected by microfiche quality
(AD-A284074) Avail: Issuing Activity (Defense Technical Information Center (DTIC))

Photogrammetrics, the science of extracting quantitative and qualitative data from multiple sequential recorded images, has been an integral part of flight test and evaluation at the Naval Air Warfare Center Aircraft Division (NAWCAD) at Patuxent River, MD for over 35 years. Photogrammetrics analysis is used for evaluation of stores separation, carrier suitability, range tracking, overhead impact scoring, and mishap reconstruction. The NAWCAD photogrammetrics team is pursuing strategies to reduce the time and increase the accuracies of solution processes that historically have been labor-intensive, prone to repetition of effort, and difficult to present This paper describes how NAWCAD scientists have applied a clearly defined process for photogrammetrics efforts, and have implemented state-of-the-art hardware and software methodologies that reduce the turnaround time, increase the accuracy, and facilitate the delivery of custom formatted products to the flight test engineer's desktop. DTIC

N95-19124 Department of the Navy, Washington, DC.
LOW NOISE FIBER GYROSCOPE SYSTEM WHICH INCLUDES EXCESS NOISE SUBTRACTION Patent
Robert P. Moeller, inventor (to Navy) and William K. Burns, inventor (to Navy) 19 Jul. 1994 10 p Filed 30 Nov. 1992
(AD-D016556; US-Patent-5,331,404; US-Patent-Appl-SN-983335; US-Patent-Class-356-350) Avail: US Patent and Trademark Office

A system and method for subtracting excess noise from a high sensitivity gyroscope system in which a laser diode array is focused into an Nd-doped active fiber. A resultant gyro signal is polarized, detected, and amplified. A noise signal is polarized, delayed, detected, and amplified such that the noise signal is polarized parallel to the gyro signal and delayed by a fiber delay, of a length equal to a length of a gyroscope fiber coil. The excess noise component in the amplified gyro signal is reduced by modulating the amplified noise signal with a portion of the amplified gyro signal and subtracting the amplitude-modulated noise signal from the amplified gyro signal to produce a reduced noise gyro signal. DTIC

N95-19229# Los Alamos National Lab., NM.
HIGH FRAME RATE CCD CAMERAS WITH FAST OPTICAL SHUTTERS FOR MILITARY AND MEDICAL IMAGING APPLICATIONS
N. S. P. King, K. Albright, S. A. Jaramillo, T. E. McDonald, G. J. Yates, and B. T. Turko (California Univ., Berkeley. Lawrence Berkeley Lab, CA.) 1994 6 p Presented at the Annual Meeting of the Society of Photo-Optical Instrumentation Engineers, San Diego, CA, 24-29 Jul. 1994
(Contract W-7405-eng-36)
(DE94-018316; LA-UR-94-2898; CONF-940723-21) Avail: CASI HC A02/MF A01

Los Alamos National Laboratory has designed and prototyped high-frame rate intensified/shuttered Charge-Coupled-Device (CCD) cameras capable of operating at kilohertz frame rates (non-interlaced mode) with optical shutters capable of acquiring nanosecond-to-microsecond exposures each frame. These cameras utilize an Interline Transfer CCD, Loral Fairchild CCD-222 with 244 (times) 380 pixels operated at pixel rates approaching 100 Mhz. Initial prototype designs demonstrated single-port serial readout rates exceeding 3.97 Kilohertz with greater than 51 p/mm spatial resolution at shutter speeds as short as 5 ns. Readout was achieved by using a truncated format of 128 (times) 128 pixels by partial masking of the CCD and then subclocking the array at approximately 65 Mhz pixel rate. Shuttering was accomplished with a proximity focused microchannel plate (MCP) image intensifier (MCPII) that incorporated a high strip current MCP and a design modification for high-speed stripline gating geometry to provide both fast shuttering and high repetition rate capabilities. Later camera designs use a close-packed quadruple head geometry fabricated using an array of four separate CCDs (pseudo 4-port device). This design provides four video outputs with optional parallel or time-phased sequential readout modes. The quad head format was designed with flexibility for coupling to various image intensifier configurations, including individual intensifiers for each CCD imager, a single intensifier with fiber optic or lens/prism coupled fanout of the input image to be shared by the four CCD imagers or a large diameter phosphor screen of a gateable framing type intensifier for time sequential relaying of a complete new input image to each CCD imager. Camera designs and their potential use in ongoing military and medical time-resolved imaging applications are discussed. DOE

N95-19233# Oak Ridge National Lab., TN.
SUBGROUP REPORT ON HARD X-RAY MICROPROBES
G. E. Ice, T. Barbee (Lawrence Livermore National Lab., Livermore, CA.), R. Bionta (Lawrence Livermore National Lab., Livermore, CA.), M. Howells (California Univ., Berkeley. Lawrence Berkeley Lab, CA.), A. C. Thompson (California Univ., Berkeley. Lawrence Berkeley Lab, CA.), and W. Yun (Argonne National Lab., IL.) 1994 9 p Presented at the X-Ray Optics in the National Laboratories Workshop, Half Moon Bay, CA, 28-29 Oct. 1992
(Contract DE-AC05-84OR-21400)
(DE94-018708; CONF-9210478-1) Avail: CASI HC A02/MF A01

The increasing availability of synchrotron x-ray sources has stimulated the development of advanced hard x-ray (E greater than or equal to 5 keV) microprobes. New x-ray optics have been demonstrated which show promise for achieving intense submicron hard x-ray probes. These probes will be used for extraordinary elemental detection by x-ray fluorescence/absorption and for microdiffraction to identify phase and strain. The inherent elemental and crystallographic sensitivity of an x-ray microprobe and its inherently nondestructive and penetrating nature makes the development of an advanced hard x-ray microprobe an important national goal. In this workshop state-of-the-art hard x-ray microprobe optics were described and future directions were discussed. Gene Ice, Oak Ridge National Laboratory (ORNL), presented an overview of the current status of hard x-ray microprobe optics and described the use of crystal spectrometers to improve minimum detectable limits in fluorescent microprobe experiments. Al Thompson, Lawrence Berkeley Laboratory (LBL), described work at the Center for X-ray Optics to develop a hard x-ray microprobe based on Kirkpatrick-Baez (KB) optics. Al Thompson also showed the results of some experimental measurements with their KB optics. Malcolm Howells presented a method for bending elliptical mirrors and Troy Barbee commented on the use of graded d spacings to achieve highest efficiency in KB multilayer microfocusing. Richard Bionta, Lawrence Livermore National Laboratory (LLNL), described the development of the first hard x-ray zone plates and future promise of so called 'jelly roll' or sputter slice zone plates. Wenbing Yun, Argonne National Laboratory (ANL), described characterization of jelly roll and lithographically produced zone plates and described the application of zone plates to focus extremely narrow bandwidths by nuclear resonance. This report summarizes the presentations of the workshop subgroup on hard x-ray microprobes. DOE

N95-19236*# McDonnell-Douglas Aerospace, Saint Louis, MO.
FIBER OPTIC CONTROL SYSTEM INTEGRATION FOR ADVANCED AIRCRAFT. ELECTRO-OPTIC AND SENSOR FABRICATION, INTEGRATION, AND ENVIRONMENTAL TESTING FOR FLIGHT CONTROL SYSTEMS Final Report
Daniel W. Seal, Thomas L. Weaver, Bradley L. Kessler, Carlos A. Bedoya, and Robert E. Mattes Nov. 1994 127 p
(Contract NAS3-25796; RTOP 505-62-50)
(NASA-CR-191194; E-8151; NAS 1.26:191194) Avail: CASI HC A07/MF A02

This report describes the design, development, and testing of passive fiber optic sensors and a multiplexing electro-optic architecture (EOA) for installation and flight test on a NASA-owned F-18 aircraft. This hardware

was developed under the Fiber Optic Control Systems for Advanced Aircraft program, part of a multiyear NASA initiative to design, develop, and demonstrate through flight test 'fly-by-light' systems for application to advanced aircraft flight and propulsion control. This development included the design and production of 10 passive optical sensors and associated multiplexed EOA hardware based on wavelength division multiplexed (WDM) technology. A variety of sensor types (rotary position, linear position, temperature, and pressure) incorporating a broad range of sensor technologies (WDM analog, WDM digital, analog microbend, and fluorescent time rate of decay) were obtained from different manufacturers and functionally integrated with an independently designed EOA. The sensors were built for installation in a variety of aircraft locations, placing the sensors in a variety of harsh environments. The sensors and EOA were designed and built to have the resulting devices be as close as practical to a production system. The integrated system was delivered to NASA for flight testing on a NASA-owned F-18 aircraft. Development and integration testing of the system provided valuable information as to which sensor types were simplest to design and build for a military aircraft environment and which types were simplest to operate with a multiplexed EOA. Not all sensor types met the full range of performance and environmental requirements. EOA development problems provided information on directions to pursue in future fly-by-light flight control development programs. Lessons learned in the development of the EOA and sensor hardware are summarized. Author (revised)

N95-19394# Los Alamos National Lab., NM.
HIGH-FRAME-RATE INTENSIFIED FAST OPTICALLY SHUTTERED TV CAMERAS WITH SELECTED IMAGING APPLICATIONS
G. J. Yates and N. S.P. King 1994 25 p Presented at the OE/LASE 1994: Conference on Optics, Electro-Optics, and Laser Applications in Science and Engineering, Los Angeles, CA, 22-29 Jan. 1994
(Contract W-7405-eng-36)
(DE94-016098; LA-UR-94-2557; CONF-940142-44) Avail: CASI HC A03/MF A01

This invited paper focuses on high speed electronic/electro-optic camera development by the Applied Physics Experiments and Imaging Measurements Group (P-15) of Los Alamos National Laboratory's Physics Division over the last two decades. The evolution of TV and image intensifier sensors and fast readout fast shuttered cameras are discussed. Their use in nuclear, military, and medical imaging applications are presented. Several salient characteristics and anomalies associated with single-pulse and high repetition rate performance of the cameras/sensors are included from earlier studies to emphasize their effects on radiometric accuracy of electronic framing cameras. The Group's test and evaluation capabilities for characterization of imaging type electro-optic sensors and sensor components including Focal Plane Arrays, gated Image Intensifiers, microchannel plates, and phosphors are discussed. Two new unique facilities, the High Speed Solid State Imager Test Station (HSTS) and the Electron Gun Vacuum Test Chamber (EGTC) arc described. A summary of the Group's current and developmental camera designs and R&D initiatives are included. DOE

N95-19553# Westinghouse Hanford Co., Richland, WA.
ACCEPTANCE/OPERATIONAL TEST PROCEDURE 101-SY TANK CAMERA PURGE SYSTEM AND IN TANK COLOR CAMERA VIDEO IMAGING SYSTEM
S. M. Werry 1994 12 p
(Contract DE-AC06-87RL-10930)
(DE95-000344; WHC-SD-WM-OTP-158) Avail: CASI HC A03/MF A01

This Acceptance/Operational Test Procedure will document the satisfactory operation of the 101-SY color camera purge control system and color camera video imaging system. DOE

N95-19711# Lawrence Livermore National Lab., Livermore, CA.
GAIN UNIFORMITY, LINEARITY, SATURATION AND DEPLETION IN GATED MICROCHANNEL-PLATE X-RAY FRAMING CAMERAS
O. L. Landen, P. M. Bell, J. J. Satariano, J. A. Oertel (Los Alamos National Lab., NM.), and D. K. Bradley (Rochester Univ., NY.) 20 Jul. 1994 14 p Presented at the Annual Meeting of the Society of Photo-Optical Instrumentation Engineers (SPIE), San Diego, CA, 11-16 Jul. 1993
(Contract W-7405-eng-48)
(DE94-018596; UCRL-JC-112384; CONF-930722-60) Avail: CASI HC A03/MF A01

The pulsed characteristics of gated, stripline configuration microchannel-plate (MCP) detectors used in X-ray framing cameras deployed on laser plasma experiments worldwide are examined in greater detail. The detectors are calibrated using short (20 ps) and long (500 ps) pulse X-ray irradiation and 3-60 ps, deep UV (202 and 213 nm), spatially-smoothed laser irradiation. Two-dimensional unsaturated gain profiles showless than 5% long-range transverse variations but up to 3 dB/cm drop in gain parallel to the pulse propagation direction. Up to 50% gain enhancements due to voltage reflection from the bends of a meander stripline geometry and from the ends of conventional straight striplines are also observed. Reproducible gate profiles are obtained with either picosecond X-ray or UV bursts and FWHM extracted with 3 picosecond accuracy. A novel single-shot method for measuring local gate propagation speeds using a tilted MCP is also demonstrated. Detailed output versus input studies indicate a linear dynamic range of 300. At higher irradiances, the gradual transition from linear behavior to hard saturation is gathered over a range of 10(exp 5) in irradiation and fitted using a discrete dynode model. Finally, a pump-probe experiment quantifying for the first time long-suspected gain depletion by strong localized irradiation was performed. The mechanism for the extra voltage and hence gain degradation is shown to be associated with intense MCP irradiation in the presence of the voltage pulse, at a fluence at least an order of magnitude above that necessary for saturation. Results obtained for both constant pump area and constant pump fluence are presented. The data are well modeled by calculating the instantaneous electrical energy loss due to the intense charge extraction at the pump site and then recalculating the gain downstream at the probe site given the pump-dependent degradation in voltage amplitude. DOE

N95-19794*# National Aeronautics and Space Administration. Lewis Research Center, Cleveland, OH.
IMPROVED SPEED CONTROL SYSTEM FOR THE 87,000 HP WIND TUNNEL DRIVE
Edward A. Becks (NYMA, Inc., Brook Park, OH.), Timothy J. Bencic, and Philip Z. Blumenthal (NYMA, Inc., Brook Park, OH.) Jan. 1995 13 p Presented at the 41st International Instrumentation Symposium, Denver, CO, 7-11 May 1995; sponsored by Instrument Society of America
(Contract NAS3-27186; RTOP 505-62-82)
(NASA-TM-106840; E-9404; NAS 1.15:106840) Avail: CASI HC A03/MF A01

This paper describes the design, installation, and integrated systems tests for a new drive motor speed control system which was part of a recent rehab project for the NASA Lewis 8x6 Supersonic Wind Tunnel. The tunnel drive consists of three mechanically-coupled 29,000 HP wound rotor induction motors driving an axial flow compressor. Liquid rheostats are used to vary the impedance of the rotor circuits, thus varying the speed of the drive system. The new design utilizes a distributed digital control system with a dual touch screen CRT operator console to provide alarm monitoring, logging, and trending. The liquid rheostats are driven by brushtype servomotor systems with magnetostrictive linear displacement transducers used for position feedback. The new system achieved all goals for speed variations with load, motor load balance, and control of total power. Author

N95-19871# California Inst. of Tech., Pasadena, CA. Dept. of Electrical Engineering.
THREE-D OPTICAL MEMORY DISK Technical Report, 1 Jul. 1993 - 28 Feb. 1994
Demetri Psaltis 22 Apr. 1994 13 p
(Contract F49620-92-J-0400)
(AD-A280002; AFOSR-94-0335TR) Avail: CASI HC A03/MF A01

Recently, a new method of multiplexing holograms by rotating the material, or equivalently, the recording beams was invented. This method is called Peristropic (Greek for rotation) multiplexing and is briefly described. Peristropic multiplexing can be combined with other multiplexing methods to increase the storage density of holographic storage systems such as the previously reported 3-D disk. Peristropic multiplexing was experimentally demonstrating using DuPont's HRF-150 photopolymer film. A total of 395 holograms were multiplexed in the 38-micrometer thick photopolymer disk by combining peristropic multiplexing with angle multiplexing. In addition, it is shown that combining both angle and peristropic multiplexing the storage density of 3-D disks is greatly enhanced. DTIC

N95-18181*# Florida Inst. of Tech., Melbourne, FL. Program in Aerospace Engineering.
MODELING AND MEASUREMENT OF THE PERFORMANCE OF A BRANCHED CONDUIT SAMPLING SYSTEM IN A MASS SPECTROMETER LEAK DETECTOR
John M. Russell *In* Univ. of Central Florida, NASA/ASEE Summer Faculty Fellowship Program. 1994 Research Reports Oct. 1994 p 419-448 (For primary document see N95-18166 05-80)
Avail: CASI HC A03/MF A04

N95-19190*# Peterson (Robert B.), Houston, TX.
CHARGE COLLECTION DURING HYPERVELOCITY PENETRATIONS OF THIN FOILS Abstract Only
Robert B. Peterson *In* Lunar and Planetary Inst., Workshop on Particle Capture, Recovery and Velocity/Trajectory Measurement Technologies 1994 p 64-76 (For primary document see N95-19172 05-90)
Avail: CASI HC A03/MF A02

N95-19192*# Washington Univ., Saint Louis, MO. Center for the Space Sciences.
PENETRATION OF MULTIPLE THIN FILMS IN MICROMETEORITE CAPTURE CELLS Abstract Only
Charles G. Simon *In* Lunar and Planetary Inst., Workshop on Particle Capture, Recovery and Velocity/Trajectory Measurement Technologies 1994 p 77-79 (For primary document see N95-19172 05-90)
(Grant NAGw-1603)
Avail: CASI HC A01/MF A02

N95-19193*# Baylor Univ., Waco, TX. Space Science Lab.
ASSESSMENT OF VELOCITY/TRAJECTORY MEASUREMENT TECHNOLOGIES DURING A PARTICLE CAPTURE EVENT Abstract Only
William G. Tanner, Carl R. Maag (Science Applications International Corp., Glendora, CA.), W. M. Alexander, and Stepheni Stephenson *In* Lunar and Planetary Inst., Workshop on Particle Capture, Recovery and Velocity/Trajectory Measurement Technologies 1994 p 79-83 (For primary document see N95-19172 05-90)
Avail: CASI HC A01/MF A02

N95-19194*# Jet Propulsion Lab., California Inst. of Tech., Pasadena, CA.
NONDESTRUCTIVE TIME-OF-CAPTURE, LOCATION AND VELOCITY SENSING IN INTACT CAPTURE Abstract Only
Peter Tsou *In* Lunar and Planetary Inst., Workshop on Particle Capture, Recovery and Velocity/Trajectory Measurement Technologies 1994 p 84-85 (For primary document see N95-19172 05-90)
Avail: CASI HC A01/MF A02

N95-19254# Coimbra Univ. (Portugal). Grupo de Mecanica dos Fluidos.
CALIBRATION AND USE OF A NON-NULLING SEVEN-HOLE PRESSURE PROBE
M. C. G. Silva and D. X. Viegas *In* AGARD, Wall Interference, Support Interference and Flow Field Measurements Jul. 1994 7 p (For primary document see N95-19251 05-34)
Copyright Avail: CASI HC A02/MF A04

N95-19255# Institute for Aerospace Research, Ottawa (Ontario).
APPLICATIONS OF THE FIVE-HOLE PROBE TECHNIQUE FOR FLOW FIELD SURVEYS AT THE INSTITUTE FOR AEROSPACE RESEARCH
L. H. Ohman (De Havilland Aircraft Co. of Canada Ltd., Downsview, Ontario.) and V. D. Nguyen *In* AGARD, Wall Interference, Support Interference and Flow Field Measurements Jul. 1994 15 p Original contains color illustrations (For primary document see N95-19251 05-34)
Copyright Avail: CASI HC A03/MF A04

N95-19256# Von Karman Inst. for Fluid Dynamics, Rhode-Saint-Genese (Belgium).
IMPROVEMENT AND VALIDATION OF AN LDV SYSTEM TO PERFORM MEASUREMENTS IN LAMINAR SUPERSONIC FLOWS
Luca Bertuccioli and Gerard Degrez *In* AGARD, Wall Interference, Support Interference and Flow Field Measurements Jul. 1994 8 p
(For primary document see N95-19251 05-34)
(Contracts CEC-Aero-0027-C; CEC-ERB-CHBI-CT-92049)
Copyright Avail: CASI HC A02/MF A04

36 LASERS AND MASERS

Includes parametric amplifiers.
For related information see also *76 Solid-State Physics.*

N95-17956 Rockwell International Corp., Canoga Park, CA. Rocketdyne Div.
NCl(b) BASED SHORT WAVELENGTH CHEMICAL LASER Final Report, 15 Oct. 1992 - 14 Feb. 1994
T. T. Yang, V. T. Gylys, and R. N. Hindy 14 Feb. 1994 36 p Limited Reproducibility: More than 20% of this document may be affected by microfiche quality
(Contract F49620-93-C-0003)
(AD-A284213; AFOSR-94-0475TR) Avail: Issuing Activity (Defense Technical Information Center (DTIC))

Based on the results of this work, the prospects of development of a visible chemical laser based on NCl(b) are promising. NCl, in the electronically excited b-state, emits to the ground state at 665 nm. The NCl b-state is generated by energy-pooling of NCl(a) and excited iodine atoms, I*. All of these species can be generated from chemical reactions solely. This work has shown that: (1) In the generation of NCl, the branching ratio for NCl(a) is high. Sixty-five percent of the HN3 ends up in the NCl(a) state; (2) The rate constant for the energy-pooling reaction NCl(a) + I* yields NCl(b) is quite favorably large, approximately 10-11 cu cm/sec; (3) A gain on the order of 1 x 10(exp 4)/cm was obtained; and (4) Variations of the cavity ring-down experiment showed that virtually no NCl(x) is formed via reaction. DTIC

N95-18061 Helsinki Univ. of Technology, Espoo (Finland). Inst. of Metrology Research.
NEW METHOD FOR HOMODYNE LASER LINEWIDTH MEASUREMENTS WITH A SHORT DELAY FIBER
H. Ludvigsen and E. Bodtker 1994 7 p Limited Reproducibility: More than 20% of this document may be affected by microfiche quality
(PB94-202629; MIR-4/94) Avail: CASI HC A02/MF A01

A new versatile method for homodyne laser line width measurements is presented. The acousto-optic modulator used in the standard self-heterodyne technique is replaced by electronic upconversion. This results in reduced optical loss and a simpler setup. The dependence of the detected homodyne signal on the mean phase difference between the mixed beams was averaged out with a phase modulator on the delay fiber. A delay fiber shorter than the coherence length of the laser can then be used. NTIS

N95-18123# California Univ., Berkeley. Lawrence Berkeley Lab, CA.
THE EFFECTS OF CAVITY TOPOLOGY ON INSTABILITIES IN ADDITIVE-PULSE MODELOCKED LASERS
G. Sucha, S. R. Bolton, and D. S. Chemla May 1994 8 p Presented at the CLEO 1994: Conference on Lasers and Electro-Optics, Anaheim, CA, 8-13 May 1994
(Contract DE-AC03-76SF-00098)
(DE94-018193; LBL-35221; CONF-940582-5) Avail: CASI HC A02/MF A01

We compare the stability properties of the Michelson and Fabry-Perot APM lasers. With excessive Kerr nonlinearity, the Fabry-Perot APM exhibits period-doubling while maintaining an autocorrelation of deceptively high quality. The Michelson APM never exhibits period-doubling, but is prone to multiple-pulsing. DOE

N95-18126# Los Alamos National Lab., NM.
OVERVIEW OF LASER TECHNOLOGY AT LOS ALAMOS NATIONAL LABORATORY
G. K. Lewis and D. A. Cremers 1994 12 p Presented at the Applications of Lasers and Electro-Optics, Orlando, FL, 17-20 Oct. 1994
(Contract W-7405-eng-36)
(DE94-018307; LA-UR-94-2846; CONF-9410189-3) Avail: CASI HC A03/MF A01

Los Alamos National Laboratory has had a long history of involvement

in laser sciences and has been recognized both for its large laser programs and smaller scale developments in laser technology and applications. The first significant program was with the Rover nuclear-based rocket propulsion system in 1968 to study laser initiated fusion. From here applications spread to programs in laser isotope separation and development of large lasers for fusion. These programs established the technological human resource base of highly trained laser physicists, engineers, and chemists that remain at the Laboratory today. Almost every technical division at Los Alamos now has some laser capability ranging from laser development, applications, studies on nonlinear processes, modeling and materials processing. During the past six years over eight R&D-100 Awards have been received by Los Alamos for development of laser-based techniques and instrumentation. Outstanding examples of technology developed include LIDAR applications to environmental monitoring, single molecule detection using fluorescence spectroscopy, a laser-based high kinetic energy source of oxygen atoms produced by a laser-sustained plasma, laser-induced breakdown spectroscopy (LIBS) for compositional, analysis, thin film high temperature superconductor deposition, multi-station laser welding, and direct metal deposition and build-up of components by fusing powder particles with a laser beam. DOE

N95-18322* National Aeronautics and Space Administration. Langley Research Center, Hampton, VA.
REDUCTION OF PARASITIC LASING Patent
Mark E. Storm, inventor (to NASA) 29 Nov. 1994 12 p Filed 11 Aug. 1993 Supersedes N94-15942 (32 - 3, p 1039)
(NASA-Case-LAR-14645-1-SB; US-Patent-5,369,662; US-Patent-Appl-SN-105528; US-Patent-Class-372-99; US-Patent-Class-372-12; US-Patent-Class-372-25; Int-Patent-Class-H01S-3/10; Int-Patent-Class-H01S-3/11) Avail: US Patent and Trademark Office

A technique was developed which carefully retro-reflects precisely controlled amounts of light back into a laser system thereby intentionally forcing the laser system components to oscillate in a new resonator called the parasitic oscillator. The parasitic oscillator uses the laser system to provide the gain and an external mirror is used to provide the output coupling of the new resonator. Any change of gain or loss inside the new resonator will directly change the lasing threshold of the parasitic oscillator. This change in threshold can be experimentally measured as a change in the absolute value of reflectivity, provided by the external mirror, necessary to achieve lasing in the parasitic oscillator. Discrepancies between experimental data and a parasitic oscillator model are direct evidence of optical misalignment or component performance problems. Any changes in the optical system can instantly be measured as a change in threshold for the parasitic oscillator. This technique also enables aligning the system for maximum parasitic suppression with the system fully operational.
Official Gazette of the U.S. Patent and Trademark Office

N95-18349# Washington State Univ., Pullman, WA. Dept. of Physics.
UV LASER-SURFACE INTERACTIONS RELEVANT TO ANALYTIC SPECTROSCOPY OF WIDE BAND GAP MATERIALS
J. T. Dickinson 1993 10 p
(Contract DE-FG06-92ER-14252)
(DE94-016180; DOE/ER-14252/1) Avail: CASI HC A02/MF A01

Laser ablation has application in materials analysis, surface modification, and thin film deposition. Processes that lead to emission and formation of particles when wide band gap materials are irradiated with pulsed UV laser light. These materials are often difficult to transport into the gas phase for analysis. Such materials are alkali halides, MgO. DOE

N95-18350# Washington State Univ., Pullman, WA. Dept. of Physics.
UV LASER-SURFACE INTERACTIONS RELEVANT TO ANALYTIC SPECTROSCOPY OF WIDE BAND GAP MATERIALS
J. T. Dickinson 1994 4 p
(Contract DE-FG06-92ER-14252)
(DE94-016181; DOE/ER-14252/2) Avail: CASI HC A01/MF A01

Laser ablation has application in materials analysis, particularly for refractory materials and for fast screening environmental analysis. Wide bandgap materials are often difficult to transport into the gas phase. Our work was concentrated on desorption and ablation of material from nominally transparent, wide bandgap materials by uv excimer radiation at modest fluences which depends on strongly absorbing lattice defects. The materials were MgO, NaNO3. DOE

N95-18357# Lawrence Livermore National Lab., Livermore, CA.
HIGH POWER PHASE CONJUGATED SOLID STATE LASERS
L. A. Hackel, C. B. Dane, L. E. Zapata, and M. R. Hermann Jul. 1994 46 p
(Contract W-7405-eng-48)
(DE94-016633; UCRL-ID-117785) Avail: CASI HC A03/MF A01

Three laser systems that are being developed for use in x-ray generation which incorporate SBS phase conjugate mirrors are described. A 25J/pulse Nd:glass laser is being developed for commercial proximity print x-ray lithography; a 0.5J/pulse, 1.3 kHz pulse repetition frequency laser is being built for soft x-ray projection lithography; and a 1 kJ/pulse laser driver for a table top x-ray laser has been designed. The results of prototypical experimental investigations are presented and the basic design principles for high average power phase conjugated laser systems shared by each of these lasers are discussed. DOE

N95-18382 Institute for Defense Analyses, Alexandria, VA.
IDA GAMMA RAY LASER Annual Report, Jan. - Dec. 1993
Bohdan Balko and Irwin W. Kay Feb. 1994 44 p Limited Reproducibility: More than 20% of this document may be affected by microfiche quality
(Contract MDA903-89-C-0003)
(AD-A284322; IDA-D-1483; IDA/HQ-94-45195; AD-E501831) Avail: Issuing Activity (Defense Technical Information Center (DTIC))

This document consists of a collection of papers published in the open literature in FY 1993. The first paper was published in Phys. Rev. B and describes the limitations of the Bonifacio-Lugiato model of superfluorescence. The second paper deals with the feasibility of nuclear superfluorescence. It was presented at the Lasers '92 Conference in Houston and published in the Proceedings. Paper Number 3 describes a nuclear superfluorescence model. It was presented at the Physics in Ukraine Conference in Kiev in June 1993 and published in the Proceedings. Paper Number 4 is a comment on a paper published in Phys. Rev. B, which we found to be wrong and which stated a misleading conclusion regarding the effect of homogeneous broadening on an inhomogeneously broadened system. Our comment is followed by the author's reply, which was also published in the Comments section of Phys. Rev. B. We include our response to the author's reply. DTIC

N95-18408 Jackson State Univ., Jackson, MS. Dept. of Mathematics.
MATHEMATICAL ANALYSIS OF THREE FREE-ELECTRON-LASER ISSUES Final Report, 1 Dec. 1990 - 30 Nov. 1993
Shayne Johnston 30 Nov. 1993 11 p Limited Reproducibility: More than 20% of this document may be affected by microfiche quality
(Contract F49620-91-C-0013)
(AD-A284122; AFOSR-94-0544TR) Avail: CASI HC A03

The central idea underlying this project was that sideband instabilities could be controlled by optical guiding effects through the radiation of slippage between electron bunches and the radiation field. However, none of the related six research objectives in the original proposal to AFOSR has been truly complete. The principal advances made during the period of AFOSR support include: the recognition that enhanced radiation pressure can produce disruptive velocity changes in the presence of slippage (ITR1), the viability of an electron macroparticle model of sideband instabilities (ITR2), and an analysis (including radiative reaction) of the analogous problem of resonance scattering (ITR2). The recognition that electrostatic waves could correlate repelling particles on a length scale much shorter than a wavelength (ITR2) led the PI to an important application to anomalous transport in turbulent plasma. DTIC

N95-18502 Technische Univ., Delft (Netherlands).
LIGHT TRANSPORT FOR MEDICAL LASER TREATMENTS Ph.D. Thesis
M. Keijzer 6 Dec. 1993 212 p
(PB94-201498) Copyright Avail: Issuing Activity

Theoretical dosimetry of laser light in biological tissues is discussed. The predicted light doses are evaluated to optimize the parameters of the laser beam for a specific treatment, or to investigate the feasibility of a new diagnostic method. Only stationary problems are treated. The sources are continuous wave laser beams (or long pulses). The aim of the research described in the thesis is to calculate stationary light doses in laser/tissue

geometries that are two or three dimensional. In chapter 2 the basic equation of tissue optics is discussed: the equation of transfer. Boundary conditions to that equation are derived for the different interfaces that occur. In section 2.4 an overview is given of the main methods to approximate the solution to the equation of transfer in a two or three dimensional geometry. Chapters 3 and 4 concern two of these solution methods: the Monte Carlo method and the diffusion approximation. In Chapter 5 the authors give the results of an application of the last method. NTIS

N95-18585 Department of the Navy, Washington, DC.
COMPACT, EFFICIENT, SCALABLE NEODYMIUM LASER CO-DOPED WITH ACTIVATOR IONS AND PUMPED BY VISIBLE LASER DIODES Patent
Richard Scheps, inventor (to Navy) 8 Feb. 1994 19 p Filed 22 Feb. 1993
(AD-D016237; US-Patent-5,285,467; US-Patent-Appl-SN-021948; US-Patent-Class-372-69) Avail: US Patent and Trademark Office

Efficient, low threshold laser emission from a laser crystal doped with chromium and neodymium ions is obtained when pumped by visible laser diodes in the range of 610 nm to 680 nm. A typical laser Cr,Nd:GSGG crystal having an extraordinarily broad absorption bandwidth allows high pump efficiencies when using visible laser diodes, particularly in comparison to the Nd:YAG laser. The broad absorption bandwidth tolerance of the Cr,Nd:GSGG crystal to the pumping wavelengths allows visible diode pumping of the neodymium transition without regard to the wavelength of the visible diodes. Longitudinal or end-pumping to take advantage of the emission properties of the visible laser diodes, a nearly hemispherical laser resonator configuration and other co-doped Cr,Nd laser host materials are disclosed. DTIC

N95-18635 Department of the Navy, Washington, DC.
METHOD FOR LASER-ASSISTED SILICON ETCHING USING HALOCARBON AMBIENTS Patent
Stephen D. Russell, inventor (to Navy), Douglas A. Sexton, inventor (to Navy), and Richard J. Orazi, inventor (to Navy) 30 Nov. 1993 23 p Filed 12 Dec. 1991
(AD-D016239; US-Patent-5,266,532; US-Patent-Appl-SN-807015; US-Patent-Class-437-242) Avail: US Patent and Trademark Office

An etching process allows a selective single-step patterning of silicon devices in a noncorrosive environment. The etching of silicon relies on a maskless laser-assisted technique in a gaseous halocarbon ambient, such as the gaseous chlorofluorocarbons, dichlorodifluoromethane and chloropentafluoroethane. Laser-assisted photothermal chemical etching reactions on silicon occur in these ambients when the incident fluence from an excimer laser at 248 nm exceeds the melt threshold (approximately 0.75 J/sq cm). When incident fluence exceeds the ablation threshold (approximately 2.2 J/sq cm) an undesirable, increased surface roughness is observed. Etch rates as large as approximately 15 A per pulse are attained within predetermined processing windows. This provides a means for thin membrane formation in silicon, rapid etches and processing of packaged devices or partially fabricated dies. DTIC

N95-18642# Institute of Electrical and Electronics Engineers, Piscataway, NJ.
14TH IEEE INTERNATIONAL SEMICONDUCTOR LASER CONFERENCE
23 Sep. 1994 279 p Conference held in Maui, HI, 19-23 Sep. 1994
(Contract N00014-94-1-0981)
(AD-A285569) Avail: CASI HC A13/MF A03

Partial Contents: Review of Recent Advances in Semiconductor Lasers: Mode Locking; Strained QW Lasers; Integrated Sources; DFB Lasers; Carrier Dynamics; Quantum Confined Lasers. DTIC

N95-19096# Lawrence Livermore National Lab., Livermore, CA.
SOLID STATE LASER DRIVER FOR EXTREME ULTRAVIOLET LITHOGRAPHY
L. E. Zapata, J. Honig, P. Reichert, and L. A. Hackel May 1994 6 p
(Contract W-7405-eng-48)
(DE94-016971; UCRL-JC-117000-Rev-1) Avail: CASI HC A02/MF A01

We describe the design and initial performance of a Nd:YAG laser master oscillator/phase conjugated power amplifier as a driver for extreme ultraviolet lithography. The design provides 0.5 to 1 joule per pulse with about 5 ns pulse width and excellent beam quality up through 1.5 kHz repetition frequency. DOE

N95-19243# Brookhaven National Lab., Upton, NY.
THE VISIBLE SMITH-PURCELL RADIATION SEARCH
R. C. Fernow, H. G. Kirk, S. Ulc, and X. Wang Mar. 1994 35 p
(Contract DE-AC02-76CH-00016)
(DE94-017514; BNL-60498; CAP-107-94R) Avail: CASI HC A03/MF A01

We report here the results of an experiment at the Accelerator Test Facility at Brookhaven National Laboratory to search for the production of visible radiation from the Smith-Purcell effect using a 3 MeV electron beam. After running the experiment under a variety of conditions we were unable to isolate a definite signal from Smith-Parcell effect. Any Smith-Purcell signal present in the measured radiation was less than 10% of the background signal. DOE

N95-19247# Lawrence Livermore National Lab., Livermore, CA.
HYPERFINE SPLITTINGS, PREPULSE TECHNIQUE, AND OTHER NEW RESULTS FOR COLLISIONAL EXCITATION NEON-LIKE X RAY LASERS
J. Nilsen, J. C. Moreno, J. A. Koch, J. H. Scofield, B. J. MacGowan, and L. B. DaSilva Jun. 1994 10 p Presented at the 4th International Colloquium on X Ray Lasers, Williamsburg, VA, 16-20 May 1994
(Contract W-7405-eng-48)
(DE94-016443; UCRL-JC-116926; CONF-940592-6) Avail: CASI HC A02/MF A01

The observation of hyperfine splitting on an x-ray laser transition is presented and the impact on the laser gain is discussed. We measure the lineshape of the 3p yields 3s (J = 0 yields 1) transition in neon-like niobium and zirconium and observe a 28 m-Angstrom splitting between the two largest hyperfine components in the niobium (Z = 41) line at 145.9 Angstrom, in good agreement with theory. In zirconium (Z = 40) no splitting is predicted or observed since the hyperfine effect is proportional to the nuclear moment and this is present primarily in elements with odd Z. The hyperfine splitting is used to explain why the low-Z ions with odd Z have not lased. We discuss the use of a prepulse technique to achieve lasing in low-Z neon-like ions from Z = 22 to 32 on the 3p yields 3s (J = 0 yields 1) transition with wavelengths from 326 to 196 Angstrom. Using this technique on selenium (Z = 34) we show a large enhancement of the J = 0 yields 1 transition at 182 Angstrom. Using a series of short pulses to drive selenium we observe the 182 Angstrom line to dominate completely the spectra. In an effort to reduce the large density gradients associated with hydrodynamic expansion, we discuss the use of low density foams for the laser target and present results which show lasing in zirconium aerogel with an initial density of 20 mg/cm(exp 3). Finally, we discuss recent double slab experiments with ruthenium (Z = 44) targets in which we observe lasing at 117 and 118 Angstrom for the first time. DOE

N95-19248# Lawrence Livermore National Lab., Livermore, CA.
MEASUREMENTS OF LINE OVERLAP FOR RESONANT SPOILING OF X RAY LASING TRANSITIONS
P. Beiersdorfer, S. R. Elliott, B. J. MacGowan, and J. Nilsen Jun. 1994 7 p Presented at the 4th International Colloquium on X Ray Lasers, Williamsburg, VA, 16-20 May 1994
(Contract W-7405-eng-48)
(DE94-016444; UCRL-JC-116837; CONF-940592-2) Avail: CASI HC A02/MF A01

High-precision measurements are presented of candidate line pairs for resonant spoiling of x-ray lasing transitions in the nickel-like W(sup 46+), the neon-like Fe(sup 16+), and the neon-like La(sup 47+) x-ray lasers. Our measurements were carried out with high-resolution crystal spectrometers, and a typical precision of 20 to 50 ppM was achieved. While most resonances appear insufficient for effective photo-spoiling, two resonance pairs are identified that provide a good overlap. These are the 4p(sub 1/2) yields 3d(sub 3/2) transition in nickel-like W(sup 46+) with the 2p(sub 3/2) yields 1s(sub 1/2) transition in hydrogenic Al(sup 12+), and the 3s(sub 1/2) yields 2p(sub 3/2) transition in neon-like La(sup 47+) with the 1(sup 1)S(sub 0)-2(sup 1)P(sub 1) line in helium-like Ti(sup 20+). DOE

N95-19398# Lawrence Livermore National Lab., Livermore, CA.
PROPAGATION OF INTENSE, ULTRASHORT LASER PULSES THROUGH METAL VAPOR: REFRACTIVE INTENSITY LIMITS AND SPECTRAL EFFECTS
P. R. Bolton, A. B. Ritchie, and R. E. Stewart Jun. 1994 5 p Presented at the Optical Society of America Conference on High Field Interactions, Saint Malo, France, 21-25 Aug. 1994
(Contract W-7405-eng-48)
(DE94-016365; UCRL-JC-117522; CONF-9408121-2) Avail: CASI HC A01/MF A01

Fundamental understanding of high intensity ultrashort laser pulse propagation through media that is critical to applications such as harmonic generation and development of recombination type, xuv/x-ray lasers driven by optical field ionization is discussed in this short communication. DOE

N95-19507# Lawrence Livermore National Lab., Livermore, CA.
INTER-AMPLIFIER PUPIL RELAY SYSTEMS FOR A HIGH AVERAGE POWER DYE LASER AT LAWRENCE LIVERMORE NATIONAL LABORATORY
S. J. Cohen Jun. 1994 9 p Presented at the Optical Society of America Meeting on Diffractive Optics: Design, Fabrication and Applications, Rochester, NY, 6-8 Jun. 1994 Revised
(Contract W-7405-eng-48)
(DE94-016544; UCRL-JC-116056-Rev-1; CONF-9406116-4-Rev-1) Avail: CASI HC A02/MF A01

The current configuration of inter-amplifier pupil relay systems for our high average power laser are compared and contrasted with previous and alternate families of designs. DOE

N95-19508# Lawrence Livermore National Lab., Livermore, CA.
PERFORMANCE IMPROVEMENTS IN DIODE LASER ARRAYS
R. J. Beach, M. A. Emanuel, B. L. Freitas, W. J. Benett, J. A. Skidmore, N. W. Carlson, and R. W. Solarz Jun. 1994 5 p Presented at the Annual Conference of the Optical Society of America and Exhibit, Boston, MA, 30 Oct. - 4 Nov. 1994
(Contract W-7405-eng-48)
(DE94-016547; UCRL-JC-117358; CONF-941006-2) Avail: CASI HC A01/MF A01

The average power performance capability of semiconductor laser diode arrays has improved dramatically over the past several years. Additionally, optical conditioning technologies have been developed that increase the effective radiance of stacked two-dimensional arrays by nearly two orders of magnitude. These performance improvements have been accompanied by cost reductions that now make feasible the replacement of flashlamp pump sources by laser diode arrays in a large variety of military and commercial solid state laser systems. DOE

N95-19551# Lawrence Livermore National Lab., Livermore, CA.
ISOTOPE SEPARATION AND ADVANCED MANUFACTURING TECHNOLOGY Semiannual Report No. 4
J. Carpenter, ed. and T. Kan, ed. 1994 46 p
(Contract W-7405-eng-48)
(DE95-000313; UCRL-LR-111984-94-2) Avail: CASI HC A03/MF A01

This is the fourth issue of a semiannual report for the Isotope Separation and Advanced Materials Manufacturing (ISAM) Technology Program at Lawrence Livermore National Laboratory. Primary objectives include: (1) the Uranium Atomic Vapor Laser Isotope Separation (UAVLIS) process, which is being developed and prepared for deployment as an advanced uranium enrichment capability; (2) Advanced manufacturing technologies, which include industrial laser and E-beam material processing and new manufacturing technologies for uranium, plutonium, and other strategically important materials in support of DOE and other national applications. This report features progress in the ISAM Program from October 1993 through March 1994. DOE

N95-19708# Lawrence Livermore National Lab., Livermore, CA.
FUTURE TRENDS IN OPTICAL COATINGS FOR HIGH-POWER LASER APPLICATIONS
M. R. Kozlowski and I. M. Thomas Jul. 1994 6 p Presented at the Annual Meeting of the Society of Photo-Optical Instrumentation Engineers, San Diego, CA, 24-29 Jul. 1994
(Contract W-7405-eng-48)
(DE94-018592; UCRL-JC-115941; CONF-940723-22) Avail: CASI HC A02/MF A01

Inertial Confinement Fusion (ICF) research has historically been a driver in the development of high performance, high damage threshold optical coatings. This is particularly the case now as the ICF community develops plans for a proposed 1.8 mega-joule solid state (Nd(+3)-phosphate glass) laser system. The new system, the National Ignition Facility, is possible in part due to advances in optical coatings technology including the laser-conditioning of multilayer dielectrics and broadened applications for room-temperature deposited coatings. Sol-gel AR coatings are the standard for large, high-power laser optics and sol-gel HR coatings are being developed. For mirror and polarizer coatings, e-beam-deposited dielectric continue to provide the highest damage threshold coatings, but their laser damage thresholds and optical performance are limited by (mu)m-scale defects and poor control over layer thickness, respectively. More energetic deposition techniques such as IAD and IBS, now popular in the commercial market, offer both advantages and disadvantages in this high-damage-threshold coatings market. DOE

N95-19722# Lawrence Livermore National Lab., Livermore, CA.
DAMAGE FROM PULSES WITH ARBITRARY TEMPORAL SHAPES
J. B. Trenholme Jun. 1994 22 p
(Contract W-7405-eng-48)
(DE94-018606; UCRL-ID-118113) Avail: CASI HC A03/MF A01

In fusion laser designs, the laser pulse has a complicated temporal shape which undergoes significant change as it passes through the laser. Our damage data, however, was taken with pulses whose temporal shapes were (more or less) Gaussian. We want to determine the damage propensity of a material exposed to a pulse of arbitrary temporal shape, given data taken with Gaussian pulses of different pulse widths. To do so, we must adopt a physical model of damage. This model will contain some number of parameters that depend on material properties, geometry, and so forth. We determine the parameters of the model appropriate to each material by fitting the model to the Gaussian data for that material. The resulting normalized model is then applied, using the appropriate pulse shape, to find the damage level for a specific material subjected to a specific pulse. The model we shall assume is related to diffusion, although (as we shall see) the experimental results do not fit any simple diffusion model. Initially, we will discuss simple diffusion models. We then examine some experimental data, and then develop a modified diffusive model from that data. That modified model is then used to predict damage levels in various portions of the NIF laser design. DOE

N95-19727# Argonne National Lab., IL.
MICROCAVITY STRUCTURES
R. L. Kustom, D. Grudzien, and A. D. Feinerman (Illinois Univ., Chicago, IL.) 1994 6 p Presented at the 17th International LINAC Conference, Tsukuba, Japan, 21-26 Aug. 1994
(Contract W-31-109-eng-38)
(DE95-001096; ANL/ASD/CP-84092; CONF-9408125-35) Avail: CASI HC A02/MF A01

The feasibility of building mm-wave cavities using deep x ray lithography techniques is being investigated. These cavities could be considered for linac accelerating structures, undulators, free electron lasers, or mm-wave amplifiers. The construction process includes making precision x ray masks, x ray exposure of poly-methyl-methacrylate (PMMA), removal of PMMA, and electroplating a metal. Highly precise two-dimensional features can be machined onto wafers by this technique. The challenge is to fabricate the wafers onto three-dimensional RF structures. Rectangular cavity geometry is best suited to this fabrication technique. Status of wafer manufacture, fabrication and alignment techniques using capillaries bonded in precision grooves, 2(pi)/3 120-GHz linac structures, heat extraction analysis, and beam dynamics in a 5-meter-long 50-MeV linac will be discussed. Measurements made on 10X larger scale models that were built with conventional techniques will also be discussed. DOE

N95-19845 Naval Research Lab., Washington, DC.
X-RAY LASER PROGRAM Final Report, Fiscal Year 1993
John P. Apruzese 25 Apr. 1994 59 p Limited Reproducibility: More than 20% of this document may be affected by microfiche quality

(AD-A279213; NRL/MR/6721-94-7453) Avail: Issuing Activity (Defense Technical Information Center (DTIC))

This report details the progress achieved by the Radiation Hydrodynamics Branch in X-Ray Laser experiments and modeling during FY93. Some of the experimental work discussed was carried out at Sandia National Laboratories in collaboration with NRL. It is divided into an executive summary and sections whose authors are separately identified. The individual sections describe progress in photopumped x ray laser research, inversions and gain in plasmas which can be created by ultraintense subpicosecond lasers, and prospects for achieving a Ly alpha laser. DTIC

N95-19258# Centre d'Etudes et de Recherches, Toulouse (France). Dept. d'Etudes et de Recherches en Aero-Thermodynamique.

EXPERIMENTAL TECHNIQUES FOR MEASURING TRANSONIC FLOW WITH A THREE DIMENSIONAL LASER VELOCIMETRY SYSTEM. APPLICATION TO DETERMINING THE DRAG OF A FUSELAGE [TECHNIQUE EXPERIMENTALE DE MESURE EN ECOULEMENT TRANSSONIQUE AVEC UN SYSTEME DE VELOCIMETRIE LASER TRIDIMENSIONNEL. APPLICATION A LA DETERMINATION DE LA TRAINEE D'UN FUSELAGE]

A. Seraudie, A. Mignosi, J. B. Dor, and S. Prudhomme *In* AGARD, Wall Interference, Support Interference and Flow Field Measurements Jul. 1994 6 p In FRENCH Original contains color illustrations (For primary document see N95-19251 05-34)

Copyright Avail: CASI HC A02/MF A04

37 MECHANICAL ENGINEERING

Includes auxiliary systems (nonpower); machine elements and processes; and mechanical equipment.

N95-17995 Kansas State Univ., Manhattan, KS.

KANSAS STATE UNIVERSITY DOE/KEURP SITE OPERATOR USER TASK FORCE

J. Hague 28 Jun. 1994 23 p Limited Reproducibility: More than 20% of this document may be affected by microfiche quality

(Contract DE-FC07-91ID-13074)

(DE94-014331; DOE/ID-13074/T12) Avail: CASI HC A03

This program relates to demonstration use of electric-powered vehicles. KSU has two electric cars (conversion vehicles) from Soleq. Corp., and is purchasing 4 Chevy trucks for conversion. This document discusses the participating groups, program plan, events, vehicles and components, operations, and procurement. DOE

N95-18010 Kulite Semi-Conductor Products, Inc., Leonia, NJ.

ADVANCED PACKAGING AND INTEGRATION TECHNOLOGIES FOR MICROSENSORS, PHASE 1 Final Report, Feb. - Jul. 1994

A. A. Ned and A. D. Kurtz 12 Aug. 1994 39 p Limited Reproducibility: More than 20% of this document may be affected by microfiche quality

(AD-A283613) Avail: CASI HC A03

Advanced microfabrication processes have been developed for producing a hermetic cover wafer with low resistance dielectrically isolated through-wafer interconnects. The feasibility of manufacturing encapsulated pressure sensors, utilizing the cover-wafer approach, has been demonstrated. Such pressure sensors represent a new generation of environmentally protected, cost effective devices. The accomplishments of Phase 1 include the following: (1) the study of conversion of single crystal silicon into porous silicon; (2) the study of conversion of porous silicon into oxide; (3) process for producing through-wafer interconnects has been established; and (4) the stresses in the cover wafer have been investigated, which enabled the fabrication of flat cover-wafers. The surface and cross-sectional morphology of the cover wafer was investigated, the hermeticity and dielectric isolation of the oxidized rings was verified, the sensors compatible with the cover-wafer approach were fabricated and tested, and a new generation of sensors designed. DTIC

N95-18041*# Detroit Diesel Allison, MI.

ADVANCED DIESEL ENGINE COMPONENT DEVELOPMENT PROGRAM, TASKS 4-14 Final Report

Tony S. Kaushal and Karen E. Weber Nov. 1994 182 p Sponsored by DOE Original contains color illustrations

(Contract DEN3-329; RTOP 778-34-2A)

(NASA-CR-191203; E-8198; DOE/NASA/0329-2; NAS 1.26:191203; DDC-RO1-ADECD-NAS) Avail: CASI HC A09/MF A02; 6 functional color pages

This report summarizes the Advanced Diesel Engine Component Development (ADECD) Program to develop and demonstrate critical technology needed to advance the heavy-duty low heat rejection engine concept. Major development activities reported are the design, analysis, and fabrication of monolithic ceramic components; vapor phase and solid film lubrication; electrohydraulic valve actuation; and high pressure common rail injection. An advanced single cylinder test bed was fabricated as a laboratory tool in studying these advanced technologies. This test bed simulates the reciprocator for a system having no cooling system, turbo compounding, Rankine bottoming cycle, common rail injection, and variable valve actuation to achieve fuel consumption of 160 g/kW-hr (.26 lb/hp-hr). The advanced concepts were successfully integrated into the test engine. All ceramic components met their functional and reliability requirements. The firedeck, cast-in-place ports, valves, valve guides, piston cap, and piston ring were made from silicon nitride. Breakthroughs required to implement a 'ceramic' engine included the fabrication of air-gap cylinder heads, elimination of compression gaskets, machining of ceramic valve seats within the ceramic firedeck, fabrication of cast-in-place ceramic port liners, implementation of vapor phase lubrication, and elimination of the engine coolant system. Silicon nitride valves were successfully developed to meet several production abuse test requirements and incorporated into the test bed with a ceramic valve guide and solid film lubrication. The ADECD cylinder head features ceramic port shields to increase insulation and exhaust energy recovery. The combustion chamber includes a ceramic firedeck and piston cap. The tribological challenge posed by top ring reversal temperatures of 550 C was met through the development of vapor phase lubrication using tricresyl phosphate at the ring-liner interface. A solenoid-controlled, variable valve actuation system that eliminated the conventional camshaft was demonstrated on the test bed. High pressure fuel injection via a common rail system was also developed to reduce particulate emissions. Author

N95-18056*# Texas Univ., El Paso, TX. Dept. of Metallurgical and Materials Engineering.

A STUDY OF GAS FLOW PATTERN, UNDERCUTTING AND TORCH MODIFICATION IN VARIABLE POLARITY PLASMA ARC WELDING Final Report

John C. McClure and Haihui Ron Hou 31 Aug. 1994 88 p

(Contract NAS8-39602)

(NASA-CR-196537; NAS 1.26:196537) Avail: CASI HC A05/MF A01

A study on the plasma and shield gas flow patterns in variable polarity plasma arc (VPPA) welding was undertaken by shadowgraph techniques. Visualization of gas flow under different welding conditions was obtained. Undercutting is often present with aluminum welds. The effects of torch alignment, shield gas flow rate and gas contamination on undercutting were investigated and suggestions made to minimize the defect. A modified shield cup for the welding torch was fabricated which consumes much less shield gas while maintaining the weld quality. The current torch was modified with a trailer flow for Al-Li welding, in which hot cracking is a critical problem. The modification shows improved weldablility on these alloys. Author

N95-18152# Naval Command, Control and Ocean Surveillance Center, San Diego, CA. Research, Development, Technology and Evaluation Div.

MATHEMATICAL ANALYSIS OF ACTUATOR FORCES IN A SCISSOR LIFT Final Report

H. Spackman May 1994 20 p

(AD-A283906; NRAD-TD-2643) Avail: CASI HC A03/MF A01

In 1985, NCCOSC began development of a tele-operated vehicle as part of the U.S. Marine Corps' Ground-Air Tele-Robotics Systems Program. One of the required vehicle components was a rigid, light-weight, and compact lift mechanism capable of deploying a surveillance package 10 feet above the vehicle bed. The lift mechanism that was eventually built and implemented was a 3-level scissor lift. In order to analyze the forces throughout the lift structure, a set of mathematical equations was derived. From these equations it was discovered that prudent placement of a lift's actuator can significantly reduce the forces required of the actuator and the stress levels in the adjacent scissor members. The purpose of this

paper is to present the equations that were derived for analyzing the actuator forces. Using these equations, a designer can quickly determine the optimal locations for mounting an actuator and the resulting forces. DTIC

N95-18317 Department of the Navy, Washington, DC.
ELECTROMAGNETIC PUMP Patent
Richard L. Bonin, inventor (to Navy) 15 Feb. 1994 13 p Filed 6 May 1993
(AD-D016260; US-Patent-5,286,176; US-Patent-Appl-SN-058018;
US-Patent-Class-417-413) Avail: US Patent and Trademark Office

A pump having a stator that forms a cylindrical chamber defined by a wall and a plurality of independently energizable magnetic field generators. A compression roller comprising a magnetic material is disposed within the wall and is free to move with respect to the stator. A flexible diaphragm is intermediate the stator and the compression roller and disposed along the wall portion. The flexible diaphragm to be pumped has an input port and an outlet port for the fluid being pumped. An energizing control at any given instant energizes a plurality of adjacent ones of the magnetic field generators. The magnetic field generators are organized into overlapping sets that can be energized as sets in sequence thereby to produce a rotating, axially extending magnetic field within the wall. The compression roller follows the rotating field thereby to compress adjacent positions of the flexible diaphragm to pump fluid from the diaphragm through the inlet port to the outlet port. DTIC

N95-18325* National Aeronautics and Space Administration. Marshall Space Flight Center, Huntsville, AL.
TUNED MASS DAMPER FOR INTEGRALLY BLADED TURBINE ROTOR Patent
John J. Marra, inventor (to NASA) 20 Dec. 1994 6 p Filed 12 Oct. 1993 Supersedes N94-29353 (32 - 8, p 3298)
(NASA-Case-MFS-28697-1; US-Patent-5,373,922;
US-Patent-Appl-SN-134443; US-Patent-Class-188-379;
US-Patent-Class-416-144; US-Patent-Class-74-573R;
US-Patent-Class-74-574; Int-Patent-Class-F16F-7/10) Avail: US Patent and Trademark Office

The invention is directed to a damper ring for damping the natural vibration of the rotor blades of an integrally bladed rocket turbine rotor. The invention consists of an integral damper ring which is fixed to the underside of the rotor blade platform of a turbine rotor. The damper ring includes integral supports which extend radially outwardly therefrom. The supports are located adjacent to the base portion and directly under each blade of the rotor. Vibration damping is accomplished by action of tuned mass damper beams attached at each end to the supports. These beams vibrate at a predetermined frequency during operation. The vibration of the beams enforce a local node of zero vibratory amplitude at the interface between the supports and the beam. The vibration of the beams create forces upon the supports which forces are transmitted through the rotor blade mounting platform to the base of each rotor blade. When these forces attain a predetermined design frequency and magnitude and are directed to the base of the rotor blades, vibration of the rotor blades is effectively counteracted.
Official Gazette of the U.S. Patent and Trademark Office

N95-18335 Department of the Navy, Washington, DC.
POSITIVE DISPLACEMENT ROTARY PUMP Patent
Paul E. Moody, inventor (to Navy) 5 Apr. 1994 6 p Filed 1 Dec. 1992
(AD-D016412; US-Patent-5,299,922; US-Patent-Appl-SN-983951;
US-Patent-Class-418-45) Avail: US Patent and Trademark Office

An eccentric drive rotates inside a ring that is hinged to a plate and an elastomeric curtain is wrapped around the ring and across an articulated plate. The curtain moves along a cylindrical wall inside the pump cavity to move fluid from an inlet to an outlet end of the chamber. Two or more chambers can be coupled in series or in parallel with one another. DTIC

N95-18541*# State Univ. of New York, Binghamton, NY. Dept. of Mechanical and Industrial Engineering.
STUDY OF THE KINEMATIC AND LOAD SHARING PROPERTIES OF WORMGEARING WITH NON-SYMMETRIC TOOTH PROFILES Final Report
D. C. Sun and Qin Yuan Cleveland, OH NASA Jan. 1995 62 p
(Grant NAG3-1316; RTOP 505-62-OJ; DA Proj. 1L1-61102-AH-45)
(NASA-CR-195414; E-9303; NAS 1.26:195414; ARL-CR-220) Avail: CASI HC A04/MF A01

The geometry of non-symmetric tooth profiles, i.e. tooth profiles with different pressure angles on the two sides of the tooth, is studied. A feasible non-symmetric tooth profile for application in helicopter transmissions is laid out as the best compromise among several conflicting factors. The non-symmetric tooth profile is then compared with the symmetric tooth profile studied previously. Based on the detailed comparisons it is concluded that the use of the non-symmetric tooth profile would severely limit the face width of the worm, consequently reduce the number of meshing teeth and cause much higher normal load on the individual gear teeth. Author

N95-18594 Department of the Navy, Washington, DC.
TORSIONAL DEVICE FOR REMOTE CONTROL STEERING SYSTEM Patent
Anthony H. Koyamatsu, inventor (to Navy), Owen T. Ono, inventor (to Navy), and Warren L. Hahn, inventor (to Navy) 28 Dec. 1993 7 p Filed 28 May 1992
(AD-D016426; US-Patent-5,272,932; US-Patent-Appl-SN-892057;
US-Patent-Class-74-492) Avail: US Patent and Trademark Office

A steering simulation device provides torsional resistance and a 'center return' function to a remote control steering mechanism experiencing bidirectional (clockwise or counterclockwise) rotational movement. A compact design is provided by utilizing a series of rotationally elastic couplings that permit an adjustable turning resistance, (torsional resistance), an adjustable, bidirectional rotary range (clockwise or counter-clockwise), and a self-centering capability. DTIC

N95-18741* National Aeronautics and Space Administration. Pasadena Office, CA.
METHOD FOR SURMOUNTING AN OBSTACLE BY A ROBOT VEHICLE Patent
Brian H. Wilcox, inventor (to NASA) (Jet Propulsion Lab., California Inst. of Tech., Pasadena, CA.) and Timothy R. Ohm, inventor (to NASA) (Jet Propulsion Lab., California Inst. of Tech., Pasadena, CA.) 13 Dec. 1994 7 p Filed 1 Oct. 1992 Supersedes N93-17272 (31 - 5, p 1179)
(NASA-Case-NPO-18764-1-CU; US-Patent-5,372,211;
US-Patent-Appl-SN-956684; US-Patent-Class-180-8.2;
US-Patent-Class-180-8.3; US-Patent-Class-280-5.28;
Int-Patent-Class-B62D-57/24) Avail: US Patent and Trademark Office

Surmounting obstacles in the path of a robot vehicle is accomplished by rotating the wheel forks of the vehicle about their transverse axes with respect to the vehicle body so as to shift most of the vehicle weight onto the rear wheels, and then driving the vehicle forward so as to drive the now lightly-loaded front wheels (only) over the obstacle. Then, after the front wheels have either surmounted or completely passed the obstacle (depending upon the length of the obstacle), the forks are again rotated about their transverse axes so as to shift most of the vehicle weight onto the front wheels. Then the vehicle is again driven forward so as to drive the now lightly-loaded rear wheels over the obstacle. Once the obstacle has been completely cleared and the vehicle is again on relatively level terrain, the forks are again rotated so as to uniformly distribute the vehicle weight between the front and rear wheels.
Official Gazette of the U.S. Patent and Trademark Office

N95-18901 Cornell Univ., Ithaca, NY.
WAVE CYCLE DESIGN FOR WAVE ROTOR ENGINES WITH LIMITED NITROGEN OXIDE EMISSIONS Ph.D. Thesis
Mohamed Razi Nalim 1994 200 p
Avail: Univ. Microfilms Order No. DA9416705

Direct work exchange between gases in wave rotors can be used to create topping cycles for gas turbine engines with peak temperatures and pressures exceeding the limits that restrict the performance of present day turbomachinery. Analytical methods are used for preliminary design and evaluation of a class of wave rotor cycles that involve large-amplitude nonsteady expansions of hot combustion products in the wave channels. A computer code is then employed to calculate the detailed time-evolution of the channel flow field. It uses the method of characteristics for one-dimensional inviscid flow, extended to treat strong shocks, entropy gradients and discontinuities, and their interactions. Several wave rotor

engine cycles are designed suitable for supersonic aircraft propulsion at Mach 2.6. One is a five-port topping cycle with wave expansion provided to accommodate both the temperature limit imposed by a low-NO(x) combustor, and the limit for cooled turbine blades. Performance improvement equivalent to a 50-150 K increase in turbine inlet temperature is obtained, for turboshaft core engines. Reverse-flow expansion of the hot gas is found to be superior for this cycle. A second type of cycle involves staged rich-lean combustion with expansion-wave cooling of very hot primary rich (phi approximately equal to 1.2-1.5) combustion products to a temperature (below 2000 K) permitting NO(x) reduction through hydrocarbon addition when necessary. Combustion is completed by rapid mixing of secondary air, similar to the two-stage rich-quench-lean (RQL) low-NO(x) combustor being evaluated at NASA Lewis for high speed propulsion, but at a lower temperature. This cycle provides an equivalent turbine-inlet-temperature improvement of about 250 K, while reducing peak temperature in the critical mixing zone by 250-400 K, compared to an equally efficient conventional cycle with RQL combustion. A through-flow expansion wave cycle is presented for this scheme. Both types of engine cycles involve bypass flows for optimal performance. Dissert. Abstr.

N95-18935*# National Aeronautics and Space Administration. Lewis Research Center, Cleveland, OH.

THERMAL BEHAVIOR SPIRAL BEVEL GEARS Ph.D. Thesis - Case Western Univ., Aug. 1993

Robert F. Handschuh (Army Research Lab., Cleveland, OH.) Jan. 1995 195 p Prepared in cooperation with Army Research Lab., Cleveland, OH

(RTOP 505-62-10; DA Proj. 1L1-62211-A-47-A)

(NASA-TM-106518; E-7584; NAS 1.15:106518; ARL-TR-403) Avail: CASI HC A09/MF A03

An experimental and analytical study of the thermal behavior of spiral bevel gears is presented. Experimental data were taken using thermocoupled test hardware and an infrared microscope. Many operational parameters were varied to investigate their effects on the thermal behavior. The data taken were also used to validate the boundary conditions applied to the analytical model. A finite element-based solution sequence was developed. The three-dimensional model was developed based on the manufacturing process for these gears. Contact between the meshing gears was found using tooth contact analysis to describe the location, curvatures, orientations, and surface velocities. This information was then used in a three-dimensional Hertzian contact analysis to predict contact ellipse size and maximum pressure. From these results, an estimate of the heat flux magnitude and the location on the finite element model was made. The finite element model used time-averaged boundary conditions to permit the solution to attain steady state in a computationally efficient manner.Then time- and position-varying boundary conditions were applied to the model to analyze the cyclic heating and cooling due to the gears meshing and transferring heat to the surroundings, respectively. The model was run in this mode until the temperature behavior stabilized. The transient flash temperature on the surface was therefore described. The analysis can be used to predict the overall expected thermal behavior of spiral bevel gears. The experimental and analytical results were compared for this study and also with a limited number of other studies. The experimental and analytical results attained in the current study were basically within 10% of each other for the cases compared. The experimental comparison was for bulk thermocouple locations and data taken with an infrared microscope. The results of a limited number of other studies were compared with those obtained herein and predicted the same basic behavior. Author

N95-19121 Department of the Navy, Washington, DC.

SAG COMPENSATED VIBRATION ISOLATION MOUNT Patent

Stuart C. Dickinson, inventor (to Navy) 12 Jul. 1994 6 p Filed 2 Aug. 1993

(AD-D016541; US-Patent-5,328,141; US-Patent-Appl-SN-100798; US-Patent-Class-248-550) Avail: US Patent and Trademark Office

A sag-compensated vibration isolation mount includes a cylindrical rubber body element and a circular band extending around the body element. The band is formed from a shape-memory alloy metal which has a predetermined transition temperature. The band is operative for restricting outward bulging and sagging of the body element when the body element is subjected to an axial load at a temperature above the transition temperature. The band has a first length at a temperature above the transition temperature and it is stretchable to a second length at a temperature below the transition temperature. At temperatures below the transition temperature, the body element normally stretches the band to its second length. However, when the band is heated above its transition temperature, the band rapidly decreases in length to its first length to forcibly compress the body element and restrict outward bulging of the body element. DTIC

N95-19125*# National Aeronautics and Space Administration. Lewis Research Center, Cleveland, OH.

DETECTING GEAR TOOTH FRACTURE IN A HIGH CONTACT RATIO FACE GEAR MESH

James J. Zakrajsek, Robert F. Handschuh (Army Research Lab., Cleveland, OH.), David G. Lewicki (Army Research Lab., Cleveland, OH.), and Harry J. Decker (Army Research Lab., Cleveland, OH.) Jan. 1995 13 p Presented at the 49th Meeting of the Society for Machinery Failure Prevention Technology, Virginia Beach, VA, 18-20 Apr. 1995; sponsored by Vibration Inst., ONR, and ARL Prepared in cooperation with Army Research Lab., Cleveland, OH

(RTOP 505-62-36; DA Proj. 1L1-62211-A-47-A)

(NASA-TM-106822; E-9366; NAS 1.15:106822; ARL-TR-600) Avail: CASI HC A03/MF A01

This paper summarized the results of a study in which three different vibration diagnostic methods were used to detect gear tooth fracture in a high contact ratio face gear mesh. The NASA spiral bevel gear fatigue test rig was used to produce unseeded fault, natural failures of four face gear specimens. During the fatigue tests, which were run to determine load capacity and primary failure mechanisms for face gears, vibration signals were monitored and recorded for gear diagnostic purposes. Gear tooth bending fatigue and surface pitting were the primary failure modes found in the tests. The damage ranged from partial tooth fracture on a single tooth in one test to heavy wear, severe pitting, and complete tooth fracture of several teeth on another test. Three gear fault detection techniques, FM4, NA4*, and NB4, were applied to the experimental data. These methods use the signal average in both the time and frequency domain. Method NA4* was able to conclusively detect the gear tooth fractures in three out of the four fatigue tests, along with gear tooth surface pitting and heavy wear. For multiple tooth fractures, all of the methods gave a clear indication of the damage. It was also found that due to the high contact ratio of the face gear mesh, single tooth fractures did not significantly affect the vibration signal, making this type of failure difficult to detect. Author

N95-19238*# National Aeronautics and Space Administration. Lewis Research Center, Cleveland, OH.

TRANSIENT AND STEADY-STATE TESTS OF THE SPACE POWER RESEARCH ENGINE WITH RESISTIVE AND MOTOR LOADS

Jeffrey S. Rauch (NYMA, Inc., Brook Park, OH.) and M. David Kankam Jan. 1995 147 p

(RTOP 583-02-21)

(NASA-TM-106832; E-9391; NAS 1.15:106832) Avail: CASI HC A07/MF A02

The NASA Lewis Research Center (LeRC) has been testing free-piston Stirling engine/linear alternators (FPSE/LA) to develop advanced power convertors for space-based electrical power generation. Tests reported herein were performed to evaluate the interaction and transient behavior of FPSE/LA-based power systems with typical user loads. Both resistive and small induction motor loads were tested with the space power research engine (SPRE) power system. Tests showed that the control system could maintain constant long term voltage and stable periodic operation over a large range of engine operating parameters and loads. Modest resistive load changes were shown to cause relatively large voltage and, therefore, piston and displacer amplitude excursions. Starting a typical small induction motor was shown to cause large and, in some cases, deleterious voltage transients. The tests identified the need for more effective controls, if FPSE/LAs are to be used for stand-alone power systems. The tests also generated a large body of transient dynamic data useful for analysis code validation. Author

N95-19567*# State Univ. of New York, Binghamton, NY. Dept. of Mechanical Engineering.
WORMGEAR GEOMETRY ADOPTED FOR IMPLEMENTING HYDROSTATIC LUBRICATION AND FORMULATION OF THE LUBRICATION PROBLEM Final Report
D. C. Sun and Qin Yuan Cleveland, OH NASA Jan. 1995 49 p
(Grant NAG3-1316; RTOP 505-62-OJ; DA Proj. 1L1-61102-AH-45)
(NASA-CR-195416; E-9345; NAS 1.26:195416; ARL-CR-219) Avail: CASI HC A03/MF A01

The geometrical parameters for a wormgear intended to be used as the transmission in advanced helicopters are finalized. The resulting contact pattern of the meshing tooth surfaces is suitable for the implementation of hydrostatic lubrication Fluid film lubrication of the contact is formulated considering external pressurization as well as hydrodynamic wedge and squeeze actions. The lubrication analysis is aimed at obtaining the oil supply pressure needed to separate the worm and gear surfaces by a prescribed minimum film thickness. The procedure of solving the mathematical problem is outlined. Author

N95-19593# Babcock and Wilcox Co., Lynchburg, VA.
DESIGN OF A FLEXIBLE ROBOTIC ARC WELDING SYSTEM, TASK 3. VOLUME 1: SYSTEM OVERVIEW Final Report, Jan. - Dec. 1988
Martin D. Kline, Larry Cagle, Michael Frazier, Mark Kilpatrick, and Grady Powers Sep. 1993 45 p
(Contract DAAA08-87-C-0096)
(AD-A285116; RIA/SE-93-01) Avail: CASI HC A03/MF A01

This report represents the 100 percent completion of the technical data package (TDP) for Task 3 of the Flexible Robotic Arc Welding System. The system design was developed to allow a diverse group of steel weldments to be fixtured, preheated, robotically arc welded manually inspected, repaired, and moved by an automatic guided vehicle throughout the welding system. The system is monitored and operated by a systems computer in a distributed control environment. The two welding robots are individually controlled by their own robotic controller but downloaded from the systems computer depending on the bar coded information that follows the fixtured weldment mounted on universal pallets. The report consists of three volumes of design specifications with a fourth volume of technical supporting information that will be supplied upon specific request only. DTIC

N95-19809 BKM, Inc., San Diego, CA.
ADVANCED DIESEL ELECTRONIC FUEL INJECTION AND TURBOCHARGING Final Report, Jul. 1990 - Dec. 1993
N. J. Beck, R. L. Barkhimer, D. C. Steinmeyer, and J. E. Kelly Dec. 1993 237 p Limited Reproducibility: More than 20% of this document may be affected by microfiche quality
(Contract DAAE07-90-C-R030)
(AD-A279176; F-632; TACOM-13603) Avail: Issuing Activity (Defense Technical Information Center (DTIC))

The program investigated advanced diesel air charging and fuel injection systems to improve specific power, fuel economy, noise, exhaust emissions, and cold startability. The techniques explored included variable fuel injection rate shaping, variable injection timing, full-authority electronic engine control, turbo-compound cooling, regenerative air circulation as a cold start aid, and variable geometry turbocharging. A Servojet electronic fuel injection system was designed and manufactured for the Cummins VTA-903 engine. A special Servojet twin turbocharger exhaust system was also installed. A series of high speed combustion flame photos was taken using the single cylinder optical engine at Michigan Technological University. Various fuel injection rate shapes and nozzle configurations were evaluated. Single-cylinder bench tests were performed to evaluate regenerative inlet air heating techniques as an aid to cold starting. An exhaust-driven axial cooling air fan was manufactured and tested on the VTA-903 engine. DTIC

N95-18169*# University of Central Florida, Orlando, FL. Dept. of Mechanical and Aerospace Engineering.
AUTOMATED PATH PLANNING OF THE PAYLOAD INSPECTION AND PROCESSING SYSTEM
Robert M. Byers *In its* NASA/ASEE Summer Faculty Fellowship Program. 1994 Research Reports Oct. 1994 p 61-90 (For primary document see N95-18166 05-80)
Avail: CASI HC A03/MF A04

N95-18177*# North Carolina Univ., Charlotte, NC. Dept. of Mechanical Engineering and Engineering Science.
DESIGN OPTIMIZATION OF A BRUSH TURBINE WITH A CLEANER/WATER BASED SOLUTION
Rhyn H. Kim *In* Univ. of Central Florida, NASA/ASEE Summer Faculty Fellowship Program. 1994 research reports Oct. 1994 p 313-338 (For primary document see N95-18166 05-80)
Avail: CASI HC A03/MF A04

N95-18178*# Tuskegee Inst., AL. Dept. of Mechanical Engineering.
RACK INSERTION END EFFECTOR (RIEE) GUIDANCE
Narasimha S. Malladi *In* Univ. of Central Florida, NASA/ASEE Summer Faculty Fellowship Program. 1994 Research Reports Oct. 1994 p 339-348 (For primary document see N95-18166 05-80)
Avail: CASI HC A02/MF A04

N95-19667# National Technical Univ., Athens (Greece). Thermal Engineering Section.
INVESTIGATION OF MECHANICAL EROSION IN FUEL PIPELINES
M. Founti and A. Klipfel *In* AGARD, Erosion, Corrosion and Foreign Object Damage Effects in Gas Turbines Nov. 1994 7 p (For primary document see N95-19653 05-07)
Copyright Avail: CASI HC A02/MF A03

38 QUALITY ASSURANCE AND RELIABILITY

Includes product sampling procedures and techniques; and quality control.

N95-18583*# National Aeronautics and Space Administration. Lewis Research Center, Cleveland, OH.
AN NDE APPROACH FOR CHARACTERIZING QUALITY PROBLEMS IN POLYMER MATRIX COMPOSITES
Don J. Roth, George Y. Baaklini, James K. Sutter, James R. Bodis (Cleveland State Univ., OH.), Todd A. Leonhardt (NYMA, Inc., Brook Park, OH.), and Elizabeth A. Crane (John Carroll Univ., Cleveland, OH.) Dec. 1994 15 p Presented at the 40th International Symposium and Exhibition, Anaheim, CA, 8-11 May 1995; sponsored by Society for the Advancement of Materials and Process Engineering
(RTOP 505-63-12)
(NASA-TM-106807; E-9292; NAS 1.15:106807) Avail: CASI HC A03/MF A01

Polymer matrix composite (PMC) materials are periodically identified appearing optically uniform but containing a higher than normal level of global nonuniformity as indicated from preliminary ultrasonic scanning. One such panel was thoroughly examined by nondestructive (NDE) and destructive methods to quantitatively characterize the nonuniformity. The NDE analysis of the panel was complicated by the fact that the panel was not uniformly thick. Mapping of ultrasonic velocity across a region of the panel in conjunction with an error analysis was necessary to (1) characterize properly the porosity gradient that was discovered during destructive analyses and (2) account for the thickness variation effects. Based on this study, a plan for future NDE characterization of PMC's is presented to the PMC community. Author

N95-18737*# Research Inst. for Advanced Computer Science, Moffett Field, CA.
MESH QUALITY CONTROL FOR MULTIPLY-REFINED TETRAHEDRAL GRIDS
Rupak Biswas and Roger Strawn (Army Aviation Systems Command, Moffett Field, CA.) Nov. 1994 16 p Submitted for publication
(Contract NAS2-13721)
(NASA-CR-197595; NAS 1.26:197595; RIACS-TR-94-19) Avail: CASI HC A03/MF A01

A new algorithm for controlling the quality of multiply-refined tetrahedral meshes is presented in this paper. The basic dynamic mesh adaption procedure allows localized grid refinement and coarsening to efficiently capture aerodynamic flow features in computational fluid dynamics problems;

however, repeated application of the procedure may significantly deteriorate the quality of the mesh. Results presented show the effectiveness of this mesh quality algorithm and its potential in the area of helicopter aerodynamics and acoustics. Author

N95-19010*# Alabama A & M Univ., Huntsville, AL. Dept. of Mathematics.
THE PROBABILITY OF FLAW DETECTION AND THE PROBABILITY OF FALSE CALLS IN NONDESTRUCTIVE EVALUATION EQUIPMENT
Enoch C. Temple *In* Alabama Univ., Research Reports: 1994 NASA/ASEE Summer Faculty Fellowship Program Oct. 1994 6 p (For primary document see N95-18967 05-80)
Avail: CASI HC A02/MF A03

39 STRUCTURAL MECHANICS

Includes structural element design and weight analysis; fatigue; and thermal stress.

For applications see *05 Aircraft Design, Testing and Performance* and *18 Spacecraft Design, Testing and Performance.*

N95-18080 Rensselaer Polytechnic Inst., Troy, NY.
THE RELIABILITY OF LASER REFLOWED Sn-Ag SOLDER JOINTS Quarterly Report No. 2
C. H. Raeder, D. L. Millard, and R. W. Messler 31 Aug. 1994 8 p Limited Reproducibility: More than 20% of this document may be affected by microfiche quality
(Contract N00014-93-1-1295)
(AD-A284732) Avail: Issuing Activity (Defense Technical Information Center (DTIC))

This is the second quarterly report of a project aimed at determining the reliability of electronic interconnects made with Sn-3.5wt percent Ag solder alloy. Isothermal creep testing is now complete. The testing procedure is outlined in Report 1. Only results will be given here. Each creep curve was decomposed assuming linear addition of three strain components: elastic, transient, and steady state strain. Young's modulus values of pure Sn as a function of temperature were taken from Drapkin and Kononenko. These data were fit linearly resulting in the equation given below which was used to calculate the elastic strain for a given test. DTIC

N95-18081 Southwest Research Inst., San Antonio, TX.
MICROSTRUCTURE-BASED FATIGUE LIFE PREDICTION METHODS FOR NAVAL STEEL STRUCTURES Final Report, 15 Jul. 1991 - 15 Jul. 1994
R. C. McClung, K. S. Chan, D. L. Davidson, and T. Y. Torng 12 Sep. 1994 163 p Limited Reproducibility: More than 20% of this document may be affected by microfiche quality
(Contract N00014-91-C-0214)
(AD-A284735; SWRI-06-4414/3) Avail: CASI HC A08

The goal of the subject program has been to develop fundamental understandings of the relationships between microstructure and fatigue damage in structural steels of interest to naval applications. Quantitative descriptions of these relationships have been incorporated within practical engineering models for the prediction of fatigue life. Fatigue damage associated with microcrack nucleation and growth has been studied experimentally with S-N fatigue specimens of HSLA-80 steel. Some microstructures were modified with appropriate heat treatments, and the effects of microstructure on microcrack nucleation and growth have been characterized. Microstructural scaling laws have been developed and verified for both fatigue crack growth (FCG) and smooth specimen total life in a wide range of steels. The effects of microstructure on FCG have been described by a dimensionless microstructural parameter which is defined in terms of stress, fatigue ductility, dislocation cell size, and dislocation barrier spacing. FCG data from large and small flaws have been critically compared on the basis of engineering models for FCG rates, and the implications of this comparison for engineering fatigue life prediction are explored. A probabilistic treatment of the micromechanical scaling laws for FCG has been derived, permitting a direct evaluation of the relationship between microstructural variation and variability in FCG rates. DTIC

N95-18199*# National Aeronautics and Space Administration. Lewis Research Center, Cleveland, OH.
COMPLETED BELTRAMI-MICHELL FORMULATION FOR ANALYZING RADIALLY SYMMETRICAL BODIES
Igor Kaljevic (Ohio Aerospace Inst., Cleveland, OH.), Sunil Saigal (Carnegie-Mellon Univ., Pittsburgh, PA.), Dale A. Hopkins, and Surya N. Patnaik (Ohio Aerospace Inst., Cleveland, OH.) Dec. 1994 22 p
(RTOP 505-63-53)
(NASA-TM-4593; E-8825; NAS 1.15:4593) Avail: CASI HC A03/MF A01

A force method formulation, the completed Beltrami-Michell formulation (CBMF), has been developed for analyzing boundary value problems in elastic continua. The CBMF is obtained by augmenting the classical Beltrami-Michell formulation with novel boundary compatibility conditions. It can analyze general elastic continua with stress, displacement, or mixed boundary conditions. The CBMF alleviates the limitations of the classical formulation, which can solve stress boundary value problems only. In this report, the CBMF is specialized for plates and shells. All equations of the CBMF, including the boundary compatibility conditions, are derived from the variational formulation of the integrated force method (IFM). These equations are defined only in terms of stresses. Their solution for kinematically stable elastic continua provides stress fields without any reference to displacements. In addition, a stress function formulation for plates and shells is developed by augmenting the classical Airy's formulation with boundary compatibility conditions expressed in terms of the stress function. The versatility of the CBMF and the augmented stress function formulation is demonstrated through analytical solutions of several mixed boundary value problems. The example problems include a composite circular plate and a composite circular cylindrical shell under the simultaneous actions of mechanical and thermal loads. Author

N95-18363# Naval Postgraduate School, Monterey, CA.
FINITE ELEMENT MODELING OF PARTIALLY DELAMINATED COMPOSITE BEAMS WITH CONTACT-IMPACT CONDITIONS M.S. Thesis
Haluk Aygunes Jun. 1994 49 p
(AD-A283726) Avail: CASI HC A03/MF A01

A new finite element modeling is presented to investigate the static and dynamic behavior of laminated composite beams with partial delamination. In this study, a newly developed rectangular beam element is used. The element has lateral and axial displacements as degrees of freedom but no rotation. For simplicity, linear shape functions are used for the beam element. As a result, the element has six degrees of freedom, four of which are the axial displacements at the corner points and two are the lateral displacements at the ends. In addition, contact-impact conditions are applied to the finite element modeling to avoid overlapping of the upper and lower portions of a delaminated section. The numerical study shows that depending on existence of an embedded delamination crack and its size, the response is different for a beam with a crack and subjected to a short impulse load. Author (DTIC)

N95-18388*# Virginia Polytechnic Inst. and State Univ., Blacksburg, VA. Dept. of Aerospace and Ocean Engineering.
COMPRESSION STRENGTH OF COMPOSITE PRIMARY STRUCTURAL COMPONENTS Semiannual Report, 1 May - 31 Oct. 1994
Eric R. Johnson Dec. 1994 65 p
(Grant NAG1-537)
(NASA-CR-197554; NAS 1.26:197554) Avail: CASI HC A04/MF A01

The linear elastic response is determined for an internally pressurized, long circular cylindrical shell stiffened on the inside by a regular arrangement of identical stringers and identical rings. Periodicity of this configuration permits the analysis of a portion of the shell wall centered over a generic stringer-ring joint; i.e., a unit cell model. The stiffeners are modeled as discrete beams, and the stringer is assumed to have a symmetrical cross section and the ring an asymmetrical section. Asymmetery causes out-of-plane bending and torsion of the ring. Displacements are assumed as truncated double Fourier series plus simple terms in the axial coordinate to account for the closed and pressure vessel effect (a non-periodic effect). The interacting line loads between the stiffeners and the inside shell wall are Lagrange multipliers in the formulation, and they are also assumed as truncated Fourier series. Displacement continuity constraints between the stiffeners and shell along the contact lines are satisfied point-wise.

Equilibrium is imposed by the principle of virtual work. A composite material crown panel from the fuselage of a large transport aircraft is the numerical example. The distributions of the interacting line loads, and the out-of-plane bending moment and torque in the ring, are strongly dependent on modeling the deformations due to transverse shear and cross-sectional warping of the ring in torsion. This paper contains the results from the semiannual report on research on 'Pressure Pillowing of an Orthogonally Stiffened Cylindrical Shell'. The results of the new work are illustrated in the included appendix. Author (revised)

N95-18456# Department of the Navy, Washington, DC.
A SHOCK ISOLATION METHOD AND APPARATUS Patent Application
Michael Tucchio, inventor (to Navy) and Robert LaFreniere, inventor (to Navy) 2 May 1994 16 p
(AD-D016471; US-Patent-Appl-SN-236856; Navy-Case-74739) Avail: CASI HC A02/MF A01

A shock isolation device for supporting the weight of an object and providing shock and isolation vibration is disclosed which includes a compressible elastomeric material. Apertures are drilled in the compressible elastomeric material for receiving buckling fibers. The buckling fibers are supported in the respective apertures by a buckling support plate positioned on a bottom surface of the compressible elastomeric material. The fibers extend above the top surface of the compressible elastomeric material to support an object above the top surface under normal conditions when no shocks occur. When a shock occurs, the buckling fibers are elastically or plastically buckled under an applied force caused by acceleration of the object and the object contacts the compressible elastomeric material to isolate the shock. A plurality of the buckling fibers are spaced evenly throughout the elastomeric material to support objects of different sizes and weights. DTIC

N95-18472 Materials Research Labs., Ascot Vale (Australia).
BEAM: A FINITE ELEMENT PROGRAM FOR THE COLLAPSE ANALYSIS OF VEHICLE STRUCTURES
S. J. Cimpoeru Jun. 1994 36 p Limited Reproducibility: More than 20% of this document may be affected by microfiche quality
(AD-A285547; MRL-TR-94-6; DODA-AR-008-636) Avail: Issuing Activity (Defense Technical Information Center (DTIC))

BEAM (Beam Element Analysis with Mechanisms) is a finite element program for the analysis of the collapse of vehicle structures. BEAM can quickly estimate the collapse load and plastic hinge locations in three-dimensional thin-walled frames that would collapse in bending. Such information can be combined with separate rigid-plastic modelling to enable the large-deflection design of vehicle frameworks so that their collapse in roll-over accidents, for instance, can be prevented. One advantage of BEAM is that it allows a user to define his own experimentally or analytically determined loads and moments as failure criteria. The theory and operation of BEAM are presented and its application to the modelling of a collapsing two-dimensional frame is described. Author (DTIC)

N95-18608# Queensland Univ., Brisbane (Australia). Dept. of Civil Engineering.
PLATE VIBRATION WITH ARBITRARILY ORIENTED STIFFENERS BASED ON MINDLIN-ENGESSER FORMULATION
Y. Xiang, S. Kitipornchai, K. M. Liew (Nanyang Technological Inst., Singapore.), and M. K. Lim (Nanyang Technological Inst., Singapore.) Jul. 1993 35 p
(RR-CE143; ISBN-0-86776-503-8) Avail: CASI HC A03/MF A01

This paper investigates the free vibration analysis of moderately thick plates with arbitrarily oriented stiffeners. Formulation of the energy functional incorporates the Mindlin theory to account for the effects of shear deformation and rotary inertia of plates, and the Engesser theory is used to account for the shear deformation of stiffeners with the inclusion of torsion effect. The Ritz minimization procedure with a set of pb-2 shape functions is employed for solution. Numerical investigations using stiffened plates of various shapes have been undertaken to illustrate the applicability and versatility of this procedure. A detailed parametric study of the effects of geometric parameters on the vibratory characteristics is reported. In the paper, the simplicity and accuracy of the proposed solution method are highlighted. Author

N95-18613# California Inst. of Tech., Pasadena, CA. Graduate Aeronautical Labs.
DYNAMIC DECOHESION OF BIMATERIALS: EXPERIMENTAL OBSERVATIONS AND FAILURE CRITERIA
John Lambros and Ares J. Rosakis Feb. 1994 51 p Submitted for publication
(Contract N00014-90-J-1340; NSF MSS-90-24838)
(GALCIT-94-2; AD-A279808) Avail: CASI HC A04/MF A01

Some results of high speed interferometric measurements of dynamically propagating interfacial cracks are presented. PMMA/Steel bimaterial specimens of the one point bend type are used. They are impact loaded using either a drop weight tower device or a high speed gas gun. This results in two distinct groups of experiments at different loading rates. In all cases very high crack propagation speeds are seen. In gas gun experiments, terminal crack tip speeds of up to 1.5C(sub S)(exp PMMA), where C(sub S)(exp PMMA) is the shear wave speed of PMMA, are measured. In addition, high accelerations (approximately equals 10(exp 7)g, where g is the acceleration of gravity) are observed and reported. Theoretically predicted near tip fields are used to extract experimental values of the dynamic complex stress intensity factor histories in each test. Using the fitted histories of the complex stress intensity factor, a dynamic crack growth criterion relating the energy release rate to phase angle and crack tip velocity is proposed and discussed. Author

N95-18909*# National Aeronautics and Space Administration. Lewis Research Center, Cleveland, OH.
COMPLETED BELTRAMI-MICHELL FORMULATION FOR ANALYZING MIXED BOUNDARY VALUE PROBLEMS IN ELASTICITY
Surya N. Patnaik (Ohio Aerospace Inst., Brook Park.), Igor Kaljevic (Ohio Aerospace Inst., Brook Park.), Dale A. Hopkins, and Sunil Saigal (Carnegie-Mellon Univ., Pittsburgh, PA.) Jan. 1995 29 p
(RTOP 505-63-53)
(NASA-TM-106809; E-9296; NAS 1.15:106809) Avail: CASI HC A03/MF A01

In elasticity, the method of forces, wherein stress parameters are considered as the primary unknowns, is known as the Beltrami-Michell formulation (BMF). The existing BMF can only solve stress boundary value problems; it cannot handle the more prevalent displacement of mixed boundary value problems of elasticity. Therefore, this formulation, which has restricted application, could not become a true alternative to the Navier's displacement method, which can solve all three types of boundary value problems. The restrictions in the BMF have been alleviated by augmenting the classical formulation with a novel set of conditions identified as the boundary compatibility conditions. This new method, which completes the classical force formulation, has been termed the completed Beltrami-Michell formulation (CBMF). The CBMF can solve general elasticity problems with stress, displacement, and mixed boundary conditions in terms of stresses as the primary unknowns. The CBMF is derived from the stationary condition of the variational functional of the integrated force method. In the CBMF, stresses for kinematically stable structures can be obtained without any reference to the displacements either in the field or on the boundary. This paper presents the CBMF and its derivation from the variational functional of the integrated force method. Several examples are presented to demonstrate the applicability of the completed formulation for analyzing mixed boundary value problems under thermomechanical loads. Selected example problems include a cylindrical shell wherein membrane and bending responses are coupled, and a composite circular plate. Author

N95-18917 Texas Univ., Austin, TX.
A BOUNDARY ELEMENT METHOD FOR TWO DIMENSIONAL LINEAR ELASTIC FRACTURE ANALYSIS Ph.D. Thesis
Chungchu Chang 1993 137 p
Avail: Univ. Microfilms Order No. DA9413454

A boundary element method is developed for the analysis of fractures in two-dimensional solids. The solids are assumed to be linearly elastic and isotropic, and both bounded and unbounded domains are treated. The boundary integral equations upon which the method is based are developed directly from Somigliana's identity, and each of them consists of the conventional ordinary boundary terms and two additional terms which can be identified as a distribution of point loads and a distribution of point dislocations along the crack lines. The strategy for establishing the integral equations is first outlined in terms of real variables, but for convenience,

complex variable techniques are adopted for the detailed development. In the numerical implementation of the formulation, the ordinary boundary integrals are treated with standard boundary element techniques, while a novel numerical procedure is developed to treat the crack line integrals. The resulting numerical procedure is used to solve several sample problems for embedded and surface-breaking cracks, and it is demonstrated that the technique is both accurate and efficient. Finally, an alternative procedure for use in treating a restricted class of problems is developed. This procedure is based upon fundamental solutions which explicitly account for certain (simple) inhomogeneities in unbounded domains, and as a consequence it provides a highly accurate and efficient means for solving fracture problems associated with these domains. Dissert. Abstr.

N95-18919 Virginia Polytechnic Inst. and State Univ., Blacksburg, VA.
ON STATIONARY AND NONSTATIONARY FATIGUE LOAD MODELING USING AUTOREGRESSIVE MOVING AVERAGE (ARMA) MODELS Ph.D. Thesis
Christoph Leser 1993 184 p
Avail: Univ. Microfilms Order No. DA9414078

The concise description of one- and multidimensional stationary and nonstationary vehicle loading histories for fatigue analysis using stochastic process theory is presented in this study. The load history is considered to have stationary random and nonstationary mean and variance content. The stationary variations are represented by a class of time series referred to as Autoregressive Moving Average (ARMA) models, while a Fourier series is used to account for the variation of the mean and variance. Due to the use of random phase angles in the Fourier series, an ensemble of mean and variance variations is obtained. The methods of nonparametric statistics are used to determine the success of the modeling of nonstationarity. Justification of the method is obtained through comparison of rainflow cycle distributions and resulting fatigue lives of original and simulated loadings. Due to the relatively small number of Fourier coefficients needed together with the use of ARMA models, a concise description of complex loadings is achieved. The overall frequency content and sequential information of the load history is statistically preserved. An ensemble of load histories can be constructed on-line with minimal computer storage capacity as used in testing equipment. The method can be used in a diversity of fields where a concise representation of random loadings is desired. Dissert. Abstr.

N95-18922 Michigan Technological Univ., Houghton, MI.
ON THE THEORY OF STICK-SLIP FRACTURE Ph.D. Thesis
Thomas William Webb 1993 110 p
Avail: Univ. Microfilms Order No. DA9411234

A stick-slip fracture model based on a modified equation of motion for the crack tip and a nonconvex fracture toughness velocity curve is presented. An extra term consisting of a second order time derivative of the crack length is introduced into the usual equation of motion for the crack tip to capture the nonsteady crack growth which occurs during stick-slip fracture. The extra term is referred to as the crack tip 'inertia' and its coefficient is referred to as the effective 'mass' of the crack. Based on this modified equation of motion for the crack tip and a differential equation describing the time rate of change of the energy release rate under constant applied extension rate loading conditions, stick-slip fracture oscillations are described by a limit cycle in the energy release rate-crack tip velocity plane. The general characteristics of stick-slip fracture are examined using common approaches in nonlinear dynamics and by performing numerical experiments on the governing equations. Numerical results are presented and compared with experimental stick-slip fracture measurements and observations. Dissert. Abstr.

N95-19501*# National Aeronautics and Space Administration. Lewis Research Center, Cleveland, OH.
TECHNOLOGY BENEFIT ESTIMATOR (T/BEST): USER'S MANUAL
Edward R. Generazio, Christos C. Chamis, and Galib Abumeri (NYMA, Inc., Brook Park, OH.) Dec. 1994 214 p
(Contract NAS3-27186; RTOP 505-63-5B)
(NASA-TM-106785; E-9239; NAS 1.15:106785) Avail: CASI HC A10/MF A03

The Technology Benefit Estimator (T/BEST) system is a formal method to assess advanced technologies and quantify the benefit contributions for prioritization. T/BEST may be used to provide guidelines to identify and prioritize high payoff research areas, help manage research and limited resources, show the link between advanced concepts and the bottom line, i.e., accrued benefit and value, and to communicate credibly the benefits of research. The T/BEST software computer program is specifically designed to estimating benefits, and benefit sensitivities, of introducing new technologies into existing propulsion systems. Key engine cycle, structural, fluid, mission and cost analysis modules are used to provide a framework for interfacing with advanced technologies. An open-ended, modular approach is used to allow for modification and addition of both key and advanced technology modules. T/BEST has a hierarchical framework that yields varying levels of benefit estimation accuracy that are dependent on the degree of input detail available. This hierarchical feature permits rapid estimation of technology benefits even when the technology is at the conceptual stage. As knowledge of the technology details increases the accuracy of the benefit analysis increases. Included in T/BEST's framework are correlations developed from a statistical data base that is relied upon if there is insufficient information given in a particular area, e.g., fuel capacity or aircraft landing weight. Statistical predictions are not required if these data are specified in the mission requirements. The engine cycle, structural fluid, cost, noise, and emissions analyses interact with the default or user material and component libraries to yield estimates of specific global benefits: range, speed, thrust, capacity, component life, noise, emissions, specific fuel consumption, component and engine weights, pre-certification test, mission performance engine cost, direct operating cost, life cycle cost, manufacturing cost, development cost, risk, and development time. Currently, T/BEST operates on stand-alone or networked workstations, and uses a UNIX shell or script to control the operation of interfaced FORTRAN based analyses. T/BEST's interface structure works equally well with non-FORTRAN or mixed software analysis. This interface structure is designed to maintain the integrity of the expert's analyses by interfacing with expert's existing input and output files. Parameter input and output data (e.g., number of blades, hub diameters, etc.) are passed via T/BEST's neutral file, while copious data (e.g., finite element models, profiles, etc.) are passed via file pointers that point to the expert's analyses output files. In order to make the communications between the T/BEST's neutral file and attached analyses codes simple, only two software commands, PUT and GET, are required. This simplicity permits easy access to all input and output variables contained within the neutral file. Both public domain and proprietary analyses codes may be attached with a minimal amount of effort, while maintaining full data and analysis integrity, and security. T/BESt's sotware framework, status, beginner-to-expert operation, interface architecture, analysis module addition, and key analysis modules are discussed. Representative examples of T/BEST benefit analyses are shown. Author

N95-19504 Materials Research Labs., Ascot Vale (Australia).
SHOCK PULSE GENERATION USING EXPLOSIVE DRIVEN METAL DRIVERS: PRACTICAL CONSIDERATIONS
George M. Weston, G. Fred Whitty, and Eric Northeast Aug. 1993 21 p
(MRL-TR-93-3; AR-008-255) Copyright Avail: Issuing Activity

The present paper examines the practical aspects of using the mousetrap plane wave generator design to shock harden metal targets of iron and copper. The paper investigates three driver plate designs and two plate sizes and compares the experimental x-ray plate profile with that provided by the modelling code Dyna 3D for the same run conditions. For the larger driver plate series of 110 mm square, the central planar area available for shock hardening using the full plate compared favorably with that provided by the driver design incorporating steel edge confinement. Drivers using explosive overhang as driver edge confinement provided the smallest central planar area for shock hardening. Shock hardening was not possible with smaller drives of 55 mm square due to the degree of plate curvature experienced before target impact. The modelling code Dyna 3D provided close agreement with experiment for the smaller driver series except where steel edge confinement was used, while for the larger driver series the modelling code consistently predicted greater plate curvature for all three designs than was experienced in practice. Author

N95-19522# CSA Engineering, Inc., Palo Alto, CA.
USING NEURAL NETWORKS IN THE MAPPING OF MIXED DISCRETE/CONTINUOUS DESIGN SPACES WITH APPLICATION TO STRUCTURAL DESIGN Final Report, 8 Sep. 1993 - 31 Jan. 1994

Stephen M. Batill, John E. Renaud, and Richard S. Sellar Feb. 1994 46 p
(Contract F33615-90-C-3211)
(AD-A285328; ASIAC-TR-94-21; WL-TR-94-3115) Avail: CASI HC A03/MF A01

The objective of this task was to extend recent research efforts in order to evaluate the suitability of using artificial neural networks to provide quantitative design space representations for structural concepts with combined continuous and discrete design variables. For a simple structural problem containing both discrete and continuous design variables it was demonstrated that the character of the design space could be well represented with a relatively small amount of training data. It was also shown that design methods are available which can be used for mixed discrete/continuous design variable problems. These methods are however limited by the discontinuous nature of the discrete design problem and by the ability to predict system characteristics in an efficient manner. Using an approach with feed-forward, back-propagation neural networks an efficient method for the design of mixed discrete/continuous systems can be obtained. DTIC

N95-19649*# National Aeronautics and Space Administration. Lewis Research Center, Cleveland, OH.
CLOSED-FORM STATIC ANALYSIS WITH INERTIA RELIEF AND DISPLACEMENT-DEPENDENT LOADS USING A MSC/NASTRAN DMAP ALTER
Alan R. Barnett (Analex Corp., Brook Park, OH.), Timothy W. Widrick (Analex Corp., Brook Park, OH.), and Damian R. Ludwiczak Jan. 1995 16 p Presented at the 1995 World Users' Conference, Los Angeles, CA, 8-12 May 1995; sponsored by MacNeal-Schwendler Corp.
(Contract NAS3-25776)
(NASA-TM-106836; E-9398; NAS 1.15:106836) Avail: CASI HC A03/MF A01

Solving for the displacements of free-free coupled systems acted upon by static loads is commonly performed throughout the aerospace industry. Many times, these problems are solved using static analysis with inertia relief. This solution technique allows for a free-free static analysis by balancing the applied loads with inertia loads generated by the applied loads. For some engineering applications, the displacements of the free-free coupled system induce additional static loads. Hence, the applied loads are equal to the original loads plus displacement-dependent loads. Solving for the final displacements of such systems is commonly performed using iterative solution techniques. Unfortunately, these techniques can be time-consuming and labor-intensive. Since the coupled system equations for free-free systems with displacement-dependent loads can be written in closed-form, it is advantageous to solve for the displacements in this manner. Implementing closed-form equations in static analysis with inertia relief is analogous to implementing transfer functions in dynamic analysis. Using a MSC/NASTRAN DMAP Alter, displacement-dependent loads have been included in static analysis with inertia relief. Such an Alter has been used successfully to solve efficiently a common aerospace problem typically solved using an iterative technique. Author

N95-19804 Federal Aviation Administration, Atlanta, GA.
STRESS-INTENSITY FACTOR SOLUTIONS FOR CRACKS AT COUNTERSUNK RIVET HOLES UNDER UNIAXIAL TENSION Final Report
P. W. Tan, C. A. Bigelow, P. E. ODonoghue, and S. N. Atluri Feb. 1994 30 p Limited Reproducibility: More than 20% of this document may be affected by microfiche quality
(AD-A279163; DOT/FAA/CT-93/68) Avail: Issuing Activity (Defense Technical Information Center (DTIC))

To predict crack growth and fracture strengths of riveted joints subjected to widespread fatigue damage, accurate stress and fracture analyses of corner and surface cracks at a rivet hole are needed. The results presented in this report focus on the computation of stress-intensity factor solutions for rivet holes with cracks. The stress-intensity factor solutions for surface and corner cracks at countersunk rivet holes in a plate were obtained using the finite-element-alternating technique. A range of crack shapes, crack sizes, and crack locations under remote tension were considered. DTIC

N95-18972*# Alabama A & M Univ., Huntsville, AL. Dept. of Engineering Technology.
RESIDUAL STRESSES IN WELDED PLATES
Edward L. Bernstein *In* Alabama Univ., Research Reports: 1994 NASA/ASEE Summer Faculty Fellowship Program Oct. 1994 6 p (For primary document see N95-18967 05-80)
Avail: CASI HC A02/MF A03

N95-19003*# Alabama Univ., Huntsville, AL. Dept. of Civil and Environmental Engineering.
CRACKING CHARACTERISTICS OF A HABITABLE MODULE PRESSURE WALL FOLLOWING ORBITAL DEBRIS PENETRATION
William P. Schonberg *In* Alabama Univ., Research Reports: 1994 NASA/ASEE Summer Faculty Fellowship Program Oct. 1994 6 p (For primary document see N95-18967 05-80)
Avail: CASI HC A02/MF A03

N95-19161# Wright Lab., Wright-Patterson AFB, OH. Acoustics and Sonic Fatigue Section.
THERMO-ACOUSTIC FATIGUE DESIGN FOR HYPERSONIC VEHICLE SKIN PANELS
Kenneth R. Wentz, Robert D. Blevins (Rohr Industries, Inc., Chula Vista, CA.), and Ian Holehouse (Rohr Industries, Inc., Chula Vista, CA.) *In* AGARD, Impact of Acoustic Loads on Aircraft Structures Sep. 1994 9 p (For primary document see N95-19142 05-71)
Copyright Avail: CASI HC A02/MF A03

N95-19165# Defence Research Agency, Farnborough, Hampshire (England).
ADVANCED STATISTICAL ENERGY ANALYSIS
K. H. Heron *In* AGARD, Impact of Acoustic Loads on Aircraft Structures Sep. 1994 8 p (For primary document see N95-19142 05-71)
Copyright Avail: CASI HC A02/MF A03

N95-19185*# National Aeronautics and Space Administration. Lyndon B. Johnson Space Center, Houston, TX.
PENETRATION EXPERIMENTS IN ALUMINUM AND TEFLON TARGETS OF WIDELY VARIABLE THICKNESS Abstract Only
F. Hoerz, Mark J. Cintala, R. P. Bernhard (Lockheed Engineering and Sciences Co., Houston, TX.), and T. H. See (Lockheed Engineering and Sciences Co., Houston, TX.) *In* Lunar and Planetary Inst., Workshop on Particle Capture, Recovery and Velocity/Trajectory Measurement Technologies 1994 p 42-48 (For primary document see N95-19172 05-90)
Avail: CASI HC A02/MF A02

N95-19470*# Rockwell International Corp., Downey, CA. Space Sytems Div.
FATIGUE LOADS SPECTRA DERIVATION FOR THE SPACE SHUTTLE: SECOND CYCLE
Raphael Ortasse *In* NASA. Langley Research Center, FAA/NASA International Symposium on Advanced Structural Integrity Methods for Airframe Durability and Damage Tolerane, Part 2 Sep. 1994 p 517-545 (For primary document see N95-19468 05-03)
Avail: CASI HC A03/MF A04

N95-19471*# Laboratory for Strength of Materials Components and Structures, Puspiptek (Indonesia).
PREDICTION OF FATIQUE CRACK GROWTH UNDER FLIGHT-SIMULATION LOADING WITH THE MODIFIED CORPUS MODEL
U. H. Padmadinata and J. Schijve (Technische Hogeschool, Delft, Netherlands.) *In* NASA. Langley Research Center, FAA/NASA International Symposium on Advanced Structural Integrity Methods for Airframe Durability and Damage Tolerance, Part 2 Sep. 1994 p 547-562 (For primary document see N95-19468 05-03)
Avail: CASI HC A03/MF A04

N95-19472*# National Aeronautics and Space Administration. Langley Research Center, Hampton, VA.
THE CHARACTERIZATION OF WIDESPREAD FATIGUE DAMAGE IN FUSELAGE STRUCTURE
Robert S. Piascik, Scott A. Willard (Lockheed Engineering and Sciences

Co., Hampton, VA.), and Matthew Miller (Boeing Commercial Airplane Co., Seattle, WA.) *In its* FAA/NASA International Symposium on Advanced Structural Integrity Methods for Airframe Durability and Damage Tolerance, Part 2 Sep. 1994 p 563-579 (For primary document see N95-19468 05-03)
Avail: CASI HC A03/MF A04

N95-19473*# Georgia Inst. of Tech., Atlanta, GA. Computational Modeling Center.
DISCRETE CRACK GROWTH ANALYSIS METHODOLOGY FOR THROUGH CRACKS IN PRESSURIZED FUSELAGE STRUCTURES
David O. Potyondy, Paul A. Wawrzynek (Cornell Univ., Ithaca, NY.), and Anthony R. Ingraffea (Cornell Univ., Ithaca, NY.) *In* NASA. Langley Research Center, FAA/NASA International Symposium on Advanced Structural Integrity Methods for Airframe Durability and Damage Tolerance, Part 2 Sep. 1994 p 581-601 (For primary document see N95-19468 05-03)
(Grant NAG1-1184)
Avail: CASI HC A03/MF A04

N95-19474*# Victoria Univ. (British Columbia).
A NEW STOCHASTIC SYSTEMS APPROACH TO STRUCTURAL INTEGRITY
James W. Provan and Khalil Farhangdoost (McGill Univ., Montreal, Quebec.) *In* NASA. Langley Research Center, FAA/NASA International Symposium on Advanced Structural Integrity Methods for Airframe Durability and Damage Tolerance, Part 2 Sep. 1994 p 603-619 (For primary document see N95-19468 05-03)
Avail: CASI HC A03/MF A04

N95-19475*# Central Aerohydrodynamics Inst., Zhukovsky (Russia).
FATIGUE AND DAMAGE TOLERANCE SCATTER MODELS
Veniamin L. Raikher *In* NASA. Langley Research Center, FAA/NASA International Symposium on Advanced Structural Integrity Methods for Airframe Durability and Damage Tolerance, Part 2 Sep. 1994 p 621-633 (For primary document see N95-19468 05-03)
Avail: CASI HC A03/MF A04

N95-19476*# Purdue Univ., West Lafayette, IN. School of Mechanical Engineering.
A PROBABILISTIC FATIGUE ANALYSIS OF MULTIPLE SITE DAMAGE
S. M. Rohrbaugh, D. Ruff, B. M. Hillberry, G. McCabe, and A. F. Grandt, Jr. *In* NASA. Langley Research Center, FAA/NASA International Symposium on Advanced Structural Integrity Methods for Airframe Durability and Damage Tolerance, Part 2 Sep. 1994 p 635-651 (For primary document see N95-19468 05-03)
(Contract F49620-93-1-0377)
Avail: CASI HC A03/MF A04

N95-19477*# Foster-Miller Associates, Inc., Waltham, MA.
EVALUATION OF THE FUSELAGE LAP JOINT FATIGUE AND TERMINATING ACTION REPAIR
Gopal Samavedam, Douglas Thomson, and David Y. Jeong (Department of Transportation, Cambridge, MA.) *In* NASA. Langley Research Center, FAA/NASA International Symposium on Advanced Structural Integrity Methods for Airframe Durability and Damage Tolerance, Part 2 Sep. 1994 p 653-663 Sponsored by FAA (For primary document see N95-19468 05-03)
Avail: CASI HC A03/MF A04

N95-19481*# College of New Jersey, Pomona, NJ.
THE LOAD SEPARATION TECHNIQUE IN THE ELASTIC-PLASTIC FRACTURE ANALYSIS OF TWO- AND THREE-DIMENSIONAL GEOMETRIES
Monir H. Sharobeam *In* NASA. Langley Research Center, FAA/NASA International Symposium on Advanced Structural Integrity Methods for Airframe Durability and Damage Tolerance, Part 2 Sep. 1994 p 703-724 (For primary document see N95-19468 05-03)
Avail: CASI HC A03/MF A04

N95-19483*# Boeing Commercial Airplane Co., Seattle, WA.
THE APPLICATION OF NEWMAN CRACK-CLOSURE MODEL TO PREDICTING FATIGUE CRACK GROWTH
Erjian Si (Shanghai Aircraft Research Inst., Shanghai, China.) *In* NASA. Langley Research Center, FAA/NASA International Symposium on Advanced Structural Integrity Methods for Airframe Durability and Damage Tolerance, Part 2 Sep. 1994 p 741-753 (For primary document see N95-19468 05-03)
Avail: CASI HC A03/MF A04

N95-19484*# Bahrain Univ., Issa Town (Bharain). College of Engineering.
FATIGUE CRACK GROWTH UNDER VARIABLE AMPLITUDE LOADING
Jihad A. Sidawi *In* NASA. Langley Research Center, FAA/NASA International Symposium on Advanced Structural Integrity Methods for Airframe Durability and Damage Tolerance, Part 2 Sep. 1994 p 755-770 (For primary document see N95-19468 05-03)
Avail: CASI HC A03/MF A04

N95-19487*# Agency for the Assessment and Application of Technology (Indonesia).
NEAR TIP STRESS AND STRAIN FIELDS FOR SHORT ELASTIC CRACKS
A. H. Soediono, G. A. Kardomateas (Georgia Inst. of Tech., Atlanta, GA.), and R. L. Carlson (Georgia Inst. of Tech., Atlanta, GA.) *In* NASA. Langley Research Center, FAA/NASA International Symposium on Advanced Structural Integrity Methods for Airframe Durability and Damage Tolerance, Part 2 Sep. 1994 p 801-828 (For primary document see N95-19468 05-03)
(Contract F09603-85-G-3104)
Avail: CASI HC A03/MF A04

N95-19492*# Open Univ., Milton Keynes (England). Fracture Research Group.
ON THE MEASUREMENT OF THE CRACK TIP STRESS FIELD AS A MEANS OF DETERMINING DELTA K(SUB eff) UNDER CONDITIONS OF FATIGUE CRACK CLOSURE
Ian R. Wallhead, Lyndon Edwards, and Peter Poole (Defence Research Agency, Farnborough, Hampshire, England.) *In* NASA. Langley Research Center, FAA/NASA International Symposium on Advanced Structural Integrity Methods for Airframe Durability and Damage Tolerance, Part 2 Sep. 1994 p 933-946 Sponsored by Dept. of Trade and Industry (For primary document see N95-19468 05-03)
Avail: CASI HC A03/MF A04

N95-19493*# Southwest Research Inst., San Antonio, TX. Aerospace and Reliability Engineering Dept.
ANALYSIS OF COLD WORKED HOLES FOR STRUCTURAL LIFE EXTENSION
David H. Wieland, Jon T. Cutshall, O. Hal Burnside, and Joseph W. Cardinal *In* NASA. Langley Research Center, FAA/NASA International Symposium on Advanced Structural Integrity Methods for Airframe Durability and Damage Tolerance, Part 2 Sep. 1994 p 947-961 (For primary document see N95-19468 05-03)
Avail: CASI HC A03/MF A04

N95-19496*# Aluminum Co. of America, Alcoa Center, PA.
PREDICTION OF R-CURVES FROM SMALL COUPON TESTS
J. R. Yeh, G. H. Bray, R. J. Bucci, and Y. Macheret *In* NASA. Langley Research Center, FAA/NASA International Symposium on Advanced Structural Integrity Methods for Airframe Durability and Damage Tolerance, Part 2 Sep. 1994 p 999-1013 (For primary document see N95-19468 05-03)
Avail: CASI HC A03/MF A04

N95-19498*# National Aeronautics and Space Administration. Langley Research Center, Hampton, VA.
STRESS INTENSITY FACTORS FOR SURFACE AND CORNER CRACKS EMANATING FROM A WEDGE-LOADED HOLE
W. Zhao (South Carolina Univ., Columbia, SC.), M. A. Sutton (South Carolina Univ., Columbia, SC.), K. N. Shivakumar (North Carolina Agricultural and Technical State Univ., Greensboro, NC.), and J. C. Newman, Jr. *In its*

FAA/NASA International Symposium on Advanced Structural Integrity Methods for Airframe Durability and Damage Tolerance, Part 2 Sep. 1994 p 1029-1043 (For primary document see N95-19468 05-03)
(Grant NAG1-1489)
Avail: CASI HC A03/MF A04

N95-19500*# West Coast Industries, Inc., Seattle, WA.
SPLIT MANDREL VERSUS SPLIT SLEEVE COLDWORKING: DUAL METHODS FOR EXTENDING THE FATIGUE LIFE OF METAL STRUCTURES
Geoffrey A. Rodman and Matthew Creager (Structural Integrity Engineering, Chatsworth, CA.) *In* NASA. Langley Research Center, FAA/NASA International Symposium on Advanced Structural Integrity Methods for Airframe Durability and Damage Tolerance, Part 2 Sep. 1994 p 1077-1086 (For primary document see N95-19468 05-03)
Avail: CASI HC A02/MF A04

42 GEOSCIENCES (GENERAL)

N95-18145# Pacific Northwest Lab., Richland, WA.
EMEFS: LESSONS LEARNED 2, MODEL EVALUATION
W. R. Barchet and R. L. Dennis (National Oceanic and Atmospheric Administration, Research Triangle Park, NC.) Nov. 1993 7 p Presented at the International Conference on Regional Photochemical Air Quality Measurement and Modeling Studies, San Diego, CA, 9-11 Nov. 1993
(Contract DE-AC06-76RL-01830)
(DE94-017468; PNL-SA-23179; CONF-931130-1) Avail: CASI HC A02/MF A01

Responsibility for the design, implementation and interpretation of an evaluation of the Regional Acid Deposition Model and the Acid Deposition and Oxidant Model was given to the Model Evaluation Team. This paper presents lessons learned from the design and implementation of the Eulerian Model Evaluation Field Study (EMEFS) protocol for model evaluation, and the interpretation of evaluation results. These lessons can benefit future model evaluation efforts. The EMEFS model evaluation protocol required a blend of operational and diagnostic testing to meet the needs of the applications of the model(s). Multiple tests and tests over multiple chemical systems were needed to stress the model and gain diagnostic insight into model performance. The protocol provided a frame of reference but not rigid procedures for testing the models. Scatter plots comparing model output with observations that included a tendency line an confidence intervals were found most informative. Spatial commensurability between observations and simulations was much more difficult to achieve than temporal commensurability. We found that fundamental features of the design of the model give rise to inherent biases in comparisons to observations. Participation of model developers allowed for rapid modification of models in response to evaluation findings. The combination of operational and diagnostic evaluation and close involvement of model developers in the evaluation process made possible a complete cycle of evaluation, revision, and retesting before the model was applied. DOE

43 EARTH RESOURCES AND REMOTE SENSING

Includes remote sensing of earth resources by aircraft and spacecraft; photogrammetry; and aerial photography.
For instrumentation see *35 Instrumentation and Photography.*

N95-17971# Ohio State Univ., Columbus. Dept. of Geodetic Science and Surveying.
DEFINITION AND REALIZATION OF A GLOBAL VERTICAL DATUM
Nagarajan Balasubramania Apr. 1994 109 p
(Contract F19628-93-K-0033)
(AD-A283303; TR-427; PL-TR-94-2144; SR-1) Avail: CASI HC A06/MF A01

The requirements for defining and realizing a global vertical datum (GVD) with a precision on the dm, or even cm, level has become essential now, due to the improved measurement accuracy provided by the space geodetic techniques. This study identifies the different approaches in which such a global vertical datum could be evolved. The first approach, which can be considered as an ideal approach, uses the best available geocentric station positions from present and future space geodetic networks, highly accurate geopotential model, and surface gravity data around the space stations for defining and realizing a global vertical datum. The other simplified approach, which can be considered more of an operational development with a short time framework, is mainly dependent on the widely available GPS and DORIS tracking networks and accurate geoid height models for the GVD development. After a review of the various heights and height systems that are in use today, detailed mathematical procedures for setting up the observation equations to define a global vertical datum in a least-squares sense, under different data scenarios, are discussed. A test computation to realize the first iteration global vertical datum with available data at 17 space geodetic stations in six regional vertical datums is also included. The gravimetric height anomaly/undulation computations at the space geodetic stations required in the test computation have been performed using both modified Stokes' technique and least-squares collocation technique combining surface gravity data in a small cap around the stations with potential coefficients from OSU91A model. DTIC

N95-18005# Instituto de Pesquisas Espaciais, Sao Jose dos Campos (Brazil).
COMPARATIVE ANALYSIS OF MULTISENSOR (TM/LANDSAT AND SAR/ERS-1) AND MULTITEMPORAL SCENES OF GUAIRA REGION, SAO PAULO STATE, BRAZIL M.S. Thesis [ANALISE COMPARATIVA DE IMAGENS MULTISSENSORES (TM/LANDSAT E SAR/ERS-1) E MULTITEMPORAIS, NA REGIAO DE GUAIRA, SP]
Darcton Policarpo Damiao Apr. 1994 121 p In PORTUGESE
(INPE-5581-TDI/544) Avail: CASI HC A06/MF A02

The present work is intended to analyze and compare two data sets of different sensor systems, acquired in a short period of time and in two opposite seasons (winter and summer). To establish the comparison, two approaches were adopted: the first, qualitative, after visual interpretation of the data allied with information obtained from field work; and the second, a quantitative approach, in which the Kappa coefficient was applied and tested after the visual interpretation. The results of the first approach matched those obtained with the second ones, showing that merging multisensor imagery is a powerful technique, especially considering its use with some other approaches, like principal component and intensity-hue-saturation (IHS) transforms. One of the conclusions is that it's essential to avoid, as far as possible, large temporal gaps among the merging images. Furthermore, it's critical to make an efficient registration, taking into account that the reference image must be the one acquired by the optical sensor system. Finally, the analysis of main results showed that the SAR/ERS-1 scenes used in this work appear to be more sensitive to permittivity than to roughness, contrary to what was expected. Perhaps this is because of an imprecise pre-processing of the images.
Author (revised)

N95-18035# German Military Geophysical Office, Traben-Trarbach (Germany).
ESTIMATION OF SATELLITE DERIVED TEMPERATURE AND MOISTURE FIELDS OVER EUROPE FROM TOVS DATA USING 3I AND ITPP ALGORITHMS Final Report, Nov. 1990 - Jun. 1992
K. D. Klaes 18 Apr. 1994 48 p
(AF Proj. 6670)
(AD-A284581; PL-TR-94-2192; AD-E202165) Avail: CASI HC A03/MF A01

The results of two TOVS retrieval algorithms in determining the three-dimensional temperature and water vapor fields from NOAA polar orbiting satellite data are presented. Derived products, specifically the 500 to 1000 mb thickness field and the integrated tropospheric water vapor (precipitable water) field, are derived for the northwestern European area on 13 August 1990. Comparisons with the in-situ radiosonde measurements and numerical weather analysis products are made. Overall the fields agree well with the German Weather Service synoptic products and additionally mesoscale features associated with cloud clusters are contained in the satellite derived fields. DTIC

N95-18078 Naval Research Lab., Bay Saint Louis, MS.
DIGITAL MAPPING, CHARTING, AND GEODESY ANALYSIS PROGRAM TECHNICAL REVIEW OF DIGITAL AERONAUTICAL FLIGHT INFORMATION DATA PROTOTYPE 1.0 ON CD-ROM Final Report
Hillary Mesick, Kevin Shaw, Susan Carter, Ruth Guidry, and Steven Kuder 12 Aug. 1994 12 p Limited Reproducibility: More than 20% of this document may be affected by microfiche quality
(AD-A284728; NRL/MR/7441-94-7549) Avail: CASI HC A03

The Naval Research Laboratory's Digital Mapping, Charting, and Geodesy Analysis Program (DMAP) has performed a technical review of Prototype 1.0 of Digital Aeronautical Flight Information Data (DAFID). For the first time, this information is available on Compact Disk-Read Only Memory. The DAFID database was created to allow quicker access to the data due to its format standardization and more divided structure. It also includes a digital 28-day Global Positioning System almanac and programs in FORTRAN and BASIC for calculating magnetic data. A few recommendations for improvement are made by DMAP. DTIC

N95-18214# Instituto de Pesquisas Espaciais, Sao Jose dos Campos (Brazil).
HEURISTIC INFERENCE ABOUT FLOW DIRECTIONS IN RIVER NETWORKS M.S. Thesis [INFERENCIA HEURISTICA SOBRE DIRECOES DE FLUXO EM REDES DE DRENAGEM]
Joao ArgemirodeCarvalhoPaiva Nov. 1994 106 p In PORTUGESE
(INPE-5588-TDI/550) Avail: CASI HC A06/MF A02

Humans are very good in deriving flow directions of a river network from such representations as photographs or remotely sensed images. Apparently, the 2-dimensional geometry of the network is in most cases sufficient to derive its sources and destinations by reasoning about the flow directions of a river network, and they need no additional information about slopes or heights. Formalizing the problem such that it can be automatically solved, however, has proven to be an extremely difficult task. Within the realm of the inference process about flow directions in river networks, a particularly important problem is the analysis of relevant hydrological features. This thesis work describes the development of a study for river networks and formalizes the features in terms of a graph. It is shown how certain reasoning processes, simplifying the complexity of a river network, can be expressed as graph operations. Besides, a computational model to derive the destination of a river network is proposed. It is based on the connectivity of channels and the angles at which channels intersect at junctions. Author

N95-18215# Instituto de Pesquisas Espaciais, Sao Jose dos Campos (Brazil).
THEMATIC CLASSIFICATION OF ZONE COASTAL: A METHODOLOGIC CONTRIBUTION M.S. Thesis [CLASSIFICACAO TEMATICA DE AREAS LITORANEAS: UMA CONTRIBUICAO METODOLOGICA]
Heraldo Soares Caldeira Sep. 1994 145 p In PORTUGESE
(INPE-5586-TDI/548) Avail: CASI HC A07/MF A02

In this study, Remote Sensing techniques and Geographical Information System (GIS) were used for land use and vegetation cover classification over coastal zones. The results give support to the elaboration and updating of nautical charts. The study was carried out using TM/Landsat imagery and aerial photographs over the Itaoca region, located in the State of Espirito Santo. Three classification algorithms were used: supervised, non-supervised and hybrids. The Kappa statistics was used to evaluate the accuracy of the results from the different methods. Author

N95-18216# Instituto de Pesquisas Espaciais, Sao Paulo (Brazil). Div. de Processamento de Imagens.
ON THE OPTIMIZATION OF SPECKLE FILTERING TECHNIQUES FOR ERS-1 IMAGES OVER ARGENTINA
Alejandro Cortese (Buenos Aires Univ., Argentina.), Laura Frulla (CAERCEM, Buenos Aires, Argentina.), Julio JacoboBerlles (Buenos Aires Univ., Argentina.), Alejandro C. Frery, and Marta Mejail (Buenos Aires Univ., Argentina.) 30 Sep. 1994 8 p Presented at the International Symposium on Resource and Environment Monitoring, Rio de Janeiro, Brazil, 26-30 Sept. 1994
(INPE-5578-PRE/1806) Avail: CASI HC A02/MF A01

SAR images provide detailed information about the target surface, though it is obscured by the well-known speckle effect. One alternative of speckle reduction is by filtering the image, but this demands some assumptions about the speckle behavior. However, it is important to take into account that noise reduction filters tend to blur the edges and sharp features of the images, since they always introduce some kind of low pass effect. Several filters have been developed for the speckle reduction, and most of them are of the form of a window that slides over the image. But there is no automatic process to determine the window size, a relevant parameter that depends, among other things, on the features of the studied area. Given a filter, it can be applied to the SAR image for different windows then it is possible to estimate the so-called speckle index as a measure that provides the best speckle reduction in accordance to the degree of heterogeneity of the region under study. In this paper the type of filter which better reduces the speckle in homogeneous and heterogeneous regions is determined. Moreover, it is possible to draw conclusions about the optimal window size used when the filter is applied. Author

N95-18368# Instituto de Pesquisas Espaciais, Sao Jose dos Campos (Brazil).
REMOTE SENSING PRODUCTS EVALUATION FOR CARTOGRAPHIC UPDATING PURPOSES M.S. Thesis [AVALIACAO DE PRODUTOS DE SENSORIAMENTO REMOTO PARA FINS DE ATUALIZACAO CARTOGRAFICA]
Oscar Ricardo Vergara Apr. 1994 151 p In PORTUGESE Original contains color illustrations
(INPE-5584-TDI/546) Avail: CASI HC A08/MF A02

The lack of updated cartographic documents shows the need of developing methodologies for updating cartographic maps which may decrease time and resource expenditures. Considering the advantages derived from the use of satellite Remote Sensing data for cartographic purposes, the objective of this work is to evaluate the performance of orbital images generated by INPE, in the context of methodologies for cartographic updating. In order to accomplish this task, the information content of different data sets for updating of 1:50,000 scale topographic maps is assessed: (Band 3 and color composition BGR 2,3,4 TM-Landsat; panchromatic and multispectral BGR 1,2,3 HRV-SPOT; hybrids products). Also studied is the geometric accuracy attainable through the use of these products in an analogical and digital format, when integrated with PROCOM-2 and SITIM/SGI systems, respectively. The results show that, in spite of some restrictions, these images provide a considerable amount of thematic information present in topographic maps at the scale of this work. The geometric evaluations show that mapping on a 1:50,000 scale cartographic base, corrected TM-Landsat and level 1B HRV-SPOT slides allow the accomplishment of cartographic updating in 1:250,000 scale. There is also the possibility of working in 1:100,000 scale. Digital images MRV-SPOT (level 1B) geometrically corrected through image/map registration, allow the achievement of geometric accuracy of class A, 1:50,000 scale topographic maps. Author (revised)

N95-18369# Instituto de Pesquisas Espaciais, Sao Jose dos Campos (Brazil).
THE PHOTOGRAPHIC SYSTEM GLOBAL EVALUATION FOR GENERATION OF INPE TM LANDSAT IMAGE M.S. Thesis [AVALIACAO GLOBAL DO SISTEMA FOTOGRAFICO PARA GERACAO DE IMAGEM LANDSAT TM DO INPE]
Luis Geraldo Ferreira Jan. 1994 135 p In PORTUGESE
(INPE-5571-TDI/542) Avail: CASI HC A07/MF A02

This paper includes a study turned to the quality of the orbital photographic product related to interferences of the photographic processing on radiometric value recorded on the final product. The proposal was to perform the following items: (1) to evaluate the photographic Landsat image production flow of INPE (Brazilian Institute for Space Research); (2) to discuss the whole production process stage by stage; (3) to compare proceedings and quality control parameter of the most significant Landsat data distribution centers of the world; (4) to discuss the processing conditions by means of densitometric evaluations and measurements of Modulation Transfer Function (MTF); (5) to recommend a new production on densitometric curve of the photographic master and a new evaluation of the densitometric parameters for monitoring the Black and White Film Transparency product; and (6) to recommend photographic materials and supplies to form images on photographic papers aiming better records of information and details. Author

N95-18372 Norwegian Hydrodynamic Labs., Trondheim (Norway).
PREDICTION OF BUOYANT OUTFLOW IN LAKES AND FJORDS WITH A QUASI 3D NUMERICAL MODEL
B. Broers 26 Nov. 1993 42 p Prepared in cooperation with Selskapet for Industriell og Teknisk Forskning, Trondheim, Norway
(PB94-206984; STF60-A93095) Avail: Issuing Activity (National Technical Information Service (NTIS))

A quasi three-dimensional model is presented and applied to some problems related to outflow of rivers into a recipient with different density. A finite element formulation is used. The predictions of a salt wedge and a surface plume of brackish water into the sea are in good agreement with available data. Different types of river outflow (along the surface, along a pycnocline or along the bottom) into a lake is demonstrated with and without Coriolis effects. NTIS

N95-18465*# National Aeronautics and Space Administration. Langley Research Center, Hampton, VA.
MISSION DESCRIPTION AND IN-FLIGHT OPERATIONS OF ERBE INSTRUMENTS ON ERBS AND NOAA 10 SPACECRAFT, FEBRUARY 1987 - FEBRUARY 1990
Kathryn A. Busch (Science Applications International Corp., Hampton, VA.) and Keith T. Degnan (Science Applications International Corp., Hampton, VA.) Nov. 1994 464 p
(RTOP 665-45-20-01)
(NASA-RP-1325; L-17335; NAS 1.61:1325) Avail: CASI HC A20/MF A04

Instruments of the Earth Radiation Budget Experiment (ERBE) are operating on three different Earth-orbiting spacecraft. The Earth Radiation Budget Satellite (ERBS) is operated by the National Aeronautics and Space Administration (NASA), and the NOAA 9 and NOAA 10 weather satellites are operated by the National Oceanic and Atmospheric Administration (NOAA). This paper is the third in a series that describes the ERBE mission in-orbit environments, instrument design and operational features, and data processing and validation procedures. This paper describes the in-flight operations for the ERBE instruments aboard the ERBS and NOAA 10 spacecraft for the period from February 1987 through February 1990. Validation and archival of radiation measurements made by ERBE instruments during this period were completed in May 1992. This paper covers normal and special operations of the spacecraft and instruments, operational anomalies, and the responses of the instruments to in-orbit and seasonal variations in the solar environment. Author

N95-18556 Oak Ridge National Lab., TN.
IMAGE ACCURACY AND REPRESENTATIONAL ENHANCEMENT THROUGH LOW-LEVEL, MULTI-SENSOR INTEGRATION TECHNIQUES
J. E. Baker 1994 18 p Presented at the Society of Photo-Optical Instrumentation Engineers (SPIE) OE/Aerospace Science and Sensing Meeting, Orlando, FL, 11-16 Apr. 1993 Limited Reproducibility: More than 20% of this document may be affected by microfiche quality
(Contract DE-AC05-84OR-21400)
(DE94-018661; CONF-930445-29) Avail: CASI HC A03

Multi-Sensor Integration (MSI) is the combining of data and information from more than one source in order to generate a more reliable and consistent representation of the environment. The need for MSI derives largely from basic ambiguities inherent in our current sensor imaging technologies. These ambiguities exist as long as the mapping from reality to image is not 1-to-1. That is, if different 'realities' lead to identical images, a single image cannot reveal the particular reality which was the truth. MSI techniques attempt to resolve some of these ambiguities by appropriately coupling complementary images to eliminate possible inverse mappings. What constitutes the best MSI technique is dependent on the given application domain, available sensors, and task requirements. MSI techniques can be divided into three categories based on the relative information content of the original images with that of the desired representation: (1) 'detail enhancement,' wherein the relative information content of the original images is less rich than the desired representation; (2) 'data enhancement,' wherein the MSI techniques are concerned with improving the accuracy of the data rather than either increasing or decreasing the level of detail; and (3) 'conceptual enhancement,' wherein the image contains more detail than is desired, making it difficult to easily recognize objects of interest. In conceptual enhancement one must group pixels corresponding to the same conceptual object and thereby reduce the level of extraneous detail. DOE

N95-18614# Army Topographic Engineering Center, Fort Belvoir, VA.
SPECTRAL REFLECTANCE PROPERTIES OF WETLANDS PLANTS
John E. Anderson Aug. 1994 10 p
(AD-A283546; R-234) Avail: CASI HC A02/MF A01

Wetlands occupy a unique position on the landscape. Being neither fully aquatic nor terrestrial, they are poorly understood from a standpoint of seasonal characterization and detection using spectral sensors. Wetlands ecotones and their associated plant communities offer a seasonally dynamic ecology which is governed primarily by fluctuations in local hydrologic regimes. Biogeochemical dynamics, caused by fluctuations in hydrology, work to manifest changes in plant physiology and provide a challenge for the spectral characterization and detection of wetlands. This paper presents information on the spectral reflectance characteristics of wetland plants and attempts to relate changes in spectral reflectance to the seasonal stresses experienced by wetlands plant communities. DTIC

N95-18739*# University of South Florida, Saint Petersburg, FL. Dept. of Marine Science.
VISIBLE-INFRARED REMOTE-SENSING MODEL AND APPLICATIONS FOR OCEAN WATERS Ph.D. Thesis
Zhongping Lee Dec. 1994 163 p
(Contract NAS5-31716)
(NASA-CR-197602; NAS 1.26:197602) Avail: CASI HC A01/MF A01

Remote sensing has become important in the ocean sciences, especially for research involving large spatial scales. To estimate the in-water constituents through remote sensing, whether carried out by satellite or airplane, the signal emitted from beneath the sea surface, the so called water-leaving radiance (L(w)), is of prime importance. The magnitude of L(w) depends on two terms: one is the intensity of the solar input, and the other is the reflectance of the in-water constituents. The ratio of the water-leaving radiance to the downwelling irradiance (E(d)) above the sear surface (remote-sensing reflectance, R(sub rs)) is independent of the intensity of the irradiance input, and is largely a function of the optical properties of the in-water constituents. In this work, a model is developed to interpret r(sub rs) for ocean water in the visible-infrared range. In addition to terms for the radiance scattered from molecules and particles, the model includes terms that describe contributions from bottom reflectance, fluorescence of gelbstoff or colored dissolved organic matter (CDOM), and water Raman scattering. By using this model, the measured R(sub rs) of waters from the West Florida Shelf to the Mississippi River plume, which covered a (concentration of chlorophyll a) range of 0.07 - 50 mg/cu m, were well interpreted. The average percentage difference (a.p.d.) between the measured and modeled R(sub rs) is 3.4%, and, for the shallow waters, the model-required water depth is within 10% of the chart depth. Simple mathematical simulations for the phytoplankton pigment absorption coefficient (a(sub theta)) are suggested for using the R(sub rs) model. The inverse problem of R(sub rs), which is to analytically derive the in-water constituents from R(sub rs) data alone, can be solved using the a(sub theta) functions without prior knowledge of the in-water optical properties. More importantly, this method avoids problems associated with a need for knowledge of the shape and value of the chlorophyll-specific absorption coefficient. The simulation was tested for a wide range of water types, including waters from Monterey Bay, the West Florida Shelf, and the Mississippi River plume. Using the simulation, the R(sub rs)-derived in-water absorption coefficients were consistent with the values from in-water measurements (r(exp 2) greater than 0.94, slope approximately 1.0). In the remote-sensing applications, a new approach is suggested for the estimation of primary production based on remote sensing. Using this approach, the calculated primary production (PP) values based upon remotely sensed data were very close to the measured values for the euphotic zone (r(exp 2) = 0.95, slope 1.26, and 32% average difference), while traditional, pigment-based PP model provided values only one-third the size of the measured data. This indicates a potential to significantly improve the accuracy of the estimation of primary production based upon remote sensing. Author

N95-18952*# Colorado Univ., Boulder, CO. Cooperative Inst. for Research in Environmental Sciences.

ICE SURFACE TEMPERATURE RETRIEVAL FROM AVHRR, ATSR, AND PASSIVE MICROWAVE SATELLITE DATA: ALGORITHM DEVELOPMENT AND APPLICATION Semiannual report no. 2

Jeff Key, James Maslanik, and Konrad Steffen 15 Nov. 1994 13 p (Grant NAGw-3437)

(NASA-CR-197542; NAS 1.26:197542) Avail: CASI HC A03/MF A01

During the first half of our second project year we have accomplished the following: (1) acquired a new AVHRR data set for the Beaufort Sea area spanning an entire year; (2) acquired additional ATSR data for the Arctic and Antarctic now totaling over seven months; (3) refined our AVHRR Arctic and Antarctic ice surface temperature (IST) retrieval algorithm, including work specific to Greenland; (4) developed ATSR retrieval algorithms for the Arctic and Antarctic, including work specific to Greenland; (5) investigated the effects of clouds and the atmosphere on passive microwave 'surface' temperature retrieval algorithms; (6) generated surface temperatures for the Beaufort Sea data set, both from AVHRR and SSM/I; and (7) continued work on compositing GAC data for coverage of the entire Arctic and Antarctic. During the second half of the year we will continue along these same lines, and will undertake a detailed validation study of the AVHRR and ATSR retrievals using LEADEX and the Beaufort Sea year-long data. Cloud masking methods used for the AVHRR will be modified for use with the ATSR. Methods of blending in situ and satellite-derived surface temperature data sets will be investigated. Author

N95-19126*# Purdue Univ., West Lafayette, IN. School of Electrical Engineering.

HYPERSPECTRAL DATA ANALYSIS PROCEDURES WITH REDUCED SENSITIVITY TO NOISE

David A. Landgrebe 1993 6 p Presented at the Workshop on Atmospheric Correction of Landsat Imagery, Torrance, CA, 29 Jun. - 1 Jul. 1993

(Grant NAGw-925)

(NASA-CR-197621; NAS 1.26:197621) Avail: CASI HC A02/MF A01

Multispectral sensor systems have become steadily improved over the years in their ability to deliver increased spectral detail. With the advent of hyperspectral sensors, including imaging spectrometers, this technology is in the process of taking a large leap forward, thus providing the possibility of enabling delivery of much more detailed information. However, this direction of development has drawn even more attention to the matter of noise and other deleterious effects in the data, because reducing the fundamental limitations of spectral detail on information collection raises the limitations presented by noise to even greater importance. Much current effort in remote sensing research is thus being devoted to adjusting the data to mitigate the effects of noise and other deleterious effects. A parallel approach to the problem is to look for analysis approaches and procedures which have reduced sensitivity to such effects. We discuss some of the fundamental principles which define analysis algorithm characteristics providing such reduced sensitivity. One such analysis procedure including an example analysis of a data set is described, illustrating this effect. Author (revised)

N95-19733 Naval Research Lab., Bay Saint Louis, MS.

DIGITAL MAPPING, CHARTING, AND GEODESY ANALYSIS PROGRAM TECHNICAL REVIEW OF RASTER PRODUCT FORMAT (RPF) AND SCANNED MAP (SMap) Final Report

H. V. Miller, Tom Fetterer, Danette Coughlan, Kevin Shaw, and Susan Carter 25 Jul. 1994 10 p Limited Reproducibility: More than 20% of this document may be affected by microfiche quality

(AD-A284267; NRL/MR/7441-94-7538) Avail: CASI HC A02

As part of its effort to adopt a triad of standards for vector, text, and raster data sets, the Defense Mapping Agency, via the Oceanographer of the Navy, has requested input from the Naval Research Laboratory's Digital Mapping, Charting, and Analysis Program (DMAP) regarding the raster product format (RPF). This format is intended to satisfy the requirement for a raster standard, and to complement the already-existing vector product format (VPF) and proposed text product standard. In its evaluation, DMAP addresses several issues, ranging from specific editorial comments about the documents to more general comments on interoperability with other standards. DMAP reports that RPF, as a stand-alone format, is acceptable; however, from the triad point-of-view, RPF should more closely resemble the VPF, particularly with respect to metadata management. An implementation of the RPF, namely Scanned Map, is also analyzed by DMAP. DTIC

N95-19734 Army Topographic Engineering Center, Fort Belvoir, VA.

ISSSR TUTORIAL 1: INTRODUCTION TO SPECTRAL REMOTE SENSING Scientific Paper

John Rinker Aug. 1994 41 p Limited Reproducibility: More than 20% of this document may be affected by microfiche quality

(AD-A284268; USATEC-R-238) Avail: CASI HC A03

This tutorial, the first of a linked set of four, provides an introduction to remote sensing as a tool for studying the earth, its land, water bodies, cultural components, and surrounding atmosphere. The basis for this capability is the recording of reflected, emitted, and luminesced photons, usually in the form of images, and the subsequent interpretation of image patterns for terrain information (manual analysis), and of spectral patterns for targeting, monitoring, and change detection (computer and digital analysis). Included are brief reviews of: radiation characteristics such as bandwidth, interference, absorption, reflectance, emittance, and luminescence; optical attributes such as focus and resolution; research in spectral measurements; and application examples from various remote sensing systems. This leads to Tutorial 2 on spectral measurements, thence to Tutorial 3 on the digital analysis of imaging spectrometer data, and to Tutorial 4 on the characteristics of available remote sensing systems. DTIC

N95-19016*# University of Western Carolina, Cullowhee, NC. Dept. of mathematics and Computer Science.

A TECHNIQUE FOR DETERMINING CLOUD FREE VERSUS CLOUD CONTAMINATED PIXELS IN SATELLITE IMAGERY

Richard A. Wohlman *In* Alabama Univ., Research Reports: 1994 NASA/ASEE Summer Faculty Fellowship Program Oct. 1994 5 p (For primary document see N95-18967 05-80)

Avail: CASI HC A01/MF A03

44 ENERGY PRODUCTION AND CONVERSION

Includes specific energy conversion systems, e.g., fuel cells; global sources of energy; geophysical conversion; and windpower.

For related information see also *07 Aircraft Propulsion and Power, 20 Spacecraft Propulsion and Power,* and *28 Propellants and Fuels.*

N95-17945# National Renewable Energy Lab., Golden, CO.

THERMOPHOTOVOLTAICS BIBLIOGRAPHY

L. Broman Sep. 1994 23 p

(Contract DE-AC36-83CH-10093)

(DE94-011898; NREL/TP-412-6845) Avail: CASI HC A03/MF A01

A bibliography containing 180 entries on thermophotovoltaic conversion of energy between 1950 and 1994 has been compiled. The entries are categorized with respect to type and contents. DOE

N95-18011 Spire Corp., Bedford, MA.

InP SOLAR CELL DEVELOPMENT ON INEXPENSIVE SILICON SUBSTRATES Quarterly Progress Report, 22 Feb. - 22 May 1994

Steven J. Wojtczuk 16 Aug. 1994 9 p Limited Reproducibility: More than 20% of this document may be affected by microfiche quality

(Contract N00014-94-C-2030)

(AD-A283624) Avail: CASI HC A02

Optimize Emitter/Base Dopants - In this section, we describe some of the differences between Spire's previous N-on-P technology and the P-on-N technology being developed for this program. Results of a 17% P/N InP cell, the best made to date are also summarized. The main reason for the change to a P/N cell is that P/N heteroepitaxial InP cells on Si wafers do not have an unintentional back-biased junction at the InP/Si interface that occurs in N/P heteroepitaxial cells. For the same emitter thickness, a P/N InP cell has about 100X higher sheet resistance than the N/P cell. In Phase 1, Spire attempted to keep the sheet resistance loss of the new P/N cells approximately the same as the 19% N/P cells with 300 A emitters and gridlines on 700 micrometers center-to-center spacings. This resulted in P/N cells with approx. 2400 A emitter thicknesses and 250

micrometers grid spacings. The P/N cells had an 8X thicker emitter, and with the closer gridline spacing had only (250/700) or about 1/3 the photocurrent of the N/P cell flowing to each set of gridlines, so that the closer gridlines reduced the I(squared)R loss by the square of this, or about 8X. DTIC

N95-18435 Naval Postgraduate School, Monterey, CA.
INTERMEDIATE DESIGN AND ANALYSIS OF THE PANSAT ELECTRICAL POWER SUBSYSTEM M.S. Thesis
Gregory F. Hand Mar. 1994 156 p Limited Reproducibility: More than 20% of this document may be affected by microfiche quality
(AD-A283610) Avail: CASI HC A08

This thesis examined three primary components of the electrical power subsystem (EPS) for the Petite Amateur Navy Satellite (PANSAT): (1) the solar array; (2) the power conditioning and control subsystem (PCCS); and (3) the batteries. The emphasis was to analyze the output performance of the solar array. Additionally, the derivation of the hybrid PCCS proposed for the EPS was examined and the use of nickel-cadmium batteries as a candidate for the secondary power source was discussed. The investigation of the solar array's output performance led to PANSAM (PANSAT Solar Array Model), a computer model which simulates the power output of the solar array. The user can specify the sun's declination, the orbit's inclination, and the satellite's orientation and rate of rotation about each of its three axes. Once a simulation is complete, PANSAM provides the effective surface area illuminated by the sun, and the output current and power. The average effective area determined by PANSAM was 17.6% less than the 1259/sq cm originally proposed by the PANSAT staff. This contributed to a substantial reduction in predicted power. A preliminary transient thermal analysis of PANSAT was also conducted to provide temperature data for PANSAM. DTIC

N95-18463# National Renewable Energy Lab., Golden, CO.
PROGRESS IN THE DEVELOPMENT OF ADVANCED SOLAR REFLECTORS
C. Kennedy and G. Jorgensen Jan. 1994 14 p Presented at the 7th International Vacuum Web Coating Conference, Miami, FL, 10-12 Nov. 1994
(Contract DE-AC36-83CH-10093)
(DE94-000264; NREL/TP-471-6092; CONF-941125-1) Avail: CASI HC A03/MF A01

Solar thermal technologies require large mirrors to provide concentrated sunlight for renewable power generation. Such materials must be inexpensive and maintain high specular reflectance for extended lifetimes in severe outdoor environments. Polymer reflectors are lighter than glass mirrors, offer greater system design flexibility, and have the potential for lower cost. During the past year, collaborative cost-shared research and development between the National Renewable Energy Laboratory (NREL) and industrial partners has identified candidate materials that perform better than the state-of-the-art commercial silvered-polymer reflectors in terms of corrosion degradation and resistance to delamination failure. Additional cooperative efforts will produce new alternative materials with reduced costs due to high speed production line capability. NREL welcomes continued and expanded interest and web coating industry involvement in developing advanced solar reflector materials. DOE

N95-18572*# National Aeronautics and Space Administration. Lewis Research Center, Cleveland, OH.
PULSED LASER ILLUMINATION OF PHOTOVOLTAIC CELLS
Jane A. Yater, Roland A. Lowe (Kent State Univ., OH.), Phillip P. Jenkins (NYMA, Inc., Brook Park, OH.), and Geoffrey A. Landis (NYMA, Inc., Brook Park, OH.) Jan. 1995 6 p Presented at the 1st World Conference on Photvoltaic Energy Conversion, Waikoloa, HI, 5-9 Dec. 1994; sponsored by IEEE, PVSEC-Japan, PVSEC-Europe
(RTOP 233-01-OA)
(NASA-TM-106820; E-9362; NAS 1.15:106820) Avail: CASI HC A02/MF A01

In future space missions, free electron lasers (FEL) may be used to illuminate photovoltaic receivers to provide remote power. Both the radio-frequency (RF) and induction FEL produce pulsed rather than continuous output. In this work we investigate cell response to pulsed laser light which simulates the RF FEL format. The results indicate that if the pulse repetition is high, cell efficiencies are only slightly reduced compared to constant illumination at the same wavelength. The frequency response of the cells is weak, with both voltage and current outputs essentially dc in nature. Comparison with previous experiments indicates that the RF FEL pulse format yields more efficient photovoltaic conversion than does an induction FEL format. Author

N95-18587*# National Aeronautics and Space Administration. Lewis Research Center, Cleveland, OH.
THE EFFECT OF TEMPERATURE ON THE RADIATIVE PERFORMANCE OF Ho-YAG THIN FILM SELECTIVE EMITTERS
Roland A. Lowe (Kent State Univ., OH.), Donald L. Chubb, and Brian S. Good Jan. 1995 6 p Presented at the 1st World Conference on Photovoltaic Energy Conversion, Waikoloa, HI, 5-9 Dec. 1994; sponsored by IEEE, PVSEC-Japan and PVSEC- Europe
(RTOP 233-01-0A)
(NASA-TM-106830; E-9380; NAS 1.15:106830) Avail: CASI HC A02/MF A01

We present the emitter efficiency results for the thin film 25 percent Ho YAG (Yttrium Aluminum Garnet, Y3Al5O12) selective emitter from 1000 to 1700 K with a platinum substrate. Spectral emittance and emissive power measurements were made (1.2 less than lambda less than 3.2 microns) and used to calculate the radiative efficiency. The radiative efficiency and power density of rare earth doped selective emitters are strongly dependent on temperature and experimental results indicate an optimum temperature (1650 K for Ho YAG) for thermophotovoltaic (TPV) applications. Author

N95-18894# Duke Univ., Durham, NC. Dept. of Mechanical Engineering and Materials Science.
NOVEL CARBON-ION FUEL CELLS
F. H. Cocks and H. LaViers 19 Apr. 1994 7 p
(Contract DE-FG22-93PC-93219)
(DE94-017390; DOE/PC-93219/T2) Avail: CASI HC A02/MF A01

Apparatuses are being constructed to create pressed and sintered rare-earth carbide pellets for carbon-ion conduction testing. Attempts were made to determined the temperature of crystalline phase transformation of the CeC2 and LaC2 where they change from the alpha CaC2 structure to the beta CaF2 structure. DOE

N95-19074# Argonne National Lab., IL.
MOLTEN CARBONATE FUEL CELL WITH HIGH POWER DENSITY
M. Krumpelt, M. F. Roche, I. Bloom, H. Geyer, and S. Johnson 1994 3 p Presented at the Fuel Cells 1994, Morgantown, WV, 17-19 Aug. 1994
(Contract W-31-109-eng-38)
(DE94-017080; ANL/CMT/CP-83637; CONF-940883-5) Avail: CASI HC A01/MF A01

The objective of this research is a doubling of the current density of the molten carbonate fuel cell (MCFC) from the present value of 1600A/sq m to 3200 A/sq m and a similar increase in the volumetric power density. This project is linked to other projects concerning MCFC's (one on the multiply manifolded MCFC's, the other on lithium ferrate and lithium cobaltate cathodes for MCFC's). DOE

N95-19115# Argonne National Lab., IL.
SEALANT MATERIALS FOR THE SOLID OXIDE FUEL CELL
M. Krumpelt, R. Kumar, I. Bloom, and K. Ley 1994 7 p Presented at the Fuel Cells 1994, Morgantown, WV, 17-19 Aug. 1994
(Contract W-31-109-eng-38)
(DE94-017073; ANL/CMT/CP-83784; CONF-940883-2) Avail: CASI HC A02/MF A01

The objective of this work is to develop sealing materials for solid oxide fuel cells (SOFC's). A suitable sealant must form strong, dense bonds with SOFC components, be chemically stable and mechanically compatible with the components at the operating temperature and over the temperature range of interest, be chemically stable in the operating environment of the SOFC (i.e. H2 and H2O on the anode side, O2 on the cathode side), and must be electrically insulating. DOE

N95-19116# Argonne National Lab., IL.
PITTING CORROSION OF ALUMINIZED SEALS IN MOLTEN CARBONATE FUEL CELLS

M. Krumpelt, M. F. Roche, and I. Bloom 1994 3 p Presented at the Fuel Cells 1994, Morgantown, WV, 17-19 Aug. 1994
(Contract W-31-109-eng-38)
(DE94-017075; ANL/CMT/CP-83647; CONF-940883-4) Avail: CASI HC A01/MF A01

The objective of this research is to gain a better understanding of the corrosion of the aluminized type 316 stainless steel employed in the seal areas of the molten carbonate fuel cell. The seals are formed between the aluminized Type 316 SS surface and the electrolyte (generally a mixture of molten alkali carbonates and lithium aluminate). DOE

N95-19117# Argonne National Lab., IL.
LITHIUM FERRATE AND LITHIUM COBALTATE CATHODES FOR MOLTEN CARBONATE FUEL CELLS
M. Krumpelt, M. Roche, I. Bloom, J. E. Indacochea, and G. Kucera 1994 3 p Presented at the Fuel Cells 1994, Morgantown, WV, 17-19 Aug. 1994
(Contract W-31-109-eng-38)
(DE94-017079; ANL/CMT/CP-83638; CONF-940883-3) Avail: CASI HC A01/MF A01

The objective of this research is to develop cathodes for the molten carbonate fuel cells (MCFC) having a performance approaching that of the lithiated nickel oxide cathode and a significantly greater life, particularly in pressurized MCFC's. To meet this objective, cathodes containing either doubly doped lithium ferrate or lithium cobaltate are being developed. In this project, the authors are optimizing the composition, microstructure, and loading density of the doubly doped lithium ferrate cathode and the lithium cobaltate cathodes. DOE

N95-19388# Spire Corp., Bedford, MA.
InP SOLAR CELL DEVELOPMENT ON INEXPENSIVE SILICON SUBSTRATES Quarterly Report, 22 May - 22 Aug. 1994
Steven J. Wojtczuk 1 Nov. 1994 4 p
(Contract N00014-94-C-2030)
(AD-A286254; SPIRE-QR-10158.02) Avail: CASI HC A01/MF A01

In Phase 1, P/N InP control cells on InP wafers had substantially less photocurrent than N/P InP counterparts. The suspected culprit was diffusion of the zinc dopant, creating a thicker emitter than intended. Secondary ion mass spectroscopy (SIMS) data confirmed this hypothesis. The primary findings are: P/N InP cells were grown with both 200 and 400 A thick emitters; however, the SIMS profiles showed both cells have virtually the same junction depth, or approximately 2000 A thick emitters, about 5 to 10 times larger than expected. The excess Zn is diffusing in from the 3000 A thick P(++) In(0.53)Ga(0.47)As contact layer on top of the cell. P/N InP cells on InP wafers or Si wafers had virtually the same diffusion profiles, with only a barely noticeable enhancement of the Zn diffusion in higher defect density InP/Si wafers, which is good news. DTIC

N95-19554# California Univ., Berkeley, CA. Dept. of Civil Engineering.
SYSTEMS AND ECONOMIC ANALYSIS OF MICROALGAE PONDS FOR CONVERSION OF CO2 TO BIOMASS
J. R. Benemann and W. J. Oswald 30 May 1994 70 p
(Contract DE-FG22-93PC-93204)
(DE95-000406; DOE/PC-93204/T1) Avail: CASI HC A04/MF A01

In the section entitled 'Photobioreactors for Mic roalgae Production of Fuels and Chemicals' the authors consider the current and potential commercial products that can be derived from microalgae during a process of CO2 utilization, alternative photobioreactor designs, and the fundamental biological and bioengineering issues in microalgae production. They emphasize the long term potential of microalgae production of low value commodities, specifically alternative fuels, which would have the greatest potential for large-scale CO2 utilization. Section 2 discusses the development of low cost technologies for macro algae harvesting. First a brief review of the current experience in algae harvesting in large-scale commercial operations is presented. This is followed by a general discussion of various algae harvesting processes, followed by a comparative evaluation of the various processes and discussion of future prospects. DOE

N95-19591# Pacific Northwest Lab., Richland, WA.
ALTERNATIVE MATERIALS FOR SOLID OXIDE FUEL CELLS
J. W. Stevenson and T. R. Armstrong Aug. 1994 10 p Presented at the Fuel Cells 1994, Morgantown, WV, 17-19 Aug. 1994
(Contract DE-AC06-76RL-01830)
(DE94-018452; PNL-SA-24680; CONF-940883-6) Avail: CASI HC A02/MF A01

The purpose of this research is to develop alternative materials for solid oxide fuel cell (SOFC) interconnections and electrodes with improved electrical, thermal, and electrochemical properties. A second objective is to develop synthesis and fabrication methods for these materials whereby they can be processed in air into SOFC's. The approach is to: (1) develop modifications of the current, state-of-the-art materials used in SOFC's; (2) minimize the number of cations used in the SOFC materials to reduce potential deleterious interactions; (3) improve thermal, electrical, and electrochemical properties; (4) develop methods to synthesize both state-of-the-art and alternative materials for the simultaneous fabrication and consolidation in air of the interconnections and electrodes with the solid electrolyte; and (5) understand electrochemical reactions at materials interfaces and the effects of component composition and processing on those reactions. This paper summarizes a comprehensive study that assessed the effect of ambient oxygen partial pressure on the stability of air-sinterable chromites and the sintering behavior of doped lanthanum manganites. DOE

N95-19832# National Renewable Energy Lab., Golden, CO.
RESEARCH ON STABLE, HIGH-EFFICIENCY AMORPHOUS SILICON MULTIJUNCTION MODULES Final Subcontract Report, 1 Jan. 1991 - 31 Aug. 1994
S. Guha (United Solar Systems Corp., Troy, MI.) Oct. 1994 96 p
(Contract DE-AC36-83CH-10093)
(DE95-000215; NREL/TP-411-7190) Avail: CASI HC A05/MF A01

The principal objective of this program is to conduct research on semiconductor materials and non-semiconductor materials to enhance the performance of multibandgap, multijunction, large-area amorphous silicon-based alloy modules. The goal for this program is to demonstrate stabilized module efficiency of 12% for multijunction modules of area greater than 900 cm(sup 2). Double-junction and triple-junction cells are made on Ag/ZnO back reflector deposited on stainless steel substrates. The top cell uses a-Si alloy; a-SiGe alloy is used for the i layer in the middle and the bottom cells. After evaporation of antireflection coating, silver grids and bus bars are put on the top surface, and the panel is encapsulated in an ethylene vinyl acetate (EVA)/Tefzel structure to make a one-square-foot monolithic module. DOE

N95-19854# National Renewable Energy Lab., Golden, CO.
TAPPING INTO THE SUN: TODAY'S APPLICATIONS OF PHOTOVOLTAIC TECHNOLOGY
Jul. 1994 21 p
(Contract DE-AC36-83CH-10093)
(DE93-000075; DOE/CH-10093/203) Avail: CASI HC A03/MF A01

Today solar-generated electricity serves people living in the most isolated spots on earth and in the center of our biggest cities. First used in the space program, PV systems are now generating electricity to pump water, light up the night, activate switches, charge batteries, supply the electric utility grid, and more. Whether you are a homeowner, planner, architect, or just someone who pays electric utility bills, photovoltaics may already touch your life in some way. DOE

N95-19855# National Renewable Energy Lab., Golden, CO.
EVIDENCE THAT AERODYNAMIC EFFECTS, INCLUDING DYNAMIC STALL, DICTATE HAWT STRUCTURAL LOADS AND POWER GENERATION IN HIGHLY TRANSIENT TIME FRAMES
D. E. Shipley (Colorado Univ., Boulder, CO.), M. S. Miller (Colorado Univ., Boulder, CO.), M. C. Robinson (Colorado Univ., Boulder, CO.), M. W. Luttges (Colorado Univ., Boulder, CO.), and D. A. Simms Aug. 1994 14 p Presented at the American Wind Energy Association Annual Conference and Exhibition, Minneapolis, MN, 9-13 May 1994
(Contract DE-AC36-83CH-10093)
(DE94-011865; NREL/TP-441-7080; CONF-940548-7) Avail: CASI HC A03/MF A01

Aerodynamic data collected from the National Renewable Energy Laboratory's Combined Experiment have shown three distinct performance regimes when the turbine is operated under relatively steady flow conditions. Operating at blade angles of attack below static stall, excellent agreement is achieved with two-dimensional wind tunnel data. Around the static stall

angle, the cycle average normal force produced is greater than the static test data. Span locations near the hub produce extremely large values of normal force coefficient, well in excess of the two-dimensional data results. These performance regimes have been shown to be a function of the three-dimensional flow structure and cycle averaged dynamic stall effects. Power generation and root bending moments have also been shown to be directly dependent on the inflow wind velocity. Aerodynamic data, including episodes of dynamic stall, have been correlated on a cycle by cycle basis with the structural and power generation characteristics of a horizontal axis wind turbine. Instantaneous unsteady forces and resultant power generation indicate that peak transient levels can significantly exceed cycle averaged values. Strong coupling between transient aerodynamic and resonant response of the turbine was also observed. These results provide some initial insight into the contribution of unsteady aerodynamics on undesirable turbine structural response and fatigue life. DOE

N95-19856# National Renewable Energy Lab., Golden, CO.
SUMMARY INFORMATION AND DATA SETS FOR THE HBCU SOLAR MEASUREMENTS NETWORK
W. Marion Aug. 1994 62 p
(Contract DE-AC36-83CH-10093)
(DE94-011872; NREL/TP-463-7090) Avail: CASI HC A04/MF A01

Since 1985, the National Renewable Energy Laboratory (NREL), formerly the Solar Energy Research Institute (SERI), has operated a solar radiation measurement network of six stations located at Historically Black Colleges and Universities (HBCU's) in the southeastern United States. NREL initiated this network to provide better regional coverage and to comply with President Reagan's Executive Order 12320, dated September 15, 1981, directing all federal agencies to implement programs to strengthen the nation's HBCU's. Funding for the HBCU network has been provided by the Department of Energy's (DOE's) Resource Assessment Program, Photovoltaic Program, and Solar Thermal Program, and it is currently funded by the Solar Radiation Resource Assessment Project. The objectives of the HBCU network are (1) To significantly improve the assessment of solar radiation resources in the southeastern United States; (2) To enlist the help of the HBCU's in collecting high-quality solar radiation data; (3) To encourage the distribution of solar radiation resource information and the development of solar energy applications in the Southeast; (4) To encourage the development of academic and research programs in solar energy at HBCU's. DOE

N95-19857# National Renewable Energy Lab., Golden, CO.
NREL PHOTOVOLTAIC PROGRAM, FY 1993
Aug. 1994 344 p
(Contract DE-AC36-83CH-10093)
(DE94-011880; NREL/TP-410-6285) Avail: CASI HC A15/MF A03

This report reviews the in-house and subcontracted research and development (R&D) activities under the National Renewable Energy Laboratory (NREL) Photovoltaic (PV) Program from October 1, 1992, through September 30, 1993 (fiscal year (FY) 1993). The NREL PV Program is part of the U.S. Department of Energy's (DOE's) National Photovoltaics Program, as described in the DOE Photovoltaics Program Plan, FY 1991 - FY 1995. The FY 1993 budget authority (BA) for carrying out the NREL PV Program was $40.1 million in operating funds and $0.9 million in capital equipment funds. An additional $4.8 million in capital equipment funds were made available for the new Solar Energy Research Facility (SERF) that will house the in-house PV laboratories beginning in FY 1994. Subcontract activities represent a major part of the NREL PV Program, with more than $23.7 million (nearly 59%) of the FY 1993 operating funds going to 70 subcontractors. In FY 1993, DOE assigned certain other PV subcontracting efforts to the DOE Golden Field Office (DOE/GO), and assigned responsibility for their technical support to the NREL PV Program. An example is the PV:BONUS (Building Opportunities in the U.S. for Photovoltaics) Project. These DOE/GO efforts are also reported in this document. DOE

N95-19858# Brookhaven National Lab., Upton, NY.
CORRELATION OF POLYCRYSTALLINE Cu(In,Ga)Se2 DEVICE EFFICIENCY WITH HOMOJUNCTION DEPTHAND INTERFACIAL STRUCTURE: X-RAY PHOTOEMISSION AND POSITRON ANNIHILATION SPECTROSCOPIC CHARACTERIZATION
A. J. Nelson (National Renewable Energy Lab., Golden, CO.), P. E. Sobol (National Renewable Energy Lab., Golden, CO.), A. M. Gabor (National Renewable Energy Lab., Golden, CO.), M. A. Contreras (National Renewable Energy Lab., Golden, CO.), P. Asoka-Kumar, and K. G. Lynn 1994 4 p Presented at the 1st World Conference on Photovoltaic Energy Conversion, Waikoloa, HI, 5-9 Dec. 1994
(Contract DE-AC02-76CH-00016)
(DE94-013543; BNL-60422; CONF-941203-1) Avail: CASI HC A01/MF A01

Angled-resolved high resolution photoemission measurements on valence band electronic structure and Cu 2p, In 3d, Ga 2p, and Se 3d core lines were used to evaluate surface and near-surface chemistry of CuInSe2 and Cu(In,Ga)Se2 device grade thin films. XPS compositional depth profiles were also acquired from the near-surface region, and bonding of the Cu, In, Ga, and Se was determined as a function of depth. A Cu-poor region was found, indicating CuIn5Se8 or a CuIn3Se5-In2Se3 mixture. Correlation between the depth of the Cu-poor region/bulk interface and device efficiency showed that the depth was 115 angstroms for a 16.4% CIGS device, 240 angstroms for a 15.0% CIGS, and 300 angstroms for 14.0% CIGS, with similar trends for CIS films. The surface region is n-type, the bulk is p-type, with a 0.5 eV valence band offset. Depth of homojunction may be the determining factor in device performance. Positron annihilation spectroscopy gave similarly illuminating results. DOE

N95-19859# Sandia National Labs., Albuquerque, NM.
A SIMPLE SINGLE-PHOTOMASK PROCESS FOR FABRICATION OF HIGH-EFFICIENCY MULTICRYSTALLINE SILICON SOLAR CELLS
W. K. Schubert, D. S. Ruby, P. A. Basore, J. M. Gee, M. E. Buck, and H. L. Tardy 1994 3 p Presented at the 1st World Conference on Photovoltaic Energy Conversion, Waikoloa, HI, 5-9 Dec. 1994
(Contract DE-AC04-94AL-85000)
(DE94-014251; SAND-94-1574C; CONF-941203-3) Avail: CASI HC A01/MF A01

We have developed a simplified process sequence for fabrication of high-efficiency multicrystalline silicon (mc-Si) solar cells. Photolithography is required only to define the evaporated metal gridlines. We use this fast turn-around, high-yield baseline process to evaluate different mc-Si materials and new processing procedures. The process uses a one-step emitter diffusion/drive-in and an aluminum-alloyed back surface field to provide a well-passivated cell with excellent blue and red response. Laser-scribed cell-isolation grooves are used to define both moderate-area (4 cm(sup 2)) and large-area (42 cm(sup 2)) cells. We have been able to achieve minority-carrier diffusion lengths well over 300 (mu)m in 2-(Omega)cm mc-Si material and have achieved efficiencies of 16.2% in 4-cm(sup 2) cells. This was accomplished without hydrogenation to passivate bulk defects or texturing to reduce reflectance. By using the same fabrication process for both small-area and large-area cells, we intend to determine and minimize the effect of areal inhomogeneities on large-area mc-Si cell performance. DOE

N95-19873# Sandia National Labs., Albuquerque, NM.
GETTERING IN MULTICRYSTALLINE SILICON: A DESIGN-OF-EXPERIMENTS APPROACH
W. K. Schubert 1994 4 p Presented at the 1st World Conference on Photovoltaic Energy Conversion, Waikoloa, HI, 5-9 Dec. 1994
(Contract DE-AC04-94AL-85000)
(DE94-014289; SAND-94-1528C; CONF-941203-4) Avail: CASI HC A01/MF A01

Design-of-experiment methods were used to study gettering due to phosphorus diffusion and aluminum alloying in four industrial multicrystalline silicon materials: Silicon-Film material from AstroPower, heat-exchanger method (HEM) material from Crystal Systems, edge-defined film-fed growth (EFG) material from Mobil Solar, and cast material from Solarex. Time and temperature for the diffusion and alloy processes were chosen for a four-factor quadratic interaction experiment. Simple diagnostic devices were used to evaluate the gettering. Only EFG and HEM materials exhibited statistically significant gettering effects within the ranges used for the various parameters. Diffusion and alloying temperature were significant for HEM material; also there was a second-order interaction between the diffusion time and temperature. There was no interaction between the diffusion and alloying processes in HEM material. EFG material showed a first-order dependence on diffusion temperature and a second-order interaction between the diffusion temperature and the alloying time. Gettering recommendations for the HEM material were used to produce the best-yet

Sandia cells on this material, but correlation with the gettering experiment was not strong. Some of the discrepancy arises from necessary processing differences between the diagnostic devices and regular solar cells. This issue and other lessons learned concerning this type of experiment are discussed. DOE

N95-19878# National Renewable Energy Lab., Golden, CO.
GROWTH AND DEVELOPMENT OF GaInAsP FOR HIGH-EFFICIENCY SOLAR CELLS Final Subcontract Report, 1 Jul. 1991 - 30 Dec. 1993
P. R. Sharps (Research Triangle Inst., Research Triangle Park, NC.) Oct. 1994 38 p
(Contract DE-AC36-83CH-10093)
(DE94-000210; NREL/TP-451-7166) Avail: CASI HC A03/MF A01

This report describes accomplishments during Phase 3 of this subcontract. The overall goals of the subcontract were (1) to develop the necessary technology to grow high-efficiency GaInAsP layers that are lattice-matched to GaAs and Ge; (2) to demonstrate high efficiency GaInAsP single-junction solar cells; and (3) to demonstrate GaInAsP/Ge cascade solar cells suitable for operation under concentrated (500X) sunlight. The major accomplishments during Phase 3 include (1) demonstrating a GaInAsP tunnel diode for use as an interconnect in the GaInAsP/Ge cascade cell, and (2) demonstrating a GaInAsP/Ge cascade cell. The development of the GaInAsP tunnel diode is a major accomplishment because it allows for the GaInAsP and Ge cells to be connected without optical losses for the bottom Ge cell, such as a Ge tunnel diode would cause. The GaInAsP/Ge cascade cell development is significant because of the demonstration of a cascade cell with a new materials system. DOE

N95-19880# National Renewable Energy Lab., Golden, CO.
ADVANCED PROCESSING TECHNOLOGY FOR HIGH-EFFICIENCY, THIN-FILM CuInSe2 AND CdTe SOLAR CELLS Annual Subcontractors Report, 1 Mar. 1993 - 28 Feb. 1994
D. L. Morel (University of South Florida, Tampa, FL.) and C. S. Ferekides (University of South Florida, Tampa, FL.) Jul. 1994 46 p
(Contract DE-AC36-83CH-10093)
(DE94-011838; NREL/TP-451-6638) Avail: CASI HC A03/MF A01

This annual report details activities in research on advanced processing technology for high-effiency, thin-film solar cells. DOE

N95-19882# National Renewable Energy Lab., Golden, CO.
SILICON-FILM (TRADEMARK) PHOTOVOLTAIC MANUFACTURING TECHNOLOGY
S. R. Collins (Astropower, Inc., Newark, DE.) and R. B. Hall (Astropower, Inc., Newark, DE.) Sep. 1994 34 p
(Contract DE-AC36-83CH-10093)
(DE94-011899; NREL/TP-411-7170) Avail: CASI HC A03/MF A01

This report describes work to develop an advanced, low-cost manufacturing process for a now utility-scale, flat-plate module. This process starts with the production of continuous sheets of thin-film, polycrystalline silicon using the Silicon-Film (trademark) process. Sheets are cut into wafers that are nominally 15 cm on a side. Fifty-six of these wafers are then fabricated into solar cells that are strung together into a 170-W module. Twelve of these modules form a 2-kW array. The program has three main components: (1) development of a Silicon-Film (trademark) wafer machine that is capable of manufacturing wafers that are 225 cm(exp 2) in size at a rate of 3.0 MW/yr, with a total product cost reduction of 70%; (2) development of an advanced solar cell manufacturing process that is capable of turning the Silicon-Film (trademark) wafer into a 3.25 W solar cell; and (3) development of an advanced module design based on these large-area silicon solar cells with an average power of 170 W for 56 solar cells and 113 W for 36 solar cells. DOE

45 ENVIRONMENT POLLUTION

Includes atmospheric, noise, thermal, and water pollution.

N95-17937# Microelectronics Center of North Carolina, Research Triangle Park, NC. Supercomputing Center.
DEPENDENCIES AND SENSITIVITY OF TROPOSPHERIC OXIDANTS TO PRECURSOR CONCENTRATIONS OVER THE NORTHEAST UNITED STATES: A MODEL STUDY Report, Apr. 1992 - May 1993
Rohit Mathur, Kenneth L. Schere (National Oceanic and Atmospheric Administration, Research Triangle Park, NC.), and Anuradha Nathan (Computer Sciences Corp., Research Triangle Park, NC.) 20 May 1994 21 p Repr. from Journal of Geophysical Research, v. 99, no. D5, 20 May 1994 p 10535-10552
(Grant EPA-R-816496) (ISSN 0148-0227)
(PB94-192770; EPA/600/J-94/310; Paper-93JD03580) Avail: CASI HC A03/MF A01

Several important issues related to the distribution and production of photochemical species are examined through an analysis of results obtained from applications of a comprehensive three-dimensional regional scale photochemical model over the northeast United States. The regional oxidant model (ROM) is used to simulate the response of various photochemical species to specific anthropogenic emissions strategies involving NO(x) and hydrocarbon reductions for an episodic period during July 1988. Domain and temporal averages of predicted concentrations are examined for various species. Their relative influence on oxidant chemistry over the modeled domain is investigated. Further, spatial distributions of ozone (O3) with respect to those of NO(x), NO(y), and hydrocarbons over the modeled domain are examined and the variations in O3 levels for different chemical regimes classified by characteristic NO(x)/ROG and NO(x)/NO(y) ratios are investigated. The relative benefits of reductions in NO(x) and hydrocarbon emissions on predicted O3 levels are also examined. In general, for this modeled domain, reductions in NO(x) emissions with or without reductions in hydrocarbon emissions have more impact on reducing predicted O3 levels compared to reductions only in hydrocarbon emissions. NTIS

N95-17943# National Renewable Energy Lab., Golden, CO.
RENEWABLE ENERGY AND ITS POTENTIAL FOR CARBON EMISSIONS REDUCTIONS IN DEVELOPING COUNTRIES: METHODOLOGY FOR TECHNOLOGY EVALUATION
D. Corbus, M. Martinez, L. Rodriguez, and J. Mark Aug. 1994 47 p
(Contract DE-AC36-83CH-10093)
(DE94-011870; NREL/TP-463-6504) Avail: CASI HC A03/MF A01

Many projects have been proposed to promote and demonstrate renewable energy technologies (RET's) in developing countries on the basis of their potential to reduce carbon emissions. However, no uniform methodology has been developed for evaluating RET's in terms of their future carbon emissions reduction potential. This study outlines a methodology for identifying RET's that have the potential for achieving large carbon emissions reductions in the future, while also meeting key criteria for commercialization and acceptability in developing countries. In addition, this study evaluates the connection between technology identification and the selection of projects that are designed to demonstrate technologies with a propensity for carbon emission reductions (e.g., Global Environmental Facility projects). Although this report applies the methodology to Mexico in a case study format, the methodology is broad based and could be applied to any developing country, as well as to other technologies. The methodology used in this report is composed of four steps: technology screening, technology identification, technology deployment scenarios, and estimates of carbon emissions reductions. The four technologies with the highest ranking in the technology identification process for the on-grid category were geothermal, biomass cogeneration, wind, and micro-/mini-hydro. Compressed natural gas (CNG) was the alternative that received the highest ranking for the transportation category. DOE

N95-17944# National Renewable Energy Lab., Golden, CO.
POTENTIAL IMPACTS ON AIR QUALITY OF THE USE OF ETHANOL AS AN ALTERNATIVE FUEL Final Report
J. S. Gaffney (Argonne National Lab., IL.) and N. A. Marley (Argonne National Lab., IL.) Sep. 1994 67 p
(Contract DE-AC36-83CH-10093)
(DE94-011881; NREL/TP-425-6956) Avail: CASI HC A04/MF A01

The use of ethanol/gasoline mixtures in motor vehicles has been proposed as an alternative fuel strategy that might improve air quality while minimizing US dependence on foreign oil. New enzymatic production methodologies are being explored to develop ethanol as a viable, economic fuel. In an attempt to reduce urban carbon monoxide (CO) and ozone levels, a number of cities are currently mandating the use of ethanol/gasoline blends. However, it is not at all clear that these blended fuels will help to abate urban pollution. In fact, the use of these fuels may lead to increased levels of other air pollutants, specifically aldehydes and peroxyacyl nitrates.

Although these pollutants are not currently regulated, their potential health and environmental impacts must be considered when assessing the impacts of alternative fuels on air quality. Indeed, formaldehyde has been identified as an important air pollutant that is currently being considered for control strategies by the State of California. This report focuses on measurements taken in Albuquerque, New Mexico during the summer of 1993 and the winter of 1994 as an initial attempt to evaluate the air quality effects of ethanol/gasoline mixtures. The results of this study have direct implications for the use of such fuel mixtures as a means to reduce CO emissions and ozone in a number of major cities and to bring these urban centers into compliance with the Clean Air Act. DOE

N95-17985 Stanford Research Inst., Menlo Park, CA.
THE SEVENTH IONOSPHERIC EFFECTS SYMPOSIUM
J. M. Goodman, ed., J. F. Thomason, ed., J. A. Klobuchar, ed., R. G. Joiner, ed., and H. Soicher, ed. 1993 699 p Symposium held in Washington, DC, 4-6 May 1993 Prepared for NRL, Washington, DC; sponsored by Phillips Lab., Kirkland AFB, NM; Los Alamos National Lab., Los Alamos, NM and Voice of America, Washington, DC Limited Reproducibility: More than 20% of this document may be affected by microfiche quality
(PB94-191930) Avail: CASI HC A99

Given the major advances in the understanding and the predictability of ionospheric effects, and in the development of an Automatic Link Establishment (ALE) standard for automating the traditional mystical process of channel selection, High Frequency (HF) should be actively increasing its usage and applications worldwide. Instead, the authors find the growth of HF communication applications hobbled by a variety of factors. Veterans of HF communications may be quick to dismiss this as simply the latest cycle of satellite euphoria and HF is dead. While many such false starts have occurred in the cyclical history of HF, a rational examination of the technologies, politics, and economics of HF versus non-HF media suggests that the future of HF may have reached a critical point in history where it will cease to be a primary communications medium for many traditional applications. A set of candidate technologies and actions are identified for reinvigorating the HF medium. Author

N95-18002# Rijksinstituut voor Volksgezondheid en Milieuhygieene, Bilthoven (Netherlands).
CATALOG OF ENVIRONMENTAL DATA SETS OF EUROPE AT THE RIVM
J. D. Dorf, R. J. VandeVelde, J. A. Bakkes, and R. Roozendaal Apr. 1993 119 p
(PB94-202710; RIVM-422501002) Avail: CASI HC A06/MF A02

The report is a catalog of foreign data sets held by the Dutch National Institute of Public Health and Environmental Protection (RIVM) for environmental research and reporting. The data sets are described in terms from the NASA Document Interchange Format (DIF) description standard. The data sets are available in digital form at present or within months and originate from RIVM or from outside sources. Included are input data to RIVM rather than results from its model calculations, etc. About sixty data sets are described comprising, as a rule, data on five to ten subjects each. The scope of most of the data is Europe; a lesser number relate to the world. NTIS

N95-18003# Instituto de Pesquisas Espaciais, Sao Jose dos Campos (Brazil).
RADIATION BALANCE IN THREE AMAZONIAN ECOSYSTEMS: CAMPINA, CAMPINARANA AND MATA DENSA Ph.D. Thesis
[BALANCO DE RADIACAO EM TRES ECOSSISTEMAS DA FLORESTA AMAZONICA: CAMPINA, CAMPINARANA E MATA DENSA]
Mario deMirandaVilasBoasRamosLeitao 1994 156 p In PORTUGESE
(INPE-5587-TDI/549) Avail: CASI HC A08/MF A02

The radiation fluxes in three Amazonian ecosystems are analyzed: 'campina' and 'campinarana' localized at 'Estacao Experimental de Silvicultura Tropical' (2 deg 34 min S; 60 deg 2 min W) and 'mata densa' at 'Reserva Florestal Ducke' (2 deg 57 min S; 59 deg 57 min W) on September 1991 and August/September 1993. In each study area on top of a tower, a set of equipments composed of pyranometers to measure the incident and reflected shortwave and infrared radiation fluxes, besides a net radiometer were installed. Next to the soil's surface, under the canopy, 16 radiometers to measure incident shortwave radiation, 16 to measure reflected short-wave radiation and 16 to measure photosynthetic active radiation (PAR) were used. The acquisition of the data was made using two 21X and one CR-10 microloggers, which allowed the obtaining of one-minute averages from values sampled every 3 seconds from 5:50 to 18:00 h, for all the observed parameters. At the 16 radiation observation points, hemispheric photographs were taken, using a Nikon camera equipped with a fish eye 8 mm lens. Complementing the radiation measures, the quantity of sunflecks was determined. The behavior of the radiation balance components and the application of Steege's proposed method (1994), which permits vegetation indexes and climatic parameters estimation through the interpretation of hemispheric photographs, were examined in detail. No differences between the short-wave albedo of the three canopies ('campinarana'-10.4 percent, 'mata densa' and 'campina'-11.3 percent) were noted. The visible-range's albedo was 1.5, 1.4, and 2 percent at the 'campinarana', 'campina' and 'mata densa', respectively, while the near infrared spectral range's albedo was 20.2, 22, and 21.2 percent at the 'campinarana', 'campina' and 'mata densa', respectively. At the basis of the canopy of the 'campina' it was verified that 5 times more short-wave and infrared radiation is received, and 6 times more PAR, than at the basis of the canopy of 'mata densa'. The radiation measurements at the basis of the canopies showed great spatial and temporal variation. Equations obtained show that the albedo modeled in terms of the sun's elevation angle, and the radiation and longwave radiation's balance estimated in terms of the incident short-wave radiation have an excellent accuracy. Finally, the use of the hemispheric photographies interpretation method is a very important tool in the study of regeneration inside canopies because, apart from allowing estimations of climatic parameters, it has the advantage of permitting the non destructive determination of parameters such as canopies leaf area index (LAI) and cover. Author (revised)

N95-18022# East Anglia Univ., Norwich (England). Climatic Research Unit.
DETECTION OF GREENHOUSE-GAS-INDUCED CLIMATIC CHANGE
T. M. L. Wigley and P. D. Jones 1 Jul. 1994 42 p
(Contract DE-FG02-86ER-60397)
(DE94-015044; DOE/ER-60397/T8) Avail: CASI HC A03/MF A01

In addition to changes due to variations in greenhouse gas concentrations, the global climate system exhibits a high degree of internally-generated and externally-forced natural variability. To detect the enhanced greenhouse effect, its signal must be isolated from the 'noise' of this natural climatic variability. A high quality, spatially extensive data base is required to define the noise and its spatial characteristics. To facilitate this, available land and marine data bases will be updated and expanded. The data will be analyzed to determine the potential effects on climate of greenhouse gas concentration changes and other factors. Analyses will be guided by a variety of models, from simple energy balance climate models to ocean General Circulation Models. Appendices A--G contain the following seven papers: (A) Recent global warmth moderated by the effects of the Mount Pinatubo eruption; (B) Recent warming in global temperature series; (C) Correlation methods in fingerprint detection studies; (D) Balancing the carbon budget: Implications for projections of future carbon dioxide concentration changes; (E) A simple model for estimating methane concentration and lifetime variations; (F) Implications for climate and sea level of revised IPCC emissions scenarios; and (G) Sulfate aerosol and climatic change. DOE

N95-18048* National Aeronautics and Space Administration. Goddard Space Flight Center, Greenbelt, MD.
EVOLUTION OF THE SOUTHERN HEMISPHERE OZONE HOLE AS SEEN BY TOMS FROM AUGUST 1979 TO DECEMBER 1991 (Videotape)
3 Aug. 1994 Videotape: 5 min. 45 sec. running time, in color, no sound
(NASA-TM-110116; NONP-NASA-VT-95-37003) Avail: CASI VHS A02/BETA A22

The computerized color images of the Total Ozone Mapping Spectrometer (TOMS) showed the ozone distribution and levels in the Earth's southern hemisphere from August 1979 to December 1991 in this video. The annual variations were presented in a monthly format and the ozone levels were measured in Dobson units. CASI

N95-18085# Army Engineer Waterways Experiment Station, Vicksburg, MS.

CUMULATIVE IMPACT ANALYSIS OF WETLANDS USING HYDROLOGIC INDICES Final Report

John M. Nestler and Katherine S. Long Sep. 1994 48 p

(AD-A284759; WES/TR/WRP-SM-3) Avail: CASI HC A03/MF A01

In order to make informed decisions concerning cumulative impact analysis of wetlands, the Corps of Engineers Districts and other wetlands professionals need data often not directly available. Cumulative impact assessment of wetlands includes relating historic patterns of flow, derived from the stream's flow record, to changes in the watershed associated with that stream. Harmonic analysis and time-scale analysis were applied to selected stream records to ascertain their potential for describing cumulative impacts. The study area chosen included selected streams in the White River basin, Arkansas/Missouri. The Cache River received particular emphasis because a significant amount of information was readily available concerning it and its surroundings. Daily flow values were retrieved from each of the streams. Using nonlinear, harmonic analysis as well as time-scale analysis (a technique adapted from fractal geometry) to reveal the time-dependent patterns in the respective samples, the results were compared decade-by-decade to discern changes in the historic, seasonal patterns. Other streams in the White River basin were analyzed in the same manner and compared with the Cache River, noting historic changes in land use and stream regulation. The study identifies methods with the potential to differentiate historic time frames in which disruptions were likely to have occurred. The methods appear to be translatable to other geographic areas where streamflow is typically seasonal. DTIC

N95-18091 Defence Science and Technology Organization, Melbourne (Australia).

POTENTIAL REPLACEMENTS FOR SOLVENTS THAT ARE OZONE DEPLETING SUBSTANCES

Lyn E. Fletcher Sep. 1994 33 p Limited Reproducibility: More than 20% of this document may be affected by microfiche quality

(AD-A285442; DSTO-TR-0046; DODA-AR-008-906) Avail: CASI HC A03

The discovery of the hole in the ozone layer over Antarctica and the global drop in stratospheric ozone has prompted the banning of CFC-113 and 1,1,1-trichloroethane, which are common solvents used for degreasing and cleaning electronic components. The Royal Australian Navy uses these substances in a variety of applications and has initiated a replacement program. Two applications, cleaning baluns after lightning strikes and cleaning electrical motors have been selected as priorities under this program. This paper assesses the suitability of various solvents for these applications. DTIC

N95-18132*# National Aeronautics and Space Administration. Langley Research Center, Hampton, VA.

COMPENDIUM OF NASA DATA BASE FOR THE GLOBAL TROPOSPHERIC EXPERIMENT'S ARCTIC BOUNDARY LAYER EXPERIMENTS ABLE-3A AND ABLE-3B

Gerald L. Gregory and A. Donald Scott, Jr. Nov. 1994 268 p

(RTOP 464-52-07-71)

(NASA-TM-109161; NAS 1.15:109161) Avail: CASI HC A12/MF A03

The report provides a compendium of NASA aircraft data that are available from NASA's Global Tropospheric Experiment's (GTE) Arctic Boundary Layer Experiments (ABLE) conducted in July and August of 1988 (ABLE-3A) and 1990 (ABLE-3B). ABLE-3A flight experiments were based at Barrow and Bethel, Alaska, and included survey/transit flights to Thule, Greenland. ABLE-3B flight experiments were based at North Bay (Ontario) and Goose Bay, Canada, and included flights northward to Frobisher Bay, Canada. The primary purposes of the experiments were (1) the measurement of the flux of various trace gases from high-arctic ecosystems, (2) the elucidation of factors important to the production and destruction of ozone, and (3) the documentation of source and chemical signature of air common to and transported into the regions. The report provides a representation, in the form of selected data plots, of aircraft data that are available in archived format via NASA Langley's Distributed Active Archive Center. The archived data bases include data for other species measured on the aircraft as well as numerous supporting data, including meteorological observations/products, results from surface studies, satellite observations, and sondes releases. Author

N95-18140 Sorbent Technologies Corp., Twinsburg, OH.

CONTROLLING COMBUSTION-SOURCE EMISSIONS AT AIR FORCE SITES WITH A NEW FILTER CONCEPT, PHASE 1 Final Technical Report, May - Nov. 1993

Sidney G. Nelson, David A. VanStone, Brian W. Nelson, and Kenneth A. Peterson Apr. 1994 56 p Limited Reproducibility: More than 20% of this document may be affected by microfiche quality

(Contract F08635-93-C-0104)

(AD-A283674; AL/EQ-TR-1994-0006) Avail: CASI HC A04

The U.S. Air Force employs many combustion sources at its facilities, including boilers, diesel engines, turbines, incinerators, and motor vehicles, that produce exhaust gases containing undesirable components. Components of concern include nitrogen oxides (NOx), carbon monoxide (CO), PM-10 particulate matter, sulfur dioxide (SO2), and a long list of compounds considered toxic by nature. Recently, Sorbent Technologies Corporation (Sorbtech) developed a new filter technology for the Air Force to control emissions from jet engine test cells. The objective was to conduct a preliminary evaluation of other possible Air Force applications of the new filter technology. The project was conducted at Sorbtech's laboratories in Ohio and at McClellan AFB in California. Of more than 10 combustion waste-gas streams at McClellan AFB, seven were characterized and three were selected for initial study by Sorbtech. A special filter-test apparatus was designed, constructed, and evaluated in the laboratory. It was then installed and employed at McClellan AFB to treat waste-gas slipstreams in the three applications. The applications were: (1) a large, stationary diesel engine; (2) a natural-gas-fired burner-heater; and (3) a mobile diesel generator. DTIC

N95-18375# Rijksinstituut voor Volksgezondheid en Milieuhygieene, Bilthoven (Netherlands).

METHANE: THE OTHER GREENHOUSE GAS. RESEARCH AND POLICY IN THE NETHERLANDS

A. R. vanAmstel, R. J. Swart, M. S. Krol, J. P. Beck, and A. F. Bouwman Apr. 1993 118 p See also DE94-722022 and PB92-209097 Sponsored by Ministerie van Volkshuisvesting, Ruimtelijke Ordening en Milieubeheer

(PB94-207149; RIVM-481507001) Avail: CASI HC A06/MF A02

The report shows emissions of methane calculated for the Netherlands for the years 1989, 1990, 1991 and 1992, using IPCC (Intergovernmental Panel for Climate Change) methodology. Results are compared with earlier estimates. Developments in the emissions for the years up to 2015 are estimated. To do this, scenarios from the third National Environmental Outlook are used. The governments aim for methane reduction is 10% of the 1990 level by the year 2000. This reduction can be concluded to take place only when waste policies and policies to reduce acid deposition and the manure surplus are effective. It is also concluded that additional policy measures for methane mitigation are feasible in the recovery of landfill gas and in the extra use of otherwise vented gas on platforms in the North Sea. Additional policies reducing cattle numbers (e.g. smaller milk quota) can be effective in methane reductions. Finally this report shows that emissions from manure are higher than earlier estimates. Measurements taken on farms will be necessary to reduce the uncertainties in this field in the Netherlands. NTIS

N95-18389# Oak Ridge National Lab., TN. Carbon Dioxide Information Analysis Center.

TRENDS 1993: A COMPENDIUM OF DATA ON GLOBAL CHANGE

Thomas A. Boden, ed., Dale P. Kaiser, ed., Robert J. Sepanski, ed., Frederick W. Stoss, ed., and Gay Marie Logsdon, ed. Sep. 1994 994 p

(Contract DE-AC05-84OR-21400)

(ORNL/CDIAC-65; ESD-4195) Avail: CASI HC A99/MF A10

This document provides synopses of frequently used global-change data. This third issue of the Trends series presents historical and modern records of atmospheric concentrations of carbon dioxide (CO2), methane (CH4), nitrous oxide (N2O), two chlorofluorocarbons (CFC-11 and CFC-12), a hydrochlorofluorocarbon (HCFC-22), and two halons (H-1301 and H-1211) from an expanded number of globally distributed data sets. Virtually all of the modern records extend into the 1990's, some into 1994. Additional trace gas data presented in Trends '93 include historical atmospheric CO2, CH4, and N2O records derived from ice cores. Trends '93 also includes revised and updated estimates through 1991 for global, regional, and national CO2 emissions produced from the burning of fossil fuels, gas flaring, and the production of cement. Updated global emissions estimates through

1992 are also presented for CFC-11 and CFC-12. In addition, Trends '93 updates and expands the presentation of long-term temperature records, whose spatial coverage ranges from an individual Antarctic (ice core) site to the entire globe and from the Earth's surface to the lower stratosphere. New subject matter appearing in Trends '93 includes a chapter for long-term regional precipitation records, several time-series records for atmospheric aerosols, and isotopic C-14 measurements for atmospheric CO2 from several sites. Data records are presented in multipage formats, each dealing with a specific site, region, or emissions species. The data records include tables; graphs; discussions of methods for collecting, measuring, and reporting the data; trends in the data, and references to literature providing further information. Author

N95-18445 Georgia Inst. of Tech., Atlanta, GA.
A MODEL STUDY OF THE INFLUENCE OF NMHC AND NO(x) EMISSIONS ON RURAL O3 CONCENTRATIONS IN GEORGIARGIA Ph.D. Thesis
Jiangfen Zheng 1993 181 p
Avail: Univ. Microfilms Order No. DA9415678

Ambient concentrations of O3, NO(x), NO, HNO3, PAN, NO(y), C4-Cl0 hydrocarbons including isoprene, and some meteorological parameters were measured at a rural site in Georgia from June 24 to July 15, 1990. Two days with the early evening ozone concentrations of about 80 ppb are identified and chosen for our model study. The rural 'background' concentrations and the distribution of O3 and its precursors over the region of our study are simulated first with an embedded 'plumes' model. It is predicted that, for the period of our simulation, the rural 'background' O3 concentrations are below 60 ppb and only 12% of the region has O3 above 80 ppb. It is also found that, due to large amount of NO(x), released into the urban and power plant areas, the maximum concentrations of O3, PAN and HNO3 tend to occur 0-8 hours downwind of these major emission areas. The maximum H2O2 is likely found in the rural area because of the NO titration of HO2. The comparison between this 'plumes' model, which has multi-box structure, and the one-dimensional vertical model, which has no horizontal resolution, demonstrates the non-linearity possessed by the chemical system. A multi-level Lagrangian model of turbulent diffusion and photochemistry in the boundary layer is then applied to trace the oxidant formation in the air parcel arriving at Elberton, the rural site located 120 miles northeast of Atlanta. On the selected two days, the calculated Elberton pollutant levels are compared with observations. The comparison indicates that the Lagrangian model predicts reasonably good pollutant levels. The impact of Atlanta anthropogenic emissions on this rural site is demonstrated. The sensitivity studies indicate that ozone concentrations at Elberton and in area downwind of Atlanta are more sensitive to NO(x) emission reductions. It is also found that in area downwind of Atlanta 9-10 molecules of ozone can be formed when one molecule of NO(x) is consumed, which gives an estimation of summer time anthropogenic ozone production of 2.1 x 10(exp 28) molecule s-l over the southeastern United States. Author (revised)

N95-18647# Lawrence Livermore National Lab., Livermore, CA.
REAL-TIME MODELING OF COMPLEX ATMOSPHERIC RELEASES IN URBAN AREAS
R. L. Baskett (EG and G Energy Measurements, Inc., Pleasanton, CA.), J. S. Ellis, and T. J. Sullivan Aug. 1994 5 p Presented at the International Workshop on Scientific Bases for Decision Making After a Radioactive Contamination of an Urban Environment, Rio de Janeiro, Brazil, 29 Aug. - 2 Sep. 1994
(Contracts W-7405-eng-48; DE-AC08-93NV-11265)
(DE94-018063; UCRL-JC-115998; CONF-9408145-1) Avail: CASI HC A01/MF A01

If a nuclear installation in or near an urban area has a venting, fire, or explosion, airborne radioactivity becomes the major concern. Dispersion models are the immediate tool for estimating the dose and contamination. Responses in urban areas depend on knowledge of the amount of the release, representative meteorological data, and the ability of the dispersion model to simulate the complex flows as modified by terrain or local wind conditions. A centralized dispersion modeling system can produce realistic assessments of radiological accidents anywhere in a country within several minutes if it is computer-automated. The system requires source-term, terrain, mapping and dose-factor databases, real-time meteorological data acquisition, three-dimensional atmospheric transport and dispersion models, and experienced staff. Experience with past responses in urban areas by the Atmospheric Release Advisory Capability (ARAC) program at Lawrence Livermore National Laboratory illustrate the challenges for three-dimensional dispersion models. DOE

N95-18664# Lawrence Livermore National Lab., Livermore, CA.
ASSESSMENT OF CO2 PROJECTIONS
I. G. Enting, T. M. L. Wigley, and M. Heimann Jul. 1994 70 p
(Contract W-7405-eng-48)
(DE94-017484; UCRL-ID-118062) Avail: CASI HC A04/MF A01

Various projections of the relation between future CO2 concentrations and future emissions were undertaken as part of the scientific assessment for Working Group 1 of the Intergovernmental Panel on Climate Change. There were three types of calculation: (1) forward projections, calculating the atmospheric CO2 concentrations resulting from specified emission scenarios; (2) inverse calculations determining the emission rates that would be required to achieve stabilization of CO2 concentrations via specified pathways; and (3) impulse response function calculations required for determining Global Warming Potentials. The use of a standardized set of conditions allows an intercomparison of models. The ocean models used in the calculations presented here span a range of forms from response function descriptions to general circulation models. The general issue for all levels of modelling is whether the model parameters can reasonably be regarded as being the same in the future as at present. Sensitivity studies explore other aspects of the uncertainties of such projections. This report documents the specifications, the models that were used and the results that were obtained. Some preliminary interpretations of the results are included. DOE

N95-18665# McGill Univ., Montreal (Quebec). Dept. of Atmospheric and Oceanic Sciences.
THE ROLE OF LARGE-SCALE, EXTRATROPICAL DYNAMICS IN CLIMATE CHANGE
T. G. Shepherd, ed. Feb. 1994 219 p Presented at the 17th Stanstead Seminar, Lennoxville, Quebec, 13-18 Jun. 1993
(Contract DE-AI02-93ER-61578)
(DE94-017651; DOE/ER-61578/1; CONF-9306361) Avail: CASI HC A10/MF A03

The climate modeling community has focused recently on improving our understanding of certain processes, such as cloud feedbacks and ocean circulation, that are deemed critical to climate-change prediction. Although attention to such processes is warranted, emphasis on these areas has diminished a general appreciation of the role played by the large-scale dynamics of the extratropical atmosphere. Lack of interest in extratropical dynamics may reflect the assumption that these dynamical processes are a non-problem as far as climate modeling is concerned, since general circulation models (GCM's) calculate motions on this scale from first principles. Nevertheless, serious shortcomings in our ability to understand and simulate large-scale dynamics exist. Partly due to a paucity of standard GCM diagnostic calculations of large-scale motions and their transports of heat, momentum, potential vorticity, and moisture, a comprehensive understanding of the role of large-scale dynamics in GCM climate simulations has not been developed. Uncertainties remain in our understanding and simulation of large-scale extratropical dynamics and their interaction with other climatic processes, such as cloud feedbacks, large-scale ocean circulation, moist convection, air-sea interaction and land-surface processes. To address some of these issues, the 17th Stanstead Seminar was convened at Bishop's University in Lennoxville, Quebec. The purpose of the Seminar was to promote discussion of the role of large-scale extratropical dynamics in global climate change. Abstracts of the talks are included in this volume. On the basis of these talks, several key issues emerged concerning large-scale extratropical dynamics and their climatic role. Individual records are indexed separately for the database. DOE

N95-18666# Oak Ridge National Lab., TN.
ONE STRATEGY FOR ESTIMATING THE POTENTIAL SOIL CARBON STORAGE DUE TO CO2 FERTILIZATION
K. G. Harrison and G. Bonani (Eidgenoessische Technische Hochschule, Zurich, Switzerland.) 1 Jun. 1994 28 p Presented at the Snowmass Global Change Institute Conference on the Global Carbon Cycle, Snowmass, CO, 19-30 Jul. 1993

(Contract DE-AC05-84OR-21400)
(DE94-017895; CONF-9307181-2) Avail: CASI HC A03/MF A01

Soil radiocarbon measurements can be used to estimate soil carbon turnover rates and inventories. A labile component of soil carbon has the potential to respond to perturbations such as CO2 fertilization, changing climate, and changing land use. Soil carbon has influenced past and present atmospheric CO2 levels and will influence future levels. A model is used to calculate the amount of additional carbon stored in soil because of CO2 fertilization. DOE

N95-18683 Army Construction Engineering Research Lab., Champaign, IL.

ENVIRONMENTAL COMPLIANCE ASSESSMENT SYSTEM (ECAS) Final Report

Carolyn ORourke and Lisa A. Gifford Aug. 1994 301 p Limited Reproducibility: More than 20% of this document may be affected by microfiche quality
(Contract MIPR-1223)
(AD-A283950; CERL-SR-EC-94/27) Avail: CASI HC A14

In response to the growing number of environmental laws and regulations worldwide, the U.S. Army has adopted an environmental compliance program that identifies compliance problems before they are cited as violations by the U.S. Environmental Protection Agency (USEPA). Beginning in 1985, Major Army Commands (MACOMs) were required to conduct comprehensive environmental assessments at all installations on a 4-year cycle. The installations must also conduct a mid-cycle internal assessment. Because each MACOM was developing a separate assessment system, the Army mandated, through Army Regulation 200.1, one unified Army-wide assessment mechanism. The resulting system combines Federal, Department of Defense (DOD), and Army environmental regulations, along with good management practices and risk management information, into a series of checklists that show (1) legal requirements and (2) which specific items or operations to review. Each assessment protocol lists a point of contact to help assessors review the checklist items as effectively as possible. The Environmental Compliance Assessment System (ECAS) manual incorporates existing checklists from USEPA and private industry. The Washington Supplement was developed to be used in conjunction with the U.S. ECAS manual, using existing Washington state environmental legislation and regulations as well as suggested management practices. DTIC

N95-18722 Royal Netherlands Meteorological Inst., De Bilt.

ATMOSPHERIC EFFECTS OF HIGH-FLYING SUBSONIC AIRCRAFT: A CATALOGUE OF PERTURBING INFLUENCES

Wieger Fransen Jun. 1994 97 p Sponsored by Ministry of Transport
(ISSN 0169-1651)
(KNMI-SR-94-03; ISBN-90-369-2054-X) Copyright Avail: Issuing Activity

Forecasts of global air transport demand predict an average annual growth rate between 5 and 7 percent until 2010. This implies that in 2005 the number of passenger-kilometers performed will at least be doubled compared to the situation in 1990. Since aircraft emit components which are both greenhouse gases and ozone precursors, this forecast of a substantial world-wide increase in air traffic aroused new interest, from both scientists and policy-makers, in the atmospheric effects of aircraft exhaust. But although a great deal of work in both fields has been done on investigating and how to deal with the effects of air traffic at and around airports and of future supersonic flights in the stratosphere, little is known about the effects of subsonic aircraft during cruise. This reports' objective is to contribute to fill this gap. By merging the results of many studies which directly or indirectly aimed at elucidating one aspect of the complex problem of how high-flying aircraft influence atmospheric processes, an attempt is made to give the readers some insight in, and sense of the seriousness of, the effects of high-flying aircraft. Author

N95-18742*# National Aeronautics and Space Administration, Washington, DC.

REMOTE SENSING/GLOBAL CHANGE. A SPECIAL BIBLIOGRAPHY

Nov. 1994 97 p
(NASA-TM-110038; NAS 1.15:110038; AD-B192484L) Avail: CASI HC A05/MF A02

The first portion of this bibliography contains citations (with abstracts, when available) to unclassified literature contained in the NASA STI Database. These citations also appeared in issues of the abstract journal 'Scientific and Technical Aerospace Reports (STAR)', or in other announcement products offered by the NASA STI Program. The citations appear in ascending accession number order. A second section provides several indexes to the citations. They are subject term, personal author, report number, and accession number. The citations are included for the following disciplines as they relate to remote sensing and global change: astronautics, engineering, geosciences, life sciences, mathematical and computer sciences, social sciences, and space sciences. Transl. by

N95-18895# Lawrence Livermore National Lab., Livermore, CA.

A MULTIPLE TIME SCALE SOLUTION FOR THE CHAPMAN MECHANISM

B. Chang Jun. 1994 12 p
(Contract W-7405-eng-48)
(DE94-017491; UCRL-ID-116663) Avail: CASI HC A03/MF A01

The rate equations representing the Chapman mechanism are solved analytically in the Multiple Time Scale Approximation by the exploitation of their stiffness. The widely different time scales of the reactions in the mechanism can be used to disentangle their effects on the solution. The reactions which bring oxygen into equilibrium with ozone are responsible for the overall stiffness, because their time scales are on the extreme ends of time scale spectrum for the reactions comprising the Chapman mechanism. Since catalytic cycles have similar equilibration reactions which may have time scales bordering the time scales of other reactions involving the catalysts, the method of multiple time scales can also be used to cured the stiffness in the rate equations governing these cycles. These analytical solutions may be incorporated into a numerical algorithm to improve its efficiency for the computation of the rate equations governing the chemistry of the atmosphere. DOE

N95-19033*# California Inst. of Tech., Pasadena, CA. Lab. of Experimental Geophysics.

SHOCK-INDUCED DEVOLATIZATION OF CALCIUM SULFATE AND IMPLICATIONS FOR K-T EXTINCTIONS

Guangqing Chen, James A. Tyburczy (Arizona State Univ., Tempe, AZ.), and Thomas J. Ahrens 22 Nov. 1993 30 p Sponsored by NASA, Washington
(NASA-CR-197608; NAS 1.26:197608; Contrib-5350) Avail: CASI HC A03/MF A01

Calcium sulfate devolatization during the impact at Chicxulub, Mexico and dispersal in the stratosphere of the resultant sulfuric acid aerosol have been suggested as a possible mechanism for the Cretaceous-Tertiary extinctions. In this paper, we investigated two shock-induced devolatization reactions of calcium sulfate up to 42 GPa in the laboratory: CaSO4 + SiO2 yields CaSiO3 + SO3(degassed) and CaSO4 yields CaO + SO2(degassed) + 1/2 O2(degassed). We found both to proceed to a much less extent than calculated by equilibrium thermodynamic calculations. Reaction products are found to be 10(exp -2) times those calculated for equilibrium. Consequently our estimate of the amount of sulfur oxides degassed into the atmosphere from shock devolatization of CaS04 in the Chicxulub lithographic section (6x10(exp 15)-2x10(exp 16)g in sulfur mass) is lower by a factor of 70 to 400 than previous estimates; the related environmental stress arising from the resultant global cooling of approximately 4 K and fallout of acid rain does not appear to suffice to explain the widespread K-T extinctions. Derived from text

N95-19112# Michigan Univ., Ann Arbor, MI. School of Natural Resources and Environment.

CHANGES IN THE FLUX OF CARBON BETWEEN PLANTS AND SOIL MICROORGANISMS AT ELEVATED CO2: PHYSIOLOGICAL PROCESSES WITH ECOSYSTEM-LEVEL IMPLICATIONS

Donald R. Zak and Kurt S. Pregitzer (Michigan Technological Univ., Houghton, MI.) 15 May 1994 8 p
(Contract DE-FG02-93ER-61666)
(DE94-017067; DOE/ER-61666/1) Avail: CASI HC A02/MF A01

Our ability to interpret ecosystem response to elevated atmospheric CO2 is contingent on under standing and integrating a complex of physiological and ecological processes. However, we have a limited understanding of the combined effects of changes in plant carbon (C) allocation, microbial activity, and nitrogen (N) dynamics on the long-term response of terrestrial ecosystems to elevated CO2. Individually, these factors are potent modifiers of C and N dynamics, and an in depth

understanding of their interactions should provide insight into ecosystem-level responses to global climate change. Our research is aimed at quantifying the physiological mechanisms leading to increased fine root production, microbial biomass and rates of N cycling at elevated atmospheric CO2. More specifically, we will experimentally manipulate soil nitrogen availability and atmospheric CO2 to understand how changes in plant resource availability influence the cycling of carbon between plants and soil microorganisms. DOE

N95-19403# Research Triangle Inst., Research Triangle Park, NC. Center for Economics Research.

ECONOMIC IMPACT ANALYSIS FOR PROPOSED EMISSION STANDARDS AND GUIDELINES FOR MUNICIPAL WASTE COMBUSTORS: A DESCRIPTION OF THE BASIS FOR, AND IMPACTS OF, PROPOSED REVISIONS TO AIR POLLUTANT EMISSION REGULATIONS FOR NEW AND EXISTING MUNICIPAL WASTE COMBUSTORS UNDER CLEAN AIR ACT SECTIONS 111(B), 111(D), AND 129 Final Report

B. L. Jellicorse and J. L. Dempsey Mar. 1994 182 p

(Contract EPA-68-D1-0143)

(PB94-213543; RTI/5681/57; EPA/450/3-91/029) Avail: CASI HC A09/MF A02

EPA is proposing revised and expanded air pollutant emission standards for new, and guidelines for existing, municipal waste combustors (MWC's), pursuant to Sections 111(b), 111(d), and 129 of the Clean Air Act of 1990. The regulations will replace or supplement those promulgated by EPA on February 11, 1991. The standards and guidelines will apply to MWC's with a capacity to combust 35 or more Mg of municipal solid waste per day. The pollutants to be regulated are particulate matter (total and fine), opacity, sulfur dioxide, hydrogen chloride, oxides of nitrogen, carbon monoxide, lead, cadmium mercury, and dibenzofurans and dioxins. The report describes the standards and guidelines, their potential economic impacts, and related matters. EPA estimates the national annual cost of the standards in 1994 will be $44 million, plus the cost of the 1991 standards, $157 million, for a total of $201 million. EPA estimates the equivalent cost of the guidelines at $280 million plus $168 million for a total of $448 million. NTIS

N95-19406# Environmental Protection Agency, Research Triangle Park, NC. Office of Air Quality Planning and Standards.

ALTERNATIVE CONTROL TECHNIQUES DOCUMENT: NO(x) EMISSIONS FROM GLASS MANUFACTURING

W. J. Neuffer Jun. 1994 160 p See also PB88-101795

(PB94-214079; EPA/453/R-94/037) Avail: CASI HC A08/MF A02

This alternative control techniques (ACT) document describes available control techniques for reducing NO(x) emissions from glass furnaces. Control techniques include low NO(x) burners, oxy-firing, modified furnace, cullet preheat, electric boost, selective catalytic reduction, and selective noncatalytic reduction. Achievable controlled NO(x) emission levels, costs, and cost effectiveness and environmental and energy impacts for these controls are discussed. NO(x) formation and uncontrolled NO(x) emission levels are also discussed. NTIS

N95-19556# Oak Ridge National Lab., TN.

HISTORIC PATTERNS OF CO2 EMISSIONS FROM FOSSIL FUELS: IMPLICATIONS FOR STABILIZATION OF EMISSIONS

R. J. Andres and G. Marland 1994 16 p Presented at the Annual Meeting and Exhibition of the Air and Waste Management Association, Cincinnati, OH, 19-24 Jun. 1994

(Contracts DE-AC05-84OR-21400; DE-AC05-76OR-00033)

(DE95-000489; CONF-940632-25) Avail: CASI HC A03/MF A01

This paper examines the historical record of greenhouse gas emissions since 1950, reviews the prospects for emissions in the future, and projects what would be the short-term outcome if the stated targets of the FCCC were in fact achieved. The examination focuses on the most important of the greenhouse gases, CO2. The extensive record of historic CO2 emissions is explored to ascertain if it is an adequate basis for useful extrapolation into the near future. Global carbon dioxide emissions from fossil fuel consumption have been documented. Emissions grew at 4.3% per year from 1950 until the time of the 1973 oil crisis. Another disruption in growth followed the oil price increases of 1979. Global total emissions have been increasing steadily since the 1982-1983 minimum and have grown by more than 20% since then. At present, emission of CO2 from fossil fuel burning is dominated by a few countries: the U.S., the former Soviet Union, China, the developed countries of Europe and Japan. Only 20 countries emit 84% of emissions from all countries. However, rates of growth in many of the developed countries are now very low. In contrast, energy use has grown rapidly over the last 20 years in some of the large, developing economies. Emissions from fossil fuel consumption are now nearly 4 times those from land use change and are the primary cause of measured increases in the atmospheric concentration of CO2. The increasing concentration of atmospheric CO2 has led to rising concern about the possibility of impending changes in the global climate system. In an effort to limit or mitigate potential negative effects of global climate change, 154 countries signed the United Nations Framework Convention on Climate Change (FCCC) in Rio de Janeiro in June, 1992. The FCCC asks all countries to conduct an inventory of their current greenhouse gas emissions setting non-binding targets. DOE

N95-19582# Energy and Environmental Analysis, Inc., Arlington, VA.

AIR POLLUTION MITIGATION MEASURES FOR AIRPORTS AND ASSOCIATED ACTIVITY

May 1994 206 p Prepared in cooperation with K. T. Analytics, Inc., Frederick, MD

(Contract ARB-A132-168)

(PB94-207610; ARB-R-94/534) Avail: CASI HC A10/MF A03

This report is a reference guide to emission mitigation techniques that can be applied to aircraft and their operations, the ground support equipment that service aircraft at airports, and other airport on-road and off-road emission sources such as maintenance, passenger, and employee vehicles. Each measure is described along with guidelines for its use and constraints that may limit its effectiveness. The information can be used to quantify emission reductions that result from operational, procedural, or technological changes to these sources. Projects and plans to reduce air pollution at U.S. and European airports are described. A detailed description of procedures used to calculate aircraft emissions is provided in an appendix. NTIS

N95-19685# Air Force Inst. of Tech., Wright-Patterson AFB, OH. School of Engineering.

DEVELOPING AN EMISSION FACTOR FOR HAZARDOUS AIR POLLUTANTS FOR AN F-16 USING JP-8 FUEL M.S. Thesis

Donald J. VanSchaack Sep. 1994 99 p

(AD-A284802; AFIT/GEE/ENS/94S-26) Avail: CASI HC A05/MF A02

The 1990 Clean Air Act amendments drastically changed the legislation of hazardous air pollutants (HAPs) or air toxics. Title 3 of the act which specifically addresses HAPs now lists 189 substances which may require regulation as air toxics. Consequently, the reporting of HAP emissions from all Air Force operations will be required in the future. However, the Department of Defense (DoD) does not have methods available to report this information. This thesis develops emission factors for selected HAPs from an F-16 C&D aircraft/F110 engine operating on JP-8 fuel. The methodology included: determining which HAPs should be selected, using past aircraft emission studies to estimate HAP concentrations for the F110 engine using JP-8 fuel, determining an emission factor formula to calculate emission factors for each HAP, and testing the developed emission factors on an airfield operation. The estimated emission factors for each HAP for the F110 engine are low for all engine modes mainly because the F110 is a newer engine with high combustion efficiency. The resultant emission inventory shows that many HAPs would be classified as major sources under current Title 3 legislation. Thus, it is important to assess airfield operations to ensure they remain in compliance with the upcoming Title 3 legislation. DTIC

N95-19686# Air Force Inst. of Tech., Wright-Patterson AFB, OH. School of Engineering.

DEVELOPMENT OF A COMPREHENSIVE BASE-LEVEL ENVIRONMENTAL TRAINING PROGRAM FOR TOTAL ENVIRONMENTAL COMPLIANCE M.S. Thesis

William M. Barrett, Jr. Sep. 1994 119 p

(AD-A284806; AFIT/GEE/ENV/94S-03) Avail: CASI HC A06/MF A02

The leadership of the Air Force has established a goal of total environmental compliance because it is the right and necessary thing to do. Commitment to this goal can be accomplished through strong leadership;

however, achieving this goal can only be accomplished through effective training. The lack of consistent guidance for developing and executing comprehensive base-level environmental training programs has forced bases to develop these training programs by whatever means available to them. This has resulted in a broad variation in the thoroughness of base-level training programs throughout the Air Force. This research effort investigates the relationship between the thoroughness of base-level environmental training programs and base environmental compliance and identifies training program improvements which will help the Air Force achieve its goal. Existing base-level environmental training programs were graded with a quality score based upon a measurement of the training content and the target audiences' functional level. A statistical correlation between the training quality score and environmental compliance status was assessed in light of other possible influences using an analysis of covariance method. The analysis showed significant potential for improving base-level training and the need for major command policies regarding environmental training of base-level personnel. DTIC

N95-19779*# Colorado Univ., Boulder, CO. Cryospheric and Polar Processes Div.

ASSESSMENT OF CLIMATE VARIABILITY OF THE GREENLAND ICE SHEET: INTEGRATION OF IN SITU AND SATELLITE DATA Annual Progress Report, 30 May - 5 Jun. 1993

K. Steffen, W. Abdalati, J. Stroeve, and J. Key Jan. 1994 28 p (Grant NAGw-2158)

(NASA-CR-197604; NAS 1.26:197604) Avail: CASI HC A03/MF A01

The proposed research involves the application of multispectral satellite data in combination with ground truth measurements to monitor surface properties of the Greenland Ice Sheet which are essential for describing the energy and mass of the ice sheet. Several key components of the energy balance are parameterized using satellite data and in situ measurements. The analysis will be done for a ten year time period in order to get statistics on the seasonal and interannual variations of the surface processes and the climatology. Our goal is to investigate to what accuracy and over what geographic areas large scale snow properties and radiative fluxes can be derived based upon a combination of available remote sensing and meteorological data sets. Operational satellite sensors are calibrated based on ground measurements and atmospheric modeling prior to large scale analysis to ensure the quality of the satellite data. Further, several satellite sensors of different spatial and spectral resolution are intercompared to access the parameter accuracy. Proposed parameterization schemes to derive key component of the energy balance from satellite data are validated. For the understanding of the surface processes a field program was designed to collect information on spectral albedo, specular reflectance, soot content, grain size and the physical properties of different snow types. Further, the radiative and turbulent fluxes at the ice/snow surface are monitored for the parameterization and interpretation of the satellite data. The expected results include several baseline data sets of albedo, surface temperature, radiative fluxes, and different snow types of the entire Greenland Ice Sheet. These climatological data sets will be of potential use for climate sensitivity studies in the context of future climate change. Author

N95-19808 Army Engineer Waterways Experiment Station, Vicksburg, MS. Environmental Lab.

HEAVY METAL SOIL CONTAMINATION AT US ARMY INSTALLATIONS: PROPOSED RESEARCH AND STRATEGY FOR TECHNOLOGY DEVELOPMENT Final Report

R. M. Bricka, Clint W. Williford, and Larry W. Jones Mar. 1994 81 p Limited Reproducibility: More than 20% of this document may be affected by microfiche quality

(AD-A279171; WES/TR/EL-IRRP-94-1) Avail: Issuing Activity (Defense Technical Information Center (DTIC))

This document represents a research strategy to develop new and innovative technologies for treatment of heavy metal-contaminated soils on U.S. Army installations. For a technology to be considered, it must be effective, economically feasible, and available for implementation within 5 years. The activities undertaken to develop the research strategy are also described in this report. A survey of U.S. Army installations shows that soils contaminated by heavy metals are a common problem. Over 50 percent of the installations surveyed have potential heavy metal problems that may prove to be costly and/or beyond current technology to remediate. Of the six analytes found most often as contaminants in a U.S. Army Environmental Center (USAEC) database, five are classified as heavy metals. Chrome, lead, and cadmium are the most common metal contaminants. Further, the variety of contaminated media (e.g., water, soils, and structure) at military installations makes it likely that a variety of cleanup technologies will be required. The scientific basis of the interaction of heavy metals with different soils is briefly discussed in this report to provide an understanding of the efficacy of potential soil remediation techniques. Consideration is given to a 1987 review of soil remediation technologies produced by Roy F. Weston, Inc., for USAEC; to the results of the deliberations of an advisory panel empaneled specifically to address metal/soil cleanup technologies, and to site visits and inquiries by personnel of the U.S. Army Engineer Waterways Experiment Station (WES) Environmental Laboratory. DTIC

N95-19860 Army Construction Engineering Research Lab., Champaign, IL.

ENVIRONMENTAL COMPLIANCE ASSESSMENT SYSTEM (ECAS). SOUTH CAROLINA SUPPLEMENT: US ARMY Final Report

Carolyn ORourke and Lisa A. Gifford Apr. 1994 403 p Limited Reproducibility: More than 20% of this document may be affected by microfiche quality

(AD-A279244; CERL-SR-EC-94/17) Avail: Issuing Activity (Defense Technical Information Center (DTIC))

In response to the growing number of environmental laws and regulations worldwide, the U.S. Army has adopted an environmental compliance program that identifies compliance problems before they are cited as violations by the U.S. Environmental Protection Agency (USEPA). Beginning in 1985, Major Army Commands (MACOM's) were required to conduct comprehensive environmental assessments at all installations on a 4-year cycle. The installations must also conduct a mid-cycle internal assessment. Because each MACOM was developing a separate assessment system, the Army mandated, through Army Regulation 200-1, one unified Army-wide assessment mechanism. The resulting system combines Federal, Department of Defense (DOD), and Army environmental regulations, along with good management practices and risk management information, into a series of checklists that show legal requirements and which specific items or operations to review. Each assessment protocol lists a point of contact to help assessors review the checklist items as effectively as possible. The Environmental Compliance Assessment System (ECAS) manual incorporates existing checklists from USEPA and private industry. The South Carolina Supplement was developed to be used in conjunction with the U.S. ECAS manual, using existing South Carolina state environmental legislation and regulations as well as suggested management practices. DTIC

N95-19879# State Univ. of New York, Albany, NY. Atmospheric Sciences Research Center.

A REPORT ON WORKSHOPS: GENERAL CIRCULATION MODEL STUDY OF CLIMATE: CHEMISTRY INTERACTION

Wang Wei-Chyung and Ivar S. A. Isaksen (Oslo Univ., Norway.) 1993 10 p Presented at the Workshop on General Circulation Model Study: Climate-chemistry Interactions; Workshop on General Circulation Model Study: Climate-chemistry Interactions, Oslo (Norway); Albany, NY, 19-21 Aug. 1992; 26-27 May 1993

(Contract DE-FG02-92ER-61447)

(DE94-010252; DOE/ER-61447/1; CONF-9208255-Summ; CONF-9305343-Summ) Avail: CASI HC A02/MF A01

This report summarizes the discussion on General Circulation Model Study of Climate-Chemistry Interaction from two workshops, the first held 19-21 August 1992 at Oslo, Norway and the second 26-27 May 1993 at Albany, New York, USA. The workshops are the IAMAP activities under the Trace Constituent Working Group. The main objective of the two workshops was to recommend specific general circulation model (GCM) studies of the ozone distribution and the climatic effect of its changes. The workshops also discussed the climatic implications of increasing sulfate aerosols because of its importance to regional climate. The workshops were organized into four working groups: observation of atmospheric O3; modeling of atmospheric chemical composition; modeling of sulfate aerosols; and aspects of climate modeling. DOE

N95-18991*# Georgia Univ., Athens. Dept. of Geography.
A GIS APPROACH TO URBAN HEAT ISLAND RESEARCH: THE CASE OF HUNTSVILLE, ALABAMA
Chor Pong Lo *In* Alabama Univ., Research Reports: 1994 NASA/ASEE Summer Faculty Fellowship Program Oct. 1994 6 p (For primary document see N95-18967 05-80)
Avail: CASI HC A02/MF A03

46 GEOPHYSICS

Includes aeronomy; upper and lower atmosphere studies; ionospheric and magnetospheric physics; and geomagnetism.
For space radiation see *93 Space Radiation.*

N95-17946# Los Alamos National Lab., NM.
MAGNETOTELLURIC MAPPING OF UPPER CRUSTAL ISOTHERMS BENEATH THE VALLES CALDERA HYDROTHERMAL SYSTEM
George R. Jiracek (San Diego State Univ., San Diego, CA.), Christopher L. Kinn (San Diego State Univ., San Diego, CA.), Clark L. Scott (San Diego State Univ., San Diego, CA.), Scott A. Curran (San Diego State Univ., San Diego, CA.), and Martha G. Kuykendall (California Inst. of Tech., Pasadena, CA.) 1993 5 p
(Contract W-7405-eng-36)
(DE94-013606; LA-SUB-94-38) Avail: CASI HC A01/MF A01

Magnetotelluric (MT) soundings across the western margin of the Valles Caldera hydrothermal system in New Mexico have revealed a striking correlation between depth of the electrically conductive portion of the upper crust and isotherms projected from deep geothermal test wells. The crust is highly resistive (approximately greater than 1000 ohm-m) in the range of 2 to 4 km depth where temperatures of over 300 C have been logged in test wells. However, at greater depths the upper crust becomes increasingly conductive; in this range, the conductivity contours closely match the projected isotherms. The inferred geoelectric section was obtained by two-dimensional inversion after shallow three-dimensional distortion corrections were applied to the data. Inversions were constrained to depths as great as 4 km by borehole electric logs which highly compatible with the nearby MT soundings. Possible reasons for the positive correlation between the conductive depth patterns and the isotherms are: (1) fluid accumulation within the thermally controlled brittle-ductile transition and (2) a halo of conductive mineralization (e.g., connected sulfide films) surrounding a still cooling, shallow intrusive. DOE

N95-17947# Los Alamos National Lab., NM.
TRACE ELEMENT CHARACTERISTICS OF LITHOSPHERIC AND ASTHENOSPHERIC MANTLE IN THE RIO GRANDE RIFT REGION
F. V. Perry (New Mexico Univ., Albuquerque, NM.) 1994 5 p
(Contract W-7405-eng-36)
(DE94-013609; LA-SUB-94-76) Avail: CASI HC A01/MF A01

Trace element analyses of 10 mafic volcanic rocks from the Colorado Plateau transition zone, Colorado Plateau, Rio Grande rift, and Great Plains were obtained to characterize the trace element characteristics of asthenospheric and lithospheric mantle beneath these regions. Characterization of these mantle reservoirs using the trace element contents of basalts allows one to track the response of the lithosphere to continental rifting and extension. DOE

N95-17967 Washington Univ., Seattle, WA.
TWO AND THREE DIMENSIONAL MAGNETOTELLURIC INVERSION
J. R. Booker 1994 4 p Limited Reproducibility: More than 20% of this document may be affected by microfiche quality
(Contract DE-FG06-92ER-14231)
(DE94-014820; DOE/ER-14231/1) Avail: CASI HC A01

Improved imaging of underground electrical structure has wide practical importance in exploring for groundwater, mineral, and geothermal resources, and in characterizing oil fields and waste sites. Because the electromagnetic inverse problem for natural sources is generally multidimensional, most imaging algorithms saturate available computer power long before they can deal with complete data sets. We have developed an algorithm to directly invert large multidimensional magnetotelluric data sets that is orders of magnitude faster than competing methods. In the past year, we have extended the two-dimensional (2D) version to permit incorporation of geological constraints, have developed ways to assess model resolution, and have completed work on an accurate and fast three-dimensional (3D) forward algorithm. We are proposing to further enhance the capabilities of the 2D code and to incorporate the 3D forward code in a fully 3D inverse algorithm. Finally, we will embark on an investigation of related EM imaging techniques which may have the potential for further increasing resolution. DOE

N95-18115# Army Research Lab., White Sands Missle Range, NM. Battlefield Environment Directorate.
ENERGY BALANCE MODEL FOR iMAGERY AND ELECTROMAGNETIC PROPAGATION Final Report
Henry Rachele and Arnold Tunick Jul. 1994 58 p Revised
(AD-A284552; ARL-TR-522) Avail: CASI HC A04/MF A01

The optical turbulence structure parameter C(sup 2) sub n typically appears in equations used to estimate the effects of temperature and moisture (gradients) on imagery and electromagnetic propagation. Temperature and moisture gradients can be approximated from sensible and latent heat flux estimates, by the application of basic Obukhov similarity theory parameterizations, and the fluxes can be obtained from radiation/energy balance equations. Numerous energy balance models exist requiring different kinds and numbers of inputs. The semiempirical model developed and presented was constrained to require a minimum number of conventional measurements at a reference level (2 m). There measurements include temperature, pressure, relative humidity, and windspeed. The model also requires a judgment of soil type and moisture (dry, moist, or saturated), cloud characteristics (tenths of cloud cover and density and an estimate of cloud height), day of the year, time of day, and longitude and latitude of the site. Model estimates of net radiation, sensible, ground, and latent heat fluxes are compared with measured values. Comparisons of C(sup 2) sub n estimates computed from measured versus modeled energy fluxes are also made. DTIC

N95-18125# Los Alamos National Lab., NM.
OBSERVATIONS OF TEC FLUCTUATIONS FROM AN EXPLOSION ON THE EARTH'S SURFACE
R. S. Massey, R. C. Carlos, A. R. Jacobson, and G. Wu 1994 5 p Presented at the International Beacon Satellite Symposium, Aberystwyth, Wales, 11-15 Jul. 1994
(Contract W-7405-eng-36)
(DE94-018278; LA-UR-94-2777; CONF-9407124-2) Avail: CASI HC A01/MF A01

The authors report observations of perturbations in the ionosphere total electron content (TEC) caused by acoustic waves propagating from a large chemical explosion in southern New Mexico at the earth's surface. Fluctuations in TEC were measured by two arrays of receivers that monitor the phase of the 136 MHz beacons on two geostationary satellites. One array, located in northern New Mexico, observed fluctuations in the region where acoustic waves from the blast impinged directly on the ionosphere, while the second array, in Texas, was located to observe fluctuations caused by ducted acoustic waves. The TEC disturbance at the New Mexico array had an amplitude of about 2x10(exp 14) m(sup -2) (more than 10 times the array noise level), while the amplitude at the Texas array, at a range of 900 km, was only a few times the instrumental noise level. Noise background analysis shows that the probability that a comparable or larger response at the New Mexico array might have been caused by a background noise event was less than 1%. The corresponding probability for the Texas array was 3%. DOE

N95-18148# Los Alamos National Lab., NM.
RESULTS FROM THE NORTHERN NEW MEXICO SATELLITE-BEACON RADIO INTERFEROMETER
R. Carlos, A. Jacobson, R. Massey, and G. Wu 1994 5 p Presented at the International Beacon Satellite Symposium, Aberystwyth, Wales, 11-15 Jul. 1994
(Contract W-7405-eng-36)
(DE94-018310; LA-UR-94-2951; CONF-9407124-1) Avail: CASI HC A01/MF A01

An interferometer described in the Boston, 1992, meeting of the Beacon Satellite Symposium has been in full operation for over a year now. It consists of four autonomous stations; three are in a triangle 70 km on a side and one is in the center. The stations receive the VHF beacons from

two geosynchronous satellites, GOES-2 and ATS-3. The phases of the beacons are tracked at each station by referring them to an extremely stable rubidium oscillator. The studies of the two satellites are virtually separate experiments. The received phase of the beacon is retarded by the increased Total-Electron-Content of the dense regions of waves in the ionosphere. By comparing the phase history at four spatially separated stations, the authors can determine the two-dimensional propagation vector of the waves. This array is optimal for wavelengths of 70-300 km (periods of 300-3,000 seconds). Since the measurement is of the phase of the signal rather than the difference between the O-mode and X-mode phases, and since the beacons are in the VHF rather than in the L-band of GPS beacons, the array is very sensitive. It has a noise level of 10(exp 13) electrons/m(exp 2), or 10(sup -4) of the normal daytime TEC. This has been verified by operating two stations in the same location, so that they saw the same ionosphere. The first interesting results from a year's study is that the authors do not see the same TID's when looking at the two satellites. One conclusion they draw is that they do not see evidence of ionospheric winds. DOE

N95-18390# Instituto de Pesquisas Espaciais, Sao Jose dos Campos (Brazil).

IMAGERY CORRECTION FOR ATMOSPHERIC EFFECTS USING SOUNDING DATA M.S. Thesis [CORRECAO DE UMA IMAGEM PARA OS EFEITOS ATMOSFERICOS UTILIZANDO DADOS DE RADIOSSONDA]

Luiz Carlos Barbosa Ribeiro May 1992 91 p In PORTUGESE
(INPE-5506-TDI/518) Avail: CASI HC A05/MF A01

The upwelling radiation received by a sensor has three distinct components: target radiation directly transmitted through the atmosphere, diffuse radiation from the background and the diffuse atmospheric radiation. The sum of the last two components is called path radiance, whose effects reduce the spatial and spectral variability of the image. So, in order to remove these effects (haze), a method based on radiative transfer equations was used to estimate spurious radiation reaching the sensor. The atmospheric parameters were collected by a sounding device, and a code, LOWTRAN-6, was used to obtain spectral transmittance in the visible and near-IR ranges. A computer program was developed to improve the quality of the images using calculated data. Appreciable results were achieved. Author

N95-18413 South Dakota School of Mines and Technology, Rapid City, SD.

THE NUMERICAL SIMULATION OF MARINE BOUNDARY LAYER CLOUDS Annual Report, 1 Sep. 1993 - 31 Aug. 1994

Harold D. Orville 31 Aug. 1994 8 p Limited Reproducibility: More than 20% of this document may be affected by microfiche quality
(Contract N00014-91-J-4017)
(AD-A284149) Avail: Issuing Activity (Defense Technical Information Center (DTIC))

The primary objectives of the research are to numerically simulate stratus, stratocumulus, and cumulus clouds in the marine boundary layer. This includes the formation, evolution, and dissolution of the clouds and the area covered, then the change from one type of cloud to another would be investigated. Also the change from open cell to closed cell type convection and the formation of cloud streets could investigated. DTIC

N95-18444*# Massachusetts Inst. of Tech., Cambridge. Research Lab. of Electronics.

ATMOSPHERIC INFRARED SOUNDER Semiannual Progress Report, 15 Jun. 1994 - 15 Dec. 1994

Philip W. Rosenkranz and David H. Staelin 21 Dec. 1994 7 p
(Contract NAS5-31376)
(NASA-CR-197573; NAS 1.26:197573) Avail: CASI HC A02/MF A01

The microwave 'first-guess' algorithm was run on the cloudy test simulations. Eight datasets were considered in the cloudy test, comprising approximately 360 retrievals, of which one failed to converge. Retrievals were done on the AMSU-A grid. Examination of the true profiles (provided for the A, C and D tracks) showed numerous cases of very pronounced temperature inversion layers in the troposphere which the retrieval does not have enough vertical resolution to reproduce. A typical example with an inversion layer near 700 mbar is shown in Figure 1. The inversion layers also exhibit strong vertical gradients of water vapor which are not resolved in the retrieval. (Water vapor volume density is given in g/sq cm per layer. Layer thickness is 20 mb from 200 to 400 mb, and 25 mb from 400 to 1,000 mb.) The retrievals do reproduce the overall smoothed shape of the profiles, and therefore as a first guess should be within the range of linear methods for IR retrievals using AIRS. Author

N95-18452 Mission Research Corp., Nashua, NH.

INNOVATIVE DEVELOPMENT AND APPLICATION OF MODELS FOR WEAKLY IONIZED IONOSPHERIC PLASMAS Final Report, 15 May 1990 - 30 Nov. 1993

J. V. Eccles, James Hingst, and Russell Armstrong Nov. 1993 76 p
Limited Reproducibility: More than 20% of this document may be affected by microfiche quality
(Contract F19628-90-C-0118)
(AD-A284583; PL-TR-93-2238; AD-E202162) Avail: CASI HC A05

Artificial modifications of the ionosphere through chemical releases and ionospheric heating experiments are examined with models of chemistry and transport to advance understanding of ion chemistry of the upper atmosphere. The specific releases investigated were the SF6 released of the CRRES-at-Kwajalein rocket campaign and the CO2 releases of the Red Air 1 program. Both the SF6 and CO2 releases experienced freezing or clustering of the molecules. This must be accounted for in the composition and airglow observations. In addition, HF heating effects in the E and F region were examined through modeling of energy deposition and resulting chemistry. NO(x) production in a HF ionospheric heater beam is estimated and compared with natural sources of NO(x). Global effects of HF operation are very small but the local effects can be large enough to permit observable modulation to this environment. DTIC

N95-18476*# New Hampshire Univ., Durham. Inst. for the Study of Earth Oceans and Space.

PARTICLE ACCELERATION AND TRANSPORT IN THE TAIL AND AT THE FRONT SIDE OF THE MAGNETOSPHERE, TASK 1 AND 2 Final Report, 19 Feb. 1991 - 30 Sep. 1994

Lynn M. Kistler, Eberhard Moebius, and Martin A. Lee Dec. 1994 12 p
(Grant NAG5-1548)
(NASA-CR-197575; NAS 1.26:197575) Avail: CASI HC A03/MF A01

The work under this grant involved studies of: (1) the acceleration and heating of ions in the course of magnetospheric substorms and the spatial distributions of the ion populations in the magnetotail; and (2) the comparison in in-situ acceleration at the bow shock and the leakage of energetic particles from the magnetosphere as source of energetic ions upstream of the Earth's bow shock. Author

N95-18623# Naval Postgraduate School, Monterey, CA.

MULTISPECTRAL NOAA MARINE ATMOSPHERIC BOUNDARY LAYER (MABL) ESTIMATES DURING VOCAR M.S. Thesis

David J. Walsh Jun. 1994 115 p
(AD-A283702) Avail: CASI HC A06/MF A02

Satellite derived images of surface relative humidity and boundary layer height are generated from AVHRR data collected in a coastal region during the Variability of Coastal Atmospheric Refractivity (VOCAR) IOP (24 August - 3 September 1993) for comparison with in-situ data. The technique, proposed by Kren (1987) and verified by Smolinski (1988) uses channels 1, 4, and 5 via the relationship between radiative extinction and relative humidity. The input variables measured are sea surface temperature, and total atmospheric water vapor, from the split-window technique in addition to aerosol optical depth, inferred from Channel 1 radiance. The assumption of total atmospheric water vapor confined to the MABL is relaxed. Satellite-derived boundary layer heights are brought into agreement with radiosonde measurements by varying the amount of water vapor confined to the MABL. Agreement between satellite and radiosonde measured heights and slopes is good. Spatial and temporal variability of refractive conditions over the region is large. The method appears capable of tracking the bottom of a trapping layer, associated with the inversion at the top of the MABL, inferred from radiosonde measurements. Comparison with the IR Duct Technique, an empirical method which applies to cloudy areas, shows promise for integration with this technique for clear areas. DTIC

N95-18640 Selskapet for Industriell og Teknisk Forskning, Trondheim (Norway). Div. of Geotechnical Engineering.
LONG-TERM PROCESSES IN GEOMATERIALS. A THREE-DIMENSIONAL VISCO-ELASTIC SOIL MODEL
A. Kavli 10 Nov. 1993 19 p Sponsored by Royal Norwegian Council for Scientific and Industrial Research
(PB94-207180; STF69-A93026) Avail: Issuing Activity (National Technical Information Service (NTIS))

A visco-elastic strain hardening creep model based on a Kelvin body coupled in series with a Hookean spring, is implemented into the finite element program GEOnac. The model is to some extent tested and is found to produce time-deformation curves of similar shape as often seen from laboratory tests on soils. Even though there is a time delay in the deformation, the deformation due to a closed load loop will after infinite time return to the state before the load was applied. This is the definition of visco-elastic behavior. Further model correlations to laboratory measured soil behavior is not done within this project. The work behind this report is performed under the subproject 'Long-term Processes in Geomaterials' of the Norwegian Research Council supported program 'Analysis of Concrete and Geomaterials'. The viscous-elastic behavior model presented in this report can mainly be used for analyzing static loads. NTIS

N95-18731 Georgia Inst. of Tech., Atlanta, GA.
LABORATORY STUDIES OF STRATOSPHERIC BROMINE CHEMISTRY: KINETICS OF THE REACTIONS OF BROMINE MONOXIDE WITH NITROGEN DIOXIDE AND ATOMIC OXYGEN Ph.D. Thesis
Robert Peyton Thorn 1993 259 p
Avail: Univ. Microfilms Order No. DA9415672

A laser flash photolysis - long path absorption - technique has been employed to study the kinetics of the reaction BrO+NO2+M(k(sub 16)) yields products as a function of temperature (248-346 K), pressure (16-800 Torr), and buffer gas identity (N2, CF4). 351 nm photolysis of NO2/Br2/N2 mixtures generated BrO. The BrO decay in the presence of excess NO2 was followed by UV absorption at 338.3 nm. The reaction is in the falloff regime between third and second order over the entire range of conditions investigated. This is the first study where temperature dependent measurements of k(sub 16)(P,T) have been reported at pressures greater than 12 Torr; hence, these results help constrain choices of k(sub 16)(P,T) for use in modeling stratospheric BrO(x) chemistry. The kinetics of the important stratospheric reaction BrO+O(P-3)(k(sub 14)) yields Br+O2 in N2 buffer gas have been studied as a function of temperature (233-328 K) and pressure (25-150 Torr) using a novel dual laser flash photolysis/long path absorption/resonance fluorescence technique. 248 nm pulsed laser photolysis of Br2/O3/N2 mixtures produces O atoms in excess over Br2. After a delay sufficient for BrO to be generated, a 532 nm laser pulse photolysis a small fraction of the O3 to generate O(P-3). The decay of O(P-3) in the presence of an excess, known concentration of BrO, as determined by UV absorption at 338.3 nm and by numerical simulation, is then followed by time-resoved atomic resonance fluorescence spectroscopy. The experimental results have shown the reaction kinetics to be independent of pressure, to increase with decreasing temperature, and to be faster than suggested by the only previous (indirect) measurement. The resulting Anhenius expression for k(sub 14)(T) is k(sub 14)(T) = 1.64 x 10(exp -11) exp(263/T) cm(exp 3) molecule(exp-1)s(exp -1). The absolute accuracy of k(sub 14)(T) at any temperature within the range studied is estimated to be +/- 25%. Possible kinetic interferences from production of vibrationally or electronically excited O2 are discussed. The effect of the faster reaction rate coefficients that are reported for the BrO + NO2 + M and BrO + O(P-3) reactions upon bromine partitioning and ozone depletion in the stratosphere is discussed. Dissert. Abstr.

N95-19032*# New Hampshire Univ., Durham. Dept. of Physics.
CROSS-TAIL CURRENT, FIELD-ALIGNED CURRENT, AND B(y)
Richard L. Kaufmann, Chen Lu, and Douglas J. Larson 1994 60 p
(Grants NAGw-1625; NSF ATM-92-02126)
(NASA-CR-197624; NAS 1.26:197624) Avail: CASI HC A04/MF A01

Orbits of individual charged particles were traced in a one-dimensional magnetic field model that included a uniform cross-tail component B(sub yo). The effects of B(sub yo) on the cross-tail current distribution j(sub y)(z), the average cross-tail drift velocity(nu(sub y)z), and the average pitch angle change(delta alpha) experienced during current sheet encounters were calculated. The addition of a B(sub yo) that exceeded several tenths of one nanotesla completely eliminated all resonance effects for odd-N orbits. An odd-N resonance involves ions that enter and exit the current sheet on the same side. Pitch angles of nearly all such ions changed substantially during a typical current sheet interaction, and there was no region of large cross-tail drift velocity in the presence of a modest B(sub yo). the addition of a very large B(sub yo) guide field in the direction that enhances the natural drift produces a large j(y) and small (Delta alpha) for ions with all energies. The addition of a modest B(sub yo) had less effect near even-N resonances. In this case, ions in a small energy range were found to undergo so little change in pitch angle that particles which originated in the ionosphere would pass through the current sheet and return to the conjugate ionosphere. Finally, the cross-tail drift of ions from regions dominated by stochastic orbits to regions dominated by either resonant or guiding center orbits was considered. The ion drift speed changed substantially during such transitions. The accompanying electrons obey the guiding center equations, so electron drift is more uniform. Any difference between gradients in the fluxes associated with electron and ion drifts requires the presence of a Birkeland current in order to maintain charge neutrality. This plasma sheet region therefore serves as a current generator. The analysis predicts that the resulting Birkeland current connects to the lowest altitude equatorial regions in which ions drift to or from a point at which stochastic orbits predominate. The proposed mechanism appears only in analyses that include non-guiding-center effects. Author

N95-19083# Naval Postgraduate School, Monterey, CA.
DOPPLER SHIFT AND SPREAD STUDY FOR IONOSPHERICALLY PROPAGATED SIGNALS M.S. Thesis
Nickolaos Malachias Jun. 1994 70 p
(AD-A284610) Avail: CASI HC A04/MF A01

Modern, High Frequency (HF) communication techniques, such as spread spectrum and frequency hopping, require precise signal frequency information. The predominant HF propagation path is via the ionosphere, which often produces Doppler frequency shift and spread. This study examined the frequency spectra of selected HF signals traversing short and long mid-latitude paths and one high-latitude auroral zone path. Signal amplitude and Doppler shifts and spreads observed show diurnal, carrier frequency and ionospheric path dependencies. Higher frequency signals experienced more Doppler shift, especially during the daytime. Spectrum spreading was more pronounced at night and was affected by multiple reflections, the auroral oval and field-aligned ionization. Additional signal observations are needed to cover seasonal variations, disturbed ionospheric conditions and solar cycle variations. The impact of Doppler shift and spread on wide-spectrum HF communications also needs to be examined. DTIC

N95-19086# Naval Postgraduate School, Monterey, CA.
FIRST PRINCIPLES USED IN ORBITAL PREDICTION AND AN ATMOSPHERIC MODEL COMPARISON M.S. Thesis
Brian E. Bowden 16 Jun. 1994 71 p
(AD-A284636) Avail: CASI HC A04/MF A01

This thesis develops an orbital prediction model based on fundamental principles of orbital dynamics and drag. A FORTRAN based orbital prediction scheme was designed to provide accurate ephemerides for a particular DOD satellite program. The satellite program under study has satellites at 650 and 800 kilometers with high inclinations. In order to obtain the highest accuracy possible, a comparison of atmospheric models had to be conducted in order to determine which model was more accurate. Mathematical formulation for three widely used earth atmospheric models are presented; the JACCHIA 60, JACCHIA 7 1, and MSIS 86 atmospheric models. The MSIS 86 atmospheric model was not evaluated due to computer problems. Comparison of the two JACCHIA models proved that the JACCHIA 71 model provided much more accurate ephemerides. It is believed that this is due not only to the incorporation of variations in density caused by solar flux, but also geomagnetic activity and a better modeling of the polar regions. Further work on this project would include incorporation of the MSIS 86 model for evaluation, incorporation of the full WGS-84 geopotential model, and using more accurate observed vectors in order to obtain a better comparison. Incorporating a subroutine which will vary the B-factor as a function of latitude will greatly increase accuracy. This is a major deviation from current operational practice, in that the B-factor is often used as an error catch-all and does not truly represent its dynamical purpose. DTIC

N95-19105# Boston Univ., MA. Center for Space Physics.
NEW APPLICATIONS OF THE PHILLIPS LABORATORY. THEORETICAL IONOSPHERIC MODEL AND STUDIES OF NEUTRAL DENSITY WAVES
Matthew W. Fox, Xiaoqing Pi, and Jeffrey M. Forbes Apr. 1994 66 p
(Contract F19628-93-K-0012)
(AD-A284663; PL-TR-94-2161; AD-E202181) Avail: CASI HC A04/MF A01

Firstly, a series of new applications for the PHILLIPS Laboratory ionospheric model have been developed; a version has been prepared that allows restarts from specified background conditions, and runs have been made of both impulsive (e.g., storm onset) and periodic (e.g., atmospheric wave) perturbed conditions. Comparison studies are the subject of ongoing work. Secondly, tests of a new plasmaspheric model have been conducted with a view to merging it with the PL model in a new version of PRISM. Thirdly, the PL model has been applied to a study of the low latitude ionosphere involving comparisons of the observed longitudinal and seasonal morphology of irregularities. Next, a version of the model has been prepared that permits a study of the effects of substorms through modifications of the vertical drift and neutral wind fields. Case studies at different longitudes identified increases in TEC with substorm expansion phases and decreases with substorm subsidence. Finally, SETA measurements of neutral density variations have been utilized in a study of both small-scale (up to 2500 km) larger scale wave phenomena, including descriptions of diurnal and magnetic activity dependencies. DTIC

N95-19129*# Pennsylvania State Univ., University Park, PA. Dept. of Meteorology.
NASA GODDARD EARTH SCIENCES GRADUATE STUDENT PROGRAM Final Technical Report
Thomas P. Ackerman 27 Oct. 1994 91 p
(Grant NAG5-1810)
(NASA-CR-197130; NAS 1.26:197130) Avail: CASI HC A05/MF A01

The evolution of synoptic-scale dynamics associated with a middle and upper tropospheric cloud event that occurred on 26 November 1991 is examined. The case under consideration occurred during the FIRE CIRRUS-II Intensive Field Observing Period held in Coffeyville, KS during Nov. and Dec., 1991. Using data from the wind profiler demonstration network and a temporally and spatially augmented radiosonde array, emphasis is given to explaining the evolution of the kinematically-derived ageostrophic vertical circulations and correlating the circulation with the forcing of an extensively sampled cloud field. This is facilitated by decomposing the horizontal divergence into its component parts through a natural coordinate representation of the flow. Ageostrophic vertical circulations are inferred and compared to the circulation forcing arising from geostrophic confluence and shearing deformation derived from the Sawyer-Eliassen Equation. It is found that a thermodynamically indirect vertical circulation existed in association with a jet streak exit region. The circulation was displaced to the cyclonic side of the jet axis due to the orientation of the jet exit between a deepening diffluent trough and building ridge. The cloud line formed in the ascending branch of the vertical circulation with the most concentrated cloud development occurring in conjunction with the maximum large-scale vertical motion. The relationship between the large scale dynamics and the parameterization of middle and upper tropospheric clouds in large-scale models is discussed and an example of ice water contents derived from a parameterization forced by the diagnosed vertical motions and observed water vapor contents is presented. Author

N95-19387# Technion - Israel Inst. of Tech., Haifa (Israel). Space Research Inst.
INVESTIGATION OF THE IONOSPHERIC SHORT-TERM VARIABILITY Final Report, Sep. 1993 - Aug. 1994
Zwi Houminer Oct. 1994 48 p
(Contract DAJA45-93-C-0035)
(AD-A286253; R/D-7059-EE-01) Avail: CASI HC A03/MF A01

Both the total electron content of the ionosphere (TEC) and the critical frequency of the F2 layer (foF2) exhibit large day-to-day variations during quiet and active geomagnetic periods. It is of great interest to ascertain whether good correlation exists between TEC daily variability about the monthly mean and foF2 variations. With the availability of the global GPS constellation to provide instantaneous time-delay values such a correlation may enable the improvement of HF short-term predictions using passive monitoring of TEC. To determine the correlation, a pilot study was conducted using several months of TEC data taken in Haifa, Israel, during 1980 as well as GPS time-delay measurements taken during the summer of 1992 in Jerusalem, Israel. The corresponding foF2 measurements were from Cape Zevgary, Cyprus. DTIC

N95-19560# Colorado School of Mines, Golden, CO. Center for Wave Phenomena.
A 2D DEPTH MIGRATION IN TRANSVERSELY ISOTROPIC MEDIA USING EXPLICIT OPERATORS
O. Uzcategui Apr. 1994 27 p Presented at the CWP Annual Project Review Meeting, Breckenridge, CO, 11-14 May 1993
(Contract DE-FG02-89ER-14079)
(DE95-000645; DOE/ER-14079/34; CWP-154P; CONF-9305377-3) Avail: CASI HC A03/MF A01

Stable, explicit depth-extrapolation filters can be used to propagate plane waves corresponding to the qP and qSV (quasi-P and quasi-SV propagation) modes for transversely isotropic (TI) media. The author discusses and compares results of two different methods for obtaining the filters for TI media with a vertical axis of symmetry (VTI). The first, a modified Taylor series method, is used to calculate the N-coefficients of a finite-length filter such that the Taylor expansion around vertical propagation matches the spatial Fourier transform of the downward-continuation operator for VTI media. Second, a least-squares method is used to calculate the filter coefficients such that the amplitude and phase departures from the ideal response of the downward-continuation operator for VTI media are minimized over a range of frequencies and propagation angles. In both methods, the amplitude response of the filter is forced to be less than unity in the evanescent region in order to achieve stability. In general, as exemplified in all the cases studied here, the constrained least-squares method produced filters with accurate wavefield extrapolation for a wider range of propagation angles than that obtained for the modified Taylor series method. In both methods, the maximum angle that can be accurately propagated depends on the ratio of frequency to vertical phase velocity (f/V(sub v)), and on the length of the filter. However, for a fixed filter length and for a given ratio f/V(sub v), the maximum angle propagated with accuracy depends on the elastic constants of the medium. The accuracy of the filters degrades as the degree of anisotropy becomes more extreme. DOE

47 METEOROLOGY AND CLIMATOLOGY

Includes weather forecasting and modification.

N95-17938# National Telecommunications and Information Administration, Annapolis, MD.
MEASUREMENTS OF WIND PROFILER EMC CHARACTERISTICS
D. Law, F. Sanders, G. Patrick, and M. Richmond Mar. 1994 72 p Prepared in cooperation with National Oceanic and Atmospheric Administration, Boulder, CO
(PB94-194107; NTIA-93-301) Avail: CASI HC A04/MF A01

The report provides the results of measurements that were conducted on a 404.37 MHz wind profiler located in Platteville, Colorado. These measurements included radiated spectra (both high and low mode), radiated harmonic and subharmonic power measurements, characterization of the antenna frequency response, determination of the radiated antenna gain values near ground level, susceptibility of profiler performance to interference from selected emission waveforms, and the effects on a typical land mobile/amateur operation from wind profiler emissions. In addition, the report presents detailed wind profiler system description including operations/functions, system hardware, digital signal processing, as well as an analytical estimation of the interference effects on profiler performance. The information contained within the report can serve as an aid in conducting electromagnetic compatibility (EMC) analysis to determine compatibility between wind profilers and other systems. NTIS

N95-17952# National Oceanic and Atmospheric Administration, Boulder, CO. Forecast Systems Lab.
PRODUCT USAGE EVALUATION OF THE AVIATION GRIDDED FORECAST SYSTEM WORKSTATION AT THE DENVER CENTER WEATHER SERVICE UNIT

Mary M. Cairns, Jun Chen, and Ronald J. Miller Jun. 1994 38 p
(PB94-195922; NOAA-TM-ERL-FSL-9) Avail: CASI HC A03/MF A01

This report describes the evaluation of an experimental prototype of the Aviation Gridded Forecast System (AGFS) workstation. The AGFS program, sponsored by the Federal Aviation Administration, was established to provide more timely and accurate forecasts of aviation weather (e.g., ceiling, visibility, icing, and turbulence) to the aviation community. In February 1993, the prototype AGFS was installed at the Denver Center Weather Service Unit (CWSU), and since then has been in use by the CWSU meteorologists in their day-to-day forecast process. In order to better understand the types of meteorological products required by the forecasters and to develop workstation requirements for future prototype AGFS workstations, the products selected on the experimental AGFS workstation were evaluated for the period of 11 February through 31 December 1993. Usage logs, the primary analysis tool, are automatically-recorded logs of nearly every selection made on the workstation graphic displays. Products were grouped by type (e.g., radar, surface, and satellite) and scale (e.g., national and regional), and the evaluation covered hourly and monthly totals of products selected. NTIS

N95-17955 Utah Univ., Salt Lake City, UT. Dept. of Meteorology.
MODELING OF CLOUD AND RADIATION PROCESSES FOR LARGE-SCALE CLOUDS AND TROPICAL ANVILS Final Report, 1 Nov. 1991 - 31 Mar. 1994
K. N. Liou, Q. Fu, S. Krueger, J. L. Lee, S. C. Ou, and Y. Takano 31 May 1994 146 p Limited Reproducibility: More than 20% of this document may be affected by microfiche quality
(Grant AF-AFOSR-0039-91)
(AD-A284212) Avail: CASI HC A07

This final report includes five reprints and preprints of papers associated with the modeling of cloud/radiation processes for large-scale clouds and tropical anvils. These papers present (1) a three-dimensional large-scale cloud model for testing the role of radiative heating and ice phase processes, (2) parameterization of the radiative properties of cirrus clouds, (3) discussion of the scattering and absorption properties of ice crystals in relation to numerical modeling, (4) improvements of an ice-phase microphysics parameterization for use in cloud models, and (5) physical discussions on the interactions of radiation and convection in simulated tropical cloud clusters using a cumulus ensemble model. DTIC

N95-17992# National Weather Service, Kansas City, MO. Scientific Services Div.
USE OF PROFILER DATA FOR ANALYSIS AND NOWcasting OF A WINTER SEASON EXTRATROPICAL CYCLONE
B. S. Small Jun. 1994 20 p
(PB94-187804; NOAA-TM-NWS-CR-106) Avail: CASI HC A03/MF A01

In the early 1990's an experimental network of wind profilers was deployed across the central United States. Base profiler data in the form of time-height cross sections and standard pressure plan review have been available to the Weather Service Forecast Office (WSFO) St. Louis staff since late in 1991. Wind profiler information is currently run automatically by Watchdog on AFOS every hour if the forecaster desires. Since the entire profiler network has not been established until recently, relatively few papers have been published utilizing profiler data. The paper will describe the evolution of a winter storm which produced between three and six inches of snow from central Oklahoma to central Illinois. Specifically, it will be shown how profiler data is used to (1) diagnose several meteorological processes during the evolution of a winter storm event and (2) aid the forecasters in producing a short-term forecast or NOWcast. Features discussed will include jet streak formation, the advection of cold air through the depth of the atmosphere, conveyer belt circulations and a significant overrunning episode. Author

N95-17993# National Weather Service, Milwaukee, WI. Forecast Office.
FORECASTING SNOWFALL USING MIXING RATIOS ON AN ISENTROPIC SURFACE: AN EMPIRICAL STUDY
C. Garcia May 1994 36 p
(PB94-188760; NOAA-TM-NWS-CR-105) Avail: CASI HC A03/MF A01

This study attempts to correlate isentropic mixing ratios and the amount of snowfall produced by different snow events. During the course of the study, a forecast technique was developed that utilized realtime quantitative moisture to predict maximum snowfall during the ensuing 12-hour period. The forecast technique lists seven steps for analyzing isentropic plots and associated cross sections. These steps are necessary in order to isolate the mixing ratios which will be most pertinent to a forecasted or ongoing snow event. From empirical evidence gathered during the six years of study, a scale was developed that directly related mixing ratios on an isentropic surface to maximum snowfall using an approximate 2 to 1 ratio. Included are three case studies detailing snow events ranging from light to heavy snowfall. Author

N95-18006# Instituto de Pesquisas Espaciais, Sao Jose dos Campos (Brazil).
OBSERVATIONAL STUDIES AND MODELLING OF INTERCEPTION LOSS OF GROSS RAINFALL IN THE AMAZONIAN RAINFOREST M.S. Thesis [EXPERIMENTOS OBSERVACIONAIS E MODELAGEM DAS PERDAS POR INTERCEPTACAO DA PRECIPITACAO NA FLORESTA AMAZONICA]
Vinicius Nobrega Ubarana Sep. 1994 108 p In PORTUGESE
(INPE-5583-TDI/545) Avail: CASI HC A06/MF A02

In this work the process of interception of gross rainfall by the vegetative cover of Amazonian rainforest in terra firme forest is studied. Numerical models are used with well defined physical basis for the simulation of the process in obtaining of a medium value of the interception loss in the region of Reservations Ducke near Manaus/AM, Amazonia Central. The models used are the SiB (Simple Biosphere Model), calibrated for the site by Sellers, et al., (1989); and the model for the process of interception, Rutter model implemented for the site by Lloyd, et al., (1988). The objective of this part of the work is to compare the results obtained by both models. In addition an observational experiment is conducted to get the interception loss of two different points in the Amazonia: one in the Reserva Biologica do Jaru in Ji-Parana/RO, Amazonia Ocidental and the other in the Reserva da Vale do Rio Doce in Maraba/PA, Amazonia Oriental. The methodology is based on the work of Lloyd and Marques (1988). The results obtained with the modeling process indicated a behavior very similar to the model results although with an overestimated value for the region. The difference, however, is within the error limit in the determination of the observed value. For the period studied the SiB's model estimated an interception loss equivalent to 10.9 percent of total precipitation and the Rutter model estimated 12.9 percent. For the Ji-Parana region, 12.5 percent of interception loss was observed during the period August 1992 to July 1993. In Maraba the interception represented 13 percent of the gross rainfall during the period September 1992 to June 1993. It is proposed that we carry on the observational experiment for at least one more year. Author (revised)

N95-18014 Air Force Environmental Technical Applications Center, Scott AFB, IL.
CLIMATE AND WEATHER OF CENTRAL AFRICA. EXECUTIVE SUMMARY
Kenneth R. Walters, Sr., Christopher A. Donahue, Gary L. Welch, and Andrew C. Henderson Aug. 1994 110 p Limited Reproducibility: More than 20% of this document may be affected by microfiche quality
(AD-A283647; USAFETAC/TN-94/004) Avail: Issuing Activity (Defense Technical Information Center (DTIC))

A brief executive summary that describes the weather and climatology of Central Africa, an area that comprises Kenya, Tanzania, Uganda Rwanda, Burundi, and Zaire. For the purposes of this study, Zimbabwe (in southern Africa) has been added. Appendices provide summarized airfield weather data, paradrop weather, and cloud ceiling frequencies. Author (DTIC)

N95-18038 National Weather Service, Silver Spring, MD. Techniques Development Lab.
MISCELLANEOUS DISK UTILITY APPLICATION PROGRAMS FOR THE AFOS BACKGROUND PARTITION
R. A. Beasley Apr. 1994 23 p See also PB94-143245 Limited Reproducibility: More than 20% of this document may be affected by microfiche quality
(PB94-181328; NOAA-NWS-TDL-CP-94-2) Avail: Issuing Activity (National Technical Information Service (NTIS))

The document provides information and instructions for the collection of programs, CHECKDISK, DELOBYT, and CHECKLINKS, which allow miscellaneous Real Time Disk Operating System (RDOS) tasks to be performed on the background partition of the National Weather Service's (NWS) Automation of Field Operations and Services (AFOS) computer

system. CHECKDISK allows an AFOS site to monitor its disk space on any drive or in any partition. DELOBYT allows sites to easily remove unwanted zero byte count files, which each needlessly take up an RDOS block. CHECKLINKS allows offices to remove unresolved links. Author

N95-18076 Florida State Univ., Tallahassee, FL. Center for Ocean-Atmosphre Prediction Studies.

MARGINAL PROBABILITIES OF THE EXTREMES OF ENSO EVENTS FOR TEMPERATURE AND PRECIPITATION IN THE SOUTHEASTERN UNITED STATES

James J. OBrien Aug. 1994 126 p Limited Reproducibility: More than 20% of this document may be affected by microfiche quality

(AD-A284716) Avail: CASI HC A07

The changes in seasonal average maximum and temperature and seasonal mean monthly precipitation during El Nino/Southern Oscillation (ENSO) events are assessed at 36 stations in the southeastern United States by classifying 40 years (1948-1987) of monthly climate data as occurring during an El Nino (anomalously warm equatorial Pacific Ocean), El Viejo (anomalously cold equatorial Pacific Ocean), or neutral event using sea surface temperature data from the equatorial Pacific Ocean. The statistical distributions of the seasonal data are estimated by repeated sampling of available monthly data (a 'bootstrap technique'). The difference in means among the El Nino, El Viejo and neutral events are determined. The marginal probability is defined as the probability of a three-month seasonal average exceeding one standard deviation from the mean of all 40 years in the research period for a climate variable given an El Nino or El Viejo event is occurring. These are calculated for every station and each of ten different three-month seasons during an 'ENSO year', defined as running from October through the following September. The results indicate the southeastern United States tends to be cooler and wetter during El Nino events and warmer and drier during El Viego events. In contrast to previous studies, the magnitude of the cooling does not seem to be meaningful for El Nino events. Thus, the cold ENSO extreme called El Viejo seems to be most important for the extreme southeastern states of Florida, Georgia and South Carolina. DTIC

N95-18093*# Alabama Univ., Huntsville, AL. Earth System Science Lab.

FIELD AND DATA ANALYSIS STUDIES RELATED TO THE ATMOSPHERIC ENVIRONMENT Final Report, 21 Feb. 1991 - 1 Mar. 1994

Stanley Kidder, Douglas Mach, Jeff Bailey, Michael Stewart, Dave Slaton, Dennis Buechler, Michael Botts, and Laurie Collins Mar. 1994 7 p

(Contract NAS8-38776)

(NASA-CR-196543; NAS 1.26:196543) Avail: CASI HC A02/MF A01

This report summarizes work on a broad array of projects including: (1) applications of meteorological and/or oceanographic satellites; (2) improvement of the current set of NASA/USAF lightning related launch commit criteria rules; (3) the design, building, testing and deployment of a set of cylindrical field mills for aircraft use; (4) the study of marginal electrification storm conditions in relationship to the current launch commit rules for the space shuttle and various other launch vehicles using an instrumented aircraft; (5) support of the DC-8 and ER-2 lightning instrument package as part of both the Tropical Ocean - Global Atmospheric/Coupled Ocean-Atmospheric Response Experiment and the Convection and Moisture Experiment; (6) design of electronic circuitry and microprocessor firmware for the NASA Advanced Ground Based Field Mill; (7) design and testing of electronic and computer instrumentation for atmospheric electricity measurements; (8) simulating observations from a lightning imaging sensor on the Tropical Rainfall Measuring satellite; and (9) supporting scientific visualization and the development of computer software tools.

Derived from text

N95-18114# Naval Postgraduate School, Monterey, CA.

INTRASEASONAL OSCILLATIONS OVER THE TROPICAL WESTERN PACIFIC AND EASTERN INDIAN OCEAN FOR THE NORTHERN SUMMERS OF 1989-1991 M.S. Thesis

Jorge A. CardenasAmores Jun. 1994 116 p

(AD-A284527) Avail: CASI HC A06/MF A02

We used data analyzed by the Navy Operational Global Analysis and Prediction System to study the intraseasonal oscillations other than Madden and Julian oscillation over the tropical western Pacific and eastern Indian ocean. The period of study is May-September of 1989, 1990, and 1991. Multiple-set canonical correlation (MCC), single point correlation, and composite analyses were used to determine the structure of the disturbances. The results show that MCC mode 1 describes both the seasonal change and a near 20 day oscillation with a zonal half-wavelength around 3000-4000 km. The single point correlation and composites indicate that these oscillations are in gradient wind balance, transporting moisture northward, having upper level divergence over a surface low, and a warm-core structure. The seasonal change composite shows a quasistationary oscillation with May and June corresponding to the negative phase of MCC mode 1, and August corresponding to the positive phase of MCC mode 1. The near 20 day composite describes a westward propagation of 2.5-3 deg per day, with phase 2 corresponding to the negative phase of MCC mode 1 and phase 5 corresponding to the positive phase of MCC mode 1. DTIC

N95-18117# Army Research Lab., White Sands Missle Range, NM. Battlefield Environment Directorate.

A TECHNICAL DEMONSTRATION MOBILE PROFILER SYSTEM Final Report

James L. Cogan Aug. 1994 59 p

(AD-A284562; ARL-TR-523) Avail: CASI HC A04/MF A01

A near, real time sounding of the atmosphere from the surface to greater than or equal to 30 km over a battlefield may be obtained by combining atmospheric profiles from meteorological (MET), satellite, and ground-based instruments. This type of capability is essential for optimum use of Army resources such as artillery and defense against biological and chemical attack. The technical demonstration (TD) mobile profiler system (MPS) has this capability and plays an important role in a variety of civilian applications, including detailed analysis of MET variables for research and operations over mesoscale areas (regional pollution studies and severe storm forecasting). This report provides a brief description of the TD MPS and the method for merging data from the satellite and ground-based remote sensing systems. Results presented from a month-long field test indicate the ability of the present version of the TD MPS to generate useful atmospheric soundings in the format of an artillery MET message and a variety of other formats and displays. Comparisons made with data from rawinsondes nearly coincident in space and time indicate the level of accuracy of the data. An intercomparison between two rawinsonde systems on site suggest possible errors in the rawinsonde data. DTIC

N95-18141 Sparta, Inc., Lexington, MA.

A SENSITIVITY ANALYSIS OF UPWELLING RADIANCES IN THE 3-5 MICROMETERS REGION AS A FUNCTION OF ATMOSPHERIC CONDITIONS

David R. Longtin and John R. Hummel 17 Jun. 1994 28 p Limited Reproducibility: More than 20% of this document may be affected by microfiche quality

(Contract F19628-91-C-0093)

(AD-A283678; AD-E202154; LTR94-002; TR-94-2181; SR-9) Avail: CASI HC A03

Under the direction of the Remote Sensing Branch of the Naval Research Laboratory (NRL), SPARTA, Inc. calculated upwelling ground-to-space radiances and kernel functions for model atmospheres under different viewing and atmospheric conditions. These sensitivity calculations were then used by NRL personnel in a feasibility study which examined the possibility of obtaining information about atmospheric constituents from a remote sensing platform as it looks through the atmosphere at a source of a known blackbody temperature. In the current sensitivity study, upwelling radiances were calculated for selected bandpasses in the 3-5 micrometers region (1920-3330 1/cm). The results indicated that upwelling radiances are governed by the blackbody temperature at the surface. The impacts of the carbon dioxide profile, sensor platform altitude, surface visibility, and solar contributions (day/night variations) are small or insignificant. The impact of the water vapor profile depends on where in the atmosphere the perturbations exist, the surface blackbody temperature, the viewing angle, and the sensor bandpass. Broadband kernel functions generally peak in the 2-4 km altitude region.

DTIC

N95-18201*# National Aeronautics and Space Administration. Goddard Space Flight Center, Greenbelt, MD.

OPTICAL RAIN GAUGE PERFORMANCE: SECOND WORKSHOP ON OPTICAL RAIN GAUGE MEASUREMENTS

David A. Short, ed., Otto W. Thiele, ed., and Michael J. McPhaden, ed. (National Oceanic and Atmospheric Administration, Seattle, WA.) Washington Dec. 1994 77 p Workshop held in Greenbelt, MD, 21-22 Apr. 1994
(RTOP 461-54-15; RTOP 461-56-50)
(NASA-CP-3288; Rept-95B00023; NAS 1.55:3288) Avail: CASI HC A05/MF A01

The primary focus of the workshop was on the performance and reliability of STi mini-Optical Rain Gauges in a number of environments, including deployments on ships and buoys in the western equatorial Pacific Ocean during the TOGA/COARE field experiment, deployments on buoys in U.S. coastal waters, and comparisons with other types of rain gauges on the Virginia coast and in Florida. The workshop was attended by 20 investigators, representing 10 different institutions, who gathered to present new results obtained since the first workshop (April 1993), to discuss problems, to consider solutions, and to chart future directions. Post-TOGA/COARE calibration studies were also presented. For individual titles, see N95-18202 through N95-18210.

N95-18202*# National Oceanic and Atmospheric Administration, Seattle, WA. Pacific Marine Environmental Lab.
MOORED RAINFALL MEASUREMENTS DURING COARE
Michael J. McPhaden *In* NASA. Goddard Space Flight Center, Optical Rain Gauge Performance: Second Workshop on Optical Rain Gauge Measurements Dec. 1994 p 5-9 (For primary document see N95-18201 05-47)
Avail: CASI HC A01/MF A01

This presentation discusses mini-ORG rainfall estimates collected from an array of six moornings in the western equatorial Pacific during the TOGA-COARE experiment. The moorings were clustered in the vicinity of the COARE intensive flux array (IFA) centered near 2 deg S, 156 deg E. The basic data set consisted of hourly means computed from 5-second samples. Derived from text

N95-18203*# National Oceanic and Atmospheric Administration, Seattle, WA. Pacific Marine Environmental Lab.
UPDATE ON TAO MOORED ORG ARRAY
H. Paul Freitag *In* NASA. Goddard Space Flight Center, Optical Rain Gauge Performance: Second Workshop on Optical Rain Gauge Measurements Dec. 1994 p 11-14 (For primary document see N95-18201 05-47)
Avail: CASI HC A01/MF A01

During the Coupled Ocean Atmosphere Response Experiment (COARE) six TAO moorings were equipped with optical rain gauges (ORG's). In late 1993 moorings deployed on the equator at 154E and 157.5E were recovered and not redeployed as they were augmentations to the TAO array for COARE only. In December 1993, four TAO moorings were equipped with ORG's: one each at 2N, 156E and 2S, 156E and ORG doublets on the equator at 0, 156E and 0, 165E. The 2N, 156E mooring has been lost. By the end of April all sites will have been serviced and six refurbished sensors will again be deployed in the same locations. Derived from text

N95-18204*# Miami Univ., FL. Cooperative Inst. for Marine and Atmospheric Studies.
INTER-COMPARISON OF AUTOMATIC RAIN GAUGES
Jeffrey A. Nystuen *In* NASA. Goddard Space Flight Center, Optical Rain Gauge Performance: Second Workshop on Optical Rain Gauge Measurements Dec. 1994 p 15-26 Prepared in cooperation with National Oceanic and Atmospheric Administration, Miami, FL (For primary document see N95-18201 05-47)
Avail: CASI HC A03/MF A01

The Ocean Acoustics Division (OAD) of the Atlantic Oceanographic and Meteorological Laboratory (AOML), in cooperation with NOAA/NESDIS and NASA, has deployed six rain gauges for calibration and intercomparison purposes. These instruments include: (1) a weighing rain gauge, (2) a RM Young Model 50202 capacitance rain gauge, (3) a ScTI ORG-705 (long path) optical rain gauge, (4) a ScTI ORG-105 (mini-ORG) optical rain gauge, (5) a Belfort Model 382 tipping bucket rain gauge, and (6) a Distromet RD-69 disdrometer. The system has been running continuously since July 1993. During this time period, roughly 150 events with maximum rainfall rate over 10 mm/hr and 25 events with maximum rainfall rates over 100 mm/hr have been recorded. All rain gauge types have performed well, with intercorrelations 0.9 or higher. However, limitations for each type of rain gauge have been observed. Derived from text

N95-18205*# Scientific Technology, Inc., Rockville, MD.
WALLOPS ISLAND NATURAL RAIN DATA ANALYSIS
Ting-I. Wang *In* NASA. Goddard Space Flight Center, Optical Rain Gauge Performance: Second Workshop on Optical Rain Gauge Measurements Dec. 1994 p 27-36 (For primary document see N95-18201 05-47)
Avail: CASI HC A02/MF A01

ScTI has performed a detailed analysis of four optical rain gauge ORG-105 sensors tested by Wallops Island on 8 May 1992. The four ORG's tested were S/N 2236, 2237, 2239, and 2241. Shown is a 30 minute time series of the individual ORG's, the ORG average, and the weighing gauge. The sensors tracked well with rainrates (RR) up to 45 mm/hr for the period. Also shown is a plot of accumulated rainfall over the same period. It can be seen that even though the ORG's tracked well, some ORG's tended to read higher and some read lower during the event. Author

N95-18206*# National Aeronautics and Space Administration. Goddard Space Flight Center, Greenbelt, MD.
VIBRATION (?) SPIKES DURING NATURAL RAIN EVENTS
David A. Short *In its* Optical Rain Gauge Performance: Second Workshop on Optical Rain Gauge Measurements Dec. 1994 p 37-41 (For primary document see N95-18201 05-47)
Avail: CASI HC A01/MF A01

Limited analysis of optical rain gauge (ORG) data from shipboard and ground based sensors has shown the existence of spikes, possibly attributable to sensor vibration, while rain is occurring. An extreme example of this behavior was noted aboard the PRC#5 on the evening of December 24, 1992 as the ship began repositioning during a rain event in the TOGA/COARE IFA. The spikes are readily evident in the one-second resolution data, but may be indistinguishable from natural rain rate fluctuations in subsampled or averaged data. Such spikes result in increased rainfall totals. Derived from text

N95-18207*# Texas Technological Univ., Lubbock, TX. Atmospheric Sciences Group.
A COMPARISON OF OPTICAL RAIN GAUGE AND RADAR DATA FROM TOGA/COARE
Linda Galusha *In* NASA. Goddard Space Flight Center, Optical Rain Gauge Performance: Second Workshop on Optical Rain Gauge Measurements Dec. 1994 p 43-48 (For primary document see N95-18201 05-47)
Avail: CASI HC A02/MF A01

A comparison between rain gauge data and radar data from the Tropical Oceans Global Atmosphere/Coupled Ocean Atmosphere Response Experiment (TOGA/COARE) was studied. The rain gauge data from an echo that passed over the Xiangyanghong #5 on December 24, 1992 was compared to what the MIT radar saw at this location from the R/V Vickers, 103.4 km to the east. The precipitation measured by the rain gauge peaked at 108 mm/hr 92 seconds into the period before tapering off 11 1/2 minutes later. This sharp gradient was evident in a PPI plot of the radar reflectivities and the percentage area-rainfall for the radar data statistics. The percentage area curve was converted to rain rates using a GATE Z-R and compared to a percentage time curve of rain rates according to the rain gauge. A four minute running average applied to the rain gauge rates improved the comparison of peak rates between the rain gauge and radar. Differences in peaks between rain rates observed by the rain gauge and reflectivities observed by the radar could be due to variations in rainfall rates within a single radar data bin. For example, two measurements of reflectivity such as 37 and 47 dBZ within the same bin would result in a 44 dBZ average. This range in rates from 12 mm/hr to 74 mm/hr is observed in 30 seconds by the rain gauges within the first two minutes of the radar echo passage. Author

N95-18208*# National Aeronautics and Space Administration. Goddard Space Flight Center, Greenbelt, MD.
CAN SALT ON AN OPTICAL RAIN GAUGE LENS AFFECT PERFORMANCE?

Larry F. Bliven *In its* Optical Rain Gauge Performance: Second Workshop on Optical Rain Gauge Measurements Dec. 1994 p 49-52 (For primary document see N95-18201 05-47)
Avail: CASI HC A01/MF A01

The optical rain gauge (ORG) by ScTI is designed to be tolerant to reduction of infrared beam intensity due to a dirty lens. Recently there is interest in long term use of optical gauges onboard buoys at sea. Because of logistics, these systems are serviced infrequently, i.e., every several months. Due to the proximity of the gauges to the sea surface, salt can be expected to be deposited on the lens. To obtain an indication of the potential for dirty lens to affect the ORG calibration, two simple experiments were conducted. In the control experiment, a sample ORG was compared to three other ORG's during natural rain events. Next a translucent mask was placed on the transmitter lens of the sample ORG and again data were collected under natural rain conditions. The mask reduced the gain of the perturbed ORG by about 30%. The perturbed ORG operated rather well in that the mask only causes a change in the gain and does not cause data drop out at low rain rates. However, the reduced gain would seriously impact an assessment of rain statistics. CASI

N95-18209*# National Environmental Satellite Service, Camp Springs, MD. Satellite Research Lab.
RAIN GAUGE CALIBRATION AND TESTING
John Wilkerson *In* NASA. Goddard Space Flight Center, Optical Rain Gauge Performance: Second Workshop on Optical Rain Gauge Measurements Dec. 1994 p 53-61 (For primary document see N95-18201 05-47)
Avail: CASI HC A02/MF A01

Prior to the Tropical Oceans Global Atmosphere-Coupled Ocean Atmosphere Response Experiment (TOGA-COARE), 42 Model 100 series optical gauges were tested in the rain simulator facility at Wallops Island before shipment to the field. Baseline measurements at several rain rates were made simultaneously with collector cans, tipping bucket, and a precision weighing gauge and held for post-COARE evaluation with a repeat set of measurements that were to be recorded after the instruments were returned. This was done as a means of detecting any calibration changes that might have occurred while deployed. Although it was known that the artificial rain in the simulator did not contain the required exponential distribution for accurate optical rain gauge rate measurements, use of the facility was necessary because it was the only means available for taking controlled observations with instruments that were received, tested, and shipped out in groups over a period of months. At that point, it was believed that these measurements would be adequately precise for detecting performance changes over time. However, analysis of the data by STI now indicates that this may not be true. Further study of the data will be undertaken to resolve this. Author (revised)

N95-18210*# Ministry of Posts and Telecommunications, Tokyo (Japan). Communications Research Lab.
EFFECT OF HEAVY RAIN TO THE TOTAL RECEIVED POWER Abstract Only
Toshio Iguchi *In* NASA. Goddard Space Flight Center, Optical Rain Gauge Performance: Second Workshop on Optical Rain Gauge Measurements Dec. 1994 p 63 (For primary document see N95-18201 05-47)
Avail: CASI HC A01/MF A01

If the average power at the receiver is substantially reduced by heavy rain, the AGC (automatic gain control) circuit of the rain gauge will try to compensate this reduction by increasing the gain. If this happens, then the pulses created by rain drops are amplified more than they should be and the rainfall rate may be overestimated. If the effective diameter (blocking efficiency) of a particle is 2 mm and if the beam width is 2 cm, each particle will reduce the received power by 10 percent when it crosses the beam. Since the beam is blocked by water drops 75 percent of the total time according to the above calculation, the total received power may be reduced by 7.5 percent. To compensate this reduction to the reference value, the gain of amplifier will be increased by 8.1 percent. This increase of gain will increase all pulse sizes by the same fraction and result in the overestimate of the rainfall rate. Derived from text

N95-18384 Massachusetts Inst. of Tech., Lexington. Lincoln Lab.
IMPLEMENTATION OF THE 1992 TERMINAL AREA-LOCAL ANALYSIS AND PREDICTION SYSTEM (T-LAPS) Project Report
S. H. Olson, C. D. McLain, and S. Yao 22 Aug. 1994 56 p Limited Reproducibility: More than 20% of this document may be affected by microfiche quality
(Contract DTFA01-91-Z-02036)
(AD-A284334; ATC-219) Avail: Issuing Activity (Defense Technical Information Center (DTIC))

The Integrated Terminal Weather System (ITWS) development program was initiated by the Federal Aviation Administration (FAA) to produce a fully automated, integrated terminal weather information system to improve the safety, efficiency and capacity of terminal area aviation operations. The ITWS will acquire data from FAA and National Weather Service (NWS) sensors as well as from aircraft in flight in the terminal area. The ITWS will provide air traffic personnel with products that are immediately usable without further meteorological interpretation. These products include current terminal area weather and short-term (0-30 minute) predictions of significant weather phenomena. The Terminal area-Local Analysis and Prediction System (T-LAPS) is being evaluated as a possible provider of the Terminal Winds Product for the ITWS. T-LAPS is a direct descendant of the Local Analysis and Prediction System (LAPS) developed at the National Oceanic and Atmospheric Administration's (NOAA's) Forecast Systems Laboratory (FSL). T-LAPS takes meteorological data from a wide variety of data sources as input and provides a gridded, three-dimensional (3-D) analysis of the state of the local atmosphere in the terminal area as output. For the 1992 system, the output was a gridded 3-D analysis of the horizontal winds. This information is intended to be used by the Terminal Air Traffic Control Automation (TATCA) program to estimate the effects of winds on aircraft in the terminal area. The 1993 and 1994 T-LAPS systems will incorporate more sophisticated wind analysis algorithms. DTIC

N95-18392 Royal Netherlands Meteorological Inst., De Bilt.
THE EFFECT OF SPATIAL AVERAGING ON THRESHOLD EXCEEDANCES OF DAILY PRECIPITATION AMOUNTS
T. A. Buishand, B. vanMourik, and A. M. G. Klein Tank 1993 18 p Sponsored by Dutch National Research Program on Global Air Pollution and Climate Change
(ISSN 0169-1708)
(KNMI-TR-154; ISBN-90-369-2036-1) Copyright Avail: Issuing Activity

The effect of spatial averaging on the number of days with a precipitation amount greater than or equal to 0.1, greater than or equal to 1.0 and greater than or equal to 10.0 mm is investigated, using daily precipitation amounts in the Netherlands (approximately 40,000 sq km); 320 rainfall stations) for the 10-year period 1981-1990. The average seasonal and annual exceedance frequencies for point precipitation are compared with the country-wide average. This comparison is also made for regions with an area of about 10,000 sq km and a region with an area of about 1000 sq km. Because the spatial average daily precipitation amount shows less variation than point precipitation, the number of exceedances of the 10.0 mm threshold is smaller for the spatial average, whereas for the 0.1 and 1.0 mm thresholds the opposite holds. The largest differences between the exceedance frequencies of point and areal average precipitation (up to 50% for the country-wide average) are found for the summer season, due to the occurrence of small scale convective storms. The effect of the size of the region on the threshold exceedances is also stronger for summer than for the other seasons. For the 10 mm threshold this effect is partly obscured, however, by the large random errors, resulting from the small number of exceedances in the relatively short 10-year period. The exceedance frequencies for the Netherlands are compared with those in the Canadian Climate Center second-generation GCM. For the two land grid points near the Netherlands the exceedance frequencies of the three thresholds differ strongly from those in the real climate. These differences cannot be explained by spatial averaging alone. The fact that the average precipitation amounts are too large in the model also contributes to the differences in exceedance frequencies. The large systematic differences make the use of GCM predicted precipitation at a single grid point questionable. Author

N95-18393 Royal Netherlands Meteorological Inst., De Bilt.
STORM ACTIVITY OVER THE NORTH SEA AND THE NETHERLANDS IN TWO CLIMATE MODELS COMPARED WITH OBSERVATIONS

Jules J. Beersma Feb. 1994 47 p
(ISSN 0169-1651)
(KNMI-WR-94-02; ISBN-90-369-2050-7) Copyright Avail: Issuing Activity

An intercomparison of wind characteristics over the North Sea and the Netherlands is made between the observations, the control runs of the Canadian Climate Center (CCC) second generation (GCM and the ECHAM coupled ocean-atmosphere GCM, and the enhanced CO2 runs of these models. Wind direction, wind speed, the frequency of gales (clusters of high wind speeds), the storm track (the time filtered variability of the 500 hPa height) and Empirical Orthogonal Functions (EOF's) of the 500 hPa circulation are considered. In general the differences between the control run and the observations are large. The ECHAM model very poorly reproduces the wind direction distribution and the CCC model strongly underestimates the mean wind speed over sea during summer. The gale frequency is reasonable over land in the ECHAM model but too small over sea in both models. The storm track is in both models less pronounced than in the observations and in the ECHAM model shifted to the south. The average annual amplitudes of the second and third EOF's in the CCC model and those of the three principal EOF's in the ECHAM model differ significantly from the observed ones. The comparison of the control run and increased CO2 runs of the models shows in only a few cases a statistical significant change in the wind characteristics. These differences are usually small compared to the differences between the control run and the observations. Author

N95-18394 Royal Netherlands Meteorological Inst., De Bilt.
CONCEPTUAL MODELS OF SEVERE CONVECTIVE WEATHER IN THE NETHERLANDS
Dong Hongnian 1993 39 p
(ISSN 0169-1651)
(KNMI-WR-93-05; ISBN-90-369-2043-4) Copyright Avail: Issuing Activity

Fifty cases of severe convective weather in the Netherlands have been analyzed. According to their circulation type they can be classified in five classes. Accordingly five conceptual models of severe convective weather are presented including average circulation type, average value of surface potential wetbulb temperature (Omega (sub SW)) and stability parameter (Delta T), a synthetical illustration of its causes and conditions for its occurrence. These conceptual models can be used as a basis for forecasting and also for understanding severe convective weather. Author

N95-18395 Royal Netherlands Meteorological Inst., De Bilt.
A SYNOPTIC CLIMATOLOGY OF CONVECTIVE WEATHER IN THE NETHERLANDS
Dong Hongnian 1993 38 p
(ISSN 0169-1651)
(KNMI-WR-93-04; ISBN-90-369-2042-6) Copyright Avail: Issuing Activity

Six kinds of convective weather phenomena, i.e. thunderstorm, tornado, hail, heavy shower, wind gust and lightning strike, have been examined to compile a synoptic climatology of convective weather in the Netherlands by: (1) determining a climatology of convective weather; and (2) establishing a relationship between convective weather and circulations pattern. Extreme values of the different convective weather parameters have been established. Information gathered on the loss of property and life are presented in this report. We found the following yearly occurrence of severe convective weather phenomena: (1) 2.64 tornadoes, 2.2 tornadic days on average per year; (2) heavy rain (greater than or equal to 80 mm/day): 1.75 days per year; (3) wind gust (greater than or equal to 20 m/s): 11 days per year; (4) heavy showers (greater than or equal to 10 mm/h): 8.2 days; (greater than or equal to 25 mm/h): 1.8 days per year; (5) hail size greater than or equal to no. 3 (marble size): 15.5 days; greater than or equal to no. 4 (walnut): 3.8 days per year; and (6) lightning strikes: 653 per year on 54.5 days per year on average. Temporal (yearly, monthly and hourly) and spatial variation of convective weather were also investigated. The relationship between circulation pattern and convective weather indicates that most convective weather occurred in only three main circulation patterns and five sub patterns. Author

N95-18399 Auckland Univ. (New Zealand).
ATMOSPHERIC CHEMISTRY OF BIOGENIC SULFUR IN THE SOUTHERN HEMISPHERE Ph.D. Thesis
David John Wylie 1993 330 p
Avail: Univ. Microfilms Order No. DA9411866

Measurements of atmospheric dimethylsulfide (DMS), as well as methanesulfonic acid (MSA) and non sea salt sulfate (NSSS) concentrations in atmospheric aerosol, rain water and Antarctic snow and ice core samples carried out between December 1990 and January 1993. Major ions in rain water, aerosol and snow samples were also determined. Samples were collected in the marine troposphere at two coastal North Island sites (Leigh and Baring Head) in New Zealand, and at coastal (McDonald Beach) and remote (East Antarctic Plateau) sites on the Antarctic continent. The air masses sampled were predominately of a marine origin and allowed the comparison between DMS and sulfur aerosol concentrations over a wide range of environmental conditions and with respect to latitude. Atmospheric DMS, MSA and NSSS concentrations in rain water and aerosol samples were observed to vary seasonally and latitudinally. At the New Zealand sites, seasonal atmospheric DMS concentrations ranged from the detection limit (0.25 nmol m(sup -3)) to 14.9 nmol m(sup -3) (median 3.15 nmol m(sup -3)) with a spring maximum. An atmospheric DMS diurnal variation factor of approximately 1.7 was observed. Marine aerosol MSA concentrations ranged seasonally from 0.02 to 1.40 nmol m(sup -3) (combined site median 0.30 nmol m(sup -3)) also with a spring maximum. The marine MSA/NSSS molar ratios ranged from 2.38 to 22.3% (median 6.40%) for rain water and from 0.82 to 21.4% (median 3.27%) for aerosol samples. At McDonald Beach, in Antarctica, atmospheric DMS concentrations ranged from 2.98 to 19.2 nmol m(sup -3) (median 6.27 nmol m(sup -3)) during the austral summer. Aerosol concentrations ranged from 0.60 to 3.46 nmol m(sup -3) (median 1.68 nmol m(sup -3)) for MSA and from 3.05 to 11.6 nmol m(sup -3) (median 6.77 nmol m(sup -3)) for NSSS. A remote site on the East Antarctic Plateau also showed elevated aerosol MSA concentrations (0.09 to 0.43 nmol m(sup -3), median 0.14 nmol m(sup -3)). The aerosol MSA/NSSS molar ratios ranged from 6.54 to 40.4% (combined median 24%) for these sites. Ice core, snow pit and surface snow samples from the East Antarctic Plateau site showed concentrations ranging from 0.01 to 0.31 mu eq L(sup -1) (median 0.04 mu eq L(sup -1)) for MSA and from 0.54 to 29.5 mu eq L(sup -1) (median 2.96 mu eq L(sup -1)) for NSSS. Some generalizations as to the importance of DMS and the wet and dry sulfur deposition of MSA and NSSS at these sites are made. The atmospheric DMS concentrations at coastal New Zealand and Antarctic sites are comparable to other remote Southern Hemisphere sites suggesting some uniformity over the South West Pacific troposphere. However, between the Antarctic and New Zealand sites there are large variations in the MSA and NSSS depositional rates, the aerosol MSA size distribution and the ratio of MSA/NSSS. Author

N95-18607# Queensland Univ., Brisbane (Australia). Dept. of Civil Engineering.
INCORPORATING UNCERTAINTY AND RISK IN RAINFALL-BASED FLOOD ESTIMATES
W. J. C. Meynink and D. K. Brady Jul. 1993 43 p
(RR-CE144; ISBN-0-86776-514-3) Avail: CASI HC A03/MF A01

An approach for defining the variance of the design flood risk distribution for rainfall-based methods of flood estimation is proposed. This approach facilitates the inclusion of catchment response variability and the uncertainty associated with the estimation of catchment response parameters. It is demonstrated, using the additive properties of variance, that the design flood distribution variance is always greater than the design rainfall distribution variance, and that if the design rainfall is applied to a natural or urban catchment response model with 'best fit' parameters, then the risk of hydrological failure can be substantially greater than indicated by the selected design rainfall. This approach also facilitates quantitative evaluation of the worth of additional hydrological data. Author

N95-18721# National Environmental Satellite Service, Washington, DC. Office of Research and Applications.
OFFICE OF RESEARCH AND APPLICATIONS: RESEARCH PROGRAMS
Dec. 1994 168 p Original contains color illustrations
Avail: CASI HC A08/MF A02

This book describes research and development activities at the Office of Research and Applications (ORA). It is a completely new edition of the ORA Research Programs book first published in 1989. ORA is a component of the National Oceanic and Atmospheric Administration's (NOAA) National Environmental Satellite and Information Service (NESDIS). NESDIS is responsible for the Nation's civil operational environmental satellite system. This system consists of two Polar-orbiting Operational Environmental

Satellites and two Geostationary Operational Environment Satellite spacecraft. The remote-sensing instruments on these satellites provide real-time global observations of the atmosphere, oceans, and land. NOAA needs these observations to issue weather warnings and forecasts, predict ocean conditions, and assess climate variations. ORA conducts a broad program of satellite remote sensing research. ORA scientists develop algorithms for deriving geophysical variables from satellite observations, monitor instrument calibration, validate satellite products, demonstrate the application of satellite data to important environmental problems, and plan future instruments. The first four sections of this book are organized according to the elements of NOAA's Strategic Plan that are supported by satellite observations. These are: (1) advance short-term forecast and warning services, (2) implement seasonal to interannual climate forecasts, (3) predict and assess decadal-to-centennial change, and (4) coastal ecosystems health. The last section covers various cross-cutting activities. The sections are comprised of research topics, each consisting of a brief narrative and accompanying illustration. Author

N95-18732 Virginia Univ., Charlottesville, VA.
DEPENDENCE OF MEDIUM-RANGE FORECAST ERROR ON PATTERNS IN THE INITIAL STATE Ph.D. Thesis
David Robert Walker 1994 303 p
Avail: Univ. Microfilms Order No. DA9415593

A study of the once daily (0000 UTC) 1000 mb error fields of the National Meteorological Center's 80-wave Medium-Rang Forecast (MRF) model are presented. Time and space mean error fields over integration length and period of record are diagnosed. A reduction in the model biases show the improvement in model long wave radiational cooling calculations. Potential skill, as measured by the anomaly correlation, shows less variability over the period of record but large changes over integration length. Principal component analysis of the 429 variable error covariance matrices for the cool and warm seasons reduces to six orthogonal variables that explain over 60 percent of the original error variance. The primary modes of error variability are spatially coherent over the ten integration lengths. The dominant error modes are related to behavioral problems in the MRF model. The error patterns are associated with orographic features (Alberta and Colorado Rockies), storm tracks and baroclinic zones (Gulf stream region and United States-Canadian border) and persistent atmospheric features (Hudson Bay low, eastern Pacific subtropical high and Desert Southwest heat low). This historical data base of 80-wave MRF model integrations is used to determine if different initial states produce distinctly different model forecast errors. Teleconnection indices defined by the 500 mb height field are used to identify patterns in the initial state of individual model integrations. The mean error patterns in the 80-wave MRF are significantly different at day-7 and day-10 using the Western Pacific, Western Atlantic and Eurasian teleconnection indices to distinguish between initial states. Model error patterns are also sensitive to Lejenas' Blocking !ndex at 30 deg and 140 deg W. The presence or absence of a low pressure system in the forecast is information used to reduce the model forecast error. Dependent data sets are used for correction scheme development and independent data sets are used for correction scheme testing. The improvement in the skill of the forecast increases substantially in the 6 to 10 day forecast range. The application of the corrections produce 10 day forecasts with skill scores comparable to 8 day forecasts. Dissert. Abstr.

N95-18926 Royal Netherlands Meteorological Inst., De Bilt.
AN ANALYTIC CONCEPTUAL MODEL OF EXTRATROPICAL CYCLONES
L. C. Heijboer 1993 50 p
(ISSN 0169-1651)
(KNMI-WR-93-03; ISBN-90-369-2041-8) Copyright Avail: Issuing Activity

An analytic conceptual model has been developed describing the nonlinear development of small and large scale extratropical cyclones towards the mature stage. The model shows the self-development and self-limiting processes of an extratropical cyclone and reveals the existence of A- and B-development, as described by Petterssen and Smebye. Even a so-called 'synoptic bomb' can be simulated. The model also describes the essential subsynoptic scale features, such as warm and cold frontal zones, together with the associated conveyor belts, as well as the overrunning of the descending high tropospheric and low stratospheric air over the warm conveyor belt, together with the tropopause fold caused by the descending air. A linear stability analysis has been carried out with the equations. For the unstable modes the results agree with those of the classical linear stability theory for rectangular sine-waves. Asymptotic expressions for the most unstable mode for large time have been obtained for the maximum windspeed of the disturbance and the amount of spiralling of the thermal field as function of the radius, the Coriolis parameter, the layer thickness, the static stability and the thermal wind of the background flow. Because the analytic solution consists of elementary mathematical functions, the model can easily be run on a personal computer. This, together with the conceptual nature of the model, contributes considerably to the understanding of the behavior and (sub)synoptic structure of extratropical cyclones and makes the model well suited for educational purposes. As an application the model has been used for the estimation of the vertical transport of trace gases. Calculations and statistical observational evidence, indicate that in the Northern Hemisphere depressions generate a mean downwards ozone flux from the lower stratosphere of about 5x10(exp 14) molecules ozone per second and squared meter. Moreover, calculated upward vertical velocities suggest that molecules with a residence time of the order of days, originally in the boundary layer, participate in the chemistry of the upper troposphere. Author

N95-19407# National Academy of Sciences - National Research Council, Washington, DC. Commission on Engineering and Technical Systems.
TOWARD A NEW NATIONAL WEATHER SERVICE: WEATHER FOR THOSE WHO FLY Annual Report
Mar. 1994 111 p
(Contract NOAA-50-DGNW-0-00041)
(PB94-214418) Copyright Avail: CASI HC A06/MF A02

Weather has significant impacts on the safety and efficiency of aviation. Some one-quarter to one-half of all aviation accidents are weather related. The present-day aviation weather system is obsolete, the aviational needs for modern weather information systems are manifold and urgent. However, the study finds that it must be coupled with related programs of the FAA focused on aviation weather needs and on improving the presentation of aviation weather information. Major improvements are possible today but are not expected to be implemented by the federal government for many years. Further, the study indicates that to reduce accidents, improved weather education for pilots is needed and should be based on the realities of weather impacts on flight, emphasizing the conditions and phenomena that can surprise pilots. NTIS

N95-19521# Naval Command, Control and Ocean Surveillance Center, San Diego, CA.
SURFACE AND UPPER-AIR METEOROLOGICAL MEASUREMENTS SUPPORTING THE NATO/AC243/PANEL 3 RESEARCH STUDY GROUPS 8 AND 21 CAMPAIGN IN LORIENT, FRANCE (SEPTEMBER 1993) Final Report, Sep. 1993 - Aug. 1994
Kenneth D. Anderson Aug. 1994 43 p
(AD-A285326; NRAD-TR-1668) Avail: CASI HC A03/MF A01

Two weeks of surface and upper-air meteorological measurements are presented. These measurements were part of an international effort, consisting of contributions from Canada, France, The Netherlands, Germany, and the USA, coordinated by NATO/AC243/Panel 3 Research Study Groups 8 and 21. This effort was designed to assess the effects of the lower atmosphere on the propagation of the electromagnetic phase front at frequencies from 10 to 94 GHz. Radio frequency propagation and meteorological measurements were made between the island of Ile de Groix and the town of Gavres, France. The results from this coordinated effort should lead to significant improvement in the understanding of low-altitude target acquisition and tracking. DTIC

N95-19581# National Weather Service, Bohemia, NY. Scientific Services Div.
SYNOPTIC AND MESOSCALE EXAMINATION OF THE NORTHERN NEW ENGLAND WINTER STORM OF JANUARY 29-30, 1990
R. A. Marine (National Weather Service, Portland, MA.) and S. J. Capriola (National Weather Service, Portland, MA.) Jul. 1994 44 p
(PB94-209426; NOAA-TM-NWS-ER-88) Avail: CASI HC A03/MF A01

On 29-30 Jan. 1990, a low pressure system tracked parallel to the New England coastline and produced up to 20 inches of snow over portions of Maine, New Hampshire, and Vermont. This detailed study will examine the synoptic and mesoscale features that led to this heavy snow event. In

addition, the use of various local forecast techniques and 'rules of thumb' will be shown to be an effective way to improve upon dynamical model forecasts. NTIS

N95-19596# Naval Postgraduate School, Monterey, CA.
SYNOPTIC-SCALE INFLUENCE ON THE MONTEREY BAY SEA-BREEZE M.S. Thesis
Michael Charles Knapp Sep. 1994 109 p
(AD-A285129) Avail: CASI HC A06/MF A02

The diurnal fluctuations of the surface ambient wind associated with the sea-breeze are analyzed for the period May 1 through September 30, 1993 from a single station, Monterey airport, located on the southern Monterey Bay coast. Data analyzed included time series of wind speed, wind direction, clouds, precipitation and locally generated 3 hourly surface pressure analyses of California and the Pacific northwest. The characteristics of the sea-breeze circulation under varying synoptic-scale patterns are evaluated to determine the modifying roles of boundary layer stability, surface inversion strength, and low-level cloud amount on the resultant time of onset and peak intensity of the Monterey Bay sea-breeze. The primary modifying factor under all synoptic-scale pressure patterns was the boundary layer depth and stability with the differential heating taking longer to destabilize the boundary layer during the Trough regime. DTIC

N95-19701# Physical Optics Corp., Torrance, CA. Research and Development Div.
A NOVEL TECHNIQUE FOR 4-DIMENSIONAL ATMOSPHERIC AND OCEANOGRAPHIC IRRADIANCE MEASUREMENTS USING 3-D SPATIAL FILTERING Final Report, 14 Apr. - 30 Sep. 1994
Steve Ackelson 30 Sep. 1994 20 p
(Contract N00014-94-C-0099)
(AD-A285658) Avail: CASI HC A03/MF A01

In this project, POC advanced and optimized a spatial filtering technique for measuring irradiance spatial density. The key component of the novel technique is a pixel filter placed at the image focal plane. The pixel filter design includes a wavefront-matched filter, a microlens, and a point detector. The pixel filter allows the light from the in-focus volume to pass, suppressing the light from out-of-focus areas. Three objectives were established for the Phase 1 project and its Option Task. This report does not concern the Option Task since that task has not been performed yet. The objectives were: (1) numerically analyze and characterize the properties of an imaging system using the proposed 3-D spatial filtering technique, and determine optimal system design parameters; (2) construct a single pixel filter, and experimentally demonstrate the proof-of-concept of the technique; and (3) identify work to be performed in Phase 2 of this research. DTIC

N95-19712# Materials Research Labs., Ascot Vale (Australia).
A REVIEW OF LAND SURFACE TEMPERATURE AND HUMIDITY CONDITIONS SPECIFIED FOR AUSTRALIA IN DEF (AUST) 5168 AND STANAG 2895
L. M. Barrington Mar. 1994 33 p
(AD-A284258; MRL-GD-0058; DODA-AR-008-623) Avail: CASI HC A03/MF A01

Australian Ordnance Council (AOC) Task 154 'Definition of the Australian Environmental Conditions Affecting the Design of Military Material' was accepted by the Explosives Environmental and Service Life Advisory Committee (EESLAC) in 1990 to provide a concise definition of the possible manufacture to target environments to which material designed for the ADF could be exposed. This task was divided into two discrete areas of work by EESLAC, namely a study of surface transport vibration levels and a comparative analysis of available meteorological data and the contents of DEF (AUST) 5168. This paper discusses the latter analysis, expanded to include a review of STANAG 2895 also. In general, the available data suggests that the operational and storage diurnal cycles defined in the two standards reasonably represent the conditions likely to be experienced in Australia. However, the effects of direct solar radiation on material must also be considered in determining the maximum temperature which the material surface is likely to attain. DTIC

N95-19870 Florida State Univ., Tallahassee, FL. Dept. of Meteorology.
PREDICTION OF GLOBAL CLOUD COVER WITH A VERY HIGH RESOLUTION GLOBAL SPECTRAL MODEL Final Report, 15 Nov. 1990 - 14 Feb. 1994
T. N. Krishnamurti 3 May 1994 115 p Limited Reproducibility: More than 20% of this document may be affected by microfiche quality
(Grant AF-AFOSR-0023-91)
(AD-A279944; AFOSR-94-0334TR) Avail: Issuing Activity (Defense Technical Information Center (DTIC))

The completed research is in the area of cloud prediction with a high resolution global model. We have extended our studies on the handling of implicit clouds (i.e. clouds specified as a function of prevailing humidity). We have also examined this problem in the context of rainfall initialization (called physical initialization). We demonstrate a strong positive impact on cloud forecasts from such an initialization. We have also made a start on the problem of explicit cloud forecasts using cloud water mixing ratio and cloud fractions as basic forecast variables. Our preliminary results, described in the final report, are very encouraging. Mannoji (1994) has in fact noted a slight superiority of the explicit over the implicit scheme. That work was performed using a low resolution global model. Further work on the improvement of the explicit scheme at higher resolution is required. DTIC

N95-18172*# Texas Technological Univ., Lubbock, TX. Dept. of Geosciences.
EXPERIMENTS WITH THE MESOSCALE ATMOSPHERIC SIMULATION SYSTEM (MASS) USING THE SYNTHETIC RELATIVE HUMIDITY
Chia-Bo Chang *In* Univ. of Central Florida, NASA/ASEE Summer Faculty Fellowship Program. 1994 Research Reports Oct. 1994 p 139-158 (For primary document see N95-18166 05-80)
Avail: CASI HC A03/MF A04

N95-18174*# Pennsylvania State Univ., University Park, PA. Dept. of Meteorology.
LIGHTNING STUDIES USING LDAR AND COMPANION DATA SETS
Gregory S. Forbes *In* Univ. of Central Florida, NASA/ASEE Summer Faculty Fellowship Program. 1994 Research Reports Oct. 1994 p 205-235 (For primary document see N95-18166 05-80)
Avail: CASI HC A03/MF A04

N95-18977*# Pennsylvania State Univ., University Park, PA. Dept. of Meteorology.
IMPLICATIONS OF SUMMERTIME MARINE STRATOCUMULUS ON THE NORTH AMERICAN CLIMATE
John H. E. Clark *In* Alabama Univ., Research Reports: 1994 NASA/ASEE Summer Faculty Fellowship Program Oct. 1994 6 p (For primary document see N95-18967 05-80)
Avail: CASI HC A02/MF A03

N95-19001*# Wisconsin Univ., Whitewater, WI. Dept. of Mechanics and Computer Science.
TWO SPACE SCATTERER FORMALISM CALCULATION OF BULK PARAMETERS OF THUNDERCLOUDS
Dieudonne D. Phanord *In* Alabama Univ., Research Reports: 1994 NASA/ASEE Summer Faculty Fellowship Program Oct. 1994 6 p (For primary document see N95-18967 05-80)
Avail: CASI HC A02/MF A03

48 OCEANOGRAPHY

Includes biological, dynamic, and physical oceanography; and marine resources.

For related information see also *43 Earth Resources and Remote Sensing.*

N95-17951# Geological Survey, Woods Hole, MA.
GEOLOGIC STUDIES: EXECUTIVE SUMMARY REPORT
Peter Popenoe 1994 51 p Sponsored by Bureau of Land Management
(PB94-187481) Avail: CASI HC A04/MF A01

The general objectives of the geological oceanography program in 1976-1977 were to (1) measure the rate, direction, and forcing mechanisms of sediment mobility over the sea bed, and to monitor resultant changes in bottom morphology or texture; (2) determine the concentration, distribution, and flux of suspended particulate matter in the water column; (3) determine the vertical distribution of trace metals in the near-surface sediment at

selected locations; (4) evaluate potential geological hazards to oil and gas development due to surface and intermediate depth structure and mass sediment transport events; (5) identify and evaluate the distribution and significance of outcrop and reefal structures; and (6) support the activities of the chemical/biological contractor by obtaining information on sediment texture and composition, particularly as it relates to the physical, biological, and chemical processes of the shelf. The report presents a summation of principal findings and conclusions from this initial effort. NTIS

N95-18012 Naval Postgraduate School, Monterey, CA.
THE DIURNAL CYCLE OF HIGH-FREQUENCY TEMPERATURE VARIABILITY AT 0 DEG 140 DEG W ON SEASONAL AND INTERANNUAL TIME SCALES Ph.D. Thesis
Russell E. Brainard Jun. 1994 169 p Limited Reproducibility: More than 20% of this document may be affected by microfiche quality
(AD-A283640) Avail: Issuing Activity (Defense Technical Information Center (DTIC))

The diurnal cycle of high-frequency temperature fluctuations attributable to turbulence and internal waves in the upper central equatorial Pacific Ocean is found to persist over most of the period November 1983 - October 1987. Moored temperature and velocity data in the upper 300 m at 0 deg, 140 deg W during this four-year period were used to: (1) determine the vertical extent of the diurnal cycle of turbulence and internal waves and evaluate its contribution to the equatorial zonal momentum balance; and (2) determine whether the diurnal cycle of turbulence and internal waves varied seasonally and interannually in response to varying surface forcing and ambient stability conditions. Using 15-minute spot-sampled temperature data at 35 m, 60 m, 100 m, 140 m, 200 m, and 300 m, isotherm displacement variance (IDV) was computed for each six-hour time period as a proxy for vertical overturning and displacement associated with turbulence and internal waves. The time series of monthly mean IDV for each of the six-hour time bins showed the magnitude of the diurnal cycle of turbulence and internal waves (Delta(IDV)) as a function of season and depth. The diurnal change in IDV was pronounced at both the 35-m and the 60-m depths, with nighttime IDV significantly greater than daytime IDV. This result is consistent with TROPIC HEAT microstructure observations over two periods of a few days to weeks, showing that IDV is a useful proxy for turbulence and internal wave energy during periods when microstructure measurements are not available. DTIC

N95-18153# Naval Postgraduate School, Monterey, CA. Dept. of Oceanography.
COASTAL ACOUSTIC TOMOGRAPHY DATA CONSTRAINTS APPLIED TO A COASTAL OCEAN CIRCULATION MODEL Final Report, Jun. 1993 - Mar. 1994
Le N. Ly and Ching-Sang Chiu Apr. 1994 92 p
(AD-A283911; NPS-OC-94-001) Avail: CASI HC A05/MF A01

A direct insertion scheme for assimilating coastal acoustic tomographic (CAT) vertical temperature sections into a multilevel, coastal primitive equation model for the Gulf of Sirte (Lybia) is investigated using computer simulation experiments. Although the model was developed for the whole Mediterranean Sea (MED), only a model sub-domain covering the Gulf of Sirte was used in this study. The model has realistic coastlines and bottom topography, and a coastal-following, curvilinear, nearly orthogonal, horizontal coordinate system with a horizontal resolution of about 10 by 10 km. The grid of the model was designed using a grid generation/focusing technique. The model has complete thermodynamics, second order turbulence closure, and 16 bottom-following (sigma) vertical levels. To generate the true ocean for this study, the model was first spun up for 30 days with the Levitus temperature and salinity and ECMWF wind climatologies, and then run for one year and more. The last 60 days of this control run were taken to represent actuality. DTIC

N95-18160# Coastal Engineering Research Center, Vicksburg, MS.
COASTAL MODELING SYSTEM (CMS) USER'S MANUAL. SUPPLEMENT 3 TO SEPTEMBER 1991 MANUAL Instruction Report
Mary A. Cialone, David J. Mark, Lucia W. Chou, David A. Leenknecht, and Jack E. Davis Aug. 1994 200 p
(AD-A283922; CERC-91-1-Suppl-3) Avail: CASI HC A09/MF A03

The Coastal Modeling System (CMS) is a software package aimed at organizing the Coastal Engineering Research Center's larger numerical models and their supporting software into a user-friendly system that is available to all Corps elements having a need to apply the supported modeling technology. Since some of the models share similar input requirements, output capability, and procedural implementation, efforts are made to standardize these portions of the models as much as possible. FORTRAN 77 programming language is used exclusively in the system software to ensure portability of the models and supporting programs to other computer systems. Graphics programs also make use of DISSPLA software. Models selected for inclusion in CMS are well advanced in their development and have been rigorously tested over a wide range of conditions. The models in CMS can be considered tested, reliable, and mature. The numerical models documented here include: SPH, WIFM, RCPWAVE, CLHYD, SHALWV, STWAVE, and HARBD. Numerical model SPH is a parametric model for representing wind and atmospheric pressure fields generated by hurricanes. Numerical model WIFM solves the vertically integrated Navier-Stokes equations in stretched Cartesian coordinates. The model simulates shallow-water, long-wave hydrodynamics such as tidal circulation, storm surges, and tsunami propagation. DTIC

N95-18468 Naval Postgraduate School, Monterey, CA.
ENVIRONMENTAL FORCING OF AMBIENT NOISE IN THE NANSEN AND AMUNDSEN BASINS OF THE ARCTIC OCEAN M.S. Thesis
David Feller 22 Sep. 1994 187 p Limited Reproducibility: More than 20% of this document may be affected by microfiche quality
(AD-A285540; NPS-OC-94-05) Avail: CASI HC A09

The AREA 1992 experiment inserted three ANMET buoys on separate ice floes about 600 km north of Franz Josef Land. The buoys drifted in unison for most of the experiment and provided 12-19 months of hourly ambient noise data between 5 and 4000 Hz while obtaining limited weather data. The drift pattern was neatly divided into five legs of nearly uniform ice velocities in response to major changes in the wind field. The annual median spectra of each buoy were nearly identical at or above 200 Hz but diverged below 200 Hz. The largest differences were recorded between the two closest buoys. The annual spectra were 10 dB greater than the long term Eurasian Basin median spectra at all frequencies. The annual median spectra was 6-7 dB greater than the CEAREX 1988/1989 median spectra below 100 Hz but was quieter than CEAREX above 100 Hz. Ice speed was the best environmental correlate with ambient noise from 5-10 Hz, wind speed was best from 32-100 Hz, and wind stress was best above 100 Hz. Three periods of extreme noise levels (two loud, one quiet), each lasting for several days, were investigated in detail to establish the role of wind forcing on ambient noise generation. Periods of loud noise were associated with periods of high wind/ice speed coupled with rapid changes in direction, i.e., loud noise levels are the result of large ice convergence and shearing moment. Quiet periods occur when the buoy drift speed is slow. One of the loud noise events showed the periods of ice convergence on nearby land will increase the noise level, even during times of moderate wind speeds. DTIC

N95-18470# Coastal Engineering Research Center, Vicksburg, MS.
KINGS BAY COASTAL AND ESTUARINE PHYSICAL MONITORING AND EVALUATION PROGRAM: COASTAL STUDIES. VOLUME 1: MAIN TEXT AND APPENDIX A Final Report
Nicholas C. Kraus, Laurel T. Gorman, and Joan Pope Aug. 1994 308 p Sponsored by Office of the Chief of Naval Operations
(AD-A285542; CERC-TR-94-9-Vol-1) Avail: CASI HC A14/MF A01

The objective of this study was to assess the impacts of U.S. Navy-sponsored navigation channel modification and maintenance activities conducted from 1985-1992 on the shoreline in the vicinity of the traditionally called St. Marys Entrance. This inlet, separating Cumberland Island, Georgia, to the north and Amelia Island, Florida, to the south contains a large estuary, a commercial and recreational port, Fernandina Harbor, Florida, and, since the 1970s, a U.S. Navy submarine base located at Kings Bay, Georgia. A study of the coastal area included the following components: (1) Review of historical data and previous studies; (2) Numerical simulation of waves and shoreline change; and (3) Monitoring of waves, water level, shoreline position, beach profile and sediments, and ebb-tidal bathymetry over the period 1988-1992. No adverse impact on the beaches of Cumberland Island and Amelia Island by U.S. Navy navigation channel modification and maintenance at St. Marys Entrance could be detected in any of the analyses or monitoring performed in this study. DTIC

N95-18617# Naval Postgraduate School, Monterey, CA.
CALIBRATION AND SEDIMENT LOAD ALGORITHMS FOR AN ACOUSTIC SEDIMENT FLUX PROBE M.S. Thesis
Weston J. Anderson Jun. 1994 95 p
(AD-A283655) Avail: CASI HC A05/MF A01

A method to infer sediment concentrations from acoustic backscatter levels has been implemented for a prototype acoustic sediment flux probe. This required calibrations of the acoustic transceiver systems and direct measurements of the system response to typical sediment size distributions over a wide range of concentrations. The sensitivities of the 1.3 MHz and 5.2 MHz transducers of an acoustic sediment probe were measured using the backscatter amplitudes from stainless steel wires of four different radii. A two-frequency inversion algorithm estimating the geometric mean radius and variance about the mean of suspended sediment with an assumed lognormal size distribution and the sediment mass concentration was developed and tested in a laboratory setting. The sensitivity of the 5.2 MHz transducer for each wire was consistent within 10%. The sensitivity of the 1.3 MHz transducer calculated for each wire was not consistent and is believed to be due to a strong angular dependence between the wire orientation and the 1.3 MHz transducer face. The sensitivities of each of the four transducers were, however, inferred from the system's response to the controlled sediment backscatter measurements. DTIC

N95-18622# Naval Postgraduate School, Monterey, CA.
A NUMERICAL SIMULATION OF SEASONAL CIRCULATION IN THE SOUTH CHINA SEA M.S. Thesis
Ching-Chung Li Mar. 1994 84 p
(AD-A283701) Avail: CASI HC A05/MF A01

The circulation in the South China Sea (SCS) is mainly determined by the monsoons. This monsoon-induced circulation is connected with the circulation in the Pacific Ocean to a small extent and linked with that of the Indian Ocean only by the Timor Current. During winter, the water enters the South China Sea at the north through Formosa Strait and Luzon Strait, and exits at the south through Karimata Strait. During summer, the circulation reverses, the water enters at the south and exits at the north. Water from the north is generally cooler than water from the south. The northward (southward) flow induces warm (cold) advection. Therefore, the seasonal cycle of the circulation in the South China Sea becomes a major factor controlling the seasonal cycle of the sea surface temperature, which might effect the seasonal variation of the Eastern Asian monsoon system. In the preliminary results, the seasonal circulation and temperature patterns simulated by the primitive equation model are similar to those reported by Wyrtki(1961). Yet, our model is better than the Pohlmann (1987) shallow-water model and shows more details. DTIC

N95-18951*# Mississippi State Univ., Bay Saint Louis, MS. Center for Air Sea Technology.
USERS MANUAL FOR THE MOODS DATA MANAGEMENT SYSTEM (MDMS), VERSION 1.0
Aug. 1994 48 p
(Contract NAS13-330)
(NASA-CR-197015; NAS 1.26:197015; AD-A283757) Avail: CASI HC A03/MF A01

The MOODS Data Management System (MDMS) provides access to the Master Oceanographic Observation Data Set (MOODS) maintained by NAVOCEANO. This manual provides instructions to users of this system. DTIC

N95-19503 Materials Research Labs., Ascot Vale (Australia).
THE STOKES (VERSION 4) NORMAL-MODE SHALLOW WATER TRANSMISSION LOSS PROGRAM
Marshall V. Hall Jun. 1993 60 p
(MRL-CP-1; AR-008-263) Copyright Avail: Issuing Activity

The STOKES program calculates the normal-mode-sum solution to the acoustic wave equation for an arbitrary sound-speed profile in a water column overlying a seabed that consists of a liquid layer and a solid half-space. The water column sound-speed profile may be arbitrary except that the sound-speed adjacent to the sea-floor must not be significantly greater than that at the depths of the sound transducers. For the seabed, the user can either supply values for each geoacoustic parameter, or if the seabed is unconsolidated sediment, supply the mean grain-size. In the latter case, STOKES uses published regression equations and models to estimate the geoacoustic parameters. The mode phase-speed eigenvalues are the zeroes of a characteristic function that depends on the depth function at the sea-floor and the reflectivity of the sea-floor. STOKES calculates the mode eigenvalues to great accuracy, and is superior to SNAP if the seabed has a significant shear-speed. STOKES has been successfully run for realistic cases with bottom depths of from 60 to 120 m, and for frequencies from 32 Hz to 2 kHz. It has also performed very well when compared with bench-marks. At very low frequencies, near the cut-off frequency of the sound-speed profile as a whole (usually of the order of 10 Hz in practical cases), the imaginary part of any eigenvalue is large, and in some cases this prevents STOKES, which uses a simple root finding procedure, from finding any mode. In such a case the transmission loss (at ranges of at least a few kilometers) would be exceptionally high, and its precise value would not be of practical interest. Author

N95-19523# Colorado Univ., Boulder, CO.
NONLINEAR OCEAN WAVES Final Report, 1 Jan. 1992 - 30 Sep. 1994
Mark J. Ablowitz, James H. Curry, Joe L. Hammack, and Harvey Segur 30 Sep. 1994 81 p
(Contract N00014-92-J-1274)
(AD-A285331) Avail: CASI HC A05/MF A01

The dynamics of waves in deep water and in shallow water are quite different. In shallow water, we have shown experimentally the existence of a family of finite-amplitude waves that propagate practically without change of form in shallow water of uniform depth. The surface patterns of these waves are genuinely two-dimensional, and periodic. The waves are easy to generate experimentally, and they seem to be stable to perturbations. They are described with reasonable accuracy by an 8-parameter family of exact solutions of the Kadomtsev-Petviahsvili equation. The situation is quite different in deep water, where much of our knowledge is based on numerical simulations. An approximate model of one-dimensional, nearly monochromatic waves in deep water is the nonlinear Schrodinger equation. We find that for certain ranges of parameters in initial data, numerical solutions of the equation are so unstable that long-time simulations of the equation are not reproducible, and are quite unreliable. DTIC

N95-19540# Army Engineer Waterways Experiment Station, Vicksburg, MS.
ADCIRC: AN ADVANCED THREE-DIMENSIONAL CIRCULATION MODEL FOR SHELVES, COASTS, AND ESTUARIES. REPORT 5: A TROPICAL STORM DATABASE FOR THE EAST AND GULF OF MEXICO COASTS OF THE UNITED STATES Technical Report No. 5, 1 Sep. 1992 - 1 Apr. 1994
Norman W. Scheffner, David J. Mark, C. A. Blain (Notre Dame Univ., IN.), J. J. Westerink (Notre Dame Univ., IN.), and R. A. Luettich, Jr. (North Carolina Univ., Chapel Hill, NC.) Aug. 1994 315 p
(AD-A285576; WES/TR/DRP-92-6) Avail: CASI HC A14/MF A03

This report summarizes results of a numerical storm surge study conducted for the east coast of the United States and the Gulf of Mexico. The report describes a database of surge elevations and currents produced from the numerical simulation of 134 historically based tropical storm events and their maximum water level surge impact at 486 discrete locations along the east and gulf coasts of the United States and Puerto Rico. A visual indication of the spatial distribution of the peak surge elevation is provided in the form of an atlas of storm track and maximum storm surge corresponding to a 246-station nearshore subset of the 486-location database. The simulated events used to generate the results contained in this report are not intended to be hindcasts of historic events. The goal was to provide a database of events similar to historic events which can be used to evaluate project response to, or protection afforded from, events which are realistic in both magnitude and duration for a specific location. If use of the database indicates a more detailed study is necessary, then the modeling techniques described in this report can be used to hindcast specific events. This hindcasting procedure requires detailed verification of the storm event by comparing computed results to prototype data, a procedure which was beyond the scope of this study. DTIC

N95-19563# Naval Surface Warfare Center, Dahlgren, VA. Strategic and Space Systems Dept.
SEAFLOOR POSITIONING ACROSS JUAN DE FUCA RIDGE Final Report

Patrick Fell and C. Harris Seay Apr. 1994 53 p
(AD-A285049; NSWCDD/TR-93/643) Avail: CASI HC A04/MF A01

The results of an analysis of a complex data set acquired during the United States Geological Survey's Marine Crustal Deformation Study are presented. The experiment, which commenced in the spring of 1992 in a region of the Pacific known as the Juan de Fuca ridge, represents a first attempt to monitor locally plate dynamics in the marine environment using a network of tripod-mounted, dual-frequency acoustic transponders. The aim is to collect over a period of years time-series measurements of extension rates along the southern Juan de Fuca ridge. In addition, by collecting a combination of Global Positioning System satellite tracking data, low-frequency acoustics data, and water column pressure, conductivity, and temperature at depth, it was possible to extend geodetic control from land onto the seafloor. The methods to accomplish this latter goal of the experiment are described, as well as the final results. Baseline comparisons between several of the solutions obtained during this analysis are presented along with recommendations for additional data collection and analysis.
DTIC

N95-19577*# National Aeronautics and Space Administration. Goddard Space Flight Center, Greenbelt, MD.
SeaWiFS TECHNICAL REPORT SERIES. VOLUME 18: SeaWiFS TECHNICAL REPORT SERIES CUMULATIVE INDEX: VOLUMES 1-17
Elaine R. Firestone, ed. (General Sciences Corp., Laurel, MD.) and Stanford B. Hooker, ed. Feb. 1995 50 p
(NASA-TM-104566-Vol-18; Rept-95B00038-Vol-18; NAS 1.15:104566-Vol-18) Avail: CASI HC A03/MF A01

The Sea-viewing Wide field-of-view Sensor (SeaWiFS) is the follow-on ocean color instrument to the Coastal Zone Color Scanner (CZCS) which ceased operations in 1986 after an eight-year mission. SeaWiFS is expected to be launched in 1995 on the SeaStar satellite, being built by Orbital Sciences Corporation (OSC). The SeaWiFS Project at the National Aeronautics and Space Administration's (NASA) Goddard Space Flight Center (GSFC), has undertaken the responsibility of documenting all aspects of this mission, which is critical to the ocean color and marine science communities. This documentation, entitled the SeaWiFS Technical Report Series, is in the form of NASA Technical Memorandum Number 104566. All reports published are volumes within the series. This particular volume serves as a reference, or guidebook, to the previous 17 volumes and consists of 6 sections including: an errata, an addendum (summaries of various SeaWiFS Working Group Bio-optical Algorithm and Protocols Subgroups Workshops, and other auxiliary information), an index to key words and phrases, a list of all references cited, and lists of acronyms and symbols used. It is the editor's intention to publish a cumulative index of this type after every five volumes in the series. Each index covers the topics published in all previous editions, that is, each new index includes all of the information contained in the preceding indices. Author

N95-19728 Hawaii Univ., Honolulu, HI. School of Ocean and Earth Science and Technology.
DENSITY STRUCTURE OF THE UPPER OCEANIC CRUST AT ZERO POROSITY Final Report
25 Aug. 1994 2 p Limited Reproducibility: More than 20% of this document may be affected by microfiche quality
(Contract N00014-92-J-1763)
(AD-A284235) Avail: Issuing Activity (Defense Technical Information Center (DTIC))

We obtained data on the density of about forty samples of submarine midocean ridge basalt (MORB). These data were obtained using a pychnometer after careful hand-picking of glass shards and have a precision better than +/- 0.05 g/cu cm. A very surprising result is that the measured densities have a much greater range (2.7-2.95 g/cu cm) than expected densities calculated from their chemical composition (2.85-2.97). While we cannot yet rule out the effects of volatiles (H2O and CO2), microcracks, and slight alteration of glasses, we hope to be able to do so soon. DTIC

N95-19818# Naval Research Lab., Bay Saint Louis, MS.
COASTAL BENTHIC BOUNDARY LAYER SPECIAL RESEARCH PROGRAM: A REVIEW OF THE FIRST YEAR. VOLUME 1 Final Report
Michael D. Richardson 6 Apr. 1994 325 p
(Proj. R31-03)
(AD-A280034) Avail: CASI HC A14/MF A03

The coastal benthic boundary layer special research program (CBBLSRP) is a 5-year Office of Naval Research program that addresses the physical characterization and modeling of benthic boundary layer processes and the impact of these processes on seafloor structure, properties, and behavior. In volume 1 of this report, we present preliminary results from the first years' experiments that were conducted on the gas-rich soft sediments of Eckernfoerde Bay (Baltic Sea) and on the sandy sediments of the northeastern Gulf of Mexico. Year-end reports for the 21 projects supported by the CBBLSRP are included along with a summary of the first years' accomplishments. Volume 2 will include four updated cruise reports along with sample descriptions, locations, and maps that will be provided for reference.
DTIC

51 LIFE SCIENCES (GENERAL)

N95-18371# Pacific Northwest Lab., Richland, WA.
MECHANISMS OF INTERACTION AND BIOLOGICAL EFFECTS OF EXTREMELY-LOW-FREQUENCY ELECTROMAGNETIC FIELDS
T. S. Tenforde 1994 10 p Presented at the US-Japan Science Seminar, Sapporo, Japan, 28 Jun. - 1 Jul. 1994
(Contract DE-AC06-76RL-01830)
(DE94-015200; PNL-SA-24287; CONF-9406207-1) Avail: CASI HC A02/MF A01

Evidence is mounting, that environmental electric and magnetic fields in the extremely-low-frequency (ELF) band below 300 Hz can influence biological functions by mechanisms that are only poorly understood at the present time. The primary objectives of this paper are to review the physical properties of ELF fields, their interactions with living systems at the tissue, cellular, and subcellular levels, and the key role of cell membranes in the transduction of signals from imposed ELF fields. Topics of discussion include signal-to-noise ratios for single cells and cell aggregates, resonance phenomena involving a combination of static and ELF magnetic fields, and the possible influence of ELF fields on molecular signaling pathways that involve membrane receptors and cytoplasmic second messengers. The implications of these findings for promotion of tumor growth by ELF fields are also reviewed.
DOE

N95-18439 Colorado State Univ., Fort Collins, CO. Dept. of Anatomy and Neurobiology.
CELLULAR NEUROPHYSIOLOGY OF THE RAT SUPRACHIASMATIC NUCLEUS: ELECTRICAL PROPERTIES, NEUROTRANSMISSION, AND MECHANISMS OF SYNCHRONIZATION Annual Report, 1 Jul. 1993 - 30 Jun. 1994
F. E. Dudek 29 Jul. 1994 108 p Limited Reproducibility: More than 20% of this document may be affected by microfiche quality
(Contract F49620-93-1-0302)
(AD-A284111; AFOSR-94-0513TR) Avail: Issuing Activity (Defense Technical Information Center (DTIC))

The general aim of this research has been to understand the electrophysiological properties and synaptic mechanisms of supra-chiasmatic nucleus (SCN) neurons. Our earlier experiments included sharp-intracellular-electrode analyses of amino-acid-mediated synaptic transmission and intrinsic membrane properties, focussing on the degree to which SCN neurons are homogenous or heterogenous. This work showed that GABA (in addition to glutamate) plays a critical role in fast synaptic transmission in the SCN, and that SCN neurons are not homogenous in terms of their electrophysiological properties, although they could not be grouped into distinct neuron classes. More recently, multiple-unit extracellular recordings have shown synchronous bursts of action potentials in the SCN in low (Ca(2+)) solutions containing amino-acid-receptor antagonists demonstrated to block chemical synapses, thus suggesting that SCN neurons can communicate through nonsynaptic mechanisms. Our more recent studies using whole-cell patch-clamp techniques in the thin-slice preparation have shown evidence for local GABA-ergic communication among SCN neurons, and have begun to define the different types of K(+) currents present in SCN neurons.
DTIC

N95-18734*# National Aeronautics and Space Administration. Ames Research Center, Moffett Field, CA.
EFFECT OF HEAT ACCLIMATION ON SITTING ORTHOSTATIC TOLERANCE IN THE HEAT AFTER 48 AND 96 HOUR BED REST IN MEN
J. E. Greenleaf and M. Matter, Jr. Jan. 1995 10 p
(RTOP 199-18-12-07)
(NASA-TM-108861; A-95026; NAS 1.15:108861) Avail: CASI HC A02/MF A01

The purpose of this pilot study was to investigate sitting orthostatic tolerance and determine potentially adverse signs and symptoms that would incapacitate subjects in a hot environment (Gemini reentry cabin temperature profile) after 48 hr and 96 hr of horizontal bed rest (BR), which simulated microgravity deconditioning. Six college men (23-29 yr) were allocated into two groups: heat acclimated (three subjects: No. 1- control, No. 2- 48 hr BR, and No. 3- 96 hr BR) and nonheat acclimated (three subjects: No. 4- control, No. 5- 48 hr BR, and No. 6- 96 hr BR). After BR they sat in an ambient temperature of 57 C (135 F) for 30 min which then was decreased to 49 C (120 F) for up to 480 min. Tolerance time in the heat with seated orthostatic stress was 480 min (subject No. 1) and 180 min (subject No. 4) in the two ambulatory men, but was reduced to 22-150 min in the four bed-rested men irrespective of their heat acclimation status. Although heat acclimation appeared to enhance tolerance and attenuate accompanying physiological responses, as well as ameliorate the frequency and intensity of adverse signs and symptoms at termination of exposure, tolerance was reduced in the bed-rest deconditioned subjects regardless of their acclimation level. Thus, these few collective findings do not indicate an unequivocal positive effect of acute heat acclimation on sitting orthostatic tolerance in acute bed-rest deconditioned subjects. Author (revised)

N95-19140*# National Aeronautics and Space Administration. Ames Research Center, Moffett Field, CA.
DRINK COMPOSITION AND CYCLE-ERGOMETER ENDURANCE IN MEN: CARBOHYDRATE, Na(+), OSMOLALITY
J. E. Greenleaf, R. Looft-Wilson, J. L. Wisherd, N. Marchman, T. Wells, P. R. Barnes, and L. G. Wong (Shaklee US, Inc., San Francisco, CA.) Dec. 1994 16 p
(RTOP 199-18-12-07)
(NASA-TM-4650; A-94137; NAS 1.15:4650) Avail: CASI HC A03/MF A01

Cycle-ergometer endurance performance was determined in 5 untrained men (22-39 yr, 62.4-100.5 kg, 29-55 mL x min(exp -1) x kg(exp -1) peak oxygen uptake) after consuming Nothing (N) or two fluid formulations (10 mL x kg(exp -1), 555-998 mL). Performance 1 (P1), a multi-ionic-glucose rehydration drink, contains 55 mEq/L Na(exp +), 416 mg/dL citrate, 2,049 mg/dL glucose, and 365 mOsm/kgH2O. HyperAde (HA), a sodium chloride-citrate hyperhydration drink, contains 164 mEq/L Na(exp +), 854 mg/dL citrate, less than 0.5 mg/dL glucose, and 253 mOsm/kgH2O. Endurance at a load of 87-91 percent of peak VO2 was 30.50 +/- SE 3.44 min with HA; 24.55 +/- 1.09 min with P1 (p greater than 0.10 from HA); and 24.68 +/- 1.50 min with N (p less than 0.05 from HA). The attenuated endurance performance with P1 and N could not be attributed to differences in exercise metabolism, change or absolute level of rectal and mean skin temperature, or change in perceived exertion. The greater increase in resting plasma volume with HA, compared with P1 or N, probably contributed to the greater endurance with HA. ARC

N95-19536# Naval Research Lab., Washington, DC.
PROCEEDINGS OF NATURAL SCIENCES SYMPOSIUM
Jul. 1994 84 p Symposium held in Washington, DC, 14 Jun. 1993
(AD-A285452; NRL/PU/6000-94-252) Avail: CASI HC A05/MF A01

This symposium included seven Nobel Laureates' presentations: Prospects for the Physical Sciences; Creativity and Managed Research; Science -- The Preeminent Random Process; Dealing with Genes; Understanding Life as Chemistry; The Impossible Takes a Little Longer; and Reflections of an Era. This last presentation is made by Dr. Jerome Karle, Nobel Laureate, Chemistry, 1985, for whom the conference marked a 75th birthday and 45th year in government service. The focus of these talks was an outlook on the 'Future Implications of Current Advances in the Natural Sciences'. CASI

N95-19613# Department of Energy, Washington, DC. Office of Energy Research.
[ACTIVITIES OF THE DIVISION OF ENERGY BIOSCIENCES] Annual Summary Report, FY 1994
Sep. 1994 172 p
(DE95-001046; DOE/ER-0621P) Avail: CASI HC A08/MF A02

The Energy Biosciences program was initiated in 1979 for the purpose of fulfilling the need of basic information about plants and microorganisms relating to varied energy matters. The program generates basic information that contributes significantly to future technologies involving alternate fuel generation, petroleum replacements, sustained industrial activities along with means of improving environmental conditions. The Energy Biosciences program during Fiscal Year 1994 received 139 new research applications following the screening of numerous preapplications. Of the applications received, 21 projects were funded. DOE

N95-18173*# Maryland Univ., College Park, MD. Dept. of Horticulture.
PHYSIOLOGICAL AND GENETIC CHARACTERIZATION OF PLANT GROWTH AND GRAVITROPISM IN LED LIGHT SOURCES
Gerald F. Deitzer *In* Univ. of Central Florida, NASA/ASEE Summer Faculty Fellowship Program. 1994 Research Reports Oct. 1994 p 159-203 (For primary document see N95-18166 05-80)
Avail: CASI HC A03/MF A04

N95-18179*# Colorado State Univ., Fort Collins, CO. Dept. of Agricultural and Chemical Engineering.
ETHYLENE DYNAMICS IN THE CELSS BIOMASS PRODUCTION CHAMBER
Allen L. Rakow *In* Univ. of Central Florida, NASA/ASEE Summer Faculty Fellowship Program. 1994 Research Reports Oct. 1994 p 349-378 (For primary document see N95-18166 05-80)
Avail: CASI HC A03/MF A04

N95-18997*# Alabama Univ., Huntsville, AL. Dept. of Biological Sciences.
CONCENTRATION AND TEMPERATURE EFFECTS ON OVOSTATIN ACTIVITY
Debra M. Moriarity *In* Alabama Univ., Research Reports: 1994 NASA/ASEE Summer Faculty Fellowship Program Oct. 1994 6 p (For primary document see N95-18967 05-80)
Avail: CASI HC A02/MF A03

N95-19014*# Calhoun Community Coll., Decatur, AL. Dept. of Natural Sciences.
CAPILLARY ELECTROPHORESIS: BIOTECHNOLOGY FOR SEPARATION OF DNA AND CHROMOSOMES
George O. Williams, Jr. *In* Alabama Univ., Research Reports: 1994 NASA/ASEE Summer Faculty Fellowship Program Oct. 1994 5 p (For primary document see N95-18967 05-80)
Avail: CASI HC A01/MF A03

52 AEROSPACE MEDICINE

Includes physiological factors; biological effects of radiation; and effects of weightlessness on man and animals.

N95-17949# National Library of Medicine, Bethesda, MD. Office of the Director.
NATIONAL LIBRARY OF MEDICINE PROGRAMS AND SERVICES, FISCAL YEAR 1991 Final Annual Report, 1 Oct. 1990 - 30 Sep. 1991
Mar. 1992 80 p
(PB94-188026; NLM/OD-94/01) Avail: CASI HC A05/MF A01

The report provides statistical and narrative information regarding the National Library of Medicine's (NLM's) activities during FY 1990. Coverage includes information on: library operations, specialized information services, the Lister Hill National Center for Biomedical Communications, the National Center for Biotechnology Information, extramural programs, the Office of Computer and Communications Systems, international programs, and the administration. In addition, there is information about NLM special initiatives, including outreach, the unified medical language system, paper preservation, and high performance computing and communications. Appendices include

a staff bibliography; extramural-supported publications; lists of members of various NLM advisory bodies including the Board of Regents, Board of Scientific Counselors, Biomedical Library Review Committee, and the Literature Selection Technical Review Committee; and a list of acronyms, abbreviations, and initialisms. NTIS

N95-17950# National Library of Medicine, Bethesda, MD. Office of the Director.
NATIONAL LIBRARY OF MEDICINE PROGRAMS AND SERVICES, FISCAL YEAR 1992 Final Annual Report, 1 Oct. 1991 - 30 Sep. 1992
Mar. 1993 84 p
(PB94-188034) Avail: CASI HC A05/MF A01

The report provides statistical and narrative information regarding the National Library of Medicine's (NLM's) activities during FY 1990. Coverage includes information on: library operations, specialized information services, the Lister Hill National Center for Biomedical Communications, the National Center for Biotechnology Information, extramural programs, the Office of Computer and Communications Systems, international programs, and the administration. In addition, there is information about NLM special initiatives, including outreach, health services research, and high performance computing and communications. Appendices include a staff bibliography; extramural-supported publications; lists of members of various NLM advisory bodies including the Board of Regents, Board of Scientific Counselors, Biomedical Library Review Committee, and the Literature Selection Technical Review Committee; and a list of acronyms, abbreviations, and initialisms. NTIS

N95-17998# JAYCOR, San Diego, CA.
HEALTH HAZARDS ASSESSMENT FOR BLAST OVERPRESSURE EXPOSURES Report, 2 Nov. 1992 - 31 May 1994
James H. Stuhmiller 1 Jun. 1994 49 p
(Contract DAMD17-93-C-3005)
(AD-A283352) Avail: CASI HC A03/MF A01

The Army needs to set blast overpressure exposure standards that will protect soldiers in training against adverse effects from blast coming from a variety of weapons in a variety of surroundings. JAYCOR is developing biomechanical models that compute the tissues level response due to external blast loading and correlations of that response to pathology and lethality. To validate the models, animal test data has been organized into a database. Trends in the data have been determined that are independent of the models and agreement between the correlations and observations have been good for all level of blasts and animal species. The future work will refine the pathology prediction by location and provide a probabilistically-based methodology for making health hazards assessment. DTIC

N95-18138 Naval Aerospace Medical Research Lab., Pensacola, FL.
EFFECTS OF WEIGHT LIFTING ON INTRATHORACIC PRESSURES GENERATED BY ANTI-G STRAINING MANEUVERS
L. G. Meyer, J. D. Grissett, and J. G. Lamberth 1994 19 p Limited Reproducibility: More than 20% of this document may be affected by microfiche quality
(DA Proj. M00-96)
(AD-A283651; NAMRL-1393) Avail: Issuing Activity (Defense Technical Information Center (DTIC))

The purpose of this study was to assess the effects of physical fitness program on the ability to perform an anti-G straining maneuver (AGSM). We used mouth-generated intrathoracic pressure (IP) as an index of effectiveness of the AGSM. We compared changes in IP in experimental subjects who performed the AGSM 5 times per week and participated in a weight lifting exercise program to IP's in control subjects who performed the AGSM 10 times per week and did not participate in a weight training program. Initial mean IP's were 169 mmHg and 167 mmHg for the experimental and control groups respectively. After 6 weeks of exercise and AGSM training, mean IP for the experimental subjects was 213 mmHg (26% increase). After 3 weeks of AGSM training, mean IP for the control group was 202 mmHg (21% increase). The difference in pre- and post-IP's between groups was not significant, but both groups significantly increased their IP's with training. Multiple linear regression analysis showed that pulmonary vital capacity and the strength of several muscle groups were significant predictors of IP in the experimental group. We conclude that strength and anaerobic fitness may be important for the performance of an effective AGSM. However, the AGSM training alone appeared to improve the performance of the AGSM as indicated by the increased IP's. DTIC

N95-18400 California Univ., San Diego, La Jolla, CA. Dept. of Psychiatry.
EXTRATHALAMIC MODULATION OF CORTICAL RESPONSIVENESS Annual Report, 1 Jul. 1993 - 30 Jun. 1994
Stephen L. Foote 1 Aug. 1994 23 p Limited Reproducibility: More than 20% of this document may be affected by microfiche quality
(Contract F49620-93-1-0402)
(AD-A284100; AFOSR-94-0514TR) Avail: Issuing Activity (Defense Technical Information Center (DTIC))

The overall goal of the proposed studies is to further elucidate the mechanisms by which the brainstem noradrenergic (NA) nucleus, locus coeruleus (LC), is capable of altering forebrain electrophysiological activity. The proposed studies have the following Specific Aims: (1) To examine the relationship between the intensity of LC neuronal activity, forebrain EEG activation, and rates of NA release in neocortex and hippocampus using microdialysis; (2) To test the hypothesis that LC-induced activation of forebrain EEG is mediated by LC/NA actions on septal and basal forebrain neurons; (3) To examine, in unanesthetized monkey, the effects of activating or inactivating the LC/NA system on forebrain EEG and on dialysis measures of NA and acetylcholine release in neocortex and hippocampus. The effects on these dialysis measures of systemic adrenergic drugs that alter cognitive performance will also be determined; (4) To examine, in monkey, the effects of activating or inactivating the LC/NA system on cortical and hippocampal EEG measures and on complex, bimanual motor behavior. DTIC

N95-18512 Massachusetts General Hospital, Boston, MA.
CELLULAR ANALYSIS OF CIRCADIAN RHYTHMICITY IN CULTURED SCN NEURONS Annual Report, 1 Jul. 1993 - 31 Jul. 1994
Steven M. Reppert and David K. Welsh 28 Jul. 1994 4 p Limited Reproducibility: More than 20% of this document may be affected by microfiche quality
(Contract F49620-93-1-0434)
(AD-A284167; AFOSR-94-0495TR) Avail: Issuing Activity (Defense Technical Information Center (DTIC))

Circadian rhythms are generated by brain cells located in the suprachiasmatic nuclei (SCN) of the mammalian hypothalamus, but it is not clear how individual cells contribute to the operation of the circadian clock. SCN neurons dissociated from newborn rat SCN were characterized by immunocytochemistry and by patch recording of spontaneous action potentials and synaptic currents. Inhibitory synaptic interactions were prevalent among neurons, increasing progressively with time in culture. Evidence was found for presence of gap junctions between glial cells but not between neurons. To assess circadian rhythmicity, long-term multielectrode recordings of spontaneous action potentials were obtained from neurons cultured for 1-6 weeks on Glass plates containing a flat array of 61 microelectrodes. Firing rates of some but not all individual neurons exhibited clear circadian rhythms with periods of nearly 24 hrs. Within a culture, cells expressing circadian rhythms showed no short-term firing synchrony. The phase of the circadian rhythm varied among cultures and, in most cases, among different cells within the same culture. With the ability to record circadian rhythms from individual SCN neurons, experimental analysis can now proceed to detailed study of circadian pacemaker neurons and their interactions. DTIC

N95-18515 New England Medical Center Hospitals, Boston, MA.
RETINAL INJURIES FROM SINGLE AND MULTIPLE PICOSECOND LASER PULSES Annual Report, 1 May 1993 - 30 Apr. 1994
Carmen A. Puliafito 30 Apr. 1994 10 p Limited Reproducibility: More than 20% of this document may be affected by microfiche quality
(Contract F49620-93-1-0337)
(AD-A284173) Avail: Issuing Activity (Defense Technical Information Center (DTIC))

We investigate laser-induced shock waves from melanin particles as a possible cause of retinal injury from ultrashort pulse laser exposures. Melanin granules were isolated from calf retina and suspended in gels. The melanin particles were irradiated with 100 psec laser pulses from an amplified, mode-locked Nd:YAG laser and shock waves were observed under a

microscope using a time-delayed strobe pulse. Spherical shock fronts were observed at incident laser fluences 4J/sq cm and were imaged as close as 20 micrometers from the melanin particles. Multiple shock fronts were resolved when several melanin particles were irradiated simultaneously. Shock front radii were measured as a function of photographic delay time and laser fluence. Average shock from velocities during the first 10 nsec ranged from 2500 to 4000 m/sec. A velocity of 3000 m/sec corresponds to a shock pressure of 11 kbars. These results indicate that shock wave emission from melanin particles in the retinal pigment epithelium is a potential cause of retinal injury from ultrashort laser pulses. DTIC

N95-18518 SRI International Corp., Menlo Park, CA.
IN VITRO SYSTEM FOR STUDYING METABOLISM OF ENVIRONMENTAL CHEMICALS IN HUMAN CELLS Annual Report, 30 Apr. 1993 - 29 Apr. 1994
Carol E. Green 25 Jul. 1994 24 p Limited Reproducibility: More than 20% of this document may be affected by microfiche quality
(Contract F49620-91-C-0050)
(AD-A284174; AFOSR-94-0508TR) Avail: Issuing Activity (Defense Technical Information Center (DTIC))

The objective of the project is to establish and use an in vitro liver model from rodents and humans to develop quantitative data on the metabolism of toxic chemicals. In the third year of the project, liver slices from rat and human liver were compared to evaluate their capacity for chloroform metabolism. It was observed that the weight (an indication of the slice thickness) of the liver slices was inversely related to the rate of chloroform metabolism, suggesting that metabolism was limited by diffusion into the tissue in the thicker slices. Using the thinnest slices possible, the kinetic constants for chloroform metabolism by rat and human liver slices were determined. The V max values for chloriform in metabolism were 2.82 +/- 0.79 nmol/mi n/g tissue and 2.91 + or 0. 99 nmol/min/g tissue, with rat and human liver, respectively and the K values were 25.5 +/- 18.4 nmol/flask and 8.33 +/- 1.9 nmol/flask, rat and human liver, respectively. Rat hepatocytes incubated under similar conditions metabolized chloroform with a V max of 10 nmol/min/g and a K m of 93 nmol/flask. In summary, the liver slice system was readily adaptable to investigation of the metabolism of volatile chemicals. DTIC

N95-18618# Army Research Inst. of Environmental Medicine, Natick, MA.
DESIGN CONCEPTS FOR AN INTEGRATED ENVIRONMENTAL MEDICINE WORKSTATION FOR PREDICTION, SIMULATION AND TRAINING
Matthew J. Reardon Dec. 1993 53 p
(AD-A283686) Avail: CASI HC A04/MF A01

A design concept is developed for a comprehensive multimedia software-based environmental medicine and physiology workstation for military health care planners and providers for use in both operational and training settings. This will be based on integrating a core of predictive models for soldier responses to hot, cold, and high altitude stress. Overlying this core is a layer of on-line documentation to provide assistance and guidance as well as support training modes. The user interactive information resource will incorporate USARIEM's cumulative database in hot, cold, and altitude stress as well as nutrition, human performance, and injury prevention. The outer layer of the workstation is a flexible, user friendly, graphical interface. It may also be tailored as an environmental medicine computer-based training module for medical students and residents. DTIC

N95-18626 Indiana Univ., Bloomington, IN. Hearing and Communication Lab.
PERCEPTION OF COMPLEX AUDITORY PATTERNS Annual Report, 15 Sep. 1992 - 14 Sep. 1993
Charles S. Watson 14 Sep. 1993 16 p Limited Reproducibility: More than 20% of this document may be affected by microfiche quality
(Contract F49620-92-J-0506)
(AD-A284189; AFOSR-94-0503TR) Avail: Issuing Activity (Defense Technical Information Center (DTIC))

This report describes research progress in three areas: the perception of complex sounds, including tonal sequences and bursts of frozen Gaussian noise; models for the discrimination of complex sounds; and the perception of speech sounds, under various degrees of stimulus uncertainty and levels of training. Major accomplishments during this period include: the finding that the ability to detect very small frequency changes in single components of tonal sequences, previously assumed to be accomplished only after lengthy training on the specific discrimination task in question, is largely the result of familiarity with the stimulus and is relatively independent of the manner in which that familiarity was acquired; the previously described PTD rule for auditory pattern discrimination predicts the discrimination of changes in temporal as well as spectral properties of patterns, and a new model of auditory pattern discrimination that combines elements of Jeffress leaky integrator and the Durlach-Braida equalization-cancellation models is quite successful in describing the results of noise-burst discrimination experiments, including the PTD phenomena mentioned above. DTIC

N95-18656 Hahnemann Medical Coll. and Hospital, Philadelphia, PA.
CEREBELLAR CIRCUIT MECHANISMS WHICH ACCOMPANY COORDINATED LIMB TRAJECTORY PATTERNS IN THE RAT: USE OF A MODEL OF SPONTANEOUS CHANGES IN LIMB COORDINATION Annual Report, Feb. 1993 - Mar. 1994
Sheryl S. Smith 1 Aug. 1994 7 p Limited Reproducibility: More than 20% of this document may be affected by microfiche quality
(Contract F49620-93-1-0136)
(AD-A284023; AFOSR-94-0542TR) Avail: Issuing Activity (Defense Technical Information Center (DTIC))

The olivo-cerebellar circuit plays a role in the coordination of the distal limbs. The present study was proposed to determine the behavior of individual neurons in this circuit, recorded chronically as ensembles of 10-20 during tests of limb coordination across spontaneous changes in limb coordination. Hormone (estrous) and circadian cycles are known to be associated with improvements in the speed and accuracy of limb trajectory, and will be used in this study as a model of changes in performance. Underlying circuit properties which accompany changes in performance will be assessed during performance paradigms. Rats, chronically implanted with microwires in the dorsal accessory olive and arrays of Purkinje cells in the paravermal cerebellum will be monitored during treadmill paradigms employing constant speed, variable acceleration and perturbed gait. Single unit discharge will then be analyzed and correlated with changes in performance associated with hormone state. The following parameters will be assessed: (1) step-cycle correlated discharge; (2) the strength of olivo-cerebellar connections, using cross-correlation techniques; (3) the degree of synchronized olivary oscillatory discharge, a putative timing mechanism for rapid movements; and (4) changes in center-surround properties of adjacent arrays of Purkinje cells. DTIC

N95-18661 Southeastern Center for Electrical Engineering Education, Inc., Saint Cloud, FL.
THE CROSS-VALIDATION OF THE UNITED STATES AIR FORCE SUBMAXIMAL CYCLE ERGOMETER TEST TO ESTIMATE AEROBIC CAPACITY Interim Report, Jun. 1993 - Jun. 1994
Michael L. Pollock, Linda Garzarella, Diego DeHoyos, William Brechue, and Matt Beekley Jun. 1994 157 p Prepared in cooperation with Florida Univ., Gainesville, FL Limited Reproducibility: More than 20% of this document may be affected by microfiche quality
(Contract F33615-90-D-0606; AF Proj. 7930)
(AD-A284055; AL/CF-TR-1994-0046) Avail: Issuing Activity (Defense Technical Information Center (DTIC))

Two hundred and seven subjects (males, n=103; females, n=104) between the ages of 18 and 54 volunteered for this study to determine the accuracy of the USAF submaximal cycle ergometry (SCE) test versus treadmill (TM). The analysis shows that USAF SCE VO(sub 2max) estimates are valid for males and females in this age range. For males, baseline SCE underpredicted VO(sub 2max) by 2.2 ml/kg/min, had a moderately high correlation (r=0.85), and acceptably low standard error of the estimate (SEE, 6.7 ml/kg/min). For females, baseline SCE overestimated VO(sub 2max) by 2.2 ml/kg/min. For females, correlation was moderately high (r=0.85) with a relatively low SEE (5.5 ml/kg/min, 16.6%). Repeat SCE did not increase accuracy. Adjusting power output to achieve higher steady state heart rates improved correlations and lowered SEE. SCE was more closely related to TM VO(sub 2max) than to maximal cycle measures. Finally, 102 subjects completed a YMCA SCE test. For males, the YMCA test overpredicted VO(sub max). Correlation and SEE were not satisfactory (r=0.63 and SEE=9.8 ml/kg/min). For females, the YMCA test was equally good or slightly better than the USAF SCE in estimating VO sub 2max.

USAF SCE sensitivity was 75%. Specificity was 96%. Suggestions to further improve USAF SCE validity and accuracy are offered. DTIC

N95-19239* National Aeronautics and Space Administration, Washington, DC.
AEROSPACE MEDICINE AND BIOLOGY: A CONTINUING BIBLIOGRAPHY WITH INDEXES (SUPPLEMENT 398)
Feb. 1995 41 p
(NASA-SP-7011(398); NAS 1.21:7011(398)) Avail: CASI HC A03

This bibliography lists 66 reports, articles and other documents introduced into the NASA Scientific and Technical Information System during Feb. 1995. Subject coverage includes: aerospace medicine, life sciences, behavioral sciences, man/system technology and life support, and space biology. Author

N95-19244# Oak Ridge National Lab., TN.
NUCLEAR MEDICINE PROGRAM Quarterly Progress Report, period ending 30 Jun. 1994
F. F. Knapp, Jr., K. R. Ambrose, A. L. Beets, C. R. Lambert, D. W. McPherson, S. Mirzadeh, and H. Luo Aug. 1994 17 p
(Contract DE-AC05-84OR-21400)
(DE94-017530; ORNL/TM-12789) Avail: CASI HC A03/MF A01

We describe the first successful synthesis and in vivo evaluation of a fluorinated analog of the IQNP muscarinic-cholinergic receptor ligand. Unanticipated synthetic hurdles lead to several unsuccessful approaches before the synthesis of a model compound was achieved. The successful route involved introduction of the fluoroethyl moiety at an early stage of the synthesis by alkylation of ethyl 1,3-dithiane-2-carboxylate with 1-fluoro-2-bromoethane. Subsequent unmasking of the carbonyl, followed by introduction of the phenyl group with phenylmagnesium bromide and subsequent transesterification with racemic quinuclidinol afforded the target compound, 1-azabicyclo(2.2.2)oct-3-yl alpha-(1-fluoroethan-2-yl)-alpha-hydroxy- alpha-phenylacetate (QNF). Pretreatment of Fisher rats with QNF one hour prior to the intravenous administration of the (I-131)-Z-(R,R) IQNP isomer demonstrated that the new fluoro analog blocked uptake of iodine-131 in those regions of the brain rich in muscarinic-cholinergic receptors measured three hours after injection. As an example, the control values for group of nontreated animals were (5 animals; mean +/- SD): cortex, 1.20 +/- 0.27; striatum, 0.73 +/- 0.19; pons, 0.70 +/- 0.20; cerebellum, 0.43 +/- 0.114. Brains from animals pretreated with the fluoro analogue had the following values (mean +/- SD; % decrease): cortex, 0.67 +/- 0.15 (65%); striatum, 0.35 +/- 0.114 (52%); pons, 0.40 +/- 0.08 (43%); cerebellum, 0.16 +/- 0.09 (63%). Also during this period several tungsten-188/rhenium-188 generators and tin-117m samples were provided for collaborative studies. DOE

N95-19384# Hilton Systems, Inc., Cherry Hill, NJ.
AGE 60 STUDY. PART 3: CONSOLIDATED DATABASE EXPERIMENTS Final Report
Edwin J. Kay (Lehigh Univ., Bethlehem, PA.), Donald J. Hillman (Lehigh Univ., Bethlehem, PA.), Diane T. Hyland (Lehigh Univ., Bethlehem, PA.), Robert S. Voros (Lehigh Univ., Bethlehem, PA.), Regina M. Harris, and Jim D. Deimler Oct. 1994 99 p
(Contract DTFA02-90-C-90125)
(AD-A286247; RN-8025-3C(R2)-Pt-3; DOT/FAA/AM-94/22-Pt-3) Avail: CASI HC A05/MF A02

This report was a primary deliverable from the research contract with Hilton Systems, Inc. on the FAA's mandatory retirement for pilots operating under Federal Aviation Regulations Part 121, the Age 60 Rule. The purpose of this study was to examine existing data to assess the relationship between pilot age, accident rate, and experience. Three existing data bases were integrated on a single computer platform: (1) the FAA Airmen Certification file, (2) the FAA Medical History file, and (3) the National Transportation Safety Board (NTSB) Accident data base. The report presents a discussion of the methodological issues with studies in aging and reviews prior research. Limitations of utilizing these data sets are discussed. The methodological approach was developed from these considerations. Hilton Systems replicated and extended analyses from previous studies, including statistical analyses. The report describes outcomes from analyses conducted to answer a series of questions examining the relationship between age and accident rates for pilots holding Class 1, Class 2, and Class 3 medical certificates. Recent and total flight time are utilized as a measure of risk exposure. The results present a converging body of evidence which fail to support a hypothesis that accident rates increase at or about the age of 60 years. DTIC

N95-19385# Hilton Systems, Inc., Cherry Hill, NJ.
AGE 60 STUDY. PART 4: EXPERIMENTAL EVALUATION OF PILOT PERFORMANCE Final Report
Diane T. Hyland, Edwin J. Kay, and Jim D. Deimler Oct. 1994 66 p
(Contract DTFA02-90-C-90125)
(AD-A286248; RN-8025-4B-Pt-4; DOT/FAA/AM-94/23-Pt-4) Avail: CASI HC A04/MF A01

This report was a deliverable from the research contract with Hilton Systems, Inc. on the FAA's mandatory retirement for pilots operating under Federal Aviation Regulations Part 121, the Age 60 Rule. The purpose of this study was to examine the feasibility of developing an individually-based pilot performance assessment, as well as design an experimental methodology to empirically examine the relationship between pilot aging and performance. Pilot performance was measured with both domain-dependent as well as domain-independent assessments to test a decrement with compensation model of expertise and aging. Computerized cognitive test batteries, COGSREEN and WOMBAT, were selected as the domain-independent measures. Flitescript and whole task performance in the B-727 simulator were domain-dependent measures. Forty B-727-rated pilots were recruited from air carriers and the FAA. Pilots were males between the ages of 41 and 71 years (M=53.9, sd=8.1). DTIC

N95-19413# Advisory Group for Aerospace Research and Development, Neuilly-Sur-Seine (France). Aerospace Medical Panel.
THE CLINICAL BASIS FOR AEROMEDICAL DECISION MAKING [LES BASES CLINIQUES POUR LA PRISE DE DECISION DANS LE DOMAINE AEROMEDICAL]
Sep. 1994 257 p In ENGLISH and FRENCH Symposium held in Palma de Mallorca, Spain, Apr. 1994
(AGARD-CP-553; ISBN-92-836-0003-7) Copyright Avail: CASI HC A12/MF A03

This symposium addressed the rationale behind aeromedical decisions. Lack of available data required decision-makers to be conservative when deciding who should fly or not. Papers in this symposium updated available data and provided a focal point for discussion and re-evaluation of aeromedical selection and retention standards. Discussion periods allowed for open exchange on particular topics of concern, i.e., cardiovascular and neurological problems and HIV. Our purpose was to exchange data, experience, and management rationales dealing with the very difficult task of aeromedical decision-making. Information sharing would enable nations to update management protocols based upon experience and collectively more powerful data. The elimination of costly redundant research, the focusing of future research, and collaborative efforts between AGARD member nations is the hope of this exchange. For individual titles, see N95-19414 through N95-19443.

N95-19414# Air Force Systems Command, Bolling AFB, Washington, DC. Medical Operations Agency.
AEROMEDICAL RISK MANAGEMENT FOR AIRCREW
T. M. Gibson (Royal Air Force, Farnborough, England.) and P. M. Giovanetti *In* AGARD, The Clinical Basis for Aeromedical Decision Making Sep. 1994 8 p (For primary document see N95-19413 05-52)
Copyright Avail: CASI HC A02/MF A03

Medical waivers for aircrew are exceptions to aeromedical standards which have operational justification. The goal of the waiver process is to preserve flying experience to the fullest extent while preserving flight safety, individual health and mission completion. Unfortunately, the flight surgeon has historically been forced to be conservative in deciding who was or who was not fit to fly because of a paucity of relevant scientific data. Moreover, the waiver process has not always been applied logically or consistently. The US Air Force has recently applied the philosophy of aeromedical risk management to produce a waiver guide for flight surgeons. The guide lists the aeromedical concerns for selected chronic conditions met by the flight surgeon. Advice is given on the workup required for each waiver request and a discussion section examine the rationale for the aeromedical disposition. For each condition, an indication is given of the

US Air Force waiver experience over the last few years. This paper examines the basic philosophy and describes the use of the waiver guide. Author

N95-19415# Belgian Air Force, Brussels (Belgium).
THE WAY TO WAIVERS IN THE BAF
J. P. Vastesaeger and P. Vandenbosch *In* AGARD, The Clinical Basis for Aeromedical Decision Making Sep. 1994 4 p (For primary document see N95-19413 05-52)
Copyright Avail: CASI HC A01/MF A03

The medical and physical examinations our pilots go in for at recruiting and during their annual revision become more extended and accurate thanks to new medical techniques. On the other hand we notice that the importance of human factors as a cause of flight accidents increases. Therefore, the medical Commission (GCGLUD) responsible for declaring pilots fit to fly has to describe the affections regarding to risks and prognosis in more detail, and has to impose flight restrictions adapted to the type of airplane and the function of the pilot involved. The medical Commission for suitability to fly's decision thus has an important influence on the further career of the pilot in question and on flight safety in common. The Commission has to find a balance between common and personal interest. The main intention of this study was to critically evaluate the procedures followed by the Commission, based on an investigation on the cases of all pilots, in the Belgian Airforce, who were restricted definitely during the year of 1992. The population, the different kinds of affections and the resulting flight restrictions were studied. These data will be followed by a critical view on the method of procedure of the Commission. Author

N95-19416# Naval Aerospace Medical Inst., Pensacola, FL.
THE WAIVER PROCESS AND DISQUALIFYING MEDICAL CONDITIONS IN US NAVAL AVIATION PERSONNEL
Dean A. Bailey, Louis G. Gilleran, and P. Glenn Merchant *In* AGARD, The Clinical Basis for Aeromedical Decision Making Sep. 1994 11 p (For primary document see N95-19413 05-52)
Copyright Avail: CASI HC A03/MF A03

In the United States Navy, many diagnoses are considered disqualifying for aviation duty but may be 'waived' to return to flight duties after resolution of the disease or appropriate treatment of the condition. Personnel with waivers are usually subject to more frequent physical examinations and/or special diagnostic procedures. Although the Naval Aerospace and Operational Medical Institute promulgates written aeromedical guidelines that delineate which disease conditions may be waived and which may not, waivers are granted on a case-by-case basis considering not only the diagnosis, but the age, experience, and type of aviation duty of the individual in question. This study was undertaken to determine which conditions were most and least likely to be waived. We reviewed all cases entered in the Naval Aviation Medical Data Bank who had been diagnosed with a condition considered disqualifying for aviation duty, totaling over 39,000 records. Cases were stratified by diagnosis and aviation duty and the percentage waived was calculated for major diagnostic groups. Approximately 66% of all cases with a disqualifying diagnosis were recommended for a waiver. Otolaryngologic, ophthalmologic and musculoskeletal disorders accounted for over 50% of diagnoses in personnel recommended for a waiver. Fear of flying, personality disorders and adjustment disorders were the three diagnoses least likely to be granted a waiver. The most common disqualifying diagnoses of aviation personnel not recommended for waiver were disorders of refraction and accommodation, obesity, allergic rhinitis, alcohol dependence, and hypertension. Designated aviation personnel were significantly more likely to be waived than students. Author

N95-19417# Naval Aerospace Medical Inst., Pensacola, FL.
THE EFFECT OF SPECIAL BOARDS OF FLIGHT SURGEONS ON THE EVOLUTION OF US NAVAL FLIGHT STANDARDS
K. L. Gallagher and E. A. Bower *In* AGARD, The Clinical Basis for Aeromedical Decision Making Sep. 1994 5 p (For primary document see N95-19413 05-52)
Copyright Avail: CASI HC A01/MF A03

The flight surgeon is frequently asked to make a determination on the 'fitness to fly' of a member of his or her squadron. Common medical conditions that are transient, unlikely to progress in the operational environment, and have no sequelae that could compromise safety of flight do not result in the physical disqualification of the aviator. These simple cases lend themselves to a prompt aeromedical disposition and are routinely handled by the squadron flight surgeon through the issuance of temporary grounding notices. Following resolution of the acute illness, the aviator can immediately return to full flight status. If any of these prerequisites are not met, however, the aeromedical disposition becomes more complex. Medical conditions that may have significant sequeale, require long term follow up, or those that require chronic medication are not compatible with existing Naval aviation physical standards. If the aviator's career is to be preserved, a waiver of physical standards must be obtained. These challenging cases are generally handled by the squadron flight surgeon, with input from higher medical authorities. These recommendations are forwarded to the Bureau of Personnel for final action. The line community is the final arbiter of standards, and will issue a waiver for flight status based on the needs of the service. Since 1956, the U.S. Navy aeromedical community has officially recognized the need for an approach to evaluate aviators with significant fitness for flight questions. In 1957, the Chief of Naval Air Training established a reviewing body of speciality trained flight surgeons at the Naval Aviation Medical Center in Pensacola, Florida. This group became known as the Special Board of Flight Surgeons. The Senior Board of Flight Surgeons can make recommendations that supersede the recommendations of the Special Board of Flight Surgeons, and in effect can serve as the court of last resort for aviators seeking another hearing of their case prior to final recommendation. A Special Board of Flight Surgeons is requested by an aviator's commanding officer. Medical information is supplied to the clinical departments at the Naval Aerospace and Operational Medical Institute (NAMI) and a recommendation on the merits of hearing the case is then made to the commanding officer of NAMI. All special board cases presented at NAMI from 1 January 1984 until 31 December 1993 were reviewed. There were 119 special board cases involving 116 individuals. These individuals appeared before the board on two separate occasions. Pertinent demographic data were entered into a computerized database program (dBase III, Ashton-Tate Inc.) for trend analysis. The rationale for the aeromedical conclusions reached in each of the 119 cases presented in the past ten years was explored in detail. No statistical analyses were attempted on the data. The effect of sex and race on board outcome were considered, however, there were only two females and few minorities during the time frame considered negating any statistical significance. Author

N95-19418# Centro de Instruccion de Medicina Aeroespatial, Madrid (Spain).
FIT TO FLY: ANALYSIS OF THE AEROMEDICAL DISPOSITION IN AIRCREWMEMBERS OF THE SPANISH ARMED FORCES
Francisco Rios, Jose A. Azofra, Patrick P. Miles, Juan J. Canton, Vicente Velamazan, and Jose B. delValle *In* AGARD, The Clinical Basis for Aeromedical Decision Making Sep. 1994 14 p (For primary document see N95-19413 05-52)
Copyright Avail: CASI HC A03/MF A03

Medical fitness is an essential part of air safety. Aircrews undergo their regular medical review to ensure their physical and mental status will enable them to carry out their onboard functions in both normal and exceptional circumstances. Medical screening during the selection process followed by continued medical vigilance over the health of aircrews has been the major contributor to air safety by reducing the risk of potential incapacitation during flying duty. Because preexisting disease has been described as a contributor to aircraft mishaps military aviators undergo detailed initial flying physical examinations designed to find those with physical defects or disabilities that could potentially compromise flying safety. Another major objective of the physical examination is to periodically reevaluate conditions already known to the pilot and flight surgeon which may or may not have required the granting of a waiver previously, as there are many medical problems or conditions which are not static but may become improved or worsened over the time interval since the last periodic check up. The decision whether to let a pilot fly again is always a difficult one, especially since the airman involved is usually very keen to return to duty and will do his utmost to convince those who make these decisions that he is capable of flying. Flight surgeons have the responsibility to confirm this capability prior to putting a pilot back in the cockpit. The purpose of this study was: (1) to review the aeromedical disposition of Spanish military personnel through the first half of 1993 and identify the major reasons for permanent or temporary disqualification; (2) to determine the incidence or various medical causes for permanent or restricted status;

and (3) to determine the incidence and reasons for restrictions or temporary disqualification among aviators who, after appropriate follow-up were returned to flying duties. ESDU

N95-19419# Naval Aerospace Medical Inst., Pensacola, FL.
AMDRS: A RESOURCE FOR INTELLIGENT AEROMEDICAL DECISION-MAKING
C. J. Nickle *In* AGARD, The Clinical Basis for Aeromedical Decision Making Sep. 1994 6 p (For primary document see N95-19413 05-52)
Copyright Avail: CASI HC A02/MF A03

The Aviation Medical Data Retrieval System (AMDRS) is a dynamic, expanding database that currently contains information on 150,000 individuals, and approximately 75,000 separate complete examinations. The Naval Aerospace and Operational Medical Institute (NAMI) developed AMDRS in March 1989. The Aviation Epidemiological Data Register (AEDR), developed by the US Army Aeromedical Research Laboratory, is the temporary repository of information from which the AMDRS develops. After the medical record is completed by reviewers, information is transferred for permanent storage in the Aviation Medical Data Base (AMDB). The purpose of this paper will be to provide detail about the information available in the database, examples of previous studies completed, and propose specific areas for future study. Author

N95-19420# Institute of Aviation Medicine, Fuerstenfeldbruck (Germany).
RELEVANCE OF LABORATORY TESTS IN AEROMEDICAL DECISIONS
K. Reichenbach-Klinke *In* AGARD, The Clinical Basis for Aeromedical Decision Making Sep. 1994 3 p (For primary document see N95-19413 05-52)
Copyright Avail: CASI HC A01/MF A03

Laboratory tests in body fluids are an essential part of the aeromedical examination. It helps to find objective data in a poor anamnesis. Nearly all pilots tell us they feel healthy and fit for flying duty. The chemical finding sometimes give surprising results. Measurements are of a high technical standard, quality control guarantees reliability. So no-one can ignore an abnormal laboratory measure, the range of test profiles in aeromedical examination in civil and military regulations is different. Our laboratory program for pilots is now reformed and will be part of the regulations for the aeromedical examination. The selection of laboratory screening test follows some criteria: (1) relevance for a safety relevant disorder; (2) test is sufficient specific and sensitive; and (3) test can be automated and economically performed. Specials in military duty asymptomatic chronic diseases, which may be aggravated in extreme climate, must be excluded. Author

N95-19421# Italian Air Force Forensic Medical Inst., Rome (Italy).
TSH DETERMINATION IN SUBJECTS WITH MEDIUM-LOW LEVELS OF SERUM THYROXINE
D. Danese, F. Viaggi, and O. Sarlo *In* AGARD, The Clinical Basis for Aeromedical Decision Making Sep. 1994 13 p (For primary document see N95-19413 05-52)
Copyright Avail: CASI HC A03/MF A03

The prevalence of thyroid diseases is almost 5 to 7%. Hypothyroidism, whether primary (thyroidal) or secondary (hypothyrotropic and, rarely, hypothalamic) occurs at all ages and is more common in women. Its frequency varies depending on the population studied. The prevalence of overt hypothyroidism is 0.5 to 2%. Even though hypothyroidism is an uncommon cause of disease, it nevertheless decreases psychological and physiological efficiency, modifying the aeromedical standards. Hypothyroidism is an involved clinical, metabolic condition supported by inadequate thyroid function. Elevation of thyrotropin blood levels is a sensitive indicator of decreased thyroid gland function (primary hypothyroidism). In this study we evaluated the prevalence of subclinical hypothyroidism, characterized by an elevation of TSH levels with low levels of serum thyoxine and medium-low levels of free tiroxine, in subjects examined at the Forensic Medical Institute of IAF, during ordinary checkups. Author

N95-19422# Service de Medecine Aeronautique, Versailles (France).
EKG IN FLIGHT: USEFULNESS AND LIMITS FOR AIRCREW REHABILITATION
A. Seigneuric, J. P. Burlaton, F. Didelot, R. Carlioz, and P. E. Bertran *In* AGARD, The Clinical Basis for Aeromedical Decision Making Sep. 1994 5 p (For primary document see N95-19413 05-52)
Copyright Avail: CASI HC A01/MF A03

During the last 16 years, we have performed 86 in-flight EKG's on french aircrew members in order to have additional arguments for fitness decisions. Fighter pilots were the most important group (39%) followed by helicopter pilots (27%), transport pilots (13%) and student pilots (9%). The most important reasons were EKG disturbances and in particular excitability disorders. Cardiac troubles like coronary or valvular disease were more rare. This examination provided positive indication of flying fitness in 70% of cases, negative indications in 15% and no indication in 15% of cases. It is a useful complement to conventional cardiac investigations before medical decision in certain cases. Author

N95-19423# Centro de Instruccion de Medicina Aeroespatial, Madrid (Spain).
EVALUATION OF THE EKG'S ISOELECTRIC T WAVE IN AIR FORCE PILOTS
M. A. Gomez-Marino, F. Rios-Tejada, and V. VelamazanPerdomo *In* AGARD, The Clinical Basis for Aeromedical Decision Making Sep. 1994 7 p (For primary document see N95-19413 05-52)
Copyright Avail: CASI HC A02/MF A03

171 out of 5126 performed EKG's from aircrew members (3.33%), showed some ST-T wave abnormalities. We studied 23 out of the 171 with isoelectric (low amplitude or moderate inversion, but less than 1 mm) in all leads but not in V2-V3 where the T wave were normal. Six of those, had T wave inversion in III and avF leads. All 23 are healthy males, between 30-55 years old (43.6 plus or minus .3), without associated EKG disorders, ionic alterations, and no one regularly practiced heavy exercise. Each one had had between 3 and 21 (11.5 plus or minus 6.5) EKG recordings along a following period of 3 to 20 years (13.0 plus or minus 6.3). All of them has been evaluated through treadmill test (Bruce protocol, submaximal greater than 90%), Doppler-Echocardiography and 24 hours Holter monitoring. We found in 22 cases (95.6%), echocardiographic criteria of left ventricular hypertrophy (IV septum more than 13 mm). 15 out of 15 were symmetric and 6 were asymmetric. 19 cases (86.4%) had a mitral filling flow pattern typical of left ventricular compliance disorder, with atrial wave (A) bigger than fast filling wave (E). Only 3 cases (13.6%) had normal mitral flow Doppler pattern. Valvular or subvalvular aortic gradient was not found in any case. Bruce test results were negative in all cases, but in 21 of those (91.3%), during exercise or the first minute of recovery, T waves became normal, returning to be isoelectrics before 10 minutes. We conclude that asymptomatic flyers without coronary risk factors with isoelectric T waves in all EKG leads (but normals T waves in V2-V3), with or without T inversion in III and avF leads, should be adequately tested in order to rule-out mild hypertrophic myocardiopathy, by Doppler-Echocardiography, and not focus attention in trying to find coronary artery diseases. Author

N95-19424# Laboratoire de Medecine Aerospatiale, Bretigny-sur-Orge (France).
CENTRIFUGE TESTS OF THE MEDICAL CONDITION OF FRENCH FIGHTER PILOTS [EPREUVE EN CENTRIFUGEUSE DANS LE CADRE DE L'APTITUDE MEDICALE DES PILOTES DE CHASSE FRANCAIS]
G. Ossard, A. Seigneuric (Service de Medecine Aeronautique, Versailles, France.), J. M. Clere, and J. P. Burlaton (Service de Medecine Aeronautique, Versailles, France.) *In* AGARD, The Clinical Basis for Aeromedical Decision Making Sep. 1994 8 p In FRENCH (For primary document see N95-19413 05-52)
Copyright Avail: CASI HC A02/MF A03

The performance of piloting may be involved with processes of which the etiology is not well known today. In the French Air Force, after a serious illness, the pilots undergo a medical examination of their condition to resume flying. Therefore, in order to insure that no risk remains due to accelerations, the pilots undergo a standardized centrifuge test in the Aerospace Medicine Laboratory. From 1983 to 1993, 112 centrifuge tests were conducted. The requirement for having a centrifuge test is largely predominated by illness of loss of consciousness and cardio-vadcular disturbances which are essentially transitory electrocardiograph anomalies. In certain cases, the disorders have been reproduced and analyzed. The centrifuge test frequently permit avoidance of a disqualification which would

have grave consequences for the pilot, based on physiological findings, and for the savings to the Air Force of an investment in operational status. Author

N95-19425# Royal Norwegian Air Force, Oslo (Norway). Inst. of Aviation Medicine.

IS THE PILOT FIT FOR FLYING AFTER AN ACCIDENT?

Grete Myhre *In* AGARD, The Clinical Basis for Aeromedical Decision Making Sep. 1994 3 p (For primary document see N95-19413 05-52)

Copyright Avail: CASI HC A01/MF A03

It has been recommended that a pilot should fly as soon as possible after an aviation accident or incident, provided he is medically fit. This tradition has been successful in many cases and has therefore been accepted as the right thing to do in the flying society. New knowledge about post traumatic reactions related to accidents has led to new procedures in the Royal Norwegian Air Force in the wake of a crash. Since an accident necessarily affects many persons, much like rings in the water after throwing a pebble, the new post accident debriefing procedures cover the involved parts after a survivable accident in addition to the rest of the squadron. A considerable problem with post traumatic emotional reactions are that they are not usually detected right after the accident, but are elements in a process rather than immediate results of the acute event. So far this program has demonstrated two effects: (1) maintaining the confidence level the aviator had prior to the accident, and (2) demystifying normal emotional reactions in flying personnel, which in itself is a very important accomplishment. In conclusion, the pilot is fit for flying when he has been made aware of the emotions connected with an accident and what to do if and when they appear. The pilot will be able to continue his duties if he has a supportive team that he can lean on in the first period of time after his traumatic experience. For most people it is an advantage to get back to work and resume the normal activities as soon as possible. The aviator will be able to execute his duties without limitations, knowing that the emotions he has gone through are normal and expected, provided the flight surgeon has performed this part of his job carefully. Author

N95-19426# Naval Aerospace Medical Inst., Pensacola, FL.

THE CONCEPT OF AERONAUTICAL ADAPTABILITY AS DEVELOPED BY THE US NAVY

P. G. Merchant and J. C. Baggett *In* AGARD, The Clinical Basis for Aeromedical Decision Making Sep. 1994 7 p (For primary document see N95-19413 05-52)

Copyright Avail: CASI HC A02/MF A03

Physicians working in the field of aviation medicine have known from the earliest days of the specialty that the psychological fitness of aviators was a critical element in minimizing aircraft accidents. Studies, spanning 8 decades of aviation, have demonstrated that the majority of aviation accidents have been the result of human factors. Selection of psychologically fit candidates and monitoring the status of designated Naval Aviation personnel has thus been one of the major tasks performed by Naval Flight Surgeons. To guide them, the concept of Aeronautical Adaptability has been developed. Composed of two similar but separate concepts, the first one requires the flight surgeon to evaluate the motivation, temperment, flexibility, and appropriate psychological defense mechanisms of aviation candidates. The second concept accepts that once designated, an aviator has proven his ability to adapt to the rigors of aviation. Still, it requires monitoring of the experienced aviator's pattern of coping with the stresses of aviation, and provides the means to find designated personnel not Aeronautically Adaptable should maladaptive behavior affect the safety of flight. This paper will explore the early psychological standards in the U.S. Navy, then discuss Aeronautical Adaptability as it evolved over the last 15 years. It will discuss the rational behind the current concept and show how Aeronautical Adaptability provides a fair, timely system of review to help the U.S. Naval Flight Surgeon process difficult cases that could present an unacceptable safety risk in Naval Aviation. Author

N95-19427# Organisatie voor Toegepast Natuurwetenschappelijk Onderzoek, Soesterberg (Netherlands). Human Factors Research Inst.

VESTIBULAR EXAMINATION IN PILOTS SUSCEPTIBLE TO MOTION SICKNESS

Willem Bles, Bernd deGraaf, and Jelte E. Bos *In* AGARD, The Clinical Basis for Aeromedical Decision Making Sep. 1994 8 p (For primary document see N95-19413 05-52)

Copyright Avail: CASI HC A02/MF A03

An analysis is presented of data obtained from vestibular examinations on student pilots prone to airsickness. It is shown that those pilots who were most susceptible during the initial flight training course, in the laboratory even suffered from mild conditions of the Coriolis test. Abnormal postural behavior in the tilting room test, or long time constants of the nystagmus decay after sudden stops from constant velocity rotation, do not contra-indicate a successful desensitization program. A Practical Flying Selection considerably diminishes the number of student pilots suffering from airsickness. Those who pass this test, but got nevertheless into motion sickness trouble during the pilot training, were successfully treated with a desensitization program. Author

N95-19428# Naval Aerospace Medical Inst., Pensacola, FL.

THE NAMI SYNCOPE TEST BATTERY AND CLINICAL DECISION-MAKING IN AVIATORS WITH SYNCOPE

J. R. DeVoll and E. W. Hopkins *In* AGARD, The Clinical Basis for Aeromedical Decision Making Sep. 1994 9 p (For primary document see N95-19413 05-52)

Copyright Avail: CASI HC A02/MF A03

The Syncope Test Battery (STB) was adopted in 1988 at the Naval Aerospace and Operational Medicine Institute (NAMI) to provide a coherent and consistent methodology for the evaluation of physiologic or secondary syncope. Records from 1988-1992 that utilized the STB were reviewed, and STB results were compared against final diagnostic categories of physiologic or secondary syncope ($n=55$). Analysis of the STB showed a sensitivity of 20.6 percent, specificity 100 percent, predictive value positive 100 percent, predictive value negative 43.8 percent, and concordance 50.9 percent. These results failed to support the effectiveness of the STB, and the STB did not result in any change between the preliminary and final diagnoses as made on other clinical bases. The evaluation and disposition of syncopal aviators is reviewed in the light of general and aerospace medical literature. It is concluded that the STB is not a useful tool in evaluating syncope in the US Navy aviation population. A step-wise algorithmic approach is recommended for the evaluation of syncopal aviators, but the eventual disposition must still be individualized and remains problematic for the flight surgeon. Author

N95-19429# Royal Norwegian Air Force, Oslo (Norway). Inst. of Aviation Medicine.

THINK HEALTH NOT DISEASE

Harald T. Andersen *In* AGARD, The Clinical Basis for Aeromedical Decision Making Sep. 1994 5 p (For primary document see N95-19413 05-52)

Copyright Avail: CASI HC A01/MF A03

At air crew selection time many important medical decisions are made, most of them relying on simple clinical methods such as preliminary case history and physical examination. Information obtained using sophisticated laboratory methods may give crucial information when results are evaluated against occupational hazards, but it is important to keep in mind that such procedures are not clinically indicated. Health management of those successfully trained is not performed towards a background of disease but to the contrary, in order to promote health. Retention of those treated for illness is a decision of fitness to fly after evaluation of treatment. Clinicians may be satisfied with the treatment of a patient, flight surgeons may or may not be happy with the result considering the occupational hazards of military aviation. It follows that selection, health management and retention of aviators are in principle considerations of health not of disease. Examinations performed on asymptomatic military aviators using diagnostic high technology instrumentation may not contribute essentially to medical decision making. Author

N95-19430# Divisione Aerea Studi Ricerche e Sperimentazioni, Pratica di Mare (Italy).

NEUROPSYCHOPHYSIOLOGIC SEQUELAE OF MILD HEAD INJURY

Antonio Belli, Silvio Porcu, and Andrea Bellatreccia *In* AGARD, The Clinical Basis for Aeromedical Decision Making Sep. 1994 11 p (For primary document see N95-19413 05-52)

Copyright Avail: CASI HC A03/MF A03

Psychologic or neuropsychologic consequences of severe closed head

injury have received much attention in both clinical and experimental studies. Nevertheless, it has been clearly established that even mild closed head-injured patients may develop psychologic or even psychiatric sequelae of clinical relevance, including poor social adjustments as well as cognitive impairment. Symptoms such as dizziness, fatigue, irritability, headaches, insomnia, anxiety, and amnesia are also frequently reported, these being usually the major features of post-concussion syndrome. Cognitive impairment is responsible of attention and concentration capability disorders, with consequent difficulty in retrieving acquired information and performing usual tasks. Full or satisfactory recovery from such symptoms is normally achieved in few months, with persistence in a minority of cases with distinct risk factors (age, gender, multiple trauma, history of previous head injuries). Such manifestations of head trauma are satisfactorily detected and followed up by means of specific neuropsychologic tests in several studies, while CT-scan fails to provide but scarce prognostic reliability. The role of neurophysiology is controversial, although opinions are that it should be referred to in selected cases and in a multidisciplinary approach. Finally, an interesting and significant correspondence of neuropsychologic tests, behavioral data and MRI or SPECT findings casts a new light on both clinical and research aspects of the question. Making a decision whether returning a head-injured pilot to flight activity or not certainly constitutes an additional problem for the risk of epilepsy and of other neurological or neurosurgical complications is to be considered of primary importance even for mild head trauma (which accounts 75 percent or more of the total, with an annual incidence of about 150 per 100,000 population). Neuropsychologic sequelae themselves do require a restriction from flying duties for months or years. It is advisable to await normalization of neuropsychologic and neurophysiologic parameters, in absence of neuroimaging (i.e. MRI) signs, before returning the patient to flight activity. Neurophysiology (EEG, evoked potentials) provides cost-effective, sensible and reproducible means for diagnosis and follow-up and its value could be boosted by the implantation of an individual neurophysiological database for all the flying personnel. Author

N95-19431# German Air Force, Fuerstenfeldbruk (Germany). Inst. of Aviation Medicine.

NEUROLOGICAL DECISION MAKING IN AVIATION MEDICINE BASED ON ELECTROPHYSIOLOGICAL METHODS

H. Glaser and W. Freund *In* AGARD, The Clinical Basis for Aeromedical Decision Making Sep. 1994 7 p (For primary document see N95-19413 05-52)

Copyright Avail: CASI HC A02/MF A03

The task of neurology in aviation medicine is to determine whether a person is without disturbances of the nervous system's function and without elevated probability to show relevant disturbances in future. Besides medical history and clinical examination, decisions are based on technical methods. Concerning image generating methods, testing of higher brain functions, and sonotopographic methods neurology for the most part utilizes the service of the specialities radiology, psychology, and angiology, while application of electro-physiological methods like electroencephalography, electromyography, neurography or examination of evoked potentials are the neurological specialities own methods. The main task of electroence-phalography in aviation medicine in our opinion is to identify persons with an individually higher electrophysiological lability, which is a lower threshold for abnormal activity of the brain. These persons under conditions of military duty bear a higher risk of developing epileptic phenomena, even if they stay asymptomatic under conditions of everyday life. Author

N95-19432# Portuguese Air Force Aeromedical Center, Lisbon (Portugal).

THE EEG IN THE EVALUATION OF APPLICANTS TO AIRCREW MEMBERS

Nuno Pedro Ribeiro *In* AGARD, The Clinical Basis for Aeromedical Decision Making Sep. 1994 4 p (For primary document see N95-19413 05-52)

Copyright Avail: CASI HC A01/MF A03

The E.E.G. has been used since its beginning as a tool in selection of aircrew personnel. Knowing that even in epileptic patients the E.E.G. in a great majority of cases doesn't show abnormalities, the problem is raised on the meaning of such method in the selection of aircrew candidates. On the other hand we must agree in the definition of a 'normal' E.E.G., and what are the meanings of certain abnormalities in an individual that says that he/she is healthy and denies in his/her clinical history, epilepsy, febrile convulsions, headaches and head traumas. Acording to Niedermeyer and Lops da Silva, the usefulness of the E.E.G. in aircrew selection is that we'll have a record to compare in case of need of repetition of E.E.G. In the Portuguese Air Force the selection is seriated, the neurological observation being one of the last ones and only one small part of all applicants submitted to it. The evaluation consists on a clinical history, in which the denial of all pathology is the rule (they are all voluntary), neurological examination and an E.E.G., 30 minutes duration, in the 10-20 system (since 1990), with two hyperventilations and one photic stimulation. Author (revised)

N95-19433# Queens Medical Centre, Nottingham (England). Dept. of Neurosurgery.

CLINICAL BASIS FOR AEROMEDICAL DECISION-MAKING: THE EEG EXAMPLE

J. L. Firth *In* AGARD, The Clinical Basis for Aeromedical Decision Making Sep. 1994 8 p (For primary document see N95-19413 05-52)

Copyright Avail: CASI HC A02/MF A03

The EEG, electroencephalogram, is used as a test in aircrew selection. Given that the natural history of the seizure disorders has been described, the validity of this practice is questioned and potentially more rewarding applications of the EEG suggested. System reliability is a major component of aircraft system performance. In military aviation both are central nervous system dependent. In aircrew assessment and management the EEG, electroencephalogram, has traditionally played a major role. Advances in technology, data retrieval, storage, presentation, processing, interpretation and assessment make this an appropriate time to review the place of the EEG in aeromedical decision-making and research. Author

N95-19434# Centro de Instruccion de Medicina Aeroespatial, Madrid (Spain).

SPINE INJURIES: UP TO DATE EVALUATION IN AIRCRAFT EJECTIONS

Francisco Rios, Jose A. Azofra, Patrick P. Miles, Carlos Velasco, Juan Sieiro, and Alfredo Cuevas *In* AGARD, The Clinical Basis for Aeromedical Decision Making Sep. 1994 6 p (For primary document see N95-19413 05-52)

Copyright Avail: CASI HC A02/MF A03

Spinal injury during aircraft egress has been a well known phenomenon since the early days of flying, though at that time usually secondary to ground impact. However, the development of High Performance Aircraft (HPA) has forced the consequent development of high performance ejection mechanisms. These modern ejection systems have functioned superbly with the latest generation mechanism allowing 91.1 percent survivability when egress takes place above 500 ft from ground level and 79.2 percent pilot survival rate when egress is undertaken at flying level less than 500 ft. However, while the overall success rate of 88 percent has resulted in many more pilots surviving an egress experience, 21 percent of these flyers have been shown to suffer some degree of significant spinal injury (vertebral compression-fracture) during egress, potentially threatening their ability to return to the cockpit. Modern HPA, with their ability to inflict immediate and sustained high +Gz forces to the cockpit environment challenge the flight surgeon now as never before to carefully and successfully evaluate the pilot who has suffered egress-related spinal injury in order to determine whether it will be safe for the flyer to return to such an environment. This challenge is made even more pressing by the fact that pilots who eject are often well-trained, experienced flyers whose potential lost services, either due to permanent disqualification from flying duties or due to further, additional spinal injury, represent a significant potential loss of valuable human resources to NATO Air Forces, already facing the loss of key personnel and resources due to today's economic pressures. These factors make it imperative that all of the modern medical means at hand be utilized in the analysis of post-ejection spinal injuries. Author

N95-19435# German Air Force, Fuerstenfeldbruk (Germany). Specialized Group Orthopedics.

CLINICAL PRACTICE, DIAGNOSIS AND THERAPY OF INTERVERTEBRAL DISK LESION: IMPORTANCE TO FITNESS FOR MILITARY FLYING DUTIES

T. Pippig *In* AGARD, The Clinical Basis for Aeromedical Decision Making Sep. 1994 6 p (For primary document see N95-19413 05-52)

Copyright Avail: CASI HC A02/MF A03

The intervertebral disk, central element of the motion segment, may be exposed to high strains which occur when piloting a jet aircraft or a helicopter. Isolated traumatic ID lesions due to flying strains do probably not come into existence neither ID degeneration according to our actual findings and knowledge of the matter. When there is an accurate diagnosis as to ID prolapse considering clinical and radiological findings, ability for military flying duties is exempted for the next six months. Adequate therapy, either by conservative or surgical treatment, is to be initiated. In the case of cervical ID prolapse however, we do not recognize ability for military flying duties for pilots of jet aircraft seated on an ejection seat and for helicopter pilots, even after good results of treatment. After lumbar ID prolapse and good results of treatment we consider the ability for military flying duties as being restored. Thereafter and when the first flying strains set in, the responsible flight surgeon should examine the pilot regularly, at least in the beginning. Author

N95-19436# German Air Force, Fuerstenfeldbruk (Germany). Inst. of Aviation Medicine.

SPINAL NERVE SYNDROMES: THE NEED TO CONFIRM THE DIAGNOSIS WITH NEUROPHYSIOLOGICAL EXAMINATIONS

Wolfgang Freund and H.-J. Glaser *In* AGARD, The Clinical Basis for Aeromedical Decision Making Sep. 1994 8 p (For primary document see N95-19413 05-52)

Copyright Avail: CASI HC A02/MF A03

Because even the normally healthy pilots suffer from the usual aging and degeneration of the spine, sudden g-stress may lead to compressions of spinal nerves if degenerated intervertebral discs protrude into the intraspinal space. To avoid risks to general flight-safety as well as to the pilot's health, back-pain and sciadic syndromes have to be evaluated aeromedically. The common methods to investigate the cause of spinal-nerve affections can be divided into three steps: first the intensified interrogation and clinical examination of the pilot, which usually leads to the rough specification of the location of the lesion as well as a first hypothesis of the cause (e.g.: A probably traumatic lesion of the left first thoracal nerve). Second usually come radiological methods such as X-ray of the spine and, more promising, a X-ray computer-tomography (CT) and in difficult cases magnetic-resonance-imaging (MRI), which can differentiate between tumors and protusions of intervertebral discs. In the third step the extent of the damage is evaluated by neurophysiological methods. From the viewpoint of aeromedical decision-making this step is the most critical. Of the suitable methods there are the following used the GAF Institute of Aviation-Medicine (GAFIAM): Electromyography: Fast, rather accurate and reliable, though it covers only the motorical part of the nerve-root); Neurography (F-wave measurements can detect lesions in the motorical part of the nerve-root); Somatosensory Evoked Potentials (SEP) (though time-consuming and demanding they offer the only way to measure sensory deficits); and Magnetically Evoked Potentials. To illustrate the decision-making process, examples are demonstrated. Author

N95-19437# Aerospace Medical Research Labs., Brooks AFB, TX. Internal Medicine Branch.

THE AEROMEDICAL IMPLICATIONS OF SUPRAVENTRICULAR TACHYCARDIA

Londe A. Richardson and Paul V. Celio *In* AGARD, The Clinical Basis for Aeromedical Decision Making Sep. 1994 5 p (For primary document see N95-19413 05-52)

Copyright Avail: CASI HC A01/MF A03

Supraventricular tachycardia (SVT) is uncommon in healthy screened populations and has an overall prevalence of 0.02 percent and a maximal prevalence 0f 0.1 percent on routine screening electrocardiograms (2-8), 4.6 percent on Holter monitors (9-12) and approximately 0.6 percent on treadmills (13, 14). A review of the clinical literature reveals that occupational and aeromedical risks for aviators with SVT remains inadequately addressed. Long term follow-up data in aviators with SVT is limited to a single small series by Matthewson and Varnam who followed four aviators for 14 years and found no deaths or coronary events. The Aeromedical Consultation Service (ACS) is a centralized United States Air Force (USAF) referral center which performs aeromedical evaluations in aviators to determine their fitness for flying. The ACS has evaluated aviators with SVT since 1955. In 1973, the ACS developed a protocol permitting resumption of flying duties in aviators with SVT; waivers were granted in selected low aeromedical risk cases. We have continued to provide clinical follow-up of aviators with SVT to insure that waivers for SVT are recommended only in low aeromedical risk cases. Although uncommon, SVT can present suddenly with presyncope, syncope or sudden death with potentially catastrophic results during flying duties. Aviators with SVT were disqualified historically because of these risks. Medical standards must be conservative to insure that USAF aviators are free of such conditions. However, this conservative approach has disqualified many asymptomatic aviators who may have safety flown if data had been available demonstrating that certain subsets had an acceptably low aeromedical risk. When evaluating an aviator with SVT, waiver authorities must determine the extent of aeromedical risk, the level of risk acceptable for continued flying duties and which waiver restrictions should be applied. This paper provides outcome data, acquired from aviators with various SVT presentation profiles to assist in that risk stratification. With these data, a safe return to flying duties for those aviators with acceptably low levels of aeromedical risk can be achieved. Author

N95-19438# Aerospace Medical Research Labs., Brooks AFB, TX. Internal Medicine Branch.

SARCOIDOSIS IN US MILITARY AVIATORS

Robert Munson, B. Tuomala, Paul V. Celio, and Londe A. Richardson *In* AGARD, The Clinical Basis for Aeromedical Decision Making Sep. 1994 3 p (For primary document see N95-19413 05-52)

Copyright Avail: CASI HC A01/MF A03

Sarcoidosis is a systemic granulomatous disease of unknown etiology and is generally a benign, self-limiting disorder. Myocardial involvement has been known since 1929, but several articles published in the early 1970's indicated that myocardial involvement was a more common and serious problem. In 1974, Fleming reported on 50 cases of myocardial sarcoidosis with cardiac involvement confirmed in 20 cases by necropsy. He suggested that myocardial sarcoid was probably underdiagnosed and was not a rare condition. In 1984, he also suggested that sarcoidosis was frequently overlooked until sudden death occurs, often in relatively young people, 25-54 years of age. In 1976, Matsui, et al., reported in a Japanese population on 72 individuals with sarcoidosis at autopsy. Fifty-eight percent of these individuals died because of myocardial involvement. Most of these deaths were sudden and the diagnosis was generally not suspected during life. In addition, myocardial involvement was apparently a late complication and was not predicted by progressive pulmonary involvement. In 1977, Roberts et al., reported on 113 patients found to have myocardial sarcoidosos at autopsy. Seventy-nine percent had cardiac dysfunction due to myocardial involvement, 67 percent experienced sudden death, and 23 percent developed congestive heart failure. Most patients with myocardial sarcoid presented initially with cardiac symptoms and most had little or no evidence of other organ involvement. In 16 percent sudden death was the initial manifestation of sarcoidosos. In view of the possible catastrophic consequences of sudden unexpected death or sudden incapacitation of a military aviator, the United States Air Force (USAF) became concerned about the implication of myocardial sarcoidosis. Prior to 1978, all USAF flyers with sarcoidosis were evaluated at the local flight surgeon's office. After they became stable and the findings of sarcoid resolved, they were returned to flying duties with a local waiver. The details of the local evaluation were not prescribed by protocol and were based solely on the judgment of the local physician. In 1978, the USAF initiated the sarcoidosis study group. This program was initiated to solve 2 basic problems. First clinical studies indicated that a more thorough evaluation was required to examine the possibility that an individual with a history of pulmonary sarcoidosis may have asymptomatic butsignificant myocardial granulomas. This program also provided a mechanism for recurrent periodic evaluations to ensure the aviator's continued fitness for flying. The second objective of the sarcoid study group was to perform these evaluations in a systematic fashion with periodic review to determine the outcome of individuals with a history of sarcoidosis to insure that the prognosis of this grop was consistent with continued flying duties. Author

N95-19439# Aerospace Medical Research Labs., Brooks AFB, TX. Clinical Sciences Div.

THE AEROMEDICAL RISK ASSOCIATED WITH ASYMPTOMATIC CHOLELITHIASIS IN USAF PILOTS AND NAVIGATORS

G. W. Saboe, J. W. Slauson, R. Johnson, and T. H. Loecker *In* AGARD, The Clinical Basis for Aeromedical Decision Making Sep. 1994 6 p (For primary document see N95-19413 05-52)
Copyright Avail: CASI HC A02/MF A03

The USAF aeromedical policy regarding incidentially discovered, asymptomatic cholelithiasis requires the aircrew to undergo cholecystectomy prior to being considered for return to flying duties. The merit of continuing this USAF policy was evaluated at the request of the USAF Surgeon General. A review of the medical literature predicted a 1 percent to 4 percent annual event rate of acute cholecystitis in individuals with previous asymptomatic cholelithiasis. The prevalence of asymptomatic cholelithiasis in USAF pilots and navigators was determined to be 2 percent to 3 percent, based on data acquired at the Ellingson Aerospace Medicine Consultation Service (ACS). Of 11.685 pilots and navigators evaluated at the ACS, 0.7 percent (n = 880) were diagnosed with cholelithiasis or previous cholecystectomy. Between 1972 to 1992, 16,232 man years of pilot and navigator exposure to asymptomatic cholelithiasis was estimated to have occurred; however, only 50 cases with a diagnosis of cholecystectomy or cholelithiasis were reported in the USAF Surgeon General waiver file. Mortality and morbidity associated with cholecystectomy by either open or laparoscopic technique were reported as 0.2 percent and 5 percent, respectively. Using 1994 USAF pilot and navigator manpower data and the worse case scenario of a 0.7 percent occurrence for the onset of acute symptoms associated with previously asymptomatic cholelithiasis, up to five aircrew would be expected to experience acute symptomatology at some time during 1994. However, if every pilot and navigator flew 200 to 1,000 flying hours during 1994, 0.1 to 0.6 individuals, or essentially none, would be predicted to experience acute symptoms related to gallstones inflight. The natural history of cholelithiasis in USAF pilots and navigators is more favorable than suggested by the clinical literature. The inflight risk of experiencing acute symptoms associated with previously asymptomatic cholelithiasis is essentially nonexistent in USAF aircrew. Author

N95-19440# Centro de Instruccion de Medicina Aeroespatial, Madrid (Spain).
CLINICAL BASIS FOR AEROMEDICAL DECISIONS IN AIRCREW HIV POSITIVE
Jose A. Azofra, Francisco Rios, Juan J. Canton, Patrick P. Miles, Carlos Velasco, and V. Velamazan *In* AGARD, The Clinical Basis for Aeromedical Decision Making Sep. 1994 3 p (For primary document see N95-19413 05-52)
Copyright Avail: CASI HC A01/MF A03

There has been appropriate concern regarding HIV infection and its effect on aviation safety. Among reasons cited is the consideration that the nervous system is involved early in HIV infection and that dementia in its early stages may be subtle and difficult to detect, on opinion not currently supported by the medical literature. Others have felt that seropositivity alone did not constitute an unacceptable risk to aviation safety, suggesting that other criteria be used, such as the development of AIDS related symptoms, or laboratory abnormalities, prior to grounding a flyer. Discussion and controversy will continue in this area until specific studies of asymptomatic seropositive individuals' performance in real and simulated flying environments are carried out by the aeromedical community. As the prevalence of this disease continues to grow exponentially in the general population the answers to these questions will become increasingly more important. Author

N95-19441# Aerospace Medical Research Labs., Brooks AFB, TX. Ophthalmology Branch.
COLOR VISION ISSUES IN MODERN MILITARY AVIATION OR THE SEARCH FOR THE ABOMINABLE CONEMAN
Douglas J. Ivan, J. Terry Yates, Thomas J. Tredici, and John M. Gooch *In* AGARD, The Clinical Basis for Aeromedical Decision Making Sep. 1994 17 p (For primary document see N95-19413 05-52)
Copyright Avail: CASI HC A03/MF A03

Visual information provided to the modern military aircrew member accounts for the preponderance of data contributing to situational awareness. Although long recognized as a critical factor in aviation, as a result of advancing technological developments, color vision is emerging as an ever-increasing critical requirement in modern and future cockpits. Despite that premise, the modern battlefield is characterized by a vast array of technological weaponry that increases the threat to the visual system and dictates effective countermeasures that compromise visual performance in general and color perception in specific. This paper will review the aeromedical basis of color testing developments and issues that effect aeromedical decisions in color standards and performance as they relate to the modern military aircrew member. It will include an update on color vision issues raised by protective equipment such as selective waveband filters that include sunglass materials and laser protective eyewear/visors. Color-related aircraft accident issues will be addressed. Author

N95-19442# Aerospace Medical Research Labs., Brooks AFB, TX. Ophthalmology Branch.
PHOTOREFRACTIVE KERATECTOMY (PRK) IN THE MILITARY AVIATOR: AN AEROMEDICAL EXPOSE
Douglas J. Ivan *In* AGARD, The Clinical Basis for Aeromedical Decision Making Sep. 1994 18 p (For primary document see N95-19413 05-52)
Copyright Avail: CASI HC A03/MF A03

Refractive surgery to correct rehabilitate refractive errors of the eye continues to evolve at a significant pace and is here to stay. The surgical manipulation of the cornea by carefully planned incisions, as in radial keratotomy, represented the first technological procedure to evolve for the correction of ametropia and is an area of continued active development and improvement. More recently, photorefractive keratectomy (PRK) using laser technology to ablate and recon-tour the corneal surface has emerged as a viable modality. This paper explores the aeromedical factors surrounding this new revolutionary procedure and discusses the issues relevant to evaluating its applicability to the modern aviator as well as reviewing results of the latest clinical trials currently in progress. The goal is to provide the aeromedical community with the fundamental information required to formulate aeromedical decision- and policy-making in regard to a new procedure that is certain to have tremendous impact on future aircrew candidates. Author

N95-19443# Institute of Aviation Medicine, Prague (Czechoslovakia).
MEDICATION IN THE COURSE OF ACTIVE FLYING DUTY
M. Rada, A. Dvorak, and J. Sulc *In* AGARD, The Clinical Basis for Aeromedical Decision Making Sep. 1994 8 p (For primary document see N95-19413 05-52)
Copyright Avail: CASI HC A02/MF A03

The Czech Institute of Aviation Medicine deals with the practice of medication of airmen without the prohibition of active flying over 25 years. The experience with medical treatment of 420 airmen during the 1982-1993 period is presented in details. Main reason for employment of this policy follows from the successful management of initial stages of primary hypertension as well as of other health disturbances. Hypertension counts for 57.9 percent of all cases liable to medication, being most often started in the second half of the fifth and first half of the sixth decade. Mean duration of medication took 3, 4 years leading to the overall prolongation of active flying for 2, 9 years. A combination of two antihypertensive agents, viz. the diuretic and the beta-blocking agent appears to be the most effective method. Among other frequently applied pharmaceuticals hypolipidaemic and hepato-protective agents along with vitamin compound remedies should be included. The introduction of medication must precede a thorough medical and psychological examination, repeated prior to waivered certification. Regular observation performed by a flight surgeon or a licensed aeromedical examiner is mandatory. With observance of responsible policy the preservation of an airman in active duty despite his/her medication brings significant economic as well as social benefits without the flight safety impairment. Author

N95-19537# Physics and Electronics Lab. TNO, The Hague (Netherlands).
HIGH PERFORMANCE COMPUTING FOR MEDICAL IMAGE INTERPRETATION
A. C. Dumay Oct. 1993 72 p
(AD-A285457; FEL-93-B160; TDCK-93-2783) Avail: CASI HC A04/MF A01

Medical image processing aims at improvement of the image quality in order to support the medical diagnosis and therapy. Globally, there can be four subjects distinguished for image processing, including: (1) data fusion, (2) object/feature extraction, (3) analysis, and (4) visualization. Data fusion,

or registration, concerns the combination of images acquired with various imaging modalities into a single image. Object/feature extraction, or segmentation, aims at the recognition and extraction of objects and object features from image data. And the analysis involves the interpretation of the object features from which conclusions can be drawn. Visualization is of utmost importance for each of the forementioned subjects. With the introduction of computer tomography (CT) and magnetic resonance imaging (MRI) three-dimensional images can be acquired from patients. The processing of 3D images such that the time required for that purpose is in acceptable limits makes the use of high performance computing (HPC) techniques desirable. Currently (commercially) available implementations do not satisfy the performance requirements for routine use in a clinical setting. As a result, such systems will not be used at all or at high costs of personnel. High performance computing medical image interpretation includes data fusion, object/feature extraction, analysis, and visualization of 3D medical images. Modules for these purposes may be integrated in existing medical systems to support interactive visualization, quantitative analysis, radiotherapy planning, and neurosurgery planning. Integrated into a high performance computing medical image interpretation system (HPMI(sup 2)S), one has the tools for developing anatomical models for simulation and training for example minimal access surgery (MAS) and triage. DTIC

N95-19695# Keele Univ. (England). Dept. of Chemistry.
PHOTOBIOLOGY IN MEDICINE Final Proceedings Report, 30 Sep. - 13 Oct. 1993
T. George Truscott, ed. 13 Oct. 1993 200 p Sponsored by European Office of Aerospace Research and Development
(AD-A284843; CSP-93-1041) Avail: CASI HC A09/MF A03

Man has recognized an association of light with life and medicine for over 3000 years. Today the major challenges to this topic include the elucidation of photochemical reactions involved in photobiology at the molecular level. This includes the use of a variety of modern probing techniques that directly measure the reactivity of excited states and free radicals involved in biological reactions. This textbook is based on such an approach and has arisen from some of the lectures delivered at the NATO ASI held at Hotel Capo Caccia near the Centre for Advanced Research in Photobiology (CARP) in Cardegia, Italy. The ASI took place from 30 Sep. - 13 Oct. 93 and involved a total membership of 90. Photobiology in medicine is a wide-ranging subject that obviously cannot be totally covered comprehensively in one book alone. Rather, chosen topics of current interest in photomedicine were focused upon and these are linked to the major underlying themes and techniques in photophysics and photochemistry. DTIC

N95-19698# Alabama Univ., Birmingham, AL.
CUMULATIVE EFFECTS OF REPEATED BRIEF CEREBRAL ISCHEMIA Final Report
H. P. Hetherington and K. A. Conger 1994 48 p
(Contract F49620-92-J-0362)
(AD-A284234; AFOSR-94-0481TR) Avail: CASI HC A03/MF A01

The purpose of this grant was to investigate the metabolic and physiological factors determining the extent of the ischemic damage in a model of brief repetitive cerebral ischemia. The model is intended to simulate the effects of Gz induced blackout experienced by fighter pilots undergoing high gravitational stress maneuvers. To achieve this goal a rat model was developed whereby the ischemia was remotely induced by inflation (under computer control) of an occlusive cuff placed about the common carotid artery. Metabolic parameters were determined using in vivo NMR spectroscopy measurements throughout the ischemic and reflow periods. Lactate production was found to be highly reproducible and not limited by blood glucose levels. High energy phosphate decreases were correlated with loss of high frequency EEG. To evaluate the correlation between histologic damage and measures of regional metabolism we have carried out H-1 spectroscopic imaging experiments with histologic evaluations of the brain three hours after reperfusion. These studies were acquired with 5 minute (two dimensional mapping across the cortex) and 16 sec time resolution (one dimensional mapping) during the ischemia and reflow. Preliminary results of regional clearance kinetics of lactate shows a strong correlation with the presence of histologic damage. DTIC

N95-19714# Rothe Development, Inc., San Antonio, TX.
ECHO IMAGING TECHNIQUES DETERMINE THE SIZE OF INTRAVASCULAR BUBBLES IN DECOMPRESSION SICKNESS Final Report
Robert M. Olson Jul. 1994 30 p
(Contract F33615-89-D-0604)
(AD-A284849; AL/CF-TR-1994-0033) Avail: CASI HC A03/MF A01

The size of altitude induced intravenous bubbles was determined. These bubbles, referred to as venous gas emboli (VGE), are thought to be a major factor in the onset and severity of decompression sickness (DCS). Ten volunteer subjects were monitored for altitude induced VGE in the inferior vena cava (IVC) with a HP Sonos 1000 echo imaging system. Bubble size was determined indirectly and by in-vitro sizing methods because ultrasonic images do not necessarily represent true VGE size. Stratification of bubbles of known size in a water filled mechanical analog of the IVC determined the upper size limit, which was 300 microns in these experiments; bubbles larger than 300 microns roll along the top of the vessel. The lower size limit was the size of the smallest bubbles which the Sonos 1000 could image, determined indirectly by in-vitro microbubble flotation rates and survival times measured ultrasonically and calibrated microscopically. The diameter of the smallest VGE which echo imaging systems can detect in the IVC was found to be 30-40 microns. Used in this determination was the fact that these microbubbles are too small to float; they survive less than a minute. In conclusion, the size of the ultrasonically detected VGE in the interior of the IVC of decompressed subjects can be measured; for subjects at 29,500 ft. bubble size varied from 30-300 microns. DTIC

N95-19746* National Aeronautics and Space Administration, Washington, DC.
AEROSPACE MEDICINE AND BIOLOGY: A CONTINUING BIBLIOGRAPHY WITH INDEXES (SUPPLEMENT 397)
Jan. 1995 57 p
(NASA-SP-7011(397); NAS 1.21:7011(397)) Avail: CASI HC A04

This bibliography lists 122 reports, articles and other documents introduced into the NASA Scientific and Technical Information System during Jan. 1995. Subject coverage includes: aerospace medicine and physiology, life support systems and man/system technology, protective clothing, exobiology and extraterrestrial life, planetary biology, and flight crew behavior and performance. Author

N95-19811 Army Research Inst. of Environmental Medicine, Natick, MA.
DISTRIBUTED MEDICAL DATABASE SYSTEM FOR REAL-TIME MONITORING OF THE HEALTH AND RISK EXPOSURE OF MILITARY RESEARCH STUDY VOLUNTEERS AT USARIEM
Matthew J. Reardon and Donna Cardinal May 1994 67 p Limited Reproducibility: More than 20% of this document may be affected by microfiche quality
(AD-A279193; USARIEM-T94-13) Avail: Issuing Activity (Defense Technical Information Center (DTIC))

This report describes a computerized medical database system designed to track the health and study related risk exposures and adverse incidents of soldiers participating as volunteer test subjects in USARIEM human-use research studies. This database system was implemented as an Oracle application on the USARIEM DEC VAX. The data collected at remote computer terminals are transmitted via modem and LAN to secure digital storage media at USARIEM. Database file access is controlled using methods to ensure test subject confidentiality and anonymity with regard to medical information. Only physician users are allowed access to medical details in the database. This database system was designed to improve the tracking of research study related risks and medical incidents as well as improve the coordination of medical care provided to test subjects by USARIEM physicians. DTIC

N95-19827 Army Research Inst. of Environmental Medicine, Natick, MA.
ANNUAL HISTORICAL REPORT, CALENDAR YEAR 1993
Apr. 1994 174 p Limited Reproducibility: More than 20% of this document may be affected by microfiche quality
(AD-A280178) Avail: CASI HC A08

This report contains information concerning the mission, organization, key staff, overall funding and significant research accomplishments of the US Army Research Institute of Environmental Medicine, a subordinate

element of the US Army Medical Research and Development Command, for calendar year 1992. Also included are listings of published reports, abstracts, presentations and key briefings for each Research Division of the Institute and significant accomplishments and appointments of the professional staff. DTIC

N95-18971*# Oakwood Coll., Huntsville, AL. Dept.of Chemistry, Biochemistry and Allied Health.
THE ASSESSMENT OF VIRTUAL REALITY FOR HUMAN ANATOMY INSTRUCTION
Karen P. Benn *In* Alabama Univ., Research Reports: 1994 NASA/ASEE Summer Faculty Fellowship Program Oct. 1994 6 p (For primary document see N95-18967 05-80)
Avail: CASI HC A01/MF A03

53 BEHAVIORAL SCIENCES

Includes psychological factors; individual and group behavior; crew training and evaluation; and psychiatric research.

N95-18084 Air Force Materials Lab., Wright-Patterson AFB, OH. Crew Systems Directorate.
SITUATION AWARENESS: PAPERS AND ANNOTATED BIBLIOGRAPHY Interim Report, 15 Jan. 1992 - 6 Jun. 1994
Michael Vidulich, Cynthia Dominguez, Eric Vogel, and Grant McMillan Jun. 1994 167 p Limited Reproducibility: More than 20% of this document may be affected by microfiche quality
(AF Proj. 7184)
(AD-A284752; AL/CF-TR-1994-0085) Avail: CASI HC A08

This report combines an annotated bibliography about situation awareness (SA) with four papers that discuss central issues for SA research. The report was compiled to support the Armstrong Laboratory's Situation Awareness Integration (SAINT) team. The annotated bibliography includes the citations and reviews of over 200 articles that discuss SA research or the role of SA in operational systems. These articles are indexed by keyword and author(s). The four papers address the definition of SA, the cognitive processes involved in SA, the operational role of SA, and the initial results of the SA research program conducted by the SAINT team. DTIC

N95-18094 Maryland Univ., College Park, MD. Computer Vision Lab.
THE SYNTHESIS OF VISION AND ACTION
Cornelia Fermueller and Yiannis Aloimonos 1993 40 p Limited Reproducibility: More than 20% of this document may be affected by microfiche quality
(Contract N00014-93-1-0257)
(AD-A285453) Avail: CASI HC A03

Our efforts to reconstruct the world using visual information have led to the insight that the study of Vision should not be separated from the study of a system's actions and purposes. In computational terms this relates to approaching the analysis of perceptual information processing systems through the modelling of the observer and world in a synergistic manner, not through the isolated modelling of observer and world as closed systems. The question still remains: how should such a synergistic modelling be realized? This chapter addresses the question by providing a methodology for synthesizing vision systems and integrating perception and action. In particular, we outline an architecture for purposive vision systems and present a hierarchy of navigational competences based on computational models of increasing complexity, employing representations of motion, shape, form and space. Pure computational considerations will not tell us what visual competences and representations are important to vision systems performing a set of tasks. Interaction, however, with empirical sciences such as Neurobiology, Physiology, Psychology, Ethology, etc., can give us inspiration about the visual categories relevant to systems existing in real world environments. Throughout the chapter, we describe biological findings and how they affect the choice of computational models and representations needed for the synthesis of a hierarchy of navigational competences in a working system. DTIC

N95-18095# Army Research Inst. for the Behavioral and Social Sciences, Alexandria, VA.
CREATION OF NEW ITEMS AND FORMS FOR THE PROJECT A ASSEMBLING OBJECTS TEST Final Report, Oct. 1990 - Jan. 1994
Henry H. Busciglio, Dale R. Palmer, Ivey H. King, and Clinton B. Walker Aug. 1994 48 p
(AD-A285522; ARI-TR-1004) Avail: CASI HC A03/MF A01

The Army's Project A was a comprehensive effort to improve the selection and classification of enlisted personnel. The Assembling Objects (AO) test was a major product of this effort. Previous research has shown AO to be an excellent measure of both overall spatial ability and complex, g-loaded problem-solving skills. In view of the great potential usefulness of the AO measure, researchers from the U.S. Army Research Institute for the Behavioral and Social Sciences examined the original test to develop precise, comprehensive item specifications. Using these specifications, they developed new draft items that were psychometrically tested in a field setting. The researchers then chose the best of the new items and combined them into three complete new forms that were further tested. Analyses showed that all three new forms displayed acceptable (or better) psychometric properties, at both the item and total score level, thus supporting the usefulness of the item specifications for creating new AO items and forms. These efforts should help to make the Assembling Objects test a valuable addition to the testing programs of the Army and the other armed services. DTIC

N95-18151# Defence and Civil Inst. of Environmental Medicine, Downsview (Ontario).
IMPLEMENTATION OF A HUMAN INFORMATION PROCESSING MODEL FOR TASK NETWORK SIMULATION
Keith C. Hendy May 1994 47 p
(AD-A283903; DCIEM-94-40) Avail: CASI HC A03/MF A01

Task network simulation is an analytical technique that is widely used to predict operator performance and/or workload during early stages of systems design. Task network simulation is based on traditional time-line analysis methods, but allows possibility of non-deterministic task characteristics such as completion times, sequences, outcomes etc. Many simulation environments allow task parameters to vary with various network states, which supports complex logical relationships, and the varying network behaviors. This report outlines the implementation of a theoretical framework for a new model of the human information processor for using task network simulation. The development and validation of the Information Processing (IP) Model is described in detail elsewhere. This report deals only with those aspects that are necessary to take the ideas of the IP Model and adapt them for direct application task network simulation. The material contained in this report provides the bridge between the conceptual descriptions of the Model, and the software requirements necessary to put that concept into practice. As part of this process, many parameters are defined and assigned tentative values so that the model can be run within the task network simulation environment. DTIC

N95-18401 Yale Univ., New Haven, CT. Dept. of Psychology.
A PARALLEL PROCESSING HYPOTHESIS FOR SHORT-TERM AND LONG-TERM MEMORY IN APLYSIA Annual Report, 1 May 1993 - 30 Apr. 1994
Thomas J. Carew 30 Apr. 1994 7 p Limited Reproducibility: More than 20% of this document may be affected by microfiche quality
(Contract F49620-93-1-0273)
(AD-A284101; AFOSR-94-0499TR) Avail: Issuing Activity (Defense Technical Information Center (DTIC))

The primary focus of this program of research is a mechanistic analysis of the relationship between short-term and long-term information processing in central neural circuits of the marine mollucs Aplysia. During the last year we have completed several projects in this program; these projects fall into two broad classes which focus on facilitatory and, more recently, inhibitory information processing. We have identified several forms of behaviorally relevant cellular and circuit modifications which involve both facilitatory and inhibitory information processing. Our goal for the current year is to analyze each of these processes mechanistically, and determine their interaction in both short-term and long-term storage of information in identified neural networks. DTIC

N95-18403 Pittsburgh Univ., Pittsburgh, PA.
VISUO-OCULAR PERFORMANCE DURING VESTIBULAR STIMULATION Annual Report, 1 Jul. 1993 - 30 Jun. 1994
Joseph M. Furman and James A. Carl 30 Jun. 1994 6 p Limited Reproducibility: More than 20% of this document may be affected by microfiche quality
(Contract F49620-93-1-0261)
(AD-A284103; AFOSR-94-0510TR) Avail: Issuing Activity (Defense Technical Information Center (DTIC))

The objective of this study is to enhance knowledge regarding spatial orientation and disorientation in environments characterized by combined stress, namely simultaneous visual and vestibular stimulation. This study will test the hypothesis that target acquisition, ocular tracking, and visual search are degraded by vestibular stimulation using off-vertical axis rotation. Target acquisition stimuli will consist of a spot moving suddenly to a new location in a pseudo-random fashion; ocular tracking stimuli will consist of constant velocity target motion. Visual search will combine these stimuli. Eye movements will be recorded using the magnetic scleral search coil method. Analysis of the data will yield measures of saccadic latency and accuracy, and ocular pursuit gain. Calculated performance measures will be compared across visual and vestibular stimulus conditions with analysis of variance. The goal of the first year of research was to develop protocols and assess visual-vestibular interaction. As proposed for the first year, 15 normal subjects (8F, 7M) have been tested with the entire protocol of vestibular, visual, and visual-vestibular stimuli. With these first year studies completed, studies for the second year have begun. DTIC

N95-18414 Naval Aerospace Medical Research Lab., Pensacola, FL.
COMPUTER-BASED PSYCHOMOTOR TESTS IN OPTIMAL TRAINING TRACK ASSIGNMENT OF STUDENT NAVAL AVIATORS
D. R. Street, Jr. and D. L. Dolgin Feb. 1994 18 p Limited Reproducibility: More than 20% of this document may be affected by microfiche quality
(DA Proj. M00-96)
(AD-A283720; NAMRL-1391) Avail: Issuing Activity (Defense Technical Information Center (DTIC))

The purpose of our investigation was to determine if computer-based selection tests could predict training track assignment for student naval aviators. This study evaluated the predictive efficacy of an experimental battery of computer-based pilot selection tests for training classification. Student naval aviators are currently assigned to an aircraft training track based primarily on performance in primary training. Students were tested on the experimental test battery and classified into one of three aircraft training tracks based on their test scores. The resulting classifications were compared to actual selections made as the students progressed through naval aviation training. Using a sample of 237 students, linear analyses were conducted to evaluate the efficacy of predicted decisions. The unique contribution of the experimental battery was determined by comparing scores on the experimental battery to scores on the Navy/Marine Corps Aviation Selection Test Battery, a paper-and-pencil pilot selection test used by the United States Navy and Marine Corps, and student primary flight training grades. A significant classification model including one of the experimental selection tests was derived. The model was able to significantly predict fast attack pipeline selections before flight training. DTIC

N95-18440 Naval Biodynamics Lab., New Orleans, LA.
NAVAL BIODYNAMICS LABORATORY 1993 COMMAND HISTORY
1993 58 p Limited Reproducibility: More than 20% of this document may be affected by microfiche quality
(AD-A284358) Avail: CASI HC A04

The Naval Biodynamics Laboratory (NBDL) was established as the Naval Aerospace Medical Research Laboratory Detachment (NAMRLD) in April 1971 by the Bureau of Medicine and Surgery. NAMRLD was a detachment of the Naval Aerospace Medical Research Laboratory which is located at the Naval Air Station, Pensacola, Florida. The initial purpose of the Detachment was to study human response to impact acceleration. In 1975, the mission was expanded to include human response to vibration, ship motion, and to study human performance. NBDL was designated a separate command by the Secretary of the Navy in February, 1980, and officially established on 28 February 1980. NBDL is under the command of Naval Medical Research and Development Command (NMRDC) and receives primary support from the Chief, Bureau of Medicine and Surgery, Washington, DC. DTIC

N95-18530# Michigan State Univ., East Lansing, MI.
EFFECTIVE TEAM PERFORMANCE UNDER STRESS AND NORMAL CONDITIONS: AN EXPERIMENTAL PARADIGM, THEORY AND DATA FOR STUDYING TEAM DECISION MAKING IN HIERARCHICAL TEAMS WITH DISTRIBUTED EXPERTISE Final Report, 15 Mar. 1990 - 31 Aug. 1993
Daniel R. Ilgen and John R. Hollenbeck Aug. 1993 85 p
(Contract N00014-90-J-1786)
(AD-A284683) Avail: CASI HC A05/MF A01

The report describes a program of research addressing decision making in hierarchical teams with distributed expertise. A theory of such decision making is presented along with empirical research related to the theory. Then a team simulation exercise was developed to address team decision for four person teams. This exercise presents teams with problems that require gathering and sharing information prior to reaching a team decision and also allow for the assignment of team members to roles that differ in areas of expertise. This exercise, performed on four networked computers, allows for the assessment of a large number of team behaviors. Along with the exercise, repeated measures regression is used as a means of analyzing team data by taking advantage of the statistical power available at various levels of analysis. Several studies were conducted to assess the viability of theory and to look at a number of other issues of decision making. DTIC

N95-19068 Carnegie-Mellon Univ., Pittsburgh, PA. Dept. of Computer Science.
ASSESSMENT OF THE ACSE SCIENCE LEARNING ENVIRONMENT AND THE IMPACT OF MOVIES AND SIMULATIONS
John F. Pane 1 Jun. 1994 21 p Limited Reproducibility: More than 20% of this document may be affected by microfiche quality
(Grant NSF MDR-91-50211)
(AD-A284071; CMU-CS-94-162) Avail: CASI HC A03

This paper describes an empirical study that assesses a multimedia science learning environment, and the impact on student learning of movies and simulations as lesson components. The study measures summative effects on student performance and satisfaction, and gathers formative data about student use of the environment for iterative improvement to the system and lessons. Two lessons containing movies and simulations were compared with lessons that used static graphics to present the same material. Preliminary results show that participants using the lesson with movies and simulations spend significantly more time working through the material, and score higher on questions that target material that is presented with simulation. Analysis of usage patterns identifies features of the system that are effective, underutilized, misunderstood or problematic. DTIC

N95-19538# Institute for Human Factors TNO, Soesterberg (Netherlands).
LEARNING EFFECTS ON STRATEGY SELECTION IN A DYNAMIC TASK ENVIRONMENT AS A FUNCTION OF TIME PRESSURE
J. H. Kerstholt Jun. 1994 17 p
(AD-A285458; TNO-TM-1994-B-12; TDCK-94-0055) Avail: CASI HC A03/MF A01

Previous research on strategy selection in dynamic task environments indicated that subjects preferred to request information first, before an action was applied, even when the straightforward application of actions would have resulted in more optimal performance. Furthermore, this strategy was also used when subjects only had limited time for diagnosis. In the present experiment it was investigated whether the amount of training could account for the limited use that subjects made of the task dynamics. Subjects were required to monitor the changing fitness level of an athlete, by means of a graph on a computer screen, and to apply treatments whenever necessary. They could request various symptoms that would provide an indication for the cause underlying a possible fitness decline. The subjects either received limited training or elaborate training and they had either sufficient time for diagnosis, or worked under time pressure. The results showed that the amount of training did not affect the strategy that subjects used: half of the subjects used a judgment-oriented strategy and the other half used an action-oriented strategy in both training conditions. However, the well trained subjects were superior in selecting information

and they processed the information at a faster rate than the subjects with only minimal training. The time pressure effects replicated previous findings: subjects used the same strategy and speeded up information processing. A high level of time pressure only deteriorated the information integration processes of the subjects who had received only minimal training, but not that of the well-trained subjects. DTIC

N95-19564# Army Aeromedical Research Lab., Fort Rucker, AL. Aircrew Health and Performance Div.
COLLECTION OF REAL-TIME, MULTICHANNEL EEG DATA FROM HELICOPTER PILOTS IN FLIGHT: A FEASIBILITY STUDY Final Report
John A. Caldwell, Jr., James A. Lewis, Stephen R. Darling, Robert M. Dillard, and Parley P. Johnson May 1994 61 p
(AD-A285050; USAARL-94-26) Avail: CASI HC A04/MF A01

An initial assessment of whether valid electroencephalographic (EEG) data could be collected on helicopter pilots in flight was conducted using 20 volunteers. Each subject provided a brief eyes-open and eyes-closed EEG in the laboratory and then in a helicopter. During helicopter flights, data were monitored and recorded on the ground in real-time via a radio telemetry system. Initial hardware problems resulted in the exclusion of several records, but these problems were resolved toward the end of the study. Analysis of the remaining acceptable EEG records indicated that the typical increase in alpha activity (7.5-13.0 Hz) due to eye closure was clearly observable at every analyzed electrode site regardless of whether the testing occurred in the laboratory or in the helicopter. Further examinations of delta, theta, and beta bands showed that the EEG data were not overly contaminated by artifacts, although it was much more difficult to find 'clean' segments on records collected in the helicopter than in the laboratory. It was concluded that it is possible to record and telemeter useable EEG from the in-flight helicopter environment. DTIC

N95-19583# Prins Maurits Lab. TNO, Rijswijk (Netherlands).
MULTIPLE-TASK PERFORMANCE: A CRITICAL REVIEW OF THE LITERATURE AND A COGNITIVE NEUROSCIENCE FRAMEWORK
J. E. Korteling 10 Mar. 1994 91 p
(AD-A285133; IZF-1994-B-5; TDCK-94-0043) Avail: CASI HC A05/MF A01

In our modern society, technological developments have altered the nature of jobs and tasks. In many work situations, operators are required to monitor, control, and manipulate information via complex technological systems. Such systems typically involve performance of several tasks in a limited period of time. In order to be able to optimize such technological systems, knowledge with regard to complex-task performance is needed, based on which technical products, processes, and systems involved in daily life can be matched to the capabilities and limitations of people. DTIC

N95-19602# New York Univ., New York, NY. Dept. of Psychology.
FACILITATION AND INTERFERENCE IN IDENTIFICATION OF PICTURES AND WORDS Final Report, 1 Dec. 1991 - 31 May 1994
Joan G. Snodgrass 5 Oct. 1994 54 p
(Contract F49620-92-J-0119)
(AD-A285882; AFOSR-94-0670TR) Avail: CASI HC A04/MF A01

This research is concerned with long-term facilitation and short-term interference and facilitation in identification of pictures and words. The long-term facilitation occurs when subjects are exposed to some representation of the item during a study episode, and then show improved identification of that item during a retention test. This type of facilitation is known as priming (or long-term priming) and the retention test is known as an implicit or indirect test because subjects are not instructed to think back to the prior study episode during the test. Much of our recent research has concerned the relationship between performance on the implicit test of picture fragment completion and the explicit test of recognition memory. Our major interest has been on the importance of maintaining the same surface features between study and test on performance in both implicit and explicit tests. Contrary to previous findings that explicit tests are impervious to surface changes and only sensitive to changes in meaning, we have found performance decrements from changes in surface features in explicit as well as implicit tests. These surface changes have been as subtle as differences in the level of fragmentation between study and test and as extreme as differences in the form of item (picture vs. word) between study and test. The research carried out under the grant has exploited this similarity between explicit and implicit tests within a components-of-information model of memory which accommodates both associations and dissociations between the two classes of tests. DTIC

N95-19740 Rice Univ., Houston, TX.
COMPARING PERFORMANCE ON IMPLICIT MEMORY TESTS Annual Technical Report, 1 Aug. 1993 - 31 Jul. 1994
Henry Roediger, III 31 Aug. 1994 9 p Limited Reproducibility: More than 20% of this document may be affected by microfiche quality
(Contract F49620-92-J-0437)
(AD-A284861; AFOSR-94-0577TR) Avail: CASI HC A02

The second year of this grant saw progress on nine projects. In particular, in the past year five papers or chapters have been published, six are in press, three are in preparation, and data are being collected on several new projects. We have completed projects on the following topics: (1) effects of imagery on nonverbal implicit tests; (2) effects of high priority events on implicit tests; (3) specificity of priming on verbal and nonverbal perceptual tests; (4) direct comparison of two methods of testing for contamination of implicit tests by conscious recollection; (5) the experimental basis of serial position effects; and (6) a new paradigm for the study of false memories. Four or five other projects should be completed during the final year of the grant. DTIC

54 MAN/SYSTEM TECHNOLOGY AND LIFE SUPPORT

Includes human engineering; biotechnology; and space suits and protective clothing.

For related information see also *16 Space Transportation.*

N95-18029# Army Research Lab., White Sands Missle Range, NM. Battlefield Environment Directorate.
NIGHT VISION GOGGLES (NVG) SOFTWARE USER'S GUIDE, VERSION 5.1 Final Report
David Sauter and Gavino Zertuche Jun. 1994 37 p
(AD-A284563; ARL-TR-524) Avail: CASI HC A03/MF A01

Numerous military applications utilize night vision devices (NVD). Aviation and ground transportation are two applications that the computer program Night Vision Goggles (NVG) is intended to support. Aviators and vehicle drivers must have an idea of what the ambient light levels are before using NVD's. Not enough light precludes safe use of the devices, while enough light allows for adequate performance of the required tasks by the unaided eye. The weather also effects natural illumination. NVG is intended to provide users of NVD's with forecasts of favorable and unfavorable times of use. The criteria for NVD use times are specified by the user in terms of lunar altitude and percent illumination as well as illumination level to ensure wide application of the software in terms of the different NVD's and different services. The illumination level for user specified times can also be determined. Current or forecast meteorological conditions or climatology may be input to realistically account for the effects of clouds, fog, precipitation, and surface reflectivity. The user friendly program is menu driven for ease of operation. DTIC

N95-18077 Army Aeromedical Research Lab., Fort Rucker, AL.
DESIGN AND DEVELOPMENT OF AN ENHANCED BIODYNAMIC MANIKIN, PHASE 1 Final Report
Paul H. Frisch and William Boulay Aug. 1994 106 p Limited Reproducibility: More than 20% of this document may be affected by microfiche quality
(AD-A284725; USAARL-CR-94-1) Avail: CASI HC A06

Manikins have been used as substitutes for human subject in biodynamic testing since 1944. The original manikin was a simple wooden form to provide an equivalent weight to body mass for testing an ejection seat in a German DO335 aircraft. Since then, manikins have undergone a gradual evolution trying to achieve the goal of a biofidelic human analog. Standard Hybrid 3-type manikins have a rigid thoracic and lumbar spine, limiting the response of the manikin's back in a dynamic environment. The predominant injury in survivable U.S. Army rotary-wing mishaps often is spinal injury. The U.S. Army wants to procure a manikin with an enhanced spinal biofidelity with self-contained data acquisition and storage capabilities. The proposed

evolution in manikin design to meet the needs of the Army is discussed. A standard Hybrid 3-type manikin will be modified. A standard DOT part 572 head and Hybrid III flexible neck will be used. The spinal column includes a flexible spine with multiple vertebral segments, adjustment blocks, biodynamic load cells and sensors, and mountings for the neck and shoulder. DTIC

N95-18086# Texas Univ., Austin, TX. Computer and Vision Research Center.

FUSION OF MULTIPLE SENSING MODALITIES FOR MACHINE VISION Final Report, 1 Feb. 1991 - 31 May 1994

J. K. Aggarwal 31 May 1994 39 p

(Contract DAAL03-91-G-0050)

(AD-A284762) Avail: CASI HC A03/MF A01

We report on a broad program of research in machine vision to develop an approach based upon synergistically combining diverse sensing modalities. The research projects fall into four general categories: (1) Outdoor Scene interpretation via the Fusion of Multiple Imaging Modalities; (2) Motion Computation and Object Recognition Using Range Images; (3) Structure and Identity Based on Color and Shape Information; and (4) Autonomous Navigation. Accomplishments include the development of the AIMS (automatic interpretation using multiple sensors) knowledge-based system to interpret registered laser radar and thermal images for the detection and recognition of man-made objects in outdoor rural scenes; the development of a new approach for the detection of large man-made objects using perceptual organization techniques; new algorithms for object recognition and motion estimation, including improved algorithms for using three-dimensional (range) images to compute structure and motion; a CAD-based object recognition system; a decision-theoretical algorithm to estimate 3D structures from extended sequences of 2D images taken by a moving camera; an algorithm for matching line segments based on perceptual grouping relaxation labeling; and the construction of an autonomous mobile robot, Robo-Tex, as a testbed for navigation algorithms. DTIC

N95-18189*# National Aeronautics and Space Administration. Lyndon B. Johnson Space Center, Houston, TX.

GEOMETRY AND GRAVITY INFLUENCES ON STRENGTH CAPABILITY

Jeffrey Poliner (Lockheed Engineering and Sciences Co., Houston, TX.), Robert P. Wilmington (Lockheed Engineering and Sciences Co., Houston, TX.), and Glenn K. Klute Dec. 1994 26 p

(Contract NAS9-17900)

(NASA-TP-3511; S-784; NAS 1.60:3511) Avail: CASI HC A03/MF A01

Strength, defined as the capability of an individual to produce an external force, is one of the most important determining characteristics of human performance. Knowledge of strength capabilities of a group of individuals can be applied to designing equipment and workplaces, planning procedures and tasks, and training individuals. In the manned space program, with the high risk and cost associated with spaceflight, information pertaining to human performance is important to ensuring mission success and safety. Knowledge of individual's strength capabilities in weightlessness is of interest within many areas of NASA, including workplace design, tool development, and mission planning. The weightless environment of space places the human body in a completely different context. Astronauts perform a variety of manual tasks while in orbit. Their ability to perform these tasks is partly determined by their strength capability as demanded by that particular task. Thus, an important step in task planning, development, and evaluation is to determine the ability of the humans performing it. This can be accomplished by utilizing quantitative techniques to develop a database of human strength capabilities in weightlessness. Furthermore, if strength characteristics are known, equipment and tools can be built to optimize the operators' performance. This study examined strength in performing a simple task, specifically, using a tool to apply a torque to a fixture. Author

N95-18385 Air Force Inst. of Tech., Wright-Patterson AFB, OH.

CROSSHIFT VIBROMETRY: BIOMARKER FOR ERGONOMIC STRESS Ph.D. Thesis

Edward J. Klinenberg Sep. 1994 244 p Limited Reproducibility: More than 20% of this document may be affected by microfiche quality

(AD-A284337; AFIT/CI/CIA-94-035D) Avail: Issuing Activity (Defense Technical Information Center (DTIC))

Identification of a reliable and sensitive biomarker for ergonomic stress would be important for the early identification of high risk tasks that may lead to the development of carpal tunnel syndrome. This dissertation consisted of three field studies conducted at a large aircraft repair facility which looked into the use of multi-frequency vibrotactile thresholds changes over the workday (crosshift vibrometry) as a potential biomarker for ergonomic stress. In the first study, 121 industrial workers (82 male, 39 female) from a variety of occupations had their vibrotactile thresholds measured at four frequencies (31.5 Hz, 125 Hz, 250 Hz, 500 Hz) in the morning and afternoon. Fingertip skin temperature, demographic information, time of test, hand/wrist pain, and task information were recorded for each worker. Overall, vibration sensitivity increased as the day progressed. The effect was small and frequency dependent with higher frequencies producing greater effects. Crosshift vibrometry was significantly associated with fingertip skin temperature differences and exposure duration, but only at the highest frequencies (250, 500 Hz). Crosshift vibrometry was not associated with sex or age at any frequency. In the second study, 52 workers from five shops (36 male, 16 female) were tested on two separate days. At the lowest frequency tested (31.5 Hz), crosshift vibrometry was associated with the shops that employees worked in (sheetmetal repair, engine repair, grocery scanners). DTIC

N95-18531# Virginia Univ., Charlottesville, VA. School of Engineering and Applied Science.

IMPROVED FILTRATION MATERIALS AND MODELING Final Report, Jun. 1990 - Jun. 1993

M. D. LeVan Jul. 1994 101 p

(Contract DAAA15-90-C-0012)

(AD-A284684; ERDEC-CR-132) Avail: CASI HC A06/MF A02

The objective of this work was to develop new approaches to identify, measure, and correlate relevant data and derive appropriate mathematical models for designing and evaluating regenerable adsorbent-based air filtration systems. The contract contained two tasks: (1) the measurement and interpretation of single and multicomponent adsorption equilibria of vapors of organic compounds and water on BPL activated carbon; and (2) the construction and testing of a generic mathematical model for pressure swing adsorption (PSA) incorporating the adsorption isotherms and including rate phenomena and thermal effects. This final report discusses research accomplishments in two areas and the current status of knowledge in the areas. The contract work proceeded as planned, was coordinated with the U.S. Army Edgewood Research, Development and Engineering Center personnel at all times, and was consistent with the contract schedule. DTIC

N95-19061*# National Aeronautics and Space Administration. Marshall Space Flight Center, Huntsville, AL.

ANALYTICAL CONTROL TEST PLAN AND MICROBIOLOGICAL METHODS FOR THE WATER RECOVERY TEST

M. S. Traweek, ed. and J. D. Tatara, ed. (ION Electronics, Hunsville, AL.) Washington Dec. 1994 194 p

(NASA-TM-108473; NAS 1.15:108473) Avail: CASI HC A09/MF A03

Qualitative and quantitative laboratory results are important to the decision-making process. In some cases, they may represent the only basis for deciding between two or more given options or processes. Therefore, it is essential that handling of laboratory samples and analytical operations employed are performed at a deliberate level of conscientious effort. Reporting erroneous results can lead to faulty interpretations and result in misinformed decisions. This document provides analytical control specifications which will govern future test procedures related to all Water Recovery Test (WRT) Phase 3 activities to be conducted at the National Aeronautics and Space Administration/Marshall Space Flight Center (NASA/MSFC). This document addresses the process which will be used to verify analytical data generated throughout the test period, and to identify responsibilities of key personnel and participating laboratories, the chains of communication to be followed, and ensure that approved methodology and procedures are used during WRT activities. This document does not outline specifics, but provides a minimum guideline by which sampling protocols, analysis methodologies, test site operations, and laboratory operations should be developed. Author

N95-19412 Selskapet for Industriell og Teknisk Forskning, Trondheim (Norway). Div. for Informatics.
GUIDELINES FOR REDUCTION OF HUMAN ERRORS DURING MAINTENANCE OF SAFETY SYSTEMS; MAINTAINABILITY AND MAINTENANCE SUPPORT
L. Bodsberg, R. Rosness, and K. Oeien 18 Mar. 1994 45 p
(PB94-215597; STF75-A93065) Avail: Issuing Activity

Guidance on reduction of human errors during maintenance of process control and safety systems are presented. The guidance is presented on three levels: (1) General design principles; (2) General requirements (maintainability and maintenance support of systems in general); (3) and Specific requirements (maintainability and maintenance support of safety systems in particular). The document covers the maintainability and maintenance support aspect of the safety systems availability performance. The report serves as a collection and transfer of operational experience from operating companies to vendors of process control and safety systems, to those in the operating companies responsible for writing system specifications, and to those responsible for the management and organization of the maintenance activities. NTIS

N95-19502 Materials Research Labs., Ascot Vale (Australia).
EVALUATION OF PUREAU WATER FOR USE AS EMERGENCY DRINKING WATER FOR ADF AIRCRAFT
G. E. Driver Dec. 1993 14 p
(MRL-TN-648; AR-008-562) Copyright Avail: Issuing Activity

A commercially available, purified water packed in PET bottles has been tested for suitability as an emergency drinking water for ADF aircraft. The water meets chemical and organoleptic requirements of the ADF, and is preferred to the current product on the basis of taste and the lower permeability of the package to water. The product failed to meet the ADF's stringent microbiological specifications. Further testing is required to determine the ability of the package to withstand the forces of ejection, and the high temperatures within the cockpit of aircraft parked in the sun in tropical areas of Australia. Author

N95-18990*# East Carolina Univ., Greenville, NC. School of Human Environmental Sciences.
DEVELOPMENT OF MICROGRAVITY, FULL BODY FUNCTIONAL REACH ENVELOPE USING 3-D COMPUTER GRAPHIC MODELS AND VIRTUAL REALITY TECHNOLOGY
Patricia F. Lindsey *In* Alabama Univ., Research Reports: 1994 NASA/ASEE Summer Faculty Fellowship Program Oct. 1994 6 p (For primary document see N95-18967 05-80)
Avail: CASI HC A02/MF A03

N95-19627*# Kent State Univ., OH.
ON THE DEVELOPMENT OF AN EXPERT SYSTEM FOR WHEELCHAIR SELECTION
Gregory R. Madey, Charlotte A. Bhansin (Cleveland Clinic Foundation, OH.), Sulaiman A. Alaraini, and Mohamed A. Nour *In* NASA. Johnson Space Center, Third CLIPS Conference Proceedings, Volume 1 Nov. 1994 p 2-12 (For primary document see N95-19625 05-61)
Avail: CASI HC A03/MF A03

55 SPACE BIOLOGY

Includes exobiology; planetary biology; and extraterrestrial life.

N95-18569*# National Aeronautics and Space Administration. Ames Research Center, Moffett Field, CA.
US EXPERIMENTS FLOWN ON THE SOVIET BIOSATELLITE COSMOS 2044. VOLUME 1: MISSION DESCRIPTION, EXPERIMENTS K-7-01 - K-7-15 Final Report
James P. Connolly, ed., Richard E. Grindeland, ed., and Rodney W. Ballard, ed. Sep. 1994 487 p
(RTOP 199-08-12)
(NASA-TM-108802-Vol-1; A-94031-Vol-1; NAS 1.15:108802-Vol-1) Avail: CASI HC A21/MF A04

Cosmos 2044 was launched on September 15, 1989, containing radiation dosimetry experiments and a biological payload including two young male rhesus monkeys, ten adult male Wistar rats, insects, amphibians, protozoa, cell cultures, worms, plants and fish. The biosatellite was launched from the Plesetsk Cosmodrome in the Soviet Union for a mission duration of 14 days, as planned. The major research objectives were: (1) Study adaptive response mechanisms of mammals during flight; (2) Study physiological mechanisms underlying vestibular, motor system and brain function in primates during early and later adaptation phases; (3) Study the tissue regeneration processes of mammals; (4) Study the development of single-celled organisms, cell cultures and embryos in microgravity; (5) Study radiation characteristics during the mission and investigate doses, fluxes and spectra of cosmic radiation for various types of shielding. American and Soviet specialists jointly conducted 29 experiments on this mission including extensive preflight and post flight studies with rhesus monkeys, and tissue processing and cell culturing post flight. Biosamples and data were subsequently transferred to the United States. The U.S. responsibilities for this flight included development of flight and ground-based hardware, the preparation of rat tissue sample procedures, the verification testing of hardware and experiment procedures, and the post flight analysis of biospecimens and data for the joint experiments. The U.S. investigations included four primate experiments, 24 rat experiments, and one radiation dosimetry experiment. Three scientists investigated tissue repair during flight for a subgroup of rats injured preflight by surgical intervention. A description of the Cosmos 2044 mission is presented in this report including preflight, on-orbit and post flight activities. The flight and ground-based bioinstrumentation which was developed by the U.S. and U.S.S.R. is also described, along with the associated preflight testing of the U.S. hardware. Author

59 MATHEMATICAL AND COMPUTER SCIENCES (GENERAL)

No abstracts in this category.

60 COMPUTER OPERATIONS AND HARDWARE

Includes hardware for computer graphics, firmware, and data processing.

For components see *33 Electronics and Electrical Engineering.*

N95-17939 Princeton Univ., NJ. Dept. of Mechanical and Aerospace Engineering.
STUDY OF A NAVIER-STOKES COMPUTER Final Report, 1 Feb. 1992 - 31 Jan. 1994
Daniel Nosenchuck 14 Jul. 1994 6 p Limited Reproducibility: More than 20% of this document may be affected by microfiche quality
(Contract F49620-92-J-0151)
(AD-A284196; AFOSR-94-0489TR) Avail: CASI HC A02

During the past year, research has progressed along three fronts: (1) development of a high-performance FORTRAN compiler for the Navier-Stokes computer (NSC); (2) identification of appropriate application codes; and (3) study of an upgrade to the NSC architecture and hardware to produce a next-generation node. DTIC

N95-18517 Department of the Navy, Washington, DC.
LASER OPTICAL MOUSE Patent
Frank J. Snow, inventor (to Navy) 28 Dec. 1993 8 p Filed 15 Aug. 1991
(AD-D016273; US-Patent-5,274,361; US-Patent-Appl-SN-756261) Avail: US Patent and Trademark Office

An apparatus for determining distance coordinates along two orthogonal axes for a computer system, where the coordinates represent the position of a cursor on a screen of a display unit of the computer system. The apparatus includes a pair of velocity detectors and an operating device such as a CPU. When the velocity detectors are moved by an operator, each of the velocity detectors detects velocities along a respective one of

the orthogonal axes. The detected velocities are converted into moving distances representative of the coordinates through a calculation of the operating device. DTIC

N95-18659 Carnegie-Mellon Univ., Pittsburgh, PA. Dept. of Computer Science.
A REDUNDANT DISK ARRAY ARCHITECTURE FOR EFFICIENT SMALL WRITES
Daniel Stodolsky, Mark Holland, William V. Courtright, II, and Garth A. Gibson 29 Jul. 1994 27 p Limited Reproducibility: More than 20% of this document may be affected by microfiche quality
(Grant NSF ECD-07068-89; ARPA Order 7330)
(AD-A284048; CMU-CS-94-170) Avail: Issuing Activity (Defense Technical Information Center (DTIC))

Parity encoded redundant disk arrays provide highly reliable, cost effective secondary storage with high performance for reads and large writes. Their performance on small writes, however, is much worse than mirrored disks - the traditional, highly reliable, but expensive organization for secondary storage. Unfortunately, small writes are a substantial portion of the I/O workload of many important, demanding applications such as on-line transaction processing. This paper presents parity logging, a novel solution to the small write problem for redundant disk arrays. Parity logging applies journalling techniques to substantially reduce the cost of small writes. We provide detailed models of parity logging and competing schemes - mirroring, floating storage, and RAID level 5 - and verify these models by simulation. Parity logging provides performance competitive with mirroring, but with capacity overhead close to the minimum offered by RAID level 5. Finally, parity logging can exploit data caching more effectively than all three alternative approaches. DTIC

N95-18963* National Aeronautics and Space Administration. Pasadena Office, CA.
INTEGRATED, NONVOLATILE, HIGH-SPEED ANALOG RANDOM ACCESS MEMORY Patent
Romney R. Katti, inventor (to NASA) (Jet Propulsion Lab., California Inst. of Tech., Pasadena, CA.), Jiin-Chuan Wu, inventor (to NASA) (Jet Propulsion Lab., California Inst. of Tech., Pasadena, CA.), and Henry L. Stadler, inventor (to NASA) (Jet Propulsion Lab., California Inst. of Tech., Pasadena, CA.) 20 Dec. 1994 9 p Filed 24 Sep. 1993 Continuation of abandoned US-Patent-Appl-SN-653578, filed 11 Feb. 1991
(NASA-Case-NPO-17998-2-CU; US-Patent-5,375,082;
US-Patent-Appl-SN-129001; US-Patent-Appl-SN-653578;
US-Patent-Class-365-45; US-Patent-Class-365-48; US-Patent-Class-365-145;
US-Patent-Class-365-171; US-Patent-Class-365-158;
Int-Patent-Class-G11C-27/00) Avail: US Patent and Trademark Office

This invention provides an integrated, non-volatile, high-speed random access memory. A magnetically switchable ferromagnetic or ferrimagnetic layer is sandwiched between an electrical conductor which provides the ability to magnetize the magnetically switchable layer and a magneto resistive or Hall effect material which allows sensing the magnetic field which emanates from the magnetization of the magnetically switchable layer. By using this integrated three-layer form, the writing process, which is controlled by the conductor, is separated from the storage medium in the magnetic layer and from the readback process which is controlled by the magnetoresistive layer. A circuit for implementing the memory in CMOS or the like is disclosed.
Official Gazette of the U.S. Patent and Trademark Office

N95-19875# State Univ. of New York, Stony Brook, NY.
HIGH PERFORMANCE COMPUTING EQUIPMENT FOR ENVIRONMENTAL REMEDIATION MODELING AND FIRST PRINCIPLES SIMULATION OF MATERIALS PROPERTIES
J. Glimm and W. B. Lindquist Aug. 1994 12 p
(Contract DE-FG02-93ER-25158)
(DE95-000497; DOE/ER-25158/T1) Avail: CASI HC A03/MF A01

A 56-node Intel Paragon parallel computer was purchased with major support provided by this grant, and installed in July, 1993, in the Center for Scientific Computing, Department of Applied Mathematics and Statistics, SUNY - Stony Brook. The targeted research funded by this proposal consists of work to support the Stony Brook and Brookhaven National Laboratory contributions to the Partnership in Computational Science (PICS) program; namely environmental remediation modeling of ground water transport, Car-Parrinello first principles molecular dynamics calculations, and the supporting development of the parallelized VolVis graphics package. Research accomplishments to date for this targeted research is discussed in section 2. This computer has also enabled or enhanced many other projects conducted both by the Center for Scientific Computing and by the Department of Applied Mathematics and Statistics. These other projects include two- and three-dimensional gas dynamics using front tracking, other molecular dynamics applications, kidney modeling, and global optimization techniques applied to DNA-protein interactions. Technical summaries of these additional projects are presented in section 3. The targeted research includes users from the Departments of Applied Mathematics and Computer Science at SUNY - Stony Brook, as well as staff scientists from the Departments of Physics and Applied Sciences at Brookhaven National Laboratory. The additional projects involve university faculty from the above departments as well as the Departments of Physics and Chemistry. Regular users of this machine currently include 10 faculty members, 8 postdoctoral fellows, more that 12 PhD students and approximately 8 staff members from BNL. DOE

61 COMPUTER PROGRAMMING AND SOFTWARE

Includes computer programs, routines, alogorithms, and specific applications, e.g., CAD/CAM.

N95-17935 Newcastle-upon-Tyne Univ., Newcastle (England). Dept. of Computing Science.
PRE-PROCESSING IN SADE: STAGE 3
L. Rapanotti and G. M. Megson Feb. 1994 34 p See also PB94-168002
(PB94-201571; TRS-471) Copyright Avail: Issuing Activity (National Technical Information Service (NTIS))

This report is part of a series on the synthesis of regular array designs from high-level specifications in the Systolic Algorithm Design Environment (SADE). We have previously shown how to map a specification in the form of a set of nested DO-loops in a (restricted) Pascal program to a system of Conditional Recurrence Equations and how to reduce such a system of equations to its normal form by the separation of its inputs, outputs and computations. In this report we illustrate how the data dependencies of the system can be made uniform, allowing the derivation of purely systolic array designs. NTIS

N95-17940 Harvard Univ., Cambridge, MA. Dept. of Psychology.
COOPERATIVITY AND 3-D REPRESENTATION Final Report, 1 Feb. 1993 - 28 Feb. 1994
Patrick Cavanagh 26 Jul. 1994 17 p Limited Reproducibility: More than 20% of this document may be affected by microfiche quality
(Grant AF-AFOSR-0169-91)
(AD-A284203; AFOSR-94-0485TR) Avail: CASI HC A03

Recent evidence indicates that the early stages in visual processing may be broken into several parallel streams that are specialized for the analysis of different visual attributes. A contour localization task showed that all attributes can contribute equally to border localization - no particular attribute dominated position decisions. A series of experiments on transparency perception showed that transparency is analyzed rapidly (within 60 msec) and influences early levels of visual processing. We have also investigated the early stages that lead from the initial 2D representation to object recognition. Visual priming studies have been completed which suggest that object recognition begins, not with the construction of a 3-D model, but with a crude match of 2-D views to internal prototypes. Visual search studies have shown that some scene features may be rapidly suppressed. For example, shadows appear to be identified early and discounted in order to allow object contours to be processed. Finally, long-term practice in visual search tasks leads to learning of both object-centered and retinotopic properties of the stimuli. DTIC

N95-17972 Technische Univ., Delft (Netherlands).
APPLICATIONS OF QUATERNIONS TO DYNAMICAL SIMULATION, COMPUTER GRAPHICS AND BIOMECHANICS Ph.D. Thesis [TOEPASSINGEN VAN QUATERNIONEN OP DYNAMISCHE SIMULATIE, COMPUTER GRAPHICS EN BIOMECHNIKA]
J. R. Mebius 11 Jan. 1994 282 p Limited Reproducibility: More than 20% of this document may be affected by microfiche quality
(PB94-201456) Copyright Avail: Issuing Activity

At the heart of this thesis is the ARTIBODIES system for computer-aided modeling and visualization of spatial articulated bodies. Spatial rotations and orientations are in the ARTIBODIES system represented by quaternions. General spatial displacements are represented as a rotation followed by a translation. Chapter 2 contains a group-theoretic treatment of the concepts of location, position, and orientation. Chapters 3 - 6 contain a construction of the theory of quaternions aimed at the representation of spatial rotations by quaternions. Some applications of the ARTIBODIES system to orthopedics, dance and ballet, and sign languages for the deaf are treated in Chapter 10. The application to dynamical simulation, in particular to the simulation of the rotation of a rigid body about a fixed point, is treated extensively in Chapter 11. An application of quaternions to computer graphics, viz. to the problem of the generation of a smooth spatial rotational motion passing through prescribed orientations at prescribed times, the rotation animation problem, is the subject of Chapter 7. In Chapter 8 a kinematical interpretation of one of the geometrical aspects of Chapter 7 is presented. NTIS

N95-17978# Argonne National Lab., IL.
A DOMAIN DECOMPOSITION ALGORITHM FOR ELLIPTIC PROBLEMS IN THREE DIMENSIONS
B. F. Smith 1994 14 p
(Contract W-31-109-eng-38)
(DE94-019265; ANL/MCS/PP-71520) Avail: CASI HC A03/MF A01

Most domain decomposition algorithms have been developed for problems in two dimensions. One reason for this is the difficulty in devising a satisfactory, easy-to-implement, robust method of providing global communication of information for problems in three dimensions. Several methods that work well in two dimensions do not perform satisfactorily in three dimensions. A new iteractive substructuring algorithm for three dimensions is proposed. It is shown that the condition number of the resulting preconditioned problem is bounded independently of the number of subdomains and that the growth is quadratic in the logarithm of the number of degrees of freedom associated with a subdomain. The condition number is also bounded independently of the jumps in the coefficients of the differential equation between subdomains. The new algorithm also has more potential parallelism than the iterative substructuring methods previously proposed for problems in three dimensions. DOE

N95-18000 Technische Hogeschool, Twente (Netherlands). Dept. of Computer Science.
ALTERNATIVE FORMULATION OF COCKE-YOUNGER-KASAMI'S ALGORITHM
P. R. J. Asveld Dec. 1993 7 p Limited Reproducibility: More than 20% of this document may be affected by microfiche quality
(PB94-202751; Memo-INF-93-48) Avail: CASI HC A02

We provide a reformulation of Cocke-Younger-Kasami's algorithm for recognizing context-free languages in which there are no references either to indices of table entries or to the length of the input string. Some top-down analogues of this functional approach are discussed as well. NTIS

N95-18013 Naval Postgraduate School, Monterey, CA.
LINEAR OPTIMIZATION AND IMAGE RECONSTRUCTION M.S. Thesis
Christopher A. Rhoden Jun. 1994 110 p Limited Reproducibility: More than 20% of this document may be affected by microfiche quality
(AD-A283641) Avail: Issuing Activity (Defense Technical Information Center (DTIC))

The Simplex algorithm, developed by George B. Dantzig in 1947 represents a quantum leap in the ability of applied scientists to solve complicated linear optimization problems. Subsequently, its utility in solving finite models, including applications in transportation, production planning, and scheduling, have made the algorithm an indispensable tool to many operations researchers. This thesis is primarily an exploration of the simplex algorithm, and a discussion of the utility of the algorithm in unconventional optimization problems. The mathematical theory upon which the algorithm is based and a general description of the algorithm are presented. The reader is assumed to have little exposure to convexity, duality, or the Simplex algorithm itself. More important to the thesis are the examples that accompany the discussion of the Simplex algorithm. Herein are a variety of unusual applications for the algorithm, including applications in infinite dimensional vector spaces, uniform approximation, and computer assisted tomographic image reconstruction. These examples serve both to facilitate a better understanding of the algorithm, and to present it in unusual settings. DTIC

N95-18015 Naval Postgraduate School, Monterey, CA.
IMPROVING SOFTWARE CHARACTERISTICS OF A REAL-TIME SYSTEM USING REENGINEERING TECHNIQUES M.S. Thesis
Scott A. Book Mar. 1994 117 p Limited Reproducibility: More than 20% of this document may be affected by microfiche quality
(AD-A283659) Avail: Issuing Activity (Defense Technical Information Center (DTIC))

The major problem addressed by this research is how to improve an existing real-time software system's readability, maintainability, stability and portability using reengineering techniques. A fundamental portion of the Model-based Mobile robot Language (MML) was the real-time system chosen as the basis for this study. The approach taken was to create a new system design. The new design was based on system specifications obtained by conducting static and dynamic analysis on the existing system. The results are that a new core system was implemented using a design that focused on creating independent software sub-systems while encapsulating data. Hardware dependencies were localized and assembly code minimized. The new system is easier to understand and modify and is portable to other hardware platforms. DTIC

N95-18017 Naval Postgraduate School, Monterey, CA.
A FORMAL METHOD FOR SEMANTICS-BASED CHANGE-MERGING OF SOFTWARE PROTOTYPES Ph.D. Thesis
David A. Dampier Jun. 1994 221 p Limited Reproducibility: More than 20% of this document may be affected by microfiche quality
(AD-A283668) Avail: Issuing Activity (Defense Technical Information Center (DTIC))

This dissertation addresses the need for a formal method to support the merging of changes in independently developed versions of a prototype in a computer-aided rapid prototyping system. The goal is to provide the prototype developer with the ability to combine independently developed enhancements to a prototype, check for consistency, and automatically update all derived versions of a prototype with changes made to the base version. A useful semantics-based method is provided for change-merging that is guaranteed to detect all conflicts. Prototype slicing is used to capture the affected parts of each variation and the preserved part of the base in both variations. We then combine the affected parts with the preserved part using our model, which includes the first use of Brouwerian Algebras to formalize the merging of hard real time constraints. Our Slicing Theorem guarantees that this method produces a prototype that correctly exhibits the significant behavior of each of the input versions, provided the changes do not conflict. The method achieves correctness by comparing the slice of the change-merged version with respect to each affected part against the same slice of the appropriate changed version. If the slices are the same, the change-merge is correct, otherwise a diagnostic message results. A preliminary conditional method for change-merging while programs is also provided that is strictly more accurate than previous methods. This dissertation contributes to computer-aided software maintenance by providing a model, algorithm and implementation for an automated change-merging tool for PSDL (Prototype System Descriptive Language) prototypes. Preliminary testing shows that this tool will enhance the ability of the prototype developer to deliver a prototype in less time by enabling more concurrency in the development effort. DTIC

N95-18018 Naval Postgraduate School, Monterey, CA.
A PLATFORM INDEPENDENT APPLICATION OF LUX ILLUMINATION PREDICTION ALGORITHMS M.S. Thesis
Michael T. Lester Jun. 1994 126 p Limited Reproducibility: More than 20% of this document may be affected by microfiche quality
(AD-A283669) Avail: CASI HC A07

Naval Aviators require prior knowledge of the time and location of astronomical phenomena in order to properly plan and execute combat and training operations during the hours of darkness using Night Vision Devices (NVD's). This thesis presents a computer application of illumination prediction algorithms which predict the time of selected astronomical phenomena. This computer program is platform independent (given the proper libraries), event-driven, object-oriented, and utilizes a Graphical User Interface (GUI). Using this application, operators in the field will be able to determine the time of selected phenomena and the quantity of illumination, measured in Lux, for a given time and date. DTIC

N95-18030# Unisys Corp., Reston, VA.
PORTABLE, REUSABLE, INTEGRATED SOFTWARE MODULES (PRISM) DOCUMENTATION LIBRARY MODEL DOCUMENT RELEASE 1.0: CENTRAL ARCHIVE FOR REUSABLE DEFENSE SOFTWARE (CARDS)
Aleisa Petracca and Les Hayhurst 3 Dec. 1993 41 p
(Contract F19628-93-C-0130)
(AD-A284567; STARS-VC-B015/000/00) Avail: CASI HC A03/MF A01

This Portable, Reusable, Integrated Software Modules (PRISM) Documentation Library Release 1.0 Model Document was created by the Central Archive for Reusable Defense Software (CARDS) Program to help disseminate PRISM documentation and knowledge. It represents the current state of the PRISM documentation library model. It is a 'living' document and will be updated with every library release. This document describes library modeling and examines modeling concepts and specialization/aggregation hierarchies. This document is specific to PRISM Documentation Library Model Release 1.0 in its description of document types, actual documents available, and future direction of this model. The intended audience is anyone desiring an understanding of the PRISM documentation library model and wanting a description of this current library release. The reader should have an understanding of CARDS and PRISM. DTIC

N95-18031# Unisys Corp., Reston, VA.
LIBRARY CAPABILITY DEMONSTRATION. CENTRAL ARCHIVE FOR REUSABLE DEFENSE SOFTWARE (CARDS)
Scott A. Hissam 30 Sep. 1993 30 p
(Contract F19628-93-C-0130)
(AD-A284568; STARS-VC-B018/001/00) Avail: CASI HC A03/MF A01

This demonstration was developed under the Central Archive for Reusable Defense Software (CARDS) Program to help facilitate advances in software reuse methods. This demonstration illustrates techniques for incorporating commercial off-the-shelf (COTS) software into the CARDS reuse library framework. DTIC

N95-18032# Unisys Corp., Reston, VA.
LIBRARY CAPABILITY DEMONSTRATION. CENTRAL ARCHIVE FOR REUSABLE DEFENSE SOFTWARE (CARDS)
Daniel Nichols 24 Mar. 1994 21 p
(Contract F19628-93-C-0130)
(AD-A284569; STARS-VC-B018/004/00) Avail: CASI HC A03/MF A01

This is the fourth library capability demonstration under this contract. Each demonstration provides information about the Central Archive for Reusable Defense Software (CARDS) operational library capabilities. The goals of this demonstration are to show how CARDS: (1) made the command center library (CCL) model easier to navigate; (2) made the CCL model easier to conceptualize; (3) made the CCL model more maintainable; and (4) improved the CCL performance in the reuse library framework (RLF) graphical browser. DTIC

N95-18033# Unisys Corp., Reston, VA.
LIBRARY DEVELOPMENT HANDBOOK. CENTRAL ARCHIVE FOR REUSABLE DEFENSE SOFTWARE (CARDS)
Brian Curfman, Steven Lewis, and Jay Reddy 29 Oct. 1993 101 p
(Contract F19628-93-C-0130)
(AD-A284570; STARS-VC-B005/001/00) Avail: CASI HC A06/MF A02

The process of developing a domain-oriented reuse library is elaborate. This library development handbook provides an overview of the phases involved in developing such a library: domain analysis, library encoding, and library population. This handbook presents a generic library population process that has been developed by the Central Archive for Reusable Defense Software library development team. This handbook enumerates specific instructions and examples for populating a domain-oriented reuse library, based on this library population process. We are currently assessing the implications of legal issues on our policies and procedures. Appropriate risk reduction procedures will be detailed in subsequent releases. DTIC

N95-18034# Unisys Corp., Reston, VA.
LIBRARY CAPABILITY DEMONSTRATION. CENTRAL ARCHIVE FOR REUSABLE DEFENSE SOFTWARE (CARDS)
Gene Humphrey and Brian Massey 28 Jan. 1994 28 p
(Contract F19628-93-C-0130)
(AD-A284572; STARS-VC-B018/002/00) Avail: CASI HC A03/MF A01

This demonstration was developed under the Central Archive for Reusable Defense Software (CARDS) Program to demonstrate CARDS ability to support heterogeneous computing environments of the DoD. This demonstration illustrates the capability for a remote user to view, via the library, a demonstration of a component running on a non-Unix platform, such as a 386/486 class PC. DTIC

N95-18079 Illinois Univ., Urbana, IL. Center for Reliable and High-Performance Computing.
A NOVEL SYSTEM LEVEL APPROACH TO FAULT TOLERANCE IN DISTRIBUTED MEMORY MULTICOMPUTERS Final Report, 1 Oct. 1990 - 30 Sep. 1993
Prithviraj Banergee Sep. 1994 13 p Limited Reproducibility: More than 20% of this document may be affected by microfiche quality
(Contract N00014-91-J-1096)
(AD-A284729) Avail: CASI HC A03

The objective of this research was to develop new, cost-effective techniques for fault tolerance in multicomputer architectures. The requirements for high performance and fault tolerance are seemingly contradictory: parallel architectures and algorithms developed for high performance attempt to achieve maximum utilization of each of the processors, while fault tolerance requires redundant computations and checks to ensure that the results of the applied to highly parallel multicomputer architectures. Our unique approach to achieve fault tolerance in multicomputer parallel architectures is to use an algorithm-based tolerance (ABFT) technique which is an on-line system-level method for detection of faults followed by a system level approach to reconfiguration and recovery of a parallel processor system. DTIC

N95-18089 Electronics Research Lab., Salisbury (Australia).
A VISUAL APPROACH TO THE ANALYSIS OF LARGE SOFTWARE SYSTEMS
Philip Dart, Gina Kingston, Rudi Vernik, and Stefan Landherr Jul. 1994 25 p Limited Reproducibility: More than 20% of this document may be affected by microfiche quality
(AD-A285440; ERL-0838-RN; DODA-AR-009-029) Avail: CASI HC A03

Analyzing a large software system is a difficult and time consuming task, even with current automated assistance. Measures taken of software systems may be too abstract, applicable only to a particular class of system or simply too subjective. This paper examines problems associated with using existing tools and measures, and then presents an alternative approach to the analysis of large software systems based on system views that have been designed for a specific analysis task. We detail various abstract and concrete views of static system structure, and describe a software analysis environment developed to experiment with this approach. The concepts reported in this paper were developed during early enabling research undertaken as part of the SMAT task. Many of the concepts have already been included in other components of this task, including the SEE-Ada tool for software evaluation. DTIC

N95-18155# Carnegie-Mellon Univ., Pittsburgh, PA. Dept. of Computer Science.
REPRESENTING AND REFORMULATING DIAGONALIZATION METHODS
Erica Melis Jul. 1994 21 p
(AD-A283916; CMU-CS-94-174) Avail: CASI HC A03/MF A01

Finding an appropriate representation of planning operators is crucial for theorem provers that work with proof planning. We show a new representation of operators and demonstrate how diagonalization can be represented by operators. We explain how a diagonalization operator used

in one proof-plan can be analogically transferred to an operator used in another proof-plan. Finally, we find an operator that is common to all the proof-plans and thus might be considered as the Diagonal Method. DTIC

N95-18161# Army Construction Engineering Research Lab., Champaign, IL.

R.MAPCALC: AN ALGEBRA FOR GIS AND IMAGE PROCESSING Final Report

Michael Shapiro and James Westervelt Apr. 1994 27 p

(AD-A283923; USACERL-TR-EC-94/13) Avail: CASI HC A03/MF A01

As geographic information systems are enhanced with more robust query capabilities, they evolve from basic spatial data storage, retrieval, and display systems to more powerful spatial modeling systems. Languages that empower a user to design and create spatial models will advance this development even further. This study describes a map algebra language that can form the foundation for overlay and neighborhood analyses in both raster geographic information systems and image-processing systems. The language combines maps and images in expressions with arithmetic and logical operators and mathematical functions to produce new maps and images. This algebra has been implemented in the Geographical Resources analysis Support System r.mapcalc module. The language syntax is first described and then examples relevant to geographic information systems and image-processing applications are presented. DTIC

N95-18343# Unisys Corp., Reston, VA. Technology Center.

TECHNICAL CONCEPT DOCUMENT. CENTRAL ARCHIVE FOR REUSABLE DEFENSE SOFTWARE (CARDS)

James L. Estep and Scott A. Hissam 28 Feb. 1994 78 p

(Contract F19628-93-C-0130)

(AD-A284430; STARS-VC-B009/001/00) Avail: CASI HC A05/MF A01

The Central Archive for Reusable Defense Software (CARDS) program is a concerted DOD initiative to transition advances in the techniques and technology of library-aided, architecture-centric, domain-specific software reuse into mainstream DOD software procurement. This technology transition effort involves the development of a domain-specific reuse library for researching technologies and methodologies for creating reuse libraries. This document describes the technical concepts employed towards the development of the CARDS Command Center Library. It is an update to a previous version published on February 26, 1993. CARDS views a reuse library as reusable software components, a library model and supporting library applications. This view, and it's consequences on library development are presented in this document. A discussion of model-based reuse library infrastructure presents a model-based view of library development, with an emphasis on distinctions between domain and library modeling. The component qualification process is presented as an integral part of the library development process. Modeling of the command center library has evolved to support development and integration of various reuse library applications. The CARDS system composition and component qualification tools are discussed. DTIC

N95-18344# Unisys Corp., Reston, VA. Technology Center.

LIBRARY OPERATIONS POLICIES AND PROCEDURES. VOLUME 2: CENTRAL ARCHIVE FOR REUSABLE DEFENSE SOFTWARE (CARDS)

Ricardo Cortes and Mark Quick 28 Feb. 1994 173 p

(Contract F19628-93-C-0130)

(AD-A284431; STARS-VC-B004/002/01-Vol-2) Avail: CASI HC A08/MF A02

The Central Archive for Reusable Defense Software (CARDS) Program is a DOD initiative to transfer the technologies of library-assisted, domain-specific reuse into other DOD software procedures and procurements. Volume Two of the library Operation Policies and Procedures (LOPP) provides detailed operating instructions for day-to-day operation and maintenance of the library. Volume Two targets the technical individual who will be implementing the policies and procedures of the LOPP, Volume One. Volume Two provides detailed descriptions of the day-to-day tasks for operating and maintaining a reuse library. This document also provides quick access to the specific areas or interest and is designed to allow the reader to retrieve only information specific to their area of interest or concern. In addition to outlining the CARDS daily operations, Volume Two contains those forms reference. In Volume One. Volume Two focuses on the CARDS library as its model implementation environment. To allow the library implementor to use this document as a reference guide, Volume Two is intentionally organized to be free of a specific management structure. DTIC

N95-18354# Argonne National Lab., IL.

FAST NUMERICAL DETERMINATION OF SYMMETRIC SPARSITY PATTERNS

R. G. Carter (Minnesota Univ., Minneapolis, MN.) 1994 28 p

(Contract W-31-109-eng-38)

(DE94-016344; ANL/MCS/PP-77610) Avail: CASI HC A03/MF A01

The author considers a function g: R(sup n) (yields) R(sup n) for which the Jacobian is symmetric and sparse. Such functions often arise, for instance, in numerical optimization, where g is the gradient of some objective function f so that the Jacobian of g is the Hessian of f. In many such applications one can generate extremely efficient algorithms by taking advantage of the sparsity structure of the problem if this pattern is known a priori. Unfortunately, determining such sparsity structures by hand is often difficult and prone to error. If one suspects a mistake has been made, or if g is a 'black box' so that the true structure is completely unknown, one often has no alternative but to compute the entire matrix by finite differences - a prohibitively expensive task for large problems. The author shows that it is possible to numerically determine symmetric sparsity patterns using a relatively small number of g evaluations. Numerical results are shown for n up to 100,000 in which all nonzeros in the Jacobian are correctly identified in about one-hundredth of the time required to estimate the sparsity structure by a full finite difference calculation. When a good initial guess for the sparsity structure is available, numerical results are presented for n up to 500,000, in which all missing nonzeros are correctly located almost five-thousand times faster than would be possible with a full finite difference calculation. DOE

N95-18364# Carnegie-Mellon Univ., Pittsburgh, PA. Software Engineering Inst.

MAPPING A DOMAIN MODEL AND ARCHITECTURE TO A GENERIC DESIGN Final Report

A. S. Peterson and Jay L. Stanley, Jr. May 1994 142 p

(Contract F19628-90-C-0003)

(AD-A283747; CMU/SEI-94-TR-8; ESC-TR-94-008) Avail: CASI HC A07/MF A02

In contrast to the number of reports on domain analysis, little work has been done in describing the utilization of domain analysis results in the development of generic designs for building applications in a domain. This report describes a process for mapping domain information in Feature-Oriented Domain Analysis (FODA) into a generic design for a domain. The design includes supporting code components that conform to the Object Connection Architecture (OCA), a model for structuring software systems. A process for the use of the design in implementing applications is included. The processes and products described herein augment the final phase of domain analysis (or engineering) described in the original FODA report. This report also documents the continuing work of applying FODA to the movement control domain. The design and Ada code examples for the domain used in the document are from prototype software, created in part to test the processes presented. DTIC

N95-18365# Wright Lab., Wright-Patterson AFB, OH.

UNIVERSAL WIND TUNNEL DATA ACQUISITION AND REDUCTION SOFTWARE Final Report, Jan. 1990 - Apr. 1993

Glenn W. Williams Jan. 1994 128 p

(AF Proj. 2404)

(AD-A283897; WL-TR-94-3063) Avail: CASI HC A07/MF A02

A software system was designed to support the data acquisition and reduction requirements of six wind tunnels (three continuous flow and three blow down) and a force/pressure laboratory. In order to make it easier for users to identify and select the command options available, a drop down menu was developed for use as the primary interface between the operator and the software. This drop down menu was developed before window terminals were available, and thus it works on VT100 type terminals. Because some operations/procedures are recurring during a specific test and include a series of menu commands, a macro feature was included as a user maintainable function in order to reduce a set of commands/operations to a single keystroke. The facility hardware

configuration and data output formats are coded into the system by editing text files, no compilation or linking is required. DTIC

N95-18419 Unisys Corp., Reston, VA.
ENGINEER'S HANDBOOK. CENTRAL ARCHIVE FOR REUSABLE DEFENSE SOFTWARE (CARDS)
Chris Fronczek, George Jackelen, and Stephen Riesbeck 28 Feb. 1994 89 p Limited Reproducibility: More than 20% of this document may be affected by microfiche quality
(Contract F19628-93-C-0130)
(AD-A284341; STARS-VC-B002/002/00) Avail: Issuing Activity (Defense Technical Information Center (DTIC))

This Engineer's Handbook was developed under the Central Archive for Reusable Defense Software (CARDS) Program to help facilitate advances in software reuse techniques and technologies. This document provides guidance to government System Program Office (SPO) Engineers on envisioned changes to their duties and responsibilities as domain-specific software reuse becomes incorporated into mainstream DOD system/software acquisition and engineering processes. DTIC

N95-18420 Unisys Corp., Reston, VA.
ACQUISITION HANDBOOK: UPDATE. COMPREHENSIVE APPROACH TO REUSABLE DEFENSIVE SOFTWARE (CARDS)
Leandro V. Delgado, Robert J. Bowes, Theresa R. Huber, and Robert O. Saisi 25 Mar. 1994 199 p Limited Reproducibility: More than 20% of this document may be affected by microfiche quality
(Contract F19628-93-C-0130)
(AD-A284342; STARS-VC-B011/001/00) Avail: CASI HC A09

The Acquisition Handbook is aimed towards all Government Program Managers and their support personnel, such as Contracting Officers and Administrators, procurement attorneys, and program control, involved in systems, subsystems and component acquisition and maintenance. The concepts discussed assume that the reader has at least three years experience in acquisition. This guidebook will assist them in incorporating software reuse into all phases of the acquisition life cycle, from concept exploration to Post Deployment Software Support (PDSS). It is not a 'cookbook' for every possible reuse issue or strategy, rather it is meant to help you develop and tailor reuse programs. The goal of the Acquisition Handbook is to encourage software reuse during the acquisition and maintenance portions of the life cycle process, ranging from planning the acquisition strategy through awarding the contract to managing the effort and follow-on support. Software reuse guidance will be presented by providing methods, examples, recommendations and techniques to implement various reuse strategies throughout the acquisition life cycle. The implications and affects of software reuse on the technical, management, cost, schedule, and risk aspects of a program/system during the acquisition process will be the foundation of this document. DTIC

N95-18421# Unisys Corp., Reston, VA. Technology Center.
TRAINING PLAN. CENTRAL ARCHIVE FOR REUSABLE DEFENSE SOFTWARE (CARDS)
Harry J. Facemire and Kerrin Smith 29 Jan. 1994 138 p
(Contract F19628-93-C-0130)
(AD-A284343; STARS-VC-B003/001/00) Avail: CASI HC A07/MF A02

The Central Archive for Reusable Defense Software (CARDS) Training Plan serves as a comprehensive guide for creating training courses and training materials on domain-specific reuse for Department of Defense (DOD) organizations, DOD contractors, system engineers, and university professors. The Training Plan provides guidance for conducting three different domain-specific software reuse training courses for four different audiences. The intent of the courses in the Training Plan is to demonstrate how software reuse can reduce development and maintenance time and costs, reduce project risks, and increase productivity. DTIC

N95-18422# Unisys Corp., Reston, VA. Technology Center.
FRANCHISE PLAN. CENTRAL ARCHIVE FOR REUSABLE DEFENSE SOFTWARE (CARDS)
Rose Marie Armstrong 28 Feb. 1994 75 p
(Contract F19628-93-C-0130)
(AD-A284344; STARS-VC-B010/001/00) Avail: CASI HC A04/MF A01

The Central Archive for Reusable Defense Software (CARDS) Franchise Plan is a tool to help management, with assistance from CARDS, develop a detailed, tailored implementation plan which will prepare the organization to begin the process of software reuse. The CARDS Franchise Plan is targeted toward management level personnel and is meant to introduce reuse and obtain assistance from programs such as CARDS to do reuse. The Franchise Plan presents a planning processes for building a reuse infrastructure. To establish a reuse infrastructure the Franchise Plan will describe the steps that need to be accomplished: (1) Establish management commitment for reuse; (2) Develop an organizational assessment which defines an organization's current state of affairs, and assesses its potential for reuse; (3) Develop a requirement/implementation study which determines the organization's requirements for instituting reuse; and (4) Develop a reuse implementation plan which describes those steps necessary to implement a reuse infrastructure. DTIC

N95-18423# Unisys Corp., Reston, VA. Technology Center.
LIBRARY USER'S GUIDE. COMPREHENSIVE APPROACH TO REUSABLE DEFENSIVE SOFTWARE (CARDS)
Tom Bock 24 May 1994 20 p
(Contract F19628-93-C-0130)
(AD-A284345; STARS-VC-B006/003/00) Avail: CASI HC A03/MF A01

This Command Center Library (CCL) User's Guide was developed under the Comprehensive Approach to Reusable Defense Software (CARDS) Program to help disseminate the Portable Reusable Integrated Software Modules (PRISM) Program documentation and knowledge. It represents the current state of the CCL Models. It is a 'living' document and will be updated with every CCL release. This document describes the method needed to access the CCL Models. This Guide is specific to CCL Model Release 4.0. The intended audience is anyone desiring an understanding of, or wanting access to, the current release of the CCL Models. DTIC

N95-18437 Cognitech, Inc., Santa Monica, CA.
RECONSTRUCTION OF SHAPES FROM SHADING AND SHAPE BASED IMAGE RECONSTRUCTION USING MODERN NONLINEAR ANALYSIS Final Report, 15 Sep. 1991 - 29 Apr. 1994
Stanley Osher 20 Jun. 1994 19 p Limited Reproducibility: More than 20% of this document may be affected by microfiche quality
(Contract F49620-91-C-0083)
(AD-A284107; TR-31; AFOSR-94-0518TR) Avail: CASI HC A03

Shape based restoration, frame fusion, stereo matching, reconstruction of shapes from shading, and photometric stereo and video processing were successfully integrated into a partial differential equations based framework. Tools from the theory of viscosit/ solutions, nonoscillatory approximations, and calculus of variations were used to develop state-of-the-art algorithms in these areas. DTIC

N95-18447 Unisys Corp., Reston, VA.
PORTABLE, REUSABLE, INTEGRATED SOFTWARE MODULES (PRISM) DOCUMENTATION LIBRARY VERSION DESCRIPTION DOCUMENT RELEASE 1.0. CENTRAL ARCHIVE FOR REUSABLE DEFENSE SOFTWARE (CARDS)
George Jackelen and Larry McCutchan 3 Dec. 1993 27 p Limited Reproducibility: More than 20% of this document may be affected by microfiche quality
(Contract F19628-93-C-0130)
(AD-A284571; STARS-VC-B007/000/01) Avail: CASI HC A03

This Version Description Document has been prepared for CARDS (Central Archive for Reusable Defense Software) Portable, Reusable, Integrated Software Modules (PRISM) Documentation Library (PDL) Release 1.0 and describes: (1) Since there were no previous release, there are no changes; (2) Known problems and work arounds (where possible); (3) Installation instructions; (4) A list of files for this release; and (5) A release tape file list. This VDD is part of the CARDS library release package which includes the actual release, a library user's manual, and a library model document. DTIC

N95-18449 Unisys Corp., Reston, VA.
METRICS CONCEPT REPORT. CENTRAL ARCHIVE FOR REUSABLE DEFENSE SOFTWARE (CARDS)
Anita Berns 31 Mar. 1994 47 p Limited Reproducibility: More than 20% of this document may be affected by microfiche quality
(Contract F19628-93-C-0130)
(AD-A284573; STARS-VC-B019/004/00) Avail: CASI HC A03

In February 1993 the Defense Information Systems Agency/Center for Information Management (DISA/CIM) sponsored a Software Reuse Metrics Workshop. The primary goal of these meetings was to develop a set of questions that would indicate what measurements should be collected in support of the DISA/CIM Software Reuse Program. These proceedings indicate that DISA/CIM's Software Reuse Metrics Plan will be used as a foundation for developing a DOD Software Reuse Metrics Plan. The DISA/CIM plan serves as a major input into the DOD-wide plan, and DISA/CIM will be conducting pilot prototypes of their recommendations. The CARDS (Central Archive for Reusable Defense Software) metrics efforts should also provide valuable information that can be feed into the DOD-wide Software Reuse Metrics Plan. As stated in the DOD Software Vision and Strategy Document, the DOD must establish a baseline upon which to gauge success and measure improvement that serve as a basis for comparison among alternative approaches. Therefore, the CARDS metrics effort is two-fold: (1) use metrics within the CARDS Program to measure and improve processes, products, and services; and (2) monitor and provide possible contributions to the DOD Software Reuse Metrics Plan. DTIC

N95-18450 Unisys Corp., Reston, VA.

LIBRARY CAPABILITY DEMONSTRATION. CENTRAL ARCHIVE FOR REUSABLE DEFENSE SOFTWARE (CARDS)

Jim Petro 29 Jan. 1994 26 p Limited Reproducibility: More than 20% of this document may be affected by microfiche quality

(Contract F19628-93-C-0130)

(AD-A284574; STARS-VC-B018/003/00) Avail: CASI HC A03

This is the third library capability demonstration under this contract. Each demonstration provides information about the Central Archive for Reusable Defense Software (CARDS) operational library capabilities. The goal of this demonstration are to show how CARDS: (1) Has simplified access to assets; (2) Has captured the Portable, Reusable, Integrated Software Modules (PRISM) Program concepts in the CARDS Command Center Library (CCL); and (3) Provides access to prototypes of CARDS framework enhancements. DTIC

N95-18487*# Institute for Computer Applications in Science and Engineering, Hampton, VA.

A SIMPLE HYPERBOLIC MODEL FOR COMMUNICATION IN PARALLEL PROCESSING ENVIRONMENTS Final Report

Ion Stoica (Old Dominion Univ., Norfolk, VA.), Florin Sultan (Old Dominion Univ., Norfolk, VA.), and David Keyes (Old Dominion Univ., Norfolk, VA.) Hampton, VA NASA Sep. 1994 40 p Submitted for publication

(Contract NAS1-19480; RTOP 505-90-52-01)

(NASA-CR-195984; NAS 1.26:195984; ICASE-94-78) Avail: CASI HC A03/MF A01

We introduce a model for communication costs in parallel processing environments called the 'hyperbolic model,' which generalizes two-parameter dedicated-link models in an analytically simple way. Dedicated interprocessor links parameterized by a latency and a transfer rate that are independent of load are assumed by many existing communication models; such models are unrealistic for workstation networks. The communication system is modeled as a directed communication graph in which terminal nodes represent the application processes that initiate the sending and receiving of the information and in which internal nodes, called communication blocks (CBs), reflect the layered structure of the underlying communication architecture. The direction of graph edges specifies the flow of the information carried through messages. Each CB is characterized by a two-parameter hyperbolic function of the message size that represents the service time needed for processing the message. The parameters are evaluated in the limits of very large and very small messages. Rules are given for reducing a communication graph consisting of many to an equivalent two-parameter form, while maintaining an approximation for the service time that is exact in both large and small limits. The model is validated on a dedicated Ethernet network of workstations by experiments with communication subprograms arising in scientific applications, for which a tight fit of the model predictions with actual measurements of the communication and synchronization time between end processes is demonstrated. The model is then used to evaluate the performance of two simple parallel scientific applications from partial differential equations: domain decomposition and time-parallel multigrid. In an appropriate limit, we also show the compatibility of the hyperbolic model with the recently proposed LogP model. Author

N95-18564# California Univ., Los Angeles, CA. Flight Systems Research Center.

MINIMAL TIME DETECTION ALGORITHMS AND APPLICATIONS TO FLIGHT SYSTEMS

Alexander Tartakovsky Dec. 1993 86 p

(TR-2-FSRC-93) Avail: CASI HC A05/MF A01

The report focuses on sequential algorithms to detect changes in statistical models of observed random data when these occur at unknown points in time and statistical properties of observations after change occurrence depend on change time. Besides it is assumed that the samples are non-identically distributed and the amount of a change is unknown. The development of well-known results in change-point detection problems for such a model has great importance for various applications, for example for testing of flight systems. A maximum likelihood detection algorithm (with respect to an unknown change time) is investigated for independent non-identically distributed observations. It is proved that this procedure is asymptotically optimal with respect to expect detection delay (i.e., is a minimal time-detection algorithm) when the mean time until false alarm (or between false detections) tends to infinity. Several asymptotically optimal and non-optimal simple modifications of the maximum likelihood algorithm are also considered. For the case of an unknown amount of change two approaches are proposed. The first one consists of the testing of multiple hypotheses. The second approach is based on the use of the double maximum likelihood principle both for unknown change in time and unknown parameter after change. An asymptotically optimal (minimal time) multialternative sequential algorithm is constructed and analyzed. In contrast to the adaptive algorithm the multialternative one ensures minimal detection delay only for several isolated points, but does not require estimation of an unknown amount and hence can be used for moderate sample size. Finally, proposed minimal time detection algorithms are applied in the problem of identification of aircraft system parameters from flight test data during flight control. Author

N95-18584*# Institute for Computer Applications in Science and Engineering, Hampton, VA.

SCALABILITY OF PARALLEL SPATIAL DIRECT NUMERICAL SIMULATION CODE ON IBM SP1 PARALLEL SUPERCOMPUTER Final Report

Ulf R. Hanebutte, Ronald D. Joslin (National Aeronautics and Space Administration. Langley Research Center, Hampton, VA.), and Mohammad Zubair (IBM Watson Research Center, Yorktown Heights, NY.) Hampton, VA NASA Aug. 1994 20 p Submitted for publication

(Contract NAS1-19480; RTOP 505-90-52-01)

(NASA-CR-194975; NAS 1.26:194975; ICASE-94-80) Avail: CASI HC A03/MF A01

The implementation and the performance of a parallel spatial direct numerical simulation (PSDNS) code are reported for the IBM SP1 supercomputer. The spatially evolving disturbances that are associated with laminar-to-turbulent in three-dimensional boundary-layer flows are computed with the PS-DNS code. By remapping the distributed data structure during the course of the calculation, optimized serial library routines can be utilized that substantially increase the computational performance. Although the remapping incurs a high communication penalty, the parallel efficiency of the code remains above 40% for all performed calculations. By using appropriate compile options and optimized library routines, the serial code achieves 52-56 Mflops on a single node of the SP1 (45% of theoretical peak performance). The actual performance of the PSDNS code on the SP1 is evaluated with a 'real world' simulation that consists of 1.7 million grid points. One time step of this simulation is calculated on eight nodes of the SP1 in the same time as required by a Cray Y/MP for the same simulation. The scalability information provides estimated computational costs that match the actual costs relative to changes in the number of grid points. Author

N95-18652# Sandia National Labs., Albuquerque, NM.

ALARM ANNUNCIATION IN A GRAPHICAL ENVIRONMENT

D. G. Adams 1994 4 p Presented at the Institute of Nuclear Materials Management Annual Meeting, Naples, FL, 17-20 Jul. 1994

(Contract DE-AC04-94AL-85000)

(DE94-015761; SAND-94-1156C; CONF-940748-14) Avail: CASI HC A01/MF A01

Well-designed graphical user interfaces, such as Microsoft

Windows(trademark) or UNIX(trademark) -- based X-Windows, provide a capability for enhanced display of security alarm information. Conversely, a poorly designed interface can quickly overwhelm an operator. This paper describes types of graphical information that can be displayed and offers guidance on how to best display that information. Limits are proposed for the complexity of the user interface, and guidelines are suggested for the display of maps and sensors. DOE

N95-18668 Selskapet for Industriell og Teknisk Forskning, Trondheim (Norway). Div. for Information Technology.
SICOMP, THE SINTEF DATA COMPRESSION LIBRARY (VERSION 1.0) REFERENCE MANUAL
E. Arge and C. Tarrou 7 Jan. 1994 46 p
(PB94-207107; STF33-A94001) Avail: Issuing Activity (National Technical Information Service (NTIS))

SICOMP is a toolkit for data compression. More precisely, it is a collection of C routines that applies to certain kinds of data. Two general types of data are handled by SICOMP, that is, either vectors of 2D points representing piecewise linear curves, or matrices of real numbers representing surfaces on uniform grids. By data compression we mean manipulating the data in such a way that the storage requirements decrease. The routines for the compression of piecewise linear curves consist of implementations based on well known methods. These methods produce vectors of 2D points representing piecewise linear curves containing fewer points than the original curves. In addition, routines for compact representation of these 2D points, based on quantization, is implemented. The part of SICOMP which handles compression of uniform grids consists of routines based on decomposition techniques, as well as routines for quantization and Huffman encoding. The manual describes the main routines in SICOMP. Most of the descriptions provide examples of use. NTIS

N95-18676 Carnegie-Mellon Univ., Pittsburgh, PA. Dept. of Computer Science.
PROGRAM VERIFICATION FOR OPTIMIZED BYTE COPY
Edoardo S. Biagioni Jul. 1994 21 p Limited Reproducibility: More than 20% of this document may be affected by microfiche quality
(Contract F19628-91-C-0168; ARPA Order 8313)
(AD-A283915; CMU-CS-94-172) Avail: CASI HC A03

We present a program to copy bytes, together with a formal specification and a proof that the code satisfies the specification. The program, which is in the critical path for a network implementation, has been tuned carefully over a period of time; the proof covers the entire program, and is easily updated if the program is modified. The program is written in the Standard ML programming language and was produced as part of the Fox Project implementation of the TCP/IP protocol suite. DTIC

N95-18899*# National Aeronautics and Space Administration. Langley Research Center, Hampton, VA.
DYNAMIC STABILITY INSTRUMENTATION SYSTEM (DSIS). VOLUME 1: HARDWARE DESCRIPTION
L. Jordan, T. S. Daniels, D. A. Hare, R. P. Boyden, and D. A. Dress Nov. 1994 91 p
(RTOP 505-59-54-02)
(NASA-TM-109160-Vol-1; NAS 1.15:109160-Vol-1) Avail: CASI HC A05/MF A01

This paper is a hardware description manual for the Dynamic Stability Instrumentation System that is used in specific NASA Langley wind tunnels. The instrumentation system performs either a synchronous demodulation or a fast Fourier transform on dynamic balance strain gage signals, and ultimately computes aerodynamic coefficients. The DSIS consists of a double rack of instruments, a remote motor-generator set, two special stings each with motor driven shafts, and specially designed balances. The major components in the instrumentation rack include a personal computer, digital signal processor microcomputers, computer-controlled signal conditioners, function generator, digital multimeter, and an optional fast Fourier transform analyzer. Author

N95-18924 Boston Univ., MA.
A GENERAL THEORY OF SEMI-UNIFICATION Ph.D. Thesis
Said Jahama 1994 112 p
Avail: Univ. Microfilms Order No. DA9415025

An extended study of the theory of semi-unification is presented. Various restrictions on the terms allowed for substitution give rise to different cases of semi-unification. Semi-unification on finite and regular terms has already been considered in the literature. This thesis introduces a general case of semi-unification where substitutions are allowed on non-regular terms, and the equivalence of this general case to a well-known undecidable data base dependency problem is proved, thus establishing the undecidability of general semi-unification. Type reconstruction for the simply typed lambda calculus with polymorphic recursion is closely related to semi-unification. It has already been proved that semi-unification on finite terms is equivalent to this type reconstruction problem when only finite types are permitted. The equivalence of semi-unification on regular terms to type reconstruction when recursive types are permitted is proved, which proves the undecidability of this type reconstruction problem. For reasons of language design, recursive types are sometimes restricted to be positive in the literature. The thesis also proves the equivalence of the type reconstruction problem with positive recursive types to a semi-unification problem where substitutions are restricted to some special regular terms. Also presented is a unified way of looking at the various problems of semi-unification, as well as a presentation of some properties that are common to all the cases of semi-unification. Differences between the cases of semi-unification are discussed. The principality issue and the solution set for those problems are studied. It is proved that semiunification on general terms has the principality property. Finally, a recursive inseparability result between semi-unifIcation on regular terms and semi-unification on general terms is presented. Dissert. Abstr.

N95-18931*# Institute for Computer Applications in Science and Engineering, Hampton, VA.
ON EXTENDING PARALLELISM TO SERIAL SIMULATORS Final Report
David Nicol (College of William and Mary, Williamsburg, VA.) and Philip Heidelberger (IBM Watson Research Center, Yorktown Heights, NY.) Dec. 1994 18 p Submitted for publication
(Contract NAS1-19480; RTOP 505-90-52-01; NSF CCR-92-01195)
(NASA-CR-195011; NAS 1.26:195011; ICASE-94-95) Avail: CASI HC A03/MF A01

This paper describes an approach to discrete event simulation modeling that appears to be effective for developing portable and efficient parallel execution of models of large distributed systems and communication networks. In this approach, the modeler develops submodels using an existing sequential simulation modeling tool, using the full expressive power of the tool. A set of modeling language extensions permit automatically synchronized communication between submodels; however, the automation requires that any such communication must take a nonzero amount off simulation time. Within this modeling paradigm, a variety of conservative synchronization protocols can transparently support conservative execution of submodels on potentially different processors. A specific implementation of this approach, U.P.S. (Utilitarian Parallel Simulator), is described, along with performance results on the Intel Paragon. Author

N95-19027*# Institute for Computer Applications in Science and Engineering, Hampton, VA.
EMPIRICAL STUDY OF PARALLEL LRU SIMULATION ALGORITHMS Final Report
Eric Carr (College of William and Mary, Williamsburg, VA.) and David M. Nicol (Carleton Coll., Northfield, MN.) Oct. 1994 16 p Submitted for publication
(Contract NAS1-19480; RTOP 505-90-52-01; NSF CCR-92-01195)
(NASA-CR-194995; NAS 1.26:194995; ICASE-94-87) Avail: CASI HC A03/MF A01

This paper reports on the performance of five parallel algorithms for simulating a fully associative cache operating under the LRU (Least-Recently-Used) replacement policy. Three of the algorithms are SIMD, and are implemented on the MasPar MP-2 architecture. Two other algorithms are parallelizations of an efficient serial algorithm on the Intel Paragon. One SIMD algorithm is quite simple, but its cost is linear in the cache size. The two other SIMD algorithm are more complex, but have costs that are independent on the cache size. Both the second and third SIMD algorithms compute all stack distances; the second SIMD algorithm is completely general, whereas the third SIMD algorithm presumes and takes advantage of bounds on the range of reference tags. Both MIMD algorithm implemented on the Paragon are general and compute all stack distances; they differ in one step that may affect their respective scalability. We

assess the strengths and weaknesses of these algorithms as a function of problem size and characteristics, and compare their performance on traces derived from execution of three SPEC benchmark programs. Author

N95-19028*# Institute for Computer Applications in Science and Engineering, Hampton, VA.
ON k-ARY n-CUBES: THEORY AND APPLICATIONS Final Report
Weizhen Mao (College of William and Mary, Williamsburg, VA.) and David M. Nicol (College of William and Mary, Williamsburg, VA.) Oct. 1994 30 p Submitted for publication
(Contract NAS1-19480; RTOP 505-90-52-01; NSF CCR-92-10372; NSF CCR-90-01195)
(NASA-CR-194996; NAS 1.26:194996; ICASE-94-88) Avail: CASI HC A03/MF A01

Many parallel processing networks can be viewed as graphs called k-ary n-cubes, whose special cases include rings, hypercubes and toruses. In this paper, combinatorial properties of k-ary n-cubes are explored. In particular, the problem of characterizing the subgraph of a given number of nodes with the maximum edge count is studied. These theoretical results are then used to compute a lower bounding function in branch-and-bound partitioning algorithms and to establish the optimality of some irregular partitions. Author

N95-19106# Unisys Corp., Reston, VA.
SOFTWARE TECHNOLOGY FOR ADAPTABLE, RELIABLE SYSTEMS (STARS). SOFTWARE ARCHITECTURE SEMINAR REPORT: CENTRAL ARCHIVE FOR REUSABLE DEFENSE SOFTWARE (CARDS)
H. J. Facemire, Aleisa Petracca, and Stephen Riesbeck 29 Jan. 1994 326 p
(Contract F19628-93-C-0130)
(AD-A284668) Avail: CASI HC A15/MF A03

In order to increase awareness, explore current research into software architectures as a means of implementing software reuse, and examine current practices and issues involving architectures, the Central Archive for Reusable Defense Software (CARDS) Program sponsored a Software Architecture Seminar and Workshop at West Virginia University's Concurrent Engineering Research Center (CERC) facility in Morgantown, West Virginia on November 16 and 17, 1993. The goals of the Seminar and Workshop were to understand the various meanings of software architecture, current research in the field of architecture, and current efforts applying software architecture. This document contains an overview of the proceedings of the Architecture Seminar on Tuesday, November 16 and the Architecture Workshop on Wednesday, November 17. This includes issues discussed, questions and answers, working group discussions, and references. This document also contains presentation slides from the Seminar, the Seminar panel discussion, and the Workshop. DTIC

N95-19397# Argonne National Lab., IL.
XAMATH: AN XAFS ANALYSIS PACKAGE BASED ON MATHEMATICA(TM)
S. R. Wasserman 11 Jul. 1994 7 p Presented at the 8th International Conference on X Ray Absorption Fine Structure, Berlin, Germany, 28 Aug. - 2 Sep. 1994
(Contract W-31-109-eng-38)
(DE94-016346; ANL/CHM/CP-82280; CONF-9408131-2) Avail: CASI HC A02/MF A01

XAMath is a graphics-based interactive package written with the Mathematica(R) system for the analysis of XAFS data. Mathematica(R) offers the advantage of use on several computer platforms, including Unix, IBM Windows, and Macintosh, without any modification of the program. The portability and flexibility of this software has some cost in speed of execution. DOE

N95-19409 Selskapet for Industriell og Teknisk Forskning, Trondheim (Norway). Div. of Production Engineering.
SIMULATION IN MANUFACTURING
J. O. Strandhagen 9 Jul. 1993 16 p
(PB94-215563; STF20-A93119) Avail: Issuing Activity

The importance of numerical simulation can be described by the viewpoint that there are three pillars in scientific and technology research; (1) analytic methods; (2) experimental methods; and (3) numerical simulation. The report will give an introduction to the world of simulation in manufacturing. The word simulation is now being used in a much wider context than only a few years back. The author will link it to Production Engineering and Production Management and state where in these complicated and multi-skilled fields simulation is applicable. NTIS

N95-19545# Carnegie-Mellon Univ., Pittsburgh, PA. Software Engineering Inst.
DRAFT SEI PROGRAM PLANS: 1995-1999 Final Report
Aug. 1994 242 p
(Contract F19628-90-C-0003)
(AD-A285047; CMU/SEI-94-SR-19) Avail: CASI HC A11/MF A03

This document presents the Software Engineering Institute (SEI) strategy and one-year implementation plan for calendar year (CY) 1995, together with the SEI five-year program plan. This document is, in essence, a proposal. It describes the strategic directions and offers detailed options for the coming year. Until the proposed options are selected and budget allocations are approved by the sponsor, the SEI cannot commit to specific work or supporting schedules. DTIC

N95-19625*# National Aeronautics and Space Administration. Lyndon B. Johnson Space Center, Houston, TX.
THIRD CLIPS CONFERENCE PROCEEDINGS, VOLUME 1
Gary Riley, ed. Nov. 1994 201 p Conference held in Houston, TX, 12-14 Sep. 1994; sponsored by NASA. Johnson Space Center and I-NET, Inc., Houston, TX
(NASA-CP-10162-Vol-1; S-785-Vol-1; NAS 1.55:10162-Vol-1) Avail: CASI HC A10/MF A03

Expert systems are computed programs which emulate human expertise in well defined problem domains. The potential payoff from expert systems is high: valuable expertise can be captured and preserved, repetitive and/or mundane tasks requiring human expertise can be automated, and uniformity can be applied in decision making processes. The C Language Integrated Production Systems (CLIPS) is an expert system building tool, developed at the Johnson Space Center, which provides a complete environment for the development and delivery of rule and/or object based expert systems. CLIPS was specifically designed to provide a low cost option for developing and deploying expert system applications across a wide range of hardware platforms. The development of CLIPS has helped to improve the ability to deliver expert systems technology throughout the public and private sectors for a wide range of applications and diverse computing environments. For individual titles, see N95-19626 through N95-19647.

N95-19626*# Harris Space Systems Corp., Rockledge, FL.
THE BUFFER DIAGNOSTIC PROTOTYPE: A FAULT ISOLATION APPLICATION USING CLIPS Abstract Only
Ken Porter *In* NASA. Johnson Space Center, Third CLIPS Conference Proceedings, Volume 1 Nov. 1994 p 1 (For primary document see N95-19625 05-61)
Avail: CASI HC A01/MF A03

This paper describes problem domain characteristics and development experiences from using CLIPS 6.0 in a proof-of-concept troubleshooting application called the Buffer Diagnostic Prototype. The problem domain is a large digital communications subsystems called the real-time network (RTN), which was designed to upgrade the launch processing system used for shuttle support at KSC. The RTN enables up to 255 computers to share 50,000 data points with millisecond response times. The RTN's extensive built-in test capability but lack of any automatic fault isolation capability presents a unique opportunity for a diagnostic expert system application. The Buffer Diagnostic Prototype addresses RTN diagnosis with a multiple strategy approach. A novel technique called 'faulty causality' employs inexact qualitative models to process test results. Experimental knowledge provides a capability to recognize symptom-fault associations. The implementation utilizes rule-based and procedural programming techniques, including a goal-directed control structure and simple text-based generic user interface that may be reusable for other rapid prototyping applications. Although limited in scope, this project demonstrates a diagnostic approach that may be adapted to troubleshoot a broad range of equipment. Author

N95-19627*# Kent State Univ., OH.
ON THE DEVELOPMENT OF AN EXPERT SYSTEM FOR WHEELCHAIR SELECTION **c54**

Gregory R. Madey, Charlotte A. Bhansin (Cleveland Clinic Foundation, OH.), Sulaiman A. Alaraini, and Mohamed A. Nour *In* NASA. Johnson Space Center, Third CLIPS Conference Proceedings, Volume 1 Nov. 1994 p 2-12 (For primary document see N95-19625 05-61)
Avail: CASI HC A03/MF A03

The presentation of wheelchairs for the Multiple Sclerosis (MS) patients involves the examination of a number of complicated factors including ambulation status, length of diagnosis, and funding sources, to name a few. Consequently, only a few experts exist in this area. To aid medical therapists with the wheelchair selection decision, a prototype medical expert system (ES) was developed. This paper describes and discusses the steps of designing and developing the system, the experiences of the authors, and the lessons learned from working on this project. Wheelchair Advisor, programmed in CLIPS, serves as diagnosis, classification, prescription, and training tool in the MS field. Interviews, insurance letters, forms, and prototyping were used to gain knowledge regarding the wheelchair selection problem. Among the lessons learned are that evolutionary prototyping is superior to the conventional system development life-cycle (SDLC), the wheelchair selection is a good candidate for ES applications, and that ES can be applied to other similar medical subdomains. Author

N95-19628*# Center for Genetic Services, Corpus Christi, TX.
EXPERT WITNESS: A SYSTEM FOR DEVELOPING EXPERT MEDICAL TESTIMONY
Raymond Lewandowski, David Perkins (Texas A&M Univ., Corpus Christi, TX.), and David Leasure (Texas A&M Univ., Corpus Christi, TX.) *In* NASA. Johnson Space Center, Third CLIPS Conference Proceedings, Volume 1 Nov. 1994 p 13-17 (For primary document see N95-19625 05-61)
Avail: CASI HC A01/MF A03

Expert Witness in an expert system designed to assist attorneys and medical experts in determining the merit of medical malpractice claims in the area of obstetrics. It substitutes the time of the medical expert with the time of a paralegal assistant guided by the expert system during the initial investigation of the medical records and patient interviews. The product of the system is a narrative transcript containing important data, immediate conclusions from the data, and overall conclusions of the case that the attorney and medical expert use to make decisions about whether and how to proceed with the case. The transcript may also contain directives for gathering additional information needed for the case. The system is a modified heuristic classifier and is implemented using over 600 CLIPS rules together with a C-based user interface. The data abstraction and solution refinement are implemented directly using forward chaining production and matching. The use of CLIPS and C is essential to delivering a system that runs on a generic PC platform. The direct implementation in CLIPS together with locality of inference ensures that the system will scale gracefully. Two years of use has revealed no errors in the reasoning. Author

N95-19629*# California Univ., Los Angeles, CA. Dept. of Computer Science.
THE DESIGN AND IMPLEMENTATION OF EPL: AN EVENT PATTERN LANGUAGE FOR ACTIVE DATABASES **c82**
G. Giuffrida and C. Zaniolo *In* NASA. Johnson Space Center, Third CLIPS Conference Proceedings, Volume 1 Nov. 1994 p 21-28 Sponsored in cooperation with Hughes Aircraft Corp. (For primary document see N95-19625 05-61)
Avail: CASI HC A02/MF A03

The growing demand for intelligent information systems requires closer coupling of rule-based reasoning engines, such as CLIPS, with advanced data base management systems (DBMS). For instance, several commercial DBMS now support the notion of triggers that monitor events and transactions occurring in the database and fire induced actions, which perform a variety of critical functions, including safeguarding the integrity of data, monitoring access, and recording volatile information needed by administrators, analysts, and expert systems to perform assorted tasks; examples of these tasks include security enforcement, market studies, knowledge discovery, and link analysis. At UCLA, we designed and implemented the event pattern language (EPL) which is capable of detecting and acting upon complex patterns of events which are temporally related to each other. For instance, a plant manager should be notified when a certain pattern of overheating repeats itself over time in a chemical process; likewise, proper notification is required when a suspicious sequence of bank transactions is executed within a certain time limit. The EPL prototype is built in CLIPS to operate on top of Sybase, a commercial relational DBMS, where actions can be triggered by events such as simple database updates, insertions, and deletions. The rule-based syntax of EPL allows the sequences of goals in rules to be interpreted as sequences of temporal events; each goal can correspond to either (1) a simple event, or (2) a (possibly negated) event/condition predicate, or (3) a complex event defined as the disjunction and repetition of other events. Various extensions have been added to CLIPS in order to tailor the interface with Sybase and its open client/server architecture. Author

N95-19630*# Texas Univ., Austin, TX. Tactical Simulation Div.
CLIPS++: EMBEDDING CLIPS INTO C++
Lance Obermeyer and Daniel P. Miranker *In* NASA. Lyndon B. Johnson Space Center, Third CLIPS Conference Proceedings, Volume 1 Nov. 1994 p 29-33 (For primary document see N95-19625 05-61)
(Contract DABT63-92-0042)
Avail: CASI HC A01/MF A03

This paper describes a set of C++ extensions to the CLIPS language and their embodiment in CLIPS++. These extensions and the implementation approach of CLIPS++ provide a new level of embeddability with C and C++. These extensions are a C++ include statement and a defcontainer construct; (include (c++-header-file.h)) and (defcontainer (c++-type)). The include construct allows C++ functions to be embedded in both the LHS and RHS of CLIPS rules. The header file in an include construct is the same header file the programmer uses for his/her own C++ code, independent of CLIPS. The defcontainer construct allows the inference engine to treat C++ class instances as CLIPS deftemplate facts. Consequently existing C++ class libraries may be transparently imported into CLIPS. These C++ types may use advanced features like inheritance, virtual functions, and templates. The implementation has been tested with several class libraries, including Rogue Wave Software's Tools.h++, GNU's libg++, and USL's C++ Standard Components. The execution speed of CLIPS++ has been determined to be 5 to 700 times the execution speed of CLIPS 6.0 (10 to 20X typical). Author

N95-19631*# California Univ., Los Angeles, CA. Dept. of Computer Science.
EXPERT SYSTEM SHELL TO REASON ON LARGE AMOUNTS OF DATA **c82**
Gionanni Giuffrida *In* NASA. Johnson Space Center, Third CLIPS Conference Proceedings, Volume 1 Nov. 1994 p 34-42 (For primary document see N95-19625 05-61)
Avail: CASI HC A02/MF A03

The current data base management systems (DBMS's) do not provide a sophisticated environment to develop rule based expert systems applications. Some of the new DBMS's come with some sort of rule mechanism; these are active and deductive database systems. However, both of these are not featured enough to support full implementation based on rules. On the other hand, current expert system shells do not provide any link with external databases. That is, all the data are kept in the system working memory. Such working memory is maintained in main memory. For some applications the reduced size of the available working memory could represent a constraint for the development. Typically these are applications which require reasoning on huge amounts of data. All these data do not fit into the computer main memory. Moreover, in some cases these data can be already available in some database systems and continuously updated while the expert system is running. This paper proposes an architecture which employs knowledge discovering techniques to reduce the amount of data to be stored in the main memory; in this architecture a standard DBMS is coupled with a rule-based language. The data are stored into the DBMS. An interface between the two systems is responsible for inducing knowledge from the set of relations. Such induced knowledge is then transferred to the rule-based language working memory.
Author (revised)

N95-19632*# RECOM Technologies, Inc., Moffett Field, CA. AI Research Branch.
AI AND WORKFLOW AUTOMATION: THE PROTOTYPE ELECTRONIC PURCHASE REQUEST SYSTEM **c81**
Michael M. Compton and Shawn R. Wolfe *In* NASA. Johnson Space

Center, Third CLIPS Conference Proceedings, Volume 1 Nov. 1994 p 45-51 (For primary document see N95-19625 05-61)
Avail: CASI HC A02/MF A03

Automating 'paper' workflow processes with electronic forms and email can dramatically improve the efficiency of those processes. However, applications that involve complex forms that are used for a variety of purposes or that require numerous and varied approvals often require additional software tools to ensure that (1) the electronic form is correctly and completely filled out, and (2) the form is routed to the proper individuals and organizations for approval. The prototype electronic purchase request (PEPR) system, which has been in pilot use at NASA Ames Research Center since December 1993, seamlessly links a commercial electronics forms package and a CLIPS-based knowledge system that first ensures that electronic forms are correct and complete, and then generates an 'electronic routing slip' that is used to route the form to the people who must sign it. The PEPR validation module is context-sensitive, and can apply different validation rules at each step in the approval process. The PEPR system is form-independent, and has been applied to several different types of forms. The system employs a version of CLIPS that has been extended to support AppleScript, a recently-released scripting language for the Macintosh. This 'scriptability' provides both a transparent, flexible interface between the two programs and a means by which a single copy of the knowledge base can be utilized by numerous remote users. Author

N95-19633*# Princeton Univ., NJ. Dept. of Mechanical and Aerospace Engineering.
A KNOWLEDGE-BASED SYSTEM FOR CONTROLLING AUTOMOBILE TRAFFIC **c81**
Alexander Maravas and Robert F. Stengel *In* NASA. Johnson Space Center, Third CLIPS Conference Proceedings, Volume 1 Nov. 1994 p 52-60 (For primary document see N95-19625 05-61)
(Grant NSF ECS-92-16450)
Avail: CASI HC A02/MF A03

Transportation network capacity variations arising from accidents, roadway maintenance activity, and special events as well as fluctuations in commuters' travel demands complicate traffic management. Artificial intelligence concepts and expert systems can be useful in framing policies for incident detection, congestion anticipation, and optimal traffic management. This paper examines the applicability of intelligent route guidance and control as decision aids for traffic management. Basic requirements for managing traffic are reviewed, concepts for studying traffic flow are introduced, and mathematical models for modeling traffic flow are examined. Measures for quantifying transportation network performance levels are chosen, and surveillance and control strategies are evaluated. It can be concluded that automated decision support holds great promise for aiding the efficient flow of automobile traffic over limited-access roadways, bridges, and tunnels.
Author

N95-19634*# Tennessee Technological Univ., Cookeville, TN.
DEVELOPMENT OF AN EXPERT SYSTEM FOR POWER QUALITY ADVISEMENT USING CLIPS 6.0 **c33**
A. Chandrasekaran, P. R. R. Sarma, and Ashok Sundaram (Electric Power Research Inst., Palo Alto, CA.) *In* NASA. Johnson Space Center, Third CLIPS Conference Proceedings, Volume 1 Nov. 1994 p 61-66 (For primary document see N95-19625 05-61)
Avail: CASI HC A02/MF A03

Proliferation of power electronic devices has brought in its wake both deterioration in and demand for quality power supply from the utilities. The power quality problems become apparent when the user's equipment or systems maloperate or fail. Since power quality concerns arise from a wide variety of sources and the problem fixes are better achieved from the expertise of field engineers, development of an expert system for power quality advisement seems to be a very attractive and cost-effective solution for utility applications. An expert system thus developed gives an understanding of the adverse effects of power quality related problems on the system and could help in finding remedial solutions. The paper reports the design of a power quality advisement expert system being developed using CLIPS 6.0. A brief outline of the power quality concerns is first presented. A description of the knowledge base is next given and details of actual implementation include screen output from the program. Author

N95-19635*# Pratt and Whitney Aircraft, East Hartford, CT.
QPA-CLIPS: A LANGUAGE AND REPRESENTATION FOR PROCESS CONTROL
Thomas G. Freund *In* NASA. Johnson Space Center, Third CLIPS Conference Proceedings, Volume 1 Nov. 1994 p 67-77 Sponsored in cooperation with the National Center for Mfg. Sciences, Allen-Bradley Co., and Erie Press Systems (For primary document see N95-19625 05-61)
Avail: CASI HC A03/MF A03

QPA-CLIPS is an extension of CLIPS oriented towards process control applications. Its constructs define a dependency network of process actions driven by sensor information. The language consists of three basic constructs: TASK, SENSOR, and FILTER. TASK's define the dependency network describing alternative state transitions for a process. SENSOR's and FILTER's define sensor information sources used to activate state transitions within the network. Deftemplate's define these constructs and their run-time environment is an interpreter knowledge base, performing pattern matching on sensor information and so activating TASK's in the dependency network. The pattern matching technique is based on the repeatable occurrence of a sensor data pattern. QPA-CIPS has been successfully tested on a SPARCStation providing supervisory control to an Allen-Bradley PLC 5 controller driving molding equipment. Author

N95-19636*# Aerospace Corp., Los Angeles, CA.
FUZZY EXPERT SYSTEMS USING CLIPS
Thach C. Le *In* NASA. Johnson Space Center, Third CLIPS Conference Proceedings, Volume 1 Nov. 1994 p 81-91 (For primary document see N95-19625 05-61)
Avail: CASI HC A03/MF A03

This paper describes a CLIPS-based fuzzy expert system development environment called FCLIPS and illustrates its application to the simulated cart-pole balancing problem. FCLIPS is a straightforward extension of CLIPS without any alteration to the CLIPS internal structures. It makes use of the object-oriented and module features in CLIPS version 6.0 for the implementation of fuzzy logic concepts. Systems of varying degrees of mixed Boolean and fuzzy rules can be implemented in CLIPS. Design and implementation issues of FCLIPS will also be discussed. Author

N95-19637*# National Aeronautics and Space Administration. Marshall Space Flight Center, Huntsville, AL.
NEURAL NET CONTROLLER FOR INLET PRESSURE CONTROL OF ROCKET ENGINE TESTING **c63**
Luis C. Trevino *In* NASA. Johnson Space Center, Third CLIPS Conference Proceedings, Volume 1 Nov. 1994 p 92-104 (For primary document see N95-19625 05-61)
Avail: CASI HC A03/MF A03

Many dynamic systems operate in select operating regions, each exhibiting characteristic modes of behavior. It is traditional to employ standard adjustable gain proportional-integral-derivative (PID) loops in such systems where no apriori model information is available. However, for controlling inlet pressure for rocket engine testing, problems in fine tuning, disturbance accommodation, and control gains for new profile operating regions (for research and development) are typically encountered. Because of the capability of capturing I/O peculiarities, using NETS, a back propagation trained neural network is specified. For select operating regions, the neural network controller is simulated to be as robust as the PID controller. For a comparative analysis, the higher order moment neural array (HOMNA) method is used to specify a second neural controller by extracting critical exemplars from the I/O data set. Furthermore, using the critical exemplars from the HOMNA method, a third neural controller is developed using NETS back propagation algorithm. All controllers are benchmarked against each other. Author

N95-19638*# State Univ. of Southeastern Oklahoma, Durant, OK. Dept. of Computer Science.
CLIPS TEMPLATE SYSTEM FOR PROGRAM UNDERSTANDING
Ronald B. Finkbine *In* NASA. Johnson Space Center, Third CLIPS Conference Proceedings, Volume 1 Nov. 1994 p 105-111 (For primary document see N95-19625 05-61)
Avail: CASI HC A02/MF A03

Program understanding is a subfield of software reengineering and attempts to recognize the run-time behavior of source code. To this point, success in this area has been limited to very small code segments. An

expert system, HLAR (High-Level Algorithm Recognizer), has been written in CLIPS and recognizes three sorting algorithms, selection sort, quicksort, and heapsort. This paper describes the HLAR system in general and, in depth, the CLIPS templates used for program representation and understanding. Author

N95-19639*# Honeywell, Inc., Clearwater, FL. Military Avionics Div.
USING EXPERT SYSTEMS TO ANALYZE ATE DATA
Jim Harrington *In* NASA. Johnson Space Center, Third CLIPS Conference Proceedings, Volume 1 Nov. 1994 p 115-122 (For primary document see N95-19625 05-61)
Avail: CASI HC A02/MF A03

The proliferation of automatic test equipment (ATE) is resulting in the generation of large amounts of component data. Some of this component data is not accurate due to the presence of noise. Analyzing this data requires the use of new techniques. This paper describes the process of developing an expert system to analyze ATE data and provides an example rule in the CLIPS language for analyzing trip thresholds for high gain/high speed comparators. Author

N95-19640*# RECOM Technologies, Inc., Moffett Field, CA.
REAL-TIME REMOTE SCIENTIFIC MODEL VALIDATION
Richard Frainier and Nicolas Groleau *In* NASA. Johnson Space Center, Third CLIPS Conference Proceedings, Volume 1 Nov. 1994 p 123-130 (For primary document see N95-19625 05-61)
Avail: CASI HC A02/MF A03

This paper describes flight results from the use of a CLIPS-based validation facility to compare analyzed data from a space life sciences (SLS) experiment to an investigator's preflight model. The comparison, performed in real-time, either confirms or refutes the model and its predictions. This result then becomes the basis for continuing or modifying the investigator's experiment protocol. Typically, neither the astronaut crew in Spacelab nor the ground-based investigator team are able to react to their experiment data in real time. This facility, part of a larger science advisor system called Principal Investigator in a Box, was flown on the space shuttle in October, 1993. The software system aided the conduct of a human vestibular physiology experiment and was able to outperform humans in the tasks of data integrity assurance, data analysis, and scientific model validation. Of twelve preflight hypotheses associated with investigator's model, seven were confirmed and five were rejected or compromised. Author

N95-19641*# Kent State Univ., OH.
A CLIPS-BASED EXPERT SYSTEM FOR THE EVALUATION AND SELECTION OF ROBOTS
Mohamed A. Nour, Felix O. Offodile, and Gregory R. Madey *In* NASA. Johnson Space Center, Third CLIPS Conference Proceedings, Volume 1 Nov. 1994 p 131-140 (For primary document see N95-19625 05-61)
Avail: CASI HC A02/MF A03

This paper describes the development of a prototype expert system for intelligent selection of robots for manufacturing operations. The paper first develops a comprehensive, three-stage process to model the robot selection problem. The decisions involved in this model easily lend themselves to an expert system application. A rule-based system, based on the selection model, is developed using the CLIPS expert system shell. Data about actual robots is used to test the performance of the prototype system. Further extensions to the rule-based system for data handling and interfacing capabilities are suggested. Author

N95-19642*# LB and M Associates, Inc., Lawton, OK.
ADDING INTELLIGENT SERVICES TO AN OBJECT ORIENTED SYSTEM
Bret R. Robideaux and Theodore A. Metzler *In* NASA. Johnson Space Center, Third CLIPS Conference Proceedings, Volume 1 Nov. 1994 p 143-152 (For primary document see N95-19625 05-61)
Avail: CASI HC A02/MF A03

As today's software becomes increasingly complex, the need grows for intelligence of one sort or another to becomes part of the application, often an intelligence that does not readily fit the paradigm of one's software development. There are many methods of developing software, but at this time, the most promising is the object oriented (OO) method. This method involves an analysis to abstract the problem into separate 'objects' that are unique in the data that describe them and the behavior that they exhibit, and eventually to convert this analysis into computer code using a programming language that was designed (or retrofitted) for OO implementation. This paper discusses the creation of three different applications that are analyzed, designed, and programmed using the Shlaer/Mellor method of OO development and C++ as the programming language. All three, however, require the use of an expert system to provide an intelligence that C++ (or any other 'traditional' language) is not directly suited to supply. The flexibility of CLIPS permitted us to make modifications to it that allow seamless integration with any of our applications that require an expert system. We illustrate this integration with the following applications: (1) an after action review (AAR) station that assists a reviewer in watching a simulated tank battle and developing an AAR to critique the performance of the participants in the battle; (2) an embedded training system and over-the-shoulder coach for howitzer crewmen; and (3) a system to identify various chemical compounds from their infrared absorption spectra. Author

N95-19643*# RECOM Technologies, Inc., Moffett Field, CA. AI Research Branch.
CLIPS, AppleEvents, AND AppleScript: INTEGRATING CLIPS WITH COMMERCIAL SOFTWARE
Michael M. Compton and Shawn R. Wolfe *In* NASA. Johnson Space Center, Third CLIPS Conference Proceedings, Volume 1 Nov. 1994 p 153-161 (For primary document see N95-19625 05-61)
Avail: CASI HC A02/MF A03

Many of today's intelligent systems are comprised of several modules, perhaps written in different tools and languages, that together help solve the user's problem. These systems often employ a knowledge-based component that is not accessed directly by the user, but instead operates 'in the background' offering assistance to the user as necessary. In these types of modular systems, an efficient, flexible, and eady-to-use mechanism for sharing data between programs is crucial. To help permit transparent integration of CLIPS with other Macintosh applications, the AI Research Branch at NASA Ames Research Center has extended CLIPS to allow it to communicate transparently with other applications through two popular data-sharing mechanisms provided by the Macintosh operating system: Apple Events (a 'high-level' event mechanism for program-to-program communication), and AppleScript, a recently-released scripting language for the Macintosh. This capability permits other applications (running on either the same or a remote machine) to send a command to CLIPS, which then responds as if the command were typed into the CLIPS dialog window. Any result returned by the command is then automatically returned to the program that sent it. Likewise, CLIPS can send several types of Apple Events directly to other local or remote applications. This CLIPS system has been successfully integrated with a variety of commercial applications, including data collection programs, electronics forms packages, DBMS's, and email programs. These mechanisms can permit transparent user access to the knowledge base from within a commercial application, and allow a single copy of the knowledge base to service multiple users in a networked environment. Author

N95-19644*# Maharishi International Univ., Fairfield, IA. Dept. of Computer Science.
TARGET'S ROLE IN KNOWLEDGE ACQUISITION, ENGINEERING, VALIDATION, AND DOCUMENTATION c82
Keith R. Levi *In* NASA. Johnson Space Center, Third CLIPS Conference Proceedings, Volume 1 Nov. 1994 p 162-168 (For primary document see N95-19625 05-61)
Avail: CASI HC A02/MF A03

We investigate the use of the TARGET task analysis tool for use in the development of rule-based expert systems. We found TARGET to be very helpful in the knowledge acquisition process. It enabled us to perform knowledge acquisition with one knowledge engineer rather than two. In addition, it improved communication between the domain expert and knowledge engineer. We also found it to be useful for both the rule development and refinement phases of the knowledge engineering process. Using the network in these phases required us to develop guidelines that enabled us to easily translate the network into production rules. A significant requirement for TARGET remaining useful throughout the knowledge engineering process was the need to carefully maintain consistency between the network and the rule representations. Maintaining consistency not only

benefited the knowledge engineering process, but also has significant payoffs in the areas of validation of the expert system and documentation of the knowledge in the system. Author

N95-19645*# Raytheon Co., Marlborough, MA.
AN EXPERT SYSTEM FOR CONFIGURING A NETWORK FOR A MILSTAR TERMINAL **c62**
Melissa J. Mahoney and Elizabeth J. Wilson *In* NASA. Johnson Space Center, Third CLIPS Conference Proceedings, Volume 1 Nov. 1994 p 171-179 (For primary document see N95-19625 05-61)
Avail: CASI HC A02/MF A03

This paper describes a rule-based expert system which assists the user in configuring a network for Air Force terminals using the Milstar satellite system. The network configuration expert system approach uses CLIPS. The complexity of network configuration is discussed, and the methods used to model it are described. Author

N95-19646*# National Aeronautics and Space Administration. Lyndon B. Johnson Space Center, Houston, TX.
EXPERT SYSTEM TECHNOLOGIES FOR SPACE SHUTTLE DECISION SUPPORT: TWO CASE STUDIES **c82**
Christopher J. Ortiz and David A. Hasan (LinCom Corp., Houston, TX.) *In its* Third CLIPS Conference Proceedings, Volume 1 Nov. 1994 p 180-190 (For primary document see N95-19625 05-61)
Avail: CASI HC A03/MF A03

This paper addresses the issue of integrating the C Language Integrated Production System (CLIPS) into distributed data acquisition environments. In particular, it presents preliminary results of some ongoing software development projects aimed at exploiting CLIPS technology in the new mission control center (MCC) being built at NASA Johnson Space Center. One interesting aspect of the control center is its distributed architecture; it consists of networked workstations which acquire and share data through the NASA/JSC-developed information sharing protocol (ISP). This paper outlines some approaches taken to integrate CLIPS and ISP in order to permit the development of intelligent data analysis applications which can be used in the MCC. Three approaches to CLIPS/IPS integration are discussed. The initial approach involves clearly separating CLIPS from ISP using user-defined functions for gathering and sending data to and from a local storage buffer. Memory and performance drawbacks of this design are summarized. The second approach involves taking full advantage of CLIPS and the CLIPS Object-Oriented Language (COOL) by using objects to directly transmit data and state changes from ISP to COOL. Any changes within the object slots eliminate the need for both a data structure and external function call thus taking advantage of the object matching capabilities within CLIPS 6.0. The final approach is to treat CLIPS and ISP as peer toolkits. Neither is embedded in the other; rather the application interweaves calls to each directly in the application source code. Author

N95-19647*# Ensco, Inc., Melbourne, FL. Applied Research and Systems Div.
THE METEOROLOGICAL MONITORING SYSTEM FOR THE KENNEDY SPACE CENTER/CAPE CANAVERAL AIR STATION **c82**
Allan V. Dianic *In* NASA. Johnson Space Center, Third CLIPS Conference Proceedings, Volume 1 Nov. 1994 p 191-200 (For primary document see N95-19625 05-61)
Avail: CASI HC A02/MF A03

The Kennedy Space Center (KSC) and Cape Canaveral Air Station (CCAS) are involved in many weather-sensitive operations. Manned and unmanned vehicle launches, which occur several times each year, are obvious example of operations whose success and safety are dependent upon favorable meteorological conditions. Other operations involving NASA, Air Force, and contractor personnel, including daily operations to maintain facilities, refurbish launch structures, prepare vehicles for launch, and handle hazardous materials, are less publicized but are no less weather-sensitive. The Meteorological Monitoring System (MMS) is a computer network which acquires, processes, disseminates, and monitors near real-time and forecast meteorological information to assist operational personnel and weather forecasters with the task of minimizing the risk to personnel, materials, and the surrounding population. CLIPS has been integrated into the MMS to provide quality control analysis and data monitoring. This paper describes aspects of the MMS relevant to CLIPS including requirements, actual implementation details, and results of performance testing. Author

N95-19688# Naval Air Warfare Center, Patuxent River, MD. Aircraft Div.
THE USE OF GENETIC ALGORITHMS FOR FLIGHT TEST AND EVALUATION OF ARTIFICIAL INTELLIGENCE AND COMPLEX SOFTWARE SYSTEMS
Elizabeth Davies, John McMaster, and Mary Stark 1994 6 p
(AD-A284824) Avail: CASI HC A02/MF A01

Artificial intelligence (AI) technologies are emerging from research laboratories into industry, particularly into the field of aviation. One such application is the ARPA/USAF Pilot's Associate, a set of cooperating expert systems designed to aid the tactical pilot in a combat situation. There are currently no rigorous methods for the test and evaluation of such tactical airborne expert systems. The focus of this program, sponsored in part by the Office of Naval Technology, is the development of a test and evaluation facility for tactical airborne systems which incorporate artificial intelligence. In particular, the subject of this paper is the development of a genetic algorithm (GA) which will automatically find those test cases for which the system under test performs most poorly. DTIC

N95-19742 Naval Research Lab., Bay Saint Louis, MS.
PAK: A PROCESSING SYSTEM FOR VECTORIZED TIME-SERIES DATA Final Report
Sarah H. Peckinpaugh and Peter M. Smith 17 Aug. 1994 24 p Limited Reproducibility: More than 20% of this document may be affected by microfiche quality
(AD-A284881; NRL/MR/7240-94-7542) Avail: CASI HC A03

This document describes the PAK function and how to use it. The function is written in MATLAB. The function is designed for processing vectorized data. Options are provided for creating, viewing, and processing the data. DTIC

N95-19747*# National Aeronautics and Space Administration. Lyndon B. Johnson Space Center, Houston, TX.
THIRD CLIPS CONFERENCE PROCEEDINGS, VOLUME 2
Gary Riley, ed. Nov. 1994 200 p Conference held in Houston, TX, 12-14 Sep. 1994; sponsored by NASA. Johnson Space Center and I-NET, Inc., Houston, TX
(NASA-CP-10162-Vol-2; S-785-Vol-2; NAS 1.55:10162-Vol-2) Avail: CASI HC A09/MF A03

Expert systems are computer programs which emulate human expertise in well defined problem domains. The C Language Integrated Production System (CLIPS) is an expert system building tool, developed at the Johnson Space Center, which provides a complete environment for the development and delivery of rule and/or object based expert systems. CLIPS was specifically designed to provide a low cost option for developing and deploying expert system applications across a wide range of hardware platforms. The development of CLIPS has helped to improve the ability to deliver expert system technology throughout the public and private sectors for a wide range of applications and diverse computing environments. The Third Conference on CLIPS provided a forum for CLIPS users to present and discuss papers relating to CLIPS applications, uses, and extensions. For individual titles, see N95-19748 through N95-19768.

N95-19748*# California Polytechnic State Univ., San Luis Obispo, CA. Dept. of Computer Science.
USING PVM TO HOST CLIPS IN DISTRIBUTED ENVIRONMENTS
Leonard Myers and Kym Pohl *In* NASA. Johnson Space Center, Third CLIPS Conference Proceedings, Volume 2 Nov. 1994 p 203-211 (For primary document see N95-19747 05-61)
Avail: CASI HC A02/MF A03

It is relatively easy to enhance CLIPS (C Language Integrated Production System) to support multiple expert systems running in a distributed environment with heterogeneous machines. The task is minimized by using the PVM (Parallel Virtual Machine) code from Oak Ridge Labs to provide the distributed utility. PVM is a library of C and FORTRAN subprograms that supports distributive computing on many different UNIX platforms. A PVM deamon is easily installed on each CPU that enters the virtual machine environment. Any user with rsh or rexec access to a machine can use the one PVM deamon to obtain a generous set of distributed facilities. The ready availability of both CLIPS and PVM makes the combination of software particularly attractive for budget conscious experimentation of heterogeneous distributive computing with multiple CLIPS executables. This paper presents

a design that is sufficient to provide essential message passing functions in CLIPS and enable the full range of PVM facilities. Author

N95-19749*# National Aeronautics and Space Administration. Lewis Research Center, Cleveland, OH.

A PARALLEL STRATEGY FOR IMPLEMENTING REAL-TIME EXPERT SYSTEMS USING CLIPS

Laszlo A. Ilyes (Cleveland State Univ., OH.), F. Eugenio Villaseca (Cleveland State Univ., OH.), and John DeLaat *In* NASA. Johnson Space Center, Third CLIPS Conference Proceedings, Volume 2 Nov. 1994 p 212-219 (For primary document see N95-19747 05-61)

(Contract NCC3-257)

Avail: CASI HC A02/MF A03

As evidenced by current literature, there appears to be a continued interest in the study of real-time expert systems. It is generally recognized that speed of execution is only one consideration when designing an effective real-time expert system. Some other features one must consider are the expert system's ability to perform temporal reasoning, handle interrupts, prioritize data, contend with data uncertainty, and perform context focusing as dictated by the incoming data to the expert system. This paper presents a strategy for implementing a real time expert system on the iPSC/860 hypercube parallel computer using CLIPS. The strategy takes into consideration not only the execution time of the software, but also those features which define a true real-time expert system. The methodology is then demonstrated using a practical implementation of an expert system which performs diagnostics on the Space Shuttle Main Engine (SSME). This particular implementation uses an eight node hypercube to process ten sensor measurements in order to simultaneously diagnose five different failure modes within the SSME. The main program is written in ANSI C and embeds CLIPS to better facilitate and debug the rule based expert system. Author

N95-19750*# Swiss Scientific Computing Center, Manno (Switzerland). Section of Research and Development.

USING CLIPS IN THE DOMAIN OF KNOWLEDGE-BASED MASSIVELY PARALLEL PROGRAMMING c62

Jiri J. Dvorak *In* NASA. Johnson Space Center, Third CLIPS Conference Proceedings, Volume 2 Nov. 1994 p 220-229 (For primary document see N95-19747 05-61)

Avail: CASI HC A02/MF A03

The Program Development Environment (PDE) is a tool for massively parallel programming of distributed-memory architectures. Adopting a knowledge-based approach, the PDE eliminates the complexity introduced by parallel hardware with distributed memory and offers complete transparency in respect of parallelism exploitation. The knowledge-based part of the PDE is realized in CLIPS. Its principal task is to find an efficient parallel realization of the application specified by the user in a comfortable, abstract, domain-oriented formalism. A large collection of fine-grain parallel algorithmic skeletons, represented as COOL objects in a tree hierarchy, contains the algorithmic knowledge. A hybrid knowledge base with rule modules and procedural parts, encoding expertise about application domain, parallel programming, software engineering, and parallel hardware, enables a high degree of automation in the software development process. In this paper, important aspects of the implementation of the PDE using CLIPS and COOL are shown, including the embedding of CLIPS with C++-based parts of the PDE. The appropriateness of the chosen approach and of the CLIPS language for knowledge-based software engineering are discussed. Author

N95-19751*# Royal Military Coll. of Saint-Jean, Richelain (Quebec). Group of Applied Research in Management Support Systems.

TRANSPORT AIRCRAFT LOADING AND BALANCING SYSTEM: USING A CLIPS EXPERT SYSTEM FOR MILITARY AIRCRAFT LOAD PLANNING

J. Richardson, M. Labbe, Y. Belala, and Vincent Leduc *In* NASA. Johnson Space Center, Third CLIPS Conference Proceedings, Volume 2 Nov. 1994 p 233-240 (For primary document see N95-19747 05-61)

Avail: CASI HC A02/MF A03

The requirement for improving aircraft utilization and responsiveness in airlift operations has been recognized for quite some time by the Canadian Forces. To date, the utilization of scarce airlift resources has been planned mainly through the employment of manpower-intensive manual methods in combination with the expertise of highly qualified personnel. In this paper, we address the problem of facilitating the load planning process for military aircraft cargo planes through the development of a computer-based system. We introduce TALBAS (Transport Aircraft Loading and BAlancing System), a knowledge-based system designed to assist personnel involved in preparing valid load plans for the C130 Hercules aircraft. The main features of this system which are accessible through a convivial graphical user interface, consists of the automatic generation of valid cargo arrangements given a list of items to be transported, the user-definition of load plans and the automatic validation of such load plans. Author

N95-19752*# Mississippi State Univ., Mississippi State, MS. Dept. of Computer Science.

PREDICTING AND EXPLAINING THE MOVEMENT OF MESOSCALE OCEANOGRAPHIC FEATURES USING CLIPS

Susan Bridges, Liang-Chun Chen, and Matthew Lybanon (Naval Research Lab., Bay Saint Louis, MS.) *In* NASA. Johnson Space Center, Third CLIPS Conference Proceedings, Volume 2 Nov. 1994 p 241-245 (For primary document see N95-19747 05-61)

(Contract NAS13-330)

Avail: CASI HC A01/MF A03

The Naval Research Laboratory has developed an oceanographic expert system that describes the evolution of mesoscale features in the Gulf Stream region of the northwest Atlantic Ocean. These features include the Gulf Stream current and the warm and cold core eddies associated with the Gulf Stream. An explanation capability was added to the eddy prediction component of the expert system in order to allow the system to justify the reasoning process it uses to make predictions. The eddy prediction and explanation components of the system have recently been redesigned and translated from OPS83 to C and CLIPS and the new system is called WATE (Where Are Those Eddies). The new design has improved the system's readability, understandability and maintainability and will also allow the system to be incorporated into the Semi-Automated Mesoscale Analysis System which will eventually be embedded into the Navy's Tactical Environmental Support System, Third Generation, TESS(3). Author

N95-19753*# University of Central Florida, Orlando, FL. Intelligent Simulation Lab.

KNOWLEDGE BASED TRANSLATION AND PROBLEM SOLVING IN AN INTELLIGENT INDIVIDUALIZED INSTRUCTION SYSTEM

Namho Jung and John E. Biegel *In* NASA. Johnson Space Center, Third CLIPS Conference Proceedings, Volume 2 Nov. 1994 p 246-252 (For primary document see N95-19747 05-61)

Avail: CASI HC A02/MF A03

An Intelligent Individualized Instruction I(sup 3) system is being built to provide computerized instruction. We present the roles of a translator and a problem solver in an intelligent computer system. The modular design of the system provides for easier development and allows for future expansion and maintenance. CLIPS modules and classes are utilized for the purpose of the modular design and inter module communications. CLIPS facts and rules are used to represent the system components and the knowledge base. CLIPS provides an inferencing mechanism to allow the I(sup 3) system to solve problems presented to it in English. Author (revised)

N95-19754*# Saint Thomas Univ., Houston, TX. Management Information Systems.

MIRO: A DEBUGGING TOOL FOR CLIPS INCORPORATING HISTORICAL RETE NETWORKS

Sharon M. Tuttle and Christoph F. Eick (Houston Univ., TX.) *In* NASA. Johnson Space Center, Third CLIPS Conference Proceedings, Volume 2 Nov. 1994 p 255-262 (For primary document see N95-19747 05-61)

Avail: CASI HC A02/MF A03

At the last CLIPS conference, we discussed our ideas for adding a temporal dimension to the Rete network used to implement CLIPS. The resulting historical Rete network could then be used to store 'historical' information about a run of a CLIPS program, to aid in debugging. MIRO, a debugging tool for CLIPS built on top of CLIPS, incorporates such a historical Rete network and uses it to support its prototype question-answering capability. By enabling CLIPS users to directly ask debugging-related questions about the history of a program run, we hope to reduce the amount of single-stepping and program tracing required to debug a CLIPS program. In this paper, we briefly describe MIRO's architecture and

implementation, and the current question-types that MIRO supports. These question-types are further illustrated using an example, and the benefits of the debugging tool are discussed. We also present empirical results that measure the run-time and partial storage overhead of MIRO, and discuss how MIRO may also be used to study various efficiency aspects of CLIPS programs. Author

N95-19755*# Hughes Information Technology Co., Reston, VA.
OPTIMAL PATTERN DISTRIBUTIONS IN RETE-BASED PRODUCTION SYSTEMS
Stephen L. Scott *In* NASA. Johnson Space Center, Third CLIPS Conference Proceedings, Volume 2 Nov. 1994 p 263-272 (For primary document see N95-19747 05-61)
Avail: CASI HC A02/MF A03

Since its introduction into the AI community in the early 1980's, the Rete algorithm has been widely used. This algorithm has formed the basis for many AI tools, including NASA's CLIPS. One drawback of Rete-based implementation, however, is that the network structures used internally by the Rete algorithm make it sensitive to the arrangement of individual patterns within rules. Thus while rules may be more or less arbitrarily placed within source files, the distribution of individual patterns within these rules can significantly affect the overall system performance. Some heuristics have been proposed to optimize pattern placement, however, these suggestions can be conflicting. This paper describes a systematic effort to measure the effect of pattern distribution on production system performance. An overview of the Rete algorithm is presented to provide context. A description of the methods used to explore the pattern ordering problem area are presented, using internal production system metrics such as the number of partial matches, and coarse-grained operating system data such as memory usage and time. The results of this study should be of interest to those developing and optimizing software for Rete-based production systems. Author

N95-19756*# National Aeronautics and Space Administration. Marshall Space Flight Center, Huntsville, AL.
SIMULATION IN A DYNAMIC PROTOTYPING ENVIRONMENT: PETRI NETS OR RULES?
Loretta A. Moore (Auburn Univ., AL.), Shannon W. Price (Auburn Univ., AL.), and Joseph P. Hale *In* NASA. Johnson Space Center, Third CLIPS Conference Proceedings, Volume 2 Nov. 1994 p 273-281 (For primary document see N95-19747 05-61)
(Contract NAS8-39131)
Avail: CASI HC A02/MF A03

An evaluation of a prototyped user interface is best supported by a simulation of the system. A simulation allows for dynamic evaluation of the interface rather than just a static evaluation of the screen's appearance. This allows potential users to evaluate both the look (in terms of the screen layout, color, objects, etc.) and feel (in terms of operations and actions which need to be performed) of a system's interface. Because of the need to provide dynamic evaluation of an interface, there must be support for producing active simulations. The high-fidelity training simulators are normally delivered too late to be effectively used in prototyping the displays. Therefore, it is important to build a low fidelity simulator, so that the iterative cycle of refining the human computer interface based upon a user's interactions can proceed early in software development. Author

N95-19757*# Lehigh Univ., Bethlehem, PA. Dept. of Electrical Engineering and Computer Science.
COLLABORATIVE ENGINEERING-DESIGN SUPPORT SYSTEM
Dong Ho Lee and D. Richard Decker *In* NASA. Johnson Space Center, Third CLIPS Conference Proceedings, Volume 2 Nov. 1994 p 285-295 Sponsored by Semiconductor Research Corp. (For primary document see N95-19747 05-61)
Avail: CASI HC A03/MF A03

Designing engineering objects requires many engineers' knowledge from different domains. There needs to be cooperative work among engineering designers to complete a design. Revisions of a design are time consuming, especially if designers work at a distance and with different design description formats. In order to reduce the design cycle, there needs to be a sharable design describing the engineering community, which can be electronically transportable. Design is a process of integrating that is not easy to define definitively. This paper presents Design Script which is a generic engineering design knowledge representation scheme that can be applied in any engineering domain. The Design Script is developed through encapsulation of common design activities and basic design components based on problem decomposition. It is implemented using CLIPS with a Windows NT graphical user interface. The physical relationships between engineering objects and their subparts can be constructed in a hierarchical manner. The same design process is repeatedly applied at each given level of hierarchy and recursively into lower levels of the hierarchy. Each class of the structure can be represented using the Design Script. Author

N95-19758*# Texas Univ., San Antonio, TX.
CHARACTER SELECTING ADVISOR FOR A ROLE-PLAYING GAME
Carol L. Redfield and Felicia Berlanga (Berlanga, Felicia, San Antonio, TX.) *In* NASA. Johnson Space Center, Third CLIPS Conference Proceedings, Volume 2 Nov. 1994 p 296-302 Sponsored in part by NSF (For primary document see N95-19747 05-61)
Avail: CASI HC A02/MF A03

Role-playing games have been a source of much pleasure and merriment for people of all ages. The process of developing a character for a role-playing game is usually very, very time consuming, delaying what many players consider the most entertaining part of the game. An expert system has been written to assist a player in creating a character by guiding the player through a series of questions. This paper discusses the selection of this topic, the knowledge engineering, the software development, and the resulting program that cuts the time of character development from about 4 hours to 30 minutes. The program was written on a PC and an Apollo in CLIPS 4.3 and currently runs on the Apollo. Author

N95-19759*# Yalif (Guy U.), MA.
THE COMPUTER AIDED AIRCRAFT-DESIGN PACKAGE (CAAP)
Guy U. Yalif *In* NASA. Johnson Space Center, Third CLIPS Conference Proceedings, Volume 2 Nov. 1994 p 303-314 (For primary document see N95-19747 05-61)
Avail: CASI HC A03/MF A03

The preliminary design of an aircraft is a complex, labor-intensive, and creative process. Since the 1970's, many computer programs have been written to help automate preliminary airplane design. Time and resource analyses have identified, 'a substantial decrease in project duration with the introduction of an automated design capability'. Proof-of-concept studies have been completed which establish 'a foundation for a computer-based airframe design capability', Unfortunately, today's design codes exist in many different languages on many, often expensive, hardware platforms. Through the use of a module-based system architecture, the Computer aided Aircraft-design Package (CAAP) will eventually bring together many of the most useful features of existing programs. Through the use of an expert system, it will add an additional feature that could be described as indispensable to entry level engineers and students: the incorporation of 'expert' knowledge into the automated design process. Author

N95-19760*# National Aeronautics and Space Administration. Marshall Space Flight Center, Huntsville, AL.
RULE BASED DESIGN OF CONCEPTUAL MODELS FOR FORMATIVE EVALUATION
Loretta A. Moore (Auburn Univ., AL.), Kai Chang (Auburn Univ., AL.), Joseph P. Hale, Terri Bester (Auburn Univ., AL.), Thomas Rix (Auburn Univ., AL.), and Yaowen Wang (Auburn Univ., AL.) *In* NASA. Johnson Space Center, Third CLIPS Conference Proceedings, Volume 2 Nov. 1994 p 317-325 (For primary document see N95-19747 05-61)
(Contract NAS8-39131)
Avail: CASI HC A02/MF A03

A Human-Computer Interface (HCI) Prototyping Environment with embedded evaluation capability has been investigated. This environment will be valuable in developing and refining HCI standards and evaluating program/project interface development, especially Space Station Freedom on-board displays for payload operations. This environment, which allows for rapid prototyping and evaluation of graphical interfaces, includes the following four components: (1) a HCI development tool, (2) a low fidelity simulator development tool, (3) a dynamic, interactive interface between the HCI and the simulator, and (4) an embedded evaluator that evaluates the adequacy of a HCI based on a user's performance. The embedded evaluation tool collects data while the user is interacting with the system

and evaluates the adequacy of an interface based on a user's performance. This paper describes the design of conceptual models for the embedded evaluation system using a rule-based approach. Author

N95-19761*# California Univ., Irvine, CA. Dept. of Information and Computer Science.
AUTOMATED RULE-BASE CREATION VIA CLIPS-INDUCE
Patrick M. Murphy *In* NASA. Johnson Space Center, Third CLIPS Conference Proceedings, Volume 2 Nov. 1994 p 326-333 (For primary document see N95-19747 05-61)
Avail: CASI HC A02/MF A03

Many CLIPS rule-bases contain one or more rule groups that perform classification. In this paper we describe CLIPS-Induce, an automated system for the creation of a CLIPS classification rule-base from a set of test cases. CLIPS-Induce consists of two components, a decision tree induction component and a CLIPS production extraction component. ID3, a popular decision tree induction algorithm, is used to induce a decision tree from the test cases. CLIPS production extraction is accomplished through a top-down traversal of the decision tree. Nodes of the tree are used to construct query rules, and branches of the tree are used to construct classification rules. The learned CLIPS productions may easily be incorporated into a large CLIPS system that perform tasks such as accessing a database or displaying information. Author

N95-19762*# California Univ., Irvine, CA. Dept. of Information and Computer Science.
AUTOMATED REVISION OF CLIPS RULE-BASES
Patrick M. Murphy and Michael J. Pazzani *In* NASA. Johnson Space Center, Third CLIPS Conference Proceedings, Volume 2 Nov. 1994 p 334-342 (For primary document see N95-19747 05-61)
(Contracts F49620-92-J-0430; F49620-93-1-0569; NSF IRI-93-10413)
Avail: CASI HC A02/MF A03

This paper describes CLIPS-R, a theory revision system for the revision of CLIPS rule-bases. CLIPS-R may be used for a variety of knowledge-base revision tasks, such as refining a prototype system, adapting an existing system to slightly different operating conditions, or improving an operational system that makes occasional errors. We present a description of how CLIPS-R revises rule-bases, and an evaluation of the system on three rule-bases. Author

N95-19763*# Royal Military Coll. of Saint-Jean, Richelain (Quebec). Groupe de Recherche en Intelligence Artificielle Distribuee.
DAI-CLIPS: DISTRIBUTED, ASYNCHRONOUS, INTERACTING CLIPS
Denis Gagne and Alain Garant *In* NASA. Johnson Space Center, Third CLIPS Conference Proceedings, Volume 2 Nov. 1994 p 345-355 (For primary document see N95-19747 05-61)
Avail: CASI HC A03/MF A03

DAI-CLIPS is a distributed computational environment within which each CLIPS is an active independent computational entity with the ability to communicate freely with other CLIPS. Furthermore, new CLIPS can be created, others can be deleted or modify their expertise, all dynamically in an asynchronous and independent fashion during execution. The participating CLIPS are distributed over a network of heterogeneous processors taking full advantage of the available processing power. We present the general framework encompassing DAI-CLIPS and discuss some of its advantages and potential applications. Author

N95-19764*# University of South Florida, Tampa, FL. Dept. of Computer Science and Engineering.
PCLIPS: PARALLEL CLIPS **c62**
Lawrence O. Hall, Bonnie H. Bennett (Honeywell, Inc., Minneapolis, MN.), and Ivan Tello *In* NASA. Johnson Space Center, Third CLIPS Conference Proceedings, Volume 2 Nov. 1994 p 356-362 Sponsored in cooperation with Honeywell and Florida High Technology and Research Council (For primary document see N95-19747 05-61)
Avail: CASI HC A02/MF A03

A parallel version of CLIPS 5.1 has been developed to run on Intel Hypercubes. The user interface is the same as that for CLIPS with some added commands to allow for parallel calls. A complete version of CLIPS runs on each node of the hypercube. The system has been instrumented to display the time spent in the match, recognize, and act cycles on each node. Only rule-level parallelism is supported. Parallel commands enable the assertion and retraction of facts to/from remote nodes working memory. Parallel CLIPS was used to implement a knowledge-based command, control, communications, and intelligence (C(sup 3)I) system to demonstrate the fusion of high-level, disparate sources. We discuss the nature of the information fusion problem, our approach, and implementation. Parallel CLIPS has also be used to run several benchmark parallel knowledge bases such as one to set up a cafeteria. Results show from running Parallel CLIPS with parallel knowledge base partitions indicate that significant speed increases, including superlinear in some cases, are possible. Author

N95-19765*# LinCom Corp., Houston, TX.
USING CLIPS TO REPRESENT KNOWLEDGE IN A VR SIMULATION
Mark L. Engelberg *In* NASA. Johnson Space Center, Third CLIPS Conference Proceedings, Volume 2 Nov. 1994 p 363-371 (For primary document see N95-19747 05-61)
Avail: CASI HC A02/MF A03

Virtual reality (VR) is an exciting use of advanced hardware and software technologies to achieve an immersive simulation. Until recently, the majority of virtual environments were merely 'fly-throughs' in which a user could freely explore a 3-dimensional world or a visualized dataset. Now that the underlying technologies are reaching a level of maturity, programmers are seeking ways to increase the complexity and interactivity of immersive simulations. In most cases, interactivity in a virtual environment can be specified in the form 'whenever such-and-such happens to object X, it reacts in the following manner.' CLIPS and COOL provide a simple and elegant framework for representing this knowledge-base in an efficient manner that can be extended incrementally. The complexity of a detailed simulation becomes more manageable when the control flow is governed by CLIPS' rule-based inference engine as opposed to by traditional procedural mechanisms. Examples in this paper will illustrate an effective way to represent VR information in CLIPS, and to tie this knowledge base to the input and output C routines of a typical virtual environment. Author

N95-19766*# North Carolina Agricultural and Technical State Univ., Greensboro, NC. Dept. of Computer Science.
REFLEXIVE REASONING FOR DISTRIBUTED REAL-TIME SYSTEMS
David Goldstein *In* NASA. Johnson Space Center, Third CLIPS Conference Proceedings, Volume 2 Nov. 1994 p 372-374 (For primary document see N95-19747 05-61)
Avail: CASI HC A01/MF A03

This paper discusses the implementation and use of reflexive reasoning in real-time, distributed knowledge-based applications. Recently there has been a great deal of interest in agent-oriented systems. Implementing such systems implies a mechanism for sharing knowledge, goals and other state information among the agents. Our techniques facilitate an agent examining both state information about other agents and the parameters of the knowledge-based system shell implementing its reasoning algorithms. The shell implementing the reasoning is the Distributed Artificial Intelligence Toolkit, which is a derivative of CLIPS. Author

N95-19767*# Reticular Systems, Inc., San Diego, CA.
PalymSys (TM): AN EXTENDED VERSION OF CLIPS FOR CONSTRUCTION AND REASONING USING BLACKBOARDS
Travis Bryson and Dan Ballard *In* NASA. Johnson Space Center, Third CLIPS Conference Proceedings, Volume 2 Nov. 1994 p 377-387 (For primary document see N95-19747 05-61)
Avail: CASI HC A03/MF A03

This paper describes PalymSys(TM) -- an extended version of the CLIPS language that is designed to facilitate the implementation of blackboard systems. The paper first describes the general characteristics of blackboards and shows how a control blackboard architecture can be used by AI systems to examine their own behavior and adapt to real-time problem-solving situations by striking a balance between domain and control reasoning. The paper then describes the use of PalymSys in the development of a situation assessment subsystem for use aboard Army helicopters. This system performs real-time inferencing about the current battlefield situation using multiple domain blackboards as well as a control blackboard. A description of the control and domain blackboards and their implementation is presented. The paper also describes modifications made to the standard CLIPS 6.02 language in PalymSys(TM) 2.0. These include: (1) a dynamic Dempster-Shafer belief network whose structure is completely specifiable at run-time in the consequent of a PalymSys(TM) rule, (2) extension of the

run command including a continuous run feature that enables the system to run even when the agenda is empty, and (3) a built-in communications link that uses shared memory to communicate with other independent processes. Author

N95-19768*# Cengeloglu (Yilmaz), Winter Park, FL.
DYNACLIPS (DYNAmic CLIPS): A DYNAMIC KNOWLEDGE EXCHANGE TOOL FOR INTELLIGENT AGENTS
Yilmaz Cengeloglu, Soheil Khajenoori (Embry-Riddle Aeronautical Univ., Daytona Beach, FL.), and Darrell Linton (University of Central Florida, Orlando, FL.) *In* NASA. Johnson Space Center, Third CLIPS Conference Proceedings, Volume 2 Nov. 1994 p 388-400 (For primary document see N95-19747 05-61)
Avail: CASI HC A03/MF A03

In a dynamic environment, intelligent agents must be responsive to unanticipated conditions. When such conditions occur, an intelligent agent may have to stop a previously planned and scheduled course of actions and replan, reschedule, start new activities and initiate a new problem solving process to successfully respond to the new conditions. Problems occur when an intelligent agent does not have enough knowledge to properly respond to the new situation. DYNACLIPS is an implementation of a framework for dynamic knowledge exchange among intelligent agents. Each intelligent agent is a CLIPS shell and runs a separate process under SunOS operating system. Intelligent agents can exchange facts, rules, and CLIPS commands at run time. Knowledge exchange among intelligent agents at run times does not effect execution of either sender and receiver intelligent agent. Intelligent agents can keep the knowledge temporarily or permanently. In other words, knowledge exchange among intelligent agents would allow for a form of learning to be accomplished. Author

N95-19803 Software Productivity Consortium, Herndon, VA.
PROCESS DEFINITION AND MODELING GUIDEBOOK. VOLUME 1: CONCEPTS AND PRINCIPLES OF MPDM. VERSION 02.00.02
R. Bechtold, J. Brackett, and S. Redwine Mar. 1994 112 p Limited Reproducibility: More than 20% of this document may be affected by microfiche quality
(Contract MDA972-92-J-1018)
(AD-A279162; SPC-92041-CMC-Vol-1) Avail: Issuing Activity (Defense Technical Information Center (DTIC))

This two volume guidebook provides guidance on efficiently developing and evolving a quality set of process definitions that will direct and improve the ways you develop software. This guidebook is particularly helpful for those persons who must fulfill a software process improvement action plan calling for definition of part or all of their software process. This guidebook provides a flexible set of templates and techniques for capturing and representing processes and explains how to use the template-based information to produce guidebooks training materials and models. Basic usage principles and techniques are presented in Volume 1; advanced usage concepts are presented in Volume 2. DTIC

N95-19813 Software Productivity Consortium, Herndon, VA.
PROCESS DEFINITION AND MODELING GUIDEBOOK. VOLUME 2: ADVANCED APPLICATIONS OF MPDM
R. Bechtold, J. Brackett, and S. Redwine Mar. 1994 186 p Limited Reproducibility: More than 20% of this document may be affected by microfiche quality
(Contract MDA972-92-J-1018)
(AD-A279199; SPC-92041-CMC-Vol-2) Avail: Issuing Activity (Defense Technical Information Center (DTIC))

This two volume guidebook provides guidance on efficiently developing and evolving a quality set of process definitions that will direct and improve the ways you develop software. This guidebook is particularly helpful for those persons who must fulfill a software process improvement action plan calling for definition of part or all of their software process. This guidebook provides a flexible set of templates and techniques for capturing and representing processes and explains how to use the template-based information to produce guidebooks training materials and models. Basic usage principles and techniques are presented in Volume 1; advanced usage concepts are presented in Volume 2. DTIC

N95-19821 Wickersheimer Engineers, Inc., Champaign, IL.
TUTORIAL GUIDE: COMPUTER-AIDED STRUCTURAL MODELING (CASM), VERSION 5.00 Final Report
David Wickersheimer, Gene McDermott, Ken Taylor, and Carl Roth Apr. 1994 305 p Limited Reproducibility: More than 20% of this document may be affected by microfiche quality
(Contract DACA39-86-C-0024)
(AD-A280147; WES/IR/ITL-94-1) Avail: Issuing Activity (Defense Technical Information Center (DTIC))

The Computer-Aided Structural Modeling (CASM) computer program is designed to aid the structural engineer in the preliminary design and evaluation of structural building systems by the use of three-dimensional (3-D) interactive graphics. CASM allows the structural engineer to quickly evaluate various framing alternatives in order to make more informed decisions in the initial structural evaluation process. The program was developed by the Information Technology Laboratory in conjunction with the Computer Aided Structural Engineering (CASE) Project, Building Systems Task Group. This release of the CASM is designed to aid the user with design criteria, building loads, and structural framing and design. The various parts of the program are: (1) Basic design criteria-- The user can enter information directly or retrieve information from a user-definable database. The design criteria include information about the project, regional design information, and site-specific design information. (2) Building geometry-- The user can assemble the building shape using 3-D primitives (cubes, prisms, spheres, cylinders, etc.) in an easy manner using pull-down menus, icons, and a mouse. (3) Dead and live loads-- The user can select and construct dead and live loads from several user-definable menus of building materials and load conditions. These loads can then be applied to any desired area of the building volume. DTIC

N95-18186*# Missouri Univ., Rolla, MO. Dept. of Computer Science.
PERFORMANCE EVALUATION OF THE NASA/KSC CAD/CAE AND OFFICE AUTOMATION LAN'S
George W. Zobrist *In* Univ. of Central Florida, NASA/ASEE Summer Faculty Fellowship Program. 1994 Research Reports Oct. 1994 p 545-567 (For primary document see N95-18166 05-80)
Avail: CASI HC A03/MF A04

N95-19004*# Texas A&I Univ., Kingsville, TX. Dept. of Electrical Engineering and Computer Science.
EVALUATION OF THE EFFICIENCY AND RELIABILITY OF SOFTWARE GENERATED BY CODE GENERATORS
Barbara Schreur *In* Alabama Univ., Research Reports: 1994 NASA/ASEE Summer Faculty Fellowship Program Oct. 1994 6 p (For primary document see N95-18967 05-80)
Avail: CASI HC A02/MF A03

62 COMPUTER SYSTEMS

Includes computer networks and special application computer systems.

N95-17936 Newcastle-upon-Tyne Univ., Newcastle (England). Dept. of Computing Science.
REFORMULATED PRECONDITIONED CONJUGATE GRADIENT SQUARED METHOD. PART 1: THE ALGORITHM
R. Cook and C. Phillips Mar. 1994 15 p
(PB94-201589; TRS-473-Pt-1) Copyright Avail: Issuing Activity (National Technical Information Service (NTIS))

The authors are concerned with the solution of the system of linear equations Ax = b, with A an n x n matrix and x and b conforming n-vectors. Of particular interest is the situation in which n is large (or the order of 1000's) and A is sparse; linear systems with such properties arise from, for example, 'the discretization' of elliptic partial differential equations using finite difference or finite element techniques. It is theoretically possible to solve systems of this form using direct methods based on elimination techniques, but this approach can be very expensive both in terms of storage requirements and computation. This is a direct consequence of the fill-in that may occur. An alternative, and frequently used, approach which avoids these drawbacks is based on the use of iteration, leading to

a family of (Krylov subspace) methods which cover the various particular forms that A may take. NTIS

N95-17989# National Inst. of Standards and Technology, Gaithersburg, MD. Systems and Software Technology Div.
USER PROFILE FOR RESEARCHERS STUDYING OBJECTS: IMPLICATIONS FOR COMPUTER SYSTEMS
J. Moline Apr. 1994 25 p See also PB-235952
(PB94-188463; NISTIR-5415) Avail: CASI HC A03/MF A01

A group of twenty-five researchers who study objects was observed over a four year period. A variety of methods of data collection was used: observation, interview, questionnaires, and analysis of published materials. This report identifies the features needed in computer systems to facilitate the research of those who study objects. The researchers need to link objects with text, work with a variety of data types, and collaborate with colleagues over a computer network. Author

N95-18039 Technische Univ., Twente (Netherlands). Tele-Informatics and Open Systems Group.
DESIGN AND ANALYSIS OF DYNAMIC LEADER ELECTION PROTOCOLS IN BROADCAST NETWORKS
J. Brunekreef (Amsterdam Univ., Netherlands.), J. P. Katoen, R. Koymans (Philips Gloeilampenfabrieken N.V., Eindhoven, Netherlands.), and S. Mauw (Technische Hogeschool, Eindhoven, Netherlands.) 8 Sep. 1993 79 p
(PB94-202728; TIOS-93-43) Copyright Avail: Issuing Activity

The well-known problem of leader election in distributed systems is considered in a dynamic context where processes may participate and crash spontaneously. Processes communicate by means of buffered broadcasting as opposed to usual point-to-point communication. In this paper the authors design a leader election protocol in such a dynamic system. As the problem at hand is considerably complex they adopt a step-wise refinement design method starting from a simple leader election protocol. In a first refinement a symmetric solution is obtained and eventually a fault-tolerant protocol is constructed. This gives rise to three protocols. The worst case message complexity of all protocols is analyzed. A formal approach to the verification of the leader election protocols is adopted. The requirements are specified in a property-oriented way, and the protocols are denoted by means of extended finite state machines. It is proven using linear-time temporal logic that the protocols satisfy their requirements. Furthermore, the protocols are specified in more detail in the process algebra formalism Algebra of Communicating Processes (ACP). NTIS

N95-18050# California Univ., Berkeley, CA.
CONSTRUCTION OF A CONNECTIONIST NETWORK SUPERCOMPUTER Technical Progress Report, 1 May - 31 Jul. 1994
31 Jul. 1994 4 p
(Contract N00014-92-J-1617)
(AD-A283354) Avail: CASI HC A02/MF A01

We have made progress in several areas in this quarter: considerable progress in both high low level software aspects of the project, work on a CNS-O system, to be based on the nearly completed TO processor, and continue to make progress in the application of analog VLSI to speech preprocessors. DTIC

N95-18055*# Illinois Univ., Urbana-Champaign, IL.
NASA/DOD AEROSPACE KNOWLEDGE DIFFUSION RESEARCH PROJECT. PAPER 47: THE VALUE OF COMPUTER NETWORKS IN AEROSPACE
Ann Peterson Bishop and Thomas E. Pinelli (National Aeronautics and Space Administration. Langley Research Center, Hampton, VA.) 1995 8 p Presented at the 33d Aerospace Meeting and Exhibit, Reno, NV, 9-12 Jan. 1995; sponsored by AIAA
(NASA Order L-58104-D)
(NASA-CR-197591; NAS 1.26:197591; AIAA Paper 95-0703) Avail: CASI HC A02/MF A01

This paper presents data on the value of computer networks that were obtained from a national survey of 2000 aerospace engineers that was conducted in 1993. Survey respondents reported the extent to which they used computer networks in their work and communication and offered their assessments of the value of various network types and applications. They also provided information about the positive impacts of networks on their work, which presents another perspective on value. Finally, aerospace engineers' recommendations on network implementation present suggestions for increasing the value of computer networks within aerospace organizations. Author

N95-18106 Purdue Univ., West Lafayette, IN. Dept. of Electrical Engineering.
SOFTWARE TECHNIQUES FOR BALANCING COMPUTATION AND COMMUNICATION IN PARALLEL SYSTEMS Final Report, Aug. 1992 - Dec. 1993
John K. Antonio Jul. 1994 52 p Limited Reproducibility: More than 20% of this document may be affected by microfiche quality
(Contract F30602-92-C-0108; AF Proj. 5581)
(AD-A285536; RL-TR-94-98) Avail: CASI HC A04

The work presented in this report is the result of collaboration between Rome Laboratory and Purdue University. The work is divided into two main parts. The first part describes a new mapping technique developed under this effort called the hypersphere mapper, for the hypercube embedding problem. Solving the hypercube embedding problem involves finding the best mapping (i.e., assignment) of software tasks onto the processing elements of a parallel computer having a hypercube inter-connection network. The second part of the work describes a new software engineering tool called OMARS (Optimal Mapping Alternate Routing System). OMARS is an interactive tool that aids the software engineer in deciding how to best map multiple software tasks onto the processors of message passing parallel architectures. Hypersphere mapper is one of several mapping algorithms that is integrated into OMARS. DTIC

N95-18129# Oak Ridge National Lab., TN.
EARLY EXPERIENCES AND PERFORMANCE OF THE INTEL PARAGON
T. H. Dunigan Aug. 1994 24 p
(Contract DE-AC05-84OR-21400)
(DE94-018061; ORNL/TM-12194) Avail: CASI HC A03/MF A01

Experiences and performance figures are reported from early tests of the 512-node Intel Paragon XPS35 at Oak Ridge National Laboratory. Computation performance of the 50 MHz i860XP processor as well as communication performance of the 200 megabyte/second mesh are reported and compared with other multiprocessors. Single and multiple hop communication bandwidths and latencies are measured. Concurrent communication speeds and speed under network load are also measured. File I/O performance of the mesh-attached Parallel File System is measured. Early experiences with OSF/Mach and SUNMOS operating systems are reported, as well results from porting various distributed-memory applications. This report also summarizes the second phase of a Cooperative Research and Development Agreement between Oak Ridge National Laboratory and Intel in evaluating a 66-node Intel Paragon XPS5. DOE

N95-18137 Naval Postgraduate School, Monterey, CA.
A SCALABLE DECENTRALIZED GROUP MEMBERSHIP SERVICE FOR AN ASYNCHRONOUS ENVIRONMENT M.S. Thesis
David S. Neely Jun. 1994 194 p Limited Reproducibility: More than 20% of this document may be affected by microfiche quality
(AD-A283633) Avail: Issuing Activity (Defense Technical Information Center (DTIC))

This thesis presents a globally scalable, decentralized group membership service to manage client process groups operating in a distributed, asynchronous environment. This group membership service is totally scalable, handling process groups spanning a single LAN to groups spanning the entire global Internet equally well. It provides for nested and overlapping groups, as well as multiple groups residing on a single LAN. It also provides various Quality of Service selections which permit individual groups to be configured for an optimal balance between high quality with strong consistency semantics for group membership, and weaker consistency semantics with reduced complexity and latency. This thesis describes the complete design of the protocol used to implement the group membership service. It presents the design requirements and goals, and underlying assumptions about the network. The various Quality of Service selections provided by the group membership service are described in detail, as well as the interface between the process groups, the membership service, and the underlying network. The use of a hierarchical architecture to obtain the desired scalibility, flexibility, and robustness is explained. A proof of correctness for the protocol is presented, and a partial implementation of the group membership service is described. DTIC

N95-18158# Wisconsin Univ., Milwaukee, WI. Dept. of Electrical Engineering and Computer Science.
FAIR PETRI NETS AND STRUCTURAL INDUCTION FOR RINGS OF PROCESSES
Ichiro Suzuki, Jianan Li, and Masafumi Yamashita Dec. 1994 28 p
(Contract N00014-94-1-0284; NSF CCR-90-04346; NSF IRI-93-07506)
(AD-A283920) Avail: CASI HC A03/MF A01

We present a structural induction theorem for rings consisting of an arbitrary number of identical components. The components of a ring are modeled using a fair Petri net, in which the firing of a prespecified set of transitions is assumed to occur fairly, i.e., any of these transitions that becomes firable infinitely often must fire infinitely often. Specifically, we introduce the concept of similarity between rings of different sizes, and give a condition under which the similarity between the rings of sizes two and three guarantees the similarity among the rings of all sizes. So if the given condition is satisfied, then the correctness of a ring of any large size can be inferred from the correctness of a ring having only a few components. The usefulness of the theorem is demonstrated using the examples of token-passing mutual exclusion and a simple producer-consumer system. DTIC

N95-18159# Wisconsin Univ., Milwaukee, WI. Dept. of Electrical Engineering and Computer Science.
A PRACTICAL ALGORITHM FOR INTEGER SORTING ON A MESH-CONNECTED COMPUTER (PRELIMINARY VERSION)
Sumanta Guha 5 May 1994 14 p
(Contract N00014-94-1-0284; NSF IRI-93-07506; NSF CCR-90-04346)
(AD-A283921) Avail: CASI HC A03/MF A01

This paper presents count-sort, a parallel algorithm for mesh-connected computers to sort integers where the range of inputs is known. A straightforward counting technique that has not been implemented previously in parallel sorting algorithms is presented. On a mesh-connected computer with square root N x square root N processors we are able to sort N integers in the range 1... square root N in time c square root N where c is very small. For practical values of N, the algorithm is extremely fast. Further, it is possible to expand the range by a factor k to 1 ... k square root N so that the slowdown is less than k. We produce an implementation of count-sort on the SIMD MasPar MP-1 with 8192 processors that sorts 8-bit integers significantly faster than the manufacturer's current library routine for sorting 8-bit integers. DTIC

N95-18454 Rome Lab., Griffiss AFB, NY.
GLOBAL TIME TRANSFORMATIONS
Jon B. Valente and Robert J. Vaeth Jul. 1994 68 p Limited Reproducibility: More than 20% of this document may be affected by microfiche quality
(AF Proj. 5581)
(AD-A285539; RL-TR-94-87) Avail: CASI HC A04

This report on global time transformations comes from an in-house research effort in the area of distributed-parallel computing. The distributed-parallel computing environments are multiple clock systems interconnected by communications networks. The global time transformation maps the data from these different systems into a common (i.e., global) clock for an analysis. The derivation of the global time transformation is given. The primary components of the global time transformation are the clock rate and clock offset. These components and the measurement techniques for measuring these components are discussed. To demonstrate the accuracy of the global time transformation, a set of measurements were taken to compare with the transformation predictions. DTIC

N95-18521*# Duke Univ., Durham, NC. Dept. of Computer Science.
CHARACTERIZING PARALLEL FILE-ACCESS PATTERNS ON A LARGE-SCALE MULTIPROCESSOR
Apratim Purakayastha, Carla Schlatter Ellis, David Kotz (Dartmouth Coll., Hanover, NH.), Nils Nieuwejaar (Dartmouth Coll., Hanover, NH.), and Michael Best (Massachusetts Inst. of Tech., Cambridge.) 24 Oct. 1994 31 p Sponsored by Thinking Machines Corp.
(Contract NCC2-849; NSF CCR-91-13170)
(NASA-CR-197568; NAS 1.26:197568; CS-1994-33) Avail: CASI HC A03/MF A01

Rapid increases in the computational speeds of multiprocessors have not been matched by corresponding performance enhancements in the I/O subsystem. To satisfy the large and growing I/O requirements of some parallel scientific applications, we need parallel file systems that can provide high-bandwidth and high-volume data transfer between the I/O subsystem and thousands of processors. Design of such high-performance parallel file systems depends on a thorough grasp of the expected workload. So far there have been no comprehensive usage studies of multiprocessor file systems. Our CHARISMA project intends to fill this void. The first results from our study involve an iPSC/860 at NASA Ames. This paper presents results from a different platform, the CM-5 at the National Center for Supercomputing Applications. The CHARISMA studies are unique because we collect information about every individual read and write request and about the entire mix of applications running on the machines. The results of our trace analysis lead to recommendations for parallel file system design. First the file system should support efficient concurrent access to many files, and I/O requests from many jobs under varying load conditions. Second, it must efficiently manage large files kept open for long periods. Third, it should expect to see small requests predominantly sequential access patterns, application-wide synchronous access, no concurrent file-sharing between jobs appreciable byte and block sharing between processes within jobs, and strong interprocess locality. Finally, the trace data suggest that node-level write caches and collective I/O request interfaces may be useful in certain environments. Author

N95-18532*# Cornell Univ., Ithaca, NY. Dept. of Computer Science.
THE ISIS PROJECT: FAULT-TOLERANCE IN LARGE DISTRIBUTED SYSTEMS Final Research and Development Status Report No. 8, 1 Jan. 1992 - 30 Jun. 1992
Kenneth P. Birman and Keith Marzullo 1 Jan. 1993 16 p Sponsored by DARPA
(Grant NAG2-593)
(NASA-CR-197561; NAS 1.26:197561) Avail: CASI HC A03/MF A01

This final status report covers activities of the Isis project during the first half of 1992. During the report period, the Isis effort has achieved a major milestone in its effort to redesign and reimplement the Isis system using Mach and Chorus as target operating system environments. In addition, we completed a number of publications that address issues raised in our prior work; some of these have recently appeared in print, while others are now being considered for publication in a variety of journals and conferences. Derived from text

N95-18581*# Dartmouth Coll., Hanover, NH. Dept. of Computer Science.
DYNAMIC FILE-ACCESS CHARACTERISTICS OF A PRODUCTION PARALLEL SCIENTIFIC WORKLOAD
David Kotz and Nils Nieuwejaar 1994 10 p Repr. from IEEE, v. 1063, no. 9535, 1994 p 640-649
(Contract NCC2-849)
(NASA-CR-197570; NAS 1.26:197570) Copyright Avail: CASI HC A02/MF A01

Multiprocessors have permitted astounding increases in computational performance, but many cannot meet the intense I/O requirements of some scientific applications. An important component of any solution to this I/O bottleneck is a parallel file system that can provide high-bandwidth access to tremendous amounts of data in parallel to hundreds or thousands of processors. Most successful systems are based on a solid understanding of the expected workload, but thus far there have been no comprehensive workload characterizations of multiprocessor file systems. This paper presents the results of a three week tracing study in which all file-related activity on a massively parallel computer was recorded. Our instrumentation differs from previous efforts in that it collects information about every I/O request and about the mix of jobs running in a production environment. We also present the results of a trace-driven caching simulation and recommendations for designers of multiprocessor file systems. Author

N95-18615# Naval Postgraduate School, Monterey, CA. Dept. of Computer Science.
THROUGHPUT ANALYSIS BETWEEN HIGH END WORKSTATIONS ACROSS AN FDDI NETWORK M.S. Thesis
Mark A. Schivley 16 Jun. 1994 159 p
(AD-A283608) Avail: CASI HC A08/MF A02

Recently developed high speed networks are capable of transmitting data at rates of 100 Mbps or more. One such network protocol is Fiber

Distributed Data Interface (FDDI). This network has a physical transmission rate of 100 Mbps. Analytical and simulation studies have shown that the FDDI protocol should provide actual throughput of 80% to 95% of this physical rate. Can the end user expect to see this kind of performance? If not, then what kind of throughput can actually be expected and where are the bottle necks? In order to answer these and other related questions, two areas were studied: First, a performance comparison between a 40MHz SPARCstation 10 workstation and a 50MHz SPARCstation 10 workstation was conducted using the Neal Nelson commercial benchmark tool. Next, a well-known network measurement tool, ttcp, was used to obtain data transfer rates while varying several tunable operating system and network parameters. The parameters varied were: Target Token Rotation Time, TCP/IP window size, NFS asynchronous threads. Logical Link buffer size and Maximum Transfer Unit size. The results from the commercial benchmark analysis were used to determine if there are any differences which can affect transfer rates between the two workstations. The results from the commercial benchmark tool clearly showed that the newer, higher speed processor is faster. The network tool ttcp showed that the TCP/IP window size had the largest impact on throughput performance. Throughput more than doubles from a window size of 4k to a window size of 20k. DTIC

N95-18892 Carnegie-Mellon Univ., Pittsburgh, PA. Dept. of Computer Science.

RESEARCH IN PARALLEL COMPUTING Final Report, 1987 - 1990

C. H. Chien, T. Gross, R. Rashid, Z. Segall, and P. Steenkiste 5 Aug. 1994 56 p Limited Reproducibility: More than 20% of this document may be affected by microfiche quality

(Contract N00039-87-C-0251; ARPA Order 4864)

(AD-A283983; CMU-CS-94-180) Avail: CASI HC A04

This report chronicles an integrated research program conducted at Carnegie Mellon's Computer Science Department during the contract period 1987 to 1990. This research produced the iWarp System, a homogeneous multiprocessor that provides both high-speed computation and communication; a high-performance, fiberoptic interface board and a crossbar switch for high-speed, heterogeneous computing; a parallel operating system as well as software for analyzing and debugging its performance; and an environment for building. DTIC

N95-19513# Clarkson Univ., Potsdam, NY. Dept. of Electrical and Computer Engineering.

ADVANCED TECHNIQUES FOR ANALYSIS AND EVALUATION OF ROBUST PROTOCOLS Final Report, Aug. 1992 - Nov. 1993

Robert A. Meyer and David A. Perreault (Boston Univ., MA.) Aug. 1994 22 p

(Contract F30602-92-C-0074)

(AD-A285682; RL-TR-94-151) Avail: CASI HC A03/MF A01

The objective of this effort was to study new algorithms for robust communication network protocols and to develop techniques for analysis and evaluation of these protocol algorithms. These techniques are necessary to provide an objective basis on which to judge the effectiveness of these new algorithms for future C3I Air Force networks. A primary contribution of this work was to assist in the transfer of technology from on-going contract research efforts to the Rome Laboratory Network Design Facility. This report describes the testbed environment used during this study, presents an example of a typical protocol algorithm study, and illustrates the analysis and evaluation methodology with this example protocol. Sample experimental results that were used to identify certain problems with this protocol are also included. DTIC

N95-19524# Syracuse Univ., NY. Dept. of Electrical and Computer Engineering.

ENHANCING THE ARCHITECTURAL CHARACTERIZATION OF PARALLEL PROTO Final Report, Oct. 1992 - Oct. 1993

Daniel J. Pease Aug. 1994 26 p

(Contract F30602-92-C-0062)

(AD-A285678; RL-TR-94-147) Avail: CASI HC A03/MF A01

The objective of the work presented in this report was to determine the feasibility of integrating the architectural database of the Parallel Assessment Window System (PAWS) into the database of the Parallel Proto (PPROTO) tool. PAWS and PPROTO are Rome Laboratory developed tools. The PAWS tool is an experimental system for performing machine evaluation and comparisons. The tool provides the user with the ability to predict the performance of an application on a number of selected parallel architectures. PPROTO is a software engineering environment that allows a user to validate and analyze the requirements of parallel and distributed systems using rapid prototyping techniques. The benefit of being able to integrate the PAWS database into the PPROTO database is that high level performance prediction can be performed at the requirements phase of the software engineering lifecycle. This would provide users the capability of determining which parallel architecture would be most suitable for their particular problem domain. DTIC

N95-19526# Clarkson Univ., Potsdam, NY. Dept. of Electrical and Computer Engineering.

PST: A SIMULATION TOOL FOR PARALLEL SYSTEMS Final Report, Feb. 1993 - May 1994

David J. Potter, William A. Rivet, and Hisham Awad Aug. 1994 102 p

(Contract F30602-93-C-0055)

(AD-A285680; RL-TR-94-111) Avail: CASI HC A06/MF A02

The objective of this research effort was to develop a tool to simulate various parallel computer systems. The tools would give users insight into the differ classes of parallel machines in terms of architecture, software, synchronization, communication, efficiency, connectivity, and application specialties. In addition it would give valuable information towards the development of languages and tools which can be used independently of the machine architecture. This work would contribute to objectives set by the Software for High Performance Computers Group at Rome Laboratory, namely: (1) developing technology for general purpose parallel computing and (2) developing methods for predicting parallel software performance. The tool would be compatible with the Parallel Experimentation and Evaluation Platform (PEEP) at Rome, in particular totally compatible with X Windows workstations. DTIC

N95-19592# Argonne National Lab., IL. Mathematics and Computer Science Div.

THE QED WORKSHOP

G. W. Pieper Jul. 1994 10 p Workshop held in Argonne, IL, 18-20 May 1994

(Contract W-31-109-eng-38)

(DE94-018499; ANL/MCS/TM-191; CONF-9405215-Summ) Avail: CASI HC A02/MF A01

On May 18-20, 1994, Argonne National Laboratory hosted the QED Workshop. The workshop was supported by special funding from the Office of Naval Research. The purpose of the workshop was to assemble a group of researchers to consider whether it is desirable and feasible to build a proof-checked encyclopedia of mathematics, with an associated facility for theorem proving and proof checking. Among the projects represented were Coq, Eves, HOL, ILF, Imps, MathPert, Mizar, NQTHM, NuPrl, OTTER, Proof Pad, Qu-Prolog, and RRL. Although the content of the QED project is highly technical rigorously proof-checked mathematics of all sorts the discussions at the workshop were rarely technical. No prepared talks or papers were given. Instead, the discussions focused primarily on such political, sociological, practical, and aesthetic questions, such as Why do it? Who are the customers? How can one get mathematicians interested? What sort of interfaces are desirable? The most important conclusion of the workshop was that QED is an idea worthy pursuing, a statement with which virtually all the participants agreed. In this document, the authors capture some of the discussions and outline suggestions for the start of a QED scientific community. DOE

N95-19605# University of Southern California, Marina del Rey, CA. Information Sciences Inst.

GENERATING PARALLEL EXECUTION PLANS WITH A PARTIAL ORDER PLANNER

Craig A. Knoblock May 1994 9 p

(Contract F30602-91-C-0081)

(AD-A285888; ISI/RR-94-380) Avail: CASI HC A02/MF A01

Many real-world planning problems require generating plans that maximize the parallelism inherent in a problem. There are a number of partial-order planners that generate such plans; however, in most of these planners it is unclear under what conditions the resulting plans will be correct and whether the planner can even find a plan if one exists. This paper identifies the underlying assumptions about when a partial plan can be executed in parallel, defines the classes of parallel plans that can be generated by

different partial-order planners, and describe the changes required to turn UCPOP into a parallel execution planner. In addition, we describe how this planner can be applied to the problem of query access planning, where parallel execution produces substantial reductions in overall execution. DTIC

N95-19689# Louisiana State Univ., Baton Rouge, LA. Dept. of Computer Science.
A GENERAL THEORY OF SIGNAL INTEGRATION FOR FAULT TOLERANT DISTRIBUTED SENSOR NETWORKS Report, 1 Oct. 1993 - 30 Sep. 1994
S. S. Iyengar and B. Jones 30 Sep. 1994 8 p
(Contract N00014-91-J-1306)
(AD-A284825) Avail: CASI HC A02/MF A01

The computational issues relating to information integration by multisensor systems and distributed sensor networks are an area of intense ongoing research. Many significant advances have been made recently in the field of sensor integration. This interest in Distributed Sensor Networks (DSNs) technology for information gathering is at least partially due to: (1) the development of new technology making DSNs economically feasible to implement and (2) the growing complexity of information gathering applications. The extraction and fusion of accurate information from the noisy and faulty signals returned by many sensors requires the resolution of many problems including: (1) the architecture of fault-tolerant and robust distributed sensor networks, (2) the reliable synchronization of sensor signals, (3) the efficient integration of information in order to minimize communications and processing overhead, and (4) the development of efficient computational tools for abstract representation and integration of sensor data. The sensor fusion process is of interest for the process of human decision making as well as for its applications within automated systems. DTIC

N95-19692# California Inst. of Tech., Pasadena, CA.
PARALLEL COMPUTATION Final Report
K. M. Chandy 6 Sep. 1994 11 p
(Contract N00014-89-J-3201)
(AD-A284831) Avail: CASI HC A03/MF A01

In this project we have worked on three problems: (1) designing a theory of the modular design of parallel reactive systems, (2) an application of parallel systems of importance to the Navy-parallel discrete-event simulation, and (3) parallel languages that integrate task and data parallelism. DTIC

N95-19831 Oak Ridge National Lab., TN. Mathematical Science Section.
SOLUTION OF POTENTIAL FLOW PROBLEMS ON A NETWORK OF WORKSTATIONS
B. D. Semeraro 14 Jun. 1994 8 p Presented at the 33rd American Institute of Aeronautics and Astronautics (AIAA) Aerospace Sciences Meeting, Reno, NV, 9-12 Jan. 1995 Limited Reproducibility: More than 20% of this document may be affected by microfiche quality
(Contract DE-AC05-84OR-21400)
(DE94-017861; CONF-950130-1) Avail: CASI HC A02

This paper deals with the solution of potential flow problems via a panel or boundary element method on a network of scientific workstations. The idea is to treat the workstation network as a relatively course grained parallel computer and to distribute the work of constructing the influence coefficient matrix over the network. We make use of the Parallel Virtual Machine (PVM) software developed at the Oak Ridge National Laboratory to do the interprocess communications. We specifically address the problem of how to distribute the data across the network as well as the implementation of the parallel linear system solver. DOE

N95-19834 Tampere Univ. of Technology (Finland). Electricity and Magnetism Lab.
SOLUTIONS OF TEAM PROBLEM NO. 13 USING INTEGRAL EQUATIONS IN A SEQUENTIAL AND PARALLEL COMPUTING ENVIRONMENT
Lauri Kettunen, Kimmo Forsman, David Levine (Argonne National Lab., IL.), and William Gropp (Argonne National Lab., IL.) 1993 4 p Presented at the 4th International TEAM Workshop, Miami, FL, 5-6 Nov. 1993 Limited Reproducibility: More than 20% of this document may be affected by microfiche quality
(Contract W-31-109-eng-38)
(DE95-001472; ANL/MCS/CP-84282; CONF-9311255-1) Avail: Issuing Activity (Department of Energy (DOE))

In this paper a brief discussion of h-type volume integral formulations implemented in GFUNET/CORAL code is given and solutions of TEAM benchmark No. 13 are shown. GFUNET/CORAL is a general purpose code for 2D and 3D magnetostatics. Solutions of TEAM problem No. 13 are computed using both a sequential and parallel version of GFUNET/CORAL. DOE

N95-19843 California Univ., Berkeley, CA.
CONNECTIONIST NETWORK SUPERCOMPUTER PROJECT
John Wawrzynek Mar. 1994 14 p Prepared in cooperation with International Computer Science Inst., Berkeley, CA Sponsored by ONR, NSF, and the ministries of research of Germany, Italy, and Sweden, and cooperating companies Limited Reproducibility: More than 20% of this document may be affected by microfiche quality
(AD-A279206) Avail: Issuing Activity (Defense Technical Information Center (DTIC))

The project consists of the following: (1) a tool for artificial neural network research; (2) training large nets (up to 10 to the 9th power parameters); (3) experiments with real-world I/O (new work in speech and vision); and (4) research and education in parallel architectures. DTIC

N95-19645*# Raytheon Co., Marlborough, MA.
AN EXPERT SYSTEM FOR CONFIGURING A NETWORK FOR A MILSTAR TERMINAL
Melissa J. Mahoney and Elizabeth J. Wilson *In* NASA. Johnson Space Center, Third CLIPS Conference Proceedings, Volume 1 Nov. 1994 p 171-179 (For primary document see N95-19625 05-61)
Avail: CASI HC A02/MF A03

N95-19750*# Swiss Scientific Computing Center, Manno (Switzerland). Section of Research and Development.
USING CLIPS IN THE DOMAIN OF KNOWLEDGE-BASED MASSIVELY PARALLEL PROGRAMMING
Jiri J. Dvorak *In* NASA. Johnson Space Center, Third CLIPS Conference Proceedings, Volume 2 Nov. 1994 p 220-229 (For primary document see N95-19747 05-61)
Avail: CASI HC A02/MF A03

N95-19764*# University of South Florida, Tampa, FL. Dept. of Computer Science and Engineering.
PCLIPS: PARALLEL CLIPS
Lawrence O. Hall, Bonnie H. Bennett (Honeywell, Inc., Minneapolis, MN.), and Ivan Tello *In* NASA. Johnson Space Center, Third CLIPS Conference Proceedings, Volume 2 Nov. 1994 p 356-362 Sponsored in cooperation with Honeywell and Florida High Technology and Research Council (For primary document see N95-19747 05-61)
Avail: CASI HC A02/MF A03

63 CYBERNETICS

Includes feedback and control theory, artificial intelligence, robotics and expert systems.

For related information see also *54 Man/System Technology and Life Support.*

N95-17948# Sandia National Labs., Albuquerque, NM.
ADAPTIVE ROBOT PATH PLANNING IN CHANGING ENVIRONMENTS
P. C. Chen 1994 7 p Presented at the 1994 Institute of Electrical and Electronics Engineers Conference on Tolls With Artificial Intelligence, New Orleans, LA, 6 Nov. 1994
(Contract DE-AC04-94AL-85000)
(DE94-016564; SAND-94-2006C; CONF-9411103-1) Avail: CASI HC A02/MF A01

Path planning needs to be fast to facilitate real-time robot programming. Unfortunately, current planning techniques are still too slow to be effective, as they often require several minutes, if not hours of computation. To overcome this difficulty, we present an adaptive algorithm that uses past experience to speed up future performance. It is a learning algorithm

suitable for incrementally-changing environments such as those encountered in manufacturing of evolving products and waste-site remediation. The algorithm allows the robot to adapt to its environment by having two experience manipulation schemes: For minor environmental change, we use an object-attached experience abstraction scheme to increase the flexibility of the learned experience; for major environmental change, we use an on-demand experience repair scheme to retain those experiences that remain valid and useful. Using this algorithm, we can effectively reduce the overall robot planning time by re-using the computation result for one task to plan a path for another. DOE

N95-18023# Naval Postgraduate School, Monterey, CA.
TIME-OPTIMAL CONTROL OF A THIRD ORDER REGULATOR M.S. Thesis
Serhat Balkan Jun. 1994 64 p
(AD-A283307) Avail: CASI HC A04/MF A01

The time-optimal control law as a function of the states for second and third-order linear regulators with real eigenvalues was derived. Notions of a switching curve for the second-order system and switching surface for the third-order system was introduced. A set of states was found which divided the state space into two distinct regions, in one of which the time-optimal control was +1 and in the other of which the time-optimal control was -1. DTIC

N95-18057# Maryland Univ., College Park, MD. Center for Automation Research.
ROBUST IMAGE UNDERSTANDING. TECHNIQUES AND APPLICATIONS Technical Report, 1989 - 1992
Azriel Rosenfeld Oct. 1993 25 p
(Contract DACA76-89-C-0019)
(AD-A283427; TEC-0050) Avail: CASI HC A03/MF A01

The research for this report deals with the following topics: (1) feature detection, including both edge detection and line slope estimation; (2) Robust and Bayesian estimation of image parameters; (3) image and pattern matching; (4) region segmentation and shape recognition; (5) shape recovery and pose estimation; (6) robot hand-eye coordination; (7) robot navigation and path planning; (8) visibility and navigation on terrain; (9) motion transparency and motion parameter estimation; and (10) structure from motion, using both feature-based and normal-flow-based methods and regularization techniques. DTIC

N95-18157# Wisconsin Univ., Milwaukee, WI. Dept. of Electrical Engineering and Computer Science.
DISTRIBUTED METHODS FOR CONTROLLING MULTIPLE MOBILE ROBOTS
Ichiro Suzuki 1 Apr. 1994 6 p
(Contract N00014-94-1-0284; NSF IRI-93-07506)
(AD-A283919) Avail: CASI HC A02/MF A01

This project is supported jointly by ONR Grant N00014-94-1-0284 and NSF Grant IRI-9307506. Although the official starting date of the ONR grant was November 1, 1993, the work started when the NSF grant arrived in August 1993. So in the following, we report the activities since August 1993. However, since UWM received the official notification and the ONR grant number in late January, 1994, we were not able to acknowledge the support from ONR in some of the articles mentioned in this report. The intent of the project is to study the fundamentals of the distributed control method for multiple mobile robots and develop a theory for applying the method effectively. In this method, at every tick of its local clock,, each robot observes the positions of all the robots and moves to a new position determined by the given algorithm. Typically, we assume that the robots are anonymous (they all execute the same algorithm and they cannot be distinguished by their appearances), initially they do not have a common x-y coordinate system, and their local clocks may not be synchronized. A basic problem for such a robot system is to design an algorithm that, when executed individually by the robots, allows the robots as a group to achieve the given goal. DTIC

N95-18218 Rensselaer Polytechnic Inst., Troy, NY.
AN ANALOG COMPUTING APPROACH TO STRUCTURAL ANALYSIS AND OPTIMAL DESIGN THROUGH ARTIFICIAL NEURAL NETWORKS Ph.D. Thesis
Biao Fu 1993 153 p
Avail: Univ. Microfilms Order No. DA9420319

There has been significant research activity in the general area of neural computing, or more specifically, artificial neural networks. This thesis investigates the applicability of distinctly different architectures of neural networks in structural analysis and optimal design. Specific topics investigated in this work include: (1) Adaptive Resonance Theory (ART) based neural networks in automated conceptual design of structural systems; (2) Hopfield neural networks and a variant of this network referred to as the deformable template model in the solution of combinatorial optimization problems; (3) Development of a measure referred to as generalized cross validation for determining the quality of a function approximation obtained through the use of regularization neural networks; and (4) The use of regularization networks in structural damage monitoring. The results of these studies clearly demonstrate the usefulness of the neural network based computing paradigm in problems of structural engineering and design. In addition to this demonstrated potential in providing acceptable solutions to genetically difficult optimization problems, neural networks offer a significant function approximation capability for reducing the computational effort in an iterative design environment. The approach presented in this thesis provides a rational approach for controlling the quality of function approximations from the regularization network. Another important contribution of the present work is to show how the pattern recognition feature of neural networks, particularly the ART network, can be used to create the framework for a conceptual design system, in a manner similar to that available in the rule-based expert systems. Dissert. Abstr.

N95-18313* National Aeronautics and Space Administration. Pasadena Office, CA.
THREE-PARAMETER TUNABLE TILT-INTEGRAL-DERIVATIVE (TID) CONTROLLER Patent
Boris J. Lurie, inventor (to NASA) (Jet Propulsion Lab., California Inst. of Tech., Pasadena, CA.) 6 Dec. 1994 12 p Filed 1 Feb. 1993
Supersedes N93-29176 (31 - 11, p 3542)
(NASA-Case-NPO-18492-1-CU; US-Patent-5,371,670;
US-Patent-Appl-SN-023253; US-Patent-Class-364-160;
US-Patent-Class-364-148; US-Patent-Class-364-162;
Int-Patent-Class-G05B-13/02) Avail: US Patent and Trademark Office

A feedback control system compensator of the PID type is provided, wherein the proportional component of the compensator is replaced with a tilted component having a transfer function s to the power of -1/n. The resulting transfer function of the entire compensator more closely approximates an optimal transfer function, thereby achieving improved feedback controller. Further, as compared to conventional PID compensators, the TID compensator allows for simpler tuning, better disturbance rejection ratio, and smaller effects of plant parameter variations on closed loop response. Official Gazette of the U.S. Patent and Trademark Office

N95-18441 SAM Technology, Inc., San Francisco, CA.
SIGNET-SOFTWARE TOOLS FOR SIGNAL IDENTIFICATION USING NEURAL NETWORKS Final Report, 1 Mar. 1989 - 28 Feb. 1994
H. M. Leong and A. S. Gevins 15 Jul. 1994 37 p Limited Reproducibility: More than 20% of this document may be affected by microfiche quality
(Contract F49620-89-C-0049)
(AD-A284362; AFOSR-94-0477TR) Avail: CASI HC A03

We are developing a software signal processing workbench named SIGNET that simplifies exploratory analysis of multi-channel time series data. We have demonstrated, for the first time, the feasibility of building a signal-processing system around an object-oriented database (OODB). This provides a graphical means for users to create, compare, and manipulate complex data structures while maintaining system wide understanding of these structures. This understanding enables the system to provide database queries by content, data subset extraction with retention of important relationships, traceable self-documenting data, insurance that only appropriate data is fed to signal processing functions, etc. The end result is that users have a high degree of flexibility to manipulate data while data integrity and validity is protected. Over the course of the project, we completed a detailed system design, evaluated existing database technologies and chose an OODB upon which to build SIGNET. We built a prototype that implemented the essential framework of SIGNET and provided a platform with which to test the basic technical issues underlying our design. Signal review and exploratory signal analysis software was

enhanced for incorporation into the SIGNET framework. We have also tested and analyzed the prototype and have found that the major drawback to our initial design was the speed of system response. lie major factors causing this have been identified and speed-up solutions have been designed. We conclude that OODB technology provides a powerful and appropriate framework to model the data and processes that are used in exploratory multidimensional signal-processing applications. We are determining the commercial viability of developing the prototype into a full commercial system. DTIC

N95-18649# Sandia National Labs., Albuquerque, NM.
QuikForm: INTELLIGENT DEFORMATION PROCESSING OF STRUCTURAL ALLOYS
R. J. Bourcier and G. W. Wellman 1994 12 p Presented at the 41st Sagamore Conference on Intelligent Processing of Materials, Plymouth, MA, 29 Aug. - 1 Sep. 1994
(Contract DE-AC04-94AL-85000)
(DE94-018739; SAND-94-2261C; CONF-9408164-1) Avail: CASI HC A03/MF A01

There currently exists a critical need for tools to enhance the industrial competitiveness and agility of US industries involved in deformation processing of structural alloys. In response to this need, Sandia National Laboratories has embarked upon the QuikForm Initiative. The goal of this program is the development of computer-based tools to facilitate the design of deformation processing operations. The authors are currently focusing their efforts on the definition/development of a comprehensive system for the design of sheet metal stamping operations. The overall structure of the proposed QuikForm system is presented, and the focus of their thrust in each technical area is discussed. DOE

N95-18675 Illinois Univ., Urbana, IL.
ANNUAL ALLERTON CONFERENCE ON COMMUNICATION, CONTROL AND COMPUTING
Dilip V. Sarwate and Paul VanDooren 1 Oct. 1993 11 p The 31st Conference was held in Monticello, IL, 29 Sep. - 1 Oct. 1993 Limited Reproducibility: More than 20% of this document may be affected by microfiche quality
(AD-A283892) Avail: Issuing Activity (Defense Technical Information Center (DTIC))

A system consisting of multiple mobile robots in which the robots can see each other by their eye sensors but are not equipped with any communication system, can be viewed as a distributed system in which the components (i.e., robots) can 'communicate' with each other only by means of their moves. We use this system to investigate, through a case study of a number of problems on the formation of geometric figures in the plane, the power and limitations of the distributed control method for mobile robots. In the distributed control method, at every tick of its local clock, each robot observes the positions of all the robots and moves to a new position determined by the given algorithm. The robots are anonymous in the sense that they all execute the same algorithm and they cannot be, distinguished by appearances. The local clocks of the robots are not necessarily synchronized, and initially, the robots do not have a common x-y coordinate system. The problems we discuss include the following: (1) converging the robots to a single point; (2) moving the robots to a single point; (3) agreement on a single point; (4) agreement on the unit distance; (5) agreement on direction; and (6) leader election. We develop algorithms for solving some of these problems under various conditions. Some impossibility results are also presented. DTIC

N95-18740* National Aeronautics and Space Administration. Pasadena Office, CA.
ADAPTIVE NEURON MODEL: AN ARCHITECTURE FOR THE RAPID LEARNING OF NONLINEAR TOPOLOGICAL TRANSFORMATIONS Patent
Raoul Tawel, inventor (to NASA) (Jet Propulsion Lab., California Inst. of Tech., Pasadena, CA.) 6 Dec. 1994 20 p Filed 28 Aug. 1992 Supersedes N93-11174 (31 - 2, p 420)
(NASA-Case-NPO-18579-1-CU; US-Patent-5,371,834;
US-Patent-Appl-SN-937335; US-Patent-Class-395-23;
US-Patent-Class-395-21; US-Patent-Class-395-24; US-Patent-Class-395-25;
Int-Patent-Class-G06F-15/18) Avail: US Patent and Trademark Office

A method for the rapid learning of nonlinear mappings and topological transformations using a dynamically reconfigurable artificial neural network is presented. This fully-recurrent Adaptive Neuron Model (ANM) network was applied to the highly degenerate inverse kinematics problem in robotics, and its performance evaluation is bench-marked. Once trained, the resulting neuromorphic architecture was implemented in custom analog neural network hardware and the parameters capturing the functional transformation downloaded onto the system. This neuroprocessor, capable of 10(exp 9) ops/sec, was interfaced directly to a three degree of freedom Heathkit robotic manipulator. Calculation of the hardware feed-forward pass for this mapping was benchmarked at approximately 10 microsec.
Official Gazette of the U.S. Patent and Trademark Office

N95-18875# Ministry of Science and Development, Jerusalem (Israel).
INTERNATIONAL CONFERENCE ON CONTROL THEORY AND ITS APPLICATIONS
Ruby Musrie, ed. Oct. 1993 165 p Conference held in Kibbutz Maale HaChamisha, Israel, 18-21 Oct. 1993
(DE94-626221; INIS-mf-13778; CONF-9310325) Avail: CASI HC A08/MF A02 (US Sales Only)

Various presentations on robotics and control theory and computer codes are included. DOE

N95-18889 Wisconsin Univ., Milwaukee, WI. Dept. of Electrical Engineering and Computer Science.
DISTRIBUTED ALGORITHMS FOR CONTROLLING MULTIPLE MOBILE ROBOTS
Kazuo Sugihara (Hawaii Univ., Manoa, HI.) and Ichiro Suzuki 14 Jan. 1994 26 p Limited Reproducibility: More than 20% of this document may be affected by microfiche quality
(Contract N00014-94-1-0284; NSF CCR-90-04346; NSF IRI-93-07506)
(AD-A283975) Avail: CASI HC A03

We discuss a method for controlling a group of mobile robots in a distributed manner. The method is fully distributed in the sense that each robot plans its motion individually based upon a given goal of the group and the observed positions of other robots. We illustrate the method by showing how a large number of robots can form an approximation of a circle, a simple polygon or a line segment in the plane. We also show how the robots can distribute themselves nearly uniformly within a circle or a convex polygon in the plane. Finally, we show how the robots can be divided into two or more groups. It turns out that in many cases most robots execute an identical, simple algorithm. The performance of the method is demonstrated by simulation. DTIC

N95-19062* National Aeronautics and Space Administration. Pasadena Office, CA.
SLIDING MODE CONTROL METHOD HAVING TERMINAL CONVERGENCE IN FINITE TIME Patent
Subramanian T. Venkataraman, inventor (to NASA) (Jet Propulsion Lab., California Inst. of Tech., Pasadena, CA.) and Sandeep Gulati, inventor (to NASA) (Jet Propulsion Lab., California Inst. of Tech., Pasadena, CA.) 6 Dec. 1994 15 p Filed 18 Jun. 1992 Supersedes N93-11177 (31 - 2, p 324)
(NASA-Case-NPO-18584-1-CU; US-Patent-5,371,669;
US-Patent-Appl-SN-921192; US-Patent-Class-364-160;
US-Patent-Class-364-148; US-Patent-Class-395-96;
Int-Patent-Class-G05B-13/02) Avail: US Patent and Trademark Office

An object of this invention is to provide robust nonlinear controllers for robotic operations in unstructured environments based upon a new class of closed loop sliding control methods, sometimes denoted terminal sliders, where the new class will enforce closed-loop control convergence to equilibrium in finite time. Improved performance results from the elimination of high frequency control switching previously employed for robustness to parametric uncertainties. Improved performance also results from the dependence of terminal slider stability upon the rate of change of uncertainties over the sliding surface rather than the magnitude of the uncertainty itself for robust control. Terminal sliding mode control also yields improved convergence where convergence time is finite and is to be controlled. A further object is to apply terminal sliders to robot manipulator control and benchmark performance with the traditional computed torque control method and provide for design of control parameters.
Derived from text

N95-19118# Wright Lab., Wright-Patterson AFB, OH. Avionics Directorate.
MACHINE LEARNING: A COMPARATIVE STUDY OF PATTERN THEORY AND C4.5 Final Report, 1 Dec. 1993 - 1 Jun. 1994
Jeffery A. Goldman Jun. 1994 129 p
(AF Proj. 0100)
(AD-A285582; WL-TR-94-1102) Avail: CASI HC A07/MF A02

The Machine Learning field has identified several different inductive bias classes with Occam's Razor being held as an accepted paradigm. C4.5, an extension of ID3, is one of the leaders in this class of learning systems with which other systems measure their ability. A completely different approach, yet still a method in the class of Occam biased learning mechanisms, is Pattern Theory. This approach seeks to recognize patterns in a robust manner using function decomposition. FLASH, the embodiment of Pattern Theory is itself, an inductive learning system. In this study, we hope to show that the Pattern Theoretic approach is not only as good as the classic decision tree methods, but also it exhibits strong promise to be a robust technique to identifying patterns. We will compare C4.5 and Pattern Theory against a special benchmark set of patterns intended to illustrate many types of potential concepts to be learned. The comparisons will be made by constructing learning curves for each system. DTIC

N95-19512# Harris Corp., Melbourne, FL. Government Communication Systems Div.
NEURAL NETWORK COMMUNICATIONS SIGNAL PROCESSING Final Report, Sep. 1992 - May 1994
Dennis Tebbe, John Doner, and Tom Billhartz Aug. 1994 129 p
(Contract F30602-92-C-0051)
(AD-A285681; RL-TR-94-150) Avail: CASI HC A07/MF A02

This final technical report describes the research and development-results of the Neural Network Communications Signal Processing (NNCSP) Program. The objectives of the NNCSP program are to: (1) develop and implement a neural network and communications signal processing simulation system for the purpose of exploring the applicability of neural network technology to communications signal processing; (2) demonstrate several configurations of the simulation to illustrate the system's ability to model many types of neural network based communications systems; and (3) use the simulation to identify the neural network configurations to be included in the conceptual design of a neural network transceiver that could be implemented in a follow-on program. DTIC

N95-19572# Naval Postgraduate School, Monterey, CA.
CONSTRUCTING A REAL-TIME MOBILE ROBOT SOFTWARE SYSTEM M.S. Thesis
Kevin L. Huggins Sep. 1994 107 p
(AD-A285969) Avail: CASI HC A06/MF A02

The problem with the Model-based Mobile robot Language (MML) processor is that the code is unstructured, causing the system to be unstable; it is very difficult to read because of deficient source code documentation; and because of poorly defined function interfaces and extensive functional coupling, the system is hard to maintain. To fix the MML processor, we performed a manual static analysis of the existing source code to understand its structure. Next, based on the analysis, the software system was restructured and the functionality enhanced. Finally, explicit source code documentation was added in the form of comments. There are several results with the new system. First, global variables are reduced from 152 to zero. Secondly, function interfaces are clearly defined and function coupling is enhanced. Finally, the source code is extensively documented. Following from these results, the new system is more stable, easier to read and understand, and simpler to modify. DTIC

N95-19599# University of Southern California, Marina del Rey, CA. Information Sciences Inst.
EVALUATING THE TRADE-OFFS IN PARTIAL-ORDER PLANNING ALGORITHMS
Craig A. Knoblock and Qiang Yang (Waterloo Univ., Ontario.) May 1994 12 p
(Contract F30602-91-C-0081)
(AD-A285876; ISI/RR-381) Avail: CASI HC A03/MF A01

Most practical partial-order planning systems employ some form of goal protection. However, it is not clear from previous work what the tradeoffs are between the different goal protection strategies. Is it better to protect against all threats to a subgoal, some threats, or no threats at all? In this paper, we consider three well-known planning algorithms, SNLP, NONLIN, and TWEAK. Each algorithm makes use of a different goal protection strategy. Through a comparison of the three algorithms, we provide a detailed analysis of different goal protection methods, in order to identify the facts that determine the performance of the systems. The analysis clearly shows that the relative performance of the different goal-protection methods used by the systems, depends on the characteristics of the problems being solved. One of the main determining factors of performance is the ratio of the number of negative threats to the number of positive threats. We present an artificial domain where we can control this ratio and show that in fact the planners show radically different performance as the ratio is varied. The implication of this result for someone implementing a planning system is that the most appropriate algorithm will depend on the types of problems to be solved by the planner. DTIC

N95-19601# University of Southern California, Marina del Rey, CA. Information Sciences Inst.
MULTI-METHOD PLANNING Ph.D. Thesis
Soowon Lee Apr. 1994 156 p
(Contract N00014-92-K-2015)
(AD-A285878; ISI/RR-94-390) Avail: CASI HC A08/MF A02

The ability to find a low execution-cost plan efficiently over a wide domain of applicability is the core of domain-independent planning systems. The approach investigated here to building such a planning system begins with two hypotheses: (1) no single method will satisfy both sufficiency and efficiency for all situations; and (2) multi-method planning can out-perform single-method planning in terms of sufficiency and efficiency. To evaluate these hypotheses, a set of single-method planners for the domains investigated show that these planners have trouble performing efficiently over a wide range of problems. As an alternative to single-method planning, multi-method planning is investigated in this thesis. A multi-method planner consists of a coordinated set of methods which have different performance and scope. Given a set of created methods, the key issue in multi-method planning is how to coordinate individual methods in an efficiency manner so that the multi-method planner can have high performance. The multi-method framework presented here provides one was to do this based on the notion of bias-relaxation. In a bias-relaxation multi-method planner, planning starts by trying highly restricted and efficient methods, and then successively relaxes restrictions until a sufficient method is found. DTIC

N95-18183*# Wake Forest Univ., Winston-Salem, NC. Dept. of Mathematics and Computer Science.
ENHANCEMENTS TO THE KATE MODEL-BASED REASONING SYSTEM
Stan J. Thomas *In* Univ. of Central Florida, NASA/ASEE Summer Faculty Fellowship Program. 1994 Research Reports Oct. 1994 p 485-508 (For primary document see N95-18166 05-80)
Avail: CASI HC A03/MF A04

N95-18992*# Texas A&M Univ., College Station, TX.
NEURAL NETWORKS APPLICATIONS TO CONTROL AND COMPUTATIONS
Leon A. Luxemburg *In* Alabama Univ., Research Reports: 1994 NASA/ASEE Summer Faculty Fellowship Program Oct. 1994 6 p (For primary document see N95-18967 05-80)
Avail: CASI HC A02/MF A03

N95-18999*# Mercer Univ., Macon, GA. Dept. of Electrical and Computer Engineering.
A NEW PISTON CONTROL STRATEGY FOR SEGMENTED MIRRORS
Philip D. Olivier *In* Alabama Univ., Research Reports: 1994 NASA/ASEE Summer Faculty Fellowship Program Oct. 1994 6 p (For primary document see N95-18967 05-80)
Avail: CASI HC A02/MF A03

N95-19637*# National Aeronautics and Space Administration. Marshall Space Flight Center, Huntsville, AL.
NEURAL NET CONTROLLER FOR INLET PRESSURE CONTROL OF ROCKET ENGINE TESTING
Luis C. Trevino *In* NASA. Johnson Space Center, Third CLIPS Conference Proceedings, Volume 1 Nov. 1994 p 92-104 (For primary document

see N95-19625 05-61)
Avail: CASI HC A03/MF A03

64 NUMERICAL ANALYSIS

Includes iteration, difference equations, and numerical approximation.

N95-17977# Argonne National Lab., IL.
SINGULAR PERTURBATION PROBLEM GOVERNED BY SYSTEM OF CONSERVATION LAWS
M. Garbey 1994 13 p
(Contract W-31-109-eng-38)
(DE94-019264; ANL/MCS/PP-71512) Avail: CASI HC A03/MF A01

The author presents an asymptotic analysis of a parabolic-hyperbolic singular perturbation problem driven by a system of conservation laws. The main part of the analysis concerns the construction of shock layers associated with discontinuities of the hyperbolic problem. The formal method applies to a general class of partial differential equations and can be used as a tool to design asymptotic-induced numerical methods. DOE

N95-18108*# Institute for Computer Applications in Science and Engineering, Hampton, VA.
AN ALGORITHM FOR SOLVING THE SYSTEM-LEVEL PROBLEM IN MULTILEVEL OPTIMIZATION Final Report
R. J. Balling (Brigham Young Univ., Provo, UT.) and J. Sobieszczanski-Sobieski (National Aeronautics and Space Administration. Langley Research Center, Hampton, VA.) Dec. 1994 26 p Submitted for publication
(Contract NAS1-19480; RTOP 505-90-52-01)
(NASA-CR-195015; NAS 1.26:195015; ICASE-94-96) Avail: CASI HC A03/MF A01

A multilevel optimization approach which is applicable to nonhierarchic coupled systems is presented. The approach includes a general treatment of design (or behavior) constraints and coupling constraints at the discipline level through the use of norms. Three different types of norms are examined: the max norm, the Kreisselmeier-Steinhauser (KS) norm, and the 1(sub p) norm. The max norm is recommended. The approach is demonstrated on a class of hub frame structures which simulate multidisciplinary systems. The max norm is shown to produce system-level constraint functions which are non-smooth. A cutting-plane algorithm is presented which adequately deals with the resulting corners in the constraint functions. The algorithm is tested on hub frames with increasing number of members (which simulate disciplines), and the results are summarized. Author

N95-18109*# Institute for Computer Applications in Science and Engineering, Hampton, VA.
OPTIMIZATION OF COUPLED SYSTEMS: A CRITICAL OVERVIEW OF APPROACHES Final Report
R. J. Balling (Brigham Young Univ., Provo, UT.) and J. Sobieszczanski-Sobieski (National Aeronautics and Space Administration. Langley Research Center, Hampton, VA.) Dec. 1994 32 p Submitted for publication
(Contract NAS1-19480; RTOP 505-90-52-01)
(NASA-CR-195019; NAS 1.26:195019; ICASE-94-100) Avail: CASI HC A03/MF A01

A unified overview is given of problem formulation approaches for the optimization of multidisciplinary coupled systems. The overview includes six fundamental approaches upon which a large number of variations may be made. Consistent approach names and a compact approach notation are given. The approaches are formulated to apply to general nonhierarchic systems. The approaches are compared both from a computational viewpoint and a managerial viewpoint. Opportunities for parallelism of both computation and manpower resources are discussed. Recommendations regarding the need for future research are advanced. Author

N95-18110*# Institute for Computer Applications in Science and Engineering, Hampton, VA.
FLOATING SHOCK FITTING VIA LAGRANGIAN ADAPTIVE MESHES Final Report
John VanRosendale Nov. 1994 24 p Submitted for publication
(Contract NAS1-19480; RTOP 505-90-52-01)
(NASA-CR-194997; NAS 1.26:194997; ICASE-94-89) Avail: CASI HC A03/MF A01

In recent works we have formulated a new approach to compressible flow simulation, combining the advantages of shock-fitting and shock-capturing. Using a cell-centered Roe scheme discretization on unstructured meshes, we warp the mesh while marching to steady state, so that mesh edges align with shocks and other discontinuities. This new algorithm, the Shock-fitting Lagrangian Adaptive Method (SLAM) is, in effect, a reliable shock-capturing algorithm which yields shock-fitted accuracy at convergence. Shock-capturing algorithms like this, which warp the mesh to yield shock-fitted accuracy, are new and relatively untried. However, their potential is clear. In the context of sonic booms, accurate calculation of near-field sonic boom signatures is critical to the design of the High Speed Civil Transport (HSCT). SLAM should allow computation of accurate N-wave pressure signatures on comparatively coarse meshes, significantly enhancing our ability to design low-boom configurations for high-speed aircraft. Author

N95-18120# Oak Ridge National Lab., TN.
STATIC AND DYNAMIC NUCLEAR MANY-BODY DESCRIPTIONS ON PARALLEL ARCHITECTURES
C. R. Chinn, A. S. Umar, M. R. Strayer, and M. Vallieres 1994 26 p Presented at the Supercomputing 1994 Meeting, Washington, DC, 14-18 Nov. 1994
(Contract DE-AC05-84OR-21400)
(DE94-018134; CONF-941118-7) Avail: CASI HC A03/MF A01

Numerical methods used to solve the system of stiff, nonlinear partial differential equations in static Hartree-Fock descriptions of many-body nuclear systems are presented along with an extension of the time dependent Hartree-Fock solution to linear response theory. A full three dimensional representation is obtained by using a collocation basis spline spatial lattice. Numerical procedures used for parallel applications are discussed. Comparisons are presented for MIMD massively computers, including the Intel Paragon and the iPSC/860 hypercube. Algorithms used to improve communication overhead, especially pipelining the Gramm-Schmidt orthogonalization routine, and difficulties with limited node memory will be discussed. DOE

N95-18131# Oak Ridge National Lab., TN.
ARBITRARILY HIGH ORDER NODAL AND CHARACTERISTIC METHODS
Y. Y. Azmy 1994 8 p Presented at the Winter Meeting of the American Nuclear Society, Washington, DC, 13-18 Nov. 1994
(Contract DE-AC05-84OR-21400)
(DE94-018130; CONF-941102-21) Avail: CASI HC A02/MF A01

The quest for higher computational efficiency initially led researchers in the neutron transport area to develop and implement high-order approximations for solving the linear Boltzmann equation. This drive aimed at achieving higher accuracy on coarse meshes, thereby resulting in a net savings of computational resources represented by execution time and memory. Many endeavors succeeded in reaching this goal, producing a variety of elegent, albeit complicated, formalisms, that proved extremely accurate and efficient in solving test, as well as practical applications, problems. The two main classes of high order transport methods that received the most attention are the Nodal and Characteristic methods. A de facto linear order standard for the spatial approximation (even though Quadratic Nodal Methods were also considered) was dictated by the algebraic complexity of the derivation of the discrete variable equations, the programming complexity of implementing and verifying them in codes, and limitations on computational resources available to run such codes. The significant advances in computational resources in terms of hardware capacity and speed, as well as architectural innovations such as vector and parallel processing, all but eliminated the third (above) obstacle towards the development and implementation of even higher order methods. The algebraic and programming complexities, on the other hand, were alleviated to some extent by the development of Arbitrarily High Order Transport methods of the Nodal and the Characteristic types, which are discussed in this report. DOE

N95-18346# Los Alamos National Lab., NM.
LOWER BOUNDS FOR IDENTIFYING SUBSET MEMBERS WITH SUBSET QUERIES
E. Knill Apr. 1994 13 p Presented at the Symposium on Foundations of Computer Science, Santa Fe, NM, 20-22 Nov. 1994
(Contract W-7405-eng-36)
(DE94-014296; LA-UR-94-2014; CONF-941178-1) Avail: CASI HC A03/MF A01

An instance of a group testing problem is a set of objects (Omicron)and an unknown subset P of (Omicron). The task is to determine P by using queries of the type 'does P intersect Q', where Q is a subset of (Omicron). This problem occurs in areas such as fault detection, multiaccess communications, optimal search, blood testing and chromosome mapping. Consider the two stage algorithm for solving a group testing problem where in the first stage, a predetermined set of queries, are asked in parallel, and in the second stage, P is determined by testing individual objects. Let n = (vert bar)(Omicron)(vert bar). Suppose that P is generated by independently adding each (chi) (element of)(Omicron) to P with probability p/n. Let q(sub 1) (q(sub 2)) be the number of queries asked in the first (second) stage of this algorithm. We show that if q(sub 1) = o(log(n) log(n)/log log(n)), then Exp(q(sub 2)) = n(sup l)-0(1)), while there exist algorithms with q(sub 1) = O(log(n)log(n)/loglog(n)) and Exp(q(sub 2)) = o(l). The proof involves a relaxation technique which can be used with arbitrary distributions. The best previously known bound is q(sub 1) + Exp(q(sub 2)) = (Omega)(p log(n)). For general group testing algorithms, our results imply that if the average number of queries over the course of n(sup (gamma)) ((gamma) greater than 0) independent experiments is O n(sup l)-(element of)), then with high probability (Omega)(log(n)log(n)/loglog(n)) non-singleton subsets are queried. This settles a conjecture of Bill Bruno and David Torney and has important consequences for the use of group testing in screening DNA libraries and other applications where its is more cost effective to use non-adaptive algorithms and/or expensive to prepare a subset Q for its first test. DOE

N95-18374 Selskapet for Industriell og Teknisk Forskning, Trondheim (Norway). Div. for Information Technology.
DECOMPOSITION OF PARAMETRIC CURVES
M. Daehlen 16 Dec. 1993 23 p Presented at the 3rd Conference on Geometric Design, Tempe, AZ Prepared in cooperation with Oslo Univ., Norway and Royal Norwegian Council for Scientific and Industrial Research, Oslo, Norway
(PB94-207024; STF33-A93037) Avail: Issuing Activity (National Technical Information Service (NTIS))

This is a tutorial on data reduction and decomposition techniques for curves and surfaces. It was presented at the 34th conference on Geometric Design in Tempe, Arizona, October 31, 1993. NTIS

N95-18479*# Institute for Computer Applications in Science and Engineering, Hampton, VA.
AN INVERSE PROBLEM IN THERMAL IMAGING Final Report
Kurt Bryan (Rose-Hulman Inst. of Tech., Terre Haute, IN.) and Lester F. Caudill, Jr. (Kentucky Univ., Lexington, KY.) Dec. 1994 35 p Submitted for publication
(Contract NAS1-19480; RTOP 505-90-52-01)
(NASA-CR-195018; NAS 1.26:195018; ICASE-94-99) Avail: CASI HC A03/MF A01

This paper examines uniqueness and stability results for an inverse problem in thermal imaging. The goal is to identify an unknown boundary of an object by applying a heat flux and measuring the induced temperature on the boundary of the sample. The problem is studied both in the case in which one has data at every point on the boundary of the region and the case in which only finitely many measurements are available. An inversion procedure is developed and used to study the stability of the inverse problem for various experimental configurations. Author

N95-18482# Maryland Univ., College Park, MD. Inst. for Physical Science and Technology.
SUBSPACE CORRECTION METHODS FOR THE ITERATIVE SOLUTION OF HIERARCHIC PLATE MODELS. 1: HEAT TRANSFER PROBLEMS
C. Schwab and I. Babuska Apr. 1994 43 p
(Contracts N00014-90-J-1030; F49620-92-J-0100; NSF DMS-91-20877)
(AD-A285712; TN-BN-1169) Avail: CASI HC A03/MF A01

A class of iterative methods for solving the system of partial differential equations stemming from hierarchic models of the heat conduction problem in orthotropic laminated plates is analyzed. The analysis leads to sharp explicit expressions for the rate of the convergence depending on the shape or director functions used in the derivations of the hierarchic models. DTIC

N95-18511 Nebraska Univ., Lincoln, NE.
A NEW MULTI-DIMENSIONAL TRANSFORM FOR DIGITAL SIGNAL PROCESSING USING GENERALIZED ASSOCIATION SCHEMES Final Annual Report, 1 Jun. 1992 - 31 May 1994
Prabir Bhattacharya 31 May 1994 19 p Limited Reproducibility: More than 20% of this document may be affected by microfiche quality
(AD-A284166; AFOSR-94-0490TR) Avail: Issuing Activity (Defense Technical Information Center (DTIC))

Our research focused on the development of a multi-dimensional discrete transform using a new algebra of multi-dimensional arrays. The proposed transform for the n-dimensional can compute en block the transforms of a family of (n-1) dimensional arrays. Also, the number of multiplications is relatively low. The definition of the transform (for the 3-dimensional case) uses the concept of an inverse pair for a pair of 3-dimensional arrays. We have developed methods to compute such inverse pairs and it has been shown there is an abundant supplies of such pairs which could then profitably be used to define various types of 3-dimensional transforms. We have also investigated the properties of the ternary algebra associated with the 3-dimensional arrays. Further, the multi-dimensional approach has been used by us to the representation of uncertain information in conjunction with the Dempster-Schafer theory. It has been shown how to compute the information regarding the probability of occurrences of the variables as certain matrix products. DTIC

N95-18658 Carnegie-Mellon Univ., Pittsburgh, PA. Dept. of Computer Science.
IMPROVED APPROXIMATION GUARANTEES FOR MINIMUM-WEIGHT k-TREES AND PRIZE-COLLECTING SALESMEN
Baruch Awerbuch, Yossi Azar, and Avrim Blum Aug. 1994 11 p Limited Reproducibility: More than 20% of this document may be affected by microfiche quality
(Contracts DABT63-93-C-0038; DAAL03-86-K-0171; N00014-J-92-1799; AF-AFOSR-0078-86; NSF CCR-91-14440)
(AD-A284042; CMU-CS-94-173) Avail: Issuing Activity (Defense Technical Information Center (DTIC))

Consider a salesperson that must sell some quota of brushes in order to win a trip to Hawaii. This salesperson has a map (a weighted graph) in which each city has an attached demand specifying the number of brushes that can be sold in that city. What is the best route to take to sell the quota while traveling the least distance possible? Notice that unlike the standard traveling salesman problem, not only do we need to figure out the order in which to visit the cities, but we must decide the more fundamental question: which cities do we want to visit? In this paper we give the first approximation algorithms with poly-logarithmic performance guarantees for this problem, as well as for the slightly more general PCTSP problem of Balas, and a variation we call the bank-robber problem (also called the orienteering problem by Golden, Levi, and Vohra). We do this by providing an O(log(2)k) approximation to the k-MST problem which is defined as follows. Given an undirected graph on n nodes with non-negative edge weights and an integer k less than or equal n, find the tree of least weight that spans k vertices. (If desired, one may specify in the problem a root vertex that must be in the tree as well.) Our result improves on the previous best bound of O(k squared) of Ravi et al. and comes quite close to the bound of O(log k) of Garg and Hochbaum for the special case of points in 2-dimensional Euclidean space. DTIC

N95-18679 Naval Command, Control and Ocean Surveillance Center, San Diego, CA. Research, Development, Technology and Evaluation Div.
A DIRECT DECOMPOSITION METHOD FOR THE SOLUTION OF SPARSE LINEAR LEAST SQUARES PROBLEMS Final Report
A. K. Kevorkian Jun. 1994 40 p Limited Reproducibility: More than 20% of this document may be affected by microfiche quality
(AD-A284060; NRAD-TR-1653) Avail: Issuing Activity (Defense Technical Information Center (DTIC))

Given a sparse nonsquare system of linear equations Mx = b where

M(T)M is either dense or full, we present a direct method that generates a least squares solution of the original system by solving a smaller least squares problem. The method accomplishes this decomposition by applying orthogonal transformations to a restructured form of the original system of equations Mx = b. The algorithms derived from the decomposition result are well suited for both sequential and parallel architecture machines. In a specific Navy signal processing application, the presented algorithm computed on a Sun SPARC 10 workstation a least squares solution of a rank deficient system comprising 703 equations and 592 variables in a number of floating point computations tenfold smaller than a method that does not exploit the sparsity structure of M. DTIC

N95-18736*# Research Inst. for Advanced Computer Science, Moffett Field, CA.

WEIGHTED GRAPH BASED ORDERING TECHNIQUES FOR PRECONDITIONED CONJUGATE GRADIENT METHODS

Simon S. Clift (Queens Univ., Kingston, Ontario.) and Wei-Pai Tang (Waterloo Univ., Ontario.) Dec. 1994 25 p Sponsored by Natural Sciences and Engineering Research Council of Canada and Information Technology Center

(Contract NAS2-13721)

(NASA-CR-197597; NAS 1.26:197597; RIACS-TR-94-20) Avail: CASI HC A03/MF A01

We describe the basis of a matrix ordering heuristic for improving the incomplete factorization used in preconditioned conjugate gradient techniques applied to anisotropic PDE's. Several new matrix ordering techniques, derived from well-known algorithms in combinatorial graph theory, which attempt to implement this heuristic, are described. These ordering techniques are tested against a number of matrices arising from linear anisotropic PDE's, and compared with other matrix ordering techniques. A variation of RCM is shown to generally improve the quality of incomplete factorization preconditioners. Author

N95-18876# Joint Inst. for Nuclear Research, Dubna (USSR). Lab. of Theoretical Physics.

COVARIANT DIFFERENTIAL COMPLEXES OF QUANTUM LINEAR GROUPS

A. P. Isaev and P. N. Pyatov 1993 23 p Submitted for publication

(DE94-626640; JINR-E-2-93-416) Avail: CASI HC A03/MF A01 (US Sales Only)

We consider the possible covariant external algebra structures for Cartan's 1-forms (Omega) on GL (sub q)(N) and SL(sub q)(N). Our starting point is that (Omega) s realize an adjoint representation of quantum group and all nonomials of (Omega) s possess the unique ordering. For the obtained external algebras we define the differential mapping d possessing the usual nilpotence condition, and the generally deformed version of Leibnitz rules. The status of the known examples of GL(sub q)(N)- differential calculi in the proposed classification scheme and the problems of SL(sub q)(N)-reducti on are discussed. DOE

N95-18878# Centro Brasileiro de Pesquisas Fisicas, Rio de Janeiro.

LIE ALGEBRAS FOR THE DIRAC-CLIFFORD RING

J. A. Mignaco and C. A. Linhares (Centro Tecnico Aerospacial, San Jose dos Campos, Brazil.) 1992 27 p

(DE94-626643; CBPF-NF-037/92) Avail: CASI HC A03/MF A01 (US Sales Only)

It is shown in a general way that the Dirac-Clifford ring formed by the Dirac matrices and all their products, for all even and odd spacetime dimensions D, span the cumulation algebras SU(2(sup D/2)) for even D and SU(2(sup (D-)1(sup)/2)) + SU(2(sup (D-1)/2)) for odd D. Some physical consequences of these results are discussed. DOE

N95-18896# Sandia National Labs., Albuquerque, NM. Cubit Development Team.

CUBIT MESH GENERATION ENVIRONMENT

Ted D. Blacker, William J. Bohnhoff, Tony L. Edwards, James R. Hipp, Randy R. Lober, Scott A. Mitchell, Gregory D. Sjaardema, Timothy J. Tautges, Tammy J. Wilson, and William R. Oakes (Oak Ridge National Lab., TN.) et al May 1994 160 p

(Contract DE-AC04-94AL-85000)

(DE94-017496; SAND-94-1100) Avail: CASI HC A09/MF A02

The CUBIT mesh generation environment is a two- and three-dimensional finite element mesh generation tool which is being developed to pursue the goal of robust and unattended mesh generation--effectively automating the generation of quadrilateral and hexahedral elements. It is a solid-modeler based preprocessor that meshes volume and surface solid models for finite element analysis. A combination of techniques including paving, mapping, sweeping, and various other algorithms being developed are available for discretizing the geometry into a finite element mesh. CUBIT also features boundary layer meshing specifically designed for fluid flow problems. Boundary conditions can be applied to the mesh through the geometry and appropriate files for analysis generated. CUBIT is specifically designed to reduce the time required to create all-quadrilateral and all-hexahedral meshes. This manual is designed to serve as a reference and guide to creating finite element models in the CUBIT environment. DOE

N95-19169 Technische Univ., Delft (Netherlands). Faculty of Technical Mathematics and Informatics.

ALGORITHMS AND APPLICATIONS IN TIMED DISCRETE EVENT SYSTEMS Ph.D. Thesis

J. G. Braker 22 Dec. 1993 194 p Limited Reproducibility: More than 20% of this document may be affected by microfiche quality

(PB94-201423; ISBN-90-9006669-1) Avail: CASI HC A09

The thesis is concerned with the max-plus algebra approach to Discrete Event Dynamic Systems (DEDS). It begins with a general introduction to max-plus algebra. It then deals with the modelling and analysis of transportation networks that are subject to timetables. An aspect of the similarity of linear algebra and max-plus algebra is reflected in an algorithm for the determination of eigenvectors. A generalization of max-plus algebra is discussed, and an extension of an existing algorithm for the determination of the eigenvalue in max-plus algebra is investigated. The notion of structural stability of an autonomous system is introduced. Finally, the eigenvector control problem is presented, where an initial state must be steered to an eigenvector. NTIS

N95-19190 Institut des Hautes Etudes Scientifiques, Bures-sur-Yvette (France).

PLANE JACOBIAN CONJECTURE

S. Friedland Mar. 1994 16 p Prepared in cooperation with Illinois Univ. Limited Reproducibility: More than 20% of this document may be affected by microfiche quality

(PB94-192341; IHES/M/94/19) Avail: CASI HC A03

Let F = (F(sub 1).., F(sub n)) : C(sup n) approaches C(sup n) be a polynomial map. Assume that F is a local diffeomorphism. Then the Jacobian conjecture claims that F is a diffeomorphism. The authors summarize briefly the content of the paper. Section 1 discusses the known properties of dominating polynomial maps F : C(sup n) approaches C(sup n) which are needed later. In Section 2 the authors discuss the homology and cohomology monodromy of a regular fiber of a primitive polynomial in two variables. Section 3 discusses a first order differential operator L with polynomial coefficients determined by a primitive dominating polynomial map phi : C(sup n) approaches C(sup n-1). They show that ker(L) and coker(L) are finite dimensional. Moreover, the dimension of coker(L) is the rank of the first homology of the generic fiber phi(sup -1)(xc). In the last section they prove the plane Jacobian conjecture for the local polynomial diffeomorphism F = (F(sup 1), F(sub 2)) for which the generic fiber F(sub 1) = t is a rational curve. NTIS

N95-19375# Institut des Hautes Etudes Scientifiques, Bures-sur-Yvette (France).

ANTISYMMETRIC TENSOR FIELD INTERACTIONS AND NEUTRON STAR MODELS

T. Damour and N. Pinto-Neto (Paris VI Univ., France.) 4 Mar. 1994 21 p Submitted for publication

(PB94-215605; IHES/P/94/16) Avail: CASI HC A03/MF A01

Gravity theories involving, besides the usual Einsteinian metric field, a macroscopically coupled, finite range antisymmetric tensor field B(sub mu nu) are studied as foils to the strong gravitational field predictions of general relativity. The authors consider the minimal class of such models among the multiparameter gravity theories recently introduced by Damour, Deser and McCarthy. In the limiting case where the range mu(exp -1) of the B field is much larger than the characteristic size of the system, this class comprises two arbitrary parameters: the coupling length lambda, which

measures the coupling of B(sub mu nu) to the baryon rest-mass density; and a dimensionless parameter b characterizing the deviation of the 'physical' metric from the Einstein value. The authors show that when lambda is a few kilometers and b of order unity this class of models predicts strong-field deviations of order unity in the overall characteristics of neutron stars: radius, binding energy, surface red-shift and maximum mass. NTIS

N95-19408# Technische Univ., Twente (Netherlands). Faculty of Applied Mathematics.
CLASSIFICATION OF GRADED, FINITE-DIMENSIONAL LIE ALGEBRAS OF VECTOR FIELDS
G. F. Post Dec. 1993 23 p
(PB94-215449) Avail: CASI HC A03/MF A01

We study finite-dimensional Lie algebras of vector fields on R(exp n), that contain the elements partial derivative with respect to X(sub i) and X(sub i) partial derivative with respect to X(sub i) for i = 1...n. To any Lie algebra L of this class, we associate an N-valued n x n-matrix A and a set of special elements S included in (1,...,n). We prove that the pair (A,S) necessarily satisfies 2 properties. Conversely, to any pair (A,S) satisfying those 2 properties we associate a Lie algebra L(A,S), such that L(A,S) is maximal in the class of all L with matrix A and special elements S. NTIS

N95-19609# Arizona Univ., Tucson, AZ.
SINGULARITIES AND SYMMETRIES OF NONLINEAR ORDINARY AND PARTIAL DIFFERENTIAL EQUATIONS
1994 6 p
(Contract DE-FG02-92ER-25123)
(DE95-000904; DOE/ER-25123/T1) Avail: CASI HC A02/MF A01

In this project we have studied singularities as both fundamental mathematical objects in their own right determining, for example, integrable and nonintegrable properties of nonlinear differential equations; and the determining mechanism of crucial physical processes such as self-focusing singularities and current sheet formation. This approach defines broad based, interdisciplinary research program relevant to the DOE/AMS mission. DOE

N95-19717# Institut des Hautes Etudes Scientifiques, Bures-sur-Yvette (France).
TOWARDS A CLASSIFICATION OF SU(2)(DIRECT SUM)...(DIRECT SUM)SU(2) MODULAR INVARIANT PARTITION FUNCTIONS
T. Gannon Mar. 1994 37 p See also PB94-167657 Sponsored in part by the Natural Sciences and Engineering Research Council of Canada
(PB94-217247; IHES/P/94/21) Avail: CASI HC A03/MF A01

The complete classification of WZNW modular invariant partition functions is known for very few affine algebras and levels, the most significant being all levels of A(sub 1) and A(sub 2) and level 1 of all simple algebras. Here, the authors address the classification problem for the nicest high rank semisimple affine algebras: A(sub 1, sup (1))(sup (circle +)r). Among other things, they explicitly find all automorphism invariants, for all levels k = (k(sub 1), ..., k(sub r)), and complete the classification for A(sub 1, sup (1)) (circled +) A(sub 1, sup (1)), for all levels k(sub 1), k(sub 2). They also solve the classification problem for A(sub 1, sup (1))(sup (circle +)r), for any levels k(sub i). In addition, they find some physical invariants which seem to be new. NTIS

N95-19718# Institut des Hautes Etudes Scientifiques, Bures-sur-Yvette (France).
COULOMB GAS REPRESENTATION OF THE SU(2) WZW CORRELATORS AT HIGHER GENERA
K. Gawedzki Apr. 1994 9 p See also PB94-217262
(PB94-217254; IHES/P/94/25) Avail: CASI HC A02/MF A01

The authors extend the analysis of PB94-217262 to the case with insertion points. The result allows expression of the correlation functions of the SU(2) WZW conformed field theory on Riemann surfaces of genus greater than 1 by finite dimensional integrals. NTIS

N95-19719 Institut des Hautes Etudes Scientifiques, Bures-sur-Yvette (France).
SU(2) WZW THEORY AT HIGHER GENERA
K. Gawedzki Feb. 1994 43 p See also PB94-148467 and PB94-217254
(PB94-217262; IHES/P/94/10) Avail: Issuing Activity

We compute, by free field techniques, the scalar product of the SU(2) Chern-Simons states on genus greater than 1 surfaces. The result is a finite-dimensional integral over positions of 'screening charges' and one complex modular parameter. It uses an effective description of the CS states closely related to the one worked out by Bertram. The scalar product formula allows expression of the higher genus partition functions of the WZW conformal field theory by finite-dimensional integrals. It should provide the hermitian metric preserved by the Knizhnik - Zamolodchikov - Bernard connection describing the variations of the CS states under the change of the complex structure of the surface. NTIS

N95-19735 Yale Univ., New Haven, CT. Dept. of Computer Science.
HIGH-ORDER CORRECTED TRAPEZOIDAL RULES FOR SINGULAR FUNCTIONS
Sharad Kapur and Vladimir Rokhlin Aug. 1994 38 p Limited Reproducibility: More than 20% of this document may be affected by microfiche quality
(Contract N00014-89-J-1527)
(AD-A284269; YaleU/DCS/RR-1042) Avail: CASI HC A03

A group of quadrature formulae is presented applicable to both nonsingular functions and functions with end-point singularities, generalizing the classical end-point corrected trapezoidal quadrature rules. We present an algorithm for the construction of very high-order end-point corrected trapezoidal rules, taking advantage of functional information outside the interval of integration. The scheme applies not only to nonsingular functions, but also for a wide class of functions with monotonic singularities. Numerical experiments are presented demonstrating the practical usefulness of the new class of quadratures. Tables of quadrature weights are included for singularities of the form s(x) = log(absolute value of x), s(x) = absolute value of x to the lambda power for a variety of values of lambda.
Author (DTIC)

N95-19819# Gdansk Technical Univ. (Poland). Dept. of Electronics.
SOLUTION OF MAXWELL'S EQUATIONS USING THE TIME DOMAIN METHOD OF MOMENTS. SUPPLEMENT: PUBLICATIONS AND REPORTS Final Technical Report
Michal Mrozowski May 1994 54 p
(Contracts DAJA45-92-C-0032; KBN-3-0687-91-01)
(AD-A280143; R/D-6840-EE-01-Suppl) Avail: CASI HC A04/MF A01

A new approach to the analysis of Maxwell's equations in the time domain is presented. The salient feature of the method discussed is that they are based on the expansion of unknown functions into infinite series of entire domain or entire subdomain basis functions and the expansion coefficients are found by means of the method of moments procedure. Four new explicit algorithms are introduced and discussed. The stability condition is derived in the general way based on the functional analysis techniques. A fast and efficient absorbing boundary condition is proposed. The results of the numerical tests are presented showing that new algorithms can achieve greater speed than a traditional FDTD technique. DTIC

N95-19820# Gdansk Technical Univ. (Poland). Dept. of Electronics.
SOLUTION OF MAXWELL'S EQUATIONS USING THE TIME DOMAIN METHOD OF MOMENTS Final Technical Report, Nov. 1992 - Apr. 1994
Michal Mrozowski May 1994 5 p
(Contract DAJA45-92-C-0032)
(AD-A280144; R/D-6940-EE-01; ERO-92-MM-01) Avail: CASI HC A01/MF A01

New algorithms for the time domain analysis of electromagnetic waves in shielded structures are presented. Electromagnetic fields inside a structure under investigation are expanded into series of basis functions and the expansion coefficients are found by means of the method of moments. Numerical cost of algorithms and their stability is discussed and cost efficient hybrid approach combining the new technique with classical FDTD algorithms is proposed. Numerical tests show that significant speed up can be obtained for structures with homogeneous regions. A very fast, low return loss absorbing boundary condition (ABC) is proposed which accounts for the highly dispersive character of the structure. A very good performance of the ABC is demonstrated. DTIC

N95-19869 Washington Univ., Saint Louis, MO.
THEORY AND APPLICATIONS OF THE PHI TRANSFORM WAVELETS Final Report, 1 Jul. 1990 - 31 Dec. 1993

Guido Weiss 31 Dec. 1993 12 p Limited Reproducibility: More than 20% of this document may be affected by microfiche quality
(Grant AF-AFOSR-0323-90)
(AD-A279943; AFOSR-94-0327TR) Avail: Issuing Activity (Defense Technical Information Center (DTIC))

A fundamental idea in Fourier analysis is that the Fourier Transform gives a simultaneous diagonalization of a small but very important class of operators including differentiation and integration. On the other hand, the Fourier Transform is not well suited for studying Multiplication operators. The wavelet transform (and related transforms give excellent simultaneous almost diagonalization of a very large class of operators which includes differentiation, integration, and multiplication: in fact, more-generally singular integral operators and pseudo-differential operators. Professor Rochberg's recent work has been to use this fact to study such operators. Some work has been in the real variable tradition, other parts have involved operators on spaces of analytic functions. DTIC

65 STATISTICS AND PROBABILITY

Includes data sampling and smoothing; Monte Carlo method; and stochastic processes.

N95-18007# Naval Postgraduate School, Monterey, CA.
DOUBLE EULERIAN CYCLES ON DE BRUIJN DIGRAPHS M.S. Thesis
Gary W. Krahn Jun. 1994 135 p
(AD-A283334) Avail: CASI HC A07/MF A01

A binary de Bruijn sequence has the property that every n-tuple is distinct on a given period of length 2n. An efficient algorithm to generate a class of classical de Bruijn sequences is given based upon the distance between cycles within the Good - de Bruijn digraph. The de Bruijn property on binary sequences is shown to be a randomness property of the ZERO and ONE run sequences. Utilizing this randomness we find additional new structure in de Bruijn sequences. We analyze binary sequences that are not de Bruijn but instead possess the sufficient structure so that every distinct binary n-tuple can be systematically combed out of the sequence. These complete or nonclassical de Bruijn sequences are a generalization of the well-known de Bruijn cycle. Our investigation focuses on binary sequences, called double Eulerian cycles, that define a cycle along a graph (digraph) visiting each edge (arc) exactly twice. A new algorithm to generate a class of double Eulerian cycles on graphs and digraphs is found. Double Eulerian cycles along the binary Good - de Bruijn digraph are partitioned by the run structure of their defining sequences. This partition allows for a statistical analysis to determine the relative size of the set of complete cycles defined by the sequences we study. A measure that categorizes double Eulerian cycles along graphs (digraphs) by the distance between the two visitations of each edge (arc) is provided. An algorithm to generate double Eulerian cycles of minimum measure is given. DTIC

N95-18020 Phillips Lab., Kirtland AFB, NM.
A FAST RECURSIVE ALGORITHM TO COMPUTE THE PROBABILITY OF M-OUT-OF-N EVENTS Final Report, 1 Aug. 1993 - 1 Jan. 1994
G. E. Radke, Jr. and J. Evanoff (Ball Aerospace Systems Div., Albuquerque, NM.) May 1994 14 p Limited Reproducibility: More than 20% of this document may be affected by microfiche quality
(AF Proj. 3647)
(AD-A283679; AD-E202151; PL-TR-94-1003) Avail: CASI HC A03

The successful performance of systems (power plants, aircraft, missiles, spacecraft, etc.) while degraded due to either man-made or natural stimuli is currently of interest to the survivability/vulnerability assessment communities. The fault tree model has long been used to qualify and quantify the likelihood of these degraded states. This report details the use of a particular recursive algorithm which is based on the 2-out-of-3 principle for M-out-of-N gates. Software currently available to calculate M-out-of-N gates is usually based on a cut set methodology for quantification. However, when N is too large, the number of cut sets becomes unmanageable. This algorithm provides a technique to calculate an exact probability when N is too large for cut set techniques. DTIC

N95-18113# Naval Postgraduate School, Monterey, CA. Dept. of Electrical and Computer Engineering.
TLS-BASED PREFILTERING TECHNIQUE FOR TIME-DOMAIN ARMA MODELING Final Report, 1 Oct. 1993 - 30 Sep. 1994
Monique P. Fargues 15 Aug. 1994 19 p
(AD-A284525; NPS-EC-94-009) Avail: CASI HC A03/MF A01

Modeling time-series with linear pole-zero autoregressive-moving average (ARMA) models has numerous applications in signal processing. This problem is in general nonlinear and most ARMA modeling techniques are iterative in nature. The iterative prefiltering (IP) method has the advantage of computing potential nonminimum phase representations which may be useful in time-domain modeling. The original IP minimization procedure is an ill-conditioned problem which has classically been solved using a least-squares approach. This work presents a modification of the classical IP technique in which the least-squares iteration step is replaced by a total least squares (TLS) step to take advantage of the statistical properties of the TLS method. Results show that improvements in the modeling performances may be obtained by using the TLS-based IP method when modeling signals distorted by white Gaussian noise. DTIC

N95-18653# Sandia National Labs., Albuquerque, NM.
CAN INFORMATION SURETY BE ASSESSED WITH HIGH CONFIDENCE?
J. J. Lim, S. K. Fletcher, R. D. Halbgewachs, R. M. Jansma, P. D. Sands, P. A. Watterberg, and G. D. Wyss 1994 13 p Presented at the High Consequence Operations Safety Symposium, Albuquerque, NM, 12-14 Jul. 1994
(Contract DE-AC04-94AL-85000)
(DE94-015805; SAND-94-1796C; CONF-940788-3) Avail: CASI HC A03/MF A01

Several basic reasons are given to support the position that an integrated, systems methodology entailing probabilistic assessment offers the best means for addressing the problems in software safety. The recognized hard problems in software safety, or safety per se, and some of the techniques for hazard identification and analysis are then discussed relative to their specific strengths and limitations. The paper notes that it is the combination of techniques that will lead to safer systems, and that more experience, examples, and applications of techniques are needed to understand the limits to which software safety can be assessed. Lastly, some on-going project work at Sandia National Laboratories on developing a solution methodology is presented. DOE

N95-18672 Office of Naval Research, Arlington, VA.
EIGENVALUE TESTS AND DISTRIBUTIONS FOR SMALL SAMPLE ORDER DETERMINATION FOR COMPLEX WISHART MATRICES Final Report, 1984 - 1994
Curtis I. Caldwell 13 Aug. 1994 935 p Limited Reproducibility: More than 20% of this document may be affected by microfiche quality
(AD-A283825) Avail: Issuing Activity (Defense Technical Information Center (DTIC))

This thesis looks at tests to determine how many signal sources exist in the medium when constrained to using only a few samples. It applies classical hypothesis testing assuming complex multivariate Gaussian random variables. The critical issue is the derivation of probability density functions of appropriate test statistics. This thesis includes a comprehensive development of the tools of statistics of complex variables for engineers and physicists. This includes complex matrix derivatives, changes of complex variables, and properties of the characteristic function of a complex multivariate random variable. Probability density functions are derived for: the set of eigenvalues satisfying the generalized eigenvalue problem of two complex Wishart matrices, the matrix complex Normal distribution, a joint distribution needed to derive the density for the sphericity test statistic, ratio of averages of disjoint sums of sequential eigenvalues of a complex Wishart matrix, and several tests based on the ratio of an arbitrary eigenvalue. DTIC

N95-19065 Naval Undersea Warfare Center, Newport, RI.
STATISTICS OF COMPLEX CROSS SPECTRUM ESTIMATE FOR SINUSOIDAL SIGNALS AND ARBITRARY NOISE SPECTRA
Albert H. Nuttall 27 Jul. 1994 59 p Limited Reproducibility: More than 20% of this document may be affected by microfiche quality
(AD-A283984; NUWC-NPt-TR-10709) Avail: CASI HC A04

The joint characteristic function of the real and imaginary parts of the complex cross spectrum estimate is derived in closed form for sinusoidal signals and arbitrary noise spectra. The corresponding joint probability density function for noise-only is also obtained in closed form, while that for signal present requires a numerical procedure involving a two-dimensional fast Fourier transform. These results are used to obtain the mean and deflection of the magnitude cross spectrum estimate. Comparisons are made with the deflection of an auto spectrum estimate available from the two channels by weighted summation. Potential limitations of restricting attention to the deflection criterion as a detectability measure are pointed out. DTIC

N95-19104 Minnesota Univ., Minneapolis, MN. Inst. for Mathematics and Its Applications.

FINITE MARKOV CHAINS AND RANDOM DISCRETE STRUCTURES Final Report, 15 Oct. 1993 - 14 Apr. 1994

Avner Friedman and Willard Miller, Jr. 26 Jul. 1994 5 p Limited Reproducibility: More than 20% of this document may be affected by microfiche quality

(Contract F49620-94-1-0009)

(AD-A284192; IMA-1; AFOSR-94-0520TR) Avail: Issuing Activity (Defense Technical Information Center (DTIC))

This grant from the Air Force Office of Scientific Research supported the research related to the two IMA Workshops Finite Markov Chain Renaissance held on October 18-22, 1993 and Random Discrete Structures held on November 15-19, 1993. The first workshop was organized by Persi Diaconis and David Aldous, while the second one by David Aldous and Robin Pemantle. Both workshops were integral parts of the IMA 1993-1994 year-long program on 'EMERGING APPLICATIONS OF PROBABILITY'. The October workshop addressed the following issues: Theoretical computer science examples: successes and open problems; computation-Bayesian statistics; Classical probability examples: successes and open problems; Mathematical theory and other aspects of Markov Chains. The November workshop explored examples from Jung's work on synchronicity to recent studies of parapsychology; random graphs; random permutations and Stein's method. In addition this workshop addressed new questions concerning probability on discrete infinite structures. The services of J. Michael Steele, a senior fellow was partially supported by this grant. Steele provided over-all direction for the entire probability program. Similarity, the grant supported 8 one-month visitors and 21 workshop participants. Grant AF/F49620-94-1-009 also supported the publication of the technical research reports submitted by the workshop participants for inclusion in the the IMA Preprint Series, and two IMA Proceedings Volumes. DTIC

66 SYSTEMS ANALYSIS

Includes mathematical modeling; network analysis; and operations research.

No abstracts in this category.

67 THEORETICAL MATHEMATICS

Includes topology and number theory.

N95-19030*# Fermi National Accelerator Lab., Batavia, IL. NASA/Fermilab Astrophysics Center.

SECOND-ORDER RECONSTRUCTION OF THE INFLATIONARY POTENTIAL

Andrew R. Liddle (Sussex Univ., Brighton, England.) and Michael S. Turner (Chicago Univ., Chicago, IL.) 1994 20 p Submitted for publication Sponsored by Royal Society and DOE

(Grant NAGw-2381)

(NASA-CR-197629; NAS 1.26:197629; FERMILAB-Pub-93/399-A; SUSSEX-AST-94/2-1; Astro-Ph/9402021) Avail: CASI HC A03/MF A01

To first order in the deviation from scale invariance the inflationary potential and its first two derivatives can be expressed in terms of the spectral indices of the scalar and tensor perturbations, n and n(sub T), and their contributions to the variance of the quadrupole CBR temperature anisotropy, S and T. In addition, there is a 'consistency relation' between these quantities: n(sub T) = (-1/ 7)(T/S). We derive the second-order expressions for the inflationary potential and its first two derivatives and the first-order expression for its third derivative, in terms, of n, n(sub T), S, T, and dn/d ln gamma. We also obtain the second-order consistency relation, n(sub T) = (-1/7)(T/S)(1 + 0.11(T/S) + 0.15(n-1)). As an example we consider the exponential potential, the only known case where exact analytic solutions for the perturbation spectra exist. We reconstruct the potential via Taylor expansion (with coefficients calculated at both first and second order), and introduce the Pade approximate as a greatly improved alternative. Author

N95-19288*# Stanford Univ., CA.

VISUALIZING SECOND ORDER TENSOR FIELDS WITH HYPERSTREAMLINES

Thierry Delmarcelle and Lambertus Hesselink 15 Mar. 1993 22 p

(Contract NCA2-781; NSF ECS-88-15815)

(NASA-CR-197619; NAS 1.26:197619) Avail: CASI HC A03/MF A01

Hyperstreamlines are a generalization to second order tensor fields of the conventional streamlines used in vector field visualization. As opposed to point icons commonly used in visualizing tensor fields, hyperstreamlines form a continuous representation of the complete tensor information along a three-dimensional path. This technique is useful in visulaizing both symmetric and unsymmetric three-dimensional tensor data. Several examples of tensor field visualization in solid materials and fluid flows are provided. Dissert. Abstr.

N95-19348*# Kansas Univ., Lawrence, KS. Dept. of Physics and Astronomy.

TESTING HIGHER-ORDER LAGRANGIAN PERTURBATION THEORY AGAINST NUMERICAL SIMULATION. 1: PANCAKE MODELS

T. Buchert (Max-Planck-Inst. fuer Astrophysik, Garching, Germany.), A. L. Melott, and A. G. Weiss (Max-Planck-Inst. fuer Astrophysik, Garching, Germany.) 1993 26 p Sponsored by DFG and National Center for Superconducting Applications

(Grants NAGw-2923; NSF AST-90-21414; NSF OSR-92-55223)

(NASA-CR-197611; NAS 1.26:197611) Avail: CASI HC A03/MF A01

We present results showing an improvement of the accuracy of perturbation theory as applied to cosmological structure formation for a useful range of quasi-linear scales. The Lagrangian theory of gravitational instability of an Einstein-de Sitter dust cosmogony investigated and solved up to the third order is compared with numerical simulations. In this paper we study the dynamics of pancake models as a first step. In previous work the accuracy of several analytical approximations for the modeling of large-scale structure in the mildly non-linear regime was analyzed in the same way, allowing for direct comparison of the accuracy of various approximations. In particular, the Zel'dovich approximation (hereafter ZA) as a subclass of the first-order Lagrangian perturbation solutions was found to provide an excellent approximation to the density field in the mildly non-linear regime (i.e. up to a linear r.m.s. density contrast of sigma is approximately 2). The performance of ZA in hierarchical clustering models can be greatly improved by truncating the initial power spectrum (smoothing the initial data). We here explore whether this approximation can be further improved with higher-order corrections in the displacement mapping from homogeneity. We study a single pancake model (truncated power-spectrum with power-spectrum with power-index n = -1) using cross-correlation statistics employed in previous work. We found that for all statistical methods used the higher-order corrections improve the results obtained for the first-order solution up to the stage when sigma (linear theory) is approximately 1. While this improvement can be seen for all spatial scales, later stages retain this feature only above a certain scale which is increasing with time. However, third-order is not much improvement over second-order at any stage. The total breakdown of the perturbation approach is observed at the stage, where sigma (linear theory) is approximately 2, which corresponds to the onset of hierarchical clustering. This success is found at a considerable higher non-linearity than is usual for perturbation theory. Whether a truncation of the initial power-spectrum in hierarchical models retains this improvement will be analyzed in a forthcoming work. Author (revised)

N95-19603# Army Research Lab., Aberdeen Proving Ground, MD.
THE TENSOR EQUATION AX+XA=PHI (A, H) WITH APPLICATIONS TO KINEMATICS OF CONTINUA Final Report, Mar. 1992 - Mar. 1993
Michael J. Scheidler Sep. 1994 44 p
(AD-A285886; ARL-TR-582) Avail: CASI HC A03/MF A01

The (second-order) tensor equation AX + XA = Phi (A,H) is studied for certain isotropic functions Phi (A,H) which are linear in H. Qualitative properties of the solution X and relations between the solutions for forms of Phi are established for an inner product space of arbitrary dimension. These results, together with Rivlin's identities for tensor polynomials in two variables, are applied in three dimension to obtain new explicit formulas for X in direct tensor notation as well as new derivations of previously known formulas. Several applications to the kinematics of continua are considered. DTIC

70 PHYSICS (GENERAL)

For precision time and time interval (PTTI) see *35 Instrumentation and Photography;* for geophysics, astrophysics or solar physics see *46 Geophysics, 90 Astrophysics,* or *92 Solar Physics.*

N95-17983# Johns Hopkins Univ., Laurel, MD. Applied Physics Lab.
FUNDAMENTAL ADVANCES FOR CHARACTERIZING CATHODIC PROTECTION SYSTEMS Annual Report, Aug. 1992 - Jul. 1993
R. Srinivasan, P. R. Zarriello, P. Gopalan, and J. C. Murphy Mar. 1994 61 p See also PB93-125003 Sponsored by Gas Research Inst., Chicago, IL
(Contract GRI-5091-260-2118)
(PB94-180692; GRI-93/0367) Avail: CASI HC A04/MF A01

This research is developing a corrosion rate measurement to assist in (1) identifying in greater detail why corrosion occurs in pipelines that are nominally cathodically protected and (2) determining more specifically the requirements for cathodic protection. Present corrosion rate methods are limited to culmative changes such as weight loss. Under this project a new, instantaneous and nondestructive, technique has been developed to measure corrosion rate of metals under cathodic protection.
Author (revised)

N95-18127# Oak Ridge National Lab., TN.
STUDY OF FRUSTRATED SYSTEMS VIA DISSIPATIVE MAPS
G. S. Canright and G. I. Watson Apr. 1994 6 p Presented at the 7th Annual Conference on Computer Simulation Studies in Condensed Matter Physics, Athens, GA, 21-25 Feb. 1994
(Contract DE-AC05-84OR-21400)
(DE94-017754; CONF-940299-1) Avail: CASI HC A02/MF A01

The authors briefly describe a method for finding complex metastables states for frustrated classical systems, using a dissipative dynamical map. They show by example that this technique can give states which are very competitive in energy with the ground state, and with other, simpler states which are found by exhaustive search. The problem the authors look at is a two-body interaction F representing the repulsion between uniform layers of flux lines in a layered superconductor. DOE

N95-18916 Stanford Univ., CA.
NUMERICAL ANALYSIS OF DISSIPATIVE DYNAMICAL SYSTEMS IN SOLID AND FLUID MECHNAICS, WITH A SPECIAL EMPHASIS ON COUPLED PROBLEMS Ph.D. Thesis
Francisco ArmeroRovira 1994 386 p
Avail: Univ. Microfilms Order No. DA9414530

The goals of this dissertation are the formulation, analysis and implementation of efficient time-stepping algorithms that optimally represent the dissipative properties of a number of systems in solid and fluid mechanics, with special emphasis on coupled problems. The first part focuses on coupled thermomechanical problems in solid mechanics, ranging from linearized thermoelasticity to finite strain thermoplasticity. A-priori stability estimates are derived for the continuum problems, identifying the dissipative structure of these systems. Given their coupled character, computational efficiency requires fractional-step (staggered) methods, characterized by a modular and low-cost implementation. However, standard staggered schemes are only conditionally stable. The analysis presented here in the context of the classical theory of operator splits points out the cause of this limitation; namely, the previously identified dissipative structure is broken by the split. Moreover, this approach allows the formulation and analysis of a new class of nonlinear unconditionally stable staggered time-stepping algorithms, the first of this kind. The extension to other coupled systems in solid mechanics is indicated. The second part concentrates on incompressible Navier-Stokes and coupled magnetohydrodynamics (MHD). These systems possess an asymptotic long-term dissipative structure characterized by an absorbing set and a global attractor. Time-stepping algorithms are analyzed in this context. Rigorous nonlinear stability and long-term analyses are presented for the time semidiscrete and the fully discrete mixed finite element systems. Direct and projection methods (that is, fractional-step methods designed to enforce the incompressibility constraint) are considered. A class of time-stepping schemes presenting nonlinear stability and optimally dissipative long-term properties is identified which, in addition, is linear within the time step. The existence of an algorithmic attractor is proven for a characteristic member of this class. The combination of these results with the strategy outlined above for thermomechanical problems leads to the formulation of new monolithic and staggered algorithms for coupled MHD that exhibit these same properties. The efficiency of all these time-stepping algorithms is demonstrated via a number of numerical simulations that employ both standard and non-standard finite element methods. Dissert. Abstr.

N95-19234# Sandia National Labs., Albuquerque, NM.
GIANT EFFECTIVE MASS DEVIATIONS NEAR THE MAGNETIC FIELD-INDUCED MINIGAP IN DOUBLE QUANTUM WELLS
N. E. Harff, J. A. Simmons, S. K. Lyo, J. F. Klem, and S. M. Goodnick (Oregon State Univ., Corvallis, OR.) 1994 4 p Presented at the 22nd International Conference on Physics of Semiconductors, Vancouver, British Columbia, 15-19 Aug. 1994
(Contract DE-AC04-94AL-85000)
(DE94-018889; SAND-94-2099C; CONF-9408155-6) Avail: CASI HC A01/MF A01

The authors report major deviations in the electron effective mass m* near the partial energy gap, or minigap, formed in strongly coupled double quantum wells (QW's) by an anticrossing of the two QW dispersion curves. The anticrossing and minigap are induced by an in-plane magnetic field B(sub parallel) and give rise to large distortions in the Fermi surface and density of states, including a Van Hove singularity. Sweeping B(sub parallel) moves the minigap through the Fermi level, with the upper and lower gap edges producing a sharp maximum and minimum in the low-temperature in-plane conductance, in agreement with theoretical calculations. The temperature dependence of Shubnikov-de Haas (SdH) oscillations appearing in a tilted magnetic field yield a decreased m* less than or equal to 1/3 m*(sub GaAs) near the upper gap edge, and indicate an increase in m* near the lower gap edge. DOE

N95-19704# Argonne National Lab., IL.
THE INTERACTION OF TWO NARROW MAGNETS AND A MOVING CONDUCTING SLIP
Z. Wang, S. R. Winkleman, T. M. Mulcahy, H. T. Coffey, D. M. Rote, and J. R. Hull Jul. 1994 18 p
(Contract W-31-109-eng-38)
(DE94-018575; ANL/ESD/TM-70) Avail: CASI HC A03/MF A01

Measurements were made of the forces experienced by two narrow but relatively long permanent magnets positioned above a moving, electrically conducting surface. The intent was to determine the accuracy of various means of computing these forces. It was found that the behavior at very high speeds can be approximated by using elementary methods and making the assumption that magnetic images are formed in the conductor. At lower speeds, a published formulation that uses Fourier transform techniques is quite reliable for the parameters of the experiments. A commercial computer code that uses a finite-element method of analysis is also in good agreement The results are relevant to the design of high-speed magnetically levitated (maglev) ground transportation vehicles having multiple magnets, where the guideway consists of a continuous-sheet conductor.
DOE

N95-19195*# Jet Propulsion Lab., California Inst. of Tech., Pasadena, CA.
THE PHYSICS OF INTACT CAPTURE Abstract Only
Peter Tsou, D. J. Griffiths (Oregon State Univ., Corvallis, OR.), and A. L.

Albee (California Inst. of Tech., Pasadena, CA.) *In* Lunar and Planetary Inst., Workshop on Particle Capture, Recovery and Velocity/Trajectory Measurement Technologies 1994 p 85-88 (For primary document see N95-19172 05-90)
Avail: CASI HC A01/MF A02

71 ACOUSTICS

Includes sound generation, transmission and attenuation.
For noise pollution see *45 Environmental Pollution.*

N95-18083 Washington Univ., Seattle, WA. Applied Physics Lab.
TIME SPREAD AND FREQUENCY COHERENCE IN ACOUSTIC FORWARD SCATTERING FROM THE SEA SURFACE
Peter H. Dahl and Azmi Al-Kurd Aug. 1994 25 p Limited Reproducibility: More than 20% of this document may be affected by microfiche quality
(Contracts N00039-88-C-0051; N00039-91-C-0072)
(AD-A284736; APL-UW-TR-9405; PSU/ARL-S89-2) Avail: CASI HC A03

Measurements of the characteristic time spread L (in seconds) of surface forward scattering were made from the research platform FLIP in January 1992. These data were compared with a model for L and matched the model to within an average relative error of 30 percent. The inverse, L-1 (inhertz), is a measure of the coherence bandwidth of the channel and therefore important in both designing waveforms and determining signal-processing strategies. Using the model for L, simulators can assess realistic magnitudes of the coherence bandwidth of the surface channel as a function of source/receiver geometry and environmental conditions. DTIC

N95-18379 Edgewood Research Development and Engineering Center, Aberdeen Proving Ground, MD.
DESIGN OF SPHERICAL AEROSOL PARTICLES TO MAXIMIZE SOUND ATTENUATION Final Report, Jul. - Oct. 1993
Janon F. Embury Jun. 1994 20 p Limited Reproducibility: More than 20% of this document may be affected by microfiche quality
(AD-A284313; ERDEC-TR-169) Avail: CASI HC A03

Analytic expressions for the audible sound absorption and scatter cross sections of an aerosol consisting of spherical particles are identified. The acoustic cross sections per aerosol mass and volume are explored as functions of three independent variables (sound frequency, particle diameter, and particle density) to determine regions of strong attenuation of audible sound. Optimum diameters, and densities that maximize cross sections per mass and volume at specific frequencies are found by reading contour plots contained in the figures of this report. Corresponding expected levels of acoustic attenuation are also contemplated. To a small extent, it is possible to scatter audible acoustic radiation with aerosol particles while aerosol absorption of sound can be significant. Comparing the levels of audible sound attenuation by atmospheric gases plus water vapor with the levels of attenuation achievable with an aerosol, we find that aerosol absorption of sound can greatly exceed that of the intervening air. DTIC

N95-18542 Duke Univ., Durham, NC.
ACOUSTIC RADIATION DAMPING OF FLAT RECTANGULAR PLATES SUBJECTED TO SUBSONIC FLOWS Ph.D. Thesis
Karen Heitman Lyle 1993 118 p
Avail: Univ. Microfilms Order No. DA9414114

The acoustic radiation damping for various isotropic and laminated composite plates and semi-infinite strips subjected to a uniform subsonic and steady flow has been predicted. The predictions are based on the linear vibration of a flat plate. The fluid loading is characterized as the perturbation pressure derived from the linearized Bernoulli and continuity equations. Parameters varied in the analysis include Mach number, mode number and plate size, aspect ratio and mass. The predictions are compared with existing theoretical results and experimental data. The analytical results show that the fluid loading can significantly affect realistic plate responses. Generally, graphite/epoxy and carbon/carbon plates have higher acoustic radiation damping values than similar aluminum plates, except near plate divergence conditions resulting from aeroelastic instability. Universal curves are presented where the acoustic radiation damping normalized by the mass ratio is a linear function of the reduced frequency. A separate curve is required for each Mach number and plate aspect ratio. In addition, acoustic radiation damping values can be greater than or equal to the structural component of the modal critical damping ratio (assumed as 0.01) for the higher subsonic Mach numbers. New experimental data were acquired for comparison with the analytical results. Dissert. Abstr.

N95-18566 British Broadcasting Corp., Tadworth (England). Research and Development Dept.
A WIDEBAND ABSORBER FOR TELEVISION STUDIOS
M. D. M. Baird 1994 14 p
(BBC-RD-1994/12) Copyright Avail: Issuing Activity (BBC, Kingswood Warren, Tadworth, Surrey, England)

The acoustic treatment in BBC television has taken various forms to date, all of which have been relatively expensive, some of which provide inadequate absorption. An investigation has been conducted into the possibilities of producing a new type of wideband absorber which would be more economic, also taking installation time into account, than earlier designs. This Report describes the absorption coefficient measurements made on various combinations of materials, from which a wideband sound absorber has been developed. The absorber works efficiently between 50 Hz and 10 kHz, is simple and easy to construct using readily available materials, and is fire resistant. The design lends itself, if necessary, to on-site fine tuning, and savings in the region of 50 percent can be achieved in terms of cost and space with respect to previous designs. Author

N95-18673 Massachusetts Inst. of Tech., Cambridge. Dept. of Ocean Engineering.
AN ANALYSIS OF NOISE REDUCTION IN VARIABLE RELUCTANCE MOTORS USING PULSE POSITION RANDOMIZATION M.S. Thesis
Melissa C. Smoot May 1994 103 p Limited Reproducibility: More than 20% of this document may be affected by microfiche quality
(Contract N00123-89-G-0580)
(AD-A283846) Avail: CASI HC A06

The design and implementation of a control system to introduce randomization into the control of a variable reluctance motor (VRM) is presented. The goal is to reduce noise generated by radial vibrations of the stator. Motor phase commutation angles are dithered by 1 or 2 mechanical degrees to investigate the effect of randomization on acoustic noise. VRM commutation points are varied using a uniform probability density function and a 4 state Markov chain among other methods. The theory of VRM and inverter operation and a derivation of the major source of acoustic noise are developed. The experimental results show the effects of randomization. Uniform dithering and Markov chain dithering both tend to spread the noise spectrum, reducing peak noise components. No clear evidence is found to determine which is the optimum randomization scheme. The benefit of commutation angle randomization in reducing VRM loudness as perceived by humans is found to be questionable. DTIC

N95-18890 Iowa Univ., Iowa City, IA. Dept. of Physics and Astronomy.
SOUND SPEED PROFILES FROM VERTICAL ARRAY DATA
David H. Berman 22 Mar. 1994 58 p Limited Reproducibility: More than 20% of this document may be affected by microfiche quality
(Contract N00014-93-1-2004)
(AD-A283978) Avail: CASI HC A04

A scheme for extracting sound speed information from vertical arrays in shallow water is examined. The scheme hinges on the covariance matrix of the pressures received at the array being diagonal in the modes of the water column, and involves computing second derivatives of the covariance. Conditions under which the covariance might be mode-diagonal are examined. It is found that without attenuation, it is unlikely to find mode-diagonal covariances. However with reasonable attenuations, the covariance will be dominated by the lowest mode. The scheme described here is applied to vertical array data taken in 1985. DTIC

N95-18930*# Georgia Inst. of Tech., Atlanta, GA. Acoustics, Aerodynamics and Advanced Vehicles Div.
ACOUSTIC PROPERTIES AND DURABILITY OF LINER MATERIALS AT NON-STANDARD ATMOSPHERIC CONDITIONS
K. K. Ahuja, R. J. Gaeta, Jr., and J. S. Hsu Nov. 1994 194 p
(Contract NAS1-19061; RTOP 505-59-52-01)
(NASA-CR-195010; NAS 1.26:195010; GTRI-A-8612-015) Avail: CASI HC A09/MF A03

This report documents the results of an experimental study on how

acoustic properties of certain absorbing liner materials are affected by nonstandard atmospheric conditions. This study was motivated by the need to assess risks associated with incorporating acoustic testing capability in wind tunnels with semicryogenic high Reynolds number aerodynamic and/or low pressure capabilities. The study consisted of three phases: 1) measurement of acoustic properties of selected liner materials at subatmospheric pressure conditions, 2) periodic cold soak and high pressure exposure of liner materials for 250 cycles, and 3) determination of the effect of periodic cold soak on the acoustic properties of the liner materials at subatmospheric conditions and the effect on mechanical resiliency. The selected liner materials were Pyrell foam, Fiberglass, and Kevlar. A vacuum facility was used to create the subatmospheric environment in which an impedance tube was placed to measure acoustic properties of the test materials. An automated cryogenic cooling system was used to simulate periodic cold soak and high pressure exposure. It was found that lower ambient pressure reduced the absorption effectiveness of the liner materials to varying degrees. Also no significant change in the acoustic properties occurred after the periodic cold soak. Furthermore, mechanical resiliency tests indicated no noticeable change. Author

N95-19046 British Broadcasting Corp., Tadworth (England). Research and Development Dept.

HIGH FREQUENCY ROOM RESPONSES: ACOUSTIC DESIGN AND THE CONTROL OF STEREOPHONIC IMAGE QUALITY

R. Walker 1994 17 p

(BBC-RD-1994/11) Copyright Avail: Issuing Activity (BBC, Kingswood Warren, Tadworth, Surrey, England)

Aspects to mid and high frequency acoustic design are described, mainly in the context of relatively small rooms. The factors affecting the design and some of the difficulties which may be encountered are also discussed. The primary means of evaluating the quality of reproduced sound is the studio control room (and its associated equipment). This Report is written primarily in terms of the design of control rooms, but is directly applicable to other small spaces and, to a lesser extent, to larger spaces. Author

N95-19048 British Broadcasting Corp., Tadworth (England). Research and Development Dept.

ACOUSTIC NOISE CRITERIA FOR LISTENING ROOMS AND CONTROL ROOMS

R. Walker 1994 13 p

(BBC-RD-1994/06) Copyright Avail: Issuing Activity (BBC, Kingswood Warren, Tadworth, Surrey, England)

This Report is based on a submission document to both EBU G1(LIST) and ITU-R TG 10/3 drafting committees. It describes background noise criteria for high-quality listening environments from a number of different organizations and the derivation of a compromise criterion for the continuous background noise levels. The outcome of the work, and the proposal submitted to those technical groups, was the choice of an appropriate Noise Rating curve as a common standard NRIO was found to fit well with other organizations' criteria. Some problems relating to the apparent demise of the former ISO Noise Rating curves are also discussed. Author

N95-19054 British Broadcasting Corp., Tadworth (England). Research Dept.

DYNAMIC RANGE CONTROL OF AUDIO SIGNALS BY DIGITAL SIGNAL PROCESSING

N. H. C. Gilchrist 1993 12 p

(BBC-RD-1993/7) Copyright Avail: Issuing Activity (BBC, Kingswood Warren, Tadworth, Surrey, England)

It is often necessary to reduce the dynamic range of musical programs, particularly those comprising orchestral and choral music, for them to be received satisfactorily by listeners to conventional FM and AM broadcasts. With the arrival of DAB (Digital Audio Broadcasting) a much wider dynamic range will become available for radio broadcasting, although some listeners may prefer to have a signal with a reduced dynamic range. This report describes a digital processor developed by the BBC to control the dynamic range of musical programs in a manner similar to that of a trained Studio Manager. It may be used prior to transmission in conventional broadcasting, replacing limiters or other compression equipment. In DAB, it offers the possibility of providing a dynamic range control signal to be sent to the receiver via an ancillary data channel, simultaneously with the uncompressed audio, giving the listener the option of the full dynamic range or a reduced dynamic range. Author

N95-19057 Materials Research Labs., Ascot Vale (Australia).

THE EVALUATION OF TRANSMISSION EFFICIENCY AND COUPLING LOSS FACTOR OF STRUCTURAL JUNCTIONS

Yan K. Tso Aug. 1993 30 p

(MRL-TR-93-1; AR-008-252) Copyright Avail: Issuing Activity

The evaluation of transmission efficiency of structural junctions forms an important part in the study of structure-born noise as it provides the basis for identifying and quantifying the vibration paths in the structure. In this report, analytical methods for evaluating the transmission efficiency of structural junctions including plate-plate and plate-beam junction are described. The calculation of coupling loss factor from the transmission efficiency of a junction for Statistical Energy Analysis (SEA) is also described. Sample calculations of transmission efficiencies on a number of structural junctions are presented. It is found that for typical naval ship constructions that consist of plates coupled to light thin beams, the elastic vibrations of the beams have a significant effect on the transmission efficiency. Author

N95-19142# Advisory Group for Aerospace Research and Development, Neuilly-Sur-Seine (France). Structures and Materials Panel.

IMPACT OF ACOUSTIC LOADS ON AIRCRAFT STRUCTURES [IMPACT DES SOLICITATIONS ACOUSTIQUES SUR LES STRUCTURES D'AERONEFS]

Sep. 1994 265 p In ENGLISH and FRENCH Symposium held in Lillehammer, Norway, May 1994 Original contains color illustrations

(AGARD-CP-549; ISBN-92-836-0001-0) Copyright Avail: CASI HC A12/MF A03

A broad band of different activities was addressed in the Specialists' Meeting held by the Structures and Materials Panel of AGARD in May 1994: Topics dealt with the acoustic environment in subsonic and hypersonic flow regimes, innovative structural design techniques and materials for fatigue resistant structures, and experimental and analytical tools for evaluation of the behavior of structures in an acoustically and thermally adverse environment. For individual titles, see N95-19143 through N95-19167.

N95-19143# British Aerospace Aircraft Group, Warton (England). Military Aircraft Div.

CURRENT AND FUTURE PROBLEMS IN STRUCTURAL ACOUSTIC FATIGUE

P. D. Green *In* AGARD, Impact of Acoustic Loads on Aircraft Structures Sep. 1994 5 p (For primary document see N95-19142 05-71)

Copyright Avail: CASI HC A01/MF A03

Acoustic fatigue failures can be caused by the dynamic response of aircraft structures to unsteady pressure loading from aerodynamic and engine acoustic sources. The life of structures is often difficult to assess accurately and may be greatly affected by steady thermal, in-plane and out-of-plane loads. Furthermore, currently available methods do not enable fatigue life assessment of the substructure to be made, despite these failures occurring regularly in service. This paper discusses current problems associated with structural acoustic fatigue and extends upon this to account for likely clearance philosophies and configurations for future aircraft. Author

N95-19144# Eurocopter Deutschland G.m.b.H., Munich (Germany).

HELICOPTER INTERNAL NOISE

G. Niesl and E. Laudien (Daimler-Benz A.G., Munick, Germany.) *In* AGARD, Impact of Acoustic Loads on Aircraft Structures Sep. 1994 12 p Sponsored in part by BRITE/EURAM (For primary document see N95-19142 05-71)

(Proj. RHINO)

Copyright Avail: CASI HC A03/MF A03

Compared to fixed wing aircraft, helicopter interior noise is higher, and subjectively more annoying. This is mainly due to discrete frequencies by the main transmission system, and also from other components like main and tail rotor, engines, or cooling fans. Up to now, mainly passive measures have been used for interior noise reduction. Despite intensive experimental and theoretical investigation to improve acoustic treatment, their weight penalties remain high especially in the low frequency range. Here, active noise control offers additional capacities without excessive weight efforts.

Loud-speaker based systems are sufficiently well developed for implementing a prototype system in the helicopter. Two other principles are in development: active panel control which introduces mechanical actuators to excite the cabin walls, and active control of gearbox struts with actuators in the load path between gearbox and fuselage. Author

N95-19145# Dassault Aviation, Saint-Cloud (France).
AEROACOUSTIC QUALIFICATION OF HERMES SHINGLES [DIMENSIONNEMENT ET QUALIFICATION AEROACOUSTIQUE DES TUILES HERMES]
C. Petiau and A. Paret *In* AGARD, Impact of Acoustic Loads on Aircraft Structures Sep. 1994 17 p In ENGLISH and FRENCH (For primary document see N95-19142 05-71)
Copyright Avail: CASI HC A03/MF A03

General problems of aeroacoustic analysis are presented, taking as an example shingle studies of the HERMES space shuttle. Analysis of shingle behavior meets this problem in a particularly difficult way (very hard environment, specific difficulties due to design of shingles). Available analysis tools include: (1) calculation means, which are mainly those of aeroelasticity, and (2) ground test means (wind tunnel, progressive wave tubes, shaker,...). None of these means can alone satisfy the needs of structural dimensioning and qualification; in particular the calculation of turbulent sources is not possible today, and they are very difficult to simulate with ground testing of actual structural parts. In spite of these difficulties, and referring to the preliminary tests and calculations of HERMES shingles, a rational strategy is proposed for aeroacoustic dimensioning and qualification of structural parts. This leads to a succession of tests, the conditions of which are determined by calculations, calculation models being themselves validated by comparison with test results. Author

N95-19146# Wright Lab., Wright-Patterson AFB, OH. Structural Dynamics Branch.
WEAPONS BAY ACOUSTIC ENVIRONMENT
L. L. Shaw and R. M. Shimovetz *In* AGARD, Impact of Acoustic Loads on Aircraft Structures Sep. 1994 10 p (For primary document see N95-19142 05-71)
Copyright Avail: CASI HC A02/MF A03

An aircraft weapons bay exposed to freestream flow experiences an intense aeroacoustic environment in and around the bay. Experience has taught that the intensity of this environment can be severe enough to result in damage to a store, its internal equipment, or the structure of the weapons bay itself. To ensure that stores and sensitive internal equipment can withstand this hazardous environment and successfully complete the mission, they must be qualified to the most severe sound pressure levels anticipated for the mission. If the qualification test levels are too high, the store and its internal equipment will be over designed, resulting in unnecessary costs and possible performance penalties. If the qualification levels are below those experienced in flight, the store or its internal equipment may catastrophically fail during performance of the mission. Thus, it is desirable that the expected levels in weapons bays be accurately predicted. A large number of research efforts have been directed toward understanding flow-induced cavity oscillations. However, the phenomena are still not adequately understood to allow one to predict the fluctuating pressure levels for various configurations and flow conditions. This is especially true at supersonic flow speeds, where only a small amount of data are available. This paper will give a background of flow induced cavity oscillations and discuss predictions, control and suppression, and the future of weapons bay acoustic environments. A large number of research efforts have been directed toward understanding flow-induced cavity oscillations. However, the phenomena are still not adequately understood to allow one to predict the fluctuating pressure levels for various configurations and flow conditions. This is especially true at supersonic flow speeds, where only a small amount of data are available. This paper will give a background of flow induced cavity oscillations and discuss predictions, control and suppression, and the future of weapons bay acoustic environments. Author

N95-19147# Alenia, Turin (Italy).
IMPACT OF NOISE ENVIRONMENT ON ENGINE NACELLE DESIGN
R. Giuzio, E. Dalle-Mura, and G. Giuffre *In* AGARD, Impact of Acoustic Loads on Aircraft Structures Sep. 1994 11 p (For primary document see N95-19142 05-71)
Copyright Avail: CASI HC A03/MF A03

The present paper describes the general philosophy and the followed methodology in engine nacelle design, usually resulting in the embodiment of acoustic treatment in intake and exhaust ducts to make the relevant aircraft compliant with noise certification requirements. A general description of conventional acoustic liners currently in service, and liners of innovative design currently being investigated is also included, giving emphasis to the methodology for the selection of the proper acoustic treatment. Finally the Alenia software package (ALNOIS), ad hoc developed to cover the complete engine nacelle acoustic design and to support the acoustic panels manufacturing, is briefly described. Author

N95-19148*# National Aeronautics and Space Administration. Langley Research Center, Hampton, VA.
IMPACT OF DYNAMIC LOADS ON PROPULSION INTEGRATION
J. M. Seiner *In* AGARD, Impact of Acoustic Loads on Aircraft Structures Sep. 1994 14 p (For primary document see N95-19142 05-71)
Copyright Avail: CASI HC A03/MF A03

Aircraft dynamic loads produced by engine exhaust plumes are examined for a class of military fighter and bomber configurations in model and full scale. The configurations examined are associated with the USAF F-15 and B-1B aircraft, and the US F-18 HARV and ASTOVL programs. The experience gained as a result of these studies is used to formulate a level of understanding concerning this phenomena that could be useful at the preliminary stage of propulsion/airframe design. Author

N95-19149# Wright Lab., Wright-Patterson AFB, OH. Chief, Structural Integrity Branch.
HIGH-TEMPERATURE ACOUSTIC TEST FACILITIES AND METHODS
Jerome Pearson *In* AGARD, Impact of Acoustic Loads on Aircraft Structures Sep. 1994 9 p (For primary document see N95-19142 05-71)
Copyright Avail: CASI HC A02/MF A03

The Wright Laboratory is the Air Force center for air vehicles, responsible for developing advanced technology and incorporating it into new flight vehicles and for continuous technological improvement of operational air vehicles. Part of that responsibility is the problem of acoustic fatigue. With the advent of jet aircraft in the 1950's, acoustic fatigue of aircraft structure became a significant problem. In the 1960's the Wright Laboratory constructed the first large acoustic fatigue test facilities in the United States, and the laboratory has been a dominant factor in high-intensity acoustic testing since that time. This paper discusses some of the intense environments encountered by new and planned Air Force flight vehicles, and describes three new acoustic test facilities of the Wright Laboratory designed for testing structures in these dynamic environments. These new test facilities represent the state of the art in high-temperature, high-intensity acoustic testing and random fatigue testing. They will allow the laboratory scientists and engineers to test the new structures and materials required to withstand the severe environments of captive-carry missiles, augmented lift wings and flaps, exhaust structures of stealth aircraft, and hypersonic vehicle structures well into the twenty-first century. Author

N95-19150# Industrieanlagen-Betriebsgesellschaft m.b.H., Ottobrunn (Germany).
DESIGN AND OPERATION OF A THERMOACOUSTIC TEST FACILITY
c09
G. Bayerdoerfer and L. Freyberg *In* AGARD, Impact of Acoustic Loads on Aircraft Structures Sep. 1994 5 p Sponsored in cooperation with BMFT and the Deutsche Agentur fuer Raumfahrtangelegenheite G.m.b.H., Bonn, Germany (For primary document see N95-19142 05-71)
Copyright Avail: CASI HC A01/MF A03

Aerothermal environments as encountered during the missions of reusable spacecraft, hypersonic vehicles, advanced launchers, etc. are the major design driver for an advanced Thermal Protection System (TPS) technology. In developing such materials and structures ground testing under simulated operational conditions is of eminent importance. In order to meet these requirements IABG has designed a thermoacoustic facility which was recently put into operation. The facility is able to produce surface temperatures up to 1300 C and sound pressure levels up to 160 dB. The design approach and operational aspects from test work performed so far are described. Author

N95-19151# Wright Lab., Wright-Patterson AFB, OH.
NONLINEAR DYNAMIC RESPONSE OF AIRCRAFT STRUCTURES TO ACOUSTIC EXCITATION **c05**
H. F. Wolfe and R. G. White (Southampton Univ., England.) *In* AGARD, Impact of Acoustic Loads on Aircraft Structures Sep. 1994 10 p (For primary document see N95-19142 05-71)
Copyright Avail: CASI HC A02/MF A03

Acoustic fatigue failure in aerospace structures has been a concern for many years. New prediction techniques are needed for the new materials and structural concepts of interest and higher sound pressure levels encountered. The objective of this program of work is to improve the fundamental understanding of the nonlinear behavior of beams and plates excited from low to high levels of excitation. Experiments have been conducted utilizing a clamped-clamped (C-C) beam statically tested and shaker driven at increasing levels of excitation. Similarly, C-C-C-C plates were excited by a vibration shaker and in a progressive wave tube. The total strains and the components, bending and axial, and the displacements were measured with increasing levels of excitation. Bistable behavior was observed with sinusoidal excitation for both the beams and plates. The measured axial or membrane strains were very low compared to the bending strains for high levels of excitation. The beams randomly excited exhibited a slight frequency shift and peak broadening, which can be attributed to an increased stiffening or hard spring nonlinearity. The plates randomly excited exhibited a greater frequency shift and peak broadening than the beams. The dynamic tests resulted in a nonlinear relationship between the response strains and displacements and the excitation levels. A multimodal model is discussed to estimate the mean square stress response due to high levels of excitation. Author

N95-19152# Rome Univ. (Italy). Dept. of Aerospace.
ACOUSTICS OF SPACE STRUCTURES
P. Santini, F. Morganti (Alenia Spazio S.p.A., Rome, Italy.), and R. Giovannucci *In* AGARD, Impact of Acoustic Loads on Aircraft Structures Sep. 1994 13 p Sponsored in cooperation with the Italian Ministero per la Universita e per la ricerca Scientifica e Technologica (For primary document see N95-19142 05-71)
Copyright Avail: CASI HC A03/MF A03

The problem of the response of a panel belonging to a space structure or to a launcher is considered. By using a modal approach in the frequency domain, the structure is described through a finite element model, and the acoustic field through Green's function. The presence of the air is considered, and it leads to an addition to the mass matrix and to the damping matrix of the relevant terms. The transfer function is then applied to the case of random inputs, for which an analytical expression is provided. Some numerical examples show the effect of the additional terms on the spectral distribution and on the relevant RMS value. Author

N95-19153# Science Applications International Corp., Fort Washington, PA.
PREDICTION OF FLUCTUATING PRESSURE AND POWER SPECTRA IN ATTACHED AND SEPARATED COMPRESSIBLE FLOW **c34**
A. L. Laganelli, K. R. Wentz (Rohr Industries, Inc., Chula Vista, CA.), and H. F. Wolfe (Rohr Industries, Inc., Chula Vista, CA.) *In* AGARD, Impact of Acoustic Loads on Aircraft Structures Sep. 1994 12 p (For primary document see N95-19142 05-71)
(Contract F33615-87-C-3227)
Copyright Avail: CASI HC A03/MF A03

A brief review is presented of work by the authors to provide an engineering prediction technique for power intensity (rms fluctuating pressure) and power spectral density (PSD) for attached and separated compressible flow. The review process also considers recent shock/turbulent boundary layer interaction work conducted at the University of Texas at Mach 5. It is shown that prediction techniques are hampered as the result of the requirement to know parameters of flow interactions a priori; in particular, the choice of characteristic length and velocity scales. A technique is presented, based on the Houbolt spectra assumption, that appears to provide engineering solutions to the design resolution of complex flow problems. The method is based on a first moment type of PSD (f.phi(f)/(Rho sub OA)squared) that has a fixed value for attached and separated flows. Moreover, when applying the concept with the Houbolt spectra, an excellent comparison is shown to PSD data for shock/turbulent boundary layer interactions. Author (revised)

N95-19154# Wright Lab., Wright-Patterson AFB, OH.
MODELLING STRUCTURALLY DAMAGING TWIN-JET SCREECH **c05**
Mary Kae Lockwood, Steven H. Walker, and Alan B. Cain (McDonnell-Douglas Corp., Saint Louis, MO.) *In* AGARD, Impact of Acoustic Loads on Aircraft Structures Sep. 1994 8 p (For primary document see N95-19142 05-71)
Copyright Avail: CASI HC A02/MF A03

Closely spaced twin jet aircraft have been known to be susceptible to aft-end structural damage due to the high sound pressure levels resulting from twin jet screech. An initial engineering workstation tool to predict the occurence of screech, ultimately allowing the design of configurations which will not result in screech, is presented here. The model has been developed in a modular fashion to facilitate upgrades. The implementation takes advantage of a graphical interface, yielding predictions of screech amplitude versus frequency within a few seconds once the initial flowfield is defined. The four physically based modules in the code, for the instability waves, shock-vortex interaction, acoustic feedback and receptivity, are based on analytical, computational and experimental research. Preliminary results for 2-D jets illustrate the effects freestream Mach number and shear layer growth rate have on the screech amplitude and frequency. Author

N95-19155# Construcciones Aeronauticas S.A., Madrid (Spain). Structural Dynamics Dept.
APPLICATION OF THE PSD TECHNIQUE TO ACOUSTIC FATIGUE STRESS CALCULATIONS IN COMPLEX SUBSTRUCTURES
H. Climent and J. Casalengua *In* AGARD, Impact of Acoustic Loads on Aircraft Structures Sep. 1994 11 p (For primary document see N95-19142 05-71)
Copyright Avail: CASI HC A03/MF A03

A method for stress calculation using the Power Spectral Density (PSD) technique for acoustic fatigue evaluation is presented. The sound pressure levels (SPL) are converted to acoustic pressures PSD and applied to a finite element model representation of the substructure. This technique can cover: complex geometries in substructures, detailed effects of reinforcements and the contribution of several normal modes, improving the previous procedure based on ESDU data sheets that accounts for simple geometries and only contributions of the first mode are considered. The method is used to predict stresses at substructures subjected to a severe acoustic environment. Comparison with acoustic fatigue test results show good correlation between experimental data and theoretical analyses in terms of stresses and accelerations providing an encouraging basis for further work in this direction. Author

N95-19156# Deutsche Aerospace A.G., Bremen (Germany).
ACOUSTIC FATIGUE TESTING ON DIFFERENT MATERIALS AND SKIN-STRINGER ELEMENTS
Klaus Koenig *In* AGARD, Impact of Acoustic Loads on Aircraft Structures Sep. 1994 11 p (For primary document see N95-19142 05-71)
Copyright Avail: CASI HC A03/MF A03

Within a comparative study, 29 different coupons covering 8 different designs and 6 different materials were fatigued by an excitation of 30 g(exp 2)/Hz on a shaker. The selected designs and materials represent realistic alternatives of an aircraft surface structure. The investigation led to the following conclusion: (1) Besides classical aluminium, CFRP is the best material with regard to sonic fatigue. (2) Al/Li, ARALL and Al layer materials showed shorter life times than the classical Al. (3) The most striking improvement in design for the dimensions selected here was achieved with separate doublers between skin and stringer. (4) The modal damping found was most often smaller than the 1.7 percent of the critical as known from ESDU for Al. (5) Pure CFRP without rivets showed the smallest damping: 0.6 - 0.9 percent. Author

N95-19157# McDonnell-Douglas Corp., Saint Louis, MO.
ACOUSTIC FATIGUE CHARACTERISTICS OF ADVANCED MATERIALS AND STRUCTURES
J. H. Jacobs and M. A. Ferman (Saint Louis Univ., Cahokia, IL.) *In* AGARD, Impact of Acoustic Loads on Aircraft Structures Sep. 1994 9 p (For primary document see N95-19142 05-71)
Copyright Avail: CASI HC A02/MF A03

A summary of McDonnell Douglas Aerospace's (MDA) capability for treating acoustic loading on modern fighter aircraft structure is given. A brief overview of techniques that have been developed since the mid-70's

are presented. In metallic structure fabrication concepts such as Super Plastic Formed/Diffusion Bonding (SPF/DB) suddenly required new analysis procedures. In addition, the 1980's brought the additional complications of structures exposed to high thermal and acoustic environments on such vehicles as the AV-8V Harrier II and National Aerospace Plane (NASP). Methods developed to handle these new material forms, intense noise, and thermal loads are discussed. The influences of nonlinear structural responses on fatigue life due to combined load environments are also discussed. Additional developments in thermal-acoustic testing capability are also discussed. Author

N95-19158# Daimler-Benz A.G., Munick (Germany).
ACOUSTIC FATIGUE OF CARBON FIBRE STRUCTURES
G. Mueller and M. Gruenewald *In* AGARD, Impact of Acoustic Loads on Aircraft Structures Sep. 1994 7 p (For primary document see N95-19142 05-71)
Copyright Avail: CASI HC A02/MF A03

Based on the acoustic fatigue endurance curve of CFRP-probes (Carbon Fibre Reinforced Plastic) obtained within the BRITE EURAM PROGRAMME - ACOUFAT further investigations have been carried out with respect to (1) nonlinearities in the measurements for the calibration of the different transducers; (2) effects of residual strength for the coupons; (3) effects of moisture and temperature in the material due to storage and testing in humid environment. For one chosen coupon type, the sum of these effects leads to a reduction of the allowable strain in the range of high cycles by a factor of approximately 4 compared to the value obtained originally for the coupon using the 2 percent failure criterion and tested at room temperature. The modifications are considered step by step and the resulting curve is given in this paper. Author

N95-19159# Dassault Aviation, Saint-Cloud (France). Structures Div.
BRITE-EURAM PROGRAMME: ACOUFAT ACOUSTIC FATIGUE AND RELATED DAMAGE TOLERANCE OF ADVANCED COMPOSITE AND METALLIC STRUCTURES
D. Tougard *In* AGARD, Impact of Acoustic Loads on Aircraft Structures Sep. 1994 12 p Sponsored in cooperation with the European Community and ACOUFAT (For primary document see N95-19142 05-71)
Copyright Avail: CASI HC A03/MF A03

The Brite/Euram programme ACOUFAT is concerned with 'Acoustic fatigue and related damage tolerance of advanced composite and metallic structure'. Three main fields of the ACOUFAT results are discussed: (1) The use of a 'frequency degradation' criterion, usually applied to classical metallic materials and early Carbon Fiber Reinforced Plastic (CFRP) materials, is not considered suitable, as the only parameter, for determination of CFRP specimen 'failure' in acoustic fatigue. It is suggested that a suitable criterion should be based, in further work, upon the degradation of the mechanical properties of the specimens; (2) On the basis of Wind-Tunnel (WT) calibration tests, a semi-empirical model of the spatio-temporal characteristics of the aero-acoustic loads exerted on a flat panel by the turbulent field created by a flap has been developed and utilized as 'Load Data Input' for Finite Element (FE) calculations. The WT tests have been reasonably well presented: the development of this semi-empirical model is an encouraging initial success. The results from the initial modelling suggest that this can be extended to the modelling of the acoustic loads in Progressive Wave Tubes (PWT); and (3) The excitation of structures by aero-acoustic loads may not be simulated fully in PWT by simply modifying and correctly shaping the spectral content. The effect of the spatial distribution of the loading is clearly different in both cases and the tested specimen endurance may be significantly different. It is clear that a theoretical approach based on a correct prediction of the responses to both types of environment is required. Author

N95-19160# Fokker B.V., Schipol-Oost (Netherlands).
ACOUSTIC FATIGUE BEHAVIOUR OF GLARE COMPOSITES
P. T. Elangovan, H. Ottens (National Aerospace Lab., Marknesse, Netherlands.), and G. Bayerdorfer (Industrieanlagen-Betriebsgesellschaft m.b.H., Ottobrunn, Germany.) *In* AGARD, Impact of Acoustic Loads on Aircraft Structures Sep. 1994 8 p Sponsored in part by ACOUFAT (For primary document see N95-19142 05-71)
Copyright Avail: CASI HC A02/MF A03

The GLARE (Glass Aluminum Reinforced) laminates, a new type of fiber metal laminates with promising fatigue behavior, are evaluated for their acoustic fatigue properties. In this investigation, the endurance data are developed by using shaker test specimens. Since the GLARE laminates make use of lay-ups and metal bonding, the influence of the laminate lay-up configuration and temperature on the acoustic fatigue strength is investigated from the shaker test results. Four types of shaker specimens are used in this investigation: plain cantilever, riveted skin-stringer, bonded skin-stringer, and rib-mode vibration specimens. Two stiffened GLARE skin panels are tested in the Progressive Wave Tube (PWT) at IABG. The panel testing indicates the importance of the secondary structure in the acoustic environment, although the GLARE skin itself does not show any damage. Author (revised)

N95-19161# Wright Lab., Wright-Patterson AFB, OH. Acoustics and Sonic Fatigue Section.
THERMO-ACOUSTIC FATIGUE DESIGN FOR HYPERSONIC VEHICLE SKIN PANELS **c39**
Kenneth R. Wentz, Robert D. Blevins (Rohr Industries, Inc., Chula Vista, CA.), and Ian Holehouse (Rohr Industries, Inc., Chula Vista, CA.) *In* AGARD, Impact of Acoustic Loads on Aircraft Structures Sep. 1994 9 p (For primary document see N95-19142 05-71)
Copyright Avail: CASI HC A02/MF A03

Thermo-vibro-acoustic analysis and test of skin panels for airbreathing hypersonic vehicles is made for a generic vehicle and trajectory. Aerothermal analysis shows that impingement of the bow shock wave on the vehicle and engine noise produce high fluctuating pressures and local heat fluxes. Maximum temperatures will exceed 2700 F (1480 C) at the top of the ascent trajectory and engine sound levels will exceed 170 dB at takeoff. As a result, loads due to engine acoustics and shock impingement dominate the design of many transatmospheric vehicle skin panels. Author

N95-19162# British Aerospace Aircraft Group, Bristol (England).
APPLICATION OF SUPERPLASTICALLY FORMED AND DIFFUSION BONDED STRUCTURES IN HIGH INTENSITY NOISE ENVIRONMENTS
R. J. Cummins and J. P. C. Wong *In* AGARD, Impact of Acoustic Loads on Aircraft Structures Sep. 1994 10 p (For primary document see N95-19142 05-71)
Copyright Avail: CASI HC A02/MF A03

Two specimens, representing an aircraft control surface and an access door, have been tested under high intensity acoustic excitation. The access door was also subjected to an elevated temperature environment of 150 C during this test. These specimens were manufactured as multi-cell box configurations by superplastic forming and diffusion bonding (SPFDB) to a similar structural weight as existing aircraft components produced by alternative means of construction. The influence of the spandrel-shaped void, formed at the skin/stringer intersection, on the acoustic fatigue performance is considered. Author (revised)

N95-19163# Alenia Spazio S.p.A., Turin (Italy).
AN OVERALL APPROACH OF COCKPIT NOISE VERIFICATION IN A MILITARY AIRCRAFT
R. Giuzio and M. Norese (Aeronautica Macchi S.p.A., Varese, Italy.) *In* AGARD, Impact of Acoustic Loads on Aircraft Structures Sep. 1994 12 p (For primary document see N95-19142 05-71)
Copyright Avail: CASI HC A03/MF A03

The present paper describes the applicable concepts for cockpit noise verification in military aircraft. A design-to-noise procedure is outlined and the overall requirements for medical, intelligibility and operational aspects are discussed, including the proposition of an adequate index to quantify the quality of noise at the pilot's ear. Guidelines for cockpit noise control, to be applied during the design phase of the project, are given together with the expected benefits. Advanced noise control measures and noise measuring techniques are also dealt with and a specific case of cockpit noise verification is described. Author (revised)

N95-19164# National Research Council of Canada, Ottawa (Ontario). Inst. for Aerospace Research.
NOISE TRANSMISSION AND REDUCTION IN TURBOPROP AIRCRAFT
Douglas G. MacMartin, Gordon L. Basso, and Barry Leigh (De Havilland Aircraft Co. of Canada Ltd., Downsview, Ontario.) *In* AGARD, Impact of Acoustic Loads on Aircraft Structures Sep. 1994 9 p (For primary document see N95-19142 05-71)
Copyright Avail: CASI HC A02/MF A03

There is considerable interest in reducing the cabin noise environment in turboprop aircraft. Various approaches have been considered at deHaviland Inc., including passive tuned-vibration absorbers, speaker-based noise cancellation, and structural vibration control of the fuselage. These approaches will be discussed briefly. In addition to controlling the noise, a method of predicting the internal noise is required both to evaluate potential noise reduction approaches, and to validate analytical design models. Instead of costly flight tests, or carrying out a ground simulation of the propeller pressure field, a much simpler reciprocal technique can be used. A capacitive scanner is used to measure the fuselage vibration response on a deHaviland Dash-8 fuselage, due to an internal noise source. The approach is validated by comparing this reciprocal noise transmission measurement with the direct measurement. The fuselage noise transmission information is then combined with computer predictions of the propeller pressure field data to predict the internal noise at two points. Author

N95-19165# Defence Research Agency, Farnborough, Hampshire (England).
ADVANCED STATISTICAL ENERGY ANALYSIS **c39**
K. H. Heron *In* AGARD, Impact of Acoustic Loads on Aircraft Structures Sep. 1994 8 p (For primary document see N95-19142 05-71)
Copyright Avail: CASI HC A02/MF A03

A high-frequency theory (advanced statistical energy analysis (ASEA)) is developed which takes account of the mechanism of tunnelling and uses a ray theory approach to track the power flowing around a plate or a beam network and then uses statistical energy analysis (SEA) to take care of any residual power. ASEA divides the energy of each sub-system into energy that is freely available for transfer to other sub-systems and energy that is fixed within the sub-systems that are physically separate and can be interpreted as a series of mathematical models, the first of which is identical to standard SEA and subsequent higher order models are convergent on an accurate prediction. Using a structural assembly of six rods as an example, ASEA is shown to converge onto the exact results while SEA is shown to overpredict by up to 60 dB. Author

N95-19166# LMS International, Leuven (Belgium).
IDENTIFICATION AND ANALYSIS OF AIR- AND STRUCTURE-BORNE NOISE AND VIBRATION PATHS
Herman VanderAuweraer, Katrien Wyckaert, and Peter vanderLinden *In* AGARD, Impact of Acoustic Loads on Aircraft Structures Sep. 1994 11 p Sponsored in cooperation with the European Commission (For primary document see N95-19142 05-71)
Copyright Avail: CASI HC A03/MF A03

In order to investigate the contribution of individual sources and source transmission paths, a method referred to as 'Transfer Path Analysis' has been developed. Its formulation to address structure-born noise problems is outlined in detail and illustrated with an example from the car industry. Current research in this context is briefly reviewed, including the case of reciprocity techniques and the air-born noise problem. Author

N95-19167# National Research Council of Canada, Ottawa (Ontario). Structures and Materials Lab.
SPECTROGRAM DIAGNOSIS OF AIRCRAFT DISASTERS **c03**
F. W. Slingerland *In* AGARD, Impact of Acoustic Loads on Aircraft Structures Sep. 1994 6 p Original contains color illustrations (For primary document see N95-19142 05-71)
Copyright Avail: CASI HC A02/MF A03

Impulsive forces applied to an aircraft fuselage generate radial vibration waves in the structure analogous to those in a classical thin shell. It has been found that these waves are detected by the cockpit area microphone, and that spectrogram analysis of the microphone recording can provide information on the nature, origin and strength of the source, whether an explosion or a sudden decompression. Author

N95-19514# Naval Undersea Warfare Center, Newport, RI.
TRANSDUCER ARRAY INTERACTION MODELING USING VARIATIONAL PRINCIPLES Final Report
Harold C. Robinson 29 Sep. 1994 15 p Presented at the 127th Meeting of the Acoustical Society of America, Cambridge, MA, Jun. 1994
(AD-A285687; NUWC-NPT-TD-10-749) Avail: CASI HC A03/MF A01

This document will detail a method for calculating the radiation interaction effects between active transducers in an array, commonly known as the radiation impedance, using variational methods. A brief review of previous treatments of the radiation impedance for single mode and multimode transducers will be given. These interaction treatments will be modified, using the variational principle, to yield expressions for the self and mutual radiation impedance which do not require exact solutions for the surface pressure of the radiator. Specific calculations of the self and mutual impedances for baffled pistons and flexural disks will be presented and compared with previous theoretical treatments. The extension of these variational expressions to flextensional transducers will be briefly discussed. DTIC

N95-19770 Materials Research Labs., Ascot Vale (Australia).
ACOUSTIC TRANSMISSION LOSS AND STRUCTUREBORNE NOISE TRANSMISSION TESTS ON A LASCOR AND A REFERENCE STEEL PANEL
C. J. Norwood Sep. 1993 31 p
(MRL-TN-623; AR-008-225) Copyright Avail: Issuing Activity

LASCOR is a laser welded corrugated steel sandwich developed as a lightweight construct for ship superstructures. Tests were performed to measure acoustic transmission loss and structureborne noise transmission for both a LASCOR panel and a reference conventional rib-stiffened steel panel. This report outlines the test methods used and compares the results for the two panels. Author

N95-19802 Stanford Univ., CA.
TUNNELING ACOUSTIC MICROSCOPY Final Technical Report, 1 Apr. 1990 - 31 Dec. 1993
Calvin F. Quate and B. T. Khuri-Yakub 31 Dec. 1993 193 p Limited Reproducibility: More than 20% of this document may be affected by microfiche quality
(Contract N00014-90-J-1635)
(AD-A279160) Avail: Issuing Activity (Defense Technical Information Center (DTIC))

We have demonstrated the use of a near-field scanning acoustic microscope in a noncontact mode using electrostriction to generate acoustic waves from a subwavelength dimension spot. Noncontact images have been obtained using the electrostrictive acoustic signal as the sole feedback signal. 5 micrometer lateral resolution in this mode has been demonstrated using 11 micrometer acoustic wavelength. Due to the nonlinear force interaction between the tip and the sample, frequency doubling is observed in the electrostrictive mode. During imaging, the tip and sample are excited by an RF signal at 350 MHz and the image is composed of a signal at 700 MHz. DTIC

N95-19850 Pennsylvania State Univ., University Park, PA. Materials Research Lab.
MATERIALS FOR ADAPTIVE STRUCTURAL ACOUSTIC CONTROL, VOLUME 3 Annual Report, 1 Feb. 1993 - 31 Jan. 1994
L. E. Cross 11 Apr. 1994 198 p Limited Reproducibility: More than 20% of this document may be affected by microfiche quality
(Contract N00014-92-J-1510)
(AD-A279223) Avail: Issuing Activity (Defense Technical Information Center (DTIC))

The research goals of this ONR sponsored University Research Initiative entitled Materials for Adaptive Structural Acoustics Control relate directly to the sensing and actuating material which must be integrated to function in adaptive control of acoustic structures. This report documents work in the second year of the program and for convenience the activities are grouped under the headings General Summary Papers, Materials Studies, Composite Sensors, Actuator Studies, Integration Issues, Processing Studies, and Thin Film Ferroelectrics. The general papers cover a new comprehensive description of ferroelectric ceramics and their applications, analysis of high temperature piezoelectric sensors and the possible application of nonlinearity in enhancing the smartness of ceramics and composites. Scale effects on ferroics are of increasing interest and the manner in which nano-scale polar regions control the properties of relaxor ferroelectrics is again emphasized. For material studies the detailed examination of the evolution of diffuse, then relaxor behavior in lanthanum modified lead titanate has been completed. Interest in the soft PZT's, relaxor and phase switching materials continues, with a new thrust developing towards a more complete description of domain walls and morphotropic phase boundaries in perovskites. Materials issues in the wear out and fatigue effects in polarization

switching systems have been subjected to detailed evaluation and the precautions necessary to fabricate long lasting materials which will stand 109 switches without any fatigue are delineated. DTIC

72 ATOMIC AND MOLECULAR PHYSICS

Includes atomic structure, electron properties, and molecular spectra.

N95-17974# California Univ., Santa Barbara, CA. Dept. of Physics.
ATOMIC SCALE FORCE MAPPING WITH THE ATOMIC FORCE MICROSCOPE
J. P. Cleveland, M. Radmacher, and P. K. Hansma Sep. 1994 10 p
(Contract N00014-92-J-1260)
(AD-A284940; TR-13) Avail: CASI HC A02/MF A01

The ability to recognize differences between atoms in topographically similar positions has been a long-standing goal in Atomic Force Microscopy especially in a biological context. Mapping of forces (often attractive) at very small (less than 5 A) tip-sample separations is one plausible way to achieve this. We have measured these types of forces above crystalline surfaces in water. Atomic resolution on attractive forces is demonstrated on the cleavage planes of calcite and muscovite mica. Atomic scale variations in the force between the tip and sample as a function of lateral position are observed on calcite. DTIC

N95-17976# Texas Univ., Austin, TX. Dept. of Physics.
LASER WAKEFIELD EXCITATION AND MEASUREMENT ON A FEMTOSECOND TIME SCALE: THEORY AND EXPERIMENT Progress Report, 1 Sep. 1993 - 31 Aug. 1994
T. Tajima and M. Downer Mar. 1994 7 p
(Contract DE-FG05-92ER-40739)
(DE94-019198; DOE/ER-40739/2) Avail: CASI HC A02/MF A01

This is a progress report describing work on laser generated wakefields, which can be applied to particle acceleration. The authors have carried out simulation studies in one and two dimensions, and experimental studies of the generation of such fields. The authors also report on the propagation studies of femtosecond laser pulses in atmospheric density gases, and work on developing such high power laser sources, with well controlled pointing and spectral characteristics. The project has involved collaboration with Japanese and Russian researchers. DOE

N95-18049# Stanford Univ., CA. Linear Accelerator Center.
THE LEFT-RIGHT FORWARD-BACKWARD ASYMMETRY FOR B QUARKS AT THE SLD Ph.D. Thesis - Massachusets Inst. of Technology
D. C. Williams May 1994 199 p
(Contract DE-AC03-76SF-00515)
(DE94-014508; SUAC-445) Avail: CASI HC A09/MF A03

The left-right asymmetry for B quarks, A(sub b), is precisely predicted by the Weinberg-Salam-Glashow model of particle interactions, now the standard model for high-energy particle physics. As a test of this model, A(sub b) is directly measured at the SLC Large Detector (SLD) by taking advantage of the unique polarized electron beam at the Stanford Linear Collider (SLC) and measuring the left-right forward-backward asymmetry of B quarks. To measure the asymmetry, B quarks are identified using muons of high total and transverse momenta. The result for the 1993 data sample of 37,843 hadronic Z's is A(sub b) = 0.91 (plus/minus) 0.19 (plus/minus) 0.06, where the first error is statistical and the second systematic. This result is in agreement with the standard model prediction of A(sub b) = 0.935. Author

N95-18062# Queens Univ., Belfast (Northern Ireland). Dept. of Applied Mathematics and Theoretical Physics.
ION-MOLECULE COLLISIONS, ELECTRON MOLECULE COLLISIONS, EXCITATION AND IONIZATION OF ATOMS Final Report, 15 Apr. 1991 - 14 Apr. 1994
Kenneth L. Bell and Robert H. Reid 8 Jul. 1994 26 p
(Grant AF-AFOSR-0261-91; AF Proj. 2303)
(AD-A284584; PL-TR-94-2213; AD-E202182) Avail: CASI HC A03/MF A01

Corrected values of the dissociative recombination rate coefficient for N2(+)(v) have been deduced from an analysis of published experimental data. The theory of the dissociative recombination of polyatomic ions has been developed with particular reference to the branching ratios of the exothermic channels. The role of single-electron transitions in dissociative recombination has been discussed and it has been shown that the radiationless transition probability is indeed very high. Research on the dissociative recombination of CHO(+), H3(+), and D3(+) has led to the discovery of a new mechanism for dissociative recombination, characterized by the radiationless transition being of the single-electron type and by the absence of any crossing. It takes place through a multistep process and is generally very rapid. Despite having been discovered only recently, it is of common occurrence. Extensive calculations on tidal thermolecular ionic recombination have been performed. The discrepancies between the various results on CH3(+) + H2 and CH3(+) + D2 association have been discussed. The emission of the 557.7 nm line of O I, the Herzberg I bands of O2, and the atmospheric bands of O2 have been satisfactorily explained. Rocket results on the emission of the 557.7 nm and 630.0 nm lines of O I from the nocturnal F-region have been analyzed. A new theory of the nightglow's green continuum has been proposed: metastable oxygen molecules collide with the ambient gas molecules to form complexes that dissociate by allowed radiative transitions. DTIC

N95-18124# Wyoming Univ., Laramie, WY.
EXOTIC ATOMS: MUONIC ATOMS INTO VACUUM FROM SOLID HYDROGEN
R. Kunselman 1993 12 p Presented at the High Energy Physics and Nuclear Structure Conference, Perugia, Italy, 28 Jun. - 2 Jul. 1993
(Contract DE-FG02-87ER-40333)
(DE94-018255; CONF-9306365-1; COO-2197-140) Avail: CASI HC A03/MF A01

The experiments use various solid hydrogen layers to form various muonic hydrogen isotopes that escape into vacuum. The method relies on transfer of the muon from protium to either a deuteron or a triton. The resulting muonic deuterium or muonic tritium will not immediately thermalize because of the very low elastic cross sections, and may be emitted from the surface of the layer. Measurements which detect decay electrons, muonic x-rays, and fusion products have been used to study the processes. A target has been constructed which exploits muonic atom emission in order to learn more about the energy dependence of transfer and muon molecular formation. DOE

N95-18144# Sandia National Labs., Albuquerque, NM.
ION EMISSION INTENSITY RATIOS AS A FUNCTION OF ELECTRODE GAP, MELTING CURRENT, AND PRESSURE DURING LOW CURRENT VACUUM ARC REMELTING
R. L. Williamson and S. M. Grose (Inco Alloys International, Inc., Huntington, WV.) 1994 13 p Presented at the Symposium on Liquid Metal Processing and Casting, Santa Fe, NM, 11-14 Sep. 1994
(Contract DE-AC04-94AL-85000)
(DE94-017407; SAND-94-1674C; CONF-940978-3) Avail: CASI HC A03/MF A01

The arc energy distribution in the electrode gap plays a central role in the vacuum arc remelting (VAR) process. However, very little has been done to investigate the response of this important process variable to changes in process parameters. Emission spectroscopy was used to investigate variations in arc energy in the annulus of a VAR furnace during melting of 0.43 m diameter Alloy 718 electrode into 0.51 in diameter ingot. Time averaged (1 second) intensity data from various chromium atom and ion (Cr(+)) emission lines were simultaneously collected and selected intensity ratios were subsequently used as air energy indicators. These studies were carried out as a function of melting current, electrode gap, and CO partial pressure. The data were modeled and the ion electronic energy was found to be a function of electrode gap, the energy content of the ionic vapor decreasing with increasing gap length; the ion ratios were not found to be sensitive to pressure. On the other hand, the chromium atom electronic energy was difficult to model in the factor space investigated, but was determined to be sensitive, to pressure. The difference in character of the chromium ion and atom energy fluctuations in the furnace annulus are attributed to the difference in the origins of these arc species and the non-equilibrium nature of the metal vapor arc. Most of the ion population is emitted directly from cathode spots, whereas much of the atomic vapor arises due to vaporization from the electrode and pool surfaces. Also, the

positively charged ionic species interact more strongly with the electron gas than the neutral atomic species, the two distributions never equilibrating due to the low pressure. DOE

N95-18324* National Aeronautics and Space Administration. Pasadena Office, CA.

ELECTRON REVERSAL IONIZER FOR DETECTION OF TRACE SPECIES USING A SPHERICAL CATHODE Patent

Said Boumsellek, inventor (to NASA) (Jet Propulsion Lab., California Inst. of Tech., Pasadena, CA.) and Ara Chutjian, inventor (to NASA) (Jet Propulsion Lab., California Inst. of Tech., Pasadena, CA.) 20 Dec. 1994 12 p Filed 15 Sep. 1993 Supersedes N94-17329 (32 - 3, p 1185)
(NASA-Case-NPO-18870-1-CU; US-Patent-5,374,828; US-Patent-Appl-SN-127653; US-Patent-Class-250-427; US-Patent-Class-250-288; Int-Patent-Class-H01J-37/08; Int-Patent-Class-H01J-49/00; Int-Patent-Class-B01D-59/44) Avail: US Patent and Trademark Office

A reversal electron, high-current ionizer capable of focusing a beam of electrons to a reversal region employs an indirectly heated cathode having a concave emitting surface of width of W less than 2r, where r is the radius of curvature and preferably a ratio of width to radius approximately equal to one for optimum high current for a given cathode width.
Official Gazette of the U.S. Patent and Trademark Office

N95-18329# Instituto de Fisica Teorica, Sao Paulo (Brazil).

EVIDENCE FOR COEXISTENCE OF TWO PHASES IN RELATIVISTIC HEAVY ION COLLISIONS AND COMPARISON WITH LATTICE RESULTS

Jishnu Dey, G. Krein, Lauro Tomio, and T. Frederico (Centro Tecnico Aerospacial, San Jose dos Campos, Brazil.) Jan. 1994 13 p
(DE94-626672; IFT-P-005/94) Avail: CASI HC A03/MF A01 (US Sales Only)

The combined CERN and Brookhaven heavy ion (H.I.) data supports a scenario of hadron gas which is in chemical and thermal equilibrium at a temperature T of about 140 MeV. Using the Brown-Stachel-Welke model (which gives 150 MeV), it is shown that in this scenario, the hot nucleons have mass 3 pi T and the pi and rho mesons have masses close to pi T and 2 pi T. This provides a possible connection with Euclidean time lattice masses of quarks. A simple model with pions and quarks supports the coexistence of two phases in these heavy ion experiments, suggesting a second order phase transition. DOE

N95-18334# Florida Agricultural and Mechanical Univ., Tallahassee, FL. Dept. of Physics.

ELECTRON INTERACTIONS WITH NON-LINEAR POLYATOMIC MOLECULES AND THEIR RADICALS Final Report, 7 Jun. 1990 - 6 Jun. 1993

Ashok K. Jain and Charles A. Weatherford Dec. 1993 172 p
(Contract F33615-90-C-2032)
(AD-A283952; WL-TR-94-2036) Avail: CASI HC A08/MF A02

The work involved the computation of collision cross sections for electron collisions with non-linear polyatomic molecules and their radicals and ions. A reliable set of cross section data for elastic and inelastic processes in these systems has been produced without resorting to a fitting procedure. The computational model employed the adiabatic nuclei approximation for electron scattering from molecules in the gas phase. In addition, a method for calculating the required cross sections by solving the Schroedinger equation as a partial differential equation using a finite difference discretization has been developed. DTIC

N95-18356# Centro Brasileiro de Pesquisas Fisicas, Rio de Janeiro.

DIQUARKS IN DEEP INELASTIC SCATTERING AND THE GOTTFRIED SUM RULE

F. Caruso and E. Leader 1992 10 p
(DE94-626685; CBPF-NF-031/92) Avail: CASI HC A02/MF A01 (US Sales Only)

Previous attempts to invoke diquarks in deep inelastic scattering are based upon a specific model of the proton wave-function, involving either a pure quark-diquark structure or a superposition of three-quark and quark-diquark structures. In this paper diquarks are introduced in a general way without recourse to any wave-functions. Allowance is made both for their elastic and their inelastic scattering. It is argued that previous attempts to do this are incorrect. It is demonstrated, with complete generality, that diquarks cannot resolve the current disagreement between theory and experiment in the Gottfried sum rule. DOE

N95-18360# Joint Inst. for Nuclear Research, Dubna (USSR). Lab. of Theoretical Physics.

THE BEHAVIOR OF THE SLOPE OF ELASTIC NUCLEON SCATTERING AT SMALL TRANSFER MOMENTA AND RECENT U A 4/2 DATA

S. V. Goloskokov, S. P. Kuleshov, and O. V. Selyugin 1993 4 p Submitted for publication
(DE94-626687; JINR-E-2-93-433) Avail: CASI HC A01/MF A01 (US Sales Only)

Theoretical predictions for the behavior of the slope of the nucleon-nucleon scattering and other parameters of the differential cross sections in the framework of the dynamic model are compared with the recent U A 4/2 data at small transfer momenta and at a center-of-mass energy of 541 GeV. Predictions at superhigh energies are considered. DOE

N95-18366# Centro Brasileiro de Pesquisas Fisicas, Rio de Janeiro.

FEYNMAN-x AND TRANSVERSE MOMENTUM DEPENDENCE OF D(SUP (+-)) AND D(SUP 0), D-BAR(SUP 0) PRODUCTION IN 250 GeV (PI)(SUP -) - NUCLEON INTERACTIONS

G. A. Alves, S. Amato, J. C. Anjos, J. A. Appel, S. B. Bracker, L. M. Cremaldi, C. L. Darling, R. L. Dixon, D. Errede, and H. C. Fenker et al 1992 15 p
(DE94-626698; CBPF-NF-034/92; Fermilab-Pub-92/208E) Avail: CASI HC A03/MF A01 (US Sales Only)

The differential cross-section with respect to Feynman-x (x(sub F)) and transverse momentum (P(sub (Tau))) for charm meson production using targets of Be, Al, Cu, and W are measured. In the range 0.1 less than x(sub F) less than 0.7, d(sigma)/d x(sub F) is well fit by the form (1-x(sub F))(sup n) with n = 3.9 +/- 0.2. The difference between n values for D(sup -) and D(sup +) is 1.1 +/- 0.4. However, an asymmetry of 0.18 +/- 0.04 favoring the production of D(sup -) compared to D(sup +) is found. In the lower P(sub (Tau)) range, less than 2 GeV, d(sigma)/d P(sub (Tau))(sup 2) is well fit by the form exp(-b x P(sub (Tau))(sup 2)) with b = 1.03 +/- 0.04 GeV(exp -2), while in the higher P(sub (Tau)) range, 0.8 to 3.6 GeV, it is well fit by the form exp(-b(sup ') x P(sub (Tau))) with b(sup ') = 2.76 +/- 0.06 GeV(exp -1). The shape of the differential cross-section has no significant dependence on atomic mass of the target material. DOE

N95-18427# Argonne National Lab., IL.

IONIZATION OF ATOMS BY HIGH ENERGY PHOTONS

M. Y. Amusia and A. F. Ioffe (Physical-Technical Inst., Leningrad, USSR.) 1994 15 p Presented at the Workshop on Atomic Physics At High Brilliance Light Sources, Argonne, IL, 23-24 Apr. 1994
(Contract W-31-109-eng-38)
(DE94-018356; ANL/PHY/CP-84007; CONF-9404198-2) Avail: CASI HC A03/MF A01

Photoionization of atoms by high energy photons is considered. It is emphasized that in this frequency region the cross section and other characteristics of the process are strongly effected by electron shell polarization and rearrangement effects, including that due to inner vacancy Auger decay. In the effects of nuclear structure could be important and noticeable, i.e. of virtual or real excitation of the nucleus degrees of freedom and of the Quantum Electrodynamics vacuum. Ionization accompanied by secondary photon emission (Compton ionization) is analyzed in the considered domain of energies. DOE

N95-18428# Argonne National Lab., IL.

PION OBSERVABLES AND QCD

C. D. Roberts 1994 10 p Presented at the Workshop on Chiral Dynamics: Theory and Experiments, Cambridge, MA, 25-19 Jul. 1994
(Contract W-31-109-eng-38)
(DE94-018357; ANL/PHY/CP-84024; CONF-9407125-1) Avail: CASI HC A02/MF A01

The Dyson-Schwinger equations (DSE's) are a tower of coupled integral equations that relate the Green functions of QCD to one another. Solving these equations provides the solution of QCD. This tower of equations includes the equation for the quark self-energy, which is the analogue of

the gap equation in superconductivity, and the Bethe-Salpeter equation, the solution of which is the quark-antiquark bound state amplitude in QCD. The application of this approach to solving Abelian and non-Abelian gauge theories is reviewed. The nonperturbative DSE approach is being developed as both: (1) a computationally less intensive alternative; and (2) a complement to numerical simulations of the lattice action of QCD. In recent years, significant progress has been made with the DSE approach so that it is now possible to make sensible and direct comparisons between quantities calculated using this approach and the results of numerical simulations of Abelian gauge theories. Herein the application of the DSE approach to the calculation of pion observables is described: the (pi)-(pi) scattering lengths (a(sub 0)(sup 0), a(sub 0)(sup 2), A(sub 1)(sup 1), a(sub 2)(sup 2)) and associated partial wave amplitudes; the (pi)(sup 0) approaches (gamma)(gamma) decay width; and the charged pion form factor, F(sub (pi))(q(sup 2)). Since this approach provides a straightforward, microscopic description of dynamical chiral symmetry breaking (D(sub X)SB) and confinement, the calculation of pion observables is a simple and elegant illustrative example of its power and efficacy. The relevant DSE's are discussed in the calculation of pion observables and concluding remarks are presented. DOE

N95-18438 Georgia Univ., Athens.
PHOTOGENERATION AND CHARACTERIZATION OF ENERGETIC MOLECULES IN SUPERSONIC MOLECULAR BEAMS Final Report
Michael A. Duncan 24 Jun. 1994 16 p Limited Reproducibility: More than 20% of this document may be affected by microfiche quality
(Grant AF-AFOSR-0001-91)
(AD-A284108; AFOSR-94-0483TR) Avail: CASI HC A03

A variety of weakly bound and/or metastable molecules have been investigated in the environment of a pulsed supersonic molecular beam. Experiments were attempted with little success for the production of metastable oxygen ring systems. Other experiments focused on metal ion and metal neutral complexes with small molecules or rare gas atoms. Spectroscopic studies were successful for magnesium ion complexes with the rare gases and with carbon dioxide, water, and nitrogen. Aluminum atom van der Waals complexes were studied with high resolution photoelectron spectroscopy. These studies obtained a variety of new data on metal condensation energetics and the structure of the initial phases of condensation. DTIC

N95-18473# Pennsylvania State Univ., University Park, PA. Dept. of Chemistry.
AN ATOMIC VIEW OF MOTION ON SURFACES Technical Report, 1 Jun. 1994 - 31 May 1995
P. S. Weiss, M. J. Abrams, M. T. Cygan, J. H. Ferris, and M. M. Kamna 10 Oct. 1994 25 p
(Contract N00014-91-J-1630)
(AD-A285565; TR-19-ONR) Avail: CASI HC A02/MF A01

We use the scanning tunneling microscope to obtain an atomic scale view of the motion of adsorbates on surfaces. For sufficiently slow diffusion, we follow this motion in real time. For faster adsorbate motion we are able to observe the partial and transient occupancy of surface sites on the time scale of our measurements. For lateral motion induced by surface processes such as adsorption or chemical reaction, we are able to analyze the final positions of the adsorbates or reaction products in order to measure the distances covered and to elucidate the means by which energy is accommodated to the surface. Author (DTIC)

N95-18474 Clemson Univ., SC. Physics Lab.
INVESTIGATION OF SINGLE EVENTS UPSETS IN SILICON AND GaAs STRUCTURES USING REACTION CALCULATIONS Technical Report, 1 Oct. 1988 - 10 Mar. 1992
Peter J. McNulty 1 Sep. 1994 329 p Limited Reproducibility: More than 20% of this document may be affected by microfiche quality
(Contract DNA001-88-C-0189)
(AD-A285581; DNA-TR-92-163) Avail: CASI HC A15

Two procedures were developed to obtain the dimensions of the sensitive volume: one using charge collection measurements and the other proton Seu cross sections measured at different energies and angles of incidence. The CUPID simulation codes play an important role. They have been made user friendly and received adequate documentation. The methodology has been extended to single event latch-up and displacement damage. DTIC

N95-18519 Army Research Lab., Adelphi, MD.
AN INVESTIGATION OF NONUNIFORM DOSE DEPOSITION FROM AN ELECTRON BEAM Final Report, Jun. 1993
William Lilley and Kieu X. Luu Aug. 1994 17 p Limited Reproducibility: More than 20% of this document may be affected by microfiche quality
(AD-A284175; ARL-TR-481) Avail: Issuing Activity (Defense Technical Information Center (DTIC))

In a search for an explanation of nonuniform electron-beam dose deposition, the integrated tiger series (ITS) of coupled electron/photon Monte Carlo transport codes was used to calculate energy deposition in the package materials of an application-specific integrated circuit (ASIC) while the thicknesses of some of the materials were varied. The thicknesses of three materials that were in the path of an electron-beam pulse were varied independently so that analysis could determine how the radiation dose measurements using thermoluminescent dosimeters (TLD's) would be affected. The three materials were chosen because they could vary during insertion of the die into the package or during the process of taking dose measurements. The materials were aluminum, HIPEC (a plastic), and silver epoxy. The calculations showed that with very small variations in thickness, the silver epoxy had a large effect on the dose uniformity over the area of the die. DTIC

N95-18548# Argonne National Lab., IL.
CAN AN INFRARED-VANISHING GLUON PROPAGATOR CONFINE QUARKS?
C. D. Roberts 1994 10 p Presented at the Workshop on Quantum Infrared Physics, Paris, France, Jun. 1994
(Contract W-31-109-eng-38)
(DE94-018388; ANL/PHY/CP-83992; CONF-9406248-3) Avail: CASI HC A02/MF A01

It is shown that the solution of the quark Dyson-Schwinger equation in QCD obtained with a gluon propagator of the form D(q) approximately equal to q(exp 2)/(q(exp 4)+b(exp 4)) and a quark-gluon vertex that is free of kinematic singularities does not describe a confined particle and that there is always a value of b(exp 2) = b(sub c)(exp 2) such that chiral symmetry is not dynamically broken for b(exp 2) greater than b(sub c)(exp 2). DOE

N95-18550# Argonne National Lab., IL.
SUMMARY OF THE WORKING GROUP ON TESTS OF QCD
V. Papavassiliou 1994 8 p Presented at the Workshop on the Future of High Sensitivity Charm Experiments, Batavia, IL, 7-9 Jun. 1994
(Contract W-31-109-eng-38)
(DE94-018390; ANL/PHY/CP-83915; CONF-9406242-2) Avail: CASI HC A02/MF A01

The working group discussed several topics related to charm production that can provide important input for our understanding of QCD. It was recognized that studies of both open and hidden charm in a high-statistics experiment will be essential in order to understand the production mechanisms. Nuclear effects were also discussed and a connection was made to similar effects observed in other reactions. DOE

N95-18551# Argonne National Lab., IL.
HIGHER-ORDER LIPATOV KERNELS AND THE QCD POMERON
A. R. White 12 Aug. 1994 10 p Presented at the Workshop on Quantum Infrared Physics, Paris, France, Jun. 1994
(Contract W-31-109-eng-38)
(DE94-018395; ANL-HEP-CP-94-49; CONF-9406248-2) Avail: CASI HC A02/MF A01

Three closely related topics are covered: the derivation of O(g(exp 4)) Lipatov kernels in pure glue QCD; the significance of quarks for the physical Pomeron in QCD; and the possible inter-relation of Pomeron dynamics with Electroweak symmetry breaking. DOE

N95-18554# Washington Univ., Seattle, WA. Inst. for Nuclear Theory.
EXACT m(SUB QUARK) DOES NOT EQUAL 0 CONDENSATES IN QCD(1+1)(N(SUB C) YIELDS INFINITY
M. Burkardt 1994 6 p Presented at the Workshop on Quantum Infrared Physics, Paris, France, Jun. 1994

(Contract DE-FG06-90ER-40561)
(DE94-018581; DOE/ER-40561/156; CONF-9406248-1) Avail: CASI HC A02/MF A01

In the limit of an infinite number of colors, we derive an analytic expression for the quark condensation in QCD(sub 1+1) as a function of the quark mass and the gauge coupling constant. For zero quark mass, a nonvanishing quark condensate is obtained. Nevertheless, we prove that there is no phase transition as a function of the quark mass. It is furthermore shown that the expansion of /0(bar) -psi psi (bar)0/ in the gauge coupling has zero radius of convergence but that the perturbation series is Borel summable with finite radius of convergence. The nonanalytic behavior m(sub q) yields 0 approximately - N(sub C)(radical)G(exp 2) can only be obtained by summing the perturbation series to infinite order. DOE

N95-18643 Rutherford Appleton Lab., Chilton (England).
GENERATION PERMUTATION SYMMETRY AND THE QUARK MIXING MATRIX
P. F. Harrison and W. G. Scott Jun. 1994 11 p Prepared in cooperation with London Univ., London, England
(PB95-108189; RAL-94-072) Avail: Issuing Activity (National Technical Information Service (NTIS))

We propose a new discrete symmetry in the generation space of the fundamental fermions, consistent with the observed fermion mass spectrum. In the case of the quarks, the symmetry leads to the unique prediction of flat CKM matrix at high energy. We explore the possibility that evolution due to quantum corrections leads to the observed hierarchical form of the CKM matrix at low energies. NTIS

N95-18644# California Inst. of Tech., Pasadena, CA.
PROPERTIES OF NUCLEI AND ELEMENTARY PARTICLES AT LOW AND INTERMEDIATE ENERGIES
F. Boehm 1993 134 p
(Contract DE-FG03-88ER-40397)
(DE94-008502; DOE/ER-40397/T1) Avail: CASI HC A07/MF A02

Work reported relate to: a 12 ton low energy neutrino detector for neutrino oscillation studies at the San Onofre Reactor Station; new limits on the 17 keV neutrino; time reversal and parity tests for hindered nuclear gamma transitions; and theory of nuclear structure and its application. Derived from text

N95-18655 International Business Machines Corp., San Jose, CA. Research Div.
MOLECULAR DYNAMICS STUDY OF AQUEOUS ELECTROLYTE SOLUTIONS NEAR A STRUCTURED SPHERE
Sheng-Bai Zhu, Michael R. Philpott, and James N. Glosli 22 Aug. 1994 14 p Limited Reproducibility: More than 20% of this document may be affected by microfiche quality
(Contract N00014-92-C-0173)
(AD-A284010; TR-12) Avail: Issuing Activity (Defense Technical Information Center (DTIC))

Molecular dynamics studies of water and ions around a charged small compact globular object are described. The hypothetical molecular ion C(--) sub 60 is used as the globular model. It is found that the cesium cation is in physical contact on the spherical surface much of the time with an incomplete hydration shell. The chloride ion spends part of the time in a solvent-separated adsorption configuration and part of the time in the diffuse region. No adsorption of the sodium ion onto the spherical surface is observed. DTIC

N95-18874# University of Western Michigan, Kalamazoo, MI.
CORRELATED CHARGE-CHANGING ION-ATOM COLLISIONS
J. A. Tanis Apr. 1994 9 p
(Contract DE-FG02-87ER-13778)
(DE94-017355; DOE/ER-13778/62) Avail: CASI HC A02/MF A01

This report summarizes the progress and accomplishments of research supported by DOE. This work involves the experimental investigation of fundamental atomic processes in collisions of few-electron, charged projectile ions with neutral gas targets or electrons. The major emphasis is the study of collision processes involving two active electrons, and particularly those in which the electron-electron interaction plays a role. New results have been obtained for studies involving: (1) continuum-electron emission; (2) double ionization of helium and Li(+); and (3) resonant recombination of atom ic ions. Experiments were conducted using accelerators at Western Michigan University, Michigan State University, Indiana University, Lawrence Livermore Laboratory, and the Institute of Nuclear Research, Debrecen, Hungary. Brief summaries of work completed and work in progress are given. DOE

N95-18882# Joint Inst. for Nuclear Research, Dubna (USSR). Lab. of Theoretical Physics.
BOHR'S QUANTIZATION RULE IN THE WORLD OF RESONANCES OF ELEMENTARY PARTICLES
F. A. Gareev, Yu. L. Ratis, and E. A. Strokovskij 1993 16 p Submitted for publication
(DE94-626721; JINR-E-2-93-426) Avail: CASI HC A03/MF A01 (US Sales Only)

Quantization based on general quantum mechanical arguments is carried out for asymptotic values of momenta of decay products of hadronic resonances. Mass formula for hadronic resonances is obtained with making use of the above mentioned quantization conditions. Calculated spectra having a structure similar to that of the Balmer series are compared with the experimental data; the corresponding mass formula can be used for predictions of new possible resonances and their searches. DOE

N95-18883# China Nuclear Information Centre, Beijing (China).
AN UNIFIED PROGRAM FOR CALCULATING THE FAST NEUTRON NUCLEAR DATA FOR MIDDLE-HEAVY NUCLEI (MUP-3)
Ziqiang Yu (Nankai Univ., Tiangjin, China.), Xiaocheng Zhang (Nankai Univ., Tiangjin, China.), Hongmo Zhou (Nankai Univ., Tiangjin, China.), Yixin Zuo (Nankai Univ., Tiangjin, China.), Shunuan Wang (Chinese Nuclear Data Center, Beijing.), Jishang Zhang (Chinese Nuclear Data Center, Beijing.), and Xiangjun Shi (Chinese Nuclear Data Center, Beijing.) Mar. 1993 6 p
(DE94-626822; CNIC-00730; NKU-0001) Avail: CASI HC A02/MF A01 (US Sales Only)

MUP-3 program is used to calculate the fast neutron data of middle-heavy nuclei in energy range from 1 keV to 20 MeV. Its theoretical framework includes the optical model, width fluctuation corrected Hauser-Feshbach formula, evaporation model and pre-equilibrium statistical theory based on the generalized exciton model. MUP-3 is designed by the module structure and adopts some new techniques to raise its running speed. DOE

N95-18884# Joint Inst. for Nuclear Research, Dubna (USSR). Lab. of Nuclear Problems.
ON MEASUREMENT OF CROSS SECTIONS FOR SCATTERING OF p(MU)- AND d(MU)-ATOMS IN HYDROGEN AND DEUTERIUM
V. M. Bystritskij 1993 11 p Submitted for publication
(DE94-626957; JINR-E-1-93-450) Avail: CASI HC A03/MF A01 (US Sales Only)

The paper is a brief review of all experiments on measurement of cross sections for scattering of p(mu)-atoms in hydrogen and d(mu)-atoms in hydrogen and deuterium. The experimental results are analyzed and compared both with one another and with calculated results. A program for further investigation of scattering of muonic atoms of hydrogen isotopes is proposed in order to clarify the nature of discrepancies between some experimental results and to get more precise information about the above processes. DOE

N95-18912# Deutsche Forschungsanstalt fuer Luft- und Raumfahrt, Goettingen (Germany). Inst. fuer Stroemungsmechanik.
FLOW FIELD INVESTIGATION IN A FREE JET - FREE JET CORE SYSTEM FOR THE GENERATION OF HIGH INTENSITY MOLECULAR BEAMS Ph.D. Thesis [UNTERSUCHUNG DER STROEMUNG IN EINEM FREISTRAHL-KERNFREISTRAHL-SYSTEM ZUR ERZEUGUNG INTENSIVER MOLEKULARSTRAHLEN]
Bent Fritsche 1994 219 p In GERMAN Original contains color illustrations
(ISSN 0939-2963)
(DLR-FB-94-11) Avail: CASI HC A10/MF A03

In a free jet - free jet core system the first skimmer is (unlike in conventional molecular beam systems) operated in continuum flow. This until now rarely examined concept is treated in detail experimentally and theoretically. Investigated are the influence of skimmer geometry, pumping capacity, gas properties, Mach and Knudsen number, skimmer boundary

layer and condensation. The main emphasis of the work is put on the treatment of the arising shocks. This leads to criteria for optimizing the system as a source for molecular beams with previously not achieved intensities and as a wind tunnel for the experimental investigation of gas-surface interactions under orbital conditions. Author

N95-19077# Fermi National Accelerator Lab., Batavia, IL.
ASYMMETRIC ANTIPROTON DEBUNCHER: NO BAD MIXING, MORE GOOD MIXING
V. Visnjic Jul. 1994 12 p
(Contract DE-AC02-76CH-03000)
(DE94-017171; FNAL-TM-1897) Avail: CASI HC A03/MF A01

An asymmetric lattice for the Fermilab Antiproton Debuncher is designed. The lattice has zero mixing between the pickups and the kickers (bad mixing) while the mixing in the rest of the machine (good mixing) can be varied (even during the operation of the machine) in order to optimize the stochastic cooling. As an example, a lattice with zero bad mixing and twice the good mixing is presented. The betatron cooling rate in this lattice is twice its present value. DOE

N95-19078# Texas Univ., Austin, TX. Inst. for Fusion Studies.
STUDY OF ALPHA PHYSICS RELATED TO ITER PROJECT
H. L. Berk Aug. 1994 7 p
(Contract DE-FG05-80ET-53088)
(DE94-017329; DOE/ET-53088/T6) Avail: CASI HC A02/MF A01

A critical issue in the controlled fusion program is the understanding of alpha particle confinement in an ignited tokamak plasma. The standard ignition scenario in a burning plasma is that alpha particles are born at 3.5 MeV, and heat the background plasma as they transfer this energy by electron drag during the time they slow down. However, several experiments have already demonstrated that if Alfven waves are excited by the presence of fast particles, the wave fields can cause rapid particle loss through radial diffusion. If such processes arise in a reactor, the entire methodology of planning what ignition conditions should be like, needs to be strongly modified. Hence, the understanding of the Alfven-alpha particle interaction is one of the most significant issues that can be addressed as the plasma physics community prepares for an ITER experiment to demonstrate controlled fusion conditions. Should Alfven wave excitations be present in a burning reactor, an appropriate method of analysis needs to be developed. The past year, the research team, working with the P.I. of this contract, has developed a method of analysis that should be appropriate for this problem. During the past year a numerical tool was successfully developed for a model problem that contains physics properties similar to the Alfven-alpha particle problem. Work is now in progress for simulating the more realistic Alfven-alpha particle problem. DOE

N95-19199# Sandia National Labs., Albuquerque, NM.
LEVIS ION SOURCE AND BEAM CHARACTERIZATION ON PBFA-2
T. J. Renk, G. C. Tisone, R. G. Adams, J. E. Bailey, A. B. Filuk, D. J. Johnson, and T. D. Pointon 1993 6 p Presented at the 10th International Conference on High Power Particle Beams, San Diego, CA, 20-24 Jun. 1994
(Contract DE-AC04-94AL-85000)
(DE94-015802; SAND-93-3813C; CONF-940634-12) Avail: CASI HC A02/MF A01

We report on the continuing development of the LEVIS (Laser Evaporation Ion Source) lithium active ion source for the 15-cm radial focussing ion diode on PBFA-11. We found previously that DC-heating of the anode surface to 150 C maximum for 5 hrs resulted in a pure lithium beam. This paper discusses the characterization of LEVIS source uniformity by Faraday cup arrays and multiple lines of sight for visible light spectroscopy. These diagnostics give some evidence of nonuniformity in both A-K gap electric fields and ion current density. Despite this, however, the measured focal spot size appears smaller than with a passive LiF source operated in the same magnetic field topology. Experiments using a curved anode for vertical beam focussing show reduced ion beam turn-on delay by 5 ns by altering the magnetic field topology as well as anode curvature. Another 3-5 ns reduction was achieved by switching from a passive LiF to the active LEVIS source. DOE

N95-19228# Oak Ridge National Lab., TN.
IMPURITY BEHAVIOR DURING ION-BERNSTEIN WAVE HEATING IN PBX-M
R. C. Isler, A. P. Post-Zwicker, S. F. Paul (Princeton Univ., NJ.), W. Tighe (Princeton Univ., NJ.), M. Ono (Princeton Univ., NJ.), B. P. LeBlanc (Princeton Univ., NJ.), R. Bell (Princeton Univ., NJ.), H. W. Kugel (Princeton Univ., NJ.), and R. Kaita (Princeton Univ., NJ.) 1994 5 p Presented at the European Conference on Controlled Fusion and Plasma Physics, Marseilles, France, 26 Jun. - 1 Jul. 1994
(Contract DE-AC05-84OR-21400)
(DE94-018114; CONF-940635-13) Avail: CASI HC A01/MF A01

Ion-Bernstein-wave heating (IBWH) has been tested in several tokamaks. In some cases the results have been quite positive, producing temperature increases and also improving both energy and particle confinement times, whereas in others, no distinctive changes were observed. Most recently, IBWH has been utilized in the Princeton Beta Experiment-Modified (PBX-M) where the long-range goal is the achievement of operation in the second stable region by current and pressure profile control. Investigations have been performed in this machine using IBWH as the sole source of auxiliary power or using IBWH in conjunction with neutral-beam injection (NBI) or with lower-hybrid current drive (LHCD). Impurity studies seem particularly important for IBWH since not only have influxes often been observed to increase, but the global impurity confinement time has also been shown to lengthen as the confinement of the working gas improved. The authors present here a set of characteristic experimental results regarding the impurity behavior in PBX-M; in general, these are consonant with previous observations in other tokamaks. DOE

N95-19232# Oak Ridge National Lab., TN.
ION MIXING IN OXIDE-SAPPHIRE SYSTEMS
D. L. Joslin, C. W. White, and C. J. McHargue (Tennessee Univ., Knoxville, TN.) 1994 12 p Presented at the Nuclear Instruments and Methods in Physics Research on Radiation Effects in Insulators, Nagoya, Japan, 5-10 Sep. 1993
(Contract DE-AC05-84OR-21400)
(DE94-018660; CONF-9309259-7) Avail: CASI HC A03/MF A01

Ion beam mixing of thin oxide films on sapphire substrates has been studied in order to examine any role of equilibrium thermodynamic parameters on the mixing process. Mixing experiments were performed with polycrystalline oxide films deposited on single crystalline (alpha)-Al2O3 substrates. According to the equilibrium phase diagrams, Cr2O3 is completely soluble in (alpha)-Al2O3, while ZrO2 is insoluble. The couples were irradiated with Cr ions (160 and 340 keV) or Kr ions to fluences of 4 x 10(exp 16) ions/sq cm at temperatures between 20 and 900 C. Rutherford backscattering spectrometry, X-ray photoelectron spectroscopy, and transmission electron microscopy were used to analyze samples before and after irradiation to determine the extent and nature of interface modifications. No long-range mixing was detected under any condition studied; the width of the 'mixed' region in each case was consistent with recoil mixing. The absence of long-range mixing is rationalized in terms of the different ranges of oxygen ions and cations. DOE

N95-19245# Washington Univ., Seattle, WA. Inst. for Nuclear Theory.
FAMILY SYMMETRIES AND PROTON DECAY
Hitoshi Murayama (California Univ., Berkeley. Lawrence Berkeley Lab, CA.) and D. B. Kaplan 1994 13 p
(Contract DE-FG06-90ER-40561)
(DE94-017575; DOE/ER-40561/148) Avail: CASI HC A03/MF A01

The proton decay modes p yields K(sup 0) e(sup +) and p yields K(sup 0) mu(sup +) may be visible in certain supersymmetric theories, and if seen would provide evidence for new flavor physics at extremely short distances. These decay modes can arise from the dimension five operator (Q(sub 1)Q(sub 1)Q(sub 2)L(sub 1,2)), where Q(sub i) and L(sub i) are i'th generation quark and lepton superfields respectively. Such an operator is not generated at observable levels due to gauge or Higgs boson exchange in a minimal GUT. However in theories that explain the fermion mass hierarchy, it may be generated at the Planck scale with a strength such that the decays p yields K(sup 0) l(sup +) are both compatible with the proton lifetime and visible at Super-Kamiokande. Observable proton decay can even occur in theories without unification. DOE

N95-19376 Institut des Hautes Etudes Scientifiques, Bures-sur-Yvette (France).
NON LOCALIZABILITY OF THE PHOTON KEYSTONE TO A REMODELLING OF PHYSICS [NON LOCALISABILITE DU PHOTON, CLEF DE VOUTE D'UNE REFONTE DE LA PHYSIQUE]
H. Bacry Feb. 1994 13 p In FRENCH
(PB94-217213; IHES/P/94/12) Avail: Issuing Activity

If the authors try to solve the problem of the non-localizability of the photon, they are led to modify slightly almost all chapters of Physics.
NTIS

N95-19557# Oak Ridge National Lab., TN.
NEUTRON SCATTERING STUDY OF DILUTE SUPERCRITICAL SOLUTIONS
H. D. Cochran, G. D. Wignall, V. M. Shah (Tennessee Univ., Knoxville, TN.), J. D. Londono (Tennessee Univ., Knoxville, TN.), and P. R. Bienkowski (Tennessee Univ., Knoxville, TN.) 1994 8 p Presented at the 3d International Symposium on Supercritical Fluids, Strasbourg, France, 17-19 Oct. 1994
(Contract DE-AC05-84OR-21400)
(DE95-000493; CONF-9410114-2) Avail: CASI HC A02/MF A01

Dilute solutions in supercritical solvents exhibit interesting microstructures that are related to their dramatic macroscopic behavior. In typical attractive solutions, solutes are believed to be surrounded by clusters of solvent molecules, and solute molecules are believed to congregate in the vicinity of one another. Repulsive solutions, on the other hand, exhibit a local region of reduced solvent density around the solute with solute-solute congregation. Such microstructures influence solubility, partial molar volume, reaction kinetics, and many other properties. We have undertaken to observe these interesting microstructures directly by neutron scattering experiments on dilute noble gas systems including Ar. The three partial structure factors for such systems and the corresponding pair correlation functions can be determined by using the isotope substitution technique. The systems studied are uniquely suited for our objectives because of the large coherent neutron scattering length of the isotope (sup 36)Ar and because of the accurate potential energy functions that are available for use in molecular simulations and theoretical calculations to be compared with the scattering results. We will describe our experiment, the unique apparatus we have built for it, and the neutron scattering results from our initial allocations of beam time. We will also describe planned scattering experiments to follow those with noble gases, including study of long-chain molecules in supercritical solvents. Such studies will involve hydrocarbon mixtures with and without deuteration to provide contrast.
DOE

N95-19562# Louisiana State Univ., Baton Rouge, LA.
EMBEDDED MICROCLUSTERS IN ZEOLITES AND CLUSTER BEAM SPUTTERING: SIMULATION ON PARALLEL COMPUTERS
P. Vashishta, R. K. Kalia, and D. L. Greenwell Sep. 1994 14 p
(Contract DE-FG05-92ER-45477)
(DE95-000662; DOE/ER-45477/2) Avail: CASI HC A03/MF A01

We have designed a time-space multiresolution approach for large-scale molecular-dynamics (MD) simulations involving long-range Coulomb forces and three-body interactions. This approach has been implemented on various parallel architectures including the 512-node Intel Touchstone Delta at Caltech and the 128-processor IBM SP1 at Argonne National Laboratory. Parallel MD simulations involving 1.12-million particles have been performed to investigate the pore interface growth and the roughness of fracture surfaces in porous silica. When the mass density is reduced to a critical value, pores grow catastrophically to cause fracture. The roughness exponent for internally fractured surfaces, (alpha) = 0.87 +/- 0.02, supports experimental claims about the universality of (alpha). A reliable interatomic potential has been developed for MD simulations of Si3N4. The nature of phonon densities-of-states due to low-energy floppy modes in crystalline and glassy states has been investigated. Floppy modes appear continuously in the glass as the connectivity of the system is reduced. In the crystal, they appear suddenly at 30% volume expansion. The density-of-states due to floppy modes varies linearly with energy, and the specific heat is significantly enhanced by these modes. Thermal conductivities of ceramic materials are calculated with a nonequilibrium MD method and the Kubo-Greenwood formula using a parallel eigensolver and the parallel MD approach. The calculations for amorphous silica agree well with experiments over a very wide range of temperatures above the plateau region. Currently, we are investigating thermal transport mechanisms in technologically important materials - porous glasses, nanophase ceramics, and zeolites.
DOE

N95-19587# California Univ., Berkeley. Lawrence Berkeley Lab, CA.
BARYON STOPPING IN 200 GeV/A S+Au COLLISIONS
J. T. Mitchell Jun. 1994 5 p Presented at the Intersections of Particle and Nuclear Physics, Saint Petersburg, FL, 31 May - 6 Jun. 1994
(Contract DE-AC03-76SF-00098)
(DE94-018215; LBL-35810; CONF-940514-13) Avail: CASI HC A01/MF A01

Measurements of rapidity and transverse momentum distributions of negative hadrons and of 'protons' obtained by subtracking negative hadron distributions from positive hadron distributions are presented for 200 GeV/A S+Au collisions. The distributions are shown as a function of event centrality and are indicative of a system exhibiting a large degree of nuclear stopping.
DOE

N95-19590# Pacific Northwest Lab., Richland, WA.
INTRINSIC BARRIERS FOR H-ATOM TRANSFER REACTIONS INVOLVING HYDROCARBONS
D. M. Camaioni, S. T. Autrey, and J. A. Franz Aug. 1994 16 p Presented at the 208th American Chemical Society National Meeting, Washington, DC, 21-26 Aug. 1994
(Contract DE-AC06-76RL-01830)
(DE94-018451; PNL-SA-24420; CONF-940813-21) Avail: CASI HC A03/MF A01

Intrinsic barriers (formally the barrier in the absence of driving force) for H-atom transfer reactions are key parameters in Evans-Polyanyi and Marcus equations for estimating exothermic reaction barriers and are fundamentally significant for the insight they provide about bond reorganization energies for formation of transition state structures. Although knowable from experiment, relatively few of these barriers have been measured due to experimental difficulties in measuring rates for identity reactions. Thus, the authors have used semiempirical Molecular Orbital theoretical methods (MNDO/PM3) to calculate barriers for a series of H-atom transfer identity reactions involving alkyl, alkenyl, arylalkyl and hydroaryl radicals and donors. Briefly stated, they find that barriers decrease with the degree of alkyl substitution at the radical site whereas barriers increase with the degree of conjugation with the radical site. Details of the methodology and analyses of how these barrier heights correlate with reactant and transition state properties will be presented and discussed.
DOE

N95-19597# Wisconsin Univ., Madison, WI.
SPECTROSCOPY AND DYNAMICS OF VIBRATIONALLY EXCITED MOLECULES Annual Technical Report, May 1992 - Apr. 1993
F. F. Crim 5 Oct. 1994 2 p
(Contract F49620-92-J-0073)
(AD-A285874; AFOSR-94-0666TR) Avail: CASI HC A01/MF A01

This report describes the progress of student supported by an AASERT award. The fields of study concerned spectroscopy and dynamics of vibrationally excited molecules.
Author (DTIC)

N95-19705# Washington Univ., Seattle, WA.
LIMITS ON CP NONCONSERVING INTERACTIONS FROM ELECTRIC DIPOLE MOMENTS
W. C. Haxton 1994 18 p
(Contract DE-FG06-90ER-40561)
(DE94-018582; DOE/ER-40561/158) Avail: CASI HC A03/MF A01

I discuss bounds on CP-nonconserving (CPNC) and parity-nonconserving (PNC) hadronic interactions that result from measurements of atomic electric dipole moments. In most models of hadronic CPNC, the nuclear edm arises primarily from the polarization of the ground state by the CPNC PNC NN interaction, rather than from the edms of valence nucleons. When the atom is placed in an external field, the nucleus is fully shielded apart from nuclear finite size effects and relativistic corrections arising from hyperfine interactions, so that careful atomic calculations must be performed to deduce the residual sensitivity to the nuclear edm. I describe these shielding effects qualitatively, and present results from more detailed calculations. Atomic limits, when translated into effective bounds on the neutron edm, have now reached sensitivities that are comparable to direct

neutron edm limits. I also discuss limits that can be extracted on CPNC parity-conserving (PC) hadronic interactions. Such interactions can generate atomic edms when combined with weak radiative corrections. DOE

N95-19706# Massachusetts Inst. of Tech., Cambridge.
THE VERY LOW ENERGY SOLAR FLUX OF ELECTRON AND HEAVY-FLAVOR NEUTRINOS AND ANTINEUTRINOS
Wei Lin and W. C. Haxton (Washington Univ., Seattle, WA.) 1994 14 p
(Contracts DE-FG06-90ER-40561; DE-AC02-76ER-03069; DE-FC02-94ER-40818)
(DE94-018583; DOE/ER-40561/159) Avail: CASI HC A03/MF A01

We have calculated the thermal flux of low-energy solar neutrinos and antineutrinos of all flavors. The principal process, neutrino pair emission from free-bound atomic transitions in iron and other solar metals, produces a peak flux density per flavor approximately 10(exp 11)/sq cm /sec/MeV at E(sub (nu)) approximately 1 keV, a value comparable to the peak of the pp electron neutrino density. This flux carries information on the temperature and metallicity of the solar core and on heavy flavor neutrino masses for m(sub (nu))(sub (mu)) or m(sub (nu))(sub tau) approximately greater than 1 keV. DOE

N95-19709# Lawrence Livermore National Lab., Livermore, CA.
SCINTILLATING-FIBER IMAGING DETECTOR FOR 14-MeV NEUTRONS
D. Ress, R. A. Lerche, R. J. Ellis, G. W. Heaton, M. B. Nelson, G. Mant, and D. E. Lehr 25 Jul. 1994 20 p Presented at the Annual Meeting of the Society of Photo-Optical Instrumentation Engineers, San Diego, CA, 24-29 Jul. 1994
(Contract W-7405-eng-48)
(DE94-018593; UCRL-JC-115596; CONF-940723-24) Avail: CASI HC A03/MF A01

The authors have created a detector to image the neutrons emitted by imploded inertial-confinement fusion targets. The 14-MeV neutrons, which are produced by deuterium-tritium fusion events in the target, pass through an aperture to create an image on the detector. The neutron radiation is converted to blue light (430 nm) with a 20-cm-square array of plastic scintillating fibers. Each fiber is 10-cm long with a 1-mm-square cross section; approximately 35-thousand fibers make up the array. The resulting blue-light image is reduced and amplified by a sequence of fiber-optic tapers and image intensifiers, then acquired by a CCD camera. The fiber-optic readout system was tested optically for overall throughput the resolution. The authors plan to characterize the scintillator array reusing an ion-beam neutron source as well as DT-fusion neutrons emitted by inertial confinement targets. Characterization experiments will measure the light-production efficiency, spatial resolution, and neutron scattering within the detector. Several neutron images of laser-fusion targets have been obtained with the detector. Several neutron images of laser-fusion targets have been obtained with the detector. They describe the detector and their characterization methods, present characterization results, and give examples of the neutron images. DOE

N95-19726# Argonne National Lab., IL.
PRINCIPAL-VALUE RESUMMATION FOR DILEPTON PRODUCTION
H. Contopanagos, L. Alvero (State Univ. of New York, Stony Brook, NY.), and G. Sterman (State Univ. of New York, Stony Brook, NY.) 1994 6 p Presented at the Meeting of the Division of Particles and Fields of the American Physical Society, Albuquerque, NM, 2-6 Aug. 1994
(Contract W-31-109-eng-38)
(DE95-001094; ANL-HEP-CP-94-53; ITP-SB-94-40; CONF-940816-35)
Avail: CASI HC A02/MF A01

We present a new method of resummation of QCD threshold distributions to the hard scattering function of the dilepton production cross section in hadron-hadron collisions. Our formulation by-passes the infrared singularities of the QCD running coupling through a principal value prescription, and does not require an explicit infrared cut-off. The resulting large corrections exponentiate, and we discuss asymptotic properties of the exponent. We present a closed analytical formula for the resummed hard part in momentum space, and give predictions, at fixed-target energies, for the resulting cross section which is a bounded function of its kinematic variables in the entire partonic phase space. DOE

N95-19786# Argonne National Lab., IL.
THE INTERACTIONS OF HIGH-ENERGY, HIGHLY CHARGED Xe IONS WITH FULLERENES
T. LeBrun, H. G. Berry, S. Cheng, R. W. Dunford, H. Esbensen, D. S. Gemmell, E. P. Kanter, and W. Bauer (Michigan State Univ., East Lansing, MI.) 1994 8 p Presented at the 7th International Conference on Physics of Highly Charged Ions, Vienna, Austria, 19-23 Sep. 1994
(Contract W-31-109-eng-38)
(DE95-001440; ANL/PHY/CP-82861; CONF-940922-1) Avail: CASI HC A02/MF A01

Ionization and fragmentation have been measured for C60 molecules bombarded in the vapor phase by Xe(sup 35+) and Xe(sup 18+) ions with energies in the range 420-625 MeV. The CM energies exceeded those used in previous studies by several orders of magnitude. We present the observed mass distribution of positively-charged fragments together with a theoretical model indicating that the total interaction cross section contains roughly equal contributions from (1) excitation of the giant plasmon resonance, and (2) large-energy-transfer processes that lead to multiple fragmentation of the molecule. DOE

N95-19787# Argonne National Lab., IL. Physics Div.
SPECTRAL DISTRIBUTION OF THE TWO-PHOTON DECAY OF He-LIKE KRYPTON
R. Ali, I. Ahmad, H. G. Berry, R. W. Dunford, D. S. Gemmell, E. P. Kanter, P. H. Mokler (Gesellschaft fuer Schwerionenforschung m.b.H., Darmstadt, Germany.), A. E. Livingston (Notre Dame Univ., IN.), S. Cheng (Toledo Univ., OH.), and L. J. Curtis (Toledo Univ., OH.) 1994 17 p Presented at the 7th International Conference on Physics of Highly Charged Ions, Vienna, Austria, 19-23 Sep. 1994
(Contracts W-31-109-eng-38; DE-FG05-88ER-13958; DE-FG02-92ER-14283)
(DE95-001442; ANL/PHY/CP-82860; CONF-940922-2) Avail: CASI HC A03/MF A01

We report progress on a measurement of the spectral distribution of photons from the two-photon decay of the 2(sup 1)S(sub 0) level in heliumlike krypton. A measurement of the exact shape of the continuum singles spectrum of the two-photon decay in heliumlike ions provides a sensitive probe of the calculation of the transition probability. In our experiment a beam of Kr(sup 34+) ions is excited using a thin carbon foil and the subsequent decays are observed in an array of four x ray detectors. DOE

N95-19835 Fermi National Accelerator Lab., Batavia, IL.
STUDIES OF PROMPT PHOTON PRODUCTION AND MULTIJET PRODUCTION AT THE TEVATRON COLLIDER
E. Buckley-Geer Sep. 1994 6 p Presented at the 27th International Conference on High Energy Physics, Glasgow, 21-27 Jul. 1994 Limited Reproducibility: More than 20% of this document may be affected by microfiche quality
(Contract DE-AC02-76CH-03000)
(DE95-002216; FNAL/C-94-336-E; CONF-940722-29) Avail: CASI HC A02

We present measurements of inclusive isolated prompt photon production in p(-p) collisions at a center-of-mass energy of 1.8 TeV from the Fermilab experiments CDF and D0. Precision measurements of prompt photon production from CDF constrain the gluon distribution, and recent results from D0 agree with CDF and QCD predictions. We also present studies of events with up to six jets in the final state from the CDF experiment. The mass distributions and mass ratio for these events is well described by the HERWIG parton shower Monte Carlo and by leading order QCD. Finally we present studies by both CDF and D0 of events with three jets in the final state. DOE

73 NUCLEAR AND HIGH-ENERGY PHYSICS

Includes elementary and nuclear particles; and reactor theory. For space radiation see *93 Space Radiation*.

N95-18146# General Atomics Co., San Diego, CA.
FUELED EMITTER, TFE VERIFICATION PROGRAM Final Test Report

Jul. 1994 77 p
(Contract DE-AC03-86SF-16298; GA Proj. 3450)
(DE94-017557; GA-A-21594) Avail: CASI HC A05/MF A01

The program objective is to demonstrate the technology readiness of a TFE suitable for use as the basic element in a thermionic reactor with electric power output in the 0.5 to 5.0 MW(e) range, and a full-power life of 7 years. The TFE Verification Program built directly on the technology and data base developed in the 1960s and early 1970s in an AEC/NASA program, and in the SP-100 program conducted in 1983, 1984 and 1985. In the SP-100 program, the attractive features of thermionic power conversion technology were recognized but concern was expressed over the lack of fast reactor irradiation data. The TFE Verification Program addressed that concern. DOE

N95-18147# General Atomics Co., San Diego, CA.
TFE DESIGN PACKAGE, TFE VERIFICATION PROGRAM Final Report
Jun. 1994 73 p
(Contract DE-AC03-86SF-16298; AG Proj. 3450)
(DE94-017558; GA-A-21597) Avail: CASI HC A04/MF A01

The program objective is to demonstrate the technology readiness of a TFE suitable for use as the basic element in a thermionic reactor with electric power output in the 0.5 to 5.0 MW(e) range, and a full-power life of 7 years. A TFE for a megawatt class system is described. Only six cells are considered for simplicity; a megawatt class TFE would have many more cells, the exact number dependent on optimization trade studies. DOE

N95-18217*# New Mexico Univ., Albuquerque, NM. Inst. for Space and Nuclear Power.
A REVIEW OF NUCLEAR THERMAL PROPULSION CARBIDE FUEL CORROSION AND KEY ISSUES Final Report
Dennis G. Pelaccio and Mohamed S. El-Genk Nov. 1994 58 p
(Grants NAG3-1346; NGT-40019)
(NASA-CR-197533; NAS 1.26:197533; UNM-ISNPS-5-1994) Avail: CASI HC A04/MF A01

Corrosion (mass loss) of carbide nuclear fuels due to their exposure to hot hydrogen in nuclear thermal propulsion engine systems greatly impacts the performance, thrust-to-weight and life of such systems. This report provides an overview of key issues and processes associated with the corrosion of carbide materials. Additionally, past pertinent development reactor test observations, as well as related experimental work and analysis modeling efforts are reviewed. At the conclusion, recommendations are presented, which provide the foundation for future corrosion modeling and verification efforts. Author

N95-18370*# Constellation Technology Corp., Saint Petersburg FL.
[SIMULATION OF GAMMA-RAY SPECTRA FOR A VARIETY OF USER-SPECIFIED DETECTOR DESIGNS] Semiannual Technical Report, 1 Mar. - 31 Aug. 1994
A. C. Rester, Jr. 15 Dec. 1994 32 p Sponsored by ARPA and AF
(Contract NAS5-32586; Proj. 194001)
(NASA-CR-197551; NAS 1.26:197551) Avail: CASI HC A03/MF A01

The gamma-ray spectrum simulation program BSIMUL was designed to allow the operator to follow the path of a gamma-ray through a detector, shield and collimator whose dimensions are entered by the operator. It can also be used to simulate spectra that would be generated by a detector. Several improvements have been made to the program within the last few months. The detector, shield and collimator dimensions can now be entered through an interactive menu whose options are discussed below. In addition, spectra containing more than one gamma-ray energy can now be generated with the menu - for isotopes listed in the program. Adding isotopes to the main routine is also quite easy. Subroutines have been added to enable the operator to specify the material and dimensions of a collimator. This report details the progress made in simulating gamma-ray spectra for a variety of user-specified detector designs. In addition, a short discussion of work done in the related areas of pulse shape analysis and the spectral analysis is included. The pulse shape analysis and spectral analysis work is being performed pursuant to the requirements of contract F-94-C-0006, for the Advanced Research Projects Agency and the U.S. Air Force. Derived from text

N95-18552# Illinois Univ., Urbana, IL.
STUDY OF HIGH GAIN SPHERICAL SHELL ICF TARGETS CONTAINING UNIFORM LAYERS OF LIQUID DEUTERIUM TRITIUM FUEL
E. M. Simpson and Kyekyoon Kim May 1994 125 p Prepared for Lawrence Livermore National Lab., Livermore, CA
(Contract W-7405-eng-48)
(DE94-018550; UCRL-CR-118128) Avail: CASI HC A06/MF A02

A numerical model has been developed to describe the thermally induced behavior of a liquid layer of hydrogen isotopes inside a spherical Inertial Confinement Fusion (ICF) target and to calculate the far-field temperature gradient which will sustain a uniform liquid layer. This method is much faster than the trial-and-error method previously employed. The governing equations are the equations of continuity, momentum, energy, mass diffusion-convection, and conservation of the individual isotopic species. Ordinary and thermal diffusion equations for the diffusion of fluxes of the species are included. These coupled equations are solved by a finite-difference method using upwind schemes, variable mesh, and rigorous boundary conditions. The solution methodology unique to the present problem is discussed in detail. In particular, the significance of the surface tension gradient driven flows (also called Marangoni flows) in forming uniform liquid layers inside ICF targets is demonstrated. Using the theoretical model, the values of the externally applied thermal gradients that give rise to uniform liquid layers of hydrogen inside a cryogenic spherical-shell ICF target are calculated, and the results compared with the existing experimental data. DOE

N95-18881# Joint Inst. for Nuclear Research, Dubna (USSR).
STUDY OF STRANGENESS PRODUCTION IN RELATIVISTIC NUCLEUS BEAMS AT JINR
E. O. Okonov 1993 11 p Presented at the International Courses of the NATO Advanced Study Institute: Hot and Dense Nuclear Matter, Bodrum, Turkey, 26 Sep. - 9 Oct. 1993
(DE94-626720; JINR-E-1-93-443) Avail: CASI HC A03/MF A01 (US Sales Only)

The experimental data on strangeness production in nucleus-nucleus collisions at 3.4 - 3.7 A GeV are analyzed and compared with more recent results of BNL and CERN at higher energies. The main attention is given to remarkable changes in properties of produced (Lambda)- and K-particles when a degree of the collision centrality increases: the flattening of their angular distributions up to nearly isotropic ones; the enhancement of the relative yields of (Lambda)'s with P(sub T) greater than or equal to 1 GeV/c (i.e. beyond a background from N N-interactions) by a factor of about 10; the occurrence of a considerable portion of (Lambda)'s ((approx) 10%) with anomalously high P(sub T); the increase of Boltzmann temperatures T(sub (Lambda),K) from 75 MeV with approaching a plateau at T(sub (Lambda),K) (approx) 160 MeV, which corresponds to the inverse slope parameter T(sub 0) (approx equal) 200 MeV and is near to the predicted critical temperature for the phase transition into quark-gluon plasma (QGP). The found effects confirmed by the data of BNL and CERN experiments, are expected as signals of a stopping, thermalization and heating of hadron matter with a formation of a hot and dense fireball/mixed phase via first order phase transition. Although more detailed studies and searches for alternative interpretations (beside QGP) are necessary to make a final conclusion, the considered results provide a strong evidence for a creation of a high excited fireball which is predicted to be a prolific source of strange objects formed. Programs of analyses are elaborated to examine anomalous events form central nucleus-nucleus collisions detected in streamer spectrometers, in order to look for light states of strange quark/hypernuclear matter. DOE

N95-18893# Maryland Univ., College Park, MD. Dept. of Physics.
ADVANCED METHODS FOR THE COMPUTATION OF PARTICLE BEAM TRANSPORT AND THE COMPUTATION OF ELECTROMAGNETIC FIELDS AND BEAM-CAVITY INTERACTIONS
A. J. Dragt and R. L. Gluckstern Aug. 1994 22 p
(Contract DE-FG05-92ER-40748)
(DE94-017359; DOE/ER-40748/2) Avail: CASI HC A03/MF A01

The University of Maryland Dynamical Systems and Accelerator Theory Group has been carrying out long-term research work in the general area of Dynamical Systems with a particular emphasis on applications to Accelerator Physics. This work is broadly divided into two tasks: the

computation of charged particle beam transport and the computation of electromagnetic fields and beam-cavity interactions. Each of these tasks is described briefly. Work is devoted both to the development of new methods and the application of these methods to problems of current interest in accelerator physics including the theoretical performance of present and proposed high energy machines. In addition to its research effort, the Dynamical Systems and Accelerator Theory Group is actively engaged in the education of students and postdoctoral research associates. Substantial progress in research has been made during the past year. DOE

N95-18897# Sandia National Labs., Albuquerque, NM.
HEISHI: A FUEL PERFORMANCE MODEL FOR SPACE NUCLEAR APPLICATIONS
M. F. Young Aug. 1994 53 p
(Contract DE-AC04-94AL-85000)
(DE94-017497; SAND-94-0169) Avail: CASI HC A04/MF A01

HEISHI is a Fortran computer model designed to aid in analysis, prediction, and optimization of fuel characteristics for use in Space Nuclear Thermal Propulsion (SNTP). Calculational results include fission product release rate, fuel failure fraction, mode of fuel failure, stress-strain state, and fuel material morphology. HEISHI contains models for decay chain calculations of retained and released fission products, based on an input power history and release coefficients. Decay chain parameters such as direct fission yield, decay rates, and branching fractions are obtained from a database. HEISHI also contains models for stress-strain behavior of multilayered fuel particles with creep and differential thermal expansion effects, transient particle temperature profile, grain growth, and fuel particle failure fraction. Grain growth is treated as a function of temperature; the failure fraction depends on the coating tensile strength, which in turn is a function of grain size. The HEISHI code is intended for use in analysis of coated fuel particles for use in particle bed reactors; however, much of the code is geometry-independent and applicable to fuel geometries other than spherical. DOE

N95-18957* National Aeronautics and Space Administration. Pasadena Office, CA.
THREE-GRID ACCELERATOR SYSTEM FOR AN ION PROPULSION ENGINE Patent
John R. Brophy, inventor (to NASA) (Jet Propulsion Lab., California Inst. of Tech., Pasadena, CA.) 6 Dec. 1994 7 p Filed 23 May 1994 Continuation of abandoned US-Patent-Appl-SN-066829, filed 21 May 1993
(NASA-Case-NPO-18391-2-CU; US-Patent-5,369,953;
US-Patent-Appl-SN-247611; US-Patent-Appl-SN-066829;
US-Patent-Class-60-202; US-Patent-Class-313-359.1;
US-Patent-Class-315-5.37; US-Patent-Class-315-111.01;
Int-Patent-Class-H05H-1/00) Avail: US Patent and Trademark Office

An apparatus is presented for an ion engine comprising a three-grid accelerator system with the decelerator grid biased negative of the beam plasma. This arrangement substantially reduces the charge-exchange ion current reaching the accelerator grid at high tank pressures, which minimizes erosion of the accelerator grid due to charge exchange ion sputtering, known to be the major accelerator grid wear mechanism. An improved method for life testing ion engines is also provided using the disclosed apparatus. In addition, the invention can also be applied in materials processing. Official Gazette of the U.S. Patent and Trademark Office

N95-18965*# Fermi National Accelerator Lab., Batavia, IL. NASA/Fermilab Astrophysics Center.
COSMIC RAY MODELS FOR EARLY GALACTIC LITHIUM, BERYLLIUM, AND BORON PRODUCTION
Brian D. Fields (Chicago Univ., Chicago, IL.), Keith A. Olive (Minnesota Univ., Minneapolis, MN.), and David N. Schramm (Chicago Univ., Chicago, IL.) Jan. 1994 58 p Submitted for publication Sponsored by NSF and Presidental Young Investigator Award
(Contract NAGw-2381; DE-AC02-93ER-40105)
(NASA-CR-197626; NAS 1.26:197626; FERMILAB-Pub-94/010-A) Avail: CASI HC A04/MF A01

To better understand the early galactic production of Li, Be, and B by cosmic ray spallation and fusion reactions, the dependence of these production rates on cosmic ray models and model parameters is examined. The sensitivity of elemental and isotropic production to the cosmic ray pathlength magnitude and energy dependence, source spectrum spallation kinematics, and cross section uncertainties is studied. Changes in these model features, particularly those features related to confinement, are shown to alter the Be- and B-versus-Fe slopes from a naive quadratic relation. The implications of our results for the diffuse gamma-ray background are examined, and the role of chemical evolution and its relation to our results is noted. It is also noted that the unmeasured high energy behavior of alpha + alpha fusion can lead to effects as large as a factor of 2 in the resultant yields. Future data should enable Population II Li, Be, and B abundances to constrain cosmic ray models for the early Galaxy. Author

N95-19561# Fermi National Accelerator Lab., Batavia, IL.
PHYSICS AT THE FERMILAB TEVATRON PROTON-ANTIPROTON COLLIDER
S. Geer Aug. 1994 44 p Presented at the 5th BCSPIN Summer School in Physics, Kathmandu, Nepal, 22 May - 7 Jul. 1994
(Contract DE-AC02-76CH-03000)
(DE95-000648; FNAL/C-94/275-E; CONF-9405237-1) Avail: CASI HC A03/MF A01

These lectures discuss a selection of QCD and Electroweak results from the CDF and DO experiments at the Fermilab Tevatron Proton-Antiproton Collider. Results are presently based on data samples of about 20 pb(exp -1) at a center-of-mass energy of 1.8 TeV. Results discussed include jet production, direct photon production, W mass and width measurements, the triboson coupling, and most exciting of all, evidence for top quark production. DOE

N95-19584# California Univ., Berkeley. Lawrence Berkeley Lab, CA.
CHARACTERIZATION OF THE 50 MeV ALS LINAC BEAM WITH OPTICAL TRANSITION RADIATION
M. J. deLoos, S. B. vanderGeer, and W. P. Leemans Jun. 1994 3 p Presented at the 4th European Particle Accelerator Conference, London, England, 27 Jun. - 1 Jul. 1994
(Contract DE-AC03-76SF-00098)
(DE94-018208; LBL-34973; CONF-940618-77) Avail: CASI HC A01/MF A01

First experimental results of the optical transition radiation diagnostic at the Beam Test Facility (BTF) are presented. The BTF uses the 50 MeV Advanced Light Source (ALS) injector. Using sensitive CCD cameras single shot energies, spot sizes and divergences can be measured for the InC/bunch electron beam. The emittance was determined by analyzing optical transition radiation data for various currents of a quadrupole lens. DOE

N95-19588# Lawrence Livermore National Lab., Livermore, CA.
CONTRIBUTIONS OF THE NATIONAL IGNITION FACILITY TO THE DEVELOPMENT OF INERTIAL FUSION ENERGY
M. Tobin, G. Logan, T. DiazDeLaRubia, V. Schrock (California Univ., Berkeley, CA.), K. Schultz (General Atomics Co., San Diego, CA.), Robert E. Tokheim (SRI International Corp., Menlo Park, CA.), M. Abdou (California Univ., Los Angeles, CA.), and R. Bangerter (California Univ., Berkeley. Lawrence Berkeley Lab, CA.) Jun. 1994 24 p Presented at the ISFNT-3: 3rd International Symposium on Fusion Nuclear Technology, Los Angeles, CA, 27 Jun. - 1 Jul. 1994
(Contract W-7405-eng-48)
(DE94-018335; UCRL-JC-117698; CONF-940664-26) Avail: CASI HC A03/MF A01

The Department of Energy is proposing to construct the National Ignition Facility (NIF) to embark on a program to achieve ignition and modest gain in the laboratory early in the next century. The NIF will use a (ge) 1.8-MJ, 0.35-mm laser with 192 independent beams, a fifty-fold increase over the energy of the Nova laser. System performance analyses suggest yields as great as 20 MJ may be achievable. The benefits of a micro-fusion capability in the laboratory include: essential contributions to defense programs, resolution of important Inertial Fusion Energy issues, and unparalleled conditions of energy density for basic science and technology research. We have begun to consider the role the National Ignition Facility will fill in the development of Inertial Fusion Energy. While the achievement of ignition and gain speaks for itself in terms of its impact on developing IFE, we believe there are areas of IFE development such as fusion power technology, IFE target design and fabrication, and understanding chamber dynamics, that would significantly benefit from NIF experiments. In the area of IFE target physics, ion targets will be designed using the NIF

laser, and feasibility of high gain targets will be confirmed. Target chamber dynamics experiments will benefit from x-ray and debris energies that mimic in-IFE-chamber conditions. Fusion power technology will benefit from using single-shot neutron yields to measure spatial distribution of neutron heating, activation, and tritium breeding in relevant materials. IFE target systems will benefit from evaluating low-cost target fabrication techniques by testing such targets on NIF. Additionally, we believe it is feasible to inject up to four targets and engage them with the NIF laser by triggering the beams in groups of approximately 50 separated in time by approximately 0.1 s. Sub-ignition neutron yields would allow an indication of symmetry achieved in such proof-of-principle rep-rate experiments. DOE

N95-19784# Continuous Electron Beam Accelerator Facility, Newport New, VA.
THE FOUNDING OF CEBAF, 1979 TO 1987
Catherine Westfall (Michigan State Univ., East Lansing, MI.) Sep. 1994 43 p
Avail: CASI HC A03/MF A01

A history of the founding, design effort, construction, and funding of the Continuous Electron Beam Accelerator Facility is presented. The contributions made by individuals and technical design groups are discussed. CASI

N95-19841 Stanford Linear Accelerator Center, CA. Synchrontron Radiation Lab.
ALGORITHMS FOR ORBIT CONTROL ON SPEAR
J. Corbett, D. Keeley, R. Hettel, I. Linscott, and J. Sebek Jun. 1994 3 p Presented at the 4th European Particle AcceleratorConference, London, United Kingdom, 27 Jun. - 1 Jul. 1994 Limited Reproducibility: More than 20% of this document may be affected by microfiche quality
(Contract DE-AC03-76SF-00515)
(DE95-002868; SU-SLAC-PUB-6517; SU-SLAC/SSRL-0077; CONF-940618-90) Avail: CASI HC A01

A global orbit feedback system has been installed on SPEAR to help stabilize the position of the photon beams. The orbit control algorithms depend on either harmonic reconstruction of the orbit or eigenvector decomposition. The orbit motion is corrected by dipole corrector kicks determined from the inverse corrector-to-bpm response matrix. This paper outlines features of these control algorithms as applied to SPEAR. DOE

N95-19874# Japan Atomic Energy Research Inst., Tokyo (Japan).
DEVELOPMENT OF AN AMORPHOUS SURGE BLOCKER FOR A HIGH VOLTAGE ACCELERATION POWER SUPPLY OF THE NEUTRAL BEAM INJECTORS
Makoto Mizuno (Japan Atomic Energy Research Inst., Naka, Japan.), Yoshihiro Ohara (Japan Atomic Energy Research Inst., Naka, Japan.), Kazuhiro Watanabe (Japan Atomic Energy Research Inst., Naka, Japan.), and Akira Ozaki Oct. 1993 18 p
(DE94-770648; JAERI-M-93-214) Avail: CASI HC A03/MF A01

An amorphous surge blocker for a high voltage acceleration power supply for the neutral beam injectors has been developed. Since the saturation magnetic flux density of the amorphous core is higher than that of the ferrite core, the surge blocker made of amorphous cores can be reduced in size appreciably compared to the conventional ferrite surge blocker. A 350 kV, 0.05 volt-second amorphous surge blocker was designed, fabricated and tested. The amorphous core was made by winding an amorphous tape with a film for the layer insulation and was heat-treated to recover the magnetic characteristics. The core is molded by epoxy resin and installed in a FRP insulator tube filled with SF6 gas for the insulation. The volt-second measured was higher than the designed value and the electrical breakdown along the cores and between layers was not observed. This test result shows that the amorphous surge blocker is applicable for a dc acceleration power supply for high energy neutral beam injectors. DOE

74 OPTICS

Includes light phenomena; and optical devices.
For lasers see *36 Lasers and Masers.*

N95-18067# Rome Lab., Griffiss AFB, NY.
GIGABIT OPTICAL INTERCONNECTS: SYSTEM AND COMPONENT ANALYSIS, DESIGN AND DEVELOPMENT
Raymond K. Boncek, Mark F. Krol, Michael J. Hayduk, John L. Stacy, and Steven T. Johns Jul. 1994 26 p
(AF Proj. 4600)
(AD-A285536; RL-TR-94-86) Avail: CASI HC A03/MF A01

This report describes the results of experiments performed in various areas of technology required to develop gigabit optical interconnects for communication at 1.3 micrometer wavelength. First, we will summarize the analysis of optical correlation switches (i.e. optical AND gates) for use in time-division optical interconnects. Next, we describe the design and characterization of an all-optical, 30db contrast ratio GaAlInAs multiple quantum well asymmetric reflection modulator. Then, we comment on the characterization of polarization-dependent, strained-layer InGaAs/GaAs materials useful for light emitters and modulators. Finally, we report on the development of an optically transparent ATM packet switch testbed operating at 1.24416 Gbit/s. This work is a continuation of in-house efforts begun under 62702F, JON 4600P201 and summarized in RL-TR-91-398. DTIC

N95-18100 Washington Univ., Saint Louis, MO.
DESIGN AND FABRICATION OF N x N OPTICAL COUPLERS BASED ON ORGANIC POLYMER OPTICAL WAVEGUIDES Final Report, Jan. 1993 - Jan. 1994
Robert R. Krchnavek and Daniel L. Rode Aug. 1994 44 p Limited Reproducibility: More than 20% of this document may be affected by microfiche quality
(Contract F30602-93-C-0004; AF Proj. 4600)
(AD-A285530; RL-TR-94-142) Avail: CASI HC A03

In this report, we examine the design and fabrication of a planar, 10x10 optical coupler utilizing photopolymerizable organic polymers. Background information on the theory of operation of the coupler culminating in a set of design equations is presented. The details of the material processing are described, including the preparation of monomer mixtures that result in single-mode polymer waveguides (lambda = 1300 nm) that have core dimensions approximately equal to those of single-mode fiber. This is necessary to insure high coupling efficiency between the planar device and optical fiber. A unique method of aligning and attaching optical fibers to the coupler is demonstrated. This method relies on patterned alignment ways, a transcision cut, and single-mode D-fiber. A theoretical analysis of the in situ monitoring technique used to fabricate the single-mode D-fiber is presented and compared favorably with the experimental results. Finally, the 10x10 coupler is characterized. We have measured an excess loss of approximately 8 dB. Author (DTIC)

N95-18102 Cornell Univ., Ithaca, NY.
EVALUATION OF THE CURRENT BIASED INTEGRATED OPTICAL PROCESSORS BASED ON BISTABLE DODE ELEMENTS Final Report, Mar. - Jul. 1993
C. L. Tang, P. D. Swanson, M. A. Parker (Rome Lab., Griffiss AFB, NY.), and S. I. Libby (Rome Lab., Griffiss AFB, NY.) Jul. 1994 20 p Limited Reproducibility: More than 20% of this document may be affected by microfiche quality
(Contract F30602-93-C-0068; AF Proj. 4600)
(AD-A285532; RL-TR-94-97) Avail: CASI HC A03

Three optical switching elements have been designed, fabricated and tested for use in an integrated, optical signal processor. The first, and optical NOR logic gate, uses gain quenching as a means of allowing one (or more) light beam (s) to control the output light. This technique, along with the use of a two-pad bistable output laser, is used in the demonstration of the feasibility of the second device, an all optical RS flip-flop. The third device consists of a broad area orthogonal mode switch laser, whose corollary outputs correspond to the sign of the voltage difference between its two high impedance electrical inputs. This device also has possible memory applications if bistable mode switching within the broad area laser can be achieved. DTIC

N95-18104 Rensselaer Polytechnic Inst., Troy, NY.
DEVELOPMENT OF ULTRASHORT OPTICAL PULSE SOURCES NEAR 1.3 AND 1.5 MICRONS WITH AN EMPHASIS ON STABILITY, HIGH REPETITION RATE, AND PARALLELISM Final Report, May 1993 - May 1994
R. L. Fork Aug. 1994 31 p Limited Reproducibility: More than 20% of this document may be affected by microfiche quality
(Contract F30602-93-D-0104; AF Proj. 4600)
(AD-A285535; RL-TR-94-137) Avail: CASI HC A03

We use experiment and numerical simulation to study performance of a harmonically modelocked laser that includes an electronic modulator and an intracavity Fabry-Perot etalon. We experimentally generate trains of pulses of 40 ps duration at 1.3 Ghz. We also study introduction of nonlinear optical shaping in the form of a NOLM loop. Numerical simulation indicates that NOLM loop, or similar nonlinear optical pulse shaping, can reduce the pulse duration to subpicosecond values. Experiment shows that the added length of a NOLM loop, however, has a destabilizing influence in that its nonlinear shaping that is not susceptible to this destabilization are examined. Dynamics of this type of laser, including NOLM loops, are simulated in a manner that predicts the rate of approach to stability. DTIC

N95-18142 Army Research Lab., Aberdeen Proving Ground, MD.
MIDINFRARED OPTICAL PROPERTIES OF PETROLEUM OIL AEROSOLS Final Report
K. P. Gurton and C. W. Bruce Aug. 1994 36 p Limited Reproducibility: More than 20% of this document may be affected by microfiche quality
(AD-A283689; ARL-TR-255) Avail: CASI HC A03

The mass normalized absorption and extinction coefficients were measured for fog oil aerosol at 3.4 micrometers with a combined photoacoustic and transmissometer system. An extinction spectral profile was determined over a range of infrared (IR) wavelengths from 2.7 to 4.0 micrometers by an IR scanning transmissometer. The extinction spectrum was mass normalized by referencing it to the photoacoustic portion of the experiment. A corresponding Mie calculation was conducted and compared with the above measurements. Agreement is good for the most recent optical coefficients. An extrapolation of this data to other similar petroleum products such as kerosene or diesel fuel that exhibit similar bulk absorption characteristics were briefly examined. DTIC

N95-18154# Wright Lab., Wright-Patterson AFB, OH.
ERROR MEASUREMENTS IN AN ACOUSTO-OPTIC TUNABLE FILTER-FIBER BRAGG GRATING SENSOR SYSTEM Final Report, Aug. 1991 - Jan. 1994
Antonio Crespo May 1994 103 p
(AF Proj. 2001)
(AD-A283912; WL-TR-94-5023) Avail: CASI HC A06/MF A02

This final report is a thesis submitted to the University of P.R., Mayaguez Campus. This research analyzed theoretically and experimentally an Acousto-Optic Tunable Filter--Fiber Bragg Grating (AOTF-FBG) system. This analysis was targeted to investigate the measurement error in the AOTF-FBG system. DTIC

N95-18342# Naval Command, Control and Ocean Surveillance Center, San Diego, CA. RDT and E Div.
LIQUID CRYSTAL TUNABLE FILTER Final Report
G. L. Adams Mar. 1994 83 p
(AD-A284383; NRAD-TR-1643) Avail: CASI HC A05/MF A01

The objective was to manufacture and test a tunable birefringent filter made using liquid crystal variable phase plates. In FY 92, a six stage tunable birefringent filter was purchased from Meadowlark Optical, Inc. of Longmont, CO. The filter design is a variation on the well known Lynot-Solc birefringent filter design. The filter was tested using resources available in the Code 843 Receiver laboratory. Preliminary analysis indicates that the liquid crystal variable phase plates operated as expected and did not seem to degrade the filter performance appreciably. The filter stages were characterized individually and assembled into a composite filter. Testing measured the filter's performance and agreement with theory that included characterization of the bandpass, field of view, peak transmission, out-of-band rejection, and transmission uniformity. The filter performance is still being assessed, and the final report will be available as an NRaD technical report in 1994. In general, the measured filter performance agreed well with predicted performance, resulting in a filter that was tunable over the specified range with a bandwidth that varied from 1.5 to 3 nm. DTIC

N95-18345 Institute of Electrical and Electronics Engineers, Piscataway, NJ. Lasers and Electro-Optics Society.
1994 IEEE NONLINEAR OPTICS: MATERIALS FUNDAMENTAL AND APPLICATIONS CONFERENCE
29 Jul. 1994 479 p Conference held at Waikoloa, HI, 25-29 Jul. 1994; sponsored by Optical Society of America Limited Reproducibility: More than 20% of this document may be affected by microfiche quality
(Contract N00014-94-1-0548)
(AD-A285769; IEEE-94CH3370-4; LC-93-61269; ISBN-0-7803-1473-5; ISBN-0-7803-1474-3; ISBN-0-7803-1475-1) Avail: CASI HC A21

The following topics are discussed: (1) Nonlinear organic materials; (2) Novel NLO effects; (3) Nonlinear frequency conversion; (4) Quantum wells & Semiconductors; (5) Ultrafast spectroscopy; (6) Ultrashort pulse sources and high intensity phenomena; (7) Photorefractive applications; (8) Photorefractive materials and solitons; (9) Nonlinear optical effects in fibers; (10) Holographic optical storage; and (11) Fundamental quantum process in NLO. DTIC

N95-18404 Imperial Coll. of Science and Technology, London (England).
LIGHT SCATTERING FROM ROUGH SURFACES Final Report
J. C. Dainty 17 Aug. 1994 55 p Limited Reproducibility: More than 20% of this document may be affected by microfiche quality
(Contract DAJA45-90-C-0026)
(AD-A284112; R/D-6409-EE-01) Avail: Issuing Activity (Defense Technical Information Center (DTIC))

A randomly rough surface illuminated by a parallel laser beam at some angle theta produces a speckle pattern in space. If the angle of illumination is changed to theta + change of theta then the speckle pattern changes in two ways: it translates in angle and changes its form in a manner that depends on the detailed surface characteristics and the angles involved. We have made experimental measurements of the angular correlation of speckle for two-dimensional Gaussian surfaces of low and high root-mean-square slope. In comparing with theory we have distinguished between surfaces for which single scattering is valid (very low slope) and those for which Kirchhoff theory is valid (larger rms slopes). A numerical ray-tracing approach has been implemented for two-dimensional surfaces that includes shadowing and polarization in a limited way. A conceptual, heuristic model is developed that explains the essential physical features. Author (DTIC)

N95-18409 Thermo Electron Technologies Corp., San Diego, CA.
ATOMIC LINE FILTER FOR SDI APPLICATIONS Final Report, Mar. 1989 - Sep. 1993
Jim Menders, S. H. Bloom, Eric Korevaar, M. Rivers, and C. S. Liu 13 Apr. 1994 70 p Limited Reproducibility: More than 20% of this document may be affected by microfiche quality
(Contract N00014-89-C-0068)
(AD-A284125; TTC-2847-R) Avail: CASI HC A04

When optical signals are embedded in background noise, narrowband optical filters are needed for receivers to achieve quantum limited performance. Such is typically the case with daytime optical communications and lidar. Narrowband filtered detectors. with acceptance bands of just a few picometers (pm) and high out of band rejection are well suited for these applications. The main thrust of this program has been the development of two means for narrowband detection: the Fast Atomic Line Filter/Field Ion Detector (FALF/FID) and the Faraday magneto-optic filter. The FALF/FIDs transduce optical radiation within a narrow band directly into electrical signals. They are laser pumped filters based on the spectroscopy of atomic vapors. We designed, built and tested an infrared FALF/FID with an rise time of under 10 ns and a quantum efficiency of greater than 25%. Faraday filters are imaging magneto-optic filters with passbands of a few pm. Faraday filters with passbands in the visable and the near infra-red were constructed and tested. Transmission spectra were measured, and found to agree closely with theoretical predictions. Both of these narrowband detection schemes must be used in conjunction with a tuned narrowband laser source. We developed a frequency locked alexandrite laser designed to match the acceptance band of a rubidium based filter. Finally, a preliminary demonstration of a laser interrogator

using a tuned infrared diode laser in conjunction with a filtered receiver was demonstrated. DTIC

N95-18424 Naval Postgraduate School, Monterey, CA.
DIRECT DETECTION AND COHERENT OPTICAL SYSTEMS EMPLOYING ERROR-CORRECTION CODING M.S. Thesis
Eui-Sik Hwang Jun. 1994 37 p Limited Reproducibility: More than 20% of this document may be affected by microfiche quality
(AD-A284350) Avail: Issuing Activity (Defense Technical Information Center (DTIC))

We evaluate the bit error probability of coded lightwave systems employing direct detection with OOK modulation, and coherent systems with FSK modulation and noncoherent detection. Block codes, convolutional codes, and concatenated codes are investigated. For direct systems, both hard and soft decoding are considered. Only hard decoding is employed in coherent optical systems. DTIC

N95-18459# Department of the Navy, Washington, DC.
A FIBER OPTIC COUPLER Patent Application
Thomas Iwanski, inventor (to Navy) and James Doucet, inventor (to Navy) 2 May 1994 12 p
(AD-D016473; US-Patent-Appl-SN-236823; Navy-Case-75012) Avail: CASI HC A02/MF A01

There is presented a fiber optic coupler for disposition in an underwater bulkhead, the coupler comprising a hydraulic fitting portion of substantially cylindrical configuration and having first threads on an exterior portion thereof. A first shank portion extends axially from the fitting portion and has formed thereon as an integral portion thereof a collar portion configured as a nut. A second shank portion extends axially from the collar portion, and a hub portion extends axially from the second shank portion and has second threads thereon. A tubular portion extends axially from the fitting portion in a direction opposite from the first shank portion. A bore extends through the tubular portion, fitting portion, first shank portion, second shank portion, and hub portion and is configured to receive known fiber optic terminators. DTIC

N95-18460# Department of the Navy, Washington, DC.
FIBER OPTIC PRESSURE AND/OR VIBRATION DETECTOR Patent Application
Frank W. Cuomo, inventor (to Navy) 18 May 1994 23 p
(AD-D016474; US-Patent-Appl-SN-246900; Navy-Case-76275) Avail: CASI HC A02/MF A01

A fiber optic pressure/vibration sensor for measuring pressure variations due to acoustic waves or the like and/or measuring vibrations of a body under test is described. The sensor includes a light source, a multimode single optical fiber for transmission of light from the light source from one end thereof to a fiber optic probe having a reflector at the other end of the optic fiber. The movement of the reflector under the influence of impinge acoustic waves or the vibrations of a body under test modulates of the light. The reflected light is carried by the same single optical fiber to a fiber optic couple which sends the reflected light through another coupled optical fiber on to a photodetector to generate and measure the electrical signals produced due to the pressure variations or vibrations of the body under test. DTIC

N95-18478# Maryland Univ., College Park, MD. Center for Automation Research.
ON THE GEOMETRY OF VISUAL CORRESPONDENCE
Cornelia Fermueller and Yiannis Aloimonos Jul. 1994 40 p Prepared in cooperation with Royal Inst. of Tech., Stockholm, Sweden
(Contracts N00014-93-1-0257; DACA76-92-C-0009; NSF IRI-90-57934; ARPA Order 8459)
(AD-A285700; CAR-TR-732; CS-TR-3341) Avail: CASI HC A03/MF A01

Image displacement fields-optical flow fields, stereo disparity fields, normal flow fields-due to rigid motion possess a global geometric structure which is independent of the scene in view. Motion vectors of certain lengths and directions are constrained to lie on the imaging surface at particular loci whose location and form depends solely on the 3D motion parameters. If optical flow fields or stereo disparity fields are considered, then equal vectors are shown to lie on conic sections. Similarly, for normal motion fields, equal vectors lie within regions whose boundaries also constitute conics. By studying various properties of these curves and regions and their relationships, a characterization of the structure of rigid motion fields is given. The goal of this paper is to introduce a concept underlying the global structure of image displacement fields. This concept gives rise to various constraints that could form the basis of algorithms for the recovery of visual information from multiple views. DTIC

N95-18480# Maryland Univ., College Park, MD. Center for Automation Research.
VISION AND ACTION
Cornelia Fermueller and Yiannis Aloimonos Jun. 1994 43 p
(Contracts N00014-93-1-0257; DACA76-92-C-0009; NSF IRI-90-57934; ARPA Order 8459)
(AD-A285701; CAR-TR-722; CS-TR-3305) Avail: CASI HC A03/MF A01

Our work on Active Vision has recently focused on the computational modelling of navigational tasks, where our investigations were guided by the idea of approaching vision for behavioral systems in form of modules that are directly related to perceptual tasks. These studies led us to branch in various directions and inquire into the problems that have to be addressed in order to obtain an overall understanding of perceptual systems. In this paper we present our views about the architecture of vision systems, about how to tackle the design and analysis of perceptual systems, and promising future research directions. Our suggested approach for understanding behavioral vision to realize the relationship of perception and action builds on two earlier approaches; the Medusa philosophy 3 and the Synthetic approach 15. The resulting framework calls for synthesizing an artificial vision system by studying vision competences of increasing complexity and at the same time pursuing the integration of the perceptual components with action and learning modules. We expect that Computer Vision research in the future will progress in tight collaboration with many other disciplines that are concerned with empirical approaches to vision, i.e. the understanding of biological vision. Throughout the paper we describe biological findings that motivate computational arguments which we believe will influence studies of Computer Vision in the near future. DTIC

N95-18484# Naval Command, Control and Ocean Surveillance Center, San Diego, CA. Electromagnetic Propagation Div.
MARINE BOUNDARY LAYER REFRACTIVE EFFECTS IN THE INFRARED
R. Feinberg, H. V. Hitney, and H. G. Hughes Oct. 1994 81 p
(AD-A285717; NRAD-TD-2706) Avail: CASI HC A05/MF A01

An experiment was conducted to determine whether ducting phenomena (gradients in refractivity) occur close to the ocean surface at infrared wavelengths. A CO2 laser beam (10.6 microns) was transmitted and received over an 8.5 km path in San Diego Bay. For the cases investigated (sea warmer than the air), the results of the study indicate that for air temperature gradients less than 1 C/meter, the distance to the infrared horizon was only 60 percent of the normal geometrical horizon. DTIC

N95-18509 Texas Univ., Austin, TX.
LOCAL SPATIO-TEMPORAL ANALYSIS IN VISION SYSTEMS Annual Report No. 1, 1 May 1993 - 31 May 1994
Wilson S. Geisler, Alan Bovik, Lawrence Cormack, Joydeep Ghosh, and David Gildeen 31 Jul. 1994 31 p Limited Reproducibility: More than 20% of this document may be affected by microfiche quality
(Contract F49620-93-1-0307)
(AD-A284162; AFOSR-94-0504TR) Avail: Issuing Activity (Defense Technical Information Center (DTIC))

The aims of this project are the following: (1) develop a physiologically and psychophysically based model of low-level human visual processing (a key component of which are local frequency coding mechanisms); (2) develop image models and image-processing methods based upon local frequency coding; (3) develop algorithms for performing certain complex visual tasks based upon local frequency representations, (4) develop models of human performance in certain complex tasks based upon our understanding of low-level processing; and (5) develop a computational testbed for implementing, evaluating and visualizing the proposed models and algorithms, using a massively parallel computer. Progress has been substantial on all aims. The highlights include the following: (1) completion of a number of psychophysical and physiological experiments revealing new, systematic and exciting properties of the primate (human and monkey) visual system; (2) further development of image models that can accurately represent the local frequency structure in complex images; (3) near

completion in the construction of the Texas Active Vision Testbed; (4) development and testing of several new computer vision algorithms dealing with shape-from-texture, shape-from-stereo, and depth-from-focus; (5) implementation and evaluation of several new models of human visual performance; and (6) evaluation, purchase and installation of a MasPar parallel computer. DTIC

N95-18529# Department of the Navy, Washington, DC.
INFRARED-TO-VISIBLE CONVERTER Patent Application
Eric S. Snow, inventor (to Navy) 29 Jun. 1994 38 p
(AD-D016443; US-Patent-Appl-SN-267697; Navy-Case-74808) Avail: CASI HC A03/MF A01

A quantum well infrared photodetector comprises multiple quantum well detectors formed within a single P-N structure forward-biased by an external voltage source, for directly converting infrared radiation having a wavelength in the range of approximately 4-15 micrometers into visible radiation or near infrared radiation. Multiple quantum well detectors disposed between the P-N contact layers are comprised of alternating gallium arsenide (GaAs) quantum well layers, aluminum gallium arsenide (AlGaAs) barrier layers and alternatively, a blocking layer of aluminum arsenide (AlAs) positioned between a last aluminum gallium arsenide (AlGaAs) barrier layer and the N contact layer; and are forward-biased by the external voltage source in order to produce band-gap luminescence by radiative recombination of excess carriers representative of electrons and holes in the N contact layer when the P contact layer is illuminated with optical energy of incident infrared radiation. DTIC

N95-18560 Department of the Navy, Washington, DC.
MULTI-LINE PASSIVE FIBER OPTIC SLIPRING Patent
Darrell T. Abney, inventor (to Navy) 7 Jun. 1994 8 p Filed 30 Sep. 1993
(AD-D016430; US-Patent-5,319,726; US-Patent-Appl-SN-129725; US-Patent-Class-385-26) Avail: US Patent and Trademark Office

A multi-line, passive fiber optic slipring is provided. A plurality of transmitting optical fibers are terminated in a plurality of focusing lenses. The fibers and focusing lens are free to rotate about an axis rotation. A plurality of ellipsoidal mirrors are stacked on top of one another beneath the focusing lenses such that the axis of rotation passes through a first focal point of each of the plurality of ellipsoidal mirrors. Each of the focusing lenses focuses optical signals through the first focal point of a corresponding one of the ellipsoidal mirrors. The optical signals reflect from each corresponding mirror to a second focal point of the corresponding mirror. Each mirror is further provided with an optical aperture along the axis of rotation to allow the optical signals not focused on the first focal point of the corresponding mirror to pass therethrough. Each of a plurality of receiving optical fibers is fixed at a corresponding one of the second focal points. DTIC

N95-18563 Department of the Navy, Washington, DC.
FIBER OPTIC FLEXURAL DISK ACCELEROMETER Patent
David A. Brown, inventor (to Navy), Steven L. Garrett, inventor (to Navy), and Thomas J. Hofler, inventor (to Navy) 7 Jun. 1994 10 p Filed 7 Feb. 1991
(AD-D016444; US-Patent-5,317,929; US-Patent-Appl-SN-651856; US-Patent-Class-73-517R) Avail: US Patent and Trademark Office

An accelerometer or seismometer has a pair of flat spirals of optical fiber and has one or more elastic disks bearing a mass and supported for flexure. Each spiral is fixedly attached to a corresponding disk side so that disk flexure lengthens a spiral on one disk side and shortens a spiral on an oppositely facing disk side, the spirals being connected as legs of a fiber optic interferometer so that the interferometer provides an output corresponding to the flexure. A pair of the disks may be mounted oppositely of a sealed body with a pair of the spirals arranged to minimize the effect of pressure changes on the sensor, and a pair of the spirals may be mounted oppositely of a thermally conducting disk to minimize temperature differences between the spirals. The mass may be centrally mounted on a disk with the disk peripherally supported, or the mass may be distributed around the disk periphery with the disk centrally supported for isolation from mounting strain. Several of the disks may be coaxially mounted to provide increased sensitivity. DTIC

N95-18593 Department of the Navy, Washington, DC.
ANNULAR COMPUTED TOMOGRAPHY Patent
James E. Prindiville, inventor (to Navy), Michael P. Skipalis, inventor (to Navy), and Hayden G. Martin, inventor (to Navy) 17 May 1994 8 p Filed 11 May 1993
(AD-D016424; US-Patent-5,313,513; US-Patent-Appl-SN-059846; US-Patent-Class-378-4) Avail: US Patent and Trademark Office

A Computed Tomography system for obtaining annular views of cylindrical objects, in which x-ray scanning is done of an annulus of the objects, and the computation necessary to derive the reconstructed image in polar coordinates is limited to the annulus of the objects, ignoring the other areas. Normalization is done to adjust the reconstructed image to the number of scans made of the various areas of the object. DTIC

N95-18628 Department of the Navy, Washington, DC.
DISENGAGABLE ADAPTER FOR AN OPTICAL FIBER CONNECTION Patent
Gair D. Brown, inventor (to Navy), Michael A. Richardson, inventor (to Navy), and Gary A. Burcham, inventor (to Navy) 22 Mar. 1994 8 p Filed 18 Mar. 1993
(AD-D016231; US-Patent-5,297,227; US-Patent-Appl-SN-033223; US-Patent-Class-385-56) Avail: US Patent and Trademark Office

A disengagable adapter for mechanically coupling optical fibers is provided. The disengagable adapter separates into two complementary receptacle parts. Each receptacle part receives through a bore a single optical-fiber located within an optical-fiber connector plug. Each receptacle part attaches to and securely holds a different connector plug. The receptacle parts mate with each other in a complementary fashion and thereby connect the two optical fiber connector plugs together. These connector plugs accordingly align the two optical fibers located within the plugs. The optical fibers can be separated either by demating the complementary parts or by disconnecting one side of the adapter from its connector plug. Mounting the complementary parts to a plate facilitates multiple, simultaneous connections. DTIC

N95-18682 Stanford Univ., CA. Optical Communications Research Lab.
ADVANCED OPTICAL FIBER COMMUNICATIONS SYSTEMS Final Report, 1 Sep. 1991 - 31 Aug. 1994
Leonid G. Kazovsky 31 Aug. 1994 164 p Limited Reproducibility: More than 20% of this document may be affected by microfiche quality
(Contract N00014-91-J-1857)
(AD-A283942) Avail: CASI HC A08

Part 1 describes our work on high dynamic range optical analog links. Within Part 1, Chapter 1 covers linewidth-insensitive coherent amplitude-modulated links and Chapter 2 covers coherent angle-modulated links and linewidth-insensitive interferometric links. Part 2 describes our work on dynamic wavelength division multiplexing (WDM) networks. Within Part 2, Chapter 3 covers the physical layer of STARNET, a coherent WDM communication network built at Stanford. Chapter 4 addresses the impact of semiconductor laser linewidth on STARNET physical layer performance. Chapter 5 covers the electronic interface architecture of STARNET. Part 3 describes our work with nonlinear effects in fiber. Within Part 3, Chapter 6 covers the impact of fiber nonlinearities such as four-wave mixing (FWM), cross-phase modulation (XPM), stimulated Brillouin scattering (SBS), and fiber-induced parasitic phase modulation on optical communication systems. This report ends with conclusions and a list of publications generated during this project. DTIC

N95-19085# Army Research Lab., White Sands Missle Range, NM.
LARGE AREA THERMAL TARGET BOARD: AN IMPROVEMENT TO ENVIRONMENTAL EFFECTS AND SYSTEM PARAMETERS CHARACTERIZATION Final Report
Wendell R. Watkins, Brent L. Bean, and Peter D. Munding Jun. 1994 38 p
(AD-A284614; ARL-TR-283) Avail: CASI HC A03/MF A01

Recent field tests have provided excellent opportunities to use a new characterization tool associated with the Mobile Imaging Spectroscopy Laboratory (MISL) of the Battlefield Environment Directorate, formerly the U.S. Army Atmospheric Sciences Laboratory. The MISL large area (1.8 by 1.8 m, uniform temperature, thermal target) was used for characterization and isolation of phenomena which impact target contrast. By viewing the target board from closeup and distant ranges simultaneously with the MISL

thermal imagers, the inherent scene content could be calibrated and the degrading effects of atmospheric propagation could be isolated. The target board is equipped with several spatial frequency bar patterns, but only the largest 3.5-cycle full area bar pattern was used for the distant range of 1.6 km. The quantities measured with the target board include the inherent background change, the contrast transmission, and the atmospheric modulation transfer function. The MISL target board has a unique design which makes it lightweight with near perfect transition between the hot and cold portions of the bar pattern. The heated portion of the target is an elongated rectangular even which is tilted back at a 30 deg angle to form a 1.8 by 1.8 m square when viewed from the front. The cold bars we positioned in front of the heated oven surface and can be oriented in either the vertical or horizontal direction. The oven is mounted on a lightweight trailer for one- or two-man positioning. An attached metal and canvas structure is used to shield the entire target from both solar loading and cooling winds. The target board has a thin aluminum sheet front surface which is insulated from the oven's heating structure. DTIC

N95-19088# GTE Labs., Inc., Waltham, MA.
METHODS AND COMPONENTS FOR OPTICAL CONTENTION RESOLUTION IN HIGH SPEED NETWORKS Interim Report, 23 May - 23 Aug. 1994
Paul Melman and Han Kim 23 Aug. 1994 11 p
(Contract MDA972-93-C-0057)
(AD-A284674) Avail: CASI HC A03/MF A01

During the fourth quarter of the CORD Project substantial effort was devoted to refinement and interworking of the various system functions required to resolve network contentions optically. The system group at Stanford University continued the design and development of the CORD prototype and subsystems. This includes the subcarrier-multiplexing header transceiver, the pilot tone clock transceiver and the payload data transceiver. Substantial progress has also been made on the digital logic subsystems as well as the digital logic and analog/digital interface circuits for the 2.488 Gbps payload data channel. DTIC

N95-19389 Department of the Navy, Washington, DC.
TORQUE-BALANCED EXTENDABLE FIBER OPTIC CABLE Patent
Gregory A. Simonds, inventor (to Navy) and Louis E. Sansone, inventor (to Navy) 16 Aug. 1994 4 p Filed 6 Oct. 1993
(AD-D016496; US-Patent-5,339,378; US-Patent-Appl-SN-134192; US-Patent-Class-385-100) Avail: US Patent and Trademark Office

An extendable fiber optic cable includes an inner tubular core, a viscous gel received in the tubular core, a plurality of optical fibers suspended in the gel, reinforcing fibers which are braided around the inner core, and an elastomeric outer cover which is received over the reinforcing fibers. The cable is first formed in a straight configuration and then formed into a plurality of coiled segments wherein adjacent coiled segments are wound in alternating directions, i.e. clockwise, counterclockwise, clockwise, etc. Straight segments of wire are provided between the coiled segments wherein the cable is stretchable up to 50% of its relaxed length. The alternating coil segments prevent the cable from twisting and transmitting torque forces to the optical fibers. DTIC

N95-19710# Lawrence Livermore National Lab., Livermore, CA.
PULSEWIDTH-DEPENDENT DAMAGE MEASUREMENTS OF DIELECTRIC MATERIALS
B. C. Stuart, S. Herman, B. W. Shore, and M. D. Perry Jun. 1994 5 p Presented at the Topical Meeting on High Field Interactions and Short Wavelength Generation, Saint Malo, France, 22-24 Aug. 1994
(Contract W-7405-eng-48)
(DE94-018594; UCRL-JC-118115; CONF-940889-3) Avail: CASI HC A01/MF A01

The application of chirped pulse amplification to short-pulse lasers has led to a dramatic increase in the number of high-power, sub-picosecond laser systems. Accordingly, knowledge of the short-pulse damage thresholds of optical components and the scaling of the damage thresholds with pulsewidth has become increasingly important. The development of high energy, (e.g. kilojoule class) short-pulse lasers is contingent on the ability to produce optical components capable of withstanding high fluence nanosecond and femtosecond pulses. In this paper, the authors report on their measurements of the front-surface damage threshold of many different dielectric materials including windows, multilayer mirrors, and diffraction gratings over the pulsewidth range of 0.1 to 3,000 ps. DOE

N95-19732 SRI International Corp., Menlo Park, CA.
IR MATERIALS PRODUCIBILITY Quarterly Technical Report No. 8, 1 May - 31 Aug. 1994
A. Sher, M. A. Berding, and S. Krishnamurthy 1 Sep. 1994 24 p Limited Reproducibility: More than 20% of this document may be affected by microfiche quality
(Contract MDA972-92-C-0053; ARPA Order 8557)
(AD-A284263) Avail: CASI HC A03

The work summarized covers the eighth quarter of a program with a goal that is threefold: first, to study the properties of native point defects in infrared focal-plane array (IRFPA) active and substrate materials; second, to study the properties of native point defects in two classes of photonic materials, the wide-gap II-VI compounds (ZnSe as the prototype for which impurity properties will also be calculated) and the nonlinear optical materials (LiNbO3 as the prototype); the third, to study the properties of HgZnTe as a very-long-wave infrared (VLWIR) detector material. We have continued the refinement of the calculation of the tellurium antisite-mercury vacancy pair in HgCdTe. We find a binding energy of more than 1 eV. We have developed a strategy for calculating the ionization energies of defects in semiconductors, and have tested the strategy on the arsenic antisite in GaAs with good results. We have begun the calculation of the ionization energies in CdTe and ZnSe, and preliminary results are reported. Transport-related properties have been calculated for HgCdTe and HgZnTe and compared with results using the effective mass approximation. DTIC

N95-19862 Phillips Lab., Hanscom AFB, MA.
PROCEEDINGS OF THE 15TH ANNUAL CONFERENCE ON ATMOSPHERIC TRANSMISSION MODELS
Michael L. Hoke and Leonard W. Abreu 18 May 1994 377 p Conference held in Bedford, MA, 2-3 Jun. 1992 Limited Reproducibility: More than 20% of this document may be affected by microfiche quality
(AF Proj. 3054)
(AD-A279919; PL-TR-94-2135; ERP-1149) Avail: Issuing Activity (Defense Technical Information Center (DTIC))

This document contains the viewgraphs and other materials for the 26 papers presented at the 15th Annual Review Conference On Atmospheric Transmission Models held at the Geophysics Directorate, Phillips Laboratory (AFMC), Hanscom AFB, MA. DTIC

N95-18167*# South Dakota State Univ., Brookings, SD. Dept. of Electrical Engineering.
THE DEVELOPMENT OF A FIBER OPTICS COMMUNICATION NETWORK FOR CONTROLLING A MULTIDEGREE-OF-FREEDOM SERPENTINE TRUSS
Alfred S. Andrawis *In* Univ. of Central Florida, NASA/ASEE Summer Faculty Fellowship Program. 1994 Research Reports Oct. 1994 p 1-29 (For primary document see N95-18166 05-80)
Avail: CASI HC A03/MF A04

N95-18969*# Missouri Univ., Rolla, MO. Dept. of Physics.
A COMPARISON BETWEEN USING INCOHERENT OR COHERENT SOURCES TO ALIGN AND TEST AN ADAPTIVE OPTICAL TELESCOPE
Richard Anderson *In* Alabama Univ., Research Reports: 1994 NASA/ASEE Summer Faculty Fellowship Program Oct. 1994 6 p (For primary document see N95-18967 05-80)
Avail: CASI HC A02/MF A03

N95-18984*# Northwest Shoals Community Coll., Phil Campbell, AL. Dept. of Electro-Optics.
SURFACE ROUGHNESS MEASUREMENTS
Thomas G. Howard *In* Alabama Univ., Research Reports: 1994 NASA/ASEE Summer Faculty Fellowship Program Oct. 1994 3 p (For primary document see N95-18967 05-80)
Avail: CASI HC A01/MF A03

N95-18995*# Marquette Univ., Milwaukee, WI. Dept. of Physics.
MANN: A PROGRAM TO TRANSFER DESIGNS FOR DIFFRACTIVE OPTICAL ELEMENTS TO A MANN PHOTOLITHOGRAPHIC MASK GENERATOR

Donald R. Matthys *In* Alabama Univ., Research Reports: 1994 NASA/ASEE Summer Faculty Fellowship Program Oct. 1994 6 p (For primary document see N95-18967 05-80)
Avail: CASI HC A02/MF A03

N95-19006*# Chicago State Univ., Chicago, IL. Dept. of Mathematics and Computer Science.
SCATTERING OF POINT SOURCE ILLUMINATION BY AN ARBITRARY CONFIGURATION
Richard Solakiewicz *In* Alabama Univ., Research Reports: 1994 NASA/ASEE Summer Faculty Fellowship Program Oct. 1994 6 p (For primary document see N95-18967 05-80)
Avail: CASI HC A02/MF A03

N95-19009*# University of the Pacific, Stockton, CA. Dept. of Physics.
PRISM PROJECT OPTICAL INSTRUMENT
Charles R. Taylor *In* Alabama Univ., Research Reports: 1994 NASA/ASEE Summer Faculty Fellowship Program Oct. 1994 6 p (For primary document see N95-18967 05-80)
Avail: CASI HC A02/MF A03

N95-19253# Von Karman Inst. for Fluid Dynamics, Rhode-Saint-Genese (Belgium).
PARTICLE IMAGE VELOCIMETRY: PRINCIPLES, CURRENT APPLICATIONS AND FUTURE PROSPECTS
M. L. Riethmuller *In* AGARD, Wall Interference, Support Interference and Flow Field Measurements Jul. 1994 12 p (For primary document see N95-19251 05-34)
Copyright Avail: CASI HC A03/MF A04

N95-19274# Central Aerohydrodynamics Inst., Zhukovsky (Russia).
OPTICAL SURFACE PRESSURE MEASUREMENTS: ACCURACY AND APPLICATION FIELD EVALUATION
A. Bukov, V. Mosharov, A. Orlov, V. Pesetsky, V. Radchenko, S. Phonov, S. Matyash, M. Kuzmin (Moscow M. V. Lomonosov Inst. of the Technology of Fine Chemicals, USSR.), and N. Sadovskii (Moscow M. V. Lomonosov Inst. of the Technology of Fine Chemicals, USSR.) *In* AGARD, Wall Interference, Support Interference and Flow Field Measurements Jul. 1994 9 p (For primary document see N95-19251 05-34)
Copyright Avail: CASI HC A02/MF A04

75 PLASMA PHYSICS

Includes magnetohydrodynamics and plasma fusion.

For ionospheric plasmas see *46 Geophysics*. For space plasmas see *90 Astrophysics*.

N95-17965 Los Alamos National Lab., NM.
DETECTION OF ALPHA PARTICLES VIA OBSERVATION OF He II LINE EMISSION IN THE LITHIUM PELLET CLOUD DURING DT OPERATION IN TFTR
G. A. Wurden, M. Sasao (National Inst. for Fusion Science, Nagoya, Japan.), and D. K. Mansfield (Princeton Univ., NJ.) 1994 5 p Presented at the 21st European Conference on Controlled Fusion and Plasma Physics, Marseilles, 26 Jun. - 1 Jul. 1994 Limited Reproducibility: More than 20% of this document may be affected by microfiche quality
(Contracts W-7405-eng-36; DE-AC02-76CH-03073)
(DE94-014485; LA-UR-94-2223; CONF-940635-1) Avail: CASI HC A01

The purpose of this diagnostic is to detect alpha particles in DT plasmas via spectroscopy, using injected lithium pellets as a source of charge exchange particles. As of June 1994, we have not seen alpha signals above the bremsstrahlung background via this technique in TFTR DT plasmas. This paper discusses the basis for the measurement, shows existing data, and describes possible actions to improve the measurement attempt on TFTR. Expected core alpha concentrations are of order 10(exp 11) cm(exp -3) during high power neutral beam-heated TFTR supershots. The various charge states in the cloud of a 0.5 km/sec 'high-speed' lithium pellet can provide a dense target for charge exchange of fast alphas born in the DT plasma. By directly observing the light emission from the resulting excited, singly-ionized He(+) particles, we can detect the presence of alphas which have undergone a single charge exchange collision. This light emission will be strongly Doppler-broadened, and a spectral measurement of the n=4 yields 3 visible transition yields the alpha velocity distribution at the pellet radial location. One achieves a tremendous source enhancement over other techniques which rely on low density atomic beams for charge exchange neutrals. Of course, this enhancement does not come for free. When using lithium pellet spectroscopy, the alpha population will only be sampled from regions traversed by the lithium pellet, and only on timescales of less than 1 millisecond duration, corresponding to the pellet lifetime. In addition, enhanced bremsstrahlung light from the pellet cloud may be a serious source of background light. In principle, if the pellet cloud densities are known as a function of plasma radius, one could infer the fast alpha population density with a few centimeter spatial resolution across the same plasma radius. DOE

N95-17969# Los Alamos National Lab., NM.
CONCEPTUAL DESIGN FOR A SCINTILLATING-FIBER NEUTRON DETECTOR FOR FUSION REACTOR PLASMA DIAGNOSTICS
W. C. Sailor, C. W. Barnes, R. E. Chrien, and G. A. Wurden 1994 8 p Presented at the 10th Topical Conference on High-Temperature Plasma Diagnostics, Rochester, NY, 8-12 May 1994
(Contract W-7405-eng-36)
(DE94-014716; LA-UR-94-1505; CONF-940552-12) Avail: CASI HC A02/MF A01

A conceptual design for a 'pointing' neutron detector that is capable of delivering 10(exp 4) -10(exp 5) Hz countrate of T(D,n) events from triton burnup at a deuterium-burning tokamak is described. The detector consists of collimated bundles of scintillating fibers that are separated by metal or polyethylene. These bundles in turn are set into a larger collimator that has some of the bundles set in 'unplugged' holes and others in 'plugged' holes whose countrate difference gives the net countrate. It is computed that the use of a 6 MeV(sub ee) (electron equivalent) discriminator will allow 14-MeV neutron countrates of 2x10(exp 4) Hz in a DD machine or 3 MHz in a DT machine, while effectively rejecting the gamma background. The efficiency-area product for 14-MeV neutrons will be approximatly 0.014 cm(sup 2). The angular resolution is computed to be 4.5(degree) HWHM for a 35 cm long collimator. DOE

N95-18119# General Atomics Co., San Diego, CA.
PROGRESS ON THE MULTIPULSE THOMSON SCATTERING DIAGNOSTIC ON D3-D
R. E. Stockdale, T. N. Carlstrom, C. L. Hsieh, and C. C. Makariou May 1994 17 p Presented at the 10th Topical Conference on High-Temperature Plasma Diagnostics, Rochester, NY, 8-12 May 1994
(Contract DE-AC03-89ER-51114)
(DE94-017515; GA-A-21704; CONF-940552-25) Avail: CASI HC A03/MF A01

The DIII-D Thomson scattering diagnostic, operational since 1990, uses 8 Nd:YAG 20 Hz lasers to measure electron temperature and density profiles (40 spatial points) throughout the plasma discharge. Recent progress has enabled a new set of operating modes to better fulfill varying plasma physics requirements. Custom circuitry for laser control (programmable with 1 micron precision) has successfully replaced a previous scheme which used real-time 68030 software. Two new modes of operation have been demonstrated. Burst Mode is useful to study a transient plasma event: a series of laser pulses axe fired at a rate less than to equal to 10 kHz after an external asynchronous event trigger. Burst Mode is also useful to synchronize the Thomson lasers with other systems, such as an asynchronous Michelson ECE diagnostic scanning near 40 Hz. Group Mode allows a programmed set of lasers to fire simultaneously into the same (65 nanosecond) data acquisition gate. Improved signal/noise then yields smaller statistical errors in the profile results. This provides profile data for lower density plasmas, such as those anticipated during fast wave current drive experiments. Plans for a new CCD-based laser alignment system for position monitoring and feedback control will also be presented. DOE

N95-18353# Dartmouth Coll., Hanover, NH.
NONLINEAR MAGNETOHYDRODYNAMICS
D. C. Montgomery 30 Jul. 1994 13 p
(Contract DE-FG02-85ER-53194)
(DE94-016223; DOE/ER-53194/4) Avail: CASI HC A03/MF A01

Work has continued to focus on resistive, viscous, magnetohydrodynamic

(MHD) steady states that model tokamak configurations. Recent emphasis has been on the subject of plasma rotation, and the stabilizing effects it has on the kind of MHD activity that results when current thresholds are exceeded in non-rotating configurations. The author believes that relatively superficial consequences of the effects of rotation (e.g., the 'velocity shear layer,' which must result when any fluid of whatever nature is rotated in the presence of a material boundary) have been assigned causative effects that do not belong to them, in the presently-dominant perspective on the subject. Output from the author's three-dimensional spectral-method numerical code has shown how rotation may be made to suppress helical deformations of the current channel and paired helical vortices in a supercritical magnetofluid column. A velocity 'shear layer' results if and when there is wall friction. The role of ion parallel viscosity (rather than shear viscosity) in determining stability boundaries in current-carrying magnetofluids is being investigated. A lattice-Boltzmann equation method of computing three-dimensional magnetohydrodynamic toroidal effects is under consideration. DOE

N95-18547# Argonne National Lab., IL.
EROSION OF MELT LAYERS DEVELOPED DURING A PLASMA DISRUPTION
A. Hassanein, A. Konkashbaev (Academy of Sciences, USSR, Moscow, USSR.), and I. Konkashbaev (Academy of Sciences, USSR, Moscow, USSR.) Aug. 1994 5 p Presented at the 18th European Symposium on Fusion Technology, Karlsruhe, Germany, 22-26 Aug. 1994
(Contract W-31-109-eng-38)
(DE94-018362; ANL/TD/CP-82442; CONF-940843-5) Avail: CASI HC A01/MF A01

Material erosion of plasma-facing components during a tokamak disruption is a serious problem that limits reactor operation and economical reactor lifetime. In particular, metallic low-Z components such as Be will be subjected to severe melting during disruptions and edge localized models (ELM's). Loss of the developed melt layer will critically shorten the lifetime of these components, severely contaminate the plasma, and seriously inhibit successful and reliable operation of the reactor. In this study mechanisms responsible for melt-layer loss during a disruption are modeled and evaluated. Implications of melt-layer loss on the performance of metallic facing components in the reactor environment are discussed. DOE

N95-18557 Oak Ridge National Lab., TN.
GLOBAL WAVE MODELING OF ELECTRON INTERACTIONS WITH FAST MAGNETOSONIC WAVES
E. F. Jaeger, D. B. Batchelor, and M. Murakami 1994 5 p Presented at the 10th Topical Conference on Radio Frequency Power in Plasmas, Boston, MA, 1-3 Apr. 1993 Limited Reproducibility: More than 20% of this document may be affected by microfiche quality
(Contract DE-AC05-84OR-21400)
(DE94-018942; CONF-9304112-25) Avail: CASI HC A01

Electron interactions with fast magnetosonic waves are of interest for both direct electron heating and fast-wave current drive (FWCD) in tokamaks. Here the authors apply the full-wave ICRF code PICES to examples of both of these applications. To realistically account for the actual D-shaped magnetic geometry of present-day tokamaks, PICES is interfaced with the 3-D MHD equilibrium code VMEC. Likewise, to correctly model the real toroidal structure of both source and image currents in ICRF current drive antennas, PICES is interfaced with the 2-D recessed antenna impedance code RANT. Both current drive and electron heating by fast waves can be strongly altered through modification of the kappa(sub (parallel))-spectrum by the poloidal magnetic field. A poloidal mode expansion in PICES allows such variations in kappa(sub (parallel)) to be included correctly. In this paper, comparisons are made to observations of the direct electron heating profile on TFTR and to the FWCD efficiency on DIII-D. They also extrapolate to make predictions for future tokamaks such as TPX and ITER. DOE

N95-18885# China Nuclear Information Centre, Beijing (China).
THE EXPERIMENTAL INVESTIGATION OF PLASMA CONFIGURATION IN MM-4U DEVICE
Linzhou Ming (Southwestern Inst. of Physics, Leshan, China.), Guanjun Wu (Southwestern Inst. of Physics, Leshan, China.), Zhicai Li (Southwestern Inst. of Physics, Leshan, China.), Rubin Ye (Southwestern Inst. of Physics, Leshan, China.), Jihai Wang (Southwestern Inst. of Physics, Leshan, China.), Guoping Zhao (Southwestern Inst. of Physics, Leshan, China.), and Liyun Xu (Southwestern Inst. of Physics, Leshan, China.) May 1993 7 p In CHINESE
(DE94-626964; CNIC-00757; SIP-0062) Avail: CASI HC A02/MF A01 (US Sales Only)

The experimental results of axial magnetic field profiles in some mirror ratios are given. The experimental results are in good agreement with the theoretical calculations. The axial plasma potential profiles in four mirror ratios have been measured. It shows that the tandem mirror confinement configuration of barrier-like axisymmetric negative potential can be established in various mirror ratios and the central cell plasma potential absolute value increases with the decreasing of mirror ratio. The measured plasma density profile is similar to that of the potential. The typical values of plasma parameter are as follows: The plasma potential in eastern and western end cells and in the central cell are -126 V, -105 V and -50 V, respectively. The corresponding electron densities are 4 x 10(exp 10) cm(exp -3), 3.6 x 10(exp 10) cm(exp -3) and 2.0 x 10(exp 10) cm(exp -3) and the electro temperature is 43 eV. The measured electron temperature is proportional to the injected electron energy. When the injected electron energy is increased, the plasma potential is dropping and the electron density is increasing. The electron density is proportional to the square magnetic field. The discussion of the above results is also presented. DOE

N95-18886# China Nuclear Information Centre, Beijing (China).
SIMPLIFIED IDEAL MHD NORMAL MODE EQUATIONS FOR TOROIDAL AXISYMMETRIC PLASMAS
Bingren Shi (Southwestern Inst. of Physics, Leshan, China.) Mar. 1993 12 p
(DE94-627004; CNIC-00732; SIP-0058) Avail: CASI HC A03/MF A01 (US Sales Only)

The ideal MHD normal mode equations for general toroidal axisymmetric plasmas can be significantly simplified by properly treating the compressibility term in two limiting cases. The simplified equations, describing the general global modes (the low n, m mode), contain only two scalar functions. For tokamak plasmas, a further simplification, the shear Alfven approximation, is introduced, it makes possible to describe the global mode by a simplified eigenmode equation with only one scalar function. This eigenequation, similar to the reduced tokamak equations widely used in recent literatures, provides and unified way to analyze the kink, Alfven spectrum and MHD TAE (toroidal Alfven eigenmode) modes. DOE

N95-18887# China Nuclear Information Centre, Beijing (China).
STUDY ON HEAT FLUX OF PLASMA SCRAPE-OFF LAYER IN HL-1 TOKAMAK
Guodong Li (Southwestern Inst. of Physics, Leshan, China.), Yuanxian Xu (Southwestern Inst. of Physics, Leshan, China.), and Xiaodong Gong (Southwestern Inst. of Physics, Leshan, China.) May 1993 7 p In CHINESE
(DE94-627009; CNIC-00737; SIP-0059) Avail: CASI HC A02/MF A01 (US Sales Only)

A study of the heat flux of plasma scrape-off layer (SOL) in HL-1 tokamak has been performed by a probe shielded with circular graphite tube. The radial distribution of heat flux was obtained in the ion-drift side and electron-drift side of the SOL. By using thermocouples, the heat load on the graphite tiles of pump limiter head and its non-homogeneous poloidal distribution have been measured. The heat load on the limiter head and on the neutralizer plate of diverter was significantly reduced owing to the puffing at the head of plate. Some performances of the plasma also were improved. DOE

N95-18888 Purdue Univ., West Lafayette, IN. School of Nuclear Engineering.
ENGINEERING CONSIDERATIONS FOR THE SELF-ENERGIZING MAGNETOPLASMADYNAMIC (MPD) - TYPE FUSION PLASMA THRUSTER Final Report, Jul. 1992 - Dec. 1993
Chan K. Choi and Larry T. Cox, Jr. Aug. 1994 98 p Limited Reproducibility: More than 20% of this document may be affected by microfiche quality
(Contract F04611-90-K-0054)
(AD-A283968; PL-TR-94-3037) Avail: CASI HC A05

With a Dense Plasma Focus (DPF) device as the central concept, studies have been done to determine its feasibility as a propulsion system

for space. In this report, past work in the areas of propulsion system code development is discussed, as well as the recent work dealing with stability analysis and scaling laws in the pinch region. A modeling based on a tokamak-like m=O instability relating to the electron drift velocity wavelength is established. Magnetic field and kinetic temperature profiles are calculated based in certain assumptions about the plasma. It is found that the results of the pinch equilibrium profiles agree with the assumed current-squared scaling of kinetic temperature density, and that the total fusion power released from the pinch scales as: Pf Ip(5.4). This is found to correlate well with the reaction rate parameter data for the utilized fuel of deuterium and helium -3. The resulting profile shape for kinetic temperature agrees in form with the proposed modeling. Using the more detailed pinch calculations in the already existent DPF propulsion code, it is found that for optimal performance a current range of 30 to 40 (MA) is needed to obtain results found in earlier work. DTIC

N95-18905 Clemson Univ., SC.
RADIO WAVE HEATING OF THE LOWER IONOSPHERE Ph.D. Thesis
Matthew Jack Freeman 1993 87 p
Avail: Univ. Microfilms Order No. DA9419684

The interaction of high power, high frequency radio waves with the lower ionosphere is becoming an area of considerable theoretical and experimental interest. In particular, significant ohmic heating of the collisional, weakly ionized ionospheric plasma is possible, which can change the absorptive and conductive properties of the plasma in a nonlinear fashion. Precisely controlled heating may have applications to the production of ELF/VLF waves in the ionosphere by the stimulation when inferring the physical parameters of the sources. The necessary generalizations to the standard synchrotron self-Compton theory are presented. Relativistic induced Compton scattering is very sensitive to the number of mildly relativistic electrons in the source, and so may be a useful probe to this portion of the electron energy distribution. Dissert. Abstr.

N95-18906 Auburn Univ., AL.
DETERMINATION OF THE ELECTRON DENSITY AND THE ELECTRON TEMPERATURE IN A HIGH-PRESSURE MICROWAVE DISCHARGE Ph.D. Thesis
Tony Charles Lashley 1994 89 p
Avail: Univ. Microfilms Order No. DA9420252

The electron temperature and electron density have been measured in a helium microwave discharge plasma for operational pressures in the range one to fifty torr. These measurements demonstrate a pressure dependence which indicates there is an optimum pressure region in which there is a maximum average electron density. Radial measurements indicate the presence of a low electron temperature and density region along the axis of the discharge. These observations are used to suggest criteria for the design and use of microwave discharge plasmas at elevated pressures. Dissert. Abstr.

N95-18907 Delaware Univ., Newark, DE.
LATTICE GAS AND LATTICE BOLTZMANN METHODS FOR SIMULATION OF HYDRODYNAMICS AND MAGNETOHYDRODYNAMICS Ph.D. Thesis
Daniel Osvaldo Martinez 1993 165 p
Avail: Univ. Microfilms Order No. DA9419552

Lattice Gas Automata (LGA) methods and their extensions, Lattice Boltzmann (LB) methods, have emerged in recent years as tools for modeling fluid dynamics and other systems described by partial differential equations. These schemes do not attempt to directly solve the equations, but rather to create a dynamics of fictitious particles in a lattice, whose macroscopic behavior corresponds to the Navier-Stokes equations, magneto-hydrodynamics (MHD) equations, or the equations of interest. In this thesis, the general principles are explained for the LGA methods first in the context of incompressible hydrodynamics, and then attempts to model MHD are described. Numerical simulations in the context of MHD are included. Likewise, we discuss the LB approach and describe the sequence of improvements that led to today's efficient models. Effective MHD LB models are also accounted for, along with the calculation of their transport properties. Comparisons of numerical experiments using LB methods and spectral methods that show the accuracy of the LB methods are included. Dissert. Abstr.

N95-19079# Texas Univ., Austin, TX. Inst. for Fusion Studies.
ESTABLISHMENT OF AN INSTITUTE FOR FUSION STUDIES
R. D. Hazeltine Jul. 1994 32 p
(Contract DE-FG05-80ET-53088)
(DE94-017330; DOE/ET-53088/T5) Avail: CASI HC A03/MF A01

The Institute for Fusion Studies is a national center for theoretical fusion plasma physics research. Its purposes are: (1) to conduct research on theoretical questions concerning the achievement of controlled fusion energy by means of magnetic confinement, including both fundamental problems of long-range significance, as well as shorter-term issues; (2) to serve as a national and international center for information exchange by hosting exchange visits, conferences, and workshops; and (3) to train students and postdoctoral research personnel for the fusion energy program and plasma physics research areas. The theoretical research results obtained by the Institute contribute to the progress of nuclear fusion research, whose goal is the development of fusion power as a basic energy source. Close collaborative relationships have been developed with other university and national laboratory fusion groups, both in the US and abroad. In addition to its primary focus on mainstream fusion physics, the Institute is also involved with research in fusion-sidestream fields, such as advanced computing techniques, nonlinear dynamics, space plasmas and astrophysics, statistical mechanics, fluid dynamics, and accelerator physics. Important research discoveries are briefly described. DOE

N95-19092# Texas Univ., Austin, TX. Inst. for Fusion Studies.
ION ORBIT LOSS AND THE POLOIDAL ELECTRIC FIELD IN A TOKAMAK
H. Xiao, R. D. Hazeltine, and P. M. Valanju 29 Jul. 1994 24 p
(Contract DE-FG05-80ET-53088)
(DE94-016860; DOE/ET-53088/666; IFSR-666) Avail: CASI HC A03/MF A01

Monte Carlo simulation studies for ion orbit loss in limiter tokamaks show a poloidal asymmetry in ion loss arising from differences in ion orbit geometry. Since electron loss to the limiter is uniformly distributed because of its tiny orbit width, the nonuniform ion loss could cause a poloidal electric field that would tend to make the ion loss to the limiter more uniform. A simple analytical derivation of this poloidal electric field and a discussion of its effects on movement and transport are also presented. DOE

N95-19201# Sandia National Labs., Albuquerque, NM.
COMPLETE MODE-SET STABILITY ANALYSIS OF MAGNETICALLY INSULATED ION DIODE EQUILIBRIA
S. A. Slutz and R. W. Lemke 1993 4 p Presented at the 10th International Conference on High Power Particle Beams, San Diego, CA, 20-24 Jun. 1994
(Contract DE-AC04-94AL-85000)
(DE94-015275; SAND-93-3812C; CONF-940634-10) Avail: CASI HC A01/MF A01

We present the first analysis of the stability of magnetically insulated ion diodes that is fully relativistic and includes electromagnetic perturbations both parallel and perpendicular to the applied magnetic field. Applying this formalism to a simple diode equilibrium model that neglects velocity shear and density gradients, we find a fast growing mode that has all of the important attributes of the low frequency mode observed in numerical simulations of magnetically insulated ion diodes, which may be a major cause of ion divergence. We identify this mode as a modified two-stream instability. Previous stability analyses indicate a variety of unstable modes, but none of these exhibit the same behavior as the low frequency mode observed in the simulations. In addition, we analyze a realistic diode equilibrium model that includes velocity shear and an electron density profile consistent with that observed in the numerical simulations. We find that the diocotron instability is reduced, but not fully quenched by the extension of the electron sheath to the anode. However, the inclusion of perturbations parallel to the applied magnetic field with a wavelength smaller than the diode height does eliminate growth of this instability. This may explain why the diocotron mode has been observed experimentally with proton sources, but not with LiF, since the turn on of LiF is not uniform. DOE

N95-19241# China Nuclear Information Centre, Beijing (China).
THEORETICAL INVESTIGATION OF MATCHING BETWEEN PLASMA HEATING AND FUELING IN HL-1M MACHINE
Shuyin Guo (Qinghua Univ., China.) 1993 11 p In CHINESE
(DE94-627019; CNIC-00742; SIP-0061) Avail: CASI HC A03/MF A01 (US Sales Only)

In addition to ohmic heating, the auxiliary heating such as ICR, ECR and LHR will be used in HL-1M machine. The pellet injection is considered as a possible method to increase the plasma density. The purpose of this article is to analyse matching problem between heating and fueling. The condition under which the auxiliary heating is effective depends on the plasma density. The plasma density will be changing during pellet injection. The high plasma temperature resulting from the auxiliary heating affects the rate of pellet ablation. There is an optimum choice for pellet size to match the plasma density and temperature. Finally, the permissible size and the injection frequency of the pellet are also given. DOE

N95-19250# Lawrence Livermore National Lab., Livermore, CA.
25-PS NEUTRON DETECTOR FOR MEASURING ICF-TARGET BURN HISTORY
R. A. Lerche, D. W. Phillion, and G. L. Tietbohl 2 May 1994 14 p Presented at the 10th Topical Conference on High-Temperature Plasma Diagnostics, Rochester, NY, 8-12 May 1994
(Contract W-7405-eng-48)
(DE94-016450; UCRL-JC-116183; CONF-940552-21) Avail: CASI HC A03/MF A01

We have developed a fast, sensitive neutron detector for recording the fusion reaction-rate history of inertial-confinement fusion (ICF) experiments. The detector is based on the fast rise-time of a commercial plastic scintillator (BC-422) and has a response less than 25 ps FWHM. A thin piece of scintillator material acts as a neutron-to-light converter. A zoom lens images scintillator light to a high-speed (15 ps) optical streak camera for recording. A retractable nose cone positions the scintillator between 1 and 50 cm from a target. A simultaneously recorded optical fiducial pulse allows the streak camera time base to be calibrated relative to the incident laser power. Burn histories have been measured for deuterium-tritium filled targets with yields ranging between 10(exp 8) and 2 x 10(exp 13) neutrons. DOE

N95-19378# General Atomics Co., San Diego, CA.
DEVELOPMENT OF LITHIUM BEAM EMISSION SPECTROSCOPY AS AN EDGE FLUCTUATION DIAGNOSTIC FOR D3-D
D. M. Thomas May 1994 25 p Presented at the 10th Topical Conference on High-Temperature Plasma Diagnostics, Rochester, NY, 8-12 May 1994
(Contracts DE-AC03-89ER-51114; DE-FG03-90ER-54081)
(DE94-017517; GA-A-21718; CONF-940552-24) Avail: CASI HC A03/MF A01

As part of the D3-D diagnostic complement designed to address L-H transition physics issues, we have developed and commissioned a diagnostic neutral lithium beam and multichannel fluorescence detection system to investigate the edge plasma density and its associated fluctuations. The use of lithium offers several advantages for tokamak edge beam emission spectroscopy (BES) studies, including large excitation cross sections which are relatively insensitive to temperature variation, the availability of the 670.8 nm resonance line well separated from most plasma line emission, and the suitability of modest beam energies and currents to probe even dense H-mode plasmas. These features permit measurements of collisionally induced fluctuations to be obtained with good spatial (less than 1 cm) and temporal (less than 10 microns) resolution. The improvements over previous lithium beam diagnostics which were required to successfully make these measurements in a large, remotely controlled machine environment will be discussed, along with the present state of the diagnostic system and our plans for future improvements of this technique. DOE

N95-19379# General Atomics Co., San Diego, CA.
2-D TOMOGRAPHY WITH BOLOMETRY IN D3-D
A. W. Leonard, W. H. Meyer (Lawrence Livermore National Lab., Livermore, CA.), B. Geer (Lawrence Livermore National Lab., Livermore, CA.), D. M. Behne (Lawrence Livermore National Lab., Livermore, CA.), and D. N. Hill (Lawrence Livermore National Lab., Livermore, CA.) Jul. 1994 13 p Presented at the 10th Topical Conference on High-Temperature Plasma Diagnostics, Rochester, NY, 8-12 May 1994
(Contracts DE-AC03-89ER-51114; W-7405-eng-48)
(DE94-017520; GA-A-21703; CONF-940552-29) Avail: CASI HC A03/MF A01

We have installed a 48-channel platinum-foil bolometer system on DIII-D achieve better spatial and temporal resolution of the radiated power in diverted discharges. Two 24-channel arrays provide complete plasma coverage with optimized views of the divertor. We have measured the divertor radiation profile for a series of radiative divertor and power balance experiments. We observe a rapid change in the magnitude and distribution of divertor radiation with heavy gas puffing. Unfolding the radiation profile with only two views requires us to treat the core and divertor radiation separately. The core radiation is fitted to a function of magnetic flux and is then subtracted from the divertor viewing chords. The divertor profile is then fit to a 2-D spline as a function of magnetic flux and poloidal angle. DOE

N95-19509# Lawrence Livermore National Lab., Livermore, CA.
NOVEL X RAY IMAGING METHODS AT THE NOVA LASER FACILITY
D. Ress, L. B. DaSilva, R. A. London, J. E. Trebes, R. A. Lerche, and D. K. Bradley (Rochester Univ., NY.) Jun. 1994 30 p Presented at the 10th Topical Conference on High-Temperature Plasma Diagnostics, Rochester, NY, 8-12 May 1994
(Contract W-7405-eng-48)
(DE94-016548; UCRL-JC-116820; CONF-940552-20) Avail: CASI HC A03/MF A01

We are pursuing several novel x-ray imaging schemes to measure plasma parameters in inertial-confinement fusion experiments. This paper will review two quite successful approaches, the soft x-ray moire deflectometer, and the annular (ring) coded-aperture microscope. The deflectometer is the newer diagnostic, and this paper will concentrate on this topic. We will describe the operating principles of moire deflectometry, give the motivations for soft x-ray probing, describe the physical apparatus in detail, and present some sample images and results. The ring coded-aperture microscope has been described previously, so here we will only briefly review the principle of the instrument. We will concentrate on the signal-to-noise ratio calculations that motivate the use of annular coded apertures, and describe recent work to predict and measure the resolution of the instrument. DOE

N95-19527# Lawrence Livermore National Lab., Livermore, CA.
THREE-DIMENSIONAL RADIATION TRANSPORT HYDRODYNAMICS
David E. Fyfe (Naval Research Lab., Washington, DC.), Jill P. Dahlburg (Naval Research Lab., Washington, DC.), John H. Gardner (Naval Research Lab., Washington, DC.), and Steven W. Haan Jul. 1994 5 p Presented at the 15th International Conference on the Numerical Simulation of Plasmas, Valley Forge, PA, 7-9 Sep. 1994
(Contract W-7405-eng-48)
(DE94-018337; UCRL-JC-117711; CONF-9409105-3) Avail: CASI HC A01/MF A01

Radiation transport hydrodynamics codes have many applications in high-temperature physics, including the study of laser matter interactions (LMI) with applications ranging from design of high-gain inertial confinement fusion (ICF) pellets to the design and diagnosis of near-term laboratory experiments at such facilities as the NRL Nike KrF Laser Facility and the NOVA laser at LLNL. Realistic LMI simulations offer one of the best means of learning how to control the ablative Rayleigh-Taylor (RT) instability, which is one of the most dangerous hydrodynamic instabilities of laser fusion. We here report the development of the RAD3D-CM radiation transport hydrodynamics code, and the first results from well-resolved multimode simulations of the evolution of the laser-driven, ablative Rayleigh-Taylor instability on planar, plastic targets. RAD3D-CM is a compressible hydrodynamics code which contains the following effects relevant for the simulation of high-temperature plasmas such as ICF-regime RT unstable laser targets: inverse bremsstrahlung laser energy deposition; classical Spitzer thermal conduction; real (table look-up) equation-of-state with either separate or identical electron and ion temperatures; and, multigroup varioable Eddington radiation transport. We are able to simulate a wide range of three-dimensional multimode LMI problems that have hitherto been impossible. Derived from text

N95-19549# National Inst. for Fusion Science, Nagoya (Japan).
DIRECT ENERGY CONVERSION SYSTEM FOR D(3)-He FUSION

Y. Tomita, L. Y. Shu, and H. Momota Nov. 1993 14 p
(DE94-770773; NIFS-252) Avail: CASI HC A03/MF A01

A novel and highly efficient direct energy conversion system is proposed for utilizing D(3)-He fueled fusion. In order to convert kinetic energy of ions, we applied a pair of direct energy conversion systems each of which has a cusp-type DEC and a traveling wave DEC (TWDEC). In a cusp-type DEC, electrons are separated from the escaping ions at the first line-cusp and the energy of thermal ion components is converted at the second cusp DEC. The fusion protons go through the cusp-type DEC and arrive at the TWDEC, which principle is similar to 'LINAC'. The energy of fusion protons is recovered to electricity with an efficiency of more than 70%. These DEC's bring about the high efficient fusion plant. DOE

N95-19552# Lawrence Livermore National Lab., Livermore, CA.
INERTIAL CONFINEMENT FUSION Quarterly Report
1994 49 p
(Contract W-7405-eng-48)
(DE95-000314; UCRL-LR-105821-94-2) Avail: CASI HC A03/MF A01

This issue of the ICF Quarterly Report contains five articles describing recent advances in research in the Inertial Confinement Fusion (ICF) Program at Lawrence Livermore National Laboratory. These articles cover topics in target fabrication and technology, heavy-ion fusion, x ray laser science, and laser science. Titles of the five articles are: production of multi-terawatt laser pulses in Cr:LiSrAlF6; development of short pulse x ray lasers for plasma probing; surface finish of plasma polymer ablator layers; ray and wave optics modeling of laboratory x ray lasers; and a comparison of driver concepts for heavy-ion fusion. Separate abstracts will be prepared for articles from this report. DOE

N95-19690# Air Force Inst. of Tech., Wright-Patterson AFB, OH.
A THREE REGION ANALYSIS OF A BOUNDED PLASMA USING PARTICLE IN CELL AND FLUID TECHNIQUES Ph.D. Thesis
Don F. Nichols Sep. 1994 218 p
(AD-A284826; AFIT/DS/ENP/94-03) Avail: CASI HC A10/MF A03

A detailed collisionless sheath theory and a three-region collisional model of a bounded plasma are presented, and the suitability of the collisional model for analysis of ignited mode thermionic converters is investigated. The sheath theory extends previous analyses to regimes in which the sheath potential and electron temperatures are comparable in magnitude. In all operating regimes typical of an ignited mode thermionic converter, the predicted sheaths extend several mean-free paths. The apparent collisionality of the sheaths prompted development of a collisional, three-region model of the converter plasma. By interfacing particle-in-cell regions (for the sheaths) and fluid regions (for the bulk of the plasma), a time-dependent, wall-to-wall model of the plasma in the inter-electrode space is created. The components of the model are tested and validated against analytic solutions and against one another, then applied to the analysis of an ignited mode thermionic converter. Under ignited mode operating conditions, the electron velocity distribution at the plasma/sheath boundary is found to be inconsistent with that assumed in the model development, and the calculation diverges. The observed distribution is analyzed and a new basis set of distribution functions is suggested that should permit application of the hybrid model to ignited mode thermionic converters. DTIC

N95-19700# California Univ., Los Angeles, CA. Plasma Physics Group.
PROPERTIES OF ALFVEN WAVES WITH TRANSVERSE SCALE ON THE ORDER OF SKIN-DEPTH
G. J. Morales, R. S. Loritsch, and J. E. Maggs Oct. 1994 6 p Presented at the International Conference on Plasma Physics, Foz do Iguaca, Brazil, 31 Oct. - 4 Nov. 1994 Sponsored by ONR
(AD-A285657; PPG-1525) Avail: CASI HC A02/MF A01

It is widely perceived that shear Alfven waves propagate electromagnetic disturbances strictly along the ambient magnetic field. This feature is a consequence of the neglect of the parallel electric field, an approximation appropriate for large perpendicular wavelengths. However, for small transverse scales, the parallel electron currents cannot be neglected. This analytical study examines shear Alfven waves whose scale across the magnetic field is on the order of the electron skin-depth. This physical situation is motivated by the interest in spontaneous filamentation in magnetized plasmas, studies of axial relaxation of transport currents, and models of electron acceleration in space plasmas. At the basic level, this study addresses how a microscopic current channel spreads. DTIC

N95-19837 Brasilia Univ. (Brazil). Dept. of Fisica.
GENERALIZED RELAXATION THEORY AND VORTICES IN PLASMAS
S. R. Oliveira and Toshiki Tajima (Texas Univ., Austin, TX.) Sep. 1994 26 p Limited Reproducibility: More than 20% of this document may be affected by microfiche quality
(Contract DE-FG05-80ET-53088)
(DE95-002615; DOE/ET-53088/672; IFSR-672) Avail: CASI HC A03

The authors present a generalization of the relaxation theory based in the canonical momentum of each species fluid in a multicomponent plasma The generalized helicity, as a topological quantity, has a lifetime larger than the lifetime of the energy. The proposed variational principle suggests vortices structures. They study localized solutions, assuming the existence of a separatrix. Two-dimensional and three-dimensional solutions are studied for an electron-positron-proton plasma. Ideal magnetohydrodynamic (MHD) three-dimensional localized vortices are studied as well. Possible cosmological implications are discussed. DOE

N95-19844 Naval Research Lab., Washington, DC.
ADVANCED CONCEPTS THEORY Final Annual Report, 1993
25 Apr. 1994 109 p Limited Reproducibility: More than 20% of this document may be affected by microfiche quality
(AD-A279212; NRL/MR/6722-94-7460) Avail: Issuing Activity (Defense Technical Information Center (DTIC))

This report details the work of the Radiation Hydrodynamics Branch conducted in FY93 with respect to several critical problems concerning the design and analysis of DECADE z-pinch experiments. Separate sections describe progress in: (1) the evaluation of DECADE's predicted PRS performance; (2) the analysis and scaling of z-pinch experiments using phenomenological turbulence transport parameters in 1-D calculations; (3) the analysis of gas puff nozzle designs and large radius implosion stability; (4) the development of a DECADE transmission line model to study power flow, POS/PRS interactions, and energy coupling to PRS loads in DECADE; (5) the development of diagnostics with which to analyze experimental and theoretical PRS data; and (6) the development of L-shell atomic models. DTIC

N95-19846 Naval Research Lab., Washington, DC.
POWER FLOW AND PRS OPTIMIZATION ON PHOENIX
Robert E. Terry and Frederick L. Cochran 28 Mar. 1994 34 p Limited Reproducibility: More than 20% of this document may be affected by microfiche quality
(AD-A279214; NRL/MR/6720-94-7428) Avail: Issuing Activity (Defense Technical Information Center (DTIC))

The DNA Phoenix program has investigated the power flow in the front end magnetically insulated transmission line (MITL) and PRS load assembly, to identify any losses, and model them, and the optimum injection angle and mass loading for a specific puff gas nozzle assembly. An optimum PRS mass loading can convert about 10-15% of the energy delivered to the front end into load kinetic energy over a range of 4.65 - 5.7 nH of initial PRS loading inductance. Specific kinetic energy per ion tends to fall off monotonically as the PRS length exceeds 4.5 cm. The gas puff optimization investigated nozzle designs which could optimize the uniformity of the implosion through high Mach number and tilting. The best yields for Argon were found at 12 deg for a Mach 4 nozzle, and 7.5 deg for a Mach 5 nozzle. The yield at the optimum tilt angle does not vary strongly with Mach number. DTIC

N95-19847 Naval Research Lab., Washington, DC.
PRS PROJECTIONS FOR DECADE
K. G. Whitney, J. W. Thornhill, J. L. Giuliani, Jr., and J. Davis 25 Apr. 1994 32 p Limited Reproducibility: More than 20% of this document may be affected by microfiche quality
(AD-A279215; NRL/MR/6722-94-7459) Avail: Issuing Activity (Defense Technical Information Center (DTIC))

Two approaches are described for predicting and evaluating the potential range of PRS performance on DECADE. On the one hand, the DECADE generator is represented as a lumped electrical circuit coupled to an inductive PRS load using slug model dynamics for the load. The nonlinearly coupled circuit equations determine the energy transfer from the Marx bank to the

load as a function of the circuit parameters, enabling one to predict the efficiency for converting Marx bank energy into load kinetic energy. Newly experimentally confirmed scaling relations then allow one to predict the conversion fraction of this kinetic energy into K-shell x rays. Both aluminum and titanium should be able to generate in excess of 100 kJ/cm of K-shell radiation based on the DECADE circuit model used in this report. On the other hand, power flow from the Marx generator to the load is taken as a given, and a number of specific issues related to PRS load dynamics are calculated using detailed (non-slug) models of the load MHD dynamics. A number of such issues are discussed. They need to be addressed because of their potential to either degrade or enhance the load yield performance predicted on the basis of kinetic energy and x ray scaling laws alone. These issues also deal with matters of x ray simulation fidelity that will be an important part of DECADE's function. It is argued that the capability to carry out aluminum radiative collapse experiments on DECADE is significantly greater than on existing simulators, and that these experiments may offer a range of opportunity for improving simulation fidelity beyond that offered by kinetic energy scaling alone. This represents a compelling reason for giving DECADE a PRS capability. DTIC

76 SOLID-STATE PHYSICS

Includes superconductivity.

For related information, see also *33 Electronics and Electrical Engineering* and *36 Lasers and Masers.*

N95-17960 Spire Corp., Bedford, MA.
DEFECT REDUCTION AND BACK CHANNEL DEGRADATION IN SIMOX
Technical Report, 31 Aug. 1990 - 30 Sep. 1993
Fereydoon Namavar 1 Aug. 1994 101 p Limited Reproducibility: More than 20% of this document may be affected by microfiche quality
(Contract DNA001-90-C-0080)
(AD-A284231; SPIRE-FR-10131; DNA-TR-93-102) Avail: CASI HC A06

Because of potential back channel leakage problems and parasitic bipolar effects in silicon-on-insulator (SOI) metal-oxide-semiconductor (MOS) devices, especially n-channel MOS devices which must operate in an ionizing radiation environment, it is desirable to produce separation by implantation of oxygen (SIMOX) wafers which have a layer of poor quality silicon near the Si/buried SiO2 interface. Also, for device fabrication these wafers must have low defect, high quality silicon near the wafer surface. We have demonstrated that by Ge implantation and solid phase epitaxy regrowth, the surface region of the Si top layer of the SIMOX wafer is improved and the region adjacent to the buried SiO2 is degraded. N-MOSFET's with and without Ge implantation were fabricated on SIMOX and Si wafers. Our results show that Ge implantation into SIMOX significantly reduced off-state leakage and parasitic bipolar effects. In addition, gate-induced drain leakage of n-MOSFET's was greatly suppressed and the source-to-drain breakdown voltage was improved. All devices were irradiated with 100 krad x-ray at RADC. Our measurements show that for devices fabricated on SIMOX with Ge implantation the off-state leakage current was up to 1000 times less than for devices fabricated on SIMOX without Ge implantation. DTIC

N95-18053# Minnesota Univ., Minneapolis, MN. School of Physics and Astronomy.
TUNNELING AND TRANSPORT IN MESOSCOPIC STRUCTURES
Technical Report, 1 Mar. 1993 - 28 Feb. 1994
Allen M. Goldman 1 Mar. 1994 9 p
(Contract N00014-92-J-1368)
(AD-A283426) Avail: CASI HC A02/MF A01

This program is focused on developing processes for the fabrication of arrays of side-by-side tunneling junctions and single side-by-side junctions. The approach combines the use of electron beam lithography, ion milling, and reactive ion etching to produce structures on Si wafers which can serve as contact shadow masks for low-temperature, with an angled vapor deposition step which is used to complete the array by forming junctions. We have produced shadow masks with 300 A-wide channels at the National Nanofabrication Facility at Cornell. We have configured our deposition system so as to achieve precision alignment of the direction of the vapor stream relative to the array structure, and proceeding with the fabrication and electrical characterization arrays. Electron microscope studies indicate that we have achieved an acceptable level of alignment for the purposes of the project, and low temperature depositions are under way at this writing. DTIC

N95-18064 Los Alamos National Lab., NM.
FABRICATION OF BIAXIALLY ORIENTED YBCO ON (001) BIAXIALLY ORIENTED YTTRIA-STABILIZED-ZIRCONIA ON POLYCRYSTALLINE SUBSTRATES
P. Arendt, S. Foltyn, Xin Di Wu, J. Townsend, C. Adams, M. Hawley, P. Tiwari, M. Maley, J. Willis, and D. Moseley et al 1994 7 p Presented at the Materials Research Society Meeting, Pittsburgh, PA, Apr. 1994 Limited Reproducibility: More than 20% of this document may be affected by microfiche quality
(Contract W-7405-eng-36)
(DE94-014808; LA-UR-94-1614; CONF-9404189-1) Avail: Issuing Activity (Department of Energy (DOE))

Ion-assisted, ion-beam sputter deposition is used to obtain (001) biaxially oriented films of cubic yttria stabilized zirconia (YSZ) on polycrystalline metal substrates. Yttrium barium copper oxide (YBCO) is then heteroepitaxially pulse laser deposited onto the YSZ. Phi scans of the films show the full-width-half maxima of the YSZ (202) and the YBCO (103) reflections to be 14 deg and 10 deg, respectively. Our best dc transport critical current density measurement for the YBCO is 800,000 A/sq cm at 75 K and 0 T. At 75 K, the total dc transport current in a 1 cm wide YBCO film is 23 A. DOE

N95-18122# California Univ., Berkeley. Lawrence Berkeley Lab, CA.
ULTRAFAST NONLINEAR OPTICAL RESPONSE OF FANO RESONANCES IN GALLIUM ARSENIDE UNDER HIGH MAGNETIC FIELD
U. Siegner, M. A. Mycek, and D. S. Chemla May 1994 8 p Presented at the International Quantum Electronics Conference, Anaheim, CA, 8-13 May 1994
(Contract DE-AC03-76SF-00098)
(DE94-018181; LBL-35201; CONF-9405219-6) Avail: CASI HC A02/MF A01

Fano interference results from the coupling between a discrete energy level and a continuum of states whose energies overlap. In the linear absorption spectrum, a Fano resonance manifests itself in an asymmetric lineshape with a minimum at the energy where the contributions of the discrete state and the continuum interfere destructively. Using femtosecond spectroscopy, the authors study for the first time, the dynamics of the coherent emission from Fano resonances and compare it to that from an isolated Lorentzian line. They find that despite the very narrow frequency lineshape, the coupling to the continuum induces an almost instantaneous nonlinear optical response. Experiments are carried out in bulk GaAs, where an applied magnetic field leads to the formation of discrete magneto-exciton states. The higher-order magneto-excitons energetically overlap with the 1-dimensional continua of states with k parallel to the field and Fano resonances are formed. The zero field absorption spectrum of the sample shows that the heavy hole (hh) and light hole (lh) exciton resonances are split due to uniaxial strain. The typical Fano lineshape is clearly observed both for hh and lh magneto-excitons at B = 10T. The temporal behavior of the polarization stimulated from Fano and Lorentzian resonances is studied by transient four-wave-mixing (FWM) experiments with co-circularly polarized 100-fs pulses. DOE

N95-18330# Instituto de Fisica Teorica, Sao Paulo (Brazil).
SU4(SUB L) X U1(SUB N) MODEL FOR THE ELECTROWEAK INTERACTIONS
F. Pisano and V. Pleitez Jan. 1994 12 p
(DE94-626675; IFT-P-003/94) Avail: CASI HC A03/MF A01 (US Sales Only)

Assuming the existence of right-handed neutrinos, an electroweak model based on the gauge symmetry SU4(sub L) x U1(sub N) is considered. We study the neutral currents coupled to all neutral vector bosons present in the theory. There are no flavor changing neutral currents at tree level, coupled with the lightest neutral vector boson. DOE

N95-18373 Selskapet for Industriell og Teknisk Forskning, Trondheim (Norway). Div. of Applied Physics.
SIZE DISTRIBUTION OF ONE-, TWO- AND THREE-DIMENSIONAL VORONOI CELLS
K. Marthinsen 3 Mar. 1994 23 p
(PB94-207008; STF19-A94005) Avail: Issuing Activity (National Technical Information Service (NTIS))

The present report gives a presentation of the different cell size distributions obtained by computer simulations of random Voronoi cell structures in one-, two- and three-dimensional space. The random Voronoi cells are constructed from cell centroids randomly distributed along a string, in the plane and in three-dimensional space, respectively. The size distributions are based on 2-3 x 10(sup 4) cells. For the spacial polyhedra both the distribution of volumes, areas and radii are presented, and the two latter quantities are compared to the distributions of areas and radii from a planar section through the three-dimensional structure, as well as to the corresponding distributions obtained from a pure two-dimensional cell structure. NTIS

N95-18453*# National Aeronautics and Space Administration. Lewis Research Center, Cleveland, OH.
MINORITY-CARRIER LIFETIME IN InP AS A FUNCTION OF LIGHT BIAS
Jane A. Yater, I. Weinberg, Phillip P. Jenkins (NYMA, Inc., Brook Park, OH.), and Geoffrey A. Landis (NYMA, Inc., Brook Park, OH.) Jan. 1995 6 p Presented at the 1st World Conference on Photovoltaic Energy Conversion, Waikoloa, HI, 5-9 Dec. 1994; sponsored by IEEE, PVSEC-Japan, PVSEC-Europe
(RTOP 233-01-OA)
(NASA-TM-106821; E-9363; NAS 1.15:106821) Avail: CASI HC A02/MF A01

Minority-carrier lifetime in InP is studied as a function of doping level and laser intensity using time-resolved photoluminescence. A continuous wave diode laser illuminates bulk InP and acts as a light bias, injecting a steady-state concentration of carriers. A 200 ps laser pulse produces a small transient signal on top of the steady-state luminescence, allowing lifetime to be measured directly as a function of incident intensity. For p-InP, lifetime increases with light bias up to a maximum value. Bulk recombination centers are presumably filled to saturation, allowing minority carriers to live longer. The saturation bias scales with dopant concentration for a particular dopant species. As light bias is increased for n-InP, minority-carrier lifetime increases slightly but then decreases, suggesting radiative recombination as a dominant decay mechanism. Author

N95-18527# Department of the Navy, Washington, DC.
PROCESS FOR FORMING EPITAXIAL BaF2 ON GaAs Patent Application
Francisco Santiago, inventor (to Navy), Tak-Kin Chy, inventor (to Navy), and Michael F. Stumberg, inventor (to Navy) 19 May 1994 15 p
(AD-D016439; US-Patent-Appl-SN-246209; Navy-Case-76233) Avail: CASI HC A03/MF A01

A process for growing single crystal epitaxial BaF2 layers on gallium arsenide substrates by slowly reacting BaF2 vapor with the clean, hot GaAs substrate at 500 to 700 C in high vacuum until a uniform, thin (approx. 12A) layer of reaction product is formed and then vapor depositing BaF2 onto the reaction layer at room temperature to 400 C to form the single crystal, epitaxial BaF2 layer. DTIC

N95-18543 Department of the Navy, Washington, DC.
METHOD OF DOPING SINGLE CRYSTAL DIAMOND FOR ELECTRONIC DEVICES Patent
Lawrence T. Kabacoff, inventor (to Navy) and John Barkyoumb, inventor (to Navy) 29 Mar. 1994 4 p Filed 8 Jul. 1991
(AD-D016267; US-Patent-5,298,106; US-Patent-Appl-SN-726489) Avail: US Patent and Trademark Office

A method of doping diamond by: (1) ion implanting carbon into the diamond to create a damage zone of opaque, nondiamond material; (2) ion implanting a semiconductor dopant material that is a pentavalent donor dopant or a trivalent acceptor dopant into the damage zone of opaque, nondiamond carbon material; (3) melting the opaque, nondiamond carbon material by lased light; and (4) allowing the carbon melt to cool and crystallize homoepitaxially as diamond from the diamond surfaces during which the dopant material is incorporated into the new diamond lattice. DTIC

N95-18559 Department of the Navy, Washington, DC.
METHOD FOR FORMING JOSEPHSON BREAK JUNCTIONS Patent
Ignacio M. Perez, inventor (to Navy) and William R. Scott, inventor (to Navy) 14 Jun. 1994 8 p Filed 17 Sep. 1992
(AD-D016427; US-Patent-5,321,004; US-Patent-Appl-SN-947022; US-Patent-Class-505-329) Avail: US Patent and Trademark Office

A Josephson break junction device suitable for highly sensitive electronic detecting systems is described. A superconductor film such as YBa2Cu3O7 is deposited on a substrate such as a single-crystal MgO. Ice film is fractured across a narrow strip by at least one indentation in the substrate juxtaposed from the strip to form a break junction. A transducer is affixed to the substrate for applying a bending movement to the substrate to regulate the distance across the gap formed at the fracture to produce a Josephson turned junction effect. Alternatively or in addition to the transducer, a bridge of a novel metal is applied across the gap to produce a weak-link junction. DTIC

N95-18627 Department of the Navy, Washington, DC.
METHOD OF FORMING PLATINUM AND PLATINUM SILICIDE SCHOTTKY CONTACTS ON BETA-SILICON CARBIDE Patent
Nicolas A. Papanicolaou, inventor (to Navy) 14 Dec. 1993 5 p Filed 28 Jul. 1992
(AD-D016221; US-Patent-5,270,252; US-Patent-Appl-SN-920738; US-Patent-Class-437-176) Avail: US Patent and Trademark Office

Platinum Schottky contacts remaining stable up to 800 C have been produced. The adhesion of the platinum deposited at slightly elevated temperatures is good. Platinum provides a metallization that is physically rugged and thermally stable. The Schottky contacts are made on B-Silicon carbide. DTIC

N95-18633 Department of the Navy, Washington, DC.
ATOMIC LAYER EPITAXY (ALE) APPARATUS FOR GROWING THIN FILMS OF ELEMENTAL SEMICONDUCTORS Patent
Max N. Yoder, inventor (to Navy) 25 Jan. 1994 16 p Filed 4 Feb. 1993
(AD-D016236; US-Patent-5,281,274; US-Patent-Appl-SN-013386; US-Patent-Class-118-697) Avail: US Patent and Trademark Office

An apparatus for and a method of growing thin films of the elemental semiconductors (group IVB), i.e., silicon, germanium, tin, lead, and, especially diamond, using modified atomic layer epitaxial (ALE) growth techniques are disclosed. In addition, stoichiometric and non-stoichiometric compounds of the group IVB elements are also grown by a variation of the method according to the present invention. The ALE growth of diamond thin films is carried-out, inter alia, by exposing a plurality of diamond or like substrates alternately to a halocarbon reactant gas, e.g., carbon tetrafluoride (CF4), and a hydrocarbon reactant gas, e.g., methane (CH4), at substrate temperatures between 300 and 650 C. DTIC

N95-18650 Sandia National Labs., Albuquerque, NM.
MAGNETO-OPTICAL STUDIES OF COMPOUND SEMICONDUCTORS
E. D. Jones, J. F. Klem, and S. K. Lyo 1994 13 p Presented at the 1994 Conference on Magneto-Optic Materials, Los Alamos, NM, 16 Jun. 1994 Limited Reproducibility: More than 20% of this document may be affected by microfiche quality
(Contract DE-AC04-94AL-85000)
(DE94-018743; SAND-94-2115C; CONF-9406259-1) Avail: CASI HC A03

A simultaneous determination of both the conduction and valence-band dispersion curves (and masses) from a single compound semiconductor quantum-well structure using magnetoluminescence is discussed. Data from InGaAs/GaAs strained-single-quantum wells and GaAs/AlGaAs lattice matched quantum wells are presented. The conduction bands are found to be parabolic for densities approaching densities of 1 (times) 10(exp 12) cm(exp -2). However, the valence bands are highly nonparabolic and strongly affected by heavy-hole light-hole interactions. DOE

N95-18685 California Univ., Santa Barbara, CA. Coll. of Engineering.
HIGH TEMPERATURE STABILITY OF BINARY MICROSTRUCTURES DERIVED FROM LIQUID PRECURSORS Final Report, 15 Dec. 1990 - 30 Jun. 1994
Fred F. Lange 30 Jun. 1994 99 p Limited Reproducibility: More than 20% of this document may be affected by microfiche quality
(Grant AF-AFOSR-0125-91)
(AD-A283960; AFOSR-94-0522TR) Avail: CASI HC A05

This program has emphasized two topics: (1) the crystallization of metastable, solid-solution structures, their partitioning into equilibrium structures and compositions, and the role of the metastable phase and its partitioning on forming unique, nanometer microstructures important to the mechanics of structural ceramics and their composites; and (2) the formation of single crystal thin films via spin coating single crystal substrates with solution precursors. Results for the first topic are now, namely, the discovery that diffusion limited crystallization concepts used in rapid solidification directly applies to precursors that crystallize at low temperatures during heating. This discovery is significant because solid-solutions can be greatly extended relative to high temperature synthesis and processing routes where equilibrium conditions are rapidly achieved and solid-solutions can be severely limited. Extension of solid-solution fields (and thus defect chemistries) in compositional space is important to synthesize now materials with optical and electronic properties controlled by defect chemistry and/or metastable compositions. Results for the second topic have shown that single crystal thin films can be formed on single crystal substrates with spin-on liquid precursors despite large differences in lattice parameters and/or crystal structures. Several mechanisms have been identified for the growth of single crystal thin films which are very different to the well know vapor phase epitaxy mechanisms. DTIC

N95-18908 State Univ. of New York, Buffalo, NY.
HIGH-PRESSURE STUDIES OF DEEP IMPURITIES IN GaAs, ZnSe, AND RELATED LAYERED STRUCTURES Ph.D. Thesis
Ming Li 1993 209 p
Avail: Univ. Microfilms Order No. DA9420185

This thesis contains three parts of experimental works. In the first part, the energy levels of dilute Si and S impurities in GaAs are investigated under pressure up to 45 kbar by means of far infrared laser and photoluminescence spectroscopy using cryogenic diamond-anvil cells. In both samples, the substitutional donors interact strongly with a deep localized state that emerges from resonance with the conduction band at high pressures. For pressures near the interaction regions, the intensity of near band-edge luminescence is observed to dip sharply and then rise with further increase of pressure. Evidence is found in GaAs:Si sample that the 1s-2p(+) absorption undergoes a splitting before being totally quenched above 28 kbar. Variable temperature measurements suggest that this localized state is not subject to large lattice relaxation. The observed behavior of this localized state is consistent with an A(sub 1) symmetry assignment, and a qualitative picture is discussed and compared with previous findings. Dissert. Abstr.

N95-18928 Pennsylvania Univ., Philadelphia, PA.
DISCRETE AND CONTINUUM ELASTIC PROPERTIES OF INTERFACES Ph.D. Thesis
Elliott Solomon Alber 1993 166 p
Avail: Univ. Microfilms Order No. DA9413790

The microstructure of defects in solids, e.g. interfaces, is heterogeneous and, consequently, so are the elastic properties. The complete anisotropic fourth-order tensors of both the discrete and the effective elastic moduli are defined in the interfacial region. To examine the meaning of discrete elastic constants, (1) a piecewise-continuous medium is considered where individual phases occupy the Voronoi polyhedra and have the elastic moduli associated with individual atoms, and (2) the relationship between natural vibrations of the discrete systems and continuum waves is explored. Questions of local energy changes and stability are addressed in terms of continuum properties of the moduli, particularly positive definiteness and strong ellipticity. Comparisons between the atomistic results (exact effective moduli) and those for the continuum analog (bounds) establish the validity of the definition of elastic properties for heterogeneous structures at atomic scales and lead to criteria to assess the stability of a given microstructure. Homogenization of interfacial properties gives heterogeneous transition zone (or interphase) model. Interface phenomena in macrosystems (composites) and microsystems (grain boundaries) is explained by inner layer conditions between homogeneous bulk regions. Dynamical membrane and spring models of the imperfect interfaces are shown to be limiting models (similar to Reuss and Voigt bounding approximations in multiphase composite mechanics) for asymptotic expansions of stress and strain fields, respectively. Asymptotic expansion of both fields (in terms of small parameter h-thickness of the layer) produces mixed-type, exact approximation of the first order in h. Derived models of imperfect interface are used for investigation of interface waves in anisotropic bicrystals and for comparison with corresponding acoustical modes in phonon spectra. Localized interface waves are explained as general inhomogeneous plane waves in subsonic, transonic and supersonic regions of the solid. Velocities for subsonic, transonic and supersonic ranges are calculated by complex variable techniques using Stroh's formalism. The dispersion curves are obtained for each model of imperfect interface. Dispersion at the interface is demonstrated to be the result of dispersive boundary conditions contrary to the dispersion in nonlinear elastic medium. Dissert. Abstr.

N95-19075# Argonne National Lab., IL. Energy Technology Div.
DEFORMATION OF HIGH-TEMPERATURE SUPERCONDUCTORS
K. C. Goretta, J. L. Routbort, D. J. Miller, Nan Chen, A. Dominguez-Rodriguez (Seville Univ., Spain.), M. Jimenez-Melendo (Seville Univ., Spain.), and A. R. DeArellano-Lopez (Seville Univ., Spain.) Aug. 1994 10 p Presented at the Conference on Plastic Deformation of Ceramics, Snowbird, UT, 7-12 Aug. 1994
(Contract W-31-109-eng-38)
(DE94-017085; ANL/ET/CP-83876; CONF-940865-1) Avail: CASI HC A02/MF A01

Of the many families of high-temperature superconductors, only the properties of those discovered prior to 1989, Y-Ba-Cu-O, Tl-Ba(Sr)-Ca-Cu-O, and Bi(Pb)-Sr-Ca-Cu-O, have been studied extensively. Deformation tests have been performed on YBa2Cu3O(x) (Y-123), YBa2Cu4O(x) (Y-124), TlBa2Ca2Cu3O(x) (Bi-2223). The tests have revealed that plasticity is generally limited in these compounds and that the rate-controlling diffusional kinetics for creep are very slow. Nevertheless, hot forming has proved to be quite successful for fabrication of bulk high-temperature superconductors, so long as deformation rates are low or large hydrostatic stresses are applied. Steady-state creep data have proved to be useful in designing optimal heat treatments for superconductors and in support of more-fundamental diffusion experiments. The high-temperature superconductors are highly complex oxides, and it is a challenge to understand their deformation responses. In this paper, results of interest and operant creep mechanisms will be reviewed. DOE

N95-19091# Brookhaven National Lab., Upton, NY.
CRYSTALLINE BEAMS: THE STRING
A. F. Haffmans, D. Maletic, and A. G. Ruggiero 30 Apr. 1994 23 p
(Contract DE-AC02-76CH-00016)
(DE94-016806; BNL-60619) Avail: CASI HC A03/MF A01

The authors study the possibility of storing a string of charged particles in a magnetic ring. They define the equilibrium configuration, and examine the confinement conditions. Subsequent, they derive the transfer matrix for motion through a drift, a quadrupole, and a dipole. They finally study the stability of the string as the space-charge force is increased. DOE

N95-19094# Argonne National Lab., IL.
DEFORMATION OF NONSTOICHIOMETRIC CuO POLYCRYSTALS
M. A. Boling-Risser, K. C. Goretta, and J. L. Routbort Jul. 1994 10 p Presented at the Conference on Plastic Deformation of Ceramics, Snowbird, UT, 7-12 Aug. 1994
(Contract W-31-109-eng-38)
(DE94-016907; ANL/ET/CP-82163; CONF-940865-2) Avail: CASI HC A02/MF A01

The current interest in fabrication methods for high temperature superconductors has fostered heightened interest in the precursor materials. It has been shown that the reaction kinetics for formation of Bi2Sr2CaCu2O(x), (Bi,Pb)(2)Sr2Ca2Cu3O(x) and YBa2Cu3O(x) are related to the copper oxide precursor through both the size of the starting powder and the oxidation state, with finer CuO powders reacting faster. Many proposed fabrication methods include a high temperature mechanical working step during the reaction process. However, little is known about the diffusional and mechanical properties of CuO at the fabrication temperatures

of interest. The literature indicates only that the electrical conductivity of CuO is independent of the oxygen partial pressure PO2. Therefore, only intrinsic ionization occurs for CuO. Thus, for a given temperature, the concentrations of electrons and holes are fixed. In this study, compression creep was employed to shed light upon the diffusion of rate-controlling defects in nonstoichiometric CuO. Tests were performed on polycrystalline samples over a range of temperature (T), PO2, and strain rate (epsilon). Data were analyzed with standard equations for steady-state creep. Electron microscopy was used in conjunction with the data analysis to identify the operative creep mechanisms. These results for CuO will be contrasted with previous work performed on another copper oxide compound, Cu2O. DOE

N95-19113# Argonne National Lab., IL.
BRAGG TRANSMISSION PHASE PLATES FOR THE PRODUCTION OF CIRCULARLY POLARIZED X-RAYS
J. C. Lang and G. Srajer 1994 12 p Presented at the International Meeting on Synchrotron Radiation Instrumentation, Stony Brook, NY, 18-22 Jul. 1994
(Contract W-31-109-eng-38)
(DE94-017072; ANL/XFD/CP-82781; CONF-940714-15) Avail: CASI HC A03/MF A01

A thin-crystal Si (400) Bragg transmission x-ray phase plate has been constructed for the production of 5 to 12 keV circularly polarized x-rays. Using multiple beam diffraction from a GaAs crystal, a direct measurement of the degree of circular polarization as a function of off-Bragg position was made. These measurements indicated nearly complete circular polarization ((vert bar)P(sub c)(vert bar) (ge) 0.95) and full helicity reversal on opposite sides of the rocking curve. DOE

N95-19122 Department of the Navy, Washington, DC.
GRADED BANDGAP SEMICONDUCTOR DEVICE FOR REAL-TIME IMAGING Patent
Veerendra K. Mathur, inventor (to Navy) 6 Sep. 1994 5 p Filed 15 Apr. 1991
(AD-D016543; US-Patent-5,345,093; US-Patent-Appl-SN-687603; US-Patent-Class-257-80) Avail: US Patent and Trademark Office

Spectral shift between different wavelength spectra by restricted narrow bandgap absorption of incident radiation at one location on a semiconductor body, under electrical bias causing release of radiation at another emission location as a result of radiative electron-hole recombination. The semiconductor body is a graded bandgap establishing composition of two selected compounds alloyed to a variable, position-dependent degree between the respective radiation and emission locations at which the respective narrow and wide bandgap properties of the compounds prevail. DTIC

N95-19235# Sandia National Labs., Albuquerque, NM.
OPTICAL DETERMINATION OF CONDUCTION AND VALENCE-BAND DISPERSION CURVES IN STRAINED SINGLE-QUANTUM WELLS
E. D. Jones, L. R. Dawson, J. F. Klem, S. K. Lyo, D. Heiman (Massachusetts Inst. of Tech., Cambridge.), and X. C. Liu (Massachusetts Inst. of Tech., Cambridge.) 1994 5 p Presented at the 22nd International Conference on Physics of Semiconductors, Vancouver, British Columbia, 15-19 Aug. 1994
(Contract DE-AC04-94AL-85000)
(DE94-018892; SAND-94-1976C; CONF-9408155-5) Avail: CASI HC A01/MF A01

Conduction and valence-band dispersion curves determined by magnetoluminescence are presented for n-type InGaAs/GaAs strained-single-quantum well structures. The magnetic field range was 0 to 30 tesla, and the temperature varied between 4.2 and 77.4 K. DOE

N95-19242# Instituto de Pesquisas Energeticas e Nucleares, Sao Paulo (Brazil).
STUDY OF THE FERRIMAGNETIC AND PARAMAGNETIC PHASES OF MAGNETITE MEASURED BY MULTIPLE NEUTRON DIFFRACTION Ph.D. Thesis [ESTUDO DAS FASES FERRI- E PARAMAGNETICA DA MAGNETITA MEDIDAS COM DIFRACAO MULTIPLA DE NEUTRONS]
V. L. Mazzocchi 1992 137 p In PORTUGESE
(DE94-627031; INIS-BR-3332) Avail: CASI HC A07/MF A02 (US Sales Only)

Structural parameters of the ferrimagnetic and paramagnetic phases of magnetite have been refined from neutron multiple diffraction data. Experimental multiple diffraction patterns used in the refinement, were obtained by measuring the 111 primary reflection of a natural single crystal of this compound, at room temperature for the ferrimagnetic phase and 703(sup 0) C for the paramagnetic phase. Corresponding theoretical patterns for both phases have been calculated by the program MULTI which uses the iterative method for the intensity calculations in neutron multiple diffraction. In this method intensities are calculated as Taylor series expansions summed up to an order sufficient for a good approximation. A step by step process has been used in the refinements according to the parameter-shift method. Both isotropic and anisotropic thermal parameters were used in the calculation of the temperature factor. DOE

N95-19511# Arizona State Univ., Tempe, AZ. Center for Solid State Science.
HETEROEPITAXY OF TERNARY SiGeC ALLOYS ON Si FOR BIPOLAR TRANSISTORS Final Report
James W. Mayer 14 Jul. 1994 12 p
(Contract F49620-93-C-0022)
(AD-A285317; AFOSR-94-0629TR) Avail: CASI HC A03/MF A01

The final report covers: (1) the development of synthetic methods and detailed phase and compositional characterization of our cubic SiC-GeC solid solutions and diamond structured SiGeC thin films; (2) our preliminary findings on bandgap measurements; and (3) the development of a novel technique for in situ observation of SiGeC CVD in an environmental electron microscope. We used this technique to deposit films that are lattice matched to Silicon. The work was carried out in the Chemical Vapor Deposition Laboratory (by graduate student Michael Todd, postdoctoral research associate Philippe Bonneau, and Professor John Kouvetakis) and the Ion Beam Facility (Barry Wilkens), with assistance from the staff of the High Resolution Electron Microscopy Group (Dr. Renu Sharma, and Professor David Smith) at Arizona State University. Vibrational characterization and bandgap studies were carried out by Nigel Cave at Motorola Phoenix. DTIC

N95-19541# Oregon Univ., Eugene, OR.
MICROSCOPIC ORIGINS OF METASTABLE EFFECTS IN a-Si:H AND DEEP DEFECT CHARACTERIZATION IN a-Si,Ge:H ALLOYS
J. D. Cohen Sep. 1994 45 p Prepared for National Renewable Energy Lab., Golden, CO
(Contract DE-AC36-83CH-10093)
(DE94-011887; NREL/TP-451-7163) Avail: CASI HC A03/MF A01

This research supported by NREL Subcontract XG-1-10063-1 over the past three years has involved, first of all, a fairly complete characterization of a two series of a-Si(1-x)Ge(x):H samples: a series of 9 films grown at the University of Delaware by the photo-CVD method (for 0.29 less than or equal to x less than or equal to 0.62) and series of 6 films grown at U.S.S.C. by the glow discharge method (for 0.20 less than or equal to x less than or equal to 0.50). Both these series of samples seem to represent what is close to the 'state-of-the-art' in current a-Si,Ge:H alloys. The authors detailed comparison of the properties of the glow discharge material with the photo-CVD samples show remarkable similarities rather than significant differences. In particular, measurements of these samples: (1) allowed the assignment of defect energy levels from a detailed analysis of transient sub-band-gap photocapacitance and photocurrent spectra. (2) The authors found the density of deep defects to increase exponentially with the germanium content. (3) The authors found that the trapping lifetimes related (mu)(tau) products for holes decrease in direct proportion to the density of midgap defects in these samples, at least up to Ge fractions of 50at.%. (4) The authors have also made significant progress toward identifying both the optical and thermal defect transitions in the a-Si,Ge:H alloys. DOE

N95-19569# California Univ., Berkeley. Lawrence Berkeley Lab, CA.
ELECTRONIC STRUCTURE OF C60 FULLERITES AND NANOTUBES
S. G. Louie May 1994 6 p Presented at the 1994 International Winterschool on Electronic Properties of Novel Materials, Kirchberg/Tirol, Austria, 5-21 Mar. 1994
(Contract DE-AC03-76SF-00098)
(DE95-000784; LBL-35673; CONF-9403164-1) Avail: CASI HC A02/MF A01

The authors present results on the electron excitation energies of solid C60 calculated using a first-principles quasiparticle theory. The effects of electron correlations and molecular orientational disorders are included. The single-particle properties of solid C60 are found to be well described in a quasiparticle band picture with orientation disorders. Electron-hole interactions are shown to be very strong in optical processes resulting in Frenkel excitons and sizable difference between the optical and photoemission gaps. The electronic and structural properties of carbon and other nanotubes are also investigated. Total energy results predict that the tubules are stable with respect to the formation of strips down to very small radii. Hybridization of the (sigma)(sup *) and (pi)(sup *) states is shown to be as important as band-folding effects in determining the metallicity of small radius tubules. DOE

N95-19585# California Univ., Berkeley. Lawrence Berkeley Lab, CA.
DEEP LEVELS IN AgGaSe2
I. H. Choi and P. Y. Yu Aug. 1994 10 p Presented at the 6th International Conference on High Pressures in Semiconductor Physics, Vancouver, British Columbia, 22-24 Aug. 1994
(Contract DE-AC03-76SF-00098)
(DE94-018209; LBL-35942; CONF-940846-2) Avail: CASI HC A02/MF A01

The photoluminescence spectra of AgGaSe2 obtained at 77 K is reported. Two emission peaks have been observed and their pressure dependence studied. One of these peaks has been identified with emission involving one of the two deep level peak D(sub 1) and D(sub 2) observed previously in absorption measurement (App. Phys. Lett. 64,1717 (1994)). A simple model for the capture of carriers into these deep levels has been proposed. DOE

N95-19586# California Univ., Berkeley. Lawrence Berkeley Lab, CA.
ENERGIES OF X CONDUCTION BAND MINIMA IN DISORDERED AND ORDERED GaInP2 ALLOYS
K. Uchida (California Univ., Berkeley, CA.), P. Y. Yu, and E. R. Weber Jul. 1994 4 p Presented at the 22d International Conference on Physics of Semiconductors, Vancouver, British Columbia, 15-19 Aug. 1994
(Contract DE-AC03-76SF-00098)
(DE94-018211; LBL-35941; CONF-9408155-1) Avail: CASI HC A01/MF A01

A pressure-induced change from a direct bandgap to an indirect bandgap semiconductor has been observed in both partially ordered and disordered GaInP2. By extrapolating back to ambient pressure the indirect Gamma-X band gap energy has been deduced. It was found that the Gamma-X conduction band separation remains almost constant between the ordered and disordered phases. A phenomenological model is proposed to explains this result. DOE

N95-19598# Neocera, Inc., College Park, MD.
HIGH TEMPERATURE SUPERCONDUCTOR (HTS) SUPERCONDUCTING QUANTUM INTERFERENCE DEVICE (SQUID) MICROSCOPE Monthly Progress Report No. 1
21 Oct. 1994 2 p
(Contract N00014-94-C-0120)
(AD-A285875) Avail: CASI HC A01/MF A01

The goal of this SBIR Phase 1 project is to establish the feasibility of designing a High Temperature Superconductor (HTS) Superconducting QUantum Interference Device (SQUID) microscope in order to detect defects, and verify customizations and repairs in MCM substrates. The overall goal of this SBIR program is to market an HTS SQUID microscope dedicated to the inspection of MCM substrates in a manufacturing environment. Author (DTIC)

N95-19608# Los Alamos National Lab., NM.
DEVELOPMENT OF MATERIALS FOR HIGH TEMPERATURE SUPERCONDUCTOR JOSEPHSON JUNCTIONS
R. J. Houlton, D. W. Reagor, M. E. Hawley, K. N. Springer, Q. X. Jia, C. B. Mombourquette, F. H. Garzon, and X. D. Wu 1994 5 p Presented at the Applied Superconductivity Conference, Boston, MA, 16-21 Oct. 1994
(Contract W-7405-eng-36)
(DE95-000896; LA-UR-94-3080; CONF-941013-1) Avail: CASI HC A01/MF A01

We have conducted a systematic optimization of deposition parameters for fabrication of multilayered oxide films to be used in the development of high temperature superconducting SNS Functions. These films were deposited by off-axis sputtering using a custom fabricated multi-gun planar magnetron system. Each material and the various combinations of materials were optimized for epitaxial lattice match, crystal quality, film uniformity, electrical properties, and surface microstructure. In addition to the standard procedures commonly used to sputter deposit epitaxial oxide films, a variety of insitu and exsitu procedures were used to produce high quality multilayer devices, including varying the nucleation temperature from the actual film growth temperature, location of the substrate during the deposition process, constant rotation of the substrate, and timing of the oxygen anneal. The unprocessed films and devices in process were characterized with Atomic Force Microscopy and Scanning Tunneling Microscopy as well as other common materials characterization techniques. Completed multilayer devices were patterned and packaged for electrical characterization. Relation between material properties and electrical characteristics is discussed. DOE

N95-19615# California Univ., Berkeley. Lawrence Berkeley Lab, CA.
PHYSICS WITH ISOTOPICALLY CONTROLLED SEMICONDUCTORS
E. E. Haller Aug. 1994 8 p Presented at the 22d International Conference on Physics of Semiconductors, Vancouver, British Columbia, 15-19 Aug. 1994
(Contract DE-AC03-76SF-00098)
(DE95-000789; LBL-35356; CONF-9408155-7) Avail: CASI HC A02/MF A01

Control of the isotopic composition of semiconductors offers a wide range of new scientific opportunities. In this paper a number of recent results obtained with isotopically pure as well as deliberately mixed diamond and Ge bulk single crystals and Ge isotope superlattices will be reviewed. Isotopic composition affects several properties such as phonon energies, bandstructure and lattice constant in subtle but theoretically well understood ways. Large effects are observed for thermal conductivity, local vibrational modes of impurities and after neutron transmutation doping (NTD). Several experiments which could profit greatly from isotope control are proposed. DOE

N95-19620# Los Alamos National Lab., NM.
PIEZOELECTRIC EFFECTS IN DOUBLE BARRIER RESONANT TUNNELING STRUCTURES
L. Cong (Minnesota Univ., Minneapolis, MN.), J. D. Albrecht (Minnesota Univ., Minneapolis, MN.), M. I. Nathan (Minnesota Univ., Minneapolis, MN.), P. P. Ruden (Minnesota Univ., Minneapolis, MN.), and D. L. Smith 1994 5 p Presented at the 22nd International Conference on Physics of Semiconductors, Vancouver, British Columbia, 15-19 Aug. 1994
(Contract W-7405-eng-36)
(DE95-000850; LA-UR-94-2984; CONF-9408155-8) Avail: CASI HC A01/MF A01

It is shown that piezoelectric effects can give rise to internal electric fields that modify the conventional current vs. voltage characteristics of 3-5 semiconductor double barrier resonant tunneling devices, if suitable stresses are applied. We measured current vs. voltage characteristics of symmetric, (001)-oriented AlAs/GaAs/AlAs double barrier structures as a function of external stress. Uniaxial stress was applied parallel to the (110), the (110), and the (001) directions. In order to understand the experimental results we calculated the current vs. voltage characteristics of resonant tunneling structures under uniaxial stress, including pressure effects on the band alignment and the effects associated with the piezoelectric nature of the constituent materials. Stresses along the (110) or (110 parallel) directions give rise to polarization charges at the interfaces, due to differences in the piezoelectric constants of the materials. The resulting internal electric fields are found to modulate the 1-5 characteristics, in good agreement with our experimental data. DOE

N95-19621# Los Alamos National Lab., NM.
WENTZEL-BARDEEN SINGULARITY IN COUPLED LUTTINGER LIQUIDS: TRANSPORT PROPERTIES
T. Martin 26 Aug. 1994 15 p Presented at the Quantum Complexity in Mesoscopic Systems, Los Alamos, NM, 16-20 May 1994
(Contract W-7405-eng-36)
(DE95-000856; LA-UR-94-3148; CONF-9405204-2) Avail: CASI HC A03/MF A01

The recent progress on 1 D interacting electrons systems and their applications to study the transport properties of quasi one dimensional wires is reviewed. We focus on strongly correlated electrons coupled to low energy acoustic phonons in one dimension. The exponents of various response functions are calculated, and their striking sensitivity to the Wentzel-Bardeen singularity is discussed. For the Hubbard model coupled to phonons the equivalent of a phase diagram is established. By increasing the filling factor towards half filling the WB singularity is approached. This in turn suppresses antiferromagnetic fluctuations and drives the system towards the superconducting regime, via a new intermediate (metallic) phase. The implications of this phenomenon on the transport properties of an ideal wire as well as the properties of a wire with weak or strong scattering are analyzed in a perturbative renormalization group calculation. This allows to recover the three regimes predicted from the divergence criteria of the response functions. DOE

N95-19697# Duke Univ., Durham, NC. Dept. of Mechanical Engineering and Materials Science.

INVESTIGATION OF SUPERLATTICE DISORDERING AND DIFFUSION MECHANISMS IN GaAs Final Report

T. Y. Tan and U. Gosele 8 Aug. 1994 15 p

(Contract DAAL03-89-K-0119)

(AD-A284847; P-28297-EL) Avail: CASI HC A03/MF A01

Accomplishment of research conducted under support of contract DAAL03-89-K-0119 is reported. A total of six categories of studies, designated for convenience, have been performed. The first five categories of studies concern the point defects and diffusion mechanisms of elements occupying the group 3 sublattice of GaAs and/or AlAs/GaAs superlattice materials, and one category of studies concerns the group V sublattice acceptor carbon in AlAs/GaAs superlattices. Our knowledge of point defects and diffusion mechanisms of elements occupying the group 3 sublattice of GaAs and/or AlAs/GaAs superlattice materials have now become substantially complete in the sense that interpretations of almost all experimental results are self-consistent and mutually-consistent. DTIC

N95-19713# University of Southern California, Los Angeles, CA. Dept. of Materials Science and Engineering.

MICROSTRUCTURE AND CRYSTAL DEFECTS IN PEROVSKITE CRYSTALS WITH A-SITE CATION ORDERING Final Technical Report, 1 Jun. 1990 - 31 May 1994

Edward Goo 26 Aug. 1994 88 p

(Contract N00014-90-J-1900)

(AD-A284261) Avail: CASI HC A05/MF A01

Microstructure of ordered A-site perovskites has been studied by transmission electron microscopy and electron diffraction. Determination of the diffuseness of the ferroelectric phase transition as a function of temperature allows the diameter of the microregions (Kanzig regions) to be determined. DTIC

N95-19715# Air Force Inst. of Tech., Wright-Patterson AFB, OH.

THE OPTICAL EMISSION AND ABSORPTION PROPERTIES OF SILICON-GERMANIUM SUPERLATTICE STRUCTURES GROWN ON NON-CONVENTIONAL SILICON SUBSTRATE ORIENTATION Ph.D. Thesis

Theodore L. Kreifels Aug. 1994 187 p

(AD-A284852; AFIT/DS/ENP/94-04) Avail: CASI HC A09/MF A02

Optical emission and absorption properties of Si(1-x)Ge(x)/Si superlattices grown on (100), (110), and (111) Si substrates were investigated to determine the optimal growth conditions for these structures to be used as infrared detectors. Fully-strained Si(1-x)Ge(x)/Si superlattices were grown by molecular beam epitaxy (MBE) and examined using low-temperature photoluminescence (PL) to identify no-phonon and phonon-replica interband transitions across the alloy bandgap. Phonon-resolved emission was most intense for undoped quantum wells grown at 710 C for all three silicon orientations. Room temperature absorption measurements were conducted on (100) and (110) Si(1-x)Ge(x)/Si superlattices using Fourier transform spectroscopy while varying incident electric field polarization. Strong intersubband absorption was observed at 7.8 micrometer from a sample composed of 15 quantum wells of 40 A Si(0.8)Ge(0.2) separated by 300 A of Si grown on (100) Si by MBE at 550 C. Valence band wells were doped 5 x 10(exp 19)/cu cm with boron. This transition, identified as HH1 (reversible transition) HH2, exhibited strong polarization dependence according to (100) Si selection rules. No subband transitions were observed on similar (110) Si(1-x)Ge(x)/Si superlattices ranging in boron dopant concentration from 1-8 x 1O(exp 19)/cu cm. Selection rules for (110) Si indicate an HHI (reversible transition) LH2 transition is allowed within the transmission bandpass of the experimental apparatus at both parallel and normal incident electric field polarizations; however, this peak was most likely masked by free-carrier absorption which dominated the spectrum. Intersubband absorption transitions were observed only for doped superlattices grown at 550 C. DTIC

N95-19724# Argonne National Lab., IL.

MASSIVELY PARALLEL FULL CONFIGURATION INTERACTION. BENCHMARK ELECTRONIC STRUCTURE CALCULATIONS ON THE INTEL TOUCHSTONE DELTA

R. J. Harrison and E. A. Stahlberg (Pacific Northwest Lab., Richland, WA.) 1994 34 p

(Contracts W-31-109-eng-38; DE-AC06-76RL-01830)

(DE95-001064; ANL/CHM/PP-76079) Avail: CASI HC A03/MF A01

We describe an implementation of the benchmark ab initio electronic structure full configuration interaction model on the Intel Touchstone Delta. Its performance is demonstrated with several calculations, the largest of which (95 million configurations, 418 million determinants) is the largest full-CI calculation yet completed. The feasibility of calculations with over one billion configurations is discussed. A sustained computation rate in excess of 4 GFLOP/s on 512 processors is achieved, with an average aggregate communication rate of 155 Mbytes/s. Data-compression techniques and a modified diagonalization method were required to minimize I/O. The object-oriented design has increased portability and provides the distinction between local and non-local data essential for use of a distributed-data model. DOE

N95-19737 Boston Univ., MA. Dept. of Electrical Computer and Systems Engineering.

GROWTH AND DOPING OF Al(x)Ga(1-x)N FILMS BY ELECTRON CYCLOTRON RESONANCE ASSISTED MOLECULAR BEAM EPITAXY Final Report, 1 May 1992 - 30 Apr. 1994

Theodore D. Moustakas 31 Aug. 1994 109 p Limited Reproducibility: More than 20% of this document may be affected by microfiche quality

(AD-A284838) Avail: CASI HC A06

The work focused on the heteroepitaxial growth, doping, and structural and optoelectronic characterization of GaN and AlN films by the method of electron cyclotron resonance microwave plasma-assisted molecular beam epitaxy (ECR-MBE). The effect of charged species in the ECR discharge in the growth and properties of the films was investigated. Conditions were identified to grow atomically smooth films (layer-by-layer growth) in semi-insulating form (p = 10(exp 12) ohms x cm). Such films were doped p- and n-type with Mg and Si respectively at the level of 10(exp 19)/cu cm. Reactive ion etching and metallic contacts to GaN were developed. From these studies we concluded that surface states are not present in the gap of GaN and thus dislocation should not effect the device performance. The role of hydrogen in the doping of GaN was investigated and p-n junction LED's were fabricated and tested. The defects in these materials were investigated by transport, photoluminescence, and optical studies. DTIC

N95-19738# Stanford Univ., CA.

MEGA-SCALE SIMULATION OF MULTI-LAYER DEVICES: FORMULATION, KINETICS, AND VISUALIZATION Final Report, 1 Jun. 1991 - 31 May 1994

Robert W. Dutton 28 Jul. 1994 98 p

(Contract DAAL03-91-G-0152)

(AD-A284848; SU-P-28297-EL) Avail: CASI HC A05/MF A02

A new energy transport model including both carrier and lattice temperatures has been developed and implemented in PISCES 2ET. Major capabilities in physical models for compound semiconductor devices include: heterojunction interfaces, deep level trapping, and new mobility models. Applications of PISCES 2ET in the modeling of GaAs MESFET sidegating and electronic effects in light-emitting structures have been achieved. The GaAs MESFET modeling of dc and ac effects have been confirmed experimentally at Stanford and in collaboration with industry. The LED and vertical cavity laser modeling is being applied by Hewlett-Packard in both their research laboratories and product divisions. Algorithms developed for

improved accuracy and efficiency in device modeling include: ac analysis for microwave devices, multiprocessor direct solvers, and massively parallel iterative solvers. Supported under the high-performance computing (HPC) initiative, a prototype version of PISCES-MEP running on Intel, Thinking Machines, and IBM parallel machines has demonstrated order-of-magnitude speed enhancements compared to the single processor version. The parallel iterative solver in the STRIDE 3D code has solved device problems with 15 million equations in 20 minutes on a 520 processor Intel machine. A mixed-mode analysis capability that couples PISCES and SPICE has been demonstrated and applied to SRAM and OEIC applications. DTIC

N95-19806 Duke Univ., Durham, NC. Dept. of Chemistry.
SYNTHESIS AND CHARACTERIZATION OF A NEUTRAL SIX-COORDINATE TRIS-ADDUCT OF AN INDIUM(3) TRIHALIDE. X RAY CRYSTAL STRUCTURE OF InCl3(THF)3
Richard L. Wells, Shreyas S. Kher, Ryan A. Baldwin, and Peter S. White 5 May 1994 14 p Limited Reproducibility: More than 20% of this document may be affected by microfiche quality
(Contract N00014-89-J-1545)
(AD-A279169; DU/DC/TR-41) Avail: Issuing Activity (Defense Technical Information Center (DTIC))

The reaction of InCl3 with excess THF afforded the adduct InCl3(THF)3 in a good yield (77.1% based on InCl3), and the X ray crystal structure shows it to be a hexa-coordinated tris-adduct of indium(III) chloride. The crystal structure consists of discrete monomeric units with no abnormally short intermolecular separations. The geometry about the indium atom approximates to octahedral with the three chlorine atoms (mean In-Cl = 2.422 A) and the oxygen atoms of each THF molecule (mean In-O = 2.254 A) residing in the meridional conformation. Crystals of InCl3(THF)3 belong to the monoclinic space group P 2(sub 1)/c with unit cell parameters a = 8.1863(2)A, b = 12.5141(2) A, c =16.815(4) A, Beta = 93.84(4) deg, V = 1718.8(7) A3 for Z = 4. Full-matrix least-squares refinement based on 1603 reflections with I (greater than) 2.5(sigma) (I) converged at R(sub w) = 0.062 (R sub w = 0.084). IR spectroscopic measurements gave absorption bands near 1027 and 857/cm, which are consistent with coordinated THF molecules. Variable temperature NMR studies showed that the tris-adduct was stable to disproportionation in solution between 20-60 C. DTIC

N95-19807 Duke Univ., Durham, NC. Dept. of Chemistry.
ISOLATION AND CHARACTERIZATION OF AN INDIUM-MIXED-PNICOGEN FOUR-MEMBERED RING COMPOUND: CRYSTAL STRUCTURE OF (Me3SiCH2)2InAs(SiMe3)2 In(CH2SiMe3)2P(SiMe3)2
Richard L. Wells, Andrew T. McPhail, and Leonidas J. Jones, III 5 May 1994 16 p Limited Reproducibility: More than 20% of this document may be affected by microfiche quality
(Contract N00014-89-J-1545)
(AD-A279170; DU/DC/TR-40) Avail: Issuing Activity (Defense Technical Information Center (DTIC))

The first four-membered ring containing two indium atoms with bridging by two different group 15 elements, (Me3SiCH2)2InAs-(SiMe3)2In(CH2SiMe3)2P(SiMe3)2 (1), to be characterized completely was prepared by the equilibration of (Me3SiCH2)2InP(SiMe3)22 (2) with (Me3SiCH2)2InAs(SiMe3)22 (3) in a 1:1 mole ratio. X ray crystallographic analysis showed the In-As-In-P ring of 1 to be planar. Crystals of 1 belong to the orthorhombic system, in the space group Pbcn (D14/2h), with four molecules in a unit cell of dimensions a = 12.848 (1) A, b = 21.558 (1) A, c = 18.736 (1) A, and are isomorphous with those of 2 and 3. The electron ionization (20 eV) mass spectrum of 1 shows a fragmentation pattern indicative of this compound and no peaks 510 m/z consistent with either 2 or 3. Clusters assigned to specific ions in the mass spectrum show appropriate isotopic patterns as calculated for the atoms present. DTIC

N95-19812 Duke Univ., Durham, NC. Dept. of Chemistry.
SYNTHESIS AND CHARACTERIZATION OF ALUMINUM-PHOSPHORUS ADDUCTS: X-RAY CRYSTAL STRUCTURES OF Cl3Al (DOT) P(SiMe3)3 (DOT) C7H8 AND Br3Al (DOT) P(SiMe3)3 (DOT) C7H8
Richard L. Wells, Andrew T. McPhail, Janeen A. Laske, and Peter S. White 5 May 1994 23 p Limited Reproducibility: More than 20% of this document may be affected by microfiche quality
(Contracts N00014-89-J-1545; N00014-93-1-0860)
(AD-A279194; DU/DC/TR-42/AASERT-01) Avail: Issuing Activity (Defense Technical Information Center (DTIC))

The attempted dehalosilylation reactions between AlX3 (X = Cl, Br) and P(SiMe3)3 in toluene in 1:1 mole ratios afforded only the adducts Cl3Al(dot)P(SiMe3)3 (1) and Br3Al(dot)P(SiMe3)3 (2), respectively. Compounds 1 and 2 were characterized by (1)H, (13)C, (27)Al, and (31)P solution NMR spectroscopy, as well as partial elemental analysis. In addition, the solid state structures of the toluene solvates of 1 and 2 were determined by single-crystal X-ray analysis. Characterization revealed that the solid solvated adducts 1 and 2 are isostructural and their crystals are isomorphous. In each compound, the Al and the P atoms reside in tetrahedral environments, with each X3Al(dot)P(SiMe3)3 (X = Cl, Br) molecule associated with one interstitial toluene molecule in the crystals. These adducts are noteworthy in that they possess extremely short, essentially equal Al-P bond lengths (For 1: Al-P 2.392(4) A, and for 2: Al-P = 2.391(6) A), which are the shortest found to date in aluminum-phosphorus molecular species. DTIC

N95-19815 Stanford Univ., CA. Dept. of Applied Physics.
HIGH TEMPERATURE SUPERCONDUCTING FILMS AND CRYSTALS Final Report, 15 Jan. 1991 - 14 Nov. 1993
A. Kapitulnik and T. H. Geballe 14 Nov. 1993 7 p Limited Reproducibility: More than 20% of this document may be affected by microfiche quality
(Grant AF-AFOSR-0145-91)
(AD-A279201; AFOSR-94-0283TR) Avail: Issuing Activity (Defense Technical Information Center (DTIC))

The work carried out under this grant has been the investigation of thin films and single crystals of the layered cuprate high-temperature superconductors, as well as other model systems. A primary objective in the program was the development of a better understanding of the limits of the occurrence of superconductors with high transition temperature (above liquid nitrogen temperature). The work is thus composed of an empirical part that searches for superconductivity by similarities and chemical guidance as well as critical tests for various theories of the high-Tc mechanism. Another aspect of the program was to study the superconducting and normal state properties in applied magnetic fields, in particular we studied the coupling between the Cu-O layers in superlattices. We employed the artificially layered Superconductor/insulator system of MoGe/Ge which have in-plane and out-of plane anisotropies which bracket those found in the layered cuprates model system. DTIC

N95-19816 EPIR Ltd., Oakbrook, IL.
INDUSTRIAL EXPLOITATION OF A ALTERNATE TECHNOLOGY FOR THE PRODUCTION OF HgCdTe EPILAYERS, STRUCTURES AND DEVICES Final Report
Jean-Pierre Faurie 14 Feb. 1994 72 p Limited Reproducibility: More than 20% of this document may be affected by microfiche quality
(Contract F49620-91-C-0007)
(AD-A279202; AFOSR-94-0281TR) Avail: Issuing Activity (Defense Technical Information Center (DTIC))

The program goals were the following: (1) estimate the total cost to produce an MBE-grown HgCdTe epitaxial wafer suitable for the industrial manufacture of an IR photo diode detector array;(2) establish manufacturing procedures for MBE-grown HgCdTe epitaxial layers in order to bring to the market a product which is suitable for FPAs; and (3) Grow high quality HgCdTe single epilayers and heterostructures with extremely uniform physical properties. These characteristics were expected to be reached at the end of this program. DTIC

N95-19817 Illinois Univ., Chicago, IL. Dept. of Physics.
MBE GROWTH, CHARACTERIZATION AND ELECTRONIC DEVICE PROCESSING OF Hg-BASED SEMICONDUCTOR ALLOYS AND HETEROSTRUCTURES Final Report, 17 Sep. 1990 - 16 Dec. 1993
Jean-Pierre Faurie 16 Dec. 1993 52 p Limited Reproducibility: More than 20% of this document may be affected by microfiche quality
(Contract F49620-90-C-0090; ARPA Order 5940)
(AD-A279203; AFOSR-94-0282TR) Avail: Issuing Activity (Defense Technical Information Center (DTIC))

The main objective of this contract was to improve the crystal quality of CdTe(111)B grown directly on silicon (100) substrate. At the starting date of this contract (Sep. 1990) the best CdTe(111)B grown on Si(100)

had double crystal x-ray rocking curves (DCRC) FWHM of 460 arcsec. These layers were exhibiting double domains and wer plagued by microtwins. At the end of this contact we are routinely growing single-domain twin-free CdTe(111)B epilayers on Si(100). The best DCRC FWHM are of 100 arcsec which is equivalent of better to th at of CdTe grown on Si with a buffer layer such as GaAs or (Ca,Ba)F2. The drastic improvement is due to a systematic investigation of the Si substrate tilt, an understanding of the driving forces for double-domain and microtwin suppression along with a precise control of the growth parameters. DTIC

N95-19828# Scientific Research Associates, Inc., Glastonbury, CT.
THE PHYSICS AND OPERATION OF ULTRA-SUBMICRON LENGTH SEMICONDUCTOR DEVICES Final Report
May 1994 95 p
(Contract N00014-86-C-0780)
(AD-A280181; FR-R-9231F) Avail: CASI HC A05/MF A01

This document summarizes activities under ONR Contract: N00014-86-C-0780, under which equilibrium and nonequilibrium electron and hole transport in micron and submicron structures were studied via a wide range of numerical procedures. These included Monte Carlo methods, moments of the Boltzmann transport equation, Schrodinger's equation and the quantum Liouville equation in the coordinate representation. While all of the studies have resulted in a large collection of publications, the basic theme of the studies was the determination of the physics of device operation and the influence of small structure size on this operation. The most recent activities have involved the quantum Liouville equation with emphasis on dissipation and the calculation of current. This document includes a description of quantum transport via the quantum Liouville equation, as we now understand it, as well as a brief summary of the previous activities involving larger submicron devices. While the principle goal of this study was elucidating the physics and operation of nanoscale devices, a continuing requirement was that all algorithms be menu driven and accessible to device scientists and engineers. The quantum transport algorithm is accessible on UNIX workstations and in a PC Windows format. DTIC

N95-19829# Scientific Research Associates, Inc., Glastonbury, CT. Center for Solid State Electonics.
MODELING OF QUANTUM TRANSPORT IN SEMICONDUCTOR DEVICES
David K. Ferry (Arizona State Univ., Tempe, AZ.) and Harold L. Grubin May 1994 213 p Repr. from The Physics and Operation of Ultra-Submicron Length Semiconductor Devices, May 1994 213 p Sponsored by ONR, ARO and AFOSR
(AD-A280182) Avail: CASI HC A10/MF A03

The evolutionary decrease in the size of an individual semiconductor device continues with no apparent end of the process in sight. As a consequence, it is quite likely that critical dimensions will soon be comparable to quantum coherence lengths for the particles involved in the transport within the device. Generally, quantum transport differs from semi-classical transport in the utilization of a quantum kinetic equation (as opposed to the Boltzmann transport equation). These quantum kinetic equations can be developed for the density matrix, the Wigner distribution function, and real-time Green's functions, as well as for many reduced approximations to these quantities. In this review, we study how these various approaches are connected as well as how they offer different views into the quantum behavior within devices. DTIC

N95-19838 Lawrence Livermore National Lab., Livermore, CA.
GENERATION AND SOLUTION OF EFFECTIVE MANY-BODY HAMILTONIANS FOR RARE EARTH AND TRANSITION METAL COMPOUNDS
A. K. McMahan Aug. 1994 21 p Presented at the Electronic Structure of Solids Using Cluster Methods Workshop, East Lansing, MI, 17-19 Jul. 1994 Limited Reproducibility: More than 20% of this document may be affected by microfiche quality
(Contract W-7405-eng-48)
(DE95-002402; UCRL-JC-118407; CONF-9407115-2) Avail: CASI HC A03

This paper gives an overview of the local density approximate (LDA) generation of effective Hamiltonians for a series of d and f electron Mott insulators and reviews their approximate solution for periodic clusters. The (charge-transfer insulator) materials considered are CeO2 and PrO2, the high-(Tc) parent La2CuO4, and three isostructural compounds, K2CuF4, K2NiF4, and La2NiO4. This paper first introduces the effective Hamiltonians in stages by considering first the Coulomb operator for a single atom or ion, and then introduces the additional hopping parameters required for a collection of atoms. Then an improved treatment of screening effects is considered, noting that Hartree-Fock calculations with screened interactions provide approximately correct insulating gaps for charge-transfer insulators. Essential spin correlations and their impact on quasiparticle dispersion are discussed, based on configuration interaction calculations for clusters. The range of validity of the present effective Hamiltonians is discussed. Conclusions are offered. DOE

N95-19015*# State Univ. of East Tennessee, Johnson City, TN. Dept. of Chemistry.
SALT-INDUCED AGGREGATION OF LYSOZYME: IMPLICATIONS FOR CRYSTAL GROWTH
Lori J. Wilson *In* Alabama Univ., Research Reports: 1994 NASA/ASEE Summer Faculty Fellowship Program Oct. 1994 6 p (For primary document see N95-18967 05-80)
Avail: CASI HC A02/MF A03

77 THERMODYNAMICS AND STATISTICAL PHYSICS

Includes quantum mechanics; theoretical physics; and Bose and Fermi statistics.

For related information see also *25 Inorganic and Physical Chemistry* and *34 Fluid Mechanics and Heat Transfer.*

N95-17996 Los Alamos National Lab., NM.
APPLICATIONS OF QUANTUM ENTROPY TO STATISTICS
R. N. Silver and H. F. Martz 1994 10 p Presented at the American Statistical Association, Toronto, Ontario, 14-18 Aug. 1994 Limited Reproducibility: More than 20% of this document may be affected by microfiche quality
(Contract W-7405-eng-36)
(DE94-014416; LA-UR-94-2168; CONF-9408107-2) Avail: CASI HC A02

This paper develops two generalizations of the maximum entropy (ME) principle. First, Shannon classical entropy is replaced by von Neumann quantum entropy to yield a broader class of information divergences (or penalty functions) for statistics applications. Negative relative quantum entropy enforces convexity, positivity, non-local extensivity and prior correlations such as smoothness. This enables the extension of ME methods from their traditional domain of ill-posed in-verse problems to new applications such as non-parametric density estimation. Second, given a choice of information divergence, a combination of ME and Bayes rule is used to assign both prior and posterior probabilities. Hyperparameters are interpreted as Lagrange multipliers enforcing constraints. Conservation principles are proposed to act statistical regularization and other hyperparameters, such as conservation of information and smoothness. ME provides an alternative to hierarchical Bayes methods. DOE

N95-18009# Scientific Research Associates, Inc., Glastonbury, CT.
LARGE SIGNAL TIME DEPENDENT QUANTUM MECHANICAL TRANSPORT IN QUANTUM PHASE BASED DEVICES Final Report, 15 Dec. 1990 - 15 Feb. 1994
Harold L. Grubin 10 Jun. 1994 245 p
(Contract F49620-91-C-0016)
(AD-A283338; R9133-F; AFOSR-94-0453TR) Avail: CASI HC A11/MF A01

This document summarizes studies performed under AFOSR Contract: F49620-91-C-0016. In this study equilibrium and nonequilibrium electron and hole transport in quantum scale structures were studied via solutions to the quantum Liouville equation in the coordinate representation. The coordinate representation density matrix solutions are the first to provide the quantum distribution function for electrons and holes in nanoscale devices coupled to model dependent dissipation. Illustrations of the use of the algorithm for quantum and classical devices are presented. A discussion of the quantum hydrodynamic equations is included because of its importance

in studying dissipation. A summary of the transient studies and the initiation of two-dimensional studies is also discussed. A considerable number of publications have emerged from this study, all of which are included in this document. DTIC

N95-18328# Joint Inst. for Nuclear Research, Dubna (USSR). Lab. of Theoretical Physics.
ZERO MODES OF FIRST CLASS SECONDARY CONSTRAINTS IN GAUGE THEORIES
A. Khvedelidze and V. Pervushin 1993 22 p Submitted for publication
(DE94-626659; JINR-E-2-93-439) Avail: CASI HC A03/MF A01 (US Sales Only)

Zero modes of first class secondary constraints in the two-dimensional electrodynamics and the four-dimensional SU(2) Yang-Mills theory are considered by the method of reduced phase space quantization in the context of the problem of a stable vacuum. We compare the description of these modes in the Dirac extended method and reveal their connection with the topological structure of the gauge symmetry group. Within the framework of the 'reduced' quantization we construct a new global realization of the homotopy group representation in the Yang-Mills theory, where the role of the stable vacuum with a finite action plays the Prasad-Sommerfeld solution. DOE

N95-18333# Centro Brasileiro de Pesquisas Fisicas, Rio de Janeiro.
COMPARISON OF THE ANOMALOUS AND NON-ANOMALOUS GENERALIZED SCHWINGER MODELS VIA FUNCTIONAL FORMALISM
A. deSouzaDutra 1992 33 p
(DE94-626684; CBPF-NF-030/92) Avail: CASI HC A03/MF A01 (US Sales Only)

The Green functions of the two versions of the generalized Schwinger model, the anomalous and the nonanomalous one, in their higher order Lagrangian density form are calculated. Furthermore it is shown through a sequence of transformations that the bosonized Lagrangian density is equivalent to the former, at least for the bosonic correlation functions. The introduction of the sources from the beginning, leading to a gauge-invariant source term, is also considered. It is verified that the two models have the same correlation functions only if the gauge-invariant sector is taken into account. Presented is a generalization of the Wess-Zumino term, and its physical consequences are studied, in particular the appearance of gauge-dependent massive excitations. DOE

N95-18352# Instituto de Fisica Teorica, Sao Paulo (Brazil).
FLATTENING OF THE RESONANCE SPECTRUM OF HADRONS FROM KAPPA-DEFORMED POINCARE ALGEBRA
Jishnu Dey, Paulo Leal Ferreira, Lauro Tomio, and Rajkumar Roy Choudhury (Indian Statistical Inst., Calcutta.) Feb. 1994 15 p
(DE94-626686; IFT-P-009/94) Avail: CASI HC A03/MF A01 (US Sales Only)

Recently, Lukierski, et. al., defined a kappa-deformed Poincare algebra which is characterized by having the energy-momentum and angular momentum subalgebras not deformed. Further Biedenharn showed that on gauging the kappa-deformed electron with the electromagnetic field, one can set a limit on the allowed value of the deformation parameter epsilon identical to 1/kappa is less than 1 fm. It is shown that one gets Regge like angular excitations, J, of the mesons, nonstrange and strange baryons, with a value of epsilon approximately 0.082 fm and predicts a flattening with J of the corresponding trajectories. The Regge fit improves on including deformation, particularly for the baryon spectrum. DOE

N95-18879# Joint Inst. for Nuclear Research, Dubna (USSR). Lab. of Theoretical Physics.
TO THE THEORY OF THE MANAGEMENT OF THE RESONANCE WIDTHS
B. N. Zakharev 1993 7 p In RUSSIAN Submitted for publication
(DE94-626645; JINR-R-4-93-427) Avail: CASI HC A02/MF A01 (US Sales Only)

A simple physical explanation is given of the potential transformation which is necessary to increase (decrease) the probability of the decay of the chosen quasi-stationary state when the half-lives of all other states remain unchanged. The arbitrary changes of the resonances widths are provided by the special auxiliary 'carriers' (narrow local attractive wells) which are able to shift separately the chosen states through the potential barrier nearer to its outer end increasing the decay rate. The possibility to manage the form of wave functions for construction of quantum systems with the desired transition rates for the arbitrary chosen discrete spectrum is considered. DOE

N95-18949*# Kansas Univ., Lawrence, KS. Dept. of Physics and Astronomy.
QUANTITATIVE ANALYSIS OF VOIDS IN PERCOLATING STRUCTURES IN TWO-DIMENSIONAL N-BODY SIMULATIONS
Patrick M. Harrington, Adrian L. Melott, and Sergei F. Shandarin 1993 12 p
(Grants NAGw-2923; NSF AST-90-21414; NSF OSR-92-55223)
(NASA-CR-197612; NAS 1.26:197612) Avail: CASI HC A03/MF A01

We present in this paper a quantitative method for defining void size in large-scale structure based on percolation threshold density. Beginning with two-dimensional gravitational clustering simulations smoothed to the threshold of nonlinearity, we perform percolation analysis to determine the large scale structure. The resulting objective definition of voids has a natural scaling property, is topologically interesting, and can be applied immediately to redshift surveys. Author

N95-19037*# Kansas Univ., Lawrence, KS. Dept. of Physics and Astronomy.
OPTIMIZING THE ZELDOVICH APPROXIMATION
Adrian L. Melott, Todd F. Pellman, and Sergei F. Shandarin [1994] 22 p
(Grants NAGw-2923; NSF AST-90-21414; NSF OSR-92-55223)
(NASA-CR-197606; NAS 1.26:197606) Avail: CASI HC A03/MF A01

We have recently learned that the Zeldovich approximation can be successfully used for a far wider range of gravitational instability scenarios than formerly proposed; we study here how to extend this range. In previous work (Coles, Melott and Shandarin 1993, hereafter CMS) we studied the accuracy of several analytic approximations to gravitational clustering in the mildly nonlinear regime. We found that what we called the 'truncated Zeldovich approximation' (TZA) was better than any other (except in one case the ordinary Zeldovich approximation) over a wide range from linear to mildly nonlinear (sigma approximately 3) regimes. TZA was specified by setting Fourier amplitudes equal to zero for all wavenumbers greater than k(sub nl), where k(sub nl) marks the transition to the nonlinear regime. Here, we study the cross correlation of generalized TZA with a group of n-body simulations for three shapes of window function: sharp k-truncation (as in CMS), a tophat in coordinate space, or a Gaussian. We also study the variation in the crosscorrelation as a function of initial truncation scale within each type. We find that k-truncation, which was so much better than other things tried in CMS, is the worst of these three window shapes. We find that a Gaussian window e(exp(-k(exp 2)/2k(exp 2, sub G))) applied to the initial Fourier amplitudes is the best choice. It produces a greatly improved crosscorrelation in those cases which most needed improvement, e.g. those with more small-scale power in the initial conditions. The optimum choice of kG for the Gaussian window is (a somewhat spectrum-dependent) 1 to 1.5 times k(sub nl). Although all three windows produce similar power spectra and density distribution functions after application of the Zeldovich approximation, the agreement of the phases of the Fourier components with the n-body simulation is better for the Gaussian window. We therefore ascribe the success of the best-choice Gaussian window to its superior treatment of phases in the nonlinear regime. We also report on the accuracy of particle positions and velocities produced by TZA. Author

N95-19340*# Kansas Univ., Lawrence, KS. Dept. of Physics and Astronomy.
QUASI-LINEAR REGIME OF GRAVITATIONAL INSTABILITY: IMPLICATION TO DENSITY-VELOCITY RELATION
Sergei F. Shandarin 1993 11 p Presented at the Cosmic Velocity Fields Conference, Paris, France, July 1993
(Grants NAGw-2923; NSF AST-90-21414; NSF OSR-92-55223)
(NASA-CR-197616; NAS 1.26:197616) Avail: CASI HC A03/MF A01

The well known linear relation between density and peculiar velocity distributions is a powerful tool for studying the large-scale structure in the Universe. Potentially it can test the gravitational instability theory and measure Omega. At present it is used in both ways: the velocity is reconstructed, provided the density is given, and vice versa. Reconstructing the density from the velocity field usually makes use of the Zel'dovich approximation.

However, the standard linear approximation in Eulerian space is used when the velocity is reconstructed from the density distribution. I show that the linearized Zel'dovich approximation, in other words the linear approximation in the Lagrangian space, is more accurate for reconstructing velocity. In principle, a simple iteration technique can recover both the density and velocity distributions in Lagrangian space, but its practical application may need an additional study. Author

N95-19358*# Kansas Univ., Lawrence, KS. Dept. of Physics and Astronomy.
A TEST OF THE ADHESION APPROXIMATION FOR GRAVITATIONAL CLUSTERING
Adrian L. Melott, Sergei Shandarin, and David H. Weinberg (Institute for Advanced Study, Princeton, NJ.) 1993 17 p Sponsored by W. M. Keck Foundation
(Grants NAGw-2923; NSF AST-90-21414; NSF OSR-92-55223; NSF PHY-92-45317)
(NASA-CR-197610; NAS 1.26:197610) Avail: CASI HC A03/MF A01

We quantitatively compare a particle implementation of the adhesion approximation to fully non-linear, numerical 'N-body' simulations. Our primary tool, cross-correlation of N-body simulations with the adhesion approximation, indicates good agreement, better than that found by the same test performed with the Zel-dovich approximation (hereafter ZA). However, the cross-correlation is not as good as that of the truncated Zel-dovich approximation (TZA), obtained by applying the Zel'dovich approximation after smoothing the initial density field with a Gaussian filter. We confirm that the adhesion approximation produces an excessively filamentary distribution. Relative to the N-body results, we also find that: (a) the power spectrum obtained from the adhesion approximation is more accurate than that from ZA or TZA, (b) the error in the phase angle of Fourier components is worse than that from TZA, and (c) the mass distribution function is more accurate than that from ZA or TZA. It appears that adhesion performs well statistically, but that TZA is more accurate dynamically, in the sense of moving mass to the right place. Author

N95-19363*# Kansas Univ., Lawrence, KS. Dept. of Physics and Astronomy.
COMPARISON OF DYNAMICAL APPROXIMATION SCHEMES FOR NON-LINEAR GRAVITATIONAL CLUSTERING
Adrian L. Melott 1994 11 p Sponsored by DFG, MURST and CINECA Computing Center
(Grants NAGw-2923; NSF AST-90-21414; NSF PHY-92-45317)
(NASA-CR-197609; NAS 1.26:197609) Avail: CASI HC A03/MF A01

We have recently conducted a controlled comparison of a number of approximations for gravitational clustering against the same n-body simulations. These include ordinary linear perturbation theory (Eulerian), the adhesion approximation, the frozen-flow approximation, the Zel'dovich approximation (describable as first-order Lagrangian perturbation theory), and its second-order generalization. In the last two cases we also created new versions of approximation by truncation, i.e., smoothing the initial conditions by various smoothing window shapes and varying their sizes. The primary tool for comparing simulations to approximation schemes was crosscorrelation of the evolved mass density fields, testing the extent to which mass was moved to the right place. The Zel'dovich approximation, with initial convolution with a Gaussian e(exp -k(exp 2)/k(exp 2, sub G)) where k(sub G) is adjusted to be just into the nonlinear regime of the evolved model (details in text) worked extremely well. Its second-order generalization worked slightly better. All other schemes, including those proposed as generalizations of the Zel'dovich approximation created by adding forces, were in fact generally worse by this measure. By explicitly checking, we verified that the success of our best-choice was a result of the best treatment of the phases of nonlinear Fourier components. Of all schemes tested, the adhesion approximation produced the most accurate nonlinear power spectrum and density distribution, but its phase errors suggest mass condensations were moved to slightly the wrong location. Due to its better reproduction of the mass density distribution function and power spectrum, it might be preferred for some uses. We recommend either n-body simulations or our modified versions of the Zel'dovich approximation, depending upon the purpose. The theoretical implication is that pancaking is implicit in all cosmological gravitational clustering, at least from Gaussian initial conditions, even when subcondensations are present. Author

N95-19852 Pennsylvania Univ., Philadelphia, PA. Dept. of Chemistry.
THE FORMULATION OF QUANTUM STATISTICAL MECHANICS BASED ON THE FEYNMAN PATH CENTROID DENSITY. 3: PHASE SPACE FORMALISM AND ANALYSIS OF CENTROID MOLECULAR DYNAMICS Technical Report, May 1993 - May 1994
Jianshu Cao and Gregory A. Voth 6 May 1994 35 p Limited Reproducibility: More than 20% of this document may be affected by microfiche quality
(Contract N00014-92-J-1243)
(AD-A279233; TR-8-3) Avail: Issuing Activity (Defense Technical Information Center (DTIC))

The formulation of quantum statistical mechanics based on the path centroid variable in Feynman path integration is generalized to a phase space perspective, thereby including the momentum as an independent dynamical variable. By virtue of this approach, operator averages and imaginary time correlation functions can be expressed in terms of an averaging over the multidimensional phase space centroid density. The imaginary time centroid-constrained correlation function matrix for the phase space variables is then found to define the effective thermal width of the phase space centroid variable. These developments also make it possible to rigorously analyze the centroid molecular dynamics method for computing quantum dynamical time correlation functions. As a result, the centroid time correlation function as calculated from centroid molecular dynamics is shown to be a well-defined approximation to the exact Kubo transformed position correlation function. This analysis thereby clarifies the underlying role of the equilibrium path centroid variable in the quantum dynamical position correlation function and provides a sound theoretical basis for the centroid molecular dynamics method. DTIC

N95-19853 Pennsylvania Univ., Philadelphia, PA. Dept. of Chemistry.
THE FORMULATION OF QUANTUM STATISTICAL MECHANICS BASED ON THE FEYNMAN PATH CENTROID DENSITY. 4: ALGORITHMS FOR CENTROID MOLECULAR DYNAMICS Technical Report, May 1993 - May 1994
Jianshu Cao and Gregory A. Voth 6 May 1994 56 p Limited Reproducibility: More than 20% of this document may be affected by microfiche quality
(Contract N00014-92-J-1243)
(AD-A279234; TR-9-4) Avail: Issuing Activity (Defense Technical Information Center (DTIC))

Numerical algorithms are developed for the centroid molecular dynamics (centroid MD) method to calculate dynamical time correlation functions for general many-body quantum systems. Approaches based on the normal mode path integral molecular dynamics and staging path integral Monte Carlo methods are described to carry out a direct calculation of the force on the centroid variables in the centroid MD algorithm. A more efficient, but approximate, scheme to compute the centroid force is devised which is based on the locally optimized harmonic approximation for the centroid potential. The centroid MD equations in the latter method can be solved with the help of an iterative procedure or through extended Lagrangian dynamics. A third algorithm introduces an effective centroid pseudopotential to approximate the full many-body centroid mean force potential by effective pairwise centroid interactions. Numerical simulations for both prototype models and more realistic many-body systems are performed to explore the feasibility and limitations of each algorithm. DTIC

80 SOCIAL SCIENCES (GENERAL)

Includes educational matters.

N95-18166*# University of Central Florida, Orlando, FL. Dept. of Mechanical and Aerospace Engineering.
NASA/ASEE SUMMER FACULTY FELLOWSHIP PROGRAM. 1994 RESEARCH REPORTS
Loren A. Anderson, ed., E. Ramon Hosler, ed., and Warren Camp, ed. (National Aeronautics and Space Administration. John F. Kennedy Space Center, Cocoa Beach, FL.) Oct. 1994 567 p Fellowship program held in Cocoa Beach, FL, 31 May - 5 Aug. 1994 Prepared in cooperation with NASA. Kennedy Space Center, Cocoa Beach, FL
(Grant NGT-60002)
(NASA-CR-197448; NAS 1.26:197448) Avail: CASI HC A24/MF A04

This document is a collection of technical reports on research conducted by the participants in the 1994 NASA/ASEE Summer Faculty Fellowship Program at Kennedy Space Center (KSC). This was the tenth year that a NASA/ASEE program has been conducted at KSC. The 1994 program was administered by the University of Central Florida in cooperation with KSC. The program was operated under the auspices of the American Society for Engineering Education (ASEE) with sponsorship and funding from the Office of Educational Affairs, NASA Headquarters, Washington, D.C. The KSC Program was one of nine such Aeronautics and Space Research Programs funded by NASA Headquarters in 1994. The NASA/ASEE program is intended to be a two-year program to allow in-depth research by the University faculty member. The editors of this document were responsible for selecting appropriately qualified faculty to address some of the many problems of current interest to NASA/KSC. For individual titles, see N95-18167 through N95-18186.

N95-18167*# South Dakota State Univ., Brookings, SD. Dept. of Electrical Engineering.

THE DEVELOPMENT OF A FIBER OPTICS COMMUNICATION NETWORK FOR CONTROLLING A MULTIDEGREE-OF-FREEDOM SERPENTINE TRUSS **c74**

Alfred S. Andrawis *In* Univ. of Central Florida, NASA/ASEE Summer Faculty Fellowship Program. 1994 Research Reports Oct. 1994 p 1-29 (For primary document see N95-18166 05-80)

Avail: CASI HC A03/MF A04

The problem addressed by this report is the large size and heavy weight of the cable bundle, used for controlling a Multidegree-Of-Freedom Serpentine Truss Manipulator arm, which imposes limitations on the manipulator arm maneuverability. This report covers a design of an optical fiber network to replace the existing copper wire network of the Serpentine Truss Manipulator. This report proposes a fiber network design which significantly reduces the bundle size into two phases. The first phase does not require any modifications for the manipulator architecture, while the other requires major modifications. Design philosophy, hardware details and schematic diagrams are presented. Author

N95-18168*# Jackson State Univ., Jackson, MS. Dept. of Technology.

SPACE STATION RACKS WEIGHT AND CG MEASUREMENT USING THE RACK INSERTION END-EFFECTOR **c18**

William V. Brewer *In* Univ. of Central Florida, NASA/ASEE Summer Faculty Fellowship Program. 1994 Research Reports Oct. 1994 p 31-60 (For primary document see N95-18166 05-80)

Avail: CASI HC A03/MF A04

The objective was to design a method to measure weight and center of gravity (C.G.) location for Space Station Modules by adding sensors to the existing Rack Insertion End Effector (RIEE). Accomplishments included alternative sensor placement schemes organized into categories. Vendors were queried for suitable sensor equipment recommendations. Inverse mathematical models for each category determine expected maximum sensor loads. Sensors are selected using these computations, yielding cost and accuracy data. Accuracy data for individual sensors are inserted into forward mathematical models to estimate the accuracy of an overall sensor scheme. Cost of the schemes can be estimated. Ease of implementation and operation are discussed. Author (revised)

N95-18169*# University of Central Florida, Orlando, FL. Dept. of Mechanical and Aerospace Engineering.

AUTOMATED PATH PLANNING OF THE PAYLOAD INSPECTION AND PROCESSING SYSTEM **c37**

Robert M. Byers *In its* NASA/ASEE Summer Faculty Fellowship Program. 1994 Research Reports Oct. 1994 p 61-90 (For primary document see N95-18166 05-80)

Avail: CASI HC A03/MF A04

The Payload Changeout Room Inspection and Processing System (PIPS) is a highly redundant manipulator intended for performing tasks in the crowded and sensitive environment of the Space Shuttle Orbiter payload bay. Its dexterity will be exploited to maneuver the end effector in a workspace populated with obstacles. A method is described by which the end effector of a highly redundant manipulator is directed toward a target via a Lyapunov stability function. A cost function is constructed which represents the distance from the manipulator links to obstacles. Obstacles are avoided by causing the vector of joint parameters to move orthogonally to the gradient of the workspace cost function. A C language program implements the algorithm to generate a joint history. The resulting motion is graphically displayed using the Interactive Graphical Robot Instruction Program (IGRIP) produced by Deneb Robotics. The graphical simulation has the potential to be a useful tool in path planning for the PIPS in the Shuttle Payload Bay environment. Author

N95-18170*# Randolph-Macon Coll., Ashland, VA. Dept. of Chemistry.

EVALUATION OF INORGANIC ZINC-RICH PRIMERS USING ELECTROCHEMICAL IMPEDANCE SPECTROSCOPY (EIS) IN COMBINATION WITH ATMOSPHERIC EXPOSURE **c25**

Luz M. Calle *In* Univ. of Central Florida, NASA/ASEE Summer Faculty Fellowship Program. 1994 Research Reports Oct. 1994 p 91-112 (For primary document see N95-18166 05-80)

Avail: CASI HC A03/MF A04

This investigation explored the use of Electrochemical Impedance Spectroscopy (EIS) in combination with atmospheric exposure as a short term method for analyzing the performance of twenty-one commercially available zinc-rich primers. The twenty-one zinc-rich primers were: Carboline CZ-11, Ameron Devoe-Marine Catha-Coat 304, Briner V-65, Ameron D-21-9, Sherwin Williams Zinc Clad II, Carboline CZ-D7, Ameron D-4, Dupont Ganicin 347WB, Porter TQ-4374H, Inorganic Coatings IC-531, Subox Galvanox IV, Southern Coatings Chemtec 600, GLidden Glidzinc 5530, Byco SP-101, Tnemec 90E-75, Devoe Catha-Coat 302H, Glidden Glidzinc 5536, Koppers 701, Ameron D-21-5, Coronado 935-152, and Subox Galvanox V. Data were also collected on galvanized steel for comparison purposes. A library of Bode magnitude plots was generated for each coating including curves for the initial time and after each week of atmospheric exposure at the Beach Corrosion Test site near the Space Shuttle launch pad at the Kennedy Space Center for up to four weeks. Subsequent measurements were collected after 8 weeks and after one year of atmospheric exposure. Analysis of the impedance data was performed with the purpose of identifying parameters that could be used to predict the long-term performance of zinc-rich primers. It has been shown that there is a correlation between the long-term performance of zinc-rich primers and several parameters obtained from EIS measurements in combination with atmospheric exposure. The equivalent circuit R2(R2C(R3W)) provided a satisfactory fit for the EIS data. The corrosion potential and the R2 resistance are parameters indicative of the galvanic mechanism of protection. The capacitance of the coating is related to the barrier mechanism of protection. Author

N95-18171*# Florida International Univ., Miami, FL. Dept. of Industrial and Systems Engineering.

ASSESSMENT OF THE SFC DATABASE FOR ANALYSIS AND MODELING **c82**

Martha A. Centeno *In* Univ. of Central Florida, NASA/ASEE Summer Faculty Fellowship Program. 1994 Research Reports Oct. 1994 p 113-137 (For primary document see N95-18166 05-80)

Avail: CASI HC A03/MF A04

SFC is one of the four clusters that make up the Integrated Work Control System (IWCS), which will integrate the shuttle processing databases at Kennedy Space Center (KSC). The IWCS framework will enable communication among the four clusters and add new data collection protocols. The Shop Floor Control (SFC) module has been operational for two and a half years; however, at this stage, automatic links to the other 3 modules have not been implemented yet, except for a partial link to IOS (CASPR). SFC revolves around a DB/2 database with PFORMS acting as the database management system (DBMS). PFORMS is an off-the-shelf DB/2 application that provides a set of data entry screens and query forms. The main dynamic entity in the SFC and IOS database is a task; thus, the physical storage location and update privileges are driven by the status of the WAD. As we explored the SFC values, we realized that there was much to do before actually engaging in continuous analysis of the SFC data. Half way into this effort, it was realized that full scale analysis would have to be a future third phase of this effort. So, we concentrated on getting to know the contents of the database, and in establishing an initial set of tools to start the continuous analysis process. Specifically, we set out to: (1) provide specific procedures for statistical models, so as to enhance the TP-OAO office analysis and modeling capabilities; (2) design a data exchange interface; (3) prototype the interface to provide inputs to SCRAM; and (4) design a modeling database. These objectives were set with the expectation that, if met, they would provide former TP-OAO

engineers with tools that would help them demonstrate the importance of process-based analyses. The latter, in return, will help them obtain the cooperation of various organizations in charting out their individual processes. Derived from text

N95-18172*# Texas Technological Univ., Lubbock, TX. Dept. of Geosciences.

EXPERIMENTS WITH THE MESOSCALE ATMOSPHERIC SIMULATION SYSTEM (MASS) USING THE SYNTHETIC RELATIVE HUMIDITY c47

Chia-Bo Chang *In* Univ. of Central Florida, NASA/ASEE Summer Faculty Fellowship Program. 1994 Research Reports Oct. 1994 p 139-158 (For primary document see N95-18166 05-80)

Avail: CASI HC A03/MF A04

This study is intended to examine the impact of the synthetic relative humidity on the model simulation of mesoscale convective storm environment. The synthetic relative humidity is derived from the National Weather Services surface observations, and non-conventional sources including aircraft, radar, and satellite observations. The latter sources provide the mesoscale data of very high spatial and temporal resolution. The synthetic humidity data is used to complement the National Weather Services rawinsonde observations. It is believed that a realistic representation of initial moisture field in a mesoscale model is critical for the model simulation of thunderstorm development, and the formation of non-convective clouds as well as their effects on the surface energy budget. The impact will be investigated based on a real-data case study using the mesoscale atmospheric simulation system developed by Mesoscale Environmental Simulations Operations, Inc. The mesoscale atmospheric simulation system consists of objective analysis and initialization codes, and the coarse-mesh and fine-mesh dynamic prediction models. Both models are a three dimensional, primitive equation model containing the essential moist physics for simulating and forecasting mesoscale convective processes in the atmosphere. The modeling system is currently implemented at the Applied Meteorology Unit, Kennedy Space Center. Two procedures involving the synthetic relative humidity to define the model initial moisture fields are considered. It is proposed to perform several short-range (approximately 6 hours) comparative coarse-mesh simulation experiments with and without the synthetic data. They are aimed at revealing the model sensitivities should allow us both to refine the specification of the observational requirements, and to develop more accurate and efficient objective analysis schemes. The goal is to advance the MASS (Mesoscal Atmospheric Simulation System) modeling expertise so that the model output can provide reliable guidance for thunderstorm forecasting. Author

N95-18173*# Maryland Univ., College Park, MD. Dept. of Horticulture.

PHYSIOLOGICAL AND GENETIC CHARACTERIZATION OF PLANT GROWTH AND GRAVITROPISM IN LED LIGHT SOURCES c51

Gerald F. Deitzer *In* Univ. of Central Florida, NASA/ASEE Summer Faculty Fellowship Program. 1994 Research Reports Oct. 1994 p 159-203 (For primary document see N95-18166 05-80)

Avail: CASI HC A03/MF A04

Among the many problems of growing plants in completely controlled environments, such as those anticipated for the space station and the CELSS program, is the need to provide light that is both adequate for photosynthesis and of proper quality for normal growth and development. NASA scientists and engineers have recently become interested in the possibility of utilizing densely packed, solid state, light emitting diodes (LED's) as a source for this light. Unlike more conventional incandescent or electrical discharge lamps, these sources are highly monochromatic and lack energy in spectral regions thought to be important for normal plant development. In addition, a recent observation by NASA scientist has suggested that infra-red LED's, that are routinely used as photographic safelights for plants grown in darkness, may interact with the ability of plants to detect gravity. In order to establish how plants respond to light from these LED light sources we carried out a series of experiments with known pigment mutants of the model mustard plant, Arabidopsis thaliana, growing in either a gravity field or on a clinostat to simulate a micro-gravity environment. Results indicate that only red light from the 665 nm LED's disrupts the ability of normal wildtype seedlings to detect a gravity stimulus. There was no consistent effect found for the far-red (735 nm) LED's or either of the infrared (880 nm or 935 nm) LED sources but both showed some effect in one or more of the genotypes tested. Of these five members of the phytochrome multigene family in Arabidopsis, only the phytochrome B pigment mutant (hy3) lacked the ability to detect gravity under all conditions. There was no effect of either micro-gravity (clinostat) or the infra-red LED's on the light induced inhibition of hypocotyl elongation. Measurements of the pigment phytochrome in oats also showed no photoconversion by 15 min irradiations with the infra-red LED's. We conclude that phytochrome B is required for the perception of gravity and that only red light is able to disrupt this perception. The infra-red LED's also do not appear to interact with gravity perception in Arabidopsis, but caution should be exercised if infra-red LED's are to be used as photographic safelights for these types of experiments. Author

N95-18174*# Pennsylvania State Univ., University Park, PA. Dept. of Meteorology.

LIGHTNING STUDIES USING LDAR AND COMPANION DATA SETS c47

Gregory S. Forbes *In* Univ. of Central Florida, NASA/ASEE Summer Faculty Fellowship Program. 1994 Research Reports Oct. 1994 p 205-235 (For primary document see N95-18166 05-80)

Avail: CASI HC A03/MF A04

Research was conducted to use the KSC Lightning Detection and Ranging (LDAR) system, together with companion data, in four subprojects: weather forecasting and advisory applications of LDAR, LDAR in relation to field mill readings, lightning flash and stroke detection using LDAR, and LDAR in relation to radar reflectivity patterns and KSC wind profiler vertical velocities. The research is aimed at developing rules, algorithms, and training materials that can be used by the operational weather forecasters who issue weather advisories for daily ground operations and launches by NASA and the United States Air Force. During the summer of 1993, LDAR data was examined on an hourly basis from 14 thunderstorm days and compared to ground strike data measured by the Lightning Location and Protection (LLP) system. These data were re-examined during 1994 to identify, number, and track LDAR-detected storms continually throughout the day and avoid certain interpretation problems arising from the use of hourly files. An areal storm growth factor was incorporated into a scheme to use current mappings of LDAR-defined thunderstorms to predict future ground strikes. During the summer of 1994, extensive sets of LDAR and companion data have been collected for 16 thunderstorm days, including a variety of meteorological situations. Detailed case studies are being conducted to relate the occurence of LDAR to the radar structure and evolution of thunderstorms. Field mill (LPWS) data are being examined to evaluate the complementary nature of LDAR and LPLWS data in determining the time of beginning and ending of the ground strike threat at critical sites. A computerized lightning flash and stroke discrimination algorithm has been written that can be used to help locate the points of origin of the electrical discharges, help distinguish in-cloud, cloud-ground, and upward flashes, and perhaps determine when the threat of ground strikes has ceased. Surface wind tower (mesonet), radar, sounding, and KSC wind profiler data will be used to develop schemes to help anticipate the timing and location of new thunderstorm development. Analysis of this data will continue in graduate student research projects. Author

N95-18175*# California State Polytechnic Univ., Pomona, CA. Dept. of Chemical and Materials Engineering.

INVESTIGATION OF NEW HYPERGOL SCRUBBER TECHNOLOGY c25

Barbara H. Glasscock *In* Univ. of Central Florida, NASA/ASEE Summer Faculty Fellowship Program. 1994 Research Reports Oct. 1994 p 235-262 (For primary document see N95-18166 05-80)

Avail: CASI HC A03/MF A04

The ultimate goal of this work is to minimize the liquid waste generated from the scrubbing of hypergolic vent gases. In particular, nitrogen tetroxide, a strong oxidizer used in hypergolic propellant systems, is currently scrubbed with a sodium hydroxide solution resulting in a hazardous liquid waste. This study investigated the use of a solution of potassium hydroxide and hydrogen peroxide for the nitrogen textroxide vent scrubber system. The potassium nitrate formed would be potentially usable as a fertilizer. The hydrogen peroxide is added to convert the potassium nitrite that is formed into more potassium nitrate. Smallscale laboratory tests were conducted to establish the stability of hydrogen peroxide in the proposed scrubbing solution and to evaluate the effectiveness of hydrogen peroxide in converting nitrite to nitrate. Author

N95-18176*# La Salle Univ., Philadelphia, PA.
APPLYING COSTS, RISKS AND VALUES EVALUATION (CRAVE) METHODOLOGY TO ENGINEERING SUPPORT REQUEST (ESR) PRIORITIZATION **c81**
Prafulla N. Joglekar *In* Univ. of Central Florida, NASA/ASEE Summer Faculty Fellowship Program. 1994 Research Reports Oct. 1994 p 263-311 (For primary document see N95-18166 05-80)
Avail: CASI HC A03/MF A04

Given limited budget, the problem of prioritization among Engineering Support Requests (ESR's) with varied sizes, shapes, and colors is a difficult one. At the Kennedy Space Center (KSC), the recently developed 4-Matrix (4-M) method represents a step in the right direction as it attempts to combine the traditional criteria of technical merits only with the new concern for cost-effectiveness. However, the 4-M method was not adequately successful in the actual prioritization of ESRs for the fiscal year 1995 (FY95). This research identifies a number of design issues that should help us to develop better methods. It emphasizes that given the variety and diversity of ESR's one should not expect that a single method could help in the assessment of all ESR's. One conclusion is that a methodology such as Costs, Risks, and Values Evaluation (CRAVE) should be adopted. It also is clear that the development of methods such as 4-M requires input not only from engineers with technical expertise in ESR's but also from personnel with adequate background in the theory and practice of cost-effectiveness analysis. At KSC, ESR prioritization is one part of the Ground Support Working Teams (GSWT) Integration Process. It was discovered that the more important barriers to the incorporation of cost-effectiveness considerations in ESR prioritization lie in this process. The culture of integration, and the corresponding structure of review by a committee of peers, is not conducive to the analysis and confrontation necessary in the assessment and prioritization of ESR's. Without assistance from appropriately trained analysts charged with the responsibility to analyze and be confrontational about each ESR, the GSWT steering committee will continue to make its decisions based on incomplete understanding, inconsistent numbers, and at times, colored facts. The current organizational separation of the prioritization and the funding processes is also identified as an important barrier to the pursuit of cost-effectiveness. Perhaps the greatest barrier is that, at the working level, KSC's culture is so preoccupied with technical concerns that it seems almost oblivious to any cost concerns, let alone cost-effectiveness concerns. It is recommended that we must urgently begin to change that culture and seek a better balance between these two concerns. Author

N95-18177*# North Carolina Univ., Charlotte, NC. Dept. of Mechanical Engineering and Engineering Science.
DESIGN OPTIMIZATION OF A BRUSH TURBINE WITH A CLEANER/WATER BASED SOLUTION **c37**
Rhyn H. Kim *In* Univ. of Central Florida, NASA/ASEE Summer Faculty Fellowship Program. 1994 research reports Oct. 1994 p 313-338 (For primary document see N95-18166 05-80)
Avail: CASI HC A03/MF A04

Recently, a fluid turbine which has a brush attached to it has been designed and tested with water as fluid. The purpose of the turbine-brush is to clean up fouling in a tube. The Montreal Protocol prohibits the use of CFC products from refrigeration industry or from industry in general as a cleanser in 1996. Alternatives for the cleansers, devices or a combination of alternative devices with a cleanser should be found. One of the methods is to develop a device which cleans fouling with a cleaning medium. In this paper, we describe a turbine connected with a brush. However, the turbine with the brush should be simple and easy to install. This device is a combined small liquid turbine with a brush. The turbine is activated by the liquid flowing through the tube. Then the turbine turns the brush cleaning fouling along the tube. Based on the energy conservation and the Bernoulli equation along with an empirical relationship of drag force obtained from an experimental apparatus, a relationship of the rotational speed, the number of blades, and geometric variables of the turbine-brush was obtained. The predicted rotational speeds were compared with the experimental observations. Further work was recommended for improvements. Author

N95-18178*# Tuskegee Inst., AL. Dept. of Mechanical Engineering.
RACK INSERTION END EFFECTOR (RIEE) GUIDANCE **c37**
Narasimha S. Malladi *In* Univ. of Central Florida, NASA/ASEE Summer Faculty Fellowship Program. 1994 Research Reports Oct. 1994 p 339-348 (For primary document see N95-18166 05-80)
Avail: CASI HC A02/MF A04

NASA-KSC has developed a mechanism to handle and insert Racks into the Space Station Logistic Modules. This mechanism consists of a Base with 3 motorized degrees of freedom, a 3 section motorized Boom that goes from 15 to 44 feet in length, and a Rack Insertion End Effector (RIEE) with 5 hand wheels for precise alignment. During the 1993 NASA-ASEE Summer Faculty Fellowship Program at KSC, I designed an Active Vision (Camera) Arrangement and developed an algorithm to determine (1) the displacements required by the Room for its initial positioning and (2) the rotations required at the five hand-wheels of the RIEE, for the insertion of the Rack, using the centroids fo the Camera Images of the Location Targets in the Logistic Module. Presently, during the summer of '94, I completed the preliminary design of an easily portable measuring instrument using encoders to obtain the 3-Dimensional Coordinates of Location Targets in the Logistics Module relative to the RIEE mechanism frame. The algorithm developed in '93 can use the output of this instrument also. Simplification of the '93 work and suggestions for the future work are discussed. Author

N95-18179*# Colorado State Univ., Fort Collins, CO. Dept. of Agricultural and Chemical Engineering.
ETHYLENE DYNAMICS IN THE CELSS BIOMASS PRODUCTION CHAMBER **c51**
Allen L. Rakow *In* Univ. of Central Florida, NASA/ASEE Summer Faculty Fellowship Program. 1994 Research Reports Oct. 1994 p 349-378 (For primary document see N95-18166 05-80)
Avail: CASI HC A03/MF A04

A material balance model for ethylene was developed and applied retrospectively to data obtained in the Biomass Production Chamber of CELSS in order to calculate true plant production rates of ethylene. Four crops were analyzed: wheat, lettuce, soybean, and potato. The model represents an effort to account for each and every source and sink for ethylene in the system. The major source of ethylene is the plant biomass and the major sink is leakage to the surroundings. The result, expressed in the units of ppd/day, were converted to nl of ethylene per gram of plant dry mass per hour and compare favorably with recent glasshouse to belljar experiments. Author

N95-18180*# Puerto Rico Univ., Mayaguez. Dept. of Mechanical Engineering.
MECHANICAL BEHAVIOR OF PRECIPITATION HARDENABLE STEELS EXPOSED TO HIGHLY CORROSIVE ENVIRONMENT **c26**
Ferdinand Rosa *In* Univ. of Central Florida, NASA/ASEE Summer Faculty Fellowship Program. 1994 Research Reports Oct. 1994 p 379-417 (For primary document see N95-18166 05-80)
Avail: CASI HC A03/MF A04

Unexpected occurrences of failures, due to stress corrosion cracking (SCC) of structural components, indicate a need for improved characterization of materials and more advanced analytical procedures for reliably predicting structures performance. Accordingly, the purpose of this study was to determine the stress corrosion susceptibility of 15 - 5 PH steel over a wide range of applied strain rates in a highly corrosive environment. The selected environment for this investigation was a 3.5 percent NaCl aqueous solution. The material selected for the study was 15 - 5 PH steel in the H 900 condition. The Slow Strain Rate technique was used to test the metallic specimens. Author

N95-18181*# Florida Inst. of Tech., Melbourne, FL. Program in Aerospace Engineering.
MODELING AND MEASUREMENT OF THE PERFORMANCE OF A BRANCHED CONDUIT SAMPLING SYSTEM IN A MASS SPECTROMETER LEAK DETECTOR **c35**
John M. Russell *In* Univ. of Central Florida, NASA/ASEE Summer Faculty Fellowship Program. 1994 Research Reports Oct. 1994 p 419-448 (For primary document see N95-18166 05-80)
Avail: CASI HC A03/MF A04

In the leak testing of a large engineering system, one may distinguish three stages, namely leakage measurement by an overall enclosure, leak location, and leakage measurement by a local enclosure. Sniffer probes attached to helium mass spectrometer leak detectors are normally designed

for leak location, a qualitative inspection technique intended to pinpoint where a leak is but not to quantify its rate of discharge. The main conclusion of the present effort is that local leakage measurement by a leak detector with a sniffer probe is feasible provided one has: (1) quantitative data on the performance of the mass separator cell (a device interior to the unit where the stream of fluid in the sample line branches); and (2) a means of stabilizing the mass transfer boundary layer that is created near a local leak site when a sniffer probe is placed in its immediate vicinity. Theoretical models of the mass separator cell are provided and measurements of the machine-specific parameters in the formulas are presented. A theoretical model of a porous probe end for stabilizing the mass transfer boundary is also presented. Author

N95-18182*# Embry-Riddle Aeronautical Univ., Daytona Beach, FL. Dept. of Aviation Business Administration.

ASSESSMENT OF A CAREER DEVELOPMENT PROGRAM FOR EXECUTIVE AMD MID-LEVEL MANAGERS

James R. Swanson, Sr. *In* Univ. of Central Florida, NASA/ASEE Summer Faculty Fellowship Program. 1994 Research Reports Oct. 1994 p 449-472 (For primary document see N95-18166 05-80)
Avail: CASI HC A03/MF A04

This project sought to validate the competencies required of mid-level and executive managers at the Kennedy Space Center (KSC), in order to enable an assessment of the Resident Management Education Program (RMEP). Forty (40) statements describing management competencies were presented to a sample of 37 KSC managers, who judged each as essential, useful but not essential, or not needed at each of two management levels. A content validity ratio (CVR) was calculated for each competency statement at the two management levels. There was general agreement on the validity of 36 or the 40 competency statements. Based on the content validity ratios and comments from respondents, recommendations for improvement of the RMEP were made. Author

N95-18183*# Wake Forest Univ., Winston-Salem, NC. Dept. of Mathematics and Computer Science.

ENHANCEMENTS TO THE KATE MODEL-BASED REASONING SYSTEM c63

Stan J. Thomas *In* Univ. of Central Florida, NASA/ASEE Summer Faculty Fellowship Program. 1994 Research Reports Oct. 1994 p 485-508 (For primary document see N95-18166 05-80)
Avail: CASI HC A03/MF A04

KATE (Knowledge-based Autonomous Test Engineer) is a model-based software system developed in the Artificial Intelligence Laboratory at the Kennedy Space Center for monitoring, fault detection, and control of launch vehicles and ground support systems. This report describes two software efforts which enhance the functionality and usability of KATE. The first addition, a flow solver, adds to KATE a tool for modeling the flow of liquid in a pipe system. The second addition adds support for editing KATE knowledge base files to the Emacs editor. The body of this report discusses design and implementation issues having to do with these two tools. It will be useful to anyone maintaining or extending either the flow solver or the editor enhancements. Author

N95-18184*# North Carolina Univ., Charlotte, NC. Dept. of Engineering Tech.

OUTGASSING OF SOLID MATERIAL INTO VACUUM THERMAL INSULATION SPACES c24

Pao-Lien Wang *In* Univ. of Central Florida, NASA/ASEE Summer Faculty Fellowship Program. 1994 Research Reports Oct. 1994 p 509-520 (For primary document see N95-18166 05-80)
Avail: CASI HC A03/MF A04

Many cryogenic storage tanks use vacuum between inner and outer tank for thermal insulation. These cryogenic tanks also use a radiation shield barrier in the vacuum space to prevent radiation heat transfer. This shield is usually constructed by using multiple wraps of aluminized mylar and glass paper as inserts. For obtaining maximum thermal performance, a good vacuum level must be maintained with the insulation system. It has been found that over a period of time solid insulation materials will vaporize into the vacuum space and the vacuum will degrade. In order to determine the degradation of vacuum, the rate of outgassing of the insulation materials must be determined. Outgassing rate of several insulation materials obtained from literature search were listed in tabular form. Author

N95-18185*# Southern Coll. of Technology, Marietta, GA. Dept. of Electrical and Computer Engineering Technology.

FEASIBILITY STUDY OF TRANSMISSION OF OTV CAMERA CONTROL INFORMATION IN THE VIDEO VERTICAL BLANKING INTERVAL c32

Preston A. White, III *In* Univ. of Central Florida, NASA/ASEE Summer Faculty Fellowship Program. 1994 Research Reports Oct. 1994 p 521-543 (For primary document see N95-18166 05-80)
Avail: CASI HC A03/MF A04

The Operational Television system at Kennedy Space Center operates hundreds of video cameras, many remotely controllable, in support of the operations at the center. This study was undertaken to determine if commercial NABTS (North American Basic Teletext System) teletext transmission in the vertical blanking interval of the genlock signals distributed to the cameras could be used to send remote control commands to the cameras and the associated pan and tilt platforms. Wavelength division multiplexed fiberoptic links are being installed in the OTV system to obtain RS-250 short-haul quality. It was demonstrated that the NABTS transmission could be sent over the fiberoptic cable plant without excessive video quality degradation and that video cameras could be controlled using NABTS transmissions over multimode fiberoptic paths as long as 1.2 km. Author

N95-18186*# Missouri Univ., Rolla, MO. Dept. of Computer Science.

PERFORMANCE EVALUATION OF THE NASA/KSC CAD/CAE AND OFFICE AUTOMATION LAN'S c61

George W. Zobrist *In* Univ. of Central Florida, NASA/ASEE Summer Faculty Fellowship Program. 1994 Research Reports Oct. 1994 p 545-567 (For primary document see N95-18166 05-80)
Avail: CASI HC A03/MF A04

This study's objective is the performance evaluation of the existing CAD/CAE (Computer Aided Design/Computer Aided Engineering) network at NASA/KSC. This evaluation also includes a similar study of the Office Automation network, since it is being planned to integrate this network into the CAD/CAE network. The Microsoft mail facility which is presently on the CAD/CAE network was monitored to determine its present usage. This performance evaluation of the various networks will aid the NASA/KSC network managers in planning for the integration of future workload requirements into the CAD/CAE network and determining the effectiveness of the planned FDDI (Fiber Distributed Data Interface) migration. Author

N95-18967*# Alabama Univ., Tuscaloosa, AL. Dept. of Aerospace Engineering.

RESEARCH REPORTS: 1994 NASA/ASEE SUMMER FACULTY FELLOWSHIP PROGRAM Final Report

L. Michael Freeman, ed., Charles R. Chappell, ed. (National Aeronautics and Space Administration. Marshall Space Flight Center, Huntsville, AL.), Frank Six, ed. (National Aeronautics and Space Administration. Marshall Space Flight Center, Huntsville, AL.), and Gerald R. Karr, ed. (Alabama Univ., Huntsville, AL.) Oct. 1994 302 p Fellowship program held in Huntsville, AL, 31 May - 4 Aug. 1994
(Grant NGT-01-002-099)
(NASA-CR-196533; NAS 1.26:196533) Avail: CASI HC A14/MF A03

For the 30th consecutive year, a NASA/ASEE Summer Faculty Fellowship Program was conducted at the Marshall Space Flight Center (MSFC). The basic objectives of the programs, which are in the 31st year of operation nationally, are (1) to further the professional knowledge of qualified engineering and science faculty members; (2) to stimulate an exchange of ideas between participants and NASA; (3) to enrich and refresh the research and teaching activities of participants' institutions; and (4) to contribute to the research objectives of the NASA centers. The Faculty Fellows spent 10 weeks at MSFC engaged in a research project compatible with their interests and background and worked in collaboration with a NASA/MSFC colleague. This document is a compilation of Fellows' reports on their research during the summer of 1994. For individual titles, see N95-18968 through N95-19016.

N95-18968*# Alabama Univ., Huntsville, AL. Dept. of Computer Science.

MSFC INSTITUTIONAL AREA NETWORK AND ATM TECHNOLOGY c32

Ashok T. Amin *In* Alabama Univ., Research Reports: 1994 NASA/ASEE Summer Faculty Fellowship Program Oct. 1994 6 p (For primary

document see N95-18967 05-80)
Avail: CASI HC A02/MF A03

The New Institutional Area Network (NEWIAN) at Marshall supports over 5000 end users with access to 26 file servers providing work presentation services. It is comprised of some 150 Ethernet LAN's interconnected by bridges/routers which are in turn connected to servers over two dual FDDI rings. The network supports various higher level protocols such as IP, IPX, AppleTalk (AT), and DECNet. At present IPX and AT protocols packets are routed, and IP protocol packets are bridged; however, work is in progress to route all IP packets. The impact of routing IP packets on network operation is examined. Broadband Integrated Services Data Network (BISDN), presently at various stages of development, is intended to provide voice, video, and data transfer services over a single network. BISDN will use asynchronous transfer mode (ATM) as a data transfer technique which provides for transmission, multiplexing, switching, and relaying of small size data units called cells. Limited ATM Wide Area Network (WAN) services are offered by Wiltel, AT&T, Sprint, and others. NASA is testing a pilot ATM WAN with a view to provide Program Support Communication Network services using ATM. ATM supports wide range of data rates and quality of service requirements. It is expected that ATM switches will penetrate campus networks as well. However, presently products in these areas are at various stages of development and standards are not yet complete. We examine development of ATM to help assess its role in the evolution of NEWIAN. Derived from text

N95-18969*# Missouri Univ., Rolla, MO. Dept. of Physics.
A COMPARISON BETWEEN USING INCOHERENT OR COHERENT SOURCES TO ALIGN AND TEST AN ADAPTIVE OPTICAL TELESCOPE **c74**
Richard Anderson *In* Alabama Univ., Research Reports: 1994 NASA/ASEE Summer Faculty Fellowship Program Oct. 1994 6 p (For primary document see N95-18967 05-80)
Avail: CASI HC A02/MF A03

The concept in the initial alignment of the segmented mirror adaptive optics telescope called the phased array mirror extendable large aperture telescope (Pamela) is to produce an optical transfer function (OTF) which closely approximates the diffraction limited value which would correspond to a system pupil function that is unity over the aperture and zero outside. There are differences in the theory of intensity measurements between coherent and incoherent radiation. As a result, some of the classical quantities which describe the performance of an optical system for incoherent radiation can not be defined for a coherent field. The most important quantity describing the quality of an optical system is the OTF and for a coherent source the OTF is not defined. Instead a coherent transfer function (CTF) is defined. The main conclusion of the paper is that an incoherent collimated source and not a collimated laser source is preferred to calibrate the Hartmann wavefront sensor (WFS) of an aligned adaptive optical system. A distant laser source can be used with minimum problems to correct the system for atmospheric turbulence. The collimation of the HeNe laser alignment source can be improved by using a very small pin hole in the spatial filter so only the central portion of the beam is transmitted and the beam from the filter is nearly constant in amplitude. The size of this pin hole will be limited by the sensitivity of the lateral effect diode (LEDD) elements. Derived from text

N95-18970*# Tennessee Univ. Space Inst., Tullahoma, TN. Dept. of Engineering Science and Mechanics.
BUBBLE FORMATION IN MICROGRAVITY **c29**
Basil N. Antar *In* Alabama Univ., Research Reports: 1994 NASA/ASEE Summer Faculty Fellowship Program Oct. 1994 6 p (For primary document see N95-18967 05-80)
Avail: CASI HC A02/MF A03

Two KC-135 flight campaigns have been conducted to date which are specifically dedicated to study bubble formation in microgravity. The first flight was conducted during March 14-18, 1994, and the other during June 20-24, 1994. The results from the June 1994 flight have not been analyzed yet, while the results from the March flight have been partially analyzed. In the first flight three different experiments were performed, one with the specific aim at determining whether or not cavitation can take place during any of the fluid handling procedures adopted in the shuttle bioprocessing experiments. The other experiments were concerned with duplicating some of the procedures that resulted in bubble formation, namely the NCS filling procedure and the needle scratch of a solid surface. The results from this set of experiments suggest that cavitation did not take place during any of the fluid handling procedures. The results clearly indicate that almost all were generated as a result of the breakup of the gas/liquid interface. This was convincingly demonstrated in the scratch tests as well as in the liquid fill tests. Derived from text

N95-18971*# Oakwood Coll., Huntsville, AL. Dept.of Chemistry, Biochemistry and Allied Health.
THE ASSESSMENT OF VIRTUAL REALITY FOR HUMAN ANATOMY INSTRUCTION **c52**
Karen P. Benn *In* Alabama Univ., Research Reports: 1994 NASA/ASEE Summer Faculty Fellowship Program Oct. 1994 6 p (For primary document see N95-18967 05-80)
Avail: CASI HC A01/MF A03

This research project seeks to meet the objective of science training by developing, assessing, and validating virtual reality as a human anatomy training medium. In ideal situations, anatomic models, computer-based instruction, and cadaver dissection are utilized to augment the traditional methods of instruction. At many institutions, lack of financial resources limits anatomy instruction to textbooks and lectures. However, human anatomy is three dimensional, unlike the one dimensional depiction found in textbooks and the two dimensional depiction found on the computer. Virtual reality is a breakthrough technology that allows one to step through the computer screen into a three dimensional world. This technology offers many opportunities to enhance science education. Therefore, a virtual testing environment of the abdominopelvic region of a human cadaver was created to study the placement of body parts within the nine anatomical divisions of the abdominopelvic region and the four abdominal quadrants. Derived from text

N95-18972*# Alabama A & M Univ., Huntsville, AL. Dept. of Engineering Technology.
RESIDUAL STRESSES IN WELDED PLATES **c39**
Edward L. Bernstein *In* Alabama Univ., Research Reports: 1994 NASA/ASEE Summer Faculty Fellowship Program Oct. 1994 6 p (For primary document see N95-18967 05-80)
Avail: CASI HC A02/MF A03

The purpose of this project was to develop a simple model which could be used to study residual stress. The mechanism that results in residual stresses in the welding process starts with the deposition of molten weld metal which heats the immediately adjacent material. After solidification of weld material, normal thermal shrinkage is resisted by the adjacent, cooler material. When the thermal strain exceeds the elastic strain corresponding to the yield point stress, the stress level is limited by this value, which decreases with increasing temperature. Cooling then causes elastic unloading which is restrained by the adjoining material. Permanent plastic strain occurs, and tension is caused in the region immediately adjacent to the weld material. Compression arises in the metal farther from the weld in order to maintain overall static equilibrium. Subsequent repair welds may add to the level of residual stresses. The level of residual stress is related to the onset of fracture during welding. Thus, it is of great importance to be able to predict the level of residual stresses remaining after a weld procedure, and to determine the factors, such as weld speed, temperature, direction, and number of passes, which may affect the magnitude of remaining residual stress. It was hoped to use traditional analytical modeling techniques so that it would be easier to comprehend the effect of these variables on the resulting stress. This approach was chosen in place of finite element methods so as to facilitate the understanding of the physical processes. The accuracy of the results was checked with some existing experimental studies giving residual stress levels found from x-ray diffraction measurements. Derived from text

N95-18973*# Union Coll., Schenectady, NY. Dept. of Mechanical Engineering.
FOREIGN BODY IMPACT EVENT DAMAGE FORMATION IN COMPOSITE STRUCTURES **c24**
Ronald B. Bucinell *In* Alabama Univ., Research Reports: 1994 NASA/ASEE Summer Faculty Fellowship Program Oct. 1994 6 p (For primary document see N95-18967 05-80)
Avail: CASI HC A02/MF A03

This report discusses a methodology that can be used to assess the

effect of foreign body impacts on composite structural integrity. The described effort focuses on modeling the effect of a central impact on a 5 3/4 inch filament wound test article. The discussion will commence with details of the material modeling that was used to establish the input properties for the analytical model. This discussion is followed by an overview of the impact assessment methodology. The progress on this effort to date is reviewed along with a discussion of tasks that have yet to be completed.

Derived from text

N95-18974*# Alabama Univ., Huntsville, AL. Dept. of Civil and Environmental Engineering.

A FINITE ELEMENT CODE FOR ELECTRIC MOTOR DESIGN c33

C. Warren Campbell *In* Alabama Univ., Research Reports: 1994 NASA/ASEE Summer Faculty Fellowship Program Oct. 1994 6 p (For primary document see N95-18967 05-80)

Avail: CASI HC A02/MF A03

FEMOT is a finite element program for solving the nonlinear magnetostatic problem. This version uses nonlinear, Newton first order elements. The code can be used for electric motor design and analysis. FEMOT can be embedded within an optimization code that will vary nodal coordinates to optimize the motor design. The output from FEMOT can be used to determine motor back EMF, torque, cogging, and magnet saturation. It will run on a PC and will be available to anyone who wants to use it.

Derived from text

N95-18975*# Marquette Univ., Milwaukee, WI. Dept. of Mechanical and Industrial Engineering.

CONCEPT OF USING A BENCHMARK PART TO EVALUATE RAPID PROTOTYPE PROCESSES c31

Vikram Cariapa *In* Alabama Univ., Research Reports: 1994 NASA/ASEE Summer Faculty Fellowship Program Oct. 1994 6 p (For primary document see N95-18967 05-80)

Avail: CASI HC A02/MF A03

A conceptual benchmark part for guiding manufacturers and users of rapid prototyping technologies is proposed. This is based on a need to have some tool to evaluate the development of this technology and to assist the user in judiciously selecting a process. The benchmark part is designed to have unique product details and features. The extent to which a rapid prototyping process can reproduce these features becomes a measure of the capability of the process. Since rapid prototyping is a dynamic technology, this benchmark part should be used to continuously monitor process capability of existing and developing technologies. Development of this benchmark part is, therefore, based on an understanding of the properties required from prototypes and characteristics of various rapid prototyping processes and measuring equipment that is used for evaluation.

Derived from text

N95-18976*# University of Southern Illinois, Carbondale, IL. Dept. of Mechanical Engineering and Energy Processes.

COMPOSITE STRUCTURES FOR MAGNETOSPHERE IMAGER SPACECRAFT c18

Tsuchin Chu *In* Alabama Univ., Research Reports: 1994 NASA/ASEE Summer Faculty Fellowship Program Oct. 1994 6 p (For primary document see N95-18967 05-80)

Avail: CASI HC A02/MF A03

Results of a trade study addressing the issues and benefits in using carbon fiber reinforced composites for the Magnetosphere Imager (MI) spacecraft are presented. The MI mission is now part of the Sun/Earth Connection Program. To qualify for this category, new technology and innovative methods to reduce the cost and size have to be considered. Topics addressed cover: (1) what is a composite, including advantages and disadvantages of composites and carbon/graphite fibers; and (2) structural design for MI, including composite design configuration, material selection, and analysis of composite structures.

CASI

N95-18977*# Pennsylvania State Univ., University Park, PA. Dept. of Meteorology.

IMPLICATIONS OF SUMMERTIME MARINE STRATOCUMULUS ON THE NORTH AMERICAN CLIMATE c47

John H. E. Clark *In* Alabama Univ., Research Reports: 1994 NASA/ASEE Summer Faculty Fellowship Program Oct. 1994 6 p (For primary document see N95-18967 05-80)

Avail: CASI HC A02/MF A03

This study focuses on the effects of summertime stratocumulus over the eastern Pacific. This cloud is linked to the semi-permanent sub-tropical highs that dominate the low-level circulation over the Pacific and Atlantic. Subsidence on the eastern flank of these highs creates an inversion based about 800 m above sea level that caps moist air near the surface. This air overlies cool waters driven by upwelling along the coastal regions of North America. Strong surface north-westerlies mix the boundary layer enough to saturate the air just below the capping inversion. Widespread stratocumulus is thus formed. All calculations were carried out using the GENESIS general circulation model that was run at MSFC. Among the more important properties of the model is that it includes radiative forcing due to absorption of solar radiation and the emission of infrared radiation, interactive clouds (both stratocumulus and cumulus types), exchanges of heat and moisture with the lower boundary. Clouds are interactive in the sense that they impact the circulation by modifying the fields of radiative heating and turbulent fluxes of heat and moisture in the boundary layer. In turn, clouds are modified by the winds through the advection of moisture. In order to isolate the effects of mid- and high-latitude stratocumulus, two runs were made with the model: one with and the other without stratocumulus. The runs were made for a year, but with perpetual July conditions, i.e., solar forcing was fixed. The diurnal solar cycle, however, was allowed for. The sea surface temperature distribution was fixed in both runs to represent climatological July conditions. All dependent variables were represented at 12 surfaces of constant sigma = p/p(sub O), where p is pressure and p(sub O) is surface pressure. To facilitate analysis, model output was transformed to constant pressure surfaces. Structures no smaller in size than 7.5 degrees longitude and 4.5 degrees in latitude were resolved. Smaller features of the circulation were parameterized. The model thus captures synoptic- and planetary-scale circulation features.

Derived from text

N95-18978*# Oklahoma Univ., Norman, OK. School of Electrical Engineering.

PERFORMANCE EVALUATION OF THE ENGINEERING ANALYSIS AND DATA SYSTEMS (EADS) 2 c82

Linda S. DeBrunner *In* Alabama Univ., Research Reports: 1994 NASA/ASEE Summer Faculty Fellowship Program Oct. 1994 6 p (For primary document see N95-18967 05-80)

Avail: CASI HC A02/MF A03

The Engineering Analysis and Data System (EADS)II (1) was installed in March 1993 to provide high performance computing for science and engineering at Marshall Space Flight Center (MSFC). EADS II increased the computing capabilities over the existing EADS facility in the areas of throughput and mass storage. EADS II includes a Vector Processor Compute System (VPCS), a Virtual Memory Compute System (CFS), a Common Output System (COS), as well as Image Processing Station, Mini Super Computers, and Intelligent Workstations. These facilities are interconnected by a sophisticated network system. This work considers only the performance of the VPCS and the CFS. The VPCS is a Cray YMP. The CFS is implemented on an RS 6000 using the UniTree Mass Storage System. To better meet the science and engineering computing requirements, EADS II must be monitored, its performance analyzed, and appropriate modifications for performance improvement made. Implementing this approach requires tool(s) to assist in performance monitoring and analysis. In Spring 1994, PerfStat 2.0 was purchased to meet these needs for the VPCS and the CFS. PerfStat(2) is a set of tools that can be used to analyze both historical and real-time performance data. Its flexible design allows significant user customization. The user identifies what data is collected, how it is classified, and how it is displayed for evaluation. Both graphical and tabular displays are supported. The capability of the PerfStat tool was evaluated, appropriate modifications to EADS II to optimize throughput and enhance productivity were suggested and implemented, and the effects of these modifications on the systems performance were observed. In this paper, the PerfStat tool is described, then its use with EADS II is outlined briefly. Next, the evaluation of the VPCS, as well as the modifications made to the system are described. Finally, conclusions are drawn and recommendations for future worked are outlined.

Derived from text

N95-18979*# Alabama Univ., Huntsville, AL. Dept. of Mechanical and Aerospace Engineering.

OPTICAL MEASUREMENTS IN ROCKET ENGINE LIQUID SPRAYS **c20**

Douglas A. Feikema *In* Alabama Univ., Research Reports: 1994 NASA/ASEE Summer Faculty Fellowship Program Oct. 1994 6 p (For primary document see N95-18967 05-80)

Avail: CASI HC A02/MF A03

The performance of liquid propellant rocket engines is dependent upon many elements of the entire system. One of the most fundamental and most critical is the performance of the injector elements. Their characterization is an important part of the development of combustion devices. Optical measurements within these environments have proven to be invaluable tools in quantifying the physical environment of two phase flows. The effort reported herein involves the measurement of drop velocity, drop size, and most importantly mass flux using Phase-Doppler Particle Anemometry within a spray generated by a single swirl injector element operating in atmospheric pressure conditions. The mass flux has been determined and validated by mechanical patternation methods and by profile integration of the mass flux. Derived from text

N95-18980*# Ohio Univ., Athens. Dept. of Industrial and Systems Engineering.

DATA DRIVEN PROPULSION SYSTEM WEIGHT PREDICTION MODEL **c20**

Richard J. Gerth *In* Alabama Univ., Research Reports: 1994 NASA/ASEE Summer Faculty Fellowship Program Oct. 1994 6 p (For primary document see N95-18967 05-80)

Avail: CASI HC A02/MF A03

The objective of the research was to develop a method to predict the weight of paper engines, i.e., engines that are in the early stages of development. The impetus for the project was the Single Stage To Orbit (SSTO) project, where engineers need to evaluate alternative engine designs. Since the SSTO is a performance driven project the performance models for alternative designs were well understood. The next tradeoff is weight. Since it is known that engine weight varies with thrust levels, a model is required that would allow discrimination between engines that produce the same thrust. Above all, the model had to be rooted in data with assumptions that could be justified based on the data. The general approach was to collect data on as many existing engines as possible and build a statistical model of the engines weight as a function of various component performance parameters. This was considered a reasonable level to begin the project because the data would be readily available, and it would be at the level of most paper engines, prior to detailed component design. Derived from text

N95-18981*# Kansas Univ., Lawrence, KS. Dept. of Mechanical Engineering.

REAL-TIME THICKNESS MEASUREMENT OF MCC ABLATOR MATERIAL **c24**

R. Bryan Greenway, Jr. *In* Alabama Univ., Research Reports: 1994 NASA/ASEE Summer Faculty Fellowship Program Oct. 1994 6 p (For primary document see N95-18967 05-80)

Avail: CASI HC A02/MF A03

One of the most favorable characteristics of the Space Shuttle Program is the reusability of two of its primary components: the orbiter itself and the Solid Rocket Boosters (SRB). The SRB's provide the primary source of propulsion for the Space Shuttle during take-off after which they are recovered for refurbishment and reuse. During refurbishment, the SRB's are stripped of all remaining ablative (heat resistant) coating. A new layer is applied to the appropriate sections (nose cone, frustum, forward skirt, and aft skirt). It is the process of applying the ablative coating which provided the impetus for this project. The thickness of this protective layer is considered to be of primary importance to the level of thermal protection provided. The objectives of this effort are to investigate possible techniques for measuring the thickness of MCC, and if possible to test the specific capabilities of those considered good candidates for implementation. The system would be able to take measurements in real-time as close to the spray gun as possible. This will allow the information to be used in the control of the process without an inordinate time delay between a measurement and its appropriate response. The thickness of the deposited material is to be measured with less than 0.100 in if uncertainty. This is the defined tolerance window for the ablator thickness. Finally, it must operate within the confines of the chamber which encloses the turntable, robot, and spray system, and therefore is required to be insensitive to, or at least maintainable in, that environment. Derived from text

N95-18982*# Auburn Univ., AL. Dept. of Aerospace Enginerring.

STEADY AND UNSTEADY BLADE STRESSES WITHIN THE SSME ATD/HPOTP INDUCER **c20**

R. Steven Gross *In* Alabama Univ., Research Reports: 1994 NASA/ASEE Summer Faculty Fellowship Program Oct. 1994 6 p (For primary document see N95-18967 05-80)

Avail: CASI HC A02/MF A03

There were two main goals of the ATD HPOTP (alternate turbopump development)(high pressure oxygen turbopump). First, determine the steady and unsteady inducer blade surface strains produced by hydrodynamic sources as a function of flow capacity (Q/N), suction specific speed (Nss), and Reynolds number (Re). Second, to identify the hydrodynamic source(s) of the unsteady blade strains. The reason the aforementioned goals are expressed in terms of blade strains as opposed to blade hydrodynamic pressures is because of the interest regarding the high cycle life of the inducer blades. This report focuses on the first goal of the test program which involves the determination of the steady and unsteady strain (stress) values at various points within the inducer blades. Strain gages were selected as the strain measuring devices. Concurrent with the experimental program, an analytical study was undertaken to produce a complete NASTRAN finite-element model of the inducer. Computational fluid dynamics analyses were utilized to provide the estimated steady-state blade surface pressure loading needed as load input to the NASTRAN inducer model. Derived from text

N95-18983*# Oregon Graduate Center for Study and Research, Beaverton, OR. Dept. of Electrical Engineering and Applied Physics.

SPECIAL RELATIVITY EFFECTS FOR SPACE-BASED COHERENT LIDAR EXPERIMENTS **c33**

V. S. RaoGudimetla *In* Alabama Univ., Research Reports: 1994 NASA/ASEE Summer Faculty Fellowship Program Oct. 1994 6 p (For primary document see N95-18967 05-80)

Avail: CASI HC A02/MF A03

There is a great need to develop a system that can measure accurately atmospheric wind profiles because an accurate data of wind profiles in the atmosphere constitutes single most input for reliable simulations of global climate numerical methods. Also such data helps us understand atmospheric circulation and climate dynamics better. Because of this need for accurate wind measurements, a space-based Laser Atmospheric Winds Sounder (LAWS) is being designed at MSFC to measure wind profiles in the lower atmosphere of the earth with an accuracy of 1 m/s at lower altitudes to 5m/s at higher altitudes. This system uses an orbiting spacecraft with a pulsed laser source and measures the Doppler shift between the transmitted and received frequencies to estimate the atmospheric wind velocities. If a significant return from the ground (sea) is possible, the spacecraft speed and height are estimated from it and these results and the Doppler shift are then used to estimate the wind velocities in the atmosphere. It is expected that at the proposed wavelengths, there will be enough backscatter from the aerosols but there may no be significant return from the ground. So a coherent (heterodyne) detection system is being proposed for signal processing because it can provide high signal to noise ratio and sensitivity and thus make the best use of low ground return. However, for a heterodyne detection scheme to provide the best results, it is important that the receiving aperture be aligned properly for the proposed wind sounder, this amounts to only a few microradians tolerance in alignment. It is suspected that the satellite motion relative to the ground may introduce errors in the order of a few microradians because of special relativity. Hence, the problem of laser scattering off a moving fixed target when the source and receiver are moving, which was not treated in the past in the literature, was analyzed in the following, using relativistic electrodynamics and applied to the case of the space-based coherent lidar, assuming flat ground. Here an interest in developing analytical expression for the location of the receiving point for the return with respect to the satellite, receiving angle and Doppler shift in frequency and amount of tip, all as measured in the satellite moving coordinate system and the diffuse scattering angle at the ground which does not require any compensation. All the three cases of retro-reflection, specular reflection and diffuse scattering by the ground

should be treated though retro-reflection and diffuse scattering are more important. Derived from text

N95-18984*# Northwest Shoals Community Coll., Phil Campbell, AL. Dept. of Electro-Optics.
SURFACE ROUGHNESS MEASUREMENTS **c74**
Thomas G. Howard *In* Alabama Univ., Research Reports: 1994 NASA/ASEE Summer Faculty Fellowship Program Oct. 1994 3 p (For primary document see N95-18967 05-80)
Avail: CASI HC A01/MF A03

The Optics Division is currently in the research phase of producing grazing-incidence mirrors to be used in x-ray detector applications. The traditional method of construction involves labor-intensive glass grinding. This also culminates in a relatively heavy mirror. For lower resolution applications, the mirrors may be of a replicated design which involves milling a mandrel as a negative of the final shape and electroplating the cylindrical mirror onto it. The mirror is then separated from the mandrel by cooling. The mandrel will shrink more than the 'shell' (mirror) allowing it to be pulled from the mandrel. Ulmer (2) describes this technique and its variations in more detail. To date, several mirrors have been tested at MSFC by the Optical Fabrication Branch by focusing x-ray energy onto a detector with limited success. Little is known about the surface roughness of the actual mirror. Hence, the attempt to gather data on these surfaces. The test involves profiling the surface of a sample, replicating the surface as described above, and then profiling the replicated surface. Derived from text

N95-18985*# Catawba Coll., Salisbury, NC. Dept. of Chemistry.
PROBING THE CHEMISTRY OF NICKEL/METAL HYDRIDE BATTERY CELLS USING ELECTROCHEMICAL IMPEDANCE SPECTROSCOPY **c33**
Bryan J. Isaac *In* Alabama Univ., Research Reports: 1994 NASA/ASEE Summer Faculty Fellowship Program Oct. 1994 6 p (For primary document see N95-18967 05-80)
Avail: CASI HC A02/MF A03

Electrochemical Impedance Spectroscopy (EIS) is a valuable tool for investigating the chemical and physical processes occurring at electrode surfaces. It offers information about electron transfer at interfaces, kinetics of reactions, and diffusion characteristics of the bulk phase between the electrodes. For battery cells, this technique offers another advantage in that it can be done without taking the battery apart. This non-destructive analysis technique can thus be used to gain a better understanding of the processes occurring within a battery cell. This also raises the possibility of improvements in battery design and identification or prediction of battery characteristics useful in industry and aerospace applications. EIS as a technique is powerful and capable of yielding significant information about the cell, but it also requires that the many parameters under investigation can be resolved. This implies an understanding of the processes occurring in a battery cell. Many battery types were surveyed in this work, but the main emphasis was on nickel/metal hydride batteries. Derived from text

N95-18986*# Alabama Univ., Tuscaloosa, AL. Dept. of Electrical Engineering.
A HYPERTEXT-BASED INTERNET-ASSESSABLE DATABASE FOR THE MSFC TECHNOLOGY TRANSFER OFFICE **c82**
Jeff Jackson *In its* Research Reports: 1994 NASA/ASEE Summer Faculty Fellowship Program Oct. 1994 6 p (For primary document see N95-18967 05-80)
Avail: CASI HC A02/MF A03

There exists a continuing need to disseminate technical information and facilities capabilities from NASA field centers in an effort to promote the successful transfer of technologies developed with public funds to the private sector. As technology transfer is a stated NASA mission, there exists a critical need for NASA centers to document technology capabilities and disseminate this information on as wide a basis as possible. Certainly local and regional dissemination is critical, but global dissemination of scientific and engineering facilities and capabilities gives NASA centers the ability to contribute to technology transfer on a much broader scale. Additionally, information should be disseminated in a complete and rapidly available form. To accomplish this information dissemination, the unique capabilities of the Internet are being exploited. The Internet allows widescale information distribution in a rapid fashion to aid in the accomplishment of technology transfer goals established by the NASA/MSFC Technology Transfer Office. Rapid information retrieval coupled with appropriate electronic feedback, allows the scientific and technical capabilities of Marshall Space Flight Center, often unique in the world, to be explored by a large number of potential benefactors of NASA (or NASA-derived) technologies. Electronic feedback, coupled with personal contact with the MSFC Technology Transfer Office personnel, allows rapid responses to technical requests from industry and academic personnel as well as private citizens. The remainder of this report gives a brief overview of the Mosaic software and a discussion of technology transfer office and laboratory facilities data that have been made available on the Internet to promote technology transfer. Derived from text

N95-18987*# Auburn Univ., AL. Dept. of Aerospace Engineering.
A PRELIMINARY ANALYSIS OF LOW FREQUENCY PRESSURE OSCILLATIONS IN HYBRID ROCKET MOTORS **c20**
Rhonald M. Jenkins *In* Alabama Univ., Research Reports: 1994 NASA/ASEE Summer Faculty Fellowship Program Oct. 1994 6 p (For primary document see N95-18967 05-80)
Avail: CASI HC A02/MF A03

Past research with hybrid rockets has suggested that certain motor operating conditions are conducive to the formation of pressure oscillations, or flow instabilities, within the motor combustion chamber. These combustion-related vibrations or pressure oscillations may be encountered in virtually any type of rocket motor and typically fall into three frequency ranges: low frequency oscillations (0-300 Hz); intermediate frequency oscillations (400-1000 Hz); and high frequency oscillations (greater than 1000 Hz). In general, combustion instability is characterized by organized pressure oscillations occurring at well-defined intervals with pressure peaks that may maintain themselves, grow, or die out. Usually, such peaks exceed +/- 5% of the mean chamber pressure. For hybrid motors, these oscillations have been observed to grow to a limiting amplitude which may be dependent on factors such as fuel characteristics, oxidizer injector characteristics, average chamber pressure, oxidizer mass flux, combustion chamber length, and grain geometry. The approach taken in the present analysis is to develop a modified chamber length, L, instability theory which accounts for the relationship between pressure and oxidizer to fuel concentration ratio in the motor. Derived from text

N95-18988*# North Carolina Agricultural and Technical State Univ., Greensboro, NC. Dept. of Mechanical Engineering.
DEVELOPMENT OF CFD MODEL FOR AUGMENTED CORE TRIPROPELLANT ROCKET ENGINE **c20**
Kenneth M. Jones *In* Alabama Univ., Research Reports: 1994 NASA/ASEE Summer Faculty Fellowship Program Oct. 1994 6 p (For primary document see N95-18967 05-80)
Avail: CASI HC A02/MF A03

The Space Shuttle era has made major advances in technology and vehicle design to the point that the concept of a single-stage-to-orbit (SSTO) vehicle appears more feasible. NASA presently is conducting studies into the feasibility of certain advanced concept rocket engines that could be utilized in a SSTO vehicle. One such concept is a tripropellant system which burns kerosene and hydrogen initially and at altitude switches to hydrogen. This system will attain a larger mass fraction because LOX-kerosene engines have a greater average propellant density and greater thrust-to-weight ratio. This report describes the investigation to model the tripropellant augmented core engine. The physical aspects of the engine, the CFD code employed, and results of the numerical model for a single modular thruster are discussed. Derived from text

N95-18989*# Alabama Univ., Huntsville, AL. Dept. of Mechanical and Aerospace Engineering.
COMPUTATIONAL SIMULATION OF LIQUID FUEL ROCKET INJECTORS **c20**
D. Brian Landrum *In* Alabama Univ., Research Reports: 1994 NASA/ASEE Summer Faculty Fellowship Program Oct. 1994 6 p (For primary document see N95-18967 05-80)
Avail: CASI HC A02/MF A03

A major component of any liquid propellant rocket is the propellant injection system. Issues of interest include the degree of liquid vaporization and its impact on the combustion process, the pressure and temperature fields in the combustion chamber, and the cooling of the injector face and

chamber walls. The Finite Difference Navier-Stokes (FDNS) code is a primary computational tool used in the MSFC Computational Fluid Dynamics Branch. The branch has dedicated a significant amount of resources to development of this code for prediction of both liquid and solid fuel rocket performance. The FDNS code is currently being upgraded to include the capability to model liquid/gas multi-phase flows for fuel injection simulation. An important aspect of this effort is benchmarking the code capabilities to predict existing experimental injection data. The objective of this MSFC/ASEE Summer Faculty Fellowship term was to evaluate the capabilities of the modified FDNS code to predict flow fields with liquid injection. Comparisons were made between code predictions and existing experimental data. A significant portion of the effort included a search for appropriate validation data. Also, code simulation deficiencies were identified. Derived from text

N95-18990*# East Carolina Univ., Greenville, NC. School of Human Environmental Sciences.

DEVELOPMENT OF MICROGRAVITY, FULL BODY FUNCTIONAL REACH ENVELOPE USING 3-D COMPUTER GRAPHIC MODELS AND VIRTUAL REALITY TECHNOLOGY **c54**

Patricia F. Lindsey *In* Alabama Univ., Research Reports: 1994 NASA/ASEE Summer Faculty Fellowship Program Oct. 1994 6 p (For primary document see N95-18967 05-80)

Avail: CASI HC A02/MF A03

In microgravity conditions mobility is greatly enhanced and body stability is difficult to achieve. Because of these difficulties, optimum placement and accessibility of objects and controls can be critical to required tasks on board shuttle flights or on the proposed space station. Anthropometric measurement of the maximum reach of occupants of a microgravity environment provide knowledge about maximum functional placement for tasking situations. Calculations for a full body, functional reach envelope for microgravity environments are imperative. To this end, three dimensional computer modeled human figures, providing a method of anthropometric measurement, were used to locate the data points that define the full body, functional reach envelope. Virtual reality technology was utilized to enable an occupant of the microgravity environment to experience movement within the reach envelope while immersed in a simulated microgravity environment. Derived from text

N95-18991*# Georgia Univ., Athens. Dept. of Geography.

A GIS APPROACH TO URBAN HEAT ISLAND RESEARCH: THE CASE OF HUNTSVILLE, ALABAMA **c45**

Chor Pong Lo *In* Alabama Univ., Research Reports: 1994 NASA/ASEE Summer Faculty Fellowship Program Oct. 1994 6 p (For primary document see N95-18967 05-80)

Avail: CASI HC A02/MF A03

The urban heat island represents a case of inadvertent human modification of climate in an urban environment. Urbanization changes the nature of the surface and atmospheric properties of a region. As a result, radiation balance in the urban areas is altered and sensible heat is added to the point that urban areas are warmer than surrounding rural areas. At the boundary between the rural and urban area, a sharp rise in temperature occurs, culminating to a peak temperature at the central business district of the city, hence the name 'urban heat island'. The extent and intensity of the urban heat island are a function of population size, land use, and topography. Because the urban heat island exhibits spatial variations of temperatures, the use of Geographic Information System (GIS) is appropriate. The research on the urban heat island focuses on the acquisition of 15 bands of visible and thermal infrared data (ranging from 0.45 to 12.2 microns) from an aerial platform using NASA's ATLAS (Airborne Thermal/Visible Land Application Sensor) over Huntsville, Alabama. The research reported in this paper is an analysis of the impact of population, land use, and topography on the shape of the urban heat island that could be developed in Huntsville using the GIS approach. The outcome of this analysis can then be verified using the acquired remotely sensed data. Derived from text

N95-18992*# Texas A&M Univ., College Station, TX.

NEURAL NETWORKS APPLICATIONS TO CONTROL AND COMPUTATIONS **c63**

Leon A. Luxemburg *In* Alabama Univ., Research Reports: 1994 NASA/ASEE Summer Faculty Fellowship Program Oct. 1994 6 p (For primary document see N95-18967 05-80)

Avail: CASI HC A02/MF A03

Several interrelated problems in the area of neural network computations are described. First an interpolation problem is considered, then a control problem is reduced to a problem of interpolation by a neural network via Lyapunov function approach, and finally a new, faster method of learning as compared with the gradient descent method, was introduced. Derived from text

N95-18993*# State Univ. of New York, Oneonta, NY. Dept. of Physics and Astronomy.

A CMC DATABASE FOR USE IN THE NEXT GENERATION LAUNCH VEHICLES (ROCKETS) **c15**

Kamala Mahanta *In* Alabama Univ., Research Reports: 1994 NASA/ASEE Summer Faculty Fellowship Program Oct. 1994 6 p (For primary document see N95-18967 05-80)

Avail: CASI HC A02/MF A03

Ceramic matrix composites (CMC's) are being envisioned as the state-of-the-art material capable of handling the tough structural and thermal demands of advanced high temperature structures for programs such as the SSTO (Single Stage to Orbit), HSCT (High Speed Civil Transport), etc. as well as for evolution of the industrial heating systems. Particulate, whisker and continuous fiber ceramic matrix (CFCC) composites have been designed to provide fracture toughness to the advanced ceramic materials which have a high degree of wear resistance, hardness, stiffness, and heat and corrosion resistance but are notorious for their brittleness and sensitivity to microscopic flaws such as cracks, voids and impurity. Author

N95-18994*# Vanderbilt Univ., Nashville, TN. Dept. of Mechanical Engineering.

LEAN SPACECRAFT AVIONICS TRADE STUDY **c19**

John A. Main *In* Alabama Univ., Research Reports: 1994 NASA/ASEE Summer Faculty Fellowship Program Oct. 1994 6 p (For primary document see N95-18967 05-80)

Avail: CASI HC A02/MF A03

Spacecraft design is generally an exercise in design trade-offs: fuel vs. weight, power vs. solar cell area, radiation exposure vs. shield weight, etc. Proper analysis of these trades is critical in the development of lightweight, efficient, 'lean' satellites. The modification of the launch plans for the Magnetosphere Imager (MI) to a Taurus launcher from the much more powerful Delta has forced a reduction in spacecraft weight availability into the mission orbit from 1300 kg to less than 500 kg. With weight now a driving factor it is imperative that the satellite design be extremely efficient and lean. The accuracy of engineering trades now takes on an added importance. An understanding of spacecraft subsystem interactions is critical in the development of a good spacecraft design, yet it is a challenge to define these interactions while the design is immature. This is currently an issue in the development of the preliminary design of the MI. The interaction and interfaces between this spacecraft and the instruments it carries are currently unclear since the mission instruments are still under development. It is imperative, however, to define these interfaces so that avionics requirements ideally suited to the mission's needs can be determined. Derived from text

N95-18995*# Marquette Univ., Milwaukee, WI. Dept. of Physics.

MANN: A PROGRAM TO TRANSFER DESIGNS FOR DIFFRACTIVE OPTICAL ELEMENTS TO A MANN PHOTOLITHOGRAPHIC MASK GENERATOR **c74**

Donald R. Matthys *In* Alabama Univ., Research Reports: 1994 NASA/ASEE Summer Faculty Fellowship Program Oct. 1994 6 p (For primary document see N95-18967 05-80)

Avail: CASI HC A02/MF A03

There are two basic areas of interest for diffractive optics. In the first, the property of wavefront division is exploited for achieving optical fanout, analogous to the more familiar electrical fanout of electronic circuitry. The basic problem here is that when using a simple uniform diffraction grating the energy input is divided unevenly among the output beams. The other area of interest is the use of diffractive elements to replace or supplement standard refractive elements such as lenses. Again, local grating variations can be used to control the amount of bending imparted to optical rays, and the efficiency of the diffractive element will depend on how closely the element can be matched to the design requirements. In general,

production restrictions limit how closely the element approaches the design, and for the common case of photolithographic production, a series of binary masks is required to achieve high efficiency. The actual design process is much more involved than in the case of elements for optical fanout, as the desired phase of the optical wavefront over some reference plane must be specified and the phase alteration to be introduced at each point by the diffraction element must be known. This generally requires the utilization of a standard optical design program. Two approaches are possible. In the first approach, the diffractive element is treated as a special type of lens and the ordinary optical design equations are used. Optical design programs tend to follow a second approach, namely, using the equations of optical interference derived from holographic theory and then allowing the introduction of phase front corrections in the form of polynomial equations. By using either of these two methods, diffractive elements can be used not only to compensate for distortions such as chromatic or spherical aberration, but also to perform the work of a variety of other optical elements such as null correctors, beam shapers, etc. The main focus of the project described in this report is how the design information from the lens design program is incorporated into the photolithographic process. It is shown that the MANN program, a photolithographic mask generator, fills the need for a link between lens design programs and mask generation controllers.The generated masks can be used to expose a resist-coated substrate which is etched and then must be re-coated, re-exposed, and re-etched for making copies, just as in the electronics industry. Derived from text

N95-18996*# Texas Christian Univ., Fort Worth, TX. Dept. of Engineering.

DESIGN OF HIGH PRESSURE WATERJET NOZZLES **c34**

Andre P. Mazzoleni *In* Alabama Univ., Research Reports: 1994 NASA/ASEE Summer Faculty Fellowship Program Oct. 1994 6 p (For primary document see N95-18967 05-80)
Avail: CASI HC A02/MF A03

The Hydroblast Research Cell at Marshall Space Flight Center is used to investigate the use of high pressure waterjets to strip paint, grease, adhesive and thermal spray coatings from various substrates. Current methods of cleaning often use ozone depleting chemicals (ODC) such as chlorinated solvents. High pressure waterjet cleaning has proven to be a viable alternative to the use of solvents. A popular method of waterjet cleaning involves the use of a rotating, multijet, high pressure water nozzle which is robotically controlled. This method enables rapid cleaning of a large area, but problems such as incomplete coverage and damage to the substrate from the waterjet have been observed. This report summarizes research consisting of identifying and investigating the basic properties of rotating, multijet, high pressure water nozzles, and how particular designs and modes of operation affect such things as stripping rate, standoff distance and completeness of coverage. The study involved computer simulations, an extensive literature review, and experimental studies of different nozzle designs. Author (revised)

N95-18997*# Alabama Univ., Huntsville, AL. Dept. of Biological Sciences.

CONCENTRATION AND TEMPERATURE EFFECTS ON OVOSTATIN ACTIVITY **c51**

Debra M. Moriarity *In* Alabama Univ., Research Reports: 1994 NASA/ASEE Summer Faculty Fellowship Program Oct. 1994 6 p (For primary document see N95-18967 05-80)
Avail: CASI HC A02/MF A03

Light scattering experiments performed at Mississippi State University using MSFC ovostatin preparations indicated that at low ovostatin concentrations, below 0.2 mg/ml, the protein was dissociating from a tetramer into dimers. Since the proposed mechanism of action involved the tetrameric form of the protein, we hypothesized that perhaps under the conditions of our assays at various O/T ratios the ovostatin was becoming dissociated into an inactive dimer. To examine this possibility we assayed the ovostatin activity as a function of ovostatin concentration and of temperature of the assay. Data are presented that show the results of these assays at 23 C, 30 C, 37 C and 42 C respectively. The data are highly suggestive that there is a decrease in ovostatin activity as the concentration of the protein falls below 0.06 mg/ml. This may not be of any physiological importance, however, since the concentration of ovostatin in the egg is about 0.5 mg/ml. Curiously, the dissociation of the tetramer into dimers does not show a significant temperature dependence as would be expected for an equilibrium reaction. Whether this is in fact the case, or whether the differences are so small as to not be discerned from the current data remains to be seen. Another aspect to consider is that in the egg the primary role of the ovostatin may or may not be as a protease inhibitor. Although the inhibition of collagenase by ovostatin may be an important aspect of embryogenesis, it is also possible that it functions as a binding protein for some substance. In this regard, all ovostatin preparations from MSFC have shown an approximately 88,000 MW protein associated with the ovostatin. The identity of this protein is not currently known and may be the subject of future studies. Author

N95-18998*# Tuskegee Inst., AL. Dept. of Electrical Engineering.

ERROR CODING SIMULATIONS IN C **c17**

Viveca K. Noble *In* Alabama Univ., Research Reports: 1994 NASA/ASEE Summer Faculty Fellowship Program Oct. 1994 5 p (For primary document see N95-18967 05-80)
Avail: CASI HC A01/MF A03

When data is transmitted through a noisy channel, errors are produced within the data rendering it indecipherable. Through the use of error control coding techniques, the bit error rate can be reduced to any desired level without sacrificing the transmission data rate. The Astrionics Laboratory at Marshall Space Flight Center has decided to use a modular, end-to-end telemetry data simulator to simulate the transmission of data from flight to ground and various methods of error control. The simulator includes modules for random data generation, data compression, Consultative Committee for Space Data Systems (CCSDS) transfer frame formation, error correction/detection, error generation and error statistics. The simulator utilizes a concatenated coding scheme which includes CCSDS standard (255,223) Reed-Solomon (RS) code over GF(2(exp 8)) with interleave depth of 5 as the outermost code, (7, 1/2) convolutional code as an inner code and CCSDS recommended (n, n-16) cyclic redundancy check (CRC) code as the innermost code, where n is the number of information bits plus 16 parity bits. The received signal-to-noise for a desired bit error rate is greatly reduced through the use of forward error correction techniques. Even greater coding gain is provided through the use of a concatenated coding scheme. Interleaving/deinterleaving is necessary to randomize burst errors which may appear at the input of the RS decoder. The burst correction capability length is increased in proportion to the interleave depth. The modular nature of the simulator allows for inclusion or exclusion of modules as needed. This paper describes the development and operation of the simulator, the verification of a C-language Reed-Solomon code, and the possibility of using Comdisco SPW(tm) as a tool for determining optimal error control schemes. Derived from text

N95-18999*# Mercer Univ., Macon, GA. Dept. of Electrical and Computer Engineering.

A NEW PISTON CONTROL STRATEGY FOR SEGMENTED MIRRORS **c63**

Philip D. Olivier *In* Alabama Univ., Research Reports: 1994 NASA/ASEE Summer Faculty Fellowship Program Oct. 1994 6 p (For primary document see N95-18967 05-80)
Avail: CASI HC A02/MF A03

One approach to the adaptive control of large segmented mirrors involves sending tilt commands to each segment and allowing each segment to minimize the distance between its edges and those of (all or some of) its neighbors. This approach has been adopted in the Phased Array Mirror, Extendible Large Aperture (PAMELA) testbed now located at NASA's Marshall Space Flight Center, Huntsville, AL. This approach minimizes (1) the communication between the sensors and the segment actuators and (2) computations required by the central controlling computer. This report discusses issues that large segmented mirrors built around the PAMELA concept (such as SELENE) will face when they migrate to integrated, and presumably to digital, on-segment computational ability and high bandwidth response. Derived from text

N95-19000*# University of Western Kentucky, Bowling Green, KY. Dept. of Chemistry.

GROWTH OF THIN FILMS OF DICYANOVINYLANISOLE ON QUARTZ AND TEFLON-COATED QUARTZ BY PHYSICAL VAPOR TRANSPORT **c27**

Earl F. Pearson *In* Alabama Univ., Research Reports: 1994 NASA/ASEE

Summer Faculty Fellowship Program Oct. 1994 7 p (For primary document see N95-18967 05-80)
Avail: CASI HC A02/MF A03

Organic compounds offer the possibility of molecular engineering in order to optimize the nonlinearity and minimize damage due to the high-power lasers used in nonlinear optical devices. Recently dicyanovinylanisole (DIVA), ((2-methoxyphenyl) methylenepropanedinitrile) has been shown to have a second order nonlinearity 40 times that of alpha-quartz. Debe et. al. have shown that a high degree of orientational order exists for thin films of phthalocyanine grown by physical vapor transport in microgravity. The microgravity environment eliminates convective flow and was critical to the formation of highly ordered dense continuous films in these samples. This work seeks to discover the parameters necessary for the production of thin continuous films of high optical quality in Earth gravity. These parameters must be known before the experiment can be planned for growing DIVA in a microgravity environment. The microgravity grown films are expected to be denser and of better optical quality than the unit gravity films as was observed in the phthalocyanine films. Derived from text

N95-19001*# Wisconsin Univ., Whitewater, WI. Dept. of Mechanics and Computer Science.
TWO SPACE SCATTERER FORMALISM CALCULATION OF BULK PARAMETERS OF THUNDERCLOUDS c47
Dieudonne D. Phanord *In* Alabama Univ., Research Reports: 1994 NASA/ASEE Summer Faculty Fellowship Program Oct. 1994 6 p (For primary document see N95-18967 05-80)
Avail: CASI HC A02/MF A03

In a previous study, we used a modified two-space scatterer formalism of Twersky to establish for a cloud modeled as a statistically homogeneous distribution of spherical water droplets, the dispersion relations that determine its bulk propagation numbers and bulk indexes of refraction in terms of the vector equivalent scattering amplitude and the dyadic scattering amplitude of the single water droplet in isolation. The results were specialized to the forward direction of scattering while demanding that the scatterers preserve the incident polarization. We apply this approach to obtain specific numerical values for the macroscopic parameters of the cloud. We work with a cloud of density rho = 100 cm(exp -3), a wavelength lambda = 0.7774 microns, and with spherical water droplets of common radius alpha = 10 microns. In addition, the scattering medium is divided into three parts, the medium outside the cloud, moist air (the medium inside the cloud but outside the droplets), and the medium inside the spherical water droplets. The results of this report are applicable to a cloud of any geometry since the boundary does not interfere with the calculations. Also, it is important to notice the plane wave nature of the incidence wave in the moist atmosphere. Derived from text

N95-19002*# Christian Brothers Coll., Memphis, TN. Dept. of Mechanical Engineering.
EVALUATION OF SSME TEST DATA REDUCTION METHODS c20
L. Michael Santi *In* Alabama Univ., Research Reports: 1994 NASA/ASEE Summer Faculty Fellowship Program Oct. 1994 6 p (For primary document see N95-18967 05-80)
Avail: CASI HC A02/MF A03

Accurate prediction of hardware and flow characteristics within the Space Shuttle Main Engine (SSME) during transient and main-stage operation requires a significant integration of ground test data, flight experience, and computational models. The process of integrating SSME test measurements with physical model predictions is commonly referred to as data reduction. Uncertainties within both test measurements and simplified models of the SSME flow environment compound the data integration problem. The first objective of this effort was to establish an acceptability criterion for data reduction solutions. The second objective of this effort was to investigate the data reduction potential of the ROCETS (Rocket Engine Transient Simulation) simulation platform. A simplified ROCETS model of the SSME was obtained from the MSFC Performance Analysis Branch . This model was examined and tested for physical consistency. Two modules were constructed and added to the ROCETS library to independently check the mass and energy balances of selected engine subsystems including the low pressure fuel turbopump, the high pressure fuel turbopump, the low pressure oxidizer turbopump, the high pressure oxidizer turbopump, the fuel preburner, the oxidizer preburner, the main combustion chamber coolant circuit, and the nozzle coolant circuit. A sensitivity study was then conducted to determine the individual influences of forty-two hardware characteristics on fourteen high pressure region prediction variables as returned by the SSME ROCETS model. Derived from text

N95-19003*# Alabama Univ., Huntsville, AL. Dept. of Civil and Environmental Engineering.
CRACKING CHARACTERISTICS OF A HABITABLE MODULE PRESSURE WALL FOLLOWING ORBITAL DEBRIS PENETRATION c39
William P. Schonberg *In* Alabama Univ., Research Reports: 1994 NASA/ASEE Summer Faculty Fellowship Program Oct. 1994 6 p (For primary document see N95-18967 05-80)
Avail: CASI HC A02/MF A03

All long-duration spacecraft in low-earth-orbit are subject to high speed impacts by meteoroids and pieces of orbital debris. The threat of damage from such impacts is a significant design consideration in the development of long duration earth-orbiting spacecraft. This report presents the results of a study whose objective was to develop an empirical model to predict the magnitude of the various cracking and through-hole creation phenomena accompanying a habitable module penetration. The significance of the work performed is that the model predictions can be fed directly into a survivability analysis to determine whether or not module unzipping would occur under a specific set of impact conditions. The likelihood of module unzipping over a structure's lifetime can also be determined in such an analysis. In addition, effective hole size predictions can be used as part of a survivability analysis to determine the time available for module evacuation prior to the onset of incapacitation due to air loss. Some of the phenomena considered include maximum petal length, maximum tip-to-tip crack distance, depth of petal deformation, number of cracks formed, orientation of the maximum tip-to-tip distance with respect to the inner wall grain direction, and the effective inner wall hole diameter. Derived from text

N95-19004*# Texas A&I Univ., Kingsville, TX. Dept. of Electrical Engineering and Computer Science.
EVALUATION OF THE EFFICIENCY AND RELIABILITY OF SOFTWARE GENERATED BY CODE GENERATORS c61
Barbara Schreur *In* Alabama Univ., Research Reports: 1994 NASA/ASEE Summer Faculty Fellowship Program Oct. 1994 6 p (For primary document see N95-18967 05-80)
Avail: CASI HC A02/MF A03

There are numerous studies which show that CASE Tools greatly facilitate software development. As a result of these advantages, an increasing amount of software development is done with CASE Tools. As more software engineers become proficient with these tools, their experience and feedback lead to further development with the tools themselves. What has not been widely studied, however, is the reliability and efficiency of the actual code produced by the CASE Tools. This investigation considered these matters. Three segments of code generated by MATRIXx, one of many commercially available CASE Tools, were chosen for analysis: ETOFLIGHT, a portion of the Earth to Orbit Flight software, and ECLSS and PFMC, modules for Environmental Control and Life Support System and Pump Fan Motor Control, respectively. Derived from text

N95-19005*# Tennessee State Univ., Nashville, TN. Dept. of Physics, mathematics and Computer Science.
A REPORT OF WORK ACTIVITIES ON THE NASA SPACELINK PUBLIC ELECTRONIC LIBRARY c82
Willard A. Smith *In* Alabama Univ., Research Reports: 1994 NASA/ASEE Summer Faculty Fellowship Program Oct. 1994 6 p (For primary document see N95-18967 05-80)
Avail: CASI HC A02/MF A03

NASA Spacelink is a comprehensive electronic data base of NASA and other source educational and informational materials. This service originates at Marshall Space Flight Center (MSFC) in Huntsville, Alabama. This is an education service of NASA Headquarters, through the MSFC Education Office, that first began in February of 1988. The new NASA Spacelink Public Electronic Library was the result of a study conducted to investigate an upgrade or redesign of the original NASA Spacelink. The UNIX Operating System was chosen to be the host operating system for the new NASA Spacelink Public Electronic Library. The UNIX system was selected for this project because of the strengths built into the embedded communication system and for its simple and direct file handling capabilities. The host hardware of the new system is a Sun Microsystems SPARCserver

1000 computer system. The configuration has four 50-MHz SuperSPARC processors with 128 megabytes of shared memory; three SB800 serial ports allowing 24 cable links for phone communications; 4.1 gigabytes of on-line disk storage; and ten (10) CD-ROM drives. Communications devices on the system are sufficient to support the expected number of users through the Internet, the local dial services, long distance dial services; the MSFC PABX, and the NPSS (NASA Packet Switching System) and 1-800 access service for the registered teachers. Derived from text

N95-19006*# Chicago State Univ., Chicago, IL. Dept. of Mathematics and Computer Science.

SCATTERING OF POINT SOURCE ILLUMINATION BY AN ARBITRARY CONFIGURATION **c74**

Richard Solakiewicz *In* Alabama Univ., Research Reports: 1994 NASA/ASEE Summer Faculty Fellowship Program Oct. 1994 6 p (For primary document see N95-18967 05-80)

Avail: CASI HC A02/MF A03

The problem of electromagnetic scattering of an incident plane wave by an arbitrary configuration of obstacles was solved by Twersky. In this report, the results are extended to point source incidence corresponding to a Hertz dipole. Knowledge of the response of a fixed configuration of scatterers excited by a point source may provide insight to improve the accuracy of the values of bulk parameters for clouds which have been found using plane wave excitation. Derived from text

N95-19007*# Wichita State Univ., Wichita, KS. Dept. of Mechanical Engineering.

MICROSTRUCTURAL ANALYSIS OF CRACKS GENERATED DURING WELDING OF 2195 ALUMINUM-LITHIUM ALLOY **c26**

George E. Talia *In* Alabama Univ., Research Reports: 1994 NASA/ASEE Summer Faculty Fellowship Program Oct. 1994 6 p (For primary document see N95-18967 05-80)

Avail: CASI HC A02/MF A03

This research summarizes a series of studies conducted at Marshall Space Flight Center to characterize the properties of 2195 Al-Li alloy. 2195 Al-Li alloy, developed by Martin Marietta laboratories, is designated as a replacement of 2219 Al-Cu alloy for the External Tank (E.T.) of the space shuttle. 2195 Al-Li alloy with its advantage of increased strength per weight over its predecessor, 2219 Al-Cu alloy, also challenges current technology. 2195 Al-Li has a greater tendency to crack than its predecessor. The present study began with the observation of pore formation in 2195 Al-Li alloy in a thermal aging process. In preliminary studies, Talia and Nunes found that most of the two pass welds studied exhibited round and crack-like porosity at the weld roots. Furthermore, the porosity observed was associated with the grain boundaries. The porosity level can be increased by thermal treatment in the air. A solid state reaction proceeding from dendritic boundaries in the weld fusion zone was observed to correlate with the generation of the porosity. Derived from text

N95-19008*# State Univ. of New York, Farmingdale, NY. Mfg. and Mechanical Research Div.

QUALITY OPTIMIZATION OF THERMALLY SPRAYED COATINGS PRODUCED BY THE JP-5000 (HVOF) GUN USING MATHEMATICAL MODELING **c27**

Hazem Tawfik *In* Alabama Univ., Research Reports: 1994 NASA/ASEE Summer Faculty Fellowship Program Oct. 1994 9 p (For primary document see N95-18967 05-80)

Avail: CASI HC A02/MF A03

Currently, thermal barrier coatings (TBC) of gas-turbine blades and similar applications have centered around the use of zirconia as a protective coating for high thermal applications. The advantages of zirconia include low thermal conductivity and good thermal shock resistance. Thermally sprayed tungsten carbide hardface coatings are used for a wide range of applications spanning both the aerospace and other industrial markets. Major aircraft engine manufacturers and repair facilities use hardface coatings for original engine manufacture (OEM), as well as in the overhaul of critical engine components. The principle function of these coatings is to resist severe wear environments for such wear mechanisms as abrasion, adhesion, fretting, and erosion. The (JP-5000) thermal spray gun is the most advanced in the High Velocity Oxygen Fuel (HVOF) systems. Recently, it has received considerable attention because of its relative low cost and its production of quality coatings that challenge the very successful but yet very expensive Vacuum Plasma Spraying (VPS) system. The quality of thermal spray coatings is enhanced as porosity, oxidation, residual stress, and surface roughness are reduced or minimized. Higher densification, interfacial bonding strength, hardness and wear resistance of coating are desirable features for quality improvement. Derived from text

N95-19009*# University of the Pacific, Stockton, CA. Dept. of Physics.

PRISM PROJECT OPTICAL INSTRUMENT **c74**

Charles R. Taylor *In* Alabama Univ., Research Reports: 1994 NASA/ASEE Summer Faculty Fellowship Program Oct. 1994 6 p (For primary document see N95-18967 05-80)

Avail: CASI HC A02/MF A03

The scientific goal of the Passively-cooled Reconnaissance of the InterStellar Medium (PRISM) project is to map the emission of molecular hydrogen at 17.035 micrometers and 28.221 micrometers. Since the atmosphere is opaque at these infrared wavelengths, an orbiting telescope is being studied. The availability of infrared focal plane arrays enables infrared imaging spectroscopy at the molecular hydrogen wavelengths. The array proposed for PRISM is 128 pixels square, with a pixel size of 75 micrometers. In order to map the sky in a period of six months, and to resolve the nearer molecular clouds, each pixel must cover 0.5 arcminutes. This sets the focal length at 51.6 cm. In order for the pixel size to be half the diameter of the central diffraction peak at 28 micrometers would require a telescope aperture of 24 cm; an aperture of 60 cm has been selected for the PRISM study for greater light gathering power. Derived from text

N95-19010*# Alabama A & M Univ., Huntsville, AL. Dept. of Mathematics.

THE PROBABILITY OF FLAW DETECTION AND THE PROBABILITY OF FALSE CALLS IN NONDESTRUCTIVE EVALUATION EQUIPMENT **c38**

Enoch C. Temple *In* Alabama Univ., Research Reports: 1994 NASA/ASEE Summer Faculty Fellowship Program Oct. 1994 6 p (For primary document see N95-18967 05-80)

Avail: CASI HC A02/MF A03

The space industry has developed many composite materials that have high durability in proportion to their weights. Many of these materials have a likelihood for flaws that is higher than in traditional metals. There are also coverings (such as paint) that develop flaws that may adversely affect the performance of the system in which they are used. Therefore there is a need to monitor the soundness of composite structures. To meet this monitoring need, many nondestructive evaluation (NDE) systems have been developed. An NDE system is designed to detect material flaws and make flaw measurements without destroying the inspected item. Also, the detection operation is expected to be performed in a rapid manner in a field or production environment. Some of the most recent video-based NDE methodologies are shearography, holography, thermography, and video image correlation. Derived from text

N95-19011*# California Polytechnic State Univ., San Luis Obispo, CA. Dept. of Materials Engineering.

THE EFFECT OF FABRICATION ON CORROSION IN ALUMINUM 2195: ENVIRONMENTAL AND MICROSTRUCTURAL CONSIDERATIONS **c26**

Daniel W. Walsh *In* Alabama Univ., Research Reports: 1994 NASA/ASEE Summer Faculty Fellowship Program Oct. 1994 6 p (For primary document see N95-18967 05-80)

Avail: CASI HC A02/MF A03

Aluminum alloys containing lithium are particularly attractive to the aerospace structural designer. Lithium's density is only 0.53 g/cc, thus an addition of one weight percent lithium not only increases yield strength, but decreases the density by almost three percent while increasing the modulus by over six percent. The fact that lithium improves these physical properties simultaneously has led to intense study and development of the alloy system. Heretofore, problems in large scale alloy production have retarded commercial development. During the last fifteen years, advances in production technology have rekindled interest in Al-Li alloys, and aluminum suppliers have developed many candidate aerospace materials. However, if these alloys are to be employed successfully, a more complete understanding of their nonequilibrium metallurgy is required. Peel and Starke have each pointed out that an understanding of the weldability of these alloys is a critical step in their implementation. This study addresses the critical lack of information on the environmental compatibility of welded Al

2195 components. Corrosion data for these systems is incomplete, particularly for welded materials exposed to sea water or sea water condensate. Derived from text

N95-19012*# Alabama A & M Univ., Huntsville, AL. Dept. of Physics.
NUMERICAL FORMULATION OF COMPOSITION SEGREGATION AT CURVED SOLID-LIQUID INTERFACE DURING STEADY STATE SOLIDIFICATION PROCESS **c25**
Jai-Ching Wang *In* Alabama Univ., Research Reports: 1994 NASA/ASEE Summer Faculty Fellowship Program Oct. 1994 6 p (For primary document see N95-18967 05-80)
Avail: CASI HC A02/MF A03

The lateral solute segregation that results from a curved solid-liquid interface shape during steady state unidirectional solidification of a binary alloy system has been studied both analytically and numerically by Coriell, Bosivert, Rehm, and Sekerka. The system under their study is a two dimensional rectangular system. However, most real growth systems are cylindrical systems. Thus, in a previous study, we have followed Coriell etc. formalism and obtained analytical results for lateral solute segregation for an azimuthal symmetric cylindrical binary melt system during steady state solidification process. The solid-liquid interface shape is expressed as a series combination of Bessel functions. In this study a computer program has been developed to simulate the lateral solute segregation. Derived from text

N95-19013*# Alabama Univ., Huntsville, AL.
EFFECTS OF VIBRATION (G-JITTERS) ON CONVECTION IN MICRO-GRAVITY **c29**
Francis C. Wang *In* Alabama Univ., Research Reports: 1994 NASA/ASEE Summer Faculty Fellowship Program Oct. 1994 9 p (For primary document see N95-18967 05-80)
Avail: CASI HC A02/MF A03

To obtain high quality crystals, it is desirable to maintain a diffusion-limited transport process in a planar solidification surface between the solid and the melt during the crystal growth process. Due to the presence of buoyancy-driven convection, however, this situation is difficult to maintain on Earth. The microgravity environment of an orbiting space laboratory presents an alternative worth pursuing. With reduced gravity, convections very much suppressed in a space laboratory, making the environment more conducive for growing crystals with better quality. However, a space laboratory is not immune from any undesirable disturbances. Nonuniform and transient accelerations such as vibrations, g-jitters, and impulsive accelerations exist as a result of crew activities, space maneuvering, and the operations of on-board equipment. Measurements conducted on-board a U.S. Spacelab mission showed the existence of vibrations in the frequency range of 1 to 100 Hz. It was reported that a dominant mode of 17 Hz and harmonics of 54 Hz were observed and these were attributed to antenna operations. The vibration is not limited to any single plane but exists in all directions. Some data from the Russian MIR space station indicates the existence of vibration also at this frequency range. Derived from text

N95-19014*# Calhoun Community Coll., Decatur, AL. Dept. of Natural Sciences.
CAPILLARY ELECTROPHORESIS: BIOTECHNOLOGY FOR SEPARATION OF DNA AND CHROMOSOMES **c51**
George O. Williams, Jr. *In* Alabama Univ., Research Reports: 1994 NASA/ASEE Summer Faculty Fellowship Program Oct. 1994 5 p (For primary document see N95-18967 05-80)
Avail: CASI HC A01/MF A03

Electrophoresis has been used for the separation of particles, ions, and molecules for a number of years. The technology for separation and detection of the results has many applications in the life sciences. One of the major goals of the scientific community is to separate DNA molecules and intact chromosomes based upon their different lengths or number of base pairs. This may be achieved by using some of the commercially available and widely used methods, but these processes require a considerable amount of time. The challenge is to achieve separation of intact chromosomes in a short time, preferably in a matter of minutes. Derived from text

N95-19015*# State Univ. of East Tennessee, Johnson City, TN. Dept. of Chemistry.
SALT-INDUCED AGGREGATION OF LYSOZYME: IMPLICATIONS FOR CRYSTAL GROWTH **c76**
Lori J. Wilson *In* Alabama Univ., Research Reports: 1994 NASA/ASEE Summer Faculty Fellowship Program Oct. 1994 6 p (For primary document see N95-18967 05-80)
Avail: CASI HC A02/MF A03

Crystallization of proteins is a prerequisite for structural analysis by x-ray crystallography. While improvements in protein crystals have been obtained in microgravity onboard the U.S. Space Shuttle, attempts to improve the crystal growth process both on the ground and in space have been limited by our lack of understanding of the mechanisms involved. Almost all proteins are crystallized with the aid of a precipitating agent. Many of the common precipitating agents are inorganic salts. An understanding of the role of salts on the aggregation of protein monomers is the key to the elucidation of the mechanisms involved in protein crystallization. In order for crystallization to occur individual molecules must self-associate into aggregates. Detection and characterization of aggregates in supersaturated protein solutions is the first step in understanding salt-induced crystallization. Derived from text

N95-19016*# University of Western Carolina, Cullowhee, NC. Dept. of mathematics and Computer Science.
A TECHNIQUE FOR DETERMINING CLOUD FREE VERSUS CLOUD CONTAMINATED PIXELS IN SATELLITE IMAGERY **c43**
Richard A. Wohlman *In* Alabama Univ., Research Reports: 1994 NASA/ASEE Summer Faculty Fellowship Program Oct. 1994 5 p (For primary document see N95-18967 05-80)
Avail: CASI HC A01/MF A03

Weather forecasting has been called the second oldest profession. To do so accurately and with some consistency requires an ability to understand the processes which create the clouds, drive the winds, and produce the ever changing atmospheric conditions. Measurement of basic parameters such as temperature, water vapor content, pressure, windspeed and wind direction throughout the three dimensional atmosphere form the foundation upon which a modern forecast is created. Doppler radar, and space borne remote sensing have provided forecasters the new tools with which to ply their trade. Derived from text

81 ADMINISTRATION AND MANAGEMENT

Includes management planning and research.

N95-17986# Small Business Administration, Washington, DC. Office of Advocacy.
SMALL BUSINESS RESEARCH SUMMARIES, NUMBERS 51-100
1994 131 p See also PB94-179959
(PB94-179967) Avail: CASI HC A07/MF A02

Small business Research Summaries are brief, one- or two-page abstracts of research on small business that has been funded by the U.S. Small Business Administrations's Office of Advocacy. Each one highlights the scope, methodology, and findings of a single research report. Research Summaries numbered 51 through 100 cover those reports issued from December 1986 to May 1991. Author

N95-17987 Small Business Administration, Washington, DC. Office of Advocacy.
SMALL BUSINESS RESEARCH SUMMARIES, NUMBERS 1-50
1994 124 p See also PB94-179967 Limited Reproducibility: More than 20% of this document may be affected by microfiche quality
(PB94-179959) Avail: CASI HC A06

Small Business research summaries are brief, one- or two-page abstracts of research on small business that has been funded by the U.S. Small Business Administration's Office of Advocacy. Each one highlights the scope, methodology, and findings of a single research report. Research summaries numbered 1 through 50 cover those reports issued from February 1981 through December 1986. Author

N95-17988 International Trade Administration, Washington, DC.
US INDUSTRIAL OUTLOOK, 1994: AN ALMANAC OF INDUSTRY, TECHNOLOGY AND SERVICES. 35TH ANNUAL EDITION. FORECASTS FOR SELECTED MANUFACTURING AND SERVICE INDUSTRIES
Jan. 1994 641 p See also PB93-111276, PB92-100163 and PB94-113966 Limited Reproducibility: More than 20% of this document may be affected by microfiche quality
(PB94-107844) Avail: CASI HC A99

U.S. Industrial Outlook 1994 covers the major manufacturing, high-technology, and service industries. The industry-by-industry overviews provide economic analyses and projections for 1994 and beyond. The document serves as a tool for planning growth, investment, negotiations, and marketing, and offers these features: industry forecasts for 1994; latest data in 450 tables and charts; profiles of international competitiveness; international trade forecasts; and environmental reviews. Author

N95-18060 Newcastle-upon-Tyne Univ., Newcastle (England). Dept. of Computing Science.
REPLICA MANAGEMENT SYSTEM: A SCHEME FOR FLEXIBLE AND DYNAMIC REPLICATION
M. C. Little and D. L. McCue Mar. 1994 16 p
(PB94-201597; TRS-472) Copyright Avail: Issuing Activity (National Technical Information Service (NTIS))

The paper describes the design and implementation of the Replica Management System (RMS), which allows a programmer to specify the quality of service required for replica groups in terms of availability and performance. From the quality of service specification, information about the replication protocol to be used, and data about the characteristics of the underlying distributed system, the RMS computes an initial placement and replication level. As machines and communications systems are detected to have failed or recovered, or performance characteristics change, the RMS can be re-invoked to compute an updated mapping of replicas which preserves the desired quality of service. The result is a flexible, dynamic and dependable replication system. NTIS

N95-18416 Naval Air Warfare Center, Patuxent River, MD. Aircraft Div.
RESOURCES AUTOMATED MANAGEMENT SYSTEM
1994 3 p Limited Reproducibility: More than 20% of this document may be affected by microfiche quality
(AD-A284153) Avail: Issuing Activity (Defense Technical Information Center (DTIC))

The Resources Automated Management System (RAMS) was developed for the Naval Air Warfare Center Aircraft Division (NAWC AD) to support the informational needs of resource managers and National Environmental Policy Act (NEPA) specialists. RAMS is a set of automated tools that has at its core a geographical information system (GIS). The GIS software provides the capability for geographically linking different types of data to a particular feature or map location. The development of RAMS began in October 1992 with the objective of managing the resources data for all NAWC AD sites and mission activities. RAMS currently maintains over 50 data layers for the Patuxent River Naval Air Station in Maryland, the Chesapeake Bay region, and the Special Use Airspace where NAWC AD activities conduct their missions on the East Coast. RAMS currently supports users with responsibility for environmental protection, natural and cultural resources preservation, security, emergency response, disaster preparedness, range and aviation safety, and facilities management. DTIC

N95-18578# General Accounting Office, Washington, DC. National Security and International Affairs Div.
EUROPEAN AERONAUTICS: STRONG GOVERNMENT PRESENCE IN INDUSTRY STRUCTURE AND RESEARCH AND DEVELOPMENT SUPPORT. REPORT TO CONGRESSIONAL REQUESTERS
Mar. 1994 60 p
(GAO/NSIAD-94-71; B-255687; AD-A279220) Avail: CASI HC A04/MF A01; GAO, PO Box 6015, Gaithersburg, MD 20884-6015 HC

The structure of the aeronautical industries of France, Germany, and the United Kingdom, their government's support towards aeronautical research and development, and the organization of each country's respective aeronautical research and development establishments are the topics of this GAO report. Information on aeronautical research and development efforts by the European community and its member nations are also included. Due to industrial consolidation, it was found that there is only one major assembler/airframe manufacturer of large civil transport aircraft in each of the three major countries studied. Also, each country had only one or two large civil aircraft engine manufacturers, again due to industrial consolidation. Although there are international collaborative efforts by each of the manufacturers, these efforts do not generally involve joint research nor information sharing of aeronautical information, perhaps due to national security concerns and/or from the companies' unwillingness to share data due to competition within the industry. Derived from text

N95-18595# General Accounting Office, Washington, DC. General Government Div.
GOVERNMENT CONTRACTORS: MEASURING COSTS OF SERVICE CONTRACTORS VERSUS FEDERAL EMPLOYEES. REPORT TO THE CHAIRMAN, SUBCOMMITTEE ON FEDERAL SERVICES, POST OFFICE AND CIVIL SERVICE, COMMITTEE ON GOVERNMENTAL AFFAIRS, US SENATE
Mar. 1994 32 p
(GAO/GGD-94-95; B-256459) Avail: CASI HC A03/MF A01; GAO, PO Box 6015, Gaithersburg, MD 20884-6015 HC

An analysis of previous reports and testimonies has been conducted. These prior reports and testimonies were conducted to compare the cost of utilizing service contractors versus Federal employees to perform services. Although agencies have not been required to make cost comparisons for advisory and assistance services, studies made by GAO, DOD's IG, and DOE's IG have indicated that cost comparisons can be a useful management tool. Noncosts factors were also considered. These include whether the services are short term and nonrecurring; the quality and timeliness of service, and the availability of Federal employees. The methodologies and limitations of the prior reports were examined to see whether they were large or comprehensive enough to permit generalization to other situations in the government, and if all possible cost factors were incorporated. Recommendations were made that the Office of Management and Budget should extend a cost comparison requirement to advisory and assistance services. Derived from text

N95-18596# General Accounting Office, Washington, DC. National Security and International Affairs Div.
OVERHEAD COSTS: COSTS CHARGED BY MCDONNELL DOUGLAS AEROSPACE'S SPACE STATION DIVISION. REPORT TO THE CHAIRMAN, LEGISLATION AND NATIONAL SECURITY SUBCOMMITTEE, COMMITTEE ON GOVERNMENT OPERATIONS, HOUSE OF REPRESENTATIVES
Jun. 1994 11 p
(GAO/NSIAD-94-150; B-255081) Avail: CASI HC A03/MF A01; GAO, PO Box 6015, Gaithersburg, MD 20884-6015 HC

A review of the overhead costs submissions of McDonnell Douglas Aerospace's Station Division, Huntington Beach, California, was conducted to determine if the company included unallowable costs in its submissions, and the extent to which overhead costs were sustained during annual indirect expense rate negotiations. The review focuses on the accounts included in the overhead costs submissions that are vulnerable to mischarges. These accounts include lobbying, advertising, consulting services, and employee educational expenses. Derived from text

N95-19133*# National Aeronautics and Space Administration, Washington, DC.
NASA DIRECTIVES: MASTER LIST AND INDEX
9 May 1994 122 p
(NHB-1410.13N; NAS 1.18:1410.13N) Avail: CASI HC A06/MF A02

This Handbook sets forth in two parts the following information for the guidance of users of the NASA Management Directives System. Chapter 1 contains introductory information material on how to use this Handbook. Chapter 2 is a complete master list of Agency-wide management directives, describing each directive by type, number, effective date, expiration date, title, and organization code of the office responsible for the directive. Chapter 3 includes a consolidated numerical list of all delegations of authority and a breakdown of such delegation by the office of Installation to which special authority is assigned. Chapter 4 sets forth a consolidated list of all NASA Handbooks (NHB's) and important footnotes covering the control and ordering of such documents. Chapter 5 is a consolidated list of NASA management directives applicable to the Jet Propulsion Laboratory. Chapter 6 is a consolidated list of NASA management directives published in the

code of Federal Regulations. Complementary manuals to the NASA Management Directives System are described in Chapter 7. Part B contains an in-depth alphabetical index to all NASA management directives other than Handbooks. Author

N95-19141# General Accounting Office, Washington, DC. National Security and International Affairs Div.
NASA PROPERTY: POOR LENDING PRACTICES AND CONTROLS AT THE JET PROPULSION LABORATORY. REPORT TO CONGRESSIONAL REQUESTERS
Apr. 1994 17 p
(GAO/NSIAD-94-116; B-253238) Avail: CASI HC A03/MF A01; GAO, PO Box 6015, Gaithersburg, MD 20884-6015 HC

This report provides the following information: (1) a review of the relationship between NASA and Caltech for managing and performing research and development at JPL; (2) a report on property management weaknesses at JPL (primarily equipment loaned to JPL employees and equipment provided to Caltech). Derived from text

N95-18176*# La Salle Univ., Philadelphia, PA.
APPLYING COSTS, RISKS AND VALUES EVALUATION (CRAVE) METHODOLOGY TO ENGINEERING SUPPORT REQUEST (ESR) PRIORITIZATION
Prafulla N. Joglekar *In* Univ. of Central Florida, NASA/ASEE Summer Faculty Fellowship Program. 1994 Research Reports Oct. 1994 p 263-311 (For primary document see N95-18166 05-80)
Avail: CASI HC A03/MF A04

N95-19632*# RECOM Technologies, Inc., Moffett Field, CA. AI Research Branch.
AI AND WORKFLOW AUTOMATION: THE PROTOTYPE ELECTRONIC PURCHASE REQUEST SYSTEM
Michael M. Compton and Shawn R. Wolfe *In* NASA. Johnson Space Center, Third CLIPS Conference Proceedings, Volume 1 Nov. 1994 p 45-51 (For primary document see N95-19625 05-61)
Avail: CASI HC A02/MF A03

N95-19633*# Princeton Univ., NJ. Dept. of Mechanical and Aerospace Engineering.
A KNOWLEDGE-BASED SYSTEM FOR CONTROLLING AUTOMOBILE TRAFFIC
Alexander Maravas and Robert F. Stengel *In* NASA. Johnson Space Center, Third CLIPS Conference Proceedings, Volume 1 Nov. 1994 p 52-60 (For primary document see N95-19625 05-61)
(Grant NSF ECS-92-16450)
Avail: CASI HC A02/MF A03

82 DOCUMENTATION AND INFORMATION SCIENCE

Includes information management; information storage and retrieval technology; technical writing; graphic arts; and micrography.

For computer documentation see *61 Computer Programming and Software.*

N95-18004# Instituto de Pesquisas Espaciais, Sao Jose dos Campos (Brazil).
SOME STATISTICAL TOOLS FOR SAR IMAGE SYNTHESIS, ANALYSIS AND PROCESSING Ph.D. Thesis [ALGUMAS FERRAMENTAS ESTATISTICAS NA SINTESE, PROCESSAMENTO E ANALISE DE IMAGENS DE RADAR DE ABERTURA SINTETICA]
Alajandro Cesar Frer Orgambide 10 Dec. 1993 242 p In PORTUGESE
(INPE-5548-TDI/534) Avail: CASI HC A11/MF A03

Computational tools, derived from statistical modeling, for the synthesis, analysis and processing of synthetic aperture radar (SAR) images are presented. Several problems arising in image processing are posed in a unified manner, within the Bayesian framework. The Potts-Strauss model is used as the a priori distribution for the classes and the following topics are studied: the maximum pseudo likelihood estimation, the convergence properties of cluster flip algorithms, and the invariance Markovian property of the a posteriori distribution of a random field given its blurred and noisy version. Specifically, the pseudo likelihood estimators for the Potts-Strauss model and an arbitrary number of classes are calculated in a tractable computational form. The convergence properties are studied using a Monte Carlo experiment, using the pseudo likelihood estimators as stopping rules. An extension of a theorem by Geman and Geman is presented; this extension allows the modeling of images with multiplicative noise, among others. Using these results about the Potts-Strauss model, a computational tool for the simulation of optical and SAR images is presented. Several distributions for the noise present in coherent illuminated images are studied, along with estimation techniques for their parameters. A modification of a Markovian algorithm (ICM) for the segmentation of SAR and optical images is presented, where all the required parameters are iteratively estimated from the data through the use of pseudo likelihood estimators allowing, thus, an automated operation. The speckle noise reduction in one look amplitude images is posed as an estimation problem; and robust filters, based on the Rayleigh distribution, are proposed for this task. A computational tool for two goodness-of-fit tests for images is presented; that information is used as a discriminating factor for land use. The influence of byte data format on these tests is evaluated through the use of Monte Carlo techniques. Author

N95-18025# Aerospace Medical Research Labs., Brooks AFB, TX. Medicine Directorate.
VARIABLE NAME DICTIONARY FOR THE AIR FORCE HEALTH STUDY 1987 PHYSICAL EXAMINATION DATA TAPE, VOLUME 1 Interim Special Report, Jun. - Jul. 1994
William H. Wolfe, Joel E. Michalek, and Judson C. Miner Aug. 1994 114 p
(AD-A283319; AL/AO-SR-1994-0010-Vol-1) Avail: CASI HC A06/MF A01

The Air Force Health Study is a 20-year cohort study of the health, mortality, and reproductive outcomes of veterans of Operation Ranch Hand, the unit responsible for aerial spraying of herbicides in Vietnam during the period 1961 to 1971. The study is designed to determine whether herbicides or their contaminant, 2,3,7,8-tetrachlorodibenzo p-dioxin (dioxin) is associated with adverse health. Air Force veterans who served in Southeast Asia during the same period that the Ranch Hand unit was operational and who were not occupationally exposed to herbicides serve as a control group. Study participants were physically examined in 1982, 1985, 1987, and 1992. At each examination, participants were administered questionnaires and psychological tests. This data tape contains data collected at the 1987 (Cycle 3) physical examination. The data files include all variables analyzed in the 1987 summary report of findings. DTIC

N95-18026# Aerospace Medical Research Labs., Brooks AFB, TX. Medicine Directorate.
VARIABLE NAME DICTIONARY FOR THE AIR FORCE HEALTH STUDY 1987 PHYSICAL EXAMINATION DATA TAPE, VOLUME 2 Interim Special Report, Jun. - Jul. 1994
William H. Wolfe, Joel E. Michalek, and Judson C. Miner Aug. 1994 24 p
(AD-A283320; AL/AO-SR-1994-0010-Vol-2) Avail: CASI HC A02/MF A01

The Air Force Health Study is a 20-year cohort study of the health, mortality, and reproductive outcomes of veterans of Operation Ranch Hand, the unit responsible for aerial spraying of herbicides in Vietnam during the period 1961 to 1971. The study is designed to determine whether herbicides or their contaminant, 2,3,7,8-tetrachlorodibenzo p-dioxin (dioxin) is associated with adverse health. Air Force veterans who served in Southeast Asia during the same period that the Ranch Hand unit was operational and who were not occupationally exposed to herbicides serve as control group. Study participants were physically examined in 1982, 1985, 1987, and 1992. At each examination, participants were administered questionnaires and psychological tests. This data tape contains data collected at the 1987 (Cycle 3) physical examination. The data files include all variables analyzed in the 1987 summary report of findings. DTIC

N95-18040*# Science Applications International Corp., McLean, VA.
A SPACE AND ATMOSPHERIC VISUALIZATION SCIENCE SYSTEM Final Report

E. P. Szuszczewicz, P. Blanchard, A. Mankofsky, C. Goodrich, D. Kamins, R. Kulkarni, D. McNabb, and M. Moroh 31 Oct. 1994 84 p Original contains color illustrations
(Contracts NAS5-32337; NAS5-31352; RTOP 656-65-07; USRA-C-555512) (NASA-CR-189390; NAS 1.26:189390) Avail: CASI HC A05/MF A01; 10 functional color pages

SAVS (a Space and Atmospheric Visualization Science system) is an integrated system with user-friendly functionality that employs a 'push-button' software environment that mimics the logical scientific processes in data acquisition, reduction, analysis, and visualization. All of this is accomplished without requiring a detailed understanding of the methods, networks, and modules that link the tools and effectively execute the functions. This report describes SAVS and its components, followed by several applications based on generic research interests in interplanetary and magnetospheric physics (IMP/ISTP), active experiments in space (CRRES), and mission planning focused on the earth's thermospheric, ionospheric, and mesospheric domains (TIMED). The final chapters provide a user-oriented description of interface functionalities, hands-on operations, and customized modules, with details of the primary modules presented in the appendices. The overall intent of the report is to reflect the accomplishments of the three-year development effort and to introduce potential users to the power and utility of the integrated data acquisition, analysis, and visualization system. Author

N95-18051*# Massachusetts Inst. of Tech., Cambridge. Artificial Intelligence Lab.
TOPOGRAPHY FROM SHADING AND STEREO Final Report
Berthold K. P. Horn Nov. 1994 190 p
(Contracts NAS5-32337; NAS5-31352; RTOP 656-65-07; USRA-C-5555-10) (NASA-CR-189389; NAS 1.26:189389) Avail: CASI HC A09/MF A02

Methods exploiting photometric information in images that have been developed in machine vision can be applied to planetary imagery. Integrating shape from shading, binocular stereo, and photometric stereo yields a robust system for recovering detailed surface shape and surface reflectance information. Such a system is useful in producing quantitative information from the vast volume of imagery being received, as well as in helping visualize the underlying surface. Author

N95-18063 Los Alamos National Lab., NM.
INDEPENDENT VALIDATION AND VERIFICATION OF AUTOMATED INFORMATION SYSTEMS IN THE DEPARTMENT OF ENERGY
W. J. Hunteman and R. Caldwell 1994 11 p Presented at the 17th National Computer Security Conference, Baltimore, MD, 11-14 Oct. 1994 Limited Reproducibility: More than 20% of this document may be affected by microfiche quality
(Contract W-7405-eng-36)
(DE94-014460; LA-UR-94-2128; CONF-9410140-1) Avail: CASI HC A03

The Department of Energy (DOE) has established an independent validation and verification (IV&V) program for all classified automated information systems (AIS) operating in compartmented or multilevel modes. The IV&V program was established in DOE Order 5639.6A and described in the manual associated with the order. This paper describes the DOE IV&V program, the IV&V process and activities, the expected benefits from an IV&V, and the criteria and methodologies used during an IV&V. The first IV&V under this program was conducted on the integrated computing network (ICN) at Los Alamos National Laboratory and several lessons learned are presented. The DOE IV&V program is based on the following definitions. An IV&V is defined as the use of expertise from outside an AIS organization to conduct validation and verification studies on a classified AIS. Validation is defined as the process of applying the specialized security test and evaluation procedures, tools, and equipment needed to establish acceptance for joint usage of an AIS by one or more departments or agencies and their contractors. Verification is the process of comparing two levels of an AIS specification for proper correspondence (e.g., security policy model with top-level specifications, top-level specifications with source code, or source code with object code). DOE

N95-18096# Naval Postgraduate School, Monterey, CA.
SECURE DISTRIBUTED FILE SYSTEMS M.S. Thesis
Tracy Michael Conroy and Winslow Hurlburt Buxton Sep. 1994 118 p
(AD-A285525) Avail: CASI HC A06/MF A01

Secure information distribution is a strategic capability as significant as weapons systems and tactics to military operations. The Department of Defense has recognized the importance of establishing and maintaining secure distributed file systems and explores the practicality and applicability of one such system, Trusted Ficus File System (TRUFFLES), in the DOD infrastructure. Integrated into this research are discussions of Privacy Enhanced Mail (PEM), which is currently an integral part of the TRUFFLES implementation. This thesis concludes with a discussion of the actual installation of a PEM reference implementation, and future requirements for the TRUFFLES installation at the Naval Postgraduate School. DTIC

N95-18099# Naval Postgraduate School, Monterey, CA.
AUTOMATIC IDENTIFICATION TECHNOLOGY (AIT): THE DEVELOPMENT OF FUNCTIONAL CAPABILITY AND CARD APPLICATION MATRICES M.S. Thesis
Leslie Anne Bower Sep. 1994 207 p
(AD-A285528) Avail: CASI HC A10/MF A01

Automatic identification technology (AIT), also known as automated data collection (ADC) technology, has been in use in various industry and government applications. The present AIT resources are magnetic ink character recognition, optical character recognition, bar code, magnetic stripe, radio frequency, optical laser memory, integrated circuit (IC), biometric and voice data collection, and machine vision. Smart card, super smart card, and magnetic memory card technology (e.g., PCMCIA) are integrated circuit technology. Personnel selecting, acquiring, implementing and using these technologies should possess a knowledge of the capabilities and applications of the AIT resources to obtain the best AIT system to meet their mission requirements. In order to facilitate an understanding of the AIT resources and their applications, two matrices were developed. An AIT Functional Capability Matrix was developed to identify and assess the capabilities of the AIT resources. An AIT Application Matrix was developed to identify the automation of various applications with these technologies. The matrices can assist system designers, system integrators, information systems management personnel, users, and consumers of AIT resources understand the functional capabilities and the applications of these technologies in a concise format. The matrices can be used for selection and acquisition of AIT systems and to track and address migration of the AIT systems throughout their life cycles. DTIC

N95-18446 Loral Systems, Inc., Orlando, FL. Adst Program Office.
DISTRIBUTED INTERACTIVE SIMULATION INTERFACE LIBRARY VERSION DESCRIPTION DOCUMENT
26 Aug. 1994 15 p Limited Reproducibility: More than 20% of this document may be affected by microfiche quality
(Contract N61339-91-D-0001)
(AD-A284470; ADST/WDL/TR-W-003322A) Avail: CASI HC A03

This document provides version descriptions for each component of the Distributed Interactive Simulation (DIS) Interface Library (DIL) and instructions for installing the DIL on a target system. DTIC

N95-18526# Department of the Navy, Washington, DC.
METHOD OF DISPLAYING TIME SERIES DATA ON FINITE RESOLUTION DISPLAY DEVICE Patent Application
Gregory Jones, inventor (to Navy), Joseph Lopes, inventor (to Navy), and Gerald Martel, inventor (to Navy) 19 May 1994 14 p
(AD-D016438; US-Patent-Appl-SN-246901; Navy-Case-75642) Avail: CASI HC A03/MF A01

The method of the present invention minimizes the time required to display a portion of a time sampled data file. A plurality of compressed data files are generated based on the time sampled data file. Each of the compressed data files is defined by a corresponding unique compression ratio such that each compressed data file contains fewer data points than the original time sampled data file. Each compressed data file characterizes the original time sampled data file. The compressed data files are stored in a data storage device for subsequent retrieval. A resolution factor is defined for each of the compressed data files. One of the compressed data files is then selected based on the resolution factor and the portion of the time sampled data file requested for display. The selected compressed data file is transferred from the data storage device to the display device. DTIC

N95-18544 Department of the Navy, Washington, DC.
VARIABLE RATE TRANSFER OF OPTICAL INFORMATION Patent

Sonlinh Phuvan, inventor (to Navy) 22 Feb. 1994 8 p Filed 24 Mar. 1993
(AD-D016268; US-Patent-5,289,304; US-Patent-Appl-SN-046254) Avail: US Patent and Trademark Office

Two-dimensional optical data is transferred at a variable rate through an optical delay module formed by spatial light modulators of the ferroelectric liquid crystal type interconnected in series for data transmission by a beam splitter through which laser radiation is introduced. Operation of the light modulators is controllably interrelated to control the variable delayed transfer rate of the module. DTIC

N95-18573*# National Aeronautics and Space Administration, Washington, DC.
NASA HIGH PERFORMANCE COMPUTING AND COMMUNICATIONS PROGRAM Annual Report, 1993
Lee Holcomb, Paul Smith, and Paul Hunter Nov. 1994 121 p
(NASA-TM-4653; NAS 1.15:4653) Avail: CASI HC A06/MF A02

The National Aeronautics and Space Administration's HPCC program is part of a new Presidential initiative aimed at producing a 1000-fold increase in supercomputing speed and a 1(X)-fold improvement in available communications capability by 1997. As more advanced technologies are developed under the HPCC program, they will be used to solve NASA's 'Grand Challenge' problems, which include improving the design and simulation of advanced aerospace vehicles, allowing people at remote locations to communicate more effectively and share information, increasing scientists' abilities to model the Earth's climate and forecast global environmental trends, and improving the development of advanced spacecraft. NASA's HPCC program is organized into three projects which are unique to the agency's mission: the Computational Aerosciences (CAS) project, the Earth and Space Sciences (ESS) project, and the Remote Exploration and Experimentation (REE) project. An additional project, the Basic Research and Human Resources (BRHR) project, exists to promote long term research in computer science and engineering and to increase the pool of trained personnel in a variety of scientific disciplines. This document presents an overview of the objectives and organization of these projects, as well as summaries of early accomplishments and the significance, status, and plans for individual research and development programs within each project. Areas of emphasis include benchmarking, testbeds, software and simulation methods. Author

N95-18654 Army Engineer Waterways Experiment Station, Vicksburg, MS. Information Technology Lab.
DEVELOPMENT OF EXECUTIVE INFORMATION SYSTEMS Final Report
Ernest H. Boswell, Jr. Aug. 1994 44 p Limited Reproducibility: More than 20% of this document may be affected by microfiche quality
(AD-A284005; WES/TR/ITL-94-6) Avail: Issuing Activity (Defense Technical Information Center (DTIC))

Executive Information Systems have been one of the key information management objectives for many organizations for over a decade. As personal computer hardware and software capabilities have grown, the potential for a useful and meaningful system has increased dramatically. Specifically, as the Microsoft Windows environment has become a de facto standard for personal computer development environments, many different software tools and methods have become available. This report investigates a representative set of Microsoft Windows-based software products to determine their applicability to Executive Information Systems development projects. A sample application is developed using each product, and the results are tabulated. DTIC

N95-18680 Naval Command, Control and Ocean Surveillance Center, San Diego, CA. Research, Development, Technology and Evaluation Div.
TECHNICAL INFORMATION DIVISION OPEN LITERATURE DATABASE (TOLD) OPERATING INSTRUCTIONS Final Report
E. R. Ratliff Jun. 1994 40 p Limited Reproducibility: More than 20% of this document may be affected by microfiche quality
(AD-A284061; NRAD-TD-2650) Avail: CASI HC A03

The Technical Information Division (TID) Open Literature Database (TOLD) is a program used to maintain records of technical papers, articles, books, and presentations prepared for publication or delivery outside of NRaD. The primary purpose is to assist TID personnel in ensuring the results of NRaD work are sent to the Defense Technical Information Center (DTIC) for further distribution. TID prepares a Report Documentation Page (SF 298) for each release and forwards the form to DTIC. DTIC

N95-18681 Naval Command, Control and Ocean Surveillance Center, San Diego, CA. Research, Development, Technology and Evaluation Div.
GRAPHICS MIS/SHOP STORE PROGRAM: USER'S MANUAL Final Report
E. R. Ratliff Sep. 1993 55 p Limited Reproducibility: More than 20% of this document may be affected by microfiche quality
(AD-A284062; NRAD-TD-2659) Avail: CASI HC A04

This manual provides instructions for the Management Information System (MIS)/Shop Store Program. The MIS/Shop Store Program maintains records of graphics work, provides statistical information on that work, and facilitates the use of a small shop store at NCCOSC's RDT&E Division (NRaD). It consists of application programs running within the FoxPro 2.5 database program and is used in a group that produces graphics products at NRaD. The program features on-screen instructions that lead the operator through most routine tasks associated with the MIS and shop store functions. DTIC

N95-18872# Sandia National Labs., Albuquerque, NM.
BUILDING A BRIDGE WITH THE CUSTOMER TO FACILITATE COLLECTING AND VALIDATING INFORMATION IN MODELING SESSIONS
S. M. Eaton 21 Jul. 1994 18 p Presented at the NIAM-ISDM 1994 Conference, Albuquerque, NM, 24-26 Aug. 1994
(Contract DE-AC04-94AL-85000)
(DE94-017338; SAND-94-2010C; CONF-9408115-2) Avail: CASI HC A03/MF A01

To build a bridge with customers, we balance the linear modeling process with the dynamics of the individuals we serve, who may feel unfamiliar, even confused, with that process. While it is recognized that human factors engineers improve the physical aspect of the workplace, they also work to integrate customers' cognitive styles, feelings, and concerns into the workplace tools. We take customers' feelings into consideration and integrate their expressed needs and concerns into the modeling sessions. After establishing an agreeable, professional relationship, we use a simple, portable CASE tool to reveal the effectiveness of NIAM. This tool, Modeler's Assistant, is friendly enough to use directly with people who know nothing of NIAM, yet it captures all the information necessary to create complete models. The Modeler's Assistant succeeds because it organizes the detailed information in an enhanced text format for customer validation. Customer cooperation results from our modeling sessions as they grow comfortable and become enthused about providing information. DOE

N95-18873# Sandia National Labs., Albuquerque, NM.
LOSSLESS COMPRESSION OF WEIGHT VECTORS FROM AN ADAPTIVE FILTER
M. V. Bredemann, G. R. Elliott, and S. D. Stearns 1994 4 p Presented at the 37th Midwest Symposium on Circuits and Systems, Lafayette, LA, 2-5 Aug. 1994
(Contract DE-AC04-94AL-85000)
(DE94-017350; SAND-94-1987C; CONF-9408126-2) Avail: CASI HC A01/MF A01

Techniques for lossless waveform compression can be applied to the transmission of weight vectors from an orbiting satellite. The vectors, which are a part of a hybrid analog/digital adaptive filter, are a representation of the radio frequency background seen by the satellite. An approach is used which treats each adaptive weight as a time-varying waveform. DOE

N95-18914# General Accounting Office, Washington, DC. Resources, Community and Economic Development Div.
INFORMATION SUPERHIGHWAY: ISSUES AFFECTING DEVELOPMENT. REPORT TO THE CONGRESS
Sep. 1994 73 p
(GAO/RCED-94-285; B-258041) Avail: CASI HC A04/MF A01; GAO, PO Box 6015, Gaithersburg, MD 20884-6015 HC

The term 'National Information Infrastructure' commonly known as the 'Information Superhighway' refers collectively to the hardware, software, standards, personnel, and training facilities that will one day form an information infrastructure that will place vast quantities of voice, video, and

data at users' fingertips. Delivery of these services is being made possible by advances in digital communications, which allow voice, video, and data to travel together over any type of telecommunications medium. Increased competition in telecommunications could spur private investors to build the superhighway, but existing telecommunications legislation and court orders limit or prohibit certain types of telecommunications competition. This report provides an overview of several major issues facing the Congress as it considers the telecommunications legislation, like: (1) managing the transition to a more competitive local telecommunications marketplace; (2) ensuring universal service in a competitive marketplace; and (3) ensuring network security, privacy, reliability, and interoperability. Derived from text

N95-18936*# National Aeronautics and Space Administration. Langley Research Center, Hampton, VA.

A STRATEGY FOR ELECTRONIC DISSEMINATION OF NASA LANGLEY TECHNICAL PUBLICATIONS

Donna G. Roper, Mary K. McCaskill, Scott D. Holland, Joanne L. Walsh, Michael L. Nelson, Susan L. Adkins, Manjula Y. Ambur, and Bryan A. Campbell Dec. 1994 94 p

(NASA-TM-109172; NAS 1.15:109172) Avail: CASI HC A05/MF A01

To demonstrate NASA Langley Research Center's relevance and to transfer technology to external customers in a timely and efficient manner, Langley has formed a working group to study and recommend a course of action for the electronic dissemination of technical reports (EDTR). The working group identified electronic report requirements (e.g., accessibility, file format, search requirements) of customers in U.S. industry through numerous site visits and personal contacts. Internal surveys were also used to determine commonalities in document preparation methods. From these surveys, a set of requirements for an electronic dissemination system was developed. Two candidate systems were identified and evaluated against the set of requirements: the Full-Text Electronic Documents System (FEDS), which is a full-text retrieval system based on the commercial document management package Interleaf, and the Langley Technical Report Server (LTRS), which is a Langley-developed system based on the publicly available World Wide Web (WWW) software system. Factors that led to the selection of LTRS as the vehicle for electronic dissemination included searching and viewing capability, current system operability, and client software availability for multiple platforms at no cost to industry. This report includes the survey results, evaluations, a description of the LTRS architecture, recommended policy statement, and suggestions for future implementations. Author

N95-18950*# National Aeronautics and Space Administration. Langley Research Center, Hampton, VA.

NASA/DOD AEROSPACE KNOWLEDGE DIFFUSION RESEARCH PROJECT. REPORT 26: THE TECHNICAL COMMUNICATION PRACTICES OF AEROSPACE ENGINEERING STUDENTS: RESULTS OF THE PHASE 3 AIAA NATIONAL STUDENT SURVEY

Thomas E. Pinelli, Laura M. Hecht (Indiana Univ., Bloomington, IN.), Rebecca O. Barclay (Rensselaer Polytechnic Inst., Troy, NY.), and John M. Kennedy (Indiana Univ., Bloomington, IN.) Dec. 1994 59 p

(RTOP 505-90-00)

(NASA-TM-109121; NAS 1.15:109121) Avail: CASI HC A04/MF A01

This report describes similarities and differences between undergraduate and graduate engineering students in the context of two general aspects of the educational experience. First, we explore the extent to which students differ regarding the factors that lead to the choice of becoming an engineer, current satisfaction with that choice, and career-related goals and objectives. Second, we look at the technical communication practices, habits, and training of aerospace engineering students. The reported data were obtained from a survey of student members of the American Institute of Aeronautics and Astronautics (AIAA). The survey was undertaken as a phase 3 activity of the NASA/DoD Aerospace Knowledge Diffusion Research Project. Data are reported for the following categories: student demographics; skill importance, skill training, and skill helpfulness; collaborative writing; computer and information technology use and importance; use of electronic networks; use and importance of libraries and library services; use and importance of information sources and products; use of foreign language technical reports; and foreign language (reading and speaking) skills. Author

N95-18953*# National Aeronautics and Space Administration. Langley Research Center, Hampton, VA.

NASA/DOD AEROSPACE KNOWLEDGE DIFFUSION RESEARCH PROJECT. REPORT 29: A COMPARISON OF THE TECHNICAL COMMUNICATIONS PRACTICES OF JAPANESE AND US AEROSPACE ENGINEERS AND SCIENTISTS

Thomas E. Pinelli, Rebecca O. Barclay (Rensselaer Polytechnic Inst., Troy, NY.), and John M. Kennedy (Indiana Univ., Bloomington, IN.) Dec. 1994 54 p

(RTOP 505-90-00)

(NASA-TM-109164; NAS 1.15:109164) Avail: CASI HC A04/MF A01

As part of Phase 4 of the NASA/DoD Aerospace Knowledge Diffusion Research Project, two studies were conducted that investigated the technical communications practices of Japanese and U.S. aerospace engineers and scientists. Both studies have the same seven objectives: first, to solicit the opinions of aerospace engineers and scientists regarding the importance of technical communications to their profession; second, to determine the use and production of technical communications by aerospace engineers and scientists; third; to seek their views about the appropriate content of an undergraduate course in technical communications; fourth, to determine aerospace engineers' and scientists' use of libraries, technical information centers, and on-line data bases; fifth, to determine the use and importance of computer and information technology to them; sixth, to determine their use of electronic networks; and seventh, to determine their use of foreign and domestically produced technical reports. A self-administered questionnaire was distributed to aerospace engineers and scientists in Japan and at the NASA Ames Research Center and the NASA Langley Research Center. The completion rates for the Japanese and U.S. surveys were 85 and 61 percent, respectively. Responses of the Japanese and U.S. participants to selected questions are presented in this report. Author

N95-19038*# National Aeronautics and Space Administration. Langley Research Center, Hampton, VA.

NASA/DOD AEROSPACE KNOWLEDGE DIFFUSION RESEARCH PROJECT. PAPER 46: TECHNICAL COMMUNICATIONS IN AEROSPACE: A COMPARISON ACROSS FOUR COUNTRIES

John M. Kennedy (Indiana Univ., Bloomington, IN.), Thomas E. Pinelli, Laura Frye Hecht (Indiana Univ., Bloomington, IN.), and Rebecca O. Barclay (Rensselaer Polytechnic Inst., Troy, NY.) 1995 12 p Presented at the 33d Aerospace Sciences Meeting and Exhibit of the American Inst. of Aeronautics and Astronautics (AIAA), Reno, NV, 11 Jan. 1995

(NASA-TM-110056; NAS 1.15:110056; AIAA Paper 95-0075) Avail: CASI HC A03/MF A01

In this paper we describe the preliminary analysis of four groups of aerospace engineering and science students -- student members of the American Institute of Aeronautics and Astronautics (AIAA) and students from universities in Japan, Russia, and Great Britain. We compare: (1) the demographic characteristics of the students; (2) factors that affected their career decision; (3) their career goals and aspirations; (4) their training in technical communication; and (5) their training in techniques for finding and using aerospace scientific and technical information (STI). Many employers in the US aerospace industry think there is a need for increased training of engineering students in technical communication. Engineers in the US and other countries believe that technical communication skills are critical for engineers' professional success. All students in our study agree about the importance of technical communication training for professional success, yet relatively few are happy with the instruction they receive. Overall, we conclude that additional instruction in technical communication and accessing STI would make it easier for students to achieve their career goals. Author

N95-19056* National Aeronautics and Space Administration. Langley Research Center, Hampton, VA.

STAND-ALONE DIGITAL DATA STORAGE CONTROL SYSTEM INCLUDING USER CONTROL INTERFACE Patent

Kenneth D. Wright, II, inventor (to NASA) and David L. Gray, inventor (to NASA) 20 Dec. 1994 84 p Filed 27 Nov. 1991 Supersedes N92-30386 (30 - 21, p 3734)

(NASA-Case-LAR-14651-1; US-Patent-5,375,211; US-Patent-Appl-SN-799571; US-Patent-Class-395-425; US-Patent-Class-364-DIG.1; US-Patent-Class-364-238.3;

US-Patent-Class-364-239.2; Int-Patent-Class-G06F-13/10) Avail: US Patent and Trademark Office

A storage control system is presented which includes an apparatus and method for user control of a storage interface to operate a storage medium to store data obtained by a real-time data acquisition system. Digital data received in serial format from the data acquisition system is first converted to a parallel format and then provided to the storage interface. The operation of the storage interface is controlled in accordance with instructions based on user control input from a user. Also, a user status output is displayed in accordance with storage data obtained from the storage interface. By allowing the user to control and monitor the operation of the storage interface, a stand-alone, user-controllable data storage system is provided for storing the digital data obtained by a real-time data acquisition system. Official Gazette of the U.S. Patent and Trademark Office

N95-19127*# National Aeronautics and Space Administration. Langley Research Center, Hampton, VA.

NASA/DOD AEROSPACE KNOWLEDGE DIFFUSION RESEARCH PROJECT. PAPER 45: A COMPARISON OF THE INFORMATION-SEEKING BEHAVIORS OF THREE GROUPS OF US AEROSPACE ENGINEERS

John M. Kennedy (Indiana Univ., Bloomington, IN.), Thomas E. Pinelli, and Rebecca O. Barclay (Rensselaer Polytechnic Inst., Troy, NY.) 1995 13 p Presented at the 33d Aerospace Sciences Meeting and Exhibit of the American Inst. of Aeronautics and Astronautics (AIAA), Reno, NV, 12 Jan. 1995

(NASA-TM-109839; NAS 1.15:109839; AIAA Paper 95-0706) Avail: CASI HC A03/MF A01

To understand the transfer of scientific and technical information (STI) in aerospace, it is necessary to understand the characteristics and behaviors of those who create and use STI. In this paper, we analyze the similarities and differences in the scientific and technical information-seeking behaviors of three groups of US aerospace engineers and scientists. We describe some of their demographic characteristics and their duties and responsibilities as a method of understanding their STI use patterns. There is considerable diversity among aerospace engineers in their use of STI. In general, engineers engaged in research use more STI than those who are in design/development and manufacturing/production. Research engineers also use different standards to determine the STI sources and products that they will use. Author

N95-19589# Pacific Northwest Lab., Richland, WA.

INFORMATION SYSTEM ARCHITECTURE TO SUPPORT TRANSPARENT ACCESS TO DISTRIBUTED, HETEROGENEOUS DATA SOURCES

J. C. Brown Aug. 1994 15 p Presented at the 11th Office Information Technology Conference, Chicago, IL, 23-25 Aug. 1994

(Contract DE-AC06-76RL-01830)

(DE94-018450; PNL-SA-24743; CONF-940873-4) Avail: CASI HC A03/MF A01

Quality situation assessment and decision making require access to multiple sources of data and information. Insufficient accessibility to data exists for many large corporations and government agencies. By utilizing current advances in computer technology, today's situation analyst's have a wealth of information at their disposal. There are many potential solutions to the information accessibility problem using today's technology. The United States Department of Energy (US-DOE) faced this problem when dealing with one class of problem in the US. The result of their efforts has been the creation of the Tank Waste Information Network System -- TWINS. The TWINS solution combines many technologies to address problems in several areas such as User Interfaces, Transparent Access to Multiple Data Sources, and Integrated Data Access. Data related to the complex is currently distributed throughout several US-DOE installations. Over time, each installation has adopted their own set of standards as related to information management. Heterogeneous hardware and software platforms exist both across the complex and within a single installation. Standards for information management vary between US-DOE mission areas within installations. These factors contribute to the complexity of accessing information in a manner that enhances the performance and decision making process of the analysts. This paper presents one approach taken by the DOE to resolve the problem of distributed, heterogeneous, multi-media information management for the HLW Tank complex. The information system architecture developed for the DOE by the TWINS effort is one that is adaptable to other problem domains and uses. DOE

N95-19604# University of Southern California, Marina del Rey, CA. Information Sciences Inst.

COOPERATING AGENTS FOR INFORMATION RETRIEVAL

Craig A. Knoblock, Yigal Arens, and Chu-Nan Hsu May 1994 16 p

(Contract F30602-91-C-0081; NSF IRI-93-13993)

(AD-A285887; ISI/RR-94-382) Avail: CASI HC A03/MF A01

With the vast number of information resources available today, a critical problem is how to locate, retrieve and process information. It would be impractical to build a single unified system that combines all of these information resources. A more promising approach is to build specialized information retrieval agents that provide access to a subset of the information resources and can send requests to other information retrieval agents when appropriate. In this paper we present the architecture of the individual information retrieval agents and describe how this architecture supports a network of cooperating information agents. We describe how these information agents represent their knowledge, communicate with other agents, dynamically construct information retrieval plans, and learn about other agents to improve efficiency. We have already built a small network of agents that have these capabilities and provide access to information for transportation planning. DTIC

N95-19876# Sandia National Labs., Albuquerque, NM.

AUTOMATICALLY GENERATING PROCEDURE CODE AND DATABASE MAINTENANCE SCRIPTS

J. W. Hatley 1994 11 p Presented at the 1994 Ingres World, Chicago, IL, 2-6 Oct. 1994

(Contract DE-AC04-94AL-85000)

(DE95-000545; SAND-94-2524C; CONF-9410204-1) Avail: CASI HC A03/MF A01

Over the past couple of years the Information Technology Department at Sandia Laboratories has developed software to automatically generate database/4gl procedure code and database maintenance scripts based on database table information. With this software developers simply enter table and referential integrity information and the software generates code and scripts as required. The generated procedure code includes simple insert/delete/update procedures, transaction logging procedures as well as referential integrity procedures. The generated database maintenance scripts include scripts to modify structures, update remote databases, create views, and create indexes. Additionally, the software can generate EPSI representations of Binder diagrams for the tables. This paper will discuss the software application and use of it in real world applications. The automated generation of procedure code and maintenance scripts allows the developers to concentrate on the development of user interface code. The technique involves generating database/4 gl procedure code and maintenance scripts automatically from the database table information. The database/4gl procedure code provides standard insert/update/delete interfaces for upper level code as well as enforces the data constraints defined in the information model. The maintenance scripts provide maintenance scripts and migration scripts. This has resulted in fully updated database applications with complete rules enforcement and database maintenance scripts within days of a database modification. DOE

N95-18171*# Florida International Univ., Miami, FL. Dept. of Industrial and Systems Engineering.

ASSESSMENT OF THE SFC DATABASE FOR ANALYSIS AND MODELING

Martha A. Centeno *In* Univ. of Central Florida, NASA/ASEE Summer Faculty Fellowship Program. 1994 Research Reports Oct. 1994 p 113-137 (For primary document see N95-18166 05-80)

Avail: CASI HC A03/MF A04

N95-18978*# Oklahoma Univ., Norman, OK. School of Electrical Engineering.

PERFORMANCE EVALUATION OF THE ENGINEERING ANALYSIS AND DATA SYSTEMS (EADS) 2

Linda S. DeBrunner *In* Alabama Univ., Research Reports: 1994 NASA/ASEE Summer Faculty Fellowship Program Oct. 1994 6 p

(For primary document see N95-18967 05-80)
Avail: CASI HC A02/MF A03

N95-18986*# Alabama Univ., Tuscaloosa, AL. Dept. of Electrical Engineering.
A HYPERTEXT-BASED INTERNET-ASSESSABLE DATABASE FOR THE MSFC TECHNOLOGY TRANSFER OFFICE
Jeff Jackson *In its* Research Reports: 1994 NASA/ASEE Summer Faculty Fellowship Program Oct. 1994 6 p (For primary document see N95-18967 05-80)
Avail: CASI HC A02/MF A03

N95-19005*# Tennessee State Univ., Nashville, TN. Dept. of Physics, mathematics and Computer Science.
A REPORT OF WORK ACTIVITIES ON THE NASA SPACELINK PUBLIC ELECTRONIC LIBRARY
Willard A. Smith *In* Alabama Univ., Research Reports: 1994 NASA/ASEE Summer Faculty Fellowship Program Oct. 1994 6 p (For primary document see N95-18967 05-80)
Avail: CASI HC A02/MF A03

N95-19629*# California Univ., Los Angeles, CA. Dept. of Computer Science.
THE DESIGN AND IMPLEMENTATION OF EPL: AN EVENT PATTERN LANGUAGE FOR ACTIVE DATABASES
G. Giuffrida and C. Zaniolo *In* NASA. Johnson Space Center, Third CLIPS Conference Proceedings, Volume 1 Nov. 1994 p 21-28 Sponsored in cooperation with Hughes Aircraft Corp. (For primary document see N95-19625 05-61)
Avail: CASI HC A02/MF A03

N95-19631*# California Univ., Los Angeles, CA. Dept. of Computer Science.
EXPERT SYSTEM SHELL TO REASON ON LARGE AMOUNTS OF DATA
Gionanni Giuffrida *In* NASA. Johnson Space Center, Third CLIPS Conference Proceedings, Volume 1 Nov. 1994 p 34-42 (For primary document see N95-19625 05-61)
Avail: CASI HC A02/MF A03

N95-19644*# Maharishi International Univ., Fairfield, IA. Dept. of Computer Science.
TARGET'S ROLE IN KNOWLEDGE ACQUISITION, ENGINEERING, VALIDATION, AND DOCUMENTATION
Keith R. Levi *In* NASA. Johnson Space Center, Third CLIPS Conference Proceedings, Volume 1 Nov. 1994 p 162-168 (For primary document see N95-19625 05-61)
Avail: CASI HC A02/MF A03

N95-19646*# National Aeronautics and Space Administration. Lyndon B. Johnson Space Center, Houston, TX.
EXPERT SYSTEM TECHNOLOGIES FOR SPACE SHUTTLE DECISION SUPPORT: TWO CASE STUDIES
Christopher J. Ortiz and David A. Hasan (LinCom Corp., Houston, TX.) *In its* Third CLIPS Conference Proceedings, Volume 1 Nov. 1994 p 180-190 (For primary document see N95-19625 05-61)
Avail: CASI HC A03/MF A03

N95-19647*# Ensco, Inc., Melbourne, FL. Applied Research and Systems Div.
THE METEOROLOGICAL MONITORING SYSTEM FOR THE KENNEDY SPACE CENTER/CAPE CANAVERAL AIR STATION
Allan V. Dianic *In* NASA. Johnson Space Center, Third CLIPS Conference Proceedings, Volume 1 Nov. 1994 p 191-200 (For primary document see N95-19625 05-61)
Avail: CASI HC A02/MF A03

83 ECONOMICS AND COST ANALYSIS

Includes cost effectiveness studies.

No abstracts in this category.

84 LAW, POLITICAL SCIENCE AND SPACE POLICY

Includes NASA appropriation hearings; aviation law; space law and policy; international law; international cooperation; and patent policy.

No abstracts in this category.

85 URBAN TECHNOLOGY AND TRANSPORTATION

Includes applications of space technology to urban problems; technology transfer; technology assessment; and surface and mass transportation.

For related information see also *03 Air Transportation and Safety, 16 Space Transportation,* and *44 Energy Production and Conversion.*

No abstracts in this category.

88 SPACE SCIENCES (GENERAL)

No abstracts in this category.

89 ASTRONOMY

Includes radio, gamma-ray, and infrared astronomy, and astrometry.

N95-17981*# Johns Hopkins Univ., Baltimore, MD. Dept. of Physics and Astronomy.
ROCKET AND LABORATORY STUDIES IN ASTRONOMY Status Report, 1 Sep. 1993 - 31 Aug. 1994
Paul D. Feldman 6 Dec. 1994 6 p
(Grant NAG5-619)
(NASA-CR-197531; NAS 1.26:197531) Avail: CASI HC A02/MF A01

This report covers the period from September 1, 1993 to August 31, 1994. During the reporting period we launched the Faint Object Telescope to measure the absolute flux of a hot white dwarf star in the spectral range below 1200 A. This experiment was not successful due to a failure of an electronics unit in the onboard TV acquisition system. The source of the failure has been identified and corrected and is described in detail below. The payload was recovered in excellent condition and we are planning to refurbish it for flight during the November 1995 Australia campaign. We have continued our laboratory studies of the ultraviolet performance of charge-coupled-detector (CCD) arrays and plan to include a UV-sensitive CCD in a new payload that was assembled during the current period. The objective of the experiment is the ultraviolet imaging of

Jupiter and we are scheduled to launch the payload, 36.115UG, in May-June 1995. We have also begun the design of a high-resolution FUV spectrograph for a future flight of the FOT and have just recently received a high line density grating fabricated by Jobin-Yvon, S.A. (France) for evaluation. Work has continued on the analysis of data from previous rocket experiments.
Derived from text

N95-18001 Massachusetts Univ., Amherst, MA.
THE 2 MICRON ALL SKY SURVEY
W. Pughe, S. Kleinmann, M. Skrutskie, M. Weinberg, and J. Huchra 1994 10 p Limited Reproducibility: More than 20% of this document may be affected by microfiche quality
(AD-A283515) Avail: CASI HC A02

The 2 micron All Sky Survey, or 2MASS, will cover the sky at three near-infrared wavelengths with a pixellation of approx. 2.0 microns. One of the primary scientific goals of the survey is to produce a catalogue of galaxies limited between K=13 and K=14 (equivalent to B=16-17) to within 10 deg of the galactic plane. The 2Mass Galaxy Catalogue is expected to contain over a million galaxies and will be an invaluable aid to mapping the local density field out to z=0.1
DTIC

N95-18361# Naval Postgraduate School, Monterey, CA.
DESIGN, VALIDATION AND PROTOTYPE TESTING OF A HIGH RESOLUTION ALL-REFLECTION MICHELSON INTERFEROMETER FOR SOLAR OCCULTATION MEASUREMENTS OF THE OI 1304-A TRIPLET EMISSION M.S. Thesis
Michael W. Gill Jun. 1994 94 p
(AD-A283705) Avail: CASI HC A05/MF A01

A prototype All-Reflection Michelson Interferometer (AMI) was tested using two different diffraction gratings and a variety of light sources. The original design used a focusing lens, a pinhole aperture and an off-axis parabolic mirror for collimation, a plane diffraction grating and two plane mirrors to divide and recombine the light and a CCD camera to record the interference pattern. Interference patterns were recorded and analyzed in the Interactive Data Language (IDL) using Fourier transform techniques. The design was then modified to approximate an actual instrument for remote observations of the atomic oxygen 1304-A triplet emission. The results of numerous experiments using both the original and modified instruments verified the feasibility of using the AMI as a compact, lightweight, high resolution instrument for use on sounding rocket or satellite platforms.
DTIC

N95-18391*# Lockheed Missiles and Space Co., Palo Alto, CA.
THE QUIESCENT AND FLARING EUV SPECTRUM OF ALGOL AND ITS RELATIONSHIP TO OTHER ACTIVE CORONAE. EUV SPECTROSCOPY OF BRIGHT HYADES CORONAE: 71 TAURI AND THETA 1 TAURI Final Report
Robert A. Stern 15 Dec. 1994 28 p
(Contract NAS5-32492)
(NASA-CR-197538; NAS 1.26:197538) Avail: CASI HC A03/MF A01

This program involves analysis and interpretation of EUVE spectrometer observations of the active stars Algol (beta Per) and 71 Tauri. The EUVE satellite spectrometers observed the prototype eclipsing binary Algol over nearly 1.5 orbital periods. Effective exposure times were 100 ksec and 89 ksec in the short wave (70-180 A) and medium wave (140-370 A) channels. High temperature (up to 20 MK) Fe XVI-XXIV emission lines are clearly detected in the overall spectrum. In addition, a quiescent continuum is present which increases towards shorter wavelengths. Using synthesized spectra of optically thin line and continuum emission folded through the instrumental response, we have examined constraints on the (Fe/H) coronal abundance in Algol. We find that the coronal Fe is underabundant by factors that approximately equal 2-4 relative to solar photospheric values, unless an unreasonably large quantity of coronal plasma at T greater than 30 MK is present in the quiescent spectrum. The latter possibility is, however, inconsistent with available X-ray data. Lightcurves of the high temperature EUV lines compared to line emission at He II 304 A show considerable differences, with much deeper minima present in the He II line during both primary and secondary eclipses. Toward the end of the observation a moderate flare lasting approximately 6 hours was detected in the high temperature Fe emission lines. The 71 Tau observation, for about the same exposure time, revealed only a handful of weak emission lines; however, the strongest lines were also those of Fe XXIII/XX, suggesting a hot coronal plasma. No obvious flaring or other variation was present in the 71 Tau Deep Survey lightcurve.
Author

N95-19617# California Univ., Berkeley. Lawrence Berkeley Lab, CA.
CORRELATION FUNCTION ANALYSIS OF THE COBE DIFFERENTIAL MICROWAVE RADIOMETER SKY MAPS Ph.D. Thesis
C. H. Lineweaver Aug. 1994 156 p
(Contract DE-AC03-76SF-00098)
(DE95-000795; LBL-36026) Avail: CASI HC A08/MF A02

The Differential Microwave Radiometer (DMR) aboard the COBE satellite has detected anisotropies in the cosmic microwave background (CMB) radiation. A two-point correlation function analysis which helped lead to this discovery is presented in detail. The results of a correlation function analysis of the two year DMR data set is presented. The first and second year data sets are compared and found to be reasonably consistent. The positive correlation for separation angles less than approximately 20 deg is robust to Galactic latitude cuts and is very stable from year to year. The Galactic latitude cut independence of the correlation function is strong evidence that the signal is not Galactic in origin. The statistical significance of the structure seen in the correlation function of the first, second and two year maps is respectively greater than 9(sigma), greater than 10(sigma) and greater than 18(sigma) above the noise. The noise in the DMR sky maps is correlated at a low level. The structure of the pixel temperature covariance matrix is given. The noise covariance matrix of a DMR sky map is diagonal to an accuracy of better than 1%. For a given sky pixel, the dominant noise covariance occurs with the ring of pixels at an angular separation of 60 deg due to the 60 deg separation of the DMR horns. The mean covariance of 60 deg is 0.45%(sub -0.14)(sup +0.18) of the mean variance. The noise properties of the DMR maps are thus well approximated by the noise properties of maps made by a single-beam experiment. Previously published DMR results are not significantly affected by correlated noise.
DOE

N95-19301*# Harvard-Smithsonian Center for Astrophysics, Cambridge, MA.
ASTRONOMICAL OBSERVATIONS OF PHENOMENA IN DISKS Abstract Only
L. Hartmann *In* Lunar and Planetary Inst., Papers Presented to the Conference on Chondrules and the Protoplanetary Disk 1994 p 11
(For primary document see N95-19289 05-90)
Avail: CASI HC A01/MF A01

90 ASTROPHYSICS

Includes cosmology; celestial mechanics; space plasmas; and interstellar and interplanetary gases and dust.

For related information see also *75 Plasma Physics.*

N95-18213# Instituto de Pesquisas Espaciais, Sao Jose dos Campos (Brazil).
EFFECTS OF METEOR SHOWERS IN THE EARTH IONOSPHERE Ph.D. Thesis [EFEITOS DAS CHUVAS DE METEOROS NA IONOSFERA TERRESTRE]
Neusa Maria PaesLeme Sep. 1994 187 p In PORTUGESE
(INPE-5591-TDI/552) Avail: CASI HC A09/MF A02

This work studies the interaction of meteor showers with the low terrestrial ionosphere. The analysis uses the VLF (Very Low Frequency, 10-30 kHz) radiopropagation technique and covers the period from 1966 to 1994. This technique enables the study of meteoroid interaction with the region from 60 to 90 km height, of which there is very poor information. The analysis of transequatorial VLF signals allows the monitoring of the main meteor showers at southern and northern hemispheres. The obtained results were compared with those detected by meteoric radar, for the more significant showers. The 28 years of continuous data monitoring of VLF signals allowed the study of the variability of the streams associated to the meteor showers, as well as the estimation of the physical and chemical parameters of the meteoric particles and of the considered region.
Author

N95-18451 Phillips Lab., Hanscom AFB, MA.
CRRESPRO DOCUMENTATION

Jeralyn D. Meffert and M. S. Gussenhoven 28 Jul. 1994 36 p Limited Reproducibility: More than 20% of this document may be affected by microfiche quality
(AD-A284578; AD-E202183; PL-TR-94-2218; ERP-1158) Avail: CASI HC A03

This technical report documents the software package CRRESPRO developed by the Phillips Laboratory. The CRRESPRO utility calculates proton omnidirectional fluence and integral omnidirectional fluence over the energy range 1-100 MeV for orbits specified by the user. Proton fluence is calculated from proton flux models created using data measured by the proton telescope (PROTEL) on the Combined Release and Radiation Effects Satellite (CRRES), which flew in a geosynchronous transfer orbit for 14 months during solar maximum. Because the March 1991 magnetic storm caused a reconfiguration of the inner magnetosphere resulting in double proton belts for certain energies, two CRRES models were constructed. The quiet (single proton belt) model uses PROTEL data from July 1990 to March 1991, and the active (double proton belt) model uses data from March 1991 to October 1991. CRRESPRO is best applied to orbits with altitudes greater than 1000 km. Unlike its sister program, CRRESRAD, CRRESPRO gives 100 percent coverage for orbits of any inclination.
DTIC

N95-18496 Pennsylvania Univ., Philadelphia, PA.
TESTING THE INFLATIONARY PARADIGM: INFLATION AND THE COSMIC MICROWAVE BACKGROUND ANISOTROPY Ph.D. Thesis
Robert Glen Crittenden 1993 154 p
Avail: Univ. Microfilms Order No. DA9413820

We introduce a new method for experimentally testing the inflationary paradigm: the suggestion that the universe underwent a period of superluminal expansion early in its history. Inflation naturally produces both density fluctuations, which are thought to have seeded structure formation, and a spectrum of primordial gravitational waves (tensor metric perturbations), which have yet to be discovered. Most inflationary scenarios predict a strict relationship between the ratio of the tensor to scalar fluctuations and the spectral index of the density fluctuations, n, which describes how their amplitude varies with wavelength. (P(k) varies as k(sup n) where P(k) is the power in the fluctuations with wavenumber k.) The detection of these gravitational waves with the proper amplitude is a critical test of inflation. We suggest a possible method for detecting these tensor fluctuations. If their amplitude is comparable to that of the density fluctuations, their presence will be evidenced by their effects on the spectrum of anisotropies in the Cosmic Microwave Background. We investigate the prospects and possible methods for performing this kind of measurement. Author

N95-18498 Virginia Univ. Hospital, Charlottesville, VA.
AN OPTICAL STUDY OF COMPACT STEEP SPECTRUM RADIO SOURCES Ph.D. Thesis
Richard Fredrick Gelderman 1994 170 p
Avail: Univ. Microfilms Order No. DA9415553

This thesis presents results from an extensive optical study of a sample of Compact Steep-Spectrum (CSS) radio galaxies and quasars. The distinguishing characteristic of the CSS class is that the objects contain powerful steep-spectrum radio sources which are confined within the dimensions of the host galaxy. Previous studies have suggested that these sources may be good candidates for finding strong interactions between the radio source and the interstellar medium of the host galaxy. Both low and high dispersion spectra and broad bang images have been obtained for a sample of 19 northern hemisphere CSS sources as well as a sample of related objects with dominant kiloparsec-scale steep-specrum radio emission. Our spectra provide measurements of emission line flux, flux ratios, equivalent widths, and continuum properties, as well as measurements of the (OIII) lambda 5007 and H(Beta) emission line profile shapes. As a class, the CSS sources have remarkably broad, structured (OIII) lambda 5007 profiles. We argue that the powerful subgalactic radio structure provides the perturbing acceleration to the ionized gas. CSS sources also appear to have relatively strong, high equivalent width, high excitation line emission, consistent with the presence of a substantial covering factor in the NLR. We conclude that the gas is photoionized by the active nucleus, and are unable to find convincing evidence that the radio jet plays a direct role in the ionization. Our images indicate that galaxy-galaxy interactions are an important aspect of the CSS phenomenon for every member of our sample. In summary, our data support a picture in which the CSS radio sources are interacting with a considerable amount of gas in their NLR. Author

N95-18499 Columbia Univ., New York, NY.
DEVELOPMENT OF A HIGH-RESOLUTION LIQUID XENON DETECTOR FOR GAMMA-RAY ASTROPHYSICS Ph.D. Thesis
Reshmi Mukherjee 1993 214 p
Avail: Univ. Microfilms Order No. DA9412819

It has been shown here that liquid xenon is one of the most promising detector media for future gamma-ray detectors, owing to an excellent combination of physical properties. The feasibility of the construction of a high resolution liquid xenon detector as a gamma-ray detector for astrophysics has been demonstrated. Up to 3.5 liters of liquid xenon has been successfully purified and using both small and large volume prototypes, the charge and the energy resolution response of such detectors to gamma-rays, internal conversion electrons and alpha particles have been measured. The best energy resolution measured was 4.5 percent FWHM at 1 MeV. Cosmic ray tracks have been imaged using a 2-dimensional liquid xenon multiwire imaging chamber. The spatial resolution along the direction of the drifting electrons was 180 microns rms. Experiments have been performed to study the scintillation light in liquid xenon, as the prompt scintillation signal in the liquid is an electron-ion pair in liquid krypton was measured for the first time with a pulsed ionization chamber to be 18.4 plus or minus 0.3 eV. Dissert. Abstr.

N95-18500 Texas Univ., Austin, TX.
PURE-ROTATIONAL EMISSION FROM MOLECULAR HYDROGEN IN OMC-1 Ph.D. Thesis
Parvinder Singh Parmar 1993 177 p
Avail: Univ. Microfilms Order No. DA9413568

Measurements of several mid-infrared pure-rotational emission lines of molecular hydrogen were obtained in two regions associated with recent star formation in OMC-1. Since these lines are optically thin and thermalized, they provide an important probe of physical conditions within the regions. In the Orion Bar photodissociation region, observations of H2J = 3-1 and 4-2 lines lead to the derivation of the kinetic gas temperature and molecular column density distributions on a spatial scale of 2 inches or approximately 0.005 pc. When compared with models in the literature, the results support the scenario that the H2 emission originates on the warm photodissociated surfaces of many dense (approximately greater than 10(exp 6) cm(exp -3)) clumps of molecular gas embedded with a small volume filling factor in a lower-density (approximately less than 5 x 10(exp 4) cm(exp -3)) cooler atomic medium. In the shock-excited region that surrounds BN-KL, observations of H2J = 3-1, 4-2, 5-3, 9-7, and 11-9 lines are interpreted in terms of a two-shock model in which the low-JH2 emission originates from molecules (with temperature about 500 K and column density about 4 x 10(exp 21) cm(exp -2)) reformed after passage of a hydrodynamic shock, and the high-J H2 emission originates from molecules (with temperature 2000-3000 K and column density about 6 x 10(exp 19) cm(exp -2)) heated in a magnetohydrodynamic shock. The think dense shell of swept-up material separating the two shocks may be moving into a clumpy medium whose density contrast is approximately 100 and whose area-filling factor is approximately 0.2. comparison of the wing emission of lines shows that the extinction within the outflow is not large. A persuasive explanation of the high-velocity wing emission remains elusive, however, and will require observations with higher spectral resolution. Dissert. Abstr.

N95-18728 McMaster Univ., Hamilton (Ontario).
DYNAMICS OF LMC CLUSTERS Ph.D. Thesis
Philippe Fischer 1993 177 p
(ISBN-0-315-84911-8) Avail: Univ. Microfilms Order No. DANN84911

The dynamics of three populous Large Magellanic Cloud (LMC) star clusters NGC 1866, NGC 1978, and NGC 1850, have been examined using a combination of BV charge-coupled device (CCD) images and high-precision radial velocities of individual member stars. NGL 1866 V-band CCD images of the young LMC cluster NGC 1866 out to a projected radius R equal to approximately 100 pc were obtained using 1.0 m telescope. The luminosity profile is described by a power-law. The total cluster luminosity is L(V)infinity = 6.5 +/- 0.3 x 10(exp 5) L(solar). In the region 4 less than or equal to R (pc) less than or equal to 12, the cluster has a mean ellipticity of epsilon = 0.17 +/- 0.06 and a minor axis position angle alpha = 125 +/- 5 deg. NGC 1866 has a systemic velocity of v(sub ave)

= 301.2 +/- 1.0 km s(exp -1) and is rotating around an axis at a position angle of 100 +/- 25 deg with a peak velocity of 1.3 +/- 0.5 km s(exp -1). The best estimate for the average slope of the mass function is x = 1.3 +/- 0.15 (r = 2.0 x 10(exp 8) years). BC CCD images of the elliptical LMC cluster NGC 1978 out to a projected radius R equal to approximately 100 pc were obtained using the 1.0 m telescope. After star-subtraction and median-filtering the ellipticity of the surface brightness distribution was determined to be epsilon = 0.30 +/- 0.03 and the major axis position angle to be PA = 152 +/- 7 deg. Single and multi-mass anisotropic King-Michie models and single-mass rotating and non-rotating oblate spheroid models were fitted to both the surface luminosity profiles and the radial velocity data. The total cluster luminosity is L(B) = 3.1-3.7 +/- 0.2 x 10(exp 5) L(B)solar magnitude and L(V) = 3.0-3.5 +/- 0.2 x 10(exp 5) L(V)solar magnitude. The single-mass models tended to give better agreement with the luminosity profiles. We found no significant differences between the M/L's derived with oblate spheroid models and those derived with spherical models. We have examined the age and internal dynamics of the young binary LMC cluster NGC 1850. Isochrone fits to BV color-magnitude diagram revealed that the primary cluster has an age of r = 90 +/- 30 Myr. The total cluster luminosity varied from L(B) = 2.60-2.65 x 10(exp 6) L(B)solar and L(B) = 1.25-1.35 x 10(exp 6). Of the 52 stars with echell spectra, a subset of 36 were used to study the cluster dynamics. Values for the slope of the mass function were determined using the derived M/L, theoretical mass-luminosity relationships, and several forms for the IMF. Dissert. Abstr.

N95-18746*# Fermi National Accelerator Lab., Batavia, IL.
A TYPE 2 SUPERNOVAE CONSTRAINT ON NEUTRINO(SUB e) - NEUTRINO(SUB s) MIXING
X. Shi (Chicago Univ., Chicago, IL.) and G. Sigl (Chicago Univ., Chicago, IL.) Dec. 1993 14 p Submitted for publication Sponsored by DOE; NSF; and Alexander-von-Humboldt Foundation
(Grant NAGw-2381)
(NASA-CR-197630; NAS 1.26:197630; FERMILAB-Pub-93/401-A) Avail: CASI HC A03/MF A01

The role of a resonant nu(e) - nu(s) oscillation is discussed in the event of a supernova explosion. It is concluded that a significant nu(e) - nu(s) mixing may hinder the ability of the supernova to explode. It may also cool the proto-neutron star too quickly with respect to the observed cooling time of several seconds. The constraints on the nu(e) - nu(s) mixing parameters based on the above arguments are calculated. Author

N95-18877# Joint Inst. for Nuclear Research, Dubna (USSR). Lab. of Theoretical Physics.
GENERAL RELATIVITY AND DARK MATTER
A. B. Pestov 1993 10 p Submitted for publication
(DE94-626641; JINR-E-2-93-424) Avail: CASI HC A02/MF A01 (US Sales Only)

It is shown that from the first principles of General Relativity it follows that there exists a new type of interactions which are tightly connected with the gravitational interactions. New particles representing a new form of interactions do not interact electromagnetically, strongly and weakly with the known elementary particles. Physics of the new particles is defined by the Planck scales. DOE

N95-18964*# Fermi National Accelerator Lab., Batavia, IL. NASA/Fermilab Astrophysics Center.
IS A MASSIVE TAU NEUTRINO JUST WHAT COLD DARK MATTER NEEDS?
Scott Dodelson, Geza Gyuk (Chicago Univ., Chicago, IL.), and Michael S. Turner (Chicago Univ., Chicago, IL.) 1994 15 p Sponsored by DOE and NSF
(Grant NAGw-2381)
(NASA-CR-197627; NAS 1.26:197627; FERMILAB-Pub-94/026-A; Astro-Ph/9402028) Avail: CASI HC A03/MF A01

The cold dark matter (CDM) scenario for structure formation in the Universe is very attractive and has many successes; however, when its spectrum of density perturbations is normalized to the COBE anisotropy measurement the level of inhomogeneity predicted on small scales is too large. This can be remedied by a tau neutrino of mass 1 MeV - 10MeV and lifetime 0.1 sec - 100 sec whose decay products include electron neutrinos because it allows the total energy density in relativistic particles to be doubled without interfering with nucleosynthesis. The anisotropies predicted on the degree scale for 'tau CDM' are larger than standard CDM. Experiments at e(sup +/-) collides may be able to probe such a mass range. Dissert. Abstr.

N95-18966*# Kansas Univ., Lawrence, KS. Dept. of Physics and Astronomy.
TESTING THE FROZEN FLOW APPROXIMATION
Francesco Lucchin (Padua Univ., Italy.), Sabino Matarrese (Padua Univ., Italy.), Adrian L. Melott, and Lauro Moscardini (Padua Univ., Italy.) 1993 20 p Sponsored by MURST
(Grants NAGw-2923; NSF AST-90-21414; NSF OSR-92-55223)
(NASA-CR-197614; NAS 1.26:197614) Avail: CASI HC A03/MF A01

We investigate the accuracy of the frozen-flow approximation (FFA), recently proposed by Matarrese, et al. (1992), for following the nonlinear evolution of cosmological density fluctuations under gravitational instability. We compare a number of statistics between results of the FFA and n-body simulations, including those used by Melott, Pellman & Shandarin (1993) to test the Zel'dovich approximation. The FFA performs reasonably well in a statistical sense, e.g. in reproducing the counts-in-cell distribution, at small scales, but it does poorly in the crosscorrelation with n-body which means it is generally not moving mass to the right place, especially in models with high small-scale power. Author

N95-19031*# Fermi National Accelerator Lab., Batavia, IL. NASA/Fermilab Astrophysics Center.
MASS AND RADIUS OF COSMIC BALLOONS
Yun Wang Jan. 1994 18 p Revised Sponsored by DOE
(Grant NAGw-2381)
(NASA-CR-197628; NAS 1.26:197628; FERMILAB-Pub-93/378-A-Rev)
Avail: CASI HC A03/MF A01

Cosmic balloons are spherical domain walls with relativistic particles trapped inside. We derive the exact mass and radius relations for a static cosmic balloon using Gauss-Codazzi equations. The cosmic balloon mass as a function of its radius, M(R), is found to have a functional form similar to that of fermion soliton stars, with a fixed point at 2GM(R)/R approximately or equal to 0.486 which corresponds to the limit of infinite central density. We derive a simple analytical approximation for the mass density of a spherically symmetric relativistic gas star. When applied to the computation of the mass and radius of a cosmic balloon, the analytical approximation yields fairly good agreement with the exact numerical solutions. Author

N95-19172*# Lunar and Planetary Inst., Houston, TX.
WORKSHOP ON PARTICLE CAPTURE, RECOVERY AND VELOCITY/TRAJECTORY MEASUREMENT TECHNOLOGIES Abstracts Only
Michael E. Zolensky, ed. 1994 113 p Workshop held in Houston, TX, 27-28 Sep. 1993
(Contract NASw-4574)
(NASA-CR-197592; NAS 1.26:197592; LPI-TR-94-05) Avail: CASI HC A06/MF A02

A workshop on particle capture, recovery, and velocity/trajectory measurement technologies was held. The primary areas covered were: (1) parent-daughter orbit divergence; (2) trajectory sensing; (3) capture medium development: laboratory experiments, and (4) future flight opportunities. For individual titles, see N95-19173 through N95-19197.

N95-19173*# California Inst. of Tech., Pasadena, CA.
COMET COMA SAMPLE RETURN INSTRUMENT Abstract Only
A. L. Albee, Don E. Brownlee (Washington Univ., Seattle, WA.), Donald S. Burnett, Peter Tsou (Jet Propulsion Lab., California Inst. of Tech., Pasadena, CA.), and K. T. Uesugi (Tokyo Univ., Sagamihara, Japan.) *In* Lunar and Planetary Inst., Workshop on Particle Capture, Recovery and Velocity/Trajectory Measurement Technologies 1994 p 5-7 (For primary document see N95-19172 05-90)
Avail: CASI HC A02/MF A02

The sample collection technology and instrument concept for the Sample of Comet Coma Earth Return Mission (SOCCER) are described. The scientific goals of this Flyby Sample Return are to return to coma dust and volatile samples from a known comet source, which will permit accurate elemental and isotopic measurements for thousands of individual solid particles and volatiles, detailed analysis of the dust structure, morphology, and mineralogy

of the intact samples, and identification of the biogenic elements or compounds in the solid and volatile samples. Having these intact samples, morphologic, petrographic, and phase structural features can be determined. Information on dust particle size, shape, and density can be ascertained by analyzing penetration holes and tracks in the capture medium. Time and spatial data of dust capture will provide understanding of the flux dynamics of the coma and the jets. Additional information will include the identification of cosmic ray tracks in the cometary grains, which can provide a particle's process history and perhaps even the age of the comet. The measurements will be made with the same equipment used for studying micrometeorites for decades past; hence, the results can be directly compared without extrapolation or modification. The data will provide a powerful and direct technique for comparing the cometary samples with all known types of meteorites and interplanetary dust. This sample collection system will provide the first sample return from a specifically identified primitive body and will allow, for the first time, a direct method of matching meteoritic materials captured on Earth with known parent bodies. Author

N95-19174*# California Inst. of Tech., Pasadena, CA.
SOCCER: COMET COMA SAMPLE RETURN MISSION Abstract Only
A. L. Albee, K. T. Uesugi (Tokyo Univ., Sagamihara, Japan.), and Peter Tsou (Jet Propulsion Lab., California Inst. of Tech., Pasadena, CA.) *In* Lunar and Planetary Inst., Workshop on Particle Capture, Recovery and Velocity/Trajectory Measurement Technologies 1994 p 7-11 (For primary document see N95-19172 05-90)
Avail: CASI HC A01/MF A02

Comets, being considered the most primitive bodies in the solar system, command the highest priority among solar system objects for studying solar nebula evolution and the evolution of life through biogenic elements and compounds. Sample Of Comet Coma Earth Return (SOCCER), a joint effort between NASA and the Institute of Space and Astronautical Science (ISAS) in Japan, has two primary science objectives: (1) the imaging of the comet nucleus and (2) the return to Earth of samples of volatile species and intact dust. This effort makes use of the unique strengths and capabilities of both countries in realizing this important quest for the return of samples from a comet. This paper presents an overview of SOCCER's science payloads, engineering flight system, and its mission operations. Author

N95-19175*# Baylor Univ., Waco, TX. Space Science Lab.
THE STATUS OF MEASUREMENT TECHNOLOGIES CONCERNING MICROMETER AND SUBMICROMETER SPACE ARTICULATE MATTER CAPTURE, RECOVERY, VELOCITY AND TRAJECTORY Abstract Only
W. M. Alexander, William G. Tanner, R. A. McDonald, G. E. Schaub, Stepheni L. Stephenson, J. A. M. McDonnell (Kent Univ., Canterbury, England.), and Carl R. Maag (Science Applications International Corp., Glendora, CA.) *In* Lunar and Planetary Inst., Workshop on Particle Capture, Recovery and Velocity/Trajectory Measurement Technologies 1994 p 11-16 (For primary document see N95-19172 05-90)
Avail: CASI HC A02/MF A02

The return of a pristine sample from a comet would lead to greater understanding of cometary structures, as well as offering insights into exobiology. The paper presented at the Discovery Program Workshop outlined a set of measurements for what was identified as a SOCCER-like interplanetary mission. Several experiments comprised the total instrumentation. This paper presents a summary of CCSR with an overview of three of the four major instruments. Details of the major dust dynamics experiment including trajectory are given in this paper. The instrument proposed here offers the opportunity for the return of cometary dust particles gathered in situ. The capture process has been employed aboard the space shuttle with successful results in returning samples to Earth for laboratory analysis. In addition, the sensors will measure the charge, mass, velocity, and size of cometary dust grains during the encounter. This data will help our understanding of dusty plasmas. Author

N95-19176*# California Inst. of Tech., Pasadena, CA. Seismological Lab.
PHYSICS OF SPACECRAFT-BASED INTERPLANETARY DUST COLLECTION BY IMPACT INTO LOW-DENSITY MEDIA Abstract Only
William W. Anderson and T. J. Ahrens *In* Lunar and Planetary Inst., Workshop on Particle Capture, Recovery and Velocity/Trajectory Measurement Technologies 1994 p 16-21 (For primary document see N95-19172 05-90)
(Grants NsG-7129; NGL-05-002-105)
Avail: CASI HC A02/MF A02

A spacecraft encountering an interplanetary dust particle (IDP) at a relative velocity of several kilometers per second may be used to capture that particle for in situ analysis or for analysis upon Earth return. In this paper we study the impact of a dust particle into a low-density medium (i.e., a foam) such that the foam dissipates the kinetic energy of impact over a sufficient distance to stop the particle without destroying it. Author

N95-19177*# A & M Associates, Lanham, MD.
PLASMA PRODUCED BY IMPACTS OF FAST DUST PARTICLES ON A THIN FILM Abstract Only
Siegfried Auer *In* Lunar and Planetary Inst., Workshop on Particle Capture, Recovery and Velocity/Trajectory Measurement Technologies 1994 p 21-24 (For primary document see N95-19172 05-90)
(NASA Order T-8495-S)
Avail: CASI HC A01/MF A02

The thin-film impact plasma detector was pioneered by Berg for detecting small cosmic dust particles and measuring their approximate velocities in a time-of-flight configuration. While Berg's device was highly successful in establishing the flux of interplanetary dust, the accuracy of measuring the velocities of individual particles was a moderate 18 percent in magnitude and 27 degrees in angle. A much greater accuracy of less than or equal to 1 percent in determining the velocity components appears desirable in order to associate a particle with its parent body. In order to meet that need, research was initiated to determine if a thin-film detector can be designed to provide such accurate velocity measurements. Previous laboratory investigations of the impact plasma uncovered two difficulties: (1) solid or liquid spray is ejected from a primary impact crater and strikes neighboring walls where it produces secondary impact craters and plasma clouds; as a result, both quantity and time of detection of the plasma can vary significantly with the experiment configuration. Particles from an accelerator rarely have speeds v greater than or equal to 10-15 km/s, while cosmic dust particles typically impact at v = 10-72 km/s. The purpose of the tests discussed in this paper was to resolve the two difficulties mentioned. That is, the experiment configuration was designed to reduce the contribution of plasma from secondary impacts. In addition, most particles with v less than or equal to 25 km/s and all particles with v less than or equal to 10 km/s were eliminated from the beam. Author

N95-19178*# A & M Associates, Lanham, MD.
HIGHLY TRANSPARENT AND RUGGED SENSOR FOR VELOCITY DETERMINATIONS OF COSMIC DUST PARTICLES Abstract Only c19
Siegfried Auer and F. O. vonBun *In* Lunar and Planetary Inst., Workshop on Particle Capture, Recovery and Velocity/Trajectory Measurement Technologies 1994 p 25-29 (For primary document see N95-19172 05-90)
(Contract NAS9-18368)
Avail: CASI HC A01/MF A02

In order to understand the evolution of interplanetary dust, numerous dust particles have been collected and analyzed. An analysis of the composition often provides information on the particle's origin. So does its origin. Composition and orbit data complement each other and should be determined together. If the last orbit of a particle can be determined, its orbital history can often be calculated backward in time and associated with its parent body. To determine the last orbit, the velocity needs to be measured before the particle is collected. The precision required in determining the velocity components relative to the spacecraft should be 1 percent or better. A sensor for naturally charged cosmic dust particles is discussed. Two models of the sensor were tested, one with a free-falling steel ball and the other with particles accelerated to high speed. Analytic expressions of the sensor signals are presented and compared with the test results. The errors in speed and angle were estimated to be about 0.3 percent and 0.2 degrees respectively. Author

N95-19179*# Centre National de la Recherche Scientifique, Orsay (France). Inst. d'Astrophysique Spatiale.
MAIN CHARACTERISTICS OF THE COMET/COMRADE EXPERIMENTS Abstract Only
J. Borg, J.-P. Bibring, and Carl R. Maag (Science Applications International Corp., Glendora, CA.) *In* Lunar and Planetary Inst., Workshop on Particle

Capture, Recovery and Velocity/Trajectory Measurement Technologies 1994 p 29-32 (For primary document see N95-19172 05-90)
Avail: CASI HC A01/MF A02

Both the COMET (Collection en Orbite de Matiere Extra Terrestre) and the COMRADE (Collection of Micrometeorites, Residue and Debris Ejecta) programs are developed to the collection and analysis of the particles of various origins orbiting around the Earth at low altitudes (between approx. 300 and approx. 500 km). The COMET experiment is more specifically designed to be flown for a short period of time (a few days), in concordance with a meteor stream crossing the Earth. Thus, it results in a considerable enrichment in the collection of grains related to a given comet. The COMRADE experiment has been selected as a proposal for long-duration flights (a few months), in order to gain information on all sizes of particles present on low Earth orbits, including submicrometer grains. It has been accepted by ESA authorities for use on the EURECA 2 platform. The objectives of these studies are multiple. The use of passive detectors gives access to the chemical and isotopical properties of the grains in the micrometer size range, by analyzing either the particle remnant mixed with the target material, or the intact particle captured in a specific low-density material. The particle remnants of the micrometer-sized extraterrestrial grains, having impacted on purposely designed metallic collectors, are identified for complete and detailed chemical, isotopic, and organic analysis, thereby determining grain composition as well as the existence of organic and inorganic molecules, to be related with the possible cometary origin of the grains. Micrometer/submicrometer dust grains are also captured in a manner that ensures minimal particle degradation. The captured intact particles are returned to Earth for complete and detailed chemical, isotopic, spectral, mineralogical, and organic analysis. Author

N95-19180*# Kent Univ., Canterbury (England). Unit for Space Sciences.
THE HYPERVELOCITY IMPACT FACILITIES AT THE UNIVERSITY OF KENT AT CANTERBURY, UK Abstract Only **c14**
Mark J. Burchell, J. A. M. McDonnell, M. J. Cole, and P. R. Ratcliff *In* Lunar and Planetary Inst., Workshop on Particle Capture, Recovery and Velocity/Trajectory Measurement Technologies 1994 p 32-35 (For primary document see N95-19172 05-90)
Avail: CASI HC A01/MF A02

The University of Kent at Canterbury facilities for production of hypervelocity impacts are discussed. Meteoroids are simulated by electrostatic acceleration of small (10(exp -12) - 10(exp -17) kg) particles using a 2-MV Van de Graaff accelerator. This machine has been operational for many years; both the machine and experimental area are currently being upgraded. Larger particles (10(exp -10) - 10(exp -14) kg) are accelerated using a more recently installed light gas gun. The status of all hardware (including experimental areas) is given, along with brief details of recent, current, and future projects making use of them. Author

N95-19181*# Florida Univ., Gainesville, FL. Dept. of Astronomy.
IRAS OBSERVATIONS SHOW THAT THE EARTH IS EMBEDDED IN A SOLAR RING OF ASTEROIDAL DUST PARTICLES IN RESONANT LOCK WITH THE PLANET Abstract Only
Stanley F. Dermott, S. Jayaraman, Y.-L. Xu, and J.-C. Liou *In* Lunar and Planetary Inst., Workshop on Particle Capture, Recovery and Velocity/Trajectory Measurement Technologies 1994 p 35-36 (For primary document see N95-19172 05-90)
Avail: CASI HC A01/MF A02

We have analyzed all the infrared observations of the zodiacal cloud obtained in 1983 by the Infrared Astronomical Satellite (IRAS) and shown that when viewed at a constant elongation angle of 90 degrees, the elliptic brightness of the cloud is systematically greater by approx. 3 percent in the trailing direction than in the leading direction. This asymmetry is observed at all times of the year and in all three of the IRAS wavebands in which the zodiacal cloud is clearly observed. The orbits of cometary particles are highly eccentric and these particles are unlikely to be trapped in corotational resonances. Thus, the IRAS observations are evidence that the Earth is embedded in a ring of asteroidal particles. Similar rings are expected to be associated with Mars and Venus. The existence of asteroidal families and their associated dust bands (also discovered by IRAS) are evidence that the asteroid belt is a significant and maybe the dominant source of dust in the zodiacal cloud. These new observations give quantitative information both on the rate of transport of asteroidal dust to the Earth and on the rate of grinding down of the asteroid belt. Without resonant trapping most dust particles spiral past the Earth without striking the planet. However, most particles trapped in resonances are released from these resonances due to close encounter with the Earth. Thus, the ring may act as a funnel through which asteroidal particles are deposited in the Earth's atmosphere. This could have implications for the efficiency of the transport of carbonaceous material from the asteroid belt to the Earth and for the origin of life on the planet. Author

N95-19182*# State Univ. of New York, Plattsburgh, NY. Dept. of Physics.
COLLECTION REQUIREMENTS FOR TRACE-ELEMENT ANALYSES OF EXTRATERRESTRIAL SAMPLES Abstract Only
George J. Flynn and S. R. Sutton (Chicago Univ., Chicago, IL.) *In* Lunar and Planetary Inst., Workshop on Particle Capture, Recovery and Velocity/Trajectory Measurement Technologies 1994 p 36-37 (For primary document see N95-19172 05-90)
Avail: CASI HC A01/MF A02

Trace-element abundances have proven important in understanding the evolution of and interrelationships between different meteorites. Preliminary investigations of the trace-element contents of interplanetary dust particles indicate that trace-element abundances will prove equally important in distinguishing between micrometeorites of different types, comparing the interplanetary dust to the meteorites, and assessing the degree of thermal alteration experienced either on the parent body or during the collection process. Sample collection, delivery, and curation must be accomplished in a manner to avoid contamination with even trace amounts of the elements to be analyzed. The present SXRF sensitivity for micrometeorite analysis is of order 1 femtogram, but anticipated improvements in sensitivity will require sample contamination substantially below this level. Sample collection and handling equipment should be constructed from materials selected for ultrahigh purity, and serious consideration should be given in selecting the particular set of elements from which the collection apparatus is composed so as not to compromise useful information. Author

N95-19183*# Tokyo Univ., Sagamihara (Japan). Inst. of Space and Astronautical Science.
LABORATORY SIMULATION OF INTACT CAPTURE OF COMETARY AND ASTEROIDAL DUST PARTICLES IN ISAS Abstract Only **c14**
A. Fujiwara, A. Nakamura, and T. Kadono *In* Lunar and Planetary Inst., Workshop on Particle Capture, Recovery and Velocity/Trajectory Measurement Technologies 1994 p 38-39 (For primary document see N95-19172 05-90)
Avail: CASI HC A01/MF A02

In order to develop a collector for intact capturing of cometary dust particles in the SOCCER mission and regolith dust particles released from asteroid surfaces by the impact of projectiles launched from a flying-by spacecraft, various kinds of materials as the collector candidates have been exposed to hypervelocity projectiles in our laboratory. Data based on the penetration characteristics of various materials (penetration depth, hole profile, effectiveness for intact capturing) are greatly increased. The materials tested for these simulation experiments include various kinds of low-density media and multisheet stacks; these are foamed plastics (polystyrene 0.01 g/cc), silica aerogels (0.04 g/cc), air (0.001 g/cc), liquid, and multisheet stack consisting of thin Al sheets (thickness 0.002 to 0.1 mm) or polyethylene sheets. Projectiles used are spheres or cylinders of nylon, polycarbonate, basalt, copper, iron, and volatile organics (e.g.,paradichlorobenzene) of size ranging from 30 micrometers to 1 cm launched by a two-stage light gas gun and a rail gun in ISAS at velocity up to about 7 km/s. Some results obtained by using nylon projectiles of velocity less than about 5 km/s are presented; the penetration depth vs. bulk density of the collector material for several kinds of materials and the velocity at which the projectiles begin to fragment vs. material density for foamed polystyrene. Author

N95-19184*# Perkin-Elmer Corp., Pomona, CA. Applied Science Operation.
TECHNIQUES FOR IN SITU COLLECTION AND MEASUREMENT OF VOLATILES RELEASED DURING HYPERVELOCITY IMPACT Abstract Only **c14**
R. A. Heppner, William Niu, and Carl R. Maag (Science Applications International Corp., Glendora, CA.) *In* Lunar and Planetary Inst., Workshop on Particle Capture, Recovery and Velocity/Trajectory Measurement

Technologies 1994 p 39-42 (For primary document see N95-19172 05-90)
Avail: CASI HC A01/MF A02

The capability of the gas capture cell to collect particles and semivolatile species which were released during impact is examined. The proposed Comet Coma Sample Return (CCSR) payload contains a variety of instrumentation for characterizing and collecting cometary dust. In this suite of instruments the Gas Capture Cell (GCC) is unique in that it not only collects the vaporization products resulting from the dust particle impacts, but also provides chemical characterization information prior to return of the dust particles for analysis on Earth. The GCC provides near real-time characterization of the volatile species, such as low- and medium-molecular-weight organic compounds that evolve from dust particles on impact with metal targets. Instrument sensitivity is sufficient for analyzing the volatile impact products resulting from single, individual dust particles. This capability will enable characterization of near-pristine dust particles, including the CHON particles, to be performed at a level not previously possible. Its design concept, operation and performance are detailed.

Author

N95-19185*# National Aeronautics and Space Administration. Lyndon B. Johnson Space Center, Houston, TX.

PENETRATION EXPERIMENTS IN ALUMINUM AND TEFLON TARGETS OF WIDELY VARIABLE THICKNESS Abstract Only **c39**

F. Hoerz, Mark J. Cintala, R. P. Bernhard (Lockheed Engineering and Sciences Co., Houston, TX.), and T. H. See (Lockheed Engineering and Sciences Co., Houston, TX.) *In* Lunar and Planetary Inst., Workshop on Particle Capture, Recovery and Velocity/Trajectory Measurement Technologies 1994 p 42-48 (For primary document see N95-19172 05-90)
Avail: CASI HC A02/MF A02

The morphologies and detailed dimensions of hypervelocity craters and penetration holes on space-exposed surfaces faithfully reflect the initial impact conditions. However, current understanding of this postmortem evidence and its relation to such first-order parameters as impact velocity or projectile size and mass is incomplete. While considerable progress is being made in the numerical simulation of impact events, continued impact simulations in the laboratory are needed to obtain empirical constraints and insights. This contribution summarizes such experiments with Al and Teflon targets that were carried out in order to provide a better understanding of the crater and penetration holes reported from the Solar Maximum Mission (SMM) and the Long Duration Exposure Facility (LDEF) satellites. A 5-mm light gas gun was used to fire spherical soda-lime glass projectiles from 50 to 3175 microns in diameter (D(sub P)), at a nominal 6 km/s, into Al (1100 series; annealed) and Teflon (Teflon(sup TFE)) targets. Targets ranged in thickness (T) from infinite halfspace targets (T approx. equals cm) to ultrathin foils (T approx. equals micron), yielding up to 3 degrees of magnitude variation in absolute and relative (D(sub P)/T) target thickness. This experimental matrix simulates the wide range in D(sub P)/T experienced by a space-exposed membrane of constant T that is being impacted by projectiles of widely varying sizes.

Author

N95-19186*# National Aeronautics and Space Administration. Lyndon B. Johnson Space Center, Houston, TX.

SOME CONSIDERATIONS ON VELOCITY VECTOR ACCURACY IN DUST TRAJECTORY ANALYSIS Abstract Only

A. A. Jackson (Lockheed Engineering and Sciences Co., Houston, TX.) and Herbert A. Zook *In* Lunar and Planetary Inst., Workshop on Particle Capture, Recovery and Velocity/Trajectory Measurement Technologies 1994 p 48-54 (For primary document see N95-19172 05-90)
Avail: CASI HC A02/MF A02

The relative contributions of comets and asteroids to the reservoir of dust in the interplanetary medium is not known. There are direct observations of dust released from comets and there is evidence to associate the IRAS dust bands with possible collisions of asteroids in the main belt. A means towards sorting out the parent sources has been proposed in the establishment of a dust collector in orbit about the Earth. The purpose of such a facility would be to collect not only cosmic dust particles intact but also the state vectors, as they arrive at the detector, the idea being that one may combine analytical laboratory analysis of the physics and chemistry of the captured particles with orbital data in order to help distinguish between bodies and identify parent bodies. The theoretical study of dust particle orbits in the solar system takes on greatly more importance if we use collected trajectory data. The orbital motion of dust when radiation and forces alone are acting is well understood. When gravitational forces due to the planets are included, the motion can become quite complex. In order to characterize the orbits of particles as they crossed the Earth's orbits, a study of the long-time dust orbital evolution was undertaken. We have considered various parameters associated with these dust orbits to see if one may in a general way discriminate between particles evolved from comets and asteroids. We proceed in this study as we have done previously. That is, we considered the dust particles as ideal black bodies, of density 1 gm/cc, spherical, with radii 10-100 microns. Particles of this size are affected by radiation forces, photon pressure, and Poynting-Robertson drag. Account was also taken of solar wind drag, which amounts to about 30 percent of the Poynting-Robertson drag negligible. The gravitational forces due to the planets are included, unlike in our previous study; the planetary orbits are those of true n-body interaction so that the possibility of secular resonance is included. Our method was to calculate explicitly by a numerical procedure the orbits of dust particles after they left their parent bodies. The motion is determined numerically with the implicit Runge-Kutta integrator using Gauss-Radau spacings.

Author

N95-19187*# Florida Univ., Gainesville, FL.

VELOCITY DISTRIBUTION OF EARTH-CROSSING ASTEROID GRAINS Abstract Only

Jer-Chyi Liou and Stanley F. Dermott *In* Lunar and Planetary Inst., Workshop on Particle Capture, Recovery and Velocity/Trajectory Measurement Technologies 1994 p 54-56 (For primary document see N95-19172 05-90)
Avail: CASI HC A01/MF A02

We have systematically studied the evolution of 4- and 9-micrometer-diameter dust particles from three prominent asteroid families, Eos, Koronis, and Themis, until they reach the Earth. We have found that they are quite distinguishable in their (I cos omega, I sin omega) phase space. The different distributions in the inclination space have several important observational consequences, which can be used to identify the origins of these dust particles. We convert the orbital elements of these Earth-crossing dust grains to distinguish them by using any one single velocity component. We conclude that in order to identify the origins of the Earth-crossing dust grains we need all three velocity components to get their orbital elements and find their positions in the inclination space.

Author

N95-19188*# Science Applications International Corp., Glendora, CA.

THE INTACT CAPTURE OF HYPERVELOCITY DUST PARTICLES USING UNDERDENSE FOAMS Abstract Only

Carl R. Maag, J. Borg (Centre National de la Recherche Scientifique, Orsay, France.), William G. Tanner (Baylor Univ., Waco, TX.), T. J. Stevenson (Mare Crisium, Tetsworth,, England.), and J.-P. Bibring (Mare Crisium, Tetsworth,, England.) *In* Lunar and Planetary Inst., Workshop on Particle Capture, Recovery and Velocity/Trajectory Measurement Technologies 1994 p 56-61 (For primary document see N95-19172 05-90)
Avail: CASI HC A02/MF A02

The impact of a hypervelocity projectile (greater than 3 km/s) is a process that subjects both the impactor and the impacted material to a large transient pressure distribution. The resultant stresses cause a large degree of fragmentation, melting, vaporization, and ionization (for normal densities). The pressure regime magnitude, however, is directly related to the density relationship between the projectile and target materials. As a consequence, a high-density impactor on a low-density target will experience the lowest level of damage. Historically, there have been three different approaches toward achieving the lowest possible target density. The first employs a projectile impinging on a foil or film of moderate density, but whose thickness is much less than the particle diameter. This results in the particle experiencing a pressure transient with both a short duration and a greatly reduced destructive effect. A succession of these films, spaced to allow nondestructive energy dissipation between impacts, will reduce the impactor's kinetic energy without allowing its internal energy to rise to the point where destruction of the projectile mass will occur. An added advantage to this method is that it yields the possibility of regions within the captured particle where a minimum of thermal modification has taken place. Polymer foams have been employed as the primary method

of capturing particles with minimum degradation. The manufacture of extremely low bulk density materials is usually achieved by the introduction of voids into the material base. It must be noted, however, that a foam structure only has a true bulk density of the mixture at sizes much larger than the cell size, since for impact processes this is of paramount importance. The scale at which the bulk density must still be close to that of the mixture is approximately equal to the impactor. When this density criterion is met, shock pressures during impact are minimized, which in turn maximizes the probability of survival for the impacting particle. The primary objectives of the experiment are to (1) Examine the morphology of primary and secondary hypervelocity impact craters. Primary attention will be paid to craters caused by ejecta during hypervelocity impacts of different substrates. (2) Determine the size distribution of ejecta by means of witness plates and collect fragments of ejecta from craters by means of momentum-sensitive micropore foam. (3) Assess the directionality of the flux by means of penetration-hole alignment of thin films placed above the cells. (4) Capture intact the particles that perforated the thin film and entered the cell. Capture media consisted of both previously flight-tested micropore foams and aerogel. The foams had different latent heats of fusion and, accordingly, will capture particles over a range of momenta. Aerogel was incorporated into the cells to determine the minimum diameter than can be captured intact. Author

N95-19189*# Search for Extraterrestrial Intelligence Inst., Mountain View, CA.

SPICE: AN INNOVATIVE, FLEXIBLE INSTRUMENT CONCEPT Abstract Only **c19**

Kenji Nishioka, D. P. Cauffman (Lockheed Missiles and Space Co., Palo Alto, CA.), B. Jurcevich (Lockheed Missiles and Space Co., Palo Alto, CA.), David J. Mendez (Lockheed Missiles and Space Co., Palo Alto, CA.), and James T. Ryder (Lockheed Missiles and Space Co., Palo Alto, CA.) *In* Lunar and Planetary Inst., Workshop on Particle Capture, Recovery and Velocity/Trajectory Measurement Technologies 1994 p 61-64 (For primary document see N95-19172 05-90)

Avail: CASI HC A01/MF A02

Studies and plans for orbital capture of cosmic dust and interplanetary dust particles (IDP's) looked very bright with the advent of space station Freedom (SSF) and formal selection of Cosmic Dust Collection Facility (CDCF) as an attached payload in 1990. Unfortunately it has been downhill since its selection, culminating in CDCF being dropped as attached payload in the SSF redesign process this year. This action was without any input from the science or cosmic dust communities. The Exobiology Intact Capture Experiment (Exo-ICE) as an experiment on CDCF was also lost. Without CDCF, no facility-class instrument for cosmic dust studies is available or planned. When CDCF (and Exo-ICE) was selected as a SSF attached payload, an exercise called the small particle intact capture experiment (SPICE) was started for Exo-ICE to develop an understanding and early testing of the necessary expertise and technology for intact capture of cosmic dust and IDP's. This SPICE activity looks to fly small, meter square or less, collection area experiments on early orbital platforms of opportunity such as EURECA, MIR, WESTAR, and others, including the shuttle. The SPICE activity has focused on developing techniques and instrument concepts to capture particles intact and without inadvertent contamination. It began with a survey and screening of available capture media concepts and then focused on the development of a capture medium that can meet these requirements. Evaluation and development of the chosen capture medium, aerogel (a silicon oxide gel), has so far lived up to the expectations of meeting the requirements and is highlighted in a companion paper at this workshop. Others such as McDonnell's Timeband Capture Cell Experiment (TICCE) on EuReCa and Tsuo's GAS-CAN lid experiments on STS 47 and 57 have flown aerogel, but without addressing the contamination issue/requirement, especially regarding organics. Horz, Zolenskym and others have studied and have also been advocates for its development. The SPICE instrument's experiment design builds on the knowledge gained from these efforts to meet the intact capture, noncontamination requirements. An overview of a possible SPICE experimental instrument concept using the MIR space station as a host platform for cosmic dust collection is provided in this paper. The SPICE concept is nonplatform-specified and can fly on any platform that provides a mode for experiment recovery. Author

N95-19190*# Peterson (Robert B.), Houston, TX.

CHARGE COLLECTION DURING HYPERVELOCITY PENETRATIONS OF THIN FOILS Abstract Only **c35**

Robert B. Peterson *In* Lunar and Planetary Inst., Workshop on Particle Capture, Recovery and Velocity/Trajectory Measurement Technologies 1994 p 64-76 (For primary document see N95-19172 05-90)

Avail: CASI HC A03/MF A02

The following represents trajectory sensor development work for the space-station-based Cosmic Dust Collection Facility (CDCF). This facility-class payload was to expose some 7 sq m of NASA-provided general-user instruments in addition to three instruments provided by formally selected principal investigators. The preferred trajectory sensor for this general-user instrument envisioned the detection of impact-triggered plasma for both velocity measurement and location instruments. Space station developments in late 1992/early 1993 lead to cancellation of this potential flight project, for both technical and fiscal reasons. This precipitated termination of all plasma detection work at JSC on behalf of CDCF's general-user instrument. The following comprises three informal reports that summarize the CDCF efforts regarding plasma sensing for trajectory determinations. The reports were initially written for internal CDCF use and were not widely distributed. Because no formal publications are envisioned at present, the three reports are included in full in this document. They not only demonstrate that substantial progress was accomplished in the development of plasma trajectory sensors during 1990-1992, but the results are hopefully of interest and use to others who may continue these developments. The chronological sequence of these three reports is reversed, with the first containing the latest information. Author

N95-19191*# Tokyo Univ., Sagamihara (Japan). Inst. of Space and Aeronautical Science.

SCIENTIFIC OBJECTIVES OF THE PRIMITIVE BODY SAMPLE RETURN MISSIONS: AN APPROACH FROM THE LIGHT-INDUCED EFFECT ON WATER VAPOR Abstract Only **c12**

Mikio Shimizu *In* Lunar and Planetary Inst., Workshop on Particle Capture, Recovery and Velocity/Trajectory Measurement Technologies 1994 p 76-77 (For primary document see N95-19172 05-90)

Avail: CASI HC A01/MF A02

Water is undoubtedly one of the most crucial components of the solar nebula for determining planetary composition: planets were formed from the accretion of the dust particles in the nebula, and the redox state of Fe in the particles can be determined by the reaction of Fe with water vapor diffused into the interior of the particle in the early stage of solar system formation. It has been discussed from various observations that the cores of Mercury, Venus, and the Earth might be metallic Fe, although the core of the Earth may be somewhat oxidized by the high pressure and temperature reaction of liquid Fe with perovskite at the boundary of the mantle and the core, whereas the core of Mars may be highly oxidized, as suggested by its low density. Isotopic anomalies of various elements have frequently been observed in the solar system (in planetary atmospheres and in meteorites) and some of them can be attributed to the injection of exotic particles formed in other stars into the solar nebula. Hydrogen and D anomalies in planetary atmospheres were frequently believed to correlate with the differential escape of H and D from the exospheres of Venus and Mars, although no one knows the primordial D/H ratios before thermal escape. This paper explains the decrease of the observed D/H ratios with distance from the sun by considering the light-induced drift effect to displace H2(16)O alone to the outside in the solar nebula. Author

N95-19192*# Washington Univ., Saint Louis, MO. Center for the Space Sciences.

PENETRATION OF MULTIPLE THIN FILMS IN MICROMETEORITE CAPTURE CELLS Abstract Only **c35**

Charles G. Simon *In* Lunar and Planetary Inst., Workshop on Particle Capture, Recovery and Velocity/Trajectory Measurement Technologies 1994 p 77-79 (For primary document see N95-19172 05-90)

(Grant NAGw-1603)

Avail: CASI HC A01/MF A02

As part of a continuing effort to develop cosmic dust detectors/collectors for use in space, we performed a series of hypervelocity impact experiments on combined sensor/capture-cell assemblies using 10-200-micron-diameter glass projectiles and olivine crystals at velocities of 0.9-14.4 km/s. The design objective of the space-flight instrument is to measure the trajectories

of individual particles with sufficient accuracy to permit identification of their parent bodies and to capture enough impactor material to allow chemical and isotopic analyses of samples returned to Earth. Three different multiple-film small-particle capture cell designs (0.1-100-micron-thick Al foils with approx. 10, 100, and 1800 micron spacing) were evaluated for their ability to capture impactor fragments and residue. Their performances were compared to two other types of capture cells, foil covered Ge crystals, and 0.50 and 0.120 g/cu cm aerogels. All capture cells were tested behind multifilm (1.4-6.0-micron-thick) polyvinylidene fluoride (PVDF) velocity/trajectory sensor devices. Several tests were also done without the PVDF sensors for comparison. The results of this study were reported by Simon in a comprehensive report in which the morphology of impacts and impactor residues in various types of capture cells after passage through two PVDF sensor films is discussed. Impactor fragments in selected capture cells from impacts at velocities up to 6.4 km/s were identified using scanning electron microscopy with energy dispersive spectroscopy (SEM/EDS). Author

N95-19193*# Baylor Univ., Waco, TX. Space Science Lab.

ASSESSMENT OF VELOCITY/TRAJECTORY MEASUREMENT TECHNOLOGIES DURING A PARTICLE CAPTURE EVENT Abstract Only **c35**

William G. Tanner, Carl R. Maag (Science Applications International Corp., Glendora, CA.), W. M. Alexander, and Stepheni Stephenson *In* Lunar and Planetary Inst., Workshop on Particle Capture, Recovery and Velocity/Trajectory Measurement Technologies 1994 p 79-83 (For primary document see N95-19172 05-90)

Avail: CASI HC A01/MF A02

Since the early 1960s, the means to measure the time of flight (TOF) of dust grain within a mechanical detection array has existed, first in the laboratory and then in space experiments. Laboratory hypervelocity dust particle accelerators have used electrostatic detection of charge on accelerated particles for TOF and particle mass detections. These laboratory studies have led to the development of ultra-thin-film sensors that have been used for TOF measurements in dust particle space experiments. The prototypes for such devices were ultra-thin-film capacitors that were used in the OGO series of satellites. The main goal of the experimental work to be described is the development of the capability to determine the velocity vector or trajectory of a dust grain traversing an integrated dust detection array. The results of these studies have shown that the capability of detecting the charge liberated by hypervelocity dust grains with diameters in the micrometer range can be detected. Based on these results, detection systems have been designed to provide a precise analysis of the physical and dynamic properties of micrometer and submicrometer dust grains, namely the design verification unit (DVU). Through unique combinations of in situ detection systems, direct measurements of particle surface charge, velocity, momentum, kinetic energy, and trajectory have been achieved. From these measurements, the remaining physical parameters of mass, size, and density can be determined. Author

N95-19194*# Jet Propulsion Lab., California Inst. of Tech., Pasadena, CA.

NONDESTRUCTIVE TIME-OF-CAPTURE, LOCATION AND VELOCITY SENSING IN INTACT CAPTURE Abstract Only **c35**

Peter Tsou *In* Lunar and Planetary Inst., Workshop on Particle Capture, Recovery and Velocity/Trajectory Measurement Technologies 1994 p 84-85 (For primary document see N95-19172 05-90)

Avail: CASI HC A01/MF A02

Velocity sensing of hypervelocity particles was a significant field of interest from the 1960s to 1970s. Generically, velocity sensing has been approached by either of two methods: first, detecting direct plasma or light emissions onto a solid surface, or second, performing time-of-flight by film penetration, or by detecting charged particles passing a static electric field. Impact plasma techniques required the destruction of the particles. Multiple-film penetrations were also destructive, especially for small particles. There is a need for an integrated, reliable, and simple location and velocity sensor compatible to our intact capture underdense medium without contributing additional damage to the captured particle. Since cometary dust, like cosmic dust, is essentially randomly distributed, knowing the time of the dust capture and the location of the capture on the collector permits the identification of the specific dust particle captured. Velocity information helps to determine the trajectory of the dust particle. Our discovery of a very suitable acoustic sensor and fruitful experimental results have led to the realization of a flight velocity sensor with intact capture underdense media. Author

N95-19195*# Jet Propulsion Lab., California Inst. of Tech., Pasadena, CA.

THE PHYSICS OF INTACT CAPTURE Abstract Only **c70**

Peter Tsou, D. J. Griffiths (Oregon State Univ., Corvallis, OR.), and A. L. Albee (California Inst. of Tech., Pasadena, CA.) *In* Lunar and Planetary Inst., Workshop on Particle Capture, Recovery and Velocity/Trajectory Measurement Technologies 1994 p 85-88 (For primary document see N95-19172 05-90)

Avail: CASI HC A01/MF A02

The ability to capture projectiles intact at hypervelocities in underdense media open a new area of study in physics. Underdense material behaves markedly different than solid, liquid, or gas upon hypervelocity impact. This new phenomenon enables applications in science that would either not be possible or would be very costly by other means. This phenomenon has been fully demonstrated in the laboratory and validated in space. Even more interesting is the fact that this hypervelocity intact capture was accomplished passively. A better understanding of the physics of intact capture will lead to improvements in intact capture. A collection of physical observations of this phenomenon is presented here. Author

N95-19196*# Chicago Univ., Chicago, IL. Lab. for Astrophysics and Space Research.

PVDF FLUX/MASS/VELOCITY/TRAJECTORY SYSTEMS AND THEIR APPLICATIONS IN SPACE Abstract Only **c19**

Anthony J. Tuzzolino *In* Lunar and Planetary Inst., Workshop on Particle Capture, Recovery and Velocity/Trajectory Measurement Technologies 1994 p 89-94 (For primary document see N95-19172 05-90)

(Contracts NAGw-3078; JPL-959531; N00014-91-J-1716)

Avail: CASI HC A02/MF A02

The current status of the University of Chicago Polyvinylidene Fluoride (PVDF) flux/mass/velocity/trajectory instrumentation is summarized. The particle response and thermal stability characteristics of pure PVDF and PVDF copolymer sensors are described, as well as the characteristics of specially constructed two-dimensional position-sensing PVDF sensors. The performance of high-flux systems and of velocity/trajectory systems using these sensors is discussed, and the objectives and designs of a PVDF velocity/trajectory dust instrument for launch on the Advanced Research and Global Observation Satellite (ARGOS) in 1995 and of a high-flux dust instrument for launch on the Cassini spacecraft to Saturn in 1997 are summarized. Author

N95-19197*# National Aeronautics and Space Administration. Lyndon B. Johnson Space Center, Houston, TX.

THE USE OF SILICA AEROGEL TO COLLECT INTERPLANETARY DUST IN SPACE Abstract Only **c27**

Michael E. Zolensky, Ruth A. Barrett (Lockheed Engineering and Sciences Co., Houston, TX.), and F. Hoerz *In* Lunar and Planetary Inst., Workshop on Particle Capture, Recovery and Velocity/Trajectory Measurement Technologies 1994 p 94-98 (For primary document see N95-19172 05-90)

Avail: CASI HC A01/MF A02

We report on impact experiments to evaluate the suitability of silica aerogel as a capture medium for interplanetary dust particles in space. The structure of silica aerogel is such that even micrometer-sized hypervelocity particles may sense it as a target of very low density; consequently shock stresses and temperatures due to impact should be minimized. We performed impact experiments in a light gas gun that employed projectiles manufactured from forsterite, pyrrhotite, and calcite. From these experiments we have developed techniques that will permit the successful extrication of interplanetary dust particles from aerogel. We note a rough correlation between increasing particle penetration lengths and decreasing aerogel density, and there is a poor correlation of track lengths with impact velocity at laboratory-attainable velocities of 5-7 km/s. We conclude that aerogel track length should not be used even as (crude) velocity indicators. Transmission electron microscope studies show the re covered particulate residues are encased in melted silica aerogel, which possibly protects the residue from some impact damage. Individual minerals within interplanetary dust are expected to exhibit differential survival, and

may be vaporized, melted, dehydrated, or structurally reordered. However, some mineral grains should successfully be captured in an unmelted state at encounter velocities less than 8 km/s. Author

N95-19249# Lawrence Livermore National Lab., Livermore, CA.
NEW ASTROPHYSICAL OPACITIES AND THEIR EFFECTS ON STELLAR MODELS
F. J. Rogers and C. A. Iglesias 17 Jun. 1994 13 p Presented at the Oji International Seminar, Tomakomai, Japan, 27 Jun. - 1 Jul. 1994
(Contract W-7405-eng-48)
(DE94-016445; UCRL-JC-117695; CONF-9406235-1) Avail: CASI HC A03/MF A01

Recent advances in astrophysical opacity calculations are discussed. A description and comparison of results from two new independent efforts is given. The large increases in the calculated opacity in the few hundred-thousand degree range have led to improved agreement with a wide range of observations. Some directions for future work are suggested. DOE

N95-19289*# Lunar and Planetary Inst., Houston, TX.
PAPERS PRESENTED TO THE CONFERENCE ON CHONDRULES AND THE PROTOPLANETARY DISK Abstracts Only
1994 58 p Conference held in Albuquerque, NM, 13-15 Oct. 1994
(Contract NASw-4574)
(NASA-CR-197121; NAS 1.26:197121; LPI-Contrib-844) Avail: CASI HC A04/MF A01

The following topics are covered in the presented papers: (1) producing chondrules; (2) carbons, CAI's, and chondrules; (3) large scale processes in the solar nebula; (4) chondrule-matrix relationships in chondritic meteorites; (5) overview of nebula models; (6) constraints placed on the nature of chondrule precursors; (7) turbulent diffusion and concentration of chondrules in the protoplanetary nebula; (8) heating and cooling in the solar nebula; (9) crystallization trends of precursor pyroxene in ordinary chondrites; (10) precipitation induced vertical lightning in the protoplanetary nebula; (11) the role of chondrules in nebular fractionations of volatiles and other elements; (12) astronomical observations of phenomena in disks; (13) experimental constraints on models for origins of chondrules, and various other topics. For individual titles, see N95-19290 through N95-19339.

N95-19290*# Washington Univ., Saint Louis, MO. Center for Space Studies.
PRODUCING CHONDRULES BY RECYCLING AND VOLATILE LOSS Abstract Only
C. M. O. Alexander *In* Lunar and Planetary Inst., Papers Presented to the Conference on Chondrules and the Protoplanetary Disk 1994 p 1 Prepared in cooperation with Carnegie Institution of Washington, Washington, DC (For primary document see N95-19289 05-90)
Avail: CASI HC A01/MF A01

Interelement correlations observed in bulk chondrule INAA data, particularly between the refractory lithophiles, have led to the now generally accepted conclusion that the chondrule precursors were nebular condensates. However, it has been recently suggested that random sampling of fragments from a previous generation of chondrules could reproduce much of the observed range of bulk chondrule composition. Derived from text

N95-19291*# Open Univ., Milton Keynes (England). Dept. of Earth Sciences.
CARBON, CAIs AND CHONDRULES Abstract Only
R. D. Ash and S. S. Russell *In* Lunar and Planetary Inst., Papers Presented to the Conference on Chondrules and the Protoplanetary Disk 1994 p 2 (For primary document see N95-19289 05-90)
Avail: CASI HC A01/MF A01

It has been shown that C is present in CAI's and chondrules. It can be distinguished from matrix C both by its thermal stability and isotopic composition, which implies that it was not introduced after parent body accretion. It is concluded that C must have been present in the chondrule and CAI precursor material. Therefore any models of chondrule and CAI formation and inferences drawn about solar system conditions during these events must take into account the consequences of the presence of C on inclusion chemistry, mineralogy, and oxidation state. Derived from text

N95-19292*# Carnegie Institution of Washington, Washington, DC. Dept. of Terrestrial Magnetism.
LARGE-SCALE PROCESSES IN THE SOLAR NEBULA Abstract Only
c92
A. P. Boss *In* Lunar and Planetary Inst., Papers Presented to the Conference on Chondrules and the Protoplanetary Disk 1994 p 2-3 (For primary document see N95-19289 05-90)
Avail: CASI HC A01/MF A01

Theoretical models of the structure of a minimum mass solar nebula should be able to provide the physical context to help evaluate the efficacy of any mechanism proposed for the formation of chondrules or Ca, Al-rich inclusions (CAI's). These models generally attempt to use the equations of radiative hydrodynamics to calculate the large-scale structure of the solar nebula throughout the planet-forming region. In addition, it has been suggested that chondrules and CAI's (=Ch&CAI's) may have been formed as a direct result of large-scale nebula processing such as passage of material through high-temperature regions associated with the global structure of the nebula. In this report we assess the status of global models of solar nebula structure and of various related mechanisms that have been suggested for Ch and CAI formation. Derived from text

N95-19293*# New Mexico Univ., Albuquerque, NM. Inst. of Meteoritics.
CHONDRULE-MATRIX RELATIONSHIPS IN CHONDRITIC METEORITES Abstract Only
A. J. Brearley *In* Lunar and Planetary Inst., Papers Presented to the Conference on Chondrules and the Protoplanetary Disk 1994 p 3-4 (For primary document see N95-19289 05-90)
Avail: CASI HC A01/MF A01

The relationship between chondrules and matrix (fine grained material with a grain size less than 5 micrometers) in chondritic meteorites has been the subject of considerable controversy and no consensus currently exists. The coexistence of these two components in meteorites with bulk compositions that deviate only slightly from CI abundances suggests that cosmochemically their origins are closely linked. Any consideration of the relationship between chondrules and matrix hinges to a large degree on the origin of matrix. The entire spectrum of models exists from matrix as a nebular product to derivation entirely from chondrules. Early models of solar nebular evolution viewed chondrites as a two-component mixture of high- and low-temperature condensates. However, this model has been challenged by the recognition that the nebula was probably not uniformly vaporized. Derived from text

N95-19294*# National Aeronautics and Space Administration. Ames Research Center, Moffett Field, CA.
OVERVIEW OF NEBULA MODELS: POTENTIAL CHONDRULE-FORMING ENVIRONMENTS Abstract Only
P. Cassen *In* Lunar and Planetary Inst., Papers Presented to the Conference on Chondrules and the Protoplanetary Disk 1994 p 4-5 (For primary document see N95-19289 05-90)
Avail: CASI HC A01/MF A01

Observations of T Tauri stars and their circumstellar disks, combined with broadly applied theoretical principles, permit the construction of solar nebular models that are potentially useful for the interpretation of meteoritic data. Quantitative comparisons of model results with meteoritic and planetary data is used to test several propositions regarding the bulk properties of chondrites and chondrule precursor material. Derived from text

N95-19295*# Rutgers Univ., New Brunswick, NJ. Dept. of Geological Sciences.
CONSTRAINTS PLACED ON THE NATURE OF CHONDRULE PRECURSORS Abstract Only
H. C. Connolly, Jr. and R. H. Hewins *In* Lunar and Planetary Inst., Papers Presented to the Conference on Chondrules and the Protoplanetary Disk 1994 p 5-6 (For primary document see N95-19289 05-90)
Avail: CASI HC A01/MF A01

The melting conditions and cooling rates experienced by chondrules have been experimentally investigated and reviewed. A discussion of experiments that have studied the nature of chondrule precursors and what constraints these experiments have placed on chondrule precursors is presented. Topics discussed include the following: (1) physical characteristics of starting compositions; (2) chemical characteristics of

starting compositions; and (3) constraints on chondrule precursors.
Derived from text

N95-19296*# National Aeronautics and Space Administration. Ames Research Center, Moffett Field, CA.
TURBULENT DIFFUSION AND CONCENTRATION OF CHONDRULES IN THE PROTOPLANETARY NEBULA Abstract Only
J. N. Cuzzi, A. R. Dobrovolskis (California Univ., Santa Cruz, CA.), and R. C. Hogan (Synernet Corp., Fremont, CA.) *In* Lunar and Planetary Inst., Papers Presented to the Conference on Chondrules and the Protoplanetary Disk 1994 p 6-7 (For primary document see N95-19289 05-90)
Avail: CASI HC A01/MF A01

Turbulence is known to possess structure on many scales. The largest or integral scale L is usually taken to be the largest dimension of the system. Two different turbulent regimes are likely to be of importance. Early stage convective turbulence in a hot nebula probably extends over the entire nebula scale height, and probably has typical eddy frequency comparable to the orbit frequency. At a later stage, midplane shear layer turbulence can be driven by the presence of a differently rotating, densely settled particle layer, with different length and timescales.
Derived from text

N95-19297*# Chicago Univ., Chicago, IL. Inst. for Nuclear Studies.
HEATING AND COOLING IN THE SOLAR NEBULA: CONSTRAINTS FROM REFRACTORY INCLUSIONS Abstract Only **c92**
A. M. Davis and G. J. MacPherson (National Museum of Natural History, Washington, DC.) *In* Lunar and Planetary Inst., Papers Presented to the Conference on Chondrules and the Protoplanetary Disk 1994 p 7-8 (For primary document see N95-19289 05-90)
Avail: CASI HC A01/MF A01

The following topics are discussed: (1) CAI classification; (2) maximum temperatures; (3) cooling rates; and (4) transient heating events.
Derived from text

N95-19298*# Kyoto Univ., Sakyoku (Japan). Dept. of Geology and Mineralogy.
CRYSTALLIZATION TRENDS OF PRECURSOR PYROXENE IN ORDINARY CHONDRITES: IMPLICATIONS FOR IGNEOUS ORIGIN OF PRECURSOR Abstract Only
T. Fujita and M. Kitamura *In* Lunar and Planetary Inst., Papers Presented to the Conference on Chondrules and the Protoplanetary Disk 1994 p 8-9 (For primary document see N95-19289 05-90)
Avail: CASI HC A01/MF A01

Various observations suggest that the precursor of the fine fragments and the relict pyroxene was formed by an igneous process in a grandparent body of the chondrite. Furthermore, the fact that the precursors appear as fragments in the matrix as well as relicts in the chondrule suggests a shock origin for the chondrite by collision of two or more bodies, which had already to some extent undergone igneous differentiation.
Derived from text

N95-19299*# Arizona Univ., Tucson, AZ.
ON THE POSSIBILITY OF PRECIPITATION-INDUCED VERTICAL LIGHTNING IN THE PROTOPLANETARY NEBULA Abstract Only
S. G. Gibbard and E. H. Levy *In* Lunar and Planetary Inst., Papers Presented to the Conference on Chondrules and the Protoplanetary Disk 1994 p 9-10 (For primary document see N95-19289 05-90)
Avail: CASI HC A01/MF A01

Many primitive meteorites contain high concentrations of chondrules - millimeter-sized beads of glassy silicate - in a matrix of essentially unprocessed material. These chondrules were apparently melted by some transient high-energy event, then cooled rapidly on timescales of minutes to hours. Among the phenomena that have been suggested as driving mechanisms for the heating event are: (1) high-velocity impacts; (2) magnetic flares; (3) aerodynamic drag heating; and (4) lightning. Although nebular lightning has been made of the efficiency of such lightning in melting chondrule precursors, a quantitative treatment of processes that might produce nebular lightning has not been attempted. We have developed a one-dimensional nebular lightning model that utilizes a spectrum of particle sizes. This model has also been applied to the Earth as a test of its predictive ability. Particles grow to an initial size distribution, then undergo elastic charge-separating collisions. Charge separation is opposed by the mobile free charge in the nebula, which can either accumulate on and neutralize the charged ice particles or move to cancel the large scale electric field. Since the free charge density depends on the grain size distribution, it is determined self-consistently as the particle distribution changes.
Derived from text

N95-19300*# Geological Survey, Reston, VA.
THE ROLE OF CHONDRULES IN NEBULAR FRACTIONATIONS OF VOLATILES AND OTHER ELEMENTS Abstract Only
J. N. Grossman *In* Lunar and Planetary Inst., Papers Presented to the Conference on Chondrules and the Protoplanetary Disk 1994 p 10-11 (For primary document see N95-19289 05-90)
Avail: CASI HC A01/MF A01

For at least 30 years, cosmochemists have been grappling with the question of how and why groups of geochemically and volatility related elements became fractionated in the major chondrite groups. At least five relatively independent fractionations are known. Virtually everyone who has thought about these facts has been attempted to attribute at least some of the fractionations to the physical separation or mixing of the visible components. By far the most abundant of these components in meteorites is chondrules, and indeed chondrules have long been suspected of playing a direct role in fractionation of volatile elements. The question addressed here is whether chondrules formed before or after chemical components became separated is of fundamental importance to our understanding of the early solar system, as the answer constrains how, when, where, and from what chondrules formed, and tells us about how materials were processed in the nebula.
Derived from text

N95-19301*# Harvard-Smithsonian Center for Astrophysics, Cambridge, MA.
ASTRONOMICAL OBSERVATIONS OF PHENOMENA IN DISKS Abstract Only **c89**
L. Hartmann *In* Lunar and Planetary Inst., Papers Presented to the Conference on Chondrules and the Protoplanetary Disk 1994 p 11 (For primary document see N95-19289 05-90)
Avail: CASI HC A01/MF A01

Astronomical constraints on disks around young stellar objects are reviewed in this abstract. Since disks around the youngest stars cannot generally be resolved spatially, most results are based on analyses of the infrared and radio emission from circumstellar dust and gas. At least half of all young stars seem to have substantial circumstellar disks at an age of approximately 10(exp 6) yr. The young objects without disks tend to be binary stellar systems, though not exclusively, and some close binaries may have outer disks that are not tidally disrupted. Probably most, if not all, stars formed originally with circumstellar disks, but evolutionary timescales may differ dramatically. All the results, disk disappearance, disk mass around young stars, and long-wavelength dust opacities, are subject to the additional uncertainty of the effects of infalling dusty envelopes, which produce the disks in the first place.
Derived from text

N95-19302*# Rutgers Univ., Piscataway, NJ. Dept. of Geological Sciences.
EXPERIMENTAL CONSTRAINTS ON MODELS FOR ORIGINS OF CHONDRULES: PEAK TEMPERATURES Abstract Only
R. H. Hewins and H. C. Connolly, Jr. *In* Lunar and Planetary Inst., Papers Presented to the Conference on Chondrules and the Protoplanetary Disk 1994 p 11-12 (For primary document see N95-19289 05-90)
Avail: CASI HC A01/MF A01

Chondrule peak temperature constraints for mathematical models pertaining to chondrule origin are discussed in this article. The peak temperatures experienced by chondrules provide a parameter that may allow discrimination between alternative heating mechanisms. Successful mechanisms must provide just enough energy to reach such temperatures and not overshoot them. In principle, determination of peak temperatures from chondrule textures and experiments that duplicate them should be very easy. However, this approach is complicated by the fact that there are several different experimental paths that reproduce chondrule properties. The key texture depends not only on the peak temperature but also on the heating time and, in the case of totally molten droplets, on interactions with other particles. Addressed here are different types of peak temperature constraints; (1) near-liquidus melting; (2) flash melting; (3) dust seeding; (4)

volatile element constraints; and (5) barred olivine chondrules.
Derived from text

N95-19303*# Arizona Univ., Tucson, AZ. Lunar and Planetary Lab.
MODELS FOR MULTIPLE HEATING MECHANISMS Abstract Only
L. L. Hood and D. Kring *In* Lunar and Planetary Inst., Papers Presented to the Conference on Chondrules and the Protoplanetary Disk 1994 p 12-13 (For primary document see N95-19289 05-90)
Avail: CASI HC A01/MF A01

Current meteoritic and astrophysical evidence (especially FU Orionis events) suggests that large-scale gas-dynamics shocks penetrating to the nebular midplane represent a promising class of multiple heating mechanisms for the formation of chondrules. Initial numerical models have shown that shock heating of chondrule precursor grains in optically thick clouds of grains is especially efficient. Shocks generated by infalling molecular cloud clumps and shocks separating different mass elements in a time dependently and axially asymmetrically evolving disk are possibilities deserving further attention. Meteoritic constraints, astrophysical considerations and multiple heating mechanisms are addressed. Derived from text

N95-19304*# Colorado Univ., Boulder, CO. Lab. for Atmospheric and Space Physics.
CHONDRULE FORMATION IN LIGHTNING DISCHARGES Abstract Only
M. Horanyi *In* Lunar and Planetary Inst., Papers Presented to the Conference on Chondrules and the Protoplanetary Disk 1994 p 13-14 (For primary document see N95-19289 05-90)
Avail: CASI HC A01/MF A01

Chondrules represent a significant mass fraction of primitive meteorites. These millimeter-sized glassy droplets appear to be the products of intensive transient heating events. Their size distribution, chemical and mineral composition, texture, isotope composition suggest that chondrules were produced as a result of short-duration melting followed by rapid cooling of solid precursor particles. Gas-dynamics heating, magnetic reconnection, and electrostatic discharges are thought to be the leading candidates to explain chondrule formation. In this paper we summarize our recent theoretical progress on the effects of 'lightning' in the early solar system and also report on preliminary results from our laboratory experiments. Differential settling of various sized dust particles toward the midplane of the nebula is suspected to build large-scale charge separations that episodically relax via the electric breakdown of the nebular gas. The electrostatic discharge os analogous to lightning in the Earth's atmosphere. Derived from text

N95-19305*# California Inst. of Tech., Pasadena, CA. Div. of Geology and Planetary Science.
THE EARLY SUN AND THE FORMATION OF CHONDRULES Abstract Only
G. R. Huss *In* Lunar and Planetary Inst., Papers Presented to the Conference on Chondrules and the Protoplanetary Disk 1994 p 14-15 (For primary document see N95-19289 05-90)
(Grant NAGw-3040)
Avail: CASI HC A01/MF A01

The early Sun and its proposed role in chondrule formation is presented in this report. The early Sun is an energy source that potentially provides a mechanism for chondrule formation and an explanation for the systematics of chondrule populations. Earlier workers have shown that a T Tauri sun would not supply enough energy to melt dust at the radius of the asteroids. However, recent observations indicate that the T Tauri phase is actually the waning stage of pre-main sequence activity. Pre-main-sequence stars are surrounded by accretion disks and are powered by accretional energy. While still embedded in a molecular-cloud core, these stars often drive massive bipolar outflows of molecular gas that has been swept up and accelerated to tens of km s(exp -1) by a high-velocity stellar wind (hundreds of km s(exp -1)). Derived from text

N95-19306*# Museum of Natural History, London (England). Mineralogy Dept.
CHONDRULES AND THEIR ASSOCIATES IN ORDINARY CHONDRITES Abstract Only
R. Hutchison *In* Lunar and Planetary Inst., Papers Presented to the Conference on Chondrules and the Protoplanetary Disk 1994 p 15-16 (For primary document see N95-19289 05-90)
Avail: CASI HC A01/MF A01

A theory for the origin of the ordinary chondrites (OC's) must account for the origin(s) of their constituents. If the OC's accreted in a protoplanetary disk, their components represent the variety of materials that coexisted in it, which constrains their possible origins. The following discussion excludes gas-rich meteorites that formed after any disk had dissipated. This discussion entails: (1) ordinary chondrites' physical properties; (2) textural relationships between chondrules; (3) textures within chondrules; (4) chemical composition; (5) igneous fragments; (6) chondrule rims and interchonrule matrix; and (7) ages of chondrites and inclusions. Derived from text

N95-19307*# New Mexico Univ., Albuquerque, NM. Inst. of Meteoritics.
RELICT GRAINS IN CHONDRULES: EVIDENCE FOR CHONDRULE RECYCLING Abstract Only
R. H. Jones *In* Lunar and Planetary Inst., Papers Presented to the Conference on Chondrules and the Protoplanetary Disk 1994 p 16-17 (For primary document see N95-19289 05-90)
Avail: CASI HC A01/MF A01

The presence of relict grains in chondrules, which offers some insight into the degree to which chondrule material was recycled in the chondrule-forming region, is discussed in this report. Relics are grains that clearly did not crystallize in situ in the host chondrule. They represent coarse-grained precursor material that did not melt during chondrule formation, and provide the only tangible record of chondrule precursor grains. Relics are commonly identified by a large difference in size, textural differences, and/or significant compositional differences compared with normal grains in the host chondrule. Two important types of relics are: (1) 'dusty,' metal-bearing grains of olivine and pyroxene; and (2) forsterite (Mg-rich olivine) grains present in FeO-rich chondrules. Derived from text

N95-19308*# Kyoto Univ. (Japan). Dept. of Geology and Mineralogy.
COLLISION OF COMETLIKE AND SLIGHTLY DIFFERENTIATED BODIES AS AN ORIGIN FOR ORDINARY CHONDRITES Abstract Only
M. Kitamura and A. Tsuchiyama (Osaka Univ., Toyonaka, Japan.) *In* Lunar and Planetary Inst., Papers Presented to the Conference on Chondrules and the Protoplanetary Disk 1994 p 17 (For primary document see N95-19289 05-90)
Avail: CASI HC A01/MF A01

One of the keys to understanding the origins of chondrites is given by the characteristics of relict minerals in chondrules that survived chondrule formation. Some of the relic materials show shock deformation textures, such as high dislocation densities in relict olivine and stacking faults in relict pyroxene. The textures suggest that shock deformation was the cause of melting of the chondrules. Some of the olivine and pyroxene fragments in the matrix of the chondrites have been shown to have a composition closer to the relict minerals than minerals crystallized during the chondrule formation. This suggests that some of the fragments originated from the precursor materials of the chondrules. A proposed origin for chondrites is discussed here along with supporting observations and conclusions.
Derived from text

N95-19309*# California Univ., Los Angeles, CA. Inst. of Geophysics and Planetary Physics.
MICROCHONDRULES IN ORDINARY CHONDRITES: IMPLICATIONS FOR CHONDRULE FORMATION Abstract Only
A. N. Krot (Hawaii Univ., Manoa, HI.) and A. E. Rubin *In* Lunar and Planetary Inst., Papers Presented to the Conference on Chondrules and the Protoplanetary Disk 1994 p 17-18 (For primary document see N95-19289 05-90)
Avail: CASI HC A01/MF A01

The occurrence of numerous microchondrules in several matrix-rich clasts and chondrule rims as described in this article has important implications for the origin of chondrules. It implies that fine-grained materials existed in the immediate vicinity of the microchondrules when they formed and that the chondrule-formation mechanism must have been highly localized. Microchondrules on OC have been reported in two principal settings: (1) as rare individuals in the fine-grained matrices of many type-3 chondrites and in the clastic matrix of the Dimmitt H regolith breccia; and (2) as the predominant or exclusive chondrule size in a few unequilibrated clasts in LL3.4 Piancaldoli, the Rio Negro L regolith breccia, L3.7 Mezo-Madaras, and LL3.1 Krymka. Derived from text

N95-19310*# Commonwealth Scientific and Industrial Research Organization, Highett, Victoria (Australia).
THE JET MODEL OF CHONDRULE FORMATION Abstract Only
K. Liffman *In* Lunar and Planetary Inst., Papers Presented to the Conference on Chondrules and the Protoplanetary Disk 1994 p 18-19 Prepared in cooperation with Melbourne Univ., Parkville, Australia (For primary document see N95-19289 05-90)
Avail: CASI HC A01/MF A01

We estimate the size range of particles that are ejected from a protostellar accretion disk by a protostellar jet. An n-body code is used to determine the subsequent motion of the ejected particles, where the particles are subject to two forces: the gravitational attraction from the protostar; and the gas drag from the halo gas of the accretion disk. Derived from text

N95-19311*# National Aeronautics and Space Administration. Lyndon B. Johnson Space Center, Houston, TX.
EXPERIMENTAL CONSTRAINTS ON MODELS FOR THE ORIGIN OF CHONDRULES: COOLING RATES Abstract Only
G. E. Lofgren *In* Lunar and Planetary Inst., Papers Presented to the Conference on Chondrules and the Protoplanetary Disk 1994 p 19-20 (For primary document see N95-19289 05-90)
Avail: CASI HC A01/MF A01

How chondrules cool and how long was the chondrule-forming event are the questions addressed in this report. This study tries to help explain these phenomena and the reasons around them. Derived from text

N95-19312*# Hawaii Univ., Manoa, HI. Inst. of Geophysics and Planetology.
IMPLICATIONS OF A PHASE-TRANSITION THERMOSTAT FOR CHONDRULE MELTING Abstract Only
S. G. Love *In* Lunar and Planetary Inst., Papers Presented to the Conference on Chondrules and the Protoplanetary Disk 1994 p 20-21 (For primary document see N95-19289 05-90)
Avail: CASI HC A01/MF A01

It is widely accepted that chondrules were formed in brief, localized nebular heating episodes. Given the apparent (at least local) high efficiency of chondrule formation, these thermal events seem to have occurred at a large number of different times and/or azimuthal locations in the solar nebula. It is reasonable to expect that the chondrule-forming events, whatever their underlying cause, were not all identical, but instead occurred with some spread of heating intensities. If this was so, it is puzzling that compositional and textural evidence points to peak temperatures certainly within 1400 - 1750 C, and in most cases within 1500 - 1550 C. This problem is addressed in this article and a possible explanation for this restricted range of peak temperatures is discussed. Derived from text

N95-19313*# Hawaii Univ., Manoa, HI. Inst. of Geophysics and Planetology.
FORMATION OF CHONDRULES BY ELECTRICAL DISCHARGE HEATING Abstract Only
S. G. Love, K. Keil, and E. R. D. Scott *In* Lunar and Planetary Inst., Papers Presented to the Conference on Chondrules and the Protoplanetary Disk 1994 p 21-22 (For primary document see N95-19289 05-90)
Avail: CASI HC A01/MF A01

A possible mechanism for making chondrules in the solar nebula is electrical discharge ('lightning') heating, which can create high-temperature (greater than 1600 K), short-duration (approximately 10 s) thermal events as indicated by the chondritic record. Lightning occurs in many diverse terrestrial and planetary settings, and may have occurred in the solar nebula; it is thus worthwhile to investigate its implications for chondrule formation. Nebular discharges do not appear a viable source of heat for melting chondrule precursors, regardless of the uncertainty in the details of the mode. Nonetheless, we believe nebular lightning worthy of further investigation than what is presented here. Experiments analogous to those currently underway to investigate terrestrial thunderstorm lightning could be fruitful in refining nebular lightning models, and would be double interesting in application to nonthunderstorm and planetary lightnings.
Derived from text

N95-19314*# National Museum of Natural History, Washington, DC. Dept. of Mineral Sciences.
CHRONOLOGY OF CHRONDRULE AND CAI FORMATION: Mg-Al ISOTOPIC EVIDENCE Abstract Only
G. J. MacPherson and A. M. Davis (Chicago Univ., Chicago, IL.) *In* Lunar and Planetary Inst., Papers Presented to the Conference on Chondrules and the Protoplanetary Disk 1994 p 22-23 (For primary document see N95-19289 05-90)
Avail: CASI HC A01/MF A01

Details of the chondrule and Ca-Al-rich inclusion (CAI) formation during the earliest history of the solar system are imperfectly known. Because CAI's are more 'refractory' than ferromagnesian chondrules and have the lowest recorded initial Sr-87/Sr-86 ratios of any solar system materials, the expectation is that CAI's formed earlier than chondrules. But it is not known, for example, if CAI formation had stopped by the time chondrule formation began. Conventional (absolute) age-dating techniques cannot adequately resolve small age differences (less than 10(exp 6) years) between objects of such antiquity. One approach has been to look at systematic differences in the daughter products of short-lived radionuclides such as Al-26 and I-129. Unfortunately, neither system appears to be 'well-behaved.' One possible reason for this circumstance is that later secondary events have partially reset the isotopic systems, but a viable alternative continues to be large-scale (nebular) heterogeneity in initial isotopic abundances, which would of course render the systems nearly useless as chronometers. In the past two years the nature of this problem has been redefined somewhat. Examination of the Al-Mg isotopic database for all CAI's suggests that the vast majority of inclusions originally had the same initial Al-26/Al-27 abundance ratio, and that the ill-behaved isotopic systematics now observed are the results of later partial reequilibration due to thermal processing. Isotopic heterogeneities did exist in the nebula, as demonstrated by the existence of so-called FUN inclusions in CV3 chondrites and isotopically anomalous hibonite grains in CM2 chondrites, which had little or no live Al-26 at the time of their formation. But, among the population of CV3 inclusions at least, FUN inclusions appear to have been a relatively minor nebular component. Derived from text

N95-19315*# Humboldt Univ., Berlin (German D.R.). Inst. fuer Mineralogie und Petrographie.
CONSTRAINTS ON CHONDRULE AGGLOMERATION FROM FINE-GRAINED CHONDRULE RIMS Abstract Only
K. Metzler and A. Bischoff (Muenster Univ., Germany.) *In* Lunar and Planetary Inst., Papers Presented to the Conference on Chondrules and the Protoplanetary Disk 1994 p 23-24 (For primary document see N95-19289 05-90)
Avail: CASI HC A01/MF A01

Fine-grained rims around chondrules, Ca,Al-rich inclusions, and other coarse-grained components occur in most types of unequilibrated chondrites, most prominently in carbonaceous chondrites of the CM group. Based on mineralogical and petrographic investigations, it was suggested that rim structures in unequilibrated ordinary chondrites could have formed in the solar nebula by accretion of dust on the surfaces of the chondrules. Dust mantles in CM chondrites seem to have formed by accretion of dust on the surfaces of chondrules and other components during their passage through dust-rich regions in the solar nebula. Concentric mantles with compositionally different layers prove the existence of various distinct dust reservoirs in the vicinity of the accreting parent body. Despite mineralogical and chemical differences, fine-grained rims from other chondrite groups principally show striking similarities to dust mantle textures in CM chondrite. This implies that the formation of dust mantles was a cosmically significant event like the chondrule formation itself. Dust mantles seem to have formed chronologically between chondrule-producing transient heating events and the agglomeration of chondritic parent bodies. For this reason the investigation of dust mantle structures may help to answer the question of how a dusty solar nebula was transformed into a planetary system.
Derived from text

N95-19316*# Kobe Univ. (Japan).
THE ORIGIN OF REFRACTORY PRECURSOR COMPONENTS OF CHONDRULES Abstract Only
K. Misawa and N. Nakamura *In* Lunar and Planetary Inst., Papers Presented to the Conference on Chondrules and the Protoplanetary Disk

1994 p 24-25 (For primary document see N95-19289 05-90)
Avail: CASI HC A01/MF A01

A percentage of all chondrules from carbonaceous chondrites are intermediate in major-element composition between the rare Ca,Al-rich chondrules and the more abundant ferromagnesian chondrules. Some of them possess fractionated REE and trace-element patterns similar to those in CAI's (Ca-Al-rich inclusions). The abundance patterns are controlled primarily by volatilities expected from a solar composition. On the basis of refractory lithophile fractionations, it is suggested that one of the refractory precursors of C chondrules is a condensate from the nebular gas or an evaporative residue of primitive dust clumps. Derived from text

N95-19317*# Tokyo Univ. (Japan). Geological Inst.
CONSTRAINTS ON CHONDRULE AND CAI ORIGINS FROM VAPOR-LIQUID-SOLID EXPERIMENTS Abstract Only
H. Nagahara *In* Lunar and Planetary Inst., Papers Presented to the Conference on Chondrules and the Protoplanetary Disk 1994 p 25-26 (For primary document see N95-19289 05-90)
Avail: CASI HC A01/MF A01

It has been widely accepted that evaporation played an important role in the formation of chondritic constituents and elemental and isotopic fractionation in the solar nebula. Although many workers consider that evaporation is just the opposite of condensation, it is true only when the process is in equilibrium. When the process is not in equilibrium, e.g., local evaporation, where generated gas moves away from the residual solids, the fractionation path is quite different from the opposite of condensation of the gas with the solar system elemental abundances. The degree of elemental, particularly isotopic, fractionation is strongly dependent on the evaporation rate of the element when evaporation takes place from solid materials. The phase relations and the rate of evaporation of chondrite-forming minerals give constraints on partial pressure of the dust components, total pressure of the nebular gas, and heating rate of the materials. Author (revised)

N95-19318*# City Univ. of New York, Brooklyn, NY. Dept. of Geology.
PORPHYRITIC VERSUS NONPORPHYRITIC CHONDRULES Abstract Only
C. E. Nehru (American Museum of Natural History, New York, NY.), M. K. Weisberg (American Museum of Natural History, New York, NY.), and M. Prinz (American Museum of Natural History, New York, NY.) *In* Lunar and Planetary Inst., Papers Presented to the Conference on Chondrules and the Protoplanetary Disk 1994 p 26-27 (For primary document see N95-19289 05-90)
Avail: CASI HC A01/MF A01

Chondrules can be divided into two broad textural types: porphyritic and nonporphyritic. Porphyritic chondrules are the most common in most chondrites and range texturally from olivine-rich (PO) to intermediate (POP) to pyroxene-rich (PP). Barred olivine (BO) chondrules can be considered a special case of porphyritic. Compositionally they can be divided into type I and II. Nonporphyritic are less abundant than porphyritic chondrules in most chondrites -- they make up approximately 125% of the chondrules in ordinary chondrites -- and range texturally from glassy (g) to cryptocrystalline (C) to radial pyroxene (RP). Compositionally nonporphyritic differ from porphyritic chondrules and within this group they are very similar to one another. Here we (1) review and contrast the characteristics of the nonporphyritic and porphyritic chondrules; (2) specify some of the problems associated with the origins of the textural and compositional differences between them; and (3) suggest a possible scenario for their origin, which may have important implications for the evolution of chondrules.
Author (revised)

N95-19319*# New Mexico Univ., Albuquerque, NM. Inst. of Meteorites.
SIDEROPHILE ELEMENTS AND METAL-SILICATE FRACTIONATION IN THE SOLAR NEBULA Abstract Only **c92**
H. E. Newsom *In* Lunar and Planetary Inst., Papers Presented to the Conference on Chondrules and the Protoplanetary Disk 1994 p 27-28 (For primary document see N95-19289 05-90)
Avail: CASI HC A01/MF A01

The most important nebular fractionation affecting the siderophile elements is the metal-silicate fractionation process and its relationship to the chondrule formation process is poorly understood. Understanding these processes is important in terms of understanding the expected compositional range for planetary building blocks. In a general way the composition of chondrites can be derived from the composition of the CI chondrites by addition or subtraction of a refractory component similar to CAI's (in some cases with a Mg2SiO4 component) and by addition or subtraction of Fe metal. Thus normalization to Fe produces the least spread in the normalized abundances of most siderophile elements relative to CI abundances. Detailed bulk chemical studies of chondrules have shown that their siderophile elements have refractory-element siderophile-element signatures (for example, Ir/Ni) that are similar to the bulk meteorites, but distinct among the different chondrite groups. This data suggests that the chondrules were not supplied to the chondrule groups from a single homogeneous source, and that each chondrite group's characteristic siderophile-element signature was established before chondrule formation. These authors make a further inference that all siderophile-lithophile-element fractionation occurred before chondrule formation, but recent discoveries and observations suggest this is not true. The discovery of the metal-rich CH meteorites, the recognition of the role of aerodynamic forces in the solar nebula, and the possible role of metal-silicate segregation during the chondrule formation process suggests that metal-silicate fractionation occurred before, during and after chondrule formation. Derived from text

N95-19320*# National Aeronautics and Space Administration. Lyndon B. Johnson Space Center, Houston, TX.
Mn-Cr ISOTOPIC SYSTEMATICS OF CHAINPUR CHONDRULES AND BULK ORDINARY CHONDRITES Abstract Only
L. Nyquist, D. Lindstrom, H. Wiesmann (Lockheed Engineering and Sciences Co., Houston, TX.), B. Bansal (Lockheed Engineering and Sciences Co., Houston, TX.), C.-Y. Shih (Lockheed Engineering and Sciences Co., Houston, TX.), D. Mittlefehldt (Lockheed Engineering and Sciences Co., Houston, TX.), R. Martinez (Lockheed Engineering and Sciences Co., Houston, TX.), and S. Wentworth (Lockheed Engineering and Sciences Co., Houston, TX.) *In* Lunar and Planetary Inst., Papers Presented to the Conference on Chondrules and the Protoplanetary Disk 1994 p 28-30 (For primary document see N95-19289 05-90)
Avail: CASI HC A01/MF A01

We report on ongoing study of the Mn-Cr systematics of individual Chainpur (LL3.4) chondrules and compare the results to those for bulk ordinary chondrites. Twenty-eight chondrules were surveyed for abundances of Mn, Cr, Na, Fe, Sc, Hf, Ir, and Zn by INAA. Twelve were chosen for SEM/EDX and high-precision Cr-isotopic studies on the basis of LL-chondrite-normalized Mn(LL), Sc(LL), (Mn/Fe)(LL), and (Sc/Fe)(LL) as well as their Mn/Cr ratios. Classification into textural types follows from SEM/EDX examination of interior surfaces. Derived from text

N95-19321*# Cologne Univ. (Germany). Mineralogisch-Petrographisches Inst.
FORMATION OF CHONDRULES AND CAIs BY NEBULAR PROCESSES Abstract Only
H. Palme *In* Lunar and Planetary Inst., Papers Presented to the Conference on Chondrules and the Protoplanetary Disk 1994 p 30 (For primary document see N95-19289 05-90)
Avail: CASI HC A01/MF A01

Chondrules are essential components of most chondritic meteorites. Carbonaceous chondrites, with the exception of CI chondrites, contain 30-50% chondrules, ordinary and enstatite chondrites even more. A better understanding of chondrule formation will therefore lead to an improved understanding of the origin of meteorites. Most studies of chondrules are, however, concerned with their texture and mineralogy. As chondrules, by definition, passed through a molten stage, their present texture and mineralogy can only provide information on conditions of crystallization from a melt and the subsequent solid-state cooling history. Information concerning chondrule formation is contained in their chemical and isotopic composition. The two most important observations relevant to the chemistry of the chondrules are their generally low Fe content and the large compositional variability of chondrules from a single meteorite, reflected in major variations of Mg/Si ratios, of Al and other refractory element abundances, total Fe, metal (Fe, Ni), and sulfide. This large compositional variability is surprising considering the uniform and nearly solar composition of bulk chondrites, which, in some cases, consist of more than 90% of chondrules. Derived from text

N95-19322*# National Aeronautics and Space Administration. Ames Research Center, Moffett Field, CA.

A CERAMIC/SLAG INTERFACE AS AN ANALOG FOR ACCRETION OF HOT REFRACTORY OBJECTS AND RIM FORMATION Abstract Only

J. M. Paque (Search for Extraterrestrial Intelligence Inst., Mountain View, CA.) and T. E. Bunch *In* Lunar and Planetary Inst., Papers Presented to the Conference on Chondrules and the Protoplanetary Disk 1994 p 31 (For primary document see N95-19289 05-90)

Avail: CASI HC A01/MF A01

Refractory inclusions or Ca-Al-rich inclusions (CAI's) from carbonaceous chondrites span a wide range of bulk compositions that cannot be explained either by segregation from a gas of solar composition at different points in the condensation sequence or by fractional crystallization from a parent liquid. CAI's are commonly rimmed by Wark-Lovering (W-L) rims, a series of nearly monomineralic layers that have been a source of controversy since the variety of rim sequences occurring on different types of CAI's from Allende were described. The origin of these distinctive features has not yet been resolved, with proponents of accretion, condensation, flash heating, ablation, evaporation, etc. Rims have generated considerable interest because they potentially contain clues to conditions experienced by CAI's after the formation of the inclusion and prior to incorporation into the parent body. Ceramic bricks in contact with hot steel slag may produce reaction products in rimlike fashion similar to those found in CAI's. The similarity between the mineralogy of blast furnace slags and CAI's has long been recognized, with both containing unusual phases not found in terrestrial materials. We provide here a comparison between a ceramic brick/slag multiple-layered interface and a multiple-layered interface between a melilite-perovskite object and a melilite-spinel object in the Allende inclusion USNM 4691-1. These results have implications in interpreting the origin of rims and the textures and compositions of CAI's. Derived from text

N95-19323*# California Univ., Los Angeles, CA. Inst. of Geophysics and Planetary Physics.

CHONDRULE REMELTING: EVIDENCE FROM COARSE-GRAINED CHONDRULE RIMS AND COMPOUND CHONDRULES Abstract Only

A. E. Rubin and A. N. Krot (Hawaii Univ., Manoa, HI.) *In* Lunar and Planetary Inst., Papers Presented to the Conference on Chondrules and the Protoplanetary Disk 1994 p 31-32 (For primary document see N95-19289 05-90)

Avail: CASI HC A01/MF A01

The meteorites that best preserve the nebular record are the type 3 ordinary (OC) and carbonaceous chondrites; their major components include chondrules and chondrule fragments, refractory and mafic inclusions, FeO-rich silicate matrix material. Many chondrules are surrounded by rims; these can be divided into two major types: (1) fine-grained rims, which are composed of matrix material; and (2) igneous or coarse-grained rims, which have igneous textures and larger, less-ferroan mafic silicate grains. Fine-grained rims surround most of the chondrules in the least-equilibrated type 3 ordinary and carbonaceous chondrites. They were most likely derived via collapse of clumps of nebular dust that accreted around coarse objects such as chondrules and inclusions. Coarse-grined or igneous rims surround approximately 10% of the chondrules in type 3 OC and approximately 50% of the chondrules in CV3 chondrites as well as some chondrule fragments and isolated mineral grains. They probably formed by partly melting finer-grained dust-rich precursors and admixed chondrule fragments. Derived from text

N95-19324*# Arizona Univ., Tucson, AZ.

CHONDRULE FORMATION IN THE RADIATIVE ACCRETIONAL SHOCK Abstract Only

T. V. Ruzmaikina and W. Ip (Max-Planck-Inst. fuer Aeronomie, Katlenburg-Lindau, Germany.) *In* Lunar and Planetary Inst., Papers Presented to the Conference on Chondrules and the Protoplanetary Disk 1994 p 32-34 (For primary document see N95-19289 05-90)

Avail: CASI HC A01/MF A01

The physical, mineralogical, and isotopic properties of chondrules strongly indicate that they were formed by the rapid melting and resolidification of preexisting solids composed of primitive material. The chondrule precursors were heated to temperatures of about 1800 K in short high-temperature events, followed by cooling with a rate of 10(exp 2)-10(exp 3) K/hr. A heat input of about 1500 J/g is required to heat chondrule precursors to such a temperature and melt them. Lightning discharges and flares in the solar nebula, and heating of the chondrule precursors by friction with gas decelerated in the accretional shock or in a shock (of unspecified origin) within the solar nebula, have been discussed as possible mechanisms for chondrule formation. One advantage of chondrule formation in large-scale shocks is that a lot of dust material can be processed. An accretional shock, which is produced by infalling gas of the presolar cloud when it collides with the solar nebula, belongs to this type of shock. In 1984 Wood considered the possibility of chondrule formation in the accretional shock by heating of chondrule precursors by gas drag. He concluded that the density in the accreting material is much lower than needed to melt silicates at the distance of the asteroid belt if the accreting matter had the cosmic ratio of dust to gas, and the mass of the solar nebula did not exceed 2 solar mass units. Melting of chondrule precursors is difficult because of their effective cooling by thermal radiation. Suppression of the radiative cooling of individual grains in dust swarms, which are opaque to thermal emission, was considered to be the only possible means of chondrule formation in solar nebula shocks. Previous models of solid grain melting in solar nebula shocks have neglected gas cooling behind the shock front, i.e., they considered adiabatic shocks. In this paper we show that large dust grains could be heated much stronger than was supposed by these authors, because of effects associated with the gas cooling.

Derived from text

N95-19325*# Trinity Coll., Dublin (Ireland). Dept. of Geology.

THE CIRCUMPLANETARY NEBULAR ENVIRONMENT: A POSSIBLE SOURCE REGION FOR CHONDRULES Abstract Only

I. S. Sanders *In* Lunar and Planetary Inst., Papers Presented to the Conference on Chondrules and the Protoplanetary Disk 1994 p 34 (For primary document see N95-19289 05-90)

Avail: CASI HC A01/MF A01

Hypotheses for the origin of chondrules fall into two broad groups: nebular and planetary. Arguments against the latter have prevailed in recent years such that, by default, the less testable nebular setting for chondrule formation is now generally favored. However, the recognition in ordinary chondrites of igneous clasts that probably formed on, or in, small planetoids hints that some parent bodies were still accreting after others had evolved magmatically and lost material to space, presumably by impact. If melting of planetoids can predate accretion, could the same early melting even be related to chondrule production? My affirmative response to this interesting question is expanded here in a chondrule-forming scenario, which incorporates both planetary and nebular features. Derived from text

N95-19326*# Tokyo Univ. (Japan). Geological Inst.

HEATING DURING SOLAR NEBULA FORMATION AND Mg ISOTOPIC FRACTIONATION IN PRECURSOR GRAINS OF CAIs AND CHONDRULES Abstract Only **c92**

S. Sasaki, H. Nagahara, K. Kitagami, and Y. Nakagawa *In* Lunar and Planetary Inst., Papers Presented to the Conference on Chondrules and the Protoplanetary Disk 1994 p 35-36 (For primary document see N95-19289 05-90)

Avail: CASI HC A01/MF A01

In some Ca-Al-rich inclusion (CAI) grains, mass-dependent isotopic fractionations of Mg, Si, and O are observed and large Mg isotopic fractionation is interpreted to have been produced by cosmochemical processes such as evaporation and condensation. Mass-dependent Mg isotopic fractionation was found in olivine chondrules of Allende meteorites. Presented is an approximate formula for the temperature of the solar nebula that depends on heliocentric distance and the initial gas distribution. Shock heating during solar nebula formation can cause evaporative fractionation within interstellar grains involved in a gas at the inner zone (a less than 3 AU) of the disk. Alternatively collision of late-accreting gas blobs might cause similar heating if Sigma(sub s) and Sigma are large enough. Since the grain size is small, the solid/gas mass ratio is low and solar (low P(sub O2)), and the ambient gas pressure is low, this heating event could not produce chondrules themselves. Chondrule formation should proceed around the disk midplane after dust grains would grow and sediment to increase the solid/gas ratio there. The heating source there is uncertain, but transient rapid accretion through the disk could release a large amount of heat, which would be observed as FU Orionis events.

Derived from text

N95-19327*# Hawaii Univ., Honolulu, HI. Inst. of Geophysics and Planetology.

VARIATIONS AMONG CHONDRITE GROUPS: CONSTRAINTS ON NEBULAR PROCESSES Abstract Only

E. R. D. Scott, S. G. Love, and I. D. Hutcheon (Lawrence Livermore National Lab., Livermore, CA.) *In* Lunar and Planetary Inst., Papers Presented to the Conference on Chondrules and the Protoplanetary Disk 1994 p 36-37 (For primary document see N95-19289 05-90)

Avail: CASI HC A01/MF A01

Diverse proportions of the four major ingredients are found in the 13 chondrite groups. Ca-Al-rich inclusions (CAI) include amoeboid-olivine aggregates, which contain refractory nodules. Matrix material forms aggregates and rims on other constituents and contains micrometer-sized grains and a small, uniform concentration of presolar grains. Fe, Ni grains are mostly derived from hot chondrules. Although bulk nonvolatile chondritic elemental ratios are typically within 30% of solar values, individual CAI and some chondrules shown large deviations. Derived from text

N95-19328*# Arkansas Univ., Fayetteville, AR. Cosmochemistry Group.

OPEN-SYSTEM BEHAVIOR DURING CHONDRULE FORMATION Abstract Only

D. W. G. Sears, H. Shaoxiong, and P. H. Benoit *In* Lunar and Planetary Inst., Papers Presented to the Conference on Chondrules and the Protoplanetary Disk 1994 p 37-38 (For primary document see N95-19289 05-90)

(Grant NAGw-3519)

Avail: CASI HC A01/MF A01

The question of whether chondrules behaved as open systems during formation is crucial to our understanding of both chondrule and chondrite formation. The very large range of chondrule types is best summarized by the compositional classification scheme, wherein the primitive chondrule groups (i.e., those not produced by metamorphic processes) are A1, A2, A5, and B1. In the Semarkona (LL3.0) chondrite, 10.5%, 25.0%, 5.0%, and 56.9% (by number) of the chondrules are groups A1, A2, A5, and B1, respectively. We argue that groups A1 and A2 were produced by reduction and evaporation during chondrule formation of material originally resembling group B1 chondrules. Derived from text

N95-19329*# Arizona Univ., Tucson, AZ. Lunar and Planetary Lab.

I-Xe STUDIES OF INDIVIDUAL CHONDRULES: WHAT CAN THEY TELL US ABOUT CHONDRULE FORMATION? Abstract Only

T. D. Swindle and C. M. Hohenberg (Washington Univ., Saint Louis, MO.) *In* Lunar and Planetary Inst., Papers Presented to the Conference on Chondrules and the Protoplanetary Disk 1994 p 38-39 (For primary document see N95-19289 05-90)

Avail: CASI HC A01/MF A01

In the past 14 years, I-Xe studies have been performed on nearly 100 individual chondrules from five different meteorites. More than half the studied chondrules come from the unequilibrated ordinary chondrites (UOC's) Chainpur, Semarkona, and Tieschitz. However, 'unequilibrated' does not necessarily mean 'unaltered,' and the I-Xe studies of chondrules from UOC's have ultimately been interpreted in terms of postformation alteration. Two types of constraints on chondrule formation are discussed: (1) the duration, location, and timing of postformation alteration (in solids over a 50-m.y. span); and (2) the ages of the earliest formed chondrules (a few million years after the earliest solids). Derived from text

N95-19330*# California Univ., San Diego, La Jolla, CA. Dept. of Chemistry.

CHEMICAL PRODUCTION OF CHONDRULE OXYGEN ISOTOPIC COMPOSITION Abstract Only

M. H. Thiemens *In* Lunar and Planetary Inst., Papers Presented to the Conference on Chondrules and the Protoplanetary Disk 1994 p 39-41 (For primary document see N95-19289 05-90)

Avail: CASI HC A01/MF A01

Defining the source of observed meteoritic O isotopic anomalies remains a fundamental challenge. The O isotopic composition of chondrules are particularly striking. There are at least three types of chemical processes that produce the isotopic compositions observed in chondrules and Ca-Al-rich inclusions (CAI's). The processes are rather general, viz, they require no specialized processes and the processes associated with chondrule production are likely to produce the observed compositions. Derived from text

N95-19331*# Osaka Univ., Toyonaka (Japan). Dept. of Earth and Space Science.

ESTABLISHMENT OF REDOX CONDITIONS DURING PLANETARY COLLISIONS AS AN ORIGIN OF CHONDRITES Abstract Only

A. Tsuchiyama and M. Kitamura (Kyoto Univ., Japan.) *In* Lunar and Planetary Inst., Papers Presented to the Conference on Chondrules and the Protoplanetary Disk 1994 p 41-42 (For primary document see N95-19289 05-90)

Avail: CASI HC A01/MF A01

Collisions between a 'cometlike' body (mixtures of chondritic materials and ice) and a slightly differentiated body were proposed for shock origin of ordinary chondrites. In this model, chondrules were formed with shock melting, and matrices were formed both by fracturing of materials and by recondensation of evaporated materials. This model can explain different redox conditions of chondrite formations by ice evaporation. Although this model was originally proposed for ordinary chondrites, we assume here that the model can be extended to chondrite formation in general. In this paper, redox conditions during chondrite formation by collisions will be discussed in the light of phase diagrams for solid-vapor equilibria. Derived from text

N95-19332*# California Univ., Los Angeles, CA. Inst. of Geophysics and Planetary Physics.

CHONDRULE ORIGINS: CONSTRAINTS FROM CHONDRULE PROPERTIES AND COSMOCHEMISTRY Abstract Only

J. T. Wasson *In* Lunar and Planetary Inst., Papers Presented to the Conference on Chondrules and the Protoplanetary Disk 1994 p 42-43 (For primary document see N95-19289 05-90)

Avail: CASI HC A01/MF A01

The origin of chondrules is a problem for the ages. Yet even though a detailed formation mechanism remains elusive, the constraints on possible mechanisms become more stringent with each systematic examination of chondrules that involves a higher level of resolution. Constraints presented here are mainly based on studies of chondrules in unequilibrated ordinary chondrites because these have been studied much more than other primitive chondrites. These constraints are listed in six categories: the first four are constraints of chondrule origin and the last two reflect the constraints chondrule properties place on the ambient nebula. Derived from text

N95-19333*# California Univ., Los Angeles, CA. Inst. of Geophysics and Planetary Physics.

THE FINE NEBULA DUST COMPONENT: A KEY TO CHONDRULE FORMATION BY LIGHTNING Abstract Only

J. T. Wasson and K. L. Rasmussen (Odense Univ., Denmark.) *In* Lunar and Planetary Inst., Papers Presented to the Conference on Chondrules and the Protoplanetary Disk 1994 p 43 (For primary document see N95-19289 05-90)

Avail: CASI HC A01/MF A01

Our assessment indicates that chondrule formation by lightning is indeed possible in the solar nebula. Previously the overriding objection to the lightning process of chondrule formation has been that low nebula pressures prevented the buildup of large potential differences. The breakdown potential is controlled by the mean free live distance of an electron. We calculate the mean free live distance in pure H2 gas at 2 AU to be approximately 500 m. A fine dust load constituting 4 wt% of the dust in the dusty midplane region leads to a reduced mean free live distance of only 7 m. Very conservatively we estimate the breakdown potential to be at least 10, 1.8, and 0.7 V/cm at 1, 2, and 3 AU respectively. We set the radius of the lightning bolt equal to the kinetic mean free path of the gas. Our calculations based on electron drift velocities in a fully ionized H2 gas show that first strike durations are 0.96, 3.4, and 7.0 ms at 1, 2, and 3 AU respectively, in much better accordance with the meteoritic evidence than previous estimates of 10-100 s. Derived from text

N95-19334*# Technische Univ., Darmstadt (Germany). Dept. of Material Sciences.

COOLING RATES OF CHONDRULES: A NEW APPROACH Abstract Only

S. Weinbruch and W. F. Mueller *In* Lunar and Planetary Inst., Papers

Presented to the Conference on Chondrules and the Protoplanetary Disk 1994 p 43-44 (For primary document see N95-19289 05-90)
Avail: CASI HC A01/MF A01

Mineralogy and texture of chondrules have been reproduced experimentally and it was demonstrated that the abundance of heterogeneous nuclei is an important factor controlling chondrule textures. Cooling rates of chondrules were estimated from the zoning patterns of olivine. Low cooling rates (less than 100 C/h) yielded chemically homogeneous olivine crystals, whereas higher cooling rates, between 100 and 2000 C/h, produced olivine compositions similar to those observed in natural chondrules. We present a new approach to determining cooling rates of chondrules based on the microstructure of chondrule clinopyroxene and plagioclase. All observations were made on Allende chondrules. Two independent processes (Ca and Mg diffusion in pyroxene and Al/Si ordering in plagioclase) yield similar cooling rates on the order of 10-1 C/h for granular olivine pyroxene (GOP) chondrules in Allende. Our cooling rates are at least one order of magnitude lower than those derived from dynamic crystallization experiments. Derived from text

N95-19335*# American Museum of Natural History, New York, NY. Dept. of Mineral Science.
IMPLICATIONS FOR THE EVOLUTION OF CHONDRULES FROM AGGLOMERATIC OLIVINE CHONDRULES Abstract Only
M. K. Weisberg and M. Prinz *In* Lunar and Planetary Inst., Papers Presented to the Conference on Chondrules and the Protoplanetary Disk 1994 p 44-45 (For primary document see N95-19289 05-90)
Avail: CASI HC A01/MF A01

There is considerable evidence that chondrules formed by the melting of solid materials and, by default, the early solar nebula is the preferred location for chondrule formation. Agglomeratic olivine (AO) chondrules supply perhaps the most intriguing, direct evidence for chondrule formation from agglomeration of solids. We review the characteristics of AO chondrules and discuss their implications for understanding chondrule precursors and chondrule evolution. Derived from text

N95-19336*# Harvard-Smithsonian Center for Astrophysics, Cambridge, MA.
MAJOR UNRESOLVED ISSUES IN THE FORMATION OF CHONDRULES AND CAIs Abstract Only
J. A. Wood *In* Lunar and Planetary Inst., Papers Presented to the Conference on Chondrules and the Protoplanetary Disk 1994 p 45-46 (For primary document see N95-19289 05-90)
Avail: CASI HC A01/MF A01

So much has been learned and published about chondrites and so many models have been floated (but neither proven nor refuted) that the subject has become extremely diffuse and amorphous. It is impossible to remain simultaneously aware of all the many constraints, from many different subdisciplines, that bear on nebular processes. This paper attempts to impose some structure on the situation and loosen the interpretational logjam by breaking the chondrite problem into a series of well-defined questions. Most are open questions; those that some might consider closed by now may deserve formal reexamination. Derived from text

N95-19337*# Rutgers Univ., Piscataway, NJ. Dept. of Geological Sciences.
FLASH HEATING IS REQUIRED TO MINIMIZE SODIUM LOSSES FROM CHONDRULES Abstract Only
Y. Yu, R. H. Hewins, and H. C. Connolly, Jr. *In* Lunar and Planetary Inst., Papers Presented to the Conference on Chondrules and the Protoplanetary Disk 1994 p 46-47 (For primary document see N95-19289 05-90)
Avail: CASI HC A01/MF A01

Chondrules were formed by high-temperature melting events, but do not always show Na depletion compared to CI chondrites, though extensive Na loss has been found in previous isothermal experiments. While Na loss can be prevented by high partial pressure of Na in the nebula, many people favor a flash-heating mechanism to reduce the Na loss from chondrule melts. To examine the validity of the flash-heating hypothesis, we have conducted a series of flash-heating experiments and observed Na loss rate under different conditions. Our results support the flash heating as a plausible heating mechanism to form chondrules. Derived from text

N95-19338*# National Museum of Natural History, Paris (France).
CHONDRULE PRECURSORS AND COOLING PATHS: THE SULFUR EVIDENCE Abstract Only
B. Zanda (Centre National de la Recherche Scientifique, Orsay, France.), Y. Yu (Rutgers Univ., Piscataway, NJ.), M. Bourot-Denise (Centre National de la Recherche Scientifique, Orsay, France.), R. H. Hewins (Rutgers Univ., Piscataway, NJ.), and H. C. Connolly, Jr. (Rutgers Univ., Piscataway, NJ.) *In* Lunar and Planetary Inst., Papers Presented to the Conference on Chondrules and the Protoplanetary Disk 1994 p 47-48 (For primary document see N95-19289 05-90)
Avail: CASI HC A01/MF A01

The behavior of moderately volatile elements (Na and S) is controversial but critical in understanding chondrule precursors and heating processes. Sulfide appeared to be present in most chondrules, but S should have been vaporized during chondrule formation. In fact, S is extensively redistributed in the course of metamorphism, and its abundance at the end of chondrule formation can only be inferred from the least equilibrated chondrites. Our study of 530 chondrules from Renazzo (CR2) and Semarkona (LL3.0) shows partial volatilization of S during chondrule formation and our melting experiments define conditions for total loss or partial retention of S. Derived from text

N95-19339*# Moscow State Univ. (Russia). Dept. of Petrology.
TEXTURAL VARIABILITY OF ORDINARY CHONDRITE CHONDRULES: IMPLICATIONS OF THEIR FORMATION Abstract Only
N. G. Zinovieva, O. B. Mitreikina, and L. B. Granovsky *In* Lunar and Planetary Inst., Papers Presented to the Conference on Chondrules and the Protoplanetary Disk 1994 p 48-50 Sponsored by International Science Foundation and Russian Fund of Fundamental Researches (For primary document see N95-19289 05-90)
Avail: CASI HC A01/MF A01

Scanning electron microscopy (SEM) and microprobe examination of the Raguli H3-4, Saratov L3, and Fucbin L5-6 ordinary chondrites and the analysis of preexisted data on other meteorites have shown that the variety of textural types of chondrules depends on the chemical composition of the chondrules. The comparison of bulk-rock chemistries of the chondrules by major components demonstrates that they apparently fall, like basic-ultrabasic rock, into groups of dunitic and pyroxenitic composition. This separation is further validated by the character of zoning in chondrules of the intermediate, peridotitic type. The effect is vividly demonstrated by the 'chondrule-in-chondrule' structure. Derived from text

N95-19341*# Kansas Univ., Lawrence, KS. Dept. of Physics and Astronomy.
QUASI-LINEAR REGIME OF GRAVITATIONAL INSTABILITY AS A CLUE TO UNDERSTANDING THE LARGE-SCALE STRUCTURE IN THE UNIVERSE
Sergei F. Shandarin 1992 17 p Presented at the Dedication Seminar for the Devayni Complex of Institutional Buildings of IUCAA, Pune, India, 29-30 Dec. 1992
(Grants NAGw-2923; NSF AST-90-21414)
(NASA-CR-197613; NAS 1.26:197613) Avail: CASI HC A03/MF A01

In the late seventies, an image of the large-scale structure in the Universe began to emerge as a result of the accumulation of the galaxy redshifts. Most of the galaxies are found to concentrate in large filaments and perhaps sheets leaving most of the volume empty. Similar structures were predicted theoretically in the frame of the adiabatic theory of galaxy formation (Zeldovich) and later in the hot dark matter cosmology. However, both scenarios have been ruled out by the observations. With these scenarios the dynamical part of the scenario was also erroneously rejected by many as well. In this talk, I derive the Zeldovich approximation from the exact dynamic equations and show that it is always better than the standard linear approximation. The advantage of the Zeldovich approximation is the greatest in the quasi-linear regime when delta(sub rms) is less than 1 (delta identical to delta(rho)/rho), but the displacement of the matter is essential. The range of scales in the quasi-linear regime depends upon the slope of the initial spectrum and increases with decreasing n, where n is the exponent, if the initial spectrum is approximated by a simple power law P(k) varies as k(exp n). Author

N95-19570# California Univ., Berkeley. Lawrence Berkeley Lab, CA.
A CRYSTALLINE QUARK-HADRON MIXED PHASE IN NEUTRON STARS
N. K. Glendenning 31 Aug. 1994 12 p Presented at the Nordic Workshop on Relativistic Heavy Ion Reaction Theory, Bergen, Norway, 11-15 Jun. 1993
(Contract DE-AC03-76SF-00098)
(DE95-000787; LBL-34361; CONF-9306374-1) Avail: CASI HC A03/MF A01

The mixed phase of a substance undergoing a first order phase transition has entirely different behavior according as the substance has more than one conserved charge or only one, as in the text book examples. In the latter case the pressure and nature of the phases are constants throughout the coexistence phase. For systems with more than one conserved charge (or independent component) we prove two theorems: (1) The pressure and the nature of the phases in equilibrium change continuously as the proportion of the phases varies from one pure phase to the other. (2) If one of the conserved charges is the Coulomb force, an intermediate-range order will be created by the competition between Coulomb and surface interface energy. Their sum is minimized when the coexistence phase assumes a Coulomb lattice of one phase immersed in the other. The geometry will vary continuously as the proportion of phases. We illustrate the theorems for a simple description of the hadron to quark phase transition in neutron stars and find a crystalline phase many kilometers thick. However the theorems are general and pertain to chemical mixtures, nuclear systems, either static as in stars or dynamic as in collisions, and have possible application to phase transitions in the early universe. DOE

N95-19575*# Lowell Observatory, Flagstaff, AZ.
NEAR-EARTH ASTEROID RETURNED SAMPLE (NEARS) Final Technical Report
Eugene M. Shoemaker and Andrew F. Cheng 1994 147 p
(Grant NAG9-701)
(NASA-CR-197297; NAS 1.26:197297) Avail: CASI HC A07/MF A02

The concept of the Near-Earth Asteroid Returned Sample (NEARS) mission is to return to Earth 10-100 g from each of four to six sites on a near-Earth asteroid and to perform global characterization of the asteroid and measure mass, volume, and density to ten percent. The target asteroid for the mission is 4660 Nereus, probably a primitive C-type asteroid, with the alternate target being 1989ML, an extremely accessible asteroid of unknown type. Launch dates will be 1998, 2000, 2002, and 2004 on the Delta II-7925 launch vehicle. The mission objectives are three-fold. (1) Provide first direct and detailed petrological, chemical, age, and isotopic characterization of a near-Earth asteroid and relate it to terrestrial, lunar, and meteoritic materials. (2) Sample the asteroid regolith and characterize any exotic fragments. (3) Identify heterogeneity in the asteroid's isotopic properties, age, and elemental chemistry. Derived from text

N95-19612# Los Alamos National Lab., NM.
A QUANTUM-DRIVE-TIME (QDT) QUANTIZATION OF THE TAUB COSMOLOGY
W. A. Miller and A. Kheyfets 1994 5 p Presented at the 7th Marcel Grossman Meeting on General Relativity, Stanford, CA, 24-29 Jul. 1994
(Contract W-7405-eng-36)
(DE95-001014; LA-UR-94-3328; CONF-9407129-2) Avail: CASI HC A01/MF A01

We present here an application of a new quantization scheme. We quantize the Taub cosmology by quantizing only the anisotropy parameter (beta) and imposing the super-Hamiltonian constraint as an expectation-value equation to recover the relationship between the scale factor (Omega) and time t. This approach appears to avoid the problem of time. DOE

N95-19773# Aircraft Research Association Ltd., Bedford (England).
EVALUATION OF THREE TURBULENCE MODELS FOR AFTERBODY/JET FLOWS, INCLUDING REYNOLDS STRESS CLOSURE
Nicholas E. May Jun. 1994 10 p Presented at the 2nd European Computational Fluid Dynamics Conference, Stuttgart, Germany, 5-8 Sep. 1994 Sponsored by British Aerospace (Military Aircraft) Limited and United Kingdom Ministry of Defence
(ARA-Memo-408) Avail: CASI HC A02/MF A01

Turbulent Navier-Stokes solutions for axisymmetric, transonic afterbody/jet flows are presented. The predictive capabilities of three turbulence models, namely a zero-equation model, a two-equation model and an algebraic Reynolds stress model are assessed by comparison with experiment. The algebraic Reynolds stress model gives superior predictions, particularly for separated flow regions. However, this improvement must be weighed against the reduced robustness of the algebraic Reynolds stress model and increased computer run-times. Author

91 LUNAR AND PLANETARY EXPLORATION

Includes planetology; and manned and unmanned flights.
For spacecraft design or space stations see *18 Spacecraft Design, Testing and Performance.*

N95-18579*# Stanford Univ., CA. Center for Radar Astronomy.
INVESTIGATION OF ATMOSPHERIC WAVES ON NEPTUNE Final Technical Report, 1 Mar. 1991 - 31 Aug. 1994
Von R. Eshleman and David P. Hinson 31 Aug. 1994 27 p
(Grant NAGw-2442)
(NASA-CR-197537; NAS 1.26:197537; SU-SPO-8729) Avail: CASI HC A03/MF A01

This document constitutes the final report for grant NAGW-2442 of the Neptune Data Analysis Program, which supported research concerning atmospheric dynamics on Neptune. Professor Von R. Eshleman was the principal investigator. David P. Hinson was a Co-Investigator. The grant covered the period 1 March 1991 through 31 August 1994, including a six month no-cost extension. Funding from this grant resulted in publication of one journal article and one book chapter as well as presentation of results at two conferences and in numerous seminars. A complete bibliography is given below. A copy of the journal article is attached along with abstracts from the book chapter and the conference presentations. With support from this grant we extended our analysis and interpretation of the Voyager Project. This research contributed to an improvement in our basic understanding of atmospheric dynamics on Neptune. The highlight was the discovery and characterization of inertio-gravity waves in the troposphere and stratosphere. Results include measures of basic wave properties, such as amplitudes and vertical wavelengths, as well as estimates of the effect of the waves on the photochemistry and momentum balance of the stratosphere. This investigation also yielded a better understanding of the potential of radio occultation experiments for studies of atmospheric waves. At the same time we developed new methods of data analysis for exploiting these capabilities. These are currently being applied to radio occultation data obtained with the Magellan spacecraft to study waves in the atmosphere of Venus. Future planetary missions, such as Mars Global Surveyor and Cassini, will benefit from these accomplishments. Author

N95-19045* National Aeronautics and Space Administration. Lyndon B. Johnson Space Center, Houston, TX.
MERCURY: EXPLORATION OF A PLANET (Videotape)
1976 Videotape: 22 min. playing time, in color, with sound
(NASA-TM-110489; NONP-NASA-VT-95-39134) Avail: CASI VHS A02/BETA A22

The flight of the Mariner 10 spacecraft to Venus and Mercury is detailed in animation and photography. Views of Mercury are featured. Also included is animation on the origin of the solar system. Dr. Bruce C. Murray, director of the Jet Propulsion Laboratory, comments on the mission. JSC

N95-19134*# National Academy of Sciences - National Research Council, Washington, DC. Committee on Planetary and Lunar Exploration.
AN INTEGRATED STRATEGY FOR THE PLANETARY SCIENCES: 1995 - 2010
1994 208 p
(Contract NASw-4627)
(NASA-CR-197145; NAS 1:26:197145; LC-94-69692) Copyright Avail: CASI HC A10/MF A03

In 1992, the National Research Council's Space Studies Board charged its Committee on Planetary and Lunar Exploration (COMPLEX) to: (1) summarize current understanding of the planets and the solar system; (2) pose the most significant scientific questions that remain; and (3) establish the priorities for scientific exploration of the planets for the period from 1995 to 2010. The broad scientific goals of solar system exploration include: (1) understanding how physical and chemical processes determine the

major characteristics of the planets, and thereby help us to understand the operation of Earth; (2) learning about how planetary systems originate and evolve; (3) determining how life developed in the solar system, particularly on Earth, and in what ways life modifies planetary environments; and (4) discovering how relatively simple, basic laws of physics and chemistry can lead to the diverse phenomena observed in complex systems. COMPLEX maintains that the most useful new programs to emphasize in the period from 1995 to 2010 are detailed investigations of comets, Mars, and Jupiter and an intensive search for, and characterization of, extrasolar planets.

Author

N95-19287*# Alabama Univ., Huntsville, AL.
STUDY FOR THE ANALYSIS OF THE OBSERVATIONS, AND NUMERICAL DATA REPRESENTING THE PLANETS AS FAR-INFRARED CALIBRATION SOURCES Final Report
Shi Tsan Wu and Minggang Zhou 12 Sep. 1994 6 p
(Contract NAS8-38609)
(NASA-CR-196542; NAS 1.26:196542) Avail: CASI HC A02/MF A01

The existing radiative transfer and inversion programs will be modified for application to the atmospheres of Uranus, Neptune, and Jupiter. The programs will be employed for analysis of KAO planetary observations in order to develop far infrared photometric calibration standards. This work will be carried out on MSFC computers. The expected end product of this task is a working program for analysis of the observations, and numerical data representing the planets as far-infrared calibration sources.

Dissert. Abstr.

N95-19739# Naval Academy, Annapolis, MD.
MODELING THE DIURNALLY PRECESSING JOVIAN MAGNETOSPHERIC FIELD
Todd D. Bode 19 May 1994 48 p
(AD-A284857; USNA-TSPR-212) Avail: CASI HC A03/MF A01

A functional representation of the magnetic field contribution of the solar-wind-driven electric currents on the magnetopause of Jupiter is presented. The representation accounts for the precession of the magnetic axis and the consequential diurnal variation of the shape of the magnetopause. Existing models of the two interior field sources (planetary dipole and currents of trapped plasma) were incorporated into a set of eight three-dimensional static models. Each model assumed a 10 deg tilt of the magnetic axis with respect to Jupiter's rotation axis. This set includes representations published for a tilt toward (Alpha = 0 deg) and away from (Alpha = 180 deg) the Sun in the noon-midnight meridian plane, as well as six complementary analogous models for azimuthal angles of 45 deg, 90 deg, 135 deg, 225 deg, 270 deg, and 315 deg. The representations were connected by replacing expansion coefficients with continuous functions which replicated each of the eight original static models and interpolated between them. The result is a time-dependent functional representation of the magnetic potential of the magnetopause surface currents in terms of an expansion in associated Legendre functions. This model yields predicted magnetic field components for any location within the magnetosphere as Jupiter's magnetic axis precesses during the course of a Jovian day (9h 55m 41s).

DTIC

92 SOLAR PHYSICS

Includes solar activity, solar flares, solar radiation and sunspots. For related information see *93 Space Radiation*.

N95-17979# Iowa Univ., Iowa City, IA. Dept. of Physics and Astronomy.
HELIOSPHERIC 2-3 kHz RADIO EMISSIONS AND THEIR RELATIONSHIP TO LARGE FORBUSH DECREASES
D. A. Gurnett and W. S. Kurth Oct. 1994 31 p Presented at the 30th Scientific Assembly, Hamburg, Germany, 11-24 Jul. 1994 Submitted for publication
(Contract JPL-959193)
(U-of-Iowa-94-19) Avail: CASI HC A03/MF A01

Two intense heliospheric 2-3 kHz radio emission events have been observed by Voyager 1 and 2, the first in 1983-84 and the second in 1992-93. These radio emission events occurred about 400 days after large Forbush decreases in mid-1982 and mid-1991. Since Forbush decreases are indicative of a strong interplanetary shock propagating outward through the heliosphere, this temporal relationship provides strong evidence that the radio emissions are triggered by the interaction of a shock with one of the outer boundaries of the heliosphere. From the travel time and the known speed of the shock, the distance to the interaction region can be estimated and is well beyond 100 AU. At this great distance the plasma frequency at the terminal shock (100 to 200 Hz) is believed to be too small to explain the observed emission frequencies, which extend up to 3.6 kHz. For this reason, we have proposed that the interaction takes place at or near the heliopause, where remote sensing measurements show that the plasma frequency is in a suitable range (approximately 3 kHz) for explaining the radio emission. From the travel time and shock propagation speed, the radial distance to the heliopause has been calculated for various candidate solar events. After taking into account the likely deceleration of the shock, the heliopause is estimated to be in the range from about 110 to 160 AU.

Author

N95-17980*# Alabama Univ., Huntsville, AL. Center of Microgravity and Materials Research.
DYNAMICS AND STATICS OF NONAXISYMMETRIC LIQUID BRIDGES Annual Report No. 2, 18 Nov. 1993 - 18 Nov. 1994
J. Iwan D. Alexander, Andy Resnick, Yiqiang Zhang, and A. Fedoseyev 18 Nov. 1994 42 p
(Grant NAG3-1384)
(NASA-CR-197520; NAS 1.26:197520) Avail: CASI HC A03/MF A01

We finished the construction of the experimental apparatus and the design and testing of some of the visualization and data acquisition techniques. Experimental work focused on three areas: force measurements, loss of stability to nonaxisymmetric bridges, and vibration behavior. The experimental work is summarized in section 2. Selected results from our force measurement experiments are outlined in section 3. In addition we worked on the theory of the dynamic stability of axisymmetric bridges and undertook numerical simulation of the effects of inclined gravity vectors on the minimum volume stability limit for static bridges. The results and status of our theoretical work and numerical simulation are described in section 4. Papers published and in preparation, conference presentations, etc., are described in section 5. Work planned for the third year is discussed in section 6. References cited in the report are listed in section 7.

Derived from text

N95-18376*# Lockheed Missiles and Space Co., Palo Alto, CA.
CORONAL ABUNDANCES AND THEIR VARIATION Semiannual Progress Report, 15 Apr. - Dec. 1994
Julia L. R. Saba 15 Dec. 1994 32 p
(Contract NASw-4814)
(NASA-CR-197553; NAS 1.26:197553) Avail: CASI HC A03/MF A01

This contract supports the investigation of elemental abundances in the solar corona, principally through analysis of high-resolution software X-ray spectra from the Flat Crystal Spectrometer on NASA's Solar Maximum Mission. The goals of the study are a characterization of the mean values of relative abundances of elements accessible in the FCS data, and information on the extent and circumstances of their variability. This report is a summation of the data analysis and reporting activities which occurred since the last report, submitted two months early, in April 1994, to facilitate evaluation of the first year's progress for contract renewal. Hence this report covers the period 15 April 1994 - 15 December 1994. A list of publications resulting from this research is included.

Author

N95-18497 Hawaii Univ., Honolulu, HI.
DYNAMIC EVOLUTION OF EMERGING MAGNETIC FLUX TUBES IN THE SOLAR CONVECTIVE ENVELOPE Ph.D. Thesis
Yuhong Fan 1993 166 p
Avail: Univ. Microfilms Order No. DA9416045

Given the present consensus that the solar cycle dynamo is operating in a thin 'overshoot layer' between the convection zone and the radiative interior, this dissertation studies the dynamics of transporting toroidal magnetic flux from the dynamo layer to the Sun's photosphere. I have carried out numerical simulations of the buoyant rise of toroidal magnetic flux tubes through the convection zone in the form of emerging loops, whose footprints remain anchored in the overshoot layer. My major conclusions are: (1) as each loop rises due to buoyancy, the Coriolis force transports mass out of the leading leg (leading in the direction of rotation) into the following leg of the loop, and causes the field strength in the

loop's leading leg to be twice that in the following. This field strength asymmetry naturally explains the observed more compact and less fragmented morphology of the leading polarity of an active region compared to its following polarity. (2) the Coriolis force induced by the diverging east-west velocity near the apex of a rising loop acts to twist the loop, and produces a tilt angle upon emergence. For reasonable choices of toroidal field strength 3 x 10(exp 4) G less than or equal to B(sub 0) less than or equal to 9 x 10(exp 4) G, the computed tilt angles are consistent with the sign, magnitude and latitudinal variation of the observed active region tilt angles. The variation of the computed tilt angle alpha with the characteristic field strength B, latitude theta, and the total flux Phi of the loop can be described by the scaling law: alpha varies as sin theta B(exp -(5/4) Theta(exp 1/4). However, for toroidal fields B(sub 0) approximately less than 2 x 10(exp 4) G, loops emerge with tilts that are opposite from those of most active regions. (3) The latitudes of loop emergence are consistent with the observed butterfly diagram assuming a dynamo wave propagating from 30 deg latitude to the equator at the base of the convection zone. In the case of solid-body rotation, a toroidal field B(sub 0) approximately greater than 6 x 10(exp 4) G is required to avoid a significant equatorial gap, but if differential rotation is included, B(sub 0) approximately greater than 3 x 10(exp 4) G leads to an acceptable butterfly diagram. Author

N95-18954*# Hughes STX, Inc., Lanham, MD.
ANALYSIS OF SOLAR SPECTRAL IRRADIANCE MEASUREMENTS FROM THE SBUV/2-SERIES AND THE SSBUV INSTRUMENTS
Semiannual Progress Report, 1 Sep. 1994 - 28 Feb. 1995
Richard P. Cebula, Matthew P. DeLand, and Ernest Hilsenrath 12 Dec. 1994 9 p
(Contract NASw-4864)
(NASA-CR-197544; NAS 1.26:197544) Avail: CASI HC A02/MF A01

The measurements of the solar ultraviolet spectral irradiance by the two Upper Atmosphere Research Satellite (UARS) solar instruments are validated to agree within their 2-Sigma calibration uncertainties of about 7 percent, as well as with measurements from the two solar instruments on the Shuttle Atmospheric Laboratory for Applications and Science (ATLAS) missions. Additionally, the precision of the two UARS data sets is better than the original 2 percent goal, especially at wavelengths greater than 160 nm. This excellent agreement can be credited to accurate pre-flight calibrations, comprehensive in-flight calibrations to track instrument degradation, and a coordinated validation program among the UARS and ATLAS solar instrument teams. The solar irradiance results presented here include those derived from UARS SUSIM, UARS SOLSTICE, ATLAS SUSIM and ATLAS SSBUV measurements on 29 March 1992 during the ATLAS-1 mission and on 15 April 1993 during the ATLAS-2 mission. Two ultraviolet spectra from 119 to 410 nm are derived as the weighted average of the UARS SOLSTICE and SUSIM measurements and are recommended as representative solar spectra for the period of the ATLAS-1 and ATLAS-2 missions. The ATLAS-1 mission occurred during the initial phase of the solar cycle 22 decline when solar activity was moderately high. The ATLAS-2 mission occurred later during the declining phase of the solar cycle 22 when solar activity was more moderate. Author

N95-19034*# Lawrence Livermore National Lab., Livermore, CA. Inst. of Geophysics and Planetary Physics.
SOLAR FLARE MODEL ATMOSPHERES
Suzanne L. Hawley and George H. Fisher (California Univ., Berkeley, CA.) [1993] 59 p
(Contracts NAS5-26555; NAGw-2547; NAGw-2969; NAGw-3429; W-7405-eng-48; NSF ATM-90-22385; NSF AST-92-18085)
(NASA-CR-197607; NAS 1.26:197607) Avail: CASI HC A04/MF A01

Solar flare model atmospheres computed under the assumption of energetic equilibrium in the chromosphere are presented. The models use a static, one-dimensional plane parallel geometry and are designed within a physically self-consistent coronal loop. Assumed flare heating mechanisms include collisions from a flux of non-thermal electrons and x-ray heating of the chromosphere by the corona. The heating by energetic electrons accounts explicitly for variations of the ionized fraction with depth in the atmosphere. X-ray heating of the chromosphere by the corona incorporates a flare loop geometry by approximating distant portions of the loop with a series of point sources, while treating the loop leg closest to the chromospheric footpoint in the plane-parallel approximation. Coronal flare heating leads to increased heat conduction, chromospheric evaporation and subsequent changes in coronal pressure; these effects are included self-consistently in the models. Cooling in the chromosphere is computed in detail for the important optically thick HI, CaII and MgII transitions using the non-LTE prescription in the program MULTI. Hydrogen ionization rates from x-ray photo-ionization and collisional ionization by non-thermal electrons are included explicitly in the rate equations. The models are computed in the 'impulsive' and 'equilibrium' limits, and in a set of intermediate 'evolving' states. The impulsive atmospheres have the density distribution frozen in pre-flare configuration, while the equilibrium models assume the entire atmosphere is in hydrostatic and energetic equilibrium. The evolving atmospheres represent intermediate stages where hydrostatic equilibrium has been established in the chromosphere and corona, but the corona is not yet in energetic equilibrium with the flare heating source. Thus, for example, chromospheric evaporation is still in the process of occurring. Author

N95-19404# National Geophysical Data Center, Boulder, CO.
SOLAR-GEOPHYSICAL DATA NUMBER 599, JULY 1994. PART 1: (PROMPT REPORTS). DATA FOR JUNE, MAY 1994, AND LATE DATA
Helen E. Coffey, ed. Jul. 1994 119 p See also PB94-208824 and PB94-213980
(PB94-213972; SGD-599-Pt-1) Avail: CASI HC A06/MF A02

Contents: Data for June 1994; Solar-Terrestrial Environment-Plots of GOES satellite X-rays, Particles and Magnetometer data with ground-based Boulder Magnetometer and Deep River Neutron Monitor; IUWDS Alert Periods (Advance and Worldwide); Solar Activity Indices - Daily Sunspot Numbers (12 Months), Daily 2800 MHz Solar Flux (12 Months), Daily Solar Indices (Sunspot Numbers and Solar Flux); Solar Flares - H-alpha Solar Flares, Intervals of No Flare Patrol; and Solar Radio Emission. NTIS

N95-19405# National Geophysical Data Center, Boulder, CO.
SOLAR-GEOPHYSICAL DATA NUMBER 599, JULY 1994. PART 2: (COMPREHENSIVE REPORTS). DATA FOR JANUARY 1994, AND MISCELLANEOUS
Helen E. Coffey, ed. Jul. 1994 87 p See also PB94-208832 and PB94-213972
(PB94-213980; SGD-599-Pt-2) Avail: CASI HC A05/MF A01

Contents: Data for January 1994; Solar Flares- H- alpha Solar Flare Groups, Intervals of No Flare Patrol Observation, Number of Solar Flares January 1965-present; Solar Radio Bursts at Fixed Frequencies; Solar X-ray Radiation from GOES Satellite Graphs; Mass Ejections from the Sun; and Active Prominences and Filaments. NTIS

N95-19619# Los Alamos National Lab., NM.
RESULTS FROM SAGE 2
J. S. Nico 1994 4 p Presented at the 27th International Conference on High Energy Physics, Glasgow, Scotland, 21-27 Jul. 1994
(Contract W-7405-eng-36)
(DE95-000849; LA-UR-94-2995; CONF-940722-24) Avail: CASI HC A01/MF A01

The Russian-American Gallium solar neutrino Experiment (SAGE) began the second phase of operation (SAGE 2) in September of 1992. Monthly measurements of the integral flux of solar neutrinos have been made with 55 tonnes of gallium. The K-peak results of the first nine runs of SAGE 2 give a capture rate of 66(sub -13)(sup +18) (stat) (sub -7)(sup +5) (sys) SNU. Combined with the SAGE 1 result of 73(sub -16)(sup +18) (stat) (sub -7)(sup 5) (sys) SNU, the capture rate is 69(sub -11)(sup +11) (stat) (sub -7)(sup +5) (sys) SNU. This represents only 52% - 56% of the capture rate predicted by different Standard Solar Models. DOE

N95-19791*# National Aeronautics and Space Administration. Goddard Space Flight Center, Greenbelt, MD.
RELATIVE ELEMENTAL ABUNDANCE AND HEATING CONSTRAINTS DETERMINED FOR THE SOLAR CORONA FROM SERTS MEASUREMENTS
David A. Falconer (Universities Space Research Association, Greenbelt, MD.) Dec. 1994 96 p
(RTOP 879-11-38; RTOP 170-38-52)
(NASA-TM-104616; Rept-95B00027; NAS 1.15:104616) Avail: CASI HC A05/MF A01

Intensities of EUV spectral lines were measured as a function of radius off the solar limb by two flights of Goddard's Solar EUV Rocket

Telescope and Spectrograph (SERTS) for three quiet sun regions. The density scale height, line-ratio densities, line-ratio temperatures, and emission measures were determined. The line-ratio temperature determined from the ionization balances of Arnaud and Rothenflug (1985) were more self-consistent than the line-ratio temperatures obtained from the values of Arnaud and Raymond (1992). Limits on the filling factor were determined from the emission measure and the line-ratio densities for all three regions. The relative abundances of silicon, aluminum, and chromium to iron were determined. Results did agree with standard coronal relative elemental abundances for one observation, but did not agree for another. Aluminum was overabundant while silicon was underabundant. Heating was required above 1.15 solar radii for all three regions studied. For two regions, local nonconductive heating is needed for any filling factor, and in all three regions for filling factor of 0.1. Author

N95-19292*# Carnegie Institution of Washington, Washington, DC. Dept. of Terrestrial Magnetism.
LARGE-SCALE PROCESSES IN THE SOLAR NEBULA Abstract Only
A. P. Boss *In* Lunar and Planetary Inst., Papers Presented to the Conference on Chondrules and the Protoplanetary Disk 1994 p 2-3 (For primary document see N95-19289 05-90)
Avail: CASI HC A01/MF A01

N95-19297*# Chicago Univ., Chicago, IL. Inst. for Nuclear Studies.
HEATING AND COOLING IN THE SOLAR NEBULA: CONSTRAINTS FROM REFRACTORY INCLUSIONS Abstract Only
A. M. Davis and G. J. MacPherson (National Museum of Natural History, Washington, DC.) *In* Lunar and Planetary Inst., Papers Presented to the Conference on Chondrules and the Protoplanetary Disk 1994 p 7-8 (For primary document see N95-19289 05-90)
Avail: CASI HC A01/MF A01

N95-19319*# New Mexico Univ., Albuquerque, NM. Inst. of Meteorites.
SIDEROPHILE ELEMENTS AND METAL-SILICATE FRACTIONATION IN THE SOLAR NEBULA Abstract Only
H. E. Newsom *In* Lunar and Planetary Inst., Papers Presented to the Conference on Chondrules and the Protoplanetary Disk 1994 p 27-28 (For primary document see N95-19289 05-90)
Avail: CASI HC A01/MF A01

N95-19326*# Tokyo Univ. (Japan). Geological Inst.
HEATING DURING SOLAR NEBULA FORMATION AND Mg ISOTOPIC FRACTIONATION IN PRECURSOR GRAINS OF CAIs AND CHONDRULES Abstract Only
S. Sasaki, H. Nagahara, K. Kitagami, and Y. Nakagawa *In* Lunar and Planetary Inst., Papers Presented to the Conference on Chondrules and the Protoplanetary Disk 1994 p 35-36 (For primary document see N95-19289 05-90)
Avail: CASI HC A01/MF A01

93 SPACE RADIATION

Includes cosmic radiation; and inner and outer earth's radiation belts.

For biological effects of radiation see *52 Aerospace Medicine.* For theory see *73 Nuclear and High-Energy Physics.*

N95-18351 California Univ., Berkeley. Lawrence Berkeley Lab, CA.
GAMQUEST, A COMPUTER PROGRAM TO IDENTIFY GAMMA RAYS
E. Brown May 1994 17 p Limited Reproducibility: More than 20% of this document may be affected by microfiche quality
(Contract DE-AC03-76SF-00098)
(DE94-016217; LBL-35715) Avail: CASI HC A03

This paper describes the application of the computer program GAMQUEST to the study of gamma-ray spectra. The program is especially suited to the analysis of samples produced by neutron activation, and of environmental samples containing radioactive pollutants. GAMQUEST searches a large database (with data for over 60,000 gamma rays) to identify the various spectral lines from samples. The program runs on the VAX/6610 computer cluster of the Lawrence Berkeley Laboratory, and can be accessed from individual accounts or through Hepnet, Internet, or World Wide Web networks. DOE

N95-18464*# Alabama Univ., Huntsville, AL. Cosmic Ray Labs.
AN INSTRUMENT TO MEASURE THE CHARGE, AND ENERGY SPECTRUM (20-1000 GeV/a) OF THE COSMIC RAY SPECIES OXYGEN TO IRON Semiannual Report No. 2, 1 Mar. - Sep. 1994
J. C. Gregory and A. E. Smith 30 Sep. 1994 21 p
(Grant NAGw-2023)
(NASA-CR-197555; NAS 1.26:197555) Avail: CASI HC A03/MF A01

BUGS-4 (Bristol University Gas Scintillator-4) made its maiden engineering flight from Fort Summer (NM) on the 29th of September 1993. The instrument was consumed by fire after striking a power line during landing following 24 hours at float. The analysis of the telemetered data from this sophisticated instrument is a demanding task. Early analysis was compromised by electronic artifacts. Unravelling these problems has been difficult and time consuming, especially as the flight hardware was burned beyond salvage, but is is an essential preliminary to analysis. During this report period we have concentrated on a small sub-set of data (the first 30,000 events; 90 minutes at float), and developed software algorithms to correct systematic errors. Using these corrected events we have begun to develop the analysis algorithms. Although the analysis is preliminary, and restricted to the first 30,000 events, the results are encouraging, and suggest the design concepts are well matched to this application. Further work will refine the analysis, and allow quantitative evaluation of the concepts employed in BUGS-4 for applicability to future instruments. We believe this work will justify fabrication of a new instrument employing techniques deployed on BUGS-4. Author

N95-18729 Columbia Univ., New York, NY.
THE ORIGIN OF THE DIFFUSE X-RAY BACKGROUND Ph.D. Thesis
Thomas Theodore Hamilton 1988 56 p
Avail: Univ. Microfilms Order No. DA9412876

An analysis of the arcminute scale fluctuations in the extragalactic diffuse X-ray background has been undertaken using the Deep Survey data gathered by the Einstein Observatory. These data provide a direct measure of the relative contributions to the unresolved X-ray background of point sources (such as quasars) and effectively diffuse emission (such as intercluster gas or a source population with a surface density greater than approximately 5000 deg(exp -2)). A statistical measure of the granularity in each of the several long-exposure, high-galactic latitude Einstein fields has been computed and compared to the granularity predicted by various Monte Carlo models. It is demonstrated that the observed small-scale anisotropy in the 1-3 KeV band cannot be understood in the context of the known X-ray point source luminosity function without invoking a log N-log S relationship which extends down to sources with fluxes of less than approximately 8 x 10(exp -15) ergs cm(exp -2) s(exp -1), a factor of 3-4 fainter than the Einstein Deep Survey sensitivity limit. However, we also show that the log N-log S slope must turn over at or near this value. For an N(S) alpha S(exp 1.5) distribution, the most likely cutoff for faint point sources is found to be 6.5 x 10(exp -15) ergs cm(exp -2) s(exp -1), with a lower limit of 5 x 10(exp -15). These cutoffs correspond to integrated point-source fluxes ranging from 40 percent to 55 percent of the total nominal X-ray background. Further results constraining the slope of the point source log N-log S relation below the Deep Survey threshold are also presented. It is argued that no reasonable extrapolation of the known population of X-ray emitting quasars can compose the entire diffuse X-ray background. These results are independent of assumptions regarding the X-ray-to-optical luminosity ratios of active galactic nuclei (AGN) and the nature of quasar evolution. We conclude that the dominant contribution to the unresolved component of the X-ray background originates in a population of numerous, low-luminosity X-ray emitters distinct from the known classes of active galactic nuclei. Dissert. Abstr.

N95-18730 Alabama Univ., Huntsville, AL.
SPATIAL AND TEMPORAL CONSTRAINTS ON THE OBSERVED DISTRIBUTION OF GAMMA-RAY BURSTS DETECTED BY BATSE Ph.D. Thesis
John M. Horack 1993 203 p
Avail: Univ. Microfilms Order No. DA9415109

The Burst and Transient Source Experiment (BATSE) on-board NASA's Compton Gamma Ray Observatory has shown that the distribution of

gamma-ray bursts on the sky is consistent with isotropy, however they also possess an inhomogeneous density distribution. These results contradict previous theories that the bursts are somehow associated with neutron stars in the disk of the galaxy. In this dissertation, we place meaningful spatial and temporal constraints on the distribution of gamma-ray bursts observed by BATSE. We begin with an analysis of the effect of location uncertainties on the observed distribution of bursts, and place constraints on the ability of BATSE to detect anisotropies in their angular distribution. This allows one to limit the allowable size of galactic halo burst models. Typical core radii must exceed approximately 40 kpc if the dipole anisotropy of a galactocentric halo is not to be detected by BATSE. Implications for various published galactic halo models are discussed. We also attempt to identify a counterpart object to the gamma-ray bursts utilizing the Earth as an occulting disk and searching for non-bursts radiation from the burst locations using BATSE. Examination of the locations 0f 70 intense bursts in a 112-day interval yields no detectable emission between 20 keV and 2 MeV at the level of approximately 0.15 Crab or higher. This intensity is nearly a factor of 1,000 below the typical intensities of the bursts used in the search. We also use the same technique to search for immediate pre-burst emission, or prompt post-burst emission. No emission is found from the 35 most intense BATSE gamma-ray bursts at a similar intensity level. These findings have important implications for burst models and timescales of emission from burst sources. For the first time, we have applied an integral moment analysis to the BATSE-observed intensity distribution. This technique provides direct measurement of properties such as the mean, variance, and skewness of the convolved luminosity-number density distribution, as well as associated uncertainties. Using this method, one obtains insight into the nature of the source distributions unavailable through computation of traditional single parameters such as (V/V(sub max)). This method also provides for an excellent means of testing the compatibility of hypothetical source distributions, regardless of the particular scenario, and requires no Monte Carlo simulations or statistical methods comparing distributions. As such, an integral moment analysis of the intensity distribution of gamma-ray bursts provides for the most complete analytic description of the source distribution available from the data, and offers the most comprehensive test of the comptability of a given hypothesized distribution with observation. Dissert. Abstr.

N95-18747*# Kansas Univ., Lawrence, KS. Dept. of Physics and Astronomy.

DECAYING NEUTRINOS IN GALAXY CLUSTERS

Adrian L. Melott, Randall J. Splinter, Massimo Persic (SISSA, Trieste, Italy.), and Paolo Salucci (SISSA; Trieste, Italy.) [1993] 16 p

(Grants NAGw-2923; NSF AST-90-21414; NSF OSR-92-55223)

(NASA-CR-197615; NAS 1.26:197615) Avail: CASI HC A03/MF A01

The DM profile in clusters of galaxies was studied and simulated using the Harrison-Zel'dovich spectrum of density fluctuations, and an amplitude previously derived from numerical simulations and in agreement with microwave background fluctuations. Neutrino DM densities, with this amplitude normalization cluster, are comparable to observed cluster DM values. It was concluded that given this normalization, the cluster DM should be al least largely composed of neutrinos. The constraint of Davidson et al., who argued that the failure to detect uv photons from the dark matter (DM) in cluster A665 excludes the decaying neutrino hypothesis, could be somewhat weakened by the presence of baryonic DM; but it cannot be eliminated given our assumptions. Derived from text

N95-18880# Instituto de Pesquisas Energeticas e Nucleares, Sao Paulo (Brazil).

ASSEMBLY AND CALIBRATION OF A NEW EXPERIMENTAL APPARATUS FOR PRODUCTION AND UTILIZATION OF CAPTURE GAMMA RAYS M.S. Thesis

R. Semmler 1993 73 p In PORTUGESE

(DE94-626650; INIS-BR-3334) Avail: CASI HC A04/MF A01 (US Sales Only)

A new experimental apparatus has been mounted at the tangential beam tube B H 4/12 of the IPEN IEA-R1 (2 MW) reactor, for production and utilization of capture gamma rays. In this type of experiment, monochromatic gamma radiation, with energy resolution of about 10 eV, is produced by thermal neutron capture in several materials placed near the reactor core. By changing the target material it was possible to obtain up to 30 gamma lines in the 5 to 11 MeV energy range and so, the present experimental arrangement may be considered as an excellent gamma ray source for photonuclear reactions studies in low excitation energies. DOE

N95-19283# Washington Univ., Seattle, WA. Inst. for Nuclear Theory.

COMMENT ON THE PREPRINT NEUTRINO FLAVOR EVOLUTION NEAR A SUPERNOVA'S CORE (ASTRO-PH 9405008) BY J. PANTALEONE

Yong-Zhong Qian and G. M. Fuller (California Univ., San Diego, CA.) 1994 7 p

(Contract DE-FG06-90ER-40561)

(DE94-017576; DOE/ER-40561/149) Avail: CASI HC A02/MF A01

The revised version of the widely circulated preprint 'Neutrino Flavor Evolution Near A Supernova's Core' by J. Pantaleone is wrong. It contains two errors which lead to incorrect conclusions regarding neutrino flavor transformation in the supernova environment. In this short note we discuss these errors. DOE

99 GENERAL

N95-19128# Japan Information Center of Science and Technology, Tokyo (Japan).

THE JAPAN INFORMATION CENTER OF SCIENCE AND TECHNOLOGY Annual Report, fiscal year 1992

1994 68 p Original contains color illustrations

Avail: CASI HC A04/MF A01

This annual report of the Japan Information Center of Science and Technology is a summary of our activities conducted and their results during FY1992. In FY1992, we have developed an advanced system called JOIS (JICST on-line information system) to improve its serviceability by adding menu functions through which users who do not have knowledge about retrieval commands can easily select and retrieve the pertinent da' , and output the desired information they need. This service was started in April, 1993. We also have prepared a practically usable machine translation system to promote international distribution of scientific and technical information, and by utilizing it for preparing a database of public data in English, we have accelerated our international activities. We also are endeavoring to develop the preceding technologies such as R&D with a prototype of a full-text database system in Japanese aiming to provide promptly the contents of original papers. Author

Typical Subject Index Listing

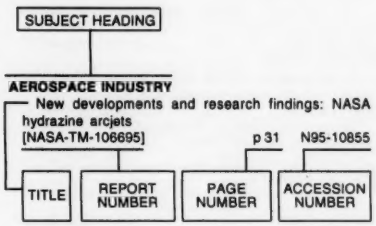

The subject heading is a key to the subject content of the document. Titles, report numbers, and accession numbers of pertinent documents are provided under each subject heading. When the title is insufficiently descriptive of the document content, a title extension is added, separated from the title by three hyphens. The report number helps to indicate the type of document cited (e.g., NASA report, NASA translation, NASA contractor report). The accession number is the number by which the document abstracts are arranged in this journal and by which the document is sold or requested. The page number helps you locate the citation in the abstract section. The titles, with title extensions if present, are arranged under each subject heading in ascending accession number order. The subject headings have been selected from the latest revision of the *NASA Thesaurus*.

A

ABLATION
Erosion of melt layers developed during a plasma disruption
[DE94-018362] p 1144 N95-18547

ABLATIVE MATERIALS
Real-time thickness measurement of MCC ablator material p 972 N95-18981

ABRASION
Quality optimization of thermally sprayed coatings produced by the JP-5000 (HVOF) gun using mathematical modeling p 989 N95-19008

ABRASIVES
Multilayer anti-erosion coatings p 954 N95-19679

ABSORBENTS
Metal-framed partitions with reduced thicknesses. Part 2: Built-in acoustic treatment
[BBC-RD-1993/6-PT-2] p 993 N95-19137

ABSORBERS (MATERIALS)
Standard reference materials: Glass filters as a standard reference material for spectrophotometry. Selection, preparation, certification and use of SRM 930 and SRM 1930
[PB94-188844] p 973 N95-17994
A wideband absorber for television studios
[BBC-RD-1994/12] p 1123 N95-18566
Acoustic properties and durability of liner materials at non-standard atmospheric conditions
[NASA-CR-195010] p 1123 N95-18930
Metal-framed partitions with reduced thicknesses. Part 2: Built-in acoustic treatment
[BBC-RD-1993/6-PT-2] p 993 N95-19137
Performance of an artificial absorber for truncating FEM meshes p 1006 N95-19801

ABSORPTION
The Solvent Absorption-Extractive Distillation (SAED) process for ethanol recovery from gas/vapor streams
[DE94-013112] p 974 N95-18637
High frequency room responses: Acoustic design and the control of stereophonic image quality
[BBC-RD-1994/11] p 1124 N95-19046

ABSORPTION CROSS SECTIONS
Design of spherical aerosol particles to maximize sound attenuation
[AD-A284313] p 1123 N95-18379

ABSORPTION SPECTRA
XAMath: An XAFS analysis package based on Mathematica(tm)
[DE94-016346] p 1100 N95-19397

ABSORPTION SPECTROSCOPY
Silicon carbide photoconductive switches
[AD-A284310] p 1008 N95-18378
X-ray absorption spectroscopy in high temperature oxidation of metals and alloys p 955 N95-19682

ABSORPTIVITY
Visible-infrared remote-sensing model and applications for ocean waters
[NASA-CR-197602] p 1051 N95-18739

ABSTRACTS
Small Business Research Summaries, numbers 51-100
[PB94-179967] p 1170 N95-17986
Small Business Research Summaries, numbers 1-50
[PB94-179959] p 1170 N95-17987

ABUNDANCE
Coronal abundances and their variation
[NASA-CR-197553] p 1195 N95-18376
Cosmic ray models for early galactic lithium, beryllium, and boron production
[NASA-CR-197626] p 1137 N95-18965
Siderophile elements and metal-silicate fractionation in the solar nebula p 1190 N95-19319
Formation of chondrules and CAIs by nebular processes p 1190 N95-19321
Relative elemental abundance and heating constraints determined for the solar corona from SERTS measurements
[NASA-TM-104616] p 1196 N95-19791

ACCELERATED LIFE TESTS
An artifical corrosion protocol for lap-splices in aircraft skin p 937 N95-19482

ACCELERATION
Summary report of mission acceleration measurements for STS-60, SPACEHAB2, launched 11 February 1994
[NASA-TM-106797] p 991 N95-19788

ACCELERATION TOLERANCE
Effects of weight lifting on intrathoracic pressures generated by anti-g straining maneuvers
[AD-A283651] p 1078 N95-18138
Naval Biodynamics Laboratory 1993 command history
[AD-A284358] p 1089 N95-18440

ACCELEROMETERS
The linear dynamics of a microsensor accelerometer modeled as a cantilever beam with an end mass
[DE94-019108] p 1031 N95-17963
Fluid dynamic linear accelerometer
[AD-D016413] p 956 N95-18553
Fiber optic flexural disk accelerometer
[AD-D016444] p 1141 N95-18563
Summary report of mission acceleration measurements for STS-60, SPACEHAB2, launched 11 February 1994
[NASA-TM-106797] p 991 N95-19788

ACCEPTABILITY
Development of an improved ballistic acceptance test for high hard armor steel plate: MIL-A-46100
[ARL-TR-509] p 979 N95-18939

ACCIDENT PREVENTION
Modern transport engine experience with environmental ingestion effects p 951 N95-19660

ACCOMMODATION
Modal Identification Experiment accommodations review
[NASA-CR-195009] p 964 N95-18105

ACCRETION DISKS
Astronomical observations of phenomena in disks p 1178 N95-19301
Models for multiple heating mechanisms p 1188 N95-19303
The early Sun and the formation of chondrules p 1188 N95-19305
Chondrules and their associates in ordinary chondrites p 1188 N95-19306

ACCUMULATIONS
Collection efficiency and ice accretion calculations for a sphere, a swept MS(1)-317 wing, a swept NACA-0012 wing tip, an axisymmetric inlet, and a Boeing 737-300
[NASA-TM-106831] p 933 N95-18582

ACCURACY
Standard reference materials: Glass filters as a standard reference material for spectrophotometry. Selection, preparation, certification and use of SRM 930 and SRM 1930
[PB94-188844] p 973 N95-17994

ACETATES
Ferroelectric thin film bismuth titanate prepared from acetate precursors
[DE95-000538] p 988 N95-19558

ACETIC ACID
Ferroelectric thin film bismuth titanate prepared from acetate precursors
[DE95-000538] p 988 N95-19558

ACETYLENE
Method of lowering the reaction exotherm in thermally polymerized acetylene terminated resins
[AD-D016276] p 985 N95-18430

ACID RAIN
Methane: The other greenhouse gas. Research and policy in the Netherlands
[PB94-207149] p 1058 N95-18375

ACOUSTIC ATTENUATION
Design of spherical aerosol particles to maximize sound attenuation
[AD-A284313] p 1123 N95-18379
Sound speed profiles from vertical array data
[AD-A283978] p 1123 N95-18890
High frequency room responses: Acoustic design and the control of stereophonic image quality
[BBC-RD-1994/11] p 1124 N95-19046
Metal-framed partitions with reduced thicknesses. Part 2: Built-in acoustic treatment
[BBC-RD-1993/6-PT-2] p 993 N95-19137
Acoustic transmission loss and structureborne noise transmission tests on a LASCOR and a reference steel panel
[MRL-TN-623] p 1128 N95-19770

ACOUSTIC DELAY LINES
True time delay beamforming
[AD-A285683] p 1003 N95-19516

ACOUSTIC EMISSION
Acoustic method of damage sensing in composite materials
[NASA-CR-196538] p 969 N95-18135
Nondestructive time-of-capture, location and velocity sensing in intact capture p 1036 N95-19194

ACOUSTIC EXCITATION
Impact of Acoustic Loads on Aircraft Structures
[AGARD-CP-549] p 1124 N95-19142
Nonlinear dynamic response of aircraft structures to acoustic excitation p 946 N95-19151
Acoustics of space structures p 1126 N95-19152
Brite-Euram programme: ACOUFAT acoustic fatigue and related damage tolerance of advanced composite and metallic structures p 1127 N95-19159

ACOUSTIC FATIGUE
Impact of Acoustic Loads on Aircraft Structures
[AGARD-CP-549] p 1124 N95-19142
Current and future problems in structural acoustic fatigue p 1124 N95-19143
High-temperature acoustic test facilities and methods p 1125 N95-19149
Nonlinear dynamic response of aircraft structures to acoustic excitation p 946 N95-19151
Application of the PSD technique to acoustic fatigue stress calculations in complex substructures p 1126 N95-19155
Acoustic fatigue testing on different materials and skin-stringer elements p 1126 N95-19156
Acoustic fatigue characteristics of advanced materials and structures p 1126 N95-19157
Acoustic fatigue of carbon fibre structures p 1127 N95-19158

Brite-Euram programme: ACOUFAT acoustic fatigue and related damage tolerance of advanced composite and metallic structures p 1127 N95-19159
Acoustic fatigue behaviour of GLARE composites p 1127 N95-19160
Thermo-acoustic fatigue design for hypersonic vehicle skin panels p 1047 N95-19161
Application of superplastically formed and diffusion bonded structures in high intensity noise environments p 1127 N95-19162

ACOUSTIC IMAGING
Echo imaging techniques determine the size of intravascular bubbles in decompression sickness
[AD-A284849] p 1087 N95-19714

ACOUSTIC IMPEDANCE
Transducer array interaction modeling using variational principles
[AD-A285687] p 1128 N95-19514

ACOUSTIC MEASUREMENT
Imagery correction for atmospheric effects using sounding data
[INPE-5506-TDI/518] p 1064 N95-18390
Calibration and sediment load algorithms for an acoustic sediment flux probe
[AD-A283655] p 1075 N95-18617
Maximal-length sequence methods: Acoustic measurements in the presence of high levels of extraneous noise
[BBC-RD-1994/5] p 1001 N95-19049
Identification and analysis of air- and structure-borne noise and vibration paths p 1128 N95-19166

ACOUSTIC MICROSCOPES
Tunneling acoustic microscopy
[AD-A279160] p 1128 N95-19802

ACOUSTIC PROPAGATION
Acoustic transmission loss and structureborne noise transmission tests on a LASCOR and a reference steel panel
[MRL-TN-623] p 1128 N95-19770

ACOUSTIC PROPERTIES
Coastal acoustic tomography data constraints applied to a coastal ocean circulation model
[AD-A283911] p 1074 N95-18153
Acoustic properties and durability of liner materials at non-standard atmospheric conditions
[NASA-CR-195010] p 1123 N95-18930
Materials for adaptive structural acoustic control, volume 3
[AD-A279223] p 1128 N95-19850

ACOUSTIC SCATTERING
Time spread and frequency coherence in acoustic forward scattering from the sea surface
[AD-A284736] p 1123 N95-18083

ACOUSTIC SIMULATION
Design and operation of a thermoacoustic test facility p 960 N95-19150

ACOUSTIC VELOCITY
Sound speed profiles from vertical array data
[AD-A283978] p 1123 N95-18890
The STOKES (Version 4) normal-mode shallow water transmission loss program
[MRL-CP-1] p 1075 N95-19503

ACOUSTICS
Improved efficiency and power density for thermoacoustic coolers
[AD-A283946] p 992 N95-18165
A wideband absorber for television studios
[BBC-RD-1994/12] p 1123 N95-18566
High frequency room responses: Acoustic design and the control of stereophonic image quality
[BBC-RD-1994/11] p 1124 N95-19046
Materials for adaptive structural acoustic control, volume 3
[AD-A279223] p 1128 N95-19850

ACOUSTO-OPTICS
Error measurements in an Acousto-Optic Tunable Filter-Fiber Bragg Grating Sensor System
[AD-A283912] p 1139 N95-18154
Fiber optic pressure and/or vibration detector
[AD-D016474] p 1140 N95-18460
True time delay beamforming
[AD-A285683] p 1003 N95-19516

ACQUIRED IMMUNODEFICIENCY SYNDROME
Clinical basis for aeromedical decisions in aircrew HIV positive p 1086 N95-19440

ACRYLIC ACID
Obtention of cationic polymeric membranes by radiation-induced grafting method
[DE94-629193] p 983 N95-17942

ACRYLIC RESINS
Optical measurements in rocket engine liquid sprays p 968 N95-18979
Macromolecular characterization and solution behavior of polymer additives
[AD-A284845] p 988 N95-19696

ACTIVATED CARBON
Controlling combustion-source emissions at Air Force sites with a new filter concept, phase 1
[AD-A283674] p 1058 N95-18140

ACTIVATION
Compact, efficient, scalable neodymium laser co-doped with activator ions and pumped by visible laser diodes
[AD-D016237] p 1038 N95-18585

ACTIVATION ENERGY
Reaction channel competition in vibrational overtone activation: 1-methylcyclopropene
[AD-A280185] p 976 N95-19830

ACTIVE CONTROL
Streamlined design and self reliant hardware for active control of precision space structures
[NASA-CR-4637] p 964 N95-18580
Annual Allerton Conference on Communication, Control and Computing
[AD-A283892] p 1114 N95-18675
Active control of instabilities in laminar boundary-layer flow. Part 1: An overview
[NASA-CR-195016-PT-1] p 1020 N95-18958
Helicopter internal noise p 1124 N95-19144

ACTIVE GALACTIC NUCLEI
An optical study of compact steep spectrum radio sources p 1179 N95-18498

ACTUATORS
Mathematical analysis of actuator forces in a scissor lift
[AD-A283906] p 1040 N95-18152
Applications catalog of pyrotechnically actuated devices/systems
[NASA-TM-106810] p 962 N95-18387
A new piston control strategy for segmented mirrors p 1115 N95-18999
Materials for adaptive structural acoustic control, volume 3
[AD-A279223] p 1128 N95-19850

ADAPTATION
Adaptive robot path planning in changing environments
[DE94-016564] p 1112 N95-17948
Adaptive wind tunnel walls versus wall interference correction methods in 2D flows at high blockage ratios p 960 N95-19267

ADAPTERS
Disengagable adapter for an optical fiber connection
[AD-D016231] p 1141 N95-18628

ADAPTIVE CONTROL
Real-time adaptive control of mixing in a plane shear layer
[AD-A285541] p 1018 N95-18469
A new piston control strategy for segmented mirrors p 1115 N95-18999
Adaptive detection and copy of coherent narrowband waveforms with uncalibrated arrays
[AD-A285125] p 1004 N95-19594
Materials for adaptive structural acoustic control, volume 3
[AD-A279223] p 1128 N95-19850

ADAPTIVE FILTERS
Locally connected adaptive Gabor filter for real-time motion compensation
[AD-A285726] p 1009 N95-18485
Lossless compression of weight vectors from an adaptive filter
[DE94-017350] p 1174 N95-18873
Adaptive detection and copy of coherent narrowband waveforms with uncalibrated arrays
[AD-A285125] p 1004 N95-19594

ADAPTIVE OPTICS
A comparison between using incoherent or coherent sources to align and test an adaptive optical telescope p 1142 N95-18969
A new piston control strategy for segmented mirrors p 1115 N95-18999

ADDITIVES
DC-conductivity and magnetoresistance of inherently conducting polymers. Polyacetylene and poly(3-alkylthiophenes)
[PB94-184587] p 1007 N95-18037
Evaluation of an unlighted swinging airport sign
[AD-A284763] p 958 N95-18087
Method of doping single crystal diamond for electronic devices
[AD-D016267] p 1149 N95-18543
Method for fabricating complementary enhancement and depletion mode field effect transistors on a single substrate
[AD-D016270] p 1010 N95-18546
Macromolecular characterization and solution behavior of polymer additives
[AD-A284845] p 988 N95-19696
Polymer based materials for additive processing of high temperature electronics packaging
[AD-A285962] p 988 N95-19745

ADDUCTS
Synthesis and characterization of a neutral six-coordinate tris-adduct of an indium(3) trihalide. X ray crystal structure of InCl3(THF)3
[AD-A279169] p 1154 N95-19806
Synthesis and characterization of aluminum-phosphorus adducts: X-ray crystal structures of Cl3Al (dot) P(SiMe3)3 (dot) C7H8 and Br3Al (dot) P(SiMe3)3 (dot) C7H8
[AD-A279194] p 1154 N95-19812

ADHESION
Method of making a membrane having hydrophilic and hydrophobic surfaces for adhering cells or antibodies by using atomic oxygen or hydroxyl radicals
[NASA-CASE-MSC-21529-1] p 983 N95-18134
Adhesion, friction, and wear behavior of clean metal-ceramic couples
[NASA-TM-106815] p 989 N95-19783
Use of titanate coupling agents in Kevlar (trade name)/phenolic composites
[AD-A279200] p 972 N95-19814

ADHESION TESTS
A constant-depth scratch test for the measurement of adhesion at film-substrate interfaces
[AD-A283660] p 983 N95-18016
Method and device for determining bond separation strength using induction heating
[NASA-CASE-LAR-14678-1] p 960 N95-18961

ADHESIVE BONDING
A constant-depth scratch test for the measurement of adhesion at film-substrate interfaces
[AD-A283660] p 983 N95-18016
Ultrasonic techniques for repair of aircraft structures with bonded composite patches p 937 N95-19486

ADSORPTION
Application of conducting polymers to electroanalysis
[DE94-015204] p 984 N95-18348
Surface phases, surface defects and the initial stages of oxidation
[DE94-016947] p 979 N95-18358
An atomic view of motion on surfaces
[AD-A285565] p 1131 N95-18473
Development of a colloidal redox system containing a smectite clay for control of reactivity and reaction selectivity
[AD-A285958] p 974 N95-19515

ADVANCED VERY HIGH RESOLUTION RADIOMETER
Multispectral NOAA Marine Atmospheric Boundary Layer (MABL) estimates during VOCAR
[AD-A283702] p 1064 N95-18623

ADVECTION
A numerical simulation of seasonal circulation in the South China Sea
[AD-A283701] p 1075 N95-18622

AERIAL PHOTOGRAPHY
Thematic classification of zone coastal: A methodologic contribution
[INPE-5586-TDI/548] p 1050 N95-18215

AEROACOUSTICS
Evaluation of boundary conditions for computational aeroacoustics
[NASA-TM-109989] p 1015 N95-18149
On the Lighthill relationship and sound generation from isotropic turbulence
[NASA-CR-195005] p 1016 N95-18191
Aeroacoustic qualification of HERMES shingles p 1125 N95-19145
Weapons bay acoustic environment p 1125 N95-19146
Impact of noise environment on engine nacelle design p 1125 N95-19147
Impact of dynamic loads on propulsion integration p 1125 N95-19148
Modelling structurally damaging twin-jet screech p 946 N95-19154
Identification and analysis of air- and structure-borne noise and vibration paths p 1128 N95-19166
Unsteady aerodynamic analyses for turbomachinery aeroelastic predictions p 949 N95-19381

AEROBES
The cross-validation of the United States Air Force submaximal cycle ergometer test to estimate aerobic capacity
[AD-A284055] p 1079 N95-18661

AERODYNAMIC CHARACTERISTICS
Documentation and archiving of the Space Shuttle wind tunnel test data base. Volume 1: Background and description
[NASA-TM-104806-VOL-1] p 965 N95-19237
Aerodynamic investigation of the flow field in a 180 deg turn channel with sharp bend p 1021 N95-19257
Interaction of a three strut support on the aerodynamic characteristics of a civil aviation model p 933 N95-19279

Documentation and archiving of the Space Shuttle wind tunnel test data base. Volume 2: User's Guide to the Archived Data Base
[NASA-TM-104806-VOL-2] p 965 N95-19624
Evidence that aerodynamic effects, including dynamic stall, dictate HAWT structural loads and power generation in highly transient time frames
[DE94-011865] p 1054 N95-19855

AERODYNAMIC COEFFICIENTS
Sectional prediction of 3D effects for separated flow on rotating blades
[PB94-201696] p 928 N95-18503
Static aerodynamics CFD analysis for 120-mm hypersonic KE projectile design
[ARL-MR-184] p 929 N95-18611
Dynamic Stability Instrumentation System (DSIS). Volume 1: Hardware description
[NASA-TM-109160-VOL-1] p 1099 N95-18899
2-D and 3-D oscillating wing aerodynamics for a range of angles of attack including stall
[NASA-TM-4632] p 931 N95-19119

AERODYNAMIC CONFIGURATIONS
A selection of experimental test cases for the validation of CFD codes. Supplement: Datasets A-E
[AGARD-AR-303-SUPPL] p 929 N95-18539
Documentation and archiving of the Space Shuttle wind tunnel test data base. Volume 1: Background and description
[NASA-TM-104806-VOL-1] p 965 N95-19237
Interference corrections for a centre-line plate mount in a porous-walled transonic wind tunnel
p 933 N95-19280
Panel methods p 1027 N95-19448
Documentation and archiving of the Space Shuttle wind tunnel test data base. Volume 2: User's Guide to the Archived Data Base
[NASA-TM-104806-VOL-2] p 965 N95-19624
A 20k payload launch vehicle fast track development concept using an RD-180 engine and a Centaur upper stage
[NASA-TM-108475] p 963 N95-19648
The aerodynamic design of an integrated wing lower surface and pylons for reduced drag
[ARA-MEMO-406] p 946 N95-19789

AERODYNAMIC DRAG
Experimental techniques for measuring transonic flow with a three dimensional laser velocimetry system. Application to determining the drag of a fuselage
p 1022 N95-19258
An investigation of drag repeatability in half model testing in the ARA Transonic Wind Tunnel
[ARA-MEMO-392] p 931 N95-19546
The aerodynamic design of an integrated wing lower surface and pylons for reduced drag
[ARA-MEMO-406] p 946 N95-19789

AERODYNAMIC FORCES
Hydrofoil force balance
[AD-D016475] p 1033 N95-18461
Gyroscopic and propeller aerodynamic effects on engine mounts dynamic loads in turbulence conditions
p 946 N95-18599

AERODYNAMIC HEAT TRANSFER
Documentation and archiving of the Space Shuttle wind tunnel test data base. Volume 1: Background and description
[NASA-TM-104806-VOL-1] p 965 N95-19237
Documentation and archiving of the Space Shuttle wind tunnel test data base. Volume 2: User's Guide to the Archived Data Base
[NASA-TM-104806-VOL-2] p 965 N95-19624

AERODYNAMIC INTERFERENCE
Background noise levels measured in the NASA Lewis 9- by 15-foot low-speed wind tunnel
[NASA-TM-106817] p 958 N95-18054
Wall Interference, Support Interference and Flow Field Measurements
[AGARD-CP-535] p 1020 N95-19251
The crucial role of wall interference, support interference and flow field measurements in the development of advanced aircraft configurations p 1021 N95-19252
Boundary-flow measurement methods for wall interference assessment and correction: Classification and review p 1022 N95-19262
Estimating wind tunnel interference due to vectored jet flows p 1023 N95-19265
Adaptive wind tunnel walls versus wall interference correction methods in 2D flows at high blockage ratios
p 960 N95-19267
Interference determination for wind tunnels with slotted walls p 960 N95-19269
Transonic wind tunnel boundary interference correction p 960 N95-19271
Calculation of low speed wind tunnel wall interference from static pressure pipe measurements
p 1024 N95-19273
The traditional and new methods of accounting for the factors distorting the flow over a model in large transonic wind tunnels p 1025 N95-19275
Calculation of wall effects of flow on a perforated wall with a code of surface singularities
p 1025 N95-19277
Evaluation of combined wall- and support-interference on wind tunnel models p 932 N95-19278
Interaction of a three strut support on the aerodynamic characteristics of a civil aviation model
p 933 N95-19279

AERODYNAMIC LOADS
Aircraft Loads due to Turbulence and their Impact on Design and Certification
[AGARD-R-798] p 956 N95-18597
Design limit loads based upon statistical discrete gust methodology p 946 N95-18603
Pressure measurements on an F/A-18 twin vertical tail in buffeting flow. Volume 4, part 2: Buffet cross spectral densities
[AD-A285555] p 957 N95-18641
Wind turbine blade aerodynamics: The combined experiment
[DE94-011866] p 929 N95-18645
Wind turbine blade aerodynamics: The analysis of field test data
[DE94-011867] p 929 N95-18646
Determination of stores pointing error due to wing flexibility under flight load
[NASA-TM-4646] p 945 N95-19044
The accuracy of parameter estimation in system identification of noisy aircraft load measurement
[NASA-CR-197516] p 945 N95-19130
Brite-Euram programme: ACOUFAT acoustic fatigue and related damage tolerance of advanced composite and metallic structures p 1127 N95-19159
Prediction of fatique crack growth under flight-simulation loading with the modified CORPUS model
p 934 N95-19471
Development of load spectra for Airbus A330/A340 full scale fatigue tests p 936 N95-19479

AERODYNAMIC NOISE
On the Lighthill relationship and sound generation from isotropic turbulence
[NASA-CR-195005] p 1016 N95-18191

AERODYNAMIC STABILITY
A spectrally accurate boundary-layer code for infinite swept wings
[NASA-CR-195014] p 1014 N95-18042
Integrated aerodynamic fin and stowable TVC vane system
[AD-D016457] p 967 N95-19073
Determination of stability and control derivatives from the NASA F/A-18 HARV from flight data using the maximum likelihood method
[NASA-CR-197320] p 958 N95-19576

AERODYNAMIC STALLING
Numerical simulation of dynamic-stall suppression by tangential blowing
[AD-A284887] p 931 N95-19110
2-D and 3-D oscillating wing aerodynamics for a range of angles of attack including stall
[NASA-TM-4632] p 931 N95-19119
Evidence that aerodynamic effects, including dynamic stall, dictate HAWT structural loads and power generation in highly transient time frames
[DE94-011865] p 1054 N95-19855

AERODYNAMICS
Parachute inflation: A problem in aeroelasticity
[AD-A284375] p 928 N95-18340
Remote sensing/global change. A special bibliography
[NASA-TM-110038] p 1060 N95-18742
Aeronautical engineering: A continuing bibliography with indexes (supplement 313)
[NASA-SP-7037(313)] p 927 N95-19168
Aeronautical engineering: A continuing bibliography with indexes (supplement 314)
[NASA-SP-7037(314)] p 927 N95-19357
CFD: Advances and Applications, part 1
[NAL-SP-9322-PT-1] p 1026 N95-19444

AEROELASTICITY
Parachute inflation: A problem in aeroelasticity
[AD-A284375] p 928 N95-18340
A linear system identification and validation of an AH-64 Apache aeroelastic simulation model
p 959 N95-18903
Unsteady aerodynamic analyses for turbomachinery aeroelastic predictions p 949 N95-19381

AEROEMBOLISM
Echo imaging techniques determine the size of intravascular bubbles in decompression sickness
[AD-A284849] p 1087 N95-19714

AEROGELS
The use of silica aerogel to collect interplanetary dust in space p 989 N95-19197

AERONAUTICAL ENGINEERING
Aeronautical engineering: A continuing bibliography with indexes (supplement 313)
[NASA-SP-7037(313)] p 927 N95-19168
Aeronautical engineering: A continuing bibliography with indexes (supplement 314)
[NASA-SP-7037(314)] p 927 N95-19357

AERONAUTICS
Aeronautical engineering: A continuing bibliography with indexes (supplement 314)
[NASA-SP-7037(314)] p 927 N95-19357

AEROSOLS
Midinfrared optical properties of petroleum oil aerosols
[AD-A283689] p 1139 N95-18142
Design of spherical aerosol particles to maximize sound attenuation
[AD-A284313] p 1123 N95-18379
Trends 1993: A compendium of data on global change
[ORNL/CDIAC-65] p 1058 N95-18389
Atmospheric chemistry of biogenic sulfur in the Southern Hemisphere p 1071 N95-18399
Shock-induced devolatization of calcium sulfate and implications for K-T extinctions
[NASA-CR-197608] p 1060 N95-19033

AEROSPACE ENGINEERING
NASA/DOD Aerospace Knowledge Diffusion Research Project. Paper 47: The value of computer networks in aerospace
[NASA-CR-197591] p 1109 N95-18055
NASA/ASEE Summer Faculty Fellowship Program. 1994 research reports
[NASA-CR-197448] p 1157 N95-18166
NASA High Performance Computing and Communications program
[NASA-TM-4653] p 1174 N95-18573
Remote sensing/global change. A special bibliography
[NASA-TM-110038] p 1060 N95-18742
NASA/DOD Aerospace Knowledge Diffusion Research Project. Report 26: The technical communication practices of aerospace engineering students: Results of the phase 3 AIAA National Student Survey
[NASA-TM-109121] p 1175 N95-18950
NASA/DOD Aerospace Knowledge Diffusion Research Project. Report 29: A comparison of the technical communications practices of Japanese and US aerospace engineers and scientists
[NASA-TM-109164] p 1175 N95-18953
Research reports: 1994 NASA/ASEE Summer Faculty Fellowship Program
[NASA-CR-196533] p 1161 N95-18967
NASA/DOD Aerospace Knowledge Diffusion Research Project. Paper 46: Technical communications in aerospace: A comparison across four countries
[NASA-TM-110056] p 1175 N95-19038
NASA/DOD Aerospace Knowledge Diffusion Research Project. Paper 45: A comparison of the information-seeking behaviors of three groups of US aerospace engineers
[NASA-TM-109839] p 1176 N95-19127
NASA Lewis Research Center Workshop on Forced Response in Turbomachinery
[NASA-CP-10147] p 949 N95-19380

AEROSPACE ENVIRONMENTS
Summary report of mission acceleration measurements for STS-60, SPACEHAB2, launched 11 February 1994
[NASA-TM-106797] p 991 N95-19788

AEROSPACE INDUSTRY
European aeronautics: Strong government presence in industry structure and research and development support. Report to Congressional Requesters
[GAO/NSIAD-94-71] p 1171 N95-18578
Split mandrel versus split sleeve coldworking: Dual methods for extending the fatigue life of metal structures
p 940 N95-19500

AEROSPACE MEDICINE
Naval Biodynamics Laboratory 1993 command history
[AD-A284358] p 1089 N95-18440
US experiments flown on the Soviet biosatellite Cosmos 2044. Volume 1: Mission description, experiments K-7-01 - K-7-15
[NASA-TM-108802-VOL-1] p 1092 N95-18569
Effect of heat acclimation on sitting orthostatic tolerance in the heat after 48 and 96 hour bed rest in men
[NASA-TM-108861] p 1077 N95-18734
Drink composition and cycle-ergometer endurance in men: Carbohydrate, Na(+), osmolality
[NASA-TM-4650] p 1077 N95-19140
Aerospace medicine and biology: A continuing bibliography with indexes (supplement 398)
[NASA-SP-7011(398)] p 1080 N95-19239
The Clinical Basis for Aeromedical Decision Making
[AGARD-CP-553] p 1080 N95-19413
Aeromedical risk management for aircrew
p 1080 N95-19414
The way to waivers in the BAF p 1081 N95-19415
The waiver process and disqualifying medical conditions in US Naval aviation personnel p 1081 N95-19416

The effect of special boards of flight surgeons on the evolution of US Naval flight standards
p 1081 N95-19417
Fit to fly: Analysis of the aeromedical disposition in aircrewmembers of the Spanish Armed Forces
p 1081 N95-19418
AMDRS: A resource for intelligent aeromedical decision-making p 1082 N95-19419
Relevance of laboratory tests in aeromedical decisions p 1082 N95-19420
TSH determination in subjects with medium-low levels of serum thyroxine p 1082 N95-19421
EKG in flight: Usefulness and limits for aircrew rehabilitation p 1082 N95-19422
Evaluation of the EKG's isoelectric T wave in Air Force pilots p 1082 N95-19423
The concept of aeronautical adaptability as developed by the US Navy p 1083 N95-19426
The NAMI syncope test battery and clinical decision-making in aviators with syncope
p 1083 N95-19428
Neuropsychophysiologic sequelae of mild head injury
p 1083 N95-19430
Neurological decision making in aviation medicine based on electrophysiological methods p 1084 N95-19431
Clinical basis for aeromedical decision-making: The EEG example p 1084 N95-19433
The aeromedical implications of supraventricular tachycardia p 1085 N95-19437
Sarcoidosis in US military aviators
p 1085 N95-19438
The aeromedical risk associated with asymptomatic cholelithiasis in USAF pilots and navigators
p 1085 N95-19439
Clinical basis for aeromedical decisions in aircrew HIV positive p 1086 N95-19440
Color vision issues in modern military aviation or the search for the Abominable Coneman
p 1086 N95-19441
Photorefractive Keratectomy (PRK) in the military aviator: An aeromedical expose p 1086 N95-19442
Medication in the course of active flying duty
p 1086 N95-19443
Aerospace medicine and biology: A continuing bibliography with indexes (supplement 397)
[NASA-SP-7011(397)] p 1087 N95-19746

AEROSPACE SYSTEMS
Conference on Aerospace Transparent Materials and Enclosures, volume 1
[AD-A283925] p 944 N95-18677

AEROSPACE TECHNOLOGY TRANSFER
NASA/DOD Aerospace Knowledge Diffusion Research Project. Paper 45: A comparison of the information-seeking behaviors of three groups of US aerospace engineers
[NASA-TM-109839] p 1176 N95-19127

AEROSPACE VEHICLES
Communication with reentry vehicle through modulated plasma
[AD-D016476] p 997 N95-18462
Environmental effects on composite airframes: A study conducted for the ARM UAV Program (Atmospheric Radiation Measurement Unmanned Aerospace Vehicle)
[DE94-015351] p 971 N95-19579

AEROTHERMODYNAMICS
Hypersonic wind tunnel test techniques
[AD-A284057] p 929 N95-18663
Design and operation of a thermoacoustic test facility
p 960 N95-19150
Thermo-acoustic fatigue design for hypersonic vehicle skin panels p 1047 N95-19161
Aero-thermodynamic distortion induced structured dynamic response
[AD-A279931] p 955 N95-19864

AEROZINE
Regenerative cooling for liquid propellant rocket thrust chambers
[INPE-5565-TDI/540] p 967 N95-18720

AFFINITY
The Solvent Absorption-Extractive Distillation (SAED) process for ethanol recovery from gas/vapor streams
[DE94-013112] p 974 N95-18637

AFRICA
Climate and weather of Central Africa. Executive summary
[AD-A283647] p 1067 N95-18014

AFTERBODIES
Numerical computations of supersonic base flow with special emphasis on turbulence modeling
[AD-A283688] p 930 N95-18670
Transonic and supersonic flowfield measurements about axisymmetric afterbodies for validation of advanced CFD codes p 932 N95-19260
Evaluation of three turbulence models for afterbody/jet flows, including Reynolds stress closure
[ARA-90] p 932 N95-19574
Evaluation of three turbulence models for afterbody/jet flows, including Reynolds stress closure
[ARA-MEMO-408] p 1194 N95-19773

AGE FACTOR
Age 60 study. Part 3: Consolidated database experiments
[AD-A286247] p 1080 N95-19384
Age 60 study. Part 4: Experimental evaluation of pilot performance
[AD-A286248] p 1080 N95-19385

AGENA ROCKET VEHICLES
Gemini 8, This is Houston, flight
[NASA-TM-110490] p 965 N95-19039

AGGLOMERATION
Constraints on chondrule agglomeration from fine-grained chondrule rims p 1189 N95-19315
Implications for the evolution of chondrules from Agglomeratic olivine chondrules p 1193 N95-19335

AGGREGATES
Mechanisms of interaction and biological effects of extremely-low-frequency electromagnetic fields
[DE94-015200] p 1076 N95-18371

AGING (BIOLOGY)
Age 60 study. Part 3: Consolidated database experiments
[AD-A286247] p 1080 N95-19384
Age 60 study. Part 4: Experimental evaluation of pilot performance
[AD-A286248] p 1080 N95-19385

AGING (MATERIALS)
Complex oxidation effects in polymer degradation
[DE94-018903] p 986 N95-18651
Thermo-oxidative stability of graphite/PMR-15 composites: Effect of fiber surface modification on composite shear properties
[NASA-TM-4608] p 981 N95-19652

AH-64 HELICOPTER
A linear system identification and validation of an AH-64 Apache aeroelastic simulation model
p 959 N95-18903

AIR CARGO
Transport aircraft loading and balancing system: Using a CLIPS expert system for military aircraft load planning
p 1105 N95-19751

AIR CURRENTS
Advanced diesel electronic fuel injection and turbocharging
[AD-A279176] p 1043 N95-19809

AIR FILTERS
Controlling combustion-source emissions at Air Force sites with a new filter concept, phase 1
[AD-A283674] p 1058 N95-18140
Improved filtration materials and modeling
[AD-A284684] p 1091 N95-18531

AIR FLOW
The stability of two-phase flow over a swept-wing
[NASA-CR-194994] p 1016 N95-18190
A selection of experimental test cases for the validation of CFD codes. Supplement: Datasets A-E
[AGARD-AR-303-SUPPL] p 929 N95-18539
Hypervelocity air flows with finite rate chemistry
[AD-A284727] p 931 N95-19109
VENTCF2: An algorithm and associated FORTRAN 77 subroutine for calculating flow through a horizontal ceiling/floor vent in a zone-type compartment fire model
[PB94-210127] p 993 N95-19402
An investigation of drag repeatability in half model testing in the ARA Transonic Wind Tunnel
[ARA-MEMO-392] p 931 N95-19546
Prediction of wind tunnel effects on the installed F/A-18A inlet flow field at high angles-of-attack
[NASA-CR-195429] p 950 N95-19651

AIR INTAKES
Protective coatings for compressor gas path components p 954 N95-19675

AIR POLLUTION
Potential impacts on air quality of the use of ethanol as an alternative fuel
[DE94-011881] p 1056 N95-17944
Application of conducting polymers to electroanalysis
[DE94-015204] p 984 N95-18348
Methane: The other greenhouse gas. Research and policy in the Netherlands
[PB94-207149] p 1058 N95-18375
A model study of the influence of NMHC and NO(x) emissions on rural O3 concentrations in Georgiargia
p 1059 N95-18445
Atmospheric effects of high-flying subsonic aircraft: A catalogue of perturbing influences
[KNMI-SR-94-03] p 1060 N95-18722
Economic impact analysis for proposed emission standards and guidelines for municipal waste combustors: A description of the basis for, and impacts of, proposed revisions to air pollutant emission regulations for new and existing municipal waste combustors under Clean Air Act Sections 111(b), 111(d), and 129
[PB94-213543] p 1061 N95-19403
Alternative control techniques document: NO(x) emissions from glass manufacturing
[PB94-214079] p 1061 N95-19406
Air pollution mitigation measures for airports and associated activity
[PB94-207610] p 1061 N95-19582
Damage of high temperature components by dust-laden air p 953 N95-19673
Gas turbine compressor corrosion and erosion in Western Europe p 954 N95-19678
Developing an emission factor for hazardous air pollutants for an F-16 using JP-8 fuel
[AD-A284802] p 1061 N95-19685

AIR QUALITY
Potential impacts on air quality of the use of ethanol as an alternative fuel
[DE94-011881] p 1056 N95-17944
Economic impact analysis for proposed emission standards and guidelines for municipal waste combustors: A description of the basis for, and impacts of, proposed revisions to air pollutant emission regulations for new and existing municipal waste combustors under Clean Air Act Sections 111(b), 111(d), and 129
[PB94-213543] p 1061 N95-19403

AIR SAMPLING
Atmospheric chemistry of biogenic sulfur in the Southern Hemisphere p 1071 N95-18399

AIR TO SURFACE MISSILES
Application of photogrammetry of F-14D store separation
[AD-A284154] p 943 N95-18417

AIR TRAFFIC
Atmospheric effects of high-flying subsonic aircraft: A catalogue of perturbing influences
[KNMI-SR-94-03] p 1060 N95-18722
On-line handling of air traffic: Management, guidance and control
[AGARD-AG-321] p 941 N95-18927

AIR TRAFFIC CONTROL
Heliport/vertiport MLS precision approaches
[AD-A283505] p 940 N95-18059
An analysis of tower (local) controller-pilot voice communications
[AD-A283718] p 996 N95-18436
On-line handling of air traffic: Management, guidance and control
[AGARD-AG-321] p 941 N95-18927

AIR TRAFFIC CONTROLLERS (PERSONNEL)
Implementation of the 1992 Terminal area-Local Analysis and Prediction System (T-LAPS)
[AD-A284334] p 1070 N95-18384
An analysis of tower (local) controller-pilot voice communications
[AD-A283718] p 996 N95-18436

AIR WATER INTERACTIONS
Storm activity over the North Sea and the Netherlands in two climate models compared with observations
[KNMI-WR-94-02] p 1070 N95-18393
The numerical simulation of marine boundary layer clouds
[AD-A284149] p 1064 N95-18413
Marine boundary layer refractive effects in the infrared
[AD-A285717] p 1140 N95-18484
Multispectral NOAA Marine Atmospheric Boundary Layer (MABL) estimates during VOCAR
[AD-A283702] p 1064 N95-18623
The role of large-scale, extratropical dynamics in climate change
[DE94-017651] p 1059 N95-18665

AIRBORNE EQUIPMENT
An airborne monitoring system for FOD and erosion faults p 953 N95-19668

AIRBORNE SURVEILLANCE RADAR
AN/APS-137 Forward Looking Airborne Radar (FLAR) evaluation
[AD-A284672] p 1002 N95-19087

AIRCRAFT ACCIDENT INVESTIGATION
Spectrogram diagnosis of aircraft disasters
p 940 N95-19167
Special investigation report: Maintenance anomaly resulting in dragged engine during landing rollout. Northwest Airlines Flight 18, Boeing 747-251B, N637US, New Tokyo International Airport, Narita, Japan, 1 Mar. 1994
[PB94-917006] p 940 N95-19793

AIRCRAFT ACCIDENTS
Spectrogram diagnosis of aircraft disasters
p 940 N95-19167

Age 60 study. Part 3: Consolidated database experiments
[AD-A286247] p 1080 N95-19384
Toward a new national weather service: Weather for those who fly
[PB94-214418] p 1072 N95-19407
Is the pilot fit for flying after an accident? p 1083 N95-19425
The concept of aeronautical adaptability as developed by the US Navy p 1083 N95-19426
Special investigation report: Maintenance anomaly resulting in dragged engine during landing rollout. Northwest Airlines Flight 18, Boeing 747-251B, N637US, New Tokyo International Airport, Narita, Japan, 1 Mar. 1994
[PB94-917006] p 940 N95-19793

AIRCRAFT ANTENNAS
Design considerations for an archimedean slot spiral antenna p 1006 N95-19798

AIRCRAFT COMPARTMENTS
Helicopter internal noise p 1124 N95-19144
Weapons bay acoustic environment p 1125 N95-19146
Noise transmission and reduction in turboprop aircraft p 1127 N95-19164

AIRCRAFT CONFIGURATIONS
Comparison of stochastic and deterministic nonlinear gust analysis methods to meet continuous turbulence criteria p 946 N95-18602
Panel methods p 1027 N95-19448
Validation and evaluation of the advanced aeronautical CFD system SAUNA: A method developer's view
[ARA-MEMO-390] p 1030 N95-19774
Verification of the CFD simulation system SAUNA for complex aircraft configurations
[ARA-MEMO-401] p 1031 N95-19776
Inviscid and viscous flow modelling of complex aircraft configurations using the CFD simulation system sauna
[ARA-MEMO-403] p 1031 N95-19777

AIRCRAFT CONSTRUCTION MATERIALS
Influence of high pressure hydrogen environment on creep deformation of Mo-Re, Haynes 188, and NARloy-Z alloys
[NASA-CR-197572] p 978 N95-18046
Conference on Aerospace Transparent Materials and Enclosures. Volume 2: Sessions 5-9
[AD-A283926] p 942 N95-18162
Conference on Aerospace Transparent Materials and Enclosures, volume 1
[AD-A283925] p 944 N95-18677
Acoustic fatigue behaviour of GLARE composites p 1127 N95-19160
Thermo-acoustic fatigue design for hypersonic vehicle skin panels p 1047 N95-19161

AIRCRAFT CONTROL
Plant and controller optimization by convex methods
[AD-A283700] p 944 N95-18621
Fiber Optic Control System integration for advanced aircraft. Electro-optic and sensor fabrication, integration, and environmental testing for flight control systems: Laboratory test results
[NASA-CR-195408] p 1034 N95-18938
Fiber Optic Control System integration for advanced aircraft. Electro-optic and sensor fabrication, integration, and environmental testing for flight control systems
[NASA-CR-191194] p 1034 N95-19236
Determination of stability and control derivatives from the NASA F/A-18 HARV from flight data using the maximum likelihood method
[NASA-CR-197320] p 958 N95-19576
The use of genetic algorithms for flight test and evaluation of artificial intelligence and complex software systems
[AD-A284824] p 1104 N95-19688
Automation of hardware-in-the-loop testing of control systems for unmanned air vehicles
[AD-A284833] p 945 N95-19693
Airship applications of modern flight test techniques
[AD-A284253] p 945 N95-19731

AIRCRAFT DESIGN
Wing design for a civil tiltrotor transport aircraft
[NASA-CR-197523] p 942 N95-18090
Aircraft Loads due to Turbulence and their Impact on Design and Certification
[AGARD-R-798] p 956 N95-18597
Design limit loads based upon statistical discrete gust methodology p 946 N95-18603
A review of gust load calculation methods at de Havilland p 932 N95-18604
Ageing nuclear power plant management: An aeronautical viewpoint
[NAL-PD-SN-9306] p 927 N95-18606
Course module for AA201: Wing structural design project
[AD-A283618] p 944 N95-18616
Plant and controller optimization by convex methods
[AD-A283700] p 944 N95-18621
E-6A hardness assurance, maintenance and surveillance program
[AD-A283994] p 945 N95-19067
Impact of noise environment on engine nacelle design p 1125 N95-19147
Modelling structurally damaging twin-jet screech p 946 N95-19154
Proceedings of the USAF Structural Integrity Program Conference
[AD-A285684] p 945 N95-19517
The Computer Aided Aircraft-design Package (CAAP) p 1106 N95-19759
The aerodynamic design of an integrated wing lower surface and pylons for reduced drag
[ARA-MEMO-406] p 946 N95-19789

AIRCRAFT ENGINES
Gyroscopic and propeller aerodynamic effects on engine mounts dynamic loads in turbulence conditions p 946 N95-18599
Wave cycle design for wave rotor engines with limited nitrogen oxide emissions p 1041 N95-18901
Quality optimization of thermally sprayed coatings produced by the JP-5000 (HVOF) gun using mathematical modeling p 989 N95-19008
Mathematical Models of Gas Turbine Engines and their Components
[AGARD-LS-198] p 948 N95-19017
Proceedings of the USAF Structural Integrity Program Conference
[AD-A285684] p 945 N95-19517
Air pollution mitigation measures for airports and associated activity
[PB94-207610] p 1061 N95-19582
Erosion, Corrosion and Foreign Object Damage Effects in Gas Turbines
[AGARD-CP-558] p 950 N95-19653
Out of area experiences with the RB199 in Toronto p 950 N95-19654
The operation of gas turbine engines in hot and sandy conditions: Royal Air Force experiences in the Gulf conflict p 950 N95-19655
Navy foreign object damage and its impact on future gas turbine engine low pressure compression systems p 951 N95-19658
Scandinavian Airlines Systems experience on erosion, corrosion and foreign object damage effects on gas turbines p 951 N95-19659
Modern transport engine experience with environmental ingestion effects p 951 N95-19660
Design of fan blades subjected to bird impact p 953 N95-19669
Testing considerations for military aircraft engines in corrosive environments (a Navy perspective) p 955 N95-19684
Developing an emission factor for hazardous air pollutants for an F-16 using JP-8 fuel
[AD-A284802] p 1061 N95-19685

AIRCRAFT EQUIPMENT
Preliminary evaluation of the F/A-18 quantity/multiple envelope expansion
[AD-A284119] p 943 N95-18407

AIRCRAFT GUIDANCE
On-line handling of air traffic: Management, guidance and control
[AGARD-AG-321] p 941 N95-18927
Research requirements for future visual guidance systems
[AD-A279188] p 941 N95-19810

AIRCRAFT ICING
Collection efficiency and ice accretion calculations for a sphere, a swept MS(1)-317 wing, a swept NACA-0012 wing tip, an axisymmetric inlet, and a Boeing 737-300
[NASA-TM-106831] p 933 N95-18582
Methods for scaling icing test conditions
[NASA-TM-106827] p 934 N95-19284

AIRCRAFT INSTRUMENTS
Flight parameters monitoring system for tracking structural integrity of rotary-wing aircraft p 934 N95-19469

AIRCRAFT MAINTENANCE
Ultrasonic techniques for repair of aircraft structures with bonded composite patches p 937 N95-19486
Air pollution mitigation measures for airports and associated activity
[PB94-207610] p 1061 N95-19582
Erosion, Corrosion and Foreign Object Damage Effects in Gas Turbines
[AGARD-CP-558] p 950 N95-19653
Out of area experiences with the RB199 in Toronto p 950 N95-19654
The operation of gas turbine engines in hot and sandy conditions: Royal Air Force experiences in the Gulf conflict p 950 N95-19655
Navy foreign object damage and its impact on future gas turbine engine low pressure compression systems p 951 N95-19658
Scandinavian Airlines Systems experience on erosion, corrosion and foreign object damage effects on gas turbines p 951 N95-19659
Special investigation report: Maintenance anomaly resulting in dragged engine during landing rollout. Northwest Airlines Flight 18, Boeing 747-251B, N637US, New Tokyo International Airport, Narita, Japan, 1 Mar. 1994
[PB94-917006] p 940 N95-19793

AIRCRAFT MODELS
Interaction, bursting and control of vortices of a cropped double-delta wing at high angle of attack
[AD-A283656] p 930 N95-18669
Estimating wind tunnel interference due to vectored jet flows p 1023 N95-19265

AIRCRAFT NOISE
Helicopter internal noise p 1124 N95-19144
Impact of noise environment on engine nacelle design p 1125 N95-19147
Modelling structurally damaging twin-jet screech p 946 N95-19154
An overall approach of cockpit noise verification in a military aircraft p 1127 N95-19163
Noise transmission and reduction in turboprop aircraft p 1127 N95-19164

AIRCRAFT PERFORMANCE
Six degree of freedom flight dynamic and performance simulation of a remotely-piloted vehicle
[AERO-TN-9301] p 942 N95-18097
Design limit loads based upon statistical discrete gust methodology p 946 N95-18603

AIRCRAFT PILOTS
Age 60 study. Part 3: Consolidated database experiments
[AD-A286247] p 1080 N95-19384
Age 60 study. Part 4: Experimental evaluation of pilot performance
[AD-A286248] p 1080 N95-19385
Fit to fly: Analysis of the aeromedical disposition in aircrewmembers of the Spanish Armed Forces p 1081 N95-19418
Is the pilot fit for flying after an accident? p 1083 N95-19425
The concept of aeronautical adaptability as developed by the US Navy p 1083 N95-19426
Vestibular examination in pilots susceptible to motion sickness p 1083 N95-19427
The NAMI syncope test battery and clinical decision-making in aviators with syncope p 1083 N95-19428
Think health not disease p 1083 N95-19429
The aeromedical implications of supraventricular tachycardia p 1085 N95-19437
Photorefractive Keratectomy (PRK) in the military aviator: An aeromedical expose p 1086 N95-19442
Collection of real-time, multichannel EEG data from helicopter pilots in flight: A feasibility study
[AD-A285050] p 1090 N95-19564

AIRCRAFT RELIABILITY
Residual life and strength estimates of aircraft structural components with MSD/MED p 937 N95-19485

AIRCRAFT SAFETY
A study of the effect of store unsteady aerodynamics on gust and turbulence loads p 946 N95-18601
Ageing nuclear power plant management: An aeronautical viewpoint
[NAL-PD-SN-9306] p 927 N95-18606
On-line handling of air traffic: Management, guidance and control
[AGARD-AG-321] p 941 N95-18927
Safety study: Commuter airline safety
[PB94-917004] p 933 N95-19132
Age 60 study. Part 3: Consolidated database experiments
[AD-A286247] p 1080 N95-19384
Toward a new national weather service: Weather for those who fly
[PB94-214418] p 1072 N95-19407
Spine injuries: Up to date evaluation in aircraft ejections p 1084 N95-19434
Modern transport engine experience with environmental ingestion effects p 951 N95-19660
Special investigation report: Maintenance anomaly resulting in dragged engine during landing rollout. Northwest Airlines Flight 18, Boeing 747-251B, N637US, New Tokyo International Airport, Narita, Japan, 1 Mar. 1994
[PB94-917006] p 940 N95-19793

AIRCRAFT SPECIFICATIONS
Six degree of freedom flight dynamic and performance simulation of a remotely-piloted vehicle
[AERO-TN-9301] p 942 N95-18097

AIRCRAFT STRUCTURES
Course module for AA201: Wing structural design project
[AD-A283618] p 944 N95-18616
Pressure measurements on an F/A-18 twin vertical tail in buffeting flow. Volume 4, part 2: Buffet cross spectral densities
[AD-A285555] p 957 N95-18641
The accuracy of parameter estimation in system identification of noisy aircraft load measurement
[NASA-CR-197516] p 945 N95-19130
Impact of Acoustic Loads on Aircraft Structures
[AGARD-CP-549] p 1124 N95-19142
Current and future problems in structural acoustic fatigue p 1124 N95-19143
Impact of noise environment on engine nacelle design p 1125 N95-19147
High-temperature acoustic test facilities and methods p 1125 N95-19149
Nonlinear dynamic response of aircraft structures to acoustic excitation p 946 N95-19151
Acoustic fatigue testing on different materials and skin-stringer elements p 1126 N95-19156
Acoustic fatigue characteristics of advanced materials and structures p 1126 N95-19157
Application of superplastically formed and diffusion bonded structures in high intensity noise environments p 1127 N95-19162
FAA/NASA International Symposium on Advanced Structural Integrity Methods for Airframe Durability and Damage Tolerance, part 2
[NASA-CP-3274-PT-2] p 934 N95-19468
Discrete crack growth analysis methodology for through cracks in pressurized fuselage structures p 935 N95-19473
Aircraft stress sequence development: A complex engineering process made simple p 936 N95-19480
Residual life and strength estimates of aircraft structural components with MSD/MED p 937 N95-19485
Ultrasonic techniques for repair of aircraft structures with bonded composite patches p 937 N95-19486
Widespread fatigue damage monitoring: Issues and concerns p 938 N95-19488
Aircraft fatigue and crack growth considering loads by structural component p 939 N95-19497
Proceedings of the USAF Structural Integrity Program Conference
[AD-A285684] p 945 N95-19517

AIRCRAFT SURVIVABILITY
Assessing aircraft survivability to high frequency transient threats
[AD-A283999] p 944 N95-18726

AIRCRAFT WAKES
Aircraft wake vortex takeoff tests at O'Hara International Airport
[AD-A283828] p 929 N95-18624

AIRFOIL OSCILLATIONS
Unsteady flow testing in a passive low-correction wind tunnel p 960 N95-19272

AIRFOIL PROFILES
In-flight lift-drag characteristics for a forward-swept wing aircraft and comparisons with contemporary aircraft)
[NASA-TP-3414] p 929 N95-18565
Protective coatings for compressor gas path components p 954 N95-19675

AIRFOILS
Fatigue in single crystal nickel superalloys
[AD-A285727] p 978 N95-18068
Hydrofoil force balance
[AD-D016475] p 1033 N95-18461
Solution of full potential equation on an airfoil by multigrid technique
[NAL-TM-CSS-9303] p 930 N95-18904
Numerical simulation of dynamic-stall suppression by tangential blowing
[AD-A284887] p 931 N95-19110
2-D and 3-D oscillating wing aerodynamics for a range of angles of attack including stall
[NASA-TM-4632] p 931 N95-19119
Development of pneumatic test techniques for subsonic high-lift and in-ground-effect wind tunnel investigations p 932 N95-19268
Analysis of test section sidewall effects on a two dimensional airfoil: Experimental and numerical investigations p 1025 N95-19276
Ice accretion with varying surface tension
[NASA-TM-106826] p 934 N95-19285

AIRFRAME MATERIALS
Acoustic fatigue testing on different materials and skin-stringer elements p 1126 N95-19156
Acoustic fatigue characteristics of advanced materials and structures p 1126 N95-19157
Environmental effects on composite airframes: A study conducted for the ARM UAV Program (Atmospheric Radiation Measurement Unmanned Aerospace Vehicle)
[DE94-015351] p 971 N95-19579

AIRFRAMES
The generic simulation executive at Manned Flight Simulator
[AD-A283997] p 959 N95-18724
FAA/NASA International Symposium on Advanced Structural Integrity Methods for Airframe Durability and Damage Tolerance, part 2
[NASA-CP-3274-PT-2] p 934 N95-19468
Development of load spectra for Airbus A330/A340 full scale fatigue tests p 936 N95-19479
Proceedings of the USAF Structural Integrity Program Conference
[AD-A285684] p 945 N95-19517

AIRLINE OPERATIONS
Safety study: Commuter airline safety
[PB94-917004] p 933 N95-19132
Air pollution mitigation measures for airports and associated activity
[PB94-207610] p 1061 N95-19582

AIRPORTS
Evaluation of an unlighted swinging airport sign
[AD-A284763] p 958 N95-18087
Aircraft wake vortex takeoff tests at O'Hara International Airport
[AD-A283828] p 929 N95-18624
On-line handling of air traffic: Management, guidance and control
[AGARD-AG-321] p 941 N95-18927
Air pollution mitigation measures for airports and associated activity
[PB94-207610] p 1061 N95-19582
Research requirements for future visual guidance systems
[AD-A279188] p 941 N95-19810

AIRSHIPS
Airship applications of modern flight test techniques
[AD-A284253] p 945 N95-19731

AIRSPACE
Resources Automated Management System
[AD-A284153] p 1171 N95-18416

ALCOHOLS
The Solvent Absorption-Extractive Distillation (SAED) process for ethanol recovery from gas/vapor streams
[DE94-013112] p 974 N95-18637

ALGAE
Systems and economic analysis of microalgae ponds for conversion of CO2 to biomass
[DE95-000406] p 1054 N95-19554

ALGEBRA
Flattening of the resonance spectrum of hadrons from kappa-deformed Poincare algebra
[DE94-626686] p 1156 N95-18352
A new multi-dimensional transform for digital signal processing using generalized association schemes
[AD-A284166] p 1117 N95-18511
Covariant differential complexes of quantum linear groups
[DE94-626640] p 1118 N95-18876
Lie algebras for the Dirac-Clifford ring
[DE94-626643] p 1118 N95-18878
Classification of graded, finite-dimensional lie algebras of vector fields
[PB94-215449] p 1119 N95-19408

ALGORITHMS
Pre-processing in SADE: Stage 3
[PB94-201571] p 1093 N95-17935
Reformulated preconditioned conjugate gradient squared method. Part 1: The algorithm
[PB94-201589] p 1108 N95-17936
A domain decomposition algorithm for elliptic problems in three dimensions
[DE94-019265] p 1094 N95-17978
Semiconductor measurement technology: Design and testing guides for the COMOS and lateral bipolar-on-SOI test library
[PB94-178019] p 1007 N95-17984
Alternative formulation of Cocke-Younger-Kasami's algorithm
[PB94-202751] p 1094 N95-18000
Linear optimization and image reconstruction
[AD-A283641] p 1094 N95-18013
A platform independent application of Lux illumination prediction algorithms
[AD-A283669] p 1094 N95-18018
A fast recursive algorithm to compute the probability of M-out-of-N events
[AD-A283679] p 1120 N95-18020
Modular implementation of feature extraction and matching algorithms for photogrammetric stereo imagery
[AD-A285422] p 1032 N95-18065
An algorithm for solving the system-level problem in multilevel optimization
[NASA-CR-195015] p 1116 N95-18108
Lower bounds for identifying subset members with subset queries
[DE94-014296] p 1117 N95-18346
Fast numerical determination of symmetric sparsity patterns
[DE94-016344] p 1096 N95-18354
Atmospheric Infrared Sounder
[NASA-CR-197573] p 1064 N95-18444
Radial basis function neural networks applied to NASA SSME data
[NASA-CR-195417] p 962 N95-18467
Minimal time detection algorithms and applications to flight systems
[TR-2-FSRC-93] p 1098 N95-18564
Calibration and sediment load algorithms for an acoustic sediment flux probe
[AD-A283655] p 1075 N95-18617
Improved approximation guarantees for minimum-weight k-trees and prize-collecting salesmen
[AD-A284042] p 1117 N95-18658
A direct decomposition method for the solution of sparse linear least squares problems
[AD-A284060] p 1117 N95-18679
Mesh quality control for multiply-refined tetrahedral grids
[NASA-CR-197595] p 1043 N95-18737
Distributed algorithms for controlling multiple mobile robots
[AD-A283975] p 1114 N95-18889
CUBIT mesh generation environment
[DE94-017496] p 1118 N95-18896
Empirical study of parallel LRU simulation algorithms
[NASA-CR-194995] p 1099 N95-19027
On k-ary n-cubes: Theory and applications
[NASA-CR-194996] p 1100 N95-19028
Representing visibility for siting problems
[AD-A284076] p 993 N95-19036
An assessment of the adaptive unstructured tetrahedral grid, Euler Flow Solver Code FELISA
[NASA-TP-3526] p 930 N95-19041
Algorithms and applications in timed discrete event systems
[PB94-201423] p 1118 N95-19169
VENTCF2: An algorithm and associated FORTRAN 77 subroutine for calculating flow through a horizontal ceiling/floor vent in a zone-type compartment fire model
[PB94-210127] p 993 N95-19402
General procedures employed in the generation of three-dimensional hybrid structured/unstructured meshes
[ARA-MEMO-400] p 1030 N95-19506
Evaluating the trade-offs in partial-order planning algorithms
[AD-A285876] p 1115 N95-19599
Parallel computations in hydro acoustics
[AD-A285900] p 1030 N95-19607
High-order corrected trapezoidal rules for singular functions
[AD-A284269] p 1119 N95-19735
Optimal pattern distributions in Rete-based production systems p 1106 N95-19755
Application of three-dimensional hybrid structured/unstructured grids to land, sea and air vehicles
[ARA-MEMO-399] p 1031 N95-19775
Verification of the CFD simulation system SAUNA for complex aircraft configurations
[ARA-MEMO-401] p 1031 N95-19776
The application of the SAUNA CFD system to high and low speed vehicles
[ARA-MEMO-402] p 1031 N95-19778
Solution of Maxwell's equations using the time domain Method of Moments. Supplement: Publications and reports
[AD-A280143] p 1119 N95-19819
Solution of Maxwell's equations using the time domain Method of Moments
[AD-A280144] p 1119 N95-19820
Algorithms for orbit control on SPEAR
[DE95-002868] p 1138 N95-19841
The formulation of quantum statistical mechanics based on the Feynman path centroid density. 4: Algorithms for centroid molecular dynamics
[AD-A279234] p 1157 N95-19853

ALIGNMENT
A comparison between using incoherent or coherent sources to align and test an adaptive optical telescope p 1142 N95-18969

ALKALI HALIDES
UV laser-surface interactions relevant to analytic spectroscopy of wide band gap materials
[DE94-016180] p 1037 N95-18349

ALKALINE EARTH METALS
Polyurethane self-priming topcoats
[AD-D016264] p 984 N95-18320
Polyurethane self-priming topcoats
[AD-D016234] p 985 N95-18631

ALL SKY PHOTOGRAPHY
The 2 Micron All Sky Survey
[AD-A283515] p 1178 N95-18001
ALLENDE METEORITE
Cooling rates of chondrules: A new approach
p 1192 N95-19334
ALLOCATIONS
Space Station: Plans to expand research community do not match available resources. Report to the Ranking Minority Member, Subcommittee on Oversight of Government Management, Committee on Government Affairs, US Senate
[GAO/NSIAD-95-33] p 965 N95-19131
ALLOTROPY
Novel catalysts for methane activation
[DE95-001179] p 976 N95-19785
ALLOYING
Alloying effects on the high-temperature oxidation resistance of Cr-Cr2Nb
[DE94-018146] p 978 N95-18121
Fundamental studies of passivity and passivity breakdown
[DE94-016954] p 987 N95-19095
Weldability of iron aluminides
[DE95-000686] p 981 N95-19568
ALLOYS
Method for making a non-magnetic alloy
[AD-D016233] p 979 N95-18630
QuikForm: Intelligent deformation processing of structural alloys
[DE94-018739] p 1114 N95-18649
ALPHA PARTICLES
Detection of alpha particles via observation of He II line emission in the lithium pellet cloud during DT operation in TFTR
[DE94-014485] p 1143 N95-17965
Study of alpha physics related to ITER Project
[DE94-017329] p 1133 N95-19078
ALTERNATING CURRENT
Mitigation of EMI generated by a variable-frequency-drive controller for an AC induction motor
[AD-A286045] p 1012 N95-19573
ALTITUDE SICKNESS
Echo imaging techniques determine the size of intravascular bubbles in decompression sickness
[AD-A284849] p 1087 N95-19714
ALUMINIDES
Weldability of iron aluminides
[DE95-000686] p 981 N95-19568
New Trends in coatings developments for turbine blades: Materials processing and repair p 954 N95-19676
ALUMINUM
Preparation of an electrocatalytic cathode for an aluminum-hydrogen peroxide battery
[AD-D016262] p 1008 N95-18318
Trivalent chromium conversion coatings for aluminum
[AD-D016274] p 978 N95-18332
Adherend surface effects on epoxy cure by NMR
[AD-A284774] p 985 N95-18442
Trivalent chromium solutions for sealing anodized aluminum
[AD-D016472] p 979 N95-18458
Characterization of metal matrix composites
[NASA-CR-195381] p 970 N95-18940
The effect of fabrication on corrosion in aluminum 2195: Environmental and microstructural considerations
p 982 N95-19011
Pitting corrosion of aluminized seals in molten carbonate fuel cells
[DE94-017075] p 1053 N95-19116
Acoustic fatigue behaviour of GLARE composites
p 1127 N95-19160
Penetration experiments in aluminum and Teflon targets of widely variable thickness p 1047 N95-19185
Propagation of intense, ultrashort laser pulses through metal vapor: Refractive intensity limits and spectral effects
[DE94-016365] p 1039 N95-19398
Synthesis and structural properties of new metallic phases exhibiting non-crystallographic symmetries
[AD-A284882] p 982 N95-19743
Relative elemental abundance and heating constraints determined for the solar corona from SERTS measurements
[NASA-TM-104616] p 1196 N95-19791
PRS projections for DECADE
[AD-A279215] p 1147 N95-19847
ALUMINUM ALLOYS
Alloying effects on the high-temperature oxidation resistance of Cr-Cr2Nb
[DE94-018146] p 978 N95-18121
On the crack growth resistance and strength of the B2 iron aluminides Fe-40Al, Fe-45Al, and Fe-10Ni-40Al (at. %)
[DE94-017857] p 978 N95-18128
Microstructural analysis of cracks generated during welding of 2195 aluminum-lithium alloy
p 982 N95-19007
The effect of fabrication on corrosion in aluminum 2195: Environmental and microstructural considerations
p 982 N95-19011
Nonstoichiometry of Al-Zr intermetallic phases
[DE94-016877] p 979 N95-19093
Warm formability of aluminum-magnesium alloys
[DE94-016170] p 980 N95-19396
Deformation texture studies in Fe3Al alloys
[DE94-017709] p 980 N95-19400
Damage monitoring in metallic and composite structures using piezoelectric thin film sensors
[ARL-RR-4] p 971 N95-19467
The application of Newman crack-closure model to predicting fatigue crack growth p 937 N95-19483
Fatigue crack growth in 2024-T3 aluminum under tensile and transverse shear stresses p 938 N95-19490
Fracture behavior of large-scale thin-sheet aluminum alloy p 939 N95-19494
Prediction of R-curves from small coupon tests
p 939 N95-19496
Modified Cu-Mn-Al high damping alloys
[AD-A285460] p 980 N95-19539
Study of laser resonance ionization mass spectrometry using a glow discharge source
[DE94-018566] p 981 N95-19703
ALUMINUM ARSENIDES
Magneto-optical studies of compound semiconductors
[DE94-018743] p 1149 N95-18650
Investigation of superlattice disordering and diffusion mechanisms in GaAs
[AD-A284847] p 1153 N95-19697
ALUMINUM CHLORIDES
Electrochemical and spectroscopy studies of selected inorganic and organic systems in molten halides
[AD-A284171] p 974 N95-18514
ALUMINUM COMPOUNDS
Electrochemical and spectroscopy studies of selected inorganic and organic systems in molten halides
[AD-A284171] p 974 N95-18514
ALUMINUM GALLIUM ARSENIDES
Magneto-optical studies of compound semiconductors
[DE94-018743] p 1149 N95-18650
Vacuum microelectronic emitters and their applications using compound semiconductor technology
[AD-A284811] p 1013 N95-19687
ALUMINUM ISOTOPES
Chronology of chrondrule and CAI formation: Mg-Al isotopic evidence p 1189 N95-19314
ALUMINUM NITRIDES
Growth and doping of Al(x)Ga(1-x)N films by electron cyclotron resonance assisted molecular beam epitaxy
[AD-A284838] p 1153 N95-19737
ALUMINUM OXIDES
Preparation and surface characterization of metal doped alumina catalyst
[PB94-175296] p 973 N95-17991
Adherend surface effects on epoxy cure by NMR
[AD-A284774] p 985 N95-18442
ALUMINUM SILICATES
Sodium sulfate corrosion of silicon carbide fiber-reinforced calcium aluminosilicate glass-ceramic matrix composites
[AD-A283703] p 969 N95-18021
ALUMINUM-LITHIUM ALLOYS
Microstructural analysis of cracks generated during welding of 2195 aluminum-lithium alloy
p 982 N95-19007
AMAZON REGION (SOUTH AMERICA)
Radiation balance in three Amazonian ecosystems: Campina, campinarana and mata densa
[INPE-5587-TDI/549] p 1057 N95-18003
Observational studies and modelling of interception loss of gross rainfall in the Amazonian rainforest
[INPE-5583-TDI/545] p 1067 N95-18006
AMBIENCE
Environmental forcing of ambient noise in the Nansen and Amundsen Basins of the Arctic Ocean
[AD-A285540] p 1074 N95-18468
AMBIENT TEMPERATURE
Status of vanadium alloy development for fusion first wall/blanket applications
[DE95-001067] p 982 N95-19725
AMINES
Adherend surface effects on epoxy cure by NMR
[AD-A284774] p 985 N95-18442
AMMONIUM PERCHLORATES
Enantiomeric separation of chiral alpha-(1-naphthyl)ethyl ammonium perchlorate by silica gel-bound chiral pyridino-18-crown-6 ligands
[AD-A280156] p 969 N95-19822
AMMONIUM PICRATES
Molecular recognition as shown by the solvent extraction of (R)- and (S)-alpha-(1-naphthyl)ethyl ammonium picrate or orange 2 by chiral pyridino-crown ethers
[AD-A280157] p 969 N95-19823
AMMONIUM SULFATES
Gas turbine compressor corrosion and erosion in Western Europe p 954 N95-19678
AMORPHOUS MATERIALS
International Conference on Deformation, Yield and Fracture of Polymers
[AD-A284354] p 984 N95-18339
Synthesis and structural properties of new metallic phases exhibiting non-crystallographic symmetries
[AD-A284882] p 982 N95-19743
AMORPHOUS SEMICONDUCTORS
Computational modeling of properties
[NASA-CR-197558] p 1010 N95-18925
AMORPHOUS SILICON
Research on stable, high-efficiency amorphous silicon multijunction modules
[DE95-000215] p 1054 N95-19832
AMPLITUDE MODULATION
Implementation of amplitude modulation companding using a digital signal processor
[BBC-RD-1994/1] p 998 N95-18536
Advanced optical fiber communications systems
[AD-A283942] p 1141 N95-18682
Signal enhancement in AM-FM interference
[AD-A285114] p 1004 N95-19565
ANALOG CIRCUITS
Locally connected adaptive Gabor filter for real-time motion compensation
[AD-A285726] p 1009 N95-18485
Adaptive Neuron Model: An architecture for the rapid learning of nonlinear topological transformations
[NASA-CASE-NPO-18579-1-CU] p 1114 N95-18740
ANALOG DATA
Signal processor having multiple distributed data buffers
[AD-D016259] p 995 N95-18315
ANALOG SIMULATION
An analog computing approach to structural analysis and optimal design through artificial neural networks
p 1113 N95-18218
ANALOG TO DIGITAL CONVERTERS
Superconductive signal-processing circuits
[AD-A285533] p 1008 N95-18103
Radar sector blanker
[AD-D016275] p 996 N95-18429
Digital circuit for the introduction and later removal of dither from an analog signal
[AD-D016462] p 1011 N95-19171
ANALOGIES
Facilitation and interference in identification of pictures and words
[AD-A285882] p 1090 N95-19602
ANALOGS
Alternative formulation of Cocke-Younger-Kasami's algorithm
[PB94-202751] p 1094 N95-18000
ANALYSIS OF VARIANCE
Visuo-ocular performance during vestibular stimulation
[AD-A284103] p 1089 N95-18403
ANALYTIC FUNCTIONS
Theory and applications of the phi transform wavelets
[AD-A279943] p 1119 N95-19869
ANALYTICAL CHEMISTRY
Activities of the Analytical Chemistry Laboratory
[DE95-000834] p 975 N95-19618
ANALYZERS
Electron reversal ionizer for detection of trace species using a spherical cathode
[NASA-CASE-NPO-18870-1-CU] p 1130 N95-18324
ANATOMY
The assessment of virtual reality for human anatomy instruction p 1088 N95-18971
ANECHOIC CHAMBERS
Background noise levels measured in the NASA Lewis 9- by 15-foot low-speed wind tunnel
[NASA-TM-106817] p 958 N95-18054
ANEMOMETERS
Aircraft wake vortex takeoff tests at O'Hara International Airport
[AD-A283828] p 929 N95-18624
ANGLE OF ATTACK
Wind tunnel performance comparative test results of a circular cylinder and 50 percent ellipse tailboom for circulation control antitorque applications
[AD-A283335] p 941 N95-18008
Interaction, bursting and control of vortices of a cropped double-delta wing at high angle of attack
[AD-A283656] p 930 N95-18669
2-D and 3-D oscillating wing aerodynamics for a range of angles of attack including stall
[NASA-TM-4632] p 931 N95-19119

Velocity measurements with hot-wires in a vortex-dominated flowfield p 932 N95-19261
Prediction of wind tunnel effects on the installed F/A-18A inlet flow field at high angles-of-attack
[NASA-CR-195429] p 950 N95-19651

ANGULAR CORRELATION
Light scattering from rough surfaces
[AD-A284112] p 1139 N95-18404

ANGULAR DISTRIBUTION
Spatial and temporal constraints on the observed distribution of gamma-ray bursts detected by BATSE p 1197 N95-18730
Study of strangeness production in relativistic nucleus beams at JINR
[DE94-626720] p 1136 N95-18881

ANGULAR MOMENTUM
Flattening of the resonance spectrum of hadrons from kappa-deformed Poincare algebra
[DE94-626686] p 1156 N95-18352

ANILINE
Application of conducting polymers to electroanalysis
[DE94-015204] p 984 N95-18348

ANISOTROPIC PLATES
Driving force analysis in an infinite anisotropic plate with multiple crack interactions
[NASA-TM-106838] p 972 N95-19782

ANISOTROPY
Testing the inflationary paradigm: Inflation and the cosmic microwave background anisotropy p 1179 N95-18496
Spatial and temporal constraints on the observed distribution of gamma-ray bursts detected by BATSE p 1197 N95-18730
Second-order reconstruction of the inflationary potential
[NASA-CR-197629] p 1121 N95-19030
A 2D depth migration in transversely isotropic media using explicit operators
[DE95-000645] p 1066 N95-19560
A Quantum-Drive-Time (QDT) quantization of the Taub cosmology
[DE95-001014] p 1194 N95-19612
Correlation function analysis of the COBE differential microwave radiometer sky maps
[DE95-000795] p 1178 N95-19617

ANNEALING
Nonstoichiometry of Al-Zr intermetallic phases
[DE94-016877] p 979 N95-19093
Characterization of the deformation and annealing of 304L stainless steel
[DE94-018584] p 981 N95-19707

ANNOTATIONS
Situation awareness: Papers and annotated bibliography
[AD-A284752] p 1088 N95-18084

ANNUAL VARIATIONS
The diurnal cycle of high-frequency temperature variability at 0 deg 140 deg W on seasonal and interannual time scales
[AD-A283640] p 1074 N95-18012
Climate and weather of Central Africa. Executive summary
[AD-A283647] p 1067 N95-18014
Evolution of the Southern Hemisphere ozone hole as seen by TOMS from August 1979 to December 1991
[NASA-TM-110116] p 1057 N95-18048
Moored rainfall measurements during COARE p 1069 N95-18202
A synoptic climatology of convective weather in the Netherlands
[KNMI-WR-93-04] p 1071 N95-18395
Mission description and in-flight operations of ERBE instruments on ERBS and NOAA 10 spacecraft, February 1987 - February 1990
[NASA-RP-1325] p 1051 N95-18465
A numerical simulation of seasonal circulation in the South China Sea
[AD-A283701] p 1075 N95-18622
Assessment of climate variability of the Greenland Ice Sheet: Integration of in situ and satellite data
[NASA-CR-197604] p 1062 N95-19779

ANNULAR FLOW
Measurement of gust response on a turbine cascade
[NASA-TM-106776] p 928 N95-18457

ANNULI
Annular computed tomography
[AD-D016424] p 1141 N95-18593

ANODES
Sealant materials for the solid oxide fuel cell
[DE94-017073] p 1053 N95-19115

ANODIZING
Trivalent chromium solutions for sealing anodized aluminum
[AD-D016472] p 979 N95-18458

ANTARCTIC REGIONS
Potential replacements for solvents that are ozone depleting substances
[AD-A285442] p 1058 N95-18091

ANTENNA ARRAYS
Phase and amplitude controlled micropatch antenna
[AD-A284191] p 1002 N95-19103
True time delay beamforming
[AD-A285683] p 1003 N95-19516
Analysis and synthesis of (SAR) waveguide phased array antennas
[AD-A285336] p 1004 N95-19535
Barium strontium titanate and non-ferroelectric oxide ceramic composites for use in phased array antennas
[AD-A279225] p 972 N95-19851

ANTENNA COMPONENTS
Phase and amplitude controlled micropatch antenna
[AD-A284191] p 1002 N95-19103

ANTENNA DESIGN
Phase and amplitude controlled micropatch antenna
[AD-A284191] p 1002 N95-19103
Analysis and synthesis of (SAR) waveguide phased array antennas
[AD-A285336] p 1004 N95-19535
Design considerations for an archimedean slot spiral antenna p 1006 N95-19798

ANTENNA FEEDS
Inband radar cross section of phased arrays with parallel feeds
[AD-A284249] p 1005 N95-19730
Simulation of thin slot spirals and dual circular patch antennas using the finite element method with mixed elements
[NASA-CR-197671] p 1005 N95-19796
Design considerations for an archimedean slot spiral antenna p 1006 N95-19798
An efficient and accurate model of the coax cable feeding structure for FEM simulations p 1006 N95-19799
Arbitrarily shaped dual-stacked patch antennas: A hybrid FEM simulation p 1006 N95-19800

ANTENNA RADIATION PATTERNS
Measurements of wind profiler EMC characteristics
[PB94-194107] p 1066 N95-17938
Geometrical and topological methods in time domain antenna synthesis
[AD-A284208] p 994 N95-17954
Synthesis of notched antenna patterns for wide bandwidth processing
[AD-A284004] p 1000 N95-18727
Analysis and synthesis of (SAR) waveguide phased array antennas
[AD-A285336] p 1004 N95-19535
Radar antenna characterization using polarization measurements
[AD-A284840] p 1005 N95-19694
Arbitrarily shaped dual-stacked patch antennas: A hybrid FEM simulation p 1006 N95-19800

ANTHRACENE
Electrochemical and spectroscopy studies of selected inorganic and organic systems in molten halides
[AD-A284171] p 974 N95-18514

ANTHROPOMETRY
Development of microgravity, full body functional reach envelope using 3-D computer graphic models and virtual reality technology p 1092 N95-18990

ANTIFERROMAGNETISM
Study of frustrated systems via dissipative maps
[DE94-017754] p 1122 N95-18127
Wentzel-Bardeen singularity in coupled Luttinger liquids: Transport properties
[DE95-000856] p 1152 N95-19621

ANTIGRAVITY
Effects of weight lifting on intrathoracic pressures generated by anti-g straining maneuvers
[AD-A283651] p 1078 N95-18138

ANTIMISSILE DEFENSE
A triangulation method for passive ranging
[AD-A284180] p 998 N95-18522

ANTINEUTRINOS
The very low energy solar flux of electron and heavy-flavor neutrinos and antineutrinos
[DE94-018583] p 1135 N95-19706

ANTIPROTONS
Asymmetric antiproton debuncher: No bad mixing, more good mixing
[DE94-017171] p 1133 N95-19077

ANTIREFLECTION COATINGS
Investigation of the microstructure of coatings for high power lasers by non-optical techniques
[DE94-017697] p 987 N95-19227
Future trends in optical coatings for high-power laser applications
[DE94-018592] p 1039 N95-19708

ANVIL CLOUDS
Modeling of cloud and radiation processes for large-scale clouds and tropical anvils
[AD-A284212] p 1067 N95-17955

APERTURES
A shock isolation method and apparatus
[AD-D016471] p 1045 N95-18456
PRISM project optical instrument p 1143 N95-19009

APOLLO FLIGHTS
Time of Apollo
[NASA-TM-110488] p 961 N95-19060

APOLLO PROJECT
Legacy of Gemini
[NASA-TM-110486] p 961 N95-19058
Time of Apollo
[NASA-TM-110488] p 961 N95-19060

APOLLO TELESCOPE MOUNT
Skylab: The second manned mission. A scientific harvest
[NASA-TM-110487] p 961 N95-19059

APPLICATION SPECIFIC INTEGRATED CIRCUITS
An investigation of nonuniform dose deposition from an electron beam
[AD-A284175] p 1131 N95-18519

APPLICATIONS PROGRAMS (COMPUTERS)
Long wavelength propagation capacity, version 1.1 (computer diskette)
[AD-M200254] p 994 N95-17964
A platform independent application of Lux illumination prediction algorithms
[AD-A283669] p 1094 N95-18018
Night Vision Goggles (NVG) software user's guide, version 5.1
[AD-A284563] p 1090 N95-18029
A Space and Atmospheric Visualization Science System
[NASA-CR-189390] p 1172 N95-18040
Coastal Modeling System (CMS) user's manual. Supplement 3 to September 1991 manual
[AD-A283922] p 1074 N95-18160
Numerical predictions of turbulent flow around a cube via the k-epsilon model
[DE94-018361] p 1017 N95-18443
CRRESPRO documentation
[AD-A284578] p 1178 N95-18451
IONCAP prediction-based Automatic Link Establishment (ALE) frequency selection for a ten-node Australian high-frequency network
[AD-A283698] p 999 N95-18619
The generic simulation executive at Manned Flight Simulator
[AD-A283997] p 959 N95-18724
Enhanced capabilities and modified users manual for axial-flow compressor conceptual design code CSPAN
[NASA-TM-106833] p 930 N95-18933
A finite element code for electric motor design p 1014 N95-18974
Evaluation of the efficiency and reliability of software generated by code generators p 1108 N95-19004
ODP based UPT model
[PB94-215589] p 1003 N95-19411
Aircraft stress sequence development: A complex engineering process made simple p 936 N95-19480
The STOKES (Version 4) normal-mode shallow water transmission loss program
[MRL-CP-1] p 1075 N95-19503
CLIPS, AppleEvents, and AppleScript: Integrating CLIPS with commercial software p 1103 N95-19643
Unit cell geometry of multiaxial preforms for structural composites
[NASA-CR-197294] p 971 N95-19650
Mega-scale simulation of multi-layer devices: Formulation, kinetics, and visualization
[AD-A284848] p 1153 N95-19738
Using CLIPS in the domain of knowledge-based massively parallel programming p 1105 N95-19750
Centrifugal and axial pump design and off-design performance prediction
[NASA-TM-106745] p 968 N95-19795
Tutorial guide: Computer-Aided Structural Modeling (CASM), version 5.00
[AD-A280147] p 1108 N95-19821

APPROACH
Heliport/vertiport MLS precision approaches
[AD-A283505] p 940 N95-18059

APPROPRIATIONS
Space Station: Plans to expand research community do not match available resources. Report to the Ranking Minority Member, Subcommittee on Oversight of Government Management, Committee on Government Affairs, US Senate
[GAO/NSIAD-95-33] p 965 N95-19131

APPROXIMATION
Linear optimization and image reconstruction
[AD-A283641] p 1094 N95-18013

Improved approximation guarantees for minimum-weight k-trees and prize-collecting salesmen
[AD-A284042] p 1117 N95-18658
On the convergence of local approximations to pseudodifferential operators with applications
[NASA-TM-106792] p 1019 N95-18898
Testing the frozen flow approximation
[NASA-CR-197614] p 1180 N95-18966

AQUEOUS SOLUTIONS
Mechanical behavior of precipitation hardenable steels exposed to highly corrosive environment
p 982 N95-18180
Trivalent chromium conversion coatings for aluminum
[AD-D016274] p 978 N95-18332
Trivalent chromium solutions for sealing anodized aluminum
[AD-D016472] p 979 N95-18458
Molecular dynamics study of aqueous electrolyte solutions near a structured sphere
[AD-A284010] p 1132 N95-18655

ARC JET ENGINES
Arcjet thruster research and technology, phase 2
[NASA-CR-182276] p 927 N95-18044

ARC MELTING
Ion emission intensity ratios as a function of electrode gap, melting current, and pressure during low current vacuum arc remelting
[DE94-017407] p 1129 N95-18144

ARC WELDING
Design of a flexible robotic arc welding system, task 3. Volume 1: System overview
[AD-A285116] p 1043 N95-19593

ARCHITECTURE (COMPUTERS)
Study of a Navier-Stokes computer
[AD-A284196] p 1092 N95-17939
Improving software characteristics of a real-time system using reengineering techniques
[AD-A283659] p 1094 N95-18015
Miscellaneous disk utility application programs for the AFOS background partition
[PB94-181328] p 1067 N95-18038
A novel system level approach to fault tolerance in distributed memory multicomputers
[AD-A284729] p 1095 N95-18079
Early experiences and performance of the Intel Paragon
[DE94-018061] p 1109 N95-18129
Mapping a domain model and architecture to a generic design
[AD-A283747] p 1096 N95-18364
Vision and action
[AD-A285701] p 1140 N95-18480
Virtual reality, an air combat T and E perspective
[AD-A284161] p 959 N95-18508
NASA High Performance Computing and Communications program
[NASA-TM-4653] p 1174 N95-18573
A direct decomposition method for the solution of sparse linear least squares problems
[AD-A284060] p 1117 N95-18679
Advanced optical fiber communications systems
[AD-A283942] p 1141 N95-18682
Performance evaluation of the Engineering Analysis and Data Systems (EADS) 2 p 1163 N95-18978
Software Technology for Adaptable, Reliable Systems (STARS). Software architecture seminar report: Central Archive for Reusable Defense Software (CARDS)
[AD-A284668] p 1100 N95-19106
Real time simulator with Ti floating point digital signal processor
[DE94-016372] p 1012 N95-19246
ODP based UPT model
[PB94-215589] p 1003 N95-19411
Enhancing the architectural characterization of parallel proto
[AD-A285678] p 1111 N95-19524
Information system architecture to support transparent access to distributed, heterogeneous data sources
[DE94-018450] p 1176 N95-19589
Cooperating agents for information retrieval
[AD-A285887] p 1176 N95-19604
Predicting and explaining the movement of mesoscale oceanographic features using CLIPS
p 1105 N95-19752
Rule based design of conceptual models for formative evaluation p 1106 N95-19760

ARCTIC OCEAN
Environmental forcing of ambient noise in the Nansen and Amundsen Basins of the Arctic Ocean
[AD-A285540] p 1074 N95-18468

ARCTIC REGIONS
Compendium of NASA data base for the Global Tropospheric Experiment's Arctic Boundary Layer Experiments ABLE-3A and ABLE-3B
[NASA-TM-109161] p 1058 N95-18132
The use of two-station ionosonde data for IONCAP/ASAPS model validation on transpolar two-hop, high-frequency skywave radio links
[AD-A284270] p 1005 N95-19736

ARMED FORCES
Fit to fly: Analysis of the aeromedical disposition in aircrewmembers of the Spanish Armed Forces
p 1081 N95-19418

ARMED FORCES (UNITED STATES)
Variable name dictionary for the Air Force health study 1987 physical examination data tape, volume 1
[AD-A283319] p 1172 N95-18025
Variable name dictionary for the Air Force health study 1987 physical examination data tape, volume 2
[AD-A283320] p 1172 N95-18026

ARMOR
Development of an improved ballistic acceptance test for high hard armor steel plate: MIL-A-46100
[ARL-TR-509] p 979 N95-18939
Design of advanced steels for armor applications
[ARL-CR-175] p 979 N95-18948

ARPA COMPUTER NETWORK
Interferometric synthetic aperture radar and the Data Collection System Digital Terrain Elevation Demonstration
[AD-A284024] p 999 N95-18657
Zoned Analog Personal Teleconferencing (ZAPT)
[AD-A285877] p 1004 N95-19600

ARRAYS
Transducer array interaction modeling using variational principles
[AD-A285687] p 1128 N95-19514

ARTIFICIAL INTELLIGENCE
Adaptive robot path planning in changing environments
[DE94-016564] p 1112 N95-17948
QuikForm: Intelligent deformation processing of structural alloys
[DE94-018739] p 1114 N95-18649
Multi-method planning
[AD-A285878] p 1115 N95-19601
Expert system shell to reason on large amounts of data p 1101 N95-19631
AI and workflow automation: The prototype electronic purchase request system p 1101 N95-19632
A knowledge-based system for controlling automobile traffic p 1102 N95-19633
Adding intelligent services to an object oriented system p 1103 N95-19642
The use of genetic algorithms for flight test and evaluation of artificial intelligence and complex software systems
[AD-A284824] p 1104 N95-19688
Optimal pattern distributions in Rete-based production systems p 1106 N95-19755
Character selecting advisor for a role-playing game
p 1106 N95-19758
Reflexive reasoning for distributed real-time systems
p 1107 N95-19766

ARTIFICIAL SATELLITES
Personal communications services: Improving theater deployable communications for the 21st century
[AD-A283465] p 994 N95-18058

ASSESSMENTS
The way to waivers in the BAF p 1081 N95-19415

ASTEROID MISSIONS
Near-Earth Asteroid Returned Sample (NEARS)
[NASA-CR-197297] p 1194 N95-19575

ASTEROIDS
Velocity distribution of Earth-crossing asteroid grains
p 1183 N95-19187
The circumplanetary nebular environment: A possible source region for chondrules p 1191 N95-19325
Near-Earth Asteroid Returned Sample (NEARS)
[NASA-CR-197297] p 1194 N95-19575

ASTRONAUT PERFORMANCE
Geometry and gravity influences on strength capability
[NASA-TP-3511] p 1091 N95-18189

ASTRONOMICAL CATALOGS
The 2 Micron All Sky Survey
[AD-A283515] p 1178 N95-18001

ASTRONOMICAL COORDINATES
A platform independent application of Lux illumination prediction algorithms
[AD-A283669] p 1094 N95-18018

ASTRONOMICAL MODELS
Spatial and temporal constraints on the observed distribution of gamma-ray bursts detected by BATSE
p 1197 N95-18730
Cosmic ray models for early galactic lithium, beryllium, and boron production
[NASA-CR-197626] p 1137 N95-18965
Cross-tail current, field-aligned current, and B(y)
[NASA-CR-197624] p 1065 N95-19032
Collision of cometlike and slightly differentiated bodies as an origin for ordinary chondrites
p 1188 N95-19308
The jet model of chondrule formation
p 1189 N95-19310
Testing higher-order Lagrangian perturbation theory against numerical simulation. 1: Pancake models
[NASA-CR-197611] p 1121 N95-19348

ASTROPHYSICS
Development of a high-resolution liquid xenon detector for gamma-ray astrophysics p 1179 N95-18499
The role of chondrules in nebular fractionations of volatiles and other elements p 1187 N95-19300
Astronomical observations of phenomena in disks
p 1178 N95-19301
Models for multiple heating mechanisms
p 1188 N95-19303
Chondrule formation in lightning discharges
p 1188 N95-19304
Chondrules and their associates in ordinary chondrites
p 1188 N95-19306
Relative elemental abundance and heating constraints determined for the solar corona from SERTS measurements
[NASA-TM-104616] p 1196 N95-19791

ASYMMETRY
The left-right forward-backward asymmetry for B quarks at the SLD
[DE94-014508] p 1129 N95-18049
Compression strength of composite primary structural components
[NASA-CR-197554] p 1044 N95-18388
Waveguide switches using asymmetric coupled quantum wells
[AD-A284056] p 1010 N95-18662
Asymmetric antiproton debuncher: No bad mixing, more good mixing
[DE94-017171] p 1133 N95-19077
Multicast tree construction in network topologies with asymmetric link loads
[AD-A285679] p 1003 N95-19525

ASYMPTOTIC METHODS
Bohr's quantization rule in the world of resonances of elementary particles
[DE94-626721] p 1132 N95-18882

ASYMPTOTIC SERIES
Singular perturbation problem governed by system of conservation laws
[DE94-019264] p 1116 N95-17977
Studies on high pressure and unsteady flame phenomena
[AD-A284126] p 973 N95-18410

ATLANTIC OCEAN
Geologic studies: Executive summary report
[PB94-187481] p 1073 N95-17951

ATLANTIS (ORBITER)
Debris/ice/TPS assessment and integrated photographic analysis of Shuttle mission STS-66
[NASA-TM-110141] p 963 N95-19790

ATMOSPHERIC BOUNDARY LAYER
Compendium of NASA data base for the Global Tropospheric Experiment's Arctic Boundary Layer Experiments ABLE-3A and ABLE-3B
[NASA-TM-109161] p 1058 N95-18132
The numerical simulation of marine boundary layer clouds
[AD-A284149] p 1064 N95-18413
Marine boundary layer refractive effects in the infrared
[AD-A285717] p 1140 N95-18484

ATMOSPHERIC CHEMISTRY
Dependencies and sensitivity of tropospheric oxidants to precursor concentrations over the northeast United States: A model study
[PB94-192770] p 1056 N95-17937
Ion-molecule collisions, electron molecule collisions, excitation and ionization of atoms
[AD-A284584] p 1129 N95-18062
Compendium of NASA data base for the Global Tropospheric Experiment's Arctic Boundary Layer Experiments ABLE-3A and ABLE-3B
[NASA-TM-109161] p 1058 N95-18132
EMEFS: Lessons learned 2, model evaluation
[DE94-017468] p 1049 N95-18145
Methane: The other greenhouse gas. Research and policy in the Netherlands
[PB94-207149] p 1058 N95-18375
Atmospheric chemistry of biogenic sulfur in the Southern Hemisphere p 1071 N95-18399
Laboratory studies of stratospheric bromine chemistry: Kinetics of the reactions of bromine monoxide with nitrogen dioxide and atomic oxygen p 1065 N95-18731
A GIS approach to urban heat island research: The case of Huntsville, Alabama p 1063 N95-18991
A report on workshops: General circulation model study of climate: Chemistry interaction
[DE94-010252] p 1062 N95-19879

ATMOSPHERIC CIRCULATION
Evolution of the Southern Hemisphere ozone hole as seen by TOMS from August 1979 to December 1991
[NASA-TM-110116] p 1057 N95-18048
Intraseasonal oscillations over the tropical western Pacific and eastern Indian ocean for the northern summers of 1989-1991
[AD-A284527] p 1068 N95-18114
EMEFS: Lessons learned 2, model evaluation
[DE94-017468] p 1049 N95-18145
Meteor 3/TOMS launch of 15 August 1991 in Plesetsk, USSR
[NASA-TM-110115] p 962 N95-18150
Implementation of the 1992 Terminal area-Local Analysis and Prediction System (T-LAPS)
[AD-A284334] p 1070 N95-18384
A synoptic climatology of convective weather in the Netherlands
[KNMI-WR-93-04] p 1071 N95-18395
Numerical predictions of turbulent flow around a cube via the k-epsilon model
[DE94-018361] p 1017 N95-18443
Atmospheric Infrared Sounder
[NASA-CR-197573] p 1064 N95-18444
Real-time modeling of complex atmospheric releases in urban areas
[DE94-018063] p 1059 N95-18647
NASA Goddard Earth Sciences Graduate Student Program --- FIRE CIRRUS-II examination of coupling between an upper tropospheric cloud system and synoptic-scale dynamics
[NASA-CR-197130] p 1066 N95-19129
ADCIRC: An advanced three-dimensional circulation model for shelves, coasts, and estuaries. Report 5: A tropical storm database for the east and Gulf of Mexico coasts of the United States
[AD-A285576] p 1075 N95-19540
Synoptic-scale influence on the Monterey Bay sea-breeze
[AD-A285129] p 1073 N95-19596

ATMOSPHERIC COMPOSITION
Detection of greenhouse-gas-induced climatic change
[DE94-015044] p 1057 N95-18022
Potential replacements for solvents that are ozone depleting substances
[AD-A285442] p 1058 N95-18091
Compendium of NASA data base for the Global Tropospheric Experiment's Arctic Boundary Layer Experiments ABLE-3A and ABLE-3B
[NASA-TM-109161] p 1058 N95-18132
A sensitivity analysis of upwelling radiances in the 3-5 micrometers region as a function of atmospheric conditions
[AD-A283678] p 1068 N95-18141
Trends 1993: A compendium of data on global change
[ORNL/CDIAC-65] p 1058 N95-18389
Atmospheric chemistry of biogenic sulfur in the Southern Hemisphere p 1071 N95-18399
Assessment of CO2 projections
[DE94-017484] p 1059 N95-18664
Changes in the flux of carbon between plants and soil microorganisms at elevated CO2: Physiological processes with ecosystem-level implications
[DE94-017067] p 1060 N95-19112

ATMOSPHERIC DENSITY
Laser wakefield excitation and measurement on a femtosecond time scale: Theory and experiment
[DE94-019198] p 1129 N95-17976

ATMOSPHERIC EFFECTS
The Seventh Ionospheric Effects Symposium
[PB94-191930] p 1057 N95-17985
Performance evaluation of ground based radar systems
[AD-A283654] p 995 N95-18139
Effects of meteor showers in the Earth ionosphere
[INPE-5591-TDI/552] p 1178 N95-18213
Imagery correction for atmospheric effects using sounding data
[INPE-5506-TDI/518] p 1064 N95-18390
Atmospheric effects of high-flying subsonic aircraft: A catalogue of perturbing influences
[KNMI-SR-94-03] p 1060 N95-18722
Hyperspectral data analysis procedures with reduced sensitivity to noise
[NASA-CR-197621] p 1052 N95-19126
Surface and upper-air meteorological measurements supporting the NATO/AC243/Panel 3 research study groups 8 and 21 campaign in Lorient, France (September 1993)
[AD-A285326] p 1072 N95-19521

ATMOSPHERIC GENERAL CIRCULATION MODELS
EMEFS: Lessons learned 2, model evaluation
[DE94-017468] p 1049 N95-18145
A report on workshops: General circulation model study of climate: Chemistry interaction
[DE94-010252] p 1062 N95-19879

ATMOSPHERIC MODELS
Dependencies and sensitivity of tropospheric oxidants to precursor concentrations over the northeast United States: A model study
[PB94-192770] p 1056 N95-17937
Modeling of cloud and radiation processes for large-scale clouds and tropical anvils
[AD-A284212] p 1067 N95-17955
The Seventh Ionospheric Effects Symposium
[PB94-191930] p 1057 N95-17985
Detection of greenhouse-gas-induced climatic change
[DE94-015044] p 1057 N95-18022
A sensitivity analysis of upwelling radiances in the 3-5 micrometers region as a function of atmospheric conditions
[AD-A283678] p 1068 N95-18141
Coastal Modeling System (CMS) user's manual. Supplement 3 to September 1991 manual
[AD-A283922] p 1074 N95-18160
Experiments with the Mesoscale Atmospheric Simulation System (MASS) using the synthetic relative humidity p 1073 N95-18172
Microburst vertical wind estimation from horizontal wind measurements
[NASA-TP-3460] p 942 N95-18198
Storm activity over the North Sea and the Netherlands in two climate models compared with observations
[KNMI-WR-94-02] p 1070 N95-18393
Conceptual models of severe convective weather in the Netherlands
[KNMI-WR-93-05] p 1071 N95-18394
A model study of the influence of NMHC and NO(x) emissions on rural O3 concentrations in Georgiargia p 1059 N95-18445
Real-time modeling of complex atmospheric releases in urban areas
[DE94-018063] p 1059 N95-18647
One strategy for estimating the potential soil carbon storage due to CO2 fertilization
[DE94-017895] p 1059 N95-18666
An analytic conceptual model of extratropical cyclones
[KNMI-WR-93-03] p 1072 N95-18926
Solar flare model atmospheres
[NASA-CR-197607] p 1196 N95-19034
First principles used in orbital prediction and an atmospheric model comparison
[AD-A284636] p 1065 N95-19086
New applications of the Phillips Laboratory. Theoretical ionospheric model and studies of neutral density waves
[AD-A284663] p 1066 N95-19105
NASA Goddard Earth Sciences Graduate Student Program --- FIRE CIRRUS-II examination of coupling between an upper tropospheric cloud system and synoptic-scale dynamics
[NASA-CR-197130] p 1066 N95-19129

ATMOSPHERIC MOISTURE
Estimation of satellite derived temperature and moisture fields over Europe from TOVS data using 3I and ITPP algorithms
[AD-A284581] p 1049 N95-18035
Energy balance model for imagery and electromagnetic propagation
[AD-A284552] p 1063 N95-18115
Experiments with the Mesoscale Atmospheric Simulation System (MASS) using the synthetic relative humidity p 1073 N95-18172
Multispectral NOAA Marine Atmospheric Boundary Layer (MABL) estimates during VOCAR
[AD-A283702] p 1064 N95-18623

ATMOSPHERIC OPTICS
Energy balance model for imagery and electromagnetic propagation
[AD-A284552] p 1063 N95-18115

ATMOSPHERIC PHYSICS
Investigation of atmospheric waves on Neptune
[NASA-CR-197537] p 1194 N95-18579
New applications of the Phillips Laboratory. Theoretical ionospheric model and studies of neutral density waves
[AD-A284663] p 1066 N95-19105

ATMOSPHERIC PRESSURE
Studies on high pressure and unsteady flame phenomena
[AD-A284126] p 973 N95-18410
Optical measurements in rocket engine liquid sprays p 968 N95-18979
Solar flare model atmospheres
[NASA-CR-197607] p 1196 N95-19034

ATMOSPHERIC RADIATION
Radiation balance in three Amazonian ecosystems: Campina, campinarana and mata densa
[INPE-5587-TDI/549] p 1057 N95-18003
Real-time modeling of complex atmospheric releases in urban areas
[DE94-018063] p 1059 N95-18647
Thermochemical IR sources: COCHISE and FACELIF experiments
[AD-A279940] p 977 N95-19868

ATMOSPHERIC REFRACTION
Method and system for inferring the radio refractive index structure of the atmosphere from radio measurements
[AD-D016436] p 999 N95-18561
Multispectral NOAA Marine Atmospheric Boundary Layer (MABL) estimates during VOCAR
[AD-A283702] p 1064 N95-18623
Surface and upper-air meteorological measurements supporting the NATO/AC243/Panel 3 research study groups 8 and 21 campaign in Lorient, France (September 1993)
[AD-A285326] p 1072 N95-19521
Proceedings of the 15th Annual Conference on Atmospheric Transmission Models
[AD-A279919] p 1142 N95-19862

ATMOSPHERIC SCATTERING
Two space scatterer formalism calculation of bulk parameters of thunderclouds p 1073 N95-19001
Scattering of point source illumination by an arbitrary configuration p 1143 N95-19006
Proceedings of the 15th Annual Conference on Atmospheric Transmission Models
[AD-A279919] p 1142 N95-19862

ATMOSPHERIC SOUNDING
Estimation of satellite derived temperature and moisture fields over Europe from TOVS data using 3I and ITPP algorithms
[AD-A284581] p 1049 N95-18035
A technical demonstration Mobile Profiler System
[AD-A284562] p 1068 N95-18117

ATMOSPHERIC TEMPERATURE
Estimation of satellite derived temperature and moisture fields over Europe from TOVS data using 3I and ITPP algorithms
[AD-A284581] p 1049 N95-18035
Marginal probabilities of the extremes of ENSO events for temperature and precipitation in the southeastern United States
[AD-A284716] p 1068 N95-18076
Energy balance model for imagery and electromagnetic propagation
[AD-A284552] p 1063 N95-18115
A review of land surface temperature and humidity conditions specified for Australia in DEF (AUST) 5168 and STANAG 2895
[AD-A284258] p 1073 N95-19712

ATMOSPHERIC TURBULENCE
Energy balance model for imagery and electromagnetic propagation
[AD-A284552] p 1063 N95-18115
Numerical predictions of turbulent flow around a cube via the k-epsilon model
[DE94-018361] p 1017 N95-18443
Aircraft Loads due to Turbulence and their Impact on Design and Certification
[AGARD-R-798] p 956 N95-18597
The impact of non-linear flight control systems on the prediction of aircraft loads due to turbulence p 956 N95-18598
Gyroscopic and propeller aerodynamic effects on engine mounts dynamic loads in turbulence conditions p 946 N95-18599
Treatment of non-linear systems by timeplane-transformed CT methods: The spectral gust method p 956 N95-18600
A study of the effect of store unsteady aerodynamics on gust and turbulence loads p 946 N95-18601
Comparison of stochastic and deterministic nonlinear gust analysis methods to meet continuous turbulence criteria p 946 N95-18602
Special effects of gust loads on military aircraft p 946 N95-18605
Computer simulation of wave propagation through turbulent media
[AD-A283695] p 1000 N95-18671
New applications of the Phillips Laboratory. Theoretical ionospheric model and studies of neutral density waves
[AD-A284663] p 1066 N95-19105

ATOMIC CLOCKS
Quartz crystal resonators and oscillators for frequency control and timing applications. A tutorial
[AD-A284995] p 1012 N95-19519

ATOMIC CLUSTERS
Atomistic and elastic analyses of defects and small structures
[DE94-017047] p 980 N95-19111
An atomic view of surface diffusion on metal surfaces
[DE94-016150] p 980 N95-19395

ATOMIC COLLISIONS
Ionization of atoms by high energy photons
[DE94-018356] p 1130 N95-18427

ATOMIC ENERGY LEVELS
Ultrafast nonlinear optical response of Fano resonances in gallium arsenide under high magnetic field
[DE94-018181] p 1148 N95-18122
ATOMIC EXCITATIONS
Ultrafast nonlinear optical response of Fano resonances in gallium arsenide under high magnetic field
[DE94-018181] p 1148 N95-18122
Ionization of atoms by high energy photons
[DE94-018356] p 1130 N95-18427
Atomic Layer Epitaxy (ALE) apparatus for growing thin films of elemental semiconductors
[AD-D016236] p 1149 N95-18633
A photoionization study of OH and OD from 680A to 950A: An analysis of the Rydberg series
[NASA-CR-196970] p 974 N95-18744
ATOMIC PHYSICS
Ionization of atoms by high energy photons
[DE94-018356] p 1130 N95-18427
Correlated charge-changing ion-atom collisions
[DE94-017355] p 1132 N95-18874
ATOMIC STRUCTURE
Electronic structure of C60 fullerites and nanotubes
[DE95-000784] p 1151 N95-19569
Massively parallel full configuration interaction. Benchmark electronic structure calculations on the Intel Touchstone Delta
[DE95-001064] p 1153 N95-19724
ATOMIZING
Study of laser resonance ionization mass spectrometry using a glow discharge source
[DE94-018566] p 981 N95-19703
ATOMS
Atomic scale force mapping with the atomic force microscope
[AD-A284940] p 1129 N95-17974
Atomic line filter for SDI applications
[AD-A284125] p 1139 N95-18409
An atomic view of motion on surfaces
[AD-A285565] p 1131 N95-18473
An atomic view of surface diffusion on metal surfaces
[DE94-016150] p 980 N95-19395
Isotope separation and advanced manufacturing technology
[DE95-000313] p 1039 N95-19551
Advanced concepts theory
[AD-A279212] p 1147 N95-19844
ATTITUDE (INCLINATION)
Visuo-ocular performance during vestibular stimulation
[AD-A284103] p 1089 N95-18403
AUDIO EQUIPMENT
Calibration and sediment load algorithms for an acoustic sediment flux probe
[AD-A283655] p 1075 N95-18617
DAB: Multiplex and system support features
[BBC-RD-1994/9] p 1001 N95-19050
Digital audio broadcasting: Comparison of coverage at different frequencies and with different bandwidths
[BBC-RD-1993/11] p 1002 N95-19135
AUDIO FREQUENCIES
Optimum dimension ratios for studios, control rooms and listening rooms
[BBC-RD-1993/8] p 993 N95-19053
AUDIO SIGNALS
DAB: Multiplex and system support features
[BBC-RD-1994/9] p 1001 N95-19050
Dynamic range control of audio signals by digital signal processing
[BBC-RD-1993/7] p 1124 N95-19054
AUDITORY SIGNALS
Perception of complex auditory patterns
[AD-A284189] p 1079 N95-18626
AUGMENTATION
Real-time adaptive control of mixing in a plane shear layer
[AD-A285541] p 1018 N95-18469
Aeromechanics technology, volume 1. Task 1: Three-dimensional Euler/Navier-Stokes Aerodynamic Method (TEAM) enhancements
[AD-A285713] p 943 N95-18483
Enhancement of creep resistance of a sintered Si3N4 ceramic by microwave annealing
[DE94-017688] p 967 N95-19399
Use of titanate coupling agents in Kevlar (trade name)/phenolic composites
[AD-A279200] p 972 N95-19814
AUSTENITIC STAINLESS STEELS
Weldability of iron aluminides
[DE95-000686] p 981 N95-19568
AUSTRALIA
A review of land surface temperature and humidity conditions specified for Australia in DEF (AUST) 5168 and STANAG 2895
[AD-A284258] p 1073 N95-19712
AUTOGYROS
Wind tunnel tests of a 42 inch diameter self-starting autogyro rotor
[AD-A279922] p 932 N95-19863
AUTOMATIC CONTROL
Operational And Supportability Implementation System (OASIS) test and evaluation master plan
[AD-A284765] p 941 N95-18088
VSTOL Systems Research Aircraft (VSRA) Harrier
[NASA-TM-110117] p 941 N95-18347
Resources Automated Management System
[AD-A284153] p 1171 N95-18416
Streamlined design and self reliant hardware for active control of precision space structures
[NASA-CR-4637] p 964 N95-18580
NASA develops new digital flight control system
[NASA-NEWS-RELEASE-94-47] p 958 N95-19029
AUTOMATIC GAIN CONTROL
Effect of heavy rain to the total received power
p 1070 N95-18210
AUTOMATIC TEST EQUIPMENT
Using expert systems to analyze ATE data
p 1103 N95-19639
AUTOMATIC WEATHER STATIONS
Use of profiler data for analysis and NOWcasting of a winter season extratropical cyclone
[PB94-187804] p 1067 N95-17992
AUTOMOBILE FUELS
Potential impacts on air quality of the use of ethanol as an alternative fuel
[DE94-011881] p 1056 N95-17944
AUTOMOBILES
Application of three-dimensional hybrid structured/unstructured grids to land, sea and air vehicles
[ARA-MEMO-399] p 1031 N95-19775
AUTOMORPHISMS
Towards a classification of su(2)(direct sum)...(direct sum)su(2) modular invariant partition functions
[PB94-217247] p 1119 N95-19717
AUTONOMOUS NAVIGATION
Fusion of multiple sensing modalities for machine vision
[AD-A284762] p 1091 N95-18086
AUTONOMY
Algorithms and applications in timed discrete event systems
[PB94-201423] p 1118 N95-19169
Cooperating agents for information retrieval
[AD-A285887] p 1176 N95-19604
AUTOREGRESSIVE PROCESSES
TLS-based prefiltering technique for time-domain ARMA modeling
[AD-A284525] p 1120 N95-18113
On stationary and nonstationary fatigue load modeling using autoregressive moving average (ARMA) models
p 1046 N95-18919
AVIATION METEOROLOGY
Product usage evaluation of the aviation gridded forecast system workstation at the Denver Center Weather Service Unit
[PB94-195922] p 1066 N95-17952
Microburst vertical wind estimation from horizontal wind measurements
[NASA-TP-3460] p 942 N95-18198
Toward a new national weather service: Weather for those who fly
[PB94-214418] p 1072 N95-19407
The meteorological monitoring system for the Kennedy Space Center/Cape Canaveral Air Station
p 1104 N95-19647
AVIONICS
New technologies for space avionics
[NASA-CR-197574] p 966 N95-18196
KC-135 cockpit modernization study. Phase 1: Equipment evaluation
[AD-A284099] p 942 N95-18398
Strategic avionics technology definition studies. Subtask 3-1A3: Electrical Actuation (ELA) Systems Test Facility
[NASA-CR-188360] p 956 N95-18567
AXIAL FLOW PUMPS
Centrifugal and axial pump design and off-design performance prediction
[NASA-TM-106745] p 968 N95-19795
AXIAL LOADS
Sag compensated vibration isolation mount
[AD-D016541] p 1042 N95-19121
Results of uniaxial and biaxial tests on riveted fuselage lap joint specimens p 938 N95-19491
AXISYMMETRIC FLOW
Marangoni convection in a gravity-free silicon float zone
[NASA-CR-197600] p 991 N95-18913
Evaluation of three turbulence models for afterbody/jet flows, including Reynolds stress closure
[ARA-90] p 932 N95-19574
Evaluation of three turbulence models for afterbody/jet flows, including Reynolds stress closure
[ARA-MEMO-408] p 1194 N95-19773
AZOLES
Novel polymeric composites through molecular engineering
[AD-A284168] p 985 N95-18513

B

BACK INJURIES
Design and development of an enhanced biodynamic manikin, phase 1
[AD-A284725] p 1090 N95-18077
Spine injuries: Up to date evaluation in aircraft ejections p 1084 N95-19434
BACKGROUND NOISE
Background noise levels measured in the NASA Lewis 9- by 15-foot low-speed wind tunnel
[NASA-TM-106817] p 958 N95-18054
Atomic line filter for SDI applications
[AD-A284125] p 1139 N95-18409
Maximal-length sequence methods: Acoustic measurements in the presence of high levels of extraneous noise
[BBC-RD-1994/5] p 1001 N95-19049
BACKGROUND RADIATION
Testing the inflationary paradigm: Inflation and the cosmic microwave background anisotropy
p 1179 N95-18496
The origin of the diffuse x-ray background
p 1197 N95-18729
Cosmic ray models for early galactic lithium, beryllium, and boron production
[NASA-CR-197626] p 1137 N95-18965
BACKSCATTERING
Calibration and sediment load algorithms for an acoustic sediment flux probe
[AD-A283655] p 1075 N95-18617
Special relativity effects for space-based coherent lidar experiments p 1014 N95-18983
BACKWARD DIFFERENCING
A spectrally accurate boundary-layer code for infinite swept wings
[NASA-CR-195014] p 1014 N95-18042
BALANCE
Helicopter Performance Evaluation (HELPE) computer model
[AD-A284319] p 942 N95-18381
Hydrofoil force balance
[AD-D016475] p 1033 N95-18461
BALANCING
Software techniques for balancing computation and communication in parallel systems
[AD-A285536] p 1109 N95-18106
Transport aircraft loading and balancing system: Using a CLIPS expert system for military aircraft load planning
p 1105 N95-19751
BALLISTICS
Thermocouples for interior ballistic temperature measurements
[AD-A283699] p 1033 N95-18620
BALLOONS
Mass and radius of cosmic balloons
[NASA-CR-197628] p 1180 N95-19031
BALTIC SEA
Coastal benthic boundary layer special research program: A review of the first year. Volume 1
[AD-A280034] p 1076 N95-19818
BANDPASS FILTERS
Standard reference materials: Glass filters as a standard reference material for spectrophotometry. Selection, preparation, certification and use of SRM 930 and SRM 1930
[PB94-188844] p 973 N95-17994
BANDWIDTH
Liquid crystal tunable filter
[AD-A284383] p 1139 N95-18342
Synthesis of notched antenna patterns for wide bandwidth processing
[AD-A284004] p 1000 N95-18727
Digital audio broadcasting: Comparison of coverage at different frequencies and with different bandwidths
[BBC-RD-1993/11] p 1002 N95-19135
Sandia National Laboratories' high power electromagnetic impulse sources
[DE95-000423] p 1004 N95-19555
BARIUM FLUORIDES
Process for forming epitaxial BaF2 on GaAs
[AD-D016439] p 1149 N95-18527
BARIUM TITANATES
Barium strontium titanate and non-ferroelectric oxide ceramic composites for use in phased array antennas
[AD-A279225] p 972 N95-19851

BARRIER LAYERS
Application of conducting polymers to electroanalysis
[DE94-015204] p 984 N95-18348
BARYONS
Baryon stopping in 200 GeV/A S+Au collisions
[DE94-018215] p 1134 N95-19587
BASALT
Trace element characteristics of lithospheric and asthenospheric mantle in the Rio Grande rift region
[DE94-013609] p 1063 N95-17947
Density structure of the upper oceanic crust at zero porosity
[AD-A284235] p 1076 N95-19728
BASE FLOW
A note on the wave action density of a viscous instability mode on a laminar free-shear flow
[NASA-TM-106771] p 1016 N95-18212
Numerical computations of supersonic base flow with special emphasis on turbulence modeling
[AD-A283688] p 930 N95-18670
BATCH PROCESSING
Requirements analysis for safety-critical systems: A chemical batch processing example
[PB94-201563] p 991 N95-17934
BAYES THEOREM
Some statistical tools for SAR image synthesis, analysis and processing
[INPE-5548-TDI/534] p 1172 N95-18004
Robust image understanding. Techniques and applications
[AD-A283427] p 1113 N95-18057
BAYS (STRUCTURAL UNITS)
Weapons bay acoustic environment
p 1125 N95-19146
BEACON SATELLITES
Results from the northern New Mexico satellite-beacon radio interferometer
[DE94-018310] p 1063 N95-18148
BEAM CURRENTS
Development of lithium beam emission spectroscopy as an edge fluctuation diagnostic for D3-D
[DE94-017517] p 1146 N95-19378
BEAM INJECTION
Development of an amorphous surge blocker for a high voltage acceleration power supply of the neutral beam injectors
[DE94-770648] p 1138 N95-19874
BEAMFORMING
True time delay beamforming
[AD-A285683] p 1003 N95-19516
Signal enhancement in AM-FM interference
[AD-A285114] p 1004 N95-19565
BEAMS (SUPPORTS)
Finite element modeling of partially delaminated composite beams with contact-impact conditions
[AD-A283726] p 1044 N95-18363
The evaluation of transmission efficiency and coupling loss factor of structural junctions
[MRL-TR-93-1] p 1124 N95-19057
BEARING ALLOYS
Nanostructured bearing alloy studies
[AD-A283328] p 978 N95-18027
BED REST
Effect of heat acclimation on sitting orthostatic tolerance in the heat after 48 and 96 hour bed rest in men
[NASA-TM-106861] p 1077 N95-18734
BENDING
Study of failure in fibrous composites subjected to bending loads
[AD-A283330] p 969 N95-18028
Discrete crack growth analysis methodology for through cracks in pressurized fuselage structures
p 935 N95-19473
BENDING FATIGUE
Detecting gear tooth fracture in a high contact ratio face gear mesh
[NASA-TM-106822] p 1042 N95-19125
BENDING VIBRATION
Large amplitude motions, especially isomerization and tunneling in polyatomic molecule spectra: Novel experimental, pattern recognition, and theoretical methods
[AD-A284194] p 985 N95-18636
BENZENE
Novel polymeric composites through molecular engineering
[AD-A284168] p 985 N95-18513
BENZOIC ACID
Polyurethane self-priming topcoats
[AD-D016264] p 984 N95-18320
Polyurethane self-priming topcoats
[AD-D016234] p 985 N95-18631
BERNOULLI THEOREM
Design optimization of a brush turbine with a cleaner/water based solution p 1043 N95-18177
Acoustic radiation damping of flat rectangular plates subjected to subsonic flows p 1123 N95-18542
BERYLLIUM
Cosmic ray models for early galactic lithium, beryllium, and boron production
[NASA-CR-197626] p 1137 N95-18965
BESSEL FUNCTIONS
Signal processing via Fourier-Bessel series expansion
[AD-A285316] p 1003 N95-19510
BETATRONS
Asymmetric antiproton debuncher: No bad mixing, more good mixing
[DE94-017171] p 1133 N95-19077
BETHE-SALPETER EQUATION
Pion observables and QCD
[DE94-018357] p 1130 N95-18428
BIAS
Evaluation of the current biased integrated optical processors based on bistable dode elements
[AD-A285532] p 1138 N95-18102
BIBLIOGRAPHIES
Thermophotovoltaics bibliography
[DE94-011898] p 1052 N95-17945
Situation awareness: Papers and annotated bibliography
[AD-A284752] p 1088 N95-18084
Remote sensing/global change. A special bibliography
[NASA-TM-110038] p 1060 N95-18742
Aeronautical engineering: A continuing bibliography with indexes (supplement 313)
[NASA-SP-7037(313)] p 927 N95-19168
Documentation and archiving of the Space Shuttle wind tunnel test data base. Volume 1: Background and description
[NASA-TM-104806-VOL-1] p 965 N95-19237
Aerospace medicine and biology: A continuing bibliography with indexes (supplement 398)
[NASA-SP-7011(398)] p 1080 N95-19239
Aeronautical engineering: A continuing bibliography with indexes (supplement 314)
[NASA-SP-7037(314)] p 927 N95-19357
Aerospace medicine and biology: A continuing bibliography with indexes (supplement 397)
[NASA-SP-7011(397)] p 1087 N95-19746
BIG BANG COSMOLOGY
A Type 2 supernovae constraint on neutrino(sub e) - neutrino(sub s) mixing
[NASA-CR-197630] p 1180 N95-18746
Is a massive tau neutrino just what cold dark matter needs?
[NASA-CR-197627] p 1180 N95-18964
BINARY ALLOYS
Numerical formulation of composition segregation at curved solid-liquid interface during steady state solidification process p 977 N95-19012
Warm formability of aluminum-magnesium alloys
[DE94-016170] p 980 N95-19396
BINARY CODES
Imagery correction for atmospheric effects using sounding data
[INPE-5506-TDI/518] p 1064 N95-18390
BINARY DATA
High temperature stability of binary microstructures derived from liquid precursors
[AD-A283960] p 1150 N95-18685
Phase stability and elastic properties of C15 compounds HfV2+Nb
[DE95-000940] p 981 N95-19611
BINARY STARS
Astronomical observations of phenomena in disks
p 1178 N95-19301
BINARY SYSTEMS (MATERIALS)
A review of nuclear thermal propulsion carbide fuel corrosion and key issues
[NASA-CR-197533] p 1136 N95-18217
Dynamic decohesion of bimaterials: Experimental observations and failure criteria
[GALCIT-94-2] p 1045 N95-18613
BINDERS (MATERIALS)
Polyurethane self-priming topcoats
[AD-D016234] p 985 N95-18631
BIOASSAY
US experiments flown on the Soviet biosatellite Cosmos 2044. Volume 1: Mission description, experiments K-7-01 - K-7-15
[NASA-TM-108802-VOL-1] p 1092 N95-18569
BIOCHEMISTRY
Drink composition and cycle-ergometer endurance in men: Carbohydrate, Na(+), osmolality
[NASA-TM-4650] p 1077 N95-19140
Activities of the Division of Energy Biosciences
[DE95-001046] p 1077 N95-19613
Photobiology in medicine
[AD-A284843] p 1087 N95-19695
BIODYNAMICS
Applications of quaternions to dynamical simulation, computer graphics and biomechanics
[PB94-201456] p 1094 N95-17972
Health hazards assessment for blast overpressure exposures
[AD-A283352] p 1078 N95-17998
Design and development of an enhanced biodynamic manikin, phase 1
[AD-A284725] p 1090 N95-18077
Naval Biodynamics Laboratory 1993 command history
[AD-A284358] p 1089 N95-18440
BIOELECTRICITY
Cellular neurophysiology of the rat suprachiasmatic nucleus: Electrical properties, neurotransmission, and mechanisms of synchronization
[AD-A284111] p 1076 N95-18439
BIOGEOCHEMISTRY
Is a massive tau neutrino just what cold dark matter needs?
[NASA-CR-197627] p 1180 N95-18964
BIOLOGICAL EFFECTS
Mechanisms of interaction and biological effects of extremely-low-frequency electromagnetic fields
[DE94-015200] p 1076 N95-18371
Light transport for medical laser treatments
[PB94-201498] p 1037 N95-18502
BIOMASS
Ethylene dynamics in the CELSS biomass production chamber p 1077 N95-18179
Systems and economic analysis of microalgae ponds for conversion of CO2 to biomass
[DE95-000406] p 1054 N95-19554
Activities of the Division of Energy Biosciences
[DE95-001046] p 1077 N95-19613
BIOTECHNOLOGY
Capillary electrophoresis: Biotechnology for separation of DNA and chromosomes p 1077 N95-19014
Activities of the Division of Energy Biosciences
[DE95-001046] p 1077 N95-19613
BIPOLAR TRANSISTORS
Heteroepitaxy of ternary SiGeC alloys on Si for bipolar transistors
[AD-A285317] p 1151 N95-19511
BIPOLARITY
Semiconductor measurement technology: Design and testing guides for the COMOS and lateral bipolar-on-SOI test library
[PB94-178019] p 1007 N95-17984
Development of a bipolar lead/acid battery for the more electric aircraft
[AD-A284050] p 1010 N95-18660
Sandia National Laboratories' high power electromagnetic impulse sources
[DE95-000423] p 1004 N95-19555
BIRD-AIRCRAFT COLLISIONS
Design of fan blades subjected to bird impact
p 953 N95-19669
BIREFRINGENCE
Liquid crystal tunable filter
[AD-A284383] p 1139 N95-18342
BIRKELAND CURRENTS
Cross-tail current, field-aligned current, and B(y)
[NASA-CR-197624] p 1065 N95-19032
BISMUTH COMPOUNDS
Ferroelectric thin film bismuth titanate prepared from acetate precursors
[DE95-000538] p 988 N95-19558
BISPHENOLS
Adherend surface effects on epoxy cure by NMR
[AD-A284774] p 985 N95-18442
BISTABLE CIRCUITS
Partition method for the determination of multiple DC operating points
[PB94-201480] p 1009 N95-18501
BIT ERROR RATE
Digital video compression: Standardisation of scalable coding schemes
[BBC-RD-1994/10] p 1001 N95-19047
Bit-rate reduction of digital television for transmission: An introductory review
[BBC-RD-1994/2] p 1001 N95-19052
BIT SYNCHRONIZATION
RINSE: A digitally implemented flywheel sync regenerator for improved video synchroniser performance
[BBC-RD-1993/14] p 999 N95-18538
BLACK AND WHITE PHOTOGRAPHY
The photographic system global evaluation for generation of INPE TM Landsat image
[INPE-5571-TDI/542] p 1050 N95-18369
BLACK BODY RADIATION
A sensitivity analysis of upwelling radiances in the 3-5 micrometers region as a function of atmospheric conditions
[AD-A283678] p 1068 N95-18141

BLADE TIPS
Performance deterioration of axial compressors due to blade defects p 952 N95-19665
Erosion of T56 5th stage rotor blades due to bleed hole overtip flow p 952 N95-19666
BLAST LOADS
Health hazards assessment for blast overpressure exposures
[AD-A283352] p 1078 N95-17998
Data acquisition from blast overpressure trials
[MRL-TN-628] p 1020 N95-19139
BLEEDING
On supersonic-inlet boundary-layer bleed flow
[NASA-CR-195426] p 955 N95-19769
BLOCK COPOLYMERS
Multi-functional pi-conjugated macromolecules based on poly (phenylene vinylene)
[AD-A284163] p 985 N95-18510
Fracture toughness of polymer/polymer bimaterial interface reinforced with block copolymers
p 986 N95-18923
Macromolecular characterization and solution behavior of polymer additives
[AD-A284845] p 988 N95-19696
BLOCKING
Adaptive wind tunnel walls versus wall interference correction methods in 2D flows at high blockage ratios
p 960 N95-19267
BLOOD
Lower bounds for identifying subset members with subset queries
[DE94-014296] p 1117 N95-18346
BLOOD CIRCULATION
Cumulative effects of repeated brief cerebral ischemia
[AD-A284234] p 1087 N95-19698
BLOWDOWN WIND TUNNELS
Operating capability and current status of the reactivated NASA Lewis Research Center Hypersonic Tunnel Facility
[NASA-TM-106808] p 960 N95-19286
BODY MEASUREMENT (BIOLOGY)
Evaluation of the EKG's isoelectric T wave in Air Force pilots p 1082 N95-19423
BODY-WING CONFIGURATIONS
The aerodynamic design of an integrated wing lower surface and pylons for reduced drag
[ARA-MEMO-406] p 946 N95-19789
BOEING 747 AIRCRAFT
Special investigation report: Maintenance anomaly resulting in dragged engine during landing rollout. Northwest Airlines Flight 18, Boeing 747-251B, N637US, New Tokyo International Airport, Narita, Japan, 1 Mar. 1994
[PB94-917006] p 940 N95-19793
BOHR THEORY
Bohr's quantization rule in the world of resonances of elementary particles
[DE94-626721] p 1132 N95-18882
BOLOMETERS
2-D tomography with bolometry in D3-D
[DE94-017520] p 1146 N95-19379
BOLTZMANN TRANSPORT EQUATION
Arbitrarily high order nodal and characteristic methods
[DE94-018130] p 1116 N95-18131
The 3d International Workshop on Computational Electronics
[AD-A284678] p 1011 N95-19089
The physics and operation of ultra-submicron length semiconductor devices
[AD-A280181] p 1155 N95-19828
BONDED JOINTS
Method and device for determining bond separation strength using induction heating
[NASA-CASE-LAR-14678-1] p 960 N95-18961
Application of superplastically formed and diffusion bonded structures in high intensity noise environments
p 1127 N95-19162
BONDING
Sealant materials for the solid oxide fuel cell
[DE94-017073] p 1053 N95-19115
BOOTS (FOOTWEAR)
A review of footwear for cold/wet scenarios. Part 2: Socks, liners, and insoles
[AD-A279937] p 989 N95-19866
BORON
On the crack growth resistance and strength of the B2 iron aluminides Fe-40Al, Fe-45Al, and Fe-10Ni-40Al (at. %)
[DE94-017857] p 978 N95-18128
Cosmic ray models for early galactic lithium, beryllium, and boron production
[NASA-CR-197626] p 1137 N95-18965
BORON-EPOXY COMPOSITES
Ultrasonic techniques for repair of aircraft structures with bonded composite patches p 937 N95-19486
BOSONS
SU4(sub L) x U1(sub N) model for the electroweak interactions
[DE94-626675] p 1148 N95-18330
BOTTLES
Evaluation of Pureau water for use as emergency drinking water for ADF aircraft
[MRL-TN-648] p 1092 N95-19502
BOUNDARIES
Waveform bounding and combination techniques for direct drive testing
[AD-A284075] p 1000 N95-19035
Boundary-flow measurement methods for wall interference assessment and correction: Classification and review p 1022 N95-19262
Transonic wind tunnel boundary interference correction p 960 N95-19271
BOUNDARY CONDITIONS
A spectrally accurate boundary-layer code for infinite swept wings
[NASA-CR-195014] p 1014 N95-18042
Evaluation of boundary conditions for computational aeroacoustics
[NASA-TM-109989] p 1015 N95-18149
Low-dissipation and -dispersion Runge-Kutta schemes for computational acoustics
[NASA-CR-195022] p 1018 N95-18488
Study of high gain spherical shell ICF targets containing uniform layers of liquid deuterium tritium fuel
[DE94-018550] p 1136 N95-18552
Wall correction method with measured boundary conditions for low speed wind tunnels
p 1023 N95-19263
Determination of solid/porous wall boundary conditions from wind tunnel data for computational fluid dynamics codes p 1023 N95-19266
Analysis of test section sidewall effects on a two dimensional airfoil: Experimental and numerical investigations p 1025 N95-19276
Turbulence modeling for CFD, part 2
p 1030 N95-19466
On supersonic-inlet boundary-layer bleed flow
[NASA-CR-195426] p 955 N95-19769
BOUNDARY ELEMENT METHOD
A boundary element method for two dimensional linear elastic fracture analysis p 1045 N95-18917
Fracture toughness of polymer/polymer bimaterial interface reinforced with block copolymers
p 986 N95-18923
BOUNDARY INTEGRAL METHOD
A boundary element method for two dimensional linear elastic fracture analysis p 1045 N95-18917
Slot spiral antenna modeling using hybrid/mixed FE-BI technique p 1006 N95-19797
An efficient and accurate model of the coax cable feeding structure for FEM simulations
p 1006 N95-19799
Arbitrarily shaped dual-stacked patch antennas: A hybrid FEM simulation p 1006 N95-19800
BOUNDARY LAYER CONTROL
Parametric study on laminar flow for finite wings at supersonic speeds
[NASA-TM-108852] p 928 N95-18101
Active control of instabilities in laminar boundary-layer flow. Part 1: An overview
[NASA-CR-195016-PT-1] p 1020 N95-18958
On supersonic-inlet boundary-layer bleed flow
[NASA-CR-195426] p 955 N95-19769
BOUNDARY LAYER EQUATIONS
A spectrally accurate boundary-layer code for infinite swept wings
[NASA-CR-195014] p 1014 N95-18042
BOUNDARY LAYER FLOW
The stability of two-phase flow over a swept-wing
[NASA-CR-194994] p 1016 N95-18190
Effect of crossflow on Goertler instability in incompressible boundary layers
[NASA-CR-195007] p 1016 N95-18193
Active control of instabilities in laminar boundary-layer flow. Part 1: An overview
[NASA-CR-195016-PT-1] p 1020 N95-18958
Solution of Navier-Stokes equations using high accuracy monotone schemes p 948 N95-19019
Boundary-flow measurement methods for wall interference assessment and correction: Classification and review p 1022 N95-19262
Viscous flow past aerofoils axisymmetric bodies and wings p 933 N95-19457
On supersonic-inlet boundary-layer bleed flow
[NASA-CR-195426] p 955 N95-19769
BOUNDARY LAYER SEPARATION
Sectional prediction of 3D effects for separated flow on rotating blades
[PB94-201696] p 928 N95-18503
Theoretical investigations of shock/boundary layer interactions on a Ma(infinity) = 8 waverider
[DLR-FB-94-12] p 930 N95-18910
BOUNDARY LAYER STABILITY
Parametric study on laminar flow for finite wings at supersonic speeds
[NASA-TM-108852] p 928 N95-18101
Effect of crossflow on Goertler instability in incompressible boundary layers
[NASA-CR-195007] p 1016 N95-18193
Active control of instabilities in laminar boundary-layer flow. Part 1: An overview
[NASA-CR-195016-PT-1] p 1020 N95-18958
Synoptic-scale influence on the Monterey Bay sea-breeze
[AD-A285129] p 1073 N95-19596
BOUNDARY LAYER TRANSITION
Method and system for identifying the onset of a turbulent boundary layer induced by a body moving through a fluid medium
[AD-D016434] p 1018 N95-18525
Hypersonic wind tunnel test techniques
[AD-A284057] p 929 N95-18663
Active control of instabilities in laminar boundary-layer flow. Part 1: An overview
[NASA-CR-195016-PT-1] p 1020 N95-18958
Hypervelocity air flows with finite rate chemistry
[AD-A284727] p 931 N95-19109
BOUNDARY LAYERS
The numerical simulation of marine boundary layer clouds
[AD-A284149] p 1064 N95-18413
Numerical simulation of shock/shock and shock/boundary-layer interactions in chemically reacting hypersonic flows
[DLR-94-04] p 1019 N95-18609
Multispectral NOAA Marine Atmospheric Boundary Layer (MABL) estimates during VOCAR
[AD-A283702] p 1064 N95-18623
Stratified carrier electroviscous fluids and apparatus
[AD-D016238] p 1019 N95-18634
CUBIT mesh generation environment
[DE94-017496] p 1118 N95-18896
Coastal benthic boundary layer special research program: A review of the first year. Volume 1
[AD-A280034] p 1076 N95-19818
BOUNDARY VALUE PROBLEMS
Completed Beltrami-Michell formulation for analyzing radially symmetrical bodies
[NASA-TM-4593] p 1044 N95-18199
Completed Beltrami-Michell formulation for analyzing mixed boundary value problems in elasticity
[NASA-TM-106809] p 1045 N95-18909
A boundary element method for two dimensional linear elastic fracture analysis p 1045 N95-18917
Optimization of layered metal matrix composite cylinders p 970 N95-18920
BOUSSINESQ APPROXIMATION
Turbulence modeling for CFD, part 2
p 1030 N95-19466
BOW WAVES
Particle acceleration and transport in the tail and at the front side of the magnetosphere, task 1 and 2
[NASA-CR-197575] p 1064 N95-18476
BRAGG ANGLE
Bragg transmission phase plates for the production of circularly polarized x-rays
[DE94-017072] p 1151 N95-19113
BRAGG CELLS
True time delay beamforming
[AD-A285683] p 1003 N95-19516
BRAIDED COMPOSITES
TEXCAD: Textile Composite Analysis for Design. Version 1.0: User's manual
[NASA-CR-4639] p 970 N95-18466
BRAIN
Cellular analysis of circadian rhythmicity in cultured SCN neurons
[AD-A284167] p 1078 N95-18512
Nuclear medicine program
[DE94-017530] p 1080 N95-19244
BRAZIL
Comparative analysis of multisensor (TM/Landsat and SAR/ERS-1) and multitemporal scenes of Guaira region, Sao Paulo State, Brazil
[INPE-5581-TDI/544] p 1049 N95-18005
BRAZING
Braze repair possibilities for hot section gas turbine parts p 954 N95-19677
BRECCIA
The circumplanetary nebular environment: A possible source region for chondrules p 1191 N95-19325
BRIDGMAN METHOD
NiAl and NiAl-based composites directionally solidified by a containerless zone process
[NASA-CR-195430] p 982 N95-19792

BRIGHTNESS
Night Vision Goggles (NVG) software user's guide, version 5.1
[AD-A284563] p 1090 N95-18029
BRIGHTNESS DISTRIBUTION
Dynamics of LMC clusters
[ISBN-0-315-84911-8] p 1179 N95-18728
BRISTOL-SIDDELEY BS 53 ENGINE
An analysis of the costs and benefits in improving F402-RR-406A High Pressure Turbine, second stage blades under the aircraft engine Component Improvement Program (CIP)
[AD-A285127] p 950 N95-19595
BROADBAND
Numerically efficient use of frequency domain MoM codes for wideband radiation and scattering problems. An application: Scattering from a microstrip patch
[AD-A284561] p 995 N95-18116
A wideband absorber for television studios
[BBC-RD-1994/12] p 1123 N95-18566
Measurements of wideband multipath propagation at 531 MHz and 1.265 GHz
[BBC-RD-1994/3] p 1001 N95-19051
Digital audio broadcasting: Comparison of coverage at different frequencies and with different bandwidths
[BBC-RD-1993/11] p 1002 N95-19135
BROADCASTING
Design and analysis of dynamic leader election protocols in broadcast networks
[PB94-202728] p 1109 N95-18039
The development of the switched-horn radio-camera system
[BBC-RD-1993/13] p 997 N95-18494
RACE project 1036: WTDM broadband customer premises network
[BBC-RD-1993/15] p 998 N95-18537
RINSE: A digitally implemented flywheel sync regenerator for improved video synchroniser performance
[BBC-RD-1993/14] p 999 N95-18538
Predicted coverage of a COFDM single frequency network for UHF digital terrestrial TV broadcasting
[BBC-RD-1993/12] p 999 N95-18540
DAB: Multiplex and system support features
[BBC-RD-1994/9] p 1001 N95-19050
Measurements of wideband multipath propagation at 531 MHz and 1.265 GHz
[BBC-RD-1994/3] p 1001 N95-19051
Optimum dimension ratios for studios, control rooms and listening rooms
[BBC-RD-1993/8] p 993 N95-19053
Engineering review, January 1993 - March 1994
p 1001 N95-19055
Digital audio broadcasting: Comparison of coverage at different frequencies and with different bandwidths
[BBC-RD-1993/11] p 1002 N95-19135
BROKEN SYMMETRY
Family symmetries and proton decay
[DE94-017575] p 1133 N95-19245
BROMINE
Laboratory studies of stratospheric bromine chemistry: Kinetics of the reactions of bromine monoxide with nitrogen dioxide and atomic oxygen p 1065 N95-18731
BROMINE COMPOUNDS
Laboratory studies of stratospheric bromine chemistry: Kinetics of the reactions of bromine monoxide with nitrogen dioxide and atomic oxygen p 1065 N95-18731
BRUSHES
Design optimization of a brush turbine with a cleaner/water based solution p 1043 N95-18177
Improved approximation guarantees for minimum-weight k-trees and prize-collecting salesmen
[AD-A284042] p 1117 N95-18658
BUBBLES
Time-evolving bubbles in two-dimensional stokes flow
[NASA-CR-194998] p 1015 N95-18188
Observation of flow and temperature oscillations around a bubble on a solid surface subject to a vertical temperature gradient
[NASA-CR-197593] p 1017 N95-18327
Evolution of a collection of bubbles with application to wakes, bubble screens, and cloud noise
[AD-A283597] p 1017 N95-18434
Bubble formation in microgravity p 991 N95-18970
Echo imaging techniques determine the size of intravascular bubbles in decompression sickness
[AD-A284849] p 1087 N95-19714
BUDGETING
Draft SEI program plans: 1995-1999
[AD-A285047] p 1100 N95-19545
BUFFETING
Pressure measurements on an F/A-18 twin vertical tail in buffeting flow. Volume 4, part 2: Buffet cross spectral densities
[AD-A285555] p 957 N95-18641
BULKHEADS
A fiber optic coupler
[AD-D016473] p 1140 N95-18459
BUOYANCY
Prediction of buoyant outflow in lakes and fjords with a quasi 3D numerical model
[PB94-206984] p 1051 N95-18372
Effects of vibration (G-jitters) on convection in micro-gravity p 991 N95-19013
BURNING RATE
Studies on high pressure and unsteady flame phenomena
[AD-A284126] p 973 N95-18410

C

C (PROGRAMMING LANGUAGE)
SICOMP, the SINTEF data compression library (version 1.0) reference manual
[PB94-207107] p 1099 N95-18668
Error coding simulations in C p 963 N95-18998
Third CLIPS Conference Proceedings, volume 1
[NASA-CP-10162-VOL-1] p 1100 N95-19625
Expert system technologies for Space Shuttle decision support: Two case studies p 1104 N95-19646
Third CLIPS Conference Proceedings, volume 2
[NASA-CP-10162-VOL-2] p 1104 N95-19747
Using PVM to host CLIPS in distributed environments p 1104 N95-19748
A parallel strategy for implementing real-time expert systems using CLIPS p 1105 N95-19749
Using CLIPS in the domain of knowledge-based massively parallel programming p 1105 N95-19750
MIRO: A debugging tool for CLIPS incorporating historical Rete networks p 1105 N95-19754
Optimal pattern distributions in Rete-based production systems p 1106 N95-19755
Automated rule-base creation via CLIPS-Induce p 1107 N95-19761
Automated revision of CLIPS rule-bases p 1107 N95-19762
DAI-CLIPS: Distributed, Asynchronous, Interacting CLIPS p 1107 N95-19763
C++ (PROGRAMMING LANGUAGE)
CLIPS++: Embedding CLIPS into C++ p 1101 N95-19630
Adding intelligent services to an object oriented system p 1103 N95-19642
C-130 AIRCRAFT
KC-130 ANVIS/HUD assessment and symbology rationale
[AD-A284155] p 943 N95-18504
C-135 AIRCRAFT
KC-135 cockpit modernization study. Phase 1: Equipment evaluation
[AD-A284099] p 942 N95-18398
An artifical corrosion protocol for lap-splices in aircraft skin p 937 N95-19482
CADMIUM SULFIDES
Fabrication of biomimetic molecular level composites
[AD-A284204] p 969 N95-17941
CADMIUM TELLURIDES
IR materials producibility
[AD-A284263] p 1142 N95-19732
Advanced processing technology for high-efficiency, thin-film CuInSe2 and CdTe solar cells
[DE94-011838] p 1056 N95-19880
CALCITE
Atomic scale force mapping with the atomic force microscope
[AD-A284940] p 1129 N95-17974
CALCIUM
Obtention of cationic polymeric membranes by radiation-induced grafting method
[DE94-629193] p 983 N95-17942
Sodium sulfate corrosion of silicon carbide fiber-reinforced calcium aluminosilicate glass-ceramic matrix composites
[AD-A283703] p 969 N95-18021
CALCIUM COMPOUNDS
Heterogeneous nucleation of calcium oxalate on native oxide surfaces
[DE94-018725] p 986 N95-18648
Shock-induced devolatization of calcium sulfate and implications for K-T extinctions
[NASA-CR-197608] p 1060 N95-19033
CALIBRATING
AASERT-93: New high-pressure diagnostic technique
[AD-A284943] p 973 N95-17975
Optical Rain Gauge Performance: Second Workshop on Optical Rain Gauge Measurements
[NASA-CP-3288] p 1068 N95-18201
Rain gauge calibration and testing p 1070 N95-18209
Aeromechanics technology, volume 1. Task 1: Three-dimensional Euler/Navier-Stokes Aerodynamic Method (TEAM) enhancements
[AD-A285713] p 943 N95-18483
Calibration and sediment load algorithms for an acoustic sediment flux probe
[AD-A283655] p 1075 N95-18617
Metrology: Calibration and measurement processes guidelines
[NASA-RP-1342] p 992 N95-18745
Assembly and calibration of a new experimental apparatus for production and utilization of capture gamma rays
[DE94-626650] p 1198 N95-18880
Calibration and testing of a large-scale electric gun for shock Hugoniot measurements
[MRL-TR-93-24] p 959 N95-18942
A comparison between using incoherent or coherent sources to align and test an adaptive optical telescope p 1142 N95-18969
Digital monopulse
[AD-D016447] p 1002 N95-19072
Calibration and use of a non-nulling seven-hole pressure probe p 1021 N95-19254
Applications of the five-hole probe technique for flow field surveys at the Institute for Aerospace Research p 1021 N95-19255
Gain uniformity, linearity, saturation and depletion in gated microchannel-plate x-ray framing cameras
[DE94-018596] p 1035 N95-19711
CAMERAS
High frame rate CCD cameras with fast optical shutters for military and medical imaging applications
[DE94-018316] p 1034 N95-19229
Acceptance/operational test procedure 101-SY tank camera purge system and in tank color camera video imaging system
[DE95-000344] p 1035 N95-19553
CANARD CONFIGURATIONS
Velocity measurements with hot-wires in a vortex-dominated flowfield p 932 N95-19261
CANTILEVER BEAMS
The linear dynamics of a microsensor accelerometer modeled as a cantilever beam with an end mass
[DE94-019108] p 1031 N95-17963
CAPACITORS
Induction heating coupler and annealer
[NASA-CASE-LAR-14277-1] p 1011 N95-18962
Power terminal protection device
[AD-D016528] p 1011 N95-19120
CAPE KENNEDY LAUNCH COMPLEX
The meteorological monitoring system for the Kennedy Space Center/Cape Canaveral Air Station p 1104 N95-19647
CAPILLARY FLOW
Observation of flow and temperature oscillations around a bubble on a solid surface subject to a vertical temperature gradient
[NASA-CR-197593] p 1017 N95-18327
CAPTURE EFFECT
Floating shock fitting via Lagrangian adaptive meshes
[NASA-CR-194997] p 1116 N95-18110
Assembly and calibration of a new experimental apparatus for production and utilization of capture gamma rays
[DE94-626650] p 1198 N95-18880
CARBIDES
A review of nuclear thermal propulsion carbide fuel corrosion and key issues
[NASA-CR-197533] p 1136 N95-18217
Novel carbon-ion fuel cells
[DE94-017390] p 1053 N95-18894
Heteroepitaxy of ternary SiGeC alloys on Si for bipolar transistors
[AD-A285317] p 1151 N95-19511
CARBOHYDRATES
Drink composition and cycle-ergometer endurance in men: Carbohydrate, Na(+), osmolality
[NASA-TM-4650] p 1077 N95-19140
CARBON
Renewable energy and its potential for carbon emissions reductions in developing countries: Methodology for technology evaluation
[DE94-011870] p 1056 N95-17943
Method of doping single crystal diamond for electronic devices
[AD-D016267] p 1149 N95-18543
One strategy for estimating the potential soil carbon storage due to CO2 fertilization
[DE94-017895] p 1059 N95-18666
Changes in the flux of carbon between plants and soil microorganisms at elevated CO2: Physiological processes with ecosystem-level implications
[DE94-017067] p 1060 N95-19112

Impurity behavior during ion-Bernstein wave heating in PBX-M
[DE94-018114] p 1133 N95-19228
Papers presented to the Conference on Chondrules and the Protoplanetary Disk
[NASA-CR-197121] p 1186 N95-19289
Carbon, CAIs and chondrules p 1186 N95-19291
Nozzle Initiative Industry Advisory Committee on Standardization of Carbon-Phenolic Test Methods and Specifications
[NASA-CR-197529] p 967 N95-19566
Novel catalysts for methane activation
[DE95-001179] p 976 N95-19785
Characterization of inactive carbon in GaAs
[DE95-002352] p 976 N95-19836

CARBON COMPOUNDS
Composites research in support of the NASP Institute for Composites (NIC)
[NASA-CR-197580] p 970 N95-18471

CARBON DIOXIDE
Trends 1993: A compendium of data on global change
[ORNL/CDIAC-65] p 1058 N95-18389
Innovative development and application of models for weakly ionized ionospheric plasmas
[AD-A284583] p 1064 N95-18452
Assessment of CO2 projections
[DE94-017484] p 1059 N95-18664
One strategy for estimating the potential soil carbon storage due to CO2 fertilization
[DE94-017895] p 1059 N95-18666
Changes in the flux of carbon between plants and soil microorganisms at elevated CO2: Physiological processes with ecosystem-level implications
[DE94-017067] p 1060 N95-19112
Systems and economic analysis of microalgae ponds for conversion of CO2 to biomass
[DE95-000406] p 1054 N95-19554
Historic patterns of CO2 emissions from fossil fuels: Implications for stabilization of emissions
[DE95-000489] p 1061 N95-19556
Novel catalysts for methane activation
[DE95-001179] p 976 N95-19785

CARBON DIOXIDE CONCENTRATION
Storm activity over the North Sea and the Netherlands in two climate models compared with observations
[KNMI-WR-94-02] p 1070 N95-18393
Changes in the flux of carbon between plants and soil microorganisms at elevated CO2: Physiological processes with ecosystem-level implications
[DE94-017067] p 1060 N95-19112

CARBON FIBER REINFORCED PLASTICS
Composite structures for magnetosphere imager spacecraft p 966 N95-18976
Acoustic fatigue of carbon fibre structures p 1127 N95-19158
Brite-Euram programme: ACOUFAT acoustic fatigue and related damage tolerance of advanced composite and metallic structures p 1127 N95-19159
A mechanism for blistering of carbon fiber composites
[AD-A286252] p 971 N95-19386

CARBON FIBERS
A real-time vision system to monitor/analyze the changes in composite specimens during mechanical testing
[ARL-TR-344] p 970 N95-18612
A mechanism for blistering of carbon fiber composites
[AD-A286252] p 971 N95-19386
Damage monitoring in metallic and composite structures using piezoelectric thin film sensors
[ARL-RR-4] p 971 N95-19467

CARBON ISOTOPES
Trends 1993: A compendium of data on global change
[ORNL/CDIAC-65] p 1058 N95-18389

CARBON MONOXIDE
Potential impacts on air quality of the use of ethanol as an alternative fuel
[DE94-011881] p 1056 N95-17944
Electrochemical interfaces and electrode processes: Electrochemical oxidation of small organisms
[AD-A284873] p 1013 N95-19741

CARBON-PHENOLIC COMPOSITES
Coupled finite element analysis of decomposing poroelastic polymeric composites and structures with subsequent thermal and gas diffusion p 986 N95-18918
Nozzle Initiative Industry Advisory Committee on Standardization of Carbon-Phenolic Test Methods and Specifications
[NASA-CR-197529] p 967 N95-19566

CARBONACEOUS CHONDRITES
Constraints on chondrule agglomeration from fine-grained chondrule rims p 1189 N95-19315
The origin of refractory precursor components of chondrules p 1189 N95-19316
Formation of chondrules and CAIs by nebular processes p 1190 N95-19321
A ceramic/slag interface as an analog for accretion of hot refractory objects and rim formation p 1191 N95-19322

CARBONATES
Molten carbonate fuel cell with high power density
[DE94-017080] p 1053 N95-19074
Pitting corrosion of aluminized seals in molten carbonate fuel cells
[DE94-017075] p 1053 N95-19116
Lithium ferrate and lithium cobaltate cathodes for molten carbonate fuel cells
[DE94-017079] p 1054 N95-19117

CARBOXYLIC ACIDS
Obtention of cationic polymeric membranes by radiation-induced grafting method
[DE94-629193] p 983 N95-17942
The Solvent Absorption-Extractive Distillation (SAED) process for ethanol recovery from gas/vapor streams
[DE94-013112] p 974 N95-18637

CARDIAC VENTRICLES
The aeromedical implications of supraventricular tachycardia p 1085 N95-19437

CARDS
Automatic Identification Technology (AIT): The development of functional capability and card application matrices
[AD-A285528] p 1173 N95-18099

CARRIER FREQUENCIES
Doppler shift and spread study for ionospherically propagated signals
[AD-A284610] p 1065 N95-19083

CARRIER LIFETIME
Minority-carrier lifetime in InP as a function of light bias
[NASA-TM-106821] p 1149 N95-18453

CASCADE FLOW
A three-dimensional structured/unstructured hybrid Navier-Stokes method for turbine blade rows
[NASA-TM-106813] p 1016 N95-18200
Measurement of gust response on a turbine cascade
[NASA-TM-106776] p 928 N95-18457
Enhanced capabilities and modified users manual for axial-flow compressor conceptual design code CSPAN
[NASA-TM-106833] p 930 N95-18933
Simulation of steady and unsteady viscous flows in turbomachinery p 949 N95-19023

CASE HISTORIES
AMDRS: A resource for intelligent aeromedical decision-making p 1082 N95-19419
Think health not disease p 1083 N95-19429

CATALOGS (PUBLICATIONS)
Small Business Research Summaries, numbers 51-100
[PB94-179967] p 1170 N95-17986
Small Business Research Summaries, numbers 1-50
[PB94-179959] p 1170 N95-17987
Catalog of environmental data sets of Europe at the RIVM
[PB94-202710] p 1057 N95-18002
Applications catalog of pyrotechnically actuated devices/systems
[NASA-TM-106810] p 962 N95-18387

CATALYSIS
Transition metal oxides deposited on rhodium and platinum: Surface chemistry and catalysis
[DE95-000793] p 975 N95-19616

CATALYSTS
Preparation and surface characterization of metal doped alumina catalyst
[PB94-175296] p 973 N95-17991
Development of a colloidal redox system containing a smectite clay for control of reactivity and reaction selectivity
[AD-A285958] p 974 N95-19515
Novel catalysts for methane activation
[DE95-001179] p 976 N95-19785

CATALYTIC ACTIVITY
Transition metal oxides deposited on rhodium and platinum: Surface chemistry and catalysis
[DE95-000793] p 975 N95-19616

CATHODE RAY TUBES
An evaluation of aircraft CRT and dot-matrix display legibility requirements
[AD-A283933] p 947 N95-18164

CATHODES
Preparation of an electrocatalytic cathode for an aluminum-hydrogen peroxide battery
[AD-D016262] p 1008 N95-18318
Electron reversal ionizer for detection of trace species using a spherical cathode
[NASA-CASE-NPO-18870-1-CU] p 1130 N95-18324

CATHODIC COATINGS
Fundamental advances for characterizing cathodic protection systems
[PB94-180692] p 1122 N95-17983

CATIONS
Microstructure and crystal defects in perovskite crystals with A-site cation ordering
[AD-A284261] p 1153 N95-19713

CAUSTICS (OPTICS)
On the measurement of the crack tip stress field as a means of determining Delta K(sub eff) under conditions of fatigue crack closure p 938 N95-19492

CAVITATION FLOW
Evolution of a collection of bubbles with application to wakes, bubble screens, and cloud noise
[AD-A283597] p 1017 N95-18434
Bubble formation in microgravity p 991 N95-18970

CAVITIES
The effects of cavity topology on instabilities in additive-pulse modelocked lasers
[DE94-018193] p 1036 N95-18123
Microcavity structures
[DE95-001096] p 1039 N95-19727
An efficient and accurate model of the coax cable feeding structure for FEM simulations p 1006 N95-19799

CAVITY FLOW
Weapons bay acoustic environment p 1125 N95-19146

CELL CATHODES
Lithium ferrate and lithium cobaltate cathodes for molten carbonate fuel cells
[DE94-017079] p 1054 N95-19117

CELL MEMBRANES (BIOLOGY)
Mechanisms of interaction and biological effects of extremely-low-frequency electromagnetic fields
[DE94-015200] p 1076 N95-18371

CELLS (BIOLOGY)
Mechanisms of interaction and biological effects of extremely-low-frequency electromagnetic fields
[DE94-015200] p 1076 N95-18371

CENTAUR LAUNCH VEHICLE
A 20k payload launch vehicle fast track development concept using an RD-180 engine and a Centaur upper stage
[NASA-TM-108475] p 963 N95-19648

CENTER OF GRAVITY
Space Station racks weight and CG measurement using the rack insertion end-effector p 966 N95-18168

CENTER OF MASS
Physics at the Fermilab Tevatron Proton-Antiproton Collider
[DE95-000648] p 1137 N95-19561

CENTRAL PROCESSING UNITS
Dynamic range control of audio signals by digital signal processing
[BBC-RD-1993/7] p 1124 N95-19054

CENTRIFUGAL CASTING
Centrifugal casting of reinforced articles
[AD-D016277] p 992 N95-18431

CENTRIFUGAL PUMPS
Centrifugal and axial pump design and off-design performance prediction
[NASA-TM-106745] p 968 N95-19795

CENTRIFUGES
Centrifuge tests of the medical condition of French fighter pilots p 1082 N95-19424
Summary report of mission acceleration measurements for STS-60, SPACEHAB2, launched 11 February 1994
[NASA-TM-106797] p 991 N95-19788

CENTROIDS
The formulation of quantum statistical mechanics based on the Feynman path centroid density. 3: Phase space formalism and analysis of centroid molecular dynamics
[AD-A279233] p 1157 N95-19852
The formulation of quantum statistical mechanics based on the Feynman path centroid density. 4: Algorithms for centroid molecular dynamics
[AD-A279234] p 1157 N95-19853

CERAMIC BONDING
Adhesion, friction, and wear behavior of clean metal-ceramic couples
[NASA-TM-106815] p 989 N95-19783

CERAMIC COATINGS
Reliability Without Hermeticity (RWOH) for Integrated Circuits (IC)
[AD-A284340] p 1009 N95-18418
Protective coatings for compressor gas path components p 954 N95-19675
Thermal testing of high performance thermal barrier coatings for turbine blades p 955 N95-19681

CERAMIC MATRIX COMPOSITES
Sodium sulfate corrosion of silicon carbide fiber-reinforced calcium aluminosilicate glass-ceramic matrix composites
[AD-A283703] p 969 N95-18021
Development of radiation-hardened ceramic composites for fusion applications
[DE94-016182] p 985 N95-18638

A CMC database for use in the next generation launch vehicles (rockets) p 963 N95-18993
Barium strontium titanate and non-ferroelectric oxide ceramic composites for use in phased array antennas [AD-A279225] p 972 N95-19851

CERAMICS
Advanced diesel engine component development program, tasks 4-14 [NASA-CR-191203] p 1040 N95-18041
Novel polymeric composites through molecular engineering [AD-A284168] p 985 N95-18513
Composite structures having organic matrices and duplex zinc/ceramic fire barriers [AD-D016232] p 970 N95-18629
Heterogeneous nucleation of calcium oxalate on native oxide surfaces [DE94-018725] p 986 N95-18648
A ceramic/slag interface as an analog for accretion of hot refractory objects and rim formation p 1191 N95-19322
Enhancement of creep resistance of a sintered Si3N4 ceramic by microwave annealing [DE94-017688] p 987 N95-19399
Recent progress on ECVD Project [DE94-016773] p 988 N95-19580
Resistance of silicon nitride turbine components to erosion and hot corrosion/oxidation attack p 955 N95-19683
Investigation of microscopic mechanisms of failure of electronic smart materials/systems [AD-A284830] p 988 N95-19691
Proceedings of the Eighth Annual Conference on Fossil Energy Materials [DE95-001055] p 981 N95-19723
Adhesion, friction, and wear behavior of clean metal-ceramic couples [NASA-TM-106815] p 989 N95-19783
Materials for adaptive structural acoustic control, volume 3 [AD-A279223] p 1128 N95-19850
Barium strontium titanate and non-ferroelectric oxide ceramic composites for use in phased array antennas [AD-A279225] p 972 N95-19851

CEREBELLUM
Cerebellar circuit mechanisms which accompany coordinated limb trajectory patterns in the rat: Use of a model of spontaneous changes in limb coordination [AD-A284023] p 1079 N95-18656

CEREBRAL CORTEX
Cerebellar circuit mechanisms which accompany coordinated limb trajectory patterns in the rat: Use of a model of spontaneous changes in limb coordination [AD-A284023] p 1079 N95-18656

CEREBRUM
Cumulative effects of repeated brief cerebral ischemia [AD-A284234] p 1087 N95-19698

CERMETS
High velocity oxygen fuel spraying of erosion and wear resistant coatings on jet engine parts p 954 N95-19680

CESIUM PLASMA
A three region analysis of a bounded plasma using particle in cell and fluid techniques [AD-A284826] p 1147 N95-19690

CH-47 HELICOPTER
Design and flight test of a simplified control system for a transport helicopter p 958 N95-18902

CHANGE DETECTION
Minimal time detection algorithms and applications to flight systems [TR-2-FSRC-93] p 1098 N95-18564

CHANNEL FLOW
Aerodynamic investigation of the flow field in a 180 deg turn channel with sharp bend p 1021 N95-19257

CHANNELS (DATA TRANSMISSION)
Processing multilevel secure test and evaluation information [AD-A284073] p 1001 N95-19069
Alleviation of co-channel interference at Poole relay station [BBC-RD-1993/4] p 1003 N95-19136

CHAOS
Synchronization of nonautonomous chaotic systems [AD-D016440] p 1010 N95-18528

CHARACTER RECOGNITION
Facilitation and interference in identification of pictures and words [AD-A285882] p 1090 N95-19602

CHARACTERIZATION
Gigabit optical interconnects: System and component analysis, design and development [AD-A285536] p 1138 N95-18067
Spectral reflectance properties of wetlands plants [AD-A283546] p 1051 N95-18614
LEVIS ion source and beam characterization on PBFA-2 [DE94-015802] p 1133 N95-19199
Heteroepitaxy of ternary SiGeC alloys on Si for bipolar transistors [AD-A285317] p 1151 N95-19511
Novel e-o polymers: NLO materials with superior temporal stability [AD-A285872] p 988 N95-19614
CVD silicon carbide characterization [AD-A285667] p 972 N95-19702
Isolation and characterization of an indium-mixed-pnicogen Four-membered ring compound: Crystal structure of (Me3SiCH2)2InAs(SiMe3)2 In(CH2SiMe3)2P(SiMe3)2 [AD-A279170] p 1154 N95-19807
MBE growth, characterization and electronic device processing of Hg-based semiconductor alloys and heterostructures [AD-A279203] p 1154 N95-19817

CHARGE CARRIERS
DC-conductivity and magnetoresistance of inherently conducting polymers. Polyacetylene and poly(3-alkylthiophenes) [PB94-184587] p 1007 N95-18037

CHARGE COUPLED DEVICES
Progress on the multipulse Thomson scattering diagnostic on D3-D [DE94-017515] p 1143 N95-18119
High frame rate CCD cameras with fast optical shutters for military and medical imaging applications [DE94-018316] p 1034 N95-19229

CHARGE TRANSFER
Three-grid accelerator system for an ion propulsion engine [NASA-CASE-NPO-18391-2-CU] p 1137 N95-18957
Assessment of velocity/trajectory measurement technologies during a particle capture event p 1036 N95-19193

CHARGED PARTICLES
Advanced methods for the computation of particle beam transport and the computation of electromagnetic fields and beam-cavity interactions [DE94-017359] p 1136 N95-18893
Crystalline beams: The string [DE94-016806] p 1150 N95-19091
Ion orbit loss and the poloidal electric field in a tokamak [DE94-016860] p 1145 N95-19092
Impurity behavior during ion-Bernstein wave heating in PBX-M [DE94-018114] p 1133 N95-19228

CHARM (PARTICLE PHYSICS)
Feynman-x and transverse momentum dependence of D(sup (+-)) and D(sup 0), D-bar(sup 0) production in 250 GeV (pi)(sup -) - nucleon interactions [DE94-626698] p 1130 N95-18366
Summary of the working group on tests of QCD [DE94-018390] p 1131 N95-18550

CHARTS
Digital mapping, charting, and geodesy analysis program technical review of Digital Aeronautical Flight Information Data Prototype 1.0 on CD-ROM [AD-A284728] p 1050 N95-18078

CHECKOUT
A parallel strategy for implementing real-time expert systems using CLIPS p 1105 N95-19749
MIRO: A debugging tool for CLIPS incorporating historical Rete networks p 1105 N95-19754

CHELATES
Polymer-based separations: Synthesis and application of polymers for ionic and molecular recognition [DE94-016427] p 984 N95-18355

CHEMICAL ANALYSIS
Midinfrared optical properties of petroleum oil aerosols [AD-A283689] p 1139 N95-18142
Application of conducting polymers to electroanalysis [DE94-015204] p 984 N95-18348
GAMQUEST, a computer program to identify gamma rays [DE94-016217] p 1197 N95-18351
TSH determination in subjects with medium-low levels of serum thyroxine p 1082 N95-19421
Activities of the Analytical Chemistry Laboratory [DE95-000834] p 975 N95-19618
Synthesis and characterization of aluminum-phosphorus adducts: X-ray crystal structures of Cl3Al (dot) P(SiMe3)3 (dot) C7H8 and Br3Al (dot) P(SiMe3)3 (dot) C7H8 [AD-A279194] p 1154 N95-19812

CHEMICAL COMPOSITION
Solid fuel ramjet composition [AD-D016458] p 990 N95-19090
Investigation of the microstructure of coatings for high power lasers by non-optical techniques [DE94-017697] p 987 N95-19227
The role of chondrules in nebular fractionations of volatiles and other elements p 1187 N95-19300
Chondrule formation in lightning discharges p 1188 N95-19304
Chondrules and their associates in ordinary chondrites p 1188 N95-19306
Thermochemical IR sources: COCHISE and FACELIF experiments [AD-A279940] p 977 N95-19868

CHEMICAL EFFECTS
Effects of meteor showers in the Earth ionosphere [INPE-5591-TDI/552] p 1178 N95-18213

CHEMICAL ELEMENTS
Synthesis and characterization of aluminum-phosphorus adducts: X-ray crystal structures of Cl3Al (dot) P(SiMe3)3 (dot) C7H8 and Br3Al (dot) P(SiMe3)3 (dot) C7H8 [AD-A279194] p 1154 N95-19812

CHEMICAL ENGINEERING
The Solvent Absorption-Extractive Distillation (SAED) process for ethanol recovery from gas/vapor streams [DE94-013112] p 974 N95-18637

CHEMICAL EVOLUTION
On the possibility of precipitation-induced vertical lightning in the protoplanetary nebula p 1187 N95-19299
Experimental constraints on models for origins of chondrules: Peak temperatures p 1187 N95-19302
Chondrule formation in lightning discharges p 1188 N95-19304
Collision of cometlike and slightly differentiated bodies as an origin for ordinary chondrites p 1188 N95-19308

CHEMICAL EXPLOSIONS
Observations of TEC fluctuations from an explosion on the Earth's surface [DE94-018278] p 1063 N95-18125

CHEMICAL FRACTIONATION
Enantiomeric separation of chiral alpha-(1-naphthyl)ethyl ammonium perchlorate by silica gel-bound chiral pyridino-18-crown-6 ligands [AD-A280156] p 969 N95-19822

CHEMICAL LASERS
NCl(b) based short wavelength chemical laser [AD-A284213] p 1036 N95-17956

CHEMICAL REACTION CONTROL
Development of a colloidal redox system containing a smectite clay for control of reactivity and reaction selectivity [AD-A285958] p 974 N95-19515

CHEMICAL REACTIONS
Difunctional monomers based on perfluoropropylene telomers [AD-A283677] p 983 N95-18019
Sodium sulfate corrosion of silicon carbide fiber-reinforced calcium aluminosilicate glass-ceramic matrix composites [AD-A283703] p 969 N95-18021
An atomic view of motion on surfaces [AD-A285565] p 1131 N95-18473
Method for laser-assisted silicon etching using halocarbon ambients [AD-D016239] p 1038 N95-18635
Intrinsic barriers for H-atom transfer reactions involving hydrocarbons [DE94-018451] p 1134 N95-19590
Alternative materials for solid oxide fuel cells [DE94-018452] p 1054 N95-19591
Reaction channel competition in vibrational overtone activation: 1-methylcyclopropene [AD-A280185] p 976 N95-19830

CHEMICAL REACTORS
Palladium-based membranes for hydrogen separation [PB94-207156] p 973 N95-18377

CHEMICAL TESTS
Relevance of laboratory tests in aeromedical decisions p 1082 N95-19420

CHIPS (ELECTRONICS)
Radar sector blanker [AD-D016275] p 996 N95-18429
Development of high reliability planar chip inductors [DE94-018589] p 1012 N95-19231

CHIPS (MEMORY DEVICES)
Semiconductor measurement technology: Design and testing guides for the COMOS and lateral bipolar-on-SOI test library [PB94-178019] p 1007 N95-17984

CHIRAL DYNAMICS
Comparison of the anomalous and non-anomalous generalized Schwinger models via functional formalism [DE94-626684] p 1156 N95-18333

CHLORIDES
NCl(b) based short wavelength chemical laser [AD-A284213] p 1036 N95-17956

Synthesis and characterization of a neutral six-coordinate tris-adduct of an indium(3) trihalide. X ray crystal structure of InCl3(THF)3
[AD-A279169] p 1154 N95-19806

CHLORINE
Synthesis and characterization of a neutral six-coordinate tris-adduct of an indium(3) trihalide. X ray crystal structure of InCl3(THF)3
[AD-A279169] p 1154 N95-19806

CHLOROFLUOROCARBONS
Trends 1993: A compendium of data on global change
[ORNL/CDIAC-65] p 1058 N95-18389
Method for laser-assisted silicon etching using halocarbon ambients
[AD-D016239] p 1038 N95-18635
Thermoelectric properties of conducting polymers
[AD-A284058] p 986 N95-18678

CHLOROFLUOROMETHANE
Method for laser-assisted silicon etching using halocarbon ambients
[AD-D016239] p 1038 N95-18635

CHONDRITES
Papers presented to the Conference on Chondrules and the Protoplanetary Disk
[NASA-CR-197121] p 1186 N95-19289
Chondrule-matrix relationships in chondritic meteorites p 1186 N95-19293
Overview of nebula models: Potential chondrule-forming environments p 1186 N95-19294
Crystallization trends of precursor pyroxene in ordinary chondrites: Implications for igneous origin of precursor p 1187 N95-19298
Chondrules and their associates in ordinary chondrites p 1188 N95-19306
Collision of cometlike and slightly differentiated bodies as an origin for ordinary chondrites p 1188 N95-19308
Microchondrules in ordinary chondrites: Implications for chondrule formation p 1188 N95-19309
Constraints on chondrule and CAI origins from vapor-liquid-solid experiments p 1190 N95-19317
Mn-Cr isotopic systematics of Chainpur chondrules and bulk ordinary chondrites p 1190 N95-19320
Chondrule remelting: Evidence from coarse-grained chondrule rims and compound chondrules p 1191 N95-19323
Variations among chondrite groups: Constraints on nebular processes p 1192 N95-19327
Open-system behavior during chondrule formation p 1192 N95-19328
I-Xe studies of individual chondrules: What can they tell us about chondrule formation? p 1192 N95-19329
Chemical production of chondrule oxygen isotopic composition p 1192 N95-19330
Establishment of redox conditions during planetary collisions as an origin of chondrites p 1192 N95-19331
Chondrule origins: Constraints from chondrule properties and cosmochemistry p 1192 N95-19332
Major unresolved issues in the formation of chondrules and CAIs p 1193 N95-19336
Flash heating is required to minimize sodium losses from chondrules p 1193 N95-19337
Chondrule precursors and cooling paths: The sulfur evidence p 1193 N95-19338
Textural variability of ordinary chondrite chondrules: Implications of their formation p 1193 N95-19339

CHONDRULE
Papers presented to the Conference on Chondrules and the Protoplanetary Disk
[NASA-CR-197121] p 1186 N95-19289
Producing chondrules by recycling and volatile loss p 1186 N95-19290
Carbon, CAIs and chondrules p 1186 N95-19291
Large-scale processes in the solar nebula p 1186 N95-19292
Chondrule-matrix relationships in chondritic meteorites p 1186 N95-19293
Overview of nebula models: Potential chondrule-forming environments p 1186 N95-19294
Constraints placed on the nature of chondrule precursors p 1186 N95-19295
Turbulent diffusion and concentration of chondrules in the protoplanetary nebula p 1187 N95-19296
Crystallization trends of precursor pyroxene in ordinary chondrites: Implications for igneous origin of precursor p 1187 N95-19298
On the possibility of precipitation-induced vertical lightning in the protoplanetary nebula p 1187 N95-19299
The role of chondrules in nebular fractionations of volatiles and other elements p 1187 N95-19300
Experimental constraints on models for origins of chondrules: Peak temperatures p 1187 N95-19302
Models for multiple heating mechanisms p 1188 N95-19303
Chondrule formation in lightning discharges p 1188 N95-19304
The early Sun and the formation of chondrules p 1188 N95-19305
Chondrules and their associates in ordinary chondrites p 1188 N95-19306
Relict grains in chondrules: Evidence for chondrule recycling p 1188 N95-19307
Collision of cometlike and slightly differentiated bodies as an origin for ordinary chondrites p 1188 N95-19308
Microchondrules in ordinary chondrites: Implications for chondrule formation p 1188 N95-19309
The jet model of chondrule formation p 1189 N95-19310
Experimental constraints on models for the origin of chondrules: Cooling rates p 1189 N95-19311
Implications of a phase-transition thermostat for chondrule melting p 1189 N95-19312
Formation of chondrules by electrical discharge heating p 1189 N95-19313
Chronology of chrondrule and CAI formation: Mg-Al isotopic evidence p 1189 N95-19314
Constraints on chondrule agglomeration from fine-grained chondrule rims p 1189 N95-19315
The origin of refractory precursor components of chondrules p 1189 N95-19316
Constraints on chondrule and CAI origins from vapor-liquid-solid experiments p 1190 N95-19317
Porphyritic versus nonporphyritic chondrules p 1190 N95-19318
Siderophile elements and metal-silicate fractionation in the solar nebula p 1190 N95-19319
Mn-Cr isotopic systematics of Chainpur chondrules and bulk ordinary chondrites p 1190 N95-19320
Formation of chondrules and CAIs by nebular processes p 1190 N95-19321
Chondrule remelting: Evidence from coarse-grained chondrule rims and compound chondrules p 1191 N95-19323
Chondrule formation in the radiative accretional shock p 1191 N95-19324
The circumplanetary nebular environment: A possible source region for chondrules p 1191 N95-19325
Heating during solar nebula formation and Mg isotopic fractionation in precursor grains of CAIs and chondrules p 1191 N95-19326
Variations among chondrite groups: Constraints on nebular processes p 1192 N95-19327
Open-system behavior during chondrule formation p 1192 N95-19328
I-Xe studies of individual chondrules: What can they tell us about chondrule formation? p 1192 N95-19329
Chemical production of chondrule oxygen isotopic composition p 1192 N95-19330
Establishment of redox conditions during planetary collisions as an origin of chondrites p 1192 N95-19331
Chondrule origins: Constraints from chondrule properties and cosmochemistry p 1192 N95-19332
The fine nebula dust component: A key to chondrule formation by lightning p 1192 N95-19333
Cooling rates of chondrules: A new approach p 1192 N95-19334
Implications for the evolution of chondrules from Agglomeratic olivine chondrules p 1193 N95-19335
Major unresolved issues in the formation of chondrules and CAIs p 1193 N95-19336
Flash heating is required to minimize sodium losses from chondrules p 1193 N95-19337
Chondrule precursors and cooling paths: The sulfur evidence p 1193 N95-19338
Textural variability of ordinary chondrite chondrules: Implications of their formation p 1193 N95-19339

CHROMIUM
Ion emission intensity ratios as a function of electrode gap, melting current, and pressure during low current vacuum arc remelting
[DE94-017407] p 1129 N95-18144
Trivalent chromium conversion coatings for aluminum
[AD-D016274] p 978 N95-18332
Trivalent chromium solutions for sealing anodized aluminum
[AD-D016472] p 979 N95-18458
Compact, efficient, scalable neodymium laser co-doped with activator ions and pumped by visible laser diodes
[AD-D016237] p 1038 N95-18585
Relative elemental abundance and heating constraints determined for the solar corona from SERTS measurements
[NASA-TM-104616] p 1196 N95-19791
Heavy metal soil contamination at US Army installations: Proposed research and strategy for technology development
[AD-A279171] p 1062 N95-19808

CHROMIUM ALLOYS
Alloying effects on the high-temperature oxidation resistance of Cr-Cr2Nb
[DE94-018146] p 978 N95-18121

CHROMIUM CARBIDES
Tribology and microstructure of PS212 with a Cr2O3 seal coat
[NASA-TM-106768] p 969 N95-18448

CHROMIUM ISOTOPES
Mn-Cr isotopic systematics of Chainpur chondrules and bulk ordinary chondrites p 1190 N95-19320

CHROMIUM OXIDES
Tribology and microstructure of PS212 with a Cr2O3 seal coat
[NASA-TM-106768] p 969 N95-18448
Ion mixing in oxide-sapphire systems
[DE94-018660] p 1133 N95-19232
Alternative materials for solid oxide fuel cells
[DE94-018452] p 1054 N95-19591

CHROMOPHORES
Novel e-o polymers: NLO materials with superior temporal stability
[AD-A285872] p 988 N95-19614

CHROMOSOMES
Lower bounds for identifying subset members with subset queries
[DE94-014296] p 1117 N95-18346
Capillary electrophoresis: Biotechnology for separation of DNA and chromosomes p 1077 N95-19014

CHROMOSPHERE
Solar flare model atmospheres
[NASA-CR-197607] p 1196 N95-19034

CHRONOLOGY
Chronology of chrondrule and CAI formation: Mg-Al isotopic evidence p 1189 N95-19314

CIRCADIAN RHYTHMS
Cellular analysis of circadian rhythmicity in cultured SCN neurons
[AD-A284167] p 1078 N95-18512
Cerebellar circuit mechanisms which accompany coordinated limb trajectory patterns in the rat: Use of a model of spontaneous changes in limb coordination
[AD-A284023] p 1079 N95-18656

CIRCUIT BOARDS
Semiconductor measurement technology: Design and testing guides for the COMOS and lateral bipolar-on-SOI test library
[PB94-178019] p 1007 N95-17984
Real time simulator with Ti floating point digital signal processor
[DE94-016372] p 1012 N95-19246
AUTO: Automatic script generation system
[AD-A285897] p 1012 N95-19606

CIRCUIT DIAGRAMS
Semiconductor measurement technology: Design and testing guides for the COMOS and lateral bipolar-on-SOI test library
[PB94-178019] p 1007 N95-17984

CIRCUIT PROTECTION
Development of an amorphous surge blocker for a high voltage acceleration power supply of the neutral beam injectors
[DE94-770648] p 1138 N95-19874

CIRCUIT RELIABILITY
High-frequency skywave signal power measurement system
[AD-A284382] p 996 N95-18341

CIRCUITS
Superconductor microelectronic devices and circuits and a method of fabricating therefor
[AD-D016280] p 1009 N95-18433
The future use of DSCS and commercial satellites in the US Navy
[AD-A285707] p 997 N95-18481
Cerebellar circuit mechanisms which accompany coordinated limb trajectory patterns in the rat: Use of a model of spontaneous changes in limb coordination
[AD-A284023] p 1079 N95-18656
Current loop signal conditioning: Practical applications
[NASA-TM-4636] p 1033 N95-18735
Precision gold conductors for HMCs
[DE94-018558] p 1012 N95-19230
PRS projections for DECADE
[AD-A279215] p 1147 N95-19847

CIRCULAR CYLINDERS
Wind tunnel performance comparative test results of a circular cylinder and 50 percent ellipse tailboom for circulation control antitorque applications
[AD-A283335] p 941 N95-18008

CIRCULAR PLATES
Completed Beltrami-Michell formulation for analyzing mixed boundary value problems in elasticity
[NASA-TM-106809] p 1045 N95-18909

CIRCULAR POLARIZATION
Bragg transmission phase plates for the production of circularly polarized x-rays
[DE94-017072] p 1151 N95-19113
CIRCULATION CONTROL AIRFOILS
Wind tunnel performance comparative test results of a circular cylinder and 50 percent ellipse tailboom for circulation control antitorque applications
[AD-A283335] p 941 N95-18008
CIRCULATION DISTRIBUTION
A synoptic climatology of convective weather in the Netherlands
[KNMI-WR-93-04] p 1071 N95-18395
CIRRUS CLOUDS
Modeling of cloud and radiation processes for large-scale clouds and tropical anvils
[AD-A284212] p 1067 N95-17955
CITIES
A GIS approach to urban heat island research: The case of Huntsville, Alabama p 1063 N95-18991
CIVIL AVIATION
European aeronautics: Strong government presence in industry structure and research and development support. Report to Congressional Requesters
[GAO/NSIAD-94-71] p 1171 N95-18578
Federal aviation regulations, part 91. General operating and flight rules. Change 8
[PB94-217445] p 940 N95-19720
Application of three-dimensional hybrid structured/unstructured grids to land, sea and air vehicles
[ARA-MEMO-399] p 1031 N95-19775
CLADDING
Weldability of iron aluminides
[DE95-000686] p 981 N95-19568
The metallurgical integrity of the frit vent assembly diffusion bond
[DE95-000610] p 968 N95-19877
CLASSICAL MECHANICS
Study of frustrated systems via dissipative maps
[DE94-017754] p 1122 N95-18127
CLASSIFICATIONS
Creation of new items and forms for the Project A Assembling Objects test
[AD-A285522] p 1088 N95-18095
Thematic classification of zone coastal: A methodologic contribution
[INPE-5586-TDI/548] p 1050 N95-18215
Hypersonic flow-field measurements: Intrusive and nonintrusive
[AD-A283867] p 930 N95-18674
Classification of graded, finite-dimensional lie algebras of vector fields
[PB94-215449] p 1119 N95-19408
Towards a classification of su(2)(direct sum)...(direct sum)su(2) modular invariant partition functions
[PB94-217247] p 1119 N95-19717
Automated rule-base creation via CLIPS-Induce p 1107 N95-19761
CLAYS
Development of a colloidal redox system containing a smectite clay for control of reactivity and reaction selectivity
[AD-A285958] p 974 N95-19515
CLEANING
Ion beam surface treatment: A new capability for surface enhancement
[DE94-014663] p 977 N95-17968
Potential replacements for solvents that are ozone depleting substances
[AD-A285442] p 1058 N95-18091
Investigation of new hypergol scrubber technology p 977 N95-18175
Design optimization of a brush turbine with a cleaner/water based solution p 1043 N95-18177
Design of high pressure waterjet nozzles p 1031 N95-18996
CLIMATE
Climate and weather of Central Africa. Executive summary
[AD-A283647] p 1067 N95-18014
Detection of greenhouse-gas-induced climatic change
[DE94-015044] p 1057 N95-18022
A GIS approach to urban heat island research: The case of Huntsville, Alabama p 1063 N95-18991
A review of land surface temperature and humidity conditions specified for Australia in DEF (AUST) 5168 and STANAG 2895
[AD-A284258] p 1073 N95-19712
A report on workshops: General circulation model study of climate: Chemistry interaction
[DE94-010252] p 1062 N95-19879
CLIMATE CHANGE
Detection of greenhouse-gas-induced climatic change
[DE94-015044] p 1057 N95-18022
Methane: The other greenhouse gas. Research and policy in the Netherlands
[PB94-207149] p 1058 N95-18375
Trends 1993: A compendium of data on global change
[ORNL/CDIAC-65] p 1058 N95-18389
Assessment of CO2 projections
[DE94-017484] p 1059 N95-18664
The role of large-scale, extratropical dynamics in climate change
[DE94-017651] p 1059 N95-18665
One strategy for estimating the potential soil carbon storage due to CO2 fertilization
[DE94-017895] p 1059 N95-18666
Office of Research and Applications: Research Programs p 1071 N95-18721
A GIS approach to urban heat island research: The case of Huntsville, Alabama p 1063 N95-18991
Assessment of climate variability of the Greenland Ice Sheet: Integration of in situ and satellite data
[NASA-CR-197604] p 1062 N95-19779
A report on workshops: General circulation model study of climate: Chemistry interaction
[DE94-010252] p 1062 N95-19879
CLIMATE MODELS
Storm activity over the North Sea and the Netherlands in two climate models compared with observations
[KNMI-WR-94-02] p 1070 N95-18393
CLIMATOLOGY
Climate and weather of Central Africa. Executive summary
[AD-A283647] p 1067 N95-18014
A synoptic climatology of convective weather in the Netherlands
[KNMI-WR-93-04] p 1071 N95-18395
The role of large-scale, extratropical dynamics in climate change
[DE94-017651] p 1059 N95-18665
Implications of summertime marine stratocumulus on the North American climate p 1073 N95-18977
Proceedings of the 15th Annual Conference on Atmospheric Transmission Models
[AD-A279919] p 1142 N95-19862
CLINICAL MEDICINE
The Clinical Basis for Aeromedical Decision Making
[AGARD-CP-553] p 1080 N95-19413
Aeromedical risk management for aircrew p 1080 N95-19414
Neuropsychophysiologic sequelae of mild head injury p 1083 N95-19430
Clinical basis for aeromedical decision-making: The EEG example p 1084 N95-19433
Sarcoidosis in US military aviators p 1085 N95-19438
CLOSED ECOLOGICAL SYSTEMS
Ethylene dynamics in the CELSS biomass production chamber p 1077 N95-18179
CLOUD COVER
Climate and weather of Central Africa. Executive summary
[AD-A283647] p 1067 N95-18014
Atmospheric Infrared Sounder
[NASA-CR-197573] p 1064 N95-18444
Ice surface temperature retrieval from AVHRR, ATSR, and passive microwave satellite data: Algorithm development and application
[NASA-CR-197542] p 1052 N95-18952
Implications of summertime marine stratocumulus on the North American climate p 1073 N95-18977
Prediction of global cloud cover with a very high resolution global spectral model
[AD-A279944] p 1073 N95-19870
CLOUD GLACIATION
Modeling of cloud and radiation processes for large-scale clouds and tropical anvils
[AD-A284212] p 1067 N95-17955
CLOUD PHYSICS
Modeling of cloud and radiation processes for large-scale clouds and tropical anvils
[AD-A284212] p 1067 N95-17955
CLOUDS (METEOROLOGY)
Scattering of point source illumination by an arbitrary configuration p 1143 N95-19006
NASA Goddard Earth Sciences Graduate Student Program --- FIRE CIRRUS-II examination of coupling between an upper tropospheric cloud system and synoptic-scale dynamics
[NASA-CR-197130] p 1066 N95-19129
CLUSTER ANALYSIS
Radial basis function neural networks applied to NASA SSME data
[NASA-CR-195417] p 962 N95-18467
CLUSTERS
Mass spectrometric studies of clusters and surfaces
[AD-A283992] p 974 N95-19066
CLUTTER
Synthesis of notched antenna patterns for wide bandwidth processing
[AD-A284004] p 1000 N95-18727
COANDA EFFECT
Wind tunnel performance comparative test results of a circular cylinder and 50 percent ellipse tailboom for circulation control antitorque applications
[AD-A283335] p 941 N95-18008
Static investigation of two fluidic thrust-vectoring concepts on a two-dimensional convergent-divergent nozzle
[NASA-TM-4574] p 931 N95-19042
COASTAL PLAINS
Thematic classification of zone coastal: A methodologic contribution
[INPE-5586-TDI/548] p 1050 N95-18215
COASTAL WATER
Coastal acoustic tomography data constraints applied to a coastal ocean circulation model
[AD-A283911] p 1074 N95-18153
COASTS
Thematic classification of zone coastal: A methodologic contribution
[INPE-5586-TDI/548] p 1050 N95-18215
Resources Automated Management System
[AD-A284153] p 1171 N95-18416
Kings Bay coastal and estuarine physical monitoring and evaluation program: Coastal studies. Volume 1: Main text and Appendix A
[AD-A285542] p 1074 N95-18470
Coastal benthic boundary layer special research program: A review of the first year. Volume 1
[AD-A280034] p 1076 N95-19818
COATING
Polyurethane self-priming topcoats
[AD-D016264] p 984 N95-18320
Real-time thickness measurement of MCC ablator material p 972 N95-18981
High velocity oxygen fuel spraying of erosion and wear resistant coatings on jet engine parts p 954 N95-19680
COATINGS
Preparation of an electrocatalytic cathode for an aluminum-hydrogen peroxide battery
[AD-D016262] p 1008 N95-18318
Precision gold conductors for HMCs
[DE94-018558] p 1012 N95-19230
COAXIAL CABLES
An efficient and accurate model of the coax cable feeding structure for FEM simulations p 1006 N95-19799
COBALT
Preparation and surface characterization of metal doped alumina catalyst
[PB94-175296] p 973 N95-17991
COCKPIT SIMULATORS
Programmable cockpit research simulator
[AD-A279219] p 960 N95-19848
COCKPITS
KC-135 cockpit modernization study. Phase 1: Equipment evaluation
[AD-A284099] p 942 N95-18398
The generic simulation executive at Manned Flight Simulator
[AD-A283997] p 959 N95-18724
An overall approach of cockpit noise verification in a military aircraft p 1127 N95-19163
Programmable cockpit research simulator
[AD-A279219] p 960 N95-19848
CODING
Direct detection and coherent optical systems employing error-correction coding
[AD-A284350] p 1140 N95-18424
Local spatio-temporal analysis in vision systems
[AD-A284162] p 1140 N95-18509
Predicted coverage of a COFDM single frequency network for UHF digital terrestrial TV broadcasting
[BBC-RD-1993/12] p 999 N95-18540
COEFFICIENTS
Plane Jacobian conjecture
[PB94-192341] p 1118 N95-19198
COGNITION
Multiple-task performance: A critical review of the literature and a cognitive neuroscience framework
[AD-A285133] p 1090 N95-19583
COGNITIVE PSYCHOLOGY
Comparing performance on implicit memory tests
[AD-A284861] p 1090 N95-19740
COHERENT LIGHT
Direct detection and coherent optical systems employing error-correction coding
[AD-A284350] p 1140 N95-18424
COLD WORKING
Analysis of cold worked holes for structural life extension p 939 N95-19493

COLLAPSE
BEAM: A finite element program for the collapse analysis of vehicle structures
[AD-A285547] p 1045 N95-18472
COLLECTION
Building a bridge with the customer to facilitate collecting and validating information in modeling sessions
[DE94-017338] p 1174 N95-18872
COLLISION AVOIDANCE
Method for surmounting an obstacle by a robot vehicle
[NASA-CASE-NPO-18764-1-CU] p 1041 N95-18741
COLLISIONAL PLASMAS
Radio wave heating of the lower ionosphere
p 1145 N95-18905
A three region analysis of a bounded plasma using particle in cell and fluid techniques
[AD-A284826] p 1147 N95-19690
COLLISIONLESS PLASMAS
A three region analysis of a bounded plasma using particle in cell and fluid techniques
[AD-A284826] p 1147 N95-19690
COLLISIONS
Correlated charge-changing ion-atom collisions
[DE94-017355] p 1132 N95-18874
Study of strangeness production in relativistic nucleus beams at JINR
[DE94-626720] p 1136 N95-18881
Principal-value resummation for dilepton production
[DE95-001094] p 1135 N95-19726
COLLOIDS
Development of a colloidal redox system containing a smectite clay for control of reactivity and reaction selectivity
[AD-A285958] p 974 N95-19515
COLOR
Acceptance/operational test procedure 101-SY tank camera purge system and in tank color camera video imaging system
[DE95-000344] p 1035 N95-19553
COLOR TELEVISION
Acceptance/operational test procedure 101-SY tank camera purge system and in tank color camera video imaging system
[DE95-000344] p 1035 N95-19553
COLOR VISION
Color vision issues in modern military aviation or the search for the Abominable Coneman
p 1086 N95-19441
COLUMBIA (ORBITER)
STS-65 Space Shuttle mission report
[NASA-CR-197598] p 963 N95-18610
COMBAT
Virtual reality, an air combat T and E perspective
[AD-A284161] p 959 N95-18508
COMBINATORIAL ANALYSIS
Weighted graph based ordering techniques for preconditioned conjugate gradient methods
[NASA-CR-197597] p 1118 N95-18736
On k-ary n-cubes: Theory and applications
[NASA-CR-194996] p 1100 N95-19028
COMBINED STRESS
Visuo-ocular performance during vestibular stimulation
[AD-A284103] p 1089 N95-18403
COMBUSTION
Observations of methane and ethylene diffusion flames stabilized around a blowing porous sphere under microgravity conditions
[NASA-TM-106766] p 990 N95-18211
Study of alpha physics related to ITER Project
[DE94-017329] p 1133 N95-19078
Historic patterns of CO2 emissions from fossil fuels: Implications for stabilization of emissions
[DE95-000489] p 1061 N95-19556
COMBUSTION CHAMBERS
One-dimensional flow description for the combustion chamber of a scramjet
[DLR-FB-94-06] p 948 N95-18911
A preliminary analysis of low frequency pressure oscillations in hybrid rocket motors p 968 N95-18987
COMBUSTION EFFICIENCY
Alternative control techniques document: NO(x) emissions from glass manufacturing
[PB94-214079] p 1061 N95-19406
COMBUSTION PHYSICS
Ignition and combustion of bulk metals in a microgravity environment
[NASA-CR-197519] p 990 N95-18082
VENTCF2: An algorithm and associated FORTRAN 77 subroutine for calculating flow through a horizontal ceiling/floor vent in a zone-type compartment fire model
[PB94-210127] p 993 N95-19402
Flamespreading in granular solid propellant: Initial results
[AD-A284245] p 976 N95-19729
COMBUSTION PRODUCTS
Controlling combustion-source emissions at Air Force sites with a new filter concept, phase 1
[AD-A283674] p 1058 N95-18140
Wave cycle design for wave rotor engines with limited nitrogen oxide emissions p 1041 N95-18901
Developing an emission factor for hazardous air pollutants for an F-16 using JP-8 fuel
[AD-A284802] p 1061 N95-19685
COMBUSTION STABILITY
A preliminary analysis of low frequency pressure oscillations in hybrid rocket motors p 968 N95-18987
COMETARY ATMOSPHERES
Comet coma sample return instrument
p 1180 N95-19173
The status of measurement technologies concerning micrometer and submicrometer space articulate matter capture, recovery, velocity and trajectory
p 1181 N95-19175
COMETARY COLLISIONS
Establishment of redox conditions during planetary collisions as an origin of chondrites
p 1192 N95-19331
COMETS
Main characteristics of the COMET/COMRADE experiments p 1181 N95-19179
COMMAND AND CONTROL
US Navy SHF SATCOM: Past, present and future
[AD-A283704] p 996 N95-18359
Design of a radio frequency data link for the unmanned ground vehicle technology test bed demonstration program
[AD-A284997] p 1004 N95-19534
COMMAND GUIDANCE
Naval Biodynamics Laboratory 1993 command history
[AD-A284358] p 1089 N95-18440
COMMERCE
Small Business Research Summaries, numbers 51-100
[PB94-179967] p 1170 N95-17986
Small Business Research Summaries, numbers 1-50
[PB94-179959] p 1170 N95-17987
COMMERCIAL SPACECRAFT
Issues in military use of commercial satellites
[AD-A283707] p 964 N95-18362
The future use of DSCS and commercial satellites in the US Navy
[AD-A285707] p 997 N95-18481
COMMONWEALTH OF INDEPENDENT STATES
The current status of Russian/CIS communication satellites
[AD-A285526] p 963 N95-18098
COMMUNICATION
Early experiences and performance of the Intel Paragon
[DE94-018061] p 1109 N95-18129
Annual Allerton Conference on Communication, Control and Computing
[AD-A283892] p 1114 N95-18675
COMMUNICATION CABLES
Torque-balanced extendable fiber optic cable
[AD-D016496] p 1142 N95-19389
COMMUNICATION NETWORKS
Design and analysis of dynamic leader election protocols in broadcast networks
[PB94-202728] p 1109 N95-18039
Gigabit optical interconnects: System and component analysis, design and development
[AD-A285538] p 1138 N95-18067
Secure distributed file systems
[AD-A285525] p 1173 N95-18096
The development of a fiber optics communication network for controlling a Multidegree-Of-Freedom Serpentine Truss p 1142 N95-18167
Global time transformations
[AD-A285539] p 1110 N95-18454
RACE project 1036: WTDM broadband customer premises network
[BBC-RD-1993/15] p 998 N95-18537
Predicted coverage of a COFDM single frequency network for UHF digital terrestrial TV broadcasting
[BBC-RD-1993/12] p 999 N95-18540
Advanced optical fiber communications systems
[AD-A283942] p 1141 N95-18682
The 23 Gigahertz (GHz) digital Low Density Radio Communications Link (LDRCL) Operational Test and Evaluation (OT/E) integration and OT/E operation
[AD-A283963] p 1000 N95-18686
Information Superhighway: Issues affecting development. Report to the Congress
[GAO/RCED-94-285] p 1174 N95-18914
MSFC institutional area network and ATM technology
p 1007 N95-18968
On k-ary n-cubes: Theory and applications
[NASA-CR-194996] p 1100 N95-19028
ODP based UPT model
[PB94-215589] p 1003 N95-19411
Multicast tree construction in network topologies with asymmetric link loads
[AD-A285679] p 1003 N95-19525
The Buffer Diagnostic Prototype: A fault isolation application using CLIPS p 1100 N95-19626
An expert system for configuring a network for a Milstar terminal p 1104 N95-19645
COMMUNICATION SATELLITES
The current status of Russian/CIS communication satellites
[AD-A285526] p 963 N95-18098
MIKON 94. International Microwave Conference. Invited papers, volume 3
[AD-A284353] p 1008 N95-18338
US Navy SHF SATCOM: Past, present and future
[AD-A283704] p 996 N95-18359
Issues in military use of commercial satellites
[AD-A283707] p 964 N95-18362
The future use of DSCS and commercial satellites in the US Navy
[AD-A285707] p 997 N95-18481
A systems analysis and project management plan for the Petite Amateur Navy Satellite (PANSAT)
[AD-A285968] p 965 N95-19571
COMMUTATION
An analysis of noise reduction in variable reluctance motors using pulse position randomization
[AD-A283846] p 1123 N95-18673
COMMUTER AIRCRAFT
Safety study: Commuter airline safety
[PB94-917004] p 933 N95-19132
COMPACT GALAXIES
An optical study of compact steep spectrum radio sources p 1179 N95-18498
COMPANDING
Implementation of amplitude modulation companding using a digital signal processor
[BBC-RD-1994/1] p 998 N95-18536
COMPARATOR CIRCUITS
Radar sector blanker
[AD-D016275] p 996 N95-18429
COMPARATORS
Fault protection circuit for power switching device
[AD-D016466] p 1009 N95-18455
COMPARISON
Inter-comparison of automatic rain gauges
p 1069 N95-18204
COMPENSATORS
Three-parameter tunable Tilt-Integral-Derivative (TID) controller
[NASA-CASE-NPO-18492-1-CU] p 1113 N95-18313
COMPETITION
A crystalline quark-hadron mixed phase in neutron stars
[DE95-000787] p 1194 N95-19570
COMPILERS
Study of a Navier-Stokes computer
[AD-A284196] p 1092 N95-17939
COMPLEX COMPOUNDS
Photogeneration and characterization of energetic molecules in supersonic molecular beams
[AD-A284108] p 1131 N95-18438
COMPLEX SYSTEMS
Thermochemical IR sources: COCHISE and FACELIF experiments
[AD-A279940] p 977 N95-19868
COMPLEX VARIABLES
Eigenvalue tests and distributions for small sample order determination for complex Wishart matrices
[AD-A283825] p 1120 N95-18672
Statistics of complex cross spectrum estimate for sinusoidal signals and arbitrary noise spectra
[AD-A283984] p 1120 N95-19065
Theory and applications of the phi transform wavelets
[AD-A279943] p 1119 N95-19869
COMPONENT RELIABILITY
Residual life and strength estimates of aircraft structural components with MSD/MED p 937 N95-19485
COMPOSITE MATERIALS
Fabrication of biomimetic molecular level composites
[AD-A284204] p 969 N95-17941
Fatigue in single crystal nickel superalloys
[AD-A285727] p 978 N95-18068
Conference on Aerospace Transparent Materials and Enclosures. Volume 2: Sessions 5-9
[AD-A283926] p 942 N95-18162
A real-time vision system to monitor/analyze the changes in composite specimens during mechanical testing
[ARL-TR-344] p 970 N95-18612
Conference on Aerospace Transparent Materials and Enclosures, volume 1
[AD-A283925] p 944 N95-18677

Mass spectrometric studies of clusters and surfaces
[AD-A283992] p 974 N95-19066
Superstrength metal composite material and process for making the same
[AD-D016555] p 971 N95-19123
Environmental effects on composite airframes: A study conducted for the ARM UAV Program (Atmospheric Radiation Measurement Unmanned Aerospace Vehicle)
[DE94-015351] p 971 N95-19579
Unit cell geometry of multiaxial preforms for structural composites
[NASA-CR-197294] p 971 N95-19650

COMPOSITE STRUCTURES
Wing design for a civil tiltrotor transport aircraft
[NASA-CR-197523] p 942 N95-18090
Acoustic method of damage sensing in composite materials
[NASA-CR-196538] p 969 N95-18135
Finite element modeling of partially delaminated composite beams with contact-impact conditions
[AD-A283726] p 1044 N95-18363
Compression strength of composite primary structural components
[NASA-CR-197554] p 1044 N95-18388
Corrosivity sensor
[AD-D016422] p 1033 N95-18524
Optimization of layered metal matrix composite cylinders p 970 N95-18920
Foreign body impact event damage formation in composite structures p 972 N95-18973
Composite structures for magnetosphere imager spacecraft p 966 N95-18976
The probability of flaw detection and the probability of false calls in nondestructive evaluation equipment p 1044 N95-19010
Impact of Acoustic Loads on Aircraft Structures
[AGARD-CP-549] p 1124 N95-19142
Acoustic fatigue of carbon fibre structures p 1127 N95-19158
Damage monitoring in metallic and composite structures using piezoelectric thin film sensors
[ARL-RR-4] p 971 N95-19467

COMPOUND A
Magneto-optical studies of compound semiconductors
[DE94-018743] p 1149 N95-18650

COMPRESSIBILITY
Simplified ideal MHD normal mode equations for toroidal axisymmetric plasmas
[DE94-627004] p 1144 N95-18886

COMPRESSIBLE BOUNDARY LAYER
A spectrally accurate boundary-layer code for infinite swept wings
[NASA-CR-195014] p 1014 N95-18042

COMPRESSIBLE FLOW
Floating shock fitting via Lagrangian adaptive meshes
[NASA-CR-194997] p 1116 N95-18110
Numerical simulation of dynamic-stall suppression by tangential blowing
[AD-A284887] p 931 N95-19110
Prediction of fluctuating pressure and power spectra in attached and separated compressible flow p 1031 N95-19153
Basic equations of fluid dynamics p 1026 N95-19445
Computation of compressible flows: Implicit methods p 1027 N95-19452
Pressure based finite volume algorithm for viscous flow computation p 1029 N95-19461
Parallel computations in hydro acoustics
[AD-A285900] p 1030 N95-19607
On supersonic-inlet boundary-layer bleed flow
[NASA-CR-195426] p 955 N95-19769
Validation and evaluation of the advanced aeronautical CFD system SAUNA: A method developer's view
[ARA-MEMO-390] p 1030 N95-19774
The application of the SAUNA CFD system to high and low speed vehicles
[ARA-MEMO-402] p 1031 N95-19778

COMPRESSION LOADS
Split mandrel versus split sleeve coldworking: Dual methods for extending the fatigue life of metal structures p 940 N95-19500

COMPRESSION RATIO
LVQ and backpropagation neural networks applied to NASA SSME data
[NASA-CR-195418] p 962 N95-18045

COMPRESSIVE STRENGTH
Compression strength of composite primary structural components
[NASA-CR-197554] p 1044 N95-18388

COMPRESSOR BLADES
Performance deterioration of axial compressors due to blade defects p 952 N95-19665
Erosion of T56 5th stage rotor blades due to bleed hole overtip flow p 952 N95-19666
High velocity oxygen fuel spraying of erosion and wear resistant coatings on jet engine parts p 954 N95-19680

COMPRESSOR EFFICIENCY
Performance deterioration of axial compressors due to blade defects p 952 N95-19665

COMPRESSOR ROTORS
The calculation of erosion in a gas turbine compressor rotor p 952 N95-19664

COMPRESSORS
Damage of high temperature components by dust-laden air p 953 N95-19673
Protective coatings for compressor gas path components p 954 N95-19675
Gas turbine compressor corrosion and erosion in Western Europe p 954 N95-19678
Multilayer anti-erosion coatings p 954 N95-19679

COMPUTATION
Fusion of multiple sensing modalities for machine vision
[AD-A284762] p 1091 N95-18086
Research in parallel computing
[AD-A283983] p 1111 N95-18892
Advanced methods for the computation of particle beam transport and the computation of electromagnetic fields and beam-cavity interactions
[DE94-017359] p 1136 N95-18893

COMPUTATIONAL ASTROPHYSICS
Quantitative analysis of voids in percolating structures in two-dimensional N-body simulations
[NASA-CR-197612] p 1156 N95-18949
Cosmic ray models for early galactic lithium, beryllium, and boron production
[NASA-CR-197626] p 1137 N95-18965
Testing the frozen flow approximation
[NASA-CR-197614] p 1180 N95-18966
Second-order reconstruction of the inflationary potential
[NASA-CR-197629] p 1121 N95-19030
Mass and radius of cosmic balloons
[NASA-CR-197628] p 1180 N95-19031
Cross-tail current, field-aligned current, and B(y)
[NASA-CR-197624] p 1065 N95-19032
Antisymmetric tensor field interactions and neutron star models
[PB94-215605] p 1118 N95-19375

COMPUTATIONAL FLUID DYNAMICS
Study of a Navier-Stokes computer
[AD-A284196] p 1092 N95-17939
Evaluation of boundary conditions for computational aeroacoustics
[NASA-TM-109989] p 1015 N95-18149
A three-dimensional structured/unstructured hybrid Navier-Stokes method for turbine blade rows
[NASA-TM-106813] p 1016 N95-18200
A note on the wave action density of a viscous instability mode on a laminar free-shear flow
[NASA-TM-106771] p 1016 N95-18212
Parachute inflation: A problem in aeroelasticity
[AD-A284375] p 928 N95-18340
Searching for stationary stable solutions of Euler's equation
[KNMI-WR-93-01] p 1017 N95-18396
A note on singularities of the 3-D Euler equation
[NASA-CR-195006] p 1017 N95-18397
Parallelization of the fluid dynamics equations on unstructured grids
[AD-A284116] p 1017 N95-18406
Numerical predictions of turbulent flow around a cube via the k-epsilon model
[DE94-018361] p 1017 N95-18443
Aeromechanics technology, volume 1. Task 1: Three-dimensional Euler/Navier-Stokes Aerodynamic Method (TEAM) enhancements
[AD-A285713] p 943 N95-18483
A selection of experimental test cases for the validation of CFD codes. Supplement: Datasets A-E
[AGARD-AR-303-SUPPL] p 929 N95-18539
A numerical analysis of smoothed particle hydrodynamics
[AD-A284698] p 1019 N95-18562
NASA High Performance Computing and Communications program
[NASA-TM-4653] p 1174 N95-18573
Static aerodynamics CFD analysis for 120-mm hypersonic KE projectile design
[ARL-MR-184] p 929 N95-18611
Numerical computations of supersonic base flow with special emphasis on turbulence modeling
[AD-A283688] p 930 N95-18670
Hypersonic flow-field measurements: Intrusive and nonintrusive
[AD-A283867] p 930 N95-18674
Mesh quality control for multiply-refined tetrahedral grids
[NASA-CR-197595] p 1043 N95-18737
Solution of full potential equation on an airfoil by multigrid technique
[NAL-TM-CSS-9303] p 930 N95-18904
Lattice gas and lattice Boltzmann methods for simulation of hydrodynamics and magnetohydrodynamics p 1145 N95-18907
Theoretical investigations of shock/boundary layer interactions on a Ma(infinity) = 8 waverider
[DLR-FB-94-12] p 930 N95-18910
One-dimensional flow description for the combustion chamber of a scramjet
[DLR-FB-94-06] p 948 N95-18911
Flow field investigation in a free jet - free jet core system for the generation of high intensity molecular beams
[DLR-FB-94-11] p 1132 N95-18912
Marangoni convection in a gravity-free silicon float zone
[NASA-CR-197600] p 991 N95-18913
Parallel Navier-Stokes computations on shared and distributed memory architectures
[NASA-TM-106823] p 1019 N95-18941
Computational simulation of liquid fuel rocket injectors p 968 N95-18989
On the CFD monotone high accuracy methods p 948 N95-19018
Solution of Navier-Stokes equations using high accuracy monotone schemes p 948 N95-19019
An assessment of the adaptive unstructured tetrahedral grid, Euler Flow Solver Code FELISA
[NASA-TP-3526] p 930 N95-19041
Static investigation of two fluidic thrust-vectoring concepts on a two-dimensional convergent-divergent nozzle
[NASA-TM-4574] p 931 N95-19042
Determination of stores pointing error due to wing flexibility under flight load
[NASA-TM-4646] p 945 N95-19044
Hypervelocity air flows with finite rate chemistry
[AD-A284727] p 931 N95-19109
Numerical simulation of dynamic-stall suppression by tangential blowing
[AD-A284887] p 931 N95-19110
Navier-Stokes, flight, and wind tunnel flow analysis for the F/A-18 aircraft
[NASA-TP-3478] p 931 N95-19114
Determination of solid/porous wall boundary conditions from wind tunnel data for computational fluid dynamics codes p 1023 N95-19266
Unsteady aerodynamic analyses for turbomachinery aeroelastic predictions p 949 N95-19381
Steady potential solver for unsteady aerodynamic analyses p 949 N95-19382
VENTCF2: An algorithm and associated FORTRAN 77 subroutine for calculating flow through a horizontal ceiling/floor vent in a zone-type compartment fire model
[PB94-210127] p 993 N95-19402
CFD: Advances and Applications, part 1
[NAL-SP-9322-PT-1] p 1026 N95-19444
Computation of inviscid flows: Full potential method p 1027 N95-19447
Panel methods p 1027 N95-19448
Numerical grid generation p 1027 N95-19449
Difference schemes for hyperbolic system of Conservation Laws p 1027 N95-19450
Finite volume method using Runge-Kutta time-stepping for solution of Euler equations p 1027 N95-19451
Computation of compressible flows: Implicit methods p 1027 N95-19452
Introduction to multigrid methods p 1028 N95-19453
Applications of multigrid methods to problems in CFD p 1028 N95-19454
CFD: Advances and Applications, 1994
[NAL-SP-9412] p 1028 N95-19455
Viscous flow past aerofoils axisymmetric bodies and wings p 933 N95-19457
Turbulence modeling for CFD, part 1 p 1028 N95-19458
Spectral methods for fluid flow p 1028 N95-19459
Discrete vortex method for computation of viscous incompressible flows p 1029 N95-19460
Pressure based finite volume algorithm for viscous flow computation p 1029 N95-19461
Hypersonic viscous flow computations p 1029 N95-19463
CFD on parallel computers p 1029 N95-19465
Turbulence modeling for CFD, part 2 p 1030 N95-19466
Evaluation of three turbulence models for afterbody/jet flows, including Reynolds stress closure
[ARA-90] p 932 N95-19574
Parallel computations in hydro acoustics
[AD-A285900] p 1030 N95-19607
On supersonic-inlet boundary-layer bleed flow
[NASA-CR-195426] p 955 N95-19769

Evaluation of three turbulence models for afterbody/jet flows, including Reynolds stress closure
[ARA-MEMO-408] p 1194 N95-19773
Validation and evaluation of the advanced aeronautical CFD system SAUNA: A method developer's view
[ARA-MEMO-390] p 1030 N95-19774
Application of three-dimensional hybrid structured/unstructured grids to land, sea and air vehicles
[ARA-MEMO-399] p 1031 N95-19775
Verification of the CFD simulation system SAUNA for complex aircraft configurations
[ARA-MEMO-401] p 1031 N95-19776
Inviscid and viscous flow modelling of complex aircraft configurations using the CFD simulation system sauna
[ARA-MEMO-403] p 1031 N95-19777
The application of the SAUNA CFD system to high and low speed vehicles
[ARA-MEMO-402] p 1031 N95-19778
Solution of potential flow problems on a network of workstations
[DE94-017861] p 1112 N95-19831

COMPUTATIONAL GRIDS
Floating shock fitting via Lagrangian adaptive meshes
[NASA-CR-194997] p 1116 N95-18110
A three-dimensional structured/unstructured hybrid Navier-Stokes method for turbine blade rows
[NASA-TM-106813] p 1016 N95-18200
The effect of spatial averaging on threshold exceedances of daily precipitation amounts
[KNMI-TR-154] p 1070 N95-18392
Atmospheric Infrared Sounder
[NASA-CR-197573] p 1064 N95-18444
Scalability of parallel spatial direct numerical simulation code on IBM SP1 parallel supercomputer
[NASA-CR-194975] p 1098 N95-18584
SICOMP, the SINTEF data compression library (version 1.0) reference manual
[PB94-207107] p 1099 N95-18668
Computer simulation of wave propagation through turbulent media
[AD-A283695] p 1000 N95-18671
Weighted graph based ordering techniques for preconditioned conjugate gradient methods
[NASA-CR-197597] p 1118 N95-18736
Mesh quality control for multiply-refined tetrahedral grids
[NASA-CR-197595] p 1043 N95-18737
CUBIT mesh generation environment
[DE94-017496] p 1118 N95-18896
Development of CFD model for augmented core tripropellant rocket engine p 968 N95-18988
The mathematical models of flow passage for gas turbine engines and their components p 948 N95-19020
Application of multicomponent models to flow passage simulation in multistage turbomachines and whole gas turbine engines p 948 N95-19022
An assessment of the adaptive unstructured tetrahedral grid, Euler Flow Solver Code FELISA
[NASA-TP-3526] p 930 N95-19041
Numerical simulation of dynamic-stall suppression by tangential blowing
[AD-A284887] p 931 N95-19110
CFD: Advances and Applications, part 1
[NAL-SP-9322-PT-1] p 1026 N95-19444
Numerical grid generation p 1027 N95-19449
Introduction to multigrid methods p 1028 N95-19453
Applications of multigrid methods to problems in CFD p 1028 N95-19454
General procedures employed in the generation of three-dimensional hybrid structured/unstructured meshes
[ARA-MEMO-400] p 1030 N95-19506
Design of fan blades subjected to bird impact p 953 N95-19669
Ice-impact analysis of blades p 953 N95-19672
Validation and evaluation of the advanced aeronautical CFD system SAUNA: A method developer's view
[ARA-MEMO-390] p 1030 N95-19774
Application of three-dimensional hybrid structured/unstructured grids to land, sea and air vehicles
[ARA-MEMO-399] p 1031 N95-19775
Verification of the CFD simulation system SAUNA for complex aircraft configurations
[ARA-MEMO-401] p 1031 N95-19776
The application of the SAUNA CFD system to high and low speed vehicles
[ARA-MEMO-402] p 1031 N95-19778
Performance of an artificial absorber for truncating FEM meshes p 1006 N95-19801

COMPUTER AIDED DESIGN
Semiconductor measurement technology: Design and testing guides for the COMOS and lateral bipolar-on-SOI test library
[PB94-178019] p 1007 N95-17984
A formal method for semantics-based change-merging of software prototypes
[AD-A283668] p 1094 N95-18017
A fast recursive algorithm to compute the probability of M-out-of-N events
[AD-A283679] p 1120 N95-18020
Wing design for a civil tiltrotor transport aircraft
[NASA-CR-197523] p 942 N95-18090
An algorithm for solving the system-level problem in multilevel optimization
[NASA-CR-195015] p 1116 N95-18108
Performance evaluation of the NASA/KSC CAD/CAE and office automation LAN's p 1108 N95-18186
MIKON 94. International Microwave Conference. Invited papers, volume 3
[AD-A284353] p 1008 N95-18338
MIKON 94. International Microwave Conference. Volume 1: Conference proceedings
[AD-A284351] p 1009 N95-18425
MIKON 94. International Microwave Conference. Conference proceedings, volume 2
[AD-A284352] p 1009 N95-18426
QuikForm: Intelligent deformation processing of structural alloys
[DE94-018739] p 1114 N95-18649
SICOMP, the SINTEF data compression library (version 1.0) reference manual
[PB94-207107] p 1099 N95-18668
EEsoF MICAD and ACADEMY macro files for coplanar waveguide and finite ground plan coplanar waveguide
[NASA-TM-106800] p 1000 N95-18733
Building a bridge with the customer to facilitate collecting and validating information in modeling sessions
[DE94-017338] p 1174 N95-18872
Enhanced capabilities and modified users manual for axial-flow compressor conceptual design code CSPAN
[NASA-TM-106833] p 930 N95-18933
Design of advanced steels for armor applications
[ARL-CR-175] p 979 N95-18948
A finite element code for electric motor design p 1014 N95-18974
Steady and unsteady blade stresses within the SSME ATD/HPOTP inducer p 968 N95-18982
Application of multidisciplinary models to the cooled turbine rotor design p 949 N95-19024
Perspective problems of gas turbine engines simulation p 949 N95-19026
Optimum dimension ratios for studios, control rooms and listening rooms
[BBC-RD-1993/8] p 993 N95-19053
Modelling structurally damaging twin-jet screech p 946 N95-19154
ODP based UPT model
[PB94-215589] p 1003 N95-19411
Using neural networks in the mapping of mixed discrete/continuous design spaces with application to structural design
[AD-A285328] p 1046 N95-19522
AUTO: Automatic script generation system
[AD-A285897] p 1012 N95-19606
Design of fan blades subjected to bird impact p 953 N95-19669
Ice-impact analysis of blades p 953 N95-19672
Collaborative engineering-design support system p 1106 N95-19757
The Computer Aided Aircraft-design Package (CAAP) p 1106 N95-19759
Rule based design of conceptual models for formative evaluation p 1106 N95-19760
PalymSys (TM): An extended version of CLIPS for construction and reasoning using blackboards p 1107 N95-19767
Tutorial guide: Computer-Aided Structural Modeling (CASM), version 5.00
[AD-A280147] p 1108 N95-19821

COMPUTER AIDED MANUFACTURING
Concept of using a benchmark part to evaluate rapid prototype processes p 994 N95-18975
Simulation in manufacturing
[PB94-215563] p 1100 N95-19409

COMPUTER AIDED MAPPING
Digital mapping, charting, and geodesy analysis program technical review of Digital Aeronautical Flight Information Data Prototype 1.0 on CD-ROM
[AD-A284728] p 1050 N95-18078
Digital mapping, charting, and geodesy analysis program technical review of Raster Product Format (RPF) and Scanned Map (SMap)
[AD-A284267] p 1052 N95-19733

COMPUTER AIDED TOMOGRAPHY
Linear optimization and image reconstruction
[AD-A283641] p 1094 N95-18013
Coastal acoustic tomography data constraints applied to a coastal ocean circulation model
[AD-A283911] p 1074 N95-18153

COMPUTER ASSISTED INSTRUCTION
Technical concept document. Central Archive for Reusable Defense Software (CARDS)
[AD-A284430] p 1096 N95-18343
Computer-based psychomotor tests in optimal training track assignment of student naval aviators
[AD-A283720] p 1089 N95-18414
Library user's guide. Comprehensive Approach to Reusable Defensive Software (CARDS)
[AD-A284345] p 1097 N95-18423
Portable, Reusable, Integrated Software Modules (PRISM) documentation library version description document release 1.0. Central Archive for Reusable Defense Software (CARDS)
[AD-A284571] p 1097 N95-18447
Library capability demonstration. Central Archive for Reusable Defense Software (CARDS)
[AD-A284574] p 1098 N95-18450
The assessment of virtual reality for human anatomy instruction p 1088 N95-18971
Assessment of the ACSE science learning environment and the impact of movies and simulations
[AD-A284071] p 1089 N95-19068
AUTO: Automatic script generation system
[AD-A285897] p 1012 N95-19606

COMPUTER DESIGN
Development of executive information systems
[AD-A284005] p 1174 N95-18654

COMPUTER GRAPHICS
Linear optimization and image reconstruction
[AD-A283641] p 1094 N95-18013
Evolution of the Southern Hemisphere ozone hole as seen by TOMS from August 1979 to December 1991
[NASA-TM-110116] p 1057 N95-18048
An evaluation of aircraft CRT and dot-matrix display legibility requirements
[AD-A283933] p 947 N95-18164
Simulation of gamma-ray spectra for a variety of user-specified detector designs
[NASA-CR-197551] p 1136 N95-18370
Distributed interactive simulation interface library version description document
[AD-A284470] p 1173 N95-18446
QuikForm: Intelligent deformation processing of structural alloys
[DE94-018739] p 1114 N95-18649
Alarm annunciation in a graphical environment
[DE94-015761] p 1098 N95-18652
Graphics MIS/Shop Store Program: User's manual
[AD-A284062] p 1174 N95-18681
Development of microgravity, full body functional reach envelope using 3-D computer graphic models and virtual reality technology p 1092 N95-18990
Representing visibility for siting problems
[AD-A284076] p 993 N95-19036
Assessment of the ACSE science learning environment and the impact of movies and simulations
[AD-A284071] p 1089 N95-19068
XAMath: An XAFS analysis package based on Mathematica(tm)
[DE94-016346] p 1100 N95-19397

COMPUTER INFORMATION SECURITY
Independent validation and verification of automated information systems in the Department of Energy
[DE94-014460] p 1173 N95-18063
Secure distributed file systems
[AD-A285525] p 1173 N95-18096

COMPUTER NETWORKS
User profile for researchers studying objects: Implications for computer systems
[PB94-188463] p 1109 N95-17989
Use of profiler data for analysis and NOWcasting of a winter season extratropical cyclone
[PB94-187804] p 1067 N95-17992
Construction of a connectionist network supercomputer
[AD-A283354] p 1109 N95-18050
NASA/DOD Aerospace Knowledge Diffusion Research Project. Paper 47: The value of computer networks in aerospace
[NASA-CR-197591] p 1109 N95-18055
Early experiences and performance of the Intel Paragon
[DE94-018061] p 1109 N95-18129
A scalable decentralized group membership service for an asynchronous environment
[AD-A283633] p 1109 N95-18137
Implementation of a human information processing model for task network simulation
[AD-A283903] p 1088 N95-18151

Distributed interactive simulation interface library version description document
[AD-A284470] p 1173 N95-18446
Global time transformations
[AD-A285539] p 1110 N95-18454
The Isis project: Fault-tolerance in large distributed systems
[NASA-CR-197561] p 1110 N95-18532
Advanced optical fiber communications systems
[AD-A283942] p 1141 N95-18682
Research in parallel computing
[AD-A283983] p 1111 N95-18892
Parallel Navier-Stokes computations on shared and distributed memory architectures
[NASA-TM-106823] p 1019 N95-18941
MSFC institutional area network and ATM technology p 1007 N95-18968
Methods and components for optical contention resolution in high speed networks
[AD-A284674] p 1142 N95-19088
Neural network communications signal processing
[AD-A285681] p 1115 N95-19512
Advanced techniques for analysis and evaluation of robust protocols
[AD-A285682] p 1111 N95-19513
The QED Workshop
[DE94-018499] p 1111 N95-19592
Cooperating agents for information retrieval
[AD-A285887] p 1176 N95-19604
The Buffer Diagnostic Prototype: A fault isolation application using CLIPS p 1100 N95-19626
Expert system technologies for Space Shuttle decision support: Two case studies p 1104 N95-19646
Solution of potential flow problems on a network of workstations
[DE94-017861] p 1112 N95-19831
High speed optical links between LLNL and Berkeley
[DE95-000552] p 1006 N95-19833
Connectionist Network Supercomputer Project
[AD-A279206] p 1112 N95-19843

COMPUTER PROGRAMMING
Linear optimization and image reconstruction
[AD-A283641] p 1094 N95-18013
Improving software characteristics of a real-time system using reengineering techniques
[AD-A283659] p 1094 N95-18015
A visual approach to the analysis of large software systems
[AD-A285440] p 1095 N95-18089
Software techniques for balancing computation and communication in parallel systems
[AD-A285536] p 1109 N95-18106
Implementation of a human information processing model for task network simulation
[AD-A283903] p 1088 N95-18151
Mapping a domain model and architecture to a generic design
[AD-A283747] p 1096 N95-18364
Guidance, Navigation and Control Digital Emulation Technology Laboratory
[AD-A284339] p 996 N95-18386
Program verification for optimized byte copy
[AD-A283915] p 1099 N95-18676
EEsoF MICAD and ACADEMY macro files for coplanar waveguide and finite ground plan coplanar waveguide
[NASA-TM-106800] p 1000 N95-18733
Evaluation of the efficiency and reliability of software generated by code generators p 1108 N95-19004
NAWCAD photogrammetrics: Methods and applications for aviation test and evaluation
[AD-A284074] p 1034 N95-19071
Software Technology for Adaptable, Reliable Systems (STARS). Software architecture seminar report: Central Archive for Reusable Defense Software (CARDS)
[AD-A284668] p 1100 N95-19106
VENTCF2: An algorithm and associated FORTRAN 77 subroutine for calculating flow through a horizontal ceiling/floor vent in a zone-type compartment fire model
[PB94-210127] p 993 N95-19402
Constructing a real-time mobile robot software system
[AD-A285969] p 1115 N95-19572
CLIPS++: Embedding CLIPS into C++ p 1101 N95-19630
Optimal pattern distributions in Rete-based production systems p 1106 N95-19755
Process definition and modeling guidebook. Volume 1: Concepts and principles of MPDM. Version 02.00.02
[AD-A279162] p 1108 N95-19803
Process definition and modeling guidebook. Volume 2: Advanced applications of MPDM
[AD-A279199] p 1108 N95-19813
Automatically generating procedure code and database maintenance scripts
[DE95-000545] p 1176 N95-19876

COMPUTER PROGRAMS
Requirements analysis for safety-critical systems: A chemical batch processing example
[PB94-201563] p 991 N95-17934
Fusion of correlated sensor observations
[AD-A284224] p 994 N95-17958
Catalog of environmental data sets of Europe at the RIVM
[PB94-202710] p 1057 N95-18002
A constant-depth scratch test for the measurement of adhesion at film-substrate interfaces
[AD-A283660] p 983 N95-18016
A platform independent application of Lux illumination prediction algorithms
[AD-A283669] p 1094 N95-18018
Operational And Supportability Implementation System (OASIS) test and evaluation master plan
[AD-A284765] p 941 N95-18088
A visual approach to the analysis of large software systems
[AD-A285440] p 1095 N95-18089
Enhancements to the KATE model-based reasoning system p 1115 N95-18183
Technical concept document. Central Archive for Reusable Defense Software (CARDS)
[AD-A284430] p 1096 N95-18343
GAMQUEST, a computer program to identify gamma rays
[DE94-016217] p 1197 N95-18351
Nonlinear magnetohydrodynamics
[DE94-016223] p 1143 N95-18353
Simulation of gamma-ray spectra for a variety of user-specified detector designs
[NASA-CR-197551] p 1136 N95-18370
Imagery correction for atmospheric effects using sounding data
[INPE-5506-TDI/518] p 1064 N95-18390
Library user's guide. Comprehensive Approach to Reusable Defensive Software (CARDS)
[AD-A284345] p 1097 N95-18423
SIGNET-software tools for signal identification using neural networks
[AD-A284362] p 1113 N95-18441
Portable, Reusable, Integrated Software Modules (PRISM) documentation library version description document release 1.0. Central Archive for Reusable Defense Software (CARDS)
[AD-A284571] p 1097 N95-18447
Metrics concept report. Central Archive for Reusable Defense Software (CARDS)
[AD-A284573] p 1097 N95-18449
Library capability demonstration. Central Archive for Reusable Defense Software (CARDS)
[AD-A284574] p 1098 N95-18450
Scalability of parallel spatial direct numerical simulation code on IBM SP1 parallel supercomputer
[NASA-CR-194975] p 1098 N95-18584
IONCAP prediction-based Automatic Link Establishment (ALE) frequency selection for a ten-node Australian high-frequency network
[AD-A283698] p 999 N95-18619
Can information surety be assessed with high confidence?
[DE94-015805] p 1120 N95-18653
Technical Information Division Open Literature Database (TOLD) operating instructions
[AD-A284061] p 1174 N95-18680
Regenerative cooling for liquid propellant rocket thrust chambers
[INPE-5565-TDI/540] p 967 N95-18720
EEsoF MICAD and ACADEMY macro files for coplanar waveguide and finite ground plan coplanar waveguide
[NASA-TM-106800] p 1000 N95-18733
International Conference on Control Theory and its Applications
[DE94-626221] p 1114 N95-18875
Hypersonic flight testing
[AD-A283981] p 944 N95-18891
An assessment of the adaptive unstructured tetrahedral grid, Euler Flow Solver Code FELISA
[NASA-TP-3526] p 930 N95-19041
Optimum dimension ratios for studios, control rooms and listening rooms
[BBC-RD-1993/8] p 993 N95-19053
NAWCAD photogrammetrics: Methods and applications for aviation test and evaluation
[AD-A284074] p 1034 N95-19071
Evaluation of scanners for C-scan imaging in nondestructive inspection of aircraft
[DE94-012473] p 990 N95-19100
Software Technology for Adaptable, Reliable Systems (STARS). Software architecture seminar report: Central Archive for Reusable Defense Software (CARDS)
[AD-A284668] p 1100 N95-19106
Data acquisition from blast overpressure trials
[MRL-TN-628] p 1020 N95-19139
The jet model of chondrule formation p 1189 N95-19310
Unsteady aerodynamic analyses for turbomachinery aeroelastic predictions p 949 N95-19381
XAMath: An XAFS analysis package based on Mathematica(tm)
[DE94-016346] p 1100 N95-19397
Technology Benefit Estimator (T/BEST): User's manual
[NASA-TM-106785] p 1046 N95-19501
Draft SEI program plans: 1995-1999
[AD-A285047] p 1100 N95-19545
Information system architecture to support transparent access to distributed, heterogeneous data sources
[DE94-018450] p 1176 N95-19589
The QED Workshop
[DE94-018499] p 1111 N95-19592
Generating parallel execution plans with a partial order planner
[AD-A285888] p 1111 N95-19605
Design of fan blades subjected to bird impact p 953 N95-19669
Global equation of state for a glassy material: Fused silica
[DE94-018598] p 988 N95-19721
MIRO: A debugging tool for CLIPS incorporating historical Rete networks p 1105 N95-19754
Process definition and modeling guidebook. Volume 1: Concepts and principles of MPDM. Version 02.00.02
[AD-A279162] p 1108 N95-19803
Process definition and modeling guidebook. Volume 2: Advanced applications of MPDM
[AD-A279199] p 1108 N95-19813
Connectionist Network Supercomputer Project
[AD-A279206] p 1112 N95-19843
Proceedings of the 15th Annual Conference on Atmospheric Transmission Models
[AD-A279919] p 1142 N95-19862

COMPUTER STORAGE DEVICES
Performance evaluation of the Engineering Analysis and Data Systems (EADS) 2 p 1163 N95-18978
Stand-alone digital data storage control system including user control interface
[NASA-CASE-LAR-14651-1] p 1175 N95-19056

COMPUTER SYSTEMS DESIGN
Miscellaneous disk utility application programs for the AFOS background partition
[PB94-181328] p 1067 N95-18038
Design and analysis of dynamic leader election protocols in broadcast networks
[PB94-202728] p 1109 N95-18039
Independent validation and verification of automated information systems in the Department of Energy
[DE94-014460] p 1173 N95-18063
A scalable decentralized group membership service for an asynchronous environment
[AD-A283633] p 1109 N95-18137
Characterizing parallel file-access patterns on a large-scale multiprocessor
[NASA-CR-197568] p 1110 N95-18521
The Isis project: Fault-tolerance in large distributed systems
[NASA-CR-197561] p 1110 N95-18532
Information system architecture to support transparent access to distributed, heterogeneous data sources
[DE94-018450] p 1176 N95-19589

COMPUTER SYSTEMS PERFORMANCE
Library capability demonstration. Central Archive for Reusable Defense Software (CARDS)
[AD-A284569] p 1095 N95-18032
Parallel Navier-Stokes computations on shared and distributed memory architectures
[NASA-TM-106823] p 1019 N95-18941
PST: A simulation tool for parallel systems
[AD-A285680] p 1111 N95-19526

COMPUTER SYSTEMS PROGRAMS
The Seventh Ionospheric Effects Symposium
[PB94-191930] p 1057 N95-17985
Improving software characteristics of a real-time system using reengineering techniques
[AD-A283659] p 1094 N95-18015
Design and analysis of dynamic leader election protocols in broadcast networks
[PB94-202728] p 1109 N95-18039
Metrics concept report. Central Archive for Reusable Defense Software (CARDS)
[AD-A284573] p 1097 N95-18449
Characterizing parallel file-access patterns on a large-scale multiprocessor
[NASA-CR-197568] p 1110 N95-18521
The Isis project: Fault-tolerance in large distributed systems
[NASA-CR-197561] p 1110 N95-18532
The generic simulation executive at Manned Flight Simulator
[AD-A283997] p 959 N95-18724

Technology Benefit Estimator (T/BEST): User's manual
[NASA-TM-106785] p 1046 N95-19501
PST: A simulation tool for parallel systems
[AD-A285680] p 1111 N95-19526

COMPUTER SYSTEMS SIMULATION
Implementation of a human information processing model for task network simulation
[AD-A283903] p 1088 N95-18151
PST: A simulation tool for parallel systems
[AD-A285680] p 1111 N95-19526

COMPUTER TECHNIQUES
Enhancement of fluorescence detection in chromatographic methods by computer analysis of second order data
[DE94-014682] p 973 N95-17966
Applications of quaternions to dynamical simulation, computer graphics and biomechanics
[PB94-201456] p 1094 N95-17972
A formal method for semantics-based change-merging of software prototypes
[AD-A283668] p 1094 N95-18017
A platform independent application of Lux illumination prediction algorithms
[AD-A283669] p 1094 N95-18018
A fast recursive algorithm to compute the probability of M-out-of-N events
[AD-A283679] p 1120 N95-18020
A Space and Atmospheric Visualization Science System
[NASA-CR-189390] p 1172 N95-18040
A practical algorithm for integer sorting on a mesh-connected computer (preliminary version)
[AD-A283921] p 1110 N95-18159
Design concepts for an integrated environmental medicine workstation for prediction, simulation and training
[AD-A283686] p 1079 N95-18618
CFD: Advances and Applications, 1994
[NAL-SP-9412] p 1028 N95-19455
High performance computing for medical image interpretation
[AD-A285457] p 1086 N95-19537
Third CLIPS Conference Proceedings, volume 1
[NASA-CP-10162-VOL-1] p 1100 N95-19625
Third CLIPS Conference Proceedings, volume 2
[NASA-CP-10162-VOL-2] p 1104 N95-19747
Transport aircraft loading and balancing system: Using a CLIPS expert system for military aircraft load planning
p 1105 N95-19751
Predicting and explaining the movement of mesoscale oceanographic features using CLIPS
p 1105 N95-19752
Knowledge based translation and problem solving in an intelligent individualized instruction system
p 1105 N95-19753
Optimal pattern distributions in Rete-based production systems p 1106 N95-19755
The Computer Aided Aircraft-design Package (CAAP)
p 1106 N95-19759
Automated revision of CLIPS rule-bases
p 1107 N95-19762
PalymSys (TM): An extended version of CLIPS for construction and reasoning using blackboards
p 1107 N95-19767

COMPUTER VISION
Cooperativity and 3-D representation
[AD-A284203] p 1093 N95-17940
Topography from shading and stereo
[NASA-CR-189389] p 1173 N95-18051
Fusion of multiple sensing modalities for machine vision
[AD-A284762] p 1091 N95-18086
Vision and action
[AD-A285701] p 1140 N95-18480

COMPUTERIZED SIMULATION
Six degree of freedom flight dynamic and performance simulation of a remotely-piloted vehicle
[AERO-TN-9301] p 942 N95-18097
The current status of Russian/CIS communication satellites
[AD-A285526] p 963 N95-18098
Coastal acoustic tomography data constraints applied to a coastal ocean circulation model
[AD-A283911] p 1074 N95-18153
Automated path planning of the Payload Inspection and Processing System p 1043 N95-18169
Experiments with the Mesoscale Atmospheric Simulation System (MASS) using the synthetic relative humidity p 1073 N95-18172
Enhancements to the KATE model-based reasoning system p 1115 N95-18183
Finite element method for eigenvalue problems in electromagnetics
[NASA-TP-3485] p 995 N95-18187
Simulation of gamma-ray spectra for a variety of user-specified detector designs
[NASA-CR-197551] p 1136 N95-18370
Size distribution of one-, two- and three-dimensional Voronoi cells
[PB94-207008] p 1149 N95-18373
Helicopter Performance Evaluation (HELPE) computer model
[AD-A284319] p 942 N95-18381
Studies on high pressure and unsteady flame phenomena
[AD-A284126] p 973 N95-18410
Atmospheric Infrared Sounder
[NASA-CR-197573] p 1064 N95-18444
A model study of the influence of NMHC and NO(x) emissions on rural O3 concentrations in Georgiargia
p 1059 N95-18445
Distributed interactive simulation interface library version description document
[AD-A284470] p 1173 N95-18446
TEXCAD: Textile Composite Analysis for Design. Version 1.0: User's manual
[NASA-CR-4639] p 970 N95-18466
Vision and action
[AD-A285701] p 1140 N95-18480
Aeromechanics technology, volume 1. Task 1: Three-dimensional Euler/Navier-Stokes Aerodynamic Method (TEAM) enhancements
[AD-A285713] p 943 N95-18483
NASA High Performance Computing and Communications program
[NASA-TM-4653] p 1174 N95-18573
Scalability of parallel spatial direct numerical simulation code on IBM SP1 parallel supercomputer
[NASA-CR-194975] p 1098 N95-18584
Low voltage electron beam lithography
[AD-A284181] p 1010 N95-18625
Real-time modeling of complex atmospheric releases in urban areas
[DE94-018063] p 1059 N95-18647
Computer simulation of wave propagation through turbulent media
[AD-A283695] p 1000 N95-18671
The generic simulation executive at Manned Flight Simulator
[AD-A283997] p 959 N95-18724
Building a bridge with the customer to facilitate collecting and validating information in modeling sessions
[DE94-017338] p 1174 N95-18872
Distributed algorithms for controlling multiple mobile robots
[AD-A283975] p 1114 N95-18889
HEISHI: A fuel performance model for space nuclear applications
[DE94-017497] p 1137 N95-18897
An analytic conceptual model of extratropical cyclones
[KNMI-WR-93-03] p 1072 N95-18926
On extending parallelism to serial simulators
[NASA-CR-195011] p 1099 N95-18931
Special relativity effects for space-based coherent lidar experiments p 1014 N95-18983
Computational simulation of liquid fuel rocket injectors
p 968 N95-18989
Development of microgravity, full body functional reach envelope using 3-D computer graphic models and virtual reality technology p 1092 N95-18990
Perspective problems of gas turbine engines simulation p 949 N95-19026
Empirical study of parallel LRU simulation algorithms
[NASA-CR-194995] p 1099 N95-19027
Assessment of the ACSE science learning environment and the impact of movies and simulations
[AD-A284071] p 1089 N95-19068
Complete mode-set stability analysis of magnetically insulated ion diode equilibria
[DE94-015275] p 1145 N95-19201
Real time simulator with Ti floating point digital signal processor
[DE94-016372] p 1012 N95-19246
Simulation in manufacturing
[PB94-215563] p 1100 N95-19409
Fatigue loads spectra derivation for the Space Shuttle: Second cycle p 934 N95-19470
Neural network communications signal processing
[AD-A285681] p 1115 N95-19512
PST: A simulation tool for parallel systems
[AD-A285680] p 1111 N95-19526
Three-dimensional radiation transport hydrodynamics
[DE94-018337] p 1146 N95-19527
Embedded microclusters in zeolites and cluster beam sputtering: Simulation on parallel computers
[DE95-000662] p 1134 N95-19562
Design of fan blades subjected to bird impact
p 953 N95-19669
Ice-impact analysis of blades p 953 N95-19672
Parallel computation
[AD-A284831] p 1112 N95-19692
Mega-scale simulation of multi-layer devices: Formulation, kinetics, and visualization
[AD-A284848] p 1153 N95-19738
Using CLIPS to represent knowledge in a VR simulation p 1107 N95-19765
Arbitrarily shaped dual-stacked patch antennas: A hybrid FEM simulation p 1006 N95-19800

COMPUTERS
Evaluation of scanners for C-scan imaging in nondestructive inspection of aircraft
[DE94-012473] p 990 N95-19100

CONCRETES
Long-term processes in geomaterials. A three-dimensional visco-elastic soil model
[PB94-207180] p 1065 N95-18640

CONCURRENT ENGINEERING
Optimization of coupled systems: A critical overview of approaches
[NASA-CR-195019] p 1116 N95-18109
Fair Petri nets and structural induction for rings of processes
[AD-A283920] p 1110 N95-18158
New technologies for space avionics
[NASA-CR-197574] p 966 N95-18196
A 20k payload launch vehicle fast track development concept using an RD-180 engine and a Centaur upper stage
[NASA-TM-108475] p 963 N95-19648

CONDUCTING POLYMERS
DC-conductivity and magnetoresistance of inherently conducting polymers. Polyacetylene and poly(3-alkylthiophenes)
[PB94-184587] p 1007 N95-18037
Application of conducting polymers to electroanalysis
[DE94-015204] p 984 N95-18348
Thermoelectric properties of conducting polymers
[AD-A284058] p 986 N95-18678

CONDUCTION BANDS
Energies of X conduction band minima in disordered and ordered GaInP2 alloys
[DE94-018211] p 1152 N95-19586

CONDUCTIVE HEAT TRANSFER
Rewetting of monogroove heat pipe in Space Station radiators
[NASA-CR-197579] p 1014 N95-18092
Subspace correction methods for the iterative solution of hierarchic plate models. 1: Heat transfer problems
[AD-A285712] p 1117 N95-18482
Coupled finite element analysis of decomposing poroelastic polymeric composites and structures with subsequent thermal and gas diffusion
p 986 N95-18918
Relative elemental abundance and heating constraints determined for the solar corona from SERTS measurements
[NASA-TM-104616] p 1196 N95-19791

CONDUCTIVITY
Optical determination of conduction and valence-band dispersion curves in strained single-quantum wells
[DE94-018892] p 1151 N95-19235

CONDUCTORS
Integrated, nonvolatile, high-speed analog random access memory
[NASA-CASE-NPO-17998-2-CU] p 1093 N95-18963
Precision gold conductors for HMCs
[DE94-018558] p 1012 N95-19230

CONFERENCES
The Seventh Ionospheric Effects Symposium
[PB94-191930] p 1057 N95-17985
Conference on Aerospace Transparent Materials and Enclosures. Volume 2: Sessions 5-9
[AD-A283926] p 942 N95-18162
NASA/ASEE Summer Faculty Fellowship Program. 1994 research reports
[NASA-CR-197448] p 1157 N95-18166
MIKON 94. International Microwave Conference. Invited papers, volume 3
[AD-A284353] p 1008 N95-18338
International Conference on Deformation, Yield and Fracture of Polymers
[AD-A284354] p 984 N95-18339
1994 IEEE Nonlinear Optics: Materials Fundamental and Applications Conference
[AD-A285769] p 1139 N95-18345
MIKON 94. International Microwave Conference. Volume 1: Conference proceedings
[AD-A284351] p 1009 N95-18425
MIKON 94. International Microwave Conference. Conference proceedings, volume 2
[AD-A284352] p 1009 N95-18426
Metrics concept report. Central Archive for Reusable Defense Software (CARDS)
[AD-A284573] p 1097 N95-18449

7th International Symposium on Applications of Laser Techniques to Fluid Mechanics, volume 2
[AD-A285685] p 1018 N95-18477
Aircraft Loads due to Turbulence and their Impact on Design and Certification
[AGARD-R-798] p 956 N95-18597
14th IEEE International Semiconductor Laser Conference
[AD-A285569] p 1038 N95-18642
The role of large-scale, extratropical dynamics in climate change
[DE94-017651] p 1059 N95-18665
Annual Allerton Conference on Communication, Control and Computing
[AD-A283892] p 1114 N95-18675
Conference on Aerospace Transparent Materials and Enclosures, volume 1
[AD-A283925] p 944 N95-18677
International Conference on Control Theory and its Applications
[DE94-626221] p 1114 N95-18875
Mathematical Models of Gas Turbine Engines and their Components
[AGARD-LS-198] p 948 N95-19017
Establishment of an Institute for Fusion Studies
[DE94-017330] p 1145 N95-19079
Workshop on Particle Capture, Recovery and Velocity/Trajectory Measurement Technologies
[NASA-CR-197582] p 1180 N95-19172
Wall Interference, Support Interference and Flow Field Measurements
[AGARD-CP-535] p 1020 N95-19251
Papers presented to the Conference on Chondrules and the Protoplanetary Disk
[NASA-CR-197121] p 1186 N95-19289
NASA Lewis Research Center Workshop on Forced Response in Turbomachinery
[NASA-CP-10147] p 949 N95-19380
The Clinical Basis for Aeromedical Decision Making
[AGARD-CP-553] p 1080 N95-19413
CFD: Advances and Applications, 1994
[NAL-SP-9412] p 1028 N95-19455
FAA/NASA International Symposium on Advanced Structural Integrity Methods for Airframe Durability and Damage Tolerance, part 2
[NASA-CP-3274-PT-2] p 934 N95-19468
Proceedings of the USAF Structural Integrity Program Conference
[AD-A285684] p 945 N95-19517
Proceedings of Natural Sciences Symposium
[AD-A285452] p 1077 N95-19536
Nozzle Initiative Industry Advisory Committee on Standardization of Carbon-Phenolic Test Methods and Specifications
[NASA-CR-197529] p 967 N95-19566
Third CLIPS Conference Proceedings, volume 1
[NASA-CP-10162-VOL-1] p 1100 N95-19625
Erosion, Corrosion and Foreign Object Damage Effects in Gas Turbines
[AGARD-CP-558] p 950 N95-19653
Proceedings of the Eighth Annual Conference on Fossil Energy Materials
[DE95-001055] p 981 N95-19723
Third CLIPS Conference Proceedings, volume 2
[NASA-CP-10162-VOL-2] p 1104 N95-19747
Second International Semiconductor Device Research Symposium (ISDRS-1993)
[AD-A279221] p 1013 N95-19849
Proceedings of the 15th Annual Conference on Atmospheric Transmission Models
[AD-A279919] p 1142 N95-19862

CONFIGURATION INTERACTION
Massively parallel full configuration interaction. Benchmark electronic structure calculations on the Intel Touchstone Delta
[DE95-001064] p 1153 N95-19724

CONFIGURATION MANAGEMENT
Replica management system: A scheme for flexible and dynamic replication
[PB94-201597] p 1171 N95-18060

CONFINEMENT
Numerical mixing calculations of confined reacting jet flows in a cylindrical duct
[NASA-TM-106736] p 947 N95-18133
Study of alpha physics related to ITER Project
[DE94-017329] p 1133 N95-19078
Crystalline beams: The string
[DE94-016806] p 1150 N95-19091
Impurity behavior during ion-Bernstein wave heating in PBX-M
[DE94-018114] p 1133 N95-19228
Three-dimensional radiation transport hydrodynamics
[DE94-018337] p 1146 N95-19527

CONFORMAL MAPPING
Study of frustrated systems via dissipative maps
[DE94-017754] p 1122 N95-18127
Adaptive Neuron Model: An architecture for the rapid learning of nonlinear topological transformations
[NASA-CASE-NPO-18579-1-CU] p 1114 N95-18740
Towards a classification of su(2)(direct sum)...(direct sum)su(2) modular invariant partition functions
[PB94-217247] p 1119 N95-19717
SU(2) WZW theory at higher genera
[PB94-217262] p 1119 N95-19719

CONGRESSIONAL REPORTS
Information Superhighway: Issues affecting development. Report to the Congress
[GAO/RCED-94-285] p 1174 N95-18914
Space Station: Plans to expand research community do not match available resources. Report to the Ranking Minority Member, Subcommittee on Oversight of Government Management, Committee on Government Affairs, US Senate
[GAO/NSIAD-95-33] p 965 N95-19131

CONICS
On the geometry of visual correspondence
[AD-A285700] p 1140 N95-18478

CONJUGATE GRADIENT METHOD
Reformulated preconditioned conjugate gradient squared method. Part 1: The algorithm
[PB94-201589] p 1108 N95-17936
Weighted graph based ordering techniques for preconditioned conjugate gradient methods
[NASA-CR-197597] p 1118 N95-18736

CONJUGATION
High power phase conjugated solid state lasers
[DE94-016633] p 1037 N95-18357

CONNECTORS
Disengagable adapter for an optical fiber connection
[AD-D016231] p 1141 N95-18628

CONSERVATION EQUATIONS
Design optimization of a brush turbine with a cleaner/water based solution p 1043 N95-18177

CONSERVATION LAWS
Singular perturbation problem governed by system of conservation laws
[DE94-019264] p 1116 N95-17977
The space-time solution element method: A new numerical approach for the Navier-Stokes equations
[NASA-TM-106818] p 1014 N95-18036
CFD: Advances and Applications, part 1
[NAL-SP-9322-PT-1] p 1026 N95-19444
Basic equations of fluid dynamics p 1026 N95-19445
Difference schemes for hyperbolic system of Conservation Laws p 1027 N95-19450

CONSTRAINTS
Experimental constraints on models for the origin of chondrules: Cooling rates p 1189 N95-19311

CONSTRUCTION
Singular perturbation problem governed by system of conservation laws
[DE94-019264] p 1116 N95-17977
Construction of a connectionist network supercomputer
[AD-A283354] p 1109 N95-18050
Sandia National Laboratories' high power electromagnetic impulse sources
[DE95-000423] p 1004 N95-19555
Microcavity structures
[DE95-001096] p 1039 N95-19727

CONSTRUCTION MATERIALS
The sound insulations of metal-framed partitions having structural loadbearing properties
[BBC-RD-1994/8] p 992 N95-18533
QuikForm: Intelligent deformation processing of structural alloys
[DE94-018739] p 1114 N95-18649
Metal-framed partitions with reduced thicknesses. Part 2: Built-in acoustic treatment
[BBC-RD-1993/6-PT-2] p 993 N95-19137

CONTAINERLESS MELTS
Plasma heating for containerless and microgravity materials processing
[NASA-CASE-NPO-18819-1-CU] p 991 N95-18326

CONTAMINANTS
GAMQUEST, a computer program to identify gamma rays
[DE94-016217] p 1197 N95-18351
A model study of the influence of NMHC and NO(x) emissions on rural O3 concentrations in Georgiargia p 1059 N95-18445
Economic impact analysis for proposed emission standards and guidelines for municipal waste combustors: A description of the basis for, and impacts of, proposed revisions to air pollutant emission regulations for new and existing municipal waste combustors under Clean Air Act Sections 111(b), 111(d), and 129
[PB94-213543] p 1061 N95-19403
Future directions in helicopter protection system configuration p 951 N95-19657
Heavy metal soil contamination at US Army installations: Proposed research and strategy for technology development
[AD-A279171] p 1062 N95-19808

CONTAMINATION
A study of gas flow pattern, undercutting and torch modification in variable polarity plasma arc welding
[NASA-CR-196537] p 1040 N95-18056
Can salt on an optical rain gauge lens affect performance? p 1069 N95-18208
A technique for determining cloud free versus cloud contaminated pixels in satellite imagery p 1052 N95-19016
Out of area experiences with the RB199 in Toronto p 950 N95-19654
Heavy metal soil contamination at US Army installations: Proposed research and strategy for technology development
[AD-A279171] p 1062 N95-19808

CONTEXT FREE LANGUAGES
Alternative formulation of Cocke-Younger-Kasami's algorithm
[PB94-202751] p 1094 N95-18000

CONTINENTAL SHELVES
Geologic studies: Executive summary report
[PB94-187481] p 1073 N95-17951

CONTINUITY (MATHEMATICS)
A 2D depth migration in transversely isotropic media using explicit operators
[DE95-000645] p 1066 N95-19560

CONTINUITY EQUATION
Acoustic radiation damping of flat rectangular plates subjected to subsonic flows p 1123 N95-18542
Basic equations of fluid dynamics p 1026 N95-19445

CONTINUOUS SPECTRA
Spectral distribution of the two-photon decay of He-like krypton
[DE95-001442] p 1135 N95-19787

CONTINUUM FLOW
Hypersonic wind tunnel test techniques
[AD-A284057] p 929 N95-18663
Flow field investigation in a free jet - free jet core system for the generation of high intensity molecular beams
[DLR-FB-94-11] p 1132 N95-18912

CONTINUUM MECHANICS
Experimental verification of a progressive damage model for composite laminates based on continuum damage mechanics
[NASA-CR-195020] p 971 N95-19043
The tensor equation AX+XA=Phi (A, H) with applications to kinematics of continua
[AD-A285886] p 1122 N95-19603

CONTINUUM MODELING
Experimental verification of a progressive damage model for composite laminates based on continuum damage mechanics
[NASA-CR-195020] p 971 N95-19043

CONTINUUMS
Ultrafast nonlinear optical response of Fano resonances in gallium arsenide under high magnetic field
[DE94-018181] p 1148 N95-18122
Discrete and continuum elastic properties of interfaces p 1150 N95-18928

CONTRACT MANAGEMENT
Overhead costs: Costs charged by McDonnell Douglas Aerospace's Space Station Division. Report to the Chairman, Legislation and National Security Subcommittee, Committee on Government Operations, House of Representatives
[GAO/NSIAD-94-150] p 1171 N95-18596

CONTRACTORS
Training plan. Central Archive for Reusable Defense Software (CARDS)
[AD-A284343] p 1097 N95-18421
Government contractors: Measuring costs of service contractors versus federal employees. Report to the Chairman, Subcommittee on Federal Services, Post Office and Civil Service, Committee on Governmental Affairs, US Senate
[GAO/GGD-94-95] p 1171 N95-18595
Overhead costs: Costs charged by McDonnell Douglas Aerospace's Space Station Division. Report to the Chairman, Legislation and National Security Subcommittee, Committee on Government Operations, House of Representatives
[GAO/NSIAD-94-150] p 1171 N95-18596

CONTRACTS
Government contractors: Measuring costs of service contractors versus federal employees. Report to the Chairman, Subcommittee on Federal Services, Post Office and Civil Service, Committee on Governmental Affairs, US Senate
[GAO/GGD-94-95] p 1171 N95-18595

CONTROL
Strategic avionics technology definition studies. Subtask 3-1A3: Electrical Actuation (ELA) Systems Test Facility [NASA-CR-188360] p 956 N95-18567
International Conference on Control Theory and its Applications [DE94-626221] p 1114 N95-18875
CONTROL BOARDS
On-line handling of air traffic: Management, guidance and control [AGARD-AG-321] p 941 N95-18927
CONTROL EQUIPMENT
The development of a fiber optics communication network for controlling a Multidegree-Of-Freedom Serpentine Truss p 1142 N95-18167
CONTROL SIMULATION
Automation of hardware-in-the-loop testing of control systems for unmanned air vehicles [AD-A284833] p 945 N95-19693
CONTROL SURFACES
Plant and controller optimization by convex methods [AD-A283700] p 944 N95-18621
An atomic view of surface diffusion on metal surfaces [DE94-016150] p 980 N95-19395
CONTROL SYSTEMS DESIGN
Microgravity isolation system design: A modern control synthesis framework [NASA-TM-106805] p 927 N95-18197
Three-parameter tunable Tilt-Integral-Derivative (TID) controller [NASA-CASE-NPO-18492-1-CU] p 1113 N95-18313
Microgravity isolation system design: A modern control analysis framework [NASA-TM-106803] p 927 N95-18486
Streamlined design and self reliant hardware for active control of precision space structures [NASA-CR-4637] p 964 N95-18580
The impact of non-linear flight control systems on the prediction of aircraft loads due to turbulence p 956 N95-18598
Plant and controller optimization by convex methods [AD-A283700] p 944 N95-18621
Design and flight test of a simplified control system for a transport helicopter p 958 N95-18902
Stand-alone digital data storage control system including user control interface [NASA-CASE-LAR-14651-1] p 1175 N95-19056
Sliding mode control method having terminal convergence in finite time [NASA-CASE-NPO-18584-1-CU] p 1114 N95-19062
Alternative control techniques document: NO(x) emissions from glass manufacturing [PB94-214079] p 1061 N95-19406
Automation of hardware-in-the-loop testing of control systems for unmanned air vehicles [AD-A284833] p 945 N95-19693
Improved speed control system for the 87,000 HP wind tunnel drive [NASA-TM-106840] p 1035 N95-19794
CONTROL THEORY
Time-optimal control of a third order regulator [AD-A283307] p 1113 N95-18023
Distributed methods for controlling multiple mobile robots [AD-A283919] p 1113 N95-18157
International Conference on Control Theory and its Applications [DE94-626221] p 1114 N95-18875
CONTROL UNITS (COMPUTERS)
Dynamic range control of audio signals by digital signal processing [BBC-RD-1993/7] p 1124 N95-19054
CONTROLLED ATMOSPHERES
Weldability of iron aluminides [DE95-000686] p 981 N95-19568
CONTROLLED FUSION
Study of alpha physics related to ITER Project [DE94-017329] p 1133 N95-19078
Establishment of an Institute for Fusion Studies [DE94-017330] p 1145 N95-19079
CONTROLLERS
New technologies for space avionics [NASA-CR-197574] p 966 N95-18196
Three-parameter tunable Tilt-Integral-Derivative (TID) controller [NASA-CASE-NPO-18492-1-CU] p 1113 N95-18313
Radar sector blanker [AD-D016275] p 996 N95-18429
Microgravity isolation system design: A modern control analysis framework [NASA-TM-106803] p 927 N95-18486
Streamlined design and self reliant hardware for active control of precision space structures [NASA-CR-4637] p 964 N95-18580
Plant and controller optimization by convex methods [AD-A283700] p 944 N95-18621
Gas storage and recovery system [NASA-CASE-MSC-22091-1] p 992 N95-18738
Lean spacecraft avionics trade study p 966 N95-18994
Sliding mode control method having terminal convergence in finite time [NASA-CASE-NPO-18584-1-CU] p 1114 N95-19062
Mitigation of EMI generated by a variable-frequency-drive controller for an AC induction motor [AD-A286045] p 1012 N95-19573
Neural net controller for inlet pressure control of rocket engine testing p 1102 N95-19637
Battery and charge controller evaluations in small stand-alone PV systems [DE94-014252] p 1013 N95-19872
CONVECTION
Conceptual models of severe convective weather in the Netherlands [KNMI-WR-93-05] p 1071 N95-18394
A synoptic climatology of convective weather in the Netherlands [KNMI-WR-93-04] p 1071 N95-18395
Dynamic evolution of emerging magnetic flux tubes in the solar convective envelope p 1195 N95-18497
Effects of vibration (G-jitters) on convection in micro-gravity p 991 N95-19013
Turbulent diffusion and concentration of chondrules in the protoplanetary nebula p 1187 N95-19296
CONVECTION CURRENTS
Experiments with the Mesoscale Atmospheric Simulation System (MASS) using the synthetic relative humidity p 1073 N95-18172
CONVECTIVE HEAT TRANSFER
Coupled finite element analysis of decomposing poroelastic polymeric composites and structures with subsequent thermal and gas diffusion p 986 N95-18918
Verification of multidisciplinary models for turbomachines p 949 N95-19025
CONVENTIONS
Effects of vibration (G-jitters) on convection in micro-gravity p 991 N95-19013
CONVERGENCE
Some statistical tools for SAR image synthesis, analysis and processing [INPE-5548-TDI/534] p 1172 N95-18004
On the convergence of local approximations to pseudodifferential operators with applications [NASA-TM-106792] p 1019 N95-18898
CONVERGENT-DIVERGENT NOZZLES
Static investigation of two fluidic thrust-vectoring concepts on a two-dimensional convergent-divergent nozzle [NASA-TM-4574] p 931 N95-19042
CONVEXITY
Applications of quantum entropy to statistics [DE94-014416] p 1155 N95-17996
Plant and controller optimization by convex methods [AD-A283700] p 944 N95-18621
COOL STARS
A Type 2 supernovae constraint on neutrino(sub e) - neutrino(sub s) mixing [NASA-CR-197630] p 1180 N95-18746
COOLERS
Improved efficiency and power density for thermoacoustic coolers [AD-A283946] p 992 N95-18165
A numerical simulation of seasonal circulation in the South China Sea [AD-A283701] p 1075 N95-18622
COOLING
Asymmetric antiproton debuncher: No bad mixing, more good mixing [DE94-017171] p 1133 N95-19077
Constraints placed on the nature of chondrule precursors p 1186 N95-19295
Heating and cooling in the solar nebula: Constraints from refractory inclusions p 1187 N95-19297
Experimental constraints on models for the origin of chondrules: Cooling rates p 1189 N95-19311
Cooling rates of chondrules: A new approach p 1192 N95-19334
COOLING SYSTEMS
Geometrical vapor blocker for parallel condensation tubes requiring subcooling [NASA-CASE-MSC-22090-1] p 1017 N95-18323
Thermoelectric properties of conducting polymers [AD-A284058] p 986 N95-18678
Regenerative cooling for liquid propellant rocket thrust chambers [INPE-5565-TDI/540] p 967 N95-18720
Application of multidisciplinary models to the cooled turbine rotor design p 949 N95-19024
COORDINATES
Annual Allerton Conference on Communication, Control and Computing [AD-A283892] p 1114 N95-18675
Special relativity effects for space-based coherent lidar experiments p 1014 N95-18983
COORDINATION
Robust image understanding. Techniques and applications [AD-A283427] p 1113 N95-18057
Cerebellar circuit mechanisms which accompany coordinated limb trajectory patterns in the rat: Use of a model of spontaneous changes in limb coordination [AD-A284023] p 1079 N95-18656
COPLANARITY
EEsoF MICAD and ACADEMY macro files for coplanar waveguide and finite ground plan coplanar waveguide [NASA-TM-106800] p 1000 N95-18733
COPOLYMERS
Obtention of cationic polymeric membranes by radiation-induced grafting method [DE94-629193] p 983 N95-17942
Multi-functional pi-conjugated macromolecules based on poly (phenylene vinylene) [AD-A284163] p 985 N95-18510
Novel polymeric composites through molecular engineering [AD-A284168] p 985 N95-18513
PVDF flux/mass/velocity/trajectory systems and their applications in space p 966 N95-19196
COPPER
Preparation and surface characterization of metal doped alumina catalyst [PB94-175296] p 973 N95-17991
COPPER ALLOYS
Microstructural analysis of cracks generated during welding of 2195 aluminum-lithium alloy p 982 N95-19007
Modified Cu-Mn-Al high damping alloys [AD-A285460] p 980 N95-19539
Study of laser resonance ionization mass spectrometry using a glow discharge source [DE94-018566] p 981 N95-19703
COPPER OXIDES
Deformation of nonstoichiometric CuO polycrystals [DE94-016907] p 1150 N95-19094
High temperature superconducting films and crystals [AD-A279201] p 1154 N95-19815
COPPER SELENIDES
Correlation of polycrystalline Cu(In,Ga)Se2 device efficiency with homojunction depthand interfacial structure: X-ray photoemission and positron annihilation spectroscopic characterization [DE94-013543] p 1055 N95-19858
Advanced processing technology for high-efficiency, thin-film CuInSe2 and CdTe solar cells [DE94-011838] p 1056 N95-19880
CORE SAMPLING
Atmospheric chemistry of biogenic sulfur in the Southern Hemisphere p 1071 N95-18399
CORIOLIS EFFECT
Prediction of buoyant outflow in lakes and fjords with a quasi 3D numerical model [PB94-206984] p 1051 N95-18372
Dynamic evolution of emerging magnetic flux tubes in the solar convective envelope p 1195 N95-18497
An analytic conceptual model of extratropical cyclones [KNMI-WR-93-03] p 1072 N95-18926
Vestibular examination in pilots susceptible to motion sickness p 1083 N95-19427
CORNER FLOW
Corner vortex suppressor [AD-D016423] p 928 N95-18337
CORONAL LOOPS
Solar flare model atmospheres [NASA-CR-197607] p 1196 N95-19034
CORRECTION
Subspace correction methods for the iterative solution of hierarchic plate models. 1: Heat transfer problems [AD-A285712] p 1117 N95-18482
Boundary-flow measurement methods for wall interference assessment and correction: Classification and review p 1022 N95-19262
Wall correction method with measured boundary conditions for low speed wind tunnels p 1023 N95-19263
Adaptive wind tunnel walls versus wall interference correction methods in 2D flows at high blockage ratios p 960 N95-19267
Transonic wind tunnel boundary interference correction p 960 N95-19271
Calculation of wall effects of flow on a perforated wall with a code of surface singularities p 1025 N95-19277

Interference corrections for a centre-line plate mount in a porous-walled transonic wind tunnel
p 933 N95-19280
Correction of support influences on measurements with sting mounted wind tunnel models p 933 N95-19281

CORRELATION
Applications of quantum entropy to statistics
[DE94-014416] p 1155 N95-17996
Producing chondrules by recycling and volatile loss
p 1186 N95-19290
Electronic structure of C60 fullerites and nanotubes
[DE95-000784] p 1151 N95-19569
Correlation function analysis of the COBE differential microwave radiometer sky maps
[DE95-000795] p 1178 N95-19617
Coulomb gas representation of the SU(2) WZW correlators at higher genera
[PB94-217254] p 1119 N95-19718

CORROSION
Corrosivity sensor
[AD-D016422] p 1033 N95-18524
The effect of fabrication on corrosion in aluminum 2195: Environmental and microstructural considerations
p 982 N95-19011
Fundamental studies of passivity and passivity breakdown
[DE94-016954] p 987 N95-19095
Pitting corrosion of aluminized seals in molten carbonate fuel cells
[DE94-017075] p 1053 N95-19116
Corrosion fatigue of iron-chromium-nickel alloys: Fracture mechanics, microstructure and chemistry
[DE95-000909] p 981 N95-19610
Erosion, Corrosion and Foreign Object Damage Effects in Gas Turbines
[AGARD-CP-558] p 950 N95-19653
Out of area experiences with the RB199 in Toronto
p 950 N95-19654
Gas turbine compressor corrosion and erosion in Western Europe p 954 N95-19678
Testing considerations for military aircraft engines in corrosive environments (a Navy perspective)
p 955 N95-19684

CORROSION PREVENTION
Polyurethane self-priming topcoats
[AD-D016420] p 984 N95-18336
Future directions in helicopter protection system configuration p 951 N95-19657

CORROSION RESISTANCE
Fundamental advances for characterizing cathodic protection systems
[PB94-180692] p 1122 N95-17983
Alloying effects on the high-temperature oxidation resistance of Cr-Cr2Nb
[DE94-018146] p 978 N95-18121
Polyurethane self-priming topcoats
[AD-D016264] p 984 N95-18320
Trivalent chromium conversion coatings for aluminum
[AD-D016274] p 978 N95-18332
Polyurethane self-priming topcoats
[AD-D016420] p 984 N95-18336
Trivalent chromium solutions for sealing anodized aluminum
[AD-D016472] p 979 N95-18458
Progress in the development of advanced solar reflectors
[DE94-000264] p 1053 N95-18463
Polyurethane self-priming topcoats
[AD-D016234] p 985 N95-18631
Method for laser-assisted silicon etching using halocarbon ambients
[AD-D016239] p 1038 N95-18635
A CMC database for use in the next generation launch vehicles (rockets) p 963 N95-18993
FAA/NASA International Symposium on Advanced Structural Integrity Methods for Airframe Durability and Damage Tolerance, part 2
[NASA-CP-3274-PT-2] p 934 N95-19468
Weldability of iron aluminides
[DE95-000686] p 981 N95-19568
Resistance of silicon nitride turbine components to erosion and hot corrosion/oxidation attack
p 955 N95-19683

CORROSION TESTS
Fundamental advances for characterizing cathodic protection systems
[PB94-180692] p 1122 N95-17983
Evaluation of inorganic zinc-rich primers using Electrochemical Impedance Spectroscopy (EIS) in combination with atmospheric exposure
p 977 N95-18170
A review of nuclear thermal propulsion carbide fuel corrosion and key issues
[NASA-CR-197533] p 1136 N95-18217
An artifical corrosion protocol for lap-splices in aircraft skin p 937 N95-19482
Testing considerations for military aircraft engines in corrosive environments (a Navy perspective)
p 955 N95-19684

CORRUGATED PLATES
Acoustic transmission loss and structureborne noise transmission tests on a LASCOR and a reference steel panel
[MRL-TN-623] p 1128 N95-19770

COSMIC BACKGROUND EXPLORER SATELLITE
Correlation function analysis of the COBE differential microwave radiometer sky maps
[DE95-000795] p 1178 N95-19617

COSMIC DUST
SOCCER: Comet Coma Sample Return Mission
p 1181 N95-19174
Plasma produced by impacts of fast dust particles on a thin film p 1181 N95-19177
Highly transparent and rugged sensor for velocity determinations of cosmic dust particles
p 966 N95-19178
Main characteristics of the COMET/COMRADE experiments p 1181 N95-19179
Laboratory simulation of intact capture of cometary and asteroidal dust particles in ISAS p 962 N95-19183
Some considerations on velocity vector accuracy in dust trajectory analysis p 1183 N95-19186
Velocity distribution of Earth-crossing asteroid grains
p 1183 N95-19187
The intact capture of hypervelocity dust particles using underdense foams p 1183 N95-19188
SPICE: An innovative, flexible instrument concept
p 966 N95-19189
Charge collection during hypervelocity penetrations of thin foils p 1036 N95-19190
Penetration of multiple thin films in micrometeorite capture cells p 1036 N95-19192
Nondestructive time-of-capture, location and velocity sensing in intact capture p 1036 N95-19194
The physics of intact capture p 1122 N95-19195
Chondrule formation in the radiative accretional shock
p 1191 N95-19324

COSMIC GASES
Mass and radius of cosmic balloons
[NASA-CR-197628] p 1180 N95-19031

COSMIC PLASMA
Charge collection during hypervelocity penetrations of thin foils p 1036 N95-19190

COSMIC RAYS
An instrument to measure the charge, and energy spectrum (20-1000 GeV/a) of the cosmic ray species oxygen to iron
[NASA-CR-197555] p 1197 N95-18464
STS-68 mission highlights resource tape
[NASA-TM-110049] p 961 N95-18568
Cosmic ray models for early galactic lithium, beryllium, and boron production
[NASA-CR-197626] p 1137 N95-18965

COSMOCHEMISTRY
The role of chondrules in nebular fractionations of volatiles and other elements p 1187 N95-19300
Relict grains in chondrules: Evidence for chondrule recycling p 1188 N95-19307
Collision of cometlike and slightly differentiated bodies as an origin for ordinary chondrites
p 1188 N95-19308
Microchondrules in ordinary chondrites: Implications for chondrule formation p 1188 N95-19309
Experimental constraints on models for the origin of chondrules: Cooling rates p 1189 N95-19311
Implications of a phase-transition thermostat for chondrule melting p 1189 N95-19312
Heating during solar nebula formation and Mg isotopic fractionation in precursor grains of CAIs and chondrules
p 1191 N95-19326
Variations among chondrite groups: Constraints on nebular processes p 1192 N95-19327
Chemical production of chondrule oxygen isotopic composition p 1192 N95-19330
Establishment of redox conditions during planetary collisions as an origin of chondrites
p 1192 N95-19331
Chondrule origins: Constraints from chondrule properties and cosmochemistry p 1192 N95-19332
Implications for the evolution of chondrules from Agglomeratic olivine chondrules p 1193 N95-19335
Major unresolved issues in the formation of chondrules and CAIs p 1193 N95-19336
Flash heating is required to minimize sodium losses from chondrules p 1193 N95-19337
Chondrule precursors and cooling paths: The sulfur evidence p 1193 N95-19338

COSMOLOGY
Relict grains in chondrules: Evidence for chondrule recycling p 1188 N95-19307
Implications of a phase-transition thermostat for chondrule melting p 1189 N95-19312
A Quantum-Drive-Time (QDT) quantization of the Taub cosmology
[DE95-001014] p 1194 N95-19612

COST ANALYSIS
Applying Costs, Risks and Values Evaluation (CRAVE) methodology to Engineering Support Request (ESR) prioritization p 1160 N95-18176
Government contractors: Measuring costs of service contractors versus federal employees. Report to the Chairman, Subcommittee on Federal Services, Post Office and Civil Service, Committee on Governmental Affairs, US Senate
[GAO/GGD-94-95] p 1171 N95-18595
Technology Benefit Estimator (T/BEST): User's manual
[NASA-TM-106785] p 1046 N95-19501
An analysis of the costs and benefits in improving F402-RR-406A High Pressure Turbine, second stage blades under the aircraft engine Component Improvement Program (CIP)
[AD-A285127] p 950 N95-19595

COST EFFECTIVENESS
Applying Costs, Risks and Values Evaluation (CRAVE) methodology to Engineering Support Request (ESR) prioritization p 1160 N95-18176
Government contractors: Measuring costs of service contractors versus federal employees. Report to the Chairman, Subcommittee on Federal Services, Post Office and Civil Service, Committee on Governmental Affairs, US Senate
[GAO/GGD-94-95] p 1171 N95-18595
A redundant disk array architecture for efficient small writes
[AD-A284048] p 1093 N95-18659

COST ESTIMATES
Technology Benefit Estimator (T/BEST): User's manual
[NASA-TM-106785] p 1046 N95-19501

COST REDUCTION
Progress in the development of advanced solar reflectors
[DE94-000264] p 1053 N95-18463
Phase and amplitude controlled micropatch antenna
[AD-A284191] p 1002 N95-19103
Split mandrel versus split sleeve coldworking: Dual methods for extending the fatigue life of metal structures
p 940 N95-19500

COSTS
Overhead costs: Costs charged by McDonnell Douglas Aerospace's Space Station Division. Report to the Chairman, Legislation and National Security Subcommittee, Committee on Government Operations, House of Representatives
[GAO/NSIAD-94-150] p 1171 N95-18596
Industrial exploitation of a alternate technology for the production of HgCdTe epilayers, structures and devices
[AD-A279202] p 1154 N95-19816

COUPLED MODES
Numerical analysis of dissipative dynamical systems in solid and fluid mechnaics, with a special emphasis on coupled problems p 1122 N95-18916

COUPLERS
Design and fabrication of N x N optical couplers based on organic polymer optical waveguides
[AD-A285530] p 1138 N95-18100
A fiber optic coupler
[AD-D016473] p 1140 N95-18459
Induction heating coupler and annealer
[NASA-CASE-LAR-14277-1] p 1011 N95-18962

COUPLING
Optimization of coupled systems: A critical overview of approaches
[NASA-CR-195019] p 1116 N95-18109
The evaluation of transmission efficiency and coupling loss factor of structural junctions
[MRL-TR-93-1] p 1124 N95-19057

COUPLING CIRCUITS
Design and fabrication of N x N optical couplers based on organic polymer optical waveguides
[AD-A285530] p 1138 N95-18100

COUPLINGS
A fiber optic coupler
[AD-D016473] p 1140 N95-18459

COVERINGS
The probability of flaw detection and the probability of false calls in nondestructive evaluation equipment
p 1044 N95-19010

CRACK CLOSURE
Fracture toughness of polymer/polymer bimaterial interface reinforced with block copolymers
p 986 N95-18923
Prediction of fatique crack growth under flight-simulation loading with the modified CORPUS model
p 934 N95-19471

Discrete crack growth analysis methodology for through cracks in pressurized fuselage structures
p 935 N95-19473
A new stochastic systems approach to structural integrity p 935 N95-19474
The application of Newman crack-closure model to predicting fatigue crack growth p 937 N95-19483
On the measurement of the crack tip stress field as a means of determining Delta K(sub eff) under conditions of fatigue crack closure p 938 N95-19492

CRACK GEOMETRY
The load separation technique in the elastic-plastic fracture analysis of two- and three-dimensional geometries p 936 N95-19481

CRACK INITIATION
The characterization of widespread fatigue damage in fuselage structure p 935 N95-19472
A probabilistic fatigue analysis of multiple site damage p 935 N95-19476
Evaluation of the fuselage lap joint fatigue and terminating action repair p 936 N95-19477
Fatigue life until small cracks in aircraft structures: Durability and damage tolerance p 936 N95-19478
Results of uniaxial and biaxial tests on riveted fuselage lap joint specimens p 938 N95-19491
Aircraft fatigue and crack growth considering loads by structural component p 939 N95-19497

CRACK OPENING DISPLACEMENT
Fracture toughness of polymer/polymer bimaterial interface reinforced with block copolymers
p 986 N95-18923
Fatigue life until small cracks in aircraft structures: Durability and damage tolerance p 936 N95-19478
Near tip stress and strain fields for short elastic cracks p 937 N95-19487

CRACK PROPAGATION
Microstructure-based fatigue life prediction methods for naval steel structures
[AD-A284735] p 1044 N95-18081
On the crack growth resistance and strength of the B2 iron aluminides Fe-40Al, Fe-45Al, and Fe-10Ni-40Al (at. %)
[DE94-017857] p 978 N95-18128
Dynamic decohesion of bimaterials: Experimental observations and failure criteria
[GALCIT-94-2] p 1045 N95-18613
Complex oxidation effects in polymer degradation
[DE94-018903] p 986 N95-18651
On the theory of stick-slip fracture
p 1046 N95-18922
Prediction of fatique crack growth under flight-simulation loading with the modified CORPUS model
p 934 N95-19471
The characterization of widespread fatigue damage in fuselage structure p 935 N95-19472
Discrete crack growth analysis methodology for through cracks in pressurized fuselage structures
p 935 N95-19473
A new stochastic systems approach to structural integrity p 935 N95-19474
Fatigue and damage tolerance scatter models
p 935 N95-19475
A probabilistic fatigue analysis of multiple site damage
p 935 N95-19476
Evaluation of the fuselage lap joint fatigue and terminating action repair p 936 N95-19477
Fatigue life until small cracks in aircraft structures: Durability and damage tolerance p 936 N95-19478
The load separation technique in the elastic-plastic fracture analysis of two- and three-dimensional geometries p 936 N95-19481
The application of Newman crack-closure model to predicting fatigue crack growth p 937 N95-19483
Fatigue crack growth under variable amplitude loading
p 937 N95-19484
Near tip stress and strain fields for short elastic cracks p 937 N95-19487
Fatigue crack growth in 2024-T3 aluminum under tensile and transverse shear stresses p 938 N95-19490
Analysis of cold worked holes for structural life extension p 939 N95-19493
Fatigue and residual strength investigation of ARALL(R) -3 and GLARE(R) -2 panels with bonded stringers
p 939 N95-19495
Aircraft fatigue and crack growth considering loads by structural component p 939 N95-19497
Impact loading of compressor stator vanes by hailstone ingestion p 953 N95-19670
CVD silicon carbide characterization
[AD-A285667] p 972 N95-19702
Stress-intensity factor solutions for cracks at countersunk rivet holes under uniaxial tension
[AD-A279163] p 1047 N95-19804

CRACK TIPS
On the theory of stick-slip fracture
p 1046 N95-18922
Discrete crack growth analysis methodology for through cracks in pressurized fuselage structures
p 935 N95-19473
The application of Newman crack-closure model to predicting fatigue crack growth p 937 N95-19483
On the measurement of the crack tip stress field as a means of determining Delta K(sub eff) under conditions of fatigue crack closure p 938 N95-19492

CRACKING (FRACTURING)
International Conference on Deformation, Yield and Fracture of Polymers
[AD-A284354] p 984 N95-18339
Finite element modeling of partially delaminated composite beams with contact-impact conditions
[AD-A283726] p 1044 N95-18363
A boundary element method for two dimensional linear elastic fracture analysis p 1045 N95-18917
Cracking characteristics of a habitable module pressure wall following orbital debris penetration
p 1047 N95-19003
Evaluation of the fuselage lap joint fatigue and terminating action repair p 936 N95-19477
The load separation technique in the elastic-plastic fracture analysis of two- and three-dimensional geometries p 936 N95-19481
Investigation of microscopic mechanisms of failure of electronic smart materials/systems
[AD-A284830] p 988 N95-19691

CRACKS
Dynamic decohesion of bimaterials: Experimental observations and failure criteria
[GALCIT-94-2] p 1045 N95-18613
On the theory of stick-slip fracture
p 1046 N95-18922
Microstructural analysis of cracks generated during welding of 2195 aluminum-lithium alloy
p 982 N95-19007
Experimental verification of a progressive damage model for composite laminates based on continuum damage mechanics
[NASA-CR-195020] p 971 N95-19043
A probabilistic fatigue analysis of multiple site damage
p 935 N95-19476
Evaluation of the fuselage lap joint fatigue and terminating action repair p 936 N95-19477
Fracture behavior of large-scale thin-sheet aluminum alloy p 939 N95-19494
Nonlinear analysis of damaged stiffened fuselage shells subjected to combined loads p 939 N95-19499
Driving force analysis in an infinite anisotropic plate with multiple crack interactions
[NASA-TM-106838] p 972 N95-19782

CRASHES
Is the pilot fit for flying after an accident?
p 1083 N95-19425

CREEP PROPERTIES
Influence of high pressure hydrogen environment on creep deformation of Mo-Re, Haynes 188, and NARloy-Z alloys
[NASA-CR-197572] p 978 N95-18046
The reliability of laser reflowed Sn-Ag solder joints
[AD-A284732] p 1044 N95-18080
Characterization of metal matrix composites
[NASA-CR-195381] p 970 N95-18940
Deformation of high-temperature superconductors
[DE94-017085] p 1150 N95-19075
Warm formability of aluminum-magnesium alloys
[DE94-016170] p 980 N95-19396

CREEP STRENGTH
Enhancement of creep resistance of a sintered Si3N4 ceramic by microwave annealing
[DE94-017688] p 987 N95-19399
NiAl and NiAl-based composites directionally solidified by a containerless zone process
[NASA-CR-195430] p 982 N95-19792

CREEP TESTS
Influence of high pressure hydrogen environment on creep deformation of Mo-Re, Haynes 188, and NARloy-Z alloys
[NASA-CR-197572] p 978 N95-18046
The reliability of laser reflowed Sn-Ag solder joints
[AD-A284732] p 1044 N95-18080
Enhancement of creep resistance of a sintered Si3N4 ceramic by microwave annealing
[DE94-017688] p 987 N95-19399

CRETACEOUS-TERTIARY BOUNDARY
Shock-induced devolatization of calcium sulfate and implications for K-T extinctions
[NASA-CR-197608] p 1060 N95-19033

CRITERIA
Acoustic noise criteria for listening rooms and control rooms
[BBC-RD-1994/06] p 1124 N95-19048

CRITICAL FREQUENCIES
Investigation of the ionospheric short-term variability
[AD-A286253] p 1066 N95-19387

CRITICAL LOADING
Fatigue loads spectra derivation for the Space Shuttle: Second cycle p 934 N95-19470

CRITICAL VELOCITY
Effect of crossflow on Goertler instability in incompressible boundary layers
[NASA-CR-195007] p 1016 N95-18193

CROP GROWTH
Ethylene dynamics in the CELSS biomass production chamber p 1077 N95-18179

CROP VIGOR
Ethylene dynamics in the CELSS biomass production chamber p 1077 N95-18179

CROSS CORRELATION
Cerebellar circuit mechanisms which accompany coordinated limb trajectory patterns in the rat: Use of a model of spontaneous changes in limb coordination
[AD-A284023] p 1079 N95-18656
Testing the frozen flow approximation
[NASA-CR-197614] p 1180 N95-18966
Optimizing the Zeldovich approximation
[NASA-CR-197606] p 1156 N95-19037

CROSS FLOW
Effect of crossflow on Goertler instability in incompressible boundary layers
[NASA-CR-195007] p 1016 N95-18193

CROSSED FIELDS
Complete mode-set stability analysis of magnetically insulated ion diode equilibria
[DE94-015275] p 1145 N95-19201

CROSSLINKING
Study of the effect of ionizing radiation on the structure of natural rubber latex by positron annihilation technique
[DE94-631466] p 975 N95-19550

CRRES (SATELLITE)
CRRESPRO documentation
[AD-A284578] p 1178 N95-18451

CRUDE OIL
Midinfrared optical properties of petroleum oil aerosols
[AD-A283689] p 1139 N95-18142
Activities of the Division of Energy Biosciences
[DE95-001046] p 1077 N95-19613

CRUSTAL FRACTURES
Seafloor positioning across Juan de Fuca ridge
[AD-A285049] p 1075 N95-19563

CRYOGENIC FLUID STORAGE
Outgassing of solid material into vacuum thermal insulation spaces p 972 N95-18184

CRYOGENIC ROCKET PROPELLANTS
Advanced small rocket chambers. Basic program and option 2: Fundamental processes and material evaluation
[NASA-CR-195349] p 966 N95-18192
Airborne rotary separator study
[NASA-CR-191045] p 967 N95-18743

CRYOGENIC WIND TUNNELS
Acoustic properties and durability of liner materials at non-standard atmospheric conditions
[NASA-CR-195010] p 1123 N95-18930

CRYOGENICS
Second International Semiconductor Device Research Symposium (ISDRS-1993)
[AD-A279221] p 1013 N95-19849

CRYSTAL DEFECTS
UV laser-surface interactions relevant to analytic spectroscopy of wide band gap materials
[DE94-016181] p 1037 N95-18350
Collision of cometlike and slightly differentiated bodies as an origin for ordinary chondrites
p 1188 N95-19308
Microscopic origins of metastable effects in a-Si:H and deep defect characterization in a-Si,Ge:H alloys
[DE94-011887] p 1151 N95-19541
Microstructure and crystal defects in perovskite crystals with A-site cation ordering
[AD-A284261] p 1153 N95-19713
Characterization of inactive carbon in GaAs
[DE95-002352] p 976 N95-19836

CRYSTAL FILTERS
Liquid crystal tunable filter
[AD-A284383] p 1139 N95-18342

CRYSTAL GROWTH
Fabrication of biomimetic molecular level composites
[AD-A284204] p 969 N95-17941
Size distribution of one-, two- and three-dimensional Voronoi cells
[PB94-207008] p 1149 N95-18373
Effects of vibration (G-jitters) on convection in micro-gravity p 991 N95-19013
Salt-induced aggregation of lysozyme: Implications for crystal growth p 1155 N95-19015
Microscopic origins of metastable effects in a-Si:H and deep defect characterization in a-Si,Ge:H alloys
[DE94-011887] p 1151 N95-19541

Energies of X conduction band minima in disordered and ordered GaInP2 alloys
[DE94-018211] p 1152 N95-19586
Growth and development of GaInAsP for high-efficiency solar cells
[DE94-000210] p 1056 N95-19878

CRYSTAL OSCILLATORS
Quartz crystal resonators and oscillators for frequency control and timing applications. A tutorial
[AD-A284995] p 1012 N95-19519

CRYSTAL STRUCTURE
Deformation texture studies in Fe3Al alloys
[DE94-017709] p 980 N95-19400
Synthesis and characterization of a neutral six-coordinate tris-adduct of an indium(3) trihalide. X ray crystal structure of InCl3(THF)3
[AD-A279169] p 1154 N95-19806
Isolation and characterization of an indium-mixed-pnicogen Four-membered ring compound: Crystal structure of (Me3SiCH2)2InAs(SiMe3)2 In(CH2SiMe3)2P(SiMe3)2
[AD-A279170] p 1154 N95-19807
Synthesis and characterization of aluminum-phosphorus adducts: X-ray crystal structures of Cl3Al (dot) P(SiMe3)3 (dot) C7H8 and Br3Al (dot) P(SiMe3)3 (dot) C7H8
[AD-A279194] p 1154 N95-19812

CRYSTALLINITY
Novel carbon-ion fuel cells
[DE94-017390] p 1053 N95-18894
Crystalline beams: The string
[DE94-016806] p 1150 N95-19091
A crystalline quark-hadron mixed phase in neutron stars
[DE95-000787] p 1194 N95-19570

CRYSTALLIZATION
High temperature stability of binary microstructures derived from liquid precursors
[AD-A283960] p 1150 N95-18685
Salt-induced aggregation of lysozyme: Implications for crystal growth p 1155 N95-19015
Crystallization trends of precursor pyroxene in ordinary chondrites: Implications for igneous origin of precursor p 1187 N95-19298

CRYSTALLOGRAPHY
Salt-induced aggregation of lysozyme: Implications for crystal growth p 1155 N95-19015
Isolation and characterization of an indium-mixed-pnicogen Four-membered ring compound: Crystal structure of (Me3SiCH2)2InAs(SiMe3)2 In(CH2SiMe3)2P(SiMe3)2
[AD-A279170] p 1154 N95-19807

CRYSTALS
Effects of vibration (G-jitters) on convection in micro-gravity p 991 N95-19013
Salt-induced aggregation of lysozyme: Implications for crystal growth p 1155 N95-19015
Bragg transmission phase plates for the production of circularly polarized x-rays
[DE94-017072] p 1151 N95-19113
Deformation texture studies in Fe3Al alloys
[DE94-017709] p 980 N95-19400
Development of materials for high temperature superconductor Josephson junctions
[DE95-000896] p 1152 N95-19608
MBE growth, characterization and electronic device processing of Hg-based semiconductor alloys and heterostructures
[AD-A279203] p 1154 N95-19817

CUBIC LATTICES
Analysis of the erosion of cubic centered and face centered metallic materials p 953 N95-19674

CULTURAL RESOURCES
Resources Automated Management System
[AD-A284153] p 1171 N95-18416

CULTURE TECHNIQUES
Method of making a membrane having hydrophilic and hydrophobic surfaces for adhering cells or antibodies by using atomic oxygen or hydroxyl radicals
[NASA-CASE-MSC-21529-1] p 983 N95-18134

CUMULATIVE DAMAGE
A probabilistic fatigue analysis of multiple site damage p 935 N95-19476
An artifical corrosion protocol for lap-splices in aircraft skin p 937 N95-19482
Cumulative effects of repeated brief cerebral ischemia
[AD-A284234] p 1087 N95-19698

CUMULONIMBUS CLOUDS
Two space scatterer formalism calculation of bulk parameters of thunderclouds p 1073 N95-19001

CURING
Ultrasonic techniques for repair of aircraft structures with bonded composite patches p 937 N95-19486

CURRENT AMPLIFIERS
High current amplifier utilizing a Josephson junction Schottky diode three terminal device
[AD-D016278] p 1009 N95-18432

CURRENT CONVERTERS (AC TO DC)
Power conversion system modification to permit use of DC power source
[AD-D016421] p 1010 N95-18523

CURRENT DENSITY
Alternative volume integral equation formulations applied to dielectric cylinders
[AD-A285537] p 995 N95-18066
Engineering considerations for the self-energizing magnetoplasmadynamic (MPD) - type fusion plasma thruster
[AD-A283968] p 1144 N95-18888
Molten carbonate fuel cell with high power density
[DE94-017080] p 1053 N95-19074
LEVIS ion source and beam characterization on PBFA-2
[DE94-015802] p 1133 N95-19199
Field-emitter arrays for RF vacuum microelectronics
[AD-A279932] p 1013 N95-19865

CURRENT SHEETS
Cross-tail current, field-aligned current, and B(y)
[NASA-CR-197624] p 1065 N95-19032

CURTAINS
Positive displacement rotary pump
[AD-D016412] p 1041 N95-18335

CURVED BEAMS
LEVIS ion source and beam characterization on PBFA-2
[DE94-015802] p 1133 N95-19199

CURVED PANELS
Evaluation of the fuselage lap joint fatigue and terminating action repair p 936 N95-19477

CURVES (GEOMETRY)
Decomposition of parametric curves
[PB94-207024] p 1117 N95-18374

CYANO COMPOUNDS
Growth of thin films of dicyanovinylanisole on quartz and teflon-coated quartz by physical vapor transport p 989 N95-19000

CYCLES
Double Eulerian cycles on de Bruijn digraphs
[AD-A283334] p 1120 N95-18007
A multiple time scale solution for the Chapman mechanism
[DE94-017491] p 1060 N95-18895

CYCLIC COMPOUNDS
Reaction channel competition in vibrational overtone activation: 1-methylcyclopropene
[AD-A280185] p 976 N95-19830

CYCLIC LOADS
Near tip stress and strain fields for short elastic cracks p 937 N95-19487
Fatigue crack growth in 2024-T3 aluminum under tensile and transverse shear stresses p 938 N95-19490
Damage of high temperature components by dust-laden air p 953 N95-19673

CYCLOHEXANE
Elemental fluorine based syntheses of pentafluoro phenly and other aromatic perfluoropolyether polymers
[AD-A284102] p 984 N95-18402

CYCLONES
Use of profiler data for analysis and NOWcasting of a winter season extratropical cyclone
[PB94-187804] p 1067 N95-17992
An analytic conceptual model of extratropical cyclones
[KNMI-WR-93-03] p 1072 N95-18926

CYCLOTRON RESONANCE
Mass spectrometric studies of clusters and surfaces
[AD-A283992] p 974 N95-19066
Theoretical investigation of matching between plasma heating and fueling in HL-1M machine
[DE94-627019] p 1146 N95-19241
Growth and doping of Al(x)Ga(1-x)N films by electron cyclotron resonance assisted molecular beam epitaxy
[AD-A284838] p 1153 N95-19737

CYCLOTRON RESONANCE DEVICES
High-power microwave transmission and mode conversion program
[DE94-017046] p 1002 N95-19097

CYLINDRICAL BODIES
Field and data analysis studies related to the atmospheric environment
[NASA-CR-196543] p 1068 N95-18093
Numerical mixing calculations of confined reacting jet flows in a cylindrical duct
[NASA-TM-106736] p 947 N95-18133
A fiber optic coupler
[AD-D016473] p 1140 N95-18459
Annular computed tomography
[AD-D016424] p 1141 N95-18593
Numerical computations of supersonic base flow with special emphasis on turbulence modeling
[AD-A283688] p 930 N95-18670
Surface roughness measurements p 1142 N95-18984
Numerical formulation of composition segregation at curved solid-liquid interface during steady state solidification process p 977 N95-19012
Sag compensated vibration isolation mount
[AD-D016541] p 1042 N95-19121

CYLINDRICAL CHAMBERS
Electromagnetic pump
[AD-D016260] p 1041 N95-18317

CYLINDRICAL SHELLS
Compression strength of composite primary structural components
[NASA-CR-197554] p 1044 N95-18388
Completed Beltrami-Michell formulation for analyzing mixed boundary value problems in elasticity
[NASA-TM-106809] p 1045 N95-18909

CYLINDRICAL TANKS
Free vibration analysis of partially filled liquid storage tanks
[DE94-012456] p 1020 N95-19098

CYTOPLASM
Mechanisms of interaction and biological effects of extremely-low-frequency electromagnetic fields
[DE94-015200] p 1076 N95-18371

D

DAMAGE
Debris/ice/TPS assessment and integrated photographic analysis of Shuttle mission STS-68
[NASA-TM-109207] p 963 N95-18047
Fundamental studies of passivity and passivity breakdown
[DE94-016954] p 987 N95-19095
Brite-Euram programme: ACOUFAT acoustic fatigue and related damage tolerance of advanced composite and metallic structures p 1127 N95-19159
Widespread fatigue damage monitoring: Issues and concerns p 938 N95-19488
Navy foreign object damage and its impact on future gas turbine engine low pressure compression systems p 951 N95-19658
Scandinavian Airlines Systems experience on erosion, corrosion and foreign object damage effects on gas turbines p 951 N95-19659
Experimental and numerical simulations of the effects of ingested particles in gas turbine engines p 952 N95-19662
Damage of high temperature components by dust-laden air p 953 N95-19673
Pulsewidth-dependent damage measurements of dielectric materials
[DE94-018594] p 1142 N95-19710
Damage from pulses with arbitrary temporal shapes
[DE94-018606] p 1039 N95-19722

DAMAGE ASSESSMENT
Cumulative impact analysis of wetlands using hydrologic indices
[AD-A284759] p 1058 N95-18085
Acoustic method of damage sensing in composite materials
[NASA-CR-196538] p 969 N95-18135
Foreign body impact event damage formation in composite structures p 972 N95-18973
Fatigue and damage tolerance scatter models p 935 N95-19475

DAMPING
Modal Identification Experiment accommodations review
[NASA-CR-195009] p 964 N95-18105
Modified Cu-Mn-Al high damping alloys
[AD-A285460] p 980 N95-19539

DARK MATTER
Decaying neutrinos in galaxy clusters
[NASA-CR-197615] p 1198 N95-18747
General relativity and dark matter
[DE94-626641] p 1180 N95-18877
Is a massive tau neutrino just what cold dark matter needs?
[NASA-CR-197627] p 1180 N95-18964

DATA ACQUISITION
A constant-depth scratch test for the measurement of adhesion at film-substrate interfaces
[AD-A283660] p 983 N95-18016
Variable name dictionary for the Air Force health study 1987 physical examination data tape, volume 1
[AD-A283319] p 1172 N95-18025
Variable name dictionary for the Air Force health study 1987 physical examination data tape, volume 2
[AD-A283320] p 1172 N95-18026
A Space and Atmospheric Visualization Science System
[NASA-CR-189390] p 1172 N95-18040

Automatic Identification Technology (AIT): The development of functional capability and card application matrices
[AD-A285528] p 1173 N95-18099
Assessment of the SFC database for analysis and modeling p 1158 N95-18171
Universal wind tunnel data acquisition and reduction software
[AD-A283897] p 1096 N95-18365
Strategic avionics technology definition studies. Subtask 3-1A3: Electrical Actuation (ELA) Systems Test Facility
[NASA-CR-188360] p 956 N95-18567
Interferometric synthetic aperture radar and the Data Collection System Digital Terrain Elevation Demonstration
[AD-A284024] p 999 N95-18657
Dynamic Stability Instrumentation System (DSIS). Volume 1: Hardware description
[NASA-TM-109160-VOL-1] p 1099 N95-18899
Stand-alone digital data storage control system including user control interface
[NASA-CASE-LAR-14651-1] p 1175 N95-19056
Data acquisition from blast overpressure trials
[MRL-TN-628] p 1020 N95-19139
Main characteristics of the COMET/COMRADE experiments p 1181 N95-19179
Flight parameters monitoring system for tracking structural integrity of rotary-wing aircraft p 934 N95-19469
Seafloor positioning across Juan de Fuca ridge
[AD-A285049] p 1075 N95-19563
Handbook for the extremely low frequency (ELF) data acquisition and analysis system
[DSTO-GD-0021] p 1005 N95-19622
TARGET's role in knowledge acquisition, engineering, validation, and documentation p 1103 N95-19644
Multiport pressure measurements on continuously moving wind tunnel models
[ARA-MEMO-391] p 932 N95-19772
Current Hybrid Electric Vehicle performance based on temporal data from the world's largest HEV fleet
[DE94-011859] p 1014 N95-19881

DATA BASE MANAGEMENT SYSTEMS
Assessment of the SFC database for analysis and modeling p 1158 N95-18171
Building a bridge with the customer to facilitate collecting and validating information in modeling sessions
[DE94-017338] p 1174 N95-18872
The QED Workshop
[DE94-018499] p 1111 N95-19592
The design and implementation of EPL: An event pattern language for active databases p 1101 N95-19629
Expert system shell to reason on large amounts of data p 1101 N95-19631
Distributed medical database system for real-time monitoring of the health and risk exposure of military research study volunteers at USARIEM
[AD-A279193] p 1087 N95-19811

DATA BASES
User profile for researchers studying objects: Implications for computer systems
[PB94-188463] p 1109 N95-17989
Catalog of environmental data sets of Europe at the RIVM
[PB94-202710] p 1057 N95-18002
Digital mapping, charting, and geodesy analysis program technical review of Digital Aeronautical Flight Information Data Prototype 1.0 on CD-ROM
[AD-A284728] p 1050 N95-18078
Compendium of NASA data base for the Global Tropospheric Experiment's Arctic Boundary Layer Experiments ABLE-3A and ABLE-3B
[NASA-TM-109161] p 1058 N95-18132
Assessment of the SFC database for analysis and modeling p 1158 N95-18171
Coronal abundances and their variation
[NASA-CR-197553] p 1195 N95-18376
SIGNET-software tools for signal identification using neural networks
[AD-A284362] p 1113 N95-18441
A selection of experimental test cases for the validation of CFD codes. Supplement: Datasets A-E
[AGARD-AR-303-SUPPL] p 929 N95-18539
Real-time modeling of complex atmospheric releases in urban areas
[DE94-018063] p 1059 N95-18647
Technical Information Division Open Literature Database (TOLD) operating instructions
[AD-A284061] p 1174 N95-18680
Graphics MIS/Shop Store Program: User's manual
[AD-A284062] p 1174 N95-18681
HEISHI: A fuel performance model for space nuclear applications
[DE94-017497] p 1137 N95-18897
Design of advanced steels for armor applications
[ARL-CR-175] p 979 N95-18948
A hypertext-based Internet-assessable database for the MSFC Technology Transfer Office p 1165 N95-18986
A CMC database for use in the next generation launch vehicles (rockets) p 963 N95-18993
Age 60 study. Part 3: Consolidated database experiments
[AD-A286247] p 1080 N95-19384
Solar-geophysical data number 599, July 1994. Part 1: (Prompt reports). Data for June, May 1994, and late data
[PB94-213972] p 1196 N95-19404
The waiver process and disqualifying medical conditions in US Naval aviation personnel p 1081 N95-19416
AMDRS: A resource for intelligent aeromedical decision-making p 1082 N95-19419
Enhancing the architectural characterization of parallel proto
[AD-A285678] p 1111 N95-19524
ADCIRC: An advanced three-dimensional circulation model for shelves, coasts, and estuaries. Report 5: A tropical storm database for the east and Gulf of Mexico coasts of the United States
[AD-A285576] p 1075 N95-19540
Documentation and archiving of the Space Shuttle wind tunnel test data base. Volume 2: User's Guide to the Archived Data Base
[NASA-TM-104806-VOL-2] p 965 N95-19624
Heavy metal soil contamination at US Army installations: Proposed research and strategy for technology development
[AD-A279171] p 1062 N95-19808
Distributed medical database system for real-time monitoring of the health and risk exposure of military research study volunteers at USARIEM
[AD-A279193] p 1087 N95-19811
Proceedings of the 15th Annual Conference on Atmospheric Transmission Models
[AD-A279919] p 1142 N95-19862
Automatically generating procedure code and database maintenance scripts
[DE95-000545] p 1176 N95-19876

DATA COLLECTION PLATFORMS
Performance evaluation of the Engineering Analysis and Data Systems (EADS) 2 p 1163 N95-18978

DATA COMPRESSION
LVQ and backpropagation neural networks applied to NASA SSME data
[NASA-CR-195418] p 962 N95-18045
SICOMP, the SINTEF data compression library (version 1.0) reference manual
[PB94-207107] p 1099 N95-18668

DATA CORRELATION
Inter-comparison of automatic rain gauges p 1069 N95-18204

DATA INTEGRATION
A general theory of signal integration for fault tolerant distributed sensor networks
[AD-A284825] p 1112 N95-19689

DATA LINKS
A simple hyperbolic model for communication in parallel processing environments
[NASA-CR-195984] p 1098 N95-18487
The 23 Gigahertz (GHz) digital Low Density Radio Communications Link (LDRCL) Operational Test and Evaluation (OT/E) integration and OT/E operation
[AD-A283963] p 1000 N95-18686
Design of a radio frequency data link for the unmanned ground vehicle technology test bed demonstration program
[AD-A284997] p 1004 N95-19534

DATA MANAGEMENT
Replica management system: A scheme for flexible and dynamic replication
[PB94-201597] p 1171 N95-18060
Assessment of the SFC database for analysis and modeling p 1158 N95-18171
Technical Information Division Open Literature Database (TOLD) operating instructions
[AD-A284061] p 1174 N95-18680
Users manual for the Moods Data Management System (MDMS), version 1.0
[NASA-CR-197015] p 1075 N95-18951
The Clinical Basis for Aeromedical Decision Making
[AGARD-CP-553] p 1080 N95-19413
Digital mapping, charting, and geodesy analysis program technical review of Raster Product Format (RPF) and Scanned Map (SMap)
[AD-A284267] p 1052 N95-19733

DATA PROCESSING
Use of profiler data for analysis and NOWcasting of a winter season extratropical cyclone
[PB94-187804] p 1067 N95-17992
The synthesis of vision and action
[AD-A285453] p 1088 N95-18094
Results from the northern New Mexico satellite-beacon radio interferometer
[DE94-018310] p 1063 N95-18148
Implementation of a human information processing model for task network simulation
[AD-A283903] p 1088 N95-18151
Modular signal processing unit
[AD-D016258] p 995 N95-18314
A parallel processing hypothesis for short-term and long-term memory in Aplysia
[AD-A284101] p 1088 N95-18401
Mission description and in-flight operations of ERBE instruments on ERBS and NOAA 10 spacecraft, February 1987 - February 1990
[NASA-RP-1325] p 1051 N95-18465
Radial basis function neural networks applied to NASA SSME data
[NASA-CR-195417] p 962 N95-18467
Lossless compression of weight vectors from an adaptive filter
[DE94-017350] p 1174 N95-18873
Representing visibility for siting problems
[AD-A284076] p 993 N95-19036
Data acquisition from blast overpressure trials
[MRL-TN-628] p 1020 N95-19139
Flight parameters monitoring system for tracking structural integrity of rotary-wing aircraft p 934 N95-19469
Using expert systems to analyze ATE data p 1103 N95-19639
PAK: A processing system for vectorized time-series data
[AD-A284881] p 1104 N95-19742

DATA REDUCTION
A Space and Atmospheric Visualization Science System
[NASA-CR-189390] p 1172 N95-18040
Decomposition of parametric curves
[PB94-207024] p 1117 N95-18374
The Gravity Probe B niobium bird experiment: Experimental verification of a data reduction scheme with a prototypical dc SQUID readout system p 1033 N95-18929
Evaluation of SSME test data reduction methods p 968 N95-19002
Hyperspectral data analysis procedures with reduced sensitivity to noise
[NASA-CR-197621] p 1052 N95-19126
Real-time remote scientific model validation p 1103 N95-19640

DATA RETRIEVAL
Method of displaying time series data on finite resolution display device
[AD-D016438] p 1173 N95-18526

DATA STORAGE
Stand-alone digital data storage control system including user control interface
[NASA-CASE-LAR-14651-1] p 1175 N95-19056

DATA STRUCTURES
Signal processor having multiple distributed data buffers
[AD-D016259] p 995 N95-18315
SIGNET-software tools for signal identification using neural networks
[AD-A284362] p 1113 N95-18441
Scalability of parallel spatial direct numerical simulation code on IBM SP1 parallel supercomputer
[NASA-CR-194975] p 1098 N95-18584
CLIPS template system for program understanding p 1102 N95-19638

DATA SYSTEMS
Performance evaluation of the Engineering Analysis and Data Systems (EADS) 2 p 1163 N95-18978
Data driven propulsion system weight prediction model p 968 N95-18980

DATA TRANSFER (COMPUTERS)
Dynamic file-access characteristics of a production parallel scientific workload
[NASA-CR-197570] p 1110 N95-18581
MSFC institutional area network and ATM technology p 1007 N95-18968

DATA TRANSMISSION
Signal processor having multiple distributed data buffers
[AD-D016259] p 995 N95-18315
Variable rate transfer of optical information
[AD-D016268] p 1173 N95-18544
Lossless compression of weight vectors from an adaptive filter
[DE94-017350] p 1174 N95-18873
Information Superhighway: Issues affecting development. Report to the Congress
[GAO/RCED-94-285] p 1174 N95-18914
MSFC institutional area network and ATM technology p 1007 N95-18968
Information system architecture to support transparent access to distributed, heterogeneous data sources
[DE94-018450] p 1176 N95-19589

DATUM (ELEVATION)
Definition and realization of a global vertical datum
[AD-A283303] p 1049 N95-17971
DBR LASERS
14th IEEE International Semiconductor Laser Conference
[AD-A285569] p 1038 N95-18642
DC 8 AIRCRAFT
Aircraft wake vortex takeoff tests at O'Hara International Airport
[AD-A283828] p 929 N95-18624
DC 9 AIRCRAFT
Users guide for NASA Lewis Research Center DC-9 Reduced-Gravity Aircraft Program
[NASA-TM-106755] p 959 N95-18586
DEBRIS
Debris/ice/TPS assessment and integrated photographic analysis of Shuttle mission STS-68
[NASA-TM-109207] p 963 N95-18047
Scandinavian Airlines Systems experience on erosion, corrosion and foreign object damage effects on gas turbines p 951 N95-19659
Debris/ice/TPS assessment and integrated photographic analysis of Shuttle mission STS-66
[NASA-TM-110141] p 963 N95-19790
DECAY
Properties of nuclei and elementary particles at low and intermediate energies
[DE94-008502] p 1132 N95-18644
DECAY RATES
HEISHI: A fuel performance model for space nuclear applications
[DE94-017497] p 1137 N95-18897
DECISION MAKING
Effective team performance under stress and normal conditions: An experimental paradigm, theory and data for studying team decision making in hierarchical teams with distributed expertise
[AD-A284683] p 1089 N95-18530
On-line handling of air traffic: Management, guidance and control
[AGARD-AG-321] p 941 N95-18927
The Clinical Basis for Aeromedical Decision Making
[AGARD-CP-553] p 1080 N95-19413
Fit to fly: Analysis of the aeromedical disposition in aircrewmembers of the Spanish Armed Forces p 1081 N95-19418
AMDRS: A resource for intelligent aeromedical decision-making p 1082 N95-19419
Relevance of laboratory tests in aeromedical decisions p 1082 N95-19420
EKG in flight: Usefulness and limits for aircrew rehabilitation p 1082 N95-19422
The NAMI syncope test battery and clinical decision-making in aviators with syncope p 1083 N95-19428
Think health not disease p 1083 N95-19429
Neurological decision making in aviation medicine based on electrophysiological methods p 1084 N95-19431
Clinical basis for aeromedical decision-making: The EEG example p 1084 N95-19433
Learning effects on strategy selection in a dynamic task environment as a function of time pressure
[AD-A285458] p 1089 N95-19538
DECISION THEORY
Character selecting advisor for a role-playing game p 1106 N95-19758
Automated rule-base creation via CLIPS-Induce p 1107 N95-19761
DECOMPOSITION
A domain decomposition algorithm for elliptic problems in three dimensions
[DE94-019265] p 1094 N95-17978
Decomposition of parametric curves
[PB94-207024] p 1117 N95-18374
A direct decomposition method for the solution of sparse linear least squares problems
[AD-A284060] p 1117 N95-18679
Coupled finite element analysis of decomposing poroelastic polymeric composites and structures with subsequent thermal and gas diffusion p 986 N95-18918
DECOMPRESSION SICKNESS
Echo imaging techniques determine the size of intravascular bubbles in decompression sickness
[AD-A284849] p 1087 N95-19714
DEEP WATER
Nonlinear ocean waves
[AD-A285331] p 1075 N95-19523
DEFECTS
Computational modeling of properties
[NASA-CR-197558] p 1010 N95-18925
The probability of flaw detection and the probability of false calls in nondestructive evaluation equipment p 1044 N95-19010
Atomistic and elastic analyses of defects and small structures
[DE94-017047] p 980 N95-19111
Deep levels in AgGaSe2
[DE94-018209] p 1152 N95-19585
Performance deterioration of axial compressors due to blade defects p 952 N95-19665
An atomic-resolution study of overlayer formation and interfacial mixing in the interaction of phosphorus with Si(001)
[AD-A280159] p 976 N95-19825
DEFENSE COMMUNICATIONS SYSTEM (DCS)
The future use of DSCS and commercial satellites in the US Navy
[AD-A285707] p 997 N95-18481
DEFENSE PROGRAM
Portable, Reusable, Integrated Software Modules (PRISM) documentation library model document release 1.0: Central Archive for Reusable Defense Software (CARDS)
[AD-A284567] p 1095 N95-18030
Library capability demonstration. Central Archive for Reusable Defense Software (CARDS)
[AD-A284568] p 1095 N95-18031
Library capability demonstration. Central Archive for Reusable Defense Software (CARDS)
[AD-A284569] p 1095 N95-18032
Library Development Handbook. Central Archive for Reusable Defense Software (CARDS)
[AD-A284570] p 1095 N95-18033
Library capability demonstration. Central Archive for Reusable Defense Software (CARDS)
[AD-A284572] p 1095 N95-18034
Technical concept document. Central Archive for Reusable Defense Software (CARDS)
[AD-A284430] p 1096 N95-18343
Library operations policies and procedures. Volume 2: Central Archive for Reusable Defense Software (CARDS)
[AD-A284431] p 1096 N95-18344
Engineer's handbook. Central Archive for Reusable Defense Software (CARDS)
[AD-A284341] p 1097 N95-18419
Training plan. Central Archive for Reusable Defense Software (CARDS)
[AD-A284343] p 1097 N95-18421
Library user's guide. Comprehensive Approach to Reusable Defensive Software (CARDS)
[AD-A284345] p 1097 N95-18423
Metrics concept report. Central Archive for Reusable Defense Software (CARDS)
[AD-A284573] p 1097 N95-18449
Interferometric synthetic aperture radar and the Data Collection System Digital Terrain Elevation Demonstration
[AD-A284024] p 999 N95-18657
Environmental Compliance Assessment System (ECAS)
[AD-A283950] p 1060 N95-18683
Assessing aircraft survivability to high frequency transient threats
[AD-A283999] p 944 N95-18726
Environmental Compliance Assessment System (ECAS). South Carolina supplement: US Army
[AD-A279244] p 1062 N95-19860
DEFLECTION
Evaluation of an unlighted swinging airport sign
[AD-A284763] p 958 N95-18087
Determination of stores pointing error due to wing flexibility under flight load
[NASA-TM-4646] p 945 N95-19044
Estimating wind tunnel interference due to vectored jet flows p 1023 N95-19265
DEFLUORINATION
Elemental fluorine based syntheses of pentafluoro phenly and other aromatic perfluoropolyether polymers
[AD-A284102] p 984 N95-18402
DEFORMATION
International Conference on Deformation, Yield and Fracture of Polymers
[AD-A284354] p 984 N95-18339
Plate vibration with arbitrarily oriented stiffeners based on Mindlin-Engesser formulation
[RR-CE143] p 1045 N95-18608
QuikForm: Intelligent deformation processing of structural alloys
[DE94-018739] p 1114 N95-18649
Deformation of high-temperature superconductors
[DE94-017085] p 1150 N95-19075
Deformation of nonstoichiometric CuO polycrystals
[DE94-016907] p 1150 N95-19094
Deformation texture studies in Fe3Al alloys
[DE94-017709] p 980 N95-19400
Characterization of the deformation and annealing of 304L stainless steel
[DE94-018584] p 981 N95-19707
DEGRADATION
Microscopic origins of metastable effects in a-Si:H and deep defect characterization in a-Si,Ge:H alloys
[DE94-011887] p 1151 N95-19541
Environmental effects on composite airframes: A study conducted for the ARM UAV Program (Atmospheric Radiation Measurement Unmanned Aerospace Vehicle)
[DE94-015351] p 971 N95-19579
Protective coatings for compressor gas path components p 954 N95-19675
Multilayer anti-erosion coatings p 954 N95-19679
DEGREES OF FREEDOM
A domain decomposition algorithm for elliptic problems in three dimensions
[DE94-019265] p 1094 N95-17978
Six degree of freedom flight dynamic and performance simulation of a remotely-piloted vehicle
[AERO-TN-9301] p 942 N95-18097
Rack Insertion End Effector (RIEE) guidance p 1043 N95-18178
Application of photogrammetry of F-14D store separation
[AD-A284154] p 943 N95-18417
DEHYDROGENATION
Palladium-based membranes for hydrogen separation
[PB94-207156] p 973 N95-18377
DELAMINATING
Finite element modeling of partially delaminated composite beams with contact-impact conditions
[AD-A283726] p 1044 N95-18363
Experimental verification of a progressive damage model for composite laminates based on continuum damage mechanics
[NASA-CR-195020] p 971 N95-19043
DELTA LAUNCH VEHICLE
Electrodynamic behavior of PMG-Delta
[AD-A283930] p 964 N95-18163
Near-Earth Asteroid Returned Sample (NEARS)
[NASA-CR-197297] p 1194 N95-19575
Radar cross-section measurements and simulation of a tethered satellite. The small expendable deployer system end-mass payload
[NASA-TM-4613] p 1005 N95-19781
DELTA WINGS
Overview of unsteady transonic wind tunnel test on a semispan straked delta wing oscillating in pitch
[AD-A284097] p 928 N95-18380
Aeromechanics technology, volume 1. Task 1: Three-dimensional Euler/Navier-Stokes Aerodynamic Method (TEAM) enhancements
[AD-A285713] p 943 N95-18483
Interaction, bursting and control of vortices of a cropped double-delta wing at high angle of attack
[AD-A283656] p 930 N95-18669
The utilization of a high speed reflective visualization system in the study of transonic flow over a delta wing p 932 N95-19259
Velocity measurements with hot-wires in a vortex-dominated flowfield p 932 N95-19261
DEMOGRAPHY
Catalog of environmental data sets of Europe at the RIVM
[PB94-202710] p 1057 N95-18002
DENSE PLASMAS
Engineering considerations for the self-energizing magnetoplasmadynamic (MPD) - type fusion plasma thruster
[AD-A283968] p 1144 N95-18888
Development of lithium beam emission spectroscopy as an edge fluctuation diagnostic for D3-D
[DE94-017517] p 1146 N95-19378
DENSITY DISTRIBUTION
Spatial and temporal constraints on the observed distribution of gamma-ray bursts detected by BATSE p 1197 N95-18730
Decaying neutrinos in galaxy clusters
[NASA-CR-197615] p 1198 N95-18747
Quantitative analysis of voids in percolating structures in two-dimensional N-body simulations
[NASA-CR-197612] p 1156 N95-18949
Quasi-linear regime of gravitational instability: Implication to density-velocity relation
[NASA-CR-197616] p 1156 N95-19340
Quasi-linear regime of gravitational instability as a clue to understanding the large-scale structure in the Universe
[NASA-CR-197613] p 1193 N95-19341
Testing higher-order Lagrangian perturbation theory against numerical simulation. 1: Pancake models
[NASA-CR-197611] p 1121 N95-19348
A test of the adhesion approximation for gravitational clustering
[NASA-CR-197610] p 1157 N95-19358
Comparison of dynamical approximation schemes for non-linear gravitational clustering
[NASA-CR-197609] p 1157 N95-19363

DENSITY MEASUREMENT
Density structure of the upper oceanic crust at zero porosity
[AD-A284235] p 1076 N95-19728
DEOXYRIBONUCLEIC ACID
Capillary electrophoresis: Biotechnology for separation of DNA and chromosomes p 1077 N95-19014
Power flow and PRS optimization on Phoenix
[AD-A279214] p 1147 N95-19846
DEPLETION
Gain uniformity, linearity, saturation and depletion in gated microchannel-plate x-ray framing cameras
[DE94-018596] p 1035 N95-19711
DEPLOYMENT
Personal communications services: Improving theater deployable communications for the 21st century
[AD-A283465] p 994 N95-18058
DEPOSITION
Ion beam surface treatment: A new capability for surface enhancement
[DE94-014663] p 977 N95-17968
UV laser-surface interactions relevant to analytic spectroscopy of wide band gap materials
[DE94-016180] p 1037 N95-18349
An investigation of nonuniform dose deposition from an electron beam
[AD-A284175] p 1131 N95-18519
Erosion, Corrosion and Foreign Object Damage Effects in Gas Turbines
[AGARD-CP-558] p 950 N95-19653
Particle deposition in gas turbine blade film cooling holes p 951 N95-19661
DEPOSITS
Gas turbine compressor corrosion and erosion in Western Europe p 954 N95-19678
DEPTH
A 2D depth migration in transversely isotropic media using explicit operators
[DE95-000645] p 1066 N95-19560
DEPTH MEASUREMENT
A constant-depth scratch test for the measurement of adhesion at film-substrate interfaces
[AD-A283660] p 983 N95-18016
DERIVATION
Sound speed profiles from vertical array data
[AD-A283978] p 1123 N95-18890
Second-order reconstruction of the inflationary potential
[NASA-CR-197629] p 1121 N95-19030
Classification of graded, finite-dimensional lie algebras of vector fields
[PB94-215449] p 1119 N95-19408
DESCENT
Wind tunnel tests of a 42 inch diameter self-starting autogyro rotor
[AD-A279922] p 932 N95-19863
DESIGN ANALYSIS
Personal communications services: Improving theater deployable communications for the 21st century
[AD-A283465] p 994 N95-18058
Independent validation and verification of automated information systems in the Department of Energy
[DE94-014460] p 1173 N95-18063
An algorithm for solving the system-level problem in multilevel optimization
[NASA-CR-195015] p 1116 N95-18108
Optimization of coupled systems: A critical overview of approaches
[NASA-CR-195019] p 1116 N95-18109
Mathematical analysis of actuator forces in a scissor lift
[AD-A283906] p 1040 N95-18152
Conference on Aerospace Transparent Materials and Enclosures. Volume 2: Sessions 5-9
[AD-A283926] p 942 N95-18162
Design optimization of a brush turbine with a cleaner/water based solution p 1043 N95-18177
An analog computing approach to structural analysis and optimal design through artificial neural networks p 1113 N95-18218
High power phase conjugated solid state lasers
[DE94-016633] p 1037 N95-18357
TEXCAD: Textile Composite Analysis for Design. Version 1.0: User's manual
[NASA-CR-4639] p 970 N95-18466
Microgravity isolation system design: A modern control analysis framework
[NASA-TM-106803] p 927 N95-18486
Strategic avionics technology definition studies. Subtask 3-1A3: Electrical Actuation (ELA) Systems Test Facility
[NASA-CR-188360] p 956 N95-18567
Design limit loads based upon statistical discrete gust methodology p 946 N95-18603
Conference on Aerospace Transparent Materials and Enclosures, volume 1
[AD-A283925] p 944 N95-18677
System engineering toolbox for design-oriented engineers
[NASA-RP-1358] p 962 N95-18932
High frequency room responses: Acoustic design and the control of stereophonic image quality
[BBC-RD-1994/11] p 1124 N95-19046
Proceedings of the USAF Structural Integrity Program Conference
[AD-A285684] p 945 N95-19517
Using neural networks in the mapping of mixed discrete/continuous design spaces with application to structural design
[AD-A285328] p 1046 N95-19522
Constructing a real-time mobile robot software system
[AD-A285969] p 1115 N95-19572
DESORPTION
UV laser-surface interactions relevant to analytic spectroscopy of wide band gap materials
[DE94-016181] p 1037 N95-18350
DETECTION
Fusion of multiple sensing modalities for machine vision
[AD-A284762] p 1091 N95-18086
Lightning studies using LDAR and companion data sets p 1073 N95-18174
Detection performance of generalized likelihood ratio processors for random signals of unknown location, structure, extent, and strength
[AD-A285589] p 997 N95-18475
Corrosivity sensor
[AD-D016422] p 1033 N95-18524
Workshop on Particle Capture, Recovery and Velocity/Trajectory Measurement Technologies
[NASA-CR-197592] p 1180 N95-19172
Materials for adaptive structural acoustic control, volume 3
[AD-A279223] p 1128 N95-19850
DETECTORS
Electron reversal ionizer for detection of trace species using a spherical cathode
[NASA-CASE-NPO-18870-1-CU] p 1130 N95-18324
DEUTERIUM
Exotic atoms: Muonic atoms into vacuum from solid hydrogen
[DE94-018255] p 1129 N95-18124
Study of high gain spherical shell ICF targets containing uniform layers of liquid deuterium tritium fuel
[DE94-018550] p 1136 N95-18552
On measurement of cross sections for scattering of p(mu)- and d(mu)-atoms in hydrogen and deuterium
[DE94-626957] p 1132 N95-18884
Engineering considerations for the self-energizing magnetoplasmadynamic (MPD) - type fusion plasma thruster
[AD-A283968] p 1144 N95-18888
Direct energy conversion system for D(3)-He fusion
[DE94-770773] p 1146 N95-19549
DEVELOPING NATIONS
Renewable energy and its potential for carbon emissions reductions in developing countries: Methodology for technology evaluation
[DE94-011870] p 1056 N95-17943
DIAGNOSIS
Radial basis function neural networks applied to NASA SSME data
[NASA-CR-195417] p 962 N95-18467
The waiver process and disqualifying medical conditions in US Naval aviation personnel p 1081 N95-19416
Clinical practice, diagnosis and therapy of intervertebral disk lesion: Importance to fitness for military flying duties p 1084 N95-19435
Spinal nerve syndromes: The need to confirm the diagnosis with neurophysiological examinations p 1085 N95-19436
DIALYSIS
Extrathalamic modulation of cortical responsiveness
[AD-A284100] p 1078 N95-18400
DIAMINES
Difunctional monomers based on perfluoropropylene telomers
[AD-A283677] p 983 N95-18019
DIAMOND FILMS
Atomic Layer Epitaxy (ALE) apparatus for growing thin films of elemental semiconductors
[AD-D016236] p 1149 N95-18633
DIAMONDS
Method of doping single crystal diamond for electronic devices
[AD-D016267] p 1149 N95-18543
Physics with isotopically controlled semiconductors
[DE95-000789] p 1152 N95-19615
DICTIONARIES
Variable name dictionary for the Air Force health study 1987 physical examination data tape, volume 1
[AD-A283319] p 1172 N95-18025
Variable name dictionary for the Air Force health study 1987 physical examination data tape, volume 2
[AD-A283320] p 1172 N95-18026
DIELECTRIC PROPERTIES
Advanced packaging and integration technologies for microsensors, phase 1
[AD-A283613] p 1040 N95-18010
Multi-functional pi-conjugated macromolecules based on poly (phenylene vinylene)
[AD-A284163] p 985 N95-18510
DIELECTRICS
Method of moments analysis of artificial media composed of dielectric wire objects
[AD-A283318] p 994 N95-18024
Alternative volume integral equation formulations applied to dielectric cylinders
[AD-A285537] p 995 N95-18066
Wavelets and scattering
[AD-A284131] p 996 N95-18411
Pulsewidth-dependent damage measurements of dielectric materials
[DE94-018594] p 1142 N95-19710
DIESEL ENGINES
Advanced diesel engine component development program, tasks 4-14
[NASA-CR-191203] p 1040 N95-18041
DIESEL FUELS
Midinfrared optical properties of petroleum oil aerosols
[AD-A283689] p 1139 N95-18142
Advanced diesel electronic fuel injection and turbocharging
[AD-A279176] p 1043 N95-19809
DIFFERENTIAL EQUATIONS
A domain decomposition algorithm for elliptic problems in three dimensions
[DE94-019265] p 1094 N95-17978
The space-time solution element method: A new numerical approach for the Navier-Stokes equations
[NASA-TM-106818] p 1014 N95-18036
Covariant differential complexes of quantum linear groups
[DE94-626640] p 1118 N95-18876
Free vibration analysis of partially filled liquid storage tanks
[DE94-012456] p 1020 N95-19098
Plane Jacobian conjecture
[PB94-192341] p 1118 N95-19198
Computation of compressible flows: Implicit methods p 1027 N95-19452
DIFFERENTIAL PRESSURE
Fluid dynamic linear accelerometer
[AD-D016413] p 956 N95-18553
Pressure measurements on an F/A-18 twin vertical tail in buffeting flow. Volume 4, part 2: Buffet cross spectral densities
[AD-A285555] p 957 N95-18641
DIFFRACTION
PRISM project optical instrument p 1143 N95-19009
High-power microwave transmission and mode conversion program
[DE94-017046] p 1002 N95-19097
DIFFRACTION PATHS
MANN: A program to transfer designs for diffractive optical elements to a MANN photolithographic mask generator p 1142 N95-18995
DIFFRACTION PATTERNS
Study of the ferrimagnetic and paramagnetic phases of magnetite measured by multiple neutron diffraction
[DE94-627031] p 1151 N95-19242
DIFFUSION
In vitro system for studying metabolism of environmental chemicals in human cells
[AD-A284174] p 1079 N95-18518
High temperature stability of binary microstructures derived from liquid precursors
[AD-A283960] p 1150 N95-18685
Damage from pulses with arbitrary temporal shapes
[DE94-018606] p 1039 N95-19722
Diffusion of water vapour through cold Gore-Tex (trademark)
[AD-A279939] p 989 N95-19867
DIFFUSION FLAMES
Observations of methane and ethylene diffusion flames stabilized around a blowing porous sphere under microgravity conditions
[NASA-TM-106766] p 990 N95-18211
Studies on high pressure and unsteady flame phenomena
[AD-A284126] p 973 N95-18410
DIFFUSION WELDING
The metallurgical integrity of the frit vent assembly diffusion bond
[DE95-000610] p 988 N95-19877

DIGITAL DATA
Digital mapping, charting, and geodesy analysis program technical review of Digital Aeronautical Flight Information Data Prototype 1.0 on CD-ROM
[AD-A284726] p 1050 N95-18078
Remote sensing products evaluation for cartographic updating purposes
[INPE-5584-TDI/546] p 1050 N95-18368
Predicted coverage of a COFDM single frequency network for UHF digital terrestrial TV broadcasting
[BBC-RD-1993/12] p 999 N95-18540
Interferometric synthetic aperture radar and the Data Collection System Digital Terrain Elevation Demonstration
[AD-A284024] p 999 N95-18657
Stand-alone digital data storage control system including user control interface
[NASA-CASE-LAR-14651-1] p 1175 N95-19056
Handbook for the extremely low frequency (ELF) data acquisition and analysis system
[DSTO-GD-0021] p 1005 N95-19622
Digital mapping, charting, and geodesy analysis program technical review of Raster Product Format (RPF) and Scanned Map (SMap)
[AD-A284267] p 1052 N95-19733

DIGITAL ELECTRONICS
Digital circuit for the introduction and later removal of dither from an analog signal
[AD-D016462] p 1011 N95-19171
Real time simulator with Ti floating point digital signal processor
[DE94-016372] p 1012 N95-19246

DIGITAL SYSTEMS
Digital mapping, charting, and geodesy analysis program technical review of Digital Aeronautical Flight Information Data Prototype 1.0 on CD-ROM
[AD-A284726] p 1050 N95-18078
Modular signal processing unit
[AD-D016258] p 995 N95-18314
Implementation of amplitude modulation companding using a digital signal processor
[BBC-RD-1994/1] p 998 N95-18536
A real-time vision system to monitor/analyze the changes in composite specimens during mechanical testing
[ARL-TR-344] p 970 N95-18612
NASA develops new digital flight control system
[NASA-NEWS-RELEASE-94-47] p 958 N95-19029
Measurements of wideband multipath propagation at 531 MHz and 1.265 GHz
[BBC-RD-1994/3] p 1001 N95-19051
Digital monopulse
[AD-D016447] p 1002 N95-19072
Digital audio broadcasting: Comparison of coverage at different frequencies and with different bandwidths
[BBC-RD-1993/11] p 1002 N95-19135
Improvement of a high current DC power supply system for testing the large scaled superconducting cables and magnets
[DE94-770767] p 1012 N95-19548
Mitigation of EMI generated by a variable-frequency-drive controller for an AC induction motor
[AD-A286045] p 1012 N95-19573

DIGITAL TECHNIQUES
RINSE: A digitally implemented flywheel sync regenerator for improved video synchroniser performance
[BBC-RD-1993/14] p 999 N95-18538

DIGITAL TELEVISION
Digital video compression: Standardisation of scalable coding schemes
[BBC-RD-1994/10] p 1001 N95-19047
Bit-rate reduction of digital television for transmission: An introductory review
[BBC-RD-1994/2] p 1001 N95-19052

DIISOCYANATES
Difunctional monomers based on perfluoropropylene telomers
[AD-A283677] p 983 N95-18019

DIMENSIONAL ANALYSIS
Penetration experiments in aluminum and Teflon targets of widely variable thickness p 1047 N95-19185

DIMENSIONAL STABILITY
Searching for stationary stable solutions of Euler's equation
[KNMI-WR-93-01] p 1017 N95-18396
Novel e-o polymers: NLO materials with superior temporal stability
[AD-A285872] p 988 N95-19614

DIMENSIONLESS NUMBERS
Microstructure-based fatigue life prediction methods for naval steel structures
[AD-A284735] p 1044 N95-18081

DIMERS
Direct dimer-by-dimer identification of clean and monohydride dimers on the Si(001) surface by scanning tunneling microscopy
[AD-A280158] p 976 N95-19824

DIODES
Complete mode-set stability analysis of magnetically insulated ion diode equilibria
[DE94-015275] p 1145 N95-19201

DIPOLE MOMENTS
Limits on CP nonconserving interactions from electric dipole moments
[DE94-018582] p 1134 N95-19705

DIRAC EQUATION
Lie algebras for the Dirac-Clifford ring
[DE94-626643] p 1118 N95-18878

DIRECT CURRENT
Partition method for the determination of multiple DC operating points
[PB94-201480] p 1009 N95-18501
Power conversion system modification to permit use of DC power source
[AD-D016421] p 1010 N95-18523

DIRECTIONAL ANTENNAS
The development of the switched-horn radio-camera system
[BBC-RD-1993/13] p 997 N95-18494
Predicted coverage of a COFDM single frequency network for UHF digital terrestrial TV broadcasting
[BBC-RD-1993/12] p 999 N95-18540

DISCRETE FUNCTIONS
Design limit loads based upon statistical discrete gust methodology p 946 N95-18603

DISEASES
TSH determination in subjects with medium-low levels of serum thyroxine p 1082 N95-19421

DISK OPERATING SYSTEM (DOS)
Miscellaneous disk utility application programs for the AFOS background partition
[PB94-181328] p 1067 N95-18038

DISORIENTATION
Visuo-ocular performance during vestibular stimulation
[AD-A284103] p 1089 N95-18403

DISPLACEMENT
Rack Insertion End Effector (RIEE) guidance p 1043 N95-18178
Positive displacement rotary pump
[AD-D016412] p 1041 N95-18335

DISPLAY DEVICES
An evaluation of aircraft CRT and dot-matrix display legibility requirements
[AD-A283933] p 947 N95-18164
Method of displaying time series data on finite resolution display device
[AD-D016438] p 1173 N95-18526
Rule based design of conceptual models for formative evaluation p 1106 N95-19760

DISSIPATION
Large signal time dependent quantum mechanical transport in quantum phase based devices
[AD-A283338] p 1155 N95-18009
Study of frustrated systems via dissipative maps
[DE94-017754] p 1122 N95-18127
Low-dissipation and -dispersion Runge-Kutta schemes for computational acoustics
[NASA-CR-195022] p 1018 N95-18488

DISTANCE
An atomic view of motion on surfaces
[AD-A285565] p 1131 N95-18473

DISTORTION
Giant effective mass deviations near the magnetic field-induced minigap in double quantum wells
[DE94-018889] p 1122 N95-19234
Aero-thermodynamic distortion induced structured dynamic response
[AD-A279931] p 955 N95-19864

DISTRIBUTED FEEDBACK LASERS
14th IEEE International Semiconductor Laser Conference
[AD-A285569] p 1038 N95-18642

DISTRIBUTED PARAMETER SYSTEMS
Distributed methods for controlling multiple mobile robots
[AD-A283919] p 1113 N95-18157

DISTRIBUTED PROCESSING
Library capability demonstration. Central Archive for Reusable Defense Software (CARDS)
[AD-A284572] p 1095 N95-18034
Secure distributed file systems
[AD-A285525] p 1173 N95-18096
A scalable decentralized group membership service for an asynchronous environment
[AD-A283633] p 1109 N95-18137
Signal processor having multiple distributed data buffers
[AD-D016259] p 995 N95-18315
Global time transformations
[AD-A285539] p 1110 N95-18454
The Isis project: Fault-tolerance in large distributed systems
[NASA-CR-197561] p 1110 N95-18532
Scalability of parallel spatial direct numerical simulation code on IBM SP1 parallel supercomputer
[NASA-CR-194975] p 1098 N95-18584
ODP based UPT model
[PB94-215589] p 1003 N95-19411
Using PVM to host CLIPS in distributed environments p 1104 N95-19748
DAI-CLIPS: Distributed, Asynchronous, Interacting CLIPS p 1107 N95-19763
Solution of potential flow problems on a network of workstations
[DE94-017861] p 1112 N95-19831

DISTRIBUTION (PROPERTY)
Optimal pattern distributions in Rete-based production systems p 1106 N95-19755

DISTRIBUTION FUNCTIONS
Large signal time dependent quantum mechanical transport in quantum phase based devices
[AD-A283338] p 1155 N95-18009

DITHERS
Digital circuit for the introduction and later removal of dither from an analog signal
[AD-D016462] p 1011 N95-19171

DIURNAL VARIATIONS
The diurnal cycle of high-frequency temperature variability at 0 deg 140 deg W on seasonal and interannual time scales
[AD-A283640] p 1074 N95-18012
The effect of spatial averaging on threshold exceedances of daily precipitation amounts
[KNMI-TR-154] p 1070 N95-18392
A synoptic climatology of convective weather in the Netherlands
[KNMI-WR-93-04] p 1071 N95-18395
Synoptic-scale influence on the Monterey Bay sea-breeze
[AD-A285129] p 1073 N95-19596
Modeling the diurnally precessing Jovian magnetospheric field
[AD-A284857] p 1195 N95-19739

DIVERGENCE
Applications of quantum entropy to statistics
[DE94-014416] p 1155 N95-17996
Workshop on Particle Capture, Recovery and Velocity/Trajectory Measurement Technologies
[NASA-CR-197592] p 1180 N95-19172

DIVERTERS
2-D tomography with bolometry in D3-D
[DE94-017520] p 1146 N95-19379

DOCUMENT STORAGE
A strategy for electronic dissemination of NASA Langley technical publications
[NASA-TM-109172] p 1175 N95-18936

DOPED CRYSTALS
Preparation and surface characterization of metal doped alumina catalyst
[PB94-175296] p 973 N95-17991
DC-conductivity and magnetoresistance of inherently conducting polymers. Polyacetylene and poly(3-alkylthiophenes)
[PB94-184587] p 1007 N95-18037
Minority-carrier lifetime in InP as a function of light bias
[NASA-TM-106821] p 1149 N95-18453
Compact, efficient, scalable neodymium laser co-doped with activator ions and pumped by visible laser diodes
[AD-D016237] p 1038 N95-18585
The effect of temperature on the radiative performance of Ho-YAG thin film selective emitters
[NASA-TM-106830] p 1053 N95-18587
Novel e-o polymers: NLO materials with superior temporal stability
[AD-A285872] p 988 N95-19614
Investigation of superlattice disordering and diffusion mechanisms in GaAs
[AD-A284847] p 1153 N95-19697
Characterization of inactive carbon in GaAs
[DE95-002352] p 976 N95-19836

DOPPLER EFFECT
Special relativity effects for space-based coherent lidar experiments p 1014 N95-18983
Doppler shift and spread study for ionospherically propagated signals
[AD-A284610] p 1065 N95-19083

DOSAGE
An investigation of nonuniform dose deposition from an electron beam
[AD-A284175] p 1131 N95-18519

DOWNTIME
Navy foreign object damage and its impact on future gas turbine engine low pressure compression systems
p 951 N95-19658
DRAG
In-flight lift-drag characteristics for a forward-swept wing aircraft and comparisons with contemporary aircraft)
[NASA-TP-3414] p 929 N95-18565
DRAG COEFFICIENTS
Static aerodynamics CFD analysis for 120-mm hypersonic KE projectile design
[ARL-MR-184] p 929 N95-18611
DRAG MEASUREMENT
Interference corrections for a centre-line plate mount in a porous-walled transonic wind tunnel
p 933 N95-19280
An investigation of drag repeatability in half model testing in the ARA Transonic Wind Tunnel
[ARA-MEMO-392] p 931 N95-19546
DRAG REDUCTION
The aerodynamic design of an integrated wing lower surface and pylons for reduced drag
[ARA-MEMO-406] p 946 N95-19789
DRINKING
Drink composition and cycle-ergometer endurance in men: Carbohydrate, Na(+), osmolality
[NASA-TM-4650] p 1077 N95-19140
DRIVES
Shock pulse generation using explosive driven metal drivers: Practical considerations
[MRL-TR-93-3] p 1046 N95-19504
DROP SIZE
Inter-comparison of automatic rain gauges
p 1069 N95-18204
Optical measurements in rocket engine liquid sprays
p 968 N95-18979
DROP TESTS
Dynamic decohesion of bimaterials: Experimental observations and failure criteria
[GALCIT-94-2] p 1045 N95-18613
Optical measurements in rocket engine liquid sprays
p 968 N95-18979
DRUGS
Medication in the course of active flying duty
p 1086 N95-19443
DUCTED FLOW
Solution of Navier-Stokes equations using high accuracy monotone schemes p 948 N95-19019
DUCTILITY
Superstrength metal composite material and process for making the same
[AD-D016555] p 971 N95-19123
Warm formability of aluminum-magnesium alloys
[DE94-016170] p 980 N95-19396
Multilayer anti-erosion coatings p 954 N95-19679
DURABILITY
Acoustic properties and durability of liner materials at non-standard atmospheric conditions
[NASA-CR-195010] p 1123 N95-18930
FAA/NASA International Symposium on Advanced Structural Integrity Methods for Airframe Durability and Damage Tolerance, part 2
[NASA-CP-3274-PT-2] p 934 N95-19468
Proceedings of the USAF Structural Integrity Program Conference
[AD-A285684] p 945 N95-19517
DUST
Constraints on chondrule agglomeration from fine-grained chondrule rims p 1189 N95-19315
The origin of refractory precursor components of chondrules p 1189 N95-19316
Out of area experiences with the RB199 in Toronto
p 950 N95-19654
The operation of gas turbine engines in hot and sandy conditions: Royal Air Force experiences in the Gulf conflict p 950 N95-19655
US Army rotorcraft turboshaft engines sand and dust erosion considerations p 951 N95-19656
Future directions in helicopter protection system configuration p 951 N95-19657
Damage of high temperature components by dust-laden air p 953 N95-19673
DUST COLLECTORS
Workshop on Particle Capture, Recovery and Velocity/Trajectory Measurement Technologies
[NASA-CR-197592] p 1180 N95-19172
Comet coma sample return instrument
p 1180 N95-19173
The status of measurement technologies concerning micrometer and submicrometer space articulate matter capture, recovery, velocity and trajectory
p 1181 N95-19175
Physics of spacecraft-based interplanetary dust collection by impact into low-density media
p 1181 N95-19176
Collection requirements for trace-element analyses of extraterrestrial samples p 1182 N95-19182
Laboratory simulation of intact capture of cometary and asteroidal dust particles in ISAS p 962 N95-19183
Techniques for in situ collection and measurement of volatiles released during hypervelocity impact
p 962 N95-19184
The intact capture of hypervelocity dust particles using underdense foams p 1183 N95-19188
SPICE: An innovative, flexible instrument concept
p 966 N95-19189
Charge collection during hypervelocity penetrations of thin foils p 1036 N95-19190
Penetration of multiple thin films in micrometeorite capture cells p 1036 N95-19192
Assessment of velocity/trajectory measurement technologies during a particle capture event
p 1036 N95-19193
Nondestructive time-of-capture, location and velocity sensing in intact capture p 1036 N95-19194
The use of silica aerogel to collect interplanetary dust in space p 989 N95-19197
Particle trajectories in gas turbine engines
p 952 N95-19663
DWELL
Microstructurally based variations on the dwell fatgue life of titanium alloy IMI 834 p 938 N95-19489
DYE LASERS
Inter-amplifier pupil relay systems for a high average power dye laser at Lawrence Livermore National Laboratory
[DE94-016544] p 1039 N95-19507
DYNAMIC CHARACTERISTICS
Standard reference materials: Glass filters as a standard reference material for spectrophotometry. Selection, preparation, certification and use of SRM 930 and SRM 1930
[PB94-188844] p 973 N95-17994
First principles used in orbital prediction and an atmospheric model comparison
[AD-A284636] p 1065 N95-19086
Main characteristics of the COMET/COMRADE experiments p 1181 N95-19179
Spectroscopy and dynamics of vibrationally excited molecules
[AD-A285874] p 1134 N95-19597
DYNAMIC CONTROL
Development of a multicomponent force and moment balance for water tunnel applications, volume 1
[NASA-CR-4642-VOL-1] p 1020 N95-18955
DYNAMIC LOADS
Gyroscopic and propeller aerodynamic effects on engine mounts dynamic loads in turbulence conditions
p 946 N95-18599
Dynamic decohesion of bimaterials: Experimental observations and failure criteria
[GALCIT-94-2] p 1045 N95-18613
Impact of dynamic loads on propulsion integration
p 1125 N95-19148
Evidence that aerodynamic effects, including dynamic stall, dictate HAWT structural loads and power generation in highly transient time frames
[DE94-011865] p 1054 N95-19855
DYNAMIC MODELS
The linear dynamics of a microsensor accelerometer modeled as a cantilever beam with an end mass
[DE94-019108] p 1031 N95-17963
The behavior of the slope of elastic nucleon scattering at small transfer momenta and recent U A 4/2 data
[DE94-626687] p 1130 N95-18360
A review of gust load calculation methods at de Havilland p 932 N95-18604
A linear system identification and validation of an AH-64 Apache aeroelastic simulation model
p 959 N95-18903
Complete mode-set stability analysis of magnetically insulated ion diode equilibria
[DE94-015275] p 1145 N95-19201
DYNAMIC PRESSURE
Pressure measurements on an F/A-18 twin vertical tail in buffeting flow. Volume 4, part 2: Buffet cross spectral densities
[AD-A285555] p 957 N95-18641
DYNAMIC RANGE
Dynamic range control of audio signals by digital signal processing
[BBC-RD-1993/7] p 1124 N95-19054
DYNAMIC RESPONSE
Modal Identification Experiment accommodations review
[NASA-CR-195009] p 964 N95-18105
Parachute inflation: A problem in aeroelasticity
[AD-A284375] p 928 N95-18340
Finite element modeling of partially delaminated composite beams with contact-impact conditions
[AD-A283726] p 1044 N95-18363
A review of gust load calculation methods at de Havilland p 932 N95-18604
Special effects of gust loads on military aircraft
p 946 N95-18605
SSI effects for a tank containing two liquids
[DE94-012457] p 1020 N95-19099
Changes in the flux of carbon between plants and soil microorganisms at elevated CO2: Physiological processes with ecosystem-level implications
[DE94-017067] p 1060 N95-19112
Current and future problems in structural acoustic fatigue p 1124 N95-19143
Nonlinear dynamic response of aircraft structures to acoustic excitation p 946 N95-19151
Acoustics of space structures p 1126 N95-19152
Forced response of mistuned bladed disks
p 950 N95-19383
Documentation and archiving of the Space Shuttle wind tunnel test data base. Volume 2: User's Guide to the Archived Data Base
[NASA-TM-104806-VOL-2] p 965 N95-19624
Aero-thermodynamic distortion induced structured dynamic response
[AD-A279931] p 955 N95-19864
DYNAMIC STABILITY
Dynamics and statics of nonaxisymmetric liquid bridges
[NASA-CR-197520] p 1195 N95-17980
Dynamic Stability Instrumentation System (DSIS). Volume 1: Hardware description
[NASA-TM-109160-VOL-1] p 1099 N95-18899
Investigation of the microstructure of coatings for high power lasers by non-optical techniques
[DE94-017697] p 987 N95-19227
DYNAMIC STRUCTURAL ANALYSIS
Parachute inflation: A problem in aeroelasticity
[AD-A284375] p 928 N95-18340
Plate vibration with arbitrarily oriented stiffeners based on Mindlin-Engesser formulation
[RR-CE143] p 1045 N95-18608
A preliminary analysis of low frequency pressure oscillations in hybrid rocket motors p 968 N95-18987
Free vibration analysis of partially filled liquid storage tanks
[DE94-012456] p 1020 N95-19098
Acoustics of space structures p 1126 N95-19152
Application of the PSD technique to acoustic fatigue stress calculations in complex substructures
p 1126 N95-19155
Advanced statistical energy analysis
p 1047 N95-19165
Documentation and archiving of the Space Shuttle wind tunnel test data base. Volume 2: User's Guide to the Archived Data Base
[NASA-TM-104806-VOL-2] p 965 N95-19624
DYNAMIC TESTS
V-22 simulator evaluation for shipboard operations
[AD-A284156] p 943 N95-18505
Development of a multicomponent force and moment balance for water tunnel applications, volume 2
[NASA-CR-4642-VOL-2] p 1020 N95-18956
Calculation of support interference in dynamic wind-tunnel tests p 933 N95-19282
DYNAMICAL SYSTEMS
Applications of quaternions to dynamical simulation, computer graphics and biomechanics
[PB94-201456] p 1094 N95-17972
Advanced methods for the computation of particle beam transport and the computation of electromagnetic fields and beam-cavity interactions
[DE94-017359] p 1136 N95-18893
Numerical analysis of dissipative dynamical systems in solid and fluid mechnaics, with a special emphasis on coupled problems p 1122 N95-18916
Algorithms and applications in timed discrete event systems
[PB94-201423] p 1118 N95-19169
DYSON THEORY
Pion observables and QCD
[DE94-018357] p 1130 N95-18428

E

EARLY STARS
Astronomical observations of phenomena in disks
p 1178 N95-19301
EARTH ALBEDO
Radiation balance in three Amazonian ecosystems: Campina, campinarana and mata densa
[INPE-5587-TDI/549] p 1057 N95-18003
EARTH ATMOSPHERE
Evolution of the Southern Hemisphere ozone hole as seen by TOMS from August 1979 to December 1991
[NASA-TM-110116] p 1057 N95-18048

Trends 1993: A compendium of data on global change
[ORNL/CDIAC-65] p 1058 N95-18389

EARTH CRUST
Magnetotelluric mapping of upper crustal isotherms beneath the Valles Caldera hydrothermal system
[DE94-013606] p 1063 N95-17946
Density structure of the upper oceanic crust at zero porosity
[AD-A284235] p 1076 N95-19728

EARTH IONOSPHERE
Ion-molecule collisions, electron molecule collisions, excitation and ionization of atoms
[AD-A284584] p 1129 N95-18062
Results from the northern New Mexico satellite-beacon radio interferometer
[DE94-018310] p 1063 N95-18148
Electrodynamic behavior of PMG-Delta
[AD-A283930] p 964 N95-18163
Effects of meteor showers in the Earth ionosphere
[INPE-5591-TDI/552] p 1178 N95-18213
Design, validation and prototype testing of a high resolution all-reflection Michelson interferometer for solar occultation measurements of the O! 1304-a triplet emission
[AD-A283705] p 1178 N95-18361
New applications of the Phillips Laboratory. Theoretical ionospheric model and studies of neutral density waves
[AD-A284663] p 1066 N95-19105

EARTH MAGNETOSPHERE
Particle acceleration and transport in the tail and at the front side of the magnetosphere, task 1 and 2
[NASA-CR-197575] p 1064 N95-18476

EARTH MANTLE
Trace element characteristics of lithospheric and asthenospheric mantle in the Rio Grande rift region
[DE94-013609] p 1063 N95-17947

EARTH OBSERVATIONS (FROM SPACE)
Comparative analysis of multisensor (TM/Landsat and SAR/ERS-1) and multitemporal scenes of Guaira region, Sao Paulo State, Brazil
[INPE-5581-TDI/544] p 1049 N95-18005
STS-68 mission highlights resource tape
[NASA-TM-110049] p 961 N95-18568
Legacy of Gemini
[NASA-TM-110486] p 961 N95-19058
Skylab: The second manned mission. A scientific harvest
[NASA-TM-110487] p 961 N95-19059

EARTH ORBITAL ENVIRONMENTS
Mission description and in-flight operations of ERBE instruments on ERBS and NOAA 10 spacecraft, February 1987 - February 1990
[NASA-RP-1325] p 1051 N95-18465
Spacecraft environments interactions: Protecting against the effects of spacecraft charging
[NASA-RP-1354] p 965 N95-19780

EARTH ORBITS
Orbital tests of relativistic gravity using artificial satellites
[PB94-217239] p 965 N95-19377

EARTH RADIATION BUDGET
Radiation balance in three Amazonian ecosystems: Campina, campinarana and mata densa
[INPE-5587-TDI/549] p 1057 N95-18003

EARTH RESOURCES
Resources Automated Management System
[AD-A284153] p 1171 N95-18416

EARTH RESOURCES PROGRAM
Skylab: The second manned mission. A scientific harvest
[NASA-TM-110487] p 961 N95-19059

EARTH RESOURCES SURVEY PROGRAM
Skylab: The first 40 days
[NASA-TM-110491] p 961 N95-19040

EARTH TERMINALS
An expert system for configuring a network for a Milstar terminal p 1104 N95-19645

EARTHQUAKE DAMAGE
Sloshing roof impact tests of a rectangular tank
[DE94-012462] p 1018 N95-18549

ECLIPSING BINARY STARS
The quiescent and flaring EUV spectrum of Algol and its relationship to other active coronae. EUV spectroscopy of bright hyades coronae: 71 Tauri and Theta 1 Tauri
[NASA-CR-197538] p 1178 N95-18391

ECONOMIC ANALYSIS
US Industrial Outlook, 1994: An almanac of industry, technology and services. 35th annual edition. Forecasts for selected manufacturing and service industries
[PB94-107844] p 1171 N95-17988
Systems and economic analysis of microalgae ponds for conversion of CO2 to biomass
[DE95-000406] p 1054 N95-19554

ECONOMIC IMPACT
Economic impact analysis for proposed emission standards and guidelines for municipal waste combustors: A description of the basis for, and impacts of, proposed revisions to air pollutant emission regulations for new and existing municipal waste combustors under Clean Air Act Sections 111(b), 111(d), and 129
[PB94-213543] p 1061 N95-19403

ECOSYSTEMS
Renewable energy and its potential for carbon emissions reductions in developing countries: Methodology for technology evaluation
[DE94-011870] p 1056 N95-17943
Radiation balance in three Amazonian ecosystems: Campina, campinarana and mata densa
[INPE-5587-TDI/549] p 1057 N95-18003
Changes in the flux of carbon between plants and soil microorganisms at elevated CO2: Physiological processes with ecosystem-level implications
[DE94-017067] p 1060 N95-19112

EDDY CURRENTS
Evaluation of scanners for C-scan imaging in nondestructive inspection of aircraft
[DE94-012473] p 990 N95-19100

EDDY VISCOSITY
Turbulence modeling for CFD, part 1
p 1028 N95-19458
Turbulence modeling for CFD, part 2
p 1030 N95-19466

EDGE DETECTION
Cooperativity and 3-D representation
[AD-A284203] p 1093 N95-17940
Robust image understanding. Techniques and applications
[AD-A283427] p 1113 N95-18057
An inverse problem in thermal imaging
[NASA-CR-195018] p 1117 N95-18479

EDUCATION
Training plan. Central Archive for Reusable Defense Software (CARDS)
[AD-A284343] p 1097 N95-18421
Design concepts for an integrated environmental medicine workstation for prediction, simulation and training
[AD-A283686] p 1079 N95-18618
Research reports: 1994 NASA/ASEE Summer Faculty Fellowship Program
[NASA-CR-196533] p 1161 N95-18967
The assessment of virtual reality for human anatomy instruction p 1088 N95-18971
Assessment of the ACSE science learning environment and the impact of movies and simulations
[AD-A284071] p 1089 N95-19068
Activities of the Analytical Chemistry Laboratory
[DE95-000834] p 975 N95-19618
Development of a comprehensive base-level environmental training program for total environmental compliance
[AD-A284806] p 1061 N95-19686

EFFECTS
The effect of special boards of flight surgeons on the evolution of US Naval flight standards
p 1081 N95-19417

EGRESS
Spine injuries: Up to date evaluation in aircraft ejections p 1084 N95-19434

EIGENVALUES
Finite element method for eigenvalue problems in electromagnetics
[NASA-TP-3485] p 995 N95-18187
Eigenvalue tests and distributions for small sample order determination for complex Wishart matrices
[AD-A283825] p 1120 N95-18672
Statistics of complex cross spectrum estimate for sinusoidal signals and arbitrary noise spectra
[AD-A283984] p 1120 N95-19065

EIGENVECTORS
Method of moments analysis of artificial media composed of dielectric wire objects
[AD-A283318] p 994 N95-18024
Algorithms and applications in timed discrete event systems
[PB94-201423] p 1118 N95-19169

EINSTEIN EQUATIONS
General relativity and dark matter
[DE94-626641] p 1180 N95-18877

EJECTION INJURIES
Clinical practice, diagnosis and therapy of intervertebral disk lesion: Importance to fitness for military flying duties
p 1084 N95-19435

EJECTION SEATS
Design and development of an enhanced biodynamic manikin, phase 1
[AD-A284725] p 1090 N95-18077
Preliminary evaluation of the F/A-18 quantity/multiple envelope expansion
[AD-A284119] p 943 N95-18407
Spine injuries: Up to date evaluation in aircraft ejections p 1084 N95-19434

EL NINO
Marginal probabilities of the extremes of ENSO events for temperature and precipitation in the southeastern United States
[AD-A284716] p 1068 N95-18076

ELASTIC BODIES
Completed Beltrami-Michell formulation for analyzing radially symmetrical bodies
[NASA-TM-4593] p 1044 N95-18199
A boundary element method for two dimensional linear elastic fracture analysis p 1045 N95-18917
Coupled finite element analysis of decomposing poroelastic polymeric composites and structures with subsequent thermal and gas diffusion
p 986 N95-18918

ELASTIC DEFORMATION
Fluid dynamic linear accelerometer
[AD-D016413] p 956 N95-18553
Determination of stores pointing error due to wing flexibility under flight load
[NASA-TM-4646] p 945 N95-19044
Impact loading of compressor stator vanes by hailstone ingestion p 953 N95-19670

ELASTIC PROPERTIES
The reliability of laser reflowed Sn-Ag solder joints
[AD-A284732] p 1044 N95-18080
Completed Beltrami-Michell formulation for analyzing mixed boundary value problems in elasticity
[NASA-TM-106809] p 1045 N95-18909
Optimization of layered metal matrix composite cylinders p 970 N95-18920
Discrete and continuum elastic properties of interfaces
p 1150 N95-18928
Atomistic and elastic analyses of defects and small structures
[DE94-017047] p 980 N95-19111
Sag compensated vibration isolation mount
[AD-D016541] p 1042 N95-19121
A 2D depth migration in transversely isotropic media using explicit operators
[DE95-000645] p 1066 N95-19560
Phase stability and elastic properties of C15 compounds HfV2 + Nb
[DE95-000940] p 981 N95-19611

ELASTIC SCATTERING
The behavior of the slope of elastic nucleon scattering at small transfer momenta and recent U A 4/2 data
[DE94-626687] p 1130 N95-18360

ELASTIC WAVES
Wavelets and scattering
[AD-A284131] p 996 N95-18411
The evaluation of transmission efficiency and coupling loss factor of structural junctions
[MRL-TR-93-1] p 1124 N95-19057

ELASTOMERS
Positive displacement rotary pump
[AD-D016412] p 1041 N95-18335
A shock isolation method and apparatus
[AD-D016471] p 1045 N95-18456
Thermoelectric properties of conducting polymers
[AD-A284058] p 986 N95-18678

ELASTOPLASTICITY
Characterization of metal matrix composites
[NASA-CR-195381] p 970 N95-18940
The load separation technique in the elastic-plastic fracture analysis of two- and three-dimensional geometries p 936 N95-19481

ELECTRIC BATTERIES
Preparation of an electrocatalytic cathode for an aluminum-hydrogen peroxide battery
[AD-D016262] p 1008 N95-18318
Development of a bipolar lead/acid battery for the more electric aircraft
[AD-A284050] p 1010 N95-18660
Probing the chemistry of nickel/metal hydride battery cells using electrochemical impedance spectroscopy
p 1014 N95-18985
Battery and charge controller evaluations in small stand-alone PV systems
[DE94-014252] p 1013 N95-19872

ELECTRIC CONTACTS
Advanced packaging and integration technologies for microsensors, phase 1
[AD-A283613] p 1040 N95-18010
Method of forming platinum and platinum silicide Schottky contacts on beta-silicon carbide
[AD-D016221] p 1149 N95-18627

ELECTRIC CURRENT
Electrodynamic behavior of PMG-Delta
[AD-A283930] p 964 N95-18163

Development of a bulk current injection direct-drive system to test system level components with stress waveforms that are encountered during full threat indirect effects lightning
[AD-A284160] p 933 N95-18507
Radiation-induced noise in UMPC-type current probes: IEMP response of the curruent measurement system
[AD-A284176] p 998 N95-18520

ELECTRIC DIPOLES
Limits on CP nonconserving interactions from electric dipole moments
[DE94-018582] p 1134 N95-19705

ELECTRIC DISCHARGES
Probing the chemistry of nickel/metal hydride battery cells using electrochemical impedance spectroscopy
p 1014 N95-18985

ELECTRIC FIELDS
Junction Field Effect Transistor with lateral Gate Voltage Swing (GVS-JFET)
[AD-D016353] p 1032 N95-17970
Ion orbit loss and the poloidal electric field in a tokamak
[DE94-016860] p 1145 N95-19092
Piezoelectric effects in double barrier resonant tunneling structures
[DE95-000850] p 1152 N95-19620
Properties of Alfven waves with transverse scale on the order of skin-depth
[AD-A285657] p 1147 N95-19700

ELECTRIC GENERATORS
Power conversion system modification to permit use of DC power source
[AD-D016421] p 1010 N95-18523

ELECTRIC MOTOR VEHICLES
Kansas State University DOE/KEURP Site Operator User Task Force
[DE94-014331] p 1040 N95-17995
Current Hybrid Electric Vehicle performance based on temporal data from the world's largest HEV fleet
[DE94-011859] p 1014 N95-19881

ELECTRIC MOTORS
A finite element code for electric motor design
p 1014 N95-18974

ELECTRIC NETWORKS
Partition method for the determination of multiple DC operating points
[PB94-201480] p 1009 N95-18501

ELECTRIC POTENTIAL
Pulsed laser illumination of photovoltaic cells
[NASA-TM-106820] p 1053 N95-18572
Constant current loop impedance measuring system that is immune to the effects of parasitic impedances
[NASA-CASE-ARC-11988-1] p 1011 N95-18959
Piezoelectric effects in double barrier resonant tunneling structures
[DE95-000850] p 1152 N95-19620
Barium strontium titanate and non-ferroelectric oxide ceramic composites for use in phased array antennas
[AD-A279225] p 972 N95-19851

ELECTRIC POWER SUPPLIES
Solar-electrochemical power system for a Mars mission
[NASA-TM-106606] p 967 N95-18570

ELECTRIC PROPULSION
Arcjet thruster research and technology, phase 2
[NASA-CR-182276] p 927 N95-18044
High performance storable propellant resistojet
[NASA-CR-191128] p 967 N95-18195

ELECTRIC RELAYS
Characteristics and development report for the MC3994 and MC3994A relays
[DE95-002952] p 1013 N95-19842

ELECTRIC SWITCHES
Radar sector blanker
[AD-D016275] p 996 N95-18429

ELECTRIC WIRE
Method of moments analysis of artificial media composed of dielectric wire objects
[AD-A283318] p 994 N95-18024

ELECTRICAL ENGINEERING
Current loop signal conditioning: Practical applications
[NASA-TM-4636] p 1033 N95-18735

ELECTRICAL FAULTS
Development of an expert system for power quality advisement using CLIPS 6.0 p 1014 N95-19634

ELECTRICAL IMPEDANCE
Constant current loop impedance measuring system that is immune to the effects of parasitic impedances
[NASA-CASE-ARC-11988-1] p 1011 N95-18959

ELECTRICAL MEASUREMENT
Final results of the Advanced Photovoltaic Experiment flight test
[NASA-TM-106828] p 967 N95-18571
Constant current loop impedance measuring system that is immune to the effects of parasitic impedances
[NASA-CASE-ARC-11988-1] p 1011 N95-18959

ELECTRICAL PROPERTIES
Characterization of rechargeable lithium cells. Part 1: Lithium/niobium triselenide chemistry
[AD-A284229] p 1007 N95-17959
Stratified carrier electroviscous fluids and apparatus
[AD-D016238] p 1019 N95-18634
Power terminal protection device
[AD-D016528] p 1011 N95-19120
Development of materials for high temperature superconductor Josephson junctions
[DE95-000896] p 1152 N95-19608

ELECTRICAL RESISTIVITY
Magnetotelluric mapping of upper crustal isotherms beneath the Valles Caldera hydrothermal system
[DE94-013606] p 1063 N95-17946
Junction Field Effect Transistor with lateral Gate Voltage Swing (GVS-JFET)
[AD-D016353] p 1032 N95-17970
DC-conductivity and magnetoresistance of inherently conducting polymers. Polyacetylene and poly(3-alkylthiophenes)
[PB94-184587] p 1007 N95-18037
Corrosivity sensor
[AD-D016422] p 1033 N95-18524
Computational modeling of properties
[NASA-CR-197558] p 1010 N95-18925
Deformation of nonstoichiometric CuO polycrystals
[DE94-016907] p 1150 N95-19094

ELECTRIFICATION
Field and data analysis studies related to the atmospheric environment
[NASA-CR-196543] p 1068 N95-18093

ELECTRO-OPTICS
Multi-functional pi-conjugated macromolecules based on poly (phenylene vinylene)
[AD-A284163] p 985 N95-18510
Thermal relaxation processes and stability in poled electro-optic polymers
[AD-A283948] p 987 N95-19102
Fiber Optic Control System integration for advanced aircraft. Electro-optic and sensor fabrication, integration, and environmental testing for flight control systems
[NASA-CR-191194] p 1034 N95-19236
High-frame-rate intensified fast optically shuttered TV cameras with selected imaging applications
[DE94-016098] p 1035 N95-19394
Second International Semiconductor Device Research Symposium (ISDRS-1993)
[AD-A279221] p 1013 N95-19849

ELECTROCARDIOGRAPHY
EKG in flight: Usefulness and limits for aircrew rehabilitation p 1082 N95-19422
Evaluation of the EKG's isoelectric T wave in Air Force pilots p 1082 N95-19423

ELECTROCATALYSTS
Methane conversion by solid electrolyte membranes
[PB94-191781] p 973 N95-17982
Electrochemical interfaces and electrode processes: Electrochemical oxidation of small organisms
[AD-A284873] p 1013 N95-19741

ELECTROCHEMICAL CELLS
Metal/hydrogen energy storage: Selected technical issues
[AD-A283355] p 1008 N95-18052

ELECTROCHEMICAL CORROSION
A mechanism for blistering of carbon fiber composites
[AD-A286252] p 971 N95-19386

ELECTROCHEMICAL OXIDATION
Electrochemical interfaces and electrode processes: Electrochemical oxidation of small organisms
[AD-A284873] p 1013 N95-19741

ELECTROCHEMISTRY
Methane conversion by solid electrolyte membranes
[PB94-191781] p 973 N95-17982
Fundamental advances for characterizing cathodic protection systems
[PB94-180692] p 1122 N95-17983
Evaluation of inorganic zinc-rich primers using Electrochemical Impedance Spectroscopy (EIS) in combination with atmospheric exposure
p 977 N95-18170
Preparation of an electrocatalytic cathode for an aluminum-hydrogen peroxide battery
[AD-D016262] p 1008 N95-18318
Spectroelectrochemical investigations of molten halide solutions
[AD-A284147] p 974 N95-18412
Electrochemical and spectroscopy studies of selected inorganic and organic systems in molten halides
[AD-A284171] p 974 N95-18514
Probing the chemistry of nickel/metal hydride battery cells using electrochemical impedance spectroscopy
p 1014 N95-18985
Development of a colloidal redox system containing a smectite clay for control of reactivity and reaction selectivity
[AD-A285958] p 974 N95-19515
Using electrochemistry in device processing on poly(tetrafluoroethylene) substrates
[DE95-000541] p 975 N95-19559
Alternative materials for solid oxide fuel cells
[DE94-018452] p 1054 N95-19591
Electrochemical interfaces and electrode processes: Electrochemical oxidation of small organisms
[AD-A284873] p 1013 N95-19741

ELECTRODES
Ion emission intensity ratios as a function of electrode gap, melting current, and pressure during low current vacuum arc remelting
[DE94-017407] p 1129 N95-18144
Handbook for the extremely low frequency (ELF) data acquisition and analysis system
[DSTO-GD-0021] p 1005 N95-19622
Electrochemical interfaces and electrode processes: Electrochemical oxidation of small organisms
[AD-A284873] p 1013 N95-19741

ELECTRODYNAMICS
Electrodynamic behavior of PMG-Delta
[AD-A283930] p 964 N95-18163
Zero modes of first class secondary constraints in gauge theories
[DE94-626659] p 1156 N95-18328

ELECTROENCEPHALOGRAPHY
Extrathalamic modulation of cortical responsiveness
[AD-A284100] p 1078 N95-18400
Neurological decision making in aviation medicine based on electrophysiological methods p 1084 N95-19431
The EEG in the evaluation of applicants to aircrew members p 1084 N95-19432
Clinical basis for aeromedical decision-making: The EEG example p 1084 N95-19433
Collection of real-time, multichannel EEG data from helicopter pilots in flight: A feasibility study
[AD-A285050] p 1090 N95-19564

ELECTROLESS DEPOSITION
Using electrochemistry in device processing on poly(tetrafluoroethylene) substrates
[DE95-000541] p 975 N95-19559

ELECTROLYTES
Molecular dynamics study of aqueous electrolyte solutions near a structured sphere
[AD-A284010] p 1132 N95-18655
Lithium electrode/polyacrylonitrile based polymer electrolyte interface
[AD-A283947] p 986 N95-19064

ELECTROLYTIC CELLS
Metal/hydrogen energy storage: Selected technical issues
[AD-A283355] p 1008 N95-18052

ELECTROMAGNETIC ABSORPTION
Silicon carbide photoconductive switches
[AD-A284310] p 1008 N95-18378
The optical emission and absorption properties of silicon-germanium superlattice structures grown on non-conventional silicon substrate orientation
[AD-A284852] p 1153 N95-19715

ELECTROMAGNETIC COMPATIBILITY
Measurements of wind profiler EMC characteristics
[PB94-194107] p 1066 N95-17938

ELECTROMAGNETIC FIELDS
Mechanisms of interaction and biological effects of extremely-low-frequency electromagnetic fields
[DE94-015200] p 1076 N95-18371
Advanced methods for the computation of particle beam transport and the computation of electromagnetic fields and beam-cavity interactions
[DE94-017359] p 1136 N95-18893
General information for operation of the high-temperature electromagnetic containerless vacuum induction furnace
[DE94-017170] p 991 N95-19076
Asymmetric antiproton debuncher: No bad mixing, more good mixing
[DE94-017171] p 1133 N95-19077
Solution of Maxwell's equations using the time domain Method of Moments
[AD-A280144] p 1119 N95-19820

ELECTROMAGNETIC INTERACTIONS
The Green's function in the Bloch-Nordsieck model for QED3
[DE94-626680] p 996 N95-18331
Complete mode-set stability analysis of magnetically insulated ion diode equilibria
[DE94-015275] p 1145 N95-19201

ELECTROMAGNETIC INTERFERENCE
Mitigation of EMI generated by a variable-frequency-drive controller for an AC induction motor
[AD-A286045] p 1012 N95-19573

ELECTROMAGNETIC MISSILES
Geometrical and topological methods in time domain antenna synthesis
[AD-A284208] p 994 N95-17954
ELECTROMAGNETIC NOISE
Hyperspectral data analysis procedures with reduced sensitivity to noise
[NASA-CR-197621] p 1052 N95-19126
ELECTROMAGNETIC PROPERTIES
Geometrical and topological methods in time domain antenna synthesis
[AD-A284208] p 994 N95-17954
ELECTROMAGNETIC PULSES
Radiation-induced noise in UMPC-type current probes: IEMP response of the curruent measurement system
[AD-A284176] p 998 N95-18520
Assessing aircraft survivability to high frequency transient threats
[AD-A283999] p 944 N95-18726
Waveform bounding and combination techniques for direct drive testing
[AD-A284075] p 1000 N95-19035
E-6A hardness assurance, maintenance and surveillance program
[AD-A283994] p 945 N95-19067
ELECTROMAGNETIC PUMPS
Electromagnetic pump
[AD-D016260] p 1041 N95-18317
ELECTROMAGNETIC RADIATION
Radiation-induced noise in UMPC-type current probes: IEMP response of the curruent measurement system
[AD-A284176] p 998 N95-18520
Hypersonic wind tunnel test techniques
[AD-A284057] p 929 N95-18663
Computer simulation of wave propagation through turbulent media
[AD-A283695] p 1000 N95-18671
ELECTROMAGNETIC SCATTERING
Alternative volume integral equation formulations applied to dielectric cylinders
[AD-A285537] p 995 N95-18066
Wavelets and scattering
[AD-A284131] p 996 N95-18411
Two space scatterer formalism calculation of bulk parameters of thunderclouds p 1073 N95-19001
Scattering of point source illumination by an arbitrary configuration p 1143 N95-19006
Inband radar cross section of phased arrays with parallel feeds
[AD-A284249] p 1005 N95-19730
ELECTROMAGNETIC SHIELDING
Power terminal protection device
[AD-D016528] p 1011 N95-19120
ELECTROMAGNETIC SPECTRA
ISSSR tutorial 1: Introduction to spectral remote sensing
[AD-A284268] p 1052 N95-19734
ELECTROMAGNETIC WAVE TRANSMISSION
Energy balance model for imagery and electromagnetic propagation
[AD-A284552] p 1063 N95-18115
Wavelets and scattering
[AD-A284131] p 996 N95-18411
Surface and upper-air meteorological measurements supporting the NATO/AC243/Panel 3 research study groups 8 and 21 campaign in Lorient, France (September 1993)
[AD-A285326] p 1072 N95-19521
ELECTROMAGNETISM
Finite element method for eigenvalue problems in electromagnetics
[NASA-TP-3485] p 995 N95-18187
Hypersonic wind tunnel test techniques
[AD-A284057] p 929 N95-18663
ELECTROMYOGRAPHY
Neurological decision making in aviation medicine based on electrophysiological methods p 1084 N95-19431
ELECTRON ACCELERATION
Properties of Alfven waves with transverse scale on the order of skin-depth
[AD-A285657] p 1147 N95-19700
ELECTRON ACCELERATORS
Study of the effect of ionizing radiation on the structure of natural rubber latex by positron annihilation technique
[DE94-631466] p 975 N95-19550
The founding of CEBAF, 1979 to 1987 p 1138 N95-19784
ELECTRON BEAMS
The left-right forward-backward asymmetry for B quarks at the SLD
[DE94-014508] p 1129 N95-18049
Tunneling and transport in mesoscopic structures
[AD-A283426] p 1148 N95-18053
An investigation of nonuniform dose deposition from an electron beam
[AD-A284175] p 1131 N95-18519
Low voltage electron beam lithography
[AD-A284181] p 1010 N95-18625
The visible Smith-Purcell radiation search
[DE94-017514] p 1038 N95-19243
Study of the effect of ionizing radiation on the structure of natural rubber latex by positron annihilation technique
[DE94-631466] p 975 N95-19550
Characterization of the 50 MeV ALS linac beam with optical transition radiation
[DE94-018208] p 1137 N95-19584
ELECTRON BUNCHING
Asymmetric antiproton debuncher: No bad mixing, more good mixing
[DE94-017171] p 1133 N95-19077
ELECTRON CYCLOTRON HEATING
Global wave modeling of electron interactions with fast magnetosonic waves
[DE94-018942] p 1144 N95-18557
ELECTRON DENSITY (CONCENTRATION)
Observations of TEC fluctuations from an explosion on the Earth's surface
[DE94-018278] p 1063 N95-18125
Design, validation and prototype testing of a high resolution all-reflection Michelson interferometer for solar occultation measurements of the OI 1304-a triplet emission
[AD-A283705] p 1178 N95-18361
Determination of the electron density and the electron temperature in a high-pressure microwave discharge p 1145 N95-18906
ELECTRON EMISSION
The left-right forward-backward asymmetry for B quarks at the SLD
[DE94-014508] p 1129 N95-18049
Vacuum microelectronic emitters and their applications using compound semiconductor technology
[AD-A284811] p 1013 N95-19687
ELECTRON ENERGY
Progress on the multipulse Thomson scattering diagnostic on D3-D
[DE94-017515] p 1143 N95-18119
Determination of the electron density and the electron temperature in a high-pressure microwave discharge p 1145 N95-18906
Electronic structure of C60 fullerites and nanotubes
[DE95-000784] p 1151 N95-19569
ELECTRON MASS
Giant effective mass deviations near the magnetic field-induced minigap in double quantum wells
[DE94-018889] p 1122 N95-19234
ELECTRON MICROSCOPES
An atomic view of motion on surfaces
[AD-A285565] p 1131 N95-18473
ELECTRON MOBILITY
The physics and operation of ultra-submicron length semiconductor devices
[AD-A280181] p 1155 N95-19828
ELECTRON PARAMAGNETIC RESONANCE
Spectroelectrochemical investigations of molten halide solutions
[AD-A284147] p 974 N95-18412
ELECTRON SCATTERING
DC-conductivity and magnetoresistance of inherently conducting polymers. Polyacetylene and poly(3-alkylthiophenes)
[PB94-184587] p 1007 N95-18037
Ion-molecule collisions, electron molecule collisions, excitation and ionization of atoms
[AD-A284584] p 1129 N95-18062
Electron interactions with non-linear polyatomic molecules and their radicals
[AD-A283952] p 1130 N95-18334
Global wave modeling of electron interactions with fast magnetosonic waves
[DE94-018942] p 1144 N95-18557
ELECTRON SOURCES
Electron reversal ionizer for detection of trace species using a spherical cathode
[NASA-CASE-NPO-18870-1-CU] p 1130 N95-18324
ELECTRON TRANSFER
Large signal time dependent quantum mechanical transport in quantum phase based devices
[AD-A283338] p 1155 N95-18009
Electrochemical and spectroscopy studies of selected inorganic and organic systems in molten halides
[AD-A284171] p 974 N95-18514
Probing the chemistry of nickel/metal hydride battery cells using electrochemical impedance spectroscopy p 1014 N95-18985
ELECTRON TRANSITIONS
Ion-molecule collisions, electron molecule collisions, excitation and ionization of atoms
[AD-A284584] p 1129 N95-18062
Hyperfine splittings, prepulse technique, and other new results for collisional excitation neon-like x ray lasers
[DE94-016443] p 1038 N95-19247
Measurements of line overlap for resonant spoiling of x ray lasing transitions
[DE94-016444] p 1038 N95-19248
ELECTRON TUNNELING
An atomic view of motion on surfaces
[AD-A285565] p 1131 N95-18473
ELECTRONIC AIRCRAFT
E-6A hardness assurance, maintenance and surveillance program
[AD-A283994] p 945 N95-19067
ELECTRONIC CONTROL
Advanced diesel electronic fuel injection and turbocharging
[AD-A279176] p 1043 N95-19809
ELECTRONIC EQUIPMENT
Electronics for the Si detectors in APEX
[DE94-015078] p 1007 N95-17961
Method for forming Josephson break junctions
[AD-D016427] p 1149 N95-18559
The 3d International Workshop on Computational Electronics
[AD-A284678] p 1011 N95-19089
ELECTRONIC EQUIPMENT TESTS
Digital audio broadcasting: Comparison of coverage at different frequencies and with different bandwidths
[BBC-RD-1993/11] p 1002 N95-19135
ELECTRONIC MAIL
AI and workflow automation: The prototype electronic purchase request system p 1101 N95-19632
ELECTRONIC PACKAGING
Polymer based materials for additive processing of high temperature electronics packaging
[AD-A285962] p 988 N95-19745
ELECTRONIC WARFARE
Radar antenna characterization using polarization measurements
[AD-A284840] p 1005 N95-19694
Wind tunnel tests of a 42 inch diameter self-starting autogyro rotor
[AD-A279922] p 932 N95-19863
ELECTRONICS
Technological and organizational diversity and technical advance in the early history of the American semiconductor industry
[PB94-175700] p 1007 N95-17999
ELECTRONS
Electronics for the Si detectors in APEX
[DE94-015078] p 1007 N95-17961
Large signal time dependent quantum mechanical transport in quantum phase based devices
[AD-A283338] p 1155 N95-18009
Correlated charge-changing ion-atom collisions
[DE94-017355] p 1132 N95-18874
Cross-tail current, field-aligned current, and B(y)
[NASA-CR-197624] p 1065 N95-19032
Giant effective mass deviations near the magnetic field-induced minigap in double quantum wells
[DE94-018889] p 1122 N95-19234
Direct energy conversion system for D(3)-He fusion
[DE94-770773] p 1146 N95-19549
Wentzel-Bardeen singularity in coupled Luttinger liquids: Transport properties
[DE95-000856] p 1152 N95-19621
ELECTROPHORESIS
Enhancement of fluorescence detection in chromatographic methods by computer analysis of second order data
[DE94-014682] p 973 N95-17966
Capillary electrophoresis: Biotechnology for separation of DNA and chromosomes p 1077 N95-19014
ELECTROPHYSIOLOGY
Extrathalamic modulation of cortical responsiveness
[AD-A284100] p 1078 N95-18400
Cellular neurophysiology of the rat suprachiasmatic nucleus: Electrical properties, neurotransmission, and mechanisms of synchronization
[AD-A284111] p 1076 N95-18439
Neurological decision making in aviation medicine based on electrophysiological methods p 1084 N95-19431
ELECTROSTATIC SHIELDING
Field-emitter arrays for RF vacuum microelectronics
[AD-A279932] p 1013 N95-19865
ELECTROSTATICS
Potential distributions for ellipsoidal bodies in uniform fields
[MRL-TR-92-48] p 1005 N95-19771
ELECTROSTRICTION
Tunneling acoustic microscopy
[AD-A279160] p 1128 N95-19802
ELECTROWEAK INTERACTIONS (FIELD THEORY)
SU4(sub L) x U1(sub N) model for the electroweak interactions
[DE94-626675] p 1148 N95-18330
Higher-order Lipatov kernels and the QCD Pomeron
[DE94-018395] p 1131 N95-18551

Physics at the Fermilab Tevatron Proton-Antiproton Collider
[DE95-000648] p 1137 N95-19561

ELECTROWEAK MODEL
SU4(sub L) x U1(sub N) model for the electroweak interactions
[DE94-626675] p 1148 N95-18330

ELEMENTARY EXCITATIONS
Electronic structure of C60 fullerites and nanotubes
[DE95-000784] p 1151 N95-19569
Generation and solution of effective many-body Hamiltonians for rare earth and transition metal compounds
[DE95-002402] p 1155 N95-19838

ELEMENTARY PARTICLE INTERACTIONS
Studies of prompt photon production and multijet production at the Tevatron Collider
[DE95-002216] p 1135 N95-19835

ELEMENTARY PARTICLES
Properties of nuclei and elementary particles at low and intermediate energies
[DE94-008502] p 1132 N95-18644
Bohr's quantization rule in the world of resonances of elementary particles
[DE94-626721] p 1132 N95-18882

ELLIPSOIDS
Potential distributions for ellipsoidal bodies in uniform fields
[MRL-TR-92-48] p 1005 N95-19771

ELLIPTIC DIFFERENTIAL EQUATIONS
Reformulated preconditioned conjugate gradient squared method. Part 1: The algorithm
[PB94-201589] p 1108 N95-17936

ELLIPTICITY
Discrete and continuum elastic properties of interfaces p 1150 N95-18928

EMBEDDING
Embedded microclusters in zeolites and cluster beam sputtering: Simulation on parallel computers
[DE95-000662] p 1134 N95-19562

EMBRYOLOGY
Concentration and temperature effects on ovostatin activity p 1077 N95-18997

EMERGENCY LOCATOR TRANSMITTERS
Federal aviation regulations, part 91. General operating and flight rules. Change 8
[PB94-217445] p 940 N95-19720

EMISSION SPECTRA
A spectral study of a radio-frequency plasma-generated flux of atomic oxygen
[NASA-TM-4612] p 1032 N95-18194
The quiescent and flaring EUV spectrum of Algol and its relationship to other active coronae. EUV spectroscopy of bright hyades coronae: 71 Tauri and Theta 1 Tauri
[NASA-CR-197538] p 1178 N95-18391
Pure-rotational emission from molecular hydrogen in OMC-1 p 1179 N95-18500
Large amplitude motions, especially isomerization and tunneling in polyatomic molecule spectra: Novel experimental, pattern recognition, and theoretical methods
[AD-A284194] p 985 N95-18636
Development of lithium beam emission spectroscopy as an edge fluctuation diagnostic for D3-D
[DE94-017517] p 1146 N95-19378
Deep levels in AgGaSe2
[DE94-018209] p 1152 N95-19585

EMITTANCE
Exotic atoms: Muonic atoms into vacuum from solid hydrogen
[DE94-018255] p 1129 N95-18124
The effect of temperature on the radiative performance of Ho-YAG thin film selective emitters
[NASA-TM-106830] p 1053 N95-18587
Characterization of the 50 MeV ALS linac beam with optical transition radiation
[DE94-018208] p 1137 N95-19584

EMITTERS
The effect of temperature on the radiative performance of Ho-YAG thin film selective emitters
[NASA-TM-106830] p 1053 N95-18587
InP solar cell development on inexpensive silicon substrates
[AD-A286254] p 1054 N95-19388
Vacuum microelectronic emitters and their applications using compound semiconductor technology
[AD-A284811] p 1013 N95-19687

EMOTIONAL FACTORS
Is the pilot fit for flying after an accident? p 1083 N95-19425

END EFFECTORS
Space Station racks weight and CG measurement using the rack insertion end-effector p 966 N95-18168
Automated path planning of the Payload Inspection and Processing System p 1043 N95-18169
Rack Insertion End Effector (RIEE) guidance p 1043 N95-18178

ENDOTHERMIC REACTIONS
Electrochemical and spectroscopy studies of selected inorganic and organic systems in molten halides
[AD-A284171] p 974 N95-18514

ENERGETIC PARTICLES
Particle acceleration and transport in the tail and at the front side of the magnetosphere, task 1 and 2
[NASA-CR-197575] p 1064 N95-18476

ENERGY BUDGETS
Energy balance model for imagery and electromagnetic propagation
[AD-A284552] p 1063 N95-18115
Helicopter Performance Evaluation (HELPE) computer model
[AD-A284319] p 942 N95-18381

ENERGY CONVERSION
Direct energy conversion system for D(3)-He fusion
[DE94-770773] p 1146 N95-19549

ENERGY CONVERSION EFFICIENCY
Pulsed laser illumination of photovoltaic cells
[NASA-TM-106820] p 1053 N95-18572

ENERGY GAPS (SOLID STATE)
Graded bandgap semiconductor device for real-time imaging
[AD-D016543] p 1151 N95-19122
Giant effective mass deviations near the magnetic field-induced minigap in double quantum wells
[DE94-018889] p 1122 N95-19234
Optical determination of conduction and valence-band dispersion curves in strained single-quantum wells
[DE94-018892] p 1151 N95-19235
Energies of X conduction band minima in disordered and ordered GaInP2 alloys
[DE94-018211] p 1152 N95-19586

ENERGY LEVELS
Study of frustrated systems via dissipative maps
[DE94-017754] p 1122 N95-18127
Ionization of atoms by high energy photons
[DE94-018356] p 1130 N95-18427
High-pressure studies of deep impurities in GaAs, ZnSe, and related layered structures p 1150 N95-18908

ENERGY METHODS
Advanced statistical energy analysis p 1047 N95-19165

ENERGY SOURCES
Renewable energy and its potential for carbon emissions reductions in developing countries: Methodology for technology evaluation
[DE94-011870] p 1056 N95-17943

ENERGY SPECTRA
An instrument to measure the charge, and energy spectrum (20-1000 GeV/a) of the cosmic ray species oxygen to iron
[NASA-CR-197555] p 1197 N95-18464

ENERGY STORAGE
Metal/hydrogen energy storage: Selected technical issues
[AD-A283355] p 1008 N95-18052

ENERGY TECHNOLOGY
Renewable energy and its potential for carbon emissions reductions in developing countries: Methodology for technology evaluation
[DE94-011870] p 1056 N95-17943
Proceedings of the Eighth Annual Conference on Fossil Energy Materials
[DE95-001055] p 981 N95-19723
NREL Photovoltaic Program, FY 1993
[DE94-011880] p 1055 N95-19857

ENERGY TRANSFER
Innovative development and application of models for weakly ionized ionospheric plasmas
[AD-A284583] p 1064 N95-18452
An investigation of nonuniform dose deposition from an electron beam
[AD-A284175] p 1131 N95-18519
Spectroscopy and dynamics of vibrationally excited molecules
[AD-A285874] p 1134 N95-19597
Impact loading of compressor stator vanes by hailstone ingestion p 953 N95-19670
PRS projections for DECADE
[AD-A279215] p 1147 N95-19847

ENGINE AIRFRAME INTEGRATION
Impact of dynamic loads on propulsion integration p 1125 N95-19148

ENGINE CONTROL
Transient and steady-state tests of the space power research engine with resistive and motor loads
[NASA-TM-106832] p 1042 N95-19238
Neural net controller for inlet pressure control of rocket engine testing p 1102 N95-19637
Advanced diesel electronic fuel injection and turbocharging
[AD-A279176] p 1043 N95-19809

ENGINE DESIGN
Advanced diesel engine component development program, tasks 4-14
[NASA-CR-191203] p 1040 N95-18041
Wave cycle design for wave rotor engines with limited nitrogen oxide emissions p 1041 N95-18901
Data driven propulsion system weight prediction model p 968 N95-18980
Steady and unsteady blade stresses within the SSME ATD/HPOTP inducer p 968 N95-18982
Development of CFD model for augmented core tripropellant rocket engine p 968 N95-18988
Application of multidisciplinary models to the cooled turbine rotor design p 949 N95-19024
Perspective problems of gas turbine engines simulation p 949 N95-19026
Future directions in helicopter protection system configuration p 951 N95-19657
Navy foreign object damage and its impact on future gas turbine engine low pressure compression systems p 951 N95-19658
Design of fan blades subjected to bird impact p 953 N95-19669

ENGINE FAILURE
Modern transport engine experience with environmental ingestion effects p 951 N95-19660

ENGINE INLETS
Collection efficiency and ice accretion calculations for a sphere, a swept MS(1)-317 wing, a swept NACA-0012 wing tip, an axisymmetric inlet, and a Boeing 737-300
[NASA-TM-106831] p 933 N95-18582
Prediction of wind tunnel effects on the installed F/A-18A inlet flow field at high angles-of-attack
[NASA-CR-195429] p 950 N95-19651

ENGINE MONITORING INSTRUMENTS
An airborne monitoring system for FOD and erosion faults p 953 N95-19668

ENGINE PARTS
Advanced diesel engine component development program, tasks 4-14
[NASA-CR-191203] p 1040 N95-18041
Quality optimization of thermally sprayed coatings produced by the JP-5000 (HVOF) gun using mathematical modeling p 989 N95-19008
Mathematical Models of Gas Turbine Engines and their Components
[AGARD-LS-198] p 948 N95-19017

ENGINE TESTS
Unmanned aerial vehicle heavy fuel engine test
[AD-A284332] p 947 N95-18383
Airborne rotary separator study
[NASA-CR-191045] p 967 N95-18743
Neural net controller for inlet pressure control of rocket engine testing p 1102 N95-19637
Damage of high temperature components by dust-laden air p 953 N95-19673
Testing considerations for military aircraft engines in corrosive environments (a Navy perspective) p 955 N95-19684

ENGINEERS
NASA/DOD Aerospace Knowledge Diffusion Research Project. Report 26: The technical communication practices of aerospace engineering students: Results of the phase 3 AIAA National Student Survey
[NASA-TM-109121] p 1175 N95-18950
NASA/DOD Aerospace Knowledge Diffusion Research Project. Report 29: A comparison of the technical communications practices of Japanese and US aerospace engineers and scientists
[NASA-TM-109164] p 1175 N95-18953
NASA/DOD Aerospace Knowledge Diffusion Research Project. Paper 46: Technical communications in aerospace: A comparison across four countries
[NASA-TM-110056] p 1175 N95-19038

ENGINES
Data driven propulsion system weight prediction model p 968 N95-18980

ENTROPY
Applications of quantum entropy to statistics
[DE94-014416] p 1155 N95-17996

ENTROPY (STATISTICS)
Applications of quantum entropy to statistics
[DE94-014416] p 1155 N95-17996

ENVIRONMENT EFFECTS
Potential impacts on air quality of the use of ethanol as an alternative fuel
[DE94-011881] p 1056 N95-17944
One strategy for estimating the potential soil carbon storage due to CO2 fertilization
[DE94-017895] p 1059 N95-18666
Large area thermal target board: An improvement to environmental effects and system parameters characterization
[AD-A284614] p 1141 N95-19085

Alternative control techniques document: NO(x) emissions from glass manufacturing
[PB94-214079] p 1061 N95-19406
Modern transport engine experience with environmental ingestion effects p 951 N95-19660

ENVIRONMENT MANAGEMENT
Resources Automated Management System
[AD-A284153] p 1171 N95-18416
Development of a comprehensive base-level environmental training program for total environmental compliance
[AD-A284806] p 1061 N95-19686

ENVIRONMENT MODELS
High performance computing equipment for environmental remediation modeling and first principles simulation of materials properties
[DE95-000497] p 1093 N95-19875

ENVIRONMENT POLLUTION
Economic impact analysis for proposed emission standards and guidelines for municipal waste combustors: A description of the basis for, and impacts of, proposed revisions to air pollutant emission regulations for new and existing municipal waste combustors under Clean Air Act Sections 111(b), 111(d), and 129
[PB94-213543] p 1061 N95-19403

ENVIRONMENT PROTECTION
Catalog of environmental data sets of Europe at the RIVM
[PB94-202710] p 1057 N95-18002
Resources Automated Management System
[AD-A284153] p 1171 N95-18416
Environmental Compliance Assessment System (ECAS)
[AD-A283950] p 1060 N95-18683
Development of a comprehensive base-level environmental training program for total environmental compliance
[AD-A284806] p 1061 N95-19686
Environmental Compliance Assessment System (ECAS). South Carolina supplement: US Army
[AD-A279244] p 1062 N95-19860

ENVIRONMENT SIMULATION
Rain gauge calibration and testing
p 1070 N95-18209

ENVIRONMENTAL CONTROL
Analytical control test plan and microbiological methods for the water recovery test
[NASA-TM-108473] p 1091 N95-19061

ENVIRONMENTAL ENGINEERING
Annual historical report, calendar year 1993
[AD-A280178] p 1087 N95-19827

ENVIRONMENTAL MONITORING
Catalog of environmental data sets of Europe at the RIVM
[PB94-202710] p 1057 N95-18002
Assessment of CO2 projections
[DE94-017484] p 1059 N95-18664
Environmental Compliance Assessment System (ECAS)
[AD-A283950] p 1060 N95-18683
Economic impact analysis for proposed emission standards and guidelines for municipal waste combustors: A description of the basis for, and impacts of, proposed revisions to air pollutant emission regulations for new and existing municipal waste combustors under Clean Air Act Sections 111(b), 111(d), and 129
[PB94-213543] p 1061 N95-19403
Alternative control techniques document: NO(x) emissions from glass manufacturing
[PB94-214079] p 1061 N95-19406

ENVIRONMENTAL TESTS
Midinfrared optical properties of petroleum oil aerosols
[AD-A283689] p 1139 N95-18142
A real-time vision system to monitor/analyze the changes in composite specimens during mechanical testing
[ARL-TR-344] p 970 N95-18612
Effect of heat acclimation on sitting orthostatic tolerance in the heat after 48 and 96 hour bed rest in men
[NASA-TM-108861] p 1077 N95-18734
High-temperature acoustic test facilities and methods
p 1125 N95-19149
Design and operation of a thermoacoustic test facility
p 960 N95-19150

EPHEMERIDES
First principles used in orbital prediction and an atmospheric model comparison
[AD-A284636] p 1065 N95-19086

EPITAXY
Defect reduction and back channel degradation in SIMOX
[AD-A284231] p 1148 N95-17960
InP solar cell development on inexpensive silicon substrates
[AD-A283624] p 1052 N95-18011
Process for forming epitaxial BaF2 on GaAs
[AD-D016439] p 1149 N95-18527
Method of doping single crystal diamond for electronic devices
[AD-D016267] p 1149 N95-18543
Atomic Layer Epitaxy (ALE) apparatus for growing thin films of elemental semiconductors
[AD-D016236] p 1149 N95-18633
Heteroepitaxy of ternary SiGeC alloys on Si for bipolar transistors
[AD-A285317] p 1151 N95-19511
Industrial exploitation of a alternate technology for the production of HgCdTe epilayers, structures and devices
[AD-A279202] p 1154 N95-19816

EPOXY RESINS
Adherend surface effects on epoxy cure by NMR
[AD-A284774] p 985 N95-18442
Damage monitoring in metallic and composite structures using piezoelectric thin film sensors
[ARL-RR-4] p 971 N95-19467

EQUATIONS OF MOTION
General relativity and dark matter
[DE94-626641] p 1180 N95-18877
Particle trajectories in gas turbine engines
p 952 N95-19663

EQUATIONS OF STATE
Determination of stability and control derivatives from the NASA F/A-18 HARV from flight data using the maximum likelihood method
[NASA-CR-197320] p 958 N95-19576
Global equation of state for a glassy material: Fused silica
[DE94-018598] p 988 N95-19721

EQUILIBRIUM EQUATIONS
Partition method for the determination of multiple DC operating points
[PB94-201480] p 1009 N95-18501

EQUIPMENT
NASA property: Poor lending practices and controls at the Jet Propulsion Laboratory. Report to Congressional Requesters
[GAO/NSIAD-94-116] p 1172 N95-19141

EQUIPMENT SPECIFICATIONS
User profile for researchers studying objects: Implications for computer systems
[PB94-188463] p 1109 N95-17989
Mission description and in-flight operations of ERBE instruments on ERBS and NOAA 10 spacecraft, February 1987 - February 1990
[NASA-RP-1325] p 1051 N95-18465

EQUIVALENT CIRCUITS
Resonator/oscillator response to liquid loading
[DE94-013442] p 1012 N95-19240

ERGOMETERS
The cross-validation of the United States Air Force submaximal cycle ergometer test to estimate aerobic capacity
[AD-A284055] p 1079 N95-18661

EROSION
Erosion of melt layers developed during a plasma disruption
[DE94-018362] p 1144 N95-18547
Erosion, Corrosion and Foreign Object Damage Effects in Gas Turbines
[AGARD-CP-558] p 950 N95-19653
The operation of gas turbine engines in hot and sandy conditions: Royal Air Force experiences in the Gulf conflict p 950 N95-19655
US Army rotorcraft turboshaft engines sand and dust erosion considerations p 951 N95-19656
Experimental and numerical simulations of the effects of ingested particles in gas turbine engines
p 952 N95-19662
Particle trajectories in gas turbine engines
p 952 N95-19663
The calculation of erosion in a gas turbine compressor rotor p 952 N95-19664
Erosion of T56 5th stage rotor blades due to bleed hole overtip flow p 952 N95-19666
Investigation of mechanical erosion in fuel pipelines
p 952 N95-19667
An airborne monitoring system for FOD and erosion faults p 953 N95-19668
Analysis of the erosion of cubic centered and face centered metallic materials p 953 N95-19674
Gas turbine compressor corrosion and erosion in Western Europe p 954 N95-19678
High velocity oxygen fuel spraying of erosion and wear resistant coatings on jet engine parts
p 954 N95-19680
Resistance of silicon nitride turbine components to erosion and hot corrosion/oxidation attack
p 955 N95-19683

ERROR ANALYSIS
Error measurements in an Acousto-Optic Tunable Filter-Fiber Bragg Grating Sensor System
[AD-A283912] p 1139 N95-18154
Direct detection and coherent optical systems employing error-correction coding
[AD-A284350] p 1140 N95-18424
An analysis of tower (local) controller-pilot voice communications
[AD-A283718] p 996 N95-18436
Predicted coverage of a COFDM single frequency network for UHF digital terrestrial TV broadcasting
[BBC-RD-1993/12] p 999 N95-18540
The cross-validation of the United States Air Force submaximal cycle ergometer test to estimate aerobic capacity
[AD-A284055] p 1079 N95-18661
Dependence of medium-range forecast error on patterns in the initial state p 1072 N95-18732
Error coding simulations in C p 963 N95-18998
Digital monopulse
[AD-D016447] p 1002 N95-19072
Calibration and use of a non-nulling seven-hole pressure probe p 1021 N95-19254
Optical surface pressure measurements: Accuracy and application field evaluation p 1025 N95-19274
Simulation of wave propagation in three-dimensional random media
[NASA-CR-197605] p 1004 N95-19547
Measurement and proper equalization of range sidelobes using a spherical satellite as a reflector
[AD-A285955] p 1005 N95-19744

ERROR CORRECTING CODES
Digital video compression: Standardisation of scalable coding schemes
[BBC-RD-1994/10] p 1001 N95-19047
Bit-rate reduction of digital television for transmission: An introductory review
[BBC-RD-1994/2] p 1001 N95-19052

ERRORS
Determination of stores pointing error due to wing flexibility under flight load
[NASA-TM-4646] p 945 N95-19044
Development of pneumatic test techniques for subsonic high-lift and in-ground-effect wind tunnel investigations
p 932 N95-19268
Guidelines for reduction of human errors during maintenance of safety systems; maintainability and maintenance support
[PB94-215597] p 1092 N95-19412

ESCAPE SYSTEMS
Spine injuries: Up to date evaluation in aircraft ejections p 1084 N95-19434

ESTIMATES
Incorporating uncertainty and risk in rainfall-based flood estimates
[RR-CE144] p 1071 N95-18607
Multispectral NOAA Marine Atmospheric Boundary Layer (MABL) estimates during VOCAR
[AD-A283702] p 1064 N95-18623
The cross-validation of the United States Air Force submaximal cycle ergometer test to estimate aerobic capacity
[AD-A284055] p 1079 N95-18661

ESTIMATING
Detection performance of generalized likelihood ratio processors for random signals of unknown location, structure, extent, and strength
[AD-A285589] p 997 N95-18475
One strategy for estimating the potential soil carbon storage due to CO2 fertilization
[DE94-017895] p 1059 N95-18666
The accuracy of parameter estimation in system identification of noisy aircraft load measurement
[NASA-CR-197516] p 945 N95-19130
Estimating wind tunnel interference due to vectored jet flows p 1023 N95-19265

ESTUARIES
Kings Bay coastal and estuarine physical monitoring and evaluation program: Coastal studies. Volume 1: Main text and Appendix A
[AD-A285542] p 1074 N95-18470

ETALONS
Development of ultrashort optical pulse sources near 1.3 and 1.5 microns with an emphasis on stability, high repetition rate, and parallelism
[AD-A285535] p 1139 N95-18104

ETCHING
Tunneling and transport in mesoscopic structures
[AD-A283426] p 1148 N95-18053
Method for laser-assisted silicon etching using halocarbon ambients
[AD-D016239] p 1038 N95-18635
Using electrochemistry in device processing on poly(tetrafluoroethylene) substrates
[DE95-000541] p 975 N95-19559

ETHERS
Elemental fluorine based syntheses of pentafluoro phenly and other aromatic perfluoropolyether polymers [AD-A284102] p 984 N95-18402
Adherend surface effects on epoxy cure by NMR [AD-A284774] p 985 N95-18442
ETHYL ALCOHOL
The Solvent Absorption-Extractive Distillation (SAED) process for ethanol recovery from gas/vapor streams [DE94-013112] p 974 N95-18637
ETHYLENE
Ethylene dynamics in the CELSS biomass production chamber p 1077 N95-18179
Observations of methane and ethylene diffusion flames stabilized around a blowing porous sphere under microgravity conditions [NASA-TM-106766] p 990 N95-18211
Lithium electrode/polyacrylonitrile based polymer electrolyte interface [AD-A283947] p 986 N95-19064
ETIOLOGY
Centrifuge tests of the medical condition of French fighter pilots p 1082 N95-19424
EULER EQUATIONS OF MOTION
Searching for stationary stable solutions of Euler's equation [KNMI-WR-93-01] p 1017 N95-18396
A note on singularities of the 3-D Euler equation [NASA-CR-195006] p 1017 N95-18397
Theoretical investigations of shock/boundary layer interactions on a Ma(infinity) = 8 waverider [DLR-FB-94-12] p 930 N95-18910
The mathematical models of flow passage for gas turbine engines and their components p 948 N95-19020
An assessment of the adaptive unstructured tetrahedral grid, Euler Flow Solver Code FELISA [NASA-TP-3526] p 930 N95-19041
Basic equations of fluid dynamics p 1026 N95-19445
Computation of inviscid flows: Various approximations p 1027 N95-19446
Difference schemes for hyperbolic system of Conservation Laws p 1027 N95-19450
Finite volume method using Runge-Kutta time-stepping for solution of Euler equations p 1027 N95-19451
Computation of compressible flows: Implicit methods p 1027 N95-19452
Finite-volume upwind schemes for inviscid gas dynamics p 1028 N95-19456
Validation and evaluation of the advanced aeronautical CFD system SAUNA: A method developer's view [ARA-MEMO-390] p 1030 N95-19774
Verification of the CFD simulation system SAUNA for complex aircraft configurations [ARA-MEMO-401] p 1031 N95-19776
EURECA (ESA)
Main characteristics of the COMET/COMRADE experiments p 1181 N95-19179
EUROPE
Microgravity fluid science research in Europe [PB94-201720] p 990 N95-17973
EUROPEAN SPACE PROGRAMS
Main characteristics of the COMET/COMRADE experiments p 1181 N95-19179
EUTECTIC ALLOYS
NiAl and NiAl-based composites directionally solidified by a containerless zone process [NASA-CR-195430] p 982 N95-19792
EUTECTIC COMPOSITES
NiAl and NiAl-based composites directionally solidified by a containerless zone process [NASA-CR-195430] p 982 N95-19792
EVALUATION
EMEFS: Lessons learned 2, model evaluation [DE94-017468] p 1049 N95-18145
Helicopter Performance Evaluation (HELPE) computer model [AD-A284319] p 942 N95-18381
Evaluation of scanners for C-scan imaging in nondestructive inspection of aircraft [DE94-012473] p 990 N95-19100
Evaluation of powder metallurgy plates made by Sylvania Electric Products, Incorporated [DE94-017911] p 980 N95-19401
EVAPORATION
An unified program for calculating the fast neutron nuclear data for middle-heavy nuclei (MUP-3) [DE94-626822] p 1132 N95-18883
Constraints on chondrule and CAI origins from vapor-liquid-solid experiments p 1190 N95-19317
EVAPORATION RATE
Constraints on chondrule and CAI origins from vapor-liquid-solid experiments p 1190 N95-19317
EVOKED RESPONSE (PSYCHOPHYSIOLOGY)
Neurological decision making in aviation medicine based on electrophysiological methods p 1084 N95-19431
EVOLUTION (DEVELOPMENT)
Porphyritic versus nonporphyritic chondrules p 1190 N95-19318
Formation of chondrules and CAIs by nebular processes p 1190 N95-19321
EXCITATION
Laser wakefield excitation and measurement on a femtosecond time scale: Theory and experiment [DE94-019198] p 1129 N95-17976
Theoretical interpretation of the fluorescence spectra of toluene and p-cresol [AD-A284314] p 974 N95-19170
Electronic structure of C60 fullerites and nanotubes [DE95-000784] p 1151 N95-19569
Thermochemical IR sources: COCHISE and FACELIF experiments [AD-A279940] p 977 N95-19868
EXCITONS
An unified program for calculating the fast neutron nuclear data for middle-heavy nuclei (MUP-3) [DE94-626822] p 1132 N95-18883
EXHAUST EMISSION
Controlling combustion-source emissions at Air Force sites with a new filter concept, phase 1 [AD-A283674] p 1058 N95-18140
Assessment of CO2 projections [DE94-017484] p 1059 N95-18664
Atmospheric effects of high-flying subsonic aircraft: A catalogue of perturbing influences [KNMI-SR-94-03] p 1060 N95-18722
Wave cycle design for wave rotor engines with limited nitrogen oxide emissions p 1041 N95-18901
Alternative control techniques document: NO(x) emissions from glass manufacturing [PB94-214079] p 1061 N95-19406
Historic patterns of CO2 emissions from fossil fuels: Implications for stabilization of emissions [DE95-000489] p 1061 N95-19556
Air pollution mitigation measures for airports and associated activity [PB94-207610] p 1061 N95-19582
Developing an emission factor for hazardous air pollutants for an F-16 using JP-8 fuel [AD-A284802] p 1061 N95-19685
Advanced diesel electronic fuel injection and turbocharging [AD-A279176] p 1043 N95-19809
EXHAUST GASES
Controlling combustion-source emissions at Air Force sites with a new filter concept, phase 1 [AD-A283674] p 1058 N95-18140
Atmospheric effects of high-flying subsonic aircraft: A catalogue of perturbing influences [KNMI-SR-94-03] p 1060 N95-18722
Impact of dynamic loads on propulsion integration p 1125 N95-19148
Economic impact analysis for proposed emission standards and guidelines for municipal waste combustors: A description of the basis for, and impacts of, proposed revisions to air pollutant emission regulations for new and existing municipal waste combustors under Clean Air Act Sections 111(b), 111(d), and 129 [PB94-213543] p 1061 N95-19403
Alternative control techniques document: NO(x) emissions from glass manufacturing [PB94-214079] p 1061 N95-19406
Historic patterns of CO2 emissions from fossil fuels: Implications for stabilization of emissions [DE95-000489] p 1061 N95-19556
Developing an emission factor for hazardous air pollutants for an F-16 using JP-8 fuel [AD-A284802] p 1061 N95-19685
EXHAUST NOZZLES
Development of CFD model for augmented core tripropellant rocket engine p 968 N95-18988
EXHAUST SYSTEMS
Advanced diesel electronic fuel injection and turbocharging [AD-A279176] p 1043 N95-19809
EXOBIOLOGY
Aerospace medicine and biology: A continuing bibliography with indexes (supplement 397) [NASA-SP-7011(397)] p 1087 N95-19746
EXOTHERMIC REACTIONS
Method of lowering the reaction exotherm in thermally polymerized acetylene terminated resins [AD-D016276] p 985 N95-18430
Electrochemical and spectroscopy studies of selected inorganic and organic systems in molten halides [AD-A284171] p 974 N95-18514
EXPANSION
Investigation of mechanical erosion in fuel pipelines p 952 N95-19667
EXPERIMENT DESIGN
The 2 Micron All Sky Survey [AD-A283515] p 1178 N95-18001
SPICE: An innovative, flexible instrument concept p 966 N95-19189
Real-time remote scientific model validation p 1103 N95-19640
EXPERT SYSTEMS
Fusion of multiple sensing modalities for machine vision [AD-A284762] p 1091 N95-18086
Third CLIPS Conference Proceedings, volume 1 [NASA-CP-10162-VOL-1] p 1100 N95-19625
The Buffer Diagnostic Prototype: A fault isolation application using CLIPS p 1100 N95-19626
On the development of an expert system for wheelchair selection p 1092 N95-19627
Expert Witness: A system for developing expert medical testimony p 1101 N95-19628
The design and implementation of EPL: An event pattern language for active databases p 1101 N95-19629
CLIPS++: Embedding CLIPS into C++ p 1101 N95-19630
Expert system shell to reason on large amounts of data p 1101 N95-19631
AI and workflow automation: The prototype electronic purchase request system p 1101 N95-19632
A knowledge-based system for controlling automobile traffic p 1102 N95-19633
Development of an expert system for power quality advisement using CLIPS 6.0 p 1014 N95-19634
QPA-CLIPS: A language and representation for process control p 1102 N95-19635
Fuzzy expert systems using CLIPS p 1102 N95-19636
CLIPS template system for program understanding p 1102 N95-19638
Using expert systems to analyze ATE data p 1103 N95-19639
A CLIPS-based expert system for the evaluation and selection of robots p 1103 N95-19641
Adding intelligent services to an object oriented system p 1103 N95-19642
TARGET's role in knowledge acquisition, engineering, validation, and documentation p 1103 N95-19644
An expert system for configuring a network for a Milstar terminal p 1104 N95-19645
Expert system technologies for Space Shuttle decision support: Two case studies p 1104 N95-19646
The meteorological monitoring system for the Kennedy Space Center/Cape Canaveral Air Station p 1104 N95-19647
The use of genetic algorithms for flight test and evaluation of artificial intelligence and complex software systems [AD-A284824] p 1104 N95-19688
Third CLIPS Conference Proceedings, volume 2 [NASA-CP-10162-VOL-2] p 1104 N95-19747
Using PVM to host CLIPS in distributed environments p 1104 N95-19748
A parallel strategy for implementing real-time expert systems using CLIPS p 1105 N95-19749
Transport aircraft loading and balancing system: Using a CLIPS expert system for military aircraft load planning p 1105 N95-19751
Predicting and explaining the movement of mesoscale oceanographic features using CLIPS p 1105 N95-19752
Knowledge based translation and problem solving in an intelligent individualized instruction system p 1105 N95-19753
Character selecting advisor for a role-playing game p 1106 N95-19758
The Computer Aided Aircraft-design Package (CAAP) p 1106 N95-19759
Automated revision of CLIPS rule-bases p 1107 N95-19762
PCLIPS: Parallel CLIPS p 1107 N95-19764
Reflexive reasoning for distributed real-time systems p 1107 N95-19766
PalymSys (TM): An extended version of CLIPS for construction and reasoning using blackboards p 1107 N95-19767
DYNACLIPS (DYNAmic CLIPS): A dynamic knowledge exchange tool for intelligent agents p 1108 N95-19768
EXPLOITATION
A multiple time scale solution for the Chapman mechanism [DE94-017491] p 1060 N95-18895
Industrial exploitation of a alternate technology for the production of HgCdTe epilayers, structures and devices [AD-A279202] p 1154 N95-19816
EXPLOSIONS
A Type 2 supernovae constraint on neutrino(sub e) - neutrino(sub s) mixing [NASA-CR-197630] p 1180 N95-18746
Phase and amplitude controlled micropatch antenna [AD-A284191] p 1002 N95-19103

EXPLOSIVE DEVICES
Applications catalog of pyrotechnically actuated devices/systems
[NASA-TM-106810] p 962 N95-18387
EXPONENTS
Embedded microclusters in zeolites and cluster beam sputtering: Simulation on parallel computers
[DE95-000662] p 1134 N95-19562
Wentzel-Bardeen singularity in coupled Luttinger liquids: Transport properties
[DE95-000856] p 1152 N95-19621
EXPOSURE
Health hazards assessment for blast overpressure exposures
[AD-A283352] p 1078 N95-17998
Retinal injuries from single and multiple picosecond laser pulses
[AD-A284173] p 1078 N95-18515
Distributed medical database system for real-time monitoring of the health and risk exposure of military research study volunteers at USARIEM
[AD-A279193] p 1087 N95-19811
EXTERNAL STORES
Flight testing high lateral asymmetries on highly augmented Fighter/Attack aircraft
[AD-A284206] p 941 N95-17953
A study of the effect of store unsteady aerodynamics on gust and turbulence loads p 946 N95-18601
EXTERNAL TANKS
Microstructural analysis of cracks generated during welding of 2195 aluminum-lithium alloy
p 982 N95-19007
EXTINCTION
Shock-induced devolatization of calcium sulfate and implications for K-T extinctions
[NASA-CR-197608] p 1060 N95-19033
EXTRAPOLATION
Hypersonic flight testing
[AD-A283981] p 944 N95-18891
Historic patterns of CO2 emissions from fossil fuels: Implications for stabilization of emissions
[DE95-000489] p 1061 N95-19556
EXTRASENSORY PERCEPTION
Finite Markov chains and random discrete structures
[AD-A284192] p 1121 N95-19104
EXTRATERRESTRIAL ENVIRONMENTS
Fatigue loads spectra derivation for the Space Shuttle: Second cycle p 934 N95-19470
EXTRATERRESTRIAL MATTER
IRAS observations show that the Earth is embedded in a solar ring of asteroidal dust particles in resonant lock with the planet p 1182 N95-19181
Collection requirements for trace-element analyses of extraterrestrial samples p 1182 N95-19182
The intact capture of hypervelocity dust particles using underdense foams p 1183 N95-19188
EXTREME ULTRAVIOLET RADIATION
The quiescent and flaring EUV spectrum of Algol and its relationship to other active coronae. EUV spectroscopy of bright hyades coronae: 71 Tauri and Theta 1 Tauri
[NASA-CR-197538] p 1178 N95-18391
On orbit performance of the ALEXIS EUV telescopes
[DE94-016197] p 964 N95-18639
Relative elemental abundance and heating constraints determined for the solar corona from SERTS measurements
[NASA-TM-104616] p 1196 N95-19791
EXTREMELY LOW FREQUENCIES
Mechanisms of interaction and biological effects of extremely-low-frequency electromagnetic fields
[DE94-015200] p 1076 N95-18371
Handbook for the extremely low frequency (ELF) data acquisition and analysis system
[DSTO-GD-0021] p 1005 N95-19622
EYE PROTECTION
Color vision issues in modern military aviation or the search for the Abominable Coneman
p 1086 N95-19441

F

F 2 REGION
Investigation of the ionospheric short-term variability
[AD-A286253] p 1066 N95-19387
F-14 AIRCRAFT
Application of photogrammetry of F-14D store separation
[AD-A284154] p 943 N95-18417
F-16 AIRCRAFT
Developing an emission factor for hazardous air pollutants for an F-16 using JP-8 fuel
[AD-A284802] p 1061 N95-19685
F-18 AIRCRAFT
Flight testing high lateral asymmetries on highly augmented Fighter/Attack aircraft
[AD-A284206] p 941 N95-17953
Pressure measurements on an F/A-18 twin vertical tail in buffeting flow. Volume 4, part 2: Buffet cross spectral densities
[AD-A285555] p 957 N95-18641
Fiber Optic Control System integration for advanced aircraft. Electro-optic and sensor fabrication, integration, and environmental testing for flight control systems: Laboratory test results
[NASA-CR-195408] p 1034 N95-18938
Navier-Stokes, flight, and wind tunnel flow analysis for the F/A-18 aircraft
[NASA-TP-3478] p 931 N95-19114
Prediction of wind tunnel effects on the installed F/A-18A inlet flow field at high angles-of-attack
[NASA-CR-195429] p 950 N95-19651
F-4 AIRCRAFT
Application of photogrammetry of F-14D store separation
[AD-A284154] p 943 N95-18417
FABRICATION
Design and fabrication of N x N optical couplers based on organic polymer optical waveguides
[AD-A285530] p 1138 N95-18100
Superconductor microelectronic devices and circuits and a method of fabricating therefor
[AD-D016280] p 1009 N95-18433
The effect of fabrication on corrosion in aluminum 2195: Environmental and microstructural considerations
p 982 N95-19011
Inertial confinement fusion
[DE95-000314] p 1147 N95-19552
A simple single-photomask process for fabrication of high-efficiency multicrystalline silicon solar cells
[DE94-014251] p 1055 N95-19859
Advanced processing technology for high-efficiency, thin-film CuInSe2 and CdTe solar cells
[DE94-011838] p 1056 N95-19880
Silicon-Film (trademark) photovoltaic manufacturing technology
[DE94-011899] p 1056 N95-19882
FABRY-PEROT INTERFEROMETERS
The effects of cavity topology on instabilities in additive-pulse modelocked lasers
[DE94-018193] p 1036 N95-18123
FACE CENTERED CUBIC LATTICES
An atomic view of surface diffusion on metal surfaces
[DE94-016150] p 980 N95-19395
FAILURE
BEAM: A finite element program for the collapse analysis of vehicle structures
[AD-A285547] p 1045 N95-18472
Fracture behavior of large-scale thin-sheet aluminum alloy p 939 N95-19494
FAILURE ANALYSIS
Dynamic decohesion of bimaterials: Experimental observations and failure criteria
[GALCIT-94-2] p 1045 N95-18613
Can information surety be assessed with high confidence?
[DE94-015805] p 1120 N95-18653
FAILURE MODES
Study of failure in fibrous composites subjected to bending loads
[AD-A283330] p 969 N95-18028
Can information surety be assessed with high confidence?
[DE94-015805] p 1120 N95-18653
HEISHI: A fuel performance model for space nuclear applications
[DE94-017497] p 1137 N95-18897
Detecting gear tooth fracture in a high contact ratio face gear mesh
[NASA-TM-106822] p 1042 N95-19125
Soft body impact on titanium fan blades
p 953 N95-19671
Damage of high temperature components by dust-laden air p 953 N95-19673
FAINT OBJECTS
Rocket and laboratory studies in astronomy
[NASA-CR-197531] p 1177 N95-17981
FAN BLADES
Design of fan blades subjected to bird impact
p 953 N95-19669
Soft body impact on titanium fan blades
p 953 N95-19671
FAR FIELDS
Correction of support influences on measurements with sting mounted wind tunnel models p 933 N95-19281
FAR INFRARED RADIATION
Study for the analysis of the observations, and numerical data representing the planets as far-infrared calibration sources
[NASA-CR-196542] p 1195 N95-19287
FAST FOURIER TRANSFORMATIONS
Waveform bounding and combination techniques for direct drive testing
[AD-A284075] p 1000 N95-19035
A new stochastic systems approach to structural integrity p 935 N95-19474
Signal processing via Fourier-Bessel series expansion
[AD-A285316] p 1003 N95-19510
FAST NEUTRONS
An unified program for calculating the fast neutron nuclear data for middle-heavy nuclei (MUP-3)
[DE94-626822] p 1132 N95-18883
FAST NUCLEAR REACTORS
Fueled emitter, TFE Verification Program
[DE94-017557] p 1135 N95-18146
FASTENERS
Analysis of cold worked holes for structural life extension p 939 N95-19493
Split mandrel versus split sleeve coldworking: Dual methods for extending the fatigue life of metal structures
p 940 N95-19500
FATIGUE (MATERIALS)
Fatigue in single crystal nickel superalloys
[AD-A285727] p 978 N95-18068
Microstructure-based fatigue life prediction methods for naval steel structures
[AD-A284735] p 1044 N95-18081
On stationary and nonstationary fatigue load modeling using autoregressive moving average (ARMA) models
p 1046 N95-18919
Enhancement of creep resistance of a sintered Si3N4 ceramic by microwave annealing
[DE94-017688] p 987 N95-19399
FAA/NASA International Symposium on Advanced Structural Integrity Methods for Airframe Durability and Damage Tolerance, part 2
[NASA-CP-3274-PT-2] p 934 N95-19468
Fatigue loads spectra derivation for the Space Shuttle: Second cycle p 934 N95-19470
Prediction of fatique crack growth under flight-simulation loading with the modified CORPUS model
p 934 N95-19471
The characterization of widespread fatigue damage in fuselage structure p 935 N95-19472
Residual life and strength estimates of aircraft structural components with MSD/MED p 937 N95-19485
Near tip stress and strain fields for short elastic cracks p 937 N95-19487
Widespread fatigue damage monitoring: Issues and concerns p 938 N95-19488
Fatigue crack growth in 2024-T3 aluminum under tensile and transverse shear stresses p 938 N95-19490
On the measurement of the crack tip stress field as a means of determining Delta K(sub eff) under conditions of fatigue crack closure p 938 N95-19492
Fatigue and residual strength investigation of ARALL(R) -3 and GLARE(R) -2 panels with bonded stringers
p 939 N95-19495
Aircraft fatigue and crack growth considering loads by structural component p 939 N95-19497
Corrosion fatigue of iron-chromium-nickel alloys: Fracture mechanics, microstructure and chemistry
[DE95-000909] p 981 N95-19610
Investigation of microscopic mechanisms of failure of electronic smart materials/systems
[AD-A284830] p 988 N95-19691
Stress-intensity factor solutions for cracks at countersunk rivet holes under uniaxial tension
[AD-A279163] p 1047 N95-19804
FATIGUE LIFE
Microstructure-based fatigue life prediction methods for naval steel structures
[AD-A284735] p 1044 N95-18081
Current and future problems in structural acoustic fatigue p 1124 N95-19143
Brite-Euram programme: ACOUFAT acoustic fatigue and related damage tolerance of advanced composite and metallic structures p 1127 N95-19159
Prediction of fatique crack growth under flight-simulation loading with the modified CORPUS model
p 934 N95-19471
Discrete crack growth analysis methodology for through cracks in pressurized fuselage structures
p 935 N95-19473
Fatigue and damage tolerance scatter models
p 935 N95-19475
A probabilistic fatigue analysis of multiple site damage
p 935 N95-19476
Fatigue life until small cracks in aircraft structures: Durability and damage tolerance p 936 N95-19478

The application of Newman crack-closure model to predicting fatigue crack growth p 937 N95-19483
Residual life and strength estimates of aircraft structural components with MSD/MED p 937 N95-19485
Microstructurally based variations on the dwell fatgue life of titanium alloy IMI 834 p 938 N95-19489
Analysis of cold worked holes for structural life extension p 939 N95-19493
Split mandrel versus split sleeve coldworking: Dual methods for extending the fatigue life of metal structures p 940 N95-19500

FATIGUE TESTS
Detecting gear tooth fracture in a high contact ratio face gear mesh
[NASA-TM-106822] p 1042 N95-19125
High-temperature acoustic test facilities and methods p 1125 N95-19149
Acoustic fatigue testing on different materials and skin-stringer elements p 1126 N95-19156
Acoustic fatigue of carbon fibre structures p 1127 N95-19158
Brite-Euram programme: ACOUFAT acoustic fatigue and related damage tolerance of advanced composite and metallic structures p 1127 N95-19159
Acoustic fatigue behaviour of GLARE composites p 1127 N95-19160
Prediction of fatique crack growth under flight-simulation loading with the modified CORPUS model p 934 N95-19471
Evaluation of the fuselage lap joint fatigue and terminating action repair p 936 N95-19477
Development of load spectra for Airbus A330/A340 full scale fatigue tests p 936 N95-19479
An artifical corrosion protocol for lap-splices in aircraft skin p 937 N95-19482
Fatigue crack growth under variable amplitude loading p 937 N95-19484
Ultrasonic techniques for repair of aircraft structures with bonded composite patches p 937 N95-19486
Results of uniaxial and biaxial tests on riveted fuselage lap joint specimens p 938 N95-19491

FATTY ACIDS
The Solvent Absorption-Extractive Distillation (SAED) process for ethanol recovery from gas/vapor streams
[DE94-013112] p 974 N95-18637

FAULT DETECTION
LVQ and backpropagation neural networks applied to NASA SSME data
[NASA-CR-195418] p 962 N95-18045
Enhancements to the KATE model-based reasoning system p 1115 N95-18183
Lower bounds for identifying subset members with subset queries
[DE94-014296] p 1117 N95-18346
Radial basis function neural networks applied to NASA SSME data
[NASA-CR-195417] p 962 N95-18467
Detecting gear tooth fracture in a high contact ratio face gear mesh
[NASA-TM-106822] p 1042 N95-19125
The Buffer Diagnostic Prototype: A fault isolation application using CLIPS p 1100 N95-19626
An airborne monitoring system for FOD and erosion faults p 953 N95-19668

FAULT TOLERANCE
A fast recursive algorithm to compute the probability of M-out-of-N events
[AD-A283679] p 1120 N95-18020
A novel system level approach to fault tolerance in distributed memory multicomputers
[AD-A284729] p 1095 N95-18079
The Isis project: Fault-tolerance in large distributed systems
[NASA-CR-197561] p 1110 N95-18532
A general theory of signal integration for fault tolerant distributed sensor networks
[AD-A284825] p 1112 N95-19689

FAULT TREES
A fast recursive algorithm to compute the probability of M-out-of-N events
[AD-A283679] p 1120 N95-18020
Can information surety be assessed with high confidence?
[DE94-015805] p 1120 N95-18653
Improved approximation guarantees for minimum-weight k-trees and prize-collecting salesmen
[AD-A284042] p 1117 N95-18658

FEASIBILITY
Feasibility study of transmission of OTV camera control information in the video vertical blanking interval p 1006 N95-18185
The formulation of quantum statistical mechanics based on the Feynman path centroid density. 4: Algorithms for centroid molecular dynamics
[AD-A279234] p 1157 N95-19853

FEATHERING
Wind tunnel tests of a 42 inch diameter self-starting autogyro rotor
[AD-A279922] p 932 N95-19863

FEEDBACK
A hypertext-based Internet-assessable database for the MSFC Technology Transfer Office p 1165 N95-18986
Tunneling acoustic microscopy
[AD-A279160] p 1128 N95-19802

FEEDBACK CONTROL
Three-parameter tunable Tilt-Integral-Derivative (TID) controller
[NASA-CASE-NPO-18492-1-CU] p 1113 N95-18313
Real-time adaptive control of mixing in a plane shear layer
[AD-A285541] p 1018 N95-18469
Microgravity isolation system design: A modern control analysis framework
[NASA-TM-106803] p 927 N95-18486
Plant and controller optimization by convex methods
[AD-A283700] p 944 N95-18621
Steady and unsteady blade stresses within the SSME ATD/HPOTP inducer p 968 N95-18982
Sliding mode control method having terminal convergence in finite time
[NASA-CASE-NPO-18584-1-CU] p 1114 N95-19062
Improvement of a high current DC power supply system for testing the large scaled superconducting cables and magnets
[DE94-770767] p 1012 N95-19548
Algorithms for orbit control on SPEAR
[DE95-002868] p 1138 N95-19841

FEEDFORWARD CONTROL
Neural networks applications to control and computations p 1115 N95-18992

FERMIONS
Generation permutation symmetry and the quark mixing matrix
[PB95-108189] p 1132 N95-18643

FERRATES
Lithium ferrate and lithium cobaltate cathodes for molten carbonate fuel cells
[DE94-017079] p 1054 N95-19117

FERRIMAGNETIC MATERIALS
Integrated, nonvolatile, high-speed analog random access memory
[NASA-CASE-NPO-17998-2-CU] p 1093 N95-18963
Study of the ferrimagnetic and paramagnetic phases of magnetite measured by multiple neutron diffraction
[DE94-627031] p 1151 N95-19242

FERROELECTRICITY
Ferroelectric thin film bismuth titanate prepared from acetate precursors
[DE95-000538] p 988 N95-19558
Investigation of microscopic mechanisms of failure of electronic smart materials/systems
[AD-A284830] p 988 N95-19691
Materials for adaptive structural acoustic control, volume 3
[AD-A279223] p 1128 N95-19850
Barium strontium titanate and non-ferroelectric oxide ceramic composites for use in phased array antennas
[AD-A279225] p 972 N95-19851

FERROMAGNETIC MATERIALS
Integrated, nonvolatile, high-speed analog random access memory
[NASA-CASE-NPO-17998-2-CU] p 1093 N95-18963

FERTILIZATION
One strategy for estimating the potential soil carbon storage due to CO2 fertilization
[DE94-017895] p 1059 N95-18666

FIBER COMPOSITES
Sodium sulfate corrosion of silicon carbide fiber-reinforced calcium aluminosilicate glass-ceramic matrix composites
[AD-A283703] p 969 N95-18021
Study of failure in fibrous composites subjected to bending loads
[AD-A283330] p 969 N95-18028
Composites research in support of the NASP Institute for Composites (NIC)
[NASA-CR-197580] p 970 N95-18471
Further measurements of the sound insulations of metal-framed partitions
[BBC-RD-1994/7] p 998 N95-18534
Development of radiation-hardened ceramic composites for fusion applications
[DE94-016182] p 985 N95-18638
A CMC database for use in the next generation launch vehicles (rockets) p 963 N95-18993
Damage monitoring in metallic and composite structures using piezoelectric thin film sensors
[ARL-RR-4] p 971 N95-19467
Thermo-oxidative stability of graphite/PMR-15 composites: Effect of fiber surface modification on composite shear properties
[NASA-TM-4608] p 981 N95-19652

FIBER OPTICS
Polymer fibers for nonlinear optics
[AD-A284216] p 983 N95-17957
Gigabit optical interconnects: System and component analysis, design and development
[AD-A285538] p 1138 N95-18067
Error measurements in an Acousto-Optic Tunable Filter-Fiber Bragg Grating Sensor System
[AD-A283912] p 1139 N95-18154
The development of a fiber optics communication network for controlling a Multidegree-Of-Freedom Serpentine Truss p 1142 N95-18167
Feasibility study of transmission of OTV camera control information in the video vertical blanking interval p 1006 N95-18185
A fiber optic coupler
[AD-D016473] p 1140 N95-18459
Fiber optic pressure and/or vibration detector
[AD-D016474] p 1140 N95-18460
Multi-line passive fiber optic slipring
[AD-D016430] p 1141 N95-18560
Fiber optic flexural disk accelerometer
[AD-D016444] p 1141 N95-18563
Disengagable adapter for an optical fiber connection
[AD-D016231] p 1141 N95-18628
Advanced optical fiber communications systems
[AD-A283942] p 1141 N95-18682
Fiber Optic Control System integration for advanced aircraft. Electro-optic and sensor fabrication, integration, and environmental testing for flight control systems: Laboratory test results
[NASA-CR-195408] p 1034 N95-18938
Fiber Optic Control System integration for advanced aircraft. Electro-optic and sensor fabrication, integration, and environmental testing for flight control systems
[NASA-CR-191194] p 1034 N95-19236
Torque-balanced extendable fiber optic cable
[AD-D016496] p 1142 N95-19389
Scintillating-fiber imaging detector for 14-MeV neutrons
[DE94-018593] p 1135 N95-19709
High speed optical links between LLNL and Berkeley
[DE95-000552] p 1006 N95-19833

FIBER STRENGTH
Study of failure in fibrous composites subjected to bending loads
[AD-A283330] p 969 N95-18028
Development of radiation-hardened ceramic composites for fusion applications
[DE94-016182] p 985 N95-18638

FIBER-MATRIX INTERFACES
Thermo-oxidative stability of graphite/PMR-15 composites: Effect of fiber surface modification on composite shear properties
[NASA-TM-4608] p 981 N95-19652

FIELD COILS
Handbook for the extremely low frequency (ELF) data acquisition and analysis system
[DSTO-GD-0021] p 1005 N95-19622

FIELD EFFECT TRANSISTORS
Fault protection circuit for power switching device
[AD-D016466] p 1009 N95-18455
Method for fabricating complementary enhancement and depletion mode field effect transistors on a single substrate
[AD-D016270] p 1010 N95-18546
Second International Semiconductor Device Research Symposium (ISDRS-1993)
[AD-A279221] p 1013 N95-19849

FIELD OF VIEW
Liquid crystal tunable filter
[AD-A284383] p 1139 N95-18342
SeaWiFS technical report series. Volume 18: SeaWiFS technical report series cumulative index: Volumes 1-17
[NASA-TM-104566-VOL-18] p 1076 N95-19577

FIELD STRENGTH
Dynamic evolution of emerging magnetic flux tubes in the solar convective envelope p 1195 N95-18497

FIELD THEORY (PHYSICS)
Static and dynamic nuclear many-body descriptions on parallel architectures
[DE94-018134] p 1116 N95-18120
Towards a classification of su(2)(direct sum)...(direct sum)su(2) modular invariant partition functions
[PB94-217247] p 1119 N95-19717
Coulomb gas representation of the SU(2) WZW correlators at higher genera
[PB94-217254] p 1119 N95-19718
SU(2) WZW theory at higher genera
[PB94-217262] p 1119 N95-19719

Potential distributions for ellipsoidal bodies in uniform fields
[MRL-TR-92-48] p 1005 N95-19771

FIELDS
Improved approximation guarantees for minimum-weight k-trees and prize-collecting salesmen
[AD-A284042] p 1117 N95-18658

FIGHTER AIRCRAFT
Application of photogrammetry of F-14D store separation
[AD-A284154] p 943 N95-18417
Aircraft stress sequence development: A complex engineering process made simple p 936 N95-19480
Proceedings of the USAF Structural Integrity Program Conference
[AD-A285684] p 945 N95-19517

FILM COOLING
Particle deposition in gas turbine blade film cooling holes p 951 N95-19661

FILTRATION
Controlling combustion-source emissions at Air Force sites with a new filter concept, phase 1
[AD-A283674] p 1058 N95-18140
Improved filtration materials and modeling
[AD-A284684] p 1091 N95-18531

FINITE DIFFERENCE THEORY
Fast numerical determination of symmetric sparsity patterns
[DE94-016344] p 1096 N95-18354
Low-dissipation and -dispersion Runge-Kutta schemes for computational acoustics
[NASA-CR-195022] p 1018 N95-18488
Study of high gain spherical shell ICF targets containing uniform layers of liquid deuterium tritium fuel
[DE94-018550] p 1136 N95-18552
A numerical analysis of smoothed particle hydrodynamics
[AD-A284698] p 1019 N95-18562
Numerical simulation of shock/shock and shock/boundary-layer interactions in chemically reacting hypersonic flows
[DLR-94-04] p 1019 N95-18609
Static aerodynamics CFD analysis for 120-mm hypersonic KE projectile design
[ARL-MR-184] p 929 N95-18611
Thermal behavior spiral bevel gears
[NASA-TM-106518] p 1042 N95-18935
Computational simulation of liquid fuel rocket injectors p 968 N95-18989
Computation of inviscid flows: Full potential method p 1027 N95-19447
Difference schemes for hyperbolic system of Conservation Laws p 1027 N95-19450
Computation of compressible flows: Implicit methods p 1027 N95-19452
Spectral methods for fluid flow p 1028 N95-19459

FINITE ELEMENT METHOD
Finite element method for eigenvalue problems in electromagnetics
[NASA-TP-3485] p 995 N95-18187
Finite element modeling of partially delaminated composite beams with contact-impact conditions
[AD-A283726] p 1044 N95-18363
Prediction of buoyant outflow in lakes and fjords with a quasi 3D numerical model
[PB94-206984] p 1051 N95-18372
BEAM: A finite element program for the collapse analysis of vehicle structures
[AD-A285547] p 1045 N95-18472
A review of gust load calculation methods at de Havilland p 932 N95-18604
Long-term processes in geomaterials. A three-dimensional visco-elastic soil model
[PB94-207180] p 1065 N95-18640
QuikForm: Intelligent deformation processing of structural alloys
[DE94-018739] p 1114 N95-18649
CUBIT mesh generation environment
[DE94-017496] p 1118 N95-18896
Coupled finite element analysis of decomposing poroelastic polymeric composites and structures with subsequent thermal and gas diffusion p 986 N95-18918
Thermal behavior spiral bevel gears
[NASA-TM-106518] p 1042 N95-18935
A finite element code for electric motor design p 1014 N95-18974
Steady and unsteady blade stresses within the SSME ATD/HPOTP inducer p 968 N95-18982
Simulation of multidisciplinary problems for the thermostress state of cooled high temperature turbines p 948 N95-19021
Acoustics of space structures p 1126 N95-19152
Application of the PSD technique to acoustic fatigue stress calculations in complex substructures p 1126 N95-19155
Discrete crack growth analysis methodology for through cracks in pressurized fuselage structures p 935 N95-19473
Near tip stress and strain fields for short elastic cracks p 937 N95-19487
Widespread fatigue damage monitoring: Issues and concerns p 938 N95-19488
Fatigue crack growth in 2024-T3 aluminum under tensile and transverse shear stresses p 938 N95-19490
Prediction of R-curves from small coupon tests p 939 N95-19496
Using neural networks in the mapping of mixed discrete/continuous design spaces with application to structural design
[AD-A285328] p 1046 N95-19522
Unit cell geometry of multiaxial preforms for structural composites
[NASA-CR-197294] p 971 N95-19650
Soft body impact on titanium fan blades p 953 N95-19671
Ice-impact analysis of blades p 953 N95-19672
Simulation of thin slot spirals and dual circular patch antennas using the finite element method with mixed elements
[NASA-CR-197671] p 1005 N95-19796
Slot spiral antenna modeling using hybrid/mixed FE-BI technique p 1006 N95-19797
An efficient and accurate model of the coax cable feeding structure for FEM simulations p 1006 N95-19799
Arbitrarily shaped dual-stacked patch antennas: A hybrid FEM simulation p 1006 N95-19800
Performance of an artificial absorber for truncating FEM meshes p 1006 N95-19801

FINITE VOLUME METHOD
Finite volume method using Runge-Kutta time-stepping for solution of Euler equations p 1027 N95-19451
Finite-volume upwind schemes for inviscid gas dynamics p 1028 N95-19456
Pressure based finite volume algorithm for viscous flow computation p 1029 N95-19461

FINS
Integrated aerodynamic fin and stowable TVC vane system
[AD-D016457] p 967 N95-19073

FIRE (CLIMATOLOGY)
NASA Goddard Earth Sciences Graduate Student Program --- FIRE CIRRUS-II examination of coupling between an upper tropospheric cloud system and synoptic-scale dynamics
[NASA-CR-197130] p 1066 N95-19129

FIRE EXTINGUISHERS
Handheld delivery system for modified boron-type fire extinguishment agent
[AD-A283955] p 992 N95-18684

FIRE PREVENTION
Ignition and combustion of bulk metals in a microgravity environment
[NASA-CR-197519] p 990 N95-18082

FIRES
Handheld delivery system for modified boron-type fire extinguishment agent
[AD-A283955] p 992 N95-18684
On the conduct of fast cookoff tests in Australia
[AD-A284260] p 975 N95-19699

FIRING (IGNITING)
On the conduct of fast cookoff tests in Australia
[AD-A284260] p 975 N95-19699

FISSION
Lunar surface fission power supplies: Radiation issues
[DE94-014439] p 966 N95-17997

FISSION PRODUCTS
HEISHI: A fuel performance model for space nuclear applications
[DE94-017497] p 1137 N95-18897

FITTING
Floating shock fitting via Lagrangian adaptive meshes
[NASA-CR-194997] p 1116 N95-18110
A fiber optic coupler
[AD-D016473] p 1140 N95-18459

FIXTURES
Fixture for pressure testing sight glasses
[AD-D016263] p 1032 N95-18319

FLAME HOLDERS
Computation of vortex breakdown p 1029 N95-19462

FLAME PROPAGATION
Observations of methane and ethylene diffusion flames stabilized around a blowing porous sphere under microgravity conditions
[NASA-TM-106766] p 990 N95-18211
Flame position ultrasonic interferometer
[AD-D016235] p 967 N95-18632
VENTCF2: An algorithm and associated FORTRAN 77 subroutine for calculating flow through a horizontal ceiling/floor vent in a zone-type compartment fire model
[PB94-210127] p 993 N95-19402
Flamespreading in granular solid propellant: Initial results
[AD-A284245] p 976 N95-19729

FLAME RETARDANTS
Composite structures having organic matrices and duplex zinc/ceramic fire barriers
[AD-D016232] p 970 N95-18629

FLAME STABILITY
Observations of methane and ethylene diffusion flames stabilized around a blowing porous sphere under microgravity conditions
[NASA-TM-106766] p 990 N95-18211

FLAME TEMPERATURE
On the conduct of fast cookoff tests in Australia
[AD-A284260] p 975 N95-19699

FLAMMABILITY
Technology demonstration of single hydraulic fluid for armored ground vehicle systems
[AD-A280170] p 989 N95-19826

FLAPPING
Wind tunnel tests of a 42 inch diameter self-starting autogyro rotor
[AD-A279922] p 932 N95-19863

FLASH LAMPS
Performance improvements in diode laser arrays
[DE94-016547] p 1039 N95-19508

FLASH POINT
Technology demonstration of single hydraulic fluid for armored ground vehicle systems
[AD-A280170] p 989 N95-19826

FLASHING (VAPORIZING)
Flash heating is required to minimize sodium losses from chondrules p 1193 N95-19337

FLAT PLATES
The stability of two-phase flow over a swept-wing
[NASA-CR-194994] p 1016 N95-18190
Acoustic radiation damping of flat rectangular plates subjected to subsonic flows p 1123 N95-18542
Incompressible flow of a Newtonian fluid past a vertical plate with thermal and magnetic stresses
[AD-A284856] p 1030 N95-19716

FLATTENING
Study of strangeness production in relativistic nucleus beams at JINR
[DE94-626720] p 1136 N95-18881

FLAVOR (PARTICLE PHYSICS)
Family symmetries and proton decay
[DE94-017575] p 1133 N95-19245
Comment on the preprint Neutrino Flavor Evolution Near a Supernova's Core (Astro-Ph 9405008) by J. Pantaleone
[DE94-017576] p 1198 N95-19283
Baryon stopping in 200 GeV/A S+Au collisions
[DE94-018215] p 1134 N95-19587

FLEXIBILITY
Determination of stores pointing error due to wing flexibility under flight load
[NASA-TM-4646] p 945 N95-19044

FLEXIBLE BODIES
Streamlined design and self reliant hardware for active control of precision space structures
[NASA-CR-4637] p 964 N95-18580

FLEXING
Hydrofoil force balance
[AD-D016475] p 1033 N95-18461
Fiber optic flexural disk accelerometer
[AD-D016444] p 1141 N95-18563

FLIGHT ALTITUDE
Atmospheric effects of high-flying subsonic aircraft: A catalogue of perturbing influences
[KNMI-SR-94-03] p 1060 N95-18722

FLIGHT CHARACTERISTICS
Six degree of freedom flight dynamic and performance simulation of a remotely-piloted vehicle
[AERO-TN-9301] p 942 N95-18097
Flight parameters monitoring system for tracking structural integrity of rotary-wing aircraft p 934 N95-19469
Airship applications of modern flight test techniques
[AD-A284253] p 945 N95-19731

FLIGHT CONDITIONS
Product usage evaluation of the aviation gridded forecast system workstation at the Denver Center Weather Service Unit
[PB94-195922] p 1066 N95-17952
Helicopter Performance Evaluation (HELPE) computer model
[AD-A284319] p 942 N95-18381
Comparison of frequency response and perturbation methods to extract linear models from a nonlinear simulation
[AD-A284115] p 958 N95-18405

Flight parameters monitoring system for tracking structural integrity of rotary-wing aircraft
p 934 N95-19469

FLIGHT CONTROL
Flight testing high lateral asymmetries on highly augmented Fighter/Attack aircraft
[AD-A284206] p 941 N95-17953
VSTOL Systems Research Aircraft (VSRA) Harrier
[NASA-TM-110117] p 941 N95-18347
Fluid dynamic linear accelerometer
[AD-D016413] p 956 N95-18553
The impact of non-linear flight control systems on the prediction of aircraft loads due to turbulence
p 956 N95-18598
Treatment of non-linear systems by timeplane-transformed CT methods: The spectral gust method p 956 N95-18600
Design and flight test of a simplified control system for a transport helicopter p 958 N95-18902
Integrated aerodynamic fin and stowable TVC vane system
[AD-D016457] p 967 N95-19073
The use of genetic algorithms for flight test and evaluation of artificial intelligence and complex software systems
[AD-A284824] p 1104 N95-19688
Automation of hardware-in-the-loop testing of control systems for unmanned air vehicles
[AD-A284833] p 945 N95-19693

FLIGHT CREWS
Fit to fly: Analysis of the aeromedical disposition in aircrewmembers of the Spanish Armed Forces
p 1081 N95-19418
EKG in flight: Usefulness and limits for aircrew rehabilitation p 1082 N95-19422
Evaluation of the EKG's isoelectric T wave in Air Force pilots p 1082 N95-19423
Neuropsychophysiologic sequelae of mild head injury
p 1083 N95-19430
The EEG in the evaluation of applicants to aircrew members p 1084 N95-19432
Clinical basis for aeromedical decision-making: The EEG example p 1084 N95-19433
Spine injuries: Up to date evaluation in aircraft ejections p 1084 N95-19434
Clinical practice, diagnosis and therapy of intervertebral disk lesion: Importance to fitness for military flying duties
p 1084 N95-19435
Spinal nerve syndromes: The need to confirm the diagnosis with neurophysiological examinations
p 1085 N95-19436
Sarcoidosis in US military aviators
p 1085 N95-19438
Clinical basis for aeromedical decisions in aircrew HIV positive p 1086 N95-19440
Color vision issues in modern military aviation or the search for the Abominable Coneman
p 1086 N95-19441
Photorefractive Keratectomy (PRK) in the military aviator: An aeromedical expose p 1086 N95-19442
Medication in the course of active flying duty
p 1086 N95-19443

FLIGHT ENVELOPES
Flight testing high lateral asymmetries on highly augmented Fighter/Attack aircraft
[AD-A284206] p 941 N95-17953
Course module for AA201: Wing structural design project
[AD-A283618] p 944 N95-18616

FLIGHT FITNESS
Clinical practice, diagnosis and therapy of intervertebral disk lesion: Importance to fitness for military flying duties
p 1084 N95-19435
Spinal nerve syndromes: The need to confirm the diagnosis with neurophysiological examinations
p 1085 N95-19436
The aeromedical implications of supraventricular tachycardia p 1085 N95-19437
Sarcoidosis in US military aviators
p 1085 N95-19438
The aeromedical risk associated with asymptomatic cholelithiasis in USAF pilots and navigators
p 1085 N95-19439
Clinical basis for aeromedical decisions in aircrew HIV positive p 1086 N95-19440
Color vision issues in modern military aviation or the search for the Abominable Coneman
p 1086 N95-19441
Photorefractive Keratectomy (PRK) in the military aviator: An aeromedical expose p 1086 N95-19442
Medication in the course of active flying duty
p 1086 N95-19443

FLIGHT HAZARDS
Waveform bounding and combination techniques for direct drive testing
[AD-A284075] p 1000 N95-19035
Toward a new national weather service: Weather for those who fly
[PB94-214418] p 1072 N95-19407

FLIGHT SAFETY
Users guide for NASA Lewis Research Center DC-9 Reduced-Gravity Aircraft Program
[NASA-TM-106755] p 959 N95-18586
A study of the effect of store unsteady aerodynamics on gust and turbulence loads p 946 N95-18601
On-line handling of air traffic: Management, guidance and control
[AGARD-AG-321] p 941 N95-18927
Safety study: Commuter airline safety
[PB94-917004] p 933 N95-19132
Toward a new national weather service: Weather for those who fly
[PB94-214418] p 1072 N95-19407
The concept of aeronautical adaptability as developed by the US Navy p 1083 N95-19426
The NAMI syncope test battery and clinical decision-making in aviators with syncope
p 1083 N95-19428
Spinal nerve syndromes: The need to confirm the diagnosis with neurophysiological examinations
p 1085 N95-19436
The aeromedical risk associated with asymptomatic cholelithiasis in USAF pilots and navigators
p 1085 N95-19439
Clinical basis for aeromedical decisions in aircrew HIV positive p 1086 N95-19440
Color vision issues in modern military aviation or the search for the Abominable Coneman
p 1086 N95-19441
Medication in the course of active flying duty
p 1086 N95-19443
Federal aviation regulations, part 91. General operating and flight rules. Change 8
[PB94-217445] p 940 N95-19720

FLIGHT SIMULATION
Six degree of freedom flight dynamic and performance simulation of a remotely-piloted vehicle
[AERO-TN-9301] p 942 N95-18097
KC-135 cockpit modernization study. Phase 1: Equipment evaluation
[AD-A284099] p 942 N95-18398
Comparison of frequency response and perturbation methods to extract linear models from a nonlinear simulation
[AD-A284115] p 958 N95-18405
Virtual reality, an air combat T and E perspective
[AD-A284161] p 959 N95-18508
Age 60 study. Part 4: Experimental evaluation of pilot performance
[AD-A286248] p 1080 N95-19385
Development of load spectra for Airbus A330/A340 full scale fatigue tests p 936 N95-19479

FLIGHT SIMULATORS
Comparison of frequency response and perturbation methods to extract linear models from a nonlinear simulation
[AD-A284115] p 958 N95-18405
V-22 simulator evaluation for shipboard operations
[AD-A284156] p 943 N95-18505
F/A-18 simulation validation and verification: Making a good product even better
[AD-A283995] p 944 N95-18723
The generic simulation executive at Manned Flight Simulator
[AD-A283997] p 959 N95-18724
Helicopter in-flight simulation development and use in test pilot training
[AD-A283998] p 959 N95-18725
Assessing aircraft survivability to high frequency transient threats
[AD-A283999] p 944 N95-18726
A linear system identification and validation of an AH-64 Apache aeroelastic simulation model
p 959 N95-18903

FLIGHT STRESS (BIOLOGY)
US experiments flown on the Soviet biosatellite Cosmos 2044. Volume 1: Mission description, experiments K-7-01 - K-7-15
[NASA-TM-108802-VOL-1] p 1092 N95-18569

FLIGHT SURGEONS
Aeromedical risk management for aircrew
p 1080 N95-19414
The way to waivers in the BAF p 1081 N95-19415
The effect of special boards of flight surgeons on the evolution of US Naval flight standards
p 1081 N95-19417
Fit to fly: Analysis of the aeromedical disposition in aircrewmembers of the Spanish Armed Forces
p 1081 N95-19418

FLIGHT TESTS
Flight testing high lateral asymmetries on highly augmented Fighter/Attack aircraft
[AD-A284206] p 941 N95-17953
KC-135 cockpit modernization study. Phase 1: Equipment evaluation
[AD-A284099] p 942 N95-18398
Preliminary evaluation of the F/A-18 quantity/multiple envelope expansion
[AD-A284119] p 943 N95-18407
Tilt Rotor Unmanned Air Vehicle System (TRUS) demonstrator flight test program
[AD-A284151] p 943 N95-18415
KC-130 ANVIS/HUD assessment and symbology rationale
[AD-A284155] p 943 N95-18504
V-22 simulator evaluation for shipboard operations
[AD-A284156] p 943 N95-18505
Virtual reality, an air combat T and E perspective
[AD-A284161] p 959 N95-18508
Final results of the Advanced Photovoltaic Experiment flight test
[NASA-TM-106828] p 967 N95-18571
F/A-18 simulation validation and verification: Making a good product even better
[AD-A283995] p 944 N95-18723
Helicopter in-flight simulation development and use in test pilot training
[AD-A283998] p 959 N95-18725
Hypersonic flight testing
[AD-A283981] p 944 N95-18891
Design and flight test of a simplified control system for a transport helicopter p 958 N95-18902
NAWCAD photogrammetrics: Methods and applications for aviation test and evaluation
[AD-A284074] p 1034 N95-19071
Navier-Stokes, flight, and wind tunnel flow analysis for the F/A-18 aircraft
[NASA-TP-3478] p 931 N95-19114
Fiber Optic Control System integration for advanced aircraft. Electro-optic and sensor fabrication, integration, and environmental testing for flight control systems
[NASA-CR-191194] p 1034 N95-19236
The use of genetic algorithms for flight test and evaluation of artificial intelligence and complex software systems
[AD-A284824] p 1104 N95-19688
Airship applications of modern flight test techniques
[AD-A284253] p 945 N95-19731

FLIGHT TRAINING
Computer-based psychomotor tests in optimal training track assignment of student naval aviators
[AD-A283720] p 1089 N95-18414
Vestibular examination in pilots susceptible to motion sickness p 1083 N95-19427

FLIR DETECTORS
Proceedings of the 15th Annual Conference on Atmospheric Transmission Models
[AD-A279919] p 1142 N95-19862

FLOAT ZONES
Marangoni convection in a gravity-free silicon float zone
[NASA-CR-197600] p 991 N95-18913

FLOOD PREDICTIONS
Incorporating uncertainty and risk in rainfall-based flood estimates
[RR-CE144] p 1071 N95-18607

FLOODS
Incorporating uncertainty and risk in rainfall-based flood estimates
[RR-CE144] p 1071 N95-18607

FLOW CHARACTERISTICS
Numerical mixing calculations of confined reacting jet flows in a cylindrical duct
[NASA-TM-106736] p 947 N95-18133
A selection of experimental test cases for the validation of CFD codes. Supplement: Datasets A-E
[AGARD-AR-303-SUPPL] p 929 N95-18539
Navier-Stokes, flight, and wind tunnel flow analysis for the F/A-18 aircraft
[NASA-TP-3478] p 931 N95-19114
Discrete vortex method for computation of viscous incompressible flows p 1029 N95-19460

FLOW DISTORTION
The traditional and new methods of accounting for the factors distorting the flow over a model in large transonic wind tunnels p 1025 N95-19275

FLOW DISTRIBUTION
The diurnal cycle of high-frequency temperature variability at 0 deg 140 deg W on seasonal and interannual time scales
[AD-A283640] p 1074 N95-18012
A study of gas flow pattern, undercutting and torch modification in variable polarity plasma arc welding
[NASA-CR-196537] p 1040 N95-18056

An application of a two-equation model of turbulence to three-dimensional chemically reacting flows
[NASA-CR-195411] p 1015 N95-18107
Floating shock fitting via Lagrangian adaptive meshes
[NASA-CR-194997] p 1116 N95-18110
Numerical mixing calculations of confined reacting jet flows in a cylindrical duct
[NASA-TM-106736] p 947 N95-18133
Heuristic inference about flow directions in river networks
[INPE-5588-TDI/550] p 1050 N95-18214
Evolution of a collection of bubbles with application to wakes, bubble screens, and cloud noise
[AD-A283597] p 1017 N95-18434
On the geometry of visual correspondence
[AD-A285700] p 1140 N95-18478
Hypersonic flow-field measurements: Intrusive and nonintrusive
[AD-A283867] p 930 N95-18674
Computational simulation of liquid fuel rocket injectors
p 968 N95-18989
The crucial role of wall interference, support interference and flow field measurements in the development of advanced aircraft configurations p 1021 N95-19252
Applications of the five-hole probe technique for flow field surveys at the Institute for Aerospace Research
p 1021 N95-19255
Improvement and validation of an LDV system to perform measurements in laminar supersonic flows
p 1021 N95-19256
Aerodynamic investigation of the flow field in a 180 deg turn channel with sharp bend p 1021 N95-19257
The utilization of a high speed reflective visualization system in the study of transonic flow over a delta wing
p 932 N95-19259
Transonic and supersonic flowfield measurements about axisymmetric afterbodies for validation of advanced CFD codes p 932 N95-19260
Velocity measurements with hot-wires in a vortex-dominated flowfield p 932 N95-19261
Determination of solid/porous wall boundary conditions from wind tunnel data for computational fluid dynamics codes p 1023 N95-19266
Calculation of low speed wind tunnel wall interference from static pressure pipe measurements
p 1024 N95-19273
Evaluation of the EKG's isoelectric T wave in Air Force pilots p 1082 N95-19423
Parabolized Navier-Stokes solution of supersonic/hypersonic flows p 933 N95-19464
Parallel computations in hydro acoustics
[AD-A285900] p 1030 N95-19607
An oil flow study of the reference Shuttle-C configuration
[NASA-RP-1352] p 932 N95-19623
Prediction of wind tunnel effects on the installed F/A-18A inlet flow field at high angles-of-attack
[NASA-CR-195429] p 950 N95-19651

FLOW EQUATIONS
Steady potential solver for unsteady aerodynamic analyses p 949 N95-19382

FLOW GEOMETRY
Heuristic inference about flow directions in river networks
[INPE-5588-TDI/550] p 1050 N95-18214
Application of multicomponent models to flow passage simulation in multistage turbomachines and whole gas turbine engines p 948 N95-19022

FLOW MEASUREMENT
Method and flowmeter for unsteady fluid flow study
[AD-D016432] p 1015 N95-18112
7th International Symposium on Applications of Laser Techniques to Fluid Mechanics, volume 2
[AD-A285685] p 1018 N95-18477
Wall Interference, Support Interference and Flow Field Measurements
[AGARD-CP-535] p 1020 N95-19251
The crucial role of wall interference, support interference and flow field measurements in the development of advanced aircraft configurations p 1021 N95-19252
Particle Image Velocimetry: Principles, current applications and future prospects p 1021 N95-19253
Calibration and use of a non-nulling seven-hole pressure probe p 1021 N95-19254
Applications of the five-hole probe technique for flow field surveys at the Institute for Aerospace Research
p 1021 N95-19255
Improvement and validation of an LDV system to perform measurements in laminar supersonic flows
p 1021 N95-19256
Aerodynamic investigation of the flow field in a 180 deg turn channel with sharp bend p 1021 N95-19257
Experimental techniques for measuring transonic flow with a three dimensional laser velocimetry system. Application to determining the drag of a fuselage
p 1022 N95-19258
Transonic and supersonic flowfield measurements about axisymmetric afterbodies for validation of advanced CFD codes p 932 N95-19260

FLOW REGULATORS
Geometrical vapor blocker for parallel condensation tubes requiring subcooling
[NASA-CASE-MSC-22090-1] p 1017 N95-18323

FLOW STABILITY
The stability of two-phase flow over a swept-wing
[NASA-CR-194994] p 1016 N95-18190
A note on the wave action density of a viscous instability mode on a laminar free-shear flow
[NASA-TM-106771] p 1016 N95-18212
A numerical analysis of smoothed particle hydrodynamics
[AD-A284698] p 1019 N95-18562
The effect of stable stratification on three-dimensional structure in shear layers p 1019 N95-18921

FLOW VELOCITY
A study of gas flow pattern, undercutting and torch modification in variable polarity plasma arc welding
[NASA-CR-196537] p 1040 N95-18056
The application of the SAUNA CFD system to high and low speed vehicles
[ARA-MEMO-402] p 1031 N95-19778

FLOW VISUALIZATION
Overview of unsteady transonic wind tunnel test on a semispan straked delta wing oscillating in pitch
[AD-A284097] p 928 N95-18380
Hypersonic flow-field measurements: Intrusive and nonintrusive
[AD-A283867] p 930 N95-18674
Static investigation of two fluidic thrust-vectoring concepts on a two-dimensional convergent-divergent nozzle
[NASA-TM-4574] p 931 N95-19042
Hypervelocity air flows with finite rate chemistry
[AD-A284727] p 931 N95-19109
The crucial role of wall interference, support interference and flow field measurements in the development of advanced aircraft configurations p 1021 N95-19252
The utilization of a high speed reflective visualization system in the study of transonic flow over a delta wing
p 932 N95-19259
An oil flow study of the reference Shuttle-C configuration
[NASA-RP-1352] p 932 N95-19623

FLOWMETERS
Method and flowmeter for unsteady fluid flow study
[AD-D016432] p 1015 N95-18112

FLUENCE
CRRESPRO documentation
[AD-A284578] p 1178 N95-18451

FLUID BOUNDARIES
Stratified carrier electroviscous fluids and apparatus
[AD-D016238] p 1019 N95-18634

FLUID DYNAMICS
Evolution of a collection of bubbles with application to wakes, bubble screens, and cloud noise
[AD-A283597] p 1017 N95-18434
Method and system for identifying the onset of a turbulent boundary layer induced by a body moving through a fluid medium
[AD-D016434] p 1018 N95-18526
Fluid dynamic linear accelerometer
[AD-D016413] p 956 N95-18553
Establishment of an Institute for Fusion Studies
[DE94-017330] p 1145 N95-19079
Basic equations of fluid dynamics
p 1026 N95-19445
Computation of inviscid flows: Various approximations
p 1027 N95-19446
Computation of vortex breakdown
p 1029 N95-19462
Investigation of mechanical erosion in fuel pipelines
p 952 N95-19667
Incompressible flow of a Newtonian fluid past a vertical plate with thermal and magnetic stresses
[AD-A284856] p 1030 N95-19716

FLUID FILMS
Rewetting of monogroove heat pipe in Space Station radiators
[NASA-CR-197579] p 1014 N95-18092
Wormgear geometry adopted for implementing hydrostatic lubrication and formulation of the lubrication problem
[NASA-CR-195416] p 1043 N95-19567

FLUID FLOW
Hydrofoil force balance
[AD-D016475] p 1033 N95-18461
7th International Symposium on Applications of Laser Techniques to Fluid Mechanics, volume 2
[AD-A285685] p 1018 N95-18477
Fluid dynamic linear accelerometer
[AD-D016413] p 956 N95-18553
Spectral methods for fluid flow p 1028 N95-19459
Computation of vortex breakdown
p 1029 N95-19462
An oil flow study of the reference Shuttle-C configuration
[NASA-RP-1352] p 932 N95-19623

FLUID MECHANICS
Microgravity fluid science research in Europe
[PB94-201720] p 990 N95-17973
7th International Symposium on Applications of Laser Techniques to Fluid Mechanics, volume 2
[AD-A285685] p 1018 N95-18477
Aeromechanics technology, volume 1. Task 1: Three-dimensional Euler/Navier-Stokes Aerodynamic Method (TEAM) enhancements
[AD-A285713] p 943 N95-18483
Stratified carrier electroviscous fluids and apparatus
[AD-D016238] p 1019 N95-18634
Numerical analysis of dissipative dynamical systems in solid and fluid mechnaics, with a special emphasis on coupled problems p 1122 N95-18916

FLUID PRESSURE
Fixture for pressure testing sight glasses
[AD-D016263] p 1032 N95-18319

FLUID-SOLID INTERACTIONS
Investigation of mechanical erosion in fuel pipelines
p 952 N95-19667

FLUIDICS
Static investigation of two fluidic thrust-vectoring concepts on a two-dimensional convergent-divergent nozzle
[NASA-TM-4574] p 931 N95-19042

FLUORESCENCE
Enhancement of fluorescence detection in chromatographic methods by computer analysis of second order data
[DE94-014682] p 973 N95-17966
Visible-infrared remote-sensing model and applications for ocean waters
[NASA-CR-197602] p 1051 N95-18739
Theoretical interpretation of the fluorescence spectra of toluene and p-cresol
[AD-A284314] p 974 N95-19170

FLUORINE
Elemental fluorine based syntheses of pentafluoro phenly and other aromatic perfluoropolyether polymers
[AD-A284102] p 984 N95-18402

FLUORO COMPOUNDS
Difunctional monomers based on perfluoropropylene telomers
[AD-A283677] p 983 N95-18019

FLUX DENSITY
Study for the analysis of the observations, and numerical data representing the planets as far-infrared calibration sources
[NASA-CR-196542] p 1195 N95-19287
The very low energy solar flux of electron and heavy-flavor neutrinos and antineutrinos
[DE94-018583] p 1135 N95-19706

FLY BY LIGHT CONTROL
Fiber Optic Control System integration for advanced aircraft. Electro-optic and sensor fabrication, integration, and environmental testing for flight control systems: Laboratory test results
[NASA-CR-195408] p 1034 N95-18938
Fiber Optic Control System integration for advanced aircraft. Electro-optic and sensor fabrication, integration, and environmental testing for flight control systems
[NASA-CR-191194] p 1034 N95-19236

FLY BY WIRE CONTROL
Development of a bipolar lead/acid battery for the more electric aircraft
[AD-A284050] p 1010 N95-18660
NASA develops new digital flight control system
[NASA-NEWS-RELEASE-94-47] p 958 N95-19029

FLYBY MISSIONS
Workshop on Particle Capture, Recovery and Velocity/Trajectory Measurement Technologies
[NASA-CR-197592] p 1180 N95-19172
SOCCER: Comet Coma Sample Return Mission
p 1181 N95-19174
The status of measurement technologies concerning micrometer and submicrometer space articulate matter capture, recovery, velocity and trajectory
p 1181 N95-19175

FLYING PERSONNEL
The waiver process and disqualifying medical conditions in US Naval aviation personnel p 1081 N95-19416
AMDRS: A resource for intelligent aeromedical decision-making p 1082 N95-19419

FOAMS
Physics of spacecraft-based interplanetary dust collection by impact into low-density media
p 1181 N95-19176
The intact capture of hypervelocity dust particles using underdense foams p 1183 N95-19188

FOCAL PLANE DEVICES
IR materials producibility
[AD-A284263] p 1142 N95-19732
FOCUSING
Multi-line passive fiber optic slipring
[AD-D016430] p 1141 N95-18560
FOG
Midinfrared optical properties of petroleum oil aerosols
[AD-A283689] p 1139 N95-18142
FOILS (MATERIALS)
Charge collection during hypervelocity penetrations of thin foils p 1036 N95-19190
FORBUSH DECREASES
Heliospheric 2-3 kHz radio emissions and their relationship to large Forbush decreases
[U-OF-IOWA-94-19] p 1195 N95-17979
FORCE DISTRIBUTION
Hydrofoil force balance
[AD-D016475] p 1033 N95-18461
FORCED VIBRATION
Vibration (?) spikes during natural rain events p 1069 N95-18206
Forced response of mistuned bladed disks p 950 N95-19383
FORECASTING
US Industrial Outlook, 1994: An almanac of industry, technology and services. 35th annual edition. Forecasts for selected manufacturing and service industries
[PB94-107844] p 1171 N95-17988
FOREIGN BODIES
Erosion, Corrosion and Foreign Object Damage Effects in Gas Turbines
[AGARD-CP-558] p 950 N95-19653
FORM FACTORS
He-4 electromagnetic structure in unitary and analytic VMD model with strict OZI rule
[DE94-626716] p 996 N95-18367
FORMALISM
Using CLIPS in the domain of knowledge-based massively parallel programming p 1105 N95-19750
The formulation of quantum statistical mechanics based on the Feynman path centroid density. 3: Phase space formalism and analysis of centroid molecular dynamics
[AD-A279233] p 1157 N95-19852
FORMAT
Digital mapping, charting, and geodesy analysis program technical review of Raster Product Format (RPF) and Scanned Map (SMap)
[AD-A284267] p 1052 N95-19733
Programmable cockpit research simulator
[AD-A279219] p 960 N95-19848
FORMATION
The early Sun and the formation of chondrules p 1188 N95-19305
FORSTERITE
Relict grains in chondrules: Evidence for chondrule recycling p 1188 N95-19307
FORTRAN
Study of a Navier-Stokes computer
[AD-A284196] p 1092 N95-17939
Digital mapping, charting, and geodesy analysis program technical review of Digital Aeronautical Flight Information Data Prototype 1.0 on CD-ROM
[AD-A284728] p 1050 N95-18078
HEISHI: A fuel performance model for space nuclear applications
[DE94-017497] p 1137 N95-18897
FORWARD SCATTERING
Time spread and frequency coherence in acoustic forward scattering from the sea surface
[AD-A284736] p 1123 N95-18083
FOSSIL FUELS
Historic patterns of CO2 emissions from fossil fuels: Implications for stabilization of emissions
[DE95-000489] p 1061 N95-19556
Proceedings of the Eighth Annual Conference on Fossil Energy Materials
[DE95-001055] p 981 N95-19723
FOSSILS
Proceedings of the Eighth Annual Conference on Fossil Energy Materials
[DE95-001055] p 981 N95-19723
FOUR-WAVE MIXING
AASERT-93: New high-pressure diagnostic technique
[AD-A284943] p 973 N95-17975
Ultrafast nonlinear optical response of Fano resonances in gallium arsenide under high magnetic field
[DE94-018181] p 1148 N95-18122
FOURIER ANALYSIS
Low-dissipation and -dispersion Runge-Kutta schemes for computational acoustics
[NASA-CR-195022] p 1018 N95-18488
Theory and applications of the phi transform wavelets
[AD-A279943] p 1119 N95-19869
FOURIER SERIES
Compression strength of composite primary structural components
[NASA-CR-197554] p 1044 N95-18388
Spectral methods for fluid flow p 1028 N95-19459
Signal processing via Fourier-Bessel series expansion
[AD-A285316] p 1003 N95-19510
FOURIER TRANSFORMATION
Design, validation and prototype testing of a high resolution all-reflection Michelson interferometer for solar occultation measurements of the OI 1304-a triplet emission
[AD-A283705] p 1178 N95-18361
A new multi-dimensional transform for digital signal processing using generalized association schemes
[AD-A284166] p 1117 N95-18511
Statistics of complex cross spectrum estimate for sinusoidal signals and arbitrary noise spectra
[AD-A283984] p 1120 N95-19065
Mass spectrometric studies of clusters and surfaces
[AD-A283992] p 974 N95-19066
A 2D depth migration in transversely isotropic media using explicit operators
[DE95-000645] p 1066 N95-19560
The interaction of two narrow magnets and a moving conducting slip
[DE94-018575] p 1122 N95-19704
Theory and applications of the phi transform wavelets
[AD-A279943] p 1119 N95-19869
FRACTIONATION
The role of chondrules in nebular fractionations of volatiles and other elements p 1187 N95-19300
Constraints on chondrule and CAI origins from vapor-liquid-solid experiments p 1190 N95-19317
Siderophile elements and metal-silicate fractionation in the solar nebula p 1190 N95-19319
Heating during solar nebula formation and Mg isotopic fractionation in precursor grains of CAIs and chondrules p 1191 N95-19326
FRACTOGRAPHY
The characterization of widespread fatigue damage in fuselage structure p 935 N95-19472
FRACTURE MECHANICS
Composites research in support of the NASP Institute for Composites (NIC)
[NASA-CR-197580] p 970 N95-18471
A real-time vision system to monitor/analyze the changes in composite specimens during mechanical testing
[ARL-TR-344] p 970 N95-18612
Dynamic decohesion of bimaterials: Experimental observations and failure criteria
[GALCIT-94-2] p 1045 N95-18613
Development of radiation-hardened ceramic composites for fusion applications
[DE94-016182] p 985 N95-18638
A boundary element method for two dimensional linear elastic fracture analysis p 1045 N95-18917
On the theory of stick-slip fracture p 1046 N95-18922
J-integral characterization of the nozzle steels from intermediate test vessels IV-5 and IV-9
[DE95-001066] p 979 N95-18934
FAA/NASA International Symposium on Advanced Structural Integrity Methods for Airframe Durability and Damage Tolerance, part 2
[NASA-CP-3274-PT-2] p 934 N95-19468
Fatigue and damage tolerance scatter models p 935 N95-19475
The load separation technique in the elastic-plastic fracture analysis of two- and three-dimensional geometries p 936 N95-19481
The application of Newman crack-closure model to predicting fatigue crack growth p 937 N95-19483
Fatigue crack growth under variable amplitude loading p 937 N95-19484
Fracture behavior of large-scale thin-sheet aluminum alloy p 939 N95-19494
Corrosion fatigue of iron-chromium-nickel alloys: Fracture mechanics, microstructure and chemistry
[DE95-000909] p 981 N95-19610
Driving force analysis in an infinite anisotropic plate with multiple crack interactions
[NASA-TM-106838] p 972 N95-19782
NiAl and NiAl-based composites directionally solidified by a containerless zone process
[NASA-CR-195430] p 982 N95-19792
FRACTURE STRENGTH
On the theory of stick-slip fracture p 1046 N95-18922
Fracture toughness of polymer/polymer bimaterial interface reinforced with block copolymers p 986 N95-18923
J-integral characterization of the nozzle steels from intermediate test vessels IV-5 and IV-9
[DE95-001066] p 979 N95-18934
Design of advanced steels for armor applications
[ARL-CR-175] p 979 N95-18948
A CMC database for use in the next generation launch vehicles (rockets) p 963 N95-18993
Prediction of R-curves from small coupon tests p 939 N95-19496
NiAl and NiAl-based composites directionally solidified by a containerless zone process
[NASA-CR-195430] p 982 N95-19792
Stress-intensity factor solutions for cracks at countersunk rivet holes under uniaxial tension
[AD-A279163] p 1047 N95-19804
FRACTURES (MATERIALS)
A boundary element method for two dimensional linear elastic fracture analysis p 1045 N95-18917
Detecting gear tooth fracture in a high contact ratio face gear mesh
[NASA-TM-106822] p 1042 N95-19125
FRACTURING
International Conference on Deformation, Yield and Fracture of Polymers
[AD-A284354] p 984 N95-18339
Fracture behavior of large-scale thin-sheet aluminum alloy p 939 N95-19494
Embedded microclusters in zeolites and cluster beam sputtering: Simulation on parallel computers
[DE95-000662] p 1134 N95-19562
NiAl and NiAl-based composites directionally solidified by a containerless zone process
[NASA-CR-195430] p 982 N95-19792
FRAGMENTATION
The interactions of high-energy, highly charged Xe ions with fullerenes
[DE95-001440] p 1135 N95-19786
FRAGMENTS
Facilitation and interference in identification of pictures and words
[AD-A285882] p 1090 N95-19602
FRAMES
The sound insulations of metal-framed partitions having structural loadbearing properties
[BBC-RD-1994/8] p 992 N95-18533
Further measurements of the sound insulations of metal-framed partitions
[BBC-RD-1994/7] p 998 N95-18534
FRAMING CAMERAS
Implementation of 40-ps high-speed gated-microchannel-plate based x-ray framing cameras on reentrant SIM's for Nova
[DE94-018597] p 1033 N95-18555
High-frame-rate intensified fast optically shuttered TV cameras with selected imaging applications
[DE94-016098] p 1035 N95-19394
Gain uniformity, linearity, saturation and depletion in gated microchannel-plate x-ray framing cameras
[DE94-018596] p 1035 N95-19711
FREE ELECTRON LASERS
Mathematical analysis of three free-electron-laser issues
[AD-A284122] p 1037 N95-18408
Pulsed laser illumination of photovoltaic cells
[NASA-TM-106820] p 1053 N95-18572
Microcavity structures
[DE95-001096] p 1039 N95-19727
FREE JETS
Flow field investigation in a free jet - free jet core system for the generation of high intensity molecular beams
[DLR-FB-94-11] p 1132 N95-18912
FREE VIBRATION
Plate vibration with arbitrarily oriented stiffeners based on Mindlin-Engesser formulation
[RR-CE143] p 1045 N95-18608
Free vibration analysis of partially filled liquid storage tanks
[DE94-012456] p 1020 N95-19098
FREE-PISTON ENGINES
Transient and steady-state tests of the space power research engine with resistive and motor loads
[NASA-TM-106832] p 1042 N95-19238
FREQUENCIES
Time spread and frequency coherence in acoustic forward scattering from the sea surface
[AD-A284736] p 1123 N95-18083
High power phase conjugated solid state lasers
[DE94-016633] p 1037 N95-18357
Local spatio-temporal analysis in vision systems
[AD-A284162] p 1140 N95-18509
IONCAP prediction-based Automatic Link Establishment (ALE) frequency selection for a ten-node Australian high-frequency network
[AD-A283698] p 999 N95-18619
Digital audio broadcasting: Comparison of coverage at different frequencies and with different bandwidths
[BBC-RD-1993/11] p 1002 N95-19135

Sandia National Laboratories' high power electromagnetic impulse sources
[DE95-000423] p 1004 N95-19555
Field-emitter arrays for RF vacuum microelectronics
[AD-A279932] p 1013 N95-19865

FREQUENCY CONTROL
Phase and amplitude controlled micropatch antenna
[AD-A284191] p 1002 N95-19103
Quartz crystal resonators and oscillators for frequency control and timing applications. A tutorial
[AD-A284995] p 1012 N95-19519

FREQUENCY CONVERTERS
1994 IEEE Nonlinear Optics: Materials Fundamental and Applications Conference
[AD-A285769] p 1139 N95-18345

FREQUENCY DIVISION MULTIPLEXING
Double-loop frequency selective surfaces for multi frequency division multiplexing in a dual reflector antenna
[NASA-CASE-NPO-18701-2-CU] p 1000 N95-18960

FREQUENCY HOPPING
Doppler shift and spread study for ionospherically propagated signals
[AD-A284610] p 1065 N95-19083

FREQUENCY MODULATION
Implementation of amplitude modulation companding using a digital signal processor
[BBC-RD-1994/1] p 998 N95-18536
Quartz crystal resonators and oscillators for frequency control and timing applications. A tutorial
[AD-A284995] p 1012 N95-19519
Signal enhancement in AM-FM interference
[AD-A285114] p 1004 N95-19565

FREQUENCY RESPONSE
Comparison of frequency response and perturbation methods to extract linear models from a nonlinear simulation
[AD-A284115] p 958 N95-18405
Pulsed laser illumination of photovoltaic cells
[NASA-TM-106820] p 1053 N95-18572
Comparison of stochastic and deterministic nonlinear gust analysis methods to meet continuous turbulence criteria p 946 N95-18602
Current loop signal conditioning: Practical applications
[NASA-TM-4636] p 1033 N95-18735
Optimum dimension ratios for studios, control rooms and listening rooms
[BBC-RD-1993/8] p 993 N95-19053

FREQUENCY SHIFT
Doppler shift and spread study for ionospherically propagated signals
[AD-A284610] p 1065 N95-19083

FREQUENCY STANDARDS
Quartz crystal resonators and oscillators for frequency control and timing applications. A tutorial
[AD-A284995] p 1012 N95-19519

FRICTION
Nonlinear magnetohydrodynamics
[DE94-016223] p 1143 N95-18353
Adhesion, friction, and wear behavior of clean metal-ceramic couples
[NASA-TM-106815] p 989 N95-19783
Use of titanate coupling agents in Kevlar (trade name)/phenolic composites
[AD-A279200] p 972 N95-19814

FRIT
The metallurgical integrity of the frit vent assembly diffusion bond
[DE95-000610] p 968 N95-19877

FUEL CAPSULES
The metallurgical integrity of the frit vent assembly diffusion bond
[DE95-000610] p 968 N95-19877

FUEL CELLS
Methane conversion by solid electrolyte membranes
[PB94-191781] p 973 N95-17982
Novel carbon-ion fuel cells
[DE94-017390] p 1053 N95-18894
Molten carbonate fuel cell with high power density
[DE94-017080] p 1053 N95-19074
Sealant materials for the solid oxide fuel cell
[DE94-017073] p 1053 N95-19115
Pitting corrosion of aluminized seals in molten carbonate fuel cells
[DE94-017075] p 1053 N95-19116
Lithium ferrate and lithium cobaltate cathodes for molten carbonate fuel cells
[DE94-017079] p 1054 N95-19117
Alternative materials for solid oxide fuel cells
[DE94-018452] p 1054 N95-19591

FUEL COMBUSTION
A preliminary analysis of low frequency pressure oscillations in hybrid rocket motors p 968 N95-18987
Computational simulation of liquid fuel rocket injectors p 968 N95-18989
On the conduct of fast cookoff tests in Australia
[AD-A284260] p 975 N95-19699

FUEL CONSUMPTION
Historic patterns of CO2 emissions from fossil fuels: Implications for stabilization of emissions
[DE95-000489] p 1061 N95-19556
Protective coatings for compressor gas path components p 954 N95-19675

FUEL CONTROL
New technologies for space avionics
[NASA-CR-197574] p 966 N95-18196
Neural net controller for inlet pressure control of rocket engine testing p 1102 N95-19637

FUEL CORROSION
A review of nuclear thermal propulsion carbide fuel corrosion and key issues
[NASA-CR-197533] p 1136 N95-18217

FUEL INJECTION
Advanced diesel engine component development program, tasks 4-14
[NASA-CR-191203] p 1040 N95-18041
A preliminary analysis of low frequency pressure oscillations in hybrid rocket motors p 968 N95-18987
Computational simulation of liquid fuel rocket injectors p 968 N95-18989
Advanced diesel electronic fuel injection and turbocharging
[AD-A279176] p 1043 N95-19809

FUEL PUMPS
Centrifugal and axial pump design and off-design performance prediction
[NASA-TM-106745] p 968 N95-19795

FUEL TANKS
Evaluation of powder metallurgy plates made by Sylvania Electric Products, Incorporated
[DE94-017911] p 980 N95-19401

FUEL TESTS
Unmanned aerial vehicle heavy fuel engine test
[AD-A284332] p 947 N95-18383
On the conduct of fast cookoff tests in Australia
[AD-A284260] p 975 N95-19699

FUEL VALVES
Advanced diesel engine component development program, tasks 4-14
[NASA-CR-191203] p 1040 N95-18041

FUELS
Unmanned aerial vehicle heavy fuel engine test
[AD-A284332] p 947 N95-18383
Investigation of mechanical erosion in fuel pipelines p 952 N95-19667

FULL SCALE TESTS
Wall interaction effects for a full-scale helicopter rotor in the NASA Ames 80- by 120-foot wind tunnel p 932 N95-19270
Evaluation of the fuselage lap joint fatigue and terminating action repair p 936 N95-19477
Development of load spectra for Airbus A330/A340 full scale fatigue tests p 936 N95-19479
Testing considerations for military aircraft engines in corrosive environments (a Navy perspective) p 955 N95-19684

FULLERENES
Novel catalysts for methane activation
[DE95-001179] p 976 N95-19785
The interactions of high-energy, highly charged Xe ions with fullerenes
[DE95-001440] p 1135 N95-19786

FUNCTIONAL ANALYSIS
Correlation function analysis of the COBE differential microwave radiometer sky maps
[DE95-000795] p 1178 N95-19617
Solution of Maxwell's equations using the time domain Method of Moments. Supplement: Publications and reports
[AD-A280143] p 1119 N95-19819
Solution of Maxwell's equations using the time domain Method of Moments
[AD-A280144] p 1119 N95-19820

FUNCTIONAL DESIGN SPECIFICATIONS
Mathematical analysis of actuator forces in a scissor lift
[AD-A283906] p 1040 N95-18152
The impact of non-linear flight control systems on the prediction of aircraft loads due to turbulence p 956 N95-18598
Design limit loads based upon statistical discrete gust methodology p 946 N95-18603

FUNCTIONS (MATHEMATICS)
Correlation function analysis of the COBE differential microwave radiometer sky maps
[DE95-000795] p 1178 N95-19617

FUSELAGES
Application of photogrammetry of F-14D store separation
[AD-A284154] p 943 N95-18417
Experimental techniques for measuring transonic flow with a three dimensional laser velocimetry system. Application to determining the drag of a fuselage p 1022 N95-19258
The characterization of widespread fatigue damage in fuselage structure p 935 N95-19472
Discrete crack growth analysis methodology for through cracks in pressurized fuselage structures p 935 N95-19473
Evaluation of the fuselage lap joint fatigue and terminating action repair p 936 N95-19477
Development of load spectra for Airbus A330/A340 full scale fatigue tests p 936 N95-19479
Results of uniaxial and biaxial tests on riveted fuselage lap joint specimens p 938 N95-19491
Prediction of R-curves from small coupon tests p 939 N95-19496
Nonlinear analysis of damaged stiffened fuselage shells subjected to combined loads p 939 N95-19499

FUSION REACTORS
Conceptual design for a scintillating-fiber neutron detector for fusion reactor plasma diagnostics
[DE94-014716] p 1143 N95-17969
Erosion of melt layers developed during a plasma disruption
[DE94-018362] p 1144 N95-18547

FUZZY SYSTEMS
Fuzzy expert systems using CLIPS p 1102 N95-19636

G

GALACTIC CLUSTERS
Decaying neutrinos in galaxy clusters
[NASA-CR-197615] p 1198 N95-18747
Optimizing the Zeldovich approximation
[NASA-CR-197606] p 1156 N95-19037
A test of the adhesion approximation for gravitational clustering
[NASA-CR-197610] p 1157 N95-19358
Comparison of dynamical approximation schemes for non-linear gravitational clustering
[NASA-CR-197609] p 1157 N95-19363

GALACTIC EVOLUTION
Testing the inflationary paradigm: Inflation and the cosmic microwave background anisotropy p 1179 N95-18496
Quantitative analysis of voids in percolating structures in two-dimensional N-body simulations
[NASA-CR-197612] p 1156 N95-18949
Is a massive tau neutrino just what cold dark matter needs?
[NASA-CR-197627] p 1180 N95-18964
Testing the frozen flow approximation
[NASA-CR-197614] p 1180 N95-18966
Mass and radius of cosmic balloons
[NASA-CR-197628] p 1180 N95-19031
A test of the adhesion approximation for gravitational clustering
[NASA-CR-197610] p 1157 N95-19358
Comparison of dynamical approximation schemes for non-linear gravitational clustering
[NASA-CR-197609] p 1157 N95-19363

GALAXIES
The 2 Micron All Sky Survey
[AD-A283515] p 1178 N95-18001

GALERKIN METHOD
Spectral methods for fluid flow p 1028 N95-19459

GALLIUM
Fundamental studies of passivity and passivity breakdown
[DE94-016954] p 987 N95-19095
Results from SAGE 2
[DE95-000849] p 1196 N95-19619

GALLIUM ARSENIDES
InP solar cell development on inexpensive silicon substrates
[AD-A283624] p 1052 N95-18011
Gigabit optical interconnects: System and component analysis, design and development
[AD-A285538] p 1138 N95-18067
Ultrafast nonlinear optical response of Fano resonances in gallium arsenide under high magnetic field
[DE94-018181] p 1148 N95-18122
Investigation of single events upsets in silicon and GaAs structures using reaction calculations
[AD-A285581] p 1131 N95-18474
Process for forming epitaxial BaF2 on GaAs
[AD-D016439] p 1149 N95-18527
Solar-electrochemical power system for a Mars mission
[NASA-TM-106606] p 967 N95-18570
Magneto-optical studies of compound semiconductors
[DE94-018743] p 1149 N95-18650

High-pressure studies of deep impurities in GaAs, ZnSe, and related layered structures p 1150 N95-18908
Giant effective mass deviations near the magnetic field-induced minigap in double quantum wells [DE94-018889] p 1122 N95-19234
Optical determination of conduction and valence-band dispersion curves in strained single-quantum wells [DE94-018892] p 1151 N95-19235
Vacuum microelectronic emitters and their applications using compound semiconductor technology [AD-A284811] p 1013 N95-19687
Investigation of superlattice disordering and diffusion mechanisms in GaAs [AD-A284847] p 1153 N95-19697
Characterization of inactive carbon in GaAs [DE95-002352] p 976 N95-19836
Growth and development of GaInAsP for high-efficiency solar cells [DE94-000210] p 1056 N95-19878

GALLIUM NITRIDES

Growth and doping of Al(x)Ga(1-x)N films by electron cyclotron resonance assisted molecular beam epitaxy [AD-A284838] p 1153 N95-19737

GALLIUM PHOSPHIDES

Energies of X conduction band minima in disordered and ordered GaInP2 alloys [DE94-018211] p 1152 N95-19586
Growth and development of GaInAsP for high-efficiency solar cells [DE94-000210] p 1056 N95-19878

GALLIUM SELENIDES

Deep levels in AgGaSe2 [DE94-018209] p 1152 N95-19585
Correlation of polycrystalline Cu(In,Ga)Se2 device efficiency with homojunction depthand interfacial structure: X-ray photoemission and positron annihilation spectroscopic characterization [DE94-013543] p 1055 N95-19858

GAMMA RAY BURSTS

Spatial and temporal constraints on the observed distribution of gamma-ray bursts detected by BATSE p 1197 N95-18730

GAMMA RAY LASERS

IDA gamma ray laser [AD-A284322] p 1037 N95-18382

GAMMA RAY SPECTRA

GAMQUEST, a computer program to identify gamma rays [DE94-016217] p 1197 N95-18351
Simulation of gamma-ray spectra for a variety of user-specified detector designs [NASA-CR-197551] p 1136 N95-18370

GAMMA RAYS

Obtention of cationic polymeric membranes by radiation-induced grafting method [DE94-629193] p 983 N95-17942
GAMQUEST, a computer program to identify gamma rays [DE94-016217] p 1197 N95-18351
Development of a high-resolution liquid xenon detector for gamma-ray astrophysics p 1179 N95-18499
Assembly and calibration of a new experimental apparatus for production and utilization of capture gamma rays [DE94-626650] p 1198 N95-18880
Cosmic ray models for early galactic lithium, beryllium, and boron production [NASA-CR-197626] p 1137 N95-18965

GAPS

Ion emission intensity ratios as a function of electrode gap, melting current, and pressure during low current vacuum arc remelting [DE94-017407] p 1129 N95-18144
Method for forming Josephson break junctions [AD-D016427] p 1149 N95-18559

GAS ANALYSIS

Two-stage gas measurement system [NASA-CASE-LAR-14791-1] p 1032 N95-18316
Electron reversal ionizer for detection of trace species using a spherical cathode [NASA-CASE-NPO-18870-1-CU] p 1130 N95-18324
Techniques for in situ collection and measurement of volatiles released during hypervelocity impact p 962 N95-19184

GAS COMPOSITION

Detection of greenhouse-gas-induced climatic change [DE94-015044] p 1057 N95-18022
Two-stage gas measurement system [NASA-CASE-LAR-14791-1] p 1032 N95-18316

GAS COOLING

Chondrule formation in the radiative accretional shock p 1191 N95-19324

GAS DETECTORS

Modeling and measurement of the performance of a branched conduit sampling system in a mass spectrometer leak detector p 1036 N95-18181
Two-stage gas measurement system [NASA-CASE-LAR-14791-1] p 1032 N95-18316

GAS DYNAMICS

Simulation of multidisciplinary problems for the thermostress state of cooled high temperature turbines p 948 N95-19021
Application of multidisciplinary models to the cooled turbine rotor design p 949 N95-19024
Models for multiple heating mechanisms p 1188 N95-19303
Chondrule formation in lightning discharges p 1188 N95-19304
CFD: Advances and Applications, 1994 [NAL-SP-9412] p 1028 N95-19455
Finite-volume upwind schemes for inviscid gas dynamics p 1028 N95-19456
Hypersonic viscous flow computations p 1029 N95-19463

GAS FLOW

A study of gas flow pattern, undercutting and torch modification in variable polarity plasma arc welding [NASA-CR-196537] p 1040 N95-18056
Flow field investigation in a free jet - free jet core system for the generation of high intensity molecular beams [DLR-FB-94-11] p 1132 N95-18912
Mathematical Models of Gas Turbine Engines and their Components [AGARD-LS-198] p 948 N95-19017
The mathematical models of flow passage for gas turbine engines and their components p 948 N95-19020
Application of multicomponent models to flow passage simulation in multistage turbomachines and whole gas turbine engines p 948 N95-19022
Application of multidisciplinary models to the cooled turbine rotor design p 949 N95-19024
Parabolized Navier-Stokes solution of supersonic/hypersonic flows p 933 N95-19464

GAS IONIZATION

Solar flare model atmospheres [NASA-CR-197607] p 1196 N95-19034

GAS JETS

The jet model of chondrule formation p 1189 N95-19310

GAS METERS

An instrument to measure the charge, and energy spectrum (20-1000 GeV/a) of the cosmic ray species oxygen to iron [NASA-CR-197555] p 1197 N95-18464

GAS RECOVERY

Gas storage and recovery system [NASA-CASE-MSC-22091-1] p 992 N95-18738

GAS TRANSPORT

An analytic conceptual model of extratropical cyclones [KNMI-WR-93-03] p 1072 N95-18926

GAS TURBINE ENGINES

Wave cycle design for wave rotor engines with limited nitrogen oxide emissions p 1041 N95-18901
Mathematical Models of Gas Turbine Engines and their Components [AGARD-LS-198] p 948 N95-19017
The mathematical models of flow passage for gas turbine engines and their components p 948 N95-19020
Application of multicomponent models to flow passage simulation in multistage turbomachines and whole gas turbine engines p 948 N95-19022
Proceedings of the USAF Structural Integrity Program Conference [AD-A285684] p 945 N95-19517
Erosion, Corrosion and Foreign Object Damage Effects in Gas Turbines [AGARD-CP-558] p 950 N95-19653
Out of area experiences with the RB199 in Toronto p 950 N95-19654
The operation of gas turbine engines in hot and sandy conditions: Royal Air Force experiences in the Gulf conflict p 950 N95-19655
US Army rotorcraft turboshaft engines sand and dust erosion considerations p 951 N95-19656
Navy foreign object damage and its impact on future gas turbine engine low pressure compression systems p 951 N95-19658
Experimental and numerical simulations of the effects of ingested particles in gas turbine engines p 952 N95-19662
Particle trajectories in gas turbine engines p 952 N95-19663
An airborne monitoring system for FOD and erosion faults p 953 N95-19668
Aero-thermodynamic distortion induced structured dynamic response [AD-A279931] p 955 N95-19864

GAS TURBINES

Fatigue in single crystal nickel superalloys [AD-A285727] p 978 N95-18068
Numerical mixing calculations of confined reacting jet flows in a cylindrical duct [NASA-TM-106736] p 947 N95-18133
Scandinavian Airlines Systems experience on erosion, corrosion and foreign object damage effects on gas turbines p 951 N95-19659
Particle deposition in gas turbine blade film cooling holes p 951 N95-19661
The calculation of erosion in a gas turbine compressor rotor p 952 N95-19664
Erosion of T56 5th stage rotor blades due to bleed hole overtip flow p 952 N95-19666
Protective coatings for compressor gas path components p 954 N95-19675
Braze repair possibilities for hot section gas turbine parts p 954 N95-19677
Gas turbine compressor corrosion and erosion in Western Europe p 954 N95-19678
Multilayer anti-erosion coatings p 954 N95-19679

GAS-METAL INTERACTIONS

Influence of high pressure hydrogen environment on creep deformation of Mo-Re, Haynes 188, and NARloy-Z alloys [NASA-CR-197572] p 978 N95-18046
A review of nuclear thermal propulsion carbide fuel corrosion and key issues [NASA-CR-197533] p 1136 N95-18217
X-ray absorption spectroscopy in high temperature oxidation of metals and alloys p 955 N95-19682

GASEOUS DIFFUSION

Coupled finite element analysis of decomposing poroelastic polymeric composites and structures with subsequent thermal and gas diffusion p 986 N95-18918

GASOHOL (FUEL)

Potential impacts on air quality of the use of ethanol as an alternative fuel [DE94-011881] p 1056 N95-17944

GATES (CIRCUITS)

Junction Field Effect Transistor with lateral Gate Voltage Swing (GVS-JFET) [AD-D016353] p 1032 N95-17970
Method for fabricating complementary enhancement and depletion mode field effect transistors on a single substrate [AD-D016270] p 1010 N95-18546

GAUGE INVARIANCE

Zero modes of first class secondary constraints in gauge theories [DE94-626659] p 1156 N95-18328
SU4(sub L) x U1(sub N) model for the electroweak interactions [DE94-626675] p 1148 N95-18330
Comparison of the anomalous and non-anomalous generalized Schwinger models via functional formalism [DE94-626684] p 1156 N95-18333

GAUGE THEORY

Zero modes of first class secondary constraints in gauge theories [DE94-626659] p 1156 N95-18328
Comparison of the anomalous and non-anomalous generalized Schwinger models via functional formalism [DE94-626684] p 1156 N95-18333

GEAR TEETH

Study of the kinematic and load sharing properties of wormgearing with non-symmetric tooth profiles [NASA-CR-195414] p 1041 N95-18541
Thermal behavior spiral bevel gears [NASA-TM-106518] p 1042 N95-18935
Detecting gear tooth fracture in a high contact ratio face gear mesh [NASA-TM-106822] p 1042 N95-19125
Wormgear geometry adopted for implementing hydrostatic lubrication and formulation of the lubrication problem [NASA-CR-195416] p 1043 N95-19567

GEARS

Thermal behavior spiral bevel gears [NASA-TM-106518] p 1042 N95-18935
Detecting gear tooth fracture in a high contact ratio face gear mesh [NASA-TM-106822] p 1042 N95-19125
Wormgear geometry adopted for implementing hydrostatic lubrication and formulation of the lubrication problem [NASA-CR-195416] p 1043 N95-19567

GEMINI FLIGHTS

Legacy of Gemini [NASA-TM-110486] p 961 N95-19058

GEMINI SPACECRAFT

Gemini 8, This is Houston, flight [NASA-TM-110490] p 965 N95-19039

GEMINI 8 FLIGHT

Gemini 8, This is Houston, flight [NASA-TM-110490] p 965 N95-19039

GENETIC ALGORITHMS
The use of genetic algorithms for flight test and evaluation of artificial intelligence and complex software systems
[AD-A284824] p 1104 N95-19688
GENETIC ENGINEERING
Proceedings of Natural Sciences Symposium
[AD-A285452] p 1077 N95-19536
GEOCHEMISTRY
Microchondrules in ordinary chondrites: Implications for chondrule formation p 1188 N95-19309
GEODESY
Definition and realization of a global vertical datum
[AD-A283303] p 1049 N95-17971
Digital mapping, charting, and geodesy analysis program technical review of Digital Aeronautical Flight Information Data Prototype 1.0 on CD-ROM
[AD-A284728] p 1050 N95-18078
GEODETIC ACCURACY
Definition and realization of a global vertical datum
[AD-A283303] p 1049 N95-17971
GEODETIC SURVEYS
Definition and realization of a global vertical datum
[AD-A283303] p 1049 N95-17971
Seafloor positioning across Juan de Fuca ridge
[AD-A285049] p 1075 N95-19563
GEOELECTRICITY
Magnetotelluric mapping of upper crustal isotherms beneath the Valles Caldera hydrothermal system
[DE94-013606] p 1063 N95-17946
GEOGRAPHIC INFORMATION SYSTEMS
R.MAPCALC: An algebra for GIS and image processing
[AD-A283923] p 1096 N95-18161
A GIS approach to urban heat island research: The case of Huntsville, Alabama p 1063 N95-18991
GEOIDS
Definition and realization of a global vertical datum
[AD-A283303] p 1049 N95-17971
GEOLOGICAL FAULTS
Trace element characteristics of lithospheric and asthenospheric mantle in the Rio Grande rift region
[DE94-013609] p 1063 N95-17947
GEOLOGY
Geologic studies: Executive summary report
[PB94-187481] p 1073 N95-17951
Remote sensing/global change. A special bibliography
[NASA-TM-110038] p 1060 N95-18742
GEOMAGNETISM
Investigation of the ionospheric short-term variability
[AD-A286253] p 1066 N95-19387
GEOMETRIC ACCURACY
Remote sensing products evaluation for cartographic updating purposes
[INPE-5584-TDI/546] p 1050 N95-18368
GEOMETRICAL OPTICS
High-power microwave transmission and mode conversion program
[DE94-017046] p 1002 N95-19097
GEOPHYSICS
Image accuracy and representational enhancement through low-level, multi-sensor integration techniques
[DE94-018661] p 1051 N95-18556
Remote sensing/global change. A special bibliography
[NASA-TM-110038] p 1060 N95-18742
Solar-geophysical data number 599, July 1994. Part 1: (Prompt reports). Data for June, May 1994, and late data
[PB94-213972] p 1196 N95-19404
Solar-geophysical data number 599, July 1994. Part 2: (Comprehensive reports). Data for January 1994, and miscellaneous
[PB94-213980] p 1196 N95-19405
Proceedings of the 15th Annual Conference on Atmospheric Transmission Models
[AD-A279919] p 1142 N95-19862
GEOPOTENTIAL HEIGHT
Definition and realization of a global vertical datum
[AD-A283303] p 1049 N95-17971
GEOSYNCHRONOUS ORBITS
CRRESPRO documentation
[AD-A284578] p 1178 N95-18451
GEOTECHNICAL ENGINEERING
Long-term processes in geomaterials. A three-dimensional visco-elastic soil model
[PB94-207180] p 1065 N95-18640
GERMANIUM
Defect reduction and back channel degradation in SIMOX
[AD-A284231] p 1148 N95-17960
Solar-electrochemical power system for a Mars mission
[NASA-TM-106606] p 967 N95-18570
Heteroepitaxy of ternary SiGeC alloys on Si for bipolar transistors
[AD-A285317] p 1151 N95-19511
The optical emission and absorption properties of silicon-germanium superlattice structures grown on non-conventional silicon substrate orientation
[AD-A284852] p 1153 N95-19715
GERMANIUM ALLOYS
Microscopic origins of metastable effects in a-Si:H and deep defect characterization in a-Si,Ge:H alloys
[DE94-011887] p 1151 N95-19541
GETTERS
Gettering in multicrystalline silicon: A design-of-experiments approach
[DE94-014289] p 1055 N95-19873
GLARE
An evaluation of aircraft CRT and dot-matrix display legibility requirements
[AD-A283933] p 947 N95-18164
GLASS
Standard reference materials: Glass filters as a standard reference material for spectrophotometry. Selection, preparation, certification and use of SRM 930 and SRM 1930
[PB94-188844] p 973 N95-17994
Sodium sulfate corrosion of silicon carbide fiber-reinforced calcium aluminosilicate glass-ceramic matrix composites
[AD-A283703] p 969 N95-18021
Fixture for pressure testing sight glasses
[AD-D016263] p 1032 N95-18319
GLASS FIBER REINFORCED PLASTICS
Acoustic fatigue behaviour of GLARE composites p 1127 N95-19160
GLASS LASERS
Future trends in optical coatings for high-power laser applications
[DE94-018592] p 1039 N95-19708
GLOBAL AIR POLLUTION
Trends 1993: A compendium of data on global change
[ORNL/CDIAC-65] p 1058 N95-18389
GLOBAL POSITIONING SYSTEM
Heliport/vertiport MLS precision approaches
[AD-A283505] p 940 N95-18059
Digital mapping, charting, and geodesy analysis program technical review of Digital Aeronautical Flight Information Data Prototype 1.0 on CD-ROM
[AD-A284728] p 1050 N95-18078
AN/APS-137 Forward Looking Airborne Radar (FLAR) evaluation
[AD-A284672] p 1002 N95-19087
Seafloor positioning across Juan de Fuca ridge
[AD-A285049] p 1075 N95-19563
GLOBAL WARMING
Detection of greenhouse-gas-induced climatic change
[DE94-015044] p 1057 N95-18022
Assessment of CO2 projections
[DE94-017484] p 1059 N95-18664
GLOW DISCHARGES
Microscopic origins of metastable effects in a-Si:H and deep defect characterization in a-Si,Ge:H alloys
[DE94-011887] p 1151 N95-19541
Study of laser resonance ionization mass spectrometry using a glow discharge source
[DE94-018566] p 981 N95-19703
GLUONS
Can an infrared-vanishing gluon propagator confine quarks?
[DE94-018388] p 1131 N95-18548
GOERTLER INSTABILITY
Effect of crossflow on Goertler instability in incompressible boundary layers
[NASA-CR-195007] p 1016 N95-18193
GOLD
Precision gold conductors for HMCs
[DE94-018558] p 1012 N95-19230
Development of high reliability planar chip inductors
[DE94-018589] p 1012 N95-19231
GOVERNMENT PROCUREMENT
Government contractors: Measuring costs of service contractors versus federal employees. Report to the Chairman, Subcommittee on Federal Services, Post Office and Civil Service, Committee on Governmental Affairs, US Senate
[GAO/GGD-94-95] p 1171 N95-18595
GOVERNMENT/INDUSTRY RELATIONS
Small Business Research Summaries, numbers 51-100
[PB94-179967] p 1170 N95-17986
Small Business Research Summaries, numbers 1-50
[PB94-179959] p 1170 N95-17987
Using federal technology policy to strength the US microelectronics industry
[DE94-017293] p 1008 N95-18143
European aeronautics: Strong government presence in industry structure and research and development support. Report to Congressional Requesters
[GAO/NSIAD-94-71] p 1171 N95-18578
GRAFTING
Obtention of cationic polymeric membranes by radiation-induced grafting method
[DE94-629193] p 983 N95-17942
GRAIN BOUNDARIES
Discrete and continuum elastic properties of interfaces p 1150 N95-18928
Modified Cu-Mn-Al high damping alloys
[AD-A285460] p 980 N95-19539
GRAIN SIZE
Size distribution of one-, two- and three-dimensional Voronoi cells
[PB94-207008] p 1149 N95-18373
Chondrule-matrix relationships in chondritic meteorites p 1186 N95-19293
Microchondrules in ordinary chondrites: Implications for chondrule formation p 1188 N95-19309
Constraints on chondrule agglomeration from fine-grained chondrule rims p 1189 N95-19315
Chondrule remelting: Evidence from coarse-grained chondrule rims and compound chondrules p 1191 N95-19323
Chondrule formation in the radiative accretional shock p 1191 N95-19324
GRAPH THEORY
Double Eulerian cycles on de Bruijn digraphs
[AD-A283334] p 1120 N95-18007
Weighted graph based ordering techniques for preconditioned conjugate gradient methods
[NASA-CR-197597] p 1118 N95-18736
On k-ary n-cubes: Theory and applications
[NASA-CR-194996] p 1100 N95-19028
Finite Markov chains and random discrete structures
[AD-A284192] p 1121 N95-19104
GRAPHICAL USER INTERFACE
Fusion of correlated sensor observations
[AD-A284224] p 994 N95-17958
A platform independent application of Lux illumination prediction algorithms
[AD-A283669] p 1094 N95-18018
Alarm annunciation in a graphical environment
[DE94-015761] p 1098 N95-18652
XAMath: An XAFS analysis package based on Mathematica(tm)
[DE94-016346] p 1100 N95-19397
Information system architecture to support transparent access to distributed, heterogeneous data sources
[DE94-018450] p 1176 N95-19589
Rule based design of conceptual models for formative evaluation p 1106 N95-19760
GRAPHITE
Study on heat flux of plasma scrape-off layer in HL-1 tokamak
[DE94-627009] p 1144 N95-18887
Thermo-oxidative stability of graphite/PMR-15 composites: Effect of fiber surface modification on composite shear properties
[NASA-TM-4608] p 981 N95-19652
GRAPHITE-EPOXY COMPOSITES
Study of failure in fibrous composites subjected to bending loads
[AD-A283330] p 969 N95-18028
Acoustic method of damage sensing in composite materials
[NASA-CR-196538] p 969 N95-18135
Experimental verification of a progressive damage model for composite laminates based on continuum damage mechanics
[NASA-CR-195020] p 971 N95-19043
GRATINGS (SPECTRA)
MANN: A program to transfer designs for diffractive optical elements to a MANN photolithographic mask generator p 1142 N95-18995
Spectroscopy and dynamics of vibrationally excited molecules
[AD-A285874] p 1134 N95-19597
GRAVIMETRY
Diffusion of water vapour through cold Gore-Tex (trademark)
[AD-A279939] p 989 N95-19867
GRAVITATION
Definition and realization of a global vertical datum
[AD-A283303] p 1049 N95-17971
Orbital tests of relativistic gravity using artificial satellites
[PB94-217239] p 965 N95-19377
GRAVITATION THEORY
Quasi-linear regime of gravitational instability as a clue to understanding the large-scale structure in the Universe
[NASA-CR-197613] p 1193 N95-19341
GRAVITATIONAL EFFECTS
Dynamics and statics of nonaxisymmetric liquid bridges
[NASA-CR-197520] p 1195 N95-17980

Ignition and combustion of bulk metals in a microgravity environment
[NASA-CR-197519] p 990 N95-18082
Rewetting of monogroove heat pipe in Space Station radiators
[NASA-CR-197579] p 1014 N95-18092
Physiological and genetic characterization of plant growth and gravitropism in LED light sources
p 1077 N95-18173
Geometry and gravity influences on strength capability
[NASA-TP-3511] p 1091 N95-18189
Quasi-linear regime of gravitational instability: Implication to density-velocity relation
[NASA-CR-197616] p 1156 N95-19340
Comparison of dynamical approximation schemes for non-linear gravitational clustering
[NASA-CR-197609] p 1157 N95-19363
Antisymmetric tensor field interactions and neutron star models
[PB94-215605] p 1118 N95-19375
Spinal nerve syndromes: The need to confirm the diagnosis with neurophysiological examinations
p 1085 N95-19436

GRAVITATIONAL FIELDS
Comparison of dynamical approximation schemes for non-linear gravitational clustering
[NASA-CR-197609] p 1157 N95-19363
Antisymmetric tensor field interactions and neutron star models
[PB94-215605] p 1118 N95-19375

GRAVITATIONAL PHYSIOLOGY
Cumulative effects of repeated brief cerebral ischemia
[AD-A284234] p 1087 N95-19698

GRAVITATIONAL WAVES
Testing the inflationary paradigm: Inflation and the cosmic microwave background anisotropy
p 1179 N95-18496
Second-order reconstruction of the inflationary potential
[NASA-CR-197629] p 1121 N95-19030

GRAVITROPISM
Physiological and genetic characterization of plant growth and gravitropism in LED light sources
p 1077 N95-18173

GRAVITY PROBE B
The Gravity Probe B niobium bird experiment: Experimental verification of a data reduction scheme with a prototypical dc SQUID readout system
p 1033 N95-18929

GRAVITY WAVES
The diurnal cycle of high-frequency temperature variability at 0 deg 140 deg W on seasonal and interannual time scales
[AD-A283640] p 1074 N95-18012
Investigation of atmospheric waves on Neptune
[NASA-CR-197537] p 1194 N95-18579

GRAZING INCIDENCE
Surface roughness measurements
p 1142 N95-18984

GREEN'S FUNCTIONS
Alternative volume integral equation formulations applied to dielectric cylinders
[AD-A285537] p 995 N95-18066
The Green's function in the Bloch-Nordsieck model for QED3
[DE94-626680] p 996 N95-18331
Comparison of the anomalous and non-anomalous generalized Schwinger models via functional formalism
[DE94-626684] p 1156 N95-18333
Acoustics of space structures p 1126 N95-19152
Modeling of quantum transport in semiconductor devices
[AD-A280182] p 1155 N95-19829

GREENHOUSE EFFECT
Renewable energy and its potential for carbon emissions reductions in developing countries: Methodology for technology evaluation
[DE94-011870] p 1056 N95-17943
Detection of greenhouse-gas-induced climatic change
[DE94-015044] p 1057 N95-18022
Methane: The other greenhouse gas. Research and policy in the Netherlands
[PB94-207149] p 1058 N95-18375
Historic patterns of CO2 emissions from fossil fuels: Implications for stabilization of emissions
[DE95-000489] p 1061 N95-19556

GRID GENERATION (MATHEMATICS)
A three-dimensional structured/unstructured hybrid Navier-Stokes method for turbine blade rows
[NASA-TM-106813] p 1016 N95-18200
Scalability of parallel spatial direct numerical simulation code on IBM SP1 parallel supercomputer
[NASA-CR-194975] p 1098 N95-18584
QuikForm: Intelligent deformation processing of structural alloys
[DE94-018739] p 1114 N95-18649
Mesh quality control for multiply-refined tetrahedral grids
[NASA-CR-197595] p 1043 N95-18737
CUBIT mesh generation environment
[DE94-017496] p 1118 N95-18896
Simulation of multidisciplinary problems for the thermostress state of cooled high temperature turbines
p 948 N95-19021
An assessment of the adaptive unstructured tetrahedral grid, Euler Flow Solver Code FELISA
[NASA-TP-3526] p 930 N95-19041
CFD: Advances and Applications, part 1
[NAL-SP-9322-PT-1] p 1026 N95-19444
Numerical grid generation p 1027 N95-19449
General procedures employed in the generation of three-dimensional hybrid structured/unstructured meshes
[ARA-MEMO-400] p 1030 N95-19506
Validation and evaluation of the advanced aeronautical CFD system SAUNA: A method developer's view
[ARA-MEMO-390] p 1030 N95-19774
Application of three-dimensional hybrid structured/unstructured grids to land, sea and air vehicles
[ARA-MEMO-399] p 1031 N95-19775
Verification of the CFD simulation system SAUNA for complex aircraft configurations
[ARA-MEMO-401] p 1031 N95-19776
Inviscid and viscous flow modelling of complex aircraft configurations using the CFD simulation system sauna
[ARA-MEMO-403] p 1031 N95-19777
The application of the SAUNA CFD system to high and low speed vehicles
[ARA-MEMO-402] p 1031 N95-19778
Performance of an artificial absorber for truncating FEM meshes p 1006 N95-19801

GRIDS
Parallelization of the fluid dynamics equations on unstructured grids
[AD-A284116] p 1017 N95-18406

GROOVES
Rewetting of monogroove heat pipe in Space Station radiators
[NASA-CR-197579] p 1014 N95-18092

GROUND EFFECT (AERODYNAMICS)
Tilt Rotor Unmanned Air Vehicle System (TRUS) demonstrator flight test program
[AD-A284151] p 943 N95-18415
Development of pneumatic test techniques for subsonic high-lift and in-ground-effect wind tunnel investigations
p 932 N95-19268

GROUND EFFECT (COMMUNICATIONS)
Performance evaluation of ground based radar systems
[AD-A283654] p 995 N95-18139

GROUND OPERATIONAL SUPPORT SYSTEM
Lightning studies using LDAR and companion data sets p 1073 N95-18174

GROUND STATE
Theoretical interpretation of the fluorescence spectra of toluene and p-cresol
[AD-A284314] p 974 N95-19170

GROUND STATIONS
Performance evaluation of ground based radar systems
[AD-A283654] p 995 N95-18139
Expert system technologies for Space Shuttle decision support: Two case studies p 1104 N95-19646

GROUND TESTS
Hypersonic flight testing
[AD-A283981] p 944 N95-18891

GROUND TRUTH
Assessment of climate variability of the Greenland Ice Sheet: Integration of in situ and satellite data
[NASA-CR-197604] p 1062 N95-19779

GROUND WATER
High performance computing equipment for environmental remediation modeling and first principles simulation of materials properties
[DE95-000497] p 1093 N95-19875

GROUND-AIR-GROUND COMMUNICATION
STS-68 mission highlights resource tape
[NASA-TM-110049] p 961 N95-18568

GROUP DYNAMICS
Effective team performance under stress and normal conditions: An experimental paradigm, theory and data for studying team decision making in hierarchical teams with distributed expertise
[AD-A284683] p 1089 N95-18530

GROUP 4B COMPOUNDS
Atomic Layer Epitaxy (ALE) apparatus for growing thin films of elemental semiconductors
[AD-D016236] p 1149 N95-18633

GUIDANCE (MOTION)
Rack Insertion End Effector (RIEE) guidance
p 1043 N95-18178
Guidance, Navigation and Control Digital Emulation Technology Laboratory
[AD-A284339] p 996 N95-18386

GULF OF MEXICO
Coastal benthic boundary layer special research program: A review of the first year. Volume 1
[AD-A280034] p 1076 N95-19818

GUN PROPELLANTS
Flamespreading in granular solid propellant: Initial results
[AD-A284245] p 976 N95-19729

GUST LOADS
The impact of non-linear flight control systems on the prediction of aircraft loads due to turbulence
p 956 N95-18598
A study of the effect of store unsteady aerodynamics on gust and turbulence loads p 946 N95-18601
Comparison of stochastic and deterministic nonlinear gust analysis methods to meet continuous turbulence criteria p 946 N95-18602
A review of gust load calculation methods at de Havilland p 932 N95-18604
Special effects of gust loads on military aircraft
p 946 N95-18605

GUSTS
Measurement of gust response on a turbine cascade
[NASA-TM-106776] p 928 N95-18457
Treatment of non-linear systems by timeplane-transformed CT methods: The spectral gust method p 956 N95-18600
Design limit loads based upon statistical discrete gust methodology p 946 N95-18603
A review of gust load calculation methods at de Havilland p 932 N95-18604
Special effects of gust loads on military aircraft
p 946 N95-18605

GYROSCOPES
The Gravity Probe B niobium bird experiment: Experimental verification of a data reduction scheme with a prototypical dc SQUID readout system
p 1033 N95-18929
Low noise fiber gyroscope system which includes excess noise subtraction
[AD-D016556] p 1034 N95-19124

GYROSCOPIC STABILITY
Gyroscopic and propeller aerodynamic effects on engine mounts dynamic loads in turbulence conditions
p 946 N95-18599

H

H-INFINITY CONTROL
Automation of hardware-in-the-loop testing of control systems for unmanned air vehicles
[AD-A284833] p 945 N95-19693

HADRONS
Evidence for coexistence of two phases in relativistic heavy ion collisions and comparison with lattice results
[DE94-626672] p 1130 N95-18329
Flattening of the resonance spectrum of hadrons from kappa-deformed Poincare algebra
[DE94-626686] p 1156 N95-18352
Study of strangeness production in relativistic nucleus beams at JINR
[DE94-626720] p 1136 N95-18881
Bohr's quantization rule in the world of resonances of elementary particles
[DE94-626721] p 1132 N95-18882
Limits on CP nonconserving interactions from electric dipole moments
[DE94-018582] p 1134 N95-19705

HAFNIUM OXIDES
Investigation of the microstructure of coatings for high power lasers by non-optical techniques
[DE94-017697] p 987 N95-19227

HAIL
Impact loading of compressor stator vanes by hailstone ingestion p 953 N95-19670

HALIDES
Spectroelectrochemical investigations of molten halide solutions
[AD-A284147] p 974 N95-18412
Electrochemical and spectroscopy studies of selected inorganic and organic systems in molten halides
[AD-A284171] p 974 N95-18514

HALOCARBONS
Method for laser-assisted silicon etching using halocarbon ambients
[AD-D016239] p 1038 N95-18635

HALOGEN COMPOUNDS
Trends 1993: A compendium of data on global change
[ORNL/CDIAC-65] p 1058 N95-18389

HAMILTONIAN FUNCTIONS
Limits on CP nonconserving interactions from electric dipole moments
[DE94-018582] p 1134 N95-19705
Generation and solution of effective many-body Hamiltonians for rare earth and transition metal compounds
[DE95-002402] p 1155 N95-19838
HANDBOOKS
Engineer's handbook. Central Archive for Reusable Defense Software (CARDS)
[AD-A284341] p 1097 N95-18419
Acquisition handbook: Update. Comprehensive Approach to Reusable Defensive Software (CARDS)
[AD-A284342] p 1097 N95-18420
NASA directives: Master list and index
[NHB-1410.13N] p 1171 N95-19133
Handbook for the extremely low frequency (ELF) data acquisition and analysis system
[DSTO-GD-0021] p 1005 N95-19622
HARDENING (MATERIALS)
Shock pulse generation using explosive driven metal drivers: Practical considerations
[MRL-TR-93-3] p 1046 N95-19504
HARDNESS
A CMC database for use in the next generation launch vehicles (rockets) p 963 N95-18993
E-6A hardness assurance, maintenance and surveillance program
[AD-A283994] p 945 N95-19067
Analysis of the erosion of cubic centered and face centered metallic materials p 953 N95-19674
HARMONIC ANALYSIS
Cumulative impact analysis of wetlands using hydrologic indices
[AD-A284759] p 1058 N95-18085
HARMONIC GENERATIONS
Propagation of intense, ultrashort laser pulses through metal vapor: Refractive intensity limits and spectral effects
[DE94-016365] p 1039 N95-19398
HARRIER AIRCRAFT
VSTOL Systems Research Aircraft (VSRA) Harrier
[NASA-TM-110117] p 941 N95-18347
An analysis of the costs and benefits in improving F402-RR-406A High Pressure Turbine, second stage blades under the aircraft engine Component Improvement Program (CIP)
[AD-A285127] p 950 N95-19595
HARTREE APPROXIMATION
Static and dynamic nuclear many-body descriptions on parallel architectures
[DE94-018134] p 1116 N95-18120
HAZARDS
Health hazards assessment for blast overpressure exposures
[AD-A283352] p 1078 N95-17998
HEAD (ANATOMY)
Neuropsychophysiologic sequelae of mild head injury p 1083 N95-19430
HEAD-UP DISPLAYS
VSTOL Systems Research Aircraft (VSRA) Harrier
[NASA-TM-110117] p 941 N95-18347
HEALTH
Health hazards assessment for blast overpressure exposures
[AD-A283352] p 1078 N95-17998
Variable name dictionary for the Air Force health study 1987 physical examination data tape, volume 1
[AD-A283319] p 1172 N95-18025
Variable name dictionary for the Air Force health study 1987 physical examination data tape, volume 2
[AD-A283320] p 1172 N95-18026
Design concepts for an integrated environmental medicine workstation for prediction, simulation and training
[AD-A283686] p 1079 N95-18618
Think health not disease p 1083 N95-19429
The EEG in the evaluation of applicants to aircrew members p 1084 N95-19432
Medication in the course of active flying duty p 1086 N95-19443
Distributed medical database system for real-time monitoring of the health and risk exposure of military research study volunteers at USARIEM
[AD-A279193] p 1087 N95-19811
HEALTH PHYSICS
Aeromedical risk management for aircrew p 1080 N95-19414
HEARING
Design of spherical aerosol particles to maximize sound attenuation
[AD-A284313] p 1123 N95-18379
HEART DISEASES
The aeromedical implications of supraventricular tachycardia p 1085 N95-19437
Sarcoidosis in US military aviators p 1085 N95-19438
HEART RATE
Effects of weight lifting on intrathoracic pressures generated by anti-g straining maneuvers
[AD-A283651] p 1078 N95-18138
HEAT ACCLIMATIZATION
Effect of heat acclimation on sitting orthostatic tolerance in the heat after 48 and 96 hour bed rest in men
[NASA-TM-108861] p 1077 N95-18734
HEAT EXCHANGERS
Improved efficiency and power density for thermoacoustic coolers
[AD-A283946] p 992 N95-18165
Airborne rotary separator study
[NASA-CR-191045] p 967 N95-18743
HEAT FLUX
Study on heat flux of plasma scrape-off layer in HL-1 tokamak
[DE94-627009] p 1144 N95-18887
The very low energy solar flux of electron and heavy-flavor neutrinos and antineutrinos
[DE94-018583] p 1135 N95-19706
Assessment of climate variability of the Greenland Ice Sheet: Integration of in situ and satellite data
[NASA-CR-197604] p 1062 N95-19779
HEAT GENERATION
Thermal behavior spiral bevel gears
[NASA-TM-106518] p 1042 N95-18935
HEAT ISLANDS
A GIS approach to urban heat island research: The case of Huntsville, Alabama p 1063 N95-18991
HEAT MEASUREMENT
Complex oxidation effects in polymer degradation
[DE94-018903] p 986 N95-18651
HEAT OF SOLUTION
Design of advanced steels for armor applications
[ARL-CR-175] p 979 N95-18948
HEAT PIPES
Rewetting of monogroove heat pipe in Space Station radiators
[NASA-CR-197579] p 1014 N95-18092
HEAT PUMPS
Lunar base heat pump, phase 1
[NASA-CR-188300] p 1015 N95-18111
Norwegian heat pump status and policy review
[PB94-206992] p 992 N95-18667
HEAT RESISTANT ALLOYS
Influence of high pressure hydrogen environment on creep deformation of Mo-Re, Haynes 188, and NARloy-Z alloys
[NASA-CR-197572] p 978 N95-18046
Fatigue in single crystal nickel superalloys
[AD-A285727] p 978 N95-18068
Ion emission intensity ratios as a function of electrode gap, melting current, and pressure during low current vacuum arc remelting
[DE94-017407] p 1129 N95-18144
New Trends in coatings developments for turbine blades: Materials processing and repair p 954 N95-19676
HEAT SOURCES
Models for multiple heating mechanisms p 1188 N95-19303
HEAT TRANSFER
TFE design package, TFE Verification Program
[DE94-017558] p 1136 N95-18147
Subspace correction methods for the iterative solution of hierarchic plate models. 1: Heat transfer problems
[AD-A285712] p 1117 N95-18482
Hypersonic wind tunnel test techniques
[AD-A284057] p 929 N95-18663
Hypersonic flight testing
[AD-A283981] p 944 N95-18891
Marangoni convection in a gravity-free silicon float zone
[NASA-CR-197600] p 991 N95-18913
Thermal behavior spiral bevel gears
[NASA-TM-106518] p 1042 N95-18935
Application of multidisciplinary models to the cooled turbine rotor design p 949 N95-19024
An investigation of drag repeatability in half model testing in the ARA Transonic Wind Tunnel
[ARA-MEMO-392] p 931 N95-19546
HEAT TREATMENT
Sodium sulfate corrosion of silicon carbide fiber-reinforced calcium aluminosilicate glass-ceramic matrix composites
[AD-A283703] p 969 N95-18021
Microstructure-based fatigue life prediction methods for naval steel structures
[AD-A284735] p 1044 N95-18081
Design of advanced steels for armor applications
[ARL-CR-175] p 979 N95-18948
Weldability of iron aluminides
[DE95-000686] p 981 N95-19568
HEATING
Study of strangeness production in relativistic nucleus beams at JINR
[DE94-626720] p 1136 N95-18881
Solar flare model atmospheres
[NASA-CR-197607] p 1196 N95-19034
Theoretical investigation of matching between plasma heating and fueling in HL-1M machine
[DE94-627019] p 1146 N95-19241
Heating and cooling in the solar nebula: Constraints from refractory inclusions p 1187 N95-19297
Chondrule formation in lightning discharges p 1188 N95-19304
Formation of chondrules by electrical discharge heating p 1189 N95-19313
Heating during solar nebula formation and Mg isotopic fractionation in precursor grains of CAIs and chondrules p 1191 N95-19326
Flash heating is required to minimize sodium losses from chondrules p 1193 N95-19337
HEAVY IONS
Evidence for coexistence of two phases in relativistic heavy ion collisions and comparison with lattice results
[DE94-626672] p 1130 N95-18329
HEAVY NUCLEI
An unified program for calculating the fast neutron nuclear data for middle-heavy nuclei (MUP-3)
[DE94-626822] p 1132 N95-18883
HEAVY WATER
A photoionization study of OH and OD from 680A to 950A: An analysis of the Rydberg series
[NASA-CR-196970] p 974 N95-18744
HELICOPTER CONTROL
Design and flight test of a simplified control system for a transport helicopter p 958 N95-18902
HELICOPTER ENGINES
US Army rotorcraft turboshaft engines sand and dust erosion considerations p 951 N95-19656
Future directions in helicopter protection system configuration p 951 N95-19657
HELICOPTER PERFORMANCE
Helicopter Performance Evaluation (HELPE) computer model
[AD-A284319] p 942 N95-18381
HELICOPTER PROPELLER DRIVE
Study of the kinematic and load sharing properties of wormgearing with non-symmetric tooth profiles
[NASA-CR-195414] p 1041 N95-18541
HELICOPTERS
Heliport/vertiport MLS precision approaches
[AD-A283505] p 940 N95-18059
Helicopter Performance Evaluation (HELPE) computer model
[AD-A284319] p 942 N95-18381
Tilt Rotor Unmanned Air Vehicle System (TRUS) demonstrator flight test program
[AD-A284151] p 943 N95-18415
Helicopter in-flight simulation development and use in test pilot training
[AD-A283998] p 959 N95-18725
Helicopter internal noise p 1124 N95-19144
Collection of real-time, multichannel EEG data from helicopter pilots in flight: A feasibility study
[AD-A285050] p 1090 N95-19564
Particle trajectories in gas turbine engines p 952 N95-19663
The calculation of erosion in a gas turbine compressor rotor p 952 N95-19664
Multilayer anti-erosion coatings p 954 N95-19679
HELIOSPHERE
Heliospheric 2-3 kHz radio emissions and their relationship to large Forbush decreases
[U-OF-IOWA-94-19] p 1195 N95-17979
HELIPORTS
Heliport/vertiport MLS precision approaches
[AD-A283505] p 940 N95-18059
HELIUM
Gas storage and recovery system
[NASA-CASE-MSC-22091-1] p 992 N95-18738
Engineering considerations for the self-energizing magnetoplasmadynamic (MPD) - type fusion plasma thruster
[AD-A283968] p 1144 N95-18888
HELIUM IONS
Particle acceleration and transport in the tail and at the front side of the magnetosphere, task 1 and 2
[NASA-CR-197575] p 1064 N95-18476
HELIUM ISOTOPES
He-4 electromagnetic structure in unitary and analytic VMD model with strict OZI rule
[DE94-626716] p 996 N95-18367
HELIUM PLASMA
Determination of the electron density and the electron temperature in a high-pressure microwave discharge p 1145 N95-18906

HERMES MANNED SPACEPLANE
Aeroacoustic qualification of HERMES shingles
p 1125 N95-19145
HERMETIC SEALS
Advanced packaging and integration technologies for microsensors, phase 1
[AD-A283613] p 1040 N95-18010
HETEROCYCLIC COMPOUNDS
Application of conducting polymers to electroanalysis
[DE94-015204] p 984 N95-18348
HETEROGENEITY
Heterogeneous nucleation of calcium oxalate on native oxide surfaces
[DE94-018725] p 986 N95-18648
Discrete and continuum elastic properties of interfaces
p 1150 N95-18928
HETEROJUNCTIONS
Mega-scale simulation of multi-layer devices: Formulation, kinetics, and visualization
[AD-A284848] p 1153 N95-19738
HEURISTIC METHODS
Improved efficiency and power density for thermoacoustic coolers
[AD-A283946] p 992 N95-18165
Heuristic inference about flow directions in river networks
[INPE-5588-TDI/550] p 1050 N95-18214
Light scattering from rough surfaces
[AD-A284112] p 1139 N95-18404
Weighted graph based ordering techniques for preconditioned conjugate gradient methods
[NASA-CR-197597] p 1118 N95-18736
HIERARCHIES
The synthesis of vision and action
[AD-A285453] p 1088 N95-18094
HIGH ALTITUDE
Design concepts for an integrated environmental medicine workstation for prediction, simulation and training
[AD-A283686] p 1079 N95-18618
HIGH CURRENT
High frame rate CCD cameras with fast optical shutters for military and medical imaging applications
[DE94-018316] p 1034 N95-19229
Improvement of a high current DC power supply system for testing the large scaled superconducting cables and magnets
[DE94-770767] p 1012 N95-19548
HIGH DEFINITION TELEVISION
Multi-channel sound for HDTV: Subjective tests on sound channel configuration
[BBC-RD-1994/4] p 998 N95-18535
Digital video compression: Standardisation of scalable coding schemes
[BBC-RD-1994/10] p 1001 N95-19047
HIGH ENERGY FUELS
Solid fuel ramjet composition
[AD-D016458] p 990 N95-19090
HIGH ENERGY INTERACTIONS
Pion observables and QCD
[DE94-018357] p 1130 N95-18428
HIGH FREQUENCIES
The Seventh Ionospheric Effects Symposium
[PB94-191930] p 1057 N95-17985
The future use of DSCS and commercial satellites in the US Navy
[AD-A285707] p 997 N95-18481
High frequency direct drive generation using white noise sources
[AD-A284158] p 997 N95-18506
Assessing aircraft survivability to high frequency transient threats
[AD-A283999] p 944 N95-18726
Radio wave heating of the lower ionosphere
p 1145 N95-18905
High frequency room responses: Acoustic design and the control of stereophonic image quality
[BBC-RD-1994/11] p 1124 N95-19046
Doppler shift and spread study for ionospherically propagated signals
[AD-A284610] p 1065 N95-19083
The use of two-station ionosonde data for IONCAP/ASAPS model validation on transpolar two-hop, high-frequency skywave radio links
[AD-A284270] p 1005 N95-19736
HIGH GRAVITY ENVIRONMENTS
Cumulative effects of repeated brief cerebral ischemia
[AD-A284234] p 1087 N95-19698
HIGH POWER LASERS
Inter-amplifier pupil relay systems for a high average power dye laser at Lawrence Livermore National Laboratory
[DE94-016544] p 1039 N95-19507
Future trends in optical coatings for high-power laser applications
[DE94-018592] p 1039 N95-19708
HIGH PRESSURE
AASERT-93: New high-pressure diagnostic technique
[AD-A284943] p 973 N95-17975
Influence of high pressure hydrogen environment on creep deformation of Mo-Re, Haynes 188, and NARloy-Z alloys
[NASA-CR-197572] p 978 N95-18046
Studies on high pressure and unsteady flame phenomena
[AD-A284126] p 973 N95-18410
High-pressure studies of deep impurities in GaAs, ZnSe, and related layered structures p 1150 N95-18908
Design of high pressure waterjet nozzles
p 1031 N95-18996
An analysis of the costs and benefits in improving F402-RR-406A High Pressure Turbine, second stage blades under the aircraft engine Component Improvement Program (CIP)
[AD-A285127] p 950 N95-19595
HIGH RESOLUTION
High-frequency skywave signal power measurement system
[AD-A284382] p 996 N95-18341
High radar range resolution with the step frequency waveform
[AD-A284611] p 1002 N95-19084
Prediction of global cloud cover with a very high resolution global spectral model
[AD-A279944] p 1073 N95-19870
HIGH REYNOLDS NUMBER
On the Lighthill relationship and sound generation from isotropic turbulence
[NASA-CR-195005] p 1016 N95-18191
Acoustic properties and durability of liner materials at non-standard atmospheric conditions
[NASA-CR-195010] p 1123 N95-18930
Unsteady aerodynamic analyses for turbomachinery aeroelastic predictions p 949 N95-19381
HIGH SPEED
Storm activity over the North Sea and the Netherlands in two climate models compared with observations
[KNMI-WR-94-02] p 1070 N95-18393
Dynamic decohesion of bimaterials: Experimental observations and failure criteria
[GALCIT-94-2] p 1045 N95-18613
Throughput analysis between high end workstations across an FDDI network
[AD-A283608] p 1110 N95-18615
Thermocouples for interior ballistic temperature measurements
[AD-A283699] p 1033 N95-18620
Hypersonic flight testing
[AD-A283981] p 944 N95-18891
High frame rate CCD cameras with fast optical shutters for military and medical imaging applications
[DE94-018316] p 1034 N95-19229
Advanced diesel electronic fuel injection and turbocharging
[AD-A279176] p 1043 N95-19809
HIGH STRENGTH
Computer simulation of wave propagation through turbulent media
[AD-A283695] p 1000 N95-18671
HIGH STRENGTH STEELS
J-integral characterization of the nozzle steels from intermediate test vessels IV-5 and IV-9
[DE95-001066] p 979 N95-18934
HIGH TEMPERATURE
Lunar base heat pump, phase 1
[NASA-CR-188300] p 1015 N95-18111
Palladium-based membranes for hydrogen separation
[PB94-207156] p 973 N95-18377
Composites research in support of the NASP Institute for Composites (NIC)
[NASA-CR-197580] p 970 N95-18471
High temperature stability of binary microstructures derived from liquid precursors
[AD-A283960] p 1150 N95-18685
General information for operation of the high-temperature electromagnetic containerless vacuum induction furnace
[DE94-017170] p 991 N95-19076
Deformation of nonstoichiometric CuO polycrystals
[DE94-016907] p 1150 N95-19094
Theoretical investigation of matching between plasma heating and fueling in HL-1M machine
[DE94-627019] p 1146 N95-19241
Development of materials for high temperature superconductor Josephson junctions
[DE95-000896] p 1152 N95-19608
Damage of high temperature components by dust-laden air p 953 N95-19673
New Trends in coatings developments for turbine blades: Materials processing and repair p 954 N95-19676
X-ray absorption spectroscopy in high temperature oxidation of metals and alloys p 955 N95-19682
Status of vanadium alloy development for fusion first wall/blanket applications
[DE95-001067] p 982 N95-19725
Polymer based materials for additive processing of high temperature electronics packaging
[AD-A285962] p 988 N95-19745
NiAl and NiAl-based composites directionally solidified by a containerless zone process
[NASA-CR-195430] p 982 N95-19792
High temperature superconducting films and crystals
[AD-A279201] p 1154 N95-19815
Materials for adaptive structural acoustic control, volume 3
[AD-A279223] p 1128 N95-19850
HIGH TEMPERATURE SUPERCONDUCTORS
Deformation of high-temperature superconductors
[DE94-017085] p 1150 N95-19075
Deformation of nonstoichiometric CuO polycrystals
[DE94-016907] p 1150 N95-19094
High Temperature Superconductor (HTS) superconducting quantum interference device (SQUID) microscope
[AD-A285875] p 1152 N95-19598
Development of materials for high temperature superconductor Josephson junctions
[DE95-000896] p 1152 N95-19608
Activities of the Analytical Chemistry Laboratory
[DE95-000834] p 975 N95-19618
High temperature superconducting films and crystals
[AD-A279201] p 1154 N95-19815
HIGH TEMPERATURE TESTS
Influence of high pressure hydrogen environment on creep deformation of Mo-Re, Haynes 188, and NARloy-Z alloys
[NASA-CR-197572] p 978 N95-18046
High-temperature acoustic test facilities and methods
p 1125 N95-19149
Design and operation of a thermoacoustic test facility
p 960 N95-19150
HIGH VOLTAGES
Preparation of an electrocatalytic cathode for an aluminum-hydrogen peroxide battery
[AD-D016262] p 1008 N95-18318
Development of an amorphous surge blocker for a high voltage acceleration power supply of the neutral beam injectors
[DE94-770648] p 1138 N95-19874
HISTORIES
Technological and organizational diversity and technical advance in the early history of the American semiconductor industry
[PB94-175700] p 1007 N95-17999
Historic patterns of CO2 emissions from fossil fuels: Implications for stabilization of emissions
[DE95-000489] p 1061 N95-19556
HOLDERS
Background noise levels measured in the NASA Lewis 9- by 15-foot low-speed wind tunnel
[NASA-TM-106817] p 958 N95-18054
HOLE MOBILITY
The physics and operation of ultra-submicron length semiconductor devices
[AD-A280181] p 1155 N95-19828
HOLES
Erosion of T56 5th stage rotor blades due to bleed hole overtip flow p 952 N95-19666
HOLES (ELECTRON DEFICIENCIES)
Electronic structure of C60 fullerites and nanotubes
[DE95-000784] p 1151 N95-19569
HOLES (MECHANICS)
Analysis of cold worked holes for structural life extension p 939 N95-19493
Split mandrel versus split sleeve coldworking: Dual methods for extending the fatigue life of metal structures
p 940 N95-19500
Particle deposition in gas turbine blade film cooling holes p 951 N95-19661
Stress-intensity factor solutions for cracks at countersunk rivet holes under uniaxial tension
[AD-A279163] p 1047 N95-19804
HOLLOW CATHODES
Electrodynamic behavior of PMG-Delta
[AD-A283930] p 964 N95-18163
HOLMIUM
The effect of temperature on the radiative performance of Ho-YAG thin film selective emitters
[NASA-TM-106830] p 1053 N95-18587
HOLOGRAPHY
Three-D optical memory disk
[AD-A280002] p 1035 N95-19871
HOMING DEVICES
Guidance, Navigation and Control Digital Emulation Technology Laboratory
[AD-A284339] p 996 N95-18386

HOMODYNE RECEPTION
New method for homodyne laser linewidth measurements with a short delay fiber
[PB94-202629] p 1036 N95-18061
HOMOGENEITY
Modified Cu-Mn-Al high damping alloys
[AD-A285460] p 980 N95-19539
HOMOGENIZING
Discrete and continuum elastic properties of interfaces p 1150 N95-18928
Atomistic and elastic analyses of defects and small structures
[DE94-017047] p 980 N95-19111
HOMOJUNCTIONS
Correlation of polycrystalline Cu(In,Ga)Se2 device efficiency with homojunction depthand interfacial structure: X-ray photoemission and positron annihilation spectroscopic characterization
[DE94-013543] p 1055 N95-19858
HOMOLOGY
Plane Jacobian conjecture
[PB94-192341] p 1118 N95-19198
HOT CORROSION
Sodium sulfate corrosion of silicon carbide fiber-reinforced calcium aluminosilicate glass-ceramic matrix composites
[AD-A283703] p 969 N95-18021
A review of nuclear thermal propulsion carbide fuel corrosion and key issues
[NASA-CR-197533] p 1136 N95-18217
New Trends in coatings developments for turbine blades: Materials processing and repair p 954 N95-19676
X-ray absorption spectroscopy in high temperature oxidation of metals and alloys p 955 N95-19682
Resistance of silicon nitride turbine components to erosion and hot corrosion/oxidation attack p 955 N95-19683
HOT PRESSING
Nanostructured bearing alloy studies
[AD-A283328] p 978 N95-18027
HOT WORKING
Deformation of high-temperature superconductors
[DE94-017085] p 1150 N95-19075
HUGONIOT EQUATION OF STATE
Calibration and testing of a large-scale electric gun for shock Hugoniot measurements
[MRL-TR-93-24] p 959 N95-18942
HUMAN BEHAVIOR
Extrathalamic modulation of cortical responsiveness
[AD-A284100] p 1078 N95-18400
HUMAN BEINGS
Design and development of an enhanced biodynamic manikin, phase 1
[AD-A284725] p 1090 N95-18077
Drink composition and cycle-ergometer endurance in men: Carbohydrate, Na(+), osmolality
[NASA-TM-4650] p 1077 N95-19140
HUMAN BODY
The assessment of virtual reality for human anatomy instruction p 1088 N95-18971
HUMAN FACTORS ENGINEERING
Conference on Aerospace Transparent Materials and Enclosures, volume 1
[AD-A283925] p 944 N95-18677
Building a bridge with the customer to facilitate collecting and validating information in modeling sessions
[DE94-017338] p 1174 N95-18872
An overall approach of cockpit noise verification in a military aircraft p 1127 N95-19163
The concept of aeronautical adaptability as developed by the US Navy p 1083 N95-19426
On the development of an expert system for wheelchair selection p 1092 N95-19627
HUMAN IMMUNODEFICIENCY VIRUS
Clinical basis for aeromedical decisions in aircrew HIV positive p 1086 N95-19440
HUMAN PERFORMANCE
Implementation of a human information processing model for task network simulation
[AD-A283903] p 1088 N95-18151
Naval Biodynamics Laboratory 1993 command history
[AD-A284358] p 1089 N95-18440
Local spatio-temporal analysis in vision systems
[AD-A284162] p 1140 N95-18509
Effective team performance under stress and normal conditions: An experimental paradigm, theory and data for studying team decision making in hierarchical teams with distributed expertise
[AD-A284683] p 1089 N95-18530
Design concepts for an integrated environmental medicine workstation for prediction, simulation and training
[AD-A283686] p 1079 N95-18618
Learning effects on strategy selection in a dynamic task environment as a function of time pressure
[AD-A285458] p 1089 N95-19538
Multiple-task performance: A critical review of the literature and a cognitive neuroscience framework
[AD-A285133] p 1090 N95-19583
HUMAN REACTIONS
Is the pilot fit for flying after an accident? p 1083 N95-19425
HUMAN TOLERANCES
Effect of heat acclimation on sitting orthostatic tolerance in the heat after 48 and 96 hour bed rest in men
[NASA-TM-108861] p 1077 N95-18734
Drink composition and cycle-ergometer endurance in men: Carbohydrate, Na(+), osmolality
[NASA-TM-4650] p 1077 N95-19140
HUMAN-COMPUTER INTERFACE
Laser optical mouse
[AD-D016273] p 1092 N95-18517
Method of displaying time series data on finite resolution display device
[AD-D016438] p 1173 N95-18526
Simulation in a dynamic prototyping environment: Petri nets or rules? p 1106 N95-19756
Rule based design of conceptual models for formative evaluation p 1106 N95-19760
Using CLIPS to represent knowledge in a VR simulation p 1107 N95-19765
HUMIDITY
Energy balance model for imagery and electromagnetic propagation
[AD-A284552] p 1063 N95-18115
Experiments with the Mesoscale Atmospheric Simulation System (MASS) using the synthetic relative humidity p 1073 N95-18172
Multispectral NOAA Marine Atmospheric Boundary Layer (MABL) estimates during VOCAR
[AD-A283702] p 1064 N95-18623
A review of land surface temperature and humidity conditions specified for Australia in DEF (AUST) 5168 and STANAG 2895
[AD-A284258] p 1073 N95-19712
Prediction of global cloud cover with a very high resolution global spectral model
[AD-A279944] p 1073 N95-19870
HURRICANES
ADCIRC: An advanced three-dimensional circulation model for shelves, coasts, and estuaries. Report 5: A tropical storm database for the east and Gulf of Mexico coasts of the United States
[AD-A285576] p 1075 N95-19540
HYBRID COMPOSITES
Aryl gels and related materials. Synthesis and characterization of a new class of microporous materials
[AD-A285044] p 987 N95-19544
HYBRID ROCKET ENGINES
A preliminary analysis of low frequency pressure oscillations in hybrid rocket motors p 968 N95-18987
HYDRAULIC ANALOGIES
Verification of multidisciplinary models for turbomachines p 949 N95-19025
HYDRAULIC FLUIDS
Technology demonstration of single hydraulic fluid for armored ground vehicle systems
[AD-A280170] p 989 N95-19826
HYDRAULIC JETS
Design of high pressure waterjet nozzles p 1031 N95-18996
HYDRAULIC TEST TUNNELS
Corner vortex suppressor
[AD-D016423] p 928 N95-18337
Development of a multicomponent force and moment balance for water tunnel applications, volume 1
[NASA-CR-4642-VOL-1] p 1020 N95-18955
Development of a multicomponent force and moment balance for water tunnel applications, volume 2
[NASA-CR-4642-VOL-2] p 1020 N95-18956
HYDRIDES
Direct dimer-by-dimer identification of clean and monohydride dimers on the Si(001) surface by scanning tunneling microscopy
[AD-A280158] p 976 N95-19824
HYDROCARBONS
Dependencies and sensitivity of tropospheric oxidants to precursor concentrations over the northeast United States: A model study
[PB94-192770] p 1056 N95-17937
A model study of the influence of NMHC and NO(x) emissions on rural O3 concentrations in Georgiargia p 1059 N95-18445
Intrinsic barriers for H-atom transfer reactions involving hydrocarbons
[DE94-018451] p 1134 N95-19590
Electrochemical interfaces and electrode processes: Electrochemical oxidation of small organisms
[AD-A284873] p 1013 N95-19741
Novel catalysts for methane activation
[DE95-001179] p 976 N95-19785
HYDRODYNAMIC EQUATIONS
A numerical analysis of smoothed particle hydrodynamics
[AD-A284698] p 1019 N95-18562
Large-scale processes in the solar nebula p 1186 N95-19292
HYDRODYNAMICS
Dynamics and statics of nonaxisymmetric liquid bridges
[NASA-CR-197520] p 1195 N95-17980
A numerical analysis of smoothed particle hydrodynamics
[AD-A284698] p 1019 N95-18562
Lattice gas and lattice Boltzmann methods for simulation of hydrodynamics and magnetohydrodynamics p 1145 N95-18907
SSI effects for a tank containing two liquids
[DE94-012457] p 1020 N95-19099
Three-dimensional radiation transport hydrodynamics
[DE94-018337] p 1146 N95-19527
Advanced concepts theory
[AD-A279212] p 1147 N95-19844
X-ray laser program
[AD-A279213] p 1039 N95-19845
HYDROFOILS
Hydrofoil force balance
[AD-D016475] p 1033 N95-18461
HYDROGEN
A review of nuclear thermal propulsion carbide fuel corrosion and key issues
[NASA-CR-197533] p 1136 N95-18217
Palladium-based membranes for hydrogen separation
[PB94-207156] p 973 N95-18377
Pure-rotational emission from molecular hydrogen in OMC-1 p 1179 N95-18500
On measurement of cross sections for scattering of p(mu)- and d(mu)-atoms in hydrogen and deuterium
[DE94-626957] p 1132 N95-18884
PRISM project optical instrument p 1143 N95-19009
Precision gold conductors for HMCs
[DE94-018558] p 1012 N95-19230
The fine nebula dust component: A key to chondrule formation by lightning p 1192 N95-19333
Weldability of iron aluminides
[DE95-000686] p 981 N95-19568
Intrinsic barriers for H-atom transfer reactions involving hydrocarbons
[DE94-018451] p 1134 N95-19590
HYDROGEN ATOMS
On measurement of cross sections for scattering of p(mu)- and d(mu)-atoms in hydrogen and deuterium
[DE94-626957] p 1132 N95-18884
HYDROGEN EMBRITTLEMENT
Influence of high pressure hydrogen environment on creep deformation of Mo-Re, Haynes 188, and NARloy-Z alloys
[NASA-CR-197572] p 978 N95-18046
HYDROGEN FUELS
Airborne rotary separator study
[NASA-CR-191045] p 967 N95-18743
HYDROGEN ISOTOPES
On measurement of cross sections for scattering of p(mu)- and d(mu)-atoms in hydrogen and deuterium
[DE94-626957] p 1132 N95-18884
HYDROGEN OXYGEN FUEL CELLS
Solar-electrochemical power system for a Mars mission
[NASA-TM-106606] p 967 N95-18570
HYDROGEN PEROXIDE
Investigation of new hypergol scrubber technology p 977 N95-18175
Preparation of an electrocatalytic cathode for an aluminum-hydrogen peroxide battery
[AD-D016262] p 1008 N95-18318
HYDROGENATION
Palladium-based membranes for hydrogen separation
[PB94-207156] p 973 N95-18377
HYDROLOGICAL CYCLE
Observational studies and modelling of interception loss of gross rainfall in the Amazonian rainforest
[INPE-5583-TDI/545] p 1067 N95-18006
HYDROLOGY
Prediction of buoyant outflow in lakes and fjords with a quasi 3D numerical model
[PB94-206984] p 1051 N95-18372
HYDROLOGY MODELS
Observational studies and modelling of interception loss of gross rainfall in the Amazonian rainforest
[INPE-5583-TDI/545] p 1067 N95-18006
Heuristic inference about flow directions in river networks
[INPE-5588-TDI/550] p 1050 N95-18214

High performance computing equipment for environmental remediation modeling and first principles simulation of materials properties
[DE95-000497] p 1093 N95-19875

HYDROPHONES
Signal processor having multiple distributed data buffers
[AD-D016259] p 995 N95-18315

HYDROSTATIC PRESSURE
Study of the kinematic and load sharing properties of wormgearing with non-symmetric tooth profiles
[NASA-CR-195414] p 1041 N95-18541
Fluid dynamic linear accelerometer
[AD-D016413] p 956 N95-18553

HYDROSTATICS
Dynamics and statics of nonaxisymmetric liquid bridges
[NASA-CR-197520] p 1195 N95-17980
Deformation of high-temperature superconductors
[DE94-017085] p 1150 N95-19075
Wormgear geometry adopted for implementing hydrostatic lubrication and formulation of the lubrication problem
[NASA-CR-195416] p 1043 N95-19567

HYDROTHERMAL SYSTEMS
Magnetotelluric mapping of upper crustal isotherms beneath the Valles Caldera hydrothermal system
[DE94-013606] p 1063 N95-17946

HYDROXYL RADICALS
Method of making a membrane having hydrophilic and hydrophobic surfaces for adhering cells or antibodies by using atomic oxygen or hydroxyl radicals
[NASA-CASE-MSC-21529-1] p 983 N95-18134
A photoionization study of OH and OD from 680A to 950A: An analysis of the Rydberg series
[NASA-CR-196970] p 974 N95-18744

HYGROSCOPICITY
Gas turbine compressor corrosion and erosion in Western Europe p 954 N95-19678

HYPERBOLIC DIFFERENTIAL EQUATIONS
Geometrical and topological methods in time domain antenna synthesis
[AD-A284208] p 994 N95-17954
Difference schemes for hyperbolic system of Conservation Laws p 1027 N95-19450

HYPERBOLIC FUNCTIONS
A simple hyperbolic model for communication in parallel processing environments
[NASA-CR-195984] p 1098 N95-18487
Finite-volume upwind schemes for inviscid gas dynamics p 1028 N95-19456

HYPERCUBE MULTIPROCESSORS
Software techniques for balancing computation and communication in parallel systems
[AD-A285536] p 1109 N95-18106
A parallel strategy for implementing real-time expert systems using CLIPS p 1105 N95-19749
PCLIPS: Parallel CLIPS p 1107 N95-19764

HYPERFINE STRUCTURE
Hyperfine splittings, prepulse technique, and other new results for collisional excitation neon-like x ray lasers
[DE94-016443] p 1038 N95-19247

HYPERGOLIC ROCKET PROPELLANTS
Investigation of new hypergol scrubber technology p 977 N95-18175

HYPERSONIC FLIGHT
Hypersonic flight testing
[AD-A283981] p 944 N95-18891

HYPERSONIC FLOW
Numerical simulation of shock/shock and shock/boundary-layer interactions in chemically reacting hypersonic flows
[DLR-94-04] p 1019 N95-18609
Hypersonic flow-field measurements: Intrusive and nonintrusive
[AD-A283867] p 930 N95-18674
Theoretical investigations of shock/boundary layer interactions on a Ma(infinity) = 8 waverider
[DLR-FB-94-12] p 930 N95-18910
Hypersonic viscous flow computations p 1029 N95-19463
Parabolized Navier-Stokes solution of supersonic/hypersonic flows p 933 N95-19464

HYPERSONIC VEHICLES
Influence of high pressure hydrogen environment on creep deformation of Mo-Re, Haynes 188, and NARloy-Z alloys
[NASA-CR-197572] p 978 N95-18046
Hypersonic wind tunnel test techniques
[AD-A284057] p 929 N95-18663
Thermo-acoustic fatigue design for hypersonic vehicle skin panels p 1047 N95-19161

HYPERSONIC WIND TUNNELS
Hypersonic wind tunnel test techniques
[AD-A284057] p 929 N95-18663
Operating capability and current status of the reactivated NASA Lewis Research Center Hypersonic Tunnel Facility
[NASA-TM-106808] p 960 N95-19286

HYPERSONICS
Static aerodynamics CFD analysis for 120-mm hypersonic KE projectile design
[ARL-MR-184] p 929 N95-18611

HYPERVELOCITY FLOW
Hypervelocity air flows with finite rate chemistry
[AD-A284727] p 931 N95-19109

HYPERVELOCITY GUNS
Calibration and testing of a large-scale electric gun for shock Hugoniot measurements
[MRL-TR-93-24] p 959 N95-18942

HYPERVELOCITY IMPACT
Cracking characteristics of a habitable module pressure wall following orbital debris penetration p 1047 N95-19003
Physics of spacecraft-based interplanetary dust collection by impact into low-density media p 1181 N95-19176
Plasma produced by impacts of fast dust particles on a thin film p 1181 N95-19177
The hypervelocity impact facilities at the University of Kent at Canterbury, UK p 961 N95-19180
Techniques for in situ collection and measurement of volatiles released during hypervelocity impact p 962 N95-19184
Penetration experiments in aluminum and Teflon targets of widely variable thickness p 1047 N95-19185
The intact capture of hypervelocity dust particles using underdense foams p 1183 N95-19188
Penetration of multiple thin films in micrometeorite capture cells p 1036 N95-19192
The use of silica aerogel to collect interplanetary dust in space p 989 N95-19197

HYPERVELOCITY PROJECTILES
Penetration experiments in aluminum and Teflon targets of widely variable thickness p 1047 N95-19185
The intact capture of hypervelocity dust particles using underdense foams p 1183 N95-19188
The physics of intact capture p 1122 N95-19195
The use of silica aerogel to collect interplanetary dust in space p 989 N95-19197

HYPOTHESES
A parallel processing hypothesis for short-term and long-term memory in Aplysia
[AD-A284101] p 1088 N95-18401
Eigenvalue tests and distributions for small sample order determination for complex Wishart matrices
[AD-A283825] p 1120 N95-18672

I

ICE
Ice accretion with varying surface tension
[NASA-TM-106826] p 934 N95-19285
Ice-impact analysis of blades p 953 N95-19672

ICE ENVIRONMENTS
Assessment of climate variability of the Greenland Ice Sheet: Integration of in situ and satellite data
[NASA-CR-197604] p 1062 N95-19779

ICE FLOES
Environmental forcing of ambient noise in the Nansen and Amundsen Basins of the Arctic Ocean
[AD-A285540] p 1074 N95-18468

ICE FORMATION
Debris/ice/TPS assessment and integrated photographic analysis of Shuttle mission STS-68
[NASA-TM-109207] p 963 N95-18047
Ice accretion with varying surface tension
[NASA-TM-106826] p 934 N95-19285
Debris/ice/TPS assessment and integrated photographic analysis of Shuttle mission STS-66
[NASA-TM-110141] p 963 N95-19790

IDENTIFYING
Lower bounds for identifying subset members with subset queries
[DE94-014296] p 1117 N95-18346

IGNEOUS ROCKS
Trace element characteristics of lithospheric and asthenospheric mantle in the Rio Grande rift region
[DE94-013609] p 1063 N95-17947

IGNITION
Ignition and combustion of bulk metals in a microgravity environment
[NASA-CR-197519] p 990 N95-18082
Thermocouples for interior ballistic temperature measurements
[AD-A283699] p 1033 N95-18620
Study of alpha physics related to ITER Project
[DE94-017329] p 1133 N95-19078
Contributions of the National Ignition Facility to the development of Inertial Fusion Energy
[DE94-018335] p 1137 N95-19588

ILLUMINATING
Light scattering from rough surfaces
[AD-A284112] p 1139 N95-18404
KC-130 ANVIS/HUD assessment and symbology rationale
[AD-A284155] p 943 N95-18504

ILLUMINATION
A platform independent application of Lux illumination prediction algorithms
[AD-A283669] p 1094 N95-18018

IMAGE ANALYSIS
Atomic scale force mapping with the atomic force microscope
[AD-A284940] p 1129 N95-17974
Some statistical tools for SAR image synthesis, analysis and processing
[INPE-5548-TDI/534] p 1172 N95-18004
Comparative analysis of multisensor (TM/Landsat and SAR/ERS-1) and multitemporal scenes of Guaira region, Sao Paulo State, Brazil
[INPE-5581-TDI/544] p 1049 N95-18005
On the optimization of speckle filtering techniques for ERS-1 images over Argentina
[INPE-5578-PRE/1806] p 1050 N95-18216
A real-time vision system to monitor/analyze the changes in composite specimens during mechanical testing
[ARL-TR-344] p 970 N95-18612
ISSSR tutorial 1: Introduction to spectral remote sensing
[AD-A284268] p 1052 N95-19734

IMAGE CORRELATORS
Imagery correction for atmospheric effects using sounding data
[INPE-5506-TDI/518] p 1064 N95-18390

IMAGE ENHANCEMENT
Imagery correction for atmospheric effects using sounding data
[INPE-5506-TDI/518] p 1064 N95-18390
Image accuracy and representational enhancement through low-level, multi-sensor integration techniques
[DE94-018661] p 1051 N95-18556

IMAGE FILTERS
On the optimization of speckle filtering techniques for ERS-1 images over Argentina
[INPE-5578-PRE/1806] p 1050 N95-18216

IMAGE INTENSIFIERS
Image intensifier system resolution based on laboratory measured parameters
[AD-A283917] p 1008 N95-18156
High frame rate CCD cameras with fast optical shutters for military and medical imaging applications
[DE94-018316] p 1034 N95-19229
High-frame-rate intensified fast optically shuttered TV cameras with selected imaging applications
[DE94-016098] p 1035 N95-19394
Scintillating-fiber imaging detector for 14-MeV neutrons
[DE94-018593] p 1135 N95-19709

IMAGE PROCESSING
Cooperativity and 3-D representation
[AD-A284203] p 1093 N95-17940
Applications of quantum entropy to statistics
[DE94-014416] p 1155 N95-17996
The 2 Micron All Sky Survey
[AD-A283515] p 1178 N95-18001
Some statistical tools for SAR image synthesis, analysis and processing
[INPE-5548-TDI/534] p 1172 N95-18004
R.MAPCALC: An algebra for GIS and image processing
[AD-A283923] p 1096 N95-18161
On the optimization of speckle filtering techniques for ERS-1 images over Argentina
[INPE-5578-PRE/1806] p 1050 N95-18216
Remote sensing products evaluation for cartographic updating purposes
[INPE-5584-TDI/546] p 1050 N95-18368
The photographic system global evaluation for generation of INPE TM Landsat image
[INPE-5571-TDI/542] p 1050 N95-18369
Reconstruction of shapes from shading and shape based image reconstruction using modern nonlinear analysis
[AD-A284107] p 1097 N95-18437
Local spatio-temporal analysis in vision systems
[AD-A284162] p 1140 N95-18509
Image accuracy and representational enhancement through low-level, multi-sensor integration techniques
[DE94-018661] p 1051 N95-18556
Annular computed tomography
[AD-D016424] p 1141 N95-18593

A real-time vision system to monitor/analyze the changes in composite specimens during mechanical testing
[ARL-TR-344] p 970 N95-18612
On orbit performance of the ALEXIS EUV telescopes
[DE94-016197] p 964 N95-18639
Lossless compression of weight vectors from an adaptive filter
[DE94-017350] p 1174 N95-18873
Performance evaluation of the Engineering Analysis and Data Systems (EADS) 2 p 1163 N95-18978
NAWCAD photogrammetrics: Methods and applications for aviation test and evaluation
[AD-A284074] p 1034 N95-19071
High frame rate CCD cameras with fast optical shutters for military and medical imaging applications
[DE94-018316] p 1034 N95-19229
Novel x ray imaging methods at the Nova Laser Facility
[DE94-016548] p 1146 N95-19509
High performance computing for medical image interpretation
[AD-A285457] p 1086 N95-19537
Parallel computations in hydro acoustics
[AD-A285900] p 1030 N95-19607

IMAGE RECONSTRUCTION
Linear optimization and image reconstruction
[AD-A283641] p 1094 N95-18013
Reconstruction of shapes from shading and shape based image reconstruction using modern nonlinear analysis
[AD-A284107] p 1097 N95-18437

IMAGE RESOLUTION
High performance computing for medical image interpretation
[AD-A285457] p 1086 N95-19537
Embedded microclusters in zeolites and cluster beam sputtering: Simulation on parallel computers
[DE95-000662] p 1134 N95-19562

IMAGERY
The Seventh Ionospheric Effects Symposium
[PB94-191930] p 1057 N95-17985
Modular implementation of feature extraction and matching algorithms for photogrammetric stereo imagery
[AD-A285422] p 1032 N95-18065

IMAGES
Electronic structure of C60 fullerites and nanotubes
[DE95-000784] p 1151 N95-19569

IMAGING TECHNIQUES
Two and three dimensional magnetotelluric inversion
[DE94-014820] p 1063 N95-17967
Atomic scale force mapping with the atomic force microscope
[AD-A284940] p 1129 N95-17974
Fusion of multiple sensing modalities for machine vision
[AD-A284762] p 1091 N95-18086
On the geometry of visual correspondence
[AD-A285700] p 1140 N95-18478
Development of a high-resolution liquid xenon detector for gamma-ray astrophysics p 1179 N95-18499
Image accuracy and representational enhancement through low-level, multi-sensor integration techniques
[DE94-018661] p 1051 N95-18556
A real-time vision system to monitor/analyze the changes in composite specimens during mechanical testing
[ARL-TR-344] p 970 N95-18612
Evaluation of scanners for C-scan imaging in nondestructive inspection of aircraft
[DE94-012473] p 990 N95-19100
Graded bandgap semiconductor device for real-time imaging
[AD-D016543] p 1151 N95-19122
High frame rate CCD cameras with fast optical shutters for military and medical imaging applications
[DE94-018316] p 1034 N95-19229
High-frame-rate intensified fast optically shuttered TV cameras with selected imaging applications
[DE94-016098] p 1035 N95-19394
Novel x ray imaging methods at the Nova Laser Facility
[DE94-016548] p 1146 N95-19509
High performance computing for medical image interpretation
[AD-A285457] p 1086 N95-19537
Acceptance/operational test procedure 101-SY tank camera purge system and in tank color camera video imaging system
[DE95-000344] p 1035 N95-19553
A novel technique for 4-dimensional atmospheric and oceanographic irradiance measurements using 3-D spatial filtering
[AD-A285658] p 1073 N95-19701
Scintillating-fiber imaging detector for 14-MeV neutrons
[DE94-018593] p 1135 N95-19709

IMPACT
Particle deposition in gas turbine blade film cooling holes p 951 N95-19661

IMPACT DAMAGE
Acoustic method of damage sensing in composite materials
[NASA-CR-196538] p 969 N95-18135
Foreign body impact event damage formation in composite structures p 972 N95-18973
Cracking characteristics of a habitable module pressure wall following orbital debris penetration p 1047 N95-19003
Experimental verification of a progressive damage model for composite laminates based on continuum damage mechanics
[NASA-CR-195020] p 971 N95-19043
An airborne monitoring system for FOD and erosion faults p 953 N95-19668
Design of fan blades subjected to bird impact p 953 N95-19669
Impact loading of compressor stator vanes by hailstone ingestion p 953 N95-19670
Soft body impact on titanium fan blades p 953 N95-19671
Ice-impact analysis of blades p 953 N95-19672

IMPACT LOADS
Impact loading of compressor stator vanes by hailstone ingestion p 953 N95-19670

IMPACT RESISTANCE
Conference on Aerospace Transparent Materials and Enclosures. Volume 2: Sessions 5-9
[AD-A283926] p 942 N95-18162
Mixed high explosives for insensitive booster compositions
[MRL-TR-92-22] p 990 N95-19505

IMPACT TESTS
Sloshing roof impact tests of a rectangular tank
[DE94-012462] p 1018 N95-18549
Calibration and testing of a large-scale electric gun for shock Hugoniot measurements
[MRL-TR-93-24] p 959 N95-18942
Laboratory simulation of intact capture of cometary and asteroidal dust particles in ISAS p 962 N95-19183
Soft body impact on titanium fan blades p 953 N95-19671

IMPEDANCE MATCHING
Analysis and synthesis of (SAR) waveguide phased array antennas
[AD-A285336] p 1004 N95-19535

IMPEDANCE MEASUREMENT
Evaluation of inorganic zinc-rich primers using Electrochemical Impedance Spectroscopy (EIS) in combination with atmospheric exposure p 977 N95-18170
Constant current loop impedance measuring system that is immune to the effects of parasitic impedances
[NASA-CASE-ARC-11988-1] p 1011 N95-18959

IMPLOSIONS
Advanced concepts theory
[AD-A279212] p 1147 N95-19844

IMPULSES
Sandia National Laboratories' high power electromagnetic impulse sources
[DE95-000423] p 1004 N95-19555

IMPURITIES
High-pressure studies of deep impurities in GaAs, ZnSe, and related layered structures p 1150 N95-18908
Impurity behavior during ion-Bernstein wave heating in PBX-M
[DE94-018114] p 1133 N95-19228
Modified Cu-Mn-Al high damping alloys
[AD-A285460] p 980 N95-19539
Microscopic origins of metastable effects in a-Si:H and deep defect characterization in a-Si,Ge:H alloys
[DE94-011887] p 1151 N95-19541

IN SITU MEASUREMENT
Fundamental advances for characterizing cathodic protection systems
[PB94-180692] p 1122 N95-17983
Workshop on Particle Capture, Recovery and Velocity/Trajectory Measurement Technologies
[NASA-CR-197592] p 1180 N95-19172
Techniques for in situ collection and measurement of volatiles released during hypervelocity impact p 962 N95-19184
Assessment of climate variability of the Greenland Ice Sheet: Integration of in situ and satellite data
[NASA-CR-197604] p 1062 N95-19779

IN-FLIGHT MONITORING
EKG in flight: Usefulness and limits for aircrew rehabilitation p 1082 N95-19422
Flight parameters monitoring system for tracking structural integrity of rotary-wing aircraft p 934 N95-19469

INCIDENCE
Investigation of single events upsets in silicon and GaAs structures using reaction calculations
[AD-A285581] p 1131 N95-18474

INCIDENT RADIATION
Radiation balance in three Amazonian ecosystems: Campina, campinarana and mata densa
[INPE-5587-TDI/549] p 1057 N95-18003
Graded bandgap semiconductor device for real-time imaging
[AD-D016543] p 1151 N95-19122

INCLUSIONS
Heating and cooling in the solar nebula: Constraints from refractory inclusions p 1187 N95-19297
Chronology of chrondrule and CAI formation: Mg-Al isotopic evidence p 1189 N95-19314
A ceramic/slag interface as an analog for accretion of hot refractory objects and rim formation p 1191 N95-19322
Chondrule remelting: Evidence from coarse-grained chondrule rims and compound chondrules p 1191 N95-19323

INCOMPRESSIBLE BOUNDARY LAYER
Effect of crossflow on Goertler instability in incompressible boundary layers
[NASA-CR-195007] p 1016 N95-18193

INCOMPRESSIBLE FLOW
A note on the wave action density of a viscous instability mode on a laminar free-shear flow
[NASA-TM-106771] p 1016 N95-18212
A note on singularities of the 3-D Euler equation
[NASA-CR-195006] p 1017 N95-18397
On the geometry of visual correspondence
[AD-A285700] p 1140 N95-18478
Basic equations of fluid dynamics p 1026 N95-19445
Turbulence modeling for CFD, part 1 p 1028 N95-19458
Discrete vortex method for computation of viscous incompressible flows p 1029 N95-19460
Pressure based finite volume algorithm for viscous flow computation p 1029 N95-19461
Parallel computations in hydro acoustics
[AD-A285900] p 1030 N95-19607
Incompressible flow of a Newtonian fluid past a vertical plate with thermal and magnetic stresses
[AD-A284856] p 1030 N95-19716

INCOMPRESSIBLE FLUIDS
Incompressible flow of a Newtonian fluid past a vertical plate with thermal and magnetic stresses
[AD-A284856] p 1030 N95-19716

INDEPENDENT VARIABLES
Design of spherical aerosol particles to maximize sound attenuation
[AD-A284313] p 1123 N95-18379
The formulation of quantum statistical mechanics based on the Feynman path centroid density. 3: Phase space formalism and analysis of centroid molecular dynamics
[AD-A279233] p 1157 N95-19852

INDEXES (DOCUMENTATION)
Aeronautical engineering: A continuing bibliography with indexes (supplement 313)
[NASA-SP-7037(313)] p 927 N95-19168
Aeronautical engineering: A continuing bibliography with indexes (supplement 314)
[NASA-SP-7037(314)] p 927 N95-19357
Solar-geophysical data number 599, July 1994. Part 1: (Prompt reports). Data for June, May 1994, and late data
[PB94-213972] p 1196 N95-19404

INDIAN OCEAN
Intraseasonal oscillations over the tropical western Pacific and eastern Indian ocean for the northern summers of 1989-1991
[AD-A284527] p 1068 N95-18114
A numerical simulation of seasonal circulation in the South China Sea
[AD-A283701] p 1075 N95-18622

INDIUM
Synthesis and characterization of a neutral six-coordinate tris-adduct of an indium(3) trihalide. X ray crystal structure of InCl3(THF)3
[AD-A279169] p 1154 N95-19806
Isolation and characterization of an indium-mixed-pnicogen Four-membered ring compound: Crystal structure of (Me3SiCH2)2InAs(SiMe3)2 In(CH2SiMe3)2P(SiMe3)2
[AD-A279170] p 1154 N95-19807

INDIUM ARSENIDES
Optical determination of conduction and valence-band dispersion curves in strained single-quantum wells
[DE94-018892] p 1151 N95-19235

Growth and development of GaInAsP for high-efficiency solar cells
[DE94-000210] p 1056 N95-19878

INDIUM COMPOUNDS
Advanced processing technology for high-efficiency, thin-film CuInSe2 and CdTe solar cells
[DE94-011838] p 1056 N95-19880

INDIUM GALLIUM ARSENIDES
Magneto-optical studies of compound semiconductors
[DE94-018743] p 1149 N95-18650

INDIUM PHOSPHIDES
InP solar cell development on inexpensive silicon substrates
[AD-A283624] p 1052 N95-18011
Minority-carrier lifetime in InP as a function of light bias
[NASA-TM-106821] p 1149 N95-18453
InP solar cell development on inexpensive silicon substrates
[AD-A286254] p 1054 N95-19388
Energies of X conduction band minima in disordered and ordered GaInP2 alloys
[DE94-018211] p 1152 N95-19586
Growth and development of GaInAsP for high-efficiency solar cells
[DE94-000210] p 1056 N95-19878

INDUCTANCE
Power flow and PRS optimization on Phoenix
[AD-A279214] p 1147 N95-19846

INDUCTION HEATING
Method and device for determining bond separation strength using induction heating
[NASA-CASE-LAR-14678-1] p 960 N95-18961
Induction heating coupler and annealer
[NASA-CASE-LAR-14277-1] p 1011 N95-18962

INDUCTION MOTORS
Mitigation of EMI generated by a variable-frequency-drive controller for an AC induction motor
[AD-A286045] p 1012 N95-19573
Improved speed control system for the 87,000 HP wind tunnel drive
[NASA-TM-106840] p 1035 N95-19794

INDUCTORS
Development of high reliability planar chip inductors
[DE94-018589] p 1012 N95-19231

INDUSTRIES
US Industrial Outlook, 1994: An almanac of industry, technology and services. 35th annual edition: Forecasts for selected manufacturing and service industries
[PB94-107844] p 1171 N95-17988
Technological and organizational diversity and technical advance in the early history of the American semiconductor industry
[PB94-175700] p 1007 N95-17999
Using federal technology policy to strength the US microelectronics industry
[DE94-017293] p 1008 N95-18143
Second International Semiconductor Device Research Symposium (ISDRS-1993)
[AD-A279221] p 1013 N95-19849

INELASTIC SCATTERING
Diquarks in deep inelastic scattering and the Gottfried sum rule
[DE94-626685] p 1130 N95-18356

INERTIA
On the theory of stick-slip fracture
p 1046 N95-18922
Closed-form static analysis with inertia relief and displacement-dependent loads using a MSC/NASTRAN DMAP Alter
[NASA-TM-106836] p 1047 N95-19649

INERTIAL CONFINEMENT FUSION
Study of high gain spherical shell ICF targets containing uniform layers of liquid deuterium tritium fuel
[DE94-018550] p 1136 N95-18552
25-ps neutron detector for measuring ICF-target burn history
[DE94-016450] p 1146 N95-19250
Inertial confinement fusion
[DE95-000314] p 1147 N95-19552
Contributions of the National Ignition Facility to the development of Inertial Fusion Energy
[DE94-018335] p 1137 N95-19588
Future trends in optical coatings for high-power laser applications
[DE94-018592] p 1039 N95-19708
Scintillating-fiber imaging detector for 14-MeV neutrons
[DE94-018593] p 1135 N95-19709
Damage from pulses with arbitrary temporal shapes
[DE94-018606] p 1039 N95-19722

INERTIAL FUSION (REACTOR)
Contributions of the National Ignition Facility to the development of Inertial Fusion Energy
[DE94-018335] p 1137 N95-19588

INFORMATION
The synthesis of vision and action
[AD-A285453] p 1088 N95-18094

INFORMATION ADAPTIVE SYSTEM
A scalable decentralized group membership service for an asynchronous environment
[AD-A283633] p 1109 N95-18137

INFORMATION DISSEMINATION
NASA/DOD Aerospace Knowledge Diffusion Research Project. Paper 47: The value of computer networks in aerospace
[NASA-CR-197591] p 1109 N95-18055
A strategy for electronic dissemination of NASA Langley technical publications
[NASA-TM-109172] p 1175 N95-18936
NASA/DOD Aerospace Knowledge Diffusion Research Project. Report 26: The technical communication practices of aerospace engineering students: Results of the phase 3 AIAA National Student Survey
[NASA-TM-109121] p 1175 N95-18950
NASA/DOD Aerospace Knowledge Diffusion Research Project. Report 29: A comparison of the technical communications practices of Japanese and US aerospace engineers and scientists
[NASA-TM-109164] p 1175 N95-18953
A hypertext-based Internet-assessable database for the MSFC Technology Transfer Office p 1165 N95-18986
NASA/DOD Aerospace Knowledge Diffusion Research Project. Paper 45: A comparison of the information-seeking behaviors of three groups of US aerospace engineers
[NASA-TM-109839] p 1176 N95-19127
The Japan Information Center of Science and Technology p 1198 N95-19128

INFORMATION FLOW
A simple hyperbolic model for communication in parallel processing environments
[NASA-CR-195984] p 1098 N95-18487
NASA/DOD Aerospace Knowledge Diffusion Research Project. Paper 45: A comparison of the information-seeking behaviors of three groups of US aerospace engineers
[NASA-TM-109839] p 1176 N95-19127

INFORMATION MANAGEMENT
User profile for researchers studying objects: Implications for computer systems
[PB94-188463] p 1109 N95-17989
Portable, Reusable, Integrated Software Modules (PRISM) documentation library model document release 1.0: Central Archive for Reusable Defense Software (CARDS)
[AD-A284567] p 1095 N95-18030
Library capability demonstration. Central Archive for Reusable Defense Software (CARDS)
[AD-A284568] p 1095 N95-18031
Library capability demonstration. Central Archive for Reusable Defense Software (CARDS)
[AD-A284569] p 1095 N95-18032
Library Development Handbook. Central Archive for Reusable Defense Software (CARDS)
[AD-A284570] p 1095 N95-18033
Metrics concept report. Central Archive for Reusable Defense Software (CARDS)
[AD-A284573] p 1097 N95-18449
Development of executive information systems
[AD-A284005] p 1174 N95-18654
Graphics MIS/Shop Store Program: User's manual
[AD-A284062] p 1174 N95-18681
Environmental Compliance Assessment System (ECAS)
[AD-A283950] p 1060 N95-18683
Processing multilevel secure test and evaluation information
[AD-A284073] p 1001 N95-19069
Information system architecture to support transparent access to distributed, heterogeneous data sources
[DE94-018450] p 1176 N95-19589
Cooperating agents for information retrieval
[AD-A285887] p 1176 N95-19604
Environmental Compliance Assessment System (ECAS). South Carolina supplement: US Army
[AD-A279244] p 1062 N95-19860

INFORMATION PROCESSING (BIOLOGY)
Cooperativity and 3-D representation
[AD-A284203] p 1093 N95-17940
Learning effects on strategy selection in a dynamic task environment as a function of time pressure
[AD-A285458] p 1089 N95-19538
Multiple-task performance: A critical review of the literature and a cognitive neuroscience framework
[AD-A285133] p 1090 N95-19583

INFORMATION RETRIEVAL
Library capability demonstration. Central Archive for Reusable Defense Software (CARDS)
[AD-A284572] p 1095 N95-18034
A strategy for electronic dissemination of NASA Langley technical publications
[NASA-TM-109172] p 1175 N95-18936
Users manual for the Moods Data Management System (MDMS), version 1.0
[NASA-CR-197015] p 1075 N95-18951
Cooperating agents for information retrieval
[AD-A285887] p 1176 N95-19604

INFORMATION SYSTEMS
National Library of Medicine programs and services, fiscal year 1991
[PB94-188026] p 1077 N95-17949
National Library of Medicine programs and services, fiscal year 1992
[PB94-188034] p 1078 N95-17950
Semiconductor measurement technology: Design and testing guides for the COMOS and lateral bipolar-on-SOI test library
[PB94-178019] p 1007 N95-17984
User profile for researchers studying objects: Implications for computer systems
[PB94-188463] p 1109 N95-17989
Independent validation and verification of automated information systems in the Department of Energy
[DE94-014460] p 1173 N95-18063
Automatic Identification Technology (AIT): The development of functional capability and card application matrices
[AD-A285528] p 1173 N95-18099
Implementation of the 1992 Terminal area-Local Analysis and Prediction System (T-LAPS)
[AD-A284334] p 1070 N95-18384
Resources Automated Management System
[AD-A284153] p 1171 N95-18416
Metrics concept report. Central Archive for Reusable Defense Software (CARDS)
[AD-A284573] p 1097 N95-18449
Alarm annunciation in a graphical environment
[DE94-015761] p 1098 N95-18652
Development of executive information systems
[AD-A284005] p 1174 N95-18654
Users manual for the Moods Data Management System (MDMS), version 1.0
[NASA-CR-197015] p 1075 N95-18951
NASA/DOD Aerospace Knowledge Diffusion Research Project. Report 29: A comparison of the technical communications practices of Japanese and US aerospace engineers and scientists
[NASA-TM-109164] p 1175 N95-18953
A report of work activities on the NASA Spacelink public electronic library p 1168 N95-19005
NASA/DOD Aerospace Knowledge Diffusion Research Project. Paper 45: A comparison of the information-seeking behaviors of three groups of US aerospace engineers
[NASA-TM-109839] p 1176 N95-19127
The Japan Information Center of Science and Technology p 1198 N95-19128
Aerospace medicine and biology: A continuing bibliography with indexes (supplement 398)
[NASA-SP-7011(398)] p 1080 N95-19239
Aeronautical engineering: A continuing bibliography with indexes (supplement 314)
[NASA-SP-7037(314)] p 927 N95-19357
Toward a new national weather service: Weather for those who fly
[PB94-214418] p 1072 N95-19407
Multicast tree construction in network topologies with asymmetric link loads
[AD-A285679] p 1003 N95-19525
Information system architecture to support transparent access to distributed, heterogeneous data sources
[DE94-018450] p 1176 N95-19589
Zoned Analog Personal Teleconferencing (ZAPT)
[AD-A285877] p 1004 N95-19600
The design and implementation of EPL: An event pattern language for active databases p 1101 N95-19629

INFORMATION TRANSFER
Secure distributed file systems
[AD-A285525] p 1173 N95-18096
NASA/DOD Aerospace Knowledge Diffusion Research Project. Report 29: A comparison of the technical communications practices of Japanese and US aerospace engineers and scientists
[NASA-TM-109164] p 1175 N95-18953
NASA/DOD Aerospace Knowledge Diffusion Research Project. Paper 45: A comparison of the information-seeking behaviors of three groups of US aerospace engineers
[NASA-TM-109839] p 1176 N95-19127
Knowledge based translation and problem solving in an intelligent individualized instruction system
p 1105 N95-19753
Collaborative engineering-design support system
p 1106 N95-19757
DYNACLIPS (DYNAmic CLIPS): A dynamic knowledge exchange tool for intelligent agents
p 1108 N95-19768

INFRARED ASTRONOMY
Study for the analysis of the observations, and numerical data representing the planets as far-infrared calibration sources
[NASA-CR-196542] p 1195 N95-19287
INFRARED DETECTORS
A triangulation method for passive ranging
[AD-A284180] p 998 N95-18522
The optical emission and absorption properties of silicon-germanium superlattice structures grown on non-conventional silicon substrate orientation
[AD-A284852] p 1153 N95-19715
IR materials producibility
[AD-A284263] p 1142 N95-19732
INFRARED IMAGERY
Ice surface temperature retrieval from AVHRR, ATSR, and passive microwave satellite data: Algorithm development and application
[NASA-CR-197542] p 1052 N95-18952
A GIS approach to urban heat island research: The case of Huntsville, Alabama p 1063 N95-18991
Large area thermal target board: An improvement to environmental effects and system parameters characterization
[AD-A284614] p 1141 N95-19085
INFRARED INSTRUMENTS
Atmospheric Infrared Sounder
[NASA-CR-197573] p 1064 N95-18444
Proceedings of the 15th Annual Conference on Atmospheric Transmission Models
[AD-A279919] p 1142 N95-19862
INFRARED LASERS
Atomic line filter for SDI applications
[AD-A284125] p 1139 N95-18409
INFRARED RADIATION
Midinfrared optical properties of petroleum oil aerosols
[AD-A283689] p 1139 N95-18142
Application of photogrammetry of F-14D store separation
[AD-A284154] p 943 N95-18417
Marine boundary layer refractive effects in the infrared
[AD-A285717] p 1140 N95-18484
Infrared-to-visible converter
[AD-D016443] p 1141 N95-18529
Can an infrared-vanishing gluon propagator confine quarks?
[DE94-018388] p 1131 N95-18548
PRISM project optical instrument
p 1143 N95-19009
Principal-value resummation for dilepton production
[DE95-001094] p 1135 N95-19726
Thermochemical IR sources: COCHISE and FACELIF experiments
[AD-A279940] p 977 N95-19868
INFRARED SIGNATURES
A triangulation method for passive ranging
[AD-A284180] p 998 N95-18522
Large area thermal target board: An improvement to environmental effects and system parameters characterization
[AD-A284614] p 1141 N95-19085
INFRARED SPECTRA
Midinfrared optical properties of petroleum oil aerosols
[AD-A283689] p 1139 N95-18142
Visible-infrared remote-sensing model and applications for ocean waters
[NASA-CR-197602] p 1051 N95-18739
PRISM project optical instrument
p 1143 N95-19009
INGESTION (ENGINES)
Modern transport engine experience with environmental ingestion effects p 951 N95-19660
Experimental and numerical simulations of the effects of ingested particles in gas turbine engines
p 952 N95-19662
INHIBITORS
Concentration and temperature effects on ovostatin activity p 1077 N95-18997
INJECTION
Development of a bulk current injection direct-drive system to test system level components with stress waveforms that are encountered during full threat indirect effects lightning
[AD-A284160] p 933 N95-18507
Theoretical investigation of matching between plasma heating and fueling in HL-1M machine
[DE94-627019] p 1146 N95-19241
Power flow and PRS optimization on Phoenix
[AD-A279214] p 1147 N95-19846
INJECTORS
Optical measurements in rocket engine liquid sprays
p 968 N95-18979
INJURIES
Neuropsychophysiologic sequelae of mild head injury
p 1083 N95-19430
INLET FLOW
Wind turbine blade aerodynamics: The combined experiment
[DE94-011866] p 929 N95-18645
Wind turbine blade aerodynamics: The analysis of field test data
[DE94-011867] p 929 N95-18646
Gas storage and recovery system
[NASA-CASE-MSC-22091-1] p 992 N95-18738
Prediction of wind tunnel effects on the installed F/A-18A inlet flow field at high angles-of-attack
[NASA-CR-195429] p 950 N95-19651
INLET PRESSURE
Neural net controller for inlet pressure control of rocket engine testing p 1102 N95-19637
INMARSAT SATELLITES
The future use of DSCS and commercial satellites in the US Navy
[AD-A285707] p 997 N95-18481
INNER RADIATION BELT
CRRESPRO documentation
[AD-A284578] p 1178 N95-18451
INOCULATION
Investigation of the microstructure of coatings for high power lasers by non-optical techniques
[DE94-017697] p 987 N95-19227
INORGANIC COATINGS
Reliability Without Hermeticity (RWOH) for Integrated Circuits (IC)
[AD-A284340] p 1009 N95-18418
INORGANIC COMPOUNDS
Aryl gels and related materials. Synthesis and characterization of a new class of microporous materials
[AD-A285044] p 987 N95-19544
INORGANIC MATERIALS
Fabrication of biomimetic molecular level composites
[AD-A284204] p 969 N95-17941
INPUT/OUTPUT ROUTINES
TEXCAD: Textile Composite Analysis for Design. Version 1.0: User's manual
[NASA-CR-4639] p 970 N95-18466
Characterizing parallel file-access patterns on a large-scale multiprocessor
[NASA-CR-197568] p 1110 N95-18521
Dynamic file-access characteristics of a production parallel scientific workload
[NASA-CR-197570] p 1110 N95-18581
INSOLATION
Summary information and data sets for the HBCU Solar Measurements Network
[DE94-011872] p 1055 N95-19856
INSPECTION
Debris/ice/TPS assessment and integrated photographic analysis of Shuttle mission STS-68
[NASA-TM-109207] p 963 N95-18047
Modeling and measurement of the performance of a branched conduit sampling system in a mass spectrometer leak detector p 1036 N95-18181
INSTALLING
TEXCAD: Textile Composite Analysis for Design. Version 1.0: User's manual
[NASA-CR-4639] p 970 N95-18466
INSTRUMENT APPROACH
Heliport/vertiport MLS precision approaches
[AD-A283505] p 940 N95-18059
INSTRUMENT ORIENTATION
A comparison between using incoherent or coherent sources to align and test an adaptive optical telescope
p 1142 N95-18969
INSTRUMENT PACKAGES
Field and data analysis studies related to the atmospheric environment
[NASA-CR-196543] p 1068 N95-18093
INSULATED STRUCTURES
The sound insulations of metal-framed partitions having structural loadbearing properties
[BBC-RD-1994/8] p 992 N95-18533
Further measurements of the sound insulations of metal-framed partitions
[BBC-RD-1994/7] p 998 N95-18534
Metal-framed partitions with reduced thicknesses. Part 1: Narrower studs and cavities
[BBC-RD-1993/5-PT-1] p 993 N95-19138
INSULATION
The sound insulations of metal-framed partitions having structural loadbearing properties
[BBC-RD-1994/8] p 992 N95-18533
Further measurements of the sound insulations of metal-framed partitions
[BBC-RD-1994/7] p 998 N95-18534
Metal-framed partitions with reduced thicknesses. Part 2: Built-in acoustic treatment
[BBC-RD-1993/6-PT-2] p 993 N95-19137
Metal-framed partitions with reduced thicknesses. Part 1: Narrower studs and cavities
[BBC-RD-1993/5-PT-1] p 993 N95-19138
INTAKE SYSTEMS
Prediction of wind tunnel effects on the installed F/A-18A inlet flow field at high angles-of-attack
[NASA-CR-195429] p 950 N95-19651
INTEGRAL EQUATIONS
The space-time solution element method: A new numerical approach for the Navier-Stokes equations
[NASA-TM-106818] p 1014 N95-18036
Alternative volume integral equation formulations applied to dielectric cylinders
[AD-A285537] p 995 N95-18066
An inverse problem in thermal imaging
[NASA-CR-195018] p 1117 N95-18479
High-order corrected trapezoidal rules for singular functions
[AD-A284269] p 1119 N95-19735
Solutions of TEAM Problem No. 13 using integral equations in a sequential and parallel computing environment
[DE95-001472] p 1112 N95-19834
Theory and applications of the phi transform wavelets
[AD-A279943] p 1119 N95-19869
INTEGRALS
Coulomb gas representation of the SU(2) WZW correlators at higher genera
[PB94-217254] p 1119 N95-19718
SU(2) WZW theory at higher genera
[PB94-217262] p 1119 N95-19719
INTEGRATED CIRCUITS
Automatic Identification Technology (AIT): The development of functional capability and card application matrices
[AD-A285528] p 1173 N95-18099
Superconductive signal-processing circuits
[AD-A285533] p 1008 N95-18103
High power phase conjugated solid state lasers
[DE94-016633] p 1037 N95-18357
Reliability Without Hermeticity (RWOH) for Integrated Circuits (IC)
[AD-A284340] p 1009 N95-18418
MIKON 94. International Microwave Conference. Volume 1: Conference proceedings
[AD-A284351] p 1009 N95-18425
INTELLIGENCE
Modular implementation of feature extraction and matching algorithms for photogrammetric stereo imagery
[AD-A285422] p 1032 N95-18065
INTELSAT SATELLITES
The future use of DSCS and commercial satellites in the US Navy
[AD-A285707] p 997 N95-18481
INTERACTIONAL AERODYNAMICS
Sectional prediction of 3D effects for separated flow on rotating blades
[PB94-201696] p 928 N95-18503
Pressure measurements on an F/A-18 twin vertical tail in buffeting flow. Volume 4, part 2: Buffet cross spectral densities
[AD-A285555] p 957 N95-18641
INTERATOMIC FORCES
Atomic scale force mapping with the atomic force microscope
[AD-A284940] p 1129 N95-17974
Embedded microclusters in zeolites and cluster beam sputtering: Simulation on parallel computers
[DE95-000662] p 1134 N95-19562
INTERFACES
A constant-depth scratch test for the measurement of adhesion at film-substrate interfaces
[AD-A283660] p 983 N95-18016
INTERFACIAL TENSION
Time-evolving bubbles in two-dimensional stokes flow
[NASA-CR-194998] p 1015 N95-18188
Fracture toughness of polymer/polymer bimaterial interface reinforced with block copolymers
p 986 N95-18923
Ice accretion with varying surface tension
[NASA-TM-106826] p 934 N95-19285
INTERFERENCE IMMUNITY
Combiner for two dimensional adaptive interference suppression system
[AD-D016272] p 997 N95-18516
Signal enhancement in AM-FM interference
[AD-A285114] p 1004 N95-19565
INTERFEROMETERS
Fiber optic flexural disk accelerometer
[AD-D016444] p 1141 N95-18563
Flame position ultrasonic interferometer
[AD-D016235] p 967 N95-18632
INTERFEROMETRY
Dynamic decohesion of bimaterials: Experimental observations and failure criteria
[GALCIT-94-2] p 1045 N95-18613

Interferometric synthetic aperture radar and the Data Collection System Digital Terrain Elevation Demonstration
[AD-A284024] p 999 N95-18657

INTERMETALLICS
Nonstoichiometry of Al-Zr intermetallic phases
[DE94-016877] p 979 N95-19093
Deformation texture studies in Fe3Al alloys
[DE94-017709] p 980 N95-19400
Braze repair possibilities for hot section gas turbine parts p 954 N95-19677
NiAl and NiAl-based composites directionally solidified by a containerless zone process
[NASA-CR-195430] p 982 N95-19792

INTERNAL FLOW
One-dimensional flow description for the combustion chamber of a scramjet
[DLR-FB-94-06] p 948 N95-18911
Determination of solid/porous wall boundary conditions from wind tunnel data for computational fluid dynamics codes p 1023 N95-19266
The application of the SAUNA CFD system to high and low speed vehicles
[ARA-MEMO-402] p 1031 N95-19778

INTERNAL PRESSURE
Nonlinear analysis of damaged stiffened fuselage shells subjected to combined loads p 939 N95-19499

INTERNAL WAVES
The diurnal cycle of high-frequency temperature variability at 0 deg 140 deg W on seasonal and interannual time scales
[AD-A283640] p 1074 N95-18012

INTERNATIONAL COOPERATION
Meteor 3/TOMS launch of 15 August 1991 in Plesetsk, USSR
[NASA-TM-110115] p 962 N95-18150
US experiments flown on the Soviet biosatellite Cosmos 2044. Volume 1: Mission description, experiments K-7-01 - K-7-15
[NASA-TM-108802-VOL-1] p 1092 N95-18569
European aeronautics: Strong government presence in industry structure and research and development support. Report to Congressional Requesters
[GAO/NSIAD-94-71] p 1171 N95-18578

INTERNATIONAL SPACE STATION
Space Station: Plans to expand research community do not match available resources. Report to the Ranking Minority Member, Subcommittee on Oversight of Government Management, Committee on Government Affairs, US Senate
[GAO/NSIAD-95-33] p 965 N95-19131

INTERNATIONAL TRADE
US Industrial Outlook, 1994: An almanac of industry, technology and services. 35th annual edition. Forecasts for selected manufacturing and service industries
[PB94-107844] p 1171 N95-17988

INTERNETS
A scalable decentralized group membership service for an asynchronous environment
[AD-A283633] p 1109 N95-18137
A hypertext-based Internet-assessable database for the MSFC Technology Transfer Office p 1165 N95-18986
A report of work activities on the NASA Spacelink public electronic library p 1168 N95-19005

INTERPLANETARY DUST
Physics of spacecraft-based interplanetary dust collection by impact into low-density media p 1181 N95-19176
Plasma produced by impacts of fast dust particles on a thin film p 1181 N95-19177
Highly transparent and rugged sensor for velocity determinations of cosmic dust particles p 966 N95-19178
Collection requirements for trace-element analyses of extraterrestrial samples p 1182 N95-19182
Techniques for in situ collection and measurement of volatiles released during hypervelocity impact p 962 N95-19184
Some considerations on velocity vector accuracy in dust trajectory analysis p 1183 N95-19186
Velocity distribution of Earth-crossing asteroid grains p 1183 N95-19187
The intact capture of hypervelocity dust particles using underdense foams p 1183 N95-19188
Assessment of velocity/trajectory measurement technologies during a particle capture event p 1036 N95-19193
The use of silica aerogel to collect interplanetary dust in space p 989 N95-19197
The fine nebula dust component: A key to chondrule formation by lightning p 1192 N95-19333

INTERPLANETARY SPACECRAFT
SOCCER: Comet Coma Sample Return Mission p 1181 N95-19174

INTERPOLATION
Neural networks applications to control and computations p 1115 N95-18992

INTERPROCESSOR COMMUNICATION
A simple hyperbolic model for communication in parallel processing environments
[NASA-CR-195984] p 1098 N95-18487
Characterizing parallel file-access patterns on a large-scale multiprocessor
[NASA-CR-197568] p 1110 N95-18521
Parallel Navier-Stokes computations on shared and distributed memory architectures
[NASA-TM-106823] p 1019 N95-18941
On k-ary n-cubes: Theory and applications
[NASA-CR-194996] p 1100 N95-19028
Neural network communications signal processing
[AD-A285681] p 1115 N95-19512
Advanced techniques for analysis and evaluation of robust protocols
[AD-A285682] p 1111 N95-19513
Using PVM to host CLIPS in distributed environments p 1104 N95-19748
PalymSys (TM): An extended version of CLIPS for construction and reasoning using blackboards p 1107 N95-19767
Solution of potential flow problems on a network of workstations
[DE94-017861] p 1112 N95-19831

INTERSTELLAR MATTER
PRISM project optical instrument p 1143 N95-19009
The early Sun and the formation of chondrules p 1188 N95-19305

INTERSTICES
Metal-framed partitions with reduced thicknesses. Part 1: Narrower studs and cavities
[BBC-RD-1993/5-PT-1] p 993 N95-19138

INTERVERTEBRAL DISKS
Clinical practice, diagnosis and therapy of intervertebral disk lesion: Importance to fitness for military flying duties p 1084 N95-19435
Spinal nerve syndromes: The need to confirm the diagnosis with neurophysiological examinations p 1085 N95-19436

INTRAVASCULAR SYSTEM
Echo imaging techniques determine the size of intravascular bubbles in decompression sickness
[AD-A284849] p 1087 N95-19714

INTRAVENOUS PROCEDURES
Nuclear medicine program
[DE94-017530] p 1080 N95-19244

INVARIANCE
Limits on CP nonconserving interactions from electric dipole moments
[DE94-018582] p 1134 N95-19705

INVENTORIES
The generic simulation executive at Manned Flight Simulator
[AD-A283997] p 959 N95-18724

INVERSE KINEMATICS
Adaptive Neuron Model: An architecture for the rapid learning of nonlinear topological transformations
[NASA-CASE-NPO-18579-1-CU] p 1114 N95-18740

INVERSIONS
An inverse problem in thermal imaging
[NASA-CR-195018] p 1117 N95-18479

INVISCID FLOW
Computation of inviscid flows: Various approximations p 1027 N95-19446
Computation of inviscid flows: Full potential method p 1027 N95-19447
Finite volume method using Runge-Kutta time-stepping for solution of Euler equations p 1027 N95-19451
CFD: Advances and Applications, 1994
[NAL-SP-9412] p 1028 N95-19455
Finite-volume upwind schemes for inviscid gas dynamics p 1028 N95-19456
Viscous flow past aerofoils axisymmetric bodies and wings p 933 N95-19457
Validation and evaluation of the advanced aeronautical CFD system SAUNA: A method developer's view
[ARA-MEMO-390] p 1030 N95-19774
Verification of the CFD simulation system SAUNA for complex aircraft configurations
[ARA-MEMO-401] p 1031 N95-19776
Inviscid and viscous flow modelling of complex aircraft configurations using the CFD simulation system sauna
[ARA-MEMO-403] p 1031 N95-19777

IODINE
DC-conductivity and magnetoresistance of inherently conducting polymers. Polyacetylene and poly(3-alkylthiophenes)
[PB94-184587] p 1007 N95-18037

IODINE ISOTOPES
I-Xe studies of individual chondrules: What can they tell us about chondrule formation? p 1192 N95-19329

IODINE 131
Nuclear medicine program
[DE94-017530] p 1080 N95-19244

ION ACCELERATORS
Three-grid accelerator system for an ion propulsion engine
[NASA-CASE-NPO-18391-2-CU] p 1137 N95-18957

ION BEAMS
Ion beam surface treatment: A new capability for surface enhancement
[DE94-014663] p 977 N95-17968
Tunneling and transport in mesoscopic structures
[AD-A283426] p 1148 N95-18053
LEVIS ion source and beam characterization on PBFA-2
[DE94-015802] p 1133 N95-19199
Ion mixing in oxide-sapphire systems
[DE94-018660] p 1133 N95-19232

ION CURRENTS
Three-grid accelerator system for an ion propulsion engine
[NASA-CASE-NPO-18391-2-CU] p 1137 N95-18957
LEVIS ion source and beam characterization on PBFA-2
[DE94-015802] p 1133 N95-19199

ION CYCLOTRON RADIATION
Global wave modeling of electron interactions with fast magnetosonic waves
[DE94-018942] p 1144 N95-18557
Mass spectrometric studies of clusters and surfaces
[AD-A283992] p 974 N95-19066

ION EMISSION
Ion emission intensity ratios as a function of electrode gap, melting current, and pressure during low current vacuum arc remelting
[DE94-017407] p 1129 N95-18144

ION ENGINES
TFE design package, TFE Verification Program
[DE94-017558] p 1136 N95-18147
Three-grid accelerator system for an ion propulsion engine
[NASA-CASE-NPO-18391-2-CU] p 1137 N95-18957

ION EXCHANGE RESINS
Obtention of cationic polymeric membranes by radiation-induced grafting method
[DE94-629193] p 983 N95-17942
Polymer-based separations: Synthesis and application of polymers for ionic and molecular recognition
[DE94-016427] p 984 N95-18355

ION EXCHANGING
Ion exchange polymers and method for making
[NASA-CASE-LEW-15576-1] p 984 N95-18321

ION IMPLANTATION
Defect reduction and back channel degradation in SIMOX
[AD-A284231] p 1148 N95-17960
Method of doping single crystal diamond for electronic devices
[AD-D016267] p 1149 N95-18543

ION PROPULSION
Three-grid accelerator system for an ion propulsion engine
[NASA-CASE-NPO-18391-2-CU] p 1137 N95-18957

ION RECOMBINATION
Ion-molecule collisions, electron molecule collisions, excitation and ionization of atoms
[AD-A284584] p 1129 N95-18062

ION SOURCES
LEVIS ion source and beam characterization on PBFA-2
[DE94-015802] p 1133 N95-19199

IONIC COLLISIONS
Evidence for coexistence of two phases in relativistic heavy ion collisions and comparison with lattice results
[DE94-626672] p 1130 N95-18329
Ion mixing in oxide-sapphire systems
[DE94-018660] p 1133 N95-19232

IONIC REACTIONS
Innovative development and application of models for weakly ionized ionospheric plasmas
[AD-A284583] p 1064 N95-18452
A photoionization study of OH and OD from 680A to 950A: An analysis of the Rydberg series
[NASA-CR-196970] p 974 N95-18744

IONIZATION
Deformation of nonstoichiometric CuO polycrystals
[DE94-016907] p 1150 N95-19094
Study of laser resonance ionization mass spectrometry using a glow discharge source
[DE94-018566] p 981 N95-19703
The interactions of high-energy, highly charged Xe ions with fullerenes
[DE95-001440] p 1135 N95-19786

IONIZATION POTENTIALS
Mass spectrometric studies of clusters and surfaces
[AD-A283992] p 974 N95-19066

IONIZERS
Electron reversal ionizer for detection of trace species using a spherical cathode
[NASA-CASE-NPO-18870-1-CU] p 1130 N95-18324
IONIZING RADIATION
Study of the effect of ionizing radiation on the structure of natural rubber latex by positron annihilation technique
[DE94-631466] p 975 N95-19550
IONOSONDES
The use of two-station ionosonde data for IONCAP/ASAPS model validation on transpolar two-hop, high-frequency skywave radio links
[AD-A284270] p 1005 N95-19736
IONOSPHERES
Observations of TEC fluctuations from an explosion on the Earth's surface
[DE94-018278] p 1063 N95-18125
Doppler shift and spread study for ionospherically propagated signals
[AD-A284610] p 1065 N95-19083
IONOSPHERIC DISTURBANCES
Results from the northern New Mexico satellite-beacon radio interferometer
[DE94-018310] p 1063 N95-18148
New applications of the Phillips Laboratory. Theoretical ionospheric model and studies of neutral density waves
[AD-A284663] p 1066 N95-19105
IONOSPHERIC ELECTRON DENSITY
Results from the northern New Mexico satellite-beacon radio interferometer
[DE94-018310] p 1063 N95-18148
Investigation of the ionospheric short-term variability
[AD-A286253] p 1066 N95-19387
IONOSPHERIC HEATING
Innovative development and application of models for weakly ionized ionospheric plasmas
[AD-A284583] p 1064 N95-18452
Radio wave heating of the lower ionosphere
p 1145 N95-18905
IONOSPHERIC PROPAGATION
The Seventh Ionospheric Effects Symposium
[PB94-191930] p 1057 N95-17985
IONCAP prediction-based Automatic Link Establishment (ALE) frequency selection for a ten-node Australian high-frequency network
[AD-A283698] p 999 N95-18619
The use of two-station ionosonde data for IONCAP/ASAPS model validation on transpolar two-hop, high-frequency skywave radio links
[AD-A284270] p 1005 N95-19736
IONOSPHERICS
The Seventh Ionospheric Effects Symposium
[PB94-191930] p 1057 N95-17985
IONS
Cross-tail current, field-aligned current, and B(y)
[NASA-CR-197624] p 1065 N95-19032
Direct energy conversion system for D(3)-He fusion
[DE94-770773] p 1146 N95-19549
The interactions of high-energy, highly charged Xe ions with fullerenes
[DE95-001440] p 1135 N95-19786
Spectral distribution of the two-photon decay of He-like krypton
[DE95-001442] p 1135 N95-19787
IRIDIUM ALLOYS
The metallurgical integrity of the frit vent assembly diffusion bond
[DE95-000610] p 968 N95-19877
IRON
Surface phases, surface defects and the initial stages of oxidation
[DE94-016947] p 979 N95-18358
Coronal abundances and their variation
[NASA-CR-197553] p 1195 N95-18376
An instrument to measure the charge, and energy spectrum (20-1000 GeV/a) of the cosmic ray species oxygen to iron
[NASA-CR-197555] p 1197 N95-18464
Impurity behavior during ion-Bernstein wave heating in PBX-M
[DE94-018114] p 1133 N95-19228
The very low energy solar flux of electron and heavy-flavor neutrinos and antineutrinos
[DE94-018583] p 1135 N95-19706
Relative elemental abundance and heating constraints determined for the solar corona from SERTS measurements
[NASA-TM-104616] p 1196 N95-19791
IRON ALLOYS
On the crack growth resistance and strength of the B2 iron aluminides Fe-40Al, Fe-45Al, and Fe-10Ni-40Al (at. %)
[DE94-017857] p 978 N95-18128
Deformation texture studies in Fe3Al alloys
[DE94-017709] p 980 N95-19400
Weldability of iron aluminides
[DE95-000686] p 981 N95-19568
Study of laser-resonance ionization mass spectrometry using a glow discharge source
[DE94-018566] p 981 N95-19703
IRON CHLORIDES
DC-conductivity and magnetoresistance of inherently conducting polymers. Polyacetylene and poly(3-alkylthiophenes)
[PB94-184587] p 1007 N95-18037
IRRADIANCE
Nonlinear response of the photocathode of an x-ray streak camera to UV light
[DE94-018073] p 1032 N95-18130
Visible-infrared remote-sensing model and applications for ocean waters
[NASA-CR-197602] p 1051 N95-18739
A novel technique for 4-dimensional atmospheric and oceanographic irradiance measurements using 3-D spatial filtering
[AD-A285658] p 1073 N95-19701
IRRADIATION
Development of radiation-hardened ceramic composites for fusion applications
[DE94-016182] p 985 N95-18638
Study of the effect of ionizing radiation on the structure of natural rubber latex by positron annihilation technique
[DE94-631466] p 975 N95-19550
ISCHEMIA
Cumulative effects of repeated brief cerebral ischemia
[AD-A284234] p 1087 N95-19698
ISENTROPIC PROCESSES
Forecasting snowfall using mixing ratios on an isentropic surface: An empirical study
[PB94-188760] p 1067 N95-17993
ISOLATION
A shock isolation method and apparatus
[AD-D016471] p 1045 N95-18456
Isolation and characterization of an indium-mixed-pnicogen Four-membered ring compound: Crystal structure of (Me3SiCH2)2InAs(SiMe3)2 In(CH2SiMe3)2P(SiMe3)2
[AD-A279170] p 1154 N95-19807
ISOMERIZATION
Large amplitude motions, especially isomerization and tunneling in polyatomic molecule spectra: Novel experimental, pattern recognition, and theoretical methods
[AD-A284194] p 985 N95-18636
Reaction channel competition in vibrational overtone activation: 1-methylcyclopropene
[AD-A280185] p 976 N95-19830
ISOMERS
Elemental fluorine based syntheses of pentafluoro phenyl and other aromatic perfluoropolyether polymers
[AD-A284102] p 984 N95-18402
Molecular recognition as shown by the solvent extraction of (R)- and (S)-alpha-(1-naphthyl)ethyl ammonium picrate or orange 2 by chiral pyridino-crown ethers
[AD-A280157] p 969 N95-19823
ISOTHERMAL PROCESSES
Thermo-oxidative stability of graphite/PMR-15 composites: Effect of fiber surface modification on composite shear properties
[NASA-TM-4608] p 981 N95-19652
ISOTHERMS
Magnetotelluric mapping of upper crustal isotherms beneath the Valles Caldera hydrothermal system
[DE94-013606] p 1063 N95-17946
ISOTOPE SEPARATION
Isotope separation and advanced manufacturing technology
[DE95-000313] p 1039 N95-19551
ISOTOPES
Carbon, CAIs and chondrules p 1186 N95-19291
Physics with isotopically controlled semiconductors
[DE95-000789] p 1152 N95-19615
ISOTOPIC LABELING
Nuclear medicine program
[DE94-017530] p 1080 N95-19244
Mn-Cr isotopic systematics of Chainpur chondrules and bulk ordinary chondrites p 1190 N95-19320
Formation of chondrules and CAIs by nebular processes p 1190 N95-19321
ISOTROPIC MEDIA
A 2D depth migration in transversely isotropic media using explicit operators
[DE95-000645] p 1066 N95-19560
ISOTROPIC TURBULENCE
On the Lighthill relationship and sound generation from isotropic turbulence
[NASA-CR-195005] p 1016 N95-18191
Experimental studies of Reynolds number dependence of turbulent mixing and transport
[DE94-015338] p 1030 N95-19578
ISOTROPY
Fatigue in single crystal nickel superalloys
[AD-A285727] p 978 N95-18068
Study of strangeness production in relativistic nucleus beams at JINR
[DE94-626720] p 1136 N95-18881
ITERATION
TLS-based prefiltering technique for time-domain ARMA modeling
[AD-A284525] p 1120 N95-18113
The formulation of quantum statistical mechanics based on the Feynman path centroid density. 4: Algorithms for centroid molecular dynamics
[AD-A279234] p 1157 N95-19853
ITERATIVE SOLUTION
A domain decomposition algorithm for elliptic problems in three dimensions
[DE94-019265] p 1094 N95-17978
Subspace correction methods for the iterative solution of hierarchic plate models. 1: Heat transfer problems
[AD-A285712] p 1117 N95-18482

J

J INTEGRAL
J-integral characterization of the nozzle steels from intermediate test vessels IV-5 and IV-9
[DE95-001066] p 979 N95-18934
The load separation technique in the elastic-plastic fracture analysis of two- and three-dimensional geometries p 936 N95-19481
Fatigue crack growth under variable amplitude loading
p 937 N95-19484
JACKS (LIFTS)
Mathematical analysis of actuator forces in a scissor lift
[AD-A283906] p 1040 N95-18152
JAMMING
Radar sector blanker
[AD-D016275] p 996 N95-18429
JAPAN
Using federal technology policy to strength the US microelectronics industry
[DE94-017293] p 1008 N95-18143
NASA/DOD Aerospace Knowledge Diffusion Research Project. Paper 46: Technical communications in aerospace: A comparison across four countries
[NASA-TM-110056] p 1175 N95-19038
JAPANESE SPACE PROGRAM
SOCCER: Comet Coma Sample Return Mission
p 1181 N95-19174
JET AIRCRAFT
Preliminary evaluation of the F/A-18 quantity/multiple envelope expansion
[AD-A284119] p 943 N95-18407
JET CONTROL
New technologies for space avionics
[NASA-CR-197574] p 966 N95-18196
JET ENGINES
Developing an emission factor for hazardous air pollutants for an F-16 using JP-8 fuel
[AD-A284802] p 1061 N95-19685
JET FLOW
Numerical mixing calculations of confined reacting jet flows in a cylindrical duct
[NASA-TM-106736] p 947 N95-18133
Flow field investigation in a free jet - free jet core system for the generation of high intensity molecular beams
[DLR-FB-94-11] p 1132 N95-18912
Evaluation of three turbulence models for afterbody/jet flows, including Reynolds stress closure
[ARA-90] p 932 N95-19574
Evaluation of three turbulence models for afterbody/jet flows, including Reynolds stress closure
[ARA-MEMO-408] p 1194 N95-19773
JET MIXING FLOW
One-dimensional flow description for the combustion chamber of a scramjet
[DLR-FB-94-06] p 948 N95-18911
JET VANES
Integrated aerodynamic fin and stowable TVC vane system
[AD-D016457] p 967 N95-19073
JFET
Junction Field Effect Transistor with lateral Gate Voltage Swing (GVS-JFET)
[AD-D016353] p 1032 N95-17970
JOINTS (JUNCTIONS)
The evaluation of transmission efficiency and coupling loss factor of structural junctions
[MRL-TR-93-1] p 1124 N95-19057
Evaluation of scanners for C-scan imaging in nondestructive inspection of aircraft
[DE94-012473] p 990 N95-19100

JOSEPHSON JUNCTIONS
Superconductive signal-processing circuits
[AD-A285533] p 1008 N95-18103
High current amplifier utilizing a Josephson junction Schottky diode three terminal device
[AD-D016278] p 1009 N95-18432
Method for forming Josephson break junctions
[AD-D016427] p 1149 N95-18559
Development of materials for high temperature superconductor Josephson junctions
[DE95-000896] p 1152 N95-19608
JP-4 JET FUEL
Regenerative cooling for liquid propellant rocket thrust chambers
[INPE-5565-TDI/540] p 967 N95-18720
Airborne rotary separator study
[NASA-CR-191045] p 967 N95-18743
JP-5 JET FUEL
Unmanned aerial vehicle heavy fuel engine test
[AD-A284332] p 947 N95-18383
Regenerative cooling for liquid propellant rocket thrust chambers
[INPE-5565-TDI/540] p 967 N95-18720
JP-8 JET FUEL
Unmanned aerial vehicle heavy fuel engine test
[AD-A284332] p 947 N95-18383
Developing an emission factor for hazardous air poliutants for an F-16 using JP-8 fuel
[AD-A284802] p 1061 N95-19685
JUNCTION DIODES
Electronics for the Si detectors in APEX
[DE94-015078] p 1007 N95-17961
High current amplifier utilizing a Josephson junction Schottky diode three terminal device
[AD-D016278] p 1009 N95-18432
JUPITER (PLANET)
Rocket and laboratory studies in astronomy
[NASA-CR-197531] p 1177 N95-17981
Modeling the diurnally precessing Jovian magnetospheric field
[AD-A284857] p 1195 N95-19739
JUPITER ATMOSPHERE
Study for the analysis of the observations, and numerical data representing the planets as far-infrared calibration sources
[NASA-CR-196542] p 1195 N95-19287

K

K-EPSILON TURBULENCE MODEL
An application of a two-equation model of turbulence to three-dimensional chemically reacting flows
[NASA-CR-195411] p 1015 N95-18107
Numerical predictions of turbulent flow around a cube via the k-epsilon model
[DE94-018361] p 1017 N95-18443
Numerical computations of supersonic base flow with special emphasis on turbulence modeling
[AD-A283688] p 930 N95-18670
Development of CFD model for augmented core tripropellant rocket engine p 968 N95-18988
KALMAN FILTERS
The Gravity Probe B niobium bird experiment: Experimental verification of a data reduction scheme with a prototypical dc SQUID readout system
p 1033 N95-18929
KERNEL FUNCTIONS
Higher-order Lipatov kernels and the QCD Pomeron
[DE94-018395] p 1131 N95-18551
A numerical analysis of smoothed particle hydrodynamics
[AD-A284698] p 1019 N95-18562
KEROSENE
Midinfrared optical properties of petroleum oil aerosols
[AD-A283689] p 1139 N95-18142
KEVLAR (TRADEMARK)
Acoustic method of damage sensing in composite materials
[NASA-CR-196538] p 969 N95-18135
Use of titanate coupling agents in Kevlar (trade name)/phenolic composites
[AD-A279200] p 972 N95-19814
KINEMATICS
Study of the kinematic and load sharing properties of wormgearing with non-symmetric tooth profiles
[NASA-CR-195414] p 1041 N95-18541
The tensor equation AX+XA=Phi (A, H) with applications to kinematics of continua
[AD-A285886] p 1122 N95-19603
KINETIC ENERGY
Static aerodynamics CFD analysis for 120-mm hypersonic KE projectile design
[ARL-MR-184] p 929 N95-18611
Direct energy conversion system for D(3)-He fusion
[DE94-770773] p 1146 N95-19549
Power flow and PRS optimization on Phoenix
[AD-A279214] p 1147 N95-19846
PRS projections for DECADE
[AD-A279215] p 1147 N95-19847
KINETICS
Deformation of high-temperature superconductors
[DE94-017085] p 1150 N95-19075
KNOWLEDGE BASED SYSTEMS
CLIPS, AppleEvents, and AppleScript: Integrating CLIPS with commercial software p 1103 N95-19643
KNOWLEDGE BASES (ARTIFICIAL INTELLIGENCE)
Enhancements to the KATE model-based reasoning system p 1115 N95-18183
Expert system shell to reason on large amounts of data p 1101 N95-19631
AI and workflow automation: The prototype electronic purchase request system p 1101 N95-19632
TARGET's role in knowledge acquisition, engineering, validation, and documentation p 1103 N95-19644
PCLIPS: Parallel CLIPS p 1107 N95-19764
DYNACLIPS (DYNAmic CLIPS): A dynamic knowledge exchange tool for intelligent agents
p 1108 N95-19768
KNOWLEDGE REPRESENTATION
Cooperating agents for information retrieval
[AD-A285887] p 1176 N95-19604
QPA-CLIPS: A language and representation for process control p 1102 N95-19635
CLIPS template system for program understanding
p 1102 N95-19638
TARGET's role in knowledge acquisition, engineering, validation, and documentation p 1103 N95-19644
Collaborative engineering-design support system
p 1106 N95-19757
Character selecting advisor for a role-playing game
p 1106 N95-19758
Using CLIPS to represent knowledge in a VR simulation p 1107 N95-19765
KRYPTON
Ion mixing in oxide-sapphire systems
[DE94-018660] p 1133 N95-19232
Spectral distribution of the two-photon decay of He-like krypton
[DE95-001442] p 1135 N95-19787

L

LABORATORIES
Sandia National Laboratories' high power electromagnetic impulse sources
[DE95-000423] p 1004 N95-19555
X-ray laser program
[AD-A279213] p 1039 N95-19845
LAGRANGE MULTIPLIERS
Compression strength of composite primary structural components
[NASA-CR-197554] p 1044 N95-18388
Free vibration analysis of partially filled liquid storage tanks
[DE94-012456] p 1020 N95-19098
LAGRANGIAN FUNCTION
Floating shock fitting via Lagrangian adaptive meshes
[NASA-CR-194997] p 1116 N95-18110
Comparison of the anomalous and non-anomalous generalized Schwinger models via functional formalism
[DE94-626684] p 1156 N95-18333
A model study of the influence of NMHC and NO(x) emissions on rural O3 concentrations in Georgiargia
p 1059 N95-18445
A numerical analysis of smoothed particle hydrodynamics
[AD-A284698] p 1019 N95-18562
Quasi-linear regime of gravitational instability: Implication to density-velocity relation
[NASA-CR-197616] p 1156 N95-19340
Testing higher-order Lagrangian perturbation theory against numerical simulation. 1: Pancake models
[NASA-CR-197611] p 1121 N95-19348
Comparison of dynamical approximation schemes for non-linear gravitational clustering
[NASA-CR-197609] p 1157 N95-19363
LAMBERT SURFACE
Reconstruction of shapes from shading and shape based image reconstruction using modern nonlinear analysis
[AD-A284107] p 1097 N95-18437
LAMINAR BOUNDARY LAYER
Parametric study on laminar flow for finite wings at supersonic speeds
[NASA-TM-108852] p 928 N95-18101
Active control of instabilities in laminar boundary-layer flow. Part 1: An overview
[NASA-CR-195016-PT-1] p 1020 N95-18958
LAMINAR FLOW
Parametric study on laminar flow for finite wings at supersonic speeds
[NASA-TM-108852] p 928 N95-18101
Studies on high pressure and unsteady flame phenomena
[AD-A284126] p 973 N95-18410
Numerical simulation of shock/shock and shock/boundary-layer interactions in chemically reacting hypersonic flows
[DLR-94-04] p 1019 N95-18609
Numerical simulation of dynamic-stall suppression by tangential blowing
[AD-A284887] p 931 N95-19110
Improvement and validation of an LDV system to perform measurements in laminar supersonic flows
p 1021 N95-19256
LAMINATES
Study of failure in fibrous composites subjected to bending loads
[AD-A283330] p 969 N95-18028
Finite element modeling of partially delaminated composite beams with contact-impact conditions
[AD-A283726] p 1044 N95-18363
Optimization of layered metal matrix composite cylinders p 970 N95-18920
Experimental verification of a progressive damage model for composite laminates based on continuum damage mechanics
[NASA-CR-195020] p 971 N95-19043
Acoustic fatigue behaviour of GLARE composites
p 1127 N95-19160
LAND SURFACE TEMPERATURE
Ice surface temperature retrieval from AVHRR, ATSR, and passive microwave satellite data: Algorithm development and application
[NASA-CR-197542] p 1052 N95-18952
A review of land surface temperature and humidity conditions specified for Australia in DEF (AUST) 5168 and STANAG 2895
[AD-A284258] p 1073 N95-19712
LAND USE
Cumulative impact analysis of wetlands using hydrologic indices
[AD-A284759] p 1058 N95-18085
Thematic classification of zone coastal: A methodologic contribution
[INPE-5586-TDI/548] p 1050 N95-18215
One strategy for estimating the potential soil carbon storage due to CO2 fertilization
[DE94-017895] p 1059 N95-18666
A GIS approach to urban heat island research: The case of Huntsville, Alabama p 1063 N95-18991
LANDING SIMULATION
Development of load spectra for Airbus A330/A340 full scale fatigue tests p 936 N95-19479
LANTHANUM OXIDES
Alternative materials for solid oxide fuel cells
[DE94-018452] p 1054 N95-19591
LAP JOINTS
Evaluation of the fuselage lap joint fatigue and terminating action repair p 936 N95-19477
Fatigue life until small cracks in aircraft structures: Durability and damage tolerance p 936 N95-19478
An artifical corrosion protocol for lap-splices in aircraft skin p 937 N95-19482
Results of uniaxial and biaxial tests on riveted fuselage lap joint specimens p 938 N95-19491
Nonlinear analysis of damaged stiffened fuselage shells subjected to combined loads p 939 N95-19499
LASER ABLATION
UV laser-surface interactions relevant to analytic spectroscopy of wide band gap materials
[DE94-016180] p 1037 N95-18349
UV laser-surface interactions relevant to analytic spectroscopy of wide band gap materials
[DE94-016181] p 1037 N95-18350
Pulsewidth-dependent damage measurements of dielectric materials
[DE94-018594] p 1142 N95-19710
LASER ANEMOMETERS
Transonic and supersonic flowfield measurements about axisymmetric afterbodies for validation of advanced CFD codes p 932 N95-19260
LASER APPLICATIONS
Overview of laser technology at Los Alamos National Laboratory
[DE94-018307] p 1036 N95-18126
7th International Symposium on Applications of Laser Techniques to Fluid Mechanics, volume 2
[AD-A285685] p 1018 N95-18477
Light transport for medical laser treatments
[PB94-201498] p 1037 N95-18502
Laser optical mouse
[AD-D016273] p 1092 N95-18517

Method for laser-assisted silicon etching using halocarbon ambients
[AD-D016239] p 1038 N95-18635
A comparison between using incoherent or coherent sources to align and test an adaptive optical telescope
p 1142 N95-18969
Future trends in optical coatings for high-power laser applications
[DE94-018592] p 1039 N95-19708

LASER ARRAYS
Performance improvements in diode laser arrays
[DE94-016547] p 1039 N95-19508

LASER BEAMS
New method for homodyne laser linewidth measurements with a short delay fiber
[PB94-202629] p 1036 N95-18061
Effect of heavy rain to the total received power
p 1070 N95-18210
Light scattering from rough surfaces
[AD-A284112] p 1139 N95-18404
Light transport for medical laser treatments
[PB94-201498] p 1037 N95-18502

LASER DOPPLER VELOCIMETERS
Improvement and validation of an LDV system to perform measurements in laminar supersonic flows
p 1021 N95-19256
Aerodynamic investigation of the flow field in a 180 deg turn channel with sharp bend p 1021 N95-19257
Experimental techniques for measuring transonic flow with a three dimensional laser velocimetry system. Application to determining the drag of a fuselage
p 1022 N95-19258
Transonic and supersonic flowfield measurements about axisymmetric afterbodies for validation of advanced CFD codes p 932 N95-19260

LASER MATERIALS
NCl(b) based short wavelength chemical laser
[AD-A284213] p 1036 N95-17956
Measurements of line overlap for resonant spoiling of x ray lasing transitions
[DE94-016444] p 1038 N95-19248

LASER MODE LOCKING
Development of ultrashort optical pulse sources near 1.3 and 1.5 microns with an emphasis on stability, high repetition rate, and parallelism
[AD-A285535] p 1139 N95-18104
14th IEEE International Semiconductor Laser Conference
[AD-A285569] p 1038 N95-18642

LASER OUTPUTS
Reduction of parasitic lasing
[NASA-CASE-LAR-14645-1-SB] p 1037 N95-18322
UV laser-surface interactions relevant to analytic spectroscopy of wide band gap materials
[DE94-016180] p 1037 N95-18349
Compact, efficient, scalable neodymium laser co-doped with activator ions and pumped by visible laser diodes
[AD-D016237] p 1038 N95-18585
Solid state laser driver for extreme ultraviolet lithography
[DE94-016971] p 1038 N95-19096
X-ray laser program
[AD-A279213] p 1039 N95-19845

LASER PLASMAS
Gain uniformity, linearity, saturation and depletion in gated microchannel-plate x-ray framing cameras
[DE94-018596] p 1035 N95-19711

LASER PUMPING
High power phase conjugated solid state lasers
[DE94-016633] p 1037 N95-18357
Compact, efficient, scalable neodymium laser co-doped with activator ions and pumped by visible laser diodes
[AD-D016237] p 1038 N95-18585
Solid state laser driver for extreme ultraviolet lithography
[DE94-016971] p 1038 N95-19096

LASER RANGE FINDERS
Overview of laser technology at Los Alamos National Laboratory
[DE94-018307] p 1036 N95-18126

LASER SPECTROSCOPY
Silicon carbide photoconductive switches
[AD-A284310] p 1008 N95-18378
Development of laser-ion beam photodissociation methods
[DE95-002800] p 977 N95-19840

LASER TARGET INTERACTIONS
UV laser-surface interactions relevant to analytic spectroscopy of wide band gap materials
[DE94-016180] p 1037 N95-18349
UV laser-surface interactions relevant to analytic spectroscopy of wide band gap materials
[DE94-016181] p 1037 N95-18350
Light transport for medical laser treatments
[PB94-201498] p 1037 N95-18502
Three-dimensional radiation transport hydrodynamics
[DE94-018337] p 1146 N95-19527

LASER TARGETS
Study of high gain spherical shell ICF targets containing uniform layers of liquid deuterium tritium fuel
[DE94-018550] p 1136 N95-18552
25-ps neutron detector for measuring ICF-target burn history
[DE94-016450] p 1146 N95-19250
Contributions of the National Ignition Facility to the development of Inertial Fusion Energy
[DE94-018335] p 1137 N95-19588

LASERS
Laser wakefield excitation and measurement on a femtosecond time scale: Theory and experiment
[DE94-019198] p 1129 N95-17976
The reliability of laser reflowed Sn-Ag solder joints
[AD-A284732] p 1044 N95-18080
The effects of cavity topology on instabilities in additive-pulse modelocked lasers
[DE94-018193] p 1036 N95-18123
Overview of laser technology at Los Alamos National Laboratory
[DE94-018307] p 1036 N95-18126
Reduction of parasitic lasing
[NASA-CASE-LAR-14645-1-SB] p 1037 N95-18322
Liquid crystal tunable filter
[AD-A284383] p 1139 N95-18342
7th International Symposium on Applications of Laser Techniques to Fluid Mechanics, volume 2
[AD-A285685] p 1018 N95-18477
Aircraft wake vortex takeoff tests at O'Hara International Airport
[AD-A283828] p 929 N95-18624
Isotope separation and advanced manufacturing technology
[DE95-000313] p 1039 N95-19551
Contributions of the National Ignition Facility to the development of Inertial Fusion Energy
[DE94-018335] p 1137 N95-19588
Damage from pulses with arbitrary temporal shapes
[DE94-018606] p 1039 N95-19722

LASING
Reduction of parasitic lasing
[NASA-CASE-LAR-14645-1-SB] p 1037 N95-18322
Hyperfine splittings, prepulse technique, and other new results for collisional excitation neon-like x ray lasers
[DE94-016443] p 1038 N95-19247
Measurements of line overlap for resonant spoiling of x ray lasing transitions
[DE94-016444] p 1038 N95-19248

LATERAL CONTROL
Determination of stability and control derivatives from the NASA F/A-18 HARV from flight data using the maximum likelihood method
[NASA-CR-197320] p 958 N95-19576

LATEX
Study of the effect of ionizing radiation on the structure of natural rubber latex by positron annihilation technique
[DE94-631466] p 975 N95-19550

LATTICE PARAMETERS
Methane conversion by solid electrolyte membranes
[PB94-191781] p 973 N95-17982

LATTICES (MATHEMATICS)
Lattice gas and lattice Boltzmann methods for simulation of hydrodynamics and magnetohydrodynamics
p 1145 N95-18907

LAUNCH VEHICLE CONFIGURATIONS
A 20k payload launch vehicle fast track development concept using an RD-180 engine and a Centaur upper stage
[NASA-TM-108475] p 963 N95-19648

LAUNCH VEHICLES
Field and data analysis studies related to the atmospheric environment
[NASA-CR-196543] p 1068 N95-18093
An oil flow study of the reference Shuttle-C configuration
[NASA-RP-1352] p 932 N95-19623

LAUNCHERS
Comparison of the folded stripline and stacked stripline concepts to the folded waveguide launcher
[DE94-018951] p 999 N95-18558

LAUNCHING
Field and data analysis studies related to the atmospheric environment
[NASA-CR-196543] p 1068 N95-18093

LAW (JURISPRUDENCE)
Acquisition handbook: Update. Comprehensive Approach to Reusable Defensive Software (CARDS)
[AD-A284342] p 1097 N95-18420
Environmental Compliance Assessment System (ECAS)
[AD-A283950] p 1060 N95-18683
Environmental Compliance Assessment System (ECAS). South Carolina supplement: US Army
[AD-A279244] p 1062 N95-19860

LAYOUTS
Programmable cockpit research simulator
[AD-A279219] p 960 N95-19848

LEAD ACID BATTERIES
Development of a bipolar lead/acid battery for the more electric aircraft
[AD-A284050] p 1010 N95-18660
Battery and charge controller evaluations in small stand-alone PV systems
[DE94-014252] p 1013 N95-19872

LEAD OXIDES
Deformation of high-temperature superconductors
[DE94-017085] p 1150 N95-19075

LEADING EDGES
Impact loading of compressor stator vanes by hailstone ingestion p 953 N95-19670
Soft body impact on titanium fan blades
p 953 N95-19671
Ice-impact analysis of blades p 953 N95-19672

LEAKAGE
Ethylene dynamics in the CELSS biomass production chamber p 1077 N95-18179
Modeling and measurement of the performance of a branched conduit sampling system in a mass spectrometer leak detector p 1036 N95-18181

LEARNING
Learning effects on strategy selection in a dynamic task environment as a function of time pressure
[AD-A285458] p 1089 N95-19538

LEARNING THEORY
Learning effects on strategy selection in a dynamic task environment as a function of time pressure
[AD-A285458] p 1089 N95-19538

LEAST SQUARES METHOD
TLS-based prefiltering technique for time-domain ARMA modeling
[AD-A284525] p 1120 N95-18113
The accuracy of parameter estimation in system identification of noisy aircraft load measurement
[NASA-CR-197516] p 945 N95-19130

LECTURES
Physics at the Fermilab Tevatron Proton-Antiproton Collider
[DE95-000648] p 1137 N95-19561

LEGAL LIABILITY
Expert Witness: A system for developing expert medical testimony p 1101 N95-19628

LEGENDRE FUNCTIONS
Spectral methods for fluid flow p 1028 N95-19459

LEGIBILITY
An evaluation of aircraft CRT and dot-matrix display legibility requirements
[AD-A283933] p 947 N95-18164

LENSES
Can salt on an optical rain gauge lens affect performance? p 1069 N95-18208
Multi-line passive fiber optic slipring
[AD-D016430] p 1141 N95-18560
MANN: A program to transfer designs for diffractive optical elements to a MANN photolithographic mask generator p 1142 N95-18995

LEPTONS
Principal-value resummation for dilepton production
[DE95-001094] p 1135 N95-19726

LESIONS
Clinical practice, diagnosis and therapy of intervertebral disk lesion: Importance to fitness for military flying duties
p 1084 N95-19435
Spinal nerve syndromes: The need to confirm the diagnosis with neurophysiological examinations
p 1085 N95-19436
Sarcoidosis in US military aviators
p 1085 N95-19438

LETHALITY
Health hazards assessment for blast overpressure exposures
[AD-A283352] p 1078 N95-17998

LEVITATION
The interaction of two narrow magnets and a moving conducting slip
[DE94-018575] p 1122 N95-19704

LEVITATION MELTING
Plasma heating for containerless and microgravity materials processing
[NASA-CASE-NPO-18819-1-CU] p 991 N95-18326

LIAPUNOV FUNCTIONS
Neural networks applications to control and computations p 1115 N95-18992

LIBRARIES
National Library of Medicine programs and services, fiscal year 1991
[PB94-188026] p 1077 N95-17949

National Library of Medicine programs and services, fiscal year 1992
[PB94-188034] p 1078 N95-17950
Technical concept document. Central Archive for Reusable Defense Software (CARDS)
[AD-A284430] p 1096 N95-18343
Library operations policies and procedures. Volume 2: Central Archive for Reusable Defense Software (CARDS)
[AD-A284431] p 1096 N95-18344
Library user's guide. Comprehensive Approach to Reusable Defensive Software (CARDS)
[AD-A284345] p 1097 N95-18423
Distributed interactive simulation interface library version description document
[AD-A284470] p 1173 N95-18446
Portable, Reusable, Integrated Software Modules (PRISM) documentation library version description document release 1.0. Central Archive for Reusable Defense Software (CARDS)
[AD-A284571] p 1097 N95-18447
Library capability demonstration. Central Archive for Reusable Defense Software (CARDS)
[AD-A284574] p 1098 N95-18450
NASA/DOD Aerospace Knowledge Diffusion Research Project. Report 26: The technical communication practices of aerospace engineering students: Results of the phase 3 AIAA National Student Survey
[NASA-TM-109121] p 1175 N95-18950
A report of work activities on the NASA Spacelink public electronic library p 1168 N95-19005

LIE GROUPS
Lie algebras for the Dirac-Clifford ring
[DE94-626643] p 1118 N95-18878
Classification of graded, finite-dimensional lie algebras of vector fields
[PB94-215449] p 1119 N95-19408

LIFE (DURABILITY)
Enhancement of creep resistance of a sintered Si3N4 ceramic by microwave annealing
[DE94-017688] p 987 N95-19399
FAA/NASA International Symposium on Advanced Structural Integrity Methods for Airframe Durability and Damage Tolerance, part 2
[NASA-CP-3274-PT-2] p 934 N95-19468

LIFE SCIENCES
Aerospace medicine and biology: A continuing bibliography with indexes (supplement 398)
[NASA-SP-7011(398)] p 1080 N95-19239
Aerospace medicine and biology: A continuing bibliography with indexes (supplement 397)
[NASA-SP-7011(397)] p 1087 N95-19746

LIFE SUPPORT SYSTEMS
Aerospace medicine and biology: A continuing bibliography with indexes (supplement 398)
[NASA-SP-7011(398)] p 1080 N95-19239
Aerospace medicine and biology: A continuing bibliography with indexes (supplement 397)
[NASA-SP-7011(397)] p 1087 N95-19746

LIFT
In-flight lift-drag characteristics for a forward-swept wing aircraft and comparisons with contemporary aircraft)
[NASA-TP-3414] p 929 N95-18565

LIFTOFF (LAUNCHING)
Meteor 3/TOMS launch of 15 August 1991 in Plesetsk, USSR
[NASA-TM-110115] p 962 N95-18150

LIGANDS
Polymer-based separations: Synthesis and application of polymers for ionic and molecular recognition
[DE94-016427] p 984 N95-18355
Molecular recognition as shown by the solvent extraction of (R)- and (S)-alpha-(1-naphthyl)ethyl ammonium picrate or orange 2 by chiral pyridino-crown ethers
[AD-A280157] p 969 N95-19823

LIGHT (VISIBLE RADIATION)
Infrared-to-visible converter
[AD-D016443] p 1141 N95-18529
Analysis of solar spectral irradiance measurements from the SBUV/2-series and the SSBUV instruments
[NASA-CR-197544] p 1196 N95-18954
The visible Smith-Purcell radiation search
[DE94-017514] p 1038 N95-19243
Photobiology in medicine
[AD-A284843] p 1087 N95-19695

LIGHT AMPLIFIERS
Waveguide switches using asymmetric coupled quantum wells
[AD-A284056] p 1010 N95-18662
Methods and components for optical contention resolution in high speed networks
[AD-A284674] p 1142 N95-19088

LIGHT EMISSION
Detection of alpha particles via observation of He II line emission in the lithium pellet cloud during DT operation in TFTR
[DE94-014485] p 1143 N95-17965
Scientific objectives of the primitive body sample return missions: An approach from the light-induced effect on water vapor p 961 N95-19191
The visible Smith-Purcell radiation search
[DE94-017514] p 1038 N95-19243
The optical emission and absorption properties of silicon-germanium superlattice structures grown on non-conventional silicon substrate orientation
[AD-A284852] p 1153 N95-19715

LIGHT EMITTING DIODES
Physiological and genetic characterization of plant growth and gravitropism in LED light sources p 1077 N95-18173

LIGHT MODULATION
Gigabit optical interconnects: System and component analysis, design and development
[AD-A285538] p 1138 N95-18067
Variable rate transfer of optical information
[AD-D016268] p 1173 N95-18544

LIGHT SCATTERING
Light scattering from rough surfaces
[AD-A284112] p 1139 N95-18404

LIGHT SOURCES
Physiological and genetic characterization of plant growth and gravitropism in LED light sources p 1077 N95-18173
Fiber optic pressure and/or vibration detector
[AD-D016474] p 1140 N95-18460
Characterization of the 50 MeV ALS linac beam with optical transition radiation
[DE94-018208] p 1137 N95-19584

LIGHT TRANSMISSION
Silicon carbide photoconductive switches
[AD-A284310] p 1008 N95-18378
Light transport for medical laser treatments
[PB94-201498] p 1037 N95-18502

LIGHTHILL METHOD
On the Lighthill relationship and sound generation from isotropic turbulence
[NASA-CR-195005] p 1016 N95-18191

LIGHTING EQUIPMENT
KC-130 ANVIS/HUD assessment and symbology rationale
[AD-A284155] p 943 N95-18504

LIGHTNING
Field and data analysis studies related to the atmospheric environment
[NASA-CR-196543] p 1068 N95-18093
Lightning studies using LDAR and companion data sets p 1073 N95-18174
Development of a bulk current injection direct-drive system to test system level components with stress waveforms that are encountered during full threat indirect effects lightning
[AD-A284160] p 933 N95-18507
On the possibility of precipitation-induced vertical lightning in the protoplanetary nebula p 1187 N95-19299
Chondrule formation in lightning discharges p 1188 N95-19304
Formation of chondrules by electrical discharge heating p 1189 N95-19313
The fine nebula dust component: A key to chondrule formation by lightning p 1192 N95-19333

LIKELIHOOD RATIO
Detection performance of generalized likelihood ratio processors for random signals of unknown location, structure, extent, and strength
[AD-A285589] p 997 N95-18475

LINE SPECTRA
GAMQUEST, a computer program to identify gamma rays
[DE94-016217] p 1197 N95-18351
Relative elemental abundance and heating constraints determined for the solar corona from SERTS measurements
[NASA-TM-104616] p 1196 N95-19791

LINEAR ACCELERATORS
Fluid dynamic linear accelerometer
[AD-D016413] p 956 N95-18553
Characterization of the 50 MeV ALS linac beam with optical transition radiation
[DE94-018208] p 1137 N95-19584
Microcavity structures
[DE95-001096] p 1039 N95-19727
The founding of CEBAF, 1979 to 1987 p 1138 N95-19784

LINEAR ALTERNATORS
Transient and steady-state tests of the space power research engine with resistive and motor loads
[NASA-TM-106832] p 1042 N95-19238

LINEAR ARRAYS
Inband radar cross section of phased arrays with parallel feeds
[AD-A284249] p 1005 N95-19730

LINEAR EQUATIONS
Reformulated preconditioned conjugate gradient squared method. Part 1: The algorithm
[PB94-201589] p 1108 N95-17936
An inverse problem in thermal imaging
[NASA-CR-195018] p 1117 N95-18479
A direct decomposition method for the solution of sparse linear least squares problems
[AD-A284060] p 1117 N95-18679
The tensor equation AX+XA=Phi (A, H) with applications to kinematics of continua
[AD-A285886] p 1122 N95-19603

LINEAR EVOLUTION EQUATIONS
Testing the frozen flow approximation
[NASA-CR-197614] p 1180 N95-18966

LINEAR PROGRAMMING
Linear optimization and image reconstruction
[AD-A283641] p 1094 N95-18013

LINEAR QUADRATIC REGULATOR
Time-optimal control of a third order regulator
[AD-A283307] p 1113 N95-18023

LINEAR SYSTEMS
The reliability of laser reflowed Sn-Ag solder joints
[AD-A284732] p 1044 N95-18080

LINEAR VIBRATION
Acoustic radiation damping of flat rectangular plates subjected to subsonic flows p 1123 N95-18542

LININGS
Acoustic properties and durability of liner materials at non-standard atmospheric conditions
[NASA-CR-195010] p 1123 N95-18930
A review of footwear for cold/wet scenarios. Part 2: Socks, liners, and insoles
[AD-A279937] p 989 N95-19866

LIOUVILLE EQUATIONS
Large signal time dependent quantum mechanical transport in quantum phase based devices
[AD-A283338] p 1155 N95-18009
The physics and operation of ultra-submicron length semiconductor devices
[AD-A280181] p 1155 N95-19828

LIQUEFIED GASES
Development of a high-resolution liquid xenon detector for gamma-ray astrophysics p 1179 N95-18499

LIQUID BRIDGES
Dynamics and statics of nonaxisymmetric liquid bridges
[NASA-CR-197520] p 1195 N95-17980

LIQUID CHROMATOGRAPHY
Enhancement of fluorescence detection in chromatographic methods by computer analysis of second order data
[DE94-014682] p 973 N95-17966

LIQUID CRYSTALS
Liquid crystal tunable filter
[AD-A284383] p 1139 N95-18342
Workshop on Synthesis of Macromolecules with Precisely Controlled Structure for New Materials
[AD-A285321] p 987 N95-19520

LIQUID FUELS
Study of high gain spherical shell ICF targets containing uniform layers of liquid deuterium tritium fuel
[DE94-018550] p 1136 N95-18552
On the conduct of fast cookoff tests in Australia
[AD-A284260] p 975 N95-19699

LIQUID INJECTION
Bubble formation in microgravity p 991 N95-18970
Computational simulation of liquid fuel rocket injectors p 968 N95-18989

LIQUID OXYGEN
Airborne rotary separator study
[NASA-CR-191045] p 967 N95-18743

LIQUID PHASE SINTERING
Polymer based materials for additive processing of high temperature electronics packaging
[AD-A285962] p 988 N95-19745

LIQUID PHASES
Elemental fluorine based syntheses of pentafluoro phenly and other aromatic perfluoropolyether polymers
[AD-A284102] p 984 N95-18402

LIQUID PROPELLANT ROCKET ENGINES
Advanced small rocket chambers. Basic program and option 2: Fundamental processes and material evaluation
[NASA-CR-195349] p 966 N95-18192
Optical measurements in rocket engine liquid sprays p 968 N95-18979
Development of CFD model for augmented core tripropellant rocket engine p 968 N95-18988
Computational simulation of liquid fuel rocket injectors p 968 N95-18989

A 20k payload launch vehicle fast track development concept using an RD-180 engine and a Centaur upper stage
[NASA-TM-108475] p 963 N95-19648
Centrifugal and axial pump design and off-design performance prediction
[NASA-TM-106745] p 968 N95-19795

LIQUID ROCKET PROPELLANTS
Development of CFD model for augmented core tripropellant rocket engine p 968 N95-18988

LIQUID SLOSHING
Sloshing roof impact tests of a rectangular tank
[DE94-012462] p 1018 N95-18549

LIQUID WASTES
Investigation of new hypergol scrubber technology p 977 N95-18175

LIQUID-VAPOR INTERFACES
Bubble formation in microgravity p 991 N95-18970

LIQUIDS
Microgravity fluid science research in Europe
[PB94-201720] p 990 N95-17973
SSI effects for a tank containing two liquids
[DE94-012457] p 1020 N95-19099
Resonator/oscillator response to liquid loading
[DE94-013442] p 1012 N95-19240
Wentzel-Bardeen singularity in coupled Luttinger liquids: Transport properties
[DE95-000856] p 1152 N95-19621

LITHIUM
Characterization of rechargeable lithium cells. Part 1: Lithium/niobium triselenide chemistry
[AD-A284229] p 1007 N95-17959
Detection of alpha particles via observation of He II line emission in the lithium pellet cloud during DT operation in TFTR
[DE94-014485] p 1143 N95-17965
Cosmic ray models for early galactic lithium, beryllium, and boron production
[NASA-CR-197626] p 1137 N95-18965
The effect of fabrication on corrosion in aluminum 2195: Environmental and microstructural considerations p 982 N95-19011
Lithium electrode/polyacrylonitrile based polymer electrolyte interface
[AD-A283947] p 986 N95-19064
Molten carbonate fuel cell with high power density
[DE94-017080] p 1053 N95-19074
Lithium ferrate and lithium cobaltate cathodes for molten carbonate fuel cells
[DE94-017079] p 1054 N95-19117
Development of lithium beam emission spectroscopy as an edge fluctuation diagnostic for D3-D
[DE94-017517] p 1146 N95-19378

LITHIUM ALLOYS
Microstructural analysis of cracks generated during welding of 2195 aluminum-lithium alloy p 982 N95-19007
The effect of fabrication on corrosion in aluminum 2195: Environmental and microstructural considerations p 982 N95-19011
Nonstoichiometry of Al-Zr intermetallic phases
[DE94-016877] p 979 N95-19093

LITHIUM NIOBATES
IR materials producibility
[AD-A284263] p 1142 N95-19732

LITHOGRAPHY
Tunneling and transport in mesoscopic structures
[AD-A283426] p 1148 N95-18053
Low voltage electron beam lithography
[AD-A284181] p 1010 N95-18625
Solid state laser driver for extreme ultraviolet lithography
[DE94-016971] p 1038 N95-19096
Using electrochemistry in device processing on poly(tetrafluoroethylene) substrates
[DE95-000541] p 975 N95-19559
Microcavity structures
[DE95-001096] p 1039 N95-19727

LITHOSPHERE
Trace element characteristics of lithospheric and asthenospheric mantle in the Rio Grande rift region
[DE94-013609] p 1063 N95-17947

LIVER
In vitro system for studying metabolism of environmental chemicals in human cells
[AD-A284174] p 1079 N95-18518

LOAD DISTRIBUTION (FORCES)
Transport aircraft loading and balancing system: Using a CLIPS expert system for military aircraft load planning p 1105 N95-19751

LOAD TESTS
Dynamic decohesion of bimaterials: Experimental observations and failure criteria
[GALCIT-94-2] p 1045 N95-18613
Experimental verification of a progressive damage model for composite laminates based on continuum damage mechanics
[NASA-CR-195020] p 971 N95-19043
Development of load spectra for Airbus A330/A340 full scale fatigue tests p 936 N95-19479

LOADING OPERATIONS
Transport aircraft loading and balancing system: Using a CLIPS expert system for military aircraft load planning p 1105 N95-19751

LOADS (FORCES)
BEAM: A finite element program for the collapse analysis of vehicle structures
[AD-A285547] p 1045 N95-18472
Calibration and sediment load algorithms for an acoustic sediment flux probe
[AD-A283655] p 1075 N95-18617
Power terminal protection device
[AD-D016528] p 1011 N95-19120
The load separation technique in the elastic-plastic fracture analysis of two- and three-dimensional geometries p 936 N95-19481
Aircraft fatigue and crack growth considering loads by structural component p 939 N95-19497
Nonlinear analysis of damaged stiffened fuselage shells subjected to combined loads p 939 N95-19499
Power flow and PRS optimization on Phoenix
[AD-A279214] p 1147 N95-19846
PRS projections for DECADE
[AD-A279215] p 1147 N95-19847

LOCAL AREA NETWORKS
A scalable decentralized group membership service for an asynchronous environment
[AD-A283633] p 1109 N95-18137
Performance evaluation of the NASA/KSC CAD/CAE and office automation LAN's p 1108 N95-18186
Distributed medical database system for real-time monitoring of the health and risk exposure of military research study volunteers at USARIEM
[AD-A279193] p 1087 N95-19811

LOCI
On the geometry of visual correspondence
[AD-A285700] p 1140 N95-18478

LOGARITHMS
A domain decomposition algorithm for elliptic problems in three dimensions
[DE94-019265] p 1094 N95-17978

LOGIC CIRCUITS
Power conversion system modification to permit use of DC power source
[AD-D016421] p 1010 N95-18523
Digital circuit for the introduction and later removal of dither from an analog signal
[AD-D016462] p 1011 N95-19171

LOGIC DESIGN
Fair Petri nets and structural induction for rings of processes
[AD-A283920] p 1110 N95-18158

LOGIC PROGRAMMING
A general theory of semi-unification p 1099 N95-18924

LOGISTICS
Applying Costs, Risks and Values Evaluation (CRAVE) methodology to Engineering Support Request (ESR) prioritization p 1160 N95-18176
E-6A hardness assurance, maintenance and surveillance program
[AD-A283994] p 945 N95-19067

LOGISTICS MANAGEMENT
Graphics MIS/Shop Store Program: User's manual
[AD-A284062] p 1174 N95-18681

LONG WAVE RADIATION
Midinfrared optical properties of petroleum oil aerosols
[AD-A283689] p 1139 N95-18142

LONGITUDINAL CONTROL
Determination of stability and control derivatives from the NASA F/A-18 HARV from flight data using the maximum likelihood method
[NASA-CR-197320] p 958 N95-19576

LOOP TRANSFER FUNCTIONS
Current loop signal conditioning: Practical applications
[NASA-TM-4636] p 1033 N95-18735

LORENTZ TRANSFORMATIONS
Special relativity effects for space-based coherent lidar experiments p 1014 N95-18983

LOSSES
Ion orbit loss and the poloidal electric field in a tokamak
[DE94-016860] p 1145 N95-19092
Producing chondrules by recycling and volatile loss p 1186 N95-19290

LOW ALTITUDE
Multilayer anti-erosion coatings p 954 N95-19679

LOW CONDUCTIVITY
Quality optimization of thermally sprayed coatings produced by the JP-5000 (HVOF) gun using mathematical modeling p 989 N95-19008

LOW COST
Progress in the development of advanced solar reflectors
[DE94-000264] p 1053 N95-18463
Assessing aircraft survivability to high frequency transient threats
[AD-A283999] p 944 N95-18726
InP solar cell development on inexpensive silicon substrates
[AD-A286254] p 1054 N95-19388
Programmable cockpit research simulator
[AD-A279219] p 960 N95-19848

LOW DENSITY MATERIALS
Physics of spacecraft-based interplanetary dust collection by impact into low-density media p 1181 N95-19176
Laboratory simulation of intact capture of cometary and asteroidal dust particles in ISAS p 962 N95-19183
The intact capture of hypervelocity dust particles using underdense foams p 1183 N95-19188
Nondestructive time-of-capture, location and velocity sensing in intact capture p 1036 N95-19194
The physics of intact capture p 1122 N95-19195
The use of silica aerogel to collect interplanetary dust in space p 989 N95-19197

LOW FREQUENCIES
Long wavelength propagation capacity, version 1.1 (computer diskette)
[AD-M200254] p 994 N95-17964
Optimum dimension ratios for studios, control rooms and listening rooms
[BBC-RD-1993/8] p 993 N95-19053

LOW NOISE
Low noise fiber gyroscope system which includes excess noise subtraction
[AD-D016556] p 1034 N95-19124

LOW SPEED
Velocity measurements with hot-wires in a vortex-dominated flowfield p 932 N95-19261

LOW SPEED WIND TUNNELS
Background noise levels measured in the NASA Lewis 9- by 15-foot low-speed wind tunnel
[NASA-TM-106817] p 958 N95-18054
Wall correction method with measured boundary conditions for low speed wind tunnels p 1023 N95-19263
Calculation of low speed wind tunnel wall interference from static pressure pipe measurements p 1024 N95-19273

LOW TEMPERATURE TESTS
Characterization of rechargeable lithium cells. Part 1: Lithium/niobium triselenide chemistry
[AD-A284229] p 1007 N95-17959

LOW VOLTAGE
Low voltage electron beam lithography
[AD-A284181] p 1010 N95-18625

LOWER ATMOSPHERE
Surface and upper-air meteorological measurements supporting the NATO/AC243/Panel 3 research study groups 8 and 21 campaign in Lorient, France (September 1993)
[AD-A285326] p 1072 N95-19521

LOWER IONOSPHERE
Radio wave heating of the lower ionosphere p 1145 N95-18905

LUBRICATION
Advanced diesel engine component development program, tasks 4-14
[NASA-CR-191203] p 1040 N95-18041
Wormgear geometry adopted for implementing hydrostatic lubrication and formulation of the lubrication problem
[NASA-CR-195416] p 1043 N95-19567

LUMINESCENCE
Optical surface pressure measurements: Accuracy and application field evaluation p 1025 N95-19274

LUMINOSITY
The origin of the diffuse x-ray background p 1197 N95-18729

LUMINOUS INTENSITY
Night Vision Goggles (NVG) software user's guide, version 5.1
[AD-A284563] p 1090 N95-18029
Scientific objectives of the primitive body sample return missions: An approach from the light-induced effect on water vapor p 961 N95-19191

LUNAR BASES
Lunar surface fission power supplies: Radiation issues
[DE94-014439] p 966 N95-17997
Lunar base heat pump, phase 1
[NASA-CR-188300] p 1015 N95-18111

LUNAR EXPLORATION
Time of Apollo
[NASA-TM-110488] p 961 N95-19060
An integrated strategy for the planetary sciences: 1995 - 2010
[NASA-CR-197145] p 1194 N95-19134
LUNAR LANDING
Time of Apollo
[NASA-TM-110488] p 961 N95-19060
LUNAR ROCKS
Lunar surface fission power supplies: Radiation issues
[DE94-014439] p 966 N95-17997
LUNAR SURFACE
Lunar surface fission power supplies: Radiation issues
[DE94-014439] p 966 N95-17997
LYSOZYME
Salt-induced aggregation of lysozyme: Implications for crystal growth p 1155 N95-19015

M

MACH NUMBER
Measurement of gust response on a turbine cascade
[NASA-TM-106776] p 928 N95-18457
Parallel computations in hydro acoustics
[AD-A285900] p 1030 N95-19607
MACHINE LEARNING
LVQ and backpropagation neural networks applied to NASA SSME data
[NASA-CR-195418] p 962 N95-18045
Adaptive Neuron Model: An architecture for the rapid learning of nonlinear topological transformations
[NASA-CASE-NPO-18579-1-CU] p 1114 N95-18740
Machine learning: A comparative study of pattern theory and C4.5
[AD-A285582] p 1115 N95-19118
MACHINE TRANSLATION
Knowledge based translation and problem solving in an intelligent individualized instruction system
p 1105 N95-19753
MACINTOSH PERSONAL COMPUTERS
CLIPS, AppleEvents, and AppleScript: Integrating CLIPS with commercial software p 1103 N95-19643
MACROMOLECULES
Multi-functional pi-conjugated macromolecules based on poly (phenylene vinylene)
[AD-A284163] p 985 N95-18510
Workshop on Synthesis of Macromolecules with Precisely Controlled Structure for New Materials
[AD-A285321] p 987 N95-19520
Macromolecular characterization and solution behavior of polymer additives
[AD-A284845] p 988 N95-19696
MAGELLANIC CLOUDS
Dynamics of LMC clusters
[ISBN-0-315-84911-8] p 1179 N95-18728
MAGNESIUM
Coronal abundances and their variation
[NASA-CR-197553] p 1195 N95-18376
MAGNESIUM ALLOYS
Warm formability of aluminum-magnesium alloys
[DE94-016170] p 980 N95-19396
MAGNESIUM CHLORIDES
Gas turbine compressor corrosion and erosion in Western Europe p 954 N95-19678
MAGNESIUM ISOTOPES
Chronology of chrondrule and CAI formation: Mg-Al isotopic evidence p 1189 N95-19314
Heating during solar nebula formation and Mg isotopic fractionation in precursor grains of CAIs and chondrules
p 1191 N95-19326
MAGNESIUM OXIDES
UV laser-surface interactions relevant to analytic spectroscopy of wide band gap materials
[DE94-016180] p 1037 N95-18349
UV laser-surface interactions relevant to analytic spectroscopy of wide band gap materials
[DE94-016181] p 1037 N95-18350
MAGNETIC COILS
The US 100 T Magnet Project
[DE94-016099] p 1011 N95-19200
MAGNETIC DISKS
A selection of experimental test cases for the validation of CFD codes. Supplement: Datasets A-E
[AGARD-AR-303-SUPPL] p 929 N95-18539
MAGNETIC DISPERSION
Optical determination of conduction and valence-band dispersion curves in strained single-quantum wells
[DE94-018892] p 1151 N95-19235
MAGNETIC FIELD CONFIGURATIONS
The experimental investigation of plasma configuration in MM-4U device
[DE94-626964] p 1144 N95-18885
LEVIS ion source and beam characterization on PBFA-2
[DE94-015802] p 1133 N95-19199
MAGNETIC FIELD INVERSIONS
Two and three dimensional magnetotelluric inversion
[DE94-014820] p 1063 N95-17967
MAGNETIC FIELDS
Ultrafast nonlinear optical response of Fano resonances in gallium arsenide under high magnetic field
[DE94-018181] p 1148 N95-18122
Electromagnetic pump
[AD-D016260] p 1041 N95-18317
Cross-tail current, field-aligned current, and B(y)
[NASA-CR-197624] p 1065 N95-19032
The US 100 T Magnet Project
[DE94-016099] p 1011 N95-19200
Complete mode-set stability analysis of magnetically insulated ion diode equilibria
[DE94-015275] p 1145 N95-19201
Giant effective mass deviations near the magnetic field-induced minigap in double quantum wells
[DE94-018889] p 1122 N95-19234
Direct energy conversion system for D(3)-He fusion
[DE94-770773] p 1146 N95-19549
Handbook for the extremely low frequency (ELF) data acquisition and analysis system
[DSTO-GD-0021] p 1005 N95-19622
Properties of Alfven waves with transverse scale on the order of skin-depth
[AD-A285657] p 1147 N95-19700
Incompressible flow of a Newtonian fluid past a vertical plate with thermal and magnetic stresses
[AD-A284856] p 1030 N95-19716
Potential distributions for ellipsoidal bodies in uniform fields
[MRL-TR-92-48] p 1005 N95-19771
MAGNETIC FLUX
Method and flowmeter for unsteady fluid flow study
[AD-D016432] p 1015 N95-18112
Study of frustrated systems via dissipative maps
[DE94-017754] p 1122 N95-18127
Superconductor microelectronic devices and circuits and a method of fabricating therefor
[AD-D016280] p 1009 N95-18433
Dynamic evolution of emerging magnetic flux tubes in the solar convective envelope p 1195 N95-18497
MAGNETIC INDUCTION
Magnetotelluric mapping of upper crustal isotherms beneath the Valles Caldera hydrothermal system
[DE94-013606] p 1063 N95-17946
General information for operation of the high-temperature electromagnetic containerless vacuum induction furnace
[DE94-017170] p 991 N95-19076
MAGNETIC MATERIALS
Method for making a non-magnetic alloy
[AD-D016233] p 979 N95-18630
MAGNETIC PERMEABILITY
Alternative volume integral equation formulations applied to dielectric cylinders
[AD-A285537] p 995 N95-18066
MAGNETIC STORMS
CRRESPRO documentation
[AD-A284578] p 1178 N95-18451
Particle acceleration and transport in the tail and at the front side of the magnetosphere, task 1 and 2
[NASA-CR-197575] p 1064 N95-18476
MAGNETIC SURVEYS
Magnetotelluric mapping of upper crustal isotherms beneath the Valles Caldera hydrothermal system
[DE94-013606] p 1063 N95-17946
Two and three dimensional magnetotelluric inversion
[DE94-014820] p 1063 N95-17967
MAGNETITE
Study of the ferrimagnetic and paramagnetic phases of magnetite measured by multiple neutron diffraction
[DE94-627031] p 1151 N95-19242
MAGNETIZATION
Method for making a non-magnetic alloy
[AD-D016233] p 979 N95-18630
MAGNETO-OPTICS
Atomic line filter for SDI applications
[AD-A284125] p 1139 N95-18409
Magneto-optical studies of compound semiconductors
[DE94-018743] p 1149 N95-18650
MAGNETOACOUSTIC WAVES
Global wave modeling of electron interactions with fast magnetosonic waves
[DE94-018942] p 1144 N95-18557
MAGNETOHYDRODYNAMIC FLOW
A study of gas flow pattern, undercutting and torch modification in variable polarity plasma arc welding
[NASA-CR-196537] p 1040 N95-18056
MAGNETOHYDRODYNAMIC WAVES
Study of alpha physics related to ITER Project
[DE94-017329] p 1133 N95-19078
Properties of Alfven waves with transverse scale on the order of skin-depth
[AD-A285657] p 1147 N95-19700
MAGNETOHYDRODYNAMICS
Nonlinear magnetohydrodynamics
[DE94-016223] p 1143 N95-18353
Global wave modeling of electron interactions with fast magnetosonic waves
[DE94-018942] p 1144 N95-18557
Simplified ideal MHD normal mode equations for toroidal axisymmetric plasmas
[DE94-627004] p 1144 N95-18886
Lattice gas and lattice Boltzmann methods for simulation of hydrodynamics and magnetohydrodynamics
p 1145 N95-18907
Numerical analysis of dissipative dynamical systems in solid and fluid mechnaics, with a special emphasis on coupled problems p 1122 N95-18916
A three region analysis of a bounded plasma using particle in cell and fluid techniques
[AD-A284826] p 1147 N95-19690
Generalized relaxation theory and vortices in plasmas
[DE95-002615] p 1147 N95-19837
MAGNETOPAUSE
Modeling the diurnally precessing Jovian magnetospheric field
[AD-A284857] p 1195 N95-19739
MAGNETOPLASMADYNAMICS
Engineering considerations for the self-energizing magnetoplasmadynamic (MPD) - type fusion plasma thruster
[AD-A283968] p 1144 N95-18888
MAGNETORESISTIVITY
DC-conductivity and magnetoresistance of inherently conducting polymers. Polyacetylene and poly(3-alkylthiophenes)
[PB94-184587] p 1007 N95-18037
MAGNETOSPHERES
Cross-tail current, field-aligned current, and B(y)
[NASA-CR-197624] p 1065 N95-19032
MAGNETOSTATICS
A finite element code for electric motor design
p 1014 N95-18974
Potential distributions for ellipsoidal bodies in uniform fields
[MRL-TR-92-48] p 1005 N95-19771
Solutions of TEAM Problem No. 13 using integral equations in a sequential and parallel computing environment
[DE95-001472] p 1112 N95-19834
MAGNETRONS
Development of materials for high temperature superconductor Josephson junctions
[DE95-000896] p 1152 N95-19608
MAGNETS
The US 100 T Magnet Project
[DE94-016099] p 1011 N95-19200
Improvement of a high current DC power supply system for testing the large scaled superconducting cables and magnets
[DE94-770767] p 1012 N95-19548
MAIN SEQUENCE STARS
New astrophysical opacities and their effects on stellar models
[DE94-016445] p 1186 N95-19249
MAINTAINABILITY
KC-135 cockpit modernization study. Phase 1: Equipment evaluation
[AD-A284099] p 942 N95-18398
Navy foreign object damage and its impact on future gas turbine engine low pressure compression systems
p 951 N95-19658
New Trends in coatings developments for turbine blades: Materials processing and repair p 954 N95-19676
MAINTENANCE
Acquisition handbook: Update. Comprehensive Approach to Reusable Defensive Software (CARDS)
[AD-A284342] p 1097 N95-18420
Kings Bay coastal and estuarine physical monitoring and evaluation program: Coastal studies. Volume 1: Main text and Appendix A
[AD-A285542] p 1074 N95-18470
E-6A hardness assurance, maintenance and surveillance program
[AD-A283994] p 945 N95-19067
Performance deterioration of axial compressors due to blade defects p 952 N95-19665
An airborne monitoring system for FOD and erosion faults p 953 N95-19668
Braze repair possibilities for hot section gas turbine parts p 954 N95-19677
Automatically generating procedure code and database maintenance scripts
[DE95-000545] p 1176 N95-19876

MALFUNCTIONS
Gemini 8, This is Houston, flight
[NASA-TM-110490] p 965 N95-19039
MAN MACHINE SYSTEMS
Aerospace medicine and biology: A continuing bibliography with indexes (supplement 398)
[NASA-SP-7011(398)] p 1080 N95-19239
Aerospace medicine and biology: A continuing bibliography with indexes (supplement 397)
[NASA-SP-7011(397)] p 1087 N95-19746
MANAGEMENT
Assessment of a career development program for executive amd mid-level managers
p 1161 N95-18182
MANAGEMENT INFORMATION SYSTEMS
Graphics MIS/Shop Store Program: User's manual
[AD-A284062] p 1174 N95-18681
Environmental Compliance Assessment System (ECAS)
[AD-A283950] p 1060 N95-18683
AMDRS: A resource for intelligent aeromedical decision-making p 1082 N95-19419
Environmental Compliance Assessment System (ECAS). South Carolina supplement: US Army
[AD-A279244] p 1062 N95-19860
MANAGEMENT METHODS
Applying Costs, Risks and Values Evaluation (CRAVE) methodology to Engineering Support Request (ESR) prioritization p 1160 N95-18176
Assessment of a career development program for executive amd mid-level managers
p 1161 N95-18182
NASA directives: Master list and index
[NHB-1410.13N] p 1171 N95-19133
The Clinical Basis for Aeromedical Decision Making
[AGARD-CP-553] p 1080 N95-19413
Technology Benefit Estimator (T/BEST): User's manual
[NASA-TM-106785] p 1046 N95-19501
MANAGEMENT SYSTEMS
Replica management system: A scheme for flexible and dynamic replication
[PB94-201597] p 1171 N95-18060
Resources Automated Management System
[AD-A284153] p 1171 N95-18416
On-line handling of air traffic: Management, guidance and control
[AGARD-AG-321] p 941 N95-18927
NASA directives: Master list and index
[NHB-1410.13N] p 1171 N95-19133
Aeromedical risk management for aircrew
p 1080 N95-19414
Acceptance/operational test procedure 101-SY tank camera purge system and in tank color camera video imaging system
[DE95-000344] p 1035 N95-19553
A knowledge-based system for controlling automobile traffic p 1102 N95-19633
MANDRELS
Surface roughness measurements
p 1142 N95-18984
Split mandrel versus split sleeve coldworking: Dual methods for extending the fatigue life of metal structures
p 940 N95-19500
MANEUVERABILITY
The development of a fiber optics communication network for controlling a Multidegree-Of-Freedom Serpentine Truss p 1142 N95-18167
MANGANESE
Preparation and surface characterization of metal doped alumina catalyst
[PB94-175296] p 973 N95-17991
Warm formability of aluminum-magnesium alloys
[DE94-016170] p 980 N95-19396
MANGANESE ALLOYS
Modified Cu-Mn-Al high damping alloys
[AD-A285460] p 980 N95-19539
MANGANESE ISOTOPES
Mn-Cr isotopic systematics of Chainpur chondrules and bulk ordinary chondrites p 1190 N95-19320
MANGANESE OXIDES
Alternative materials for solid oxide fuel cells
[DE94-018452] p 1054 N95-19591
MANIPULATORS
The development of a fiber optics communication network for controlling a Multidegree-Of-Freedom Serpentine Truss p 1142 N95-18167
Automated path planning of the Payload Inspection and Processing System p 1043 N95-18169
MANNED MANEUVERING UNITS
Skylab: The second manned mission. A scientific harvest
[NASA-TM-110487] p 961 N95-19059
MANNED SPACE FLIGHT
Legacy of Gemini
[NASA-TM-110486] p 961 N95-19058
Skylab: The second manned mission. A scientific harvest
[NASA-TM-110487] p 961 N95-19059
MANUFACTURING
US Industrial Outlook, 1994: An almanac of industry, technology and services. 35th annual edition. Forecasts for selected manufacturing and service industries
[PB94-107844] p 1171 N95-17988
European aeronautics: Strong government presence in industry structure and research and development support. Report to Congressional Requesters
[GAO/NSIAD-94-71] p 1171 N95-18578
Simulation in manufacturing
[PB94-215563] p 1100 N95-19409
Isotope separation and advanced manufacturing technology
[DE95-000313] p 1039 N95-19551
A CLIPS-based expert system for the evaluation and selection of robots p 1103 N95-19641
Silicon-Film (trademark) photovoltaic manufacturing technology
[DE94-011899] p 1056 N95-19882
MANURES
Methane: The other greenhouse gas. Research and policy in the Netherlands
[PB94-207149] p 1058 N95-18375
MANY BODY PROBLEM
Static and dynamic nuclear many-body descriptions on parallel architectures
[DE94-018134] p 1116 N95-18120
Quantitative analysis of voids in percolating structures in two-dimensional N-body simulations
[NASA-CR-197612] p 1156 N95-18949
Testing the frozen flow approximation
[NASA-CR-197614] p 1180 N95-18966
Optimizing the Zeldovich approximation
[NASA-CR-197606] p 1156 N95-19037
The jet model of chondrule formation
p 1189 N95-19310
A test of the adhesion approximation for gravitational clustering
[NASA-CR-197610] p 1157 N95-19358
Comparison of dynamical approximation schemes for non-linear gravitational clustering
[NASA-CR-197609] p 1157 N95-19363
Generation and solution of effective many-body Hamiltonians for rare earth and transition metal compounds
[DE95-002402] p 1155 N95-19838
The formulation of quantum statistical mechanics based on the Feynman path centroid density. 4: Algorithms for centroid molecular dynamics
[AD-A279234] p 1157 N95-19853
MAPPING
Software techniques for balancing computation and communication in parallel systems
[AD-A285536] p 1109 N95-18106
Real-time modeling of complex atmospheric releases in urban areas
[DE94-018063] p 1059 N95-18647
MARANGONI CONVECTION
Marangoni convection in a gravity-free silicon float zone
[NASA-CR-197600] p 991 N95-18913
MARINE METEOROLOGY
Marine boundary layer refractive effects in the infrared
[AD-A285717] p 1140 N95-18484
Office of Research and Applications: Research Programs p 1071 N95-18721
ADCIRC: An advanced three-dimensional circulation model for shelves, coasts, and estuaries. Report 5: A tropical storm database for the east and Gulf of Mexico coasts of the United States
[AD-A285576] p 1075 N95-19540
MARINER 10 SPACE PROBE
Mercury: Exploration of a planet
[NASA-TM-110489] p 1194 N95-19045
MARITIME SATELLITES
The future use of DSCS and commercial satellites in the US Navy
[AD-A285707] p 997 N95-18481
MARKET RESEARCH
Quality optimization of thermally sprayed coatings produced by the JP-5000 (HVOF) gun using mathematical modeling p 989 N95-19008
MARKETING
US Industrial Outlook, 1994: An almanac of industry, technology and services. 35th annual edition. Forecasts for selected manufacturing and service industries
[PB94-107844] p 1171 N95-17988
MARKOV CHAINS
Finite Markov chains and random discrete structures
[AD-A284192] p 1121 N95-19104
A new stochastic systems approach to structural integrity p 935 N95-19474
MARTENSITE
Design of advanced steels for armor applications
[ARL-CR-175] p 979 N95-18948
MASKS
Microcavity structures
[DE95-001096] p 1039 N95-19727
MASS DISTRIBUTION
A test of the adhesion approximation for gravitational clustering
[NASA-CR-197610] p 1157 N95-19358
MASS FLOW
Simulation of multidisciplinary problems for the thermostress state of cooled high temperature turbines
p 948 N95-19021
VENTCF2: An algorithm and associated FORTRAN 77 subroutine for calculating flow through a horizontal ceiling/floor vent in a zone-type compartment fire model
[PB94-210127] p 993 N95-19402
MASS SPECTRA
Study of laser resonance ionization mass spectrometry using a glow discharge source
[DE94-018566] p 981 N95-19703
MASS SPECTROMETERS
Modeling and measurement of the performance of a branched conduit sampling system in a mass spectrometer leak detector p 1036 N95-18181
MASS SPECTROSCOPY
Mass spectrometric studies of clusters and surfaces
[AD-A283992] p 974 N95-19066
Development of laser-ion beam photodissociation methods
[DE95-002800] p 977 N95-19840
MASS TRANSFER
Modeling and measurement of the performance of a branched conduit sampling system in a mass spectrometer leak detector p 1036 N95-18181
MASSIVELY PARALLEL PROCESSORS
Local spatio-temporal analysis in vision systems
[AD-A284162] p 1140 N95-18509
Dynamic file-access characteristics of a production parallel scientific workload
[NASA-CR-197570] p 1110 N95-18581
Empirical study of parallel LRU simulation algorithms
[NASA-CR-194995] p 1099 N95-19027
Massively parallel full configuration interaction. Benchmark electronic structure calculations on the Intel Touchstone Delta
[DE95-001064] p 1153 N95-19724
Using CLIPS in the domain of knowledge-based massively parallel programming p 1105 N95-19750
MATERIAL BALANCE
Ethylene dynamics in the CELSS biomass production chamber p 1077 N95-18179
MATERIALS TESTS
Regenerative cooling for liquid propellant rocket thrust chambers
[INPE-5565-TDI/540] p 967 N95-18720
Current loop signal conditioning: Practical applications
[NASA-TM-4636] p 1033 N95-18735
Thermal behavior spiral bevel gears
[NASA-TM-106518] p 1042 N95-18935
MATHEMATICAL MODELS
Observational studies and modelling of interception loss of gross rainfall in the Amazonian rainforest
[INPE-5583-TDI/545] p 1067 N95-18006
A constant-depth scratch test for the measurement of adhesion at film-substrate interfaces
[AD-A283660] p 983 N95-18016
A formal method for semantics-based change-merging of software prototypes
[AD-A283668] p 1094 N95-18017
The left-right forward-backward asymmetry for B quarks at the SLD
[DE94-014508] p 1129 N95-18049
Energy balance model for imagery and electromagnetic propagation
[AD-A284552] p 1063 N95-18115
Numerical mixing calculations of confined reacting jet flows in a cylindrical duct
[NASA-TM-106736] p 947 N95-18133
Coastal acoustic tomography data constraints applied to a coastal ocean circulation model
[AD-A283911] p 1074 N95-18153
Image intensifier system resolution based on laboratory measured parameters
[AD-A283917] p 1008 N95-18156
Coastal Modeling System (CMS) user's manual. Supplement 3 to September 1991 manual
[AD-A283922] p 1074 N95-18160
Assessment of the SFC database for analysis and modeling p 1158 N95-18171
Heuristic inference about flow directions in river networks
[INPE-5588-TDI/550] p 1050 N95-18214

Fast numerical determination of symmetric sparsity patterns
[DE94-016344] p 1096 N95-18354
Finite element modeling of partially delaminated composite beams with contact-impact conditions
[AD-A283726] p 1044 N95-18363
Prediction of buoyant outflow in lakes and fjords with a quasi 3D numerical model
[PB94-206984] p 1051 N95-18372
Compression strength of composite primary structural components
[NASA-CR-197554] p 1044 N95-18388
Imagery correction for atmospheric effects using sounding data
[INPE-5506-TDI/518] p 1064 N95-18390
A model study of the influence of NMHC and NO(x) emissions on rural O3 concentrations in Georgiargia p 1059 N95-18445
TEXCAD: Textile Composite Analysis for Design. Version 1.0: User's manual
[NASA-CR-4639] p 970 N95-18466
Aeromechanics technology, volume 1. Task 1: Three-dimensional Euler/Navier-Stokes Aerodynamic Method (TEAM) enhancements
[AD-A285713] p 943 N95-18483
A simple hyperbolic model for communication in parallel processing environments
[NASA-CR-195984] p 1098 N95-18487
Improved filtration materials and modeling
[AD-A284684] p 1091 N95-18531
Sloshing roof impact tests of a rectangular tank
[DE94-012462] p 1018 N95-18549
Minimal time detection algorithms and applications to flight systems
[TR-2-FSRC-93] p 1098 N95-18564
The impact of non-linear flight control systems on the prediction of aircraft loads due to turbulence p 956 N95-18598
Long-term processes in geomaterials. A three-dimensional visco-elastic soil model
[PB94-207180] p 1065 N95-18640
Regenerative cooling for liquid propellant rocket thrust chambers
[INPE-5565-TDI/540] p 967 N95-18720
Weighted graph based ordering techniques for preconditioned conjugate gradient methods
[NASA-CR-197597] p 1118 N95-18736
A linear system identification and validation of an AH-64 Apache aeroelastic simulation model p 959 N95-18903
On stationary and nonstationary fatigue load modeling using autoregressive moving average (ARMA) models p 1046 N95-18919
An analytic conceptual model of extratropical cyclones
[KNMI-WR-93-03] p 1072 N95-18926
Thermal behavior spiral bevel gears
[NASA-TM-106518] p 1042 N95-18935
Characterization of metal matrix composites
[NASA-CR-195381] p 970 N95-18940
Testing the frozen flow approximation
[NASA-CR-197614] p 1180 N95-18966
Residual stresses in welded plates p 1047 N95-18972
Foreign body impact event damage formation in composite structures p 972 N95-18973
Data driven propulsion system weight prediction model p 968 N95-18980
Steady and unsteady blade stresses within the SSME ATD/HPOTP inducer p 968 N95-18982
Mathematical Models of Gas Turbine Engines and their Components
[AGARD-LS-198] p 948 N95-19017
The mathematical models of flow passage for gas turbine engines and their components p 948 N95-19020
Simulation of multidisciplinary problems for the thermostress state of cooled high temperature turbines p 948 N95-19021
Application of multicomponent models to flow passage simulation in multistage turbomachines and whole gas turbine engines p 948 N95-19022
Application of multidisciplinary models to the cooled turbine rotor design p 949 N95-19024
Second-order reconstruction of the inflationary potential
[NASA-CR-197629] p 1121 N95-19030
Mass and radius of cosmic balloons
[NASA-CR-197628] p 1180 N95-19031
Cross-tail current, field-aligned current, and B(y)
[NASA-CR-197624] p 1065 N95-19032
Experimental verification of a progressive damage model for composite laminates based on continuum damage mechanics
[NASA-CR-195020] p 971 N95-19043
SSI effects for a tank containing two liquids
[DE94-012457] p 1020 N95-19099
Algorithms and applications in timed discrete event systems
[PB94-201423] p 1118 N95-19169
Large-scale processes in the solar nebula p 1186 N95-19292
On the possibility of precipitation-induced vertical lightning in the protoplanetary nebula p 1187 N95-19299
The jet model of chondrule formation p 1189 N95-19310
Experimental constraints on models for the origin of chondrules: Cooling rates p 1189 N95-19311
Testing higher-order Lagrangian perturbation theory against numerical simulation. 1: Pancake models
[NASA-CR-197611] p 1121 N95-19348
Antisymmetric tensor field interactions and neutron star models
[PB94-215605] p 1118 N95-19375
Unsteady aerodynamic analyses for turbomachinery aeroelastic predictions p 949 N95-19381
Forced response of mistuned bladed disks p 950 N95-19383
ODP based UPT model
[PB94-215589] p 1003 N95-19411
Prediction of fatigue crack growth under flight-simulation loading with the modified CORPUS model p 934 N95-19471
Discrete crack growth analysis methodology for through cracks in pressurized fuselage structures p 935 N95-19473
A new stochastic systems approach to structural integrity p 935 N95-19474
Fatigue and damage tolerance scatter models p 935 N95-19475
A probabilistic fatigue analysis of multiple site damage p 935 N95-19476
The tensor equation AX+XA=Phi (A, H) with applications to kinematics of continua
[AD-A285886] p 1122 N95-19603
Unit cell geometry of multiaxial preforms for structural composites
[NASA-CR-197294] p 971 N95-19650
Particle trajectories in gas turbine engines p 952 N95-19663
The calculation of erosion in a gas turbine compressor rotor p 952 N95-19664
Design of fan blades subjected to bird impact p 953 N95-19669
Soft body impact on titanium fan blades p 953 N95-19671
Ice-impact analysis of blades p 953 N95-19672
Damage of high temperature components by dust-laden air p 953 N95-19673
Analysis of the erosion of cubic centered and face centered metallic materials p 953 N95-19674
A three region analysis of a bounded plasma using particle in cell and fluid techniques
[AD-A284826] p 1147 N95-19690
Mega-scale simulation of multi-layer devices: Formulation, kinetics, and visualization
[AD-A284848] p 1153 N95-19738
On supersonic-inlet boundary-layer bleed flow
[NASA-CR-195426] p 955 N95-19769
Slot spiral antenna modeling using hybrid/mixed FE-BI technique p 1006 N95-19797
Modeling of quantum transport in semiconductor devices
[AD-A280182] p 1155 N95-19829
High performance computing equipment for environmental remediation modeling and first principles simulation of materials properties
[DE95-000497] p 1093 N95-19875

MATHEMATICAL PROGRAMMING

Representing and reformulating diagonalization methods
[AD-A283916] p 1095 N95-18155

MATRICES (MATHEMATICS)

Reformulated preconditioned conjugate gradient squared method. Part 1: The algorithm
[PB94-201589] p 1108 N95-17936
Fast numerical determination of symmetric sparsity patterns
[DE94-016344] p 1096 N95-18354
Plant and controller optimization by convex methods
[AD-A283700] p 944 N95-18621
Eigenvalue tests and distributions for small sample order determination for complex Wishart matrices
[AD-A283825] p 1120 N95-18672
Weighted graph based ordering techniques for preconditioned conjugate gradient methods
[NASA-CR-197597] p 1118 N95-18736
Crystalline beams: The string
[DE94-016806] p 1150 N95-19091
The tensor equation AX+XA=Phi (A, H) with applications to kinematics of continua
[AD-A285886] p 1122 N95-19603

MATRIX MATERIALS

Polymer-based separations: Synthesis and application of polymers for ionic and molecular recognition
[DE94-016427] p 984 N95-18355
Method for making a non-magnetic alloy
[AD-D016233] p 979 N95-18630
Experimental verification of a progressive damage model for composite laminates based on continuum damage mechanics
[NASA-CR-195020] p 971 N95-19043
Superstrength metal composite material and process for making the same
[AD-D016555] p 971 N95-19123
Chondrule-matrix relationships in chondritic meteorites p 1186 N95-19293

MAXIMUM ENTROPY METHOD

Applications of quantum entropy to statistics
[DE94-014416] p 1155 N95-17996

MAXIMUM LIKELIHOOD ESTIMATES

Some statistical tools for SAR image synthesis, analysis and processing
[INPE-5548-TDI/534] p 1172 N95-18004
Detection performance of generalized likelihood ratio processors for random signals of unknown location, structure, extent, and strength
[AD-A285589] p 997 N95-18475
Minimal time detection algorithms and applications to flight systems
[TR-2-FSRC-93] p 1098 N95-18564
Determination of stability and control derivatives from the NASA F/A-18 HARV from flight data using the maximum likelihood method
[NASA-CR-197320] p 958 N95-19576

MAXWELL EQUATION

Geometrical and topological methods in time domain antenna synthesis
[AD-A284208] p 994 N95-17954
Solution of Maxwell's equations using the time domain Method of Moments. Supplement: Publications and reports
[AD-A280143] p 1119 N95-19819
Solution of Maxwell's equations using the time domain Method of Moments
[AD-A280144] p 1119 N95-19820

MEASURE AND INTEGRATION

The formulation of quantum statistical mechanics based on the Feynman path centroid density. 3: Phase space formalism and analysis of centroid molecular dynamics
[AD-A279233] p 1157 N95-19852

MEASUREMENT

A Quantum-Drive-Time (QDT) quantization of the Taub cosmology
[DE95-001014] p 1194 N95-19612

MEASURING INSTRUMENTS

Hypersonic flight testing
[AD-A283981] p 944 N95-18891
On the measurement of the crack tip stress field as a means of determining Delta K(sub eff) under conditions of fatigue crack closure p 938 N95-19492

MECHANICAL DRIVES

Positive displacement rotary pump
[AD-D016412] p 1041 N95-18335
Development of a bulk current injection direct-drive system to test system level components with stress waveforms that are encountered during full threat indirect effects lightning
[AD-A284160] p 933 N95-18507

MECHANICAL ENGINEERING

Strategic avionics technology definition studies. Subtask 3-1A3: Electrical Actuation (ELA) Systems Test Facility
[NASA-CR-188360] p 956 N95-18567

MECHANICAL PROPERTIES

Alloying effects on the high-temperature oxidation resistance of Cr-Cr2Nb
[DE94-018146] p 978 N95-18121
On the crack growth resistance and strength of the B2 iron aluminides Fe-40Al, Fe-45Al, and Fe-10Ni-40Al (at. %)
[DE94-017857] p 978 N95-18128
Novel polymeric composites through molecular engineering
[AD-A284168] p 985 N95-18513
Course module for AA201: Wing structural design project
[AD-A283618] p 944 N95-18616
Environmental effects on composite airframes: A study conducted for the ARM UAV Program (Atmospheric Radiation Measurement Unmanned Aerospace Vehicle)
[DE94-015351] p 971 N95-19579
Recent progress on ECVD Project
[DE94-016773] p 988 N95-19580
CVD silicon carbide characterization
[AD-A285667] p 972 N95-19702

MEDICAL EQUIPMENT
Design and development of an enhanced biodynamic manikin, phase 1
[AD-A284725] p 1090 N95-18077
MEDICAL SCIENCE
National Library of Medicine programs and services, fiscal year 1991
[PB94-188026] p 1077 N95-17949
National Library of Medicine programs and services, fiscal year 1992
[PB94-188034] p 1078 N95-17950
Naval Biodynamics Laboratory 1993 command history
[AD-A284358] p 1089 N95-18440
Light transport for medical laser treatments
[PB94-201498] p 1037 N95-18502
Photobiology in medicine
[AD-A284843] p 1087 N95-19695
Annual historical report, calendar year 1993
[AD-A280178] p 1087 N95-19827
MEDICAL SERVICES
High performance computing for medical image interpretation
[AD-A285457] p 1086 N95-19537
On the development of an expert system for wheelchair selection p 1092 N95-19627
Expert Witness: A system for developing expert medical testimony p 1101 N95-19628
Distributed medical database system for real-time monitoring of the health and risk exposure of military research study volunteers at USARIEM
[AD-A279193] p 1087 N95-19811
Annual historical report, calendar year 1993
[AD-A280178] p 1087 N95-19827
MELANIN
Retinal injuries from single and multiple picosecond laser pulses
[AD-A284173] p 1078 N95-18515
MELTING
Constraints placed on the nature of chondrule precursors p 1186 N95-19295
Experimental constraints on models for origins of chondrules: Peak temperatures p 1187 N95-19302
Chondrule formation in lightning discharges p 1188 N95-19304
Chondrule remelting: Evidence from coarse-grained chondrule rims and compound chondrules p 1191 N95-19323
Chondrule formation in the radiative accretional shock p 1191 N95-19324
The circumplanetary nebular environment: A possible source region for chondrules p 1191 N95-19325
MELTING POINTS
Superstrength metal composite material and process for making the same
[AD-D016555] p 971 N95-19123
MELTS (CRYSTAL GROWTH)
Implications of a phase-transition thermostat for chondrule melting p 1189 N95-19312
MEMBRANES
Method of making a membrane having hydrophilic and hydrophobic surfaces for adhering cells or antibodies by using atomic oxygen or hydroxyl radicals
[NASA-CASE-MSC-21529-1] p 983 N95-18134
Ion exchange polymers and method for making
[NASA-CASE-LEW-15576-1] p 984 N95-18321
Palladium-based membranes for hydrogen separation
[PB94-207156] p 973 N95-18377
MEMORY
A parallel processing hypothesis for short-term and long-term memory in Aplysia
[AD-A284101] p 1088 N95-18401
Facilitation and interference in identification of pictures and words
[AD-A285882] p 1090 N95-19602
Comparing performance on implicit memory tests
[AD-A284861] p 1090 N95-19740
MEMORY (COMPUTERS)
A novel system level approach to fault tolerance in distributed memory multicomputers
[AD-A284729] p 1095 N95-18079
Automatic Identification Technology (AIT): The development of functional capability and card application matrices
[AD-A285528] p 1173 N95-18099
MENTAL PERFORMANCE
Age 60 study. Part 4: Experimental evaluation of pilot performance
[AD-A286248] p 1080 N95-19385
Neuropsychophysiologic sequelae of mild head injury p 1083 N95-19430
Comparing performance on implicit memory tests
[AD-A284861] p 1090 N95-19740
MERCURY (PLANET)
Mercury: Exploration of a planet
[NASA-TM-110489] p 1194 N95-19045
MERCURY CADMIUM TELLURIDES
Industrial exploitation of a alternate technology for the production of HgCdTe epilayers, structures and devices
[AD-A279202] p 1154 N95-19816
MERCURY ISOTOPES
Multi-channel, covert, non-line-of-sight UV communication
[AD-D016269] p 999 N95-18545
MERCURY TELLURIDES
IR materials producibility
[AD-A284263] p 1142 N95-19732
MESOMETEOROLOGY
Estimation of satellite derived temperature and moisture fields over Europe from TOVS data using 3I and ITPP algorithms
[AD-A284581] p 1049 N95-18035
Synoptic and mesoscale examination of the northern New England winter storm of January 29-30, 1990
[PB94-209426] p 1072 N95-19581
MESONS
Feynman-x and transverse momentum dependence of D(sup (+-)) and D(sup 0), D-bar(sup 0) production in 250 GeV (pi)(sup -) - nucleon interactions
[DE94-626698] p 1130 N95-18366
Summary of the working group on tests of QCD
[DE94-018390] p 1131 N95-18550
MESOSCALE PHENOMENA
Estimation of satellite derived temperature and moisture fields over Europe from TOVS data using 3I and ITPP algorithms
[AD-A284581] p 1049 N95-18035
Experiments with the Mesoscale Atmospheric Simulation System (MASS) using the synthetic relative humidity p 1073 N95-18172
Predicting and explaining the movement of mesoscale oceanographic features using CLIPS p 1105 N95-19752
MESSAGE PROCESSING
A simple hyperbolic model for communication in parallel processing environments
[NASA-CR-195984] p 1098 N95-18487
Advanced techniques for analysis and evaluation of robust protocols
[AD-A285682] p 1111 N95-19513
METABOLISM
In vitro system for studying metabolism of environmental chemicals in human cells
[AD-A284174] p 1079 N95-18518
Drink composition and cycle-ergometer endurance in men: Carbohydrate, Na(+), osmolality
[NASA-TM-4650] p 1077 N95-19140
Cumulative effects of repeated brief cerebral ischemia
[AD-A284234] p 1087 N95-19698
METAL BONDING
Application of superplastically formed and diffusion bonded structures in high intensity noise environments p 1127 N95-19162
Adhesion, friction, and wear behavior of clean metal-ceramic couples
[NASA-TM-106815] p 989 N95-19783
METAL CLUSTERS
Photogeneration and characterization of energetic molecules in supersonic molecular beams
[AD-A284108] p 1131 N95-18438
METAL COATINGS
Preparation of an electrocatalytic cathode for an aluminum-hydrogen peroxide battery
[AD-D016262] p 1008 N95-18318
Trivalent chromium conversion coatings for aluminum
[AD-D016274] p 978 N95-18332
Method of forming platinum and platinum silicide Schottky contacts on beta-silicon carbide
[AD-D016221] p 1149 N95-18627
Composite structures having organic matrices and duplex zinc/ceramic fire barriers
[AD-D016232] p 970 N95-18629
METAL COMBUSTION
Ignition and combustion of bulk metals in a microgravity environment
[NASA-CR-197519] p 990 N95-18082
METAL FATIGUE
Microstructure-based fatigue life prediction methods for naval steel structures
[AD-A284735] p 1044 N95-18081
Warm formability of aluminum-magnesium alloys
[DE94-016170] p 980 N95-19396
A new stochastic systems approach to structural integrity p 935 N95-19474
A probabilistic fatigue analysis of multiple site damage p 935 N95-19476
Evaluation of the fuselage lap joint fatigue and terminating action repair p 936 N95-19477
The application of Newman crack-closure model to predicting fatigue crack growth p 937 N95-19483
Fatigue crack growth under variable amplitude loading p 937 N95-19484
METAL FILMS
Trivalent chromium conversion coatings for aluminum
[AD-D016274] p 978 N95-18332
Propagation of intense, ultrashort laser pulses through metal vapor: Refractive intensity limits and spectral effects
[DE94-016365] p 1039 N95-19398
METAL FOILS
2-D tomography with bolometry in D3-D
[DE94-017520] p 1146 N95-19379
METAL HYDRIDES
Metal/hydrogen energy storage: Selected technical issues
[AD-A283355] p 1008 N95-18052
Probing the chemistry of nickel/metal hydride battery cells using electrochemical impedance spectroscopy p 1014 N95-18985
METAL IONS
Photogeneration and characterization of energetic molecules in supersonic molecular beams
[AD-A284108] p 1131 N95-18438
Compact, efficient, scalable neodymium laser co-doped with activator ions and pumped by visible laser diodes
[AD-D016237] p 1038 N95-18585
Measurements of line overlap for resonant spoiling of x ray lasing transitions
[DE94-016444] p 1038 N95-19248
METAL MATRIX COMPOSITES
Centrifugal casting of reinforced articles
[AD-D016277] p 992 N95-18431
Composites research in support of the NASP Institute for Composites (NIC)
[NASA-CR-197580] p 970 N95-18471
Optimization of layered metal matrix composite cylinders p 970 N95-18920
Characterization of metal matrix composites
[NASA-CR-195381] p 970 N95-18940
METAL OXIDE SEMICONDUCTORS
Defect reduction and back channel degradation in SIMOX
[AD-A284231] p 1148 N95-17960
Fault protection circuit for power switching device
[AD-D016466] p 1009 N95-18455
Method for fabricating complementary enhancement and depletion mode field effect transistors on a single substrate
[AD-D016270] p 1010 N95-18546
METAL OXIDES
Power terminal protection device
[AD-D016528] p 1011 N95-19120
Transition metal oxides deposited on rhodium and platinum: Surface chemistry and catalysis
[DE95-000793] p 975 N95-19616
METAL PLATES
Development of an improved ballistic acceptance test for high hard armor steel plate: MIL-A-46100
[ARL-TR-509] p 979 N95-18939
Residual stresses in welded plates p 1047 N95-18972
METAL POLISHING
Ion beam surface treatment: A new capability for surface enhancement
[DE94-014663] p 977 N95-17968
METAL SHEETS
Fracture behavior of large-scale thin-sheet aluminum alloy p 939 N95-19494
Prediction of R-curves from small coupon tests p 939 N95-19496
METAL SURFACES
Ion beam surface treatment: A new capability for surface enhancement
[DE94-014663] p 977 N95-17968
Preparation and surface characterization of metal doped alumina catalyst
[PB94-175296] p 973 N95-17991
Trivalent chromium conversion coatings for aluminum
[AD-D016274] p 978 N95-18332
Adherend surface effects on epoxy cure by NMR
[AD-A284774] p 985 N95-18442
Fundamental studies of passivity and passivity breakdown
[DE94-016954] p 987 N95-19095
An atomic view of surface diffusion on metal surfaces
[DE94-016150] p 980 N95-19395
X-ray absorption spectroscopy in high temperature oxidation of metals and alloys p 955 N95-19682
METAL VAPORS
Propagation of intense, ultrashort laser pulses through metal vapor: Refractive intensity limits and spectral effects
[DE94-016365] p 1039 N95-19398
METALLIC GLASSES
Synthesis and structural properties of new metallic phases exhibiting non-crystallographic symmetries
[AD-A284882] p 982 N95-19743

METALLICITY
Electronic structure of C60 fullerites and nanotubes
[DE95-000784] p 1151 N95-19569
METALLIZING
Using electrochemistry in device processing on poly(tetrafluoroethylene) substrates
[DE95-000541] p 975 N95-19559
METALS
The probability of flaw detection and the probability of false calls in nondestructive evaluation equipment
p 1044 N95-19010
Fundamental studies of passivity and passivity breakdown
[DE94-016954] p 987 N95-19095
Metal-framed partitions with reduced thicknesses. Part 2: Built-in acoustic treatment
[BBC-RD-1993/6-PT-2] p 993 N95-19137
Metal-framed partitions with reduced thicknesses. Part 1: Narrower studs and cavities
[BBC-RD-1993/5-PT-1] p 993 N95-19138
Adhesion, friction, and wear behavior of clean metal-ceramic couples
[NASA-TM-106815] p 989 N95-19783
Heavy metal soil contamination at US Army installations: Proposed research and strategy for technology development
[AD-A279171] p 1062 N95-19808
METASTABLE STATE
Photogeneration and characterization of energetic molecules in supersonic molecular beams
[AD-A284108] p 1131 N95-18438
High temperature stability of binary microstructures derived from liquid precursors
[AD-A283960] p 1150 N95-18685
Nonstoichiometry of Al-Zr intermetallic phases
[DE94-016877] p 979 N95-19093
Microscopic origins of metastable effects in a-Si:H and deep defect characterization in a-Si,Ge:H alloys
[DE94-011887] p 1151 N95-19541
METEORITE COLLISIONS
Collision of cometlike and slightly differentiated bodies as an origin for ordinary chondrites
p 1188 N95-19308
METEORITES
Papers presented to the Conference on Chondrules and the Protoplanetary Disk
[NASA-CR-197121] p 1186 N95-19289
Chondrule-matrix relationships in chondritic meteorites
p 1186 N95-19293
Experimental constraints on models for origins of chondrules: Peak temperatures p 1187 N95-19302
Models for multiple heating mechanisms
p 1188 N95-19303
Chondrule formation in lightning discharges
p 1188 N95-19304
Relict grains in chondrules: Evidence for chondrule recycling p 1188 N95-19307
Experimental constraints on models for the origin of chondrules: Cooling rates p 1189 N95-19311
METEORITIC COMPOSITION
Papers presented to the Conference on Chondrules and the Protoplanetary Disk
[NASA-CR-197121] p 1186 N95-19289
Producing chondrules by recycling and volatile loss
p 1186 N95-19290
Carbon, CAIs and chondrules p 1186 N95-19291
Large-scale processes in the solar nebula
p 1186 N95-19292
Chondrule-matrix relationships in chondritic meteorites
p 1186 N95-19293
Turbulent diffusion and concentration of chondrules in the protoplanetary nebula p 1187 N95-19296
On the possibility of precipitation-induced vertical lightning in the protoplanetary nebula
p 1187 N95-19299
The role of chondrules in nebular fractionations of volatiles and other elements p 1187 N95-19300
Experimental constraints on models for origins of chondrules: Peak temperatures p 1187 N95-19302
Chondrules and their associates in ordinary chondrites
p 1188 N95-19306
Relict grains in chondrules: Evidence for chondrule recycling p 1188 N95-19307
Collision of cometlike and slightly differentiated bodies as an origin for ordinary chondrites
p 1188 N95-19308
Microchondrules in ordinary chondrites: Implications for chondrule formation p 1188 N95-19309
The jet model of chondrule formation
p 1189 N95-19310
Experimental constraints on models for the origin of chondrules: Cooling rates p 1189 N95-19311
Implications of a phase-transition thermostat for chondrule melting p 1189 N95-19312
Chronology of chrondrule and CAI formation: Mg-Al isotopic evidence p 1189 N95-19314
Constraints on chondrule agglomeration from fine-grained chondrule rims p 1189 N95-19315
The origin of refractory precursor components of chondrules p 1189 N95-19316
Constraints on chondrule and CAI origins from vapor-liquid-solid experiments p 1190 N95-19317
Porphyritic versus nonporphyritic chondrules
p 1190 N95-19318
Siderophile elements and metal-silicate fractionation in the solar nebula p 1190 N95-19319
Mn-Cr isotopic systematics of Chainpur chondrules and bulk ordinary chondrites p 1190 N95-19320
Formation of chondrules and CAIs by nebular processes p 1190 N95-19321
A ceramic/slag interface as an analog for accretion of hot refractory objects and rim formation
p 1191 N95-19322
Chondrule remelting: Evidence from coarse-grained chondrule rims and compound chondrules
p 1191 N95-19323
Chondrule formation in the radiative accretional shock
p 1191 N95-19324
The circumplanetary nebular environment: A possible source region for chondrules p 1191 N95-19325
Heating during solar nebula formation and Mg isotopic fractionation in precursor grains of CAIs and chondrules
p 1191 N95-19326
Variations among chondrite groups: Constraints on nebular processes p 1192 N95-19327
Open-system behavior during chondrule formation
p 1192 N95-19328
I-Xe studies of individual chondrules: What can they tell us about chondrule formation? p 1192 N95-19329
Chemical production of chondrule oxygen isotopic composition p 1192 N95-19330
Chondrule origins: Constraints from chondrule properties and cosmochemistry p 1192 N95-19332
The fine nebula dust component: A key to chondrule formation by lightning p 1192 N95-19333
Cooling rates of chondrules: A new approach
p 1192 N95-19334
Implications for the evolution of chondrules from Agglomeratic olivine chondrules p 1193 N95-19335
Major unresolved issues in the formation of chondrules and CAIs p 1193 N95-19336
Flash heating is required to minimize sodium losses from chondrules p 1193 N95-19337
Chondrule precursors and cooling paths: The sulfur evidence p 1193 N95-19338
Textural variability of ordinary chondrite chondrules: Implications of their formation p 1193 N95-19339
METEORITIC MICROSTRUCTURES
Relict grains in chondrules: Evidence for chondrule recycling p 1188 N95-19307
Microchondrules in ordinary chondrites: Implications for chondrule formation p 1188 N95-19309
Cooling rates of chondrules: A new approach
p 1192 N95-19334
METEOROID HAZARDS
Cracking characteristics of a habitable module pressure wall following orbital debris penetration
p 1047 N95-19003
METEOROID SHOWERS
Effects of meteor showers in the Earth ionosphere
[INPE-5591-TDI/552] p 1178 N95-18213
METEOROLOGICAL INSTRUMENTS
Metrology: Calibration and measurement processes guidelines
[NASA-RP-1342] p 992 N95-18745
METEOROLOGICAL PARAMETERS
Climate and weather of Central Africa. Executive summary
[AD-A283647] p 1067 N95-18014
Imagery correction for atmospheric effects using sounding data
[INPE-5506-TDI/518] p 1064 N95-18390
Environmental forcing of ambient noise in the Nansen and Amundsen Basins of the Arctic Ocean
[AD-A285540] p 1074 N95-18468
Real-time modeling of complex atmospheric releases in urban areas
[DE94-018063] p 1059 N95-18647
Surface and upper-air meteorological measurements supporting the NATO/AC243/Panel 3 research study groups 8 and 21 campaign in Lorient, France (September 1993)
[AD-A285326] p 1072 N95-19521
METEOROLOGICAL RADAR
Measurements of wind profiler EMC characteristics
[PB94-194107] p 1066 N95-17938
A technical demonstration Mobile Profiler System
[AD-A284562] p 1068 N95-18117
A comparison of optical rain gauge and radar data from TOGA/COARE p 1069 N95-18207
METEOROLOGICAL SATELLITES
Field and data analysis studies related to the atmospheric environment
[NASA-CR-196543] p 1068 N95-18093
Meteor 3/TOMS launch of 15 August 1991 in Plesetsk, USSR
[NASA-TM-110115] p 962 N95-18150
METEOROLOGICAL SERVICES
Product usage evaluation of the aviation gridded forecast system workstation at the Denver Center Weather Service Unit
[PB94-195922] p 1066 N95-17952
Use of profiler data for analysis and NOWcasting of a winter season extratropical cyclone
[PB94-187804] p 1067 N95-17992
Implementation of the 1992 Terminal area-Local Analysis and Prediction System (T-LAPS)
[AD-A284334] p 1070 N95-18384
Toward a new national weather service: Weather for those who fly
[PB94-214418] p 1072 N95-19407
METEOROLOGY
Forecasting snowfall using mixing ratios on an isentropic surface: An empirical study
[PB94-188760] p 1067 N95-17993
A Space and Atmospheric Visualization Science System
[NASA-CR-189390] p 1172 N95-18040
Implementation of the 1992 Terminal area-Local Analysis and Prediction System (T-LAPS)
[AD-A284334] p 1070 N95-18384
The effect of spatial averaging on threshold exceedances of daily precipitation amounts
[KNMI-TR-154] p 1070 N95-18392
Conceptual models of severe convective weather in the Netherlands
[KNMI-WR-93-05] p 1071 N95-18394
Dependence of medium-range forecast error on patterns in the initial state p 1072 N95-18732
A technique for determining cloud free versus cloud contaminated pixels in satellite imagery
p 1052 N95-19016
METHANE
Methane conversion by solid electrolyte membranes
[PB94-191781] p 973 N95-17982
Observations of methane and ethylene diffusion flames stabilized around a blowing porous sphere under microgravity conditions
[NASA-TM-106766] p 990 N95-18211
Methane: The other greenhouse gas. Research and policy in the Netherlands
[PB94-207149] p 1058 N95-18375
Trends 1993: A compendium of data on global change
[ORNL/CDIAC-65] p 1058 N95-18389
Airborne rotary separator study
[NASA-CR-191045] p 967 N95-18743
Novel catalysts for methane activation
[DE95-001179] p 976 N95-19785
METHOD OF CHARACTERISTICS
Arbitrarily high order nodal and characteristic methods
[DE94-018130] p 1116 N95-18131
METHOD OF MOMENTS
Method of moments analysis of artificial media composed of dielectric wire objects
[AD-A283318] p 994 N95-18024
Numerically efficient use of frequency domain MoM codes for wideband radiation and scattering problems. An application: Scattering from a microstrip patch
[AD-A284561] p 995 N95-18116
Solution of Maxwell's equations using the time domain Method of Moments. Supplement: Publications and reports
[AD-A280143] p 1119 N95-19819
Solution of Maxwell's equations using the time domain Method of Moments
[AD-A280144] p 1119 N95-19820
METHODOLOGY
User profile for researchers studying objects: Implications for computer systems
[PB94-188463] p 1109 N95-17989
METHYL COMPOUNDS
Lithium electrode/polyacrylonitrile based polymer electrolyte interface
[AD-A283947] p 986 N95-19064
Reaction channel competition in vibrational overtone activation: 1-methylcyclopropene
[AD-A280185] p 976 N95-19830
METROLOGY
Metrology: Calibration and measurement processes guidelines
[NASA-RP-1342] p 992 N95-18745
MICHELSON INTERFEROMETERS
The effects of cavity topology on instabilities in additive-pulse modelocked lasers
[DE94-018193] p 1036 N95-18123

Design, validation and prototype testing of a high resolution all-reflection Michelson interferometer for solar occultation measurements of the OI 1304-a triplet emission
[AD-A283705] p 1178 N95-18361

MICROANALYSIS
Subgroup report on hard x-ray microprobes
[DE94-018708] p 1034 N95-19233

MICROBALANCES
Resonator/oscillator response to liquid loading
[DE94-013442] p 1012 N95-19240

MICROBIOLOGY
Analytical control test plan and microbiological methods for the water recovery test
[NASA-TM-108473] p 1091 N95-19061

MICROBURSTS (METEOROLOGY)
Microburst vertical wind estimation from horizontal wind measurements
[NASA-TP-3460] p 942 N95-18198

MICROCHANNEL PLATES
Implementation of 40-ps high-speed gated-microchannel-plate based x-ray framing cameras on reentrant SIM's for Nova
[DE94-018597] p 1033 N95-18555
Gain uniformity, linearity, saturation and depletion in gated microchannel-plate x-ray framing cameras
[DE94-018596] p 1035 N95-19711

MICROCRACKS
Microstructure-based fatigue life prediction methods for naval steel structures
[AD-A284735] p 1044 N95-18081
Fatigue life until small cracks in aircraft structures: Durability and damage tolerance p 936 N95-19478
Impact loading of compressor stator vanes by hailstone ingestion p 953 N95-19670
Investigation of microscopic mechanisms of failure of electronic smart materials/systems
[AD-A284830] p 988 N95-19691

MICROELECTRONICS
The linear dynamics of a microsensor accelerometer modeled as a cantilever beam with an end mass
[DE94-019108] p 1031 N95-17963
Using federal technology policy to strength the US microelectronics industry
[DE94-017293] p 1008 N95-18143
Superconductor microelectronic devices and circuits and a method of fabricating therefor
[AD-D016280] p 1009 N95-18433
Precision gold conductors for HMCs
[DE94-018558] p 1012 N95-19230
Vacuum microelectronic emitters and their applications using compound semiconductor technology
[AD-A284811] p 1013 N95-19687
Field-emitter arrays for RF vacuum microelectronics
[AD-A279932] p 1013 N95-19865

MICROGRAVITY
Microgravity fluid science research in Europe
[PB94-201720] p 990 N95-17973
Physiological and genetic characterization of plant growth and gravitropism in LED light sources
p 1077 N95-18173
Microgravity isolation system design: A modern control synthesis framework
[NASA-TM-106805] p 927 N95-18197
Observations of methane and ethylene diffusion flames stabilized around a blowing porous sphere under microgravity conditions
[NASA-TM-106766] p 990 N95-18211
Microgravity isolation system design: A modern control analysis framework
[NASA-TM-106803] p 927 N95-18486
Users guide for NASA Lewis Research Center DC-9 Reduced-Gravity Aircraft Program
[NASA-TM-106755] p 959 N95-18586
Effect of heat acclimation on sitting orthostatic tolerance in the heat after 48 and 96 hour bed rest in men
[NASA-TM-108861] p 1077 N95-18734
Marangoni convection in a gravity-free silicon float zone
[NASA-CR-197600] p 991 N95-18913
Bubble formation in microgravity p 991 N95-18970
Development of microgravity, full body functional reach envelope using 3-D computer graphic models and virtual reality technology p 1092 N95-18990
Effects of vibration (G-jitters) on convection in micro-gravity p 991 N95-19013
Summary report of mission acceleration measurements for STS-60, SPACEHAB2, launched 11 February 1994
[NASA-TM-106797] p 991 N95-19788

MICROGRAVITY APPLICATIONS
Plasma heating for containerless and microgravity materials processing
[NASA-CASE-NPO-18819-1-CU] p 991 N95-18326
US experiments flown on the Soviet biosatellite Cosmos 2044. Volume 1: Mission description, experiments K-7-01 - K-7-15
[NASA-TM-108802-VOL-1] p 1092 N95-18569

MICROMECHANICS
Optimization of layered metal matrix composite cylinders p 970 N95-18920

MICROMETEORITES
The hypervelocity impact facilities at the University of Kent at Canterbury, UK p 961 N95-19180
Penetration of multiple thin films in micrometeorite capture cells p 1036 N95-19192

MICROORGANISMS
Changes in the flux of carbon between plants and soil microorganisms at elevated CO2: Physiological processes with ecosystem-level implications
[DE94-017067] p 1060 N95-19112
Systems and economic analysis of microalgae ponds for conversion of CO2 to biomass
[DE95-000406] p 1054 N95-19554
Activities of the Division of Energy Biosciences
[DE95-001046] p 1077 N95-19613

MICROPHONES
Background noise levels measured in the NASA Lewis 9- by 15-foot low-speed wind tunnel
[NASA-TM-106817] p 958 N95-18054

MICROPROCESSORS
Early experiences and performance of the Intel Paragon
[DE94-018061] p 1109 N95-18129

MICROSTRIP ANTENNAS
Numerically efficient use of frequency domain MoM codes for wideband radiation and scattering problems. An application: Scattering from a microstrip patch
[AD-A284561] p 995 N95-18116
Slot spiral antenna modeling using hybrid/mixed FE-BI technique p 1006 N95-19797
An efficient and accurate model of the coax cable feeding structure for FEM simulations
p 1006 N95-19799
Arbitrarily shaped dual-stacked patch antennas: A hybrid FEM simulation p 1006 N95-19800

MICROSTRIP TRANSMISSION LINES
Comparison of the folded stripline and stacked stripline concepts to the folded waveguide launcher
[DE94-018951] p 999 N95-18558

MICROSTRUCTURE
Influence of high pressure hydrogen environment on creep deformation of Mo-Re, Haynes 188, and NARloy-Z alloys
[NASA-CR-197572] p 978 N95-18046
Microstructure-based fatigue life prediction methods for naval steel structures
[AD-A284735] p 1044 N95-18081
Tribology and microstructure of PS212 with a Cr2O3 seal coat
[NASA-TM-106768] p 969 N95-18448
An NDE approach for characterizing quality problems in polymer matrix composites
[NASA-TM-106807] p 1043 N95-18583
High temperature stability of binary microstructures derived from liquid precursors
[AD-A283960] p 1150 N95-18685
Discrete and continuum elastic properties of interfaces
p 1150 N95-18928
Microstructural analysis of cracks generated during welding of 2195 aluminum-lithium alloy
p 982 N95-19007
The effect of fabrication on corrosion in aluminum 2195: Environmental and microstructural considerations
p 982 N95-19011
Investigation of the microstructure of coatings for high power lasers by non-optical techniques
[DE94-017697] p 987 N95-19227
Microstructurally based variations on the dwell fatgue life of titanium alloy IMI 834 p 938 N95-19489
Neutron scattering study of dilute supercritical solutions
[DE95-000493] p 1134 N95-19557
Development of materials for high temperature superconductor Josephson junctions
[DE95-000896] p 1152 N95-19608
Corrosion fatigue of iron-chromium-nickel alloys: Fracture mechanics, microstructure and chemistry
[DE95-000909] p 981 N95-19610
Analysis of the erosion of cubic centered and face centered metallic materials p 953 N95-19674
Investigation of microscopic mechanisms of failure of electronic smart materials/systems
[AD-A284830] p 988 N95-19691
Microstructure and crystal defects in perovskite crystals with A-site cation ordering
[AD-A284261] p 1153 N95-19713
Synthesis and structural properties of new metallic phases exhibiting non-crystallographic symmetries
[AD-A284882] p 982 N95-19743
Direct dimer-by-dimer identification of clean and monohydride dimers on the Si(001) surface by scanning tunneling microscopy
[AD-A280158] p 976 N95-19824
An atomic-resolution study of overlayer formation and interfacial mixing in the interaction of phosphorus with Si(001)
[AD-A280159] p 976 N95-19825

MICROWAVE AMPLIFIERS
Microcavity structures
[DE95-001096] p 1039 N95-19727

MICROWAVE CIRCUITS
MIKON 94. International Microwave Conference. Invited papers, volume 3
[AD-A284353] p 1008 N95-18338

MICROWAVE EQUIPMENT
MIKON 94. International Microwave Conference. Invited papers, volume 3
[AD-A284353] p 1008 N95-18338

MICROWAVE IMAGERY
Ice surface temperature retrieval from AVHRR, ATSR, and passive microwave satellite data: Algorithm development and application
[NASA-CR-197542] p 1052 N95-18952

MICROWAVE LANDING SYSTEMS
Heliport/vertiport MLS precision approaches
[AD-A283505] p 940 N95-18059
Processing multilevel secure test and evaluation information
[AD-A284073] p 1001 N95-19069

MICROWAVE RADIOMETERS
A technical demonstration Mobile Profiler System
[AD-A284562] p 1068 N95-18117
Correlation function analysis of the COBE differential microwave radiometer sky maps
[DE95-000795] p 1178 N95-19617

MICROWAVE RESONANCE
Determination of the electron density and the electron temperature in a high-pressure microwave discharge
p 1145 N95-18906

MICROWAVE SCATTERING
Numerically efficient use of frequency domain MoM codes for wideband radiation and scattering problems. An application: Scattering from a microstrip patch
[AD-A284561] p 995 N95-18116

MICROWAVE SENSORS
MIKON 94. International Microwave Conference. Invited papers, volume 3
[AD-A284353] p 1008 N95-18338

MICROWAVE SPECTRA
Ice surface temperature retrieval from AVHRR, ATSR, and passive microwave satellite data: Algorithm development and application
[NASA-CR-197542] p 1052 N95-18952

MICROWAVE TRANSMISSION
Comparison of the folded stripline and stacked stripline concepts to the folded waveguide launcher
[DE94-018951] p 999 N95-18558
High-power microwave transmission and mode conversion program
[DE94-017046] p 1002 N95-19097

MICROWAVES
MIKON 94. International Microwave Conference. Invited papers, volume 3
[AD-A284353] p 1008 N95-18338
MIKON 94. International Microwave Conference. Volume 1: Conference proceedings
[AD-A284351] p 1009 N95-18425
MIKON 94. International Microwave Conference. Conference proceedings, volume 2
[AD-A284352] p 1009 N95-18426
Atmospheric Infrared Sounder
[NASA-CR-197573] p 1064 N95-18444
Correlation function analysis of the COBE differential microwave radiometer sky maps
[DE95-000795] p 1178 N95-19617

MID-OCEAN RIDGES
Density structure of the upper oceanic crust at zero porosity
[AD-A284235] p 1076 N95-19728

MIGRATION
A 2D depth migration in transversely isotropic media using explicit operators
[DE95-000645] p 1066 N95-19560

MILITARY AIRCRAFT
Development of a bulk current injection direct-drive system to test system level components with stress waveforms that are encountered during full threat indirect effects lightning
[AD-A284160] p 933 N95-18507
Application of three-dimensional hybrid structured/unstructured grids to land, sea and air vehicles
[ARA-MEMO-399] p 1031 N95-19775

MILITARY AVIATION
Virtual reality, an air combat T and E perspective
[AD-A284161] p 959 N95-18508
The waiver process and disqualifying medical conditions in US Naval aviation personnel p 1081 N95-19416
The effect of special boards of flight surgeons on the evolution of US Naval flight standards
p 1081 N95-19417
MILITARY HELICOPTERS
US Army rotorcraft turboshaft engines sand and dust erosion considerations p 951 N95-19656
MILITARY OPERATIONS
Secure distributed file systems
[AD-A285525] p 1173 N95-18096
Interferometric synthetic aperture radar and the Data Collection System Digital Terrain Elevation Demonstration
[AD-A284024] p 999 N95-18657
Development of a comprehensive base-level environmental training program for total environmental compliance
[AD-A284806] p 1061 N95-19686
Annual historical report, calendar year 1993
[AD-A280178] p 1087 N95-19827
Alternative solvents/technologies for paint stripping: Phase 1
[AD-A279918] p 989 N95-19861
MILITARY PSYCHOLOGY
Situation awareness: Papers and annotated bibliography
[AD-A284752] p 1088 N95-18084
MILITARY SPACECRAFT
Issues in military use of commercial satellites
[AD-A283707] p 964 N95-18362
MILITARY TECHNOLOGY
US Navy SHF SATCOM: Past, present and future
[AD-A283704] p 996 N95-18359
Proceedings of Natural Sciences Symposium
[AD-A285452] p 1077 N95-19536
MILLIMETER WAVES
MIKON 94. International Microwave Conference. Invited papers, volume 3
[AD-A284353] p 1008 N95-18338
MIKON 94. International Microwave Conference. Volume 1: Conference proceedings
[AD-A284351] p 1009 N95-18425
MIKON 94. International Microwave Conference. Conference proceedings, volume 2
[AD-A284352] p 1009 N95-18426
Microcavity structures
[DE95-001096] p 1039 N95-19727
MIMD (COMPUTERS)
CFD on parallel computers p 1029 N95-19465
MINERALOGY
Chondrule formation in the radiative accretional shock
p 1191 N95-19324
MINORITY CARRIERS
Minority-carrier lifetime in InP as a function of light bias
[NASA-TM-106821] p 1149 N95-18453
MIRRORS
Progress in the development of advanced solar reflectors
[DE94-000264] p 1053 N95-18463
Multi-line passive fiber optic slipring
[AD-D016430] p 1141 N95-18560
On orbit performance of the ALEXIS EUV telescopes
[DE94-016197] p 964 N95-18639
Surface roughness measurements
p 1142 N95-18984
A new piston control strategy for segmented mirrors
p 1115 N95-18999
MISSILE CONFIGURATIONS
A selection of experimental test cases for the validation of CFD codes. Supplement: Datasets A-E
[AGARD-AR-303-SUPPL] p 929 N95-18539
Application of three-dimensional hybrid structured/unstructured grids to land, sea and air vehicles
[ARA-MEMO-399] p 1031 N95-19775
MISSILE CONTROL
Multipath-induced, low-angle tracking error at 140 GHz
[AD-A283630] p 995 N95-18136
Integrated aerodynamic fin and stowable TVC vane system
[AD-D016457] p 967 N95-19073
MISSILES
Solid fuel ramjet composition
[AD-D016458] p 990 N95-19090
MISSION PLANNING
Automatic Identification Technology (AIT): The development of functional capability and card application matrices
[AD-A285528] p 1173 N95-18099
Mission description and in-flight operations of ERBE instruments on ERBS and NOAA 10 spacecraft, February 1987 - February 1990
[NASA-RP-1325] p 1051 N95-18465
Solar-electrochemical power system for a Mars mission
[NASA-TM-106606] p 967 N95-18570
Fatigue loads spectra derivation for the Space Shuttle: Second cycle p 934 N95-19470
Near-Earth Asteroid Returned Sample (NEARS)
[NASA-CR-197297] p 1194 N95-19575
SeaWiFS technical report series. Volume 18: SeaWiFS technical report series cumulative index: Volumes 1-17
[NASA-TM-104566-VOL-18] p 1076 N95-19577
MIXING
A Type 2 supernovae constraint on neutrino(sub e) - neutrino(sub s) mixing
[NASA-CR-197630] p 1180 N95-18746
Ion mixing in oxide-sapphire systems
[DE94-018660] p 1133 N95-19232
MIXING LAYERS (FLUIDS)
Numerical mixing calculations of confined reacting jet flows in a cylindrical duct
[NASA-TM-106736] p 947 N95-18133
Studies on high pressure and unsteady flame phenomena
[AD-A284126] p 973 N95-18410
MIXING RATIOS
Forecasting snowfall using mixing ratios on an isentropic surface: An empirical study
[PB94-188760] p 1067 N95-17993
MIXTURES
Spectroelectrochemical investigations of molten halide solutions
[AD-A284147] p 974 N95-18412
MOBILE COMMUNICATION SYSTEMS
Personal communications services: Improving theater deployable communications for the 21st century
[AD-A283465] p 994 N95-18058
MODULATION
Extrathalamic modulation of cortical responsiveness
[AD-A284100] p 1078 N95-18400
Direct detection and coherent optical systems employing error-correction coding
[AD-A284350] p 1140 N95-18424
Field-emitter arrays for RF vacuum microelectronics
[AD-A279932] p 1013 N95-19865
MODULATION TRANSFER FUNCTION
The photographic system global evaluation for generation of INPE TM Landsat image
[INPE-5571-TDI/542] p 1050 N95-18369
MODULATORS
Development of ultrashort optical pulse sources near 1.3 and 1.5 microns with an emphasis on stability, high repetition rate, and parallelism
[AD-A285535] p 1139 N95-18104
MODULES
Modular implementation of feature extraction and matching algorithms for photogrammetric stereo imagery
[AD-A285422] p 1032 N95-18065
Vision and action
[AD-A285701] p 1140 N95-18480
MODULUS OF ELASTICITY
Discrete and continuum elastic properties of interfaces
p 1150 N95-18928
MOISTURE
Acoustic fatigue of carbon fibre structures
p 1127 N95-19158
MOLECULAR BEAM EPITAXY
Growth and doping of Al(x)Ga(1-x)N films by electron cyclotron resonance assisted molecular beam epitaxy
[AD-A284838] p 1153 N95-19737
MBE growth, characterization and electronic device processing of Hg-based semiconductor alloys and heterostructures
[AD-A279203] p 1154 N95-19817
MOLECULAR BEAMS
Photogeneration and characterization of energetic molecules in supersonic molecular beams
[AD-A284108] p 1131 N95-18438
Flow field investigation in a free jet - free jet core system for the generation of high intensity molecular beams
[DLR-FB-94-11] p 1132 N95-18912
MOLECULAR BIOLOGY
Photobiology in medicine
[AD-A284843] p 1087 N95-19695
MOLECULAR DIFFUSION
Investigation of superlattice disordering and diffusion mechanisms in GaAs
[AD-A284847] p 1153 N95-19697
MOLECULAR DYNAMICS
Molecular dynamics study of aqueous electrolyte solutions near a structured sphere
[AD-A284010] p 1132 N95-18655
Embedded microclusters in zeolites and cluster beam sputtering: Simulation on parallel computers
[DE95-000662] p 1134 N95-19562
The formulation of quantum statistical mechanics based on the Feynman path centroid density. 3: Phase space formalism and analysis of centroid molecular dynamics
[AD-A279233] p 1157 N95-19852
The formulation of quantum statistical mechanics based on the Feynman path centroid density. 4: Algorithms for centroid molecular dynamics
[AD-A279234] p 1157 N95-19853
High performance computing equipment for environmental remediation modeling and first principles simulation of materials properties
[DE95-000497] p 1093 N95-19875
MOLECULAR EXCITATION
Reaction channel competition in vibrational overtone activation: 1-methylcyclopropene
[AD-A280185] p 976 N95-19830
Excited state processes in transition metal complexes. Redox splitting in soluble polymers
[DE95-002690] p 977 N95-19839
MOLECULAR GASES
Pure-rotational emission from molecular hydrogen in OMC-1 p 1179 N95-18500
PRISM project optical instrument
p 1143 N95-19009
MOLECULAR INTERACTIONS
Electron interactions with non-linear polyatomic molecules and their radicals
[AD-A283952] p 1130 N95-18334
MOLECULAR IONS
Particle acceleration and transport in the tail and at the front side of the magnetosphere, task 1 and 2
[NASA-CR-197575] p 1064 N95-18476
Molecular dynamics study of aqueous electrolyte solutions near a structured sphere
[AD-A284010] p 1132 N95-18655
Impurity behavior during ion-Bernstein wave heating in PBX-M
[DE94-018114] p 1133 N95-19228
MOLECULAR ORBITALS
Intrinsic barriers for H-atom transfer reactions involving hydrocarbons
[DE94-018451] p 1134 N95-19590
MOLECULAR SPECTROSCOPY
Development of laser-ion beam photodissociation methods
[DE95-002800] p 977 N95-19840
MOLECULAR STRUCTURE
Elemental fluorine based syntheses of pentafluoro phenly and other aromatic perfluoropolyether polymers
[AD-A284102] p 984 N95-18402
Adherend surface effects on epoxy cure by NMR
[AD-A284774] p 985 N95-18442
Thermal relaxation processes and stability in poled electro-optic polymers
[AD-A283948] p 987 N95-19102
Workshop on Synthesis of Macromolecules with Precisely Controlled Structure for New Materials
[AD-A285321] p 987 N95-19520
Intrinsic barriers for H-atom transfer reactions involving hydrocarbons
[DE94-018451] p 1134 N95-19590
Macromolecular characterization and solution behavior of polymer additives
[AD-A284845] p 988 N95-19696
MOLECULAR WEIGHT
Multi-functional pi-conjugated macromolecules based on poly (phenylene vinylene)
[AD-A284163] p 985 N95-18510
MOLECULES
Neutron scattering study of dilute supercritical solutions
[DE95-000493] p 1134 N95-19557
Spectroscopy and dynamics of vibrationally excited molecules
[AD-A285874] p 1134 N95-19597
The interactions of high-energy, highly charged Xe ions with fullerenes
[DE95-001440] p 1135 N95-19786
Isolation and characterization of an indium-mixed-pnicogen Four-membered ring compound: Crystal structure of (Me3SiCH2)2InAs(SiMe3)2 In(CH2SiMe3)2P(SiMe3)2
[AD-A279170] p 1154 N95-19807
MOMENTUM
Feynman-x and transverse momentum dependence of D(sup (+-)) and D(sup 0), D-bar(sup 0) production in 250 GeV (pi)(sup -) - nucleon interactions
[DE94-626698] p 1130 N95-18366
The formulation of quantum statistical mechanics based on the Feynman path centroid density. 3: Phase space formalism and analysis of centroid molecular dynamics
[AD-A279233] p 1157 N95-19852

MONITORS
Application of conducting polymers to electroanalysis
[DE94-015204] p 984 N95-18348
MONOCHROMATIC RADIATION
Assembly and calibration of a new experimental apparatus for production and utilization of capture gamma rays
[DE94-626650] p 1198 N95-18880
MONOMERS
Difunctional monomers based on perfluoropropylene telomers
[AD-A283677] p 983 N95-18019
Polymer-based separations: Synthesis and application of polymers for ionic and molecular recognition
[DE94-016427] p 984 N95-18355
MONOPULSE RADAR
Multipath-induced, low-angle tracking error at 140 GHz
[AD-A283630] p 995 N95-18136
Digital monopulse
[AD-D016447] p 1002 N95-19072
MONOTONE FUNCTIONS
On the CFD monotone high accuracy methods
p 948 N95-19018
MONSOONS
A numerical simulation of seasonal circulation in the South China Sea
[AD-A283701] p 1075 N95-18622
MONTE CARLO METHOD
Some statistical tools for SAR image synthesis, analysis and processing
[INPE-5548-TDI/534] p 1172 N95-18004
An investigation of nonuniform dose deposition from an electron beam
[AD-A284175] p 1131 N95-18519
A probabilistic fatigue analysis of multiple site damage
p 935 N95-19476
The formulation of quantum statistical mechanics based on the Feynman path centroid density. 4: Algorithms for centroid molecular dynamics
[AD-A279234] p 1157 N95-19853
MONTEREY BAY (CA)
Synoptic-scale influence on the Monterey Bay sea-breeze
[AD-A285129] p 1073 N95-19596
MONTMORILLONITE
Development of a colloidal redox system containing a smectite clay for control of reactivity and reaction selectivity
[AD-A285958] p 974 N95-19515
MOON
Time of Apollo
[NASA-TM-110488] p 961 N95-19060
MORPHOLOGY
HEISHI: A fuel performance model for space nuclear applications
[DE94-017497] p 1137 N95-18897
MOSSBAUER EFFECT
IDA gamma ray laser
[AD-A284322] p 1037 N95-18382
MOTION
Multiport pressure measurements on continuously moving wind tunnel models
[ARA-MEMO-391] p 932 N95-19772
MOTION SICKNESS
Vestibular examination in pilots susceptible to motion sickness p 1083 N95-19427
MOTION SIMULATION
Development of microgravity, full body functional reach envelope using 3-D computer graphic models and virtual reality technology p 1092 N95-18990
MOUNTING
Mathematical analysis of actuator forces in a scissor lift
[AD-A283906] p 1040 N95-18152
MRCA AIRCRAFT
Out of area experiences with the RB199 in Toronto
p 950 N95-19654
MUFFLERS
The sound insulations of metal-framed partitions having structural loadbearing properties
[BBC-RD-1994/8] p 992 N95-18533
MULTICHANNEL COMMUNICATION
Multi-channel, covert, non-line-of-sight UV communication
[AD-D016269] p 999 N95-18545
MULTIDISCIPLINARY DESIGN OPTIMIZATION
NASA High Performance Computing and Communications program
[NASA-TM-4653] p 1174 N95-18573
MULTIGRID METHODS
A simple hyperbolic model for communication in parallel processing environments
[NASA-CR-195984] p 1098 N95-18487
Solution of full potential equation on an airfoil by multigrid technique
[NAL-TM-CSS-9303] p 930 N95-18904
CFD: Advances and Applications, part 1
[NAL-SP-9322-PT-1] p 1026 N95-19444
Introduction to multigrid methods
p 1028 N95-19453
Applications of multigrid methods to problems in CFD
p 1028 N95-19454
Inviscid and viscous flow modelling of complex aircraft configurations using the CFD simulation system sauna
[ARA-MEMO-403] p 1031 N95-19777
MULTIMEDIA
Design concepts for an integrated environmental medicine workstation for prediction, simulation and training
[AD-A283686] p 1079 N95-18618
Assessment of the ACSE science learning environment and the impact of movies and simulations
[AD-A284071] p 1089 N95-19068
Zoned Analog Personal Teleconferencing (ZAPT)
[AD-A285877] p 1004 N95-19600
MULTIPATH TRANSMISSION
Multipath-induced, low-angle tracking error at 140 GHz
[AD-A283630] p 995 N95-18136
The development of the switched-horn radio-camera system
[BBC-RD-1993/13] p 997 N95-18494
Predicted coverage of a COFDM single frequency network for UHF digital terrestrial TV broadcasting
[BBC-RD-1993/12] p 999 N95-18540
Measurements of wideband multipath propagation at 531 MHz and 1.265 GHz
[BBC-RD-1994/3] p 1001 N95-19051
MULTIPLEXING
Predicted coverage of a COFDM single frequency network for UHF digital terrestrial TV broadcasting
[BBC-RD-1993/12] p 999 N95-18540
Fiber Optic Control System integration for advanced aircraft. Electro-optic and sensor fabrication, integration, and environmental testing for flight control systems: Laboratory test results
[NASA-CR-195408] p 1034 N95-18938
DAB: Multiplex and system support features
[BBC-RD-1994/9] p 1001 N95-19050
Three-D optical memory disk
[AD-A280002] p 1035 N95-19871
MULTIPROCESSING (COMPUTERS)
Reformulated preconditioned conjugate gradient squared method. Part 1: The algorithm
[PB94-201589] p 1108 N95-17936
A novel system level approach to fault tolerance in distributed memory multicomputers
[AD-A284729] p 1095 N95-18079
Characterizing parallel file-access patterns on a large-scale multiprocessor
[NASA-CR-197568] p 1110 N95-18521
Dynamic file-access characteristics of a production parallel scientific workload
[NASA-CR-197570] p 1110 N95-18581
Research in parallel computing
[AD-A283983] p 1111 N95-18892
MULTISENSOR APPLICATIONS
Image accuracy and representational enhancement through low-level, multi-sensor integration techniques
[DE94-018661] p 1051 N95-18556
Hyperspectral data analysis procedures with reduced sensitivity to noise
[NASA-CR-197621] p 1052 N95-19126
MULTISENSOR FUSION
Fusion of correlated sensor observations
[AD-A284224] p 994 N95-17958
A technical demonstration Mobile Profiler System
[AD-A284562] p 1068 N95-18117
A general theory of signal integration for fault tolerant distributed sensor networks
[AD-A284825] p 1112 N95-19689
MUONS
Exotic atoms: Muonic atoms into vacuum from solid hydrogen
[DE94-018255] p 1129 N95-18124
MUSCLES
Effects of weight lifting on intrathoracic pressures generated by anti-g straining maneuvers
[AD-A283651] p 1078 N95-18138
MUSCOVITE
Atomic scale force mapping with the atomic force microscope
[AD-A284940] p 1129 N95-17974
MUSCULAR STRENGTH
Geometry and gravity influences on strength capability
[NASA-TP-3511] p 1091 N95-18189
MYOCARDIUM
Sarcoidosis in US military aviators
p 1085 N95-19438

N

N-TYPE SEMICONDUCTORS
Minority-carrier lifetime in InP as a function of light bias
[NASA-TM-106821] p 1149 N95-18453
Growth and doping of Al(x)Ga(1-x)N films by electron cyclotron resonance assisted molecular beam epitaxy
[AD-A284838] p 1153 N95-19737
NACELLES
Impact of noise environment on engine nacelle design
p 1125 N95-19147
NARROWBAND
Adaptive detection and copy of coherent narrowband waveforms with uncalibrated arrays
[AD-A285125] p 1004 N95-19594
NASA PROGRAMS
NASA High Performance Computing and Communications program
[NASA-TM-4653] p 1174 N95-18573
Research reports: 1994 NASA/ASEE Summer Faculty Fellowship Program
[NASA-CR-196533] p 1161 N95-18967
General information for operation of the high-temperature electromagnetic containerless vacuum induction furnace
[DE94-017170] p 991 N95-19076
NASA SPACE PROGRAMS
SOCCER: Comet Coma Sample Return Mission
p 1181 N95-19174
NASTRAN
Closed-form static analysis with inertia relief and displacement-dependent loads using a MSC/NASTRAN DMAP Alter
[NASA-TM-106836] p 1047 N95-19649
NATIONAL AIRSPACE SYSTEM
Operational And Supportability Implementation System (OASIS) test and evaluation master plan
[AD-A284765] p 941 N95-18088
NATURAL GAS
Methane: The other greenhouse gas. Research and policy in the Netherlands
[PB94-207149] p 1058 N95-18375
NAVIER-STOKES EQUATION
Study of a Navier-Stokes computer
[AD-A284196] p 1092 N95-17939
The space-time solution element method: A new numerical approach for the Navier-Stokes equations
[NASA-TM-106818] p 1014 N95-18036
A three-dimensional structured/unstructured hybrid Navier-Stokes method for turbine blade rows
[NASA-TM-106813] p 1016 N95-18200
Static aerodynamics CFD analysis for 120-mm hypersonic KE projectile design
[ARL-MR-184] p 929 N95-18611
Numerical computations of supersonic base flow with special emphasis on turbulence modeling
[AD-A283688] p 930 N95-18670
Theoretical investigations of shock/boundary layer interactions on a Ma(infinity) = 8 waverider
[DLR-FB-94-12] p 930 N95-18910
Marangoni convection in a gravity-free silicon float zone
[NASA-CR-197600] p 991 N95-18913
Numerical analysis of dissipative dynamical systems in solid and fluid mechnaics, with a special emphasis on coupled problems p 1122 N95-18916
Parallel Navier-Stokes computations on shared and distributed memory architectures
[NASA-TM-106823] p 1019 N95-18941
Computational simulation of liquid fuel rocket injectors
p 968 N95-18989
Solution of Navier-Stokes equations using high accuracy monotone schemes p 948 N95-19019
Simulation of steady and unsteady viscous flows in turbomachinery p 949 N95-19023
Numerical simulation of dynamic-stall suppression by tangential blowing
[AD-A284887] p 931 N95-19110
Unsteady aerodynamic analyses for turbomachinery aeroelastic predictions p 949 N95-19381
Basic equations of fluid dynamics
p 1026 N95-19445
Computation of inviscid flows: Various approximations
p 1027 N95-19446
Computation of compressible flows: Implicit methods
p 1027 N95-19452
Applications of multigrid methods to problems in CFD
p 1028 N95-19454
Parabolized Navier-Stokes solution of supersonic/hypersonic flows p 933 N95-19464
Evaluation of three turbulence models for afterbody/jet flows, including Reynolds stress closure
[ARA-90] p 932 N95-19574

Evaluation of three turbulence models for afterbody/jet flows, including Reynolds stress closure
[ARA-MEMO-408] p 1194 N95-19773
Inviscid and viscous flow modelling of complex aircraft configurations using the CFD simulation system sauna
[ARA-MEMO-403] p 1031 N95-19777
The application of the SAUNA CFD system to high and low speed vehicles
[ARA-MEMO-402] p 1031 N95-19778

NAVIGATION
Robust image understanding. Techniques and applications
[AD-A283427] p 1113 N95-18057
Guidance, Navigation and Control Digital Emulation Technology Laboratory
[AD-A284339] p 996 N95-18386
Kings Bay coastal and estuarine physical monitoring and evaluation program: Coastal studies. Volume 1: Main text and Appendix A
[AD-A285542] p 1074 N95-18470

NAVIGATORS
The aeromedical risk associated with asymptomatic cholelithiasis in USAF pilots and navigators
p 1085 N95-19439

NAVY
The future use of DSCS and commercial satellites in the US Navy
[AD-A285707] p 997 N95-18481

NEAR FIELDS
Correction of support influences on measurements with sting mounted wind tunnel models p 933 N95-19281
Tunneling acoustic microscopy
[AD-A279160] p 1128 N95-19802

NEAR INFRARED RADIATION
The 2 Micron All Sky Survey
[AD-A283515] p 1178 N95-18001
Infrared-to-visible converter
[AD-D016443] p 1141 N95-18529

NEBULAE
Papers presented to the Conference on Chondrules and the Protoplanetary Disk
[NASA-CR-197121] p 1186 N95-19289
Large-scale processes in the solar nebula
p 1186 N95-19292
Overview of nebula models: Potential chondrule-forming environments p 1186 N95-19294
Turbulent diffusion and concentration of chondrules in the protoplanetary nebula p 1187 N95-19296
On the possibility of precipitation-induced vertical lightning in the protoplanetary nebula
p 1187 N95-19299
The role of chondrules in nebular fractionations of volatiles and other elements p 1187 N95-19300

NEGATIVE FEEDBACK
AASERT-93: New high-pressure diagnostic technique
[AD-A284943] p 973 N95-17975

NEODYMIUM
Compact, efficient, scalable neodymium laser co-doped with activator ions and pumped by visible laser diodes
[AD-D016237] p 1038 N95-18585

NEODYMIUM LASERS
High power phase conjugated solid state lasers
[DE94-016633] p 1037 N95-18357
Compact, efficient, scalable neodymium laser co-doped with activator ions and pumped by visible laser diodes
[AD-D016237] p 1038 N95-18585
Future trends in optical coatings for high-power laser applications
[DE94-018592] p 1039 N95-19708

NEON
Coronal abundances and their variation
[NASA-CR-197553] p 1195 N95-18376

NEPTUNE (PLANET)
Investigation of atmospheric waves on Neptune
[NASA-CR-197537] p 1194 N95-18579

NEPTUNE ATMOSPHERE
Investigation of atmospheric waves on Neptune
[NASA-CR-197537] p 1194 N95-18579
Study for the analysis of the observations, and numerical data representing the planets as far-infrared calibration sources
[NASA-CR-196542] p 1195 N95-19287

NERVES
Cellular neurophysiology of the rat suprachiasmatic nucleus: Electrical properties, neurotransmission, and mechanisms of synchronization
[AD-A284111] p 1076 N95-18439

NETHERLANDS
The effect of spatial averaging on threshold exceedances of daily precipitation amounts
[KNMI-TR-154] p 1070 N95-18392
Storm activity over the North Sea and the Netherlands in two climate models compared with observations
[KNMI-WR-94-02] p 1070 N95-18393
Conceptual models of severe convective weather in the Netherlands
[KNMI-WR-93-05] p 1071 N95-18394
A synoptic climatology of convective weather in the Netherlands
[KNMI-WR-93-04] p 1071 N95-18395

NETWORK ANALYSIS
Partition method for the determination of multiple DC operating points
[PB94-201480] p 1009 N95-18501

NETWORK CONTROL
A scalable decentralized group membership service for an asynchronous environment
[AD-A283633] p 1109 N95-18137

NEURAL NETS
LVQ and backpropagation neural networks applied to NASA SSME data
[NASA-CR-195418] p 962 N95-18045
An analog computing approach to structural analysis and optimal design through artificial neural networks
p 1113 N95-18218
A parallel processing hypothesis for short-term and long-term memory in Aplysia
[AD-A284101] p 1088 N95-18401
SIGNET-software tools for signal identification using neural networks
[AD-A284362] p 1113 N95-18441
Radial basis function neural networks applied to NASA SSME data
[NASA-CR-195417] p 962 N95-18467
Adaptive Neuron Model: An architecture for the rapid learning of nonlinear topological transformations
[NASA-CASE-NPO-18579-1-CU] p 1114 N95-18740
Neural networks applications to control and computations p 1115 N95-18992
The accuracy of parameter estimation in system identification of noisy aircraft load measurement
[NASA-CR-197516] p 945 N95-19130
Neural network communications signal processing
[AD-A285681] p 1115 N95-19512
Using neural networks in the mapping of mixed discrete/continuous design spaces with application to structural design
[AD-A285328] p 1046 N95-19522
Neural net controller for inlet pressure control of rocket engine testing p 1102 N95-19637
Connectionist Network Supercomputer Project
[AD-A279206] p 1112 N95-19843

NEUROLOGY
Neurological decision making in aviation medicine based on electrophysiolcgical methods p 1084 N95-19431

NEUROMUSCULAR TRANSMISSION
Cellular neurophysiology of the rat suprachiasmatic nucleus: Electrical properties, neurotransmission, and mechanisms of synchronization
[AD-A284111] p 1076 N95-18439

NEURONS
Extrathalamic modulation of cortical responsiveness
[AD-A284100] p 1078 N95-18400
Cellular neurophysiology of the rat suprachiasmatic nucleus: Electrical properties, neurotransmission, and mechanisms of synchronization
[AD-A284111] p 1076 N95-18439
Cellular analysis of circadian rhythmicity in cultured SCN neurons
[AD-A284167] p 1078 N95-18512
Adaptive Neuron Model: An architecture for the rapid learning of nonlinear topological transformations
[NASA-CASE-NPO-18579-1-CU] p 1114 N95-18740

NEUROPHYSIOLOGY
Extrathalamic modulation of cortical responsiveness
[AD-A284100] p 1078 N95-18400
A parallel processing hypothesis for short-term and long-term memory in Aplysia
[AD-A284101] p 1088 N95-18401
Cellular neurophysiology of the rat suprachiasmatic nucleus: Electrical properties, neurotransmission, and mechanisms of synchronization
[AD-A284111] p 1076 N95-18439
Neuropsychophysiologic sequelae of mild head injury
p 1083 N95-19430
Spinal nerve syndromes: The need to confirm the diagnosis with neurophysiological examinations
p 1085 N95-19436

NEUTRAL ATMOSPHERES
New applications of the Phillips Laboratory. Theoretical ionospheric model and studies of neutral density waves
[AD-A284663] p 1066 N95-19105

NEUTRAL BEAMS
Development of lithium beam emission spectroscopy as an edge fluctuation diagnostic for D3-D
[DE94-017517] p 1146 N95-19378
Development of an amorphous surge blocker for a high voltage acceleration power supply of the neutral beam injectors
[DE94-770648] p 1138 N95-19874

NEUTRAL CURRENTS
SU4(sub L) x U1(sub N) model for the electroweak interactions
[DE94-626675] p 1148 N95-18330

NEUTRINOS
SU4(sub L) x U1(sub N) model for the electroweak interactions
[DE94-626675] p 1148 N95-18330
Properties of nuclei and elementary particles at low and intermediate energies
[DE94-008502] p 1132 N95-18644
Decaying neutrinos in galaxy clusters
[NASA-CR-197615] p 1198 N95-18747
Is a massive tau neutrino just what cold dark matter needs?
[NASA-CR-197627] p 1180 N95-18964
Comment on the preprint Neutrino Flavor Evolution Near a Supernova's Core (Astro-Ph 9405008) by J. Pantaleone
[DE94-017576] p 1198 N95-19283
The very low energy solar flux of electron and heavy-flavor neutrinos and antineutrinos
[DE94-018583] p 1135 N95-19706

NEUTRON COUNTERS
Conceptual design for a scintillating-fiber neutron detector for fusion reactor plasma diagnostics
[DE94-014716] p 1143 N95-17969
Exotic atoms: Muonic atoms into vacuum from solid hydrogen
[DE94-018255] p 1129 N95-18124
25-ps neutron detector for measuring ICF-target burn history
[DE94-016450] p 1148 N95-19250
Scintillating-fiber imaging detector for 14-MeV neutrons
[DE94-018593] p 1135 N95-19709

NEUTRON DIFFRACTION
Study of the ferrimagnetic and paramagnetic phases of magnetite measured by multiple neutron diffraction
[DE94-627031] p 1151 N95-19242

NEUTRON SCATTERING
Neutron scattering study of dilute supercritical solutions
[DE95-000493] p 1134 N95-19557

NEUTRON SPECTRA
High frame rate CCD cameras with fast optical shutters for military and medical imaging applications
[DE94-018316] p 1034 N95-19229

NEUTRON STARS
Antisymmetric tensor field interactions and neutron star models
[PB94-215605] p 1118 N95-19375
A crystalline quark-hadron mixed phase in neutron stars
[DE95-000787] p 1194 N95-19570

NEUTRONS
Assembly and calibration of a new experimental apparatus for production and utilization of capture gamma rays
[DE94-626650] p 1198 N95-18880
Limits on CP nonconserving interactions from electric dipole moments
[DE94-018582] p 1134 N95-19705
Scintillating-fiber imaging detector for 14-MeV neutrons
[DE94-018593] p 1135 N95-19709

NEW ENGLAND (US)
Synoptic and mesoscale examination of the northern New England winter storm of January 29-30, 1990
[PB94-209426] p 1072 N95-19581

NEWTONIAN FLUIDS
Incompressible flow of a Newtonian fluid past a vertical plate with thermal and magnetic stresses
[AD-A284856] p 1030 N95-19716

NICKEL
Preparation and surface characterization of metal doped alumina catalyst
[PB94-175296] p 973 N95-17991
Preparation of an electrocatalytic cathode for an aluminum-hydrogen peroxide battery
[AD-D016262] p 1008 N95-18318
Surface phases, surface defects and the initial stages of oxidation
[DE94-016947] p 979 N95-18358
Probing the chemistry of nickel/metal hydride battery cells using electrochemical impedance spectroscopy
p 1014 N95-18985
Impurity behavior during ion-Bernstein wave heating in PBX-M
[DE94-018114] p 1133 N95-19228

NICKEL ALLOYS
Fatigue in single crystal nickel superalloys
[AD-A285727] p 978 N95-18068

NICKEL CADMIUM BATTERIES
Metal/hydrogen energy storage: Selected technical issues
[AD-A283355] p 1008 N95-18052
Intermediate design and analysis of the PANSAT electrical power subsystem
[AD-A283610] p 1053 N95-18435
NIGHT VISION
A platform independent application of Lux illumination prediction algorithms
[AD-A283669] p 1094 N95-18018
Night Vision Goggles (NVG) software user's guide, version 5.1
[AD-A284563] p 1090 N95-18029
KC-130 ANVIS/HUD assessment and symbology rationale
[AD-A284155] p 943 N95-18504
NIGHTGLOW
Ion-molecule collisions, electron molecule collisions, excitation and ionization of atoms
[AD-A284584] p 1129 N95-18062
NIOBIUM
The Gravity Probe B niobium bird experiment: Experimental verification of a data reduction scheme with a prototypical dc SQUID readout system
p 1033 N95-18929
General information for operation of the high-temperature electromagnetic containerless vacuum induction furnace
[DE94-017170] p 991 N95-19076
Hyperfine splittings, prepulse technique, and other new results for collisional excitation neon-like x ray lasers
[DE94-016443] p 1038 N95-19247
NIOBIUM COMPOUNDS
Characterization of rechargeable lithium cells. Part 1: Lithium/niobium triselenide chemistry
[AD-A284229] p 1007 N95-17959
NITRIC ACID
A model study of the influence of NMHC and NO(x) emissions on rural O3 concentrations in Georgiargia
p 1059 N95-18445
NITROGEN
Changes in the flux of carbon between plants and soil microorganisms at elevated CO2: Physiological processes with ecosystem-level implications
[DE94-017067] p 1060 N95-19112
NITROGEN COMPOUNDS
NCl(b) based short wavelength chemical laser
[AD-A284213] p 1036 N95-17956
NITROGEN DIOXIDE
Laboratory studies of stratospheric bromine chemistry: Kinetics of the reactions of bromine monoxide with nitrogen dioxide and atomic oxygen p 1065 N95-18731
NITROGEN OXIDES
Dependencies and sensitivity of tropospheric oxidants to precursor concentrations over the northeast United States: A model study
[PB94-192770] p 1056 N95-17937
Numerical mixing calculations of confined reacting jet flows in a cylindrical duct
[NASA-TM-106736] p 947 N95-18133
A model study of the influence of NMHC and NO(x) emissions on rural O3 concentrations in Georgiargia
p 1059 N95-18445
Wave cycle design for wave rotor engines with limited nitrogen oxide emissions p 1041 N95-18901
Alternative control techniques document: NO(x) emissions from glass manufacturing
[PB94-214079] p 1061 N95-19406
NITROGEN TETROXIDE
Investigation of new hypergol scrubber technology
p 977 N95-18175
NITROSYLS
Excited state processes in transition metal complexes. Redox splitting in soluble polymers
[DE95-002690] p 977 N95-19839
NITROUS OXIDES
Trends 1993: A compendium of data on global change
[ORNL/CDIAC-65] p 1058 N95-18389
NOISE
The accuracy of parameter estimation in system identification of noisy aircraft load measurement
[NASA-CR-197516] p 945 N95-19130
NOISE (SOUND)
Environmental forcing of ambient noise in the Nansen and Amundsen Basins of the Arctic Ocean
[AD-A285540] p 1074 N95-18468
Acoustic noise criteria for listening rooms and control rooms
[BBC-RD-1994/06] p 1124 N95-19048
Maximal-length sequence methods: Acoustic measurements in the presence of high levels of extraneous noise
[BBC-RD-1994/5] p 1001 N95-19049
Identification and analysis of air- and structure-borne noise and vibration paths p 1128 N95-19166
NOISE INTENSITY
Radiation-induced noise in UMPC-type current probes: IEMP response of the curruent measurement system
[AD-A284176] p 998 N95-18520
Acoustic noise criteria for listening rooms and control rooms
[BBC-RD-1994/06] p 1124 N95-19048
An overall approach of cockpit noise verification in a military aircraft p 1127 N95-19163
NOISE MEASUREMENT
Background noise levels measured in the NASA Lewis 9- by 15-foot low-speed wind tunnel
[NASA-TM-106817] p 958 N95-18054
MIKON 94. International Microwave Conference. Invited papers, volume 3
[AD-A284353] p 1008 N95-18338
NOISE PREDICTION
On the Lighthill relationship and sound generation from isotropic turbulence
[NASA-CR-195005] p 1016 N95-18191
NOISE PREDICTION (AIRCRAFT)
Modelling structurally damaging twin-jet screech
p 946 N95-19154
NOISE PROPAGATION
Noise transmission and reduction in turboprop aircraft
p 1127 N95-19164
Advanced statistical energy analysis
p 1047 N95-19165
Acoustic transmission loss and structureborne noise transmission tests on a LASCOR and a reference steel panel
[MRL-TN-623] p 1128 N95-19770
NOISE REDUCTION
Background noise levels measured in the NASA Lewis 9- by 15-foot low-speed wind tunnel
[NASA-TM-106817] p 958 N95-18054
On the optimization of speckle filtering techniques for ERS-1 images over Argentina
[INPE-5578-PRE/1806] p 1050 N95-18216
The sound insulations of metal-framed partitions having structural loadbearing properties
[BBC-RD-1994/8] p 992 N95-18533
Further measurements of the sound insulations of metal-framed partitions
[BBC-RD-1994/7] p 998 N95-18534
An analysis of noise reduction in variable reluctance motors using pulse position randomization
[AD-A283846] p 1123 N95-18673
Hyperspectral data analysis procedures with reduced sensitivity to noise
[NASA-CR-197621] p 1052 N95-19126
Helicopter internal noise p 1124 N95-19144
Impact of noise environment on engine nacelle design
p 1125 N95-19147
An overall approach of cockpit noise verification in a military aircraft p 1127 N95-19163
Noise transmission and reduction in turboprop aircraft
p 1127 N95-19164
Using expert systems to analyze ATE data
p 1103 N95-19639
NOISE SPECTRA
An analysis of noise reduction in variable reluctance motors using pulse position randomization
[AD-A283846] p 1123 N95-18673
Statistics of complex cross spectrum estimate for sinusoidal signals and arbitrary noise spectra
[AD-A283984] p 1120 N95-19065
NONDESTRUCTIVE TESTS
Fundamental advances for characterizing cathodic protection systems
[PB94-180692] p 1122 N95-17983
Acoustic method of damage sensing in composite materials
[NASA-CR-196538] p 969 N95-18135
Wavelets and scattering
[AD-A284131] p 996 N95-18411
An inverse problem in thermal imaging
[NASA-CR-195018] p 1117 N95-18479
An NDE approach for characterizing quality problems in polymer matrix composites
[NASA-TM-106807] p 1043 N95-18583
Annular computed tomography
[AD-D016424] p 1141 N95-18593
Probing the chemistry of nickel/metal hydride battery cells using electrochemical impedance spectroscopy
p 1014 N95-18985
The probability of flaw detection and the probability of false calls in nondestructive evaluation equipment
p 1044 N95-19010
Evaluation of powder metallurgy plates made by Sylvania Electric Products, Incorporated
[DE94-017911] p 980 N95-19401
NONEQUILIBRIUM FLOW
Hypervelocity air flows with finite rate chemistry
[AD-A284727] p 931 N95-19109
NONINTRUSIVE MEASUREMENT
Wall Interference, Support Interference and Flow Field Measurements
[AGARD-CP-535] p 1020 N95-19251
The crucial role of wall interference, support interference and flow field measurements in the development of advanced aircraft configurations p 1021 N95-19252
Particle Image Velocimetry: Principles, current applications and future prospects p 1021 N95-19253
NONLINEAR EQUATIONS
Static and dynamic nuclear many-body descriptions on parallel architectures
[DE94-018134] p 1116 N95-18120
Singularities and symmetries of nonlinear ordinary and partial differential equations
[DE95-000904] p 1119 N95-19609
NONLINEAR OPTICS
Polymer fibers for nonlinear optics
[AD-A284216] p 983 N95-17957
AASERT-93: New high-pressure diagnostic technique
[AD-A284943] p 973 N95-17975
1994 IEEE Nonlinear Optics: Materials Fundamental and Applications Conference
[AD-A285769] p 1139 N95-18345
Growth of thin films of dicyanovinylanisole on quartz and teflon-coated quartz by physical vapor transport
p 989 N95-19000
Aryl gels and related materials. Synthesis and characterization of a new class of microporous materials
[AD-A285044] p 987 N95-19544
Novel e-o polymers: NLO materials with superior temporal stability
[AD-A285872] p 988 N95-19614
NONLINEAR SYSTEMS
Synchronization of nonautonomous chaotic systems
[AD-D016440] p 1010 N95-18528
The impact of non-linear flight control systems on the prediction of aircraft loads due to turbulence
p 956 N95-18598
Treatment of non-linear systems by timeplane-transformed CT methods: The spectral gust method p 956 N95-18600
Nonlinear dynamic response of aircraft structures to acoustic excitation p 946 N95-19151
NONLINEARITY
1994 IEEE Nonlinear Optics: Materials Fundamental and Applications Conference
[AD-A285769] p 1139 N95-18345
Nonlinear magnetohydrodynamics
[DE94-016223] p 1143 N95-18353
Comparison of stochastic and deterministic nonlinear gust analysis methods to meet continuous turbulence criteria p 946 N95-18602
Adaptive Neuron Model: An architecture for the rapid learning of nonlinear topological transformations
[NASA-CASE-NPO-18579-1-CU] p 1114 N95-18740
An analytic conceptual model of extratropical cyclones
[KNMI-WR-93-03] p 1072 N95-18926
Quantitative analysis of voids in percolating structures in two-dimensional N-body simulations
[NASA-CR-197612] p 1156 N95-18949
Unsteady aerodynamic analyses for turbomachinery aeroelastic predictions p 949 N95-19381
Nonlinear analysis of damaged stiffened fuselage shells subjected to combined loads p 939 N95-19499
Nonlinear ocean waves
[AD-A285331] p 1075 N95-19523
Singularities and symmetries of nonlinear ordinary and partial differential equations
[DE95-000904] p 1119 N95-19609
Novel e-o polymers: NLO materials with superior temporal stability
[AD-A285872] p 988 N95-19614
NONUNIFORMITY
An NDE approach for characterizing quality problems in polymer matrix composites
[NASA-TM-106807] p 1043 N95-18583
LEVIS ion source and beam characterization on PBFA-2
[DE94-015802] p 1133 N95-19199
NORMAL DENSITY FUNCTIONS
Quasi-linear regime of gravitational instability as a clue to understanding the large-scale structure in the Universe
[NASA-CR-197613] p 1193 N95-19341
A test of the adhesion approximation for gravitational clustering
[NASA-CR-197610] p 1157 N95-19358
NORTH SEA
Storm activity over the North Sea and the Netherlands in two climate models compared with observations
[KNMI-WR-94-02] p 1070 N95-18393
NOTCHES
Synthesis of notched antenna patterns for wide bandwidth processing
[AD-A284004] p 1000 N95-18727

NOVA LASER SYSTEM
Implementation of 40-ps high-speed gated-microchannel-plate based x-ray framing cameras on reentrant SIM's for Nova
[DE94-018597] p 1033 N95-18555
NOZZLE DESIGN
J-integral characterization of the nozzle steels from intermediate test vessels IV-5 and IV-9
[DE95-001066] p 979 N95-18934
Design of high pressure waterjet nozzles
p 1031 N95-18996
Advanced concepts theory
[AD-A279212] p 1147 N95-19844
Power flow and PRS optimization on Phoenix
[AD-A279214] p 1147 N95-19846
NOZZLE FLOW
Flow field investigation in a free jet - free jet core system for the generation of high intensity molecular beams
[DLR-FB-94-11] p 1132 N95-18912
NUCLEAR ELECTRIC PROPULSION
Design considerations for a Space Station radiation shield for protection from both man-made and natural sources
[NASA-CR-195298] p 964 N95-18495
NUCLEAR FUEL ELEMENTS
Fueled emitter, TFE Verification Program
[DE94-017557] p 1135 N95-18146
TFE design package, TFE Verification Program
[DE94-017558] p 1136 N95-18147
The metallurgical integrity of the frit vent assembly diffusion bond
[DE95-000610] p 968 N95-19877
NUCLEAR FUELS
A review of nuclear thermal propulsion carbide fuel corrosion and key issues
[NASA-CR-197533] p 1136 N95-18217
NUCLEAR INTERACTIONS
Study of strangeness production in relativistic nucleus beams at JINR
[DE94-626720] p 1136 N95-18881
NUCLEAR MAGNETIC RESONANCE
Adherend surface effects on epoxy cure by NMR
[AD-A284774] p 985 N95-18442
Nozzle Initiative Industry Advisory Committee on Standardization of Carbon-Phenolic Test Methods and Specifications
[NASA-CR-197529] p 967 N95-19566
Synthesis and characterization of aluminum-phosphorus adducts: X-ray crystal structures of Cl3Al (dot) P(SiMe3)3 (dot) C7H8 and Br3Al (dot) P(SiMe3)3 (dot) C7H8
[AD-A279194] p 1154 N95-19812
NUCLEAR MEDICINE
Nuclear medicine program
[DE94-017530] p 1080 N95-19244
NUCLEAR MODELS
IDA gamma ray laser
[AD-A284322] p 1037 N95-18382
NUCLEAR PHYSICS
Mass spectrometric studies of clusters and surfaces
[AD-A283992] p 974 N95-19066
NUCLEAR POWER REACTORS
Ageing nuclear power plant management: An aeronautical viewpoint
[NAL-PD-SN-9306] p 927 N95-18606
NUCLEAR PROPULSION
A review of nuclear thermal propulsion carbide fuel corrosion and key issues
[NASA-CR-197533] p 1136 N95-18217
HEISHI: A fuel performance model for space nuclear applications
[DE94-017497] p 1137 N95-18897
NUCLEAR REACTIONS
Baryon stopping in 200 GeV/A S+Au collisions
[DE94-018215] p 1134 N95-19587
NUCLEAR RESEARCH
Correlated charge-changing ion-atom collisions
[DE94-017355] p 1132 N95-18874
NUCLEAR ROCKET ENGINES
TFE design package, TFE Verification Program
[DE94-017558] p 1136 N95-18147
Design considerations for a Space Station radiation shield for protection from both man-made and natural sources
[NASA-CR-195298] p 964 N95-18495
NUCLEAR SCATTERING
IDA gamma ray laser
[AD-A284322] p 1037 N95-18382
NUCLEAR STRUCTURE
Properties of nuclei and elementary particles at low and intermediate energies
[DE94-008502] p 1132 N95-18644
NUCLEATION
Heterogeneous nucleation of calcium oxalate on native oxide surfaces
[DE94-018725] p 986 N95-18648
NUCLEI (NUCLEAR PHYSICS)
Properties of nuclei and elementary particles at low and intermediate energies
[DE94-008502] p 1132 N95-18644
NUCLEON-NUCLEON INTERACTIONS
Limits on CP nonconserving interactions from electric dipole moments
[DE94-018582] p 1134 N95-19705
NUCLEON-NUCLEON SCATTERING
The behavior of the slope of elastic nucleon scattering at small transfer momenta and recent U A 4/2 data
[DE94-626687] p 1130 N95-18360
NUCLEONS
Diquarks in deep inelastic scattering and the Gottfried sum rule
[DE94-626685] p 1130 N95-18356
Feynman-x and transverse momentum dependence of D(sup (+-)) and D(sup 0), D-bar(sup 0) production in 250 GeV (pi)(sup -) - nucleon interactions
[DE94-626698] p 1130 N95-18366
NUCLIDES
Bohr's quantization rule in the world of resonances of elementary particles
[DE94-626721] p 1132 N95-18882
Is a massive tau neutrino just what cold dark matter needs?
[NASA-CR-197627] p 1180 N95-18964
NUMERICAL ANALYSIS
The space-time solution element method: A new numerical approach for the Navier-Stokes equations
[NASA-TM-106818] p 1014 N95-18036
Development of ultrashort optical pulse sources near 1.3 and 1.5 microns with an emphasis on stability, high repetition rate, and parallelism
[AD-A285535] p 1139 N95-18104
Fast numerical determination of symmetric sparsity patterns
[DE94-016344] p 1096 N95-18354
Decaying neutrinos in galaxy clusters
[NASA-CR-197615] p 1198 N95-18747
Numerical analysis of dissipative dynamical systems in solid and fluid mechnaics, with a special emphasis on coupled problems p 1122 N95-18916
Quantitative analysis of voids in percolating structures in two-dimensional N-body simulations
[NASA-CR-197612] p 1156 N95-18949
Orbital tests of relativistic gravity using artificial satellites
[PB94-217239] p 965 N95-19377
NUMERICAL CONTROL
Data acquisition from blast overpressure trials
[MRL-TN-628] p 1020 N95-19139
Improved speed control system for the 87,000 HP wind tunnel drive
[NASA-TM-106840] p 1035 N95-19794
NUMERICAL INTEGRATION
High-order corrected trapezoidal rules for singular functions
[AD-A284269] p 1119 N95-19735
NYSTAGMUS
Vestibular examination in pilots susceptible to motion sickness p 1083 N95-19427

O

OASES
Operational And Supportability Implementation System (OASIS) test and evaluation master plan
[AD-A284765] p 941 N95-18088
OBJECT-ORIENTED PROGRAMMING
ODP based UPT model
[PB94-215589] p 1003 N95-19411
Adding intelligent services to an object oriented system p 1103 N95-19642
Expert system technologies for Space Shuttle decision support: Two case studies p 1104 N95-19646
OBLIQUE SHOCK WAVES
Improvement and validation of an LDV system to perform measurements in laminar supersonic flows
p 1021 N95-19256
OCCUPATION
Crosshift vibrometry: Biomarker for ergonomic stress
[AD-A284337] p 1091 N95-18385
OCEAN BOTTOM
Geologic studies: Executive summary report
[PB94-187481] p 1073 N95-17951
The STOKES (Version 4) normal-mode shallow water transmission loss program
[MRL-CP-1] p 1075 N95-19503
Seafloor positioning across Juan de Fuca ridge
[AD-A285049] p 1075 N95-19563
Density structure of the upper oceanic crust at zero porosity
[AD-A284235] p 1076 N95-19728
Coastal benthic boundary layer special research program: A review of the first year. Volume 1
[AD-A280034] p 1076 N95-19818
OCEAN CURRENTS
Coastal acoustic tomography data constraints applied to a coastal ocean circulation model
[AD-A283911] p 1074 N95-18153
ADCIRC: An advanced three-dimensional circulation model for shelves, coasts, and estuaries. Report 5: A tropical storm database for the east and Gulf of Mexico coasts of the United States
[AD-A285576] p 1075 N95-19540
OCEAN DYNAMICS
Nonlinear ocean waves
[AD-A285331] p 1075 N95-19523
OCEAN MODELS
Coastal acoustic tomography data constraints applied to a coastal ocean circulation model
[AD-A283911] p 1074 N95-18153
Coastal Modeling System (CMS) user's manual. Supplement 3 to September 1991 manual
[AD-A283922] p 1074 N95-18160
Visible-infrared remote-sensing model and applications for ocean waters
[NASA-CR-197602] p 1051 N95-18739
OCEAN SURFACE
Time spread and frequency coherence in acoustic forward scattering from the sea surface
[AD-A284736] p 1123 N95-18083
Marine boundary layer refractive effects in the infrared
[AD-A285717] p 1140 N95-18484
Visible-infrared remote-sensing model and applications for ocean waters
[NASA-CR-197602] p 1051 N95-18739
Synoptic-scale influence on the Monterey Bay sea-breeze
[AD-A285129] p 1073 N95-19596
OCEANOGRAPHIC PARAMETERS
Users manual for the Moods Data Management System (MDMS), version 1.0
[NASA-CR-197015] p 1075 N95-18951
OCEANOGRAPHY
Geologic studies: Executive summary report
[PB94-187481] p 1073 N95-17951
Field and data analysis studies related to the atmospheric environment
[NASA-CR-196543] p 1068 N95-18093
SeaWiFS technical report series. Volume 18: SeaWiFS technical report series cumulative index: Volumes 1-17
[NASA-TM-104566-VOL-18] p 1076 N95-19577
A novel technique for 4-dimensional atmospheric and oceanographic irradiance measurements using 3-D spatial filtering
[AD-A285658] p 1073 N95-19701
OCEANS
Long wavelength propagation capacity, version 1.1 (computer diskette)
[AD-M200254] p 994 N95-17964
Visible-infrared remote-sensing model and applications for ocean waters
[NASA-CR-197602] p 1051 N95-18739
OFFSHORE ENERGY SOURCES
Geologic studies: Executive summary report
[PB94-187481] p 1073 N95-17951
OILS
An oil flow study of the reference Shuttle-C configuration
[NASA-RP-1352] p 932 N95-19623
OLIVINE
Relict grains in chondrules: Evidence for chondrule recycling p 1188 N95-19307
Implications for the evolution of chondrules from Agglomeratic olivine chondrules p 1193 N95-19335
OMNIDIRECTIONAL ANTENNAS
The development of the switched-horn radio-camera system
[BBC-RD-1993/13] p 997 N95-18494
Predicted coverage of a COFDM single frequency network for UHF digital terrestrial TV broadcasting
[BBC-RD-1993/12] p 999 N95-18540
ON-LINE SYSTEMS
Library capability demonstration. Central Archive for Reusable Defense Software (CARDS)
[AD-A284572] p 1095 N95-18034
A redundant disk array architecture for efficient small writes
[AD-A284048] p 1093 N95-18659
On-line handling of air traffic: Management, guidance and control
[AGARD-AG-321] p 941 N95-18927
A strategy for electronic dissemination of NASA Langley technical publications
[NASA-TM-109172] p 1175 N95-18936
The Japan Information Center of Science and Technology p 1198 N95-19128

ONBOARD EQUIPMENT
Lean spacecraft avionics trade study
p 966 N95-18994
ONE DIMENSIONAL FLOW
One-dimensional flow description for the combustion chamber of a scramjet
[DLR-FB-94-06] p 948 N95-18911
OPACITY
New astrophysical opacities and their effects on stellar models
[DE94-016445] p 1186 N95-19249
OPERATING COSTS
Protective coatings for compressor gas path components p 954 N95-19675
OPERATING SYSTEMS (COMPUTERS)
Construction of a connectionist network supercomputer
[AD-A283354] p 1109 N95-18050
Fair Petri nets and structural induction for rings of processes
[AD-A283920] p 1110 N95-18158
The generic simulation executive at Manned Flight Simulator
[AD-A283997] p 959 N95-18724
Research in parallel computing
[AD-A283983] p 1111 N95-18892
OPERATIONAL HAZARDS
Erosion, Corrosion and Foreign Object Damage Effects in Gas Turbines
[AGARD-CP-558] p 950 N95-19653
The operation of gas turbine engines in hot and sandy conditions: Royal Air Force experiences in the Gulf conflict p 950 N95-19655
OPERATIONS RESEARCH
Multi-method planning
[AD-A285878] p 1115 N95-19601
OPERATOR PERFORMANCE
Kansas State University DOE/KEURP Site Operator User Task Force
[DE94-014331] p 1040 N95-17995
Implementation of a human information processing model for task network simulation
[AD-A283903] p 1088 N95-18151
OPERATORS (MATHEMATICS)
On the convergence of local approximations to pseudodifferential operators with applications
[NASA-TM-106792] p 1019 N95-18898
Plane Jacobian conjecture
[PB94-192341] p 1118 N95-19198
Theory and applications of the phi transform wavelets
[AD-A279943] p 1119 N95-19869
OPHTHALMOLOGY
Photorefractive Keratectomy (PRK) in the military aviator: An aeromedical expose p 1086 N95-19442
OPTICAL COMMUNICATION
Gigabit optical interconnects: System and component analysis, design and development
[AD-A285538] p 1138 N95-18067
Atomic line filter for SDI applications
[AD-A284125] p 1139 N95-18409
Multi-line passive fiber optic slipring
[AD-D016430] p 1141 N95-18560
Advanced optical fiber communications systems
[AD-A283942] p 1141 N95-18682
Methods and components for optical contention resolution in high speed networks
[AD-A284674] p 1142 N95-19088
High speed optical links between LLNL and Berkeley
[DE95-000552] p 1006 N95-19833
OPTICAL COMPUTERS
Evaluation of the current biased integrated optical processors based on bistable dode elements
[AD-A285532] p 1138 N95-18102
OPTICAL DATA PROCESSING
Variable rate transfer of optical information
[AD-D016268] p 1173 N95-18544
OPTICAL DISKS
Surface roughness measurements
p 1142 N95-18984
OPTICAL EQUIPMENT
Inter-amplifier pupil relay systems for a high average power dye laser at Lawrence Livermore National Laboratory
[DE94-016544] p 1039 N95-19507
Aryl gels and related materials. Synthesis and characterization of a new class of microporous materials
[AD-A285044] p 987 N95-19544
OPTICAL FIBERS
Polymer fibers for nonlinear optics
[AD-A284216] p 983 N95-17957
Design and fabrication of N x N optical couplers based on organic polymer optical waveguides
[AD-A285530] p 1138 N95-18100
Fiber optic pressure and/or vibration detector
[AD-D016474] p 1140 N95-18460
Disengagable adapter for an optical fiber connection
[AD-D016231] p 1141 N95-18628
Advanced optical fiber communications systems
[AD-A283942] p 1141 N95-18682
Torque-balanced extendable fiber optic cable
[AD-D016496] p 1142 N95-19389
OPTICAL FILTERS
Error measurements in an Acousto-Optic Tunable Filter-Fiber Bragg Grating Sensor System
[AD-A283912] p 1139 N95-18154
Atomic line filter for SDI applications
[AD-A284125] p 1139 N95-18409
OPTICAL GYROSCOPES
Low noise fiber gyroscope system which includes excess noise subtraction
[AD-D016556] p 1034 N95-19124
OPTICAL MATERIALS
Growth of thin films of dicyanovinylanisole on quartz and teflon-coated quartz by physical vapor transport
p 989 N95-19000
Aryl gels and related materials. Synthesis and characterization of a new class of microporous materials
[AD-A285044] p 987 N95-19544
Novel e-o polymers: NLO materials with superior temporal stability
[AD-A285872] p 988 N95-19614
IR materials producibility
[AD-A284263] p 1142 N95-19732
OPTICAL MEASUREMENT
New method for homodyne laser linewidth measurements with a short delay fiber
[PB94-202629] p 1036 N95-18061
Midinfrared optical properties of petroleum oil aerosols
[AD-A283689] p 1139 N95-18142
Thermocouples for interior ballistic temperature measurements
[AD-A283699] p 1033 N95-18620
Optical measurements in rocket engine liquid sprays
p 968 N95-18979
Surface roughness measurements
p 1142 N95-18984
Optical determination of conduction and valence-band dispersion curves in strained single-quantum wells
[DE94-018892] p 1151 N95-19235
Particle Image Velocimetry: Principles, current applications and future prospects p 1021 N95-19253
Optical surface pressure measurements: Accuracy and application field evaluation p 1025 N95-19274
OPTICAL MEASURING INSTRUMENTS
Optical Rain Gauge Performance: Second Workshop on Optical Rain Gauge Measurements
[NASA-CP-3288] p 1068 N95-18201
Moored rainfall measurements during COARE
p 1069 N95-18202
Update on TAO moored ORG array
p 1069 N95-18203
Wallops Island natural rain data analysis
p 1069 N95-18205
Vibration (?) spikes during natural rain events
p 1069 N95-18206
A comparison of optical rain gauge and radar data from TOGA/COARE p 1069 N95-18207
Can salt on an optical rain gauge lens affect performance? p 1069 N95-18208
Rain gauge calibration and testing
p 1070 N95-18209
Effect of heavy rain to the total received power
p 1070 N95-18210
Real-time adaptive control of mixing in a plane shear layer
[AD-A285541] p 1018 N95-18469
Fiber optic flexural disk accelerometer
[AD-D016444] p 1141 N95-18563
Fiber Optic Control System integration for advanced aircraft. Electro-optic and sensor fabrication, iniegration, and environmental testing for flight control systems
[NASA-CR-191194] p 1034 N95-19236
Spectroscopy and dynamics of vibrationally excited molecules
[AD-A285874] p 1134 N95-19597
OPTICAL MEMORY (DATA STORAGE)
Three-D optical memory disk
[AD-A280002] p 1035 N95-19871
OPTICAL MICROSCOPES
High Temperature Superconductor (HTS) superconducting quantum interference device (SQUID) microscope
[AD-A285875] p 1152 N95-19598
OPTICAL PATHS
MANN: A program to transfer designs for diffractive optical elements to a MANN photolithographic mask generator p 1142 N95-18995
OPTICAL PROPERTIES
Development of ultrashort optical pulse sources near 1.3 and 1.5 microns with an emphasis on stability, high repetition rate, and parallelism
[AD-A285535] p 1139 N95-18104
Midinfrared optical properties of petroleum oil aerosols
[AD-A283689] p 1139 N95-18142
Mathematical analysis of three free-electron-laser issues
[AD-A284122] p 1037 N95-18408
Atomic line filter for SDI applications
[AD-A284125] p 1139 N95-18409
Multi-functional pi-conjugated macromolecules based on poly (phenylene vinylene)
[AD-A284163] p 985 N95-18510
MANN: A program to transfer designs for diffractive optical elements to a MANN photolithographic mask generator p 1142 N95-18995
Investigation of the microstructure of coatings for high power lasers by non-optical techniques
[DE94-017697] p 987 N95-19227
Aryl gels and related materials. Synthesis and characterization of a new class of microporous materials
[AD-A285044] p 987 N95-19544
CVD silicon carbide characterization
[AD-A285667] p 972 N95-19702
Proceedings of the 15th Annual Conference on Atmospheric Transmission Models
[AD-A279919] p 1142 N95-19862
OPTICAL PUMPING
Measurements of line overlap for resonant spoiling of x ray lasing transitions
[DE94-016444] p 1038 N95-19248
OPTICAL RADAR
Overview of laser technology at Los Alamos National Laboratory
[DE94-018307] p 1036 N95-18126
Atomic line filter for SDI applications
[AD-A284125] p 1139 N95-18409
Special relativity effects for space-based coherent lidar experiments p 1014 N95-18983
OPTICAL RELAY SYSTEMS
Design and fabrication of N x N optical couplers based on organic polymer optical waveguides
[AD-A285530] p 1138 N95-18100
OPTICAL RESONANCE
Large amplitude motions, especially isomerization and tunneling in polyatomic molecule spectra: Novel experimental, pattern recognition, and theoretical methods
[AD-A284194] p 985 N95-18636
Study of laser resonance ionization mass spectrometry using a glow discharge source
[DE94-018566] p 981 N95-19703
OPTICAL SWITCHING
Polymer fibers for nonlinear optics
[AD-A284216] p 983 N95-17957
Evaluation of the current biased integrated optical processors based on bistable dode elements
[AD-A285532] p 1138 N95-18102
Methods and components for optical contention resolution in high speed networks
[AD-A284674] p 1142 N95-19088
OPTICAL THICKNESS
Multispectral NOAA Marine Atmospheric Boundary Layer (MABL) estimates during VOCAR
[AD-A283702] p 1064 N95-18623
OPTICAL TRANSFER FUNCTION
A comparison between using incoherent or coherent sources to align and test an adaptive optical telescope
p 1142 N95-18969
OPTICAL TRANSITION
Characterization of the 50 MeV ALS linac beam with optical transition radiation
[DE94-018208] p 1137 N95-19584
OPTICAL WAVEGUIDES
Design and fabrication of N x N optical couplers based on organic polymer optical waveguides
[AD-A285530] p 1138 N95-18100
Waveguide switches using asymmetric coupled quantum wells
[AD-A284056] p 1010 N95-18662
OPTICS
Subgroup report on hard x-ray microprobes
[DE94-018708] p 1034 N95-19233
SeaWiFS technical report series. Volume 18: SeaWiFS technical report series cumulative index: Volumes 1-17
[NASA-TM-104566-VOL-18] p 1076 N95-19577
OPTIMAL CONTROL
Microgravity isolation system design: A modern control synthesis framework
[NASA-TM-106805] p 927 N95-18197
OPTIMIZATION
Linear optimization and image reconstruction
[AD-A283641] p 1094 N95-18013

Time-optimal control of a third order regulator
[AD-A283307] p 1113 N95-18023
An algorithm for solving the system-level problem in multilevel optimization
[NASA-CR-195015] p 1116 N95-18108
Optimization of coupled systems: A critical overview of approaches
[NASA-CR-195019] p 1116 N95-18109
Design optimization of a brush turbine with a cleaner/water based solution p 1043 N95-18177
An analog computing approach to structural analysis and optimal design through artificial neural networks p 1113 N95-18218
Program verification for optimized byte copy
[AD-A283915] p 1099 N95-18676
Optimization of layered metal matrix composite cylinders p 970 N95-18920
Performance improvements in diode laser arrays
[DE94-016547] p 1039 N95-19508

OPTOELECTRONIC DEVICES
The 3d International Workshop on Computational Electronics
[AD-A284678] p 1011 N95-19089

ORBIT PERTURBATION
Second-order reconstruction of the inflationary potential
[NASA-CR-197629] p 1121 N95-19030

ORBITAL ELEMENTS
Some considerations on velocity vector accuracy in dust trajectory analysis p 1183 N95-19186
Velocity distribution of Earth-crossing asteroid grains p 1183 N95-19187

ORBITAL MECHANICS
Optimal transfer and swing-by orbits in the two- and three-body problems p 961 N95-18900
First principles used in orbital prediction and an atmospheric model comparison
[AD-A284636] p 1065 N95-19086

ORBITAL RESONANCES (CELESTIAL MECHANICS)
IRAS observations show that the Earth is embedded in a solar ring of asteroidal dust particles in resonant lock with the planet p 1182 N95-19181

ORBITAL WORKERS
Geometry and gravity influences on strength capability
[NASA-TP-3511] p 1091 N95-18189

ORDER-DISORDER TRANSFORMATIONS
Waveguide switches using asymmetric coupled quantum wells
[AD-A284056] p 1010 N95-18662
Energies of X conduction band minima in disordered and ordered GaInP2 alloys
[DE94-018211] p 1152 N95-19586

ORGANIC COMPOUNDS
Improved filtration materials and modeling
[AD-A284684] p 1091 N95-18531
Growth of thin films of dicyanovinylanisole on quartz and teflon-coated quartz by physical vapor transport p 989 N95-19000
Aryl gels and related materials. Synthesis and characterization of a new class of microporous materials
[AD-A285044] p 987 N95-19544

ORGANIC MATERIALS
Fabrication of biomimetic molecular level composites
[AD-A284204] p 969 N95-17941
1994 IEEE Nonlinear Optics: Materials Fundamental and Applications Conference
[AD-A285769] p 1139 N95-18345
Thermoelectric properties of conducting polymers
[AD-A284058] p 986 N95-18678

ORGANIZATIONS
Training plan. Central Archive for Reusable Defense Software (CARDS)
[AD-A284343] p 1097 N95-18421
Franchise plan. Central Archive for Reusable Defense Software (CARDS)
[AD-A284344] p 1097 N95-18422
Activities of the Analytical Chemistry Laboratory
[DE95-000834] p 975 N95-19618

ORGANOMETALLIC POLYMERS
Excited state processes in transition metal complexes. Redox splitting in soluble polymers
[DE95-002690] p 977 N95-19839

ORION CONSTELLATION
Models for multiple heating mechanisms p 1188 N95-19303

ORTHOSTATIC TOLERANCE
Effect of heat acclimation on sitting orthostatic tolerance in the heat after 48 and 96 hour bed rest in men
[NASA-TM-108861] p 1077 N95-18734

OSCILLATING FLOW
Evaluation of boundary conditions for computational aeroacoustics
[NASA-TM-109989] p 1015 N95-18149

OSCILLATION DAMPERS
Tuned mass damper for integrally bladed turbine rotor
[NASA-CASE-MFS-28697-1] p 1041 N95-18325

OSCILLATIONS
Intraseasonal oscillations over the tropical western Pacific and eastern Indian ocean for the northern summers of 1989-1991
[AD-A284527] p 1068 N95-18114
Observation of flow and temperature oscillations around a bubble on a solid surface subject to a vertical temperature gradient
[NASA-CR-197593] p 1017 N95-18327
Overview of unsteady transonic wind tunnel test on a semispan straked delta wing oscillating in pitch
[AD-A284097] p 928 N95-18380
Cerebellar circuit mechanisms which accompany coordinated limb trajectory patterns in the rat: Use of a model of spontaneous changes in limb coordination
[AD-A284023] p 1079 N95-18656
Development of a multicomponent force and moment balance for water tunnel applications, volume 2
[NASA-CR-4642-VOL-2] p 1020 N95-18956

OSCILLATORS
Spectroscopy and dynamics of vibrationally excited molecules
[AD-A285874] p 1134 N95-19597

OSMIUM COMPOUNDS
Excited state processes in transition metal complexes. Redox splitting in soluble polymers
[DE95-002690] p 977 N95-19839

OSMOSIS
Drink composition and cycle-ergometer endurance in men: Carbohydrate, Na(+), osmolality
[NASA-TM-4650] p 1077 N95-19140

OUTGASSING
Outgassing of solid material into vacuum thermal insulation spaces p 972 N95-18184

OUTLET FLOW
Gas storage and recovery system
[NASA-CASE-MSC-22091-1] p 992 N95-18738

OVERPRESSURE
Health hazards assessment for blast overpressure exposures
[AD-A283352] p 1078 N95-17998
Data acquisition from blast overpressure trials
[MRL-TN-628] p 1020 N95-19139

OXALATES
Heterogeneous nucleation of calcium oxalate on native oxide surfaces
[DE94-018725] p 986 N95-18648

OXIDATION
Methane conversion by solid electrolyte membranes
[PB94-191781] p 973 N95-17982
Alloying effects on the high-temperature oxidation resistance of Cr-Cr2Nb
[DE94-018146] p 978 N95-18121
Surface phases, surface defects and the initial stages of oxidation
[DE94-016947] p 979 N95-18358
Complex oxidation effects in polymer degradation
[DE94-018903] p 986 N95-18651
Deformation of nonstoichiometric CuO polycrystals
[DE94-016907] p 1150 N95-19094
X-ray absorption spectroscopy in high temperature oxidation of metals and alloys p 955 N95-19682
Resistance of silicon nitride turbine components to erosion and hot corrosion/oxidation attack p 955 N95-19683

OXIDATION RESISTANCE
Thermo-oxidative stability of graphite/PMR-15 composites: Effect of fiber surface modification on composite shear properties
[NASA-TM-4608] p 981 N95-19652

OXIDATION-REDUCTION REACTIONS
Spectroelectrochemical investigations of molten halide solutions
[AD-A284147] p 974 N95-18412
Establishment of redox conditions during planetary collisions as an origin of chondrites p 1192 N95-19331
Development of a colloidal redox system containing a smectite clay for control of reactivity and reaction selectivity
[AD-A285958] p 974 N95-19515
Excited state processes in transition metal complexes. Redox splitting in soluble polymers
[DE95-002690] p 977 N95-19839

OXIDE FILMS
Ion mixing in oxide-sapphire systems
[DE94-018660] p 1133 N95-19232
Development of materials for high temperature superconductor Josephson junctions
[DE95-000896] p 1152 N95-19608

OXIDES
Advanced packaging and integration technologies for microsensors, phase 1
[AD-A283613] p 1040 N95-18010
Surface phases, surface defects and the initial stages of oxidation
[DE94-016947] p 979 N95-18358
Sealant materials for the solid oxide fuel cell
[DE94-017073] p 1053 N95-19115
Barium strontium titanate and non-ferroelectric oxide ceramic composites for use in phased array antennas
[AD-A279225] p 972 N95-19851

OXYGEN
Coronal abundances and their variation
[NASA-CR-197553] p 1195 N95-18376
An instrument to measure the charge, and energy spectrum (20-1000 GeV/a) of the cosmic ray species oxygen to iron
[NASA-CR-197555] p 1197 N95-18464
Development of radiation-hardened ceramic composites for fusion applications
[DE94-016182] p 985 N95-18638
A multiple time scale solution for the Chapman mechanism
[DE94-017491] p 1060 N95-18895
Sealant materials for the solid oxide fuel cell
[DE94-017073] p 1053 N95-19115
A mechanism for blistering of carbon fiber composites
[AD-A286252] p 971 N95-19386

OXYGEN ATOMS
Method of making a membrane having hydrophilic and hydrophobic surfaces for adhering cells or antibodies by using atomic oxygen or hydroxyl radicals
[NASA-CASE-MSC-21529-1] p 983 N95-18134
A spectral study of a radio-frequency plasma-generated flux of atomic oxygen
[NASA-TM-4612] p 1032 N95-18194
Laboratory studies of stratospheric bromine chemistry: Kinetics of the reactions of bromine monoxide with nitrogen dioxide and atomic oxygen p 1065 N95-18731
Synthesis and characterization of a neutral six-coordinate tris-adduct of an indium(3) trihalide. X ray crystal structure of InCl3(THF)3
[AD-A279169] p 1154 N95-19806

OXYGEN IONS
Impurity behavior during ion-Bernstein wave heating in PBX-M
[DE94-018114] p 1133 N95-19228

OXYGEN ISOTOPES
Chemical production of chondrule oxygen isotopic composition p 1192 N95-19330

OZONE
Dependencies and sensitivity of tropospheric oxidants to precursor concentrations over the northeast United States: A model study
[PB94-192770] p 1056 N95-17937
Potential replacements for solvents that are ozone depleting substances
[AD-A285442] p 1058 N95-18091
A model study of the influence of NMHC and NO(x) emissions on rural O3 concentrations in Georgiargia p 1059 N95-18445
A multiple time scale solution for the Chapman mechanism
[DE94-017491] p 1060 N95-18895
A report on workshops: General circulation model study of climate: Chemistry interaction
[DE94-010252] p 1062 N95-19879

OZONE DEPLETION
Evolution of the Southern Hemisphere ozone hole as seen by TOMS from August 1979 to December 1991
[NASA-TM-110116] p 1057 N95-18048
Compendium of NASA data base for the Global Tropospheric Experiment's Arctic Boundary Layer Experiments ABLE-3A and ABLE-3B
[NASA-TM-109161] p 1058 N95-18132
Meteor 3/TOMS launch of 15 August 1991 in Plesetsk, USSR
[NASA-TM-110115] p 962 N95-18150

OZONOSPHERE
Potential replacements for solvents that are ozone depleting substances
[AD-A285442] p 1058 N95-18091

P

P-I-N JUNCTIONS
Electronics for the Si detectors in APEX
[DE94-015078] p 1007 N95-17961

P-N JUNCTIONS
InP solar cell development on inexpensive silicon substrates
[AD-A283624] p 1052 N95-18011
InP solar cell development on inexpensive silicon substrates
[AD-A286254] p 1054 N95-19388

P-TYPE SEMICONDUCTORS
Minority-carrier lifetime in InP as a function of light bias
[NASA-TM-106821] p 1149 N95-18453
Growth and doping of Al(x)Ga(1-x)N films by electron cyclotron resonance assisted molecular beam epitaxy
[AD-A284838] p 1153 N95-19737
Characterization of inactive carbon in GaAs
[DE95-002352] p 976 N95-19836
PACIFIC OCEAN
Intraseasonal oscillations over the tropical western Pacific and eastern Indian ocean for the northern summers of 1989-1991
[AD-A284527] p 1068 N95-18114
A numerical simulation of seasonal circulation in the South China Sea
[AD-A283701] p 1075 N95-18622
PACKAGING
Reliability Without Hermeticity (RWOH) for Integrated Circuits (IC)
[AD-A284340] p 1009 N95-18418
PACKET SWITCHING
MSFC institutional area network and ATM technology p 1007 N95-18968
PACKETS (COMMUNICATION)
Signal processor having multiple distributed data buffers
[AD-D016259] p 995 N95-18315
PADE APPROXIMATION
On the convergence of local approximations to pseudodifferential operators with applications
[NASA-TM-106792] p 1019 N95-18898
PAIN
Crosshift vibrometry: Biomarker for ergonomic stress
[AD-A284337] p 1091 N95-18385
PAINTS
The probability of flaw detection and the probability of false calls in nondestructive evaluation equipment p 1044 N95-19010
Alternative solvents/technologies for paint stripping: Phase 1
[AD-A279918] p 989 N95-19861
PAIR PRODUCTION
The very low energy solar flux of electron and heavy-flavor neutrinos and antineutrinos
[DE94-018583] p 1135 N95-19706
PALLADIUM
Precision gold conductors for HMCs
[DE94-018558] p 1012 N95-19230
PALLADIUM COMPOUNDS
Palladium-based membranes for hydrogen separation
[PB94-207156] p 973 N95-18377
PANEL METHOD (FLUID DYNAMICS)
Course module for AA201: Wing structural design project
[AD-A283618] p 944 N95-18616
Calculation of support interference in dynamic wind-tunnel tests p 933 N95-19282
CFD: Advances and Applications, part 1
[NAL-SP-9322-PT-1] p 1026 N95-19444
Panel methods p 1027 N95-19448
PANELS
Thermo-acoustic fatigue design for hypersonic vehicle skin panels p 1047 N95-19161
Soft body impact on titanium fan blades p 953 N95-19671
Acoustic transmission loss and structureborne noise transmission tests on a LASCOR and a reference steel panel
[MRL-TN-623] p 1128 N95-19770
PARABOLIC FLIGHT
Users guide for NASA Lewis Research Center DC-9 Reduced-Gravity Aircraft Program
[NASA-TM-106755] p 959 N95-18586
PARACHUTES
Parachute inflation: A problem in aeroelasticity
[AD-A284375] p 928 N95-18340
PARALLEL COMPUTERS
Study of a Navier-Stokes computer
[AD-A284196] p 1092 N95-17939
Software techniques for balancing computation and communication in parallel systems
[AD-A285536] p 1109 N95-18106
A practical algorithm for integer sorting on a mesh-connected computer (preliminary version)
[AD-A283921] p 1110 N95-18159
Local spatio-temporal analysis in vision systems
[AD-A284162] p 1140 N95-18509
Scalability of parallel spatial direct numerical simulation code on IBM SP1 parallel supercomputer
[NASA-CR-194975] p 1098 N95-18584
PST: A simulation tool for parallel systems
[AD-A285680] p 1111 N95-19526
Embedded microclusters in zeolites and cluster beam sputtering: Simulation on parallel computers
[DE95-000662] p 1134 N95-19562
High performance computing equipment for environmental remediation modeling and first principles simulation of materials properties
[DE95-000497] p 1093 N95-19875
PARALLEL PROCESSING (COMPUTERS)
Reformulated preconditioned conjugate gradient squared method. Part 1: The algorithm
[PB94-201589] p 1108 N95-17936
Construction of a connectionist network supercomputer
[AD-A283354] p 1109 N95-18050
A novel system level approach to fault tolerance in distributed memory multicomputers
[AD-A284729] p 1095 N95-18079
Development of ultrashort optical pulse sources near 1.3 and 1.5 microns with an emphasis on stability, high repetition rate, and parallelism
[AD-A285535] p 1139 N95-18104
Software techniques for balancing computation and communication in parallel systems
[AD-A285536] p 1109 N95-18106
Static and dynamic nuclear many-body descriptions on parallel architectures
[DE94-018134] p 1116 N95-18120
Early experiences and performance of the Intel Paragon
[DE94-018061] p 1109 N95-18129
A practical algorithm for integer sorting on a mesh-connected computer (preliminary version)
[AD-A283921] p 1110 N95-18159
Modular signal processing unit
[AD-D016258] p 995 N95-18314
A parallel processing hypothesis for short-term and long-term memory in Aplysia
[AD-A284101] p 1088 N95-18401
Parallelization of the fluid dynamics equations on unstructured grids
[AD-A284116] p 1017 N95-18406
Global time transformations
[AD-A285539] p 1110 N95-18454
A simple hyperbolic model for communication in parallel processing environments
[NASA-CR-195984] p 1098 N95-18487
Local spatio-temporal analysis in vision systems
[AD-A284162] p 1140 N95-18509
Characterizing parallel file-access patterns on a large-scale multiprocessor
[NASA-CR-197568] p 1110 N95-18521
Dynamic file-access characteristics of a production parallel scientific workload
[NASA-CR-197570] p 1110 N95-18581
Scalability of parallel spatial direct numerical simulation code on IBM SP1 parallel supercomputer
[NASA-CR-194975] p 1098 N95-18584
A direct decomposition method for the solution of sparse linear least squares problems
[AD-A284060] p 1117 N95-18679
Research in parallel computing
[AD-A283983] p 1111 N95-18892
On extending parallelism to serial simulators
[NASA-CR-195011] p 1099 N95-18931
Parallel Navier-Stokes computations on shared and distributed memory architectures
[NASA-TM-106823] p 1019 N95-18941
Empirical study of parallel LRU simulation algorithms
[NASA-CR-194995] p 1099 N95-19027
On k-ary n-cubes: Theory and applications
[NASA-CR-194996] p 1100 N95-19028
CFD on parallel computers p 1029 N95-19465
Enhancing the architectural characterization of parallel proto
[AD-A285678] p 1111 N95-19524
PST: A simulation tool for parallel systems
[AD-A285680] p 1111 N95-19526
Generating parallel execution plans with a partial order planner
[AD-A285888] p 1111 N95-19605
Parallel computations in hydro acoustics
[AD-A285900] p 1030 N95-19607
Parallel computation
[AD-A284831] p 1112 N95-19692
Massively parallel full configuration interaction. Benchmark electronic structure calculations on the Intel Touchstone Delta
[DE95-001064] p 1153 N95-19724
A parallel strategy for implementing real-time expert systems using CLIPS p 1105 N95-19749
Using CLIPS in the domain of knowledge-based massively parallel programming p 1105 N95-19750
PCLIPS: Parallel CLIPS p 1107 N95-19764
Solution of potential flow problems on a network of workstations
[DE94-017861] p 1112 N95-19831
Solutions of TEAM Problem No. 13 using integral equations in a sequential and parallel computing environment
[DE95-001472] p 1112 N95-19834
Connectionist Network Supercomputer Project
[AD-A279206] p 1112 N95-19843
High performance computing equipment for environmental remediation modeling and first principles simulation of materials properties
[DE95-000497] p 1093 N95-19875
PARALLEL PROGRAMMING
NASA High Performance Computing and Communications program
[NASA-TM-4653] p 1174 N95-18573
Parallel computation
[AD-A284831] p 1112 N95-19692
Using CLIPS in the domain of knowledge-based massively parallel programming p 1105 N95-19750
PARAMETER IDENTIFICATION
Minimal time detection algorithms and applications to flight systems
[TR-2-FSRC-93] p 1098 N95-18564
PARAMETERIZATION
NASA Goddard Earth Sciences Graduate Student Program --- FIRE CIRRUS-II examination of coupling between an upper tropospheric cloud system and synoptic-scale dynamics
[NASA-CR-197130] p 1066 N95-19129
PARITY
A redundant disk array architecture for efficient small writes
[AD-A284048] p 1093 N95-18659
Limits on CP nonconserving interactions from electric dipole moments
[DE94-018582] p 1134 N95-19705
PARSING ALGORITHMS
Alternative formulation of Cocke-Younger-Kasami's algorithm
[PB94-202751] p 1094 N95-18000
PARTIAL DIFFERENTIAL EQUATIONS
Reformulated preconditioned conjugate gradient squared method. Part 1: The algorithm
[PB94-201589] p 1108 N95-17936
Geometrical and topological methods in time domain antenna synthesis
[AD-A284208] p 964 N95-17954
Singular perturbation problem governed by system of conservation laws
[DE94-019264] p 1116 N95-17977
Static and dynamic nuclear many-body descriptions on parallel architectures
[DE94-018134] p 1116 N95-18120
Arbitrarily high order nodal and characteristic methods
[DE94-018130] p 1116 N95-18131
Subspace correction methods for the iterative solution of hierarchic plate models. 1: Heat transfer problems
[AD-A285712] p 1117 N95-18482
Weighted graph based ordering techniques for preconditioned conjugate gradient methods
[NASA-CR-197597] p 1118 N95-18736
Difference schemes for hyperbolic system of Conservation Laws p 1027 N95-19450
Singularities and symmetries of nonlinear ordinary and partial differential equations
[DE95-000904] p 1119 N95-19609
PARTIAL PRESSURE
Deformation of nonstoichiometric CuO polycrystals
[DE94-016907] p 1150 N95-19094
Constraints on chondrule and CAI origins from vapor-liquid-solid experiments p 1190 N95-19317
PARTICLE ACCELERATION
Laser wakefield excitation and measurement on a femtosecond time scale: Theory and experiment
[DE94-019198] p 1129 N95-17976
Particle acceleration and transport in the tail and at the front side of the magnetosphere, task 1 and 2
[NASA-CR-197575] p 1064 N95-18476
The hypervelocity impact facilities at the University of Kent at Canterbury, UK p 961 N95-19180
PARTICLE BEAMS
Advanced methods for the computation of particle beam transport and the computation of electromagnetic fields and beam-cavity interactions
[DE94-017359] p 1136 N95-18893
PARTICLE COLLISIONS
Electron interactions with non-linear polyatomic molecules and their radicals
[AD-A283952] p 1130 N95-18334
Solar flare model atmospheres
[NASA-CR-197607] p 1196 N95-19034
Baryon stopping in 200 GeV/A S+Au collisions
[DE94-018215] p 1134 N95-19587
PARTICLE DECAY
Decaying neutrinos in galaxy clusters
[NASA-CR-197615] p 1198 N95-18747

Family symmetries and proton decay
[DE94-017575] p 1133 N95-19245

PARTICLE DENSITY (CONCENTRATION)
Comment on the preprint Neutrino Flavor Evolution Near a Supernova's Core (Astro-Ph 9405008) by J. Pantaleone
[DE94-017576] p 1198 N95-19283

PARTICLE FLUX DENSITY
PVDF flux/mass/velocity/trajectory systems and their applications in space p 966 N95-19196

PARTICLE IMAGE VELOCIMETRY
7th International Symposium on Applications of Laser Techniques to Fluid Mechanics, volume 2
[AD-A285685] p 1018 N95-18477
Particle Image Velocimetry: Principles, current applications and future prospects p 1021 N95-19253

PARTICLE IN CELL TECHNIQUE
A three region analysis of a bounded plasma using particle in cell and fluid techniques
[AD-A284826] p 1147 N95-19690

PARTICLE INTERACTIONS
The left-right forward-backward asymmetry for B quarks at the SLD
[DE94-014508] p 1129 N95-18049
Can an infrared-vanishing gluon propagator confine quarks?
[DE94-018388] p 1131 N95-18548
Summary of the working group on tests of QCD
[DE94-018390] p 1131 N95-18550
Higher-order Lipatov kernels and the QCD Pomeron
[DE94-018395] p 1131 N95-18551

PARTICLE MASS
Evidence for coexistence of two phases in relativistic heavy ion collisions and comparison with lattice results
[DE94-626672] p 1130 N95-18329

PARTICLE PRODUCTION
Feynman-x and transverse momentum dependence of D(sup (+-)) and D(sup 0), D-bar(sup 0) production in 250 GeV (pi)(sup -) - nucleon interactions
[DE94-626698] p 1130 N95-18366
Principal-value resummation for dilepton production
[DE95-001094] p 1135 N95-19726

PARTICLE SIZE DISTRIBUTION
The calculation of erosion in a gas turbine compressor rotor p 952 N95-19664

PARTICLE TELESCOPES
CRRESPRO documentation
[AD-A284578] p 1178 N95-18451

PARTICLE TRAJECTORIES
Some considerations on velocity vector accuracy in dust trajectory analysis p 1183 N95-19186
Charge collection during hypervelocity penetrations of thin foils p 1036 N95-19190
Penetration of multiple thin films in micrometeorite capture cells p 1036 N95-19192
PVDF flux/mass/velocity/trajectory systems and their applications in space p 966 N95-19196
Particle deposition in gas turbine blade film cooling holes p 951 N95-19661
Experimental and numerical simulations of the effects of ingested particles in gas turbine engines p 952 N95-19662
Particle trajectories in gas turbine engines p 952 N95-19663
The calculation of erosion in a gas turbine compressor rotor p 952 N95-19664

PARTICULATE SAMPLING
Comet coma sample return instrument p 1180 N95-19173
SOCCER: Comet Coma Sample Return Mission p 1181 N95-19174
The status of measurement technologies concerning micrometer and submicrometer space articulate matter capture, recovery, velocity and trajectory p 1181 N95-19175
Physics of spacecraft-based interplanetary dust collection by impact into low-density media p 1181 N95-19176
Highly transparent and rugged sensor for velocity determinations of cosmic dust particles p 966 N95-19178
Main characteristics of the COMET/COMRADE experiments p 1181 N95-19179
Laboratory simulation of intact capture of cometary and asteroidal dust particles in ISAS p 962 N95-19183
SPICE: An innovative, flexible instrument concept p 966 N95-19189
Penetration of multiple thin films in micrometeorite capture cells p 1036 N95-19192

PARTICULATES
Superstrength metal composite material and process for making the same
[AD-D016555] p 971 N95-19123

PARTITIONS (MATHEMATICS)
Partition method for the determination of multiple DC operating points
[PB94-201480] p 1009 N95-18501
On k-ary n-cubes: Theory and applications
[NASA-CR-194996] p 1100 N95-19028
Towards a classification of su(2)(direct sum)...(direct sum)su(2) modular invariant partition functions
[PB94-217247] p 1119 N95-19717

PARTITIONS (STRUCTURES)
Metal-framed partitions with reduced thicknesses. Part 2: Built-in acoustic treatment
[BBC-RD-1993/6-PT-2] p 993 N95-19137
Metal-framed partitions with reduced thicknesses. Part 1: Narrower studs and cavities
[BBC-RD-1993/5-PT-1] p 993 N95-19138

PASSIVITY
Fundamental studies of passivity and passivity breakdown
[DE94-016954] p 987 N95-19095

PATTERN RECOGNITION
Cooperativity and 3-D representation
[AD-A284203] p 1093 N95-17940
Modular implementation of feature extraction and matching algorithms for photogrammetric stereo imagery
[AD-A285422] p 1032 N95-18065
Fusion of multiple sensing modalities for machine vision
[AD-A284762] p 1091 N95-18086
An analog computing approach to structural analysis and optimal design through artificial neural networks p 1113 N95-18218
Large amplitude motions, especially isomerization and tunneling in polyatomic molecule spectra: Novel experimental, pattern recognition, and theoretical methods
[AD-A284194] p 985 N95-18636
Machine learning: A comparative study of pattern theory and C4.5
[AD-A285582] p 1115 N95-19118
Facilitation and interference in identification of pictures and words
[AD-A285882] p 1090 N95-19602

PAYLOADS
Meteor 3/TOMS launch of 15 August 1991 in Plesetsk, USSR
[NASA-TM-110115] p 962 N95-18150
Parachute inflation: A problem in aeroelasticity
[AD-A284375] p 928 N95-18340
STS-68 mission highlights resource tape
[NASA-TM-110049] p 961 N95-18568
US experiments flown on the Soviet biosatellite Cosmos 2044. Volume 1: Mission description, experiments K-7-01 - K-7-15
[NASA-TM-108802-VOL-1] p 1092 N95-18569
Lean spacecraft avionics trade study p 966 N95-18994
Near-Earth Asteroid Returned Sample (NEARS)
[NASA-CR-197297] p 1194 N95-19575
A 20k payload launch vehicle fast track development concept using an RD-180 engine and a Centaur upper stage
[NASA-TM-108475] p 963 N95-19648
Summary report of mission acceleration measurements for STS-60, SPACEHAB2, launched 11 February 1994
[NASA-TM-106797] p 991 N95-19788

PELLETS
Detection of alpha particles via observation of He II line emission in the lithium pellet cloud during DT operation in TFTR
[DE94-014485] p 1143 N95-17965
Novel carbon-ion fuel cells
[DE94-017390] p 1053 N95-18894
Theoretical investigation of matching between plasma heating and fueling in HL-1M machine
[DE94-627019] p 1146 N95-19241

PENETRATION
Cracking characteristics of a habitable module pressure wall following orbital debris penetration p 1047 N95-19003
Laboratory simulation of intact capture of cometary and asteroidal dust particles in ISAS p 962 N95-19183
Penetration experiments in aluminum and Teflon targets of widely variable thickness p 1047 N95-19185
Charge collection during hypervelocity penetrations of thin foils p 1036 N95-19190
Penetration of multiple thin films in micrometeorite capture cells p 1036 N95-19192
Assessment of velocity/trajectory measurement technologies during a particle capture event p 1036 N95-19193
Nondestructive time-of-capture, location and velocity sensing in intact capture p 1036 N95-19194
The use of silica aerogel to collect interplanetary dust in space p 989 N95-19197

PERCOLATION
Quantitative analysis of voids in percolating structures in two-dimensional N-body simulations
[NASA-CR-197612] p 1156 N95-18949

PERFORMANCE
Early experiences and performance of the Intel Paragon
[DE94-018061] p 1109 N95-18129
On orbit performance of the ALEXIS EUV telescopes
[DE94-016197] p 964 N95-18839
Performance improvements in diode laser arrays
[DE94-016547] p 1039 N95-19508

PERFORMANCE PREDICTION
Six degree of freedom flight dynamic and performance simulation of a remotely-piloted vehicle
[AERO-TN-9301] p 942 N95-18097
Performance evaluation of ground based radar systems
[AD-A283654] p 995 N95-18139
Image intensifier system resolution based on laboratory measured parameters
[AD-A283917] p 1008 N95-18156
Intermediate design and analysis of the PANSAT electrical power subsystem
[AD-A283610] p 1053 N95-18435
HEISHI: A fuel performance model for space nuclear applications
[DE94-017497] p 1137 N95-18897
Empirical study of parallel LRU simulation algorithms
[NASA-CR-194995] p 1099 N95-19027
Centrifugal and axial pump design and off-design performance prediction
[NASA-TM-106745] p 968 N95-19795

PERFORMANCE TESTS
Fundamental advances for characterizing cathodic protection systems
[PB94-180692] p 1122 N95-17983
Wind tunnel performance comparative test results of a circular cylinder and 50 percent ellipse tailboom for circulation control antitorque applications
[AD-A283335] p 941 N95-18008
Conference on Aerospace Transparent Materials and Enclosures. Volume 2: Sessions 5-9
[AD-A283926] p 942 N95-18162
Performance evaluation of the NASA/KSC CAD/CAE and office automation LAN's p 1108 N95-18186
High performance storable propellant resistojet
[NASA-CR-191128] p 967 N95-18195
Design, validation and prototype testing of a high resolution all-reflection Michelson interferometer for solar occultation measurements of the OI 1304-a triplet emission
[AD-A283705] p 1178 N95-18361
Helicopter Performance Evaluation (HELPE) computer model
[AD-A284319] p 942 N95-18381
Final results of the Advanced Photovoltaic Experiment flight test
[NASA-TM-106828] p 967 N95-18571
Concept of using a benchmark part to evaluate rapid prototype processes p 994 N95-18975
Performance evaluation of the Engineering Analysis and Data Systems (EADS) 2 p 1163 N95-18978
Evaluation of SSME test data reduction methods p 968 N95-19002
Transient and steady-state tests of the space power research engine with resistive and motor loads
[NASA-TM-106832] p 1042 N95-19238
Nozzle Initiative Industry Advisory Committee on Standardization of Carbon-Phenolic Test Methods and Specifications
[NASA-CR-197529] p 967 N95-19566
A systems analysis and project management plan for the Petite Amateur Navy Satellite (PANSAT)
[AD-A285968] p 965 N95-19571
Facilitation and interference in identification of pictures and words
[AD-A285882] p 1090 N95-19602
Current Hybrid Electric Vehicle performance based on temporal data from the world's largest HEV fleet
[DE94-011859] p 1014 N95-19881

PERIODIC VARIATIONS
Intraseasonal oscillations over the tropical western Pacific and eastern Indian ocean for the northern summers of 1989-1991
[AD-A284527] p 1068 N95-18114
Compression strength of composite primary structural components
[NASA-CR-197554] p 1044 N95-18388

PERIPHERAL EQUIPMENT (COMPUTERS)
Laser optical mouse
[AD-D016273] p 1092 N95-18517

PERMANENT MAGNETS
The interaction of two narrow magnets and a moving conducting slip
[DE94-018575] p 1122 N95-19704

PERMEABILITY
Method of moments analysis of artificial media composed of dielectric wire objects
[AD-A283318] p 994 N95-18024
PERMITTIVITY
Method of moments analysis of artificial media composed of dielectric wire objects
[AD-A283318] p 994 N95-18024
Barium strontium titanate and non-ferroelectric oxide ceramic composites for use in phased array antennas
[AD-A279225] p 972 N95-19851
PEROVSKITES
Methane conversion by solid electrolyte membranes
[PB94-191781] p 973 N95-17982
Ferroelectric thin film bismuth titanate prepared from acetate precursors
[DE95-000538] p 988 N95-19558
Microstructure and crystal defects in perovskite crystals with A-site cation ordering
[AD-A284261] p 1153 N95-19713
PEROXIDES
Preparation of an electrocatalytic cathode for an aluminum-hydrogen peroxide battery
[AD-D016262] p 1008 N95-18318
PERSONAL COMPUTERS
Development of executive information systems
[AD-A284005] p 1174 N95-18654
Zoned Analog Personal Teleconferencing (ZAPT)
[AD-A285877] p 1004 N95-19600
PERSONNEL
Variable name dictionary for the Air Force health study 1987 physical examination data tape, volume 1
[AD-A283319] p 1172 N95-18025
Variable name dictionary for the Air Force health study 1987 physical examination data tape, volume 2
[AD-A283320] p 1172 N95-18026
Creation of new items and forms for the Project A Assembling Objects test
[AD-A285522] p 1088 N95-18095
Crosshift vibrometry: Biomarker for ergonomic stress
[AD-A284337] p 1091 N95-18385
Franchise plan. Central Archive for Reusable Defense Software (CARDS)
[AD-A284344] p 1097 N95-18422
Government contractors: Measuring costs of service contractors versus federal employees. Report to the Chairman, Subcommittee on Federal Services, Post Office and Civil Service, Committee on Governmental Affairs, US Senate
[GAO/GGD-94-95] p 1171 N95-18595
NASA property: Poor lending practices and controls at the Jet Propulsion Laboratory. Report to Congressional Requesters
[GAO/NSIAD-94-116] p 1172 N95-19141
PERSONNEL DEVELOPMENT
Assessment of a career development program for executive amd mid-level managers
p 1161 N95-18182
PERSONNEL SELECTION
The Clinical Basis for Aeromedical Decision Making
[AGARD-CP-553] p 1080 N95-19413
Think health not disease p 1083 N95-19429
Neurological decision making in aviation medicine based on electrophysiological methods p 1084 N95-19431
The EEG in the evaluation of applicants to aircrew members p 1084 N95-19432
Clinical basis for aeromedical decision-making: The EEG example p 1084 N95-19433
PERTURBATION
Singular perturbation problem governed by system of conservation laws
[DE94-019264] p 1116 N95-17977
Observations of TEC fluctuations from an explosion on the Earth's surface
[DE94-018278] p 1063 N95-18125
Comparison of frequency response and perturbation methods to extract linear models from a nonlinear simulation
[AD-A284115] p 958 N95-18405
Complete mode-set stability analysis of magnetically insulated ion diode equilibria
[DE94-015275] p 1145 N95-19201
PERTURBATION THEORY
Testing the frozen flow approximation
[NASA-CR-197614] p 1180 N95-18966
Testing higher-order Lagrangian perturbation theory against numerical simulation. 1: Pancake models
[NASA-CR-197611] p 1121 N95-19348
Comparison of dynamical approximation schemes for non-linear gravitational clustering
[NASA-CR-197609] p 1157 N95-19363
PETN
Mixed high explosives for insensitive booster compositions
[MRL-TR-92-22] p 990 N95-19505
PETRI NETS
Fair Petri nets and structural induction for rings of processes
[AD-A283920] p 1110 N95-18158
Simulation in a dynamic prototyping environment: Petri nets or rules? p 1106 N95-19756
PETROLOGY
Chondrule formation in the radiative accretional shock
p 1191 N95-19324
PHASE DIAGRAMS
Establishment of redox conditions during planetary collisions as an origin of chondrites
p 1192 N95-19331
Phase stability and elastic properties of C15 compounds HfV2 + Nb
[DE95-000940] p 981 N95-19611
PHASE SHIFT
An analysis of noise reduction in variable reluctance motors using pulse position randomization
[AD-A283846] p 1123 N95-18673
Fracture toughness of polymer/polymer bimaterial interface reinforced with block copolymers
p 986 N95-18923
Propagation of intense, ultrashort laser pulses through metal vapor: Refractive intensity limits and spectral effects
[DE94-016365] p 1039 N95-19398
PHASE TRANSFORMATIONS
Phase transformations and phase relations in Ti(50)Pd(50-x)TM(x) alloys
[DE94-018999] p 977 N95-17962
Evidence for coexistence of two phases in relativistic heavy ion collisions and comparison with lattice results
[DE94-626672] p 1130 N95-18329
Implications of a phase-transition thermostat for chondrule melting p 1189 N95-19312
Microstructure and crystal defects in perovskite crystals with A-site cation ordering
[AD-A284261] p 1153 N95-19713
PHASED ARRAYS
A new piston control strategy for segmented mirrors
p 1115 N95-18999
Phase and amplitude controlled micropatch antenna
[AD-A284191] p 1002 N95-19103
Analysis and synthesis of (SAR) waveguide phased array antennas
[AD-A285336] p 1004 N95-19535
Inband radar cross section of phased arrays with parallel feeds
[AD-A284249] p 1005 N95-19730
Barium strontium titanate and non-ferroelectric oxide ceramic composites for use in phased array antennas
[AD-A279225] p 972 N95-19851
PHENOLIC RESINS
Nozzle Initiative Industry Advisory Committee on Standardization of Carbon-Phenolic Test Methods and Specifications
[NASA-CR-197529] p 967 N95-19566
PHENOMENOLOGY
Advanced concepts theory
[AD-A279212] p 1147 N95-19844
PHONONS
Physics with isotopically controlled semiconductors
[DE95-000789] p 1152 N95-19615
Wentzel-Bardeen singularity in coupled Luttinger liquids: Transport properties
[DE95-000856] p 1152 N95-19621
PHOSPHATES
Polyurethane self-priming topcoats
[AD-D016234] p 985 N95-18631
PHOSPHORUS
An atomic-resolution study of overlayer formation and interfacial mixing in the interaction of phosphorus with Si(001)
[AD-A280159] p 976 N95-19825
Gettering in multicrystalline silicon: A design-of-experiments approach
[DE94-014289] p 1055 N95-19873
PHOTOCATHODES
Nonlinear response of the photocathode of an x-ray streak camera to UV light
[DE94-018073] p 1032 N95-18130
PHOTOCHEMICAL REACTIONS
Dependencies and sensitivity of tropospheric oxidants to precursor concentrations over the northeast United States: A model study
[PB94-192770] p 1056 N95-17937
Electrochemical and spectroscopy studies of selected inorganic and organic systems in molten halides
[AD-A284171] p 974 N95-18514
Investigation of atmospheric waves on Neptune
[NASA-CR-197537] p 1194 N95-18579
Photobiology in medicine
[AD-A284843] p 1087 N95-19695
Excited state processes in transition metal complexes. Redox splitting in soluble polymers
[DE95-002690] p 977 N95-19839
PHOTOCHROMISM
Conference on Aerospace Transparent Materials and Enclosures, volume 1
[AD-A283925] p 944 N95-18677
PHOTOCONDUCTIVITY
Silicon carbide photoconductive switches
[AD-A284310] p 1008 N95-18378
Microscopic origins of metastable effects in a-Si:H and deep defect characterization in a-Si,Ge:H alloys
[DE94-011887] p 1151 N95-19541
PHOTODISSOCIATION
Pure-rotational emission from molecular hydrogen in OMC-1 p 1179 N95-18500
A photoionization study of OH and OD from 680A to 950A: An analysis of the Rydberg series
[NASA-CR-196970] p 974 N95-18744
Development of laser-ion beam photodissociation methods
[DE95-002800] p 977 N95-19840
PHOTOELECTRIC EFFECT
Nonlinear response of the photocathode of an x-ray streak camera to UV light
[DE94-018073] p 1032 N95-18130
PHOTOGEOLOGY
Topography from shading and stereo
[NASA-CR-189389] p 1173 N95-18051
PHOTOGRAMMETRY
Modular implementation of feature extraction and matching algorithms for photogrammetric stereo imagery
[AD-A285422] p 1032 N95-18065
Application of photogrammetry of F-14D store separation
[AD-A284154] p 943 N95-18417
NAWCAD photogrammetrics: Methods and applications for aviation test and evaluation
[AD-A284074] p 1034 N95-19071
PHOTOGRAPHIC MEASUREMENT
The photographic system global evaluation for generation of INPE TM Landsat image
[INPE-5571-TDI/542] p 1050 N95-18369
PHOTOGRAPHIC PROCESSING
The photographic system global evaluation for generation of INPE TM Landsat image
[INPE-5571-TDI/542] p 1050 N95-18369
PHOTOGRAPHIC RECORDING
Debris/ice/TPS assessment and integrated photographic analysis of Shuttle mission STS-66
[NASA-TM-110141] p 963 N95-19790
PHOTOINTERPRETATION
Debris/ice/TPS assessment and integrated photographic analysis of Shuttle mission STS-68
[NASA-TM-109207] p 963 N95-18047
PHOTOIONIZATION
Ion-molecule collisions, electron molecule collisions, excitation and ionization of atoms
[AD-A284584] p 1129 N95-18062
Ionization of atoms by high energy photons
[DE94-018356] p 1130 N95-18427
An optical study of compact steep spectrum radio sources p 1179 N95-18498
A photoionization study of OH and OD from 680A to 950A: An analysis of the Rydberg series
[NASA-CR-196970] p 974 N95-18744
PHOTOLITHOGRAPHY
MANN: A program to transfer designs for diffractive optical elements to a MANN photolithographic mask generator p 1142 N95-18995
A simple single-photomask process for fabrication of high-efficiency multicrystalline silicon solar cells
[DE94-014251] p 1055 N95-19859
PHOTOLUMINESCENCE
Minority-carrier lifetime in InP as a function of light bias
[NASA-TM-106821] p 1149 N95-18453
Deep levels in AgGaSe2
[DE94-018209] p 1152 N95-19585
PHOTOLYSIS
Laboratory studies of stratospheric bromine chemistry: Kinetics of the reactions of bromine monoxide with nitrogen dioxide and atomic oxygen p 1065 N95-18731
Reaction channel competition in vibrational overtone activation: 1-methylcyclopropene
[AD-A280185] p 976 N95-19830
PHOTOMAPPING
Topography from shading and stereo
[NASA-CR-189389] p 1173 N95-18051
PHOTOMASKS
A simple single-photomask process for fabrication of high-efficiency multicrystalline silicon solar cells
[DE94-014251] p 1055 N95-19859
PHOTOMETERS
Infrared-to-visible converter
[AD-D016443] p 1141 N95-18529

PHOTON BEAMS
Algorithms for orbit control on SPEAR
[DE95-002868] p 1138 N95-19841
PHOTONICS
Second International Semiconductor Device Research Symposium (ISDRS-1993)
[AD-A279221] p 1013 N95-19849
PHOTONS
Ionization of atoms by high energy photons
[DE94-018356] p 1130 N95-18427
An investigation of nonuniform dose deposition from an electron beam
[AD-A284175] p 1131 N95-18519
Decaying neutrinos in galaxy clusters
[NASA-CR-197615] p 1198 N95-18747
Non localizability of the photon keystone to a remodelling of physics
[PB94-217213] p 1134 N95-19376
Physics at the Fermilab Tevatron Proton-Antiproton Collider
[DE95-000648] p 1137 N95-19561
Spectral distribution of the two-photon decay of He-like krypton
[DE95-001442] p 1135 N95-19787
Studies of prompt photon production and multijet production at the Tevatron Collider
[DE95-002216] p 1135 N95-19835
PHOTOPRODUCTION
Studies of prompt photon production and multijet production at the Tevatron Collider
[DE95-002216] p 1135 N95-19835
PHOTOSPHERE
Dynamic evolution of emerging magnetic flux tubes in the solar convective envelope p 1195 N95-18497
PHOTOSYNTHESIS
Physiological and genetic characterization of plant growth and gravitropism in LED light sources
p 1077 N95-18173
PHOTOTHERMAL CONVERSION
Thermophotovoltaics bibliography
[DE94-011898] p 1052 N95-17945
PHOTOVOLTAGES
Silicon carbide photoconductive switches
[AD-A284310] p 1008 N95-18378
PHOTOVOLTAIC CELLS
Thermophotovoltaics bibliography
[DE94-011898] p 1052 N95-17945
Pulsed laser illumination of photovoltaic cells
[NASA-TM-106820] p 1053 N95-18572
PHOTOVOLTAIC CONVERSION
Thermophotovoltaics bibliography
[DE94-011898] p 1052 N95-17945
Intermediate design and analysis of the PANSAT electrical power subsystem
[AD-A283610] p 1053 N95-18435
Pulsed laser illumination of photovoltaic cells
[NASA-TM-106820] p 1053 N95-18572
Tapping into the Sun: Today's applications of photovoltaic technology
[DE93-000075] p 1054 N95-19854
NREL Photovoltaic Program, FY 1993
[DE94-011880] p 1055 N95-19857
PHOTOVOLTAIC EFFECT
InP solar cell development on inexpensive silicon substrates
[AD-A283624] p 1052 N95-18011
Silicon carbide photoconductive switches
[AD-A284310] p 1008 N95-18378
PHYSICAL EXAMINATIONS
The waiver process and disqualifying medical conditions in US Naval aviation personnel p 1081 N95-19416
Fit to fly: Analysis of the aeromedical disposition in aircrewmembers of the Spanish Armed Forces
p 1081 N95-19418
Relevance of laboratory tests in aeromedical decisions p 1082 N95-19420
Centrifuge tests of the medical condition of French fighter pilots p 1082 N95-19424
Think health not disease p 1083 N95-19429
Neurological decision making in aviation medicine based on electrophysiological methods p 1084 N95-19431
PHYSICAL EXERCISE
Effects of weight lifting on intrathoracic pressures generated by anti-g straining maneuvers
[AD-A283651] p 1078 N95-18138
PHYSICAL FITNESS
Effects of weight lifting on intrathoracic pressures generated by anti-g straining maneuvers
[AD-A283651] p 1078 N95-18138
PHYSICAL PROPERTIES
The physics of intact capture p 1122 N95-19195
PHYSICS
Non localizability of the photon keystone to a remodelling of physics
[PB94-217213] p 1134 N95-19376
PHYSIOLOGICAL EFFECTS
Effects of weight lifting on intrathoracic pressures generated by anti-g straining maneuvers
[AD-A283651] p 1078 N95-18138
Physiological and genetic characterization of plant growth and gravitropism in LED light sources
p 1077 N95-18173
Mechanisms of interaction and biological effects of extremely-low-frequency electromagnetic fields
[DE94-015200] p 1076 N95-18371
Drink composition and cycle-ergometer endurance in men: Carbohydrate, Na(+), osmolality
[NASA-TM-4650] p 1077 N95-19140
PHYSIOLOGICAL FACTORS
Neuropsychophysiologic sequelae of mild head injury
p 1083 N95-19430
Cumulative effects of repeated brief cerebral ischemia
[AD-A284234] p 1087 N95-19698
Aerospace medicine and biology: A continuing bibliography with indexes (supplement 397)
[NASA-SP-7011(397)] p 1087 N95-19746
PHYSIOLOGICAL RESPONSES
US experiments flown on the Soviet biosatellite Cosmos 2044. Volume 1: Mission description, experiments K-7-01 - K-7-15
[NASA-TM-108802-VOL-1] p 1092 N95-18569
PHYSIOLOGICAL TESTS
Effects of weight lifting on intrathoracic pressures generated by anti-g straining maneuvers
[AD-A283651] p 1078 N95-18138
Effect of heat acclimation on sitting orthostatic tolerance in the heat after 48 and 96 hour bed rest in men
[NASA-TM-108861] p 1077 N95-18734
Drink composition and cycle-ergometer endurance in men: Carbohydrate, Na(+), osmolality
[NASA-TM-4650] p 1077 N95-19140
EKG in flight: Usefulness and limits for aircrew rehabilitation p 1082 N95-19422
PHYSIOLOGY
Changes in the flux of carbon between plants and soil microorganisms at elevated CO2: Physiological processes with ecosystem-level implications
[DE94-017067] p 1060 N95-19112
TSH determination in subjects with medium-low levels of serum thyroxine p 1082 N95-19421
PICOSECOND PULSES
Retinal injuries from single and multiple picosecond laser pulses
[AD-A284173] p 1078 N95-18515
PIEZOELECTRICITY
Damage monitoring in metallic and composite structures using piezoelectric thin film sensors
[ARL-RR-4] p 971 N95-19467
Piezoelectric effects in double barrier resonant tunneling structures
[DE95-000850] p 1152 N95-19620
PIGMENTS
Polyurethane self-priming topcoats
[AD-D016234] p 985 N95-18631
PILOT PERFORMANCE
V-22 simulator evaluation for shipboard operations
[AD-A284156] p 943 N95-18505
Age 60 study. Part 3: Consolidated database experiments
[AD-A286247] p 1080 N95-19384
Age 60 study. Part 4: Experimental evaluation of pilot performance
[AD-A286248] p 1080 N95-19385
The NAMI syncope test battery and clinical decision-making in aviators with syncope
p 1083 N95-19428
PILOT SELECTION
Computer-based psychomotor tests in optimal training track assignment of student naval aviators
[AD-A283720] p 1089 N95-18414
PILOT TRAINING
Computer-based psychomotor tests in optimal training track assignment of student naval aviators
[AD-A283720] p 1089 N95-18414
V-22 simulator evaluation for shipboard operations
[AD-A284156] p 943 N95-18505
F/A-18 simulation validation and verification: Making a good product even better
[AD-A283995] p 944 N95-18723
Helicopter in-flight simulation development and use in test pilot training
[AD-A283998] p 959 N95-18725
Vestibular examination in pilots susceptible to motion sickness p 1083 N95-19427
Programmable cockpit research simulator
[AD-A279219] p 960 N95-19848
PILOTLESS AIRCRAFT
Unmanned aerial vehicle heavy fuel engine test
[AD-A284332] p 947 N95-18383
Environmental effects on composite airframes: A study conducted for the ARM UAV Program (Atmospheric Radiation Measurement Unmanned Aerospace Vehicle)
[DE94-015351] p 971 N95-19579
Automation of hardware-in-the-loop testing of control systems for unmanned air vehicles
[AD-A284833] p 945 N95-19693
PILOTS
Centrifuge tests of the medical condition of French fighter pilots p 1082 N95-19424
The aeromedical risk associated with asymptomatic cholelithiasis in USAF pilots and navigators
p 1085 N95-19439
PILOTS (PERSONNEL)
An analysis of tower (local) controller-pilot voice communications
[AD-A283718] p 996 N95-18436
The way to waivers in the BAF p 1081 N95-19415
PIONS
Pion observables and QCD
[DE94-018357] p 1130 N95-18428
PIPELINES
Investigation of mechanical erosion in fuel pipelines
p 952 N95-19667
PIPELINING (COMPUTERS)
Pre-processing in SADE: Stage 3
[PB94-201571] p 1093 N95-17935
PIPES (TUBES)
Optimization of layered metal matrix composite cylinders p 970 N95-18920
PITCH (INCLINATION)
Development of a multicomponent force and moment balance for water tunnel applications, volume 2
[NASA-CR-4642-VOL-2] p 1020 N95-18956
PITCHING MOMENTS
Static aerodynamics CFD analysis for 120-mm hypersonic KE projectile design
[ARL-MR-184] p 929 N95-18611
Development of a multicomponent force and moment balance for water tunnel applications, volume 1
[NASA-CR-4642-VOL-1] p 1020 N95-18955
PITOT TUBES
Hypersonic flow-field measurements: Intrusive and nonintrusive
[AD-A283867] p 930 N95-18674
PITTING
Pitting corrosion of aluminized seals in molten carbonate fuel cells
[DE94-017075] p 1053 N95-19116
Detecting gear tooth fracture in a high contact ratio face gear mesh
[NASA-TM-106822] p 1042 N95-19125
PIXELS
A technique for determining cloud free versus cloud contaminated pixels in satellite imagery
p 1052 N95-19016
A novel technique for 4-dimensional atmospheric and oceanographic irradiance measurements using 3-D spatial filtering
[AD-A285658] p 1073 N95-19701
PLANAR STRUCTURES
Development of high reliability planar chip inductors
[DE94-018589] p 1012 N95-19231
PLANE WAVES
Method of moments analysis of artificial media composed of dielectric wire objects
[AD-A283318] p 994 N95-18024
Computer simulation of wave propagation through turbulent media
[AD-A283695] p 1000 N95-18671
Shock pulse generation using explosive driven metal drivers: Practical considerations
[MRL-TR-93-3] p 1046 N95-19504
Simulation of wave propagation in three-dimensional random media
[NASA-CR-197605] p 1004 N95-19547
A 2D depth migration in transversely isotropic media using explicit operators
[DE95-000645] p 1066 N95-19560
PLANETARY COMPOSITION
Scientific objectives of the primitive body sample return missions: An approach from the light-induced effect on water vapor p 961 N95-19191
PLANETARY EVOLUTION
An integrated strategy for the planetary sciences: 1995 - 2010
[NASA-CR-197145] p 1194 N95-19134
On the possibility of precipitation-induced vertical lightning in the protoplanetary nebula
p 1187 N95-19299
Chondrules and their associates in ordinary chondrites
p 1188 N95-19306
Collision of cometlike and slightly differentiated bodies as an origin for ordinary chondrites
p 1188 N95-19308

PLANETARY MAGNETIC FIELDS
Modeling the diurnally precessing Jovian magnetospheric field
[AD-A284857] p 1195 N95-19739
PLANETARY MAGNETOSPHERES
Modeling the diurnally precessing Jovian magnetospheric field
[AD-A284857] p 1195 N95-19739
PLANETARY MAPPING
Topography from shading and stereo
[NASA-CR-189389] p 1173 N95-18051
PLANETARY NEBULAE
Papers presented to the Conference on Chondrules and the Protoplanetary Disk
[NASA-CR-197121] p 1186 N95-19289
Large-scale processes in the solar nebula p 1186 N95-19292
Heating and cooling in the solar nebula: Constraints from refractory inclusions p 1187 N95-19297
Formation of chondrules by electrical discharge heating p 1189 N95-19313
Siderophile elements and metal-silicate fractionation in the solar nebula p 1190 N95-19319
Formation of chondrules and CAIs by nebular processes p 1190 N95-19321
The circumplanetary nebular environment: A possible source region for chondrules p 1191 N95-19325
Heating during solar nebula formation and Mg isotopic fractionation in precursor grains of CAIs and chondrules p 1191 N95-19326
Variations among chondrite groups: Constraints on nebular processes p 1192 N95-19327
The fine nebula dust component: A key to chondrule formation by lightning p 1192 N95-19333
Major unresolved issues in the formation of chondrules and CAIs p 1193 N95-19336
PLANNING
Evaluating the trade-offs in partial-order planning algorithms
[AD-A285876] p 1115 N95-19599
Multi-method planning
[AD-A285878] p 1115 N95-19601
Generating parallel execution plans with a partial order planner
[AD-A285888] p 1111 N95-19605
PLANTS (BOTANY)
Physiological and genetic characterization of plant growth and gravitropism in LED light sources p 1077 N95-18173
PLASMA ARC WELDING
A study of gas flow pattern, undercutting and torch modification in variable polarity plasma arc welding
[NASA-CR-196537] p 1040 N95-18056
PLASMA CONTROL
Erosion of melt layers developed during a plasma disruption
[DE94-018362] p 1144 N95-18547
Establishment of an Institute for Fusion Studies
[DE94-017330] p 1145 N95-19079
Impurity behavior during ion-Bernstein wave heating in PBX-M
[DE94-018114] p 1133 N95-19228
Development of lithium beam emission spectroscopy as an edge fluctuation diagnostic for D3-D
[DE94-017517] p 1146 N95-19378
Novel x ray imaging methods at the Nova Laser Facility
[DE94-016548] p 1146 N95-19509
PLASMA CURRENTS
Modeling the diurnally precessing Jovian magnetospheric field
[AD-A284857] p 1195 N95-19739
PLASMA DENSITY
The experimental investigation of plasma configuration in MM-4U device
[DE94-626964] p 1144 N95-18885
Theoretical investigation of matching between plasma heating and fueling in HL-1M machine
[DE94-627019] p 1146 N95-19241
Development of lithium beam emission spectroscopy as an edge fluctuation diagnostic for D3-D
[DE94-017517] p 1146 N95-19378
Novel x ray imaging methods at the Nova Laser Facility
[DE94-016548] p 1146 N95-19509
PLASMA DIAGNOSTICS
Detection of alpha particles via observation of He II line emission in the lithium pellet cloud during DT operation in TFTR
[DE94-014485] p 1143 N95-17965
Conceptual design for a scintillating-fiber neutron detector for fusion reactor plasma diagnostics
[DE94-014716] p 1143 N95-17969
Progress on the multipulse Thomson scattering diagnostic on D3-D
[DE94-017515] p 1143 N95-18119
Implementation of 40-ps high-speed gated-microchannel-plate based x-ray framing cameras on reentrant SIM's for Nova
[DE94-018597] p 1033 N95-18555
Complete mode-set stability analysis of magnetically insulated ion diode equilibria
[DE94-015275] p 1145 N95-19201
Development of lithium beam emission spectroscopy as an edge fluctuation diagnostic for D3-D
[DE94-017517] p 1146 N95-19378
2-D tomography with bolometry in D3-D
[DE94-017520] p 1146 N95-19379
Novel x ray imaging methods at the Nova Laser Facility
[DE94-016548] p 1146 N95-19509
PLASMA FOCUS
Engineering considerations for the self-energizing magnetoplasmadynamic (MPD) - type fusion plasma thruster
[AD-A283968] p 1144 N95-18888
PLASMA FREQUENCIES
Heliospheric 2-3 kHz radio emissions and their relationship to large Forbush decreases
[U-OF-IOWA-94-19] p 1195 N95-17979
PLASMA GENERATORS
A spectral study of a radio-frequency plasma-generated flux of atomic oxygen
[NASA-TM-4612] p 1032 N95-18194
PLASMA HEATING
Radio wave heating of the lower ionosphere p 1145 N95-18905
Impurity behavior during ion-Bernstein wave heating in PBX-M
[DE94-018114] p 1133 N95-19228
Theoretical investigation of matching between plasma heating and fueling in HL-1M machine
[DE94-627019] p 1146 N95-19241
PLASMA JETS
Progress on the multipulse Thomson scattering diagnostic on D3-D
[DE94-017515] p 1143 N95-18119
PLASMA LAYERS
Study on heat flux of plasma scrape-off layer in HL-1 tokamak
[DE94-627009] p 1144 N95-18887
Cross-tail current, field-aligned current, and B(y)
[NASA-CR-197624] p 1065 N95-19032
PLASMA PHYSICS
Progress on the multipulse Thomson scattering diagnostic on D3-D
[DE94-017515] p 1143 N95-18119
Establishment of an Institute for Fusion Studies
[DE94-017330] p 1145 N95-19079
Generalized relaxation theory and vortices in plasmas
[DE95-002615] p 1147 N95-19837
PLASMA POTENTIALS
The experimental investigation of plasma configuration in MM-4U device
[DE94-626964] p 1144 N95-18885
PLASMA RADIATION
Development of lithium beam emission spectroscopy as an edge fluctuation diagnostic for D3-D
[DE94-017517] p 1146 N95-19378
PLASMA SHEATHS
A three region analysis of a bounded plasma using particle in cell and fluid techniques
[AD-A284826] p 1147 N95-19690
PLASMA SPRAYING
Composite structures having organic matrices and duplex zinc/ceramic fire barriers
[AD-D016232] p 970 N95-18629
PLASMA TEMPERATURE
Determination of the electron density and the electron temperature in a high-pressure microwave discharge p 1145 N95-18906
Theoretical investigation of matching between plasma heating and fueling in HL-1M machine
[DE94-627019] p 1146 N95-19241
PLASMA TORCHES
Plasma heating for containerless and microgravity materials processing
[NASA-CASE-NPO-18819-1-CU] p 991 N95-18326
PLASMA-PARTICLE INTERACTIONS
Three-grid accelerator system for an ion propulsion engine
[NASA-CASE-NPO-18391-2-CU] p 1137 N95-18957
PLASMAS (PHYSICS)
AASERT-93: New high-pressure diagnostic technique
[AD-A284943] p 973 N95-17975
Nonlinear magnetohydrudynamics
[DE94-016223] p 1143 N95-18353
Innovative development and application of models for weakly ionized ionospheric plasmas
[AD-A284583] p 1064 N95-18452
Communication with reentry vehicle through modulated plasma
[AD-D016476] p 997 N95-18462
Particle acceleration and transport in the tail and at the front side of the magnetosphere, task 1 and 2
[NASA-CR-197575] p 1064 N95-18476
Erosion of melt layers developed during a plasma disruption
[DE94-018362] p 1144 N95-18547
The experimental investigation of plasma configuration in MM-4U device
[DE94-626964] p 1144 N95-18885
Simplified ideal MHD normal mode equations for toroidal axisymmetric plasmas
[DE94-627004] p 1144 N95-18886
Study on heat flux of plasma scrape-off layer in HL-1 tokamak
[DE94-627009] p 1144 N95-18887
Engineering considerations for the self-energizing magnetoplasmadynamic (MPD) - type fusion plasma thruster
[AD-A283968] p 1144 N95-18888
Study of alpha physics related to ITER Project
[DE94-017329] p 1133 N95-19078
Drink composition and cycle-ergometer endurance in men: Carbohydrate, Na(+), osmolality
[NASA-TM-4650] p 1077 N95-19140
Plasma produced by impacts of fast dust particles on a thin film p 1181 N95-19177
2-D tomography with bolometry in D3-D
[DE94-017520] p 1146 N95-19379
Novel x ray imaging methods at the Nova Laser Facility
[DE94-016548] p 1146 N95-19509
Inertial confinement fusion
[DE95-000314] p 1147 N95-19552
Properties of Alfven waves with transverse scale on the order of skin-depth
[AD-A285657] p 1147 N95-19700
PLASMASPHERE
New applications of the Phillips Laboratory. Theoretical ionospheric model and studies of neutral density waves
[AD-A284663] p 1066 N95-19105
PLASTIC DEFORMATION
Prediction of fatique crack growth under flight-simulation loading with the modified CORPUS model p 934 N95-19471
Impact loading of compressor stator vanes by hailstone ingestion p 953 N95-19670
Soft body impact on titanium fan blades p 953 N95-19671
PLASTIC PROPERTIES
Deformation of high-temperature superconductors
[DE94-017085] p 1150 N95-19075
PLATE THEORY
Discrete crack growth analysis methodology for through cracks in pressurized fuselage structures p 935 N95-19473
PLATES (STRUCTURAL MEMBERS)
Completed Beltrami-Michell formulation for analyzing radially symmetrical bodies
[NASA-TM-4593] p 1044 N95-18199
The evaluation of transmission efficiency and coupling loss factor of structural junctions
[MRL-TR-93-1] p 1124 N95-19057
Evaluation of powder metallurgy plates made by Sylvania Electric Products, Incorporated
[DE94-017911] p 980 N95-19401
Shock pulse generation using explosive driven metal drivers: Practical considerations
[MRL-TR-93-3] p 1046 N95-19504
PLATES (TECTONICS)
Seafloor positioning across Juan de Fuca ridge
[AD-A285049] p 1075 N95-19563
PLATINUM
Preparation of an electrocatalytic cathode for an aluminum-hydrogen peroxide battery
[AD-D016262] p 1008 N95-18318
Method of forming platinum and platinum silicide Schottky contacts on beta-silicon carbide
[AD-D016221] p 1149 N95-18627
2-D tomography with bolometry in D3-D
[DE94-017520] p 1146 N95-19379
An atomic view of surface diffusion on metal surfaces
[DE94-016150] p 980 N95-19395
Transition metal oxides deposited on rhodium and platinum: Surface chemistry and catalysis
[DE95-000793] p 975 N95-19616
PLENUM CHAMBERS
Unsteady flow testing in a passive low-correction wind tunnel p 960 N95-19272
PLUGS
Disengagable adapter for an optical fiber connection
[AD-D016231] p 1141 N95-18628

Handheld delivery system for modified boron-type fire extinguishment agent
[AD-A283955] p 992 N95-18684

PLUMES
Prediction of buoyant outflow in lakes and fjords with a quasi 3D numerical model
[PB94-206984] p 1051 N95-18372
Impact of dynamic loads on propulsion integration p 1125 N95-19148
Estimating wind tunnel interference due to vectored jet flows p 1023 N95-19265

PLUTONIUM
Isotope separation and advanced manufacturing technology
[DE95-000313] p 1039 N95-19551

PNEUMATICS
Development of pneumatic test techniques for subsonic high-lift and in-ground-effect wind tunnel investigations p 932 N95-19268

POINCARE PROBLEM
Flattening of the resonance spectrum of hadrons from kappa-deformed Poincare algebra
[DE94-626686] p 1156 N95-18352

POINT DEFECTS
Investigation of superlattice disordering and diffusion mechanisms in GaAs
[AD-A284847] p 1153 N95-19697
IR materials producibility
[AD-A284263] p 1142 N95-19732

POINT SOURCES
The origin of the diffuse x-ray background p 1197 N95-18729
Scattering of point source illumination by an arbitrary configuration p 1143 N95-19006

POISSON EQUATION
Searching for stationary stable solutions of Euler's equation
[KNMI-WR-93-01] p 1017 N95-18396

POLARIMETRY
MIKON 94. International Microwave Conference. Invited papers, volume 3
[AD-A284353] p 1008 N95-18338
Radar antenna characterization using polarization measurements
[AD-A284840] p 1005 N95-19694

POLARIZATION
Fundamental advances for characterizing cathodic protection systems
[PB94-180692] p 1122 N95-17983
The left-right forward-backward asymmetry for B quarks at the SLD
[DE94-014508] p 1129 N95-18049
Methods and components for optical contention resolution in high speed networks
[AD-A284674] p 1142 N95-19088

POLARIZATION (CHARGE SEPARATION)
On the possibility of precipitation-induced vertical lightning in the protoplanetary nebula p 1187 N95-19299

POLARIZATION (WAVES)
Radar antenna characterization using polarization measurements
[AD-A284840] p 1005 N95-19694

POLARIZATION CHARACTERISTICS
Radar antenna characterization using polarization measurements
[AD-A284840] p 1005 N95-19694

POLICIES
Library operations policies and procedures. Volume 2: Central Archive for Reusable Defense Software (CARDS)
[AD-A284431] p 1096 N95-18344
Issues in military use of commercial satellites
[AD-A283707] p 964 N95-18362
Norwegian heat pump status and policy review
[PB94-206992] p 992 N95-18667

POLITICS
Design and analysis of dynamic leader election protocols in broadcast networks
[PB94-202728] p 1109 N95-18039

POLLUTION CONTROL
Controlling combustion-source emissions at Air Force sites with a new filter concept, phase 1
[AD-A283674] p 1058 N95-18140
Methane: The other greenhouse gas. Research and policy in the Netherlands
[PB94-207149] p 1058 N95-18375
Economic impact analysis for proposed emission standards and guidelines for municipal waste combustors: A description of the basis for, and impacts of, proposed revisions to air pollutant emission regulations for new and existing municipal waste combustors under Clean Air Act Sections 111(b), 111(d), and 129
[PB94-213543] p 1061 N95-19403
Air pollution mitigation measures for airports and associated activity
[PB94-207610] p 1061 N95-19582

POLYACETYLENE
DC-conductivity and magnetoresistance of inherently conducting polymers. Polyacetylene and poly(3-alkylthiophenes)
[PB94-184587] p 1007 N95-18037

POLYACRYLONITRILE
A model study of the influence of NMHC and NO(x) emissions on rural O3 concentrations in Georgiargia p 1059 N95-18445
Lithium electrode/polyacrylonitrile based polymer electrolyte interface
[AD-A283947] p 986 N95-19064

POLYAMIDE RESINS
Novel polymeric composites through molecular engineering
[AD-A284168] p 985 N95-18513

POLYATOMIC MOLECULES
Electron interactions with non-linear polyatomic molecules and their radicals
[AD-A283952] p 1130 N95-18334
Large amplitude motions, especially isomerization and tunneling in polyatomic molecule spectra: Novel experimental, pattern recognition, and theoretical methods
[AD-A284194] p 985 N95-18636

POLYBUTADIENE
Solid fuel ramjet composition
[AD-D016458] p 990 N95-19090

POLYCRYSTALS
Deformation of nonstoichiometric CuO polycrystals
[DE94-016907] p 1150 N95-19094
Ion mixing in oxide-sapphire systems
[DE94-018660] p 1133 N95-19232
Correlation of polycrystalline Cu(In,Ga)Se2 device efficiency with homojunction depthand interfacial structure: X-ray photoemission and positron annihilation spectroscopic characterization
[DE94-013543] p 1055 N95-19858

POLYETHYLENES
Fabrication of biomimetic molecular level composites
[AD-A284204] p 969 N95-17941
Obtention of cationic polymeric membranes by radiation-induced grafting method
[DE94-629193] p 983 N95-17942

POLYIMIDES
Thermo-oxidative stability of graphite/PMR-15 composites: Effect of fiber surface modification on composite shear properties
[NASA-TM-4608] p 981 N95-19652

POLYMER CHEMISTRY
Difunctional monomers based on perfluoropropylene telomers
[AD-A283677] p 983 N95-18019
Ion exchange polymers and method for making
[NASA-CASE-LEW-15576-1] p 984 N95-18321
Workshop on Synthesis of Macromolecules with Precisely Controlled Structure for New Materials
[AD-A285321] p 987 N95-19520

POLYMER MATRIX COMPOSITES
An NDE approach for characterizing quality problems in polymer matrix composites
[NASA-TM-106807] p 1043 N95-18583
Polymer based materials for additive processing of high temperature electronics packaging
[AD-A285962] p 988 N95-19745

POLYMERIC FILMS
Ion exchange polymers and method for making
[NASA-CASE-LEW-15576-1] p 984 N95-18321

POLYMERIZATION
Method of lowering the reaction exotherm in thermally polymerized acetylene terminated resins
[AD-D016276] p 985 N95-18430

POLYMERS
International Conference on Deformation, Yield and Fracture of Polymers
[AD-A284354] p 984 N95-18339
Polymer-based separations: Synthesis and application of polymers for ionic and molecular recognition
[DE94-016427] p 984 N95-18355
Elemental fluorine based syntheses of pentafluoro phenly and other aromatic perfluoropolyether polymers
[AD-A284102] p 984 N95-18402
Complex oxidation effects in polymer degradation
[DE94-018903] p 986 N95-18651
Thermal relaxation processes and stability in poled electro-optic polymers
[AD-A283948] p 987 N95-19102
Novel e-o polymers: NLO materials with superior temporal stability
[AD-A285872] p 988 N95-19614

POLYNOMIALS
Plane Jacobian conjecture
[PB94-192341] p 1118 N95-19198

POLYSTYRENE
Macromolecular characterization and solution behavior of polymer additives
[AD-A284845] p 988 N95-19696

POLYURETHANE RESINS
Polyurethane self-priming topcoats
[AD-D016264] p 984 N95-18320
Polyurethane self-priming topcoats
[AD-D016420] p 984 N95-18336
Polyurethane self-priming topcoats
[AD-D016234] p 985 N95-18631

POLYVINYL FLUORIDE
PVDF flux/mass/velocity/trajectory systems and their applications in space p 966 N95-19196

POMERONS
Higher-order Lipatov kernels and the QCD Pomeron
[DE94-018395] p 1131 N95-18551

PONDS
Systems and economic analysis of microalgae ponds for conversion of CO2 to biomass
[DE95-000406] p 1054 N95-19554

POPULATIONS
Catalog of environmental data sets of Europe at the RIVM
[PB94-202710] p 1057 N95-18002
A GIS approach to urban heat island research: The case of Huntsville, Alabama p 1063 N95-18991

POROSITY
Microstructural analysis of cracks generated during welding of 2195 aluminum-lithium alloy p 982 N95-19007
Embedded microclusters in zeolites and cluster beam sputtering: Simulation on parallel computers
[DE95-000662] p 1134 N95-19562

POROUS MATERIALS
Coupled finite element analysis of decomposing poroelastic polymeric composites and structures with subsequent thermal and gas diffusion p 986 N95-18918
Aryl gels and related materials. Synthesis and characterization of a new class of microporous materials
[AD-A285044] p 987 N95-19544

POROUS PLATES
The stability of two-phase flow over a swept-wing
[NASA-CR-194994] p 1016 N95-18190

POROUS WALLS
Determination of solid/porous wall boundary conditions from wind tunnel data for computational fluid dynamics codes p 1023 N95-19266
Calculation of wall effects of flow on a perforated wall with a code of surface singularities p 1025 N95-19277

PORTABLE EQUIPMENT
Handheld delivery system for modified boron-type fire extinguishment agent
[AD-A283955] p 992 N95-18684
Digital audio broadcasting: Comparison of coverage at different frequencies and with different bandwidths
[BBC-RD-1993/11] p 1002 N95-19135
XAMath: An XAFS analysis package based on Mathematica(tm)
[DE94-016346] p 1100 N95-19397

POSITION (LOCATION)
Space Station racks weight and CG measurement using the rack insertion end-effector p 966 N95-18168
BEAM: A finite element program for the collapse analysis of vehicle structures
[AD-A285547] p 1045 N95-18472
Detection performance of generalized likelihood ratio processors for random signals of unknown location, structure, extent, and strength
[AD-A285589] p 997 N95-18475
On the geometry of visual correspondence
[AD-A285700] p 1140 N95-18478
Representing visibility for siting problems
[AD-A284076] p 993 N95-19036
Non localizability of the photon keystone to a remodelling of physics
[PB94-217213] p 1134 N95-19376

POSITION ERRORS
Multipath-induced, low-angle tracking error at 140 GHz
[AD-A283630] p 995 N95-18136

POSITIONING
Rack Insertion End Effector (RIEE) guidance p 1043 N95-18178

POSITRON ANNIHILATION
Study of the effect of ionizing radiation on the structure of natural rubber latex by positron annihilation technique
[DE94-631466] p 975 N95-19550

POSITRONIUM
Study of the effect of ionizing radiation on the structure of natural rubber latex by positron annihilation technique
[DE94-631466] p 975 N95-19550

POSITRONS
Electronics for the Si detectors in APEX
[DE94-015078] p 1007 N95-17961

POSTFLIGHT ANALYSIS
US experiments flown on the Soviet biosatellite Cosmos 2044. Volume 1: Mission description, experiments K-7-01 - K-7-15
[NASA-TM-108802-VOL-1] p 1092 N95-18569
Final results of the Advanced Photovoltaic Experiment flight test
[NASA-TM-106828] p 967 N95-18571
STS-65 Space Shuttle mission report
[NASA-CR-197598] p 963 N95-18610
Debris/ice/TPS assessment and integrated photographic analysis of Shuttle mission STS-66
[NASA-TM-110141] p 963 N95-19790
POSTLAUNCH REPORTS
STS-65 Space Shuttle mission report
[NASA-CR-197598] p 963 N95-18610
POSTMISSION ANALYSIS (SPACECRAFT)
STS-65 Space Shuttle mission report
[NASA-CR-197598] p 963 N95-18610
POTABLE WATER
Evaluation of Pureau water for use as emergency drinking water for ADF aircraft
[MRL-TN-648] p 1092 N95-19502
POTASSIUM
DC-conductivity and magnetoresistance of inherently conducting polymers. Polyacetylene and poly(3-alkylthiophenes)
[PB94-184587] p 1007 N95-18037
POTASSIUM HYDROXIDES
Investigation of new hypergol scrubber technology p 977 N95-18175
POTASSIUM NITRATES
Investigation of new hypergol scrubber technology p 977 N95-18175
POTENTIAL FIELDS
Potential distributions for ellipsoidal bodies in uniform fields
[MRL-TR-92-48] p 1005 N95-19771
POTENTIAL FLOW
Solution of full potential equation on an airfoil by multigrid technique
[NAL-TM-CSS-9303] p 930 N95-18904
CFD: Advances and Applications, part 1
[NAL-SP-9322-PT-1] p 1026 N95-19444
Computation of inviscid flows: Full potential method p 1027 N95-19447
Viscous flow past aerofoils axisymmetric bodies and wings p 933 N95-19457
Solution of potential flow problems on a network of workstations
[DE94-017861] p 1112 N95-19831
POWDER (PARTICLES)
Recent progress on ECVD Project
[DE94-016773] p 988 N95-19580
POWDER METALLURGY
Nanostructured bearing alloy studies
[AD-A283328] p 978 N95-18027
Evaluation of powder metallurgy plates made by Sylvania Electric Products, Incorporated
[DE94-017911] p 980 N95-19401
POWER CONDITIONING
Intermediate design and analysis of the PANSAT electrical power subsystem
[AD-A283610] p 1053 N95-18435
Strategic avionics technology definition studies. Subtask 3-1A3: Electrical Actuation (ELA) Systems Test Facility
[NASA-CR-188360] p 956 N95-18567
POWER EFFICIENCY
Performance improvements in diode laser arrays
[DE94-016547] p 1039 N95-19508
POWER SPECTRA
Second-order reconstruction of the inflationary potential
[NASA-CR-197629] p 1121 N95-19030
Optimizing the Zeldovich approximation
[NASA-CR-197606] p 1156 N95-19037
Prediction of fluctuating pressure and power spectra in attached and separated compressible flow p 1031 N95-19153
Application of the PSD technique to acoustic fatigue stress calculations in complex substructures p 1126 N95-19155
Testing higher-order Lagrangian perturbation theory against numerical simulation. 1: Pancake models
[NASA-CR-197611] p 1121 N95-19348
A test of the adhesion approximation for gravitational clustering
[NASA-CR-197610] p 1157 N95-19358
POWER SUPPLY CIRCUITS
Intermediate design and analysis of the PANSAT electrical power subsystem
[AD-A283610] p 1053 N95-18435
Development of an expert system for power quality advisement using CLIPS 6.0 p 1014 N95-19634
Development of an amorphous surge blocker for a high voltage acceleration power supply of the neutral beam injectors
[DE94-770648] p 1138 N95-19874
PRE-MAIN SEQUENCE STARS
The early Sun and the formation of chondrules p 1188 N95-19305
PREAMPLIFIERS
Inter-amplifier pupil relay systems for a high average power dye laser at Lawrence Livermore National Laboratory
[DE94-016544] p 1039 N95-19507
PRECESSION
Modeling the diurnally precessing Jovian magnetospheric field
[AD-A284857] p 1195 N95-19739
PRECIPITATES
Nonstoichiometry of Al-Zr intermetallic phases
[DE94-016877] p 979 N95-19093
PRECIPITATION (METEOROLOGY)
Observational studies and modelling of interception loss of gross rainfall in the Amazonian rainforest
[INPE-5583-TDI/545] p 1067 N95-18006
Marginal probabilities of the extremes of ENSO events for temperature and precipitation in the southeastern United States
[AD-A284716] p 1068 N95-18076
PRECIPITATION HARDENING
Characterization of the deformation and annealing of 304L stainless steel
[DE94-018584] p 981 N95-19707
PRECIPITATION PARTICLE MEASUREMENT
Inter-comparison of automatic rain gauges p 1069 N95-18204
A comparison of optical rain gauge and radar data from TOGA/COARE p 1069 N95-18207
PREDICTION ANALYSIS TECHNIQUES
Microstructure-based fatigue life prediction methods for naval steel structures
[AD-A284735] p 1044 N95-18081
Implementation of the 1992 Terminal area-Local Analysis and Prediction System (T-LAPS)
[AD-A284334] p 1070 N95-18384
Incorporating uncertainty and risk in rainfall-based flood estimates
[RR-CE144] p 1071 N95-18607
Forced response of mistuned bladed disks p 950 N95-19383
PREDICTIONS
Design concepts for an integrated environmental medicine workstation for prediction, simulation and training
[AD-A283686] p 1079 N95-18618
Fundamental studies of passivity and passivity breakdown
[DE94-016954] p 987 N95-19095
Predicting and explaining the movement of mesoscale oceanographic features using CLIPS p 1105 N95-19752
PRS projections for DECADE
[AD-A279215] p 1147 N95-19847
PREFORMS
Unit cell geometry of multiaxial preforms for structural composites
[NASA-CR-197294] p 971 N95-19650
PREGNANCY
Expert Witness: A system for developing expert medical testimony p 1101 N95-19628
PREMIXED FLAMES
Studies on high pressure and unsteady flame phenomena
[AD-A284126] p 973 N95-18410
PREPROCESSING
Pre-processing in SADE: Stage 3
[PB94-201571] p 1093 N95-17935
PRESSURE CHAMBERS
Fixture for pressure testing sight glasses
[AD-D016263] p 1032 N95-18319
PRESSURE DISTRIBUTION
Measurement of gust response on a turbine cascade
[NASA-TM-106776] p 928 N95-18457
Aeromechanics technology, volume 1. Task 1: Three-dimensional Euler/Navier-Stokes Aerodynamic Method (TEAM) enhancements
[AD-A285713] p 943 N95-18483
Study of the kinematic and load sharing properties of wormgearing with non-symmetric tooth profiles
[NASA-CR-195414] p 1041 N95-18541
2-D and 3-D oscillating wing aerodynamics for a range of angles of attack including stall
[NASA-TM-4632] p 931 N95-19119
Analysis of test section sidewall effects on a two dimensional airfoil: Experimental and numerical investigations p 1025 N95-19276
PRESSURE EFFECTS
Acoustic properties and durability of liner materials at non-standard atmospheric conditions
[NASA-CR-195010] p 1123 N95-18930
Pressure based finite volume algorithm for viscous flow computation p 1029 N95-19461
PRESSURE GAGES
Advanced packaging and integration technologies for microsensors, phase 1
[AD-A283613] p 1040 N95-18010
PRESSURE GRADIENTS
Effect of crossflow on Goertler instability in incompressible boundary layers
[NASA-CR-195007] p 1016 N95-18193
PRESSURE MEASUREMENT
Outgassing of solid material into vacuum thermal insulation spaces p 972 N95-18184
Fiber optic pressure and/or vibration detector
[AD-D016474] p 1140 N95-18460
Thermocouples for interior ballistic temperature measurements
[AD-A283699] p 1033 N95-18620
Calibration and use of a non-nulling seven-hole pressure probe p 1021 N95-19254
Applications of the five-hole probe technique for flow field surveys at the Institute for Aerospace Research p 1021 N95-19255
Calculation of low speed wind tunnel wall interference from static pressure pipe measurements p 1024 N95-19273
Optical surface pressure measurements: Accuracy and application field evaluation p 1025 N95-19274
Multiport pressure measurements on continuously moving wind tunnel models
[ARA-MEMO-391] p 932 N95-19772
PRESSURE OSCILLATIONS
Method and system for identifying the onset of a turbulent boundary layer induced by a body moving through a fluid medium
[AD-D016434] p 1018 N95-18525
A preliminary analysis of low frequency pressure oscillations in hybrid rocket motors p 968 N95-18987
Prediction of fluctuating pressure and power spectra in attached and separated compressible flow p 1031 N95-19153
PRESSURE REDUCTION
Erosion of T56 5th stage rotor blades due to bleed hole overtip flow p 952 N95-19666
PRESSURE SENSORS
Overview of unsteady transonic wind tunnel test on a semispan straked delta wing oscillating in pitch
[AD-A284097] p 928 N95-18380
Calibration and use of a non-nulling seven-hole pressure probe p 1021 N95-19254
Applications of the five-hole probe technique for flow field surveys at the Institute for Aerospace Research p 1021 N95-19255
Optical surface pressure measurements: Accuracy and application field evaluation p 1025 N95-19274
Multiport pressure measurements on continuously moving wind tunnel models
[ARA-MEMO-391] p 932 N95-19772
PRESSURE VESSELS
Compression strength of composite primary structural components
[NASA-CR-197554] p 1044 N95-18388
J-integral characterization of the nozzle steels from intermediate test vessels IV-5 and IV-9
[DE95-001066] p 979 N95-18934
PRIMITIVE EARTH ATMOSPHERE
Scientific objectives of the primitive body sample return missions: An approach from the light-induced effect on water vapor p 961 N95-19191
PRINCIPAL COMPONENTS ANALYSIS
Dependence of medium-range forecast error on patterns in the initial state p 1072 N95-18732
PRINTED CIRCUITS
AUTO: Automatic script generation system
[AD-A285897] p 1012 N95-19606
PRISMS
PRISM project optical instrument p 1143 N95-19009
PROBABILITY DENSITY FUNCTIONS
Eigenvalue tests and distributions for small sample order determination for complex Wishart matrices
[AD-A283825] p 1120 N95-18672
PROBABILITY THEORY
A fast recursive algorithm to compute the probability of M-out-of-N events
[AD-A283679] p 1120 N95-18020
Marginal probabilities of the extremes of ENSO events for temperature and precipitation in the southeastern United States
[AD-A284716] p 1068 N95-18076

Lower bounds for identifying subset members with subset queries
[DE94-014296] p 1117 N95-18346
Aircraft wake vortex takeoff tests at O'Hara International Airport
[AD-A283828] p 929 N95-18624
Eigenvalue tests and distributions for small sample order determination for complex Wishart matrices
[AD-A283825] p 1120 N95-18672
An analysis of noise reduction in variable reluctance motors using pulse position randomization
[AD-A283846] p 1123 N95-18673
To the theory of the management of the resonance widths
[DE94-626645] p 1156 N95-18879
The probability of flaw detection and the probability of false calls in nondestructive evaluation equipment
p 1044 N95-19010
Finite Markov chains and random discrete structures
[AD-A284192] p 1121 N95-19104
A probabilistic fatigue analysis of multiple site damage
p 935 N95-19476

PROBES
Subgroup report on hard x-ray microprobes
[DE94-018708] p 1034 N95-19233

PROBLEM SOLVING
Creation of new items and forms for the Project A Assembling Objects test
[AD-A285522] p 1088 N95-18095
Software techniques for balancing computation and communication in parallel systems
[AD-A285536] p 1109 N95-18106
Representing visibility for siting problems
[AD-A284076] p 993 N95-19036
Multi-method planning
[AD-A285878] p 1115 N95-19601
Cooperating agents for information retrieval
[AD-A285887] p 1176 N95-19604
Generating parallel execution plans with a partial order planner
[AD-A285888] p 1111 N95-19605
Knowledge based translation and problem solving in an intelligent individualized instruction system
p 1105 N95-19753
PalymSys (TM): An extended version of CLIPS for construction and reasoning using blackboards
p 1107 N95-19767

PROCEDURES
NASA property: Poor lending practices and controls at the Jet Propulsion Laboratory. Report to Congressional Requesters
[GAO/NSIAD-94-116] p 1172 N95-19141
The way to waivers in the BAF p 1081 N95-19415
Environmental Compliance Assessment System (ECAS). South Carolina supplement: US Army
[AD-A279244] p 1062 N95-19860

PROCESS CONTROL (INDUSTRY)
Guidelines for reduction of human errors during maintenance of safety systems; maintainability and maintenance support
[PB94-215597] p 1092 N95-19412
QPA-CLIPS: A language and representation for process control p 1102 N95-19635

PROCUREMENT
Library operations policies and procedures. Volume 2: Central Archive for Reusable Defense Software (CARDS)
[AD-A284431] p 1096 N95-18344
Acquisition handbook: Update. Comprehensive Approach to Reusable Defensive Software (CARDS)
[AD-A284342] p 1097 N95-18420

PROCUREMENT MANAGEMENT
AI and workflow automation: The prototype electronic purchase request system p 1101 N95-19632

PROCUREMENT POLICY
Government contractors: Measuring costs of service contractors versus federal employees. Report to the Chairman, Subcommittee on Federal Services, Post Office and Civil Service, Committee on Governmental Affairs, US Senate
[GAO/GGD-94-95] p 1171 N95-18595

PRODUCT DEVELOPMENT
A wideband absorber for television studios
[BBC-RD-1994/12] p 1123 N95-18566
Character selecting advisor for a role-playing game
p 1106 N95-19758

PRODUCTION ENGINEERING
Simulation in manufacturing
[PB94-215563] p 1100 N95-19409

PROFILE METHOD (FORECASTING)
Use of profiler data for analysis and NOWcasting of a winter season extratropical cyclone
[PB94-187804] p 1067 N95-17992

PROGRAM VERIFICATION (COMPUTERS)
Program verification for optimized byte copy
[AD-A283915] p 1099 N95-18676
Representing visibility for siting problems
[AD-A284076] p 993 N95-19036
MIRO: A debugging tool for CLIPS incorporating historical Rete networks p 1105 N95-19754

PROGRAMMING ENVIRONMENTS
Fuzzy expert systems using CLIPS
p 1102 N95-19636
Using PVM to host CLIPS in distributed environments
p 1104 N95-19748
Simulation in a dynamic prototyping environment: Petri nets or rules? p 1106 N95-19756
DAI-CLIPS: Distributed, Asynchronous, Interacting CLIPS p 1107 N95-19763

PROGRAMMING LANGUAGES
A formal method for semantics-based change-merging of software prototypes
[AD-A283668] p 1094 N95-18017
R.MAPCALC: An algebra for GIS and image processing
[AD-A283923] p 1096 N95-18161
Program verification for optimized byte copy
[AD-A283915] p 1099 N95-18676
The design and implementation of EPL: An event pattern language for active databases p 1101 N95-19629
QPA-CLIPS: A language and representation for process control p 1102 N95-19635

PROGRESS
Construction of a connectionist network supercomputer
[AD-A283354] p 1109 N95-18050
Progress in the development of advanced solar reflectors
[DE94-000264] p 1053 N95-18463
Perception of complex auditory patterns
[AD-A284189] p 1079 N95-18626
X-ray laser program
[AD-A279213] p 1039 N95-19845

PROJECT MANAGEMENT
Development of an improved ballistic acceptance test for high hard armor steel plate: MIL-A-46100
[ARL-TR-509] p 979 N95-18939
A systems analysis and project management plan for the Petite Amateur Navy Satellite (PANSAT)
[AD-A285968] p 965 N95-19571

PROJECT PLANNING
Kansas State University DOE/KEURP Site Operator User Task Force
[DE94-014331] p 1040 N95-17995
Draft SEI program plans: 1995-1999
[AD-A285047] p 1100 N95-19545
A systems analysis and project management plan for the Petite Amateur Navy Satellite (PANSAT)
[AD-A285968] p 965 N95-19571

PROJECTILE CRATERING
Penetration experiments in aluminum and Teflon targets of widely variable thickness p 1047 N95-19185

PROJECTILES
Static aerodynamics CFD analysis for 120-mm hypersonic KE projectile design
[ARL-MR-184] p 929 N95-18611
Correlated charge-changing ion-atom collisions
[DE94-017355] p 1132 N95-18874

PROPAGATION MODES
A 2D depth migration in transversely isotropic media using explicit operators
[DE95-000645] p 1066 N95-19560

PROPELLANT COMBUSTION
Computational simulation of liquid fuel rocket injectors
p 968 N95-18989
Mixed high explosives for insensitive booster compositions
[MRL-TR-92-22] p 990 N95-19505

PROPELLANT SENSITIVITY
Mixed high explosives for insensitive booster compositions
[MRL-TR-92-22] p 990 N95-19505

PROPELLANT STORABILITY
Mixed high explosives for insensitive booster compositions
[MRL-TR-92-22] p 990 N95-19505

PROPELLANT TESTS
Airborne rotary separator study
[NASA-CR-191045] p 967 N95-18743
Mixed high explosives for insensitive booster compositions
[MRL-TR-92-22] p 990 N95-19505

PROPELLER BLADES
Ice-impact analysis of blades p 953 N95-19672

PROPELLER FANS
Ice-impact analysis of blades p 953 N95-19672

PROPELLER NOISE
Noise transmission and reduction in turboprop aircraft
p 1127 N95-19164

PROPELLERS
Gyroscopic and propeller aerodynamic effects on engine mounts dynamic loads in turbulence conditions
p 946 N95-18599

PROPORTIONAL CONTROL
Three-parameter tunable Tilt-Integral-Derivative (TID) controller
[NASA-CASE-NPO-18492-1-CU] p 1113 N95-18313

PROPOSALS
Space Station: Plans to expand research community do not match available resources. Report to the Ranking Minority Member, Subcommittee on Oversight of Government Management, Committee on Government Affairs, US Senate
[GAO/NSIAD-95-33] p 965 N95-19131

PROPULSION
Engineering considerations for the self-energizing magnetoplasmadynamic (MPD) - type fusion plasma thruster
[AD-A283968] p 1144 N95-18888
Operating capability and current status of the reactivated NASA Lewis Research Center Hypersonic Tunnel Facility
[NASA-TM-106808] p 960 N95-19286

PROPULSION SYSTEM CONFIGURATIONS
Data driven propulsion system weight prediction model
p 968 N95-18980
Technology Benefit Estimator (T/BEST): User's manual
[NASA-TM-106785] p 1046 N95-19501

PROPULSION SYSTEM PERFORMANCE
Airborne rotary separator study
[NASA-CR-191045] p 967 N95-18743
Data driven propulsion system weight prediction model
p 968 N95-18980
Evaluation of SSME test data reduction methods
p 968 N95-19002

PROPYLENE
Difunctional monomers based on perfluoropropylene telomers
[AD-A283677] p 983 N95-18019

PROTECTION
Fault protection circuit for power switching device
[AD-D016466] p 1009 N95-18455
Power terminal protection device
[AD-D016528] p 1011 N95-19120
Evaluating the trade-offs in partial-order planning algorithms
[AD-A285876] p 1115 N95-19599

PROTECTIVE CLOTHING
A review of footwear for cold/wet scenarios. Part 2: Socks, liners, and insoles
[AD-A279937] p 989 N95-19866

PROTECTIVE COATINGS
Sodium sulfate corrosion of silicon carbide fiber-reinforced calcium aluminosilicate glass-ceramic matrix composites
[AD-A283703] p 969 N95-18021
Evaluation of inorganic zinc-rich primers using Electrochemical Impedance Spectroscopy (EIS) in combination with atmospheric exposure
p 977 N95-18170
Trivalent chromium conversion coatings for aluminum
[AD-D016274] p 978 N95-18332
Polyurethane self-priming topcoats
[AD-D016420] p 984 N95-18336
Reliability Without Hermeticity (RWOH) for Integrated Circuits (IC)
[AD-A284340] p 1009 N95-18418
Composite structures having organic matrices and duplex zinc/ceramic fire barriers
[AD-D016232] p 970 N95-18629
Polyurethane self-priming topcoats
[AD-D016234] p 985 N95-18631
Real-time thickness measurement of MCC ablator material p 972 N95-18981
Quality optimization of thermally sprayed coatings produced by the JP-5000 (HVOF) gun using mathematical modeling p 989 N95-19008
Erosion, Corrosion and Foreign Object Damage Effects in Gas Turbines
[AGARD-CP-558] p 950 N95-19653
Protective coatings for compressor gas path components p 954 N95-19675
New Trends in coatings developments for turbine blades: Materials processing and repair p 954 N95-19676
High velocity oxygen fuel spraying of erosion and wear resistant coatings on jet engine parts
p 954 N95-19680

PROTEIN CRYSTAL GROWTH
STS-68 mission highlights resource tape
[NASA-TM-110049] p 961 N95-18568

PROTEINS
Concentration and temperature effects on ovostatin activity p 1077 N95-18997

Salt-induced aggregation of lysozyme: Implications for crystal growth p 1155 N95-19015

PROTOCOL (COMPUTERS)

Design and analysis of dynamic leader election protocols in broadcast networks
[PB94-202728] p 1109 N95-18039

A scalable decentralized group membership service for an asynchronous environment
[AD-A283633] p 1109 N95-18137

Throughput analysis between high end workstations across an FDDI network
[AD-A283608] p 1110 N95-18615

MSFC institutional area network and ATM technology p 1007 N95-18968

Advanced techniques for analysis and evaluation of robust protocols
[AD-A285682] p 1111 N95-19513

Multicast tree construction in network topologies with asymmetric link loads
[AD-A285679] p 1003 N95-19525

SeaWiFS technical report series. Volume 18: SeaWiFS technical report series cumulative index: Volumes 1-17
[NASA-TM-104566-VOL-18] p 1076 N95-19577

Expert system technologies for Space Shuttle decision support: Two case studies p 1104 N95-19646

PROTON BELTS

CRRESPRO documentation
[AD-A284578] p 1178 N95-18451

PROTONS

CRRESPRO documentation
[AD-A284578] p 1178 N95-18451

Investigation of single events upsets in silicon and GaAs structures using reaction calculations
[AD-A285581] p 1131 N95-18474

Family symmetries and proton decay
[DE94-017575] p 1133 N95-19245

Direct energy conversion system for D(3)-He fusion
[DE94-770773] p 1146 N95-19549

Baryon stopping in 200 GeV/A S+Au collisions
[DE94-018215] p 1134 N95-19587

PROTOPLANETS

On the possibility of precipitation-induced vertical lightning in the protoplanetary nebula p 1187 N95-19299

Chondrules and their associates in ordinary chondrites p 1188 N95-19306

PROTOSTARS

Models for multiple heating mechanisms p 1188 N95-19303

PROTOTYPES

A formal method for semantics-based change-merging of software prototypes
[AD-A283668] p 1094 N95-18017

New technologies for space avionics
[NASA-CR-197574] p 966 N95-18196

Design, validation and prototype testing of a high resolution all-reflection Michelson interferometer for solar occultation measurements of the OI 1304-a triplet emission
[AD-A283705] p 1178 N95-18361

The quiescent and flaring EUV spectrum of Algol and its relationship to other active coronae. EUV spectroscopy of bright hyades coronae: 71 Tauri and Theta 1 Tauri
[NASA-CR-197538] p 1178 N95-18391

Handheld delivery system for modified boron-type fire extinguishment agent
[AD-A283955] p 992 N95-18684

Concept of using a benchmark part to evaluate rapid prototype processes p 994 N95-18975

Simulation in a dynamic prototyping environment: Petri nets or rules? p 1106 N95-19756

PROVING

Library capability demonstration. Central Archive for Reusable Defense Software (CARDS)
[AD-A284574] p 1098 N95-18450

Real-time remote scientific model validation p 1103 N95-19640

PSYCHOLOGICAL EFFECTS

Is the pilot fit for flying after an accident? p 1083 N95-19425

PSYCHOLOGICAL FACTORS

Is the pilot fit for flying after an accident? p 1083 N95-19425

The concept of aeronautical adaptability as developed by the US Navy p 1083 N95-19426

Neuropsychophysiologic sequelae of mild head injury p 1083 N95-19430

PSYCHOLOGICAL TESTS

Computer-based psychomotor tests in optimal training track assignment of student naval aviators
[AD-A283720] p 1089 N95-18414

Comparing performance on implicit memory tests
[AD-A284861] p 1090 N95-19740

PSYCHOLOGY

Facilitation and interference in identification of pictures and words
[AD-A285882] p 1090 N95-19602

PSYCHOMETRICS

Creation of new items and forms for the Project A Assembling Objects test
[AD-A285522] p 1088 N95-18095

PSYCHOMOTOR PERFORMANCE

Computer-based psychomotor tests in optimal training track assignment of student naval aviators
[AD-A283720] p 1089 N95-18414

Age 60 study. Part 4: Experimental evaluation of pilot performance
[AD-A286248] p 1080 N95-19385

PUBLIC HEALTH

Catalog of environmental data sets of Europe at the RIVM
[PB94-202710] p 1057 N95-18002

PULSE CODE MODULATION

Digital circuit for the introduction and later removal of dither from an analog signal
[AD-D016462] p 1011 N95-19171

PULSE COMMUNICATION

The 23 Gigahertz (GHz) digital Low Density Radio Communications Link (LDRCL) Operational Test and Evaluation (OT/E) integration and OT/E operation
[AD-A283963] p 1000 N95-18686

PULSE DURATION

Development of ultrashort optical pulse sources near 1.3 and 1.5 microns with an emphasis on stability, high repetition rate, and parallelism
[AD-A285535] p 1139 N95-18104

Pulsewidth-dependent damage measurements of dielectric materials
[DE94-018594] p 1142 N95-19710

PULSE GENERATORS

Shock pulse generation using explosive driven metal drivers: Practical considerations
[MRL-TR-93-3] p 1046 N95-19504

Sandia National Laboratories' high power electromagnetic impulse sources
[DE95-000423] p 1004 N95-19555

PULSED LASER DEPOSITION

Fabrication of biaxially oriented YBCO on (001) biaxially oriented yttria-stabilized-zirconia on polycrystalline substrates
[DE94-014808] p 1148 N95-18064

PULSED LASERS

Laser wakefield excitation and measurement on a femtosecond time scale: Theory and experiment
[DE94-019198] p 1129 N95-17976

Retinal injuries from single and multiple picosecond laser pulses
[AD-A284173] p 1078 N95-18515

Pulsed laser illumination of photovoltaic cells
[NASA-TM-106820] p 1053 N95-18572

Inertial confinement fusion
[DE95-000314] p 1147 N95-19552

Pulsewidth-dependent damage measurements of dielectric materials
[DE94-018594] p 1142 N95-19710

Damage from pulses with arbitrary temporal shapes
[DE94-018606] p 1039 N95-19722

PULSED RADIATION

Radiation-induced noise in UMPC-type current probes: IEMP response of the current measurement system
[AD-A284176] p 998 N95-18520

PULSES

The US 100 T Magnet Project
[DE94-016099] p 1011 N95-19200

Propagation of intense, ultrashort laser pulses through metal vapor: Refractive intensity limits and spectral effects
[DE94-016365] p 1039 N95-19398

PUMPS

Positive displacement rotary pump
[AD-D016412] p 1041 N95-18335

PURGING

Acceptance/operational test procedure 101-SY tank camera purge system and in tank color camera video imaging system
[DE95-000344] p 1035 N95-19553

PYLONS

The aerodynamic design of an integrated wing lower surface and pylons for reduced drag
[ARA-MEMO-406] p 946 N95-19789

PYROTECHNICS

Applications catalog of pyrotechnically actuated devices/systems
[NASA-TM-106810] p 962 N95-18387

PYROXENES

Crystallization trends of precursor pyroxene in ordinary chondrites: Implications for igneous origin of precursor p 1187 N95-19298

Relict grains in chondrules: Evidence for chondrule recycling p 1188 N95-19307

PYRROLES

Application of conducting polymers to electroanalysis
[DE94-015204] p 984 N95-18348

Q

QUADRATURES

High-order corrected trapezoidal rules for singular functions
[AD-A284269] p 1119 N95-19735

QUALITATIVE ANALYSIS

GAMQUEST, a computer program to identify gamma rays
[DE94-016217] p 1197 N95-18351

Analytical control test plan and microbiological methods for the water recovery test
[NASA-TM-108473] p 1091 N95-19061

QUALITY CONTROL

Requirements analysis for safety-critical systems: A chemical batch processing example
[PB94-201563] p 991 N95-17934

The photographic system global evaluation for generation of INPE TM Landsat image
[INPE-5571-TDI/542] p 1050 N95-18369

Mesh quality control for multiply-refined tetrahedral grids
[NASA-CR-197595] p 1043 N95-18737

Metrology: Calibration and measurement processes guidelines
[NASA-RP-1342] p 992 N95-18745

Analytical control test plan and microbiological methods for the water recovery test
[NASA-TM-108473] p 1091 N95-19061

Relevance of laboratory tests in aeromedical decisions p 1082 N95-19420

Nozzle Initiative Industry Advisory Committee on Standardization of Carbon-Phenolic Test Methods and Specifications
[NASA-CR-197529] p 967 N95-19566

Development of an expert system for power quality advisement using CLIPS 6.0 p 1014 N95-19634

The meteorological monitoring system for the Kennedy Space Center/Cape Canaveral Air Station p 1104 N95-19647

QUANTITATIVE ANALYSIS

Enhancement of fluorescence detection in chromatographic methods by computer analysis of second order data
[DE94-014682] p 973 N95-17966

Quantitative analysis of voids in percolating structures in two-dimensional N-body simulations
[NASA-CR-197612] p 1156 N95-18949

Analytical control test plan and microbiological methods for the water recovery test
[NASA-TM-108473] p 1091 N95-19061

QUANTUM CHROMODYNAMICS

Evidence for coexistence of two phases in relativistic heavy ion collisions and comparison with lattice results
[DE94-626672] p 1130 N95-18329

Feynman-x and transverse momentum dependence of D(sup (+-)) and D(sup 0), D-bar(sup 0) production in 250 GeV (pi)(sup -) - nucleon interactions
[DE94-626698] p 1130 N95-18366

Pion observables and QCD
[DE94-018357] p 1130 N95-18428

Can an infrared-vanishing gluon propagator confine quarks?
[DE94-018388] p 1131 N95-18548

Summary of the working group on tests of QCD
[DE94-018390] p 1131 N95-18550

Higher-order Lipatov kernels and the QCD Pomeron
[DE94-018395] p 1131 N95-18551

Exact m(sub quark) does not equal 0 condensates in QCD(1+1)(N(sub C) yields infinity
[DE94-018581] p 1131 N95-18554

Physics at the Fermilab Tevatron Proton-Antiproton Collider
[DE95-000648] p 1137 N95-19561

Principal-value resummation for dilepton production
[DE95-001094] p 1135 N95-19726

QUANTUM EFFICIENCY

InP solar cell development on inexpensive silicon substrates
[AD-A283624] p 1052 N95-18011

Atomic line filter for SDI applications
[AD-A284125] p 1139 N95-18409

Research on stable, high-efficiency amorphous silicon multijunction modules
[DE95-000215] p 1054 N95-19832

QUANTUM ELECTRODYNAMICS

The Green's function in the Bloch-Nordsieck model for QED3
[DE94-626680] p 996 N95-18331

QUANTUM ELECTRONICS
Large signal time dependent quantum mechanical transport in quantum phase based devices
[AD-A283338] p 1155 N95-18009
High Temperature Superconductor (HTS) superconducting quantum interference device (SQUID) microscope
[AD-A285875] p 1152 N95-19598
QUANTUM MECHANICS
Covariant differential complexes of quantum linear groups
[DE94-626640] p 1118 N95-18876
To the theory of the management of the resonance widths
[DE94-626645] p 1156 N95-18879
The formulation of quantum statistical mechanics based on the Feynman path centroid density. 3: Phase space formalism and analysis of centroid molecular dynamics
[AD-A279233] p 1157 N95-19852
The formulation of quantum statistical mechanics based on the Feynman path centroid density. 4: Algorithms for centroid molecular dynamics
[AD-A279234] p 1157 N95-19853
QUANTUM OPTICS
Wavelets and scattering
[AD-A284131] p 996 N95-18411
QUANTUM STATISTICS
Applications of quantum entropy to statistics
[DE94-014416] p 1155 N95-17996
QUANTUM THEORY
The 3d International Workshop on Computational Electronics
[AD-A284678] p 1011 N95-19089
Non localizability of the photon keystone to a remodelling of physics
[PB94-217213] p 1134 N95-19376
Modeling of quantum transport in semiconductor devices
[AD-A280182] p 1155 N95-19829
QUANTUM WELL LASERS
14th IEEE International Semiconductor Laser Conference
[AD-A285569] p 1038 N95-18642
QUANTUM WELLS
Gigabit optical interconnects: System and component analysis, design and development
[AD-A285538] p 1138 N95-18067
1994 IEEE Nonlinear Optics: Materials Fundamental and Applications Conference
[AD-A285769] p 1139 N95-18345
Infrared-to-visible converter
[AD-D016443] p 1141 N95-18529
Magneto-optical studies of compound semiconductors
[DE94-018743] p 1149 N95-18650
Waveguide switches using asymmetric coupled quantum wells
[AD-A284056] p 1010 N95-18662
Giant effective mass deviations near the magnetic field-induced minigap in double quantum wells
[DE94-018889] p 1122 N95-19234
Optical determination of conduction and valence-band dispersion curves in strained single-quantum wells
[DE94-018892] p 1151 N95-19235
The optical emission and absorption properties of silicon-germanium superlattice structures grown on non-conventional silicon substrate orientation
[AD-A284852] p 1153 N95-19715
QUARKS
The left-right forward-backward asymmetry for B quarks at the SLD
[DE94-014508] p 1129 N95-18049
Diquarks in deep inelastic scattering and the Gottfried sum rule
[DE94-626685] p 1130 N95-18356
Can an infrared-vanishing gluon propagator confine quarks?
[DE94-018388] p 1131 N95-18548
Higher-order Lipatov kernels and the QCD Pomeron
[DE94-018395] p 1131 N95-18551
Exact m(sub quark) does not equal 0 condensates in QCD(1 + 1)(N(sub C) yields infinity
[DE94-018581] p 1131 N95-18554
Generation permutation symmetry and the quark mixing matrix
[PB95-108189] p 1132 N95-18643
Physics at the Fermilab Tevatron Proton-Antiproton Collider
[DE95-000648] p 1137 N95-19561
Baryon stopping in 200 GeV/A S + Au collisions
[DE94-018215] p 1134 N95-19587
QUARTZ CRYSTALS
Resonator/oscillator response to liquid loading
[DE94-013442] p 1012 N95-19240
Quartz crystal resonators and oscillators for frequency control and timing applications. A tutorial
[AD-A284995] p 1012 N95-19519
QUARTZ TRANSDUCERS
Resonator/oscillator response to liquid loading
[DE94-013442] p 1012 N95-19240
QUASARS
An optical study of compact steep spectrum radio sources p 1179 N95-18498
QUATERNIONS
Applications of quaternions to dynamical simulation, computer graphics and biomechanics
[PB94-201456] p 1094 N95-17972

R

RADAR
The Seventh Ionospheric Effects Symposium
[PB94-191930] p 1057 N95-17985
RADAR ANTENNAS
Radar sector blanker
[AD-D016275] p 996 N95-18429
Radar antenna characterization using polarization measurements
[AD-A284840] p 1005 N95-19694
RADAR CROSS SECTIONS
Numerically efficient use of frequency domain MoM codes for wideband radiation and scattering problems. An application: Scattering from a microstrip patch
[AD-A284561] p 995 N95-18116
Inband radar cross section of phased arrays with parallel feeds
[AD-A284249] p 1005 N95-19730
Radar cross-section measurements and simulation of a tethered satellite. The small expendable deployer system end-mass payload
[NASA-TM-4613] p 1005 N95-19781
RADAR DATA
A comparison of optical rain gauge and radar data from TOGA/COARE p 1069 N95-18207
Interferometric synthetic aperture radar and the Data Collection System Digital Terrain Elevation Demonstration
[AD-A284024] p 999 N95-18657
RADAR DETECTION
Performance evaluation of ground based radar systems
[AD-A283654] p 995 N95-18139
Adaptive detection and copy of coherent narrowband waveforms with uncalibrated arrays
[AD-A285125] p 1004 N95-19594
RADAR HOMING MISSILES
Multipath-induced, low-angle tracking error at 140 GHz
[AD-A283630] p 995 N95-18136
RADAR IMAGERY
Some statistical tools for SAR image synthesis, analysis and processing
[INPE-5548-TDI/534] p 1172 N95-18004
Comparative analysis of multisensor (TM/Landsat and SAR/ERS-1) and multitemporal scenes of Guaira region, Sao Paulo State, Brazil
[INPE-5581-TDI/544] p 1049 N95-18005
On the optimization of speckle filtering techniques for ERS-1 images over Argentina
[INPE-5578-PRE/1806] p 1050 N95-18216
RADAR MAPS
Interferometric synthetic aperture radar and the Data Collection System Digital Terrain Elevation Demonstration
[AD-A284024] p 999 N95-18657
RADAR MEASUREMENT
Measurements of wind profiler EMC characteristics
[PB94-194107] p 1066 N95-17938
Microburst vertical wind estimation from horizontal wind measurements
[NASA-TP-3460] p 942 N95-18198
A comparison of optical rain gauge and radar data from TOGA/COARE p 1069 N95-18207
Measurement and proper equalization of range sidelobes using a spherical satellite as a reflector
[AD-A285955] p 1005 N95-19744
RADAR NAVIGATION
Radar antenna characterization using polarization measurements
[AD-A284840] p 1005 N95-19694
RADAR RANGE
MIKON 94. International Microwave Conference. Invited papers, volume 3
[AD-A284353] p 1008 N95-18338
High radar range resolution with the step frequency waveform
[AD-A284611] p 1002 N95-19084
RADAR REFLECTORS
Measurement and proper equalization of range sidelobes using a spherical satellite as a reflector
[AD-A285955] p 1005 N95-19744
RADAR RESOLUTION
High radar range resolution with the step frequency waveform
[AD-A284611] p 1002 N95-19084
RADAR SCATTERING
Numerically efficient use of frequency domain MoM codes for wideband radiation and scattering problems. An application: Scattering from a microstrip patch
[AD-A284561] p 995 N95-18116
Inband radar cross section of phased arrays with parallel feeds
[AD-A284249] p 1005 N95-19730
RADAR TRACKING
Multipath-induced, low-angle tracking error at 140 GHz
[AD-A283630] p 995 N95-18136
AN/APS-137 Forward Looking Airborne Radar (FLAR) evaluation
[AD-A284672] p 1002 N95-19087
Radar cross-section measurements and simulation of a tethered satellite. The small expendable deployer system end-mass payload
[NASA-TM-4613] p 1005 N95-19781
RADAR TRANSMISSION
Performance evaluation of ground based radar systems
[AD-A283654] p 995 N95-18139
RADIAL DISTRIBUTION
Study on heat flux of plasma scrape-off layer in HL-1 tokamak
[DE94-627009] p 1144 N95-18887
RADIANCE
A sensitivity analysis of upwelling radiances in the 3-5 micrometers region as a function of atmospheric conditions
[AD-A283678] p 1068 N95-18141
RADIATION ABSORPTION
Implications of summertime marine stratocumulus on the North American climate p 1073 N95-18977
Graded bandgap semiconductor device for real-time imaging
[AD-D016543] p 1151 N95-19122
RADIATION COUNTERS
Electronics for the Si detectors in APEX
[DE94-015078] p 1007 N95-17961
Highly transparent and rugged sensor for velocity determinations of cosmic dust particles p 966 N95-19178
RADIATION DETECTORS
Development of a high-resolution liquid xenon detector for gamma-ray astrophysics p 1179 N95-18499
RADIATION DISTRIBUTION
Mathematical analysis of three free-electron-laser issues
[AD-A284122] p 1037 N95-18408
RADIATION DOSAGE
Design considerations for a Space Station radiation shield for protection from both man-made and natural sources
[NASA-CR-195298] p 964 N95-18495
Light transport for medical laser treatments
[PB94-201498] p 1037 N95-18502
US experiments flown on the Soviet biosatellite Cosmos 2044. Volume 1: Mission description, experiments K-7-01 - K-7-15
[NASA-TM-108802-VOL-1] p 1092 N95-18569
RADIATION EFFECTS
IDA gamma ray laser
[AD-A284322] p 1037 N95-18382
STS-68 mission highlights resource tape
[NASA-TM-110049] p 961 N95-18568
Transducer array interaction modeling using variational principles
[AD-A285687] p 1128 N95-19514
Study of the effect of ionizing radiation on the structure of natural rubber latex by positron annihilation technique
[DE94-631466] p 975 N95-19550
Photobiology in medicine
[AD-A284843] p 1087 N95-19695
Spacecraft environments interactions: Protecting against the effects of spacecraft charging
[NASA-RP-1354] p 965 N95-19780
RADIATION HARDENING
Defect reduction and back channel degradation in SIMOX
[AD-A284231] p 1148 N95-17960
RADIATION MEASUREMENT
Radiation balance in three Amazonian ecosystems: Campina, campinarana and mata densa
[INPE-5587-TDI/549] p 1057 N95-18003
Analysis of solar spectral irradiance measurements from the SBUV/2-series and the SSBUV instruments
[NASA-CR-197544] p 1196 N95-18954
Propagation of intense, ultrashort laser pulses through metal vapor: Refractive intensity limits and spectral effects
[DE94-016365] p 1039 N95-19398

Summary information and data sets for the HBCU Solar Measurements Network
[DE94-011872] p 1055 N95-19856

RADIATION MEASURING INSTRUMENTS
Mission description and in-flight operations of ERBE instruments on ERBS and NOAA 10 spacecraft, February 1987 - February 1990
[NASA-RP-1325] p 1051 N95-18465

RADIATION PRESSURE
Mathematical analysis of three free-electron-laser issues
[AD-A284122] p 1037 N95-18408

RADIATION PROTECTION
Spacecraft environments interactions: Protecting against the effects of spacecraft charging
[NASA-RP-1354] p 965 N95-19780

RADIATION SHIELDING
Design considerations for a Space Station radiation shield for protection from both man-made and natural sources
[NASA-CR-195298] p 964 N95-18495

RADIATION SPECTRA
Atomic line filter for SDI applications
[AD-A284125] p 1139 N95-18409
Mission description and in-flight operations of ERBE instruments on ERBS and NOAA 10 spacecraft, February 1987 - February 1990
[NASA-RP-1325] p 1051 N95-18465

RADIATION TRANSPORT
Lunar surface fission power supplies: Radiation issues
[DE94-014439] p 966 N95-17997
Three-dimensional radiation transport hydrodynamics
[DE94-018337] p 1146 N95-19527

RADIATIVE TRANSFER
Modeling of cloud and radiation processes for large-scale clouds and tropical anvils
[AD-A284212] p 1067 N95-17955
Imagery correction for atmospheric effects using sounding data
[INPE-5506-TDI/518] p 1064 N95-18390
Study for the analysis of the observations, and numerical data representing the planets as far-infrared calibration sources
[NASA-CR-196542] p 1195 N95-19287

RADICALS
Lithium electrode/polyacrylonitrile based polymer electrolyte interface
[AD-A283947] p 986 N95-19064
Intrinsic barriers for H-atom transfer reactions involving hydrocarbons
[DE94-018451] p 1134 N95-19590

RADII
Advanced concepts theory
[AD-A279212] p 1147 N95-19844

RADIO ANTENNAS
Design considerations for an archimedean slot spiral antenna p 1006 N95-19798

RADIO ASTRONOMY
Effects of meteor showers in the Earth ionosphere
[INPE-5591-TDI/552] p 1178 N95-18213
Astronomical observations of phenomena in disks p 1178 N95-19301

RADIO COMMUNICATION
Personal communications services: Improving theater deployable communications for the 21st century
[AD-A283465] p 994 N95-18058
Communication with reentry vehicle through modulated plasma
[AD-D016476] p 997 N95-18462
The 23 Gigahertz (GHz) digital Low Density Radio Communications Link (LDRCL) Operational Test and Evaluation (OT/E) integration and OT/E operation
[AD-A283963] p 1000 N95-18686
Engineering review, January 1993 - March 1994 p 1001 N95-19055
The use of two-station ionosonde data for IONCAP/ASAPS model validation on transpolar two-hop, high-frequency skywave radio links
[AD-A284270] p 1005 N95-19736

RADIO EMISSION
Heliospheric 2-3 kHz radio emissions and their relationship to large Forbush decreases
[U-OF-IOWA-94-19] p 1195 N95-17979

RADIO EQUIPMENT
Phase and amplitude controlled micropatch antenna
[AD-A284191] p 1002 N95-19103

RADIO FREQUENCIES
Automatic Identification Technology (AIT): The development of functional capability and card application matrices
[AD-A285528] p 1173 N95-18099
A spectral study of a radio-frequency plasma-generated flux of atomic oxygen
[NASA-TM-4612] p 1032 N95-18194
Method and system for inferring the radio refractive index structure of the atmosphere from radio measurements
[AD-D016436] p 999 N95-18561
Hypersonic wind tunnel test techniques
[AD-A284057] p 929 N95-18663
Lossless compression of weight vectors from an adaptive filter
[DE94-017350] p 1174 N95-18873
Development of high reliability planar chip inductors
[DE94-018589] p 1012 N95-19231
Microcavity structures
[DE95-001096] p 1039 N95-19727
Field-emitter arrays for RF vacuum microelectronics
[AD-A279932] p 1013 N95-19865

RADIO FREQUENCY INTERFERENCE
Combiner for two dimensional adaptive interference suppression system
[AD-D016272] p 997 N95-18516
Alleviation of co-channel interference at Poole relay station
[BBC-RD-1993/4] p 1003 N95-19136
Signal enhancement in AM-FM interference
[AD-A285114] p 1004 N95-19565

RADIO GALAXIES
An optical study of compact steep spectrum radio sources p 1179 N95-18498

RADIO INTERFEROMETERS
Results from the northern New Mexico satellite-beacon radio interferometer
[DE94-018310] p 1063 N95-18148

RADIO OCCULTATION
Investigation of atmospheric waves on Neptune
[NASA-CR-197537] p 1194 N95-18579

RADIO RECEIVERS
Combiner for two dimensional adaptive interference suppression system
[AD-D016272] p 997 N95-18516

RADIO SIGNALS
Combiner for two dimensional adaptive interference suppression system
[AD-D016272] p 997 N95-18516
Method and system for inferring the radio refractive index structure of the atmosphere from radio measurements
[AD-D016436] p 999 N95-18561

RADIO TELEMETRY
Collection of real-time, multichannel EEG data from helicopter pilots in flight: A feasibility study
[AD-A285050] p 1090 N95-19564

RADIO TELESCOPES
MIKON 94. International Microwave Conference. Invited papers, volume 3
[AD-A284353] p 1008 N95-18338

RADIO TRANSMISSION
Personal communications services: Improving theater deployable communications for the 21st century
[AD-A283465] p 994 N95-18058
The development of the switched-horn radio-camera system
[BBC-RD-1993/13] p 997 N95-18494
Implementation of amplitude modulation companding using a digital signal processor
[BBC-RD-1994/1] p 998 N95-18536
Method and system for inferring the radio refractive index structure of the atmosphere from radio measurements
[AD-D016436] p 999 N95-18561

RADIO WAVES
Radio wave heating of the lower ionosphere p 1145 N95-18905

RADIOACTIVE AGE DETERMINATION
I-Xe studies of individual chondrules: What can they tell us about chondrule formation? p 1192 N95-19329

RADIOACTIVE ISOTOPES
Chronology of chrondrule and CAI formation: Mg-Al isotopic evidence p 1189 N95-19314

RADIOACTIVE MATERIALS
GAMQUEST, a computer program to identify gamma rays
[DE94-016217] p 1197 N95-18351

RADIOMETRIC RESOLUTION
High-frame-rate intensified fast optically shuttered TV cameras with selected imaging applications
[DE94-016098] p 1035 N95-19394

RAIN
Optical Rain Gauge Performance: Second Workshop on Optical Rain Gauge Measurements
[NASA-CP-3288] p 1068 N95-18201
Moored rainfall measurements during COARE p 1069 N95-18202
Update on TAO moored ORG array p 1069 N95-18203
The effect of spatial averaging on threshold exceedances of daily precipitation amounts
[KNMI-TR-154] p 1070 N95-18392
Incorporating uncertainty and risk in rainfall-based flood estimates
[RR-CE144] p 1071 N95-18607

RAIN FORESTS
Observational studies and modelling of interception loss of gross rainfall in the Amazonian rainforest
[INPE-5583-TDI/545] p 1067 N95-18006

RAIN GAGES
Optical Rain Gauge Performance: Second Workshop on Optical Rain Gauge Measurements
[NASA-CP-3288] p 1068 N95-18201
Moored rainfall measurements during COARE p 1069 N95-18202
Update on TAO moored ORG array p 1069 N95-18203
Inter-comparison of automatic rain gauges p 1069 N95-18204
Wallops Island natural rain data analysis p 1069 N95-18205
Vibration (?) spikes during natural rain events p 1069 N95-18206
A comparison of optical rain gauge and radar data from TOGA/COARE p 1069 N95-18207
Can salt on an optical rain gauge lens affect performance? p 1069 N95-18208
Rain gauge calibration and testing p 1070 N95-18209
Effect of heavy rain to the total received power p 1070 N95-18210

RAINDROPS
Effect of heavy rain to the total received power p 1070 N95-18210

RAMAN SPECTRA
Visible-infrared remote-sensing model and applications for ocean waters
[NASA-CR-197602] p 1051 N95-18739

RAMJET ENGINES
Solid fuel ramjet composition
[AD-D016458] p 990 N95-19090

RANDOM ACCESS MEMORY
Integrated, nonvolatile, high-speed analog random access memory
[NASA-CASE-NPO-17998-2-CU] p 1093 N95-18963

RANDOM NOISE
Perception of complex auditory patterns
[AD-A284189] p 1079 N95-18626
Signal processing via Fourier-Bessel series expansion
[AD-A285316] p 1003 N95-19510

RANDOM PROCESSES
Proceedings of Natural Sciences Symposium
[AD-A285452] p 1077 N95-19536

RANDOM SIGNALS
Detection performance of generalized likelihood ratio processors for random signals of unknown location, structure, extent, and strength
[AD-A285589] p 997 N95-18475

RANDOM VARIABLES
Eigenvalue tests and distributions for small sample order determination for complex Wishart matrices
[AD-A283825] p 1120 N95-18672
A new stochastic systems approach to structural integrity p 935 N95-19474

RANGEFINDING
Lightning studies using LDAR and companion data sets p 1073 N95-18174
A triangulation method for passive ranging
[AD-A284180] p 998 N95-18522

RAPID QUENCHING (METALLURGY)
High temperature stability of binary microstructures derived from liquid precursors
[AD-A283960] p 1150 N95-18685

RARE EARTH COMPOUNDS
Generation and solution of effective many-body Hamiltonians for rare earth and transition metal compounds
[DE95-002402] p 1155 N95-19838

RARE EARTH ELEMENTS
Novel carbon-ion fuel cells
[DE94-017390] p 1053 N95-18894
The origin of refractory precursor components of chondrules p 1189 N95-19316

RARE GASES
Neutron scattering study of dilute supercritical solutions
[DE95-000493] p 1134 N95-19557

RASTER SCANNING
Digital mapping, charting, and geodesy analysis program technical review of Raster Product Format (RPF) and Scanned Map (SMap)
[AD-A284267] p 1052 N95-19733

RATES (PER TIME)
Throughput analysis between high end workstations across an FDDI network
[AD-A283608] p 1110 N95-18615
Experimental constraints on models for the origin of chondrules: Cooling rates p 1189 N95-19311

RAYLEIGH-RITZ METHOD
Free vibration analysis of partially filled liquid storage tanks
[DE94-012456] p 1020 N95-19098
RDX
Mixed high explosives for insensitive booster compositions
[MRL-TR-92-22] p 990 N95-19505
REACTING FLOW
An application of a two-equation model of turbulence to three-dimensional chemically reacting flows
[NASA-CR-195411] p 1015 N95-18107
Numerical mixing calculations of confined reacting jet flows in a cylindrical duct
[NASA-TM-106736] p 947 N95-18133
Numerical simulation of shock/shock and shock/boundary-layer interactions in chemically reacting hypersonic flows
[DLR-94-04] p 1019 N95-18609
Computation of vortex breakdown
p 1029 N95-19462
REACTION KINETICS
Spectroelectrochemical investigations of molten halide solutions
[AD-A284147] p 974 N95-18412
Laboratory studies of stratospheric bromine chemistry: Kinetics of the reactions of bromine monoxide with nitrogen dioxide and atomic oxygen p 1065 N95-18731
Probing the chemistry of nickel/metal hydride battery cells using electrochemical impedance spectroscopy
p 1014 N95-18985
Computational simulation of liquid fuel rocket injectors
p 968 N95-18989
Deformation of nonstoichiometric CuO polycrystals
[DE94-016907] p 1150 N95-19094
Neutron scattering study of dilute supercritical solutions
[DE95-000493] p 1134 N95-19557
The formulation of quantum statistical mechanics based on the Feynman path centroid density. 4: Algorithms for centroid molecular dynamics
[AD-A279234] p 1157 N95-19853
REACTION PRODUCTS
Shock-induced devolatization of calcium sulfate and implications for K-T extinctions
[NASA-CR-197608] p 1060 N95-19033
REACTIVITY
Tunneling and transport in mesoscopic structures
[AD-A283426] p 1148 N95-18053
Mass spectrometric studies of clusters and surfaces
[AD-A283992] p 974 N95-19066
Development of a colloidal redox system containing a smectite clay for control of reactivity and reaction selectivity
[AD-A285958] p 974 N95-19515
Transition metal oxides deposited on rhodium and platinum: Surface chemistry and catalysis
[DE95-000793] p 975 N95-19616
REACTOR CORES
Assembly and calibration of a new experimental apparatus for production and utilization of capture gamma rays
[DE94-626650] p 1198 N95-18880
REACTOR DESIGN
Fueled emitter, TFE Verification Program
[DE94-017557] p 1135 N95-18146
TFE design package, TFE Verification Program
[DE94-017558] p 1136 N95-18147
Ageing nuclear power plant management: An aeronautical viewpoint
[NAL-PD-SN-9306] p 927 N95-18606
REACTOR MATERIALS
Evaluation of powder metallurgy plates made by Sylvania Electric Products, Incorporated
[DE94-017911] p 980 N95-19401
REACTOR SAFETY
Ageing nuclear power plant management: An aeronautical viewpoint
[NAL-PD-SN-9306] p 927 N95-18606
READOUT
The Gravity Probe B niobium bird experiment: Experimental verification of a data reduction scheme with a prototypical dc SQUID readout system
p 1033 N95-18929
REAL TIME OPERATION
Adaptive robot path planning in changing environments
[DE94-016564] p 1112 N95-17948
Improving software characteristics of a real-time system using reengineering techniques
[AD-A283659] p 1094 N95-18015
A formal method for semantics-based change-merging of software prototypes
[AD-A283668] p 1094 N95-18017
Miscellaneous disk utility application programs for the AFOS background partition
[PB94-181328] p 1067 N95-18038
Two-stage gas measurement system
[NASA-CASE-LAR-14791-1] p 1032 N95-18316
Real-time adaptive control of mixing in a plane shear layer
[AD-A285541] p 1018 N95-18469
Locally connected adaptive Gabor filter for real-time motion compensation
[AD-A285726] p 1009 N95-18485
A real-time vision system to monitor/analyze the changes in composite specimens during mechanical testing
[ARL-TR-344] p 970 N95-18612
Real-time modeling of complex atmospheric releases in urban areas
[DE94-018063] p 1059 N95-18647
Real-time thickness measurement of MCC ablator material p 972 N95-18981
Stand-alone digital data storage control system including user control interface
[NASA-CASE-LAR-14651-1] p 1175 N95-19056
Digital monopulse
[AD-D016447] p 1002 N95-19072
Graded bandgap semiconductor device for real-time imaging
[AD-D016543] p 1151 N95-19122
Collection of real-time, multichannel EEG data from helicopter pilots in flight: A feasibility study
[AD-A285050] p 1090 N95-19564
Constructing a real-time mobile robot software system
[AD-A285969] p 1115 N95-19572
Real-time remote scientific model validation
p 1103 N95-19640
Unit cell geometry of multiaxial preforms for structural composites
[NASA-CR-197294] p 971 N95-19650
A parallel strategy for implementing real-time expert systems using CLIPS p 1105 N95-19749
Reflexive reasoning for distributed real-time systems
p 1107 N95-19766
PalymSys (TM): An extended version of CLIPS for construction and reasoning using blackboards
p 1107 N95-19767
Distributed medical database system for real-time monitoring of the health and risk exposure of military research study volunteers at USARIEM
[AD-A279193] p 1087 N95-19811
REAL VARIABLES
Theory and applications of the phi transform wavelets
[AD-A279943] p 1119 N95-19869
RECEIVERS
Liquid crystal tunable filter
[AD-A284383] p 1139 N95-18342
RINSE: A digitally implemented flywheel sync regenerator for improved video synchroniser performance
[BBC-RD-1993/14] p 999 N95-18538
Pulsed laser illumination of photovoltaic cells
[NASA-TM-106820] p 1053 N95-18572
RECONNAISSANCE
PRISM project optical instrument
p 1143 N95-19009
RECORDS MANAGEMENT
Miscellaneous disk utility application programs for the AFOS background partition
[PB94-181328] p 1067 N95-18038
RECRYSTALLIZATION
Size distribution of one-, two- and three-dimensional Voronoi cells
[PB94-207008] p 1149 N95-18373
RECTANGULAR PANELS
Sloshing roof impact tests of a rectangular tank
[DE94-012462] p 1018 N95-18549
RECTANGULAR PLATES
Acoustic radiation damping of flat rectangular plates subjected to subsonic flows p 1123 N95-18542
RECTANGULAR WIND TUNNELS
Corner vortex suppressor
[AD-D016423] p 928 N95-18337
RECURSIVE FUNCTIONS
A general theory of semi-unification
p 1099 N95-18924
RECYCLING
Gas storage and recovery system
[NASA-CASE-MSC-22091-1] p 992 N95-18738
Producing chondrules by recycling and volatile loss
p 1186 N95-19290
REED-SOLOMON CODES
Error coding simulations in C p 963 N95-18998
REENTRY VEHICLES
Communication with reentry vehicle through modulated plasma
[AD-D016476] p 997 N95-18462
REFINING
Study of the ferrimagnetic and paramagnetic phases of magnetite measured by multiple neutron diffraction
[DE94-627031] p 1151 N95-19242
REFLECTANCE
Progress in the development of advanced solar reflectors
[DE94-000264] p 1053 N95-18463
REFLECTED WAVES
Radiation balance in three Amazonian ecosystems: Campina, campinarana and mata densa
[INPE-5587-TDI/549] p 1057 N95-18003
REFLECTING TELESCOPES
A comparison between using incoherent or coherent sources to align and test an adaptive optical telescope
p 1142 N95-18969
REFLECTOR ANTENNAS
Double-loop frequency selective surfaces for multi frequency division multiplexing in a dual reflector antenna
[NASA-CASE-NPO-18701-2-CU] p 1000 N95-18960
REFRACTIVITY
Marine boundary layer refractive effects in the infrared
[AD-A285717] p 1140 N95-18484
Method and system for inferring the radio refractive index structure of the atmosphere from radio measurements
[AD-D016436] p 999 N95-18561
Waveguide switches using asymmetric coupled quantum wells
[AD-A284056] p 1010 N95-18662
MANN: A program to transfer designs for diffractive optical elements to a MANN photolithographic mask generator p 1142 N95-18995
Propagation of intense, ultrashort laser pulses through metal vapor: Refractive intensity limits and spectral effects
[DE94-016365] p 1039 N95-19398
REFRACTORIES
Heating and cooling in the solar nebula: Constraints from refractory inclusions p 1187 N95-19297
The origin of refractory precursor components of chondrules p 1189 N95-19316
A ceramic/slag interface as an analog for accretion of hot refractory objects and rim formation
p 1191 N95-19322
REFRIGERANTS
Lunar base heat pump, phase 1
[NASA-CR-188300] p 1015 N95-18111
REFRIGERATING MACHINERY
Norwegian heat pump status and policy review
[PB94-206992] p 992 N95-18667
REFRIGERATORS
Improved efficiency and power density for thermoacoustic coolers
[AD-A283946] p 992 N95-18165
Summary report of mission acceleration measurements for STS-60, SPACEHAB2, launched 11 February 1994
[NASA-TM-106797] p 991 N95-19788
REGENERATIVE COOLING
Regenerative cooling for liquid propellant rocket thrust chambers
[INPE-5565-TDI/540] p 967 N95-18720
REGENERATORS
RINSE: A digitally implemented flywheel sync regenerator for improved video synchroniser performance
[BBC-RD-1993/14] p 999 N95-18538
REGGE POLES
Flattening of the resonance spectrum of hadrons from kappa-deformed Poincare algebra
[DE94-626686] p 1156 N95-18352
REGOLITH
Lunar surface fission power supplies: Radiation issues
[DE94-014439] p 986 N95-17997
REGULATIONS
Safety study: Commuter airline safety
[PB94-917004] p 933 N95-19132
NASA directives: Master list and index
[NHB-1410.13N] p 1171 N95-19133
Economic impact analysis for proposed emission standards and guidelines for municipal waste combustors: A description of the basis for, and impacts of, proposed revisions to air pollutant emission regulations for new and existing municipal waste combustors under Clean Air Act Sections 111(b), 111(d), and 129
[PB94-213543] p 1061 N95-19403
Relevance of laboratory tests in aeromedical decisions p 1082 N95-19420
Federal aviation regulations, part 91. General operating and flight rules. Change 8
[PB94-217445] p 940 N95-19720
Environmental Compliance Assessment System (ECAS). South Carolina supplement: US Army
[AD-A279244] p 1062 N95-19660

REGULATORS
Time-optimal control of a third order regulator
[AD-A283307] p 1113 N95-18023
REINFORCING FIBERS
Sodium sulfate corrosion of silicon carbide fiber-reinforced calcium aluminosilicate glass-ceramic matrix composites
[AD-A283703] p 969 N95-18021
Development of radiation-hardened ceramic composites for fusion applications
[DE94-016182] p 985 N95-18638
REINFORCING MATERIALS
Centrifugal casting of reinforced articles
[AD-D016277] p 992 N95-18431
RELATIVISTIC EFFECTS
Orbital tests of relativistic gravity using artificial satellites
[PB94-217239] p 965 N95-19377
RELATIVISTIC PARTICLES
Is a massive tau neutrino just what cold dark matter needs?
[NASA-CR-197627] p 1180 N95-18964
Mass and radius of cosmic balloons
[NASA-CR-197628] p 1180 N95-19031
RELATIVISTIC THEORY
Orbital tests of relativistic gravity using artificial satellites
[PB94-217239] p 965 N95-19377
RELATIVITY
General relativity and dark matter
[DE94-626641] p 1180 N95-18877
Special relativity effects for space-based coherent lidar experiments p 1014 N95-18983
Antisymmetric tensor field interactions and neutron star models
[PB94-215605] p 1118 N95-19375
RELAXATION METHOD (MATHEMATICS)
Generalized relaxation theory and vortices in plasmas
[DE95-002615] p 1147 N95-19837
RELAXATION TIME
Thermal relaxation processes and stability in poled electro-optic polymers
[AD-A283948] p 987 N95-19102
RELAY
Inter-amplifier pupil relay systems for a high average power dye laser at Lawrence Livermore National Laboratory
[DE94-016544] p 1039 N95-19507
RELIABILITY
The reliability of laser reflowed Sn-Ag solder joints
[AD-A284732] p 1044 N95-18080
Reliability Without Hermeticity (RWOH) for Integrated Circuits (IC)
[AD-A284340] p 1009 N95-18418
Handheld delivery system for modified boron-type fire extinguishment agent
[AD-A283955] p 992 N95-18684
RELIABILITY ANALYSIS
System engineering toolbox for design-oriented engineers
[NASA-RP-1358] p 962 N95-18932
Residual life and strength estimates of aircraft structural components with MSD/MED p 937 N95-19485
RELIABILITY ENGINEERING
Development of high reliability planar chip inductors
[DE94-018589] p 1012 N95-19231
RELIC RADIATION
Is a massive tau neutrino just what cold dark matter needs?
[NASA-CR-197627] p 1180 N95-18964
RELIEF MAPS
Remote sensing products evaluation for cartographic updating purposes
[INPE-5584-TDI/546] p 1050 N95-18368
RELIEF VALVES
Gas storage and recovery system
[NASA-CASE-MSC-22091-1] p 992 N95-18738
RELUCTANCE
An analysis of noise reduction in variable reluctance motors using pulse position randomization
[AD-A283846] p 1123 N95-18673
REMOTE CONTROL
The development of a fiber optics communication network for controlling a Multidegree-Of-Freedom Serpentine Truss p 1142 N95-18167
Feasibility study of transmission of OTV camera control information in the video vertical blanking interval p 1006 N95-18185
Torsional device for remote control steering system
[AD-D016426] p 1041 N95-18594
Design of a radio frequency data link for the unmanned ground vehicle technology test bed demonstration program
[AD-A284997] p 1004 N95-19534
REMOTE SENSING
A sensitivity analysis of upwelling radiances in the 3-5 micrometers region as a function of atmospheric conditions
[AD-A283678] p 1068 N95-18141
Heuristic inference about flow directions in river networks
[INPE-5588-TDI/550] p 1050 N95-18214
Remote sensing products evaluation for cartographic updating purposes
[INPE-5584-TDI/546] p 1050 N95-18368
Office of Research and Applications: Research Programs p 1071 N95-18721
Visible-infrared remote-sensing model and applications for ocean waters
[NASA-CR-197602] p 1051 N95-18739
Remote sensing/global change. A special bibliography
[NASA-TM-110038] p 1060 N95-18742
Ice surface temperature retrieval from AVHRR, ATSR, and passive microwave satellite data: Algorithm development and application
[NASA-CR-197542] p 1052 N95-18952
ISSSR tutorial 1: Introduction to spectral remote sensing
[AD-A284268] p 1052 N95-19734
REMOTE SENSORS
SeaWiFS technical report series. Volume 18: SeaWiFS technical report series cumulative index: Volumes 1-17
[NASA-TM-104566-VOL-18] p 1076 N95-19577
REMOTELY PILOTED VEHICLES
Six degree of freedom flight dynamic and performance simulation of a remotely-piloted vehicle
[AERO-TN-9301] p 942 N95-18097
Design of a radio frequency data link for the unmanned ground vehicle technology test bed demonstration program
[AD-A284997] p 1004 N95-19534
REPLACING
Application of photogrammetry of F-14D store separation
[AD-A284154] p 943 N95-18417
REPLICAS
Replica management system: A scheme for flexible and dynamic replication
[PB94-201597] p 1171 N95-18060
REPRODUCTION (COPYING)
Program verification for optimized byte copy
[AD-A283915] p 1099 N95-18676
REQUIREMENTS
Guidelines for reduction of human errors during maintenance of safety systems; maintainability and maintenance support
[PB94-215597] p 1092 N95-19412
RESEARCH
Microgravity fluid science research in Europe
[PB94-201720] p 990 N95-17973
NASA/ASEE Summer Faculty Fellowship Program. 1994 research reports
[NASA-CR-197448] p 1157 N95-18166
Research reports: 1994 NASA/ASEE Summer Faculty Fellowship Program
[NASA-CR-196533] p 1161 N95-18967
Aero-thermodynamic distortion induced structured dynamic response
[AD-A279931] p 955 N95-19864
RESEARCH AIRCRAFT
VSTOL Systems Research Aircraft (VSRA) Harrier
[NASA-TM-110117] p 941 N95-18347
Fiber Optic Control System integration for advanced aircraft. Electro-optic and sensor fabrication, integration, and environmental testing for flight control systems: Laboratory test results
[NASA-CR-195408] p 1034 N95-18938
RESEARCH AND DEVELOPMENT
NASA/ASEE Summer Faculty Fellowship Program. 1994 research reports
[NASA-CR-197448] p 1157 N95-18166
NASA High Performance Computing and Communications program
[NASA-TM-4653] p 1174 N95-18573
European aeronautics: Strong government presence in industry structure and research and development support. Report to Congressional Requesters
[GAO/NSIAD-94-71] p 1171 N95-18578
Office of Research and Applications: Research Programs p 1071 N95-18721
Engineering review, January 1993 - March 1994 p 1001 N95-19055
NASA/DOD Aerospace Knowledge Diffusion Research Project. Paper 45: A comparison of the information-seeking behaviors of three groups of US aerospace engineers
[NASA-TM-109839] p 1176 N95-19127
The Japan Information Center of Science and Technology p 1198 N95-19128
Space Station: Plans to expand research community do not match available resources. Report to the Ranking Minority Member, Subcommittee on Oversight of Government Management, Committee on Government Affairs, US Senate
[GAO/NSIAD-95-33] p 965 N95-19131
Distributed medical database system for real-time monitoring of the health and risk exposure of military research study volunteers at USARIEM
[AD-A279193] p 1087 N95-19811
Annual historical report, calendar year 1993
[AD-A280178] p 1087 N95-19827
NREL Photovoltaic Program, FY 1993
[DE94-011880] p 1055 N95-19857
RESEARCH FACILITIES
The founding of CEBAF, 1979 to 1987 p 1138 N95-19784
RESEARCH MANAGEMENT
Space Station: Plans to expand research community do not match available resources. Report to the Ranking Minority Member, Subcommittee on Oversight of Government Management, Committee on Government Affairs, US Senate
[GAO/NSIAD-95-33] p 965 N95-19131
Proceedings of Natural Sciences Symposium
[AD-A285452] p 1077 N95-19536
RESEARCH PROJECTS
Small Business Research Summaries, numbers 51-100
[PB94-179967] p 1170 N95-17986
Small Business Research Summaries, numbers 1-50
[PB94-179959] p 1170 N95-17987
RESEARCH VEHICLES
Determination of stability and control derivatives from the NASA F/A-18 HARV from flight data using the maximum likelihood method
[NASA-CR-197320] p 958 N95-19576
RESIDUAL STRENGTH
Acoustic fatigue of carbon fibre structures p 1127 N95-19158
Residual life and strength estimates of aircraft structural components with MSD/MED p 937 N95-19485
Widespread fatigue damage monitoring: Issues and concerns p 938 N95-19488
Fracture behavior of large-scale thin-sheet aluminum alloy p 939 N95-19494
Fatigue and residual strength investigation of ARALL(R) -3 and GLARE(R) -2 panels with bonded stringers p 939 N95-19495
Prediction of R-curves from small coupon tests p 939 N95-19496
RESIDUAL STRESS
Residual stresses in welded plates p 1047 N95-18972
Analysis of cold worked holes for structural life extension p 939 N95-19493
Split mandrel versus split sleeve coldworking: Dual methods for extending the fatigue life of metal structures p 940 N95-19500
RESINS
Method of lowering the reaction exotherm in thermally polymerized acetylene terminated resins
[AD-D016276] p 985 N95-18430
Use of titanate coupling agents in Kevlar (trade name)/phenolic composites
[AD-A279200] p 972 N95-19814
RESISTOJET ENGINES
High performance storable propellant resistojet
[NASA-CR-191128] p 967 N95-18195
RESOLUTION
Methods and components for optical contention resolution in high speed networks
[AD-A284674] p 1142 N95-19088
Research requirements for future visual guidance systems
[AD-A279188] p 941 N95-19810
RESONANCE
To the theory of the management of the resonance widths
[DE94-626645] p 1156 N95-18879
Bohr's quantization rule in the world of resonances of elementary particles
[DE94-626721] p 1132 N95-18882
RESONANCE SCATTERING
Flattening of the resonance spectrum of hadrons from kappa-deformed Poincare algebra
[DE94-626686] p 1156 N95-18352
Coronal abundances and their variation
[NASA-CR-197553] p 1195 N95-18376
Mathematical analysis of three free-electron-laser issues
[AD-A284122] p 1037 N95-18408
RESONANT TUNNELING
Piezoelectric effects in double barrier resonant tunneling structures
[DE95-000850] p 1152 N95-19620

RESONATORS
Resonator/oscillator response to liquid loading
[DE94-013442] p 1012 N95-19240
Quartz crystal resonators and oscillators for frequency control and timing applications. A tutorial
[AD-A284995] p 1012 N95-19519
RESOURCES MANAGEMENT
Resources Automated Management System
[AD-A284153] p 1171 N95-18416
RETINA
Retinal injuries from single and multiple picosecond laser pulses
[AD-A284173] p 1078 N95-18515
RETIREMENT
Age 60 study. Part 3: Consolidated database experiments
[AD-A286247] p 1080 N95-19384
RETROREFLECTION
Reduction of parasitic lasing
[NASA-CASE-LAR-14645-1-SB] p 1037 N95-18322
RETROREFLECTORS
Reduction of parasitic lasing
[NASA-CASE-LAR-14645-1-SB] p 1037 N95-18322
REVERBERATION CHAMBERS
Design and operation of a thermoacoustic test facility
p 960 N95-19150
REVIEWING
Boundary-flow measurement methods for wall interference assessment and correction: Classification and review p 1022 N95-19262
REYNOLDS NUMBER
An application of a two-equation model of turbulence to three-dimensional chemically reacting flows
[NASA-CR-195411] p 1015 N95-18107
Effect of crossflow on Goertler instability in incompressible boundary layers
[NASA-CR-195007] p 1016 N95-18193
Hypersonic flow-field measurements: Intrusive and nonintrusive
[AD-A283867] p 930 N95-18674
Steady and unsteady blade stresses within the SSME ATD/HPOTP inducer p 968 N95-18982
Velocity measurements with hot-wires in a vortex-dominated flowfield p 932 N95-19261
Unsteady flow testing in a passive low-correction wind tunnel p 960 N95-19272
Introduction to multigrid methods
p 1028 N95-19453
Experimental studies of Reynolds number dependence of turbulent mixing and transport
[DE94-015338] p 1030 N95-19578
Parallel computations in hydro acoustics
[AD-A285900] p 1030 N95-19607
REYNOLDS STRESS
Turbulence modeling for CFD, part 1
p 1028 N95-19458
Evaluation of three turbulence models for afterbody/jet flows, including Reynolds stress closure
[ARA-90] p 932 N95-19574
Evaluation of three turbulence models for afterbody/jet flows, including Reynolds stress closure
[ARA-MEMO-408] p 1194 N95-19773
RHEOLOGY
Macromolecular characterization and solution behavior of polymer additives
[AD-A284845] p 988 N95-19696
RHODIUM
An atomic view of surface diffusion on metal surfaces
[DE94-016150] p 980 N95-19395
Transition metal oxides deposited on rhodium and platinum: Surface chemistry and catalysis
[DE95-000793] p 975 N95-19616
RIEMANN MANIFOLD
General relativity and dark matter
[DE94-626641] p 1180 N95-18877
Coulomb gas representation of the SU(2) WZW correlators at higher genera
[PB94-217254] p 1119 N95-19718
SU(2) WZW theory at higher genera
[PB94-217262] p 1119 N95-19719
RIGID STRUCTURES
Applications of quaternions to dynamical simulation, computer graphics and biomechanics
[PB94-201456] p 1094 N95-17972
RIMS
Constraints on chondrule agglomeration from fine-grained chondrule rims p 1189 N95-19315
A ceramic/slag interface as an analog for accretion of hot refractory objects and rim formation
p 1191 N95-19322
Chondrule remelting: Evidence from coarse-grained chondrule rims and compound chondrules
p 1191 N95-19323
RIPPLES
Preliminary evaluation of the F/A-18 quantity/multiple envelope expansion
[AD-A284119] p 943 N95-18407
RISK
Incorporating uncertainty and risk in rainfall-based flood estimates
[RR-CE144] p 1071 N95-18607
Aeromedical risk management for aircrew
p 1080 N95-19414
Fit to fly: Analysis of the aeromedical disposition in aircrewmembers of the Spanish Armed Forces
p 1081 N95-19418
The aeromedical implications of supraventricular tachycardia p 1085 N95-19437
Distributed medical database system for real-time monitoring of the health and risk exposure of military research study volunteers at USARIEM
[AD-A279193] p 1087 N95-19811
RIVER BASINS
Cumulative impact analysis of wetlands using hydrologic indices
[AD-A284759] p 1058 N95-18085
RIVETED JOINTS
Fatigue life until small cracks in aircraft structures: Durability and damage tolerance p 936 N95-19478
Results of uniaxial and biaxial tests on riveted fuselage lap joint specimens p 938 N95-19491
Stress intensity factors for surface and corner cracks emanating from a wedge-loaded hole
p 939 N95-19498
Stress-intensity factor solutions for cracks at countersunk rivet holes under uniaxial tension
[AD-A279163] p 1047 N95-19804
RIVETS
Evaluation of the fuselage lap joint fatigue and terminating action repair p 936 N95-19477
Stress-intensity factor solutions for cracks at countersunk rivet holes under uniaxial tension
[AD-A279163] p 1047 N95-19804
ROBOT ARMS
The development of a fiber optics communication network for controlling a Multidegree-Of-Freedom Serpentine Truss p 1142 N95-18167
ROBOT CONTROL
Distributed methods for controlling multiple mobile robots
[AD-A283919] p 1113 N95-18157
The development of a fiber optics communication network for controlling a Multidegree-Of-Freedom Serpentine Truss p 1142 N95-18167
Adaptive Neuron Model: An architecture for the rapid learning of nonlinear topological transformations
[NASA-CASE-NPO-18579-1-CU] p 1114 N95-18740
Method for surmounting an obstacle by a robot vehicle
[NASA-CASE-NPO-18764-1-CU] p 1041 N95-18741
Sliding mode control method having terminal convergence in finite time
[NASA-CASE-NPO-18584-1-CU] p 1114 N95-19062
ROBOT DYNAMICS
Adaptive robot path planning in changing environments
[DE94-016564] p 1112 N95-17948
ROBOTICS
Automated path planning of the Payload Inspection and Processing System p 1043 N95-18169
International Conference on Control Theory and its Applications
[DE94-626221] p 1114 N95-18875
Sliding mode control method having terminal convergence in finite time
[NASA-CASE-NPO-18584-1-CU] p 1114 N95-19062
Design of a radio frequency data link for the unmanned ground vehicle technology test bed demonstration program
[AD-A284997] p 1004 N95-19534
Design of a flexible robotic arc welding system, task 3. Volume 1: System overview
[AD-A285116] p 1043 N95-19593
ROBOTS
Adaptive robot path planning in changing environments
[DE94-016564] p 1112 N95-17948
Improving software characteristics of a real-time system using reengineering techniques
[AD-A283659] p 1094 N95-18015
Robust image understanding. Techniques and applications
[AD-A283427] p 1113 N95-18057
Annual Allerton Conference on Communication, Control and Computing
[AD-A283892] p 1114 N95-18675
Method for surmounting an obstacle by a robot vehicle
[NASA-CASE-NPO-18764-1-CU] p 1041 N95-18741
Distributed algorithms for controlling multiple mobile robots
[AD-A283975] p 1114 N95-18889
Constructing a real-time mobile robot software system
[AD-A285969] p 1115 N95-19572
Design of a flexible robotic arc welding system, task 3. Volume 1: System overview
[AD-A285116] p 1043 N95-19593
A CLIPS-based expert system for the evaluation and selection of robots p 1103 N95-19641
ROBUSTNESS (MATHEMATICS)
Advanced techniques for analysis and evaluation of robust protocols
[AD-A285682] p 1111 N95-19513
ROCKET ENGINE CONTROL
New technologies for space avionics
[NASA-CR-197574] p 966 N95-18196
ROCKET ENGINE DESIGN
Arcjet thruster research and technology, phase 2
[NASA-CR-182276] p 927 N95-18044
Advanced small rocket chambers. Basic program and option 2: Fundamental processes and material evaluation
[NASA-CR-195349] p 966 N95-18192
High performance storable propellant resistojet
[NASA-CR-191128] p 967 N95-18195
ROCKET ENGINES
Integrated aerodynamic fin and stowable TVC vane system
[AD-D016457] p 967 N95-19073
Neural net controller for inlet pressure control of rocket engine testing p 1102 N95-19637
ROCKET THRUST
Regenerative cooling for liquid propellant rocket thrust chambers
[INPE-5565-TDI/540] p 967 N95-18720
ROCKET-BORNE INSTRUMENTS
Rocket and laboratory studies in astronomy
[NASA-CR-197531] p 1177 N95-17981
ROLL
Development of a multicomponent force and moment balance for water tunnel applications, volume 2
[NASA-CR-4642-VOL-2] p 1020 N95-18956
ROLLING MOMENTS
Development of a multicomponent force and moment balance for water tunnel applications, volume 1
[NASA-CR-4642-VOL-1] p 1020 N95-18955
ROOM TEMPERATURE
Lithium electrode/polyacrylonitrile based polymer electrolyte interface
[AD-A283947] p 986 N95-19064
High Temperature Superconductor (HTS) superconducting quantum interference device (SQUID) microscope
[AD-A285875] p 1152 N95-19598
Characterization of the deformation and annealing of 304L stainless steel
[DE94-018584] p 981 N95-19707
ROOMS
High frequency room responses: Acoustic design and the control of stereophonic image quality
[BBC-RD-1994/11] p 1124 N95-19046
Acoustic noise criteria for listening rooms and control rooms
[BBC-RD-1994/06] p 1124 N95-19048
Optimum dimension ratios for studios, control rooms and listening rooms
[BBC-RD-1993/8] p 993 N95-19053
VENTCF2: An algorithm and associated FORTRAN 77 subroutine for calculating flow through a horizontal ceiling/floor vent in a zone-type compartment fire model
[PB94-210127] p 993 N95-19402
ROTARY ENGINES
Unmanned aerial vehicle heavy fuel engine test
[AD-A284332] p 947 N95-18383
ROTARY WING AIRCRAFT
Flight parameters monitoring system for tracking structural integrity of rotary-wing aircraft
p 934 N95-19469
Rotorcraft ditchings and water-related impacts that occurred from 1982 to 1989, phase 1
[AD-A279164] p 940 N95-19805
ROTARY WINGS
Design and development of an enhanced biodynamic manikin, phase 1
[AD-A284725] p 1090 N95-18077
A linear system identification and validation of an AH-64 Apache aeroelastic simulation model
p 959 N95-18903
2-D and 3-D oscillating wing aerodynamics for a range of angles of attack including stall
[NASA-TM-4632] p 931 N95-19119
Wall interaction effects for a full-scale helicopter rotor in the NASA Ames 80- by 120-foot wind tunnel
p 932 N95-19270

ROTATION
Applications of quaternions to dynamical simulation, computer graphics and biomechanics
[PB94-201456] p 1094 N95-17972
Rack insertion End Effector (RIEE) guidance
p 1043 N95-18178
Nonlinear magnetohydrodynamics
[DE94-016223] p 1143 N95-18353
Summary report of mission acceleration measurements for STS-60, SPACEHAB2, launched 11 February 1994
[NASA-TM-106797] p 991 N95-19788
Three-D optical memory disk
[AD-A280002] p 1035 N95-19871

ROTOR AERODYNAMICS
Measurement of gust response on a turbine cascade
[NASA-TM-106776] p 928 N95-18457
Sectional prediction of 3D effects for separated flow on rotating blades
[PB94-201696] p 928 N95-18503
Wind turbine blade aerodynamics: The combined experiment
[DE94-011866] p 929 N95-18645
Wind turbine blade aerodynamics: The analysis of field test data
[DE94-011867] p 929 N95-18646

ROTOR BLADES (TURBOMACHINERY)
Tuned mass damper for integrally bladed turbine rotor
[NASA-CASE-MFS-28697-1] p 1041 N95-18325
Measurement of gust response on a turbine cascade
[NASA-TM-106776] p 928 N95-18457
Verification of multidisciplinary models for turbomachines p 949 N95-19025

ROTOR DYNAMICS
Tuned mass damper for integrally bladed turbine rotor
[NASA-CASE-MFS-28697-1] p 1041 N95-18325
A linear system identification and validation of an AH-64 Apache aeroelastic simulation model
p 959 N95-18903

ROTORS
Wave cycle design for wave rotor engines with limited nitrogen oxide emissions p 1041 N95-18901
Wind tunnel tests of a 42 inch diameter self-starting autogyro rotor
[AD-A279922] p 932 N95-19863

RUBBER
Sag compensated vibration isolation mount
[AD-D016541] p 1042 N95-19121
Study of the effect of ionizing radiation on the structure of natural rubber latex by positron annihilation technique
[DE94-631486] p 975 N95-19550

RUNGE-KUTTA METHOD
Low-dissipation and -dispersion Runge-Kutta schemes for computational acoustics
[NASA-CR-195022] p 1018 N95-18488
Some considerations on velocity vector accuracy in dust trajectory analysis p 1183 N95-19186
Finite volume method using Runge-Kutta time-stepping for solution of Euler equations p 1027 N95-19451

RUNWAYS
Aircraft wake vortex takeoff tests at O'Hara International Airport
[AD-A283828] p 929 N95-18624

RUSSIAN FEDERATION
The current status of Russian/CIS communication satellites
[AD-A285526] p 963 N95-18098
NASA/DOD Aerospace Knowledge Diffusion Research Project. Paper 46: Technical communications in aerospace: A comparison across four countries
[NASA-TM-110056] p 1175 N95-19038

RUTHENIUM
Hyperfine splittings, prepulse technique, and other new results for collisional excitation neon-like x ray lasers
[DE94-016443] p 1038 N95-19247

RUTHENIUM COMPOUNDS
Excited state processes in transition metal complexes. Redox splitting in soluble polymers
[DE95-002690] p 977 N95-19839

RYDBERG SERIES
A photoionization study of OH and OD from 680A to 950A: An analysis of the Rydberg series
[NASA-CR-196970] p 974 N95-18744

S

S WAVES
Properties of Alfven waves with transverse scale on the order of skin-depth
[AD-A285657] p 1147 N95-19700

SAFETY
Requirements analysis for safety-critical systems: A chemical batch processing example
[PB94-201563] p 991 N95-17934
Status of vanadium alloy development for fusion first wall/blanket applications
[DE95-001067] p 982 N95-19725

SAFETY MANAGEMENT
System engineering toolbox for design-oriented engineers
[NASA-RP-1358] p 962 N95-18932
Safety study: Commuter airline safety
[PB94-917004] p 933 N95-19132
Guidelines for reduction of human errors during maintenance of safety systems; maintainability and maintenance support
[PB94-215597] p 1092 N95-19412
Rotorcraft ditchings and water-related impacts that occurred from 1982 to 1989, phase 1
[AD-A279164] p 940 N95-19805

SALTS
Can salt on an optical rain gauge lens affect performance? p 1069 N95-18208

SAMPLERS
Comet coma sample return instrument
p 1180 N95-19173

SAMPLING
Two-stage gas measurement system
[NASA-CASE-LAR-14791-1] p 1032 N95-18316
Near-Earth Asteroid Returned Sample (NEARS)
[NASA-CR-197297] p 1194 N95-19575

SANDS
The operation of gas turbine engines in hot and sandy conditions: Royal Air Force experiences in the Gulf conflict p 950 N95-19655
US Army rotorcraft turboshaft engines sand and dust erosion considerations p 951 N95-19656
Future directions in helicopter protection system configuration p 951 N95-19657
Erosion of T56 5th stage rotor blades due to bleed hole overtip flow p 952 N95-19666

SAPPHIRE
Ion mixing in oxide-sapphire systems
[DE94-018660] p 1133 N95-19232

SATELLITE COMMUNICATION
The current status of Russian/CIS communication satellites
[AD-A285526] p 963 N95-18098
US Navy SHF SATCOM: Past, present and future
[AD-A283704] p 996 N95-18359
Issues in military use of commercial satellites
[AD-A283707] p 964 N95-18362
The future use of DSCS and commercial satellites in the US Navy
[AD-A285707] p 997 N95-18481
On orbit performance of the ALEXIS EUV telescopes
[DE94-016197] p 964 N95-18639
An expert system for configuring a network for a Milstar terminal p 1104 N95-19645

SATELLITE DESIGN
A systems analysis and project management plan for the Petite Amateur Navy Satellite (PANSAT)
[AD-A285968] p 965 N95-19571

SATELLITE DRAG
First principles used in orbital prediction and an atmospheric model comparison
[AD-A284636] p 1065 N95-19086

SATELLITE IMAGERY
Comparative analysis of multisensor (TM/Landsat and SAR/ERS-1) and multitemporal scenes of Guaira region, Sao Paulo State, Brazil
[INPE-5581-TDI/544] p 1049 N95-18005
Thematic classification of zone coastal: A methodologic contribution
[INPE-5586-TDI/548] p 1050 N95-18215
On the optimization of speckle filtering techniques for ERS-1 images over Argentina
[INPE-5578-PRE/1806] p 1050 N95-18216
Remote sensing products evaluation for cartographic updating purposes
[INPE-5584-TDI/546] p 1050 N95-18368
The photographic system global evaluation for generation of INPE TM Landsat image
[INPE-5571-TDI/542] p 1050 N95-18369
Multispectral NOAA Marine Atmospheric Boundary Layer (MABL) estimates during VOCAR
[AD-A283702] p 1064 N95-18623
Ice surface temperature retrieval from AVHRR, ATSR, and passive microwave satellite data: Algorithm development and application
[NASA-CR-197542] p 1052 N95-18952
A technique for determining cloud free versus cloud contaminated pixels in satellite imagery
p 1052 N95-19016
SeaWiFS technical report series. Volume 18: SeaWiFS technical report series cumulative index: Volumes 1-17
[NASA-TM-104566-VOL-18] p 1076 N95-19577

SATELLITE INSTRUMENTS
Lean spacecraft avionics trade study
p 966 N95-18994
SeaWiFS technical report series. Volume 18: SeaWiFS technical report series cumulative index: Volumes 1-17
[NASA-TM-104566-VOL-18] p 1076 N95-19577

SATELLITE NETWORKS
The future use of DSCS and commercial satellites in the US Navy
[AD-A285707] p 997 N95-18481

SATELLITE OBSERVATION
Office of Research and Applications: Research Programs p 1071 N95-18721
Ice surface temperature retrieval from AVHRR, ATSR, and passive microwave satellite data: Algorithm development and application
[NASA-CR-197542] p 1052 N95-18952
Assessment of climate variability of the Greenland Ice Sheet: Integration of in situ and satellite data
[NASA-CR-197604] p 1062 N95-19779

SATELLITE ORIENTATION
Radar cross-section measurements and simulation of a tethered satellite. The small expendable deployer system end-mass payload
[NASA-TM-4613] p 1005 N95-19781

SATELLITE SOUNDING
Estimation of satellite derived temperature and moisture fields over Europe from TOVS data using 3I and ITPP algorithms
[AD-A284581] p 1049 N95-18035
A technical demonstration Mobile Profiler System
[AD-A284562] p 1068 N95-18117

SATELLITE TRACKING
Seafloor positioning across Juan de Fuca ridge
[AD-A285049] p 1075 N95-19563

SATELLITE TRANSMISSION
On orbit performance of the ALEXIS EUV telescopes
[DE94-016197] p 964 N95-18639

SCALARS
Real-time adaptive control of mixing in a plane shear layer
[AD-A285541] p 1018 N95-18469
7th International Symposium on Applications of Laser Techniques to Fluid Mechanics, volume 2
[AD-A285685] p 1018 N95-18477
Simplified ideal MHD normal mode equations for toroidal axisymmetric plasmas
[DE94-627004] p 1144 N95-18886
Visualizing second order tensor fields with hyperstreamlines
[NASA-CR-197619] p 1121 N95-19288

SCALE EFFECT
Methods for scaling icing test conditions
[NASA-TM-106827] p 934 N95-19284

SCALE MODELS
Methods for scaling icing test conditions
[NASA-TM-106827] p 934 N95-19284
Particle deposition in gas turbine blade film cooling holes p 951 N95-19661

SCALING LAWS
Microstructure-based fatigue life prediction methods for naval steel structures
[AD-A284735] p 1044 N95-18081
Methods for scaling icing test conditions
[NASA-TM-106827] p 934 N95-19284

SCANNERS
Evaluation of scanners for C-scan imaging in nondestructive inspection of aircraft
[DE94-012473] p 990 N95-19100
Tunneling acoustic microscopy
[AD-A279160] p 1128 N95-19802

SCANNING ELECTRON MICROSCOPY
Field-emitter arrays for RF vacuum microelectronics
[AD-A279932] p 1013 N95-19865

SCANNING TUNNELING MICROSCOPY
Direct dimer-by-dimer identification of clean and monohydride dimers on the Si(001) surface by scanning tunneling microscopy
[AD-A280158] p 976 N95-19824

SCATTERING
On measurement of cross sections for scattering of p(mu)- and d(mu)-atoms in hydrogen and deuterium
[DE94-626957] p 1132 N95-18884

SCATTERING AMPLITUDE
Fatigue and damage tolerance scatter models
p 935 N95-19475

SCATTERING CROSS SECTIONS
Electron interactions with non-linear polyatomic molecules and their radicals
[AD-A283952] p 1130 N95-18334
The behavior of the slope of elastic nucleon scattering at small transfer momenta and recent U A 4/2 data
[DE94-626687] p 1130 N95-18360
On measurement of cross sections for scattering of p(mu)- and d(mu)-atoms in hydrogen and deuterium
[DE94-626957] p 1132 N95-18884

SCATTERING FUNCTIONS
Principal-value resummation for dilepton production
[DE95-001094] p 1135 N95-19726

SCHOTTKY DIODES
High current amplifier utilizing a Josephson junction Schottky diode three terminal device
[AD-D016278] p 1009 N95-18432
Method of forming platinum and platinum silicide Schottky contacts on beta-silicon carbide
[AD-D016221] p 1149 N95-18627
SCHROEDINGER EQUATION
Electron interactions with non-linear polyatomic molecules and their radicals
[AD-A283952] p 1130 N95-18334
SCIENTIFIC VISUALIZATION
A Space and Atmospheric Visualization Science System
[NASA-CR-189390] p 1172 N95-18040
System engineering toolbox for design-oriented engineers
[NASA-RP-1358] p 962 N95-18932
Visualizing second order tensor fields with hyperstreamlines
[NASA-CR-197619] p 1121 N95-19288
SCIENTISTS
NASA/DOD Aerospace Knowledge Diffusion Research Project. Report 29: A comparison of the technical communications practices of Japanese and US aerospace engineers and scientists
[NASA-TM-109164] p 1175 N95-18953
SCINTILLATING FIBERS
Conceptual design for a scintillating-fiber neutron detector for fusion reactor plasma diagnostics
[DE94-014716] p 1143 N95-17969
Scintillating-fiber imaging detector for 14-MeV neutrons
[DE94-018593] p 1135 N95-19709
SCINTILLATION
Development of a high-resolution liquid xenon detector for gamma-ray astrophysics p 1179 N95-18499
SCINTILLATION COUNTERS
Conceptual design for a scintillating-fiber neutron detector for fusion reactor plasma diagnostics
[DE94-014716] p 1143 N95-17969
An instrument to measure the charge, and energy spectrum (20-1000 GeV/a) of the cosmic ray species oxygen to iron
[NASA-CR-197555] p 1197 N95-18464
25-ps neutron detector for measuring ICF-target burn history
[DE94-016450] p 1146 N95-19250
SCORING
NAWCAD photogrammetrics: Methods and applications for aviation test and evaluation
[AD-A284074] p 1034 N95-19071
SCRUBBERS
Investigation of new hypergol scrubber technology
p 977 N95-18175
SEA BREEZE
Synoptic-scale influence on the Monterey Bay sea-breeze
[AD-A285129] p 1073 N95-19596
SEA ICE
Ice surface temperature retrieval from AVHRR, ATSR, and passive microwave satellite data: Algorithm development and application
[NASA-CR-197542] p 1052 N95-18952
SEA SURFACE TEMPERATURE
Marginal probabilities of the extremes of ENSO events for temperature and precipitation in the southeastern United States
[AD-A284716] p 1068 N95-18076
A numerical simulation of seasonal circulation in the South China Sea
[AD-A283701] p 1075 N95-18622
Multispectral NOAA Marine Atmospheric Boundary Layer (MABL) estimates during VOCAR
[AD-A283702] p 1064 N95-18623
Ice surface temperature retrieval from AVHRR, ATSR, and passive microwave satellite data: Algorithm development and application
[NASA-CR-197542] p 1052 N95-18952
Implications of summertime marine stratocumulus on the North American climate p 1073 N95-18977
SEA WATER
Handbook for the extremely low frequency (ELF) data acquisition and analysis system
[DSTO-GD-0021] p 1005 N95-19622
SEALERS
Tribology and microstructure of PS212 with a Cr2O3 seal coat
[NASA-TM-106768] p 969 N95-18448
Sealant materials for the solid oxide fuel cell
[DE94-017073] p 1053 N95-19115
SEALING
Fixture for pressure testing sight glasses
[AD-D016263] p 1032 N95-18319
Trivalent chromium solutions for sealing anodized aluminum
[AD-D016472] p 979 N95-18458
Sealant materials for the solid oxide fuel cell
[DE94-017073] p 1053 N95-19115
SEARCH RADAR
AN/APS-137 Forward Looking Airborne Radar (FLAR) evaluation
[AD-A284672] p 1002 N95-19087
SEAS
A numerical simulation of seasonal circulation in the South China Sea
[AD-A283701] p 1075 N95-18622
SECONDARY FLOW
Static investigation of two fluidic thrust-vectoring concepts on a two-dimensional convergent-divergent nozzle
[NASA-TM-4574] p 931 N95-19042
SECURITY
Alarm annunciation in a graphical environment
[DE94-015761] p 1098 N95-18652
Processing multilevel secure test and evaluation information
[AD-A284073] p 1001 N95-19069
SEDIMENT TRANSPORT
Geologic studies: Executive summary report
[PB94-187481] p 1073 N95-17951
SEDIMENTS
Geologic studies: Executive summary report
[PB94-187481] p 1073 N95-17951
Calibration and sediment load algorithms for an acoustic sediment flux probe
[AD-A283655] p 1075 N95-18617
Coastal benthic boundary layer special research program: A review of the first year. Volume 1
[AD-A280034] p 1076 N95-19818
SEGMENTS
Robust image understanding. Techniques and applications
[AD-A283427] p 1113 N95-18057
SEISMOGRAPHS
Fiber optic flexural disk accelerometer
[AD-D016444] p 1141 N95-18563
SEISMOLOGY
Sloshing roof impact tests of a rectangular tank
[DE94-012462] p 1018 N95-18549
SELECTION
On the development of an expert system for wheelchair selection p 1092 N95-19627
SELECTIVE DISSEMINATION OF INFORMATION
Independent validation and verification of automated information systems in the Department of Energy
[DE94-014460] p 1173 N95-18063
SELECTIVE SURFACES
Double-loop frequency selective surfaces for multi frequency division multiplexing in a dual reflector antenna
[NASA-CASE-NPO-18701-2-CU] p 1000 N95-18960
SELENIDES
Characterization of rechargeable lithium cells. Part 1: Lithium/niobium triselenide chemistry
[AD-A284229] p 1007 N95-17959
SELENIUM
Hyperfine splittings, prepulse technique, and other new results for collisional excitation neon-like x ray lasers
[DE94-016443] p 1038 N95-19247
SELF LUBRICATING MATERIALS
Tribology and microstructure of PS212 with a Cr2O3 seal coat
[NASA-TM-106768] p 969 N95-18448
SEMANTICS
A formal method for semantics-based change-merging of software prototypes
[AD-A283668] p 1094 N95-18017
SEMICONDUCTING FILMS
Growth and doping of Al(x)Ga(1-x)N films by electron cyclotron resonance assisted molecular beam epitaxy
[AD-A284838] p 1153 N95-19737
SEMICONDUCTOR DEVICES
Technological and organizational diversity and technical advance in the early history of the American semiconductor industry
[PB94-175700] p 1007 N95-17999
MIKON 94. International Microwave Conference. Volume 1: Conference proceedings
[AD-A284351] p 1009 N95-18425
MIKON 94. International Microwave Conference. Conference proceedings, volume 2
[AD-A284352] p 1009 N95-18426
The 3d International Workshop on Computational Electronics
[AD-A284678] p 1011 N95-19089
Graded bandgap semiconductor device for real-time imaging
[AD-D016543] p 1151 N95-19122
Vacuum microelectronic emitters and their applications using compound semiconductor technology
[AD-A284811] p 1013 N95-19687
Mega-scale simulation of multi-layer devices: Formulation, kinetics, and visualization
[AD-A284848] p 1153 N95-19738
The physics and operation of ultra-submicron length semiconductor devices
[AD-A280181] p 1155 N95-19828
Modeling of quantum transport in semiconductor devices
[AD-A280182] p 1155 N95-19829
Second International Semiconductor Device Research Symposium (ISDRS-1993)
[AD-A279221] p 1013 N95-19849
SEMICONDUCTOR DIODES
Compact, efficient, scalable neodymium laser co-doped with activator ions and pumped by visible laser diodes
[AD-D016237] p 1038 N95-18585
Performance improvements in diode laser arrays
[DE94-016547] p 1039 N95-19508
SEMICONDUCTOR LASERS
New method for homodyne laser linewidth measurements with a short delay fiber
[PB94-202629] p 1036 N95-18061
14th IEEE International Semiconductor Laser Conference
[AD-A285569] p 1038 N95-18642
Advanced optical fiber communications systems
[AD-A283942] p 1141 N95-18682
SEMICONDUCTORS (MATERIALS)
Technological and organizational diversity and technical advance in the early history of the American semiconductor industry
[PB94-175700] p 1007 N95-17999
Advanced packaging and integration technologies for microsensors, phase 1
[AD-A283613] p 1040 N95-18010
1994 IEEE Nonlinear Optics: Materials Fundamental and Applications Conference
[AD-A285769] p 1139 N95-18345
Fault protection circuit for power switching device
[AD-D016466] p 1009 N95-18455
Atomic Layer Epitaxy (ALE) apparatus for growing thin films of elemental semiconductors
[AD-D016236] p 1149 N95-18633
Magneto-optical studies of compound semiconductors
[DE94-018743] p 1149 N95-18650
The 3d International Workshop on Computational Electronics
[AD-A284678] p 1011 N95-19089
Graded bandgap semiconductor device for real-time imaging
[AD-D016543] p 1151 N95-19122
Giant effective mass deviations near the magnetic field-induced minigap in double quantum wells
[DE94-018889] p 1122 N95-19234
Optical determination of conduction and valence-band dispersion curves in strained single-quantum wells
[DE94-018892] p 1151 N95-19235
Deep levels in AgGaSe2
[DE94-018209] p 1152 N95-19585
Energies of X conduction band minima in disordered and ordered GaInP2 alloys
[DE94-018211] p 1152 N95-19586
Physics with isotopically controlled semiconductors
[DE95-000789] p 1152 N95-19615
Vacuum microelectronic emitters and their applications using compound semiconductor technology
[AD-A284811] p 1013 N95-19687
IR materials producibility
[AD-A284263] p 1142 N95-19732
MBE growth, characterization and electronic device processing of Hg-based semiconductor alloys and heterostructures
[AD-A279203] p 1154 N95-19817
Research on stable, high-efficiency amorphous silicon multijunction modules
[DE95-000215] p 1054 N95-19832
Second International Semiconductor Device Research Symposium (ISDRS-1993)
[AD-A279221] p 1013 N95-19849
NREL Photovoltaic Program, FY 1993
[DE94-011880] p 1055 N95-19857
SEMISPAN MODELS
2-D and 3-D oscillating wing aerodynamics for a range of angles of attack including stall
[NASA-TM-4632] p 931 N95-19119
SENSITIVITY
A sensitivity analysis of upwelling radiances in the 3-5 micrometers region as a function of atmospheric conditions
[AD-A283678] p 1068 N95-18141
Low noise fiber gyroscope system which includes excess noise subtraction
[AD-D016556] p 1034 N95-19124

Subgroup report on hard x-ray microprobes
[DE94-018708] p 1034 N95-19233
Spectral distribution of the two-photon decay of He-like krypton
[DE95-001442] p 1135 N95-19787

SENSORS
The linear dynamics of a microsensor accelerometer modeled as a cantilever beam with an end mass
[DE94-019108] p 1031 N95-17963
Space Station racks weight and CG measurement using the rack insertion end-effector p 966 N95-18168
Determination of stores pointing error due to wing flexibility under flight load
[NASA-TM-4646] p 945 N95-19044
Highly transparent and rugged sensor for velocity determinations of cosmic dust particles p 966 N95-19178
PVDF flux/mass/velocity/trajectory systems and their applications in space p 966 N95-19196

SENSORY FEEDBACK
Building a bridge with the customer to facilitate collecting and validating information in modeling sessions
[DE94-017338] p 1174 N95-18872

SEPARATED FLOW
Prediction of fluctuating pressure and power spectra in attached and separated compressible flow p 1031 N95-19153

SEPARATION
Enantiomeric separation of chiral alpha-(1-naphthyl)ethyl ammonium perchlorate by silica gel-bound chiral pyridino-18-crown-6 ligands
[AD-A280156] p 969 N95-19822

SEPARATORS
Modeling and measurement of the performance of a branched conduit sampling system in a mass spectrometer leak detector p 1036 N95-18181
Airborne rotary separator study
[NASA-CR-191045] p 967 N95-18743
Future directions in helicopter protection system configuration p 951 N95-19657

SEQUENCING
Double Eulerian cycles on de Bruijn digraphs
[AD-A283334] p 1120 N95-18007
Decomposition of parametric curves
[PB94-207024] p 1117 N95-18374
Perception of complex auditory patterns
[AD-A284189] p 1079 N95-18626
Maximal-length sequence methods: Acoustic measurements in the presence of high levels of extraneous noise
[BBC-RD-1994/5] p 1001 N95-19049

SERIES EXPANSION
Signal processing via Fourier-Bessel series expansion
[AD-A285316] p 1003 N95-19510

SERUMS
TSH determination in subjects with medium-low levels of serum thyroxine p 1082 N95-19421

SERVICE LIFE
Battery and charge controller evaluations in small stand-alone PV systems
[DE94-014252] p 1013 N95-19872

SHAFTS (MACHINE ELEMENTS)
Wall interaction effects for a full-scale helicopter rotor in the NASA Ames 80- by 120-foot wind tunnel p 932 N95-19270

SHALLOW WATER
Sound speed profiles from vertical array data
[AD-A283978] p 1123 N95-18890
The STOKES (Version 4) normal-mode shallow water transmission loss program
[MRL-CP-1] p 1075 N95-19503
Nonlinear ocean waves
[AD-A285331] p 1075 N95-19523

SHAPE MEMORY ALLOYS
Phase transformations and phase relations in Ti(50)Pd(50-x)TM(x) alloys
[DE94-018999] p 977 N95-17962

SHAPES
Numerical formulation of composition segregation at curved solid-liquid interface during steady state solidification process p 977 N95-19012
Ice accretion with varying surface tension
[NASA-TM-106826] p 934 N95-19285
Spectral distribution of the two-photon decay of He-like krypton
[DE95-001442] p 1135 N95-19787

SHARP LEADING EDGES
Interaction, bursting and control of vortices of a cropped double-delta wing at high angle of attack
[AD-A283656] p 930 N95-18669

SHEAR LAYERS
Real-time adaptive control of mixing in a plane shear layer
[AD-A285541] p 1018 N95-18469
The effect of stable stratification on three-dimensional structure in shear layers p 1019 N95-18921

SHEAR PROPERTIES
Thermo-oxidative stability of graphite/PMR-15 composites: Effect of fiber surface modification on composite shear properties
[NASA-TM-4608] p 981 N95-19652

SHEAR STRENGTH
A constant-depth scratch test for the measurement of adhesion at film-substrate interfaces
[AD-A283660] p 983 N95-18016

SHEAR STRESS
Fatigue crack growth in 2024-T3 aluminum under tensile and transverse shear stresses p 938 N95-19490

SHELLS (STRUCTURAL FORMS)
Completed Beltrami-Michell formulation for analyzing radially symmetrical bodies
[NASA-TM-4593] p 1044 N95-18199

SHIPS
STS-68 mission highlights resource tape
[NASA-TM-110049] p 961 N95-18568

SHOCK FRONTS
Retinal injuries from single and multiple picosecond laser pulses
[AD-A284173] p 1078 N95-18515

SHOCK HEATING
Models for multiple heating mechanisms p 1188 N95-19303
Chondrule formation in the radiative accretional shock p 1191 N95-19324

SHOCK RESISTANCE
Quality optimization of thermally sprayed coatings produced by the JP-5000 (HVOF) gun using mathematical modeling p 989 N95-19008

SHOCK WAVE GENERATORS
Calibration and testing of a large-scale electric gun for shock Hugoniot measurements
[MRL-TR-93-24] p 959 N95-18942
Shock pulse generation using explosive driven metal drivers: Practical considerations
[MRL-TR-93-3] p 1046 N95-19504

SHOCK WAVE INTERACTION
Heliospheric 2-3 kHz radio emissions and their relationship to large Forbush decreases
[U-OF-IOWA-94-19] p 1195 N95-17979
Numerical simulation of shock/shock and shock/boundary-layer interactions in chemically reacting hypersonic flows
[DLR-94-04] p 1019 N95-18609
Theoretical investigations of shock/boundary layer interactions on a Ma(infinity) = 8 waverider
[DLR-FB-94-12] p 930 N95-18910
Prediction of fluctuating pressure and power spectra in attached and separated compressible flow p 1031 N95-19153

SHOCK WAVES
Particle acceleration and transport in the tail and at the front side of the magnetosphere, task 1 and 2
[NASA-CR-197575] p 1064 N95-18476
Aeromechanics technology, volume 1. Task 1: Three-dimensional Euler/Navier-Stokes Aerodynamic Method (TEAM) enhancements
[AD-A285713] p 943 N95-18483
Retinal injuries from single and multiple picosecond laser pulses
[AD-A284173] p 1078 N95-18515
Flow field investigation in a free jet - free jet core system for the generation of high intensity molecular beams
[DLR-FB-94-11] p 1132 N95-18912
Shock-induced devolatization of calcium sulfate and implications for K-T extinctions
[NASA-CR-197608] p 1060 N95-19033
Spectrogram diagnosis of aircraft disasters p 940 N95-19167
Chondrule formation in the radiative accretional shock p 1191 N95-19324

SHORELINES
Kings Bay coastal and estuarine physical monitoring and evaluation program: Coastal studies. Volume 1: Main text and Appendix A
[AD-A285542] p 1074 N95-18470

SHORT CRACKS
Near tip stress and strain fields for short elastic cracks p 937 N95-19487
Widespread fatigue damage monitoring: Issues and concerns p 938 N95-19488

SHUTTLE DERIVED VEHICLES
An oil flow study of the reference Shuttle-C configuration
[NASA-RP-1352] p 932 N95-19623

SICKNESSES
Centrifuge tests of the medical condition of French fighter pilots p 1082 N95-19424

SIDEBANDS
Mathematical analysis of three free-electron-laser issues
[AD-A284122] p 1037 N95-18408

SIDELOBES
Radar antenna characterization using polarization measurements
[AD-A284840] p 1005 N95-19694
Measurement and proper equalization of range sidelobes using a spherical satellite as a reflector
[AD-A285955] p 1005 N95-19744

SIGNAL ANALYSIS
Flame position ultrasonic interferometer
[AD-D016235] p 967 N95-18632

SIGNAL ANALYZERS
Evaluation of the current biased integrated optical processors based on bistable dode elements
[AD-A285532] p 1138 N95-18102
Modular signal processing unit
[AD-D016258] p 995 N95-18314
Signal processor having multiple distributed data buffers
[AD-D016259] p 995 N95-18315
Digital monopulse
[AD-D016447] p 1002 N95-19072

SIGNAL DETECTION
Adaptive detection and copy of coherent narrowband waveforms with uncalibrated arrays
[AD-A285125] p 1004 N95-19594

SIGNAL GENERATORS
Synchronization of nonautonomous chaotic systems
[AD-D016440] p 1010 N95-18528

SIGNAL MEASUREMENT
High-frequency skywave signal power measurement system
[AD-A284382] p 996 N95-18341

SIGNAL PROCESSING
Fusion of correlated sensor observations
[AD-A284224] p 994 N95-17958
Superconductive signal-processing circuits
[AD-A285533] p 1008 N95-18103
TLS-based prefiltering technique for time-domain ARMA modeling
[AD-A284525] p 1120 N95-18113
Modular signal processing unit
[AD-D016258] p 995 N95-18314
Signal processor having multiple distributed data buffers
[AD-D016259] p 995 N95-18315
Wavelets and scattering
[AD-A284131] p 996 N95-18411
SIGNET-software tools for signal identification using neural networks
[AD-A284362] p 1113 N95-18441
A new multi-dimensional transform for digital signal processing using generalized association schemes
[AD-A284166] p 1117 N95-18511
Combiner for two dimensional adaptive interference suppression system
[AD-D016272] p 997 N95-18516
Synchronization of nonautonomous chaotic systems
[AD-D016440] p 1010 N95-18528
Implementation of amplitude modulation companding using a digital signal processor
[BBC-RD-1994/1] p 998 N95-18536
Current loop signal conditioning: Practical applications
[NASA-TM-4636] p 1033 N95-18735
Dynamic Stability Instrumentation System (DSIS). Volume 1: Hardware description
[NASA-TM-109160-VOL-1] p 1099 N95-18899
Waveform bounding and combination techniques for direct drive testing
[AD-A284075] p 1000 N95-19035
Digital video compression: Standardisation of scalable coding schemes
[BBC-RD-1994/10] p 1001 N95-19047
DAB: Multiplex and system support features
[BBC-RD-1994/9] p 1001 N95-19050
Dynamic range control of audio signals by digital signal processing
[BBC-RD-1993/7] p 1124 N95-19054
Statistics of complex cross spectrum estimate for sinusoidal signals and arbitrary noise spectra
[AD-A283984] p 1120 N95-19065
Digital monopulse
[AD-D016447] p 1002 N95-19072
High radar range resolution with the step frequency waveform
[AD-A284611] p 1002 N95-19084
Digital circuit for the introduction and later removal of dither from an analog signal
[AD-D016462] p 1011 N95-19171
Signal processing via Fourier-Bessel series expansion
[AD-A285316] p 1003 N95-19510
Neural network communications signal processing
[AD-A285681] p 1115 N95-19512
True time delay beamforming
[AD-A285683] p 1003 N95-19516
Signal enhancement in AM-FM interference
[AD-A285114] p 1004 N95-19565

Adaptive detection and copy of coherent narrowband waveforms with uncalibrated arrays
[AD-A285125] p 1004 N95-19594
Parallel computations in hydro acoustics
[AD-A285900] p 1030 N95-19607
A general theory of signal integration for fault tolerant distributed sensor networks
[AD-A284825] p 1112 N95-19689

SIGNAL RECEPTION
Radar sector blanker
[AD-D016275] p 996 N95-18429

SIGNAL TO NOISE RATIOS
High-frequency skywave signal power measurement system
[AD-A284382] p 996 N95-18341
Radiation-induced noise in UMPC-type current probes: IEMP response of the curruent measurement system
[AD-A284176] p 998 N95-18520
Special relativity effects for space-based coherent lidar experiments p 1014 N95-18983
Maximal-length sequence methods: Acoustic measurements in the presence of high levels of extraneous noise
[BBC-RD-1994/5] p 1001 N95-19049
Measurement and proper equalization of range sidelobes using a spherical satellite as a reflector
[AD-A285955] p 1005 N95-19744

SIGNAL TRANSMISSION
Signal processor having multiple distributed data buffers
[AD-D016259] p 995 N95-18315
Tunneling acoustic microscopy
[AD-A279160] p 1128 N95-19802

SIGNATURES
An assessment of the adaptive unstructured tetrahedral grid, Euler Flow Solver Code FELISA
[NASA-TP-3526] p 930 N95-19041
Proceedings of the 15th Annual Conference on Atmospheric Transmission Models
[AD-A279919] p 1142 N95-19862

SIGNS AND SYMPTOMS
Crosshift vibrometry: Biomarker for ergonomic stress
[AD-A284337] p 1091 N95-18385

SILICA GEL
The use of silica aerogel to collect interplanetary dust in space p 989 N95-19197

SILICA GLASS
Global equation of state for a glassy material: Fused silica
[DE94-018598] p 988 N95-19721

SILICATES
Global equation of state for a glassy material: Fused silica
[DE94-018598] p 988 N95-19721

SILICIDES
Method of forming platinum and platinum silicide Schottky contacts on beta-silicon carbide
[AD-D016221] p 1149 N95-18627

SILICON
Defect reduction and back channel degradation in SIMOX
[AD-A284231] p 1148 N95-17960
The linear dynamics of a microsensor accelerometer modeled as a cantilever beam with an end mass
[DE94-019108] p 1031 N95-17963
Semiconductor measurement technology: Design and testing guides for the COMOS and lateral bipolar-on-SOI test library
[PB94-178019] p 1007 N95-17984
Advanced packaging and integration technologies for microsensors, phase 1
[AD-A283613] p 1040 N95-18010
InP solar cell development on inexpensive silicon substrates
[AD-A283624] p 1052 N95-18011
Investigation of single events upsets in silicon and GaAs structures using reaction calculations
[AD-A285581] p 1131 N95-18474
Method for fabricating complementary enhancement and depletion mode field effect transistors on a single substrate
[AD-D016270] p 1010 N95-18546
Method for laser-assisted silicon etching using halocarbon ambients
[AD-D016239] p 1038 N95-18635
Marangoni convection in a gravity-free silicon float zone
[NASA-CR-197600] p 991 N95-18913
InP solar cell development on inexpensive silicon substrates
[AD-A286254] p 1054 N95-19388
The optical emission and absorption properties of silicon-germanium superlattice structures grown on non-conventional silicon substrate orientation
[AD-A284852] p 1153 N95-19715
Relative elemental abundance and heating constraints determined for the solar corona from SERTS measurements
[NASA-TM-104616] p 1196 N95-19791
MBE growth, characterization and electronic device processing of Hg-based semiconductor alloys and heterostructures
[AD-A279203] p 1154 N95-19817
Direct dimer-by-dimer identification of clean and monohydride dimers on the Si(001) surface by scanning tunneling microscopy
[AD-A280158] p 976 N95-19824
An atomic-resolution study of overlayer formation and interfacial mixing in the interaction of phosphorus with Si(001)
[AD-A280159] p 976 N95-19825
A simple single-photomask process for fabrication of high-efficiency multicrystalline silicon solar cells
[DE94-014251] p 1055 N95-19859
Silicon-Film (trademark) photovoltaic manufacturing technology
[DE94-011899] p 1056 N95-19882

SILICON ALLOYS
Microscopic origins of metastable effects in a-Si:H and deep defect characterization in a-Si,Ge:H alloys
[DE94-011887] p 1151 N95-19541

SILICON CARBIDES
Sodium sulfate corrosion of silicon carbide fiber-reinforced calcium aluminosilicate glass-ceramic matrix composites
[AD-A283703] p 969 N95-18021
Silicon carbide photoconductive switches
[AD-A284310] p 1008 N95-18378
Method of forming platinum and platinum silicide Schottky contacts on beta-silicon carbide
[AD-D016221] p 1149 N95-18627
Development of radiation-hardened ceramic composites for fusion applications
[DE94-016182] p 985 N95-18638
Characterization of metal matrix composites
[NASA-CR-195381] p 970 N95-18940
Surface roughness measurements p 1142 N95-18984
CVD silicon carbide characterization
[AD-A285667] p 972 N95-19702

SILICON COMPOUNDS
Composites research in support of the NASP Institute for Composites (NIC)
[NASA-CR-197580] p 970 N95-18471
Heteroepitaxy of ternary SiGeC alloys on Si for bipolar transistors
[AD-A285317] p 1151 N95-19511

SILICON DIOXIDE
Novel polymeric composites through molecular engineering
[AD-A284168] p 985 N95-18513
Embedded microclusters in zeolites and cluster beam sputtering: Simulation on parallel computers
[DE95-000662] p 1134 N95-19562
Enantiomeric separation of chiral alpha-(1-naphthyl)ethyl ammonium perchlorate by silica gel-bound chiral pyridino-18-crown-6 ligands
[AD-A280156] p 969 N95-19822

SILICON FILMS
Gettering in multicrystalline silicon: A design-of-experiments approach
[DE94-014289] p 1055 N95-19873

SILICON NITRIDES
Enhancement of creep resistance of a sintered Si3N4 ceramic by microwave annealing
[DE94-017688] p 987 N95-19399
Resistance of silicon nitride turbine components to erosion and hot corrosion/oxidation attack p 955 N95-19683

SILICON OXIDES
Investigation of the microstructure of coatings for high power lasers by non-optical techniques
[DE94-017697] p 987 N95-19227

SILVER
Deep levels in AgGaSe2
[DE94-018209] p 1152 N95-19585

SILVER COMPOUNDS
Palladium-based membranes for hydrogen separation
[PB94-207156] p 973 N95-18377

SIMD (COMPUTERS)
CFD on parallel computers p 1029 N95-19465

SIMPLEX METHOD
Linear optimization and image reconstruction
[AD-A283641] p 1094 N95-18013

SIMPLIFICATION
Simplified ideal MHD normal mode equations for toroidal axisymmetric plasmas
[DE94-627004] p 1144 N95-18886

SIMULATION
Laser wakefield excitation and measurement on a femtosecond time scale: Theory and experiment
[DE94-019198] p 1129 N95-17976
Locally connected adaptive Gabor filter for real-time motion compensation
[AD-A285726] p 1009 N95-18485
Design concepts for an integrated environmental medicine workstation for prediction, simulation and training
[AD-A283686] p 1079 N95-18618
Error coding simulations in C p 963 N95-18998
Simulation of multidisciplinary problems for the thermostress state of cooled high temperature turbines p 948 N95-19021
Simulation of steady and unsteady viscous flows in turbomachinery p 949 N95-19023
Computational simulations for some tests in transonic wind tunnels p 1023 N95-19264
Determination of solid/porous wall boundary conditions from wind tunnel data for computational fluid dynamics codes p 1023 N95-19266
A probabilistic fatigue analysis of multiple site damage p 935 N95-19476
Simulation of wave propagation in three-dimensional random media
[NASA-CR-197605] p 1004 N95-19547

SIMULATORS
Real time simulator with Ti floating point digital signal processor
[DE94-016372] p 1012 N95-19246

SINE WAVES
High frequency direct drive generation using white noise sources
[AD-A284158] p 997 N95-18506
Statistics of complex cross spectrum estimate for sinusoidal signals and arbitrary noise spectra
[AD-A283984] p 1120 N95-19065
Signal enhancement in AM-FM interference
[AD-A285114] p 1004 N95-19565

SINGLE CRYSTALS
Advanced packaging and integration technologies for microsensors, phase 1
[AD-A283613] p 1040 N95-18010
Fatigue in single crystal nickel superalloys
[AD-A285727] p 978 N95-18068
Surface phases, surface defects and the initial stages of oxidation
[DE94-016947] p 979 N95-18358
Process for forming epitaxial BaF2 on GaAs
[AD-D016439] p 1149 N95-18527
Method of doping single crystal diamond for electronic devices
[AD-D016267] p 1149 N95-18543
High temperature stability of binary microstructures derived from liquid precursors
[AD-A283960] p 1150 N95-18685
Ion mixing in oxide-sapphire systems
[DE94-018660] p 1133 N95-19232
High Temperature Superconductor (HTS) superconducting quantum interference device (SQUID) microscope
[AD-A285875] p 1152 N95-19598
Physics with isotopically controlled semiconductors
[DE95-000789] p 1152 N95-19615
NiAl and NiAl-based composites directionally solidified by a containerless zone process
[NASA-CR-195430] p 982 N95-19792
High temperature superconducting films and crystals
[AD-A279201] p 1154 N95-19815

SINGLE EVENT UPSETS
Investigation of single events upsets in silicon and GaAs structures using reaction calculations
[AD-A285581] p 1131 N95-18474

SINGULARITY (MATHEMATICS)
A note on singularities of the 3-D Euler equation
[NASA-CR-195006] p 1017 N95-18397
Determination of solid/porous wall boundary conditions from wind tunnel data for computational fluid dynamics codes p 1023 N95-19266
Singularities and symmetries of nonlinear ordinary and partial differential equations
[DE95-000904] p 1119 N95-19609
High-order corrected trapezoidal rules for singular functions
[AD-A284269] p 1119 N95-19735

SINTERING
Novel carbon-ion fuel cells
[DE94-017390] p 1053 N95-18894
Enhancement of creep resistance of a sintered Si3N4 ceramic by microwave annealing
[DE94-017688] p 987 N95-19399
Alternative materials for solid oxide fuel cells
[DE94-018452] p 1054 N95-19591

SITE SELECTION
Measurements of wideband multipath propagation at 531 MHz and 1.265 GHz
[BBC-RD-1994/3] p 1001 N95-19051
SIZE (DIMENSIONS)
Investigation of the microstructure of coatings for high power lasers by non-optical techniques
[DE94-017697] p 987 N95-19227
SIZE DETERMINATION
Echo imaging techniques determine the size of intravascular bubbles in decompression sickness
[AD-A284849] p 1087 N95-19714
SIZE DISTRIBUTION
Size distribution of one-, two- and three-dimensional Voronoi cells
[PB94-207008] p 1149 N95-18373
The jet model of chondrule formation
p 1189 N95-19310
SKIN (STRUCTURAL MEMBER)
Acoustic fatigue testing on different materials and skin-stringer elements p 1126 N95-19156
Thermo-acoustic fatigue design for hypersonic vehicle skin panels p 1047 N95-19161
An artifical corrosion protocol for lap-splices in aircraft skin p 937 N95-19462
SKY SURVEYS (ASTRONOMY)
The 2 Micron All Sky Survey
[AD-A283515] p 1178 N95-18001
The origin of the diffuse x-ray background
p 1197 N95-18729
SKYLAB PROGRAM
Skylab: The first 40 days
[NASA-TM-110491] p 961 N95-19040
SKYLAB 1
Skylab: The first 40 days
[NASA-TM-110491] p 961 N95-19040
Skylab: The second manned mission. A scientific harvest
[NASA-TM-110487] p 961 N95-19059
SKYLAB 2
Skylab: The first 40 days
[NASA-TM-110491] p 961 N95-19040
SLAGS
A ceramic/slag interface as an analog for accretion of hot refractory objects and rim formation
p 1191 N95-19322
SLEEVES
Split mandrel versus split sleeve coldworking: Dual methods for extending the fatigue life of metal structures
p 940 N95-19500
SLIDING
Sliding mode control method having terminal convergence in finite time
[NASA-CASE-NPO-18584-1-CU] p 1114 N95-19062
SLOPES
Robust image understanding. Techniques and applications
[AD-A283427] p 1113 N95-18057
SLOT ANTENNAS
Simulation of thin slot spirals and dual circular patch antennas using the finite element method with mixed elements
[NASA-CR-197671] p 1005 N95-19796
Slot spiral antenna modeling using hybrid/mixed FE-BI technique p 1006 N95-19797
Design considerations for an archimedean slot spiral antenna p 1006 N95-19798
SLOTS
Interference determination for wind tunnels with slotted walls p 960 N95-19269
SLOTTED WIND TUNNELS
Interference determination for wind tunnels with slotted walls p 960 N95-19269
SMALL SCIENTIFIC SATELLITES
Composite structures for magnetosphere imager spacecraft p 966 N95-18976
SMART STRUCTURES
Phase and amplitude controlled micropatch antenna
[AD-A284191] p 1002 N95-19103
Damage monitoring in metallic and composite structures using piezoelectric thin film sensors
[ARL-RR-4] p 971 N95-19467
Investigation of microscopic mechanisms of failure of electronic smart materials/systems
[AD-A284830] p 988 N95-19691
SNOW COVER
Assessment of climate variability of the Greenland Ice Sheet: Integration of in situ and satellite data
[NASA-CR-197604] p 1062 N95-19779
SNOWSTORMS
Forecasting snowfall using mixing ratios on an isentropic surface: An empirical study
[PB94-188760] p 1067 N95-17993
Synoptic and mesoscale examination of the northern New England winter storm of January 29-30, 1990
[PB94-209426] p 1072 N95-19581
SOCIAL FACTORS
Catalog of environmental data sets of Europe at the RIVM
[PB94-202710] p 1057 N95-18002
SODIUM
Flash heating is required to minimize sodium losses from chondrules p 1193 N95-19337
SODIUM CHLORIDES
Mechanical behavior of precipitation hardenable steels exposed to highly corrosive environment
p 982 N95-18180
A mechanism for blistering of carbon fiber composites
[AD-A286252] p 971 N95-19386
Gas turbine compressor corrosion and erosion in Western Europe p 954 N95-19678
SODIUM NITRATES
UV laser-surface interactions relevant to analytic spectroscopy of wide band gap materials
[DE94-016181] p 1037 N95-18350
SODIUM SULFATES
Sodium sulfate corrosion of silicon carbide fiber-reinforced calcium aluminosilicate glass-ceramic matrix composites
[AD-A283703] p 969 N95-18021
SODIUM SULFUR BATTERIES
Solar-electrochemical power system for a Mars mission
[NASA-TM-106606] p 967 N95-18570
SOFTENING
Characterization of the deformation and annealing of 304L stainless steel
[DE94-018584] p 981 N95-19707
SOFTWARE ENGINEERING
Improving software characteristics of a real-time system using reengineering techniques
[AD-A283659] p 1094 N95-18015
Miscellaneous disk utility application programs for the AFOS background partition
[PB94-181328] p 1067 N95-18038
Construction of a connectionist network supercomputer
[AD-A283354] p 1109 N95-18050
A visual approach to the analysis of large software systems
[AD-A285440] p 1095 N95-18089
Software techniques for balancing computation and communication in parallel systems
[AD-A285536] p 1109 N95-18106
Technical concept document. Central Archive for Reusable Defense Software (CARDS)
[AD-A284430] p 1096 N95-18343
Mapping a domain model and architecture to a generic design
[AD-A283747] p 1096 N95-18364
Engineer's handbook. Central Archive for Reusable Defense Software (CARDS)
[AD-A284341] p 1097 N95-18419
Franchise plan. Central Archive for Reusable Defense Software (CARDS)
[AD-A284344] p 1097 N95-18422
Library user's guide. Comprehensive Approach to Reusable Defensive Software (CARDS)
[AD-A284345] p 1097 N95-18423
Portable, Reusable, Integrated Software Modules (PRISM) documentation library version description document release 1.0. Central Archive for Reusable Defense Software (CARDS)
[AD-A284571] p 1097 N95-18447
Library capability demonstration. Central Archive for Reusable Defense Software (CARDS)
[AD-A284574] p 1098 N95-18450
NASA High Performance Computing and Communications program
[NASA-TM-4653] p 1174 N95-18573
Software Technology for Adaptable, Reliable Systems (STARS). Software architecture seminar report: Central Archive for Reusable Defense Software (CARDS)
[AD-A284668] p 1100 N95-19106
Enhancing the architectural characterization of parallel proto
[AD-A285678] p 1111 N95-19524
Draft SEI program plans: 1995-1999
[AD-A285047] p 1100 N95-19545
Constructing a real-time mobile robot software system
[AD-A285969] p 1115 N95-19572
CLIPS template system for program understanding
p 1102 N95-19638
CLIPS, AppleEvents, and AppleScript: Integrating CLIPS with commercial software p 1103 N95-19643
Using CLIPS to represent knowledge in a VR simulation p 1107 N95-19765
Process definition and modeling guidebook. Volume 1: Concepts and principles of MPDM. Version 02.00.02
[AD-A279162] p 1108 N95-19803
Process definition and modeling guidebook. Volume 2: Advanced applications of MPDM
[AD-A279199] p 1108 N95-19813
SOFTWARE RELIABILITY
Requirements analysis for safety-critical systems: A chemical batch processing example
[PB94-201563] p 991 N95-17934
Can information surety be assessed with high confidence?
[DE94-015805] p 1120 N95-18653
Evaluation of the efficiency and reliability of software generated by code generators p 1108 N95-19004
SOFTWARE REUSE
Portable, Reusable, Integrated Software Modules (PRISM) documentation library model document release 1.0: Central Archive for Reusable Defense Software (CARDS)
[AD-A284567] p 1095 N95-18030
Library capability demonstration. Central Archive for Reusable Defense Software (CARDS)
[AD-A284568] p 1095 N95-18031
Library capability demonstration. Central Archive for Reusable Defense Software (CARDS)
[AD-A284569] p 1095 N95-18032
Library Development Handbook. Central Archive for Reusable Defense Software (CARDS)
[AD-A284570] p 1095 N95-18033
Library capability demonstration. Central Archive for Reusable Defense Software (CARDS)
[AD-A284572] p 1095 N95-18034
Technical concept document. Central Archive for Reusable Defense Software (CARDS)
[AD-A284430] p 1096 N95-18343
Engineer's handbook. Central Archive for Reusable Defense Software (CARDS)
[AD-A284341] p 1097 N95-18419
Acquisition handbook: Update. Comprehensive Approach to Reusable Defensive Software (CARDS)
[AD-A284342] p 1097 N95-18420
Training plan. Central Archive for Reusable Defense Software (CARDS)
[AD-A284343] p 1097 N95-18421
Franchise plan. Central Archive for Reusable Defense Software (CARDS)
[AD-A284344] p 1097 N95-18422
Portable, Reusable, Integrated Software Modules (PRISM) documentation library version description document release 1.0. Central Archive for Reusable Defense Software (CARDS)
[AD-A284571] p 1097 N95-18447
Metrics concept report. Central Archive for Reusable Defense Software (CARDS)
[AD-A284573] p 1097 N95-18449
Library capability demonstration. Central Archive for Reusable Defense Software (CARDS)
[AD-A284574] p 1098 N95-18450
Software Technology for Adaptable, Reliable Systems (STARS). Software architecture seminar report: Central Archive for Reusable Defense Software (CARDS)
[AD-A284668] p 1100 N95-19106
CLIPS template system for program understanding
p 1102 N95-19638
SOFTWARE TOOLS
Long wavelength propagation capacity, version 1.1 (computer diskette)
[AD-M200254] p 994 N95-17964
Some statistical tools for SAR image synthesis, analysis and processing
[INPE-5548-TDI/534] p 1172 N95-18004
A formal method for semantics-based change-merging of software prototypes
[AD-A283668] p 1094 N95-18017
Enhancements to the KATE model-based reasoning system p 1115 N95-18183
Universal wind tunnel data acquisition and reduction software
[AD-A283897] p 1096 N95-18365
The Isis project: Fault-tolerance in large distributed systems
[NASA-CR-197561] p 1110 N95-18532
Development of executive information systems
[AD-A284005] p 1174 N95-18654
SICOMP, the SINTEF data compression library (version 1.0) reference manual
[PB94-207107] p 1099 N95-18668
EEsoF MICAD and ACADEMY macro files for coplanar waveguide and finite ground plan coplanar waveguide
[NASA-TM-106800] p 1000 N95-18733
On extending parallelism to serial simulators
[NASA-CR-195011] p 1099 N95-18931
Performance evaluation of the Engineering Analysis and Data Systems (EADS) 2 p 1163 N95-18978
A hypertext-based Internet-assessable database for the MSFC Technology Transfer Office p 1165 N95-18986
Evaluation of the efficiency and reliability of software generated by code generators p 1108 N95-19004

Enhancing the architectural characterization of parallel proto
[AD-A285678] p 1111 N95-19524
The Computer Aided Aircraft-design Package (CAAP) p 1106 N95-19759
Rule based design of conceptual models for formative evaluation p 1106 N95-19760
Reflexive reasoning for distributed real-time systems p 1107 N95-19766
Automatically generating procedure code and database maintenance scripts
[DE95-000545] p 1176 N95-19876

SOI (SEMICONDUCTORS)
Defect reduction and back channel degradation in SIMOX
[AD-A284231] p 1148 N95-17960

SOIL MECHANICS
Long-term processes in geomaterials. A three-dimensional visco-elastic soil model
[PB94-207180] p 1065 N95-18640
SSI effects for a tank containing two liquids
[DE94-012457] p 1020 N95-19099

SOILS
Long-term processes in geomaterials. A three-dimensional visco-elastic soil model
[PB94-207180] p 1065 N95-18640
One strategy for estimating the potential soil carbon storage due to CO2 fertilization
[DE94-017895] p 1059 N95-18666
Changes in the flux of carbon between plants and soil microorganisms at elevated CO2: Physiological processes with ecosystem-level implications
[DE94-017067] p 1060 N95-19112
Heavy metal soil contamination at US Army installations: Proposed research and strategy for technology development
[AD-A279171] p 1062 N95-19808

SOL-GEL PROCESSES
Aryl gels and related materials. Synthesis and characterization of a new class of microporous materials
[AD-A285044] p 987 N95-19544
Future trends in optical coatings for high-power laser applications
[DE94-018592] p 1039 N95-19708

SOLAR ACTIVITY
Analysis of solar spectral irradiance measurements from the SBUV/2-series and the SSBUV instruments
[NASA-CR-197544] p 1196 N95-18954

SOLAR ACTIVITY EFFECTS
CRRESPRO documentation
[AD-A284578] p 1178 N95-18451

SOLAR ARRAYS
Intermediate design and analysis of the PANSAT electrical power subsystem
[AD-A283610] p 1053 N95-18435
Solar-electrochemical power system for a Mars mission
[NASA-TM-106606] p 967 N95-18570

SOLAR ATMOSPHERE
Solar flare model atmospheres
[NASA-CR-197607] p 1196 N95-19034

SOLAR CELLS
InP solar cell development on inexpensive silicon substrates
[AD-A283624] p 1052 N95-18011
Final results of the Advanced Photovoltaic Experiment flight test
[NASA-TM-106828] p 967 N95-18571
InP solar cell development on inexpensive silicon substrates
[AD-A286254] p 1054 N95-19388
Research on stable, high-efficiency amorphous silicon multijunction modules
[DE95-000215] p 1054 N95-19832
Tapping into the Sun: Today's applications of photovoltaic technology
[DE93-000075] p 1054 N95-19854
NREL Photovoltaic Program, FY 1993
[DE94-011880] p 1055 N95-19857
Correlation of polycrystalline Cu(In,Ga)Se2 device efficiency with homojunction depthand interfacial structure: X-ray photoemission and positron annihilation spectroscopic characterization
[DE94-013543] p 1055 N95-19858
A simple single-photomask process for fabrication of high-efficiency multicrystalline silicon solar cells
[DE94-014251] p 1055 N95-19859
Battery and charge controller evaluations in small stand-alone PV systems
[DE94-014252] p 1013 N95-19872
Gettering in multicrystalline silicon: A design-of-experiments approach
[DE94-014289] p 1055 N95-19873
Growth and development of GaInAsP for high-efficiency solar cells
[DE94-000210] p 1056 N95-19878
Advanced processing technology for high-efficiency, thin-film CuInSe2 and CdTe solar cells
[DE94-011838] p 1056 N95-19880
Silicon-Film (trademark) photovoltaic manufacturing technology
[DE94-011899] p 1056 N95-19882

SOLAR CONVECTION (ASTRONOMY)
Solar-geophysical data number 599, July 1994. Part 1: (Prompt reports). Data for June, May 1994, and late data
[PB94-213972] p 1196 N95-19404

SOLAR CORONA
Coronal abundances and their variation
[NASA-CR-197553] p 1195 N95-18376
Relative elemental abundance and heating constraints determined for the solar corona from SERTS measurements
[NASA-TM-104616] p 1196 N95-19791

SOLAR CYCLES
Dynamic evolution of emerging magnetic flux tubes in the solar convective envelope p 1195 N95-18497

SOLAR ECLIPSES
Design, validation and prototype testing of a high resolution all-reflection Michelson interferometer for solar occultation measurements of the OI 1304-a triplet emission
[AD-A283705] p 1178 N95-18361

SOLAR FLARES
Solar flare model atmospheres
[NASA-CR-197607] p 1196 N95-19034
Solar-geophysical data number 599, July 1994. Part 1: (Prompt reports). Data for June, May 1994, and late data
[PB94-213972] p 1196 N95-19404
Solar-geophysical data number 599, July 1994. Part 2: (Comprehensive reports). Data for January 1994, and miscellaneous
[PB94-213980] p 1196 N95-19405

SOLAR FLUX
Solar-geophysical data number 599, July 1994. Part 1: (Prompt reports). Data for June, May 1994, and late data
[PB94-213972] p 1196 N95-19404
The very low energy solar flux of electron and heavy-flavor neutrinos and antineutrinos
[DE94-018583] p 1135 N95-19706

SOLAR MAGNETIC FIELD
Dynamic evolution of emerging magnetic flux tubes in the solar convective envelope p 1195 N95-18497

SOLAR NEUTRINOS
A Type 2 supernovae constraint on neutrino(sub e) - neutrino(sub s) mixing
[NASA-CR-197630] p 1180 N95-18746
Results from SAGE 2
[DE95-000849] p 1196 N95-19619
The very low energy solar flux of electron and heavy-flavor neutrinos and antineutrinos
[DE94-018583] p 1135 N95-19706

SOLAR PHYSICS
Solar-geophysical data number 599, July 1994. Part 1: (Prompt reports). Data for June, May 1994, and late data
[PB94-213972] p 1196 N95-19404
Solar-geophysical data number 599, July 1994. Part 2: (Comprehensive reports). Data for January 1994, and miscellaneous
[PB94-213980] p 1196 N95-19405

SOLAR PLANETARY INTERACTIONS
Modeling the diurnally precessing Jovian magnetospheric field
[AD-A284857] p 1195 N95-19739

SOLAR PROMINENCES
Solar-geophysical data number 599, July 1994. Part 2: (Comprehensive reports). Data for January 1994, and miscellaneous
[PB94-213980] p 1196 N95-19405

SOLAR RADIATION
Analysis of solar spectral irradiance measurements from the SBUV/2-series and the SSBUV instruments
[NASA-CR-197544] p 1196 N95-18954
Implications of summertime marine stratocumulus on the North American climate p 1073 N95-18977
Relative elemental abundance and heating constraints determined for the solar corona from SERTS measurements
[NASA-TM-104616] p 1196 N95-19791
Summary information and data sets for the HBCU Solar Measurements Network
[DE94-011872] p 1055 N95-19856
Proceedings of the 15th Annual Conference on Atmospheric Transmission Models
[AD-A279919] p 1142 N95-19862

SOLAR RADIO BURSTS
Solar-geophysical data number 599, July 1994. Part 2: (Comprehensive reports). Data for January 1994, and miscellaneous
[PB94-213980] p 1196 N95-19405

SOLAR REFLECTORS
Progress in the development of advanced solar reflectors
[DE94-000264] p 1053 N95-18463

SOLAR SENSORS
Final results of the Advanced Photovoltaic Experiment flight test
[NASA-TM-106828] p 967 N95-18571

SOLAR SPECTRA
Analysis of solar spectral irradiance measurements from the SBUV/2-series and the SSBUV instruments
[NASA-CR-197544] p 1196 N95-18954

SOLAR SYSTEM EVOLUTION
Second-order reconstruction of the inflationary potential
[NASA-CR-197629] p 1121 N95-19030
Mercury: Exploration of a planet
[NASA-TM-110489] p 1194 N95-19045
Heating during solar nebula formation and Mg isotopic fractionation in precursor grains of CAIs and chondrules p 1191 N95-19326
Variations among chondrite groups: Constraints on nebular processes p 1192 N95-19327
Implications for the evolution of chondrules from Agglomeratic olivine chondrules p 1193 N95-19335

SOLAR WIND
Solar-geophysical data number 599, July 1994. Part 1: (Prompt reports). Data for June, May 1994, and late data
[PB94-213972] p 1196 N95-19404
Solar-geophysical data number 599, July 1994. Part 2: (Comprehensive reports). Data for January 1994, and miscellaneous
[PB94-213980] p 1196 N95-19405

SOLAR X-RAYS
Solar flare model atmospheres
[NASA-CR-197607] p 1196 N95-19034
Solar-geophysical data number 599, July 1994. Part 2: (Comprehensive reports). Data for January 1994, and miscellaneous
[PB94-213980] p 1196 N95-19405

SOLDERED JOINTS
The reliability of laser reflowed Sn-Ag solder joints
[AD-A284732] p 1044 N95-18080

SOLDERS
The reliability of laser reflowed Sn-Ag solder joints
[AD-A284732] p 1044 N95-18080

SOLID ELECTROLYTES
Methane conversion by solid electrolyte membranes
[PB94-191781] p 973 N95-17982

SOLID LUBRICANTS
Tribology and microstructure of PS212 with a Cr2O3 seal coat
[NASA-TM-106768] p 969 N95-18448

SOLID MECHANICS
Numerical analysis of dissipative dynamical systems in solid and fluid mechnaics, with a special emphasis on coupled problems p 1122 N95-18916

SOLID PHASES
Phase stability and elastic properties of C15 compounds HfV2 + Nb
[DE95-000940] p 981 N95-19611

SOLID PROPELLANT COMBUSTION
Solid fuel ramjet composition
[AD-D016458] p 990 N95-19090

SOLID PROPELLANT IGNITION
Flamespreading in granular solid propellant: Initial results
[AD-A284245] p 976 N95-19729

SOLID PROPELLANTS
Flamespreading in granular solid propellant: Initial results
[AD-A284245] p 976 N95-19729

SOLID SOLUTIONS
High temperature stability of binary microstructures derived from liquid precursors
[AD-A283960] p 1150 N95-18685
Heteroepitaxy of ternary SiGeC alloys on Si for bipolar transistors
[AD-A285317] p 1151 N95-19511
Multilayer anti-erosion coatings p 954 N95-19679

SOLID STATE
Lithium electrode/polyacrylonitrile based polymer electrolyte interface
[AD-A283947] p 986 N95-19064
Synthesis and characterization of aluminum-phosphorus adducts: X-ray crystal structures of Cl3Al (dot) P(SiMe3)3 (dot) C7H8 and Br3Al (dot) P(SiMe3)3 (dot) C7H8
[AD-A279194] p 1154 N95-19812

SOLID STATE LASERS
High power phase conjugated solid state lasers
[DE94-016633] p 1037 N95-18357
Solid state laser driver for extreme ultraviolet lithography
[DE94-016971] p 1038 N95-19096
Performance improvements in diode laser arrays
[DE94-016547] p 1039 N95-19508

SOLID STATE PHYSICS
The physics and operation of ultra-submicron length semiconductor devices
[AD-A280181] p 1155 N95-19828
Modeling of quantum transport in semiconductor devices
[AD-A280182] p 1155 N95-19829
SOLID SURFACES
Observation of flow and temperature oscillations around a bubble on a solid surface subject to a vertical temperature gradient
[NASA-CR-197593] p 1017 N95-18327
SOLID WASTES
Economic impact analysis for proposed emission standards and guidelines for municipal waste combustors: A description of the basis for, and impacts of, proposed revisions to air pollutant emission regulations for new and existing municipal waste combustors under Clean Air Act Sections 111(b), 111(d), and 129
[PB94-213543] p 1061 N95-19403
SOLID-SOLID INTERFACES
Discrete and continuum elastic properties of interfaces p 1150 N95-18928
Adhesion, friction, and wear behavior of clean metal-ceramic couples
[NASA-TM-106815] p 989 N95-19783
SOLIDIFICATION
Ion beam surface treatment: A new capability for surface enhancement
[DE94-014663] p 977 N95-17968
Numerical formulation of composition segregation at curved solid-liquid interface during steady state solidification process p 977 N95-19012
Effects of vibration (G-jitters) on convection in micro-gravity p 991 N95-19013
SOLITARY WAVES
Mass and radius of cosmic balloons
[NASA-CR-197628] p 1180 N95-19031
SOLUBILITY
Neutron scattering study of dilute supercritical solutions
[DE95-000493] p 1134 N95-19557
SOLUTES
Numerical formulation of composition segregation at curved solid-liquid interface during steady state solidification process p 977 N95-19012
Atomistic and elastic analyses of defects and small structures
[DE94-017047] p 980 N95-19111
Neutron scattering study of dilute supercritical solutions
[DE95-000493] p 1134 N95-19557
SOLVENT EXTRACTION
Molecular recognition as shown by the solvent extraction of (R)- and (S)-alpha-(1-naphthyl)ethyl ammonium picrate or orange 2 by chiral pyridino-crown ethers
[AD-A280157] p 969 N95-19823
SOLVENTS
Potential replacements for solvents that are ozone depleting substances
[AD-A285442] p 1058 N95-18091
Polyurethane self-priming topcoats
[AD-D016264] p 984 N95-18320
The Solvent Absorption-Extractive Distillation (SAED) process for ethanol recovery from gas/vapor streams
[DE94-013112] p 974 N95-18637
Neutron scattering study of dilute supercritical solutions
[DE95-000493] p 1134 N95-19557
Alternative solvents/technologies for paint stripping: Phase 1
[AD-A279918] p 989 N95-19861
SONIC BOOMS
Floating shock fitting via Lagrangian adaptive meshes
[NASA-CR-194997] p 1116 N95-18110
An assessment of the adaptive unstructured tetrahedral grid, Euler Flow Solver Code FELISA
[NASA-TP-3526] p 930 N95-19041
SOOT
Novel catalysts for methane activation
[DE95-001179] p 976 N95-19785
SORTING ALGORITHMS
A practical algorithm for integer sorting on a mesh-connected computer (preliminary version)
[AD-A283921] p 1110 N95-18159
SOS (SEMICONDUCTORS)
Radiation-induced noise in UMPC-type current probes: IEMP response of the current measurement system
[AD-A284176] p 998 N95-18520
SOUND DETECTING AND RANGING
Nondestructive time-of-capture, location and velocity sensing in intact capture p 1036 N95-19194
SOUND PRESSURE
Improved efficiency and power density for thermoacoustic coolers
[AD-A283946] p 992 N95-18185
Calibration and sediment load algorithms for an acoustic sediment flux probe
[AD-A283655] p 1075 N95-18617
Weapons bay acoustic environment p 1125 N95-19148
Modelling structurally damaging twin-jet screech p 946 N95-19154
SOUND TRANSMISSION
Multi-channel sound for HDTV: Subjective tests on sound channel configuration
[BBC-RD-1994/4] p 998 N95-18535
A wideband absorber for television studios
[BBC-RD-1994/12] p 1123 N95-18566
High frequency room responses: Acoustic design and the control of stereophonic image quality
[BBC-RD-1994/11] p 1124 N95-19046
Metal-framed partitions with reduced thicknesses. Part 2: Built-in acoustic treatment
[BBC-RD-1993/6-PT-2] p 993 N95-19137
Metal-framed partitions with reduced thicknesses. Part 1: Narrower studs and cavities
[BBC-RD-1993/5-PT-1] p 993 N95-19138
Identification and analysis of air- and structure-borne noise and vibration paths p 1128 N95-19166
SOUND WAVES
Observations of TEC fluctuations from an explosion on the Earth's surface
[DE94-018278] p 1063 N95-18125
Fiber optic pressure and/or vibration detector
[AD-D016474] p 1140 N95-18460
Low-dissipation and -dispersion Runge-Kutta schemes for computational acoustics
[NASA-CR-195022] p 1018 N95-18488
Further measurements of the sound insulations of metal-framed partitions
[BBC-RD-1994/7] p 998 N95-18534
Acoustic radiation damping of flat rectangular plates subjected to subsonic flows p 1123 N95-18542
The STOKES (Version 4) normal-mode shallow water transmission loss program
[MRL-CP-1] p 1075 N95-19503
Tunneling acoustic microscopy
[AD-A279160] p 1128 N95-19802
SOUNDING
Atmospheric Infrared Sounder
[NASA-CR-197573] p 1064 N95-18444
Special relativity effects for space-based coherent lidar experiments p 1014 N95-18983
SOURCE PROGRAMS
Constructing a real-time mobile robot software system
[AD-A285969] p 1115 N95-19572
SOUTHERN HEMISPHERE
Evolution of the Southern Hemisphere ozone hole as seen by TOMS from August 1979 to December 1991
[NASA-TM-110116] p 1057 N95-18048
Atmospheric chemistry of biogenic sulfur in the Southern Hemisphere p 1071 N95-18399
SOUTHERN OSCILLATION
Marginal probabilities of the extremes of ENSO events for temperature and precipitation in the southeastern United States
[AD-A284716] p 1068 N95-18076
SPACE ADAPTATION SYNDROME
US experiments flown on the Soviet biosatellite Cosmos 2044. Volume 1: Mission description, experiments K-7-01 - K-7-15
[NASA-TM-108802-VOL-1] p 1092 N95-18569
SPACE DEBRIS
Cracking characteristics of a habitable module pressure wall following orbital debris penetration p 1047 N95-19003
SPACE ENVIRONMENT SIMULATION
Development of microgravity, full body functional reach envelope using 3-D computer graphic models and virtual reality technology p 1092 N95-18990
SPACE ERECTABLE STRUCTURES
Streamlined design and self reliant hardware for active control of precision space structures
[NASA-CR-4637] p 964 N95-18580
SPACE EXPLORATION
An integrated strategy for the planetary sciences: 1995 - 2010
[NASA-CR-197145] p 1194 N95-19134
SPACE LABORATORIES
Effects of vibration (G-jitters) on convection in micro-gravity p 991 N95-19013
SPACE PLASMAS
Properties of Alfven waves with transverse scale on the order of skin-depth
[AD-A285657] p 1147 N95-19700
Spacecraft environments interactions: Protecting against the effects of spacecraft charging
[NASA-RP-1354] p 965 N95-19780
SPACE PROBES
SOCCER: Comet Coma Sample Return Mission p 1181 N95-19174
SPACE PROCESSING
Plasma heating for containerless and microgravity materials processing
[NASA-CASE-NPO-18819-1-CU] p 991 N95-18326
Microgravity isolation system design: A modern control analysis framework
[NASA-TM-106803] p 927 N95-18486
Bubble formation in microgravity p 991 N95-18970
SPACE SHUTTLE BOOSTERS
Documentation and archiving of the Space Shuttle wind tunnel test data base. Volume 1: Background and description
[NASA-TM-104806-VOL-1] p 965 N95-19237
SPACE SHUTTLE MAIN ENGINE
LVQ and backpropagation neural networks applied to NASA SSME data
[NASA-CR-195418] p 962 N95-18045
Evaluation of SSME test data reduction methods p 968 N95-19002
SPACE SHUTTLE ORBITERS
Hypersonic flight testing
[AD-A283981] p 944 N95-18891
Documentation and archiving of the Space Shuttle wind tunnel test data base. Volume 1: Background and description
[NASA-TM-104806-VOL-1] p 965 N95-19237
SPACE SHUTTLE PAYLOADS
Automated path planning of the Payload Inspection and Processing System p 1043 N95-18169
STS-65 Space Shuttle mission report
[NASA-CR-197598] p 963 N95-18610
SPACE SHUTTLES
Debris/ice/TPS assessment and integrated photographic analysis of Shuttle mission STS-68
[NASA-TM-109207] p 963 N95-18047
Field and data analysis studies related to the atmospheric environment
[NASA-CR-196543] p 1068 N95-18093
STS-65 Space Shuttle mission report
[NASA-CR-197598] p 963 N95-18610
Hypersonic flight testing
[AD-A283981] p 944 N95-18891
Documentation and archiving of the Space Shuttle wind tunnel test data base. Volume 1: Backgrour l and description
[NASA-TM-104806-VOL-1] p 965 N95-19237
Fatigue loads spectra derivation for the Space Shuttle: Second cycle p 934 N95-19470
Documentation and archiving of the Space Shuttle wind tunnel test data base. Volume 2: User's Guide to the Archived Data Base
[NASA-TM-104806-VOL-2] p 965 N95-19624
Debris/ice/TPS assessment and integrated photographic analysis of Shuttle mission STS-66
[NASA-TM-110141] p 963 N95-19790
SPACE STATION FREEDOM
Modal Identification Experiment accommodations review
[NASA-CR-195009] p 964 N95-18105
Analytical control test plan and microbiological methods for the water recovery test
[NASA-TM-108473] p 1091 N95-19061
SPACE STATIONS
Space Station racks weight and CG measurement using the rack insertion end-effector p 966 N95-18168
Design considerations for a Space Station radiation shield for protection from both man-made and natural sources
[NASA-CR-195298] p 964 N95-18495
SPACE TECHNOLOGY EXPERIMENTS
Skylab: The second manned mission. A scientific harvest
[NASA-TM-110487] p 961 N95-19059
SPACE TRANSPORTATION SYSTEM FLIGHTS
Debris/ice/TPS assessment and integrated photographic analysis of Shuttle mission STS-68
[NASA-TM-109207] p 963 N95-18047
STS-65 Space Shuttle mission report
[NASA-CR-197598] p 963 N95-18610
Debris/ice/TPS assessment and integrated photographic analysis of Shuttle mission STS-66
[NASA-TM-110141] p 963 N95-19790
SPACE-TIME FUNCTIONS
The space-time solution element method: A new numerical approach for the Navier-Stokes equations
[NASA-TM-106818] p 1014 N95-18036
Lie algebras for the Dirac-Clifford ring
[DE94-626643] p 1118 N95-18878
SPACEBORNE ASTRONOMY
Is a massive tau neutrino just what cold dark matter needs?
[NASA-CR-197627] p 1180 N95-18964
SPACEBORNE EXPERIMENTS
Microgravity fluid science research in Europe
[PB94-201720] p 990 N95-17973

Microgravity isolation system design: A modern control synthesis framework
[NASA-TM-106805] p 927 N95-18197
Observation of flow and temperature oscillations around a bubble on a solid surface subject to a vertical temperature gradient
[NASA-CR-197593] p 1017 N95-18327
US experiments flown on the Soviet biosatellite Cosmos 2044. Volume 1: Mission description, experiments K-7-01 - K-7-15
[NASA-TM-108802-VOL-1] p 1092 N95-18569
STS-65 Space Shuttle mission report
[NASA-CR-197598] p 963 N95-18610
Skylab: The first 40 days
[NASA-TM-110491] p 961 N95-19040
Skylab: The second manned mission. A scientific harvest
[NASA-TM-110487] p 961 N95-19059
SPICE: An innovative, flexible instrument concept
p 966 N95-19189
Real-time remote scientific model validation
p 1103 N95-19640
Summary report of mission acceleration measurements for STS-60, SPACEHAB2, launched 11 February 1994
[NASA-TM-106797] p 991 N95-19788

SPACEBORNE PHOTOGRAPHY
Legacy of Gemini
[NASA-TM-110486] p 961 N95-19058

SPACEBORNE TELESCOPES
On orbit performance of the ALEXIS EUV telescopes
[DE94-016197] p 964 N95-18639

SPACECRAFT CHARGING
Spacecraft environments interactions: Protecting against the effects of spacecraft charging
[NASA-RP-1354] p 965 N95-19780

SPACECRAFT CONFIGURATIONS
Fatigue loads spectra derivation for the Space Shuttle: Second cycle p 934 N95-19470

SPACECRAFT CONSTRUCTION MATERIALS
Conference on Aerospace Transparent Materials and Enclosures. Volume 2: Sessions 5-9
[AD-A283926] p 942 N95-18162
Advanced small rocket chambers. Basic program and option 2: Fundamental processes and material evaluation
[NASA-CR-195349] p 966 N95-18192
Conference on Aerospace Transparent Materials and Enclosures, volume 1
[AD-A283925] p 944 N95-18677
A CMC database for use in the next generation launch vehicles (rockets) p 963 N95-18993

SPACECRAFT DESIGN
Lean spacecraft avionics trade study
p 966 N95-18994

SPACECRAFT DOCKING
Gemini 8, This is Houston, flight
[NASA-TM-110490] p 965 N95-19039
Skylab: The first 40 days
[NASA-TM-110491] p 961 N95-19040

SPACECRAFT EQUIPMENT
Physics of spacecraft-based interplanetary dust collection by impact into low-density media
p 1181 N95-19176

SPACECRAFT INSTRUMENTS
Mission description and in-flight operations of ERBE instruments on ERBS and NOAA 10 spacecraft, February 1987 - February 1990
[NASA-RP-1325] p 1051 N95-18465
Comet coma sample return instrument
p 1180 N95-19173
The status of measurement technologies concerning micrometer and submicrometer space articulate matter capture, recovery, velocity and trajectory
p 1181 N95-19175
Highly transparent and rugged sensor for velocity determinations of cosmic dust particles
p 966 N95-19176
Main characteristics of the COMET/COMRADE experiments p 1181 N95-19179
Techniques for in situ collection and measurement of volatiles released during hypervelocity impact
p 962 N95-19184

SPACECRAFT LAUNCHING
Skylab: The first 40 days
[NASA-TM-110491] p 961 N95-19040
Debris/ice/TPS assessment and integrated photographic analysis of Shuttle mission STS-66
[NASA-TM-110141] p 963 N95-19790

SPACECRAFT MODULES
Rack Insertion End Effector (RIEE) guidance
p 1043 N95-18178

SPACECRAFT POWER SUPPLIES
Intermediate design and analysis of the PANSAT electrical power subsystem
[AD-A283610] p 1053 N95-18435
Transient and steady-state tests of the space power research engine with resistive and motor loads
[NASA-TM-106832] p 1042 N95-19238

SPACECRAFT PROPULSION
Arcjet thruster research and technology, phase 2
[NASA-CR-182276] p 927 N95-18044
Advanced small rocket chambers. Basic program and option 2: Fundamental processes and material evaluation
[NASA-CR-195349] p 966 N95-18192
High performance storable propellant resistojet
[NASA-CR-191128] p 967 N95-18195

SPACECRAFT RADIATORS
Rewetting of monogroove heat pipe in Space Station radiators
[NASA-CR-197579] p 1014 N95-18092
Geometrical vapor blocker for parallel condensation tubes requiring subcooling
[NASA-CASE-MSC-22090-1] p 1017 N95-18323

SPACECRAFT SHIELDING
Design considerations for a Space Station radiation shield for protection from both man-made and natural sources
[NASA-CR-195298] p 964 N95-18495
Debris/ice/TPS assessment and integrated photographic analysis of Shuttle mission STS-66
[NASA-TM-110141] p 963 N95-19790

SPACECRAFT STRUCTURES
Modal Identification Experiment accommodations review
[NASA-CR-195009] p 964 N95-18105
Streamlined design and self reliant hardware for active control of precision space structures
[NASA-CR-4637] p 964 N95-18580
Composite structures for magnetosphere imager spacecraft p 966 N95-18976
Cracking characteristics of a habitable module pressure wall following orbital debris penetration
p 1047 N95-19003
Aeroacoustic qualification of HERMES shingles
p 1125 N95-19145
Acoustics of space structures p 1126 N95-19152

SPATIAL DISTRIBUTION
Creation of new items and forms for the Project A Assembling Objects test
[AD-A285522] p 1088 N95-18095
A synoptic climatology of convective weather in the Netherlands
[KNMI-WR-93-04] p 1071 N95-18395

SPATIAL FILTERING
A novel technique for 4-dimensional atmospheric and oceanographic irradiance measurements using 3-D spatial filtering
[AD-A285658] p 1073 N95-19701

SPATIAL RESOLUTION
Development of a high-resolution liquid xenon detector for gamma-ray astrophysics p 1179 N95-18499
High frame rate CCD cameras with fast optical shutters for military and medical imaging applications
[DE94-018316] p 1034 N95-19229

SPECIFIC HEAT
Phase stability and elastic properties of C15 compounds HfV2 + Nb
[DE95-000940] p 981 N95-19611

SPECIFICATIONS
Guidelines for reduction of human errors during maintenance of safety systems; maintainability and maintenance support
[PB94-215597] p 1092 N95-19412

SPECIMEN GEOMETRY
A new stochastic systems approach to structural integrity p 935 N95-19474

SPECKLE PATTERNS
On the optimization of speckle filtering techniques for ERS-1 images over Argentina
[INPE-5578-PRE/1806] p 1050 N95-18216

SPECTRA
Spectral distribution of the two-photon decay of He-like krypton
[DE95-001442] p 1135 N95-19787

SPECTRAL BANDS
Silicon carbide photoconductive switches
[AD-A284310] p 1008 N95-18378

SPECTRAL LINE WIDTH
New method for homodyne laser linewidth measurements with a short delay fiber
[PB94-202629] p 1036 N95-18061

SPECTRAL METHODS
A spectrally accurate boundary-layer code for infinite swept wings
[NASA-CR-195014] p 1014 N95-18042
Treatment of non-linear systems by timeplane-transformed CT methods: The spectral gust method p 956 N95-18600
CFD: Advances and Applications, 1994
[NAL-SP-9412] p 1028 N95-19455
Spectral methods for fluid flow p 1028 N95-19459

SPECTRAL RECONNAISSANCE
ISSSR tutorial 1: Introduction to spectral remote sensing
[AD-A284268] p 1052 N95-19734

SPECTRAL REFLECTANCE
Spectral reflectance properties of wetlands plants
[AD-A283546] p 1051 N95-18614
Visible-infrared remote-sensing model and applications for ocean waters
[NASA-CR-197602] p 1051 N95-18739

SPECTRAL THEORY
Prediction of global cloud cover with a very high resolution global spectral model
[AD-A279944] p 1073 N95-19870

SPECTROMETERS
Study of strangeness production in relativistic nucleus beams at JINR
[DE94-626720] p 1136 N95-18881

SPECTROPHOTOMETRY
Standard reference materials: Glass filters as a standard reference material for spectrophotometry. Selection, preparation, certification and use of SRM 930 and SRM 1930
[PB94-188844] p 973 N95-17994

SPECTRORADIOMETERS
Final results of the Advanced Photovoltaic Experiment flight test
[NASA-TM-106828] p 967 N95-18571

SPECTROSCOPIC ANALYSIS
Evaluation of inorganic zinc-rich primers using Electrochemical Impedance Spectroscopy (EIS) in combination with atmospheric exposure
p 977 N95-18170

SPECTROSCOPY
AASERT-93: New high-pressure diagnostic technique
[AD-A284943] p 973 N95-17975
Fundamental studies of passivity and passivity breakdown
[DE94-016954] p 987 N95-19095
Spectroscopy and dynamics of vibrationally excited molecules
[AD-A285874] p 1134 N95-19597
Synthesis and characterization of aluminum-phosphorus adducts: X-ray crystal structures of Cl3Al (dot) P(SiMe3)3 (dot) C7H8 and Br3Al (dot) P(SiMe3)3 (dot) C7H8
[AD-A279194] p 1154 N95-19812

SPECTRUM ANALYSIS
Error measurements in an Acousto-Optic Tunable Filter-Fiber Bragg Grating Sensor System
[AD-A283912] p 1139 N95-18154
A spectral study of a radio-frequency plasma-generated flux of atomic oxygen
[NASA-TM-4612] p 1032 N95-18194
Simulation of gamma-ray spectra for a variety of user-specified detector designs
[NASA-CR-197551] p 1136 N95-18370
Coronal abundances and their variation
[NASA-CR-197553] p 1195 N95-18376
An instrument to measure the charge, and energy spectrum (20-1000 GeV/a) of the cosmic ray species oxygen to iron
[NASA-CR-197555] p 1197 N95-18464
An optical study of compact steep spectrum radio sources p 1179 N95-18498
Pure-rotational emission from molecular hydrogen in OMC-1 p 1179 N95-18500
Final results of the Advanced Photovoltaic Experiment flight test
[NASA-TM-106828] p 967 N95-18571
A photoionization study of OH and OD from 680A to 950A: An analysis of the Rydberg series
[NASA-CR-196970] p 974 N95-18744
Analysis of solar spectral irradiance measurements from the SBUV/2-series and the SSBUV instruments
[NASA-CR-197544] p 1196 N95-18954
Cosmic ray models for early galactic lithium, beryllium, and boron production
[NASA-CR-197626] p 1137 N95-18965
Spectrogram diagnosis of aircraft disasters
p 940 N95-19167
ISSSR tutorial 1: Introduction to spectral remote sensing
[AD-A284268] p 1052 N95-19734

SPEED CONTROL
Improved speed control system for the 87,000 HP wind tunnel drive
[NASA-TM-106840] p 1035 N95-19794

SPHERES
Collection efficiency and ice accretion calculations for a sphere, a swept MS(1)-317 wing, a swept NACA-0012 wing tip, an axisymmetric inlet, and a Boeing 737-300
[NASA-TM-106831] p 933 N95-18582
Molecular dynamics study of aqueous electrolyte solutions near a structured sphere
[AD-A284010] p 1132 N95-18655

Hypervelocity air flows with finite rate chemistry
[AD-A284727] p 931 N95-19109

SPHERICAL SHELLS
Study of high gain spherical shell ICF targets containing uniform layers of liquid deuterium tritium fuel
[DE94-018550] p 1136 N95-18552

SPHERICAL WAVES
Computer simulation of wave propagation through turbulent media
[AD-A283695] p 1000 N95-18671
Simulation of wave propagation in three-dimensional random media
[NASA-CR-197605] p 1004 N95-19547

SPHEROIDS
Potential distributions for ellipsoidal bodies in uniform fields
[MRL-TR-92-48] p 1005 N95-19771

SPINAL CORD
Spinal nerve syndromes: The need to confirm the diagnosis with neurophysiological examinations
p 1085 N95-19436

SPINE
Design and development of an enhanced biodynamic manikin, phase 1
[AD-A284725] p 1090 N95-18077
Spine injuries: Up to date evaluation in aircraft ejections p 1084 N95-19434

SPIRAL ANTENNAS
Simulation of thin slot spirals and dual circular patch antennas using the finite element method with mixed elements
[NASA-CR-197671] p 1005 N95-19796
Slot spiral antenna modeling using hybrid/mixed FE-BI technique p 1006 N95-19797
Design considerations for an archimedean slot spiral antenna p 1006 N95-19798

SPRAYED COATINGS
Tribology and microstructure of PS212 with a Cr2O3 seal coat
[NASA-TM-106768] p 969 N95-18448
Composite structures having organic matrices and duplex zinc/ceramic fire barriers
[AD-D016232] p 970 N95-18629
Quality optimization of thermally sprayed coatings produced by the JP-5000 (HVOF) gun using mathematical modeling p 989 N95-19008
High velocity oxygen fuel spraying of erosion and wear resistant coatings on jet engine parts
p 954 N95-19680

SPRAYERS
Trivalent chromium conversion coatings for aluminum
[AD-D016274] p 978 N95-18332
Design of high pressure waterjet nozzles
p 1031 N95-18996

SPRAYING
High velocity oxygen fuel spraying of erosion and wear resistant coatings on jet engine parts
p 954 N95-19680
Thermal testing of high performance thermal barrier coatings for turbine blades p 955 N95-19681

SPREAD SPECTRUM TRANSMISSION
Doppler shift and spread study for ionospherically propagated signals
[AD-A284610] p 1065 N95-19083

SPUTTERING
Fabrication of biaxially oriented YBCO on (001) biaxially oriented yttria-stabilized-zirconia on polycrystalline substrates
[DE94-014808] p 1148 N95-18064
Embedded microclusters in zeolites and cluster beam sputtering: Simulation on parallel computers
[DE95-000662] p 1134 N95-19562
Development of materials for high temperature superconductor Josephson junctions
[DE95-000896] p 1152 N95-19608

SQUID (DETECTORS)
The Gravity Probe B niobium bird experiment: Experimental verification of a data reduction scheme with a prototypical dc SQUID readout system
p 1033 N95-18929
High Temperature Superconductor (HTS) superconducting quantum interference device (SQUID) microscope
[AD-A285875] p 1152 N95-19598

STABILITY
Evaluation of the current biased integrated optical processors based on bistable dode elements
[AD-A285532] p 1138 N95-18102
Development of ultrashort optical pulse sources near 1.3 and 1.5 microns with an emphasis on stability, high repetition rate, and parallelism
[AD-A285535] p 1139 N95-18104
The effects of cavity topology on instabilities in additive-pulse modelocked lasers
[DE94-018193] p 1036 N95-18123
Helicopter in-flight simulation development and use in test pilot training
[AD-A283998] p 959 N95-18725
Atomistic and elastic analyses of defects and small structures
[DE94-017047] p 980 N95-19111
A 2D depth migration in transversely isotropic media using explicit operators
[DE95-000645] p 1066 N95-19560
Phase stability and elastic properties of C15 compounds HfV2+Nb
[DE95-000940] p 981 N95-19611

STABILITY TESTS
An analytic conceptual model of extratropical cyclones
[KNMI-WR-93-03] p 1072 N95-18926
Complete mode-set stability analysis of magnetically insulated ion diode equilibria
[DE94-015275] p 1145 N95-19201

STABILIZATION
Nonlinear magnetohydrodynamics
[DE94-016223] p 1143 N95-18353
Microgravity isolation system design: A modern control analysis framework
[NASA-TM-106803] p 927 N95-18486
Historic patterns of CO2 emissions from fossil fuels: Implications for stabilization of emissions
[DE95-000489] p 1061 N95-19556

STAINLESS STEELS
Nanostructured bearing alloy studies
[AD-A283328] p 978 N95-18027
Characterization of the deformation and annealing of 304L stainless steel
[DE94-018584] p 981 N95-19707

STANDARD DEVIATION
Marginal probabilities of the extremes of ENSO events for temperature and precipitation in the southeastern United States
[AD-A284716] p 1068 N95-18076

STANDARD MODEL (PARTICLE PHYSICS)
The left-right forward-backward asymmetry for B quarks at the SLD
[DE94-014508] p 1129 N95-18049
Family symmetries and proton decay
[DE94-017575] p 1133 N95-19245

STANDARDIZATION
The effect of special boards of flight surgeons on the evolution of US Naval flight standards
p 1081 N95-19417
Nozzle Initiative Industry Advisory Committee on Standardization of Carbon-Phenolic Test Methods and Specifications
[NASA-CR-197529] p 967 N95-19566

STANDARDS
Standard reference materials: Glass filters as a standard reference material for spectrophotometry. Selection, preparation, certification and use of SRM 930 and SRM 1930
[PB94-188844] p 973 N95-17994
Final results of the Advanced Photovoltaic Experiment flight test
[NASA-TM-106828] p 967 N95-18571
Economic impact analysis for proposed emission standards and guidelines for municipal waste combustors: A description of the basis for, and impacts of, proposed revisions to air pollutant emission regulations for new and existing municipal waste combustors under Clean Air Act Sections 111(b), 111(d), and 129
[PB94-213543] p 1061 N95-19403

STANDING WAVES
Optimum dimension ratios for studios, control rooms and listening rooms
[BBC-RD-1993/8] p 993 N95-19053

STAR CLUSTERS
Dynamics of LMC clusters
[ISBN-0-315-84911-8] p 1179 N95-18728

STAR FORMATION
Pure-rotational emission from molecular hydrogen in OMC-1 p 1179 N95-18500
Astronomical observations of phenomena in disks
p 1178 N95-19301

STATIC FIRING
High performance storable propellant resistojet
[NASA-CR-191128] p 967 N95-18195

STATIC LOADS
Course module for AA201: Wing structural design project
[AD-A283618] p 944 N95-18616
Closed-form static analysis with inertia relief and displacement-dependent loads using a MSC/NASTRAN DMAP Alter
[NASA-TM-106836] p 1047 N95-19649

STATIC MODELS
Verification of multidisciplinary models for turbomachines p 949 N95-19025

STATIC PRESSURE
Hypersonic flow-field measurements: Intrusive and nonintrusive
[AD-A283867] p 930 N95-18674
Calculation of low speed wind tunnel wall interference from static pressure pipe measurements
p 1024 N95-19273

STATIC STABILITY
Plant and controller optimization by convex methods
[AD-A283700] p 944 N95-18621
Hypersonic wind tunnel test techniques
[AD-A284057] p 929 N95-18663

STATIC TESTS
Development of a multicomponent force and moment balance for water tunnel applications, volume 1
[NASA-CR-4642-VOL-1] p 1020 N95-18955
Static investigation of two fluidic thrust-vectoring concepts on a two-dimensional convergent-divergent nozzle
[NASA-TM-4574] p 931 N95-19042

STATIONKEEPING
Arcjet thruster research and technology, phase 2
[NASA-CR-182276] p 927 N95-18044
High performance storable propellant resistojet
[NASA-CR-191128] p 967 N95-18195

STATISTICAL ANALYSIS
Some statistical tools for SAR image synthesis, analysis and processing
[INPE-5548-TDI/534] p 1172 N95-18004
Double Eulerian cycles on de Bruijn digraphs
[AD-A283334] p 1120 N95-18007
A fast recursive algorithm to compute the probability of M-out-of-N events
[AD-A283679] p 1120 N95-18020
The effect of spatial averaging on threshold exceedances of daily precipitation amounts
[KNMI-TR-154] p 1070 N95-18392
An unified program for calculating the fast neutron nuclear data for middle-heavy nuclei (MUP-3)
[DE94-626822] p 1132 N95-18883
System engineering toolbox for design-oriented engineers
[NASA-RP-1358] p 962 N95-18932
Data driven propulsion system weight prediction model
p 968 N95-18980
Advanced statistical energy analysis
p 1047 N95-19165
The jet model of chondrule formation
p 1189 N95-19310
Testing higher-order Lagrangian perturbation theory against numerical simulation. 1: Pancake models
[NASA-CR-197611] p 1121 N95-19348

STATISTICAL DISTRIBUTIONS
Marginal probabilities of the extremes of ENSO events for temperature and precipitation in the southeastern United States
[AD-A284716] p 1068 N95-18076
Minimal time detection algorithms and applications to flight systems
[TR-2-FSRC-93] p 1098 N95-18564

STATISTICAL MECHANICS
Study of frustrated systems via dissipative maps
[DE94-017754] p 1122 N95-18127
The formulation of quantum statistical mechanics based on the Feynman path centroid density. 3: Phase space formalism and analysis of centroid molecular dynamics
[AD-A279233] p 1157 N95-19852
The formulation of quantum statistical mechanics based on the Feynman path centroid density. 4: Algorithms for centroid molecular dynamics
[AD-A279234] p 1157 N95-19853

STATORS
Electromagnetic pump
[AD-D016260] p 1041 N95-18317
An analysis of noise reduction in variable reluctance motors using pulse position randomization
[AD-A283846] p 1123 N95-18673
Impact loading of compressor stator vanes by hailstone ingestion p 953 N95-19670

STEADY FLOW
Acoustic radiation damping of flat rectangular plates subjected to subsonic flows p 1123 N95-18542
Simulation of steady and unsteady viscous flows in turbomachinery p 949 N95-19023
Steady potential solver for unsteady aerodynamic analyses p 949 N95-19382
Computation of inviscid flows: Various approximations
p 1027 N95-19446

STEADY STATE
Nonlinear magnetohydrodynamics
[DE94-016223] p 1143 N95-18353
Thermal behavior spiral bevel gears
[NASA-TM-106518] p 1042 N95-18935
Steady and unsteady blade stresses within the SSME ATD/HPOTP inducer p 968 N95-18982

Numerical formulation of composition segregation at curved solid-liquid interface during steady state solidification process p 977 N95-19012

STEEL STRUCTURES

Microstructure-based fatigue life prediction methods for naval steel structures
[AD-A284735] p 1044 N95-18081

Acoustic transmission loss and structureborne noise transmission tests on a LASCOR and a reference steel panel
[MRL-TN-623] p 1128 N95-19770

STEELS

Microstructure-based fatigue life prediction methods for naval steel structures
[AD-A284735] p 1044 N95-18081

Evaluation of inorganic zinc-rich primers using Electrochemical Impedance Spectroscopy (EIS) in combination with atmospheric exposure p 977 N95-18170

Mechanical behavior of precipitation hardenable steels exposed to highly corrosive environment p 982 N95-18180

Development of an improved ballistic acceptance test for high hard armor steel plate: MIL-A-46100
[ARL-TR-509] p 979 N95-18939

Design of advanced steels for armor applications
[ARL-CR-175] p 979 N95-18948

Fatigue crack growth under variable amplitude loading p 937 N95-19484

STEERING

Torsional device for remote control steering system
[AD-D016426] p 1041 N95-18594

Synthesis of notched antenna patterns for wide bandwidth processing
[AD-A284004] p 1000 N95-18727

STELLAR CORES

A Type 2 supernovae constraint on neutrino(sub e) - neutrino(sub s) mixing
[NASA-CR-197630] p 1180 N95-18746

STELLAR CORONAS

The quiescent and flaring EUV spectrum of Algol and its relationship to other active coronae. EUV spectroscopy of bright hyades coronae: 71 Tauri and Theta 1 Tauri
[NASA-CR-197538] p 1178 N95-18391

STELLAR ENVELOPES

Astronomical observations of phenomena in disks p 1178 N95-19301

STELLAR EVOLUTION

The role of chondrules in nebular fractionations of volatiles and other elements p 1187 N95-19300

Models for multiple heating mechanisms p 1188 N95-19303

Chondrule formation in lightning discharges p 1188 N95-19304

The early Sun and the formation of chondrules p 1188 N95-19305

Microchondrules in ordinary chondrites: Implications for chondrule formation p 1188 N95-19309

Experimental constraints on models for the origin of chondrules: Cooling rates p 1189 N95-19311

Implications of a phase-transition thermostat for chondrule melting p 1189 N95-19312

STELLAR LUMINOSITY

Dynamics of LMC clusters
[ISBN-0-315-84911-8] p 1179 N95-18728

STELLAR MASS ACCRETION

Astronomical observations of phenomena in disks p 1178 N95-19301

STELLAR MASS EJECTION

Solar-geophysical data number 599, July 1994. Part 1: (Prompt reports). Data for June, May 1994, and late data
[PB94-213972] p 1196 N95-19404

Solar-geophysical data number 599, July 1994. Part 2: (Comprehensive reports). Data for January 1994, and miscellaneous
[PB94-213980] p 1196 N95-19405

STELLAR MODELS

New astrophysical opacities and their effects on stellar models
[DE94-016445] p 1186 N95-19249

Experimental constraints on models for the origin of chondrules: Cooling rates p 1189 N95-19311

Antisymmetric tensor field interactions and neutron star models
[PB94-215605] p 1118 N95-19375

STELLAR PHYSICS

A Type 2 supernovae constraint on neutrino(sub e) - neutrino(sub s) mixing
[NASA-CR-197630] p 1180 N95-18746

Decaying neutrinos in galaxy clusters
[NASA-CR-197615] p 1198 N95-18747

STELLAR RADIATION

New astrophysical opacities and their effects on stellar models
[DE94-016445] p 1186 N95-19249

STELLAR SYSTEMS

Astronomical observations of phenomena in disks p 1178 N95-19301

STEREOPHOTOGRAPHY

Topography from shading and stereo
[NASA-CR-189389] p 1173 N95-18051

STEREOSCOPY

Atomistic and elastic analyses of defects and small structures
[DE94-017047] p 980 N95-19111

STIFFENING

Compression strength of composite primary structural components
[NASA-CR-197554] p 1044 N95-18388

STIFFNESS

A multiple time scale solution for the Chapman mechanism
[DE94-017491] p 1060 N95-18895

A CMC database for use in the next generation launch vehicles (rockets) p 963 N95-18993

STIMULATED EMISSION

Large amplitude motions, especially isomerization and tunneling in polyatomic molecule spectra: Novel experimental, pattern recognition, and theoretical methods
[AD-A284194] p 985 N95-18636

STIMULATION

Visuo-ocular performance during vestibular stimulation
[AD-A284103] p 1089 N95-18403

STIRLING ENGINES

Transient and steady-state tests of the space power research engine with resistive and motor loads
[NASA-TM-106832] p 1042 N95-19238

STOCHASTIC PROCESSES

Comparison of stochastic and deterministic nonlinear gust analysis methods to meet continuous turbulence criteria p 946 N95-18602

On stationary and nonstationary fatigue load modeling using autoregressive moving average (ARMA) models p 1046 N95-18919

Forced response of mistuned bladed disks p 950 N95-19383

A new stochastic systems approach to structural integrity p 935 N95-19474

STOICHIOMETRY

Nonstoichiometry of Al-Zr intermetallic phases
[DE94-016877] p 979 N95-19093

STOKES FLOW

Time-evolving bubbles in two-dimensional stokes flow
[NASA-CR-194998] p 1015 N95-18188

STOPPING

Baryon stopping in 200 GeV/A S+Au collisions
[DE94-018215] p 1134 N95-19587

STORABLE PROPELLANTS

Advanced small rocket chambers. Basic program and option 2: Fundamental processes and material evaluation
[NASA-CR-195349] p 966 N95-18192

STORAGE BATTERIES

Characterization of rechargeable lithium cells. Part 1: Lithium/niobium triselenide chemistry
[AD-A284229] p 1007 N95-17959

STORAGE RINGS (PARTICLE ACCELERATORS)

Algorithms for orbit control on SPEAR
[DE95-002868] p 1138 N95-19841

STORAGE TANKS

Outgassing of solid material into vacuum thermal insulation spaces p 972 N95-18184

Sloshing roof impact tests of a rectangular tank
[DE94-012462] p 1018 N95-18549

Free vibration analysis of partially filled liquid storage tanks
[DE94-012456] p 1020 N95-19098

STORM SURGES

ADCIRC: An advanced three-dimensional circulation model for shelves, coasts, and estuaries. Report 5: A tropical storm database for the east and Gulf of Mexico coasts of the United States
[AD-A285576] p 1075 N95-19540

STORMS

Use of profiler data for analysis and NOWcasting of a winter season extratropical cyclone
[PB94-187804] p 1067 N95-17992

Storm activity over the North Sea and the Netherlands in two climate models compared with observations
[KNMI-WR-94-02] p 1070 N95-18393

STRAIN DISTRIBUTION

HEISHI: A fuel performance model for space nuclear applications
[DE94-017497] p 1137 N95-18897

Optimization of layered metal matrix composite cylinders p 970 N95-18920

STRAIN ENERGY RELEASE RATE

Driving force analysis in an infinite anisotropic plate with multiple crack interactions
[NASA-TM-106838] p 972 N95-19782

STRAIN GAGE BALANCES

Dynamic Stability Instrumentation System (DSIS). Volume 1: Hardware description
[NASA-TM-109160-VOL-1] p 1099 N95-18899

Development of a multicomponent force and moment balance for water tunnel applications, volume 1
[NASA-CR-4642-VOL-1] p 1020 N95-18955

Development of a multicomponent force and moment balance for water tunnel applications, volume 2
[NASA-CR-4642-VOL-2] p 1020 N95-18956

STRAIN GAGES

Hydrofoil force balance
[AD-D016475] p 1033 N95-18461

STRAIN RATE

Mechanical behavior of precipitation hardenable steels exposed to highly corrosive environment p 982 N95-18180

Warm formability of aluminum-magnesium alloys
[DE94-016170] p 980 N95-19396

STRANGENESS

Study of strangeness production in relativistic nucleus beams at JINR
[DE94-626720] p 1136 N95-18881

STRATIFICATION

The effect of stable stratification on three-dimensional structure in shear layers p 1019 N95-18921

STRATIFIED FLOW

The effect of stable stratification on three-dimensional structure in shear layers p 1019 N95-18921

STRATOCUMULUS CLOUDS

The numerical simulation of marine boundary layer clouds
[AD-A284149] p 1064 N95-18413

Implications of summertime marine stratocumulus on the North American climate p 1073 N95-18977

STRATOSPHERE

Potential replacements for solvents that are ozone depleting substances
[AD-A285442] p 1058 N95-18091

Investigation of atmospheric waves on Neptune
[NASA-CR-197537] p 1194 N95-18579

Laboratory studies of stratospheric bromine chemistry: Kinetics of the reactions of bromine monoxide with nitrogen dioxide and atomic oxygen p 1065 N95-18731

STRATUS CLOUDS

The numerical simulation of marine boundary layer clouds
[AD-A284149] p 1064 N95-18413

STREAK CAMERAS

Nonlinear response of the photocathode of an x-ray streak camera to UV light
[DE94-018073] p 1032 N95-18130

STREAMLINED BODIES

Visualizing second order tensor fields with hyperstreamlines
[NASA-CR-197619] p 1121 N95-19288

STREAMS

Cumulative impact analysis of wetlands using hydrologic indices
[AD-A284759] p 1058 N95-18085

Real-time adaptive control of mixing in a plane shear layer
[AD-A285541] p 1018 N95-18469

STRESS (BIOLOGY)

Effective team performance under stress and normal conditions: An experimental paradigm, theory and data for studying team decision making in hierarchical teams with distributed expertise
[AD-A284683] p 1089 N95-18530

STRESS ANALYSIS

Study of failure in fibrous composites subjected to bending loads
[AD-A283330] p 969 N95-18028

Completed Beltrami-Michell formulation for analyzing radially symmetrical bodies
[NASA-TM-4593] p 1044 N95-18199

Dynamic decohesion of bimaterials: Experimental observations and failure criteria
[GALCIT-94-2] p 1045 N95-18613

Completed Beltrami-Michell formulation for analyzing mixed boundary value problems in elasticity
[NASA-TM-106809] p 1045 N95-18909

Residual stresses in welded plates p 1047 N95-18972

Application of the PSD technique to acoustic fatigue stress calculations in complex substructures p 1126 N95-19155

Aircraft stress sequence development: A complex engineering process made simple p 936 N95-19480

Analysis of cold worked holes for structural life extension p 939 N95-19493

Prediction of R-curves from small coupon tests p 939 N95-19496

Driving force analysis in an infinite anisotropic plate with multiple crack interactions
[NASA-TM-106838] p 972 N95-19782

STRESS CONCENTRATION
Study of failure in fibrous composites subjected to bending loads
[AD-A283330] p 969 N95-18028
Stress-intensity factor solutions for cracks at countersunk rivet holes under uniaxial tension
[AD-A279163] p 1047 N95-19804
STRESS CORROSION
Mechanical behavior of precipitation hardenable steels exposed to highly corrosive environment
p 982 N95-18180
STRESS CORROSION CRACKING
Mechanical behavior of precipitation hardenable steels exposed to highly corrosive environment
p 982 N95-18180
STRESS DISTRIBUTION
Study of failure in fibrous composites subjected to bending loads
[AD-A283330] p 969 N95-18028
HEISHI: A fuel performance model for space nuclear applications
[DE94-017497] p 1137 N95-18897
On the measurement of the crack tip stress field as a means of determining Delta K(sub eff) under conditions of fatigue crack closure p 938 N95-19492
Prediction of R-curves from small coupon tests
p 939 N95-19496
Split mandrel versus split sleeve coldworking: Dual methods for extending the fatigue life of metal structures
p 940 N95-19500
STRESS INTENSITY FACTORS
Discrete crack growth analysis methodology for through cracks in pressurized fuselage structures
p 935 N95-19473
Fatigue crack growth under variable amplitude loading
p 937 N95-19484
On the measurement of the crack tip stress field as a means of determining Delta K(sub eff) under conditions of fatigue crack closure p 938 N95-19492
Stress intensity factors for surface and corner cracks emanating from a wedge-loaded hole
p 939 N95-19498
Driving force analysis in an infinite anisotropic plate with multiple crack interactions
[NASA-TM-106838] p 972 N95-19782
Stress-intensity factor solutions for cracks at countersunk rivet holes under uniaxial tension
[AD-A279163] p 1047 N95-19804
STRESS-STRAIN RELATIONSHIPS
BEAM: A finite element program for the collapse analysis of vehicle structures
[AD-A285547] p 1045 N95-18472
HEISHI: A fuel performance model for space nuclear applications
[DE94-017497] p 1137 N95-18897
Near tip stress and strain fields for short elastic cracks p 937 N95-19487
STRINGERS
Acoustic fatigue testing on different materials and skin-stringer elements p 1126 N95-19156
Fatigue and residual strength investigation of ARALL(R) -3 and GLARE(R) -2 panels with bonded stringers
p 939 N95-19495
STRINGS
Crystalline beams: The string
[DE94-016806] p 1150 N95-19091
STRONTIUM TITANATES
Barium strontium titanate and non-ferroelectric oxide ceramic composites for use in phased array antennas
[AD-A279225] p 972 N95-19851
STRUCTURAL ANALYSIS
Mathematical analysis of actuator forces in a scissor lift
[AD-A283906] p 1040 N95-18152
An analog computing approach to structural analysis and optimal design through artificial neural networks
p 1113 N95-18218
BEAM: A finite element program for the collapse analysis of vehicle structures
[AD-A285547] p 1045 N95-18472
Current loop signal conditioning: Practical applications
[NASA-TM-4636] p 1033 N95-18735
Completed Beltrami-Michell formulation for analyzing mixed boundary value problems in elasticity
[NASA-TM-106809] p 1045 N95-18909
Characterization of metal matrix composites
[NASA-CR-195381] p 970 N95-18940
Salt-induced aggregation of lysozyme: Implications for crystal growth p 1155 N95-19015
FAA/NASA International Symposium on Advanced Structural Integrity Methods for Airframe Durability and Damage Tolerance, part 2
[NASA-CP-3274-PT-2] p 934 N95-19468
Flight parameters monitoring system for tracking structural integrity of rotary-wing aircraft
p 934 N95-19469
Technology Benefit Estimator (T/BEST): User's manual
[NASA-TM-106785] p 1046 N95-19501
Proceedings of the USAF Structural Integrity Program Conference
[AD-A285684] p 945 N95-19517
Using neural networks in the mapping of mixed discrete/continuous design spaces with application to structural design
[AD-A285328] p 1046 N95-19522
Closed-form static analysis with inertia relief and displacement-dependent loads using a MSC/NASTRAN DMAP Alter
[NASA-TM-106836] p 1047 N95-19649
Unit cell geometry of multiaxial preforms for structural composites
[NASA-CR-197294] p 971 N95-19650
STRUCTURAL DESIGN
Wing design for a civil tiltrotor transport aircraft
[NASA-CR-197523] p 942 N95-18090
Course module for AA201: Wing structural design project
[AD-A283618] p 944 N95-18616
Composite structures for magnetosphere imager spacecraft p 966 N95-18976
The evaluation of transmission efficiency and coupling loss factor of structural junctions
[MRL-TR-93-1] p 1124 N95-19057
Impact of Acoustic Loads on Aircraft Structures
[AGARD-CP-549] p 1124 N95-19142
Current and future problems in structural acoustic fatigue p 1124 N95-19143
Aeroacoustic qualification of HERMES shingles
p 1125 N95-19145
Study of the ferrimagnetic and paramagnetic phases of magnetite measured by multiple neutron diffraction
[DE94-627031] p 1151 N95-19242
Using neural networks in the mapping of mixed discrete/continuous design spaces with application to structural design
[AD-A285328] p 1046 N95-19522
Weldability of iron aluminides
[DE95-000686] p 981 N95-19568
Tutorial guide: Computer-Aided Structural Modeling (CASM), version 5.00
[AD-A280147] p 1108 N95-19821
STRUCTURAL DESIGN CRITERIA
Aircraft Loads due to Turbulence and their Impact on Design and Certification
[AGARD-R-798] p 956 N95-18597
STRUCTURAL ENGINEERING
NASA/ASEE Summer Faculty Fellowship Program. 1994 research reports
[NASA-CR-197448] p 1157 N95-18166
An analog computing approach to structural analysis and optimal design through artificial neural networks
p 1113 N95-18218
NASA Lewis Research Center Workshop on Forced Response in Turbomachinery
[NASA-CP-10147] p 949 N95-19380
Spectroscopy and dynamics of vibrationally excited molecules
[AD-A285874] p 1134 N95-19597
Tutorial guide: Computer-Aided Structural Modeling (CASM), version 5.00
[AD-A280147] p 1108 N95-19821
STRUCTURAL FAILURE
Forced response of mistuned bladed disks
p 950 N95-19383
Damage monitoring in metallic and composite structures using piezoelectric thin film sensors
[ARL-RR-4] p 971 N95-19467
FAA/NASA International Symposium on Advanced Structural Integrity Methods for Airframe Durability and Damage Tolerance, part 2
[NASA-CP-3274-PT-2] p 934 N95-19468
Results of uniaxial and biaxial tests on riveted fuselage lap joint specimens p 938 N95-19491
Proceedings of the USAF Structural Integrity Program Conference
[AD-A285684] p 945 N95-19517
STRUCTURAL INFLUENCE COEFFICIENTS
The left-right forward-backward asymmetry for B quarks at the SLD
[DE94-014508] p 1129 N95-18049
STRUCTURAL RELIABILITY
Current and future problems in structural acoustic fatigue p 1124 N95-19143
STRUCTURAL STABILITY
Application of superplastically formed and diffusion bonded structures in high intensity noise environments
p 1127 N95-19162
Algorithms and applications in timed discrete event systems
[PB94-201423] p 1118 N95-19169
Phase stability and elastic properties of C15 compounds Hfv2 + Nb
[DE95-000940] p 981 N95-19611
STRUCTURAL VIBRATION
Modal Identification Experiment accommodations review
[NASA-CR-195009] p 964 N95-18105
Vibration (?) spikes during natural rain events
p 1069 N95-18206
Streamlined design and self reliant hardware for active control of precision space structures
[NASA-CR-4637] p 964 N95-18580
Plate vibration with arbitrarily oriented stiffeners based on Mindlin-Engesser formulation
[RR-CE143] p 1045 N95-18608
Pressure measurements on an F/A-18 twin vertical tail in buffeting flow. Volume 4, part 2: Buffet cross spectral densities
[AD-A285555] p 957 N95-18641
SSI effects for a tank containing two liquids
[DE94-012457] p 1020 N95-19099
Nonlinear dynamic response of aircraft structures to acoustic excitation p 946 N95-19151
Acoustics of space structures p 1126 N95-19152
Advanced statistical energy analysis
p 1047 N95-19165
Identification and analysis of air- and structure-borne noise and vibration paths p 1128 N95-19166
Spectrogram diagnosis of aircraft disasters
p 940 N95-19167
STRUTS
Interaction of a three strut support on the aerodynamic characteristics of a civil aviation model
p 933 N95-19279
STUDENTS
NASA/DOD Aerospace Knowledge Diffusion Research Project. Report 26: The technical communication practices of aerospace engineering students: Results of the phase 3 AIAA National Student Survey
[NASA-TM-109121] p 1175 N95-18950
NASA/DOD Aerospace Knowledge Diffusion Research Project. Paper 46: Technical communications in aerospace: A comparison across four countries
[NASA-TM-110056] p 1175 N95-19038
STUDS (STRUCTURAL MEMBERS)
Metal-framed partitions with reduced thicknesses. Part 2: Built-in acoustic treatment
[BBC-RD-1993/6-PT-2] p 993 N95-19137
Metal-framed partitions with reduced thicknesses. Part 1: Narrower studs and cavities
[BBC-RD-1993/5-PT-1] p 993 N95-19138
SUBDIVISIONS
Activities of the Analytical Chemistry Laboratory
[DE95-000834] p 975 N95-19618
SUBMARINES
Application of three-dimensional hybrid structured/unstructured grids to land, sea and air vehicles
[ARA-MEMO-399] p 1031 N95-19775
SUBMERGING
Trivalent chromium conversion coatings for aluminum
[AD-D016274] p 978 N95-18332
Trivalent chromium solutions for sealing anodized aluminum
[AD-D016472] p 979 N95-18458
Alternative solvents/technologies for paint stripping: Phase 1
[AD-A279918] p 989 N95-19861
SUBREFLECTORS
Double-loop frequency selective surfaces for multi frequency division multiplexing in a dual reflector antenna
[NASA-CASE-NPO-18701-2-CU] p 1000 N95-18960
SUBROUTINE LIBRARIES (COMPUTERS)
Portable, Reusable, Integrated Software Modules (PRISM) documentation library model document release 1.0: Central Archive for Reusable Defense Software (CARDS)
[AD-A284567] p 1095 N95-18030
Library capability demonstration. Central Archive for Reusable Defense Software (CARDS)
[AD-A284568] p 1095 N95-18031
Library capability demonstration. Central Archive for Reusable Defense Software (CARDS)
[AD-A284569] p 1095 N95-18032
Library Development Handbook. Central Archive for Reusable Defense Software (CARDS)
[AD-A284570] p 1095 N95-18033
Library capability demonstration. Central Archive for Reusable Defense Software (CARDS)
[AD-A284572] p 1095 N95-18034
SUBROUTINES
Simulation of gamma-ray spectra for a variety of user-specified detector designs
[NASA-CR-197551] p 1136 N95-18370

SICOMP, the SINTEF data compression library (version 1.0) reference manual
[PB94-207107] p 1099 N95-18668
Steady potential solver for unsteady aerodynamic analyses p 949 N95-19382
VENTCF2: An algorithm and associated FORTRAN 77 subroutine for calculating flow through a horizontal ceiling/floor vent in a zone-type compartment fire model
[PB94-210127] p 993 N95-19402

SUBSONIC AIRCRAFT
Atmospheric effects of high-flying subsonic aircraft: A catalogue of perturbing influences
[KNMI-SR-94-03] p 1060 N95-18722

SUBSONIC FLOW
Measurement of gust response on a turbine cascade
[NASA-TM-106776] p 928 N95-18457
Acoustic radiation damping of flat rectangular plates subjected to subsonic flows p 1123 N95-18542
Solution of full potential equation on an airfoil by multigrid technique
[NAL-TM-CSS-9303] p 930 N95-18904
Calculation of support interference in dynamic wind-tunnel tests p 933 N95-19282

SUBSONIC WIND TUNNELS
Unsteady flow testing in a passive low-correction wind tunnel p 960 N95-19272
Evaluation of combined wall- and support-interference on wind tunnel models p 932 N95-19278

SUBSTITUTES
Phase transformations and phase relations in Ti(50)Pd(50-x)TM(x) alloys
[DE94-018999] p 977 N95-17962
Design and development of an enhanced biodynamic manikin, phase 1
[AD-A284725] p 1090 N95-18077

SUBSTRATES
InP solar cell development on inexpensive silicon substrates
[AD-A283624] p 1052 N95-18011
A constant-depth scratch test for the measurement of adhesion at film-substrate interfaces
[AD-A283660] p 983 N95-18016
Development of a bipolar lead/acid battery for the more electric aircraft
[AD-A284050] p 1010 N95-18660
Ion mixing in oxide-sapphire systems
[DE94-018660] p 1133 N95-19232
Ferroelectric thin film bismuth titanate prepared from acetate precursors
[DE95-000538] p 988 N95-19558
Using electrochemistry in device processing on poly(tetrafluoroethylene) substrates
[DE95-000541] p 975 N95-19559
CVD silicon carbide characterization
[AD-A285667] p 972 N95-19702

SUBSTRUCTURES
Application of the PSD technique to acoustic fatigue stress calculations in complex substructures p 1126 N95-19155

SUBTRACTION
Low noise fiber gyroscope system which includes excess noise subtraction
[AD-D016556] p 1034 N95-19124

SULFATES
Atmospheric chemistry of biogenic sulfur in the Southern Hemisphere p 1071 N95-18399
Shock-induced devolatization of calcium sulfate and implications for K-T extinctions
[NASA-CR-197608] p 1060 N95-19033

SULFIDES
Atmospheric chemistry of biogenic sulfur in the Southern Hemisphere p 1071 N95-18399

SULFONES
Adherend surface effects on epoxy cure by NMR
[AD-A284774] p 985 N95-18442

SULFONIC ACID
Polymer-based separations: Synthesis and application of polymers for ionic and molecular recognition
[DE94-016427] p 984 N95-18355
Atmospheric chemistry of biogenic sulfur in the Southern Hemisphere p 1071 N95-18399

SULFUR
Surface phases, surface defects and the initial stages of oxidation
[DE94-016947] p 979 N95-18358
Atmospheric chemistry of biogenic sulfur in the Southern Hemisphere p 1071 N95-18399
Chondrule precursors and cooling paths: The sulfur evidence p 1193 N95-19338

SULFUR DIOXIDES
Gas turbine compressor corrosion and erosion in Western Europe p 954 N95-19678

SULFUR HEXAFLUORIDE
Innovative development and application of models for weakly ionized ionospheric plasmas
[AD-A284583] p 1064 N95-18452

SULFUR OXIDES
Shock-induced devolatization of calcium sulfate and implications for K-T extinctions
[NASA-CR-197608] p 1060 N95-19033

SULFURIC ACID
Shock-induced devolatization of calcium sulfate and implications for K-T extinctions
[NASA-CR-197608] p 1060 N95-19033

SUN
The early Sun and the formation of chondrules p 1188 N95-19305
Solar-geophysical data number 599, July 1994. Part 2: (Comprehensive reports). Data for January 1994, and miscellaneous
[PB94-213980] p 1196 N95-19405
Relative elemental abundance and heating constraints determined for the solar corona from SERTS measurements
[NASA-TM-104616] p 1196 N95-19791

SUNLIGHT
Progress in the development of advanced solar reflectors
[DE94-000264] p 1053 N95-18463

SUNSPOTS
IONCAP prediction-based Automatic Link Establishment (ALE) frequency selection for a ten-node Australian high-frequency network
[AD-A283698] p 999 N95-18619
Solar-geophysical data number 599, July 1994. Part 1: (Prompt reports). Data for June, May 1994, and late data
[PB94-213972] p 1196 N95-19404

SUPERCHARGERS
Advanced diesel electronic fuel injection and turbocharging
[AD-A279176] p 1043 N95-19809

SUPERCOMPUTERS
Construction of a connectionist network supercomputer
[AD-A283354] p 1109 N95-18050
NASA High Performance Computing and Communications program
[NASA-TM-4653] p 1174 N95-18573
Scalability of parallel spatial direct numerical simulation code on IBM SP1 parallel supercomputer
[NASA-CR-194975] p 1098 N95-18584
QuikForm: Intelligent deformation processing of structural alloys
[DE94-018739] p 1114 N95-18649
Connectionist Network Supercomputer Project
[AD-A279206] p 1112 N95-19843

SUPERCONDUCTING DEVICES
Superconductor microelectronic devices and circuits and a method of fabricating therefor
[AD-D016280] p 1009 N95-18433

SUPERCONDUCTING FILMS
Fabrication of biaxially oriented YBCO on (001) biaxially oriented yttria-stabilized-zirconia on polycrystalline substrates
[DE94-014808] p 1148 N95-18064
Method for forming Josephson break junctions
[AD-D016427] p 1149 N95-18559
High temperature superconducting films and crystals
[AD-A279201] p 1154 N95-19815

SUPERCONDUCTING MAGNETS
Improvement of a high current DC power supply system for testing the large scaled superconducting cables and magnets
[DE94-770767] p 1012 N95-19548
The interaction of two narrow magnets and a moving conducting slip
[DE94-018575] p 1122 N95-19704

SUPERCONDUCTIVITY
Superconductive signal-processing circuits
[AD-A285533] p 1008 N95-18103
Method for forming Josephson break junctions
[AD-D016427] p 1149 N95-18559
Improvement of a high current DC power supply system for testing the large scaled superconducting cables and magnets
[DE94-770767] p 1012 N95-19548
Development of materials for high temperature superconductor Josephson junctions
[DE95-000896] p 1152 N95-19608

SUPERCONDUCTORS (MATERIALS)
Superconductor microelectronic devices and circuits and a method of fabricating therefor
[AD-D016280] p 1009 N95-18433
High temperature superconducting films and crystals
[AD-A279201] p 1154 N95-19815

SUPERHIGH FREQUENCIES
US Navy SHF SATCOM: Past, present and future
[AD-A283704] p 996 N95-18359
The future use of DSCS and commercial satellites in the US Navy
[AD-A285707] p 997 N95-18481

SUPERLATTICES
Physics with isotopically controlled semiconductors
[DE95-000789] p 1152 N95-19615
Investigation of superlattice disordering and diffusion mechanisms in GaAs
[AD-A284847] p 1153 N95-19697
The optical emission and absorption properties of silicon-germanium superlattice structures grown on non-conventional silicon substrate orientation
[AD-A284852] p 1153 N95-19715

SUPERNOVAE
A Type 2 supernovae constraint on neutrino(sub e) - neutrino(sub s) mixing
[NASA-CR-197630] p 1180 N95-18746
Comment on the preprint Neutrino Flavor Evolution Near a Supernova's Core (Astro-Ph 9405008) by J. Pantaleone
[DE94-017576] p 1198 N95-19283

SUPERPLASTIC FORMING
Application of superplastically formed and diffusion bonded structures in high intensity noise environments p 1127 N95-19162

SUPERSONIC BOUNDARY LAYERS
Prediction of fluctuating pressure and power spectra in attached and separated compressible flow p 1031 N95-19153

SUPERSONIC COMBUSTION
Studies on high pressure and unsteady flame phenomena
[AD-A284126] p 973 N95-18410

SUPERSONIC COMBUSTION RAMJET ENGINES
One-dimensional flow description for the combustion chamber of a scramjet
[DLR-FB-94-06] p 948 N95-18911
Operating capability and current status of the reactivated NASA Lewis Research Center Hypersonic Tunnel Facility
[NASA-TM-106808] p 960 N95-19286

SUPERSONIC FLOW
Photogeneration and characterization of energetic molecules in supersonic molecular beams
[AD-A284108] p 1131 N95-18438
Numerical computations of supersonic base flow with special emphasis on turbulence modeling
[AD-A283688] p 930 N95-18670
An assessment of the adaptive unstructured tetrahedral grid, Euler Flow Solver Code FELISA
[NASA-TP-3526] p 930 N95-19041
Improvement and validation of an LDV system to perform measurements in laminar supersonic flows p 1021 N95-19256
Transonic and supersonic flowfield measurements about axisymmetric afterbodies for validation of advanced CFD codes p 932 N95-19260
Parabolized Navier-Stokes solution of supersonic/hypersonic flows p 933 N95-19464

SUPERSONIC INLETS
On supersonic-inlet boundary-layer bleed flow
[NASA-CR-195426] p 955 N95-19769

SUPERSONIC SPEED
Parametric study on laminar flow for finite wings at supersonic speeds
[NASA-TM-108852] p 928 N95-18101

SUPERSONIC WIND TUNNELS
Improved speed control system for the 87,000 HP wind tunnel drive
[NASA-TM-106840] p 1035 N95-19794

SUPERSYMMETRY
Family symmetries and proton decay
[DE94-017575] p 1133 N95-19245

SUPPORT INTERFERENCE
Wall Interference, Support Interference and Flow Field Measurements
[AGARD-CP-535] p 1020 N95-19251
The crucial role of wall interference, support interference and flow field measurements in the development of advanced aircraft configurations p 1021 N95-19252
Evaluation of combined wall- and support-interference on wind tunnel models p 932 N95-19278
Interaction of a three strut support on the aerodynamic characteristics of a civil aviation model p 933 N95-19279
Interference corrections for a centre-line plate mount in a porous-walled transonic wind tunnel p 933 N95-19280
Correction of support influences on measurements with sting mounted wind tunnel models p 933 N95-19281
Calculation of support interference in dynamic wind-tunnel tests p 933 N95-19282

SUPPORT SYSTEMS
R.MAPCALC: An algebra for GIS and image processing
[AD-A283923] p 1096 N95-18161
Activities of the Analytical Chemistry Laboratory
[DE95-000834] p 975 N95-19618

Using PVM to host CLIPS in distributed environments p 1104 N95-19748
Predicting and explaining the movement of mesoscale oceanographic features using CLIPS p 1105 N95-19752
Collaborative engineering-design support system p 1106 N95-19757

SUPPORTS
Sag compensated vibration isolation mount [AD-D016541] p 1042 N95-19121

SUPPRESSORS
Corner vortex suppressor [AD-D016423] p 928 N95-18337

SURFACE ACOUSTIC WAVE DEVICES
Signal enhancement in AM-FM interference [AD-A285114] p 1004 N95-19565

SURFACE CRACKS
Complex oxidation effects in polymer degradation [DE94-018903] p 986 N95-18651
Fracture toughness of polymer/polymer bimaterial interface reinforced with block copolymers p 986 N95-18923
The load separation technique in the elastic-plastic fracture analysis of two- and three-dimensional geometries p 936 N95-19481
Stress intensity factors for surface and corner cracks emanating from a wedge-loaded hole p 939 N95-19498

SURFACE DEFECTS
Surface phases, surface defects and the initial stages of oxidation [DE94-016947] p 979 N95-18358
Investigation of the microstructure of coatings for high power lasers by non-optical techniques [DE94-017697] p 987 N95-19227

SURFACE DIFFUSION
An atomic view of surface diffusion on metal surfaces [DE94-016150] p 980 N95-19395

SURFACE ENERGY
A crystalline quark-hadron mixed phase in neutron stars [DE95-000787] p 1194 N95-19570
Assessment of climate variability of the Greenland Ice Sheet: Integration of in situ and satellite data [NASA-CR-197604] p 1062 N95-19779

SURFACE FINISHING
Inertial confinement fusion [DE95-000314] p 1147 N95-19552

SURFACE PROPERTIES
Preparation and surface characterization of metal doped alumina catalyst [PB94-175296] p 973 N95-17991
Method of making a membrane having hydrophilic and hydrophobic surfaces for adhering cells or antibodies by using atomic oxygen or hydroxyl radicals [NASA-CASE-MSC-21529-1] p 983 N95-18134
A shock isolation method and apparatus [AD-D016471] p 1045 N95-18456
Atomistic and elastic analyses of defects and small structures [DE94-017047] p 980 N95-19111
Chondrules and their associates in ordinary chondrites p 1188 N95-19306
Experimental and numerical simulations of the effects of ingested particles in gas turbine engines p 952 N95-19662
An atomic-resolution study of overlayer formation and interfacial mixing in the interaction of phosphorus with Si(001) [AD-A280159] p 976 N95-19825

SURFACE REACTIONS
UV laser-surface interactions relevant to analytic spectroscopy of wide band gap materials [DE94-016180] p 1037 N95-18349
UV laser-surface interactions relevant to analytic spectroscopy of wide band gap materials [DE94-016181] p 1037 N95-18350
Surface phases, surface defects and the initial stages of oxidation [DE94-016947] p 979 N95-18358
Transition metal oxides deposited on rhodium and platinum: Surface chemistry and catalysis [DE95-000793] p 975 N95-19616
Experimental and numerical simulations of the effects of ingested particles in gas turbine engines p 952 N95-19662

SURFACE ROUGHNESS
Light scattering from rough surfaces [AD-A284112] p 1139 N95-18404
Surface roughness measurements p 1142 N95-18964
Embedded microclusters in zeolites and cluster beam sputtering: Simulation on parallel computers [DE95-000662] p 1134 N95-19562

SURFACE TEMPERATURE
Conceptual models of severe convective weather in the Netherlands [KNMI-WR-93-05] p 1071 N95-18394
Verification of multidisciplinary models for turbomachines p 949 N95-19025

SURFACE TREATMENT
Ion beam surface treatment: A new capability for surface enhancement [DE94-014663] p 977 N95-17968
Fundamental advances for characterizing cathodic protection systems [PB94-180692] p 1122 N95-17983

SURFACE VEHICLES
Method for surmounting an obstacle by a robot vehicle [NASA-CASE-NPO-18764-1-CU] p 1041 N95-18741
Design of a radio frequency data link for the unmanned ground vehicle technology test bed demonstration program [AD-A284997] p 1004 N95-19534

SURFACE WAVES
The diurnal cycle of high-frequency temperature variability at 0 deg 140 deg W on seasonal and interannual time scales [AD-A283640] p 1074 N95-18012

SURFACTANTS
Adherend surface effects on epoxy cure by NMR [AD-A284774] p 985 N95-18442

SURGERY
Photorefractive Keratectomy (PRK) in the military aviator: An aeromedical expose p 1086 N95-19442

SURGES
Development of an amorphous surge blocker for a high voltage acceleration power supply of the neutral beam injectors [DE94-770648] p 1138 N95-19874

SURVEILLANCE
Long wavelength propagation capacity, version 1.1 (computer diskette) [AD-M200254] p 994 N95-17964
E-6A hardness assurance, maintenance and surveillance program [AD-A283994] p 945 N95-19067

SURVEYS
Variable name dictionary for the Air Force health study 1987 physical examination data tape, volume 1 [AD-A283319] p 1172 N95-18025
Variable name dictionary for the Air Force health study 1987 physical examination data tape, volume 2 [AD-A283320] p 1172 N95-18026
The origin of the diffuse x-ray background p 1197 N95-18729
NASA/DOD Aerospace Knowledge Diffusion Research Project. Report 26: The technical communication practices of aerospace engineering students: Results of the phase 3 AIAA National Student Survey [NASA-TM-109121] p 1175 N95-18950
NASA/DOD Aerospace Knowledge Diffusion Research Project. Paper 46: Technical communications in aerospace: A comparison across four countries [NASA-TM-110056] p 1175 N95-19038
Heavy metal soil contamination at US Army installations: Proposed research and strategy for technology development [AD-A279171] p 1062 N95-19808

SURVIVAL EQUIPMENT
Evaluation of Pureau water for use as emergency drinking water for ADF aircraft [MRL-TN-648] p 1092 N95-19502

SWEEP ANGLE
Effect of crossflow on Goertler instability in incompressible boundary layers [NASA-CR-195007] p 1016 N95-18193

SWEPT FORWARD WINGS
In-flight lift-drag characteristics for a forward-swept wing aircraft and comparisons with contemporary aircraft) [NASA-TP-3414] p 929 N95-18565

SWEPT WINGS
A spectrally accurate boundary-layer code for infinite swept wings [NASA-CR-195014] p 1014 N95-18042
Collection efficiency and ice accretion calculations for a sphere, a swept MS(1)-317 wing, a swept NACA-0012 wing tip, an axisymmetric inlet, and a Boeing 737-300 [NASA-TM-106831] p 933 N95-18582
The utilization of a high speed reflective visualization system in the study of transonic flow over a delta wing p 932 N95-19259
Velocity measurements with hot-wires in a vortex-dominated flowfield p 932 N95-19261
Computational simulations for some tests in transonic wind tunnels p 1023 N95-19264

SWINGBY TECHNIQUE
Optimal transfer and swing-by orbits in the two- and three-body problems p 961 N95-18900

SWITCHES
Gigabit optical interconnects: System and component analysis, design and development [AD-A285538] p 1138 N95-18067
Silicon carbide photoconductive switches [AD-A284310] p 1008 N95-18378
Waveguide switches using asymmetric coupled quantum wells [AD-A284056] p 1010 N95-18662
Sandia National Laboratories' high power electromagnetic impulse sources [DE95-000423] p 1004 N95-19555

SWITCHING CIRCUITS
Evaluation of the current biased integrated optical processors based on bistable dode elements [AD-A285532] p 1138 N95-18102
Fault protection circuit for power switching device [AD-D016466] p 1009 N95-18455
Research in parallel computing [AD-A283983] p 1111 N95-18892
Characteristics and development report for the MC3994 and MC3994A relays [DE95-002952] p 1013 N95-19842

SYMMETRICAL BODIES
Completed Beltrami-Michell formulation for analyzing radially symmetrical bodies [NASA-TM-4593] p 1044 N95-18199

SYMMETRY
SU4(sub L) x U1(sub N) model for the electroweak interactions [DE94-626675] p 1148 N95-18330

SYNAPSES
Cellular neurophysiology of the rat suprachiasmatic nucleus: Electrical properties, neurotransmission, and mechanisms of synchronization [AD-A284111] p 1076 N95-18439

SYNCHRONISM
Synchronization of nonautonomous chaotic systems [AD-D016440] p 1010 N95-18528

SYNCHRONIZERS
RINSE: A digitally implemented flywheel sync regenerator for improved video synchroniser performance [BBC-RD-1993/14] p 999 N95-18538

SYNCHRONOUS MOTORS
Mitigation of EMI generated by a variable-frequency-drive controller for an AC induction motor [AD-A286045] p 1012 N95-19573

SYNCHROTRON RADIATION
Subgroup report on hard x-ray microprobes [DE94-018708] p 1034 N95-19233

SYNCOPE
The NAMI syncope test battery and clinical decision-making in aviators with syncope p 1083 N95-19428

SYNOPTIC METEOROLOGY
Synoptic and mesoscale examination of the northern New England winter storm of January 29-30, 1990 [PB94-209426] p 1072 N95-19581

SYNTAX
R.MAPCALC: An algebra for GIS and image processing [AD-A283923] p 1096 N95-18161

SYNTHESIS (CHEMISTRY)
Difunctional monomers based on perfluoropropylene telomers [AD-A283677] p 983 N95-18019
Ion exchange polymers and method for making [NASA-CASE-LEW-15576-1] p 984 N95-18321
Polymer-based separations: Synthesis and application of polymers for ionic and molecular recognition [DE94-016427] p 984 N95-18355
Elemental fluorine based syntheses of pentafluoro phenly and other aromatic perfluoropolyether polymers [AD-A284102] p 984 N95-18402
Excited state processes in transition metal complexes. Redox splitting in soluble polymers [DE95-002690] p 977 N95-19839

SYNTHETIC APERTURE RADAR
Some statistical tools for SAR image synthesis, analysis and processing [INPE-5548-TDI/534] p 1172 N95-18004
Comparative analysis of multisensor (TM/Landsat and SAR/ERS-1) and multitemporal scenes of Guaira region, Sao Paulo State, Brazil [INPE-5581-TDI/544] p 1049 N95-18005
On the optimization of speckle filtering techniques for ERS-1 images over Argentina [INPE-5578-PRE/1806] p 1050 N95-18216
Interferometric synthetic aperture radar and the Data Collection System Digital Terrain Elevation Demonstration [AD-A284024] p 999 N95-18657

AN/APS-137 Forward Looking Airborne Radar (FLAR) evaluation
[AD-A284672] p 1002 N95-19087
Analysis and synthesis of (SAR) waveguide phased array antennas
[AD-A285336] p 1004 N95-19535

SYNTHETIC FUELS
Activities of the Division of Energy Biosciences
[DE95-001046] p 1077 N95-19613

SYSTEM IDENTIFICATION
Comparison of frequency response and perturbation methods to extract linear models from a nonlinear simulation
[AD-A284115] p 958 N95-18405
A linear system identification and validation of an AH-64 Apache aeroelastic simulation model
p 959 N95-18903
The accuracy of parameter estimation in system identification of noisy aircraft load measurement
[NASA-CR-197516] p 945 N95-19130

SYSTEMS ANALYSIS
Requirements analysis for safety-critical systems: A chemical batch processing example
[PB94-201563] p 991 N95-17934
Use of profiler data for analysis and NOWcasting of a winter season extratropical cyclone
[PB94-187804] p 1067 N95-17992
Improving software characteristics of a real-time system using reengineering techniques
[AD-A283659] p 1094 N95-18015
Design and analysis of dynamic leader election protocols in broadcast networks
[PB94-202728] p 1109 N95-18039
A visual approach to the analysis of large software systems
[AD-A285440] p 1095 N95-18089
R.MAPCALC: An algebra for GIS and image processing
[AD-A283923] p 1096 N95-18161
The photographic system global evaluation for generation of INPE TM Landsat image
[INPE-5571-TDI/542] p 1050 N95-18369
Advanced techniques for analysis and evaluation of robust protocols
[AD-A285682] p 1111 N95-19513
Systems and economic analysis of microalgae ponds for conversion of CO2 to biomass
[DE95-000406] p 1054 N95-19554
A systems analysis and project management plan for the Petite Amateur Navy Satellite (PANSAT)
[AD-A285968] p 965 N95-19571

SYSTEMS ENGINEERING
Improving software characteristics of a real-time system using reengineering techniques
[AD-A283659] p 1094 N95-18015
Automatic Identification Technology (AIT): The development of functional capability and card application matrices
[AD-A285528] p 1173 N95-18099
Implementation of the 1992 Terminal area-Local Analysis and Prediction System (T-LAPS)
[AD-A284334] p 1070 N95-18384
SIGNET-software tools for signal identification using neural networks
[AD-A284362] p 1113 N95-18441
Progress in the development of advanced solar reflectors
[DE94-000264] p 1053 N95-18463
Strategic avionics technology definition studies. Subtask 3-1A3: Electrical Actuation (ELA) Systems Test Facility
[NASA-CR-188360] p 956 N95-18567
Development of executive information systems
[AD-A284005] p 1174 N95-18654
Engineering considerations for the self-energizing magnetoplasmadynamic (MPD) - type fusion plasma thruster
[AD-A283968] p 1144 N95-18888
Hypersonic flight testing
[AD-A283981] p 944 N95-18891
System engineering toolbox for design-oriented engineers
[NASA-RP-1358] p 962 N95-18932
Steady and unsteady blade stresses within the SSME ATD/HPOTP inducer p 968 N95-18982
Processing multilevel secure test and evaluation information
[AD-A284073] p 1001 N95-19069
Large area thermal target board: An improvement to environmental effects and system parameters characterization
[AD-A284614] p 1141 N95-19085
SPICE: An innovative, flexible instrument concept
p 966 N95-19189
LEVIS ion source and beam characterization on PBFA-2
[DE94-015802] p 1133 N95-19199
The US 100 T Magnet Project
[DE94-016099] p 1011 N95-19200
High-frame-rate intensified fast optically shuttered TV cameras with selected imaging applications
[DE94-016098] p 1035 N95-19394
Guidelines for reduction of human errors during maintenance of safety systems; maintainability and maintenance support
[PB94-215597] p 1092 N95-19412
Inter-amplifier pupil relay systems for a high average power dye laser at Lawrence Livermore National Laboratory
[DE94-016544] p 1039 N95-19507
Design of a flexible robotic arc welding system, task 3. Volume 1: System overview
[AD-A285116] p 1043 N95-19593
A novel technique for 4-dimensional atmospheric and oceanographic irradiance measurements using 3-D spatial filtering
[AD-A285658] p 1073 N95-19701
Collaborative engineering-design support system
p 1106 N95-19757

SYSTEMS MANAGEMENT
A fast recursive algorithm to compute the probability of M-out-of-N events
[AD-A283679] p 1120 N95-18020
Replica management system: A scheme for flexible and dynamic replication
[PB94-201597] p 1171 N95-18060
Automatic Identification Technology (AIT): The development of functional capability and card application matrices
[AD-A285528] p 1173 N95-18099
Assessment of the SFC database for analysis and modeling p 1158 N95-18171
Applying Costs, Risks and Values Evaluation (CRAVE) methodology to Engineering Support Request (ESR) prioritization p 1160 N95-18176
Metrics concept report. Central Archive for Reusable Defense Software (CARDS)
[AD-A284573] p 1097 N95-18449
Development of executive information systems
[AD-A284005] p 1174 N95-18654

SYSTEMS STABILITY
Standard reference materials: Glass filters as a standard reference material for spectrophotometry. Selection, preparation, certification and use of SRM 930 and SRM 1930
[PB94-188844] p 973 N95-17994

SYSTOLIC ARRAYS
Pre-processing in SADE: Stage 3
[PB94-201571] p 1093 N95-17935

T

T TAURI STARS
The quiescent and flaring EUV spectrum of Algol and its relationship to other active coronae. EUV spectroscopy of bright hyades coronae: 71 Tauri and Theta 1 Tauri
[NASA-CR-197538] p 1178 N95-18391
Overview of nebula models: Potential chondrule-forming environments p 1186 N95-19294
The early Sun and the formation of chondrules
p 1188 N95-19305

TABLES (DATA)
Climate and weather of Central Africa. Executive summary
[AD-A283647] p 1067 N95-18014

TACHYCARDIA
The aeromedical implications of supraventricular tachycardia p 1085 N95-19437

TAIL ASSEMBLIES
Pressure measurements on an F/A-18 twin vertical tail in buffeting flow. Volume 4, part 2: Buffet cross spectral densities
[AD-A285555] p 957 N95-18641

TAKEOFF
Tilt Rotor Unmanned Air Vehicle System (TRUS) demonstrator flight test program
[AD-A284151] p 943 N95-18415
Aircraft wake vortex takeoff tests at O'Hara International Airport
[AD-A283828] p 929 N95-18624

TANDEM MIRRORS
The experimental investigation of plasma configuration in MM-4U device
[DE94-626964] p 1144 N95-18885

TANKER AIRCRAFT
KC-135 cockpit modernization study. Phase 1: Equipment evaluation
[AD-A284099] p 942 N95-18398

TANKS (CONTAINERS)
SSI effects for a tank containing two liquids
[DE94-012457] p 1020 N95-19099

TARGET ACQUISITION
Visuo-ocular performance during vestibular stimulation
[AD-A284103] p 1089 N95-18403

TARGETS
Library operations policies and procedures. Volume 2: Central Archive for Reusable Defense Software (CARDS)
[AD-A284431] p 1096 N95-18344
Visuo-ocular performance during vestibular stimulation
[AD-A284103] p 1089 N95-18403
Low voltage electron beam lithography
[AD-A284181] p 1010 N95-18625
Large area thermal target board: An improvement to environmental effects and system parameters characterization
[AD-A284614] p 1141 N95-19085
Inertial confinement fusion
[DE95-000314] p 1147 N95-19552
Historic patterns of CO2 emissions from fossil fuels: Implications for stabilization of emissions
[DE95-000489] p 1061 N95-19556

TASK COMPLEXITY
Multiple-task performance: A critical review of the literature and a cognitive neuroscience framework
[AD-A285133] p 1090 N95-19583

TASKS
Vision and action
[AD-A285701] p 1140 N95-18480

TATB
Mixed high explosives for insensitive booster compositions
[MRL-TR-92-22] p 990 N95-19505

TEAMS
Effective team performance under stress and normal conditions: An experimental paradigm, theory and data for studying team decision making in hierarchical teams with distributed expertise
[AD-A284683] p 1089 N95-18530

TEARING
J-integral characterization of the nozzle steels from intermediate test vessels IV-5 and IV-9
[DE95-001066] p 979 N95-18934

TECHNOLOGIES
Using federal technology policy to strength the US microelectronics industry
[DE94-017293] p 1008 N95-18143
The Japan Information Center of Science and Technology p 1198 N95-19128

TECHNOLOGY ASSESSMENT
Technological and organizational diversity and technical advance in the early history of the American semiconductor industry
[PB94-175700] p 1007 N95-17999
NASA/DOD Aerospace Knowledge Diffusion Research Project. Paper 47: The value of computer networks in aerospace
[NASA-CR-197591] p 1109 N95-18055
Norwegian heat pump status and policy review
[PB94-206992] p 992 N95-18667

TECHNOLOGY TRANSFER
A strategy for electronic dissemination of NASA Langley technical publications
[NASA-TM-109172] p 1175 N95-18936
Research reports: 1994 NASA/ASEE Summer Faculty Fellowship Program
[NASA-CR-196533] p 1161 N95-18967
A hypertext-based Internet-assessable database for the MSFC Technology Transfer Office p 1165 N95-18986
High-frame-rate intensified fast optically shuttered TV cameras with selected imaging applications
[DE94-016098] p 1035 N95-19394

TECHNOLOGY UTILIZATION
Overview of laser technology at Los Alamos National Laboratory
[DE94-018307] p 1036 N95-18126
NASA/DOD Aerospace Knowledge Diffusion Research Project. Report 26: The technical communication practices of aerospace engineering students: Results of the phase 3 AIAA National Student Survey
[NASA-TM-109121] p 1175 N95-18950
NASA/DOD Aerospace Knowledge Diffusion Research Project. Paper 46: Technical communications in aerospace: A comparison across four countries
[NASA-TM-110056] p 1175 N95-19038
Tapping into the Sun: Today's applications of photovoltaic technology
[DE93-000075] p 1054 N95-19854

TEFLON (TRADEMARK)
Penetration experiments in aluminum and Teflon targets of widely variable thickness p 1047 N95-19185

TELECOMMUNICATION
Personal communications services: Improving theater deployable communications for the 21st century
[AD-A283465] p 994 N95-18058
Advanced optical fiber communications systems
[AD-A283942] p 1141 N95-18682

Information Superhighway: Issues affecting development. Report to the Congress
[GAO/RCED-94-285] p 1174 N95-18914
ODP based UPT model
[PB94-215589] p 1003 N95-19411

TELECONFERENCING
Zoned Analog Personal Teleconferencing (ZAPT)
[AD-A285877] p 1004 N95-19600

TELEMETRY
An instrument to measure the charge, and energy spectrum (20-1000 GeV/a) of the cosmic ray species oxygen to iron
[NASA-CR-197555] p 1197 N95-18464

TELESCOPES
PRISM project optical instrument
p 1143 N95-19009

TELEVISION CAMERAS
Feasibility study of transmission of OTV camera control information in the video vertical blanking interval
p 1006 N95-18185
High-frame-rate intensified fast optically shuttered TV cameras with selected imaging applications
[DE94-016098] p 1035 N95-19394

TELEVISION SYSTEMS
Feasibility study of transmission of OTV camera control information in the video vertical blanking interval
p 1006 N95-18185
RACE project 1036: WTDM broadband customer premises network
[BBC-RD-1993/15] p 998 N95-18537
Alleviation of co-channel interference at Poole relay station
[BBC-RD-1993/4] p 1003 N95-19136
High-frame-rate intensified fast optically shuttered TV cameras with selected imaging applications
[DE94-016098] p 1035 N95-19394

TELEVISION TRANSMISSION
Multi-channel sound for HDTV: Subjective tests on sound channel configuration
[BBC-RD-1994/4] p 998 N95-18535
Digital video compression: Standardisation of scalable coding schemes
[BBC-RD-1994/10] p 1001 N95-19047
Bit-rate reduction of digital television for transmission: An introductory review
[BBC-RD-1994/2] p 1001 N95-19052
Engineering review, January 1993 - March 1994
p 1001 N95-19055
Alleviation of co-channel interference at Poole relay station
[BBC-RD-1993/4] p 1003 N95-19136
Metal-framed partitions with reduced thicknesses. Part 1: Narrower studs and cavities
[BBC-RD-1993/5-PT-1] p 993 N95-19138

TELLURIC CURRENTS
Two and three dimensional magnetotelluric inversion
[DE94-014820] p 1063 N95-17967

TEMPERATURE CONTROL
Lunar base heat pump, phase 1
[NASA-CR-188300] p 1015 N95-18111

TEMPERATURE DEPENDENCE
Laboratory studies of stratospheric bromine chemistry: Kinetics of the reactions of bromine monoxide with nitrogen dioxide and atomic oxygen p 1065 N95-18731
Computational modeling of properties
[NASA-CR-197558] p 1010 N95-18925
New astrophysical opacities and their effects on stellar models
[DE94-016445] p 1186 N95-19249
Chondrule precursors and cooling paths: The sulfur evidence p 1193 N95-19338

TEMPERATURE DISTRIBUTION
Estimation of satellite derived temperature and moisture fields over Europe from TOVS data using 3I and ITPP algorithms
[AD-A284581] p 1049 N95-18035
A numerical simulation of seasonal circulation in the South China Sea
[AD-A283701] p 1075 N95-18622
Implications of summertime marine stratocumulus on the North American climate p 1073 N95-18977
Simulation of multidisciplinary problems for the thermostress state of cooled high temperature turbines
p 948 N95-19021
Verification of multidisciplinary models for turbomachines p 949 N95-19025
Heating during solar nebula formation and Mg isotopic fractionation in precursor grains of CAIs and chondrules
p 1191 N95-19326
Incompressible flow of a Newtonian fluid past a vertical plate with thermal and magnetic stresses
[AD-A284856] p 1030 N95-19716

TEMPERATURE EFFECTS
Energy balance model for imagery and electromagnetic propagation
[AD-A284552] p 1063 N95-18115
Innovative development and application of models for weakly ionized ionospheric plasmas
[AD-A284583] p 1064 N95-18452
The effect of temperature on the radiative performance of Ho-YAG thin film selective emitters
[NASA-TM-106830] p 1053 N95-18587
Numerical simulation of shock/shock and shock/boundary-layer interactions in chemically reacting hypersonic flows
[DLR-94-04] p 1019 N95-18609
Complex oxidation effects in polymer degradation
[DE94-018903] p 986 N95-18651
Effect of heat acclimation on sitting orthostatic tolerance in the heat after 48 and 96 hour bed rest in men
[NASA-TM-108861] p 1077 N95-18734
Thermal behavior spiral bevel gears
[NASA-TM-106518] p 1042 N95-18935
Concentration and temperature effects on ovostatin activity p 1077 N95-18997
Experimental constraints on models for origins of chondrules: Peak temperatures p 1187 N95-19302
Hypersonic viscous flow computations
p 1029 N95-19463
An investigation of drag repeatability in half model testing in the ARA Transonic Wind Tunnel
[ARA-MEMO-392] p 931 N95-19546

TEMPERATURE GRADIENTS
The diurnal cycle of high-frequency temperature variability at 0 deg 140 deg W on seasonal and interannual time scales
[AD-A283640] p 1074 N95-18012
Observation of flow and temperature oscillations around a bubble on a solid surface subject to a vertical temperature gradient
[NASA-CR-197593] p 1017 N95-18327
Marine boundary layer refractive effects in the infrared
[AD-A285717] p 1140 N95-18484
Experimental constraints on models for origins of chondrules: Peak temperatures p 1187 N95-19302

TEMPERATURE MEASUREMENT
A technical demonstration Mobile Profiler System
[AD-A284562] p 1068 N95-18117
Thermocouples for interior ballistic temperature measurements
[AD-A283699] p 1033 N95-18620

TEMPERATURE PROBES
Hypersonic flow-field measurements: Intrusive and nonintrusive
[AD-A283867] p 930 N95-18674

TEMPERATURE PROFILES
Ice surface temperature retrieval from AVHRR, ATSR, and passive microwave satellite data: Algorithm development and application
[NASA-CR-197542] p 1052 N95-18952
Implications of a phase-transition thermostat for chondrule melting p 1189 N95-19312

TEMPERATURE SENSORS
Materials for adaptive structural acoustic control, volume 3
[AD-A279223] p 1128 N95-19850

TEMPLATES
Process definition and modeling guidebook. Volume 1: Concepts and principles of MPDM. Version 02.00.02
[AD-A279162] p 1108 N95-19803

TEMPORAL DISTRIBUTION
Spatial and temporal constraints on the observed distribution of gamma-ray bursts detected by BATSE
p 1197 N95-18730

TEMPORAL RESOLUTION
High-frequency skywave signal power measurement system
[AD-A284382] p 996 N95-18341

TENSILE CREEP
Composites research in support of the NASP Institute for Composites (NIC)
[NASA-CR-197580] p 970 N95-18471

TENSILE PROPERTIES
Warm formability of aluminum-magnesium alloys
[DE94-016170] p 980 N95-19396

TENSILE STRENGTH
Development of radiation-hardened ceramic composites for fusion applications
[DE94-016182] p 985 N95-18638
Synthesis and structural properties of new metallic phases exhibiting non-crystallographic symmetries
[AD-A284882] p 982 N95-19743

TENSILE STRESS
Fatigue crack growth in 2024-T3 aluminum under tensile and transverse shear stresses p 938 N95-19490

TENSILE TESTS
Development of radiation-hardened ceramic composites for fusion applications
[DE94-016182] p 985 N95-18638
Warm formability of aluminum-magnesium alloys
[DE94-016170] p 980 N95-19396
Microstructurally based variations on the dwell fatgue life of titanium alloy IMI 834 p 938 N95-19489
Soft body impact on titanium fan blades
p 953 N95-19671

TENSOR ANALYSIS
Visualizing second order tensor fields with hyperstreamlines
[NASA-CR-197619] p 1121 N95-19288

TENSORS
General relativity and dark matter
[DE94-626641] p 1180 N95-18877
Visualizing second order tensor fields with hyperstreamlines
[NASA-CR-197619] p 1121 N95-19288
Antisymmetric tensor field interactions and neutron star models
[PB94-215605] p 1118 N95-19375
The tensor equation AX+XA=Phi (A, H) with applications to kinematics of continua
[AD-A285886] p 1122 N95-19603

TERNARY ALLOYS
Warm formability of aluminum-magnesium alloys
[DE94-016170] p 980 N95-19396
Heteroepitaxy of ternary SiGeC alloys on Si for bipolar transistors
[AD-A285317] p 1151 N95-19511

TERRAIN
Spectral reflectance properties of wetlands plants
[AD-A283546] p 1051 N95-18614

TERRAIN ANALYSIS
Real-time modeling of complex atmospheric releases in urban areas
[DE94-018063] p 1059 N95-18647
Representing visibility for siting problems
[AD-A284076] p 993 N95-19036

TERRESTRIAL DUST BELT
IRAS observations show that the Earth is embedded in a solar ring of asteroidal dust particles in resonant lock with the planet. p 1182 N95-19181

TEST CHAMBERS
High-temperature acoustic test facilities and methods
p 1125 N95-19149
Development of pneumatic test techniques for subsonic high-lift and in-ground-effect wind tunnel investigations
p 932 N95-19268
Unsteady flow testing in a passive low-correction wind tunnel p 960 N95-19272

TEST EQUIPMENT
Metrology: Calibration and measurement processes guidelines
[NASA-RP-1342] p 992 N95-18745

TEST FACILITIES
Virtual reality, an air combat T and E perspective
[AD-A284161] p 959 N95-18508
Strategic avionics technology definition studies. Subtask 3-1A3: Electrical Actuation (ELA) Systems Test Facility
[NASA-CR-188360] p 956 N95-18567
Calibration and testing of a large-scale electric gun for shock Hugoniot measurements
[MRL-TR-93-24] p 959 N95-18942
High-temperature acoustic test facilities and methods
p 1125 N95-19149
The hypervelocity impact facilities at the University of Kent at Canterbury, UK p 961 N95-19180
Development of pneumatic test techniques for subsonic high-lift and in-ground-effect wind tunnel investigations
p 932 N95-19268
Operating capability and current status of the reactivated NASA Lewis Research Center Hypersonic Tunnel Facility
[NASA-TM-106808] p 960 N95-19286
Characterization of the 50 MeV ALS linac beam with optical transition radiation
[DE94-018208] p 1137 N95-19584

TEST PILOTS
Preliminary evaluation of the F/A-18 quantity/multiple envelope expansion
[AD-A284119] p 943 N95-18407
F/A-18 simulation validation and verification: Making a good product even better
[AD-A283995] p 944 N95-18723
Helicopter in-flight simulation development and use in test pilot training
[AD-A283998] p 959 N95-18725

TEST STANDS
NASA High Performance Computing and Communications program
[NASA-TM-4653] p 1174 N95-18573

TETHERED SATELLITES
Radar cross-section measurements and simulation of a tethered satellite. The small expendable deployer system end-mass payload
[NASA-TM-4613] p 1005 N95-19781

TETHERING
Electrodynamic behavior of PMG-Delta
[AD-A283930] p 964 N95-18163

TETRAHEDRONS
Mesh quality control for multiply-refined tetrahedral grids
[NASA-CR-197595] p 1043 N95-18737
An assessment of the adaptive unstructured tetrahedral grid, Euler Flow Solver Code FELISA
[NASA-TP-3526] p 930 N95-19041
TETRAHYDROFURAN
Novel polymeric composites through molecular engineering
[AD-A284168] p 985 N95-18513
TEXTILES
TEXCAD: Textile Composite Analysis for Design. Version 1.0: User's manual
[NASA-CR-4639] p 970 N95-18466
Diffusion of water vapour through cold Gore-Tex (trademark)
[AD-A279939] p 989 N95-19867
TEXTS
A crystalline quark-hadron mixed phase in neutron stars
[DE95-000787] p 1194 N95-19570
TEXTURES
Porphyritic versus nonporphyritic chondrules p 1190 N95-19318
Formation of chondrules and CAIs by nebular processes p 1190 N95-19321
Textural variability of ordinary chondrite chondrules: Implications of their formation p 1193 N95-19339
Deformation texture studies in Fe3Al alloys
[DE94-017709] p 980 N95-19400
THEMATIC MAPPERS (LANDSAT)
Comparative analysis of multisensor (TM/Landsat and SAR/ERS-1) and multitemporal scenes of Guaira region, Sao Paulo State, Brazil
[INPE-5581-TDI/544] p 1049 N95-18005
THEMATIC MAPPING
Comparative analysis of multisensor (TM/Landsat and SAR/ERS-1) and multitemporal scenes of Guaira region, Sao Paulo State, Brazil
[INPE-5581-TDI/544] p 1049 N95-18005
Thematic classification of zone coastal: A methodologic contribution
[INPE-5586-TDI/548] p 1050 N95-18215
Remote sensing products evaluation for cartographic updating purposes
[INPE-5584-TDI/546] p 1050 N95-18368
THEOREM PROVING
Representing and reformulating diagonalization methods
[AD-A283916] p 1095 N95-18155
The QED Workshop
[DE94-018499] p 1111 N95-19592
THEOREMS
A crystalline quark-hadron mixed phase in neutron stars
[DE95-000787] p 1194 N95-19570
THEORETICAL PHYSICS
Zero modes of first class secondary constraints in gauge theories
[DE94-626659] p 1156 N95-18328
Establishment of an Institute for Fusion Studies
[DE94-017330] p 1145 N95-19079
THERAPY
Clinical practice, diagnosis and therapy of intervertebral disk lesion: Importance to fitness for military flying duties p 1084 N95-19435
THERMAL ANALYSIS
Preparation and surface characterization of metal doped alumina catalyst
[PB94-175296] p 973 N95-17991
Composite structures having organic matrices and duplex zinc/ceramic fire barriers
[AD-D016232] p 970 N95-18629
Residual stresses in welded plates p 1047 N95-18972
Thermo-acoustic fatigue design for hypersonic vehicle skin panels p 1047 N95-19161
Technology Benefit Estimator (T/BEST): User's manual
[NASA-TM-106785] p 1046 N95-19501
THERMAL CONDUCTIVITY
Quality optimization of thermally sprayed coatings produced by the JP-5000 (HVOF) gun using mathematical modeling p 989 N95-19008
THERMAL CONTROL COATINGS
Quality optimization of thermally sprayed coatings produced by the JP-5000 (HVOF) gun using mathematical modeling p 989 N95-19008
Thermal testing of high performance thermal barrier coatings for turbine blades p 955 N95-19681
THERMAL CYCLING TESTS
Thermal behavior spiral bevel gears
[NASA-TM-106518] p 1042 N95-18935
THERMAL DECOMPOSITION
Complex oxidation effects in polymer degradation
[DE94-018903] p 986 N95-18651
THERMAL DIFFUSION
Coupled finite element analysis of decomposing poroelastic polymeric composites and structures with subsequent thermal and gas diffusion p 986 N95-18918
THERMAL EMISSION
Assessment of CO2 projections
[DE94-017484] p 1059 N95-18664
Large area thermal target board: An improvement to environmental effects and system parameters characterization
[AD-A284614] p 1141 N95-19085
THERMAL ENVIRONMENTS
Hypersonic wind tunnel test techniques
[AD-A284057] p 929 N95-18663
THERMAL EXPANSION
Novel polymeric composites through molecular engineering
[AD-A284168] p 985 N95-18513
THERMAL FATIGUE
Thermal testing of high performance thermal barrier coatings for turbine blades p 955 N95-19681
THERMAL INSULATION
Outgassing of solid material into vacuum thermal insulation spaces p 972 N95-18184
Method of lowering the reaction exotherm in thermally polymerized acetylene terminated resins
[AD-D016276] p 985 N95-18430
A review of footwear for cold/wet scenarios. Part 2: Socks, liners, and insoles
[AD-A279937] p 989 N95-19866
THERMAL MAPPING
An inverse problem in thermal imaging
[NASA-CR-195018] p 1117 N95-18479
A GIS approach to urban heat island research: The case of Huntsville, Alabama p 1063 N95-18991
THERMAL NEUTRONS
Assembly and calibration of a new experimental apparatus for production and utilization of capture gamma rays
[DE94-626650] p 1198 N95-18880
THERMAL PROTECTION
Debris/ice/TPS assessment and integrated photographic analysis of Shuttle mission STS-68
[NASA-TM-109207] p 963 N95-18047
Real-time thickness measurement of MCC ablator material p 972 N95-18981
Debris/ice/TPS assessment and integrated photographic analysis of Shuttle mission STS-66
[NASA-TM-110141] p 963 N95-19790
THERMAL RESISTANCE
Real-time thickness measurement of MCC ablator material p 972 N95-18981
A CMC database for use in the next generation launch vehicles (rockets) p 963 N95-18993
THERMAL SHOCK
Quality optimization of thermally sprayed coatings produced by the JP-5000 (HVOF) gun using mathematical modeling p 989 N95-19008
Thermal testing of high performance thermal barrier coatings for turbine blades p 955 N95-19681
THERMAL STABILITY
High temperature stability of binary microstructures derived from liquid precursors
[AD-A283960] p 1150 N95-18685
Thermal relaxation processes and stability in poled electro-optic polymers
[AD-A283948] p 987 N95-19102
PVDF flux/mass/velocity/trajectory systems and their applications in space p 966 N95-19196
Carbon, CAIs and chondrules p 1186 N95-19291
Thermo-oxidative stability of graphite/PMR-15 composites: Effect of fiber surface modification on composite shear properties
[NASA-TM-4608] p 981 N95-19652
THERMAL STRESSES
Simulation of multidisciplinary problems for the thermostress state of cooled high temperature turbines p 948 N95-19021
Application of multidisciplinary models to the cooled turbine rotor design p 949 N95-19024
Incompressible flow of a Newtonian fluid past a vertical plate with thermal and magnetic stresses
[AD-A284856] p 1030 N95-19716
THERMIONIC CONVERTERS
Fueled emitter, TFE Verification Program
[DE94-017557] p 1135 N95-18146
A three region analysis of a bounded plasma using particle in cell and fluid techniques
[AD-A284826] p 1147 N95-19690
THERMIONIC EMITTERS
Fueled emitter, TFE Verification Program
[DE94-017557] p 1135 N95-18146
THERMIONIC POWER GENERATION
Fueled emitter, TFE Verification Program
[DE94-017557] p 1135 N95-18146
TFE design package, TFE Verification Program
[DE94-017558] p 1136 N95-18147
THERMOCHEMICAL PROPERTIES
Hypersonic viscous flow computations p 1029 N95-19463
THERMOCHEMISTRY
Design of advanced steels for armor applications
[ARL-CR-175] p 979 N95-18948
Thermochemical IR sources: COCHISE and FACELIF experiments
[AD-A279940] p 977 N95-19868
THERMOCOUPLES
Thermocouples for interior ballistic temperature measurements
[AD-A283699] p 1033 N95-18620
THERMODYNAMIC CYCLES
Lunar base heat pump, phase 1
[NASA-CR-188300] p 1015 N95-18111
Wave cycle design for wave rotor engines with limited nitrogen oxide emissions p 1041 N95-18901
THERMODYNAMIC PROPERTIES
Methane conversion by solid electrolyte membranes
[PB94-191781] p 973 N95-17982
International Conference on Deformation, Yield and Fracture of Polymers
[AD-A284354] p 984 N95-18339
An atomic view of motion on surfaces
[AD-A285565] p 1131 N95-18473
Thermal relaxation processes and stability in poled electro-optic polymers
[AD-A283948] p 987 N95-19102
Atomistic and elastic analyses of defects and small structures
[DE94-017047] p 980 N95-19111
THERMODYNAMICS
Characterization of metal matrix composites
[NASA-CR-195381] p 970 N95-18940
THERMOELECTRIC MATERIALS
Thermoelectric properties of conducting polymers
[AD-A284058] p 986 N95-18678
THERMOELECTRICITY
Thermoelectric properties of conducting polymers
[AD-A284058] p 986 N95-18678
Computational modeling of properties
[NASA-CR-197558] p 1010 N95-18925
THERMOLUMINESCENCE
An investigation of nonuniform dose deposition from an electron beam
[AD-A284175] p 1131 N95-18519
THERMONUCLEAR REACTIONS
Direct energy conversion system for D(3)-He fusion
[DE94-770773] p 1146 N95-19549
THERMOPLASTIC RESINS
International Conference on Deformation, Yield and Fracture of Polymers
[AD-A284354] p 984 N95-18339
THERMOSPHERE
Design, validation and prototype testing of a high resolution all-reflection Michelson interferometer for solar occultation measurements of the OI 1304-a triplet emission
[AD-A283705] p 1178 N95-18361
First principles used in orbital prediction and an atmospheric model comparison
[AD-A284636] p 1065 N95-19086
THERMOSTATS
Implications of a phase-transition thermostat for chondrule melting p 1189 N95-19312
THICK FILMS
Development of high reliability planar chip inductors
[DE94-018589] p 1012 N95-19231
THICK PLATES
Plate vibration with arbitrarily oriented stiffeners based on Mindlin-Engesser formulation
[RR-CE143] p 1045 N95-18608
THICKNESS
An NDE approach for characterizing quality problems in polymer matrix composites
[NASA-TM-106807] p 1043 N95-18583
Real-time thickness measurement of MCC ablator material p 972 N95-18981
THIN FILMS
Methane conversion by solid electrolyte membranes
[PB94-191781] p 973 N95-17982
A constant-depth scratch test for the measurement of adhesion at film-substrate interfaces
[AD-A283660] p 983 N95-18016
UV laser-surface interactions relevant to analytic spectroscopy of wide band gap materials
[DE94-016180] p 1037 N95-18349
The effect of temperature on the radiative performance of Ho-YAG thin film selective emitters
[NASA-TM-106830] p 1053 N95-18587

Atomic Layer Epitaxy (ALE) apparatus for growing thin films of elemental semiconductors
[AD-D016236] p 1149 N95-18633
Heterogeneous nucleation of calcium oxalate on native oxide surfaces
[DE94-018725] p 986 N95-18648
High temperature stability of binary microstructures derived from liquid precursors
[AD-A283960] p 1150 N95-18685
Growth of thin films of dicyanovinylanisole on quartz and teflon-coated quartz by physical vapor transport p 989 N95-19000
Lithium electrode/polyacrylonitrile based polymer electrolyte interface
[AD-A283947] p 986 N95-19064
Superstrength metal composite material and process for making the same
[AD-D016555] p 971 N95-19123
Plasma produced by impacts of fast dust particles on a thin film p 1181 N95-19177
Penetration of multiple thin films in micrometeorite capture cells p 1036 N95-19192
Assessment of velocity/trajectory measurement technologies during a particle capture event p 1036 N95-19193
Precision gold conductors for HMCs
[DE94-018558] p 1012 N95-19230
Ion mixing in oxide-sapphire systems
[DE94-018660] p 1133 N95-19232
Damage monitoring in metallic and composite structures using piezoelectric thin film sensors
[ARL-RR-4] p 971 N95-19467
Heteroepitaxy of ternary SiGeC alloys on Si for bipolar transistors
[AD-A285317] p 1151 N95-19511
Ferroelectric thin film bismuth titanate prepared from acetate precursors
[DE95-000538] p 988 N95-19558
High temperature superconducting films and crystals
[AD-A279201] p 1154 N95-19815
Materials for adaptive structural acoustic control, volume 3
[AD-A279223] p 1128 N95-19850
Correlation of polycrystalline Cu(In,Ga)Se2 device efficiency with homojunction depthand interfacial structure: X-ray photoemission and positron annihilation spectroscopic characterization
[DE94-013543] p 1055 N95-19858
Advanced processing technology for high-efficiency, thin-film CuInSe2 and CdTe solar cells
[DE94-011838] p 1056 N95-19880
Silicon-Film (trademark) photovoltaic manufacturing technology
[DE94-011899] p 1056 N95-19882

THIN LAYER CHROMATOGRAPHY
Enhancement of fluorescence detection in chromatographic methods by computer analysis of second order data
[DE94-014682] p 973 N95-17966

THIN PLATES
Residual stresses in welded plates p 1047 N95-18972
Charge collection during hypervelocity penetrations of thin foils p 1036 N95-19190
Fatigue crack growth in 2024-T3 aluminum under tensile and transverse shear stresses p 938 N95-19490

THIN WALLS
BEAM: A finite element program for the collapse analysis of vehicle structures
[AD-A285547] p 1045 N95-18472

THOMSON SCATTERING
Progress on the multipulse Thomson scattering diagnostic on D3-D
[DE94-017515] p 1143 N95-18119

THORAX
Effects of weight lifting on intrathoracic pressures generated by anti-g straining maneuvers
[AD-A283651] p 1078 N95-18138

THREE BODY PROBLEM
Optimal transfer and swing-by orbits in the two- and three-body problems p 961 N95-18900

THREE DIMENSIONAL BOUNDARY LAYER
A spectrally accurate boundary-layer code for infinite swept wings
[NASA-CR-195014] p 1014 N95-18042
Effect of crossflow on Goertler instability in incompressible boundary layers
[NASA-CR-195007] p 1016 N95-18193
Sectional prediction of 3D effects for separated flow on rotating blades
[PB94-201696] p 928 N95-18503

THREE DIMENSIONAL FLOW
An application of a two-equation model of turbulence to three-dimensional chemically reacting flows
[NASA-CR-195411] p 1015 N95-18107
A three-dimensional structured/unstructured hybrid Navier-Stokes method for turbine blade rows
[NASA-TM-106813] p 1016 N95-18200
Nonlinear magnetohydrodynamics
[DE94-016223] p 1143 N95-18353
Prediction of buoyant outflow in lakes and fjords with a quasi 3D numerical model
[PB94-206984] p 1051 N95-18372
A note on singularities of the 3-D Euler equation
[NASA-CR-195006] p 1017 N95-18397
Sectional prediction of 3D effects for separated flow on rotating blades
[PB94-201696] p 928 N95-18503
The effect of stable stratification on three-dimensional structure in shear layers p 1019 N95-18921
An assessment of the adaptive unstructured tetrahedral grid, Euler Flow Solver Code FELISA
[NASA-TP-3526] p 930 N95-19041
Validation and evaluation of the advanced aeronautical CFD system SAUNA: A method developer's view
[ARA-MEMO-390] p 1030 N95-19774

THREE DIMENSIONAL MODELS
The Green's function in the Bloch-Nordsieck model for QED3
[DE94-626680] p 996 N95-18331
Prediction of buoyant outflow in lakes and fjords with a quasi 3D numerical model
[PB94-206984] p 1051 N95-18372
Size distribution of one-, two- and three-dimensional Voronoi cells
[PB94-207008] p 1149 N95-18373
TEXCAD: Textile Composite Analysis for Design. Version 1.0: User's manual
[NASA-CR-4639] p 970 N95-18466
Long-term processes in geomaterials. A three-dimensional visco-elastic soil model
[PB94-207180] p 1065 N95-18640
Thermal behavior spiral bevel gears
[NASA-TM-106518] p 1042 N95-18935
Characterization of metal matrix composites
[NASA-CR-195381] p 970 N95-18940
Development of microgravity, full body functional reach envelope using 3-D computer graphic models and virtual reality technology p 1092 N95-18990
Cross-tail current, field-aligned current, and B(y)
[NASA-CR-197624] p 1065 N95-19032
Visualizing second order tensor fields with hyperstreamlines
[NASA-CR-197619] p 1121 N95-19288
High performance computing for medical image interpretation
[AD-A285457] p 1086 N95-19537
ADCIRC: An advanced three-dimensional circulation model for shelves, coasts, and estuaries. Report 5: A tropical storm database for the east and Gulf of Mexico coasts of the United States
[AD-A285576] p 1075 N95-19540
Simulation of wave propagation in three-dimensional random media
[NASA-CR-197605] p 1004 N95-19547
The tensor equation AX+XA=Phi (A, H) with applications to kinematics of continua
[AD-A285886] p 1122 N95-19603
Application of three-dimensional hybrid structured/unstructured grids to land, sea and air vehicles
[ARA-MEMO-399] p 1031 N95-19775

THREE DIMENSIONAL MOTION
Development of microgravity, full body functional reach envelope using 3-D computer graphic models and virtual reality technology p 1092 N95-18990
Three-dimensional radiation transport hydrodynamics
[DE94-018337] p 1146 N95-19527

THRUST AUGMENTATION
Development of CFD model for augmented core tripropellant rocket engine p 968 N95-18988

THRUST CHAMBERS
Advanced small rocket chambers. Basic program and option 2: Fundamental processes and material evaluation
[NASA-CR-195349] p 966 N95-18192
Regenerative cooling for liquid propellant rocket thrust chambers
[INPE-5565-TDI/540] p 967 N95-18720

THRUST VECTOR CONTROL
VSTOL Systems Research Aircraft (VSRA) Harrier
[NASA-TM-110117] p 941 N95-18347
Static investigation of two fluidic thrust-vectoring concepts on a two-dimensional convergent-divergent nozzle
[NASA-TM-4574] p 931 N95-19042
Integrated aerodynamic fin and stowable TVC vane system
[AD-D016457] p 967 N95-19073

THUNDERSTORMS
Two space scatterer formalism calculation of bulk parameters of thunderclouds p 1073 N95-19001

THYROID GLAND
TSH determination in subjects with medium-low levels of serum thyroxine p 1082 N95-19421

THYROXINE
TSH determination in subjects with medium-low levels of serum thyroxine p 1082 N95-19421

TILES
Aeroacoustic qualification of HERMES shingles p 1125 N95-19145

TILT ROTOR AIRCRAFT
Wing design for a civil tiltrotor transport aircraft
[NASA-CR-197523] p 942 N95-18090
Tilt Rotor Unmanned Air Vehicle System (TRUS) demonstrator flight test program
[AD-A284151] p 943 N95-18415
V-22 simulator evaluation for shipboard operations
[AD-A284156] p 943 N95-18505

TIME DEPENDENCE
Large signal time dependent quantum mechanical transport in quantum phase based devices
[AD-A283338] p 1155 N95-18009
Cumulative impact analysis of wetlands using hydrologic indices
[AD-A284759] p 1058 N95-18085
Global time transformations
[AD-A285539] p 1110 N95-18454
Minimal time detection algorithms and applications to flight systems
[TR-2-FSRC-93] p 1098 N95-18564
Marangoni convection in a gravity-free silicon float zone
[NASA-CR-197600] p 991 N95-18913
Velocity measurements with hot-wires in a vortex-dominated flowfield p 932 N95-19261
Learning effects on strategy selection in a dynamic task environment as a function of time pressure
[AD-A285458] p 1089 N95-19538
MIRO: A debugging tool for CLIPS incorporating historical Rete networks p 1105 N95-19754

TIME DIVISION MULTIPLEXING
RACE project 1036: WTDM broadband customer premises network
[BBC-RD-1993/15] p 998 N95-18537

TIME FUNCTIONS
The formulation of quantum statistical mechanics based on the Feynman path centroid density. 3: Phase space formalism and analysis of centroid molecular dynamics
[AD-A279233] p 1157 N95-19852
The formulation of quantum statistical mechanics based on the Feynman path centroid density. 4: Algorithms for centroid molecular dynamics
[AD-A279234] p 1157 N95-19853

TIME LAG
True time delay beamforming
[AD-A285683] p 1003 N95-19516

TIME MARCHING
Low-dissipation and -dispersion Runge-Kutta schemes for computational acoustics
[NASA-CR-195022] p 1018 N95-18488
Numerical computations of supersonic base flow with special emphasis on turbulence modeling
[AD-A283688] p 930 N95-18670
Finite volume method using Runge-Kutta time-stepping for solution of Euler equations p 1027 N95-19451

TIME MEASUREMENT
Time spread and frequency coherence in acoustic forward scattering from the sea surface
[AD-A284736] p 1123 N95-18083
Global time transformations
[AD-A285539] p 1110 N95-18454

TIME OF FLIGHT SPECTROMETERS
Development of laser-ion beam photodissociation methods
[DE95-002800] p 977 N95-19840

TIME OPTIMAL CONTROL
Time-optimal control of a third order regulator
[AD-A283307] p 1113 N95-18023

TIME SERIES ANALYSIS
TLS-based prefiltering technique for time-domain ARMA modeling
[AD-A284525] p 1120 N95-18113
Wallops Island natural rain data analysis p 1069 N95-18205
SIGNET-software tools for signal identification using neural networks
[AD-A284362] p 1113 N95-18441
Method of displaying time series data on finite resolution display device
[AD-D016438] p 1173 N95-18526
Signal processing via Fourier-Bessel series expansion
[AD-A285316] p 1003 N95-19510

PAK: A processing system for vectorized time-series data
[AD-A284881] p 1104 N95-19742

TISSUES (BIOLOGY)
Light transport for medical laser treatments
[PB94-201498] p 1037 N95-18502
US experiments flown on the Soviet biosatellite Cosmos 2044. Volume 1: Mission description, experiments K-7-01 - K-7-15
[NASA-TM-108802-VOL-1] p 1092 N95-18569

TITANATES
Ferroelectric thin film bismuth titanate prepared from acetate precursors
[DE95-000538] p 988 N95-19558
Use of titanate coupling agents in Kevlar (trade name)/phenolic composites
[AD-A279200] p 972 N95-19814

TITANIUM
Composites research in support of the NASP Institute for Composites (NIC)
[NASA-CR-197580] p 970 N95-18471
Precision gold conductors for HMCs
[DE94-018558] p 1012 N95-19230
Ferroelectric thin film bismuth titanate prepared from acetate precursors
[DE95-000538] p 988 N95-19558
Soft body impact on titanium fan blades
p 953 N95-19671
PRS projections for DECADE
[AD-A279215] p 1147 N95-19847

TITANIUM ALLOYS
Microstructurally based variations on the dwell fatgue life of titanium alloy IMI 834 p 938 N95-19489

TITANIUM NITRIDES
Protective coatings for compressor gas path components p 954 N95-19675

TITANIUM OXIDES
Polyurethane self-priming topcoats
[AD-D016264] p 984 N95-18320
Polyurethane self-priming topcoats
[AD-D016234] p 985 N95-18631
Heterogeneous nucleation of calcium oxalate on native oxide surfaces
[DE94-018725] p 986 N95-18648

TOKAMAK DEVICES
Erosion of melt layers developed during a plasma disruption
[DE94-018362] p 1144 N95-18547
Global wave modeling of electron interactions with fast magnetosonic waves
[DE94-018942] p 1144 N95-18557
Simplified ideal MHD normal mode equations for toroidal axisymmetric plasmas
[DE94-627004] p 1144 N95-18886
Study on heat flux of plasma scrape-off layer in HL-1 tokamak
[DE94-627009] p 1144 N95-18887
Study of alpha physics related to ITER Project
[DE94-017329] p 1133 N95-19078
Ion orbit loss and the poloidal electric field in a tokamak
[DE94-016860] p 1145 N95-19092

TOLERANCES (MECHANICS)
Brite-Euram programme: ACOUFAT acoustic fatigue and related damage tolerance of advanced composite and metallic structures p 1127 N95-19159
FAA/NASA International Symposium on Advanced Structural Integrity Methods for Airframe Durability and Damage Tolerance, part 2
[NASA-CP-3274-PT-2] p 934 N95-19468
Fatigue and damage tolerance scatter models
p 935 N95-19475
Fatigue life until small cracks in aircraft structures: Durability and damage tolerance p 936 N95-19478
Proceedings of the USAF Structural Integrity Program Conference
[AD-A285684] p 945 N95-19517

TOLLMIEN-SCHLICHTING WAVES
Active control of instabilities in laminar boundary-layer flow. Part 1: An overview
[NASA-CR-195016-PT-1] p 1020 N95-18958

TOLUENE
Theoretical interpretation of the fluorescence spectra of toluene and p-cresol
[AD-A284314] p 974 N95-19170
Synthesis and characterization of aluminum-phosphorus adducts: X-ray crystal structures of Cl3Al (dot) P(SiMe3)3 (dot) C7H8 and Br3Al (dot) P(SiMe3)3 (dot) C7H8
[AD-A279194] p 1154 N95-19812

TOMOGRAPHY
Annular computed tomography
[AD-D016424] p 1141 N95-18593
2-D tomography with bolometry in D3-D
[DE94-017520] p 1146 N95-19379

TOPOGRAPHY
Topography from shading and stereo
[NASA-CR-189389] p 1173 N95-18051
Remote sensing products evaluation for cartographic updating purposes
[INPE-5584-TDI/546] p 1050 N95-18368
Spectral reflectance properties of wetlands plants
[AD-A283546] p 1051 N95-18614
Interferometric synthetic aperture radar and the Data Collection System Digital Terrain Elevation Demonstration
[AD-A284024] p 999 N95-18657
A GIS approach to urban heat island research: The case of Huntsville, Alabama p 1063 N95-18991

TOPOLOGY
Multicast tree construction in network topologies with asymmetric link loads
[AD-A285679] p 1003 N95-19525

TORCHES
A study of gas flow pattern, undercutting and torch modification in variable polarity plasma arc welding
[NASA-CR-196537] p 1040 N95-18056

TOROIDAL PLASMAS
Simplified ideal MHD normal mode equations for toroidal axisymmetric plasmas
[DE94-627004] p 1144 N95-18886

TORQUE
Geometry and gravity influences on strength capability
[NASA-TP-3511] p 1091 N95-18189

TORSION
Torsional device for remote control steering system
[AD-D016426] p 1041 N95-18594
Course module for AA201: Wing structural design project
[AD-A283618] p 944 N95-18616

TOTAL OZONE MAPPING SPECTROMETER
Evolution of the Southern Hemisphere ozone hole as seen by TOMS from August 1979 to December 1991
[NASA-TM-110116] p 1057 N95-18048
Meteor 3/TOMS launch of 15 August 1991 in Plesetsk, USSR
[NASA-TM-110115] p 962 N95-18150

TOTAL QUALITY MANAGEMENT
System engineering toolbox for design-oriented engineers
[NASA-RP-1358] p 962 N95-18932

TOUGHNESS
Development of radiation-hardened ceramic composites for fusion applications
[DE94-016182] p 985 N95-18638
NiAl and NiAl-based composites directionally solidified by a containerless zone process
[NASA-CR-195430] p 982 N95-19792

TOXIC HAZARDS
Developing an emission factor for hazardous air pollutants for an F-16 using JP-8 fuel
[AD-A284802] p 1061 N95-19685

TOXICITY
In vitro system for studying metabolism of environmental chemicals in human cells
[AD-A284174] p 1079 N95-18518
Alternative solvents/technologies for paint stripping: Phase 1
[AD-A279918] p 989 N95-19861

TRACE CONTAMINANTS
Trends 1993: A compendium of data on global change
[ORNL/CDIAC-65] p 1058 N95-18389
Collection requirements for trace-element analyses of extraterrestrial samples p 1182 N95-19182

TRACE ELEMENTS
Trace element characteristics of lithospheric and asthenospheric mantle in the Rio Grande rift region
[DE94-013609] p 1063 N95-17947
Compendium of NASA data base for the Global Tropospheric Experiment's Arctic Boundary Layer Experiments ABLE-3A and ABLE-3B
[NASA-TM-109161] p 1058 N95-18132
Electron reversal ionizer for detection of trace species using a spherical cathode
[NASA-CASE-NPO-18870-1-CU] p 1130 N95-18324
Collection requirements for trace-element analyses of extraterrestrial samples p 1182 N95-19182
The origin of refractory precursor components of chondrules p 1189 N95-19316

TRACKING RADAR
STS-68 mission highlights resource tape
[NASA-TM-110049] p 961 N95-18568

TRADEOFFS
Evaluating the trade-offs in partial-order planning algorithms
[AD-A285876] p 1115 N95-19599

TRAFFIC
A knowledge-based system for controlling automobile traffic p 1102 N95-19633

TRAFFIC CONTROL
A knowledge-based system for controlling automobile traffic p 1102 N95-19633

TRAILING EDGES
Erosion of T56 5th stage rotor blades due to bleed hole overtip flow p 952 N95-19666

TRAINING AIRCRAFT
Aircraft stress sequence development: A complex engineering process made simple p 936 N95-19480

TRAINING ANALYSIS
Assessment of a career development program for executive amd mid-level managers
p 1161 N95-18182
Computer-based psychomotor tests in optimal training track assignment of student naval aviators
[AD-A283720] p 1089 N95-18414
Development of a comprehensive base-level environmental training program for total environmental compliance
[AD-A284806] p 1061 N95-19686

TRAINING DEVICES
Helicopter in-flight simulation development and use in test pilot training
[AD-A283998] p 959 N95-18725

TRAINING EVALUATION
Programmable cockpit research simulator
[AD-A279219] p 960 N95-19848

TRAINING SIMULATORS
Simulation in a dynamic prototyping environment: Petri nets or rules? p 1106 N95-19756

TRAJECTORIES
Cerebellar circuit mechanisms which accompany coordinated limb trajectory patterns in the rat: Use of a model of spontaneous changes in limb coordination
[AD-A284023] p 1079 N95-18656
Workshop on Particle Capture, Recovery and Velocity/Trajectory Measurement Technologies
[NASA-CR-197592] p 1180 N95-19172

TRAJECTORY ANALYSIS
Some considerations on velocity vector accuracy in dust trajectory analysis p 1183 N95-19186

TRAJECTORY CONTROL
Sliding mode control method having terminal convergence in finite time
[NASA-CASE-NPO-18584-1-CU] p 1114 N95-19062

TRAJECTORY MEASUREMENT
Assessment of velocity/trajectory measurement technologies during a particle capture event
p 1036 N95-19193

TRAJECTORY PLANNING
Adaptive robot path planning in changing environments
[DE94-016564] p 1112 N95-17948
Automated path planning of the Payload Inspection and Processing System p 1043 N95-18169

TRANSATMOSPHERIC VEHICLES
Thermo-acoustic fatigue design for hypersonic vehicle skin panels p 1047 N95-19161

TRANSDUCERS
Transducer array interaction modeling using variational principles
[AD-A285687] p 1128 N95-19514

TRANSFER ORBITS
CRRESPRO documentation
[AD-A284578] p 1178 N95-18451
Optimal transfer and swing-by orbits in the two- and three-body problems p 961 N95-18900

TRANSFORMATIONS (MATHEMATICS)
Theory and applications of the phi transform wavelets
[AD-A279943] p 1119 N95-19869

TRANSIENT HEATING
Chondrule formation in lightning discharges
p 1188 N95-19304

TRANSISTOR CIRCUITS
Partition method for the determination of multiple DC operating points
[PB94-201480] p 1009 N95-18501

TRANSITION METALS
Phase transformations and phase relations in Ti(50)Pd(50-x)TM(x) alloys
[DE94-018999] p 977 N95-17962
Transition metal oxides deposited on rhodium and platinum: Surface chemistry and catalysis
[DE95-000793] p 975 N95-19616
Electrochemical interfaces and electrode processes: Electrochemical oxidation of small organisms
[AD-A284873] p 1013 N95-19741

TRANSITION TEMPERATURE
Sag compensated vibration isolation mount
[AD-D016541] p 1042 N95-19121
High temperature superconducting films and crystals
[AD-A279201] p 1154 N95-19815

TRANSLUCENCE
Can salt on an optical rain gauge lens affect performance? p 1069 N95-18208

TRANSMISSION
Throughput analysis between high end workstations across an FDDI network
[AD-A283608] p 1110 N95-18615
TRANSMISSION EFFICIENCY
The evaluation of transmission efficiency and coupling loss factor of structural junctions
[MRL-TR-93-1] p 1124 N95-19057
TRANSMISSION ELECTRON MICROSCOPY
Phase transformations and phase relations in Ti(50)Pd(50-x)TM(x) alloys
[DE94-018999] p 977 N95-17962
Phase stability and elastic properties of C15 compounds HfV2+Nb
[DE95-000940] p 981 N95-19611
TRANSMISSION LINES
Multi-line passive fiber optic slipring
[AD-D016430] p 1141 N95-18560
Power flow and PRS optimization on Phoenix
[AD-A279214] p 1147 N95-19846
TRANSMISSION LOSS
The STOKES (Version 4) normal-mode shallow water transmission loss program
[MRL-CP-1] p 1075 N95-19503
Acoustic transmission loss and structureborne noise transmission tests on a LASCOR and a reference steel panel
[MRL-TN-623] p 1128 N95-19770
TRANSMISSIONS (MACHINE ELEMENTS)
Study of the kinematic and load sharing properties of wormgearing with non-symmetric tooth profiles
[NASA-CR-195414] p 1041 N95-18541
TRANSMITTER RECEIVERS
Flame position ultrasonic interferometer
[AD-D016235] p 967 N95-18632
TRANSMITTERS
Digital audio broadcasting: Comparison of coverage at different frequencies and with different bandwidths
[BBC-RD-1993/11] p 1002 N95-19135
Alleviation of co-channel interference at Poole relay station
[BBC-RD-1993/4] p 1003 N95-19136
TRANSONIC FLOW
Overview of unsteady transonic wind tunnel test on a semispan straked delta wing oscillating in pitch
[AD-A284097] p 928 N95-18380
Experimental techniques for measuring transonic flow with a three dimensional laser velocimetry system. Application to determining the drag of a fuselage p 1022 N95-19258
The utilization of a high speed reflective visualization system in the study of transonic flow over a delta wing p 932 N95-19259
Transonic and supersonic flowfield measurements about axisymmetric afterbodies for validation of advanced CFD codes p 932 N95-19260
Transonic wind tunnel boundary interference correction p 960 N95-19271
Evaluation of three turbulence models for afterbody/jet flows, including Reynolds stress closure
[ARA-90] p 932 N95-19574
Evaluation of three turbulence models for afterbody/jet flows, including Reynolds stress closure
[ARA-MEMO-408] p 1194 N95-19773
Validation and evaluation of the advanced aeronautical CFD system SAUNA: A method developer's view
[ARA-MEMO-390] p 1030 N95-19774
TRANSONIC SPEED
In-flight lift-drag characteristics for a forward-swept wing aircraft and comparisons with contemporary aircraft)
[NASA-TP-3414] p 929 N95-18565
Computational simulations for some tests in transonic wind tunnels p 1023 N95-19264
TRANSONIC WIND TUNNELS
Overview of unsteady transonic wind tunnel test on a semispan straked delta wing oscillating in pitch
[AD-A284097] p 928 N95-18380
Computational simulations for some tests in transonic wind tunnels p 1023 N95-19264
Interference determination for wind tunnels with slotted walls p 960 N95-19269
Transonic wind tunnel boundary interference correction p 960 N95-19271
The traditional and new methods of accounting for the factors distorting the flow over a model in large transonic wind tunnels p 1025 N95-19275
Interference corrections for a centre-line plate mount in a porous-walled transonic wind tunnel p 933 N95-19280
An investigation of drag repeatability in half model testing in the ARA Transonic Wind Tunnel
[ARA-MEMO-392] p 931 N95-19546
Multiport pressure measurements on continuously moving wind tunnel models
[ARA-MEMO-391] p 932 N95-19772
TRANSPARENCE
Conference on Aerospace Transparent Materials and Enclosures. Volume 2: Sessions 5-9
[AD-A283926] p 942 N95-18162
Novel polymeric composites through molecular engineering
[AD-A284168] p 985 N95-18513
Conference on Aerospace Transparent Materials and Enclosures, volume 1
[AD-A283925] p 944 N95-18677
TRANSPORT AIRCRAFT
Wing design for a civil tiltrotor transport aircraft
[NASA-CR-197523] p 942 N95-18090
KC-130 ANVIS/HUD assessment and symbology rationale
[AD-A284155] p 943 N95-18504
European aeronautics: Strong government presence in industry structure and research and development support. Report to Congressional Requesters
[GAO/NSIAD-94-71] p 1171 N95-18578
Proceedings of the USAF Structural Integrity Program Conference
[AD-A285684] p 945 N95-19517
Transport aircraft loading and balancing system: Using a CLIPS expert system for military aircraft load planning p 1105 N95-19751
TRANSPORT PROPERTIES
Particle acceleration and transport in the tail and at the front side of the magnetosphere, task 1 and 2
[NASA-CR-197575] p 1064 N95-18476
Experimental studies of Reynolds number dependence of turbulent mixing and transport
[DE94-015338] p 1030 N95-19578
Wentzel-Bardeen singularity in coupled Luttinger liquids: Transport properties
[DE95-000856] p 1152 N95-19621
The physics and operation of ultra-submicron length semiconductor devices
[AD-A280181] p 1155 N95-19828
Modeling of quantum transport in semiconductor devices
[AD-A280182] p 1155 N95-19829
TRANSPORT THEORY
Arbitrarily high order nodal and characteristic methods
[DE94-018130] p 1116 N95-18131
Impurity behavior during ion-Bernstein wave heating in PBX-M
[DE94-018114] p 1133 N95-19228
TRANSPORTATION
Rotorcraft ditchings and water-related impacts that occurred from 1982 to 1989, phase 1
[AD-A279164] p 940 N95-19805
TRANSPORTATION NETWORKS
Algorithms and applications in timed discrete event systems
[PB94-201423] p 1118 N95-19169
A knowledge-based system for controlling automobile traffic p 1102 N95-19633
TRAVELING IONOSPHERIC DISTURBANCES
Technical Information Division Open Literature Database (TOLD) operating instructions
[AD-A284061] p 1174 N95-18680
TRAVELING SALESMAN PROBLEM
Improved approximation guarantees for minimum-weight k-trees and prize-collecting salesmen
[AD-A284042] p 1117 N95-18658
TREADMILLS
The cross-validation of the United States Air Force submaximal cycle ergometer test to estimate aerobic capacity
[AD-A284055] p 1079 N95-18661
TREES (MATHEMATICS)
Multicast tree construction in network topologies with asymmetric link loads
[AD-A285679] p 1003 N95-19525
TREND ANALYSIS
System engineering toolbox for design-oriented engineers
[NASA-RP-1358] p 962 N95-18932
TRENDS
International Conference on Deformation, Yield and Fracture of Polymers
[AD-A284354] p 984 N95-18339
Crystallization trends of precursor pyroxene in ordinary chondrites: Implications for igneous origin of precursor p 1187 N95-19298
New Trends in coatings developments for turbine blades: Materials processing and repair p 954 N95-19676
TRIANGULATION
A triangulation method for passive ranging
[AD-A284180] p 998 N95-18522
TRIBOLOGY
Advanced diesel engine component development program, tasks 4-14
[NASA-CR-191203] p 1040 N95-18041
Tribology and microstructure of PS212 with a Cr2O3 seal coat
[NASA-TM-106768] p 969 N95-18448
TRISONIC WIND TUNNELS
Interference corrections for a centre-line plate mount in a porous-walled transonic wind tunnel p 933 N95-19280
TRITIUM
Exotic atoms: Muonic atoms into vacuum from solid hydrogen
[DE94-018255] p 1129 N95-18124
Study of high gain spherical shell ICF targets containing uniform layers of liquid deuterium tritium fuel
[DE94-018550] p 1136 N95-18552
TROPICAL METEOROLOGY
Intraseasonal oscillations over the tropical western Pacific and eastern Indian ocean for the northern summers of 1989-1991
[AD-A284527] p 1068 N95-18114
Moored rainfall measurements during COARE p 1069 N95-18202
Update on TAO moored ORG array p 1069 N95-18203
TROPICAL REGIONS
Field and data analysis studies related to the atmospheric environment
[NASA-CR-196543] p 1068 N95-18093
TROPOSPHERE
Dependencies and sensitivity of tropospheric oxidants to precursor concentrations over the northeast United States: A model study
[PB94-192770] p 1056 N95-17937
Compendium of NASA data base for the Global Tropospheric Experiment's Arctic Boundary Layer Experiments ABLE-3A and ABLE-3B
[NASA-TM-109161] p 1058 N95-18132
Investigation of atmospheric waves on Neptune
[NASA-CR-197537] p 1194 N95-18579
NASA Goddard Earth Sciences Graduate Student Program --- FIRE CIRRUS-II examination of coupling between an upper tropospheric cloud system and synoptic-scale dynamics
[NASA-CR-197130] p 1066 N95-19129
TRUCKS
Kansas State University DOE/KEURP Site Operator User Task Force
[DE94-014331] p 1040 N95-17995
TRUSSES
The development of a fiber optics communication network for controlling a Multidegree-Of-Freedom Serpentine Truss p 1142 N95-18167
TUNGSTEN CARBIDES
Quality optimization of thermally sprayed coatings produced by the JP-5000 (HVOF) gun using mathematical modeling p 989 N95-19008
TUNING
Forced response of mistuned bladed disks p 950 N95-19383
TUNNEL JUNCTIONS
High current amplifier utilizing a Josephson junction Schottky diode three terminal device
[AD-D016278] p 1009 N95-18432
TURBINE BLADES
Measurement of gust response on a turbine cascade
[NASA-TM-106776] p 928 N95-18457
Wind turbine blade aerodynamics: The combined experiment
[DE94-011866] p 929 N95-18645
Wind turbine blade aerodynamics: The analysis of field test data
[DE94-011867] p 929 N95-18646
Simulation of multidisciplinary problems for the thermostress state of cooled high temperature turbines p 948 N95-19021
Application of multidisciplinary models to the cooled turbine rotor design p 949 N95-19024
Aerodynamic investigation of the flow field in a 180 deg turn channel with sharp bend p 1021 N95-19257
An analysis of the costs and benefits in improving F402-RR-406A High Pressure Turbine, second stage blades under the aircraft engine Component Improvement Program (CIP)
[AD-A285127] p 950 N95-19595
Out of area experiences with the RB199 in Toronto p 950 N95-19654
Particle deposition in gas turbine blade film cooling holes p 951 N95-19661
Experimental and numerical simulations of the effects of ingested particles in gas turbine engines p 952 N95-19662
Damage of high temperature components by dust-laden air p 953 N95-19673
New Trends in coatings developments for turbine blades: Materials processing and repair p 954 N95-19676
Thermal testing of high performance thermal barrier coatings for turbine blades p 955 N95-19681

Resistance of silicon nitride turbine components to erosion and hot corrosion/oxidation attack p 955 N95-19683
Evidence that aerodynamic effects, including dynamic stall, dictate HAWT structural loads and power generation in highly transient time frames [DE94-011865] p 1054 N95-19855

TURBINE ENGINES
Modern transport engine experience with environmental ingestion effects p 951 N95-19660
Damage of high temperature components by dust-laden air p 953 N95-19673
New Trends in coatings developments for turbine blades: Materials processing and repair p 954 N95-19676

TURBINE PUMPS
Steady and unsteady blade stresses within the SSME ATD/HPOTP inducer p 968 N95-18982

TURBINES
Design optimization of a brush turbine with a cleaner/water based solution p 1043 N95-18177
Simulation of multidisciplinary problems for the thermostress state of cooled high temperature turbines p 948 N95-19021

TURBOCOMPRESSORS
Enhanced capabilities and modified users manual for axial-flow compressor conceptual design code CSPAN [NASA-TM-106833] p 930 N95-18933
Performance deterioration of axial compressors due to blade defects p 952 N95-19665
Impact loading of compressor stator vanes by hailstone ingestion p 953 N95-19670
Advanced diesel electronic fuel injection and turbocharging [AD-A279176] p 1043 N95-19809

TURBOJET ENGINES
Perspective problems of gas turbine engines simulation p 949 N95-19026

TURBOMACHINE BLADES
NASA Lewis Research Center Workshop on Forced Response in Turbomachinery [NASA-CP-10147] p 949 N95-19380
Forced response of mistuned bladed disks p 950 N95-19383

TURBOMACHINERY
Data driven propulsion system weight prediction model p 968 N95-18980
Application of multicomponent models to flow passage simulation in multistage turbomachines and whole gas turbine engines p 948 N95-19022
Simulation of steady and unsteady viscous flows in turbomachinery p 949 N95-19023
Verification of multidisciplinary models for turbomachines p 949 N95-19025
NASA Lewis Research Center Workshop on Forced Response in Turbomachinery [NASA-CP-10147] p 949 N95-19380
Unsteady aerodynamic analyses for turbomachinery aeroelastic predictions p 949 N95-19381
Steady potential solver for unsteady aerodynamic analyses p 949 N95-19382
Forced response of mistuned bladed disks p 950 N95-19383

TURBOPROP AIRCRAFT
Noise transmission and reduction in turboprop aircraft p 1127 N95-19164

TURBOSHAFTS
US Army rotorcraft turboshaft engines sand and dust erosion considerations p 951 N95-19656
Future directions in helicopter protection system configuration p 951 N95-19657

TURBULENCE
The diurnal cycle of high-frequency temperature variability at 0 deg 140 deg W on seasonal and interannual time scales [AD-A283640] p 1074 N95-18012
Method and system for identifying the onset of a turbulent boundary layer induced by a body moving through a fluid medium [AD-D016434] p 1018 N95-18525
Turbulent diffusion and concentration of chondrules in the protoplanetary nebula p 1187 N95-19296
Introduction to multigrid methods p 1028 N95-19453
CFD: Advances and Applications, 1994 [NAL-SP-9412] p 1028 N95-19455
Advanced concepts theory [AD-A279212] p 1147 N95-19844

TURBULENCE EFFECTS
An application of a two-equation model of turbulence to three-dimensional chemically reacting flows [NASA-CR-195411] p 1015 N95-18107
A study of the effect of store unsteady aerodynamics on gust and turbulence loads p 946 N95-18601
Comparison of stochastic and deterministic nonlinear gust analysis methods to meet continuous turbulence criteria p 946 N95-18602
Design limit loads based upon statistical discrete gust methodology p 946 N95-18603
Pressure measurements on an F/A-18 twin vertical tail in buffeting flow. Volume 4, part 2: Buffet cross spectral densities [AD-A285555] p 957 N95-18641
Computer simulation of wave propagation through turbulent media [AD-A283695] p 1000 N95-18671

TURBULENCE MODELS
Aeromechanics technology, volume 1. Task 1: Three-dimensional Euler/Navier-Stokes Aerodynamic Method (TEAM) enhancements [AD-A285713] p 943 N95-18483
Solution of Navier-Stokes equations using high accuracy monotone schemes p 948 N95-19019
Simulation of steady and unsteady viscous flows in turbomachinery p 949 N95-19023
Turbulence modeling for CFD, part 1 p 1028 N95-19458
Turbulence modeling for CFD, part 2 p 1030 N95-19466
Evaluation of three turbulence models for afterbody/jet flows, including Reynolds stress closure [ARA-90] p 932 N95-19574
Experimental studies of Reynolds number dependence of turbulent mixing and transport [DE94-015338] p 1030 N95-19578
Evaluation of three turbulence models for afterbody/jet flows, including Reynolds stress closure [ARA-MEMO-408] p 1194 N95-19773
Inviscid and viscous flow modelling of complex aircraft configurations using the CFD simulation system sauna [ARA-MEMO-403] p 1031 N95-19777
The application of the SAUNA CFD system to high and low speed vehicles [ARA-MEMO-402] p 1031 N95-19778

TURBULENT BOUNDARY LAYER
Sectional prediction of 3D effects for separated flow on rotating blades [PB94-201696] p 928 N95-18503
Method and system for identifying the onset of a turbulent boundary layer induced by a body moving through a fluid medium [AD-D016434] p 1018 N95-18525
Theoretical investigations of shock/boundary layer interactions on a Ma(infinity) = 8 waverider [DLR-FB-94-12] p 930 N95-18910
Flow field investigation in a free jet - free jet core system for the generation of high intensity molecular beams [DLR-FB-94-11] p 1132 N95-18912
Prediction of fluctuating pressure and power spectra in attached and separated compressible flow p 1031 N95-19153

TURBULENT DIFFUSION
Turbulent diffusion and concentration of chondrules in the protoplanetary nebula p 1187 N95-19296

TURBULENT FLOW
An application of a two-equation model of turbulence to three-dimensional chemically reacting flows [NASA-CR-195411] p 1015 N95-18107
Numerical predictions of turbulent flow around a cube via the k-epsilon model [DE94-018361] p 1017 N95-18443
Interaction, bursting and control of vortices of a cropped double-delta wing at high angle of attack [AD-A283656] p 930 N95-18669
Numerical computations of supersonic base flow with special emphasis on turbulence modeling [AD-A283688] p 930 N95-18670
Simulation of steady and unsteady viscous flows in turbomachinery p 949 N95-19023
Velocity measurements with hot-wires in a vortex-dominated flowfield p 932 N95-19261
Basic equations of fluid dynamics p 1026 N95-19445
Viscous flow past aerofoils axisymmetric bodies and wings p 933 N95-19457
Turbulence modeling for CFD, part 1 p 1028 N95-19458
Turbulence modeling for CFD, part 2 p 1030 N95-19466
Evaluation of three turbulence models for afterbody/jet flows, including Reynolds stress closure [ARA-90] p 932 N95-19574
Investigation of mechanical erosion in fuel pipelines p 952 N95-19667
Evaluation of three turbulence models for afterbody/jet flows, including Reynolds stress closure [ARA-MEMO-408] p 1194 N95-19773
The application of the SAUNA CFD system to high and low speed vehicles [ARA-MEMO-402] p 1031 N95-19778

TURBULENT MIXING
Experimental studies of Reynolds number dependence of turbulent mixing and transport [DE94-015338] p 1030 N95-19578

TVD SCHEMES
On the CFD monotone high accuracy methods p 948 N95-19018

TWISTED WINGS
Determination of stores pointing error due to wing flexibility under flight load [NASA-TM-4646] p 945 N95-19044

TWO BODY PROBLEM
Optimal transfer and swing-by orbits in the two- and three-body problems p 961 N95-18900

TWO DIMENSIONAL BODIES
A boundary element method for two dimensional linear elastic fracture analysis p 1045 N95-18917

TWO DIMENSIONAL FLOW
Time-evolving bubbles in two-dimensional stokes flow [NASA-CR-194998] p 1015 N95-18188
Searching for stationary stable solutions of Euler's equation [KNMI-WR-93-01] p 1017 N95-18396
Numerical simulation of dynamic-stall suppression by tangential blowing [AD-A284887] p 931 N95-19110
Numerical grid generation p 1027 N95-19449
Computation of compressible flows: Implicit methods p 1027 N95-19452

TWO DIMENSIONAL MODELS
Heuristic inference about flow directions in river networks [INPE-5588-TDI/550] p 1050 N95-18214
Size distribution of one-, two- and three-dimensional Voronoi cells [PB94-207008] p 1149 N95-18373
TEXCAD: Textile Composite Analysis for Design. Version 1.0: User's manual [NASA-CR-4639] p 970 N95-18466
Static investigation of two fluidic thrust-vectoring concepts on a two-dimensional convergent-divergent nozzle [NASA-TM-4574] p 931 N95-19042
Interference determination for wind tunnels with slotted walls p 960 N95-19269
2-D tomography with bolometry in D3-D [DE94-017520] p 1146 N95-19379

TWO FLUID MODELS
Static investigation of two fluidic thrust-vectoring concepts on a two-dimensional convergent-divergent nozzle [NASA-TM-4574] p 931 N95-19042

TWO PHASE FLOW
The stability of two-phase flow over a swept-wing [NASA-CR-194994] p 1016 N95-18190
Investigation of mechanical erosion in fuel pipelines p 952 N95-19667

U

U-2 AIRCRAFT
Field and data analysis studies related to the atmospheric environment [NASA-CR-196543] p 1068 N95-18093

ULTRAHIGH FREQUENCIES
Predicted coverage of a COFDM single frequency network for UHF digital terrestrial TV broadcasting [BBC-RD-1993/12] p 999 N95-18540
Measurements of wideband multipath propagation at 531 MHz and 1.265 GHz [BBC-RD-1994/3] p 1001 N95-19051
Alleviation of co-channel interference at Poole relay station [BBC-RD-1993/4] p 1003 N95-19136
Design of a radio frequency data link for the unmanned ground vehicle technology test bed demonstration program [AD-A284997] p 1004 N95-19534

ULTRASONIC TESTS
Acoustic method of damage sensing in composite materials [NASA-CR-196538] p 969 N95-18135
An NDE approach for characterizing quality problems in polymer matrix composites [NASA-TM-106807] p 1043 N95-18583
Echo imaging techniques determine the size of intravascular bubbles in decompression sickness [AD-A284849] p 1087 N95-19714

ULTRASONICS
Flame position ultrasonic interferometer [AD-D016235] p 967 N95-18632
Ultrasonic techniques for repair of aircraft structures with bonded composite patches p 937 N95-19486

ULTRAVIOLET ASTRONOMY
Rocket and laboratory studies in astronomy
[NASA-CR-197531] p 1177 N95-17981
The quiescent and flaring EUV spectrum of Algol and its relationship to other active coronae. EUV spectroscopy of bright hyades coronae: 71 Tauri and Theta 1 Tauri
[NASA-CR-197538] p 1178 N95-18391
Relative elemental abundance and heating constraints determined for the solar corona from SERTS measurements
[NASA-TM-104616] p 1196 N95-19791
ULTRAVIOLET EMISSION
Decaying neutrinos in galaxy clusters
[NASA-CR-197615] p 1198 N95-18747
ULTRAVIOLET RADIATION
Nonlinear response of the photocathode of an x-ray streak camera to UV light
[DE94-018073] p 1032 N95-18130
UV laser-surface interactions relevant to analytic spectroscopy of wide band gap materials
[DE94-016181] p 1037 N95-18350
Multi-channel, covert, non-line-of-sight UV communication
[AD-D016269] p 999 N95-18545
ULTRAVIOLET SPECTRA
Silicon carbide photoconductive switches
[AD-A284310] p 1008 N95-18378
The quiescent and flaring EUV spectrum of Algol and its relationship to other active coronae. EUV spectroscopy of bright hyades coronae: 71 Tauri and Theta 1 Tauri
[NASA-CR-197538] p 1178 N95-18391
Multi-channel, covert, non-line-of-sight UV communication
[AD-D016269] p 999 N95-18545
Analysis of solar spectral irradiance measurements from the SBUV/2-series and the SSBUV instruments
[NASA-CR-197544] p 1196 N95-18954
Impurity behavior during ion-Bernstein wave heating in PBX-M
[DE94-018114] p 1133 N95-19228
ULTRAVIOLET SPECTROSCOPY
Spectroelectrochemical investigations of molten halide solutions
[AD-A284147] p 974 N95-18412
Multi-functional pi-conjugated macromolecules based on poly (phenylene vinylene)
[AD-A284163] p 985 N95-18510
Electrochemical and spectroscopy studies of selected inorganic and organic systems in molten halides
[AD-A284171] p 974 N95-18514
UMBILICAL CONNECTORS
Microgravity isolation system design: A modern control synthesis framework
[NASA-TM-106805] p 927 N95-18197
UNDERGROUND STORAGE
Sloshing roof impact tests of a rectangular tank
[DE94-012462] p 1018 N95-18549
UNDERWATER ACOUSTICS
Positive displacement rotary pump
[AD-D016412] p 1041 N95-18335
Sound speed profiles from vertical array data
[AD-A283978] p 1123 N95-18890
The STOKES (Version 4) normal-mode shallow water transmission loss program
[MRL-CP-1] p 1075 N95-19503
Parallel computations in hydro acoustics
[AD-A285900] p 1030 N95-19607
UNIFORM FLOW
Acoustic radiation damping of flat rectangular plates subjected to subsonic flows p 1123 N95-18542
UNITED KINGDOM
NASA/DOD Aerospace Knowledge Diffusion Research Project. Paper 46: Technical communications in aerospace: A comparison across four countries
[NASA-TM-110056] p 1175 N95-19038
UNITED STATES
Using federal technology policy to strength the US microelectronics industry
[DE94-017293] p 1008 N95-18143
UNIVERSAL TIME
Global time transformations
[AD-A285539] p 1110 N95-18454
UNIVERSE
Testing the inflationary paradigm: Inflation and the cosmic microwave background anisotropy p 1179 N95-18496
Is a massive tau neutrino just what cold dark matter needs?
[NASA-CR-197627] p 1180 N95-18964
UNIVERSITIES
NASA/DOD Aerospace Knowledge Diffusion Research Project. Paper 46: Technical communications in aerospace: A comparison across four countries
[NASA-TM-110056] p 1175 N95-19038
UNIVERSITY PROGRAM
Research reports: 1994 NASA/ASEE Summer Faculty Fellowship Program
[NASA-CR-196533] p 1161 N95-18967
UNIX (OPERATING SYSTEM)
Alarm annunciation in a graphical environment
[DE94-015761] p 1098 N95-18652
A report of work activities on the NASA Spacelink public electronic library p 1168 N95-19005
UNSTEADY AERODYNAMICS
Overview of unsteady transonic wind tunnel test on a semispan straked delta wing oscillating in pitch
[AD-A284097] p 928 N95-18380
Sectional prediction of 3D effects for separated flow on rotating blades
[PB94-201696] p 928 N95-18503
A study of the effect of store unsteady aerodynamics on gust and turbulence loads p 946 N95-18601
Pressure measurements on an F/A-18 twin vertical tail in buffeting flow. Volume 4, part 2: Buffet cross spectral densities
[AD-A285555] p 957 N95-18641
Wind turbine blade aerodynamics: The combined experiment
[DE94-011866] p 929 N95-18645
Wind turbine blade aerodynamics: The analysis of field test data
[DE94-011867] p 929 N95-18646
Unsteady aerodynamic analyses for turbomachinery aeroelastic predictions p 949 N95-19381
Steady potential solver for unsteady aerodynamic analyses p 949 N95-19382
Evidence that aerodynamic effects, including dynamic stall, dictate HAWT structural loads and power generation in highly transient time frames
[DE94-011865] p 1054 N95-19855
UNSTEADY FLOW
Method and flowmeter for unsteady fluid flow study
[AD-D016432] p 1015 N95-18112
Overview of unsteady transonic wind tunnel test on a semispan straked delta wing oscillating in pitch
[AD-A284097] p 928 N95-18380
Pressure measurements on an F/A-18 twin vertical tail in buffeting flow. Volume 4, part 2: Buffet cross spectral densities
[AD-A285555] p 957 N95-18641
Wind turbine blade aerodynamics: The combined experiment
[DE94-011866] p 929 N95-18645
Wind turbine blade aerodynamics: The analysis of field test data
[DE94-011867] p 929 N95-18646
The mathematical models of flow passage for gas turbine engines and their components p 948 N95-19020
Simulation of steady and unsteady viscous flows in turbomachinery p 949 N95-19023
Prediction of fluctuating pressure and power spectra in attached and separated compressible flow p 1031 N95-19153
Unsteady flow testing in a passive low-correction wind tunnel p 960 N95-19272
Calculation of support interference in dynamic wind-tunnel tests p 933 N95-19282
Finite-volume upwind schemes for inviscid gas dynamics p 1028 N95-19456
UPPER ATMOSPHERE
Innovative development and application of models for weakly ionized ionospheric plasmas
[AD-A284583] p 1064 N95-18452
Thermochemical IR sources: COCHISE and FACELIF experiments
[AD-A279940] p 977 N95-19868
UPPER STAGE ROCKET ENGINES
A 20k payload launch vehicle fast track development concept using an RD-180 engine and a Centaur upper stage
[NASA-TM-108475] p 963 N95-19648
UPPER SURFACE BLOWING
Numerical simulation of dynamic-stall suppression by tangential blowing
[AD-A284887] p 931 N95-19110
UPWELLING WATER
A sensitivity analysis of upwelling radiances in the 3-5 micrometers region as a function of atmospheric conditions
[AD-A283678] p 1068 N95-18141
URANIUM
A review of nuclear thermal propulsion carbide fuel corrosion and key issues
[NASA-CR-197533] p 1136 N95-18217
URANIUM ISOTOPES
Isotope separation and advanced manufacturing technology
[DE95-000313] p 1039 N95-19551
URANUS ATMOSPHERE
Study for the analysis of the observations, and numerical data representing the planets as far-infrared calibration sources
[NASA-CR-196542] p 1195 N95-19287
URBAN TRANSPORTATION
Air pollution mitigation measures for airports and associated activity
[PB94-207610] p 1061 N95-19582
USER MANUALS (COMPUTER PROGRAMS)
Night Vision Goggles (NVG) software user's guide, version 5.1
[AD-A284563] p 1090 N95-18029
Coastal Modeling System (CMS) user's manual. Supplement 3 to September 1991 manual
[AD-A283922] p 1074 N95-18160
Portable, Reusable, Integrated Software Modules (PRISM) documentation library version description document release 1.0. Central Archive for Reusable Defense Software (CARDS)
[AD-A284571] p 1097 N95-18447
TEXCAD: Textile Composite Analysis for Design. Version 1.0: User's manual
[NASA-CR-4639] p 970 N95-18466
Users guide for NASA Lewis Research Center DC-9 Reduced-Gravity Aircraft Program
[NASA-TM-106755] p 959 N95-18586
SICOMP, the SINTEF data compression library (version 1.0) reference manual
[PB94-207107] p 1099 N95-18668
Graphics MIS/Shop Store Program: User's manual
[AD-A284062] p 1174 N95-18681
EEsoF MICAD and ACADEMY macro files for coplanar waveguide and finite ground plan coplanar waveguide
[NASA-TM-106800] p 1000 N95-18733
Enhanced capabilities and modified users manual for axial-flow compressor conceptual design code CSPAN
[NASA-TM-106833] p 930 N95-18933
Users manual for the Moods Data Management System (MDMS), version 1.0
[NASA-CR-197015] p 1075 N95-18951
Bit-rate reduction of digital television for transmission: An introductory review
[BBC-RD-1994/2] p 1001 N95-19052
Data acquisition from blast overpressure trials
[MRL-TN-628] p 1020 N95-19139
Technology Benefit Estimator (T/BEST): User's manual
[NASA-TM-106785] p 1046 N95-19501
AUTO: Automatic script generation system
[AD-A285897] p 1012 N95-19606
Unit cell geometry of multiaxial preforms for structural composites
[NASA-CR-197294] p 971 N95-19650
PAK: A processing system for vectorized time-series data
[AD-A284881] p 1104 N95-19742
Tutorial guide: Computer-Aided Structural Modeling (CASM), version 5.00
[AD-A280147] p 1108 N95-19821
USER REQUIREMENTS
User profile for researchers studying objects: Implications for computer systems
[PB94-188463] p 1109 N95-17989
Coastal Modeling System (CMS) user's manual. Supplement 3 to September 1991 manual
[AD-A283922] p 1074 N95-18160
Universal wind tunnel data acquisition and reduction software
[AD-A283897] p 1096 N95-18365

V

V-22 AIRCRAFT
V-22 simulator evaluation for shipboard operations
[AD-A284156] p 943 N95-18505
V/STOL AIRCRAFT
VSTOL Systems Research Aircraft (VSRA) Harrier
[NASA-TM-110117] p 941 N95-18347
NASA develops new digital flight control system
[NASA-NEWS-RELEASE-94-47] p 958 N95-19029
VACUUM
Outgassing of solid material into vacuum thermal insulation spaces p 972 N95-18184
Zero modes of first class secondary constraints in gauge theories
[DE94-626659] p 1156 N95-18328
Field-emitter arrays for RF vacuum microelectronics
[AD-A279932] p 1013 N95-19865
VACUUM FURNACES
General information for operation of the high-temperature electromagnetic containerless vacuum induction furnace
[DE94-017170] p 991 N95-19076

VACUUM MELTING
Ion emission intensity ratios as a function of electrode gap, melting current, and pressure during low current vacuum arc remelting
[DE94-017407] p 1129 N95-18144
VACUUM TUBES
Technological and organizational diversity and technical advance in the early history of the American semiconductor industry
[PB94-175700] p 1007 N95-17999
Vacuum microelectronic emitters and their applications using compound semiconductor technology
[AD-A284811] p 1013 N95-19687
VALENCE
Optical determination of conduction and valence-band dispersion curves in strained single-quantum wells
[DE94-018892] p 1151 N95-19235
VAN DE GRAAFF ACCELERATORS
The hypervelocity impact facilities at the University of Kent at Canterbury, UK p 961 N95-19180
VANADIUM ALLOYS
Status of vanadium alloy development for fusion first wall/blanket applications
[DE95-001067] p 982 N95-19725
VANES
Application of multidisciplinary models to the cooled turbine rotor design p 949 N95-19024
Impact loading of compressor stator vanes by hailstone ingestion p 953 N95-19670
Protective coatings for compressor gas path components p 954 N95-19675
Braze repair possibilities for hot section gas turbine parts p 954 N95-19677
VAPOR DEPOSITION
Tunneling and transport in mesoscopic structures
[AD-A283426] p 1148 N95-18053
Process for forming epitaxial BaF2 on GaAs
[AD-D016439] p 1149 N95-18527
Growth of thin films of dicyanovinylanisole on quartz and teflon-coated quartz by physical vapor transport p 989 N95-19000
Recent progress on ECVD Project
[DE94-016773] p 988 N95-19580
CVD silicon carbide characterization
[AD-A285667] p 972 N95-19702
VAPOR PHASES
Propagation of intense, ultrashort laser pulses through metal vapor: Refractive intensity limits and spectral effects
[DE94-016365] p 1039 N95-19398
The interactions of high-energy, highly charged Xe ions with fullerenes
[DE95-001440] p 1135 N95-19786
VAPORIZING
Erosion of melt layers developed during a plasma disruption
[DE94-018362] p 1144 N95-18547
VAPORS
Geometrical vapor blocker for parallel condensation tubes requiring subcooling
[NASA-CASE-MSC-22090-1] p 1017 N95-18323
Isotope separation and advanced manufacturing technology
[DE95-000313] p 1039 N95-19551
VARIABILITY
High-frequency skywave signal power measurement system
[AD-A284382] p 996 N95-18341
Investigation of the ionospheric short-term variability
[AD-A286253] p 1066 N95-19387
VARIABLE AMPLITUDE LOADING
Prediction of fatique crack growth under flight-simulation loading with the modified CORPUS model p 934 N95-19471
Fatigue crack growth under variable amplitude loading p 937 N95-19484
VARIATIONAL PRINCIPLES
Transducer array interaction modeling using variational principles
[AD-A285687] p 1128 N95-19514
VARIATIONS
Lossless compression of weight vectors from an adaptive filter
[DE94-017350] p 1174 N95-18873
VARISTORS
Power terminal protection device
[AD-D016528] p 1011 N95-19120
VECTOR ANALYSIS
PAK: A processing system for vectorized time-series data
[AD-A284881] p 1104 N95-19742
VECTOR DOMINANCE MODEL
He-4 electromagnetic structure in unitary and analytic VMD model with strict OZI rule
[DE94-626716] p 996 N95-18367
VECTOR QUANTIZATION
LVQ and backpropagation neural networks applied to NASA SSME data
[NASA-CR-195418] p 962 N95-18045
VECTORS (MATHEMATICS)
Decomposition of parametric curves
[PB94-207024] p 1117 N95-18374
VEGETATION
Thematic classification of zone coastal: A methodologic contribution
[INPE-5586-TDI/548] p 1050 N95-18215
VEGETATION GROWTH
Physiological and genetic characterization of plant growth and gravitropism in LED light sources p 1077 N95-18173
VELOCITY DISTRIBUTION
Measurement of gust response on a turbine cascade
[NASA-TM-106776] p 928 N95-18457
Environmental forcing of ambient noise in the Nansen and Amundsen Basins of the Arctic Ocean
[AD-A285540] p 1074 N95-18468
Some considerations on velocity vector accuracy in dust trajectory analysis p 1183 N95-19186
Velocity distribution of Earth-crossing asteroid grains p 1183 N95-19187
Aerodynamic investigation of the flow field in a 180 deg turn channel with sharp bend p 1021 N95-19257
Quasi-linear regime of gravitational instability: Implication to density-velocity relation
[NASA-CR-197616] p 1156 N95-19340
Quasi-linear regime of gravitational instability as a clue to understanding the large-scale structure in the Universe
[NASA-CR-197613] p 1193 N95-19341
Incompressible flow of a Newtonian fluid past a vertical plate with thermal and magnetic stresses
[AD-A284856] p 1030 N95-19716
VELOCITY MEASUREMENT
Method and flowmeter for unsteady fluid flow study
[AD-D016432] p 1015 N95-18112
7th International Symposium on Applications of Laser Techniques to Fluid Mechanics, volume 2
[AD-A285685] p 1018 N95-18477
Laser optical mouse
[AD-D016273] p 1092 N95-18517
Calibration and testing of a large-scale electric gun for shock Hugoniot measurements
[MRL-TR-93-24] p 959 N95-18942
Optical measurements in rocket engine liquid sprays p 968 N95-18979
Plasma produced by impacts of fast dust particles on a thin film p 1181 N95-19177
Highly transparent and rugged sensor for velocity determinations of cosmic dust particles p 966 N95-19178
Assessment of velocity/trajectory measurement technologies during a particle capture event p 1036 N95-19193
Nondestructive time-of-capture, location and velocity sensing in intact capture p 1036 N95-19194
PVDF flux/mass/velocity/trajectory systems and their applications in space p 966 N95-19196
Particle Image Velocimetry: Principles, current applications and future prospects p 1021 N95-19253
Improvement and validation of an LDV system to perform measurements in laminar supersonic flows p 1021 N95-19256
Aerodynamic investigation of the flow field in a 180 deg turn channel with sharp bend p 1021 N95-19257
Experimental techniques for measuring transonic flow with a three dimensional laser velocimetry system. Application to determining the drag of a fuselage p 1022 N95-19258
Velocity measurements with hot-wires in a vortex-dominated flowfield p 932 N95-19261
VENTILATION
Computational simulations for some tests in transonic wind tunnels p 1023 N95-19264
VENTS
VENTCF2: An algorithm and associated FORTRAN 77 subroutine for calculating flow through a horizontal ceiling/floor vent in a zone-type compartment fire model
[PB94-210127] p 993 N95-19402
The metallurgical integrity of the frit vent assembly diffusion bond
[DE95-000610] p 968 N95-19877
VENUS (PLANET)
Mercury: Exploration of a planet
[NASA-TM-110489] p 1194 N95-19045
VERBAL COMMUNICATION
An analysis of tower (local) controller-pilot voice communications
[AD-A283718] p 996 N95-18436
VERMICULITE
Controlling combustion-source emissions at Air Force sites with a new filter concept, phase 1
[AD-A283674] p 1058 N95-18140
VERTICAL AIR CURRENTS
Microburst vertical wind estimation from horizontal wind measurements
[NASA-TP-3480] p 942 N95-18198
An analytic conceptual model of extratropical cyclones
[KNMI-WR-93-03] p 1072 N95-18926
VERTICAL LANDING
Heliport/vertiport MLS precision approaches
[AD-A283505] p 940 N95-18059
VSTOL Systems Research Aircraft (VSRA) Harrier
[NASA-TM-110117] p 941 N95-18347
VERTICAL MOTION
NASA Goddard Earth Sciences Graduate Student Program --- FIRE CIRRUS-II examination of coupling between an upper tropospheric cloud system and synoptic-scale dynamics
[NASA-CR-197130] p 1066 N95-19129
VERTICAL TAKEOFF
VSTOL Systems Research Aircraft (VSRA) Harrier
[NASA-TM-110117] p 941 N95-18347
VERTICAL TAKEOFF AIRCRAFT
V-22 simulator evaluation for shipboard operations
[AD-A284156] p 943 N95-18505
VERY HIGH FREQUENCIES
On orbit performance of the ALEXIS EUV telescopes
[DE94-016197] p 964 N95-18639
VERY LARGE SCALE INTEGRATION
Construction of a connectionist network supercomputer
[AD-A283354] p 1109 N95-18050
Locally connected adaptive Gabor filter for real-time motion compensation
[AD-A285726] p 1009 N95-18485
Connectionist Network Supercomputer Project
[AD-A279206] p 1112 N95-19843
VERY LOW FREQUENCIES
Long wavelength propagation capacity, version 1.1 (computer diskette)
[AD-M200254] p 994 N95-17964
Effects of meteor showers in the Earth ionosphere
[INPE-5591-TDI/552] p 1178 N95-18213
VESTIBULES
Visuo-ocular performance during vestibular stimulation
[AD-A284103] p 1089 N95-18403
Vestibular examination in pilots susceptible to motion sickness p 1083 N95-19427
VIBRATION
Crosshift vibrometry: Biomarker for ergonomic stress
[AD-A284337] p 1091 N95-18385
A shock isolation method and apparatus
[AD-D016471] p 1045 N95-18456
Fiber optic pressure and/or vibration detector
[AD-D016474] p 1140 N95-18460
An analysis of noise reduction in variable reluctance motors using pulse position randomization
[AD-A283846] p 1123 N95-18673
A preliminary analysis of low frequency pressure oscillations in hybrid rocket motors p 968 N95-18987
The evaluation of transmission efficiency and coupling loss factor of structural junctions
[MRL-TR-93-1] p 1124 N95-19057
Thermochemical IR sources: COCHISE and FACELIF experiments
[AD-A279940] p 977 N95-19868
VIBRATION DAMPING
Tuned mass damper for integrally bladed turbine rotor
[NASA-CASE-MFS-28697-1] p 1041 N95-18325
Acoustic radiation damping of flat rectangular plates subjected to subsonic flows p 1123 N95-18542
Streamlined design and self reliant hardware for active control of precision space structures
[NASA-CR-4637] p 964 N95-18580
VIBRATION EFFECTS
Effects of vibration (G-jitters) on convection in micro-gravity p 991 N95-19013
VIBRATION ISOLATORS
Microgravity isolation system design: A modern control synthesis framework
[NASA-TM-106805] p 927 N95-18197
Tuned mass damper for integrally bladed turbine rotor
[NASA-CASE-MFS-28697-1] p 1041 N95-18325
Microgravity isolation system design: A modern control analysis framework
[NASA-TM-106803] p 927 N95-18486
Streamlined design and self reliant hardware for active control of precision space structures
[NASA-CR-4637] p 964 N95-18580
Sag compensated vibration isolation mount
[AD-D016541] p 1042 N95-19121
VIBRATION MEASUREMENT
Crosshift vibrometry: Biomarker for ergonomic stress
[AD-A284337] p 1091 N95-18385

Sloshing roof impact tests of a rectangular tank
[DE94-012462] p 1018 N95-18549

VIBRATION MODE
Modal Identification Experiment accommodations review
[NASA-CR-195009] p 964 N95-18105

VIBRATION TESTS
High-temperature acoustic test facilities and methods p 1125 N95-19149
Nonlinear dynamic response of aircraft structures to acoustic excitation p 946 N95-19151
Acoustic fatigue behaviour of GLARE composites p 1127 N95-19160

VIDEO COMPRESSION
Digital video compression: Standardisation of scalable coding schemes
[BBC-RD-1994/10] p 1001 N95-19047

VIDEO SIGNALS
The development of the switched-horn radio-camera system
[BBC-RD-1993/13] p 997 N95-18494
RINSE: A digitally implemented flywheel sync regenerator for improved video synchroniser performance
[BBC-RD-1993/14] p 999 N95-18538

VINYL POLYMERS
A mechanism for blistering of carbon fiber composites
[AD-A286252] p 971 N95-19386

VIRTUAL MEMORY SYSTEMS
Performance evaluation of the Engineering Analysis and Data Systems (EADS) 2 p 1163 N95-18978

VIRTUAL REALITY
Virtual reality, an air combat T and E perspective
[AD-A284161] p 959 N95-18508
The assessment of virtual reality for human anatomy instruction p 1088 N95-18971
Development of microgravity, full body functional reach envelope using 3-D computer graphic models and virtual reality technology p 1092 N95-18990
Using CLIPS to represent knowledge in a VR simulation p 1107 N95-19765

VISCOELASTIC DAMPING
Characterization of metal matrix composites
[NASA-CR-195381] p 970 N95-18940

VISCOELASTICITY
Long-term processes in geomaterials. A three-dimensional visco-elastic soil model
[PB94-207180] p 1065 N95-18640

VISCOPLASTICITY
Optimization of layered metal matrix composite cylinders p 970 N95-18920

VISCOSITY
Stratified carrier electroviscous fluids and apparatus
[AD-D016238] p 1019 N95-18634

VISCOUS FLOW
Time-evolving bubbles in two-dimensional stokes flow
[NASA-CR-194998] p 1015 N95-18188
A three-dimensional structured/unstructured hybrid Navier-Stokes method for turbine blade rows
[NASA-TM-106813] p 1016 N95-18200
A note on the wave action density of a viscous instability mode on a laminar free-shear flow
[NASA-TM-106771] p 1016 N95-18212
Solution of Navier-Stokes equations using high accuracy monotone schemes p 948 N95-19019
Simulation of steady and unsteady viscous flows in turbomachinery p 949 N95-19023
Viscous flow past aerofoils axisymmetric bodies and wings p 933 N95-19457
Discrete vortex method for computation of viscous incompressible flows p 1029 N95-19460
Pressure based finite volume algorithm for viscous flow computation p 1029 N95-19461
Hypersonic viscous flow computations p 1029 N95-19463
Inviscid and viscous flow modelling of complex aircraft configurations using the CFD simulation system sauna
[ARA-MEMO-403] p 1031 N95-19777

VISCOUS FLUIDS
Stratified carrier electroviscous fluids and apparatus
[AD-D016238] p 1019 N95-18634

VISIBILITY
Representing visibility for siting problems
[AD-A284076] p 993 N95-19036

VISIBLE SPECTRUM
Visible-infrared remote-sensing model and applications for ocean waters
[NASA-CR-197602] p 1051 N95-18739

VISUAL ACUITY
Visuo-ocular performance during vestibular stimulation
[AD-A284103] p 1089 N95-18403
Photorefractive Keratectomy (PRK) in the military aviator: An aeromedical expose p 1086 N95-19442

VISUAL AIDS
Research requirements for future visual guidance systems
[AD-A279188] p 941 N95-19810

VISUAL FLIGHT RULES
Federal aviation regulations, part 91. General operating and flight rules. Change 8
[PB94-217445] p 940 N95-19720

VISUAL PERCEPTION
Cooperativity and 3-D representation
[AD-A284203] p 1093 N95-17940
The synthesis of vision and action
[AD-A285453] p 1088 N95-18094
Fixture for pressure testing sight glasses
[AD-D016263] p 1032 N95-18319
Color vision issues in modern military aviation or the search for the Abominable Coneman p 1086 N95-19441
Facilitation and interference in identification of pictures and words
[AD-A285882] p 1090 N95-19602

VISUAL TASKS
Local spatio-temporal analysis in vision systems
[AD-A284162] p 1140 N95-18509

VOICE COMMUNICATION
An analysis of tower (local) controller-pilot voice communications
[AD-A283718] p 996 N95-18436

VOIDS
Quantitative analysis of voids in percolating structures in two-dimensional N-body simulations
[NASA-CR-197612] p 1156 N95-18949

VOLATILITY
Shock-induced devolatization of calcium sulfate and implications for K-T extinctions
[NASA-CR-197608] p 1060 N95-19033

VOLTAGE REGULATORS
Development of an amorphous surge blocker for a high voltage acceleration power supply of the neutral beam injectors
[DE94-770648] p 1138 N95-19874

VORTEX ALLEVIATION
Corner vortex suppressor
[AD-D016423] p 928 N95-18337

VORTEX BREAKDOWN
Navier-Stokes, flight, and wind tunnel flow analysis for the F/A-18 aircraft
[NASA-TP-3478] p 931 N95-19114
CFD: Advances and Applications, 1994
[NAL-SP-9412] p 1028 N95-19455
Computation of vortex breakdown p 1029 N95-19462

VORTEX FILAMENTS
Computation of vortex breakdown p 1029 N95-19462

VORTEX LATTICE METHOD
Panel methods p 1027 N95-19448

VORTEX SHEDDING
Interaction, bursting and control of vortices of a cropped double-delta wing at high angle of attack
[AD-A283656] p 930 N95-18669

VORTICES
Corner vortex suppressor
[AD-D016423] p 928 N95-18337
Aircraft wake vortex takeoff tests at O'Hara International Airport
[AD-A283828] p 929 N95-18624
Interaction, bursting and control of vortices of a cropped double-delta wing at high angle of attack
[AD-A283656] p 930 N95-18669
The effect of stable stratification on three-dimensional structure in shear layers p 1019 N95-18921
Development of a multicomponent force and moment balance for water tunnel applications, volume 1
[NASA-CR-4642-VOL-1] p 1020 N95-18955
Navier-Stokes, flight, and wind tunnel flow analysis for the F/A-18 aircraft
[NASA-TP-3478] p 931 N95-19114
Velocity measurements with hot-wires in a vortex-dominated flowfield p 932 N95-19261
CFD: Advances and Applications, 1994
[NAL-SP-9412] p 1028 N95-19455
Discrete vortex method for computation of viscous incompressible flows p 1029 N95-19460
Computation of vortex breakdown p 1029 N95-19462
Predicting and explaining the movement of mesoscale oceanographic features using CLIPS p 1105 N95-19752
Generalized relaxation theory and vortices in plasmas
[DE95-002615] p 1147 N95-19837

VORTICITY
The effect of stable stratification on three-dimensional structure in shear layers p 1019 N95-18921

VOTING
Design and analysis of dynamic leader election protocols in broadcast networks
[PB94-202728] p 1109 N95-18039

W

WAFERS
Defect reduction and back channel degradation in SIMOX
[AD-A284231] p 1148 N95-17960
Semiconductor measurement technology: Design and testing guides for the COMOS and lateral bipolar-on-SOI test library
[PB94-178019] p 1007 N95-17984
Advanced packaging and integration technologies for microsensors, phase 1
[AD-A283613] p 1040 N95-18010
InP solar cell development on inexpensive silicon substrates
[AD-A283624] p 1052 N95-18011
Tunneling and transport in mesoscopic structures
[AD-A283426] p 1148 N95-18053
Industrial exploitation of a alternate technology for the production of HgCdTe epilayers, structures and devices
[AD-A279202] p 1154 N95-19816

WAKES
Evolution of a collection of bubbles with application to wakes, bubble screens, and cloud noise
[AD-A283597] p 1017 N95-18434
Aircraft wake vortex takeoff tests at O'Hara International Airport
[AD-A283828] p 929 N95-18624

WALL FLOW
Boundary-flow measurement methods for wall interference assessment and correction: Classification and review p 1022 N95-19262
Adaptive wind tunnel walls versus wall interference correction methods in 2D flows at high blockage ratios p 960 N95-19267
Interference determination for wind tunnels with slotted walls p 960 N95-19269
Calculation of low speed wind tunnel wall interference from static pressure pipe measurements p 1024 N95-19273
Analysis of test section sidewall effects on a two dimensional airfoil: Experimental and numerical investigations p 1025 N95-19276
Calculation of wall effects of flow on a perforated wall with a code of surface singularities p 1025 N95-19277

WALL PRESSURE
Wall correction method with measured boundary conditions for low speed wind tunnels p 1023 N95-19263
Estimating wind tunnel interference due to vectored jet flows p 1023 N95-19265
Wall interaction effects for a full-scale helicopter rotor in the NASA Ames 80- by 120-foot wind tunnel p 932 N95-19270

WALL TEMPERATURE
Regenerative cooling for liquid propellant rocket thrust chambers
[INPE-5565-TDI/540] p 967 N95-18720

WALLS
Nonlinear magnetohydrodynamics
[DE94-016223] p 1143 N95-18353
Cracking characteristics of a habitable module pressure wall following orbital debris penetration p 1047 N95-19003
SSI effects for a tank containing two liquids
[DE94-012457] p 1020 N95-19099
Wall correction method with measured boundary conditions for low speed wind tunnels p 1023 N95-19263
Computational simulations for some tests in transonic wind tunnels p 1023 N95-19264
Wall interaction effects for a full-scale helicopter rotor in the NASA Ames 80- by 120-foot wind tunnel p 932 N95-19270
Status of vanadium alloy development for fusion first wall/blanket applications
[DE95-001067] p 982 N95-19725

WARFARE
F/A-18 simulation validation and verification: Making a good product even better
[AD-A283995] p 944 N95-18723

WARNING SYSTEMS
Alarm annunciation in a graphical environment
[DE94-015761] p 1098 N95-18652

WASTE TREATMENT
Environmental Compliance Assessment System (ECAS)
[AD-A283950] p 1060 N95-18683

WATER
Improved filtration materials and modeling
[AD-A284684] p 1091 N95-18531
A photoionization study of OH and OD from 680A to 950A: An analysis of the Rydberg series
[NASA-CR-196970] p 974 N95-18744
Design of high pressure waterjet nozzles
p 1031 N95-18996

WATER COLOR
Visible-infrared remote-sensing model and applications for ocean waters
[NASA-CR-197602] p 1051 N95-18739
SeaWiFS technical report series. Volume 18: SeaWiFS technical report series cumulative index: Volumes 1-17
[NASA-TM-104566-VOL-18] p 1076 N95-19577

WATER DEPTH
Nonlinear ocean waves
[AD-A285331] p 1075 N95-19523

WATER FLOW
The stability of two-phase flow over a swept-wing
[NASA-CR-194994] p 1016 N95-18190
Heuristic inference about flow directions in river networks
[INPE-5588-TDI/550] p 1050 N95-18214
Prediction of buoyant outflow in lakes and fjords with a quasi 3D numerical model
[PB94-206984] p 1051 N95-18372
Steady and unsteady blade stresses within the SSME ATD/HPOTP inducer p 968 N95-18982

WATER POLLUTION
Application of conducting polymers to electroanalysis
[DE94-015204] p 984 N95-18348

WATER RECLAMATION
Analytical control test plan and microbiological methods for the water recovery test
[NASA-TM-108473] p 1091 N95-19061

WATER TREATMENT
Ion exchange polymers and method for making
[NASA-CASE-LEW-15576-1] p 984 N95-18321

WATER TUNNEL TESTS
Interaction, bursting and control of vortices of a cropped double-delta wing at high angle of attack
[AD-A283656] p 930 N95-18669
Development of a multicomponent force and moment balance for water tunnel applications, volume 1
[NASA-CR-4642-VOL-1] p 1020 N95-18955
Development of a multicomponent force and moment balance for water tunnel applications, volume 2
[NASA-CR-4642-VOL-2] p 1020 N95-18956

WATER VAPOR
Estimation of satellite derived temperature and moisture fields over Europe from TOVS data using 3I and ITPP algorithms
[AD-A284581] p 1049 N95-18035
A sensitivity analysis of upwelling radiances in the 3-5 micrometers region as a function of atmospheric conditions
[AD-A283678] p 1068 N95-18141
Scientific objectives of the primitive body sample return missions: An approach from the light-induced effect on water vapor p 961 N95-19191
Diffusion of water vapour through cold Gore-Tex (trademark)
[AD-A279939] p 989 N95-19867

WATER WAVES
The diurnal cycle of high-frequency temperature variability at 0 deg 140 deg W on seasonal and interannual time scales
[AD-A283640] p 1074 N95-18012
Nonlinear ocean waves
[AD-A285331] p 1075 N95-19523

WATERPROOFING
Diffusion of water vapour through cold Gore-Tex (trademark)
[AD-A279939] p 989 N95-19867

WATERSHEDS
Cumulative impact analysis of wetlands using hydrologic indices
[AD-A284759] p 1058 N95-18085

WAVE DISPERSION
Low-dissipation and -dispersion Runge-Kutta schemes for computational acoustics
[NASA-CR-195022] p 1018 N95-18488

WAVE DRAG
In-flight lift-drag characteristics for a forward-swept wing aircraft and comparisons with contemporary aircraft)
[NASA-TP-3414] p 929 N95-18565

WAVE EQUATIONS
Low-dissipation and -dispersion Runge-Kutta schemes for computational acoustics
[NASA-CR-195022] p 1018 N95-18488

WAVE FRONT DEFORMATION
Collision of cometlike and slightly differentiated bodies as an origin for ordinary chondrites
p 1188 N95-19308

WAVE FUNCTIONS
Exact m(sub quark) does not equal 0 condensates in QCD(1+1)(N(sub C) yields infinity
[DE94-018581] p 1131 N95-18554
To the theory of the management of the resonance widths
[DE94-626645] p 1156 N95-18879

WAVE INTERACTION
A note on the wave action density of a viscous instability mode on a laminar free-shear flow
[NASA-TM-106771] p 1016 N95-18212

WAVE PROPAGATION
Long wavelength propagation capacity, version 1.1 (computer diskette)
[AD-M200254] p 994 N95-17964
The diurnal cycle of high-frequency temperature variability at 0 deg 140 deg W on seasonal and interannual time scales
[AD-A283640] p 1074 N95-18012
A note on the wave action density of a viscous instability mode on a laminar free-shear flow
[NASA-TM-106771] p 1016 N95-18212
Low-dissipation and -dispersion Runge-Kutta schemes for computational acoustics
[NASA-CR-195022] p 1018 N95-18488
Computer simulation of wave propagation through turbulent media
[AD-A283695] p 1000 N95-18671
Simulation of wave propagation in three-dimensional random media
[NASA-CR-197605] p 1004 N95-19547

WAVE SCATTERING
Wavelets and scattering
[AD-A284131] p 996 N95-18411
Scattering of point source illumination by an arbitrary configuration p 1143 N95-19006
Simulation of wave propagation in three-dimensional random media
[NASA-CR-197605] p 1004 N95-19547

WAVEFORMS
High frequency direct drive generation using white noise sources
[AD-A284158] p 997 N95-18506
Development of a bulk current injection direct-drive system to test system level components with stress waveforms that are encountered during full threat indirect effects lightning
[AD-A284160] p 933 N95-18507
Waveform bounding and combination techniques for direct drive testing
[AD-A284075] p 1000 N95-19035
High radar range resolution with the step frequency waveform
[AD-A284611] p 1002 N95-19084
Adaptive detection and copy of coherent narrowband waveforms with uncalibrated arrays
[AD-A285125] p 1004 N95-19594

WAVEGUIDE ANTENNAS
Analysis and synthesis of (SAR) waveguide phased array antennas
[AD-A285336] p 1004 N95-19535

WAVEGUIDES
Design and fabrication of N x N optical couplers based on organic polymer optical waveguides
[AD-A285530] p 1138 N95-18100
Finite element method for eigenvalue problems in electromagnetics
[NASA-TP-3485] p 995 N95-18187
Comparison of the folded stripline and stacked stripline concepts to the folded waveguide launcher
[DE94-018951] p 999 N95-18558
Waveguide switches using asymmetric coupled quantum wells
[AD-A284056] p 1010 N95-18662
EEsoF MICAD and ACADEMY macro files for coplanar waveguide and finite ground plan coplanar waveguide
[NASA-TM-106800] p 1000 N95-18733

WAVELENGTH DIVISION MULTIPLEXING
RACE project 1036: WTDM broadband customer premises network
[BBC-RD-1993/15] p 998 N95-18537
Advanced optical fiber communications systems
[AD-A283942] p 1141 N95-18682
Fiber Optic Control System integration for advanced aircraft. Electro-optic and sensor fabrication, integration, and environmental testing for flight control systems
[NASA-CR-191194] p 1034 N95-19236
High speed optical links between LLNL and Berkeley
[DE95-000552] p 1006 N95-19833

WAVELET ANALYSIS
Wavelets and scattering
[AD-A284131] p 996 N95-18411
Theory and applications of the phi transform wavelets
[AD-A279943] p 1119 N95-19869

WAVERIDERS
Theoretical investigations of shock/boundary layer interactions on a Ma(infinity) = 8 waverider
[DLR-FB-94-12] p 930 N95-18910

WEAPON SYSTEMS
Virtual reality, an air combat T and E perspective
[AD-A284161] p 959 N95-18508

WEAR
Tribology and microstructure of PS212 with a Cr2O3 seal coat
[NASA-TM-106768] p 969 N95-18448
Adhesion, friction, and wear behavior of clean metal-ceramic couples
[NASA-TM-106815] p 989 N95-19783

WEAR RESISTANCE
A CMC database for use in the next generation launch vehicles (rockets) p 963 N95-18993
High velocity oxygen fuel spraying of erosion and wear resistant coatings on jet engine parts
p 954 N95-19680

WEATHER
Climate and weather of Central Africa. Executive summary
[AD-A283647] p 1067 N95-18014
Implementation of the 1992 Terminal area-Local Analysis and Prediction System (T-LAPS)
[AD-A284334] p 1070 N95-18384
Conceptual models of severe convective weather in the Netherlands
[KNMI-WR-93-05] p 1071 N95-18394
A synoptic climatology of convective weather in the Netherlands
[KNMI-WR-93-04] p 1071 N95-18395
Office of Research and Applications: Research Programs p 1071 N95-18721
Toward a new national weather service: Weather for those who fly
[PB94-214418] p 1072 N95-19407

WEATHER FORECASTING
Product usage evaluation of the aviation gridded forecast system workstation at the Denver Center Weather Service Unit
[PB94-195922] p 1066 N95-17952
Forecasting snowfall using mixing ratios on an isentropic surface: An empirical study
[PB94-188760] p 1067 N95-17993
Experiments with the Mesoscale Atmospheric Simulation System (MASS) using the synthetic relative humidity p 1073 N95-18172
Lightning studies using LDAR and companion data sets p 1073 N95-18174
Conceptual models of severe convective weather in the Netherlands
[KNMI-WR-93-05] p 1071 N95-18394
Office of Research and Applications: Research Programs p 1071 N95-18721
Dependence of medium-range forecast error on patterns in the initial state p 1072 N95-18732
A technique for determining cloud free versus cloud contaminated pixels in satellite imagery
p 1052 N95-19016
Toward a new national weather service: Weather for those who fly
[PB94-214418] p 1072 N95-19407
Synoptic and mesoscale examination of the northern New England winter storm of January 29-30, 1990
[PB94-209426] p 1072 N95-19581
The meteorological monitoring system for the Kennedy Space Center/Cape Canaveral Air Station
p 1104 N95-19647

WEIGHT (MASS)
Design and development of an enhanced biodynamic manikin, phase 1
[AD-A284725] p 1090 N95-18077

WEIGHT INDICATORS
Space Station racks weight and CG measurement using the rack insertion end-effector p 966 N95-18168

WEIGHTING FUNCTIONS
Plant and controller optimization by convex methods
[AD-A283700] p 944 N95-18621

WEIGHTLESSNESS
Geometry and gravity influences on strength capability
[NASA-TP-3511] p 1091 N95-18189

WEIGHTLESSNESS SIMULATION
Users guide for NASA Lewis Research Center DC-9 Reduced-Gravity Aircraft Program
[NASA-TM-106755] p 959 N95-18586

WELDABILITY
Weldability of iron aluminides
[DE95-000686] p 981 N95-19568

WELDED JOINTS
Residual stresses in welded plates
p 1047 N95-18972
Fatigue crack growth under variable amplitude loading
p 937 N95-19484

Weldability of iron aluminides
[DE95-000686] p 981 N95-19568
The metallurgical integrity of the frit vent assembly diffusion bond
[DE95-000610] p 968 N95-19877

WELDING
Microstructural analysis of cracks generated during welding of 2195 aluminum-lithium alloy
p 982 N95-19007

WETLANDS
Cumulative impact analysis of wetlands using hydrologic indices
[AD-A284759] p 1058 N95-18085
Spectral reflectance properties of wetlands plants
[AD-A283546] p 1051 N95-18614

WETTABILITY
Method of making a membrane having hydrophilic and hydrophobic surfaces for adhering cells or antibodies by using atomic oxygen or hydroxyl radicals
[NASA-CASE-MSC-21529-1] p 983 N95-18134

WETTING
Rewetting of monogroove heat pipe in Space Station radiators
[NASA-CR-197579] p 1014 N95-18092

WHEATSTONE BRIDGES
Current loop signal conditioning: Practical applications
[NASA-TM-4636] p 1033 N95-18735

WHEELCHAIRS
On the development of an expert system for wheelchair selection p 1092 N95-19627

WHITE DWARF STARS
Rocket and laboratory studies in astronomy
[NASA-CR-197531] p 1177 N95-17981

WHITE NOISE
High frequency direct drive generation using white noise sources
[AD-A284158] p 997 N95-18506

WIND (METEOROLOGY)
Storm activity over the North Sea and the Netherlands in two climate models compared with observations
[KNMI-WR-94-02] p 1070 N95-18393

WIND PROFILES
Measurements of wind profiler EMC characteristics
[PB94-194107] p 1066 N95-17938
NASA Goddard Earth Sciences Graduate Student Program --- FIRE CIRRUS-II examination of coupling between an upper tropospheric cloud system and synoptic-scale dynamics
[NASA-CR-197130] p 1066 N95-19129

WIND SHEAR
Microburst vertical wind estimation from horizontal wind measurements
[NASA-TP-3460] p 942 N95-18198

WIND TUNNEL APPARATUS
Dynamic Stability Instrumentation System (DSIS). Volume 1: Hardware description
[NASA-TM-109160-VOL-1] p 1099 N95-18899

WIND TUNNEL CALIBRATION
The traditional and new methods of accounting for the factors distorting the flow over a model in large transonic wind tunnels p 1025 N95-19275
Analysis of test section sidewall effects on a two dimensional airfoil: Experimental and numerical investigations p 1025 N95-19276
Calculation of wall effects of flow on a perforated wall with a code of surface singularities
p 1025 N95-19277
Interference corrections for a centre-line plate mount in a porous-walled transonic wind tunnel
p 933 N95-19280
Correction of support influences on measurements with sting mounted wind tunnel models p 933 N95-19281

WIND TUNNEL DRIVES
Improved speed control system for the 87,000 HP wind tunnel drive
[NASA-TM-106840] p 1035 N95-19794

WIND TUNNEL MODELS
Evaluation of combined wall- and support-interference on wind tunnel models p 932 N95-19278
Interaction of a three strut support on the aerodynamic characteristics of a civil aviation model
p 933 N95-19279
Interference corrections for a centre-line plate mount in a porous-walled transonic wind tunnel
p 933 N95-19280
Correction of support influences on measurements with sting mounted wind tunnel models p 933 N95-19281
Calculation of support interference in dynamic wind-tunnel tests p 933 N95-19282
Multiport pressure measurements on continuously moving wind tunnel models
[ARA-MEMO-391] p 932 N95-19772

WIND TUNNEL TESTS
Wind tunnel performance comparative test results of a circular cylinder and 50 percent ellipse tailboom for circulation control antitorque applications
[AD-A283335] p 941 N95-18008
Overview of unsteady transonic wind tunnel test on a semispan straked delta wing oscillating in pitch
[AD-A284097] p 928 N95-18380
A selection of experimental test cases for the validation of CFD codes. Supplement: Datasets A-E
[AGARD-AR-303-SUPPL] p 929 N95-18539
Pressure measurements on an F/A-18 twin vertical tail in buffeting flow. Volume 4, part 2: Buffet cross spectral densities
[AD-A285555] p 957 N95-18641
Hypersonic wind tunnel test techniques
[AD-A284057] p 929 N95-18663
Static investigation of two fluidic thrust-vectoring concepts on a two-dimensional convergent-divergent nozzle
[NASA-TM-4574] p 931 N95-19042
Hypervelocity air flows with finite rate chemistry
[AD-A284727] p 931 N95-19109
Navier-Stokes, flight, and wind tunnel flow analysis for the F/A-18 aircraft
[NASA-TP-3478] p 931 N95-19114
2-D and 3-D oscillating wing aerodynamics for a range of angles of attack including stall
[NASA-TM-4632] p 931 N95-19119
Documentation and archiving of the Space Shuttle wind tunnel test data base. Volume 1: Background and description
[NASA-TM-104806-VOL-1] p 965 N95-19237
Wall Interference, Support Interference and Flow Field Measurements
[AGARD-CP-535] p 1020 N95-19251
The crucial role of wall interference, support interference and flow field measurements in the development of advanced aircraft configurations p 1021 N95-19252
Improvement and validation of an LDV system to perform measurements in laminar supersonic flows
p 1021 N95-19256
The utilization of a high speed reflective visualization system in the study of transonic flow over a delta wing
p 932 N95-19259
Transonic and supersonic flowfield measurements about axisymmetric afterbodies for validation of advanced CFD codes p 932 N95-19260
Determination of solid/porous wall boundary conditions from wind tunnel data for computational fluid dynamics codes p 1023 N95-19266
Adaptive wind tunnel walls versus wall interference correction methods in 2D flows at high blockage ratios
p 960 N95-19267
Development of pneumatic test techniques for subsonic high-lift and in-ground-effect wind tunnel investigations
p 932 N95-19268
Interference determination for wind tunnels with slotted walls p 960 N95-19269
Wall interaction effects for a full-scale helicopter rotor in the NASA Ames 80- by 120-foot wind tunnel
p 932 N95-19270
Unsteady flow testing in a passive low-correction wind tunnel p 960 N95-19272
Calculation of low speed wind tunnel wall interference from static pressure pipe measurements
p 1024 N95-19273
The traditional and new methods of accounting for the factors distorting the flow over a model in large transonic wind tunnels p 1025 N95-19275
Analysis of test section sidewall effects on a two dimensional airfoil: Experimental and numerical investigations p 1025 N95-19276
Calculation of wall effects of flow on a perforated wall with a code of surface singularities
p 1025 N95-19277
Evaluation of combined wall- and support-interference on wind tunnel models p 932 N95-19278
Interaction of a three strut support on the aerodynamic characteristics of a civil aviation model
p 933 N95-19279
Interference corrections for a centre-line plate mount in a porous-walled transonic wind tunnel
p 933 N95-19280
Correction of support influences on measurements with sting mounted wind tunnel models p 933 N95-19281
Calculation of support interference in dynamic wind-tunnel tests p 933 N95-19282
Methods for scaling icing test conditions
[NASA-TM-106827] p 934 N95-19284
An investigation of drag repeatability in half model testing in the ARA Transonic Wind Tunnel
[ARA-MEMO-392] p 931 N95-19546
An oil flow study of the reference Shuttle-C configuration
[NASA-RP-1352] p 932 N95-19623
Documentation and archiving of the Space Shuttle wind tunnel test data base. Volume 2: User's Guide to the Archived Data Base
[NASA-TM-104806-VOL-2] p 965 N95-19624
Prediction of wind tunnel effects on the installed F/A-18A inlet flow field at high angles-of-attack
[NASA-CR-195429] p 950 N95-19651
Multiport pressure measurements on continuously moving wind tunnel models
[ARA-MEMO-391] p 932 N95-19772
Wind tunnel tests of a 42 inch diameter self-starting autogyro rotor
[AD-A279922] p 932 N95-19863

WIND TUNNEL WALLS
Wall Interference, Support Interference and Flow Field Measurements
[AGARD-CP-535] p 1020 N95-19251
The crucial role of wall interference, support interference and flow field measurements in the development of advanced aircraft configurations p 1021 N95-19252
Boundary-flow measurement methods for wall interference assessment and correction: Classification and review p 1022 N95-19262
Estimating wind tunnel interference due to vectored jet flows p 1023 N95-19265
Determination of solid/porous wall boundary conditions from wind tunnel data for computational fluid dynamics codes p 1023 N95-19266
Adaptive wind tunnel walls versus wall interference correction methods in 2D flows at high blockage ratios
p 960 N95-19267
Interference determination for wind tunnels with slotted walls p 960 N95-19269
Unsteady flow testing in a passive low-correction wind tunnel p 960 N95-19272
Analysis of test section sidewall effects on a two dimensional airfoil: Experimental and numerical investigations p 1025 N95-19276
Calculation of wall effects of flow on a perforated wall with a code of surface singularities
p 1025 N95-19277
Evaluation of combined wall- and support-interference on wind tunnel models p 932 N95-19278
Prediction of wind tunnel effects on the installed F/A-18A inlet flow field at high angles-of-attack
[NASA-CR-195429] p 950 N95-19651

WIND TUNNELS
Universal wind tunnel data acquisition and reduction software
[AD-A283897] p 1096 N95-18365
Hypersonic flight testing
[AD-A283981] p 944 N95-18891
Wall correction method with measured boundary conditions for low speed wind tunnels
p 1023 N95-19263
Estimating wind tunnel interference due to vectored jet flows p 1023 N95-19265
Development of pneumatic test techniques for subsonic high-lift and in-ground-effect wind tunnel investigations
p 932 N95-19268
Wall interaction effects for a full-scale helicopter rotor in the NASA Ames 80- by 120-foot wind tunnel
p 932 N95-19270
Prediction of wind tunnel effects on the installed F/A-18A inlet flow field at high angles-of-attack
[NASA-CR-195429] p 950 N95-19651

WIND TURBINES
Wind turbine blade aerodynamics: The combined experiment
[DE94-011866] p 929 N95-18645
Wind turbine blade aerodynamics: The analysis of field test data
[DE94-011867] p 929 N95-18646
Evidence that aerodynamic effects, including dynamic stall, dictate HAWT structural loads and power generation in highly transient time frames
[DE94-011865] p 1054 N95-19855

WIND VELOCITY
Evaluation of an unlighted swinging airport sign
[AD-A284763] p 958 N95-18087
Environmental forcing of ambient noise in the Nansen and Amundsen Basins of the Arctic Ocean
[AD-A285540] p 1074 N95-18468

WIND VELOCITY MEASUREMENT
Measurements of wind profiler EMC characteristics
[PB94-194107] p 1066 N95-17938
A technical demonstration Mobile Profiler System
[AD-A284562] p 1068 N95-18117
Microburst vertical wind estimation from horizontal wind measurements
[NASA-TP-3460] p 942 N95-18198

WINDOWS (COMPUTER PROGRAMS)
User profile for researchers studying objects: Implications for computer systems
[PB94-188463] p 1109 N95-17989

TEXCAD: Textile Composite Analysis for Design. Version 1.0: User's manual
[NASA-CR-4639] p 970 N95-18466
Alarm annunciation in a graphical environment
[DE94-015761] p 1098 N95-18652

WING LOADING
Flight testing high lateral asymmetries on highly augmented Fighter/Attack aircraft
[AD-A284206] p 941 N95-17953
Determination of stores pointing error due to wing flexibility under flight load
[NASA-TM-4646] p 945 N95-19044
Development of load spectra for Airbus A330/A340 full scale fatigue tests p 936 N95-19479

WING OSCILLATIONS
2-D and 3-D oscillating wing aerodynamics for a range of angles of attack including stall
[NASA-TM-4632] p 931 N95-19119

WING PANELS
Fatigue and residual strength investigation of ARALL(R) -3 and GLARE(R) -2 panels with bonded stringers p 939 N95-19495

WING SLOTS
Numerical simulation of dynamic-stall suppression by tangential blowing
[AD-A284887] p 931 N95-19110

WING TANKS
Determination of stores pointing error due to wing flexibility under flight load
[NASA-TM-4646] p 945 N95-19044

WING-FUSELAGE STORES
The aerodynamic design of an integrated wing lower surface and pylons for reduced drag
[ARA-MEMO-406] p 946 N95-19789

WINGS
Wing design for a civil tiltrotor transport aircraft
[NASA-CR-197523] p 942 N95-18090
Parametric study on laminar flow for finite wings at supersonic speeds
[NASA-TM-108852] p 928 N95-18101
Course module for AA201: Wing structural design project
[AD-A283618] p 944 N95-18616
The accuracy of parameter estimation in system identification of noisy aircraft load measurement
[NASA-CR-197516] p 945 N95-19130
Development of load spectra for Airbus A330/A340 full scale fatigue tests p 936 N95-19479

WINTER
Use of profiler data for analysis and NOWcasting of a winter season extratropical cyclone
[PB94-187804] p 1067 N95-17992

WIRE
Wentzel-Bardeen singularity in coupled Luttinger liquids: Transport properties
[DE95-000856] p 1152 N95-19621

WIRELESS COMMUNICATION
Phase and amplitude controlled micropatch antenna
[AD-A284191] p 1002 N95-19103

WORDS (LANGUAGE)
Simulation in manufacturing
[PB94-215563] p 1100 N95-19409
Facilitation and interference in identification of pictures and words
[AD-A285882] p 1090 N95-19602

WORK HARDENING
Characterization of the deformation and annealing of 304L stainless steel
[DE94-018584] p 981 N95-19707

WORKING FLUIDS
Geometrical vapor blocker for parallel condensation tubes requiring subcooling
[NASA-CASE-MSC-22090-1] p 1017 N95-18323

WORKLOADS (PSYCHOPHYSIOLOGY)
A redundant disk array architecture for efficient small writes
[AD-A284048] p 1093 N95-18659
Multiple-task performance: A critical review of the literature and a cognitive neuroscience framework
[AD-A285133] p 1090 N95-19583
Programmable cockpit research simulator
[AD-A279219] p 960 N95-19848

WORKSTATIONS
Product usage evaluation of the aviation gridded forecast system workstation at the Denver Center Weather Service Unit
[PB94-195922] p 1066 N95-17952
Operational And Supportability Implementation System (OASIS) test and evaluation master plan
[AD-A284765] p 941 N95-18088
Throughput analysis between high end workstations across an FDDI network
[AD-A283608] p 1110 N95-18615
Design concepts for an integrated environmental medicine workstation for prediction, simulation and training
[AD-A283686] p 1079 N95-18618

WOVEN COMPOSITES
TEXCAD: Textile Composite Analysis for Design. Version 1.0: User's manual
[NASA-CR-4639] p 970 N95-18466

X

X RAY ABSORPTION
X-ray absorption spectroscopy in high temperature oxidation of metals and alloys p 955 N95-19682

X RAY ANALYSIS
Annular computed tomography
[AD-D016424] p 1141 N95-18593
Isolation and characterization of an indium-mixed-pnicogen Four-membered ring compound: Crystal structure of (Me3SiCH2)2InAs(SiMe3)2 In(CH2SiMe3)2P(SiMe3)2
[AD-A279170] p 1154 N95-19807
Synthesis and characterization of aluminum-phosphorus adducts: X-ray crystal structures of Cl3Al (dot) P(SiMe3)3 (dot) C7H8 and Br3Al (dot) P(SiMe3)3 (dot) C7H8
[AD-A279194] p 1154 N95-19812

X RAY DIFFRACTION
Ferroelectric thin film bismuth titanate prepared from acetate precursors
[DE95-000538] p 988 N95-19558

X RAY IMAGERY
Novel x ray imaging methods at the Nova Laser Facility
[DE94-016548] p 1146 N95-19509

X RAY IRRADIATION
Defect reduction and back channel degradation in SIMOX
[AD-A284231] p 1148 N95-17960

X RAY LASERS
High power phase conjugated solid state lasers
[DE94-016633] p 1037 N95-18357
Hyperfine splittings, prepulse technique, and other new results for collisional excitation neon-like x ray lasers
[DE94-016443] p 1038 N95-19247
Measurements of line overlap for resonant spoiling of x ray lasing transitions
[DE94-016444] p 1038 N95-19248
Inertial confinement fusion
[DE95-000314] p 1147 N95-19552
X-ray laser program
[AD-A279213] p 1039 N95-19845

X RAY OPTICS
Subgroup report on hard x-ray microprobes
[DE94-018708] p 1034 N95-19233

X RAY SOURCES
The origin of the diffuse x-ray background p 1197 N95-18729
Subgroup report on hard x-ray microprobes
[DE94-018708] p 1034 N95-19233

X RAY SPECTRA
Coronal abundances and their variation
[NASA-CR-197553] p 1195 N95-18376
XAMath: An XAFS analysis package based on Mathematica(tm)
[DE94-016346] p 1100 N95-19397
Propagation of intense, ultrashort laser pulses through metal vapor: Refractive intensity limits and spectral effects
[DE94-016365] p 1039 N95-19398

X RAY TELESCOPES
On orbit performance of the ALEXIS EUV telescopes
[DE94-016197] p 964 N95-18639

X RAYS
Nonlinear response of the photocathode of an x-ray streak camera to UV light
[DE94-018073] p 1032 N95-18130
GAMQUEST, a computer program to identify gamma rays
[DE94-016217] p 1197 N95-18351
Radiation-induced noise in UMPC-type current probes: IEMP response of the current measurement system
[AD-A284176] p 998 N95-18520
Implementation of 40-ps high-speed gated-microchannel-plate based x-ray framing cameras on reentrant SIM's for Nova
[DE94-018597] p 1033 N95-18555
Salt-induced aggregation of lysozyme: Implications for crystal growth p 1155 N95-19015
Bragg transmission phase plates for the production of circularly polarized x-rays
[DE94-017072] p 1151 N95-19113
Subgroup report on hard x-ray microprobes
[DE94-018708] p 1034 N95-19233
Novel x ray imaging methods at the Nova Laser Facility
[DE94-016548] p 1146 N95-19509
Gain uniformity, linearity, saturation and depletion in gated microchannel-plate x-ray framing cameras
[DE94-018596] p 1035 N95-19711
Microcavity structures
[DE95-001096] p 1039 N95-19727
Synthesis and characterization of a neutral six-coordinate tris-adduct of an indium(3) trihalide. X ray crystal structure of InCl3(THF)3
[AD-A279169] p 1154 N95-19806
Synthesis and characterization of aluminum-phosphorus adducts: X-ray crystal structures of Cl3Al (dot) P(SiMe3)3 (dot) C7H8 and Br3Al (dot) P(SiMe3)3 (dot) C7H8
[AD-A279194] p 1154 N95-19812
PRS projections for DECADE
[AD-A279215] p 1147 N95-19847

X WING ROTORS
Wall interaction effects for a full-scale helicopter rotor in the NASA Ames 80- by 120-foot wind tunnel p 932 N95-19270

X-29 AIRCRAFT
In-flight lift-drag characteristics for a forward-swept wing aircraft and comparisons with contemporary aircraft
[NASA-TP-3414] p 929 N95-18565

XENON
Development of a high-resolution liquid xenon detector for gamma-ray astrophysics p 1179 N95-18499

XENON 129
I-Xe studies of individual chondrules: What can they tell us about chondrule formation? p 1192 N95-19329

Y

YAG LASERS
Progress on the multipulse Thomson scattering diagnostic on D3-D
[DE94-017515] p 1143 N95-18119

YANG-MILLS THEORY
Zero modes of first class secondary constraints in gauge theories
[DE94-626659] p 1156 N95-18328

YARNS
Unit cell geometry of multiaxial preforms for structural composites
[NASA-CR-197294] p 971 N95-19650

YAW
Development of a multicomponent force and moment balance for water tunnel applications, volume 2
[NASA-CR-4642-VOL-2] p 1020 N95-18956

YAWING MOMENTS
Static aerodynamics CFD analysis for 120-mm hypersonic KE projectile design
[ARL-MR-184] p 929 N95-18611
Development of a multicomponent force and moment balance for water tunnel applications, volume 1
[NASA-CR-4642-VOL-1] p 1020 N95-18955

YBCO SUPERCONDUCTORS
Fabrication of biaxially oriented YBCO on (001) biaxially oriented yttria-stabilized-zirconia on polycrystalline substrates
[DE94-014808] p 1148 N95-18064
Deformation of high-temperature superconductors
[DE94-017085] p 1150 N95-19075

YIELD POINT
Fatigue life until small cracks in aircraft structures: Durability and damage tolerance p 936 N95-19478

YIELD STRENGTH
International Conference on Deformation, Yield and Fracture of Polymers
[AD-A284354] p 984 N95-18339
The effect of fabrication on corrosion in aluminum 2195: Environmental and microstructural considerations p 982 N95-19011
Microstructurally based variations on the dwell fatgue life of titanium alloy IMI 834 p 938 N95-19489

YTTRIA-STABILIZED ZIRCONIA
Fabrication of biaxially oriented YBCO on (001) biaxially oriented yttria-stabilized-zirconia on polycrystalline substrates
[DE94-014808] p 1148 N95-18064

YTTRIUM OXIDES
Thermal testing of high performance thermal barrier coatings for turbine blades p 955 N95-19681

YTTRIUM-ALUMINUM GARNET
The effect of temperature on the radiative performance of Ho-YAG thin film selective emitters
[NASA-TM-106830] p 1053 N95-18587

Z

ZEOLITES
Embedded microclusters in zeolites and cluster beam sputtering: Simulation on parallel computers
[DE95-000662] p 1134 N95-19562
ZETA PINCH
Advanced concepts theory
[AD-A279212] p 1147 N95-19844
ZINC
Preparation and surface characterization of metal doped alumina catalyst
[PB94-175296] p 973 N95-17991
Evaluation of inorganic zinc-rich primers using Electrochemical Impedance Spectroscopy (EIS) in combination with atmospheric exposure
p 977 N95-18170
Polyurethane self-priming topcoats
[AD-D016264] p 984 N95-18320
Composite structures having organic matrices and duplex zinc/ceramic fire barriers
[AD-D016232] p 970 N95-18629
Polyurethane self-priming topcoats
[AD-D016234] p 985 N95-18631
ZINC SELENIDES
High-pressure studies of deep impurities in GaAs, ZnSe, and related layered structures p 1150 N95-18908
IR materials producibility
[AD-A284263] p 1142 N95-19732
ZINC TELLURIDES
IR materials producibility
[AD-A284263] p 1142 N95-19732
ZIRCONIUM
A review of nuclear thermal propulsion carbide fuel corrosion and key issues
[NASA-CR-197533] p 1136 N95-18217
Hyperfine splittings, prepulse technique, and other new results for collisional excitation neon-like x ray lasers
[DE94-016443] p 1038 N95-19247
ZIRCONIUM ALLOYS
Nonstoichiometry of Al-Zr intermetallic phases
[DE94-016877] p 979 N95-19093
ZIRCONIUM OXIDES
Composite structures having organic matrices and duplex zinc/ceramic fire barriers
[AD-D016232] p 970 N95-18629
Quality optimization of thermally sprayed coatings produced by the JP-5000 (HVOF) gun using mathematical modeling p 989 N95-19008
Ion mixing in oxide-sapphire systems
[DE94-018660] p 1133 N95-19232
Thermal testing of high performance thermal barrier coatings for turbine blades p 955 N95-19681
ZODIACAL DUST
IRAS observations show that the Earth is embedded in a solar ring of asteroidal dust particles in resonant lock with the planet p 1182 N95-19181

PERSONAL AUTHOR INDEX

Typical Personal Author Index Listing

ACKERMAN, PHILLIP L. ..... p 147 N95-10536

PERSONAL AUTHOR | PAGE NUMBER | ACCESSION NUMBER

Listings in this index are arranged alphabetically by personal author. The page number helps you locate the citation in the abstract section. The accession number denotes the number by which the citation is identified.

A

AAGEDAL, J. O. ..... p 1003 N95-19411
AARLIEN, R. ..... p 992 N95-18667
ABBUD-MADRID, ANGEL ..... p 990 N95-18082
ABDALATI, W. ..... p 1062 N95-19779
ABDOU, M. ..... p 1137 N95-19588
ABITA, JOSEPH L. ..... p 979 N95-18630
ABLOWITZ, MARK J. ..... p 1075 N95-19523
ABNEY, DARRELL T. ..... p 1141 N95-18560
ABRAMS, M. J. ..... p 1131 N95-18473
ABREU, LEONARD W. ..... p 1142 N95-19862
ABUMERI, GALIB ..... p 1046 N95-19501
ACEVEDO, TERESA ..... p 1001 N95-19069
ACKELSON, STEVE ..... p 1073 N95-19701
ACKERMAN, THOMAS P. ..... p 1066 N95-19129
ADAMS, C. ..... p 1148 N95-18064
ADAMS, D. G. ..... p 1098 N95-18652
ADAMS, G. L. ..... p 1139 N95-18342
ADAMS, R. G. ..... p 1133 N95-19199
ADKINS, SUSAN L. ..... p 1175 N95-18936
AGARAWALA, S. ..... p 978 N95-18332
AGARWAL, R. K. ..... p 943 N95-18483
p 960 N95-19271
AGARWALA, VINOD S. ..... p 979 N95-18458
p 1033 N95-18524
AGER, J. W., III ..... p 976 N95-19836
AGGARWAL, J. K. ..... p 1091 N95-18086
AGRAWAL, SANJAY ..... p 990 N95-18211
AGRELL, JOHAN ..... p 932 N95-19260
AGRELL, NADA ..... p 1023 N95-19264
AHMAD, I. ..... p 1135 N95-19787
AHRENS, T. J. ..... p 1181 N95-19176
AHRENS, THOMAS J. ..... p 1060 N95-19033
AHUJA, K. K. ..... p 1123 N95-18930
AIBEL, DAVID W. ..... p 966 N95-18196
AL-KURD, AZMI ..... p 1123 N95-18083
ALARAINI, SULAIMAN A. ..... p 1092 N95-19627
ALBEE, A. L. ..... p 1180 N95-19173
p 1181 N95-19174
p 1122 N95-19195
ALBER, ELLIOTT SOLOMON ..... p 1150 N95-18928
ALBRECHT, J. D. ..... p 1152 N95-19620
ALBRIGHT, K. ..... p 1034 N95-19229
ALEXANDER, C. M. O. ..... p 1186 N95-19290
ALEXANDER, J. IWAN D. ..... p 1195 N95-17980
ALEXANDER, W. M. ..... p 1181 N95-19175
p 1036 N95-19193
ALEXANDRATOS, S. D. ..... p 984 N95-18355
ALFORD, CECIL O. ..... p 996 N95-18386
ALGE, T. L. ..... p 951 N95-19660
ALI, R. ..... p 1135 N95-19787
ALKHOZAM, ABDULLAH M. ..... p 930 N95-18669
ALLAIRE, P. E. ..... p 927 N95-18197
p 927 N95-18486
ALMOSNINO, D. ..... p 933 N95-19282
ALOIMONOS, YIANNIS ..... p 1088 N95-18094
p 1140 N95-18478
p 1140 N95-18480
ALPERINE, S. ..... p 954 N95-19676
ALVAREZ, RUBEN A. ..... p 989 N95-19826
ALVERO, L. ..... p 1135 N95-19726
ALVES, G. A. ..... p 1130 N95-18366
AMATO, S. ..... p 1130 N95-18366
AMBROSE, K. R. ..... p 1080 N95-19244
AMBUR, MANJULA Y. ..... p 1175 N95-18936
AMIN, ASHOK T. ..... p 1007 N95-18968
AMUSIA, M. Y. ..... p 1130 N95-18427
ANDERSEN, HARALD T. ..... p 1083 N95-19429
ANDERSEN, VICTOR A. ..... p 995 N95-18315
ANDERSON, DAVID N. ..... p 934 N95-19284
p 934 N95-19285
ANDERSON, JOHN E. ..... p 1051 N95-18614
ANDERSON, KARL F. ..... p 1033 N95-18735
p 1011 N95-18959
ANDERSON, KENNETH D. ..... p 1072 N95-19521
ANDERSON, LOREN A. ..... p 1157 N95-18166
ANDERSON, RICHARD ..... p 1142 N95-18969
ANDERSON, T. ..... p 991 N95-17934
ANDERSON, WESTON J. ..... p 1075 N95-18617
ANDERSON, WILLIAM W. ..... p 1181 N95-19176
ANDRAWIS, ALFRED S. ..... p 1142 N95-18167
ANDRES, R. J. ..... p 1061 N95-19556
ANJOS, J. C. ..... p 1130 N95-18366
ANNIS, CHARLES ..... p 978 N95-18068
ANTAR, BASIL N. ..... p 991 N95-18970
ANTLEY, MICHAEL ..... p 944 N95-18726
ANTONIO, JOHN K. ..... p 1109 N95-18106
APPEL, J. A. ..... p 1130 N95-18366
APRUZESE, JOHN P. ..... p 1039 N95-19845
ARCHAMBAUD, J. P. ..... p 1025 N95-19276
ARENDT, P. ..... p 1148 N95-18064
ARENS, YIGAL ..... p 1176 N95-19604
ARGE, E. ..... p 1099 N95-18668
ARGEMIRODECARVALHOPAIVA, JOAO
p 1050 N95-18214
ARMERO ROVIRA, FRANCISCO ..... p 1122 N95-18916
ARMSTRONG, ROSE MARIE ..... p 1097 N95-18422
ARMSTRONG, RUSSELL ..... p 1064 N95-18452
ARMSTRONG, T. R. ..... p 1054 N95-19591
ARNOLD, STEVEN M. ..... p 972 N95-19782
ARTS, TONY ..... p 1021 N95-19257
ASARO, R. J. ..... p 980 N95-19400
ASH, R. D. ..... p 1186 N95-19291
ASHILL, P. R. ..... p 1022 N95-19262
ASOKA-KUMAR, P. ..... p 1055 N95-19858
ASVELD, P. R. J. ..... p 1094 N95-18000
ATLURI, S. N. ..... p 1047 N95-19804
ATLURI, SATYA N. ..... p 937 N95-19485
ATREYA, ARVIND ..... p 990 N95-18211
AUER, SIEGFRIED ..... p 1181 N95-19177
p 966 N95-19178
AURAND, J. F. ..... p 1004 N95-19555
AUTEN, T. A. ..... p 979 N95-18934
AUTREY, S. T. ..... p 1134 N95-19590
AWAD, HISHAM ..... p 1111 N95-19526
AWERBUCH, BARUCH ..... p 1117 N95-18658
AYER, T. C. ..... p 949 N95-19381
AYERS, BERT F. ..... p 1020 N95-18955
p 1020 N95-18956
AYGUNES, HALUK ..... p 1044 N95-18363
AZAR, YOSSI ..... p 1117 N95-18658
AZMY, Y. Y. ..... p 1116 N95-18131
AZOFRA, JOSE A. ..... p 1081 N95-19418
p 1084 N95-19434
p 1086 N95-19440

B

BAAKLINI, GEORGE Y. ..... p 1043 N95-18583
BABBITT, N., III ..... p 962 N95-18932
BABUSKA, I. ..... p 1117 N95-18482
BACRY, H. ..... p 1134 N95-19376
BAGGETT, J. C. ..... p 1083 N95-19426
BAHM, CATHERINE M. ..... p 945 N95-19044
BAILEY, DEAN A. ..... p 1081 N95-19416
BAILEY, J. E. ..... p 1133 N95-19199
BAILEY, JEFF ..... p 1068 N95-18093
BAINS, JANE C. ..... p 939 N95-19499
BAIRD, M. D. M. ..... p 1123 N95-18566
BAKER, J. E. ..... p 1051 N95-18556
BAKKES, J. A. ..... p 1057 N95-18002
BALASUBRAMANIA, NAGARAJAN
p 1049 N95-17971
BALDERSON, KEITH A. ..... p 958 N95-18405
BALDWIN, JOHN R. ..... p 973 N95-17994
BALDWIN, RYAN A. ..... p 1154 N95-19806
BALKAN, SERHAT ..... p 1113 N95-18023
BALKO, BOHDAN ..... p 1037 N95-18382
BALLARD, DAN ..... p 1107 N95-19767
BALLARD, RODNEY W. ..... p 1092 N95-18569
BALLING, R. J. ..... p 1116 N95-18108
p 1116 N95-18109
BALSA, THOMAS F. ..... p 1016 N95-18212
BANDYOPADHYAY, PROMODE R. ..... p 928 N95-18337
BANERGEE, PRITHVIRAJ ..... p 1095 N95-18079
BANFORD, MICHAEL ..... p 957 N95-18641
BANGERTER, R. ..... p 1137 N95-19588
BANNINK, W. J. ..... p 932 N95-19259
BANSAL, B. ..... p 1190 N95-19320
BARBEE, T. ..... p 1034 N95-19233
BARCHET, W. R. ..... p 1049 N95-18145
BARCLAY, REBECCA O. ..... p 1175 N95-18950
p 1175 N95-18953
p 1175 N95-19038
p 1176 N95-19127
BARKER, WILLIAM P. ..... p 1033 N95-18461
BARKHIMER, R. L. ..... p 1043 N95-19809
BARKYOUMB, JOHN ..... p 1149 N95-18543
BARNES, C. W. ..... p 1143 N95-17969
BARNES, P. R. ..... p 1077 N95-19140
BARNETT, ALAN R. ..... p 1047 N95-19649
BARNETT, M. ..... p 949 N95-19381
BARR, TOM ..... p 1004 N95-19534
BARRETT, RUTH A. ..... p 989 N95-19197
BARRETT, WILLIAM M., JR. ..... p 1061 N95-19686
BARRINGTON, L. M. ..... p 975 N95-19699
p 1073 N95-19712
BARRY, B. C. ..... p 952 N95-19666
BASCIANI, M. ..... p 960 N95-19267
BASKETT, R. L. ..... p 1059 N95-18647
BASORE, P. A. ..... p 1055 N95-19859
BASSO, GORDON L. ..... p 1127 N95-19164
BASU, A. J. ..... p 1028 N95-19459
p 1029 N95-19465
BATCHELOR, D. B. ..... p 1144 N95-18557
BATILL, STEPHEN M. ..... p 1046 N95-19522
BATTEN, CARMEN E. ..... p 1032 N95-18194
BAUER, W. ..... p 1135 N95-19786
BAUERLE, DONALD G. ..... p 995 N95-18136
BAUM, HOWARD R. ..... p 990 N95-18211
BAUM, K. ..... p 983 N95-18019
BAYERDOERFER, G. ..... p 960 N95-19150
BAYERDORFER, G. ..... p 1127 N95-19160
BEACH, R. J. ..... p 1039 N95-19508
BEAN, BRENT L. ..... p 1141 N95-19085
BEASLEY, R. A. ..... p 1067 N95-18038
BECHTOLD, R. ..... p 1108 N95-19803
p 1108 N95-19813
BECK, FRED B. ..... p 995 N95-18187
BECK, J. P. ..... p 1058 N95-18375
BECK, N. J. ..... p 1043 N95-19809
BECKS, EDWARD A. ..... p 1035 N95-19794
BEDOYA, CARLOS A. ..... p 1034 N95-19236
BEEKLEY, MATT ..... p 1079 N95-18661
BEERSMA, JULES J. ..... p 1070 N95-18393
BEETS, A. L. ..... p 1080 N95-19244
BEHNE, D. M. ..... p 1146 N95-19379
BEIERSDORFER, P. ..... p 1038 N95-19248
BELALA, Y. ..... p 1105 N95-19751
BELL, C. P. ..... p 1001 N95-19051
BELL, KENNETH L. ..... p 1129 N95-18062
BELL, P. M. ..... p 1033 N95-18555
p 1035 N95-19711
BELL, R. ..... p 1133 N95-19228
BELLATRECCIA, ANDREA ..... p 1083 N95-19430
BELLI, ANTONIO ..... p 1083 N95-19430
BENCIC, TIMOTHY J. ..... p 1035 N95-19794
BENEMANI, J. R. ..... p 1054 N95-19554
BENETT, W. J. ..... p 1039 N95-19508
BENN, KAREN P. ..... p 1088 N95-18971
BENNER, WILLIAM E. ..... p 941 N95-18088
BENNETT, BONNIE H. ..... p 1107 N95-19764

BENNEY, RICHARD J. p 928 N95-18340
BENOIT, ANDRE p 941 N95-18927
BENOIT, P. H. p 1192 N95-19328
BENOY, PATRICIA A. p 969 N95-18448
BERDING, M. A. p 1142 N95-19732
BERK, H. L. p 1133 N95-19078
BERLANGA, FELICIA p 1106 N95-19758
BERLINCOURT, TED G. p 1009 N95-18433
BERMAN, DAVID H. p 1123 N95-18890
BERNHARD, R. P. p 1047 N95-19185
BERNS, ANITA p 1097 N95-18449
BERNSTEIN, EDWARD L. p 1047 N95-18972
BERRE, A. J. p 1003 N95-19411
BERRY, H. G. p 1135 N95-19786
p 1135 N95-19787
BERTACHINIDEALMEIDAPRADO, ANTONIO
FERNANDO p 961 N95-18900
BERTAMINI, L. p 955 N95-19681
BERTRAN, P. E. p 1082 N95-19422
BERTUCCIOLI, LUCA p 1021 N95-19256
BESSETTE, RUSSELL R. p 1008 N95-18318
BEST, MICHAEL p 1110 N95-18521
BESTER, TERRI p 1106 N95-19760
BETTS, R. R. p 1007 N95-17961
BEUTNER, THOMAS J. p 1023 N95-19266
BHANSIN, CHARLOTTE A. p 1092 N95-19627
BHATTACHARYA, PRABIR p 1117 N95-18511
BIAGIONI, EDOARDO S. p 1099 N95-18676
BIANCONI, PATRICIA A. p 969 N95-17941
BIBRING, J.-P. p 1181 N95-19179
p 1183 N95-19188
BIDWELL, COLIN S. p 933 N95-18582
BIEGEL, JOHN E. p 1105 N95-19753
BIENKOWSKI, P. R. p 1134 N95-19557
BIGELOW, C. A. p 1047 N95-19804
BILANIN, ALAN J. p 934 N95-19285
BILLHARTZ, TOM p 1115 N95-19512
BINIENDA, WIESLAW K. p 972 N95-19782
BIONTA, R. p 1034 N95-19233
BIRMAN, KENNETH P. p 1110 N95-18532
BISCHOFF, A. p 1189 N95-19315
BISHOP, ANN PETERSON p 1109 N95-18055
BISWAS, RUPAK p 1043 N95-18737
BLACKBURN, JAMES C. p 998 N95-18520
BLACKER, TED D. p 1118 N95-18896
BLAIN, C. A. p 1075 N95-19540
BLAKELY, J. p 979 N95-18358
BLANCHARD, P. p 1172 N95-18040
BLAUCH, DAVID N. p 974 N95-19515
BLES, WILLEM p 1083 N95-19427
BLEVINS, ROBERT D. p 1047 N95-19161
BLIVEN, LARRY F. p 1069 N95-18208
BLOCH, J. p 964 N95-18639
BLOOM, E. E. p 982 N95-19725
BLOOM, I. p 1053 N95-19074
p 1053 N95-19115
p 1053 N95-19116
p 1054 N95-19117
BLOOM, S. H. p 1139 N95-18409
BLUM, AVRIM p 1117 N95-18658
BLUM, FRANK D. p 972 N95-19814
BLUMBERG, W. A. p 977 N95-19868
BLUMENTHAL, PHILIP Z. p 1035 N95-19794
BOBIS, J. P. p 1012 N95-19246
BOCK, TOM p 1097 N95-18423
BODE, TODD D. p 1195 N95-19739
BODEN, THOMAS A. p 1058 N95-18389
BODIS, JAMES R. p 1043 N95-18583
BODSBERG, L. p 1092 N95-19412
BODTKER, E. p 1036 N95-18061
BOEHM, F. p 1132 N95-18644
BOER, RUUD G. DEN p 928 N95-18380
BOETTGER, J. C. p 988 N95-19721
BOFFA, A. B. p 975 N95-19616
BOHNHOFF, WILLIAM J. p 1118 N95-18896
BOLCH, WESLEY E. p 964 N95-18495
BOLING-RISSER, M. A. p 1150 N95-19094
BOLTON, P. R. p 1039 N95-19398
BOLTON, S. R. p 1036 N95-18123
BOLUS, R. p 999 N95-18657
BONANI, G. p 1059 N95-18666
BONCEK, RAYMOND K. p 1138 N95-18067
BONIN, RICHARD L. p 1041 N95-18317
BONNET, A. p 933 N95-19279
BOOK, SCOTT A. p 1094 N95-18015
BOOKER, A. I. E. p 1003 N95-19136
BOOKER, J. R. p 1063 N95-17967
BORDUNOV, A. V. p 969 N95-19822
BORG, J. p 1181 N95-19179
p 1183 N95-19188
BORGEN, GARY S. p 1011 N95-19171
BOS, JELTE E. p 1083 N95-19427
BOSS, A. P. p 1186 N95-19292
BOSWELL, ERNEST H., JR. p 1174 N95-18654
BOTTS, MICHAEL p 1068 N95-18093
BOULAY, WILLIAM p 1090 N95-18077
BOUMSELLEK, SAID p 1130 N95-18324
BOURCIER, R. J. p 1114 N95-18649
BOUROT-DENISE, M. p 1193 N95-19338
BOUWMAN, A. F. p 1058 N95-18375
BOVIK, ALAN p 1140 N95-18509
BOWDEN, BRIAN E. p 1065 N95-19086
BOWEN, BARRY C. p 963 N95-18047
p 963 N95-19790
BOWER, E. A. p 1081 N95-19417
BOWER, LESLIE ANNE p 1173 N95-18099
BOWES, ROBERT J. p 1097 N95-18420
BOWLES, KENNETH J. p 981 N95-19652
BOWMAN, W. A. p 981 N95-19703
BOYD, I. p 931 N95-19109
BOYDEN, R. P. p 1099 N95-18899
BOYER, ERIC B. p 1003 N95-19525
BOZIK, D. p 979 N95-18934
BRACKER, S. B. p 1130 N95-18366
BRACKETT, J. p 1108 N95-19803
p 1108 N95-19813
BRADLEY, D. K. p 1033 N95-18555
p 1146 N95-19509
p 1035 N95-19711
BRADSHAW, JERALD S. p 969 N95-19822
p 969 N95-19823
BRADY, D. K. p 1071 N95-18607
BRAINARD, RUSSELL E. p 1074 N95-18012
BRAKER, J. G. p 1118 N95-19169
BRANCH, MELVYN C. p 990 N95-18082
BRAY, G. H. p 939 N95-19496
BREARLEY, A. J. p 1186 N95-19293
BRECHUE, WILLIAM p 1079 N95-18661
BREDEMANN, M. V. p 1174 N95-18873
BREDESEN, R. p 973 N95-18377
BREITSAMTER, CHRISTIAN p 932 N95-19261
BRENNAN, SEAN p 945 N95-19731
BRENNER, GUNTHER p 1019 N95-18609
BREWER, WILLIAM V. p 966 N95-18168
BRICKA, R. M. p 1062 N95-19808
BRIDGES, SUSAN p 1105 N95-19752
BRIGHTWELL, P. J. p 1001 N95-19051
BRINK-SPALINK, J. p 956 N95-18600
BRINKER, DAVID J. p 967 N95-18571
BRINKMAN, C. R. p 987 N95-19399
BRITT, VICKI O. p 939 N95-19499
BROERS, B. p 1051 N95-18372
BROMAN, L. p 1052 N95-17945
BRONIKOWSKI, M. p 976 N95-19824
BROPHY, JOHN R. p 1137 N95-18957
BROWN, DANSEN p 957 N95-18641
BROWN, DAVID A. p 1141 N95-18563
BROWN, E. p 1197 N95-18351
BROWN, GAIR D. p 1141 N95-18628
BROWN, J. C. p 1176 N95-19589
BROWN, KENNETH G. p 1032 N95-18194
BROWN, R. p 971 N95-19386
BROWN, STEVE WESLEY p 965 N95-19237
p 965 N95-19624
BROWNING, R. p 1010 N95-18625
BROWNLEE, DON E. p 1180 N95-19173
BRUCATO, ROBERT p 947 N95-18383
BRUCE, C. W. p 1139 N95-18142
BRUNEKREEF, J. p 1109 N95-18039
BRUNER, CHRISTOPHER W. p 1017 N95-18406
BRYAN, KURT p 1117 N95-18479
BRYSON, TRAVIS p 1107 N95-19767
BUCCI, R. J. p 939 N95-19496
BUCHERT, T. p 1121 N95-19348
BUCHHEIT, R. G. p 977 N95-17968
BUCINELL, RONALD B. p 972 N95-18973
BUCK, M. E. p 1055 N95-19859
BUCKLEY-GEER, E. p 1135 N95-19835
BUECHLER, DENNIS p 1068 N95-18093
BUISHAND, T. A. p 1070 N95-18392
BUKOV, A. p 1025 N95-19274
BULL, WILLIAM B. p 967 N95-19566
BUNCH, T. E. p 1191 N95-19322
BUNKER, B. C. p 986 N95-18648
BURCHAM, GARY A. p 1141 N95-18628
BURCHELL, MARK J. p 961 N95-19180
BURDETTE, GEORGE W. p 990 N95-19090
BURKARDT, M. p 1131 N95-18554
BURKE, ROBERT W. p 973 N95-17994
BURLATON, J. P. p 1082 N95-19422
p 1082 N95-19424
BURNETT, DONALD S. p 1180 N95-19173
BURNETTE, KEITH T. p 947 N95-18164
BURNHAM, D. p 929 N95-18624
BURNS, I. F. p 931 N95-19546
BURNS, WILLIAM K. p 1034 N95-19124
BURNSIDE, O. HAL p 939 N95-19493
BURRIS, STEPHEN A. p 944 N95-18616
BURT, MARTIN p 932 N95-19260
BUSCH, KATHRYN A. p 1051 N95-18465
BUSCIGLIO, HENRY H. p 1088 N95-18095
BUSHNELL, CHRISTOPHER J. p 996 N95-18359
BUSSONNET, P. X. p 953 N95-19669
BUTTRAM, M. T. p 1004 N95-19555
BUTTS, D. G. p 936 N95-19480
BUXTON, WINSLOW HURLBURT p 1173 N95-18096
BYERS, ROBERT M. p 1043 N95-18169
BYSTRITSKIJ, V. M. p 1132 N95-18884

C

CAGLE, LARRY p 1043 N95-19593
CAI, YUN-JIA p 971 N95-19650
CAIN, ALAN B. p 946 N95-19154
CAIRNS, MARY M. p 1066 N95-17952
CALDEIRA, HERALDO SOARES p 1050 N95-18215
CALDWELL, CURTIS I. p 1120 N95-18672
CALDWELL, JOHN A., JR. p 1090 N95-19564
CALDWELL, R. p 1173 N95-18063
CALLE, LUZ M. p 977 N95-18170
CAMACHO, Y. p 946 N95-18601
CAMAIONI, D. M. p 1134 N95-19590
CAMP, WARREN p 1157 N95-18166
CAMPBELL, A. A. p 986 N95-18648
CAMPBELL, BRYAN A. p 1175 N95-18936
CAMPBELL, C. WARREN p 1014 N95-18974
CAMPBELL, L. J. p 1011 N95-19200
CANRIGHT, G. S. p 1122 N95-18127
CANTON, JUAN J. p 1081 N95-19418
p 1086 N95-19440
CAO, JIANSHU p 1157 N95-19852
p 1157 N95-19853
CAPRIOLA, S. J. p 1072 N95-19581
CARDENASAMORES, JORGE A. p 1068 N95-18114
CARDINAL, DONNA p 1087 N95-19811
CARDINAL, JOSEPH W. p 939 N95-19493
CARDOSI, KIM M. p 996 N95-18436
CAREW, THOMAS J. p 1088 N95-18401
CARIAPA, VIKRAM p 994 N95-18975
CARL, JAMES A. p 1089 N95-18403
CARLIOZ, R. p 1082 N95-19422
CARLOS, R. p 1063 N95-18148
CARLOS, R. C. p 1063 N95-18125
CARLSON, N. W. p 1039 N95-19508
CARLSON, R. L. p 937 N95-19487
CARLSTROM, T. N. p 1143 N95-18119
CARPENTER, J. p 1039 N95-19551
CARR, ERIC p 1099 N95-19027
CARROLL, FRANK T. p 955 N95-19684
CARROLL, THOMAS L. p 1010 N95-18528
CARTER, R. G. p 1096 N95-18354
CARTER, SUSAN p 1050 N95-18078
p 1052 N95-19733
CARUSO, F. p 1130 N95-18356
CASALENGUA, J. p 946 N95-18601
p 1126 N95-19155
CASON-SMITH, D. M. p 1007 N95-17959
CASSEN, P. p 1186 N95-19294
CASTRUP, HOWARD T. p 992 N95-18745
CAUDILL, LESTER F., JR. p 1117 N95-18479
CAUFFMAN, D. P. p 966 N95-19189
CAUGHMAN, J. B. O. p 999 N95-18558
CAVANAGH, PATRICK p 1093 N95-17940
CEBULA, RICHARD P. p 1196 N95-18954
CELIK, ZEKI Z. p 1023 N95-19266
CELIO, PAUL V. p 1085 N95-19437
p 1085 N95-19438
CENGELOGLU, YILMAZ p 1108 N95-19768
CENTENO, MARTHA A. p 1158 N95-18171
CHADWICK, J. p 999 N95-18657
CHAHINE, GEORGES L. p 1017 N95-18434
CHAMDANI, J. I. p 996 N95-18386
CHAMIS, C. C. p 953 N95-19672
CHAMIS, CHRISTOS C. p 1046 N95-19501
CHAMPAGNE, FRANK H. p 1018 N95-18469
CHAN, K. S. p 1044 N95-18081
CHAN, S. H. p 1014 N95-18092
CHANDRASEKARAN, A. p 1014 N95-19634
CHANDY, K. M. p 1112 N95-19692
CHANG, B. p 1060 N95-18895
CHANG, CHIA-BO p 1073 N95-18172
CHANG, CHUNG-JEN p 964 N95-18163
CHANG, CHUNGCHU p 1045 N95-18917
CHANG, KAI p 1106 N95-19760
CHANG, LANG-MANN p 976 N95-19729
CHANG, LANG-MANNN p 1033 N95-18620
CHANG, SIN-CHUNG p 1014 N95-18036
CHANG, Y. W. p 1020 N95-19098
CHAPPELL, CHARLES R. p 1161 N95-18967
CHATURVEDI, SUSHIL K. p 1032 N95-18316
CHEMLA, D. S. p 1148 N95-18122
p 1036 N95-18123
CHEN, CHARLES C. p 940 N95-19805
CHEN, GUANGQING p 1060 N95-19033
CHEN, JUN p 1066 N95-17952
CHEN, LIANG-CHUN p 1105 N95-19752
CHEN, NAN p 1150 N95-19075

CHEN, P. C. ..... p 1112 N95-17948
CHEN, TONY T. D. ..... p 1032 N95-18316
CHEN, X. ..... p 976 N95-19825
CHENG, ANDREW F. ..... p 1194 N95-19575
CHENG, S. ..... p 1135 N95-19786
p 1135 N95-19787
CHIEN, C. H. ..... p 1111 N95-18892
CHIKARAISHI, HIROTAKA ..... p 1012 N95-19548
CHILDS, P. N. ..... p 1030 N95-19774
CHILDS, PAUL N. ..... p 1030 N95-19506
CHINCHECK, ELAINE ..... p 1005 N95-19694
CHINN, C. R. ..... p 1116 N95-18120
CHIU, CHING-SANG ..... p 1074 N95-18153
CHIU, W. K. ..... p 971 N95-19467
CHOE, JOON ..... p 997 N95-18462
CHOI, CHAN K. ..... p 1144 N95-18888
CHOI, I. H. ..... p 1152 N95-19585
CHOU, LUCIA W. ..... p 1074 N95-18160
CHOUDHURY, RAJKUMAR ROY ..... p 1156 N95-18352
CHOW, R. ..... p 987 N95-19227
CHRIEN, R. E. ..... p 1143 N95-17969
CHU, BEN ..... p 988 N95-19696
CHU, F. ..... p 981 N95-19611
CHU, TSUCHIN ..... p 966 N95-18976
CHUBB, DONALD L. ..... p 1053 N95-18587
CHUN, H. J. ..... p 970 N95-18940
CHUNG, H. M. ..... p 982 N95-19725
CHUTJIAN, ARA ..... p 1130 N95-18324
CHY, TAK-KIN ..... p 1149 N95-18527
CIALONE, MARY A. ..... p 1074 N95-18160
CIMPOERU, S. J. ..... p 1045 N95-18472
CINTALA, MARK J. ..... p 1047 N95-19185
CLARK, C. M. ..... p 941 N95-17953
CLARK, JOHN H. E. ..... p 1073 N95-18977
CLEMENS, P. ..... p 962 N95-18932
CLERE, J. M. ..... p 1082 N95-19424
CLEVELAND, J. P. ..... p 1129 N95-17974
CLIFT, SIMON S. ..... p 1118 N95-18736
CLIMENT, H. ..... p 946 N95-18601
p 1126 N95-19155
CLOUGH, R. L. ..... p 986 N95-18651
COATS, TIMOTHY WILLIAM ..... p 971 N95-19043
COCHRAN, FREDERICK L. ..... p 1147 N95-19846
COCHRAN, H. D. ..... p 1134 N95-19557
COCKRELL, C. R. ..... p 995 N95-18187
COCKS, F. H. ..... p 1053 N95-18894
COFFEY, H. T. ..... p 1122 N95-19704
COFFEY, HELEN E. ..... p 1196 N95-19404
p 1196 N95-19405
COGAN, JAMES L. ..... p 1068 N95-18117
COHEN, J. D. ..... p 1151 N95-19541
COHEN, S. J. ..... p 1039 N95-19507
COHEN, W. ..... p 1007 N95-17999
COLE, M. J. ..... p 961 N95-19180
COLE, N. C. ..... p 981 N95-19723
COLES, WILLIAM A. ..... p 1004 N95-19547
COLLINS, LAURIE ..... p 1068 N95-18093
COLLINS, S. R. ..... p 1056 N95-19882
COMPTON, MICHAEL M. ..... p 1101 N95-19632
p 1103 N95-19643
CONG, L. ..... p 1152 N95-19620
CONGER, K. A. ..... p 1087 N95-19698
CONNOLLY, H. C., JR. ..... p 1186 N95-19295
p 1187 N95-19302
p 1193 N95-19337
p 1193 N95-19338
CONNOLLY, JAMES P. ..... p 1092 N95-18569
CONROY, TRACY MICHAEL ..... p 1173 N95-18096
CONTOPANAGOS, H. ..... p 1135 N95-19726
CONTRERAS, M. A. ..... p 1055 N95-19858
COOK, JOSEPH S., JR. ..... p 992 N95-18738
COOK, R. ..... p 1108 N95-17936
COOK, R. L. ..... p 973 N95-17982
COOPER, L. Y. ..... p 993 N95-19402
COOPER, THOMAS D. ..... p 945 N95-19517
COPELAND, CARL E. ..... p 960 N95-18961
p 1011 N95-18962
CORBETT, J. ..... p 1138 N95-19841
CORBUS, D. ..... p 1056 N95-17943
CORMACK, LAWRENCE ..... p 1140 N95-18509
CORNWELL, JOHN D. ..... p 1017 N95-18323
CORTES, RICARDO ..... p 1096 N95-18344
CORTESE, ALEJANDRO ..... p 1050 N95-18216
COUGHLAN, DANETTE ..... p 1052 N95-19733
COULTON, DAVID G. ..... p 932 N95-19772
COULTRIP, ROBERT H. ..... p 960 N95-18961
p 1011 N95-18962
COURNOYER, RONALD C., JR. ..... p 994 N95-18058
COURTRIGHT, WILLIAM V., II ..... p 1093 N95-18659
COWARD, ADRIAN ..... p 1016 N95-18190
COX, LARRY T., JR. ..... p 1144 N95-18888
CRANE, ELIZABETH A. ..... p 1043 N95-18583
CRANE, ROGER M. ..... p 970 N95-18629
CRAVEN, D. A. ..... p 960 N95-19848
CRAVEY, ROBIN L. ..... p 1005 N95-19781
CREAGER, MATTHEW ..... p 940 N95-19500
CREASMAN, F. ..... p 960 N95-19271
CREMALDI, L. M. ..... p 1130 N95-18366
CREMERS, D. A. ..... p 1036 N95-18126
CRESPO, ANTONIO ..... p 1139 N95-18154
CRIM, F. F. ..... p 1134 N95-19597
CRITES, R. C. ..... p 1021 N95-19252
p 960 N95-19271
CRITTENDEN, ROBERT GLEN ..... p 1179 N95-18496
CROSS, L. E. ..... p 1128 N95-19850
CROWE, W. R. ..... p 1004 N95-19555
CSANADI, OSWALD I. ..... p 1010 N95-18546
CUEVAS, ALFREDO ..... p 1084 N95-19434
CUMMINS, R. J. ..... p 1127 N95-19162
CUNNINGHAM, ATLEE M., JR. ..... p 928 N95-18380
CUOMO, FRANK W. ..... p 1140 N95-18460
CURETON, K. L. ..... p 956 N95-18567
CURFMAN, BRIAN ..... p 1095 N95-18033
CURRAN, SCOTT A. ..... p 1063 N95-17946
CURRIE, T. C. ..... p 952 N95-19666
CURRY, JAMES H. ..... p 1075 N95-19523
CURTIS, L. J. ..... p 1135 N95-19787
CUTLER, J. N. ..... p 974 N95-18744
CUTSHALL, JON T. ..... p 939 N95-19493
CUZZI, J. N. ..... p 1187 N95-19296
CYGAN, M. T. ..... p 1131 N95-18473

D

DAEHLEN, M. ..... p 1117 N95-18374
DAGLEY, IAN J. ..... p 990 N95-19505
DAHL, PETER H. ..... p 1123 N95-18083
DAHLBURG, JILL P. ..... p 1146 N95-19527
DAILY, J. W. ..... p 990 N95-18082
DAINTY, J. C. ..... p 1139 N95-18404
DALE, M. C. ..... p 974 N95-18637
DALLE-MURA, E. ..... p 1125 N95-19147
DALRYMPLE, BRUCE J. ..... p 1009 N95-18432
DAMIAO, DARCTON POLICARPO
p 1049 N95-18005
DAMOUR, T. ..... p 1118 N95-19375
p 965 N95-19377
DAMPIER, DAVID A. ..... p 1094 N95-18017
DANE, C. B. ..... p 1037 N95-18357
DANESE, D. ..... p 1082 N95-19421
DANIEL, I. M. ..... p 970 N95-18940
DANIELS, T. S. ..... p 1099 N95-18899
DANIELSON, ARNOLD O. ..... p 967 N95-19073
DARLING, C. L. ..... p 1130 N95-18366
DARLING, STEPHEN R. ..... p 1090 N95-19564
DART, PHILIP ..... p 1095 N95-18089
DASILVA, L. B. ..... p 1038 N95-19247
p 1146 N95-19509
DAVIDSON, D. L. ..... p 1044 N95-18081
DAVIES, ELIZABETH ..... p 1104 N95-19688
DAVIS, A. M. ..... p 1187 N95-19297
p 1189 N95-19314
DAVIS, ALAN J. ..... p 995 N95-18314
DAVIS, CHARLES A. ..... p 1000 N95-18671
DAVIS, J. ..... p 1147 N95-19847
DAVIS, J. BRADLEY ..... p 963 N95-18047
p 963 N95-19790
DAVIS, JACK E. ..... p 1074 N95-18160
DAVIS, R. M. ..... p 1000 N95-18727
DAWSON, L. R. ..... p 1151 N95-19235
DAY, TONY ..... p 967 N95-19566
DEARELLANO-LOPEZ, A. R. ..... p 1150 N95-19075
DEBRUNNER, LINDA S. ..... p 1163 N95-18978
DECKER, D. RICHARD ..... p 1106 N95-19757
DECKER, HARRY J. ..... p 1042 N95-19125
DEESE, J. E. ..... p 960 N95-19271
DEFACIO, BRIAN ..... p 996 N95-18411
DEGNAN, KEITH T. ..... p 1051 N95-18465
DEGRAAF, BERND ..... p 1083 N95-19427
DEGREZ, GERARD ..... p 1021 N95-19256
DEHOYOS, DIEGO ..... p 1079 N95-18661
DEIMLER, JIM D. ..... p 1080 N95-19384
p 1080 N95-19385
DEITZER, GERALD F. ..... p 1077 N95-18173
DELAAT, JOHN ..... p 1105 N95-19749
DELAND, MATTHEW P. ..... p 1196 N95-18954
DELEMOS, R. ..... p 991 N95-17934
DELGADO, LEANDRO V. ..... p 1097 N95-18420
DELLACORTE, CHRISTOPHER ..... p 969 N95-18448
DELMARCELLE, THIERRY ..... p 1121 N95-19288
DELOMBARD, RICHARD ..... p 991 N95-19788
DELOOS, M. J. ..... p 1137 N95-19584
DELUCA, DANIEL P. ..... p 978 N95-18068
DELVALLE, JOSE B. ..... p 1081 N95-19418
DEMETRIUS, L. ..... p 1013 N95-19872
DEMIRANDAVILASBOASRAMOSLEITAO, MARIO
p 1057 N95-18003
DEMPSEY, J. L. ..... p 1061 N95-19403
DENISON, G. J. ..... p 1004 N95-19555
DENNIS, R. L. ..... p 1049 N95-18145
DEPASQUALE, WILLIAM ..... p 945 N95-19067
DERMOTT, STANLEY F. ..... p 1182 N95-19181
p 1183 N95-19187
DESAI, S. S. ..... p 933 N95-19457
DESHPANDE, M. D. ..... p 1026 N95-19445
DESHPANDE, MANOHAR D. ..... p 995 N95-18187
DESOURDIS, R. I. ..... p 999 N95-18619
DESOURDIS, ROBERT I. ..... p 1005 N95-19736
DESOUZADUTRA, A. ..... p 1156 N95-18333
DEVAN, J. H. ..... p 978 N95-18121
p 981 N95-19568
DEVOLL, J. R. ..... p 1083 N95-19428
DEWIT, ROLAND ..... p 939 N95-19494
DEY, JISHNU ..... p 1130 N95-18329
p 1156 N95-18352
DHARANI, LOKESH R. ..... p 972 N95-19814
DHAWAN, ATAM P. ..... p 962 N95-18045
p 962 N95-18467
DIANIC, ALLAN V. ..... p 1104 N95-19647
DIAZDELARUBIA, T. ..... p 1137 N95-19588
DIBERARDINO, THOMAS ..... p 985 N95-18430
DICKINSON, J. T. ..... p 1037 N95-18349
p 1037 N95-18350
DICKINSON, STUART C. ..... p 1042 N95-19121
DIDELOT, F. ..... p 1082 N95-19422
DIECKMAN, S. L. ..... p 1012 N95-19246
DIGIANFRANCESCO, A. ..... p 955 N95-19681
DILLARD, ROBERT M. ..... p 1090 N95-19564
DIMARCO, PETER CHARLES ..... p 951 N95-19658
DINGUS, PETER ..... p 966 N95-18196
DINKINS, JAMES R. ..... p 1011 N95-18962
DITTMAR, JAMES H. ..... p 958 N95-18054
DIXON, R. L. ..... p 1130 N95-18366
DIYECHA, AMARNATH P. ..... p 992 N95-18431
DJOMEHRI, M. JAHED ..... p 930 N95-19041
DOBROVOLSKIS, A. R. ..... p 1187 N95-19296
DODELSON, SCOTT ..... p 1180 N95-18964
DOLGIN, D. L. ..... p 1089 N95-18414
DOMINGUEZ-RODRIGUEZ, A. ..... p 1150 N95-19075
DOMINGUEZ, CYNTHIA ..... p 1088 N95-18084
DONAHUE, CHRISTOPHER A. ..... p 1067 N95-18014
DONER, JOHN ..... p 1115 N95-19512
DONIERE, TIMOTHY F. ..... p 962 N95-18045
DONOHOE, S. R. ..... p 932 N95-19259
DOR, J. B. ..... p 1022 N95-19258
DORF, J. D. ..... p 1057 N95-18002
DOUCET, JAMES ..... p 1140 N95-18459
DOWN, M. G. ..... p 950 N95-19654
DOWNER, M. ..... p 1129 N95-17976
DRAGT, A. J. ..... p 1136 N95-18893
DRESS, D. A. ..... p 1099 N95-18899
DRIVER, G. E. ..... p 1092 N95-19502
DRNEVICH, R. F. ..... p 967 N95-18743
DRUY, M. ..... p 988 N95-19614
DU, G. W. ..... p 971 N95-19650
DUDEK, F. E. ..... p 1076 N95-18439
DUFRENE, ROMAN ..... p 1008 N95-18338
p 1009 N95-18425
p 1009 N95-18426
DUMAY, A. C. ..... p 1086 N95-19537
DUNCAN, MICHAEL A. ..... p 1131 N95-18438
DUNFORD, R. W. ..... p 1135 N95-19786
p 1135 N95-19787
DUNGAN, G. D. ..... p 941 N95-17953
DUNIGAN, T. H. ..... p 1109 N95-18129
DUNLOP, J. L. ..... p 1013 N95-19872
DUNN, ROBERT B. ..... p 1004 N95-19565
DUTTA, P. K. ..... p 1029 N95-19460
DUTTA, VIMALA ..... p 1027 N95-19452
DUTTON, ROBERT W. ..... p 1153 N95-19738
DVORAK, A. ..... p 1086 N95-19443
DVORAK, JIRI J. ..... p 1105 N95-19750
DYCK, WALTER ..... p 989 N95-19866

E

EASTWOOD, CHARLES W. ..... p 962 N95-18387
EATON, S. M. ..... p 1174 N95-18872
ECCLES, J. V. ..... p 1064 N95-18452
ECKERT, D. ..... p 933 N95-19281
EDWARDS, B. ..... p 964 N95-18639
EDWARDS, LYNDON ..... p 938 N95-19492
EDWARDS, TONY L. ..... p 1118 N95-18896
EDWARDS, VERNON R. ..... p 951 N95-19656
EGGEN, G. ..... p 992 N95-18667
EHRHART, JOHN E., JR. ..... p 942 N95-18398
EICK, CHRISTOPH F. ..... p 1105 N95-19754
EICKE, WOODWARD G. ..... p 992 N95-18745
EL-GENK, MOHAMED S. ..... p 1136 N95-18217
ELANGOVAN, P. T. ..... p 1127 N95-19160
ELDER, R. L. ..... p 952 N95-19663
ELLIOTT, G. R. ..... p 1174 N95-18873
ELLIOTT, S. R. ..... p 1038 N95-19248
ELLIS, CARLA SCHLATTER ..... p 1110 N95-18521
ELLIS, J. S. ..... p 1059 N95-18647
ELLIS, R. J. ..... p 1135 N95-19709

EMANUEL, M. A. ..... p 1039 N95-19508
EMBURY, JANON F. ..... p 1123 N95-18379
ENG, ANTHONY T. ..... p 984 N95-18320
p 984 N95-18336
p 985 N95-18631
ENGELBERG, MARK L. ..... p 1107 N95-19765
ENGLAR, ROBERT J. ..... p 932 N95-19268
ENTING, I. G. ..... p 1059 N95-18664
ERICKSON, LARRY L. ..... p 930 N95-19041
ERLEBACHER, GORDON ..... p 1020 N95-18958
ERREDE, D. ..... p 1130 N95-18366
ESBENSEN, H. ..... p 1135 N95-19786
ESHLEMAN, VON R. ..... p 1194 N95-18579
ESTEP, JAMES L. ..... p 1096 N95-18343
EVANOFF, J. ..... p 1120 N95-18020
EVANS, R. H. ..... p 997 N95-18494
EVANS, RICHARD H. ..... p 999 N95-18538
EVENMO, K. ..... p 992 N95-18667
EVERETT, WIN ..... p 943 N95-18407
EVERHART, K. ..... p 962 N95-18932
EYLER, JOHN R. ..... p 974 N95-19066
EYSSA, Y. ..... p 1011 N95-19200

F

FACEMIRE, H. J. ..... p 1100 N95-19106
FACEMIRE, HARRY J. ..... p 1097 N95-18421
FALCONER, DAVID A. ..... p 1196 N95-19791
FAN, YUHONG ..... p 1195 N95-18497
FARESE, G. E. ..... p 965 N95-19377
FARGES, C. ..... p 954 N95-19679
FARGUES, MONIQUE P. ..... p 1120 N95-18113
FARHANGDOOST, KHALIL ..... p 935 N95-19474
FASSETT, J. D. ..... p 981 N95-19703
FAURIE, JEAN-PIERRE ..... p 1154 N95-19816
p 1154 N95-19817
FEDOSEYEV, A. ..... p 1195 N95-17980
FEIKEMA, DOUGLAS A. ..... p 968 N95-18979
FEINBERG, R. ..... p 1140 N95-18484
FEINERMAN, A. D. ..... p 1039 N95-19727
FEINLEIB, RICHARD E. ..... p 1003 N95-19516
FELDMAN, PAUL D. ..... p 1177 N95-17981
FELL, C. P. ..... p 977 N95-19868
FELL, PATRICK ..... p 1075 N95-19563
FELLER, DAVID ..... p 1074 N95-18468
FELSHER, HARRY ..... p 964 N95-18495
FENKER, H. C. ..... p 1130 N95-18366
FEREKIDES, C. S. ..... p 1056 N95-19880
FERGUSON, CHRIS J. ..... p 943 N95-18417
FERMAN, M. A. ..... p 1126 N95-19157
FERMUELLER, CORNELIA ..... p 1088 N95-18094
p 1140 N95-18478
p 1140 N95-18480
FERNKRANS, LARS ..... p 1024 N95-19273
FERNOW, R. C. ..... p 1038 N95-19243
FERRANDO, WILLIAM A. ..... p 992 N95-18431
FERREIRA, LUIS GERALDO ..... p 1050 N95-18369
FERREIRA, PAULO LEAL ..... p 1156 N95-18352
FERRIS, J. H. ..... p 1131 N95-18473
FERRY, DAVID K. ..... p 1155 N95-19829
FETTERER, TOM ..... p 1052 N95-19733
FIELD, ROBERT W. ..... p 985 N95-18636
FIELDS, BRIAN D. ..... p 1137 N95-18965
FIELDS, RICHARD J. ..... p 939 N95-19494
FILICE, J. P. ..... p 1004 N95-19547
FILUK, A. B. ..... p 1133 N95-19199
FINK, DAVID W. ..... p 1030 N95-19716
FINKBINE, RONALD B. ..... p 1102 N95-19638
FIRESTONE, ELAINE R. ..... p 1076 N95-19577
FIRTH, J. L. ..... p 1084 N95-19433
FISCHER, PHILIPPE ..... p 1179 N95-18728
FISHER, DAVID T. ..... p 941 N95-18008
FISHER, GEORGE H. ..... p 1196 N95-19034
FLEETER, SANFORD ..... p 955 N95-19864
FLETCHER, J. A. ..... p 998 N95-18535
FLETCHER, LYN E. ..... p 1058 N95-18091
FLETCHER, S. K. ..... p 1120 N95-18653
FLOKAS, VASSILIOS ..... p 1005 N95-19730
FLYNN, GEORGE J. ..... p 1182 N95-19182
FOGARTY, K. M. ..... p 940 N95-19805
FOLTYN, S. ..... p 1148 N95-18064
FOOTE, STEPHEN L. ..... p 1078 N95-18400
FORBES, GREGORY S. ..... p 1073 N95-18174
FORBES, JEFFREY M. ..... p 1066 N95-19105
FORK, R. L. ..... p 1139 N95-18104
FORSMAN, ALEC E. ..... p 1034 N95-19071
FORSMAN, KIMMO ..... p 1112 N95-19834
FORSYTHE, KEITH W. ..... p 1004 N95-19594
FOUNTI, M. ..... p 952 N95-19667
FOX, DENNIS S. ..... p 955 N95-19683
FOX, MATTHEW W. ..... p 1066 N95-19105
FOX, R. J. ..... p 991 N95-19078
FOX, ROBERT L. ..... p 960 N95-18961
p 1011 N95-18962
FRAINIER, RICHARD ..... p 1103 N95-19640
FRALICK, DION T. ..... p 1005 N95-19781
FRANCINI, R. B. ..... p 937 N95-19486
FRANK, THOMAS A. ..... p 1010 N95-18523
FRANSEN, WIEGER ..... p 1060 N95-18722
FRANZ, J. A. ..... p 1134 N95-19590
FRANZ, JUDY R. ..... p 1010 N95-18925
FRASER, M. E. ..... p 977 N95-19868
FRAZIER, MICHAEL ..... p 1043 N95-19593
FRAZIER, S. ..... p 997 N95-18506
FRAZIER, SAM ..... p 933 N95-18507
FRAZIER, SAMUEL ..... p 1000 N95-19035
FRAZIER, SAMUEL J. ..... p 944 N95-18726
FREDERICO, T. ..... p 1130 N95-18329
FREEMAN, L. MICHAEL ..... p 1161 N95-18967
FREEMAN, MATTHEW JACK ..... p 1145 N95-18905
FREER, M. ..... p 1007 N95-17961
FREESTONE, M. M. ..... p 960 N95-19269
FREHLICH, R. G. ..... p 1004 N95-19547
FREITAG, H. PAUL ..... p 1069 N95-18203
FREITAS, B. L. ..... p 1039 N95-19508
FRERY, ALEJANDRO C. ..... p 1050 N95-18216
FREUND, THOMAS G. ..... p 1102 N95-19635
FREUND, W. ..... p 1084 N95-19431
FREUND, WOLFGANG ..... p 1085 N95-19436
FREYBERG, L. ..... p 960 N95-19150
FRICKE, ROBERT W., JR. ..... p 963 N95-18610
FRIEDLAND, S. ..... p 1118 N95-19198
FRIEDMAN, AVNER ..... p 1121 N95-19104
FRISCH, PAUL H. ..... p 1090 N95-18077
FRISCHBIER, J. ..... p 953 N95-19670
FRITSCHE, BENT ..... p 1132 N95-18912
FRONCZEK, CHRIS ..... p 1097 N95-18419
FRULLA, LAURA ..... p 1050 N95-18216
FU, BIAO ..... p 1113 N95-18218
FU, Q. ..... p 1067 N95-17955
FUJITA, T. ..... p 1187 N95-19298
FUJIWARA, A. ..... p 962 N95-19183
FULK, DAVID A. ..... p 1019 N95-18562
FULLER, G. M. ..... p 1198 N95-19283
FULTON, R. D. ..... p 1032 N95-18130
FURMAN, JOSEPH M. ..... p 1089 N95-18403
FURNELL, G. D. ..... p 1005 N95-19771
FYFC, DAVID E. ..... p 1146 N95-19527

G

GABOR, A. M. ..... p 1055 N95-19858
GAETA, R. J., JR. ..... p 1123 N95-18930
GAFFNEY, J. S. ..... p 1056 N95-17944
GAGNE, DENIS ..... p 1107 N95-19763
GALEA, S. C. ..... p 971 N95-19467
GALLAGHER, K. L. ..... p 1081 N95-19417
GALUSHA, LINDA ..... p 1069 N95-18207
GALWAY, ROBIN D. ..... p 933 N95-19280
GANNON, T. ..... p 1119 N95-19717
GARANT, ALAIN ..... p 1107 N95-19763
GARBEY, M. ..... p 1116 N95-17977
GARCIA-AVELLO, C. ..... p 941 N95-18927
GARCIA, C. ..... p 1067 N95-17993
GARCIA, JOSEPH AVILA ..... p 928 N95-18101
GARDNER, JOHN H. ..... p 1146 N95-19527
GARDNER, W. L. ..... p 999 N95-18558
GAREEV, F. A. ..... p 1132 N95-18882
GARRETT, STEVEN L. ..... p 1141 N95-18563
GARZARELLA, LINDA ..... p 1079 N95-18661
GARZON, F. H. ..... p 1152 N95-19608
GAUNTNER, JIM W. ..... p 949 N95-19380
GAWEDZKI, K. ..... p 1119 N95-19718
p 1119 N95-19719
GEBALLE, T. H. ..... p 1154 N95-19815
GEE, J. M. ..... p 1055 N95-19859
GEER, B. ..... p 1146 N95-19379
GEER, S. ..... p 1137 N95-19561
GEISLER, WILSON S. ..... p 1140 N95-18509
GELDERMAN, RICHARD FREDRICK ..... p 1179 N95-18498
GELLER, MYER ..... p 999 N95-18545
GEMMELL, D. S. ..... p 1135 N95-19786
p 1135 N95-19787
GENERAZIO, EDWARD R. ..... p 1046 N95-19501
GEORGALA, J. M. ..... p 1030 N95-19774
GEORGALA, JEANETTE M. ..... p 1030 N95-19506
p 1031 N95-19775
GERTH, RICHARD J. ..... p 968 N95-18980
GESELL, LESLIE H. ..... p 1003 N95-19516
GETSON, E. S. ..... p 943 N95-18417
GEVINS, A. S. ..... p 1113 N95-18441
GEYER, H. ..... p 1053 N95-19074
GHAFFARI, FARHAD ..... p 931 N95-19114
GHALEB, SAM ..... p 1002 N95-19072
GHANNADIAN, F. ..... p 996 N95-18386
GHOSH, JOYDEEP ..... p 1140 N95-18509
GIBBARD, S. G. ..... p 1187 N95-19299
GIBSON, GARTH A. ..... p 1093 N95-18659
GIBSON, T. M. ..... p 1080 N95-19414
GIELDA, T. P. ..... p 943 N95-18483
GIESKE, J. H. ..... p 990 N95-19100
GIFFORD, LISA A. ..... p 1060 N95-18683
p 1062 N95-19860
GILCHRIST, N. H. C. ..... p 1124 N95-19054
GILDEEN, DAVID ..... p 1140 N95-18509
GILL, MICHAEL W. ..... p 1178 N95-18361
GILLEN, K. T. ..... p 986 N95-18651
GILLERAN, LOUIS G. ..... p 1081 N95-19416
GILMORE, P. ..... p 1011 N95-19200
GIOVANETTI, P. M. ..... p 1080 N95-19414
GIOVANNUCCI, R. ..... p 1126 N95-19152
GIUFFRE, G. ..... p 1125 N95-19147
GIUFFRIDA, G. ..... p 1101 N95-19629
GIUFFRIDA, GIONANNI ..... p 1101 N95-19631
GIULIANI, J. L., JR. ..... p 1147 N95-19847
GIUZIO, R. ..... p 1125 N95-19147
p 1127 N95-19163
GLASER, H. ..... p 1084 N95-19431
GLASER, H.-J. ..... p 1085 N95-19436
GLASER, JOHN ..... p 932 N95-18604
GLASSCOCK, BARBARA H. ..... p 977 N95-18175
GLASSMAN, ARTHUR J. ..... p 930 N95-18933
GLENDENNING, N. K. ..... p 1194 N95-19570
GLEZER, ARI ..... p 1018 N95-18469
GLIMM, J. ..... p 1093 N95-19875
GLOSLI, JAMES N. ..... p 1132 N95-18655
GLUCKSTERN, R. L. ..... p 1136 N95-18893
GOGGIN, PATRICK J. ..... p 946 N95-18602
GOLDBERG, B. E. ..... p 962 N95-18932
GOLDMAN, ALLEN M. ..... p 1148 N95-18053
GOLDMAN, JEFFERY A. ..... p 1115 N95-19118
GOLDMAN, JEFFREY H. ..... p 1015 N95-18111
GOLDSTEIN, DAVID ..... p 1107 N95-19766
GOLOSKOKOV, S. V. ..... p 1130 N95-18360
GOMEZ-MARINO, M. A. ..... p 1082 N95-19423
GONG, JIAN ..... p 1005 N95-19796
p 1006 N95-19797
p 1006 N95-19799
p 1006 N95-19800
p 1006 N95-19801
GONG, XIAODONG ..... p 1144 N95-18887
GOO, EDWARD ..... p 1153 N95-19713
GOOCH, JOHN M. ..... p 1086 N95-19441
GOOD, BRIAN S. ..... p 1053 N95-18587
GOODMAN, J. M. ..... p 1057 N95-17985
GOODNICK, S. M. ..... p 1122 N95-19234
GOODNICK, STEPHEN M. ..... p 1011 N95-19089
GOODRICH, C. ..... p 1172 N95-18040
GOODWIN, G. M. ..... p 981 N95-19568
GOPALAN, P. ..... p 1122 N95-17983
GORETTA, K. C. ..... p 1150 N95-19075
p 1150 N95-19094
GORMAN, LAUREL T. ..... p 1074 N95-18470
GOSELE, U. ..... p 1153 N95-19697
GOVER, J. E. ..... p 1008 N95-18143
GOZZI, DANIELE ..... p 955 N95-19682
GRAFF, G. L. ..... p 986 N95-18648
GRANACKI, JOHN ..... p 1012 N95-19606
GRANDT, A. F., JR. ..... p 935 N95-19476
GRANOVSKII, A. V. ..... p 949 N95-19024
GRANOVSKY, L. B. ..... p 1193 N95-19339
GRANT, STANLEY E. ..... p 995 N95-18139
GRAVES, G. A., JR. ..... p 972 N95-19702
GRAY, DAVID L. ..... p 1175 N95-19056
GREEN, CAROL E. ..... p 1079 N95-18518
GREEN, J. E. ..... p 931 N95-19546
GREEN, P. D. ..... p 1124 N95-19143
GREENLEAF, J. E. ..... p 1077 N95-18734
p 1077 N95-19140
GREENLY, J. B. ..... p 977 N95-17968
GREENWAY, R. BRYAN, JR. ..... p 972 N95-18981
GREENWELL, D. L. ..... p 1134 N95-19562
GREGORY, GERALD L. ..... p 1058 N95-18132
GREGORY, J. C. ..... p 1197 N95-18464
GRIFFITHS, D. J. ..... p 1122 N95-19195
GRINDELAND, RICHARD E. ..... p 1092 N95-18569
GRINEVICH, OLEG ..... p 976 N95-19830
GRISSETT, J. D. ..... p 1078 N95-18138
GRODSINSKY, C. M. ..... p 927 N95-18197
p 927 N95-18486
GROLEAU, NICOLAS ..... p 1103 N95-19640
GROPP, WILLIAM ..... p 1112 N95-19834
GROSE, S. M. ..... p 1129 N95-18144
GROSS, R. STEVEN ..... p 968 N95-18982
GROSS, T. ..... p 1111 N95-18892
GROSSBECK, M. L. ..... p 982 N95-19725
GROSSMAN, J. N. ..... p 1187 N95-19300
GRUBIN, HAROLD L. ..... p 1155 N95-18009
p 1155 N95-19829
GRUDZIEN, D. ..... p 1039 N95-19727
GRUENEWALD, M. ..... p 1127 N95-19158
GUELLA, T. P. ..... p 1000 N95-18727
GUHA, S. ..... p 1054 N95-19832
GUHA, SUMANTA ..... p 1110 N95-18159
GUIDOS, BERNARD J. ..... p 929 N95-18611

GUIDRY, RUTH ..... p 1050 N95-18078
GULATI, SANDEEP ..... p 1114 N95-19062
GUO, SHUYIN ..... p 1146 N95-19241
GUREVICH, INNA ..... p 966 N95-18196
GURNETT, D. A. ..... p 1195 N95-17979
GURTON, K. P. ..... p 1139 N95-18142
GUSSENHOVEN, M. S. ..... p 1178 N95-18451
GWYN, C. W. ..... p 1008 N95-18143
GYLYS, V. T. ..... p 1036 N95-17956
GYUK, GEZA ..... p 1180 N95-18964

H

HAAN, STEVEN W. ..... p 1146 N95-19527
HACKEL, L. A. ..... p 1037 N95-18357
p 1038 N95-19096
HAFFMANS, A. F. ..... p 1150 N95-19091
HAGSTROM, THOMAS ..... p 1019 N95-18898
HAGUE, J. ..... p 1040 N95-17995
HAH, C. ..... p 1016 N95-18200
HAHN, WARREN L. ..... p 1041 N95-18594
HAHS, C. A. ..... p 991 N95-19076
HAINES, JOEL ..... p 945 N95-19067
HALBGEWACHS, R. D. ..... p 1120 N95-18653
HALE, JOSEPH P. ..... p 1106 N95-19756
p 1106 N95-19760
HALL, DAVID G. ..... p 958 N95-18054
HALL, LAWRENCE O. ..... p 1107 N95-19764
HALL, MARSHALL V. ..... p 1075 N95-19503
HALL, PHILIP ..... p 1016 N95-18190
HALL, R. B. ..... p 1056 N95-19882
HALL, R. C. ..... p 995 N95-18116
HALL, ROGER B. ..... p 996 N95-18429
HALL, WILLIAM B. ..... p 967 N95-19566
HALLER, E. E. ..... p 1152 N95-19615
p 976 N95-19836
HALTURIN, V. A. ..... p 948 N95-19021
HAMED, A. ..... p 952 N95-19662
HAMEKA, HENDRIK F. ..... p 974 N95-19170
HAMERS, R. J. ..... p 976 N95-19824
p 976 N95-19825
HAMILTON, THOMAS THEODORE
p 1197 N95-18729
HAMLYN, GARRY ..... p 1032 N95-18065
HAMMACK, JOE L. ..... p 1075 N95-19523
HAMPTON, R. D. ..... p 927 N95-18197
p 927 N95-18486
HAND, GREGORY F. ..... p 1053 N95-18435
HANDEGARD, T. ..... p 1003 N95-19411
HANDSCHUH, ROBERT F. ..... p 1042 N95-18935
p 1042 N95-19125
HANEBUTTE, ULF R. ..... p 1098 N95-18584
HANSMA, P. K. ..... p 1129 N95-17974
HANSON, R. ..... p 931 N95-19109
HAPP, TH. ..... p 1007 N95-17961
HARADA, IKI ..... p 1018 N95-18549
HARE, D. A. ..... p 1099 N95-18899
HARFF, N. E. ..... p 1122 N95-19234
HARLOFF, GARY J. ..... p 955 N95-19769
HARMON, BRUCE N. ..... p 977 N95-17962
HARNE, DONALD ..... p 939 N95-19494
HARRINGTON, JIM ..... p 1103 N95-19639
HARRINGTON, PATRICK M. ..... p 1156 N95-18949
HARRINGTON, S. R. ..... p 1013 N95-19872
HARRIS, CHARLES E. ..... p 934 N95-19468
HARRIS, P. K. ..... p 952 N95-19663
HARRIS, REGINA M. ..... p 1080 N95-19384
HARRIS, T. L. ..... p 989 N95-19861
HARRISON, K. G. ..... p 1059 N95-18666
HARRISON, P. F. ..... p 1132 N95-18643
HARRISON, R. J. ..... p 1153 N95-19724
HARTMANN, L. ..... p 1178 N95-19301
HARVEY, A. ..... p 1015 N95-18111
HARWELL, WILLIAM D. ..... p 1017 N95-18323
HASAN, DAVID A. ..... p 1104 N95-19646
HASSANEIN, A. ..... p 1144 N95-18547
HASSOON, SALAH ..... p 976 N95-19830
HATLEY, J. W. ..... p 1176 N95-19876
HATT, DAVID J. ..... p 959 N95-18942
HAWLEY, M. ..... p 1148 N95-18064
HAWLEY, M. E. ..... p 1152 N95-19608
HAWLEY, SUZANNE L. ..... p 1196 N95-19034
HAXTON, W. C. ..... p 1134 N95-19705
p 1135 N95-19706
HAYDER, M. EHTESHAM ..... p 1019 N95-18941
HAYDUK, MICHAEL J. ..... p 1138 N95-18067
HAYES, JERRY L. ..... p 992 N95-18745
HAYHURST, LES ..... p 1095 N95-18030
HAZELTINE, R. D. ..... p 1145 N95-19079
p 1145 N95-19092
HE, Z. X. ..... p 974 N95-18744
HEATON, G. W. ..... p 1135 N95-19709
HECHT, LAURA FRYE ..... p 1175 N95-19038
HECHT, LAURA M. ..... p 1175 N95-18950
HEGEDUS, CHARLES R. ..... p 984 N95-18320
p 984 N95-18336
p 985 N95-18631
HEIDELBACH, ROBERT ..... p 999 N95-18657
HEIDELBERGER, PHILIP ..... p 1099 N95-18931
HEIJBOER, L. C. ..... p 1072 N95-18926
HEIMAN, D. ..... p 1151 N95-19235
HEIMANN, M. ..... p 1059 N95-18664
HEINLE, ROBERT A. ..... p 945 N95-19044
HENDERSON, ANDREW C. ..... p 1067 N95-18014
HENDY, KEITH C. ..... p 1088 N95-18151
HENSHALL, G. A. ..... p 980 N95-19396
HEPPNER, R. A. ..... p 962 N95-19184
HERMAN, S. ..... p 1142 N95-19710
HERMANN, M. R. ..... p 1037 N95-18357
HERON, K. H. ..... p 1047 N95-19165
HERR, J. L. ..... p 965 N95-19780
HESS, K. R. ..... p 981 N95-19703
HESSE, PHILIP W. ..... p 997 N95-18462
HESSELINK, LAMBERTUS ..... p 1121 N95-19288
HETHERINGTON, H. P. ..... p 1087 N95-19698
HETTEL, R. ..... p 1138 N95-19841
HEWINS, R. H. ..... p 1186 N95-19295
p 1187 N95-19302
p 1193 N95-19337
p 1193 N95-19338
HICKEY, JOHN R. ..... p 967 N95-18571
HICKS, JOHN W. ..... p 929 N95-18565
HILDRETH, BRADLEY ..... p 1001 N95-19069
HILL, D. N. ..... p 1146 N95-19379
HILL, KEITH ..... p 967 N95-19566
HILLBERRY, B. M. ..... p 935 N95-19476
HILLIARD, KEITH D. ..... p 1004 N95-19534
HILLMAN, DONALD J. ..... p 1080 N95-19384
HILSENRATH, ERNEST ..... p 1196 N95-18954
HINDY, R. N. ..... p 1036 N95-17956
HINGST, JAMES ..... p 1064 N95-18452
HINSON, DAVID P. ..... p 1194 N95-18579
HIPP, JAMES R. ..... p 1118 N95-18896
HIRSCHON, A. S. ..... p 976 N95-19785
HIRST, DONALD J. ..... p 984 N95-18320
p 984 N95-18336
HISSAM, SCOTT A. ..... p 1095 N95-18031
p 1096 N95-18343
HITNEY, H. V. ..... p 1140 N95-18484
HITNEY, HERBERT V. ..... p 999 N95-18561
HIXON, R. ..... p 1015 N95-18149
HOELZER, D. T. ..... p 988 N95-19558
HOEPPNER, DAVID W. ..... p 938 N95-19489
HOERZ, F. ..... p 1047 N95-19185
p 989 N95-19197
HOFFER, G. ..... p 997 N95-18506
HOFFMAN, D. J. ..... p 999 N95-18558
HOFLER, THOMAS J. ..... p 992 N95-18165
p 1141 N95-18563
HOGAN, R. C. ..... p 1187 N95-19296
HOHENBERG, C. M. ..... p 1192 N95-19329
HOKE, MICHAEL L. ..... p 1142 N95-19862
HOLBROOK, D. ..... p 1007 N95-17999
HOLCOMB, LEE ..... p 1174 N95-18573
HOLCOMBE, DAVID ..... p 1013 N95-19687
HOLDEMAN, J. D. ..... p 947 N95-18133
HOLDEN, M. ..... p 931 N95-19109
HOLEHOUSE, IAN ..... p 1047 N95-19161
HOLLAND, MARK ..... p 1093 N95-18659
HOLLAND, SCOTT D. ..... p 1175 N95-18936
HOLLENBECK, JOHN R. ..... p 1089 N95-18530
HOM, IVAN ..... p 1012 N95-19606
HONGNIAN, DONG ..... p 1071 N95-18394
p 1071 N95-18395
HONIG, J. ..... p 1038 N95-19096
HOOD, L. L. ..... p 1188 N95-19303
HOOKER, STANFORD B. ..... p 1076 N95-19577
HOOVER, SCOTT M. ..... p 992 N95-18431
HOPKINS, DALE A. ..... p 1044 N95-18199
p 1045 N95-18909
HOPKINS, E. W. ..... p 1083 N95-19428
HORACK, JOHN M. ..... p 1197 N95-18730
HORANYI, M. ..... p 1188 N95-19304
HORN, BERTHOLD K. P. ..... p 1173 N95-18051
HORST, SCOTT C. ..... p 1010 N95-18662
HORTON, G. C. ..... p 952 N95-19664
HOSLER, E. RAMON ..... p 1157 N95-18166
HOU, HAIHUI RON ..... p 1040 N95-18056
HOUBOLT, JOHN C. ..... p 946 N95-18605
HOULTON, R. J. ..... p 1152 N95-19608
HOUMINER, ZWI ..... p 1066 N95-19387
HOUTS, M. G. ..... p 966 N95-17997
HOUWINK, R. ..... p 928 N95-18503
HOWARD, A. J. ..... p 975 N95-19559
HOWARD, STEPHEN L. ..... p 1033 N95-18620
p 976 N95-19729
HOWARD, THOMAS G. ..... p 1142 N95-18984
HOWELL, BARBARA ..... p 986 N95-18678
HOWELLS, M. ..... p 1034 N95-19233
HOYNIAK, DAN ..... p 949 N95-19380
p 949 N95-19382
HSIEH, C. L. ..... p 1143 N95-18119
HSU, CHU-NAN ..... p 1176 N95-19604
HSU, J. S. ..... p 1123 N95-18930
HU, F. Q. ..... p 1018 N95-18488
HUANG, T. C. ..... p 996 N95-18386
HUBER, R. J. ..... p 1012 N95-19240
HUBER, THERESA R. ..... p 1097 N95-18420
HUCHIN, J. P. ..... p 954 N95-19676
HUCHRA, J. ..... p 1178 N95-18001
HUGGINS, KEVIN L. ..... p 1115 N95-19572
HUGHES, D. A. ..... p 953 N95-19671
HUGHES, H. G. ..... p 1140 N95-18484
HUGHES, THOMAS C. ..... p 942 N95-18398
HULL, D. L. ..... p 946 N95-18603
HULL, J. R. ..... p 1122 N95-19704
HUMMEL, JOHN R. ..... p 1068 N95-18141
HUMPHREY, GENE ..... p 1095 N95-18034
HUNTEMAN, W. J. ..... p 1173 N95-18063
HUNTER, PAUL ..... p 1174 N95-18573
HURDLEBRINK, DEBRA ..... p 966 N95-18196
HURLBURT, GEORGE ..... p 1001 N95-19069
HUSS, G. R. ..... p 1188 N95-19305
HUSSAINI, M. Y. ..... p 1018 N95-18488
HUSSAINI, M. YOUSUFF ..... p 1020 N95-18958
HUSZTHY, PETER ..... p 969 N95-19822
p 969 N95-19823
HUTCHEON, I. D. ..... p 1192 N95-19327
HUTCHINSON, J. M. R. ..... p 981 N95-19703
HUTCHISON, R. ..... p 1188 N95-19306
HWANG, EUI-SIK ..... p 1140 N95-18424
HYLAND, DAVID C. ..... p 964 N95-18580
HYLAND, DIANE T. ..... p 1080 N95-19384
p 1080 N95-19385

I

ICE, G. E. ..... p 1034 N95-19233
IDEN, D. ..... p 972 N95-19702
IGLESIAS, C. A. ..... p 1186 N95-19249
IGUCHI, TOSHIO ..... p 1070 N95-18210
ILGEN, DANIEL R. ..... p 1089 N95-18530
ILYES, LASZLO A. ..... p 1105 N95-19749
IMAM, M. A. ..... p 971 N95-19123
IMMARIGEON, J. P. ..... p 954 N95-19675
INDACOCHEA, J. E. ..... p 1054 N95-19117
INGLEFIELD, PAUL T. ..... p 985 N95-18442
INGRAFFEA, ANTHONY R. ..... p 935 N95-19473
IOB, M. ..... p 960 N95-19848
IOFFE, A. F. ..... p 1130 N95-18427
IP, W. ..... p 1191 N95-19324
IRELAND, P. T. ..... p 951 N95-19661
ISAAC, BRYAN J. ..... p 1014 N95-18985
ISAEV, A. P. ..... p 1118 N95-18876
ISAKSEN, IVAR S. A. ..... p 1062 N95-19879
ISLER, R. C. ..... p 1133 N95-19228
IVAN, DOUGLAS J. ..... p 1086 N95-19441
p 1086 N95-19442
IVANOV, MIKHAIL J. ..... p 948 N95-19018
p 948 N95-19019
p 948 N95-19020
p 949 N95-19026
IWANSKI, THOMAS ..... p 1140 N95-18459
IYENGAR, S. S. ..... p 1112 N95-19689
IZATT, REED M. ..... p 969 N95-19822
p 969 N95-19823

J

JACKELEN, GEORGE ..... p 1097 N95-18419
p 1097 N95-18447
JACKSON, A. A. ..... p 1183 N95-19186
JACKSON, JEFF ..... p 1165 N95-18986
JACOBOBERLLES, JULIO ..... p 1050 N95-18216
JACOBS, J. H. ..... p 1126 N95-19157
JACOBSON, A. ..... p 1063 N95-18148
JACOBSON, A. R. ..... p 1063 N95-18125
JAEGER, E. F. ..... p 1144 N95-18557
JAHAMA, SAID ..... p 1099 N95-18924
JAIN, ASHOK K. ..... p 1130 N95-18334
JAMES, S. D. ..... p 1007 N95-17959
JANSMA, R. M. ..... p 1120 N95-18653
JARAMILLO, S. A. ..... p 1034 N95-19229
JASSOWSKI, DONALD M. ..... p 966 N95-18192
JAYARAMAN, S. ..... p 1182 N95-19181
JAYASIMHA, D. N. ..... p 1019 N95-18941
JELLICORSE, B. L. ..... p 1061 N95-19403
JENKINS, PHILLIP P. ..... p 1149 N95-18453
p 1053 N95-18572
JENKINS, RHONALD M. ..... p 968 N95-18987
JENSEN, JAMES O. ..... p 974 N95-19170
JEONG, DAVID Y. ..... p 936 N95-19477
JERINA, K. L. ..... p 978 N95-18046
JIA, Q. X. ..... p 1152 N95-19608
JIANG, QING ..... p 988 N95-19691

JIANG, WEI-NAN ..... p 1013 N95-19687
JIMENEZ-MELENDO, M. ..... p 1150 N95-19075
JIRACEK, GEORGE R. ..... p 1063 N95-17946
JOGLEKAR, PRAFULLA N. ..... p 1160 N95-18176
JOHNS, STEVEN T. ..... p 1138 N95-18067
JOHNSON, D. J. ..... p 1133 N95-19199
JOHNSON, ERIC R. ..... p 1044 N95-18388
JOHNSON, PARLEY P. ..... p 1090 N95-19564
JOHNSON, R. ..... p 1085 N95-19439
JOHNSON, S. ..... p 1053 N95-19074
JOHNSON, SAMUEL D. ..... p 960 N95-18961
p 1011 N95-18962
JOHNSTON, DAVID F. ..... p 1011 N95-18962
JOHNSTON, G. P. ..... p 977 N95-17968
JOHNSTON, SHAYNE ..... p 1037 N95-18408
JOINER, R. G. ..... p 1057 N95-17985
JONES, B. ..... p 1112 N95-19589
JONES, E. D. ..... p 1149 N95-18650
p 1151 N95-19235
JONES, GREGORY ..... p 1173 N95-18526
JONES, J. H. ..... p 982 N95-19725
JONES, KENNETH M. ..... p 968 N95-18988
JONES, LARRY W. ..... p 1062 N95-19808
JONES, LEONIDAS J., III ..... p 1154 N95-19807
JONES, P. D. ..... p 1057 N95-18022
JONES, R. H. ..... p 1188 N95-19307
JONES, T. V. ..... p 951 N95-19661
JORDAN, T. L. ..... p 1099 N95-18899
JORGENSEN, G. ..... p 1053 N95-18463
JOSLIN, D. L. ..... p 1133 N95-19232
JOSLIN, RONALD D. ..... p 1098 N95-18584
p 1020 N95-18958
JOSLIN, STEVEN M. ..... p 982 N95-19792
JOSOWICZ, M. A. ..... p 984 N95-18348
JUDKINS, R. R. ..... p 981 N95-19723
JUNG, NAMHO ..... p 1105 N95-19753
JURCEVICH, B. ..... p 966 N95-19189

K

KABACOFF, LAWRENCE T. ..... p 1149 N95-18543
KAD, B. K. ..... p 980 N95-19400
KADONO, T. ..... p 962 N95-19183
KAISER, DALE P. ..... p 1058 N95-18389
KAITA, R. ..... p 1133 N95-19228
KALIA, R. K. ..... p 1134 N95-19562
KALJEVIC, IGOR ..... p 1044 N95-18199
p 1045 N95-18909
KAMINS, D. ..... p 1172 N95-18040
KAMNA, M. M. ..... p 1131 N95-18473
KAN, T. ..... p 1039 N95-19551
KANKAM, M. DAVID ..... p 1042 N95-19238
KANTER, E. P. ..... p 1135 N95-19786
p 1135 N95-19787
KAPITULNIK, A. ..... p 1154 N95-19815
KAPLAN, D. B. ..... p 1133 N95-19245
KAPUR, SHARAD ..... p 1119 N95-19735
KARALEKAS, D. ..... p 970 N95-18940
KARASZ, FRANK E. ..... p 985 N95-18510
KARDOMATEAS, G. A. ..... p 937 N95-19487
KARMARKAR, SUBHASH D. ..... p 992 N95-18431
KARR, GERALD R. ..... p 1161 N95-18967
KATAN, J. R. ..... p 999 N95-18619
KATAN, JOSEPH R. ..... p 1005 N95-19736
KATNIK, GREGORY N. ..... p 963 N95-19790
KATOEN, J. P. ..... p 1109 N95-18039
KATTI, ROMNEY R. ..... p 1093 N95-18963
KATZ, ERIC S. ..... p 958 N95-18087
KATZ, RICHARD A. ..... p 1018 N95-18525
KAUFMANN, RICHARD L. ..... p 1065 N95-19032
KAUSHAL, TONY S. ..... p 1040 N95-18041
KAVLI, A. ..... p 1065 N95-18640
KAY, EDWIN J. ..... p 1080 N95-19384
p 1080 N95-19385
KAY, IRWIN W. ..... p 1037 N95-18382
KAZI, TAUSEEF ..... p 1012 N95-19606
KAZOVSKY, LEONID G. ..... p 1141 N95-18682
KEE-BOWLING, BONNIE ..... p 958 N95-18054
KEELEY, D. ..... p 1138 N95-19841
KEIJZER, M. ..... p 1037 N95-18502
KEIL, K. ..... p 1189 N95-19313
KELLOGG, G. L. ..... p 980 N95-19395
KELLY, J. E. ..... p 1043 N95-19809
KELNER, GALINA ..... p 1032 N95-17970
KENNEDY, C. ..... p 1053 N95-18463
KENNEDY, JOHN M. ..... p 1175 N95-18950
p 1175 N95-18953
p 1175 N95-19038
p 1176 N95-19127
KERSHAW, JAMES ..... p 1032 N95-18065
KERSTHOLT, J. H. ..... p 1089 N95-19538
KESSLER, BRADLEY L. ..... p 1034 N95-18938
p 1034 N95-19236
KETTUNEN, LAURI ..... p 1112 N95-19834
KEVORKIAN, A. K. ..... p 1117 N95-18679
KEY, J. ..... p 1062 N95-19779
KEY, JEFF ..... p 1052 N95-18952
KEYES, DAVID ..... p 1098 N95-18487
KEYSER, DAVID R. ..... p 956 N95-18553
KHAJENOORI, SOHEIL ..... p 1108 N95-19768
KHER, SHREYAS S. ..... p 1154 N95-19806
KHEYFETS, A. ..... p 1194 N95-19612
KHINOO, L. A. ..... p 959 N95-18725
KHURI-YAKUB, B. T. ..... p 1128 N95-19802
KHVEDELIDZE, A. ..... p 1156 N95-18328
KIDDER, STANLEY ..... p 1068 N95-18093
KIGGANS, J. D. ..... p 987 N95-19399
KILKENNY, J. D. ..... p 1033 N95-18555
KILPATRICK, MARK ..... p 1043 N95-19593
KIM, HAN ..... p 1142 N95-19088
KIM, KYEKYOON ..... p 1136 N95-18552
KIM, RHYN H. ..... p 1043 N95-18177
KING, IVEY H. ..... p 1088 N95-18095
KING, JAMES A. ..... p 964 N95-18580
KING, N. S. P. ..... p 1034 N95-19229
KING, N. S.P. ..... p 1035 N95-19394
KINGSTON, GINA ..... p 1095 N95-18089
KINN, CHRISTOPHER L. ..... p 1063 N95-17946
KIRK, D. R. ..... p 1020 N95-19139
KIRK, H. G. ..... p 1038 N95-19243
KISTLER, LYNN M. ..... p 1064 N95-18476
KITAGAMI, K. ..... p 1191 N95-19326
KITAMURA, M. ..... p 1187 N95-19298
p 1188 N95-19308
p 1192 N95-19331
KITIPORNCHAI, S. ..... p 1045 N95-18608
KIWAN, ABDUL R. ..... p 942 N95-18381
KLAES, K. D. ..... p 1049 N95-18035
KLEINMANN, S. ..... p 1178 N95-18001
KLEINMEYER, JAMES D. ..... p 970 N95-18612
KLEM, J. F. ..... p 1149 N95-18650
p 1122 N95-19234
p 1151 N95-19235
KLEPPER, S. ..... p 1007 N95-17999
KLICH, PHILLIP J. ..... p 964 N95-18105
KLINE, MARTIN D. ..... p 1043 N95-19593
KLINENBERG, EDWARD J. ..... p 1091 N95-18385
KLINKER, JAMES E. ..... p 1003 N95-19525
KLIPFEL, A. ..... p 952 N95-19667
KLOBUCHAR, J. A. ..... p 1057 N95-17985
KLUTE, GLENN K. ..... p 1091 N95-18189
KNAPP, F. F., JR. ..... p 1080 N95-19244
KNAPP, MICHAEL CHARLES ..... p 1073 N95-19596
KNILL, E. ..... p 1117 N95-18346
KNOBLOCK, CRAIG A. ..... p 1115 N95-19599
p 1176 N95-19604
p 1111 N95-19605
KNOSPE, C. R. ..... p 927 N95-18197
p 927 N95-18486
KO, FRANK ..... p 971 N95-19650
KOCH, J. A. ..... p 1038 N95-19247
KOENIG, KLAUS ..... p 1126 N95-19156
KOENIG, P. ..... p 953 N95-19673
KOLKMAN, H. J. ..... p 954 N95-19678
KONG, JEFFREY ..... p 945 N95-19130
KONG, L. ..... p 960 N95-19272
KONKASHBAEV, A. ..... p 1144 N95-18547
KONKASHBAEV, I. ..... p 1144 N95-18547
KOOKER, DOUGLAS E. ..... p 1033 N95-18620
p 976 N95-19729
KOONTZ, STEVEN L. ..... p 983 N95-18134
KORENYI-BOTH, ANDRAS ..... p 969 N95-18448
KOREVAAR, ERIC ..... p 1139 N95-18409
KORTELING, J. E. ..... p 1090 N95-19583
KOSTEGE, VALEREY K. ..... p 948 N95-19021
p 949 N95-19025
KOSTEGE, VALERY K. ..... p 949 N95-19024
KOTIUGA, P. R. ..... p 994 N95-17954
KOTZ, DAVID ..... p 1110 N95-18521
p 1110 N95-18581
KOYAMATSU, ANTHONY H. ..... p 1041 N95-18594
KOYMANS, R. ..... p 1109 N95-18039
KOZLOWSKI, M. R. ..... p 987 N95-19227
p 1039 N95-19708
KRAHN, GARY W. ..... p 1120 N95-18007
KRAMER, A. G. ..... p 1005 N95-19744
KRAMER, BRIAN R. ..... p 1020 N95-18955
p 1020 N95-18956
KRAUS, NICHOLAS C. ..... p 1074 N95-18470
KRCHNAVEK, ROBERT R. ..... p 1138 N95-18100
KREIFELS, THEODORE L. ..... p 1153 N95-19715
KREIN, G. ..... p 1130 N95-18329
KREMER, FRANS G. J. ..... p 948 N95-18911
KRING, D. ..... p 1188 N95-19303
KRISHNAMURTHY, S. ..... p 1142 N95-19732
KRISHNAMURTI, T. N. ..... p 1073 N95-19870
KROL, M. S. ..... p 1058 N95-18375
KROL, MARK F. ..... p 1138 N95-18067
KROT, A. N. ..... p 1188 N95-19309
p 1191 N95-19323
KRUEGER, S. ..... p 1067 N95-17955
KRUMPELT, M. ..... p 1053 N95-19074
p 1053 N95-19115
p 1053 N95-19116
p 1054 N95-19117
KRUPA, VLADISLAV G. ..... p 948 N95-19018
p 948 N95-19019
p 949 N95-19023
KUBOTA, T. ..... p 996 N95-18386
KUCERA, G. ..... p 1054 N95-19117
KUDER, STEVEN ..... p 1050 N95-18078
KUEPPER, A. ..... p 1023 N95-19263
KUGEL, H. W. ..... p 1133 N95-19228
KUK, V. H. M. ..... p 951 N95-19661
KULESHOV, S. P. ..... p 1130 N95-18360
KULKARNI, R. ..... p 1172 N95-18040
KUMAR, ANAND ..... p 1027 N95-19451
KUMAR, R. ..... p 1053 N95-19115
KUNC, J. ..... p 931 N95-19109
KUNSELMAN, R. ..... p 1129 N95-18124
KUNST, FRANK A. ..... p 964 N95-18362
KURKOV, A. P. ..... p 928 N95-18457
KURTH, W. S. ..... p 1195 N95-17979
KURTZ, A. D. ..... p 1040 N95-18010
KUSTOM, R. L. ..... p 1039 N95-19727
KUYKENDALL, MARTHA G. ..... p 1063 N95-17946
KUZMIN, M. ..... p 1025 N95-19274
KUZYK, MARK G. ..... p 983 N95-17957
KWON, O. ..... p 1016 N95-18200
KYRALA, G. A. ..... p 1032 N95-18130

L

LABBE, M. ..... p 1105 N95-19751
LACEY, PAUL I. ..... p 989 N95-19826
LAFRENIERE, ROBERT ..... p 1045 N95-18456
LAGANELLI, A. L. ..... p 1031 N95-19153
LAGOW, RICHARD J. ..... p 984 N95-18402
LAKASZOW ..... p 943 N95-18504
LAMB, JOHN D. ..... p 969 N95-19823
LAMBERT, C. R. ..... p 1080 N95-19244
LAMBERTH, J. G. ..... p 1078 N95-18138
LAMBROS, JOHN ..... p 1045 N95-18613
LANCIAULT, MARK ..... p 966 N95-18196
LANCTO, R. ..... p 972 N95-19851
LANDEN, O. ..... p 1033 N95-18555
LANDEN, O. L. ..... p 1035 N95-19711
LANDGREBE, DAVID A. ..... p 1052 N95-19126
LANDHERR, STEFAN ..... p 1095 N95-18089
LANDIS, GEOFFREY A. ..... p 1149 N95-18453
p 1053 N95-18572
LANDRUM, D. BRIAN ..... p 968 N95-18989
LANG, J. C. ..... p 1151 N95-19113
LANGE, FRED F. ..... p 1150 N95-18685
LANSING, MATTHEW ..... p 969 N95-18135
LARSON, DOUGLAS J. ..... p 1065 N95-19032
LASCHKA, BORIS ..... p 932 N95-19261
LASHLEY, TONY CHARLES ..... p 1145 N95-18906
LASKE, JANEEN A. ..... p 1154 N95-19812
LAUDIEN, E. ..... p 1124 N95-19144
LAVELLE, THOMAS M. ..... p 930 N95-18933
LAVIERS, H. ..... p 1053 N95-18894
LAW, C. K. ..... p 973 N95-18410
LAW, D. ..... p 1066 N95-17938
LAWRY, D. ..... p 997 N95-18506
LAWTON, JOSEPH ..... p 947 N95-18383
LE, THACH C. ..... p 1102 N95-19636
LEADER, E. ..... p 1130 N95-18356
LEASURE, DAVID ..... p 1101 N95-19628
LEBLANC, B. P. ..... p 1133 N95-19228
LEBRUN, T. ..... p 1135 N95-19786
LEDUC, VINCENT ..... p 1105 N95-19751
LEE, B. D. ..... p 989 N95-19861
LEE, C. L. ..... p 1031 N95-17963
LEE, DONG HO ..... p 1106 N95-19757
LEE, J. ..... p 1015 N95-18107
LEE, J. L. ..... p 1067 N95-17955
LEE, M. B. R. ..... p 999 N95-18540
LEE, MARTIN A. ..... p 1064 N95-18476
LEE, MICHAEL E. ..... p 992 N95-18684
LEE, S. K. ..... p 966 N95-17997
LEE, SOOWON ..... p 1115 N95-19601
LEE, SUNPYO ..... p 986 N95-18918
LEE, ZHONGPING ..... p 1051 N95-18739
LEEMANS, W. P. ..... p 1137 N95-19584
LEENKNECHT, DAVID A. ..... p 1074 N95-18160
LEFEBVRE, PAUL J. ..... p 1015 N95-18112
p 1033 N95-18461
LEHR, D. E. ..... p 1135 N95-19709
LEI, CHARLES ..... p 971 N95-19650
LEIGH, BARRY ..... p 1127 N95-19164
LEMAITRE, J. ..... p 941 N95-18927
LEMKE, R. W. ..... p 1145 N95-19201
LENNON, W. J. ..... p 1006 N95-19833
LEONARD, A. W. ..... p 1146 N95-19379
LEONG, H. M. ..... p 1113 N95-18441

LEONHARDT, TODD A. p 1043 N95-18583
LERCHE, R. A. p 1146 N95-19250
p 1146 N95-19509
p 1135 N95-19709
LEROY, G. p 952 N95-19664
LESER, CHRISTOPH p 1046 N95-18919
LESTER, MICHAEL T. p 1094 N95-18018
LESUER, D. R. p 980 N95-19396
LEUNG, EMILY W. p 991 N95-18326
LEVAN, M. D. p 1091 N95-18531
LEVI, KEITH R. p 1103 N95-19644
LEVINE, DAVID p 1112 N95-19834
LEVY, E. H. p 1187 N95-19299
LEWANDOWSKI, RAYMOND p 1101 N95-19628
LEWICKI, DAVID G. p 1042 N95-19125
LEWIS, BEVERLEY W. p 1032 N95-18194
LEWIS, G. K. p 1036 N95-18126
LEWIS, JAMES A. p 1090 N95-19564
LEWIS, STEVEN p 1095 N95-18033
LEY, K. p 1053 N95-19115
LI, CHING-CHUNG p 1075 N95-18622
LI, GUODONG p 1144 N95-18887
LI, HUA p 1009 N95-18485
LI, JIANAN p 1110 N95-18158
LI, MING p 1150 N95-18908
LI, ZHICAI p 1144 N95-18885
LIBBY, S. I. p 1138 N95-18102
LIDDLE, ANDREW R. p 1121 N95-19030
LIEW, K. M. p 1045 N95-18608
LIFFMAN, K. p 1189 N95-19310
LILLEY, WILLIAM p 1131 N95-18519
LIM, J. J. p 1120 N95-18653
LIM, M. K. p 1045 N95-18608
LIN, WEI p 1135 N95-19706
LINCOLN, JOHN W. p 945 N95-19517
LINDQUIST, W. B. p 1093 N95-19875
LINDSEY, PATRICIA F. p 1092 N95-18990
LINDSTROM, D. p 1190 N95-19320
LINEWEAVER, C. H. p 1178 N95-19617
LINHARES, C. A. p 1118 N95-18878
LINSCOTT, I. p 1138 N95-19841
LINTON, DARRELL p 1108 N95-19768
LIOU, J.-C. p 1182 N95-19181
LIOU, JER-CHYI p 1183 N95-19187
LIOU, K. N. p 1067 N95-17955
LITTLE, M. C. p 1171 N95-18060
LIU, C. S. p 1139 N95-18409
LIU, K. C. p 987 N95-19399
LIU, X. C. p 1151 N95-19235
LIVINGSTON, A. E. p 1135 N95-19787
LO, CHOR PONG p 1063 N95-18991
LOBER, RANDY R. p 1118 N95-18896
LOCKWOOD, MARY KAE p 946 N95-19154
LOECKER, T. H. p 1085 N95-19439
LOELLBACH, J. p 1016 N95-18200
LOEVNES, K. p 1003 N95-19411
LOFGREN, G. E. p 1189 N95-19311
LOGAN, G. p 1137 N95-19588
LOGSDON, GAY MARIE p 1058 N95-18389
LOKOS, WILLIAM A. p 945 N95-19044
LOMBARDO, GIUSEPPE p 953 N95-19668
LONDON, R. A. p 1146 N95-19509
LONDONO, J. D. p 1134 N95-19557
LONG, KATHERINE S. p 1058 N95-18085
LONGTIN, DAVID R. p 1068 N95-18141
LOOFT-WILSON, R. p 1077 N95-19140
LOOMIS, B. A. p 982 N95-19725
LOPES, JOSEPH p 1173 N95-18526
LOPEZSALDANA, I. R. p 975 N95-19550
LORBECK, J. A. p 1002 N95-19097
LORITSCH, R. S. p 1147 N95-19700
LOUAT, NORMAN P. p 971 N95-19123
LOUEY, CRAIG N. p 990 N95-19505
LOUIE, S. G. p 1151 N95-19569
LOVE, S. G. p 1189 N95-19312
p 1189 N95-19313
p 1192 N95-19327
LOVEJOY, M. L. p 975 N95-19559
LOVELL, T. p 1015 N95-18111
LOW, SAMUEL R. p 939 N95-19494
LOWE, ROLAND A. p 1053 N95-18572
p 1053 N95-18587
LU, CHEN p 1065 N95-19032
LU, YANXIA p 988 N95-19558
LUBOSCH, BERND p 945 N95-19067
LUCATORTO, T. B. p 981 N95-19703
LUCCHIN, FRANCESCO p 1180 N95-18966
LUCCI, B. L. p 928 N95-18457
LUDVIGSEN, H. p 1036 N95-18061
LUDWICZAK, DAMIAN R. p 1047 N95-19649
LUETTICH, R. A., JR. p 1075 N95-19540
LUGT, HANS J. p 991 N95-18913
LUKE, SUE p 929 N95-18565
LUNDSTROM, J. M. p 1004 N95-19555
LUO, H. p 1080 N95-19244
LURIE, BORIS J. p 1113 N95-18313
LUSEBRINK, H. p 956 N95-18600
LUTTGES, M. W. p 929 N95-18645
p 929 N95-18646
p 1054 N95-19855
LUU, KIEU X. p 1131 N95-18519
LUXEMBURG, LEON A. p 1115 N95-18992
LY, LE N. p 1074 N95-18153
LYBANON, MATTHEW p 1105 N95-19752
LYLE, KAREN HEITMAN p 1123 N95-18542
LYNCH, F. T. p 1021 N95-19252
LYNN, K. G. p 1055 N95-19858
LYO, S. K. p 1149 N95-18650
p 1122 N95-19234
p 1151 N95-19235

M

MA, DAVID C. p 1018 N95-18549
MAAG, CARL R. p 1181 N95-19175
p 1181 N95-19179
p 962 N95-19184
p 1183 N95-19188
p 1036 N95-19193
MACDONALD-SMITH, DIAN F. M. p 946 N95-19789
MACDONALD, B. D. p 979 N95-18934
MACDONALD, DIGBY D. p 987 N95-19095
MACGOWAN, B. J. p 1038 N95-19247
p 1038 N95-19248
MACH, DOUGLAS p 1068 N95-18093
MACHERET, Y. p 939 N95-19496
MACLEOD, J. D. p 954 N95-19675
MACMARTIN, DOUGLAS G. p 1127 N95-19164
MACPHERSON, G. J. p 1187 N95-19297
p 1189 N95-19314
MADDOCKS, M. C. D. p 1002 N95-19135
MADERUELO, C. p 946 N95-18601
MADEY, GREGORY R. p 1092 N95-19627
p 1103 N95-19641
MADHUKAR, MADHU S. p 981 N95-19652
MAGGIO, ANTHONY p 947 N95-18383
MAGGS, J. E. p 1147 N95-19700
MAGNEE, A. p 953 N95-19674
MAHANTA, KAMALA p 963 N95-18993
MAHONEY, MELISSA J. p 1104 N95-19645
MAIER, M. R. p 1007 N95-17961
MAIN, JOHN A. p 966 N95-18994
MAJUMDAR, SEKHAR p 1028 N95-19458
p 1029 N95-19461
p 1030 N95-19466
MAKARIOU, C. C. p 1143 N95-18119
MALACHIAS, NICKOLAOS p 1065 N95-19083
MALCOLM, GERALD N. p 1020 N95-18955
p 1020 N95-18956
MALETIC, D. p 1150 N95-19091
MALEY, M. p 1148 N95-18064
MALHOTRA, R. p 976 N95-19785
MALIK, A. A. p 983 N95-18019
MALIK, M. R. p 1016 N95-18193
MALLADI, NARASIMHA S. p 1043 N95-18178
MALLORY, MARK p 945 N95-19067
MAMANTOV, GLEB p 974 N95-18412
p 974 N95-18514
MAN, KIN F. p 991 N95-18326
MANKBADI, REDA R. p 1015 N95-18149
MANKOFSKY, A. p 1172 N95-18040
MANN, DARRELL L. p 951 N95-19657
MANSFIELD, D. K. p 1143 N95-17965
MANT, G. p 1135 N95-19709
MANTHEY, J. p 1018 N95-18488
MAO, WEIZHEN p 1100 N95-19028
MARAVAS, ALEXANDER p 1102 N95-19633
MARCHMAN, N. p 1077 N95-19140
MARIJNISSEN, G. p 954 N95-19677
MARINE, R. A. p 1072 N95-19581
MARINH E, H. p 983 N95-17942
MARION, W. p 1055 N95-19856
MARK, ALEXANDER p 992 N95-18745
MARK, DAVID J. p 1074 N95-18160
p 1075 N95-19540
MARK, J. p 1056 N95-17943
MARK, JAMES E. p 985 N95-18513
MARLAND, G. p 1061 N95-19556
MARLEY, N. A. p 1056 N95-17944
MAROLO, SAMUEL A. p 942 N95-18162
p 944 N95-18677
MARRA, JOHN J. p 1041 N95-18325
MARSEE, R. L. p 1002 N95-19087
MARSH, CATHERINE L. p 1008 N95-18318
MARSHALL, J. C. p 1007 N95-17984
MARTEL, GERALD p 1173 N95-18526
MARTHINSEN, K. p 1149 N95-18373
MARTIN, HAYDEN G. p 1141 N95-18593
MARTIN, ROBERT E. p 992 N95-18745
MARTIN, S. J. p 1012 N95-19240
MARTIN, T. p 1152 N95-19621
MARTINDALE, I. p 953 N95-19671
MARTINEZ, DANIEL OSVALDO p 1145 N95-18907
MARTINEZ, M. p 1056 N95-17943
MARTINEZ, R. p 1190 N95-19320
MARTINOU, R. p 954 N95-19676
MARTZ, H. F. p 1155 N95-17996
MARZULLO, KEITH p 1110 N95-18532
MASLANIK, JAMES p 1052 N95-18952
MASSEY, BRIAN p 1095 N95-18034
MASSEY, R. p 1063 N95-18148
MASSEY, R. S. p 1063 N95-18125
MATARRESE, SABINO p 1180 N95-18966
MATHERS, C. D. p 998 N95-18537
MATHUR, J. S. p 1027 N95-19449
MATHUR, ROHIT p 1056 N95-17937
MATHUR, VEERENDRA K. p 1151 N95-19122
MATTER, M., JR. p 1077 N95-18734
MATTES, ROBERT E. p 1034 N95-19236
MATTHEWS, R. K. p 929 N95-18663
p 930 N95-18674
p 944 N95-18891
MATTHYS, DONALD R. p 1142 N95-18995
MATYASH, S. p 1025 N95-19274
MAUS, J. R. p 944 N95-18891
MAUW, S. p 1109 N95-18039
MAVRODINEANU, RADU p 973 N95-17994
MAY, N. E. p 932 N95-19574
MAY, NICHOLAS E. p 1194 N95-19773
p 1031 N95-19775
p 1031 N95-19776
p 1031 N95-19777
p 1031 N95-19778
MAYER, JAMES W. p 1151 N95-19511
MAZIASZ, P. J. p 978 N95-18128
p 981 N95-19568
MAZZOCCHI, V. L. p 1151 N95-19242
MAZZOLENI, ANDRE P. p 1031 N95-18996
MCAULAY, ROBERT J. p 1004 N95-19565
MCCABE, G. p 935 N95-19476
MCCASKILL, MARY K. p 1175 N95-18936
MCCLUNG, R. C. p 1044 N95-18081
MCCLURE, JOHN C. p 1040 N95-18056
MCCOLLUM, M. B. p 965 N95-19780
MCCUE, D. L. p 1171 N95-18060
MCCULLOUGH, JAMES A. p 941 N95-18088
MCCUTCHAN, LARRY p 1097 N95-18447
MCDANIEL, MICHAEL p 945 N95-19731
MCDERMOTT, GENE p 1108 N95-19821
MCDONALD, R. A. p 1181 N95-19175
MCDONALD, T. E. p 1034 N95-19229
MCDONNELL, J. A. M. p 1181 N95-19175
p 961 N95-19180
MCHARGUE, C. J. p 1133 N95-19232
MCINTYRE, D. C. p 977 N95-17968
MCKAMEY, C. G. p 980 N95-19400
MCKAMEY, C. J. p 981 N95-19568
MCLAIN, C. D. p 1070 N95-18384
MCLEMORE, DONALD p 944 N95-18726
MCMAHAN, A. K. p 1155 N95-19838
MCMASTER, JOHN p 1104 N95-19688
MCMILLAN, GRANT p 1088 N95-18084
MCNABB, D. p 1172 N95-18040
MCNULTY, PETER J. p 1131 N95-18474
MCPHADEN, MICHAEL J. p 1068 N95-18201
p 1069 N95-18202
MCPHAIL, ANDREW T. p 1154 N95-19807
p 1154 N95-19812
MCPHERSON, D. W. p 1080 N95-19244
MEBIUS, J. R. p 1094 N95-17972
MEFFERT, JERALYN D. p 1178 N95-18451
MEGSON, G. M. p 1093 N95-17935
MEJAIL, MARTA p 1050 N95-18216
MELILLO, MICHAEL R. p 1000 N95-18686
MELIS, ERICA p 1095 N95-18155
MELMAN, PAUL p 1142 N95-19088
MELOTT, A. L. p 1121 N95-19348
MELOTT, ADRIAN L. p 1198 N95-18747
p 1156 N95-18949
p 1180 N95-18966
p 1156 N95-19037
p 1157 N95-19358
p 1157 N95-19363
MELVIN, C. E. p 997 N95-18494
MENDERS, JIM p 1139 N95-18409
MENDEZ, DAVID J. p 966 N95-19189
MENON, NALINI p 972 N95-19814
MERCHANT, P. G. p 1083 N95-19426
MERCHANT, P. GLENN p 1081 N95-19416
MESICK, HILLARY p 1050 N95-18078
MESSLER, R. W. p 1044 N95-18080
MESSMAN, JERRY D. p 973 N95-17994
METZLER, K. p 1189 N95-19315
METZLER, THEODORE A. p 1103 N95-19642
MEUNIER, HUBERT G. p 1008 N95-18318
MEVREL, R. p 954 N95-19676
MEWHINNEY, MICHAEL p 958 N95-19029

MEYER, L. G. p 1078 N95-18138
MEYER, ROBERT A. p 1111 N95-19513
MEYER, THOMAS J. p 977 N95-19839
MEYER, W. H. p 1146 N95-19379
MEYERS, GARY W. p 990 N95-19090
MEYERS, MICHAEL J. p 943 N95-18415
MEYNINK, W. J. C. p 1071 N95-18607
MICHALEK, JOEL E. p 1172 N95-18025
p 1172 N95-18026
MICHEL, CLAUDE D. p 1010 N95-18523
MICHONNEAU, J. F. p 1025 N95-19276
MIGNACO, J. A. p 1118 N95-18878
MIGNOSI, A. p 1022 N95-19258
p 1025 N95-19276
MILES, PATRICK P. p 1081 N95-19418
p 1084 N95-19434
p 1086 N95-19440
MILLARD, D. L. p 1044 N95-18080
MILLER, D. J. p 1150 N95-19075
MILLER, H. V. p 1052 N95-19733
MILLER, M. S. p 929 N95-18645
p 929 N95-18646
p 1054 N95-19855
MILLER, MATTHEW p 935 N95-19472
MILLER, PHILIP p 932 N95-19260
MILLER, R. V. p 959 N95-18725
MILLER, RONALD J. p 1066 N95-17952
MILLER, S. M. p 977 N95-19868
MILLER, T. p 953 N95-19673
MILLER, W. A. p 1194 N95-19612
MILLER, WILLARD, JR. p 1121 N95-19104
MINER, JUDSON C. p 1172 N95-18025
p 1172 N95-18026
MING, LINZHOU p 1144 N95-18885
MINOWA, CHIKAHIRO p 1018 N95-18549
MIRANKER, DANIEL P. p 1101 N95-19630
MIRIYALA, S. K. p 971 N95-19386
MIRZADEH, S. p 1080 N95-19244
MISAWA, K. p 1189 N95-19316
MISHRA, UMESH K. p 1013 N95-19687
MISSON, N. J. p 1001 N95-19051
MITCHELL, J. T. p 1134 N95-19587
MITCHELL, M. A. p 975 N95-19559
MITCHELL, SCOTT A. p 1118 N95-18896
MITCHELL, T. E. p 981 N95-19611
MITREIKINA, O. B. p 1193 N95-19339
MITTLEFEHLDT, D. p 1190 N95-19320
MIYOSHI, KAZUHISA p 989 N95-19783
MIZUNO, MAKOTO p 1138 N95-19874
MOATS, MICHAEL L. p 945 N95-19693
MOEBIUS, EBERHARD p 1064 N95-18476
MOEHRING, J. T. p 951 N95-19660
MOELLER, ROBERT P. p 1034 N95-19124
MOHAMMADI, JAMSHID p 934 N95-19469
MOHAN, S. R. p 960 N95-19269
MOHLER, STANLEY R., JR. p 933 N95-18582
MOISON, WILLIAM p 996 N95-18341
MOKLER, P. H. p 1135 N95-19787
MOKRY, M. p 932 N95-19278
MOLINE, J. p 1109 N95-17989
MOLL, A. J. p 976 N95-19836
MOMBOURQUETTE, C. B. p 1152 N95-19608
MOMMENS, E. J. p 989 N95-19861
MOMOTA, H. p 1146 N95-19549
MONEY, JOHN M. p 1013 N95-19849
MONGE-CADET, P. p 954 N95-19679
MONTELLI, LUCIANNA p 990 N95-19505
MONTGOMERY, D. C. p 1143 N95-18353
MOODY, PAUL E. p 1041 N95-18335
MOORE, J. H. p 1003 N95-19136
MOORE, LORETTA A. p 1106 N95-19756
p 1106 N95-19760
MORALES, G. J. p 1147 N95-19700
MORALES, NELSON p 967 N95-18570
MORDFIN, LEONARD p 939 N95-19494
MORE, K. L. p 987 N95-19399
MOREL, D. L. p 1056 N95-19680
MOREL, MICHAEL p 949 N95-19380
MORENO, J. C. p 1038 N95-19247
MORGANTI, F. p 1126 N95-19152
MORIARITY, DEBRA M. p 1077 N95-18997
MOROH, M. p 1172 N95-18040
MOSCARDINI, LAURO p 1180 N95-18966
MOSELEY, D. p 1148 N95-18064
MOSHAROV, V. p 1025 N95-19274
MOSIER-BOSS, P. A. p 1008 N95-18052
MOUSTAKAS, THEODORE D. p 1153 N95-19737
MROZOWSKI, MICHAL p 1119 N95-19819
p 1119 N95-19820
MUDKAVI, VIDYADHAR Y. p 1029 N95-19462
MUELLER, G. p 1127 N95-19158
MUELLER, W. F. p 1192 N95-19334
MUKHERJEE, RESHMI p 1179 N95-18499
MULCAHY, T. M. p 1122 N95-19704
MULLER, M. p 940 N95-19805
MUNDING, PETER D. p 1141 N95-19085
MUNSON, ROBERT p 1085 N95-19438
MUNTZ, E. P. p 931 N95-19109
MURAKAMI, M. p 1144 N95-18557
MURAYAMA, HITOSHI p 1133 N95-19245
MURPHY, J. C. p 1122 N95-17983
MURPHY, PATRICK M. p 1107 N95-19761
p 1107 N95-19762
MURPHY, T. C. p 1007 N95-17959
MURTHY, DURBHA V. p 949 N95-19380
MURTHY, P. L. N. p 953 N95-19672
MUSRIE, RUBY p 1114 N95-18875
MUTTON, PHILIP p 964 N95-18105
MYCEK, M. A. p 1148 N95-18122
MYERS, LEONARD p 1104 N95-19748
MYHRE, GRETE p 1083 N95-19425

N

NAGAHARA, H. p 1190 N95-19317
p 1191 N95-19326
NAGY, D. R. p 954 N95-19675
NAIK, RAJIV A. p 970 N95-18466
NAKAGAWA, Y. p 1191 N95-19326
NAKAMURA, A. p 962 N95-19183
NAKAMURA, N. p 1189 N95-19316
NALIM, MOHAMED RAZI p 1041 N95-18901
NAMAVAR, FEREYDOON p 1148 N95-17960
NANCE, W. R. p 1013 N95-19842
NANGIA, R. K. p 1023 N95-19265
NAPOLITANO, MARCELLO R. p 958 N95-19576
NATHAN, ANURADHA p 1056 N95-17937
NATHAN, M. I. p 1152 N95-19620
NAZARAENKO, ALEXANDER Y. p 969 N95-19823
NEAU, E. L. p 977 N95-17968
NED, A. A. p 1040 N95-18010
NEELY, DAVID S. p 1109 N95-18137
NEHRU, C. E. p 1190 N95-19318
NELSON, A. J. p 1055 N95-19858
NELSON, BRIAN W. p 1058 N95-18140
NELSON, M. B. p 1135 N95-19709
NELSON, MICHAEL L. p 1175 N95-18936
NELSON, SIDNEY G. p 1058 N95-18140
NESTLER, JOHN M. p 1058 N95-18085
NEUFFER, W. J. p 1061 N95-19406
NEWMAN, D. M. p 942 N95-18097
NEWMAN, E. H. p 994 N95-18024
NEWMAN, J. C., JR. p 939 N95-19498
NEWSOM, H. E. p 1190 N95-19319
NEWTON, PETER J. p 969 N95-18021
NEYLAND, V. M. p 1025 N95-19275
NGO, E. p 972 N95-19851
NGUYEN, V. D. p 1021 N95-19255
NICHOLS, DANIEL p 1095 N95-18032
NICHOLS, DON F. p 1147 N95-19690
NICHOLS, JAMES p 959 N95-18724
NICKERSON, EARL S., JR. p 1032 N95-18319
NICKLE, C. J. p 1082 N95-19419
NICO, J. S. p 1196 N95-19619
NICOL, DAVID p 1099 N95-18931
NICOL, DAVID M. p 1099 N95-19027
p 1100 N95-19028
NIEH, T. G. p 980 N95-19396
NIELSEN, THOMAS p 936 N95-19479
NIESL, G. p 1124 N95-19144
NIEUWEJAAR, NILS p 1110 N95-18521
p 1110 N95-18581
NIEWOEHNER, ROBERT J., JR. p 944 N95-18621
NIGMATULLIN, RAVIL Z. p 948 N95-19018
p 948 N95-19020
p 948 N95-19022
NILSEN, J. p 1038 N95-19247
p 1038 N95-19248
NINAS, LARRY E. p 963 N95-18098
NISHIOKA, KENJI p 966 N95-19189
NIU, WILLIAM p 962 N95-19184
NOBLE, VIVECA K. p 963 N95-18998
NOGUCHI, R. A. p 971 N95-19579
NOKES, C. R. p 998 N95-18536
NORESE, M. p 1127 N95-19163
NORTHEAST, ERIC p 1046 N95-19504
NORWOOD, C. J. p 1128 N95-19770
NOSENCHUCK, DANIEL p 1092 N95-17939
NOUR, MOHAMED A. p 1092 N95-19627
p 1103 N95-19641
NOWAK, R. E. p 959 N95-18508
NOWOBILSKI, J. J. p 967 N95-18743
NURNBERGER, MICHAEL W. p 1005 N95-19796
p 1006 N95-19798
NUTTALL, ALBERT H. p 997 N95-18475
p 1120 N95-19065
NYQUIST, L. p 1190 N95-19320
NYSTUEN, JEFFREY A. p 1069 N95-18204

O

OAKES, WILLIAM R. p 1118 N95-18896
OBERMEYER, LANCE p 1101 N95-19630
OBRIEN, JAMES J. p 1068 N95-18076
ODAY, M. p 972 N95-19851
ODONOGHUE, P. E. p 1047 N95-19804
OECHSLE, VICTOR L. p 947 N95-18133
OEIEN, K. p 1092 N95-19412
OERTEL, J. p 1033 N95-18555
OERTEL, J. A. p 1035 N95-19711
OFFODILE, FELIX O. p 1103 N95-19641
OGAWA, NOBUYUKI p 1018 N95-18549
OHARA, YOSHIHIRO p 1138 N95-19874
OHM, TIMOTHY R. p 1041 N95-18741
OHMAN, L. H. p 1021 N95-19255
OHRING, SAMUEL p 991 N95-18913
OKONOV, E. O. p 1136 N95-18881
OLIPHANT, A. p 998 N95-18537
OLIVE, KEITH A. p 1137 N95-18965
OLIVEIRA, S. R. p 1147 N95-19837
OLIVER, M. p 946 N95-18601
OLIVIER, PHILIP D. p 1115 N95-18999
OLKIEWICZ, CRAIG p 934 N95-19469
OLSEN, J. R. p 956 N95-18567
OLSON, GREGORY B. p 979 N95-18948
OLSON, HAROLD W. p 941 N95-19810
OLSON, ROBERT M. p 1087 N95-19714
OLSON, S. H. p 1070 N95-18384
ONCLEY, STEVEN p 1016 N95-18191
ONO, M. p 1133 N95-19228
ONO, OWEN T. p 1041 N95-18594
ORAZI, RICHARD J. p 1038 N95-18635
ORGAMBIDE, ALAJANDRO CESAR FRERY p 1172 N95-18004
ORLOV, A. p 1025 N95-19274
ORO, D. M. p 1032 N95-18130
OROURKE, CAROLYN p 1060 N95-18683
p 1062 N95-19860
ORTASSE, RAPHAEL p 934 N95-19470
ORTIZ, CHRISTOPHER J. p 1104 N95-19646
ORVILLE, HAROLD D. p 1064 N95-18413
OSBORNE, M. C. p 985 N95-18638
OSCZEVSKI, RANDALL J. p 989 N95-19867
OSHER, STANLEY p 1097 N95-18437
OSSARD, G. p 1082 N95-19424
OSTER, JOHN p 943 N95-18407
OSWALD, W. J. p 1054 N95-19554
OTTENS, H. p 1127 N95-19160
OU, S. C. p 1067 N95-17955
OUYANG, SHEWANG p 978 N95-18046
OZAKI, AKIRA p 1138 N95-19874

P

PACK, WILLIAM D. p 960 N95-19286
PADMADINATA, U. H. p 934 N95-19471
PAESLEME, NEUSA MARIA p 1178 N95-18213
PAGE, A. G. p 960 N95-19848
PALME, H. p 1190 N95-19321
PALMER, DALE R. p 1088 N95-18095
PANE, JOHN F. p 1089 N95-19068
PAPADOPOLOUS, DEMETRIOS S. p 981 N95-19652
PAPANICOLAOU, NICOLAS A. p 1149 N95-18827
PAPAVASSILIOU, V. p 1131 N95-18550
PAPROCKI, THOMAS H. p 941 N95-19810
PAQUE, J. M. p 1191 N95-19322
PARAMESWARAN, V. R. p 954 N95-19675
PARET, A. p 1125 N95-19145
PARIMUHA, EDWARD p 1000 N95-19035
PARIMUHA, EDWARD M. p 944 N95-18726
PARISH, DEBORAH R. p 955 N95-19684
PARK, JAI H. p 937 N95-19485
PARKER, M. A. p 1138 N95-18102
PARKER, ROBERT P. p 990 N95-19505
PARKIN, D. M. p 1011 N95-19200
PARKINSON, G. V. p 960 N95-19272
PARMAR, PARVINDER SINGH p 1179 N95-18500
PATNAIK, SURYA N. p 1044 N95-18199
p 1045 N95-18909
PATRICK, G. p 1066 N95-17938
PATTERSON, P. E. p 1004 N95-19555
PATTILLO, M. J. p 986 N95-18648
PAUL, S. F. p 1133 N95-19228
PAULOSE, ABRAHAM p 1002 N95-19084
PAZZANI, MICHAEL J. p 1107 N95-19762
PEACE, A. J. p 1030 N95-19774
PEACE, ANDREW J. p 1031 N95-19776
p 1031 N95-19777
p 1031 N95-19778
PEARLSTEIN, FRED p 978 N95-18332
p 979 N95-18458
p 1033 N95-18524
PEARSON, EARL F. p 989 N95-19000

PEARSON, JEROME p 1125 N95-19149
PEASE, DANIEL J. p 1111 N95-19524
PEASE, R. F. p 1010 N95-18625
PECKINPAUGH, SARAH H. p 1104 N95-19742
PECORA, LOUIS M. p 1010 N95-18528
PEDDICORD, K. LEE p 964 N95-18495
PEISEN, DEBORAH p 940 N95-18059
PELACCIO, DENNIS G. p 1136 N95-18217
PELEGRIN, M. p 941 N95-18927
PELEGRIS, GERASIMOS p 998 N95-18522
PELLERIN, F. p 954 N95-19679
PELLMAN, TODD F. p 1156 N95-19037
PELLOUX, R. M. p 970 N95-18471
PELZ, RICHARD B. p 1030 N95-19607
PENDLETON, ED p 957 N95-18641
PERARA, P. A. A. p 1007 N95-17961
PEREZ, IGNACIO M. p 1149 N95-18559
PERKINS, DAVID p 1101 N95-19628
PERNAMBUCO-WISE, P. p 1011 N95-19200
PERREAULT, DAVID A. p 1111 N95-19513
PERRY, F. V. p 1063 N95-17947
PERRY, M. D. p 1142 N95-19710
PERSIC, MASSIMO p 1198 N95-18747
PERVUSHIN, V. p 1156 N95-18328
PESETSKY, V. p 1025 N95-19274
PESTOV, A. B. p 1180 N95-18877
PETERS, M. E. p 994 N95-18024
PETERSON, A. S. p 1096 N95-18364
PETERSON, KENNETH A. p 1058 N95-18140
PETERSON, ROBERT B. p 1036 N95-19190
PETIAU, C. p 1125 N95-19145
PETRACCA, ALEISA p 1095 N95-18030
p 1100 N95-19106
PETRE, E. p 941 N95-18927
PETRO, JIM p 1098 N95-18450
PETTIT, CHRIS p 957 N95-18641
PHANORD, DIEUDONNE D. p 1073 N95-19001
PHILIPP, WARREN H. p 984 N95-18321
PHILLION, D. W. p 1146 N95-19250
PHILLIPS, C. p 1108 N95-17936
PHILLIPS, DOUGLAS J. p 964 N95-18580
PHILLIPS, W. MORRIS p 960 N95-18961
p 1011 N95-18962
PHILPOTT, MICHAEL R. p 1132 N95-18655
PHONOV, S. p 1025 N95-19274
PHUVAN, SONLINH p 1173 N95-18544
PI, XIAOQING p 1066 N95-19105
PIASCIK, ROBERT S. p 935 N95-19472
PIAT, J. F. p 1025 N95-19277
PIEPER, G. W. p 1111 N95-19592
PIERCE, DOUGLAS C. p 1010 N95-18660
PIERRE, CHRISTOPHE p 950 N95-19383
PIERS, W. J. p 928 N95-18503
PILLAY, SASI KUMAR p 1019 N95-18941
PIMENTEL, B. M. p 996 N95-18331
PINELLI, THOMAS E. p 1109 N95-18055
p 1175 N95-18950
p 1175 N95-18953
p 1175 N95-19038
p 1176 N95-19127
PINOLI, PAT C. p 967 N95-19566
PINTO-NETO, N. p 1118 N95-19375
PIPPIG, T. p 1084 N95-19435
PISANO, F. p 1148 N95-18330
PIZIALI, R. A. p 931 N95-19119
PLEITEZ, V. p 1148 N95-18330
PLUMB, G. D. p 992 N95-18533
p 998 N95-18534
p 993 N95-19137
p 993 N95-19138
POCOCK, MARK F. p 1031 N95-19775
p 1031 N95-19776
p 1031 N95-19777
POHL, KYM p 1104 N95-19748
POINTON, T. D. p 1133 N95-19199
POKORA, DARLENE C. p 932 N95-19623
POLINER, JEFFREY p 1091 N95-18189
POLLOCK, MICHAEL L. p 1079 N95-18661
PONCHAK, GEORGE E. p 1000 N95-18733
POOLE, PETER p 938 N95-19492
POOLE, RICHARD J. D. p 933 N95-19280
POON, S. J. p 982 N95-19743
POPE, D. P. p 981 N95-19611
POPE, JOAN p 1074 N95-18470
POPENOE, PETER p 1073 N95-17951
PORCU, SILVIO p 1083 N95-19430
PORTER, KEN p 1100 N95-19626
POST-ZWICKER, A. P. p 1133 N95-19228
POST, G. F. p 1119 N95-19408
POTTER, B. G. p 988 N95-19558
POTTER, DAVID J. p 1111 N95-19526
POTYONDY, DAVID O. p 935 N95-19473
POWERS, GRADY p 1043 N95-19593
PRABHU, DINESH K. p 933 N95-19464
PRASKOVSKY, ALEXANDER p 1016 N95-18191
PRATHER, W. p 997 N95-18506
PRATHER, WILLIAM p 944 N95-18726
PREGITZER, KURT S. p 1060 N95-19112
PRICE, SHANNON W. p 1106 N95-19756
PRIEDHORSKY, W. p 964 N95-18639
PRINDIVILLE, JAMES E. p 1141 N95-18593
PRINZ, M. p 1190 N95-19318
p 1193 N95-19335
PROBERT, P. H. p 999 N95-18558
PROVAN, JAMES W. p 935 N95-19474
PROVENZANO, VIRGIL p 971 N95-19123
PRUDHOMME, S. p 1022 N95-19258
PRUETT, C. DAVID p 1014 N95-18042
PSALTIS, DEMETRI p 1035 N95-19871
PUGHE, W. p 1178 N95-18001
PULIAFITO, CARMEN A. p 1078 N95-18515
PULLEN, I. R. p 1002 N95-19135
PURAKAYASTHA, APRATIM p 1110 N95-18521
PURVIS, CHRISTOPHER REECE p 958 N95-18902
PYATOV, P. N. p 1118 N95-18876

Q

QIAN, YONG-ZHONG p 1198 N95-19283
QUANTIERI, THOMAS F. p 1004 N95-19565
QUATE, CALVIN F. p 1128 N95-19802
QUEMARD, C. p 933 N95-19279
QUESNEL, E. p 954 N95-19679
QUICK, MARK p 1096 N95-18344

R

RACHELE, HENRY p 1063 N95-18115
RADA, M. p 1086 N95-19443
RADCHENKO, V. p 1025 N95-19274
RADKE, G. E., JR. p 1120 N95-18020
RADMACHER, M. p 1129 N95-17974
RADMILOVIC, V. p 979 N95-19093
RAEDER, C. H. p 1044 N95-18080
RAHMAN, ANISUR p 971 N95-19650
RAIKHER, VENIAMIN L. p 935 N95-19475
RAIS-ROHANI, MASOUD p 942 N95-18090
RAKOW, ALLEN L. p 1077 N95-18179
RANGARAJAN, R. p 1027 N95-19447
RANKIN, CHARLES C. p 939 N95-19499
RAOGUDIMETLA, V. S. p 1014 N95-18983
RAPANOTTI, L. p 1093 N95-17935
RAPOSA, JOHN R. p 1009 N95-18455
RAPTIS, A. C. p 1012 N95-19246
RASHID, R. p 1111 N95-18892
RASHIDNIA, NASSER p 1017 N95-18327
RASMUSSEN, K. L. p 1192 N95-19333
RATCLIFF, P. R. p 961 N95-19180
RATIS, YU. L. p 1132 N95-18882
RATLIFF, E. R. p 1174 N95-18680
p 1174 N95-18681
RAU, GUIDO p 1021 N95-19257
RAUCH, JEFFREY S. p 1042 N95-19238
RAUNIG, D. L. p 1002 N95-19087
RAVICHANDRAN, K. S. p 1027 N95-19450
p 1028 N95-19453
p 1028 N95-19456
RAWLINS, W. T. p 977 N95-19868
RAY, CLARK K. p 993 N95-19036
RAZAZIAN, K. p 1012 N95-19246
REAGOR, D. W. p 1152 N95-19608
REARDON, MATTHEW J. p 1079 N95-18618
p 1087 N95-19811
REDDY, C. J. p 995 N95-18187
REDDY, E. S. p 953 N95-19672
REDDY, JAY p 1095 N95-18033
REDDY, S. V. p 939 N95-19495
REDDY, WILLIAM D. p 943 N95-18505
REDFIELD, CAROL L. p 1106 N95-19758
REDWINE, S. p 1108 N95-19803
p 1108 N95-19813
REICHENBACH-KLINKE, K. p 1082 N95-19420
REICHERT, P. p 1038 N95-19096
REID, ROBERT H. p 1129 N95-18062
REITZ, RONALD P. p 1019 N95-18634
RENAUD, JOHN E. p 1046 N95-19522
RENK, T. J. p 1133 N95-19199
REPPERT, STEVEN M. p 1078 N95-18512
RESNICK, ANDY p 1195 N95-17980
RESS, D. p 1146 N95-19509
p 1135 N95-19709
RESTER, A. C., JR. p 1136 N95-18370
RHEIN, M. D. p 1007 N95-17961
RHODEN, CHRISTOPHER A. p 1094 N95-18013
RHUDY, R. W. p 929 N95-18663
RIBEIRO, LUIZ CARLOS BARBOSA p 1064 N95-18390
RIBEIRO, NUNO PEDRO p 1084 N95-19432
RICCO, A. J. p 975 N95-19559
RICH, MARKHAM K. p 965 N95-19571
RICHARDSON, J. p 1105 N95-19751
RICHARDSON, LONDE A. p 1085 N95-19437
p 1085 N95-19438
RICHARDSON, MICHAEL A. p 1141 N95-18628
RICHARDSON, MICHAEL D. p 1076 N95-19818
RICHMOND, M. p 1066 N95-17938
RICKEL, D. G. p 1011 N95-19200
RICKERBY, D. p 954 N95-19679
RIEGER, D. J. p 975 N95-19559
RIESBECK, STEPHEN p 1097 N95-18415
p 1100 N95-19106
RIETHMULLER, M. L. p 1021 N95-19253
RILEY, GARY p 1100 N95-19625
p 1104 N95-19747
RILEY, J. L. p 1001 N95-19050
RINEHART, L. F. p 1004 N95-19555
RINKER, JOHN p 1052 N95-19734
RIOS-TEJADA, F. p 1082 N95-19423
RIOS, FRANCISCO p 1081 N95-19418
p 1084 N95-19434
p 1086 N95-19440
RITCHIE, A. B. p 1039 N95-19398
RITTER, KENNETH J. p 1010 N95-18662
RIVERA, JORGE E. p 963 N95-18047
RIVERS, M. p 1139 N95-18409
RIVET, WILLIAM A. p 1111 N95-19526
RIX, THOMAS p 1106 N95-19760
ROBE, R. Q. p 1002 N95-19087
ROBERTS, C. D. p 1130 N95-18428
p 1131 N95-18548
ROBERTS, LEONARD p 1023 N95-19266
ROBERTSON, M. p 1007 N95-17961
ROBIDEAUX, BRET R. p 1103 N95-19642
ROBINSON, HAROLD C. p 1128 N95-19514
ROBINSON, M. C. p 929 N95-18645
p 929 N95-18646
p 1054 N95-19855
ROCHE, M. p 1054 N95-19117
ROCHE, M. F. p 1053 N95-19074
p 1053 N95-19116
ROCKETT, T. J. p 971 N95-19386
RODE, DANIEL L. p 1138 N95-18100
RODMAN, GEOFFREY A. p 940 N95-19500
RODRIGUEZ, L. p 1056 N95-17943
ROEDIGER, HENRY, III p 1090 N95-19740
ROGERS, F. J. p 1186 N95-19249
ROGERS, J. P. p 956 N95-18567
ROGERS, MELISSA J. B. p 991 N95-19788
ROHRBAUGH, S. M. p 935 N95-19476
ROKHLIN, VLADIMIR p 1119 N95-19735
ROMERE, PAUL O. p 965 N95-19237
p 965 N95-19624
ROOZENDAAL, R. p 1057 N95-18002
ROPER, DONNA G. p 1175 N95-18936
ROSA, FERDINAND p 982 N95-18180
ROSAKIS, ARES J. p 1045 N95-18613
ROSE, M. G. p 951 N95-19661
ROSENFELD, AZRIEL p 1113 N95-18057
ROSENKRANZ, PHILIP W. p 1064 N95-18444
ROSNESS, R. p 1092 N95-19412
ROSSMANN, A. p 953 N95-19673
ROTE, D. M. p 1122 N95-19704
ROTH, CARL p 1108 N95-19821
ROTH, DON J. p 1043 N95-18583
ROUSE, PETER L. p 951 N95-19656
ROUTBORT, J. L. p 1150 N95-19075
p 1150 N95-19094
RUBIN, A. E. p 1188 N95-19309
p 1191 N95-19323
RUBIN, RAFAEL LEVY p 967 N95-18720
RUBY, D. S. p 1055 N95-19859
RUDD, JAMES L. p 945 N95-19517
RUDD, R. F. p 1001 N95-19051
RUDEN, P. P. p 1152 N95-19620
RUEGER, M. L. p 960 N95-19271
RUFF, D. p 935 N95-19476
RUGGIERO, A. G. p 1150 N95-19091
RUIZ, C. p 953 N95-19671
RUSSELL, D. H. p 977 N95-19840
RUSSELL, JOHN M. p 1036 N95-18181
RUSSELL, S. S. p 1186 N95-19291
RUSSELL, STEPHEN D. p 1038 N95-18635
RUSSO, G. P. p 960 N95-19267
RUTAN, S. C. p 973 N95-17966
RUZMAIKINA, T. V. p 1191 N95-19324
RYAN, PHILIP F. X. p 959 N95-18942
RYDER, JAMES T. p 966 N95-19189
RYE, R. R. p 975 N95-19559

S

SABA, JULIA L. R. p 1195 N95-18376
SABOE, G. W. p 1085 N95-19439
SACKSTEDER, KURT p 990 N95-18211
SADANANDA, KUNTIMADDI p 971 N95-19123

SADDOW, STEPHEN E. p 1008 N95-18378
SADOVSKII, N. p 1025 N95-19274
SAEED, A. p 991 N95-17934
SAHU, JUBARAJ p 930 N95-18670
SAIGAL, SUNIL p 1044 N95-18199
p 1045 N95-18909
SAILOR, W. C. p 1143 N95-17969
SAISI, ROBERT O. p 1097 N95-18420
SALDEN, ROGER p 1017 N95-18396
SALTZMAN, EDWIN J. p 929 N95-18565
SALUCCI, PAOLO p 1198 N95-18747
SALZAR, ROBERT SCOTT p 970 N95-18920
SAMAVEDAM, GOPAL p 936 N95-19477
SAMMELLS, A. F. p 973 N95-17982
SAMSON, J. A. R. p 974 N95-18744
SANDERS, F. p 1066 N95-17938
SANDERS, I. S. p 1191 N95-19325
SANDS, P. D. p 1120 N95-18653
SANSONE, LOUIS E. p 1142 N95-19389
SANTI, L. MICHAEL p 968 N95-19002
SANTIAGO, FRANCISCO p 1149 N95-18527
SANTINI, P. p 1126 N95-19152
SARLO, O. p 1082 N95-19421
SARMA, P. R. R. p 1014 N95-19634
SARMIENTO REYES, L. A. p 1009 N95-18501
SARWATE, DILIP V. p 1114 N95-18675
SASAKI, S. p 1191 N95-19326
SASAO, M. p 1143 N95-17965
SASTRY, S. M. L. p 978 N95-18046
SATARIANO, J. J. p 1035 N95-19711
SAUCRAY, J. M. p 946 N95-18599
SAUTER, DAVID p 1090 N95-18029
SAWYER, BRIAN p 940 N95-18059
SAXENA, S. K. p 1029 N95-19463
SCAVONE, D. W. p 979 N95-18934
SCHAEFFLER, A. p 952 N95-19665
SCHAPPERT, G. T. p 1032 N95-18130
SCHAUB, G. E. p 1181 N95-19175
SCHEBELLA, K. J. p 975 N95-19699
SCHEFFNER, NORMAN W. p 1075 N95-19540
SCHEIDLER, MICHAEL J. p 1122 N95-19603
SCHEPS, RICHARD p 1038 N95-18585
SCHERE, KENNETH L. p 1056 N95-17937
SCHIJVE, J. p 934 N95-19471
p 936 N95-19478
SCHILLIG, J. B. p 1011 N95-19200
SCHIMA, F. J. p 981 N95-19703
SCHIVLEY, MARK A. p 1110 N95-18615
SCHLOSSER, THOMAS W. p 997 N95-18516
SCHMIDT, H.-J. p 936 N95-19479
SCHMUECKER, J. p 952 N95-19665
SCHNEIBEL, J. H. p 978 N95-18128
SCHNEIDER-MUNTAU, H. J. p 1011 N95-19200
SCHNEIDER, WALTER T. p 995 N95-18314
SCHOENFELD, S. E. p 980 N95-19400
SCHONBERG, WILLIAM P. p 1047 N95-19003
SCHOWALTER, DAVID GREGG p 1019 N95-18921
SCHRADER, K. H. p 936 N95-19480
SCHRAMM, DAVID N. p 1137 N95-18965
SCHREUR, BARBARA p 1108 N95-19004
SCHROCK, V. p 1137 N95-19588
SCHROEDER, JIM p 1003 N95-19510
SCHUBERT, W. K. p 1055 N95-19859
p 1055 N95-19873
SCHULTZ, K. p 1137 N95-19588
SCHULZ, A. L. p 989 N95-19861
SCHULZE, W. A. p 988 N95-19558
SCHWAB, C. p 1117 N95-18482
SCHWARTZ, ADAM J. p 977 N95-17962
SCHWARTZ, D. S. p 978 N95-18046
SCHWARTZ, M. p 973 N95-17982
SCOFIELD, J. H. p 1038 N95-19247
SCOTT, A. DONALD, JR. p 1058 N95-18132
SCOTT, CLARK L. p 1063 N95-17946
SCOTT, E. R. D. p 1189 N95-19313
p 1192 N95-19327
SCOTT, J. L. p 989 N95-19861
SCOTT, JAMES R. p 1014 N95-18036
SCOTT, STEPHEN L. p 1106 N95-19755
SCOTT, W. G. p 1132 N95-18643
SCOTT, WILLIAM R. p 1149 N95-18559
SEAL, DANIEL W. p 1034 N95-19236
SEARS, D. W. G. p 1192 N95-19328
SEAY, C. HARRIS p 1075 N95-19563
SEBACHER, K. p 997 N95-18506
SEBACHER, KURT p 933 N95-18507
SEBEK, J. p 1138 N95-19841
SECOR, E. D. p 983 N95-18016
SEE, T. H. p 1047 N95-19185
SEEBACH, GERALD L. p 1008 N95-18318
SEEHOLZER, THOMAS L. p 962 N95-18387
SEGALL, Z. p 1111 N95-18892
SEGUR, HARVEY p 1075 N95-19523
SEIGNEURIC, A. p 1082 N95-19422
p 1082 N95-19424
SEINER, J. M. p 1125 N95-19148
SELLAR, RICHARD S. p 1046 N95-19522
SELYUGIN, O. V. p 1130 N95-18360
SEMERARO, B. D. p 1112 N95-19831
SEMMLER, R. p 1198 N95-18880
SENAPATI, N. p 937 N95-19486
SENGUPTA, L. C. p 972 N95-19851
SEPANSKI, ROBERT J. p 1058 N95-18389
SERAUDIE, A. p 1022 N95-19258
SEXTON, DOUGLAS A. p 1038 N95-18635
SHAH, V. M. p 1134 N95-19557
SHANDARIN, SERGEI p 1157 N95-19358
SHANDARIN, SERGEI F. p 1156 N95-18949
p 1156 N95-19037
p 1156 N95-19340
p 1193 N95-19341
SHAOXIONG, H. p 1192 N95-19328
SHAPIRO, MICHAEL p 1096 N95-18161
SHAROBEAM, MONIR H. p 936 N95-19481
SHARPS, P. R. p 1056 N95-19878
SHAW, BEVIL J. p 937 N95-19482
SHAW, J. A. p 1030 N95-19774
SHAW, JONATHON A. p 1030 N95-19506
p 1031 N95-19775
p 1031 N95-19776
p 1031 N95-19777
p 1031 N95-19778
SHAW, KEVIN p 1050 N95-18078
p 1052 N95-19733
SHAW, L. L. p 1125 N95-19146
SHEA, KENNETH J. p 987 N95-19544
SHEPHERD, T. G. p 1059 N95-18665
SHER, A. p 1142 N95-19732
SHI, BINGREN p 1144 N95-18886
SHI, X. p 1180 N95-18746
SHI, XIANGJUN p 1132 N95-18883
SHIELDS, JOHN J. p 1034 N95-19071
SHIFLET, G. J. p 982 N95-19743
SHIH, C.-Y. p 1190 N95-19320
SHIH, S.-H. p 1015 N95-18149
SHIMABUKURO, RANDY L. p 1010 N95-18546
SHIMIZU, MIKIO p 961 N95-19191
SHIMOVETZ, R. M. p 1125 N95-19146
SHINODA, PATRICK M. p 932 N95-19270
SHIPLEY, D. E. p 929 N95-18645
p 929 N95-18646
p 1054 N95-19855
SHIVAKUMAR, K. N. p 939 N95-19498
SHOEMAKER, EUGENE M. p 1194 N95-19575
SHORE, B. W. p 1142 N95-19710
SHORE, CHARLES P. p 939 N95-19499
SHORT, DAVID A. p 1068 N95-18201
p 1069 N95-18206
SHU, L. Y. p 1146 N95-19549
SHUKLA, SHRIDHAR B. p 1003 N95-19525
SHUR, MICHAEL p 1032 N95-17970
p 1013 N95-19849
SI, ERJIAN p 937 N95-19483
SIDAWI, JIHAD A. p 937 N95-19484
SIEGNER, U. p 1148 N95-18122
SIEIRO, JUAN p 1084 N95-19434
SIGL, G. p 1180 N95-18746
SIKKA, V. K. p 981 N95-19568
SILBEY, ROBERT J. p 985 N95-18636
SILVA, M. C. G. p 1021 N95-19254
SILVER, ARNOLD H. p 1009 N95-18432
SILVER, R. N. p 1155 N95-17996
SIMMONS, J. A. p 1122 N95-19234
SIMMS, D. A. p 1054 N95-19855
SIMON, CHARLES G. p 1036 N95-19192
SIMON, RANDY W. p 1009 N95-18432
SIMONDS, GREGORY A. p 1142 N95-19389
SIMPSON, E. M. p 1136 N95-18552
SINGER, KENNETH D. p 987 N95-19102
SINGH, J. P. p 1028 N95-19454
SINGH, RIPUDAMAN p 937 N95-19485
SINGHAL, S. N. p 953 N95-19672
SINHA, U. N. p 1027 N95-19446
SIRS, R. C. p 950 N95-19655
SIX, FRANK p 1161 N95-18967
SJAARDEMA, GREGORY D. p 1118 N95-18896
SKIDMORE, J. A. p 1039 N95-19508
SKIPALIS, MICHAEL P. p 1141 N95-18593
SKJELLAUG, B. p 1003 N95-19411
SKRUTSKIE, M. p 1178 N95-18001
SLANE, STEVE p 986 N95-19064
SLATON, DAVE p 1068 N95-18093
SLAUSON, J. W. p 1085 N95-19439
SLINEY, HAROLD E. p 969 N95-18448
SLINGERLAND, F. W. p 940 N95-19167
SLOAN, L. R. p 975 N95-19559
SLUITER, MARCEL H. p 977 N95-17962
SLUTZ, S. A. p 1145 N95-19201
SMALL, B. S. p 1067 N95-17992
SMITH, A. E. p 1197 N95-18464
SMITH, B. F. p 1094 N95-17978
SMITH, BROOKE C. p 1020 N95-18955
p 1020 N95-18956
SMITH, CRAWFORD F. p 950 N95-19651
SMITH, D. L. p 1152 N95-19620
p 982 N95-19725
SMITH, FLOYD Z. p 962 N95-18387
SMITH, GREGORY E. p 955 N95-19769
SMITH, KERRIN p 1097 N95-18421
SMITH, MELODY V. p 973 N95-17994
SMITH, P. H. p 1007 N95-17959
SMITH, PAUL p 1174 N95-18573
SMITH, PETER M. p 1104 N95-19742
SMITH, S. H. p 937 N95-19486
SMITH, SHERYL S. p 1079 N95-18656
SMITH, SIMON p 964 N95-18495
SMITH, V. K. p 944 N95-18891
SMITH, W. H. p 981 N95-19707
SMITH, WILLARD A. p 1168 N95-19005
SMOOT, MELISSA C. p 1123 N95-18673
SMULLEN, R. R., JR. p 959 N95-18508
SNAVELY, DEANNE p 976 N95-19830
SNEAD, L. L. p 985 N95-18638
SNEL, H. p 928 N95-18503
SNODGRASS, JOAN G. p 1090 N95-19602
SNOW, ERIC S. p 1141 N95-18529
SNOW, FRANK J. p 1092 N95-18517
SOBIESZCZANSKI-SOBIESKI, J. p 1116 N95-18108
p 1116 N95-18109
SOBOL, P. E. p 1055 N95-19858
SOEDIONO, A. H. p 937 N95-19487
SOICHER, H. p 1057 N95-17985
SOLAKIEWICZ, RICHARD p 1143 N95-19006
SOLARZ, R. W. p 1039 N95-19508
SONG, L. p 986 N95-18648
SORATHIA, USMAN A. p 970 N95-18629
SOSS, DAVID A. p 967 N95-18632
SOWINSKI, D. p 1007 N95-17961
SPACKMAN, H. p 1040 N95-18152
SPAID, F. W. p 1021 N95-19252
SPARKS, W. A. p 936 N95-19480
SPATES, J. J. p 1012 N95-19240
SPAULDING, GLENN F. p 983 N95-18134
SPEECE, ROBERT F. p 963 N95-18047
SPINDT, C. A. p 1013 N95-19865
SPLINTER, RANDALL J. p 1198 N95-18747
SPRAGUE, RICHARD p 996 N95-18341
SPRINGER, ANTHONY M. p 932 N95-19623
SPRINGER, K. N. p 1152 N95-19608
SPRINKLE, DANNY R. p 1032 N95-18316
SQUILLACIOTI, RICHARD JOHN p 979 N95-18939
SRAJER, G. p 1151 N95-19113
SRINIVASA, C. p 930 N95-18904
SRINIVASAN, R. p 1122 N95-17983
SRIVASTAVA, ASHOK p 1027 N95-19448
STACY, JOHN L. p 1138 N95-18067
STADLER, HENRY L. p 1093 N95-18963
STAELIN, DAVID H. p 1064 N95-18444
STAHLBERG, E. A. p 1153 N95-19724
STANCIL, ROBERT F. p 1034 N95-19071
STANLEY, JAY L., JR. p 1096 N95-18364
STANNILAND, D. R. p 931 N95-19546
STANNILAND, DENNIS R. p 946 N95-19789
STARK, MARY p 1104 N95-19688
STARNES, JAMES H., JR. p 939 N95-19499
STEARNS, S. D. p 1174 N95-18873
STEENKISTE, P. p 1111 N95-18892
STEFANIK, RAYMOND J. p 1008 N95-18156
STEFFEN, K. p 1062 N95-19779
STEFFEN, KONRAD p 1052 N95-18952
STEFFES, PAUL R. p 962 N95-18387
STEFKO, GEORGE L. p 949 N95-19380
STEIN, KEITH R. p 928 N95-18340
STEINER, D. p 985 N95-18638
STEINMEYER, D. C. p 1043 N95-19809
STENE, J. p 992 N95-18667
STENGEL, ROBERT F. p 1102 N95-19633
STEPHENSON, STEPHENI p 1036 N95-19193
STEPHENSON, STEPHENI L. p 1181 N95-19175
STEPHENSON, TIMOTHY A. p 979 N95-18948
STERMAN, G. p 1135 N95-19726
STERN, ROBERT A. p 1178 N95-18391
STEVENS, C. O. p 987 N95-19399
STEVENS, J. W. p 1013 N95-19872
STEVENS, R. p 962 N95-18932
STEVENSON, J. W. p 1054 N95-19591
STEVENSON, T. J. p 1183 N95-19188
STEWART, MICHAEL p 1068 N95-18093
STEWART, R. E. p 1039 N95-19398
STEYSKAL, H. p 995 N95-18116
STILLWAGEN, FREDERIC H. p 964 N95-18105
STINNETT, R. W. p 977 N95-17968
STOCKDALE, R. E. p 1143 N95-18119
STODOLSKY, DANIEL p 1093 N95-18659
STOICA, ION p 1098 N95-18487
STOKES, MICHAEL p 1002 N95-19072
STOKKE, P. p 951 N95-19659
STONE, FRANK p 967 N95-19566
STORM, MARK E. p 1037 N95-18322

STOSS, FREDERICK W. ..... p 1058 N95-18389
STOUT, L. ..... p 962 N95-18932
STOWELL, S. ..... p 972 N95-19851
STRANDHAGEN, J. O. ..... p 1100 N95-19409
STRANGMEN, THOMAS E. ..... p 955 N95-19683
STRATTON, SUZANNE R. ..... p 995 N95-18136
STRAWN, ROGER ..... p 1043 N95-18737
STRAYER, M. R. ..... p 1116 N95-18120
STREET, D. R., JR. ..... p 1089 N95-18414
STREET, KENNETH W., JR. ..... p 984 N95-18321
STRIZENEC, P. ..... p 996 N95-18367
STROEVE, J. ..... p 1062 N95-19779
STROKOVSKIJ, E. A. ..... p 1132 N95-18882
STUART, B. C. ..... p 1142 N95-19710
STUDEBAKER, J. K. ..... p 1032 N95-18130
STUHMILLER, JAMES H. ..... p 1078 N95-17998
STUMBERG, MICHAEL F. ..... p 1149 N95-18527
STURISKY, SELWYN HOWARD ... p 959 N95-18903
SUAREZ, CARLOS J. ..... p 1020 N95-18955
p 1020 N95-18956
SUCHA, G. ..... p 1036 N95-18123
SUCIU, D. F. ..... p 989 N95-19861
SUGIHARA, KAZUO ..... p 1114 N95-18889
SULC, J. ..... p 1086 N95-19443
SULLIVAN, T. J. ..... p 1059 N95-18647
SULTAN, FLORIN ..... p 1098 N95-18487
SUN, D. C. ..... p 1041 N95-18541
p 1043 N95-19567
SUNDARAM, ASHOK ..... p 1014 N95-19634
SUNDER, R. ..... p 927 N95-18606
SUNDURIN, V. G. ..... p 948 N95-19021
SUTTER, JAMES K. ..... p 1043 N95-18583
SUTTON, M. A. ..... p 939 N95-19498
SUTTON, S. R. ..... p 1182 N95-19182
SUZUKI, ICHIRO ..... p 1113 N95-18157
p 1110 N95-18158
p 1114 N95-18889
SWAIM, ROBERT J. ..... p 1011 N95-18962
SWAMY, M. R. ..... p 1013 N95-19872
SWANSON, H. W., JR. ..... p 1012 N95-19231
SWANSON, JAMES R., SR. ..... p 1161 N95-18182
SWANSON, P. D. ..... p 1138 N95-18102
SWART, R. J. ..... p 1058 N95-18375
SWIERTRA, S. ..... p 941 N95-18927
SWIFT, T. ..... p 938 N95-19488
SWINDLE, T. D. ..... p 1192 N95-19329
SZPAK, S. J. ..... p 1008 N95-18052
SZUSZCZEWICZ, E. P. ..... p 1172 N95-18040

T

TABAKOFF, W. ..... p 952 N95-19662
TAHIR, H. ..... p 973 N95-17991
TAJIMA, T. ..... p 1129 N95-17976
TAJIMA, TOSHIKI ..... p 1147 N95-19837
TAKANO, Y. ..... p 1067 N95-17955
TALBOT, T. ..... p 929 N95-18624
TALBOTEC, J. ..... p 953 N95-19669
TALEFF, E. M. ..... p 980 N95-19396
TALIA, GEORGE E. ..... p 982 N95-19007
TAN, P. W. ..... p 1047 N95-19804
TAN, S. C. ..... p 952 N95-19663
TAN, T. Y. ..... p 1153 N95-19697
TANAHASHI, SHUGO ..... p 1012 N95-19548
TANG, C. L. ..... p 1138 N95-18102
TANG, WEI-PAI ..... p 1118 N95-18736
TANG, YU ..... p 1020 N95-19098
p 1020 N95-19099
TANIS, J. A. ..... p 1132 N95-18874
TANK, A. M. G. KLEIN ..... p 1070 N95-18392
TANNER, LEE E. ..... p 977 N95-17962
TANNER, WILLIAM G. ..... p 1181 N95-19175
p 1183 N95-19188
p 1036 N95-19193
TANVEER, S. ..... p 1017 N95-18397
TANVEER, SALEH ..... p 1015 N95-18188
TAPSCOTT, ROBERT E. ..... p 992 N95-18684
TARDY, H. L. ..... p 1055 N95-19859
TARROU, C. ..... p 1099 N95-18668
TARTAKOVSKY, ALEXANDER ... p 1098 N95-18564
TATARA, J. D. ..... p 1091 N95-19061
TAUTGES, TIMOTHY J. ..... p 1118 N95-18896
TAWEL, RAOUL ..... p 1114 N95-18740
TAWFIK, HAZEM ..... p 989 N95-19008
TAYLOR, CHARLES R. ..... p 1143 N95-19009
TAYLOR, JAMES L. ..... p 992 N95-18745
TAYLOR, KEN ..... p 1108 N95-19821
TAYMAN, STEVEN K. ..... p 932 N95-19863
TEBBE, DENNIS ..... p 1115 N95-19512
TELLO, IVAN ..... p 1107 N95-19764
TEMPLE, ENOCH C. ..... p 1044 N95-19010
TENCH, R. J. ..... p 987 N95-19227
TENFORDE, T. S. ..... p 1076 N95-18371
TERRY, ROBERT E. ..... p 1147 N95-19846
THIELE, OTTO W. ..... p 10b8 N95-18201
THIEMENS, M. H. ..... p 1192 N95-19330
THOMAS, D. M. ..... p 1146 N95-19378
THOMAS, EDWIN L. ..... p 987 N95-19520
THOMAS, G. ..... p 979 N95-19093
THOMAS, I. M. ..... p 1039 N95-19708
THOMAS, M. G. ..... p 1013 N95-19872
THOMAS, SCOTT R. ..... p 960 N95-19286
THOMAS, STAN J. ..... p 1115 N95-18183
THOMASON, J. F. ..... p 1057 N95-17985
THOMBLEY, R. L. ..... p 1006 N95-19833
THOMPSON, A. C. ..... p 1034 N95-19233
THOMPSON, M. O. ..... p 977 N95-17968
THOMSEN, MARK L. ..... p 938 N95-19489
THOMSON, DOUGLAS ..... p 936 N95-19477
THORN, ROBERT PEYTON ..... p 1065 N95-18731
THORNHILL, J. W. ..... p 1147 N95-19847
THURSBY, MICHAEL H. ..... p 1002 N95-19103
TIEGS, T. N. ..... p 987 N95-19399
TIETBOHL, G. L. ..... p 1146 N95-19250
TIGHE, W. ..... p 1133 N95-19228
TISONE, G. C. ..... p 1133 N95-19199
TIWARI, P. ..... p 1148 N95-18064
TOBIN, M. ..... p 1137 N95-19588
TODD, MICHAEL ..... p 988 N95-19745
TOELLE, RONALD ..... p 963 N95-19648
TOKHEIM, ROBERT E. ..... p 1137 N95-19588
TOMAZELLI, J. L. ..... p 996 N95-18331
TOMELLINI, MASSIMO ..... p 955 N95-19682
TOMIO, LAURO ..... p 1130 N95-18329
p 1156 N95-18352
TOMITA, Y. ..... p 1146 N95-19549
TORELLA, GIOVANNI ..... p 953 N95-19668
TORNG, T. Y. ..... p 1044 N95-18081
TORTORELLI, P. F. ..... p 978 N95-18121
TOUCH, JOSEPH D. ..... p 1004 N95-19600
TOUGARD, D. ..... p 1127 N95-19159
TOWNE, MATTHEW C. ..... p 931 N95-19110
TOWNSEND, J. ..... p 1148 N95-18064
TRAVEN, R. ..... p 944 N95-18723
TRAWEEK, M. S. ..... p 1091 N95-19061
TREBES, J. E. ..... p 1146 N95-19509
TREDICI, THOMAS J. ..... p 1086 N95-19441
TREFNY, CHARLES J. ..... p 960 N95-19286
TRENHOLME, J. B. ..... p 1039 N95-19722
TREVINO, LUIS C. ..... p 1102 N95-19637
TRUSCOTT, T. GEORGE ..... p 1087 N95-19695
TSANG, M. N. ..... p 989 N95-19861
TSO, YAN K. ..... p 1124 N95-19057
TSOU, PETER ..... p 1180 N95-19173
p 1181 N95-19174
p 1036 N95-19194
p 1122 N95-19195
TSUCHIYAMA, A. ..... p 1188 N95-19308
p 1192 N95-19331
TSUNG, F.-L. ..... p 1016 N95-18200
TUCCHIO, MICHAEL ..... p 1045 N95-18456
TUCKER, W. C. ..... p 971 N95-19386
TUDOR, P. N. ..... p 1001 N95-19047
TUMMALA, MURALI ..... p 1000 N95-19035
TUNICK, ARNOLD ..... p 1063 N95-18115
TUOMALA, B. ..... p 1085 N95-19438
TURKO, B. T. ..... p 1034 N95-19229
TURNER, MICHAEL S. ..... p 1180 N95-18964
p 1121 N95-19030
TUTTLE, B. A. ..... p 988 N95-19558
TUTTLE, SHARON M. ..... p 1105 N95-19754
TUZZOLINO, ANTHONY J. ..... p 966 N95-19196
TYBURCZY, JAMES A. ..... p 1060 N95-19033
TZANOS, C. P. ..... p 1017 N95-18443

U

UBARANA, VINICIUS NOBREGA ..... p 1067 N95-18006
UCHIDA, K. ..... p 1152 N95-19586
UEMATSU, HIROHIKO ..... p 1033 N95-18929
UESUGI, K. T. ..... p 1180 N95-19173
p 1181 N95-19174
UHM, HAN S. ..... p 997 N95-18462
ULC, S. ..... p 1038 N95-19243
ULRICH, G. B. ..... p 968 N95-19877
UMAR, A. S. ..... p 1116 N95-18120
UNGAR, EUGENE K. ..... p 1017 N95-18323
UPTON, CINDY G. ..... p 967 N95-19566
URQUIDI-MACDONALD, MIMA ..... p 987 N95-19095
UZCATEGUI, O. ..... p 1066 N95-19560

V

VAEKIPARTA, K. ..... p 1007 N95-18037
VAETH, ROBERT J. ..... p 1110 N95-18454
VALANJU, P. M. ..... p 1145 N95-19092
VALENTE, JON B. ..... p 1110 N95-18454
VALENTINE-FLINT, S. ..... p 1005 N95-19622
VALLIERES, M. ..... p 1116 N95-18120
VANAMSTEL, A. R. ..... p 1058 N95-18375
VANDENBOSCH, P. ..... p 1081 N95-19415
VANDERAUWERAER, HERMAN . p 1128 N95-19166
VANDERGEER, S. B. ..... p 1137 N95-19584
VANDERLINDEN, PETER ..... p 1128 N95-19166
VANDEVELDE, R. J. ..... p 1057 N95-18002
VANDOOREN, PAUL ..... p 1114 N95-18675
VANDUZER, THEODORE ..... p 1008 N95-18103
VANGESTEL, R. ..... p 954 N95-19677
VANMOURIK, B. ..... p 1070 N95-18392
VANROSENDALE, JOHN ..... p 1116 N95-18110
VANSCHAACK, DONALD J. ..... p 1081 N95-19685
VANSTONE, DAVID A. ..... p 1058 N95-18140
VANWILTENBURG, PHILIP E. ..... p 1012 N95-19573
VANZEE, JOHN W. ..... p 1008 N95-18318
VASCONCELOS, GIOVANI L. ..... p 1015 N95-18188
VASHISHTA, P. ..... p 1134 N95-19562
VASTESAEGER, J. P. ..... p 1081 N95-19415
VAUGHAN, C. E. ..... p 967 N95-18195
VEDELER, ERIK ..... p 1005 N95-19781
VELAMAZAN, V. ..... p 1086 N95-19440
VELAMAZAN, VICENTE ..... p 1081 N95-19418
VELAMAZANPERDOMO, V. ..... p 1082 N95-19423
VELASCO, CARLOS ..... p 1084 N95-19434
p 1086 N95-19440
VENEDIKTOV, V. D. ..... p 949 N95-19024
VENKATACHALAM, R. S. ..... p 980 N95-19539
VENKATARAMAN, SUBRAMANIAN T. p 1114 N95-19062
VERBEEK, A. T. J. ..... p 954 N95-19680
VERDON, JOSEPH M. ..... p 949 N95-19381
VERES, JOSEPH P. ..... p 968 N95-19795
VERGARA, OSCAR RICARDO .... p 1050 N95-18368
VERNIK, RUDI ..... p 1095 N95-18089
VERNON, R. J. ..... p 1002 N95-19097
VIAGGI, F. ..... p 1082 N95-19421
VICROY, DAN D. ..... p 942 N95-18198
VIDULICH, MICHAEL ..... p 1088 N95-18084
VIEGAS, D. X. ..... p 1021 N95-19254
VIENNEAU, ROBERT ..... p 994 N95-17958
VIG, JOHN R. ..... p 1012 N95-19519
VIGNAU, H. ..... p 952 N95-19664
VIGNOLLES, P. ..... p 953 N95-19669
VILLASECA, F. EUGENIO ..... p 1105 N95-19749
VISNJIC, V. ..... p 1133 N95-19077
VISSER, H. J. ..... p 1004 N95-19535
VIZ, MARK J. ..... p 938 N95-19490
VLIEGER, H. ..... p 938 N95-19491
VOGEL, ERIC ..... p 1088 N95-18084
VOLAKIS, JOHN L. ..... p 1005 N95-19796
p 1006 N95-19797
p 1006 N95-19798
p 1006 N95-19799
p 1006 N95-19800
p 1006 N95-19801
VONBUN, F. O. ..... p 966 N95-19178
VOROS, ROBERT S. ..... p 1080 N95-19384
VOTH, GREGORY A. ..... p 1157 N95-19852
p 1157 N95-19853
VRBANCICH, J. ..... p 1005 N95-19622
VREEBURG, J. P. B. ..... p 990 N95-17973

W

WAIBEL, MICHAEL ..... p 930 N95-18910
WALKER, CLINTON B. ..... p 1088 N95-18095
WALKER, DAVID H. ..... p 1015 N95-18111
WALKER, DAVID ROBERT ..... p 1072 N95-18732
WALKER, JAMES ..... p 969 N95-18135
WALKER, R. ..... p 1124 N95-19046
p 1124 N95-19048
p 1001 N95-19049
p 993 N95-19053
WALKER, STEVEN H. ..... p 946 N95-19154
WALLACE, H. B. ..... p 995 N95-18136
WALLHEAD, IAN R. ..... p 938 N95-19492
WALSH, DANIEL W. ..... p 982 N95-19011
WALSH, DAVID J. ..... p 1064 N95-18623
WALSH, JOANNE L. ..... p 1175 N95-18936
WALTER, DONALD ALAN ..... p 950 N95-19595
WALTERS, KENNETH R., SR. ..... p 1067 N95-18014
WALUKIEWICZ, W. ..... p 976 N95-19836
WANG, FRANCIS C. ..... p 991 N95-19013
WANG, JAI-CHING ..... p 977 N95-19012
WANG, JIHAI ..... p 1144 N95-18885
WANG, PAO-LIEN ..... p 972 N95-18184
WANG, ROSE W. ..... p 995 N95-18066
WANG, SHUNUAN ..... p 1132 N95-18883
WANG, TING-I. ..... p 1069 N95-18205
WANG, X. ..... p 1038 N95-19243
WANG, Y. ..... p 976 N95-19824
p 976 N95-19825
WANG, YAOWEN ..... p 1106 N95-19760
WANG, YUN ..... p 1180 N95-19031
WANG, Z. ..... p 1122 N95-19704

WARHAFT, Z. p 1030 N95-19578
WARMAN, R. M. p 956 N95-18598
WARNES, GORDON D. p 951 N95-19657
WASSERMAN, S. R. p 1100 N95-19397
WASSON, J. T. p 1192 N95-19332
p 1192 N95-19333
WATANABE, KAZUHIRO p 1138 N95-19874
WATKINS, WENDELL R. p 1141 N95-19085
WATSON, CHARLES S. p 1079 N95-18626
WATSON, G. I. p 1122 N95-18127
WATT, R. p 1033 N95-18555
WATTERBERG, P. A. p 1120 N95-18653
WATTS, S. p 1032 N95-18130
WAWRZYNEK, JOHN p 1112 N95-19843
WAWRZYNEK, PAUL A. p 935 N95-19473
WEATHERFORD, CHARLES A. p 1130 N95-18334
WEATHERS, JEFFREY T. p 958 N95-18405
WEAVER, THOMAS L. p 1034 N95-19236
WEBB, THOMAS WILLIAM p 1046 N95-18922
WEBER, E. R. p 1152 N95-19586
WEBER, KAREN E. p 1040 N95-18041
WEI-CHYUNG, WANG p 1062 N95-19879
WEI, R. P. p 981 N95-19610
WEINBERG, DAVID H. p 1157 N95-19358
WEINBERG, I. p 1149 N95-18453
WEINBERG, M. p 1178 N95-18001
WEINBRUCH, S. p 1192 N95-19334
WEIRICH, R. F. p 960 N95-19271
WEISBERG, M. K. p 1190 N95-19318
p 1193 N95-19335
WEISS, A. G. p 1121 N95-19348
WEISS, GUIDO p 1119 N95-19869
WEISS, P. S. p 1131 N95-18473
WELCH, GARY L. p 1067 N95-18014
WELLAND, GRANT V. p 996 N95-18411
WELLMAN, G. W. p 1114 N95-18649
WELLS, N. D. p 1001 N95-19047
p 1001 N95-19052
WELLS, RICHARD L. p 1154 N95-19806
p 1154 N95-19807
p 1154 N95-19812
WELLS, T. p 1077 N95-19140
WELSH, DAVID K. p 1078 N95-18512
WENGLAR, LYDIA p 966 N95-18196
WENTWORTH, S. p 1190 N95-19320
WENTZ, K. R. p 1031 N95-19153
WENTZ, KENNETH R. p 1047 N95-19161
WERRY, S. M. p 1035 N95-19553
WESSENDORF, K. O. p 1012 N95-19240
WESTERINK, J. J. p 1075 N95-19540
WESTERVELT, JAMES p 1096 N95-18161
WESTFALL, CATHERINE p 1138 N95-19784
WESTON, GEORGE M. p 1046 N95-19504
WHEELER, KEVIN R. p 962 N95-18467
WHITE, A. R. p 1131 N95-18551
WHITE, C. W. p 1133 N95-19232
WHITE, GARY B. p 970 N95-18612
WHITE, J. H. p 973 N95-17982
WHITE, PETER S. p 1154 N95-19806
p 1154 N95-19812
WHITE, PRESTON A., III p 1006 N95-18185
WHITE, R. G. p 946 N95-19151
WHITLEY, S. p 944 N95-18723
WHITNEY, K. G. p 1147 N95-19847
WHITTY, G. FRED p 1046 N95-19504
WICKERSHEIMER, DAVID p 1108 N95-19821
WIDMER, M. R. p 1012 N95-19230
WIDRICK, TIMOTHY W. p 1047 N95-19649
WIELAND, DAVID H. p 939 N95-19493
WIESMANN, H. p 1190 N95-19320
WIFFEN, F. p 982 N95-19725
WIGLEY, T. M. L. p 1057 N95-18022
p 1059 N95-18664
WIGNALL, G. D. p 1134 N95-19557
WIKOFF, P. M. p 989 N95-19861
WILCOX, BRIAN H. p 1041 N95-18741
WILKERSON, JOHN p 1070 N95-18209
WILLARD, SCOTT A. p 935 N95-19472
WILLAUME, J. p 933 N95-19279
WILLIAMS, D. C. p 1129 N95-18049
WILLIAMS, GEORGE O., JR. p 1077 N95-19014
WILLIAMS, GLENN W. p 1096 N95-18365
WILLIAMS, M. J. p 950 N95-19654
WILLIAMS, W. D. p 930 N95-18674
WILLIAMS, W. F. p 1001 N95-19051
WILLIAMSON, R. L. p 1129 N95-18144
WILLIFORD, CLINT W. p 1062 N95-19806
WILLIS, J. p 1148 N95-18064
WILMINGTON, ROBERT P. p 1091 N95-18189
WILSON, DALE A. p 939 N95-19495
WILSON, ELIZABETH J. p 1104 N95-19645
WILSON, LORI J. p 1155 N95-19015
WILSON, R. B. p 976 N95-19785
WILSON, TAMMY J. p 1118 N95-18896
WILT, P. R. p 1007 N95-17961
WING, DAVID J. p 931 N95-19042
WINKLEMAN, S. R. p 1122 N95-19704
WINNENBERG, THOMAS F. p 1000 N95-19035
WIPKE, K. p 1014 N95-19881
WISE, J. p 986 N95-18651
WISHERD, J. L. p 1077 N95-19140
WITHROW, COLLEEN A. p 967 N95-18570
WOHLMAN, RICHARD A. p 1052 N95-19016
WOJTCZUK, STEVEN J. p 1052 N95-18011
p 1054 N95-19388
WOLFE, H. F. p 946 N95-19151
p 1031 N95-19153
WOLFE, SHAWN R. p 1101 N95-19632
p 1103 N95-19643
WOLFE, WILLIAM H. p 1172 N95-18025
p 1172 N95-18026
WOLFS, F. L. H. p 1007 N95-17961
WONG, C. R p 980 N95-19539
WONG, J. P. C. p 1127 N95-19162
WONG, K. C. p 942 N95-18097
WONG, L. G. p 1077 N95-19140
WONG, R. p 1005 N95-19622
WOOD, J. A. p 1193 N95-19336
WOOD, MICHAEL E. p 1010 N95-18546
WOOD, W. M. p 1032 N95-18130
WOODWARD, RICHARD P. p 958 N95-18054
WOODWORTH, J. R. p 1013 N95-19872
WORKMAN, GARY L. p 969 N95-18135
WRIGHT, A. p 929 N95-18624
WRIGHT, BERNARD R. p 989 N95-19826
WRIGHT, KENNETH D., II p 1175 N95-19056
WROBEL, D. P. p 1013 N95-19842
WU, G. p 1063 N95-18125
p 1063 N95-18148
WU, GUANJUN p 1144 N95-18885
WU, H. J. p 976 N95-19785
WU, JIIN-CHUAN p 1093 N95-18963
WU, MING p 939 N95-19495
WU, SHI TSAN p 1195 N95-19287
WU, TE-KAO p 1000 N95-18960
WU, X. D. p 1152 N95-19608
WU, XIN DI p 1148 N95-18064
WURDEN, G. A. p 1143 N95-17965
p 1143 N95-17969
WYCKAERT, KATRIEN p 1128 N95-19166
WYLIE, DAVID JOHN p 1071 N95-18399
WYSS, G. D. p 1120 N95-18653

X

XIANG, Y. p 1045 N95-18608
XIAO, FEI p 986 N95-18923
XIAO, H. p 1145 N95-19092
XIONG, X. p 981 N95-19703
XU, LIYUN p 1144 N95-18885
XU, Y.-L. p 1182 N95-19181
XU, YUANXIAN p 1144 N95-18887

Y

YADLOWSKY, M. p 1004 N95-19547
YALIF, GUY U. p 1106 N95-19759
YAMADA, SHUICHI p 1012 N95-19548
YAMASHITA, MASAFUMI p 1110 N95-18158
YANG, CHARLES C. p 978 N95-18046
YANG, QIANG p 1115 N95-19599
YANG, T. T. p 1036 N95-17956
YANIEC, JOHN S. p 959 N95-18586
YANO, STEVE E. p 927 N95-18044
YAO, S. p 1070 N95-18384
YARMUS, J. p 929 N95-18624
YATER, JANE A. p 1149 N95-18453
p 1053 N95-18572
YATES, G. J. p 1034 N95-19229
p 1035 N95-19394
YATES, J. TERRY p 1086 N95-19441
YE, RUBIN p 1144 N95-18885
YEAGER, ERNEST B. p 1013 N95-19741
YEH, J. R. p 939 N95-19496
YI, YUNG K. p 1011 N95-19120
YING, SHIH-TING p 969 N95-18028
YODER, MAX N. p 1149 N95-18633
YOST, J. D. p 939 N95-19497
YOUNG, J. P. p 1013 N95-19842
YOUNG, M. F. p 1137 N95-18897
YOUNG, RICHARD D. p 939 N95-19499
YOUNG, T. S. p 929 N95-18645
p 929 N95-18646
YU, K. M. p 976 N95-19836
YU, P. Y. p 1152 N95-19585
p 1152 N95-19586
YU, Y. p 1193 N95-19337
p 1193 N95-19338
YU, ZIQIANG p 1132 N95-18883
YUAN, QIN p 1041 N95-18541
p 1043 N95-19567
YUN, W. p 1034 N95-19233

Z

ZAGHLOUL, M. E. p 1007 N95-17984
ZAK, DONALD R. p 1060 N95-19112
ZAKHAREV, B. N. p 1156 N95-18879
ZAKRAJSEK, JAMES J. p 1042 N95-19125
ZANDA, B. p 1193 N95-19338
ZANIOLO, C. p 1101 N95-19629
ZAPATA, L. E. p 1037 N95-18357
p 1038 N95-19096
ZARE, RICHARD N. p 973 N95-17975
ZARRIELLO, P. R. p 1122 N95-17983
ZEHNDER, ALAN T. p 938 N95-19490
ZERTUCHE, GAVINO p 1090 N95-18029
ZHANG, JISHANG p 1132 N95-18883
ZHANG, XIAOCHENG p 1132 N95-18883
ZHANG, YIQIANG p 1195 N95-17980
ZHAO, GUOPING p 1144 N95-18885
ZHAO, W. p 939 N95-19498
ZHENG, JIANGFEN p 1059 N95-18445
ZHOU, HONGMO p 1132 N95-18883
ZHOU, MINGGANG p 1195 N95-19287
ZHOU, YE p 1016 N95-18191
ZHU, SHENG-BAI p 1132 N95-18655
ZINOVIEVA, N. G. p 1193 N95-19339
ZOBRIST, GEORGE W. p 1108 N95-18186
ZOLENSKY, MICHAEL E. p 1180 N95-19172
p 989 N95-19197
ZOOK, HERBERT A. p 1183 N95-19186
ZOPPA, ROBERT J. p 997 N95-18481
ZUBAIR, MOHAMMAD p 1098 N95-18584
ZUBRZYCKI, J. T. p 997 N95-18494
ZUO, YIXIN p 1132 N95-18883
ZUPPARDI, G. p 960 N95-19267
ZURIGAT, Y. H. p 1016 N95-18193

Typical Corporate Source Index Listing

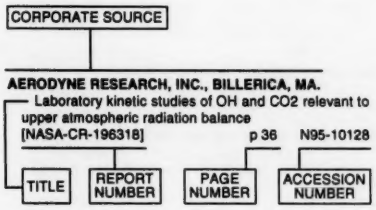

Listings in this index are arranged alphabetically by corporate source. The title of the document provides the user with a brief description of the subject matter. The report number helps to indicate the type of document cited (e.g., NASA report, translation, NASA contractor report). The accession number denotes the number by which the citation is identified. The page number helps you locate the citation in the abstract section. The titles are arranged under each corporate source in ascending accession number order.

A

A & M ASSOCIATES, LANHAM, MD.
Plasma produced by impacts of fast dust particles on a thin film p 1181 N95-19177
Highly transparent and rugged sensor for velocity determinations of cosmic dust particles p 966 N95-19178

ADVISORY GROUP FOR AEROSPACE RESEARCH AND DEVELOPMENT, NEUILLY-SUR-SEINE (FRANCE).
A selection of experimental test cases for the validation of CFD codes. Supplement: Datasets A-E
[AGARD-AR-303-SUPPL] p 929 N95-18539
Aircraft Loads due to Turbulence and their Impact on Design and Certification
[AGARD-R-798] p 956 N95-18597
On-line handling of air traffic: Management, guidance and control
[AGARD-AG-321] p 941 N95-18927
Mathematical Models of Gas Turbine Engines and their Components
[AGARD-LS-198] p 948 N95-19017
Impact of Acoustic Loads on Aircraft Structures
[AGARD-CP-549] p 1124 N95-19142
Wall Interference, Support Interference and Flow Field Measurements
[AGARD-CP-535] p 1020 N95-19251
The Clinical Basis for Aeromedical Decision Making
[AGARD-CP-553] p 1080 N95-19413
Erosion, Corrosion and Foreign Object Damage Effects in Gas Turbines
[AGARD-CP-558] p 950 N95-19653

AERONAUTICAL RESEARCH INST. OF SWEDEN, BROMMA.
Computational simulations for some tests in transonic wind tunnels p 1023 N95-19264
Calculation of low speed wind tunnel wall interference from static pressure pipe measurements p 1024 N95-19273

AERONAUTICAL RESEARCH LABS., MELBOURNE (AUSTRALIA).
Damage monitoring in metallic and composite structures using piezoelectric thin film sensors
[ARL-RR-4] p 971 N95-19467
Programmable cockpit research simulator
[AD-A279219] p 960 N95-19848

AERONAUTICAL SYSTEMS DIV., WRIGHT-PATTERSON AFB, OH.
KC-135 cockpit modernization study. Phase 1: Equipment evaluation
[AD-A284099] p 942 N95-18398

AEROSPACE CORP., LOS ANGELES, CA.
Fuzzy expert systems using CLIPS p 1102 N95-19636

AEROSPACE MEDICAL RESEARCH LABS., BROOKS AFB, TX.
Variable name dictionary for the Air Force health study 1987 physical examination data tape, volume 1
[AD-A283319] p 1172 N95-18025
Variable name dictionary for the Air Force health study 1987 physical examination data tape, volume 2
[AD-A283320] p 1172 N95-18026
The aeromedical implications of supraventricular tachycardia p 1085 N95-19437
Sarcoidosis in US military aviators p 1085 N95-19438
The aeromedical risk associated with asymptomatic cholelithiasis in USAF pilots and navigators p 1085 N95-19439
Color vision issues in modern military aviation or the search for the Abominable Coneman p 1086 N95-19441
Photorefractive Keratectomy (PRK) in the military aviator: An aeromedical expose p 1086 N95-19442

AEROSPATIALE, TOULOUSE (FRANCE).
Gyroscopic and propeller aerodynamic effects on engine mounts dynamic loads in turbulence conditions p 946 N95-18599
Interaction of a three strut support on the aerodynamic characteristics of a civil aviation model p 933 N95-19279

AGENCY FOR THE ASSESSMENT AND APPLICATION OF TECHNOLOGY (INDONESIA).
Near tip stress and strain fields for short elastic cracks p 937 N95-19487

AIR FORCE CIVIL ENGINEERING CENTER, TYNDALL AFB, FL.
Alternative solvents/technologies for paint stripping: Phase 1
[AD-A279918] p 989 N95-19861

AIR FORCE ENVIRONMENTAL TECHNICAL APPLICATIONS CENTER, SCOTT AFB, IL.
Climate and weather of Central Africa. Executive summary
[AD-A283647] p 1067 N95-18014

AIR FORCE INST. OF TECH., WRIGHT-PATTERSON AFB, OH.
Crosshift vibrometry: Biomarker for ergonomic stress
[AD-A284337] p 1091 N95-18385
A numerical analysis of smoothed particle hydrodynamics
[AD-A284698] p 1019 N95-18562
Numerical simulation of dynamic-stall suppression by tangential blowing
[AD-A284887] p 931 N95-19110
Developing an emission factor for hazardous air pollutants for an F-16 using JP-8 fuel
[AD-A284802] p 1061 N95-19685
Development of a comprehensive base-level environmental training program for total environmental compliance
[AD-A284806] p 1061 N95-19686
A three region analysis of a bounded plasma using particle in cell and fluid techniques
[AD-A284826] p 1147 N95-19690
The optical emission and absorption properties of silicon-germanium superlattice structures grown on non-conventional silicon substrate orientation
[AD-A284852] p 1153 N95-19715

AIR FORCE MATERIALS LAB., WRIGHT-PATTERSON AFB, OH.
Situation awareness: Papers and annotated bibliography
[AD-A284752] p 1088 N95-18084

AIR FORCE SYSTEMS COMMAND, BOLLING AFB, WASHINGTON, DC.
Aeromedical risk management for aircrew p 1080 N95-19414

AIRCRAFT RESEARCH ASSOCIATION LTD., BEDFORD (ENGLAND).
General procedures employed in the generation of three-dimensional hybrid structured/unstructured meshes
[ARA-MEMO-400] p 1030 N95-19506
An investigation of drag repeatability in half model testing in the ARA Transonic Wind Tunnel
[ARA-MEMO-392] p 931 N95-19546
Evaluation of three turbulence models for afterbody/jet flows, including Reynolds stress closure
[ARA-90] p 932 N95-19574
Multiport pressure measurements on continuously moving wind tunnel models
[ARA-MEMO-391] p 932 N95-19772
Evaluation of three turbulence models for afterbody/jet flows, including Reynolds stress closure
[ARA-MEMO-408] p 1194 N95-19773
Validation and evaluation of the advanced aeronautical CFD system SAUNA: A method developer's view
[ARA-MEMO-390] p 1030 N95-19774
Application of three-dimensional hybrid structured/unstructured grids to land, sea and air vehicles
[ARA-MEMO-399] p 1031 N95-19775
Verification of the CFD simulation system SAUNA for complex aircraft configurations
[ARA-MEMO-401] p 1031 N95-19776
Inviscid and viscous flow modelling of complex aircraft configurations using the CFD simulation system sauna
[ARA-MEMO-403] p 1031 N95-19777
The application of the SAUNA CFD system to high and low speed vehicles
[ARA-MEMO-402] p 1031 N95-19778
The aerodynamic design of an integrated wing lower surface and pylons for reduced drag
[ARA-MEMO-406] p 946 N95-19789

ALABAMA A & M UNIV., HUNTSVILLE, AL.
Residual stresses in welded plates p 1047 N95-18972
The probability of flaw detection and the probability of false calls in nondestructive evaluation equipment p 1044 N95-19010
Numerical formulation of composition segregation at curved solid-liquid interface during steady state solidification process p 977 N95-19012

ALABAMA UNIV., BIRMINGHAM, AL.
Cumulative effects of repeated brief cerebral ischemia
[AD-A284234] p 1087 N95-19698

ALABAMA UNIV., HUNTSVILLE, AL.
Dynamics and statics of nonaxisymmetric liquid bridges
[NASA-CR-197520] p 1195 N95-17980
Field and data analysis studies related to the atmospheric environment
[NASA-CR-196543] p 1068 N95-18093
Acoustic method of damage sensing in composite materials
[NASA-CR-196538] p 969 N95-18135
An instrument to measure the charge, and energy spectrum (20-1000 GeV/a) of the cosmic ray species oxygen to iron
[NASA-CR-197555] p 1197 N95-18464
Spatial and temporal constraints on the observed distribution of gamma-ray bursts detected by BATSE p 1197 N95-18730
Computational modeling of properties
[NASA-CR-197558] p 1010 N95-18925
MSFC institutional area network and ATM technology p 1007 N95-18968
A finite element code for electric motor design p 1014 N95-18974

Optical measurements in rocket engine liquid sprays p 968 N95-18979
Computational simulation of liquid fuel rocket injectors p 968 N95-18989
Concentration and temperature effects on ovostatin activity p 1077 N95-18997
Cracking characteristics of a habitable module pressure wall following orbital debris penetration p 1047 N95-19003
Effects of vibration (G-jitters) on convection in micro-gravity p 991 N95-19013
Study for the analysis of the observations, and numerical data representing the planets as far-infrared calibration sources
[NASA-CR-196542] p 1195 N95-19287

ALABAMA UNIV., TUSCALOOSA, AL.
Research reports: 1994 NASA/ASEE Summer Faculty Fellowship Program
[NASA-CR-196533] p 1161 N95-18967
A hypertext-based internet-assessable database for the MSFC Technology Transfer Office p 1165 N95-18986

ALCOA TECHNICAL CENTER, ALCOA CENTER, PA.
An artifical corrosion protocol for lap-splices in aircraft skin p 937 N95-19482

ALENIA, TURIN (ITALY).
Impact of noise environment on engine nacelle design p 1125 N95-19147

ALENIA SPAZIO S.P.A., TURIN (ITALY).
An overall approach of cockpit noise verification in a military aircraft p 1127 N95-19163

ALLIED-SIGNAL AEROSPACE CO., KANSAS CITY, MO.
Precision gold conductors for HMCs
[DE94-018558] p 1012 N95-19230
Development of high reliability planar chip inductors
[DE94-018589] p 1012 N95-19231
Characterization of the deformation and annealing of 304L stainless steel
[DE94-018584] p 981 N95-19707

ALUMINUM CO. OF AMERICA, ALCOA CENTER, PA.
Prediction of R-curves from small coupon tests p 939 N95-19496

AMERICAN MUSEUM OF NATURAL HISTORY, NEW YORK, NY.
Implications for the evolution of chondrules from Agglomeratic olivine chondrules p 1193 N95-19335

ANALYTICAL METHODS, INC., REDMOND, WA.
Calculation of support interference in dynamic wind-tunnel tests p 933 N95-19282

ANALYTICAL SERVICES AND MATERIALS, INC., HAMPTON, VA.
TEXCAD: Textile Composite Analysis for Design. Version 1.0: User's manual
[NASA-CR-4639] p 970 N95-18466

ARGONNE NATIONAL LAB., IL.
Electronics for the Si detectors in APEX
[DE94-015078] p 1007 N95-17961
Singular perturbation problem governed by system of conservation laws
[DE94-019264] p 1116 N95-17977
A domain decomposition algorithm for elliptic problems in three dimensions
[DE94-019265] p 1094 N95-17978
Fast numerical determination of symmetric sparsity patterns
[DE94-016344] p 1096 N95-18354
Ionization of atoms by high energy photons
[DE94-018356] p 1130 N95-18427
Pion observables and QCD
[DE94-018357] p 1130 N95-18428
Numerical predictions of turbulent flow around a cube via the k-epsilon model
[DE94-018361] p 1017 N95-18443
Erosion of melt layers developed during a plasma disruption
[DE94-018362] p 1144 N95-18547
Can an infrared-vanishing gluon propagator confine quarks?
[DE94-018388] p 1131 N95-18548
Sloshing roof impact tests of a rectangular tank
[DE94-012462] p 1018 N95-18549
Summary of the working group on tests of QCD
[DE94-018390] p 1131 N95-18550
Higher-order Lipatov kernels and the QCD Pomeron
[DE94-018395] p 1131 N95-18551
Molten carbonate fuel cell with high power density
[DE94-017080] p 1053 N95-19074
Deformation of high-temperature superconductors
[DE94-017085] p 1150 N95-19075
Deformation of nonstoichiometric CuO polycrystals
[DE94-016907] p 1150 N95-19094
Free vibration analysis of partially filled liquid storage tanks
[DE94-012456] p 1020 N95-19098
SSI effects for a tank containing two liquids
[DE94-012457] p 1020 N95-19099
Bragg transmission phase plates for the production of circularly polarized x-rays
[DE94-017072] p 1151 N95-19113
Sealant materials for the solid oxide fuel cell
[DE94-017073] p 1053 N95-19115
Pitting corrosion of aluminized seals in molten carbonate fuel cells
[DE94-017075] p 1053 N95-19116
Lithium ferrate and lithium cobaltate cathodes for molten carbonate fuel cells
[DE94-017079] p 1054 N95-19117
Real time simulator with Ti floating point digital signal processor
[DE94-016372] p 1012 N95-19246
XAMath: An XAFS analysis package based on Mathematica(tm)
[DE94-016346] p 1100 N95-19397
The QED Workshop
[DE94-018499] p 1111 N95-19592
Activities of the Analytical Chemistry Laboratory
[DE95-000834] p 975 N95-19618
The interaction of two narrow magnets and a moving conducting slip
[DE94-018575] p 1122 N95-19704
Massively parallel full configuration interaction. Benchmark electronic structure calculations on the Intel Touchstone Delta
[DE95-001064] p 1153 N95-19724
Status of vanadium alloy development for fusion first wall/blanket applications
[DE95-001067] p 982 N95-19725
Principal-value resummation for dilepton production
[DE95-001094] p 1135 N95-19726
Microcavity structures
[DE95-001096] p 1039 N95-19727
The interactions of high-energy, highly charged Xe ions with fullerenes
[DE95-001440] p 1135 N95-19786
Spectral distribution of the two-photon decay of He-like krypton
[DE95-001442] p 1135 N95-19787

ARIZONA STATE UNIV., TEMPE, AZ.
Heteroepitaxy of ternary SiGeC alloys on Si for bipolar transistors
[AD-A285317] p 1151 N95-19511

ARIZONA UNIV., TUCSON, AZ.
Real-time adaptive control of mixing in a plane shear layer
[AD-A285541] p 1018 N95-18469
On the possibility of precipitation-induced vertical lightning in the protoplanetary nebula p 1187 N95-19299
Models for multiple heating mechanisms p 1188 N95-19303
Chondrule formation in the radiative accretional shock p 1191 N95-19324
I-Xe studies of individual chondrules: What can they tell us about chondrule formation? p 1192 N95-19329
Singularities and symmetries of nonlinear ordinary and partial differential equations
[DE95-000904] p 1119 N95-19609

ARKANSAS UNIV., FAYETTEVILLE, AR.
Open-system behavior during chondrule formation p 1192 N95-19328

ARMY AEROMEDICAL RESEARCH LAB., FORT RUCKER, AL.
Design and development of an enhanced biodynamic manikin, phase 1
[AD-A284725] p 1090 N95-18077
Collection of real-time, multichannel EEG data from helicopter pilots in flight: A feasibility study
[AD-A285050] p 1090 N95-19564

ARMY AVIATION RESEARCH AND DEVELOPMENT COMMAND, MOFFETT FIELD, CA.
Wall interaction effects for a full-scale helicopter rotor in the NASA Ames 80- by 120-foot wind tunnel p 932 N95-19270

ARMY AVIATION SYSTEMS COMMAND, MOFFETT FIELD, CA.
2-D and 3-D oscillating wing aerodynamics for a range of angles of attack including stall
[NASA-TM-4632] p 931 N95-19119

ARMY AVIATION SYSTEMS COMMAND, SAINT LOUIS, MO.
US Army rotorcraft turboshaft engines sand and dust erosion considerations p 951 N95-19656

ARMY COMMUNICATIONS-ELECTRONICS COMMAND, FORT BELVOIR, VA.
Image intensifier system resolution based on laboratory measured parameters
[AD-A283917] p 1008 N95-18156

ARMY CONSTRUCTION ENGINEERING RESEARCH LAB., CHAMPAIGN, IL.
R.MAPCALC: An algebra for GIS and image processing
[AD-A283923] p 1096 N95-18161
Environmental Compliance Assessment System (ECAS)
[AD-A283950] p 1060 N95-18683
Environmental Compliance Assessment System (ECAS). South Carolina supplement: US Army
[AD-A279244] p 1062 N95-19860

ARMY ENGINEER WATERWAYS EXPERIMENT STATION, VICKSBURG, MS.
Cumulative impact analysis of wetlands using hydrologic indices
[AD-A284759] p 1058 N95-18085
Development of executive information systems
[AD-A284005] p 1174 N95-18654
ADCIRC: An advanced three-dimensional circulation model for shelves, coasts, and estuaries. Report 5: A tropical storm database for the east and Gulf of Mexico coasts of the United States
[AD-A285576] p 1075 N95-19540
Heavy metal soil contamination at US Army installations: Proposed research and strategy for technology development
[AD-A279171] p 1062 N95-19808

ARMY LAB. COMMAND, FORT MONMOUTH, NJ.
Quartz crystal resonators and oscillators for frequency control and timing applications. A tutorial
[AD-A284995] p 1012 N95-19519

ARMY MISSILE COMMAND, REDSTONE ARSENAL, AL.
Design of a radio frequency data link for the unmanned ground vehicle technology test bed demonstration program
[AD-A284997] p 1004 N95-19534

ARMY NATICK RESEARCH AND DEVELOPMENT COMMAND, MA.
Parachute inflation: A problem in aeroelasticity
[AD-A284375] p 928 N95-18340

ARMY RESEARCH INST. FOR THE BEHAVIORAL AND SOCIAL SCIENCES, ALEXANDRIA, VA.
Creation of new items and forms for the Project A Assembling Objects test
[AD-A285522] p 1088 N95-18095

ARMY RESEARCH INST. OF ENVIRONMENTAL MEDICINE, NATICK, MA.
Design concepts for an integrated environmental medicine workstation for prediction, simulation and training
[AD-A283686] p 1079 N95-18618
Distributed medical database system for real-time monitoring of the health and risk exposure of military research study volunteers at USARIEM
[AD-A279193] p 1087 N95-19811
Annual historical report, calendar year 1993
[AD-A280178] p 1087 N95-19827

ARMY RESEARCH LAB., ABERDEEN PROVING GROUND, MD.
Multipath-induced, low-angle tracking error at 140 GHz
[AD-A283630] p 995 N95-18136
Midinfrared optical properties of petroleum oil aerosols
[AD-A283689] p 1139 N95-18142
Helicopter Performance Evaluation (HELPE) computer model
[AD-A284319] p 942 N95-18381
Static aerodynamics CFD analysis for 120-mm hypersonic KE projectile design
[ARL-MR-184] p 929 N95-18611
Thermocouples for interior ballistic temperature measurements
[AD-A283699] p 1033 N95-18620
Numerical computations of supersonic base flow with special emphasis on turbulence modeling
[AD-A283688] p 930 N95-18670
The tensor equation AX+XA=Phi (A, H) with applications to kinematics of continua
[AD-A285886] p 1122 N95-19603
Flamespreading in granular solid propellant: Initial results
[AD-A284245] p 976 N95-19729

ARMY RESEARCH LAB., ADELPHI, MD.
Silicon carbide photoconductive switches
[AD-A284310] p 1008 N95-18378
An investigation of nonuniform dose deposition from an electron beam
[AD-A284175] p 1131 N95-18519
Radiation-induced noise in UMPC-type current probes: IEMP response of the curruent measurement system
[AD-A284176] p 998 N95-18520

ARMY RESEARCH LAB., CLEVELAND, OH.
Thermal behavior spiral bevel gears
[NASA-TM-106518] p 1042 N95-18935
Detecting gear tooth fracture in a high contact ratio face gear mesh
[NASA-TM-106822] p 1042 N95-19125

ARMY RESEARCH LAB., FORT MONMOUTH, NJ.
Lithium electrode/polyacrylonitrile based polymer electrolyte interface
[AD-A283947] p 986 N95-19064

ARMY RESEARCH LAB., WATERTOWN, MA.
A real-time vision system to monitor/analyze the changes in composite specimens during mechanical testing
[ARL-TR-344] p 970 N95-18612
Development of an improved ballistic acceptance test for high hard armor steel plate: MIL-A-46100
[ARL-TR-509] p 979 N95-18939
Barium strontium titanate and non-ferroelectric oxide ceramic composites for use in phased array antennas
[AD-A279225] p 972 N95-19851

ARMY RESEARCH LAB., WHITE SANDS MISSLE RANGE, NM.
Night Vision Goggles (NVG) software user's guide, version 5.1
[AD-A284563] p 1090 N95-18029
Energy balance model for imagery and electromagnetic propagation
[AD-A284552] p 1063 N95-18115
A technical demonstration Mobile Profiler System
[AD-A284562] p 1068 N95-18117
Large area thermal target board: An improvement to environmental effects and system parameters characterization
[AD-A284614] p 1141 N95-19085

ARMY TOPOGRAPHIC ENGINEERING CENTER, FORT BELVOIR, VA.
Spectral reflectance properties of wetlands plants
[AD-A283546] p 1051 N95-18614
Interferometric synthetic aperture radar and the Data Collection System Digital Terrain Elevation Demonstration
[AD-A284024] p 999 N95-18657
ISSSR tutorial 1: Introduction to spectral remote sensing
[AD-A284268] p 1052 N95-19734

ARNOLD ENGINEERING DEVELOPMENT CENTER, ARNOLD AFS, TN.
Hypersonic wind tunnel test techniques
[AD-A284057] p 929 N95-18663
Hypersonic flow-field measurements: Intrusive and nonintrusive
[AD-A283867] p 930 N95-18674
Hypersonic flight testing
[AD-A283981] p 944 N95-18891

AUBURN UNIV., AL.
Determination of the electron density and the electron temperature in a high-pressure microwave discharge
p 1145 N95-18906
Steady and unsteady blade stresses within the SSME ATD/HPOTP inducer p 968 N95-18982
A preliminary analysis of low frequency pressure oscillations in hybrid rocket motors p 968 N95-18987

AUCKLAND UNIV. (NEW ZEALAND).
Atmospheric chemistry of biogenic sulfur in the Southern Hemisphere p 1071 N95-18399

B

BABCOCK AND WILCOX CO., LYNCHBURG, VA.
Design of a flexible robotic arc welding system, task 3. Volume 1: System overview
[AD-A285116] p 1043 N95-19593

BAHRAIN UNIV., ISSA TOWN (BHARAIN).
Fatigue crack growth under variable amplitude loading
p 937 N95-19484

BATTELLE COLUMBUS LABS., OH.
Ultrasonic techniques for repair of aircraft structures with bonded composite patches p 937 N95-19486

BATTELLE MEMORIAL INST., COLUMBUS, OH.
Theoretical interpretation of the fluorescence spectra of toluene and p-cresol
[AD-A284314] p 974 N95-19170

BAYLOR UNIV., WACO, TX.
The status of measurement technologies concerning micrometer and submicrometer space articulate matter capture, recovery, velocity and trajectory
p 1181 N95-19175
Assessment of velocity/trajectory measurement technologies during a particle capture event
p 1036 N95-19193

BELGIAN AIR FORCE, BRUSSELS (BELGIUM).
The way to waivers in the BAF p 1081 N95-19415

BKM, INC., SAN DIEGO, CA.
Advanced diesel electronic fuel injection and turbocharging
[AD-A279176] p 1043 N95-19809

BOEING COMMERCIAL AIRPLANE CO., SEATTLE, WA.
The application of Newman crack-closure model to predicting fatigue crack growth p 937 N95-19483

BOSTON UNIV., MA.
Geometrical and topological methods in time domain antenna synthesis
[AD-A284208] p 994 N95-17954
A general theory of semi-unification
p 1099 N95-18924
New applications of the Phillips Laboratory. Theoretical ionospheric model and studies of neutral density waves
[AD-A284663] p 1066 N95-19105
Growth and doping of Al(x)Ga(1-x)N films by electron cyclotron resonance assisted molecular beam epitaxy
[AD-A284838] p 1153 N95-19737

BOWLING GREEN STATE UNIV., OH.
Reaction channel competition in vibrational overtone activation: 1-methylcyclopropene
[AD-A280185] p 976 N95-19830

BRASILIA UNIV. (BRAZIL).
Generalized relaxation theory and vortices in plasmas
[DE95-002615] p 1147 N95-19837

BRIGHAM YOUNG UNIV., PROVO, UT.
Enantiomeric separation of chiral alpha-(1-naphthyl)ethyl ammonium perchlorate by silica gel-bound chiral pyridino-18-crown-6 ligands
[AD-A280156] p 969 N95-19822
Molecular recognition as shown by the solvent extraction of (R)- and (S)-alpha-(1-naphthyl)ethyl ammonium picrate or orange 2 by chiral pyridino-crown ethers
[AD-A280157] p 969 N95-19823

BRITISH AEROSPACE AIRBUS LTD., BRISTOL (ENGLAND).
The impact of non-linear flight control systems on the prediction of aircraft loads due to turbulence
p 956 N95-18598

BRITISH AEROSPACE AIRCRAFT GROUP, BRISTOL (ENGLAND).
Application of superplastically formed and diffusion bonded structures in high intensity noise environments
p 1127 N95-19162

BRITISH AEROSPACE AIRCRAFT GROUP, PRESTON (ENGLAND).
Transonic and supersonic flowfield measurements about axisymmetric afterbodies for validation of advanced CFD codes p 932 N95-19260

BRITISH AEROSPACE AIRCRAFT GROUP, WARTON (ENGLAND).
Current and future problems in structural acoustic fatigue p 1124 N95-19143

BRITISH BROADCASTING CORP., TADWORTH (ENGLAND).
The development of the switched-horn radio-camera system
[BBC-RD-1993/13] p 997 N95-18494
The sound insulations of metal-framed partitions having structural loadbearing properties
[BBC-RD-1994/8] p 992 N95-18533
Further measurements of the sound insulations of metal-framed partitions
[BBC-RD-1994/7] p 998 N95-18534
Multi-channel sound for HDTV: Subjective tests on sound channel configuration
[BBC-RD-1994/4] p 998 N95-18535
Implementation of amplitude modulation companding using a digital signal processor
[BBC-RD-1994/1] p 998 N95-18536
RACE project 1036: WTDM broadband customer premises network
[BBC-RD-1993/15] p 998 N95-18537
RINSE: A digitally implemented flywheel sync regenerator for improved video synchroniser performance
[BBC-RD-1993/14] p 999 N95-18538
Predicted coverage of a COFDM single frequency network for UHF digital terrestrial TV broadcasting
[BBC-RD-1993/12] p 999 N95-18540
A wideband absorber for television studios
[BBC-RD-1994/12] p 1123 N95-18566
High frequency room responses: Acoustic design and the control of stereophonic image quality
[BBC-RD-1994/11] p 1124 N95-19046
Digital video compression: Standardisation of scalable coding schemes
[BBC-RD-1994/10] p 1001 N95-19047
Acoustic noise criteria for listening rooms and control rooms
[BBC-RD-1994/06] p 1124 N95-19048
Maximal-length sequence methods: Acoustic measurements in the presence of high levels of extraneous noise
[BBC-RD-1994/5] p 1001 N95-19049
DAB: Multiplex and system support features
[BBC-RD-1994/9] p 1001 N95-19050
Measurements of wideband multipath propagation at 531 MHz and 1.265 GHz
[BBC-RD-1994/3] p 1001 N95-19051
Bit-rate reduction of digital television for transmission: An introductory review
[BBC-RD-1994/2] p 1001 N95-19052
Optimum dimension ratios for studios, control rooms and listening rooms
[BBC-RD-1993/8] p 993 N95-19053
Dynamic range control of audio signals by digital signal processing
[BBC-RD-1993/7] p 1124 N95-19054
Engineering review, January 1993 - March 1994
p 1001 N95-19055
Digital audio broadcasting: Comparison of coverage at different frequencies and with different bandwidths
[BBC-RD-1993/11] p 1002 N95-19135
Alleviation of co-channel interference at Poole relay station
[BBC-RD-1993/4] p 1003 N95-19136
Metal-framed partitions with reduced thicknesses. Part 2: Built-in acoustic treatment
[BBC-RD-1993/6-PT-2] p 993 N95-19137
Metal-framed partitions with reduced thicknesses. Part 1: Narrower studs and cavities
[BBC-RD-1993/5-PT-1] p 993 N95-19138

BRITISH COLUMBIA UNIV., VANCOUVER (BRITISH COLUMBIA).
Unsteady flow testing in a passive low-correction wind tunnel p 960 N95-19272

BROOKHAVEN NATIONAL LAB., UPTON, NY.
Crystalline beams: The string
[DE94-016806] p 1150 N95-19091
The visible Smith-Purcell radiation search
[DE94-017514] p 1038 N95-19243
Correlation of polycrystalline Cu(In,Ga)Se2 device efficiency with homojunction depthand interfacial structure: X-ray photoemission and positron annihilation spectroscopic characterization
[DE94-013543] p 1055 N95-19858

BURNETTE ENGINEERING, FAIRBORN, OH.
An evaluation of aircraft CRT and dot-matrix display legibility requirements
[AD-A283933] p 947 N95-18164

C

CALHOUN COMMUNITY COLL., DECATUR, AL.
Capillary electrophoresis: Biotechnology for separation of DNA and chromosomes p 1077 N95-19014

CALIFORNIA INST. OF TECH., PASADENA, CA.
Dynamic decohesion of bimaterials: Experimental observations and failure criteria
[GALCIT-94-2] p 1045 N95-18613
Properties of nuclei and elementary particles at low and intermediate energies
[DE94-008502] p 1132 N95-18644
Shock-induced devolatization of calcium sulfate and implications for K-T extinctions
[NASA-CR-197608] p 1060 N95-19033
Comet coma sample return instrument
p 1180 N95-19173
SOCCER: Comet Coma Sample Return Mission
p 1181 N95-19174
Physics of spacecraft-based interplanetary dust collection by impact into low-density media
p 1181 N95-19176
The early Sun and the formation of chondrules
p 1188 N95-19305
Parallel computation
[AD-A284831] p 1112 N95-19692
Three-D optical memory disk
[AD-A280002] p 1035 N95-19871

CALIFORNIA POLYTECHNIC STATE UNIV., SAN LUIS OBISPO, CA.
The effect of fabrication on corrosion in aluminum 2195: Environmental and microstructural considerations
p 982 N95-19011
Using PVM to host CLIPS in distributed environments
p 1104 N95-19748

CALIFORNIA STATE POLYTECHNIC UNIV., POMONA, CA.
Investigation of new hypergol scrubber technology
p 977 N95-18175

CALIFORNIA UNIV., BERKELEY, CA.
Construction of a connectionist network supercomputer
[AD-A283354] p 1109 N95-18050
Superconductive signal-processing circuits
[AD-A285533] p 1008 N95-18103
Systems and economic analysis of microalgae ponds for conversion of CO2 to biomass
[DE95-000406] p 1054 N95-19554
Connectionist Network Supercomputer Project
[AD-A279206] p 1112 N95-19843

CALIFORNIA UNIV., BERKELEY. LAWRENCE BERKELEY LAB, CA.
Ultrafast nonlinear optical response of Fano resonances in gallium arsenide under high magnetic field
[DE94-018181] p 1148 N95-18122
The effects of cavity topology on instabilities in additive-pulse modelocked lasers
[DE94-018193] p 1036 N95-18123

GAMQUEST, a computer program to identify gamma rays
[DE94-016217] p 1197 N95-18351
Nonstoichiometry of Al-Zr intermetallic phases
[DE94-016877] p 979 N95-19093
Electronic structure of C60 fullerites and nanotubes
[DE95-000784] p 1151 N95-19569
A crystalline quark-hadron mixed phase in neutron stars
[DE95-000787] p 1194 N95-19570
Characterization of the 50 MeV ALS linac beam with optical transition radiation
[DE94-018208] p 1137 N95-19584
Deep levels in AgGaSe2
[DE94-018209] p 1152 N95-19585
Energies of X conduction band minima in disordered and ordered GaInP2 alloys
[DE94-018211] p 1152 N95-19586
Baryon stopping in 200 GeV/A S+Au collisions
[DE94-018215] p 1134 N95-19587
Physics with isotopically controlled semiconductors
[DE95-000789] p 1152 N95-19615
Transition metal oxides deposited on rhodium and platinum: Surface chemistry and catalysis
[DE95-000793] p 975 N95-19616
Correlation function analysis of the COBE differential microwave radiometer sky maps
[DE95-000795] p 1178 N95-19617
Characterization of inactive carbon in GaAs
[DE95-002352] p 976 N95-19836

CALIFORNIA UNIV., IRVINE, CA.
Aryl gels and related materials. Synthesis and characterization of a new class of microporous materials
[AD-A285044] p 987 N95-19544
Automated rule-base creation via CLIPS-Induce p 1107 N95-19761
Automated revision of CLIPS rule-bases p 1107 N95-19762

CALIFORNIA UNIV., LOS ANGELES, CA.
Minimal time detection algorithms and applications to flight systems
[TR-2-FSRC-93] p 1098 N95-18564
The accuracy of parameter estimation in system identification of noisy aircraft load measurement
[NASA-CR-197516] p 945 N95-19130
Microchondrules in ordinary chondrites: Implications for chondrule formation p 1188 N95-19309
Chondrule remelting: Evidence from coarse-grained chondrule rims and compound chondrules p 1191 N95-19323
Chondrule origins: Constraints from chondrule properties and cosmochemistry p 1192 N95-19332
The fine nebula dust component: A key to chondrule formation by lightning p 1192 N95-19333
The design and implementation of EPL: An event pattern language for active databases p 1101 N95-19629
Expert system shell to reason on large amounts of data p 1101 N95-19631
Properties of Alfven waves with transverse scale on the order of skin-depth
[AD-A285657] p 1147 N95-19700

CALIFORNIA UNIV., SAN DIEGO, CA.
The effect of stable stratification on three-dimensional structure in shear layers p 1019 N95-18921
Simulation of wave propagation in three-dimensional random media
[NASA-CR-197605] p 1004 N95-19547

CALIFORNIA UNIV., SAN DIEGO, LA JOLLA, CA.
Extrathalamic modulation of cortical responsiveness
[AD-A284100] p 1078 N95-18400
Chemical production of chondrule oxygen isotopic composition p 1192 N95-19330

CALIFORNIA UNIV., SANTA BARBARA, CA.
Atomic scale force mapping with the atomic force microscope
[AD-A284940] p 1129 N95-17974
High temperature stability of binary microstructures derived from liquid precursors
[AD-A283960] p 1150 N95-18685
Vacuum microelectronic emitters and their applications using compound semiconductor technology
[AD-A284811] p 1013 N95-19687

CARNEGIE INSTITUTION OF WASHINGTON, WASHINGTON, DC.
Producing chondrules by recycling and volatile loss p 1186 N95-19290
Large-scale processes in the solar nebula p 1186 N95-19292

CARNEGIE-MELLON UNIV., PITTSBURGH, PA.
Technological and organizational diversity and technical advance in the early history of the American semiconductor industry
[PB94-175700] p 1007 N95-17999
Representing and reformulating diagonalization methods
[AD-A283916] p 1095 N95-18155
Mapping a domain model and architecture to a generic design
[AD-A283747] p 1096 N95-18364
Improved approximation guarantees for minimum-weight k-trees and prize-collecting salesmen
[AD-A284042] p 1117 N95-18658
A redundant disk array architecture for efficient small writes
[AD-A284048] p 1093 N95-18659
Program verification for optimized byte copy
[AD-A283915] p 1099 N95-18676
Research in parallel computing
[AD-A283983] p 1111 N95-18892
Assessment of the ACSE science learning environment and the impact of movies and simulations
[AD-A284071] p 1089 N95-19068
Draft SEI program plans: 1995-1999
[AD-A285047] p 1100 N95-19545

CASE WESTERN RESERVE UNIV., CLEVELAND, OH.
Thermal relaxation processes and stability in poled electro-optic polymers
[AD-A283948] p 987 N95-19102
Electrochemical interfaces and electrode processes: Electrochemical oxidation of small organisms
[AD-A284873] p 1013 N95-19741

CATAWBA COLL., SALISBURY, NC.
Probing the chemistry of nickel/metal hydride battery cells using electrochemical impedance spectroscopy p 1014 N95-18985

CENGELOGLU (YILMAZ), WINTER PARK, FL.
DYNACLIPS (DYNAmic CLIPS): A dynamic knowledge exchange tool for intelligent agents p 1108 N95-19768

CENTER FOR GENETIC SERVICES, CORPUS CHRISTI, TX.
Expert Witness: A system for developing expert medical testimony p 1101 N95-19628

CENTRAL AEROHYDRODYNAMICS INST., ZHUKOVSKY (RUSSIA).
Optical surface pressure measurements: Accuracy and application field evaluation p 1025 N95-19274
Fatigue and damage tolerance scatter models p 935 N95-19475

CENTRAL INST. OF AVIATION MOTORS, MOSCOW (RUSSIA).
On the CFD monotone high accuracy methods p 948 N95-19018
Solution of Navier-Stokes equations using high accuracy monotone schemes p 948 N95-19019
The mathematical models of flow passage for gas turbine engines and their components p 948 N95-19020
Simulation of multidisciplinary problems for the thermostress state of cooled high temperature turbines p 948 N95-19021
Application of multicomponent models to flow passage simulation in multistage turbomachines and whole gas turbine engines p 948 N95-19022
Simulation of steady and unsteady viscous flows in turbomachinery p 949 N95-19023
Application of multidisciplinary models to the cooled turbine rotor design p 949 N95-19024
Verification of multidisciplinary models for turbomachines p 949 N95-19025
Perspective problems of gas turbine engines simulation p 949 N95-19026

CENTRE D'ETUDES ET DE RECHERCHES, TOULOUSE (FRANCE).
Experimental techniques for measuring transonic flow with a three dimensional laser velocimetry system. Application to determining the drag of a fuselage p 1022 N95-19258
Analysis of test section sidewall effects on a two dimensional airfoil: Experimental and numerical investigations p 1025 N95-19276

CENTRE NATIONAL DE LA RECHERCHE SCIENTIFIQUE, ORSAY (FRANCE).
Main characteristics of the COMET/COMRADE experiments p 1181 N95-19179

CENTRO BRASILEIRO DE PESQUISAS FISICAS, RIO DE JANEIRO.
Comparison of the anomalous and non-anomalous generalized Schwinger models via functional formalism
[DE94-626684] p 1156 N95-18333
Diquarks in deep inelastic scattering and the Gottfried sum rule
[DE94-626685] p 1130 N95-18356
Feynman-x and transverse momentum dependence of D(sup (+-)) and D(sup 0), D-bar(sup 0) production in 250 GeV (pi)(sup -) - nucleon interactions
[DE94-626698] p 1130 N95-18366
Lie algebras for the Dirac-Clifford ring
[DE94-626643] p 1118 N95-18878

CENTRO DE INSTRUCCION DE MEDICINA AEROESPATIAL, MADRID (SPAIN).
Fit to fly: Analysis of the aeromedical disposition in aircrewmembers of the Spanish Armed Forces p 1081 N95-19418
Evaluation of the EKG's isoelectric T wave in Air Force pilots p 1082 N95-19423
Spine injuries: Up to date evaluation in aircraft ejections p 1084 N95-19434
Clinical basis for aeromedical decisions in aircrew HIV positive p 1086 N95-19440

CENTRO SVILUPPO MATERIALI S.P.A., TRENTO (ITALY).
Thermal testing of high performance thermal barrier coatings for turbine blades p 955 N95-19681

CERAMICS AND MATERIALS PROCESSING, INC., CLARENCE, NY.
Recent progress on ECVD Project
[DE94-016773] p 988 N95-19580

CESSNA AIRCRAFT CO., WICHITA, KS.
Design limit loads based upon statistical discrete gust methodology p 946 N95-18603

CHICAGO STATE UNIV., CHICAGO, IL.
Scattering of point source illumination by an arbitrary configuration p 1143 N95-19006

CHICAGO UNIV., CHICAGO, IL.
PVDF flux/mass/velocity/trajectory systems and their applications in space p 966 N95-19196
Heating and cooling in the solar nebula: Constraints from refractory inclusions p 1187 N95-19297

CHINA NUCLEAR INFORMATION CENTRE, BEIJING (CHINA).
An unified program for calculating the fast neutron nuclear data for middle-heavy nuclei (MUP-3)
[DE94-626822] p 1132 N95-18883
The experimental investigation of plasma configuration in MM-4U device
[DE94-626964] p 1144 N95-18885
Simplified ideal MHD normal mode equations for toroidal axisymmetric plasmas
[DE94-627004] p 1144 N95-18886
Study on heat flux of plasma scrape-off layer in HL-1 tokamak
[DE94-627009] p 1144 N95-18887
Theoretical investigation of matching between plasma heating and fueling in HL-1M machine
[DE94-627019] p 1146 N95-19241

CHRISTIAN BROTHERS COLL., MEMPHIS, TN.
Evaluation of SSME test data reduction methods p 968 N95-19002

CINCINNATI UNIV., OH.
LVQ and backpropagation neural networks applied to NASA SSME data
[NASA-CR-195418] p 962 N95-18045
Radial basis function neural networks applied to NASA SSME data
[NASA-CR-195417] p 962 N95-18467
Novel polymeric composites through molecular engineering
[AD-A284168] p 985 N95-18513
Experimental and numerical simulations of the effects of ingested particles in gas turbine engines p 952 N95-19662

CITY UNIV., LONDON (ENGLAND).
Interference determination for wind tunnels with slotted walls p 960 N95-19269

CITY UNIV. OF NEW YORK, BROOKLYN, NY.
Porphyritic versus nonporphyritic chondrules p 1190 N95-19318

CLARK UNIV., WORCESTER, MA.
Adherend surface effects on epoxy cure by NMR
[AD-A284774] p 985 N95-18442

CLARKSON UNIV., POTSDAM, NY.
Advanced techniques for analysis and evaluation of robust protocols
[AD-A285682] p 1111 N95-19513
PST: A simulation tool for parallel systems
[AD-A285680] p 1111 N95-19526

CLEMSON UNIV., SC.
Investigation of single events upsets in silicon and GaAs structures using reaction calculations
[AD-A285581] p 1131 N95-18474
Radio wave heating of the lower ionosphere p 1145 N95-18905

COAST GUARD RESEARCH AND DEVELOPMENT CENTER, GROTON, CT.
AN/APS-137 Forward Looking Airborne Radar (FLAR) evaluation
[AD-A284672] p 1002 N95-19087

COASTAL ENGINEERING RESEARCH CENTER, VICKSBURG, MS.
Coastal Modeling System (CMS) user's manual. Supplement 3 to September 1991 manual
[AD-A283922] p 1074 N95-18160

Kings Bay coastal and estuarine physical monitoring and evaluation program: Coastal studies. Volume 1: Main text and Appendix A
[AD-A285542] p 1074 N95-18470

COGNITECH, INC., SANTA MONICA, CA.
Reconstruction of shapes from shading and shape based image reconstruction using modern nonlinear analysis
[AD-A284107] p 1097 N95-18437

COIMBRA UNIV. (PORTUGAL).
Calibration and use of a non-nulling seven-hole pressure probe p 1021 N95-19254

COLLEGE OF NEW JERSEY, POMONA, NJ.
The load separation technique in the elastic-plastic fracture analysis of two- and three-dimensional geometries p 936 N95-19481

COLLEGE OF WILLIAM AND MARY, WILLIAMSBURG, VA.
A spectrally accurate boundary-layer code for infinite swept wings
[NASA-CR-195014] p 1014 N95-18042

COLOGNE UNIV. (GERMANY).
Formation of chondrules and CAIs by nebular processes p 1190 N95-19321

COLORADO SCHOOL OF MINES, GOLDEN, CO.
A 2D depth migration in transversely isotropic media using explicit operators
[DE95-000645] p 1066 N95-19560

COLORADO STATE UNIV., FORT COLLINS, CO.
Ethylene dynamics in the CELSS biomass production chamber p 1077 N95-18179
Cellular neurophysiology of the rat suprachiasmatic nucleus: Electrical properties, neurotransmission, and mechanisms of synchronization
[AD-A284111] p 1076 N95-18439

COLORADO UNIV., BOULDER, CO.
Ignition and combustion of bulk metals in a microgravity environment
[NASA-CR-197519] p 990 N95-18082
Ice surface temperature retrieval from AVHRR, ATSR, and passive microwave satellite data: Algorithm development and application
[NASA-CR-197542] p 1052 N95-18952
Chondrule formation in lightning discharges p 1188 N95-19304
Nonlinear ocean waves
[AD-A285331] p 1075 N95-19523
Assessment of climate variability of the Greenland Ice Sheet: Integration of in situ and satellite data
[NASA-CR-197604] p 1062 N95-19779

COLUMBIA UNIV., NEW YORK, NY.
Development of a high-resolution liquid xenon detector for gamma-ray astrophysics p 1179 N95-18499
The origin of the diffuse x-ray background p 1197 N95-18729

COMMONWEALTH SCIENTIFIC AND INDUSTRIAL RESEARCH ORGANIZATION, HIGHETT, VICTORIA (AUSTRALIA).
The jet model of chondrule formation p 1189 N95-19310

CONNECTICUT UNIV., STORRS, CT.
Nanostructured bearing alloy studies
[AD-A283328] p 978 N95-18027

CONSTELLATION TECHNOLOGY CORP., SAINT PETERSBURG FL.
Simulation of gamma-ray spectra for a variety of user-specified detector designs
[NASA-CR-197551] p 1136 N95-18370

CONSTRUCCIONES AERONAUTICAS S.A., MADRID (SPAIN).
A study of the effect of store unsteady aerodynamics on gust and turbulence loads p 946 N95-18601
Application of the PSD technique to acoustic fatigue stress calculations in complex substructures p 1126 N95-19155

CONTINUOUS ELECTRON BEAM ACCELERATOR FACILITY, NEWPORT NEW, VA.
The founding of CEBAF, 1979 to 1987 p 1138 N95-19784

CORNELL UNIV., ITHACA, NY.
Evaluation of the current biased integrated optical processors based on bistable dode elements
[AD-A285532] p 1138 N95-18102
Surface phases, surface defects and the initial stages of oxidation
[DE94-016947] p 979 N95-18358
The Isis project: Fault-tolerance in large distributed systems
[NASA-CR-197561] p 1110 N95-18532
Wave cycle design for wave rotor engines with limited nitrogen oxide emissions p 1041 N95-18901
Fracture toughness of polymer/polymer bimaterial interface reinforced with block copolymers p 986 N95-18923
Fatigue crack growth in 2024-T3 aluminum under tensile and transverse shear stresses p 938 N95-19490
Experimental studies of Reynolds number dependence of turbulent mixing and transport
[DE94-015338] p 1030 N95-19578

CRANFIELD UNIV., BEDFORD (ENGLAND).
Particle trajectories in gas turbine engines p 952 N95-19663

CSA ENGINEERING, INC., PALO ALTO, CA.
Using neural networks in the mapping of mixed discrete/continuous design spaces with application to structural design
[AD-A285328] p 1046 N95-19522

D

DAIMLER-BENZ A.G., MUNICK (GERMANY).
Acoustic fatigue of carbon fibre structures p 1127 N95-19158

DARTMOUTH COLL., HANOVER, NH.
Nonlinear magnetohydrodynamics
[DE94-016223] p 1143 N95-18353
Dynamic file-access characteristics of a production parallel scientific workload
[NASA-CR-197570] p 1110 N95-18581

DASSAULT AVIATION, SAINT-CLOUD (FRANCE).
Aeroacoustic qualification of HERMES shingles p 1125 N95-19145
Brite-Euram programme: ACOUFAT acoustic fatigue and related damage tolerance of advanced composite and metallic structures p 1127 N95-19159

DAVIDSON COLL., NC.
Development of a colloidal redox system containing a smectite clay for control of reactivity and reaction selectivity
[AD-A285958] p 974 N95-19515

DAYTON UNIV., OH.
Conference on Aerospace Transparent Materials and Enclosures, volume 1
[AD-A283925] p 944 N95-18677

DAYTON UNIV. RESEARCH INST., OH.
Conference on Aerospace Transparent Materials and Enclosures. Volume 2: Sessions 5-9
[AD-A283926] p 942 N95-18162
CVD silicon carbide characterization
[AD-A285667] p 972 N95-19702

DE HAVILLAND AIRCRAFT CO. OF CANADA LTD., DOWNSVIEW (ONTARIO).
A review of gust load calculation methods at de Havilland p 932 N95-18604
Interference corrections for a centre-line plate mount in a porous-walled transonic wind tunnel p 933 N95-19280

DEFENCE AND CIVIL INST. OF ENVIRONMENTAL MEDICINE, DOWNSVIEW (ONTARIO).
Implementation of a human information processing model for task network simulation
[AD-A283903] p 1088 N95-18151

DEFENCE RESEARCH AGENCY, BEDFORD (ENGLAND).
Boundary-flow measurement methods for wall interference assessment and correction: Classification and review p 1022 N95-19262

DEFENCE RESEARCH AGENCY, FARNBOROUGH, HAMPSHIRE (ENGLAND).
Advanced statistical energy analysis p 1047 N95-19165
The operation of gas turbine engines in hot and sandy conditions: Royal Air Force experiences in the Gulf conflict p 950 N95-19655
The calculation of erosion in a gas turbine compressor rotor p 952 N95-19664

DEFENCE RESEARCH ESTABLISHMENT OTTAWA, OTTAWA (ONTARIO).
A review of footwear for cold/wet scenarios. Part 2: Socks, liners, and insoles
[AD-A279937] p 989 N95-19866
Diffusion of water vapour through cold Gore-Tex (trademark)
[AD-A279939] p 989 N95-19867

DEFENCE SCIENCE AND TECHNOLOGY ORGANIZATION, MELBOURNE (AUSTRALIA).
Potential replacements for solvents that are ozone depleting substances
[AD-A285442] p 1058 N95-18091
Handbook for the extremely low frequency (ELF) data acquisition and analysis system
[DSTO-GD-0021] p 1005 N95-19622

DELAWARE UNIV., NEWARK, DE.
Lattice gas and lattice Boltzmann methods for simulation of hydrodynamics and magnetohydrodynamics p 1145 N95-18907

DENVER UNIV., DENVER, CO.
Signal processing via Fourier-Bessel series expansion
[AD-A285316] p 1003 N95-19510

DEPARTMENT OF ENERGY, WASHINGTON, DC.
Activities of the Division of Energy Biosciences
[DE95-001046] p 1077 N95-19613

DEPARTMENT OF THE NAVY, WASHINGTON, DC.
Junction Field Effect Transistor with lateral Gate Voltage Swing (GVS-JFET)
[AD-D016353] p 1032 N95-17970
Method and flowmeter for unsteady fluid flow study
[AD-D016432] p 1015 N95-18112
Modular signal processing unit
[AD-D016258] p 995 N95-18314
Signal processor having multiple distributed data buffers
[AD-D016259] p 995 N95-18315
Electromagnetic pump
[AD-D016260] p 1041 N95-18317
Preparation of an electrocatalytic cathode for an aluminum-hydrogen peroxide battery
[AD-D016262] p 1008 N95-18318
Fixture for pressure testing sight glasses
[AD-D016263] p 1032 N95-18319
Polyurethane self-priming topcoats
[AD-D016264] p 984 N95-18320
Trivalent chromium conversion coatings for aluminum
[AD-D016274] p 978 N95-18332
Positive displacement rotary pump
[AD-D016412] p 1041 N95-18335
Polyurethane self-priming topcoats
[AD-D016420] p 984 N95-18336
Corner vortex suppressor
[AD-D016423] p 928 N95-18337
Radar sector blanker
[AD-D016275] p 996 N95-18429
Method of lowering the reaction exotherm in thermally polymerized acetylene terminated resins
[AD-D016276] p 985 N95-18430
Centrifugal casting of reinforced articles
[AD-D016277] p 992 N95-18431
High current amplifier utilizing a Josephson junction Schottky diode three terminal device
[AD-D016278] p 1009 N95-18432
Superconductor microelectronic devices and circuits and a method of fabricating therefor
[AD-D016280] p 1009 N95-18433
Fault protection circuit for power switching device
[AD-D016466] p 1009 N95-18455
A shock isolation method and apparatus
[AD-D016471] p 1045 N95-18456
Trivalent chromium solutions for sealing anodized aluminum
[AD-D016472] p 979 N95-18458
A fiber optic coupler
[AD-D016473] p 1140 N95-18459
Fiber optic pressure and/or vibration detector
[AD-D016474] p 1140 N95-18460
Hydrofoil force balance
[AD-D016475] p 1033 N95-18461
Communication with reentry vehicle through modulated plasma
[AD-D016476] p 997 N95-18462
Combiner for two dimensional adaptive interference suppression system
[AD-D016272] p 997 N95-18516
Laser optical mouse
[AD-D016273] p 1092 N95-18517
Power conversion system modification to permit use of DC power source
[AD-D016421] p 1010 N95-18523
Corrosivity sensor
[AD-D016422] p 1033 N95-18524
Method and system for identifying the onset of a turbulent boundary layer induced by a body moving through a fluid medium
[AD-D016434] p 1018 N95-18525
Method of displaying time series data on finite resolution display device
[AD-D016438] p 1173 N95-18526
Process for forming epitaxial BaF2 on GaAs
[AD-D016439] p 1149 N95-18527
Synchronization of nonautonomous chaotic systems
[AD-D016440] p 1010 N95-18528
Infrared-to-visible converter
[AD-D016443] p 1141 N95-18529
Method of doping single crystal diamond for electronic devices
[AD-D016267] p 1149 N95-18543
Variable rate transfer of optical information
[AD-D016268] p 1173 N95-18544
Multi-channel, covert, non-line-of-sight UV communication
[AD-D016269] p 999 N95-18545
Method for fabricating complementary enhancement and depletion mode field effect transistors on a single substrate
[AD-D016270] p 1010 N95-18546

Fluid dynamic linear accelerometer
[AD-D016413] p 956 N95-18553
Method for forming Josephson break junctions
[AD-D016427] p 1149 N95-18559
Multi-line passive fiber optic slipring
[AD-D016430] p 1141 N95-18560
Method and system for inferring the radio refractive index structure of the atmosphere from radio measurements
[AD-D016436] p 999 N95-18561
Fiber optic flexural disk accelerometer
[AD-D016444] p 1141 N95-18563
Compact, efficient, scalable neodymium laser co-doped with activator ions and pumped by visible laser diodes
[AD-D016237] p 1038 N95-18585
Annular computed tomography
[AD-D016424] p 1141 N95-18593
Torsional device for remote control steering system
[AD-D016426] p 1041 N95-18594
Method of forming platinum and platinum silicide Schottky contacts on beta-silicon carbide
[AD-D016221] p 1149 N95-18627
Disengagable adapter for an optical fiber connection
[AD-D016231] p 1141 N95-18628
Composite structures having organic matrices and duplex zinc/ceramic fire barriers
[AD-D016232] p 970 N95-18629
Method for making a non-magnetic alloy
[AD-D016233] p 979 N95-18630
Polyurethane self-priming topcoats
[AD-D016234] p 985 N95-18631
Flame position ultrasonic interferometer
[AD-D016235] p 967 N95-18632
Atomic Layer Epitaxy (ALE) apparatus for growing thin films of elemental semiconductors
[AD-D016236] p 1149 N95-18633
Stratified carrier electroviscous fluids and apparatus
[AD-D016238] p 1019 N95-18634
Method for laser-assisted silicon etching using halocarbon ambients
[AD-D016239] p 1038 N95-18635
Digital monopulse
[AD-D016447] p 1002 N95-19072
Integrated aerodynamic fin and stowable TVC vane system
[AD-D016457] p 967 N95-19073
Solid fuel ramjet composition
[AD-D016458] p 990 N95-19090
Power terminal protection device
[AD-D016528] p 1011 N95-19120
Sag compensated vibration isolation mount
[AD-D016541] p 1042 N95-19121
Graded bandgap semiconductor device for real-time imaging
[AD-D016543] p 1151 N95-19122
Superstrength metal composite material and process for making the same
[AD-D016555] p 971 N95-19123
Low noise fiber gyroscope system which includes excess noise subtraction
[AD-D016556] p 1034 N95-19124
Digital circuit for the introduction and later removal of dither from an analog signal
[AD-D016462] p 1011 N95-19171
Torque-balanced extendable fiber optic cable
[AD-D016496] p 1142 N95-19389

DETROIT DIESEL ALLISON, MI.
Advanced diesel engine component development program, tasks 4-14
[NASA-CR-191203] p 1040 N95-18041

DEUTSCHE AEROSPACE A.G., BREMEN (GERMANY).
Acoustic fatigue testing on different materials and skin-stringer elements p 1126 N95-19156

DEUTSCHE AIRBUS G.M.B.H., HAMBURG (GERMANY).
Treatment of non-linear systems by timeplane-transformed CT methods: The spectral gust method p 956 N95-18600
Development of load spectra for Airbus A330/A340 full scale fatigue tests p 936 N95-19479

DEUTSCHE FORSCHUNGSANSTALT FUER LUFT- UND RAUMFAHRT, BRUNSWICK (GERMANY).
Theoretical investigations of shock/boundary layer interactions on a Ma(infinity) = 8 wavenider
[DLR-FB-94-12] p 930 N95-18910
Wall correction method with measured boundary conditions for low speed wind tunnels p 1023 N95-19263

DEUTSCHE FORSCHUNGSANSTALT FUER LUFT- UND RAUMFAHRT, COLOGNE (GERMANY).
One-dimensional flow description for the combustion chamber of a scramjet
[DLR-FB-94-06] p 948 N95-18911

DEUTSCHE FORSCHUNGSANSTALT FUER LUFT- UND RAUMFAHRT, GOETTINGEN (GERMANY).
Numerical simulation of shock/shock and shock/boundary-layer interactions in chemically reacting hypersonic flows
[DLR-94-04] p 1019 N95-18609
Flow field investigation in a free jet - free jet core system for the generation of high intensity molecular beams
[DLR-FB-94-11] p 1132 N95-18912

DIVISIONE AEREA STUDI RICERCHE E SPERIMENTAZIONI, PRATICA DI MARE (ITALY).
Neuropsychophysiologic sequelae of mild head injury p 1083 N95-19430

DREXEL UNIV., PHILADELPHIA, PA.
Unit cell geometry of multiaxial preforms for structural composites
[NASA-CR-197294] p 971 N95-19650

DU PONT DE NEMOURS (E. I.) AND CO., WILMINGTON, DE.
Evaluation of powder metallurgy plates made by Sylvania Electric Products, Incorporated
[DE94-017911] p 980 N95-19401

DUKE UNIV., DURHAM, NC.
Characterizing parallel file-access patterns on a large-scale multiprocessor
[NASA-CR-197568] p 1110 N95-18521
Acoustic radiation damping of flat rectangular plates subjected to subsonic flows p 1123 N95-18542
Novel carbon-ion fuel cells
[DE94-017390] p 1053 N95-18894
Investigation of superlattice disordering and diffusion mechanisms in GaAs
[AD-A284847] p 1153 N95-19697
Synthesis and characterization of a neutral six-coordinate tris-adduct of an indium(3) trihalide. X ray crystal structure of InCl3(THF)3
[AD-A279169] p 1154 N95-19806
Isolation and characterization of an indium-mixed-pnicogen Four-membered ring compound: Crystal structure of (Me3SiCH2)2InAs(SiMe3)2 In(CH2SiMe3)2P(SiMe3)2
[AD-A279170] p 1154 N95-19807
Synthesis and characterization of aluminum-phosphorus adducts: X-ray crystal structures of Cl3Al (dot) P(SiMe3)3 (dot) C7H8 and Br3Al (dot) P(SiMe3)3 (dot) C7H8
[AD-A279194] p 1154 N95-19812

DYNAFLOW, INC., FULTON, MD.
Evolution of a collection of bubbles with application to wakes, bubble screens, and cloud noise
[AD-A283597] p 1017 N95-18434

E

EAST ANGLIA UNIV., NORWICH (ENGLAND).
Detection of greenhouse-gas-induced climatic change
[DE94-015044] p 1057 N95-18022

EAST CAROLINA UNIV., GREENVILLE, NC.
Development of microgravity, full body functional reach envelope using 3-D computer graphic models and virtual reality technology p 1092 N95-18990

EDGERTON, GERMESHAUSEN AND GRIER, INC., IDAHO FALLS, ID.
Alternative solvents/technologies for paint stripping: Phase 1
[AD-A279918] p 989 N95-19861

EDGEWOOD RESEARCH DEVELOPMENT AND ENGINEERING CENTER, ABERDEEN PROVING GROUND, MD.
Design of spherical aerosol particles to maximize sound attenuation
[AD-A284313] p 1123 N95-18379

EIDETICS INTERNATIONAL, INC., TORRANCE, CA.
Development of a multicomponent force and moment balance for water tunnel applications, volume 1
[NASA-CR-4642-VOL-1] p 1020 N95-18955
Development of a multicomponent force and moment balance for water tunnel applications, volume 2
[NASA-CR-4642-VOL-2] p 1020 N95-18956

ELECTRONICS RESEARCH LAB., SALISBURY (AUSTRALIA).
Modular implementation of feature extraction and matching algorithms for photogrammetric stereo imagery
[AD-A285422] p 1032 N95-18065
A visual approach to the analysis of large software systems
[AD-A285440] p 1095 N95-18089

ELTRON RESEARCH, INC., BOULDER, CO.
Methane conversion by solid electrolyte membranes
[PB94-191781] p 973 N95-17982

EMBRY-RIDDLE AERONAUTICAL UNIV., DAYTONA BEACH, FL.
Assessment of a career development program for executive amd mid-level managers p 1161 N95-18182

ENERGY AND ENVIRONMENTAL ANALYSIS, INC., ARLINGTON, VA.
Air pollution mitigation measures for airports and associated activity
[PB94-207610] p 1061 N95-19582

ENSCO, INC., MELBOURNE, FL.
The meteorological monitoring system for the Kennedy Space Center/Cape Canaveral Air Station p 1104 N95-19647

ENVIRONMENTAL PROTECTION AGENCY, RESEARCH TRIANGLE PARK, NC.
Alternative control techniques document: NO(x) emissions from glass manufacturing
[PB94-214079] p 1061 N95-19406

EPIR LTD., OAKBROOK, IL.
Industrial exploitation of a alternate technology for the production of HgCdTe epilayers, structures and devices
[AD-A279202] p 1154 N95-19816

ESSEX CORP., COLUMBIA, MD.
True time delay beamforming
[AD-A285683] p 1003 N95-19516

EUROCOPTER DEUTSCHLAND G.M.B.H., MUNICH (GERMANY).
Helicopter internal noise p 1124 N95-19144

F

FEDERAL AVIATION ADMINISTRATION, ATLANTA, GA.
Evaluation of an unlighted swinging airport sign
[AD-A284763] p 958 N95-18087
Operational And Supportability Implementation System (OASIS) test and evaluation master plan
[AD-A284765] p 941 N95-18088
Stress-intensity factor solutions for cracks at countersunk rivet holes under uniaxial tension
[AD-A279163] p 1047 N95-19804

FEDERAL AVIATION ADMINISTRATION, ATLANTIC CITY, NJ.
The 23 Gigahertz (GHz) digital Low Density Radio Communications Link (LDRCL) Operational Test and Evaluation (OT/E) integration and OT/E operation
[AD-A283963] p 1000 N95-18686

FEDERAL AVIATION ADMINISTRATION, CAMBRIDGE, MA.
An analysis of tower (local) controller-pilot voice communications
[AD-A283718] p 996 N95-18436
Aircraft wake vortex takeoff tests at O'Hara International Airport
[AD-A283828] p 929 N95-18624

FEDERAL AVIATION ADMINISTRATION, LONG BEACH, CA.
Widespread fatigue damage monitoring: Issues and concerns p 938 N95-19488

FEDERAL AVIATION ADMINISTRATION, WASHINGTON, DC.
Federal aviation regulations, part 91. General operating and flight rules. Change 8
[PB94-217445] p 940 N95-19720

FERMI NATIONAL ACCELERATOR LAB., BATAVIA, IL.
A Type 2 supernovae constraint on neutrino(sub e) - neutrino(sub s) mixing
[NASA-CR-197630] p 1180 N95-18746
Is a massive tau neutrino just what cold dark matter needs?
[NASA-CR-197627] p 1180 N95-18964
Cosmic ray models for early galactic lithium, beryllium, and boron production
[NASA-CR-197626] p 1137 N95-18965
Second-order reconstruction of the inflationary potential
[NASA-CR-197629] p 1121 N95-19030
Mass and radius of cosmic balloons
[NASA-CR-197628] p 1180 N95-19031
Asymmetric antiproton debuncher: No bad mixing, more good mixing
[DE94-017171] p 1133 N95-19077
Physics at the Fermilab Tevatron Proton-Antiproton Collider
[DE95-000648] p 1137 N95-19561
Studies of prompt photon production and multijet production at the Tevatron Collider
[DE95-002216] p 1135 N95-19835

FLORIDA AGRICULTURAL AND MECHANICAL UNIV., TALLAHASSEE, FL.
Electron interactions with non-linear polyatomic molecules and their radicals
[AD-A283952] p 1130 N95-18334

FLORIDA INST. OF TECH., MELBOURNE, FL.
Modeling and measurement of the performance of a branched conduit sampling system in a mass spectrometer leak detector p 1036 N95-18181
Phase and amplitude controlled micropatch antenna
[AD-A284191] p 1002 N95-19103

FLORIDA INTERNATIONAL UNIV., MIAMI, FL.
Assessment of the SFC database for analysis and modeling p 1158 N95-18171
FLORIDA STATE UNIV., TALLAHASSEE, FL.
Marginal probabilities of the extremes of ENSO events for temperature and precipitation in the southeastern United States
[AD-A284716] p 1068 N95-18076
Prediction of global cloud cover with a very high resolution global spectral model
[AD-A279944] p 1073 N95-19870
FLORIDA UNIV., GAINESVILLE, FL.
The cross-validation of the United States Air Force submaximal cycle ergometer test to estimate aerobic capacity
[AD-A284055] p 1079 N95-18661
Mass spectrometric studies of clusters and surfaces
[AD-A283992] p 974 N95-19066
IRAS observations show that the Earth is embedded in a solar ring of asteroidal dust particles in resonant lock with the planet p 1182 N95-19181
Velocity distribution of Earth-crossing asteroid grains p 1183 N95-19187
FLUOROCHEM, INC., AZUSA, CA.
Difunctional monomers based on perfluoropropylene telomers
[AD-A283677] p 983 N95-18019
FOKKER B.V., SCHIPOL-OOST (NETHERLANDS).
Acoustic fatigue behaviour of GLARE composites p 1127 N95-19160
FOSTER-MILLER ASSOCIATES, INC., WALTHAM, MA.
Lunar base heat pump, phase 1
[NASA-CR-188300] p 1015 N95-18111
Evaluation of the fuselage lap joint fatigue and terminating action repair p 936 N95-19477
Novel e-o polymers: NLO materials with superior temporal stability
[AD-A285872] p 988 N95-19614

G

GALAXY SCIENTIFIC CORP., PLEASANTVILLE, NJ.
Rotorcraft ditchings and water-related impacts that occurred from 1982 to 1989, phase 1
[AD-A279164] p 940 N95-19805
GDANSK TECHNICAL UNIV. (POLAND).
Solution of Maxwell's equations using the time domain Method of Moments. Supplement: Publications and reports
[AD-A280143] p 1119 N95-19819
Solution of Maxwell's equations using the time domain Method of Moments
[AD-A280144] p 1119 N95-19820
GENCORP AEROJET, SACRAMENTO, CA.
Advanced small rocket chambers. Basic program and option 2: Fundamental processes and material evaluation
[NASA-CR-195349] p 966 N95-18192
GENERAL ACCOUNTING OFFICE, WASHINGTON, DC.
European aeronautics: Strong government presence in industry structure and research and development support. Report to Congressional Requesters
[GAO/NSIAD-94-71] p 1171 N95-18578
Government contractors: Measuring costs of service contractors versus federal employees. Report to the Chairman, Subcommittee on Federal Services, Post Office and Civil Service, Committee on Governmental Affairs, US Senate
[GAO/GGD-94-95] p 1171 N95-18595
Overhead costs: Costs charged by McDonnell Douglas Aerospace's Space Station Division. Report to the Chairman, Legislation and National Security Subcommittee, Committee on Government Operations, House of Representatives
[GAO/NSIAD-94-150] p 1171 N95-18596
Information Superhighway: Issues affecting development. Report to the Congress
[GAO/RCED-94-285] p 1174 N95-18914
Space Station: Plans to expand research community do not match available resources. Report to the Ranking Minority Member, Subcommittee on Oversight of Government Management, Committee on Government Affairs, US Senate
[GAO/NSIAD-95-33] p 965 N95-19131
NASA property: Poor lending practices and controls at the Jet Propulsion Laboratory. Report to Congressional Requesters
[GAO/NSIAD-94-116] p 1172 N95-19141
GENERAL ATOMICS CO., SAN DIEGO, CA.
Progress on the multipulse Thomson scattering diagnostic on D3-D
[DE94-017515] p 1143 N95-18119
Fueled emitter, TFE Verification Program
[DE94-017557] p 1135 N95-18146
TFE design package, TFE Verification Program
[DE94-017558] p 1136 N95-18147
Development of lithium beam emission spectroscopy as an edge fluctuation diagnostic for D3-D
[DE94-017517] p 1146 N95-19378
2-D tomography with bolometry in D3-D
[DE94-017520] p 1146 N95-19379
GENERAL ELECTRIC CO., CINCINNATI, OH.
Modern transport engine experience with environmental ingestion effects p 951 N95-19660
GENERAL ELECTRIC CO., SCHENECTADY, NY.
J-integral characterization of the nozzle steels from intermediate test vessels IV-5 and IV-9
[DE95-001066] p 979 N95-18934
GEOLOGICAL SURVEY, RESTON, VA.
The role of chondrules in nebular fractionations of volatiles and other elements p 1187 N95-19300
GEOLOGICAL SURVEY, WOODS HOLE, MA.
Geologic studies: Executive summary report
[PB94-187481] p 1073 N95-17951
GEORGIA INST. OF TECH., ATLANTA, GA.
Guidance, Navigation and Control Digital Emulation Technology Laboratory
[AD-A284339] p 996 N95-18386
A model study of the influence of NMHC and NO(x) emissions on rural O3 concentrations in Georgiargia p 1059 N95-18445
Laboratory studies of stratospheric bromine chemistry: Kinetics of the reactions of bromine monoxide with nitrogen dioxide and atomic oxygen p 1065 N95-18731
A linear system identification and validation of an AH-64 Apache aeroelastic simulation model p 959 N95-18903
Acoustic properties and durability of liner materials at non-standard atmospheric conditions
[NASA-CR-195010] p 1123 N95-18930
Development of pneumatic test techniques for subsonic high-lift and in-ground-effect wind tunnel investigations p 932 N95-19268
Discrete crack growth analysis methodology for through cracks in pressurized fuselage structures p 935 N95-19473
Residual life and strength estimates of aircraft structural components with MSD/MED p 937 N95-19485
GEORGIA UNIV., ATHENS.
Photogeneration and characterization of energetic molecules in supersonic molecular beams
[AD-A284108] p 1131 N95-18438
A GIS approach to urban heat island research: The case of Huntsville, Alabama p 1063 N95-18991
GERMAN AIR FORCE, FUERSTENFELDBRUK (GERMANY).
Neurological decision making in aviation medicine based on electrophysiological methods p 1084 N95-19431
Clinical practice, diagnosis and therapy of intervertebral disk lesion: Importance to fitness for military flying duties p 1084 N95-19435
Spinal nerve syndromes: The need to confirm the diagnosis with neurophysiological examinations p 1085 N95-19436
GERMAN-DUTCH WIND TUNNEL, NORTH EAST POLDER (NETHERLANDS).
Correction of support influences on measurements with sting mounted wind tunnel models p 933 N95-19281
GERMAN MILITARY GEOPHYSICAL OFFICE, TRABEN-TRARBACH (GERMANY).
Estimation of satellite derived temperature and moisture fields over Europe from TOVS data using 3I and ITPP algorithms
[AD-A284581] p 1049 N95-18035
GTE LABS., INC., WALTHAM, MA.
Methods and components for optical contention resolution in high speed networks
[AD-A284674] p 1142 N95-19088

H

HAHNEMANN MEDICAL COLL. AND HOSPITAL, PHILADELPHIA, PA.
Cerebellar circuit mechanisms which accompany coordinated limb trajectory patterns in the rat: Use of a model of spontaneous changes in limb coordination
[AD-A284023] p 1079 N95-18656
HARRIS CORP., MELBOURNE, FL.
Streamlined design and self reliant hardware for active control of precision space structures
[NASA-CR-4637] p 964 N95-18580
Neural network communications signal processing
[AD-A285681] p 1115 N95-19512
HARRIS SPACE SYSTEMS CORP., ROCKLEDGE, FL.
The Buffer Diagnostic Prototype: A fault isolation application using CLIPS p 1100 N95-19626
HARVARD-SMITHSONIAN CENTER FOR ASTROPHYSICS, CAMBRIDGE, MA.
Astronomical observations of phenomena in disks p 1178 N95-19301
Major unresolved issues in the formation of chondrules and CAIs p 1193 N95-19336
HARVARD UNIV., CAMBRIDGE, MA.
Cooperativity and 3-D representation
[AD-A284203] p 1093 N95-17940
HAWAII UNIV., HONOLULU, HI.
Dynamic evolution of emerging magnetic flux tubes in the solar convective envelope p 1195 N95-18497
Variations among chondrite groups: Constraints on nebular processes p 1192 N95-19327
Density structure of the upper oceanic crust at zero porosity
[AD-A284235] p 1076 N95-19728
HAWAII UNIV., MANOA, HI.
Implications of a phase-transition thermostat for chondrule melting p 1189 N95-19312
Formation of chondrules by electrical discharge heating p 1189 N95-19313
HELSINKI UNIV. OF TECHNOLOGY, ESPOO (FINLAND).
DC-conductivity and magnetoresistance of inherently conducting polymers. Polyacetylene and poly(3-alkylthiophenes)
[PB94-184587] p 1007 N95-18037
New method for homodyne laser linewidth measurements with a short delay fiber
[PB94-202629] p 1036 N95-18061
HILTON SYSTEMS, INC., CHERRY HILL, NJ.
Age 60 study. Part 3: Consolidated database experiments
[AD-A286247] p 1080 N95-19384
Age 60 study. Part 4: Experimental evaluation of pilot performance
[AD-A286248] p 1080 N95-19385
HONEYWELL, INC., CLEARWATER, FL.
Using expert systems to analyze ATE data p 1103 N95-19639
HUGHES INFORMATION TECHNOLOGY CO., RESTON, VA.
Optimal pattern distributions in Rete-based production systems p 1106 N95-19755
HUGHES STX, INC., LANHAM, MD.
Analysis of solar spectral irradiance measurements from the SBUV/2-series and the SSBUV instruments
[NASA-CR-197544] p 1196 N95-18954
HUMBOLDT UNIV., BERLIN (GERMAN D.R.).
Constraints on chondrule agglomeration from fine-grained chondrule rims p 1189 N95-19315

I

ILLINOIS UNIV., CHICAGO, IL.
MBE growth, characterization and electronic device processing of Hg-based semiconductor alloys and heterostructures
[AD-A279203] p 1154 N95-19817
ILLINOIS UNIV., URBANA, IL.
A novel system level approach to fault tolerance in distributed memory multicomputers
[AD-A284729] p 1095 N95-18079
Study of high gain spherical shell ICF targets containing uniform layers of liquid deuterium tritium fuel
[DE94-018550] p 1136 N95-18552
Annual Allerton Conference on Communication, Control and Computing
[AD-A283892] p 1114 N95-18675
ILLINOIS UNIV., URBANA-CHAMPAIGN, IL.
NASA/DOD Aerospace Knowledge Diffusion Research Project. Paper 47: The value of computer networks in aerospace
[NASA-CR-197591] p 1109 N95-18055
IMPERIAL COLL. OF SCIENCE AND TECHNOLOGY, LONDON (ENGLAND).
International Conference on Deformation, Yield and Fracture of Polymers
[AD-A284354] p 984 N95-18339
Light scattering from rough surfaces
[AD-A284112] p 1139 N95-18404
INDIANA UNIV., BLOOMINGTON, IN.
Perception of complex auditory patterns
[AD-A284189] p 1079 N95-18626
INDUSTRIEANLAGEN-BETRIEBSGESELLSCHAFT M.B.H., OTTOBRUNN (GERMANY).
Design and operation of a thermoacoustic test facility p 960 N95-19150
INSTITUT DES HAUTES ETUDES SCIENTIFIQUES, BURES-SUR-YVETTE (FRANCE).
Plane Jacobian conjecture
[PB94-192341] p 1118 N95-19198
Antisymmetric tensor field interactions and neutron star models
[PB94-215605] p 1118 N95-19375

Non localizability of the photon keystone to a remodelling of physics
[PB94-217213] p 1134 N95-19376
Orbital tests of relativistic gravity using artificial satellites
[PB94-217239] p 965 N95-19377
Towards a classification of su(2)(direct sum)...(direct sum)su(2) modular invariant partition functions
[PB94-217247] p 1119 N95-19717
Coulomb gas representation of the SU(2) WZW correlators at higher genera
[PB94-217254] p 1119 N95-19718
SU(2) WZW theory at higher genera
[PB94-217262] p 1119 N95-19719

INSTITUTE FOR AEROSPACE RESEARCH, OTTAWA (ONTARIO).
Applications of the five-hole probe technique for flow field surveys at the Institute for Aerospace Research p 1021 N95-19255
Evaluation of combined wall- and support-interference on wind tunnel models p 932 N95-19278

INSTITUTE FOR COMPUTER APPLICATIONS IN SCIENCE AND ENGINEERING, HAMPTON, VA.
An algorithm for solving the system-level problem in multilevel optimization
[NASA-CR-195015] p 1116 N95-18108
Optimization of coupled systems: A critical overview of approaches
[NASA-CR-195019] p 1116 N95-18109
Floating shock fitting via Lagrangian adaptive meshes
[NASA-CR-194997] p 1116 N95-18110
Time-evolving bubbles in two-dimensional stokes flow
[NASA-CR-194998] p 1015 N95-18188
The stability of two-phase flow over a swept-wing
[NASA-CR-194994] p 1016 N95-18190
On the Lighthill relationship and sound generation from isotropic turbulence
[NASA-CR-195005] p 1016 N95-18191
Effect of crossflow on Goertler instability in incompressible boundary layers
[NASA-CR-195007] p 1016 N95-18193
A note on singularities of the 3-D Euler equation
[NASA-CR-195006] p 1017 N95-18397
An inverse problem in thermal imaging
[NASA-CR-195018] p 1117 N95-18479
A simple hyperbolic model for communication in parallel processing environments
[NASA-CR-195984] p 1098 N95-18487
Low-dissipation and -dispersion Runge-Kutta schemes for computational acoustics
[NASA-CR-195022] p 1018 N95-18488
Scalability of parallel spatial direct numerical simulation code on IBM SP1 parallel supercomputer
[NASA-CR-194975] p 1098 N95-18584
On extending parallelism to serial simulators
[NASA-CR-195011] p 1099 N95-18931
Active control of instabilities in laminar boundary-layer flow. Part 1: An overview
[NASA-CR-195016-PT-1] p 1020 N95-18958
Empirical study of parallel LRU simulation algorithms
[NASA-CR-194995] p 1099 N95-19027
On k-ary n-cubes: Theory and applications
[NASA-CR-194996] p 1100 N95-19028

INSTITUTE FOR DEFENSE ANALYSES, ALEXANDRIA, VA.
IDA gamma ray laser
[AD-A284322] p 1037 N95-18382

INSTITUTE FOR HUMAN FACTORS TNO, SOESTERBERG (NETHERLANDS).
Learning effects on strategy selection in a dynamic task environment as a function of time pressure
[AD-A285458] p 1089 N95-19538

INSTITUTE OF AVIATION MEDICINE, FUERSTENFELDBRUCK (GERMANY).
Relevance of laboratory tests in aeromedical decisions p 1082 N95-19420

INSTITUTE OF AVIATION MEDICINE, PRAGUE (CZECHOSLOVAKIA).
Medication in the course of active flying duty p 1086 N95-19443

INSTITUTE OF ELECTRICAL AND ELECTRONICS ENGINEERS, PISCATAWAY, NJ.
1994 IEEE Nonlinear Optics: Materials Fundamental and Applications Conference
[AD-A285769] p 1139 N95-18345
14th IEEE International Semiconductor Laser Conference
[AD-A285560] p 1038 N95-18642

INSTITUTO DE FISICA TEORICA, SAO PAULO (BRAZIL).
Evidence for coexistence of two phases in relativistic heavy ion collisions and comparison with lattice results
[DE94-626672] p 1130 N95-18329
SU4(sub L) x U1(sub N) model for the electroweak interactions
[DE94-626675] p 1148 N95-18330
The Green's function in the Bloch-Nordsieck model for QED3
[DE94-626680] p 996 N95-18331
Flattening of the resonance spectrum of hadrons from kappa-deformed Poincare algebra
[DE94-626686] p 1156 N95-18352

INSTITUTO DE PESQUISAS ENERGETICAS E NUCLEARES, SAO PAULO (BRAZIL).
Assembly and calibration of a new experimental apparatus for production and utilization of capture gamma rays
[DE94-626650] p 1198 N95-18880
Study of the ferrimagnetic and paramagnetic phases of magnetite measured by multiple neutron diffraction
[DE94-627031] p 1151 N95-19242

INSTITUTO DE PESQUISAS ESPACIAIS, SAO JOSE DOS CAMPOS (BRAZIL).
Radiation balance in three Amazonian ecosystems: Campina, campinarana and mata densa
[INPE-5587-TDI/549] p 1057 N95-18003
Some statistical tools for SAR image synthesis, analysis and processing
[INPE-5548-TDI/534] p 1172 N95-18004
Comparative analysis of multisensor (TM/Landsat and SAR/ERS-1) and multitemporal scenes of Guaira region, Sao Paulo State, Brazil
[INPE-5581-TDI/544] p 1049 N95-18005
Observational studies and modelling of interception loss of gross rainfall in the Amazonian rainforest
[INPE-5583-TDI/545] p 1067 N95-18006
Effects of meteor showers in the Earth ionosphere
[INPE-5591-TDI/552] p 1178 N95-18213
Heuristic inference about flow directions in river networks
[INPE-5588-TDI/550] p 1050 N95-18214
Thematic classification of zone coastal: A methodologic contribution
[INPE-5586-TDI/548] p 1050 N95-18215
Remote sensing products evaluation for cartographic updating purposes
[INPE-5584-TDI/546] p 1050 N95-18368
The photographic system global evaluation for generation of INPE TM Landsat image
[INPE-5571-TDI/542] p 1050 N95-18369
Imagery correction for atmospheric effects using sounding data
[INPE-5506-TDI/518] p 1064 N95-18390

INSTITUTO DE PESQUISAS ESPACIAIS, SAO PAULO (BRAZIL).
On the optimization of speckle filtering techniques for ERS-1 images over Argentina
[INPE-5578-PRE/1806] p 1050 N95-18216
Regenerative cooling for liquid propellant rocket thrust chambers
[INPE-5565-TDI/540] p 967 N95-18720

INTERNATIONAL BUSINESS MACHINES CORP., SAN JOSE, CA.
Molecular dynamics study of aqueous electrolyte solutions near a structured sphere
[AD-A284010] p 1132 N95-18655

INTERNATIONAL COMPUTER SCIENCE INST., BERKELEY, CA.
Connectionist Network Supercomputer Project
[AD-A279206] p 1112 N95-19843

INTERNATIONAL TRADE ADMINISTRATION, WASHINGTON, DC.
US Industrial Outlook, 1994: An almanac of industry, technology and services. 35th annual edition. Forecasts for selected manufacturing and service industries
[PB94-107844] p 1171 N95-17988

INTERTURBINE HOLDING B.V., LOMM (NETHERLANDS).
Braze repair possibilities for hot section gas turbine parts p 954 N95-19677

IOWA UNIV., IOWA CITY, IA.
Heliospheric 2-3 kHz radio emissions and their relationship to large Forbush decreases
[U-OF-IOWA-94-19] p 1195 N95-17979
Sound speed profiles from vertical array data
[AD-A283978] p 1123 N95-18890

ITALIAN AIR FORCE FORENSIC MEDICAL INST., ROME (ITALY).
TSH determination in subjects with medium-low levels of serum thyroxine p 1082 N95-19421

J

JACKSON STATE UNIV., JACKSON, MS.
Space Station racks weight and CG measurement using the rack insertion end-effector p 966 N95-18168
Mathematical analysis of three free-electron-laser issues
[AD-A284122] p 1037 N95-18408

JAPAN ATOMIC ENERGY RESEARCH INST., TOKYO (JAPAN).
Development of an amorphous surge blocker for a high voltage acceleration power supply of the neutral beam injectors
[DE94-770648] p 1138 N95-19874

JAPAN INFORMATION CENTER OF SCIENCE AND TECHNOLOGY, TOKYO (JAPAN).
The Japan Information Center of Science and Technology p 1198 N95-19128

JAYCOR, SAN DIEGO, CA.
Health hazards assessment for blast overpressure exposures
[AD-A283352] p 1078 N95-17998

JET PROPULSION LAB., CALIFORNIA INST. OF TECH., PASADENA, CA.
Three-parameter tunable Tilt-Integral-Derivative (TID) controller
[NASA-CASE-NPO-18492-1-CU] p 1113 N95-18313
Electron reversal ionizer for detection of trace species using a spherical cathode
[NASA-CASE-NPO-18870-1-CU] p 1130 N95-18324
Plasma heating for containerless and microgravity materials processing
[NASA-CASE-NPO-18819-1-CU] p 991 N95-18326
Adaptive Neuron Model: An architecture for the rapid learning of nonlinear topological transformations
[NASA-CASE-NPO-18579-1-CU] p 1114 N95-18740
Method for surmounting an obstacle by a robot vehicle
[NASA-CASE-NPO-18764-1-CU] p 1041 N95-18741
Metrology: Calibration and measurement processes guidelines
[NASA-RP-1342] p 992 N95-18745
Three-grid accelerator system for an ion propulsion engine
[NASA-CASE-NPO-18391-2-CU] p 1137 N95-18957
Double-loop frequency selective surfaces for multi frequency division multiplexing in a dual reflector antenna
[NASA-CASE-NPO-18701-2-CU] p 1000 N95-18960
Integrated, nonvolatile, high-speed analog random access memory
[NASA-CASE-NPO-17998-2-CU] p 1093 N95-18963
Sliding mode control method having terminal convergence in finite time
[NASA-CASE-NPO-18584-1-CU] p 1114 N95-19062
Nondestructive time-of-capture, location and velocity sensing in intact capture p 1036 N95-19194
The physics of intact capture p 1122 N95-19195

JOHNS HOPKINS UNIV., BALTIMORE, MD.
Rocket and laboratory studies in astronomy
[NASA-CR-197531] p 1177 N95-17981

JOHNS HOPKINS UNIV., LAUREL, MD.
Fundamental advances for characterizing cathodic protection systems
[PB94-180692] p 1122 N95-17983

JOHNSON CONTROLS, INC., MILWAUKEE, WI.
Development of a bipolar lead/acid battery for the more electric aircraft
[AD-A284050] p 1010 N95-18660

JOINT INST. FOR NUCLEAR RESEARCH, DUBNA (USSR).
Zero modes of first class secondary constraints in gauge theories
[DE94-626659] p 1156 N95-18328
The behavior of the slope of elastic nucleon scattering at small transfer momenta and recent U A 4/2 data
[DE94-626687] p 1130 N95-18360
He-4 electromagnetic structure in unitary and analytic VMD model with strict OZI rule
[DE94-626716] p 996 N95-18367
Covariant differential complexes of quantum linear groups
[DE94-626640] p 1118 N95-18876
General relativity and dark matter
[DE94-626641] p 1180 N95-18877
To the theory of the management of the resonance widths
[DE94-626645] p 1156 N95-18879
Study of strangeness production in relativistic nucleus beams at JINR
[DE94-626720] p 1136 N95-18881
Bohr's quantization rule in the world of resonances of elementary particles
[DE94-626721] p 1132 N95-18882
On measurement of cross sections for scattering of p(mu)- and d(mu)-atoms in hydrogen and deuterium
[DE94-626957] p 1132 N95-18884

K

K. T. ANALYTICS, INC. FREDERICK, MD.
Air pollution mitigation measures for airports and associated activity
[PB94-207610] p 1061 N95-19582
KAMAN SCIENCES CORP., UTICA, NY.
Fusion of correlated sensor observations
[AD-A284224] p 994 N95-17958
KANSAS STATE UNIV., MANHATTAN, KS.
Kansas State University DOE/KEURP Site Operator User Task Force
[DE94-014331] p 1040 N95-17995
KANSAS UNIV., LAWRENCE, KS.
Decaying neutrinos in galaxy clusters
[NASA-CR-197615] p 1198 N95-18747
Quantitative analysis of voids in percolating structures in two-dimensional N-body simulations
[NASA-CR-197612] p 1156 N95-18949
Testing the frozen flow approximation
[NASA-CR-197614] p 1180 N95-18966
Real-time thickness measurement of MCC ablator material p 972 N95-18981
Optimizing the Zeldovich approximation
[NASA-CR-197606] p 1156 N95-19037
Quasi-linear regime of gravitational instability: Implication to density-velocity relation
[NASA-CR-197616] p 1156 N95-19340
Quasi-linear regime of gravitational instability as a clue to understanding the large-scale structure in the Universe
[NASA-CR-197613] p 1193 N95-19341
Testing higher-order Lagrangian perturbation theory against numerical simulation. 1: Pancake models
[NASA-CR-197611] p 1121 N95-19348
A test of the adhesion approximation for gravitational clustering
[NASA-CR-197610] p 1157 N95-19358
Comparison of dynamical approximation schemes for non-linear gravitational clustering
[NASA-CR-197609] p 1157 N95-19363
KEELE UNIV. (ENGLAND).
Photobiology in medicine
[AD-A284843] p 1087 N95-19695
KENT STATE UNIV., OH.
On the development of an expert system for wheelchair selection p 1092 N95-19627
A CLIPS-based expert system for the evaluation and selection of robots p 1103 N95-19641
KENT UNIV., CANTERBURY (ENGLAND).
The hypervelocity impact facilities at the University of Kent at Canterbury, UK p 961 N95-19180
KOBE UNIV. (JAPAN).
The origin of refractory precursor components of chondrules p 1189 N95-19316
KULITE SEMI-CONDUCTOR PRODUCTS, INC., LEONIA, NJ.
Advanced packaging and integration technologies for microsensors, phase 1
[AD-A283613] p 1040 N95-18010
KYOTO UNIV. (JAPAN).
Collision of cometlike and slightly differentiated bodies as an origin for ordinary chondrites p 1188 N95-19308
KYOTO UNIV., SAKYOKU (JAPAN).
Crystallization trends of precursor pyroxene in ordinary chondrites: Implications for igneous origin of precursor p 1187 N95-19298

L

LA SALLE UNIV., PHILADELPHIA, PA.
Applying Costs, Risks and Values Evaluation (CRAVE) methodology to Engineering Support Request (ESR) prioritization p 1160 N95-18176
LA SAPIENZA UNIV., ROME (ITALY).
X-ray absorption spectroscopy in high temperature oxidation of metals and alloys p 955 N95-19682
LABORATOIRE DE MEDECINE AEROSPATIALE, BRETIGNY-SUR-ORGE (FRANCE).
Centrifuge tests of the medical condition of French fighter pilots p 1082 N95-19424
LABORATORY FOR STRENGTH OF MATERIALS COMPONENTS AND STRUCTURES, PUSPIPTEK (INDONESIA).
Prediction of fatique crack growth under flight-simulation loading with the modified CORPUS model p 934 N95-19471
LAWRENCE LIVERMORE NATIONAL LAB., LIVERMORE, CA.
Phase transformations and phase relations in Ti(50)Pd(50-x)TM(x) alloys
[DE94-018999] p 977 N95-17962
The linear dynamics of a microsensor accelerometer modeled as a cantilever beam with an end mass
[DE94-019108] p 1031 N95-17963
High power phase conjugated solid state lasers
[DE94-016633] p 1037 N95-18357
Study of high gain spherical shell ICF targets containing uniform layers of liquid deuterium tritium fuel
[DE94-018550] p 1136 N95-18552
Implementation of 40-ps high-speed gated-microchannel-plate based x-ray framing cameras on reentrant SIM's for Nova
[DE94-018597] p 1033 N95-18555
Real-time modeling of complex atmospheric releases in urban areas
[DE94-018063] p 1059 N95-18647
Assessment of CO2 projections
[DE94-017484] p 1059 N95-18664
A multiple time scale solution for the Chapman mechanism
[DE94-017491] p 1060 N95-18895
Solar flare model atmospheres
[NASA-CR-197607] p 1196 N95-19034
Solid state laser driver for extreme ultraviolet lithography
[DE94-016971] p 1038 N95-19096
Investigation of the microstructure of coatings for high power lasers by non-optical techniques
[DE94-017697] p 987 N95-19227
Hyperfine splittings, prepulse technique, and other new results for collisional excitation neon-like x ray lasers
[DE94-016443] p 1038 N95-19247
Measurements of line overlap for resonant spoiling of x ray lasing transitions
[DE94-016444] p 1038 N95-19248
New astrophysical opacities and their effects on stellar models
[DE94-016445] p 1186 N95-19249
25-ps neutron detector for measuring ICF-target burn history
[DE94-016450] p 1146 N95-19250
Warm formability of aluminum-magnesium alloys
[DE94-016170] p 980 N95-19396
Propagation of intense, ultrashort laser pulses through metal vapor: Refractive intensity limits and spectral effects
[DE94-016365] p 1039 N95-19398
Inter-amplifier pupil relay systems for a high average power dye laser at Lawrence Livermore National Laboratory
[DE94-016544] p 1039 N95-19507
Performance improvements in diode laser arrays
[DE94-016547] p 1039 N95-19508
Novel x ray imaging methods at the Nova Laser Facility
[DE94-016548] p 1146 N95-19509
Three-dimensional radiation transport hydrodynamics
[DE94-018337] p 1146 N95-19527
Isotope separation and advanced manufacturing technology
[DE95-000313] p 1039 N95-19551
Inertial confinement fusion
[DE95-000314] p 1147 N95-19552
Contributions of the National Ignition Facility to the development of Inertial Fusion Energy
[DE94-018335] p 1137 N95-19588
Future trends in optical coatings for high-power laser applications
[DE94-018592] p 1039 N95-19708
Scintillating-fiber imaging detector for 14-MeV neutrons
[DE94-018593] p 1135 N95-19709
Pulsewidth-dependent damage measurements of dielectric materials
[DE94-018594] p 1142 N95-19710
Gain uniformity, linearity, saturation and depletion in gated microchannel-plate x-ray framing cameras
[DE94-018596] p 1035 N95-19711
Damage from pulses with arbitrary temporal shapes
[DE94-018606] p 1039 N95-19722
High speed optical links between LLNL and Berkeley
[DE95-000552] p 1006 N95-19833
Generation and solution of effective many-body Hamiltonians for rare earth and transition metal compounds
[DE95-002402] p 1155 N95-19838
LB AND M ASSOCIATES, INC., LAWTON, OK.
Adding intelligent services to an object oriented system p 1103 N95-19642
LEHIGH UNIV., BETHLEHEM, PA.
Corrosion fatigue of iron-chromium-nickel alloys: Fracture mechanics, microstructure and chemistry
[DE95-000909] p 981 N95-19610
Collaborative engineering-design support system p 1106 N95-19757
LIBURDI ENGINEERING LTD., HAMILTON (ONTARIO).
Protective coatings for compressor gas path components p 954 N95-19675
LIEGE UNIV. (BELGIUM).
Analysis of the erosion of cubic centered and face centered metallic materials p 953 N95-19674
LINCOM CORP., HOUSTON, TX.
Using CLIPS to represent knowledge in a VR simulation p 1107 N95-19765
LMS INTERNATIONAL, LEUVEN (BELGIUM).
Identification and analysis of air- and structure-borne noise and vibration paths p 1128 N95-19166
LOCKHEED CORP., FORT WORTH, TX.
Overview of unsteady transonic wind tunnel test on a semispan straked delta wing oscillating in pitch
[AD-A284097] p 928 N95-18380
LOCKHEED ENGINEERING AND SCIENCES CO., HAMPTON, VA.
Modal Identification Experiment accommodations review
[NASA-CR-195009] p 964 N95-18105
LOCKHEED ENGINEERING AND SCIENCES CO., HOUSTON, TX.
STS-65 Space Shuttle mission report
[NASA-CR-197598] p 963 N95-18610
LOCKHEED MISSILES AND SPACE CO., PALO ALTO, CA.
Coronal abundances and their variation
[NASA-CR-197553] p 1195 N95-18376
The quiescent and flaring EUV spectrum of Algol and its relationship to other active coronae. EUV spectroscopy of bright hyades coronae: 71 Tauri and Theta 1 Tauri
[NASA-CR-197538] p 1178 N95-18391
LOCKHEED SANDERS, INC., NASHUA, NH.
New technologies for space avionics
[NASA-CR-197574] p 966 N95-18196
LONDON UNIV. (ENGLAND).
Generation permutation symmetry and the quark mixing matrix
[PB95-108189] p 1132 N95-18643
LORAL SYSTEMS, INC., ORLANDO, FL.
Distributed interactive simulation interface library version description document
[AD-A284470] p 1173 N95-18446
LOS ALAMOS NATIONAL LAB., NM.
Magnetotelluric mapping of upper crustal isotherms beneath the Valles Caldera hydrothermal system
[DE94-013606] p 1063 N95-17946
Trace element characteristics of lithospheric and asthenospheric mantle in the Rio Grande rift region
[DE94-013609] p 1063 N95-17947
Detection of alpha particles via observation of He II line emission in the lithium pellet cloud during DT operation in TFTR
[DE94-014485] p 1143 N95-17965
Conceptual design for a scintillating-fiber neutron detector for fusion reactor plasma diagnostics
[DE94-014716] p 1143 N95-17969
Applications of quantum entropy to statistics
[DE94-014416] p 1155 N95-17996
Lunar surface fission power supplies: Radiation issues
[DE94-014439] p 966 N95-17997
Independent validation and verification of automated information systems in the Department of Energy
[DE94-014460] p 1173 N95-18063
Fabrication of biaxially oriented YBCO on (001) biaxially oriented yttria-stabilized-zirconia on polycrystalline substrates
[DE94-014808] p 1148 N95-18064
Observations of TEC fluctuations from an explosion on the Earth's surface
[DE94-018278] p 1063 N95-18125
Overview of laser technology at Los Alamos National Laboratory
[DE94-018307] p 1036 N95-18126
Nonlinear response of the photocathode of an x-ray streak camera to UV light
[DE94-018073] p 1032 N95-18130
Results from the northern New Mexico satellite-beacon radio interferometer
[DE94-018310] p 1063 N95-18148
Lower bounds for identifying subset members with subset queries
[DE94-014296] p 1117 N95-18346
On orbit performance of the ALEXIS EUV telescopes
[DE94-018197] p 964 N95-18639
The US 100 T Magnet Project
[DE94-016099] p 1011 N95-19200
High frame rate CCD cameras with fast optical shutters for military and medical imaging applications
[DE94-018316] p 1034 N95-19229
High-frame-rate intensified fast optically shuttered TV cameras with selected imaging applications
[DE94-016098] p 1035 N95-19394

Development of materials for high temperature superconductor Josephson junctions
[DE95-000896] p 1152 N95-19608
Phase stability and elastic properties of C15 compounds HfV2+Nb
[DE95-000940] p 981 N95-19611
A Quantum-Drive-Time (QDT) quantization of the Taub cosmology
[DE95-001014] p 1194 N95-19612
Results from SAGE 2
[DE95-000849] p 1196 N95-19619
Piezoelectric effects in double barrier resonant tunneling structures
[DE95-000850] p 1152 N95-19620
Wentzel-Bardeen singularity in coupled Luttinger liquids: Transport properties
[DE95-000856] p 1152 N95-19621
Global equation of state for a glassy material: Fused silica
[DE94-018598] p 988 N95-19721

LOUISIANA STATE UNIV., BATON ROUGE, LA.
Embedded microclusters in zeolites and cluster beam sputtering: Simulation on parallel computers
[DE95-000662] p 1134 N95-19562
A general theory of signal integration for fault tolerant distributed sensor networks
[AD-A284825] p 1112 N95-19689

LOWELL OBSERVATORY, FLAGSTAFF, AZ.
Near-Earth Asteroid Returned Sample (NEARS)
[NASA-CR-197297] p 1194 N95-19575

LUNAR AND PLANETARY INST., HOUSTON, TX.
Workshop on Particle Capture, Recovery and Velocity/Trajectory Measurement Technologies
[NASA-CR-197592] p 1180 N95-19172
Papers presented to the Conference on Chondrules and the Protoplanetary Disk
[NASA-CR-197121] p 1186 N95-19289

M

MAHARISHI INTERNATIONAL UNIV., FAIRFIELD, IA.
TARGET's role in knowledge acquisition, engineering, validation, and documentation p 1103 N95-19644

MARQUETTE UNIV., MILWAUKEE, WI.
Concept of using a benchmark part to evaluate rapid prototype processes p 994 N95-18975
MANN: A program to transfer designs for diffractive optical elements to a MANN photolithographic mask generator p 1142 N95-18995

MARTIN MARIETTA LABS., BALTIMORE, MD.
Waveguide switches using asymmetric coupled quantum wells
[AD-A284056] p 1010 N95-18662

MARYLAND UNIV., COLLEGE PARK, MD.
Robust image understanding. Techniques and applications
[AD-A283427] p 1113 N95-18057
The synthesis of vision and action
[AD-A285453] p 1088 N95-18094
Physiological and genetic characterization of plant growth and gravitropism in LED light sources p 1077 N95-18173
On the geometry of visual correspondence
[AD-A285700] p 1140 N95-18478
Vision and action
[AD-A285701] p 1140 N95-18480
Subspace correction methods for the iterative solution of hierarchic plate models. 1: Heat transfer problems
[AD-A285712] p 1117 N95-18482
Advanced methods for the computation of particle beam transport and the computation of electromagnetic fields and beam-cavity interactions
[DE94-017359] p 1136 N95-18893

MASSACHUSETTS GENERAL HOSPITAL, BOSTON, MA.
Cellular analysis of circadian rhythmicity in cultured SCN neurons
[AD-A284167] p 1078 N95-18512

MASSACHUSETTS INST. OF TECH., CAMBRIDGE.
Topography from shading and stereo
[NASA-CR-189389] p 1173 N95-18051
Atmospheric Infrared Sounder
[NASA-CR-197573] p 1064 N95-18444
Composites research in support of the NASP Institute for Composites (NIC)
[NASA-CR-197560] p 970 N95-18471
Large amplitude motions, especially isomerization and tunneling in polyatomic molecule spectra: Novel experimental, pattern recognition, and theoretical methods
[AD-A284194] p 985 N95-18636
An analysis of noise reduction in variable reluctance motors using pulse position randomization
[AD-A283846] p 1123 N95-18673
Workshop on Synthesis of Macromolecules with Precisely Controlled Structure for New Materials
[AD-A285321] p 987 N95-19520
The very low energy solar flux of electron and heavy-flavor neutrinos and antineutrinos
[DE94-018583] p 1135 N95-19706

MASSACHUSETTS INST. OF TECH., LEXINGTON.
Implementation of the 1992 Terminal area-Local Analysis and Prediction System (T-LAPS)
[AD-A284334] p 1070 N95-18384
Signal enhancement in AM-FM interference
[AD-A285114] p 1004 N95-19565
Adaptive detection and copy of coherent narrowband waveforms with uncalibrated arrays
[AD-A285125] p 1004 N95-19594

MASSACHUSETTS UNIV., AMHERST, MA.
The 2 Micron All Sky Survey
[AD-A283515] p 1178 N95-18001
Multi-functional pi-conjugated macromolecules based on poly (phenylene vinylene)
[AD-A284163] p 985 N95-18510

MATERIALS RESEARCH LABS., ASCOT VALE (AUSTRALIA).
BEAM: A finite element program for the collapse analysis of vehicle structures
[AD-A285547] p 1045 N95-18472
Calibration and testing of a large-scale electric gun for shock Hugoniot measurements
[MRL-TR-93-24] p 959 N95-18942
The evaluation of transmission efficiency and coupling loss factor of structural junctions
[MRL-TR-93-1] p 1124 N95-19057
Data acquisition from blast overpressure trials
[MRL-TN-628] p 1020 N95-19139
Evaluation of Pureau water for use as emergency drinking water for ADF aircraft
[MRL-TN-648] p 1092 N95-19502
The STOKES (Version 4) normal-mode shallow water transmission loss program
[MRL-CP-1] p 1075 N95-19503
Shock pulse generation using explosive driven metal drivers: Practical considerations
[MRL-TR-93-3] p 1046 N95-19504
Mixed high explosives for insensitive booster compositions
[MRL-TR-92-22] p 990 N95-19505
On the conduct of fast cookoff tests in Australia
[AD-A284260] p 975 N95-19699
A review of land surface temperature and humidity conditions specified for Australia in DEF (AUST) 5168 and STANAG 2895
[AD-A284258] p 1073 N95-19712
Acoustic transmission loss and structureborne noise transmission tests on a LASCOR and a reference steel panel
[MRL-TN-623] p 1128 N95-19770
Potential distributions for ellipsoidal bodies in uniform fields
[MRL-TR-92-48] p 1005 N95-19771

MCDONNELL-DOUGLAS AEROSPACE, LONG BEACH, CA.
Comparison of stochastic and deterministic nonlinear gust analysis methods to meet continuous turbulence criteria p 946 N95-18602
The crucial role of wall interference, support interference and flow field measurements in the development of advanced aircraft configurations p 1021 N95-19252

MCDONNELL-DOUGLAS AEROSPACE, SAINT LOUIS, MO.
Fiber Optic Control System integration for advanced aircraft. Electro-optic and sensor fabrication, integration, and environmental testing for flight control systems: Laboratory test results
[NASA-CR-195408] p 1034 N95-18938
Fiber Optic Control System integration for advanced aircraft. Electro-optic and sensor fabrication, integration, and environmental testing for flight control systems
[NASA-CR-191194] p 1034 N95-19236
Transonic wind tunnel boundary interference correction p 960 N95-19271

MCDONNELL-DOUGLAS CORP., SAINT LOUIS, MO.
Aeromechanics technology, volume 1. Task 1: Three-dimensional Euler/Navier-Stokes Aerodynamic Method (TEAM) enhancements
[AD-A285713] p 943 N95-18483
Acoustic fatigue characteristics of advanced materials and structures p 1126 N95-19157

MCGILL UNIV., MONTREAL (QUEBEC).
The role of large-scale, extratropical dynamics in climate change
[DE94-017651] p 1059 N95-18665

MCMASTER UNIV., HAMILTON (ONTARIO).
Dynamics of LMC clusters
[ISBN-0-315-84911-8] p 1179 N95-18728

MELBOURNE UNIV., PARKVILLE (AUSTRALIA).
The jet model of chondrule formation p 1189 N95-19310

MERCER UNIV., MACON, GA.
A new piston control strategy for segmented mirrors p 1115 N95-18999

MIAMI UNIV., FL.
Inter-comparison of automatic rain gauges p 1069 N95-18204

MICHIGAN STATE UNIV., EAST LANSING, MI.
Effective team performance under stress and normal conditions: An experimental paradigm, theory and data for studying team decision making in hierarchical teams with distributed expertise
[AD-A284683] p 1089 N95-18530

MICHIGAN TECHNOLOGICAL UNIV., HOUGHTON, MI.
On the theory of stick-slip fracture p 1046 N95-18922

MICHIGAN UNIV., ANN ARBOR, MI.
Atomistic and elastic analyses of defects and small structures
[DE94-017047] p 980 N95-19111
Changes in the flux of carbon between plants and soil microorganisms at elevated CO2: Physiological processes with ecosystem-level implications
[DE94-017067] p 1060 N95-19112
Forced response of mistuned bladed disks p 950 N95-19383
Simulation of thin slot spirals and dual circular patch antennas using the finite element method with mixed elements
[NASA-CR-197671] p 1005 N95-19796
Slot spiral antenna modeling using hybrid/mixed FE-BI technique p 1006 N95-19797
Design considerations for an archimedean slot spiral antenna p 1006 N95-19798
An efficient and accurate model of the coax cable feeding structure for FEM simulations p 1006 N95-19799
Arbitrarily shaped dual-stacked patch antennas: A hybrid FEM simulation p 1006 N95-19800
Performance of an artificial absorber for truncating FEM meshes p 1006 N95-19801

MICROELECTRONICS CENTER OF NORTH CAROLINA, RESEARCH TRIANGLE PARK, NC.
Dependencies and sensitivity of tropospheric oxidants to precursor concentrations over the northeast United States: A model study
[PB94-192770] p 1056 N95-17937

MINISTRY OF POSTS AND TELECOMMUNICATIONS, TOKYO (JAPAN).
Effect of heavy rain to the total received power p 1070 N95-18210

MINISTRY OF SCIENCE AND DEVELOPMENT, JERUSALEM (ISRAEL).
International Conference on Control Theory and its Applications
[DE94-626221] p 1114 N95-18875

MINNESOTA UNIV., MINNEAPOLIS, MN.
Tunneling and transport in mesoscopic structures
[AD-A283426] p 1148 N95-18053
Finite Markov chains and random discrete structures
[AD-A284192] p 1121 N95-19104

MISSION RESEARCH CORP., NASHUA, NH.
Innovative development and application of models for weakly ionized ionospheric plasmas
[AD-A284583] p 1064 N95-18452

MISSISSIPPI STATE UNIV., BAY SAINT LOUIS, MS.
Users manual for the Moods Data Management System (MDMS), version 1.0
[NASA-CR-197015] p 1075 N95-18951

MISSISSIPPI STATE UNIV., MISSISSIPPI STATE, MS.
Wing design for a civil tiltrotor transport aircraft
[NASA-CR-197523] p 942 N95-18090
Nozzle Initiative Industry Advisory Committee on Standardization of Carbon-Phenolic Test Methods and Specifications
[NASA-CR-197529] p 967 N95-19566
Predicting and explaining the movement of mesoscale oceanographic features using CLIPS p 1105 N95-19752

MISSOURI UNIV., COLUMBIA, MO.
Wavelets and scattering
[AD-A284131] p 996 N95-18411

MISSOURI UNIV., ROLLA, MO.
Performance evaluation of the NASA/KSC CAD/CAE and office automation LAN's p 1108 N95-18186
A comparison between using incoherent or coherent sources to align and test an adaptive optical telescope p 1142 N95-18969
Use of titanate coupling agents in Kevlar (trade name)/phenolic composites
[AD-A279200] p 972 N95-19814

MITECH, INC., PLEASANTVILLE, NJ.
Research requirements for future visual guidance systems
[AD-A279188] p 941 N95-19810
MITRE CORP., BEDFORD, MA.
Synthesis of notched antenna patterns for wide bandwidth processing
[AD-A284004] p 1000 N95-18727
Measurement and proper equalization of range sidelobes using a spherical satellite as a reflector
[AD-A285955] p 1005 N95-19744
MOSCOW STATE UNIV. (RUSSIA).
Textural variability of ordinary chondrite chondrules: Implications of their formation p 1193 N95-19339
MOTOREN- UND TURBINEN-UNION MUENCHEN G.M.B.H., MUNICH (GERMANY).
Performance deterioration of axial compressors due to blade defects p 952 N95-19665
Impact loading of compressor stator vanes by hailstone ingestion p 953 N95-19670
Damage of high temperature components by dust-laden air p 953 N95-19673
MUSEUM OF NATURAL HISTORY, LONDON (ENGLAND).
Chondrules and their associates in ordinary chondrites p 1188 N95-19306

N

NANGIA ASSOCIATES, BRISTOL (ENGLAND).
Estimating wind tunnel interference due to vectored jet flows p 1023 N95-19265
NAPLES UNIV. (ITALY).
Adaptive wind tunnel walls versus wall interference correction methods in 2D flows at high blockage ratios p 960 N95-19267
NATIONAL ACADEMY OF SCIENCES - NATIONAL RESEARCH COUNCIL, WASHINGTON, DC.
An integrated strategy for the planetary sciences: 1995 - 2010
[NASA-CR-197145] p 1194 N95-19134
Toward a new national weather service: Weather for those who fly
[PB94-214418] p 1072 N95-19407
NATIONAL AERONAUTICS AND SPACE ADMINISTRATION, WASHINGTON, DC.
NASA High Performance Computing and Communications program
[NASA-TM-4653] p 1174 N95-18573
Remote sensing/global change. A special bibliography
[NASA-TM-110038] p 1060 N95-18742
NASA directives: Master list and index
[NHB-1410.13N] p 1171 N95-19133
Aeronautical engineering: A continuing bibliography with indexes (supplement 313)
[NASA-SP-7037(313)] p 927 N95-19168
Aerospace medicine and biology: A continuing bibliography with indexes (supplement 398)
[NASA-SP-7011(398)] p 1080 N95-19239
Aeronautical engineering: A continuing bibliography with indexes (supplement 314)
[NASA-SP-7037(314)] p 927 N95-19357
Aerospace medicine and biology: A continuing bibliography with indexes (supplement 397)
[NASA-SP-7011(397)] p 1087 N95-19746
NATIONAL AERONAUTICS AND SPACE ADMINISTRATION. AMES RESEARCH CENTER, MOFFETT FIELD, CA.
Parametric study on laminar flow for finite wings at supersonic speeds
[NASA-TM-108852] p 928 N95-18101
VSTOL Systems Research Aircraft (VSRA) Harrier
[NASA-TM-110117] p 941 N95-18347
US experiments flown on the Soviet biosatellite Cosmos 2044. Volume 1: Mission description, experiments K-7-01 - K-7-15
[NASA-TM-108802-VOL-1] p 1092 N95-18569
Effect of heat acclimation on sitting orthostatic tolerance in the heat after 48 and 96 hour bed rest in men
[NASA-TM-108861] p 1077 N95-18734
Constant current loop impedance measuring system that is immune to the effects of parasitic impedances
[NASA-CASE-ARC-11988-1] p 1011 N95-18959
NASA develops new digital flight control system
[NASA-NEWS-RELEASE-94-47] p 958 N95-19029
An assessment of the adaptive unstructured tetrahedral grid, Euler Flow Solver Code FELISA
[NASA-TP-3526] p 930 N95-19041
2-D and 3-D oscillating wing aerodynamics for a range of angles of attack including stall
[NASA-TM-4632] p 931 N95-19119
Drink composition and cycle-ergometer endurance in men: Carbohydrate, Na(+), osmolality
[NASA-TM-4650] p 1077 N95-19140
Wall interaction effects for a full-scale helicopter rotor in the NASA Ames 80- by 120-foot wind tunnel p 932 N95-19270
Overview of nebula models: Potential chondrule-forming environments p 1186 N95-19294
Turbulent diffusion and concentration of chondrules in the protoplanetary nebula p 1187 N95-19296
A ceramic/slag interface as an analog for accretion of hot refractory objects and rim formation p 1191 N95-19322
NATIONAL AERONAUTICS AND SPACE ADMINISTRATION. GODDARD SPACE FLIGHT CENTER, GREENBELT, MD.
Evolution of the Southern Hemisphere ozone hole as seen by TOMS from August 1979 to December 1991
[NASA-TM-110116] p 1057 N95-18048
Meteor 3/TOMS launch of 15 August 1991 in Plesetsk, USSR
[NASA-TM-110115] p 962 N95-18150
Optical Rain Gauge Performance: Second Workshop on Optical Rain Gauge Measurements
[NASA-CP-3288] p 1068 N95-18201
Vibration (?) spikes during natural rain events p 1069 N95-18206
Can salt on an optical rain gauge lens affect performance? p 1069 N95-18208
SeaWiFS technical report series. Volume 18: SeaWiFS technical report series cumulative index: Volumes 1-17
[NASA-TM-104566-VOL-18] p 1076 N95-19577
Relative elemental abundance and heating constraints determined for the solar corona from SERTS measurements
[NASA-TM-104616] p 1196 N95-19791
NATIONAL AERONAUTICS AND SPACE ADMINISTRATION. HUGH L. DRYDEN FLIGHT RESEARCH CENTER, EDWARDS, CA.
Current loop signal conditioning: Practical applications
[NASA-TM-4636] p 1033 N95-18735
NATIONAL AERONAUTICS AND SPACE ADMINISTRATION. HUGH L. DRYDEN FLIGHT RESEARCH FACILITY, EDWARDS, CA.
In-flight lift-drag characteristics for a forward-swept wing aircraft and comparisons with contemporary aircraft)
[NASA-TP-3414] p 929 N95-18565
Determination of stores pointing error due to wing flexibility under flight load
[NASA-TM-4646] p 945 N95-19044
NATIONAL AERONAUTICS AND SPACE ADMINISTRATION. JOHN F. KENNEDY SPACE CENTER, COCOA BEACH, FL.
Debris/ice/TPS assessment and integrated photographic analysis of Shuttle mission STS-68
[NASA-TM-109207] p 963 N95-18047
NASA/ASEE Summer Faculty Fellowship Program. 1994 research reports
[NASA-CR-197448] p 1157 N95-18166
Debris/ice/TPS assessment and integrated photographic analysis of Shuttle mission STS-66
[NASA-TM-110141] p 963 N95-19790
NATIONAL AERONAUTICS AND SPACE ADMINISTRATION. LYNDON B. JOHNSON SPACE CENTER, HOUSTON, TX.
Method of making a membrane having hydrophilic and hydrophobic surfaces for adhering cells or antibodies by using atomic oxygen or hydroxyl radicals
[NASA-CASE-MSC-21529-1] p 983 N95-18134
Geometry and gravity influences on strength capability
[NASA-TP-3511] p 1091 N95-18189
Geometrical vapor blocker for parallel condensation tubes requiring subcooling
[NASA-CASE-MSC-22090-1] p 1017 N95-18323
STS-68 mission highlights resource tape
[NASA-TM-110049] p 961 N95-18568
Gas storage and recovery system
[NASA-CASE-MSC-22091-1] p 992 N95-18738
Gemini 8, This is Houston, flight
[NASA-TM-110490] p 965 N95-19039
Skylab: The first 40 days
[NASA-TM-110491] p 961 N95-19040
Mercury: Exploration of a planet
[NASA-TM-110489] p 1194 N95-19045
Legacy of Gemini
[NASA-TM-110486] p 961 N95-19058
Skylab: The second manned mission. A scientific harvest
[NASA-TM-110487] p 961 N95-19059
Time of Apollo
[NASA-TM-110488] p 961 N95-19060
Penetration experiments in aluminum and Teflon targets of widely variable thickness p 1047 N95-19185
Some considerations on velocity vector accuracy in dust trajectory analysis p 1183 N95-19186
The use of silica aerogel to collect interplanetary dust in space p 989 N95-19197
Documentation and archiving of the Space Shuttle wind tunnel test data base. Volume 1: Background and description
[NASA-TM-104806-VOL-1] p 965 N95-19237
Experimental constraints on models for the origin of chondrules: Cooling rates p 1189 N95-19311
Mn-Cr isotopic systematics of Chainpur chondrules and bulk ordinary chondrites p 1190 N95-19320
Documentation and archiving of the Space Shuttle wind tunnel test data base. Volume 2: User's Guide to the Archived Data Base
[NASA-TM-104806-VOL-2] p 965 N95-19624
Third CLIPS Conference Proceedings, volume 1
[NASA-CP-10162-VOL-1] p 1100 N95-19625
Expert system technologies for Space Shuttle decision support: Two case studies p 1104 N95-19646
Third CLIPS Conference Proceedings, volume 2
[NASA-CP-10162-VOL-2] p 1104 N95-19747
NATIONAL AERONAUTICS AND SPACE ADMINISTRATION. LANGLEY RESEARCH CENTER, HAMPTON, VA.
Compendium of NASA data base for the Global Tropospheric Experiment's Arctic Boundary Layer Experiments ABLE-3A and ABLE-3B
[NASA-TM-109161] p 1058 N95-18132
Finite element method for eigenvalue problems in electromagnetics
[NASA-TP-3485] p 995 N95-18187
A spectral study of a radio-frequency plasma-generated flux of atomic oxygen
[NASA-TM-4612] p 1032 N95-18194
Microburst vertical wind estimation from horizontal wind measurements
[NASA-TP-3460] p 942 N95-18198
Two-stage gas measurement system
[NASA-CASE-LAR-14791-1] p 1032 N95-18316
Reduction of parasitic lasing
[NASA-CASE-LAR-14645-1-SB] p 1037 N95-18322
Mission description and in-flight operations of ERBE instruments on ERBS and NOAA 10 spacecraft, February 1987 - February 1990
[NASA-RP-1325] p 1051 N95-18465
Special effects of gust loads on military aircraft p 946 N95-18605
Dynamic Stability Instrumentation System (DSIS). Volume 1: Hardware description
[NASA-TM-109160-VOL-1] p 1099 N95-18899
A strategy for electronic dissemination of NASA Langley technical publications
[NASA-TM-109172] p 1175 N95-18936
NASA/DOD Aerospace Knowledge Diffusion Research Project. Report 26: The technical communication practices of aerospace engineering students: Results of the phase 3 AIAA National Student Survey
[NASA-TM-109121] p 1175 N95-18950
NASA/DOD Aerospace Knowledge Diffusion Research Project. Report 29: A comparison of the technical communications practices of Japanese and US aerospace engineers and scientists
[NASA-TM-109164] p 1175 N95-18953
Method and device for determining bond separation strength using induction heating
[NASA-CASE-LAR-14678-1] p 960 N95-18961
Induction heating coupler and annealer
[NASA-CASE-LAR-14277-1] p 1011 N95-18962
NASA/DOD Aerospace Knowledge Diffusion Research Project. Paper 46: Technical communications in aerospace: A comparison across four countries
[NASA-TM-110056] p 1175 N95-19038
Static investigation of two fluidic thrust-vectoring concepts on a two-dimensional convergent-divergent nozzle
[NASA-TM-4574] p 931 N95-19042
Stand-alone digital data storage control system including user control interface
[NASA-CASE-LAR-14651-1] p 1175 N95-19056
Navier-Stokes, flight, and wind tunnel flow analysis for the F/A-18 aircraft
[NASA-TP-3478] p 931 N95-19114
NASA/DOD Aerospace Knowledge Diffusion Research Project. Paper 45: A comparison of the information-seeking behaviors of three groups of US aerospace engineers
[NASA-TM-109839] p 1176 N95-19127
Impact of dynamic loads on propulsion integration p 1125 N95-19148
FAA/NASA International Symposium on Advanced Structural Integrity Methods for Airframe Durability and Damage Tolerance, part 2
[NASA-CP-3274-PT-2] p 934 N95-19468
The characterization of widespread fatigue damage in fuselage structure p 935 N95-19472
Stress intensity factors for surface and corner cracks emanating from a wedge-loaded hole p 939 N95-19498
Nonlinear analysis of damaged stiffened fuselage shells subjected to combined loads p 939 N95-19499

Radar cross-section measurements and simulation of a tethered satellite. The small expendable deployer system end-mass payload
[NASA-TM-4613] p 1005 N95-19781

NATIONAL AERONAUTICS AND SPACE ADMINISTRATION. LEWIS RESEARCH CENTER, CLEVELAND, OH.

The space-time solution element method: A new numerical approach for the Navier-Stokes equations
[NASA-TM-106818] p 1014 N95-18036
Background noise levels measured in the NASA Lewis 9- by 15-foot low-speed wind tunnel
[NASA-TM-106817] p 958 N95-18054
Numerical mixing calculations of confined reacting jet flows in a cylindrical duct
[NASA-TM-106736] p 947 N95-18133
Evaluation of boundary conditions for computational aeroacoustics
[NASA-TM-109989] p 1015 N95-18149
Microgravity isolation system design: A modern control synthesis framework
[NASA-TM-106805] p 927 N95-18197
Completed Beltrami-Michell formulation for analyzing radially symmetrical bodies
[NASA-TM-4593] p 1044 N95-18199
A three-dimensional structured/unstructured hybrid Navier-Stokes method for turbine blade rows
[NASA-TM-106813] p 1016 N95-18200
Observations of methane and ethylene diffusion flames stabilized around a blowing porous sphere under microgravity conditions
[NASA-TM-106766] p 990 N95-18211
A note on the wave action density of a viscous instability mode on a laminar free-shear flow
[NASA-TM-106771] p 1016 N95-18212
Ion exchange polymers and method for making
[NASA-CASE-LEW-15576-1] p 984 N95-18321
Applications catalog of pyrotechnically actuated devices/systems
[NASA-TM-106810] p 962 N95-18387
Tribology and microstructure of PS212 with a Cr2O3 seal coat
[NASA-TM-106768] p 969 N95-18448
Minority-carrier lifetime in InP as a function of light bias
[NASA-TM-106821] p 1149 N95-18453
Measurement of gust response on a turbine cascade
[NASA-TM-106776] p 928 N95-18457
Microgravity isolation system design: A modern control analysis framework
[NASA-TM-106803] p 927 N95-18486
Solar-electrochemical power system for a Mars mission
[NASA-TM-106606] p 967 N95-18570
Final results of the Advanced Photovoltaic Experiment flight test
[NASA-TM-106828] p 967 N95-18571
Pulsed laser illumination of photovoltaic cells
[NASA-TM-106820] p 1053 N95-18572
Collection efficiency and ice accretion calculations for a sphere, a swept MS(1)-317 wing, a swept NACA-0012 wing tip, an axisymmetric inlet, and a Boeing 737-300
[NASA-TM-106831] p 933 N95-18582
An NDE approach for characterizing quality problems in polymer matrix composites
[NASA-TM-106807] p 1043 N95-18583
Users guide for NASA Lewis Research Center DC-9 Reduced-Gravity Aircraft Program
[NASA-TM-106755] p 959 N95-18586
The effect of temperature on the radiative performance of Ho-YAG thin film selective emitters
[NASA-TM-106830] p 1053 N95-18587
EEsoF MICAD and ACADEMY macro files for coplanar waveguide and finite ground plan coplanar waveguide
[NASA-TM-106800] p 1000 N95-18733
On the convergence of local approximations to pseudodifferential operators with applications
[NASA-TM-106792] p 1019 N95-18898
Completed Beltrami-Michell formulation for analyzing mixed boundary value problems in elasticity
[NASA-TM-106809] p 1045 N95-18909
Enhanced capabilities and modified users manual for axial-flow compressor conceptual design code CSPAN
[NASA-TM-106833] p 930 N95-18933
Thermal behavior spiral bevel gears
[NASA-TM-106518] p 1042 N95-18935
Parallel Navier-Stokes computations on shared and distributed memory architectures
[NASA-TM-106823] p 1019 N95-18941
Detecting gear tooth fracture in a high contact ratio face gear mesh
[NASA-TM-106822] p 1042 N95-19125
Transient and steady-state tests of the space power research engine with resistive and motor loads
[NASA-TM-106832] p 1042 N95-19238
Methods for scaling icing test conditions
[NASA-TM-106827] p 934 N95-19284
Ice accretion with varying surface tension
[NASA-TM-106826] p 934 N95-19285
Operating capability and current status of the reactivated NASA Lewis Research Center Hypersonic Tunnel Facility
[NASA-TM-106808] p 960 N95-19286
NASA Lewis Research Center Workshop on Forced Response in Turbomachinery
[NASA-CP-10147] p 949 N95-19380
Steady potential solver for unsteady aerodynamic analyses p 949 N95-19382
Technology Benefit Estimator (T/BEST): User's manual
[NASA-TM-106785] p 1046 N95-19501
Closed-form static analysis with inertia relief and displacement-dependent loads using a MSC/NASTRAN DMAP Alter
[NASA-TM-106836] p 1047 N95-19649
Thermo-oxidative stability of graphite/PMR-15 composites: Effect of fiber surface modification on composite shear properties
[NASA-TM-4608] p 981 N95-19652
Ice-impact analysis of blades p 953 N95-19672
Resistance of silicon nitride turbine components to erosion and hot corrosion/oxidation attack
p 955 N95-19683
A parallel strategy for implementing real-time expert systems using CLIPS p 1105 N95-19749
Driving force analysis in an infinite anisotropic plate with multiple crack interactions
[NASA-TM-106838] p 972 N95-19782
Adhesion, friction, and wear behavior of clean metal-ceramic couples
[NASA-TM-106815] p 989 N95-19783
Summary report of mission acceleration measurements for STS-60, SPACEHAB2, launched 11 February 1994
[NASA-TM-106797] p 991 N95-19788
Improved speed control system for the 87,000 HP wind tunnel drive
[NASA-TM-106840] p 1035 N95-19794
Centrifugal and axial pump design and off-design performance prediction
[NASA-TM-106745] p 968 N95-19795

NATIONAL AERONAUTICS AND SPACE ADMINISTRATION. MARSHALL SPACE FLIGHT CENTER, HUNTSVILLE, AL.

Tuned mass damper for integrally bladed turbine rotor
[NASA-CASE-MFS-28697-1] p 1041 N95-18325
System engineering toolbox for design-oriented engineers
[NASA-RP-1358] p 962 N95-18932
Analytical control test plan and microbiological methods for the water recovery test
[NASA-TM-108473] p 1091 N95-19061
An oil flow study of the reference Shuttle-C configuration
[NASA-RP-1352] p 932 N95-19623
Neural net controller for inlet pressure control of rocket engine testing p 1102 N95-19637
A 20k payload launch vehicle fast track development concept using an RD-180 engine and a Centaur upper stage
[NASA-TM-108475] p 963 N95-19648
Simulation in a dynamic prototyping environment: Petri nets or rules? p 1106 N95-19756
Rule based design of conceptual models for formative evaluation p 1106 N95-19760
Spacecraft environments interactions: Protecting against the effects of spacecraft charging
[NASA-RP-1354] p 965 N95-19780

NATIONAL AERONAUTICS AND SPACE ADMINISTRATION. PASADENA OFFICE, CA.

Three-parameter tunable Tilt-Integral-Derivative (TID) controller
[NASA-CASE-NPO-18492-1-CU] p 1113 N95-18313
Electron reversal ionizer for detection of trace species using a spherical cathode
[NASA-CASE-NPO-18870-1-CU] p 1130 N95-18324
Plasma heating for containerless and microgravity materials processing
[NASA-CASE-NPO-18819-1-CU] p 991 N95-18326
Adaptive Neuron Model: An architecture for the rapid learning of nonlinear topological transformations
[NASA-CASE-NPO-18579-1-CU] p 1114 N95-18740
Method for surmounting an obstacle by a robot vehicle
[NASA-CASE-NPO-18764-1-CU] p 1041 N95-18741
Three-grid accelerator system for an ion propulsion engine
[NASA-CASE-NPO-18391-2-CU] p 1137 N95-18957
Double-loop frequency selective surfaces for multi frequency division multiplexing in a dual reflector antenna
[NASA-CASE-NPO-18701-2-CU] p 1000 N95-18960
Integrated, nonvolatile, high-speed analog random access memory
[NASA-CASE-NPO-17998-2-CU] p 1093 N95-18963
Sliding mode control method having terminal convergence in finite time
[NASA-CASE-NPO-18584-1-CU] p 1114 N95-19062

NATIONAL AEROSPACE LAB., AMSTERDAM (NETHERLANDS).

Microgravity fluid science research in Europe
[PB94-201720] p 990 N95-17973
Sectional prediction of 3D effects for separated flow on rotating blades
[PB94-201696] p 928 N95-18503
Results of uniaxial and biaxial tests on riveted fuselage lap joint specimens p 938 N95-19491
Gas turbine compressor corrosion and erosion in Western Europe p 954 N95-19678

NATIONAL AEROSPACE LAB., BANGALORE (INDIA).

Ageing nuclear power plant management: An aeronautical viewpoint
[NAL-PD-SN-9306] p 927 N95-18606
Solution of full potential equation on an airfoil by multigrid technique
[NAL-TM-CSS-9303] p 930 N95-18904
CFD: Advances and Applications, part 1
[NAL-SP-9322-PT-1] p 1026 N95-19444
Basic equations of fluid dynamics
p 1026 N95-19445
Computation of inviscid flows: Various approximations
p 1027 N95-19446
Computation of inviscid flows: Full potential method
p 1027 N95-19447
Panel methods p 1027 N95-19448
Numerical grid generation p 1027 N95-19449
Difference schemes for hyperbolic system of Conservation Laws p 1027 N95-19450
Finite volume method using Runge-Kutta time-stepping for solution of Euler equations p 1027 N95-19451
Computation of compressible flows: Implicit methods
p 1027 N95-19452
Introduction to multigrid methods
p 1028 N95-19453
Applications of multigrid methods to problems in CFD
p 1028 N95-19454
CFD: Advances and Applications, 1994
[NAL-SP-9412] p 1028 N95-19455
Finite-volume upwind schemes for inviscid gas dynamics p 1028 N95-19456
Viscous flow past aerofoils axisymmetric bodies and wings p 933 N95-19457
Turbulence modeling for CFD, part 1
p 1028 N95-19458
Spectral methods for fluid flow p 1028 N95-19459
Discrete vortex method for computation of viscous incompressible flows p 1029 N95-19460
Pressure based finite volume algorithm for viscous flow computation p 1029 N95-19461
Computation of vortex breakdown
p 1029 N95-19462
Hypersonic viscous flow computations
p 1029 N95-19463
Parabolized Navier-Stokes solution of supersonic/hypersonic flows p 933 N95-19464
CFD on parallel computers p 1029 N95-19465
Turbulence modeling for CFD, part 2
p 1030 N95-19466

NATIONAL ENVIRONMENTAL SATELLITE SERVICE, CAMP SPRINGS, MD.

Rain gauge calibration and testing
p 1070 N95-18209

NATIONAL ENVIRONMENTAL SATELLITE SERVICE, WASHINGTON, DC.

Office of Research and Applications: Research Programs p 1071 N95-18721

NATIONAL GEOPHYSICAL DATA CENTER, BOULDER, CO.

Solar-geophysical data number 599, July 1994. Part 1: (Prompt reports). Data for June, May 1994, and late data
[PB94-213972] p 1196 N95-19404
Solar-geophysical data number 599, July 1994. Part 2: (Comprehensive reports). Data for January 1994, and miscellaneous
[PB94-213980] p 1196 N95-19405

NATIONAL INST. FOR FUSION SCIENCE, NAGOYA (JAPAN).

Improvement of a high current DC power supply system for testing the large scaled superconducting cables and magnets
[DE94-770767] p 1012 N95-19548
Direct energy conversion system for D(3)-He fusion
[DE94-770773] p 1146 N95-19549

NATIONAL INST. OF STANDARDS AND TECHNOLOGY, GAITHERSBURG, MD.
Semiconductor measurement technology: Design and testing guides for the COMOS and lateral bipolar-on-SOI test library
[PB94-178019] p 1007 N95-17984
User profile for researchers studying objects: Implications for computer systems
[PB94-188463] p 1109 N95-17989
Standard reference materials: Glass filters as a standard reference material for spectrophotometry. Selection, preparation, certification and use of SRM 930 and SRM 1930
[PB94-188844] p 973 N95-17994
VENTCF2: An algorithm and associated FORTRAN 77 subroutine for calculating flow through a horizontal ceiling/floor vent in a zone-type compartment fire model
[PB94-210127] p 993 N95-19402
Fracture behavior of large-scale thin-sheet aluminum alloy p 939 N95-19494
Study of laser resonance ionization mass spectrometry using a glow discharge source
[DE94-018566] p 981 N95-19703

NATIONAL LIBRARY OF MEDICINE, BETHESDA, MD.
National Library of Medicine programs and services, fiscal year 1991
[PB94-188026] p 1077 N95-17949
National Library of Medicine programs and services, fiscal year 1992
[PB94-188034] p 1078 N95-17950

NATIONAL MUSEUM OF NATURAL HISTORY, PARIS (FRANCE).
Chondrule precursors and cooling paths: The sulfur evidence p 1193 N95-19338

NATIONAL MUSEUM OF NATURAL HISTORY, WASHINGTON, DC.
Chronology of chrondrule and CAI formation: Mg-Al isotopic evidence p 1189 N95-19314

NATIONAL OCEANIC AND ATMOSPHERIC ADMINISTRATION, BOULDER, CO.
Measurements of wind profiler EMC characteristics
[PB94-194107] p 1066 N95-17938
Product usage evaluation of the aviation gridded forecast system workstation at the Denver Center Weather Service Unit
[PB94-195922] p 1066 N95-17952

NATIONAL OCEANIC AND ATMOSPHERIC ADMINISTRATION, MIAMI, FL.
Inter-comparison of automatic rain gauges p 1069 N95-18204

NATIONAL OCEANIC AND ATMOSPHERIC ADMINISTRATION, SEATTLE, WA.
Moored rainfall measurements during COARE p 1069 N95-18202
Update on TAO moored ORG array p 1069 N95-18203

NATIONAL RENEWABLE ENERGY LAB., GOLDEN, CO.
Renewable energy and its potential for carbon emissions reductions in developing countries: Methodology for technology evaluation
[DE94-011870] p 1056 N95-17943
Potential impacts on air quality of the use of ethanol as an alternative fuel
[DE94-011881] p 1056 N95-17944
Thermophotovoltaics bibliography
[DE94-011898] p 1052 N95-17945
Progress in the development of advanced solar reflectors
[DE94-000264] p 1053 N95-18463
Wind turbine blade aerodynamics: The combined experiment
[DE94-011866] p 929 N95-18645
Wind turbine blade aerodynamics: The analysis of field test data
[DE94-011867] p 929 N95-18646
Microscopic origins of metastable effects in a-Si:H and deep defect characterization in a-Si,Ge:H alloys
[DE94-011887] p 1151 N95-19541
Research on stable, high-efficiency amorphous silicon multijunction modules
[DE95-000215] p 1054 N95-19832
Tapping into the Sun: Today's applications of photovoltaic technology
[DE93-000075] p 1054 N95-19854
Evidence that aerodynamic effects, including dynamic stall, dictate HAWT structural loads and power generation in highly transient time frames
[DE94-011865] p 1054 N95-19855
Summary information and data sets for the HBCU Solar Measurements Network
[DE94-011872] p 1055 N95-19856
NREL Photovoltaic Program, FY 1993
[DE94-011880] p 1055 N95-19857
Growth and development of GaInAsP for high-efficiency solar cells
[DE94-000210] p 1056 N95-19878
Advanced processing technology for high-efficiency, thin-film CuInSe2 and CdTe solar cells
[DE94-011838] p 1056 N95-19880
Current Hybrid Electric Vehicle performance based on temporal data from the world's largest HEV fleet
[DE94-011859] p 1014 N95-19881
Silicon-Film (trademark) photovoltaic manufacturing technology
[DE94-011899] p 1056 N95-19882

NATIONAL RESEARCH COUNCIL OF CANADA, OTTAWA (ONTARIO).
Noise transmission and reduction in turboprop aircraft p 1127 N95-19164
Spectrogram diagnosis of aircraft disasters p 940 N95-19167
Erosion of T56 5th stage rotor blades due to bleed hole overtip flow p 952 N95-19666

NATIONAL SEMICONDUCTOR CORP., SANTA CLARA, CA.
Reliability Without Hermeticity (RWOH) for Integrated Circuits (IC)
[AD-A284340] p 1009 N95-18418

NATIONAL TECHNICAL UNIV., ATHENS (GREECE).
Investigation of mechanical erosion in fuel pipelines p 952 N95-19667

NATIONAL TELECOMMUNICATIONS AND INFORMATION ADMINISTRATION, ANNAPOLIS, MD.
Measurements of wind profiler EMC characteristics
[PB94-194107] p 1066 N95-17938

NATIONAL TRANSPORTATION SAFETY BOARD, WASHINGTON, DC.
Safety study: Commuter airline safety
[PB94-917004] p 933 N95-19132
Special investigation report: Maintenance anomaly resulting in dragged engine during landing rollout. Northwest Airlines Flight 18, Boeing 747-251B, N637US, New Tokyo International Airport, Narita, Japan, 1 Mar. 1994
[PB94-917006] p 940 N95-19793

NATIONAL WEATHER SERVICE, BOHEMIA, NY.
Synoptic and mesoscale examination of the northern New England winter storm of January 29-30, 1990
[PB94-209426] p 1072 N95-19581

NATIONAL WEATHER SERVICE, KANSAS CITY, MO.
Use of profiler data for analysis and NOWcasting of a winter season extratropical cyclone
[PB94-187804] p 1067 N95-17992

NATIONAL WEATHER SERVICE, MILWAUKEE, WI.
Forecasting snowfall using mixing ratios on an isentropic surface: An empirical study
[PB94-188760] p 1067 N95-17993

NATIONAL WEATHER SERVICE, SILVER SPRING, MD.
Miscellaneous disk utility application programs for the AFOS background partition
[PB94-181328] p 1067 N95-18038

NAVAL ACADEMY, ANNAPOLIS, MD.
Incompressible flow of a Newtonian fluid past a vertical plate with thermal and magnetic stresses
[AD-A284856] p 1030 N95-19716
Modeling the diurnally precessing Jovian magnetospheric field
[AD-A284857] p 1195 N95-19739

NAVAL AEROSPACE MEDICAL INST., PENSACOLA, FL.
The waiver process and disqualifying medical conditions in US Naval aviation personnel p 1081 N95-19416
The effect of special boards of flight surgeons on the evolution of US Naval flight standards p 1081 N95-19417
AMDRS: A resource for intelligent aeromedical decision-making p 1082 N95-19419
The concept of aeronautical adaptability as developed by the US Navy p 1083 N95-19426
The NAMI syncope test battery and clinical decision-making in aviators with syncope p 1083 N95-19428

NAVAL AEROSPACE MEDICAL RESEARCH LAB., PENSACOLA, FL.
Effects of weight lifting on intrathoracic pressures generated by anti-g straining maneuvers
[AD-A283651] p 1078 N95-18138
Computer-based psychomotor tests in optimal training track assignment of student naval aviators
[AD-A283720] p 1089 N95-18414

NAVAL AIR DEVELOPMENT CENTER, WARMINSTER, PA.
Preliminary evaluation of the F/A-18 quantity/multiple envelope expansion
[AD-A284119] p 943 N95-18407

NAVAL AIR WARFARE CENTER, PATUXENT RIVER, MD.
Flight testing high lateral asymmetries on highly augmented Fighter/Attack aircraft
[AD-A284206] p 941 N95-17953
Comparison of frequency response and perturbation methods to extract linear models from a nonlinear simulation
[AD-A284115] p 958 N95-18405
Parallelization of the fluid dynamics equations on unstructured grids
[AD-A284116] p 1017 N95-18406
Tilt Rotor Unmanned Air Vehicle System (TRUS) demonstrator flight test program
[AD-A284151] p 943 N95-18415
Resources Automated Management System
[AD-A284153] p 1171 N95-18416
Application of photogrammetry of F-14D store separation
[AD-A284154] p 943 N95-18417
KC-130 ANVIS/HUD assessment and symbology rationale
[AD-A284155] p 943 N95-18504
V-22 simulator evaluation for shipboard operations
[AD-A284156] p 943 N95-18505
High frequency direct drive generation using white noise sources
[AD-A284158] p 997 N95-18506
Development of a bulk current injection direct-drive system to test system level components with stress waveforms that are encountered during full threat indirect effects lightning
[AD-A284160] p 933 N95-18507
Virtual reality, an air combat T and E perspective
[AD-A284161] p 959 N95-18508
F/A-18 simulation validation and verification: Making a good product even better
[AD-A283995] p 944 N95-18723
The generic simulation executive at Manned Flight Simulator
[AD-A283997] p 959 N95-18724
Helicopter in-flight simulation development and use in test pilot training
[AD-A283998] p 959 N95-18725
Assessing aircraft survivability to high frequency transient threats
[AD-A283999] p 944 N95-18726
Waveform bounding and combination techniques for direct drive testing
[AD-A284075] p 1000 N95-19035
E-6A hardness assurance, maintenance and surveillance program
[AD-A283994] p 945 N95-19067
Processing multilevel secure test and evaluation information
[AD-A284073] p 1001 N95-19069
NAWCAD photogrammetrics: Methods and applications for aviation test and evaluation
[AD-A284074] p 1034 N95-19071
The use of genetic algorithms for flight test and evaluation of artificial intelligence and complex software systems
[AD-A284824] p 1104 N95-19688
Airship applications of modern flight test techniques
[AD-A284253] p 945 N95-19731

NAVAL AIR WARFARE CENTER, TRENTON, NJ.
Unmanned aerial vehicle heavy fuel engine test
[AD-A284332] p 947 N95-18383
Navy foreign object damage and its impact on future gas turbine engine low pressure compression systems p 951 N95-19656
Testing considerations for military aircraft engines in corrosive environments (a Navy perspective) p 955 N95-19684

NAVAL BIODYNAMICS LAB., NEW ORLEANS, LA.
Naval Biodynamics Laboratory 1993 command history
[AD-A284358] p 1089 N95-18440

NAVAL COMMAND, CONTROL AND OCEAN SURVEILLANCE CENTER, SAN DIEGO, CA.
Long wavelength propagation capacity, version 1.1 (computer diskette)
[AD-M200254] p 994 N95-17964
Metal/hydrogen energy storage: Selected technical issues
[AD-A283355] p 1008 N95-18052
Mathematical analysis of actuator forces in a scissor lift
[AD-A283906] p 1040 N95-18152
High-frequency skywave signal power measurement system
[AD-A284382] p 996 N95-18341
Liquid crystal tunable filter
[AD-A284383] p 1139 N95-18342
Marine boundary layer refractive effects in the infrared
[AD-A285717] p 1140 N95-18484
A direct decomposition method for the solution of sparse linear least squares problems
[AD-A284060] p 1117 N95-18679
Technical Information Division Open Literature Database (TOLD) operating instructions
[AD-A284061] p 1174 N95-18680

Graphics MIS/Shop Store Program: User's manual
[AD-A284062] p 1174 N95-18681
Surface and upper-air meteorological measurements supporting the NATO/AC243/Panel 3 research study groups 8 and 21 campaign in Lorient, France (September 1993)
[AD-A285326] p 1072 N95-19521

NAVAL POSTGRADUATE SCHOOL, MONTEREY, CA.
Double Eulerian cycles on de Bruijn digraphs
[AD-A283334] p 1120 N95-18007
Wind tunnel performance comparative test results of a circular cylinder and 50 percent ellipse tailboom for circulation control antitorque applications
[AD-A283335] p 941 N95-18008
The diurnal cycle of high-frequency temperature variability at 0 deg 140 deg W on seasonal and interannual time scales
[AD-A283640] p 1074 N95-18012
Linear optimization and image reconstruction
[AD-A283641] p 1094 N95-18013
Improving software characteristics of a real-time system using reengineering techniques
[AD-A283659] p 1094 N95-18015
A constant-depth scratch test for the measurement of adhesion at film-substrate interfaces
[AD-A283660] p 983 N95-18016
A formal method for semantics-based change-merging of software prototypes
[AD-A283668] p 1094 N95-18017
A platform independent application of Lux illumination prediction algorithms
[AD-A283669] p 1094 N95-18018
Sodium sulfate corrosion of silicon carbide fiber-reinforced calcium aluminosilicate glass-ceramic matrix composites
[AD-A283703] p 969 N95-18021
Time-optimal control of a third order regulator
[AD-A283307] p 1113 N95-18023
Study of failure in fibrous composites subjected to bending loads
[AD-A283330] p 969 N95-18028
Personal communications services: Improving theater deployable communications for the 21st century
[AD-A283465] p 994 N95-18058
Secure distributed file systems
[AD-A285525] p 1173 N95-18096
The current status of Russian/CIS communication satellites
[AD-A285526] p 963 N95-18098
Automatic Identification Technology (AIT): The development of functional capability and card application matrices
[AD-A285528] p 1173 N95-18099
TLS-based prefiltering technique for time-domain ARMA modeling
[AD-A284525] p 1120 N95-18113
Intraseasonal oscillations over the tropical western Pacific and eastern Indian ocean for the northern summers of 1989-1991
[AD-A284527] p 1068 N95-18114
A scalable decentralized group membership service for an asynchronous environment
[AD-A283633] p 1109 N95-18137
Performance evaluation of ground based radar systems
[AD-A283654] p 995 N95-18139
Coastal acoustic tomography data constraints applied to a coastal ocean circulation model
[AD-A283911] p 1074 N95-18153
Electrodynamic behavior of PMG-Delta
[AD-A283930] p 964 N95-18163
Improved efficiency and power density for thermoacoustic coolers
[AD-A283946] p 992 N95-18165
US Navy SHF SATCOM: Past, present and future
[AD-A283704] p 996 N95-18359
Design, validation and prototype testing of a high resolution all-reflection Michelson interferometer for solar occultation measurements of the OI 1304-a triplet emission
[AD-A283705] p 1178 N95-18361
Issues in military use of commercial satellites
[AD-A283707] p 964 N95-18362
Finite element modeling of partially delaminated composite beams with contact-impact conditions
[AD-A283726] p 1044 N95-18363
Direct detection and coherent optical systems employing error-correction coding
[AD-A284350] p 1140 N95-18424
Intermediate design and analysis of the PANSAT electrical power subsystem
[AD-A283610] p 1053 N95-18435
Environmental forcing of ambient noise in the Nansen and Amundsen Basins of the Arctic Ocean
[AD-A285540] p 1074 N95-18466
The future use of DSCS and commercial satellites in the US Navy
[AD-A285707] p 997 N95-18481
A triangulation method for passive ranging
[AD-A284180] p 998 N95-18522
Throughput analysis between high end workstations across an FDDI network
[AD-A283608] p 1110 N95-18615
Course module for AA201: Wing structural design project
[AD-A283618] p 944 N95-18616
Calibration and sediment load algorithms for an acoustic sediment flux probe
[AD-A283655] p 1075 N95-18617
Plant and controller optimization by convex methods
[AD-A283700] p 944 N95-18621
A numerical simulation of seasonal circulation in the South China Sea
[AD-A283701] p 1075 N95-18622
Multispectral NOAA Marine Atmospheric Boundary Layer (MABL) estimates during VOCAR
[AD-A283702] p 1064 N95-18623
Interaction, bursting and control of vortices of a cropped double-delta wing at high angle of attack
[AD-A283656] p 930 N95-18669
Computer simulation of wave propagation through turbulent media
[AD-A283695] p 1000 N95-18671
Doppler shift and spread study for ionospherically propagated signals
[AD-A284610] p 1065 N95-19083
High radar range resolution with the step frequency waveform
[AD-A284611] p 1002 N95-19084
First principles used in orbital prediction and an atmospheric model comparison
[AD-A284636] p 1065 N95-19086
Multicast tree construction in network topologies with asymmetric link loads
[AD-A285679] p 1003 N95-19525
A systems analysis and project management plan for the Petite Amateur Navy Satellite (PANSAT)
[AD-A285968] p 965 N95-19571
Constructing a real-time mobile robot software system
[AD-A285969] p 1115 N95-19572
Mitigation of EMI generated by a variable-frequency-drive controller for an AC induction motor
[AD-A286045] p 1012 N95-19573
An analysis of the costs and benefits in improving F402-RR-406A High Pressure Turbine, second stage blades under the aircraft engine Component Improvement Program (CIP)
[AD-A285127] p 950 N95-19595
Synoptic-scale influence on the Monterey Bay sea-breeze
[AD-A285129] p 1073 N95-19596
Automation of hardware-in-the-loop testing of control systems for unmanned air vehicles
[AD-A284833] p 945 N95-19693
Inband radar cross section of phased arrays with parallel feeds
[AD-A284249] p 1005 N95-19730

NAVAL RESEARCH LAB., BAY SAINT LOUIS, MS.
Digital mapping, charting, and geodesy analysis program technical review of Digital Aeronautical Flight Information Data Prototype 1.0 on CD-ROM
[AD-A284728] p 1050 N95-18078
Digital mapping, charting, and geodesy analysis program technical review of Raster Product Format (RPF) and Scanned Map (SMap)
[AD-A284267] p 1052 N95-19733
PAK: A processing system for vectorized time-series data
[AD-A284881] p 1104 N95-19742
Coastal benthic boundary layer special research program: A review of the first year. Volume 1
[AD-A280034] p 1076 N95-19818

NAVAL RESEARCH LAB., WASHINGTON, DC.
The Seventh Ionospheric Effects Symposium
[PB94-191930] p 1057 N95-17985
Proceedings of Natural Sciences Symposium
[AD-A285452] p 1077 N95-19536
Radar antenna characterization using polarization measurements
[AD-A284840] p 1005 N95-19694
Advanced concepts theory
[AD-A279212] p 1147 N95-19844
X-ray laser program
[AD-A279213] p 1039 N95-19845
Power flow and PRS optimization on Phoenix
[AD-A279214] p 1147 N95-19846
PRS projections for DECADE
[AD-A279215] p 1147 N95-19847
Wind tunnel tests of a 42 inch diameter self-starting autogyro rotor
[AD-A279922] p 932 N95-19863

NAVAL SURFACE WARFARE CENTER, BETHESDA, MD.
Thermoelectric properties of conducting polymers
[AD-A284058] p 986 N95-18678
Marangoni convection in a gravity-free silicon float zone
[NASA-CR-197600] p 991 N95-18913
Modified Cu-Mn-Al high damping alloys
[AD-A285460] p 980 N95-19539

NAVAL SURFACE WARFARE CENTER, DAHLGREN, VA.
Seafloor positioning across Juan de Fuca ridge
[AD-A285049] p 1075 N95-19563

NAVAL SURFACE WARFARE CENTER, SILVER SPRING, MD.
Characterization of rechargeable lithium cells. Part 1: Lithium/niobium triselenide chemistry
[AD-A284229] p 1007 N95-17959

NAVAL UNDERSEA WARFARE CENTER, NEW LONDON, CT.
Detection performance of generalized likelihood ratio processors for random signals of unknown location, structure, extent, and strength
[AD-A285589] p 997 N95-18475
IONCAP prediction-based Automatic Link Establishment (ALE) frequency selection for a ten-node Australian high-frequency network
[AD-A283698] p 999 N95-18619

NAVAL UNDERSEA WARFARE CENTER, NEWPORT, RI.
Statistics of complex cross spectrum estimate for sinusoidal signals and arbitrary noise spectra
[AD-A283984] p 1120 N95-19065
Transducer array interaction modeling using variational principles
[AD-A285687] p 1128 N95-19514
The use of two-station ionosonde data for IONCAP/ASAPS model validation on transpolar two-hop, high-frequency skywave radio links
[AD-A284270] p 1005 N95-19736

NEBRASKA UNIV., LINCOLN, NE.
A new multi-dimensional transform for digital signal processing using generalized association schemes
[AD-A284166] p 1117 N95-18511
A photoionization study of OH and OD from 680A to 950A: An analysis of the Rydberg series
[NASA-CR-196970] p 974 N95-18744
Investigation of microscopic mechanisms of failure of electronic smart materials/systems
[AD-A284830] p 988 N95-19691

NEOCERA, INC., COLLEGE PARK, MD.
High Temperature Superconductor (HTS) superconducting quantum interference device (SQUID) microscope
[AD-A285875] p 1152 N95-19598

NEW ENGLAND MEDICAL CENTER HOSPITALS, BOSTON, MA.
Retinal injuries from single and multiple picosecond laser pulses
[AD-A284173] p 1078 N95-18515

NEW HAMPSHIRE UNIV., DURHAM.
Particle acceleration and transport in the tail and at the front side of the magnetosphere, task 1 and 2
[NASA-CR-197575] p 1064 N95-18476
Cross-tail current, field-aligned current, and B(y)
[NASA-CR-197624] p 1065 N95-19032

NEW MEXICO UNIV., ALBUQUERQUE, NM.
A review of nuclear thermal propulsion carbide fuel corrosion and key issues
[NASA-CR-197533] p 1136 N95-18217
Handheld delivery system for modified boron-type fire extinguishment agent
[AD-A283955] p 992 N95-18684
Chondrule-matrix relationships in chondritic meteorites p 1186 N95-19293
Relict grains in chondrules: Evidence for chondrule recycling p 1188 N95-19307
Siderophile elements and metal-silicate fractionation in the solar nebula p 1190 N95-19319

NEW YORK UNIV., NEW YORK, NY.
Facilitation and interference in identification of pictures and words
[AD-A285882] p 1090 N95-19602

NEWCASTLE-UPON-TYNE UNIV., NEWCASTLE (ENGLAND).
Requirements analysis for safety-critical systems: A chemical batch processing example
[PB94-201563] p 991 N95-17934
Pre-processing in SADE: Stage 3
[PB94-201571] p 1093 N95-17935
Reformulated preconditioned conjugate gradient squared method. Part 1: The algorithm
[PB94-201589] p 1108 N95-17936

Replica management system: A scheme for flexible and dynamic replication
[PB94-201597] p 1171 N95-18060

NORTH CAROLINA AGRICULTURAL AND TECHNICAL STATE UNIV., GREENSBORO, NC.
Development of CFD model for augmented core tripropellant rocket engine p 968 N95-18988
Reflexive reasoning for distributed real-time systems p 1107 N95-19766

NORTH CAROLINA UNIV., CHAPEL HILL, NC.
Excited state processes in transition metal complexes. Redox splitting in soluble polymers
[DE95-002690] p 977 N95-19839

NORTH CAROLINA UNIV., CHARLOTTE, NC.
Design optimization of a brush turbine with a cleaner/water based solution p 1043 N95-18177
Outgassing of solid material into vacuum thermal insulation spaces p 972 N95-18184

NORTHWEST SHOALS COMMUNITY COLL., PHIL CAMPBELL, AL.
Surface roughness measurements p 1142 N95-18984

NORTHWESTERN UNIV., EVANSTON, IL.
Characterization of metal matrix composites
[NASA-CR-195381] p 970 N95-18940
Design of advanced steels for armor applications
[ARL-CR-175] p 979 N95-18948

NORWEGIAN HYDRODYNAMIC LABS., TRONDHEIM (NORWAY).
Prediction of buoyant outflow in lakes and fjords with a quasi 3D numerical model
[PB94-206984] p 1051 N95-18372

NYMA, INC., BROOK PARK, OH.
An application of a two-equation model of turbulence to three-dimensional chemically reacting flows
[NASA-CR-195411] p 1015 N95-18107
Prediction of wind tunnel effects on the installed F/A-18A inlet flow field at high angles-of-attack
[NASA-CR-195429] p 950 N95-19651

NYMA, INC., CLEVELAND, OH.
Observation of flow and temperature oscillations around a bubble on a solid surface subject to a vertical temperature gradient
[NASA-CR-197593] p 1017 N95-18327
On supersonic-inlet boundary-layer bleed flow
[NASA-CR-195426] p 955 N95-19769

O

OAK RIDGE NATIONAL LAB., TN.
Static and dynamic nuclear many-body descriptions on parallel architectures
[DE94-018134] p 1116 N95-18120
Alloying effects on the high-temperature oxidation resistance of Cr-Cr2Nb
[DE94-018146] p 978 N95-18121
Study of frustrated systems via dissipative maps
[DE94-017754] p 1122 N95-18127
On the crack growth resistance and strength of the B2 iron aluminides Fe-40Al, Fe-45Al, and Fe-10Ni-40Al (at. %)
[DE94-017857] p 978 N95-18128
Early experiences and performance of the Intel Paragon
[DE94-018061] p 1109 N95-18129
Arbitrarily high order nodal and characteristic methods
[DE94-018130] p 1116 N95-18131
Trends 1993: A compendium of data on global change
[ORNL/CDIAC-65] p 1058 N95-18389
Image accuracy and representational enhancement through low-level, multi-sensor integration techniques
[DE94-018661] p 1051 N95-18556
Global wave modeling of electron interactions with fast magnetosonic waves
[DE94-018942] p 1144 N95-18557
Comparison of the folded stripline and stacked stripline concepts to the folded waveguide launcher
[DE94-018951] p 999 N95-18558
One strategy for estimating the potential soil carbon storage due to CO2 fertilization
[DE94-017895] p 1059 N95-18666
General information for operation of the high-temperature electromagnetic containerless vacuum induction furnace
[DE94-017170] p 991 N95-19076
Impurity behavior during ion-Bernstein wave heating in PBX-M
[DE94-018114] p 1133 N95-19228
Ion mixing in oxide-sapphire systems
[DE94-018660] p 1133 N95-19232
Subgroup report on hard x-ray microprobes
[DE94-018708] p 1034 N95-19233
Nuclear medicine program
[DE94-017530] p 1080 N95-19244
Enhancement of creep resistance of a sintered Si3N4 ceramic by microwave annealing
[DE94-017688] p 987 N95-19399
Deformation texture studies in Fe3Al alloys
[DE94-017709] p 980 N95-19400
Historic patterns of CO2 emissions from fossil fuels: Implications for stabilization of emissions
[DE95-000489] p 1061 N95-19556
Neutron scattering study of dilute supercritical solutions
[DE95-000493] p 1134 N95-19557
Weldability of iron aluminides
[DE95-000686] p 981 N95-19568
Proceedings of the Eighth Annual Conference on Fossil Energy Materials
[DE95-001055] p 981 N95-19723
Solution of potential flow problems on a network of workstations
[DE94-017861] p 1112 N95-19831

OAK RIDGE Y-12 PLANT, TN.
The metallurgical integrity of the frit vent assembly diffusion bond
[DE95-000610] p 968 N95-19877

OAKWOOD COLL., HUNTSVILLE, AL.
The assessment of virtual reality for human anatomy instruction p 1088 N95-18971

OFFICE NATIONAL D'ETUDES ET DE RECHERCHES AEROSPATIALES, MODANE (FRANCE).
Calculation of wall effects of flow on a perforated wall with a code of surface singularities p 1025 N95-19277

OFFICE OF NAVAL RESEARCH, ARLINGTON, VA.
Eigenvalue tests and distributions for small sample order determination for complex Wishart matrices
[AD-A283825] p 1120 N95-18672

OHIO AEROSPACE INST., CLEVELAND, OH.
Composites research in support of the NASP Institute for Composites (NIC)
[NASA-CR-197580] p 970 N95-18471

OHIO STATE UNIV., COLUMBUS.
Definition and realization of a global vertical datum
[AD-A283303] p 1049 N95-17971
Method of moments analysis of artificial media composed of dielectric wire objects
[AD-A283318] p 994 N95-18024

OHIO UNIV., ATHENS.
Data driven propulsion system weight prediction model p 968 N95-18980

OKLAHOMA UNIV., NORMAN, OK.
Performance evaluation of the Engineering Analysis and Data Systems (EADS) 2 p 1163 N95-18978

OLD DOMINION UNIV., NORFOLK, VA.
Experimental verification of a progressive damage model for composite laminates based on continuum damage mechanics
[NASA-CR-195020] p 971 N95-19043

OPEN UNIV., MILTON KEYNES (ENGLAND).
Carbon, CAIs and chondrules p 1186 N95-19291
On the measurement of the crack tip stress field as a means of determining Delta K(sub eff) under conditions of fatigue crack closure p 938 N95-19492

OREGON GRADUATE CENTER FOR STUDY AND RESEARCH, BEAVERTON, OR.
Special relativity effects for space-based coherent lidar experiments p 1014 N95-18983

OREGON STATE UNIV., CORVALLIS, OR.
The 3d International Workshop on Computational Electronics
[AD-A284678] p 1011 N95-19089

OREGON UNIV., EUGENE, OR.
Microscopic origins of metastable effects in a-Si:H and deep defect characterization in a-Si,Ge:H alloys
[DE94-011887] p 1151 N95-19541

ORGANISATIE VOOR TOEGEPAST NATUURWETENSCHAPPELIJK ONDERZOEK, SOESTERBERG (NETHERLANDS).
Vestibular examination in pilots susceptible to motion sickness p 1083 N95-19427

OSAKA UNIV., TOYONAKA (JAPAN).
Establishment of redox conditions during planetary collisions as an origin of chondrites p 1192 N95-19331

OSLO UNIV. (NORWAY).
Decomposition of parametric curves
[PB94-207024] p 1117 N95-18374

OXFORD UNIV., OXFORD (ENGLAND).
Particle deposition in gas turbine blade film cooling holes p 951 N95-19661
Soft body impact on titanium fan blades p 953 N95-19671

P

PACIFIC NORTHWEST LAB., RICHLAND, WA.
EMEFS: Lessons learned 2, model evaluation
[DE94-017468] p 1049 N95-18145
Application of conducting polymers to electroanalysis
[DE94-015204] p 984 N95-18348
Mechanisms of interaction and biological effects of extremely-low-frequency electromagnetic fields
[DE94-015200] p 1076 N95-18371
Heterogeneous nucleation of calcium oxalate on native oxide surfaces
[DE94-018725] p 986 N95-18648
Information system architecture to support transparent access to distributed, heterogeneous data sources
[DE94-018450] p 1176 N95-19589
Intrinsic barriers for H-atom transfer reactions involving hydrocarbons
[DE94-018451] p 1134 N95-19590
Alternative materials for solid oxide fuel cells
[DE94-018452] p 1054 N95-19591

PALERMO UNIV. (ITALY).
An airborne monitoring system for FOD and erosion faults p 953 N95-19668

PENNSYLVANIA STATE UNIV., UNIVERSITY PARK, PA.
Fabrication of biomimetic molecular level composites
[AD-A284204] p 969 N95-17941
Lightning studies using LDAR and companion data sets p 1073 N95-18174
An atomic view of motion on surfaces
[AD-A285565] p 1131 N95-18473
Coupled finite element analysis of decomposing poroelastic polymeric composites and structures with subsequent thermal and gas diffusion p 986 N95-18918
Implications of summertime marine stratocumulus on the North American climate p 1073 N95-18977
Fundamental studies of passivity and passivity breakdown
[DE94-016954] p 987 N95-19095
NASA Goddard Earth Sciences Graduate Student Program
[NASA-CR-197130] p 1066 N95-19129
Materials for adaptive structural acoustic control, volume 3
[AD-A279223] p 1128 N95-19850

PENNSYLVANIA UNIV., PHILADELPHIA, PA.
Testing the inflationary paradigm: Inflation and the cosmic microwave background anisotropy p 1179 N95-18496
Discrete and continuum elastic properties of interfaces p 1150 N95-18928
The formulation of quantum statistical mechanics based on the Feynman path centroid density. 3: Phase space formalism and analysis of centroid molecular dynamics
[AD-A279233] p 1157 N95-19852
The formulation of quantum statistical mechanics based on the Feynman path centroid density. 4: Algorithms for centroid molecular dynamics
[AD-A279234] p 1157 N95-19853

PERKIN-ELMER CORP., POMONA, CA.
Techniques for in situ collection and measurement of volatiles released during hypervelocity impact p 962 N95-19184

PETERSON (ROBERT B.), HOUSTON, TX.
Charge collection during hypervelocity penetrations of thin foils p 1036 N95-19190

PHILLIPS LAB., HANSCOM AFB, MA.
CRRESPRO documentation
[AD-A284578] p 1178 N95-18451
Proceedings of the 15th Annual Conference on Atmospheric Transmission Models
[AD-A279919] p 1142 N95-19862
Thermochemical IR sources: COCHISE and FACELIF experiments
[AD-A279940] p 977 N95-19868

PHILLIPS LAB., KIRTLAND AFB, NM.
A fast recursive algorithm to compute the probability of M-out-of-N events
[AD-A283679] p 1120 N95-18020

PHYSICAL OPTICS CORP., TORRANCE, CA.
A novel technique for 4-dimensional atmospheric and oceanographic irradiance measurements using 3-D spatial filtering
[AD-A285658] p 1073 N95-19701

PHYSICS AND ELECTRONICS LAB. TNO, THE HAGUE (NETHERLANDS).
Analysis and synthesis of (SAR) waveguide phased array antennas
[AD-A285336] p 1004 N95-19535
High performance computing for medical image interpretation
[AD-A285457] p 1086 N95-19537

PITTSBURGH UNIV., PITTSBURGH, PA.
Visuo-ocular performance during vestibular stimulation
[AD-A284103] p 1089 N95-18403
PORTUGUESE AIR FORCE AEROMEDICAL CENTER, LISBON (PORTUGAL).
The EEG in the evaluation of applicants to aircrew members p 1084 N95-19432
PRATT AND WHITNEY AIRCRAFT, EAST HARTFORD, CT.
QPA-CLIPS: A language and representation for process control p 1102 N95-19635
PRATT AND WHITNEY AIRCRAFT, WEST PALM BEACH, FL.
Fatigue in single crystal nickel superalloys
[AD-A285727] p 978 N95-18068
PRAXAIR, INC., TONAWANDA, NY.
Airborne rotary separator study
[NASA-CR-191045] p 967 N95-18743
PRINCETON UNIV., NJ.
Study of a Navier-Stokes computer
[AD-A284196] p 1092 N95-17939
Studies on high pressure and unsteady flame phenomena
[AD-A284126] p 973 N95-18410
A knowledge-based system for controlling automobile traffic p 1102 N95-19633
PRINS MAURITS LAB. TNO, RIJSWIJK (NETHERLANDS).
Multiple-task performance: A critical review of the literature and a cognitive neuroscience framework
[AD-A285133] p 1090 N95-19583
PUERTO RICO UNIV., MAYAGUEZ.
Mechanical behavior of precipitation hardenable steels exposed to highly corrosive environment p 982 N95-18180
PURDUE UNIV., WEST LAFAYETTE, IN.
Software techniques for balancing computation and communication in parallel systems
[AD-A285536] p 1109 N95-18106
The Solvent Absorption-Extractive Distillation (SAED) process for ethanol recovery from gas/vapor streams
[DE94-013112] p 974 N95-18637
Engineering considerations for the self-energizing magnetoplasmadynamic (MPD) - type fusion plasma thruster
[AD-A283968] p 1144 N95-18888
Hyperspectral data analysis procedures with reduced sensitivity to noise
[NASA-CR-197621] p 1052 N95-19126
A probabilistic fatigue analysis of multiple site damage p 935 N95-19476
Aero-thermodynamic distortion induced structured dynamic response
[AD-A279931] p 955 N95-19864

Q

QUAID-I-AZAM UNIV., ISLAMABAD (PAKISTAN).
Preparation and surface characterization of metal doped alumina catalyst
[PB94-175296] p 973 N95-17991
QUEENS MEDICAL CENTRE, NOTTINGHAM (ENGLAND).
Clinical basis for aeromedical decision-making: The EEG example p 1084 N95-19433
QUEENS UNIV., BELFAST (NORTHERN IRELAND).
Ion-molecule collisions, electron molecule collisions, excitation and ionization of atoms
[AD-A284584] p 1129 N95-18062
QUEENSLAND UNIV., BRISBANE (AUSTRALIA).
Incorporating uncertainty and risk in rainfall-based flood estimates
[RR-CE144] p 1071 N95-18607
Plate vibration with arbitrarily oriented stiffeners based on Mindlin-Engesser formulation
[RR-CE143] p 1045 N95-18608

R

RANDOLPH-MACON COLL., ASHLAND, VA.
Evaluation of inorganic zinc-rich primers using Electrochemical Impedance Spectroscopy (EIS) in combination with atmospheric exposure p 977 N95-18170
RAYTHEON CO., MARLBOROUGH, MA.
An expert system for configuring a network for a Milstar terminal p 1104 N95-19645
RECOM TECHNOLOGIES, INC., MOFFETT FIELD, CA.
AI and workflow automation: The prototype electronic purchase request system p 1101 N95-19632
Real-time remote scientific model validation p 1103 N95-19640
CLIPS, AppleEvents, and AppleScript: Integrating CLIPS with commercial software p 1103 N95-19643
RENSSELAER POLYTECHNIC INST., TROY, NY.
The reliability of laser reflowed Sn-Ag solder joints
[AD-A284732] p 1044 N95-18080
Development of ultrashort optical pulse sources near 1.3 and 1.5 microns with an emphasis on stability, high repetition rate, and parallelism
[AD-A285535] p 1139 N95-18104
An analog computing approach to structural analysis and optimal design through artificial neural networks p 1113 N95-18218
Development of radiation-hardened ceramic composites for fusion applications
[DE94-016182] p 985 N95-18638
Representing visibility for siting problems
[AD-A284076] p 993 N95-19036
RESEARCH INST. FOR ADVANCED COMPUTER SCIENCE, MOFFETT FIELD, CA.
Weighted graph based ordering techniques for preconditioned conjugate gradient methods
[NASA-CR-197597] p 1118 N95-18736
Mesh quality control for multiply-refined tetrahedral grids
[NASA-CR-197595] p 1043 N95-18737
RESEARCH TRIANGLE INST., RESEARCH TRIANGLE PARK, NC.
Economic impact analysis for proposed emission standards and guidelines for municipal waste combustors: A description of the basis for, and impacts of, proposed revisions to air pollutant emission regulations for new and existing municipal waste combustors under Clean Air Act Sections 111(b), 111(d), and 129
[PB94-213543] p 1061 N95-19403
RETICULAR SYSTEMS, INC., SAN DIEGO, CA.
PalymSys (TM): An extended version of CLIPS for construction and reasoning using blackboards p 1107 N95-19767
RHODE ISLAND UNIV., KINGSTON, RI.
A mechanism for blistering of carbon fiber composites
[AD-A286252] p 971 N95-19386
RICE UNIV., HOUSTON, TX.
Comparing performance on implicit memory tests
[AD-A284861] p 1090 N95-19740
RIJKSINSTITUUT VOOR VOLKSGEZONDHEID EN MILIEUHYGIEENE, BILTHOVEN (NETHERLANDS).
Catalog of environmental data sets of Europe at the RIVM
[PB94-202710] p 1057 N95-18002
Methane: The other greenhouse gas. Research and policy in the Netherlands
[PB94-207149] p 1058 N95-18375
ROCKET RESEARCH CORP., REDMOND, WA.
Arcjet thruster research and technology, phase 2
[NASA-CR-182276] p 927 N95-18044
High performance storable propellant resistojet
[NASA-CR-191128] p 967 N95-18195
ROCKWELL INTERNATIONAL CORP., CANOGA PARK, CA.
NCl(b) based short wavelength chemical laser
[AD-A284213] p 1036 N95-17956
ROCKWELL INTERNATIONAL CORP., DOWNEY, CA.
Strategic avionics technology definition studies. Subtask 3-1A3: Electrical Actuation (ELA) Systems Test Facility
[NASA-CR-188360] p 956 N95-18567
Fatigue loads spectra derivation for the Space Shuttle: Second cycle p 934 N95-19470
ROLLS-ROYCE LTD., BRISTOL (ENGLAND).
Out of area experiences with the RB199 in Toronto p 950 N95-19654
Future directions in helicopter protection system configuration p 951 N95-19657
ROME LAB., GRIFFISS AFB, NY.
Gigabit optical interconnects: System and component analysis, design and development
[AD-A285538] p 1138 N95-18067
Numerically efficient use of frequency domain MoM codes for wideband radiation and scattering problems. An application: Scattering from a microstrip patch
[AD-A284561] p 995 N95-18116
Global time transformations
[AD-A285539] p 1110 N95-18454
ROME UNIV. (ITALY).
Acoustics of space structures p 1126 N95-19152
ROTHE DEVELOPMENT, INC., SAN ANTONIO, TX.
Echo imaging techniques determine the size of intravascular bubbles in decompression sickness
[AD-A284849] p 1087 N95-19714
ROYAL INST. OF TECH., STOCKHOLM (SWEDEN).
On the geometry of visual correspondence
[AD-A285700] p 1140 N95-18478
ROYAL MILITARY COLL. OF SAINT-JEAN, RICHELAIN (QUEBEC).
Transport aircraft loading and balancing system: Using a CLIPS expert system for military aircraft load planning p 1105 N95-19751
DAI-CLIPS: Distributed, Asynchronous, Interacting CLIPS p 1107 N95-19763
ROYAL NETHERLANDS METEOROLOGICAL INST., DE BILT.
The effect of spatial averaging on threshold exceedances of daily precipitation amounts
[KNMI-TR-154] p 1070 N95-18392
Storm activity over the North Sea and the Netherlands in two climate models compared with observations
[KNMI-WR-94-02] p 1070 N95-18393
Conceptual models of severe convective weather in the Netherlands
[KNMI-WR-93-05] p 1071 N95-18394
A synoptic climatology of convective weather in the Netherlands
[KNMI-WR-93-04] p 1071 N95-18395
Searching for stationary stable solutions of Euler's equation
[KNMI-WR-93-01] p 1017 N95-18396
Atmospheric effects of high-flying subsonic aircraft: A catalogue of perturbing influences
[KNMI-SR-94-03] p 1060 N95-18722
An analytic conceptual model of extratropical cyclones
[KNMI-WR-93-03] p 1072 N95-18926
ROYAL NORWEGIAN AIR FORCE, OSLO (NORWAY).
Is the pilot fit for flying after an accident? p 1083 N95-19425
Think health not disease p 1083 N95-19429
ROYAL NORWEGIAN COUNCIL FOR SCIENTIFIC AND INDUSTRIAL RESEARCH, OSLO (NORWAY).
Decomposition of parametric curves
[PB94-207024] p 1117 N95-18374
RUTGERS - THE STATE UNIV., PISCATAWAY, NJ.
Parallel computations in hydro acoustics
[AD-A285900] p 1030 N95-19607
RUTGERS UNIV., NEW BRUNSWICK, NJ.
Constraints placed on the nature of chondrule precursors p 1186 N95-19295
RUTGERS UNIV., PISCATAWAY, NJ.
Experimental constraints on models for origins of chondrules: Peak temperatures p 1187 N95-19302
Flash heating is required to minimize sodium losses from chondrules p 1193 N95-19337
RUTHERFORD APPLETON LAB., CHILTON (ENGLAND).
Generation permutation symmetry and the quark mixing matrix
[PB95-108189] p 1132 N95-18643

S

SAINT THOMAS UNIV., HOUSTON, TX.
MIRO: A debugging tool for CLIPS incorporating historical Rete networks p 1105 N95-19754
SAM TECHNOLOGY, INC., SAN FRANCISCO, CA.
SIGNET-software tools for signal identification using neural networks
[AD-A284362] p 1113 N95-18441
SANDIA NATIONAL LABS., ALBUQUERQUE, NM.
Adaptive robot path planning in changing environments
[DE94-016564] p 1112 N95-17948
Ion beam surface treatment: A new capability for surface enhancement
[DE94-014663] p 977 N95-17968
Using federal technology policy to strength the US microelectronics industry
[DE94-017293] p 1008 N95-18143
Ion emission intensity ratios as a function of electrode gap, melting current, and pressure during low current vacuum arc remelting
[DE94-017407] p 1129 N95-18144
QuikForm: Intelligent deformation processing of structural alloys
[DE94-018739] p 1114 N95-18649
Magneto-optical studies of compound semiconductors
[DE94-018743] p 1149 N95-18650
Complex oxidation effects in polymer degradation
[DE94-018903] p 986 N95-18651
Alarm annunciation in a graphical environment
[DE94-015761] p 1098 N95-18652
Can information surety be assessed with high confidence?
[DE94-015805] p 1120 N95-18653
Building a bridge with the customer to facilitate collecting and validating information in modeling sessions
[DE94-017338] p 1174 N95-18872
Lossless compression of weight vectors from an adaptive filter
[DE94-017350] p 1174 N95-18873
CUBIT mesh generation environment
[DE94-017496] p 1118 N95-18896
HEISHI: A fuel performance model for space nuclear applications
[DE94-017497] p 1137 N95-18897
Evaluation of scanners for C-scan imaging in nondestructive inspection of aircraft
[DE94-012473] p 990 N95-19100

LEVIS ion source and beam characterization on PBFA-2
[DE94-015802] p 1133 N95-19199
Complete mode-set stability analysis of magnetically insulated ion diode equilibria
[DE94-015275] p 1145 N95-19201
Giant effective mass deviations near the magnetic field-induced minigap in double quantum wells
[DE94-018889] p 1122 N95-19234
Optical determination of conduction and valence-band dispersion curves in strained single-quantum wells
[DE94-018892] p 1151 N95-19235
Resonator/oscillator response to liquid loading
[DE94-013442] p 1012 N95-19240
An atomic view of surface diffusion on metal surfaces
[DE94-016150] p 980 N95-19395
Sandia National Laboratories' high power electromagnetic impulse sources
[DE95-000423] p 1004 N95-19555
Ferroelectric thin film bismuth titanate prepared from acetate precursors
[DE95-000538] p 988 N95-19558
Using electrochemistry in device processing on poly(tetrafluoroethylene) substrates
[DE95-000541] p 975 N95-19559
Environmental effects on composite airframes: A study conducted for the ARM UAV Program (Atmospheric Radiation Measurement Unmanned Aerospace Vehicle)
[DE94-015351] p 971 N95-19579
Characteristics and development report for the MC3994 and MC3994A relays
[DE95-002952] p 1013 N95-19842
A simple single-photomask process for fabrication of high-efficiency multicrystalline silicon solar cells
[DE94-014251] p 1055 N95-19859
Battery and charge controller evaluations in small stand-alone PV systems
[DE94-014252] p 1013 N95-19872
Gettering in multicrystalline silicon: A design-of-experiments approach
[DE94-014289] p 1055 N95-19873
Automatically generating procedure code and database maintenance scripts
[DE95-000545] p 1176 N95-19876

SCANDINAVIAN AIRLINES SYSTEM, OSLO (NORWAY).
Scandinavian Airlines Systems experience on erosion, corrosion and foreign object damage effects on gas turbines p 951 N95-19659

SCIENCE APPLICATIONS INTERNATIONAL CORP., FORT WASHINGTON, PA.
Prediction of fluctuating pressure and power spectra in attached and separated compressible flow p 1031 N95-19153

SCIENCE APPLICATIONS INTERNATIONAL CORP., GLENDORA, CA.
The intact capture of hypervelocity dust particles using underdense foams p 1183 N95-19188

SCIENCE APPLICATIONS INTERNATIONAL CORP., MCLEAN, VA.
A Space and Atmospheric Visualization Science System
[NASA-CR-189390] p 1172 N95-18040

SCIENTIFIC RESEARCH ASSOCIATES, INC., GLASTONBURY, CT.
Large signal time dependent quantum mechanical transport in quantum phase based devices
[AD-A283338] p 1155 N95-18009
The physics and operation of ultra-submicron length semiconductor devices
[AD-A280181] p 1155 N95-19828
Modeling of quantum transport in semiconductor devices
[AD-A280182] p 1155 N95-19829

SCIENTIFIC TECHNOLOGY, INC., ROCKVILLE, MD.
Wallops Island natural rain data analysis p 1069 N95-18205

SEARCH FOR EXTRATERRESTRIAL INTELLIGENCE INST., MOUNTAIN VIEW, CA.
SPICE: An innovative, flexible instrument concept p 968 N95-19189

SELSKAPET FOR INDUSTRIELL OG TEKNISK FORSKNING, OSLO (NORWAY).
ODP based UPT model
[PB94-215589] p 1003 N95-19411

SELSKAPET FOR INDUSTRIELL OG TEKNISK FORSKNING, TRONDHEIM (NORWAY).
Prediction of buoyant outflow in lakes and fjords with a quasi 3D numerical model
[PB94-206984] p 1051 N95-18372
Size distribution of one-, two- and three-dimensional Voronoi cells
[PB94-207008] p 1149 N95-18373
Decomposition of parametric curves
[PB94-207024] p 1117 N95-18374
Palladium-based membranes for hydrogen separation
[PB94-207156] p 973 N95-18377
Long-term processes in geomaterials. A three-dimensional visco-elastic soil model
[PB94-207180] p 1065 N95-18640
Norwegian heat pump status and policy review
[PB94-206992] p 992 N95-18667
SICOMP, the SINTEF data compression library (version 1.0) reference manual
[PB94-207107] p 1099 N95-18668
Simulation in manufacturing
[PB94-215563] p 1100 N95-19409
Guidelines for reduction of human errors during maintenance of safety systems; maintainability and maintenance support
[PB94-215597] p 1092 N95-19412

SERVICE DE MEDECINE AERONAUTIQUE, VERSAILLES (FRANCE).
EKG in flight: Usefulness and limits for aircrew rehabilitation p 1082 N95-19422

SMALL BUSINESS ADMINISTRATION, WASHINGTON, DC.
Small Business Research Summaries, numbers 51-100
[PB94-179967] p 1170 N95-17986
Small Business Research Summaries, numbers 1-50
[PB94-179959] p 1170 N95-17987

SOCIETE NATIONALE D'ETUDE ET DE CONSTRUCTION DE MOTEURS D'AVIATION, EVRY (FRANCE).
New Trends in coatings developments for turbine blades: Materials processing and repair p 954 N95-19676

SOCIETE NATIONALE D'ETUDE ET DE CONSTRUCTION DE MOTEURS D'AVIATION, MOISSY-CRAMAYEL (FRANCE).
Design of fan blades subjected to bird impact p 953 N95-19669

SOFTWARE PRODUCTIVITY CONSORTIUM, HERNDON, VA.
Process definition and modeling guidebook. Volume 1: Concepts and principles of MPDM. Version 02.00.02
[AD-A279162] p 1108 N95-19803
Process definition and modeling guidebook. Volume 2: Advanced applications of MPDM
[AD-A279199] p 1108 N95-19813

SORBENT TECHNOLOGIES CORP., TWINSBURG, OH.
Controlling combustion-source emissions at Air Force sites with a new filter concept, phase 1
[AD-A283674] p 1058 N95-18140

SOUTH DAKOTA SCHOOL OF MINES AND TECHNOLOGY, RAPID CITY, SD.
The numerical simulation of marine boundary layer clouds
[AD-A284149] p 1064 N95-18413

SOUTH DAKOTA STATE UNIV., BROOKINGS, SD.
The development of a fiber optics communication network for controlling a Multidegree-Of-Freedom Serpentine Truss p 1142 N95-18167

SOUTHEASTERN CENTER FOR ELECTRICAL ENGINEERING EDUCATION, INC., SAINT CLOUD, FL.
The cross-validation of the United States Air Force submaximal cycle ergometer test to estimate aerobic capacity
[AD-A284055] p 1079 N95-18661

SOUTHERN COLL. OF TECHNOLOGY, MARIETTA, GA.
Feasibility study of transmission of OTV camera control information in the video vertical blanking interval p 1006 N95-18185

SOUTHWEST RESEARCH INST., SAN ANTONIO, TX.
Microstructure-based fatigue life prediction methods for naval steel structures
[AD-A284735] p 1044 N95-18081
Aircraft stress sequence development: A complex engineering process made simple p 936 N95-19480
Analysis of cold worked holes for structural life extension p 939 N95-19493
Technology demonstration of single hydraulic fluid for armored ground vehicle systems
[AD-A280170] p 989 N95-19826

SPARTA, INC., LEXINGTON, MA.
A sensitivity analysis of upwelling radiances in the 3-5 micrometers region as a function of atmospheric conditions
[AD-A283678] p 1068 N95-18141

SPIRE CORP., BEDFORD, MA.
Defect reduction and back channel degradation in SIMOX
[AD-A284231] p 1148 N95-17960
InP solar cell development on inexpensive silicon substrates
[AD-A283624] p 1052 N95-18011
InP solar cell development on inexpensive silicon substrates
[AD-A286254] p 1054 N95-19388

SRI INTERNATIONAL CORP., MENLO PARK, CA.
Alternative volume integral equation formulations applied to dielectric cylinders
[AD-A285537] p 995 N95-18066
In vitro system for studying metabolism of environmental chemicals in human cells
[AD-A284174] p 1079 N95-18518
IR materials producibility
[AD-A284263] p 1142 N95-19732
Novel catalysts for methane activation
[DE95-001179] p 976 N95-19785
Field-emitter arrays for RF vacuum microelectronics
[AD-A279932] p 1013 N95-19865

STANFORD LINEAR ACCELERATOR CENTER, CA.
Algorithms for orbit control on SPEAR
[DE95-002868] p 1138 N95-19841

STANFORD RESEARCH INST., MENLO PARK, CA.
The Seventh Ionospheric Effects Symposium
[PB94-191930] p 1057 N95-17985

STANFORD UNIV., CA.
AASERT-93: New high-pressure diagnostic technique
[AD-A284943] p 973 N95-17975
The left-right forward-backward asymmetry for B quarks at the SLD
[DE94-014508] p 1129 N95-18049
Investigation of atmospheric waves on Neptune
[NASA-CR-197537] p 1194 N95-18579
Low voltage electron beam lithography
[AD-A284181] p 1010 N95-18625
Advanced optical fiber communications systems
[AD-A283942] p 1141 N95-18682
Design and flight test of a simplified control system for a transport helicopter p 958 N95-18902
Numerical analysis of dissipative dynamical systems in solid and fluid mechnaics, with a special emphasis on coupled problems p 1122 N95-18916
The Gravity Probe B niobium bird experiment: Experimental verification of a data reduction scheme with a prototypical dc SQUID readout system p 1033 N95-18929
Visualizing second order tensor fields with hyperstreamlines
[NASA-CR-197619] p 1121 N95-19288
Mega-scale simulation of multi-layer devices: Formulation, kinetics, and visualization
[AD-A284848] p 1153 N95-19738
Tunneling acoustic microscopy
[AD-A279160] p 1128 N95-19802
High temperature superconducting films and crystals
[AD-A279201] p 1154 N95-19815

STATE UNIV. OF EAST TENNESSEE, JOHNSON CITY, TN.
Salt-induced aggregation of lysozyme: Implications for crystal growth p 1155 N95-19015

STATE UNIV. OF NEW YORK, ALBANY, NY.
A report on workshops: General circulation model study of climate: Chemistry interaction
[DE94-010252] p 1062 N95-19879

STATE UNIV. OF NEW YORK, BINGHAMTON, NY.
Study of the kinematic and load sharing properties of wormgearing with non-symmetric tooth profiles
[NASA-CR-195414] p 1041 N95-18541
Wormgear geometry adopted for implementing hydrostatic lubrication and formulation of the lubrication problem
[NASA-CR-195416] p 1043 N95-19567

STATE UNIV. OF NEW YORK, BUFFALO, NY.
High-pressure studies of deep impurities in GaAs, ZnSe, and related layered structures p 1150 N95-18908

STATE UNIV. OF NEW YORK, FARMINGDALE, NY.
Quality optimization of thermally sprayed coatings produced by the JP-5000 (HVOF) gun using mathematical modeling p 989 N95-19008

STATE UNIV. OF NEW YORK, ONEONTA, NY.
A CMC database for use in the next generation launch vehicles (rockets) p 963 N95-18993

STATE UNIV. OF NEW YORK, PLATTSBURGH, NY.
Collection requirements for trace-element analyses of extraterrestrial samples p 1182 N95-19182

STATE UNIV. OF NEW YORK, STONY BROOK, NY.
Macromolecular characterization and solution behavior of polymer additives
[AD-A284845] p 988 N95-19696
High performance computing equipment for environmental remediation modeling and first principles simulation of materials properties
[DE95-000497] p 1093 N95-19875

STATE UNIV. OF SOUTHEASTERN OKLAHOMA, DURANT, OK.
CLIPS template system for program understanding p 1102 N95-19636

SWISS SCIENTIFIC COMPUTING CENTER, MANNO (SWITZERLAND).
Using CLIPS in the domain of knowledge-based massively parallel programming p 1105 N95-19750

SYDNEY UNIV. (AUSTRALIA).
Six degree of freedom flight dynamic and performance simulation of a remotely-piloted vehicle
[AERO-TN-9301] p 942 N95-18097

SYRACUSE UNIV., NY.
Enhancing the architectural characterization of parallel proto
[AD-A285678] p 1111 N95-19524
SYSTEMS AND ELECTRONICS, INC., ELK GROVE VILLAGE, IL.
Flight parameters monitoring system for tracking structural integrity of rotary-wing aircraft
p 934 N95-19469
SYSTEMS CONTROL TECHNOLOGY, INC., ARLINGTON, VA.
Heliport/vertiport MLS precision approaches
[AD-A283505] p 940 N95-18059

T

TAMPERE UNIV. OF TECHNOLOGY (FINLAND).
Solutions of TEAM Problem No. 13 using integral equations in a sequential and parallel computing environment
[DE95-001472] p 1112 N95-19834
TECHNICAL UNIV. OF LISBON (PORTUGAL).
7th International Symposium on Applications of Laser Techniques to Fluid Mechanics, volume 2
[AD-A285685] p 1018 N95-18477
TECHNION - ISRAEL INST. OF TECH., HAIFA (ISRAEL).
Investigation of the ionospheric short-term variability
[AD-A286253] p 1066 N95-19387
TECHNISCHE HOGESCHOOL, DELFT (NETHERLANDS).
Fatigue life until small cracks in aircraft structures: Durability and damage tolerance p 936 N95-19478
TECHNISCHE HOGESCHOOL, TWENTE (NETHERLANDS).
Alternative formulation of Cocke-Younger-Kasami's algorithm
[PB94-202751] p 1094 N95-18000
TECHNISCHE UNIV., DARMSTADT (GERMANY).
Cooling rates of chondrules: A new approach
p 1192 N95-19334
TECHNISCHE UNIV., DELFT (NETHERLANDS).
Applications of quaternions to dynamical simulation, computer graphics and biomechanics
[PB94-201456] p 1094 N95-17972
Partition method for the determination of multiple DC operating points
[PB94-201480] p 1009 N95-18501
Light transport for medical laser treatments
[PB94-201498] p 1037 N95-18502
Algorithms and applications in timed discrete event systems
[PB94-201423] p 1118 N95-19169
The utilization of a high speed reflective visualization system in the study of transonic flow over a delta wing
p 932 N95-19259
TECHNISCHE UNIV., MUNICH (GERMANY).
Velocity measurements with hot-wires in a vortex-dominated flowfield p 932 N95-19261
TECHNISCHE UNIV., TWENTE (NETHERLANDS).
Design and analysis of dynamic leader election protocols in broadcast networks
[PB94-202728] p 1109 N95-18039
Classification of graded, finite-dimensional lie algebras of vector fields
[PB94-215449] p 1119 N95-19408
TENNESSEE STATE UNIV., NASHVILLE, TN.
A report of work activities on the NASA Spacelink public electronic library p 1168 N95-19005
TENNESSEE TECHNOLOGICAL UNIV., COOKEVILLE, TN.
Fatigue and residual strength investigation of ARALL(R) -3 and GLARE(R) -2 panels with bonded stringers
p 939 N95-19495
Development of an expert system for power quality advisement using CLIPS 6.0 p 1014 N95-19634
TENNESSEE UNIV., KNOXVILLE, TN.
Polymer-based separations: Synthesis and application of polymers for ionic and molecular recognition
[DE94-016427] p 964 N95-18355
Spectroelectrochemical investigations of molten halide solutions
[AD-A284147] p 974 N95-18412
Electrochemical and spectroscopy studies of selected inorganic and organic systems in molten halides
[AD-A284171] p 974 N95-18514
NiAl and NiAl-based composites directionally solidified by a containerless zone process
[NASA-CR-195430] p 982 N95-19792
TENNESSEE UNIV. SPACE INST., TULLAHOMA, TN.
Bubble formation in microgravity p 991 N95-18970
TEXAS A&I UNIV., KINGSVILLE, TX.
Evaluation of the efficiency and reliability of software generated by code generators p 1108 N95-19004
TEXAS A&M UNIV., COLLEGE STATION, TX.
Design considerations for a Space Station radiation shield for protection from both man-made and natural sources
[NASA-CR-195298] p 964 N95-18495
Neural networks applications to control and computations p 1115 N95-18992
Development of laser-ion beam photodissociation methods
[DE95-002800] p 977 N95-19840
TEXAS CHRISTIAN UNIV., FORT WORTH, TX.
Design of high pressure waterjet nozzles
p 1031 N95-18996
TEXAS TECHNOLOGICAL UNIV., LUBBOCK, TX.
Experiments with the Mesoscale Atmospheric Simulation System (MASS) using the synthetic relative humidity p 1073 N95-18172
A comparison of optical rain gauge and radar data from TOGA/COARE p 1069 N95-18207
Locally connected adaptive Gabor filter for real-time motion compensation
[AD-A285726] p 1009 N95-18485
TEXAS UNIV., AUSTIN, TX.
Laser wakefield excitation and measurement on a femtosecond time scale: Theory and experiment
[DE94-019198] p 1129 N95-17976
Fusion of multiple sensing modalities for machine vision
[AD-A284762] p 1091 N95-18086
Elemental fluorine based syntheses of pentafluoro phenly and other aromatic perfluoropolyether polymers
[AD-A284102] p 984 N95-18402
Pure-rotational emission from molecular hydrogen in OMC-1 p 1179 N95-18500
Local spatio-temporal analysis in vision systems
[AD-A284162] p 1140 N95-18509
Optimal transfer and swing-by orbits in the two- and three-body problems p 961 N95-18900
A boundary element method for two dimensional linear elastic fracture analysis p 1045 N95-18917
Study of alpha physics related to ITER Project
[DE94-017329] p 1133 N95-19078
Establishment of an Institute for Fusion Studies
[DE94-017330] p 1145 N95-19079
Ion orbit loss and the poloidal electric field in a tokamak
[DE94-016860] p 1145 N95-19092
CLIPS++: Embedding CLIPS into C++
p 1101 N95-19630
TEXAS UNIV., EL PASO, TX.
A study of gas flow pattern, undercutting and torch modification in variable polarity plasma arc welding
[NASA-CR-196537] p 1040 N95-18056
TEXAS UNIV., SAN ANTONIO, TX.
Character selecting advisor for a role-playing game
p 1106 N95-19758
TEXTRON BELL HELICOPTER, FORT WORTH, TX.
Aircraft fatigue and crack growth considering loads by structural component p 939 N95-19497
THERMO ELECTRON TECHNOLOGIES CORP., SAN DIEGO, CA.
Atomic line filter for SDI applications
[AD-A284125] p 1139 N95-18409
TOKYO UNIV. (JAPAN).
Constraints on chondrule and CAI origins from vapor-liquid-solid experiments p 1190 N95 19317
Heating during solar nebula formation and Mg isotopic fractionation in precursor grains of CAIs and chondrules
p 1191 N95-19326
TOKYO UNIV., SAGAMIHARA (JAPAN).
Laboratory simulation of intact capture of cometary and asteroidal dust particles in ISAS p 962 N95-19183
Scientific objectives of the primitive body sample return missions: An approach from the light-induced effect on water vapor p 961 N95-19191
TORANAGA TECHNOLOGIES, INC., CARLSBAD, CA.
Polymer based materials for additive processing of high temperature electronics packaging
[AD-A285962] p 988 N95-19745
TRINITY COLL., DUBLIN (IRELAND).
The circumplanetary nebular environment: A possible source region for chondrules p 1191 N95-19325
TSENTRALNI AEROGIDRODINAMICHESKII INST., MOSCOW (USSR).
The traditional and new methods of accounting for the factors distorting the flow over a model in large transonic wind tunnels p 1025 N95-19275
TURBINE SUPPORT EUROPA, TILBURG (NETHERLANDS).
High velocity oxygen fuel spraying of erosion and wear resistant coatings on jet engine parts
p 954 N95-19680
TURBOMECA S.A. - BREVETS SZYDLOWSKI, BORDES (FRANCE).
Multilayer anti-erosion coatings p 954 N95-19679
TUSKEGEE INST., AL.
Rack Insertion End Effector (RIEE) guidance
p 1043 N95-18178
Error coding simulations in C p 963 N95-18998

U

UNION COLL., SCHENECTADY, NY.
Foreign body impact event damage formation in composite structures p 972 N95-18973
UNISYS CORP., RESTON, VA.
Portable, Reusable, Integrated Software Modules (PRISM) documentation library model document release 1.0: Central Archive for Reusable Defense Software (CARDS)
[AD-A284567] p 1095 N95-18030
Library capability demonstration. Central Archive for Reusable Defense Software (CARDS)
[AD-A284568] p 1095 N95-18031
Library capability demonstration. Central Archive for Reusable Defense Software (CARDS)
[AD-A284569] p 1095 N95-18032
Library Development Handbook. Central Archive for Reusable Defense Software (CARDS)
[AD-A284570] p 1095 N95-18033
Library capability demonstration. Central Archive for Reusable Defense Software (CARDS)
[AD-A284572] p 1095 N95-18034
Technical concept document. Central Archive for Reusable Defense Software (CARDS)
[AD-A284430] p 1096 N95-18343
Library operations policies and procedures. Volume 2: Central Archive for Reusable Defense Software (CARDS)
[AD-A284431] p 1096 N95-18344
Engineer's handbook. Central Archive for Reusable Defense Software (CARDS)
[AD-A284341] p 1097 N95-18419
Acquisition handbook: Update. Comprehensive Approach to Reusable Defensive Software (CARDS)
[AD-A284342] p 1097 N95-18420
Training plan. Central Archive for Reusable Defense Software (CARDS)
[AD-A284343] p 1097 N95-18421
Franchise plan. Central Archive for Reusable Defense Software (CARDS)
[AD-A284344] p 1097 N95-18422
Library user's guide. Comprehensive Approach to Reusable Defensive Software (CARDS)
[AD-A284345] p 1097 N95-18423
Portable, Reusable, Integrated Software Modules (PRISM) documentation library version description document release 1.0. Central Archive for Reusable Defense Software (CARDS)
[AD-A284571] p 1097 N95-18447
Metrics concept report. Central Archive for Reusable Defense Software (CARDS)
[AD-A284573] p 1097 N95-18449
Library capability demonstration. Central Archive for Reusable Defense Software (CARDS)
[AD-A284574] p 1098 N95-18450
Software Technology for Adaptable, Reliable Systems (STARS). Software architecture seminar report: Central Archive for Reusable Defense Software (CARDS)
[AD-A284668] p 1100 N95-19106
UNITED TECHNOLOGIES RESEARCH CENTER, EAST HARTFORD, CT.
Unsteady aerodynamic analyses for turbomachinery aeroelastic predictions p 949 N95-19381
UNIVERSIDAD AUTONOMA DEL ESTADO DE MEXICO, TOLUCA.
Obtention of cationic polymeric membranes by radiation-induced grafting method
[DE94-629193] p 983 N95-17942
Study of the effect of ionizing radiation on the structure of natural rubber latex by positron annihilation technique
[DE94-631466] p 975 N95-19550
UNIVERSITY OF CENTRAL FLORIDA, ORLANDO, FL.
NASA/ASEE Summer Faculty Fellowship Program. 1994 research reports
[NASA-CR-197448] p 1157 N95-18166
Automated path planning of the Payload Inspection and Processing System p 1043 N95-18169
Knowledge based translation and problem solving in an intelligent individualized instruction system
p 1105 N95-19753
UNIVERSITY OF SOUTH FLORIDA, SAINT PETERSBURG, FL.
Visible-infrared remote-sensing model and applications for ocean waters
[NASA-CR-197602] p 1051 N95-18739
UNIVERSITY OF SOUTH FLORIDA, TAMPA, FL.
PCLIPS: Parallel CLIPS p 1107 N95-19764

UNIVERSITY OF SOUTHERN CALIFORNIA, LOS ANGELES, CA.
Hypervelocity air flows with finite rate chemistry
[AD-A284727] p 931 N95-19109
Microstructure and crystal defects in perovskite crystals with A-site cation ordering
[AD-A284261] p 1153 N95-19713
UNIVERSITY OF SOUTHERN CALIFORNIA, MARINA DEL REY, CA.
Evaluating the trade-offs in partial-order planning algorithms
[AD-A285876] p 1115 N95-19599
Zoned Analog Personal Teleconferencing (ZAPT)
[AD-A285877] p 1004 N95-19600
Multi-method planning
[AD-A285878] p 1115 N95-19601
Cooperating agents for information retrieval
[AD-A285887] p 1176 N95-19604
Generating parallel execution plans with a partial order planner
[AD-A285888] p 1111 N95-19605
AUTO: Automatic script generation system
[AD-A285897] p 1012 N95-19606
UNIVERSITY OF SOUTHERN ILLINOIS, CARBONDALE, IL.
Composite structures for magnetosphere imager spacecraft p 966 N95-18976
UNIVERSITY OF THE PACIFIC, STOCKTON, CA.
PRISM project optical instrument
p 1143 N95-19009
UNIVERSITY OF WESTERN CAROLINA, CULLOWHEE, NC.
A technique for determining cloud free versus cloud contaminated pixels in satellite imagery
p 1052 N95-19016
UNIVERSITY OF WESTERN KENTUCKY, BOWLING GREEN, KY.
Growth of thin films of dicyanovinylanisole on quartz and teflon-coated quartz by physical vapor transport
p 989 N95-19000
UNIVERSITY OF WESTERN MICHIGAN, KALAMAZOO, MI.
Correlated charge-changing ion-atom collisions
[DE94-017355] p 1132 N95-18874
UTAH UNIV., SALT LAKE CITY, UT.
Modeling of cloud and radiation processes for large-scale clouds and tropical anvils
[AD-A284212] p 1067 N95-17955
Microstructurally based variations on the dwell fatgue life of titanium alloy IMI 834 p 938 N95-19489

V

VANDERBILT UNIV., NASHVILLE, TN.
Lean spacecraft avionics trade study
p 966 N95-18994
VICTORIA UNIV. (BRITISH COLUMBIA).
A new stochastic systems approach to structural integrity p 935 N95-19474
VIRGINIA COMMONWEALTH UNIV., RICHMOND, VA.
Enhancement of fluorescence detection in chromatographic methods by computer analysis of second order data
[DE94-014682] p 973 N95-17966
VIRGINIA POLYTECHNIC INST. AND STATE UNIV., BLACKSBURG, VA.
Compression strength of composite primary structural components
[NASA-CR-197554] p 1044 N95-18388
On stationary and nonstationary fatigue load modeling using autoregressive moving average (ARMA) models
p 1046 N95-18919
VIRGINIA UNIV., CHARLOTTESVILLE, VA.
Improved filtration materials and modeling
[AD-A284684] p 1091 N95-18531
Dependence of medium-range forecast error on patterns in the initial state p 1072 N95-18732
Optimization of layered metal matrix composite cylinders p 970 N95-18920
Synthesis and structural properties of new metallic phases exhibiting non-crystallographic symmetries
[AD-A284882] p 982 N95-19743
Second International Semiconductor Device Research Symposium (ISDRS-1993)
[AD-A279221] p 1013 N95-19849
VIRGINIA UNIV. HOSPITAL, CHARLOTTESVILLE, VA.
An optical study of compact steep spectrum radio sources p 1179 N95-18498
VON KARMAN INST. FOR FLUID DYNAMICS, RHODE-SAINT-GENESE (BELGIUM).
Particle Image Velocimetry: Principles, current applications and future prospects p 1021 N95-19253
Improvement and validation of an LDV system to perform measurements in laminar supersonic flows
p 1021 N95-19256
Aerodynamic investigation of the flow field in a 180 deg turn channel with sharp bend p 1021 N95-19257

W

WAKE FOREST UNIV., WINSTON-SALEM, NC.
Enhancements to the KATE model-based reasoning system p 1115 N95-18183
WARSAW TECHNICAL UNIV. (POLAND).
MIKON 94. International Microwave Conference. Invited papers, volume 3
[AD-A284353] p 1008 N95-18338
MIKON 94. International Microwave Conference. Volume 1: Conference proceedings
[AD-A284351] p 1009 N95-18425
MIKON 94. International Microwave Conference. Conference proceedings, volume 2
[AD-A284352] p 1009 N95-18426
WASHINGTON STATE UNIV., PULLMAN, WA.
Polymer fibers for nonlinear optics
[AD-A284216] p 983 N95-17957
UV laser-surface interactions relevant to analytic spectroscopy of wide band gap materials
[DE94-016180] p 1037 N95-18349
UV laser-surface interactions relevant to analytic spectroscopy of wide band gap materials
[DE94-016181] p 1037 N95-18350
Heterogeneous nucleation of calcium oxalate on native oxide surfaces
[DE94-018725] p 986 N95-18648
WASHINGTON UNIV., SAINT LOUIS, MO.
Influence of high pressure hydrogen environment on creep deformation of Mo-Re, Haynes 188, and NARloy-Z alloys
[NASA-CR-197572] p 978 N95-18046
Design and fabrication of N x N optical couplers based on organic polymer optical waveguides
[AD-A285530] p 1138 N95-18100
Penetration of multiple thin films in micrometeorite capture cells p 1036 N95-19192
Producing chondrules by recycling and volatile loss
p 1186 N95-19290
Theory and applications of the phi transform wavelets
[AD-A279943] p 1119 N95-19869
WASHINGTON UNIV., SEATTLE, WA.
Two and three dimensional magnetotelluric inversion
[DE94-014820] p 1063 N95-17967
Time spread and frequency coherence in acoustic forward scattering from the sea surface
[AD-A284736] p 1123 N95-18083
Exact m(sub quark) does not equal 0 condensates in QCD(1+1)(N(sub C) yields infinity
[DE94-016581] p 1131 N95-18554
Family symmetries and proton decay
[DE94-017575] p 1133 N95-19245
Comment on the preprint Neutrino Flavor Evolution Near a Supernova's Core (Astro-Ph 9405008) by J. Pantaleone
[DE94-017576] p 1198 N95-19283
Limits on CP nonconserving interactions from electric dipole moments
[DE94-018582] p 1134 N95-19705
WEST COAST INDUSTRIES, INC., SEATTLE, WA.
Split mandrel versus split sleeve coldworking: Dual methods for extending the fatigue life of metal structures
p 940 N95-19500
WEST VIRGINIA UNIV., MORGANTOWN, VA.
Determination of stability and control derivatives from the NASA F/A-18 HARV from flight data using the maximum likelihood method
[NASA-CR-197320] p 958 N95-19576
WESTINGHOUSE HANFORD CO., RICHLAND, WA.
Acceptance/operational test procedure 101-SY tank camera purge system and in tank color camera video imaging system
[DE95-000344] p 1035 N95-19553
WICHITA STATE UNIV., WICHITA, KS.
Microstructural analysis of cracks generated during welding of 2195 aluminum-lithium alloy
p 982 N95-19007
WICKERSHEIMER ENGINEERS, INC., CHAMPAIGN, IL.
Tutorial guide: Computer-Aided Structural Modeling (CASM), version 5.00
[AD-A280147] p 1108 N95-19821
WISCONSIN UNIV., MADISON, WI.
High-power microwave transmission and mode conversion program
[DE94-017046] p 1002 N95-19097
Spectroscopy and dynamics of vibrationally excited molecules
[AD-A285874] p 1134 N95-19597
Direct dimer-by-dimer identification of clean and monohydride dimers on the Si(001) surface by scanning tunneling microscopy
[AD-A280158] p 976 N95-19824
An atomic-resolution study of overlayer formation and interfacial mixing in the interaction of phosphorus with Si(001)
[AD-A280159] p 976 N95-19825
WISCONSIN UNIV., MILWAUKEE, WI.
Rewetting of monogroove heat pipe in Space Station radiators
[NASA-CR-197579] p 1014 N95-18092
Distributed methods for controlling multiple mobile robots
[AD-A283919] p 1113 N95-18157
Fair Petri nets and structural induction for rings of processes
[AD-A283920] p 1110 N95-18158
A practical algorithm for integer sorting on a mesh-connected computer (preliminary version)
[AD-A283921] p 1110 N95-18159
Distributed algorithms for controlling multiple mobile robots
[AD-A283975] p 1114 N95-18889
WISCONSIN UNIV., WHITEWATER, WI.
Two space scatterer formalism calculation of bulk parameters of thunderclouds p 1073 N95-19001
WRIGHT LAB., WRIGHT-PATTERSON AFB, OH.
Error measurements in an Acousto-Optic Tunable Filter-Fiber Bragg Grating Sensor System
[AD-A283912] p 1139 N95-18154
Universal wind tunnel data acquisition and reduction software
[AD-A283897] p 1096 N95-18365
Pressure measurements on an F/A-18 twin vertical tail in buffeting flow. Volume 4, part 2: Buffet cross spectral densities
[AD-A285555] p 957 N95-18641
Machine learning: A comparative study of pattern theory and C4.5
[AD-A285582] p 1115 N95-19118
Weapons bay acoustic environment
p 1125 N95-19146
High-temperature acoustic test facilities and methods
p 1125 N95-19149
Nonlinear dynamic response of aircraft structures to acoustic excitation p 946 N95-19151
Modelling structurally damaging twin-jet screech
p 946 N95-19154
Thermo-acoustic fatigue design for hypersonic vehicle skin panels p 1047 N95-19161
Determination of solid/porous wall boundary conditions from wind tunnel data for computational fluid dynamics codes p 1023 N95-19266
Proceedings of the USAF Structural Integrity Program Conference
[AD-A285684] p 945 N95-19517
WYOMING UNIV., LARAMIE, WY.
Exotic atoms: Muonic atoms into vacuum from solid hydrogen
[DE94-018255] p 1129 N95-18124

Y

YALE UNIV., NEW HAVEN, CT.
A parallel processing hypothesis for short-term and long-term memory in Aplysia
[AD-A284101] p 1088 N95-18401
High-order corrected trapezoidal rules for singular functions
[AD-A284269] p 1119 N95-19735
YALIF (GUY U.), MA.
The Computer Aided Aircraft-design Package (CAAP)
p 1106 N95-19759

Typical Contract Number Index Listing

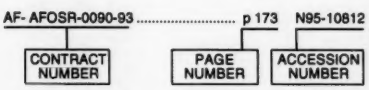

Listings in this index are arranged alphanumerically by contract number. Under each contract number the accession numbers denoting documents that have been produced as a result of research done under that contract are arranged in ascending order. The page number helps to locate the citation in the abstract section. The accession number denotes the number by which the citation is identified.

AF PROJ. R381 ..... p 1008 N95-18103
AF PROJ. 0100 ..... p 1115 N95-19118
AF PROJ. 0702 ..... p 989 N95-19861
AF PROJ. 1926 ..... p 944 N95-18677
AF PROJ. 2001 ..... p 1139 N95-18154
AF PROJ. 2303 ..... p 1129 N95-18062
AF PROJ. 2304 ..... p 995 N95-18066
p 995 N95-18116
AF PROJ. 2307 ..... p 1018 N95-18469
AF PROJ. 2401 ..... p 928 N95-18380
p 957 N95-18641
AF PROJ. 2404 ..... p 1096 N95-18365
p 943 N95-18483
AF PROJ. 2418 ..... p 945 N95-19517
AF PROJ. 3054 ..... p 1142 N95-19862
AF PROJ. 3647 ..... p 1120 N95-18020
AF PROJ. 4600 ..... p 1138 N95-18067
p 1138 N95-18100
p 1138 N95-18102
p 1139 N95-18104
AF PROJ. 5581 ..... p 1109 N95-18106
p 1110 N95-18454
AF PROJ. 6670 ..... p 1049 N95-18035
AF PROJ. 7184 ..... p 1088 N95-18084
AF PROJ. 7930 ..... p 1079 N95-18661
AF-AFOSR-0001-91 ..... p 1131 N95-18438
AF-AFOSR-0023-91 ..... p 1073 N95-19870
AF-AFOSR-0039-91 ..... p 1067 N95-17955
AF-AFOSR-0078-86 ..... p 1117 N95-18658
AF-AFOSR-0079-91 ..... p 985 N95-18636
AF-AFOSR-0125-91 ..... p 1150 N95-18685
AF-AFOSR-0145-91 ..... p 1154 N95-19815
AF-AFOSR-0169-91 ..... p 1093 N95-17940
AF-AFOSR-0251-91 ..... p 955 N95-19864
AF-AFOSR-0261-91 ..... p 1129 N95-18062
AF-AFOSR-0307-90 ..... p 996 N95-18411
AF-AFOSR-0323-90 ..... p 1119 N95-19869
AF-AFOSR-0465-89 ..... p 1018 N95-18469
AG PROJ. 3450 ..... p 1136 N95-18147
ARB-A132-168 ..... p 1061 N95-19582
ARPA ORDER 4864 ..... p 1111 N95-18892
ARPA ORDER 5940 ..... p 1154 N95-19817
ARPA ORDER 7330 ..... p 1093 N95-18659
ARPA ORDER 8162 ..... p 1013 N95-19865
ARPA ORDER 8313 ..... p 1099 N95-18676
ARPA ORDER 8459 ..... p 1140 N95-18478
p 1140 N95-18480
ARPA ORDER 8557 ..... p 1142 N95-19732
CEC-AERO-0027-C ..... p 1021 N95-19256
CEC-ERB-CHBI-CT-92049 ..... p 1021 N95-19256
DA PROJ. M00-96 ..... p 1078 N95-18138
p 1089 N95-18414
DA PROJ. 1L1-61102-AH-43 ..... p 995 N95-18136
p 1033 N95-18620
p 930 N95-18670
DA PROJ. 1L1-61102-AH-45 ..... p 1041 N95-18541
p 1043 N95-19567
DA PROJ. 1L1-61102-AH-52 ..... p 928 N95-18340
DA PROJ. 1L1-62211-A-47-A ..... p 1042 N95-18935
p 1042 N95-19125
DA PROJ. 1L1-62618-AH-80 ..... p 942 N95-18381
p 929 N95-18611
DA PROJ. 1L1-62705-AH-94 ..... p 1012 N95-19519
DA PROJ. 1L1-62786-D-283 ..... p 928 N95-18340
DA PROJ. 1O1-62622-A-553 ..... p 974 N95-19170
DAAA08-87-C-0096 ..... p 1043 N95-19593
DAAA15-90-C-0012 ..... p 1091 N95-18531
DAAB07-94-C-H601 ..... p 1000 N95-18727
DAAE07-90-C-R030 ..... p 1043 N95-19809
DAAK70-92-C-0059 ..... p 989 N95-19826
DAAL03-86-K-0171 ..... p 1117 N95-18658
DAAL03-89-K-0119 ..... p 1153 N95-19697
DAAL03-91-C-0034 ..... p 974 N95-19170
DAAL03-91-G-0040 ..... p 988 N95-19696
DAAL03-91-G-0050 ..... p 1091 N95-18086
DAAL03-91-G-0152 ..... p 1153 N95-19738
DAAL03-91-G-0161 ..... p 1013 N95-19687
DAAL03-91-G-0333 ..... p 985 N95-18442
DAAL04-91-C-0073 ..... p 979 N95-18948
DABT63-91-C-0001 ..... p 1004 N95-19600
DABT63-92-0042 ..... p 1101 N95-19630
DABT63-93-C-0038 ..... p 1117 N95-18658
DACA39-86-C-0024 ..... p 1108 N95-19821
DACA76-89-C-0019 ..... p 1113 N95-18057
DACA76-92-C-0009 ..... p 1140 N95-18478
p 1140 N95-18480
DAJA45-90-C-0026 ..... p 1139 N95-18404
DAJA45-92-C-0032 ..... p 1119 N95-19819
p 1119 N95-19820
DAJA45-93-C-0035 ..... p 1066 N95-19387
DAMD17-93-C-3005 ..... p 1078 N95-17998
DASG60-89-C-0142 ..... p 996 N95-18386
DE-AC02-76CH-00016 ..... p 1150 N95-19091
p 1038 N95-19243
p 1055 N95-19858
DE-AC02-76CH-03000 ..... p 1133 N95-19077
p 1137 N95-19561
DE-AC02-76CH-03073 ..... p 1135 N95-19835
DE-AC02-76ER-03069 ..... p 1143 N95-17965
DE-AC02-93ER-40105 ..... p 1135 N95-19706
DE-AC03-76SF-00098 ..... p 1137 N95-18965
p 1007 N95-17961
p 1148 N95-18122
p 1036 N95-18123
p 1197 N95-18351
p 979 N95-19093
p 1151 N95-19569
p 1194 N95-19570
p 1137 N95-19584
p 1152 N95-19585
p 1152 N95-19586
p 1134 N95-19587
p 1152 N95-19615
p 975 N95-19616
p 1178 N95-19617
p 976 N95-19836
DE-AC03-76SF-00515 ..... p 1129 N95-18049
p 1138 N95-19841
DE-AC03-86SF-16298 ..... p 1135 N95-18146
p 1136 N95-18147
DE-AC03-89ER-51114 ..... p 1143 N95-18119
p 1146 N95-19378
p 1146 N95-19379
DE-AC04-76DP-00613 ..... p 1012 N95-19230
p 1012 N95-19231
p 981 N95-19707
DE-AC04-94AL-85000 ..... p 1112 N95-17948
p 977 N95-17968
p 1008 N95-18143
p 1129 N95-18144
p 1114 N95-18649
p 1149 N95-18650
p 986 N95-18651
p 1098 N95-18652
p 1120 N95-18653
p 1174 N95-18872
p 1174 N95-18873
p 1118 N95-18896
p 1137 N95-18897
p 990 N95-19100
p 1133 N95-19199
p 1145 N95-19201
p 1122 N95-19234
p 1151 N95-19235
p 1012 N95-19240
p 980 N95-19395
p 1004 N95-19555
p 988 N95-19558
p 975 N95-19559
p 971 N95-19579
p 1013 N95-19842
p 1055 N95-19859
p 1013 N95-19872
p 1055 N95-19873
p 1176 N95-19876
DE-AC05-76OR-00033 ..... p 1061 N95-19556
DE-AC05-84OR-21400 ..... p 1116 N95-18120
p 978 N95-18121
p 1122 N95-18127
p 978 N95-18128
p 1109 N95-18129
p 1116 N95-18131
p 1058 N95-18389
p 1051 N95-18556
p 1144 N95-18557
p 999 N95-18558
p 1059 N95-18666
p 991 N95-19076
p 1133 N95-19228
p 1133 N95-19232
p 1034 N95-19233
p 1080 N95-19244
p 987 N95-19399
p 980 N95-19400
p 1061 N95-19556
p 1134 N95-19557
p 981 N95-19568
p 981 N95-19723
p 1112 N95-19831
DE-AC05-84OS-21400 ..... p 968 N95-19877
DE-AC06-76RL-01830 ..... p 1049 N95-18145
p 984 N95-18348
p 1076 N95-18371
p 986 N95-18648
p 1176 N95-19589
p 1134 N95-19590
p 1054 N95-19591
p 1153 N95-19724
DE-AC06-87RL-10930 ..... p 1035 N95-19553
DE-AC07-76ID-01570 ..... p 989 N95-19861
DE-AC08-93NV-11265 ..... p 1059 N95-18647
DE-AC09-76SR-00001 ..... p 980 N95-19401
DE-AC12-76SN-00052 ..... p 979 N95-18934
DE-AC22-92PC-92112 ..... p 976 N95-19785
DE-AC36-83CH-10093 ..... p 1056 N95-17943
p 1056 N95-17944
p 1052 N95-17945
p 1053 N95-18463
p 929 N95-18645
p 929 N95-18646
p 1151 N95-19541
p 1054 N95-19832
p 1054 N95-19854
p 1054 N95-19855
p 1055 N95-19856
p 1055 N95-19857
p 1056 N95-19878
p 1056 N95-19880
p 1014 N95-19881
p 1056 N95-19882
DE-AI02-93ER-61578 ..... p 1059 N95-18665
DE-AI05-86ER-60447 ..... p 981 N95-19703
DE-FC02-94ER-40818 ..... p 1135 N95-19706
DE-FC07-91ID-13074 ..... p 1040 N95-17995
DE-FG02-85CE-40772 ..... p 974 N95-18637
DE-FG02-85ER-52122 ..... p 1002 N95-19097
DE-FG02-85ER-53194 ..... p 1143 N95-18353
DE-FG02-86ER-60397 ..... p 1057 N95-18022
DE-FG02-87ER-13778 ..... p 1132 N95-18874
DE-FG02-87ER-40333 ..... p 1129 N95-18124
DE-FG02-87ER-45328 ..... p 979 N95-18358
DE-FG02-88ER-13929 ..... p 1030 N95-19578
DE-FG02-88ER-45354 ..... p 981 N95-19610
DE-FG02-88ER-45367 ..... p 980 N95-19111
DE-FG02-89ER-14079 ..... p 1066 N95-19560
DE-FG02-91ER-45461 ..... p 987 N95-19095
DE-FG02-92ER-14270 ..... p 1015 N95-18188

	p 1017	N95-18397
DE-FG02-92ER-14283	p 1135	N95-19787
DE-FG02-92ER-25123	p 1119	N95-19609
DE-FG02-92ER-54181	p 985	N95-18638
DE-FG02-92ER-61447	p 1062	N95-19879
DE-FG02-93ER-25158	p 1093	N95-19875
DE-FG02-93ER-61666	p 1060	N95-19112
DE-FG03-88ER-40397	p 1132	N95-18644
DE-FG03-90ER-54081	p 1146	N95-19378
DE-FG05-80ET-53088	p 1133	N95-19078
	p 1145	N95-19079
	p 1145	N95-19092
	p 1147	N95-19837
DE-FG05-85ER-13434	p 977	N95-19840
DE-FG05-86ER-13591	p 984	N95-18355
DE-FG05-86ER-13633	p 977	N95-19839
DE-FG05-88ER-13833	p 973	N95-17966
DE-FG05-88ER-13958	p 1135	N95-19787
DE-FG05-92ER-40739	p 1129	N95-17976
DE-FG05-92ER-40748	p 1136	N95-18893
DE-FG05-92ER-45477	p 1134	N95-19562
DE-FG06-89ER-75522	p 986	N95-18648
DE-FG06-90ER-40561	p 1131	N95-18554
	p 1133	N95-19245
	p 1198	N95-19283
	p 1134	N95-19705
	p 1135	N95-19706
DE-FG06-92ER-14231	p 1063	N95-17967
DE-FG06-92ER-14252	p 1037	N95-18349
	p 1037	N95-18350
DE-FG22-93PC-93204	p 1054	N95-19554
DE-FG22-93PC-93219	p 1053	N95-18894
DE-FG42-93R2-15556	p 988	N95-19580
DE-GM07-87ID-11026	p 989	N95-19861
DEN3-329	p 1040	N95-18041
DNA001-88-C-0189	p 1131	N95-18474
DNA001-90-C-0080	p 1148	N95-17960
DTFA01-91-Z-02036	p 1070	N95-18384
DTFA02-90-C-90125	p 1080	N95-19384
	p 1080	N95-19385
DTFA03-89-C-00043	p 940	N95-19805
DTFA03-92-Z-00018	p 939	N95-19494
EPA-R-816496	p 1056	N95-17937
EPA-68-D1-0143	p 1061	N95-19403
FMI PROJ. NAS-9614	p 1015	N95-18111
F04611-90-K-0054	p 1144	N95-18888
F08635-93-C-0104	p 1058	N95-18140
F09603-85-G-3104	p 937	N95-19487
F19628-90-C-0002	p 1004	N95-19565
	p 1004	N95-19594
F19628-90-C-0003	p 1096	N95-18364
	p 1100	N95-19545
F19628-90-C-0028	p 1010	N95-18662
F19628-90-C-0118	p 1064	N95-18452
F19628-90-K-0037	p 1008	N95-18103
F19628-91-C-0093	p 1068	N95-18141
F19628-91-C-0168	p 1099	N95-18676
F19628-93-C-0130	p 1095	N95-18030
	p 1095	N95-18031
	p 1095	N95-18032
	p 1095	N95-18033
	p 1095	N95-18034
	p 1096	N95-18343
	p 1096	N95-18344
	p 1097	N95-18419
	p 1097	N95-18420
	p 1097	N95-18421
	p 1097	N95-18422
	p 1097	N95-18423
	p 1097	N95-18447
	p 1097	N95-18449
	p 1098	N95-18450
	p 1100	N95-19106
F19628-93-K-0012	p 1066	N95-19105
F19628-93-K-0033	p 1049	N95-17971
F19628-94-C-0001	p 1005	N95-19744
F29601-84-C-0080	p 992	N95-18684
F30602-90-D-0105	p 972	N95-19702
F30602-91-C-0081	p 1115	N95-19599
	p 1176	N95-19604
	p 1111	N95-19605
F30602-91-D-0001	p 995	N95-18066
F30602-92-C-0018	p 1003	N95-19516
F30602-92-C-0051	p 1115	N95-19512
F30602-92-C-0062	p 1111	N95-19524
F30602-92-C-0074	p 1111	N95-19513
F30602-92-C-0108	p 1109	N95-18106
F30602-93-C-0004	p 1138	N95-18100
F30602-93-C-0006	p 994	N95-17958
F30602-93-C-0055	p 1111	N95-19526
F30602-93-C-0068	p 1138	N95-18102
F30602-93-D-0104	p 1139	N95-18104
F33615-84-C-3627	p 947	N95-18164
F33615-87-C-3227	p 1031	N95-19153
F33615-89-D-0604	p 1087	N95-19714
F33615-90-C-2032	p 1130	N95-18334
F33615-90-C-3211	p 1046	N95-19522
F33615-90-C-5009	p 1009	N95-18418
F33615-90-D-0606	p 1079	N95-18661
F33615-91-C-2142	p 1010	N95-18660
F33615-92-C-3400	p 942	N95-18162
	p 944	N95-18677
F33617-91-C-3004	p 943	N95-18483
F34601-90-C-1336	p 937	N95-19482
F49620-89-C-0049	p 1113	N95-18441
F49620-90-C-0090	p 1154	N95-19817
F49620-91-C-0007	p 1154	N95-19816
F49620-91-C-0013	p 1037	N95-18408
F49620-91-C-0016	p 1155	N95-18009
F49620-91-C-0050	p 1079	N95-18518
F49620-91-C-0083	p 1097	N95-18437
F49620-92-J-0056	p 994	N95-17954
F49620-92-J-0073	p 1134	N95-19597
F49620-92-J-0100	p 1117	N95-18482
F49620-92-J-0104	p 984	N95-18402
F49620-92-J-0119	p 1090	N95-19602
F49620-92-J-0151	p 1092	N95-17939
F49620-92-J-0222	p 974	N95-18412
F49620-92-J-0227	p 973	N95-18410
F49620-92-J-0296	p 969	N95-17941
F49620-92-J-0322	p 985	N95-18513
F49620-92-J-0362	p 1087	N95-19698
F49620-92-J-0379	p 987	N95-19544
F49620-92-J-0400	p 1035	N95-19871
F49620-92-J-0430	p 1107	N95-19762
F49620-92-J-0437	p 1090	N95-19740
F49620-92-J-0506	p 1079	N95-18626
F49620-93-C-0003	p 1036	N95-17956
F49620-93-C-0022	p 1151	N95-19511
F49620-93-C-0053	p 988	N95-19614
F49620-93-1-0129	p 974	N95-18514
F49620-93-1-0136	p 1079	N95-18656
F49620-93-1-0175	p 987	N95-19520
F49620-93-1-0178	p 985	N95-18510
F49620-93-1-0202	p 987	N95-19102
F49620-93-1-0255	p 983	N95-17957
F49620-93-1-0261	p 1089	N95-18403
F49620-93-1-0271	p 1003	N95-19510
F49620-93-1-0273	p 1088	N95-18401
F49620-93-1-0286	p 1002	N95-19103
F49620-93-1-0302	p 1076	N95-18439
F49620-93-1-0307	p 1140	N95-18509
F49620-93-1-0337	p 1078	N95-18515
F49620-93-1-0373	p 931	N95-19109
F49620-93-1-0377	p 935	N95-19476
F49620-93-1-0402	p 1078	N95-18400
F49620-93-1-0434	p 1078	N95-18512
F49620-93-1-0442	p 973	N95-17975
F49620-93-1-0569	p 1107	N95-19762
F49620-94-C-0074	p 988	N95-19745
F49620-94-1-0009	p 1121	N95-19104
GA PROJ. 3450	p 1135	N95-18146
GRI-5089-260-1824	p 973	N95-17982
GRI-5091-260-2118	p 1122	N95-17983
JPL-959193	p 1195	N95-17979
JPL-959531	p 966	N95-19196
KBN-3-0687-91-01	p 1119	N95-19819
MDA903-89-C-0003	p 1037	N95-18382
MDA972-91-C-0029	p 1013	N95-19865
MDA972-92-C-0053	p 1142	N95-19732
MDA972-92-J-1018	p 1108	N95-19803
	p 1108	N95-19813
MDA972-93-C-0057	p 1142	N95-19088
MIPR-1223	p 1060	N95-18683
NAGW-1603	p 1036	N95-19192
NAGW-1625	p 1065	N95-19032
NAGW-1751	p 974	N95-18744
NAGW-2023	p 1197	N95-18464
NAGW-2158	p 1062	N95-19779
NAGW-2381	p 1180	N95-18746
	p 1180	N95-18964
	p 1137	N95-18965
	p 1121	N95-19030
	p 1180	N95-19031
NAGW-2442	p 1194	N95-18579
NAGW-2547	p 1196	N95-19034
NAGW-2923	p 1198	N95-18747
	p 1156	N95-18949
	p 1180	N95-18966
	p 1156	N95-19037
	p 1156	N95-19340
	p 1193	N95-19341
	p 1121	N95-19348
	p 1157	N95-19358
	p 1157	N95-19363
NAGW-2969	p 1196	N95-19034
NAGW-3040	p 1188	N95-19305
NAGW-3078	p 966	N95-19196
NAGW-3429	p 1196	N95-19034
NAGW-3437	p 1052	N95-18952
NAGW-3519	p 1192	N95-19328
NAGW-925	p 1052	N95-19126
NAG1-1184	p 935	N95-19473
NAG1-1311	p 938	N95-19490
NAG1-1478	p 1005	N95-19796
NAG1-1489	p 939	N95-19498
NAG1-1571	p 942	N95-18090
NAG1-537	p 1044	N95-18388
NAG2-593	p 1110	N95-18532
NAG2-865	p 978	N95-18046
NAG3-1223	p 972	N95-19782
NAG3-1257	p 990	N95-18082
NAG3-1316	p 1041	N95-18541
	p 1043	N95-19567
NAG3-1346	p 1136	N95-18217
NAG3-1381	p 1014	N95-18092
NAG3-1384	p 1195	N95-17980
NAG3-876	p 982	N95-19792
NAG3-944	p 964	N95-18495
NAG3-950	p 970	N95-18940
NAG5-1548	p 1064	N95-18476
NAG5-1810	p 1066	N95-19129
NAG5-619	p 1177	N95-17981
NAG8-253	p 1004	N95-19547
NAG8-936	p 967	N95-19566
NAG9-701	p 1194	N95-19575
NASA ORDER C-32007-M	p 991	N95-18913
NASA ORDER L-58104-D	p 1109	N95-18055
NASA ORDER T-8495-S	p 1181	N95-19177
NASW-4574	p 1180	N95-19172
	p 1186	N95-19289
NASW-4627	p 1194	N95-19134
NASW-4814	p 1195	N95-18376
NASW-4864	p 1196	N95-18954
NAS1-19000	p 964	N95-18105
NAS1-19061	p 1123	N95-18930
NAS1-19299	p 1016	N95-18193
NAS1-19372	p 964	N95-18580
NAS1-19480	p 1116	N95-18108
	p 1116	N95-18109
	p 1116	N95-18110
	p 1015	N95-18188
	p 1016	N95-18190
	p 1016	N95-18191
	p 1016	N95-18193
	p 1017	N95-18397
	p 1117	N95-18479
	p 1098	N95-18487
	p 1018	N95-18488
	p 1098	N95-18584
	p 1099	N95-18931
	p 1020	N95-18958
	p 1099	N95-19027
	p 1100	N95-19028
NAS1-19656	p 1014	N95-18042
NAS1-19708	p 970	N95-18466
NAS1-19858	p 971	N95-19043
NAS13-330	p 1075	N95-18951
	p 1105	N95-19752
NAS2-13571	p 1020	N95-18955
	p 1020	N95-18956
NAS2-13721	p 1118	N95-18736
	p 1043	N95-18737
NAS3-24631	p 927	N95-18044
NAS3-24652	p 967	N95-18195
NAS3-25266	p 1015	N95-18107
NAS3-25560	p 967	N95-18743
NAS3-25646	p 966	N95-18192
NAS3-25685	p 969	N95-18448
NAS3-25776	p 962	N95-18387
	p 1047	N95-19649
NAS3-25796	p 1034	N95-18938
	p 1034	N95-19236
NAS3-25950	p 947	N95-18133
NAS3-27186	p 958	N95-18054
	p 1015	N95-18107
	p 1016	N95-18200
	p 1017	N95-18327
	p 933	N95-18582
	p 1046	N95-19501
	p 950	N95-19651
	p 955	N95-19769
	p 1035	N95-19794
NAS5-26555	p 1196	N95-19034
NAS5-31352	p 1172	N95-18040
	p 1173	N95-18051
NAS5-31376	p 1064	N95-18444
NAS5-31716	p 1051	N95-18739
NAS5-32337	p 1172	N95-18040
	p 1173	N95-18051
NAS5-32492	p 1178	N95-18391
NAS5-32586	p 1136	N95-18370
NAS7-918	p 992	N95-18745
NAS8-38609	p 969	N95-18135
	p 1010	N95-18925
	p 1195	N95-19267
NAS8-38776	p 1068	N95-18093
NAS8-39131	p 1106	N95-19756

	p 1106	N95-19760
NAS8-39602	p 1040	N95-18056
NAS9-17900	p 1091	N95-18189
NAS9-18368	p 966	N95-19178
NAS9-18819	p 1015	N95-18111
NAS9-18873	p 966	N95-18196
NAS9-18880	p 956	N95-18567
NCA2-781	p 1121	N95-19288
NCC1-138	p 971	N95-19650
NCC2-374	p 945	N95-19130
NCC2-55	p 1023	N95-19266
NCC2-759	p 958	N95-19576
NCC2-849	p 1110	N95-18521
	p 1110	N95-18581
NCC3-218	p 970	N95-18471
NCC3-233	p 1016	N95-18200
	p 1016	N95-18212
	p 1019	N95-18898
	p 1019	N95-18941
NCC3-257	p 1105	N95-19749
NCC3-308	p 962	N95-18045
	p 962	N95-18467
NCC3-365	p 927	N95-18197
	p 927	N95-18486
NGL-05-002-105	p 1181	N95-19176
NGT-01-002-099	p 1161	N95-18967
NGT-40019	p 1136	N95-18217
NGT-60002	p 1157	N95-18166
NOAA-50-DGNW-0-00041	p 1072	N95-19407
NSF AST-90-21414	p 1198	N95-18747
	p 1156	N95-18949
	p 1180	N95-18966
	p 1156	N95-19037
	p 1156	N95-19340
	p 1193	N95-19341
	p 1121	N95-19348
	p 1157	N95-19358
	p 1157	N95-19363
NSF AST-92-18085	p 1196	N95-19034
NSF ATM-90-22385	p 1196	N95-19034
NSF ATM-92-02126	p 1065	N95-19032
NSF CCR-90-01195	p 1100	N95-19028
NSF CCR-90-04346	p 1110	N95-18158
	p 1110	N95-18159
	p 1114	N95-18889
NSF CCR-91-13170	p 1110	N95-18521
NSF CCR-91-14440	p 1117	N95-18658
NSF CCR-92-01195	p 1099	N95-18931
	p 1099	N95-19027
NSF CCR-92-10372	p 1100	N95-19028
NSF DMS-91-20877	p 1117	N95-18482
NSF DMS-93-04406	p 1019	N95-18898
NSF ECD-07068-89	p 1093	N95-18659
NSF ECS-88-15815	p 1121	N95-19288
NSF ECS-92-16450	p 1102	N95-19633
NSF IRI-90-57934	p 1140	N95-18478
	p 1140	N95-18480
NSF IRI-93-07506	p 1113	N95-18157
	p 1110	N95-18158
	p 1110	N95-18159
	p 1114	N95-18889
NSF IRI-93-10413	p 1107	N95-19762
NSF IRI-93-13993	p 1176	N95-19604
NSF MDR-91-50211	p 1089	N95-19068
NSF MSS-90-24838	p 1045	N95-18613
NSF OMR-92-12658	p 974	N95-18744
NSF OSR-92-55223	p 1198	N95-18747
	p 1156	N95-18949
	p 1180	N95-18966
	p 1156	N95-19037
	p 1156	N95-19340
	p 1121	N95-19348
	p 1157	N95-19358
NSF PHY-92-45317	p 1157	N95-19358
	p 1157	N95-19363
NSG-7129	p 1181	N95-19176
N00014-J-92-1799	p 1117	N95-18658
N00014-86-C-0780	p 1155	N95-19828
N00014-87-J-1248	p 974	N95-19066
N00014-89-C-0025	p 1017	N95-18434
N00014-89-C-0068	p 1139	N95-18409
N00014-89-J-1007	p 994	N95-18024
N00014-89-J-1320	p 1030	N95-19607
N00014-89-J-1527	p 1119	N95-19735
N00014-89-J-1545	p 1154	N95-19806
	p 1154	N95-19807
	p 1154	N95-19812
N00014-89-J-3201	p 1112	N95-19692
N00014-90-J-1030	p 1117	N95-18482
N00014-90-J-1212	p 1013	N95-19741
N00014-90-J-1340	p 1045	N95-18613
N00014-90-J-1635	p 1128	N95-19802
N00014-90-J-1786	p 1089	N95-18530
N00014-90-J-1900	p 1153	N95-19713
N00014-91-C-0007	p 983	N95-18019
N00014-91-C-0124	p 978	N95-18068
N00014-91-C-0214	p 1044	N95-18081
N00014-91-J-1096	p 1095	N95-18079
N00014-91-J-1274	p 972	N95-19814
N00014-91-J-1306	p 1112	N95-19689
N00014-91-J-1328	p 971	N95-19386
N00014-91-J-1629	p 976	N95-19824
	p 976	N95-19825
N00014-91-J-1630	p 1131	N95-18473
N00014-91-J-1710	p 969	N95-19822
	p 969	N95-19823
N00014-91-J-1716	p 966	N95-19196
N00014-91-J-1857	p 1141	N95-18682
N00014-91-J-4017	p 1064	N95-18413
N00014-91-J-4130	p 976	N95-19830
N00014-92-C-0173	p 1132	N95-18655
N00014-92-J-1243	p 1157	N95-19852
	p 1157	N95-19853
N00014-92-J-1260	p 1129	N95-17974
N00014-92-J-1274	p 1075	N95-19523
N00014-92-J-1368	p 1148	N95-18053
N00014-92-J-1510	p 1128	N95-19850
N00014-92-J-1617	p 1109	N95-18050
N00014-92-J-1763	p 1076	N95-19728
N00014-92-J-1996	p 1010	N95-18625
N00014-92-K-2015	p 1115	N95-19601
N00014-93-1-0257	p 1088	N95-18094
	p 1140	N95-18478
	p 1140	N95-18480
N00014-93-1-0860	p 1154	N95-19812
N00014-93-1-1295	p 1044	N95-18080
N00014-93-1-2004	p 1123	N95-18890
N00014-94-C-0099	p 1073	N95-19701
N00014-94-C-0120	p 1152	N95-19598
N00014-94-C-2030	p 1052	N95-18011
	p 1054	N95-19388
N00014-94-1-0072	p 974	N95-19515
N00014-94-1-0077	p 1009	N95-18485
N00014-94-1-0167	p 1013	N95-19849
N00014-94-1-0284	p 1113	N95-18157
	p 1110	N95-18158
	p 1110	N95-18159
	p 1114	N95-18889
N00014-94-1-0548	p 1139	N95-18345
N00014-94-1-0981	p 1038	N95-18642
N00014-94-1-5300	p 988	N95-19691
N00039-87-C-0251	p 1111	N95-18892
N00039-88-C-0051	p 1123	N95-18083
N00039-91-C-0072	p 1123	N95-18083
N00123-89-G-0580	p 1123	N95-18673
N61339-91-D-0001	p 1173	N95-18446
N68171-94-M-5109	p 984	N95-18339
N68171-94-M-6048	p 1018	N95-18477
PE0601152	p 997	N95-18475
PROJ. RHINO	p 1124	N95-19144
PROJ. R31-03	p 1076	N95-19818
PROJ. 194001	p 1136	N95-18370
RTOP 170-38-52	p 1196	N95-19791
RTOP 199-08-12	p 1092	N95-18569
RTOP 199-18-12-07	p 1077	N95-18734
	p 1077	N95-19140
RTOP 233-01-OA	p 1149	N95-18453
	p 1053	N95-18572
RTOP 233-01-0A	p 967	N95-18571
	p 1053	N95-18587
RTOP 233-01-01-06	p 964	N95-18580
RTOP 233-03-05	p 967	N95-18570
RTOP 235-01-08	p 1000	N95-18733
RTOP 242-70-02	p 967	N95-18195
RTOP 307-51-12-04	p 1032	N95-18194
RTOP 323-17-07	p 962	N95-18387
RTOP 323-36-02	p 992	N95-18745
RTOP 461-54-15	p 1068	N95-18201
RTOP 461-56-50	p 1068	N95-18201
RTOP 464-52-07-71	p 1058	N95-18132
RTOP 488-10-12	p 964	N95-18495
RTOP 505-59-20	p 930	N95-19041
RTOP 505-59-50-02	p 1014	N95-18042
RTOP 505-59-52-01	p 1123	N95-18930
RTOP 505-59-52	p 931	N95-19119
RTOP 505-59-53	p 1020	N95-18955
	p 1020	N95-18956
RTOP 505-59-54-02	p 1099	N95-18899
RTOP 505-62-OJ	p 1041	N95-18541
	p 1043	N95-19567
RTOP 505-62-10	p 1042	N95-18935
RTOP 505-62-20	p 955	N95-19769
RTOP 505-62-30-01	p 931	N95-19042
RTOP 505-62-36	p 1042	N95-19125
RTOP 505-62-5J	p 968	N95-19795
RTOP 505-62-50	p 1034	N95-18938
	p 1034	N95-19236
RTOP 505-62-52	p 1014	N95-18036
	p 1015	N95-18107
RTOP 505-62-82	p 1035	N95-19794
RTOP 505-63-12	p 1043	N95-18583
	p 972	N95-19782
RTOP 505-63-5A	p 969	N95-18448
	p 989	N95-19783
RTOP 505-63-5B	p 928	N95-18457
	p 970	N95-18940
	p 949	N95-19380
	p 1046	N95-19501
RTOP 505-63-50-04	p 971	N95-19043
RTOP 505-63-50	p 1033	N95-18735
RTOP 505-63-52	p 982	N95-19792
RTOP 505-63-53	p 1044	N95-18199
	p 1045	N95-18909
RTOP 505-64-13-01	p 942	N95-18198
RTOP 505-64-52-04	p 995	N95-18187
RTOP 505-64-70-01	p 1005	N95-19781
RTOP 505-68-10	p 933	N95-18582
	p 934	N95-19284
	p 934	N95-19285
RTOP 505-68-30-03	p 931	N95-19114
RTOP 505-68-30	p 950	N95-19651
RTOP 505-68-50	p 929	N95-18565
RTOP 505-69-50	p 930	N95-18933
RTOP 505-70-62	p 960	N95-19286
RTOP 505-90-00	p 1175	N95-18950
	p 1175	N95-18953
RTOP 505-90-5K	p 1016	N95-18200
	p 1016	N95-18212
	p 1019	N95-18898
	p 1019	N95-18941
RTOP 505-90-52-01	p 1116	N95-18108
	p 1118	N95-18109
	p 1116	N95-18110
	p 1015	N95-18188
	p 1016	N95-18190
	p 1016	N95-18191
	p 1016	N95-18193
	p 1017	N95-18397
	p 1117	N95-18479
	p 1098	N95-18487
	p 1018	N95-18488
	p 1098	N95-18584
	p 1099	N95-18931
	p 1020	N95-18958
	p 1099	N95-19027
	p 1100	N95-19028
RTOP 506-42-31	p 927	N95-18044
RTOP 510-01-50	p 981	N95-19652
RTOP 510-02-11-07	p 970	N95-18466
RTOP 537-02-21	p 947	N95-18133
RTOP 537-07-00	p 928	N95-18101
RTOP 538-02-10-01	p 934	N95-19468
RTOP 538-03-11	p 958	N95-18054
RTOP 583-02-21	p 1042	N95-19238
RTOP 584-03-11	p 962	N95-18045
	p 962	N95-18467
RTOP 656-61-23	p 990	N95-18211
RTOP 656-65-07	p 1172	N95-18040
	p 1173	N95-18051
RTOP 665-45-20-01	p 1051	N95-18465
RTOP 694-03-0C	p 959	N95-18586
RTOP 778-34-2A	p 1040	N95-18041
RTOP 879-11-38	p 1196	N95-19791
RTOP 963-60-OD	p 991	N95-19788
RTOP 963-70-OH	p 927	N95-18197
	p 927	N95-18486
RTOP 963-89-00-01	p 964	N95-18105
SBA-5648-OA-90	p 1007	N95-17999
SMD113325	p 932	N95-19574
SPO-S-0020536	p 932	N95-19574
USRA-C-5555-10	p 1173	N95-18051
USRA-C-555512	p 1172	N95-18040
W-31-109-ENG-38	p 1007	N95-17961
	p 1116	N95-17977
	p 1094	N95-17978
	p 1096	N95-18354
	p 1130	N95-18427
	p 1130	N95-18428
	p 1017	N95-18443
	p 1144	N95-18547
	p 1131	N95-18548
	p 1018	N95-18549
	p 1131	N95-18550
	p 1131	N95-18551
	p 1053	N95-19074
	p 1150	N95-19075
	p 1150	N95-19094
	p 1020	N95-19098
	p 1020	N95-19099
	p 1151	N95-19113
	p 1053	N95-19115
	p 1053	N95-19116
	p 1054	N95-19117
	p 1012	N95-19246
	p 1100	N95-19397
	p 1111	N95-19592
	p 975	N95-19618
	p 1122	N95-19704

	p 1153	N95-19724
	p 982	N95-19725
	p 1135	N95-19726
	p 1039	N95-19727
	p 1135	N95-19786
	p 1135	N95-19787
	p 1112	N95-19834
W-7405-ENG-36	p 1063	N95-17946
	p 1063	N95-17947
	p 1143	N95-17965
	p 1143	N95-17969
	p 1155	N95-17996
	p 966	N95-17997
	p 1173	N95-18063
	p 1148	N95-18064
	p 1063	N95-18125
	p 1036	N95-18126
	p 1032	N95-18130
	p 1063	N95-18148
	p 1117	N95-18346
	p 964	N95-18639
	p 1011	N95-19200
	p 1034	N95-19229
	p 1035	N95-19394
	p 1152	N95-19608
	p 981	N95-19611
	p 1194	N95-19612
	p 1196	N95-19619
	p 1152	N95-19620
	p 1152	N95-19621
	p 988	N95-19721
W-7405-ENG-48	p 977	N95-17962
	p 1031	N95-17963
	p 1037	N95-18357
	p 1136	N95-18552
	p 1033	N95-18555
	p 1059	N95-18647
	p 1059	N95-18664
	p 1060	N95-18895
	p 1196	N95-19034
	p 1038	N95-19096
	p 987	N95-19227
	p 1038	N95-19247
	p 1038	N95-19248
	p 1186	N95-19249
	p 1146	N95-19250
	p 1146	N95-19379
	p 980	N95-19396
	p 1039	N95-19398
	p 1039	N95-19507
	p 1039	N95-19508
	p 1146	N95-19509
	p 1146	N95-19527
	p 1039	N95-19551
	p 1147	N95-19552
	p 1137	N95-19588
	p 1039	N95-19708
	p 1135	N95-19709
	p 1142	N95-19710
	p 1035	N95-19711
	p 1039	N95-19722
	p 1006	N95-19833
	p 1155	N95-19838

Typical Report Number Index Listing

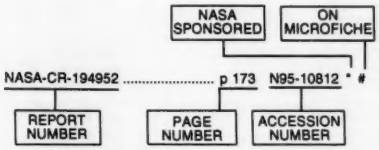

Listings in this index are arranged alphanumerically by report number. The accession number denotes the number by which the citation is identified. The page number helps to locate the citation in the abstract section. An asterisk (*) indicates that the item is a NASA report. A pound sign (#) indicates that the item is available on microfiche.

A-94031-VOL-1 ..... p 1092 N95-18569 * #
A-94053 ..... p 931 N95-19119 * #
A-94137 ..... p 1077 N95-19140 * #
A-94146 ..... p 928 N95-18101 * #
A-94147 ..... p 930 N95-19041 * #
A-95026 ..... p 1077 N95-18734 * #

AD-A279160 ..... p 1128 N95-19802
AD-A279162 ..... p 1108 N95-19803
AD-A279163 ..... p 1047 N95-19804
AD-A279164 ..... p 940 N95-19805
AD-A279169 ..... p 1154 N95-19806
AD-A279170 ..... p 1154 N95-19807
AD-A279171 ..... p 1062 N95-19808
AD-A279176 ..... p 1043 N95-19809
AD-A279188 ..... p 941 N95-19810
AD-A279193 ..... p 1087 N95-19811
AD-A279194 ..... p 1154 N95-19812
AD-A279199 ..... p 1108 N95-19813
AD-A279200 ..... p 972 N95-19814
AD-A279201 ..... p 1154 N95-19815
AD-A279202 ..... p 1154 N95-19816
AD-A279203 ..... p 1154 N95-19817
AD-A279206 ..... p 1112 N95-19843
AD-A279212 ..... p 1147 N95-19844
AD-A279213 ..... p 1039 N95-19845
AD-A279214 ..... p 1147 N95-19846
AD-A279215 ..... p 1147 N95-19847
AD-A279219 ..... p 960 N95-19848
AD-A279220 ..... p 1171 N95-18578 #
AD-A279221 ..... p 1013 N95-19849
AD-A279223 ..... p 1128 N95-19850
AD-A279225 ..... p 972 N95-19851
AD-A279233 ..... p 1157 N95-19852
AD-A279234 ..... p 1157 N95-19853
AD-A279244 ..... p 1062 N95-19860
AD-A279808 ..... p 1045 N95-18613 #
AD-A279918 ..... p 989 N95-19861
AD-A279919 ..... p 1142 N95-19862
AD-A279922 ..... p 932 N95-19863
AD-A279931 ..... p 955 N95-19864
AD-A279932 ..... p 1013 N95-19865
AD-A279937 ..... p 989 N95-19866
AD-A279939 ..... p 989 N95-19867
AD-A279940 ..... p 977 N95-19868
AD-A279943 ..... p 1119 N95-19869
AD-A279944 ..... p 1073 N95-19870
AD-A280002 ..... p 1035 N95-19871 #
AD-A280034 ..... p 1076 N95-19818 #
AD-A280114 ..... p 970 N95-18612 #
AD-A280143 ..... p 1119 N95-19819 #
AD-A280144 ..... p 1119 N95-19820 #
AD-A280147 ..... p 1108 N95-19821
AD-A280156 ..... p 969 N95-19822 #
AD-A280157 ..... p 969 N95-19823 #
AD-A280158 ..... p 976 N95-19824 #
AD-A280159 ..... p 976 N95-19825 #
AD-A280170 ..... p 989 N95-19826 #
AD-A280178 ..... p 1087 N95-19827
AD-A280181 ..... p 1155 N95-19828 #
AD-A280182 ..... p 1155 N95-19829 #
AD-A280185 ..... p 976 N95-19830 #
AD-A280187 ..... p 991 N95-18913 * #
AD-A283303 ..... p 1049 N95-17971 #
AD-A283307 ..... p 1113 N95-18023 #
AD-A283318 ..... p 994 N95-18024 #
AD-A283319 ..... p 1172 N95-18025 #
AD-A283320 ..... p 1172 N95-18026 #
AD-A283328 ..... p 978 N95-18027 #
AD-A283330 ..... p 969 N95-18028 #
AD-A283334 ..... p 1120 N95-18007 #
AD-A283335 ..... p 941 N95-18008 #
AD-A283338 ..... p 1155 N95-18009 #
AD-A283352 ..... p 1078 N95-17998 #
AD-A283354 ..... p 1109 N95-18050 #
AD-A283355 ..... p 1008 N95-18052 #
AD-A283426 ..... p 1148 N95-18053 #
AD-A283427 ..... p 1113 N95-18057 #
AD-A283465 ..... p 994 N95-18058 #
AD-A283505 ..... p 940 N95-18059 #
AD-A283515 ..... p 1178 N95-18001
AD-A283546 ..... p 1051 N95-18614 #
AD-A283597 ..... p 1017 N95-18434 #
AD-A283608 ..... p 1110 N95-18615 #
AD-A283610 ..... p 1053 N95-18435
AD-A283613 ..... p 1040 N95-18010
AD-A283618 ..... p 944 N95-18616 #
AD-A283624 ..... p 1052 N95-18011
AD-A283630 ..... p 995 N95-18136
AD-A283633 ..... p 1109 N95-18137
AD-A283640 ..... p 1074 N95-18012
AD-A283641 ..... p 1094 N95-18013
AD-A283647 ..... p 1067 N95-18014
AD-A283651 ..... p 1078 N95-18138
AD-A283654 ..... p 995 N95-18139
AD-A283655 ..... p 1075 N95-18617 #
AD-A283656 ..... p 930 N95-18669
AD-A283659 ..... p 1094 N95-18015
AD-A283660 ..... p 983 N95-18016
AD-A283668 ..... p 1094 N95-18017
AD-A283669 ..... p 1094 N95-18018
AD-A283674 ..... p 1058 N95-18140
AD-A283677 ..... p 983 N95-18019
AD-A283678 ..... p 1068 N95-18141
AD-A283679 ..... p 1120 N95-18020
AD-A283686 ..... p 1079 N95-18618 #
AD-A283688 ..... p 930 N95-18670
AD-A283689 ..... p 1139 N95-18142
AD-A283695 ..... p 1000 N95-18671
AD-A283698 ..... p 999 N95-18619 #
AD-A283699 ..... p 1033 N95-18620 #
AD-A283700 ..... p 944 N95-18621 #
AD-A283701 ..... p 1075 N95-18622 #
AD-A283702 ..... p 1064 N95-18623 #
AD-A283703 ..... p 969 N95-18021
AD-A283704 ..... p 996 N95-18359 #
AD-A283705 ..... p 1178 N95-18361 #
AD-A283707 ..... p 964 N95-18362 #
AD-A283718 ..... p 996 N95-18436
AD-A283720 ..... p 1089 N95-18414
AD-A283726 ..... p 1044 N95-18363 #
AD-A283747 ..... p 1096 N95-18364 #
AD-A283757 ..... p 1075 N95-18951 * #
AD-A283825 ..... p 1120 N95-18672
AD-A283828 ..... p 929 N95-18624 #
AD-A283846 ..... p 1123 N95-18673
AD-A283867 ..... p 930 N95-18674
AD-A283892 ..... p 1114 N95-18675
AD-A283897 ..... p 1096 N95-18365 #
AD-A283903 ..... p 1088 N95-18151 #
AD-A283906 ..... p 1040 N95-18152 #
AD-A283911 ..... p 1074 N95-18153 #
AD-A283912 ..... p 1139 N95-18154 #
AD-A283915 ..... p 1099 N95-18676
AD-A283916 ..... p 1095 N95-18155 #
AD-A283917 ..... p 1008 N95-18156 #
AD-A283919 ..... p 1113 N95-18157 #
AD-A283920 ..... p 1110 N95-18158 #
AD-A283921 ..... p 1110 N95-18159 #
AD-A283922 ..... p 1074 N95-18160 #
AD-A283923 ..... p 1096 N95-18161 #
AD-A283925 ..... p 944 N95-18677
AD-A283926 ..... p 942 N95-18162 #
AD-A283930 ..... p 964 N95-18163 #
AD-A283933 ..... p 947 N95-18164 #
AD-A283942 ..... p 1141 N95-18682
AD-A283946 ..... p 992 N95-18165 #
AD-A283947 ..... p 986 N95-19064
AD-A283948 ..... p 987 N95-19102
AD-A283950 ..... p 1060 N95-18683
AD-A283952 ..... p 1130 N95-18334 #
AD-A283955 ..... p 992 N95-18684
AD-A283960 ..... p 1150 N95-18685
AD-A283963 ..... p 1000 N95-18686
AD-A283968 ..... p 1144 N95-18888
AD-A283975 ..... p 1114 N95-18889
AD-A283978 ..... p 1123 N95-18890
AD-A283981 ..... p 944 N95-18891
AD-A283983 ..... p 1111 N95-18892
AD-A283984 ..... p 1120 N95-19065
AD-A283992 ..... p 974 N95-19066
AD-A283994 ..... p 945 N95-19067
AD-A283995 ..... p 944 N95-18723
AD-A283997 ..... p 959 N95-18724
AD-A283998 ..... p 959 N95-18725
AD-A283999 ..... p 944 N95-18726
AD-A284004 ..... p 1000 N95-18727
AD-A284005 ..... p 1174 N95-18654
AD-A284010 ..... p 1132 N95-18655
AD-A284023 ..... p 1079 N95-18656
AD-A284024 ..... p 999 N95-18657
AD-A284042 ..... p 1117 N95-18658
AD-A284048 ..... p 1093 N95-18659
AD-A284050 ..... p 1010 N95-18660
AD-A284055 ..... p 1079 N95-18661
AD-A284056 ..... p 1010 N95-18662
AD-A284057 ..... p 929 N95-18663
AD-A284058 ..... p 986 N95-18678
AD-A284060 ..... p 1117 N95-18679
AD-A284061 ..... p 1174 N95-18680
AD-A284062 ..... p 1174 N95-18681
AD-A284071 ..... p 1089 N95-19068
AD-A284073 ..... p 1001 N95-19069
AD-A284074 ..... p 1034 N95-19071
AD-A284075 ..... p 1000 N95-19035
AD-A284076 ..... p 993 N95-19036
AD-A284097 ..... p 928 N95-18380
AD-A284099 ..... p 942 N95-18398
AD-A284100 ..... p 1078 N95-18400
AD-A284101 ..... p 1088 N95-18401
AD-A284102 ..... p 984 N95-18402
AD-A284103 ..... p 1089 N95-18403
AD-A284107 ..... p 1097 N95-18437
AD-A284108 ..... p 1131 N95-18438
AD-A284111 ..... p 1076 N95-18439
AD-A284112 ..... p 1139 N95-18404
AD-A284115 ..... p 958 N95-18405
AD-A284116 ..... p 1017 N95-18406
AD-A284119 ..... p 943 N95-18407
AD-A284122 ..... p 1037 N95-18408
AD-A284125 ..... p 1139 N95-18409
AD-A284126 ..... p 973 N95-18410
AD-A284131 ..... p 996 N95-18411
AD-A284147 ..... p 974 N95-18412
AD-A284149 ..... p 1064 N95-18413
AD-A284151 ..... p 943 N95-18415
AD-A284153 ..... p 1171 N95-18416
AD-A284154 ..... p 943 N95-18417
AD-A284155 ..... p 943 N95-18504
AD-A284156 ..... p 943 N95-18505
AD-A284158 ..... p 997 N95-18506
AD-A284160 ..... p 933 N95-18507
AD-A284161 ..... p 959 N95-18508
AD-A284162 ..... p 1140 N95-18509
AD-A284163 ..... p 985 N95-18510
AD-A284166 ..... p 1117 N95-18511
AD-A284167 ..... p 1078 N95-18512
AD-A284168 ..... p 985 N95-18513
AD-A284171 ..... p 974 N95-18514
AD-A284173 ..... p 1078 N95-18515
AD-A284174 ..... p 1079 N95-18518

AD-A284175 ..... p 1131 N95-18519
AD-A284176 ..... p 998 N95-18520
AD-A284180 ..... p 998 N95-18522
AD-A284181 ..... p 1010 N95-18625
AD-A284189 ..... p 1079 N95-18626
AD-A284191 ..... p 1002 N95-19103
AD-A284192 ..... p 1121 N95-19104
AD-A284194 ..... p 985 N95-18636
AD-A284196 ..... p 1092 N95-17939
AD-A284203 ..... p 1093 N95-17940
AD-A284204 ..... p 969 N95-17941
AD-A284206 ..... p 941 N95-17953
AD-A284208 ..... p 994 N95-17954
AD-A284212 ..... p 1067 N95-17955
AD-A284213 ..... p 1036 N95-17956
AD-A284216 ..... p 983 N95-17957
AD-A284224 ..... p 994 N95-17958
AD-A284229 ..... p 1007 N95-17959
AD-A284231 ..... p 1148 N95-17960
AD-A284234 ..... p 1087 N95-19698 #
AD-A284235 ..... p 1076 N95-19728
AD-A284245 ..... p 976 N95-19729
AD-A284249 ..... p 1005 N95-19730
AD-A284253 ..... p 945 N95-19731
AD-A284258 ..... p 1073 N95-19712 #
AD-A284260 ..... p 975 N95-19699 #
AD-A284261 ..... p 1153 N95-19713 #
AD-A284263 ..... p 1142 N95-19732
AD-A284267 ..... p 1052 N95-19733
AD-A284268 ..... p 1052 N95-19734
AD-A284269 ..... p 1119 N95-19735
AD-A284270 ..... p 1005 N95-19736
AD-A284310 ..... p 1008 N95-18378 #
AD-A284313 ..... p 1123 N95-18379
AD-A284314 ..... p 974 N95-19170
AD-A284319 ..... p 942 N95-18381
AD-A284322 ..... p 1037 N95-18382
AD-A284332 ..... p 947 N95-18383
AD-A284334 ..... p 1070 N95-18384
AD-A284337 ..... p 1091 N95-18385
AD-A284339 ..... p 996 N95-18386
AD-A284340 ..... p 1009 N95-18418 #
AD-A284341 ..... p 1097 N95-18419
AD-A284342 ..... p 1097 N95-18420
AD-A284343 ..... p 1097 N95-18421 #
AD-A284344 ..... p 1097 N95-18422 #
AD-A284345 ..... p 1097 N95-18423 #
AD-A284350 ..... p 1140 N95-18424
AD-A284351 ..... p 1009 N95-18425 #
AD-A284352 ..... p 1009 N95-18426 #
AD-A284353 ..... p 1008 N95-18338 #
AD-A284354 ..... p 984 N95-18339 #
AD-A284358 ..... p 1089 N95-18440
AD-A284362 ..... p 1113 N95-18441
AD-A284375 ..... p 928 N95-18340 #
AD-A284382 ..... p 996 N95-18341 #
AD-A284383 ..... p 1139 N95-18342 #
AD-A284430 ..... p 1096 N95-18343 #
AD-A284431 ..... p 1096 N95-18344 #
AD-A284470 ..... p 1173 N95-18446
AD-A284525 ..... p 1120 N95-18113 #
AD-A284527 ..... p 1068 N95-18114 #
AD-A284552 ..... p 1063 N95-18115 #
AD-A284561 ..... p 995 N95-18116 #
AD-A284562 ..... p 1068 N95-18117 #
AD-A284563 ..... p 1090 N95-18029 #
AD-A284567 ..... p 1095 N95-18030 #
AD-A284568 ..... p 1095 N95-18031 #
AD-A284569 ..... p 1095 N95-18032 #
AD-A284570 ..... p 1095 N95-18033 #
AD-A284571 ..... p 1097 N95-18447
AD-A284572 ..... p 1095 N95-18034 #
AD-A284573 ..... p 1097 N95-18449
AD-A284574 ..... p 1098 N95-18450
AD-A284578 ..... p 1178 N95-18451
AD-A284581 ..... p 1049 N95-18035 #
AD-A284583 ..... p 1064 N95-18452
AD-A284584 ..... p 1129 N95-18062 #
AD-A284610 ..... p 1065 N95-19083 #
AD-A284611 ..... p 1002 N95-19084 #
AD-A284614 ..... p 1141 N95-19085 #
AD-A284636 ..... p 1065 N95-19086 #
AD-A284663 ..... p 1066 N95-19105 #
AD-A284668 ..... p 1100 N95-19106 #
AD-A284672 ..... p 1002 N95-19087 #
AD-A284674 ..... p 1142 N95-19088 #
AD-A284678 ..... p 1011 N95-19089 #
AD-A284683 ..... p 1089 N95-18530 #
AD-A284684 ..... p 1091 N95-18531 #
AD-A284698 ..... p 1019 N95-18562 #
AD-A284716 ..... p 1068 N95-18076
AD-A284725 ..... p 1090 N95-18077
AD-A284727 ..... p 931 N95-19109 #
AD-A284728 ..... p 1050 N95-18078
AD-A284729 ..... p 1095 N95-18079
AD-A284732 ..... p 1044 N95-18080
AD-A284735 ..... p 1044 N95-18081
AD-A284736 ..... p 1123 N95-18083
AD-A284752 ..... p 1088 N95-18084
AD-A284759 ..... p 1058 N95-18085 #
AD-A284762 ..... p 1091 N95-18086 #
AD-A284763 ..... p 958 N95-18087 #
AD-A284765 ..... p 941 N95-18088 #
AD-A284774 ..... p 985 N95-18442
AD-A284802 ..... p 1061 N95-19685 #
AD-A284806 ..... p 1061 N95-19686 #
AD-A284811 ..... p 1013 N95-19687 #
AD-A284824 ..... p 1104 N95-19688 #
AD-A284825 ..... p 1112 N95-19689 #
AD-A284826 ..... p 1147 N95-19690 #
AD-A284830 ..... p 988 N95-19691 #
AD-A284831 ..... p 1112 N95-19692 #
AD-A284833 ..... p 945 N95-19693 #
AD-A284838 ..... p 1153 N95-19737
AD-A284840 ..... p 1005 N95-19694
AD-A284843 ..... p 1087 N95-19695 #
AD-A284845 ..... p 988 N95-19696 #
AD-A284847 ..... p 1153 N95-19697 #
AD-A284848 ..... p 1153 N95-19738 #
AD-A284849 ..... p 1087 N95-19714 #
AD-A284852 ..... p 1153 N95-19715 #
AD-A284856 ..... p 1030 N95-19716 #
AD-A284857 ..... p 1195 N95-19739 #
AD-A284861 ..... p 1090 N95-19740
AD-A284873 ..... p 1013 N95-19741
AD-A284881 ..... p 1104 N95-19742
AD-A284882 ..... p 982 N95-19743
AD-A284887 ..... p 931 N95-19110
AD-A284940 ..... p 1129 N95-17974 #
AD-A284943 ..... p 973 N95-17975 #
AD-A284995 ..... p 1012 N95-19519 #
AD-A284997 ..... p 1004 N95-19534 #
AD-A285044 ..... p 987 N95-19544 #
AD-A285047 ..... p 1100 N95-19545 #
AD-A285049 ..... p 1075 N95-19563 #
AD-A285050 ..... p 1090 N95-19564 #
AD-A285114 ..... p 1004 N95-19565 #
AD-A285116 ..... p 1043 N95-19593 #
AD-A285125 ..... p 1004 N95-19594 #
AD-A285127 ..... p 950 N95-19595 #
AD-A285129 ..... p 1073 N95-19596 #
AD-A285133 ..... p 1090 N95-19583 #
AD-A285316 ..... p 1003 N95-19510 #
AD-A285317 ..... p 1151 N95-19511 #
AD-A285321 ..... p 987 N95-19520 #
AD-A285326 ..... p 1072 N95-19521 #
AD-A285328 ..... p 1046 N95-19522 #
AD-A285331 ..... p 1075 N95-19523 #
AD-A285336 ..... p 1004 N95-19535 #
AD-A285422 ..... p 1032 N95-18065
AD-A285440 ..... p 1095 N95-18089
AD-A285442 ..... p 1058 N95-18091
AD-A285452 ..... p 1077 N95-19536 #
AD-A285453 ..... p 1088 N95-18094
AD-A285457 ..... p 1086 N95-19537 #
AD-A285458 ..... p 1089 N95-19538 #
AD-A285460 ..... p 980 N95-19539 #
AD-A285522 ..... p 1088 N95-18095 #
AD-A285525 ..... p 1173 N95-18096 #
AD-A285526 ..... p 993 N95-18098 #
AD-A285528 ..... p 1173 N95-18099 #
AD-A285530 ..... p 1138 N95-18100
AD-A285532 ..... p 1138 N95-18102
AD-A285533 ..... p 1008 N95-18103 #
AD-A285535 ..... p 1139 N95-18104
AD-A285536 ..... p 1109 N95-18106
AD-A285537 ..... p 995 N95-18066 #
AD-A285538 ..... p 1138 N95-18067 #
AD-A285539 ..... p 1110 N95-18454
AD-A285540 ..... p 1074 N95-18468
AD-A285541 ..... p 1018 N95-18469 #
AD-A285542 ..... p 1074 N95-18470 #
AD-A285547 ..... p 1045 N95-18472
AD-A285555 ..... p 957 N95-18641 #
AD-A285565 ..... p 1131 N95-18473 #
AD-A285569 ..... p 1038 N95-18642 #
AD-A285576 ..... p 1075 N95-19540 #
AD-A285581 ..... p 1131 N95-18474
AD-A285582 ..... p 1115 N95-19118 #
AD-A285589 ..... p 997 N95-18475 #
AD-A285657 ..... p 1147 N95-19700 #
AD-A285658 ..... p 1073 N95-19701 #
AD-A285667 ..... p 972 N95-19702 #
AD-A285678 ..... p 1111 N95-19524 #
AD-A285679 ..... p 1003 N95-19525 #
AD-A285680 ..... p 1111 N95-19526 #
AD-A285681 ..... p 1115 N95-19512 #
AD-A285682 ..... p 1111 N95-19513 #
AD-A285683 ..... p 1003 N95-19516 #
AD-A285684 ..... p 945 N95-19517 #
AD-A285685 ..... p 1018 N95-18477
AD-A285687 ..... p 1128 N95-19514 #
AD-A285700 ..... p 1140 N95-18478 #
AD-A285701 ..... p 1140 N95-18480 #
AD-A285707 ..... p 997 N95-18481 #
AD-A285712 ..... p 1117 N95-18482 #
AD-A285713 ..... p 943 N95-18483 #
AD-A285717 ..... p 1140 N95-18484 #
AD-A285726 ..... p 1009 N95-18485 #
AD-A285727 ..... p 978 N95-18068 #
AD-A285769 ..... p 1139 N95-18345
AD-A285872 ..... p 988 N95-19614 #
AD-A285874 ..... p 1134 N95-19597 #
AD-A285875 ..... p 1152 N95-19598 #
AD-A285876 ..... p 1115 N95-19599 #
AD-A285877 ..... p 1004 N95-19600 #
AD-A285878 ..... p 1115 N95-19601 #
AD-A285882 ..... p 1090 N95-19602 #
AD-A285886 ..... p 1122 N95-19603 #
AD-A285887 ..... p 1176 N95-19604 #
AD-A285888 ..... p 1111 N95-19605 #
AD-A285897 ..... p 1012 N95-19606 #
AD-A285900 ..... p 1030 N95-19607 #
AD-A285955 ..... p 1005 N95-19744 #
AD-A285958 ..... p 974 N95-19515 #
AD-A285962 ..... p 988 N95-19745 #
AD-A285968 ..... p 965 N95-19571 #
AD-A285989 ..... p 1115 N95-19572 #
AD-A286045 ..... p 1012 N95-19573 #
AD-A286247 ..... p 1080 N95-19384 #
AD-A286248 ..... p 1080 N95-19385 #
AD-A286252 ..... p 971 N95-19386 #
AD-A286253 ..... p 1066 N95-19387 #
AD-A286254 ..... p 1054 N95-19388 #

AD-B192484L ..... p 1060 N95-18742 * #

AD-D016221 ..... p 1149 N95-18627
AD-D016231 ..... p 1141 N95-18628
AD-D016232 ..... p 970 N95-18629
AD-D016233 ..... p 979 N95-18630
AD-D016234 ..... p 985 N95-18631
AD-D016235 ..... p 967 N95-18632
AD-D016236 ..... p 1149 N95-18633
AD-D016237 ..... p 1038 N95-18585
AD-D016238 ..... p 1019 N95-18634
AD-D016239 ..... p 1038 N95-18635
AD-D016258 ..... p 995 N95-18314
AD-D016259 ..... p 995 N95-18315
AD-D016260 ..... p 1041 N95-18317
AD-D016262 ..... p 1008 N95-18318
AD-D016263 ..... p 1032 N95-18319
AD-D016264 ..... p 984 N95-18320
AD-D016267 ..... p 1149 N95-18543
AD-D016268 ..... p 1173 N95-18544
AD-D016269 ..... p 999 N95-18545
AD-D016270 ..... p 1010 N95-18546
AD-D016272 ..... p 997 N95-18516
AD-D016273 ..... p 1092 N95-18517
AD-D016274 ..... p 978 N95-18332
AD-D016275 ..... p 996 N95-18429
AD-D016276 ..... p 985 N95-18430
AD-D016277 ..... p 992 N95-18431
AD-D016278 ..... p 1009 N95-18432
AD-D016280 ..... p 1009 N95-18433
AD-D016353 ..... p 1032 N95-17970
AD-D016412 ..... p 1041 N95-18335
AD-D016413 ..... p 956 N95-18553
AD-D016420 ..... p 984 N95-18336
AD-D016421 ..... p 1010 N95-18523
AD-D016422 ..... p 1033 N95-18524
AD-D016423 ..... p 928 N95-18337
AD-D016424 ..... p 1141 N95-18593
AD-D016426 ..... p 1041 N95-18594
AD-D016427 ..... p 1149 N95-18559
AD-D016430 ..... p 1141 N95-18560
AD-D016432 ..... p 1015 N95-18112
AD-D016434 ..... p 1018 N95-18525
AD-D016436 ..... p 999 N95-18561
AD-D016438 ..... p 1173 N95-18526 #
AD-D016439 ..... p 1149 N95-18527 #
AD-D016440 ..... p 1010 N95-18528 #
AD-D016443 ..... p 1141 N95-18529 #
AD-D016444 ..... p 1141 N95-18563
AD-D016447 ..... p 1002 N95-19072
AD-D016457 ..... p 967 N95-19073
AD-D016458 ..... p 990 N95-19090
AD-D016462 ..... p 1011 N95-19171
AD-D016466 ..... p 1009 N95-18455 #
AD-D016471 ..... p 1045 N95-18456 #
AD-D016472 ..... p 979 N95-18458 #
AD-D016473 ..... p 1140 N95-18459 #
AD-D016474 ..... p 1140 N95-18460 #
AD-D016475 ..... p 1033 N95-18461 #
AD-D016476 ..... p 997 N95-18462 #
AD-D016496 ..... p 1142 N95-19389
AD-D016528 ..... p 1011 N95-19120
AD-D016541 ..... p 1042 N95-19121

AD-D016543 ..... p 1151 N95-19122
AD-D016555 ..... p 971 N95-19123
AD-D016556 ..... p 1034 N95-19124

AD-E202151 ..... p 1120 N95-18020
AD-E202154 ..... p 1068 N95-18141
AD-E202162 ..... p 1064 N95-18452
AD-E202165 ..... p 1049 N95-18035 #
AD-E202181 ..... p 1066 N95-19105 #
AD-E202182 ..... p 1129 N95-18062 #
AD-E202183 ..... p 1178 N95-18451
AD-E501831 ..... p 1037 N95-18382

AD-M200254 ..... p 994 N95-17964

ADST/WDL/TR-W-003322A ..... p 1173 N95-18446

AEDC-TR-94-5 ..... p 930 N95-18674
AEDC-TR-94-6 ..... p 929 N95-18663
AEDC-TR-94-7 ..... p 944 N95-18891

AERO-TN-9301 ..... p 942 N95-18097 #

AFB-0053-FM-9740-841 ..... p 988 N95-19614 #

AFCESA/ESL-TR-89-62 ..... p 989 N95-19861

AFIT/CI/CIA-94-035D ..... p 1091 N95-18385

AFIT/DS/AA/94-4 ..... p 931 N95-19110

AFIT/DS/ENC-94-1 ..... p 1019 N95-18562 #

AFIT/DS/ENP/94-03 ..... p 1147 N95-19690 #
AFIT/DS/ENP/94-04 ..... p 1153 N95-19715 #

AFIT/GEE/ENS/94S-26 ..... p 1061 N95-19685 #

AFIT/GEE/ENV/94S-03 ..... p 1061 N95-19686 #

AFOSR-94-0281TR ..... p 1154 N95-19816
AFOSR-94-0282TR ..... p 1154 N95-19817
AFOSR-94-0283TR ..... p 1154 N95-19815
AFOSR-94-0327TR ..... p 1119 N95-19869
AFOSR-94-0334TR ..... p 1073 N95-19870
AFOSR-94-0335TR ..... p 1035 N95-19871 #
AFOSR-94-0338TR ..... p 955 N95-19864
AFOSR-94-0453TR ..... p 1155 N95-18009 #
AFOSR-94-0475TR ..... p 1036 N95-17956
AFOSR-94-0476TR ..... p 996 N95-18411
AFOSR-94-0477TR ..... p 1113 N95-18441
AFOSR-94-0479TR ..... p 985 N95-18636
AFOSR-94-0481TR ..... p 1087 N95-19698 #
AFOSR-94-0483TR ..... p 1131 N95-18438
AFOSR-94-0485TR ..... p 1093 N95-17940
AFOSR-94-0489TR ..... p 1092 N95-17939
AFOSR-94-0490TR ..... p 1117 N95-18511
AFOSR-94-0493TR ..... p 985 N95-18513
AFOSR-94-0495TR ..... p 1078 N95-18512
AFOSR-94-0496TR ..... p 974 N95-18514
AFOSR-94-0499TR ..... p 983 N95-17957
AFOSR-94-0499TR ..... p 1088 N95-18401
AFOSR-94-0500TR ..... p 974 N95-18412
AFOSR-94-0501TR ..... p 973 N95-18410
AFOSR-94-0502TR ..... p 969 N95-17941
AFOSR-94-0503TR ..... p 1079 N95-18626
AFOSR-94-0504TR ..... p 1140 N95-18509
AFOSR-94-0507TR ..... p 985 N95-18510
AFOSR-94-0508TR ..... p 1079 N95-18518
AFOSR-94-0510TR ..... p 1089 N95-18403
AFOSR-94-0511TR ..... p 984 N95-18402
AFOSR-94-0513TR ..... p 1076 N95-18439
AFOSR-94-0514TR ..... p 1078 N95-18400
AFOSR-94-0517TR ..... p 994 N95-17954
AFOSR-94-0518TR ..... p 1097 N95-18437
AFOSR-94-0520TR ..... p 1121 N95-19104
AFOSR-94-0521TR ..... p 1002 N95-19103
AFOSR-94-0522TR ..... p 1150 N95-18685
AFOSR-94-0542TR ..... p 1079 N95-18656
AFOSR-94-0543TR ..... p 987 N95-19102
AFOSR-94-0544TR ..... p 1037 N95-18408
AFOSR-94-0557TR ..... p 987 N95-19544 #
AFOSR-94-0568TR ..... p 973 N95-17975 #
AFOSR-94-0577TR ..... p 1090 N95-19740
AFOSR-94-0579TR ..... p 931 N95-19109 #
AFOSR-94-0626TR ..... p 988 N95-19614 #
AFOSR-94-0628 ..... p 1018 N95-18469 #
AFOSR-94-0629TR ..... p 1151 N95-19511 #
AFOSR-94-0630TR ..... p 1003 N95-19510 #
AFOSR-94-0631TR ..... p 987 N95-19520 #
AFOSR-94-0666TR ..... p 1134 N95-19597 #
AFOSR-94-0670TR ..... p 1090 N95-19602 #
AFOSR-94-0672TR ..... p 988 N95-19745 #

AGARD-AG-321 ..... p 941 N95-18927 #

AGARD-AR-303-SUPPL ..... p 929 N95-18539

AGARD-CP-535 ..... p 1020 N95-19251 #
AGARD-CP-549 ..... p 1124 N95-19142 #
AGARD-CP-553 ..... p 1080 N95-19413 #
AGARD-CP-558 ..... p 950 N95-19653 #

AGARD-LS-198 ..... p 948 N95-19017 #

AGARD-R-798 ..... p 956 N95-18597 #

AIAA PAPER 94-0393 ..... p 1031 N95-19776 #
AIAA PAPER 94-0572 ..... p 990 N95-18211 * #
AIAA PAPER 94-2112 ..... p 945 N95-19044 * #
AIAA PAPER 94-3369 ..... p 1016 N95-18200 * #
AIAA PAPER 95-0038 ..... p 955 N95-19769 * #
AIAA PAPER 95-0075 ..... p 1175 N95-19038 * #
AIAA PAPER 95-0160 ..... p 1015 N95-18149 * #
AIAA PAPER 95-0538 ..... p 934 N95-19285 * #
AIAA PAPER 95-0540 ..... p 934 N95-19284 * #
AIAA PAPER 95-0577 ..... p 1019 N95-18941 * #
AIAA PAPER 95-0703 ..... p 1109 N95-18055 * #
AIAA PAPER 95-0706 ..... p 1176 N95-19127 * #
AIAA PAPER 95-0720 ..... p 958 N95-18054 * #
AIAA PAPER 95-0733 ..... p 947 N95-18133 * #
AIAA PAPER 95-0734 ..... p 1015 N95-18107 * #
AIAA PAPER 95-0755 ..... p 933 N95-18582 * #
AIAA PAPER 95-0763 ..... p 1014 N95-18036 * #
AIAA PAPER 95-0880 ..... p 1017 N95-18327 * #
AIAA PAPER 95-6146 ..... p 960 N95-19286 * #

AL/AO-SR-1994-0010-VOL-1 ..... p 1172 N95-18025 #
AL/AO-SR-1994-0010-VOL-2 ..... p 1172 N95-18026 #

AL/CF-TR-1994-0033 ..... p 1087 N95-19714 #
AL/CF-TR-1994-0046 ..... p 1079 N95-18661
AL/CF-TR-1994-0085 ..... p 1088 N95-18084

AL/EQ-TR-1994-0006 ..... p 1058 N95-18140

AMSEL-NV-TR-0112 ..... p 1008 N95-18156 #

AMSMI-TR-RD-AS-94-23 ..... p 1004 N95-19534 #

ANL-HEP-CP-94-49 ..... p 1131 N95-18551 #
ANL-HEP-CP-94-53 ..... p 1135 N95-19726 #

ANL/ACL-93/2 ..... p 975 N95-19618 #

ANL/ASD/CP-84092 ..... p 1039 N95-19727 #

ANL/CHM/CP-82280 ..... p 1100 N95-19397 #

ANL/CHM/PP-76079 ..... p 1153 N95-19724 #

ANL/CMT/CP-83637 ..... p 1053 N95-19074 #
ANL/CMT/CP-83638 ..... p 1054 N95-19117 #
ANL/CMT/CP-83647 ..... p 1053 N95-19116 #
ANL/CMT/CP-83784 ..... p 1053 N95-19115 #

ANL/ESD/TM-70 ..... p 1122 N95-19704 #

ANL/ET/CP-82163 ..... p 1150 N95-19094 #
ANL/ET/CP-83611 ..... p 1012 N95-19246 #
ANL/ET/CP-83876 ..... p 1150 N95-19075 #

ANL/MCS/CP-84282 ..... p 1112 N95-19834

ANL/MCS/PP-71512 ..... p 1116 N95-17977 #
ANL/MCS/PP-71520 ..... p 1094 N95-17978 #
ANL/MCS/PP-77610 ..... p 1096 N95-18354 #

ANL/MCS/TM-191 ..... p 1111 N95-19592 #

ANL/PHY/CP-82860 ..... p 1135 N95-19787 #
ANL/PHY/CP-82861 ..... p 1135 N95-19786 #
ANL/PHY/CP-83448 ..... p 1007 N95-17961
ANL/PHY/CP-83915 ..... p 1131 N95-18550 #
ANL/PHY/CP-83992 ..... p 1131 N95-18548 #
ANL/PHY/CP-84007 ..... p 1130 N95-18427 #
ANL/PHY/CP-84024 ..... p 1130 N95-18428 #

ANL/RE/CP-82143 ..... p 1020 N95-19098 #
ANL/RE/CP-82146 ..... p 1020 N95-19099 #
ANL/RE/CP-82360 ..... p 1018 N95-18549 #

ANL/RE/PP-79251 ..... p 1017 N95-18443 #

ANL/TD/CP-82442 ..... p 1144 N95-18547 #
ANL/TD/CP-82851 ..... p 982 N95-19725 #

ANL/XFD/CP-82781 ..... p 1151 N95-19113 #

APL-UW-TR-9405 ..... p 1123 N95-18083

AR-006-903 ..... p 990 N95-19505

AR-008-225 ..... p 1128 N95-19770
AR-008-234 ..... p 1020 N95-19139
AR-008-245 ..... p 1005 N95-19771
AR-008-252 ..... p 1124 N95-19057
AR-008-255 ..... p 1046 N95-19504
AR-008-263 ..... p 1075 N95-19503
AR-008-342 ..... p 971 N95-19467
AR-008-562 ..... p 1092 N95-19502
AR-008-932 ..... p 1005 N95-19622

ARA-MEMO-390 ..... p 1030 N95-19774 #
ARA-MEMO-391 ..... p 932 N95-19772 #
ARA-MEMO-392 ..... p 931 N95-19546 #
ARA-MEMO-399 ..... p 1031 N95-19775 #
ARA-MEMO-400 ..... p 1030 N95-19506 #
ARA-MEMO-401 ..... p 1031 N95-19776 #
ARA-MEMO-402 ..... p 1031 N95-19778 #
ARA-MEMO-403 ..... p 1031 N95-19777 #
ARA-MEMO-406 ..... p 946 N95-19789 #
ARA-MEMO-408 ..... p 1194 N95-19773 #

ARA-90 ..... p 932 N95-19574 #

ARB-R-94/534 ..... p 1061 N95-19582 #

ARI-TR-1004 ..... p 1088 N95-18095 #

ARL-CR-175 ..... p 979 N95-18948 #
ARL-CR-219 ..... p 1043 N95-19567 * #
ARL-CR-220 ..... p 1041 N95-18541 * #

ARL-MR-140 ..... p 995 N95-18136
ARL-MR-146 ..... p 1033 N95-18620 #
ARL-MR-184 ..... p 929 N95-18611 #

ARL-RR-4 ..... p 971 N95-19467

ARL-TN-49 ..... p 960 N95-19848

ARL-TR-255 ..... p 1139 N95-18142
ARL-TR-283 ..... p 1141 N95-19085 #
ARL-TR-342 ..... p 972 N95-19851
ARL-TR-344 ..... p 970 N95-18612 #
ARL-TR-366 ..... p 998 N95-18520
ARL-TR-388 ..... p 1008 N95-18378 #
ARL-TR-403 ..... p 1042 N95-18935 * #
ARL-TR-438 ..... p 930 N95-18670
ARL-TR-446 ..... p 976 N95-19729
ARL-TR-481 ..... p 1131 N95-18519
ARL-TR-489 ..... p 942 N95-18381
ARL-TR-509 ..... p 979 N95-18939 #
ARL-TR-522 ..... p 1063 N95-18115 #
ARL-TR-523 ..... p 1068 N95-18117 #
ARL-TR-524 ..... p 1090 N95-18029 #
ARL-TR-582 ..... p 1122 N95-19603 #
ARL-TR-600 ..... p 1042 N95-19125 * #
ARL-TR-73 ..... p 986 N95-19064

ASC-TR-94-5026-PHASE-1 ..... p 942 N95-18398

ASIAC-TR-94-21 ..... p 1046 N95-19522 #

ASL-94-001 ..... p 1002 N95-19103

ASTRO-PH/9402021 ..... p 1121 N95-19030 * #
ASTRO-PH/9402028 ..... p 1180 N95-18964 * #

ATC-219 ..... p 1070 N95-18384

B-253238 ..... p 1172 N95-19141 #
B-255081 ..... p 1171 N95-18596 #
B-255687 ..... p 1171 N95-18578 #
B-256459 ..... p 1171 N95-18595 #
B-258041 ..... p 1174 N95-18914 #
B-259020 ..... p 965 N95-19131 #

BBC-RD-1993/11 ..... p 1002 N95-19135
BBC-RD-1993/12 ..... p 999 N95-18540
BBC-RD-1993/13 ..... p 997 N95-18494
BBC-RD-1993/14 ..... p 999 N95-18536
BBC-RD-1993/15 ..... p 998 N95-18537
BBC-RD-1993/4 ..... p 1003 N95-19136
BBC-RD-1993/5-PT-1 ..... p 993 N95-19138
BBC-RD-1993/6-PT-2 ..... p 993 N95-19137
BBC-RD-1993/7 ..... p 1124 N95-19054
BBC-RD-1993/8 ..... p 993 N95-19053
BBC-RD-1994/06 ..... p 1124 N95-19048
BBC-RD-1994/10 ..... p 1001 N95-19047
BBC-RD-1994/11 ..... p 1124 N95-19046
BBC-RD-1994/12 ..... p 1123 N95-18566
BBC-RD-1994/1 ..... p 998 N95-18538
BBC-RD-1994/2 ..... p 1001 N95-19052
BBC-RD-1994/3 ..... p 1001 N95-19051
BBC-RD-1994/4 ..... p 998 N95-18535
BBC-RD-1994/5 ..... p 1001 N95-19049
BBC-RD-1994/7 ..... p 998 N95-18534

BBC-RD-1994/8 ..... p 992 N95-18533
BBC-RD-1994/9 ..... p 1001 N95-19050

BFLRF-298 ..... p 989 N95-19826 #

BNL-60422 ..... p 1055 N95-19858 #
BNL-60498 ..... p 1038 N95-19243 #
BNL-60519 ..... p 1150 N95-19091 #

BRL-IMR-971 ..... p 930 N95-18670

CAP-107-94R ..... p 1038 N95-19243 #

CAR-TR-722 ..... p 1140 N95-18480 #
CAR-TR-732 ..... p 1140 N95-18478 #

CARDIVNSWC-SSM-64-94/12 ..... p 986 N95-18678

CARDIVNSWC-TR-61-94-06 ..... p 980 N95-19539 #

CARDIVNSWC-94/003 ..... p 991 N95-18913 * #

CBPF-NF-030/92 ..... p 1156 N95-18333 #
CBPF-NF-031/92 ..... p 1130 N95-18356 #
CBPF-NF-034/92 ..... p 1130 N95-18366 #
CBPF-NF-037/92 ..... p 1118 N95-18878 #

CCR-94-08 ..... p 990 N95-18082 * #

CERC-TR-94-9-VOL-1 ..... p 1074 N95-18470 #

CERC-91-1-SUPPL-3 ..... p 1074 N95-18160 #

CERL-SR-EC-94/17 ..... p 1062 N95-19860
CERL-SR-EC-94/27 ..... p 1060 N95-18683

CGR/DC-19/94 ..... p 1002 N95-19087 #

CMU-CS-94-162 ..... p 1089 N95-19068
CMU-CS-94-170 ..... p 1093 N95-18659
CMU-CS-94-172 ..... p 1099 N95-18676
CMU-CS-94-173 ..... p 1117 N95-18658
CMU-CS-94-174 ..... p 1095 N95-18155 #
CMU-CS-94-180 ..... p 1111 N95-18892

CMU/SEI-94-SR-19 ..... p 1100 N95-19545 #
CMU/SEI-94-TR-8 ..... p 1096 N95-18364 #

CNIC-00730 ..... p 1132 N95-18883 #
CNIC-00732 ..... p 1144 N95-18886 #
CNIC-00737 ..... p 1144 N95-18887 #
CNIC-00742 ..... p 1146 N95-19241 #
CNIC-00757 ..... p 1144 N95-18885 #

CONF-9206255-SUMM ..... p 1062 N95-19879 #
CONF-9210478-1 ..... p 1034 N95-19233 #
CONF-9303281-1 ..... p 974 N95-18637 #
CONF-9304112-25 ..... p 1144 N95-18557
CONF-9304112-27 ..... p 999 N95-18558
CONF-930445-29 ..... p 1051 N95-18556
CONF-9305343-SUMM ..... p 1062 N95-19879 #
CONF-9305377-3 ..... p 1066 N95-19560 #
CONF-9306361 ..... p 1059 N95-18665 #
CONF-9306365-1 ..... p 1129 N95-18124 #
CONF-9306374-1 ..... p 1194 N95-19570 #
CONF-9307181-2 ..... p 1059 N95-18666 #
CONF-930722-60 ..... p 1035 N95-19711 #
CONF-930726-8 ..... p 929 N95-18645 #
CONF-9309259-7 ..... p 1133 N95-19232 #
CONF-9310325 ..... p 1114 N95-18875 #
CONF-9310328-2 ..... p 987 N95-19399 #
CONF-9311255-1 ..... p 1112 N95-19834
CONF-931130-1 ..... p 1049 N95-18145 #
CONF-940113-11 ..... p 929 N95-18646 #
CONF-940142-44 ..... p 1035 N95-19394 #
CONF-940286-2 ..... p 980 N95-19400 #
CONF-940286-4 ..... p 978 N95-18128 #
CONF-940299-1 ..... p 1122 N95-18127 #
CONF-9403164-1 ..... p 1151 N95-19569 #
CONF-9404189-1 ..... p 1148 N95-18064
CONF-9404190-1 ..... p 984 N95-18348 #
CONF-9404198-2 ..... p 1130 N95-18427 #
CONF-9404213-1 ..... p 986 N95-18648 #
CONF-940514-13 ..... p 1134 N95-19587 #
CONF-9405143-6 ..... p 978 N95-18121 #
CONF-9405143-7 ..... p 981 N95-19568 #
CONF-9405143 ..... p 981 N95-19723 #
CONF-9405199-1 ..... p 1007 N95-17961
CONF-9405204-2 ..... p 1152 N95-19621 #
CONF-9405215-SUMM ..... p 1111 N95-19592 #
CONF-9405219-6 ..... p 1148 N95-18122 #
CONF-9405237-1 ..... p 1137 N95-19561 #
CONF-940531-3 ..... p 1004 N95-19555 #
CONF-940548-7 ..... p 1054 N95-19855 #
CONF-940552-12 ..... p 1143 N95-17969 #
CONF-940552-20 ..... p 1146 N95-19509 #
CONF-940552-21 ..... p 1146 N95-19250 #
CONF-940552-24 ..... p 1146 N95-19378 #
CONF-940552-25 ..... p 1143 N95-18119 #
CONF-940552-29 ..... p 1146 N95-19379 #
CONF-940582-5 ..... p 1036 N95-18123 #
CONF-940592-2 ..... p 1038 N95-19248 #
CONF-940592-6 ..... p 1038 N95-19247 #
CONF-9406116-4-REV-1 ..... p 1039 N95-19507 #
CONF-940613-12 ..... p 1020 N95-19099 #
CONF-940613-13 ..... p 1018 N95-18549 #
CONF-940613-20 ..... p 1020 N95-19098 #
CONF-940616B-3 ..... p 987 N95-19227 #
CONF-940618-77 ..... p 1137 N95-19584 #
CONF-940618-90 ..... p 1138 N95-19841
CONF-9406207-1 ..... p 1076 N95-18371 #
CONF-9406235-1 ..... p 1186 N95-19249 #
CONF-9406242-2 ..... p 1131 N95-18550 #
CONF-9406248-1 ..... p 1131 N95-18554 #
CONF-9406248-2 ..... p 1131 N95-18551 #
CONF-9406248-3 ..... p 1131 N95-18548 #
CONF-9406259-1 ..... p 1149 N95-18650
CONF-940632-25 ..... p 1061 N95-19556 #
CONF-940634-10 ..... p 1145 N95-19201 #
CONF-940634-12 ..... p 1133 N95-19199 #
CONF-940634-9 ..... p 977 N95-17968 #
CONF-940635-13 ..... p 1133 N95-19228 #
CONF-940635-1 ..... p 1143 N95-17965
CONF-940664-26 ..... p 1137 N95-19588 #
CONF-940704-3 ..... p 977 N95-17962 #
CONF-9407108-1 ..... p 980 N95-19395 #
CONF-9407115-2 ..... p 1155 N95-19838
CONF-9407124-1 ..... p 1063 N95-18148 #
CONF-9407124-2 ..... p 1063 N95-18125 #
CONF-9407125-1 ..... p 1130 N95-18428 #
CONF-9407129-2 ..... p 1194 N95-19612 #
CONF-940714-15 ..... p 1151 N95-19113 #
CONF-940722-24 ..... p 1196 N95-19619 #
CONF-940722-29 ..... p 1135 N95-19835
CONF-940723-19 ..... p 1032 N95-18130 #
CONF-940723-21 ..... p 1034 N95-19229 #
CONF-940723-22 ..... p 1039 N95-19708 #
CONF-940723-24 ..... p 1135 N95-19709 #
CONF-940723-25 ..... p 1033 N95-18555 #
CONF-940723-9 ..... p 964 N95-18639 #
CONF-940748-14 ..... p 1098 N95-18652 #
CONF-940788-3 ..... p 1120 N95-18653 #
CONF-9408107-2 ..... p 1155 N95-17996
CONF-9408115-2 ..... p 1174 N95-18872 #
CONF-940812-11 ..... p 966 N95-17997 #
CONF-9408121-2 ..... p 1039 N95-19398 #
CONF-9408125-35 ..... p 1039 N95-19727 #
CONF-9408126-2 ..... p 1174 N95-18873 #
CONF-940813-21 ..... p 1134 N95-19590 #
CONF-9408130-1 ..... p 1012 N95-19246 #
CONF-9408131-2 ..... p 1100 N95-19397 #
CONF-9408145-1 ..... p 1059 N95-18647 #
CONF-9408155-1 ..... p 1152 N95-19586 #
CONF-9408155-5 ..... p 1151 N95-19235 #
CONF-9408155-6 ..... p 1122 N95-19234 #
CONF-9408155-7 ..... p 1152 N95-19615 #
CONF-9408155-8 ..... p 1152 N95-19620 #
CONF-940816-35 ..... p 1135 N95-19726 #
CONF-9408164-1 ..... p 1114 N95-18649 #
CONF-940831-1 ..... p 1011 N95-19200 #
CONF-940839-1 ..... p 988 N95-19558 #
CONF-940843-5 ..... p 1144 N95-18547 #
CONF-940846-2 ..... p 1152 N95-19585 #
CONF-940865-1 ..... p 1150 N95-19075 #
CONF-940865-2 ..... p 1150 N95-19094 #
CONF-940873-4 ..... p 1176 N95-19589 #
CONF-940883-2 ..... p 1053 N95-19115 #
CONF-940883-3 ..... p 1054 N95-19117 #
CONF-940883-4 ..... p 1053 N95-19116 #
CONF-940883-5 ..... p 1053 N95-19074 #
CONF-940883-6 ..... p 1054 N95-19591 #
CONF-940889-3 ..... p 1142 N95-19710 #
CONF-9409105-3 ..... p 1146 N95-19527 #
CONF-9409179-1 ..... p 980 N95-19396 #
CONF-9409179-2 ..... p 979 N95-19093 #
CONF-940922-1 ..... p 1135 N95-19786 #
CONF-940922-2 ..... p 1135 N95-19787 #
CONF-940933-7 ..... p 982 N95-19725 #
CONF-940978-3 ..... p 1129 N95-18144 #
CONF-940981-3 ..... p 976 N95-19836
CONF-941006-2 ..... p 1039 N95-19508 #
CONF-9410114-2 ..... p 1134 N95-19557 #
CONF-941013-1 ..... p 1152 N95-19608 #
CONF-9410140-1 ..... p 1173 N95-18063
CONF-9410154-2 ..... p 1006 N95-19833
CONF-9410184-2 ..... p 981 N95-19611 #
CONF-9410189-3 ..... p 1036 N95-18126 #
CONF-9410200-1 ..... p 986 N95-18651 #
CONF-9410204-1 ..... p 1176 N95-19876 #
CONF-941063-2 ..... p 1012 N95-19240 #
CONF-941063-6 ..... p 975 N95-19559 #
CONF-941102-21 ..... p 1116 N95-18131 #
CONF-9411103-1 ..... p 1112 N95-17948 #
CONF-941118-7 ..... p 1116 N95-18120 #
CONF-941125-1 ..... p 1053 N95-18463 #
CONF-941178-1 ..... p 1117 N95-18346 #
CONF-941203-1 ..... p 1055 N95-19858 #
CONF-941203-2 ..... p 1013 N95-19872 #
CONF-941203-3 ..... p 1055 N95-19859 #
CONF-941203-4 ..... p 1055 N95-19873 #
CONF-941221-2 ..... p 1014 N95-19881 #
CONF-950130-1 ..... p 1112 N95-19831

CONTRIB-5350 ..... p 1060 N95-19033 * #

COO-2197-140 ..... p 1129 N95-18124 #

CS-TR-3305 ..... p 1140 N95-18480 #
CS-TR-3341 ..... p 1140 N95-18478 #

CS-1994-33 ..... p 1110 N95-18521 * #

CSP-93-1041 ..... p 1087 N95-19695 #

CWP-154P ..... p 1066 N95-19560 #

DCIEM-94-40 ..... p 1088 N95-18151 #

DDC-RO1-ADECD-NAS ..... p 1040 N95-18041 * #

DE93-000075 ..... p 1054 N95-19854 #
DE94-000210 ..... p 1056 N95-19878 #
DE94-000264 ..... p 1053 N95-18463 #
DE94-008502 ..... p 1132 N95-18644 #
DE94-010252 ..... p 1062 N95-19879 #
DE94-011838 ..... p 1056 N95-19880 #
DE94-011859 ..... p 1014 N95-19881 #
DE94-011865 ..... p 1054 N95-19855 #
DE94-011866 ..... p 929 N95-18645 #
DE94-011867 ..... p 929 N95-18646 #
DE94-011870 ..... p 1056 N95-17943 #
DE94-011872 ..... p 1055 N95-19856 #
DE94-011880 ..... p 1055 N95-19857 #
DE94-011881 ..... p 1056 N95-17944 #
DE94-011887 ..... p 1151 N95-19541 #
DE94-011898 ..... p 1052 N95-17945 #
DE94-011899 ..... p 1056 N95-19882 #
DE94-012456 ..... p 1020 N95-19098 #
DE94-012457 ..... p 1020 N95-19099 #
DE94-012462 ..... p 1018 N95-18549 #
DE94-012473 ..... p 990 N95-19100 #
DE94-013112 ..... p 974 N95-18637 #
DE94-013442 ..... p 1012 N95-19240 #
DE94-013543 ..... p 1055 N95-19858 #
DE94-013606 ..... p 1063 N95-17946 #
DE94-013609 ..... p 1063 N95-17947 #
DE94-014251 ..... p 1055 N95-19859 #
DE94-014252 ..... p 1013 N95-19872 #
DE94-014289 ..... p 1055 N95-19873 #
DE94-014296 ..... p 1117 N95-18346 #
DE94-014331 ..... p 1040 N95-17995
DE94-014416 ..... p 1155 N95-17996
DE94-014439 ..... p 966 N95-17997 #
DE94-014460 ..... p 1173 N95-18063
DE94-014485 ..... p 1143 N95-17965
DE94-014508 ..... p 1129 N95-18049 #
DE94-014663 ..... p 977 N95-17968 #
DE94-014682 ..... p 973 N95-17966
DE94-014716 ..... p 1143 N95-17969 #
DE94-014808 ..... p 1148 N95-18064
DE94-014820 ..... p 1063 N95-17967
DE94-015044 ..... p 1057 N95-18022 #
DE94-015078 ..... p 1007 N95-17961
DE94-015200 ..... p 1076 N95-18371 #
DE94-015204 ..... p 984 N95-18348 #
DE94-015275 ..... p 1145 N95-19201 #
DE94-015338 ..... p 1030 N95-19578 #
DE94-015351 ..... p 971 N95-19579 #
DE94-015761 ..... p 1098 N95-18652 #
DE94-015802 ..... p 1133 N95-19199 #
DE94-015805 ..... p 1120 N95-18653 #
DE94-016098 ..... p 1035 N95-19394 #
DE94-016099 ..... p 1011 N95-19200 #
DE94-016150 ..... p 980 N95-19395 #
DE94-016170 ..... p 980 N95-19396 #
DE94-016180 ..... p 1037 N95-18349 #
DE94-016181 ..... p 1037 N95-18350 #
DE94-016182 ..... p 985 N95-18638 #
DE94-016197 ..... p 964 N95-18639 #
DE94-016217 ..... p 1197 N95-18351
DE94-016223 ..... p 1143 N95-18353 #
DE94-016344 ..... p 1096 N95-18354 #
DE94-016346 ..... p 1100 N95-19397 #
DE94-016365 ..... p 1039 N95-19398 #
DE94-016372 ..... p 1012 N95-19246 #
DE94-016427 ..... p 984 N95-18355 #
DE94-016443 ..... p 1038 N95-19247 #
DE94-016444 ..... p 1038 N95-19248 #

DE94-016445 ..... p 1186 N95-19249 #
DE94-016450 ..... p 1146 N95-19250 #
DE94-016544 ..... p 1039 N95-19507 #
DE94-016547 ..... p 1039 N95-19508 #
DE94-016548 ..... p 1146 N95-19509 #
DE94-016564 ..... p 1112 N95-17948 #
DE94-016633 ..... p 1037 N95-18357 #
DE94-016773 ..... p 988 N95-19580 #
DE94-016806 ..... p 1150 N95-19091 #
DE94-016860 ..... p 1145 N95-19092 #
DE94-016877 ..... p 979 N95-19093 #
DE94-016907 ..... p 1150 N95-19094 #
DE94-016947 ..... p 979 N95-18358 #
DE94-016954 ..... p 987 N95-19095 #
DE94-016971 ..... p 1038 N95-19096 #
DE94-017046 ..... p 1002 N95-19097 #
DE94-017047 ..... p 980 N95-19111 #
DE94-017067 ..... p 1060 N95-19112 #
DE94-017072 ..... p 1151 N95-19113 #
DE94-017073 ..... p 1053 N95-19115 #
DE94-017075 ..... p 1053 N95-19116 #
DE94-017079 ..... p 1054 N95-19117 #
DE94-017080 ..... p 1053 N95-19074 #
DE94-017085 ..... p 1150 N95-19075 #
DE94-017170 ..... p 991 N95-19076 #
DE94-017171 ..... p 1133 N95-19077 #
DE94-017293 ..... p 1008 N95-18143 #
DE94-017329 ..... p 1133 N95-19078 #
DE94-017330 ..... p 1145 N95-19079 #
DE94-017338 ..... p 1174 N95-18872 #
DE94-017350 ..... p 1174 N95-18873 #
DE94-017355 ..... p 1132 N95-18874 #
DE94-017359 ..... p 1136 N95-18893 #
DE94-017390 ..... p 1053 N95-18894 #
DE94-017407 ..... p 1129 N95-18144 #
DE94-017468 ..... p 1049 N95-18145 #
DE94-017484 ..... p 1059 N95-18664 #
DE94-017491 ..... p 1060 N95-18895 #
DE94-017496 ..... p 1118 N95-18896 #
DE94-017497 ..... p 1137 N95-18897 #
DE94-017514 ..... p 1038 N95-19243 #
DE94-017515 ..... p 1143 N95-18119 #
DE94-017517 ..... p 1146 N95-19378 #
DE94-017520 ..... p 1146 N95-19379 #
DE94-017530 ..... p 1080 N95-19244 #
DE94-017557 ..... p 1135 N95-18146 #
DE94-017558 ..... p 1136 N95-18147 #
DE94-017575 ..... p 1133 N95-19245 #
DE94-017576 ..... p 1198 N95-19283 #
DE94-017651 ..... p 1059 N95-18665 #
DE94-017688 ..... p 987 N95-19399 #
DE94-017697 ..... p 987 N95-19227 #
DE94-017709 ..... p 980 N95-19400 #
DE94-017754 ..... p 1122 N95-18127 #
DE94-017857 ..... p 978 N95-18128 #
DE94-017861 ..... p 1112 N95-19831
DE94-017895 ..... p 1059 N95-18666 #
DE94-017911 ..... p 980 N95-19401 #
DE94-018061 ..... p 1109 N95-18129 #
DE94-018063 ..... p 1059 N95-18647 #
DE94-018073 ..... p 1032 N95-18130 #
DE94-018114 ..... p 1133 N95-19228 #
DE94-018130 ..... p 1116 N95-18131 #
DE94-018134 ..... p 1116 N95-18120 #
DE94-018146 ..... p 978 N95-18121 #
DE94-018181 ..... p 1148 N95-18122 #
DE94-018193 ..... p 1036 N95-18123 #
DE94-018208 ..... p 1137 N95-19584 #
DE94-018209 ..... p 1152 N95-19585 #
DE94-018211 ..... p 1152 N95-19586 #
DE94-018215 ..... p 1134 N95-19587 #
DE94-018255 ..... p 1129 N95-18124 #
DE94-018278 ..... p 1063 N95-18125 #
DE94-018307 ..... p 1036 N95-18126 #
DE94-018310 ..... p 1063 N95-18148 #
DE94-018316 ..... p 1034 N95-19229 #
DE94-018335 ..... p 1137 N95-19588 #
DE94-018337 ..... p 1146 N95-19527 #
DE94-018356 ..... p 1130 N95-18427 #
DE94-018357 ..... p 1130 N95-18428 #
DE94-018361 ..... p 1017 N95-18443 #
DE94-018362 ..... p 1144 N95-18547 #
DE94-018388 ..... p 1131 N95-18548 #
DE94-018390 ..... p 1131 N95-18550 #
DE94-018395 ..... p 1131 N95-18551 #
DE94-018450 ..... p 1176 N95-19589 #
DE94-018451 ..... p 1134 N95-19590 #
DE94-018452 ..... p 1054 N95-19591 #
DE94-018499 ..... p 1111 N95-19592 #
DE94-018550 ..... p 1136 N95-18552 #
DE94-018558 ..... p 1012 N95-19230 #
DE94-018566 ..... p 981 N95-19703 #
DE94-018575 ..... p 1122 N95-19704 #
DE94-018581 ..... p 1131 N95-18554 #
DE94-018582 ..... p 1134 N95-19705 #
DE94-018583 ..... p 1135 N95-19706 #
DE94-018584 ..... p 981 N95-19707 #
DE94-018589 ..... p 1012 N95-19231 #
DE94-018592 ..... p 1039 N95-19708 #
DE94-018593 ..... p 1135 N95-19709 #
DE94-018594 ..... p 1142 N95-19710 #
DE94-018596 ..... p 1035 N95-19711 #
DE94-018597 ..... p 1033 N95-18555 #
DE94-018598 ..... p 988 N95-19721 #
DE94-018606 ..... p 1039 N95-19722 #
DE94-018660 ..... p 1133 N95-19232 #
DE94-018661 ..... p 1051 N95-18556
DE94-018708 ..... p 1034 N95-19233 #
DE94-018725 ..... p 986 N95-18648 #
DE94-018739 ..... p 1114 N95-18649 #
DE94-018743 ..... p 1149 N95-18650
DE94-018889 ..... p 1122 N95-19234 #
DE94-018892 ..... p 1151 N95-19235 #
DE94-018903 ..... p 986 N95-18651 #
DE94-018942 ..... p 1144 N95-18557
DE94-018951 ..... p 999 N95-18558
DE94-018999 ..... p 977 N95-17962 #
DE94-019108 ..... p 1031 N95-17963 #
DE94-019198 ..... p 1129 N95-17976 #
DE94-019264 ..... p 1116 N95-17977 #
DE94-019265 ..... p 1094 N95-17978 #
DE94-626221 ..... p 1114 N95-18875 #
DE94-626640 ..... p 1118 N95-18876 #
DE94-626641 ..... p 1180 N95-18877 #
DE94-626643 ..... p 1118 N95-18878 #
DE94-626645 ..... p 1156 N95-18879 #
DE94-626650 ..... p 1198 N95-18880 #
DE94-626659 ..... p 1156 N95-18328 #
DE94-626672 ..... p 1130 N95-18329 #
DE94-626675 ..... p 1148 N95-18330 #
DE94-626680 ..... p 996 N95-18331 #
DE94-626684 ..... p 1156 N95-18333 #
DE94-626685 ..... p 1130 N95-18356 #
DE94-626686 ..... p 1156 N95-18352 #
DE94-626687 ..... p 1130 N95-18360 #
DE94-626698 ..... p 1130 N95-18366 #
DE94-626716 ..... p 996 N95-18367 #
DE94-626720 ..... p 1136 N95-18881 #
DE94-626721 ..... p 1132 N95-18882 #
DE94-626822 ..... p 1132 N95-18883 #
DE94-626957 ..... p 1132 N95-18884 #
DE94-626964 ..... p 1144 N95-18885 #
DE94-627004 ..... p 1144 N95-18886 #
DE94-627009 ..... p 1144 N95-18887 #
DE94-627019 ..... p 1146 N95-19241 #
DE94-627031 ..... p 1151 N95-19242 #
DE94-629193 ..... p 983 N95-17942 #
DE94-631466 ..... p 975 N95-19550 #
DE94-770648 ..... p 1138 N95-19874 #
DE94-770767 ..... p 1012 N95-19548 #
DE94-770773 ..... p 1146 N95-19549 #
DE95-000215 ..... p 1054 N95-19832 #
DE95-000313 ..... p 1039 N95-19551 #
DE95-000314 ..... p 1147 N95-19552 #
DE95-000344 ..... p 1035 N95-19553 #
DE95-000406 ..... p 1054 N95-19554 #
DE95-000423 ..... p 1004 N95-19555 #
DE95-000489 ..... p 1061 N95-19556 #
DE95-000493 ..... p 1134 N95-19557 #
DE95-000497 ..... p 1093 N95-19875 #
DE95-000538 ..... p 988 N95-19558 #
DE95-000541 ..... p 975 N95-19559 #
DE95-000545 ..... p 1176 N95-19876 #
DE95-000552 ..... p 1006 N95-19833
DE95-000610 ..... p 968 N95-19877 #
DE95-000645 ..... p 1066 N95-19560 #
DE95-000648 ..... p 1137 N95-19561 #
DE95-000662 ..... p 1134 N95-19562 #
DE95-000686 ..... p 981 N95-19568 #
DE95-000784 ..... p 1151 N95-19569 #
DE95-000787 ..... p 1194 N95-19570 #
DE95-000789 ..... p 1152 N95-19615 #
DE95-000793 ..... p 975 N95-19616 #
DE95-000795 ..... p 1178 N95-19617 #
DE95-000834 ..... p 975 N95-19618 #
DE95-000849 ..... p 1196 N95-19619 #
DE95-000850 ..... p 1152 N95-19620 #
DE95-000856 ..... p 1152 N95-19621 #
DE95-000896 ..... p 1152 N95-19608 #
DE95-000904 ..... p 1119 N95-19609 #
DE95-000909 ..... p 981 N95-19610 #
DE95-000940 ..... p 981 N95-19611 #
DE95-001014 ..... p 1194 N95-19612 #
DE95-001046 ..... p 1077 N95-19613 #
DE95-001055 ..... p 981 N95-19723 #
DE95-001064 ..... p 1153 N95-19724 #
DE95-001066 ..... p 979 N95-18934 #
DE95-001067 ..... p 982 N95-19725 #
DE95-001094 ..... p 1135 N95-19726 #
DE95-001096 ..... p 1039 N95-19727 #
DE95-001179 ..... p 976 N95-19785 #
DE95-001440 ..... p 1135 N95-19786 #
DE95-001442 ..... p 1135 N95-19787 #
DE95-001472 ..... p 1112 N95-19834
DE95-002216 ..... p 1135 N95-19835
DE95-002352 ..... p 976 N95-19836
DE95-002402 ..... p 1155 N95-19838
DE95-002615 ..... p 1147 N95-19837
DE95-002690 ..... p 977 N95-19839
DE95-002800 ..... p 977 N95-19840
DE95-002868 ..... p 1138 N95-19841
DE95-002952 ..... p 1013 N95-19842

DLR-FB-94-06 ..... p 948 N95-18911 #
DLR-FB-94-11 ..... p 1132 N95-18912 #
DLR-FB-94-12 ..... p 930 N95-18910 #

DLR-94-04 ..... p 1019 N95-18609 #

DNA-TR-92-163 ..... p 1131 N95-18474
DNA-TR-93-102 ..... p 1148 N95-17960

DODA-AR-008-375 ..... p 960 N95-19848
DODA-AR-008-623 ..... p 1073 N95-19712 #
DODA-AR-008-636 ..... p 1045 N95-18472
DODA-AR-008-640 ..... p 975 N95-19699 #
DODA-AR-008-839 ..... p 1032 N95-18085
DODA-AR-008-906 ..... p 1058 N95-18091
DODA-AR-009-029 ..... p 1095 N95-18089

DOE/CH-10093/203 ..... p 1054 N95-19854 #

DOE/ER-0621P ..... p 1077 N95-19613 #
DOE/ER-13434/T2 ..... p 977 N95-19840
DOE/ER-13591/8 ..... p 984 N95-18355 #
DOE/ER-13633/12 ..... p 977 N95-19839
DOE/ER-13778/62 ..... p 1132 N95-18874 #
DOE/ER-13833/19 ..... p 973 N95-17966
DOE/ER-13929/5 ..... p 1030 N95-19578 #
DOE/ER-14079/34 ..... p 1066 N95-19560 #
DOE/ER-14231/1 ..... p 1063 N95-17967
DOE/ER-14252/1 ..... p 1037 N95-18349 #
DOE/ER-14252/2 ..... p 1037 N95-18350 #
DOE/ER-25123/T1 ..... p 1119 N95-19609 #
DOE/ER-25158/T1 ..... p 1093 N95-19875 #
DOE/ER-40397/T1 ..... p 1132 N95-18644 #
DOE/ER-40561/148 ..... p 1133 N95-19245 #
DOE/ER-40561/149 ..... p 1198 N95-19283 #
DOE/ER-40561/156 ..... p 1131 N95-18554 #
DOE/ER-40561/158 ..... p 1134 N95-19705 #
DOE/ER-40561/159 ..... p 1135 N95-19706 #
DOE/ER-40739/2 ..... p 1129 N95-17976 #
DOE/ER-40748/2 ..... p 1136 N95-18893 #
DOE/ER-45328/8 ..... p 979 N95-18358 #
DOE/ER-45354/6 ..... p 981 N95-19610 #
DOE/ER-45367/6 ..... p 980 N95-19111 #
DOE/ER-45461/T1 ..... p 987 N95-19095 #
DOE/ER-45477/2 ..... p 1134 N95-19562 #
DOE/ER-52122/10 ..... p 1002 N95-19097 #
DOE/ER-53194/4 ..... p 1143 N95-18353 #
DOE/ER-54181/2 ..... p 985 N95-18638 #
DOE/ER-60397/T8 ..... p 1057 N95-18022 #
DOE/ER-60447/T6 ..... p 981 N95-19703 #
DOE/ER-61447/1 ..... p 1062 N95-19879 #
DOE/ER-61578/1 ..... p 1059 N95-18665 #
DOE/ER-61666/1 ..... p 1060 N95-19112 #

DOE/ET-53088/T5 ..... p 1145 N95-19079 #
DOE/ET-53088/T6 ..... p 1133 N95-19078 #
DOE/ET-53088/666 ..... p 1145 N95-19092 #
DOE/ET-53088/672 ..... p 1147 N95-19837

DOE/ID-13074/T12 ..... p 1040 N95-17995

DOE/NASA/0329-2 ..... p 1040 N95-18041 * #

DOE/PC-92112/T5 ..... p 976 N95-19785 #
DOE/PC-93204/T1 ..... p 1054 N95-19554 #
DOE/PC-93219/T2 ..... p 1053 N95-18894 #

DOE/R2-15556/T1 ..... p 988 N95-19580 #

DOE/TIC-4500-R74 ..... p 979 N95-18934 #

DOT-VNTSC-FAA-94-11 ..... p 996 N95-18436
DOT-VNTSC-FAA-94-12 ..... p 929 N95-18624 #

DOT/FAA/AM-94/22-PT-3 ..... p 1080 N95-19384 #
DOT/FAA/AM-94/23-PT-4 ..... p 1080 N95-19385 #

DOT/FAA/CT-TN94/27 ..... p 1000 N95-18686
DOT/FAA/CT-TN94/29 ..... p 958 N95-18087 #
DOT/FAA/CT-TN94/6 ..... p 941 N95-18088 #

DOT/FAA/CT-92/13 ..... p 940 N95-19805
DOT/FAA/CT-93/49 ..... p 941 N95-19810
DOT/FAA/CT-93/68 ..... p 1047 N95-19804

DOT/FAA/RD-94-25 ..... p 929 N95-18624 #
DOT/FAA/RD-94/15 ..... p 996 N95-18436
DOT/FAA/RD-94/23 ..... p 940 N95-18059 #
DOT/FAA/RD-94/7 ..... p 942 N95-18198 * #

DPW-56-321 ..... p 980 N95-19401 #

DREO-TN-93-28-PT-2 ..... p 989 N95-19866

DREO-1202 ..... p 989 N95-19867

DSTO-GD-0021 ..... p 1005 N95-19622

DSTO-TR-0046 ..... p 1058 N95-18091

DU/DC/TR-40 ..... p 1154 N95-19807
DU/DC/TR-41 ..... p 1154 N95-19806
DU/DC/TR-42/AASERT-01 ..... p 1154 N95-19812

E-7584 ..... p 1042 N95-18935 * #
E-7825 ..... p 967 N95-18195 * #
E-8151 ..... p 1034 N95-19236 * #
E-8198 ..... p 1040 N95-18041 * #
E-8680 ..... p 964 N95-18495 * #
E-8825 ..... p 1044 N95-18199 * #
E-8885 ..... p 967 N95-18570 * #
E-8953 ..... p 981 N95-19652 * #
E-9111 ..... p 949 N95-19380 * #
E-9121 ..... p 970 N95-18940 * #
E-9157 ..... p 968 N95-19795 * #
E-9175 ..... p 959 N95-18586 * #
E-9209 ..... p 990 N95-18211 * #
E-9211 ..... p 969 N95-18448 * #
E-9219 ..... p 1016 N95-18212 * #
E-9227 ..... p 928 N95-18457 * #
E-9239 ..... p 1046 N95-19501 * #
E-9253 ..... p 1019 N95-18898 * #
E-9265 ..... p 1034 N95-18938 * #
E-9267 ..... p 991 N95-19788 * #
E-9276 ..... p 1000 N95-18733 * #
E-9278 ..... p 1015 N95-18107 * #
E-9281 ..... p 927 N95-18486 * #
E-9283 ..... p 927 N95-18197 * #
E-9292 ..... p 1043 N95-18583 * #
E-9294 ..... p 980 N95-19286 * #
E-9296 ..... p 1045 N95-18909 * #
E-9297 ..... p 962 N95-18387 * #
E-9303 ..... p 1041 N95-18541 * #
E-9332 ..... p 927 N95-18044 * #
E-9339 ..... p 1016 N95-18200 * #
E-9341 ..... p 989 N95-19783 * #
E-9345 ..... p 1043 N95-19567 * #
E-9347 ..... p 962 N95-18467 * #
E-9348 ..... p 962 N95-18045 * #
E-9349 ..... p 947 N95-18133 * #
E-9356 ..... p 958 N95-18054 * #
E-9357 ..... p 1014 N95-18036 * #
E-9362 ..... p 1053 N95-18572 * #
E-9363 ..... p 1149 N95-18453 * #
E-9366 ..... p 1042 N95-19125 * #
E-9369 ..... p 1019 N95-18941 * #
E-9375 ..... p 934 N95-19285 * #
E-9376 ..... p 934 N95-19284 * #
E-9377 ..... p 967 N95-18571 * #
E-9380 ..... p 1053 N95-18587 * #
E-9381 ..... p 933 N95-18582 * #
E-9387 ..... p 967 N95-18745 * #
E-9391 ..... p 1042 N95-19238 * #
E-9393 ..... p 955 N95-19769 * #
E-9394 ..... p 930 N95-18933 * #
E-9398 ..... p 1047 N95-19649 * #
E-9401 ..... p 972 N95-19782 * #
E-9404 ..... p 1035 N95-19794 * #
E-9416 ..... p 950 N95-19651 * #
E-9422 ..... p 982 N95-19792 * #

EGG-WTD-10299 ..... p 989 N95-19861

EPA/450/3-91/029 ..... p 1061 N95-19403 #
EPA/453/R-94/037 ..... p 1061 N95-19406 #
EPA/600/J-94/310 ..... p 1056 N95-17937 #

ERDEC-CR-132 ..... p 1091 N95-18531 #
ERDEC-CR-144 ..... p 974 N95-19170

ERDEC-TR-169 ..... p 1123 N95-18379

ERL-0800-RR ..... p 1032 N95-18065
ERL-0838-RN ..... p 1095 N95-18089

ERO-92-MM-01 ..... p 1119 N95-19820 #

ERP-1149 ..... p 1142 N95-19662
ERP-1158 ..... p 1178 N95-18451

ESC-TR-93-292 ..... p 1004 N95-19594 #
ESC-TR-93-328 ..... p 1004 N95-19565 #
ESC-TR-94-008 ..... p 1096 N95-18364 #
ESC-TR-94-196 ..... p 1005 N95-19744 #

ESD-4195 ..... p 1058 N95-18389 #

ESL-TR-88-46 ..... p 992 N95-18684

ESL-721566-3 ..... p 994 N95-18024 #

F-632 ..... p 1043 N95-19809

FEL-93-B160 ..... p 1086 N95-19537 #
FEL-94-B062 ..... p 1004 N95-19535 #

FERMILAB-PUB-92/208E ..... p 1130 N95-18366 #
FERMILAB-PUB-93/378-A-REV ... p 1180 N95-19031 * #
FERMILAB-PUB-93/399-A ..... p 1121 N95-19030 * #
FERMILAB-PUB-93/401-A ..... p 1180 N95-18746 * #
FERMILAB-PUB-94/010-A ..... p 1137 N95-18965 * #
FERMILAB-PUB-94/026-A ..... p 1180 N95-18964 * #

FMI-NAS-9614-4 ..... p 1015 N95-18111 * #

FNAL-TM-1897 ..... p 1133 N95-19077 #

FNAL/C-94-336-E ..... p 1135 N95-19835
FNAL/C-94/275-E ..... p 1137 N95-19561 #

FR-R-9231F ..... p 1155 N95-19828 #

GA-A-21594 ..... p 1135 N95-18146 #
GA-A-21597 ..... p 1136 N95-18147 #
GA-A-21703 ..... p 1146 N95-19379 #
GA-A-21704 ..... p 1143 N95-18119 #
GA-A-21718 ..... p 1146 N95-19378 #

GALCIT-94-2 ..... p 1045 N95-18613 #

GAO/GGD-94-95 ..... p 1171 N95-18595 #

GAO/NSIAD-94-116 ..... p 1172 N95-19141 #
GAO/NSIAD-94-150 ..... p 1171 N95-18596 #
GAO/NSIAD-94-71 ..... p 1171 N95-18578 #
GAO/NSIAD-95-33 ..... p 965 N95-19131 #

GAO/RCED-94-285 ..... p 1174 N95-18914 #

GRI-93/0367 ..... p 1122 N95-17983 #
GRI-94/0081 ..... p 973 N95-17982 #

GTRI-A-8612-015 ..... p 1123 N95-18930 * #

H-1913 ..... p 929 N95-18565 * #
H-2022 ..... p 945 N95-19044 * #
H-2026 ..... p 1033 N95-18735 * #
H-2030-VOL-1 ..... p 1020 N95-18955 * #
H-2030-VOL-2 ..... p 1020 N95-18956 * #

ICASE-94-100 ..... p 1116 N95-18109 * #
ICASE-94-102 ..... p 1018 N95-18488 * #
ICASE-94-78 ..... p 1098 N95-18487 * #
ICASE-94-80 ..... p 1098 N95-18584 * #
ICASE-94-86 ..... p 1016 N95-18190 * #
ICASE-94-87 ..... p 1099 N95-19027 * #
ICASE-94-88 ..... p 1100 N95-19028 * #
ICASE-94-89 ..... p 1116 N95-18110 * #
ICASE-94-90 ..... p 1015 N95-18188 * #
ICASE-94-92 ..... p 1016 N95-18191 * #
ICASE-94-93 ..... p 1017 N95-18397 * #
ICASE-94-94 ..... p 1016 N95-18193 * #
ICASE-94-95 ..... p 1099 N95-18931 * #
ICASE-94-96 ..... p 1116 N95-18108 * #
ICASE-94-97-PT-1 ..... p 1020 N95-18958 * #
ICASE-94-99 ..... p 1117 N95-18479 * #

ICOMP-94-27 ..... p 1016 N95-18212 * #
ICOMP-94-29 ..... p 1019 N95-18898 * #
ICOMP-94-31 ..... p 1016 N95-18200 * #
ICOMP-94-32 ..... p 1019 N95-18941 * #

IDA-D-1483 ..... p 1037 N95-18382

IDA/HQ-94-45195 ..... p 1037 N95-18382

IEEE-94CH3370-4 ..... p 1139 N95-18345

IFSR-666 ..... p 1145 N95-19092 #
IFSR-672 ..... p 1147 N95-19837

IFT-P-003/94 ..... p 1148 N95-18330 #
IFT-P-004/94 ..... p 996 N95-18331 #
IFT-P-005/94 ..... p 1130 N95-18329 #
IFT-P-009/94 ..... p 1156 N95-18352 #

IHES/M/94/19 ..... p 1118 N95-19198

IHES/P/94/10 ..... p 1119 N95-19719
IHES/P/94/12 ..... p 1134 N95-19376
IHES/P/94/16 ..... p 1118 N95-19375 #
IHES/P/94/21 ..... p 1119 N95-19717 #
IHES/P/94/22 ..... p 965 N95-19377 #
IHES/P/94/25 ..... p 1119 N95-19718 #

IMA-1 ..... p 1121 N95-19104

INIS-BR-3332 ..... p 1151 N95-19242 #
INIS-BR-3334 ..... p 1198 N95-18880 #

INIS-MF-13778 ..... p 1114 N95-18875 #
INIS-MF-13925 ..... p 975 N95-19550 #
INIS-MF-13928 ..... p 983 N95-17942 #

INPE-5506-TDI/518 ..... p 1064 N95-18390 #
INPE-5548-TDI/534 ..... p 1172 N95-18004 #
INPE-5565-TDI/540 ..... p 967 N95-18720 #
INPE-5571-TDI/542 ..... p 1050 N95-18369 #
INPE-5578-PRE/1806 ..... p 1050 N95-18216 #
INPE-5581-TDI/544 ..... p 1049 N95-18005 #
INPE-5583-TDI/545 ..... p 1067 N95-18006 #
INPE-5584-TDI/546 ..... p 1050 N95-18368 #
INPE-5586-TDI/548 ..... p 1050 N95-18215 #
INPE-5587-TDI/549 ..... p 1057 N95-18003 #
INPE-5588-TDI/550 ..... p 1050 N95-18214 #
INPE-5591-TDI/552 ..... p 1178 N95-18213 #

INT-FATENT-CLASS-B01D-59/44 p 1130 N95-18324 *
INT-PATENT-CLASS-B23K-10/00 p 991 N95-18326 *
INT-PATENT-CLASS-B62D-57/24 p 1041 N95-18741 *

INT-PATENT-CLASS-F16F-7/10 .. p 1041 N95-18325 *
INT-PATENT-CLASS-F28B-11/00 p 1017 N95-18323 *

INT-PATENT-CLASS-G01N-27/12 p 1032 N95-18316 *
INT-PATENT-CLASS-G01R-27/02 p 1011 N95-18959 *
INT-PATENT-CLASS-G05B-13/02 p 1113 N95-18313 *
INT-PATENT-CLASS-G05B-13/02 p 1114 N95-19062 *
INT-PATENT-CLASS-G06F-13/10 p 1175 N95-19056 *
INT-PATENT-CLASS-G06F-15/18 p 1114 N95-18740 *
INT-PATENT-CLASS-G11C-27/00 p 1093 N95-18963 *

INT-PATENT-CLASS-H01J-37/08 p 1130 N95-18324 *
INT-PATENT-CLASS-H01J-49/00 p 1130 N95-18324 *
INT-PATENT-CLASS-H01Q-19/14 p 1000 N95-18960 *
INT-PATENT-CLASS-H01S-3/10 . p 1037 N95-18322 *
INT-PATENT-CLASS-H01S-3/11 . p 1037 N95-18322 *
INT-PATENT-CLASS-H05B-6/10 . p 960 N95-18961 *
INT-PATENT-CLASS-H05B-6/14 . p 1011 N95-18962 *
INT-PATENT-CLASS-H05H-1/00 . p 1137 N95-18957 *

ISBN-0-315-84911-8 ..... p 1179 N95-18728
ISBN-0-7803-1473-5 ..... p 1139 N95-18345
ISBN-0-7803-1474-3 ..... p 1139 N95-18345
ISBN-0-7803-1475-1 ..... p 1139 N95-18345
ISBN-0-86776-503-8 ..... p 1045 N95-18608 #
ISBN-0-86776-514-3 ..... p 1071 N95-18607 #
ISBN-90-369-2035-3 ..... p 1017 N95-18396
ISBN-90-369-2036-1 ..... p 1070 N95-18392
ISBN-90-369-2041-8 ..... p 1072 N95-18926
ISBN-90-369-2042-6 ..... p 1071 N95-18395
ISBN-90-369-2043-4 ..... p 1071 N95-18394
ISBN-90-369-2050-7 ..... p 1070 N95-18393
ISBN-90-369-2054-X ..... p 1060 N95-18722
ISBN-90-6275-974-2 ..... p 1009 N95-18501
ISBN-90-9006669-1 ..... p 1118 N95-19169
ISBN-92-835-0756-8 ..... p 1020 N95-19251 #
ISBN-92-835-0758-4 ..... p 941 N95-18927 #
ISBN-92-836-0001-0 ..... p 1124 N95-19142 #
ISBN-92-836-0002-9 ..... p 956 N95-18597 #
ISBN-92-836-0003-7 ..... p 1080 N95-19413 #
ISBN-92-836-0005-3 ..... p 950 N95-19653 #
ISBN-92-836-1008-3 ..... p 948 N95-19017 #
ISBN-951-22-1760-0 ..... p 1007 N95-18037

ISI/RR-381 ..... p 1115 N95-19599 #
ISI/RR-94-380 ..... p 1111 N95-19605 #
ISI/RR-94-382 ..... p 1176 N95-19604 #
ISI/RR-94-390 ..... p 1115 N95-19601 #

ISI/SR-93-374 ..... p 1004 N95-19600 #

ISI/TM-93-389 ..... p 1012 N95-19606 #

ITP-SB-94-40 ..... p 1135 N95-19726 #

IZF-1994-B-5 ..... p 1090 N95-19583 #

JAERI-M-93-214 ..... p 1138 N95-19874 #

JINR-E-1-93-443 ..... p 1136 N95-18881 #
JINR-E-1-93-450 ..... p 1132 N95-18884 #
JINR-E-2-93-416 ..... p 1118 N95-18876 #
JINR-E-2-93-424 ..... p 1180 N95-18877 #

JINR-E-2-93-426 ..... p 1132 N95-18882 #
JINR-E-2-93-432 ..... p 996 N95-18367 #
JINR-E-2-93-433 ..... p 1130 N95-18360 #
JINR-E-2-93-439 ..... p 1156 N95-18328 #

JINR-R-4-93-427 ..... p 1156 N95-18879 #

KAPL-4744 ..... p 979 N95-18934 #

KCP-613-5376 ..... p 1012 N95-19230 #
KCP-613-5471 ..... p 981 N95-19707 #
KCP-613-5482 ..... p 1012 N95-19231 #

KNMI-SR-94-03 ..... p 1060 N95-18722

KNMI-TR-154 ..... p 1070 N95-18392

KNMI-WR-93-01 ..... p 1017 N95-18396
KNMI-WR-93-03 ..... p 1072 N95-18926
KNMI-WR-93-04 ..... p 1071 N95-18395
KNMI-WR-93-05 ..... p 1071 N95-18394
KNMI-WR-94-02 ..... p 1070 N95-18393

L-17335 ..... p 1051 N95-18465 * #
L-17336 ..... p 931 N95-19114 * #
L-17350 ..... p 931 N95-19042 * #
L-17351 ..... p 1032 N95-18194 * #
L-17376 ..... p 942 N95-18198 * #
L-17392 ..... p 995 N95-18187 * #
L-17410 ..... p 1005 N95-19781 * #
L-17432-PT-2 ..... p 934 N95-19468 * #

LA-SUB-94-38 ..... p 1063 N95-17946 #
LA-SUB-94-76 ..... p 1063 N95-17947 #

LA-UR-94-1505 ..... p 1143 N95-17969 #
LA-UR-94-1614 ..... p 1148 N95-18064
LA-UR-94-1958 ..... p 966 N95-17997 #
LA-UR-94-2014 ..... p 1117 N95-18346 #
LA-UR-94-2128 ..... p 1173 N95-18063
LA-UR-94-2168 ..... p 1155 N95-17996
LA-UR-94-2223 ..... p 1143 N95-17965
LA-UR-94-2557 ..... p 1035 N95-19394 #
LA-UR-94-2576 ..... p 1011 N95-19200 #
LA-UR-94-2612 ..... p 964 N95-18639 #
LA-UR-94-2696 ..... p 1032 N95-18130 #
LA-UR-94-2777 ..... p 1063 N95-18125 #
LA-UR-94-2846 ..... p 1036 N95-18126 #
LA-UR-94-2898 ..... p 1034 N95-19229 #
LA-UR-94-2951 ..... p 1063 N95-18148 #
LA-UR-94-2984 ..... p 1152 N95-19620 #
LA-UR-94-2995 ..... p 1196 N95-19619 #
LA-UR-94-3080 ..... p 1152 N95-19608 #
LA-UR-94-3148 ..... p 1152 N95-19621 #
LA-UR-94-3247 ..... p 981 N95-19611 #
LA-UR-94-3328 ..... p 1194 N95-19612 #

LA-12841-MS ..... p 988 N95-19721 #

LBL-34361 ..... p 1194 N95-19570 #
LBL-34973 ..... p 1137 N95-19584 #
LBL-35201 ..... p 1148 N95-18122 #
LBL-35221 ..... p 1036 N95-18123 #
LBL-35356 ..... p 1152 N95-19615 #
LBL-35433 ..... p 976 N95-19836
LBL-35673 ..... p 1151 N95-19569 #
LBL-35715 ..... p 1197 N95-18351
LBL-35725 ..... p 979 N95-19093 #
LBL-35810 ..... p 1134 N95-19587 #
LBL-35941 ..... p 1152 N95-19586 #
LBL-35942 ..... p 1152 N95-19585 #
LBL-35954 ..... p 975 N95-19616 #
LBL-36026 ..... p 1178 N95-19617 #

LC-93-61269 ..... p 1139 N95-18345
LC-94-69692 ..... p 1194 N95-19134 * #

LPI-CONTRIB-844 ..... p 1186 N95-19289 * #

LPI-TR-94-05 ..... p 1180 N95-19172 * #

LTR94-002 ..... p 1068 N95-18141

M-766 ..... p 932 N95-19623 * #
M-767 ..... p 965 N95-19780 * #
M-768 ..... p 962 N95-18932 * #

MEMO-INF-93-48 ..... p 1094 N95-18000

MIR-4/94 ..... p 1036 N95-18061

MITRE-MP-94B000007 ..... p 1000 N95-18727

MRL-CP-1 ..... p 1075 N95-19503

MRL-GD-0058 ..... p 1073 N95-19712 #

MRL-TN-623 ..... p 1128 N95-19770
MRL-TN-628 ..... p 1020 N95-19139
MRL-TN-648 ..... p 1092 N95-19502
MRL-TN-664 ..... p 975 N95-19699 #

MRL-TR-92-22 ..... p 990 N95-19505
MRL-TR-92-48 ..... p 1005 N95-19771
MRL-TR-93-1 ..... p 1124 N95-19057
MRL-TR-93-24 ..... p 959 N95-18942
MRL-TR-93-3 ..... p 1046 N95-19504
MRL-TR-94-6 ..... p 1045 N95-18472

MTR-11162 ..... p 1005 N95-19744 #

NAL-PD-SN-9306 ..... p 927 N95-18606 #

NAL-SP-9322-PT-1 ..... p 1026 N95-19444 #
NAL-SP-9412 ..... p 1028 N95-19455 #

NAL-TM-CSS-9303 ..... p 930 N95-18904 #

NAMRL-1391 ..... p 1089 N95-18414
NAMRL-1393 ..... p 1078 N95-18138

NAS 1.15:104566-VOL-18 ..... p 1076 N95-19577 * #
NAS 1.15:104616 ..... p 1196 N95-19791 * #
NAS 1.15:104806-VOL-1 ..... p 965 N95-19237 * #
NAS 1.15:104806-VOL-2 ..... p 965 N95-19624 * #
NAS 1.15:106518 ..... p 1042 N95-18935 * #
NAS 1.15:106606 ..... p 967 N95-18570 * #
NAS 1.15:106736 ..... p 947 N95-18133 * #
NAS 1.15:106745 ..... p 968 N95-19795 * #
NAS 1.15:106755 ..... p 959 N95-18586 * #
NAS 1.15:106766 ..... p 990 N95-18211 * #
NAS 1.15:106768 ..... p 969 N95-18448 * #
NAS 1.15:106771 ..... p 1016 N95-18212 * #
NAS 1.15:106776 ..... p 928 N95-18457 * #
NAS 1.15:106785 ..... p 1046 N95-19501 * #
NAS 1.15:106792 ..... p 1019 N95-18898 * #
NAS 1.15:106797 ..... p 991 N95-19788 * #
NAS 1.15:106800 ..... p 1000 N95-18733 * #
NAS 1.15:106803 ..... p 927 N95-18486 * #
NAS 1.15:106805 ..... p 927 N95-18197 * #
NAS 1.15:106807 ..... p 1043 N95-18583 * #
NAS 1.15:106808 ..... p 960 N95-19286 * #
NAS 1.15:106809 ..... p 1045 N95-18909 * #
NAS 1.15:106810 ..... p 962 N95-18387 * #
NAS 1.15:106813 ..... p 1016 N95-18200 * #
NAS 1.15:106815 ..... p 989 N95-19783 * #
NAS 1.15:106817 ..... p 958 N95-18054 * #
NAS 1.15:106818 ..... p 1014 N95-18036 * #
NAS 1.15:106820 ..... p 1053 N95-18572 * #
NAS 1.15:106821 ..... p 1149 N95-18453 * #
NAS 1.15:106822 ..... p 1042 N95-19125 * #
NAS 1.15:106823 ..... p 1019 N95-18941 * #
NAS 1.15:106826 ..... p 934 N95-19285 * #
NAS 1.15:106827 ..... p 934 N95-19284 * #
NAS 1.15:106828 ..... p 967 N95-18571 * #
NAS 1.15:106830 ..... p 1053 N95-18587 * #
NAS 1.15:106831 ..... p 933 N95-18582 * #
NAS 1.15:106832 ..... p 1042 N95-19238 * #
NAS 1.15:106833 ..... p 930 N95-18933 * #
NAS 1.15:106836 ..... p 1047 N95-19649 * #
NAS 1.15:106838 ..... p 972 N95-19782 * #
NAS 1.15:106840 ..... p 1035 N95-19794 * #
NAS 1.15:108473 ..... p 1091 N95-19061 * #
NAS 1.15:108475 ..... p 963 N95-19648 * #
NAS 1.15:108802-VOL-1 ..... p 1092 N95-18569 * #
NAS 1.15:108852 ..... p 928 N95-18101 * #
NAS 1.15:108861 ..... p 1077 N95-18734 * #
NAS 1.15:109121 ..... p 1175 N95-18950 * #
NAS 1.15:109160-VOL-1 ..... p 1099 N95-18899 * #
NAS 1.15:109161 ..... p 1058 N95-18132 * #
NAS 1.15:109164 ..... p 1175 N95-18953 * #
NAS 1.15:109172 ..... p 1175 N95-18936 * #
NAS 1.15:109207 ..... p 963 N95-18047 * #
NAS 1.15:109839 ..... p 1176 N95-19127 * #
NAS 1.15:109989 ..... p 1015 N95-18149 * #
NAS 1.15:110038 ..... p 1060 N95-18742 * #
NAS 1.15:110056 ..... p 1175 N95-19038 * #
NAS 1.15:110141 ..... p 963 N95-19790 * #
NAS 1.15:4574 ..... p 931 N95-19042 * #
NAS 1.15:4593 ..... p 1044 N95-18199 * #
NAS 1.15:4608 ..... p 981 N95-19652 * #
NAS 1.15:4612 ..... p 1032 N95-18194 * #
NAS 1.15:4613 ..... p 1005 N95-19781 * #
NAS 1.15:4632 ..... p 931 N95-19119 * #
NAS 1.15:4636 ..... p 1033 N95-18735 * #
NAS 1.15:4646 ..... p 945 N95-19044 * #
NAS 1.15:4650 ..... p 1077 N95-19140 * #
NAS 1.15:4653 ..... p 1174 N95-18573 * #
NAS 1.18:1410.13N ..... p 1171 N95-19133 * #
NAS 1.21:7011(397) ..... p 1087 N95-19746 *
NAS 1.21:7011(398) ..... p 1080 N95-19239 *
NAS 1.21:7037(313) ..... p 927 N95-19168 *
NAS 1.21:7037(314) ..... p 927 N95-19357 *

NAS 1.26:182276 ..... p 927 N95-18044 * #
NAS 1.26:188300 ..... p 1015 N95-18111 * #
NAS 1.26:188360 ..... p 956 N95-18567 * #
NAS 1.26:189389 ..... p 1173 N95-18051 * #
NAS 1.26:189390 ..... p 1172 N95-18040 * #
NAS 1.26:191045 ..... p 967 N95-18743 * #
NAS 1.26:191128 ..... p 967 N95-18195 * #
NAS 1.26:191194 ..... p 1034 N95-19236 * #
NAS 1.26:191203 ..... p 1040 N95-18041 * #
NAS 1.26:194975 ..... p 1098 N95-18584 * #
NAS 1.26:194994 ..... p 1016 N95-18190 * #
NAS 1.26:194995 ..... p 1099 N95-19027 * #
NAS 1.26:194996 ..... p 1100 N95-19028 * #
NAS 1.26:194997 ..... p 1116 N95-18110 * #
NAS 1.26:194998 ..... p 1015 N95-18188 * #
NAS 1.26:195005 ..... p 1016 N95-18191 * #
NAS 1.26:195006 ..... p 1017 N95-18397 * #
NAS 1.26:195007 ..... p 1016 N95-18193 * #
NAS 1.26:195009 ..... p 964 N95-18105 * #
NAS 1.26:195010 ..... p 1123 N95-18930 * #
NAS 1.26:195011 ..... p 1099 N95-18931 * #
NAS 1.26:195014 ..... p 1014 N95-18042 * #
NAS 1.26:195015 ..... p 1116 N95-18108 * #
NAS 1.26:195016-PT-1 ..... p 1020 N95-18958 * #
NAS 1.26:195018 ..... p 1117 N95-18479 * #
NAS 1.26:195019 ..... p 1116 N95-18109 * #
NAS 1.26:195020 ..... p 971 N95-19043 * #
NAS 1.26:195022 ..... p 1018 N95-18488 * #
NAS 1.26:195298 ..... p 964 N95-18495 * #
NAS 1.26:195349 ..... p 966 N95-18192 * #
NAS 1.26:195381 ..... p 970 N95-18940 * #
NAS 1.26:195408 ..... p 1034 N95-18938 * #
NAS 1.26:195411 ..... p 1015 N95-18107 * #
NAS 1.26:195414 ..... p 1041 N95-18541 * #
NAS 1.26:195416 ..... p 1043 N95-19567 * #
NAS 1.26:195417 ..... p 962 N95-18467 * #
NAS 1.26:195418 ..... p 962 N95-18045 * #
NAS 1.26:195426 ..... p 955 N95-19769 * #
NAS 1.26:195429 ..... p 950 N95-19651 * #
NAS 1.26:195430 ..... p 982 N95-19792 * #
NAS 1.26:195984 ..... p 1098 N95-18487 * #
NAS 1.26:196533 ..... p 1161 N95-18967 * #
NAS 1.26:196537 ..... p 1040 N95-18056 * #
NAS 1.26:196538 ..... p 969 N95-18135 * #
NAS 1.26:196542 ..... p 1195 N95-19287 * #
NAS 1.26:196543 ..... p 1068 N95-18093 * #
NAS 1.26:196970 ..... p 974 N95-18744 * #
NAS 1.26:197015 ..... p 1075 N95-18951 * #
NAS 1.26:197121 ..... p 1186 N95-19289 * #
NAS 1.26:197130 ..... p 1066 N95-19129 * #
NAS 1.26:197294 ..... p 971 N95-19650 * #
NAS 1.26:197297 ..... p 1194 N95-19575 * #
NAS 1.26:197320 ..... p 958 N95-19576 * #
NAS 1.26:197448 ..... p 1157 N95-18166 * #
NAS 1.26:197516 ..... p 945 N95-19130 * #
NAS 1.26:197519 ..... p 990 N95-18082 * #
NAS 1.26:197520 ..... p 1195 N95-17980 * #
NAS 1.26:197523 ..... p 942 N95-18090 * #
NAS 1.26:197529 ..... p 967 N95-19566 * #
NAS 1.26:197531 ..... p 1177 N95-17981 * #
NAS 1.26:197533 ..... p 1136 N95-18217 * #
NAS 1.26:197537 ..... p 1194 N95-18579 * #
NAS 1.26:197538 ..... p 1178 N95-18391 * #
NAS 1.26:197542 ..... p 1052 N95-18952 * #
NAS 1.26:197544 ..... p 1196 N95-18954 * #
NAS 1.26:197551 ..... p 1136 N95-18370 * #
NAS 1.26:197553 ..... p 1195 N95-18376 * #
NAS 1.26:197554 ..... p 1044 N95-18388 * #
NAS 1.26:197555 ..... p 1197 N95-18464 * #
NAS 1.26:197558 ..... p 1010 N95-18925 * #
NAS 1.26:197561 ..... p 1110 N95-18532 * #
NAS 1.26:197568 ..... p 1110 N95-18521 * #
NAS 1.26:197570 ..... p 1110 N95-18581 * #
NAS 1.26:197572 ..... p 978 N95-18046 * #
NAS 1.26:197573 ..... p 1064 N95-18444 * #
NAS 1.26:197574 ..... p 966 N95-18196 * #
NAS 1.26:197575 ..... p 1064 N95-18476 * #
NAS 1.26:197579 ..... p 1014 N95-18092 * #
NAS 1.26:197580 ..... p 970 N95-18471 * #
NAS 1.26:197591 ..... p 1109 N95-18055 * #
NAS 1.26:197592 ..... p 1180 N95-19172 * #
NAS 1.26:197593 ..... p 1017 N95-18327 * #
NAS 1.26:197595 ..... p 1043 N95-18737 * #
NAS 1.26:197597 ..... p 1118 N95-18736 * #
NAS 1.26:197598 ..... p 963 N95-18610 * #
NAS 1.26:197600 ..... p 991 N95-18913 * #
NAS 1.26:197602 ..... p 1051 N95-18739 * #
NAS 1.26:197604 ..... p 1062 N95-19779 * #
NAS 1.26:197605 ..... p 1004 N95-19547 * #
NAS 1.26:197606 ..... p 1156 N95-19037 * #
NAS 1.26:197607 ..... p 1196 N95-19034 * #
NAS 1.26:197608 ..... p 1060 N95-19033 * #
NAS 1.26:197609 ..... p 1157 N95-19363 * #
NAS 1.26:197610 ..... p 1157 N95-19358 * #
NAS 1.26:197611 ..... p 1121 N95-19348 * #
NAS 1.26:197612 ..... p 1156 N95-18949 * #

NAS 1.26:197613 ..... p 1193 N95-19341 * #
NAS 1.26:197614 ..... p 1180 N95-18966 * #
NAS 1.26:197615 ..... p 1198 N95-18747 * #
NAS 1.26:197616 ..... p 1156 N95-19340 * #
NAS 1.26:197619 ..... p 1121 N95-19288 * #
NAS 1.26:197621 ..... p 1052 N95-19126 * #
NAS 1.26:197624 ..... p 1065 N95-19032 * #
NAS 1.26:197626 ..... p 1137 N95-18965 * #
NAS 1.26:197627 ..... p 1180 N95-18964 * #
NAS 1.26:197628 ..... p 1180 N95-19031 * #
NAS 1.26:197629 ..... p 1121 N95-19030 * #
NAS 1.26:197630 ..... p 1180 N95-18746 * #
NAS 1.26:197671 ..... p 1005 N95-19796 * #
NAS 1.26:4637 ..... p 964 N95-18580 * #
NAS 1.26:4639 ..... p 970 N95-18466 * #
NAS 1.26:4642-VOL-1 ..... p 1020 N95-18955 * #
NAS 1.26:4642-VOL-2 ..... p 1020 N95-18956 * #
NAS 1.55:10147 ..... p 949 N95-19380 * #
NAS 1.55:10162-VOL-1 ..... p 1100 N95-19625 * #
NAS 1.55:10162-VOL-2 ..... p 1104 N95-19747 * #
NAS 1.55:3274-PT-2 ..... p 934 N95-19468 * #
NAS 1.55:3288 ..... p 1068 N95-18201 * #
NAS 1.60:3414 ..... p 929 N95-18565 * #
NAS 1.60:3460 ..... p 942 N95-18198 * #
NAS 1.60:3478 ..... p 931 N95-19114 * #
NAS 1.60:3485 ..... p 995 N95-18187 * #
NAS 1.60:3511 ..... p 1091 N95-18189 * #
NAS 1.60:3526 ..... p 930 N95-19041 * #
NAS 1.61:1325 ..... p 1051 N95-18465 * #
NAS 1.61:1342 ..... p 992 N95-18745 * #
NAS 1.61:1352 ..... p 932 N95-19623 * #
NAS 1.61:1354 ..... p 965 N95-19780 * #
NAS 1.61:1358 ..... p 962 N95-18932 * #
NAS 1.26:197145 ..... p 1194 N95-19134 * #

NAS-3988-FM-94101-639 ..... p 988 N95-19614 #
NAS-8819-FM-9614-820 ..... p 1015 N95-18111 * #

NASA-CASE-ARC-11988-1 ..... p 1011 N95-18959 *

NASA-CASE-LAR-14277-1 ..... p 1011 N95-18962 *
NASA-CASE-LAR-14645-1-SB ..... p 1037 N95-18322 *
NASA-CASE-LAR-14651-1 ..... p 1175 N95-19056 *
NASA-CASE-LAR-14678-1 ..... p 960 N95-18961 *
NASA-CASE-LAR-14791-1 ..... p 1032 N95-18316 *

NASA-CASE-LEW-15576-1 ..... p 984 N95-18321 *

NASA-CASE-MFS-28697-1 ..... p 1041 N95-18325 *

NASA-CASE-MSC-21529-1 ..... p 983 N95-18134 *
NASA-CASE-MSC-22090-1 ..... p 1017 N95-18323 *
NASA-CASE-MSC-22091-1 ..... p 992 N95-18738 *

NASA-CASE-NPO-17998-2-CU .... p 1093 N95-18963 *
NASA-CASE-NPO-18391-2-CU .... p 1137 N95-18957 *
NASA-CASE-NPO-18492-1-CU .... p 1113 N95-18313 *
NASA-CASE-NPO-18579-1-CU .... p 1114 N95-18740 *
NASA-CASE-NPO-18584-1-CU .... p 1114 N95-19062 *
NASA-CASE-NPO-18701-2-CU .... p 1000 N95-18960 *
NASA-CASE-NPO-18764-1-CU .... p 1041 N95-18741 *
NASA-CASE-NPO-18819-1-CU .... p 991 N95-18326 *
NASA-CASE-NPO-18870-1-CU .... p 1130 N95-18324 *

NASA-CP-10147 ..... p 949 N95-19380 * #
NASA-CP-10162-VOL-1 ..... p 1100 N95-19625 * #
NASA-CP-10162-VOL-2 ..... p 1104 N95-19747 * #
NASA-CP-3274-PT-2 ..... p 934 N95-19468 * #
NASA-CP-3288 ..... p 1068 N95-18201 * #

NASA-CR-182276 ..... p 927 N95-18044 * #
NASA-CR-188300 ..... p 1015 N95-18111 * #
NASA-CR-188360 ..... p 956 N95-18567 * #
NASA-CR-189389 ..... p 1173 N95-18051 * #
NASA-CR-189390 ..... p 1172 N95-18040 * #
NASA-CR-191045 ..... p 967 N95-18743 * #
NASA-CR-191128 ..... p 967 N95-18195 * #
NASA-CR-191194 ..... p 1034 N95-19236 * #
NASA-CR-191203 ..... p 1040 N95-18041 * #
NASA-CR-194975 ..... p 1098 N95-18584 * #
NASA-CR-194994 ..... p 1016 N95-18190 * #
NASA-CR-194995 ..... p 1099 N95-19027 * #
NASA-CR-194996 ..... p 1100 N95-19028 * #
NASA-CR-194997 ..... p 1116 N95-18110 * #
NASA-CR-194998 ..... p 1015 N95-18188 * #
NASA-CR-195005 ..... p 1016 N95-18191 * #
NASA-CR-195006 ..... p 1017 N95-18397 * #
NASA-CR-195007 ..... p 1016 N95-18193 * #
NASA-CR-195009 ..... p 964 N95-18105 * #
NASA-CR-195010 ..... p 1123 N95-18930 * #
NASA-CR-195011 ..... p 1099 N95-18931 * #
NASA-CR-195014 ..... p 1014 N95-18042 * #
NASA-CR-195015 ..... p 1116 N95-18108 * #
NASA-CR-195016-PT-1 ..... p 1020 N95-18958 * #
NASA-CR-195018 ..... p 1117 N95-18479 * #
NASA-CR-195019 ..... p 1116 N95-18109 * #
NASA-CR-195020 ..... p 971 N95-19043 * #
NASA-CR-195022 ..... p 1018 N95-18488 * #
NASA-CR-195298 ..... p 964 N95-18495 * #
NASA-CR-195349 ..... p 966 N95-18192 * #
NASA-CR-195381 ..... p 970 N95-18940 * #
NASA-CR-195408 ..... p 1034 N95-18938 * #
NASA-CR-195411 ..... p 1015 N95-18107 * #
NASA-CR-195414 ..... p 1041 N95-18541 * #
NASA-CR-195416 ..... p 1043 N95-19567 * #
NASA-CR-195417 ..... p 962 N95-18467 * #
NASA-CR-195418 ..... p 962 N95-18045 * #
NASA-CR-195426 ..... p 955 N95-19769 * #
NASA-CR-195429 ..... p 950 N95-19651 * #
NASA-CR-195430 ..... p 982 N95-19792 * #
NASA-CR-195984 ..... p 1098 N95-18487 * #
NASA-CR-196533 ..... p 1161 N95-18967 * #
NASA-CR-196537 ..... p 1040 N95-18056 * #
NASA-CR-196538 ..... p 969 N95-18135 * #
NASA-CR-196542 ..... p 1195 N95-19287 * #
NASA-CR-196543 ..... p 1068 N95-18093 * #
NASA-CR-196970 ..... p 974 N95-18744 * #
NASA-CR-197015 ..... p 1075 N95-18951 * #
NASA-CR-197121 ..... p 1186 N95-19289 * #
NASA-CR-197130 ..... p 1066 N95-19129 * #
NASA-CR-197145 ..... p 1194 N95-19134 * #
NASA-CR-197294 ..... p 971 N95-19650 * #
NASA-CR-197297 ..... p 1194 N95-19575 * #
NASA-CR-197320 ..... p 958 N95-19576 * #
NASA-CR-197448 ..... p 1157 N95-18166 * #
NASA-CR-197516 ..... p 945 N95-19130 * #
NASA-CR-197519 ..... p 990 N95-18082 * #
NASA-CR-197520 ..... p 1195 N95-17980 * #
NASA-CR-197523 ..... p 942 N95-18090 * #
NASA-CR-197529 ..... p 967 N95-19566 * #
NASA-CR-197531 ..... p 1177 N95-17981 * #
NASA-CR-197533 ..... p 1136 N95-18217 * #
NASA-CR-197537 ..... p 1194 N95-18579 * #
NASA-CR-197538 ..... p 1178 N95-18391 * #
NASA-CR-197542 ..... p 1052 N95-18952 * #
NASA-CR-197544 ..... p 1196 N95-18954 * #
NASA-CR-197551 ..... p 1136 N95-18370 * #
NASA-CR-197553 ..... p 1195 N95-18376 * #
NASA-CR-197554 ..... p 1044 N95-18388 * #
NASA-CR-197555 ..... p 1197 N95-18464 * #
NASA-CR-197558 ..... p 1010 N95-18925 * #
NASA-CR-197561 ..... p 1110 N95-18532 * #
NASA-CR-197568 ..... p 1110 N95-18521 * #
NASA-CR-197570 ..... p 1110 N95-18581 * #
NASA-CR-197572 ..... p 978 N95-18046 * #
NASA-CR-197573 ..... p 1064 N95-18444 * #
NASA-CR-197574 ..... p 966 N95-18196 * #
NASA-CR-197575 ..... p 1064 N95-18476 * #
NASA-CR-197579 ..... p 1014 N95-18092 * #
NASA-CR-197580 ..... p 970 N95-18471 * #
NASA-CR-197591 ..... p 1109 N95-18055 * #
NASA-CR-197592 ..... p 1180 N95-19172 * #
NASA-CR-197593 ..... p 1017 N95-18327 * #
NASA-CR-197595 ..... p 1043 N95-18737 * #
NASA-CR-197597 ..... p 1118 N95-18736 * #
NASA-CR-197598 ..... p 963 N95-18610 * #
NASA-CR-197600 ..... p 991 N95-18913 * #
NASA-CR-197602 ..... p 1051 N95-18739 * #
NASA-CR-197604 ..... p 1062 N95-19779 * #
NASA-CR-197605 ..... p 1004 N95-19547 * #
NASA-CR-197606 ..... p 1156 N95-19037 * #
NASA-CR-197607 ..... p 1196 N95-19034 * #
NASA-CR-197608 ..... p 1060 N95-19033 * #
NASA-CR-197609 ..... p 1157 N95-19363 * #
NASA-CR-197610 ..... p 1157 N95-19358 * #
NASA-CR-197611 ..... p 1121 N95-19348 * #
NASA-CR-197612 ..... p 1156 N95-18949 * #
NASA-CR-197613 ..... p 1193 N95-19341 * #
NASA-CR-197614 ..... p 1180 N95-18966 * #
NASA-CR-197615 ..... p 1198 N95-18747 * #
NASA-CR-197616 ..... p 1156 N95-19340 * #
NASA-CR-197619 ..... p 1121 N95-19288 * #
NASA-CR-197621 ..... p 1052 N95-19126 * #
NASA-CR-197624 ..... p 1065 N95-19032 * #
NASA-CR-197626 ..... p 1137 N95-18965 * #
NASA-CR-197627 ..... p 1180 N95-18964 * #
NASA-CR-197628 ..... p 1180 N95-19031 * #
NASA-CR-197629 ..... p 1121 N95-19030 * #
NASA-CR-197630 ..... p 1180 N95-18746 * #
NASA-CR-197671 ..... p 1005 N95-19796 * #
NASA-CR-4637 ..... p 964 N95-18580 * #
NASA-CR-4639 ..... p 970 N95-18466 * #
NASA-CR-4642-VOL-1 ..... p 1020 N95-18955 * #
NASA-CR-4642-VOL-2 ..... p 1020 N95-18956 * #

NASA-NEWS-RELEASE-94-47 ..... p 958 N95-19029 *

NASA-RP-1325 ..... p 1051 N95-18465 * #
NASA-RP-1342 ..... p 992 N95-18745 * #
NASA-RP-1352 ..... p 932 N95-19623 * #
NASA-RP-1354 ..... p 965 N95-19780 * #
NASA-RP-1358 ..... p 962 N95-18932 * #
NASA-SP-7011(397) ..... p 1087 N95-19746 *
NASA-SP-7011(398) ..... p 1080 N95-19239 *
NASA-SP-7037(313) ..... p 927 N95-19168 *
NASA-SP-7037(314) ..... p 927 N95-19357 *

NASA-TM-104566-VOL-18 ..... p 1076 N95-19577 * #
NASA-TM-104616 ..... p 1196 N95-19791 * #
NASA-TM-104806-VOL-1 ..... p 965 N95-19237 * #
NASA-TM-104806-VOL-2 ..... p 965 N95-19624 * #
NASA-TM-106518 ..... p 1042 N95-18935 * #
NASA-TM-106606 ..... p 967 N95-18570 * #
NASA-TM-106736 ..... p 947 N95-18133 * #
NASA-TM-106745 ..... p 968 N95-19795 * #
NASA-TM-106755 ..... p 959 N95-18586 * #
NASA-TM-106766 ..... p 990 N95-18211 * #
NASA-TM-106768 ..... p 969 N95-18448 * #
NASA-TM-106771 ..... p 1016 N95-18212 * #
NASA-TM-106776 ..... p 928 N95-18457 * #
NASA-TM-106785 ..... p 1046 N95-19501 * #
NASA-TM-106792 ..... p 1019 N95-18898 * #
NASA-TM-106797 ..... p 991 N95-19788 * #
NASA-TM-106800 ..... p 1000 N95-18733 * #
NASA-TM-106803 ..... p 927 N95-18486 * #
NASA-TM-106805 ..... p 927 N95-18197 * #
NASA-TM-106807 ..... p 1043 N95-18583 * #
NASA-TM-106808 ..... p 960 N95-19286 * #
NASA-TM-106809 ..... p 1045 N95-18909 * #
NASA-TM-106810 ..... p 962 N95-18387 * #
NASA-TM-106813 ..... p 1016 N95-18200 * #
NASA-TM-106815 ..... p 989 N95-19783 * #
NASA-TM-106817 ..... p 958 N95-18054 * #
NASA-TM-106818 ..... p 1014 N95-18036 * #
NASA-TM-106820 ..... p 1053 N95-18572 * #
NASA-TM-106821 ..... p 1149 N95-18453 * #
NASA-TM-106822 ..... p 1042 N95-19125 * #
NASA-TM-106823 ..... p 1019 N95-18941 * #
NASA-TM-106826 ..... p 934 N95-19285 * #
NASA-TM-106827 ..... p 934 N95-19284 * #
NASA-TM-106828 ..... p 967 N95-18571 * #
NASA-TM-106830 ..... p 1053 N95-18587 * #
NASA-TM-106831 ..... p 933 N95-18582 * #
NASA-TM-106832 ..... p 1042 N95-19238 * #
NASA-TM-106833 ..... p 930 N95-18933 * #
NASA-TM-106836 ..... p 1047 N95-19649 * #
NASA-TM-106838 ..... p 972 N95-19782 * #
NASA-TM-106840 ..... p 1035 N95-19794 * #
NASA-TM-108473 ..... p 1091 N95-19061 * #
NASA-TM-108475 ..... p 963 N95-19648 * #
NASA-TM-108802-VOL-1 ..... p 1092 N95-18569 * #
NASA-TM-108852 ..... p 928 N95-18101 * #
NASA-TM-108861 ..... p 1077 N95-18734 * #
NASA-TM-109121 ..... p 1175 N95-18950 * #
NASA-TM-109160-VOL-1 ..... p 1099 N95-18899 * #
NASA-TM-109161 ..... p 1058 N95-18132 * #
NASA-TM-109164 ..... p 1175 N95-18953 * #
NASA-TM-109172 ..... p 1175 N95-18936 * #
NASA-TM-109207 ..... p 963 N95-18047 * #
NASA-TM-109839 ..... p 1176 N95-19127 * #
NASA-TM-109989 ..... p 1015 N95-18149 * #
NASA-TM-110038 ..... p 1060 N95-18742 * #
NASA-TM-110049 ..... p 961 N95-18568 *
NASA-TM-110056 ..... p 1175 N95-19038 * #
NASA-TM-110115 ..... p 962 N95-18150 *
NASA-TM-110116 ..... p 1057 N95-18048 *
NASA-TM-110117 ..... p 941 N95-18347 *
NASA-TM-110141 ..... p 963 N95-19790 * #
NASA-TM-110486 ..... p 961 N95-19058 *
NASA-TM-110487 ..... p 961 N95-19059 *
NASA-TM-110488 ..... p 961 N95-19060 *
NASA-TM-110489 ..... p 1194 N95-19045 *
NASA-TM-110490 ..... p 965 N95-19039 *
NASA-TM-110491 ..... p 961 N95-19040 *
NASA-TM-4574 ..... p 931 N95-19042 * #
NASA-TM-4593 ..... p 1044 N95-18199 * #
NASA-TM-4608 ..... p 981 N95-19652 * #
NASA-TM-4612 ..... p 1032 N95-18194 * #
NASA-TM-4613 ..... p 1005 N95-19781 * #
NASA-TM-4632 ..... p 931 N95-19119 * #
NASA-TM-4636 ..... p 1033 N95-18735 * #
NASA-TM-4646 ..... p 945 N95-19044 * #
NASA-TM-4650 ..... p 1077 N95-19140 * #
NASA-TM-4653 ..... p 1174 N95-18573 * #

NASA-TP-3414 ..... p 929 N95-18565 * #
NASA-TP-3460 ..... p 942 N95-18198 * #
NASA-TP-3478 ..... p 931 N95-19114 * #
NASA-TP-3485 ..... p 995 N95-18187 * #
NASA-TP-3511 ..... p 1091 N95-18189 * #
NASA-TP-3526 ..... p 930 N95-19041 * #

NAVY-CASE-74453 ..... p 1009 N95-18455 #
NAVY-CASE-74739 ..... p 1045 N95-18456 #
NAVY-CASE-74766 ..... p 979 N95-18458 #
NAVY-CASE-74808 ..... p 1141 N95-18529 #
NAVY-CASE-74885 ..... p 1033 N95-18461 #
NAVY-CASE-75012 ..... p 1140 N95-18459 #

NAVY-CASE-75471 ..... p 997 N95-18462 #
NAVY-CASE-75496 ..... p 1010 N95-18528 #
NAVY-CASE-75642 ..... p 1173 N95-18526 #
NAVY-CASE-75647 ..... p 979 N95-18458 #
NAVY-CASE-76233 ..... p 1149 N95-18527 #
NAVY-CASE-76275 ..... p 1140 N95-18460 #

NAWCAD-SA80 ..... p 943 N95-18407

NAWCADTRN-PE-261 ..... p 947 N95-18383

NHB-1410.13N ..... p 1171 N95-19133 * #

NIFS-252 ..... p 1146 N95-19549 #
NIFS-256 ..... p 1012 N95-19548 #

NIST/SP-260/116 ..... p 973 N95-17994 #
NIST/SP-400-93 ..... p 1007 N95-17984 #

NISTIR-5415 ..... p 1109 N95-17989 #
NISTIR-5470 ..... p 993 N95-19402 #

NKU-0001 ..... p 1132 N95-18883 #

NLM/OD-94/01 ..... p 1077 N95-17949 #

NLR-TP-92409-U ..... p 928 N95-18503
NLR-TP-92426-U ..... p 990 N95-17973

NMERI-WA3-53(3.29) ..... p 992 N95-18684

NOAA-NWS-TDL-CP-94-2 ..... p 1067 N95-18038

NOAA-TM-ERL-FSL-9 ..... p 1066 N95-17952 #

NOAA-TM-NWS-CR-105 ..... p 1067 N95-17993 #
NOAA-TM-NWS-CR-106 ..... p 1067 N95-17992 #

NOAA-TM-NWS-ER-88 ..... p 1072 N95-19581 #

NONP-AGARD-SUPPL-VT-95-3838
0 ..... p 929 N95-18539

NONP-DTIC-DK-94-15236 ..... p 994 N95-17964

NONP-NASA-VT-95-37002 ..... p 941 N95-18347 *
NONP-NASA-VT-95-37003 ..... p 1057 N95-18048 *
NONP-NASA-VT-95-37004 ..... p 962 N95-18150 *
NONP-NASA-VT-95-38127 ..... p 961 N95-18568 *
NONP-NASA-VT-95-39131 ..... p 961 N95-19058 *
NONP-NASA-VT-95-39132 ..... p 961 N95-19059 *
NONP-NASA-VT-95-39133 ..... p 961 N95-19060 *
NONP-NASA-VT-95-39134 ..... p 1194 N95-19045 *
NONP-NASA-VT-95-39135 ..... p 965 N95-19039 *
NONP-NASA-VT-95-39136 ..... p 961 N95-19040 *

NPS-EC-94-009 ..... p 1120 N95-18113 #
NPS-EC-94-012 ..... p 1003 N95-19525 #

NPS-OC-94-001 ..... p 1074 N95-18153 #
NPS-OC-94-05 ..... p 1074 N95-18468

NRAD-TD-2394-CD ..... p 994 N95-17964
NRAD-TD-2643 ..... p 1040 N95-18152 #
NRAD-TD-2650 ..... p 1174 N95-18680
NRAD-TD-2659 ..... p 1174 N95-18681
NRAD-TD-2664 ..... p 996 N95-18341 #
NRAD-TD-2706 ..... p 1140 N95-18484 #

NRAD-TR-1643 ..... p 1139 N95-18342 #
NRAD-TR-1653 ..... p 1117 N95-18679
NRAD-TR-1657 ..... p 1008 N95-18052 #
NRAD-TR-1668 ..... p 1072 N95-19521 #

NREL/TP-410-6285 ..... p 1055 N95-19857 #
NREL/TP-411-7170 ..... p 1056 N95-19882 #
NREL/TP-411-7190 ..... p 1054 N95-19632 #
NREL/TP-412-6845 ..... p 1052 N95-17945 #
NREL/TP-425-6956 ..... p 1056 N95-17944 #
NREL/TP-441-7080 ..... p 1054 N95-19855 #
NREL/TP-441-7107 ..... p 929 N95-18645 #
NREL/TP-441-7108 ..... p 929 N95-18646 #
NREL/TP-451-6638 ..... p 1056 N95-19880 #
NREL/TP-451-7163 ..... p 1151 N95-19541 #
NREL/TP-451-7166 ..... p 1056 N95-19878 #
NREL/TP-463-6504 ..... p 1056 N95-17943 #
NREL/TP-463-7090 ..... p 1055 N95-19856 #
NREL/TP-471-6092 ..... p 1053 N95-18463 #
NREL/TP-473-7260 ..... p 1014 N95-19881 #

NRL/FR/5730-94-9588 ..... p 1005 N95-19694

NRL/MR/5710-94-7485 ..... p 932 N95-19863
NRL/MR/6720-94-7428 ..... p 1147 N95-19846
NRL/MR/6721-94-7453 ..... p 1039 N95-19845
NRL/MR/6722-94-7459 ..... p 1147 N95-19847

NRL/MR/6722-94-7460 ..... p 1147 N95-19844
NRL/MR/7240-94-7542 ..... p 1104 N95-19742
NRL/MR/7441-94-7538 ..... p 1052 N95-19733
NRL/MR/7441-94-7549 ..... p 1050 N95-18078

NRL/PU/6000-94-252 ..... p 1077 N95-19536 #

NSTS-08292 ..... p 963 N95-18610 * #

NSWCDD/TR-92/298 ..... p 1007 N95-17959
NSWCDD/TR-93/643 ..... p 1075 N95-19563 #

NTIA-93-301 ..... p 1066 N95-17938 #

NTSB/SIR-94/02 ..... p 940 N95-19793 #

NTSB/SS-94/02 ..... p 933 N95-19132 #

NUWC-NPT-TD-10-749 ..... p 1128 N95-19514 #

NUWC-NPT-TR-10689 ..... p 1005 N95-19736
NUWC-NPT-TR-10709 ..... p 1120 N95-19065
NUWC-NPT-TR-10739 ..... p 997 N95-18475 #

ORNL/CDIAC-65 ..... p 1058 N95-18389 #

ORNL/FMP-94/1 ..... p 981 N95-19723 #

ORNL/M-3595 ..... p 991 N95-19076 #

ORNL/TM-12194 ..... p 1109 N95-18129 #
ORNL/TM-12789 ..... p 1080 N95-19244 #

P-28297-EL ..... p 1153 N95-19697 #

PAPER-93JD03580 ..... p 1056 N95-17937 #

PB94-107844 ..... p 1171 N95-17988
PB94-175296 ..... p 973 N95-17991
PB94-175700 ..... p 1007 N95-17999 #
PB94-178019 ..... p 1007 N95-17984 #
PB94-179959 ..... p 1170 N95-17987
PB94-179967 ..... p 1170 N95-17986 #
PB94-180692 ..... p 1122 N95-17983 #
PB94-181328 ..... p 1067 N95-18038
PB94-184587 ..... p 1007 N95-18037
PB94-187481 ..... p 1073 N95-17951 #
PB94-187804 ..... p 1067 N95-17992 #
PB94-188026 ..... p 1077 N95-17949 #
PB94-188034 ..... p 1078 N95-17950 #
PB94-188463 ..... p 1109 N95-17989 #
PB94-188760 ..... p 1067 N95-17993 #
PB94-188844 ..... p 973 N95-17994 #
PB94-191781 ..... p 973 N95-17982 #
PB94-191930 ..... p 1057 N95-17985
PB94-192341 ..... p 1118 N95-19198
PB94-192770 ..... p 1056 N95-17937 #
PB94-194107 ..... p 1066 N95-17938 #
PB94-195922 ..... p 1066 N95-17952 #
PB94-201423 ..... p 1118 N95-19169
PB94-201458 ..... p 1094 N95-17972
PB94-201480 ..... p 1009 N95-18501
PB94-201498 ..... p 1037 N95-18502
PB94-201563 ..... p 991 N95-17934
PB94-201571 ..... p 1093 N95-17935
PB94-201589 ..... p 1108 N95-17936
PB94-201597 ..... p 1171 N95-18060
PB94-201696 ..... p 928 N95-18503
PB94-201720 ..... p 990 N95-17973
PB94-202629 ..... p 1036 N95-18061
PB94-202710 ..... p 1057 N95-18002 #
PB94-202728 ..... p 1109 N95-18039
PB94-202751 ..... p 1094 N95-18000
PB94-206984 ..... p 1051 N95-18372
PB94-206992 ..... p 992 N95-18667
PB94-207008 ..... p 1149 N95-18373
PB94-207024 ..... p 1117 N95-18374
PB94-207107 ..... p 1099 N95-18668
PB94-207149 ..... p 1058 N95-18375 #
PB94-207156 ..... p 973 N95-18377
PB94-207180 ..... p 1065 N95-18640
PB94-207610 ..... p 1061 N95-19582 #
PB94-209426 ..... p 1072 N95-19581 #
PB94-210127 ..... p 993 N95-19402 #
PB94-213543 ..... p 1061 N95-19403 #
PB94-213972 ..... p 1196 N95-19404 #
PB94-213980 ..... p 1196 N95-19405 #
PB94-214079 ..... p 1061 N95-19406 #
PB94-214418 ..... p 1072 N95-19407 #
PB94-215449 ..... p 1119 N95-19408 #
PB94-215563 ..... p 1100 N95-19409
PB94-215589 ..... p 1003 N95-19411
PB94-215597 ..... p 1092 N95-19412
PB94-215605 ..... p 1118 N95-19375 #
PB94-217213 ..... p 1134 N95-19376
PB94-217239 ..... p 965 N95-19377 #

PB94-217247 ..... p 1119 N95-19717 #
PB94-217254 ..... p 1119 N95-19718 #
PB94-217262 ..... p 1119 N95-19719
PB94-217445 ..... p 940 N95-19720 #
PB94-917004 ..... p 933 N95-19132 #
PB94-917006 ..... p 940 N95-19793 #
PB95-108189 ..... p 1132 N95-18643

PL-TR-93-2238 ..... p 1064 N95-18452
PL-TR-94-1003 ..... p 1120 N95-18020
PL-TR-94-2086 ..... p 977 N95-19868
PL-TR-94-2135 ..... p 1142 N95-19862
PL-TR-94-2144 ..... p 1049 N95-17971 #
PL-TR-94-2161 ..... p 1066 N95-19105 #
PL-TR-94-2192 ..... p 1049 N95-18035 #
PL-TR-94-2213 ..... p 1129 N95-18062 #
PL-TR-94-2218 ..... p 1178 N95-18451
PL-TR-94-3037 ..... p 1144 N95-18888

PNL-SA-23179 ..... p 1049 N95-18145 #
PNL-SA-23282 ..... p 986 N95-18648 #
PNL-SA-23945 ..... p 984 N95-18348 #
PNL-SA-24287 ..... p 1076 N95-18371 #
PNL-SA-24420 ..... p 1134 N95-19590 #
PNL-SA-24680 ..... p 1054 N95-19591 #
PNL-SA-24743 ..... p 1176 N95-19589 #

PPG-1525 ..... p 1147 N95-19700 #

PSRP-670 ..... p 977 N95-19868

PSU/ARL-S89-2 ..... p 1123 N95-18083

R-234 ..... p 1051 N95-18614 #

R/D-6409-EE-01 ..... p 1139 N95-18404
R/D-6840-EE-01-SUPPL ..... p 1119 N95-19819 #
R/D-6940-EE-01 ..... p 1119 N95-19820 #
R/D-7059-EE-01 ..... p 1066 N95-19387 #
R/D-7341-MS-02 ..... p 984 N95-18339 #
R/D-7346-EE-02-VOL-1 ..... p 1009 N95-18425 #
R/D-7346-EE-02-VOL-2 ..... p 1009 N95-18426 #
R/D-7346-EE-02-VOL-3 ..... p 1008 N95-18338 #
R/D-7414-AN-02-VOL-2 ..... p 1018 N95-18477

RAL-94-072 ..... p 1132 N95-18643

REPT-3 ..... p 985 N95-18636
REPT-91-R-1475 ..... p 927 N95-18044 * #
REPT-91-R-1553 ..... p 967 N95-18195 * #
REPT-92RR-28 ..... p 940 N95-18059 #
REPT-95B00023 ..... p 1068 N95-18201 * #
REPT-95B00027 ..... p 1196 N95-19791 * #
REPT-95B00038-VOL-18 ..... p 1076 N95-19577 * #

RIA/SE-93-01 ..... p 1043 N95-19593 #

RIACS-TR-94-19 ..... p 1043 N95-18737 * #
RIACS-TR-94-20 ..... p 1118 N95-18736 * #

RIVM-422501002 ..... p 1057 N95-18002 #
RIVM-481507001 ..... p 1058 N95-18375 #

RL-TR-93-221 ..... p 995 N95-18116 #
RL-TR-94-100 ..... p 995 N95-18066 #
RL-TR-94-104 ..... p 1003 N95-19516 #
RL-TR-94-111 ..... p 1111 N95-19526 #
RL-TR-94-122 ..... p 972 N95-19702 #
RL-TR-94-134 ..... p 994 N95-17958
RL-TR-94-137 ..... p 1139 N95-18104
RL-TR-94-140 ..... p 1008 N95-18103 #
RL-TR-94-142 ..... p 1138 N95-18100
RL-TR-94-147 ..... p 1111 N95-19524 #
RL-TR-94-150 ..... p 1115 N95-19512 #
RL-TR-94-151 ..... p 1111 N95-19513 #
RL-TR-94-86 ..... p 1138 N95-18067 #
RL-TR-94-87 ..... p 1110 N95-18454
RL-TR-94-92 ..... p 1010 N95-18662
RL-TR-94-97 ..... p 1138 N95-18102
RL-TR-94-98 ..... p 1109 N95-18106

RN-8025-3C(R2)-PT-3 ..... p 1080 N95-19384 #
RN-8025-4B-PT-4 ..... p 1080 N95-19385 #

RR-CE143 ..... p 1045 N95-18608 #
RR-CE144 ..... p 1071 N95-18607 #

RTI/5681/57 ..... p 1061 N95-19403 #

R9133-F ..... p 1155 N95-18009 #

S-784 ..... p 1091 N95-18189 * #
S-785-VOL-1 ..... p 1100 N95-19625 * #
S-785-VOL-2 ..... p 1104 N95-19747 * #
S-786-VOL-1 ..... p 965 N95-19237 * #
S-786-VOL-2 ..... p 965 N95-19624 * #

SAND-93-1531 ..... p 1013 N95-19842
SAND-93-2743C ..... p 1004 N95-19555 #
SAND-93-2775C ..... p 977 N95-17968 #
SAND-93-3812C ..... p 1145 N95-19201 #
SAND-93-3813C ..... p 1133 N95-19199 #
SAND-94-0169 ..... p 1137 N95-18897 #
SAND-94-0945 ..... p 990 N95-19100 #
SAND-94-1100 ..... p 1118 N95-18896 #
SAND-94-1156C ..... p 1098 N95-18652 #
SAND-94-1172C ..... p 975 N95-19559 #
SAND-94-1310C ..... p 1012 N95-19240 #
SAND-94-1528C ..... p 1055 N95-19873 #
SAND-94-1560C ..... p 1013 N95-19872 #
SAND-94-1574C ..... p 1055 N95-19859 #
SAND-94-1674C ..... p 1129 N95-18144 #
SAND-94-1681 ..... p 1008 N95-18143 #
SAND-94-1796C ..... p 1120 N95-18653 #
SAND-94-1804C ..... p 980 N95-19395 #
SAND-94-1976C ..... p 1151 N95-19235 #
SAND-94-1987C ..... p 1174 N95-18873 #
SAND-94-2008C ..... p 1112 N95-17948 #
SAND-94-2010C ..... p 1174 N95-18872 #
SAND-94-2099C ..... p 1122 N95-19234 #
SAND-94-2115C ..... p 1149 N95-18650
SAND-94-2233C ..... p 986 N95-18651 #
SAND-94-2261C ..... p 1114 N95-18649 #
SAND-94-2276C ..... p 988 N95-19558 #
SAND-94-2524C ..... p 1176 N95-19876 #
SAND-94-8210 ..... p 971 N95-19579 #

SGD-599-PT-1 ..... p 1196 N95-19404 #
SGD-599-PT-2 ..... p 1196 N95-19405 #

SIP-0058 ..... p 1144 N95-18886 #
SIP-0059 ..... p 1144 N95-18887 #
SIP-0061 ..... p 1146 N95-19241 #
SIP-0062 ..... p 1144 N95-18885 #

SLCET-TR-88-1-REV-7.0 ..... p 1012 N95-19519 #

SPC-92041-CMC-VOL-1 ..... p 1108 N95-19803
SPC-92041-CMC-VOL-2 ..... p 1108 N95-19813

SPIRE-FR-10131 ..... p 1146 N95-17960

SPIRE-QR-10158.02 ..... p 1054 N95-19388 #

SR-1 ..... p 1049 N95-17971 #
SR-9 ..... p 1068 N95-18141

SR/H-789 ..... p 980 N95-19401 #

SSD94D0298 ..... p 956 N95-18567 * #

STARS-VC-B002/002/00 ..... p 1097 N95-18419
STARS-VC-B003/001/00 ..... p 1097 N95-18421 #
STARS-VC-B004/002/01-VOL-2 . p 1096 N95-18344 #
STARS-VC-B005/001/00 ..... p 1095 N95-18033 #
STARS-VC-B006/003/00 ..... p 1097 N95-18423 #
STARS-VC-B007/000/01 ..... p 1097 N95-18447
STARS-VC-B009/001/00 ..... p 1096 N95-18343 #
STARS-VC-B010/001/00 ..... p 1097 N95-18422 #
STARS-VC-B011/001/00 ..... p 1097 N95-18420
STARS-VC-B015/000/00 ..... p 1095 N95-18030 #
STARS-VC-B018/001/00 ..... p 1095 N95-18031 #
STARS-VC-B018/002/00 ..... p 1095 N95-18034 #
STARS-VC-B018/003/00 ..... p 1098 N95-18450
STARS-VC-B018/004/00 ..... p 1095 N95-18032 #
STARS-VC-B019/004/00 ..... p 1097 N95-18449

STF11-A94005 ..... p 992 N95-18667
STF19-A94005 ..... p 1149 N95-18373
STF20-A93119 ..... p 1100 N95-19409
STF28-A93087 ..... p 973 N95-18377
STF33-A93037 ..... p 1117 N95-18374
STF33-A94001 ..... p 1099 N95-18668
STF33-A94007 ..... p 1003 N95-19411
STF60-A93095 ..... p 1051 N95-18372
STF69-A93026 ..... p 1065 N95-18640
STF75-A93065 ..... p 1092 N95-19412

SU-P-28297-EL ..... p 1153 N95-19738 #

SU-SLAC-PUB-6517 ..... p 1138 N95-19841

SU-SLAC/SSRL-0077 ..... p 1138 N95-19841

SU-SPO-8729 ..... p 1194 N95-18579 * #

SUAC-445 ..... p 1129 N95-18049 #

SUSSEX-AST-94/2-1 ..... p 1121 N95-19030 * #

SWRI-06-4414/3 ..... p 1044 N95-18081

TACOM-13603 ..... p 1043 N95-19809

TDCK-93-2783 ..... p 1086 N95-19537 #
TDCK-94-0043 ..... p 1090 N95-19583 #
TDCK-94-0055 ..... p 1089 N95-19538 #
TDCK-94-0176 ..... p 1004 N95-19535 #

TEC-0050 ..... p 1113 N95-18057 #

TIOS-93-43 ..... p 1109 N95-18039

TN-BN-1169 ..... p 1117 N95-18482 #

TNO-TM-1994-B-12 ..... p 1089 N95-19538 #

TR-12 ..... p 1132 N95-18655
TR-13 ..... p 1129 N95-17974 #
TR-154/6/93/ECE ..... p 962 N95-18467 * #
TR-156/6/93/ECE ..... p 962 N95-18045 * #
TR-15 ..... p 976 N95-19824 #
TR-15 ..... p 976 N95-19830 #
TR-16 ..... p 976 N95-19825 #
TR-19-ONR ..... p 1131 N95-18473 #
TR-2-FSRC-93 ..... p 1098 N95-18564 #
TR-27 ..... p 969 N95-19822 #
TR-29 ..... p 969 N95-19823 #
TR-31 ..... p 1097 N95-18437
TR-427 ..... p 1049 N95-17971 #
TR-8-3 ..... p 1157 N95-19852
TR-9-4 ..... p 1157 N95-19853
TR-94-2181 ..... p 1068 N95-18141
TR-993 ..... p 1004 N95-19565 #
TR-994 ..... p 1004 N95-19594 #

TRS-469 ..... p 991 N95-17934
TRS-471 ..... p 1093 N95-17935
TRS-472 ..... p 1171 N95-18060
TRS-473-PT-1 ..... p 1108 N95-17936

TTC-2847-R ..... p 1139 N95-18409

U-OF-IOWA-94-19 ..... p 1195 N95-17979 #

UCRL-CR-118128 ..... p 1136 N95-18552 #

UCRL-ID-116663 ..... p 1060 N95-18895 #
UCRL-ID-117785 ..... p 1037 N95-18357 #
UCRL-ID-118062 ..... p 1059 N95-18664 #
UCRL-ID-118113 ..... p 1039 N95-19722 #
UCRL-ID-118367 ..... p 1031 N95-17963 #

UCRL-JC-112384 ..... p 1035 N95-19711 #
UCRL-JC-115596 ..... p 1135 N95-19709 #
UCRL-JC-115941 ..... p 1039 N95-19708 #
UCRL-JC-115998 ..... p 1059 N95-18647 #
UCRL-JC-116056-REV-1 ..... p 1039 N95-19507 #
UCRL-JC-116183 ..... p 1146 N95-19250 #
UCRL-JC-116385 ..... p 977 N95-17962 #
UCRL-JC-116820 ..... p 1146 N95-19509 #
UCRL-JC-116837 ..... p 1038 N95-19248 #
UCRL-JC-116926 ..... p 1038 N95-19247 #
UCRL-JC-117000-REV-1 ..... p 1038 N95-19096 #
UCRL-JC-117193 ..... p 1033 N95-18555, #
UCRL-JC-117358 ..... p 1039 N95-19508 #
UCRL-JC-117438 ..... p 987 N95-19227 #
UCRL-JC-117522 ..... p 1039 N95-19398 #
UCRL-JC-117528 ..... p 980 N95-19396 #
UCRL-JC-117695 ..... p 1186 N95-19249 #
UCRL-JC-117698 ..... p 1137 N95-19588 #
UCRL-JC-117711 ..... p 1146 N95-19527 #
UCRL-JC-118115 ..... p 1142 N95-19710 #
UCRL-JC-118154 ..... p 1006 N95-19833
UCRL-JC-118407 ..... p 1155 N95-19838

UCRL-LR-105821-94-2 ..... p 1147 N95-19552 #
UCRL-LR-111984-94-2 ..... p 1039 N95-19551 #

UDR-TR-93-122 ..... p 972 N95-19702 #

UMICH-030601-4-T ..... p 1005 N95-19796 * #

UMR-FDB-37 ..... p 972 N95-19814

UNM-ISNPS-5-1994 ..... p 1136 N95-18217 * #

US-PATENT-APPL-SN-004004 ..... p 1011 N95-19171
US-PATENT-APPL-SN-013386 ..... p 1149 N95-18633
US-PATENT-APPL-SN-018128 ..... p 1011 N95-18959 *
US-PATENT-APPL-SN-020940 ..... p 928 N95-18337
US-PATENT-APPL-SN-021948 ..... p 1038 N95-18585
US-PATENT-APPL-SN-023253 ..... p 1113 N95-18313 *
US-PATENT-APPL-SN-033223 ..... p 1141 N95-18628
US-PATENT-APPL-SN-039602 ..... p 992 N95-18738 *
US-PATENT-APPL-SN-046254 ..... p 1173 N95-18544
US-PATENT-APPL-SN-054497 ..... p 984 N95-18320
US-PATENT-APPL-SN-058018 ..... p 1041 N95-18317
US-PATENT-APPL-SN-059770 ..... p 995 N95-18315
US-PATENT-APPL-SN-059846 ..... p 1141 N95-18593

US-PATENT-APPL-SN-060947 ..... p 1011 N95-18962 *
US-PATENT-APPL-SN-062864 ..... p 984 N95-18336
US-PATENT-APPL-SN-063844 ..... p 956 N95-18553
US-PATENT-APPL-SN-066829 ..... p 1137 N95-18957 *
US-PATENT-APPL-SN-074100 ..... p 996 N95-18429
US-PATENT-APPL-SN-081910 ..... p 984 N95-18321 *
US-PATENT-APPL-SN-083402 ..... p 960 N95-18961 *
US-PATENT-APPL-SN-086424 ..... p 1002 N95-19072
US-PATENT-APPL-SN-094541 ..... p 1010 N95-18546
US-PATENT-APPL-SN-100798 ..... p 1042 N95-19121
US-PATENT-APPL-SN-105528 ..... p 1037 N95-18322 *
US-PATENT-APPL-SN-115832 ..... p 1017 N95-18323 *
US-PATENT-APPL-SN-117514 ..... p 1018 N95-18525
US-PATENT-APPL-SN-126144 ..... p 1000 N95-18960 *
US-PATENT-APPL-SN-126869 ..... p 978 N95-18332
US-PATENT-APPL-SN-127653 ..... p 1130 N95-18324 *
US-PATENT-APPL-SN-129001 ..... p 1093 N95-18963 *
US-PATENT-APPL-SN-129725 ..... p 1141 N95-18560
US-PATENT-APPL-SN-134192 ..... p 1142 N95-19389
US-PATENT-APPL-SN-134443 ..... p 1041 N95-18325 *
US-PATENT-APPL-SN-134762 ..... p 979 N95-18458 #
US-PATENT-APPL-SN-153933 ..... p 991 N95-18326 *
US-PATENT-APPL-SN-165207 ..... p 999 N95-18545
US-PATENT-APPL-SN-223346 ..... p 1009 N95-18455 #
US-PATENT-APPL-SN-236823 ..... p 1140 N95-18459 #
US-PATENT-APPL-SN-236856 ..... p 1045 N95-18456 #
US-PATENT-APPL-SN-246209 ..... p 1149 N95-18527 #
US-PATENT-APPL-SN-246900 ..... p 1140 N95-18460 #
US-PATENT-APPL-SN-246901 ..... p 1173 N95-18526 #
US-PATENT-APPL-SN-247611 ..... p 1137 N95-18957 *
US-PATENT-APPL-SN-247827 ..... p 997 N95-18462 #
US-PATENT-APPL-SN-267696 ..... p 1010 N95-18528 #
US-PATENT-APPL-SN-267697 ..... p 1141 N95-18529 #
US-PATENT-APPL-SN-279037 ..... p 1033 N95-18461 #
US-PATENT-APPL-SN-329621 ..... p 990 N95-19090
US-PATENT-APPL-SN-474695 ..... p 967 N95-18632
US-PATENT-APPL-SN-594751 ..... p 1011 N95-19120
US-PATENT-APPL-SN-632872 ..... p 1015 N95-18112
US-PATENT-APPL-SN-651856 ..... p 1141 N95-18563
US-PATENT-APPL-SN-653578 ..... p 1093 N95-18963 *
US-PATENT-APPL-SN-666104 ..... p 967 N95-19073
US-PATENT-APPL-SN-687603 ..... p 1151 N95-19122
US-PATENT-APPL-SN-693106 ..... p 995 N95-18314
US-PATENT-APPL-SN-704563 ..... p 992 N95-18431
US-PATENT-APPL-SN-726489 ..... p 1149 N95-18543
US-PATENT-APPL-SN-745315 ..... p 1009 N95-18432
US-PATENT-APPL-SN-756261 ..... p 1092 N95-18517
US-PATENT-APPL-SN-767952 ..... p 1032 N95-17970
US-PATENT-APPL-SN-799571 ..... p 1175 N95-19056 *
US-PATENT-APPL-SN-807015 ..... p 1038 N95-18635
US-PATENT-APPL-SN-826202 ..... p 1019 N95-18634
US-PATENT-APPL-SN-828630 ..... p 971 N95-19123
US-PATENT-APPL-SN-831582 ..... p 1009 N95-18433
US-PATENT-APPL-SN-857901 ..... p 983 N95-18134 *
US-PATENT-APPL-SN-879480 ..... p 1032 N95-18316 *
US-PATENT-APPL-SN-892057 ..... p 1041 N95-18594
US-PATENT-APPL-SN-901286 ..... p 1032 N95-18319
US-PATENT-APPL-SN-904109 ..... p 997 N95-18516
US-PATENT-APPL-SN-909501 ..... p 1000 N95-18960 *
US-PATENT-APPL-SN-920738 ..... p 1149 N95-18627
US-PATENT-APPL-SN-921192 ..... p 1114 N95-19062 *
US-PATENT-APPL-SN-926112 ..... p 1010 N95-18523
US-PATENT-APPL-SN-929212 ..... p 970 N95-18629
US-PATENT-APPL-SN-931467 ..... p 1008 N95-18318
US-PATENT-APPL-SN-936983 ..... p 985 N95-18631
US-PATENT-APPL-SN-937335 ..... p 1114 N95-18740 *
US-PATENT-APPL-SN-942912 ..... p 985 N95-18430
US-PATENT-APPL-SN-942914 ..... p 1033 N95-18524
US-PATENT-APPL-SN-947022 ..... p 1149 N95-18559
US-PATENT-APPL-SN-950569 ..... p 999 N95-18561
US-PATENT-APPL-SN-956684 ..... p 1041 N95-18741 *
US-PATENT-APPL-SN-983335 ..... p 1034 N95-19124
US-PATENT-APPL-SN-983951 ..... p 1041 N95-18335
US-PATENT-APPL-SN-984637 ..... p 979 N95-18630

US-PATENT-CLASS-118-697 ..... p 1149 N95-18633
US-PATENT-CLASS-124-204 ..... p 985 N95-18631
US-PATENT-CLASS-137-485 ..... p 992 N95-18738 *
US-PATENT-CLASS-137-549 ..... p 992 N95-18738 *
US-PATENT-CLASS-137-571 ..... p 992 N95-18738 *
US-PATENT-CLASS-137-587 ..... p 992 N95-18738 *
US-PATENT-CLASS-141-114 ..... p 992 N95-18738 *
US-PATENT-CLASS-148-432 ..... p 979 N95-18630
US-PATENT-CLASS-148-573 ..... p 1011 N95-18962 *
US-PATENT-CLASS-149-19.9 ..... p 990 N95-19090
US-PATENT-CLASS-164-75 ..... p 992 N95-18431
US-PATENT-CLASS-164-97 ..... p 971 N95-19123
US-PATENT-CLASS-165-110 ..... p 1017 N95-18323 *
US-PATENT-CLASS-165-174 ..... p 1017 N95-18323 *
US-PATENT-CLASS-165-1 ..... p 1017 N95-18323 *
US-PATENT-CLASS-165-913 ..... p 1017 N95-18323 *
US-PATENT-CLASS-180-8.2 ..... p 1041 N95-18741 *
US-PATENT-CLASS-180-8.3 ..... p 1041 N95-18741 *
US-PATENT-CLASS-188-379 ..... p 1041 N95-18325 *
US-PATENT-CLASS-204-404 ..... p 1033 N95-18524
US-PATENT-CLASS-204-426 ..... p 1032 N95-18316 *

US-PATENT-CLASS-219-121.36 .. p 991 N95-18326 *
US-PATENT-CLASS-219-121.52 .. p 991 N95-18326 *
US-PATENT-CLASS-219-121.59 .. p 991 N95-18326 *
US-PATENT-CLASS-219-123 ..... p 991 N95-18326 *
US-PATENT-CLASS-219-633 ..... p 960 N95-18961 *
US-PATENT-CLASS-219-633 ..... p 1011 N95-18962 *
US-PATENT-CLASS-219-634 ..... p 1011 N95-18962 *
US-PATENT-CLASS-219-635 ..... p 960 N95-18961 *
US-PATENT-CLASS-219-635 ..... p 1011 N95-18962 *
US-PATENT-CLASS-219-659 ..... p 960 N95-18961 *
US-PATENT-CLASS-219-659 ..... p 1011 N95-18962 *
US-PATENT-CLASS-219-665 ..... p 960 N95-18961 *
US-PATENT-CLASS-220-581 ..... p 992 N95-18738 *
US-PATENT-CLASS-220-901 ..... p 992 N95-18738 *
US-PATENT-CLASS-244-130 ..... p 928 N95-18337
US-PATENT-CLASS-244-3.22 ..... p 967 N95-19073
US-PATENT-CLASS-248-550 ..... p 1042 N95-19121
US-PATENT-CLASS-250-288 ..... p 1130 N95-18324 *
US-PATENT-CLASS-250-427 ..... p 1130 N95-18324 *
US-PATENT-CLASS-252-73 ..... p 1019 N95-18634
US-PATENT-CLASS-257-286 ..... p 1032 N95-17970
US-PATENT-CLASS-257-80 ..... p 1151 N95-19122
US-PATENT-CLASS-280-5.28 ..... p 1041 N95-18741 *
US-PATENT-CLASS-29-890.037 .. p 1017 N95-18323 *
US-PATENT-CLASS-307-66 ..... p 1010 N95-18523
US-PATENT-CLASS-313-359.1 .... p 1137 N95-18957 *
US-PATENT-CLASS-315-111.01 .. p 1137 N95-18957 *
US-PATENT-CLASS-315-5.37 ..... p 1137 N95-18957 *
US-PATENT-CLASS-324-130 ..... p 1011 N95-18959 *
US-PATENT-CLASS-324-601 ..... p 1011 N95-18959 *
US-PATENT-CLASS-324-705 ..... p 1011 N95-18959 *
US-PATENT-CLASS-324-706 ..... p 1011 N95-18959 *
US-PATENT-CLASS-324-713 ..... p 1011 N95-18959 *
US-PATENT-CLASS-341-131 ..... p 1011 N95-19171
US-PATENT-CLASS-342-165 ..... p 1002 N95-19072
US-PATENT-CLASS-342-175 ..... p 996 N95-18429
US-PATENT-CLASS-342-378 ..... p 997 N95-18516
US-PATENT-CLASS-343-781CA .. p 1000 N95-18960 *
US-PATENT-CLASS-343-781P .... p 1000 N95-18960 *
US-PATENT-CLASS-343-909 ..... p 1000 N95-18960 *
US-PATENT-CLASS-356-350 ..... p 1034 N95-19124
US-PATENT-CLASS-361-144 ..... p 991 N95-18326 *
US-PATENT-CLASS-361-56 ..... p 1011 N95-19120
US-PATENT-CLASS-364-DIG.1 .... p 1175 N95-19056 *
US-PATENT-CLASS-364-148 ..... p 1113 N95-18313 *
US-PATENT-CLASS-364-148 ..... p 1114 N95-19062 *
US-PATENT-CLASS-364-160 ..... p 1113 N95-18313 *
US-PATENT-CLASS-364-160 ..... p 1114 N95-19062 *
US-PATENT-CLASS-364-162 ..... p 1113 N95-18313 *
US-PATENT-CLASS-364-238.3 .... p 1175 N95-19056 *
US-PATENT-CLASS-364-239.2 .... p 1175 N95-19056 *
US-PATENT-CLASS-364-550 ..... p 999 N95-18561
US-PATENT-CLASS-365-145 ..... p 1093 N95-18963 *
US-PATENT-CLASS-365-158 ..... p 1093 N95-18963 *
US-PATENT-CLASS-365-171 ..... p 1093 N95-18963 *
US-PATENT-CLASS-365-45 ..... p 1093 N95-18963 *
US-PATENT-CLASS-365-48 ..... p 1093 N95-18963 *
US-PATENT-CLASS-367-134 ..... p 995 N95-18315
US-PATENT-CLASS-367-1 ..... p 1018 N95-18525
US-PATENT-CLASS-372-12 ..... p 1037 N95-18322 *
US-PATENT-CLASS-372-25 ..... p 1037 N95-18322 *
US-PATENT-CLASS-372-69 ..... p 1038 N95-18585
US-PATENT-CLASS-372-99 ..... p 1037 N95-18322 *
US-PATENT-CLASS-378-4 ..... p 1141 N95-18593
US-PATENT-CLASS-385-100 ..... p 1142 N95-19389
US-PATENT-CLASS-385-26 ..... p 1141 N95-18560
US-PATENT-CLASS-385-56 ..... p 1141 N95-18628
US-PATENT-CLASS-395-21 ..... p 1114 N95-18740 *
US-PATENT-CLASS-395-23 ..... p 1114 N95-18740 *
US-PATENT-CLASS-395-24 ..... p 1114 N95-18740 *
US-PATENT-CLASS-395-25 ..... p 1114 N95-18740 *
US-PATENT-CLASS-395-425 ..... p 1175 N95-19056 *
US-PATENT-CLASS-395-800 ..... p 995 N95-18314
US-PATENT-CLASS-395-96 ..... p 1114 N95-19062 *
US-PATENT-CLASS-416-144 ..... p 1041 N95-18325 *
US-PATENT-CLASS-417-413 ..... p 1041 N95-18317
US-PATENT-CLASS-418-45 ..... p 1041 N95-18335
US-PATENT-CLASS-422-88 ..... p 1032 N95-18316 *
US-PATENT-CLASS-422-94 ..... p 1032 N95-18316 *
US-PATENT-CLASS-422-98 ..... p 1032 N95-18316 *
US-PATENT-CLASS-428-213 ..... p 970 N95-18629
US-PATENT-CLASS-435-180 ..... p 983 N95-18134 *
US-PATENT-CLASS-435-181 ..... p 983 N95-18134 *
US-PATENT-CLASS-435-240.23 .. p 983 N95-18134 *
US-PATENT-CLASS-435-240.243 p 983 N95-18134 *
US-PATENT-CLASS-435-7.92 ..... p 983 N95-18134 *
US-PATENT-CLASS-436-531 ..... p 983 N95-18134 *
US-PATENT-CLASS-436-532 ..... p 983 N95-18134 *
US-PATENT-CLASS-437-176 ..... p 1149 N95-18627
US-PATENT-CLASS-437-242 ..... p 1038 N95-18635
US-PATENT-CLASS-437-34 ..... p 1010 N95-18546
US-PATENT-CLASS-505-329 ..... p 1149 N95-18559
US-PATENT-CLASS-521-25 ..... p 984 N95-18321 *
US-PATENT-CLASS-521-27 ..... p 984 N95-18321 *
US-PATENT-CLASS-521-28 ..... p 984 N95-18321 *
US-PATENT-CLASS-521-31 ..... p 984 N95-18321 *
US-PATENT-CLASS-524-204 ..... p 984 N95-18336
US-PATENT-CLASS-525-154 ..... p 984 N95-18321 *
US-PATENT-CLASS-525-330.2 .... p 984 N95-18321 *
US-PATENT-CLASS-525-383 ..... p 984 N95-18321 *
US-PATENT-CLASS-60-202 ..... p 1137 N95-18957 *
US-PATENT-CLASS-73-35 ..... p 967 N95-18632
US-PATENT-CLASS-73-516 ..... p 956 N95-18553
US-PATENT-CLASS-73-517R ..... p 1141 N95-18563
US-PATENT-CLASS-73-827 ..... p 960 N95-18961 *
US-PATENT-CLASS-73-861.16 .... p 1015 N95-18112
US-PATENT-CLASS-73-862.628 .. p 1011 N95-18959 *
US-PATENT-CLASS-74-492 ..... p 1041 N95-18594
US-PATENT-CLASS-74-573R ..... p 1041 N95-18325 *
US-PATENT-CLASS-74-574 ..... p 1041 N95-18325 *

US-PATENT-5,266,532 ..... p 1038 N95-18635
US-PATENT-5,270,252 ..... p 1149 N95-18627
US-PATENT-5,272,908 ..... p 967 N95-18632
US-PATENT-5,272,932 ..... p 1041 N95-18594
US-PATENT-5,274,361 ..... p 1092 N95-18517
US-PATENT-5,281,274 ..... p 1149 N95-18633
US-PATENT-5,281,672 ..... p 985 N95-18430
US-PATENT-5,284,697 ..... p 970 N95-18629
US-PATENT-5,285,467 ..... p 1038 N95-18585
US-PATENT-5,286,176 ..... p 1041 N95-18317
US-PATENT-5,287,727 ..... p 1032 N95-18319
US-PATENT-5,289,194 ..... p 997 N95-18516
US-PATENT-5,289,304 ..... p 1173 N95-18544
US-PATENT-5,290,599 ..... p 984 N95-18320
US-PATENT-5,290,839 ..... p 985 N95-18631
US-PATENT-5,291,459 ..... p 995 N95-18315
US-PATENT-5,291,611 ..... p 995 N95-18314
US-PATENT-5,291,784 ..... p 956 N95-18553
US-PATENT-5,294,268 ..... p 979 N95-18630
US-PATENT-5,294,936 ..... p 996 N95-18429
US-PATENT-5,295,528 ..... p 992 N95-18431
US-PATENT-5,296,155 ..... p 1019 N95-18634
US-PATENT-5,296,429 ..... p 1008 N95-18318
US-PATENT-5,296,749 ..... p 1009 N95-18433
US-PATENT-5,297,227 ..... p 1141 N95-18628
US-PATENT-5,298,106 ..... p 1149 N95-18543
US-PATENT-5,299,922 ..... p 1041 N95-18335
US-PATENT-5,300,443 ..... p 1010 N95-18546
US-PATENT-5,301,051 ..... p 999 N95-18545
US-PATENT-5,303,882 ..... p 928 N95-18337
US-PATENT-5,304,257 ..... p 978 N95-18332
US-PATENT-5,306,927 ..... p 1009 N95-18432
US-PATENT-5,307,688 ..... p 1015 N95-18112
US-PATENT-5,308,903 ..... p 984 N95-18336
US-PATENT-5,309,007 ..... p 1032 N95-17970
US-PATENT-5,310,470 ..... p 1033 N95-18524
US-PATENT-5,311,180 ..... p 1011 N95-19171
US-PATENT-5,313,513 ..... p 1141 N95-18593
US-PATENT-5,315,304 ..... p 1002 N95-19072
US-PATENT-5,317,929 ..... p 1141 N95-18563
US-PATENT-5,319,249 ..... p 1010 N95-18523
US-PATENT-5,319,608 ..... p 1018 N95-18525
US-PATENT-5,319,726 ..... p 1141 N95-18560
US-PATENT-5,320,304 ..... p 967 N95-19073
US-PATENT-5,320,692 ..... p 990 N95-19090
US-PATENT-5,321,004 ..... p 1149 N95-18559
US-PATENT-5,327,316 ..... p 1011 N95-19120
US-PATENT-5,327,359 ..... p 999 N95-18561
US-PATENT-5,328,141 ..... p 1042 N95-19121
US-PATENT-5,331,404 ..... p 1034 N95-19124
US-PATENT-5,333,667 ..... p 971 N95-19123
US-PATENT-5,339,378 ..... p 1142 N95-19389
US-PATENT-5,345,093 ..... p 1151 N95-19122
US-PATENT-5,368,067 ..... p 992 N95-18738 *
US-PATENT-5,368,090 ..... p 1017 N95-18323 *
US-PATENT-5,369,012 ..... p 983 N95-18134 *
US-PATENT-5,369,662 ..... p 1037 N95-18322 *
US-PATENT-5,369,953 ..... p 1137 N95-18957 *
US-PATENT-5,371,110 ..... p 984 N95-18321 *
US-PATENT-5,371,469 ..... p 1011 N95-18959 *
US-PATENT-5,371,669 ..... p 1114 N95-19062 *
US-PATENT-5,371,670 ..... p 1113 N95-18313 *
US-PATENT-5,371,834 ..... p 1114 N95-18740 *
US-PATENT-5,372,211 ..... p 1041 N95-18741 *
US-PATENT-5,373,302 ..... p 1000 N95-18960 *
US-PATENT-5,373,922 ..... p 1041 N95-18325 *
US-PATENT-5,374,400 ..... p 1032 N95-18316 *
US-PATENT-5,374,801 ..... p 991 N95-18326 *
US-PATENT-5,374,808 ..... p 960 N95-18961 *
US-PATENT-5,374,809 ..... p 1011 N95-18962 *
US-PATENT-5,374,828 ..... p 1130 N95-18324 *
US-PATENT-5,375,082 ..... p 1093 N95-18963 *
US-PATENT-5,375,211 ..... p 1175 N95-19056 *

USAARL-CR-94-1 ..... p 1090 N95-18077

USAARL-94-26 ..... p 1090 N95-19564 #

USAATCOM-TR-94-A-011 ..... p 931 N95-19119 * #

USACERL-TR-EC-94/13 ..... p 1096 N95-18161 #

USAFETAC/TN-94/004 ..... p 1067 N95-18014

USARIEM-T94-13 ..... p 1087 N95-19811

USATEC-R-237 ..... p 999 N95-18657
USATEC-R-238 ..... p 1052 N95-19734

USCG-D-18-94 ..... p 1002 N95-19087 #

USNA-TSPR-212 ..... p 1195 N95-19739 #
USNA-TSPR-213 ..... p 1030 N95-19716 #

UVA/525486/EE94/101 ..... p 1013 N95-19849

WES/IR/ITL-94-1 ..... p 1108 N95-19821

WES/TR/DRP-92-6 ..... p 1075 N95-19540 #

WES/TR/EL-IRRP-94-1 ..... p 1062 N95-19808

WES/TR/ITL-94-6 ..... p 1174 N95-18654

WES/TR/WRP-SM-3 ..... p 1058 N95-18085 #

WHC-SD-WM-OTP-158 ..... p 1035 N95-19553 #

WL-TM-94-3132-VOL-4-PT-2 ..... p 957 N95-18641 #

WL-TR-91-7020 ..... p 947 N95-18164 #
WL-TR-93-3010-VOL-1 ..... p 943 N95-18483 #
WL-TR-94-1102 ..... p 1115 N95-19118 #
WL-TR-94-2025 ..... p 1010 N95-18660
WL-TR-94-2036 ..... p 1130 N95-18334 #
WL-TR-94-3017 ..... p 928 N95-18380
WL-TR-94-3063 ..... p 1096 N95-18365 #
WL-TR-94-3115 ..... p 1046 N95-19522 #
WL-TR-94-4079 ..... p 945 N95-19517 #
WL-TR-94-4083-VOL-1 ..... p 944 N95-18677
WL-TR-94-4084-VOL-2 ..... p 942 N95-18162 #
WL-TR-94-4086 ..... p 1009 N95-18418 #
WL-TR-94-5023 ..... p 1139 N95-18154 #

Y/DV-1321 ..... p 968 N95-19877 #

YALEU/DCS/RR-1042 ..... p 1119 N95-19735

APPENDIX

NASA SCIENTIFIC AND TECHNICAL INFORMATION OFFICE PRODUCTS AND SERVICES

The NASA Scientific and Technical Information (STI) Office provides for the collection and announcement of aerospace-related reports and literature obtained worldwide through agreements and exchanges. The result of the collection is the comprehensive NASA STI Database that covers aeronautics, space, and supporting disciplines.

The STI Database, documents generated or obtained by NASA, and products and services derived from or supporting the database are made available to the NASA research community and to the public. Descriptions and sources of these items are presented in the following pages.

Scientific and Technical Aerospace Reports (STAR) is an abstract journal, listing citations with abstracts for aerospace-related reports obtained from worldwide sources. *STAR* is issued on the first of each month, and announces current documents that have been entered into the NASA STI Database during the previous month. The reports are of the following types:

- NASA, NASA contractor, and NASA grantee reports;
- Reports issued by other U.S. Government agencies, domestic and foreign institutions, universities, and private firms;
- Translations in report form;
- NASA-owned patents and patent applications
- Other U.S. Government agency and foreign patents and patent applications
- Domestic and foreign dissertations and theses.

Journal, book, and conference literature, journal translations, and certain foreign dissertations having the same subject scope as *STAR* are announced in a companion journal, *NASA Open Volumes on Aerospace (NOVA). NOVA* is issued on the 15th of each month and is available from the NASA Center for AeroSpace Information, at the address below.

ELIGIBILITY AND REGISTRATION FOR NASA STI PRODUCTS AND SERVICES

Organizations of the type listed below that have registered with NASA can receive products and services.

- NASA offices and installations, contractors, subcontractors, grantees, and consultants;
- Other U.S. Government agencies and their contractors;
- Libraries in the United States that have arrangements with NASA to maintain collections of NASA documents for public reference;
- Other organizations in the United States having a need for NASA documents in work related to aeronautics and space research;
- Organizations abroad that have established reciprocal documents exchange arrangements with NASA.

The central service points—central points of document acquisition and control within qualified organizations—or individuals are eligible to register for NASA STI products and services. Domestic organizations or individuals may be eligible to receive various classes of NASA publications and services and should address their requests for registration or further information to:

ATTN: Registration Services
NASA Center for AeroSpace Information
800 Elkridge Landing Road
Linthicum Heights, MD 21090-2934
301-621-0390

Organizations abroad should direct requests to:

National Aeronautics and Space Administration
Scientific and Technical Information Office (JTT)
International STI Office
Washington, DC 20546-0001
USA
703-271-5640

SUBJECT SCOPE

The subject scope of *STAR* and *NOVA* includes all aspects of aeronautics and space research and development, supporting basic and applied research, and applications. Aerospace aspects of Earth resources, energy development, conservation, oceanography, environmental protection, urban transportation, and other topics of high national priority are also covered.

HOW TO USE *STAR* SUBJECT CATEGORIES

Abstracts in *STAR* are categorized by 10 major subject divisions that are divided further into 76 specific subject categories. The subject divisions and categories are listed in the Table of Contents together with a note for each that defines its scope and provides any cross-references. For example:

16 SPACE TRANSPORTATION

Includes passenger and cargo space transportation, e.g., shuttle operations; and space rescue techniques. For related information see also *03 Air Transportation and Safety* and *18 Spacecraft Design, Testing and Performance*. For space suits see *54 Man/System Technology and Life Support*.

CROSS-REFERENCES

Individual *STAR* abstracts are not ordinarily cross-referenced, except for certain conference reports or book translations that have had separate abstracts written for their component papers or chapters. Citations and abstracts of the components follow immediately after those of the parent document. When the subject content of a component differs sufficiently from the general content of the parent, a cross-reference citation also is printed at the end of the category to which it normally would have been assigned if it were independent.

DOCUMENTS ON MICROFICHE

Documents available on microfiche are designated by a pound sign (#) following the accession number.

LIMITED REPRODUCIBILITY

A note of limited reproducibility appears in the citation, if there are factors affecting the reproducibility of more than 20% of the document. These factors include faint or broken type, color photographs, black and white photographs, foldouts, dot matrix print, or some other factor that limits the reproducibility of the document. This notation also appears on the microfiche header.

NASA PATENTS AND PATENT APPLICATIONS

Patents and patent applications owned by NASA are announced in *STAR* under appropriate subject categories and are referenced in the *STAR* indexes. In the Report Number Index, patents are indexed by the NASA Case Number, and the U.S. Patent Class. Patent applications are indexed by the NASA Case Number and the U.S. Patent Application Serial Number.

Printed copies of patents (which are not microfiched) are available for purchase from the U.S. Patent and Trademark Office.

When ordering patents, the U.S. Patent Number should be used, and payment must be remitted in advance, by money order or check payable to the Commissioner of Patents and Trademarks. Prepaid purchase coupons for ordering are also available from the U.S. Patent and Trademark Office.

NASA patent application specifications are sold in both paper copy and microfiche by the NASA Center for AeroSpace Information (CASI). The N accession number should be used in ordering either paper copy or microfiche from CASI.

The patents and patent applications announced in *STAR* are owned by NASA and are available for royalty-free licensing. Requests for licensing terms and further information should be addressed to:

National Aeronautics and Space Administration
Associate General Counsel for Intellectual Property
Code GP
Washington, DC 20546-0001

SOURCES FOR DOCUMENTS

One or more sources from which a document announced in *STAR* is available to the public is ordinarily given on the last line of the citation. The most commonly indicated sources and their acronyms or abbreviations are listed below, and their addresses are listed on page A-6. If the publication is available from a source other than those listed, the publisher and his address will be displayed on the availability line or in combination with the corporate source line.

Avail: CASI. Sold by the NASA Center for AeroSpace Information. Prices for hard copy (HC) and microfiche (MF) are indicated by a price code following the letters HC or MF in the *STAR* citation. Current values for the price codes are given in the tables on page A-7.

NOTE ON ORDERING DOCUMENTS: When ordering publications from NASA CASI, use the N accession number or other report number. It is also advisable to cite the title and other bibliographic identification.

Avail: SOD (or GPO). Sold by the Superintendent of Documents, U.S. Government Printing Office, in hard copy.

Avail: BLL (formerly NLL): British Library Lending Division, Boston Spa, Wetherby, Yorkshire, England. Photocopies available from this organization at the price shown. (If none is given, inquiry should be addressed to the BLL.)

Avail: DOE Depository Libraries. Organizations in U.S. cities and abroad that maintain collections of Department of Energy reports, usually in microfiche form, are listed in *Energy Research Abstracts*. Services available from the DOE and its depositories are described in a booklet, *DOE Technical Information Center - Its Functions and Services* (TID-4660), which may be obtained without charge from the DOE Technical Information Center.

Avail: ESDU. Pricing information on specific data, computer programs, and details on Engineering Sciences Data Unit (ESDU) topic categories can be obtained from ESDU International Ltd. Requesters in North America should use the Virginia address while all other requesters should use the London address, both of which are on page A-6.

Avail: Fachinformationszentrum Karlsruhe. Gesellschaft für wissenschaftlich-technische Information mbH 76344 Eggenstein-Leopoldshafen, Germany.

Avail: HMSO. Publications of Her Majesty's Stationery Office are sold in the U.S. by Pendragon House, Inc. (PHI), Redwood City, CA. The U.S. price (including a service and mailing charge) is given, or a conversion table may be obtained from PHI.

Avail: Issuing Activity, or Corporate Author, or no indication of availability. Inquiries as to the availability of these documents should be addressed to the organization shown in the citation as the corporate author of the document.

Avail: NASA Public Document Rooms. Documents so indicated may be examined at or purchased from the National Aeronautics and Space Administration (JBD-4), Public Documents Room (Room 1H23), Washington, DC 20546-0001, or public document rooms located at NASA installations, and the NASA Pasadena Office at the Jet Propulsion Laboratory.

Avail: NTIS. Sold by the National Technical Information Service. Initially distributed microfiche under the NTIS SRIM (Selected Research in Microfiche) are available. For information concerning this service, consult the NTIS Subscription Section, Springfield, VA 22161.

Avail: Univ. Microfilms. Documents so indicated are dissertations selected from *Dissertation Abstracts* and are sold by University Microfilms as xerographic copy (HC) and microfilm. All requests should cite the author and the Order Number as they appear in the citation.

Avail: US Patent and Trademark Office. Sold by Commissioner of Patents and Trademarks, U.S. Patent and Trademark Office, at the standard price of $1.50 each, postage free. (See discussion of NASA patents and patent applications on page A-3.)

Avail: (US Sales Only). These foreign documents are available to users within the United States from the National Technical Information Service (NTIS). They are available to users outside the United States through the International Nuclear Information Service (INIS) representative in their country, or by applying directly to the issuing organization.

Avail: USGS. Originals of many reports from the U.S. Geological Survey, which may contain color illustrations, or otherwise may not have the quality of illustrations preserved in the microfiche or facsimile reproduction, may be examined by the public at the libraries of the USGS field offices whose addresses are listed on page A-6. The libraries may be queried concerning the availability of specific documents and the possible utilization of local copying services, such as color reproduction.

FEDERAL DEPOSITORY LIBRARY PROGRAM

In order to provide the general public with greater access to U.S. Government publications, Congress established the Federal Depository Library Program under the Government Printing Office (GPO), with 53 regional depositories responsible for permanent retention of material, inter-library loan, and reference services. At least one copy of nearly every NASA and NASA-sponsored publication, either in printed or microfiche format, is received and retained by the 53 regional depositories. A list of the regional GPO libraries, arranged alphabetically by state, appears on page A-8. These libraries are *not* sales outlets. A local library can contact a regional depository to help locate specific reports, or direct contact may be made by an individual.

PUBLIC COLLECTION OF NASA DOCUMENTS

An extensive collection of NASA and NASA-sponsored publications is maintained by the British Library Lending Division, Boston Spa, Wetherby, Yorkshire, England for public access. The British Library Lending Division also has available many of the non-NASA publications cited in *STAR*. European requesters may purchase facsimile copy or microfiche of NASA and NASA-sponsored documents, those identified by both the symbols # and * from ESA — Information Retrieval Service European Space Agency, 8-10 rue Mario-Nikis, 75738 CEDEX 15, France.

SUBMITTING DOCUMENTS

All users of this abstract service are urged to forward reports to be considered for announcement in *STAR*. This will aid NASA in its efforts to provide the fullest possible coverage of all scientific and technical publications that might support aeronautics and space research and development. If you have prepared relevant reports (other than those you will transmit to NASA, DOD, or DOE through the

usual contract- or grant-reporting channels), please send them for consideration to the NASA Center for AeroSpace Information, 800 Elkridge Landing Road, Linthicum Heights, MD 21090-2934.

Reprints of journal articles, book chapters, and conference papers are also welcome. These will be considered for announcement in *STAR's* companion journal, *NOVA*.

You may specify a particular source to be included in a report announcement if you wish; otherwise the report will be placed on a public sale at the NASA Center for AeroSpace Information. Copyrighted publications will be announced but not distributed or sold.

PURCHASE OF *STAR*

STAR is publicly available on annual subscription from the NASA Center for AeroSpace Information (CASI). 1995 *STAR* subscription prices are $100.00/domestic and $125.00/foreign. Single copy prices: $33.00/domestic, $41.00/foreign.

An annual, cumulative *STAR Index* is also available at $70.00/domestic and foreign.

STAR is available to registered users on annual subscription from the NASA Center for AeroSpace Information, ATTN: Registration Services, 800 Elkridge Landing Road, Linthicum Heights, MD 21090-2934.

ADDRESSES OF ORGANIZATIONS

British Library Lending Division
Boston Spa, Wetherby, Yorkshire
England

Commissioner of Patents and Trademarks
U.S. Patent and Trademark Office
Washington, DC 20231

Department of Energy
Technical Information Center
P.O. Box 62
Oak Ridge, TN 37830

European Space Agency-
Information Retrieval Service ESRIN
Via Galileo Galilei
00044 Frascati (Rome) Italy

Engineering Sciences Data Unit International
P.O. Box 1633
Manassas, VA 22110

Engineering Sciences Data Unit
International, Ltd.
251-259 Regent Street
London, W1R 7AD, England

Fachinformationszentrum Karlsruhe
Gesellschaft für wissenschaftlich-technische
Information mbH
76344 Eggenstein-Leopoldshafen, Germany

Her Majesty's Stationery Office
P.O. Box 569, S.E. 1
London, England

NASA Center for AeroSpace Information
800 Elkridge Landing Road
Linthicum Heights, MD 21090-2934

National Aeronautics and Space Administration
Scientific and Technical Information Office
(JTT)
Washington, DC 20546-0001

National Technical Information Service
5285 Port Royal Road
Springfield, VA 22161

Pendragon House, Inc.
899 Broadway Avenue
Redwood City, CA 94063

Superintendent of Documents
U.S. Government Printing Office
Washington, DC 20402

University Microfilms
A Xerox Company
300 North Zeeb Road
Ann Arbor, MI 48106

University Microfilms, Ltd.
Tylers Green
London, England

U.S. Geological Survey Library National Center
MS 950
12201 Sunrise Valley Drive
Reston, VA 22092

U.S. Geological Survey Library
2255 North Gemini Drive
Flagstaff, AZ 86001

U.S. Geological Survey
345 Middlefield Road
Menlo Park, CA 94025

U.S. Geological Survey Library
Box 25046
Denver Federal Center, MS914
Denver, CO 80225

NASA CASI PRICE CODE TABLE

(Effective January 1, 1995)

CASI PRICE CODE	NORTH AMERICAN PRICE	FOREIGN PRICE
A01	$ 6.00	$ 12.00
A02	9.00	18.00
A03	17.50	35.00
A04-A05	19.50	39.00
A06-A09	27.00	54.00
A10-A13	36.50	73.00
A14-A17	44.50	89.00
A18-A21	52.00	104.00
A22-A25	61.00	122.00
A99	Call For Price	Call For Price

IMPORTANT NOTICE

For users not registered at the NASA CASI, prepayment is required. Additionally, a shipping and handling fee of $1.00 per document for delivery within the United States and $9.00 per document for delivery outside the United States is charged.

For users registered at the NASA CASI, document orders may be invoiced at the end of the month, charged against a deposit account, or paid by check or credit card. NASA CASI accepts American Express, Diners' Club, MasterCard, and VISA credit cards. There are no shipping and handling charges. To register at the NASA CASI, please request a registration form through the NASA Access Help Desk at the address or numbers below.

NASA Center for AeroSpace Information
800 Elkridge Landing Road
Linthicum Heights, MD 21090-2934
Telephone: (301) 621-0390
E-mail: help@sti.nasa.gov
Fax: (301) 621-0134

FEDERAL REGIONAL DEPOSITORY LIBRARIES

ALABAMA

AUBURN UNIV. AT MONTGOMERY LIBRARY
Documents Dept.
7300 University Dr.
Montgomery, AL 36117-3596
(205) 244-3650 Fax: (205) 244-0678

UNIV. OF ALABAMA
Amelia Gayle Gorgas Library
Govt. Documents
P.O. Box 870266
Tuscaloosa, AL 35487-0266
(205) 348-6046 Fax: (205) 348-0760

ARIZONA

DEPT. OF LIBRARY, ARCHIVES, AND PUBLIC RECORDS
Research Division
Third Floor, State Capitol
1700 West Washington
Phoenix, AZ 85007
(602) 542-3701 Fax: (602) 542-4400

ARKANSAS

ARKANSAS STATE LIBRARY
State Library Service Section
Documents Service Section
One Capitol Mall
Little Rock, AR 72201-1014
(501) 682-2053 Fax: (501) 682-1529

CALIFORNIA

CALIFORNIA STATE LIBRARY
Govt. Publications Section
P.O. Box 942837 - 914 Capitol Mall
Sacramento, CA 94337-0091
(916) 654-0069 Fax: (916) 654-0241

COLORADO

UNIV. OF COLORADO - BOULDER
Libraries - Govt. Publications
Campus Box 184
Boulder, CO 80309-0184
(303) 492-8834 Fax: (303) 492-1881

DENVER PUBLIC LIBRARY
Govt. Publications Dept. BSG
1357 Broadway
Denver, CO 80203-2165
(303) 640-8846 Fax: (303) 640-8817

CONNECTICUT

CONNECTICUT STATE LIBRARY
231 Capitol Avenue
Hartford, CT 06106
(203) 566-4971 Fax: (203) 566-3322

FLORIDA

UNIV. OF FLORIDA LIBRARIES
Documents Dept.
240 Library West
Gainesville, FL 32611-2048
(904) 392-0366 Fax: (904) 392-7251

GEORGIA

UNIV. OF GEORGIA LIBRARIES
Govt. Documents Dept.
Jackson Street
Athens, GA 30602-1645
(706) 542-8949 Fax: (706) 542-4144

HAWAII

UNIV. OF HAWAII
Hamilton Library
Govt. Documents Collection
2550 The Mall
Honolulu, HI 96822
(808) 948-8230 Fax: (808) 956-5968

IDAHO

UNIV. OF IDAHO LIBRARY
Documents Section
Rayburn Street
Moscow, ID 83844-2353
(208) 885-6344 Fax: (208) 885-6817

ILLINOIS

ILLINOIS STATE LIBRARY
Federal Documents Dept.
300 South Second Street
Springfield, IL 62701-1796
(217) 782-7596 Fax: (217) 782-6437

INDIANA

INDIANA STATE LIBRARY
Serials/Documents Section
140 North Senate Avenue
Indianapolis, IN 46204-2296
(317) 232-3679 Fax: (317) 232-3728

IOWA

UNIV. OF IOWA LIBRARIES
Govt. Publications
Washington & Madison Streets
Iowa City, IA 52242-1166
(319) 335-5926 Fax: (319) 335-5900

KANSAS

UNIV. OF KANSAS
Govt. Documents & Maps Library
6001 Malott Hall
Lawrence, KS 66045-2800
(913) 864-4660 Fax: (913) 864-3855

KENTUCKY

UNIV. OF KENTUCKY
King Library South
Govt. Publications/Maps Dept.
Patterson Drive
Lexington, KY 40506-0039
(606) 257-3139 Fax: (606) 257-3139

LOUISIANA

LOUISIANA STATE UNIV.
Middleton Library
Govt. Documents Dept.
Baton Rouge, LA 70803-3312
(504) 388-2570 Fax: (504) 388-6992

LOUISIANA TECHNICAL UNIV.
Prescott Memorial Library
Govt. Documents Dept.
Ruston, LA 71272-0046
(318) 257-4962 Fax: (318) 257-2447

MAINE

UNIV. OF MAINE
Raymond H. Fogler Library
Govt. Documents Dept.
Orono, ME 04469-5729
(207) 581-1673 Fax: (207) 581-1653

MARYLAND

UNIV. OF MARYLAND - COLLEGE PARK
McKeldin Library
Govt. Documents/Maps Unit
College Park, MD 20742
(301) 405-9165 Fax: (301) 314-9416

MASSACHUSETTS

BOSTON PUBLIC LIBRARY
Govt. Documents
666 Boylston Street
Boston, MA 02117-0286
(617) 536-5400, ext. 226
Fax: (617) 536-7758

MICHIGAN

DETROIT PUBLIC LIBRARY
5201 Woodward Avenue
Detroit, MI 48202-4093
(313) 833-1025 Fax: (313) 833-0156

LIBRARY OF MICHIGAN
Govt. Documents Unit
P.O. Box 30007
717 West Allegan Street
Lansing, MI 48909
(517) 373-1300 Fax: (517) 373-3381

MINNESOTA

UNIV. OF MINNESOTA
Govt. Publications
409 Wilson Library
309 19th Avenue South
Minneapolis, MN 55455
(612) 624-5073 Fax: (612) 626-9353

MISSISSIPPI

UNIV. OF MISSISSIPPI
J.D. Williams Library
106 Old Gym Bldg.
University, MS 38677
(601) 232-5857 Fax: (601) 232-7465

MISSOURI

UNIV. OF MISSOURI - COLUMBIA
106B Ellis Library
Govt. Documents Sect.
Columbia, MO 65201-5149
(314) 882-6733 Fax: (314) 882-8044

MONTANA

UNIV. OF MONTANA
Mansfield Library
Documents Division
Missoula, MT 59812-1195
(406) 243-6700 Fax: (406) 243-2060

NEBRASKA

UNIV. OF NEBRASKA - LINCOLN
D.L. Love Memorial Library
Lincoln, NE 68588-0410
(402) 472-2562 Fax: (402) 472-5131

NEVADA

THE UNIV. OF NEVADA LIBRARIES
Business and Govt. Information Center
Reno, NV 89557-0044
(702) 784-6579 Fax: (702) 784-1751

NEW JERSEY

NEWARK PUBLIC LIBRARY
Science Div. - Public Access
P.O. Box 630
Five Washington Street
Newark, NJ 07101-7812
(201) 733-7782 Fax: (201) 733-5648

NEW MEXICO

UNIV. OF NEW MEXICO
General Library
Govt. Information Dept.
Albuquerque, NM 87131-1466
(505) 277-5441 Fax: (505) 277-6019

NEW MEXICO STATE LIBRARY
325 Don Gaspar Avenue
Santa Fe, NM 87503
(505) 827-3824 Fax: (505) 827-3888

NEW YORK

NEW YORK STATE LIBRARY
Cultural Education Center
Documents/Gift & Exchange Section
Empire State Plaza
Albany, NY 12230-0001
(518) 474-5355 Fax: (518) 474-5786

NORTH CAROLINA

UNIV. OF NORTH CAROLINA - CHAPEL HILL
Walter Royal Davis Library
CB 3912, Reference Dept.
Chapel Hill, NC 27514-8890
(919) 962-1151 Fax: (919) 962-4451

NORTH DAKOTA

NORTH DAKOTA STATE UNIV. LIB.
Documents
P.O. Box 5599
Fargo, ND 58105-5599
(701) 237-8886 Fax: (701) 237-7138

UNIV. OF NORTH DAKOTA
Chester Fritz Library
University Station
P.O. Box 9000 - Centennial and University Avenue
Grand Forks, ND 58202-9000
(701) 777-4632 Fax: (701) 777-3319

OHIO

STATE LIBRARY OF OHIO
Documents Dept.
65 South Front Street
Columbus, OH 43215-4163
(614) 644-7051 Fax: (614) 752-9178

OKLAHOMA

OKLAHOMA DEPT. OF LIBRARIES
U.S. Govt. Information Division
200 Northeast 18th Street
Oklahoma City, OK 73105-3298
(405) 521-2502, ext. 253
Fax: (405) 525-7804

OKLAHOMA STATE UNIV.
Edmon Low Library
Stillwater, OK 74078-0375
(405) 744-6546 Fax: (405) 744-5183

OREGON

PORTLAND STATE UNIV.
Branford P. Millar Library
934 Southwest Harrison
Portland, OR 97207-1151
(503) 725-4123 Fax: (503) 725-4524

PENNSYLVANIA

STATE LIBRARY OF PENN.
Govt. Publications Section
116 Walnut & Commonwealth Ave.
Harrisburg, PA 17105-1601
(717) 787-3752 Fax: (717) 783-2070

SOUTH CAROLINA

CLEMSON UNIV.
Robert Muldrow Cooper Library
Public Documents Unit
P.O. Box 343001
Clemson, SC 29634-3001
(803) 656-5174 Fax: (803) 656-3025

UNIV. OF SOUTH CAROLINA
Thomas Cooper Library
Green and Sumter Streets
Columbia, SC 29208
(803) 777-4841 Fax: (803) 777-9503

TENNESSEE

UNIV. OF MEMPHIS LIBRARIES
Govt. Publications Dept.
Memphis, TN 38152-0001
(901) 678-2206 Fax: (901) 678-2511

TEXAS

TEXAS STATE LIBRARY
United States Documents
P.O. Box 12927 - 1201 Brazos
Austin, TX 78701-0001
(512) 463-5455 Fax: (512) 463-5436

TEXAS TECH. UNIV. LIBRARIES
Documents Dept.
Lubbock, TX 79409-0002
(806) 742-2282 Fax: (806) 742-1920

UTAH

UTAH STATE UNIV.
Merrill Library Documents Dept.
Logan, UT 84322-3000
(801) 797-2678 Fax: (801) 797-2677

VIRGINIA

UNIV. OF VIRGINIA
Alderman Library
Govt. Documents
University Ave. & McCormick Rd.
Charlottesville, VA 22903-2498
(804) 824-3133 Fax: (804) 924-4337

WASHINGTON

WASHINGTON STATE LIBRARY
Govt. Publications
P.O. Box 42478
16th and Water Streets
Olympia, WA 98504-2478
(206) 753-4027 Fax: (206) 586-7575

WEST VIRGINIA

WEST VIRGINIA UNIV. LIBRARY
Govt. Documents Section
P.O. Box 6069 - 1549 University Ave.
Morgantown, WV 26506-6069
(304) 293-3051 Fax: (304) 293-6638

WISCONSIN

ST. HIST. SOC. OF WISCONSIN LIBRARY
Govt. Publication Section
816 State Street
Madison, WI 53706
(608) 264-6525 Fax: (608) 264-6520

MILWAUKEE PUBLIC LIBRARY
Documents Division
814 West Wisconsin Avenue
Milwaukee, WI 53233
(414) 286-3073 Fax: (414) 286-8074

*U.S. GOVERNMENT PRINTING OFFICE: 1995-387-253/20004

SCAN Goes Electronic!

If you have NASA Mail or if you can access the Internet, you can get biweekly issues of *SCAN* delivered to your desk—top absolutely free!

Electronic SCAN takes advantage of computer technology to alert you to the latest aerospace-related, worldwide scientific and technical information that has been published.

No more waiting while the paper copy is printed and mailed to you. You can review *Electronic SCAN* the same day it is released! And you get all 191—or any combination of—subject areas of announcements with abstracts to browse at your leisure. When you locate a publication of interest, you can print the announcement or electronically add it to your publication order list.

Electronic SCAN
Timely
Flexible
Complete
Free!

Start your free access to *Electronic SCAN* today. Over 1,000 announcements of new reports, books, conference proceedings, journal articles . . . and more—delivered to your computer every two weeks.

For instant access via Internet:
ftp.sti.nasa.gov
gopher.sti.nasa.gov
listserv@sti.nasa.gov

For additional information:
e-mail: help@sti.nasa.gov
scan@sti.nasa.gov
(Enter this address on the "To" line. Leave the subject line blank and send. You will receive an automatic reply with instructions in minutes.)

Phone: (301) 621-0390 Fax: (301) 621-0134

Write: NASA Access Help Desk
NASA STI Office
NASA Center for AeroSpace Information
800 Elkridge Landing Road
Linthicum Heights, MD 21090-2934

National Aeronautics and Space Administration
Scientific and Technical Information Office

4/95
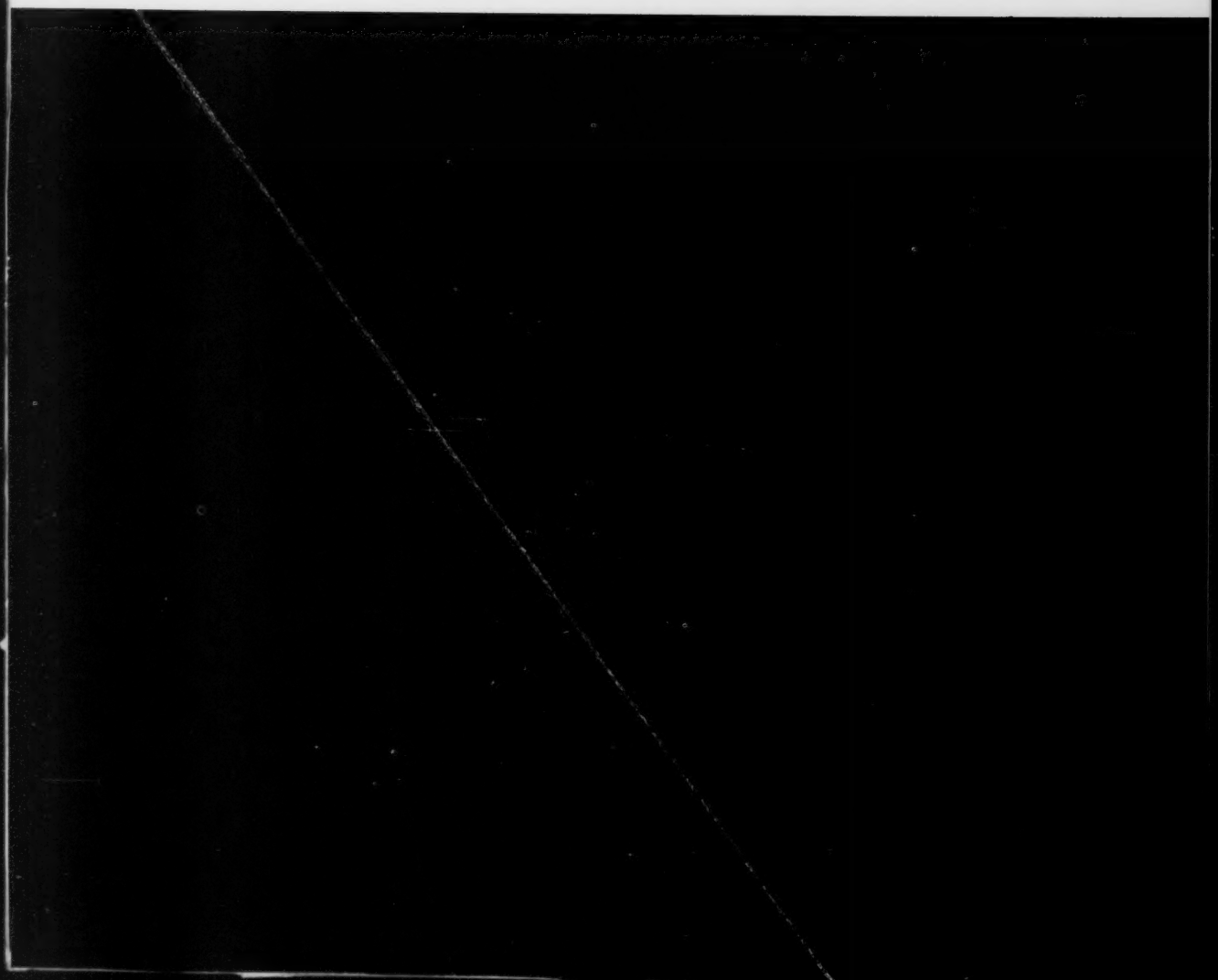
National Aeronautics and
Space Administration
Code JTT
Washington, DC 20546-0001